NUCLEAR SCIENCE ABSTRACTS

Volume 25 Number 9

Abstracts 18334-20905

May 15, 1971

UNITED STATES ATOMIC ENERGY COMMISSION
Division of Technical Information

XUM

REPORT COLLECTIONS IN THE UNITED STATES

The libraries listed below purchase and maintain microfiche collections of USAEC and foreign reports that are abstracted in *NSA*. Their collections also include *NSA* and its indexes, AEC's Technical Progress Reviews, AEC-sponsored translations, conference proceedings published by AEC, and various bibliographic tools. Most of these libraries have microfiche reader-printers or other photocopy facilities with which to reproduce enlarged copies from microfiche. Charges for reproduction services vary.

ALABAMA
Auburn, Auburn University
Tuskegee Institute, Tuskegee Institute

ALASKA
College, University of Alaska

ARIZONA
Tucson, University of Arizona

ARKANSAS
Fayetteville, University of Arkansas

CALIFORNIA
Davis, University of California
Los Angeles, University of California

COLORADO
Boulder, University of Colorado

DISTRICT OF COLUMBIA
Washington, Library of Congress (by deposit)

FLORIDA
Gainesville, University of Florida

GEORGIA
Atlanta, Georgia Institute of Technology

HAWAII
Honolulu, University of Hawaii

IDAHO
Pocatello, Idaho State University

ILLINOIS
Evanston, Northwestern University
Urbana, University of Illinois

INDIANA
Lafayette, Purdue University

IOWA
Ames, Iowa State University

KANSAS
Manhattan, Kansas State University

KENTUCKY
Lexington, University of Kentucky
Louisville, University of Louisville

LOUISIANA
Baton Rouge, Louisiana State University
New Orleans, Tulane University

MARYLAND
Baltimore, Johns Hopkins University
College Park, University of Maryland

MASSACHUSETTS
Cambridge, Massachusetts Institute of Technology
Worcester, Worcester Polytechnic Institute

MICHIGAN
Ann Arbor, University of Michigan

MISSISSIPPI
State College, Mississippi State University

MISSOURI
Kansas City, Linda Hall Library

NEVADA
Las Vegas, University of Nevada

NEW JERSEY
Princeton, Princeton University

NEW MEXICO
Albuquerque, University of New Mexico

NEW YORK
Albany, New York State Library
Albany, State University at Albany
Buffalo, State University of New York at Buffalo
Ithaca, Cornell University
New York, Columbia University
Rochester, University of Rochester
Syracuse, Syracuse University
Troy, Rensselaer Polytechnic Institute

NORTH CAROLINA
Raleigh, North Carolina State University

OHIO
Cincinnati, University of Cincinnati
Cleveland, Cleveland Public Library
Columbus, Ohio State University
Toledo, University of Toledo

OKLAHOMA
Norman, University of Oklahoma

PENNSYLVANIA
Philadelphia, University of Pennsylvania
Pittsburgh, Carnegie Library
University Park, Pennsylvania State University

PUERTO RICO
San Juan, University of Puerto Rico

SOUTH CAROLINA
Columbia, University of South Carolina

TENNESSEE
Knoxville, University of Tennessee
Nashville, Joint University Libraries
Oak Ridge, Oak Ridge Associated Universities

TEXAS
Austin, University of Texas
College Station, Texas A & M University
Houston, Rice University

UTAH
Salt Lake City, University of Utah

VIRGINIA
Blacksburg, Virginia Polytechnic Institute
Charlottesville, University of Virginia

WASHINGTON
Pullman, Washington State University
Seattle, University of Washington

WEST VIRGINIA
Morgantown, West Virginia University

WISCONSIN
Madison, University of Wisconsin

WYOMING
Laramie, University of Wyoming

The following governmental and international organizations offer for sale USAEC reports abstracted in *Nuclear Science Abstracts:*

National Technical Information Service, U. S. Department of Commerce
Springfield, Virginia 22151
International Atomic Energy Agency, Vienna, Austria
National Lending Library, Boston Spa, England

Volume 25, Number 9, May 15, 1971

NUCLEAR SCIENCE ABSTRACTS

A semimonthly publication of the USAEC Division of Technical Information, Edward J. Brunenkant, Director,
Published by the USAEC Division of Technical Information Extension, Robert L. Shannon, Extension Manager.

Nuclear Science Abstracts provides the only comprehensive abstracting and indexing coverage of international nuclear science literature. *Nuclear Science Abstracts* covers scientific and technical reports of the U. S. Atomic Energy Commission and its contractors, other U. S. Government agencies, other governments, universities, and industrial and research organizations. In addition, books, conference proceedings, individual conference papers, patents, and journal literature on a worldwide basis are abstracted and indexed. Each issue of *Nuclear Science Abstracts* includes four indexes: subject, personal author, corporate author, and report number.

The following organizations scan and abstract the nuclear science literature in their respective countries:

Atomic Energy of Canada Limited
Australian Atomic Energy Commission
Danish Atomic Energy Commission
Finnish Atomic Energy Commission
French Atomic Energy Commission
Japan Atomic Energy Bureau–Atomic Energy Research Institute
Institutt for Atomenergi (Norway)
Aktiebolaget Atomenergi (Sweden)
United Kingdom Atomic Energy Authority

Numerous organizations, societies, and publishers throughout the world provide *Nuclear Science Abstracts* with advance page-proof copy of their publications, e.g., in the United States the American Institute of Physics provides page-proof copy of its publications.

A list of the journals scanned regularly and the abbreviations used appears in Issue 1 (January 15) of each volume of *Nuclear Science Abstracts* and is supplemented in Issues 7, 13, and 19. Issue 1 of each volume also describes the scope and arrangement of the subject matter covered in *Nuclear Science Abstracts.* The subject matter covered is also described in TID-4552, *Subject Scope of Nuclear Science Abstracts,* available free from the USAEC Division of Technical Information Extension, P.O. Box 62, Oak Ridge, Tennessee 37830. An outline of the subject categories appears in the Contents of each issue.

AVAILABILITY OF PUBLICATIONS ABSTRACTED

Public availability of all U. S. Atomic Energy Commission reports is indicated in the report number indexes. The availability of other reports, when known, is also indicated. The availability of some unnumbered reports is given in the abstract.

Dissertations abstracted in *Dissertation Abstracts* and included in *Nuclear Science Abstracts* are available from University Microfilms, Inc., 315 N. First Street, Ann Arbor, Michigan 48103.

Information on the availability of the published literature and unpublished conference papers abstracted in *Nuclear Science Abstracts* can be obtained from the USAEC Division of Technical Information Extension, P.O. Box 62, Oak Ridge, Tennessee 37830.

HOW TO OBTAIN NUCLEAR SCIENCE ABSTRACTS

Nuclear Science Abstracts is available to the public on a subscription basis from the Superintendent of Documents, U. S. Government Printing Office, Washington, D. C. 20402.

For the 24 regular issues, the yearly rate is $42.00 for domestic subscribers and $52.50 for foreign subscribers. A single issue costs $1.75, domestic rates, or $2.19, foreign rates. Domestic rates apply to the United States, Canada, Mexico, and Central and South American countries except Argentina, Brazil, Guyana, French Guiana, Surinam, and British Honduras.

For a yearly subscription to the cumulative indexes, the rates are $38.00 for domestic subscribers and $47.50 for foreign subscribers.

The following cumulative indexes are available:

From Johnson Reprint Corporation, 111 Fifth Avenue, New York, N. Y. 10003:
Vols. 1–4, Subjects and Authors (1948–1950), $30.00.

From Superintendent of Documents, U. S. Government Printing Office, Washington, D. C. 20402:

Vols. 5–10, Subjects and Authors (1951–1956), $5.25.

Vols. 11–15, Subjects (1957–1961), $19.00.
Vols. 11–15, Personal Authors (1957–1961), $14.25.
Vols. 11–15, Corporate Authors (1957–1961), $2.50.

Vols. 16–20, Subjects (1962–1966), $36.00.
Vols. 16–20, Personal Authors (1962–1966), $22.50.
Vols. 16–20, Corporate Authors (1962–1966), $3.75.

Vol. 21, Subjects and Authors (1967), $16.00.
Vol. 22, Subjects and Authors (1968), $26.00.
Vol. 23, Subjects and Authors (1969), $25.75.
Vol. 24, Subjects and Authors (1970), $22.50.

Cumulative Report Number Index, Vols. 1-15 Revised, $4.00.
Cumulative Report Number Index, Vols. 16-20 Revised, $5.50.
Cumulative Report Number Index, Vols. 21-24, $4.25.

Nuclear Science Abstracts is available on an exchange basis to universities, research institutions, industrial firms, and publishers of scientific information. Government agencies may obtain *NSA* free of charge. Inquiries should be directed to the USAEC Division of Technical Information Extension, P. O. Box 62, Oak Ridge, Tennessee 37830.

XUM

INDEXES TO NSA

Comprehensive indexes appear in each issue and are cumulated quarterly and annually. Multivolume cumulations have been issued as indicated above.

All documents abstracted are indexed by subjects and personal authors. Report literature is indexed also by corporate author and report number. Each of these indexes in every issue is preceded by an introduction explaining in detail the organization of the index and the principles by which it is compiled. The reader is referred to these explanations for information not found in the brief summary below.

Personal Authors

Each author's name is indexed in the form appearing on the document abstracted:

ISHIHARA, T., Accumulation of fallout ^{137}Cs in newborn infants, 23:50538
ISHIHARA, Toyokuki, Shielding effect of paraffin, water, soil, concrete, Fe, and Pb for high-energy neutrons, 23:51748

Subjects

The subject index consisting of specific materials, objects, and processes is arranged alphabetically. Modifying phrases specific to these subjects in turn are arranged alphabetically under the subjects.

MELPHALAN
  effects on proliferation of cultured antigen-stimulated spleen cells from mice, dose-response curve for, 23:50820
MEMBRANE FILTERS
  design for removal of cell-free Streptococcus faecalus from bacteria cultures in fermentation tank, 23:49996 (UCRL-18667, pp 322-9)
MENDELEVIUM
  separation from einsteinium and fermium by electrolysis, 23:49772 (UCRL-18667, pp 277-312)
  separation from sodium acetate solutions by solvent extraction using sodium amalgam, 23:49772 (UCRL-18667, pp 277-312)
  stability of divalent state of, 23:49772 (UCRL-18667, pp 277-312)

Corporate Authors

Technical report literature is indexed from the name of the organization or institution responsible for the issuance of the report.

51093 (LA-4164) FABRICATION OF BORON CARBIDE RINGS AND DISKS. Sheinberg, H.; Herrera, T.; Kostacopoulos, J. **(Los Alamos Scientific Lab., N. Mex.).** Apr. 25, 1969. Contract W-7405-eng-36. 11p. Dep. CFSTI.

is indexed as:

LOS ALAMOS SCIENTIFIC LAB., N. MEX.
  Fabrication of boron carbide rings and disks, 23:51093 (LA-4164)

Report Numbers

Technical report literature is also indexed by report numbers. This index includes information on where individual reports may be obtained. While not reports, patents and conference papers are indexed here as a matter of convenience.

JPRS-	**(Non-AEC)**	
46949	**23-51587**	**CFSTI**
48330	**23-52305**	**CFSTI**
48331	**23-52451**	**CFSTI**
48481	**23-50889**	**CFSTI**
48743	**23-51034**	**CFSTI**
49025	**23-51706**	**CFSTI (U. S. Sales Only)**
JUL-	**(German)**	
571-RG	**23-52269**	**Dep**
578-PP	**23-51624**	**Dep. CFSTI (U. S. Sales Only)**
581-FN	**23-51079**	**Dep. CFSTI (U. S. Sales Only)**
584-RG	**23-52313**	**Dep**
586-FN	**23-51035**	**Dep. CFSTI (U. S. Sales Only)**
K-		
1777	**23-50987**	**Dep. CFSTI**
1778	**23-50988**	**Dep. CFSTI**
KFK-	**(German)**	
743	**23-52461**	**Dep**
743	**23-52447**	**For translation see EURFNR-613**
781/I	**23-52462**	**Dep**
824	**23-52397**	**Dep. CFSTI (U. S. Sales Only)**

TABLE OF CONTENTS

Volume 25, Number 9, May 15, 1971

Category *Page*

CHEMISTRY 1803
- Analytical Chemistry 1803
  - *Chemical and Spectral Procedures* 1803
  - *Isotope Dilution Procedures* 1805
  - *Radiometric and Radiochemical Procedures* 1805
  - *Activation Procedures* 1806
- Inorganic, Organic, and Physical Chemistry 1806
  - *Chemical Properties* 1806
  - *Isotope Effects and Exchange* 1808
  - *Physical Chemistry* 1812
- Radiation and Nuclear Chemistry 1812
  - *Radiation Effects* 1812
  - *Radiation Processes* 1813
  - *Radiolysis* 1816
  - *Radioisotope Production* 1819
  - *Recoil Production and Reactions* 1819
- Radiochemistry 1820
- Separation Processes 1820

EARTH SCIENCES 1824
- Geology and Hydrology 1824
- Meteorology 1824
- Mineralogy and Exploration 1824
- Oceanography 1829
- Seismology 1829

ENGINEERING 1830
- Nuclear Explosions 1830
- Facilities and Equipment 1830
- Heat Transfer and Fluid Flow 1831
- Isotope Technology 1833
- Materials Testing 1835
- Radioactive Material Handling 1836
- Vacuum Engineering 1838

INSTRUMENTATION 1839
- Radiation Detection Instruments 1839
  - *General Detectors and Monitors* 1839
  - *Nuclear Spectroscopic Instrumentation* 1847
  - *High Energy Physics Instrumentation* 1851
- Radiation Dosimeters 1853
- Radiometric Instruments 1854
- Miscellaneous Instruments and Components 1856
- Radiation Effects on Instruments and Instrument Components 1860

LIFE SCIENCES 1861
- Biochemistry, Physiology, and Molecular Biology 1861
  - *Basic Processes* 1861
  - *Metabolism, Physiology, and Toxicology* 1861
  - *Radiation Effects* 1863
  - *Immunology* 1865
- Ecology 1866
- Genetics and Cytogenetics 1868
- Health Physics and Safety 1872
  - *Radioactive Contamination and Decontamination* 1872
  - *Dosimetry and Monitoring* 1872
  - *Radiation Protection* 1876
  - *Safety Procedures* 1876

Category *Page*

LIFE SCIENCES (Cont'd.)

  - *Legal Aspects* 1877
- Medicine 1877
  - *Protective Substances* 1877
  - *Radiation Sickness and Injuries* 1878
  - *Radiodiagnosis* 1879
  - *Radiotherapy* 1881
  - *Blast and Thermal Effects* 1884
- Radiation Effects on Animals 1884
  - *Invertebrates* 1884
  - *Vertebrates* 1885
  - *Man* 1889
- Radiation Effects on Plants 1891
- Radiation Effects on Microorganisms 1891
- Radiosterilization and Radiopreservation 1892

METALS, CERAMICS, AND OTHER MATERIALS 1893
- Metals and Alloys 1893
  - *Corrosion and Erosion* 1893
  - *Preparation and Fabrication* 1894
  - *Properties Evaluations* 1895
  - *Structure and Phase Studies* 1899
  - *Radiation Effects* 1901
- Ceramics and Cermets 1902
  - *Corrosion and Erosion* 1902
  - *Preparation and Fabrication* 1902
  - *Properties Evaluations* 1904
  - *Structure and Phase Studies* 1905
  - *Radiation Effects* 1905
- Plastics and Other Materials 1906

PHYSICS (GENERAL) 1907
- Astrophysics and Cosmology 1907
  - *Cosmic Ray Exposure Ages* 1907
  - *Stars* 1907
  - *Quasi-Stellar, Radio, and X-Ray Sources* 1911
  - *Solar Phenomena* 1915
  - *Galaxies* 1920
  - *Cosmology* 1922
  - *Planetary Phenomena* 1923
- Atomic and Molecular Physics 1923
  - *Atomic, Electron, Ion, and Molecular Beams and Their Reactions* 1923
  - *Atomic and Molecular Properties* 1923
  - *Positronium, Muonium, and Mesic Atoms and Molecules* 1924
  - *Collision Phenomena* 1925
  - *Atomic Theory* 1927
- Cosmic Radiation 1928
- Direct Energy Conversion 1929
- Fluid Physics 1930
- Geophysics (Upper Atmosphere) 1933
- Low-Temperature Physics and Cryogenic Equipment 1934
  - *Superfluidity* 1934
  - *Superconductivity* 1934
  - *Equipment and Devices* 1939
- Plasma and Thermonuclear Physics 1940
  - *Confinement and Heating* 1940
  - *Diagnostics* 1941

XUM

TABLE OF CONTENTS (continued)

Category *Page*

PHYSICS (GENERAL) (Cont'd.)

- *Kinetics (General)* 1941
- *Kinetics (Experimental)* 1942
- *Kinetics (Theoretical)* 1942
- *Production* 1944
- *Stability* 1945
- *Thermonuclear Processes* 1947
- *Wave Phenomena* 1947

Shielding 1950

Solid-State Physics 1951
- *Radiation Effects* 1951
- *Physical Properties* 1965
- *Moessbauer Effects and NMR* 1966

Theoretical Physics 1967

PHYSICS (HIGH-ENERGY) 1968

Particle Interactions and Properties (Experimental) . . . 1968
- *Electromagnetic* 1968
- *Weak* 1968
- *Strong (Baryon-Induced)* 1969
- *Strong (Meson-Induced)* 1970

Particle Interactions and Properties (Theoretical) 1971
- *General* 1971
- *Electromagnetic* 1972
- *Weak* 1975
- *Strong (General)* 1975
- *Strong (Baryon No. = 0)* 1977
- *Strong (Baryon No. = 1)* 1978
- *Strong (Baryon No. ≥ 2)* 1979

Particle Invariance Principles and Symmetries 1981
- *General* 1981
- *Applications (Electromagnetic and Weak)* 1981
- *Applications (Strong)* 1982

Field Theories 1982
- *General* 1982
- *Quantum Field Theory* 1983
- *Gravitation and General Relativity* 1985

Scattering Theory 1987

Particle Accelerators 1989

PHYSICS (NUCLEAR) 1997

Neutron Interactions with Matter 1997

Nuclear Properties and Reactions, A ≤ 5 1998

PHYSICS (NUCLEAR) (Cont'd.)

Nuclear Properties and Reactions, 6 ≤ A ≤ 19 2000

Nuclear Properties and Reactions, 20 ≤ A ≤ 89 2005

Nuclear Properties and Reactions, A ≥ 90 2010

Nuclear Theory 2021

REACTOR TECHNOLOGY 2029

Commercial Power Reactors 2029
- *Operation and Economics* 2030
- *Safety and Siting* 2031
- *Steam and Power Conversion Systems* 2035

Power Reactor Development 2035
- *Kinetics and Dynamics* 2037
- *Control Systems* 2037
- *Shielding* 2038
- *Cooling Systems* 2038
- *Fuels* 2039
- *Auxiliary and Emergency Systems* 2040
- *Operation and Economics* 2040
- *Safety and Siting* 2041
- *Power Conversion Systems* 2043

Research and Test Reactors 2044

Rocket and Space Reactors 2047

Process Heat and Desalination Reactors 2047

Marine and Portable Power Reactors 2047

Production Reactors 2048

Reactor Theory 2048
- *Kinetics* 2048
- *Dynamics* 2049
- *Experimental Applications* 2049

Reactor Components, Fuels, and Accessories 2049

GENERAL 2051

CORPORATE AUTHOR INDEX INDEX-1

PERSONAL AUTHOR INDEX INDEX-10

SUBJECT INDEX INDEX-62

REPORT NUMBER INDEX INDEX-154

STAFF OF NUCLEAR SCIENCE ABSTRACTS

John W. Norris
Managing Editor

Donald D. Davis
Assistant Managing Editor

David E. Bost
Production Manager

Sidney F. Lanier
Subject Heading Specialist

J. Paul Meredith
Descriptive Cataloging Specialist

Frederick E. Marsh, Jr.
Computer Index Coordinator

Clara L. Fox
Corporate Author Specialist

Helen W. White
Report Number Specialist

Section Editors

Everett J. Hoffman
Chemistry

Robert C. Kelly
Engineering; Earth Sciences; Metals, Ceramics, and Other Materials

Lee M. Thompson
General Physics

Charles E. Stuber
High Energy Physics; Instrumentation

Donald D. Davis
Life Sciences

Lawrence T. Whitehead
Nuclear Physics

James M. Jacobs
Reactor Technology

Evaluators

Thomas S. Chapman
Rose V. Jermain
John H. Mitchell
Mary H. Newman
Polly C. Summers

Abstractors

F. S. Armstrong*
Ellis R. Bedford
Mary M. Brown
Jane G. Buchanan
D. Lamar Cason
Gloria M. Caton
David C. Cunningham
James R. Dulaney
Helga B. Gerstner
Mary C. Grissom
Phyllis C. Hansen
Carolyn D. Houston
Elaine E. Huber
Rose V. Jermain
W. Hugh Kinser, Jr.
Lisbeth C. Lieberman
Betty L. McDowell
Patricia B. McEwen
Fay M. Martin
William D. Matheny
Dora H. Moneyhun
Jean F. Peckham
Henry D. Raleigh
Mona H. Raridon
Julia S. Redford
Jessie W. Rushing
Robert W. Rutkowski
Francis L. Sachs
Lila B. Smith
Anne G. Ward
Helen L. Ward
Milton O. Whitson
Juanita Wilson

---

*Atomic Energy of Canada, Ltd.

Charles R. Bruce
Publishing Coordinator

Communication concerning the editorial policy and content of *Nuclear Science Abstracts* should be addressed to the Managing Editor, *Nuclear Science Abstracts*, USAEC Division of Technical Information Extension, P. O. Box 62, Oak Ridge, Tennessee 37830.

Use of funds for printing this publication approved by the Director of the Bureau of the Budget, June 26, 1969.

Volume 25, Number 9 May 15, 1971

NUCLEAR SCIENCE ABSTRACTS

CHEMISTRY

Analytical Chemistry

Refer also to abstracts 18870 and 19166.

18334 (CONF-680946-(Absts.)) III POLISH ANALYTICAL CONFERENCE, WARSAW, 10-14 SEPTEMBER 1968. (International Union of Pure and Applied Chemistry). 76p. (In Polish and English).

Abstracts of papers presented at the Polish Analytical Conference in Warsaw September 10-14, 1968 are presented as four sections: general problems; analysis of inorganic substances; analysis of organic substances; and techniques of analytical chemistry. (D.H.M.)

18335 BARIUM AND STRONTIUM IN SILICATES. A STUDY ON THE DEVELOPMENT OF ANALYTICAL METHODS. Ingamells, C. O.; Suhr, N. H.; Tan, F. C.; Anderson, D. H. (Pennsylvania State Univ., University Park). Anal. Chim. Acta; 53: 345-60(Feb 1971).

Barium and strontium in silicates were determined by a number of methods, and their contents in several standard samples are reported. Instrumental techniques evaluated include isotope dilution mass spectrometry, flame emission and absorption spectrometry, emission spectrography and spectrometry, x-ray fluorescence spectrography, and neutron activation analysis. Classical gravimetric methods are reported. Two x-ray fluorescence procedures were used; one involves fusion with lithium metaborate and yields only strontium values. The other uses a direct dilution technique and gives results for both barium and strontium. In practice, this method requires a suite of analyzed standards, which should be generally similar in composition to the unknown. Strontium can be satisfactorily determined by atomic absorption spectrometry in whole-rock solutions, but there are difficulties in determining barium in this way. Emission spectrometry, with a spark-solution technique and automated equipment, gives rapid and accurate results for both barium and strontium. Flame emission spectrometry, neutron activation analysis, and classical gravimetric methods are not satisfactory as practicable routine methods for barium and strontium in silicate rocks. Conclusions are that barium and strontium may be satisfactorily determined by several methods, and that refinement of these methods is possible to the point where sampling error, rather than analytical error, may often determine variance in the results. (auth)

18336 EQUIPMENT FOR SAMPLING SODIUM. Rohde, J. F. M.; Hissink, M.; Bos, L. (Central Tech. Inst. TNO, Delft, Netherlands). J. Nucl. Energ.; 24: 503-8(Dec 1970).

Equipment was developed to obtain sodium samples for analysis from a loop. Five samples in nickel crucibles may be taken at the same time. Before the samples are taken the equipment is cleaned by flushing with liquid sodium. Since sodium shows a tendency to segregate during cooling, special attention must be given to a correct representation of the bulk sodium composition by the samples. Data for oxygen are presented to demonstrate the performance of the equipment. (auth) (UK)

18337 REVERSED-PHASE THIN-LAYER CHROMATOGRAPHY OF A NUMBER OF METAL IONS IN THE SYSTEM AMBERLITE LA-2-MIXTURE OF HYDROCHLORIC ACID AND THIOCYANATE. Kuroda, Rokuro; Oguma, Koichi; Nakamura, Kenji (Univ. of Chiba, Japan). Nippon Kagaku Zasshi; 91: 1155-8(Dec 1970). (In Japanese).

Thin-layer chromatographic behavior of 48 metal ions on cellulose impregnated with Amberlite LA-2 was surveyed by using hydrochloric acid-ammonium thiocyanate mixtures as solvent. The acid concentration was mostly kept constant at 0.5 mole/l while the concentration of thiocyanate, ranging from 0.01 to 1 mole/l, was changed. For selected 18 metal ions R_f's were measured as a function of hydrochloric acid concentration (1 to 6 mole/l), where the concentration of thiocyanate was kept constant at 0.01 mole/l. In contrast to pure ammonium thiocyanate solutions, where many metal ions exhibited extremes of R_f 0 or unity, many more metal ions showed chromatographic distribution in the acid thiocyanate media. Chromatographic behavior of many metal ions as a function of thiocyanate or hydrochloric acid concentration can be explained on the basis of either ion exchange of the thiocyanato (chloro) complex anion or association of a neutral thiocyanato (chloro) complex. When the thiocyanate or hydrochloric acid concentration is properly selected, many useful separations of analytical interest can be accomplished. Thus multicomponent separations like Al-Ga-In-Tl(III), Bi(III)-U(VI)-Cd-Au(III), Ni-Cd-Zn, etc., are illustrated to demonstrate the utilization of R_f measurements. (auth)

Chemical and Spectral Procedures

Refer also to abstracts 18428, 18673, 18826, and 18863.

18338 (CEA-CONF-1725) APPLICATION OF PHOTOELECTRON SPECTROSCOPY TO CHEMICAL ANALYSIS. Lemaire, H. (Commissariat a l'Energie Atomique, Grenoble (France). Centre d'Etudes Nucleaires). 1970. 16p. (In French). (CONF-701036-1). Dep. NTIS (U. S. Sales Only).

From Conference on the Doping of Interstitial Elements and their Influence on the Properties of Metals and Alloys, Grenoble, France.

A renewed interest in the use of electron spectroscopy for chemical analysis (ESCA) results from considerable improvements made in β spectrometer resolution. Irradiation of a material with photons of energy $h\nu$ liberates groups of photoelectrons of kinetic energy C_i given by $C_i = h\nu - L_i$ where L_i is the binding energy of the electrons within the material. The ESCA spectra will thus exhibit as many lines as there are electronic levels with energies less than $h\nu$. In particular, the analysis of deep-lying levels allows quantitative and qualitative analysis of the material under consideration to be made. The entire periodic table, with the exception of hydrogen, can be covered. The positions of the levels vary slightly with the electronic environment of the atoms considered. This property allows the characteristics of the environment to be determined and differences between compounds to be observed. (France)

18339 (CEA-R-3557(2)) ANALYTICAL METHODS USED BY THE GEOCHEMICAL SECTION: WATER. Berthollet, Pierre; Cavalier, Guy (Commissariat a l'Energie Atomique, Fontenay-aux-Roses (France). Centre d'Etudes Nucleaires). Jan 1971. 189p. (In French). Dep. NTIS (U. S. Sales Only).

The analytical methods used by the C.E.A. Geochemical Section to determine the chemical composition of natural waters encountered during prospecting of uraniferous deposits or in the course of mining operations are described. Because of the diversity of the samples and the different items of information requested, methods were selected and adapted to answer to the demands peculiar to mining research. (France)

XUM

18340 (KY-626) ISOTOPIC INTEGRITY FOR UF_6 FIELD SAMPLES. Smith, R. F. (Paducah Gaseous Diffusion Plant, Ky.). 15 Jan 1971. Contract W-7405-eng-26. 8p. Dep. NTIS.

It was concluded that UF_6 cylinders differing in isotopic concentration by a factor of 4.5 may be sampled consecutively on the same system without washing it with steam or water between cylinders. The only cleaning requirement is that the sampling manifold be flushed with approximately 1800 grams of UF_6 at the same isotopic concentration as that next to be sampled. Thus, the UF_6 which is drained to the "discard position" for preserving the uranium measurement integrity will also suffice for cleaning the sampling system isotopically. (auth)

18341 (RT/CHI-(70)14) ANALYSIS OF MICRO CONSTITUENTS IN Zr MATRIX. I. SIMULTANEOUS POLAROGRAPHIC DETERMINATION OF Cu AND Mo WITHOUT PRELIMINARY SEPARATION. Borello, A.; Guidotti, G. R. (Comitato Nazionale per l'Energia Nucleare, Rome (Italy)). 1 Apr 1970. 12p. Dep. NTIS (U. S. Sales Only).

Cu and Mo contained in 0.5% Cu-0.5% Mo-Zr alloys of nuclear interest as fuel jacketing material can be determined by dc polarography without preliminary separation. The Zr alloy is dissolved with 1:1 H_2SO_4 in the presence of HNO_3 and HF as catalyst. After evaporating to copious fumes of SO_3, the residue is diluted with an aqueous solution of 0.5 M H_2SO_4-0.5 M citric acid, which acts as supporting electrolyte. Polarography is then carried out. Two diffusion-controlled waves were obtained due to Mo(VI) to Mo(V) and Cu(II) to Cu(Hg), and Mo(V) to Mo(III) reductions, respectively. Separate calibration curves for Cu (II) and Mo(V) were used in order to calculate both concentrations. The diffusion current for Cu was obtained subtracting one half of Mo(V) diffusion current to the total diffusion current of the first wave. Cu and Mo present in the concentration range 5×10^{-5} to 5×10^{-3} M in the polarographic cell were determined together with a relative error better than ±1.5%. (auth)

18342 1-(2-CARBOXY-4-SULPHONATOPHENYL)-3-HYDROXY-3-PHENYLTRIAZENE AS A SPECTROPHOTOMETRIC REAGENT FOR THE DETERMINATIONS OF COPPER(II) AND PALLADIUM(II) IN PRESENCE OF OTHER IONS AND IN TERNARY MIXTURES WITH IRON, MOLYBDENUM, AND VANADIUM. Majumdar, A. K.; Chakraborti, D. (Jadavpur Univ., Calcutta). Anal. Chim. Acta; 53: 393-400(Feb 1971).

Methods for the spectrophotometric determination of copper(II) and palladium(II) in the presence of other ions and of color-forming metal ions in ternary mixtures were developed with 1-(2-carboxy-4-sulfonatophenyl)-3-hydroxy-3-phenyltriazene as the reagent. The reagent forms 1:2 complexes with both copper(II) and palladium(II) with dissociation constants of the order of 10^{-9} and 10^{-11}, respectively. The systems obey Beer's law with optimal ranges of 0.3-3.0 ppM and 0.4-5.0 ppM; the sensitivities are 0.0043 and 0.0055 $\mu g\ cm^{-2}$ and the molar absorptivities are 15333 and 20222, respectively. The reagent is highly selective for palladium. (auth)

18343 DETECTION OF TRACES OF TRANSITION METALS BY FORMATION OF PEROXY COMPOUNDS AND SORPTION ON A CHELATING RESIN. Maura, Giancarlo; Rinaldi, Gilberto (Univ., Rome). Anal. Chim. Acta; 53: 466-8(Feb 1971).

Formation of colored peroxy compounds permits the detection of traces of some transition elements but when extremely small concentrations are used, the colors are not distinct and are sometimes unstable. However, if the reactions are carried out in the presence of a little white colored chelating resin, the peroxy compounds are adsorbed and concentrated on the resin and their colors are intensified; the sensitivity of the detection reactions is thus improved. Moreover, unstable peroxy compounds (e.g., of chromium and vanadium) are stabilized by sorption on chelating resins. Detection reactions of Ti, V, Cr, Mo, Ce, and U as peroxy compounds and their sensitivity in the presence of Dowex A-1 chelating resin are given. Peroxy compounds of Nb, Ta, and W are not absorbed in similar conditions, because the reagents regenerate the resin. (D.H.M.)

18344 IMPROVEMENTS IN THE DETERMINATION OF ^{15}N IN THE LOW CONCENTRATION RANGE BY EMISSION SPECTROSCOPY. Perschke, H.; Proksch, G.; Keroe, E. A.; Muehl, A. (International Atomic Energy Agency, Seibersdorf, Austria). Anal. Chim. Acta; 53: 459-63(Feb 1971).

Results show that the simple linear interpolation of the background $^{14}N-^{14}N$ band in the region of the $^{14}N-^{15}N$ peak is a satisfactory basis for the measurement of the size of the latter peak and with pure nitrogen, analyses for ^{15}N with a precision better than ±2% are possible in the region of natural to 1% excess ^{15}N. With proper activation of the Dumas chemicals, it is possible to obtain a sample of nitrogen from organic and inorganic nitrogenous material which is sufficiently free from impurities so that results with a precision of ±2% are possible on a routine basis from natural to 2% abundance. (auth)

18345 USE OF SILICA GEL FOR THE SEPARATION OF TRACES OF URANIUM. Sulcek, Zdenek; Sixta, Vaclav (Central Geological Survey, Prague). Anal. Chim. Acta; 53: 335-44(Feb 1971).

A simple chromatographic procedure for the separation of trace amounts of uranium was developed. From the solution, containing EDTA and tartaric acid at pH 5, uranyl ions are selectively retained on a short silica gel column and are later eluted with 3 M acetic acid. The uranium content is measured spectrophotometrically with Arsenazo III directly in the eluate without further pH adjustment. The effects of aluminum and thorium are discussed in detail. The method is applied to the determination of microgram amounts of uranium in rocks and underground waters. (auth)

18346 BIAMPEROMETRIC TITRATION OF HEXACYANOFERRATE(III), IRON(III), COPPER(II), CERIUM(IV), AND IODINE WITH MERCURY(I) PERCHLORATE. Merrer, Robert J.; Stock, John T. (Univ. of Connecticut, Storrs). Anal. Chim. Acta; 53: 233-8Feb 1971).

The biamperometric titration of hexacyanoferrate(III), iron(III), copper(II), cerium(IV), and iodine with mercury(I) perchlorate was studied. In the concentration range 50 to 1000 μN, the error rarely exceeds 2%. Although the biamperometric and RPE amperometric techniques are of comparable utility at concentrations down to 100 μN, the amperometric technique is preferable for low-concentration titrations. (auth)

18347 METHODS FOR ELECTROPHORETIC AND CHROMATOGRAPHIC ANALYSIS OF AZO COMPOUNDS. COMMUNICATION 3. SYNTHESIS AND ANALYSIS OF AZO COMPOUNDS BASED ON HETEROCYCLIC COMPONENTS. Savvin, S. B.; Rozovskii, Yu. G.; Akimova, T. G.; Sokolovskaya, L. A.; Likhonina, E. A. (Inst. of Geochemistry and Analytical Chemistry, Moscow). Zh. Anal. Khim.; 26: 164-74(Jan 1971). (In Russian).

A method has been developed for the synthesis and analysis of heterocyclic azo compounds based on 4-aminoantipyrine, 2-aminobenzothiazole, rhodanine, and thiorhodanine. The analysis includes establishing the reagent individuality, its identification by the electrophoretic method, and the determination of the concentration of the major substance by the potentiometric and vanadatometric titration methods. The reagents based on 4-aminoantipyrine can be of interest for the photometric determination of La, Zn, Cu, V, and some other elements; the reagents based on 2-aminobenzothiazole can be applied to the determination of Th, Zr, Al, Pd; the reagents based on rhodanine and thiorhodanine can be used for determining Pd. (auth)

18348 TITRIMETRIC DETERMINATION OF THE RARE EARTH ELEMENTS WITH 1,2-DIHYDROXYBENZENE-3,5-DISULPHONIC ACID. Poluektov, N. S.; Alakaeva, L. A.; Tishchenko, M. A. (Inst. of General and Inorganic Chemistry, Odessa). Zh. Anal. Khim.; 26: 181-3(Jan 1971). (In Russian).

Conditions have been found for the direct titrimetric determination of the rare earth elements by 4,5-dihydroxybenzene-1,3-disulfonic acid solution in the presence of Eriochrome Cyanine R. No interference is caused by Li, K, Na, Ca, Ba, Mg, Sr, B, Cd, Mo, W, Ge. The standard deviation of a separate determination is 0.22%. (auth)

18349 STUDY OF THE FLUORESCENT NIOBIUM COMPLEX WITH HYDROGEN PEROXIDE AND SULPHONAPHTHOLAZORESORCINOL. Pilipenko, A. T.; Volkova, A. I.; Zhebentyaev, A. I. (Inst. of General and Inorganic Chemistry, Kiev). Zh. Anal. Khim.; 26: 117-21(Jan 1971). (In Russian).

The reaction of forming a fluorescent mixed complex of niobium with N_2O_2 and dihydroxyphenylazonaphthalenesulfonic acid (SNAR) has been studied. Conditions for the complex formation and its spectrophotometric and fluorescence characteristics have been examined; the ratio of niobium and SNAR in the complex (1:1) has been found. The mixed complex Nb(IV)-N_2O_2-SNAR is a complex anion. The complex is readily extracted with butanol on adding diphenylguanidine to solutions of the complex. The fluorescence intensity of aqueous solutions of the complex is influenced by methanol (ethanol or acetone) additives. The fluorescence intensity increased at concentrations of up to 30% of methanol and up to 20% of ethanol (acetone) in aqueous solutions of the complex. The complexes break down on the further increase of the concentration of organic solvents. The possibility of a fluorimetric determination of niobium as its complex with H_2O_2 and SNAR in the presence of 15-fold amounts of tantalum is discussed. The sensitivity is 0.2 μg of Nb in 5 ml of solution. (auth)

18350 SIMULTANEOUS DETERMINATION OF PLUTONIUM(IV) AND NITRIC ACID WITH THE HELP OF DENSITY–CONDUCTIVITY MEASUREMENTS. Baumgaertel, G.; Kuhn, E. (Kernforschungszentrum, Karlsruhe, Ger.). Anal. Chim. Acta; 53: 208–10(Jan 1971). (In German).

In the concentration range of interest, density and conductivity measurements for various Pu(N)/HNO_3 ratios were made and a diagram drawn. This diagram could then be used to determine unknown concentrations of Pu(IV) and HNO_3. (M.C.G.,

18351 CHEMICAL ANALYSIS OF TELLURITE–TELLURATE COMPOUNDS. Cornwell, J. C. (Kennecott Copper Corp., Lexington, Mass.). Anal. Chim. Acta; 53: 325–33(Feb 1971).

Methods were developed for the analysis of tellurite–tellurate compounds by means of automatic amperometric and potentiometric titrations. Tellurium(VI) is determined by the classical Bunsen method; the chlorine is absorbed in an excess of potassium iodide, and the liberated iodine is titrated automatically with sodium thiosulfate to an amperometric end point. After fusion with potassium pyrosulfate total tellurium and the associated metal ion are determined by automatic potentiometric redox and EDTA titrations, respectively. (auth)

18352 SPECTROPHOTOMETRIC DETERMINATION OF URANIUM(VI) WITH 2-(5-BROMO-2-PYRIDYLAZO)-5-DIETHYLAMINOPHENOL. Johnson, D. A.; Florence, T. M. (Australian Atomic Energy Commission Research Establishment, Lucas Heights). Anal. Chim. Acta; 53: 73–9(Jan 1971).

A new reagent, 2-(5-bromo-2-pyridylazo)-5-diethylaminophenol (bromo-PADAP), is described for the spectrophotometric determination of uranium(VI). This reagent is highly sensitive towards uranium, the uranyl complex having a molar absorptivity of 74,000 at 578 nm and pH 7.6. In the presence of a mixed masking solution only a few ions interfere seriously, and the method can be made specific for uranium by a preliminary extraction of uranium into tri-n-octylphosphine oxide, and direct development of the bromo-PADAP color in the organic phase. Details are given for the determination of uranium in waters, ores, phosphoric acid and phosphate rocks, thorium oxide, and zirconium oxide. (auth)

18353 EXTRACTION SEPARATION OF MOLYBDENUM FROM RHENIUM AND ITS DETERMINATION WITH 5,7-DIBROMO-8-QUINOLINOL. Gorina, D. O.; Zharovskii, F. G. (Kiev State Univ.). Ukr. Khim. Zh.; 36: 707–9(Jul 1970). (In Russian).

Optimum conditions were found for the formation and extraction of molybdenum complexes with 5,7-dibromo-8-quinolinol. The composition and optical properties of a solution of the complex in carbon tetrachloride were studied. A method was developed for direct extraction-photometric determination of Mo with 5,7-dibromo-8-quinolinol. This method was used for determination of Mo in presence of Re. (tr-auth)

18354 ALKALINE EARTH ELEMENTS IN MARINE SEDIMENTS OFF TARAPUR COAST. Rao, S. R.; Shah, S. M. (Bhabha Atomic Research Centre, Bombay). Curr. Sci. (India); 40: 25–7 (20 Jan 1971).

Premonsoon sediment samples collected off the Tarapur coast were decomposed completely and analyzed for radium-226, strontium, and calcium. The content of each of the three elements in the sediment samples after leaching with hydrochloric acid, EDTA, ammonium citrate, and ammonium acetate is given, and a comparison of the percentage leached from each sample by the leach is made. (D.P.O.)

18355 DETERMINATION OF LOW SILVER CONTENT IN DRUGS BY LOW-ENERGY GAMMA-RAY STIMULATED CHARACTERISTIC RADIATION. Svitel, J.; Skobla, J.; Schiller, P. (Komensky Univ., Bratislava). Farm. Obz.; 38: No. 3, 83–7 (1969). (In Slovak).

The applicability of ^{125}I, ^{153}Gd, and ^{241}Am was investigated for the determination of low silver concentrations in drugs by x ray fluorescence. The sources were compared from different points of view (sensitivity of analysis, decay half-time, cost, etc.). For operating analyses the ^{153}Gd source was the most suitable. The main advantages of the described method in comparison with classical ones were speed and simplicity. In addition to pharmacy, this method is applicable in other branches as well (photochemistry, geology). (NSA of Czech)

Isotope Dilution Procedures

18356 (KR–140) CHEMICAL ANALYSIS OF HIGH BURN-UP PuO_2 FUEL. I. METHODS. Joon, K.; den Boef, R.; Haaland, J.; Stijfhoorn, D. E.; de Wit, R. (Institutt for Atomenergi, Kjeller (Norway)). Jun 1970. 25p. Dep. NTIS (U. S. Sales Only).

A scheme is described for chemical isolation and purification of Zr, Mo, Ru, Pd, Cs, Nd, Pm, Sm, Eu, and Pu from irradiated pyrocarbon–silicon carbide-coated PuO_2 fuel. The final analysis is done by isotopic dilution mass spectrometry, except in the case of Pm, which is determined by liquid scintillation counting, using the ^{149}Pm spike and gamma spectrometry for chemical yield determination. The scheme can also be applied for other types of nuclear fuel, and it can easily be extended to comprise other elements as well. (auth)

18357 (NBS-TN–546) ANALYTICAL MASS SPECTROMETRY SECTION: SUMMARY OF ACTIVITIES, JULY 1969–JUNE 1970. Shields, William R. (ed.) (National Bureau of Standards, Washington, D. C.). Nov 1970. 120p. GPO $1.25.

Research progress in mass spectrometry is discussed. Topics covered include: instrumentation, isotopic standards, trace characterization by isotope dilution analysis, high-sensitivity analysis, atomic weight research, spark-source mass spectrograph, and miscellaneous. (M.C.G.)

18358 (RT/CHI–(70)18) ISOTOPIC ANALYSIS OF UO_2 AND APPLICATION TO STREAM ANALYSIS. QUANTITATIVE DETERMINATION OF UO_2 AND BORON BY MEANS OF ISOTOPIC DILUTION. Boniforti, R. (Comitato Nazionale per l'Energia Nucleare, Rome (Italy)). 27 Apr 1970. 18p. (In Italian). Dep. NTIS (U. S. Sales Only).

Analytical methods and results are reported both for uranium isotopic analysis and quantitative determination of boron and uranium by the isotopic dilution technique. (auth)

Radiometric and Radiochemical Procedures

Refer also to abstracts 18522, 18688, 18731, 18746, 18768, 18814, and 19803.

18359 (WCAP–3385-56(Pt.2)) SAXTON CORE II FUEL PERFORMANCE EVALUATION. PART II. EVALUATION OF MASS SPECTROMETRIC AND RADIOCHEMICAL ANALYSES OF IRRADIATED SAXTON PLUTONIUM FUEL. Nodvik, R. J. (Westinghouse Electric Corp., Pittsburgh, Pa. Nuclear Fuel Div.). Jul 1970. Contract AT(30-1)-3385. 144p. Dep, NTIS.

Physics evaluations were performed with mass spectrometric, alpha spectrometric, and radiochemical data obtained from analysis of 47 samples (including 10 radial microsamples) removed from Saxton Core II Zr-clad PuO_2–UO_2 fuel rods; these rods consisted of both pelletized and vibratory compacted fuel and represented both asymptotic and nonasymptotic neutron spectra. The maximum measured values of axial samples (one-inch segments) and rod-average burnup were about 29,000 and 20,700 MWD/MTM, respectively. Comparisons of burnup values determined with two independent methods, the Heavy Element method and the ^{148}Nd fission product method, showed agreement to within two percent, thus verifying the internal consistency of the mass spectrometric data and the validity of the data-reduction methods. Pellet burnups inferred from ^{137}Cs activity showed a negative four percent bias and indicated the possibility of a few percent Cs axial migration from the center to the ends of the fuel rod. Evaluation of ^{137}Cs data from radial microsamples showed a high degree of radial migration within the pellet, with burnups inferred from Cs being seventy percent lower at the center and fifteen to twenty percent higher at the periphery than the burnups determined by the Heavy Element and ^{148}Nd methods. Comparisons between unit cell calculations and measurements for the main chain U and Pu isotopes showed agreement to within about three percent. The calculations tend to underpredict the plutonium concentration by two percent. In the case of the special isotopes (i.e., those not included in the U and Pu main chains), the unit cell calculations were in good agreement with measured values of ^{236}Pu and ^{241}Am and showed gross discrepancies for ^{237}Np, ^{238}Pu, ^{242}Cm, and ^{244}Cm. The calculations overpredicted ^{236}Pu by 8% and underpredicted ^{241}Am by 4%, both differences being well within the uncertainties of the measurements. The calculations underpredicted ^{237}Np and ^{238}Pu by about 30% and underpredicted the ^{242}Cm and ^{244}Cm isotopes by approximately 20 and 40%, respectively. (auth)

18360 CONTROL OF TRITIUM IN WATER AND SEWAGE. Haschke, J. (Hygienische Institutes der Freien und Hansestadt, Hamburg). Arch. Hyg. Bakteriol.; 153: 383–9(Oct 1969). (In German).

The possibilities of simple routine determination of the tritium in water and sewage are considered. The samples are composed of 3 ml water or sewage and 15 ml Dioxan radioactive tracer substance. The accuracy amounts to approximately 3×10^3 pCi/liter, a value lying by the factor 1000 under the maximum permissible concentration in water from a controlled area. The separation of

XUM

tritium and any disturbing nuclides can be achieved by means of a precipitation or flocculation method, the removal of suspended particles and other admixtures by filtration. Any complications involved are discussed. In a series examination of water and sewage in Hamburg, tritium could be detected and determined in one sample of sewage. (auth)

18361 SELF-VOLUME STANDARDS FOR SCHILLING TESTS AND OTHER IN VITRO BULK LIQUID COUNTING. Spencer, R. P. (Yale Univ., New Haven). Int. J. Appl. Radiat. Isotop.; 22: 54(Jan 1971).

It is suggested that instead of using a standard in a separate container with the attendant variations from the sample in geometry, sample holder thickness, and contained sediment the sample should first be assayed and then an aliquot of a standard solution added to the sample and the total count obtained. (UK)

18362 MOISTURE DETERMINATION IN SOLIDS BY NEUTRON RADIATION. Dresia, Heinrich; Bessing, Reinhold; Fischotter, Peter; Lunau, Wigand (to Rheinische Kalksteinwerke GmbH). U. S. Patent 3,532,883. 6 Oct 1970. Priority date 26 Mar 1968, Germany.

An apparatus is described for determining the moisture content of solid substances by means of fast neutrons that are slowed down by interaction with the hydrogen atoms of the water contained in the solid substance and with a hydrogen-containing reflector whereby the neutron counter is shielded against the thermal neutrons emanating from the reflector. Neutron source and counter are disposed as a unit outside the solid substance in a cavity partially formed by that substance. (auth)

18363 ALPHA-SPECTROSCOPY METHOD FOR DIRECT DETERMINATION OF THE INDIVIDUAL CONCENTRATIONS OF RADON DAUGHTERS IN AIR. Goumnerova, L.; Minev, L.; Velikov, V. (Univ. of Sofia). Compt. Rend. Acad. Bulg. Sci.; 23: 919-22(1970).

Since radon rarely occurs in air in radioactive equilibrium with its daughters, measuring the atmospheric radon concentration gives no information about the daughter concentrations. A method is suggested for the separate determination of RaA and RaC by plotting the decay curves of RaA and RaC independently of each other. The radon daughters are sampled on a charged metal plate or a membrane filter. (R.W.R.)

18364 USE OF ^{14}C AS A SECONDARY COUNTING STANDARD FOR ^{35}S. Buckley, J. P. (Radiochemical Centre, Amersham, Eng.). Int. J. Appl. Radiat. Isotop.; 22: 41-2(Jan 1971).

The discrepancy obtained if ^{35}S is measured using ^{14}C as a secondary standard without making any correction for spectral differences was determined. It was found that this was a useful practical procedure for work of moderate precision. For use as an internal standard it has the added advantage of being available in a nonquenching chemical form; i.e., hexadecane. (UK)

18365 DETERMINATION OF PERCENT CONTENTS OF URANIUM AND THORIUM IN NATURAL RADIOACTIVE ORES BY γ-RAY SPECTROMETRY. Cho, S. W. (Atomic Energy Research Inst., Seoul); Chung, M. K.; Yoo, K. J.; Hong, C. Y. J. Korean Nucl. Soc.; 2: 273-8(Dec 1970). (In Korean).

The contents of uranium and thorium in radioactive ores produced in Korea were determined by gamma spectrometry utilizing a Ge(Li) diode detector. Both methods, namely, gamma spectrometries of activated samples and nonactivated samples, were tested and compared for their accuracies and rapidness. The usefulness of the application of the Ge(Li) diode detector to the determination of uranium and thorium in ores is discussed in detail. (auth)

Activation Procedures

Refer also to abstracts 18886 and 19817.

18366 (NBS-TN-548) ACTIVATION ANALYSIS SECTION: SUMMARY OF ACTIVITIES, JULY 1969–JUNE 1970. LaFleur, Philip D.; Becker, Donald A. (eds.) (National Bureau of Standards, Washington, D. C.). Dec 1970. 164p. GPO $1.25.

Activities of the Activation Analysis Section for the period July 1969 to June 1970 are surveyed and progress made on the various projects discussed. Operating characteristics of the NBS Reactor for activation analysis are given. Special attention is given to the many practical problems encountered and the solutions to these problems, especially the analysis of trace elements in glass Standard Reference Material (SRM) and of the botanical SRM. The quantitative analysis for boron using the nuclear track technique is discussed as well as extension of the analysis for uranium using this technique. The value of 3-MeV neutrons in neutron generator activation analysis and the experimental parameters for using these neutrons are discussed. The new target and pneumatic transfer systems at the NBS LINAC for photon activation analysis are described and the application of photon activation analysis for determining thallium in glass and high-purity metals and gold, manganese, and iron in high-purity cadmium is discussed. Research into determination of nitrogen by photon activation analysis is described. A computer program, ALSPIS, for peak finding and integration is described and the application of a mini-computer to the Activation Analysis Section is noted. (auth)

18367 VIBRATIONAL ENTROPY OF THE DILUTE SILVER-GOLD SYSTEM. McGinness III, John Edward. Houston, Tex.; Rice Univ. (1970). 77p. University Microfilms Order No. 70-23,554.

Thesis.

The effusion method was used to investigate the gas–solid equilibrium of Ag–0.013% Au over a temperature range of 300°C. Neutron activation was employed to measure the small amounts of effused mass collected on nitrogen-cooled copper targets. The change in vibrational entropy ($\bar{S}_u - S_v^0$) occurring when a solvent atom is replaced by a solute atom and the corresponding enthalpy change ($\bar{H}_u - H_v^0$) were derived from the experimental data. Experimental values of the vibrational entropy obtained by other workers for binary systems are compared with the results of the Ag–Au system. (Diss. Abstr. Int., B)

18368 ANALYSIS WITH A Po–Be SOURCE: THE MEASUREMENT OF PROMPT GAMMA-RAYS. Allan, D. L.; Armitage, B. H.; Spencer, W. (Atomic Energy Research Establishment, Harwell, Eng.). Anal. Chim. Acta; 53: 401-14(Feb 1971).

Measurements of prompt γ rays arising from the neutron irradiation of nineteen elements and compounds with a Po–Be source were made with a Ge(Li) detector and also a NaI(Tl) detector. The intensities of the strongest γ rays present in each substance have been obtained in units of counts kg^{-1} min^{-1} Ci^{-1}. The effect on the γ-ray intensity of the presence of moisture in a sand (SiO_2) sample was also investigated. (auth)

18369 INTESTINAL ABSORPTION OF METALLIC MERCURY. Bornmann, G.; Henke, G.; Alfes, H.; Moellmann, H. (Univ., Muenster, Ger.). Arch. Toxikol.; 26: 203-9(1970). (In German).

It was demonstrated by means of neutron activation analysis that a small portion of orally administered metallic mercury is absorbed by rats. The animals tolerated this without visible symptoms, yet it resulted in a 10-fold or greater increase above normal values of mercury in blood and kidneys. (auth)

18370 SOME ITALIAN METEORITES TRACE ELEMENTS CONTENT BY NONDESTRUCTIVE NEUTRON ACTIVATION ANALYSIS. Orvini, Edoardo; Meloni, Sandro; Maxia, Vera; Di Casa, Michele (Univ., Pavia, Italy). Ann. Chim. (Rome); 60: 506-13(1970).

In order to obtain a more reliable chemical composition of some Italian meteorites, especially for their trace element content, a nondestructive method of activation analysis was set up and applied to the determination of sodium, manganese, chromium, scandium, copper, and cobalt. The analyzed meteorites include the following: Albareto, Alessandria, Alfianello, Assisi, Cereseto, Collescipoli, Girgenti, Monte Milone, Motta di Conti, Orvinio, Siena, Sinnai, Trenzano, Valdinizza and Vigarano. Irradiations have been carried out in the LENA Reactor of the University of Pavia. Induced activity was measured by gamma spectrometry. Precision of the method is within 10%. The results obtained are reported and compared with the existing data in the literature. A general good agreement is observed with the more recent values. Also average values for each class of the examined chondrites are given. These are in good agreement with the average class values reported by other authors for the olivine-bronzite class. There is also agreement for the olivine-hypersthene class provided Orvinio's data are not considered. It appears from the results that, at least from the chemical point of view, this chondrite should belong to the olivine-bronzite class. (auth)

Inorganic, Organic, and Physical Chemistry

Refer also to abstracts 18687, 19166, and 19473.

Chemical Properties

Refer also to abstracts 18498, 18507, 18899, and 20754.

18371 EFFECT OF IONIC MEDIA ON THE STABILITY CONSTANTS OF CHLORIDE, NITRATE, AND THIOCYANATE

COMPLEXES OF AMERICIUM(III) AND EUROPIUM(III). Khopkar, P. K.; Narayanankutty, P. (Bhabha Atomic Research Centre, Trombay, India). J. Inorg. Nucl. Chem.; 33: 495-502 (Feb 1971).

Stability constants of Am(III) and Eu(III) complexes with chloride, nitrate, and thiocyanate ions were determined in lithium, hydrogen, sodium, and ammonium ion media at 30 ± 0.1°C and unit ionic strength, by a solvent extraction method. For chloride complexes, the first stability constant K_1 was found to increase regularly with decreasing hydration of the medium cations. The effect of medium cations on the stabilities of nitrate and thiocyanate complexes was found to be much smaller. (auth) (UK)

18372 REDUCTION OF URANIUM TETRAFLUORIDE VAPORS BY CERTAIN METALS. Khripin, L. A.; Luk'yanova, L. A. Zh. Neorg. Khim.; 13: 2047-9(Aug 1968). (In Russian).

A study was made of the production of UF_3 by the reduction of UF_4 by metals at high temperatures in order to evaluate the possibility of using UF_4 greatly contaminated with impurities of low volatility (mainly UO_2) and to increase the range of metals that can be used for reducing UF_4. Results showed that when UF_4 is reduced in the vapor phase, no impurities are passed into the UF_3 formed, and that Zr, Be, and Ti reduce UF_4 vapor to the trifluoride. The yields of UF_3 were very low for Be and Ti, but Zr can be used successfully to prepare UF_3. Under the conditions used Cr, Ge, and Fe did not react appreciably with UF_4 vapor. (D.H.M.)

18373 ACID AND METAL SALT CATALYZED HYDROLYSES OF $PO_2F_2^-$ AND PO_3F^{2-}. Clark, Howell R.; Jones, Mark M. (Vanderbilt Univ., Nashville). Inorg. Chem.; 10: 28-33(Jan 1971).

A general catalytic effect is shown by Th(IV), Zr(IV), and Al(III) toward the removal of one fluoride ligand from $PO_2F_2^-$ in dilute acidic media. Release of fluoride from PO_3F^{2-} is accelerated by Th(IV) in media having a pH above 1.5; inhibition occurs under more acidic conditions. The acid hydrolysis of $PO_2F_2^-$ conforms to a series first-order rate law in which the second step proceeds approximately 1.8 times more rapidly than the first. Data were obtained for the acid-catalyzed reaction at 15, 25, and 35 in solutions ranging from 0.25 to 3.0 $\underline{M}$ HCl. A suitable rate expression for these concentrations is $(-dC/dt) = \{[a_{HCl} + K/(a_{HCl})^2]\}C$ where $C = [PO_2F_2^-] + [HPO_2F_2]$ and K = 0.45, the apparent ionization constant of HOP_2F_2. The behavior of these fluorophosphates suggests that metal ion catalyzed fluoride release is suppressed as the oxygen: fluorine ligand ratio increases about a central atom whereas acid catalysis is facilitated. Alternative hard-base coordination sites and the chelating tendency of M^{n+} (in contrast to H^+) are used in rationalizing this trend. (auth)

18374 5,7-DIHALO-8-HYDROXYQUINOLINE COMPLEXES OF U(VI). Thompson, M.; Corsini, A. (McMaster Univ., Hamilton, Ont.). J. Inorg. Nucl. Chem.; 33: 471-8(Feb 1971).

The 5,7-dihalo-8-hydroxyquinoline complexes of U(VI) precipitated from aqueous acetone solution were re-investigated and found not to have the previously assigned compositions, $UO_2(C_9H_4NOX_2)_2 \cdot C_9H_5NOX_2$ and $UO_2(C_9H_4NOX_2)_2$, where X = Cl or Br. The basic composition is $UO_2(C_9H_4NOX_2)_2 \cdot OC(CH_3)_2$ but the exact composition is difficult to assign because of the insolubility of the reagents and the presence of water in the complexes. (auth) (UK)

18375 METAL-ION CATALYZED AND METAL-ION-ASSISTED FLUORIDE HYDROLYSES. Clark, Howell Rieke. Nashville; Vanderbilt Univ. (1970). 163p. University Microfilms Order No. 70-24.855.

Thesis.

Significant increases in the rates of hydrolysis attributable to "superacid" catalysis from hard acid metal cations were obtained for the following complex fluoro anions: $PF_6^-BF_4^-$, $AsF_5(OH)^-$, AsF_6^-, $PO_2F_2^-$, and PO_3F^{2-}. Optimum catalytic conditions produced increases in reaction rates of two or more orders of magnitude over the uncatalyzed rate. Cations studied as catalysts were Zr(IV), Th(IV), Al(III), Be(II), Ti(IV), and Mg(II). A spectrophotometric technique was used to monitor fluoride concentration for the hydrolysis of AsF_5-$(OH)^-$. All other hydrolyses were studied by a potentiometric procedure using a fluoride specific ion electrode. Aqueous solutions of the nitrate or chloride salts of the desired cations were used as catalysts. Increases in the rate of hydrolysis attributable to these catalysts were shown for the following organic fluorides: benzyl fluoride, fluoroacetate, benzotrifluoride, o- and m-aminobenzotrifluoride, and o-hydroxybenzotrifluoride. Organic fluorides that did not show significant hydrolysis were tri-fluoroacetate, 3-nitro-4-chlorobenzotrifluoride, and the iso-meric fluoroanilines. Catalytic activity among hard acid metal ions generally parallels fluoro complex formation constants as anticipated by the Hard and Soft Acid-Base Theory. The order of activity for the catalyst species used may be expressed as Th(IV) ~ Zr(IV) > Al(III) > Be(II) ~ Ti(IV) > Mg(II). Because of their combined catalytic effectiveness and greater resistance to hydrolysis, Al(III) and Th(IV) were most frequently used. Experimental data support a direct interaction between the catalyst ion, M^{n+}, and the fluoro substrate, Q-F. The process of metal ion-catalyzed fluoride hydrolysis exhibits complex pH dependence. Optimum catalytic conditions involve the minimum acidity to retard hydrolysis of the aquo catalyst ion and of the fluorometallate complex formed by catalyst interaction. Alternative hard base sites on the original substrate or on stable hydrolysis intermediates further complicate the pH dependence through interaction with the catalyst ions. Catalytic displacement of fluorine from the C-F bond presently appears restricted to aliphatic species. No significant acceleration of the hydrolysis of fluorine bound to an aromatic ring can presently be attributed to metal ion catalysis. The hydrolysis of trifluoromethyl groups attached to a ring is influenced by both the nature and position of ring substituents. Electron depleted groups inhibit the hydrolysis, while enhancement results from donor substituents, particularly when the group is ortho to the $-CF_3$ group. The acid hydrolysis of $PO_2F_2^-$ conforms to a series first order rate law in which the second step proceeds approximately 1.8 times more rapidly than the first. Data obtained for the acid-catalyzed reaction at 15, 25, and 35°C in solutions ranging from 0.25-3.0 $\underline{M}$ HCl support a rate expression of the form $-(dC/dt) = \{[a_{HCl} + K/(a_{HCl})^2]\}C$ where $C = [PO_2F_2^-] + [HPO_2F_2]$, and K = 0.45, the apparent ionization constant of HPO_2F_2. Apparent Arrhenius activation energy for the reaction is 16.7 ± 0.6 kcal/mole. (Diss. Abstr. Int., B)

18376 VOLTAMMETRY OF NEPTUNIUM(VI)-PROPIONATE COMPLEXES AT THE ROTATED GLASSY CARBON ELECTRODE. Plock, C. E. (Dow Chemical Co., Golden, Colo). Anal. Chim. Acta; 53: 249-57(Feb 1971).

The voltammetry of the neptunyl-propionate complex was investigated over varying conditions of ligand concentration and pH. A reversible one-electron wave was obtained in all propionate concentration ranges investigated over the pH range to 0.0 to 6.0. The half-wave potential was independent of the pH in the range 0.0 to 1.7, but was a function of the pH in the ranges 1.7 to 3.9 and 3.9 to 6.0. The limiting current was independent of the pH in the range 0.0 to 3.9, but was a function of the pH above 3.9. The maximum metal: ligand ratio was found to be 1:3 by conductometric and amperometric titrations. The diffusion coefficient was $0.56 \cdot 10^{-5}$ $cm^2\ sec^{-1}$ at pH 2.5 and $0.50 \cdot 10^{-5}$ $cm^2\ sec^{-1}$ at pH 5.5. (auth)

18377 THERMAL STABILITY OF MONOISOPROPYLBIPHENYL. Bozhko, D. F.; Molodykh, E. I.; Novikov, V. P. Izv. Vyssh. Ucheb. Zaved., Mashinostr.; No. 5, 129-35(1968). (In Russian).

Experimental data obtained in the temperature range from 370 to 430°C, at an initial pressure of 21 to 26 atm, for 200 hr were used for determining the rate constant of formation of high-boiling residues and formation of gas during pyrolysis of monoisopropylbiphenyl. The composition of the gaseous phase and of the high-boiling residues was determined. The studies were made to determine the usefulness of this compound as a reactor moderator-coolant. (R.V.J.)

18378 THERMAL DECOMPOSITION OF BIS-HEXANITROAZOBENZENE AND PYROLYSIS OF URANIA GEL. PART I. KINETICS AND MECHANISM OF THERMAL DECOMPOSITION OF BIS-HEXANITROAZOBENZENE. PART II. PYROLYSIS AND GAS CHROMATOGRAPHIC STUDY OF URANIUM DIOXIDE GEL SHARDS AND BEADS. Choi, In Kap. Salt Lake City; Univ. of Utah (1970). 143p. University Microfilms Order No. 70-23,826.

Thesis.

The weight change parameters of bis-hexanitroazobenzene were determined isothermally in the temperature range 180 to 280°C and the residues were analyzed by gas chromatography and infrared spectroscopy. Trace amounts of ammonia were found to enhance the rate of decomposition significantly and water vapor also accelerated the reaction rate. The thermogravimetric weight loss data, infrared analysis and gas chromatographic analysis indicated rather uniform decomposition. A first-order plot fit the data for ten-hour (or up to 5%) decomposition with an activation enthalpy of 14 kcal per mole after the first hour in the temperature range of 180 and 240°C. One five-day (70%) decomposition at 240°C fit the first order plot for the entire period. Gases evolved by pyrolysis of urania gel shards and beads were analyzed qualitatively using a gas chromatograph. Samples were heated incrementally in the temperature range of 100 to 680°C in a pyrolysis unit connected to a gas chromatograph. In addition to gas chromatography, infrared spectroscopy and mass spectrometry were employed to identify the off-gases. The principal gases from the urania gels and beads were carbon dioxide and carbon monoxide. The amount of gases produced was directly related to the impurity content. (Diss. Abstr. Int., B)

18379 PRECIPITATION CONDITIONS IN THE URANYL NITRATE-AMMONIUM HYDROXIDE SYSTEM. Szego, L.; Mar-

XUM

shal, C. J. (Australian Atomic Energy Commission Research Establishment, Lucas Heights). J. Inorg. Nucl. Chem.; 33: 595-8 (Feb 1971).

An investigation of limiting conditions for precipitate formation at room temperature at various uranium concentrations in the uranyl nitrate–ammonium hydroxide system was undertaken and the composition of the initial precipitates examined. It was found impossible to obtain uranyl hydroxide over a concentration range of 0.0005 to 2.0M and it was shown that the composition of the initial precipitate was variable and never approached that of uranyl hydroxide. The results are discussed and compared with others previously reported. (UK)

18380 DECOMPOSITION OF AMMONIUM URANYL PENTAFLUORIDE ON HEATING. Sudarikov, B. N.; Seleznev, V. P.; Rakov, Z. G.; Kulyako, Yu. M. Zh. Neorg. Khim.; 15: 2773-6 (Oct 1970). (In Russian).

By x-ray and thermogravimetric methods, the scheme for thermal decomposition of $(NH_4)_3UO_2F_5$ was determined and the intermediate phase $NH_4[(UO_2)_2F_5]$ isolated and characterized. The decomposition pressures of $(NH_4)_3UO_2F_5$ and $NH_4[(UO_2)_2F_5]$ and their heats of formation were determined. (tr-auth)

18381 INVESTIGATION OF COMPLEX FORMATION IN THE SYSTEM UO_2^{2+}–H_2SO_4–HF–TOA. Lipovskii, A. A.; Nikitina, S. A. Zh. Neorg. Khim.; 15: 2793-6(Oct 1970). (In Russian).

It was established that, on dissolution of U(IV) fluorides and sulfates in solutions of trioctylamine sulfate and fluoride in benzene, the compounds $(TOAH)_3UO_2(SO_4)_2F$ and $(TOAH)_3UO_2SO_4F_3$ are formed. The electronic and ir spectra were measured and it was concluded from the spectra that the sulfate groups are bidentately coordinated to the uranium atoms. Polymer compounds were formed by participation of sulfate groups in bridge formation. (tr-auth)

18382 SYNTHESIS OF (o-OXALOPHENYLAZO)CHROMOTROPIC ACID AND THE DETERMINATION OF STABILITY CONSTANT OF ITS THORIUM CHELATE. Toei, Kyoji; Miyata, Haruo; Ozaki, Takeshi (Okayama Univ., Japan). Nippon Kagaku Zasshi; 91: 1148-51(Dec 1970). (In Japanese).

The reagent ((0–oxalophenylazo) chromotropic acid, having a –CO–COOH group in the position ortho to the phenyl group of phenylazochromotropic acid) was prepared from diazotized isatin and chromotropic acid. The color of the reagent in aqueous solution was red, and its absorption maximum was observed at 510 to 540 mμ. The acid dissociation constants ($pK_1 = 3.52$ and $pK_2 = 10.19$) were determined by means of pH titration and spectrophotometric methods at 25°C and ionic strength of 0.1(KNO_3). The reagent reacted with thorium ion in an acidic medium to form a violet 1 : 1 chelate, which exhibited an absorption maximum at 575 mμ. The stability constant, log K, was determined spectrophotometrically to be 13.5_8 at 25°C and ionic strength of 0.1. (auth)

18383 DISPROPORTIONATION COEFFICIENTS OF PLUTONIUM. Silver, G. L. (Monsanto Research Corp., Miamisburg, Ohio). J. Inorg. Nucl. Chem.; 33: 577-83(Feb 1971).

The disproportionation reactions of tetravalent and pentavalent plutonium ions are customarily written so as to include only two plutonium oxidation states as products. Experiment has demonstrated that three plutonium oxidation states result from the disproportionation reactions and disproportionation stoichiometries are illustrated that include three oxidation states as products. (UK)

18384 OXIDATION-REDUCTION PROCESSES IN THE SYSTEMS $ReCl_5$–UO_2Cl_2 ($UOCl_3$). Glukhov, I. A.; Eliseev, S. S.; El'manova, N. A. (Inst. of Chemistry, Stalinabad, USSR). Zh. Neorg. Khim.; 15: 2998-3001(Nov 1970). (In Russian).

On heating equimolar mixtures of $ReCl_5$ with UO_2Cl_2, the oxidizing-reducing reaction proceeds according to the reaction $ReCl_5 + UO_2Cl_2 \rightleftharpoons ReOCl_4 + UOCl_3$. When $UOCl_3$ is isolated and reacted with $ReCl_5$, UCl_4 is produced by the reaction: $UOCl_3 + ReCl_5 \rightleftharpoons UCl_4 + ReOCl_4$. The total reaction can be expressed by the equation: $UO_2Cl_2 + 2ReCl_5 \rightleftharpoons UCl_4 + 2ReOCl_4$. (tr-auth)

Isotope Effects and Exchange

Refer also to abstracts 18424, 18426, and 18459.

18385 (CONF-700816–(Vol.1), pp 278-88) EVALUATION OF ACTIVATED CARBON SUPPORTED ISOTOPE EXCHANGE TECHNIQUES FOR CONTAINMENT ATMOSPHERE PURIFICATION. Kovach, J. L. (North American Carbon, Inc., Columbus, Ohio); Montagnon, J. R. (International Carbon, Inc., Paris (France)).

From 11. AEC air cleaning conference; Richland, Wash. (31 Aug 1970).

In Proceedings of the eleventh AEC air cleaning conference.

Removal of $CH_3\,^{131}I$ by isotope exchange processes is reviewed. The extension of the supported isotope exchange processes from liquid or gas phase isotope exchange processes is considered feasible. The evaluation of the kinetics of the supported isotope exchange processes requires further careful study. A new carbon based catalyst GX 133 was evaluated for HTO–H_2O isotope exchange. Two carbons, GX 136 impregnated with Na_4XeO_6 and GX 121 impregnated with XeF_2, were also evaluated for ^{131}Xe–^{133}Xe exchange. The initial results indicate that isotope exchange does take place on a supported surface, however, the stability of these impregnated carbons has to be further evaluated. (auth)

18386 KINETIC ISOTOPIC EFFECT OF THE OXIDATION OF HYDROGEN ON FERRIC OXIDE. Bulgakov, N. N.; Ismagilov, Z. R.; Popovskii, V. V.; Boreskov, G. K. (Inst. of Catalysis, Novosibirsk, USSR. Novosibirsk State Univ., USSR). Kinet. Catal. (USSR) (Engl. Transl.); 11: 520-7(May-Jun 1970).

Translated from Kinet. Katal.; 11: 638-47(May-Jun 1970).

The rates, orders, and activation energies of the oxidation of protium and deuterium on ferric oxide were determined in a circulation-flow apparatus under conditions of a large excess of oxygen. It was established that the rate of oxidation of protium is higher than the rate of oxidation of deuterium; the reaction orders and activation energies are close. The simplest stepwise schemes of the reaction mechanism were considered. The kinetic data and values of the kinetic isotopic effects agree with three schemes of the mechanisms, according to which a molecule of hydrogen, weakly bound to the surface, enters into the active complex of the first stage. (auth)

18387 ISOTOPIC EXCHANGE IN CARBON MONOXIDE MOLECULES ON ZINC AND IRON OXIDES. Nekipelov, V. N.; Kasatkina, L. A. (Moscow Chemicotechnological Inst.). Kinet. Catal. (USSR) (Engl. Transl.); 11: 557-63(May-Jun 1970).

Translated from Kinet. Katal.; 11: 683-91(May-Jun 1970).

The kinetics of isotopic exchange in CO molecules on the oxides ZnO, Fe_2O_3, and Fe_3O_4 was studied in the temperature interval from −196 to 400°C at pressures of 5 to 20 mm Hg. The experimentally obtained values of the rates of exchange, activation energy, and order of the reaction with respect to the CO pressure are cited. (auth)

18388 EVALUATING THE MOBILITY OF SURFACE OXYGEN IN SEVERAL OXIDES AND THEIR MIXTURES BY MEANS OF OXYGEN ISOTOPE EXCHANGE+ I. MOBILITY OF SURFACE OXYGEN IN THE SYSTEM Bi_2O_3–MoO_3. Adamiya, T. V.; Mishchenko, Yu. A.; Gel'bshtein, A. I. (Inst. of Physical Chemistry, Moscow). Kinet. Catal. (USSR) (Engl. Transl.); 11: 599-603 (May-Jun 1970).

Translated from Kinet. Katal.; 11: 734-40(May-Jun 1970).

Heteromolecular oxygen isotope exchange was used to determine the mobility of surface oxygen in molybdenum trioxide, bismuth oxide, and bismuth molybdate of the composition $Bi_2O_3 \cdot 2MoO_3$. Surface and bulk oxygen in Bi_2O was found to be nonequivalent, as has the oxygen in bismuth molybdate, in exchange with gaseous oxygen. The oxygen in MoO_3 may be either equivalent or nonequivalent in the exchange, depending on the experimental conditions and the preliminary treatment of the oxide. The formation of bismuth molybdate of the composition $Bi_2O_3 \cdot 2MoO_3$ leads to an increase in the binding energy of surface oxygen in the Bi_2O_3–MoO_3 system. (auth)

18389 INFLUENCE OF THE CONDITIONS OF PRELIMINARY TREATMENT ON THE ENERGY OF THE BONDING OF OXYGEN ON LANTHANUM OXIDE. Sokolovskii, V. D.; Mitrofanova, G. N.; Sazonov, L. A. (Inst. of Catalysis, Novosibirsk, USSR). Kinet. Catal. (USSR) (Engl. Transl.); 11: 662-3(May-Jun 1970).

Translated from Kinet. Katal.; 11: 804-6(May-Jun 1970).

The influence of the conditions of preliminary treatment on the rate of homomolecular isotopic exchange of oxygen on lanthanum oxide was studied. It has been shown that if the vapors of lubricants and oils from the vacuum system reach the catalyst during the preliminary treatment of the specimens, the rate of exchange is decreased by a factor of several hundreds, and the activation energy increases by 10 kcal/mole. (auth)

18390 KINETICS OF COPPER(II)- AND COPPER(I)-CATALYZED DEUTERIUM EXCHANGE IN SULFURIC AND PERCHLORIC ACID SOLUTIONS. von Hahn, H. E. A.; Peters, E. (Univ. of British Columbia, Vancouver). J. Phys. Chem.; 75: 571-9(18 Feb 1971).

The cupric and cuprous ion-catalyzed exchange of deuterium with protium in sulfuric and perchloric acid solutions was studied at 160° and 5 to 15 atm of D_2 or H_2 pressure. Exchange occurred in both the D_2–H_2O and the H_2–D_2O systems. In the absence of copper ions no exchange took place. The $Cu^{(I)}$-catalyzed exchange rates were markedly greater than the $Cu^{(II)}$-catalyzed exchange rates. The exchange studies revealed a hitherto unobserved fast reaction between cuprous ions and dissolved hydrogen in perchloric acid solutions. The exchange rates were unexpectedly fast in low sulfuric acid solutions indicating the possible existence of reactive copper sulfate complexes. The rates of exchange and of $Cu^{(II)}$ reduction were measured at several levels of cuprous ion concentration. With these data and suitable derived equations, the four parameters k_1, k_{-1}/k_2, k_3, and k_{-3}/k_4 of the $Cu^{(II)}$-reduction rate law, viz. $-\frac{1}{2}(d[Cu^{II}]/dt) = (k_1[Cu^{II}]^2[H_2]/((k_{-1}/k_2)[H^+] + [Cu^{II}]) + (k_3[Cu^I][Cu^{II}]^2[H_2]/[(k_{-1}/k_2)[H^+] + [Cu^{II}]]\{(k_{-3}/k_4)[H^+] + [Cu^{II}]\})$ could be calculated for each exchange experiment. The values obtained were in satisfactory agreement with those obtained in previous studies in the H_2-H_2O system, when taking isotope effects into consideration. (auth)

18391 STRUCTURE OF NITROFORM IN VARIOUS SOLVENTS. Marshall, H. P.; Borgardt, F. G.; Noble, Paul Jr.; Bhacca, N. S. (Lockheed Palo Alto Research Lab., Calif.). J. Phys. Chem.; 75: 499-504(18 Feb 1971).

Proton exchange rates were determined for nitroform (trinitromethane) in $D_2O-D_2SO_4$ solvent up to an analytical mole fraction of $D_2O = 0.5$. The proton exchange rate for an analytical mole fraction of 0.159 of D_2O in $D_2SO_4-D_2O$ is given by $\log k$ (sec^{-1}) $= 9.38 - 19{,}200/2.303RT$ ($\Delta S^\dagger$ at 55° is −17 eu) for the temperature range of 40 to 70°. Further, the log of the rate constants was found to be proportional to the analytical mole fraction of D_2O in D_2SO_4. A mechanism for the proton exchange reaction is proposed. Proton chemical shifts for nitroform, 1,1-dinitroethane, and 1,1-dinitropropane were determined in a series of solvents. The chemical shift of nitroform ranges from δ (ppM) of 7.40 in CCl_4 to δ (ppM) of 9.18 in acetone; in the latter solvent, complex formation occurs with a $K_{eq} = 10$ (~37°) (concentration in mole fraction). Rapid proton exchange occurs between water, methanol, and 12N HCl and nitroform. Proton chemical shifts of 1,1-dinitroethane and 1,1-dinitropropane for the C-1 proton are shifted downfield by ~0.7 (ppM) in changing solvent from CCl_4 to acetone. Small shifts (~0.04 ppM) downfield were observed for the C-2 protons. Coupling constants were determined for the various protons in the dinitroalkanes and found to be independent of the solvent system. (auth)

18392 SYMMETRY COORDINATES, HARMONIC FORCE FIELD, AND MEAN AMPLITUDES FOR LIGHT AND HEAVY DIBENZENE CHROMIUM. Cyvin, S. J. (Technical Univ. of Norway, Trondheim); Brunvoll, J.; Schaefer, Lothar. J. Chem. Phys.; 54: 1517-22(15 Feb 1971).

The molecular vibrations of dibenzene chromium were analyzed in terms of the eclipsed 25 atomic model of symmetry D_{6h} with planar ligands. A complete set of symmetry coordinates was constructed and based almost entirely on conventional types of valence coordinates. A harmonic force field is given, and used to calculate the vibrational frequencies, mean amplitudes of vibration, and perpendicular amplitude correction coefficients for $(C_6H_6)_2Cr$ and $(C_6D_6)_2Cr$. (auth)

18393 UNIMOLECULAR DECOMPOSITION OF TOLUENE AND CYCLOHEPTATRIENE MOLECULAR IONS. VARIATION OF THE DEGREE OF SCRAMBLING AND ISOTOPE EFFECT WITH INTERNAL ENERGY. Howe, I.; McLafferty, F. W. (Cornell Univ., Ithaca, N. Y.). J. Amer. Chem. Soc.; 93: 99-105 (13 Jan 1971).

Quantitative measurements of the relative losses of H and D from the molecular ions of deuterated toluenes and cycloheptatrienes have been carried out for several definable ranges of precursor ion energies. The molecular ions appear to be completely scrambled in formation of the low-energy ions arising from unimolecular metastable transitions, but the degrees of scrambling decreases with increasing internal energy and hence with decreasing lifetime. The dueterium isotope effect decreases with increasing internal energy; the observed values agree well with the theoretical values calculated by Vestal. The large isotope effect observed here for low-energy ions, particularly metastables, sounds a warning about the significance of deuterium-labeling studies where primary isotope effects are involved. The close similarity in the results for toluene and cycloheptatriene is consistent with Harrison's postulation of an initial isomerization of the toluene molecular ion to that of cycloheptatriene. The greatest differences are observed at high energies, indicating that here appreciable direct decomposition may be occurring from the unscrambled toluene molecular ion. (auth)

18394 MATRIX-ISOLATION STUDY OF THE LOW-PRESSURE PYROLYSIS AND ULTRAVIOLET PHOTOLYSIS OF DIMETHYL PEROXIDES AND OF CF_3OCl. Christe, Karl O.; Pilipovich, Donald (Rocketdyne, Canoga Park, Calif.). J. Amer. Chem. Soc.; 93: 51-6(13 Jan 1971).

The low-pressure pyrolysis and uv photolysis of CH_3OOCH_3, CD_3OOCD_3, CF_3OOCF_3, and CF_3OCl were studied to obtain information on the initial decomposition steps. The decomposition products were trapped at 8°K in an argon matrix and identified by infrared spectroscopy. The main products in the pyrolysis and photolysis of CH_3OOCH_3 or CD_3OOCD_3 are formaldehyde and methanol. The pyrolysis of CF_3OOCF_3 yielded COF_2 and CO_2 as main products. In addition, a novel unstable species was produced having its strongest infrared absorptions at 1592 and 1025 cm^{-1}. The decomposition of CF_3OCl resulted in COF_2 as the only detectable product. (auth)

18395 SOLVENT ISOTOPE EFFECTS UPON PROTON TRANSFER FROM THE HYDRONIUM ION. O'Ferrall, R. A. More; Koeppl, G. W.; Kresge, A. J. (Illinois Inst. of Tech., Chicago. Rice Univ., Houston). J. Amer. Chem. Soc.; 93: 9-20(13 Jan 1971).

Model calculations of solvent isotope effects for reactions of H_3O^+ in H_2O are described. Models for H_2O and H_3O^+ take account of librational modes, and force constants are chosen to yield the constant $L = 9.0$ for the equilibrium $2D_3O^+ + 3H_2O \rightleftharpoons 2H_3O^+ + 3D_2O$. Primary and secondary isotope effects $(k_H/k_D)_I$ and $(k_H/k_D)_{II}$ for proton transfer from H_3O^+ are calculated. It is found that as the structure of the transition state is varied from reactant-like to product-like the secondary isotope effect increases monotonically, while the primary isotope effect passes through a maximum. The parameter α defined by $(k_H/k_D)_{II} = L^{-\alpha/3}$ provides a measure of the extent of proton transfer in the transition state. Contributions from "transfer" isotope effects are taken into account. Deviations from the rule of the geometric mean (RGM) for isotopic exchange equilibria are considered in detail within the framework of Bernstein's rules, and are ascribed mainly to contributions from bending vibrations. The deviations are underestimated by harmonic calculations, but calculations and experiment combined yield practical estimates for both D and T fractionation in H_2O and H_3O^+. Deviations are canceled between H_2O and H_3O^+ but cause discrepancies of up to 10% in the fractionation of single exchangeable hydrogens. Their effect upon the separation of primary and secondary kinetic isotope effects for proton transfer from H_3O^+ is tested. Maximum discrepancies between experimental methods based on (i) kinetic dependence in H_2O-D_2O mixtures, (ii) isotope distribution in the products, and (iii) tritium transfer in H_2O and D_2O are again 10% and are associated principally with fractionation of the reacting hydrogen. Neglect of deviations from the RGM does not obscure the strong correlations between isotope effects and transition state structure. (auth)

18396 SECONDARY HYDROGEN-DEUTERIUM ISOTOPE EFFECTS IN THE FLUORINE NUCLEAR MAGNETIC RESONANCE SHIFTS OF METHYL-p-FLUOROPHENYLCARBONIUM IONS. Timberlake, J. W.; Thompson, J. A.; Taft, R. W. (Univ. of California, Irvine). J. Amer. Chem. Soc.; 93: 274-6(13 Jan 1971).

In the study of the secondary β-deuterium isotope effects on the fluorine NMR shifts of p-fluorophenylmethylcarbonium ions, two lines indicate that little or no steric interaction effects are involved in the observed shifts. For the substituted groups, the isotope effect follows the electronic sequence, $NH_2 < OH < Me < H < CF_3$ rather than the steric size sequence. (B.L.M.)

18397 KINETICS OF IODINATION OF SODIUM PHENYLPROPIOLATE. Wilson, Mary H.; Berliner, Ernst (Bryn Mawr Coll., Pa.). J. Amer. Chem. Soc.; 93: 208-16(13 Jan 1971).

The addition of iodine to sodium phenylpropiolate was studied in aqueous solution. At moderate iodide ion concentrations the reaction was found to be termolecular, involving iodine, iodide ion, and sodium phenylpropiolate with an activation energy of 15.3 kcal/mole, and an activation entropy of −23.5 eu. Analysis of the rate constants at low iodide ion concentrations revealed a three-term expression $k_{obsd} = k_t(I^-)/(K_1 + I^-) + k'/(K_1 + I^-) + k''/(I^-)(K_1 + I^-)$. In this expression k_t is the rate constant for the termolecular reaction, k' the rate constant for a bimolecular reaction involving molecular iodine, and the constant k'' is the rate constant for a reaction possibly involving the hydrated iodine cation (H_2OI^+). K_1 is the equilibrium constant for the triiodide ion. Product analyses, salt effects, the relative rates of reaction of phenylpropiolic acid and its anion, the effect of pH, activation parameters, and solvent isotope effects were investigated and are not inconsistent with the proposed mechanism. (auth)

18398 REACTIONS OF ACETYLIMIDAZOLE AND ACETYLIMIDAZOLIUM ION WITH NUCLEOPHILIC REAGENTS. STRUCTURE-REACTIVITY RELATIONSHIPS. Oakenfull, David G.; Jencks, William P. (Brandeis Univ., Waltham, Mass.). J. Amer. Chem. Soc.; 93: 178-88(13 Jan 1971).

The reactions of amines with acetylimidazolium ion exhibit a large dependence on amine basicity, $\beta = 1.0$, for amines both more and less basic than the leaving imidazole. The rapid reaction of N-methylimidazole with acetylimidazolium ion (and of imidazole with acetyl-N-methylimidazolium ion) shows that concerted proton transfer is not important in these reactions. The nucleophilic reactions with tertiary amines are inhibited by very low concentrations of added imidazole. The dependence of oxyanion reactivity upon basicity varies markedly; β values decrease with increasing basicity over the entire range from approximately 1.7 to 0. The reactions of tertiary amines with free acetylimidazole are not inhibited by imidazole and represent general base catalysis of hydrolysis; the triethylenediamine reaction exhibits a solvent deuterium isotope effect $k_{H_2O}/k_{D_2O} = 2.1$. The β values for general base catalysis of hydrolysis are 0.34 for acetylimidazolium ion and 0.55 for acetylimidazole. The β value for the nucleophilic reaction of phenolate anions and free acetylimidazole is 1.3. It is argued that the nucleophilic reactions of trifluoroethoxide ion with acetylimidazole and acetylimidazolium ion cannot proceed through a tetrahedral addition intermediate that is at equilibrium with respect to proton transfer. (auth)

18399 VIBRATIONAL ANALYSES OF LIQUID WATER AND THE HYDRONIUM ION IN AQUEOUS SOLUTION. **O'Ferrall, R. A. More; Koeppl, G. W.; Kresge, A. J. (Illinois Inst. of Tech., Chicago. Rice Univ., Houston). J. Amer. Chem. Soc.; 93: 1-9 (13 Jan 1971).**

A vibrational analysis of liquid water, considered as a mixture of molecules with different numbers of hydrogen bonds, is reported. A nine-atom model consisting of H_2O surrounded tetrahedrally by two oxygens and two OH groups is used for the fully bound species. Molecules in lower states of hydrogen bonding are represented by removing one or more of the peripheral groups. Frequencies are calculated for intramolecular bending and stretching modes as well as for intermolecular stretching and bending of hydrogen bonds. Apart from discrepancies in the stretching modes of ~100 cm^{-1}, substantial agreement with experimentally based assignments for different water species, due mainly to Walrafen, is obtained. It is predicted that the HDO bending band should broaden with increasing temperature, and evidence for strong intermolecular coupling of librational modes is presented. Observed frequencies of 60 cm^{-1} and less are ascribed to intermolecular bending modes. Calculations for H_3O^+ using a comparable model are also reported and compared with measured frequencies of $H_9O_4^+Br^-$ crystals and H_3O^+ in solutions of sulfur dioxide and water. The calculated frequencies for aqueous H_3O^+ are subjected to the condition that they reproduce the equilibrium constant for the isotopic exchange process, $2D_3O^+(aq) + 3H_2O(g) \rightleftharpoons 2H_3O^+(aq) + 3D_2O(g)$. It is concluded that the reported intramolecular frequencies are too high. This supports an earlier published conclusion that in aqueous solution the vibrational spectrum of H_3O^+ is obscured by the high rate of proton transfer between solvent molecules. (auth)

18400 MECHANSIMS OF MONOFUNCTIONAL AND BIFUNCTIONAL CATALYSIS OF AN ESTER HYDROLYSIS. THE KINETICS OF METHYL 2,6-DICARBOXYBENZOATE HYDROLYSIS. **Hurst, Gail H.; Bender, Myron L. (Northwestern Univ., Evanston, Ill.). J. Amer. Chem. Soc.; 93: 704-11(10 Feb 1971).**

The pH-rate profile for the hydrolysis of methyl 2,6-dicarboxybenzoate (1) reveals reactions of the protonated ester, neutral ester, monoanion, and dianion, and of hydroxide ion with dianion. At pH 4 the hydrolysis of 1 proceeds 10^7 times faster than hydrolysis of methyl mesitoate and 10^5 times faster than hydrolysis of methyl p-nitrobenzoate. Methyl 2-carboxy-6-nitrobenzoate (2) was found to have a pH-independent reaction at low pH with a rate constant similar to that of methyl hydrogen phthalate and one-half that of the neutral ester of 1. Therefore, catalysis is assumed to be the same for these esters and to be monofunctional for the reaction of the neutral ester of 1. Carboxyl group participation occurs in the reaction of the protonated ester since the solvent deuterium isotope effect of 1.1 is too large for other mechanisms. Only a nucleophilic mechanism for catalysis explains the failure to observe a pH-independent reaction in the hydrolysis of methyl 2-carboxy-3-nitrobenzoate (4) at low pH. The monoanion of 1 hydrolyzes 12 times faster than the neutral ester and 4000 times faster than the dianion. This is interpreted in terms of rate-limiting breakdown of the tetrahedral intermediate; the low reactivity of the dianion is also observed for the anion of 2 and results from unfavorable partitioning of the intermediate. Three possible mechanisms for bifunctional catalysis of the hydrolysis of the monoanion are given. (auth)

18401 TEMPERATURE DEPENDENCE OF THE 1555 cm^{-1} INFRARED ABSORPTION BAND IN LIQUID D_2O: INFLECTION POINTS. **Oder, R.; Goring, D. A. I. (Pulp and Paper Research Inst. of Canada, Montreal. McGill Univ., Montreal). Can J. Chem.; 48: 3790-6(15 Dec 1970).**

The temperature dependence curves of the peak height, frequency, and half-width of the infrared intermolecular combination band absorbing at 1555 cm^{-1} in liquid D_2O was observed to behave sigmoidally between 5 and 70°C. No evidence of sharp discontinuities was obtained but inflection points in the rather broad temperature interval of about 25 to 40°C were observed. Results are discussed in terms of structural changes occurring in the liquid. (auth) (Canada)

18402 INFRARED AND RAMAN SPECTRA AND VIBRATIONAL ASSIGNMENT OF METHYLENE CYCLOPROPANE-h_6 AND -d_6. **Bertie, J. E.; Norton, M. G. (Univ. of Alberta, Edmonton). Can J. Chem.; 48: 3889-3902(15 Dec 1970).**

Infrared spectra were recorded in the range 4000 to 20 cm^{-1} for methylene cyclopropane-h_6 and -d_6 in the gas phase, and from 4000 to 200 cm^{-1} for methylene cyclopropane-h_6 in the liquid phase. Raman spectra were recorded for the liquid phases of both species. The fundamental modes of vibration were assigned using ir band contours and Raman depolarization ratios, with the exception of the ir inactive A_2 modes which were not observed. An interesting feature is the occurrence of remarkably small isotope shifts for certain modes. (auth) (Canada)

18403 THERMOMAGNETIC TORQUE IN DEUTERIUM GAS. **McClurg, G. R.; Adair III, T. W. (Texas A and M Univ., College Station). J. Chem. Phys.; 54: 1678-82(15 Feb 1971).**

The Scott thermomagnetic torque was measured in three ortho-para concentrations of deuterium gas at pressures of 0.45 to 1.80 torr and in magnetic fields up to 440 Oe. The temperature range covered was 100 to 350°K. The product of the torque and pressure plotted as a function of the field divided by pressure has a maximum at $(H/P)_{max} = 90$ Oe/torr. All ortho-para concentrations of deuterium gas produced the same torque in contrast to the results in hydrogen. Also, in all concentrations the torque was found to become very small as the temperature was lowered to 100°K. (auth)

18404 RESONANCE PHOSPHORESCENCE, RAMAN SCATTERING, AND DECOMPOSITION OF HEXAAMMINECHROMIUM (III) SALTS UTILIZING He-Ne LASER EXCITATION. **Long II, Thomas Veach; Penrose, Dana Jo Burge (Pennsylvania State Univ., University Park). J. Amer. Chem. Soc.; 93: 632-7(10 Feb 1971).**

He-Ne laser excitation (632.8 nm) of $Cr(NH_3)_6^{3+}$ in a conventional Raman experiment produces both a Raman spectrum and a resonance-phosphorescence spectrum containing Stokes and anti-Stokes vibronic components. The frequencies of all vibrations of the CrN_6 octahedron are measured and assigned, including the infrared- and Raman-forbidden but vibronically allowed bending mode of T_{2u} symmetry (v_6). A general valence-force-field analysis of $Cr(NH_3)_6^{3+}$ and $Co(NH_3)_6^{3+}$ yields values of f_r, the metal-ligand stretching force constant, of 1.60 and 1.72 mdyn/Å, respectively. The laser-Raman spectrum of $Cr(NH_3)_5Cl^{2+}$ is also reported. The 0-0 band of the $(^4A_{2g}-^2E_g)$ electronic transition of $Cr(NH_3)_6^{3+}$ is located, and the vibronic components of this transition are completely assigned for both emission and absorption spectra. The phosphorescence spectrum of $Cr(ND_3)_6^{3+}$ in D_2O is also reported and the shifts on deuteration are consistent with the vibronic assignments. Decomposition of the salts upon laser irradiation is observed, and, for the solid materials, this results in the formation of complexes in which the counteranion has replaced one or more ammine groups, while the previously observed green photoaquation product forms in solution. (auth)

18405 ACID-CATALYZED ISOMERIZATION OF CIS-1-PHENYL-1,3-BUTADIENE AND CIS-1-METHYL-3-PHENYL-ALLYL ALCOHOL. **Pocker, Y.; Hill, Martin J. (Univ. of Washington, Seattle). J. Amer. Chem. Soc.; 93: 691-7(10 Feb 1971).**

The kinetics of the acid-catalyzed isomerization of cis-1-phenyl-1,3-butadiene (1) and cis-1-methyl-3-phenylallyl alcohol (2) to the corresponding trans compounds in aqueous sulfuric acid as well as in 40% aqueous dioxane containing perchloric acid were investigated. Both reactions give good pseudo-first-order kinetics, and plots of log k vs. $-H_0$ give good straight lines. The rate of isomerization of 1 in deuteriosulfuric acid is slower by a factor of 2.24 to 3.15 than in aqueous sulfuric acid, although deuterium incorporation occurs exclusively at the terminal carbon atom. The rate of isomerization of 2 is accelerated in deuteriosulfuric acid by a factor of 2.5 over the aqueous acid, and there is no deuterium incorporation into the molecule except for the hydroxyl proton. The loss of ^{18}O label from labeled 2 occurs at the same rate as isomerization to trans alcohol, indicating that the loss of water from protonated 2 is rate determining in the isomerization and there is no detectable return to starting material. Similarly, the protonation of 1 to give the cis carbonium ion is found to be rate de-

XUM

termining. In each case, rapid rotation about the C_1-C_2 bond converts the cis carbonium ion directly to the trans ion before attack by solvent can occur. Thus, even under kinetic control, all products are derived from the trans carbonium ion. This is the first case of a cis allylic cation that is not stable with respect to cis–trans isomerization in aqueous solution. Due consideration to the energetic requirements is given in the discussion of these processes. (auth)

18406 SECONDARY DEUTERIUM ISOTOPE EFFECTS ON TRIPLET EXCITATION TRANSFER. DEUTERIUM POSITION AND SENSITIZER EFFECTS. Caldwell, Richard A.; Sovocool, G. W.; Peresie, R. J. (Cornell Univ., Ithaca, N. Y.). J. Amer. Chem. Soc.; 93: 779-81(10 Feb 1971).

A study was made of the isotope effects in the photosensitized trans–cis isomerization of β-methylstyrene using propiophenone, benzophenone, 2-acetonaphthone, chrysene, biacetyl, and fluorenone, and deuterium labeling in β, α, meta, or para positions. Principal conclusions are: the isotope effect on partitioning of the olefin triplet to cis and trans ground states is nil; significant involvement of remote positions in the excitation-transfer process occurs; sensitizers with widely differing types of chromophore show essentially identical isotope effects, emphasizing the similarity of the bimolecular interactions; and the origins of the deuterium isotope effect are probably more closely allied with the effect of deuterium on excitation energy than with the effect on Franck–Condon factors associated with twisting around the α,β bond in the olefin T_1 state. (D.H.M.)

18407 A ^{14}C KINETIC ISOTOPE EFFECT STUDY OF NUCLEOPHILIC SUBSTITUTION REACTIONS OF p-SUBSTITUTED BENZYL CHLORIDES. Pearson, Neal. Fayetteville, Ark.; Univ. of Arkansas (1970). 225p. University Microfilms Order No. 70-26,219.

Thesis.

A kinetic and carbon-14 kinetic isotope effect study of nucleophilic displacement reactions of p-substituted benzyl-7-^{14}C chlorides was carried out utilizing the system represented by the general equation:

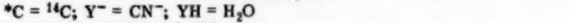

$^*C = {}^{14}C$; $Y^- = CN^-$; $YH = H_2O$
$X = CH_3O, CH_3, H, Cl, NO_3$

Reactions of benzyl chlorides are considered to be "border-line" in nature and can be shifted toward the S_N1 end of the mechanistic spectrum by electron donating substituents and toward the S_N2 end by electron withdrawing groups. It was thus hoped to correlate the magnitude of the benzyl carbon atom isotope effect with the mechanistic path. The kinetic and isotope effect results are summarized. They reflect the changing mechanism suggested by the kinetic results. Electron donating substituents shift the mechanism towards the S_N1 end of the spectrum with small isotope effects being observed. (The greater the electron donating ability of the substituent, the smaller the isotope effect.) As the electron donating ability of the substituent decreases, larger isotope effects are observed. A series of theoretical isotope effect calculations was carried out within the framework of the transition state theory employing cut-off models for reactant and S_N1 and S_N2 activated complexes. The results of these calculations indicate that the observed trends in k/k^* can be reproduced using reasonable models. These results reaffirm the idea that central atom isotope effects can be used as a mechanistic criterion in displacement reactions. (Diss. Abstr. Int., B)

18408 GREEN'S FUNCTION ANALYSIS OF SF_6 AND RELATED MOLECULES. Ramaswamy, K.; Mohan, N. (Annamalai Univ., Annamalainagar, India). J. Mol. Struct.; 7: 51-8(Jan 1971).

Isotopic rules for various substitutions of XY_6 octahedral molecules were formulated using the Green's function analysis. The molecular constants of SF_6 were determined. Some of the vibrational frequencies of the substituted molecules like SeF_6, TeF_6, SF_5Cl, SF_5CF_3, and SF_5Br were predicted using the frequencies of the parent molecule SF_6. The changes in the force constant were also calculated. (auth)

18409 EXPERIMENTAL AND THEORETICAL STUDY OF THE SECONDARY DEUTERIUM ISOTOPE EFFECTS ON THE IONIZATION IN THE BENZOIC, o-TOLUIC, MESITOIC, AND PHENYLACETIC ACID SYSTEMS. Demayo, Adrian. Ottawa; Carleton Univ. (1969).

Thesis.

The conductance method, as it is applied to the determination of the dissociation constants of weak acids is discussed, the experimental results for the dissociation constant and the thermodynamic functions for the ionization of the following acids are given: benzoic, benzoic-2-d, benzoic-d_5, o-toluic, o-toluic-d_7, m-toluic, p-toluic, mesitoic, mesitoic-d_9, phenylacetic, and phenylacetic-α-d_2. The determinations were done in aqueous solutions at temperatures between 20 and 40°C. The dissociation constants were determined by using a modified Ives-Feates-Pryor double conductance cell, an impedance bridge, and Fuoss-Shedlovsky extrapolation method. It was estimated that the dissociation constants are reliable within 0.1 to 0.2%. The thermodynamic functions of ionization were calculated by using Clarke and Glew equations. The temperature coefficient of the heat capacity of ionization found was not considered to be significant. The secondary deuterium isotope effects, K_H/K_D, were found to be constant over the temperature range employed in this work. Calculations of the Wolfsberg-Stern type were carried out in the benzoic, o-toluic, and phenylacetic acid systems in order to obtain an idea of the type of force constant changes that would lead to calculated values for the ratio K_H/K_D, in good agreement with the experimental ones. It was found that the assumption of a slight increase in the force constants of those internal coordinates of the anions which were located in the vicinity of the carboxylate group led to a good agreement between the calculated and the experimentally obtained results. (Diss. Abstr. Int., B)

18410 KINETIC ISOTOPE EFFECTS IN THE REACTIONS OF BROMINE ATOMS WITH CH_4 AND CD_4. Yokota, Toshitsugu; Timmons, Richard B. (Catholic Univ. of America, Washington, D. C.). Int. J. Chem. Kinet.; 2: 325-34(Jul 1970).

The competitive reactions of Br atoms with CH_4 and CD_4 were studied over the temperature range of 562 to 637°K. Over this temperature interval, the kinetic isotope effect, k_H/k_D, varied from 3.05 to 2.47 for the reactions $Br + CH_4 \xrightarrow{k_H} HBr + CH_3$ and $Br + CD_4 \xrightarrow{k_D} DBr + CD_3$. The rate constant ratio k_H/k_D, expressed in Arrhenius form, was found to equal (1.10 ± 0.05) exp (1030 ± 60/RT). A comparison is presented between the experimental results and the result obtained theoretically from absolute rate theory using the London-Eyring-Polanyi-Sato (LEPS) method of constructing the potential energy surface of the reaction. The agreement between theory and experiment is very poor, and believed to arise from the highly unsymmetrical nature of the potential energy surface involved in these reactions. A comparison is also presented between the k_H/k_D values obtained in the $Br + CH_4-CD_4$ experiments and the available data on the corresponding $Cl + CH_4-CD_4$ reactions. (auth)

18411 BASE-CATALYZED PROTIUM–DEUTERIUM EXCHANGE IN BICYCLO[2.2.1]HEPTANONES. Werstiuk, N. H.; Taillefer, R. (McMaster Univ., Hamilton, Ont.). Can. J. Chem.; 48: 3966-7(15 Dec 1970).

The rates of NaOD-catalyzed protium–deuterium exo exchange in fenchan-2,5-dione (2) and 1-methyl-5-oxo-camphene (3) are 200 and 7, respectively, relative to epiisofenchone (1). The endo exchange rates in 2 and 3 are 1840 and 4, respectively, relative to 1. These data give information about the relative importances of conjugative, conformational, inductive, strain, and steric effects that may arise when a carbonyl group or a double bond is situated 1,3 to an enolizable center in the 2.2.1 system. (auth) (Canada)

18412 EXCHANGE REACTIONS OF THE CENTRAL ATOMS IN LANTHANIDE–AMINOPOLYCARBOXYLATE COMPLEXES. III. KINETICAL INVESTIGATION OF ISOTOPIC EXCHANGE REACTIONS OF Tb^{3+} IONS WITH TbEDTA, TbHEDTA, AND TbDCTA COMPLEXES, RESP. Szarvas, P.; Bruecher, E. (Kossuth Univ., Debrecen, Hungary). Monatsh. Chem.; 101: 1321-9(Sep-Oct 1970). (In German).

The kinetics of isotopic exchange reactions between Tb^{3+} ions and TbEDTA, TbHEDTA as well as TbDCTA complexes, at pH's between 2.98 and 6.8 were investigated. On the basis of the determinated rate equations, the possibilities of the exchange mechanisms are discussed and some conclusions about the bonding and structural problems of the Tb—APK complexes are obtained. (auth)

18413 β-DEUTERIUM ISOTOPE EFFECT IN SOLVOLYSIS OF 1,2-DIMETHYL-EXO-2-NORBORNYL p-NITROBENZOATE. Humski, K. (Inst. Ruder Boskovic, Zagreb). Croat. Chem. Acta; 42: 501-4(1970).

Secondary β-deuterium isotope effects and product distributions in the solvolysis of 1,2-dimethyl-exo-2-norbornyl p-nitrobenzoate in dioxane–water mixtures were measured. The magnitude of the effect, k_H/k_D, increased from 1.28 to 1.35 while the amount of the elimination products changed from 36 to 66% when the solvent was changed from 50 to 70 vol % of dioxane. These results indicate that the elimination step is rate-determining. The calculated secondary β-deuterium isotope effect of 1.22 supports the contention that the ionization of the 1,2-

dimethyl-exo-2-norbornyl derivatives is not strongly assisted. (auth)

18414 RELATIVE LEAVING ABILITIES AND ISOTOPE EFFECTS IN ELECTROPHILIC AROMATIC SUBSTITUTION. Perrin, Charles L. (Univ. of California, San Diego, La Jolla). J. Org. Chem.; 36: 420-5(12 Feb 1971).

In acetic acid–acetic anhydride containing HCl, 1-chloro-1-nitro-2-keto-1,2-dihydronaphthalene undergoes both migration and loss of NO_2^+, rather than Cl^+. In contrast, the bromo analog loses Br^+. It was therefore concluded that the leaving abilities of these electrophiles increase in the order $Cl^+ < NO_2^+ < Br^+$. An order of relative leaving abilities for most of the common electrophiles is presented and justified. The factors that govern relative leaving abilities are considered. The implications of these relative leaving abilities for isotope effects and other aspects of electrophilic aromatic substitution are discussed. (auth)

Physical Chemistry

Refer also to abstract 18349.

18415 POSSIBLE USE OF POSITRON ANNIHILATION TO STUDY CHEMISORPTION. Mokrushin, A. D.; Prokop'ev, E. P.; Tsyganov, A. D. (Moscow State Pedagogical Inst.). Kinet. Catal. (USSR) (Engl. Transl.); 11: 666(May-Jun 1970). Translated from Kinet. Katal.; 11: 808-9(May-Jun 1970).

Two long-lived positrons with lifetimes of $\tau_3 = 1.4 \times 10^{-7}$ and $\tau_2 = 1.8 \times 10^{-9}$ sec were observed in certain finely dispersed powders (such as Al_2O_3, MgO, and SiO_2) under vacuum, and the lifetime τ_3 was found to correspond to the free ortho-positronium that exists in the pores of the test sample and the lifetime τ_2 was due to the annihilation of ortho-positronium by surface electrons. In this connection, some possible new methods for studying the adsorption and chemisorption of various substances are suggested. (D.H.M.)

18416 UNIFORM, NONPOROUS THORIA: THE EFFECT OF SURFACE WATER ON ADSORPTIVE PROPERTIES. Gammage, R. B.; Fuller, E. L. Jr.; Holmes, H. F. (Oak Ridge National Lab. Tenn.). J. Colloid Interface Sci.; 34: 428-35(Nov 1970).

Adsorption isotherms were measured for H_2O vapor, N_2, and Ar on a nonporous sample of ThO_2 outgassed at temperatures between 25 and 1000°C. Uniformity of the clean surface is evidenced by the multilayer stepwise adsorption of each adsorbate. Irreversibly bound H_2O has the profound effect of masking the physisorption potential of the surface and causes the step structure of the isotherms of H_2O, N_2, and Ar to be lost. The amount of N_2 or Ar adsorbed on the water-covered surface is reduced and the low apparent specific surface area suggests that there is a less than normal density of packing of these adsorbate molecules. In contrast the amount of physisorbed H_2O increases as more H_2O becomes irreversibly bound to the surface. Comparison with standard t-curves for H_2O vapor shows that "normal adsorption behavior" occurs only after several sorption cycles in H_2O vapor. On the clean surface a layer of H_2O is first chemisorbed and the following physical adsorption of H_2O has been discussed in terms of site orientation. An analysis of the character of N_2 and Ar adsorptions was also made using t-curves. (auth)

18417 VAPOR PRESSURE OF GADOLINIUM(III)-BROMIDE ACCORDING TO THE CUP METHOD OF W. FISCHER. Weigel, Fritz; Trinkl, Gabriele (Univ., Munich). Z. Anorg. Allg. Chem.; 377: 228-39(1970). (In German).

The vapor pressure of gadolinium(III) bromide was measured, using the molybdenum cup method of Fischer, Gewehr, and Wingchen. Within the 1200 to 1600°K temperature range, the experimental points may be fitted to the equation $\lg P_{atm} = -(47330/4,575 \cdot T) + 5,9672$. By extrapolation to $p = 1$ atm, a boiling point of 1,728°K (1,455°C) was obtained. The thermodynamic parameters for evaporation and sublimation were derived from vapor pressure data. Corresponding values for curium(III) bromide were estimated. (auth)

18418 SOLUBILITY OF CARBON DIOXIDE IN HEAVY WATER AT PRESSURES UP TO 40 ATM. Kratochvil, J.; Sobr, J.; Matous, J.; Pick, J. (Inst. of Chemical Tech., Prague). Collect. Czech. Chem. Commun.; 35: 3761-4(Dec 1970).

In analyzing the operation conditions of a heavy water reactor it is necessary to take into account the solubility of carbon dioxide in heavy water. Experimental data on equilibrium in this system are reported and critically evaluated. The data cover the pressure range from 1 atm to 40 atm, and temperatures 30, 50, and 80°C. (auth)

18419 LOW-FREQUENCY VIBRATIONS OF INORGANIC AND COORDINATION COMPOUNDS. Ferraro, John R. New York; Plenum Press (1971). 320p. $18.50. (TID-25660).

Information is presented on the correlation of far-infrared vibrations for molecules in inorganic and coordination compounds. Topics covered include: history, far-infrared instrumentation, sampling techniques and instrument calibration in the far-infrared region, new techniques used with far-infrared measurements, metal–oxygen vibrations, metal–halide vibration, metal–nitrogen vibrations, miscellaneous metal–ligand vibrations, and other low-frequency vibrations. (M.C.G.)

Radiation and Nuclear Chemistry

Radiation Effects

Refer also to abstracts 19164 and 19300.

18420 (COO-1385-34) ESR STUDY OF THE IO_2F^- RADICAL IN γ-IRRADIATED SINGLE CRYSTALS OF POTASSIUM OXYFLUOROIODATE. Subramanian, S.; Rogers, Max T. (Michigan State Univ., East Lansing. Dept. of Chemistry). [1970]. 23p. Dep. NTIS.

Single crystals of KIO_2F_2 γ-irradiated at room temperature, or irradiated at 77°K and allowed to warm above 140°K, gave ESR spectra characteristic of the 27-electron radical anion IO_2F^-. The g, A(^{19}F) and A(^{127}I) tensors were evaluated, and the ^{127}I quadrupole interaction parameters Q′ and Q″ were estimated, from the spectra. The unpaired electron is predominantly delocalized over the iodine and oxygen atoms and interacts only weakly with the fluorine atom. Loss of a fluorine atom from $IO_2F_2^-$ would lead to a radical structure based on a trigonal bipyramid with the electron pair and two oxygen atoms in equatorial positions and the fluorine atom and odd electron in apical positions. The ESR data are consistent with an arrangement of this type and with some involvement of iodine 5d orbitals in the bonding. (auth)

18421 (RLO-2098-1) POLYMER GRAFTING TO INORGANIC SUBSTRATES. Annual Progress Report, February 1, 1969–January 31, 1970. Raff, R. A. V.; Subramanian, R. V.; Schecter, D. J.; Adams, M. F. (Washington State Univ., Pullman. Research Div.). Contract AT(45-1)-2098. 93p. Dep. NTIS.

An exploratory study was made on the effect of gamma radiation on a number of inorganic filler-polymer resin composites. The feasibility of a masterbatch technique to prepare active fillers was explored with polystyrene–carbon black and polyethylene–aluminum oxide systems, and desirable trends were observed in the selective response of certain properties of these systems to gamma irradiation. The potential utility of gamma radiation was further confirmed by the greatly improved mechanical properties of carbon black-reinforced and glass fiber-reinforced polyethylene specimens after exposure to gamma rays. There were no major differences brought about by gamma irradiation in the properties of phenolic resin laminates with carbon or graphite cloth inserts or of glass fiber-reinforced polyester resin. Gamma irradiation was applied successfully in other areas. Thus, acrylonitrile was polymerized inside porous carbon using gamma rays. By subsequent heating of the product to cyclize and stabilize the polyacrylonitrile in the pores, an impervious carbon of superior strength and chemical resistance was obtained. Further, by irradiation of castings containing various metals embedded in epoxide resin, the metal-resin bond strengths were increased several-fold. Finally, radiation polymerization of vinyl monomers with cation or anion exchange groups was conducted in the presence of finely divided firebrick to give a material with the theoretically expected ion exchange capacities. (auth)

18422 THERMALLY STIMULATED CURRENTS FROM GAMMA-IRRADIATED ORGANIC POLYMERS: POLY(METHYL METHACRYLATE). Tamsky, Morgan Jerome. Lawrence, Kan.; Univ. of Kansas (1970). 231p. University Microfilms Order No. 70-25,416.

Thesis.

The phenomenon of thermally stimulated currents (TSC) from γ irradiation was studied for the following polymers, especially poly(methylmethacrylate (PMMA); isotactic PMMA, syndiotactic PMMA, commercial PMMA, polyethylene, polypropylene, polystyrene, polytetrafluoroethylene, polyvinylchloride, and carnauba wax. Disk shaped samples, a few cm in diameter and about one cm thick, were omnidirectionally irradiated in a ^{60}Co source to doses of 1 Mrad at 31°C. The TSC was measured by heating the samples at controlled linear rates, 1.5 to 6.3°C/min, with a vibrating reed electrometer in the same circuit with the sample. The major conclusions of the present study apply to PMMA specifically but are not restricted to only this polymer: (1) The "simple model" for TSC, described in detail, adequately accounts for the characteristics of the TSC glow curves measured in the present study. The kinetic order of the TSC appears to be first for the highly syndiotactic PMMA samples. For the isotactic PMMA sample there is some indication that the TSC may be a second order process. (2) The model of Barnes for TSC from γ-irradiated PMMA which postulated that irradiation produced electrons were trapped on impurities; and that positive charges were trapped on the side chains of PMMA molecules, being "passed" from one side chain to the next during thermal release until recombining with electrons, does not adequately explain the results of the present study. (3) Impurities are not the major trap sites for irradiation produced charges. The polymer chain is probably acting as the positive hole trap site and the polymer matrix as the ionized electron trap site. Predominantely isotactic PMMA appeared to be able to trap more irradiation produced charges than predominately syndiotactic PMMA. (4) A substantial number of the irradiation produced charges may be trapped sufficiently near each other so that the coulombic interaction between "pairs" of oppositely charged species is much larger than the influence of an external field (of the order of 1000 V/cm) on the charges of a "pair." (5) Polymer transitions are responsible for detrapping the irradiation produced charge species, which are trapped during irradiation, when an irradiated sample is heated. It appears that the polymer transition for a given polymer, which correlates "best" with the observed TSC, is that transition, which occurs at or above the irradiation temperature and which produces a change in the dielectric constant. The particular transition, which correlates best with the TSC does not appear to be limited to a given type (e.g., α, β, or melting). (6) The TSC measured with a temperature gradient and without an applied field is not thermoelectric in nature but is manifest by a more rapid rate of recombination of oppositely charged species near the hot side. This asymmetry in the rate of recombination leads to the dependence of the polarity of the TSC on the direction of the temperature gradient. It appears that the TSC measured with a temperature gradient and without an applied field involves recombinations between "pairs" of oppositely charged species bound by coulombic forces larger than the influence of an external field (of the order of 1000 V/cm). The TSC measured without a temperature gradient and with an applied field appears to involve recombination of charges not bound by strong coulombic forces to oppositely charged species and which are thus free to move under the influence of an external field. (7) The calculated activation energy for the TSC in the polymers studied ranged from about 1 to 3 eV. For PMMA the values of the activation energy were about 1.3 eV for highly isotactic samples, 0.9 eV for highly syndiotactic samples and 1.0 eV for commerical samples. (8) The polarity of the mobile charge carrier is not directly determined by the polarity of the TSC. (Diss. Abstr. Int. B)

18423 EPR STUDY ON THE STABLE HYDROGEN ATOMS ON γ-IRRADIATED CLINOPTILOLITES CONTAINING La, Mg, AND K IONS. Papp, J.; Mikheikin, I. D.; Kazanskii, V. D. (Inst. of Organic Chemistry, Moscow). Kinet. Catal. (USSR) (Eng. Transl.); 11: 671-2(May-Jun 1970).

Translated from Kinet. Katal.; 11: 812-13(May-Jun 1970).

Clinoptilolite samples containing La^{3+}, Mg^{2+}, K^+ ions introduced by ion exchange and heated in vacuo at 400, 500, 600, or 700°C for 3 to 4 hrs were exposed to γ radiation at the temperature of liquid nitrogen. Their EPR spectra consisted of intensive complex lines with a g-factor equal to about 2 and known doublets with splitting of about 500 Oe produced by hydrogen atoms; the complex lines differ in the various samples. When the samples were heated to room temperature, the intensity of the signals due to hydrogen atoms decreased and the shape altered. The EPR spectra of the hydrogen atom could also be recorded at room temperature. The concentration of hydrogen atoms produced by γ irradiation remained almost unaltered when the samples were fired before irradiation at temperatures of 400 to 500°C; when the temperature is raised to 600°C the EPR signal is reduced by a factor of 5 to 10; and the signal disappears completely when the temperature of the pretreatment equals 700°C. (D.H.M.)

18424 ORIGIN OF COMPLEX ELECTRON SPIN RESONANCE SPECTRA OF γ-IRRADIATED POLYCRYSTALLINE n-ALKYL IODIDES WITH EVEN NUMBER OF CARBON ATOMS PER MOLECULE. Egland, R. J.; Ogren, P. J.; Willard, J. E. (Univ. of Wisconsin, Madison). Contract AT(11-1)-1715. J. Phys. Chem.; 75: 467-71(18 Feb 1971).

The ESR spectra of six isotopically different γ-irradiated polycrystalline ethyl iodides ($C_2H_5{}^{127}I$, $C_2H_5{}^{129}I$, $C_2D_5{}^{127}I$, $C_2D_5{}^{129}I$, $CH_3CD_2{}^{127}I$, and $CD_3CH_2{}^{127}I$) were examined to assist in determining the origin of the unusual 1000-G wide pattern from C_2H_5I. Comparison of the spectra from C_2H_5I, C_2D_5I, CH_3CD_2I, and CD_3CH_2I confirms the contribution of hyperfine splitting by hydrogen and indicates that it is due primarily to the methyl hydrogen atoms with little or no contribution from the methylene hydrogens. Comparison of the X- and Q-band spectra of γ-irradiated polycrystalline C_2H_5I indicates that the great spectral width is not caused by anisotropic g values, reopening the question as to whether it may be the result of hyperfine splitting by iodine. This was investigated by the substitution of ^{129}I for ^{127}I. Exposure for γ-irradiated polycrystalline C_2H_5I to near-infrared radiation converted the complex ESR spectrum into the ethyl radical spectrum. Irradiation of polycrystalline C_2H_4I did not produce the spectrum obtained from C_2H_5I. Irradiation of all glassy and polycrystalline n-alkyl chlorides and bromides from C_2 to C_8, as well as the glassy iodides and odd-carbon-number polycrystalline iodides, yielded only the spectrum of the alkyl radical. The hypothesis that the complex spectra from the C_2, C_4, C_6, and C_8 n-alkyl iodides result from physically trapped electrons is considered. In this case the breadth of the spectrum results from hyperfine splitting by iodine nuclei. The difference between the spectra observed for the alkyl halides with odd and even numbers of C atoms per molecule then indicates that the branching ratio between physical trapping and dissociative capture is controlled by small differences in the crystal structure of the matrix. (auth)

18425 INVESTIGATION OF THE EFFECT OF IONIZING RADIATION ON THE STRUCTURE AND PROPERTIES OF MODIFIED CAPRON FIBERS. Spitsyn, V. I.; Goryaev, N. M.; Plavnik, G. M.; (and others) (Inst. of Physical Chemistry, Moscow). High Energy Chem. (USSR) (Engl. Transl.); 4: 330-2(Jul-Aug 1970).

Translated from Khim. Vys. Energ.; 4: 372-3(Jul-Aug 1970).

The effects of 1-MeV electrons on the structure and mechanical properties of Capron fibers and also fibers modified by radioinduced graft polymerization of vinyl monomers or by the introduction of various aromatic additives were investigated. The strength characteristics of the fibers were sensitive to radiation. Modification of the surface and introduction of additives increased radiation stability and reduced the structural sensitivity of the fibers to radiation. (M.C.G.)

18426 EVIDENCE FOR HYDROGEN ATOM ABSTRACTION BY METHYL RADICALS IN THE SOLID STATE AT 77°K. Sprague, Estel D.; Williams, Ffrancon (Univ. of Tennessee, Knoxville). Contract AT(40-1)-2968. J. Amer. Chem. Soc.; 93: 787-8(10 Feb 1971). (ORO-2968-54).

Detailed studies on the reactions of methyl radicals in γ-irradiated acetonitrile at low temperature resulted in definitive evidence for a process of hydrogen abstraction with an activation energy of only 1.4 kcal $mole^{-1}$. This result suggests either a large contribution from tunnelling at low temperature or a drastic modification of the potential energy surface for the reaction upon going to the solid state. Results also show a large primary kinetic isotope effect in the hydrogen atom abstraction process from acetonitrile. (D.H.M.)

18427 CHANGE OF PROPERTIES OF SILICA GEL UNDER ACTION OF GAMMA IRRADIATION. Ranchenkov, G. M.; Rozen, I. V.; Skoblo, V. A.; Krashin, D. I. Tr., Mosk. Inst. Neftekhim. Gazov. Prom.; No. 86, 124-5(1969). (In Russian).

Studies of the effects of γ radiation on the sorptive properties of silica gels showed that sorption increased with increased γ doses, especially, in the sorption of materials with highly developed surfaces. (R.V.J.)

Radiation Processes

Refer also to abstract 20213.

18428 (NP-18676) MASS SPECTROMETRIC STUDIES ON NEGATIVE ION-MOLECULE REACTIONS OF NITROETHYLENE. Shiga, Tetsuo; Yamaoka, Hitoshi; Sugiura, Toshio; Arakawa, Kazuo (Forskningsradens Laboratorium, Studsvik (Sweden)). 1970. 37p. (LF-33). Dep. NTIS (U. S. Sales Only).

Fragment ions from nitroethylene are formed by dissociative resonance capture. The parent ion is formed by nondissociative resonance capture with an appearance potential close to 0 eV. The cross section is estimated to be 1.3×10^{-16} cm^2. The derived mean lifetime of the parent ion is 14 μsec. Mass numbers of 99, 119, and 146 are also detected. The intensities of these ions show second order dependence on the pressure while that of the parent ion shows first order dependence. Ionization efficiency curves are similar in all cases. The formation of the dimer ion $M/e = 146$ by ion-molecule reaction suggests that the parent ion is the initiating species in the radioinduced polymerization of nitroethylene. The derived rate constant for the dimerization reaction is 3.2×10^{-13} cm^3 $molecule^{-1}$ sec^{-1}. High electron energies of

20 to 100 eV are used to obtain information on the most usual ion-molecule reactions initiated by high-energy ionizing radiation. The intensity of the parent ion shows a second order dependence on the pressure below 10^{-4} torr and a higher than second order dependence above 10^{-4} torr. The intensity of the dimer ion shows a second order dependence greater than that of the parent ion. The intensity of the parent ion is shown to be dependent on the pressure of additional rare gases. (auth) (Sweden)

18429 RADIATION INDUCED GRAFT TERPOLYMERIZATION OF POLY(ETHYLENE TEREPHTHALATE). PART III. THE MECHANISM OF TERPOLYMERIZATION IN VIEW OF THE REACTIONS OCCURRING DURING RADIOLYSIS OF THE GRAFTING SOLUTIONS. **Stolarczyk, Lech; Achmatowicz-Szmajke, Teresa (Inst. of Nuclear Research, Warsaw). Nukleonika; 15: 523-34(1970).**

Aqueous solutions of acryl- or methacrylamide and unsaturated dicarboxylic acids, which were used for grafting were radiolyzed, and the decarboxylation process as well as the disappearance of double bonds were studied. The gaseous products of radiolysis were determined by gas chromatography. Graft terpolymerization of the polyester from ethylene saturated aqueous solutions of acrylamide was performed. Based on the data presented in all three parts of this work, the mechanism of the graft terpolymerization process of the polyester is proposed. (auth)

18430 RADIATION-INDUCED POLYCONDENSATION OF FURFURAL IN THE PRESENCE OF ALKYL HALIDE. **Kaetsu, Isao; Ito, Akihiko (Japan Atomic Energy Research Inst., Takasaki). Kobunshi Kagaku; 27: 763-8(Oct 1970). (In Japanese).**

Furfural was polymerized by irradiation in the presence of alkyl halides such as chloroform, carbon tetrachloride, and bromoform. This polycondensation reaction also took place by the addition of preirradiated aklyl halides to furfural, but in these cases the rates of polycondensation were smaller than those of in-source reaction. The maximum value of the rate was observed at certain concentrations of alkyl halide in both cases of in-source and post-reactions. In a furfural–alkyl chloride system, the maximum rate was formed at a molar equivalent composition and in a furfural–alkyl bromide system, at higher alkyl halide concentration. It was deduced that radioinduced polycondensation of furfural was initiated by hydrogen halide formed through the radiolysis of alkyl halide. (auth) (Japan)

18431 INVESTIGATIONS IN THE FIELD OF RADIATION-INDUCED SOLID-STATE POLYMERIZATION. XXVI. STRUCTURAL STUDIES RELATED TO THE POLYMERIZATION OF CHOLESTERYL ACRYLATE. **Hardy, Gy.; Cser, F.; Kallo, A.; (and others) (Research Inst. for the Plastics Industry, Budapest). Acta Chim. Acad. Sci. Hung.; 65: 287-300(1970).**

The phase conditions of cholesteryl acrylate, cholesteryl acetate, and cholesteryl propionate, and the phase diagram of the two-component systems formed respectively by the latter two and the first compound were investigated. X-ray tests supplied a probable structure of the smectic state of cholesteryl acrylate (40 Å thick and 200–250 Å wide plates form a bundle of fibers. The plates are double molecular layers, the acrylate groups in the middle are coplanar). This is also supported by electron microscopic investigations. Depending on the temperature, in the polymerizing system, the polymer is isomorphous with the monomer below 0°C and becomes separated from the monomer as globular formations above 0°C. Accordingly, the polymerization-kinetic curve of the smectic liquid crystalline system is linear or shows an accelerating character, depending on the temperature. By a light-scattering method the equation describing the relationship between the viscosity and molecular weight of poly(cholesteryl acrylate) was determined. (auth)

18432 INVESTIGATIONS IN THE FIELD OF RADIATION-INDUCED-SOLID STATE POLYMERIZATION. XXVII. POLYMERIZATION OF CHOLESTERYL ACRYLATE AND ITS TWO-COMPONENT SYSTEMS. **Hardy, Gy.; Nyitrai, K. (Research Inst. for the Plastics Industry, Budapest). Acta Chim. Acad. Sci. Hung.; 65: 301-10(1970).**

The polymerization kinetics of a chloroform solution containing 0.9 mole/liter cholesteryl acrylate were studied. The overall activation energy of the liquid phase radioinduced polymerization is 4.3 kcal/mole and the process is characterized by the reaction of chain transfer to chloroform. In the smectic liquid crystalline state below 20°C, the polymerization kinetics curves are linear; above 20°C, these are of an accelerating character. In spite of this fact, polymerization occurs in the lattice, but is accelerated above 20°C because at this temperature the polymer formed no longer remains in the lattice of the monomer, but is precipitated as an amorphous product forming a separate phase. This is supported by the independence of the molecular weights of the polymers from the dose rate and conversion, and also by the laws valid for the two-component systems formed with isomorphous cholesteryl propionate and with p-benzoquinone yielding an eutectic system. (auth)

18433 COMPARISON OF THE ULTRAVIOLET SPECTRA AND POLYMERIZATION OF SOME DIMETHACRYLAMIDES AND N-ISOBUTYRYLMETHACRYLAMIDES. **Myers, George Rodney. Gainesville, Fla.; Univ. of Florida (1969). 111p. University Microfilms Order No. 70-11,747.**

Thesis.

Research was carried out to prepare a suitable 1,6-diene, the corresponding monoene, and to compare their ultraviolet spectra and their polymerization. The compounds chosen for this study were dimethacrylamide, N-isobutyrylmethacrylamide and their N-methyl and N-phenyl derivatives. The ultraviolet spectra of the compounds were determined and compared with related compounds. The compounds were polymerized in solution by free radical initiators and properties of the polymers studied in an attempt to determine their structure. The monomers are crystalline compounds that could be polymerized in the solid state by gamma rays. For this reason, another objective of this research was to irradiate the monomers and to determine the structure of the polymers. The ultraviolet spectra of the N-isobutyrylmethacrylamides and dimethacrylamides were determined and compared with the spectra of the related diisobutyramides, methacrylamides and isobutyramides. Of the compounds studied, N-isobutyrylmethacrylamide polymerizes at the fastest rate. The N-phenyl and N-methyl derivatives of N-isobutyrylmethacrylamide do not polymerize. For the dimethacrylamides, dimethacrylamide polymerizes fastest, N-phenyldimethacrylamide at a slightly lower rate, and N-methyldimethacrylamide considerably slower. The polymerization rate of N-phenyl and N-methyldimethacrylamide is slower in benzene than in DMF. Both N-isobutyrylmethacrylamide and dimethacrylamide polymerize faster in benzene, probably due to the heterogeneous nature of the system. Also, dimethacrylamide will crosslink, while the N-phenyl and N-methyl derivatives will not. The structures of the polymers produced were determined from a study of their NMR spectra. Polymerization of dimethacrylamide yields a polymer consisting primarily of six-membered rings. Five-membered rings and units resulting from linear propagation with the formation of pendent double bonds are also formed. Polymerization of N-methyldimethacrylamide gave a polymer consisting of about 90 per cent five-membered rings and 10 per cent six-membered rings. For N-phenyldimethacrylamide, the polymer seems to contain only five-membered rings. For dimethacrylamide and N-isobutyrylmethacrylamide monomer association or monomer-polymer association through hydrogen bonding could account for their increased polymerization rate. The structural differences were attributed to the steric and resonance effects of the methyl and phenyl substituents. N-isobutyrylmethacrylamide, dimethacrylamide, N-methylacrylamide, and N-phenyldimethacrylamide were polymerized by gamma rays from a ^{60}Co source. Dimethacrylamide gave an insoluble polymer consisting of six-membered rings, five-membered rings and units resulting from linear propagation without cyclization. From N-methyldimethacrylamide a soluble polymer consisting of 30 per cent six-membered rings and 70 per cent five-membered rings was obtained. The polymer from N-phenyldimethacrylamide contained five-membered rings and a small amount of six-membered rings. (Diss. Abstr. Int., B)

18434 RELATION OF RADIATION CROSS-LINKING IN SPECIAL PURPOSE ELASTOMERS TO ADDITIONS OF CHLOROALKANES OF VARIOUS STRUCTURES. **Kozlov, V. T.; Evseev, A. G.; Zubov, P. I.; (and others). Vysokomol. Soedin., Ser. B; 12: 743-5(Oct 1970). (In Russian).**

The effects of chloroalkanes with different chain lengths and various degrees of chlorination on the rate of radioinduced cross-linking of special-purpose elastomers were studied. EPR and photolysis studies showed the great value of electron capture reactions in radiation sensitization processes. (tr-auth)

18435 APPLICATION OF THE METHOD OF RADIOTHERMOLUMINESCENCE FOR THE INVESTIGATION OF HIGH-TEMPERATURE RELAXATION IN POLYETHYLENE. **Aulov, V. A.; Sukhov, F. F.; Slovokhotova, N. A.; Kargin, V. A. (Inst. of Physical Chemistry, Moscow). Vysokomol. Soedin., Ser. B; 12: 757-8(Oct 1970). (In Russian).**

For investigation of the α-maximum form, polyethylene films, 100-μ thick, were prepared by hot pressing with no further heat treatment. The irradiation was carried out in liquid nitrogen using a ^{60}Co γ source. The maximum radiothermoluminescence occurred at 51 ± 5°C, which coincides with the temperature of the α-relaxation region for this polymer. (tr-auth)

18436 ACTION OF IONIZING RADIATION ON THE STRUCTURE AND PROPERTIES OF THE COPOLYMER OF STYRENE

XUM

WITH 2-ETHYLHEXYL ACRYLATE. Vinogradova, A. P.; Egorova, Z. S.; Leshchenko, S. S.; Karpov, V. L. (Inst. of Physical Chemistry, Moscow). Vysokomol. Soedin., Ser. B; 12: 748-51(Oct 1970). (In Russian).

Changes in stability, thermomechanical properties, and solubility observed in a copolymer of styrene with 40% 2-ethylhexyl acrylate on irradiation with ^{60}Co γ radiation showed that the predominant process caused by the radiation is crosslinking. Spectral studies of the molecular changes showed that formation of the space network occurs mainly by 2-ethylhexyl acrylate branching. It was concluded that the greater sensitivity of this copolymer to radiation, in comparison to polystyrene, is related to the branchings, which increase the flexibility of the polymer chain. (tr-auth)

18437 RADIATION CURABLE POLYVINYL CHLORIDE COMPOSITION CONTAINING TRIALLYL ISOCYANURATE. Klopfer, Oskar E.; Hornbaker, Edwin D. (to Ethyl Corp.). U. S. Patent 3,539,488. 10 Nov 1970. Filed 7 Mar 1968.

A cross-linked, heat-stable vinyl halide resin is described, and a process for preparing the resin comprises irradiating a mixture of polyvinyl halide and a polyfunctional allyl or vinyl monomer, such as trimethylolpropane trimethacrylate triallyl isocyanurate, and the like. Resultant cured poly(vinyl halide) resins have heat-deflection temperatures in excess of 90°C, when irradiated at dose levels of at least 1.0 MRad. (Offic. Gaz.)

18438 RADIOTHERMAL ISOMERIZATION OF ALKYL BROMIDES. Pozdeev, V. V.; Fomina, N. V.; Kocheshkov, K. A. (Inst. of Physical Chemistry, Moscow). High Energy Chem. (USSR) (Engl. Transl.); 4: 343-4(Jul-Aug 1970).

Translated from Khim. Vys. Energ.; 4: 379-80(Jul-Aug 1970).

Radioinduced isomerization and radiolysis of alkyl bromides were studied at 150 to 240°C. Data are given on butyl bromide as an example. The data also show that the degree of isomerization decreased as the length of the hydrocarbon chain and the boiling point of the alkyl bromide increased. (M.C.G.)

18439 RADIATION CURABLE PAINT CONTAINING A VINYL ESTER BINDER RESIN HAVING PENDANT DIESTER GROUPS. Aronoff, Elihu J.; McLaughlin, Ernest O. (to Ford Motor Co.). U. S. Patent 3,542,587. 24 Nov 1970. Filed 1 Jul 1968.

A coating curable by exposure to an electron beam comprises a vinyl monomeric component and a vinyl polymeric component having 2 or more diester side chains of the following structural formula:

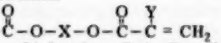

$$-\overset{\overset{\displaystyle O}{\|}}{C}-O-X-O-\overset{\overset{\displaystyle O}{\|}}{C}-\overset{\overset{\displaystyle Y}{|}}{C}=CH_2$$

in which x is a C_2 to C_{10} alkyl, C_5 to C_6 cycloalkyl, or C_2 to C_{10} polyalkyleneoxy divalent radical and Y is a hydrogen or methyl radical. The coating is polymerized by exposure to an electron beam having an average energy in the range of 100,000 to 450,000 eV. (Offic. Gaz.)

18440 KINETICS FOR THE RADIATION POLYMERIZATION OF SOLID ACRYLONITRILE IN THE REGIONS OF PHASE TRANSITIONS. Kritskaya, D. A.; Ponomarev, A. N.; Tal'roze, V. L. (Moscow State Univ.). High Energy Chem. (USSR) (Engl. Transl.); 4: 287-90(Jul-Aug 1970).

Translated from Khim. Vys. Energ.; 4: 332-6(Jul-Aug 1970).

The kinetics were studied for the radiation polymerization of frozen acrylonitrile (AN) during its irradiation by electrons having an energy of several kiloelectron volts in the regions of phase transitions by using an adiabatic microcalorimeter. It is shown that at 110°K a bimolecular rupture of the growing polymeric chains is observed. The chain development time, equal to about 10^{-2} sec for I = 0.5 Mrad/sec, was measured by the sector method. Two types of processes were observed in the phase transition at 157°K: a reaction with a chain development time of about 30 sec and monomolecular rupture and also a reaction with a short chain development time and bimolecular rupture. On the basis of the experimental data that were obtained, the rate constants were calculated for the growth and rupture of the polymeric chain at 110 and 157°K and the stationary concentrations were evaluated for the active centers which carry out the polymerization. (auth)

18441 POLYMERIZATION OF ARYLACETYLENIC COMPOUNDS. Lee, Joseph Y. C. New York; City Univ. (1970). 159p. University Microfilms Order No. 70-24,475.

Thesis.

The polymerization of diphenyldiacetylene, diphenylacetylene, phenylacetylene, and 2-ethynylnaphthalene was studied under very carefully controlled conditions to exclude oxygen, moisture, and light to which the resulting polyenes may be sensitive. The polymers thus prepared showed properties different from those prepared by other means. They have a higher molecular weight and form charge-transfer complexes with suitable π-electron acceptors. Poly(2-ethynylnaphthalene) is a new polymer. Their structures and stereochemistry are discussed. Polymerization of diphenyldiacetylene by the stereospecific Ziegler-type catalyst with carefully controlled inert atmosphere gives consistently a higher molecular weight than reported in the literature. The rate of polymerization is proportional to the square of the monomer concentration and the molecular weight of the polymer appears to be independent of the monomer concentration. It was concluded that thermal polymerization involves a bimolecular initiation and termination step. Polydiphenyldiacetylene obtained this way is always soluble in aromatic solvents so that a three-dimensional cross-linked structure can be precluded. The softening temperature is 270 to 300°C, although no sharp endotherm is observed in differential thermal analysis. They are dark-brown in color, have an electron paramagnetic resonance signal without hyperfine structures and the spin concentration increases upon formation of charge-transfer complexes. Gamma irradiation with ^{60}Co yields a dimer. Polymerization of diphenylacetylene by the stereospecific Ziegler-type catalyst gives mostly colorless trimer and some polymer. Polydiphenylacetylene obtained this way has two fractions, about 10% benzene soluble fraction and about 90% benzene insoluble fraction. Both fractions do not react with antimony trichloride to give a positive color test for a conjugated double bond system and do not give an EPR signal. Their melting points are greater than 450°C. There was no thermal polymerization up to 140°C under the experimental conditions. Gamma irradiation gave a dimer in very low yield. Phenylacetylene could be polymerized thermally or catalytically. Thermally prepared polyphenylacetylene contains a small amount of 1,2,4-triphenylbenzene and Ziegler-type catalyst initiated polymer contains some 1,3,5-triphenylbenzene, besides the expected polymer as detected by infrared spectra. Thermally prepared polymers are soluble in aromatic solvents. The catalyst prepared polymer becomes insoluble as the Al : Ti ratio increases. The presence of a long planar conjugated sequence is unlikely on the basis of ultraviolet data. Polyphenylacetylene obtained this way is orange colored, with a softening temperature of 160 to 200°C, an EPR signal without hyperfine structures and forms charge-transfer complexes with suitable π-electron acceptors. Poly(2-ethynylnaphthalene) was prepared by the Ziegler-type catalyst. The highest number average molecular weight of the polymer is 2091, corresponding to a degree of polymerization of 14 monomer units. The polymer is reddish colored, soluble in aromatic solvents and has a softening temperature slightly higher than polyphenylacetylene, at 190 to 230°C. Poly(2-ethynylnaphthalene), like polyphenylacetylene, is paramagnetic, has an EPR signal without resolved hyperfine structures. Infrared spectra and color test indicated a conjugated double bond system. However, long planar conjugated sequence is unlikely. (Diss. Abstr. Int., B)

18442 MECHANISM OF RADIATION POLYMERIZATION OF VINYL MONOMERS IN THE PRESENCE OF MINERAL ADDITIONS. Kornienko, T. P.; Zelenchukova, T. G. (Inst. of Physical Chemistry, Kiev). Teor. Eksp. Khim.; 6: 553-6(Jul-Aug 1970). (In Russian).

The effects of γ radiation on the copolymerization of styrene with methyl methacrylate were studied at room temperature. The effects of additions of silica gel and magnesium oxide and solvents of differing electronic natures were investigated. The polymerization rate was increased significantly by additions of silica gel and to a much lesser degree by additions of magnesium oxide. The effects of solvents on the process did not depend on their electronic nature. The constants calculated for the initial stages of reaction are close to those known for radical polymerization. It was concluded that the effects of the solid additions are related to the formation of radiation defects of the radical type on their surface. (tr-auth)

18443 RADIATION HARDENING OF COMMERCIAL POLYESTER RESINS. Proksch, E. (Reaktorzentrum, Seibersdorf, Austria). Kunstoffe; 60; 414-19(1970). (In German).

The effects of γ radiation, reactor irradiation, and electrons on a commercial polyester resin were studied. Sample pretreatment, effects of dose and dose rate, the polymerization mechanism, polymer decomposition, and irradiation atmosphere are discussed. (M.C.G.)

18444 INVESTIGATION OF AROMATIC HYDROCARBONS OF SUPSINSKAYA PETROLEUM AND THEIR CATALYTIC CONVERSION IN THE PRESENCE OF IRRADIATED CATALYSTS. Shakarashvili, T. S.; Bekauri, N. G.; Kutsiava, N. G.; Khorava, I. S. Tr. Gruz. Politekh. Inst.; No. 2, 13-19(1969). (In Russian).

Aromatic hydrocarbons of the 200 to 250°C fraction of Supsinskaya petroleum were investigated. The picrate method was used to identify methylethyl-, diethyl-, and butylnaphthalenes, and their catalytic conversion was performed in the presence

XUM

of a catalyst irradiated with γ rays. Irradiated catalysts decreased the conversion temperature of the hydrocarbons by 50 to 70°C. (Referativnyi Zh.) (JPRS)

18445 RADIATION-INDUCED SOLID-STATE POLYMERIZATION IN SOME METHACRYLATES. Bowden, M. J.; O'Donnell, J. H.; Sothman, R. D. (Univ. of Queensland, Brisbane). J. Macromol. Sci., Part A; 4: 1239-46(Aug 1970).

Results on the polymerization of methacrylic acid, octadecyl methacrylate, zinc methacrylate, and barium methacrylate monohydrate in the solid state were compared. Polymerization was initiated by ^{60}Co γ rays, both in-source and post-irradiation polymerization techniques being used. Electron spin resonance studies showed that the polymerization proceeded by a free radical mechanism in all cases. The initial radicals formed by irradiation at low temperatures added a first monomer unit about 100°C below the temperature of long-chain polymerization. Some radical decay occurred in the early stages of polymerization. The rate of polymerization increased rapidly, approaching the melting point or other phase change in the monomer. (auth)

18446 RADIATION-INDUCED COPOLYMERIZATION OF STYRENE AND CELLULOSE AT LOW DOSE RATES. Garnett, J. L.; Martin, E. C. (Univ. of New South Wales, Kensington, Australia). J. Macromol. Sci., Part A; 4: 1193-1214(Aug 1970).

A study was made of the radioinduced grafting of styrene to cellulose in the presence of ^{60}Co gamma irradiation at low total doses and dose rates. For copolymerization, Whatmans 41 filter paper was immersed in solutions of styrene in methanol at various monomer concentrations. The dose rates were varied from 140 to 3100 rads/hr while the total dose varied from 10^3 to 2×10^5 rads. In the presence of oxygen the grafting results showed considerable scatter, but a statistical analysis revealed that at all concentrations a linear relationship existed between total dose and graft %. Three factors contributing to the variance about the regression line were examined. Residual oxygen in the solution, while not important at high dose rates, was shown markedly to contribute to the variance in the range examined. A linear dose-rate effect involving a decrease in graft with increasing dose rate was demonstrated. A LET effect also contributed to the overall variance. Preliminary results indicate the presence of a maximum, which may be a Trommsdorff effect. (auth)

Radiolysis

Refer also to abstracts 18808, 18854, and 18906.

18447 (CALT-767-P-4-73) PUZZLES IN THE DIFFUSION KINETICS OF THE RADIATION CHEMISTRY OF AQUEOUS SOLUTIONS. Kuppermann, Aron (California Inst. of Tech., Pasadena. Arthur A. Noyes Lab. of Chemical Physics). [1970]. 28p. (CONF-700319-1). Dep. NTIS.

From International Meeting on Primary Radiation Effects in Chemistry and Biology, Buenos Aires, Argentina.

The time scale under consideration is from the passage of high-energy radiation through the system to approximately one nanosecond thereafter. The simple one-radical diffusion model in radiation chemistry is discussed along with a more generalized model. The effects of scavenger concentration, pH and isotope separation factors are considered. (M.C.G.)

18448 (CEA-N-1369) PHYSICAL CHEMISTRY SERVICE. Semiannual Progress Report, July–December 1969. (Commissariat a l'Energie Atomique, Saclay (France). Centre d'Etudes Nucleaires). Oct 1970. 60p. (In French). Dep. NTIS (U. S. Sales Only).

The principal results obtained in the following fields are reported: study of the absorption spectra of ions using pulsed radiolysis: pulsed radiolysis of NH_3; radiolysis of 2-propanol; radiolysis of p-bromophenol in ethanol; H_2 yield in the radiolysis of the $Ni(ClO_4)_2$, $NiCl_2$, $NiSO_4$, and $UO_2(ClO_4)_2$ solutions; pulsed radiolysis of the BrO_3^- and IO_3^- ions in aqueous solutions; NMR studies on radicals produced by the radiolysis of undecafluoro (trifluoromethyl) cyclohexane; NMR studies on the kinetics of the radioinduced polymerization of acrylamide; radiolysis of N_2O in vitreous tetrahydro-2-methylfuran and ethanol; desorption of O chemisorbed on graphite; and studies involving molecular beams. (France)

18449 (ORNL-tr-2386) DISCUSSION OF THE ELEMENTARY REACTIONS OF RADIOLYSIS OF METHANE IN THE GASEOUS PHASE. Fayard, Florence. Translated by R. Gregg Mansfield (Oak Ridge National Lab., Tenn.), from J. Chim. Phys.; 60: 651-8(1963). 15p. Dep. NTIS.

An abstract of this paper, prepared from the original language, appeared as NSA 17: 34005.

18450 (ORO-3519-8) RADIATION CHEMISTRY OF MONOSUBSTITUTED AROMATIC COMPOUNDS. Progress Report, January 15, 1970–January 15, 1971. Knight, J. A. Jr. (Georgia Inst. of Tech., Atlanta. Engineering Experiment Station). Contract AT(40-1)-3519. 19p. Dep. NTIS.

Studies on the radiolysis of aniline are reported. The effects of anthracene, naphthalene, biphenyl, and tetramethylparaphenylenediamine on the radiolytic products were studied. Yields of hydrogen, ammonia, benzene, diphenylamine, and amino radiolytic products are given. (J.G.B.)

18451 CHEMICAL EFFECTS OF RADIATION IN BENZENE–BROMOBENZENE SOLUTIONS. Kumar, Sampath Sadhu. Manhattan, Kan.; Kansas State Univ. (1970). 83p. University Microfilms Order No. 70-25,546.

Thesis.

The chemical effects of gamma excitation on certain organic solvents and solutions were studied. The solvents were benzene and bromobenzene. The solutions were mixtures of benzene and bromobenzene and mixtures of leucocrystal violet, bromobenzene and benzene. The yield of biphenyl was larger in the mixtures of the solvents than in either of the pure solvents. Rate constants for certain energy transfer reactions were estimated on the basis of measured product spectra and the published value of the ratio of rate constants for energy transfer and quenching. The lower limit of the value of the rate constant for dissociative electron capture by bromobenzene in benzene was estimated to be 5.66×10^9 M^{-1} sec^{-1}. In the radiolysis of bromobenzene, the decomposition of bromobenzene was estimated to be 7.75 molecules per hundred eV on the basis of product spectra and the invariance of the number of carbon atoms. In the radiolysis of solutions of leucocrystal violet in benzene–bromobenzene mixtures, significant amount of oxidation occurred under aerated conditions. In an aerated solution of benzene containing 10^{-3} $\underline{M}$ leucocrystal violet and 0.096 $\underline{M}$ bromobenzene, the estimated yields of crystal violet, biphenyl, and benzene were, respectively, 1.06, 0.75, and 0.96 molecules per hundred eV. In the same solution, under degassed conditions, the estimated yields of crystal violet and biphenyl were, respectively, 0.075 and 1.76. Benzene formation was found to be negligible. Reaction schemes, which are consistent with major observed effects, are proposed for the radiolysis of bromobenzene, a solution of benzene containing 0.096 $\underline{M}$ bromobenzene and a solution of benzene containing 0.096 $\underline{M}$ bromobenzene and 10^{-3} $\underline{M}$ leucocrystal violet, over the dose ranges employed. Some preliminary studies were made on the dosimetric aspects of the leucocrystal violet–bromobenzene system under aerated conditions. The aspects of convenience, range selection, sensitivity, and efficiency observed in the preliminary studies indicate that this system may form a basis for a chemical dosimeter. (Diss. Abstr. Int., B)

18452 EFFECT OF AMMONIA ON THE ION REACTIONS IN THE RADIOLYSIS OF ETHYLENE IN THE GAS PHASE. Niedzielski, Jan; Gawlowski, Janusz (Univ., Warsaw). Nukleonika; 15: 531-45(1970).

The ionic reactions in the radiolysis of gaseous ethylene were studied, using ammonia as a positive ion scavenger. The changes in radiation yields of some hydrocarbons due to the presence of ammonia were interpreted in terms of the proton reaction taking place between ammonia and the ions. The highly unsaturated compounds appearing in the presence of ammonia, such as vinylacetylene, allene, propyne, butadiene, are formed by a purely ionic mechanism, including competition between proton transfer reaction of the parent ion and its further condensation with ethylene. The calculated rate constants of the reactions of $C_4H_5^+$, $C_3H_5^+$, and $C_4H_7^+$ ions with ethylene are: 1×10^7, 1.9×10^9, and 8.4×10^9 $\underline{M}^{-1}$ s^{-1}, respectively. It was found that butenes and hexenes are formed partly by the ionic and partly by the free radical mechanism. Some evidence was presented for the occurrence of isomerization of the $C_4H_9^+$ butyl ions; the rate constant of this reaction was estimated as approximately 10^7 s^{-1}. Two isomers of butyl ions differ in reactivity towards ethylene, the rate constants being 6×10^8 and $\leq 1.8 \times 10^7$ $\underline{M}^{-1}$, s^{-1}, respectively. Branched alkanes or their precursors are formed in the radiolysis of pure ethylene by the ionic mechanism, probably involving neutralization of the higher order ions; however, the presence of ammonia inhibits their formation. Methane forms mainly from the dissociation of excited lower order ions. (auth)

18453 SELF-ABSORPTION OF THE CHERENKOV LIGHT AS A QUANTITATIVE INDICATOR OF RADIOLYSIS PROGRESS. Zagorski, Zbigniew Pawel; Zimek, Zbigniew (Inst. of Nuclear Research, Warsaw). Nukleonika; 15: 335-42(1970).

The phenomenon of Cherenkov light self-absorption in liquids was investigated from the point of view of the kinetics of radiolytic changes in irradiated solution. This method, when using an adequately built vessel, enables the determination of stable and intermediate products of radiolysis with sufficient accuracy. The new approach creates possibilities of carrying out measurements under circumstances unavailable for conventional methods making use of the absorption of external light. (auth)

18454 UNCHARGED TRANSIENT SPECIES IN RADIATION CHEMISTRY. HOT HYDROGEN ATOMS AND SUPEREXCITED STATES. Hatano, Yoshihiko (Tokyo Inst. of Tech.). Nippon Kagaku Zasshi; 91: 1009-21(Nov 1970). (In Japanese).

Some evidence is presented for a possible role of uncharged intermediates in radiolysis except for usual free radical reactions. It comprises the following seven parts: some debatable problems of the role of hot hydrogen atoms in radiation chemistry; some debatable problems of the role of highly excited electronic states involving superexcited states in radiation chemistry; primary processes of hydrogen formation in the gas- and liquid-phase radiolysis of olefins; theoretical calculation of the hydrogen yields in the radiolysis of olefins; excitation from superexcitation of hydrocarbons, estimation of their yields by the optical approximation; primary processes of hydrogen formation in the radiolysis of saturated hydrocarbons; and the role of hot hydrogen atoms in the radiolysis of various compounds. (auth) (Japan)

18455 NITROGEN SENSITIZED GAS PHASE γ-RADIOLYSIS OF ETHYLENE. Gawlowski, Janusz; Niedzielski, Jan (Univ., Warsaw). Nukleonika; 15: 455-62(1970).

Gamma radiolysis of gaseous ethylene–nitrogen mixutres (0.2 to 80% vol of theylene) was investigated under pressures close to normal. The dependence of the radiolytic yields of volatile products on ethylene concentration was determined. The results suggest that the reaction $N + C_2H_4 \rightarrow HCN + CH_3$ does not represent the mechanism of nitrogen atom interaction with ethylene. Instead of yielding HCN, nitrogen atoms recombine yielding excited molecules. This leads to the transfer of energy of ethylene, predominantly via the reaction $N_2^{\ddagger} + C_2H_4 \rightarrow N_2 + C_2H_2 + 2H$. From kinetic analysis of the data, it follows that the ratio of the rate constant of the transfer energy reaction to the rate constant of the decay of excited state reaction has the value of 1.66×10^{-3} liter/mole. (auth)

18456 DISSOCIATIVE ELECTRON CAPTURE PROCESS OF METHYL VINYL ETHER IN ORGANIC GLASSES. Irie, Masahiro (Kyoto Univ.); Hayashi, Koichiro; Okamura, Seizo; Yoshida, Hiroshi. J. Phys. Chem.; 75: 476-81(18 Feb 1971).

Dissociative electron capture by methyl vinyl ether was studied by electron spin resonance in 3-methylhexane and 2-methyltetrahydrofuran glasses containing methyl vinyl ether irradiated by ^{60}Co γ rays at 77°K. The yield of trapped electrons increased remarkably with increasing concentration of methyl vinyl ether in the 3-methylhexane glass, while the increase is insignificant in the 2-methyltetrahydrofuran glass. The rate of photobleaching of the trapped electrons induced by visible light decreased with the addition of methyl vinyl ether to 3-methylhexane, while it increased in 2-methyltetrahydrofuran. The bleaching of the trapped electrons results in the formation of methyl radicals by the dissociative electron capture process, $CH_3OCH=CH_2 + e \rightarrow \cdot CH_3 + CH_2=CHO^-$. In contrast to alkyl halides which capture electrons dissociatively during the γ irradiation, the dissociative electron capture process of methyl vinyl ether occurs only when the electrons are liberated from their physical traps by visible light. This is attributed to the fact that the cross section of methyl vinyl ether for physical electron trapping is larger than that for dissociative electron capture and that, under the visible light illumination, the electrons are detrapped and trapped repeatedly and finally captured by methyl vinyl ether to give methyl radicals. (auth)

18457 PHOTOISOMERIZATION OF MALEATE RADICAL ANIONS PRODUCED IN 2-METHYLTETRAHYDROFURAN BY γ IRRADIATION AT 77°K. Torikai, Ayako; Suzuki, Toshimi; Miyazaki, Tetsuo; Fueki, Kenji; Kuri, Zen-ichiro (Nagoya Univ., Japan). J. Phys. Chem.; 75: 482-6(18 Feb 1971).

Photoisomerization of γ-radioinduced maleate radical anions in MTHF was studied by electron spin resonance (ESR), optical absorption measurements, and product analysis. Irradiation of MTHF glasses of maleic acid, dimethyl and diethyl maleate at 77°K yielded the corresponding radical anions. These species changed into the fumaric acid radical anion and dimethyl and diethyl fumarate radical anions, respectively, by illumination of light. Upon illumination of γ-irradiated dimethyl maleate in MTHF glass with visible light, neither the formation of new radicals nor the change of solvent radicals was observed, and any gaseous or liquid products other than dimethyl furmarate did not increase in their amounts. Experimental results indicate that reactions other than the cis → trans isomerization are not involved in this case. (auth)

18458 SCAVENGING OF THE MOLECULAR HYDROGEN YIELD FROM WATER IRRADIATED WITH TRITIUM β PARTICLES. Appleby, A.; Gagnon, W. F. (Rutgers–The State Univ., New Brunswick, N. J.). J. Phys. Chem.; 75: 601-2(18 Feb 1971).

An attempt was made to distinguish experimentally between the properties of spurs and short tracks involved in the effects of scavengers on molecular hydrogen yields in the radiolysis of aqueous solutions. Previous theoretical studies have suggested that a major fraction of the energy deposited in water by low-energy electrons gives rise to short tracks rather than spurs. The scavenging effects of copper ions on the molecular H_2 yields produced by tritium β radiolysis (average energy of tritium β = 5.69 keV) was measured. The molecular H_2 yields were found to be significantly less scavengeable than that produced by ^{60}Co γ radiolysis. It is postulated that the large difference in scavengeability of the molecular H_2 yield, when it originates from radiations giving predominantly short tracks rather than spurs, is due to a change in the relative importance of the processes involved in the production of hydrogen. (J.G.B.)

18459 RATE CONSTANTS FOR REACTION OF HYDROGEN ATOMS IN AQUEOUS SOLUTIONS. Neta, P.; Holdren, G. R.; Schuler, Robert H. (Carnegie-Mellon Univ., Pittsburgh). J. Phys. Chem.; 75: 449-54(18 Feb 1971).

The rates for the abstraction and addition reaction of the hydrogen atoms produced in the γ irradiation of aqueous solutions were measured at pH 1 for 18 organic solutes. The rates were measured relative to the rate of formation of HD from deuterioisopropyl alcohol solutions in competitive experiments and put on an absolute scale by reference to the known rate for addition of hydrogen atoms to benzoic acid. A comparison is made with values measured previously on seven of the systems. The overall agreement is reasonable, and it is noted, in particular, that the relative rates measured by different methods agree quite well. (auth)

18460 RADIATION CHEMISTRY OF AQUEOUS SOLUTIONS OF $CFCl_3$, CF_2Cl_2, AND CF_3Cl. Balkas, Turgut I.; Fendler, J. H.; Schuler, Robert H. (Carnegie-Mellon Univ., Pittsburgh). J. Phys. Chem.; 75: 455-66(18 Feb 1971).

Radiation chemical studies of aqueous solutions of the three fluorochloromethanes indicated that the initial reaction occurs mainly via the attack of hydrated electrons on the solute to produce chloride ions. Irradiations were carried out with both ^{60}Co γ rays and 2.8 MeV Van de Graaff electrons. A rate constant of $\sim 10^{10}$ $\underline{M}^{-1}$ sec^{-1} was observed for reaction of hydrated electrons with each of the solutes. In the absence of competing reactions the halogenated radical produced as the complement of the chloride ion undergoes secondary hydrolysis reactions. In the case of $CFCl_3$, one fluoride and three chloride ions are produced for each electron which reacts with the solute. Hydrolysis was found to be complete except for experiments carried out at very high dose rates or in the presence of very reactive radical scavengers. The chloride ion yields from CF_2Cl_2 and CF_3Cl are, respectively, twice and equal to the hydrated electron yield, with the yield from CF_3Cl being notably independent of dose, dose rate, or added radical scavenger. In these cases the fluoride ion yields exhibit a very pronounced dose rate dependence and complete hydrolysis occurs only at dose rates less than 10^{13} eV g^{-1} sec^{-1}. A common dose rate dependence was observed for these two solutes, and this fact is taken to indicate that the rate-controlling steps involve the second-order reactions of a difluorinated radical, probably CF_2. The secondary hydrolysis reactions were studied on the 10^{-6} to 10^{-2} sec time scale using conductometric methods. In each case the second step in the hydrolysis occurs with a period of ~10 μsec. The third and fourth halide ions are produced in reactions which have periods ~1 msec or longer. A number of effects which illustrate the minor importance of complicating side reactions are noted and discussed in some detail. (auth)

18461 GROWTH AND DECAY OF ALKYL RADICALS IN γ-IRRADIATED ALKYL IODIDES AT 77°K. Fenrick, H. W.; Nazhat, N. B.; Ogren, P. J.; Willard, J. E. (Univ. of Wisconsin, Madison). Contract AT(11-1)-1715. J. Phys. Chem.; 75: 472-5(18 Feb 1971).

During γ irradiation of glassy ethyl iodide at 77°K the concentration of trapped ethyl radicals grows to a steady state where the rate of radical production is balanced by the rate of thermal decay plus radioinduced decay. In the absence of radiation, the fraction of the radicals which decays per unit time is independent of the initial radical concentration, but decreases with time. This and other evidence indicates that the decay is by geminate recombination of $C_2H_5 + I^-$ pairs formed by dissociative electron capture and possibly also of $C_2H_5 + I$ pairs. The rates of decay of C_2H_5 and C_2D_5 in a $C_2H_5I-C_2D_5I$ mixed matrix are equal, but decay is much slower in a C_2D_5I matrix than a C_2H_5I matrix. The

XUM

inhibiting effect of matrix deuteration on decay, coupled with the relatively small effect of the chain length of the matrix molecules (from C_2H_5I to $C_6H_{13}I$) is further evidence that radical decay in the alkyl iodide glasses is controlled by molecular vibration or rotation processes rather than by diffusion. Experiments using $CH_3{}^{13}CH_2I$ suggest that the isomerization $CH_3{}^{13}CH_2 \rightarrow CH_2{}^{13}CH_3$ does not occur in glassy ethyl iodide. (auth)

18462 ELECTRON PARAMAGNETIC RESONANCE OF ELECTRON-IRRADIATED $K_3Rh(CN)_6$ IN A KCl LATTICE. Muniz, R. P. A.; Vugman, N. V.; Danon, J. (Centro Brasileiro de Pesquisas Fisicas, Rio de Janeiro). J. Chem. Phys.; 54: 1284-8 (1 Feb 1971).

Electron irradiation of the diamagnetic $Rh(CN)_6^{3-}$ ion in a KCl host lattice produces three paramagnetic species. EPR studies reveal that one of the species can be assigned as $Rh(CN)_4Cl_2^{4-}$, of D_{4h} symmetry, $4d^7$ low spin configuration, arising from the trapping of an electron in a d_z^2 orbital followed by the substitution of two axial cyanides by chloride ions. The experimental data were interpreted in terms of a spin Hamiltonian yielding the principal values of the g and hyperfine tensors as $g_{||} = 1.995$, $g_{\perp} = 2.297$, $A_{||}^{Rh} = -40.8 \times 10^{-4}$ cm^{-1}, $A_{\perp}^{Rh} = -36.9 \times 10^{-4}$ cm^{-1}, $A_{||}^{Cl} = +27.8 \times 10^{-4}$ cm^{-1}, $A_{\perp}^{Cl} = +12.4 \times 10^{-4}$ cm^{-1}. Theoretical estimates of g values confirm this assignment. A semiempirical estimate of the unpaired electron density on the metal and ligands is presented. (auth)

18463 DETERMINATION OF THE RADIATION YIELD OF NITRITE IONS IN THE IRRADIATION OF SODIUM NITRATE SOLUTIONS IN THE SMALL-DOSE REGION. Podzorova, E. A.; Orekhov, V. D.; Vereshchinskii, I. V.; Kabakchi, A. M. (Inst. of Physical Chemistry, Moscow). High Energy Chem. (USSR) (Engl. Transl.); 4: 328-9(Jul-Aug 1970).

Translated from Khim. Vys. Energ.; 4: 370-2(Jul-Aug 1970).

The radiolysis of aqueous sodium nitrate solutions in the γ dose region lower than 1×10^{17} eV/ml was investigated. A colorimetic method, based on extraction of the azo dye being formed in a smaller volume of an organic solvent, was used to determine the nitrite ions. It was concluded that $G(NO_2^-) = 4.5$, measured in an aqueous solution, and $G(NO_2^-) = 5.8$ in an organic solvent after extraction. (M.C.G.)

18464 SPACE DISTRIBUTION OF RADICALS DURING γ-IRRADIATION OF METHANOL AT 77°K. Raitsimring, A. M.; Pomytkin, A. P.; Tsvetkov, Yu. D. (Inst. of Chemical Kinetics and Combustion, Novosibirsk, USSR). High Energy Chem. (USSR) (Engl. Transl.); 4: 326-7(Jul-Aug 1970).

Translated from Khim. Vys. Energ.; 4: 369-70(Jul-Aug 1970).

The space distribution of radical products from the radiolysis of solid methane was investigated by the electron spin echo method. Gamma rays at a dose range of 0.02 to 1.5 Mrad were used. A completely different scale of trace and track effects was observed. (M.C.G.)

18465 EFFECT OF IRRADIATION DOSE RATE AND MANNER OF PREPARATION OF SAMPLES ON THE KINETICS OF RADICAL BUILD-UP IN ANILINE. Tolkachev, V. A.; Sokolov, I. B. (Inst. of Chemical Kinetics and Combustion, Novosibirsk, USSR). High Energy Chem. (USSR) (Engl. Transl.); 4: 324-5(Jul-Aug 1970).

Translated from Khim. Vys. Energ.; 4: 367-8(Jul-Aug 1970).

Pure aniline samples were irradiated with ^{60}Co γ rays and pulsed electrons. The kinetics of radical buildup were investigated in two types of samples: degassed and sealed at atmospheric pressure. The law of accumulation of free radicals for both types of samples can be described by a single curve for γ irradiation. In β irradiation the buildup curve of the second type of samples is higher. (M.C.G.)

18466 ROLE OF CHARGED PARTICLES AND EXCITED MOLECULES IN THE RADIOLYTIC OXIDATION OF n-HEPTANE BY MOLCULAR OXYGEN. Muratbekov, M. B.; Saraeva, V. V. (Moscow State Univ.). High Energy Chem. (USSR) (Engl. Transl.); 4: 322-3(Jul-Aug 1970).

Translated from Khim. Vys. Energ.; 4: 365-7(Jul-Aug 1970).

The effects of nitrous oxide and oxygen on the product yields from the γ radiolysis of n-heptane were studied over a wide range of additive concentration at 0°C and a dose rate of 1.2×10^{16} eV/ml sec. The yield of heptyl radicals in the heptane$-N_2O(0.3\underline{M})-O_2(0.02\underline{M})$ system was 8.1 in agreement with $G = 8.7$ for the system without oxygen. When the oxygen concentration in the heptane$-N_2O-O_2$ system increased from 0.02 to 0.22$\underline{M}$, the yield of heptyl radicals was reduced, indicating the participation of oxygen in reactions with electrons. When heptane is irradiated in the presence of oxygen, the hydrogen yield is reduced to 2.6, the same value obtained with nitrous oxide (0.3$\underline{M}$). (D.H.M.)

18467 STABILIZED IONS AND THE FORMATION OF CROSS LINKS IN THE RADIOLYSIS OF POLYBUTADIENE. Novikov, G. F.; Kozlov, V. T.; Yakovlev, B. S.; Frankevich, E. L. (Moscow State Univ.). High Energy Chem. (USSR) (Engl. Transl.); 4: 291-5(Jul-Aug 1970).

Translated from Khim. Vys. Energ.; 4: 337-41(Jul-Aug 1970).

To substantiate the ionic mechanism of the formation of cross links in polybutadiene in post-radiation processes, the dependences of the concentrations of cross links and ions stabilized in low-temperature radiolysis on the time of illumination of samples with light 400 nm ≲ λ ≲ 800 nm at 77°K were investigated. It was shown that the absorption of light in γ-irradiated polybutadiene was due chiefly to ions, an increase in the concentration of which at 77°K leads to a decrease in the concentration of cross links measured after thawing. Possible mechanisms of the formation of cross links in the post-radiation conversions of polybutadiene, including the step of regeneration of the charge, were discussed. (auth)

18468 COMMENTS ON THE EPR SPECTRA OF IRRADIATED SOLID GLYCINE. Mayer, I. (Central Research Inst. for Chemistry, Budapest). Chem. Phys. Lett.; 8: 117-19(1 Jan 1971).

Comments are given on a recent interpretation of the EPR spectra of irradiated solid glycine. It is emphasized that Morton's assumption for deuterated glycines still seems necessary. Explanation is given for the changes of spectra after irradiation. (auth)

18469 THEORY OF PULSE RADIOLYSIS IN AN ELECTRIC FIELD. Chernenko, A. A.; Vinkler, E. G. (Moscow State Univ. Inst. of Electro-Chemistry, Moscow). Dokl. Akad. Nauk SSSR; 195: 650-3(21 Nov 1970). (In Russian).

The possibility of using the relaxation method for determining radiation yield and the rate of reactions between various products of radiolysis was analyzed. A formula relating the initial current through the cell with radiation-chemical yields and diffusion coefficients for charged radiolytic products was obtained. Quantitative criteria for description of chemical processes in the cell were also found. The model studied indicated that the relaxation method can determine only certain reaction rate constants. In order to obtain other constants and for separation of mobilities and radiation yields it was necessary to vary the conditions of the experiments. Calculations of a series of kinetic schemes revealed that the current relaxation curves may have qualitative differences that may be used for determining the mechanism taking place in the reaction system. (R.V.J.)

18470 γ-RADIOLYSIS OF TIN OXIDES. Bekker, A. A.; Fabrichnyi, P. B.; Pozdeev, V. V.; Babeshkin, A. M.; Nesmeyanov, An. N. (Moscow State Univ.). High Energy Chem. (USSR) (Engl. Transl.); 4: 284-6(Jul-Aug 1970).

Translated from Khim. Vys. Energ.; 4: 328-31(Jul-Aug 1970).

Tin monoxide and dioxide were irradiated with ^{60}Co γ rays at doses of 100, 300, 500, and 1000 Mrad at room temperature and were studied by the Moessbauer method and by chemical analysis. The tin dioxide was found to be stable against the irradiation, while the monoxide decays, forming the dioxide and the metal. The concentration of these products in an irradiated monoxide sample increases linearly with the dose. Radiation reduction and partial disproportionation presumably occur in the monoxide as a result of the γ radiation. (auth)

18471 EFFECT OF TEMPERATURE AND OXYGEN ON THE COMPOSITION OF THE γ-RADIOLYSIS PRODUCTS OF ISOOCTANE (2,2,4-TRIMETHYLPENTANE). Pichuzhkin, V. I.; Saraeva, V. V.; Bakh, N. A. (Moscow State Univ.). High Energy Chem. (USSR) (Engl. Transl.); 4: 275-8(Jul-Aug 1970).

Translated from Khim. Vys. Energ.; 4: 317-21(Jul-Aug 1970).

The γ-radiolysis of isooctane was studied at different temperatures in the presence and absence of oxygen. It is shown that an appreciable part of the products of rupture of the $-C-C-$bonds (e.g., isobutane and isobutene) is formed not by a radical disproportionation route but by molecular dissociation of the excited isooctane molecule. The dimeric C_{16} hydrocarbons arise as recombination products of secondary and tertiary radicals, whose formation depends on rapid reaction of the initially formed radicals with an isooctane molecule. (auth)

18472 ELIMINATION OF OXIDATION INDUCED BY GAMMA IRRADIATION IN AQUEOUS PHARMACEUTICALS. Pandula, Egon; Farkas, Erzsebet (Semmelweis Medical Univ., Budapest). Acta Pharm. Hung.; 40: 165-9(Jul 1970). (In Hungarian).

The radiolysis of aqueous solutions showed that the changes induced by gamma irradiation are mainly of oxidative character that can often be eliminated with the usual antioxidants. Sixteen different protective agents were studied in cyanocobalamin solution. Potassium pyrosulfite proved to be the most effective among them. This antioxidant was also used in 7 other solutions. It was shown that potassium pyrosulfite exerts a favorable protective action in solutions of atropine sulfate, ephedrine hydrochloride, lidocaine hydrochloride, morphine hydrochloride, hydrocodeine bitar-

XUM

trate and ascorbic acid. It was not effective in chloramphenicol solution. (JPRS)

18473 DESTRUCTION OF FREE RADICALS IN IRRADIATED ORGANIC CRYSTALS. Tolkachev, V. A. (Inst. of Chemical Kinetics and Combustion, Novosibirsk, USSR). High Energy Chem. (USSR) (Engl. Transl.); 4: 279-83(Jul-Aug 1970).

Translated from Khim. Vys. Energ.; 4: 322-7(Jul-Aug 1970).

Data on the annealing of radicals in solid crystalline organic substances, in which the mobility of the molecules and polar groups is frozen, were compared with the real and imaginary portions of the complex dielectric permeability in the region of premelting. It was concluded that the destruction of radicals may be due both to the mobility of the molecules close to defects in the crystal structure and to the appearance of a liquid phase in the crystalline samples. The proposed models explain the basic principles observed in investigations of the annealing of free radicals. (auth)

18474 SALT EFFECT DURING PULSED RADIOLYSIS OF NEUTRAL WATER AND ALKALINE SOLUTIONS. Brusentseva, S. A. (Inst. of Electrochemistry, Moscow). High Energy Chem. (USSR) (Engl. Transl.); 4: 339-40(Jul-Aug 1970).

Translated from Khim. Vys. Energ.; 4: 377-8(Jul-Aug 1970).

The influence of the ionic strength on the absolute rate constant of the disappearance of e_{hydr} in the electron pulse radiolysis of water at different pH's was investigated. The ionic strength was changed by adding $LiClO_4$. The hydrated electrons disappeared by a second-order reaction in the pH region from 12.7 to 11.4. A first-order reaction occurred in less alkaline solutions and neutral water. (M.C.G.)

18475 PRIMARY RADIOLYSIS REACTIONS OF NON-ALKALINE AQUEOUS SOLUTIONS OF PYRIMIDINE BASES. Fel, N. S.; Dolin, P. I. (Inst. of Electrochemistry, Moscow). High Energy Chem. (USSR) (Engl. Transl.); 4: 337-8(Jul-Aug 1970).

Translated from Khim. Vys. Energ.; 4: 376-7(Jul-Aug 1970).

The optical spectra of short-lived radiolysis products of aqueous thymine solutions were investigated. It was concluded that the primary attack by OH, H, and e_{aq}^- consists in rupture of the 4,5-double bond of thymine. (M.C.G.)

18476 EVIDENCE OF THE OCCURRENCE OF MONOMOLECULAR REACTIONS IN THE RADIOLYSIS OF AQUEOUS SOLUTIONS OF OXYGEN. Kabakchi, S. A.; Shubin, V. N. (Inst. of Electrochemistry, Moscow). High Energy Chem. (USSR) (Engl. Transl.); 4: 335-6(Jul-Aug 1970).

Translated from Khim. Vys. Energ.; 4: 375(Jul-Aug 1970).

It was found that the dependence of the stationary concentration of H_2O_2 in the γ radiolysis of aqueous solutions of oxygen on the oxygen concentration at a dose range of 2.7×10^{14} to 6.3×10^{16} eV/ml/sec obeys the $I^{1/2}$ law in a narrow region of oxygen concentrations, but at larger variations the $I^{1/2}$ law is not satisfied. This confirmed the occurrence of monomolecular processes in the radiolysis. (M.C.G.)

18477 AN OBSERVATION ON THE NATURE OF INTERMEDIATE PARTICLES IN THE RADIOLYSIS OF AQUEOUS SOLUTIONS OF OXYGEN. Byakov, V. M.; Kalyazin, E. T. (Moscow State Univ). High Energy Chem. (USSR) (Engl. Transl.); 4: 333-4(Jul-Aug 1970).

Translated from Khim. Vys. Energ.; 4: 373-4(Jul-Aug 1970).

The composition of products from the radiolysis of oxygen-containing water is $H_2O_{aq}^*$, H, H_2, H_2O_2. It is suggested that the originally excited molecules of $H_2O_{aq}^*$ formed enter into an acid-base interaction with the surrounding water molecules. The product of this reaction $(e^- \ldots OH)_{aq}^*$ plays a part in the volume of the solution currently ascribed to the hydrated electron and the hydroxy radical. (M.C.G.)

18478 STRUCTURE AND STABILITIES OF THE FREE RADICALS FORMED IN γ-IRRADIATED GLYCINE. Komar, I. N.; Nikolov, O. T.; Maier, I. (Kharkov State Univ.). Teor. Eksp. Khim.; 6: 561-6(Jul-Aug 1970). (In Russian).

Post-irradiation heating of glycine monocrystals and polycrystals showed that on irradiation three types of radicals are formed simultaneously: CH_2COO-, $^+NH_3CHCOO-$, and $NH_2CHCOO-$. The contents of these radicals in irradiated glycine at room temperature are 38, 58, and 4%, respectively. The $NH_2CHCOO-$ radical is the most stable and the CH_2COO- radical the most unstable. After doses of 10^5 r, the recombination of all three radicals is described by a first order process. The ESR spectra were studied. (tr-auth)

18479 RADIATION DAMAGE IN SELENATES OF DIVALENT METALS. Spitsyn, Vict. I.; Medvedev, A. S.; Gromov, V. V.; Shtanko, V. F. (Moscow Inst. of Physical Chemistry). Dokl. Akad. Nauk SSSR; 195: 643-5(21 Nov 1970). (In Russian).

Radioinduced disturbances in selenates were studied using powders of $BaSeO_4$, $CaSeO_4 \cdot 2H_2O$, and $BeSeO_4 \cdot 4H_2O$. All the salts were recrystallized and crushed before irradiation. A cobalt device with a maximum dose in the center equal to 1000 rad/sec was used as the radiation source. The EPR spectra for irradiated material at −196°C were recorded and analyzed. (R.V.J.)

Radioisotope Production

Refer also to abstracts 18501, 19054, and 20455.

18480 (BRH/DMRE-70-4) CYCLOTRON PRODUCTION OF ^{123}I: AN EVALUATION OF THE NUCLEAR RFACTIONS WHICH PRODUCE THIS ISOTOPE. Sodd, Vincent J.; Scholz, Kenneth L.; Blue, James W.; Wellman, Henry N. (Bureau of Radiological Health, Rockville, Md.). Oct 1970. 40p. NTIS.

Studied were the $^{121}Sb(^4He,2n)^{123}I$, $^{121}Sb(^3He,n)^{123}I$, $^{122}Te(d,n)^{123}I$, $^{122}Te(^4He,p2n)^{123}I$, $^{122}Te(^3He,pn)^{123}I$, and $^{123}Te(^3He,p2n)^{123}I$ reactions that produce ^{123}I directly and the $^{122}Te(^4He,3n)^{123}Xe$, $^{122}Te(^3He,2n)^{123}Xe$, and $^{123}Te(^3He,3n)^{123}Xe$ reactions that produce ^{123}I indirectly through the positron decay of 2.1 hour ^{123}Xe. The use of the gas-flow ^{123}I cyclotron target assembly for the production of ^{123}I with radiochemical purity greater than 99.995% is recommended. (11 references) (auth)

18481 ^{252}Cf AS A NEUTRON SOURCE. Hoehlein, G. (Kernforschungszentrum, Karlsruhe, Ger.). Atomwirt., Atomtech.; 15: 514-17(Nov 1970). (In German).

Properties and applicability of ^{252}Cf are reviewed. At the present time, West Germany does not possess installations in which ^{252}Cf can be produced in sufficient amounts for studies of technical applicability. In a project at Karlsruhe on actinides, various transuranium elements will be produced and ^{252}Cf will become available in milligram amounts within a few years. The basic radioisotopes, americium and curium, will be supplied by the fuel recovery installation at Karlsruhe. (H.B.G.)

18482 RAPID SEPARATION OF GENERATOR-PRODUCED ^{68}Ga FROM EDTA ELUATE. Carlton, J. E.; Hayes, R. L. (Oak Ridge Associated Universities, Inc., Tenn.). Int. J. Appl. Radiat. Isotop.; 22: 44-5(Jan 1971).

The possible medical uses of ^{68}Ga are summarized. The availability of the short-half-life daughter ^{68}Ga (78 hr) from the long-lived parent ^{68}Ge (280) days by elution is described. The eluate however is not acceptable as it contains EDTA. A rapid and efficient ion exchange apparatus and method for separation are described. The choice of anion exchange resin is discussed, recovery being 85 and 99% for different resins. The procedure takes about 15 min to perform. (UK)

Recoil Production and Reactions

Refer also to abstract 18490.

18483 (COO-1617-27) HALOGEN ATOM REACTIONS ACTIVATED BY RADIATIVE NEUTRON CAPTURE AND ^{82m}Br AND ^{130m}I ISOMERIC TRANSITION. Progress Report No. 5, February 1970–February 1971. (Nebraska Univ., Lincoln. Dept. of Chemistry). 15 Feb 1971. Contract AT(11-1)-1617. 115p. Dep. NTIS.

Modifications in the design of the radiogas chromatograph used in the laboratory are described. The kinetics of the addition process of iodine to various C_5 alkene isomers in solution at 25°C was investigated. The $^{127}I(n,\gamma)^{128}I$ induced yields in iodine or iodomethane systems of pentene, 1-pentene, trans-2-pentene, or cis-2-pentene were compared. Results were also compared with yields from the reactor irradiation of $^{131}I_2$ in solutions of the various C_5 hydrocarbon isomers. Cyclopentane, benzene, and selected alkylbenzenes were probed both in the liquid and solid phases with nuclear processes induced by the neutron activation of one or more of the following species: $^{127}I_2$, $^{129}I_2$, Br_2, ICl, and IBr. Of particular interest in each of the systems were the following: isotope effects due to (n,γ) and (IT) processes; individual and comparative scavenging effects in the liquid phase systems of the various halogens and interhalogens; crystalline structure at 77°K, and; product distributions of organic halides. Isotope and pressure effects were studied in (n,γ) and (IT) activated bromine reactions in gaseous CH_3Br. (J.G.B.)

18484 RECOIL TRITIUM REACTIONS WITH TRIMETHYLFLUOROSILANE. A STUDY ON PARAMETERS AFFECTING HOT-ATOM SUBSTITUTION REACTIONS. Daniel, S. H.; Tang, Yi-noo (Texas A and M Univ., College Station). J. Phys. Chem.; 75: 301-7(4 Feb 1971).

XUM

In the recoil tritium reactions with trimethylfluorosilane, abstraction and substitution at the CH bonds are the most predominantly observed processes while reactions at the SiC and SiF bonds are relatively minor. Primary yields of products were evaluated by correcting for the minor amount of decomposition in the gas phase. A comparison of the recoil tritium substitution at various bonds of trimethylfluorosilane and tetramethylsilane was made after their individual data were normalized with a specific activity ratio factor obtained from competition experiments. Since the residual part of both molecules is $(CH_3)_3Si$ after the T-for-F and T-for-CH_3 substitution, a comparison can be made of the two reactions to give strong support to a bond-strength effect for hot-atom substitution reactions. Other comparisons in these systems are also consistent with an inductive effect resulting from the presence of a very electronegative atom, F, in trimethylfluorosilane. (auth)

18485 THE STUDY OF EQUILIBRIUM CHARGE-STATE DISTRIBUTIONS OF BORON IONS AND NON-EQUILIBRIUM CHARGE-STATE DISTRIBUTIONS OF CARBON IONS BY RECOIL SPECTROMETRY. Volkar, Martin Anthony. Pittsburgh; Univ. of Pittsburgh (1970). 87p. University Microfilms Order No. 70-20,356.

Thesis.

Equilibrium charge state distributions for ^{10}B recoils produced in the $^{12}C(d,\alpha)^{10}B$ reaction were measured in the velocity region 10.4 to 11.2×10^8 cm/sec. The experimental mean charges and charge fractions fit in well with those reported by Nikolaev, et al., for surrounding velocity regions. The mean charges were compared with those predicted by Bohr, Lamb, and a modified phenomenological approach of Dmitriev, the latter giving agreement within 3%. The experimental charge fractions also agree fairly well with those predicted by Dmitriev's approach. The charge-state distributions for 5.01-MeV ^{12}C recoils produced by 12-MeV incident deuterons in the $^{12}C(d,d)^{12}C$ reaction were measured in VYNS targets ranging in thickness from 46.3 to 0.9 $\mu g/cm^2$. The distributions from the targets show nonequilibrium characteristics, and a statistical treatment of the data indicates a trend toward increased widths of the charge distributions and increased mean charges with decreased target thickness. (Diss. Abstr. Int., B)

18486 POLYMERIC CHROMIUM(III) COMPLEXES ARISING FROM THE NEUTRON IRRADIATION OF CRYSTALLINE POTASSIUM CHROMATE. I. SEPARATION METHODS AND SOME CHEMICAL PROPERTIES OF POLYNUCLEAR RECOIL PRODUCTS. Guetlich, P.; Froehlich, K.; Odar, S. (Technische Hochschule, Darmstadt, Ger.). J. Inorg. Nucl. Chem.; 33: 307-16(Feb 1971). (In German).

Mono- and polynuclear cationic chromium(III) complexes, labelled with ^{51}Cr, were found beside labelled chromate ions in aqueous solutions of neutron-irradiated crystals of K_2CrO_4. A separation technique on the basis of cationic exchange was developed for the separation of the various chromium complexes into several fractions with complexes of different degree of polymerization. For some complexes the composition could be determined by adding carrier to the solution to be analyzed. The activity distribution of ^{51}Cr among the various recoil products in solution was found to depend considerably upon the time of storage of the irradiated crystals at room temperature as well as the pH of the solvent. Possible reactions occurring between the recoil fragments and the solvent upon dissolution of the irradiated crystals are discussed. (auth) (UK)

18487 PROCESSES FOR THE DESTRUCTION OF THE n-HEXANE MOLECULE DUE TO THE ACTION OF TRITIUM RECOIL ATOMS. Avdonina, E. N. (Moscow State Univ.). High Energy Chem. (USSR) (Engl. Transl.); 4: 253-7(Jul-Aug 1970).

Translated from Khim. Vys. Energ.; 4: 291-6(Jul-Aug 1970).

Binary mixtures of benzene and n-hexane were irradiated with a flux of $1.2 \cdot 10^{13}$ neutrons/cm^2/sec in the presence of lithium carbonate for 15 min at 70°C and with a flux of $9 \cdot 10^{11}$ neutrons/cm^2/sec for 2 hr at −170°C. A comparison of the yield of radioactive alkanes and olefins with a short chain length, formed by the action of tritium recoil atoms on the n-hexane molecule, with the radiation yields of these products in the same experiments showed that the main paths for the formation of light hydrocarbons is different in the two processes. (auth)

18488 STUDY OF THE CHEMICAL BEHAVIOR OF RECOIL ATOMS DUE TO (γ,γ') PROCESS. Yoshihara, Kenji; Kaji, Harumi; Nagatani, Toshio (Tohoku Univ., Sendai). Kakuriken Kenkyu Hokoku; 2: 147-9(Dec 1969). (In Japanese).

The hot-atom effect of the γ-induced nuclear isomer excitation process of ^{115}In was previously studied and it was found that the In^{3+} yield rose from zero when the energy of recoil atoms exceeded a certain value called "appearance energy." The hot-atom effect is reported for Na, K, or H compounds of the indium complex. First, $Na[InY(H_2O)]2H_2O$, $K[InY(H_2O)]H_2O$ and $H[InY(H_2O)]$ were irradiated with the γ rays of various energies to induce (γ,γ') excitation, and the In^{3+} yield was measured as a function of recoil energy. In all cases, In^{3+} yield increased and reached a limiting value with increasing recoil energy. No difference in yield was observed between the Na and K compounds. On the other hand, H compounds gave high yield in comparison with Na or K compounds. The hot-atom effect of ^{115m}In, ^{114m}In, and ^{116m}In, which were formed by (γ,γ'), (γ,n), and (n,γ) processes, respectively, was compared. No difference was observed among them. (Japan)

Radiochemistry

Refer also to abstract 19473.

18489 THEORY OF CHEMICAL EFFECTS PRODUCED BY ISOMERIC TRANSITION OF ^{82m}Br IN LIQUID ORGANIC SYSTEMS. Katsanos, N. A.; Leontiadis, I. L. (Democritus Nuclear Research Centre, Athens). J. Inorg. Nucl. Chem.; 33: 295-305(Feb 1971).

An earlier hypothesis of a rapid equilibrium between complexes, formed in an organic mixture between bromine activated by isomeric transition and the two organic constituents of the mixture, was extended to explain the effect of change of concentration of elemental bromine in the mixture. A general scheme of reactions is proposed, from which linear equations were derived describing the change in retention and yields of the different products with changes in the mole fractions of the various components of a ternary mixture, containing elemental bromine and two organic liquids. These equations, in simpler forms, were first applied to the two binary mixtures of elemental bromine and each of the two organic liquids to determine the various parameters needed for quantitative analysis of the results obtained with the respective ternary mixtures. Agreement between theory and experiment was confirmed (a) by the linearity of the various experimental plots based on the above equations, and (b) by the internal consistency of the proposed scheme, as judged from the agreement between the values of the same parameters determined from different equations and different mixtures. It is probable that analogous schemes apply to other nuclear transformations. (auth) (UK)

18490 CHEMICAL EFFECTS OF THE NUCLEAR ISOMERIC TRANSFORMATION OF ^{80m}Br IN BROMOBENZENE. Choi, Jae Ho (Atomic Energy Research Inst., Seoul). J. Korean Nucl. Soc.; 2: No. 1, 3-7(Mar 1970).

The chemical fate of ^{80}Br atoms from the $^{80m}Br-^{80}Br$ isomeric transition was determined in liquid bromobenzene under varied conditions of Br_2 concentration, temperature, and sample preparation. The organic yields from $Br^{80m}Br$ in polycrystalline bromobenzene are essentially independent of Br_2 concentration over a wide range. The organic yields from Br_2 in polycrystalline $C_6H_5{}^{80m}Br$ are much higher than those from $Br^{80m}Br$ on polycrystalline bromobenzene. The total organic yields for (n,2n) and (n,γ) activation of bromine in bromobenzenes containing added bromine were found to be similar to those observed in the isomeric transition process, supporting evidence that the chemical effects are independent of the recoil energy of the activated nucleus, of the mode of nuclear formation, and of variation of fragmentation effects within the recoil track. (auth)

Separation Processes

Refer also to abstracts 18385, 18482, 18564, 18885, 19189, and 19259–19261.

18491 (AEC-tr-7190) TECHNOLOGY OF PROCESSING URANIUM ORES: A SHORT HISTORICAL SURVEY OF THE DEVELOPMENT ON TECHNOLOGY OF PROCESSING URANIUM ORES IN THE U.S.S.R. Kovda, G. A.; Laskorin, B. N.; Nevskii, B. V. Translation of Russian report. 34p. Dep. NTIS.

The history of developments in the processing of uranium ore in Russia is presented. The concentration of uranium ores, hydrometallurgical processing, adsorptive technology, extraction technology, extraction of uranium from natural waters, and schemes for processing uranium ores of different composition are discussed. (M.C.G.)

18492 (ANL-7709) PYROCHEMICAL PROCESSING OF FUEL MATERIALS AND SCRAP CONTAINING ^{238}Pu. Nelson, P. A.; Fischer, J.; Lenc, J. F.; Haley, J. R.; Schilb, J. D. (Argonne National Lab., Ill.). Jul 1970. Contract W-31-109-eng-38. 49p. Dep. NTIS.

The use of pyrochemical processing techniques was investigated as a means of recovering ^{238}Pu from various types of materials

XUM

and purifying it. One promising process tested consisted of reducing $^{238}PuO_2$ powder or microspheres with liquid Zn–Mg alloys in the presence of a molten chloride salt. A metallic ^{238}Pu product was then recovered by vacuum distillation of the solvent metals. This process was effective in removing the light-element impurities that cause neutron emission by (α,n) reactions. In an experimental test of this process, in which about 12 g of $^{238}PuO_2$ with a neutron count of 42,500 n/(sec)(g ^{238}Pu) was used as the starting material, the neutron count of the product was 2930 n/(sec)(g ^{238}Pu) [2360 n/(sec)(g Pu)]. Processes were also considered for (1) removing corrosion-product impurities from $^{238}PuO_2$ and (2) recovering ^{238}Pu from $^{238}PuO_2$–Mo and $^{238}PuO_2$–ZrO_2 fuel materials. Experiments with $^{239}PuO_2$ indicated the general feasibility of pyrochemical processes for these applications, but the procedures have not been sufficiently developed for use in production. The results of this work indicate that pyrochemical procedures that may have immediate production applications are (1) reduction of $^{238}PuO_2$ scrap material to produce impure ^{238}Pu metal for subsequent aqueous processing, (2) reduction of relatively pure $^{238}PuO_2$ to remove light-element impurities and produce ^{238}Pu metal, and (3) dissolution of $^{238}PuO_2$–Mo cermets in a $CuCl_2$-containing molten salt for aqueous processing. (auth)

18493 (CEA-Bib–191) STUDY AND DEVELOPMENT OF THE DECLADDING AND DISSOLUTION OF UO_2 AND PuO_2 FUELS, CLAD WITH STAINLESS STEEL OR ZIRCALOY. Auchapt, Jacqueline M.; Auchapt, Pierre R. (Commissariat a l'Energie Atomique, Chusclan (France). Centre de Production de Plutonium de Marcoule). Nov 1970. 185p. (In French). Dep. NTIS (U. S. Sales Only).

Processes were designed for decladding, some of them oriented toward pure research (stainless steel melting) and others capable of industrial applications (simple or complex electrolysis). Attempts were made to leach continuously the clad segments of sheared fuel and to pick the hulls out of the solution, but trials with simulated or real fuels have not been successful. The three most widely used processes are electrolysis, chemical decladding, and mechanical shear-leach. The last two processes have industrial applications. Difficulties similar to those encountered in aqueous processing are experienced. (France)

18494 (DOCKET-50201-63) WEST VALLEY REPROCESSING PLANT. Technical Specification Change No. 13, Request for Hearing. (Nuclear Fuels Services, Inc., Rockville, Md.). 11 Feb 1971. 3p. Dep. NTIS.

18495 (DOCKET-50201-64) WEST VALLEY REPROCESSING PLANT. Request for Possession Limit of 5 x 10^{-3} Curies of ^{85}Sr. (Nuclear Fuels Services, Inc., West Valley, N. Y.). 16 Jun 1970. 1p. Dep. NTIS.

18496 (DOCKET-50201-65) WEST VALLEY REPROCESSING PLANT. Comments on Nonpropriety Portion of Revision 6 to Final Safety Analysis Report. (Division of Materials [and] Licensing (AEC), Washington, D. C.). 25 Nov 1970. 3p. Dep. NTIS.

Tornado design criteria, safe shutdown, seismological considerations, and other design criteria for natural phenomena are discussed. (M.C.G.)

18497 (DOCKET-50372-3) ARC PLANT. Scheduling of Activities Related to Construction Permit Application. (Atlantic Richfield Co., Philadelphia, Pa.). 17 Feb 1971. 3p. Dep. NTIS.

Current plans are presented for the scheduling of activities related to the construction permit application. (M.C.G.)

18498 (KFK–1298) FORMATION OF CHELATES AND ADDUCT CHELATES IN THE EXTRACTION OF TRIVALENT AMERICIUM AND CALIFORNIUM. Feinauer, Dieter (Kernforschungszentrum, Karlsruhe (West Germany). Institut fuer Radiochemie). Sep 1970. 73p. (In German). Dep. NTIS (U. S. Sales Only).

In the following systems chelate formation was studied by extraction measurements and the stability constants of the chelates formed were calculated: Cf(III)/oxine (HOX), in this case the basic chelate $Cf(OH)_2(OX)$ was formed; Cf(III)/5,7-dichloro-8-hydroxyquinoline (HDCO), here the normal 1 : 3 chelate $Cf(DCO)_3$ was formed; and Am(III) and Cf(III)/thenoyltrifluoroacetone (HTTA), in this case the 1 : 3 chelates $M(TTA)_3$ were formed. The synergic efficiency of various adduct-forming agents (A) with oxygen, nitrogen, sulfur, and selenium as central atoms was also studied in the system Am(III)/HTTA. The stability constants of the 1 : 1 and 1 : 2 adducts $Am(TTA)_3 \cdot A$ and $Am(TTA)_3 \cdot 2A$ were determined graphically. With phenyl ether and diphenyl selenide, 1 : 1 adducts were formed. With butyl ether, isobutyl ether and the sulfides used, 1 : 4 adducts were obtained. All the other agents used formed 1 : 2 compounds. The stability constants calculated for the 1 : 2 adducts ranged from – 0.26 for the compound with 1-nitrobutane to +4.78 for that with di-n-butyl sulfoxide. For the systems Am(III)/HTTA and Am(III)/HTTA/methyl isobutyl ketone the Gibbs free energy, enthalpy, and entropy of the chelating and adduct formation reactions were determined by extraction measurements at various temperatures. (auth)

18499 (LIB/Trans–330) PROCESS FOR THE SEPARATION OF HAFNIUM CONTAINED IN ZIRCONIUM. Ishizuka, Hiroshi. Translated by W. Buykx (Australian Atomic Energy Commission), from French Patent 1,537,218. 12p. Dep. NTIS.

A process for the separation of the tetrachlorides of hafnium and zirconium is given. It consists of preparation of $ZrCl_4$ containing 1 to 5% hafnium, from zircon sands; fusing of an alkali metal halogenide (at >60 mole%) with the $ZrCl_4$ at 250 to 650°C and at least 30 atm, to form a double salt; reduction of the hafnium content of the double salt by bringing it into contact with $ZrCl_4$ vapor, which may or may not contain traces of hafnium, and heating the double salt after its hafnium content has been sufficiently reduced. The double salt in the molten state and containing traces of $ZrCl_4$ following $ZrCl_4$ extraction, can be used cyclically as a solvent for the dissolution of crude $ZrCl_4$ vapor and $ZrCl_4$ vapor containing large amounts of hafnium. Zirconium-poor $HfCl_4$ is formed by bringing the double salt in contact with hafnium-rich $ZrCl_4$ at 250 to 650°C at $p < 30$ atm. (Australia)

18500 (NP–18669) FUTURE OF REPROCESSING IN EUROPE. Seynaeve; Marcus; Asyee; (and others) (Forum Atomique Europeen). 1969. 136p. Dep. NTIS (U. S. Sales Only).

An analysis of the reprocessing situation in Europe is presented. Topics covered include: market situation, cost structure, ancillary factors, recommendations, reprocessing techniques and their development, existing and scheduled reprocessing plants, and assessment of technical factors and their influence on economics of LWR processing. (M.C.G.)

18501 (RCN–131) SEPARATION OF GRAM-AMOUNTS OF LANTHANIDES BY CATION EXCHANGE, USING AN AQUEOUS SOLUTION OF α-HYDROXYISOBUTYRIC ACID AS AN ELUANT. Das, H. A.; Hoede, D.; van Stigt, Ch. A.; Zonderhuis, J. (Reactor Centrum Nederland, Petten). Sep 1970. 72p. Dep. NTIS (U. S. Sales Only).

A procedure was developed for the mutual separation of gram quantities of the lanthanides present in solutions of thermal fission products. A second aim was the purification of "crude" ^{147}Pm sources. The method is based on column chromatography on Dowex-50 W (50 to 100 mesh) with an aqueous solution of α-hydroxyisobutyric acid (AHIB) as an eluant. Because of the radioactivity of the samples, the process has to be performed in a shielded glovebox. Consequently, a considerable economy was exercised with respect to the volume of the apparatus. The process was successfully tested with labeled artificial mixtures of 20 grams of the rare earths involved. The method was applied to the purification of batches of "crude" ^{147}Pm. (Netherlands)

18502 (RFP–1421) RECOVERY OF NIOBIUM FROM NIOBIUM–URANIUM ALLOYS: AN ANNOTATED BIBLIOGRAPHY. Navratil, James D. (Dow Chemical Co., Golden, Colo. Rocky Flats Div.). 4 Feb 1971. Contract AT(29-1)-1106. 43p. Dep. NTIS.

Two hundred sixty-seven references, with resumes, are presented in 4 sections: alloy dissolution, alloy separation, niobium metal preparation, and refining of niobium. A subject index, book listing, index of organizational symbols, and author index are provided. (M.C.G.)

18503 (RT/CHI–(70)25) I. PREPARATION OF RESINS WITH COMPLEX GROUPS. II. SYNTHESIS OF PHENOLIC RESINS WITH HYDROXAMIC GROUPS. Gasparini, G. M.; Vomero, S. (Comitato Nazionale per l'Energia Nucleare, Rome (Italy)). 14 Jul 1970. 30p. (In Italian). Dep. NTIS (U. S. Sales Only).

The synthesis of some phenolic resins with a hydroxamic group is described. Their chemical stability, exchange capacity, and chelating properties were evaluated. The ability of these resins to extract $^{95}Zr - ^{95}Nb$ from acid solutions makes them attractive for a final purification of uranium solutions. (auth)

18504 (UJV–2450-Ch) PROBLEMS ON SORPTION EQUILIBRIUM IN ION EXCHANGE COLUMN FOR MICROQUANTITIES OF RADIOACTIVE SOLUTION IN THE PRESENCE OF COMPETING ION. Uher, E. (Ceskoslovenska Akademie Ved, Rez. Ustav Jaderneho Vyzkumu). Nov 1970. 40p. (In Czech). Dep. NTIS (U. S. Sales Only).

The sorption of trace amounts of Sr^{2+} on a strongly acidic H^+-based cation exchanger from solutions containing an excess of strong acid and a further competing cation (Fe^{3+}) was studied. The formulas for the strontium sorption isotherm and for the strontium effective capacity were derived. These values can

XUM

be substituted into the breakthrough formulas derived by others for the case of solutions containing only one ionic component. The Sr^{2+} sorption, in case of the hydrolysis of Fe^{3+} previously retained by the sorbent, was also considered. The derivation procedure for solutions of other composition was also briefly considered. Equilibrium values were determined. (auth)

18505 (WHAN-FR-32) APPLICATION OF AQUEOUS TECHNOLOGY TO LMFBR SEPARATIONS PROCESSES. PROGRAM PLAN FOR TASK T-1: SOLVENT PERFORMANCE. Richardson, G. L. (WADCO Corp., Richland, Wash.). Dec 1970. Contract AT(45-1)-2170. 72p. Dep. NTIS.

Studies are being made to determine TBP solvent performance using a dynamic system with radioactive feed solutions as near to those expected from LMFBR as practicable. The effects of radiation dose rate and cumulative exposure on TBP solvent properties are discussed. Flowsheets are shown. (29 references). (M.C.G.)

18506 INVESTIGATION OF THE EXTRACTION OF THORIUM, LEAD, AND IRON(III) AS CAPROIC ACID COMPOUNDS. Pietsch, R. (Univ., Graz). Anal. Chim. Acta; 53: 287-94(Feb 1971). (In German).

The possibility of extracting thorium, lead, and iron(III) with caproic (n-hexanoic) acid as their caproates into chloroform is described. Experimental conditions are detailed and examples of single extraction and separation methods are given. The composition of the metal compounds in the chloroform layer was established. (auth)

18507 PRECIPITATION METHOD OF RECOVERING ELEMENT 95 FROM CONTAMINANTS. Werner, Louis B. (to United States Atomic Energy Commission). U. S. Patent 3,551,119. 29 Dec 1970. Filed 23 Aug 1946.

A precipitation method is described for separating element 95 (americium) from iron or radioactive fission products in acidic aqueous solutions. To separate element 95 from iron, the solution is made 1 $\underline{M}$ with respect to K^+ and to HF, the precipitate is recovered and dissolved in H_2SO_4, and element 95 is precipitated as the hydroxide in a substantially Fe-free state. Element 95 is separated from fission products by contacting the solution with a soluble Zr salt and a soluble phosphate compound to precipitate the zirconium phosphate along with the fission products. The solution is then neutralized with a soluble hydroxide to precipitate element 95 and rare earth fission products. After separation of the precipitate, which is then dissolved in acid, element 95 is then complexed with fluorosilicate ions, and LaF_3 is added to precipitate the carrier with associated rare earth fission products while element 95 remains in solution. (B.L.M.)

18508 HYDROCHLORIC ACID EXTRACTION OF MOLYBDENUM FROM THE TAILINGS OF UZBEKISTAN COAL ASH TREATED BY SULFURIC ACID. Mirzakarimov, A. M. (Inst. of Chemistry, Tashkent). Uzb. Khim. Zh.; No. 5, 107-9(1970). (In Russian).

Optimum conditions for Mo extraction from the tailings of sulfuric acid-treated coal ash by hydrochloric acid solutions were found to be 3% HCl solution, 20°C, and time rates of 1, 10, and 20 min. From 85.28 to 86.98% Mo extraction was obtained in relation to the insoluble residue. (R.V.J.)

18509 PURIFICATION OF POLONIUM. Kershner, Carl J.; Ellis, Robert E. (to United States Atomic Energy Commission). U. S. Patent 3,544,307. 1 Dec 1970. Filed 30 Oct 1968.

The purification and removal of oxygen from association with polonium comprises heating the material to vaporize polonium and separate oxygen from its oxide, removing oxygen from the vapor by passing the vapor through or over tantalum powder, and then collecting the purified polonium. (Offic. Gaz.)

18510 UTILIZATION OF EXTRACTION FOR SEPARATION AND ISOLATION OF RARE METALS. Bol'shakov, K. A.; Korovin, S. S. Zh. Vses. Khim. Obshchest. im. D. I. Mendeleeva; 1 15: 380-7(1970). (In Russian).

The separation of rare elements by extraction processes is discussed. Examples discussed include Rb and Cs, Ga and In, and Sc, Y, and the lanthanides. The main rules of extraction of metals, formation of coordination compounds between organic reagents and the metals, and donor-acceptor reactions were examined. The behavior of the metals in both aqueous and organic solutions was explained from the point of view of peculiarities of atomic structure. Further developments in solvent extraction processes are considered. (tr-auth)

18511 LIQUID–LIQUID EXTRACTION OF METAL-HALIDE COMPLEXES DEPENDING ON THEIR COMPOSITION AND STRUCTURE. COMMUNICATION 1. THE PART OF THE CHARGE OF THE COMPLEX. Zolotov, Yu. A. (Inst. of Geochemistry and Analytical Chemistry, Moscow). Zh. Anal. Khim.; 26: 20-5(Jan 1971). (In Russian).

The effects of the total charge of metal halide complexes on their liquid–liquid extraction have been examined. The origin of the complex charge has been estimated and certain ways for its decrease have been outlined. Molecular halides of the SbI_3 type and anionic acidocomplexes are suggested to be considered from the unified stand. It has been shown that neutral molecular halides extracted by inert organic solvents are formed by the elements which are at the end of periods III, IV, V, and VI of the periodic system. (auth)

18512 DUAL TEMPERATURE ISOTOPE EXCHANGE PROCESS. Babcock, Dale F. (to United States Atomic Energy Commission). U. S. Patent 3,549,323. 22 Dec 1970. Filed 16 Apr 1968.

A liquid and a gas each containing a desired isotope flow countercurrently through two liquid–gas contacting towers. The towers are maintained at different temperatures to enrich the liquid in the isotope at one temperature and the gas in the isotope at the other temperature. Liquid, having the natural concentration of the desired isotope, is fed into the top of the tower in which the liquid is enriched, and as an additional feed into the lower portion of the tower in which the gas is enriched. The latter feed results in a significant increase in productivity. The process is particularly applicable to the concentration of deuterium by exchange between H_2O and H_2S. (Offic. Gaz.)

18513 DUAL TEMPERATURE ISOTOPE EXCHANGE PROCESS. Babcock, Dale F. (to United States Atomic Energy Commission). U. S. Patent 3,549,324. 22 Dec 1970. Filed 16 Apr 1968.

Liquid and gas containing a desired isotope flow countercurrently through two liquid–gas contacting towers in each stage of a multiple stage process. The towers are maintained at different temperatures to enrich the liquid in the isotope at one temperature and the gas in the isotope at the other temperature. Enriched liquid or gas is fed from a first to a subsequent stage into a tower operated to enrich the respective fluid. Enriched liquid from a first stage is also fed into the lower portion of a subsequent stage tower operated to enrich the gas in the isotope. The process is particularly applicable to the concentration of deuterium by exchange between H_2S and H_2O. (Offic. Gaz.)

18514 DUAL TEMPERATURE ISOTOPE EXCHANGE PROCESS. Babcock, Dale F. (to United Atomic Energy Commission). U. S. Patent 3,549,325. 22 Dec 1970. Filed 16 Apr 1968.

A liquid and gas each containing a desired isotope are made to flow countercurrently through two liquid–gas contacting towers. The towers are maintained at different temperatures to enrich the liquid in the isotope at one temperature and to enrich the gas in the isotope at the other temperature. A portion of the enriched liquid is contacted with the full flow of the enriched gas at a temperature suited for further enriching the liquid. This liquid portion is thereafter withdrawn as product of the process or as feed to a subsequent stage. The process is particularly applicable to the concentration of deuterium by exchange between H_2S and H_2O. (Offic. Gaz.)

18515 TREATMENT AND DISPOSAL OF RADIOACTIVE WASTE. PART I. SOURCES AND KINDS OF RADIOACTIVE WASTE. Schlosser, Kurt (Oesterreichische Studiengesellschaft fuer Atomenergie GmbH, Vienna). Elektrotech. Maschinenbau; 87: 378-83(1970). (In German).

Safety considerations in the processing of radioactive waste are discussed. Sources of waste include: nuclear reactors, clinics, biological and scientific research installations, and isotope laboratories. (M.C.G.)

18516 DETERMINATION OF THE DISTRIBUTION CONSTANTS OF TRIVALENT CERIUM IN EXTRACTION BY NEUTRAL ALKYL PHOSPHONATES. Mikhlin, E. B.; Korpusov, G. V. Zh. Neorg. Khim.; 15: 2797-2802(Oct 1970). (In Russian).

The composition and distribution constants for trivalent cerium compounds in extraction by diisopentyl methylphosphonate and diisooctyl methylphosphonate were determined. On extraction, the complex $Ce(NO_3)_3 \cdot 3S$, where S = solvent, goes into the organic phase. It was found that the extraction capability of the phosphonates studied was significantly above the extraction capability of TPB. (tr-auth)

18517 PLUTONIUM TECHNOLOGY. Stoll, W. (Alpha-Chemie und -Metallurgie GmbH, Wolfgang, Ger.). Atomwirt., Atomtech.; 15: 580-4(Dec 1970). (In German).

Recovery of plutonium from spent fuel elements is discussed, as well as subsequent manufacturing procedures leading to particular chemical compounds. Mixed oxides and production of fuel elements for fast breeder or thermal reactors require, during all steps, special processes, equipment, and safety measures. At the present time, special interest centers on plutonium uranium oxides. Discussed are problems connected with their production, handling, storage, transportation, and scrap treatment. Starting from laboratory-scale experimentation, development leads to manual technical procedures and finally to automation of the most important processes and monitoring steps. This type of development is demonstrated on hand of the manufacturing of ceramic fuel material. (tr-auth)

18518 FLOCCULATION TREATMENT OF RADIOACTIVE CONTAMINATED SEA WATER. I. EXPERIMENTAL STUDIES ON FLOCCULANTS. Sakurai, A.; Nagaoka, Y.; Wadachi, Y. (Japan Atomic Energy Research Inst., Tokyo). Int. Chem. Eng.; 11: 167-71(Jan 1971).

The efficiency of the flocculation treatment of contaminated seawater containing fission products was studied. The radioisotopes studied were ^{137}Cs, ^{90}Sr$-$^{90}Y, ^{144}Ce, ^{147}Pm, ^{106}Ru, and ^{95}Zr$-$^{95}Nb. A flocculant of various concentrations (50, 200, 500, 2000 ppM) was added to contaminated brine. The sample was stirred, let stand, and the supernatant solution removed, dried, and the radioactivity counted. Results are presented in graphs. (M.C.G.)

18519 DISTRIBUTION OF Np IN NITRIC ACID SOLUTION CONTAINING URANYL ION. Steinwandter, H.; Bobleter, O.; Hecht, F. (Univ., Vienna). Monatsh. Chem.; 101: 1648-57(Nov-Dec 1970). (In German).

The distribution coefficients (D) of neptunium in the valence states (IV), (V), and (VI) between nitric acid solutions and an anion exchanger were determined. The distribution coefficient D(IV) for Np(IV) was determined after reduction of a series of samples, D(V) being taken from the literature, and D(VI) was assumed to be equal to D(V) for reasons of analogy. The ratios of the valence states in the respective solutions were determined quantitatively. From these data, the D values could also be ascertained by calculations. It was found that reduction takes place in the exchanger resin, which displaces the equilibrium towards Np(IV), and D is only determined by the portion of Np(IV). In solutions free of oxidizers, D is an additive value of all valence states and their respective concentrations. (auth)

18520 SEPARATION OF BISMUTH(III) FROM OTHER IONS BY CATION EXCHANGE CHROMATOGRAPHY. Akki, S. B.; Khopkar, S. M. (Indian Inst. of Tech., Bombay). Separ. Sci.; 5: 707-11(Dec 1970).

The cation exchange behavior of bismuth was studied on Dowex 50W-X8 with hydrochloric, sulfuric, nitric, and perchloric acids, with ammonium chloride and sodium nitrate as the eluting agents. The efficiency of eluants was evolved in terms of elution constant and volume distribution coefficient. Bismuth was separated from copper, cadmium, tin, aluminum, nickel, manganese, vanadium, magnesium, mercury, iron, zinc, silver, cobalt, barium, and calcium by the gradient elution process. It was separated from lead, uranium, antimony, and strontium by selective elution with specific eluants. The oxyanions were separated from it by the selective sorption process. The method was found to be applicable to analysis of bismuth-based alloys. (auth)

XUM

EARTH SCIENCES

Geology and Hydrology

Refer also to abstracts 18339, 18360, 18622, 18623, 18814, 18988, 19006, and 20228.

18521 (ORNL-4584, pp 1-10) FATE OF TRACE ELEMENTS AND RADIONUCLIDES IN TERRESTRIAL ENVIRONMENT. Tamura, Tsuneo; Bonner, W. P.; Francis, C. W.; (and others). (Oak Ridge National Lab., Tenn.).

From Health Physics Division annual progress report for period ending July 31, 1970.

Banding of several reference clay minerals was evaluated in a continuous density-gradient solution using zonal centrifugation. Variables examined were particle sizes, cationic saturations, and centrifugal forces. Zonal centrifugation was also used to segregate mineral fractions of several environmental samples, and then these were investigated for phosphate or radionuclide distribution. For phosphate distribution, samples were obtained from the bottom and suspended sediments of the ORIC pond and a soil whose runoff drains into the pond. The principal finding is that most of the phosphate is present in the iron and aluminum phosphate forms. For radionuclide distribution samples, bottom sediments from White Oak Lake Bed and Creek were examined. ^{137}Cs was found primarily in the clay mineral band; ^{90}Sr was found in most bands, including the bands containing calcium carbonate, which tentatively confirms earlier conclusion. Distribution of ^{137}Cs in a soil from previously tagged trees (Liriodendron forest) suggests that the mineral illite plays a dominant role in fixing this radionuclide. Water quality studies of Walker Branch Watershed were continued. Water temperatures were measured continuously at several locations in the two streams which drain the watershed. Differences in water temperatures were observed with time and location, and the differences were not predictably uniform. The differences are discussed, with reference to the source of groundwater and to air temperatures. (auth)

18522 (USGS-474-97) RADIOCHEMICAL ANALYSIS OF WATER FROM WELLS, SPRINGS, AND STREAMS IN CENTRAL NEVADA. Schroder, L. J.; Beetem, W. A.; Villasana, Edward (Geological Survey, Denver, Colo.). 1971. Contract AT(29-2)-474. 24p. Dep. NTIS.

Analyses of water samples for tritium, gross alpha activity, and gross beta activity are tabulated by increasing latitude and longitude of sampling points. Sample collection procedures, numbering system for wells and springs, and detection levels are discussed. (M.C.G.)

18523 MISCIBLE DISPLACEMENT MEASUREMENTS WITHIN LABORATORY COLUMNS USING THE GAMMA-PHOTONEUTRON METHOD. Corey, J. C.; Hawkins, R. H.; Overman, R. F.; Green, R. E. (E. I. du Pont de Nemours and Co., Aiken, S. C. Univ. of Hawaii, Honolulu). Contract (07-2)-1. Soil Sci. Soc. Amer., Proc.; 34: 854-8(Nov-Dec 1970).

When fluid in a porous medium is displaced by a second fluid that is miscible with the first, a transition zone exists between the two. The length and location of this transition zone in a soil column is difficult to measure in situ. When one of the fluids contains D_2O as the major component, a new procedure, the gamma-photoneutron method, readily measures this transition zone. This method permits precise measurements of the average concentration of heavy water (D_2O) at selected locations in a soil column. The utility of the method is illustrated by two experiments: the downward displacement of D_2O (specific gravity of 1.105 g/cm^3) by H_2O, and the downward displacement of H_2O by $D_2O + NaNO_3$ (specific gravity of 1.291 g/cm^3). The mathematical model which describes the shape of the transition zone between the miscible fluids requires the apparent diffusion coefficients to be constant. The experiment showed the apparent diffusion coefficient was not constant as the zone moved through a 100-cm column. Unstable flow due to viscosity differences between fluids was probably responsible for increases in the apparent diffusion coefficient when H_2O displaced D_2O. (auth)

18524 POSSIBILITY FOR DETERMINING POROSITY, DENSITY, AND MINERAL COMPOSITION OF ROCKS BY GAMMA-RAY ABSORPTION. Malinin, V. F. Razved. Geofiz.; No. 38, 121-6(1970). (In Russian).

The possibility of determining the porosity, density, and mineralogical composition of specimens by means of γ-radiation absorption and scattering was studied using a lead-shielded gamma source. A detector with a 20 × 40 mm NaI(Tl) crystal and FEU-35 photomultiplier was used in the experiment. The method proved to be effective for measuring using the soft or hard components of the direct or scattered γ radiation. Results of measurements of γ-radiation intensity with various energy threshold discrimination were used for determining the mineralogical composition of the dolomite or limestone rock. (R.V.J.)

Meteorology

Refer also to abstracts 18831, 18832, 18976, 18988, 18989, 19135, and 19167.

18525 (CONF-700816-(Vol.1)) PROCEEDINGS OF THE ELEVENTH AEC AIR CLEANING CONFERENCE HELD IN THE FEDERAL BUILDING, RICHLAND, WASHINGTON, AUGUST 31–SEPTEMBER 3, 1970. First, Melvin W.; Morgan, James M. Jr. (eds.) (Harvard Univ., Boston, Mass. Harvard Air Cleaning Lab. Division of Reactor Development and Technology (AEC), Washington, D. C.). Dec 1970. 458p. Dep. NTIS.

Separate abstracts were prepared on 19 papers that discuss the removal of radioactive aerosols from the environment. Three papers were abstracted previously and appeared in NSA. (C.H.)

For abstracts of individual papers see: 18385, 18559–18563, 18638, 18926, 19192, 19193, 20692, 20756–20761, 20782, and 20783.

18526 (ORNL-4584, pp 37-40) ENGINEERING, ECONOMIC, AND SAFETY EVALUATION. Jacobs, D. G.; Cowser, K. E.; Reeves III, M.; (and others). (Oak Ridge National Lab., Tenn.).

From Health Physics Division annual progress report for period ending July 31, 1970.

Investigation of factors involved in the siting and operation of nuclear facilities has continued. Radioactive production and decay processes can now be included directly in computer calculation of downwind air concentrations that result from routine release of gaseous effluents. After deposition, the movement of radionuclides in food chains can be simulated by the preliminary computer program PATHWAY. An example is used to illustrate application of this program. Information was assembled on nuclear power plant locations and the surface waters contiguous to each site for use in discussions on regional planning. (auth)

18527 PARTICIPATION OF RADIOGENIC NEON IN THE FORMATION OF THE EARTH'S ATMOSPHERE. Penchev, N. P.; Piperov, N. B. (Inst. of General and Inorganic Chemistry, Sofia). Compt. Rend. Acad. Bulg. Sci.; 23: 197-200(1970).

The isotopic composition of neon and argon in gases evolved from mineral springs in Bulgaria was studied to determine the possibility of radiogenic neon being formed in the Earth's crust. This study was combined with independently published data from other researchers to establish the possible presence of radiogenic neon in the atmosphere. It was concluded that the increase in percentage of ^{21}Ne and ^{22}Ne in the neon of high-helium-content natural gases (in relation to atmospheric neon) shows that the percentage yield of radiogenic ^{22}Ne is $^1/_{10}$ to $^1/_{20}$ as large as the ^{21}Ne yield; therefore, only about 0.2% of the atmospheric ^{22}Ne is considered to be radiogenic in origin. (L.C.L.)

18528 FIXATION AND MIGRATION IN SOILS OF THE PRINCIPAL PRODUCTS OF FISSION AND ACTIVATION. Saas, A.; Grauby, A. (CEA, Saint-Paul-les-Durance, France). Bull. Inform. Sci. Tech. (Paris); No. 151, 55-65(Sep 1970). (In French).

The work carried out by the Cadarache Radioecology Group on the subject of the fixation and migration of principal fission and activation products in soils is reviewed. This work includes a study of the factors involved during the fixation process: internal and external factors, nature of the vectors, rate of integration into the biological cycle, pedogenesis and the part played by certain dynamic constituents such as organic soil matter. This work, carried out both in the laboratory and in the field, has led to the development of a range of techniques which can be easily adapted to studies on environment and on soil pollution by chemical pollutants such as pesticides. (auth) (France)

Mineralogy and Exploration

18529 (STI/PUB-277) URANIUM EXPLORATION GEOLOGY. Panel Proceedings Series. Proceedings of a Panel Held in Vienna, 13–17 April 1970. (International Atomic Energy Agency, Vienna (Austria)). Oct 1970. 392p. (In several languages). (CONF-700429). IAEA $10.00.

A total of 25 papers were presented at the meeting. A separate abstract was prepared for each paper. (G.M.C.)

For abstracts of individual papers see: 18530–18554.

18530 URANIUM RESERVES, FUTURE DEMAND, AND THE EXTENT OF THE EXPLORATION PROBLEM. **Nininger, R. D.** (Atomic Energy Commission, Washington, D. C.). pp 3-19 of Uranium Exploration Geology. Vienna; International Atomic Energy Agency (1970).

From Panel on Uranium Exploration Geology, Vienna, Austria. See STI/PUB–277; CONF-700429.

The need for a better understanding of uranium geology and exploration guidelines may be stated simply. Known world low-cost reserves, that is, reserves which can be exploited and delivered to the world market, excluding the USSR, Eastern Europe and Mainland China, at prices of $10 or less per pound are approximately one third of the estimated requirements through the remainder of this century. Four countries, Canada, South Africa, the United States and France, control 85 to 90% of the known low-cost uranium reserves, and 13 other countries have the remainder. Since the ultimate uranium requirements are of more importance to this Panel than the immediate supply and demand situation, we should be concerned with the large number of developing countries which will not have large requirements for uranium and which have not been adequately explored. These could become important suppliers of uranium over the next 30 years while at the same time greatly improving their own economic position and standard of living. Uranium geology is now at a stage in which a flood of details about specific types of deposits is available but has not been sufficiently well digested and assimilated to bring some cohesiveness to the various concepts of regional, tectonic, lithologic and geochemical distribution of uranium. A meeting of this kind can be instrumental in integrating some of these ideas into meaningful criteria that will help guide exploration anywhere in the world. (auth)

18531 WORLD URANIUM DEPOSITS. **Bowie, S. H. U.** (Inst. of Geological Sciences, London). pp 23-33 of Uranium Exploration Geology. Vienna; International Atomic Energy Agency (1970).

From Panel on Uranium Exploration Geology, Vienna, Austria. See STI/PUB–277; CONF-700429.

Peneconcordant uranium deposits in quartz-pebble conglomerates and in medium- to coarse-grained sandstones constituted the most important concentrations of uranium known at present. Discordant occurrences of vein, pegmatite or contact metamorphic type contained smaller but significant tonnages which generally had to be relatively high grade to be worked economically. Major peneconcordant deposits are those of the Elliot Lake–Blind River area of Canada, the Colorado Plateau of the USA and the Witwatersrand basin in the Republic of South Africa. Important new deposits also occur in the Tin Mersoï basin of Niger. France, Australia and Spain have reserves of over 10,000 short tons of uranium oxide in discordant but also to variable extents in peneconcordant deposits. (auth)

18532 DISTRIBUTION OF TYPES OF URANIUM DEPOSITS AND FAVORABLE ENVIRONMENTS FOR URANIUM EXPLORATIONS. **Little, H. W.** (Geological Survey of Canada, Ottawa). pp 35-48 of Uranium Exploration Geology. Vienna; International Atomic Energy Agency (1970).

From Panel on Uranium Exploration Geology, Vienna, Austria. See STI/PUB–277; CONF-700429.

Productive uranium deposits in Canada are of four types: conglomeratic, hydrothermal veins, and disseminations with simple mineralogy, hydrothermal veins and disseminations with complex mineral associations, and pegmatitic. All occur in the Canadian Shield near its edge. Extensions of known deposits and new ore bodies adjacent to known ones were outlined recently, notably at Elliot Lake, Bancroft and Beaverlodge. In addition, promising indications of deposits in new districts, both of the types above and of new types not previously reported in Canada were uncovered in several parts of the country. Mineralization was reported in the Cypress Hills of Saskatchewan and at Padlei and Baker Lake in District of Keewatin, but little exploratory drilling was done in Keewatin. More promising discoveries were made at Rabbit Lake in Saskatchewan, Makkovik–Kaipokok area in Labrador, and at some other localities from which information is not yet available for publication. New discoveries confirmed some predictions of favorable environments for certain types of uranium deposits; for example pyritiferous conglomerates of Early Proterozoic age wherever found are in varying degrees uraniferous, but similar conglomerates of Late Proterozoic age are not. Lignitic uranium deposits are being drilled in Oligocene beds predicted to be favorable. In the Canadian Shield new discoveries were made of pegmatitic and of vein and replacement deposits in areas that were previously pointed out to be lithologically and/or structurally favorable. (auth)

18533 URANIFEROUS PRECAMBRIAN CONGLOMERATES OF SOUTH AFRICA. **Whiteside, H. C. M.** (Anglo American Corp. of South Africa Ltd., Johannesburg). pp 49-75 of Uranium Exploration Geology. Vienna; International Atomic Energy Agency (1970).

From Panel on Uranium Exploration Geology, Vienna, Austria. See STI/PUB–277; CONF-700429.

Auriferous conglomerates, some of which contain appreciable quantities of uraninite in addition to gold, occur in four systems, namely the Transvaal, the Ventersdorp, the Witwatersrand and the Dominion Reef Systems. The ages of these conglomerates are discussed and their distribution, characteristics and mineralogy are described. Gold and uraninite, as well as some other heavy minerals, are considered to be detrital in origin and it is shown that the distribution of gold is related to sedimentary features such as direction of transport and grain size. Production figures for the period 1952 to 1968 are given. (auth)

18534 SUMMARY NOTES ON THE GEOLOGY OF THE PRINCIPAL URANIFEROUS DISTRICTS STUDIED BY THE CEA. **Gangloff, A.** (CEA, Fontenay-aux-Roses, France). pp 77-105 of Uranium Exploration Geology. Vienna; International Atomic Energy Agency (1970). (In French).

From Panel on Uranium Exploration Geology, Vienna, Austria. See STI/PUB–277; CONF-700429.

The type of uranium vein deposits found in France, which seems to characterize the western part of the areas of granitization and maximum metamorphism of the Hercynian range in Europe, is also well represented in the Iberian Peninsula. This type of deposit has the following major characteristics. The veins are embedded in the granite. The uranium is mainly found in the form of pitchblende and its weathering products, and is accompanied by a paragenesis that is sparse, somewhat lacking in variety and chiefly represented by iron sulphides, lead sulphite (galena), blende and chalcopyrite. The ore bodies may be associated with a chalcedonous gangue that is fairly plentiful and of striped appearance, or form intricate networks of smaller veins, or may comprise a mass within the episyenitic rock. They show preference for location at intersections with lamprophyric dykes. The deposits are associated with granites containing two types of mica and show a tendency towards albitization and high radioactivity. The granites are usually accompanied by a peripheral aureole of tin–tungsten veins. Mineralization occurs in the neighborhood of extensive mylonitic zones. The age of the fertile granites is of the order of 300 M yr, whereas the mineralization is of the order of 250 M yr old. Geochemical studies conducted recently in some of the uranium-bearing regions have shown, among other things, that in the fertile granites the basic uranium concentrations in unaltered rock ranged from 15 to 20 ppM. Among the different types of sedimentary formations with which uranium deposits are conventionally associated, it is the detrital continental basins that were the main focus of attention in studies made both in France and abroad. Study of these basins made it possible to single out a number of common characteristics that provide a corresponding number of criteria of favorability. The continental uranium-bearing basins of sedimentary origin appear to show preference for relatively stable areas, whether they be located in cratonic zones (Agadès or Mounana) or, conversely, in folded zones (Hérault basin). These basins, at least during the period of sedimentation of the formations in question, were surrounded by crystalline reliefs. The sedimentation is of a predominantly continental nature with facies indicating deltaic, fluvio-deltaic, fluviatile, fluvio-lacustrine and lacustrine spread. Generally speaking, there is alternation of granulated and fine sediments to be observed there (Agadès). In exceptional cases fine sediments may alone be present (Hérault). The basins show signs of poor drainage which differ according to the basin, and are manifested by sedimentological facies and their relative arrangements. The geochemical evidence of containment, such as the general presence of analcime in the Agadès basin, is especially significant. The presence of traps is essential for mineralization. They are of various kinds, their structure being sedimentological, tectonic or a combination of the two. In the Agadès basin, at the level of the ore bodies, the traps are basically sedimentological structures, but the latter are often themselves a result of tectonic phenomena. At Mounana the mineralization is apparently governed by tectonic factors. In the Hérault basin the two types co-exist. As regards the genesis of the deposits, as elsewhere, most French research workers support supergene epigenetic theories. The source of the uranium, according to these, should be sought in the crystalline massifs encircling the sedimentary basins. Before being concentrated in the deposit, the uranium is leached from these massifs or is extracted from the sediments stemming from them, either as a solution or on the basis of disseminated detrital uraninite. Or the uranium may be extracted, either completely or in part, from acid volcanic ash during diagenetic processes. According to those favoring the hydrothermal epigenetic theories,

XUM

the uranium is concentrated by thermal waters resulting from acid volcanism on the basis of the previous forms of diffused uranium or else, if endogenic in origin, it is contributed by these solutions. It should be added in conclusion that when prospecting for uranium in a sedimentary medium, attention should be paid to the fact that workable deposits may be found in unusual geological contexts. Such is the case with the Bakouma deposit in the Central African Republic. There the ore bodies are formed from a fine argilo-silico-phosphate Paleocene material filling the fossil karsts in proterozoic dolomites. The uranium is present in the tetravalent state in a carbonated fluorapatite network comprising as much as 50% of the sediment. The origin of this mineralization is still something of a puzzle. (auth)

18535 URANIUM MINERALIZATION IN THE BOHEMIAN MASSIF. Pluskal, O. (Charles Univ., Prague). pp 107-15 of Uranium Exploration Geology. Vienna; International Atomic Energy Agency (1970).

From Panel on Uranium Exploration Geology, Vienna, Austria. See STI/PUB-277; CONF-700429.

Uranium mineralization in the Bohemian Massif may be compared with other uranium-bearing Variscan provinces in Europe. There are some common features, especially the close connection between mineralization and Variscan granitoids and the presence of a distinctly separated stage of uranium mineralization during the hydrothermal processes. Some exogenous deposits are very similar as well. On the other hand, the results of geological study of uranium mineralization in the Bohemian Massif indicate the important role of local geological factors. In any region, only a correct determination of their function permits the distinction to be made between barren occurrences and outcrops of deposits and permits the search for buried ore bodies. (auth)

18536 CHARACTER OF THE UNITED STATES URANIUM RESOURCES. Patterson, J. A. (Atomic Energy Commission, Washington, D. C.). pp 117-27 of Uranium Exploration Geology. Vienna; International Atomic Energy Agency (1970).

From Panel on Uranium Exploration Geology, Vienna, Austria. See STI/PUB-277; CONF-700429.

Uranium deposits are widespread in the western United States and occur in a variety of geologic environments. However, U. S. resources are preponderantly in tabular disseminated deposits in sedimentary host rocks of the Colorado Plateau and the Wyoming Basins. The deposits of the Plateau area are largely in sandstone of Jurassic or Triassic ages. In the Wyoming Basins, the deposits are in sandstones of Tertiary age. The 3100 deposits reported are log normally distributed with a median size of only 2.5 short tons U_3O_8. The 25 largest deposits (over 3000 short tons of U_3O_8 each) contain about half the U. S. resources. Most known deposits are comparatively shallow, less than 700 ft deep, but important deposits are being found at depths exceeding 2000 ft. The ores are predominately uraninite and coffinite types. (auth)

18537 URANIUM DEPOSITS IN PORTUGAL. Matos Dias, J. M. (Junta de Energia Nuclear, Lisbon); Soares de Andrade, A. A. pp 129-42 of Uranium Exploration Geology. Vienna; International Atomic Energy Agency (1970).

From Panel on Uranium Exploration Geology, Vienna, Austria. See STI/PUB-277; CONF-700429.

Portugal is built of a Hercynian basement (the western part of the Iberian Meseta) bordered with Alpine epicontinental sediments of Meso—Cenozoic age. All the uranium deposits so far known occur in the Meseta. They reveal a series of common aspects. On a regional scale, they are correlated with Hercynian younger granites with a high background of radioactivity and outcrop in neo-Cretaceous and possibly Triassic peneplains. On a local scale, they occur close to the roof or the walls of the granite bodies and are located in fractures of variable magnitude, excluding big faults. The ore bodies show a progressive disappearance with depth. On a mineralogical scale, pitchblende + pyrite (and/or marcasite) ± jasper is the most common mineral association. Gummite, black oxides, and colored secondary minerals are abundant in the upper levels. It is suggested that the pitchblende occurring in the contact metasediments and in the granites has supergenic origin. On a chemical scale, the available data allow the assumption of a supergenic origin per descensum for the Portuguese deposits. On the basis of these facts some guides for prospecting orebodies in Meseta and in the borderlands are discussed. (auth)

18538 ROESSING URANIUM DEPOSIT NEAR SWAKOPMUND, SOUTH WEST AFRICA. A PRELIMINARY REPORT. von Backstroem, J. W. (Atomic Energy Board, Pretoria). pp 143-50 of Uranium Exploration Geology. Vienna; International Atomic Energy Agency (1970).

From Panel on Uranium Exploration Geology, Vienna, Austria. See STI/PUB-277; CONF-700429.

Although South Africa's established uranium reserves are confined mainly to the conglomerates of the Witwatersrand basin, the newly discovered deposits of the Namib desert offer great future potential. The Rössing uranium deposit lies northeast of Swakopmund on the Namib plain, near the edge of the Khan river basin. It was known since before World War I that uranium and copper mineralization is associated with alaskitic pegmatites which have intruded schist, granulite, quartzite, and marble of the Damara System and Nosib Formation. Consistent radiometric age determination on uraninite, davidite, and biotite indicates an age of 510 ± 40 million years. Uranium occurs in the form of complex oxides as well as in euhedral very fine-grained uraninite in a large pegmatite body. The entire mineralized area is underlain by pegmatite, locally termed alaskite (a quartz, alkali-feldspar rock). The major radioactive mineral is uraninite and the secondary minerals derived from it consist of rössingite (a new mineral), metatorbenite, meta-haiweeite, uranophane, beta-uranophane, carnotite, thorogummite and gummite. Favorability criteria for uranium mineralization, as deduced from the above mentioned deposit, are summarized. (auth)

18539 LOW-GRADE URANIUM DEPOSITS IN AGPAITIC NEPHELINE SYENITES, SOUTH GREENLAND. Soerensen, H. (Univ. of Copenhagen). pp 151-9 of Uranium Exploration Geology. Vienna; International Atomic Energy Agency (1970).

From Panel on Uranium Exploration Geology, Vienna, Austria. See STI/PUB-277; CONF-700429.

The latest major intrusion in the Precambrian Gardar alkaline igneous province in south Greenland is the Ilímaussaq massif which is made up mainly of agpaitic nepheline syenites. The latest members of the intrusion, lujavritic nepheline syenites, are locally enriched in U and Th. Three main types of deposits are distinguished: steenstrupine and monazite/rhabdophanite in analcime-natrolite rich fine-grained lujavrites without eudialyte, 200 to 600 ppM U, 200 to 2000 ppM Th; steenstrupine, monazite/rhabdophanite and thorite in medium- to fine-grained lujavrites and their contact-metasomatically altered fine-grained lujavrites and lavas of the roof of the intrusion, 100 to 3000 ppM U and 50 to 13,000 ppM Th; and late hydrothermal veins associated with the lujavrites which are enriched in U, Th, Re, Be, Nb, Li, but are of limited extent. Mineralized fractures also occur around Ilímaussaq and other Gardar intrusions, but are not of any economic interest. (auth)

18540 OCCURRENCE OF URANIUM IN ALKALINE IGNEOUS ROCKS. Soerensen, H. (Univ. of Copenhagen). pp 161-8 of Uranium Exploration Geology. Vienna; International Atomic Energy Agency (1970).

From Panel on Uranium Exploration Geology, Vienna, Austria. See STI/PUB-277; CONF-700429.

The major types of uranium mineralization associated with alkaline rocks are briefly reviewed: disseminated mineralization in alkali granite, nepheline syenite and alkali trachyte and related vein deposits; nepheline syenite pegmatites in which radioactive minerals are associated with late zeolitization and albitization; and hydrothermal and metasomatic deposits occurring as veins and impregnations in and around alkaline rocks. The chances of finding uranium deposits are considered best in and around agpaitic nepheline syenites and peralkaline syenites and granites rich in Zr, rare earths and Nb minerals. (auth)

18541 ALIO GHELLE RADIOACTIVE MINERAL OCCURRENCE IN THE BUR REGION OF THE REPUBLIC OF SOMALIA. A BRIEF SUMMARY OF THE PRINCIPAL FEATURES. Cameron, J. (International Atomic Energy Agency, Vienna). pp 169-75 of Uranium Exploration Geology. Vienna; International Atomic Energy Agency (1970).

From Panel on Uranium Exploration Geology, Vienna, Austria. See STI/PUB-277; CONF-700429.

The Alio Ghelle radioactive mineral occurrence is situated about 200 km WNW of Mogadiscio in the Republic of Somalia. The country rock is Precambrian biotite schist-gneiss or granofels intruded by granitic-gneiss bands. Radioactive mineralization is mainly due to a thorite replacement but the nature of the ore controls were not determined. Thorium, uranium, yttrium and small amounts of ytterbium and scandium are the potentially exploitable metals. (auth)

18542 EXHALATIVE-SUPERGENIC URANIUM MINERALIZATION IN THE QUATERNARY ALKALINE VOLCANIC ROCKS OF CENTRAL ITALY. Mittempergher, M. (CNEN, Rome). pp 177-84 of Uranium Exploration Geology. Vienna; International Atomic Energy Agency (1970).

From Panel on Uranium Exploration Geology, Vienna, Austria. See STI/PUB-277; CONF-700429.

Uranium and iron sulfide exhalative-supergenic mineralization

XUM

is fairly widespread in the three volcanic districts of Vulsini, Vico, and Sabatini in central Italy. The mineralization is associated with volcanic rocks which are unique in regard to their general chemical-petrographic characteristics as well as their content of U and other associated minor elements. Prominent petrochemical characters are the exceptional abundance of K_2O and the undersaturation in SiO_2: the potash feldspathoids are frequent. The mean U content of these volcanites is 25 ppM with a maximum of 500 ppM; the Th mean is 130 ppM with a maximum of 240 ppM. The causes of such an exceptional content of radioactive elements are discussed. The U mineralization is related to magmatic H_2S exhalations and to supergenic weathering of exhalative pyrite and marcasite. Furthermore, the ore deposits are controlled by the superficial and underground hydrology. The most evident macroscopic characters of mineralized volcanites are silicification and kaolinization. The economic potentialities of the mineralization as well as the limitations arising from the exhalative-supergenic genesis are discussed. Uranium deposits related to volcanic processes are rare. Therefore the presence of these occurrences in one of the most uraniferous volcanic provinces described so far appears very significant. (auth)

18543 METALLOTECTONIC CONTROL OF URANIUM DISTRIBUTION. Gabelman, J. W. (Atomic Energy Commission, Washington, D. C.). pp 187-204 of Uranium Exploration Geology. Vienna; International Atomic Energy Agency (1970).

From Panel on Uranium Exploration Geology, Vienna, Austria. See STI/PUB-277; CONF-700429.

Zoning of particular metal deposits around alteration centers distinguishes mineral districts of certain ranges of mineralization temperature. Grouping of similar districts into adjacent linear regional zones arranged in temperature-paragenetic sequence establishes regional zoning and a mineralization temperature intensity gradient oriented across the zones. The mineral zones are correlative and coextensive with zones of deformation intensity for both compressional (orogenic) and tensional (taphrogenic) phases of tectonic activity in circumcontinental mobile belts. Mineralization intensity gradients match deformation intensity gradients. Therefore, each phase of the tectonic cycle is considered capable of generating a concurrent or somewhat later mineralization cycle. The frictional heat of shallow orogeny is believed capable of concerting all available ground fluids into hydrothermal fluids that can leach, mobilize, and redistribute elements according to their temperature stability, thus producing regional zones. Taphrogeny, which occurs dominantly in hinterlands from which low-temperature elements were flushed, involves deep faults that may tap the mantle and introduce new elements, including those of low temperature stability. Uranium is most stabilized in lowest temperature environments and thus seeks a regional zonal position at the extreme foreland end of mineralization gradients of either type. The consistency of this relation, in mobile belts throughout the Americas, justifies its extension to mobile belts of any age throughout the world to allow prediction of most uraniferous regions. Metallotectonics of the Iberian peninsula, interpreted for the first time, indicate that uranium has migrated to the lowest temperature environments possible in the central Meseta where it exists in Tertiary deposits. Without metallogenic data, the optimum regional positions for uranium in the rest of the world are predicted from tectonic analysis of mobile belts. Regions deemed most favorable by this method include the world's most significant uranium districts. (auth)

18544 GENERAL GEOSTRUCTURAL CONSIDERATIONS CONCERNING THE DISTRIBUTION OF URANIUM DEPOSITS WITH SEDIMENTARY CONTROL IN ARGENTINA AND THEIR APPLICATION IN THE REST OF SOUTH AMERICA. Stipanicic, P. N. (Comision Nacional de Energia Atomica, Buenos Aires). pp 205-16 of Uranium Exploration Geology. Vienna; International Atomic Energy Agency (1970). (In Spanish).

From Panel on Uranium Exploration Geology, Vienna, Austria. See STI/PUB-277; CONF-700429.

From the experience gained within Argentine territory, it would seem that many of the principal uranium deposits of the stratiform type contained in sedimentary rocks are very closely linked with the presence, in their vicinity, of large peneplained areas in which fertile rocks outcrop. The genesis of these deposits must in principle have entailed (apart from fulfillment of the conditions necessary for the host rock to permit uranium concentration, precipitation, and so on) leaching of the uranium, starting in the source areas; these areas are in fact the peneplains referred to above, after exposure to degradation, weathering, and so on, for lengthy periods. Since some of the geological events playing a part in the above mentioned geomorphological configurations are common to the whole of South America, which is also true in certain instances of the composition of the terrain, it is felt that the Argentine experience could be extrapolated beyond the geographical bounds of the country and be applied in prospection for uranium-bearing deposits in other parts of the continent. In this connection, and after selection of sedimentary formations with characteristics such as to make them favorable hosts, it is suggested that a regional analysis be made to ascertain the presence of neighboring peneplains that were clearly defined at any particular stage of their geological history. On the basis of the existing data on uranium deposits in Argentine territory, the most important formations could be those arising late in the Precambrian, Middle Devonian, Middle Permian, end of the Triassic, and beginning of the Tertiary periods. However, one should not disregard other diastrophic stages, such as those which either locally or regionally may have been highly active, thereby permitting development of extensive peneplain areas. (auth)

18545 URANIUM ORE ROLLS IN THE UNITED STATES. Harshman, E. N. (Geological Survey, Denver). pp 219-32 of Uranium Exploration Geology. Vienna; International Atomic Energy Agency (1970).

From Panel on Uranium Exploration Geology, Vienna, Austria. See STI/PUB-277; CONF-700429.

About 40% of the uranium ore reserves in the United States, minable at $8 per pound of contained U_3O_8, are in roll-type deposits in the State of Wyoming. The host rocks are arkosic sandstones, deposited in intermontane basins under fluvial conditions, and derived from the granitic cores of mountain ranges that flank the basins. The host rocks are Eocene and possibly Paleocene in age and are, or were, overlain by a sequence of continental tuffaceous siltstones, sandstones and conglomerates 400 to 700 m thick. Most of the ore is unoxidized and lies below the water table. It contains pyrite, uraninite, coffinite, marcasite, hematite, ferroselite, and native selenium. The ore bodies range in size from a few hundred to several hundred thousand tons of material containing 0.10 to 5% U_3O_8. As mined, the ore averages about 0.25% U_3O_8. The ore bodies are genetically related to and lie at the margins of large tongues of altered sandstone. The character of the alteration and the distribution of several elements within and near the altered sandstone suggest that the ore-bearing fluid was groundwater, neutral to slightly alkaline and oxidizing with respect to the elements being transported. Roll-type deposits in littoral and fluvial sandstones were recently discovered in the Gulf Coastal Plain area of Texas. These deposits appear to be similar to the Wyoming deposits in form, distribution of elements, and genesis. (auth)

18546 URANIUM OCCURRENCES IN SMALL SEDIMENTARY BASINS IN JAPAN. Hayashi, S. (Power Reactor and Nuclear Fuel Development Corp., Tokyo). pp 233-41 of Uranium Exploration Geology. Vienna; International Atomic Energy Agency (1970).

From Panel on Uranium Exploration Geology, Vienna, Austria. See STI/PUB-277; CONF-700429.

A brief history of uranium surveying and prospecting in Japan is given. The two most promising uranium deposits, Ningyo-toge and Tono, are described. These deposits were found in the basal part of the Neogene Tertiary underlain by Cretaceous granitic rocks. The most prevalent concepts on uranium deposition, especially about the source of uranium, are believed to be groundwater passing through granitic host rocks. A peculiar occurrence in the Toyota deposit is also outlined. Favorability criteria recognized in small basins in Japan are the presence of channel structures in basement granitic rocks (not so commonly observed in other countries); and a non-marine conglomeratic facies in the Neogene Tertiary. (auth)

18547 GENESIS OF URANIFEROUS DEPOSITS IN METASEDIMENTS IN THE PROVINCE OF SALAMANCA (SPAIN). Fernandez Polo, J. A. (Junta de Energia Nuclear, Madrid). pp 243-52 of Uranium Exploration Geology. Vienna; International Atomic Energy Agency (1970). (In Spanish).

From Panel on Uranium Exploration Geology, Vienna, Austria. See STI/PUB-277; CONF-700429.

The numerous radioactive outcrops in the Province of Salamanca, in palaeozoic metasediments with different degrees of metamorphism, required new criteria for their study as the type of uraniferous mineralization differed completely from other known occurrences. Subsequently, similar deposits were found in the Province of Cáceres and in the south of Spain (points of similarity with deposits in Portugal were also established). An analysis of the geological environment and its evolution, uraniferous and associated ores, gangue, supergene alteration, morphology of the ore bodies and certain economic characteristics is given. The possible processes of uraniferous enrichment are discussed, eliminating those which do not fit the conditions encountered in these deposits. The relation of the deposits to the geological conditions, both from the petrographic and from the tectonic and environmental points of view is considered. The

XUM

presence of mineralization in slate formations is not associated with particular stratigraphic levels nor with petrological peculiarities of the metasediments in question. However, a certain connection is observed between location and tectonic features; as regards the latter, the degree of relaxation and hence of permeability appears to be decisive. This, together with the fact that the deposits are located alongside a graben, reinforces the impression that one is here dealing with mineralization mechanisms of a supergene nature which are completely independent of lead, tin and tungsten mineralization preceding the uraniferous deposits. The geomorphology of the areas where the deposits are located is also perfectly differentiated and thus appears to have a decisive influence on the genetic processes. The geological and mining studies carried out in this region, which were really exhaustive in some areas, appear to support the assumptions set forth in the paper. (auth)

18548 CHARACTERISTICS OF URANIUM ORE GENESIS IN THE PERMIAN AND LOWER TRIASSIC OF THE ITALIAN ALPS. Mittempergher, M. (CNEN, Rome). pp 253-64 of Uranium Exploration Geology. Vienna; International Atomic Energy Agency (1970).

From Panel on Uranium Exploration Geology, Vienna, Austria. See STI/PUB-277; CONF-700429.

Uranium mineralization is always present in the volcanic products, in the continental sandstones and in the littoral-lagoonal sediments of Permian and Lower Triassic age in the Alps. In some areas, these lithological formations were metamorphosed during the Alpine orogenesis; consequently the mineralization was regenerated and redistributed. Corresponding to the different geologic and paleogeographic conditions, the uranium occurrences are characterized as: epithermal occurrences in the late paleozoic volcanites; epigenetic occurrences in continental sandy sediments of Permian age; and syngenetic occurrences in littoral sediments of permo-Triassic age. Such a uranium ore genesis takes place over a wide subsident basin in the Hercynian foreland; this basin evolved, during the Cretaceous, from the Alpine geosyncline. Structural and paleogeographic analysis of the subsident basin revealed the presence of zones with differential subsidence in the southern Alps. The most important and numerous uraniferous occurrences appear within the Lombard region, where the subsidence occurred rapidly. Furthermore, the most frequent occurrences are distributed in proximity of volcanic masses which represent the magmatism of the Saalian phase of the Hercynian orogenesis. Once again, the mineralization related to late Hercynian magmatism in Europe is confirmed. The uraniferous occurrences of the Late Paleozoic and Lower Triassic in the Alps show typical characteristics of uranium ore genesis in pre-geosyncline basins. (auth)

18549 URANIUM: ITS GEOLOGICAL OCCURRENCE AS A GUIDE TO EXPLORATION. Robertson, D. S. (David S. Robertson and Associates Ltd., Toronto). pp 267-84 of Uranium Exploration Geology. Vienna; International Atomic Energy Agency (1970).

From Panel on Uranium Exploration Geology, Vienna, Austria. See STI/PUB-277; CONF-700429.

Uranium is a lithophile element and as such it is concentrated by processes active in the crust. About 90% of the world's reserves occur in basal Huronian conglomerates and post Paleozoic sandstones. It is suggested that significant expansion of reserve under current economic conditions requires the finding of further reserve of these types. The ore deposits in the basal Huronian are of detrital origin. They are restricted in time to a period after the development of extensive acid crust but before the evolution of an oxidizing atmosphere. Because of this they are of extremely restricted occurrence. The post Paleozoic sandstone ore deposits, called Western States type, are formed by leaching of uranium from granite surfaces, volcanic sediments or arkoses, the movement of uranium in groundwater and its precipitation by organic material. It appears that the processes necessary, which continue to the present time, take place only in arid to semi-arid climates. Because of this, the areas of the earth in which such deposits can be found are limited. (auth)

18550 SOME GEOLOGICAL CONCEPTS FOR CONSIDERATION IN THE SEARCH FOR URANIUM PROVINCES AND MAJOR URANIUM DEPOSITS. Bowie, S. H. U. (Inst. of Geological Sciences, London). pp 285-300 of Uranium Exploration Geology. Vienna; International Atomic Energy Agency (1970).

From Panel on Uranium Exploration Geology, Vienna, Austria. See STI/PUB-277; CONF-700429.

The discovery of the major uranium ore provinces of the world depended more on the application of geological knowledge than on the use of the wide range of electronic appliances at the disposal of the prospector or mining company. This does not mean, however, that such instruments were not and still are of immense value in the specific location of uranium ore bodies. Isotope ratio studies showed that the ore-forming processes extended in many instances over hundreds of millions of years and this, together with mineragraphic evidence, suggests that uranium is epigenetic in the case of most major peneconcordant deposits. The most favorable environments for the discovery of new uranium provinces and major uranium deposits are considered to be intracratonic sediments, miogeosynclinal sediments, and sediments in intermontane basins in uranium provinces, particularly if there are associated acid igneous intrusive or eruptive rocks. (auth)

18551 THERMODYNAMIC CONDITIONS OF THE ORIGIN OF URANINITES. Kaspar, J.; Hejl, V. (Inst. of Experimental Mineralogy and Geochemistry, Prague). pp 301-14 of Uranium Exploration Geology. Vienna; International Atomic Energy Agency (1970).

From Panel on Uranium Exploration Geology, Vienna, Austria. See STI/PUB-277; CONF-700429.

It is well known that all uranium minerals are oxygen compounds. The only simple oxide occurring in nature is UO_2 uraninite (ulrichite or pitchblende). Its crystal structure corresponds to pure UO_2, but besides U^{4+}, it also contains a variable amount of U^{6+} up to $(U^{4+}U^{6+})\ O_{2.6}$. For this reason a study was made of the physicochemical conditions of its origin in nature. A calculation model was developed approximating the processes going on in nature. The dependence of the origin of UO_2, UO_3, and U_3O_8 on temperature (300 to 900°K) and pressure (1 to 10,000 atm) was studied. Calculations of values of free enthalpies at 1 atm showed that values of ΔG were predominantly negative. Therefore, in theory, the oxides could exist in nature. At the same time, the absolute values of ΔG were most favorable for the formation of UO_3 which, however, was not encountered in nature. UO_3 formation was most favored because the experimental reactions occurred in an environment with a surplus of oxygen. The oxides under study formed a series according to the decreasing value of ΔG, namely UO_3, U_3O_8, and UO_2. In nature, however, the origin of uraninite (in pegmatites as well as hydrothermal veins) occurred under a lack of oxygen and the above sequence was the reverse, the only oxide originating in nature being therefore UO_2. On the whole, calculations showed that the existence of UO_2, UO_3, and U_3O_8 was possible under high pressures up to 10,000 atm. However, increasing pressure influenced unfavorably the value ΔG; in other words, the formation of the uranium oxides was less probable. From the results obtained, it is clear that temperature is more important than pressure for the formation of uraninites. Another important factor was the chemical character of the environment in which uraninite originated. The reducing atmosphere supported the origin of UO_2, whereas an oxidizing medium suppressed its origin. The calculated values were checked against experimental results of hydrothermal synthesis of uraninites in autoclaves. Uraninites in nature may originate in pegmatites as well as in the zone of hypergenesis. At the same time, according to the different content of U^{6+}, uraninites may be classified as α, β, or γ uraninite I, II, and III. Chemically, it is a question of the variable amount of UO_3 in the structure of UO_2 which causes change in the unit cell dimensions in the range between $a_0 = 5.38$ and 5.49 Å. In summing up the results of the calculations and the experimental data, and comparing them with the whole paragenesis in which uraninite occurs in individual places (for instance where carbonates or sulphides prevail), it was concluded that the composition and properties of uraninites may be used as an indicator of certain genetic conditions. The results may also be applied to the prognoses of the extent of uraninite occurrence in individual deposits. (auth)

18552 SPECULATIONS ON THE URANIUM ORE FLUID. Gabelman, J. W. (Atomic Energy Commission, Washington, D. C.). pp 315-30 of Uranium Exploration Geology. Vienna; International Atomic Energy Agency (1970).

From Panel on Uranium Exploration Geology, Vienna, Austria. See STI/PUB-277; CONF-700429.

Lateral secretion by fresh meteoric groundwater is a popular theory for uranium mineralization in sedimentary rocks. However, field evidence indicates that presently migrating fresh groundwater does not mineralize its aquifers, and that uranium, copper, and vanadium deposits are formed by fluids which were corrosive enough to pervade and alter relatively impermeable rocks. Further, uranium mineralization occurred in geographically restricted areas and not in any hydrodynamic system with suitable source and reservoir rocks. Uranium districts are concentrated along the forelands of mobile belts whereas the best source rocks are in the hinterlands. Districts in regionally extensive preferred formations are localized in relation to broad tectonic features rather than the topographic surface, stratigraphy, local structures, or local hydrodynamic systems. The areally uniform uranium content presently found in the most uraniferous source rocks (granite, rhyolitic tuff, and carbonaceous shale) indicates its resistance to leaching by ordinary water. A portion of this uranium is removable by acid leaching. Uranium deposits also contain a family of minor elements in quantities up to several orders of magnitude times their level in source rocks. Some of these are not easily leached. The patterns of altered rock that invariably accompany uranium deposits do not reflect fresh-water flow but are restricted, selective among similar chemical traps, and locally transgressive, indicating a limited supply of fluid. The difficulties in concentrating a sufficient volume of ions by diffusion or water by flow to create an ore deposit invite consideration of a concentrated fluid. Fresh water analyses show contents of the family of uranium deposit elements many times less than the levels in source rocks, whereas brines have concentrations many times more, even approaching the concentration in ores. Fluid-gas inclusions in calcite in sandstone uranium deposits appear to be brines trapped at 45 to 65°C. Recent isotopic studies show many brines to be meteoric water enriched in mineral ions by percolation through heated environments. The uranium ore fluid must have corrosiveness, penetrability, concentration and selectivity; qualities which fresh groundwater does not possess. The ore fluid could be a brine composed of originally meteoric water mixed with magmatic, connate, or rock crystallization fluids and mineral ions from any source. This fluid could migrate and mineralize in response to temperature zoning. (auth)

18553 INTERPRETATION OF COLOR RELATIONS IN SANDSTONE AS A GUIDE TO URANIUM EXPLORATION AND ORE GENESIS. Adler, H. H. (Atomic Energy Commission, Washington, D. C.). pp 331-44 of Uranium Exploration Geology. Vienna; International Atomic Energy Agency (1970).

From Panel on Uranium Exploration Geology, Vienna, Austria. See STI/PUB-277; CONF-700429.

Most of the uranium mined in the United States of America occurs in red or drab fluvial sandstone and is associated with a pyritiferous carbonaceous facies formed during and shortly after sandstone deposition. Many of the ore deposits, particularly the roll-type deposits, formed by accretion of uranium along or near oxidized borders of the reduzate facies. The ore accumulated by recyclic oxidation–reduction and solution-deposition of uranium and other elements. The uranium deposits are closely related to hematite-red and limonite-drab coloring in the sandstone. The pigmentation, which is post-diagenetic and most likely related to geologically recent groundwater circulation in the sediments, results from the release of iron during oxidation of pyrite by oxygenated groundwater below the water-table. Limonite is formed initially but may subsequently dehydrate to hematite. Dehydration may be episodic since drab-red boundaries are usually sharp. The transformation is accelerated under warm climatic conditions and possibly conforms to periods during which groundwater temperatures were slightly elevated. Iron may also be taken up by montmorillonite or removed by circulating groundwaters resulting in a pale green or bleached color in the oxidation sandstone. The color of the sandstone can be used to determine the extent of the tongue of oxidative alteration and to define areas favorable for exploration. (auth)

18554 CRITERIA FOR THE SELECTION OF EXPLORATION AREAS IN THE UNITED KINGDOM. Ostle, D. (Inst. of Geological Sciences, London). pp 345-53 of Uranium Exploration Geology. Vienna; International Atomic Energy Agency (1970).

From Panel on Uranium Exploration Geology, Vienna, Austria. See STI/PUB-277; CONF-700429.

General criteria used in the selection of areas favorable to the occurrence of uranium deposits are outlined. They include the size and type of target, the nature and age of known mineralization, tectonic and lithological favorability and palaeogeography. The areas selected include those underlain by sediments of the Old Red Sandstone cuvette and surrounding crystalline rocks of northern Scotland as well as a large belt of geosynclinal sediments in the Southern Uplands of Scotland having associated volcanics, intrusive granites and uranium and other base metal mineralization related to structural features. Triassic basins of the English Midlands were selected on lithological and geochemical grounds. Palaeogeographic criteria, among others, lend support to the selection of areas underlain by basal Namurian and Cambro–Ordovician shales in north and southwest England and Wales. (auth)

18555 DIRECTION OF THE DEVELOPMENT ON A NUCLEAR FUEL CYCLE. URANIUM RESOURCES. Kamiyama, Teiji (Power Reactor and Nuclear Fuel Development Corp., Tokyo). Genshiryoku Kogyo; 16: No. 4, 47-9(Apr 1970). (In Japanese).

Future development of Japanese uranium resources must be decided on the basis of restrospective and future views on the subject. It is noted that what has been done in the area of mining and refining of the uranium ores available in the country was mainly due to efforts of the PNC. It is felt that effort should be devoted to enhancement of the mining and refining for domestic mineral deposits, and then turning to overseas resources development. Activities devoted to overseas uranium resources include contract talks and prospecting. Future efforts should include conclusion of the long-term uranium purchase agreements with oversea countries, and multiple measures for developing uranium resources outside Japan. (Japan)

Oceanography

Refer also to abstract 18939.

Seismology

Refer also to abstract 18988.

18556 (ORNL-4584, pp 41) EARTHQUAKES AND REACTOR SAFETY. McClain, W. C.; Myers, O. H. (Oak Ridge National Lab., Tenn.).

From Health Physics Division annual progress report for period ending July 31, 1970.

Routine operation of the ORNL seismograph station continued from Aug. 1969 to Aug. 1970, and included the regular reporting of data to the U.S. Coast and Geodetic Survey and the periodical issuance of a station bulletin. In addition, a seismic history of the southeast region of the United States was compiled and a study of the seismicity of this area made. (auth)

XUM

ENGINEERING

Nuclear Explosions

Refer also to abstracts 18556, 18831, 18832, and 20449.

Facilities and Equipment

Refer also to abstracts 18854, 18863, 18926, and 19279.

18557 (ANL-7677) LOAD-EQUIVALENCE PARAMETERS FOR DYNAMIC LOADING OF STRUCTURES IN THE PLASTIC RANGE. Youngdahl, Carl K. (Argonne National Lab., Ill.). May 1970. Contract W-31-109-eng-38. 71p. Dep. NTIS.

The solutions to four classical problems in dynamic plasticity—circular plate under uniform pressure, the reinforced circular cylindrical shell under uniform pressure, the free-free beam with a central concentrated force, and the circular cylindrical shell with a ring load are examined to determine the effect of pulse shape on final plastic deformation. It is found that there is a strong dependence on pulse shape for pulses having the same total impulse and maximum load; however, the effect of the pulse shape is virtually eliminated if the pulses have the same total impulse and effective load. The effective load is defined as the impulse divided by twice the mean time of the pulse, where the mean time is the interval between the onset of plastic deformation and the centroid of the pulse. (auth)

18558 (ARH-1474) CPDREV: A SPARE PARTS INVENTORY CONTROL SYSTEM. Morgenthaler, A. C. (Atlantic Richfield Hanford Co., Richland, Wash.). 21 Nov 1969. Contract AT(45-1)-2130. 54p. Dep. NTIS.

"CPDREV" is the computer program name of an inventory control system. The program is designed to operate with serially numbered inventory systems and is specifically oriented to industrial maintenance spare parts management. CPDREV uses a mathematical optimization technique known as dynamic programming in a Subroutine called SPAROP. This employs a high speed computing algorithm to find the best (optimum) inventory order quantity and order time by a recursive trial and error technique. Twenty parameters are supplied or received in correspondence between the main program and SPAROP. The algorithm requires an average time of 44 milliseconds to optimize these 20 values over all of the many reorder periods between the current date and the end of the planning period. The best combination of staggered purchases is the global optimum policy. The first of these purchases is recycled to the main control program as the current order quantity. This is then converted to a maximum and minimum stock level. Hence, future purchases as well as the present purchase are also considered in arriving at today's best order policy. Recomputation of MAX and MINs should be performed at least every 90 days. CPDREV uses a UNIVAC 1108 computer and requires 10 minutes to evaluate 8,000 items and print pertinent management reports. The system is applicable to any computer which has 63,000 words of user available core and one million words of high speed user available random access drum space (such as UNIVAC 432 drums). Results from one processing are saved and available as recycle to the next processing period. This permits faster evaluation on subsequent processings. CPDREV is highly flexible in that it permits customized treatment of single items or groups of them to conform with managerial control policies. (auth)

18559 (CONF-700816-(Vol.1), pp 128-42) PRESENT STATUS OF THE DESIGN AND TESTING OF RADIOACTIVE FILTRATION INSTALLATIONS AND ASSOCIATED AEROSOL RESEARCH. Dyment, J. (Atomic Weapons Research Establishment, Aldermaston (England)).

From 11. AEC air cleaning conference; Richland, Wash. (31 Aug 1970).

In Proceedings of the eleventh AEC air cleaning conference.

Present AWRE philosophy on safety aspects of the design of filtered ventilation systems for radioactive process buildings evolved several years ago but is now restated. Development of the sodium flame test as an in-place test is discussed and a method of producing suitable quantities of a stable aerosol for this purpose is described. For reactor applications, the effect of high temperatures on the performance of HEPA filters was examined and the need for in-place testing of units subjected to these conditions is indicated. An associated aerosol research program in which the filterability of submicron particles by high-efficiency media was investigated is reviewed. (auth)

18560 (CONF-700816-(Vol.1), pp 207-15) COMPARISON OF EQUATIONS USED IN THE DESIGN OF FISSION GAS ADSORPTION BEDS. Underhill, Dwight W. (Harvard School of Public Health, Boston, Mass.).

From 11. AEC air cleaning conference; Richland, Wash. (31 Aug 1970).

In Proceedings of the eleventh AEC air cleaning conference.

The radioactive isotopes of Kr and Xe are the most difficult fission products to contain, and measurable quantities of these isotopes may be released from nuclear reactors and fuel reprocessing plants. One method of removing the shorter lived isotopes of these materials is to pass the waste gas stream through an adsorption holdup bed. If the time of holdup is long compared to their half lives, the process of radiodecay will remove these isotopes. A comparison is made of the various equations which have been developed for evaluating the efficiency of fission gas holdup beds. It is shown that under conditions favorable for high efficiency, each of these equations leads to the same simple approximate solution. This fundamental similarity is shown to be due to the probabilistic nature of mass transfer. The limits of applicability of the approximate equation are examined and it is suggested that, in many cases of engineering design, the approximate equation will be sufficiently accurate. (auth)

18561 (CONF-700816-(Vol.1), pp 216-23) DESIGN OF FISSION GAS HOLDUP SYSTEMS. Underhill, Dwight; Yusa, Hideo; Grubner, Otto (Harvard School of Public Health, Boston, Mass.).

From 11. AEC air cleaning conference; Richland, Wash. (31 Aug 1970).

In Proceedings of the eleventh AEC air cleaning conference.

Recently the Harvard Air Cleaning Laboratory was asked to prepare a preliminary design for the fission gas holdup beds for the Fast Flux Test Facility. The staff of the Laboratory developed a set of simple equations for rapidly calculating the holdup efficiency, the temperature rise, and the pressure drop for each bed without the need for electronic computers. Because the methods used in this design may be of interest to other people in the field of nuclear safety, an outline of the approaches used in determining each of these factors is presented. (auth)

18562 (CONF-700816-(Vol.1), pp 413-24) HEAT TRANSFER OF SODIUM COMPOUNDS DEPOSITED ON SURFACES FROM AEROSOLS. First, Melvin W.; Yusa, Hideo (Harvard School of Public Health, Boston, Mass.).

From 11. AEC air cleaning conference; Richland, Wash. (31 Aug 1970).

In Proceedings of the eleventh AEC air cleaning conference.

Methods and apparatus have been developed to measure the coefficient of thermal conductivity of layers of elemental sodium combustion products deposited on heat exchange surfaces with an accuracy satisfactory for engineering design studies. (auth)

18563 (CONF-700816-(Vol.1), pp 445-58) SODIUM AEROSOL FILTRATION STUDIES. First, M. W.; Baldwin, T. (Harvard School of Public Health, Boston, Mass.).

From 11. AEC air cleaning conference; Richland, Wash. (31 Aug 1970).

In Proceedings of the eleventh AEC air cleaning conference.

Industrial cleanable cloth filters have important advantages for sodium fume collection following accidental releases from liquid metal-cooled fast breeder reactors. Glass filter fabrics have superior temperature resistance, but are attacked chemically by strong alkalies and are difficult to clean by gentle backflow. Teflon fabrics are stronger and can be cleaned of accumulated filter-cake by vigorous mechanical shaking. In addition, they have excellent chemical resistance and good cleaning characteristics. When Teflon is pretreated with an asbestos filter aid, it has high initial collection efficiency and may be cleaned satisfactorily for many cycles. This permits total filtration of large amounts of sodium fume per square foot of filter cloth. (auth)

18564 (ORNL-4629, pp 10-13) THORIUM-URANIUM RECYCLE FACILITY. (Oak Ridge National Lab., Tenn.).

In Status and progress report for thorium fuel cycle development for January 1, 1969-March 31, 1970.

The safety analysis was published and accepted, and the maintenance manual was completed. The cell used for $LiF-^{233}UF_4$ preparation was cleaned to permit direct installation of equipment for isolating ^{248}Cm. Improvements were made or sought in the in-cell fire protection system, emergency power, cell outlet filters, and waste systems. (auth)

18565 (ORNL-TM-3291) OPTIMUM TURBINE EXHAUST PRESSURE FOR USE OF A SINGLE-EFFECT, VERTICAL-TUBE STILL DESALTING PLANT WITH A STEAM TURBINE-GENERATOR. Welfare, F. G. (Oak Ridge National Lab., Tenn.). Feb 1971. Contract W-7405-eng-26. 26p. Dep. NTIS.

The optimum turbine exhaust pressure for a dual-purpose (power and water) plant employing a single-effect vertical-tube evaporator was calculated for a variety of economic conditions. The results show a possible saving due to the optimization of up to 2.5 millions of dollars or about 3.8 cents per thousand gallons of product water. (auth)

18566 (ORNL-tr-2370) SAFETY ASPECTS IN THE DESIGN OF THE WAK. Herre, F.; Schulze, K. P.; Muszynski, G.; Patzelt, A. Translated by R. Gregg Mansfield (Oak Ridge National Lab., Tenn.), from Atomwirt., Atomtech.; 15: 79-83(1970). 10p. Dep. NTIS.

The design and operation of a reprocessing plant for irradiated fuel elements (WAK) located at Karlsruhe, Germany, are described. Emphasis is placed on design features that assure radiation protection for operating personnel, such as shielding and ventilation systems. (C.H.)

18567 APPARATUS FOR DETERMINING THE POSITION OF A RADIOACTIVE SOURCE. Laloy, Paul (to Commissariat a l'Energie Atomique). British Patent 1,211,316. 4 Nov 1970. Priority date 23 Jul 1968, France.

Apparatus for accurately determining the position of a radiation source used, for example, for gammagraphic monitoring or inspection of a metal component, particularly of a cylindrical or spherical shape, is discussed. (C.E.S.)

18568 THEORY FOR FREE VIBRATION OF ORTHOTROPIC SHELLS OF REVOLUTION. Stoneking, J. E.; Boresi, A. P. (Univ. of Illinois, Urbana). Nucl. Eng. Design; 14: 271-85(Nov 1970).

A theory of free vibration for orthotropic shells of revolution including the effects of transverse shear and rotary inertia is formulated. Derived equilibrium equations are expressed in terms of the displacement vector, which is written as a truncated power series expansion in the thickness coordinate. The partition method, in conjunction with piecewise polynomials, is used to obtain a solution. The effect of transverse shear for non-axisymmetric, transverse vibrations of a cylinder and of a torus segment is indicated in several examples. Results show that transverse shear significantly affects the natural frequencies of these shells. (auth)

18569 GEOMETRY CHANGES IN THE LIMIT ANALYSIS OF AXISYMMETRIC INTERSECTING SHELLS. Sherbourne, A. N.; Perelmuter, M. (Univ. of Waterloo, Ont.). Nucl. Eng. Design; 14: 239-57(Nov 1970).

The problem of determining the carrying capacity for internal pressure loading of a shell consisting of an intersection of spherical and cylindrical shells is solved using a simple circumscribing yield surface for non-hardening Tresca material together with strain-displacement relations corresponding to those of the "large displacement" theory of thin shells. (auth)

18570 DIRECTION OF THE DEVELOPMENT ON A NUCLEAR FUEL CYCLE. FUEL REPROCESSING. Yamazaki, Masao; Nakajima, Kentaro (Power Reactor and Nuclear Fuel Development Corp., Tokyo). Genshiryoku Kogyo; 16: No. 4, 59-63(Apr 1970). (In Japanese).

The fuel reprocessing in the world is now for peaceful uses, after the stage for military purposes. In Japan, the test operation in this connection has been made in JAERI, and a reprocessing facility of practical size is about to be constructed in the PNC. The trends in fuel reprocessing in the world show transition from military to peaceful purposes. Reprocessing in the 1970's, including the amounts of spent fuels and the reprocessing capacities and procedures (the wet and the dry method, and their recent developments) are described along with direction of the reprocessing technologies, including the reprocessing of high burnup and fast reactor fuels. Economical and safe disposal of the radioactive wastes and the reduction in down time for the facilities are discussed. (Japan)

18571 CALCULATION OF EFFICIENCY OF γ-IRRADIATORS. Drozdov, V. E.; Dunaev, L. M. This paper was summarized in At. Energ. (USSR); 28: 492-3(Jun 1970) as paper No. 395/5482. (In Russian).

A method is described for calculating the efficiency of any γ-irradiation facility using line sources based on the expression $\eta = (\omega/\varphi_0) \int_{C}^{\varphi_0} \eta_i(\mu d_i;\ k_i;\ \mu b_i)\alpha_i(k_i;\ \mu b_i)d\varphi$, where ω is the fraction of the source radiation incident on the apparatus (or the relative solid angle); μd_i and μb_i are respectively the thickness of the layer and the size of the air gap between the radiator and the apparatus in the i-th direction expressed in mean free paths; $k_i = \mu H/\mu b_i + \mu\alpha_i$ (μH is the half height of the radiator in mean free paths and α_i is a correction for the air gap). Values of ω, η_i (μd_i, k_i, μb_i), and $\alpha_i(k, \mu b_i)$ were calculated for a wide selection of radiator and apparatus parameters. Using the rule of additivity and the calculated values of η_i, α_i, and ω, the efficiency of any irradiation facility employing line sources can be found by integrating the equation numerically. Studies and experiments showed that the calculation of η_i for the equation can be simplified by using the relation $\eta_i = \eta_1(\omega_1/\omega_i)$, where η_1 and ω_1 are known; the subscripts 1 and i correspond respectively to fixed and arbitrary distances of the irradiator from the apparatus. This relation can be used to calculate η even in the case of a nonuniform distribution of activity in the irradiator. (auth)

18572 METHOD AND MEANS FOR REMOVING FOREIGN MATTER FROM FILTER ELEMENTS. Naylor, Donald William; Boulter, Frank; Maynard, George Herbert (to Nuclear Design and Construction Limited). British Patent 1,222,081. 10 Feb 1971. Filed 13 Jan 1967.

A method is described for removing foreign matter collected by one or more circuit filter elements situated within a main fluid flow circuit. This is accomplished by isolating the part of the circuit containing the filter element and connecting this isolated part to a container thus constituting a branch circuit. The branch is connected to a vacuum and then, at a point near the filter unit, the branch is opened to atmosphere causing the foreign matter in the filter to be blown into the container. This invention could find application in the coolant gas flow circuit filter in a gas-cooled nuclear reactor. (UK)

18573 DISCONTINUOUS FINITE ELEMENTS IN THERMAL ANALYSIS. Thompson, J. J.; Chen, P. Y. P. (Univ. of New South Wales, Kensington, Australia). Nucl. Eng. Design; 14: 211-22(Nov 1970).

Finite element methods using discontinuous, piecewise linear or quadratic, approximating functions, were developed for transient heat flow analysis. The methods are shown to have definite advantages over the ordinary continuous finite element methods, particularly as regards the prediction of the spatial temperature moments which are needed for the ordinary finite element methods of thermal stress analysis. (auth)

18574 DIRECTION OF THE DEVELOPMENT ON REACTOR MATERIALS. STRUCTURAL MATERIALS FOR THE HEAT EXCHANGERS. Tada, Masabumi (Tokyo Shibaura Electric Co. Ltd., Kawasaki, Japan). Genshiryoku Kogyo; 16: No. 4, 86-91 (Apr 1970). (In Japanese).

A brief description of light-water reactors is given followed by discussions of the (intermediate) primary and the secondary heat exchanger in a Na-cooled fast-breeder power reactor system. The primary heat exchanger is for sodium-to-sodium coolants. Types AISI 304 and 316 SS are employed as the structural materials because of the high heat resistance and corrosion resistance. In this heat exchanger, discontinuous structure is avoided. The secondary heat exchanger is for sodium to water (steam) coolants. The materials used are austenitic stainless steel and ferrite steel. A description is given which includes an outline of the heat exchangers; selection of the materials; corrosion in the Na coolant; change in the mechanical properties in the Na environment (2¼ Cr–1 Mo steel, and 316 stainless steel); and problems in the design of heat exchangers. (Japan)

18575 FINITE ELEMENT ANALYSIS OF PLATE BENDING WITH TRANSVERSE SHEAR DEFORMATION. Greimann, L. F. (Southwest Research Inst., San Antonio); Lynn, P. P. Nucl. Eng. Design; 14: 223-30(Nov 1970).

Based on Mindlin's plate theory, a finite element stiffness approach for plate bending which includes transverse shear deformation is presented. Three different rectangular plate finite element models are developed and are used to investigate the importance of plate thickness effect in static and free vibration plate bending problems. One of the proposed displacement fields incorporates transverse shear deformations without increasing the number of nodal quantities beyond that associated with existing (classical plate theory) finite elements. The method is applicable for the analysis of thick plates or slabs which occur in Civil Engineering structures such as power plants or nuclear reactors. (auth)

Heat Transfer and Fluid Flow

Refer also to abstracts 18574, 19191, 19278, 20706, and 20790.

18576 (AEC-tr-7189) VELOCITY FIELD OF TURBULENT FLUID FLOW IN A LONGITUDINAL STREAMLINE OF CLUS-

XUM

TERS OF RODS. Subbotin, V. I.; Ushakov, P. A.; Levchenko, Yu. D.; Alexandrov, A. M. Translation of Russian report. 34p. Dep. NTIS.

In the active zones of nuclear reactors and steam generators, the flow of the cooling agent can proceed in channels with noncircular cross sections, particularly in channels with smoothly packed rods. Results of studies of velocity fields and the hydraulic resistance of turbulent flow in channels, formed by the system of smooth parallel rods, are reported. The rods formed a regular triangular package in the grid. The majority of experimental studies dedicated to the investigation of turbulent flow in channels packed with rods were directed to obtaining friction coefficients necessary for calculation of the power for passage of the cooling agent. Local flow characteristics were found basically by methods of theoretical calculation. Velocity fields, distributions of tangential stress over the perimeter of the entire channel, and data on resistance were obtained in the experiments. Measurements in the channels were carried out in the area of stabilized air flow. Results are presented in a series of figures and diagrams. (J.R.D.)

18577 (AECL-3783) A PACKAGE OF COMPUTER PROGRAMS FOR THE ANALYSIS OF TEMPERATURE DISTRIBUTION IN THREE DIMENSIONAL SYSTEMS. Carver, M. B. (Atomic Energy of Canada Ltd., Chalk River (Ontario). Chalk River Nuclear Labs.). Dec 1970. 37p. Dep. NTIS (U. S. Sales Only).

TRUMP, a computer program for transient or steady state temperature calculations in complex systems, has had wide use at CRNL for some time. The program is used to calculate the temperatures in an interconnected series of nodes using an iterative heat balance scheme. The input data required to describe intricate geometry becomes very extensive and the preparation is time consuming. The programs described have been developed to produce the various types of input required by TRUMP and include MESH—a program for generating node geometry and connection data from simple input; PLOOK—a program which extracts the thermal properties of given materials from an extensive compilation of materials; DECAY—a program which produces a heat generation vs time array for fuel removed from a reactor, given the irradiation history; and FORM—a program which computes radiation form factors between convex and concave surfaces which may have shielding surfaces partially interposed. The listings of MESH and the property files for PLOOK are extremely lengthy and no listings are included, but they are available on request. (auth)

18578 (WANL-TME-2721) W-MESHER: A COMPUTER PROGRAM TO ANALYTICALLY PARTITION A TWO-DIMENSIONAL FIGURE. Monkelis, M. R. (Westinghouse Electric Corp., Pittsburgh, Pa. Astronuclear Lab.). Jul 1970. 140p. Dep. NTIS.

A computer code is described which is used to analytically partition a two-dimensional figure, bounded by straight line and circular arc segments, into a network of mesh cells. The output is capable of being used in heat transfer codes to calculate the temperature distribution of a given geometrical configuration with known boundary conditions. (auth)

18579 NUMERICAL CALCULATION OF ONE-DIMENSIONAL UNSTATIONARY TEMPERATURE AND STRESS FIELDS. Svoboda, M. (Technical Univ., Prague). Nucl. Eng. Design; 14: 258-70(Nov 1970). (In German).

A method for numerical analysis of one-dimensional transient temperature fields and elastic thermal stress fields is outlined and a FORTRAN-program is described. Results of parametric studies are given in diagrams. The computer program is included. (auth)

18580 HEAT AND MASS TRANSFER OF RODS IN A TURBULENT LIQUID. Polyanin, L. N. This paper was summarized in At. Energ. (USSR); 26: 279-80(Mar 1969) as paper No. 263/5019. (In Russian).

A physical description of a bundle of nonuniformly heated rods is considered, with account of the heat and mass transfer among the flow regions in hydraulic cells. An estimate of the turbulent exchange coefficient between cells formed by a bundle of cylindrical rods in a triangular lattice is obtained from statistical turbulence theory: $K \approx (0.03/d)Re^{-1/12}$, which is applicable when the ratio of the distance between rod centers to the rod diameter satisfied ($\sim l/d \geq 1.1$), and is in agreement with experimental data. The coolant mass flow through the h-th cross section of the j-th cell is given by $g_j(h) = [f_j\sqrt{\gamma_j(h)/\xi_j(h)}/\Sigma_j f_j\sqrt{\gamma_j(h)/\xi_j(h)}]G_k$, where G_k is the flow of liquid through the channel, f_j is the transfer cross section of the j-th cell, γ_j is the density of the liquid, and ξ_j is the hydraulic resistance coefficient. Results are calculated for a heat-evolving assembly to illustrate the flow distribution of coolant along the height of the cells, and the influence of turbulent diffusion on the equilibration of the coolant temperature along the cross section of the channel. The height variations of the coolant flow rate in the cells of a water-moderated, water-cooled reactor can reach about 10%. The smoothing effects of turbulent diffusion cause temperature drops to decrease by 20 to 30% or more in the coolant in neighboring cells. (auth)

18581 HEAT TRANSFER VALUES FOR WATER IN STEAM GENERATORS WITH FORCED CONVECTION AND REACTOR CHANNELS AT PRESSURES OF 170 TO 215 BAR. Herkenrath, H.; Moerk-Moerkenstein, P. (EURATOM, Ispra, Italy). Atomkernenergie; 16: 207-12(1970). (In German).

Sixty diagrams are presented showing experimental results within the framework of a comprehensive program for the investigation of heat transfer in tubes through which water flowed under high pressure. The parameters are as follows: pressure, 170 to 215 bar; mass flow, 700 to 3500 kg/m^{2}sec; heat flux, 20 to 180 W/cm^2; and internal tube diameter, 10 and 20 mm. (H.B.G.)

18582 MOVEMENTS OF GENERATING VAPOUR BUBBLE IN SATURATED POOL BOILING. 1. MOVEMENTS IN NUCLEATE AND FILM BOILING. Iida, Yoshihiro (Yokohama National Univ., Japan); Kobayashi, Kiyoshi. Nippon Kikai Gakkai Rombunshu; 36: 438-45(Mar 1970). (In Japanese).

Bubble generating point density and the structure of a generating vapor bubble may be important problems in the description of boiling heat transfer. Measurements of vapor generating point density were carried out in boiling experiments with water. The structure of generating vapor bubble in nucleate and film boiling modes was also investigated through the movements of vapor voids at the local point of the heating surface in the saturated pool boiling experiment. The pool is contained by glass tube of 60 mm ID and 40 mm in height. The copper heating surface is 20 mm dia. The void detection probe can be moved up or down, left or right, and the detected void signal is observed by synchronization film. The generating point distribution was independent of heat flux, but its point was correlated with heat flux. The correlation of the generating point density and heat transfer coefficient is presented. It is also shown that the movements of generating vapor bubbles have a cyclic characteristic. (Japan)

18583 BOILING OF LIQUIDS ON FINE WIRE UNDER NATURAL CONVECTION CONDITIONS. Subbotin, V. I.; Kaznovskii, S. P.; Korotaev, S. K.; Sviridenko, V. E.; Selevanov, Yu. F. This paper was summarized in At. Energ. (USSR); 26: 448(May 1969) as paper No. 289/5014. (In Russian).

The critical thermal load in water boiling on fine wire as a function of the water composition, the diameter and material of the wire, and the conditions of thermal load application is investigated. The experiments were performed under atmospheric pressure at the saturation temperature. The experimental device consists of a 3-liter boiler, a thermostat-type condenser, current leads, and locking accessories. The boiler is provided with four windows for filming and visual observation. The measuring system of the device includes a pressure gage, a movable thermocouple for measuring the water temperature along the boiler height, and instruments for measuring the power of the experimental heaters. The experiments were performed on horizontally positioned wires made of Kh18N10T steel, tungsten, a tungsten-rhenium alloy, Nichrome, and platinum. The wire diameter varied from 0.005 to 1.8 mm (capillary tubes were used for $d > 0.8$ mm). The length of the wires with diameters of 0.005 to 0.05 mm was 20 to 25 mm, while the length of the other wires was 50 mm. The operating liquid consisted of distilled water with the following salinity values: 20; 1; less than 0.1 mg/liter; 1 mg/liter with an addition of 0.01 mg/liter hydrazine for preventing the formation of scum on the boiling surface. The wires were heated by direct transmission of ac current. The thermal load was increased to the critical value in different ways: smoothly from the start of boiling to the onset of crisis; in steps (the increments were reduced to about 0.1 q_{cr} in approaching the boiling crisis, while the time intervals between the increments varied from a few seconds to a few minutes); by instantaneous application of a 0.97 q_{cr} thermal load, which was maintained until the boiling crisis was reached. In certain experiments, boiling on wire under a thermal load of 0.5 q_{cr} lasted 30 min before the crisis was reached. The start of bubble boiling was determined visually. The onset of the boiling crisis was recorded with respect to the electric current drop and local reddening of the wire. For wire diameters smaller than 0.058 mm, the boiling crisis was always accompanied by overheating. It was found that for an impurity content of 0.1 to 1 mg/liter, the critical thermal load is independent of the wire diameter in the 0.005 to 1.8 mm range and is equal to 10^6 kcal/m^{2}hr. With an increase in salinity to 20 mg/liter, the q_{cr} value increases by about

60%. The addition of 0.01 mg/liter hydrazine for a salinity of 1 mg/liter reduces the q_{cr} value by 20 to 25%. The thermal load for which bubble boiling develops increases with a reduction in the wire diameter. For diameters of 0.012 to 0.058 mm, film boiling develops outside the bubble boiling zone, while, for diameters smaller than 0.012 mm, the crisis sets in without preliminary bubble boiling. The time of preliminary boiling on wire, the manner in which the thermal load is increased (in steps, smoothly, or by shock), or the form of the electric current do not affect the q_{cr} value. (auth)

18584 INVESTIGATION OF HEAT-TRANSFER CRISIS IN A BUNCH OF FUEL ELEMENT SIMULATORS UNDER NATURAL CIRCULATION CONDITIONS. Zenkevich, B. A.; Peskov, O. L.; Sapankevich, A. This paper was summarized in At. Energ. (USSR); 26: 446-7(May 1969) as paper No. 286/5141. (In Russian).

Results of experiments on the heat transfer crisis in natural water circulation in a bundle of simulators of twisted strip fuel elements in the reactor of the ABV-1.5 plant are presented. An analysis of the theoretical as well as experimental investigations of the heat transfer crisis in boiling coolant flow shows that the reliability of reactor operation can presently be estimated only on the basis of full-scale experiments. An expression for calculating the critical power of a single fuel element was obtained by computer processing of the results of experiments: $N_{cr} = 6.23(1 + 5l) K_1^{0.297} (W_g \cdot 10^{-2})^{0.367}$, where N_{cr} is given in kilowatts, and l in meters; $Wg = G/3600f$ kg/m^2 · sec; $K_1 = (i' - i_1)/r$ (i' is the enthalpy of water at the saturation line; i_1 is the enthalpy of water, determined with respect to the temperature of the water entering the bundle of fuel element simulators; r is the latent vaporization heat). The expression can be used for parameters such as pressure, 6 to 80 atm abs.; temperature of the entering water, 30 to 270°C; mass velocity, 200 to 900 kg/m^2 · sec; fuel element length, 0.2 to 0.6 m. Good agreement was observed between the data for simulators with uniform heat release and with stepwise heat release, which simulated the heat release in a reactor. This made it possible to use the equation for estimating the margin to the heat transfer crisis in the reactor core with respect to the power level. (auth)

18585 HEAT TRANSFER IN POOL BOILING OF WATER AND FREON-113 ON A CYLINDRICAL ROD. Dul'kin, I. N.; Rakushina, N. I.; Roizen, L. I.; Fastovskii, V. G. (All-Union Electrotechnical Inst., Moscow). Inzh.-Fiz. Zh.; 19: 637-45 (Oct 1970). (In Russian).

Heat removal regimes in boiling water and Freon-113 on non-isothermal surfaces of cylindrical rods were studied analytically and experimentally. Heat flux was supplied through a rod end face and dissipated from the surface with various pool boiling regimes. Tested were copper rods 1.4 cm in dia and 1.25 cm; 2.65 cm; 4.4 cm and 6.6 cm in length. (auth)

18586 STUDY ON CURVED PIPE STEAM GENERATOR. Kozeki, Moribumi (Mitsui Shipbuilding and Engineering Co. Ltd., Tokyo); Nariai, Hideki; Furukawa, T.; Kurosu, Kenji. Nippon Kikai Gakkaishi; 73: 538-46(Apr 1970). (In Japanese).

The transition and control of curved pipe steam generators are important characteristics in optimization of the reactor size for ships. Experiments on two-phase local boiling heat transfer, pressure drop and dryout in small heating tubes, and the over-all heat transfer, pressure drop, and transition or control in a curved pipe steam generator are described. The dryout of curved pipe occurred on low steam weight fraction at its outer region. It was seen that pressure drop is large in comparison with Martinelli–Nelson's result. For the transition and control characteristics of the steam generator, it was observed that the rapid opening or closing of the feed valve produced a peak of the superheat starting point. (Japan)

18587 REAL GAS EFFECTS IN CARBON DIOXIDE CYCLES. Angelino, G. (Politecnico, Milan). Atomkernenergie; 17: 27-33(Feb 1971).

The substantially good results achievable with CO_2 with respect to other gases are due to the real gas behavior in the vicinity of the Andrews curve. Simple cycles benefit from the reduced compression work, but their efficiency is compromised by significant losses caused by irreversible heat transfer. More complex cycle arrangements, six of which are proposed and analyzed in detail, reduce heat transfer losses while maintaining the advantage of low compression work and raise cycle efficiency to values attained only by the best steam practice. Some of the cycles presented were conceived to give a good efficiency at moderate pressure which is of particular value in direct-cycle nuclear applications. The favorable influence on heat transfer coefficients of the combined variation with pressure of mechanical, thermal and transport properties, due to real gas effects, is illustrated. Technical aspects as turbo-machines dimensions and heat transfer surfaces needed for regeneration are also considered. Cooling water requirements are found to be not much more stringent than in steam stations. (auth)

18588 HEAT TRANSFER TO A BINGHAM PLASTIC IN THE ENTRANCE REGION OF A CIRCULAR TUBE. Samant, A. B.; Marner, W. J. (South Dakota School of Mines and Tech., Rapid City). Nucl. Sci. Eng.; 43: 241-6(Mar 1971).

Heat transfer by laminar forced convection to a Bingham plastic in the entrance region of a circular tube was investigated. Uniform velocity and temperature profiles were assumed at the inlet of the constant wall temperature tube. All rheological properties were taken to be constants in the analysis. The governing conservation equations were solved using a finite difference technique for a range of the parameters of the problem—dimensionless plug radius ($\bar{a}$) and Prandtl number (Pr). The results show that the mean Nusselt numbers—beyond an initial entrance length—are higher for Bingham plastics than for Newtonian fluids. This increase in Nu_m becomes more significant with increasing dimensionless plug radius, while the entrance length $\bar{z}$ increases with decreasing Prandtl number. (auth)

18589 STEADY-STATE, TWO-DIMENSIONAL TEMPERATURE DISTRIBUTIONS IN A SINGLE FUEL ELEMENT PELLET AND ADJACENT CLADDING DUE TO AXIAL VARYING HEAT TRANSFER COEFFICIENTS. Meier, S.; Wolf, L. (Technische Univ., Berlin). Atomkernenergie; 17: 73-4(Feb 1971).

Based on results of thermal analysis it can be concluded that the assumed local variation of the heat transfer coefficient between pellet and cladding due to pellet deformations does not lead to local hot spots on the inner cladding surface. These are only induced by an axial variation of the heat transfer coefficient between cladding and coolant. The local axial temperature variations of the pellet may explain irregularities found in postirradiation examinations of fuel rods. Results of studies on variable boundary conditions between fuel and cladding in the axial direction supplemented other results dealing with circumferentially varying boundary conditions. (auth)

Isotope Technology

Refer also to abstracts 18524, 18564, 18571, 18614, 18615, 18617, 18624, 18819, 18870, 19034, and 20816.

18590 (BNWL-1308-4) PACIFIC NORTHWEST LABORATORY DIVISION OF ISOTOPE DEVELOPMENT PROGRAMS QUARTERLY REPORT: AUGUST–OCTOBER 1970. Hansen, J. E. (comp.) (Battelle-Northwest, Richland, Wash. Pacific Northwest Lab.). Nov 1970. Contract AT(45-1)-1830. 41p. Dep. NTIS.

Results of research conducted to develop isotopic fuels are reported. Information is included on progress in programs on waste Cs radiation sources, properties of fission product Rh and Pd, properties of purified fission product Xe, recovery of fission product Cs and Sr, nondestructive testing of radiation sources, advanced source development, circulatory support heat sources, and methods for seabed mineral exploration. (J.R.D.)

18591 (DP-1254) SAVANNAH RIVER LABORATORY ^{60}Co POWER AND HEAT SOURCES. Quarterly Progress Report, July–September 1970. Angerman, C. L.; Ross, C. P. (comps.) (Du Pont de Nemours (E. I.) and Co., Aiken, S. C. Savannah River Lab.). Dec 1970. Contract AT(07-2)-1. 27p. Dep. NTIS.

Activities are reported on studies to provide data that will be required for designing, fabricating, and operating ^{60}Co heat sources. Primary emphasis is on selecting materials for encapsulating cobalt fuel forms and establishing temperature limits for operation of capsules in normal and accident environments. Development of specific heat source concepts is not at present included in the scope of the program, but assistance is provided when required for developing and testing demonstration units. Results of work during the period revealed that welding the centers of the caps in rhenium capsules melted small areas of adjacent cobalt oxide wafers and caused vapor transport of rhenium within the capsule. Satisfactory capsule performance was demonstrated through 20,000 hr at 1000°C with Haynes 25, Hastelloy C, and Hastelloy X capsules. The small diameter increases observed in Haynes 25 capsules after 10,000 hr at 1000°C can be accounted for semi-quantitatively by the precipitation of cobalt-tungsten intermetallic compounds within the Haynes alloy matrix. Nine of ten superalloy capsules containing irradiated cobalt were heated for up to 10,000 hr at 1000°C and were found intact as measured by helium leak tests; the Hastelloy C capsule heated 10,000 hr had an indicated leak rate greater than that of the other capsules.

Oxidation data obtained after 3000 hr at 1000 and 1125°C on capsule and core materials for the WANL 30 kW(t) demonstration unit indicated that radial gaps between fuel pin and Nickel 201 core should be greater than 0.050 in. to prevent interference during five years of operation at normal conditions. The oxide scale formed on Haynes 188 impeded reaction with Nickel 200 at 1125°C for only about 1000 hr. (auth)

18592 (ORNL-4298) COMPATIBILITY TESTS FOR SELECTION OF RADIOISOTOPE HEAT SOURCE COMPOUNDS. Box, W. D.; Crouse, R. S. (Oak Ridge National Lab., Tenn.). Dec 1968. Contract W-7405-eng-26. 187p. Dep. NTIS.

Several compounds of three radioisotopes being studied at ORNL for future use as heat sources have been tested for compatibility with candidate container materials. The source materials consisted of cerium, strontium, and gadolinium metals, strontium titanate, strontium fluoride, strontium disilicide, strontium oxide, strontium oxide with 9% beryllium oxide, ceric oxide, cerous oxide, ceric oxide with 5% neodymium, cerium hexaboride, cerous sulfide, cerium oxysulfide, and cerous fluoride. The nonradioactive element was used in each case. The container materials included the superalloys Hastelloy X, Haynes alloy No. 25, Ni-o-nel, N-155, and Inconel X and the refractory materials molybdenum, niobium, TZM, tantalum, and tungsten. These tests were conducted at temperatures up to 1850°C for times to 10,000 hr. As a result of these tests, the following source and container material combinations are recommended for further investigation: cerous oxide-molybdenum, cerium hexaboride-tantalum, cerium oxysulfide-tungsten, cerous fluoride-molybdenum, strontium titanate-refractory metals, strontium fluoride-refractory metals, strontium oxide-molybdenum, and gadolinium-tantalum. Strontium disilicide reacted extensively with all materials investigated. (auth)

18593 (ORNL-IIC-32) LIST OF AEC RADIOISOTOPE CUSTOMERS WITH SUMMARY OF RADIOISOTOPE SHIPMENTS, FY 1970. Curl, Ruth (comp.) (Oak Ridge National Lab., Tenn.). Feb 1971. Contract W-7405-eng-26. 30p. Dep. NTIS.

An alphabetical list of customers, with isotopes purchased during the fiscal year is given. It is subdivided into domestic and foreign customers. In order to differentiate among the suppliers, the isotopes furnished by Oak Ridge National Laboratory have no other designation. Those furnished by Argonne National Laboratory are followed by (A); those by Brookhaven National Laboratory, by (B); those by Douglas-United Nuclear, Inc., by (D); those by Idaho Nuclear Corporation, by (I); those by Mound, by (M); and those by Savannah River Plant, by (S). All entries for Argonne, Douglas, and Idaho are either reactor service irradiations or cyclotron service irradiations, or both, with no processed isotopes being sold. The entries for Savannah River represent material for resale and loans. The designations CSI, RSI, and SS denote, respectively, cyclotron service irradiations, reactor service irradiations, and special services (including such items as target fabrications, source encapsulation, and preparation of special chemical forms). Targets are designated as Tgs, and fission products as FP. An alphabetical list of isotopes, cross-referenced to customer numbers and again divided into the domestic and foreign categories is included. An alphabetical list also included of states and countries, cross-referenced to customer numbers, the purpose of which is to indicate geographical concentrations of isotope users. A comprehensive table is presented which includes an alphabetical listing of the isotopes and a breakdown into shipments, quantities, and dollars for each isotope under the domestic, foreign, and project (AEC facilities) categories. There are also included the total figures for each isotope. (auth)

18594 (ORNL-TM-3292) ISOTOPE KILOWATT PROGRAM QUARTERLY PROGRESS REPORT FOR PERIOD ENDING DECEMBER 31, 1970. (Oak Ridge National Lab., Tenn.). Feb 1971. Contract W-7405-eng-26. 26p. Dep. NTIS.

The organic fluid capsule test system was constructed, the test installation was completed, the system was brought up to temperature, and endurance testing was started at 600°F on December 30, 1970. The heat pipe and associated test equipment for the thermoelectric heat transfer test were fabricated, the test installation was completed, and the shakedown tests were initiated. Some difficulty was experienced with overcooling of the condenser end of the heat pipe during the initial startup but this was overcome by changing the startup procedure. The heat pipe was started up and operated satisfactorily during the last week of December. Analyses of the relative performance characteristics of iron and nickel heat block-shield assemblies have been completed. The study shows that nickel will be required if advanced thermoelectric materials become available and are to be operated with a hot junction temperature of 1350°F, but for the rest of the systems steel will be satisfactory. Nickel is generally superior to steel, but steel is adequate for the other applications. The cost and delivery time are, of course, much greater for nickel. The 4.10-in. diameter fuel capsule for the $SrTiO_3$ source has been evaluated and a detailed report validating the capsule design with a safety analysis has been prepared. (auth)

18595 (SC-RR-70-854) EFFECTS OF LOAD CONDITIONS ON LONG TERM RADIOISOTOPE THERMOELECTRIC GENERATOR OPERATION. Waddoups, I. G. (Sandia Labs., Albuquerque, N. Mex.). Dep 1970. 64p. Dep. NTIS.

Results of the analysis performed indicate that both the effects of decreasing heat input and the system load conditions must be considered in order to obtain maximum performance at end-of-life (EOL). Furthermore, this maximum EOL performance does not occur at the same load condition for maximum beginning-of-life performance. (auth)

18596 TRANSFER PROPERTIES OF ^{252}Cf AND THEIR USE FOR SOURCE PREPARATION. Pauker, S.; Steiger-Shafrir, N. H. (Technion-Israel Inst. of Tech., Haifa). Nucl. Instrum. Methods; 91: 557-63(1971).

A detailed experimental study of the transfer properties of ^{252}Cf for the purpose of preparation of thin and uniformly deposited secondary sources is described. For the optimum use of these properties, the transfer range, the ionic charge conditions and the angular distribution of the ejected ^{252}Cf atoms were investigated. The most probable transfer range was found to be 0.25 $\mu g/cm^2$ in air, the ejected atoms prior to collisions with air molecules were found to be neutral and the angular distribution of ejection was found to be anisotropic. (auth)

18597 THEORETICAL AND EXPERIMENTAL STUDY OF CENTRIFUGATION WITHIN FIXED WALLS OF A GASEOUS BINARY MIXTURE. Guilloud, J. C. Entropie; Nos. 34-5; 23-35(Jul-Oct 1970). (In French).

A method of centrifugation in the gaseous state, is described; in contrast with ultra-centrifugation, it is the mixture to be separated which is rapidly rotated in a fixed device. The object of this study was to compare ultra-centrifugation and this possible method of isotopic separation. A physical explanation of the multiplying effect, which is the most interesting feature of ultra-centrifugation, and which does not occur in a turbulence tube, is given. Calculations on the magnitude of the differences in concentration likely when centrifuging within fixed walls are given. The experimental loop in which the observed separation effects were less than those theoretically predicted, is described. The results obtained demonstrated the inferiority of this method in comparison with gaseous diffusion. (auth) (France)

18598 AN ELECTRIC GENERATOR WITH THERMOPILES AND RADIOELEMENTS. Freund, Jean-Pierre; Stoll, Roger (to Societe Nationale d'Etude et de Construction de Moteurs d'Aviation. To Compagnie Generale de Telegraphie sans fil (CSF)). French Patent 1,595,641. 15 Jun 1970. Filed 21 Oct 1968. (In French).

An electric generator with thermopiles and using as a heat source a radioelement such as Sr is described. The generator is contained in a metallic case closed by a massive plug which constitutes the cold source. The generator consists of a Mo heat collector presenting a pressure face parallel to the internal terminal face of the plug and defining the parallel positions of the radioactive sources which are regularly distributed about an axis perpendicular to this face. The system also possesses a number of thermopiles some of which are regularly distributed along the coaxial retaining loops. Each thermopile is supported by a rod sliding in a bore perpendicular to the heat collector face and there is an elastic mechanism for pushing the thermopiles towards this face. An insulating material separates the collector from the case. Each thermopile consists of two parallel doped SiGe rods. (auth) (France)

18599 SIGNIFICANCE OF RADIOACTIVE ISOTOPES IN BUILDING STRUCTURES. Jencek, L.; Zajc, A. Gradbeni Vestn.; 3: 70-4(1969).

The theoretical bases for the backscattering of γ-rays and the idea for measurements of the density of soil or concrete are examined along with the use of fast neutron slowdown for measurements of the moisture content of soil or concrete. The results of practical measurements of the soil and in concrete penstock of the water channel for the hydroelectric power plant, Srednja Drava 1, are given. The significance of the radioactive methods for the statistics and the evaluation, respectively of the quality control of the soil or concrete is pointed out. (Bull. Sci. Sect. A)

18600 HYDROSPACE ENERGY CONVERTER. Majkrzak, Charles P. (to International Telephone and Telegraph Corp.). U. S. Patent 3,543,036. 24 Nov 1970. Filed 31 Jul 1967.

An arrangement is provided for converting energy of radiation from a radioisotopic energy source into useful electrical energy using a mercury vapor turbogenerator system, as the converter, to produce a submersible oceanographic power supply independent of the atmosphere for its operation. (Official Gazette)

18601 ABSOLUTE GAMMA-RAY INTENSITY MEASUREMENTS OF A SNAP-15A HEAT SOURCE. Reier, Melvin (Jet Propulsion Lab., Pasadena, Calif.). Nucl. Sci. Eng.; 43: 267-72(Mar 1971).

A germanium crystal was used to measure the absolute intensity of gamma rays from the decay of ^{238}Pu, ^{212}Pb, ^{212}Bi, and ^{208}Tl in a 1½-W SNAP-15A heat source. In practically all cases, agreement with other measurements was excellent. In addition, the amount of ^{236}Pu impurity orginally present in the sample can be measured with an accuracy of 4%. It is estimated that the ^{236}Pu content in a fuel sample that is several months old can easily be measured with an accuracy of 10%. (auth)

18602 PRESENT STATE AND PROBLEMS IN THE DEVELOPMENT OF GASEOUS DIFFUSION TECHNIQUE. Nakane, Ryohei (Inst. of Physical and Chemical Research, Yamato, Japan). Karyoku Hatsuden; 21: 927-37(Aug 1970). (In Japanese).

The situation of gaseous diffusion for uranium enrichment in Japan and problems for the future are reviewed. The relations of separation efficiency and diffusion-barrier pores were examined; the pores of about 100 Å radius were found to be the most efficient. The energy transfer due to the collision of molecules, counter diffusion, and the counter flow of gas affect the efficiency. The plant size to produce the 1,000 tons per year of 5 at. % enriched uranium was calculated taking these factors in consideration. The ideal cascade is square, but the number of barriers and power demands are very large. For practicality, a squared-off cascade is utilized. In Japan, the porous barriers made of alumina or teflon were studied; it was found that their permeating factor did not change in the course of use. The radius of pores attained were equivalent to less than 400 Å according to results of experiment. The fabrication of the pipes for diffusion barrier, with nickel as the supporter material is described. In this connection, plate-type barriers were also considered. The immediate problems in gaseous diffusion are to raise the barrier efficiency by bringing the pore radius down to about 100 Å, and increase the degree of gas permeation, thus reduce the total area of barriers. (Japan)

18603 DIRECTION OF THE DEVELOPMENT ON A NUCLEAR FUEL CYCLE. URANIUM ENRICHMENT. Takei, Mitsuo (Japan Energy Economic Research Inst., Tokyo). Genshiryoku Kogyo; 16: No. 4, 50-4(Apr 1970). (In Japanese).

It is generally agreed that nuclear power generation in the 1970's will be by light-water reactors. The enrichment of uranium will be a major problem in nuclear fuel cycles. The uranium enrichment is now nearly monopolized by the United States, however, the joint enrichment program by three European countries is proceeding steadily. The world state of uranium enrichment, and also its demands, are described. Information is included on uranium enrichment capacity with speculation of the future nuclear power generation in the United States. Information is also included on economic evaluation of the supply sources, dealing with the cost of uranium enrichment in the United States and in the European three-nation program; and emergence of European joint-plants based on the three-country program. (Japan)

18604 DIFFUSION COEFFICIENTS OF ISOTOPIC MIXTURES OF CO AND N_2. Vugts, H. F.; Boerboom, A. J. H.; Los, J. (FOM-Instituut voor Atoom- en Molecuulfysica, Amsterdam). Physica; 50: 593-605(31 Dec 1970).

Relative diffusion coefficients as a function of temperature have been determined for the systems $^{12}C^{18}O-^{12}C^{16}O$, $^{13}C^{16}O-^{12}C^{16}O$, $^{12}C^{18}O-N_2$, $^{13}C^{16}O-N_2$ and $^{14}N^{15}N-^{14}N_2$. The measurements have been performed in the temperature range from 230 through 425°K. The method used gives an accuracy in the values of the diffusion coefficients of 0.1%, relative to those at room temperature. By normalizing to argon, absolute values for the different mixtures could be obtained. Above 300°K the behavior of the diffusion coefficients as a function of temperature could be described with the monatomic gas theory, yielding ϵ/k values in the order of 80°K. A mutual comparison between the values for the different mixtures, however, is inconsistent with a monatomic description. Below 300°K the temperature dependence for all mixtures strongly deviates from a monatomic behavior. The results are discussed in connection with thermal diffusion. (auth)

18605 ISOTOPIC ELECTRIC GENERATOR USING THERMOELECTRIC ELEMENTS. Freund, Jean-Pierre; Stoll, Roger (to Societe Nationale d'Etude et de Construction de Moteurs d'Aviation. Compagnie Generale de Telegraphie Sans Fil). U. S. Patent 3,551,212. 29 Dec 1970. Priority date 24 Apr 1967, France.

The radioisotope-powered electric generator has a thermopile clamped between a metal housing acting as a cold source and a heat collector having an internal bore which receives the isotopic source. The collector is forced toward the thermopile by springs which bear on a support secured to said housing. Heat insulating material fills the space between the heat collector and housing. The source may be inserted into the collector through a closable opening in the housing. (Official Gazette)

18606 MEASUREMENT OF COAL DUST CONCENTRATIONS IN PIPELINES USING RADIOACTIVE ISOTOPES. Stoenner, A. (Rheinstahl Bergbau AG, Marl, Ger); Schneider, A.; Koenig, W. Mitt. Ver. Grosskesselbetr.; 50: 100-4(Apr 1970). (In German).

A system for continuous measuring of the dust concentration in mixtures of coal dust and air using ^{90}Sr is described. The method has been tested in commercial operation. It can be used for comparative measurements in parallel coal dust pipelines or also as an impulse sender for control systems. (auth)

18607 TRENDS IN THE UTILIZATION OF RADIATIONS AND RADIOISOTOPES. NEW APPLICATIONS AND THE PROBLEMS. Murakami, Yukio (Tokyo Metropolitan Univ.). Genshiryoku Kogyo; 16: No. 4, 92-7; 124(Apr 1970). (In Japanese).

The present state of the technology for the production and use of radioisotopes in Japan is reviewed. (W.H.K.)

18608 TRENDS IN THE UTILIZATION OF RADIATIONS AND RADIOISOTOPES. APPLICATIONS IN THE INDUSTRIES. Kato, Masao (Tokyo Univ.). Genshiryoku Kogyo; 16: No. 4, 98-100(Apr 1970). (In Japanese).

Industrial uses of radioisotopes in Japan are summarized. Applications include nondestructive inspection, process control, analysis, space development, oceanographic survey, and mineral resources development. Economic aspects, standardization of techniques, and instrumentation are also discussed. (TSS) (Japan)

18609 URANIUM ENRICHMENT BY GASEOUS DIFFUSION OR ULTRACENTRIFUGATION. Grenon, Michel. Sci. Progr. Decouverte; No. 3428, 23-32(Dec 1970). (In French).

The world requirements of enriched uranium, used as fuel for the almost universally adopted light water reactors, will be of the order of 40 million UTS by 1980; this figure includes 21 to 23 million UTS destined for the United States and corresponding to the saturation of the capacities of the three existing plants (Oak Ridge, Paducah, and Portsmouth). The European requirements are estimated at 12 million UTS by 1980. The most pertinent questions to be answered concern whether the new plant needed before 1980 will be constructed in the United States or in Europe, and if in Europe according to what procedure. (auth) (France)

Materials Testing

Refer also to abstracts 18567 and 18599.

18610 (DP-Report-580) QUALITY CONTROL, INSPECTION, AND TESTING OF FUEL MATERIALS FOR THE TWO UPRATED FUEL ELEMENTS. Project DRAGON. Conde, J. F. G.; Holliday, J.; Good, P. D.; Milne, J. M. (Atomic Energy Establishment, Winfrith (England)). Jul 1967. 31p. Dep. NTIS (U. S. Sales Only).

The results of quality control, inspection, and testing of the special uprated fuel elements employed in the 10 MW power run are summarized. The performance of the two graphites used for the first and second charge fuel elements was assessed. Both uprated fuel elements contained six outer rods with twice the normal fuel loading and a center rod having an uprating factor of 2.6. One element was fuelled with the standard U/Zr fuel used for the driver region of the first charge and the second with the UC-10 fuel to be similarly employed in the second charge. (auth)

18611 (HSSTP-TR-12) THREE-DIMENSIONAL ELASTIC-PLASTIC STRESS AND STRAIN ANALYSIS FOR FRACTURE MECHANICS. PHASE I. SIMPLE FLAWED SPECIMENS. Levy, N.; Marcal, P. V. (Brown Univ., Providence, R. I. Div. of Engineering). Sep 1970. Contract W-7405-eng-26. 121p. Dep. NTIS.

Development of an elastic-plastic finite element analysis for three-dimensional specimens with flaws is described. Particular attention is paid to the analysis of a semi-elliptic crack and a through crack in a plate of finite thickness. Elements developed include the three-dimensional polar, the cubic, and the cubic distorted. In addition, programs to generate the mesh of elements

XUM

and nodal points for a given problem size and specimen geometry have been written and tested. The Finite Element analysis is implemented by a computer program developed so as to handle problems with up to 10,000 degrees of freedom. As is well known, such large problems are frequently encountered in three-dimensional analysis. This capability is also required for the analysis of the stress and strain field near cracks. Results of analysis for a through crack with 4500 degrees of freedom, and for a semi-elliptic crack with 2700 degrees of freedom are shown. (auth)

18612 (LIB/Trans-324) PRACTICAL TESTING WITH COLOUR RADIOGRAPHY. Krainer, E. Translated by J. B. Hopkinson (Australian Atomic Energy Commission Research Establishment, Lucas Heights), from German report. 16p. Dep. NTIS (U. S. Sales Only).

Application of a one-film direct color radiographic process to nondestructive materials testing is described. The film was x-irradiated at 150 to 350 kV through the test sample and subjected to a development which was interrupted with exposure to colored light (treatment: initial developing 4 min; washing 2 min; intermediate exposure 0.5 min, with L551 filter; developing 4 min; washing 1 min; and bleach fixing 5 to 7 min, all at 20 ± 1°C on Agfa-Gevaert experimental color film, G24 developer and G470 bleach solution). Pre-treatment in 5% formaldehyde for $\frac{1}{2}$ to 1 min was found to be beneficial. Stepped photographs were used in the setting up of exposure charts. Lead foil amplifiers gave an increase in exposure. For welded joint-investigations the attainable picture quality was not sufficient. For complicated smaller castings, color radiography was advantageous because of the large thickness range which could be covered by one photograph. A number of examples are illustrated. (Australia)

18613 (SC-DR-70-693) ULTRASONIC CHARACTERIZATION AND COMPUTERIZED ANALYSIS OF GRAPHITE BILLETS. Baker, R. A.; Bishop, D. E.; Stoker, G. C. (Sandia Labs., Albuquerque, N. Mex.). Dec 1970. 62p. Dep. NTIS.

A computer-aided, ultrasonic test system for graphite billets was developed, the primary purpose of which was to select the optimum location within the billet of a reentry vehicle nose tip. An on-line mini-computer provides process control functions and initial data processing. Further data processing and billet quality analysis are provided by a large computer. Visualization of the internal structure is aided by the use of computer-controlled plotter. The ultrasonic test system consists of a commercial ultrasonic tester with an automatic scanning and immersion system. Position readout indicators provide scan position and part rotation information. A special interface module receives ultrasonic test data from the tester and converts this information to analog voltages, while an auxiliary function module, controlled by the mini-computer, digitizes and records the position and ultrasonic information on magnetic tape. The large computer analyzes the ultrasonic flaw data in terms of the up to 3300 possible nose-tip locations within the billet. In evaluating each particular nose-tip location, every flaw indication is assigned a weight. These weights are totaled for that cone location. The 15 positions having the lowest weights are presented to the design engineer for his final selection. The plotter is used to provide graphical pictures of the flaws within the billet to aid the engineer in his selection of the optimum position of the nose tip. Plots are made showing all of the flaws in the billet by subdividing into slabs which run parallel to the billet axis and into discs perpendicular to the axis. Such plots show the flaw distribution in a clear, concise manner. Further programs plot histograms of the data with respect to three location parameters. (auth)

18614 AN APPARATUS FOR VERIFYING WELDS AND SIMILAR WORK UNDER WATER USING γ RADIOGRAPHY. (to Societe Generale de Travaux Maritimes et Fluviaux S.A.). French Patent 1,594,560. 8 Jun 1970. Filed 1 Jul 1968. (In French).

An apparatus was developed for verifying welds under water; it consists of a watertight box with a principal compartment containing a γ source and a secondary compartment against the outer wall of which are placed the pieces to be examined. (auth) (France)

18615 NEUTRON RADIOGRAPHY. Boutaine, J. (CEA, Saclay, France). Tech. Mod.; 62: 422-23(Oct 1970). (In French).

The principles of neutron radiography are briefly reviewed and possible industrial applications discussed. (France)

18616 REACTOR STRESS ANALYSIS IN NUCLEAR ENGINEERING EDUCATION. Ma, Benjamin M. (Iowa State Univ. of Science and Tech., Ames). Nucl. Eng. Design; 14: 175-80 (Nov 1970).

The objectives, conduct and content of a sequence of graduate-level courses on reactor stress analysis applied to various nuclear-reactor components is introduced. Radiation damage, radiation effects and high temperatures change the nuclear, physical, and mechanical properties of reactor materials appreciably. Consequently, the combined radiation, thermal and mechanical stress analysis for reactor components is also quite different from the purely mechanical stress analysis for conventional structures. (auth)

18617 PORTABLE NEUTRON RADIOGRAPHIC CAMERA USING ^{252}Cf. Shaw, C. B.; Cason, J. L. (WADCO, Richland, Wash.). Mater. Eval.; 29: No. 2, 40-4(Feb 1971).

A research program is being conducted to determine the usefulness of ^{252}Cf as a source for portable thermal neutron radiography. Emphasis has been on developing a device using ^{252}Cf that could be used for laboratory, hot cell or field radiography. The use of ^{252}Cf for neutron radiography in a portable device has been evaluated both analytically and experimentally. A 268 μg ^{252}Cf source (NS-1, the first such source fabricated) was obtained from ORNL for experimental testing. This source has a neutron yield of 6.2×10^8 neutrons/sec and was used in an experimental container designed for neutron radiography. A first generation portable device which completely contains the ^{252}Cf has been designed and built and is presently being evaluated. Preliminary work included flux measurements and neutron radiographs. (auth)

18618 IMPROVEMENTS IN OR RELATING TO NEUTRON RADIOGRAPHY APPARATUS. Hendry, Innes Craig; Spowart, Alexander Rollo (to United Kingdom Atomic Energy Authority). British Patent 1,217,515. 31 Dec 1970. Filed 16 Jul 1968.

The apparatus described comprises a housing for a neutron source, a collimator for the neutrons, and means for locating neutron moderating material between the source and collimator. The distance between the source and the collimator is variable to allow variations in thickness of the moderating material; this variability permits the use of higher than thermal neutron beams for penetrating heavy absorbers. The efficiency of the neutron detection system used increased with increase in the collimated thermal neutron flux. A source capable of undergoing fast neutron fission, and a substance fissionable with thermal neutrons, are provided between the source housing and collimator, for boosting the collimated thermal neutron flux. These substances may respectively comprise ^{238}U and ^{235}U in the form of natural and enriched U-metal. Oil is then a suitable moderating material. Alternative types of neutron sources and detectors are described. (UK)

Radioactive Material Handling

Refer also to abstracts 18515, 18521, 18526, 18559–18561, 18564, 18566, 18570, 18603, 18988, 19017, 19019, 19260, and 19261.

18619 (BNL-50267) SAFEGUARDS APPLICATIONS FOR ISOTOPIC NEUTRON SOURCES. Beyster, J. R.; Kull, L. A. (Brookhaven National Lab., Upton, N. Y.). Jun 1970. 121p. Dep. NTIS.

Neutron sources including (γ,n), (α,n), and fission were examined for their usefulness in performing nondestructive assays of nuclear materials. Physical characteristics, costs, transportation requirements, and availability of each source type are reviewed and evaluated for use in proposed safeguard assays. The most promising sources are identified and all available sources are tabulated. (J.R.D.)

18620 (BNWL-1440) REAL-TIME NUCLEAR FUELS INVENTORY AND CRITICALITY CONTROL SYSTEM. Crow, V. L. (Battelle-Northwest, Richland, Wash. Pacific Northwest Lab.). Jan 1971. Contract AT(45-1)-1830. 199p. Dep. NTIS.

Accounting methods used for fissionable materials at the FFTF Fuel Fabrication Demonstration Facility are described. A digital computer system is used in such a way that each time material to be accounted for is transferred from one process station to another, information pertaining to the transfer is input using alphanumeric terminals associated with the central computing system. Each time a material transfer occurs the inventory for the involved process station is updated. In this way, real-time information about the material present at any process station can be obtained. Discussions and information are included on computer hardware, inventory and criticality control software, utility software, monitor software, and computer operation. (J.R.D.)

18621 (DP-1245) ZEOLITE PREFILTER TO REDUCE PLUGGAGE IN ZEOLITE CESIUM REMOVAL COLUMN. Hawkins, R. H.; Horton, J. H. (Du Pont de Nemours (E. I.) and Co., Aiken, S. C. Savannah River Lab.). Jan 1971. Contract AT(07-2)-1. 16p. Dep. NTIS.

Pluggage has frequently necessitated premature replacement of zeolite used to remove ^{137}Cs from Savannah River Plant waste. This pluggage is likely caused by suspended solids in the column feed or by a precipitate formed by reaction of the waste and zeolite. Laboratory tests show that a 6-inch granular, backwashable prefilter made of zeolite reduces pluggage of the zeolite cesium removal column. (auth)

18622 (ORNL–4584, pp 11-15) DISPOSAL BY HYDRAULIC FRACTURING. de Laguna, Wallace; Cowser, K. E.; Tamura, Tsuneo; Sealand, O. M. (Oak Ridge National Lab., Tenn.).

From Health Physics Division annual progress report for period ending July 31, 1970.

Operational waste injection ILW-6 was made in June 1969. Some 80,000 gal of waste, containing nearly 100,000 Ci of activity, were disposed of without incident. The work in New York State is well under way. The injection well and the four surrounding observation wells have been completed, and two test injections have been made. Both injections were into the same slot at a depth of 1450 ft. The first was made with water only in October, 1969, and apparently made a dominantly horizontal but complex fracture. The second, containing 2.7 Ci of ^{95}Zr–^{95}Nb, was made on June 26, 1970, and is already known to be horizontal. A dye, Rhodamine B, was mixed with the radioactive tracer to make a visible marker. (auth)

18623 (ORNL–4584, pp 16-36) DISPOSAL IN NATURAL SALT FORMATIONS. Bradshaw, R. L.; Blomeke, J. O.; Empson, F. M.; (and others). (Oak Ridge National Lab., Tenn.).

From Health Physics Division annual progress report for period ending July 31, 1970.

The principal effort in the current program is a study leading to the development of a conceptual design (and the required safety analyses) of a combined solidified high-level power reactor fuel-reprocessing waste repository and low-activity alpha-contaminated waste repository. This one facility should be capable of handling all waste of these two types until about the end of this century. For the high-level wastes a total (gross) salt mine area of about 850 acres, all newly mined for the purpose, will be required. The present design for the low-level facility calls for the use of an existing inactive mine which has around 40 million cubic feet of space already mined. The tentatively selected location is near Lyons, Kansas. A geologic and hydrologic study based on available information indicates that the central Kansas area meets the criteria established for the location of the first demonstration repository (e.g., salt beds at least 200 ft thick and lying at depths of no more than 2000 ft). Also the Arbuckle formation appears to be suitable for disposal of excess salt as brine. However, contacts with local salt producers have indicated the possibility for sale of the salt either as brine or as rock salt. Therefore, sale of the excess salt is considered to be the desirable disposal method, with the Arbuckle formation as a backup. A number of preliminary studies of temperatures (due to radioactive decay heat) at mine level and in the rock formations around the mine have been carried out. Based on all considerations (such as mine stability, aquifer temperature rises, etc.), it appears that 200°C peak salt temperature is neither too conservative nor too liberal for at least the initial stages of a high-level disposal facility operation. A study of salt tectonics in relation to the disposal of solidified high-level waste was made. Considering the specific case of the formation at Lyons, Kansas, it was concluded that the possibility of extensive salt deformation affecting the safety of the disposal area for a period of a few hundred thousand years can be excluded. Also the heating caused by the decay heat generated in the high-level waste would be of such short duration (from a geologic point of view) that no significant consequences would be expected. (auth)

18624 (ORNL–4629, pp 1-9) PROCESS DEMONSTRATION AND ^{233}U DISTRIBUTION. (Oak Ridge National Lab., Tenn.).

In Status and progress report for thorium fuel cycle development for January 1, 1969–March 31, 1970.

The Oak Ridge National Laboratory facility for storing and handling ^{233}U is being augmented by nine wells for storing solids and five tanks for storing solutions. This change increases the storage capacity by 80% for solids and 100% for solutions. A nitrate-to-oxide conversion line with a capacity of 22 kg ^{233}U/week is being installed. The facility received 44 kg of ^{233}U and shipped 7 kg. Experience with the TRUST (Thorium Reactor Uranium Storage Tank) facility showed that using borosilicate glass Raschig rings is practical for criticality control in large tanks of solutions of fissile isotopes. (auth)

18625 (SGAE-RT–35/1970) RECENT DEVELOPMENTS IN RADIOACTIVE WASTE MANAGEMENT. Oszuszky, F. J. P. (Oesterreichische Studiengesellschaft fuer Atomenergie G.m.b.H., Seibersdorf). [1970]. 13p. (CONF-700903–14). Dep. NTIS (U. S. Sales Only).

From 4th Foratom Congress on Industrial Aspects of the Nuclear Fuel Cycle in Europe, Stockholm, Sweden.

With the increasing installation of nuclear power in the USA and Europe special care will have to be directed towards the policy of a common, national waste management policy in respect to treatment, control, and storage of such radioactive wastes. Public opinion is forcing operators and authorities to ensure highest standards of safety in disposing of radioactive wastes to the environment. Considering the fact that within the next few years the total nuclear capacity will amount to about 30 GW(e) or 3% of the global installed capacity; waste disposal becomes more important. This fact is supported by considering that in Western Europe alone where in the same time span the increase of nuclear power will be even more than 4% of total capacity. This increasing trend will probably continue in Western Europe resulting within only one decade in an installed power of approximately 560 GW(e) of which 100 GW(e) or about 18% should be produced in nuclear reactors. (auth)

18626 (WASH–1162) SAFEGUARDS GLOSSARY. (Brookhaven National Lab., Upton, N. Y.). 1 Dec 1970. 22p. GPO $0.25.

A list of approximately 110 terms and definitions for use in activities associated with fissionable material safeguards is presented. A later dictionary is planned which will include a longer list of terms and definitions based on usage at each site. (J.R.D.)

18627 ELECTRIC EQUIPMENT FOR THE FUEL ELEMENT HANDLING AT THE ESSOR REACTOR IN THE EURATOM NUCLEAR RESEARCH CENTRE ISPRA/ITALY. Kleine-Tebbe, E.; Rueter, W. BBC-Nachr.; 52: 228-35(1970). (In German).

After a brief review of the electric handling system is described. The construction and function of the machine for charging and discharging of fuel elements is considered in particular. The coolant and washing agents for the fuel elements may constitute explosive mixtures if they come in contact with oxygen. Therefore, the electric equipment had to be explosion-proof. (auth) (INIS)

18628 PLUTONIUM BUY BACK FACILITY (15 Feb 1968) (Engineering Materials). (Richland Operations Office (AEC) Wash.). (CAPE–1752).

49 drawings.

Process hoods used in receiving, measuring, and sampling of $Pu[NO_3]_4$ solutions shipped to Hanford under the AEC's Pu Buy-Back Program are described. Equipment for weighing, measuring, blending, and loadout includes balances, tanks, filters, storage containers, a vacuum trap, truck lift, articulated arm for an impact wrench, hoist, and a lifting device for a shipping container. The flow diagram for the facility and the piping and electrical drawings are also provided. (For details see TID-4100 Suppl. 61) (F.S.)

18629 A DESTRUCTIBLE GLOVE BOX AND THE MANIPULATION ASSEMBLY USED WITH SUCH A BOX. French Patent 1,595,595. 15 Jun 1970. Filed 18 Sep 1968. (In French).

A destructible glove box is described. The box consists of a closed gas-tight container made of flexible material and possessing gas-tight fittings between the ports and external parts. The flexible container is made of a radiation impervious material forming the manipulating gloves inside the box and a transparent portion. The supporting assembly consists of a rigid U shaped frame across which the glove box is maintained taut. The glove box supports the parts communicating with the exterior. (auth) (France)

18630 STUDIES ON THE FLUIDIZED BED CALCINATION OF HIGH LEVEL RADIOACTIVE LIQUID WASTES. Mitsuishi, Nobuo (Kyushu Univ., Fukuoka); Oda, Fumihiko; Okubo, Takayoshi; Maeda, Kenjiro; Fukumoto, Tsutomu. Kyushu Daigaku Kogaku Shuho; 43: 382-5(Jun 1970). (In Japanese).

A model experiment was carried out on the fluidized bed calcination treatment of high-level radioactive liquid wastes. One of the merits of this method is that the inactive compact granular solids which are easy to handle, can be obtained. In order to carry out the operation efficiently, it is necessary to minimize the amount of particles which are released from the fluidized bed. However to decrease the velocity of the fluidizing air or the calcination temperature induces the solidification of the particles inside the column and makes continuous operation difficult. On the other hand, when the operation is continued for a long time, the diameter of the particles inside the bed becomes large, and it becomes difficult to maintain good fluidization. Therefore, it is necessary to control the size of the particles. To supply the fluidized bed with seed particles continuously, may be an effective method. It is concluded from the model experiment that the fluidized bed calcination is an efficient method of treating high-level radioactive liquid wastes. (Japan)

XUM

18631 REPROCESSING OF SPENT FUEL. Maruyama, Masatomo (Power Reactor and Nuclear Fuel Development Corp., Tokyo). Hoshasen Kagaku; 12: 190-4(Dec 1969). (In Japanese).

Environmental research has been carried out in Japan for the purpose of the construction of a reprocessing plant. The reprocessing plant at Tokai in Japan was designed similar to the Windscale plant in England and the La Hague plant in France. This plant may be operated automatically and safely even in an unexpected accident. It is one of the safest plants in the world, because the disposal limit of radioactive waste is one hundredth of the actual disposal in the Windscale plant, and the maximum concentration of radioactive gas and water at the disposal site is very low as compared with ICRP recommendations. (Japan)

18632 TRANSPORT CONTAINER FOR RADIOACTIVE MATERIALS AND OBJECTS. (to Kernforschungsanlage Julich GmbH). British Patent 1,222,196. 10 Feb 1971. Priority date 20 Apr 1968, Germany.

A transport container for radioactive materials is described which includes an outer fire-resistant shell and a radiation shielding shell consisting of at least two superimposed parts connected to form an internal space. The contact surfaces of the inner shell have a stepped configuration to prevent radiation escape from the internal space and a closure plate which fits this configuration. (J.R.D.)

18633 IMPROVEMENTS IN AND RELATING TO SHIELDING CONTAINERS. Brisac, Michael; Vertut, Jean (to Commissariat a l'Energie Atomique). British Patent 1,222,189. 10 Feb 1971. Priority date 29 Mar 1968, France.

Improved containers are described which are designed to withstand shocks and fire, and provide protection under these conditions. The protective elements comprise, alternately, zones filled with light thermally-insulating materials, and zones having heavier material with higher mechanical strength, the zones being distributed according to the shape of the container. (J.R.D.)

18634 METHOD FOR THE SOLIDIFICATION OF RADIOACTIVE WASTE. Nagakura, Tadashi (Central Research Inst. of Electric Power Industry, Chiba, Japan). Genshiryoku Kogyo; 16: No. 7, 15-19(Jul 1970). (In Japanese).

The amounts of radioactive wastes are increasing rapidly with the growth of nuclear power generation. The establishment of sound techniques for its economic and safe disposal are important. In Japan, nuclear power plants are located in coastal areas, presenting hazards in marine life. With emphasis on intermediate-level wastes from atomic power stations, the state of solidification techniques, and the problems, including developments in oversea countries, are described. An outline of the solidification technique is given along with descriptions of underground and ocean disposal, and disposal in containers. Fundamental requirements for the solidification in containers, solidification with concretes, mixing with cement and the absorption in moisture-absorbing material, and solidification with asphalt are examined. (Japan)

18635 PRINCIPLES UNDERLYING THE CONTROL OF DISCHARGE OF RADIOACTIVE WASTES TO THE ENVIRONMENT. Atom (London); 172: 36-8(Feb 1971).

The types of radioactive discharges arising from United Kingdom Atomic Energy Authority premises are considered and the arrangements for gases, liquids, and solid discharges given. The programs for sampling and analysis of both discharged samples and of the environment are discussed. Recommendations of the International Commission on Radiological Protection covering the exposure to radiation of members of the general public and the monitoring of released radioactive material are considered. The critical path of nuclides in water and the atmosphere is discussed. The computation of derived working limits and the contribution to these from sources other than waste discharges are examined. (UK)

Vacuum Engineering

Refer also to abstracts 18837, 18838, 18878, 19195, and 19469.

INSTRUMENTATION

Radiation Detection Instruments

Refer also to abstract 19038.

18636 MEASUREMENT OF ALPHA CONTAMINATION ON SURFACE OF FISSILE ELEMENT. Wolschrijn, Rolf A. (to Reactor Centrum Nederland). U. S. Patent 3,535,524. 20 Oct 1970. Filed 15 Sep 1967.

A device for measuring surface contamination by α-radiators on fissile rods consists of an ionization chamber which is equipped for carrying out measurements at a low voltage. In the ionization chamber the rods can be fastened and serve as one of two electrodes, the other electrode forming the wall of the ionization chamber. (auth)

General Detectors and Monitors

Refer also to abstracts 18799, 18805, 18840, 18868, 18880, 18898, 18995, 19005, 19053, 19828, 19835, 20163, 20173, and 20711.

18637 (AEEW-M-898) EFFICIENCY OF A ^{6}Li GLASS SCINTILLATOR DETECTOR FOR FAST REACTOR SPECTRUM MEASUREMENTS. Hardiman, J. P. (Atomic Energy Establishment, Winfrith (England)). Jan 1970. 21p. Dep. NTIS (U. S. Sales Only). UK 5s. 6d.

The efficiency of a lithium glass detector, which is used in the measurement of fast neutron energy spectra of cores assembled in the zero energy fast reactor ZEBRA, has been measured relative to (1) a calibrated Harwell long counter using the pulsed Van de Graaff, IBIS, to produce monoenergetic neutrons and (2) the calibrated Harwell Boron-Vaseline-Plug Detector using the ZEBRA time-of-flight equipment. Calculations have also been made using the transport code, TURTLE, and the Monte Carlo programme GEM. Discrepancies of 20% between calculated and observed efficiences are found in the energy region 70 to 130 keV, probably arising from inadequate nuclear and material composition data. A recommended efficiency from 100 eV to 1 MeV is given for the detector. (auth) (UK)

18638 (CONF-700816–(Vol.1), pp 143–74) CALIBRATION AND INITIAL FIELD TESTING OF ^{85}Kr DETECTORS FOR ENVIRONMENTAL MONITORING AROUND A NUCLEAR FUEL REPROCESSING PLANT. Smith, D. G.; Cochran, J. A.; Shleien, B. (Bureau of Radiological Health, Winchester, Mass. Northeastern Radiological Health Lab.).

From 11. AEC air cleaning conference; Richland, Wash. (31 Aug 1970).

In Proceedings of the eleventh AEC air cleaning conference.

In order to measure ^{85}Kr in the environment around nuclear fuel reprocessing facilities, several types of commercially available detectors were calibrated in the laboratory and then field tested. Among the detectors evaluated were several sizes of flow-through ionization chambers (with vibrating-reed electrometers), thin-walled cylindrical GM tubes, single and double thin-window GM tubes, and β scintillation detectors. A laboratory facility for calibrating all types of external β detectors against standardized ionization chambers has been developed. Following calibration all suitable instruments were field tested in the environs of an operating nuclear fuel reprocessing plant to ascertain their limits of sensitivity, reliability, and applicability. The most sensitive detector tested, a double window pancake-type GM tube, had a maximum sensitivity under field conditions of 1.8×10^{-8} μCi/cc. However, its window was extremely fragile. A more rugged, single window GM tube had a sensitivity of 3×10^{-8} μCi/cc. All successfully tested instruments are discussed with respect to appropriate environmental monitoring applications. (auth)

18639 (IFVE-SEF-69-44) DEVICE WITH A SNAP-OFF DIODE FOR COMPENSATION OF THE INFLUENCE OF THE PULSE AMPLITUDE SPREAD OF THE SCINTILLATION AND CHERENKOV COUNTERS AT THE MOMENT OF TRIGGERING THE FAST SHAPERS. Lapshin, V. G.; Rykalin, V. I.; Tsisek, Z. (Gosudarstvennyi Komitet po Ispol'zovaniyu Atomnoi Energii SSSR, Serpukhov. Institut Fiziki Vysokikh Energii). 1969. 17p. (In Russian). Dep. NTIS (U. S. Sales Only).

A device with a snap-off diode for compensation of the influence of the pulse amplitude spread on the time resolution in fast shapers is described. The results of testing this device are given. In the range of the amplitude change of the input pulses from 0.5 to 10 V the shift of the time distribution was $\Delta t \simeq 0.2$ nsec. The dead time of the device is $t_m \simeq 20$ nsec. (auth)

18640 (IFVE-SEF-70-23) TIME RESOLUTION OF SCINTILLATION COUNTERS. Donskov, S. V.; Shuvalov, R. S. (Gosudarstvennyi Komitet po Ispol'zovaniyu Atomnoi Energii SSSR, Serpukhov. Institut Fiziki Vysokikh Energii). 1970. 15p. (In Russian). Dep. NTIS (U. S. Sales Only).

In the frame of ideal photomultipliers the time resolution calculations are made for the following modes: 1) the gravity center of pulse; 2) the point of crossing by the integrated pulse current, varying proportionally to the number of the emitted photoelectrons; 3) the threshold discriminator; and 4) the threshold discriminator with the correction for the average time when approaching the given level. The calculations have been made for Poisson and uniform distributions. The best time resolution is obtained for the last of the listed modes. (auth)

18641 (IN–1446) SCANS: SPECTRA CALCULATION FROM ACTIVATED NUCLIDE SETS. Putnam, M. H.; Putnam, G. E. (Idaho Nuclear Corp., Idaho Falls). Nov 1970. Contract AT(10-1)-1230. 23p. Dep. NTIS.

The SCANS program determines the fast- (above 1 MeV) and thermal-neutron flux levels from ^{58}Co and ^{60}Co disintegration rates, given the irradiation history (operating power level versus time) of the reactor in which the activities were produced in Ni and Co wires. The program processes up to 50 pairs of disintegration rates per problem; hence, all the data from a pair of irradiated wires monitored at a number of corresponding positions can be handled. The method used to determine the flux spectrum can be generalized to handle a greater number of energy groups provided that the group fluxes can be determined in an order such that the activity used to determine a given group is independent of all of the group fluxes not yet determined. The program can be easily changed to handle other transition schemes of almost arbitrary complexity. The major features of the method are that the irradiation history (flux versus time) of the samples can be of arbitrary complexity and that absorption depletion of the nuclides in the transition schemes is automatically taken into account. (auth)

18642 (JINR-P13-5485) TWO-DIMENSIONAL ANALYZER FOR THE HALF-LIFE MEASUREMENTS OF THE NUCLEUS OF EXCITED STATES BY THE γ-γ DELAYED COINCIDENCE METHOD ON THE BASIS OF COMPUTER MINSK-2. Morozov, V. A.; Razov, V. I.; Fominykh, V. I.; Tsupko-Sitnikov, V. M. (Joint Inst. for Nuclear Research, Dubna (USSR). Lab. of Nuclear Problems). 1970. 18p. (In Russian). Dep. NTIS (U. S. Sales Only).

A coincidence circuit for two-dimensional measurements of the half-lives of nuclear excited states in the nano- and microsecond range is described. (auth)

18643 (NP–18672) PHOTOMETRIC MASS DETERMINATION IN NUCLEAR EMULSION ON COSMIC RAY CARBON. PART 1. MEASUREMENTS IN THE RESIDUAL RANGE INTERVAL $0 \leq R \leq 1$ mm. Joensson, G.; Kristiansson, K.; Malmqvist, L. (Lund Univ. (Sweden). Dept. of Physics). Jun 1969. 70p. (KS–6903). Dep. NTIS (U.S. Sales Only).

Carbon nuclei were stopped in a nuclear emulsion stack exposed to the cosmic rays in a high altitude balloon flight. The analysis is based on width measurements in the residual range interval $0 \leq R \leq 1$ mm of 37 stopping carbon tracks. The measurements were carried out with a photometer constructed for measurements with high precision in short tracks. The standard deviation of the experimentally determined mass values amounts to 0.72 ± 0.08 units of mass. This result is in good agreement with an assumption that the carbon flux is strongly dominated by one isotope only. Whether the most abundant isotope is ^{12}C or ^{13}C cannot be decided from the reported measurement. (auth) (Sweden)

18644 (ORNL–4584, pp 152–64) SPECTROMETRY RESEARCH AND DEVELOPMENT. Foston, J. W.; Thorngate, J. H.; Brown, M. D.; (and others). (Oak Ridge National Lab., Tenn.).

From Health Physics Division annual progress report for period ending July 31, 1970.

Experimental measurements of dose distributions in man-sized tissue-equivalent media were made to test the recently calculated values. A special extrapolation chamber was developed and used for measuring the dose-distribution near bone-tissue and tissue-bone interfaces in phantoms irradiated by the Health Physics Research Reactor (HPRR). Other experiments were directed to the measurement of LET in neutron-irradiated tissue phantoms utilizing recently developed counters. Measurement of the HPRR spectrum in the energy range below 0.5 MeV was accomplished. A variety of electronic instruments related

XUM

to spectrometry research were developed or improved; and zone-refining techniques were used for the purification of detector materials. (auth)

18645 (USIP–70-1) CONSTRUCTION AND EXAMINATION OF A GAS SCINTILLATION DETECTOR. Englund, Bjoern (Stockholm Univ. (Sweden). Inst. of Physics). Mar 1970. 38p. (In Swedish). Dep. NTIS (U. S. Sales Only).

A xenon gas scintillation detector, with an active volume of $12 \times 12 \times 25$ cm^3, has been constructed. The performance of the detector related to purity of xenon gas and optical components, such as reflectors, wavelength shifters and lightguides, has been investigated using α-particles and cosmic ray muons. The best results were obtained with POPOP as wavelength shifter and when the photomultiplier was directly attached to the quartz window of the detector. Using 5 MeV α-particles the detected peak had a width of 7%. The spectrum obtained from cosmic ray muons was in agreement with the calculated distribution. The possibilities of using such a detector to discriminate between highly relativistic particles is discussed. (auth)

18646 (WHAN-SA–73) GAS-FLOW METHOD FOR DETECTION OF FAST NEUTRONS IN REACTORS. Brown, D. P.; Upton, J. W. Jr.; Spear, W. G. (WADCO Corp., Richland, Wash.). 17 Nov 1970. Contracts AT(45-1)-1830; AT(45-1)-2170. 14p. (CONF-701102–8). Dep. NTIS.

From Meeting of the American Nuclear Society, Washington, D. C.

A developmental sensor for fast neutrons which eliminates the electrical cable problems and which can operate at temperatures up to 1200°F is described. Based on the ^{9}Be(n,α)^{6}He reaction, the method uses a flowing gas (helium) to carry the resulting beta emitter from an in-core sensor to a measurement cell external to the reactor. This external cell can be well shielded to prevent gamma radiations emanating from the reactor environment from interfering with the detected signal. A combination of current measurement and pulse counting should lead to a wide-range detector (10^8 to $>10^{16}$ nv). Theoretical considerations of the overall system performance show the sensitivity to be a function of several factors including the ^{6}He escape probability from the screens, gas-flow rate through the detection cell, ^{6}He collection efficiency of the fill gas, and temperature. Temperature affects the sensitivity and accuracy of the readings primarily through its effect upon the gas velocity in the exit tube connecting the in-core neutron sensor to the beta measurement cell external to the reactor. An increase in temperature results in a corresponding increase in gas velocity which reduces the transit time of ^{6}He atoms (0.8 second half life); thus, more atoms enter the measurement cell due to fewer decaying enroute. The detection time constant is anticipated to approach 0.1 sec. (auth)

18647 NEUTRON FLUX MEASUREMENT BY COUNTING THE ASSOCIATED ^{3}He PARTICLES FROM THE T(p,n) REACTION CORRESPONDING TO 500 keV NEUTRON ENERGY. Paulsen, A. (Central Bureau for Nuclear Measurements, Geel, Belg.); Widera, R.; Berlin, A.; Trapani, A. Nucl. Instrum. Methods; 91: 589-93(1971).

An earlier publication (Nucl. Instr. and Meth. 69(1969-70)) about counting associated ^{3}He particles from the T(p,n) reaction is continued. Even with a simpler experimental set-up than described there (without electrostatic separation of the Coulomb scattered protons) but the Ti–T targets having thinner Al backings (200 μg/cm^2 Al) it is possible to shift the energy of the associated neutrons down to 500 keV with a slight increase in accuracy. The results of this method were compared with those from n-p scattering in a methane-filled proportional counter. Agreement was found within 0.8%. (auth)

18648 PHOSPHORESCENT COMPONENTS IN CsI(Tl) AND CsI(Na). Francois, P. E.; Martin, D. T. (Univ. of Aston, Birmingham, Eng.). Int. J. Appl. Radiat. Isotop.; 21: 687(Nov 1970).

Crystals of thallium- and sodium-activated CsI were irradiated at room temperature under a tungsten filament lamp, strip lighting and a 3600 Å uv lamp for periods between 15 sec and a few minutes. Exponential fall off of the resulting curves indicated the existence of traps with half lives of about 1 min, 5 min and 50 min, in the CsI(Tl) crystal. The intensity of phosphorescent emission from the CsI(Na) crystal was found to be less than that from the CsI(Tl) crystal by a factor of at least three suggesting that in experiments when the disturbing effect of phosphorescence is significant, sodium activated crystals should be used. (UK)

18649 4π LIQUID-SCINTILLATION WHOLE-BODY COUNTER. II. COINCIDENCE COUNTING STUDIES. Grunewald, Ralph; Craig, E. C.; Ziemer, P. L.; Kessler, W. V.; Christian, J. E. (Purdue Univ., Lafayette, Ind.). Contract AT(11-1)-876. Int. J. Appl. Radiat. Isotop.; 21: 703-9(Dec 1970).

A 4π liquid scintillation whole body counter, consisting of two 2π detector tanks was employed to study the feasibility of using coincidence techniques to efficiently count positron emitters in large samples. The background response for the coincidence mode was first studied. A significant portion of the background was observed to result from pulses in coincidence in both detector tanks. The possibility of background suppression by anti-coincidence counting techniques was investigated but found not to be a useful method of improving counting statistics for counting ordinary gamma emitters. However, in the case of samples containing positron emitters, such as ^{22}Na and ^{58}Co, background could be greatly suppressed and counting statistics significantly improved by the use of coincidence counting techniques. The method not only reduced the background, but also discriminated against monogamma emitters such as ^{137}Cs and ^{40}K. Thus, the method lends itself to measurement of positron emitters in humans where ^{137}Cs and ^{40}K are present as an interfering background. (auth) (UK)

18650 APPLICATION OF THE MODULATION TRANSFER FUNCTION TO REDUCE UNSHARPNESS IN SCINTIGRAMS. Okumura, Y. (Memorial Hospital for Cancer and Allied Diseases, New York). Int. J. Appl. Radiat. Isotop.; 22: 49-52(Jan 1971).

The application of an iterative calculation to eliminate unsharpness in scintigrams involves a long calculation for an adequate approximation. Another approach to overcome image degradation is the use of the modulation transfer function (MTF) and the derivation of a concise mathematical expression for this is given. An example is presented of this correction applied to a scintiscan of the Picker thyroid phantom. A two dimensional plane was considered because the display of the scintigram is two dimensional. An IBM 1800 was used for the data processing and for applying the correction. The advantages over the iterative method are that the correction is performed by one calculation and that an estimate of the effective improvement in the resolution can be made by correcting the point spread function. (UK)

18651 METHOD OF AN APPARATUS FOR THE MEASUREMENT OF PHYSICAL CHARACTERISTICS OF X-RAYS, IN PARTICULAR OF γ-RAYS, AND ITS APPLICATION. Higatsberger, Michael J.; Weinzierl, Peter; Hicks, Harald P. (to Oesterreichische Studiengesellschaft fuer Atomenergie GmbH). U. S. Patent 3,535,520. 20 Oct 1970. Priority date 13 Nov 1963, Austria.

A method and apparatus of measuring the physical characteristics of x-rays, particular of gamma rays, preferably for measurements of nuclear reactor core fuel, comprising feeding primary x-ray radiation to a semiconductor detector in which the x-ray radiation undergoes a scattering interaction producing secondary radiation, the latter of which is detected and producing a first signal proportional to the energy of the secondary radiation, and sending the first signal to a coincidence circuit. The scattered primary x-ray radiation is detected in at least one selectively positioned second detector which produces a second signal as a result thereof. The second signal is sent to the coincidence circuit which is adapted to permit the first signal to pass to a measuring device when the first and second signals are substantially simultaneously received by the coincidence circuit, and measuring and classifying the first signals in the measuring device and counting predetermined first signals thereby providing a measure of the intensity of predetermined x-rays of the primary x-rays. (auth)

18652 METHOD AND APPARATUS FOR ANALYSING AN AMPLITUDE SPECTRUM. Dervieux, Bernard; Douzon, Jean; Giroury, Andre (to Commissariat a l'Energie Atomique). British Patent 1,209,512. 21 Oct 1970. Filed 26 Aug 1968.

Reference is made to a method for analyzing an amplitude spectrum that is statistically invariable in time and to a device for carrying out the analysis. Analysis of the amplitude spectrum of pulses produced at a distant point at which it is not possible to place a large unit such as a multi-channel analyzer gives rise to difficult problems when the pulses cannot be transmitted without undergoing distortions. Such a problem arises in prospecting for radioactive ores where a large unit cannot be located in the probe unit located in the borehole. The method described makes a comparison between the pulses to be analyzed and a reference signal near the point at which the pulses are produced. A direct current of predetermined value is generated and the amplitude of each pulse is compared with the value of this current; a signal is emitted responsive to each pulse whose amplitude is greater than the value of the current and the current is altered by predetermined steps at times separated by intervals during which a number of pulses are compared with the corresponding current, and the signals are separately counted for the said time intervals. In an alternative arrangement a second direct current may be generated having a second predetermined value greater than that of the first current, and a signal is emitted when the amplitude of a pulse is greater than the first value and less than the second value. The values of the two currents may be caused to vary simultaneously so that their difference remains constant, and the difference is proportional to the average of the values of the two amounts. A proportional radiation detector may be employed. (UK)

18653 SCINTILLATION SCANNING OF RADIOACTIVE ISOTOPES. (to Picker Corp.). British Patent 1,211,122. 4 Nov 1970. Priority date 15 Aug 1967, United States.

A method and device for producing a multicolored photographic record of the concentration and distribution of radioisotopes from scintillation scanning is presented. The device includes at least two sources of light each of a different color and a discriminator for selectively energizing the light sources in accordance with the amplitude of the output signal of the pulse rate measuring device. As an area is scanned by a scintillation probe, the color-sensitive photographic film is scanned by various combinations of colored light thus producing a multicolored record of the isotope distribution. (C.E.S.)

18654 EVALUATION OF AN LN_2-TEMPERATURE SOLID STATE SPECTROMETER FOR ROCKET BORNE EXPERIMENTS. MacGregor, G. A.; Turiel, I.; Bettenhausen, R.; Iantuono, A. (Univ. of California, Livermore). Rev. Sci. Instrum.; 42: 35-9 (Jan 1971).

A rocket borne solid state spectrometer was used recently during a solar flare to detect solar x-ray emissions in the energy range 4 to 40 keV. The silicon detector, cooled by liquid nitrogen and incorporating an optical feedback preamplifier, is believed to be the first such detector used in this type of experiment. The spectrometer and detection system are evaluated under laboratory and field conditions, offering calibration data and some experimental results. Suggestions are made for future experimentation. (auth)

18655 RESPONSE OF LARGE VOLUME NE-213 LIQUID SCINTILLATORS TO ELECTRONS AND PROTONS. Bertin, A. (Univ., Bologna. Istituto Nazionale di Fisica Nucleare, Bologna); Vitale, A.; Placci, A. Nucl. Instrum. Methods; 91: 649-52(1971).

The response of a large-size NE-213 liquid scintillation detector to electrons and protons was measured to calibrate the neutron detection efficiency of the detector. (W.H.K.)

18656 SCINTILLATION DECAY OF SEVERAL FAST ORGANIC SCINTILLATORS. Kunze, R.; Langkau, R. (Institut fuer Experimentalphysik, Hamburg). Nucl. Instrum. Methods; 91: 667-8(1971). (In German).

The scintillation decay of several fast organic scintillators is studied. The pulse shapes were measured by a sampling technique and corrected for instrumental time resolution. (auth)

18657 PROPERTIES OF THIN SPARK CHAMBERS WITH THE ADMIXTURE OF CARBOHYDRATES TO THE SPARK CHAMBER GAS. Heidbreder, E. (Max-Planck-Institut fuer Physik und Astrophysik, Garching, Ger.). Nucl. Instrum. Methods; 91: 653-5(1971).

It is shown that the efficiency and power of resolution of thin spark chambers are strongly improved after the addition of carbohydrates to the spark chamber gases neon and helium. (auth)

18658 FEEDBACK CONTROL OF PROPORTIONAL COUNTER GAIN. Lampton, Michael (Univ. of California, Berkeley). Rev. Sci. Instrum.; 42: 117-19(Jan 1971).

A technique is described for stabilizing the gain of a gas proportional counter system. A feedback signal is derived from an auxiliary calibration counter, which controls the high voltage applied to the detectors. Theoretical speed and accuracy limitations are discussed. Performance of an actual system is described. (auth)

18659 EFFICIENCY OF CHANNEL ELECTRON MULTIPLIERS FOR ELECTRONS OF 1 TO 50 keV. Archuleta, R. J.; DeForest, S. E. (Univ. of California, San Diego, La Jolla) Rev. Sci. Instrum.; 42: 89-91(Jan 1971).

The calibration of the University of California, San Diego (UCSD) plasma detector on board Applications Technology Satellite 5 (ATS-5) has been used to determine the shape of the efficiency vs energy curve for channel electron multipliers. Results are compared with other workers with reasonable agreement. The measured efficiencies are well expressed in the range 1 to 50 keV by $\epsilon = 1 - \{2/[3 + 6.5/(E - 0.5) + 30/(E - 0.5)^3]\}$. (auth)

18660 IMAGE ABERRATIONS PRODUCED BY MULTI-CHANNEL COLLIMATORS FOR A SCINTILLATION CAMERA. Bonte, Frederick J.; Graham, Kenneth D.; Dowdey, J. Edward (Univ. of Texas, Dallas). Radiology; 98: 329-34(Feb 1971).

An interference pattern which distorted the representation of a parallel-line phantom containing a radionuclide was observed during a study of the quality of the image produced by a commercial Anger camera equipped with "diverging" and other multichannel collimators. Discontinuities occurred in the individual phantom line images, forming a Moiré pattern. The effect was maximal close to the face of the collimator and disappeared at a distance from it. Further study has shown this to be a property of all camera collimators with thick septa between the linear arrays of collimator holes. (auth)

18661 SCINTILLATION COUNTER WITH A LiI(Eu) CRYSTAL FOR REGISTERING THERMAL NEUTRONS. Kuzminov, Ya. S. (All-Union Scientific-Research Inst. for Chemical Reagents and Specially Pure Chemical Substances, Kharkov). Instrum. Exp. Tech. (USSR) (Engl. Transl.); No. 2, 399-400(Mar-Apr 1970).

Translated from Prib. Tekh. Eksp.; No. 2, 82-3(Mar-Apr 1970).

The possibility of using a LiI(Eu) scintillation counter for registering thermal neutrons from a reactor is considered. Gamma radiation response amounts to 6 to 7% of the recorded neutron response. (auth)

18662 LOW-ACTIVATED TRIGGER CHAMBER CONTAINING ^{3}He. Dmitriev, A. B.; Vorobev, M. G.; Malyshev, E. K.; Pomerantsev, A. A. Instrum. Exp. Tech. (USSR) (Engl. Transl.); No. 2, 397-8(Mar-Apr 1970).

Translated from Prib. Tekh. Eksp.; No. 2, 80-1(Mar-Apr 1970).

The design and the characteristics of a neutron ionization chamber compensated for γ radiation are described. The chamber is made of Ti, with ^{3}He and ^{4}He serving as the filler gases. (auth)

18663 STATISTICAL ERROR OF MEASUREMENT OF THE COUNTING RATE OF A GAS-DISCHARGE COUNTER DURING PULSE SUPPLY. Volkov, A. S. (Inst. of Applied Geophysics, Moscow). Prib. Tekh. Eksp.; No. 6, 61-2(Nov-Dec 1969). (In Russian).

A formula is derived for the relative fluctuation of the voltage across the integrating cell of a counting-rate meter in the case of a gas-discharge counter having a pulsed power supply. The difference between the derived formula and the well-known formula for a dc power supply is due to the difference between the laws governing the distribution of the intervals between counter pulses. For an integrating-cell time constant that is much shorter than the interval between power-supply pulses the difference between the formulas vanishes. (auth)

18664 MEASUREMENT LIMITS OF EXPOSURE DOSE RATE BY GAS-DISCHARGE COUNTERS. Kondrasheva, E. P.; Filatov, A. I.; Chaikovskii, V. G. Prib. Tekh. Eksp.; No. 6, 63-5(Nov-Dec 1969). (In Russian).

On the basis of experimental data, calculations are made of the relations that connect a counter's dimensions, sensitivity, noise, deadtime, and range of measured dose rates; a given degree of deviation of the load characteristics from linearity is taken into consideration. (auth)

18665 SCINTILLATION CHARACTERISTICS OF PURE AND ACTIVATED CADMIUM IODIDE CRYSTALS. Zherebetskii, S. K.; Lyskovich, A. B.; Pentsak, G. M.; Chepelev, V. V. (Lvov State Univ.). Instrum. Exp. Tech. (USSR) (Engl. Transl.); No. 2, 401-3 (Mar-Apr 1970).

Translated from Prib. Tekh. Eksp.; No. 2, 84-5(Mar-Apr 1970).

The results of an investigation into the scintillation characteristics of cadmium iodide-base crystals are presented. Between 160 and 190°K, CdI_2(Pb) crystals may be satisfactorily used as scintillation detectors for ionizing radiations. (auth)

18666 TEFLON AND ALUMINUM CELLS WITH WINDOWS FOR LIQUID SCINTILLATION DETECTORS. Sharkis, A. A.; Paeda, R. I. (Vilnyus State Univ., USSR). Instrum. Exp. Tech. (USSR) (Engl. Transl.); No. 2, 407-8(Mar-Apr 1970).

Translated from Prib. Tekh. Eksp.; No. 2, 88-9(Mar-Apr 1970).

The design and properties of Teflon and aluminum cells with cemented windows are described. A technique for cementing the windows to Teflon cells is described. Such cells are designed for liquid scintillation detectors used to detect ^{110}Ag, ^{60}Co, and ^{204}Tl. The background characteristics of the cells are described. (auth)

18667 CIRCUITS FOR THE IDENTIFICATION OF NEUTRONS. Brovchenko, V. G.; Kondratev, L. G. (Inst. of Atomic Energy, Moscow). Instrum. Exp. Tech. (USSR) (Engl. Transl.); No. 2, 415-18(Mar-Apr 1970).

XUM

Translated from Prib. Tekh. Eksp.; No. 2, 95-8(Mar-Apr 1970).

Identification circuits are described which are based on comparing the charge of the fast component with the total charge of the scintillation pulse. The recording threshold of identifiable neutrons is 300 keV. The repetition intensity of blocked γ quanta is >10 sec^{-1}. The circuit is adjusted by a single controlling element. Calculations of the resolving time and the allowable value of the time constant of charge integration for the fast component are presented. (auth)

18668 AMPLIFIER FOR SEMICONDUCTOR GAMMA DETECTORS. Zhuravlev, O. K.; Leonov, V. F.; Somikov, A. V. (Inst. of Atomic Energy, Moscow). Instrum. Exp. Tech. (USSR) (Engl. Transl.); No. 2, 460-3(Mar-Apr 1970).

Translated from Prib. Tekh. Eksp.; No. 2, 131-4(Mar-Apr 1970).

A transistor spectrometric amplifier is described which is designed to operate with semiconductor γ-detectors at loads of 10^4 pulses per second. (auth)

18669 ELIMINATION OF CORRELATION EFFECTS IN THE DETECTION OF GAMMA QUANTA. Andreev, D. S. (Physical-Technical Inst., Leningrad). Instrum. Exp. Tech. (USSR) (Engl. Transl.); No. 2, 393-4(Mar-Apr 1970).

Translated from Prib. Tekh. Eksp.; No. 2, 77-8(Mar-Apr 1970).

A new method is suggested for eliminating correlation effects. Two identical detectors are mounted at the angles $\vartheta_1 = 37°20'$ and $\vartheta_2 = 79°10'$ [$P_k(\cos\vartheta_1) = -P_k(\cos\vartheta_2)$; $k = 2.4$] relative to the axis of the correlation function. The total count of the detectors mounted in this fashion is independent of the degree of correlation and is equal to the count which would be obtained in the complete absence of correlation. Such a method of eliminating correlation effects is more universal and simpler to achieve than the well-known method in which the detector is mounted at an angle of $\vartheta' = 54°45'$ [$P_2(\cos\vartheta') = 0$], and the distance to the detector is chosen on the basis of the requirement that the attenuation factor G_4 must vanish. (auth)

18670 DEVICE FOR MULTIPARAMETRIC INVESTIGATION OF NUCLEAR FISSION. Maslennikov, S. I.; Okolovich, V. N.; Pavlov, A. F. (Inst. of Nuclear Physics, Alma-Ata, USSR). Instrum. Exp. Tech. (USSR) (Engl. Transl.); No. 2, 358-60(Mar-Apr 1970).

Translated from Prib. Tekh. Eksp.; No. 2, 47-9(Mar-Apr 1970).

A description is given of a device for multiparametric investigations of various characteristics of the process of nuclear fission by means of AI-100 analyzers with automatic gain control of two independent amplifying channels. (auth)

18671 SPARK FISSION-FRAGMENT COUNTER. Gangrskii, Yu. P.; Dalkhsuren, B.; Lazarev, Yu. A.; Markov, B. N.; Nguyen Cong, Khan (Joint Inst. for Nuclear Research, Dubna, USSR). Instrum. Exp. Tech. (USSR) (Engl. Transl.); No. 2, 376-8 (Mar-Apr 1970).

Translated from Prib. Tekh. Eksp.; No. 2, 63-5(Mar-Apr 1970).

A spark fission-fragment counter is described. Results are given of measurements of the efficiency with which fragments are recorded and the resolving time for various gas mixtures based on He, Ne, Ar, Kr, Xe, and N_2. It is shown that for a number of gas mixtures, it is possible to obtain a recording efficiency for fission fragments of up to 50% while achieving an efficiency of less than 10^{-10}% for α particles. (auth)

18672 RESOLVING POWER OF SILICON SURFACE-BARRIER COUNTERS. Afanasev, V. F.; Strokan, N. B.; Tisnek, N. I. (Physical-Technical Inst., Leningrad). Instrum. Exp. Tech. (USSR) (Engl. Transl.); No. 2, 379-82(Mar-Apr 1970).

Translated from Prib. Tekh. Eksp.; No. 2, 66-8(Mar-Apr 1970).

It is seen that the energy resolution of the counters relative to α particles is determined by fluctuations of the lifetime of the current carriers and the resistivity in the original Si plates. Possible methods of revealing the separate effects of the indicated factors are considered. (auth)

18673 X-RAY SPECTRAL APPARATUS (REVIEW). Blokhin, M. A. (Rostov State Univ., Rostov-on-Don, USSR). Instrum. Exp. Tech. (USSR) (Engl. Transl.); No. 2, 313-21(Mar-Apr 1970).

Translated from Prib. Tekh. Eksp.; No. 2, 9-18(Mar-Apr 1970).

A classification of x-ray spectrometers and spectrographs is examined. Apparatus for investigating the fine structure of x-ray spectra with crystal analyzers in the wavelength region up to 26 to 28 Å and with diffraction gratings for the spectral region up to 500 Å is described briefly. Investigations permit obtaining information on the energy distribution of the density of electron states of solids, charge of atoms in compounds, and nature of the chemical bond. Mass-produced x-ray spectral apparatus for determining the average composition of materials is described in greater detail. This apparatus is used not only in laboratories but also at industrial enterprises for control of technological processes and as composition detectors for automation of production. (38 references) (auth)

18674 MEASURING AND ANALYZING METHODS WITH MULTI-CHANNEL ANALYZER VAS 4096. Gammel, Reinhold (Siemens Aktiegesellschaft, Karlsruhe, Ger.). Siemens Rev.; 37: 628-31(Dec 1970).

A lithium-drifted germanium detector system with preamplifier, amplifier, high-voltage generator, and multichannel analyzer system is described. The use of the versatile VAS 4096 multichannel analyzer in this germanium detector configuration for pulse-height analysis, multichannel scaling, sampled-voltage analysis, and averaging enhancement is discussed. (W.H.K.)

18675 SOLID STATE DETECTOR TELESCOPE FOR CHARGED PHOTOPARTICLES. Busso, L.; Costa, S.; Ferrero, L.; Pasqualini, L. (Univ., Turin). Atti Accad. Sci. Torino. I. Cl. Sci. Fis., Mat. Natur.; 104: 629-44(Nov-Dec 1970).

The design of a solid-state dE/dx telescope detector for the identification of charged particles is discussed. An experimental layout for the measurement of charged particles from the photodisintegration of carbon-12 using a 100-MeV synchrotron x-ray source is described. Results are discussed. (W.H.K.)

18676 THE Ge(Li) SPECTROMETER AS A POINT DETECTOR. Notea, A. (Technion-Israel Inst. of Tech., Haifa). Nucl. Instrum. Methods; 91: 513-15(1971).

The behaviour of a Ge(Li) spectrometer as a point detector is considered. The intrinsic peak efficiency of the point detector is suggested as a characteristic parameter. A procedure for relative calibration of photon sources and for comparison between various shape spectrometers, based on accurate corrections of solid angle as a function of photon energy, is presented. Examples of the procedure are given. (auth)

18677 ORIENTATION SYSTEM FOR BALLOON-BORNE PAYLOADS. Gokhale, G. S.; Iyengar, V. S.; Kunte, P. K. (Tata Inst. of Fundamental Research, Bombay). Nucl. Instrum. Methods; 91: 509-12(1971).

A new, simple system to orient a balloon-borne x-ray telescope about a vertical axis is described. The telescope is mounted in servo controlled gimbals; this results in a low moment of inertia for the oriented part. The servo uses a flux-gate magnetometer as a direction sensor. Pointing accuracy of ±1° has been obtained in flight. (auth)

18678 SPECTRAL DISTRIBUTIONS OF FAST AND SLOW COMPONENTS IN A LIQUID SCINTILLATOR. Amaldi, U. Jr.; Biancastelli, R.; Bosio, C.; Papadopoulos, L. (Physics Lab., Rome). Nucl. Instrum. Methods; 91: 477-80(1971).

The time dependence of the light output of a liquid scintillator (Ne 213) containing an alpha emitter was measured as a function of the wavelength. For this purpose optical interferential filters were introduced in the usual single photoelectron technique. The results show that in the range 4000 to 5000 Å the spectral distributions of the emitted light varies with time. (auth)

18679 USE OF A CHECKER BOARD COUNTER IN BLOCKING EXPERIMENTS. Fuschini, E.; Maroni, C.; Massa, I.; Uguzzoni, A.; Verondini, E. (Univ., Bologna. Istituto Nazionale di Fisica Nucleare, Bologna). Nucl. Instrum. Methods; 91: 487-92(1971).

The use of a checkerboard counter to obtain angular distributions of charged particles around crystallographic directions is described. Various experimental possibilities are discussed. Blocking patterns obtained with a Si single crystal are reported. (auth)

18680 ROCKET PAYLOAD USING FOCUSING X-RAY OPTICS FOR THE OBSERVATION OF SOFT COSMIC X-RAYS. Gorenstein, P.; Harris, B.; Gursky, H.; Giacconi, R. (American Science and Engineering, Inc., Cambridge, Mass.). Nucl. Instrum. Methods; 91: 451-9(1971).

A rocket payload utilizing focusing optics was designed and constructed for the detection and localization of cosmic x-ray sources. The instrument is designed to be used in a scanning mode. The sensitivity of the instrument covers the wavelength bands 80 Å to 44 Å and 20 Å to 10 Å with a total field of view of 2° × 8°. A telescope operating on the principle of grazing incidence reflection instantaneously focuses the x rays from a distant source in one dimension upon one member of four proportional-counter elements located in the focal plane. Location precision from a single scan is about 0.1° × 1° for the stronger sources. The telescope consists of eight nested sheets of reenforced glass whose reflecting surfaces are overcoated with an evaporated layer of chromium to improve reflection properties at the shorter wavelengths. The effective collecting area of the mirror assembly for on-axis radiation is about 160 cm^2 at 80 Å and 40 cm^2 at 10 Å. The focal-plane detector is a multiwire proportional counter with a one micron polypropylene entrance window and contains a supply of propane gas regulated to a constant pressure of 50 cm of Hg. In the wavelength range 80 Å to 10 Å the focusing technique results in greater sensitivity, better angular resolution, and improved detector reliability compared to non-focusing techniques. (auth)

18681 POSITION SENSITIVE DETECTOR FOR A MAGNETIC SPECTROGRAPH. **Miller, G. L. (Bell Telephone Labs., Murray Hill, N. J.); Williams, N.; Senator, A.; Stensgaard, R.; Fischer, J. Nucl. Instrum. Methods; 91: 389-96(1971).**

A number of position-sensitive proportional counters were constructed for use in the focal plane of a broad-range magnetic spectrograph. Position information is obtained by the use of resistive charge division. An analysis of the factors controlling the position resolution is made. Completed detectors of ≈70 cm length exhibit position resolution of ≈0.2% when operating at kilohertz rates. (auth)

18682 RADIATION DETECTION DEVICES. Spergel, Philip; Di Rocco, James V.; Grenier, Raymond P. (to Baird-Atomic Inc.). British Patent 1,218,124. 6 Jan 1971. Filed 8 Aug 1968.

A method is described for providing an array of gas-filled ionization chambers to give indications of radiation at particular points in a relatively large area, with high detection sensitivity and high spatial resolution. The chambers intercommunicate through ports for ensuring that the gas pressure in each chamber is substantially the same. Part of the wall of each chamber is made of electrically insulating material and part of conductive material. Conductive fins, carried by the insulated part of the wall, project into the chamber. Radiation entering a chamber sets up an electrical discharge between the fin and the conductive part of the wall, and means are provided whereby the location of the radiation can be detected. Various constructional and geometrical arrangements are described. The indicating circuitry is also described. (UK)

18683 METHOD AND APPARATUS FOR IMPROVING COUNTING STATISTICS IN RADIOACTIVE SAMPLING APPARATUS. Olson, Robert Elmer (to Packard Instrument Co., Inc.). British Patent 1,218,884. 13 Jan 1971. Filed 5 Apr 1968.

The apparatus described is primarily intended for use in connection with scintillation counters employing a pair of light-responsive photomultipliers positioned on opposite sides of the detection chamber, and where the sample is contained in a transparent glass or plastic vial. Such vials are often slightly out of round, have small but significant wall thickness variations, and bottoms which are not perfectly flat nor of uniform thickness. Such non-symmetric containers give rise to significant errors in scintillation counting, due to different amounts of light being observed by each photomultiplier. Non-symmetry or non-homogeneity of the sample is also a serious cause of error. The object of the apparatus is to provide means so that precision and accuracy of measurement are independent of these sources of error. Provision is made for rotating the sample about its axis in various predetermined ways. (UK)

18684 NUCLEAR RADIATION DIGITAL DOSE MEASURING SYSTEM. **Taylor, Raymond A. (to Secretary of the Navy). U. S. Patent 3,541,311. 17 Nov 1970. Filed 27 Jun 1966.**

A digital measuring system is provided for determining the amount of energy provided by a nuclear radiation field at a point per unit time. Two registers are used to store information provided by a radiation detector and an analog-to-digital converter. A timing system, consisting of a predetermined counter and a source of clock pulses, controls the readout of the storage registers. (auth)

18685 INSTRUMENT FOR DETERMINATION OF WEIGHT CONCENTRATION AND RADIOACTIVE CONCENTRATION OF AEROSOLS. **Babich, Valentin Grigorievich; Kurskii, Alexandr Kuzmich; Markov, Konstantin Petrovich; Ryabov, Nikolai Vasilievich; Stas, Konstantin Nikolaevich. British Patent 1,216,561. 23 Dec 1970. Filed 16 Jan 1968.**

Reference is made to instruments for monitoring aerosols in general and radioactive aerosols in particular. The instrument described comprises a conduit through which the sample is passed, containing a filter element, a radioactive source located upstream of the filter element, a radiation detector on the opposite side of the filter element, and a mechanism for retracting the source from the conduit. The radioactive source is preferably an α-emitter. The detector should preferably be provided with a collimator capable of partially absorbing the background radiation of the aerosol sample; this may comprise an α-particle absorbing plate with apertures. The instrument is claimed to show high sensitivity and precision, dependable performance and operation, and convenience for underground mining conditions, as well as portability. It is claimed to be possible to measure particle concentrations of the order of 1 mg/m^3 within 10 min. Employment of an α-emitter as radioactive source enables the recording of minute changes in the thickness of the filter element, these being proportional to the particle weight concentration of the aerosol. In order to measure the radioactive concentration of aerosols the α-particle source is withdrawn from the conduit for the duration of measurements. (UK)

18686 INDICATING OR DETECTING APPARATUS FOR NUCLEAR RADIATION SUCH AS GAMMA RAYS. **Loveday, George Christopher (to Ekco Electronics Ltd.). British Patent 1,213,478. 25 Nov 1970. Filed 7 Dec 1967.**

Reference is made to scintillation apparatus and more particularly to apparatus of selected intensity range. The apparatus described comprises a mosaic of scintillator elements, optically screened from one another, a number of scintillation detectors arranged to view these elements, the field of view of each detector extending over a number of elements. Each detector produces a pulse in response to a detected scintillation, the peak amplitude of which is dependent on the position of the scintillation relative to the detector. The detectors are arranged with reference to a spatial coordinate system so that they lie in a series of rows, each row being defined by a constant value of one of the coordinates, and the detectors are so spaced in the rows that they lie in a series of second rows, each second row being defined by a constant value of the other coordinate. Means are provided for summing the outputs of the detectors in each row in order to provide row output pulses, which have peak amplitudes falling within predetermined amplitude ranges, and indicating the position of the particular scintillation element in the mosaic in which any particular scintillation occurs. The coordinate system may be cartesian, the first detector rows being parallel to the Y-axis and the second rows parallel to the x-axis. Interpolator means may be provided, adapted so as to receive row output pulses and to derive therefrom an output signal having an x-channel pulse and a Y-channel pulse defining respectively the first and second rows in which a particular scintillation element is located. This interpolator means may comprise a pulse amplitude analyzer for each detector row, with a common gating means. Various arrangements of the element and detector rows are described. Means may also be provided for summing all simultaneously occurring detector output pulses, each output channel comprising means controlled by signals from this summing means so that only those pulses originating from detector pulses, the total summed amplitudes of which fall within a predetermined total amplitude range, appear in the output channels. Core storage means or magnetic tape storage may be provided to record the number of scintillations produced by each scintillator element. Means are also described to give an analog display of the position of a particular scintillation element. The scintillator elements may be screened from each other by opaque light reflecting walls. (UK)

18687 NEW GELS USED IN LIQUID SCINTILLATION. **Benakis, Achille. French Patent 1,590,762. 20 Apr 1970. Filed 5 Nov 1968. (In French).**

A new method of forming gels from the liquid scintillators used in radioactivity measurements, is described. The gelifying agents used were low molecular weight polyenes such as polyethylenes with molecular weights between 2,800 and 23,000; the optimum value being about 8,000. The new gelifying agent can be obtained in the form of a diluted polyethylene resin solution or in granular form. (auth) (France)

18688 RADIATION DETECTING DEVICE FOR CHROMATOGRAPHY OR ELECTROPHORESIS BANDS. **Espinasse, Pierre; Leroy, Marcel. French Patent 1,590,263. 13 Apr 1970. Filed 28 Oct 1968. (In French).**

A radiation detector for studying the local concentration of radioactive material on a moving band is described. Applications in chromatography or electrophoresis are envisaged. The detector consists of a sheet of radiation absorbing material with a narrow slit. The band moves at constant velocity over this sheet and past the slit. On the other side of the sheet is the parallelepiped shaped crystal scintillator of the detector. (auth) (France)

18689 STATIONARY DETECTOR FOR VISUAL DISPLAY. **Gaucher, Jean-Claude; Lansiart, Alain; Lequais, Jean; Roux, Georges (to Commissariat a l'Energie Atomique). French Patent 1,586,904. 26 Jan 1970. Filed 1 Aug 1968. (In French).**

A stationary detector for studying information carried by beta

XUM

particle and x or γ ray beams is described. The detector consists of a converter, which transforms the information carried by the beam into a visual image, a light amplifier reducing the dimensions of this image, which is situated opposite the converter, a device for calculating the coordinates of the luminous point on a screen, and a recording device. (France)

18690 AUTOMATIC SCANNER FOR NUCLEAR EMULSIONS. Stephenson, J.; Dale, P. W. (Univ. of Bradford, Eng.). Nucl. Instrum. Methods; 91: 365-76(1971).

An automatic scanner for nuclear track counting, based on a mechanically moving window, was developed. The various components and improvements in the development techniques for emulsions are described. The machine will scan at a speed approximately 30 times that of human scanners and with a comparable accuracy. (auth)

18691 APPARATUS FOR MEASURING THE LIFETIME OF INDUCED NUCLEAR CONDITIONS IN THE NANO- AND SUBNANOSECOND RANGE. Morozov, V. A.; Myuminov, T. M. (Joint Inst. for Nuclear Research, Dubna, USSR). Instrum. Exp. Tech. (USSR) (Engl. Transl.); No. 2, 364-7(Mar-Apr 1970).

Translated from Prib. Tekh. Eksp.; No. 2, 53-6(Mar-Apr 1970).

An apparatus for $e^- \gamma$ coincidence to measure the lifetime of levels in the nano- and subnanosecond range is based upon a magnetic β-spectrometer. A control system is included, which makes it possible to account for apparatus effects with an accuracy no worse than ±1%. (auth)

18692 DETECTION OF RADIATION EMITTED FROM MOVING SOURCES. I. STUDY ON RADIATION RELAYS. Saito, Hideo; Sato, Otomaru; Kato, Masao (Tokyo Univ.). Seisan Kenkyu; 22: 290-3(Jun 1970). (In Japanese).

The radiation relays which utilize moving radiation sources are expected to be applied to the various fields of industry, since they have the characteristics that remote detection is possible and that they are not influenced by dust, steam and so on. The characteristics of radiation detection when the radiation source is moving and the detector is at rest are discussed. Phosphorus-32 was used as the moving radiation source, and as the detector a Geiger Mueller counter was used. The velocity of the radiation source was varied in the range from 2.49 to 37.44 km/h. The experiment was carried out in the presence of collimation of the detector and in the absence of it. Experimental results were analyzed theoretically, and the relay behavior can be analyzed by the proposed calculation. (Japan)

18693 COMPUTER PROGRAMS FOR CALCULATION OF LIQUID-SCINTILLATION DATA FROM LONG-LIVED AND SHORT-LIVED RADIONUCLIDES USED IN SINGLE OR DUAL LABELLING. Cramer, C. F.; Nicholson, M.; Moore, C.; Teng, K. (Univ. of British Columbia, Vancouver). Int. J. Appl. Radiat. Isotop.; 22: 17-20(Jan 1971).

Computer programs were written in Fortran IV language utilizing data from any of several liquid scintillation systems with automatic Teletype punched tape output. The programs calculate disintegrations per minute, percent of administered dose and, for short-lived isotopes, radioactive decay in single or dual labeled experiments. External standard or channels ratios may be used. Any number of samples can be accommodated provided the sample number does not drop. The samples can be recycled for statistical repetition. (auth) (UK)

18694 SEMICONDUCTIVE DETECTORS OF IONIZING RADIATION. Gugic, P. (Yugoslav Academy of Arts and Sciences, Zagreb). Arh. Hig. Rada Toksikol.; 20: 385-97(1969). (In Serbo-Croation).

Recent developments of diode and transistor semiconductor detectors are briefly reviewed. A survey is given of the basic principles of operation and of the most important characteristics of these detectors with special regard to their energy discrimination and potential position sensitivity. Comparison is made with gas and scintillation detectors. Some technical compromises in design are mentioned and the most significant possibilities of application presented. (auth)

18695 CALIBRATION OF A WHOLE-BODY COUNTER SUITABLE FOR USE IN ROUTINE CLINICAL INVESTIGATIONS. Barnaby, C. F.; Smith, T. (University Coll. Hospital, London). Phys. Med. Biol.; 16: 97-104(Jan 1971).

The calibration of a clinical whole-body counter which utilizes a large area (60 × 40 × 10 cm) detector is described. A simple counting technique minimized the variation in response due to different distributions of radioactivity in the patient's trunk. The counter was calibrated for a number of radionuclides (0.32 to 1.52 MeV) uniformly dispersed in a range of phantoms, and the errors involved in the use of this technique for nonuniform distributions were estimated. In 63 measurements on patients given a variety of radionuclides, the calibration was accurate to 5% (standard deviation) even though, in many cases, the distribution of radioactivity in the body was grossly nonuniform. (auth) (UK)

18696 SCINTILLATION DECAY SPECTROMETER FOR RESOLVING SUBNANOSECOND LIFETIMES. Lambrecht, R. M.; Kelly, T. M.; Merrigan, J. A. (Eastman Kodak Co., Rochester, N. Y.). Chem. Instrum.; 2: 363-74(Apr 1970).

A state-of-the-art timing spectrometer capable of resolving fluorescence decay times down to 0.2 nsec is described. The method of fast-slow coincidence combined with single photon counting is utilized to obtain accurate scintillation lifetime spectra in a few minutes of data collection time. The experimental technique is reviewed, and factors involved in optimizing timing resolution are discussed. Examples of spectra from the fastest commercially available solid scintillator are shown. The instrument is useful for study of fluorescence lifetimes in liquids and solids where the mechanisms of chemical reactions of excited molecules are under study. (auth)

18697 TOMOGRAPHIC SCINTILLATION CAMERA. Muehllehner, G. (Nuclear-Chicago Corp., Des Plaines, Ill.). Phys. Med. Biol.; 16: 87-96(Jan 1971).

Four tomographic images were obtained simultaneously by attaching a rotating collimator and a table with a top moving in a circular motion to an Anger scintillation camera, and using a modified CRT display. The device exhibited essentially the same resolution and sensitivity as a normal camera, depending on the particular collimator used. The tomographic effect was sufficient to determine clearly the depth of an object within 2.5 cm for objects with sharp outlines. A rotational speed of up to 2 revolutions per minute, allowed tomographic scintiphotos to be taken in 30 seconds. The table and collimator could be removed in a few minutes, and the camera used either in its normal mode, or as a tomographic camera. (auth) (UK)

18698 PARTICLE DETECTOR. Lansiart, Alain (to Commissariat a l'Energie Atomique). British Patent 1,210,350. 28 Oct 1970. Priority date 1 Aug 1968, France.

A beta-gamma proportional counter is described in which the anode is composed of a number of electrically insulated segments. These segments are of equal area and are connected individually to the anode of the high-voltage source through equal high resistances. (R.W.R.)

18699 CLINICAL TESTS ON A PROTOTYPE SEMICONDUCTOR GAMMA-CAMERA. McCready, V. R. (Royal Marsden Hospital, Sutton, Eng.); Parker, R. P.; Gunnersen, E. M.; (and others). Brit. J. Radiol.; 44: 58-62(Jan 1971).

A prototype γ-camera was constructed from a slice of lithium-drifted germanium 44 × 44 mm in area and 6.5 mm in sensitive thickness. Positional information was obtained using the orthogonal strip principle, the inherent spatial resolution being 3 mm. Data are presented on energy resolution, uniformity, linearity of image and spatial resolution. The application to imaging distributions of ^{99m}Tc in rats and humans is demonstrated, and comparisons on picture quality and background made (using the identical sources) with a conventional Anger system. (auth) (UK)

18700 ATTENUATION OF PROPORTIONAL COUNTER PULSES BY PULSE SHAPING NETWORKS. Breyer, B.; Cimerman, M. (Inst. Rudjer Boskovic, Zagreb). Nucl. Instrum. Methods; 92: 19-20(1971).

Ballistic deficit for proportional counter pulses shaped by different pulse shaping networks was calculated. Networks with better signal to noise performance than the simplest CR-RC filter have been investigated with respect to attenuation of proportional counter pulses. (auth)

18701 MICROLOGIC INTEGRATED CIRCUIT FOR MONITORING CORRELATION IN PULSE SEQUENCES. Pacilio, N.; Ferrari, T.; Lorenzi, P. (CNEN, Rome). Nucl. Instrum. Methods; 92: 13-17(1971).

The problem is faced of monitoring time-correlation within pulse sequences, which are partially random but also contain events linked by a correlation law. Structure, logic operation and applications are described of an ad hoc device—called "correlation monitor"—which is capable of spotting the most significant portions of pulse sequences and of enabling the storage of data only when a conspicuous fraction of correlated events is present. This type of monitor is indispensable in order to make some neutron-noise time-analysis techniques applicable in thermal and fast nuclear reactor systems. (auth)

18702 ABSOLUTE GAMMA-RAY EFFICIENCY OF A 50 cm^3 Ge(Li) DETECTOR. Young, F. C.; Figuera, A. S.; Pfeufer, G.

XUM

(Univ. of Maryland, College Park). Nucl. Instrum. Methods; 92: 71-5(1971).

Efficiencies of a 50 cm^3 coaxial Ge(Li) detector have been determined for γ rays from 122 keV to 9.17 MeV for a source to detector distance of 10 cm. Measurements were made with radioactive sources for γ-ray energies up 3.25 MeV and with γ rays from proton-induced nuclear reactions for higher energies. Absolute efficiencies determined with calibrated radioactive sources at lower γ-ray energies are in good agreement with efficiencies determined by comparison with calculated NaI efficiencies at higher energies. (auth)

18703 LIFETIME MEASUREMENTS OF ALPHA EMITTERS IN THE MILLISECOND REGION. Erlik, A.; Felsteiner, J.; Lindeman, H.; Tatcher, M. (Technion-Israel Inst. of Tech., Haifa). Nucl. Instrum. Methods; 92: 45-9(1971).

Two independent measuring methods, namely a multichannel delayed coincidence method and a time interval analyzer method, have been employed in order to determine half-lives in the millisecond region of the α-emitters ^{215}Po, ^{214}Po, and ^{218}Rn. A description is given of a new type of ten-channel time interval analyzer. (auth)

18704 MEASUREMENT OF $^{238}U/^{235}U$ FISSION RATIOS IN ZEBRA USING SOLID STATE TRACK RECORDERS. Jowitt, D. (Atomic Energy Establishment, Winfrith, Eng.). Nucl. Instrum. Methods; 92: 37-44(1971).

The application of solid-state recorders to the determination of fission ratios in a zero power fast reactor is demonstrated. Although measurements of limited accuracy may be made by counting tracks visually, automatic track counting using a "Quantimet B" television image analyzer is shown to be capable of a precision comparable with that of the conventional foil activation technique. Measurements of the $^{238}U/^{235}U$ fission ratio in several assemblies have shown no significant differences between the results obtained by the two methods. (auth)

18705 CONSTANTS OF THE CHARGED PARTICLE IDENTIFIER. Gupta, S. K. (Bhabha Atomic Research Centre, Bombay). Nucl. Instrum. Methods; 92: 33-5(1971).

Two methods of calculating the constants F and E_0 for the charged particle identifiers using a relationship for the product $P = \Delta E(E + F\Delta E + E_0)$ have been described. Such constants have been calculated for silicon detectors. The extensions to other detectors have been pointed out, and the limitations of the methods in practical cases, have been discussed. A method of setting the constants in the actual multiplier circuits has been discussed. (auth)

18706 DEAD-TIME CORRECTION FOR ANY DISTRIBUTION OF INPUT EVENTS. Teodosic, V. (Univ., Belgrade. Boris Kidric Inst. of Nuclear Sciences, Belgrade). Nucl. Instrum. Methods; 92: 109-10(1971).

A recently developed relation is used to calculate the counting-loss in the case when one element (at the front-end or after a prescaler) of the instrumentation used is of the paralyzable type. The only necessary information about the input train of events is its probability-generating function. (auth)

18707 WIRES AS THERMAL NEUTRON PROBES. Segal, Y.; Velner, S. (Technion-Israel Inst. of Tech., Haifa). Nucl. Instrum. Methods; 92: 101-8(1971).

The apparent activities of gold, indium, dysprosium, 10% DyAl, 5% DyAl, manganese, and cobalt wires caused by thermal neutron flux are calculated as a function of their diameters. The apparent activities resulting from resonance absorption of gold (4.906 eV) and indium (1.457 eV) are also calculated. (auth)

18708 METHOD FOR DEVELOPMENT OF VOLUME TRACKS IN DIELECTRIC NUCLEAR TRACK DETECTORS. Benton, E. V. (Univ. of California, Berkeley). Nucl. Instrum. Methods; 92: 97-9(1971).

For track development in dielectric nuclear track detectors, the etchant must have access to the latent track region. Since etchants do not readily diffuse through the bulk material, only latent tracks that cross the detector surface are developed. This inability to develop volume-tracks, those that do not cross a detector surface, is perhaps the single, most serious shortcoming of these detectors. A special technique for the development of volume tracks is presented. (auth)

18709 THEORY OF RADIATION DETECTION THROUGH SUPERCOOLED LIQUID. Varshneya, N. C. (Univ. of Roorkee, India). Nucl. Instrum. Methods; 92: 147-50(1971).

It is shown that it should be possible to detect high energy radiation through its ionizing effect as tracks in a supercooled liquid. A theory for this has been presented. The basis is that the supercooling is a metastable state of the liquid and ionization can initiate crystallization in it. A preliminary report on experimental observation has been published in: Nature; 223: 826(1969). (auth)

18710 EXTENSION OF RAMO'S THEOREM AS APPLIED TO INDUCED CHARGE IN SEMICONDUCTOR DETECTORS. Cavalleri, G. (CISE, Milan. Politecnico, Milan); Gatti, E.; Fabri, G.; Svelto, V. Nucl. Instrum. Methods; 92: 137-40(1971).

Extension of Ramo's theorem to the case of presence of fixed space charge has been questioned in the past and very recently. It is shown that the authors who criticized its application, fell into some errors, which are discussed. A proof of the extended Ramo's theorem is given. Further on, in order to clarify the matter, the simple case of a unidimensional problem relevant to semiconductor detectors is fully discussed. (auth)

18711 SENSITIVE FAST RESPONSE ELECTRON DETECTOR. Kuswa, Glenn W. (Univ. of Wisconsin, Madison). Rev. Sci. Instrum.; 42: 256-7(Feb 1971).

A miniature scintillation electron detector was developed for use with a small energy analyzer working in the range of 0.5 to 1000 eV. The gain was 10^4, and the inherent risetime was ~5 nsec, given sufficient input signal. Optical coupling of the signal eliminated ground loops. (auth)

18712 TECHNIQUE FOR ATTACHING A VACUUM TIGHT WINDOW TO A CURVED SURFACE. Ritter, Evelyn F.; Koehler, Conrad F. Jr. (Brookhaven National Lab., Upton, N. Y.). Rev. Sci. Instrum.; 42: 264(Feb 1971).

A simple and efficient method is described for producing a uniform vacuum tight seal when attaching a window to curved-surface detector chamber, using readily available, inexpensive materials. (L.B.S.)

18713 SCINTILLATION DETECTOR INDICATING SYSTEM. Hindel, Robert (to Picker Corp.). U. S. Patent 3,532,927. 6 Oct 1970. Filed 25 Jun 1968.

In a scintillation detector utilizing a cathode-ray tube to present a visible spot at a point on its face corresponding to the location of a scintillation in a scintillator, signals whose relative amplitudes are indicative of the location coordinates of the scintillation are subject to controlled decay with their relative amplitude ratios being preserved. A sum or energy signal is similarly treated; and when it has decayed to a reference level, the decayed coordinate signals have properly positioned the cathode-ray-tube beam to indicate the scintillation location. (auth)

18714 METHOD TO IMPROVE THE ENERGY CALIBRATION OF A Ge(Li) SPECTROMETER. Fubini, A.; Terrasi, F.; Vata, I. (CNEN, Rome). Nucl. Instrum. Methods; 92: 309-11(1971).

A method is described which improves the precision of the energy calibration of a Ge(Li) spectrometer taking into account the relationship between cascade gamma rays. (auth)

18715 EFFICIENCY CALIBRATION OF SEMICONDUCTOR X RAY DETECTORS. Campbell, J. L.; O'Brien, P.; McNelles, L. A. (Univ. of Guelph, Ont.). Nucl. Instrum. Methods; 92: 269-75(1971).

Data on the decay characteristics of several radioactive sources suitable for efficiency calibration of Ge(Li) and Si(Li) detectors in the energy range 1 to 100 keV are compiled and discussed. The sources include ^{54}Mn, ^{57}Co, ^{58}Co, ^{65}Zn, ^{85}Sr, ^{88}Y, ^{109}Cd, ^{113}Sn, ^{137}Cs, ^{139}Ce, ^{141}Ce, ^{198}Au and ^{203}Hg. (auth)

18716 EFFECTS OF ELASTIC SCATTERING ON THE LOW ENERGY NEUTRON DETECTION EFFICIENCY OF A LITHIUM GLASS AND BORON-LOADED LIQUID SCINTILLATOR. Dalton, A. W. (Australian Atomic Energy Commission Research Establishment, Sutherland). Nucl. Instrum. Methods; 92: 221-7(1971).

The neutron detection efficiencies of a lithium glass and a boron-loaded liquid scintillation detector were calibrated over the energy range from thermal to 8 keV. The calibrations were based on the measurement of a known spectrum from the low power experimental reactor facility MOATA and detailed three-dimensional Monte Carlo calculations. For both detectors good agreement was obtained between their measured and calculated efficiencies. Elastic scattering within the lithium glass produced an enhancement of the detection efficiency in the epithermal region and this enhancement increased with energy. A significant distortion of the measured spectrum arose from the scattering of neutrons into the detectors by the surrounding shielding materials. (auth)

18717 SAMPLING BY LAMINAR FLOW ENTRAINMENT TO PREVENT WALL EFFECTS. Randolph, H. W. (E. I. du Pont de Nemours and Co., Aiken, S. C.). Contract AT(07-2)-1. Nucl. Instrum. Methods; 92: 233-5(1971).

Laminar flow of a fluid sample entrained as a core inside a column of suitable buffer fluid can be used to prevent measurement interferences from depositions of the sample on container walls. A gamma monitor cell is described that embodies this principle and does not become contaminated when used for continuous monitoring of liquid streams. The monitor is capable of measuring activity of streams containing gamma activity varying from 10^3 to 10^7 d/mml. Errors caused by sample flow variations are less than ±5% of measurement. Calculations indicate that this principle should also be applicable to high-resolution counting of alpha and low-energy-beta activity in gas streams. (auth)

18718 WIRED ARITHMETIC COMPUTER FOR PARTICLE IDENTIFICATION. **Schmit, M.; Herry, J.; Flamant, Y. (Institut d'Etudes Nucleaires, Alger, Algerie). Nucl. Instrum. Methods; 91: 321-5(1971). (In French).**

Charged-particle identification is made using a fast digitalized device composed of a simplified computing unit and a wired program. (auth)

18719 METHODS AND APPARATUS FOR TESTING THE INDIVIDUAL ACTIVITIES OF PROBE BODIES THAT HAVE BEEN IRRADIATED, FOR EXAMPLE IN A NUCLEAR REACTOR INSTALLATION. (to Siemens Aktiengesellschaft). British Patent 1,209,826. 21 Oct 1970. Priority date 11 Mar 1967, Germany.

A method of testing the individual activities of activation probe bodies that have been irradiated in-pile is described. The probe bodies are arranged in file in a conveyor tube adjacent to which a counter is placed; and they are moved in succession past the counter, as by a wire or compressed air. (R.W.R.)

18720 PRACTICAL POSSIBILITIES OF USING GALLIUM AND LITHIUM AS SOLAR NEUTRINO DETECTORS. **Pomanskii, A. A.** Kosm. Luchi; No. 10, 95-7(1969). (In Russian).

$GaCl_3$ and an aquatic solution of LiCl can be used for the solar neutrino detection. The techniques of reducing germanium-71 from $GaCl_3$ and beryllium-7 from LiCl generated by reactions $\nu + {}^{71}Ga \rightarrow {}^{71}Ge + e^-$ and $\nu + {}^{7}Li \rightarrow {}^{7}Be + e^-$ are discussed. The effect of the background processes may be neglected when necessary decontamination of the detector substances is made. The problems of recording the decay of the radioactive ^{71}Ge and ^{7}Be are considered. (auth) (Meteorol. Geoastrophys. Abstr.)

18721 APPARATUS FOR PRODUCING A VOLTAGE LOGARITHMETICALLY RELATED TO THE QUANTITY OF CHARGE DELIVERED BY AN IONISATION CHAMBER. **Burkhart, Andre; Guillot, Francois (to Commissariat a l'Energie Atomique). British Patent 1,216,061. 16 Dec 1970. Priority date 13 Dec 1967, France.**

A circuit for producing a voltage that is logarithmically related to the quantity of charge delivered by an ionization chamber is described. The circuit includes a capacitor which upon discharge triggers a sawtooth generator which produces a linear voltage which is read out on a logarithmic-scale galvanometer. (W.H.K.)

18722 SCINTILLATION-TYPE ION DETECTOR EMPLOYING A SECONDARY EMITTER TARGET SURROUNDING THE ION PATH. Strausser, Yale E. (to Varian Associates). U. S. Patent 3,538,328. 3 Nov 1970. Filed 4 Mar 1968.

A scintillation-type ion detector is disclosed. The detector includes an evacuable envelope structure containing a secondary emitter target electrode structure having a bore therethrough which is preferably of conical shape. The inside surface of the bore is bombarded by the ions to be detected and is made of a material that emits secondary electrons on being bombarded by ions. The secondary electron emission from the walls of the bore is focused onto a scintillator disposed facing the exit end of the bore to give an optical photon output which is transmitted through a window to a photo multiplier. (auth)

18723 NEW DOSE CALIBRATOR FOR NUCLEAR MEDICINE. **Mauderli, Walter; Bruno, Fred P.; Williams, Clyde M. (Univ. of Florida, Gainesville). Amer. J. Roentgenol., Radium Ther. Nucl. Med.; 111: 405-7(Feb 1971).**

An ionization chamber dose calibrator for bulk assay of millicurie levels of radioactivity and the automatic calculation of the volume of nuclide to be administered are described. Two versions are offered, a less expensive one with analog readout and a more expensive version with digital readout. In both versions the design of chamber and circuits obviates the necessity of any calculation at all by the technician. (auth)

18724 DETECTION OF ^{235}U FISSION FRAGMENTS BY THE SOLID STATE TRACK RECORDER USING CELLULOSE NITRATE. Song, Kwang Suk; Lee, Sang Soo (Atomic Energy Research Inst., Seoul). J. Korean Nucl. Soc.; 2: 223-8(Dec 1970).

A special design of the solid state track recorder or SSTR using cellulose nitrate was developed for detection of fission fragments of U-235. The cellulose nitrate film of the detector is 2mm apart from the fission source which is a thin layer of uranyl nitrate (87% enrichment of U-235) suspended in cellulose nitrate. The detector is then exposed to thermal neutron flux for induced nuclear fission, and then the film was etched in 5-N NaOH solution. The diameter of a track increased as the etching time and temperature and concentration of the etchant are increased since etching is a usual chemical reaction, however, in the present experiment the optimum conditions were found for a given room temperature. The hystogram of track diameter as measured under a microscope shows the distribution is of the typical saddle shape, which is familiar in fission physics, yet correct correlation among these saddle shapes are not derived. Also a detailed technique for preparing cellulose nitrate detector films on a mercury pool and thin films of uranyl nitrate fission source are described. (auth)

18725 SEMI-EMPIRICAL EFFICIENCY CURVE FOR A THIN Ge(Li) DETECTOR AT LOW ENERGIES. **Chung, M. K.; Suh, D. W.; Cho, S. W.; Kim, E. G. (Atomic Energy Research Inst., Seoul). J. Korean Nucl. Soc.; 2: No. 1, 9-17(Mar 1970).**

Recently several workers tried semi-empirical approach to the determination of the relative total-energy-peak efficiency, $\mathcal{E}$, in the low gamma-ray energy range. They adopted the semi-empirical formula $\mathcal{E} \propto \mathcal{T} + A\sigma \exp(-BE)$, where $\mathcal{T}$ and σ are photoelectric and Compton absorption coefficients respectively, E is the gamma-ray energy and A and B are constants determined from the measured values of detection efficiencies. In spite of the good fit to the experimental curve by this formula for higher energies, this curve deviates considerably from measured values in the range, $E < 500$ to 600 keV. By the accurate analysis of experimental data, it was found that the formula, $\mathcal{E} \propto A \cdot \exp(-BE)$, which is independent of the absorption coefficients, can account experimental data more accurately in the energy range, $E > 700$ keV. For lower energies than 700 keV, the formula, ($\mathcal{E} \propto \mathcal{T} + A\sigma E^{-B}$), shows excellent agreement with the observed data. Results show that the contribution from multiple Compton scattering to the total energy peak varies with the energies as $A\,\sigma \exp(-BE)$ for higher energies and as $A\sigma E^{-B}$ for lower energies. Also, the formula $A \cdot \exp(-BE)$ is deduced from the $\mathcal{T} + A\,\sigma \exp(-BE)$ in the case of thin detectors. Utilizing experimental results, intensity ratios of ^{198}Au and ^{116m}In γ-rays are re-calibrated: $\gamma_1(411.795\ \text{keV})/\gamma_2(675.88\ \text{keV})/\gamma_3(1087.69\ \text{keV}) = 100/0.85 \pm 0.056/0.218 \pm 0.021$ for ^{198}Au and $\gamma_1(138.32\ \text{keV})/\gamma_2(417.0\ \text{keV})/\gamma_3(818.80\ \text{keV})/\gamma_4(1097.20\ \text{keV})/\gamma_5(1293.30\ \text{keV}) = (3.00 \pm 0.41)/(20.94 \pm 1.46)/(10.98 \pm 1.14)/(61.82 \pm 6.26)/80$ for ^{116m}In gamma-rays. (auth)

18726 AN INVESTIGATION OF MULTIPLE GAMMA SCATTERING IN GERMANIUM AS APPLIED TO Ge(Li) GAMMA SPECTROMETERS. Walker, David Marshall. Atlanta; Georgia Inst. of Tech. (1970). 175p. University Microfilms Order No. 70-24,387.

Thesis.

Multiple gamma scattering in finite germanium volumes as it pertains to the understanding, optimization, and evaluation of gamma spectroscopy concepts based on multiple scattering in Ge(Li) detectors is investigated. A Monte Carlo model is developed to provide the specific information needed for the evaluation of multiple scattering Ge(Li) spectrometers, and the computed results correspond closely to the measured performance of an experimental sum–coincidence Ge(Li) spectrometer. Calculations show that a major fraction of all events in which the entire energy of the incident gamma is captured involve more than one interaction, with three or more interactions being common. For the gamma energy range of 320 keV to 2754 keV, the variation of full-energy-peak efficiency and peak-to-Compton ratio is given for selected hypothetical detectors as a function of external and internal detector geometry and of energy discrimination conditions. Calculated and measured two-parameter energy spectra for coincident events show that events representing the entire energy of the incident gamma are highly localized on the energy surface. Two-dimensional discrimination techniques on the energy surface appear to offer additional Compton interference reduction for specific spectroscopy applications. A figure-of-merit for Compton interference reduction is defined and used as a basis for comparing the performance of conventional Ge(Li) detectors to that of optimized sum–coincidence detectors and to the theoretical maximum performance of Ge(Li) detectors which require multiple gamma scattering. For cylindrical Ge(Li) detectors of up to 2 cm in length and about 25 cm^3 in volume, sum–coincidence operation was calculated to give an equivalent Compton suppression factor of about two. Only in random cases do spectrom-

XUM

eters based on sum−coincidence operation of two-region Ge(Li) detectors appear to offer superior gamma-spectroscopy capabilities over those offered by Ge(Li) spectrometers of 60 cm^3 or greater that accept all detected events. Poor relative efficiency is shown to be the major limitation to Compton interference reduction for sum−coincidence systems. The full-energy-peak efficiencies of all sum−coincidence systems of this analysis are shown to be only minor fractions of the theoretical upper efficiency limits imposed by the requirement of multiple gamma scattering. Although selective efficiency improvements can be realized by special detector configurations, it appears that alternate methods of sensing the occurrence of multiple interactions within a single Ge(Li) volume have the potential for a more general and significant reduction of Compton interference for gamma spectroscopy. (Diss. Abstr. Int., B)

18727 INVESTIGATIONS ON ALPHA RADIOGRAPHY WITH PLASTIC TRACK DETECTORS. Somogyi, Gy.; Srivastava, D. S. ATOMKI (At. Kut. Intez.) Kozlem.; 12: 101-17(Nov 1970). (In Hungarian).

The features of translucency observed in plastics (cellulose nitrate, cellulose acetate and polycarbonate) irradiated with α-particles with high track density ($>10^5$ alphas/cm^2) have been studied. Quantitative data are presented for the correlation between the optical density, etching time and track density for dielectric track detectors of different sensitivity under different irradiation conditions. A few aspects of the requirements for revealing the α-particle tracks in plastics have been theoretically investigated using an observed exponential relationship for the variation of etch rate along the particle's trajectory. The part played by some parameters (irradiation geometry, particle energy, environmental conditions etc.) in the observed α-ray patterns have also been examined. It has been found that one can make energy-selective α-radiography by using less sensitive plastics like polycarbonate. The effect of irradiation in vacuum on the optical density curves has also been studied. From these investigations it was concluded that the presence of oxygen during α-particle irradiation plays an important role in track formation. The method used for these investigations offers itself as a quick and reliable method for finding the relative sensitivities of dielectric track detectors and any change in them due to environmental conditions. (auth)

18728 AUDIOVISUAL DISCRIMINATION FOR TRACK MEASUREMENTS IN EMULSIONS. Medveczky, L. ATOMKI (At. Kut. Intez.) Kozlem.; 12: 119-21(Nov 1970).

A digitized microscope for measuring proton-recoil tracks in nuclear emulsions for neutron detection is described. (W.H.K.)

18729 PROCESSING OF THIN EMULSIONS. Medveczky, L. ATOMKI (At. Kut. Intez.) Kozlem.; 12: 123-5(Nov 1970).

Different developing procedures for 50 μm thick Ilford G5 nuclear emulsions are described. The processed plates were checked with densitometry and grain counting and results are compared. (W.H.K.)

18730 DIGITAL AND ANALOG PROCESSING OF ANGER CAMERA DATA WITH A DEDICATED COMPUTER-CONTROLLED SYSTEM. Ashburn, William L.; Moser, Kenneth M.; Guisan, Michel (University Hospital, San Diego, Calif.). J. Nucl. Med.; 11: 680-8(Nov 1970).

Probably the weakest link in γ scintiphotography is in the method of permanent storage of data. While the original recorded film image may be entirely satisfactory for interpretation in most routine cases, a significant amount of potentially valuable information is often lost and beyond retrieval if one uses direct film storage alone. A method of digital magnetic tape recording, redisplay, and processing of scintillation camera data is described, and the clinical value of these techniques is illustrated. (auth)

18731 2-SUBSTITUTED NAPHTH(1,2)OXAZOLE SCINTILLATORS. Rai, Charanjit; Szawlowski, Theodore H. (to Union Oil Co.). U. S. Patent 3,526,768. 1 Sep 1970. Filed 6 Mar 1964.

The invention covers a method of measuring the beta particle emission from a radioactive sample. The radioactive sample is contacted with a scintillator solution containing a primary and/or secondary solute of the type 2-substituted naphth(1,2)oxazole. Beta bombardment of the solute molecules cause such molecules to emit one or more primary photons. If a secondary solute is also employed, the primary photons are absorbed by the secondary solute and re-emitted. The primary and secondary photons are measured with a photomultiplier-recorder to reveal the relative beta particle emission rate. (auth)

Nuclear Spectroscopic Instrumentation

Refer also to abstracts 20148, 20207, 20374, and 20425.

18732 (AD-711531) DORF-I: GAMMA-RAY SPECTROGRAPH SHIELDING STUDIES. Van Antwerp, Walter R.; Cash, Bernard L.; Hendricks, William D.; Gardner, Alvis H. (Ballistic Research Labs., Aberdeen Proving Ground, Md.). Jul 1970. 42p. (BRL-MR-2045). NTIS.

A gamma-ray spectrograph, designed for use in very intense radiation fields generated by pulsed sources, has been tested in the mixed gamma-ray and neutron field of the Harry Diamond Laboratories pulsed reactor, DORF. Details of the instrumentation used, results on the effectiveness of the mixed field shield−collimator design, and proof of the feasibility of gamma-ray spectrum measurements in either pulsed or steady-state reactor fields are presented. Counting, rate-meter, and analog circuits each performed satisfactorily. However, the shield−collimator design was not satisfactory and it was necessary to make spectrum measurements with eight inches of water interposed between the spectrograph and the reactor core. Necessary changes in the shielding and collimator configurations are discussed. (auth)

18733 (CEA-R-4052) STUDY AND DEVELOPMENT OF CADMIUM TELLURIDE DETECTORS FOR GAMMA-RAY SPECTROMETRY. Knispel, Gerard (Commissariat a l'Energie Atomique, Grenoble (France). Centre d'Etudes Nucleaires). Jan 1971. 85p. (In French). Dep. NTIS (U. S. Sales Only).

Thesis. Submitted to Univ. of Grenoble, France.

The possibility of using CdTe as a detector in γ ray spectrometry was investigated. Detectors constructed of this material have certain advantages over the conventionally used Ge(Li). Interactions between radiations and CdTe were studied. The ranges of α and β particles and the capture cross sections for γ ray photons as a function of their energies were deduced from data tabulated for tin which has almost the same density and atomic mass. Problems related to the creation and collection of charges in CdTe structures are examined and resolution problems in nuclear spectrometry considered in terms of the different parameter characteristics of the detector. The metallurgy of CdTe is discussed and the preparation of several different types of structure described: evaporation of a CdTe layer, diffusion of Au or Cu, and semiconductor metal contact. The current voltage characteristics and capacity measurements made enabled certain parameters to be ascertained and the suitability of using CdTe detectors in nuclear spectroscopy to be examined. Range measurements made are compared with theoretical predictions. A comparison was made between the results obtained using three different detectors for α particle spectroscopy. The choice of CdTe as a detector material is justified by its ability to detect γ radiation but the results indicate that work on the material is still incomplete. (auth) (France)

18734 (INP-727) AUTOMATED SYSTEMS AND ELECTRONICS FOR THE KRAKOW-DUBNA SLOW-NEUTRON INVERTED-GEOMETRY SPECTROMETER KD SOG-1. Zaleski, Tadeusz; Sokolowski, Janusz (Institute of Nuclear Physics, Krakow (Poland)). 1970. 15p. (In Polish). Dep. NTIS (U. S. Sales Only).

The spectrometer for microdynamics of condensed matter, operating at the IBR-30 pulsed reactor at the Joint Institute for Nuclear Research in Dubna (USSR), is described. Special emphasis is placed on the problem of automation and remote control of the spectrometer kinematics and detection systems and of the physical experimental conditions. (auth)

18735 (INR-1224) MEASUREMENT OF HIGH-ENERGY γ-RAY SPECTRA IN A STRONG NEUTRON FLUX. Brzosko, J. S.; Gierlik, E.; Sottan, A. Jr.; Wilhelmi, Z. (Institute of Nuclear Research, Warsaw (Poland)). 1970. 12p. Dep. NTIS (U.S. Sales Only).

A method for measuring high-energy γ rays in a strong neutron flux is elaborated. Advantages of this method are high efficiency of the detection of the γ rays from (n,γ) reactions and maximum reduction of the γ-ray background caused by interactions of the neutrons with the surroundings (especially important in a small target room). (auth)

18736 (INR-P-1227) BETA SPECTROMETER WITH A Si(Li) DETECTOR IN HOMOGENEOUS MAGNETIC FIELD. Plochocki, A.; Belcarz, E.; Slapa, M.; Szymczak, M.; Zylicz, J. (Institute of Nuclear Research, Warsaw (Poland)). 1970. 10p. Dep. NTIS (U. S. Sales Only).

A β spectrometer is described which uses a Si(Li) detector together with a system of diaphragms in a homogeneous magnetic field. Lead shielding between the source and detector provides a partial protection of the detector against electromagnetic

XUM

radiation from the source and the diaphragms make it possible to select a desired energy range of electrons for investigations. The instrument seems to be especially useful when studying very low intensity effects in the presence of intense electron radiation of another energy. (auth)

18737 (ORO-3820-7) ON-LINE ALPHA AND PROTON DFCAY SPECTROMETRY. Annual Progress Report, 1970. Macfarlane, Ronald D. (Texas Agricultural and Mechanical Univ., College Station). 15 Jan 1971. Contract AT(40-1)-3820. 21p. Dep. NTIS.

Work already completed and still in progress is reviewed. Development work was carried out on the helium-jet recoil transport system, the recoil time-of-flight mass analyzer, and the on-line mass separator using a quadrupole mass filter. Beta-delayed alpha and proton decay was studied in the light elements. Results were obtained for ^{20}Na which bear on the existence of second-class currents in the weak interaction and second-order interference effects in the CVC. Longitudinal nuclear alignment of recoils from G-T transitions was detected in $\beta-\nu$ correlation measurements of the decay of ^{20}Na. New transitions were observed in the beta decay of ^{24}Al and ^{32}Cl. A detailed study of the properties of the ^{221}Ac nucleus using heavy ions was completed. Absolute excitation functions were obtained. A new correlation was discovered relating to the widths of the excitation functions and the dynamics of yeast level changes in successive neutron evaporations. Spectra from the ^{149}Sm(n,α) reaction were studied for different chemical compounds over a range of temperatures. The ratio of excited state of ^{146}Nd was found to be slightly dependent on the chemistry and temperature of the target nucleus. (R.W.R.)

18738 (RISO-229) THERMAL NEUTRON SPECTROSCOPY USING POSITION-SENSITIVE DETECTORS TOGETHER WITH FOURIER CORRELATION TIME-OF-FLIGHT AND SINGLE-CRYSTAL TECHNIQUES. Kjems, Joergen (Danish Atomic Energy Commission, Risoe. Research Establishment). Aug 1970. 56p. Dep. NTIS (U. S. Sales Only).

A position-sensitive thermal neutron ^{3}He-detector system with 7.8 mm resolution (FWHM) is described together with its application to two different spectrometers. One uses the time-of-flight technique, and the other uses a single crystal for the energy analysis of the scattered neutrons. The TOF-spectrometer is designed primarily for the investigation of quasielastic scattering. The scattering is measured simultaneously in an angle range of 6°. The performance of the instrument is demonstrated by measurements of critical magnetic scattering from Tb. The crystal spectrometer uses a large, single crystal for the energy analysis, which can be made simultaneously in an angle range of 18°. The properties of the instrument are demonstrated by measurements of incoherent inelastic scattering from p-$C_6H_4Cl_2$, and of coherent scattering by phonons in Zn. The two instruments are compared. The crystal spectrometer is preferred because it is more flexible, it is less susceptible to mechanical and electronic failures, and it produces results where the physical features are immediately accessible to the experimenter. (auth) (Denmark)

18739 SQUARE ROOT TRANSFORM FOR THE ANALYSIS OF QUANTUM FLUCTUATIONS IN SPECTRUM DATA. Inouye, T. (Tokyo Shibaura Electric Co., Ltd., Kawasaki, Japan). Nucl. Instrum. Methods; 91: 581-4(1971).

Statistical fluctuations of pulse height distributions are analyzed from a view-point of noise elimination. The square root transform of the spectrum data that provides an additive characteristic to the relationship between the signal and the noise component is proposed for effective filtering of the data. Numerical simulations of this technique show that smoothing of the spectrum data is more effectively carried out by this transformation. (auth)

18740 MONTE-CARLO UNFOLDING OF NEUTRON SPECTRA. Sanna, R.; O'Brien, K. (Atomic Energy Commission, New York). Nucl. Instrum. Methods; 91: 573-6(1971).

A new method of unfolding neutron spectra and its application to the multi-sphere spectrometer system is described. Spectra are unfolded for several measurements and compared with results previously obtained using the iterative unfolding scheme. (auth)

18741 NEW SPECTROMETER FOR IN-CORE NEUTRON SPECTRUM MEASUREMENTS OR LOW α ACTIVITY DETECTION. De Leeuw-Gierts, G.; De Leeuw, S. (CEN, Mol,. Belgium). Nucl. Instrum. Methods; 91: 585-7(1971).

A spectrometer is described which is designed to eliminate background in low α activity measurements by means of solid state detectors or for in-core neutron spectrum measurements by means of surface barrier detectors combined with a polythene converter. A small-hollowed, low pressure, proportional counter is set up between the particle emitter and the solid state detector. Coincidence carried out between the pulses — distributed in a rather narrow and well known energy interval — generated by the passages through the proportional counter of the particles to be analysed and the solid state detector response, eliminate most of the γ background and parasites, whose energies are completely differently distributed over the two counters. (auth)

18742 250 METER NEUTRON TIME-OF-FLIGHT FACILITY WITH MODULAR DETECTOR AND DIGITAL ELECTRONICS STABILIZATION. Stoler, P.; Yergin, P. F.; Clement, J. C.; (and others) (Rensselaer Polytechnic Inst., Troy, N. Y.). Nucl. Instrum. Methods; 91: 541-5(1971).

A 250 m neutron time-of-flight facility is described. The liquid scintillation proton recoil detector has a unique modular design, and some of its properties, including efficiency and resolution are discussed. The electronic logic, including digital electronic drift compensation, as well as some of the properties of the electron-neutron conversion target are also described. (auth)

18743 INSTRUMENT REPRESENTING MOESSBAUER SPECTRA. Meisel, Werner (to VEB Carl Zeiss Jena). British Patent 1,204.162 3 Sep 1970. Filed 16 Aug 1967.

An improved Moessbauer spectrometer is described that comprises at least two detectors for measuring the intensity of γ or secondary x irradiation, an absorber or scattering means in the radiation path to each detector, a single radiation source moveable towards or away from the absorber or scattering means, together with a motor for moving the source. The line interconnecting each detector, absorber or scattering means and radiation source encloses an angle with the direction of movement of the source. It is claimed that the instrument considerably increases the measuring capacity, despite the use of only one motor. The automatically acting parts, that coordinate the intensity with the velocity, permit the use simultaneously of several spectrometer channels. The electronic detection is less bulky and costly than provision of a second spectrometer for doubling the measuring capacity, and can be used, for example, for the simultaneous measurement of two specimens or for the simultaneous measurement of the calibration spectra, the comparison spectra, and the background radiation. (UK)

18744 PRESSURIZED GAS MONITOR FOR LOW LEVEL RADIOACTIVE GASES. Baum, John W.; Littlefield, Peter S. (to United States Atomic Energy Commission). U. S. Patent 3,531,639. 29 Sep 1970. Filed 10 Dec 1968.

A monitor for continuously measuring low concentrations of radioactive gases is described. A pressure vessel contains a labyrinth formed by a scintillating material. A photomultiplier tube adjacent a window in the pressure vessel measures the light emitted by the scintillating material. (auth)

18745 CONTRIBUTION OF THE SCINTILLATOR TO THE RESOLUTION OF A SPECTROMETER USING THE SINGLE-ELECTRON METHOD. Gulakov, I. R.; Levkovich, A. D.; Pertsev, A. N.; Tolkach, P. N. (Belorussian State Univ., Minsk). Instrum. Exp. Tech. (USSR) (Engl. Transl.); No. 2, 404-6(Mar-Apr 1970).

Translated from Prib. Tekh. Eksp.; No. 2, 86-7(Mar-Apr 1970).

The use of the single-electron component of the photomultiplier noise for studying the structure of the resolved instrumental photopeak of a scintillation spectrometer is described. (auth)

18746 DETECTION LIMITS FOR RADIONUCLIDES IN THE ANALYSIS OF MULTI-COMPONENT GAMMA RAY SPECTROMETER DATA. Pasternack, B. S.; Harley, N. H. (New York Univ., N. Y.). Nucl. Instrum. Methods; 91: 533-40(1971).

The problem of obtaining the lower limit of detection (LLD) for the concentration of a nuclide present in a mixture to be assayed by the use of a multichannel gamma-ray spectrometer is considered. The method for computing the LLD proposed is based on the usual weighted least-squares technique for analyzing pulse-height distributions. Several LLD's are computed. These are the LLD for a nuclide when no other nuclides are assumed to be present in the mixture — the library of standards contains the spectrum for the nuclide of interest only; the LLD for a nuclide when other nuclides are included in the library, but not in the mixture; the LLD for a nuclide when other known nuclides are assumed to be present in the mixture at fixed levels — the library contains the spectra for all nuclides involved. As examples of the determination of LLD's for a multi-component system, mock samples were prepared, counted, and analyzed for the three situations described. An important statistical principle underlying the relationship of the LLD of a nuclide with the other nuclides included in the library (whether or not such nuclides are present in the mixture) is stressed. The LLD of a nuclide varies inversely with the residual variation obtained when its standard spectrum is regressed on the remaining library spectra. (auth)

XUM

18747 DETERMINATION OF RELATIVE PHOTOPEAK EFFICIENCY AND SYSTEM LINEARITY FOR Ge(Li) GAMMA-RAY SPECTROMETERS. Gehrke, R. J.; Cline, J. E.; Heath, R. L. (Idaho Nuclear Corp., Idaho Falls). Nucl. Instrum. Methods; 91: 349-56(1971).

A simple, precise method is described for determining both the relative detection efficiency and the linearity of a Ge(Li) spectrometer. The method employs three readily available radioactive sources — ^{75}Se(120 d), ^{82}Br(35 h), and ^{56}Co(77 d) — that emit gamma rays covering the energy range 90 to 3500 keV. The gamma-ray energies and relative intensities for these isotopes were precisely measured. A method is suggested to set the "effective zero" of the analyzer reproducibly by using the above gamma-ray sources. (auth)

18748 AN APPARATUS FOR DETECTION AND ENERGY MEASUREMENT OF MUONIC AND PIONIC X-RAYS IN THE RANGE 1 TO 10 keV. Placci, A. (CERN, Geneva); Polacco, E.; Zavattini, E.; (and others). Nucl. Instrum. Methods; 91: 417-28(1971).

A target–X-ray-detector assembly that is particularly suitable for detecting muonic and pionic X rays in the range 1.3 to 10 keV is described. Some of the main features of the system are included. (auth)

18749 GAS RECOIL NEUTRON SPECTROMETER WITH ELECTRONIC COLLIMATION BY RISE-TIME DISCRIMINATION. Mizuho, M.; Mizoguchi, T. (Japan Atomic Energy Research Inst., Tokyo). Nucl. Instrum. Methods; 91: 439-43(1971).

A gas recoil neutron spectrometer based on a new method of electronic collimation by rise-time discrimination in a proportional counter has been reported. In the preliminary studies discussed here a similar collimation was realized in a methane-filled proportional counter. The performance was examined for monoenergetic neutrons of 0.6 to 1.5 MeV. The spectrometer is expected to have a high efficiency and many advantages. Its features include the following: the energy resolution (which depends on a degree of collimation) is adjustable to the required degree by setting parameters in an electronic system without any re-settings in a counter parameter; a conventional collimator, which is apt to cause background pulses, need not be used; and the instrument, especially the counter construction, becomes very simple in this spectrometer. The spectrometer should have a very low gamma sensitivity as the gamma pulses are mainly due to electrons from the cathode resulting in relatively slow rises. (auth)

18750 METHOD FOR IMPROVING HEAVY ION SPECTRA IN SCATTERING EXPERIMENTS. Haight, R. C.; Saladin, J. X.; Vitoux, D. (Univ. of Pittsburgh). Nucl. Instrum. Methods; 91: 445-9(1971).

Energy spectra are often not sufficiently clean in two-body scattering experiments with heavy ions where a small cross section is to be measured with good precision. Such spectra were improved by observing the angle of the recoiling nucleus in addition to the energy of the scattered projectile. By using a position-sensitive detector to detect the recoils, good angular resolution was obtained over a wide range of recoil angles. The method described here is applied to the investigation of inelastic scattering of ^{16}O by ^{24}Mg. (auth)

18751 RESONANCE RECORDING OF ^{57}Co GAMMA QUANTA. Mitrofanov, K. P.; Plotnikova, M. V.; Rokhlov, N. I. (Moscow State Univ.). Instrum. Exp. Tech. (USSR) (Engl. Transl.); No. 2, 390-2(Mar-Apr 1970).

Translated from Prib. Tekh. Eksp.; No. 2, 75-6(Mar-Apr 1970).

The parameters of a resonance counter for recording ^{57}Co γ quanta without recoil are reported. The absorption system of the counter is a single line whose width is close to the natural width. The efficiency of recording resonance γ quanta is ~15%, and their count exceeds the background level by a factor of 10. (auth)

18752 A COMPTON-SUPPRESSED LOW LEVEL GAMMA-RAY SCINTILLATION SPECTROMETER FOR THE SAMPLES OF EXTENDED GEOMETRY. Sethi, S. K. (Bhabha Atomic Research Centre, Bombay). Nucl. Instrum. Methods; 91: 397-405 (1971).

A Compton-suppressed gamma-ray scintillation spectrometer having high sensitivity and selectivity is described. The spectrometer is intended to be used for the identification and estimation of low levels of gamma radioactivity in a broad range of sample sizes containing a moderately complex mixture of gamma-emitting radionuclides. The spectrometer uses a 7.6 cm dia. × 7.6 cm thick NaI(Tl) detector having anticoincidence guard of a rectangular plastic scintillator block 38 cm × 38 cm × 30 cm placed inside a 15-cm thick lead shield. Various details of the setup are given, and the use of such a system for the analysis of complex spectra of low-level activity is discussed. The anticoincidence guard provides a gross background reduction by a factor of 2.8 for the energy interval between 50 keV and 1600 keV. Performance evaluation of the system with respect to background reduction, Compton suppression factor, peak/total ratio, and peak prominence factor are discussed. (auth)

18753 EXPERIMENTAL TECHNIQUES FOR THE INVESTIGATION OF ISOMERIC TRANSITIONS IN THE MILLI- AND MICROSECOND REGION. Uyttenhove, J.; Demuynck, J. (Rijksuniversiteit, Ghent). Nucl. Instrum. Methods; 91: 307-11(1971).

A measuring system for investigations on isomers with lifetimes in the ms and μs region is described. Energy and decay-time of the isomeric state are determined by measurements of γ-ray spectra in successive time intervals with a Ge(Li) detector. Provision is made for compensation of the γ flash and for beam inspection. (auth)

18754 SPURIOUS PEAKS PRODUCED BY COMPTON SCATTERING IN Ge(Li)–Ge(Li) COINCIDENCE GAMMA-RAY SPECTROMETER SYSTEMS. Giesler, G. C.; McHarris, Wm. C.; Warner, R. A.; Kelly, W. H. (Michigan State Univ., East Lansing). Nucl. Instrum. Methods; 91: 313-20(1971).

Compton scattering between Ge(Li) γ-ray detectors in coincidence experiments was investigated. Such scattering can generate false peaks that can be mistaken for photopeaks. The effects of varying gate position, gate width, background subtraction, and angle between detectors are discussed; and suggestions are made for recognizing and minimizing spurious effects. (auth)

18755 CALCULATED TOTAL EFFICIENCIES OF COAXIAL Ge(Li) DETECTORS. Griffiths, R. (Oxford Univ., Eng.). Nucl. Instrum. Methods; 91: 377-9(1971).

A program was written to compute the total efficiencies of coaxial Ge(Li) detectors. Graphs are presented that show how the efficiency of four typical detectors of active volumes 20, 30, 50, and 80 cm^3 varies for gamma rays of energies 0.01 to 10.0 MeV for source-to-detector distances in the range 1.0 to 25.0 cm. (auth)

18756 CHARACTERISTICS OF LARGE-AREA ION-IMPLANTED p–n JUNCTIONS FOR NUCLEAR RADIATION DETECTORS. Howes, J. H.; Knill, G. (Atomic Energy Research Establishment, Harwell, Eng.). pp 97-101 of Ion Implantation. Stevenage, Eng.; Peter Peregrinus Ltd. (1970).

From Conference on Ion Implantation, Reading, England. See CONF-700945.

A description is given of Li-compensated semiconductor detectors for nuclear spectroscopy, in which the thin entry window is fabricated by ion doping to produce uniform non-injecting contacts in p-type Si and Ge crystals. It was realised that the use of too high an ion energy causes a comparatively deep layer of doped material with excessive surface damage which only anneals out at such high temperatures that the carrier lifetimes will be substantially affected, which in turn can effect the performance of the particle detector. A further factor is the effect of lattice orientation, or channelling, in single-crystal materials. Also, the depth distribution of implanted ions is deeper in single-crystal materials, such as Si and Ge, than for amorphous or polycrystalline materials. Ga or B ions in the energy range 10 to 40 keV were used for implantation, with surface doses up to 10^{14} ions/cm^2, using the Harwell Mark I electromagnetic separator. The more penetrating nuclear radiations, while requiring a thin entry window, also require a thicker depletion layer than it is practical to produce with a reversed biased pn junction, and this requirement resulted in the use of a p-i-n structure, in which the intrinsic region between the p- and n-junctions could be up to 2 cm in thickness. In the electrically neutral intrinsic region the carriers generated by nuclear radiation are collected at the p- and n-junctions. The intrinsic region is produced in high-resistivity p-type Ge or Si by first thermally diffusing a highly doped n-type contact using Li to act as a donor. Subsequently the Li from the excess donor source, which is readily ionized at slightly elevated temperature, is drifted through the crystal by means of an applied reverse voltage. The Li ions, on drifting into the p-type semiconductor, exactly balance the p-type dopant resulting in an electrically neutral region. Hitherto, when a thin particle entry window was required the remaining p-type surface was removed and a p-type contact produced by evaporating a thin layer of Au onto the intrinsic p-type surface to form a p-type surface barrier contact. The role of ion implantation is to replace the Au p-type surface barrier contact with a more robust p-type contact formed in the bulk of the semiconductor. The evaluation of diodes as counters is discussed, and applications considered. (6 references) (UK)

XUM

18757 POSITION SENSITIVE DETECTOR TELESCOPES FOR CHARGED PARTICLES USED IN THE BOL-SYSTEM. Den Boer, J. A. (Philips Research Labs., Amsterdam); Hoeberechts, A. M. E.; Hofker, W. K.; (and others). Nucl. Instrum. Methods; 92: 173-6(1971).

A detector telescope consisting of a 0.3 mm thick, position-sensitive, surface-barrier detector (Checkerboard detector) and a 5 mm Si(Li) detector was developed for application in the scattering chamber of the BOL-system. The technological implications of the requirements set for these detectors and the performance of the telescopes are discussed. (auth)

18758 EFFICIENCY OF A 180^0 COINCIDENCE SPECTROMETER FOR EXTENDED SOURCES. Burgmer, W.; Gruhle, W.; Schmidt, W. (Univ., Cologne). Nucl. Instrum. Methods; 91: 481-5(1971). (In German).

Coincidence counting efficiencies for positron annihilation quanta are calculated for various sources between the two detectors. The method is described for arbitrary positions of a point source, and maps are presented for lines of equal efficiency. For the first time the efficiency is computed for a source distributed on a cylindrical wall of a gas target chamber. It is confirmed by a measurement with a ^{22}Na source. (auth)

18759 COINCIDENCE TECHNIQUE FOR STUDY OF Ge(Li) DETECTOR PROFILES. Campbell, J. L.; Smith, H. J.; MacKenzie, I. K. (Univ. of Guelph, Ont.). Nucl. Instrum. Methods; 92: 237-45(1971).

A device employing the 180° relationship between two annihilation gamma rays to achieve collimation was used to study the profile of a Ge(Li) x ray detector housed within a conventional cryostat. The depletion depth in the central region was measured as 5.3 ± 0.1 mm, yielding the detection efficiency for collimated beam measurements of K conversion coefficients. Values of α_K of 1.43 ± 0.05 and 1.69 ± 0.06 were obtained for the well-known E2 transitions in ^{170}Yb and ^{166}Er, in close agreement with current theory. (auth)

18760 SEMICONDUCTOR DETECTOR TELESCOPE ELECTRON SPECTROMETER. Kantele, J.; Passoja, A. (Univ. of Jyvaeskylae, Finland). Nucl. Instrum. Methods; 92: 247-51(1971).

A simple dE/dx + E type semiconductor detector telescope electron spectrometer featuring high detection efficiency and effective discrimination against γ-rays and heavy particles is described. The line shape of the spectrometer is better than that of a single detector of corresponding size; at 1 MeV, the peak-to-total ratio is approximately 0.8. The device is suited to the study of beta-ray spectra and conversion electron lines at energies above about 0.4 MeV. (auth)

18761 TWO DIFFERENT TECHNIQUE MEASUREMENTS OF THE NEUTRON SPECTRUM OF AN Am–Be SOURCE. De Guarrini, F. (Univ., Trieste, Italy); Malaroda, R. Nucl. Instrum. Methods; 92: 277-84(1971).

The neutron energy spectrum of an ^{241}Am$-^{9}$Be source was measured with nuclear emulsions and with a proton recoil spectrometer with n$-\gamma$ discrimination. A good agreement was found between the two measured spectra since in both cases peaks appeared at neutron energies of about 3.5, 4.7 and 9.7 MeV; two other peaks appeared, however, between 5 and 9 MeV. The Am$-$Be neutron spectrum was also calculated by taking into account the anisotropy of the angular distributions of neutrons from the ^{9}Be(α,n)^{12}C reaction and a comparison was made with the two measured spectra. The spectra were also compared with the data obtained from reports of other authors. (auth)

18762 ENERGY MODULATED HIGH ENERGY RESOLUTION ELECTRON SPECTROMETER. Golden, D. E.; Zecca, A. (Univ., Bari, Italy). Rev. Sci. Instrum.; 42: 210-16(Feb 1971).

A new cylindrical retarding potential difference type or energy modulated electron spectrometer was constructed with high energy resolution. For energies greater than 1 eV the ratio of beam current I to energy spread FWHM, ΔE has been found to be approximately constant so that $I/\Delta E \simeq 10^{-7}$ (A/eV) at about 20 eV. For electron energies from 0 to 1 eV the electron current increases with energy by about 10^{-7} A/eV for $\Delta E \simeq 0.1$ eV to the value given by the above expression. For energies above 1 eV the electron current is a very slowly varying function of energy. The energy resolution was checked to 0.008 eV by studying the shape of the He$^-$($^2S_{1/2}$) resonance at 19.3 eV in a transmission experiment. The over-all performance of the spectrometer was studied for electron energies from 0 to 60 eV in transmission experiments in He by studying structures in the electron scattering cross section. (auth)

18763 PROTON RECOIL MONITOR FOR NEUTRON FLUX MEASUREMENTS. Jaszczak, Ronald J. (Oak Ridge National Lab., Tenn.); Macklin, R. L.; Taylor, M. C. Rev. Sci. Instrum.; 42: 240-3(Feb 1971).

Time-of-flight techniques were used with a silicon surface barrier detector and a polyethylene radiator to determine the neutron flux from the Oak Ridge electron linear accelerator in the energy region between 200 keV and 7 MeV. The 200 mm^2 surface barrier detector at 40 m and constant fraction timing electronics are used to measure time of flight, from which the neutron energies are inferred. A Monte Carlo program was written to determine the efficiency, timing, and energy characteristics of the monitor system. (auth)

18764 STATISTICAL CHOPPER METHOD FOR SEPARATION OF ELASTIC AND INELASTIC SCATTERED NEUTRONS IN TIME-OF-FLIGHT EXPERIMENTS. Pellionisz, P. (Institut Max von Laue-Paul Langevin, Grenoble, France). Nucl. Instrum. Methods; 92: 125-35(1971).

A new experimental method is discussed for the elimination of the inelastic scattered contribution in time-of-flight measurements of elastic neutron scattering. The method is based on the introduction of a pseudo-random second chopper in front of the sample which gives the effect that at certain times there are either only inelastic scattered or elastic and inelastic scattered neutrons to be detected. For the description of the sequence of these detection areas, separator functions are introduced and the measured intensities will be stored according to these separator functions in two different memory sectors. By a continuous shift of the statistical chopper the complete inelastic, resp. elastic + inelastic scattered spectra will be measured in the memory-sectors, and a difference-spectrum between them will be directly related to the pure elastic spectrum. A generalized theory on the method is presented. The influence of the duty-cycle (opening time-fraction) of the pseudo-random chopper, that of the choppers' pulse-forms and the different forms of the separator functions are discussed. The relative statistical error of the measurement is calculated as a function of the duty-cycle for different spectra and background-properties. Concerning the technical questions of the measurement, the problem of the continuous shift and the electronic data-processing system is discussed. (auth)

18765 NEW TIME-OF-FLIGHT ANALYSER FOR NEUTRON SCATTERING. Hall, J. W.; Egelstaff, P. A. (Atomic Energy Research Establishment, Harwell, Eng.). Nucl. Instrum. Methods; 92: 51-60(1971).

A new time-of-flight data collection system is described. A mathematical analysis of the relationship of the parameters of the system is given. The characteristics are defined in terms of N, the total number of on-line channels, and R, the count rate. It is shown that the mode of operation and physical constraints of the equipment control the value of the product $N \cdot R$ that can be attained. CASSANDRA is an analyzer based on this new system. It provides 5×10^5 channels for three time-of-flight experiments running in parallel. This system has been designed to handle 450 counts/second and has a paralysis time of 20 μs per event. Facilities for remote displays of data and control information using closed circuit television allow the analyzer to be situated more than a $1/4$ mile from the experiments. CASSANDRA has been in service for more than three years and has an excellent record. (auth)

18766 COMPUTER ANALYSIS TO OBTAIN NEUTRON SPECTRA FROM AN ORGANIC SCINTILLATOR. Toms, M. E. (Naval Research Lab., Washington, D. C.). Nucl. Instrum. Methods; 92: 61-70(1971).

Neutron spectra are obtained from the conversion of pulse-height data produced by recoil protons in a scintillation detector. The FORTRAN computer code which is presented uses a method of analysis which is based on the properties of the scintillator and the scintillation process. The simplicity of the code demonstrates that this method can be adapted easily for use on a small computer. Results of analysis of data from mono-energetic neutrons are presented along with limitations of the code. The neutron spectrum obtained for neutrons from a PuBe source compares very favorably with other measurements. (auth)

18767 BETA SPECTROMETER WITH A Si(Li) DETECTOR IN A HOMOGENEOUS MAGNETIC FIELD. Plochocki, A.; Belcarz, E.; Slapa, M.; Szymczak, M.; Zylicz, J. (Inst. of Nuclear Research, Swierk, Poland). Nucl. Instrum. Methods; 92: 85-8(1971).

A β spectrometer is described which uses a Si(Li) detector together with a system of diaphragms in a homogeneous magnetic field. Lead shielding between the source and detector provides a partial protection of the detector against electromagnetic radiation from the source and the diaphragms make it possible to select a desired energy range of electrons for investigations. The instrument seems to be especially useful when studying very low

XUM

intensity effects in the presence of intense electron radiation of another energy. (auth)

18768 DETERMINATION OF RADON DAUGHTERS ON FILTERS BY A SIMPLE LIQUID SCINTILLATION TECHNIQUE. Rolle, R. (Chamber of Mines, Johannesburg). Amer. Ind. Hyg. Ass. J.; 31: 718-21(Nov-Dec 1970).

A thin-layer detection system is described which can be used to separate alpha and beta spectra sufficiently for simple measurement of low-resolution alpha peaks usually obtained from filter samples. By using nondissolving liquid scintillators all activity can be retained inside the detector volume, and 100% detection efficiency is obtained. The method requires only conventional scintillation pulse-height instrumentation with no cooling, and yet has a high accuracy. (auth)

18769 EXPERIMENTAL APPARATUS FOR THE INVESTIGATION OF THE MOESSBAUER EFFECT. Zemcik, T. (Inst. of Physical Metallurgy, Brno). Jad. Energ.; 16: 413-18 (Dec 1970). (In Czech).

The principle of the experimental investigation method of the nuclear gamma ray resonance—the Moessbauer effect—is described. The main parts of the Moessbauer spectrometers are mentioned and the features of their two principal types are compared: the constant velocity devices and those with the multichannel analyzers. Finally, the examples of their realization are given and the commercial availability is briefly mentioned. (auth)

18770 EFFECT OF THIN FOILS ON THE SPECTRUM OF MONOENERGETIC ELECTRONS. Koever, A.; Varga, D.; Berenyi, D.; Ujhelyi, Cs. ATOMKI (At. Kut. Intez.) Kozlem.; 12: 137-44(Nov 1970). (In Hungarian).

The effect of terphane foils of different thickness on the conversion electron lines of various energy (62.2, 84.2, 481.6, 624.2 and 975.6 keV) was studied with a Si(Li) semiconductor detector placing the foils in front of the source. As a final result of the measurements, the effect caused by a particular foil at certain energy is given in figures. Here the FWHM (full width at the half maximum) and the shift in the maximum of the line, respectively, are plotted as function of the thickness of the foil. On the basis of these diagrams it can be said whether a layer of matter between the source and the detector with some thickness (e.g. a source covering foil, air layer etc.) is disturbing in the measurement with a beta-spectrometer of given resolution or not. It can be stated as a rough rule that the effect of the foil can be considered as negligible on a conversion line at a semiconductor beta-spectrometer (or other beta-spectrometer of similar resolution) if the thickness of foil is about three orders of magnitude less than the range for the electrons of the energy under consideration while, as is well known, the change in the intensity of the electrons can be already neglected if the thickness is about ten times less than the range. If the resolution of the spectrometer is better, only the effect of even thinner foils is negligible at the electron line of the same energy. (auth)

18771 DISTORTING EFFECT OF THE ABSORBERS FOR THE SEMICONDUCTOR AND SCINTILLATION GAMMA-RAY SPECTRA. Srivastava, D. S.; Berenyi, D.; Svingor, E. ATOMKI (At. Kut. Intez.) Kozlem.; 12: 127-36(Nov 1970).

The distortion of the scintillation and semiconductor spectrum of gamma rays with different energies (from 88 to 835 keV) was investigated for a series of aluminum and lead absorbers (from 0.1 to 11.3 gr/cm^2 thick). (auth)

18772 Ge(Li) DETECTOR FABRICATION, A Ge(Li)–Ge(Li) MULTIPARAMETER COINCIDENCE EXPERIMENT AND THE LEVELS OF ^{185}Re. Rotolante, Ralph Allen. Nashville; Vanderbilt Univ. (1970). 188p. University Microfilms Order No. 70-24,888.

Thesis.

Equipment and techniques for the fabrication of lithium-drifted germanium [Ge(Li)] detectors are described. Also discussed in detail are the operating characteristics of solid-state detectors, with particular emphasis given to the timing characteristics of such diodes. The feasibility of performing low-energy, quantitative coincidence experiments with state-of-the-art multichannel analyzers and Ge(Li) detectors is studied. The results were extended to very low energies (~50 keV). The coincidence study was done in conjunction with the level-scheme study of the isotope ^{185}Re, and quantitative results regarding transition intensities and their interpretation are presented. Finally, a discussion of the structure of the various excited levels is given. (TSS) (Diss. Abstr. Int., B)

High Energy Physics Instrumentation

Refer also to abstracts 20177, 20180, and 20446.

18773 (JINR–P1-5540) METHOD OF SEARCHING FOR THE KINK AND DETERMINING THE TRACK PARAMETERS OF PARTICLES SCATTERED IN A BUBBLE CHAMBER. Abdurakhimov, A. U.; Kladnitskaya, E. N.; Nguyen Din Thy (Joint Inst. for Nuclear Research, Dubna (USSR). Lab. of High Energy). 1970. 19p. (In Russian). Dep. NTIS (U. S. Sales Only).

A method is suggested for an effective search for the small angles of scattering in the particle track as well as the method of reconstruction of the track parameters taking scattering into account. (auth)

18774 (JINR–P13-5529) INVESTIGATION OF THE MODEL OF THE 2-METER STREAMER CHAMBER OF THE SCM-200 ASSEMBLY. Volodin, V. D.; Glagoleva, N. S.; Karzhavin, Yu. A.; Kuznetsov, P. S.; Matyushin, A. T.; Matyushin, V. T. (Joint Inst. for Nuclear Research, Dubna (USSR)). 1970. 13p. (In Russian). Dep. NTIS (U. S. Sales Only).

Development of streamers, photographed at different angles to the electromagnetic field direction (0°, 22°, 30° and 40°), is investigated. A brief description of the equipment used is given and results are discussed. (auth)

18775 (UCRL–20042) SEMICONDUCTOR DETECTORS IN HIGH-ENERGY PHYSICS. Wiegand, Clyde E. (California Univ., Berkeley. Lawrence Radiation Lab.). Sep 1970. Contract W-7405-eng-48. 20p. (CONF-700902–6). Dep. NTIS.

From International Conference on Instrumentation for High Energy Physics, Dubna, USSR.

An outline of the present state of the development of semiconductor detectors and how they are being used in experiments at high energy accelerators is given. (W.H.K.)

18776 (USIP–70-3) HARDWARE SYSTEM FOR MEASUREMENTS OF BUBBLE CHAMBER FILMS ON-LINE. Blomqvist, G.; Holmgren, S. O.; Hulth, P. O.; Svedin, U. (Stockholm Univ. (Sweden). Inst. of Physics). Jun 1970. 48p. Dep. NTIS (U. S. Sales Only).

A hardware system was constructed to connect a measuring device for bubble chamber films, "Enetra," on-line to a CDC 8090 computer. An earlier off-line system is compared. The device consists of an operator's console with thumbwheel switches, label displays, signal lights, and counting equipment all connected via the interface to the computer. Measurement procedures and the dynamical function of the interface are provided, as well as details of the equipment. (Sweden)

18777 (USIP–70-6) STUDY OF DISTORTION EFFECTS IN GEOMETRICAL RECONSTRUCTION OF EVENTS IN THE CERN 2m HYDROGEN BUBBLE CHAMBER. Yamdagni, N. (Stockholm Univ. (Sweden). Inst. of Physics). Nov 1970. 49p. Dep. NTIS (U. S. Sales Only).

Distortion effects in the geometrical reconstruction of events in CERN 2m hydrogen bubble chamber (HBC) are investigated. A short description of the chamber and the chamber calibration program CONGEN is given. The main sources of distortion in the CERN 2m HBC are radial lens distortion, and the film plane tilts. Two fitting procedures were compared: one with known radial lens distortion and another one with seven distortion coefficients. In view of the limited number of the fiducials and their location on the windows it was found realistic to fit only a few distortion coefficients. In optimizing the geometrical parameters account should be taken of the reconstruction within the chamber. The residual distortion, the distortion remaining after correcting for the two main effects, was found to be small. (FHS) (Sweden)

18778 OPERATION OF SAMPLING SPARK CHAMBERS. Metzger, G.; Schmitt, F.; Gresser, J.; Riedinger, M.; Sutter, G. (CNRS, Strasbourg). Rev. Phys. Appl.; 5: 771-6(Oct 1970). (In French).

The operation of a sampling spark chamber is discussed. An analysis is made by considering the efficiency in terms of the voltage and the delay and by calculating the spark formation time. Within the limits imposed by the basic hypotheses, agreement between experimental and theoretical results is good. (auth) (France)

18779 ELECTRON ENERGY MEASUREMENT BY THE SHOWER SPECTROMETER. Dunaitsev, A. F.; Ivanshin, Yu. I.; Kakauridze, D. B.; (and others) (Inst. for High Energy Physics, Moscow). Nucl. Instrum. Methods; 91: 601-3(1971).

The new method of electron energy measurement by the intensity of shower particles in the shower maximum region is experimentally investigated. The measurement was done in electron beams with momenta 5, 10, 15 GeV/c and showed the possibility of energy determination with an accuracy of ≈13%. (auth)

18780 HIGH SPEED MAGNETIC-CHIP MEMORY IN A SCANNING ROBOT FOR MEASUREMENT OF CHAMBER PHOTO-

XUM

GRAPHS. Bekh, A. D.; Voitenko, Yu. G.; Zharikov, G. P.; (and others) (Joint Inst. for Nuclear Research, Dubna, USSR. Inst. of Cybernetics, Kiev). Instrum. Exp. Tech. (USSR) (Engl. Transl.); No. 2, 429-30(Mar-Apr 1970).

Translated from Prib. Tekh. Eksp.; No. 2, 106-8(Mar-Apr 1970).

A high-speed memory based on magnetic chips is considered, which is used as the buffer memory in a scanning robot that measures the photographs from bubble chambers. The capacity of the memory is 128 numbers of 24 digits each. The write cycle of the high-speed memory is equal to the read-out cycle and is equal to 0.7 μsec. (auth)

18781 SUPERHIGH-ENERGY PARTICLE DETECTOR BASED ON USING THE RADIATION OF A PARTICLE IN A LAMINAR MEDIUM. Franghyan, A. A.; Harutyunyan, F. R.; Hekimyan, G. A.; Nasaryan, A. A.; Torgomyan, G. B. (Inst. for Physical Research, Erevan). Phys. Lett.; 34B: 227-9(15 Feb 1971).

Experimental results for two types of detectors, that use resonance radiation of electrons with energies of 2.8 and 3.7 GeV in a laminar medium are presented. The detectors are tested in an experiment in selecting electrons from a π^--meson beam; about 50% efficiency is achieved. (auth)

18782 SPARK GAP FOR OPERATION WITH SPARK CHAMBERS. Knyazev, V. M. Instrum. Exp. Tech. (USSR) (Engl. Transl.); No. 2, 443-5(Mar-Apr 1970).

Translated from Prib. Tekh. Eksp.; No. 2, 118-20(Mar-Apr 1970).

A spark gap is described which is distinguished by a low inductance (10^{-7} H) of the discharge circuit attributable to the small dimensions and large external surface of the spark gap. The interelectrode distance is varied without varying the external dimensions or disturbing the sealing. The condition for breakdown in the spark gap is obtained. (auth)

18783 180-LITER XENON BUBBLE CHAMBER. Kuznetsov, E. V.; Rozanov, A. N.; Bardyukov, Yu. V.; (and others) (Inst. of Theoretical and Experimental Physics, Moscow). Instrum. Exp. Tech. (USSR) (Engl. Transl.); No. 2, 368-70(Mar-Apr 1970).

Translated from Prib. Tekh. Eksp.; No. 2, 56-9(Mar-Apr 1970).

A bubble chamber with a working volume of 180 liters intended for filling with liquid xenon is described. The efficiency of the chamber with respect to the recording of γ quanta is almost 100%. (auth)

18784 COMPUTATION OF KINEMATIC PARAMETERS OF ELECTRON TRACKS IN BUBBLE CHAMBERS. Manyukov, B. A.; Shlyapnikov, P. V. (Joint Inst. for Nuclear Research, Dubna, USSR). Instrum. Exp. Tech. (USSR) (Engl. Transl.); No. 2, 371-3 (Mar-Apr 1970).

Translated from Prib. Tekh. Eksp.; No. 2, 59-61(Mar-Apr 1970).

A new method is described for analyzing electron tracks in bubble chambers with heavy liquids. In the derivation of the equations of the curve approximating the track and of the covariation matrix, a cutoff of the spectrum of the retarding losses is used. Unlike most of the known methods, the threshhold for the cutoff is not fixed, but determined together with the kinematic parameters of the track with the use of the method of least squares. (auth)

18785 SPARK CHAMBER WITH GRAPHITE ELECTRODES. Tonapetyan, S. G.; Konovalov, O. G.; Derebchinskii, A. I.; (and others) (Physical-Technical Inst., Kharkov). Instrum. Exp. Tech. (USSR) (Engl. Transl.); No. 2, 374-5(Mar-Apr 1970).

Translated from Prib. Tekh. Eksp.; No. 2, 61-3(Mar-Apr 1970).

The construction of spark chambers designed for the measurement of the polarization of protons with an energy greater than 80 MeV is described. Graphite plates with aluminum foil stuck to the surface of the plates were used as the electrodes of the chamber. The efficiency of the spark chamber per gap was 95%. (auth)

18786 ELECTRON DETECTION WITH A SHOWER DETECTOR. Titov, Yu. I.; Severin, N. F.; Akhmerov, R. V.; (and others) (Physical-Technical Inst., Kharkov). Instrum. Exp. Tech. (USSR) (Engl. Transl.); No. 2, 383-5(Mar-Apr 1970).

Translated from Prib. Tekh. Eksp.; No. 2, 69-71(Mar-Apr 1970).

The resolution of a Cherenkov shower detector operating in combination with a magnetic analyzer has been studied. The measurements were made with detectors having lead glass plates 12.6 and 6.3 radiation lengths in thickness. Under certain kinematic conditions, electrons and pions strike the detector after passing through the magnetic analyzer. The two-plate thicknesses provide the same resolution for electrons. Electrons can be detected against a pion background much more readily by the detector with the thinner plate. (auth)

18787 CHERENKOV TOTAL-ABSORPTION SPECTROMETER WITH A KRS-6 SINGLE-CRYSTAL RADIATOR. Belousov, A. S.; Rusakov, S. V.; Tamm, E. I.; (and others) (Inst. of Physics, Moscow. State Scientific-Research and Planning Inst. of Rare Metals Industry, Moscow). Instrum. Exp. Tech. (USSR) (Engl. Transl.); No. 2, 351-2(Mar-Apr 1970).

Translated from Prib. Tekh. Eksp.; No. 2, 41-3(Mar-Apr 1970).

A KRS-6 single-crystal (a solid solution of TlCl + TlBr), in the form of a truncated cone with base diameters of 30 and 127 mm and a height of 123 mm, was used as the radiator of a Cherenkov total-absorption spectrometer. Calibration of the spectrometer on beams of monoenergetic electrons with energies from 70 to 550 MeV indicated that the amplitude of the pulse at the spectrometer output depends linearly on the energy of the electrons registered. The energy resolution (total width at half-level) varies from 30 to 18% in this energy range. (auth)

18788 DIFFERENTIAL-THRESHOLD CHERENKOV DETECTOR. Prokoshkin, Yu. D. (Inst. of High-Energy Physics, Serpukhov, USSR). Instrum. Exp. Tech. (USSR) (Engl. Transl.); No. 2, 386-9(Mar-Apr 1970).

Translated from Prib. Tekh. Eksp.; No. 2, 71-4(Mar-Apr 1970).

A modification of the Cherenkov detector—a differential-threshold Cherenkov detector—having a high resolution and a large angular aperture is discussed. Particle separation can be achieved by amplitude analysis of the signals from the detector. (auth)

18789 CONTRAST AND SHAPE OF BUBBLE IMAGES IN BUBBLE CHAMBERS WITH BRIGHTFIELD ILLUMINATION. Welford, W. T. (Imperial Coll. of Science and Tech., London). Nucl. Instrum. Methods; 91: 381-7(1971).

Computations are presented of the forms of defocused bubble images for varying bubble diameter, lens aperture, and in-focus plane; the results show how the choice of focus and lens aperture may be optimized, and they also indicate the range of variation of bubble images in size and contrast which have to be measured. (auth)

18790 LARGE-AREA WIRE SPARK CHAMBERS WITH TWO-COORDINATE READ-OUT AND FERRITE CORE MEMORY. Aubert, J. J. (CERN, Geneva); Niebergall, F.; Willitts, T. R.; (and others). Nucl. Instrum. Methods; 91: 493-8(1971).

Spark chambers with crossed wire planes and sensitive areas up to 240 × 130 cm^2 were constructed for use in an electronics experiment at the CERN Proton Synchrotron. A two-coordinate read-out, which has the advantages of lower mass/cm^2 and compactness in space, was achieved by special design of the high-voltage coupling, the ferrite-core modules, and the readout system. The spatial resolution for 1.5-mm wire spacing is ±0.5 mm and ±0.65 mm for the low- and high-voltage planes, respectively. (auth)

18791 SPARK GAP TRIGGER AMPLIFIER WITH 1-msec RECOVERY TIME. Lo, C. C. (Univ. of California, Berkeley). Nucl. Instrum. Methods; 92: 299-308(1971).

A spark-gap trigger amplifier with 1-msec recovery time was developed for experiments using spark chambers with fast recovery time. The system utilizes a spark gap operating under the ambient pressure as the high-current fast switching element, and is entirely self-contained. The system is capable of operating at 1 kHz for 1 sec burst, or 400 Hz continuously. (auth)

18792 ESTIMATION OF THE SIZE OF BUBBLES IN A BUBBLE CHAMBER BY CONTRAST MEASUREMENT. Carnell, K. H.; Welford, W. T. (Imperial Coll. of Science and Tech., London). Nucl. Instrum. Methods; 92: 229-32(1971).

The diameter of an unresolved bubble can be estimated by measuring the contrast of its image in brightfield illumination. In a test of the method eleven bubbles on a single track were measured; the results agreed with the diameter expected from the chamber temperature and pressure and the growth time. (auth)

18793 READOUT OF WIRE SPARK CHAMBER BY DELAY LINES. Kullander, S.; Landaud, G.; Lorenzi, R.; Yonnet, J. (CERN, Geneva. Univ., Caen, France). Nucl. Instrum. Methods; 92: 141-5(1971). (In French).

A read-out system constructed of lumped delay lines is used for a wire spark-chamber of dimensions 60 × 100 cm^2. The lengths of the delay-line modules are between 30 and 35 cm and the delay is typically 70 ns/mm. The sparks are localized with a precision of 0.9 mm (fwhm) and resolved beyond a separation of 2 cm. (auth)

18794 HIGH RESOLUTION DIFFERENTIAL CHERENKOV COUNTERS. Denisov, S. P.; Donskov, S. V.; Gorin, Yu. P.; (and others) (Inst. for High Energy Physics, Serpukhov, USSR). Nucl. Instrum. Methods; 92: 77-80(1971).

The paper describes differential Cherenkov counters detecting Cherenkov light at the angles of 23 and 12 mrad. The counter lengths are 5 m ($\theta = 23$ mrad) and 10 m ($\theta = 12$ mrad). The spectrum band of the counters is 2500 to 6000 Å. The counter characteristics have been investigated in 35 to 45 GeV/c beams of the 70 GeV accelerator. The velocity resolutions measured are equal to 2×10^{-6} for a 10 m counter and 6×10^{-6} for a 5 m counter. The 10 m counter can separate pions and kaons up to 200 GeV/c and kaons and protons (antiprotons) up to 350 GeV/c. (auth)

18795 ANALYSIS OF A BREAKUP USING MEAN TRACK WIDTH AND BLOB MEASUREMENTS. Ackerson, B.; Sorensen, C. M.; Katz, R. (Univ. of Nebraska, Lincoln). Nucl. Instrum. Methods; 92: 81-3(1971).

The consistency of the mean track width theory and the linear grain density theory of Katz and Kobetich is confirmed through the analysis of a breakup event composed of a primary and three visible fragments in a nuclear emulsion. (auth)

18796 EVOLUTION OF THE AUTOMATIC SPARK CHAMBERS. Charpak, G. (CERN, Geneva). Annu. Rev. Nucl. Sci.; 20: 195-254(1970).

Automatic spark chambers are discussed with respect to presently used techniques and recently proposed methods. The properties of proportional multiwire chambers are treated in detail. 106 references. (R.W.R.)

Radiation Dosimeters

Refer also to abstracts 18451, 18644, 18973, and 20134.

18797 (AERE-R-6224) CODE READING OF DOSEMETER FILMS IN AN AUTOMATIC DENSITOMETER. Rae, J. B. (Atomic Energy Research Establishment, Harwell (England)). Dec 1970. 13p. Dep. NTIS (U. S. Sales Only). UK 2s. 6d.

A method of automatically scanning and recording a binary coded identification number printed on personnel radiation monitoring films is described. The six digit number, x-rayed on the film in "2 in 5" binary coded decimal, is checked for correctness and orientation before being stored and converted to serial binary coded decimal. (auth) (UK)

18798 (KFKI-70-29-HP) NEUTRON DOSIMETRY BY SEMICONDUCTOR DETECTORS AND HYDROGENOUS RADIATOR ASSEMBLY. Deme, S. (Magyar Tudomanyos Akademia Kozponti Fizikai Kutato Intezete, Budapest). 1 Nov 1970. 7p. Dep. NTIS (U. S. Sales Only).

Two methods of applying semiconductor diodes to neutron dosimetry have been studied. In the first a homogeneous polyethylene radiator and a fully depleted semiconductor detector of dE/dx type were used and the dose in rad units was calculated from the proton spectrum obtained in the semiconductor detector. In the second the protons emerging from a multilayer, sandwiched polyethylene-aluminum radiator were counted by a semiconductor detector. The structure of the radiator was such that the dose in rad was characterized by the number of protons emerging with an energy above a given threshold. The energy dependence and accuracy of both methods were determined by calculation and direct measurement. It was found that both methods are suitable for measuring to ±10% accuracy collimated neutron beams in the energy interval from 0.5 to 10 MeV with neutron intensities higher than a few rad/hr. (auth)

18799 (ORNL-4584, pp 165-86) APPLIED DOSIMETRY RESEARCH. Becker, Klaus; Boyett, R. H.; Cheka, J. S.; (and others). (Oak Ridge National Lab., Tenn.).

From Health Physics Division annual progress report for period ending July 31, 1970.

The emphasis on thermally stimulated exoelectron emission (TSEE) has continued, with major advances made in the sensitivity and stability of detectors, especially sintered BeO. Initial studies of neutron response characteristics have been completed, and the response per unit dose as a function of photon energy has been measured for several detector types. TSEE techniques were also applied to samples of lunar material with the objective of learning more about the thermal and radiation history of the moon. Also, registration of charged-particle tracks in insulating solids has proved to be of increasing practical value, with application in autoradiography with alpha particles and radon monitoring. More basic studies of track registration were made, with emphasis on alpha-particle registration in cellulose nitrate. (auth)

18800 (SC-T-71-3009) NEUTRON DOSIMETRY IN PLANTS TREATING IRRADIATED FUELS. Tabardel-Brian, Renee; Peyresblanques, H.; Sutra-Fourcade, Y. Translated for Sandia Labs., Albuquerque, N. Mex., from pp 397-413 of Symposium on Neutron Monitoring for Radiological Protection, Vienna, Austria, August 29-September 2, 1966. 19p. (CONF-660807-41). Dep. NTIS.

The neutrons are produced primarily by the (α,n) reaction with fluorine, which is used in the final stage of the process. The problem of dose assessment was solved in two stages: (1) Measurement of the spectra by multisphere detectors with ^{6}LiI(Eu) crystal detectors which, used in conjunction with a computer programme, makes it possible to obtain flux, neutron distribution and dose as a function of energy; and (2) Comparison of these results with the figures given by portable measuring instruments and the readings of personnel dosimeters which called for interpretation of the discrepancies and for the correction. (auth)

18801 SPECTROPHOTOMETRIC MEASUREMENT OF FERRIC ION CONCENTRATION IN THE FERROUS SULPHATE (FRICKE) DOSEMETER. Scharf, Karl (National Bureau of Standards, Washington, D. C.). Phys. Med. Biol.; 16: 77-86 (Jan 1971).

A systematic error in the spectrophotometric measurement of ferric ion concentrations in the ferrous sulphate dosimeter may be made by an incorrect evaluation of a non-linear spectrophotometric calibration curve. Methods are discussed for determining the radiation-produced change in molarity from the actual calibration curve, and a method of normalization of measured absorbances is suggested. Normalization factors, converting measured absorbances into normalized values, can either be calculated by choosing a reference value of the molar extinction coefficient, or can be determined by comparative absorbance measurements on two spectrophotometers, one of them being a precision instrument. Normalized absorbances are proportional to molarity and may be considered to be free of errors due to instrumental parameters and inaccuracies in acidity and temperature of solutions, and of errors in molarity if derived by comparative measurements. (auth)

18802 MEASUREMENTS OF HIGH DOSES WITH GLASS DOSIMETERS. Freytag, E. (Deutsches Electronen-Synchrotron, Hamburg). Health Phys.; 20: 93-4(Jan 1971).

The normal measurement range of 1 to 10^4 rad of radiophotoluminescence glass (RPL) dosimeters which are 1 mm diameter and 6 mm long was extended up to 10^9 rad. A calibration curve is given, measurements made with Ceric dosimeters are included for comparison. The curves are identical. (UK)

18803 IMPROVEMENTS IN AND RELATING TO THRESHOLD DOSIMETERS. Huebner, Klaus; Prokert, Konrad; Stolz, Werner (to Veb Fluorwerke Dohna). British Patent 1,210,047. 28 Oct 1970. Filed 7 Jul 1969.

Reference is made to plastic-based threshold dosimeters for use in the irradiation sterilization of medical equipment, the irradiation pasteurization of foodstuffs, and other similar technical applications of radiation at the MR level. Conventional color change threshold dosimeters have the disadvantage of poor transparency, making photometric evaluation difficult, and some systems are very sensitive to daylight. The dosimeter system described is claimed to avoid these disadvantages, and to provide, from ordinary commercially available starting materials, a simple and inexpensive dosimeter. The system employs an indicator dyestaff, a water-soluble organic halogen compound and a water-soluble buffer embedded in a transparent polyvinyl alcohol base. The indicator may be methyl orange, the halogen compound chloral hydrate, and the buffer sodium tetraborate. In this way the dosimeter consists of a transparent yellow foil having an adsorption maximum at 455 nm. A sharp color change from yellow to red occurs at an energy dose dependent on the chloral hydrate and tetraborate contents. The color change absorption maximum is at 525 nm and the change can be controlled for the range 0.5 to 10 MR. Production methods are described. (UK)

18804 METHOD AND DEVICE FOR READING THERMOLUMINESCENT DOSIMETERS. Chenault, Roger; Porrot, Emile; Portal, Guy; Prigent, Raymond (to Commissariat a l'Energie Atomique). British Patent 1,210,984. 4 Nov 1970. Priority date 18 Apr 1968, France.

A method of reading thermoluminescent dosimeters is proposed wherein the dosimeter is heated from the initial temperature to a predetermined temperature that is higher than the range of emission of peaks that are subject to fading. The dosimeter is maintained at this temperature for a sufficient time to ensure that the emission of peaks subject to fading is complete. The temperature of the dosimeter is then progressively increased to a temperature that is sufficient to cause the emission of all significant peaks and which is lower than the temperature that causes the emission of peaks related to phenomena other than the radiation dose received. The total light emission during the temperature rise is measured. A device for carrying out this method is proposed. (C.E.S.)

18805 PROCESS AND SYSTEM FOR MEASURING RADIATION DOSES USING AN IONISATION CHAMBER. Dieval, Michel; Rigaut, Henri (to commissariat a l'Energie Atomique). British Patent 1,218,296. 6 Jan 1971. Priority date 15 Sep 1967, France.

A process is described for measuring radiation doses using an ionization chamber and an integrating capacitor in which the electric charges collected in the chamber are accumulated and effect a change in the sign of the electric charges collected in the capacitor by changing the polarity of the collecting voltage of the ionization chamber whenever the voltage at the terminals of the capacitor reaches a predetermined value. Counting the number of changes enables the total integrated dose to be determined. (C.E.S.)

18806 SILICON DETECTOR AS ABSOLUTE GAMMA DOSIMETER. Berg, C. (Technische Univ., Hanover). Nucl. Instrum. Methods; 92: 21-7(1971). (In German).

Measuring absolute dose of high energy x- or γ-rays with the standard ionization chamber is rather difficult. A method is reported of measuring the dose in a dense material by separating a volume in electron equilibrium in a surface barrier detector. The active area is defined by a guard ring and the active depth is varied by the applied voltage. The conversion factor has been determined by injecting α-particles through the back contact in comparison with α-particles injected through the front contact. To eliminate the end of the active volume without a saturation field, the dose is evaluated from the slope of a plot, which shows absorbed energy as a function of the active depth. A ratemeter for automatic plotting is described. (auth)

18807 THERMOLUMINESCENT DOSIMETER FOR REPETITIVE ANALYSIS. Weissenberg, Gustav (to Ernst Leitz GmbH). U. S. Patent 3,531,641. 29 Sep 1970. Priority date 23 Dec 1965, Germany.

A dosimeter for repeated use for the measurement of ionizing radiation, such as beta and gamma rays, formed of a foil of thermoluminescent and synthetic material is described. The foil, when heated by infrared rays directed to the portion thereof desired, produces thermoluminescent light, which can be evaluated to determine quantitatively the original ionizing irradiation. The same foil can be used repeatedly for evaluation of a single dose of ionizing irradiation by subsequently heating single portions while heat-insulating the other parts of the foil. The synthetic material must tolerate the temperature at which the foil is heated by the infrared rays and must possess at least one strong absorption band in or adjacent to the infrared spectral region. (auth)

18808 INVESTIGATION OF THE GLUCOSE AND OXALIC ACID METHODS OF γ-RADIATION DOSIMETRY. Trusova, V. P.; Bologova, G. S.; Vasil'ev, A. V. This paper was summarized in At. Energ. (USSR); 26: 457(May 1969) as Paper No. 300/4947-4928. (In Russian).

It was found that the radiation chemical yield of the decomposition of glucose in aqueous solutions is unambiguously determined by its initial concentration and the absorbed dose of γ radiation and does not depend on the concentration after irradiation. Also, it was established that the radiation chemical yield of the decomposition of oxalic acid in aqueous solutions depends on the percent of its decomposition. Formulas for dose calculations are given. (W.H.K.)

18809 DOSE EQUIVALENT METER DESIGNS BASED ON TISSUE EQUIVALENT PROPORTIONAL COUNTERS. Baum, J. W.; Kuehner, A. V.; Chase, R. L. (Brookhaven National Lab., Upton, N. Y.). Health Phys.; 19: 813-24(Dec 1970).

The spectrum of pulses obtained from a suitably designed spherical tissue equivalent proportional counter contains the information necessary to determine dose, dose equivalent, and quality factor in mixed radiation fields. Use of multi-channel analyzers and tedious data reduction can be avoided by means of specially designed operational amplifier circuits described previously. Alternate methods of operating on the pulse spectrum were investigated to achieve direct-reading dose equivalent instruments. These methods include: (a) use of multiple fixed discriminators, (b) periodically varying the discrimination level, (c) periodically varying the gas gain, (d) use of multi-detector systems with biased amplifiers, and (e) use of a single detector with current measurement plus biased amplifiers for pulse weighting. Required gain, discrimination and sensitivity functions for each method have been calculated for typical instrument designs. Advantages and limitations of each system are discussed. The single detector with current measurement and two biased amplifiers seems promising for general use since it reduces both the range of pulse sizes and the range of counting rates which must be handled in a mixed LET field and employs fairly simple circuits. (auth) (UK)

18810 RECENT IMPROVEMENTS IN FLUORO-GLASS DOSIMETER. Yokota, Ryosuke; Mutoh, Yuhei; Fukuda, Kiyoshi (Tokyo Shibaura Electric Co., Ltd.). Toshiba Rev., Int. Ed.; No. 52, 27-33(Dec 1970).

More sensitive, less energy-dependent glasses with less predose have been developed for the fluoro-glass dosimeter; independence on energy in the range of 2 MeV to 30 keV is thereby assured. The 10-mR exposure dose can be measured more accurately. Another kind of glass suitable for β-ray measurement has been developed; it can also measure β rays and γ rays separately. A method of determining the incident energy and its direction is described. Comparison of glass dosimeters and film dosimeters reveals that the former have better performance. (auth)

18811 NEW TRENDS IN PERSONNEL DOSIMETRY. Becker, Klaus (Oak Ridge National Lab., Tenn.). Oak Ridge Nat. Lab. Rev.; 3: No. 5, 1-5(Fall 1970).

A general review of personnel dosimetry is presented. Etching of alpha tracks in thin plastic foils is discussed, as well as a spark technique for rendering these holes more easily visible with the use of aluminized Mylar foil. Recent results in exoelectron dosimetry, which can be used at temperatures up to 700°C, are reviewed. (R.W.R.)

18812 THERMOLUMINESCENCE: A BETTER WAY TO MONITOR RADIATION EXPOSURE. Pearce, Clyde E. (Bethesda Memorial Hospital, Boynton Beach, Fla.). Radiol. Technol.; 42: 259-65(Jan 1971).

The development and use of thermoluminescent dosimeters for monitoring radiation exposure are described. (W.H.K.)

18813 STUDY OF THE THERMOLUMINESCENT PROPERTIES OF KOREAN NATURAL QUARTZ FOR POSSIBLE USE IN GAMMA-RAY DOSIMETRY. Lee, Hee Yong; Kim, Hi Gyu; Lee, Chul (Atomic Energy Research Inst., Seoul). J. Korean Nucl. Soc.; 2: 229-39(Dec 1970).

Various thermoluminescent properties of Korean natural quartz for possible use in γ-ray dosimetry has been studied. If the heating is exactly linear, γ-irradiated radiation sensitive (type 1) α-quartz yields a glow curve of single peak, hence glow peak height could be related to the γ-dose. Quartz crystal dosimeters exhibited the linearity of thermoluminescent intensity in the range from about 2×10^3 to 2×10^6R, and also had an advantage of low fading because of the high peak temperature (200 ± 40°C). The pulverized quartz sample having the grain size of $0.3 < \phi < 0.9$mm showed the linearity of T. L. intensity in the range from 50 to 2×10^3R. Therapeutic application of the pulverized sample for the correct measurement of the absorbed dose in a body region of a cancer patient is feasible. (auth)

Radiometric Instruments

Refer also to abstract 20228.

18814 (CSIRO-Trans-9992) SPECTROMETRIC SCINTILLATION EQUIPMENT OF COMMERCIAL APPLICATION FOR RADIOACTIVE LOGGING OF BOREHOLES IN ORE DEPOSITS. Migunov, B. B.; Kholin, V. N.; Kharitonov, S. E. Translated by G. Hitoun (Australian Atomic Energy Commission), from Geofiz. Sb., Akad. Nauk Ukr. SSR, Inst. Geofiz.; No. 23, 80-4(1968). 6p. Dep. NTIS (U. S. Sales Only).

Gamma logging, neutron-neutron logging and neutron-gamma logging with a 20 and 22 cm probe using sources ^{137}Cs (10 mCi) and ^{60}Co (6 mCi) gave well-differentiated curves, using spectrometric scintillation equipment. A block diagram of the borehole apparatus is shown. The detector is a photomultiplier tube with NaI(Te) crystal. An energy gap in regions of small gamma radiation energy is created by arithmetic adding of standardized pulses of different duration, coming simultaneously from two flip-flop circuits with differing triggering thresholds fed into a common transformer. Some composite logging results are given. (Australia)

18815 (INP-715) CALIBRATION OF RADIOMETRIC PROBES FOR SOIL DENSITY MEASUREMENTS. Czubek, Jan A. (Institute of Nuclear Research, Krakow (Poland)). Jul 1970. 17p. (CONF-700947-1). Dep. NTIS (U. S. Sales Only).

From Seminar on Soil Mechanics and Foundation Engineering, Lodz, Poland.

A semi-empirical formula for the calibration curve of the gamma-gamma probe is presented as a function of: soil bulk density, soil chemical composition, source-detector spacing, and construction parameters of the probe. The possibility of elimination of the influence of such parameters as the chemical composition of the soil and the geometrical conditions of measurement on the probe response is discussed, using the so-called two-detector probe principle. The method of application of the semi-empirical formula for density probe calibration using a small number of models is also given, using the universal calibration curve principle. (auth)

18816 APPLICATION OF ONE-DIMENSIONAL TRANSPORT THEORY TO THE SUBSURFACE GAMMA-SCATTER DENSITY PROBE. Christensen, E. R. (Technical Univ., Lyngby, Denmark). Nucl. Instrum. Methods; 91: 461-8(1971).

Theoretical calibration curves for the subsurface gamma-scatter density probe are derived. The derivation is based on solution of the one-dimensional transport equation implemented by generally available computer programmes, DTF IV and GAMLEG. Some comparisons with experiments with the BASC equipment are performed. In the BASC mode of operation with weak soil-type dependence, it is shown that good agreement between theory and experiments can be obtained, except at high densities. One experimentally determined parameter is used. In the BASC mode of operation with strong soil-type dependence, good agreement between theory and experiments may be obtained by means of two experimentally determined parameters. The gain by using the outlined method of derivation of calibration curves rather than the simpler techniques usually applied, based on semi-empirical formulas, is that the number of experimentally fitted parameters is reduced from three or more to one or two. (auth)

18817 APPARATUS FOR MEASURING CALORIFIC VALUE OF PETROLEUM. Uchida, Yoshihisa; Miyashita, Kyoichi; Takada, Mamoru (to Mitsubishi Denki Kabushiki Kaisha). British Patent 1,210,756. 28 Oct 1970. Filed 1 Oct 1968.

Apparatus is described for measuring the calorific value of petroleum flowing through a pipe-line, without the need for sampling, making use of the neutron thermalizing properties of the petroleum. A source of fast neutrons is provided, together with a thermal neutron detector. The source and detector may be located outside or inside the pipe-line. Preferably the neutron counter tube is located within the pipe-line and contains the fast neutron source and thermal neutron detector in closely spaced relationship. Means are adopted to prevent any vibration that may occur in the pipe-line from being transmitted to the source and detector. The count rate provides a measure of the amount of H per unit volume of the petroleum. The calorific value of the latter is related to the C/H ratio and by dividing the thermal neutron count rate by the n power of the specific gravity, where n depends on the geometric parameters of the pipe-line, the ratio of C to H and accordingly the calorific value per unit weight of the petroleum can be determined. (UK)

18818 RADIATION SENSITIVE NOTCH PATTERN DETECTION SYSTEM. St. John, Karl M.; Kerbel, Sheldon J. (to Hazeltine Corp.). U. S. Patent 3,541,339. 17 Nov 1970. Filed 28 Mar 1968.

Disclosed is apparatus for detecting the presence of a selected notch pattern in a moving ribbon of material as the ribbon moves through an observation position. The apparatus supplies two radiation beams, each along an axis which intersects the observation position and any ribbon moving therethrough. Another portion of the apparatus, namely a pair of radiation detectors coupled to logic circuitry, is responsive to the beams of radiation and to the effect produced thereon by the movement through the observation position of an increment of the ribbon bearing a selected notch pattern, and develops an output indication each time such an increment bearing the selected notch pattern moves through the observation position. Other embodiments are covered. (auth)

18819 IMPROVEMENTS IN OR RELATING TO TIME-KEEPING SYSTEMS WITH A RADIOACTIVE TIMEKEEPING STANDARD. Koehler, Dale Roland; Grissom, John Thomas. British Patent 1,217,271. 31 Dec 1970. Filed 20 Jun 1968.

A timekeeping system is described that comprises a standard consisting of radioactive material having a half-life of at least 10^4 years and that emits γ-particles at a high statistical rate, together with solid state means to detect the particles and produce a corresponding number of electrical pulses. Scalar means are coupled to the standard to produce a single control pulse for a predetermined number of particles, at a constant low rate, and a time register is coupled to the scalar means, responsive to the control pulses so as to produce time indications. The radioactive source may comprise ^{242}Pu or ^{233}U, but is preferably ^{237}Np, and the solid state detector may be of the diffused junction, silicon surface barrier type, or a transistor counter. The source material may be mounted on the detector, or a scintillator may be interposed between the source and detector, or the source material may be dispersed in a scintillator. Various electronic arrangements are described. (UK)

18820 RADIATION FILL GAUGE. Badgett, Charles O. (to Industrial Nucleonics Corp.). U. S. Patent 3,531,638. 29 Sep 1970. Filed 23 Oct 1965.

A radiometric material fill gage for a vessel is provided by mounting a radiation detector responsive to radiation from any direction in the center of the vessel. A coating of radioactive material is deposited around the inside walls of the vessel to direct radiation through the material, regardless of its orientation, toward the centrally located detector. In a specific embodiment, the detector comprises a sphere of scintillating material coupled to a photomultiplier to provide a signal indicative of material fill. (auth)

18821 BETA-ABSORPTION-IMPACTOR AEROSOL MASS MONITOR. Lilienfeld, Pedro (GCA Corp., Bedford, Mass.). Amer. Ind. Hyg. Ass. J.; 31: 722-9(Nov-Dec 1970).

A sensitive, real-time, airborne-dust mass monitor is developed. Its operation is based on the measurement of beta-radiation absorption by aerosol particles collected onto a small area by means of inertial impaction. The device collects particles of unity density larger than 0.3 μm in diameter with nearly 100% efficiency at a flowrate of 20 liters/minute. A typical atmospheric mass concentration of 100 $\mu g/m^3$ can be evaluated in less than one minute with the use of a one millicurie ^{14}C source. (auth)

18822 PASSIVE DEVICE FOR DETERMINING RELATIVE ROTATION. Eddy, William C. Jr.; Scheiwe, John P. (to Industrial Nucleonics Corp.). U. S. Patent 3,531,997. 6 Oct 1970. Filed 30 Jun 1967.

An inertial instrument that includes a passive source on the inertial element formed as a pattern of interstitially retained inert gas radioisotope which does not appreciably alter the mass of the inertial element is described. The inert gas radioisotope is ^{85}Kr, the atoms of which are retained in the lattice of the material of the inertial element. Detectors are positioned to sense the radioactive and non-radioactive areas of the pattern to produce an output signal which is digital and representative of the relative displacement of the inertial element. (auth)

18823 DEVICE FOR STUDYING ELECTRON BACKSCATTERING FROM LAYERS OF MATERIALS. Rudenko, V. N.; Karataev, V. D.; Kurbakov, V. I. (Tomsk Polytechnic Inst., USSR). Izv. Vyssh. Ucheb. Zaved., Fiz.; No. 10, 138-40(1970). (In Russian).

Descriptions are given of a device for studying coefficients of 0.5- to 14-MeV electron backscattering on various materials with atomic number ranging from Be to U. The device is capable of recording smooth changes of the angles of electron reflection at 30 to 165° and discrete variations of the angle of incidence from 25 to 80°. Experimental data were obtained on the dependence of the intensity of backward electron scattering on the thickness of Al, Cu, and Cd on Pb. Variations in the intensity of electron backscattering may be used for determining the thickness of coatings. (R.V.J.)

18824 THICKNESS MEASUREMENT BY RADIATION IN THE PROCESS OF MANUFACTURING AUTOMOBILE TIRES. Toyama, Masaaki; Moriya, Masatoshi (Yokogawa Electric Works, Ltd., Tokyo). Otomeshon; 15: No. 2, 38-43(Feb 1970). (In Japanese).

Proper control of automobile tire cord coating with rubber is important both in quality and manufacture-cost aspects. By way of explanation of the present method, two pairs of rollers are used; rubber material is set in the upper gap between the rollers of each pair. Rubber runs out along the circumference of one of the rollers. A rubber sheet, produced by the joining, comes out appropriately while the cord is coated. The radiation thickness measurement reported is for a rubber layer, in particular, running along the said circumferences; it is based on the backscattering of radiation from the rubber layer. The radiation used is beta rays from ^{90}Sr; the detector employs an ionization chamber. The penetration thickness measurement applied to the finished coating of a cord is also described. (Japan)

18825 FUNDAMENTAL STUDIES ON RADIATION THICKNESS GAUGE. V. GAUGING AND CONTROL OF THICKNESS OF MOVING PLATE. Koyanagi, Takami (Niigata Univ., Japan). Radioisotopes (Tokyo); 20: 72-7(Feb 1971). (In Japanese).

For thickness measurements of moving plates with radiation thickness gage, the response is varied by the spatial frequency of irregularity of thickness ν(rad/cm), and the moving speed of the plate v(cm/sec). One of the reasons is that the area and shape of cross-section of the radiation-flow acts as a kind of spatial low pass filter. This characteristic can be described by the spatial transfer function or response function. The Bode-diagrams are given with rectangular and circular cross-section. In these diagrams the gains come to zero periodically and the phases reverse at these points. Such a character is observed in many optical transfer functions, but cannot be seen in common control systems. The "dead time," such as the traveling time of rolled material between roll and thickness gage in rolling mills, is in inverse proportion to the moving speed, but in the spatial domain the time is transformed into "dead distance." It is the distance between the roll and thickness gage itself, and has no relation to the speed of the plate. The response function of normal electrical or mechanical elements can be obtained from their transfer function simply by replacing the Laplace operator's with $j\nu$. The analysis and synthesis of the control systems consisting of such elements can be easier to make in the spatial domain than in the time domain. Several exercises of synthesis are made. The results point out that the "dead distance" always exists and affects the stability of control system. (auth)

Miscellaneous Instruments and Components

Refer also to abstracts 18652–18654, 18673, 18737, 19227, 19249, 19663, 19782, 19783, 19847, 20168, 20175, and 20177.

18826 (AE–409) X-RAY POWDER DIFFRACTION WITH GUINIER–HAEGG FOCUSING CAMERAS. Brown, Allan (Aktiebolaget Atomenergi, Studsvik (Sweden)). 1970. 101p. Dep. NTIS (U. S. Sales Only).

The Guinier–Hägg focusing camera is discussed with reference to its use as an instrument for rapid phase analysis. An actual camera and the alignment procedure employed in its setting up are described. The results obtained with the instrument are compared with those obtained with Debye–Scherrer cameras and powder diffractometers. Exposure times of 15 to 30 minutes with compounds of simple structure are roughly one-sixth of those required for Debye–Scherrer patterns. Coupled with the lower background resulting from the use of a monochromatic X-ray beam, the shorter exposure time gives a ten-fold increase in sensitivity for the detection of minor phases as compared with the Debye–Scherrer camera. Attention is paid to the precautions taken to obtain reliable Bragg angles from Guinier–Hägg film measurements, with particular reference to calibration procedures. The evaluation of unit cell parameters from Guinier–Hägg data is discussed together with the application of tests for the presence of angle-dependent systematic errors. It is concluded that with proper calibration procedures and least squares treatment of the data, accuracies of the order of 0.005% are attainable. A compilation of diffraction data for a number of compounds examined in the Active Central Laboratory at Studsvik is presented to exemplify the scope of this type of powder camera. (auth)

18827 (BRH/DEP–70–31) INEXPENSIVE READOUT FOR A COMMERCIAL THERMOCOUPLE MICROWAVE POWER DENSITY PROBE. Cloke, Robert L. (Bureau of Radiological Health, Rockville, Md. Div. of Electronic Products). Dec 1970. 13p. NTIS.

An inexpensive, easy-to-build readout circuit which can be used with the Narda 8122 thermocouple microwave power density probe is described. The instrument is capable of reading full-scale power densities of 10 mW/cm^2 and 100 mW/cm^2 at frequencies of 915 MHz and 2450 MHz, and includes all of the necessary features of the Narda 8100 system. (auth)

18828 (EUR-CEA-FC–576) AN IMPROVEMENT TO THE QUANTUM YIELD OF THE PHOTOCATHODES OF THE 56 TVP PHOTOMULTIPLIERS IN THE RED PART OF THE SPECTRUM (7000 A). Hesse, M.; Tittel, O. (Commissariat a l'Energie Atomique, Fontenay-aux-Roses (France). Centre d'Etudes Nucleaires). Dec 1970. 23p. (In French). Dep. NTIS (U. S. Sales Only).

The point sensitivity of a photomultiplier was examined. When illuminated with monochromatic radiation (6900 Å), a three fold variation in sensitivity across the surface was observed. The use of an improved light input system compared to the normal central method led to a seven fold improvement in sensitivity. (auth) (France)

18829 (JINR–P9–5441) MAGNETIC FIELD OF THICK FINITE dc SOLENOIDS. Danilov, V. I.; Ianovich, M. (Joint Inst. for Nuclear Research, Dubna (USSR). Lab. of Nuclear Problems). 1970. 26p. (In Russian). Dep. NTIS (U. S. Sales Only).

The expressions of the magnetic components in/or around any thick finite dc solenoid were obtained from the expression of the vector potential of a circular current loop. The field component derivatives with respect to the spatial coordinates were also determined. From these general expressions the field of semi-infinite solenoids with zero inner radius was deduced as a particular case. (auth)

18830 (NYO–3906–12) ULTRASONIC THERMOMETRY IN LMFBR SYSTEMS. Progress Report Covering the Quarter Ending September 30, 1970. Papadakis, E. P.; Patch, D. R.; Lynnworth, L. C.; Carnevale, E. H. (Panametrics, Inc., Waltham, Mass.). Contract AT(30-1)-3906. 13p. Dep. NTIS.

The development of the FFTF simulation oven and ORTC-4 noncomposite lines is discussed, and calibration data for rhenium and tungsten/rhenium ultrasonic thermometer sensors are presented. (W.H.K.)

18831 (UCRL–50892(Vol.1)) WEAPONS EFFECTS DISPLAY SYSTEM (WEDS MOD II): MATHEMATICAL MODELS USED FOR CALCULATIONS. Berndt, C. W.; Ferguson, D. E. (California Univ., Livermore. Lawrence Radiation Lab.). Jan 1971. 26p. Dep. NTIS.

A description of the mathematical models used to develop the computer programs for both the prompt nuclear effects and the fallout calculations used by the Weapons Effects Display System (WEDS MOD II) is presented. The assumptions made to simplify these programs are noted and sources of error are discussed. Desirable features for greater utility and possible inclusion in a next generation of machines are described. (auth)

18832 (UCRL–50892(Vol.6)) WEAPONS EFFECT DISPLAY SYSTEM (WEDS MOD II): PROMPT EFFECTS COMPUTER PROGRAM. Franklin, Paul (California Univ., Livermore. Lawrence Radiation Lab.). Dec 1970. 346p. Dep. NTIS.

The prompt effects computer program that has been developed by Lawrence Radiation Laboratory for WEDS MOD II is described. The program organization, data, procedures for changing the program, and a complete listing of all prompt effects software details are given. (auth)

18833 USE OF HALL PROBES IN INHOMOGENEOUS MAGNETIC FIELDS. Turin, M. (CEN, Saclay, France). Nucl. Instrum. Methods; 91: 621-5(1971). (In French).

The user of Hall probes must be aware of specific errors appearing in strongly inhomogeneous magnetic fields. It is pointed out that if the Hall plate is not perpendicular with the magnetic field direction, the component in the plane of the plate may introduce errors greater than one per cent on the measured component although normal to the Hall plate. (auth)

18834 AUTOMATIC COMPENSATING INSTRUMENT FOR MEASURING LOW ELECTRIC DIRECT CURRENTS. Cloos, O.; Heigwer, G. (Gesellschaft fuer Strahlenforschung mbH, Frankfurt am Main). Nucl. Instrum. Methods; 91: 633-5(1971).

The circuit of an automatic compensating instrument is described. The instrument consists of two identical measuring circuits, which measure low electric direct currents by Townsend's method. The potential difference between the input of the instrument and the ground does not exceed 40 mV. This instrument allows the average values of direct currents down to 10^{-10} A to be measured, which are fluctuating. The relative error is at most 10^{-3} in automatic measurements and $<10^{-4}$ for manual measurement. (auth)

18835 MASS SPECTRAL DATA PROCESSING. 2. COMPUTER USED FOR PROCESSING A MASS SPECTRA RECORDED ON MAGNETIC TAPE. Jansson, Per-Aake; Melkersson, Sune; Ryhage, Ragnar; Wikstroem, Sten (Karolinska Institutet, Stockholm). Ark. Kem.; 31: 565-78(Aug 1970).

Analog and digital computer programs were developed for processing of mass spectral data considering background spectra and normalization of resulting data. The output alternatives are bar-graphs or table printouts. Off line procedures were adopted. Input data were recorded on digital or analog magnetic tape records as mass spectral data and information from an electronic mass marker. (Sweden)

18836 HIGH RESOLUTION STUDY OF SOFT X RAYS FROM COLLISIONS OF 1 MeV H_2^+ AND 500 keV Ar^+ WITH CARBON. Boster, T. A.; Der, R. C.; Fortner, R. J.; Kavanagh, T. M.; Khan, J. M. (Univ. of California, Livermore). Nucl. Instrum. Methods; 91: 555-6(1971).

A Johann-type spectrometer with lead stearate analyzer was used to investigate the carbon-K X-ray emission lines produced from 1 MeV $H_2^+ \rightarrow$ carbon and 500 keV $Ar^+ \rightarrow$ carbon collisions. (auth)

18837 OPERATION OF THE GAGES WITH A SCREENED COLLECTOR. Bernardet, H.; Choumoff, P. S. (Societe Generale du Vide, Paris). Vide; 25: No. 148-149, 167-71 (Jul-Oct 1970). (In French).

An ionization gage was developed which has a good sensitivity and flatter characteristics than the GROSZKOWSKI and MELFI gages or the REDHEAD extractor gage. The effect of various parameters was studied: the charge on the conductive coating of the bulb influencing the electron density at any point within the anode volume or influencing the ion extraction; and the geometry of, and the voltage on the metal screen surrounding the collector having an influence on ion extraction. The effect of the potential produced by the ionizing electrons depends upon the anode transparence. If the anode is made less transparent the variation in sensitivity diminishes e.g., 28 $torr^{-1}$ (10 mA) to 19 $torr^{-1}$ (0.1 mA) may be obtained instead of 35 $torr^{-1}$ (10 mA) and 7 $torr^{-1}$ (0.1 mA). The gage described exhibits a linear dependence of ion current on pressure between 10^{-5} and 10^{-12} torr. (auth) (France)

18838 PROPERTIES OF ULTRA HIGH VACUUM EXTRACTOR GAGES. Kocian, P.; Barz, A. (Leybold-Heraeus GmbH, Cologne). Vide; 25: No. 148-149, 172-6(Jul-Oct 1970). (In French).

Accurate measurement of pressures below 10^{-9} torr is only possible when the gage is incorporated in the system. Certain modifications are required for an extraction gage if it is to be incorporated in such a system (these modifications have been described by REDHEAD). A modified extractor gage covering a pressure range between 10^{-4} and 10^{-12} torr is described. The sensitivity of this gage is 8.5^{-1} torr for emission currents less than 5 mA. Two important factors influencing the gages performance are ion desorption and the x-ray effect. (auth) (France)

18839 METER FOR MEASURING RMS VALUES OF PULSED CURRENT SIGNALS. Visser, Age T. (to United States Atomic Energy Commission). United States Patent 3,521,165. 21 Jul 1970. Filed 20 Sep 1968.

A pulsed signal RMS meter includes, connected across the signal, a resistor which is temperature-sensitive to the RMS value of the pulsed signal and has a thermal time constant greater than the time separation of the pulsed signals to remain relatively insensitive thereto. Thermocouples monitor the temperature of the resistor and provide an output which, when recorded, is a measure of the RMS value of the applied pulsed signal. (auth)

18840 PILE-UP DISCRIMINATION TECHNIQUE. Schwartz, Robert J. (to Schlumberger Tech. Corp.). United States Patent 3,525,047. 18 Aug 1970. Filed 5 Dec 1967.

An illustrative embodiment of the invention identifies individual radiation detector signals that have merged into one pulse as a result of signal amplification. A circuit samples the amplitude of the pulse, and a variable amplitude wave generator responds at a specific time relative to the sample by producing a facsimile of a single amplified detector signal appropriate to the sampled pulse amplitude. A further circuit then subtracts the facsimile pulse from the amplifier pulse. If the two pulses are identical, as indicated by a negligible difference between them, the sampled pulse represents an individual detector signal and is not a "pile-up" of several amplified detector signals. If the residue is significant, however, the sampled pulse is a composite of several amplified and overlapping detector signals. This residue then enables a counting circuit register to indicate an additional detector signal or signals. (auth)

18841 TANDEM MASS SPECTROMETER FOR SECONDARY ION STUDIES. Benninghoven, A.; Loebach, E. (Univ., Cologne). Rev. Sci. Instrum.; 42: 49-52(Jan 1971).

An instrument permitting the study of ionization processes caused by ion and electron impact on solid surfaces under well defined conditions is described. It consists functionally of a single focusing mass spectrometer providing a monoisotopic and monoenergetic primary beam and a quadrupole mass spectrometer for the analysis of secondary ions released from a target surface. Low primary ion current densities and ultrahigh vacuum conditions allow investigations without essential alterations of the target surface during experiment. Some results demonstrating instrument performance are presented. (auth)

18842 SUPERCOLLIMATION OF NEGATIVE ION BEAMS WITH APERTURES. Armstrong, D. D. (Los Alamos Scientific Lab., N. Mex.); Wegner, H. E. Rev. Sci. Instrum.; 42: 40-4 (Jan 1971).

A technique for producing highly collimated beams of negative ions using apertures is discussed. The application of the method produced a 30 μ diam H^- beam with an angular divergence of 1.5 mdeg. The results of a study of the small angle scattering of protons from a carbon are presented. Other possible applications are outlined. (auth)

18843 STUDY OF CALIBRATION, RESOLUTION, AND TRANSMISSION OF ELECTROSTATIC VELOCITY SELECTOR. Leventhal, J. J.; North, G. R. (Univ. of Missouri, St. Louis). Rev. Sci. Instrum.; 42: 120-3(Jan 1971).

The calibration, transmission, and resolution of a 127° cylindrical electrostatic velocity selector are examined as functions of the individual voltages applied to the electrodes. The calibration and resolution calculated using first order orbit theory are compared with numerically determined orbits obtained using the exact electrostatic field within the selector. The calibration and transmission are found to be strongly dependent on the electrode potentials while the resolution is insensitive to these parameters. The experimentally determined resolution is in good agreement with the calculations. Variation of the transmission with the individually applied voltage is shown to be the result of vertical focusing. (auth)

18844 LIGHT PEN USED FOR NUCLEAR DATA PROCESSING. Morvan, P. (CEN de Saclay, Gif-sur-Yvette, France). Nucl. Instrum. Methods; 91: 657-8(1971). (In French).

A light pen for man to machine communication with graphic display especially designed for nuclear data processing is described. (auth)

18845 DATA TRANSMISSION IN THE MEASUREMENT-COMPUTING COMPLEX OF THE JOINT INSTITUTE FOR NUCLEAR RESEARCH. Zabiyakin, G. I.; Lysenko, Z. V.; Polyakov, V. N. (Joint Inst. for Nuclear Research, Dubna, USSR). Instrum. Exp. Tech. (USSR) (Engl. Transl.); No. 2, 409-14(Mar-Apr 1970).

Translated from Prib. Tekh. Eksp.; No. 2, 90-5(Mar-Apr 1970).

Problems of transmitting digital information in a system consisting of a measurement-computing complex at a physics research center are considered. The feasibility of using a symmetrical trunk cable of the MKSB type for data transmission in such systems over a distance of 5 to 7 km at a rate of ~500 kbits/sec is shown. (auth)

18846 TIME–AMPLITUDE CONVERTER FOR THE NANOSECOND RANGE. Sidorov, L. V. Instrum. Exp. Tech. (USSR) (Engl. Transl.); No. 2, 434-7(Mar-Apr 1970).

Translated from Prib. Tekh. Eksp.; No. 2, 111-14(Mar-Apr 1970).

A circuit is given for a time-amplitude converter operating in the nanosecond range in an overlap mode. The resolving time for recording $\gamma - \gamma$-coincidences from ^{60}Co (the width at the half-height) is ≃1.0 nsec for a load of $\sim 10^5$ sec^{-1} and a range on input-pulse amplitudes ≃20 V in both channels. The drift of the time scale of the converter is ≃0.4 nsec in 12.5 hr. (auth)

18847 PULSE AMPLITUDE DISCRIMINATORS BASED ON AVALANCHE TRANSISTORS. Ali-Zade, D. G.; Dyakonov, V. P. (Inst. of Petroleum and Chemistry, Baku). Instrum. Exp. Tech. (USSR) (Engl. Transl.); No. 2, 431-3(Mar-Apr 1970).

Translated from Prib. Tekh. Eksp.; No. 2, 108-10(Mar-Apr 1970).

Pulse-amplitude discriminators based on avalanche transistors having a minimum value of the discrimination threshold ~20 mV for a threshold avalanche factor equal to several hundred are described. Methods of controlling the discrimination threshold and reducing the recovery times to 100 nsec are described. Results are given of an experimental investigation of discriminator circuits. The discriminators can be used for a pulse duration of the order of several nsec or more. (auth)

18848 DISCRETE FREQUENCY SWEEP IN A SYNTHESIZER FOR NUCLEAR MAGNETIC RESONANCE SPECTROSCOPY. Zabrodin, V. A.; Solovev, V. E.; Kirillov, P. K.; Tikhonov, K. A.; Galperin, L. N. (Inst. of Chemical Physics, Moscow). Instrum. Exp. Tech. (USSR) (Engl. Transl.); No. 2, 494-8(Mar-Apr 1970).

Translated from Prib. Tekh. Eksp.; No. 2, 158-61(Mar-Apr 1970).

A synthesizer with automatic discrete variation of the frequency in the 0 to 10 kHz range in steps of 0.01 Hz or in the 0 to 100 kHz range in steps of 0.1 Hz is described. The instrument is designed for use in nuclear magnetic resonance spectroscopy. (auth)

18849 ELECTROSTATIC SPECTROMETER OF CHARGED PARTICLE BEAMS WITH RING FOCUSSING IN THE FIELD OF A CYLINDRICAL CONDENSER. Zashkvara, V. V.; Korsunskii, M. I.; Red'kin, V. S.; Masyagin, V. E. (Inst. of Nuclear Physics, Alma-Ata, USSR). Instrum. Exp. Tech. (USSR) (Engl. Transl.); No. 2, 348-50(Mar-Apr 1970).

Translated from Prib. Tekh. Eksp.; No. 2, 39-41(Mar-Apr 1970).

A spectrometer is described which differs from the existing electrostatic spectrometers with ring focussing in two special features: 1) a second order focussing in the angle of divergence of the beam of charged particles is accomplished in the spectrometer and 2) a filtering is provided for the charged particles,

XUM

the angular components of whose velocities at the entrance into the field are significantly different from zero. (auth)

18850 ELECTRON GUN HAVING AN ELECTRON OUTPUT FROM A VACUUM INTO GAS. Trokhan, A. M.; Zelikson, D. L. Instrum. Exp. Tech. (USSR) (Engl. Transl.); No. 2, 538-9(Mar-Apr 1970).

Translated from Prib. Tekh. Eksp.; No. 2, 195-6(Mar-Apr 1970).

A small-sized, removable electron gun, the electron beam of which has energy up to 40 keV and current up to 10 mA and is introduced into gas through a differential gasodynamic window with the aid of an indicator showing the beam's position relative to the window openings is described. (auth)

18851 ARE GAS-FILLED MAGNETIC SEPARATORS A USEFUL TOOL TO INVESTIGATE HEAVY FAST RECOILS FROM NUCLEAR REACTIONS. Armbruster, P.; Eidens, J.; Grueter, J. W.; (and others) (Kernforschungsanlage, Juelich, Ger.). Nucl. Instrum. Methods; 91: 499-507(1971).

Gas-filled magnetic separators have been used in recent years, mainly in experiments with fission products. The need to find new techniques to investigate heavy recoils from heavy-ion reactions raise the question whether the above technique will have further future applications. Its main specific features, as calibration, resolving power, and efficiency, are discussed. The necessity of further data on mean ionic-charge values of heavy fast ions is shown in order to get reliable extrapolations for nuclei heavier than A = 150 and faster than 0.5 MeV/nucl. If a calibration with already known nuclides is possible, gas-filled magnetic recoil separators will be a useful tool to identify new short-lived species and to investigate the reactions in which the latter are produced. Together with Wien filters, which reduce the velocity spread of the recoils to values smaller than a few percent, they may then be used to measure the energy and mass of recoils with lifetimes larger than 1 μsec produced in heavy-ion reactions. (auth)

18852 DATA ACQUISITION AND ANALYSIS SYSTEM FOR NUCLEAR PHYSICS. Wery, M.; Ring, C.; Bueb, B.; Wittmer, P. (CRN, Strasbourg). Nucl. Instrum. Methods; 91: 333-9(1971). (In French).

The logic of hard- and software interfaces for collection and analysis of nuclear data with an IBM 1800 computer is described. Data acquisition is performed either by a direct transfer from 4096-channel analyzers or from a fast paper-type reader. Both are interfaced to a digital input. A C.R.T. display, a function keyboard, and an IBM printer keyboard provide flexible and efficient facilities for data analysis. The experimentalist has easy access to these non-standard input–output units by FORTRAN CALL instructions. Thus, using such a low-cost interface system, he can build self-tailored procedures for fast and reliable acquisition, as well as for interactive data reduction. This enables him to analyze the data and obtain results during the experiment. (auth)

18853 PSEUDORANDOM PULSE GENERATOR FOR A UNIFORM AMPLITUDE DISTRIBUTION WITH DISCRETE LINES. Denert, E.; Friese, T.; Streng, W. (Hahn-Meitner-Institut fuer Kernforschung, Berlin). Nucl. Instrum. Methods; 91: 327-31(1971).

For calibrating and testing pulse-height-analyzing equipment a generator was built supplying a uniform pulse-height distribution superposed by one valley and $2^n - 2$ peaks or one peak and $2^n - 2$ valleys ($n = 1, 2, 3\ldots$). The distribution is produced by a 12-bit DAC which is controlled by pseudorandom binary numbers; these are generated as the sum of a 12-bit linear feedback shift register and a binary counter, the carry bit being suppressed. In the sequence of these binary numbers special jump heights dominate. When the DAC is followed by a lead network, the special jump heights generate shifts of 2^n blocks of the uniform distribution in such a manner that a gap opens in the middle of the distribution, while the superposition of the other block limits yields peaks. The inherent differential nonlinearity of the DAC is nearly completely blurred by the lead circuit. With a lag network peaks are changed into valleys and the middle gap becomes a peak. The method has an accuracy of about 2×10^{-4}. (auth)

18854 DEVICE FOR PRODUCING AND MONITORING HYDRATED ELECTRONS. Hart, Edwin J.; Schmidt, Klaus H. (to United States Atomic Energy Commission). U. S. Patent 3,535,087. 20 Oct 1970. Filed 28 Oct 1968.

A relatively simple photolytic device for producing and detecting hydrated electrons in sufficient quantities and with adequate sensitivity to be useful for demonstration, research and analytical purposes is described. Also a spherical mirror arrangement which increases the sensitivity of the detection system, permitting smaller quantities of hydrated electrons to be analyzed than would otherwise be possible. (auth)

18855 AUTOMATIC ADJUSTMENT OF THE SIMULATED SOURCE ON AN ANALOG REACTIVITY METER. Deiss, Marcel (to Commissariat a l'Energie Atomique). French Patent 1,588,079. 23 Feb 1970. Filed 28 Oct 1968. (In French).

A procedure for controlling the voltage simulating an apparent neutron source in an analog reactivity meter, yielding directly and instantaneously the reactivity, is described. The procedure consists of inducing a rapid variation in reactivity, producing a signal representing the derivative of the reactivity evaluated by the reactivity meter and modifying the voltage in relation to the amplitude and sign of the signal. Voltage corrections are made in a discrete way so that information arising from control voltage counter effects is preserved. In certain cases several correction sequences can be envisaged. (France)

18856 HONEYCOMB BLOCK USED FOR COLLIMATION OF RADIATIONS AND METHOD OF MANUFACTURING THE SAME. Abe, Isamu; Yashiro, Hideo; Sori, Naoyuki; Hatono, Sotaro; Katsumoto, Tomiyasu; Suzuki, Tadao (to Tokyo Shibaura Electric Co. Ltd.). British Patent 1,218,096. 6 Jan 1971. Filed 8 May 1968.

In the method of manufacture described a high density metal wire is wound around a core and the core is then withdrawn to leave a compactly wound coil member. A number of such coil members are fitted together side by side, using a bonding agent, so as to fabricate a honeycomb block. The apertures of the coil members may be circular, rectangular or polygonal in shape. (UK)

18857 STUDY OF THE CHARACTERISTICS OF IMPLANTED p–n JUNCTION BY C(V,f) MEASUREMENTS. Gislon, R.; Urli, N. B.; Spoglia, U. (CSN, Rome). pp 92-6 of Ion Implantation. Stevenage, Eng.; Peter Peregrinus Ltd. (1970).

From Conference on Ion Implantation, Reading, England. See CONF-700945.

Capacitance measurements were made on Si diodes produced by ion implantation. The samples were large area n- and p-type Si crystals, implanted with B or P ions at 15 keV to a dose of 10^{13} ions/cm^2, followed by annealing at 450°C. The capacitance measured related to the p–n junction, and the frequency range was 1 to 500 kHz. Typical sets of curves for diodes obtained by implanting B on n-type Si and P on p-type Si are shown. While the former showed a monotonic increase of capacitance, the latter showed a pronounced maximum near zero applied voltage. These maxima were due mainly to the series resistance of the diodes. An equivalent circuit for the devices is described. The difference in behavior of the two types of devices is explained by the different penetration profiles of the ions. A frequency dependence was shown by the measured capacitance for both P- and B-implanted diodes, interpretations for which are discussed. These interpretations are somewhat different for the two types of diode. (9 references) (UK)

18858 SIMPLE EXPERIMENT TO COMPARE THE SWITCHING SPEEDS OF AN IMPLANT AUTO-REGISTERED AND A DIFFUSED MIST. Maloney, C. R. C. (Smiths Industries Ltd., Cheltenham, Eng.). pp 107-8 of Ion Implantation. Stevenage, Eng.; Peter Peregrinus Ltd. (1970).

From Conference on Ion Implantation, Reading, England. See CONF-700945.

In the experiment described two transistors of identical channel design were fabricated on a Si wafer; one was fabricated by implantation and the other by diffusion. Measurements were made on both devices in the same test rig and their responses were photographed from an oscilloscope display. The implant device showed a faster response. The theoretical responses were calculated from equivalent circuits and compared with the experimental results. Comparison between the shapes of the oscilloscope displays indicated that an implant device given the same input conditions as a diffusion device switched on in two-fifths of the time. (UK)

18859 APPARATUS FOR PRODUCING AND RECORDING DIFFRACTION PATTERNS. Lansiart, Alain; Morucci, Jean-Pierre; Roux, Georges (to Commissariat a l'Energie Atomique). British Patent 1,209,788. 21 Oct 1970. Priority date 14 Dec 1966, France.

An apparatus for obtaining diffraction patterns of x or gamma rays from crystals is described. It consists of a collimator, an orientable crystal support, and a gas-type detector. The detector may be adjusted to cause sparks, which are recorded by a camera, or to prevent sparks, in which case the avalanche electrons are transmitted to an image intensifier and then to a cathode-ray tube. Diffraction patterns with this system can be obtained in a much shorter time than with conventional methods; this is especially important for substances that are sensitive to radiation. (R.W.R.)

18860 HIGH PERFORMANCE LINEAR EMITTER FOLLOWER. Leskovec, R. A.; Bevington, P. R. (Case Western Reserve Univ., Cleveland). Nucl. Instrum. Methods; 92: 313(1971).

An emitter follower for photomultiplier dynode signals is described using the feedback technique of a familiar tube circuit to improve the performance of inexpensive transistors. (auth)

18861 AUTOMATIC GONIOMETER WITH HIGH RESOLVING POWER. Donati, Jean Roger (to Electricite de France). British Patent 1,209,844. 21 Oct 1970. Priority date 17 Feb 1967, France.

An automatic goniometer with high resolving power for the study of heterogeneous solids of small specific area by the small-angle diffraction of x rays is described. An instrument of this kind is particularly useful for the study of the graphites used in reactors. (R.W.R.)

18862 MODIFICATION OF THE NLZ 716a-T PULSE HEIGHT ANALYZER IN THE NZG 312-T SPECTROMETER SET USED FOR AUTOMATIC SCANNING OF INTEGRAL SPECTRA. Marik, P.; Franc, L. (Nuclear Power Station Dept., Skoda-Plzen, Czech.). Jad. Energ.; 16: 305(Sep 1970). (In Czech).

Instructions for simple arrangement of the automatic one-channel spectrometer of the NZG 312-T type used for automatic scanning of integral spectra are given. (auth)

18863 ANALYSIS OF OXYGEN AND HYDROGEN IN SODIUM. Hissink, M. (Central Technical Inst., TNO, Delft, Netherlands). Atoomenergie Haar Toepass.; 12: 165-70(May 1970). (In Dutch).

The sodium coolant of fast reactors must be kept very pure. The sampling apparatus for determining the oxygen content of the liquid metal in the coolant circuit is flushed for three hours to remove traces of oxides. The samples are analyzed in a glove box under an argon atmosphere. The sample is dissolved in mercury, with the oxide left as residue, or is subjected to differential distillation at 360°C; then the residue is dissolved in water, and the alkalinity is determined by titration. At a concentration of 3 ppM of O_2, the standard deviation amounts to 0.1 to 0.2 ppM. Determination for hydrogen may serve as an early-warning method for steam leakage into the sodium circuit. The method is based on the rapid diffusion of H_2 through nickel membranes at 400°C. Best results are obtained by connecting the vacuum side of the membrane with a mass spectrometer set for the detection of hydrogen. A less expensive method, based on an ion-getter pump, is under investigation. The anisotropic analytical circuit with a cold and a hot loop (450° and 650°C, respectively) and an electromagnetic pump contains one H_2 monitor in each loop and an electrochemical O_2 meter. (TTT)

18864 GENERALIZED PULSE HEIGHT DISTRIBUTION FOR THE ELECTRON MULTIPLIER. Wright, W. H. (Univ. of Natal, Durban, S. Afr.). Rev. Sci. Instrum.; 42: 235-9(Feb 1971).

The generalized birth and death process is used as a model for the creation of secondary electrons in order to obtain the pulse height distribution of an electron multiplier. A recurrence relation is obtained for the distribution $P_k(n)$ of the total number n of secondaries after k stages of multiplication, which result from a single electron input. It is possible to use different birth and death functions at each dynode. Results are presented using birth and death functions based on an elementary but physically meaningful theory of the secondary emission process. (auth)

18865 MAGNETIC FIELD MEASUREMENTS USING AN ELECTRON BEAM AND AN ELECTROSTATIC ANALYZER. Risley, John S. (Univ. of Washington, Seattle). Rev. Sci. Instrum.; 42: 267-8(Feb 1971).

A procedure is described by which an electron beam in an electrostatic analyzer is used as a magnetometer. The method is applied to a cylindrical mirror analyzer. (L.B.S.)

18866 PULSE SEQUENCE IDENTIFIER. Kokes, A. (Nuclear Research Inst., Rez, Czech.). Nucl. Instrum. Methods; 92: 151-2(1971).

A simple circuit for determining the sequence of the front edge of pulses at two dc coupled inputs with the resolving time of 50 ps is described. In connection with a TPHC it allows the true and chance coincidence to be measured as well as chance coincidence spectra at the same time. (auth)

18867 STABILIZATION OF SPECTRUM WITH NO REFERENCE PEAKS. Matoba, M.; Sonoda, M. (Kyushu Univ., Fukuoka). Nucl. Instrum. Methods; 92: 153(1971).

Methods to stabilize a spectrum with no reference peaks are considered. Locating one of the two windows of a usual stabilizer in the flat region of spectrum and the other in the uppermost channel region, and setting unequally the widths or the gains of the two windows, it is found possible to stabilize the spectrum with no reference peaks by comparing the counting rates in the two windows. (auth)

18868 IMPROVED RINGING COIL PULSE ENCODERS. Barton, J. C.; Munas, A. F.; Wright, A. G. (Northern Polytechnic, London). Nucl. Instrum. Methods; 92: 89-91(1971).

The advantages of ringing coil circuits as logarithmic encoders are reviewed and the choice of optimum ringing frequency considered. Circuits are given for frequencies up to 8 MHz, and it is shown that dynamic ranges of at least 1000 : 1 are possible with an input sensitivity better than 1 pC. (auth)

18869 CIRCUIT WHICH EXPANDS THE COUNT STORAGE CAPACITY OF A MULTICHANNEL ANALYZER. Ruegg, F. C. (National Bureau of Standards, Washington, D. C.). Nucl. Instrum. Methods; 92: 7-11(1971).

A circuit has been designed which allows the experimenter to store up to 10^{10} counts/channel in a 10^5 count capacity multichannel analyzer. The circuit uses the analyzer's second subgroup to store the overflow counts of the first subgroup. The circuit was designed to be used with an analyzer operating in the multichannel scaling mode. (auth)

18870 RADIATSIONNAYA TEKHNIKA. VYPUSK 4. (Radiation Technology. Number 4). Shtan, A. S. (ed.). Moscow; Atomizdat (1970). 440p.

A collection of 64 experimental and theoretical articles on the nuclear physics basis of radiation technology is presented. Isotopic sources of radiation; radiation dosimetry; radiation protection; radiometric instruments; activation, radiometric, and other methods of nuclear analysis; isotope-fueled thermoelectric generators; irradiation devices; gamma defectoscopes; radioisotope and x-ray medical devices; neutron generators; and automation in radiation technology are discussed. New devices, equipment, and instrumentation are described. (tr-auth)

18871 DIGITAL PULSE STABILIZATION AT LOW COINCIDENCE COUNT RATES. Weber, Christian H. (Ames Lab., Iowa). Rev. Sci. Instrum.; 42: 260(Feb 1971).

A modified analog-to-digital converter is described, which provides digital pulse stabilization at low and normal coincidence count rates. (L.B.S.)

18872 DATA COLLECTOR FOR A COINCIDENCE EXPERIMENT. Ikelaar, P.; van der Wiel, M. J.; Tebra, W. (FOM-Instituut voor Atoom- en Molecuulfysica, Amsterdam). J. Phys., E (London); 4: 102-4(Feb 1971).

A data collector for an atomic collision coincidence experiment is described, which has been provided with a number of options not yet available in commercial instruments. The main features are: a bidirectional counter with controlled inputs, a freely adjustable number of channels, an automatic normalization on a monitor signal of the channel dwell period and a provision for "lock-in" type measurements. (auth) (UK)

18873 VEB RFT MESSELEKTRONIK DRESDEN LINEAR AMPLIFIER/ANALYZER VA-V-100. Berger, K.-H. (VEB RFT Messelektronik, Dresden). Kernenergie; 13: 181-3(Jun 1970). (In German).

The linear amplifier/analyzer of VA-V-100 type, manufactured by VEB RFT Messelektronik Dresden, is described. Elucidations of the properties and the principle of action of the device are complemented by hints at the possible regimes of operation and connecting sets. The technical data are given. (auth)

18874 MULTIPLE DETECTOR NEUTRON LOGGING TECHNIQUE. Dewan, John T. (to Schlumberger Technology Corp.). U. S. Patent 3,532,884. 6 Oct 1970. Filed 27 Oct 1967.

The invention corrects inaccuracies in the responses from a two-neutron detector porosity logging tool caused by changes in the borehole environment. The two signal-producing neutron detectors are spaced at different distances from the neutron source. These detector signals are combined to establish a ratio signal that is related to the apparent formation porosity. An epithermal neutron detector, however, is spaced more closely to the source than either of the porosity detectors in order to produce a corrective signal that compensates the ratio signal for the effect of changes in the borehole characteristics. (auth)

18875 APPLICATION OF ELECTROSTATIC MIRRORS IN THE ELIMINATION OF THE CHROMATIC EFFECT IN MAGNETIC SPECTROMETERS. II. ABERRATIONS. Baril, Marcel (Univ. Laval, Quebec). Can. J. Phys.; 48: 2487-98(1 Nov 1970). (In French).

Chromatic aberrations in magnetic spectrometers are studied. It is shown that in many cases at least two main aberration terms can be eliminated. Resolving powers are discussed and calculated, including intensity-distribution and peak-to-valley ratio effects. (auth)

18876 FUJI ELECTROMAGNETIC FLOWMETERS FOR LIQUID SODIUM. Yada, Hisashi (Fuji Electric Co. Ltd., Tokyo). Fuji Jiho; 43: 194-7(Feb 1970). (In Japanese).

For the development of the Japanese experimental fast breeder

XUM

reactor, two kinds of electromagnetic flowmeters are utilized, i.e., the flowmeter for liquid sodium loops and the in-core flowmeter. They have been developed by Fuji Electric and are highly evaluated for their reliability. Liquid sodium flow rate is measured electromagnetically by the application of the Faraday induction principle, and the flowmeter is essentially a d-c generator. Conductible fluid, flowing in a conduit and passing through a magnetic field, generates an electric current. Although d-c energized magnets or permanent magnets are alternatively used for the flowmeter for the liquid sodium loop, the flowmeter placed in a core must use permanent magnets because of their compactness. For the operation in sodium up to 600°C, the degradation of permanent magnets was tested, and their characteristics were elucidated. In-core flowmeters used under severe conditions, however, have many unsolved problems such as the improvement of the thermal stability in magnetic fields, performance limit, the influence of irradiation, and installation. (Japan)

18877 RADIOACTIVE AEROSOL SAMPLING DEVICE. **Andre, Garnier. French Patent 1,586,204. 5 Jan 1970. Filed 13 Sep 1968. (In French).**

A device for sampling radioactive aerosols is described. It consists of a box with an opening for the sealed mounting of a filter support and contains a battery of small accumulators. These accumulators supply the energy necessary to maintain a constant speed motor. This motor is associated with a cam which transforms the rotary motion of the spindle into the to and fro motion of the drag link. A blower is incorporated which is of a general cylindrical form having one end fixed in relation to the box in the opening of the filter mounting, and the other end soldered to the closing plate. The filter support comprises a hole connecting it to the blower which has a suction valve inside and the closing plate with its pressure valve placed externally and soldered to the drag link. (auth) (France)

18878 MEASUREMENTS AND CALIBRATIONS AT PRESSURES BETWEEN 10^{-5} AND 10^{-12} TORR. Bernardet, H.; Choumoff, P. S.; Iapteff, B. (Societe Generale du Vide, Paris). Vide; 25: 131-6(May-Jun 1970). (In French).

A system was developed for comparing and calibrating ionization gages over a pressure range of 10^{-5} to 10^{-12} torr. The various bakeable parts of the system are made of stainless steel. The ultra high vacuum part of the system consists of the pumping equipment and the test manifold. The pumping equipment consists of a 100 l/s triode ion pump with a titanium sublimator and a liquid helium pump. The overall pumping speed for N_2 is about 2000 l/s. The pumping unit is connected to the test manifold by a conductance of 100 l/s provided with six flanged apertures which may be used for the test gages. The entire vessel is double walled for cooling purposes. The gas introduction manifold possesses a reference volume at pressure Pm and is connected to the test manifold through a conductance C_1 of 0.7 cm^3/s either directly or via a variable leak, which may lead to a total conductance as low as 1/1000 of C_1. Pm is measured with a reference gage. The system possesses auxiliary pumping equipment consisting of a sorption pump and an orbitron pump for pre-evacuating the system. A final 10^{-12} torr at ambient temperatures can be achieved in the test manifold. Comparisons between gages can thus be made. Preliminary results demonstrate the necessity of using several gages, operating on different principles, to estimate the pressure: outer screened collector, hot cathode magnetron, etc. Thermal effects, limiting the use of glass gages, appear for pressures $\leq 10^{-11}$ torr. (auth) (France)

Radiation Effects on Instruments and Instrument Components

18879 RADIATION HARDENED TRANSISTOR CIRCUIT. Fletcher, Larry L.; Papenfuss, Morris E. (to Sperry Rand Corp.). United States Patent 3,524,999. 18 Aug 1970. Filed 1 Oct 1965.

A method and apparatus for rendering a transitor circuit less subject to the effects of transient ionizing radiation are presented. A compensating transistor is connected to the transistor to be compensated such that the photocurrents produced when the compensating transistor is subjected to radiation provides the photocurrent requirements of the transistor to be compensated. As such, the photocurrents do not flow through the load to effect the output signal. (auth)

18880 RADIATION RESISTANCE OF TYPE ZnS + ^{10}B DETECTORS TO NEUTRONS. Ganichev, G. I.; Kolesov, B. M.; Ovchinnikov, A. K.; Timofeeva, T. V. (All-Union Scientific-Research Inst. of Prospecting Geophysics, Leningrad). Instrum. Exp. Tech. (USSR) (Engl. Transl.); No. 2, 395-6(Mar-Apr 1970).

Translated from Prib. Tekh. Eksp.; No. 2, 78-80(Mar-Apr 1970).

The reduction in light output of ZnS + ^{10}B scintillation detectors due to radiation damage caused by thermal neutrons was studied. It is shown that the reduction of the light output of the detectors is noticeable for doses exceeding 10^{12} neutrons/cm^2. (auth)

18881 COAXIAL CABLE. **Passe, Jean (to Commissariat a l'Energie Atomique). French Patent 1,590,198. 13 Apr 1970. Filed 10 Oct 1968. (In French).**

Coaxial cable, inert to radiation coming from the core of a reactor is described. The external protective shielding contains several high atomic weight elements, weakly activable by neutrons. The electrical insulator consists of at least two materials producing deactivation currents of opposite sign. The conducting core is composed of one or several elements weakly activable by the neutrons and preferably includes one or more of the insulating materials. In general, the shielding consists of a noncorrodable, high temperature resistant material; the core, insulating material, and shielding consist of elements of increasing atomic weights; the shielding is of lead or lead oxide and is contained between two thin layers of stainless steel; the insulator consists of a magnesia aluminium mixture and the core is of nickel, iron or stainless steel. (France)

18882 CURVE POWER FACTORS AND ITS RADIATION-INDUCED CHANGES IN SILICON PHOTOVOLTAIC CELLS. Usami, Akira (Nagoya Inst. of Tech., Japan). Denshi Tsushin Gakkai Ronbunshi, C; 53: 355-62(Jun 1970). (In Japanese).

Curve power factors (CPF) of silicon solar cells have been obtained by experimental and numerical analysis methods. Both the experimentally obtained and numerically analyzed values of the CPF decrease as the junction depth, bulk resistivity and the measuring temperature decrease, and increase as the illuminating light intensity increases. The degradation of the CPF of Ni or copper-doped cells by γ-irradiation is smaller than that of the non-doped ones, especially on NP-type cells. The increase of the CPF on NP-type cells have been observed under the relatively lower dosage. (auth)

18883 PROSPECTS AND LIMITS OF EMPLOYMENT OF RESISTANCE STRAIN GAUGES IN RADIOACTIVE ENVIRONMENT. Morandi, G. (CISE, Milan). Energ. Nucl. (Milan); 18: 55-62(Jan 1971). (In Italian).

The performance characteristics of resistance strain gauges in radioactive environment are examined. The problems concerning the experimental stress analysis on the reactor internals are particularly pointed out, and the conclusion is drawn that in the typical nuclear environment the most promising applications of such a technique are those related to dynamic measurements on short periods. Static measurements over a long time are of overwhelming difficulty to the stress analyst, owing to the strong radiation field and extreme temperature and pressure conditions. Some experimental results achieved during an experimental fuel-element irradiation are also briefly described. (auth)

LIFE SCIENCES

Biochemistry, Physiology, and Molecular Biology

Basic Processes

Refer also to abstracts 18977, 19027, 19036, and 19039.

18884 DIRECTIONAL CORRELATION STUDIES OF ANOMALOUS WATER IN CARBONIC ANHYDRASE. Glass, J. C.; Graf, G. (North Dakota State Univ., Fargo). Nature (London); 226: 635-6(16 May 1970).

The technique of γ-directional correlations as applied to biological macromolecules in solution was previously described by Leifert et al. (Nature 220: 907 (1968)). The use of this technique to study internal fields of water associated with hydrated dry proteins is described. Cesium-133 was used. Formed by electron capture decay of ^{133}Ba, the 356 to 81 keV γ cascade of ^{133}Cs involves an intermediate level of nuclear spin $^5/_2$ and a half-life of 6.3 ns. A film containing the ^{133}Ba was dissolved in bovine carbonic anhydrase, the solution was frozen with liquid nitrogen, and then lyophilized to constant weight. The freeze-dried samples were then adjusted to approximately 5% and 20% water content. Measurements of enzymatic activities of the samples showed no change with respect to the original enzyme preparation. The time dependent anisotropy of the 356 to 81 keV γ-γ cascade was measured by use of a two-detector time-differential coincidence system, and was found to be perturbed over a 40ns time interval for both hydrated protein samples. For the 5% hydrated sample the behavior of the perturbation factor indicated the presence of a static electric quadrupole interaction. Since static fields are not expected in aqueous dilute solutions it seems likely that the ^{133}Ba ions occupied definite sites of axial symmetry in the carbonic anhydrase molecules, and the data indicate that all the ^{133}Ba ions occupied equivalent sites. The presence of a static interaction was also indicated for the 20% hydrated sample. Comparison with the perturbation factor for the 5% sample suggested the presence of a time dependent interaction seen by a fraction of the ^{133}Ba ions. The remainder of the ^{133}Ba ions occupied sites in the protein molecule and saw only a pure static electric quadrupole interaction. If a fraction n_1 is influenced by static fields and a fraction n_2 by time dependent fields, and if the fraction n_1 is attached to the carbonic anhydrase molecules, then the fraction n_2 must be in the water associated with these molecules. If the water is normal, time dependent interactions should not be observable, but if it is anomalous (ordered) such interactions become possible due either to fluctuating fields in the water or to propagation of the electron hole, following the electron capture decay of ^{133}Ba. It is suggested that the fraction n_2 of the ^{133}Ba ions is the anomalous water associated with the carbonic anhydrase molecules. Results indicated that the water associated with carbonic anhydrase molecules is highly ordered. (UK)

18885 USE OF RADIOISOTOPE GENERATORS IN NUCLEAR MEDICINE. Roemer, M.; Grebe, S. F. (W. C. Roentgenklinik, Giessen, Ger. Medische Poliklinik, Giessen, Ger.). Kerntechnik; 12: 442-8(Oct 1970). (In German and English).

Radioisotope generators have been increasingly used in nuclear medicine in recent years owing, in particular, to the decisive advantages which the short-lived isotopes produced present in scintigraphy compared to the formerly used nuclides. These advantages include a lower radiation load on the patients, more rapid information, better quality of scintigrams, and fewer radioactive wastes. The underlying physical principles, design, uses, and radiation hazards of three most frequently used generators of this type are discussed. These include the ^{99}Mo–^{99m}Tc, ^{113}Sn–^{113m}In, and ^{87}Y–^{87m}Sr generators. (C.H.)

18886 USES OF A RESEARCH REACTOR FOR MEDICAL INVESTIGATIONS. Kasperek, K.; Schicha, H.; Siller, V. (Kernforschungsanlage, Juelich, Ger.). Kerntechnik; 12: 436-41(Oct 1970). (In German and English).

The basic investigations possible with short- and medium-lived radionuclides produced in a research reactor in medicine and biology are discussed. Among these are activation analysis of biological specimens, studies of trace element metabolism, the preparation of tracers, and various biochemical investigations. The requirements which must be fulfilled by an irradiation facility in order to make it possible to conduct such investigations are discussed. (auth)

18887 PASSAGE OF IRON(III) CYANOFERRATE THROUGH THE GASTROINTESTINAL TRACT OF RATS. Stojadinovic, S.; Knajfl, J. (Military Medical Research and Postgraduate Inst., Hradec Kralove, Czech.). Sb. Ved. Pr. VLVDU Hradci Kralove; 41: 83-92(1969). (In Czech).

The passage of iron(III) cyanoferrate, which is commonly used to minimize radiocesium resorption, through the gastrointestinal tract of rats was studied. One hundred mg of iron(III) cyanoferrate labeled with ^{59}Fe and suspended in 1 ml of H_2O was introduced into the rat stomach after 24 hrs starvation. The animals were killed 15, 30, 60 min, and 4, 12, and 24 hrs after the application. In the last two groups feces were collected and the activity measured. The small and the large intestines were removed and divided into two and four portions of identical length, respectively. The transfer of the iron(III) cyanoferrate from the stomach followed an exponential law with a half-life of about 3.5 hrs. Portions of 9.3 and 1% cyanoferrate were observed in the stomach at 12 and 24 hrs after application, respectively. A very rapid passage was found through the first and second part of the small intestine. The compound was present in the jejunum and illeum for the first hr and after four hrs, respectively. In the first part of the large intestine a maximum amount was observed after 12 hrs. Passage through the large intestine was faster than through the small one. (NSA of Czech.)

18888 EFFECT OF 6-AZAURIDINE ON THE LABELLING INDEX AND THE MEAN GRAIN COUNT OF EHRLICH-CARCINOMA ASCITES CELLS AFTER ^{3}H-THYMIDINE INCUBATION. Magdon, E.; Delzer, W. (Institut fuer Krebsforschung, Berlin). Arch. Geschwulstforsch.; 36: 247-52(1970). (In German).

In connection with studies on the radiosensitizing action of 6-azauridine in experimental animal tumors, an examination was made of the suggestion that the sensitizing effect is caused by azauridine induced inhibition of de novo synthesis of pyrimidine nucleotides, resulting in a partial synchronization of the cell cycle. At the time interval on which the maximum sensitizing effect was obtained, the incorporation of ^{3}H-thymidine in DNA of Ehrlich cells in mice 24 hours after azauridine application was studied by microautoradiography. Under these conditions the labeling index of the ascites cells increased in the azauridine treated mice by a factor of 1.5. The results indicate that the increase of the labeling index is caused by an increase of cells entering the early S-Phase, and that the accumulation of cells in this phase is responsible for the radiosensitizing action. (auth)

Metabolism, Physiology, and Toxicology

Refer also to abstracts 18369, 18926, 18935, 18938, 18979, 18992, 18997, 19063, 19144, and 19155.

18889 (CEA-CONF–1676) BIOCHEMICAL CONSIDERATIONS ON ALVEOLAR RETENTION OF LIQUID RARE EARTH AEROSOLS. Pasquier, Ch.; Lefebvre, J. C.; Ehrhart, J. C. (Commissariat a l'Energie Atomique, Fontenay-aux-Roses (France). Centre d'Etudes Nucleaires). 1970. 9p. (In French). (CONF-700931–2). Dep. NTIS (U. S. Sales Only).

From 3rd International Symposium on Inhaled Particles, London, England.

A lipoprotein typical of the alveolar lining was observed in endobronchial liquids obtained from rats and monkeys; this lipoprotein rich in glycolipids and free fatty acids has a lipidic composition widely different from the whole alveolar film. The part it played in the retention of unpolymerized ^{140}La was demonstrated in vitro by polyacrylamide disc electrophoresis and in vivo by the combination of continuous paper chromatography and electrophoresis. The stability of the lanthanum-lipoprotein complex was tested by DTPA and its contribution in respiratory contamination discussed. (auth) (France)

18890 (COO–2044-3) $^{210}PoO_2$ METABOLISM IN RUMINANTS. Second Technical Progress Report, January 15, 1970–January 15, 1971. Watters, R. L.; Johnson, James E. (Colorado State Univ., Fort Collins. Dept. of Radiology and Radiation Biology). 29 Jan 1971. Contract AT(11-1)-2044. 52p. Dep. NTIS.

It was demonstrated that ingested $^{210}PoO_2$ is transferred in small but significant quantities into the milk and meat of goats and cows. The transfer coefficient in cows for the less soluble oxide form of polonium is approximately one-third the transfer coefficient for $^{210}PoCl_4$. The fraction of ingested $^{210}PoO_2$ secreted in goat's milk is sixty times higher than the fraction secreted in cow's milk. This suggests a greater potential hazard to the population of portions of the world where goat milk and meat are an important part of the diet should accidental pasture contamination occur. The enhanced absorption of ^{210}Po secreted in milk would result in increased body burdens of ^{210}Po and suggests that in such cases the 6% gut absorption used by the I.C.R.P. for calculation of maximum permissible concentrations of ^{210}Po in water for humans should be revised. (auth)

18891 (LF-tr-46) CONTRIBUTION TO THE STUDY OF PULMONARY RETENTION AND DISPOSAL OF PLUTONIUM OXIDE. ULTRASTRUCTURAL STUDY OF ALVEOLAR MACROPHAGES. Lutz, M.; Nolibe, Petavy, G.; Rannaud, J.-Cl. Translated by A. A. Horvath (Lovelace Foundation for Medical Education and Research, Albuquerque, N. Mex.), from Arch. Mal. Prof. Med. Trav. Secur. Sociale; 31: No. 4-5, 185-96(Apr-May 1970). 17p. Dep. NTIS.

The morphology and ultrastructure of pulmonary macrophages obtained from rabbits before and at various times following the inhalation of $^{239}PuO_2$ aerosols were studied using microscopic and autoradiographic techniques. It is pointed out that the alveolar macrophages have a direct effect on the fate of inhaled particles. Results shows that, while a substantial portion of the particles were eliminated by bronchial purification and conveyed to the gastrointestinal tract, from 5 to 15% of inhaled particles were phagocytized and transported by macrophages to the lymphatic ducts and nodes, while a certain number passed directly into the lymph system. Particles of $^{239}PuO_2$ were expected to exert both chemical and α radiation effects, however very few pathological characteristics were observed in alveolar macrophages obtained from rabbits two to four days following exposure of the animals to aerosols of 0.5 μm average diameter and emitting a total radiation dose amounting to approximately 400 pCi at time of sacrifice. (C.H.)

18892 (NP-18641) MATERIAL TRANSPORT IN PLANT FOODS WITH REGARD TO RADIOACTIVE CONTAMINATION AND DECONTAMINATION. Paulus, Klaus O. (Karlsruhe Univ. (West Germany)). Jul 1970. 105p. (In German). Dep. NTIS (U. S. Sales Only).

Thesis.

Mainly on potato tissue, the uptake of ^{137}Cs, ^{90}Sr, ^{85}Sr, ^{95}Zr, and ^{144}Ce was studied theoretically and experimentally. Radioisotope transport through living tissue could not be explained by diffusion alone; two other processes played an important role: incorporation of radioisotopes into the intercellular space because of osmotic pressure differences, and binding of radioisotopes in the tissue because of biochemical reactions. Through introduction of correction factors for the two processes, a satisfactory differential equation could be derived. With respect to decontamination, thermal treatment with organic acids, especially citric acid, was successful. Equally satisfactory was a short treatment with hot water followed by washing in cold water. It was concluded that the procedures might possess general applicability to the decontamination of plant tissue. (H.B.G.)

18893 RENAL EXCRETION OF ^{51}Cr-EDTA STUDIED WITH STOP FLOW TECHNIQUE. Eide, I. (Univ. of Oslo. Ulleval Hospital, Oslo). Scand. J. Clin. Lab. Invest.; 26: 373-80(Dec 1970).

The renal clearance of ^{51}Cr-EDTA in dogs was found to be about 10% lower than inulin clearance. To test whether this difference is caused by tubular reabsorption, stop flow experiments were performed during various types of diuresis. No evidence was found for tubular reabsorption of ^{51}Cr-EDTA. The discrepancy is probably caused by decomposition of the complex during storage. (auth)

18894 AN EXPERIMENTAL DETERMINATION OF THE FACTORS INFLUENCING THE BUILD UP OF RADIONUCLIDES IN VARIOUS MARINE SPECIES. Ancellin, J.; Vilquin, A. (CEA, Cherbourg, France). Bull. Inform. Sci. Tech. (Paris); No. 151, 17-21(Sep 1970). (In French).

Experimental contaminations of marine species by various fission products (^{137}Cs, ^{106}Ru, ^{144}Ce, ^{95}Zr) were carried out in closed-circuit aquaria. In general the build up of radioelements in the species studied varied inversely with the degree of evolution of the organisms. Amongst the species of high radioelement concentration power may be mentioned the coral algae and the ascidia. The influence of the physico-chemical form of the radioelement in the contamination processes was investigated; in the case of ruthenium the concentration factors were higher for particle forms than for soluble forms. (auth) (France)

18895 EFFECTS OF LUNG WASHING ON THE RETENTION OF INHALED PARTICLES OF PLUTONIUM OXIDE. Kunzle-Lutz, M.; Metivier, H.; Nolibe, D.; (and others) (CEA, Montrouge, France. Hotel-Dieu, Paris. CEA, Saclay, France). Arch. Mal. Prof. Med. Trav. Secur. Sociale; 31: 513-16(Sep 1970). (In French).

Baboons were contaminated by breathing an atmosphere containing particles of plutonium oxide and their lung content is followed in vivo and post mortem. Washing was carried out with a tracheal probe which isolates the two lungs. The contaminated animals were divided into three groups: untreated (reference specimens), treated by lung washing on the 5th day after contamination, treated 3 times by lung washing (5th, 11th, and 18th days). The volumes of liquid injected then recuperated and the activity removed by each washing was reported. A large percentage of the injected liquid was recovered (90%). The effectiveness of washing as a means of decontamination is demonstrated by comparing the same animal with washed or untreated lungs or by comparing treated animals with reference animals. The ratio between the quantity of noneliminated dusts and the lung content at the moment of washing is calculated. (auth) (France)

18896 RESIDUAL CONTAMINATION OF MUSSELS AFTER COOKING. Vilquin, A. (CEA, Cherbourg, France). Radioprotection; 5: 247-8(1970). (In French).

Thirty mussels were contaminated in aquaria containing 40 litres of sea water to which was added ruthenium 106 trichloride. The forms of ruthenium responsible for this contamination are essentially soluble ones, the insoluble forms which appear at the time of contamination being held back by the filtration system of the aquarium. Eight of the mussels were removed and the mean specific radioactivities of the shell and flesh measured before cooking. The remaining 22 were cooked and the radioactivity measured on the 22 mussels, 5 shells, the sauce (2 samples) and fragments of onion + garlic + parsley (2 samples). The shells lost about $\frac{1}{3}$ of their radioactivity, partly to the sauce. (auth) (France)

18897 EFFECT OF BIOLOGICAL PROPERTIES OF PLANT ON ^{90}Sr CONTENTS IN YIELD. Ivanov, S. N.; Shagalova, E. D.; Shifrina, S. S. (Belorussian Research Inst. of Soil Studies and Agriochemistry, Minsk). Dokl. Akad. Nauk BSSR; 14: 947-50 (Oct 1970). (In Russian).

Comparative studies were made of the accumulation of ^{90}Sr in harvested agricultural plants grown under identical conditions. It was shown that ^{90}Sr uptake depended on biological properties of the plants. Lupine, corn, vetch (Vecia L), clover, and timothy grass contained more ^{90}Sr per unit of dry substance than winter rye, barley and oats. Strontium-90 loss was greater from the vegetative parts than the reproductive parts. Calcium retention did not appreciably affect ^{90}Sr contents or distribution. (R.V.J.)

18898 DUAL DETECTOR SYSTEM FOR THYROID UPTAKE MEASUREMENT. Sear, R. (London Hospital). Brit. J. Radiol.; 43: 876-85(1970).

An account is given of past efforts to standardize thyroid uptake measurement techniques so as to afford reasonable accuracy and permit intercomparison of results. Particular reference is made to the work of the International Atomic Energy Agency in this field. The response to extrathyroidal activity is shown to be relatively small when well designed detectors are used. It is adequate to apply a correction derived from a phantom, without carrying out a separate measurement on each subject. A technique of measurement is described using two opposed detectors. This allows uptake determinations, with either ^{131}I or ^{132}I, to be made quickly and conveniently, whilst taking account of all the main sources of error. It is shown that such a system greatly reduces errors due to variation in the depth distribution of the activity in the neck. At the same time, as used here, it does not lead to an enhanced response to extrathyroidal activity. (auth) (UK)

18899 BINDING OF AMERICIUM AND PLUTONIUM TO BONE GLYCOPROTEINS. Chipperfield, Alan R.; Taylor, David M. (Inst. of Cancer Research, Surrey, Eng.). Eur. J. Biochem.; 17: 581-5(Dec 1970).

By means of a gel filtration technique it was found that ^{239}Pu and ^{241}Am differ in their mode of binding to two glycoproteins isolated from bovine cortical bone. Plutonium was bound more strongly than americium, plutonium binding was maximal at pH 6, and americium at pH 8, and sialic acid was involved in the binding of plutonium but not americium. The mechanisms by which these elements bind to glycoproteins in vitro are discussed. (auth)

18900 INFLUENCE OF ANTIBODY FORMATION ON THE PERMEABILITY OF ERYTHROCYTES IN REGARD TO ^{32}P AND THE AMOUNT OF SIALIC ACID. Tsolov, V.; Dryanovski, P.; Koychev, K. (Higher Inst. of Veterinary Medicine, Sofia). Compt. Rend. Acad. Bulg. Sci.; 23: 1291-3(1970).

Isologous blood was injected into four calves for immunization experiments. Procedures are described for determining the titer of antibodies in serum, determining sialic acid in serum and erythrocytes, and determining ^{32}P incorporation in erythrocytes, and measurement of ^{32}P radioactivity. Fourteen days after the injection it was found that there was an increase in permeability of erythrocytes to ^{32}P as well as an increase in the sialic acid content. It was assumed that the increase in antibodies influenced the permeability. The correlation between the permeability of erythrocytes to ^{32}P and the sialic acid content is discussed. (H.L.W.)

18901 RADIOPATHOLOGY OF ^{241}Am. 1. DISTRIBUTION OF AMERICIUM IN ADULT MICE. **Hammarstroem, Lars; Nilsson, Agnar (Kungliga Veterinarhogskolan, Stockholm). Acta Radiol., Ther., Phys., Biol.; 9: 433-42(Oct 1970).**

The distribution and retention of americium-241 after a single intravenous injection were investigated in mice by autoradiography. The distribution was predominantly characterized by an accumulation of the isotope in the bone and liver tissues. Marked accumulation was noted also in the adrenal gland, the ovary, and the dental pulp. (auth)

18902 EFFECTS OF X-IRRADIATION ON ^{14}C-PYRUVATE METABOLISM IN RAT THYMOCYTES. **Araki, Kimiko; Taguchi, Shigetoshi; Ohyama, Harumi; Yamada, Takeshi (National Inst. of Radiological Sciences, Chiba, Japan). J. Radiat. Res.; 11: 79-84(Jun 1970).**

Incorporation of ^{14}C-pyruvate into the citric acid cycle metabolites was measured in rat thymocytes x-irradiated in vitro. X irradiation caused no significant changes in ^{14}C-pyruvate incorporation into the metabolites separated by Dowex-1 formate column chromatography. Glycogen content of the cells decreased, whereas malate showed a significant accumulation after irradiation. From the results, the previously reported increase in labeling of citric acid cycle metabolites derived from ^{14}C-glucose is explained as the result of the enhanced glycolysis in the thymocytes after irradiation. (auth)

Radiation Effects

Refer also to abstracts 19024, 19025, 19031, and 19128.

18903 BIOPHYSICAL MECHANISMS OF ULTRAVIOLET RADIATION. **Rokityanskii, V. I. Kazan. Med. Zh.; No. 4, 84-8(1970). (In Russian).**

The amino acids tryptophan, tyrosine, phenylalanine, and cystine are most vulnerable to uv rays. These macromolecules are largely responsible for absorbing the rays, which have an injurious effect on cells. The quantum yield of photoinactivation of enzymes is low. Another series of reactions is induced by a second photoionization product, hydrated electrons, a powerful reducing agent, more vigorous than even atomic hydrogen, and quick to react with molecules of organic compounds. There may also be changes in the conformation of the macromolecules. Interaction of the aromatic amino-acid radical with groups of the neighboring peptide chain causes cross linking between the chains and stabilizes the impaired configuration. The nitrogeneous bases of the nuclei acids are also vulnerable to uv radiation, especially in the shortwave region. They undergo photochemical transformation, and in the process lose most of their physiological activity. When nucleic acids are exposed to uv radiation, the energy of the quantum absorbed by any of its nitrogenous bases is transmitted to the neighboring bases and then transferred throughout the chain of the macromolecule of a particular nucleic acid until it is converted into thermal energy or expended on a photochemical reaction. A discussion of the use of EPR to study the effect of uv radiation on biological materials is presented. (JPRS)

18904 BEHAVIOR OF A STABILIZED CELLULAR STRAIN CULTURED IN A MEDIUM CONTAMINATED WITH ^{137}Cs. NOTE III. QUANTITATIVE ASPECTS OF MORPHOLOGICAL CHANGES. **Rossi-Torelli, M.; Polese, E.; Ghelardi, M.; Avio, C. M. (Univ., Pisa, Italy). Med. Nucl.-Radiobiol. Lat.; 12: 33-42(1969). (In Italian).**

The size of cells, nucleoplasmic ratio, mitotic rate, and cellular formula were quantitatively investigated in a cellular strain cultured in a medium contaminated with 1 μCi/cm^3 of ^{137}Cs. The results showed that size of nuclei and cells in contaminated cultures was smaller than those in the uncontaminated ones. Cells with nuclei of equal diameter were, on the average, larger in contaminated cultures than in the control; therefore nucleoplasmic ratio was smaller. The mitotic rate was higher in contaminated cultures than in control, and cellular formula showed a notable increase in giant and polynucleated cells in culture with ^{137}Cs. Morphologic and functional changes in cells cultured in a medium with ^{137}Cs were more evident in a number of cells but the whole cellular culture suffered in the presence of the radioisotope. (auth)

18905 ARYLSULFATASE ACTIVITY IN THE URINE OF THE IRRADIATED RAT. **Marafante, E.; Scoppa, P. (CCR-EURATOM, Ispra, Italy). Med. Nucl.-Radiobiol. Lat.; 12: 43-7(1969). (In Italian).**

A study was made of the effects of whole-body x irradiation (450 R) on A and B arylsulphatase activities in the rat. A considerable increase in activity was found during the first days after irradiation. However most of the increase resulted from the state of anorexia induced by radiation, as evidenced by a comparison with pair-fasted controls. (auth)

18906 COMPARISON OF ELECTRICAL DISCHARGE WITH γ-RADIATION FOR THE PRODUCTION OF FREE RADICALS IN LYOPHILIZED PROTEINS. White, Frederick, H. Jr.; Kon, Hideo; Riesz, Peter (National Institutes of Health, Bethesda, Md.). Radiat. Res.; 45: 8-24(Jan 1971).

A technique for the production of trapped free radicals in lyophilized proteins by exposure to electrical discharge at low pressures from an externally applied Tesla coil has been explored in comparison to γ-irradiation. Radical formation by discharge exhibits a dependence upon pressure, not seen for γ-irradiation. In contrast to the exponential relationship of enzymatic activity loss to dose for γ-irradiated proteins, the activity of lysozyme on exposure to discharge decreases to approximately 70% of the specific activity of the native enzyme, and continued exposure produces little further loss. This behavior coincides with the approach of free radical content to saturation as studied by electron spin resonance. A further examination of the free radical content indicates that electrical discharge produces a primary radical population, at a temperature near that of liquid nitrogen, which rearranges at higher temperatures to the more stable secondary population, as has been observed for γ-irradiated proteins. Radical distributions in the secondary population were studied by reaction with tritiated hydrogen sulfide, followed by analysis to determine the distribution of tritium among the amino acids. Although strong resemblance was found for distributions in proteins irradiated by the two methods, a number of distinct differences were observed that were suggestive of dissimilarity in the primary as well as secondary radical distributions. (auth)

18907 γ-IRRADIATION OF DILUTE SOLUTIONS OF CHYMOTRYPSIN: PROTEIN SUBSTRATES. Lynn, K. R. (National Research Council of Canada, Ottawa). Radiat. Res.; 45: 25-34 (Jan 1971).

The reactivity of dilute solutions of chymotrypsin after γ-irradiation in atmospheres of air and nitrogen has been examined using three protein substrates. It was found that the degree of reactivity residual in chymotrypsin after irradiation with a given dose varied with the substrate employed. The enzymic activity was lost in a nonexponential manner when measured with BPA and casein. The peptides produced by catalysis with irradiated enzyme were qualitatively different from those found after proteolysis in the presence of nonirradiated chymotrypsin. Oxygen was protective for the enzyme under the conditions employed. (auth)

18908 THE INFLUENCE OF ENERGY DEPRIVATION ON THE REPAIR OF RADIATION INDUCED DNA DAMAGE. Moss, Alfred Jefferson. Little Rock, Ark.; Univ. of Arkansas (1970). 88p. University Microfilms Order No. 70-26,238.

Thesis.

The production of rejoining of x-ray induced single stranded DNA breaks was studied using the alkaline sucrose density gradient technique. L cell suspensions labeled with tritiated thymidine, a DNA precursor, were studied under both control and energy deprived conditions using 1×10^{-4} $\underline{M}$ DNP (2,4-dinitrophenol) an uncoupler of aerobic oxidative phosphorylation. Sedimentation patterns were obtained using cell suspensions irradiated with various doses from 0 to 10 K rads to determine the effect of dose on the production of single strand breaks. The rejoining of radiation induced single stranded breaks was studied in both the presence and absence of DNP. Cell suspensions were incubated at 37°C following a 10 K rad dose. Results show that the induction of single stranded breaks probably includes a nucleolytic component in addition to indirect free radical effects. A greater number of breaks were produced in the absence of DNP, indicating that depressed ATP levels reduce endogenous nucleolytic activity. The rejoining mechanism is enzymatic and requires an available ATP supply for operation. In the presence of DNP no rejoining was observed following 30 minutes incubation after 10 K rads. Single stranded DNA from L cell suspensions was found to be only partially soluble in an alkaline detergent lysing solution commonly employed for the preparation of cell lysates prior to ultracentrifugal analysis. The addition of 0.05 M EDTA (ethylenediamine tetraacetate) was found to promote the formation of a homogenous lysate. Single stranded DNA solubility is dose dependent in the absence of EDTA. This limited solubility phenomenon offers a system for the study of radiation effects on labeled cultured mammalian cells in the physiological dose region. (Diss. Abstr.)

18909 VARIATIONS IN THE MAKEUP OF LENS INSOLUBLE PROTEINS. Zigman, S.; Schultz, J.; Yulo, T. (Univ. of Rochester, N. Y.). Exp. Eye Res.; 10: 58-63(Jul 1970).

In this study differences in the composition of lens water-insoluble protein of several species were sought. Lenses of young and old rats, x irradiated rats, young and old dogfish and cows, and normal and nuclear cataractous humans were separated into cortex and nucleus from which total insoluble protein was isolated by centrifugation. Urea soluble (US) and urea insoluble (UI) portions were separated, and the amounts of protein represented by these fractions were estimated. The soluble components comprising these fractions were observed by acrylamide gel electrophoresis. In rat and dogfish lenses, UI levels increased with aging in the nucleus of the lens, while in bovine and normal human lenses US predominated in both cortex and nucleus. Human nuclear cataractous lens nuclei, however, contained much higher levels of UI than of US material. Possible modifiers of the formation of insoluble protein leading to the diversity of compositions observed are discussed. (auth)

18910 DNA SYNTHESIS AFTER IRRADIATION WITH HIGH DOSES OF X-RAYS AND SPINDLE INHIBITION. von Wangenheim, K.-H.; Walther, F.; Kern, H. (Kernforschungsanlage, Juelich, Ger.). Z. Pflantzenzuecht.; 64: 6-19(Aug-Sep 1970). (In German).

Chloro-IPC was shown after seed treatment of wheat and Oenothera hookeri to be a highly specific spindle poison. The cycle of chromosome contraction and DNA synthesis remains unchanged, so that nuclei with a high degree of polyploidy in large cells arise. At the same time the suppression of spindle activity interferes with cell extension. Chloro-IPC was used in investigating the causes of suppression of mitotic activity resulting from irradiation with the object of demonstrating DNA synthesis after irradiation. In this connection it was shown that the initiation of DNA synthesis is delayed with increasing doses of irradiation and the number of synthesizing nuclei diminishes. Nevertheless, on irradiation with unusually high doses (600 to 736 kR) nuclei are still formed which, according to their DNA content (Feulgen photometry), have passed beyond the fourth mitotic cycle. This, together with the completion of development of the cells, is taken as an indication that the suppression of mitosis by irradiation is caused not by the induction of irreversible genetic defects but by "premature differentiation," the cause of which is the continuance of cytoplasmic development during the temporary inhibition of the nucleus by irradiation. The deleterious effects exerted by "premature differentiation" on the induction of mutations are discussed. (auth)

18911 DOUBLE-STRAND BREAKS IN THE DNA OF A MAMMALIAN CELL AFTER X-IRRADIATION. Lehmann, A. R.; Ormerod, M. G. (Royal Cancer Hospital, Sutton, Eng.). Biochim. Biophys. Acta; 217: 268-77(Oct 1970).

The production of x-ray-induced double-strand breaks in the DNA of murine lymphoma cells ($L_{517}8Y$) was measured by determining the molecular weight of the DNA from x-irradiated cells. The cells were lysed on top of neutral sucrose gradients and the molecular weight of the released DNA was measured by rate sedimentation through the gradients. Several independent criteria were used to test whether the sedimenting DNA was pure and unaggregated and to show that the sedimentation behavior of the DNA provided a true measure of its molecular weight. These criteria were only fulfilled if the speed of centrifugation was less than 20,000 rev./min. Using these conditions, the results show that double-strand breaks are formed in the DNA of $L_{517}8Y$ cells as single events with an efficiency of 2900 ± 400 eV per break, and that after x-ray doses of more than 20 krads these breaks are not rejoined on post-irradiation incubation. Under appropriate conditions DNA molecules of molecular weight up to $2 \cdot 10^9$ sediment freely and the molecular weight of DNA from unirradiated cells is at least $3 \cdot 10^9$ and probably greater. (auth)

18912 PRODUCTION AND REPAIR OF RADIOCHEMICAL DAMAGE IN ESCHERICHIA COLI DEOXYRIBONUCLEIC ACID; ITS MODIFICATION BY CULTURE CONDITIONS AND RELATION TO SURVIVAL. Town, Christopher D.; Smith, Kendric C.; Kaplan, Henry S. (Stanford Univ., Calif.). J. Bacteriol.; 105: 127-35 (Jan 1971).

Late log-phase Escherichia coli B/r cells are 1.6 times more sensitive to killing by x rays than are stationary-phase cells when grown in Brain Heart Infusion (BHI) + glucose. The number of single-chain breaks formed per krad is the same for log- and stationary-phase cells. Stationary-phase cells show a somewhat greater ability to repair single-chain breaks (especially after high doses of x rays) than do log-phase cells. The rapidity and extent of postirradiation deoxyribonucleic acid (DNA) degradation are greater in log-phase cells than in stationary-phase cells. The enhanced viability exhibited by stationary-phase cells thus appears to correlate both with enhanced single-chain break repair and the reduced degradation of DNA. Cells grown to stationary phase in peptone medium (PO cells) are 3.4 times more sensitive to killing by x rays than cells grown to stationary phase in peptone medium supplemented with glucose and phosphate buffer (PG cells). The yield of single-strand breaks is the same for both types of cells (but the absolute yield is about two times higher than in the cells grown in BHI + glucose). The kinetics for the repair of single-chain breaks are the same for both types of cells for about 30 min. After this time period, further repair ceases in the PO cells but continues in the PG cells, provided that glucose is present in the medium. Postirradiation DNA degradation is both more rapid and more extensive in PO cells than in PG cells whether or not glucose is present in the postirradiation incubation medium. The survival of stationary-phase E. coli B/r grown in PO or PG medium is likewise unaffected by the presence of glucose in the plating medium, and thus correlates better with the lower DNA degradation seen in the PG cells than with the increased strand rejoining, since this latter process requires the presence of glucose. (auth)

18913 EVALUATION OF PHOTOTOXICITY OF SALICYLANILIDES AND SIMILAR COMPOUNDS BY PHOTOHEMOLYSIS. Kahn, Guinter; Fleischaker, Barbara (Univ. of Colorado, Denver). J. Invest. Dermatol.; 56: 91-7(Feb 1971).

A system is described in which red blood cell photohemolysis is induced by salicylanilides and similar compounds. The range of chemical and physical conditions at which each compound reacts defines its ability as a photosensitizer. Results are correlated with the known clinical photoactivity of these compounds. Pre-irradiation by artificial and natural sunlight produced photoproducts which were evaluated by thin layer chromatography, ultraviolet spectroscopy, osmotic fragility, pH changes and toxicity to red blood cells. (auth)

18914 RED BLOOD CELL HEMOLYSIS BY PHOTOSENSITIZING COMPOUNDS. Kahn, Guinter; Fleischaker, Barbara (Univ. of Colorado, Denver). J. Invest. Dermatol.; 56: 85-90(Feb 1971).

Irradiation (290 to 370 and 320 to 400 nm) of red blood cells in the presence of some photosensitizing compounds caused hemolysis. The extent of photohemolysis was determined to evaluate effects of these compounds on red blood cell membranes. Tested substances included porphyrins, tetracyclines, psoralens, salicylanilides, phenothiazines, anthracenes and sulfonamides. Optimal physical and chemical conditions for photohemolysis were determined for each compound. Amount of hemolysis varied with pH, solvent and buffer system and sensitizer. Strongly buffered solutions tend to inhibit the reaction. We interpret the reaction to be photoxic, presumably to the cell membrane, because the RBC is essentially devoid of organelles and the reaction rate increased as the concentration of the photosensitizer increased. Non-photosensitizing substances did not react. Effects of the test compounds on RBCs were monitored with a spectrophotometer and fragiligraph, which indicated that some drugs combine with the RBC membrane in the dark and others require light. Psoralens and tetracyclines did not induce photohemolysis. (auth)

18915 RADIOTOXIN FRACTIONATION AND INVESTIGATIONS ON THEIR BIOLOGICAL PROPERTIES. Kasymov, A.; Zakirova, L. S. (Tashkent State Univ.). Uzb. Biol. Zh.; No. 3, 6-8(1970). (In Russian).

In work by the gelfiltration method on Sephadex G-10, active radiotoxin fractions were extracted from irradiated potato tubers and an irradiated rat liver. It has been found that active radiotoxin fractions inhibit corn root growth. (auth)

18916 STUDIES ON RNA SYNTHESIS PRIMED BY γ-IRRADIATED CHROMATIN TEMPLATES. Mee, L. K.; Weiss, J. J.; Wheeler, C. M. (Univ. of Newcastle upon Tyne, Eng.). Monatsh. Chem.; 101: 1639-47(Nov-Dec 1970). (In German).

The effects of γ radiation on chromatin (calf thymus and rat liver) particularly on its function as a template for the synthesis of RNA by DNA-dependent RNA polymerase were studied. The initial effect of the radiation was found to be some enhancement of the template activity of the chromatin, although at higher doses the priming ability is progressively reduced. Kinetic studies suggest that the enhancement is not due to an increase in the number of enzyme binding sites for the RNA-polymerase, while the inhibition at higher doses is accompanied by an increased number of binding sites that are inactive in RNA synthesis. A nearest neighbor base frequency analysis of the RNA synthesized on the chromatin templates was made. This indicates that the transcription from the chromatin is asymmetric. With irradiated chromatin templates, changes in base composition of the synthesized RNA suggest a relatively greater radiation sensitivity of the adenine—thymine base pair in the chromatin DNA. (auth)

18917 EFFECTS OF ^{60}Co GAMMA RAYS ON LYSOZYME IN AQUEOUS SOLUTION. Yamamoto, Kazuhiko (Osaka Univ.). J. Radiat. Res.; 11: 85-91(Jun 1970).

Lysozyme in 0.5% aqueous solution was irradiated with several doses of ^{60}Co γ rays. The effects of γ radiation on lysozyme molecule were studied by the methods of amino acid analysis, N-terminal amino acid analysis, measurement of amide-nitrogen content, ultraviolet spectroscopy, and ultracentrifugal analysis. In a sample that lost 69% of its initial enzyme activity on irradiation of 1.4×10^6 R, no significant change was observed in amino acid composition and amide-nitrogen content. N-terminal amino acids other than lysine, which was expected to be released by peptide bond cleavage, were not detected. Ultracentrifugal analysis of the irradiated lysozyme indicated the existence of a polymerized component in addition to the intact lysozyme. Mechanisms of γ-ray inactivation on lysozyme and the role of the polymerized component are discussed. (auth)

18918 PYRUVIC ACID CONTENT OF NUCLEI AND MITOCHONDRIA IN CELLS OF COTTON PLANTS UNDER NORMAL CONDITIONS AND FOLLOWING γ-IRRADIATION. Arslanova, S. V. (Inst. of Experimental Biology of Plants, Tashkent). Uzb. Biol. Zh.; No. 5, 76-8(1970). (In Russian).

The content of pyruvic acid in the cell nuclei and mitochondria of cotton plants was studied along with the activity of the associated dehydrogenases. Germinating seeds of varieties C-1622 (late harvesting) and 1306-DV (early harvesting) cotton were exposed to 10 kR of γ radiation at a dose rate of 19 R/sec. The maximum content of pyruvic acid in nuclei and mitochondria was observed at 48 hr postirradiation. The content then decreased until day 10, at which time it again increased. Glutamine and asparagine accumulated in the tissues inhibiting their conversion to other amino acids. The associated dehydrogenases were inhibited by irradiation (mildly at first, but increasing with time). Moreover, the inhibition of the dehydrogenases was more pronounced in the rootlets than in the leaves. (E.R.B.)

Immunology

Refer also to abstracts 19127 and 19130.

18919 (RLO-2225-T-16-1) LYMPHOCYTE FORMATION, LIFE SPAN, FATE, AND POTENTIAL FOR REPOPULATING HEMOPOIETIC TISSUES OF IRRADIATED ANIMALS. Progress Report. (Washington Univ., Seattle. School of Medicine). 4 Jan 1971. Contract AT(45-1)-2225. 4p. Dep. NTIS.

The effectiveness of antilymphocytic serum of the rat in suppressing immune responses such as homograft rejection was studied. It was found that the antilymphocytic serum caused a pronounced reduction in the number of small lymphocytes. It was also found that the cells were phagocytized by the liver Kupffer cells and by phagocytes of the spleen. Tritium-labeled thymidine was used in studies on deoxycytidine and thymidine dependency of lymphocytes grown in a monolayer system in the presence of phytohemagglutinin. Results led to the suggestion that blast cells in the initial PHA cultures correspond to cells in the germinal centers of lymph nodes, and those in late PHA cultures correspond to cells in the lymph node cortex outside the centers. Studies were initiated on reversal of labeling intensity with PHA cultures using tritium-labeled deoxycytidine. Studies using parabiotic rats in which one member received multiple injections of thymidine showed that more than 95% of the large blast cells in thoracic duct lymph are formed in lymph nodes or Peyer's patches and do not recirculate from blood to lymph. A quantitative assessment was made of cellular recovery in lymphoid tissues of the guinea pig following 150 R total body irradiation. (H.L.W.)

18920 PLASMA RENIN CONCENTRATION MEASURED BY USE OF RADIOIMMUNOASSAY FOR ANGIOTENSIN I. Giese, J.; Joergensen, M.; Damkjaar Nielsen, Meta; Lund, J. O.; Munck, O. (Glostrup Hospital, Copenhagen). Scand. J. Clin. Lab. Invest.; 26: 355-67(Dec 1970).

A method for the determination of plasma renin concentration was described in which efficient inactivation of angiotensinases, use of human renin as internal standard, and radioimmunological quantitation of angiotensin I are combined. The mean recovery of angiotensin I through incubation and extraction was 84%, SD 1.3%. In normal subjects, the plasma renin concentration was on the average, 24 g units/ml, range 6 to 59. The coefficient of variation for plasma renin determinations was 12 to 15%. This included variations due to storage or dilution of plasma. The method is well suited for routine clinical use. (auth) (Norway)

18921 EFFECT OF ANTILYMPHOCYTIC SERA ON THE HEMOPOIETIC TISSUE. Kaulen, D. R.; Golovanova, T. A. (Inst. of Epidemiology and Microbiology, Moscow). Vestn. Akad. Med. Nauk SSSR; No. 7, 33-41(1970). (In Russian).

Effects of rabbit antisplenic, antithymic, and antimarrow sera on hematopoietic stem cells of mice were analyzed. The tissues of the spleen, bone marrow, and embryonic liver were incubated in vitro with various dilutions of antisera and were transplanted to a lethally irradiated (850 rad) syngeneic or semisyngeneic recipient. The number of stem cells was estimated by counting the number of colonies formed in the recipient's spleen. Results showed that the antisplenic serum intensively inhibited the stem cells. The cell suspension concentration at the time of its incubation with the antiserum was of no significance. A comparative study of the antisplenic, antithymic, and antimarrow sera showed that they inhibited the splenic stem cells to the same degree. The role of the antilymphocytic component in the antisera effects on stem cells was pointed out. Addition of the antisera to various tissues showed that sorption on erythrocytes and cells of the kidney did not influence the effectiveness of the serum. A slight fall occurred during sorption on embryonal liver cells or lymphocytes. Experimental data led to the conclusion that there are essential differences between stem and lymphoid cells. It was also concluded that the effect of the antiserum does not depend upon its cytoxicity but upon other factors. (auth)

18922 INFLUENCE OF IONIZING RADIATION ON THE NATURAL IMMUNITY AND WAYS OF ITS STIMULATION. Tumanyan, M. A.; Duplishcheva, A. P.; Chakhava, O. V.; (and others). Vestn. Akad. Med. Nauk SSSR; No. 7, 25-33(1970). (In Russian).

Data on the effects of ionizing radiation on cellular and humoral factors of natural immunity are presented. A method of stimulating natural immunity using bacterial preparations of the intestinal group is described. It was shown that the active principle of the antigen was a polysaccharide and that the polysaccharide also had a radioprotective effect. (auth)

18923 ANTIBODY INHIBITION OF THE IMMUNE RESPONSE: EXPERIMENTAL ANALYSIS OF THE SITE OF ACTION IN VIVO. Eisenberg, R. A.; Weissman, I. L. (Stanford Univ., Palo Alto, Calif.). J. Immunol.; 106: 143-9(Jan 1971).

Analysis of inhibition of the immune hemolysin response was tested in vivo, utilizing sublethally irradiated mice injected with sheep red blood cells (SRBC) in order to separate antigen processing from central cellular events. The experiments demonstrate that passive anti-SRBC antibody, given to mice 2 days after SRBC and 3 days after irradiation with 600 rads, completely suppressed the response of incubated as well as non-incubated normal isologous spleen cells injected on the same day or 1 to 3 days after SRBC, but only partially suppressed a similar response in unirradiated mice when injected 2 days after SRBC. These experiments suggest that passive antibody can suppress the immune response by acting at some step subsequent to antigen processing. (auth)

18924 PREPARATION OF NONINFECTIOUS ARBOVIRUS ANTIGENS BY SUCROSE–ACETONE EXTRACTION OF GAMMA-IRRADIATED TISSUE. Tzianabos, Theodore; Campbell, Robert C.; Wright, George G. (Medical Sciences Lab., Frederick, Md.). Proc. Soc. Exp. Biol. Med.; 136: 187-90(Jan 1971).

Gamma irradiation of arbovirus-infected suckling mouse tissue provided a means of inactivating the virus in frozen tissue and allowed safe and convenient preparations of arbovirus serologic antigens by the sucrose–acetone extraction procedure. In most cases the irradiated tissues yielded satisfactory hemagglutination (HA) and complement fixing antigens following extraction. With those viruses for which HA activity was reduced by irradiation, sonication during extraction of the dried acetone–insoluble precipitate with saline restored HA titers to levels approaching those obtained with unirradiated tissue. Irradiation avoids the hazards of extraction of infectious tissue, and the extracts may be used for serological studies in laboratories not equipped for manipulation of infectious agents. (auth)

18925 STUDIES ON THE INITIATION AND REGULATION OF ANTIBODY FORMATION TO SHEEP RED BLOOD CELLS IN MICE. Jimenez-Zamudio, Luis Antonio. New Brunswick, N. J.; Rutgers–The State Univ. (1970). 199p. University Microfilms Order No. 70-10,076.

Thesis.

XUM

A number of cellular events involved in the initiation and regulation of the antibody response were explored in vivo and in vitro studies. Inbred and random-bred mice, or lymphoid tissue derived from them, were used. Sheep red blood cells (sRBC) served as the principal antigen, and all responses were measured in terms of numbers of antibody-forming cells (AFC). One aspect of the study involved an assessment of the number of stem cells of antibody-forming spleen cell populations in normal and immune mice. It was concluded that the differences observed in the total number of AFC in spleens of stimulated or suppressed animals were due to changes in the rate of cell proliferation and not due to any alteration in the number of stem-cells. Studies conducted with animals that had been treated with colloids to block the reticuloendothelial system (RES) indicated that a participation of macrophages is required for the initiation of a normal antibody response. Administration of antigen at the time of blocking of the phagocytic activity of macrophages by thorium dioxide (thorotrast) originated a long period of specific non-responsiveness to the antigen given at the time of RES blockade. Attempt to restore such impaired responses with the aid of peritoneal cells from normal or immune donors was partially successful. When cultivation of spleen fragments was initiated, in the absence of antigen, at different times after immunization of the spleen donor, the antibody response continued very much like it would have in vivo. In contrast, when spleen cell suspensions were cultivated in antigen-free media, the antibody response continued, independent of the time that had elapsed since immunization of the donor, and reached a peak three to four days after transfer from in vivo to in vitro conditions. Studies on the kinetics of the primary response induced in spleen cell suspensions in vitro, showed a similarity of this response, both in duration and magnitude, with the typical response in vivo. A stimulation of the primary antibody response in vitro also was observed when spleen cells from several random-bred CF No. 1 mice were pooled for use in one tissue culture, and compared with the response in cultures initiated with single spleens. The results are discussed from the viewpoint that the initiation of antibody formation might represent the activation of preexisting stem-cells by an antigen-guided non-specific activator. (Diss. Abstr. Int., B) (TSS)

Ecology

Refer also to abstracts 18894, 18986, 18987, 18989, and 19103.

18926 (CONF-700816-(Vol.1), pp 49-71) RADIOIODINE FIELD STUDIES WITH SYNTHETIC AEROSOLS. McNelis, D. N.; Black, S. C.; Whittaker, E. L. (Public Health Service, Las Vegas, Nev. Southwestern Radiological Health Lab.).

From 11. AEC air cleaning conference; Richland, Wash. (31 Aug 1970).

In Proceedings of the eleventh AEC air cleaning conference.

The radioiodines are the principal source of human thyroid exposure at early times following the detonation of fission devices. The major pathway for this exposure is the forage-cow-milk chain. With the cessation of atmospheric testing and the reduction in Plowshare activities, simulation remains the primary method to study this pathway. To do this, a series of experiments was conducted in which a radioactive contaminant was released under controlled conditions to simulate the passage of a radioactive cloud over cow forage. Forage is the initial link in the forage-cow-milk-man food chain and in these studies the interrelationship of the physical, chemical and biological variables concerning the transport through that link was investigated. Na ^{131}I labeled diatomaceous earth aerosols with count median diameters ranging from 0.2–24.0 μm, a ^{131}I labeled hydrosol and elemental iodine were generated for these studies. The aerosol preparation, labeling, generation and analytical procedures are discussed. (auth)

18927 (NP-18670) RADIOACTIVITY IN THE DIET OF THE INHABITANTS OF THE BRAZILIAN REGIONS OF ELEVATED NATURAL RADIATION. Penna Franca, Eduardo (Universidade Federal do Rio de Janeiro (Brazil). Instituto de Biofisica). 1968. 163p. (In Portuguese). Dep. NTIS (U. S. Sales Only).

Thesis.

Studies are reported on populations dwelling on high natural radioactivity areas in Brazil. Two such areas studied included the monazite sand region, along the coast of the State of Espírito Santo, and the volcanic intrusive anomalies, in the State of Minas Gerais. The main objective of the study was to evaluate the extent of the radioactive intake and internal contamination of the selected populations in both regions, in order to determine whether biological effects of ionizing radiation could be identified and investigated. Two villages were surveyed in the monazite sand region: Guarapary and Meaipe. The local production of food was found to be insignificant and their radioactive contents were practically within normal ranges. No statistically significant differences were observed between average ^{226}Ra and ^{228}Th contents in teeth and placentae from inhabitants of the two villages and controls. External beta and gamma radiations from the soil are the main source of human irradiation in the region. Inhalation of dust and thoron and daughter production, are secondary sources of irradiation. In the State of Minas Gerais, the villages of Tapira and Barreiro, near Araxá, were selected for having extensive agriculture production, cultivated, to a large extent, in radioactive soil. A complete survey of the radioactive contamination of local produce demonstrated high ^{226}Ra and ^{228}Ra contents in many types of foodstuff, reaching in some cases two orders of magnitude above average normal values. A dietary inquiry was conducted in a representative sample of the population which led to classify the inhabitants in groups, according to certain ranges of radioactive intake. The inquiry demonstrated that the internal radioactive contamination of the local population was of less magnitude than the levels in food had indicated. Only 12% of the inhabitants had daily intake of alpha emitters above five times the average in normal regions. Analyses of ^{226}Ra and ^{228}Th in teeth and placentae were carried on concomitantly, as a sensitive method for the detection of people with above average radium body-burdens. Body burden in these individuals will be measured using whole-body counters. Considering the relatively low levels of external and internal radiation doses to which the inhabitants of the surveyed areas are exposed, and also the small size of the populations, it was concluded that the only biological effect of radiation that could possibly be of significance would be chromosome aberrations. (C.H.)

18928 (NYO-3446-14) RADIOACTIVE FOODCHAINS IN THE SUBARCTIC ENVIRONMENT. Annual Report, August 15, 1969–August 14, 1970. Miettinen, Jorma K. (Helsinki Univ. (Finland). Dept. of Radiochemistry). Contract AT(30-1)-3446. 100p. Dep. NTIS.

Separate abstracts were prepared on seven sections of this report. (C.H.)

For abstracts of individual sections see: 18929–18933, 18986, and 18987.

18929 (NYO-3446-14, Paper 26) POLONIUM AND RADIOLEAD IN SOME LAND ANIMALS IN FINLAND. Kauranen, P.; Miettinen, J. K.; Pulliainen, E. (Helsinki Univ. (Finland)). 10p. (CONF-700412-1).

From Meeting on the Biology and Ecology of Polonium and Radiolead, Sutton, England.

Samples of reindeer, elk, willow grouse, and rock ptarmigan as well as samples of predators such as wolverine, wolf, lynx, and bear were collected from Lapland and other parts of Finland and analyzed for polonium and radiolead. It can be seen that all samples collected from Lapland (not only those of lichen-eating reindeer) show a more or less elevated polonium level in relation to samples collected from other parts of Finland. The highest soft tissue concentrations (3900 pCi ^{210}Po and 1200 pCi ^{210}Pb per kilogram wet weight) were found in reindeer killed in winter, but the highest bone concentrations (5900 pCi of ^{210}Po and 10,800 pCi of ^{210}Pb per kg) were observed in rock ptarmigan. The ^{210}Po/^{210}Pb ratios varied between 1.2 and 120 in soft tissues and between 0.3 and 0.9 in bones. The soft tissues of predators show generally somewhat higher ^{210}Po/^{210}Pb ratios than did those of herbivores. In several cases the stomach contents of the animals were studied and in some cases also analyzed for polonium and radiolead. (auth)

18930 (NYO-3446-14, Paper 27) POLONIUM AND RADIOLEAD IN SOME AQUEOUS ECOSYSTEMS IN FINLAND. Kauranen, P.; Miettinen, J. K. (Helsinki Univ. (Finland). Dept. of Radiochemistry). 18p. (CONF-700412-2).

From Meeting on the Biology and Ecology of Polonium and Radiolead, Sutton, England.

Samples of water, invertebrates and fish from fresh and brackish waters were collected in Finland and analyzed for polonium and radiolead. The data show that polonium is strongly enriched in some aquatic food chains while radiolead is enriched to a lesser degree. In invertebrates from the Gulf of Finland the polonium concentrations varied between 0.2 and 4.0 pCi per gram wet weight and the radiolead concentrations between 0.01 and 0.15 pCi per gram wet weight. These values are more than one order of magnitude higher than those observed in fish. In fish flesh the polonium concentrations varied between 3.3 to 45 pCi/kg wet weight and the radiolead concentrations between less than 0.1 to 4.7 pCi/kg wet weight. The highest polonium as well as radiolead concentrations in fish were found in plankton-eating fish (Baltic herring, cisco) and the lowest in salmon and trout. In whole fish the concentrations seem to be from 2.5 to 10 times higher than in fish flesh. From about 50 to 75 per cent of the polonium in fish seems to be located in the entrails. While the ^{137}Cs-concentration of fish is strongly dependent on the limnological type of the lake, little or no such correlation seems to exist for polonium and radiolead. (auth)

18931 (NYO–3446-14, Paper 30) CHEMICAL AND RADIOACTIVE ENVIRONMENTAL PROBLEMS IN FINLAND. Miettinen, Jorma K. (Helsinki Univ. (Finland). Dept. of Radiochemistry). 24p.

Fallout research activities of six institutes in Finland are discussed. Results of beta activity measurements are reported from 14 recording aerosol measurement stations. The relation of high body burdens of ^{137}Cs found in Lapps to ecological conditions is discussed. Results are reported for analysis of rainwater for ^{90}Sr, ^{137}Cs, and ^{3}H and analysis of milk for ^{137}Cs and ^{90}Sr. Cereals were analyzed for ^{90}Sr and human bones and flesh were analyzed for ^{137}Cs and ^{90}Sr. Activities are described in the training of scientists for fallout research and in the development of methods for quantitative analysis of radionuclides in airfilters, rainwater, and agricultural products. Food chain research was conducted with emphasis on concentration of ^{137}Cs, ^{210}Pb, ^{210}Po, ^{55}Fe, and ^{90}Sr in lichens, reindeer, and man. The contribution to internal dose from natural sources such as ^{14}C, ^{40}K, ^{87}Rb, ^{226}Ra, ^{228}Ra, and ^{222}Rn is discussed. The artificial background radiation dose from short-lived radionuclides such as ^{95}Zr, ^{106}Ru, and ^{144}Ce was estimated. It was estimated that the total radiation dose from all sources was 260 mrem/y during the 1960's. The use of radiochemical techniques for elucidation of food chains is discussed. Studies on contamination of aquatic fauna with mercury were conducted using ^{203}Hg as a tracer. (H.L.W.)

18932 (NYO–3446-14, Paper 31) RADIONUCLIDES IN PLANTS AND REINDEER MEAT IN LAPLAND. Rahola, Tua; Miettinen, J. K. (Helsinki Univ. (Finland). Dept. of Radiochemistry). 6p.

Gamma emitting radionuclides were analyzed by γ spectrometry in plant samples collected in Lapland during 1968 and 1969. A table is presented to show contents of ^{137}Cs, ^{54}Mn, ^{95}Zr, ^{106}Ru, and ^{125}Sb in a variety of plants. Samples of reindeer meat were collected and analyzed for ^{137}Cs by γ spectrometry during 1966 to 1970. A marked decrease occurred from 1966 to 1967, while no decrease occurred from 1967 to 1970. (H.L.W.)

18933 (NYO–3446-14, Paper 32) STABLE LEAD AND RADIOLEAD IN AIR FILTER SAMPLES. Kauranen, Pentti; Laensimaeki, Marja (Helsinki Univ. (Finland). Dept. of Radiochemistry). 4p.

Since it might be possible to use ^{210}Pb as a natural tracer for that part of stable lead which is taken up by inhalation, the specific activity of lead in aerosols collected on filters and its dependence on locality, season, and weather conditions were determined. A set of aerosol samples were collected from the roof of a building in Helsinki, Finland, from a rural area in southern Finland about 40 km from Helsinki, and from a rural area in the southern part of Lapland. Results showed that the specific activity of lead in ground-level air is considerably lower in Helsinki than in rural areas and that the specific activity of airborne lead varies in wide limits (about three orders of magnitude). This limits the usefulness of ^{210}Pb as a tracer for lead in aerosols. (C.H.)

18934 (ORO–3514-10) USE OF RADIOISOTOPES FOR STUDIES ON THE ECOLOGY OF TICK VECTORS OF DISEASE. Final Progress Report, April 1, 1966–December 31, 1970. Sonenshine, Daniel E. (Old Dominion Coll., Norfolk, Va.). Contract AT(40-1)-3514. 129p. Dep. NTIS.

The following species of ticks were used in mass rearing studies: Dermacentor variabilis, D. andersoni, Amblyomma americanum, and Haemaphysalis leporispalustris. A total of 1420 ticks were inoculated with ^{14}C glucose for various field programs during a three year period. Observations were made on mortality following inoculation and average radioactivity in larvae from inoculated females during all three years. Results are presented in the form of graphs and show frequency distributions of egg numbers in egg batches from ovipositing females and frequency distributions of means of radioactivity per larval batch. The ecology of vector ticks of Rocky Mountain spotted fever was studied in two forest localities in Virginia. Host parasite relations, seasonal occurrence, and other ecological associations of ticks infesting wild mammals are described. The ecology of the lone star tick, Amblyomma americanum, was studied in two contrasting habitat types in Virginia. Larvae were labeled with radioisotopes to assist in determining relative population sizes in these areas. Results led to the conclusion that the deep woods predominantly lowland deciduous forest habitat has a high tick support capacity whereas the small, frequently cut over upland woodlots have a low or moderate tick support capacity. Studies were conducted on spermatogenesis in Dermacentor variabilis in relation to duration of feeding and the presence of chromosomal aberrations in stocks injected with ^{14}C-labeled glucose. Tick progeny were labeled by inoculation of engorged females with ^{14}C, ^{144}Ce, ^{32}P, ^{90}Sr, and tritium; this technique resulted in production of viable labeled eggs and larvae. Double labeling of the dog tick with ^{14}C and ^{90}Sr was performed by inoculation of mixtures of ^{14}C glucose and inorganic ^{90}Sr into the engorged parents. Investigations were conducted on the fertility and fecundity of Dermacentor variabilis reared from larvae labeled with ^{14}C. Field trials were conducted to investigate the potential use of ^{14}C-labeled ticks in ecological studies in natural areas in Virginia and Montana. (H.L.W.)

18935 (ORO–3905) EVALUATION OF THE FACTORS INVOLVED IN BIOACCUMULATION OF GAMMA-EMITTING RADIONUCLIDES IN WHITE-TAILED DEER (ODOCOILEUS VIRGINIANUS). Second Technical Progress Report, February 1, 1970–January 31, 1971. Jenkins, J. H.; Fendley, T. T. (Georgia Univ., Athens. School of Forest Resources). 1 Nov 1970. Contract AT-(40-1)-3905. 35p. Dep. NTIS

Samples of muscle tissue were obtained systematically from 258 deer from a variety of ecological situations throughout the Southeast during 1969. These were analyzed for all gamma-emitting radionuclides by gamma spectrometric methods. Only ^{137}Cs and ^{40}K were detected in muscle tissue. Deer muscle averaged 45,000 pCi/Kg of ^{137}Cs with some specimens ranging up to 75,000 pCi/Kg, in the Lower Coastal Plain during the winter. Piedmont animals averaged around 3,000 pCi/Kg while southern Appalachian deer were about 6,000 pCi/Kg. The averages were about the same as that during the past four years, although the highest specimens (150,000 pCi/Kg ^{137}Cs) were taken in early 1968. It is postulated, with considerable supporting data, that the sterile, moist, sandy soils of the Lower Coastal Plain in combination with high water tables and some specific radionuclide concentrating plants produce the conditions which result in high biomagnification of ^{137}Cs in deer muscle tissue. There did not appear to be a significant difference in potassium concentration in deer muscle from the different physiographic regions; however, soil and vegetation samples from the Lower Coastal Plain were most deficient in potassium. Bioaccumulation studies of ^{137}Cs in the bobcat (Lynx rufus) produced data that aid in understanding the factors responsible for bio-magnification in deer and other wildlife. Cotton rats, a major food item of bobcats, were found with ^{137}Cs concentrations up to 133,051 pCi/Kg. Because of the tiny home range of the cotton rat, it was possible to study limited areas, and document the pathways of ^{137}Cs transfer from fallout to soil-vegetation to herbivore. It was concluded that the amount of ^{137}Cs in the soil may be unrelated to the amount of uptake in plants; high uptake in plants is usually, but not always, related to high bioaccumulation of ^{137}Cs (and probably ^{90}Sr) in mammals; and that bioaccumulation is more dramatic under conditions of severe potassium deficiency. (C.H.)

18936 DEVELOPMENT OF A RADIOACTIVE MARINE PERIPHYTAL COMMUNITY. Hallopeau, C. (Institut Oceanographique, Paris). Radioprotection; 4: 259-65(1969). (In French).

The development of a marine periphytal community, contaminated with either ^{137}Cs (50 to 500 μCi/l) or ^{144}Ce (5 to 50 μCi/l) was studied. During these experiments, radioactive pollution was found to entail a decrease in productivity. The chlorophyll-A content of microsystems initially contaminated with the following concentration: ^{144}Ce : 5 μCi/l, ^{137}Cs : 500 μCi/l, ^{137}Cs : 50 μCi/l, ^{144}Ce : 50 μCi/l, gave values in a decreasing order. This effect was obtained on communities having grown for over 4 months under contaminated conditions. It was concluded that ionizing radiations at levels low for the considered species yet much higher than those predictable in the natural environment can entail unfavorable effects on ecosystems in certain conditions. (auth)

18937 POLLUTION AND HYDROBIOLOGY OF FRESH WATER. Bovard, P.; Foulquier, L. (CEA, Saint-Paul-Les-Durance, France). Bull. Inform. Sci. Tech. (Paris); No. 151, 51-4(Sep 1970).

The hydrobiological studies carried out in the Continental Radioecology Laboratory are reviewed. Experiments on the contamination of mosses, molluscs and certain fish (roach, catfish, eel) are summarized. The work was completed by experiments with the radioelements: strontium, manganese and cobalt, and with certain pesticides (lindane). The methods and techniques used in radioecology can be applied to nonradioactive contaminants. (auth) (France)

18938 TRANSFER OF RADIONUCLIDES TO PLANTS BY IRRIGATION. Delmas, J.; Grauby, A.; Disdier, R. (CEA, Saint-Paul-Les-Durance, France). Bull. Inform. Sci. Tech. (Paris); No. 151, 67-73(Sep 1970). (In French).

In order to study the contamination of plants by irrigation, an experimental model simulating the radiocontamination of cultures by sprinkling them with water was developed. The absorption and distribution of radioelements in these plants were studied, and the ratio between the contamination of the food and the water determined. The relative importance of direct and indirect contamination of various plants was determined using ^{137}Cs and ^{90}Sr. (auth) (France)

18939 IN SITU OBSERVATION OF THE CONTAMINATION OF MARINE SPECIES BY ^{106}Ru AND ^{95}Zr. Gueguenlat, P. (CEA, Cherbourg, France). Bull. Inform. Sci. Tech. (Paris); No. 151, 23-6(Sep 1970). (In French).

An account of radioactivity measurements carried out in situ in a part of La Hague sector affected by radioactive waste discharge since the plant began operating in 1965 to 1966 is given. The concentration factors for ^{106}Ru and ^{95}Zr in the algae are given. (auth) (France)

18940 STUDY OF RIVER BED POLLUTION. THE DEVELOPMENT OF EQUIPMENT SIMULATING NATURAL FLOW. Picat, P. (CEA, Saint-Paul-Les-Durance, France); Morisset, A. Bull. Inform. Sci. Tech. (Paris); No. 151, 39-49(Sep 1970). (In French).

The pollution of a river can occur in either an acute (accidental) or chronic (controlled disposal) form; the transfer is dependent on the distribution of the pollutant between water, suspended materials, and the river bed. An experimental canal was developed to study the part played by the sedimentary bed and the solid flow of the river in chronic radioactive contamination. Continuous measurements of the physical and chemical parameters of the flow were made; after sampling and recording on punched tape, all the data was processed by the computer of the Cadarache Nuclear Research Center. This device also allows the study of any form of industrial or urban pollution and the implantation of living aquatic organisms. (auth) (France)

18941 RADIOBIOLOGICAL AND RADIOECOLOGICAL ASPECTS OF RADIOACTIVE POLLUTION OF EARTH ATMOSPHERE. Dobrowolski, J. Postepy Astronaut.; 3: 133-58(1969). (In Polish).

Artificial radioactive pollution of earth atmosphere is very important for all biosphere. Causes of this pollution are: experimental nuclear explosions and radioactive wastes from nuclear power plants. The radioactive pollution of the environment is not distributed equally and radiosensitivity is different too. Intensification of radioecological and radiobiological research is very important for the prevention of genetic changes in human populations. Therefore increasing international cooperation is a necessity. (NSA of Poland)

18942 RESULTS OF 3 YEARS (1964–1966) OF MEASURING THE RADIOACTIVITY OF FOODS SAMPLED IN THE CITY AND PROVINCE OF PAVIA. Lanzola, E.; Meloni, C.; Marchetti, R. (Univ., Pavia, Italy). Ann. Sanita Pubblica; 29: 61-83(Jan-Feb 1968). (In Italian).

The results of a three-year (1964 to 1966) measurement of ^{90}Sr and ^{137}Cs in various foods in the city and province of Pavia are reported. The results obtained on milk are discussed in detail. The average values of ^{90}Sr and ^{137}Cs in milk samples collected weekly in Pavia, Made, Voghera, and Vigevano and measured monthly were compared with those of the monitoring network of the CNEN for Italy, of the Public Health Service of the United States, and of the ARCRL of Great Britain. It was found that the half-life of disappearance from milk of ^{137}Cs, on the basis of the data of the three-year study and data from the other three agencies, was 12 months whereas the half-life of ^{90}Sr disappearance from milk varied from 17 to 26 months. The difference was attributed to the diverse behavior of ^{90}Sr in soil with respect to ^{137}Cs, to the absence of atmospheric nuclear explosions, and to indirect absorption rather than direct. It was found that the values of ^{90}Sr calculated with the Russell and Barlett equation (based on the deposition of fallout on the ground) were in good agreement with the values measured. By taking into account the exponential trends of ^{90}Sr and ^{137}Cs in the absence of new atmospheric explosions, the quantity of the two nuclides that can probably be found in milk in 1970 was deduced. (tr-auth)

18943 MILK AS A VECTOR OF RADIOACTIVE NUCLIDES. PREDICTING THE CONSEQUENCES OF ACCIDENTAL POLLUTION OF PASTURES. Michon, G. Lait; 49: 250-65(May-Jun 1969). (In French).

Data were obtained from agricultural and physiological studies on radioactive pollution of a pasture with ^{137}Cs, ^{131}I, ^{89}Sr, and ^{90}Sr. The data were used for estimating changes in radionuclide content of milk, quantities ingested by man, and radiation protection methods. (auth)

18944 EXPERIMENTAL CONTAMINATION OF MARINE SPECIES BY SOLUBLE AND INSOLUBLE FORMS OF ^{106}Ru IN SEAWATER. Vilquin, A. (Groupe de Radioecologie Marine, Cherbourg, France). Radioprotection: 4: 185-92(1969). (In French).

Repeating similar experiences of contamination by ^{106}Ru, the respective contaminating abilities of the soluble and insoluble forms were determined. The results, expressed as concentration factors, demonstrated the contaminating ability for insoluble forms to be from 3 to 10 times higher than for soluble forms. The values obtained were compared with values found in the natural environment submitted to the influence of radioactive waste disposals. (auth)

Genetics and Cytogenetics

Refer also to abstracts 18980, 19096, and 19157.

18945 (UCRL–20192) ISOLATION AND GENETIC CHARACTERIZATION OF RECOMBINATION DEFICIENT MUTANTS IN SACCHAROMYCES CEREVISIAE. Rodarte-Ramon, Ubaldo Sergio (California Univ., Berkeley. Lawrence Radiation Lab.). Nov 1970. Contract W-7405-eng-48. 76p. Dep. NTIS.

Thesis.

Recombination in Saccharomyces cerevisiae has been studied genetically by selecting mutants of disomic yeast deficient in x-ray and ultraviolet light (uv) induced mitotic heteroallelic reversion. Disomics were obtained by isolation techniques based on detection of heteroallelic regions in one chromosome. They were also recovered spontaneously. Of ten identified rec mutants, seven were studied in detail. The mutants exhibit depressed frequencies of x-ray and/or uv-induced reversion in the heteroallelic region arg4-2 +/+ arg4-17 on disomic chromosome VIII. Two of the mutants are x-ray sensitive and one is both x-ray and uv-sensitive. The remaining four strains exhibit wild type response to both radiations. Each of the seven mutations segregates as one gene and is recessive. Complementation and allelism tests were performed and a minimum of four genes, denoted rec1, rec2, rec3, rec4, were identified among the seven mutants. Mutations in rec1 depress x-ray and uv-induced mitotic conversion about 20 times and do not affect either x-ray induced mitotic segregation of ade2 or meiotic intragenic or intergenic recombination. Mutations in rec2 cause x-ray sensitivity and depress x-ray induced conversion to about 20% of the normal value, but do not affect uv induction of reversion. Homozygous rec2/rec2 diploids yield only 1 to 2 percent sporulation and 10 percent spore viability. They also exhibit normal frequencies of x-ray induced mitotic crossing over of ade2. Mutations in rec3 completely suppress spontaneous and x-ray or uv-induced mitotic conversion and also suppress sporulation. X-ray induced mitotic segregation of cyh2 occurs at normal frequencies. Diploids homozygous for rec4 do not exhibit spontaneous and x-ray or uv-induced mitotic conversion. They show normal frequencies for x-ray induced mitotic crossing over in ade8. Such diploids exhibit 60 percent sporulation and 90 percent spore viability. Intragenic meiotic recombination between alleles 2 and 17 in arg4 is reduced about 500 times. Meiotic crossing over appears normal for the regions between mating type and ade8 and their respective centromeres and also in the intervals between thr1 and CUP1 and the centromere of chromosome VIII. (auth)

18946 GAMMA RADIATION EFFECTS ON PHASEOLUS VULGARIS L. AND SEED RADIOSENSITIVITY DETERMINATIONS FOR OTHER SPECIES. Mujeeb, Kazi Abdul. Manhattan, Kan.; Kansas State Univ. (1970). 142p. University Microfilms Order No. 70-25,555.

Thesis.

The mutation breeding phase of this study evaluated the variability induced in Phaseolus vulgaris L. cv. Blue Lake (Pole) after exposure to acute dosages of gamma radiation from a 4500 Ci ^{60}Co source. Gamma radiation effects in X_1 were evaluated after initial dose estimation based upon 100 percent lethality, (10 kR.). The X_1 dosages ranged from 1.0 to 10.0 kR. Significant reductions (0.05) were apparent for mean germination, survival, pods per plant, seeds per plant, and total weight. All characters were negatively correlated with increasing dose. Chlorophyll mutation scoring and macromutant selections were done in the X_2 field planting. The chlorophyll mutations observed were classed under viridis, maculata, albina, alboviridis, and xantha, with a significant (0.05) maximum of viridis. Nonsignificance was observed for maculata and albina, as well as for alboviridis and xantha, but the latter differed significantly from the former. The higher dosages offered either a greater spectrum of the mutants or greater frequencies. The second phase dealt with radiosensitivity estimations utilizing three criteria: morphological (seedling performance), cytological (abnormal anaphase), and physiological (total chlorophyll content of primary leaves). Comparisons of the latter two with the former have also been made. The morphological criteria evaluated the effects of various acute gamma radiation dosages upon seeds of *Allium cepa*, *Pisum sativum* cv. Laxton Superb and Alaska, *Vicia faba*, *Lycopersicon esculentum*, *Euphorbia lagascae* 2n and 4n, *Citrullus vulgaris*, and *Cucumis sativus*. The LD$_{50}$ values (kR.) for each were estimated to be respectively 40.5, 12.0 and 15.3, 3.5, 40.0, 17.3 and 16.0, 16.0, and 55.0. The finding that 2n *E. lagascae* was more radioresistant than 4n was surprising. Seeds of *P. vulgaris* cv. Blue Lake were exposed to acute gamma radiation dosages and the LD$_{50}$ estimated utilizing the seedling performance (4.3 kR.) and total chlorophyll (6.5 kR.) criteria as percent of control, from primary leaves at 21 days from planting. Significant (0.05) differences and decreases in the two criteria were observed as was enhanced stippling and decreased primary leaf size with increasing dosages. The LD$_{50}$ estimation was also made by utilizing root tip cytology of *P. sativum* cv. Laxton Superb seeds, subjected to varied acute gamma radiation dosages. The anaphases gave 50 percent normality at 6.2 kR. compared to the LD$_{50}$ of 12.8 kR. by the morphological criteria. The values were significantly different (0.05). (Diss. Abstr. Int., B)

18947 PRODUCING AND DETECTING PARACENTRIC CHROMOSOMAL INVERSIONS IN MICE. Roderick, Thomas H. (Jackson Lab., Bar Harbor, Me.). Mutat. Res.; 11: 59-69 (Jan 1971).

Three feasible methods for finding chromosomal inversions are discussed, and recent data obtained from each method are given. The radiation and anaphase-bridge method provided five useful paracentric inversions. The first inversion proved useful in locating locus dipeptidase-I(Dip-I); in predicting the location of the centromere in linkage group XVII; and because of the fortuitous association of marker genes, in providing a balanced lethal system to detect and retain newly induced recessive lethals. Hybrid males of the interfertile subspecies *Mus m. molossinus* and *Mus m. musculus* displayed a high frequency of first meiotic anaphase bridges and double bridges, suggesting that the chromosomal arrangements of these subspecies differ by at least two paracentric inversions. (auth)

18948 RADIATION-INDUCED TRANSLOCATIONS IN SPERMATOGONIA OF MICE. Leonard, A. (CEN-SCK, Mol, Belgium). Mutat. Res.; 11: 71-88(Jan 1971).

A review is presented of the reciprocal translocations that involve exchange of terminal segments between non-homologous chromosomes and therefore require two breaks and rejoins. During many years this type of translocation has been ascertained by analyzing the F$_1$ progeny of treated and control animals for heritable semi-sterility, but at present the translocations induced in spermatogonia are studied by cytological techniques in the derived spermatocytes because at diakinesis—first metaphase stage of meiosis the homologous chromosome segments of the rearranged and interchanged chromosomes will pair to form characteristic translocation configurations. The kinetics of the translocation inductions show that some observations fit very well with a two-event process but that others seem to be in better agreement with the postulate that translocation induction is mainly the result of a one-track process. No statistical difference between the strains of mice is observed with respect to the rate of affected cells. Some decrease in the yield of spermatocytes with translocation configurations is found for long intervals of time between irradiation and observation. The analysis of the F$_1$ progeny derived from irradiated spermatogonia shows that the frequency of translocated offspring is always much lower than expected from the rate of translocated spermatocytes in the irradiated animals. (auth)

18949 MUTAGENIC EFFECTIVENESS OF FAST NEUTRONS IN MALE AND FEMALE MICE. Searle, A. G.; Phillips, Rita J. S. (Medical Research Council, Harwell, Eng.). Mutat. Res.; 11: 97-105(Jan 1971).

Previous work has shown that protracted doses of fast neutrons induce high frequencies of specific locus mutations and of reciprocal translocations in mouse spermatogonia. However, they are mutagenically very ineffective when the dictyate oocyte is the stage at risk. The mutagenic response of similar germ-cell stages in the two sexes, namely the mitotically dividing primordial spermatogonia and oogonia with their precursors, was compared following irradiation for 1 week before the 12th day of embryonic life with a mean dose of 108.5 rad fast neutrons +20.5 R γ-contamination. The large clusters of specific locus mutations found in both series show conclusively that mutations can be readily induced in female early embryonic germ cells as well as in male. Cluster size was used to estimate the mean number of germ cells at risk, from which mutation frequencies were calculated. These were $5.3 \cdot 10^{-5}$ per locus in males and $6.4 \cdot 10^{-5}$ per locus in females, from which induced mutation rates of $42 \cdot 10^{-8}$ and $58 \cdot 10^{-8}$ per rad respectively can be calculated. If dose attenuation is allowed for, higher figures are obtained. Those given are somewhat lower than the rate after protracted fast neutron irradiation of spermatogonia in the adult ($109 \cdot 10^{-8}$ per rad) but higher than the mutation rates after low linear-energy transfer irradiation of spermatogonia and much higher than frequencies after protracted irradiation of dictyate oocytes. Air-dried preparations from testicular cell suspensions of 20 males irradiated as embryos were scored for presence of multivalent configurations indicating translocations. Two had high and two had low frequencies of translocations; in addition, one mouse proved to be XYY and another had a clone of XO cells. The overall translocation frequency was 1.2%, which is lower than would be expected with irradiation of adult spermatogonia. It is concluded that the intrinsic radiosensitivity of male and female genetic material is similar in mice and that in the male these early embryonic stages are not much less sensitive than spermatogonia in the adult. It seems likely that the immature dictyate oocyte is the only germ-cell stage in the female from which mutations cannot be recovered. (auth)

18950 CYTOGENETIC STUDIES ON THE EFFECT OF CHRONIC GAMMA IRRADIATION ON VICIA FABA. Amer, Soheir M.; Mostafa, I. Y.; Mikhael, Evon (Atomic Energy Establishment, Cairo). Biol. Plant. (Prague); 11: 432-41(1969).

Vicia faba seeds (cv. Giza 1) were planted in the Inshas γ radiation field where they were chronically irradiated during the whole life of the plant. The percentage of induced abnormal pollen mother cells (P.M.Cs), as well as the frequency of abnormal P.M.Cs in the different meiotic stages were proportional to the given doses. The main types of chromosome aberrations were anaphase and telophase bridges, fragmentation, and lagging chromosomes. The nearest plants to the source showed an inhibition of shoot growth, flower and seed sterility, and irregular branching. At the doses used, irradiation had no effect on pollen fertility. Seeds of the 1st filial generation were used for both mitotic and meiotic studies. The percentage of mitotic abnormalities was proportional to the doses. The dominant type of anomaly was the presence of micronuclei in the different stages of mitosis and in the resting cells. Irradiation also affected other types of anomalies e.g. lagging chromosomes, fragments, bridges. Meiosis and pollen fertility (2nd generation) were normal. (auth)

18951 REPAIRING PROCESSES OF CHROMOSOME ABERRATIONS INDUCED BY ^{60}Co γ RAYS IN NIGELLA DAMASCENA L. Moutschen-Dahmen, J.; Moutschen-Dahmen, M.; Gilot-Delhalle, J. (Univ., Liege). Med. Nucl.-Radiobiol. Lat.; 12: 17-32(1969). (In French).

In order to investigate several repairing processes of chromosome aberrations induced by ^{60}Co γ rays, Nigella seeds were irradiated by fractionated exposures at increased time intervals. A type of aberrations in which repairing occured rapidly i.e., between 3.20 to 5.20 min was demonstrated. This finding agreed with literature data for other materials. To modify these rapid repairing processes seeds were treated with several chelating agents (1×10^{-4} *M* for 8 hr) namely 8-hydroxyquinoline, Cupferron, 2,2′-dipyridyl, EDTA, and diethyldithiocarbamate. After a 4 krad nonfractionated exposure a drop of the total radio induced aberrations was noted. Only after EDTA treatment were all kinds of aberrations decreased which was not the case after other chemicals. In contrast, all chelating agents investigated suppressed the fractionation effect i.e., enhanced significantly the amount of all kinds of aberrations as compared with the control level. The repair process was actually suppressed. Possible mechanisms of action for these substances are discussed in relation to the possibility of direct chelation of chromosome. (auth)

18952 EFFECT OF SPACE FLIGHT FACTORS ON BARLEY SEEDS. Garina, K. P.; Romanova, N. I. Cosmic Res. (USSR) (Engl. Transl.); 8: 149-51(Jan-Feb 1970).

Translated from Kosm. Issled.; 8: 158-9(Jan-Feb 1970).

Barley seeds were placed in space flight for five days and then germinated, along with controls, in tap water. After rootlets reached a length of 8 to 10 mm they were prepared for cytological examination. A significant increase in the number of chromosome rearrangements was found in anaphase and early telophase as compared with controls. An increase in the number of cells with multiple breakages of chromosomes and other disturbances was found. It was also noted that there was a stimulating effect on germination of seeds and the growth rate of rootlets. (H.L.W.)

18953 EFFECT OF SPACE-FLIGHT FACTORS ON CREPIS-CAPILLARIS SEEDS. Dubinina, L. G.; Chernikova, O. P. Cosmic Res. (USSR) (Engl. Transl.); 8: 146-8(Jan-Feb 1970).

Translated from Kosm. Issled.; 8: 156-8(Jan-Feb 1970).

A significant increase in the number of chromosome rearrangements was observed in seeds of *Crepis capillaris* subjected to the effects of space flight. An experiment was conducted on the effects of ethylenimine on seeds that had been exposed to space flight; an increased number of mutations were found. Space flight did not affect germination and sprouting of seeds. However, with the additional treatment with ethylenimine and subsequent storage, a decrease of germination and sprouting was found. (H.L.W.)

18954 PROPERTIES OF THE MITOSIS PROCESS IN MERISTEMATIC CELLS OF COTTON UNDER THE ACTION OF GAMMA RAYS AND DIMETHYL SULFATE. Saropulu, M.; Egamberdiev, A. (Inst. of Experimental Biology of Plants, Tashkent). Uzb. Biol. Zh.; No. 4, 50-2(1970). (In Russian).

Gamma radiation (30 kR) and dimethyl sulfate were applied separately and in combination to seeds of cotton plants. It was found that a 0.1% solution of dimethyl sulfate stimulated mitotic activity in root cells but did not induce chromosome aberrations. Chromosome aberrations were observed 37 to 41 hrs following irradiation of seeds and following the combined application of radiation and the chemical mutagen. Chromatid bridges were the most common form of aberration. (auth)

18955 RADIOINDUCED ANOMALIES IN COTTON POLLEN. Rumi, V. A.; Skokova, A. A.; Asriyan, N. S. (Inst. of Experimental Biology of Plants, Tashkent). Uzb. Biol. Zh.; No. 4, 53-5 (1970). (In Russian).

Cytological changes in embryonic tissues of cotton following γ irradiation of pollen were studied. During microsporogenesis the formation of cytoplasmic bridges and disturbances in meiosis were observed. Some of the abnormalities disappeared during subsequent pollen development. (auth)

18956 TESTING FOR RECESSIVE LETHALS IN MICE. Luening, K. G. (Univ. of Stockholm). Mutat. Res.; 11: 125-32(Jan 1971).

Mutagenic effects of 14 MeV neutrons from an acclerator were studied using dose levels of 150 and 250 rad. Acute and chronic treatments were compared. Backcrossing experiments were performed, and methods for performing recessive lethal tests and isolation of possible alleles are described. Methods for maintaining a lethal line and possibilities for excluding pre-existing lethals from newly induced ones are discussed. (H.L.W.)

18957 DEFINITION OF FUNCTIONAL UNITS IN A SMALL CHROMOSOMAL SEGMENT OF THE MOUSE AND ITS USE IN INTERPRETING THE NATURE OF RADIATION-INDUCED MUTATIONS. Russell, Liane B. (Oak Ridge National Lab., Tenn.). Mutat. Res.; 11: 107-23(Jan 1971).

Complementation mapping of a small chromosomal region of the mouse has defined a linear series of functional units and has aided in the interpretation of the nature of radiation-induced genetic changes. Mutations used for this purpose were derived from specific-locus mutation-rate experiments and were detected by their visible phenotype in combination with the test-stock's linkage-group-2 markers d and se (recombination frequency 0.16%). A total of 235 mutants of this type have been recovered, and 102 of these were used in complementation tests involving over 800 combinations and about 40,000 progeny. While the original screening for mutants employed only 2 markers, the subsequent analysis has, so far, revealed 16 complementation groups spanning 8 or 9 functional units. Involvement in a mutation of 2 or more functional units is taken to indicate chromosomal aberration. All mutations are consistent with a linear map, except for 2, which appear to "skip" units but have been shown not to result from recombinationally separable changes. These 2 mutations, one of which gives conversion-like results in recombination tests, are interpreted as small rearrangements. The remaining multi-unit mutations are, for the time being, taken to be deficiencies. Although there is evidence that homozygous deficiency of either one of the marked loci gives a visible effect, this by itself is no proof against the single-unit mutations being "point" mutations (perhaps single base-pair changes). A strong effect of irradiated cell stage can be demonstrated, both on the locus-spectrum (i.e., relative frequencies of events involving d, se, or both) and on frequency of mutations that are interpreted as aberrations. The latter ranges from 13.5% in most x- or γ-rayed spermatogonia, through 42.3% in postgonial stages, to 65.6% in oocytes. Within spermatogonia, neutron irradiation and 24-h fractionation of x-rays shift the distribution in the direction of postgonial results. The rest of the irradiated spermatogonia closely resemble the control distribution. The recombinational length of most of the aberrations is very small, 75 to 86% of them spanning less than 2 crossover units. Even in those groups having a high total frequency of aberrations (postgonial stages and oocytes), no more than 23% of all mutations exceed this length, and the figure is 0% for x- or γ-rayed spermatogonia (excluding 24-h fractionation data). This finding supports W. L. Russell's conclusion that his specific-locus method measures mostly single-hit events, even in irradiated oocytes. Results from x- and γ-irradiated spermatogonia indicate a clearly restricted nature of the genetic damage. (auth)

18958 RATE OF TRANSLOCATIONS INDUCED IN SPERMATOGONIA OF MICE BY TWO X-IRRADIATION EXPOSURES SEPARATED BY VARYING TIME INTERVALS. Leonard, A.; Deknudt, Gh. (CEN-SCK, Mol, Belg.). Radiat. Res.; 45: 72-9 (Jan 1971).

The influence of fractionation intervals has been studied by scoring at the diakinesis—first metaphase stage of meiosis, the rate of translocations induced in spermatogonia by two x-irradiation exposures separated by varying time intervals. After an exposure of 500 R delivered to mouse spermatogonia in a single dose the incidence of spermatocytes carrying translocations was found to be 8.05%. The yield of translocations falls to a minimum of 5.73% at a fractionation interval of 2 hours. At a 4-hour fractionation interval the yield is significantly increased and is equal to the yield obtained with a single exposure of 500 R. The rate of translocated cells falls again to a minimum of 4.44% at the 7-hour fractionation interval and rises up to 8.40% at the 16-hour interval. Those results are interpreted in terms of differential radiosensitivity of the cell-cycle stages. (auth)

18959 NEW CONCEPT OF SPERMATOGONIAL STEM-CELL RENEWAL IN THE MOUSE AND ITS RELATIONSHIP TO GENETIC EFFECTS. Oakberg, E. F. (Oak Ridge National Lab., Tenn.). Mutat. Res.; 11: 1-7(Jan 1971).

The stem cell of the seminiferous epithelium, designated spermatogonia A_s, is radiation resistant, has a long cell cycle time, and occurs as single, isolated cells. Renewal occurs by division to form more singles; formation of a pair of cells constitutes the initial step in differentiation. This model differs from previous ones in that spermatogonial types with high sensitivity to cell killing do not contribute to the stem-cell pool, and owing to their transient nature, are relatively unimportant in overall genetic effects in spermatogonia. Only A_s spermatogonia survived single radiation doses of 150, 500, 1000, and a fractionated 1000 R exposure. A combination of [^{3}H] thymidine injection and irradiation showed equal spermatogonial labeling 8.5 and 17 days after 100 and 500 R, a decrease in percentage of labeled cells after 1000 R, and the highest value after 1000 R given as two 500 R fractions 24 h apart. These results suggest that differential cell survival may be a factor in observed mutation frequencies. The high percentage of labeled spermatogonia after 1000 R given in two 500 R fractions 24 hours apart suggests that selective action of the second exposure is an important factor in the enhanced mutation frequency observed after this treatment. The data also suggest that the spermatogonial population surviving 100 and 500 R is qualitatively similar, and that the kinetics of these cells is the same as that of A_s cells in controls. Thus extrapolation of the linear portion of the mutation rate curve would not be expected to underestimate the effect of low doses. (auth)

18960 METAPHASE CHROMOSOME ABERRATIONS IN CHINESE HAMSTER LIVER CELLS IN VIVO AFTER SINGLE ACUTE ^{60}Co EXPOSURE. Brooks, A. L.; Peters, R. F.; Rollag, M. D. (Lovelace Foundation for Medical Education and Research, Albuquerque, N. Mex.). Contract AT(29-2)-1013. Radiat. Res.; 45: 191-201(Jan 1971).

The number and types of metaphase chromosomal aberrations induced by ^{60}Co gamma irradiation in the Chinese hamster liver have been determined. Partial hepatectomy was used to stimulate mitotic activity for chromosomal evaluation. Liver cells of the Chinese hamster exhibited similar sensitivities of 0.00060, 0.00087, and 0.00067 breaks/cell/R, respectively, to aberration induction by whole-body irradiation at 1 hour prior to (−1 hour) and 24 and 48 hours after partial hepatectomy. There was a shift from chromosome to chromatid aberrations which correlated closely with the biochemically determined onset of DNA synthesis. Dose-response curves for metaphase aberrations were established with the form $Y = a + bD + cD^2$ and coefficients of $a = 0.01$, $b = 1.9 \times 10^{-4}$, and $c = 1.8 \times 10^{-6}$. These indicated that liver cells were more resistant to radiation-induced aberrations than several other metaphase systems. The total number of aberrations per cell per roentgen was similar whether the animals were hepatectomized at 1 hour or 1 week after the radiation exposure. The frequency of aberrations increased as a function of time after partial hepatectomy. This was caused by an increase in deletions while the frequency of rings plus dicentrics remained constant. The advantages of scoring metaphase cells as compared to anaphase or telophase cells are discussed. (auth)

18961 GENETIC EFFECT OF RADIATION IN MANKIND AND STATISTICAL GENETICS. Yasuda, Tokuichi (National Inst. of Radiological Sciences, Chiba, Japan). Hoshasen Kagaku; 13: 250-5(Mar 1970). (In Japanese).

Genetic effects of radiation on human populations were examined with special attention to mutations. Relationships between radiation dose and mutation rates were studied from evidences of atomic bomb casualties, patients receiving radiotherapy, and radiologists.

Biochemical and genetic manifestations of mutations may be classified as chromosome abnormalities, gross effects, and deviations in polygene characters. It was found that duplications, translocations and other abnormalities were directly proportional to the radiation dose. Mutations causing gross effects occurred at the rate of about 1 : 100,000 per generation; mutations in polygene characters were 20 to 30 times more frequent than those causing gross effects. The ratio of phenotypes to frequency of mutant genes in the population and the role of geographical movement were discussed. (TSS) (Japan)

18962 EFFECT OF FAR-RED AND BLUE LIGHT ON MALEIC HYDRAZIDE-INDUCED CHROMOSOMAL ABERRATIONS IN VICIA FABA. Butala, Sharon Smock. Pullman, Wash.; Washington State Univ. (1970). 68p. University Microfilms Order No. 70-24,977.

Thesis.

Previous data on the effect of far-red light on x-ray-induced damage have resulted in two different interpretations. One considers that far-red radiation causes a synergistic production of breaks while the other assumes that far-red radiation causes a mitotic delay and does not affect breakage and/or rejoining processes. This investigation was conducted to further elucidate these interpretations by determining the action of various wavelengths of light (far red, blue, red and green) on the production of aberrations by maleic hydrazide (MH). Secondary roots of Vicia faba were treated with a 2×10^{-4} M solution of MH and/or 10 min irradiation of far-red, blue, green or red wavelengths. The wavelengths were obtained from a large spectrograph which produced pure bands of light with midpoints at 450, 555, 650, and 725 nm. Roots were exposed to a 0.05% solution of colchicine for 3 hr immediately before fixation. They were fixed from 22 to 32 hr after MH treatment regardless of other treatment to test for the most sensitive time in the cell cycle to both light and MH. Only cells at metaphase were scored for exchanges and isochromatid deletions. Cells exposed to far-red, red-MH treatment respond in the same way as cells treated with only MH; that is, far-red, red-MH treatment produced a peak frequency of abnormal cells 24 hr later. The far-red, red reversal is a characteristic of and, therefore, implicates phytochrome in the mitotic delay response. However, irradiation of MH treated roots with red or green wavelengths produced an ambiguous response. The aberration rate was approximately equal at both 24 and 28 hr and furthermore was lower than that produced by MH alone at either hour. This perhaps indicates a different length of mitotic delay and shows a previously unknown response of cells to green light and a different response to red than to far-red, red irradiation. A delay of equal magnitude to that of far-red-MH is produced by irradiation at 450 nm. The strong response to blue light indicates involvement of the high energy reaction (HER) even though the irradiation time of 10 min was rather short. Several different models are proposed to explain the results obtained with these experiments. Although exclusive involvement of phytochrome or HER is ruled out, both could be involved in the observed results. Alternatively, a system involving a hypothetical precursor, a pigment which is inactivated by far-red and blue but activated by red irradiation, and a substance which is inactivated by red or green irradiation is proposed. Further work is necessary to confirm or refute either proposal. (Diss. Abstr. Int., B)

18963 STUDY OF CHRONIC GRANULOCYTIC LEUKEMIA WITH SPECIAL REFERENCE TO A-BOMB SURVIVORS. Tsuchimoto, Taiso; Kamada, Nanao; Ishii, Yukifumi; Ozono, Noboru; Uchino, Haruto (Hiroshima Univ.). Proc. Res. Inst. Nucl. Med. Biol.; No. 11, 132-7(1970).

Chromosome analyses and clinical and hematological studies were made on 27 cases with CGL, of which 5 were in blastic crises; 12 were A-bomb exposed patients. Ph^1 chromosomes were found in marrow cells from all patients with a frequency ranging from 62 to 100% of bone marrow cells. No difference was seen cytogenetically between the A-bomb exposed and non-exposed groups. These results failed to show a chromosome pattern peculiar to patients exposed to heavy irradiation. Most of the patients with CGL found in early stages of the disease belonged to the exposed group indicating the importance of periodic exams for A-bomb exposed people. Ph^1 chromosome was shown to be present in a high frequency even in the early stage. These results should contribute to further understanding of the etiology and development of CGL. (auth)

18964 METHOD OF OBTAINING ARTIFICIAL GENETIC IMPROVEMENTS IN PLANTS. Sparano, Ottorino. British Patent 1,212,118. 11 Nov 1970. Priority date 15 Dec 1967, Italy.

Mutations were induced in vegetables, grasses, and other plants by γ irradiation of seeds for improved growth, size and quality of fruits, flowers and roots, keeping qualities, and greater resistance to disease. The radiosensitivity of the different plants and various factors, such as moisture content of seeds, influencing the radiation dose are discussed. (H.L.W.)

18965 EVALUATION OF THE EFFECTS OF CHEMICAL MUTAGENS ON MAN: THE LONG ROAD AHEAD. Neel, James V. (Univ. of Michigan, Ann Arbor). Proc. Nat. Acad. Sci. U. S. A.; 67: 908-15(Oct 1970).

By analogy with the problem of evaluating the genetic risks of radiation, it appears that it will be extremely difficult to assess the mutagenicity for man of the wide range of chemicals to which human populations are currently exposed. Nevertheless, the potential significance of this problem calls for a major effort at such an evaluation. (auth)

18966 ULTRAVIOLET LIGHT MUTATION INDUCTION DURING SYNCHRONOUS REPLICATION IN ESCHERICHIA COLI. Johnson, Robert Carey. Lawrence, Kan.; Univ. of Kansas (1969). 121p. University Microfilms Order No. 70-11,035.

Thesis.

The possibility of differential uv-induced mutagenic action specific for the point of active DNA replication in synchronized cultures of Escherichia coli was studied. It was determined that two markers in E. coli AC2519 were reversible by low doses of ultraviolet light. These markers were well separated on the genetic map. The type of base change for each marker was determined using chemical mutagens. A significant portion of the premutational uv-induced photochemical damage for both markers was photoreversible. It was concluded that each uv-induced mutation reversion should be studied with more attention given to the type of base being changed and to the nature of the active macromolecular synthetic processes involving DNA near to that uv-induced mutation. (Diss. Abstr. Int., B) (TSS)

18967 CELL LINEAGE RELATIONSHIPS IN THE IMAGINAL WING DISC OF DROSOPHILA MELANOGASTER. Bryant, Peter J. (Univ. of California, Irvine). Develop. Biol.; 22: 389-411 (Jul 1970).

An account is given of the patterns of cell lineage in the wing and mesonotum, the derivatives of the imaginal wing disc of Drosophila melanogaster. The system was analyzed using somatic crossing over, induced by x rays at specific stages of development. Clonally related cells occupy longitudinal stripes in the wing, and this was interpreted to mean that cell divisions are oriented in the developing disc. Clonally related cells occupy irregularly shaped areas in the mesonotum, but some nonrandomness was detectable. The data indicated that, in the embryo, presumptive wing disc cells are not determined as between upper wing, lower wing, and mesonotum. In the larva, however, the anlagen of these three structures were represented by separate populations of proliferating cells within the disc. These groups of cells have distinct rates and patterns of cell division. The data were used to estimate cell numbers in the three parts of the disc at various stages of development. It appeared that the growth rates of the parts of the wing disc are constant throughout larval development. The results are discussed in relation to problems of morphogenesis in imaginal discs. (auth)

18968 TWO RADIATION-INDUCED CHROMOSOMAL INVERSIONS IN MICE (MUS MUSCULUS). Roderick, Thomas H.; Hawes, Norman L. (Jackson Lab., Bar Harbor, Me.). Contracts AT(30-1)-3671; AT(30-1)-1979. Proc. Nat. Acad. Sci. U. S. A.; 67: 961-7(Oct 1970).

Whole-body x irradiation of male mice has produced presumptive paracentric inversions in 15 animals, as evidenced by high frequencies of first meiotic anaphase bridges. Two of the highest frequencies observed were propagated through several generations and found to behave as dominant genes. Acentric fragments were observed associated with about 10% of the bridges. The first inversion, in linkage group XIII, has been designated In(13)1Rk, and the second, in linkage group XVII, In(17)2Rk. For In(13)1Rk, recombination was reduced between loci inside and outside the inverted segment. (auth)

18969 ABORTIONS, CHROMOSOMAL ABERRATIONS, AND RADIATION. Freire-Maia, Newton (Federal Univ. of Parana, Curitiba, Brazil). Soc. Biol.; 17: 102-6(Jun 1970).

A review is given on four main points: frequencies of abortions in general populations; frequencies of chromosomal aberrations in spontaneous abortions; estimates of doubling doses in the production of chromosome breakage; and frequencies of abortions in human groups exposed to artificial sources of ionizing radiation as compared to those from non-exposed groups. Due to the low doubling dose for chromosome breakage and the substantial contribution of chromosomal aberrations to the occurrence of abortions, abortions would be expected to be a very sensitive

XUM

indicator of radio-induced genetic damage in man. The reviewed investigations did not show a complete agreement, but some of them clearly suggested the presence of a radiation effect. (auth)

18970 REVERSION OF ROUGH (R) TO SMOOTH (S) FORMS IN BRUCELLA ABORTUS. I. THE MANNER OF MANIFESTATION OF R → S REVERSION. Lagowska-Zlotorzycka, Maria (Inst. of Immunology and Experimental Therapy, Wroclaw). Arch. Immunol. Ther. Exp.; 18: 357-65(1970).

Spontaneous R → S reversion in the form of S sectors in R colonies was observed in Brucella abortus strain 207. The conditions for manifestation of the reversion were studied. In liquid medium, reversion was observed in cultures in the chemostat. Mutagens such as uv, HNO_2, and acriflavine had no significant influence on the frequency of appearance of the sectors. (auth)

Health Physics and Safety

Refer also to abstracts 18566, 18629, and 19167.

18971 RADIATIONS. Alves Filho, Mario. Rev. Brasil. Med.; 25: 26-7(Jan 1968). (In Portuguese).

Observations of particular interest to the radiologists, made in the United States, about a positive correlation between the leukemogenic and cancerogenic effects and radiation, and the hazards and consequences of exposures to large amounts of radiation are presented. Special emphasis is given to the danger involved when men with no specialized training in the use of radiation deal with x ray equipment. (auth)

18972 PREVENTIVE MEDICINE IN THE NUCLEAR SUBMARINE PROGRAMME. Lambert, R. J. W. J. Roy. Nav. Med. Serv. (London); 56: 176-82(Spring 1970).

Some of the new tasks imposed on the medical branch by the advent of the nuclear submarine are described. Control of the environment becomes a major part of the medical officer's duties and, in particular, atmospheric toxicology requires a sophisticated approach. A submarine community forms a useful model for certain lines of research, and some of these are indicated. (auth)

18973 RADIATION HAZARDS IN INDUSTRY. Bellian, J. G. (VLN, Cleveland). Mach. Design; 42: 134-41(28 May 1970).

The U. S Public Health Service estimates that over 30% of the radiation producing equipment in use today is being operated unsafely. There is no way to eliminate radiation; instead there must be methods for protection against it. Radiation monitors and dosimeters were considered with regard to type, characteristics, and cost. Types of radiation emitting units used in industry and medicine are listed. Atomic Energy Commission protection requirements for utilization of radioisotopes and state and federal regulations pertaining to radiation protection for personnel are discussed. (E.E.H.)

Radioactive Contamination and Decontamination

Refer also to abstracts 18360, 18518, 18526, 18892, 18894, 18926, 18928, 18932, 18939, 18941, 18943, 18989, and 19148.

18974 (AHSB(S)R-192) RISK EVALUATION FOR ANY CURIE RELEASE SPECTRUM AND ANY DOSE-RISK RELATIONSHIP. Bell, G. D. (United Kingdom Atomic Energy Authority, Risley (England). Authority Health and Safety Branch). Dec 1970. 20p. Dep. NTIS (U. S. Sales Only).

A method is presented for calculating the frequency distribution of casualties, amongst the population surrounding a nuclear reactor site, arising from the inhalation of activity released accidentally. The calculations can be performed either for single postulated accidental releases or for releases occurring according to any arbitrary frequency distribution of release. The method may be used with any dose-risk relationship and takes account of the initial height at which the release occurs. Results are presented for the release of iodine-131 on three sites spanning the range of potential reactor sites in the U. K. (auth) (UK)

18975 (CEA-N-1365) RADIOLOGICAL ACCIDENTS: RULES TO BE OBSERVED IN THE EVENT OF ACCIDENTAL EXTERNAL IRRADIATION OR ACCIDENTAL RADIOACTIVE CONTAMINATION. Jammet, H.; Le Go, R.; Lafuma, J. (Commissariat a l'Energie Atomique, Fontenay-aux-Roses (France). Centre d'Etudes Nucleaires). Sep 1970. 61p. (In French). Dep. NTIS (U. S. Sales Only).

Radiological accidents fall into two groups: accidental external irradiation for which accidental overexposure, categories of irradiation, dosimetric information, clinical and biological rules to be observed, and therapeutic decisions are defined; and accidental radioactive contamination for which relationships between the metabolism and the physico-chemical state of the various isotopes, therapeutic procedures to be followed, and technical data-sheets for the various radioelements (^{14}C, Cs, I, Pu, Pa, Sr, U, rare earths, tritium, transplutonium elements, and fission product mixtures) are established. (France)

18976 SIZE DETERMINATION OF AIRBORNE PLUTONIUM PARTICLES BY AUTOSCINTIGRAPHY. Kelkar, D. N.; Joshi, P. V. (Bhabha Atomic Research Centre, Trombay, India). Health Phys.; 19: 529-33(Oct 1970).

Size measurements of airborne plutonium particles were made by recording the photographic image produced by scintillations from a zinc sulfide screen kept in contact with the sample. A calibration curve giving the relation between the $^{239}PuO_2$ particle size and the spot size produced under optimum exposure conditions is presented and the limitations of the method are discussed. A nomogram is also presented from which the activity of a single particle can be converted to its size for particles of plutonium, uranium and some of their compounds. This technique of measuring particle size from the size of the photographic image produced by scintillations has been termed autoscintigraphy. (auth) (UK)

Dosimetry and Monitoring

Refer also to abstracts 18638, 18644, 18649, 18695, 18931, 19038, 19067, 19092, 19115, and 20424.

18977 (AD-702155) REDUCTION OF RADIATION HAZARD IN TRITIUM METHOD OF MEASURING TOTAL BODY WATER. Final Report, July-September 1969. Logsdon, Donald F. Jr.; Green, James F.; Harper, John W. (School of Aerospace Medicine, Brooks AFB, Tex.). Nov 1969. 11p. (SAM-TR-69-82). CFSTI.

The current procedure for measurement of total body water in vivo using a 250 μCi dose of tritium-labeled water produces 18.98 mrads of total body radiation. It was found that the amount of radiation activity (number of counts) necessary for usable test results could be achieved as effectively by extending the counting time or increasing the amount of serum sampled. These changes in procedure allowed for a reduction in the total amount of tritium-labeled water administered to 25 μCi. Increasing the counting time reduced the exposure dose by a factor of 5; doubling the serum sampled decreased the exposure dose by a factor of 2; combining these two procedures decreased the total body exposure by a factor of 10. If a lower degree of test accuracy can be accepted, the amount of activity measured can be reduced and the dose of tritium-labeled water correspondingly decreased. (auth) (USGRDR)

18978 (AD-711316) NUCLEAR EMULSION RECORDINGS OF THE ASTRONAUTS' RADIATION EXPOSURE ON THE FIRST LUNAR LANDING MISSION, APOLLO XI. Schaefer, Hermann J.; Sullivan, Jeremiah J. (Naval Aerospace Medical Research Lab., Pensacola, Fla.). 29 Jun 1970. 32p. (NAMRL-1112). NTIS.

Ilford G.5 and K.2 emulsions in radiation packs carried by the astronauts on Apollo XI in their space suits were analyzed for identifying the various components of the radiation field in space and determining the total mission dose. In terms of dose equivalents, trapped protons in the radiation belt, disintegration stars in tissue, galactic heavy primaries, electrons, and neutrons contribute in that order to a total mission dose of 201 millirad or 402 millirem. In this exposure, the high-ZE particles with LET values up to 3600 keV/micron tissue constitute a radiobiologically unknown quantity since it is generally agreed upon that microbeam effects in tissue cannot be measured adequately with conventional dosimetric units. Assuming that the effects in question are limited to nuclei of Z = 22 and higher, one arrives at a total mission flux of 76 nuclei/sq cm measured on the body of the astronaut; this cannot be properly assessed in its biological significance. (auth) (NTIS)

18979 (BRH/DBE-70-5) REVIEW OF RADIUM TOXICITY STUDIES. Chiacchierini, Richard P.; Jessup, Gordon L.; Nelson, Neal S.; Telles, Norman C.; Tompkins, Edythalena; Wright, James F. (Bureau of Radiological Health, Rockville, Md.). Dec 1970. 31p. NTIS.

A review was made of the available human and animal radium studies for the purpose of determining the extent to which animal and human data are sufficient to resolve the question of a dose-response relationship. The review indicated that the animal and human radium experience to date is not sufficient to specify an unequivocal dose-response model. The data reviewed cover five human groups, including radium dial painters in England and the USA (chronic low-dose ^{226}Ra ingestion), radium chemists who accidentally ingested various doses of ^{226}Ra, patients who received injections of ^{226}Ra, and patients who received ^{224}Ra. Animal studies include dogs given single or multiple injections of ^{228}Ra and mice given injections of ^{226}Ra. The human studies attempted to relate the radiation dose to the incidence of bone sarcomas, carcinomas of the paranasal sinuses and mastoids, and leukemia and other blood dyscrasias. The animal studies attempted to relate radiation dose to the incidence of bone sarcomas. Two radium retention models were used for estimations of radiation dose and body burden, one of which was based on retention following one single injection and the other retention following continuous injection or chronic ingestion. (C.H.)

18980 (CEA-CONF-1698) HEMATOLOGICAL AND CHROMOSOMIC ASPECTS OF DOSIMETRY IN IRRADIATED MAN. Le Go, Roland (Commissariat a l'Energie Atomique, Fontenay-aux-Roses (France). Centre d'Etudes Nucleaires). [1967]. 26p. (In French). (CONF-670461-2). Dep. NTIS.

From 7th Meeting of Radiologist Doctors of Latin Origin and 1st Congress of the European Association of Radiology, Barcelone, Spain.

Hematological examinations and chromosome analyses carried out on irradiated man can be considered as a real biological dosimetry method. The values obtained are only significant if referred to the dose received, which must be expressed as a function of its anatomical distribution and its biological effects on the bone marrow. This is made possible by two new concepts of dose: the physical mean dose which expresses the integral energy transfer to the bone marrow; the biological medullary dose which expresses the percentage survival of the marrow stem cells. (France)

18981 (CEA-N-1380) BIOLOGICAL DOSIMETRY OF AN ULTRAVIOLET RADIATION SOURCE USING SACCHAROMYCES CERIVISIAE. Pompidou, Alain; Malarbet, Jean-Louis; Prudhomme, Jean; Le Go, Roland (Commissariat a l'Energie Atomique, Fontenay-aux-Roses (France). Centre d'Etudes Nucleaires). Jan 1971. 11p. (In French). Dep. NTIS (U. S. Sales Only).

Ultraviolet biological dosimetry using Saccharomyces cerivisiae is described. The irradiated material is contained in a catheter of roughly sinusoidal form, between two ultraviolet sources. Mixtures of yeast and human blood were cultured in a Petri dish and the radioactive counts taken before and after irradiation. A very strong correlation between the absorbed dose rate and yeast lethality was established. It was found that red blood cells present a good screening effect to ultraviolet radiation and it was thus possible to measure the real absorbed dose rate. (France)

18982 (CEX-65.05) RADIATION SAFETY PRACTICES: OPERATION HENRE. Butler, H. M.; Haywood, F. F. (Oak Ridge National Lab., Tenn.). Apr 1970. 34p. Dep. NTIS.

During 1967 an experiment was conducted at the Nevada Test Site using a high-yield-neutron generator supported at several elevations on a 1527-ft steel tower. Numerous personnel radiation hazards were associated with the routine operation of this generator, and specialized equipment and procedures were required. The most notable hazard resulted from handling targets for the generator, each of which contained 1500 to 2000 Ci of ^{3}H. Handling was required for target fabrication, packing and shipping, mounting onto generator, removal and transfer to storage, and disposal of wastes. This report includes area monitoring and bio-sampling techniques, internal-dose estimation, and specific procedures for limiting personnel exposure. (auth)

18983 (JAERI-Memo-4216) QUARTERLY REPORT OF HEALTH AND SAFETY AT OARAI RESEARCH ESTABLISHMENT, No. 12. (Japan Atomic Energy Research Inst., Tokyo). Nov 1970. 26p. (In Japanese). Dep. NTIS (U. S. Sales Only).

Health and safety activities at Oarai Research Establishment, Japan, for the period from July 1 to Sep. 30, 1970 are reported. (auth)

18984 (JUL-688-ME) DOSIMETRY OF INCORPORATED TRITIUM AND ^{125}I. Ertl, Harald H. (Kernforschungsanlage, Juelich (West Germany). Institut fuer Medizin). Aug 1970. 37p. (In German). Dep. NTIS (U. S. Sales Only).

Exact calculation of dose distribution is only possible for a point source with exponential absorption. In the case of beta emitters, these conditions are not valid. It can be shown, however, that the exponential absorption function can be approximated satisfactorily by dividing the energy spectrum into 18 channels of 1 keV, each of which can be treated as a monoenergetic electron source. With this method, the dose distributions from tritium and ^{125}I point sources are calculated. Also computed is the energy absorbed within a certain radius and the energy escaping this radius. (H.B.G.)

18985 (LA-4563) PLUTONIUM AND STRONTIUM IN SOIL NEAR TECHNICAL AREA 21, LOS ALAMOS SCIENTIFIC LABORATORY, LOS ALAMOS, NEW MEXICO. Kennedy, William R.; Purtymun, William D. (Los Alamos Scientific Lab., N. Mex.). Nov 1970. Contract W-7405-eng-36. 5p. Dep. NTIS.

A study was made of the content of ^{238}Pu and ^{239}Pu in soil around the location at Los Alamos Scientific Laboratory to determine amounts of plutonium deposited from laboratory ventilation stack emission. In general the plutonium concentrations decrease with increased distance from the stacks. Results were similar insofar as locations of maximum concentrations to those found in 1956. Calculations as to total amounts deposited within a radius of approximately one mile give approximately 2% of the total released from the stacks in the 24 year period of operation. Strontium analyses were made to possibly distinguish fallout from atmospheric tests from stack emission material by use of the ^{239}Pu/^{90}Sr ratio method. The method proved invalid because of trace deposition of ^{90}Sr in the soil from past activities in the area. (C.H.)

18986 (NYO-3446-14, Paper 28) ENVIRONMENTAL γ-RADIATION DOSE RATE IN FINNISH LAPLAND AND SOUTHERN FINLAND. Jaakkola, T.; Kauranen, P. (Helsinki Univ. (Finland). Dept. of Radiochemistry). 13p. (CONF-700505-16).

From 2nd Congress of the International Radiation Protection Association, Brighton, England.

The occurrence of the radionuclides ^{137}Cs, ^{55}Fe, ^{210}Pb, ^{210}Po, and ^{90}Sr in Finnish Lapland and their radiation dose rates in Lapps were calculated during 1960 to 1970. The calculation of total radiation dose to the Lapps from artificial radionuclides and background radiation was made possible by measuring the environmental γ radiation dose rate. Measurements were made using an integrating portable sensitive γ radiation dosimeter. A portable γ spectrometer system was also used. Most of the measurements of the environmental radiation dose rates were conducted inside and outside the houses of the Lapps. An attempt was made to elucidate local variations of the γ radiation dose rate. The total external irradiation caused by natural radiation sources is presented. (H.L.W.)

18987 (NYO-3446-14, Paper 29) BODY BURDEN OF ^{137}Cs AND THE RADIATION DOSE OF A POPULATION GROUP IN FINNISH LAPLAND. Rahola, Tua; Miettinen, J. K. (Helsinki Univ. (Finland). Dept. of Radiochemistry). 12p. (CONF-700505-17).

From 2nd Congress of the International Radiation Protection Association, Brighton, England.

Higher radionuclide contents in the biota of Lapland than in that of southern Finland and other non-arctic areas have been observed, despite the obviously lower fallout deposition in Lapland. Since 1961 the ^{137}Cs body burden of Finnish Lapps has been estimated by using a mobile whole-body counter. These measurements have been performed every spring but only two times also in the autumn, in 1962 and 1969. A change of seasonal variation is now noticed and reported in this paper. The average maximum whole-body burden of the highest exposed group of male reindeer herders was found in the year of maximum values, 1965, to be 1.5 μCi, while the highest individual value was about 3 μCi. In March 1969 the corresponding values were 0.52 and 1.1 μCi, in September 1969 0.45 and 1.2 μCi and in March 1970 0.49 and 1.2 μCi. The autumn value of the male reindeer herder group was now 84 percent of the spring value while it was in 1962 61 percent. The annual radiation dose of reindeer herders from ^{137}Cs was in 1969 about 60 mrem/y. The integrated dose to the present generation of reindeer herders (1955 to 1985) is estimated to be about 1 rem/30 years, if no major changes in the fallout situation will take place. The dose from other artificial fallout nuclides will be much smaller than this. For southern Finns the dose from ^{137}Cs is estimated to be 0.025 rem/30 years. An estimate of the total radiation dose to be delivered to the Lapps between 1955 to 1985 is given. The dose commitment to this population from the natural radionuclide ^{210}Po is exceptionally high, of the order of 3 rem/30 y. It can be noticed that the contribution of the natural radiation sources to the total dose of the present generation will be significantly greater than that of the artificial sources even in the group of reindeer herders. (auth)

18988 (ORNL-4584) HEALTH PHYSICS DIVISION ANNUAL PROGRESS REPORT FOR PERIOD ENDING JULY 31, 1970. (Oak Ridge National Lab., Tenn.). Oct 1970. Contract W-7405-eng-26. 255p. Dep. NTIS.

Separate abstracts were prepared for 16 sections. (W.H.K.)

For abstracts of individual sections see: 18521, 18526, 18556, 18622, 18623, 18644, 18799, 18989–18991, 19490, 19491, 19757–19759, and 20134.

18989 (ORNL-4584, pp 42-56) DOSE ESTIMATION STUDIES RELATED TO PEACEFUL USES OF NUCLEAR EXPLOSIVES. Barton, C. J.; Booth, R. S.; Cowser, K. E.; (and others). (Oak Ridge National Lab., Tenn.).

XUM

From Health Physics Division annual progress report for period ending July 31, 1970.

Radiological hazards to human populations resulting from the utilization of natural gas produced by nuclear stimulation of wells are discussed. The potential radiation dose to man from the use of Gasbuggy gas for home heating was calculated, using the home occupancy factor (the fraction of time a home is occupied by family members in various age groups) and data on the content of ^{85}Kr and tritium in Gasbuggy gas during 1969. A dose of less than 170 millirems/hr/person was calculated, assuming only direct modes of exposure through inhalation or absorption through skin. It is pointed out that natural gas is used in the production of petrochemicals and the radiological safety of the use of Gasbuggy gas for this purpose was evaluated. A safety guide was developed for the exposure of human populations to transient atomic clouds formed by the accidential release of radioisotopes during underground nuclear explosions. Methods for calculating the cumulated radiation dose (CUE) at various times are described that visualize the downwind movement of the radioactive cloud at ground surface as the source of the transient exposure. Estimates were made of the annual radiation dose to human populations of Panama residing in the vicinity of the proposed interoceanic canal in the event nuclear explosions are used for excavation. Both external exposure from contaminated landscape and internal exposure from the ingestion of fallout radioisotopes in foods and beverages were used for the calculations. (C.H.)

18990 (ORNL–4584, pp 129-51) DOSIMETRY FOR HUMAN EXPOSURES AND RADIOBIOLOGY. Poston, J. W.; Cheka, J. S.; Chen, W. L.; (and others). (Oak Ridge National Lab., Tenn.).

From Health Physics Division annual progress report for period ending July 31, 1970.

Calculations of depth-dose distributions for neutrons were extended into areas of practical application, especially for the use of ^{252}Cf in cancer therapy. Dose and LET distributions for line, point, and disk-shaped sources of neutrons having the energy spectrum of ^{252}Cf were calculated. The calculations of dose and LET distributions due to neutrons were also made for two small cylinders chosen to approximate the size of rats and rabbits respectively. Preliminary calculations were also made for the dose distributions in human fetuses exposed to radiation from the nuclear bombs exploded over Hiroshima and Nagasaki. Close liaison has been maintained with the Atomic Bomb Casualty Commission (ABCC) in Japan. Emphasis this year has been given to computation of the radiation doses received by those persons exposed near the bombs who survived because of the radiation and blast protection afforded by seismic reinforced concrete buildings. (auth)

18991 (ORNL–4584, pp 200-22) INTERNAL DOSE ESTIMATION. (Oak Ridge National Lab., Tenn.).

From Health Physics Division annual progress report for period ending July 31, 1970.

The anthropomorphic phantom and Monte Carlo computer program were used for estimation of dose due to photons that take account of the distribution of red marrow. Only doses from a monoenergetic photon emitter present in lungs are reported. As might be expected, the dose was highest for the red marrow in the rib cage and certain portions of the spine. The pelvic region contained a considerable fraction of the total red marrow, and the dose to this portion was much less, often by an order of magnitude. The Monte Carlo computer program was also used to estimate doses in many body organs. However, in some cases the estimates were statistically unreliable, particularly for small organs such as gonads or thyroid when they were far from the source organ. A buildup factor for dose in an infinite medium of water has been reported, and despite the finiteness and heterogeneity of the body, the use of this buildup factor seemed to be accurate within a factor of two in all cases tested against the Monte Carlo code. This result is being tested further, and if the limit of error is this small, the method may be useful in estimating dose to small organs. Since many radionuclides are excreted in urine, the bladder wall was irradiated by radiation originating in the urine, which constituted a pool of variable size. The dose per photon varied markedly as the bladder contents increased, partly because wall thickness was changing and also because of the inverse-square relation of dose and distance. The basic data on dose per photon were estimated for a range of bladder sizes ranging from 0 to 500 ml content. A compartmental model for metabolism of iodine has been given by Berman, but because of its complexity, it has not been directly compared with more conventional models. This was done here, and for ^{131}I the comparison was rather close. For some compartments and isotopes of iodine, differences by a factor of two may occur. The question of what happens to a radium atom when produced in bone by decay of a thorium parent continued to demand attention, because the estimate of dose to bone will vary greatly depending on the model assumed. Calculations corresponding to some hypotheses were supplemented by further cases ranging from immediate transfer of the radium atom to blood to the assumption that it remains fixed in situ until its decay. Although immersion in an infinite cloud of radioactive emitter has been a standard case considered in the past, no good estimates of the energy spectrum produced in such a case have been available. Due to this fact, no reliable estimates of dose at various depths within the body have been produced. The energy spectrum resulting from a monoenergetic photon source distributed uniformly in an infinite space of air is given. It is expected that a correction for ground effect will be forthcoming. (auth)

18992 EVALUATION OF THE DOSIMETRY OF INTRAVENOUSLY ADMINISTERED ^{67}Ga CITRATE FROM MEASUREMENTS OF THE DISTRIBUTION IN MALE AUGUST-MARSHALL HYBRID RATS. Popham, Mary G.; Taylor, D. M.; Trott, N. G. (Royal Marsden Hospital, Sutton, Eng.). Brit. J. Radiol.; 43: 807-10(Nov 1970).

An attempt was made to predict the dosimetry of ^{67}Ga citrate in man using experimental data obtained on normal male August–Marshall hybrid rats. Activity in blood, pancreas, spleen, liver, kidneys, testes, lungs, and femur, as well as whole-body retention, in the rat was measured at various times following intravenous injection. The results obtained from the rat measurements indicate that with an injected dose of 2.5 mCi no organ of the body in man should receive a radiation dose of more than 2 Rads. In addition, measurements were made on female rats bearing subcutaneously implanted tumors. There was considerable variation in tumor blood ratio, but this never exceeded the liver: spleen or kidney: blood ratios. (auth) (UK)

18993 MICRODOSIMETRY (PHYSICAL ASPECTS AND FUNDAMENTAL PROBLEMS). Ivanov, V. I. At. Energ. (USSR); 29: 195-200(Aug 1970). (In Russian).

The subject of microdosimetry covers the transfer and distribution of the ionizing radiation energy in microvolumes of matter; its goal is to predict the radiation effects on the basis of physical measurements that characterize the microscopic distribution of the absorbed energy. The data obtained must be used when the observed radiation effect is determined by damage in the microstructure of the material; e.g., radiobiological effects involving injury to cells or cell components. In some cases the amount of absorbed energy is proportional to the observed effect but after a simple measurement of the absorbed energy does not give by itself sufficient information concerning the effect of radiation and requires additional data or knowledge of the spectral distribution. H. H. Rossi is considered the founder of the science of microdosimetry; in 1959 he introduced the concept of individual events whereby he designated an event as the passage of a charged particle through a given microvolume, regardless whether energy transfer occurs or not. The local energy density is considered the microscopic analog of the dose. The science of microdosimetry is still at its beginning; it is concerned with the development of experimental methods, collection of basic data, precise determination of physical constants of the interaction between radiation and matter and analysis of energy losses by charged particles. (Review article, 12 references). (TTT)

18994 DISTRIBUTION AND DOSIMETRY OF ^{113m}In COLLOID USED FOR BONE MARROW SCANNING. Colombetti, Lelio G. (Veterans Administration Hospital, Palo Alto, Calif.); Barrall, Raymond C.; Finston, Roland A. Int. J. Appl. Radiat. Isotop.; 21: 643-7(Nov 1970).

^{113m}In is being widely used for organ scanning due to its favorable characteristics. One of these characteristics, its short half life (104 min), makes ^{113m}In an excellent tool for bone marrow studies because it allows for the administration of a sufficient dose for rapid scanning while minimizing the radiation damage to the bone marrow and other tissues of the R.E. system. A new colloid was prepared using 4 ml of eluate from a ^{113m}Sn–^{113m}In generator. To the eluate, 0.8 to 1% of gelatin and 1 ml of phosphate buffer were added. This colloid was injected in white rabbits and its distribution compared with the distribution of ^{99m}TcS colloid. The uptake of ^{113m}In colloid by the bone marrow was 0.78% dose/g tissue. Doses of 8 to 10 mc are used in humans. For the purpose of radiation dose calculation, distribution of the colloid in humans is assumed to be 80% in liver, 3% in spleen, and 10% in red bone marrow. The absorbed dose from 10 mCi of ^{113m}In is: 4.3 Rad in liver, 2.5 Rad in spleen and 0.9 Rad in bone marrow. Radionuclidic impurities, principally ^{113}Sn breakthrough, contribute an additional 50% to the patient dose. (auth) (UK)

18995 BUBBLE CHAMBER PICTURES AS A MEANS OF DEMONSTRATING RADIATION DISTRIBUTION IN BIOLOGICAL SYSTEMS. Krebs, Adolph T. (Univ. of Louisville, Ky.). Radiology; 96: 635-8(Sep 1970).

Because of the difference in density between gases and tissues, it is suggested that the bubble chamber be employed using liquids rather than gases for recording tracks of high-energy radiations. (auth)

18996 LES PROBLEMES DE PROTECTION DANS L'UTILISATION INDUSTRIELLE DES RADIO-ELEMENTS. (Problems of Protection in the Industrial Utilization of the Radioelements). Fisher, Ch. Serie 33, Monographies 8. Brussels; Bureau Eurisotop (1968). 291p.

Hazards from the use of radioactive substances and the necessity for recognizing and mastering these hazards are stressed. The properties of radioelements and radiations are outlined and the principal uses are summarized. The nature of the risks associated with the use of radioelements is discussed with respect to the biological effects and the modes of exposure. The bases for radioprotection are given and the risks are analyzed as a function of the use of the radioelement. Detection methods and detection and personnel monitoring are described. Recommendations for the protection of personnel are outlined. Rules, regulations, and legislation regulating the use and transportation of radioelements are also discussed. (J.S.R.)

18997 DIRECT COUNTING OF ^{47}Ca AND ^{85}Sr IN BIOLOGICAL SAMPLES. Harmut, Magda; Maljkovic, Tea; Kostial, Krista (Inst. for Medical Research, Zagreb). Arh. Hig. Rada Toksikol.; 19: 61-5(1968).

The radioactivity of ^{47}Ca and ^{85}Sr was determined before and after thermal ashing of various biological specimens (carcass, skeleton, urine, and feces of rats). Using a two scintillation crystal assembly and making adequate adjustments to the volume of standards, the percentage of radioactivity retained in the body and excreted in urine and feces was found to be the same (within statistical fluctuations) for both ashed and non-ashed specimens after single intraperitoneal, single oral, and continuous oral administration of the tracers. (auth)

18998 TELECOBALT THERAPY FOR CARCINOMA OF LARYNGOPHARYNX. Lalanne, C. M.; Cachin, Y.; Juillard, G.; Lefur, R. (Inst. Gustave Roussy, Villejuif, France). Amer. J. Roentgenol., Radium Ther. Nucl. Med.; 111: 78-84(Jan 1971).

In small neoplasms of the laryngopharynx, telecobalt γ therapy gives as good results as the combination of surgery and pre- and post-operative telecobalt therapy. On the other hand, in larger lesions, surgery supplemented by radiotherapy seems to be the best treatment. Surgery after telecobalt therapy in carcinoma of the laryngopharynx is difficult. This must be kept in mind when designing a preoperative irradiation program. The dose in curable lesions should not exceed 3,000 R, with a weekly dose of 1,000 R. Radiosensitivity of laryngopharynx cancers varies greatly from one patient to another. However, the best chance of cure is afforded by doses between 6,500 and 7,500 R. (auth)

18999 IRRADIATION OF THE LIVER IN CHILDREN: ACUTE EFFECTS ENHANCED BY CONCOMITANT CHEMOTHERAPEUTIC ADMINISTRATION. Tefft, Melvin (Children's Hospital Medical Center, Boston); Mitus, Anna; Jaffe, Norman. Amer. J. Roentgenol., Radium Ther. Nucl. Med.; 111: 165-73(Jan 1971).

Three cases are reported that describe experience with antitumor chemotherapeutic agents, administered either during or following irradiation to the liver in children. The scan defect that occurred acutely and the peripheral blood cell count depression led to the conclusion that these agents are toxic to liver which is irradiated in whole or in part; further, that the unirradiated segment may be adversely affected by these agents since it is in a sensitive state of compensatory hypertrophy; and that such defects can occur suddenly after the completion of irradiation when certain chemotherapeutic agents are administered within six months of the completion of irradiation. (auth)

19000 DIGITAL SEARCH METHOD FOR COMPUTING ISODOSE CURVES. Rozenfeld, Martin (Argonne Cancer Research Hospital, Chicago). Radiology; 98: 181-2(Jan 1971).

A new digital search procedure that was developed for computing isodose curves from discrete radiation sources is described. With this method about 90% of the dose computations yield data points on the isodose curves, compared to about 20% in the usual calculation for an array of points. (auth)

19001 HEAD AND NECK EXPOSURES FROM PANORAMIX ROENTGENOGRAPHY. McMahon, James J. (Dept. of Health, Education, and Welfare, Rockville, Md.). Oral Surg., Oral Med., Oral Pathol.; 31: 120-32(Jan 1971).

With the advent of intracavitary medical/dental x-ray machines designed to operate during body contact, a conflict has arisen as a result of a set of recommendations which did not foresee or intentionally prohibit this unique design. If these recommendations are enacted as law as in many states, literal interpretation of the foregoing requirements and a rigid enforcement would nullify the intended advantage of these devices for diagnostic examinations. Results are reported from an investigation to obtain accurate data concerning radiation exposures to critical organs and tissues of the head and neck of interest when intracavitary dental x-ray machines are used for oral diagnostic roentgenographic procedures. Radiation exposure levels to the tongue and palatal areas were found to be similar to reported skin exposures of the face from conventional complete-mouth procedures. The mucosa and the skin are each of ectodermal origin, a relatively nonradiosensitive structure, and are more radioresistant than the tissues of critical organs. There appeared to be good correlation, radiographically and dosimetrically, between the Rando phantom and the human subjects. Measurements impossible to assess with human subjects can be extrapolated from the phantom data. Scatter radiation levels per examination are less than 0.25 mr at the operator site and apparently less than those from a conventional complete-mouth examination. Therefore, the usual shielding requirements appear adequate. This unique intraoral x-ray source to obtain an extraoral panograph is needed by public health authorities and clinicians to appreciate better the usefulness and limitations of this device. (C.H.)

19002 SPECIFIC GAMMA-RAY CONSTANT OF RADON. Sofer, D. H. (Univ. of Melbourne). Phys. Med. Biol.; 16: 150-1(Jan 1971).

A correction factor is presented to be applied whenever a value for the specific γ ray constant of radon is derived from the corresponding constant for radium and when the activity of radon sources is determined by comparison with radon. It is estimated that about 13% of the total γ ray constant of radium is contributed by the activity of RaB and 87% by the activity of RaC. Combining these figures with the activities of RaB and RaC in a radon source leads to a value of 0.84% for the excess γ ray output of the source, and therefore the γ ray output of a one mCi radon source is 0.84% greater than that of a one mCi radium source. (UK)

19003 CALCULATION OF THE DOSE DISTRIBUTION ABOUT ^{252}Cf NEEDLES IN TISSUE. Krishnaswamy, V. (Univ. of Pennsylvania, Philadelphia). Radiology; 98: 155-60(Jan 1971).

Dose distribution around a point source of ^{252}Cf in tissue due to neutron interactions was evaluated by Monte Carlo methods. The dose due to neutron and γ rays emitted by a 2 cm needle source was calculated and compared with published experimental data. The effect of absorber size on neutron dose was also determined. (auth)

19004 COORDINATE MEASURING DEVICE FOR RADIUM APPLICATIONS. Mauderli, Walter; Fitzgerald, Lawrence T.; Gross, Cordell E. (J. Hillis Miller Health Center, Gainesville, Fla.). Radiology; 98: 161-3(Jan 1971).

A device for the automatic measurement and recording of the γ radiation dose from radium-226 interstitial and intracavitary applicators is described. Voltage measurements, proportional to the distance from a point in question to two fixed points, are recorded on IBM punch cards which are then ready for submission to a computer for processing. The calculated x−y coordinates have been found to deviate less than 0.1% from the true values. (auth)

19005 POLAROID FILM IN RADIATION DOSIMETRY AND SURVEY. LeVan, H.; Stefani, S.; Hage, S. J. (Veterans Administration Hospital, Hines, Ill. Chicago Medical School. Gottlieb Memorial Hospital, Melrose Park, Ill.). Radiology; 98: 182-3 (Jan 1971).

The use of Polaroid films in radiation dosimetry and surveys; and in particular, the response of various types of Polaroid films to radiation output from different sources were investigated. A good correlation was found between the readings from a Victoreen R-chamber and from Polaroid film, regardless of whether a 300 kVp x-ray machine or a ^{137}Cs source was used. (auth)

19006 MEASUREMENT OF ABSORBED DOSE RATE FROM TERRESTRIAL BACKGROUND RADIATION IN HONG KONG. Chuang, L. A.; Wong, C. Y.; Lau, S. Y. (Chung Chi Coll., Hong Kong). J. Radiat. Res.; 11: 53-60(Jun 1970).

Experiments were conducted to provide definite information on the absorbed dose rate from terrestrial background radiation and to test Watanabe's method for measurement of the absorbed dose rate by means of spectrometry using a plastic scintillation detector. Measurements of the absorbed dose rate from soil samples and above the soil sample site resulted in a correlation factor of 14.9 between the absorbed dose rate at one meter above the ground site measurement and that of the corresponding soil sample. The overall average values of 70.5 and 15.9 Mrad/year were obtained for the absorbed dose rates due to natural radioactivity and fallout radioactivity, respectively. The absorbed

XUM

dose rates due to the fallout differed by a factor of approximately three, between two geographically separated areas in Hong Kong, Stanley-Sau Ki Wan and Kowloon-N. T. (E.E.H.)

Radiation Protection

Refer also to abstracts 19082, 19086, and 20816.

19007 (NCRP–38) PROTECTION AGAINST NEUTRON RADIATION. (National Council on Radiation Protection and Measurements, Washington, D. C.). 4 Jan 1971. 153p. NCRP $3.00.

Recommendations of the National Council on Radiation Protection (NCRP) for protection against neutron radiation are presented. The recommendations are based on a new formulation of applicable quantities and units and changes in the maximum permissible dose equivalents recommended by the NCRP and International Commission on Radiological Protection. The general principles of neutron protection are reviewed. It is assumed that differences in the biological effects of radiation are related to differences in linear energy transfer (LET) of the charged particles that deliver the absorbed dose. The limits of radiation exposure of personnel are expressed in terms of the dose equivalent (DE), which is defined as the product of absorbed dose (D) and the quality factor (QF), which is specified as a function of LET. Neutrons are classified and their primary modes of interaction with matter and tissue are discussed; radiation quantity and radiation quality are defined; the maximum permissible dose equivalent for human skin and fetuses and for the occupational exposure of personnel is defined; hazards from γ and x radiation arising in the operation of neutron sources and radiation protection during the installation and operation of neutron sources are discussed; and the performance of neutron dosimeters and effectiveness of various shielding materials for neutron protection are discussed. Procedures to be followed in the event of accidents resulting in neutron exposure are outlined. Data are appended on: methods for neutron depth dose measurements; reactions employed in neutron production; neutron capture γ rays; neutron shielding materials; and accident dosimetry. A list of definitions is also included. (126 references.) (C.H.)

19008 (NCRP–39) BASIC RADIATION PROTECTION CRITERIA. (National Council on Radiation Protection and Measurements, Washington, D. C.). 15 Jan 1971. 135p. NCRP $2.00.

Recommendations of the National Council on Radiation Protection for the protection of man against ionizing radiations are presented. Background material is included on the effects of internal and external irradiation on man as a function of dose and dose fractionation; sources of radiation exposure of man, including natural background radiation, man-made environmental radiation, medical procedures, and occupational exposure; basic biological factors and specific effects of radiation at the cellular and whole-body level; and manifestations of overexposure to internal and external sources of radiation in adults. The genetic and somatic bases for radiation protection standards are reviewed and specific protection concepts are discussed. Recommendations for maximum permissible radiation fields, body burdens, and concentrations are presented for the general population; medical exposure as related to age, sex, and pregnancy; and occupational exposure of the skin, hands and forearms, other organs and tissues, and the whole body. Dose-limiting guidelines for special cases are included. (66 references.) (C.H.)

19009 PROBLEMS OF RADIOLOGICAL PROTECTION OF OUT-PATIENTS. Kieszkowski, Z. Pol. Przegl. Radiol. Med. Nukl.; 34: 281-9(Mar-Apr 1970). (In Polish).

Statistical and substantial observations demonstrate that an excessive number of radiological examinations is performed in the out-patients radiological departments. The unnecessary irradiation of the patients may become a serious problem. A system of approximate per cent exposure of the examined people to ionizing radiation was introduced for individual types of examinations. These approximate doses were related to the generally accepted yearly dose of 30 R. The calculations of individual exposure doses are based on specially designed tables. The per cent of the yearly dose is written down on the examination results for the information of the patient and his physician. As a result of this experiment the number of radiological examinations decreased from 40 to 10%. The demand for radiodiagnostic procedures became better justified, the patients undergoing the examination are better prepared. The number of radiological examinations decreased to the indispensable minimum. The examinations are performed with better care and in shorter time. The economy of the examination improved and better protection of the staff was possible. (auth)

19010 HOW TO PROTECT PATIENT AND PHYSICIAN DURING X-RAY EXAMINATIONS. INSTALLMENT 1. EFFECT OF RADIATION. Moseley, Robert D. Jr. (Univ. of Chicago); Twigg, Homer L.; Barnett, Mark. Amer. Fam. Physician - GP; 1: 113-28(Jan 1970).

Installment one of a two part programmed instruction course designed primarily for physicians is presented. The course will review the biological basis of radiation injury and will describe techniques to protect patients and personnel from unnecessary radiation exposure during diagnostic x-ray procedures. The first installment deals with the effects of radiation. (E.R.B.)

19011 COMMENTS ON SHIELDING BY THE LEAD SHOT METHOD. Werner, Abraham (Tel-Hashomer Government Hospital, Israel). Radiology; 98: 190-1(Jan 1971).

A simple method of shielding irregular-shaped organs from irradiation by cutting a Styrofoam form to fit the projected roentgen image of the organ and filling the cavity in the Styrofoam form with lead shot is described. This form is then interposed between a ^{60}Co γ radiation source and the patient so that the irradiated organs are shielded by the layer of lead shot during treatment. For shielding equivalent to 5 cm of solid lead, a layer of 7 cm lead shot is essential. The packing fraction is virtually independent of the radius of the spheres, provided the radius is much smaller than the dimensions of the shield. (C.H.)

Safety Procedures

Refer also to abstract 19104.

19012 (CEA-CONF–1695) COMPARATIVE STUDY ON WHOLE-BODY EXPOSURE INJURIES. Jammet, H.; Le Go, R.; Parmentier, N. (Commissariat a l'Energie Atomique, Fontenay-aux-Roses (France). Centre d'Etudes Nucleaires). 1967. 31p. (In French). (CONF-670461–1). Dep. NTIS (U. S. Sales Only).

From 7th Meeting of Radiologist Doctors of Latin Origin and 1st Congress of the European Association of Radiology, Barcelona, Spain.

The following accidents were studied with respect to dosimetry, clinical considerations, and therapy: Los Alamos (1945, 1946, 1958), Oak Ridge (1958), Vinca (1958), and Mol (1965). (France)

19013 (JAERI-Memo–4240) SURVEY LIST OF ACCIDENT, HAZARD, AND ABNORMALITY IN NUCLEAR FACILITIES. Yamazaki, Yasaburo; Ishikawa, Michio; Sako, Kiyoshi; Shiba, Mayayoshi; Adachi, Hiromichi (Japan Atomic Energy Research Inst., Tokyo). Dec 1970. 60p. (In Japanese). Dep. NTIS (U. S. Sales Only).

Data are tabulated on 347 accidents and abnormal operation experiences that resulted in the release of radiation. The data are taken from Current Nuclear Safety Literature, published at Oak Ridge National Lab., USA. (C.H.)

19014 POSSIBLE HAZARD FROM NUCLEAR SUBMARINE CORROSION PRODUCTS. Hatfield, M. J. Roy. Nav. Med. Serv. (London); 56: 183-5(1970).

There is a lack of quantitative information on the fate of radioactive corrosion products from pressurized water reactors. An experiment with rats is reported which shows that there is virtually no absorption of corrosion product cobalt from the gut. The implications in assessing radiation dose following an accidental intake of corrosion products are discussed. (auth)

19015 METHODES FONDAMENTALES POUR L'ANALYSE DE SECURITE ET LE CONTROLE DES PRODUITS ET APPAREILS CONTENANT DES RADIONUCLEIDES MIS A LA DISPOSITION DU PUBLIC. (Basic Methods for Analyzing the Safety and Control Procedures for Products and Equipment Containing Radionuclides Which are at the Disposition of the Public). Paris; European Nuclear Energy Agency (1970). 33p.

The field of application of control methods for products and equipment containing radioelements is studied. The methods for determining the external dose received or the cumulated dose delivered to members of the public (from one or several products) or to the population as a whole are described. The control methods are discussed. (France)

19016 LEAK TESTING CHROMATOGRAPHIC RADIUM SOURCES: RADON EMANATION TECHNIQUE. Crowder, Samuel E. (Army Medical Lab., Fort George C. Meade, Md.). Amer. J. Roentgenol., Radium Ther. Nucl. Med.; 111: 189-90 (Jan 1971).

A method for leak testing radium-226 sources used for contact therapy is described. Contamination caused by the decay products of escaping radon is readily detected in that the radon is salvaged for ingrowth of daughters. Even with the escape of radium salts, it is likely that contamination will be detected sooner by this technique than by wipe testing the cell surface. As a basis for presenting counting considerations, a decay scheme of radon-222 is included. The γ rays of ^{214}Pb and ^{214}Bi are counted, and whereas the radon daughters are in equilibrium with the parent, the activity has an effective half-life of 3,825 days; this allows a longer time for reading samples. (C.H.)

19017 TRANSPORT OF RADIOACTIVE MATERIAL: ACCIDENTS AND INSURANCE COVERAGE. **Rogers, Lester** (Atomic Energy Commission, Washington, D. C.). J. Amer. Med. Ass.; 215: 1333-4(22 Feb 1971).

The transportation of radioactive material, whether it is medical isotopes or irradiated nuclear fuels, is subject to the regulations of the Department of Transportation (DOT), the Atomic Energy Commission (AEC), the Post Office Department (POD), and other Federal, State, and local regulatory agencies. The packaging requirements for radioactive materials are designed to provide a high degree of protection and safety for personnel and materials both during normal transport and in accidents. These requirements are related to the radiotoxicity and the radioactivity of the radioactive material to be shipped. Very small quantities of radioactive material are exempt from special packaging for truck, rail, air, or water transport and may be shipped by mail. Somewhat larger quantities must be packaged to withstand normal conditions of transport and large quantities, including irradiated nuclear fuels, must be packaged to withstand both normal and hypothetical accident conditions. Third party liability insurance is available to cover shipments of radioactive materials. For AEC shipments over the past 19 years, 119 transportation incidents have been recorded. In 84 of these, no radioactive material was released from any package. None of the remaining 35 cases in which material was released from package resulted in any significant exposure to radiation. Only one of those cases resulted in dispersal into the air and only one case involved costly (i.e., more than a few dollars) cleanup. For non-AEC shipments, all by public carriers, 34 transportation incidents involving radioactive material have come to the attention of the AEC during the past two years. In 21 of these, no radioactive material was released; 11 incidents involved some release of radioactive material; and two produced some increase in radiation levels outside the packages. None of these resulted in significant radiation exposure and only one case involved costly cleanup. The degree of safety provided by the present methods of shipping radioactive materials is demonstrated by the excellent safety record over the past 25 years. (C.H.)

Legal Aspects

19018 IS THERE A SAFE RADIATION LIMIT? **Wick, Gerald L.** New Sci.; 47: 276-7(6 Aug 1970).

Studies of the Hiroshima and Nagasaki survivors have provided valuable information about the effects of nuclear radiation. However, there is still controversy about the maximum dose permissible for humans. If the claims of some radiologists, that no safe limit exists, are true, the setting of radiation standards should be a public issue. (auth) (UK)

19019 DEVELOPMENT OF INSPECTION METHODS AND TECHNIQUES FOR NUCLEAR FACILITIES. **Kurihara, Hiroyoshi** (Science and Tech. Agency, Tokyo). Genshiryoku Kogyo; 16: No. 5, 35-8(May 1970). (In Japanese).

With the increasing demand for a nuclear weapons non-proliferation treaty, the influence on the peaceful uses of atomic energy is attracting considerable interest. The treaty is aimed at stopping the proliferation of nuclear weapons, and it specifies measures against the application of fissionable materials for military purposes in non-nuclear-weapon countries. The efficient and rational inspection of safeguards is necessary to implement such a treaty. The safeguard inspections by IAEA are described in relation to the purpose of the safeguards, and installations involved, the present state of IAEA safeguards (inspection) in Japan; influence of the NPT on the IAEA safeguards, directions toward the safeguard (practice) improvement, purpose of the safeguard inspections, and improvements in efficiency; and the present state of research and development on inspection techniques, and the future. (Japan)

Medicine

Refer also to abstracts 18482 and 18870.

19020 EARLY USE OF XENOGRAFTS AS A BIOLOGIC DRESSING IN BURN TRAUMA. **Rappaport, I.; Pepino, A. T.; Dietrick, William** (Univ. of California, Irvine). Amer. J. Surg.; 120: 144-8(Aug 1970).

Frozen irradiated xenografts and fresh refrigerated xenografts in antibiotic solution placed on burn defects in dogs showed no significant histologic difference in the granulating beds. Vascularization of the pigskin was not observed. Heterografts were applied to 150 patients with second and third degree burns as an immediate dressing. The grafts were covered with a layer of Sulfamylon-acetate gauze. Xenografts have been an effective temporary dressing. They have provided a marked reduction in pain, particularly over second degree burns. Clinically, early xenograft application reduced sepsis and hastened eschar separations. Eschar treated with pigskin remained pliable and allowed the patient a greater degree of joint mobility. Less difficulty in maintaining core temperature was noted. It was concluded that early use of xenografts may decrease morbidity. (auth)

Protective Substances

Refer also to abstracts 18888, 18913, 18914, 18922, and 19123.

19021 CONSIDERATIONS ON THE MECHANISM OF SULFUROUS RADIATION PROTECTION AGENTS. **Haehn, J.; Proesch, U.; Siegel, G.** (Humboldt Univ., Berlin). Isotopenpraxis; 6: 241-50(Aug 1970). (In German).

Concepts concerning the principles of radiation protection with SH-compounds are reviewed. It appears that from the experimental results different protection mechanisms were derived. A combination of the evaluated chemical aspects, regarding different reacting sites and types of reaction, will stimulate further development of radiation protection agents. (auth)

19022 TIME SCALE FOR RADIOPROTECTION BY AND PERMEATION OF GLYCEROL IN ANOXIC CELLS OF E. COLI B. **Brustad, Tor; Singsaas, Bjoern** (Norsk Hydro's Inst. for Cancer Research, Montebello, Norway). Radiat. Res.; 45: 94-109(Jan 1971).

The radioprotective effect of glycerol at room temperature on anoxic cells of E. coli B has been investigated, employing rapid mixing technique with resolution time of a few milliseconds. Results are compared with those obtained under steady state conditions. No protection was observed when bacteria were irradiated 10 msec or longer before being mixed with unirradiated glycerol. On the other hand, a considerable protective effect, nearly independent of dose rates up to at least 10^{10} Rad/sec, was observed when the cells were irradiated in the presence of glycerol. This protective effect was determined as a function of the time elapsed from mixing of bacteria with glycerol to irradiation. It was found that 400 msec after the cells were subjected to a 1 M glycerol environment, the protective effect was essentially equal to that obtained for cells kept in 1 M glycerol solution for several hours prior to irradiation. It is concluded that radiation-induced radiolysis products formed extracellularly do not contribute significantly to radiation lethality. The protective effect of glycerol is consistent with the assumption that glycerol must be present at or in the immediate vicinity of vital intracellular target structures in order to exert its protective effect. In separate experiments it was shown that complexes involving strong bonds are not formed between DNA and glycerol, neither in unirradiated nor in irradiated solution of DNA and glycerol. The time course of the protective effect of glycerol appears to parallel that of simple diffusion of glycerol into the cell, assuming that the membrane acts as the main barrier. An estimate of the diffusion coefficient of glycerol in the cell membrane is obtained. (auth)

19023 COMPARISON OF THE EFFECT OF HYPERBARIC OXYGEN AND OXYGEN PLUS 5 PERCENT CO_2 ON TISSUE CIRCULATION. **Johnson, R. J. R.** (Manitoba Cancer Treatment and Research Foundation, Winnipeg). Radiology; 98: 177-81(Jan 1971).

Skin patch erythema tests were used as an indirect method for comparing the effectiveness of O_2 breathing by mask and hyperbaric O_2 for increasing the radiosensitivity of tumors during therapy. Ten of 11 patients showed increased erythema with twenty minutes of HPO, while only four breathing O_2 by mask showed increased erythema. The physiological effect of these two oxygen systems on tumor capillary circulation was investigated using xenon clearance tests. Results showed that both systems caused vasoconstriction which could prevent the oxygenation of all anoxic cells even with HPO. (auth)

19024 STIMULATED UPTAKE OF α-AMINOISOBUTYRIC ACID IN RAT LIVER FOLLOWING WHOLE-BODY γ-IRRADIATION. **Shihabi, Zakariya; Neuhaus, Otto W.** (Univ. of South Dakota, Vermillion). Contract AT(11-1)-1754. Radiat. Res.; 45: 202-9(Jan 1971).

Whole-body irradiation elicited an increase in ^{14}C-AIB uptake by the rat liver with a concomitant decrease by kidney, muscle, spleen, and testes. Aminoethylisothiouronium (AET) and cysteamine (MEA) partially prevented these changes in the liver and

XUM

kidney. The uptake of inulin and orotic acid by the liver was not affected by irradiation while that for ^{32}P and algal hydrolysate was increased. (auth)

19025 EFFECT OF ESCULAMINE ON PERMEABILITY OF THE MEMBRANES OF NUCLEI AND MITOCHONDRIA IN CELLS OF IRRADIATED ANIMALS. Gorizontova, M. P. (Inst. of Normal and Pathological Physiology, Moscow). Patol. Fiziol. Eksp. Ter.; No. 3, 22-5(May-Jun 1970). (In Russian).

Esculamine (8-β,β'-dihydroxydietiaminomethyl-4-methylesculetin) is a preparation with vitamin P activity. Its barrier effect on the action of subcellular particles in the cells of animals irradiated with x-rays was studied. For this purpose the Mg accumulation in thymus cells of rats was studied at various intervals after irradiation. One hour after irradiation, a drop in the Mg ion accumulation in thymus cells of irradiated rats treated with esculamine was found. This was explained by a decrease in the permeability of the cell membranes with respect to Mg ions. In vivo tests showed that 24 hr after irradiation, prophylactic introduction of esculamine reduced ^{54}Mn accumulation by liver mitochondria in irradiated mice. Corresponding in vitro tests showed that this is caused by a reduction in permeability of mitochondrial membrane with respect to ^{54}Mn. The data show that a barrier-protective action of esculamine exists at the vessel-tissue level, as well as at the cell-membrane level. (JPRS)

19026 ENHANCEMENT OF THE PRE-IRRADIATION ACTION OF TAB. Byron, J. W. (Christie Hospital and Holt Radium Inst., Manchester, Eng.). Nature (London); 228: 568-9(7 Nov 1970).

It is known that GRAM-negative endotoxin is able either to reduce radiation mortality or at least enhance recovery of the hemopoietic system following total body irradiation, but the mechanism is obscure. The earlier recovery of hemopoietic cells observed after endotoxin treatment may be secondary to changes that allow these tissues to tolerate better the pathophysiological effects of the acute radiation syndrome. Studies on the side effects of TAB vaccine suggest that catecholamine release may play a part in the beneficial action of TAB, and an hypothesis was formulated for the part-irradiation action based on the possibility that catecholamine depletion from tissues, and especially from the adrenals, might allow better tolerance towards bacteraemic and/or hemorrhagic shock during the acute radiation syndrome. More effective reduction of mortality is achieved if the endotoxin is given before irradiation. A suggestion that the beneficial action might be enhanced by pre-irradiation treatment with a β-ARB (adrenergic receptor blockage) and post-irradiation treatment with an α-ARB agent was tested in the described studies with mice, using various doses 300 kVp x-ray total body irradiation. The α-ARB agent used was phentolamine and the β-ARB agent was propanol hydrochloride. LD$_{50}$ and DMF (dose modifying factor) data are shown tabulated. β-ARB treatment alone enhanced the mortality reducing action of TAB vaccine, and further enhancement was achieved when post-irradiation treatment with α-ARB was combined with preirradiation treatment with β-ARB. Assuming hypoxia is partly responsible for the radioprotective action of TAB, the enhancing action of the β-ARB agent could have been due to further decreases in blood flow. An effect at the cellular level was tentatively ruled out since the β-ARB agent does not modify the in vitro x-ray survival curve of a mammalian cell line. The TAB vaccine was administered shortly before the TBR, and the long-term catecholamine depletion should add to the hypoxic of TAB, and this may explain why GRAM-negative endotoxin given before TBR is more effective in reducing radiation mortality than is post-irradiation treatment. Hypoxia reduces the effective radiation dose to the hemopoietic system. The study indicates that appropriate adrenergic receptor blocking agents may increase the capacity of GRAM-negative endotoxins to reduce radiation mortality. (UK)

19027 EFFECT OF TWEEN 80 ON STRAND BREAKS OF ESCHERICHIA COLI DNA IRRADIATED IN SITU. Titani, Yoiti; Katsube, Yutaka (Shionogi and Co., Ltd., Osaka). J. Radiat. Res.; 11: 92-7(Jun 1970).

The radioprotective action of Tween 80 against strand breaks in the DNA of E. coli irradiated in situ with ^{60}Co γ rays was investigated using an alkaline sucrose sedimentation technique. Tween 80 (0.1 M) caused the number of breaks to be decreased by a factor of 1.3, a value very close to DRF for E. coli B_{s-1} obtained from the survival studies. This DRF value was considerably lower than that expected from the DRF for E. coli B/r obtained from survival studies. When ^{3}H-TdR labeled E. coli B/r was irradiated with 15 kR, ^{3}H-release during post-irradiation incubation was 20%; while the presence of 0.1 M Tween 80 during the irradiation, decreased the ^{3}H-release to 15%, even after as much as 30 kR irradiation. These facts suggest that the action of Tween 80 not only diminished the number of breaks of DNA but also caused some change in the structural nature of the breaks so that they could be repaired in a short time without any excision of DNA fragments. (auth)

19028 RADIOPROTECTIVE EFFECTS OF PSYCHOTROPIC DRUGS. Locker, A.; Weish, P. (Reaktorzentrum, Seibersdorf, Austria). Experientia; 26: 771(15 Jul 1970).

The radioprotective effects of psychotropic drugs were investigated. Melleril (Thioridazine; 3-Methythio-10[β-1'-methyl-2'-piperidyl)-ethyl]-phenothiazine; Lidanil (Mesoridazine; methyl-1-[methyl-fulfinyl-2-dibenzothiazinyl-10)-2-ethyl]-2-piperidine; Fluanxol (Flupenthixol; 2-trifluormethyl-9-[3-(4-(2-hydroxyethyl)-1-piperazinyl)-propyliden]-thiozanthene; and Sordinol (Clopenthixol; 2-chlor-9-[3-(4-(2-hydroxyethyl)-1-piperazinyl)-propyliden]-thioxanthene were injected into mice. Whole-body irradiation was carried out with γ rays from a ^{60}Co source. Melleril, Sordinol and Fluanxol exhibited a radioprotective effect on the treated mice. Lidanil did not. Since all the compounds with the exception of Lidanil caused a decrease in metabolism and a depression in body temperature, the amount of which increased with time, it was evident that the radioprotection was, at least partly, dependent upon these processes. (E.E.H.)

19029 COMPARATIVE PROTECTIVE EFFECT OF AET AGAINST FAST NEUTRON AND X-RAY IRRADIATION ON MORTALITY, INTESTINAL DISORDERS, AND HEMATOPOIETIC INJURIES IN MICE. Antoku, Shigetoshi; Sawada, Shozo (Hiroshima Univ.). J. Radiat. Res.; 11: 70-8(Jun 1970).

The protective effects of AET on mortality, intestinal disorders, and hematopoietic injuries in mice against 14-MeV neutrons were compared with those against x-ray damages. The results showed that AET was effective against lethal and hematopoietic injuries in mice exposed to fast neutrons. The protective activity against fast neutrons was, however, significantly less than that obtained with x rays. For intestinal injuries caused by fast neutrons, MEG had no protective activity, whereas it was significantly protective against x rays. (auth)

19030 SOME BLOOD CHANGES IN DINITROCHLORBENZOL-SENSITIZED DOGS AFTER REPEATED IRRADIATION. Samygin, V. K.; Tsirin, E. Kh. Tr. 1 (Pervogo) Mosk. Med. Inst.; 58: No. 2, 11-15(1968). (In Russian).

Studies with six dogs sensitized with dinitrochlorobenzol and exposed to repeated x-radiation therapy resulted in a uniform decrease of white blood elements. The most sensitive to ionizing radiation were dogs' lymphocytes and neutrophils which is in agreement with published data on acute and chronic sickness. (R.V.J.)

19031 INFLUENCE OF IONIZING RADIATION AND RADIOPROTECTORS ON THE ANTIHYALURONIDASE ACTIVITY OF BLOOD SERUM AND TISSUE PERMEABILITY IN RATS. Fedorova, T. A.; Furaeva, L. P.; Rogozkin, V. D.; Ovakimov, V. G.; Tarasenko, A. T. (Inst. of Biophysics, Moscow). Radiobiologiya; 10: 359-63(1970). (In Russian).

After whole-body γ irradiation of rats at a dose of 850 R, an increase in the antihyaluronidase activity in the blood serum and an increase in the tissue permeability of the skin were detected after 1 and 3 hr and after 1, 3, and 7 days. Intraperitoneal injection of mercamine and serotonin into the rats 10 to 15 min before irradiation prevented the change in the antihyaluronidase activity of the blood serum and the tissue permeability of the skin. (tr-auth)

Radiation Sickness and Injuries

Refer also to abstract 19012.

19032 COURSE OF PULMONARY ASCARIASIS IN AN IRRADIATED ORGANISM. III. ATTEMPT AT THERAPY. Radvan, Rostislav. Sb. Ved. Pr. Lek. Fak. Karlovy Univ. Hradci Kralove, Suppl.; 12: 545-56(1969). (In Czech).

An attempt at therapy of ascariasis in the lungs of irradiated mice was carried out with anthelmintics, antibiotics, and by means of active immunization. The effects of some antibiotics on the larvae of Ascaris suum were tested in vitro. (auth)

19033 CLINICAL ASPECTS AND TREATMENT OF RADIATION COMBINED INJURIES (CRUSH SYNDROME AND ACUTE RADIATION DISEASE). Semenov, V. A.; Ul'yanov, M. I.; Torbenko, V. P.; (and others). Ortop., Travmatol. Prot.; 31: 11-17(Jan 1970). (In Russian).

Long-term compression of the soft tissues complicated by acute radiation sickness was investigated. The study revealed a range of peculiarities of this pathology. In the early period of crush-syndrome, the irradiated animals proved to be less susceptible to the action of injuring factors. During later observation (8th to 10th day), the state of the irradiated animals deteriorated sharply. The period of the radiation sickness climax lasted up to 20 to 25 days. Changes in the morphological and biochemical blood structure in the compression and early postcompression period in combined injuries developed at later dates than after compression in the unirradiated dogs. In the postcompression period (8th to 10th day), changes in the hematological indexes in the group of irradiated animals were more sharply pronounced than in the unirradiated ones; normalization ensued later. It is suggested that the principles of pathogenic treatment of combined radiation injury should take into consideration the features of both the crush-syndrome and the developing acute radiation sickness. (auth)

Radiodiagnosis

Refer also to abstracts 18650, 18653, 18660, 18689, 18697, 18699, 18723, 18730, 18885, 18886, 19001, and 19010.

19034 (AEC-tr-7219) INTRODUCTION TO MEDICAL NEUTRON RADIOGRAPHY. Buchet, R. Translated by Myra S. Feldman (Du Pont de Nemours (E. I.) and Co., Aiken, S. C.), from J. Radiol., Electrol., Med. Nucl.; 51: 269-78(1970). 14p. Dep. NTIS.

The possibilities and limitations of the use of neutron radiography in medicine are discussed. It is pointed out that most of the developmental studies on neutron radiography have used reactor produced neutrons having a thermal flux of 10^8 n/cm^2/sec over a small surface area. For medical uses to be feasible it will be necessary to have a portable source of moderated neutrons that can be manipulated without requiring excessive protective shielding. A portable source of thermal neutrons would have to have about 10 cm^2 of surface area to be strong enough. The possibilities of using particle accelerators as neutron generators and of using radioisotope neutron sources for medical radiography are considered. (C.H.)

19035 FOLLOW-UP OF THYROID CARCINOMA BY WHOLE-BODY COUNTING. Edmonds, C. J.; Smith, T.; Barnaby, C. F. (University Coll. Hospital, London). Brit. J. Radiol.; 43: 868-75(Dec 1970).

A simple whole-body counter was used to measure retention of ^{131}I following a test dose in 36 patients with thyroid carcinoma in whom normal thyroid tissue had been ablated. In patients with normal renal function, the fall of whole-body ^{131}I content occurred with a fast initial component (biological half-life, $T_{1/2} \simeq 12$ hours) due to iodide excretion. In all patients, even in the absence of detectable localized ^{131}I concentration, this was followed by a much slower component ($T_{1/2} > 14$ days). The size of the latter component depended on the amount of ^{131}I that was organically bound and provided a measure of the amount of ^{131}I-concentrating tissue remaining. In patients with normal renal function, a single measurement on the sixth day after the test dose indicated the magnitude of the slow component. A retention exceeding 0.31% of the dose at the sixth day was associated with localized residual ^{131}I-concentrating tissue, while with retention less than 0.15% no such tissue was demonstrable by other techniques. However, very small residues could be detected by the latter techniques in some patients with whole-body retention between 0.15 and 0.31%, so that with retentions in this range whole-body counting was less critical. Impaired renal iodide clearance or constipation considerably affected the results. Measurements of whole-body retention earlier than the sixth day can be useful in detecting delay in iodide ^{131}I excretion. A scheme is suggested for using the whole-body counter in follow-up of patients with thyroid carcinoma. (auth) (UK)

19036 SPLEEN SCINTIGRAPHY WITH ^{113m}In-LABELED ERYTHROCYTES. Imhof, H.; Umek, H. (Medical Univ., Vienna). Blut; 21: 162-7(Sep 1970). (In German).

It was tried to improve spleen scintigraphy with ^{113m}In, using simple preparation techniques for labeling erythrocytes. Methods and results are discussed. (auth)

19037 ADVANTAGES AND LIMITATIONS OF DIAGNOSTIC NUCLEAR MEDICINE. Rathje, W. Therapiewoche; 20: 2043-4; 2047-51(Sep 1970). (In German).

The present status of diagnostic nuclear medicine is briefly reviewed. Detection of bone defects with ^{85}Sr or ^{87m}Sr is compared with radiological and histological findings. In addition, disturbances of bone metabolism, as studied by double-tracer technique ^{45}Ca$-^{47}$Ca, are reviewed. Diagnosis of lung embolies and bronchial carcinomas are reviewed for the ^{131}I-albumen macroaggregate method. Similar analysis concerns diseases of the central nervous system, lymphatic system, and thyroid. Briefly discussed are isotope-labeling of hormones and neutron activation analysis. Although diagnostic nuclear medicine has not completely fulfilled early high expectations, the future can be considered optimistically. Thus far, 150 definitely valuable methods are available, of which 40% are in vitro techniques. (H.B.G.)

19038 A METHOD FOR PREDICTING BODY DOSES DUE TO DIAGNOSTIC RADIOGRAPHY. Vacirca, Salvatore John. New York; New York Univ. (1970). 216p. University Microfilms Order No. 70-21,312.

Thesis.

A method for obtaining a continuous dose distribution in a phantom exposed to x rays was developed and applied to assess the dose in man resulting from diagnostic radiographic examinations. The dosimetry system consists of radiographic film in combination with lithium fluoride (LiF) thermoluminescent microdosimeters. The dose response of film, which is variable for x-ray photon energies in the diagnostic region, is compensated by the dose response of LiF which is constant for the same energy region. At the same time the pinpoint accuracy of the LiF microdosimeters is applied to the radiographic film. Thus the combination of dosimeters form a single system which has advantages superior to either individually. (Diss. Abstr. Int., B)

19039 FIRST REMARKS ABOUT ^{113m}In-DTPA IN THE STUDY OF THE KIDNEY. Abbati, A.; Rossi, A.; Turba, E. (Ospedale Maggiore, Bologna). Boll. Soc. Ital. Biol. Sper.; 45: 989-993 (15 Aug 1969). (In Italian).

Preliminary results obtained in the use of ^{113m}In-DTPA (diethylene-triaminopentacetic acid) in the study of the kidney are reported and compared with the results obtained from the use of ^{197}Hg-chlormerodrin. The results showed that ^{113m}In-DTPA makes it possible to obtain scintigraphs of the kidneys immediately following venous injection. A more complete picture of the degree of changes in the kidney and a greater resolution was obtained with ^{113m}In-DTPA. The radiocompound was rapidly eliminated, which reduced to the minimum the dose to the organ. (J.S.R.)

19040 RADIOLOGIC PRESENTATION OF THE FORMS OF PELVIC FRACTURE. Sugar, Eva; Szy, Sandor. Magy. Radiol.; 22: 159-66(Jun 1970). (In Hungarian).

A study of 422 cases showed that the method is safe and effective for the treatment of vascular diseases and abnormalities of the vertebro-basilar system. It is especially suitable for the demonstration of the origin of subarachnoid bleeding because of the fact that right brachial arteriography also demonstrates the area of the carotid. Compared with other methods of cerebral angiography, this method may result in complications at a considerable distance from the cerebral vessels. (auth)

19041 EVIDENCE OF THYROID FUNCTION USING RADIOACTIVE IODINE IN VITRO. Ghys, R. (Hopital du Sacre-Coeur, Montreal). Union Med. Can.; 99: 1478-84 (Aug 1970). (In French).

Statistical analysis of the results of 521 radioisotopic dosages of triiodothyronine (T3) and thyroxine (T4), made from May to October 1969 on patients in the Sacred Heart Hospital in Montreal is presented. They were compared to the chemical determinations of the PBI, done in 236 of these same patients. The validity and reliability of the thyroid screening profile (T3 plus T4), which should be done routinely in internal medicine, was verified. Nevertheless the results must be interpreted as a function of sex, age, and clinical status of the patient. (auth) (Canada)

19042 SCINTIGRAPHIC DETECTION OF PATHOLOGICAL PROCESSES WITHIN THE SPINAL CORD SPACE FOLLOWING INTRAVENOUS ADMINISTRATION OF RADIOISOTOPES: INTRAVENOUS MYELOSCINTIGRAPHY. Piepgras, U.; Voets, P. (Univ., Homburg, Ger.). Fortschr. Geb. Roentgenstr. Nuklearmed.; 113: 329-36(Sep 1970). (In German).

Experience with myeloscintigraphy following the intravenous injection of radioactive substances is described. The method permits the demonstration of pathological processes in the spinal canal, even when there is no abnormality in the circulation of the cerebrospinal fluid. I-V myeloscintigraphy is a valuable addition to myelography, but does not displace it. Since it is simple and safe, the method can be used for diagnostic surveys and for exclusive purposes. Similar to brain scans, it should be carried out before examination with contrast media. (F. St.)

19043 PLACE OF ISOTOPE ENCEPHALOGRAPHY BY THE LUMBAR ROUTE IN NEUROLOGICAL DIAGNOSIS. Bannister, Roger (National Hospital, London). Proc. Roy. Soc. Med.; 63: 921-5(Sep 1970).

The use of radioisotope encephalography is discussed, the technique assessed, and its diagnostic capabilities described. The technique, involving the use of ^{131}I-labeled human serum albumin (RISA) and more recently ^{99m}Tc-labeled albumin, gained impetus through recognition of the dramatic benefit from ventriculo-atrial drainage in some cases of dementia due to communicating hydrocephalus. In diagnosing communicating hydrocephalus, the radioisotope encephalogram augments, but does not replace, the air

XUM

encephalogram. Ventricular radioactivity persisting for 48 hr or more is considered justification for ventriculo-atrial drainage. However, patients demonstrating simple cerebral atrophy without ventricular radioactivity should not be subjected to ventriculo-atrial drainage. (E.R.B.)

19044 FIRST RESULTS OF LUNG FUNCTION DIAGNOSTIC METHODS IN NUCLEAR MEDICINE. Riccabona, G.; Mathie, F.; Leitner, E. (Univ., Innsbruck). Wien. Klin. Wochenschr.; 82: 765-9(16 Oct 1970). (In German).

Results of diagnostic procedures in 46 patients with various lung diseases are reported. To determine lung function, ^{99}Tc-labeled sulfur colloid inhalation was used together with intravenously injected ^{133}Xe. It was concluded that these procedures are very efficient for determination of lung function and it was suggested that improved data evaluation and standardization of techniques will improve the diagnostic efficiency even further. (H.B.G.)

19045 SCANNING OF PLACENTA WITH ^{99m}Tc. Vaalamo, P.; Poeyhoenen, L.; Vauramo, E. (Univ. Central Hospital, Tampere, Finland). Duodecim; 86: 1100-3(1970). (In Finnish).

The localisation of placenta by gamma camera films with technetium ^{99m}Tc was performed in 99 patients following suspected placenta praevia; 15 cases of placenta praevia were diagnosed on the Caesarean section of 27 patients. Of these, 11 were preoperatively demonstrated by gamma camera. In three false negative scans the placenta was implanted on the posterior aspect of the uterus, and the false result apparently arose from weak radiation energy of technetium ^{99m}Tc. In the fourth false negative scan a rare case of placenta praevia accreta was found. Scanning with technetium ^{99m}Tc has proved to be a well-tolerated, safe and simple method for placental localisation. (auth) (Finland)

19046 SCINTILLATION CAMERA IN THE DYNAMIC EVALUATION OF RENAL DISORDERS. Weiss, E. R.; Blahd, W. H.; Winston, M. A.; Krishnamurthy, G. T.; Hartenbower, D. L.; Thomas, P. B. (Wadsworth Hospital, Los Angeles). Radiology; 98: 165-9(Jan 1971).

Scintillation camera techniques with multiple radioisotopic compounds have greatly increased diagnostic accuracy in the dynamic evaluation of renal disorders. ^{99m}Tc-pertechnetate and ^{131}I-Hippuran have proved to be excellent agents for the evaluation of renal vascular perfusion and the study of renal function and morphology. The combined use of these two agents is practical and reliable and represents no hazard to the patient. ^{203}Hg or ^{197}Hg chlormerodrin and ^{99m}Tc-iron-complex also play a part in the radioisotopic evaluation of renal disease. (auth)

19047 BRAIN AND LIVER SCANS IN THE EVALUATION OF LUNG CANCER PATIENTS. Hayes, Thomas P.; Davis, Lawrence W.; Raventos, Antolin (Univ. of Pennsylvania, Philadelphia). Cancer; 27: 362-3(Feb 1971).

In an attempt to better identify those patients with long neoplasms who are incurable by surgery or radical radiotherapy, pretreatment brain and liver scans for the localization of possible metastases were done on 41 patients. The yield of positive studies was 3.7% for brain scans and 4.7% for liver scans. It is suggested that the value of these studies may be further enhanced by doing them after the rest interval of a split-course radiotherapy regimen. (C.H.)

19048 REGIONAL PULMONARY FUNCTION IN METASTATIC CARCINOMA TO THE LUNG STUDIED WITH ^{133}Xe. Ali, M. Khalil; Howe, Clifton D.; Miller, John M. (Univ. of Texas, Houston). Cancer; 27: 460-7(Feb 1971).

Lung function was studied in 21 patients with nodular pulmonary metastases. Routine pulmonary function studies demonstrated that reduction in vital capacity and arterial PO_2, related to the degree of tumor involvement, are characteristic features of metastatic lung disease. The reduced arterial PO_2 is largely explained by increased right to left shunt. Regional pulmonary function studied with ^{133}Xe and scintillation detectors revealed frequent ventilatory defects in the vicinity of single metastases. In patients with multiple bilateral metastases, defects in pulmonary blood flow and ventilation were commonly observed in the vicinity of the tumor masses. (auth)

19049 SELENOMETHIONINE ^{75}Se THYMUS SCANS IN MYASTHENIA GRAVIS. Cowan, Robert J.; Maynard, C. Douglas; Witcofski, Richard L.; Janeway, Richard; Toole, James F. (Wake Forest Univ., Winston-Salem, N. C.). J. Amer. Med. Ass.; 215: 978-9(8 Feb 1971).

Of 200 patients with myasthenia gravis studied with ^{75}Se-selenomethionine mediastinal scans, two (10%) had positive scans. Both of these patients underwent surgery with removal of a thymoma. Since this radiopharmaceutical is accumulated in numerous tissues, false-positive studies may present some difficulty. The adult thymus, in the absence of a thymoma, does not appear to concentrate ^{75}Se-selenomethionine sufficiently for external scanning. Negative studies may therefore be of value in ruling out the presence of a thymoma. (auth)

19050 SYSTEM FOR COMPUTER PROCESSING OF RADIOPHARMACEUTICAL DISBURSEMENT INFORMATION. Nusynowitz, Martin L.; Goldsmith, William A.; Waliszewski, Jerome A.; Musarra, Joseph S. (William Beaumont General Hospital, El Paso, Texas). Amer. J. Roentgenol., Radium Ther. Nucl. Med.; 111: 191-4(Jan 1971).

A system for computer processing of information relative to radiopharmaceutical disbursement is presented. The system conveniently satisfies three administrative requirements of any busy radioisotope clinic, including preparation of inventories; computation of workloads; and maintenance of patient dosage records. This system has the potential to be expanded to meet other requirements as they arise. (auth)

19051 THYROID UPTAKE OF RADIOACTIVE IODINE. A REEVALUATION. Caplan, Robert H.; Kujak, Richard (Gundersen Clinic, Ltd., La Crosse, Wis.). J. Amer. Med. Ass.; 215: 916-18(8 Feb 1971).

Mean 24-hour thyroid uptake of ^{131}I in 44 clinically euthyroid control subjects was 12.1% ± 6.1% (SD). In a separate but related study, the 24-hour thyroid uptake of ^{131}I performed for diagnostic purposes was reviewed in 65 euthyroid, 12 hypothyroid, and 14 hyperthyroid patients; the mean uptakes were 14.3% ± 7.7%, 3.9% ± 3%, and 48.7% ± 19%, respectively (mean ± SD). Iodine kinetic studies performed in the 44 control subjects revealed elevated urinary iodine excretion and plasma inorganic iodide concentration and depressed thyroid iodide clearance. These findings indicate an increased dietary intake of iodine in the population studied and suggest that revision of normal standards for thyroid function in the populations of other localities may be necessary. (auth)

19052 XII INTERNATIONAL CONGRESS OF RADIOLOGY, OCTOBER 6-11, 1969, TOKYO. BOOK OF ABSTRACTS. Chiba, Japan; National Institute of Radiological Sciences (1969). 613p. (CONF-691021-(Absts.)).

Abstracts are included for approximately one thousand papers presented at the Congress. (C.H.)

19053 ENHANCED SCINTIGRAPHIC INFORMATION DISPLAY USING COMPUTER-GENERATED RATIO TECHNIQUES. Bell, Ronald L. (Central Research Labs., Palo Alto, Calif.); DeNardo, Gerald L. J. Nucl. Med.; 11: 655-9(Nov 1970).

A method is described for computer-assisted scintigraphic information display by the use of ratio maps to present clinically significant data in pictorial form. The method was illustrated by pulmonary washin and washout studies using ^{133}Xe in cases of bulbous emphysema and pulmonary embolisms. It appeared from the exploratory studies outlined that straightforward computational techniques may considerably enhance the value of quantitative information obtained from the scintillation camera, leading to a more precise and detailed delineation of body structures and their associated functional or anatomic abnormalities. (E.E.H.)

19054 RESEARCH, DEVELOPMENT, AND PRODUCTION OF SHORT LIVED RADIOPHARMACUETICALS. Boyd, R. E. (Australian Atomic Energy Commission Research Establishment, Lucas Heights). Australas. Bull. Med. Phys. Biophys.; No. 46, 23-31(1 Oct 1970).

Currently established A.A.E.C. production processes are discussed. Methods were given for the preparation of ^{99m}Tc-sodium pertechnetate for brain scanning, ^{99m}Tc-labeled macroaggregated $Fe(OH)_2$ for lung perfusion studies, and ^{99}Tc-labeled rhenium sulfide colloid for scanning of the reticulo-endothelial system. (Australia)

19055 MYOCARDIAL UPTAKE STUDIES WITH ^{129}Cs AND THE SCINTILLATION CAMERA. Yano, Yukio; Van Dyke, Donald; Budinger, Thomas F.; Anger, Hal O.; Chu, Patricia (Univ. of California, Berkeley). J. Nucl. Med.; 11: 663-8 (Nov 1970).

A method for the production of ^{129}Cs by cyclotron irradiation is described. The distribution of ^{129}CsCl in tissues of rats and dogs was determined for various time intervals after intravenous injection. Areas of myocardial infarction were demonstrated in dogs. Cesium-129 and the scintillation camera with suitable collimation were used to image the myocardial distribution of coronary blood flow both in normals and in patients with coronary disease. The series of studies is being extended to the acute myocardial infarction patients for assessment of the clinical practicality of imaging and following the progression or regression of myocardial infarctions. (auth)

19056 LUNG FUNCTION STUDIES USING SHORT-LIVED /sup 81m/Kr AND THE SCINTILLATION CAMERA. Yano, Y.; McRae, J.; Anger, H. O. (Univ. of California, Berkeley). J. Nucl. Med.; 11: 674-9(Nov 1970).

The use of the radioactive gas ^{81m}Kr, for pulmonary perfusion and ventilation studies was investigated. Preliminary studies were done on five normal volunteers and 11 patients to determine the type of physiological and clinical information that could be obtained by using the dynamic and static imaging capabilities of the scintillation camera. Excellent resolution of the right heart, left and right pulmonary arteries, and upper tracheo-bronchial tree was achieved. It was also possible to watch the changing distribution of activity as inhalation proceeded. Abnormalities were demonstrated in patients. Krypton-81m should be particularly useful for exploring the variations in distribution of activity within the lungs in various lung disorders with changing patterns of inhalation. A method is also presented for obtaining millicurie amounts of ^{81m}Kr from a ^{81}Rb parent. (E.E.H.)

19057 EVALUATION OF SPLEEN SIZE DURING ROUTINE LIVER IMAGING WITH /sup 99m/Tc AND THE SCINTILLATION CAMERA. Sigel, Richard M.; Becker, David V.; Hurley, James R. (New York Hospital-Cornell Medical Center, New York). J. Nucl. Med.; 11: 689-92(Nov 1970).

A study was made to determine whether spleen size could be quantitatively evaluated by simply measuring organ height on routine ^{99m}Tc-sulfur colloid liver images obtained with the scintillation camera and whether it would be possible to set clinically useful criteria for splenomegaly with this technique in the hospital population. Spleen size was evaluated with a calibrated scale in 321 routine liver scans. The upper limit of normal spleen height was found to be approximately 14 cm. (E.E.H.)

19058 SCAN EVIDENCE OF ORGAN INVOLUTION AND IMPROVEMENT OF HYPERSPLENISM IN HODGKIN'S DISEASE FOLLOWING SPLENIC ARTERY LIGATION. Nuland, Sherwin B.; Cornelius, Eugene A.; Spencer, Richard P. (Yale Univ., New Haven). J. Nucl. Med.; 11: 693-4(Nov 1970).

A case is described in which splenectomy for Hodgkin's disease was found unfeasible because of tumor involvement of the pedicle. Ligation of the splenic artery produced scan-documented diminution in splenic size as well as a marked improvement in the hypersplenic blood picture and a more normal distribution of ^{99m}Tc-sulfur colloid between liver and spleen. (auth)

19059 SCINTILLATION OF A VASCULAR RIM IN SUBDURAL HEMATOMA. Smoak, William M.; Gilson, Albert J. (Univ. of Miami, Fla). J. Nucl. Med.; 11: 695-7(Nov 1970).

A case study is presented on a patient with a proven subdural hematoma who showed a rim sign on a scintillation camera study. The rim sign was thought to be due to vascular structures that contain pertechnetate and that are altered and displaced by the subdural hematoma. The probable pathophysiology of this sign is discussed, and the difference between findings in subdural hematomas studied with ^{203}Hg-chlormerodrin and with ^{99m}Tc-pertechnetate was noted. (auth)

19060 EXPERIMENTAL STUDIES ON THE DISTRIBUTION TO THE ORGANS FOLLOWING INTRAVENOUS INJECTION OF ^{131}I-ERYTHROSINE B. Takashima, Tsutomu; Rikimaru, Shigeho; Mitani, Iwao; Ando, Atsushi (Kanazawa Univ., Japan). Nippon Igaku Hoshasen Gakkai Zasshi; 29: 1025-9(Nov 1969). (In Japanese).

The visualization of the pancreas has not, as yet, become a routine procedure, because of failure in finding a contrast media for which the pancreas has a direct affinity. In a series of experiments in cats, erythrosine B was claimed to concentrate selectively in the pancreas and to visualize the pancreas. However, the intravenous injection of erythrosine-B failed to visualize the pancreas in experiments on dogs. Studies were made on the distribution of erythrosine-B following intravenous administration of ^{131}I-labeled erythrosine B. The ratios of the concentration of radioactivity in the pancreas to the concentration in the muscle following intravenous injection of ^{131}I-erythrosine B into rats showed only low affinity, contrary to a high concentration in the liver. Even after injection of secretin, it fell short of expectations. The results indicated that erythrosine B was not effective as a contrast agent for pancreatic visualization. (auth) (Japan)

19061 GROWTH OF THE HUMAN LIVER: A PRELIMINARY SCAN STUDY. Spencer, Richard P.; Banever, Carol (Yale Univ., New Haven). J. Nucl. Med.; 11: 660-2(Nov 1970).

The estimation of growth during life has been mainly limited to external measurements and to radiographic studies of ossifying bones. Hepatic scans can provide apparent dimensions and cross-sectional areas of the liver and offer a method for potentially following liver growth in life. A series of anterior scans in children is presented along with various hepatic measurements related to age, height, weight, and estimated body-surface area. It was concluded that, when sufficient cases are available for the separate study of females and males, criteria could probably be established, with appropriate confidence limits, for estimating hepatic growth and for determining whether a particular scan on a child is within normal limits. (E.E.H.)

Radiotherapy

Refer also to abstracts 19000, 19011, 19093, 19138–19140, 19147, and 19149.

19062 (NP-18693) HYPERTHYROIDISM, RADIOIODINE AND THEREAFTER. van der Grient, Anton Jacobus (Groningen Rijksuniversiteit (Netherlands)). 1969. 148p. (In Dutch). Dep. NTIS (U. S. Sales Only).

Thesis.

The cause of hyperthyroidism is unknown. The methods available for treating this disease are thus limited to decreasing the hyperfunction of the gland by drugs, or eliminating a large part of the gland by surgical removal or radiation. Data are reviewed for 268 cases of hyperthyroidism treated with ^{131}I. The results of this treatment were studied in a retrospective survey, for which 208 patients were available. The effect of internal irradiation on function and size of the thyroid was investigated, and in addition an explanation for the incidence of hypothyroidism was sought. A possible relationship between the radiation dosage and the incidence of thyroid hypofunction was investigated. Immunological changes arising after treatment were also investigated, as were the effect of treatment on the cardiovascular system, the Achilles tendon reflex and on carbohydrate metabolism. A number of laboratory investigations directly or indirectly related to thyroid function were also made. (90 references.) (C.H.)

19063 EFFECT OF RADIOTHERAPY ON THE URINARY AMINO ACIDS. Abe, Mitsuyuki; Takeuchi, Katsumi; Kitamura, Kanae; Fukuda, Masasi (Kyoto Univ.). Nippon Igaku Hoshasen Gakkai Zasshi; 30: No. 1, 23-32(Apr 1970). (In Japanese).

Quantitative amino acid determinations were made by an amino acid analyzer during radiotherapy in 17 patients with various forms of malignant tumors. In most cases an increased urinary excretion of amino acids occurred in an early phase of radiotherapy. However, there appeared to be wide variation in both the quantitative and qualitative pattern of this excretion. No relationship between exposure dose and excretion was observed. In general, urea, threonine, glutamine acid, glycine, alanine, tryptophan, and histidine showed a significant increase with aspartic acid, serine, cystine, tyrosine, and phenylalanine being somewhat higher than preirradiation levels and the excretion of valine, methionine, isoleucine, and leucine remained essentially within the preirradiation range throughout radiotherapy. It was found that there was an increase in urinary taurine excretion in patients showing marked leukopenia, while no such taurinuria was observed in patients in which leukopenia was not significant. The observed taurinuria was followed by leukopenia and was not necessarily related to total radiation doses, number of treatments, or histological nature of tumors, but rather it was closely related to leukocyte counts. As to β-aminoisobutyric acid (BAIBA), it appeared that there was a general improvement in patients' condition (disappearance or regression of tumors) as therapy progressed in subjects showing a decrease in BAIBA excretion, whereas those showing an increase in this BAIBA excretion showed no such improvement. (auth) (Japan)

19064 HISTOLOGICAL AND CYTOLOGICAL CHANGES OF CERVICAL CANCER DURING THE LINEAR ACCELERATOR IRRADIATION THERAPY. Takahashi, Hidesuke (Fukushima Medical Coll., Japan). Fukushima Igaku Zasshi; 19: No. 2, 69-78(Apr 1969). (In Japanese).

In a series of 40 cases of cervical cancer treated with irradiation from the linear accelerator, the correlation between local changes examined by the use of punch biopsy and vaginal smear and the radiation dose was studied, and radiation effects on primary lesions were evaluated. Histological and cytological changes were comparable to changes following other types of radiotherapy. Histological examinations revealed marked changes in carcinoma cells, such as swelling, vacuolization of cytoplasm, swelling and vacuolization of nucleus, karyopyknosis, karyorrhexis, decreased mitosis, and the formation of giant nuclei. Cytological studies showed swelling and low stainability of cells, multinucleation, cellular deformation, intracytoplasmic vacuolization, swelling, vacuolization, and breakdown of nuclei. These changes were seen frequently with doses of up to 4,000 R to vaginal smears. The

XUM

effects of 6000 R doses were evaluated by the presence or absence of malignant cells. Among the 40 cases, linear acceleration irradiation was judged favorable in 27 cases and unfavorable in 13. The predictability of the radiation effect to Graham's sensitization response (SR) was good in 88%, poor in 46%, while the radiation response (RR) was good in 82%, poor in 50%. (auth) (Japan)

19065 CEREBRAL GLIOMAS. NOTE I. HISTOLOGICAL OBSERVATIONS AND RADIOBIOLOGICAL CONSIDERATIONS. Crespi Porro, R. (Ospedale di Circolo, Varese, Italy). Med. Nucl.-Radiobiol. Lat.; 12: 63-90(1969). (In Italian).

The problem of vascular proliferation in cerebral gliomas on the basis of histological observations relating to 86 cases subjected to post-operational radiant treatment was examined. This phenomenon was found to be markedly more intense and frequent in immature forms and in radio-treated forms, both as regards the tumor and in the surrounding nervous parenchyma. In 22 neoplastic recurrences subjected to further radiosurgical treatment, a significant increase in the cellular and vascular regressive phenomena was noted, among which the vascular thrombosis already suggested in literature as an aetiopathogenetic factor of the peculiar vascular proliferation. In the light of the most recent studies on the oxygen effect in radiotherapy, it was noted that the real importance of the degree of vascular proliferation in the rational radiosensitization of a cerebral neoplastic mass, is worthy of reconsideration in the controversial subject of the therapy of cerebral gliomas. (auth)

19066 WAX RETRACTION AS A TECHNIQUE FOR COMPENSATING THE EFFECT OF SURFACE IRREGULARITIES IN HIGH-ENERGY RADIOTHERAPY. Jackson, W. (Western Regional Hospital Board, Glasgow). Brit. J. Radiol.; 43: 859-67(Dec 1970).

The technique of filling an irregular body contour with tissue-equivalent wax and retracting the wax in the beam direction, without making an allowance for beam divergence, was examined from the point of view of electron contamination on the skin and errors in depth dose which arise from loss of scatter and also from any change in the path of the primary ray. Skin contamination at a given point was found to depend on the angle subtended there by the irradiated wax. This leads to the simple working rule that if a retracting distance equal to the average field dimension is chosen, the skin dose will be reduced to 50% of its value before retraction. Depth dose errors, i.e., deviations from the values as read in the normal isodose chart, were found to depend chiefly on retracting distance and the thickness of the retracted wax. The technique is feasible provided a retracting distance can be found which gives an acceptable skin dose and small depth dose errors. These may be estimated from the appropriate graphs. The conditions are most easily fulfilled for small fields. (auth) (UK)

19067 SELECTION OF CONDITIONS FOR ROTATION IRRADIATION ON THE GAMMA-THERAPEUTIC APPARATUS ROKUS. Kozlov, A. P.; Afanas'ev, B. P. (Research Inst. of Oncology, Leningrad). Vop. Onkol.; 16: No. 10, 38-43(1970). (In Russian).

Experimental characteristics of the dosage fields of the gamma-therapeutic apparatus Rokus in rotation regime of irradiation are presented, and the technique of using these data for selection and practical realization of individual plans of radiation therapy is described. The criteria of selection of rotation irradiation parameters are regularity of focal irradiation, reduction of total irradiation of the body and protection toward vital organs and tissues. (auth)

19068 FLUOROSCOPIC RADIATION AND RISK OF PRIMARY LUNG CANCER FOLLOWING PNEUMO THORAX THERAPY OF TUBERCULOSIS. Gofman, J. W.; Tamplin, A. R. (Univ. of California, Livermore). Nature (London); 227: 255-6(18 Jul 1970).

It is suggested that frequent fluoroscopies of the chest, associated with the extensive use of pneumothorax collapse therapy, may be the aetiological factor responsible for the observation that persons with a tuberculosis history showed a five- to ten-fold increase in the risk of subsequent development of primary lung cancer. Some generalized case histories are summarized, in which an air dose of about 900 R was indicated to the chest region and the dose to lung tissue must have been of that order, depending on the hardness of the x rays used. It was estimated that a dose of $\sim$50 R produces lung cancers equal to the spontaneous incidence, and hence this dose would constitute a doubling dose for primary lung cancer. In the case histories considered, it was estimated that the average patient would have received 6.2 doubling doses to the lungs. Adding the spontaneous incidence, the overall lung cancer incidence would be 7.2 times the expected spontaneous incidence. It is emphasized that the suggested hypothesis be accepted only as a guide to valuable studies than can readily be made, and not considered as a plea for reducing essential radiography or fluoroscopy in the management of pulmonary tuberculosis. (UK)

19069 PROBLEMS CONCERNING RADIOTHERAPY AND CURIETHERAPY IN DENTISTRY. Urth, A. (Univ. Libre, Brussels). Acta Stomatol. Belg.; 66: 273-328(1969). (In French).

The etiology, evolution, and prevention of cancerous lesions caused by radiotherapy and curietherapy in dentistry are discussed on the basis of a bibliographic study and the examination of a few specific cases. (162 references). (J.S.R.)

19070 RADIOISOTOPE SURGERY IN GYNECOLOGY. Gitsch, E. (Univ., Vienna). Wien. Klin. Wochenschr.; 82: 727-30 (16 Oct 1970). (In German).

The use of radioisotopes in gynecological surgery for collum carcinomas is reported. The newly developed method is described and evaluated with respect to improvement of efficiency in surgical procedures. (tr-auth)

19071 RADIATION TREATMENT OF SYNCHRONIZED TUMORS: PRELIMINARY RESULTS. Nitze, H. R.; Ganzer, U.; Vosteen, K.-H. Arch. Klin. Exp. Ohren-, Nasen- Kehlkopfheilk.; 196: 401-4(1970). (In German).

Patients with advanced carcinoma of head and neck received a twelve hour infusion of 1 g of 5-fluoro-uracil. At eight hours following infusion, when mitotic synchronization was optimal, the tumor was locally treated with 500 R of x radiation. With respect to both tumor regression and survival time, the procedure appeared promising. (H.B.G.)

19072 BETATHERAPY WITH ^{90}Sr IN PLASTIC INDURATION OF THE PENIS. Holan, T.; Miclutia, M. (Hospital No. 2, Cluj). Med. Nucl.-Radiobiol. Lat.; 12: 49-54(1969). (In French).

The results obtained in 38 patients with single or few multiple lesions having a diameter of not more than 1.5 cm are reported. In order to assess the efficacy of the treatment, both the subjective changes reported by the patients and the objective ones observed clinically were considered. It was concluded that the results obtained with the therapy could be considered satisfactory although it is not possible to report complete regression of the lesion except in rare cases. The advantages of beta therapy with ^{90}Sr are emphasized and the most important drawbacks found in the technical conditions adopted are discussed. (auth)

19073 ALOPECIA MUCINOSA (FOLLICULAR MUCINOSIS): TREATMENT AND PROGNOSIS. Shapiro, Lewis (Columbia Univ., New York). J. Amer. Med. Ass.; 214: 604-5(19 Oct 1970).

The intermittent application of grenz rays (soft x rays) for treatment of alopecia mucinosa is reported. Of all of the therapeutic modalities reported, only ionizing radiation was effective to any extent. However, there is a limit to how much x radiation may be given to any area during the course of a patient's life. (E.R.B.)

19074 MEDICAL ASPECTS OF THE USE OF LASERS. Tengroth, Bjoern. Laekartidningen; 65: 4893-6(Dec 1968). (In Swedish).

The medical use of lasers in cancer surgery, neurosurgery, and dermatology must be accompanied by a knowledge of the biological effects of lasers and their advantages and disadvantages. These are briefly reviewed. (J.S.R.)

19075 X IRRADIATION OF SYNCHRONIZED ANIMAL TUMORS. Ganzer, U.; Nitze, H. R. Arch. Klin. Exp. Ohren-, Nasen- Kehlkopfheilk.; 196: 398-400(1970). (In German).

Mice with benzopyrene-induced skin cancer were divided into five groups: untreated, twice weekly injection of 0.5 mg fluorouracil for cytostatic action, combination treatment of fluorouracil and x radiation, x radiation, and synchronization in which fluorouracil was given throughout twelve hours and followed by x radiation exactly eight hours later during the G-2 phase. Survival time was longest for the synchronized group, and shortest for the combination group. The results justified application of the synchronization treatment in humans. (H.B.G.)

19076 AFTERLOADING TECHNIQUES. Ellis, Frank (Churchill Hospital, Oxford). Proc. Roy. Soc. Med.; 63: 1034-5(Oct 1970).

The advantages of afterloading techniques are that the radiation dose to theater staff is small and that insertions can be made as deliberate as necessary without the fear of occupational irradiation of the radiotherapist or ancillary staff. Also, precalculation before loading makes possible adjustments to improve dose distribution as well as facilitating the timing of commencing the radiation so as not to prejudice healing of wounds. Removal can also be conveniently timed to improve dosage distribution. The techniques used for Ra, ^{182}Ta, ^{192}Ir, and ^{137}Cs are discussed and the relative merits of wires, needles, plastic tubes, or steel tubes are considered. Used in planned combination with surgery, beam therapy, and chemotherapy, implant therapy is probably the most successful method of obtaining local cure of cancer in difficult cases. (E.R.B.)

19077 BIOPHYSICAL ASPECTS OF HIGH LET IRRADIATION. Rossi, Harald H. (Columbia Univ., New York). Amer. J. Roentgenol., Radium Ther. Nucl. Med.; 111: 27-30(Jan 1971).

Biophysical factors that affect differences in the radiosensitivity of malignant and normal tissues during radiotherapy are discussed. It is pointed out that radiobiological research has greatly enhanced understanding of the factors that might determine optimum conditions. These include dose-effect relations, recovery, division delay, change of age distribution of cells in the division cycle, oxygen enhancement ratio, revascularization of tissues and proliferation rate. Although many of these features are understood in some detail there is still not enough numerical information to permit practical applications and, consequently, the great majority of radiotherapy treatments are carried out following methods that have been in practice for decades. A major modification of radiotherapy is the employment of different radiations. The introduction of γ teletherapy sources and high voltage accelerators for the production of very energetic x rays or electrons has, in many cases, led to a substantial improvement in dose distributions but has hardly affected the role of other biophysical factors. At the highest energies the biological effectiveness of these radiations might be decreased by perhaps 15%, but there is much less, if any, change in differential sensitivities of tumors or in the action of dose modifying factors. All of these radiations have the common property of imparting energy to irradiated tissues through the agency of high speed electrons and they are sometimes termed low LET radiations. Their action differs in many respects from that of another group of radiations that are termed high LET radiations. These expressions are vague and rather misleading. Linear energy transfer (LET) is defined and differences between low LET (<10 keV/μm) and high LET (>100 keV/μm) radiations that affect their effectiveness for use in therapy are discussed. (C.H.)

19078 NEGATIVE PIONS: THEIR POSSIBLE USE IN RADIOTHERAPY. Bond, V. P. (Brookhaven National Lab., Upton, N. Y.). Amer. J. Roentgenol., Radium Ther. Nucl. Med.; 111: 9-26(Jan 1971).

The negative π meson beam has a number of favorable characteristics which, taken collectively, make a high-output beam attractive for radiotherapy. These include: a depth-dose and dose equivalent (dose × RBE) pattern superior to those now available; a relatively low OER in the peak portion of the depth-dose curve; and less repair of sublethal cell damage in the peak portion. The clinical gain to be expected from such sharply localized radiation is difficult to assess quantitatively from presently available data, and it is not possible to predict whether the over-all improvement in morbidity and mortality is likely to be 5%, 10%, or more. (C.H.)

19079 DENTAL CARE AND ORAL HYGIENE BEFORE AND AFTER TREATMENT. RADIATION CARIES. Hinds, Edward C. (Univ. of Texas, Houston). J. Amer. Med. Ass.; 215: 964-6(8 Feb 1971).

Proper dental care and oral hygiene is of the utmost importance in a healthy mouth and in individuals afflicted with cancer of the mouth such care is critical for the successful management of the disease whether irradiation, surgery, or a combination of the two is used for treatment. Radioinduced necrosis of bones is the greatest single complication following radiotherapy of oral neoplasms and it may be further complicated by infections and trauma. There is also a marked tendency to an increased incidence of dental caries following radiotherapy. Mucositis may develop soon after radiotherapy is begun. Irradiation also slows the resorption of bone following tooth extraction and may result in sharp projections of bone. The care of the mouth before, during, and following radiotherapy is described in detail. (C.H.)

19080 PLACE OF IMPLANTATION IN TONGUE AND FLOOR OF MOUTH CANCER. Pierquin, Bernard (Faculte de Medicine, Paris); Chassagne, Daniel; Baillet, Francois; Castro, Joseph R. J. Amer. Med. Ass.; 215: 961-3(8 Feb 1971).

The technical advances of interstitial therapy with ^{192}Ir applicators in comparison to that which was possible with radium permit the attainment of almost an absolute rate of local control of cancers of the mobile tongue and floor of the mouth of less than 4-cm in diameter. With a 95% permanent local control rate, proved for 153 cases, because all recurrences appeared within six months, and for 61 cases because of all of the patients surviving after four years none has presented with a late local recurrence; and knowing that the 5% with local recurrence are related to technical errors, we are able to state that the radiobiologic problems of treatment of these cancers of the mobile tongue and floor of the mouth are totally resolved with the method of interstitial therapy. Taking count of the small proportion of patients with necroses, all of whom are restorable to good health, we are able to conclude that interstitial therapy should be considered as the optimal technique, compared to teleradiotherapy, surgery, and electrocoagulation, for the treatment of primary epidermoid carcinomas of the anterior two thirds of the tongue and floor of the mouth. (auth)

19081 RADIOTHERAPEUTIC PRINCIPLES AND VIEWPOINTS. Lampe, Isadore (Univ. of Michigan, Ann Arbor). J. Amer. Med. Ass.; 215: 959-60(8 Feb 1971).

Squamous cell carcinoma is a common cancer of the oral cavity and lower lip. The squamous cell carcinoma is a radioresponsive and radiocurable neoplasm. Therapeutic methods available include low-voltage x irradiation, orthovoltage x irradiation for advanced lesions, supervoltage x irradiation, ^{60}Co γ irradiation, low-intensity radium-226 γ applicators, and other radioisotope applicators. Results are reported for 19 patients with carcinoma of the mouth treated by radiotherapy. A 53% five-year survival rate was obtained. (C.H.)

19082 USE OF ELECTRON FILTER TO REDUCE SKIN DOSE IN COBALT TELETHERAPY. Khan, Faiz M. (Univ. of Minnesota, Minneapolis). Amer. J. Roentgenol., Radium Ther. Nucl. Med.; 111: 180-1(Jan 1971).

The use of medium atomic number absorbers (electron filters) such as tin finds a routine application in ^{60}Co γ radiation therapy set-ups in which a compensator or a lucite tray to support shielding blocks is interposed in the beam. An important practical deduction may be made from this experiment; namely, the introduction of a thin sheet of tin attached to the underside of a low atomic number absorber at a distance of about 8 cm from the skin brings the skin dose close to the value obtained with no absorber in the beam. While a 0.8 mm thick sheet of tin attenuates the useful beam by less than 3%, it remarkably reduces the skin dose. It may be mentioned that using a thickness of electron filter greater than the equilibrium thickness does not further improve the skin dose but only causes undesirable attenuation of the gamma-ray beam. (auth)

19083 COMPARATIVE EVALUATION OF THE SEQUENTIAL USE OF IRRADIATION AND SURGERY IN PRIMARY TUMORS OF THE ORAL CAVITY, OROPHARYNX, LARYNX, AND HYPOPHARYNX. Crews, Quintous E.; Fletcher, Gilbert H. (Univ. of Texas, Houston). Amer. J. Roentgenol., Radium Ther. Nucl. Med.; 111: 73-7(Jan 1971).

A comparative review of the percentage of failure of irradiation for the treatment of primary neoplasms of various anatomic sites of the mouth and throat gives guidelines for primary radiation therapy on the basis of incidence of local control and the possibility of surgical correction of irradiation failures, as well as the correction of complications. (auth)

19084 ELECTIVE IRRADIATION OF THE NECK LYMPHATICS FOR SQUAMOUS CELL CARCINOMAS OF THE NASOPHARYNX AND OROPHARYNX. Berger, David S.; Fletcher, Gilbert H.; Lindberg, Robert D.; Jesse, Richard H. Jr. (Univ. of Texas, Houston). Amer. J. Roentgenol., Radium Ther. Nucl. Med.; 111: 66-72(Jan 1971).

Eight of 469 patients (1.7 per cent) with squamous cell carcinomas of the nasopharynx and orthopharynx developed new lymph node metastases in an electively x irradiated area. Nineteen of 185 patients (10.2 per cent) with partial neck irradiation developed new nodal metastases in a marginally irradiated or unirradiated area. A tissue dose of 4,500 to 5,000 rads tumor dose in five weeks is proposed for the irradiation of elective areas. This dose produces no complications or even minor sequelae. Whole neck irradiation is indicated for squamous cell carcinomas of the nasopharynx, tonsillar fossa, base of tongue, and palatine arch. (auth)

19085 RADIATION THERAPY OF CARCINOMA OF THE TONSILLAR REGION. Fayos, Juan V.; Lampe, Isadore (Univ. of Michigan, Ann Arbor). Amer. J. Roentgenol., Radium Ther. Nucl. Med.; 111: 85-94(Jan 1971).

One hundred and two patients with a diagnosis of squamous cell carcinoma of the tonsillar region received complete ^{60}Co γ radiation treatment. The absolute five year survival was 32.4 per cent, counting as if dead of the disease one patient who was alive with disease at 5 years and one who had recurrence of the primary lesion later cured by surgery. The determinate five year survival was 39.8 per cent. The prognosis decreased as the primary lesion became larger or if there was regional metastasis. The findings in this study lend support to the use of radiation therapy as the initial form of treatment of carcinoma of the tonsillar region. (auth)

19086 METHODS FOR THE ENHANCEMENT OF SKIN SPARING IN ^{60}Co TELETHERAPY. Saylor, William L.; Quillin, Robert M. (Walter Reed Army Medical Center, Washington, D. C.). Amer. J. Roentgenol., Radium Ther. Nucl. Med.; 111: 174-9(Jan 1971).

In ^{60}Co γ teletherapy the skin sparing effect can be enhanced, for all field sizes and filter-skin distances, by use of a leaded glass electron filter having a density of at least 3.2 gm/cm^3. This will result in a 20–30 per cent decrease in relative skin dose over a lucite filter or the open beam. Leaded glass filters are as effective as pure metals in reducing the skin dose. The filter thickness needs to be just sufficient to stop all electrons arising on the source side of the filter. The relative skin dose depends upon the field size and, to a lesser degree, upon the filter-skin or collimator-skin distance. (auth)

19087 POSSIBLE UTILIZATION OF THE CARNEGIE-MELLON SYNCHROCYCLOTRON FOR CANCER THERAPY. Foss, M. H.; Fox, J. G.; Banerjee, K.; McAllister, J. D.; DiPrimio, J. (Carnegie-Mellon Univ., Pittsburgh. St. Francis General Hospital, Pittsburgh). Radiology; 98: 183-5(Jan 1971).

The 440-MeV proton beam from the Carnegie–Mellon synchrocyclotron was degraded to approximately 180 MeV energy with copper and graphite absorbers, with the intention of using the beam for cancer therapy. Experimental results showed a fairly homogeneous beam with moderate intensity. Some isodose curves and Bragg peaks obtained with an automatic isodose plotter are given. (auth)

19088 MAJOR SURGERY AFTER RADICAL RADIOTHERAPY. INDICATIONS AND COMPLICATIONS. Rafla, S. (Methodist Hospital, Brooklyn). Cancer; 27: 314-22(Feb 1971).

The study of one hundred and forty-two patients who underwent major surgery after a radical course of radiotherapy for pelvic and head and neck tumors revealed the following trends: The most important complications in the immediate postoperative period are the problem of healing for tumors of the head and neck (26%) and death (within 30 days) for pelvic tumors (10%). Late results are rather disappointing in tumors in both sites. Forty-three percent of patients with head and neck tumors suffered from local recurrence, and an additional 11% suffered from severe pain and died. Fifteen per cent of the pelvic tumors recurred; another 9% of patients continued to have residual disease, and 15 experienced severe pain and ultimately died. Only one quarter of the patients were alive and well after five years. Patients who undergo surgery because of complications of radiotherapy seem to do significantly better than those with recurrent or residual disease. The latter group has the worse results, whether in the immediate postoperative period or long term. The more limited the operation is, the better the chance of uncomplicated postoperative course and long-term survival. Younger patients have less postoperative complications and higher five-year survival, especially those with cancer of the cervix. (auth)

Blast and Thermal Effects

Refer also to abstract 18990.

19089 PRENATAL RADIATION EXPOSURE AND CHILDHOOD CANCER. Burch, P. R. J. (Leeds Infirmary, Eng.). Lancet; 2: 1189(5 Dec 1970).

In 1292 children exposed in utero to radiation at Hiroshima and Nagasaki, one death under ten years was later recorded from childhood malignancy. The number expected at Japanese national death-rates was 0.75, while the excess mortality from all childhood malignancies expected on the basis of association between these and obstetric x-rays was 36.9. It is suggested that there could be a non-causal explanation of the later figure. Correcting for the changing mutagenic efficiency with dose, the effect of cytotoxicity, taking the fetal dose at Hiroshima and Nagasaki to be 70% of the maternal dose and assuming the dose-response relationship at low dose, the estimated extra cancer deaths under 10 years should be in the range 15 to 25. Allowing for the change in radiosensitivity of the embryo/fetus with trimester, the expected extra deaths should be raised to 34 to 58.(UK)

Radiation Effects on Animals

Refer also to abstract 18909.

19090 (COO-1704-22) STUDIES ON THE RADIATION AND CHEMICAL-INDUCED MOLECULAR DAMAGES, THEIR REPAIR AND BIOLOGICAL EXPRESSION IN MAMMALIAN CELLS. Annual Technical Progress Report, June 1, 1970–May 31, 1971. Trosko, James E. (Michigan State Univ., East Lansing). Contract AT-(11-1)-1704. 22p. Dep. NTIS.

Research regarding how different exogenous environmental agents affect the repair processes in higher organisms and how these effects are manifested biochemically and biologically is reported. Specific projects reported on include: synergistic effects of uv radiation and caffeine on mutation frequency and survival in Chinese hamster cells; in vitro repair of uv-radioinduced molecular damage in nuclei of Chinese hamster cells by bacterial repair enzymes (endonuclease and photoreactivating enzyme); synergistic effects of drugs (LSD) on repair of uv-radioinduced pyrimidine dimers in cultured human cells; molecular basis of platinum-tumor inhibitions; biochemical effects of irradiated sugars on cultured human (AV$_3$) cells; molecular basis of Franconi's disease (leukemia); and molecular basis for biological damage induced by uv-irradiated tissue. Publications generated during the contract periods are listed. (E.R.B.)

19091 MITOTIC INHIBITION AND ITS RELATION TO SURVIVAL IN S-180 ASCITES TUMOR CELLS IN VIVO FOLLOWING FRACTIONATED EXPOSURES OF X-RADIATION. Evans, Titus C.; Hagemann, Ronald F.; Leeper, Dennis B. (Univ. of Iowa, Iowa City). Radiat. Res.; 45: 85-93(Jan 1971).

Mouse ascites tumor cells were irradiated in vivo and the delay in cell division determined by periodic examination of mitotic index. Fractional exposures of 200 R were given eight times for a total of 1600 R. The effect on survival was determined 9 days after an inoculation of 4000 cells which had been removed from the irradiated animal. Survival was determined by counting the cells and was expressed as percentage of controls. It was found that fraction intervals of 0.5 and of 1 hour gave minimal delay and maximal survival. As the fractional interval was increased to 3 and to 4.8 hours, the delay became directly proportional to total radiation exposure and there was little recovery from lethal action as compared to the effect of other methods of exposure. It appeared that fractionation at 4.8-hour intervals tended to partially synchronize cells into later stages of the generation cycle; increased mitotic delay; and reduced survival as compared with effects of shorter fraction intervals. (auth)

19092 RESPONSE OF MOUSE EPIDERMAL CELLS TO SINGLE AND DIVIDED DOSES OF FAST NEUTRONS. Denekamp, J.; Emery, E. W.; Field, S. B. (Hammersmith Hospital, London). Radiat. Res.; 45: 80-4(Jan 1971).

Survival of mouse epidermal cells exposed to fast neutrons has been studied in vivo by the Withers' clone technique. Over the range 0.1 to 10 surviving cells per mm^2 the survival curve has a D_0 of 109 rads. When an initial dose of 450 rads of neutrons is given, followed by a second dose 24 hours later, D_0 is not significantly changed but the total dose required to produce a given survival level is 156 rads greater than for a single dose. Over the range studied, the RBE (relative to 250 kV x-rays) varies from 2.2 at 10 surviving cells/mm^2 to 1.7 at 0.1 surviving cells/mm^2. (auth)

19093 INFLUENCE OF HYPOTHERMIA ON THE RADIATION EFFECT IN HEALTHY AND CANCER TISSUE. Reinhardt, K. (Kreiskrankenhaus, Voelklingen, Ger.). Roentgen Bl.; 21: 84-90(Feb 1968). (In German).

Some effects of hypothermia, ischemia, and tissue oxygen level are reviewed. The results obtained by hypothermia and irradiation in patients with carcinomas of the extremities are reported and discussed. In a case of osteosarcoma of the femur, no skin reactions were obtained after irradiation with doses of 1800 to 3700 R during localized hypothermia and ischemia of the irradiated area. Another patient received 900, 600, and 900 R with intervals of 15 days and 4 weeks between irradiation, during localized hypothermia and ischemia, without any skin injuries. Similar results were observed after 1000, 700, and 1000 R with intervals of 3 and 2 weeks, but there was a pronounced skin reaction 4 weeks later when 700 R was given twice within an interval of 17 days, but without ischemia. Malignant tumors of the extremities and gastric carcinomas seem to be most suited for combined irradiation and hypothermia treatments. The effects of lethal whole-body doses of irradiation on rodents were delayed until hibernation was terminated. After lethal irradiation of nonhibernating rodents during artificial hypothermia, survival rates were increased over a limited interval. Localized hypothermia and ischemia increased tissue tolerance toward irradiation. Chromosomal aberrations were increased or decreased by hypothermia in cell cultures and plant seeds, depending on their growth phase. (TSS) (BBB)

Invertebrates

Refer also to abstracts 18967 and 19159.

19094 PARTIAL-BODY IRRADIATION OF LARVAE OF TENEBRIO MOLITOR. Jayaraman, S.; Ducoff, H. S. (Univ. of Illinois, Urbana). J. Invertebr. Pathol.; 16: 317-18(1970).

Exposure of anterior, middle, or posterior thirds, or of anterior and posterior thirds of larvae of *Tenebrio molitor* to x radiation was carried out. The tabulated data indicate that exposure of either the anterior third alone, or of the anterior and posterior thirds with the middle third shielded, was as effective as whole-body irradiation in the production of lethality as well as of pupation delay. Exposure of either the middle or the posterior third resulted in some mortality prior to pupation and additional deaths during the pupal stage, but survival to eclosion was much greater than in any case in which the anterior third was exposed. It is pointed out that the critical sites for lethality and pupation delay are situated in the anterior third. (H.L.W.)

19095 EFFECT OF X RAYS ON DEVELOPING CYSTICERCOIDS OF HYMENOLEPIS MICROSTOMA. Bieler, Julianne; Jones, Arthur W. (Univ. of Tennessee, Knoxville). Contract AT(40-1)-1749. Radiat. Res.; 45: 182-90(Jan 1971).

Larvae of *Tribolium confusum* were infected with eggs of *Hymenolepis microstoma*. On successive days after infection a separate batch of beetles was exposed to 5000 R of x rays. On each day a sample of infected beetles was examined. Irradiation on each day of development, except the sixth, increased the developmental period by $1\frac{1}{2}-4\frac{1}{2}$ days, the greatest increase occurring when the cysticercoids were irradiated on days 3 or 4 of their development. Radiation also caused severe hook deformities which occurred at a very low frequency (0–11%) after all treatments except that on day 4, after which almost all worms had abnormal hooks. Failure of the scolex to withdraw, although uncommon, was observed most frequently in those cysticercoids irradiated on day 4. A period of radiation sensitivity in the development of *H. microstoma* may be related to a similar period of heat sensitivity in *H. nana*, *H. diminuta*, and *H. microstoma* observed by other workers. It is proposed that this sensitive stage represents a time of organogenesis in the cestode. (auth)

19096 CORPUS ALLATUM SIZE AND OVARIAN ENVIRONMENT IN IRRADIATED CUCUMBER FLY, DACUS CUCUMIS. Bailey, Peter; Shipp, Erik (Univ. of New South Wales, Kensington, Australia). J. Insect. Physiol.; 16: 1293-9(1970).

Ovaries transplanted from normal *Dacus cucumis*, into females γ-irradiated with 10 krad as pharate adults, developed normally, and produced eggs, but 10 krad irradiated ovaries in the reciprocal transplant did not develop. *Corpora allata* (CA) from flies treated with 500 rad, 5 krad, and 10 krad were all larger than those from normal flies. However, there was not a linear relationship between dose and CA size; those from 500 rad and 5 krad treated flies were larger than CA from 10 krad flies. The CA size of flies with either anterior or posterior parts exposed to 5 krad was not demonstrably different from whole-body irradiated flies, dissected 16 days after emergence. This suggests a non-specific effect of radiation. (auth)

19097 EFFECTS OF GAMMA RADIATION ON THE PUPAL STAGE OF THE LESSER COTTON LEAF WORM, SPODOPTERA EXIGUA (Hb). Wakid, A. M.; Zaki, M. M.; El-Badry, E. A.; Ahmed, M. Y. Y. (Atomic Energy Establishment, Inshas, Egypt). Z. Angew. Entomol.; 66: 236-41(Oct 1970).

Egg production by *Spodoptera exigua* was greatly reduced when 1- and 4-day-old pupae were exposed to γ radiation. This reduction was more evident when 1-day-old pupae were treated. Dosages ranging between 2 and 16 krads applied to full grown pupae seemed to stimulate egg production. Increasing the dose reduced egg production. Hatchability of eggs laid by adults treated as 1- and 4-day-old pupae was greatly reduced especially in the former age. In full grown pupae, there was a highly positive correlation between dose and egg hatchability. Irradiation of full grown pupae with 18 krads produced completely sterile adults. Irradiation of 1-day-old pupae did not affect clearly the produced adult longevity, while with 4-day-old pupae the adult longevity was slightly increased. (auth)

19098 EFFECT OF X-IRRADIATION ON VARIOUS STAGES OF THE BLOWFLY PHAENICIA SERICATA (MEIGEN) (DIPTERA, CALLIPHORIDAE). Al-Uthman, Hilmi Sabir (Univ. of Baghdad). Acta Entomol. Bohemoslov.; 67: 304-9(1970).

The general effects of x radiation on various stages of the blowfly, *Phaenicia sericata*, with emphasis on the sterilization effects on adults were investigated. Treated females laid a reduced number of eggs and both sexes treated with as little as 1500 to 2000 R were made nearly or completely sterile. Irradiation of the larvae did not prevent pupation except when exposures exceeded 3000 R although emergence time increased with increasing doses. A dose of 1500 to 1600 R during pupal stage of 0 to 24 hrs was sufficient to produce sterility and mortality in the adults. The pupae during the age 0 to 24 hrs were almost twice as sensitive as the larval stage of the same age. Low mitotic activity in the immature stages except in eggs or immediately prior to moulting or eclosion has been offered as a general explanation. (E.E.H.)

19099 PRELIMINARY DATA ON THE ACTIVITY OF IONIZING RADIATION ON FERTILE EGGS OF TRIATOMIDEOS-RHODNIUS PROLIXUS. Machado, J. Ottilio L.; Elias, Cezar A.; Carvalho, Fabiano C.; King Assis, Benedito G.; Mattos Assumpcao, H. Hospital (Rio de Janeiro); 77: 203-7(Jan 1970). (In Portuguese).

Preliminary data were obtained on the effects of ionizing radiation on fertile eggs of the assassin bug, *Rhodnius prolixus*. A lethal dose was obtained with 5167 roentgen in Apparel Machlett type AEG-50, 45 KVm 15 mA, with a separation distance of 3 cm, and radiation in air at ambient temperature. Effects of altered nutrition on irradiated insects were also investigated. (auth)

19100 EFFECTS OF GAMMA IRRADIATION OR THE CHEMOSTERILANT, TEPA, ON THE CITRUS RED MITE AND ITS PROGENY. Beavers, J. B.; Hampton, R. B.; Toba, H. H.; Moreno, D. S. (Dept. of Agriculture, Riverside, Calif.). J. Econ. Entomol.; 64: No. 1, 72-5(Feb 1971).

Male and female citrus red mites, *Panonychus citri* (McGregor), were sterilized at doses of 24 and 32 kr, respectively. The viability of eggs produced by treated mites and their progeny was affected by doses of 8, 16, 24, and 32 kr. An increased dose generally produced a decrease in viable eggs, and doses ranging from 4 to 80 kr apparently induced dominant lethal mutations in the sperm. Doses of 96, 112, and 128 kr caused sperm injury or inactivation. Tepa at concentrations of 0.25 and 0.5% sterilized male citrus red mite, and doses of 0.125, 0.25, and 0.5% caused a reduction in female fecundity. (auth)

19101 USE OF A LINEAR ACCELERATOR IN IRRADIATION OF DICTYOCAULUS VIVIPARUS LARVAE. Tomanek, J.; Prochazka, Z. (Veterinary Research Inst., Brno). Acta Vet. (Brno); 39: 283-6(1970).

A comparison was made of the relative biological attentuation of *Dictyocaulus viviparus* larvae irradiated by means of a linear accelerator (1.6 MeV, 10 uA, dose rate 3×10^5 rads/min.) and a x-ray machine. The degree of attenuation was expressed by the number of larvae recovered from guinea pig lungs 10 days after infection with 5000 larvae. Differences in the number of larvae between individual groups exposed to 20 to 80 kR emitted by the accelerator were negligible. Some differences, however, were found in the developmental stage of larvae between the group exposed to 20 kR and those exposed to higher kR-doses. A twofold dose of kR was required with the accelerator than with the x-ray machine to obtain the same degree of larval attenuation. Standardization of radiation doses emitted by the accelerator presented difficulties owing to the high dose rate and the short time of radiation treatment. (auth)

19102 SUPPRESSION OF POPULATIONS OF PINK BOLLWORM BY RELEASES OF GAMMA-IRRADIATED MOTHS IN FIELD CAGES. Richmond, C. A.; Graham, H. M. (Dept. of Agriculture, Brownsville, Tex.). J. Econ. Entomol.; 64: No. 1, 332-3(Feb 1971).

A study was made of the comparative effectiveness of suppression by moths treated with 15 or 25 krad of γ radiation when they were released into a fertile population. Experiments were carried out in a field cage divided into nine 0.03 acre plots. The test consisted of release of 100 pairs of unirradiated virgin moths; initial release of 100 pairs of unirradiated virgin moths plus 2500 pairs of moths irradiated at 15 krad followed by periodic releases of 1250 pairs of similarly irradiated moths; and initial release of 100 pairs of unirradiated virgin moths plus 2500 pairs of moths irradiated with 25 krad followed by periodic releases of 1250 pairs of similarly irradiated moths. No significant differences were apparent in the number of first or second generation larvae in plots receiving treated moths, but there was a significant difference between the number of larvae in plots receiving only fertile moths. However, the numbers of first generation larvae in cages receiving treated moths were greater than the initial numbers of untreated moths released in these cages. (H.L.W.)

Vertebrates

Refer also to abstracts 18887, 18891, 18902, 18905, 18919, 18921, 18923, 18925, 18947–18949, 18958, 18959, 18968, 19024–19026, 19028–19033, and 19075.

19103 (PG-Report-1013) EFFECT OF ACUTE X-IRRADIATION ON THE DEVELOPMENT OF THE EGGS OF THE PLAICE,

XUM

PLEURONECTES PLATESSA. Ward, Eileen (United Kingdom Atomic Energy Authority, Sellafield (England). Production Group); Beach, S. A.; Dyson, E. D. (Atomic Energy Research Establishment, Harwell (England)). 1970. 13p. Dep. NTIS (U. S. Sales Only).

Plaice eggs were irradiated with 80 kV peak x rays at 5% of their development from fertilization to hatching. The range of doses used was approximately 30 to 150 rads and the doses were measured with thermoluminescent dosimeters. The percentage hatch of eggs, survival of three week old larvae and survival to metamorphosis were noted. The results show that at one of the most radiosensitive stages of development, the LD-50/Metamorphosis for plaice is approximately 90 rads. There is a steep response curve where a dose of 30 rads has little effect and where doses above 150 rads kill the majority of the larvae before metamorphosis. The application of these results to the radioecology of the NE Irish Sea is discussed. (auth) (UK)

19104 EFFECT OF MICROWAVES ON REVASCULARIZATION OF THE BLOOD SUPPLY IN FREE SKIN GRAFTS. Lutsenko, S. M.; Bachurin, V. I. Ortop., Travmatol. Prot.; No. 5, 76-8(1970). (In Russian).

Rabbits were exposed to microwaves for 1 hr daily for a month, after which two skin flaps were cut from their sides and backs, exchanged, and sutured to the surrounding skin. Within two days, flaps in the irradiated animals were edematous, and the epidermis began to slough off in large patches. Newly formed capillaries began to appear after 4 to 5 days, and blood first circulated one or two days later. By the end of the first week, the vessels reached the epidermis, but they were fragile and easily ruptured. After 10 to 12 days, epidermis covered the entire flap, where edges showed signs of necrosis. In control rabbits, on the other hand, the epidermis of the grafts did not progressively desquamate. Newly formed capillaries appeared after 3 days, and the blood began to circulate the next day. Final restoration of the blood supply in the flaps occurred on the 6th or 7th day, compared with the 8th or 9th day in irradiated animals. A study of patients receiving autografts for tropic ulcers caused by varicosities, extensive injuries to soft tissues, or thrombophlebitis showed no differences in the rate of healing or time of restoration of circulation between those occupationally exposed to microwave radiation, and other types of patients. This suggests that safety precautions for those working with microwaves are adequate. (JPRS)

19105 LATE APPEARING RADIATION INJURY. I. ON MICE. Sato, Fumiaki; Muramatsu, Susumu (National Inst. of Radiological Sciences, Chiba, Japan). Seibutsu Kagaku; 21: 148-55(May 1970). (In Japanese).

A study was made on the reduction of the life span of mice by the use of x rays. The life curve of mice looks like that of man, and in the case of mice, the dose of x or γ rays and the life expectancy are in proportion to each other. When a certain dose of x-ray was given daily until death, life expectancy became shorter as the dose increased, and the relation was a straight-line. Life spans were shortened when irradiation was started at a young age. Radiation effects on the life span of mice varied according to the irradiated area when partial-body irradiation was used. Though the effect of neutron particle irradiation is similar to that of x ray, recovery from the former seemed to be late. These relations were dealt with mathematically and explained as impulse lethality function or the force of mortality. (Japan)

19106 CULTURED CELLS AND RADIOBIOLOGY. Watanabe, Ikuo (National Inst. of Radiological Sciences, Chiba, Japan). Iden; 24: No. 5, 40-5(May 1970). (In Japanese).

The study of radiation using cultured cells has made great strides and established a new field in radiobiology. It is the fundamental study of the effect of radiation on organisms, and consequently its results are applied to protection against radiation and radiotherapy. Some results of radiobiology from recent papers are quoted. The Hit theory is used as the quantitative method to represent the lethal dose of radiation. The survival ratio of the cells exposed to irradiation is dependent on the period of cell division, oxygen content and the kinds of radioactive ray. Using drugs together with radiation, the radiation effect is sometimes increased and sometimes decreased, so that the drugs have a sensitizing or protective effect. Cultured cells do not begin to die as soon as radiation is applied, but survive for a certain period. This is probably because the damage induced in cells is transmitted from generation to generation, and leads to eventual death. Recovery from damage has also been observed. Radiation effects on the synthesis of DNA in cultured cells has been elucidated, and lowering of the synthesis of DNA was found to depend upon the dose. (Japan)

19107 STUDIES ON CHANGES OF MEMBRANE PERMEABILITIES OF ERYTHROCYTES BY RADIATION. I. INFLUENCE OF RADIATION ON THE CONTENTS OF POTASSIUM AND SODIUM IN ERYTHROCYTES OF RABBIT. Sasa, Matsuko (Kansai Medical School, Osaka). Kansai Ika Daigaku Zasshi; 21: 131-9(Jun 1969). (In Japanese).

Erythrocytes of rabbits were treated by roentgen radiation in doses of 100 to 5,000 R. The content of potassium in erythrocytes irradiated in a dose of 2,000 R was decreased at the temperature of 37°C. It was assumed that the reduction in potassium content was caused by the disturbance of erythrocytic membrane by irradiation. When the erythrocytes were kept in a cold room (4°C) immediately after irradiation, the influence of radiation on erythrocytes was reduced. (auth) (Japan)

19108 EXPERIMENTAL STUDIES ON THE CORRELATION BETWEEN LETHAL EFFECT IN FRACTIONATED IRRADIATION AND THE RECOVERY OF BONE MARROW CELLS IN MICE. Naito, Yasuo (Showa Univ., Tokyo). Showa Igakkai Zasshi; 29: 518-24(Sep 1969). (In Japanese).

Bone marrow cells were counted and uptake of labeled IUdR in the cells was measured several days following whole-body irradiation in mice. Surviving fractions were counted 30 days after the second dose which was given 0 to 7 days following the first dose. These procedures make it possible to establish the recovery process at the time of the second dose. A time interval of one or two days did not reveal any split dose effect, however a three day interval revealed the effects of split dose. Assuming that the rate of surviving fraction of bone marrow cells was equal by first dose as well as by second dose, it was possible to compare the surviving number of mice to the surviving fraction of the marrow cells. The number of bone marrow cells at the time of the second dose included those that survived the first dose and proliferated before the second dose. It was likely that so called bone marrow death was directly correlated to the number of the bone marrow cells that survived and that recovery-dependent dose fractionation effect in mice lethality was also directly related to proliferation of surviving bone marrow cells. (auth) (Japan)

19109 MORPHOLOGICAL CHANGES IN THE NERVOUS SYSTEM (OF CATS) INDUCED BY IONIZING RADIATION. Aszalos, Z. Honvedorvos; 20: 174-8(Apr-Jun 1968). (In Hungarian).

Tissue disturbances of the central nervous system induced by various conditions of irradiation were classified histologically in excised pieces of brain from cats and man. Pathological changes in central nervous system morphology were demonstrated histologically. The possibility that autoimmune reactions induced by exposure to ionizing radiation and the radiosensitivity of nerve tissue is considered. (R.V.J.)

19110 EFFECT OF γ-RADIATION ON THE AMINO ACID COMPOSITION OF THE MUSCULAR TISSUE OF FISH. Maslennikova, N. V. Ryb. Khoz.; 45: No. 10, 72-4(1969). (In Russian).

Studies of ionizing radiation effects on the amino acid composition of protein in muscular tissues of fish (0.5 kg cod and 2.0 kg catfish) showed that high radiation doses destroy the protein before they destroy amino acids. (R.V.J.)

19111 EFFECT OF IONIZING RADIATION ON THE VASCULAR SYSTEM IN TRANSPLANTED RAT TUMOR. Shimazaki, Shozo (Kyoto Prefectural Univ.). Kyoto Furitsu Ika Daigaku Zasshi; 78: 746-60(Dec 1969). (In Japanese).

The effects of ionizing radiation on the vascular system in transplanted rat Walker carcinosarcomas were studied together with an investigation of the normal pattern of blood vessels in the tumor. Microangiography was performed on tumors varying in size and on irradiated tumors 24 to 120 hours after a single exposure of 2,500 R. Contrast media containing lead oxide and gelatin was injected through the abdominal aorta to anesthetized animals with contrast pressure for 15 min. A type of blood supply, i.e., peripheral vascularization with penetrating vessels, was demonstrated in this tumor. Fine and dense small vessels or capillaries were observed only in the peripheral area of the tumor. In the center of the tumor, central necrosis was usually found which was surrounded by a sinusoidal lake made by very wide blood vessels. Between the peripheral fine vessels and central necrosis, vessels were irregular and formed a netlike contour. The specific patterns of the irradiated tumors showed a disappearance of such irregular vessels and an increase of fine and dense vessels throughout the tumor. This phenomenon, i.e., so called revascularization, was most evident 72 hrs. after a single exposure of 2,500 R. The revascularization phenomena in relation to clinical radiotherapy and the technique of microangiography are discussed. (auth) (Japan)

19112 SURVIVAL AND REPOPULATION OF HEMOPOIETIC TISSUES OF IRRADIATED MICE TRANSPLANTED WITH BONE MARROW CELLS FROM CYCLOPHOSPHAMIDE TREATED DONORS. Takahashi, Hiroshi; Ohara, Kanji; Ohkita, Takeshi;

Nakanishi, Sumio (Hiroshima Univ.). Proc. Res. Inst. Nucl. Med. Biol.; No. 11, 68-83(1970). (In Japanese).

Intraperitoneal injection of mice with a lethal dose of cyclophosphamide caused profound damage to bone marrow cells. During the initial stage of bone marrow regeneration, the immature granuloid cells appeared earlier than erythroid series, subsequently the cellular composition showed an abundance of immature granuloid cells, especially of myeloblasts and promyelocytes. The transplantation effects of these bone marrow cells rich in young granuloid series, on survival and on repopulation of hemopoietic tissues of lethally ^{60}Co irradiated mice were compared with the effects of normal bone marrow. The survival of the mice irradiated and transplanted with bone marrow cells obtained from the mice injected with cyclophosphamide 5 days previously, was similar to that of mice transplanted from normal donors. But the effect of transplanted bone marrow cells obtained from donor mice treated with cyclophosphamide 4 days previously, on survival was less effective than that of transplanted normal bone marrow cells. One of possible factors which affect survival may be the smaller number of mature granulocytes contained in transplanted bone marrow. Similar patterns were obtained in the recovery of spleen weight between the mice transplanted with bone marrow cells from donor treated with cyclophosphamide 4 days previously, and those transplanted with normal bone marrow cells. The spleen weight recovered earlier than the bone marrow cellularity, and increased to more than twice the value of untreated control within 15 days after transplantation. The proliferation rate of bone marrow cells during the massively repopulating period was higher in the recipients of cyclophosphamide treated cells than in the recipients of normal cells. The repopulation of erythroid series was not so good as compared with granuloid series in either of recipient groups, although the repopulation in the recipients of cyclophosphamide treated cells was somewhat better than the recipients of normal cells. The immature granuloid cells repopulated to a greater extent in the recipient of cyclophosphamide treated cells than in the recipients of normal cells, and exceeded the control value around the 9th day of transplantation. The immature granuloid cells in latter recipient group attained the control value around the 12th day of transplantation. An excess of granuloid cells was seen in both of the recipient groups. The reticulocyte count was similar in both of the recipient groups. The granulocyte count recovered and increased much earlier in the recipients of cyclophosphamide treated cells than in the recipient of normal cells. The granulocyte count showed a great increase in both groups. These results suggest that the effective cells for repopulation of hemopoietic tissues of mice irradiated and transplanted with bone marrow cells are the differentiated cells. The results also suggest that the spleen takes more part than the bone marrow in repopulation of erythropoiesis, and bone marrow is more active in granulopoiesis than in erythropoiesis during repopulation. (auth)

19113 PATHOLOGIC EFFECTS OF CONTINUOUS ^{89}Sr INGESTION IN MICE. Wright, James Francis. Davis, Calif.; Univ. of California (1969). 131p. University Microfilms Order No. 70-25,161.

Thesis.

The significance of dose rate and age on the induction of hematopoietic neoplasms by continuous feeding of ^{89}Sr to mice for 180 days was investigated. Effects were compared among three inbred strains of mice first exposed at conception or at weaning. Over 1500 mice were utilized, as well as a smaller number of adults apart from the main experiment. There was no apparent radiation effect on litter size or on survival to six months of age. Evaluation of the data to 14 months of age showed marked differences in survival rate and cumulative incidence of hematopoietic or bone tumors. The RFM strain had a high incidence of hematopoietic neoplasms beginning at six months of age; the BALB/c and C57BL strains had negligible hematopoietic neoplasms but began developing bone tumors at 10 months of age. Of 11 tumors in C57BL mice, three were in the pelvic region; BALB/c mice had no pelvic tumors but a high number of hind limb tumors; no RFM mice developed bone tumors to 14 months of age. Female mice of all strains had higher tumor incidence and earlier mortality than male mice. The dose-rate effect was evident. The highest-level groups (60 µCi ^{89}Sr/g dietary Ca daily) had approximately twice as many hematopoietic neoplasms as did the lower level groups (20 µCi ^{89}Sr/g dietary Ca daily); there were no bone tumors in control animals, two in 6-level animals, and 30 in 7-level animals. The survival rate for high-level mice was about one-half the control survival rate. The cumulative rad dose to 14 months was 4800 rads at the high level for animals first exposed during gestation and 3900 rads for mice started at weaning. (Diss. Abstr. Int., B)

19114 ENZYMEHISTOCHEMICAL MATURATION OF THE CEREBELLAR CORTEX OF RATS AFTER EARLY POSTNATAL X IRRADIATION. Ebels, E. J. (State Univ. of Groningen, Netherlands). Histochemie; 22: 25-35(1970).

The enzymehistochemical maturation of the cerebellar cortex was studied at 8, 16, and 30 days in rats whose cerebellar area was x-irradiated with 1,000 R at 2 days of age, and was compared with that in normal animals. After irradiation, the granule cells and basket and stellate neurones were absent due to lethal damage to their precursors. Only large neurones, glial cells and blood vessels were present in a disorderly arrangement; the laminar pattern of the cortex and specialized structures such as the glomeruli did not develop. Enzymehistochemically, the absence of specialized structures such as the molecular layer and the glomeruli was reflected in a uniformly strong diffuse activity of most of the dehydrogenases studied. AMPase-activity showed a strong positive correlation with the presence of granule cells. High subcortical activity of AChE in the posterior half of the vermis was presumed to be located within mossy fibres which lacked their normal goal: the granule cells. Capillaries in the irradiated cortex showed a close spatial relation to Purkinje cells. The development of the cytoplasmic organization of the Purkinje cells as demonstrated by TPPase and AcPase activities proceeded in a normal way. Some enzymes can be used as markers of certain cell types in the irradiated cortex: ICDH and G6PDH of Bergmann glial cells, AcPase of Golgi cells. It is suggested that enzymehistochemical studies of experimentally disturbed development may lead to better understanding of normal maturation. (auth)

19115 ACUTE LETHALITY AND RECOVERY OF GOATS AFTER 1 MVp X-IRRADIATION. Taylor, James F.; Still, Edwin T.; Page, Norbert P.; Leong, George F.; Ainsworth, E. John (Naval Radiological Defense Lab., San Francisco). Radiat. Res.; 45: 110-26(Jan 1971).

The $LD_{50/60}$ and recovery pattern after a sublethal radiation exposure have been determined for the Angora goat, exposed to 1 MVp x-rays at 450 R/hour. The $LD_{50/60}$ was 327 R (95% confidence interval: 292–378). The split-dose technique was utilized for measurement of the amount of recovery from the initial conditioning exposure of 150 R. At 7 days, minimal recovery had taken place, as 84% of the initial injury remained. By 14 days, rapid recovery had occurred and the animals' LD_{50} had returned to normal. At 21 days, 16% of the initial injury remained. At 30 days, the animals exhibited a reversion in radiosensitivity to the extent that the injury present at that time appeared to be greater than that produced by the conditioning exposure. The recovery pattern in the goat is marked by three distinct phases and does not fit a simple linear or exponential pattern. Routine hematological sampling for 160 days after 150 R, while showing definite depression of the leukocytes and very slow recovery of the mononuclear cells, showed no correlation between changes in the peripheral blood elements and the animals' recovery pattern. (auth)

19116 RADIATION-INDUCED CATARACTS IN GENETICALLY DIFFERENTIATED MICE. Stadler, Janice; Nash, Donald J. (Colorado State Univ., Fort Collins). Contracts AT(11-1)-107; AT(11-1)-1125. Radiat. Res.; 45: 176-81(Jan 1971).

Inbred BALB/Gw mice and hybrid mice obtained by crossing BALB mice with a genetically determined cataract stock of mice were exposed at 46 days of age to single whole-body x-irradiation of 0, 160, 320, or 480 R. The incidence of cataracts was found not to depend on sex, maternal effects, or differences at the albino locus. In both genotypes the frequency of cataracts increased with the 1.6 to 1.7 power of the exposure, but their sensitivity to a given exposure differed 5-fold. An exposure-age interaction was present, such that at higher exposures, cataracts appeared earlier. (auth)

19117 RESPONSE OF THE $9^1/_2$-DAY-OLD-RAT EMBRYO TO VARIATIONS IN EXPOSURE RATE OF 150 R X-IRRADIATION. Brent, Robert L. (Thomas Jefferson Univ., Philadelphia). Radiat. Res.; 45: 127-36(Jan 1971).

A review of the literature dealing with irradiated rodent embryos indicates that continuous irradiation with exposure rates below .005 R/min or 5 R/day is not measurably deleterious to the surviving offspring. In the experiments described herein, 9-day-old rat embryos were irradiated with 150 R at four exposure rates (100, 34, 1.5, and 0.5 R/min). The results indicate that protection of this dose of irradiation reduces the lethal, malforming, and growth retarding effects of the irradiation. Since protraction of the radiation to the embryo reduced the severity of growth retardation and the incidence of malformation, it is reasonable to conjecture that these effects are interrelated. Thus, it would seem most appropriate to study the dynamics of irreparable growth retardation with the tools of the cell biologist before attacking the more complicated problem of the mechanism of teratogenesis. When the problem of teratogenesis is approached, the studies reported here would indicate that it would be well to concentrate on one or several malformations. These protraction studies have yielded at least five malformations that do not occur following a low exposure-rate but are present in a high exposure-rate group, both groups having received 150 R. It is by studying these special instances with the newer techniques available and by concentrating on the mechanism of irreversible growth retardation that a better understanding of differentiation may evolve. (auth)

19118 EXPERIMENTAL EVALUATION OF TUMOR BED EFFECT FOR C3H MOUSE MAMMARY CARCINOMA AND FOR C3H MOUSE FIBROSARCOMA. Urano, Muneyasu; Suit, Herman D. (Univ. of Texas, Houston. Texas Medical Center, Houston). Radiat. Res.; 45: 41-9(Jan 1971).

Tumor bed effect (TBE) was evaluated by determining the TD_{50} (number of cells expected to transplant the tumor into half of the recipients) for tumor cells transplanted into normal or previously irradiated tissues. Two animal tumor systems were employed: a C3H mouse mammary carcinoma and a C3H mouse fibrosarcoma; recipient mice were (C3H/He × C57Bl) F1. Results showed that the TD_{50} was independent of the prior radiation history of the transplantation site. Thus, there was no evidence of an effect of the irradiated normal tissue to inactivate or to kill the injected tumor cells. However, after transplantation of the mammary carcinoma into irradiated tissues, tumor growth was slowed and host survival was prolonged. (auth)

19119 X-RAY-INDUCED CHANGES IN FUNCTION AND STRUCTURE OF THE RAT PAROTID GLAND. Phillips, Rodney M. J. Oral Surg.; 28: 432-7(Jun 1970).

The effects of localized x irradiation applied to rat parotid gland on salivary flow, concentration of electrolytes, amylase activity, weight, and histologic appearance of gland are reported. Accurate and reproducible methods that minimize systemic effects are introduced. (auth)

19120 IONIZING RADIATION EFFECTS ON NEUROBLAST CULTIVATED IN VITRO. Carlesi, O.; Olivo, O. M. (Univ., Bologna). Boll. Soc. Ital. Biol. Sper.; 45: 996-8(15 Aug 1969). (In Italian).

Optic lobe sections and ganglia of chicken embryos were placed in vitro cultivation and exposed to x radiation doses of from 250 to 50,000 R. The results showed that even high doses of x radiation did not cause immediate alterations in the nerve fiber, but after a variable latency period structural modifications were observed, the severity of which depended on the radiation dose. The morphological alterations caused by the radiation did not have a specific character, but were the same observed to a lesser degree and after a longer cultivation period of in vitro cultivation of the controls. The results indicated that between 2500 and 5000 R, the neurons of the ganglia tolerate the dose well. With 10,000 R part of the neurons were injured, but the majority showed a normal regeneration of the axis neurites. With 20,000 R few fibers regenerated. (J.S.R.)

19121 THICKENING OF WOOL FIBERS UNDER THE INFLUENCE OF IONIZING RADIATION. Vsevolodov, E. B.; Urazgaliev, A.; Karabalaev, U. (Inst. of Experimental Biology, Alma-Ata, USSR). Izv. Akad. Nauk Kaz. SSR, Ser. Biol.; No. 5, 81-2(1969). (In Russian).

Effects of repeated epilating doses on the thickness of wool fibers were studied using a local and a karakul ram exposed to 1000 R at 50 R/min. After two weeks all the wool fell out in the irradiated area and grew back six to seven weeks later. The thin fibers in the irradiated area grew in both animals; however, the amount of thin hair was small in comparison to the amount of normal hair. There was an increase in the diameter of normal fibers of both local and karakul rams. The increase of fiber thickness could not be explained entirely by radiation selectivity. Preliminary data showed that the difference in the thickness did not disappear with time, and the combination of weakened competition and direct stimulation was considered to be the cause of the increase in thickness. (R.V.J.)

19122 EFFECT OF PROLONGED FRACTIONATED X-RAY IRRADIATION ON THE GENERATION CYCLE OF SMALL INTESTINE CRYPT CELLS IN MICE. Rudnicki, Tadeusz; Kochmanska, Anna Nukleonika; 15: 437-43(1970). (In Polish).

No decrease in proliferative ability of small intestine crypt cells was observed after prolonged fractionated x ray irradiation with a dose of 50 or 100 R/day. This kind of exposure induced in the cell population a new steady state which was characterized by a shortened cell cycle time. This was a compensatory phenomenon neutralizing the radiation injury of cell population. The changes in the generation time cycle in the course of prolonged fractionated exposure depended on the total accumulated dose and not on the dose fractions. (auth)

19123 EFFECT OF OXYGEN-ENRICHED INSPIRED AIR, ON THE SURVIVAL OF MICE IRRADIATED WITH 500, 550, AND 600 R. Ryzewski, Jan; Kulesza, Romuald; Lipski, Slawomir (Warsaw Inst. of Radiological and Radiobiological Protection). Acta Physiol. Pol.; 21: 521-33(Jul-Aug 1970). (In Polish).

Mice x irradiated with doses of 500, 550, and 600 R were kept for 24 and 48 h in a chamber through which air passed with a higher oxygen content (1:1). After saturation of the chamber, the total oxygen content in the air inspired amounted to 60%. The survival of animals, and the erythrocyte and leukocyte count in peripheral blood were determined for a period of 30 days. An increase in the survival of mice by 20% after an irradiation dose of 500 R, by 30 to 35% after 550 R, and by 15 to 20% after 600 R, was observed. On the second day after irradiation an increase in the number of erythrocytes was found in the peripheral blood of animals staying in an atmosphere with a higher oxygen content. No significant changes were noted in the leukocyte count, excepting an increase, on the second day after irradiation, in animals with 600 R. (auth)

19124 HISTOPATHOLOGY OF LATE LOCAL RADIOLESIONS IN THE GOAT BRAIN. Andersson, Bengt; Larsson, Boerje; Leksell, Lars; (and others) (Uppsala Univ.). Acta Radiol., Ther., Phys., Biol.; 9: 385-94(Oct 1970).

Lesions in the depth of the goat brain were produced by cross-fire irradiation with high-energy proton beams, and a long-term study was performed to determine the late histopathologic effects. No late untoward changes, such as cellular elements resembling those of neoplasms in early stage, teleangiectasis and hemorrhage, were observed. (auth) (Sweden)

19125 STUDIES OF RECOVERY OF ERYTHROPOIESIS AFTER IRRADIATION AS A FUNCTION OF THE CELLULARITY OF THE ENDOCOLONIZED SPLEEN. DeGowin, Richard L.; Miller, Suzanne H.; Grund, Frank M. (Univ. of Iowa, Iowa City). J. Lab. Clin. Med.; 77: 219-27(Feb 1971).

A relationship between the rate of cellular division and the number and type of cells present may be inferred from several studies of patients and tissue culture preparations. As most chemotherapeutic agents for leukemia act on dividing cells, we have sought greater insight about the effects of cellularity in a hemopoietic organ on cellular division and differentiation. Measurements of cellular number and tritiated thymidine labeling indices in endocolonized mouse spleens demonstrated that cells resembling medium and large lymphocytes replicated during the first 5 days after irradiation. After 5 to 6 million splenic cells had been attained and the slope of the curve describing their labeling index had diminished, erythroblastic differentiation suddenly appeared. We have interpreted these findings, in light of previous studies, as support for the concept that the induction of erythropoiesis in spleen colonies by endogenous erythropoietin is related to the number of hemopoietic cells present and their proliferative activity. (auth)

19126 FACTORS REGULATING THE PROLIFERATION AND MIGRATION OF HEMATOPOIETIC STEM CELLS. Fried, Walter; Knospe, William H.; Gregory, Stephanie A.; Trobaugh, Frank E. Jr. (Rush-Presbyterian St. Luke's Medical Center, Chicago, Ill.). J. Lab. Clin. Med.; 77: 239-46(Feb 1971).

Hematopoietic stem cells (HSC) in the marrow, blood, and spleens of mice exposed to priming irradiation (300R with a leg shielded) 7 days prior to exposure to 800R regenerated more rapidly than did the HSC in tissues of mice not given priming irradiation. HSC in marrow shielded during priming irradiation did not increase in number when the mice were given no further irradiation. However, after being exposed to 200R whole-body irradiation 7 days after priming irradiation, they regenerated at a more rapid rate than did HSC in the marrow of mice unexposed to priming irradiation. HSC in the protected marrow of mice exposed to priming irradiation 4 days previously were no more sensitive to vinblastine than HSC in normal marrow. However, those in the marrow irradiated during priming x-irradiation were significantly more sensitive to the damaging effects of vinblastine. We suggest the following hypothesis to explain these results. Irradiation damage releases a humoral substance which stimulates proliferation of surviving HSC. In nondepleted marrow spaces, cell-cell interaction prevents HSC from responding to this proliferative stimulus, whereas in irradiation-depleted marrow sites, this cell-cell interaction is overridden by the humoral stimulus to proliferation. (auth)

19127 ACCELERATED REGENERATION OF TRANSPLANTED HEMATOPOIETIC STEM CELLS IN IRRADIATED MICE PRETREATED WITH CYCLOPHOSPHAMIDE. Gregory, S. A.; Fried, W.; Knospe, W. H.; Trobaugh, F. E. Jr. (Rush Presbyterian-St. Luke's Medical Center, Chicago). Blood; 37: 196-203(Feb 1971).

Results of experiments are reported which indicate that colony-forming units (CFU) regenerate more rapidly when transplanted into the marrow of lethally irradiated hosts pretreated with cyclophosphamide (CY) than when transplanted into those pretreated with saline. This effect is probably unrelated to the immunosuppressive properties of CY because it occurs in isogeneic strains as well as in randomly bred CF_1 mice. It also does not result from an increase in the radioresistance of cells which survive after injection of CY. The data presented here are compatible with the concept that CY somehow improves the environment for hematopoietic stem cell (HSC) proliferation and thereby causes an increased rate of regeneration of transplanted HSC in the marrow cavity of the host. The possibility that this is caused by release of HSC from an inhibitory effect of cell-cell interactions on proliferation or by the release of a humoral stimulus to HSC regeneration is discussed. (auth)

19128 GLUCOSE 6-PHOSPHATASE DEFICIENCY: MECHANISMS OF GENETIC CONTROL AND BIOCHEMISTRY. Gluecksohn-Waelsch, Solome (Albert Einstein Coll. of Medicine, Bronx, N. Y.); Cori, Carl F. Biochem. Genet.; 4: 195-201(Feb 1970)

Mechanisms are discussed by which several radioinduced lethal mutations in the mouse control enzyme activity and morphogenesis. These mutations behave as alleles at the albino locus in chromosome I; furthermore, all of them suppress glucose 6-phosphatase activity, resulting in perinatal death of albino homozygotes. Additional pleiotropic effects, and the absence of a dosage effect in heterozygotes, are not easily explained by a mutational change in the structural gene for glucose 6-phosphatase. The mutations might affect membrane proteins and thus render membrane structure abnormal; such membranes may lack the ability to bind tyrosinase as well as glucose 6-phosphatase and may also be responsible for morphogenetic abnormalities. (auth)

19129 PROLIFERATION OF DONOR SPLEEN AND BONE-MARROW CELLS IN THE SPLEENS AND BONE MARROWS OF UNIRRADIATED AND IRRADIATED ADULT MICE. Takada, Akikazu; Takada, Yumiko; Ambrus, Julian L. (Roswell Park Memorial Inst., Springville, N. Y.). Proc. Soc. Exp. Biol. Med.; 136: 222-6(Jan 1971).

CBA/HT_6T_6 spleen or bone-marrow cells were injected into unirradiated or irradiated CBA/H mice, and the percentages of donor-type cells in the spleen and the bone marrow were scored at various intervals after irradiation. When CBA/HT_6T_6 spleen or bone-marrow cells were injected into unirradiated CBA/H hosts, a few donor cells were found in the bone marrows and spleens of the hosts. When CBA/HT_6T_6 bone-marrow cells were injected into CBA/H mice irradiated with 400 R, more than 90% of the dividing cells in the bone marrow were of donor origin at day 10, and more than 70% were still of donor origin at day 15. Increasing the radiation dose to 600 or 800 R resulted in exclusive proliferation of donor cells in the bone marrow at days 10 and 15. When CBA/HT_6T_6 spleen cells were injected into CBA/H mice irradiated with 400 to 600 R, more than 90% of the dividing cells in the host spleens were of donor origin at day 10, but most of the donor cells were replaced with host cells by day 15. Increasing the radiation dose to 800 R resulted in a higher precentage of donor-type cells in the spleens at day 15, but some of the mice died by day 18. When CBA/HT_6T_6 spleen cells were injected into CBA/H irradiated with 400 or 600 R less than 10% of the dividing cells in the bone marrow were of donor origin at days 10 and 15. Increasing the radiation dose resulted in dividing cells mainly of donor origin in the bone marrow at days 10 and 15, but some mice died by day 18. These results suggest that stem cells compete with one another in mitosis, and that division of stem cells is largely regulated by that of other dividing cells. (auth)

19130 MODIFICATION OF RADIOSENSITIVITY OF EHRLICH ASCITES CARCINOMA CELLS IN VIVO. PART 1. SOME BASIC EXPERIMENTS ON THE ROLE OF LETHALLY IRRADIATED TUMOR CELLS. Urano, Muneyasu; Shirakura, Ichiro; Tanaka, Norimoto (Kyoto Prefectural Univ.). J. Radiat. Res.; 11: 61-9(Jun 1970).

Experiments were performed on an animal-tumor system of Ehrlich ascites carcinoma cells in ddYF mice. All the results are presented in terms of TD_{50} or the number of cells that transplant tumor in half of the recipients. The animals responded to active immunization and to whole-body irradiation with 400 Rads with an increase and a decrease of TD_{50}, respectively. It was of interest that TD_{50} correlated negatively with the number of lethally irradiated tumor cells (LR cells) when viable cells were transplanted together with LR cells. The TD_{50} fell as the number of LR cells increased and finally approached to one viable cell. A method of drawing x-ray survival curves of tumor cells without using LR cells is discussed, and an example is given that indicated that the Ehrlich ascites tumor cells irradiated under hypoxic conditions in vitro or in situ have a radiosensitivity of $m = 2$ and $D_0 = 390$ Rads. (auth)

19131 INFLUENCE OF BIS(-3-HYDROXYPROPYL) TRISULFIDE ON THE PERIPHERAL BLOOD IN RATS IRRADIATED WITH LARGE DOSES OF X-RAYS. Zebro, Tadeusz; Kowalczykowa, Janina; Mirek, Teresa; (and others). Patol. Pol.; 21: 225-36(Apr-Jun 1970). (In Polish).

The influence of bis(-3-hydroxypropyl) trisulfide on rats irradiated with 420 R whole-body x rays was studied. Experiments were carried out with four groups of hooded rats: a group irradiated but not treated with the trisulfide, a group irradiated 8 min after receiving a dose of 50 mg/kg body weight, and a third group treated with the compound but not irradiated. The peripheral blood of the rats was examined on the day preceding irradiation and in the course of 98 days after irradiation. The blood from a control group of rats was also studied. Red and white blood cells and reticulocytes were counted, percentages of white blood cells were determined, and the hematocrit and hemoglobin were assayed. Electrophoresis of serum proteins was also performed. Administration of the trisulfide before irradiation caused a rapid increase in the numbers of lymphocytes in the peripheral blood of rats, compared with unirradiated animals, but had no significant effect on normalization of the other morphologic blood elements. (auth)

19132 VISUALLY EVOKED POTENTIALS FROM THE LASER-IRRADIATED RABBIT RETINA. Hempel, Franklin Glenn. Austin, Tex.; Univ. of Texas (1969). 249p. University Microfilms Order No. 70-10,806.

Thesis.

Few investigations have been made of the effects of retinal photocoagulation on the light evoked electrical responses of the visual system. This research was conducted to examine the electroretinogram (ERG) and the lateral geniculate nucleus (LGN) and striate cortex potentials of the rabbit before and after irradiation of the retina with a high-energy ruby laser. Dark-adapted, curare-paralyzed rabbits were secured in a stereotaxic apparatus where concentric needle electrodes were inserted into the contralateral LGN and cortex. A corneal ring electrode detected the ERG. Protocol consisted of recording the three potentials while stimulating the eye with an argon laser operated at several flash intensities, exposing the retina to a calculated ruby laser radiation dosage, and recording again the responses to photic stimulation. The data show that mild 6 mm lesions inflicted by laser radiation pulses with retinal energy densities of 1.25 to 3.2 J/cm^2 apparently act to uncouple the tonic inhibition normally imposed on the lateral geniculate nucleus and visual cortex by the retina. (Diss. Abstr. Int., B)

Man

Refer also to abstracts 18890, 18927, 18961, 18963, 18969, 18971, 18977–18979, 18999, 19007, 19008, 19010, 19018, 19064, 19065, 19071, 19077, 19079, and 19089.

19133 (NP-18714) BIOLOGICAL ASPECTS OF LASER RADIATION: A REVIEW OF HAZARDS. Moore, Wellington Jr. (Bureau of Radiological Health, Rockville, Md.). Jan 1969. 15p.

Lasers emit highly directional, spatially confined, beams of intense monochromatic radiation. This radiation is potentially harmful to man. Available data on the biological effects of laser radiation on man are reviewed. Of the possible biological effects of laser radiation studied to date, the eye appears to be the most sensitive organ to injury. The lens of the eye focuses the incident visible laser radiation upon the retina resulting in an energy density at the retina of several orders of magnitude greater than the incident level at the cornea. For this reason, corneal intensities of visible laser radiation that could produce retinal damage are many orders of magnitude less than the incident intensities required to produce skin damage. (55 references.) (C.H.)

19134 STUDIES ON THE BONE MARROW OF A-BOMB EXPOSED IN HIROSHIMA BY AUTORADIOGRAPHY. Araki, Fumio (Yamaguchi Univ., Ube, Japan); Sugihara, Yoshio. Hiroshima J. Med. Sci.; 18: 247-52(Dec 1969).

Autoradiography studies were carried out on the bone marrow of 19 people exposed to atomic bomb radiation in Hiroshima. Radioactivity was discovered in six cases. Most of these were among the younger generation. Radioactivity was also found in

XUM

the bone marrow of premature babies. This suggests that radioactivity may transfer into the fetus through the placenta. (auth) (Japan)

19135 MEASUREMENTS OF ^{131}I FALLOUT IN NORWAY AND ESTIMATION OF THE SOMATIC EFFECTS. J. Norw. Med. Ass.; 7: 688-91(1 Apr 1970). (In Norwegian).

Radioactive iodine contamination from fallout has been measured in Norway since 1956, mainly by the Norwegian Defence Research Establishment. On the basis of the ^{131}I content in milk in various parts of the country, growth of the human thyroid during childhood and adolescence, and standard values for milk consumption, doses absorbed in the thyroid gland were calculated for various ages. Maximum thyroid doses appear to have been received by those born in 1956 to 58 and amount to about 2 rads. Mean thyroid dose for all born in 1945 to 1962 is about 1.2 rad. For those born before 1945 the mean dose is about 0.5 rad. Using the most conservative estimates of thyroid sensitivity to cancer induction (a total of 100×10^{-6} cases per rad for children, and 40×10^{-6} cases per rad for adults), and for ^{131}I radiation RBE (equal to 1.0), it was calculated that an increase of about 5 cases per yr should be found in the relevant age groups. According to data from the Norwegian Cancer Registry, thyroid cancer frequency has been increasing during the last ten years. The increase is found in ages below 49 years, and predominantly in women. The total increase is about 15 to 20 cases, this is approximately double the number of cases below 49 yr of age. Various interpretations of the findings were presented. (Norway)

19136 BONE TUMOURS IN MAN AND ANIMALS. **Owen, L. N.** London; Butterworths (1969). 213p. 70s.

There are two chapters of this book in scope covering: tumours induced by external irradiation, and tumours induced by internal irradiation. Both chapters review cases reported in man and of work carried out with animals. There are 25 and 61 references, respectively. (UK)

19137 EXPOSURE OF MAN TO NATURAL AND ARTIFICIAL SOURCES OF IONIZING RADIATIONS. **Rodier, J.; Vernhes, C.; Estcurnel, R.** Maroc Med.; 49: 75-91(Feb 1969). (In French).

The sources of natural and artificial radiation to which man is exposed are described in detail. The mean dose equivalent received from each source was evaluated. In natural sources, the largest dose is received from the soil. In artificial radiations, the largest dose is received from medical irradiations, almost a third of that received from all other sources of radiation, both natural and artificial. Artificial radiation from fallout and radioactive residues from nuclear installations is, at present, only about 10% of that received from natural sources. (J.S.R.)

19138 RECTOVAGINAL FISTULA. A REVIEW OF 20 YEARS' EXPERIENCE IN A COMMUNITY HOSPITAL. **Given, Fred T. Jr.** (DePaul Hospital, Norfolk, Va.). Amer. J. Obstet. Gynecol.; 108: 41-6(1 Sep 1970).

Twenty-six fistulas were repaired, with primary closure in 21 of 26 cases (81%) and over-all closure in 24 of 26 cases (92%). Special emphasis was placed on the surgical techniques employed in the repair of these fistulas. The physiologic basis for the use of the paradoxical incision (Miller) is presented in some detail. The use of the bulbocavernosus fat flap procedure (Martius) is suggested for the difficult post-radiation fistula. (auth)

19139 MAST CELL IDENTIFICATION OF RADIATION FISTULAS. **Graham, Ruth M.; Graham, John B.** (Roswell Park Memorial Inst., Buffalo, N. Y. State Univ. of New York, Buffalo). Obstet. Gynecol.; 32: 505-7(Oct 1968).

Biopsies from the edge of a vaginal fistula in 28 patients showed an easily distinguishable, higher concentration of mast cells in the 14 caused by pelvic irradiation. This was also true in the radioinduced fistulas of long duration. (auth)

19140 RADIATION-INDUCED OSTEOGENIC SARCOMA. **Dige, Ulrik.** Ugeskr. Laeger; 132: 1271-4(2 Jul 1970). (In Danish).

A case of osteogenic sarcoma induced by radiation is described. The sarcoma developed in a clavicle following post-operative radiotherapy for cancer of the breast. The analogous cases in the literature are reviewed in the light of the expression post-radiation bone sarcoma. (auth)

19141 MATHEMATICAL MODEL FOR DOSIMETRY OF THE GASTRO-INTESTINAL TRACT. **Vacca, G.; Bazin, J. P.; Karhausen, L.** (Centre d'Etudes Nucleaires, Fontenay-aux-Roses, France). Radioprotection; 4: 295-309(1969). (In French).

A new method is proposed for the computation of the dose delivered to any level of the gastrointestinal tract after ingestion of radioactive substances. The same method is used as that proposed by I. C. R. P. The concentration of the radionuclide during the progression of the meal is the central concept of this model. A graph relates the M. P. C. with the radioactive half-life of the radionuclide and with any level of the gastrointestinal tract of adults. (auth)

19142 IMPORTANCE OF HEMATOLOGIC EXAMINATIONS IN THE ASSESSMENT OF THE CHRONIC RADIATION LOAD (WITH SMALL DOSES) OF THE RADIOLOGISTS. **Mozsa, Szabolcs.** Magy. Radiol.; 22: No. 3, 180-6(Jun 1970). (In Hungarian).

A review of radiation hematology is presented. Effects of small chronic radiation doses on the blood picture of medical personnel are discussed. A separate chapter is devoted to hematological changes in teams of research personnel exposed to radiation. (auth)

19143 RADIOACTIVITY IN THE DIET OF POPULATION OF THE KERALA COAST INCLUDING MONAZITE BEARING HIGH RADIATION AREAS. **Mistry, K. B.; Bharathan, K. G.; Gopal-Ayengar, A. R.** (Bhabha Atomic Research Centre, Bombay). Health Phys.; 19: 535-42(Oct 1970).

The food consumption pattern of the population along the Kerala coast, including the monazite bearing high radiation belt, was determined through a detailed dietary survey. The food materials that constituted the diet of this population were assayed for their radioactive content. Based on these data, the daily intake of radioactivity through diet was computed. The daily per capita dietary intake of gross α, gross β, 85 keV γ, ^{228}Ra, and ^{40}K activity was estimated to be 215, 3648, 96, 162, and 3551 pCi, respectively. (auth) (UK)

19144 OSTEODYSTROPHY AFTER INHALATION OF ^{222}Rn. **Wegener, Kurt** (Univ., Heidelberg). Virchows Arch., A; 350: 179-82(1970).

Multiple localized bone densities were radiographically spotted in a 68-year-old male patient who had worked for 5 yrs in uranium mines (Joachimsthal). They were diagnosed as metastases of a prostate carcinoma. After the autopsy, histological, radiochemical, and autoradiographic investigations disclosed that a metastasizing prostatic carcinoma had not existed, but rather a paget-like osteodystrophia caused by deposits of radioactive decay products of inhaled ^{222}Rn. It was also found that decay products are also likely to deposit in calcified atheroslerotic plaques. (auth)

19145 INFLUENCE OF SOLAR ACTIVITY ON THE BLOOD FIBRINOLYTIC SYSTEM. **Rozhdestvenskaya, E. D.; Novikova, K. F.** Klin, Med. (Moscow); 47: 65-70(Jul 1969). (In Russian).

In connection with the available data on the close relationship between the incidence of thromboembolic complications and sudden death (cardiac failure) and the geomagnetic activity, the possible influence of solar activity on the fibrinolytic system of the blood was investigated. Data on the fibrinolytic activity in patients with rheumatism for a period of three years (1965 to 1967) and indices of geomagnetic disturbances were studied during a 27 day period of solar activity. It was established that the increase of the geomagnetic perturbation in the fibrinolytic activity of the blood drops and vice versa. Mathematical treatment of data testified to the high degree of relation between the phenomena studied. A distinct tendency to inhibition of fibrinolysis was found in patients on the day of magnetic storm and 24 hours after its development. The defence reaction in patients took place only 48 hours after the magnetic storm. Intensification of plasminogen activators of the rapid action from this time occurs at a more rapid rate than in healthy persons. (auth)

19146 EFFECT OF LASER BEAM ON BONE. **Talyshinskii, R. R.** Ortop., Travmatol. Prot.; 31: 38-41(Mar 1970). (In Russian).

Experiments have been carried out on the effects of gas and solid-state lasers in 32 bones taken from cadavers. The gas laser produced charring of bones; the ruby laser at an energy output of 14 to 15 joules caused mechanical injury of the bones. A penetrating gap through the cortical layer formed after eight to ten impulses. Changes in structure (densification and plication) of the bone trabeculae have been disclosed as the result of photohydraulic effect. (auth)

19147 REPRODUCTIVE FACTORS ASSOCIATED WITH RADIOTHERAPY OF MALIGNANT LYMPHOMAS. **Sooby, Donna L.; Jackson, Herbert L.; Hass, A. Curtis** (Univ. of Iowa, Iowa City). J. Iowa Med. Soc.; 60: 636-9(Sep 1970).

The question of gonadal dose in radiotherapy is considered, particularly in the case of boys and young men suffering from the various malignant lymphomas. Since many must be treated in areas near the genitalia, the question of gonadal exposure and its possible effect upon their offspring must be considered both by the patient and his physician. At present there is no evidence of radioinduced or congenital defects in offspring produced after an irradiated male regains fertility. However, due to the various medical, psychological, social, and economical factors involved, a waiting period of two years before conception is recommended. (P.C.H.)

19148 FOURTEEN YEARS AFTER BIKINI: THE LONG TERM EFFECTS OF RADIOACTIVE FALLOUT. Nelson, Arne. Laekartidningen; 65: 1779-84(Apr 1968). (In Swedish).

Japanese fishermen were exposed to high external and internal contamination from radioactive fallout from the Bikini nuclear tests in 1954. The results of continuing monitoring of the subsequent health of these people are compiled to show the long-term effects of radioactive fallout. (J.S.R.)

19149 EFFECTS OF FAST NEUTRONS ON HUMAN SKIN. Sheline, Glenn E. (Univ. of California, San Francisco); Phillips, Theodore L.; Field, Stanley B.; Brennan, James T.; Raventos, Antolin. Amer. J. Roentgenol., Radium Ther. Nucl. Med.; 111: 31-41(Jan 1971).

The observations on patients treated with fast-neutrons from the 60 inch Berkeley cyclotron between 1938 and 1943 are reviewed and reinterpreted. This investigation is concerned only with the effects of neutrons on skin and subcutaneous tissues. Utilizing data that relate the relative biological effectiveness (RBE) for neutrons to the size of the dose-fraction, the neutron doses were converted to equivalent megavoltage x-radiation doses. When applicable, factors were introduced to account for the contribution from exit beams. The time-dose fractionation pattern varied from patient to patient and usually was inconsistent with schemes used in current radiation therapy. Therefore, the doses were calculated in terms of a nominal single dose (NSD) and a nominal six week dose (SWD). The NSD and SWD allow some comparison with conventional radiation therapy. Suitable for inclusion were 144 patients with 275 separate fields treated with the 60-inch cyclotron. Among this group were 25 survivors, with 51 treatment fields, who were observed two years or more after neutron therapy was completed. Early reactions were judged according to findings during the first two months after treatment. The late reactions were graded according to observations two or more years after therapy. The data indicate that: the x-radiation equivalent of the neutron doses applied was relatively large in comparison with conventional megavoltage roentgen-ray therapy; an early reaction was visible in all treatment fields; the late reactions were severe in most patients; tissues with a high content of fat appeared to have a greater reaction; the tolerance dose for a six week period was about 6,100 rads; and the severity of late reactions increased rapidly as a function of radiation dose. (C.H.)

19150 EVOLUTION OF AN ABNORMAL LIGHT TEST REACTION. Stern, William K. (New York Medical Coll.-Metropolitan Hospital Center, New York). Arch. Dermatol.; 103: 154-7(Feb 1971).

The evolution of abnormal reactions to ultraviolet radiation (UVR) was studied in two subjects. Both of these individuals developed abnormal reactions to UVR in the UVA (320 to 400 nm) and the UVB (290 to 320 nm) ranges. The clinical and histopathologic development of these reactions in the UVB range were studied over the course of 24 hours. There was a mild perivascular infiltrate in the upper dermis leading to a severe angiitic response and marked dermal edema at four hours after ultraviolet irradiation. At 24 hours there were, in addition to a marked angiitis, epidermal changes consisting of spongiosis, exocytosis, and liquefaction degeneration of the basal layer. It is this light test reaction at 24 hours which mimics the clinical disease state in the individual so tested. A possible pathogenetic mechanism is suggested. (auth)

Radiation Effects on Plants

Refer also to abstracts 18918, 18936, 18946, 18950, 18951, 18954, 18955, 18962, 18964, and 19093.

19151 BREEDING OF MEDICINAL PLANTS BY γ-RAY IRRADIATION. 2. STUDY OF THE MUTANT OF DATURA TATULA LINNE. Yamazaki, Tomohisa (Meiji Coll. of Pharmacy, Tokyo); Yamanishi, Kiyoshi; Kobayashi, Masao; Tsubokawa, Tadashi. Shoyakugaku Zasshi; 23: No. 2, 53-7(Dec 1969). (In Japanese).

A mutant of Datura tatula Linne (D.t.) obtained previously by 10 kR γ irradiation is discussed. The breeding of several generations of the mutant was observed together with a control test of D.t., Datura stramonium Linné (D.s.) and tetraploid D.S. The height of plants, color of stems, color and length of flowers, and length, width, and weight of leaves were compared. The progeny of the mutant were found to be tetraploid plants (2n = 48), which have green stems, white flowers, and more leaves than D.t. They usually bear fruits with a small number of seeds per fruit. This lineage was named ws-4D.t. In the total content of alkaloid, no significant differences were observed between ws-4D.t. and D.t. (Japan)

19152 MONOGENIC RECESSIVE MALE STERILITY IN OIL RAPE (BRASSICA NAPUS L.) INDUCED BY GAMMA-IRRADIATION. Takagi, Yutaka (National Inst. of Radiation Breeding, Ohmiya, Japan). Z. Pflantzenzuecht.; 64: 242-7(Nov 1970).

A monogenic recessive male sterile mutant was obtained after γ irradiation of growing plants of oil rape. The mode of segregation in F_2 from crosses between this mutant and different varieties of oil rape was in close agreement with a ratio of 3 male fertile to 1 male sterile. Male sterile plants were easily distinguishable from normal plants in the flower bud stage or during early flowering. They were characterized by narrow leaves, rather thin stems, small flowers, and abnormal anthers and pollen grains. Meiosis was fairly regular and the male sterility was assumed to be caused by an abnormal development of the anther tapetum leading to pollen abortion. The seed yield of F_1 hybrid lines between the male sterile type and different oil rape varieties was 30 to 70% higher than the average of the male parents. (auth)

19153 SOME EFFECTS OF IONIZING RADIATION OF VICIA FABA. Roy, Robert Michael McGregor. Toronto; Univ. of Toronto (1968).

Thesis.

The assimilation of $^{14}CO_2$ by control and irradiated broad bean and distribution of ^{14}C-photoassimilates among top, root, and cotyledon were measured at 4-day intervals for 28 days following irradiation with a dose of 250 kV x rays. This dose yielded approximately 50% growth inhibition (dry weight). In conjunction with these measurements chlorophyll a, b, and (a + b) were determined immediately after $^{14}CO_2$ assimilation. At 8 and 12 days following irradiation the degree of stomatal opening and the number of stomata per unit leaf area (lower epidermis) were determined. At 8 days after irradiation $^{14}CO_2$ uptake was measured in control and irradiated plants at three levels of CO_2 (0.03%, 0.06%, and 0.09%). Total $^{14}CO_2$ assimilation was less in irradiated plants from 4 to 28 days following x-ray exposure. Uptake of $^{14}CO_2$ per gram top dry weight was less in irradiated plants than in nonirradiated controls from 8 to 24 days after irradiation at the 3 light intensities; however, differences were greater at higher light intensities by 8 to 12 days after exposure. In response to increased atmospheric concentrations of CO_2, uptake of $^{14}CO_2$ increased in both control and irradiated plants at 0.06% CO_2. The relative response of $^{14}CO_2$ uptake by control and irradiated plants to increased light intensity and to increased CO_2 concentrations (8 days post irradiation) in addition to the reduced stomatal apertures of irradiated plants was interpreted as evidence of reduced CO_2 diffusion in irradiated leaves; increased diffusion resistance in irradiated leaves may be implicated in the reduced $^{14}CO_2$ uptake in irradiated plants. (TSS) (Diss. Abstr. Int., B)

Radiation Effects on Microorganisms

Refer also to abstracts 18912, 18924, 18966, 18970, 18981, 19022, 19027, and 19163.

19154 RESPONSE OF PHOTOBACTERIUM FISCHERI MAV EXPOSED TO AN ULTRA HIGH DOSE-RATE PULSED ELECTRON BEAM. Lerch, Irving A. (Univ. of Chicago. Argonne Cancer Research Hospital, Chicago). Contract AT(11-1)-69. Radiat. Res.; 45: 63-71(Jan 1971).

Cellular suspensions of Photobacterium fischeri MAV were exposed to electron irradiation from a pulsed linear accelerator. As the average dose rate per pulse was increased, modifications in the survival slopes were obtained. The parameter, D_0, was found to increase as a power function of dose rate. (auth)

19155 EXPERIMENTAL STUDIES ON THE ANALYSIS OF RADIOSENSITIVITY BY MODIFICATION OF DNA METABOLISM. Suzuki, Katsuhiko (Showa Univ., Tokyo). Showa Igakkai Zasshi; 29: 495-503(Sep 1969). (In Japanese).

Studies on the influences of aminopterin in radiosensitivity were carried out in yeast cells. Lethal effects of aminopterin treatments suggested thymidineless death. The addition of thymidine monophosphates (TMP) to the culture media following irradiation did not decrease lethality, however addition of TMP and several amino acids together with TMP did decrease the lethal effects. Some apparent discrepancies in the studies were elucidated by 2-^{14}C-thymidine labeling experiments. Aminopterin treatment produced synchronization in the cell groups; G-1 arrest

XUM

in the cells harvested from log phase culture and G-2 from stationary phase culture were observed. It was concluded that the cells were most radiosensitive when irradiated in late G-1 and early S phases. Aminopterin did not seem to enhance the radiosensitivity. The results suggested the usefulness of aminopterin combined with irradiation. (auth) (Japan)

19156 EFFECTS OF GAMMA-RADIATION ON THE PATHOGENICITY OF HISTOMONAS MELEAGRIDIS. Ruff, M. D.; Hansen, M. F. (Kansas State Univ., Manhattan). Contract AT(11-1)-1209. Avian Dis.; 4: 646-53(Nov 1970).

Gamma irradiation reduced the pathogenicity of Histomonas meleagridis for turkeys. Turkeys surviving infection with irradiated histomonads were as susceptible to a challenge infection of histomonads as controls on the basis of appearance of sulfur-yellow feces and death. All but one of the turkeys died with enterohepatitis. The strain of histomonads isolated from the initially surviving turkeys, subcultured for several generations and then reinoculated into turkeys, continued to show reduced pathogenicity. (auth)

19157 JOINT TRANSDUCTION OF SEPARATE EXTRACHROMOSOMAL DRUG RESISTANCE DETERMINANTS IN STAPHYLOCOCCUS AUREUS E169. Grubb, W. B.; O'Reilly, R. J. (Univ. of Western Australia, Perth). Biochem. Biophys. Res. Commun.; 42: 377-83(5 Feb 1971).

An analysis of tetracycline, streptomycin, penicillin, and cadmium resistance in Staphylococcus aureus E169, using uv-irradiated transducing lysotes, indicates that their determinants are all extrachromosomal. The determinants for penicillin and cadmium resistance are linked. Those for streptomycin and tetracycline resistance appear not to be linked, even though they can sometimes be co-transduced. A possible explanation is offered. (auth)

Radiosterilization and Radiopreservation

Refer also to abstracts 18803 and 19102.

19158 (NP-18679) PROGRESS REPORT ON PRESERVATION OF DATES BY γ-RADIATION. Mayahi, M. F.; Ahmed, M. S. H. (Atomic Energy Commission, Baghdad (Iraq). Nuclear Research Inst.). Oct 1970. 10p. (B-6). Dep. NTIS (U. S. Sales Only).

Gamma radiation delivered at doses from 15,000 to 500,000 rad was used for processing fresh dates to increase the storage life and also for the eradication of insects infesting dry stored dates. Irradiation in cellophane bags with a low dosage (30 to 105 Krad) following washing and drying of the dates gave best results for increasing the storage life and wholesomeness. The impact of radiation processing of dates on the economy of Iraq is discussed. (C.H.)

19159 EFFECT OF FOOD PREIRRADIATION ON THE FECUNDITY OF TWO INSECTS: MEALY BUGS (PSEUDAULACASPIS PENTAGONA TARG.) AND INDIAN-MEAL MOTHS (PLODIA INTERPUNCTELLA HUEBN.). Seuge, J.; Morere, J. L.; Ferradini, C. (Faculte des Sciences, Orsay, France. Laboratoire Curie, Paris). Radiat. Res.; 45: 210-15(Jan 1971).

When the two studied insects are reared on preirradiated food, the fecundity of mealy bugs is reduced by 42% and that of the Indian-Meal moths by 32%. Effects of food irradiation on female fecundity are dose-independent in the range 33 to 165 krad for mealy bugs. (auth)

19160 INFLUENCE OF ^{60}Co γ-RAY ON POTATO. Takai, Yuriko; Yawatari, Kei; Shimomura, Hiroko; Kuriyama, Etuko; Iwao, Hiroyuki (National Inst. of Nutrition, Tokyo). Kokuritsu Eiyo Kenkyusho Kenkyu Hokoku; 79-81(Mar 1970). (In Japanese).

Several experiments were made on the effects of ^{60}Co γ rays on germination, absorption and utilization of nutrients and optimum storage dose of potatoes. Irradiation doses of 0, 7.5, 15, and 30 krad were used. Weight loss, germination rate, starch amount, reduced sugar amount, and artificial digestive ratio were compared among the groups. In the 30 krad group, the germination rate was 30% after nine mo storage, the 2-anomerization and the artificial digestive ratio were low, and the potatoes in the group were difficult to cook. In the 7.5 krad group the influence of irradiation was not observed, but the germination ratio was 100% when it had been stored for 4 mo. In the 15 krad group, both the α-anomerization and hardness had values similar to the control group, and the decrease of water content during storage was smallest. Though their germination rate was higher than the 30 krad group, it took 9 mos for 100% germination. Therefore, from the view point of nutrition, 15 krad irradiation is most desirable. (Japan)

19161 EFFECTS OF STERILISING PROCESSES ON PLASTICS. Plester, D. W. (ICI, Welwyn Garden City, Eng.). Bio-Med. Eng.; 6: 443-7(Sep 1970).

Various sterilization and disinfection processes are described in outline, and a table is given summarizing the behaviour of the following groups of plastics when exposed to various processes, including radiosterilization: -vinyls, olefins, styrene and copolymers, acrylics, polyamides, flurocarbon polymers, polyesters, and acetals. (UK)

19162 COMBINED IRRADIATION, HEAT, AND BIPHENYL TREATMENTS FOR THE CONTROL OF PENICILLIUM-DIGITATUM IN INOCULATED CITRUS FRUITS. Barkai-Golan, Rivka (Volcani Inst. of Agricultural Research, Rehovot, Israel); Padova, R. Israel J. Agr. Res. (Ktavim); 20: 129-32(Jul 1970).

Good control of rot in Shamouti oranges inoculated with spores of Penicillium digitatum was achieved by the triple combination of irradiation (35 krad ^{60}Co γ), biphenyl (15 mg per fruit) and heat (52°C for 5 minutes). The incubation period of the fungus in fruit stored at 14°C was extended to 14 days, in comparison with 10 days in fruit treated by combinations of heat with either irradiation or biphenyl, 8 days in fruit treated by biphenyl with or without irradiation, and 6 days in non-treated fruit and in fruit treated by either irradiation or heat alone. A reduction of the radiation dose or of the heating duration did not shorten the incubation period of the fungus, but increased the percentage of decayed fruit. (auth)

19163 RADIATION SENSITIVITY AND BIOCHEMICAL CHARACTERISTICS OF MICROFLORA OF BOMBAY DUCK (HARPODON NEHEREUS). Kumta, U. S.; Mavinkurve, S. S. (Bhabha Atomic Research Centre, Bombay). J. Food Sci.; 36: 63-6(Jan-Feb 1971).

The microbial flora of unirradiated and γ irradiated (0.5 Mrad) Bombay duck (Harpodon nehereus) was differentiated into organisms as spoilers and non-spoilers based on ability to liquify gelatin; ferment glucose; and produce indole, H_2S, and urease. In spoiling unirradiated fish, there was a predominance of Vibrio, Aeromonas, and Proteus spp, while Micrococci and Achromobacter spp were the major surviving groups in irradiated Bombay duck stored for 15 days at 10°C. The predominant spoilers, Proteus vulgaris and Aeromonas hydrophila, produced large amounts of TMA and TVBN and were radiation sensitive as indicated by D_{10} values of 8.6 and 5.4 Krad respectively, Micrococcus luteus was relatively biochemically inert and radiation resistant, the D_{10} value being 88 Krad. (auth)

19164 POLYETHYLENE AMPOULES AS CONTAINERS FOR RADIATION-STERILISED PARENTERAL SOLUTIONS. Moore, P. W. (Australian Atomic Energy Commission Research Establishment, Lucas Heights). Australas. J. Pharm.; 51: S57-62(Aug 1970).

To detect and study any basic interactions occurring between plastic and solution, distilled water was γ irradiated in ampoules made from polyethylenes XDG33, DND LO351, and BASF Lupolen 2351 H. Pyrex serum bottles were used as comparison containers. No differences in the biological effects of the solutions were found. Apart from the creation of oxidizing conditions, there was no basic interaction between the water and the polyethylenes that would create any additional problems to those normally encountered with plastic containers. (Australia)

XUM

METALS, CERAMICS, AND OTHER MATERIALS

Metals and Alloys

Refer also to abstract 18591.

19165 PRESENT STATE OF THE BIBLIOGRAPHY ON Nb AND ITS ALLOYS. Jeanne, F.; Driole, J.; Bonnier, E. (Ecole Nationale Superieure d'Electrochimie et d'Electrometallurgie, Grenoble, France). Rev. Phys. Appl.; 5: 597-8(Jun 1970). (In French).

From Meeting on Niobium, Paris, France. See CONF-691046. An indexed bibliography on niobium and its alloys is presented by the Centre d'Information de Thermodynamique Chimique Minerale. (auth) (France)

19166 PLUTONIUM-DOKUMENTATION. Referate-Zeitschrift mit Anhang Transplutonium-Elemente. Dezember 1970. Band 4, Heft 12. 275 Referate (Register-Nr. 4286-4879); 59 Referate (Register-Nr. 589 T-647 T). (Plutonium-Documentation. Abstract Journal with Appendix on Transplutonium Elements. December 1970. Vol. 4, No. 12. 275 Abstracts (Register No. 4286-4879); 59 Abstracts (Register No. 589 T-647-T)). Karlsruhe, Ger.; Gesellschaft fuer Kernforschung m.b.H (1970). 170p. (In German and English).

Corrosion and Erosion

Refer also to abstracts 18574 and 18592.

19167 (AERE-R-6460) BEHAVIOUR IN THE ATMOSPHERE OF THE AEROSOL FROM A SODIUM FIRE. Clough, W. S.; Garland, J. A. (Atomic Energy Research Establishment, Harwell (England)). 1970. 14p. Dep. NTIS (U. S. Sales Only).

The chemical form and physical size of the particles or droplets formed when sodium is released into the atmosphere are modified by the oxygen, water vapor, and carbon dioxide present. The chemical form under various conditions has been predicted and the equilibrium droplet size for a given sodium compound has been calculated as a function of sodium mass and relative humidity. The formation of sodium carbonate from sodium hydroxide droplets is controlled by liquid phase diffusion of reactants in the drop and probably occurs in times less than a few minutes. The formation of sodium bicarbonate from sodium carbonate droplets is much slower and many hours may elapse before equilibrium is achieved. At high relative humidities the final state is a droplet-type solution. At humidities below 95% the final state is a particle of sodium carbonate, although droplets of hydroxide solution may be present for a time of the order of 1 minute or less. The appreciable changes in size consequent upon changes in relative humidity may lead to important changes in the residence time and deposition of the particles in the atmosphere. (auth)

19168 METHOD OF INHIBITING THE CORROSION OF TANTALUM BY LIQUID LITHIUM. Wang, James Y. N.; Figlik, Kenneth G. (to United States Atomic Energy Commission). U. S. Patent 3,547,685. 15 Dec 1970. Filed 21 Aug 1968.

A method is described of inhibiting the corrosion of tantalum by liquid lithium at high temperatures by adding 0.25 to 1.5 atom percent iridium to the lithium. (Official Gazette)

19169 OXIDATION OF MOLYBDENUM AT TEMPERATURES OF 500 TO 1000^{0}C AND OXYGEN PRESSURES OF 10^{-3} TO -1 TORR. Zaitsev, A. A.; Ignatov, D. V. Izv. Akad. Nauk SSSR, Metal.; No. 4, 218-21(Jul-Aug 1970). (In Russian).

Results of kinetic and electronographic analyses show that Mo is oxidized at 500 to 1000°C by oxygen at 10^{-3} to –1 torr by the initial formation of an MoO_2 film. This reaction is followed by formation of MoO_3 which evaporates. The rates of these two reactions are increased with temperature. The reaction constant in this pressure–temperature range is 0.6 per degree. (tr-auth)

19170 ELECTROCHEMICAL PROPERTIES OF Nb. Pagetti, Jacques; Talbot, Jean (Ecole Nationale Superieure de Chimie, Paris). Rev. Phys. Appl.; 5: 365-9(Jun 1970). (In French).

From Meeting on Niobium, Paris, France. See CONF-691046. Corrosion of niobium in various acid and alkaline media at room temperature was studied using electrochemical methods. An electrolytic polishing method was developed in order to obtain a well defined reproducible surface. The good resistance of niobium in acidic solutions, except hydrofluoric acid, was attributed to a protective film of niobium oxide. Preliminary results were obtained on the anodic behavior of niobium in deaerated sodium hydroxide. In addition, the effect of dissolved oxygen on the corrosion of niobium was examined. (auth) (France)

19171 CONTAMINATION OF Nb BY O DURING ELECTROLYTIC POLISHING AND ANNEALING UNDER VACUUM. Beranger, G. (Ecole Nationale Superieure des Mines, Paris); Boisot, P.; Lacombe, P. Rev. Phys. Appl.; 5: 383-6(Jun 1970). (In French).

From Meeting on Niobium, Paris, France. See CONF-691046. The superficial contamination of Nb by oxygen during surface treatments was studied by the microanalysis method using the $^{16}O(d,p)^{17}O$ nuclear reaction. After electrolytic polishing and/or annealing under vacuum, a superficial 60 Å oxide film was observed. This method allows the oxygen located in the superficial oxide film and the oxygen dissolved in the underlying metal to be identified separately. It is shown that during annealing under vacuum, oxygen diffusion occurs and that the metal under the oxide layer is contaminated. (auth) (France)

19172 COMPARISON BETWEEN THE OXIDATION OF Nb AND THAT OF A Nb BASE ALLOY (P353M). Fries, E.; Marhic, C. (CNRS, Meudon-Bellevue, France). Rev. Phys. Appl.; 5: 519-22 (Jun 1970). (In French).

From Meeting on Niobium, Paris, France. See CONF-691046. X-ray diffraction studies were used to compare the oxidation of pure Nb with an alloy of the following composition: Nb (being the principal component)–W (10 to 12%)–V (1.5 to 2%)–Ti (0.5 to 0.7%)–Zr (3 to 4%)–C (0.25 to 0.40%). Oxidation was achieved under atmospheric conditions at temperatures ranging between 800 and 950°C and for periods of time ranging from ½ to 100 hr. In both cases 3 forms of the oxide Nb_2O_5 were observed: a low temperature form (L.T.), a medium temperature form (M.T.), and a high temperature form (H.T.). The Nb and the P 353 M alloy behave identically in relation to the different phases and the temperatures at which they appear. The alloy, however, oxidizes less readily than the pure metal. A stabilization of the L.T. form, a delay before the appearance of the M.T. and H.T. forms, and a slower rate of growth of the M.T. and H.T. forms were observed with the alloy. (auth) (France)

19173 FORMATION AND STRUCTURE OF ALUMINIDE BASE PROTECTIVE COATINGS ON Nb AND ITS ALLOYS. Slama, G.; Vignes, A. (Ecole Nationale Superieure de la Metallurgie et de l'Idustrie des Mines, Nancy). Rev. Phys. Appl.; 5: 523-33(Jun 1970). (In French).

From Meeting on Niobium, Paris, France. See CONF-691046. Niobium and niobium alloys were aluminized by pack-cementation and hot-dipping. The structure and formation of the coatings were studied. $NbAl_3$ was the main constituent of the coatings; it was formed as a layer of equiaxed grains, as a layer of grains oriented perpendicularly to the interface, or as an inner sub-layer of oriented grains, and an outer sub-layer of equiaxed grains. The occurrence of these structures depends on the coating process (pack-cementation or hot-dipping), the temperature, the structural state of Nb, and alloying. The main result of this study is to show that for a given process, these parameters modify the ductility of the metal and therefore the stress relaxation occurring during the growth of the layers. (auth) (France)

19174 OXIDATION AND PEST PHENOMENA IN $NbAl_3$. Raisson, G.; Vignes, A. (Ecole Nationale Superieure de la Metallurgie et de l'Industrie des Mines, Nancy). Rev. Phys. Appl.; 5: 535-44(Jun 1970). (In French).

From Meeting on Niobium, Paris, France. See CONF-691046. The niobium aluminide, $NbAl_3$, is the major component of the Al-base protective coatings on Nb alloys. The oxidation behavior of this compound was studied in the temperature range 600 to 1400°C. Above 1100°C, the oxidation by diffusion occurs with the formation of two layers: an inner layer of Nb_2Al and an outer layer of alumina, $NbAl_3/Nb_2Al/Al_2O_3$. Below 1100°C, the oxidation process is more complex. Below 1200°C, $NbAl_3$ becomes brittle. Besides the oxidation a fissuration of the compound occurs with oxidation of the sides of the cracks. The rate of fissuration increases with the brittleness of the $NbAl_3$. These observations explain the degradation of this compound, known as pest. The oxidation of $NbAl_3$ layers deposited on Nb by dipping in liquid Al was also studied. (auth) (France)

19175 CEMENTATION OF Nb BY Ti AND Cr SILICIDES FOR THE PRODUCTION OF PROTECTIVE COATINGS. Albrecht, J. M.; Aubry, J.; Roques, B. (Nancy Univ.). Rev. Phys. Appl.; 5: 551-7(Jun 1970). (In French).

From Meeting on Niobium, Paris, France. See CONF-691046. The development of titanium and chromium silicide coatings suitable for the protection of Nb against oxidation is discussed. One of these coatings using Cr as a modifier exhibited interesting oxidation characteristics during preliminary tests. It was obtained by pack cementation with ^{40}Cr−^{60}Si at. % prealloyed powder using iodine as the activator. (auth) (France)

19176 PROTECTION OF Nb AGAINST OXIDATION. Stecher, P.; Lux, B.; Funk, R. (Battelle Inst., Geneva). Rev. Phys. Appl.; 5: 573-95(Jun 1970). (In French).

From Meeting on Niobium, Paris, France. See CONF-691046.

In order to protect niobium alloys against high temperature oxidation, different types of coating based on silicides were developed. The structure and endurance of self-repairing films are described. With these films, protection against fissuration is obtained by incorporating a mobile phase into the pores of the silicide film. The following systems were considered: Nb(Ti)Si_2 silicide−SnAl alloy; $MoSi_2$ silicide−borosilicate glass; Cr, Fe, Nb silicide−a plastic oxide formed by the silicide itself during oxidation; Cr, Ti, Nb silicide−SnAl alloy. The last system is described in detail. The formation of a layer of chromium−titanium silicide, the impregnation process by treatment in a Sn−Al bath, and the results of different oxidation tests including tests after impact and thermal shock resistances are discussed. Changes in the properties of the coatings due to oxidation and diffusion which affect its protection characteristics are discussed. (auth) (France)

19177 STUDY OF THE OXIDATION OF Nb. Mollimard, D.; Bardolle, J.; Simon, D.; Perrin, C.; Dalibard, G. (Orleans Univ., France. CNRS, Orleans-la-Source, France). Rev. Phys. Appl.; 5: 599-608(Jun 1970). (In French).

From Meeting on Niobium, Paris, France. See CONF-691046.

Nb oxidation was studied under various temperature and pressure conditions with respect to morphology, kinetics and the crystallographical aspects of the reaction. Results were obtained in regard to the kinetics and anisotropic growth of thin films at 350°C and under an oxygen pressure of 10 torr. The reaction proceeds with increasing velocity in the (100), (211), and (111) planes, respectively. At low pressures (10^{-4} to 10^{-6} torr) and high temperatures (550 to 950°C) reaction kinetics indicated two oxygen adsorption mechanisms with activation energies of 3 and 26 kilocalories. Nucleation phenomena were also studied. The growth of oxide films of sufficient thickness at high temperatures and at pressures of the order of 5 torr was investigated. The nature of the oxide films obtained under the various conditions was determined by x ray diffractometry. (auth) (France)

19178 ZIRCONIUM OXIDATION UNDER A LOW OXYGEN PRESSURE. Dechamps, Michel; Lehr, Pierre (CNRS, Virty-sur-Seine, France). Compt. Rend., Ser. C; 271: 1533-6(21 Dec 1970). (In French).

A semi-quantitative model is proposed for zirconium oxidation under a low oxygen pressure which takes into consideration the linearity of the initial oxidation kinetics and the duration of this linear kinetics. (auth) (France)

19179 DIRECTION OF THE DEVELOPMENT ON REACTOR MATERIALS. FUEL CLADDING. Mishima, Yoshitsugu (Tokyo Univ.). Genshiryoku Kogyo; 16: No. 4, 68-72(Apr 1970). (In Japanese).

The cladding materials employed for nuclear fuels depend on the type of reactor and its operating conditions. The cladding materials, especially in connection with the operating temperature, and the problems involved, are reviewed. To improve light-water reactors, the primary aim is to increase the steam temperature from the 300 to 500°C level. The cladding materials, corresponding to this change, are described, including the alloys of zirconium and niobium. Cladding materials at the HTGR temperature levels of 600, 800, 1200°C, including the alloys and ceramics are described. Coolant for fast reactors is mainly sodium. Compatibility of the cladding with peculiar fuels and helium gas damage of the cladding is described. (Japan)

19180 METHOD OF PREOXIDIZING NUCLEAR REACTOR COMPONENTS OF ZIRCONIUM ALLOYS. Debray, Werner; Mattern, Ullrich; Stieding, Lothar (to Siemens Aktiengesellschaft). U. S. Patent 3,556,870. 19 Jan 1971. Priority date 30 Sep 1966, Germany.

A method of preoxidation of Zr alloy nuclear reactor components using water or water vapor is described. The process characterized by a multistep treatment whereby the usual preoxidation in water vapor at 400°C is preceded by treatment in water or vapor, at 200 to 350°C and preferably 250 to 300°C over a period of 1 to 4 days. (Official Gazette)

Preparation and Fabrication

Refer also to abstracts 18502, 18509, 19268, 19269, and 20731.

19181 UTILIZATION OF ELECTROSLAG WELDING IN THE PRODUCTION OF STEEL PRESSURE VESSELS FOR NUCLEAR REACTORS. Vrbensky, J. (Welding Research Inst., Bratislava); Zeke, J.; Becka, J. At. Energy Rev.; 8: 729-887(Dec 1970).

Increasing demands for the production of large pressure vessels for both nuclear and non-nuclear applications placed a premium on improved production rates and reduced delivery times. One means of contributing to this was by using automatic welding techniques. In particular, time savings could be accomplished by electroslag welding. Broad review is given of information on utilizing electroslag welding in the fabrication of reactor pressure vessels and other nuclear equipment, as well as in the chemical, refinery, and power industries. The paper is divided into four sections. The introductory section reviews the potential applications of the process in fabricating electroslag-welded joints and in electroslag remelting of steel and other metals. The second section analyzes the technological, production, physical, metallurgical, and economic aspects of electroslag welding. The analyses of welding longitudinal and circumferential welds are of particular concern. A detailed analysis of the thermal cycle during electroslag welding and its influence on the base materials used, particularly in pressure vessels, as well as the technological characteristics of the slag and melted metal, provides an understanding of the properties required of electroslag welds and the theoretical bases for achieving them. From the economic standpoint, the advantages and disadvantages of electroslag welding are compared with those of other welding methods, and the areas where electroslag welding definitely appears technically superior are identified. Section 3 describes the factors influencing the use of electroslag welding in fabricating nuclear pressure vessels, particularly in the so-called second-generation reactor vessels. Vessel-fabrication problems are differentiated from the stand points of possible weld-joint designs and the steels and filler materials used. Properties of electroslag-welded joints are analysed as they relate to the requirements of reactor pressure vessels. Also, requirements of welding machines and auxiliary welding, heat-treatment and defectoscopic (non-destructive) testing equipment are described, and the requirements for the training and qualification of the various catagories of workers involved in electroslag welding are discussed. Section 4 presents and describes typical examples of actual uses of electroslag welding in fabricating nuclear reactor pressure vessels and their parts. Also, examples are given of the fabrication of chemical and power equipment comparable to reactor pressure vessels in their construction and technical requirements. In conclusion, a review is presented of the factors which will determine the continuing and increasing use of electroslag welding in fabricating equipment for the nuclear power industry, together with statements of problems yet to be solved for the successful further development in utilizing this progressive method. (auth)

19182 SEEKING FOR THE MERITS OF A NUCLEAR IRON MILL. Ando, Masao (Kobe Steel, Ltd., Japan). Ohm (Elec. Mag.); 57: No. 8, 46-53(Aug 1970). (In Japanese).

To cope with the problem of caking coal shortage (to produce coke), the utilization of nuclear energy is attracting interest in the iron industry. The situation in iron manufacturing in Japan is examined in connection with the utilization of nuclear energy and current methods of iron manufacture, outlined. Two examples of the use of nuclear energy in iron manufacture are described. The direct reducing method in which high-temperature He gas is produced in an HTGR. The He heats the reducing gas, and then the iron ores are reduced by hydrogen. The second method employs a blast furnace in which ordinary coal is converted to gases by nuclear energy to obtain the CO, or the waste gas is heated with a reactor to convert CO_2 to CO, in order to reduce the amount of coke. In relation to the development of HTGR's, coated-particle fuels are discussed. Finally, the site conditions of an iron-manufacturing HTGR, and the safety aspects are summarized. (Japan)

19183 MECHANICAL AND METALLURGICAL STEEL/ZIRCONIUM JUNCTIONS. Boccalari, M. (CNEN, Vercelli, Italy); Brutto, E.; Liscia, A. Energ. Nucl. (Milan); 18: 33-44(Jan 1971). (In Italian).

In the CIRENE reactor, the components of power channels, scram rod channels, and neutron flux control system channels were made of Zircaloy and their connection to end plates (stainless steel) was obtained by special ad hoc techniques. The particular types of junctions obtained for the power channel and the scram rod channel respectively by rolling (mechanical connection), and for the neutron flux control system by coextrusion, which allows connections characterized by the formation of a metallurgical bond are described. (auth)

19184 EFFECTS OF INTRODUCING NUCLEAR ENERGY INTO THE ALUMINUM INDUSTRY. Ito, Akihide (Kyushu Electric Power Co. Inc., Fukuoka). Ohm (Elec. Mag.): 57: No. 8, 40-5(Aug 1970). (In Japanese).

In manufacturing aluminum from the ore, some 25% of the total cost is attributed to that of electric power; it is then necessary to minimize the unit power cost and the power cost per unit aluminum amount. First, the state of aluminum production and the associated electricity consumption in Japan are outlined. In aluminum manufacturing, the steady operation of plants is essential. In introducing nuclear power into the aluminum industry, it is necessary to have the power plant operated jointly with a utility company or in an industrial complex. The merits of a nuclear energy industrial complex, incorporating the aluminum industry and also the iron manufacturing and petrochemical industries, are discussed, including the thermal efficiency, power cost, process steam, and water supply. (Japan)

19185 CORROSION-RESISTANT URANIUM. Petit, George S.; Wright, Ralph R. (to United States Atomic Energy Commission). U. S. Patent 3,547,709. 15 Dec 1970. Filed 14 May 1968.

Metallic uranium was provided with a surface film of uranium oxide which was highly protective against corrosion-producing agents such as dry or moist air and water. The corrosion-resistant uranium oxide film was provided by heating the uranium in an evacuated furnace to a temperature in a range of about 500 to 650°C, and then contacting the uranium with a selected quantity of dry oxygen. (Official Gazette)

19186 PREPARATION OF HIGH PURITY NIOBIUM BASE ALLOYS. Geschier, R. (Ecole Nationale Superieure de Chimie, Strasbourg); Clauss, A.; Forestier, H. Rev. Phys. Appl.; 5: 443-7(Jun 1970). (In French).

From Meeting on Niobium, Paris, France. See CONF-691046.

The preparation of Nb base alloys carried out by melting high purity metal is described. Nb–Zr and Nb–Mo alloys were prepared by electron-beam melting and Nb–Ti alloys by vacuum-arc melting. After cold-forging of the cast ingots, the alloys were either cold-rolled 1 mm thick or cold-swaged 0.3 mm in diameter. Experimental conditions are given. (auth) (France)

19187 ECONOMICS OF THE VARIOUS METHODS AVAILABLE FOR PREPARING Nb. Vanlaer, Marcel; Durand, Roger. (Ugine Kuhlman, Brignoud, France). Rev. Phys. Appl.; 5: 487-94(Jun 1970). (In French).

From Meeting on Niobium, Paris, France. See CONF-691046.

Niobium has a wide range of applications requiring different degrees of purity and manufacturing processes. The most interesting process is pyrochlore's metallothermic reduction, and then a possible chloride distillation finishing with a melting in the electron beam. The process is still expensive because of the lack of wide scale exploitation. It is hoped that the demand for Nb will become comparable with that for Zr, Mo, and Ta. (auth) (France)

19188 MOLYBDENUM-DISK-TO-GLASS SEAL. Kukral, H. Vakuum-Tech.; 19: No. 3, 48-50(1970). (In German).

A method is described by which reliable molybdenum-disk-to-glass-butt seals can be produced. Information is included on the usage of such seals, the choice of materials, the basic principles, and special fabrication techniques. (Euratom)

19189 DIRECTION OF THE DEVELOPMENT ON A NUCLEAR FUEL CYCLE. PLUTONIUM. Imai, Ryukichi (Japan Atomic Power Co., Tokyo). Genshiryoku Kogyo; 16: No. 4, 64-7(Apr 1970). (In Japanese).

Plutonium availability, and its development are described with emphasis on the case of Japan. Compared with the forecast in the 1960's concerning the price of plutonium, its reduction is unexpectedly delayed for the 1970's. The development of plutonium fuel cycles requires a system analysis. Problems include the demand-supply situation, technological development, and economy of plutonium production. The plutonium supply estimates are based on the speculation concerning the construction of nuclear power plants in the world. With emphasis on oxide fuels, Pu production irradiation experiments in Japan and other countries are reviewed. The plutonium recycle in light-water reactors or its accumulation for the future fast reactors are considered in association with the enterprises. (Japan)

Properties Evaluations

Refer also to abstracts 18367, 18562, 18573, 18594, 19276, 19861, 19869, 20759, and 20761.

19190 (AI-Trans-287) CONTRIBUTION TO THE STUDY OF THE ELECTROCHEMICAL PROPERTIES OF INDIUM AMALGAMS. Rialland, Jean-Francois; Robert, Jack. Translated for Atomics International, Canoga Park, Calif., from French report. 18p. Dep. NTIS.

Results of research are presented which support hypotheses concerning the physicochemical properties of In amalgams. Other work is reported on Hg, In–Ga alloys, and Na–O batteries. (J.R.D.)

19191 (ANL-7706) VAPORIZATION DYNAMICS OF INITIALLY STATIC SUPERHEATED SODIUM. Singer, Ralph M.; Holtz, Robert E. (Argonne National Lab., Ill.). Sep 1970. Contract W-31-109-eng-38. 34p. Dep. NTIS.

Measurements of the patterns of vapor growth resulting during the transient boiling of initially static, nonuniformly superheated sodium in a vertical channel are presented and discussed. It is demonstrated that the single-slug vapor-growth model (in which the entire channel cross section is filled with vapor, except for a thin liquid film on the walls) may not be valid when the liquid temperature gradient normal to the channel axis is large and asymmetric, and/or the incipient boiling superheat is small. Under certain conditions, void fractions as low as 0.3 to 0.5 were observed. When the incipient superheat is large, the predictions of a simple vapor-slug-growth model compare favorably with the measured results. Experimental data on the vapor growth and collapse rates and the associated pressure transients are presented for boiling pressures up to about 1 atm and superheats up to about 180°C. (auth)

19192 (CONF-700816–(Vol.1), pp 393-412) CAESIUM BEHAVIOUR IN LIQUID SODIUM: THE EFFECT OF CARBON. Clough, W. S.; Wade, S. W. (Atomic Energy Research Establishment, Harwell (England)).

From 11. AEC air cleaning conference; Richland, Wash. (31 Aug 1970).

In Proceedings of the eleventh AEC air cleaning conference.

On the basis of previous thermodynamic calculations and experimental work, Cs has been identified as the most volatile major fission product with respect to release from liquid Na into the gas phase. Sorption of the Cs by graphite was shown to be very effective in reducing the volatility of the Cs and the formation of stable Cs–graphite compounds reduces the escaping tendency of Cs to less than that of I in liquid Na. The Cs forms two compounds one of which is relatively unstable in liquid Na and is probably a surface adsorption compound. The more stable fraction of the adsorbed Cs is probably a lamellar Cs–graphite compound and is almost fully stable in vacuum at 500°C in the absence of Na. The rate of reaction for the breakdown of the more stable Cs–graphite compound in Na was measured over a range of temperatures and the corresponding activation energy was calculated. Graphite was found to be equally effective for Cs sorption when it is used in the gas phase above the liquid Na. Charcoal was shown to be even more efficient than graphite in trapping Cs and the Cs-charcoal compound which is formed is almost fully stable in Na at 500°C and in air at the same temperature. Pre-treatment of the charcoal with Na at 500°C for 3 days has little effect on its performance with respect to Cs sorption. (auth)

19193 (CONF-700816–(Vol.1), pp 425-44) OPTICAL PROPERTIES OF SODIUM AEROSOLS. Reist, Parker C.; Hinds, William C. (Harvard School of Public Health, Boston, Mass.).

From 11. AEC air cleaning conference; Richland, Wash. (31 Aug 1970).

In Proceedings of the eleventh AEC air cleaning conference.

One of the consequences of burning metallic sodium is the production of a dense white smoke. The optical properties of this aerosol are discussed; the relation between visibility, aerosol concentration and time is developed, and the light scattering properties of the cloud are identified. Black discs on white targets were used to determine the visual range at different cloud concentrations. Light transmission measurements were made using a laser. At high aerosol concentrations multiple scattering was evident. Angular light scattering measurements were made which showed that the aerosol particles scattered light very strongly in the forward direction. All data indicate the opaque nature of the aerosol cloud. At concentrations above one gram per cubic meter, vision would be restricted to four meters or less, making walking through the cloud difficult and potentially hazardous. With concentrations of 0.1 gram per cubic meter, maximum visibility would be limited to about 40 meters, or roughly into the middle of a 200 foot diameter containment vessel. Typical overhead lights could be distinguished at distances three to four times greater than nonlit objects in the same cloud concentration. At low concentrations, transmission measurements could be used to deduce the apparent aerosol particle density, which was found to be 1.2 grams per cubic centimeter. Scanning electron microscope photographs appear to confirm this conclusion. (auth)

19194 (NYO-4073-4) SLIP INITIATION AND MICRODYNAMICS OF FLOW IN TUNGSTEN AND OTHER METALS. Progress Report, January 1, 1970–December 31, 1970. Bilello, J. C. (State Univ. of New York, Stony Brook). Contract AT(30-1)-4073. 21p. Dep. NTIS.

An experimental apparatus for measuring microstrain-stress data as well as determining the continuous time derivatives of the stress and strain was completed. This facility has an ultimate strain-sensitivity of $\approx 10^{-7}$ and is capable of operating over a temperature range of 4.2° to 575°K. Work is in progress to extend this system to the compressional mode. Preliminary etch-pit analysis of tungsten revealed that slip initiation in the microregion was inhomogeneous and that source exhaustion models of microyielding were inadequate. A high temperature, 2500°C, ultra-high vacuum furnace was built to outgas tungsten single crystals to yield total interstitial concentrations estimated as less than 0.1 ppM. These crystals will be utilized to study dislocation microdynamics. Correlation of direct observation of primary and forest dislocation structures with the microstrain behavior of pure Cu and Cu-1% Si single crystals has given insight into the mechanisms of slip initiation in these materials. These results indicated a method for assessing the dislocation-solute atom interaction in cases where the binding energy of the solute was relatively weak with respect to the forest dislocation strength. This approach could provide a link between the pinning-point models invoked to explain amplitude-dependent internal friction in the kHz range and the macroflow stress contribution of solutes and impurities. (auth)

19195 (ORNL-TM-3220) COMPUTER PROGRAM FOR CALCULATING, TABULATING, AND PLOTTING OUTGASSING RATES OF SELECTED GASES. Easton, D. S.; Merriman, Sandra H.; Armstrong, Carla L.; Clausing, R. E. (Oak Ridge National Lab., Tenn.). Feb 1971. Contract W-7405-eng-26. 149p. Dep. NTIS.

A computer program was written in Fortran to be used at the Oak Ridge National Laboratory Computer Center on either an IBM 360/91 or 360/75 computer for calculating outgassing rates. The experimental method is outlined, and the procedures for computing both total outgassing rates and rates based on measurement of partial pressures of various gases are described. Outgassing rates are calculated from the pressure drop across an orifice located between the chamber and the pumping system. Data from a residual-gas analyzer and three ion gages permit the simultaneous analysis of 12 gases. Results are available in both tabular and graphic form. The computer program is given along with a simple calculation and a series of plots of outgassing rate versus time. A Calcomp program for plotting data from a series of outgassing runs at different temperatures is also given. An example of plots of outgassing rates from a series of isothermal experiments is shown. (auth)

19196 (TRG-Report-1906) SOLUBILITY OF CARBON IN SODIUM. Longson, B.; Thorley, A. W. (United Kingdom Atomic Energy Authority, Risley (England). Reactor Group). May 1970. 20p. Dep. NTIS (U. S. Sales Only).

The solubility of carbon in sodium in the temperature range 600 to 950°C may be expressed by the equation: log sol (ppM) = 7.20 − 5465/T°K. From plots of carbon activity versus concentration, and from observations that oxygen did not effect carbon solubility, it is proposed that carbon dissolves in sodium as single atoms. (auth)

19197 HEAT RESISTING METAL. Tsuruoka, Kazuo (Kawasaki Steel Corp., Chiba, Japan). FAPIG (Tokyo); No. 56, 272-80(Mar 1970). (In Japanese).

The multi-purpose utilization of super heat-resisting and refractory metals in nuclear reactors such as the HTGR, is described. Tables of chemical composition and 1000 hr creep rupture strength are given for Fe-, Ni-, and Co-base alloys. Strong and weak precipitation hardening mechanisms Fe-base super-heat-resisting alloys are described. Ni-base super heat-resisting alloys; high Mo alloys; 75 Ni−15 Cr alloys; 75 Ni−20 Cr alloys; 30−60 Ni−20 Cr−20 Co alloys; Ni−Co−Cr−Mo alloys; dispersion-strengthened Ni-alloys; and three modified alloys are discussed qualitatively. Co-base super heat-resisting forged and cast alloys are described. Excluding rare metals and low creep strength metals, Cr, Mo, W, Nb and Ta are useful at high temperature, and these are explained respectively. The materials for primary piping and heat exchanger are important. The criteria for the selection of HTGR materials with satisfactory creep rupture strength, carbon transport on the primary coolant side, and corrosion by secondary coolant gas are presented. (Japan)

19198 PLUTONIUM: ITS THERMAL UTILIZATION TECHNIQUES. Nakamura, Yasuji (Power Reactor and Nuclear Fuel Development Corp., Tokyo). Genshiryoku Kogyo: 16: No. 5, 39-44(May 1970). (In Japanese).

Plutonium, in the future, will be used in advanced thermal reactors and fast breeder reactors. It is also utilized in light-water reactors i.e., thermal utilization of plutonium. The Pu thermal utilization technology was studied. The technology itself was no different from the case of uranium fuels. The problems in the production of plutonium fuels were concerned with the intrinsic poisonous and highly fissile nature of plutonium. The procedure thus became more complex, adding to the production cost. The particular nuclear properties, i.e., resonance, high fission cross section of plutonium made the difficulties in the design of the Pu fuels different from those of uranium. In its thermal utilization, plutonium co-existed with the uranium fuel. (Japan)

19199 TIN SELF-DIFFUSION IN THE In-48 PERCENT Sn LIQUID ALLOY AT PRE-SOLIDIFICATION TEMPERATURES. Petrescu, M. Stud. Cercet. Met.; 14: 199-220(1969). (In Rumanian).

Tin self-diffusion in the liquid In−Sn eutectic alloy from zonally refined metals was investigated over a temperature range between the melting point and melt superheating by 120°C. Determinations were carried out by the method developed by Anderson and Saddington. The computation of the diffusion coefficients required a numerical tabulation of the integrated equation of Fick's second law. The statistical data pointed to a temperature variation of Sn self diffusion coefficient, i.e., $D = 21.8 \times 10^{-5}$ exp. $(-2 \times 184$ (RT) $cm^2/sec)$. The experimental evidence is discussed in terms of the various theoretical models for the liquid-state diffusion mechanism. The influence of liquid-state diffusive transport on the eutectic crystallization process is studied. (auth) (Rom. Sci. Abstr.)

19200 IRON AND STEEL USED FOR NUCLEAR REACTORS. Hasegawa, Masayoshi; Yonezawa, Toshio (Waseda Univ., Tokyo). Chutanzo; 23: No. 3, 14-19(Mar 1970). (In Japanese).

The amount of electric power newly added to nation's power distribution grid by 1976 is estimated at 83,430,000 kW, of which 12% is by atomic energy, that is, 9,510,000 kW. In this situation, the demand for iron and steel in this field will increase significantly. The iron and steel used here, however, present large problems, because of neutron irradiation embrittlement. Iron and steel are used mainly for containment vessels, pressure vessels, and cooling pipes. The kinds of steel for pressure vessels are described. Alloying elements and other gaseous elements, metallurgical processes, and welding have a large influence on irradiation embrittlement of pressure-vessel steel. The effect of hydrogen, helium, and other gases produced by the nuclear conversion of alloying elements, the behavior of stainless steel in sodium environments, etc., are reviewed. (Japan)

19201 PRECIPITATION HARDENING OF ALUMINUM−2.2wt. PERCENT LITHIUM ALLOY AFTER NEUTRON IRRADIATION. Shiraishi, Kensuke (Japan Atomic Energy Research Inst., Tokai). Trans. Jap. Inst. Metals; 11: 381-4(Nov 1970).

An age-hardening was observed in aluminum-2.2 wt % lithium alloy specimens irradiated to a neutron dose of 1.2×10^{19} cm^{-2} at 45°C. The specimens were annealed for 4 hr at 350°C prior to the irradiation. Upon heating at temperatures of 155, 170, and 191°C, the yield stress of the irradiated specimens increased in two stages following the recovery of radiation-induced hardening, while the yield stress of unirradiated specimens remained unchanged. The changes in yield stress of the irradiated specimens can be explained as follows. Precipitate particles in the overaged state were destroyed and resolved into the matrix by the irradiation; and the irradiation temperature was too low for the alloy to proceed the precipitation process during the irradiation. Hardening observed in the as-irradiated specimens was due to lattice defects produced by irradiation. Following the recovery of the hardening, precipitation hardening took place in two stages corresponding to the precipitation of spherical and rod-shaped particles. (auth)

19202 INFLUENCE OF DEFECTS IN 80 mm THICKNESS STEEL PLATES FOR WELD QUALITY. Yamada, Kaneo; Miyoshi, Shigeru; Joh, Hiroshi (Fuji Electric Co. Ltd., Tokyo). Fuji Jiho; 43: 233-41(Feb 1970). (In Japanese).

Two series of experiments on thick steel plate welding are described; i.e., the behavior of defects, including large laminations and a large number of inclusions on the restrained welding test on the steel plates and the welding test on the steel plates in which large laminations and harmful sulfide inclusions were artificially made in order to study the strength of the plates. The estimation criteria for internal defects by nondestructive testing, according to ASME Code Sec. III, ASTM Standard, is explained and commented on. Restrained welding tests were performed. Nondestructive and destructive tests were performed. In the case of welding 80 mm thickness steel plates, laminations and inclusions in the plates gave little influence on welded parts. Some artificially made sulfur and phersinite inclusions did not originate cracks. Furthermore, if defects were repaired, the strength of weld was unaffected by them. (Japan)

19203 PRESENT STATE OF NON-FERROUS METALLIC MATERIAL FOR REACTOR USE. Watanabe, Ryoji (National Research Inst. for Metals, Tokyo). Zairyo Kagaku; 7: No. 1, 32-7(Mar 1970). (In Japanese).

The choice of reactor material is based on various factors, including mechanical strength, ductility, workability, corrosion, heat conductivity, cost, neutron absorption, induced radioactivity, and radiation damage. Reactor materials are used for fuel, moderator, reflector, control, coolant, shield, and structural material. The performance or type of reactor is determined partly by the particular nuclear fuel used, therefore, the containment of fuel is extremely significant, and the material used for its cladding or canning, determines the efficiency of fuel, and hence the nuclear reactor. In this connection the following non-ferrous metallic materials for fuel cladding are described: aluminum alloy, magnesium alloy, beryllium alloy, zirconium alloy, and vanadium alloy. (Japan)

19204 RELATION OF TEMPERATURE AND CONCENTRATION IN THE RECIPROCAL DIFFUSION COEFFICIENTS FOR BINARY NIOBIUM ALLOYS. Vergasova, L. L.; Prokoshkin, D. A.; Vasil'eva, E. V. Izv. Akad. Nauk SSSR, Metal.; No. 4, 198-204(Jul-Aug 1970). (In Russian).

The reciprocal of Nb vapor diffusion with metals of groups IVA, VA and VIA at 1100 to 1800°C was investigated. Microroentgenospectral analyses were used to determine the diffusion zone widths in the substrates. Depth–concentration curves were prepared. The curves were used to calculate the reciprocal diffusion coefficients in the Nb alloy systems. The effects of alloy additions on diffusion rates in Nb solid solutions were determined by interatomic bond strengths and melting points. Molybdenum, Ta, and W increase the diffusion mobility of Nb solid solutions while Ti, Zr, and V decrease the diffusion mobility in these systems. (tr-auth)

19205 INVESTIGATION OF W–Mo–Nb ALLOYS CONTAINING 30 PERCENT W. Polyakova, R. S. Izv. Akad. Nauk SSSR, metal.; No. 4, 184-8(Jul-Aug 1970). (In Russian).

Physicochemical analytical methods were used in an investigation of W–Mo–Nb alloys containing 30 wt % W. The alloys in the composition range studied have a density of 10.27 to 17.2 g/cm^2. Results of microstructural studies of these alloys revealed complete reciprocal solubility among the components. Additions of up to 70 wt % Mo to the starting W matrix separately and together with Nb and Ta additions increases room temperature hardness. The alloys gradually soften during increasing heating. The hardest phase at 1100° is the polygranular alloy. (tr-auth)

19206 STRENGTH AND PLASTICITY OF Ti–Nb–Zr ALLOYS AT -196 AND +20°C. Mikheev, V. S.; Pustovoitova, T. G.; Sokolov, V. S.; Shnyrev, G. D. Izv. Akad. Nauk SSSR, Metal.; No. 4, 171-3(Jul-Aug 1970). (In Russian).

The mechanical properties of Ti–Zr–Nb alloys were investigated using compositions containing up to 10 at. % Zr and up to 50 at. % Nb. It was found that there is a significant increase in σ_B and $\sigma_{0.2}$ alloys in the regions of alpha and beta solid solutions at 20 and –196°C. The largest difference in values of σ_B and $\sigma_{0.2}$ is found in alloys with the alpha structure, and especially in alloys having alpha plus beta solid solutions containing 20 at. % Nb. The strength and plasticity of σ_B and $\sigma_{0.2}$ in beta solid solutions have similar values and are friable being destroyed in break tests. The best combination of properties of strength and plasticity at –196°C is Ti–doped alloys containing 3 wt % Nb, 9.9 to 9.7 at. % Zr (17.5 to 16.5 at. %). The σ_5 phase is stable under 114 to 129 kg/mm^2 stress. The delta phase contains 9 to 13% Zr. (tr-auth)

19207 RELATIONSHIP BETWEEN SURFACE POTENTIAL AND ELECTRONEGATIVITY FOR ADSORPTION ON TUNGSTEN SINGLE CRYSTALS. Sargood, A. J.; Jowett, C. W.; Hopkins, B. J. (Univ. of Southampton, Eng.). Surface Sci.; 22: 343-56 (Sep 1970).

Experimental values of the surface potentials due to the adsorption of cesium, barium, uranium, iodine, bromine, chlorine, oxygen, and water on (110), (211), (100), and (111) tungsten surfaces have been correlated with electronegativity differences. For atomic adsorption a good linear relation was found for each surface between the surface potential divided by the ionic radius of the adatom and the electronegativity of the adsorbate. The "effective" electronegativities of the (110), (211), (100) and (111) tungsten surfaces deduced from these relationships were 9.46, 8.85, 8.30, and 7.47 eV respectively, values appreciably higher than their work functions, 5.15, 4.77, 4.65, and 4.45 eV. A linear relation was found between these effective electronegativities and the work functions. It is suggested that hydrogen and nitrogen do not fit this correlation because on some faces of tungsten penetration of the adatoms below the surface may take place. (auth)

19208 INTERACTION OF N_2 WITH (100) W. Clavenna, L. R.; Schmidt, L. D. (Univ. of Minnesota, Minneapolis). Surface Sci.; 22: 365-91(Sep 1970).

The binding states and condensation and desorption kinetics of nitrogen on (100) W are studied using flash desorption mass spectrometry. At moderate exposures there exist three states, a tightly bound β_2 state and two weakly bound molecular γ states; the saturation densities for each state are 2.5×10^{14} molecules cm^{-2}. Very high nitrogen exposure at low temperatures produces in addition to these states a tightly bound ($E_d = 49$ kcal mole^{-1}) β_1 state which desorbs with first order kinetics and at 300°K has a sticking coefficient of less than 10^{-3}. Desorption kinetics for the β_2 state at high coverages can be explained quantitatively only by assuming a coverage dependent activation energy or preexponential factor; the latter is predicted if desorption is limited by surface diffusion controlled recombination of atoms. The binding states and atomic configurations are shown to be reasonable on the basis of the electronic structures of the adsorbate and the substrate; this is the basis for predicting the existence of a structure for the β_2 state in which alternate sites are occupied and agrees with the measured stoichiometry. The sticking coefficient into the β_2 state is measured as a function of coverage and substrate temperature in the interval $195°K < T < 1035°K$. Condensation appears to proceed via a weakly chemisorbed precursor. Quantitative agreement with the data is obtained using a model in which the sticking coefficient and desorption kinetics of the precursor state are completely independent of the occupation of the β_2 state. (auth)

19209 WORK FUNCTION CHANGES DUE TO THE ADSORPTION OF CHLORINE, BROMINE, AND IODINE ON TUNGSTEN SINGLE CRYSTAL SURFACES. Jowett, C. W.; Hopkins, B. J. (Univ. of Southampton, Eng.). Surface Sci.; 22: 392-410(Sep 1970).

The adsorption of chlorine, bromine and iodine onto large oriented tungsten single crystals has been studied using the Kelvin contact potential difference technique. Work function changes have been determined for the (110), (100) and (111) orientations as a function of the number of molecules incident on each surface. The surface potentials for atomic adsorption were, for chlorine, +0.26, –0.58 and –1.03 V respectively, for bromine +0.32, –0.80 and –0.88 V and for iodine +0.78, +0.18 and +0.13 V. In some cases adsorption at higher coverages revealed the presence of weakly bound phases which invariably caused a decrease in the surface potential. A qualitative interpretation of the results for atomic adsorption is discussed in terms of a simple dipole model in which three contributions to the surface potential are considered. These arise from charge transfer between adsorbate and the tungsten surface, polarization of the adsorbed halogen in the metal's external field and the smoothing of the electronic charge distribution in the adsorbed film. With such a simple model it is possible to explain qualitatively the variation in magnitude of the dipole and its reversal between different crystal planes for the same adsorbate. (auth)

19210 RESIDENCE TIME MEASUREMENTS FOR THE SURFACE IONIZATION OF K ON W: THE EFFECTS OF SURFACE CONTAMINANTS. Smith, Joe N. Jr.; Wolleswinkel, J.; Los, J. (FOM-Inst. for Atomic and Molecular Physics, Amsterdam). Surface Sci.; 22: 411-25(Sep 1970).

The surface residence time, τ, for K^+ on W is measured and the values of τ_0 and Q_i, defined by the relation $\tau = \tau_0 \exp Q_i/kT$ are derived. The effect on τ_0 and Q_i produced by contamination by carbon, oxygen, nitrogen, and hydrogen are reported. A critical analysis of these results as compared with earlier work is presented. In addition, a discussion is presented which relates the results to previous physical interpretations of τ_0 and Q_i. The results suggest that strongly bound contaminants lead to small or negligible changes in these parameters while loosely bound (mobile) gaseous contaminants lead to a decrease in Q_i and an increase in τ_0. These results are also related to contamination effects observed in the scattering of thermal energy atomic beams from surfaces. (auth)

19211 MEETING ON NIOBIUM, OCTOBER 20–21, 1969, PARIS, FRANCE. Rev. Phys. Appl.; 5: 363-610(Jun 1970). (In French). (CONF-691046).

Twenty-nine papers on the fabrication, corrosion, surface treatment, properties, and applications of Nb and its alloys were presented at the conference. A separate abstract was prepared for each of twenty-three papers. One paper appeared previously in NSA. For an abstract of this paper see 24: 36921. Papers for which no abstracts were prepared are concerned with ultrasonic testing, turbines, and superconductors. (France)

For abstracts of individual papers see: 19165, 19170–19177, 19186, 19187, 19212–19219, 19244–19246, and 19258.

19212 STUDY OF THE CHANGES IN THE MECHANICAL PROPERTIES OF Nb WITH DIFFERENT IMPURITY CONTENTS BETWEEN 20 AND 850^{0}C. Fries, J. F.; Cizeron, C.; Lacombe, P. (Paris Univ., Orsay, France). Rev. Phys. Appl.; 5: 371-81 (Jun 1970). (In French).

From Meeting on Niobium, Paris, France. See CONF-691046.

The plastic deformation and the mechanical properties of three distinct lots of niobium containing varying interstitial and substitutional impurity concentrations were investigated in the intermediate temperature range. Strain-aging phenomenon and the Portevin-Le-Chatelier effect were found in the three lots. An extensive study of these phenomena led to the interpretation of the temperature dependence of the flow stress and the elongation curves. (auth) (France)

19213 STUDY OF HARDENING DUE TO INTERSTITIALS BETWEEN 20 AND 1200^{0}C IN Nb AND Nb ALLOYS. Mazot, P. (CNRS, Paris). Rev. Phys. Appl.; 5: 387-92(Jun 1970). (In French).

From Meeting on Niobium, Paris, France. See CONF-691046.

Tensile tests were carried out on different niobium alloys from 20 to 1200°C in high vacuum; they led to a three-term flow stress decomposition. The first two are the yield strength and a strain-hardening component; the results show the influence of the structural factors (impurities, precipitates ...), and deformation parameters (strain rate, temperature) on these two terms. The third component is characteristic of hardening effects, due to interstitial-dislocation interactions; successive peaks appear in the stress-temperature curves; the study of the strain rate and oxygen concentration led to the determination of the peak magnitude, the interpretation of their displacement with temperature and their identification with respect to the different interstitials. (auth) (France)

19214 DIFFUSION IN THE BINARY SYSTEMS Ti–Nb, Zr–Nb, V–Nb, Mo–Nb, W–Nb. Roux, F.; Vignes, A. (Ecole Nationale Superieure de la Metallurgie et de l'Industrie des Mines, Nancy). Rev. Phys. Appl.; 5: 393-405(Jun 1970). (In French).

From Meeting on Niobium, Paris, France. See CONF-691046.

The interdiffusion in the binary systems Ti–Nb, Zr–Nb, V–Nb, Mo–Nb, W–Nb was studied using microprobe analysis of incremental and pure metal couples. The variation of the interdiffusion coefficient for each system was determined by the Matano method; the Hall method was used to determine the limiting values of the interdiffusion coefficient of Ti, Zr, V, Mo and W in Nb. For each element, the interdiffusion coefficient follows an Arrhenius law. But the classical theories do not allow the very large differences between the diffusion coefficient of elements in Nb and the Nb self-diffusion coefficient to be explained. A valence effect for the diffusion of transition elements in niobium was noticed. An empirical correlation is proposed; it allows the diffusion rate of an element in Nb to be determined by studying the influence of this element on the melting point of the Nb-impurity solid solution. (auth) (France)

19215 STRUCTURE AND PROPERTIES OF THE BINARY Nb–T, AND Nb–Zr SOLID SOLUTIONS. Josso, E. Societe Metallurgique d'Imphy, France). Rev. Phys. Appl.; 5: 407-13 (Jun 1970). (In French).

From Meeting on Niobium, Paris, France. See CONF-691046.

Niobium solid solutions containing 10 wt % Mo, 20 wt % Ti or 4 wt % Zr were studied. In Nb–Ti alloys, the workability is similar to that of Nb metal; in Nb–Mo and Nb–Zr alloys, the forging range is smaller. The three elements strongly harden Nb but have little effect on the work hardening characteristics. Molybdenum and zirconium increase the recrystallization temperature by at least 100°C. Titanium and zirconium give rise to an extensive interdendritic segregation. The Nb–^{20}Ti alloy shows low mechanical strength at high temperatures with nearly superplastic behavior above 1200°C. In spite of its low addition element content, the Nb–^{4}Zr alloy has a higher tensile strength than the Nb–^{10}Mo alloy above 800°C. (auth) (France)

19216 HYDROGEN EMBRITTLEMENT OF Nb BASE ALLOYS. Vercaemer, C.; Geschier, R.; Guille, J.; Clauss, A.; Forestier, H. (Ecole Nationale Superieure de Chimie, Strasbourg). Rev. Phys. Appl.; 5: 434-42(Jun 1970). (In French).

From Meeting on Niobium, Paris, France. See CONF-691046.

Hydrogen embrittlement of Nb–Mo, Nb–Zr, and Nb–Ti alloys was studied at room temperature. A correlation was observed between the effect of substitutional solutes on the increase in ductile-to-brittle transition temperature and the effect of these substitutional solutes on hydrogen embrittlement. Interstitial solutes (O and N) increase hydrogen embrittlement. The presence of water vapor suppresses this phenomenon. The results obtained are discussed. (auth) (France)

19217 DEFORMATION AND RUPTURE OF Nb BETWEEN -196^{0}C AND 20^{0}C. Houssin, B.; Fries, J. F.; Cizeron, C.; Lacombe, P. (Paris Univ., Orsay, France). Rev. Phys. Appl.; 5: 467-76(Jun 1970). (In French).

From Meeting on Niobium, Paris, France. See CONF-691046.

The plastic deformation of three distinct lots of niobium containing different interstitial and substitutional impurities was studied at temperatures below 20°C. A qualitative interpretation of the temperature dependence of the mechanical properties determined by tensile tests was proposed. This interpretation was based on both the microfractographic observations (using replica techniques and the flying spot electron microscope) and the various modes of deformation. (auth) (France)

19218 RESEARCH AND DEVELOPMENT OF NEW HIGH TEMPERATURE RESISTANT Nb ALLOYS. Alheritiere, E.; Syre, R. (Trefimetaux, Argenteuil, France). Rev. Phys. Appl.; 5: 477-86 (Jun 1970). (In French).

From Meeting on Niobium, Paris, France. See CONF-691046.

Nb base alloys suitable for high temperature applications were developed. The two alloys appearing favorable were WD 15 (Nb-9 W-6 Mo-4 Hf-0.2 C) and W 6 B (Nb-6 W-2 Zr-2 Hf-0.2 C-0.2 B). The first alloy when heat treated for 2 hr at 2000°C and oil quenched ruptures after 100 hr when subjected to 19.6 hbars. Elongation before rupture is over ten percent at any temperature. The second alloy has an excellent workability. When in the form of rolled sheets, which have been heat treated for 2 hr at 2000°C and then oil quenched, rupture occurs after 100 hr when subjected to 14.5 hbars. (auth) (France)

19219 Nb BASE SUPERCONDUCTORS. Bethoux, O. (CNRS, Grenoble, France). Rev. Phys. Appl.; 5: 495-503(Jun 1970). (In French).

From Meeting on Niobium, Paris, France. See CONF-691046.

The effect of microstructure on the most important properties of superconductors is discussed. The superconducting behavior of ductile Nb alloys (Nb–Ti, Nb–Zr, Nb–Hf, Nb–Sn) and intermetallic Nb compounds is examined as a function of metallurgical treatment. Causes of instability in high critical current superconductors and its technological solutions are discussed. (auth) (France)

19220 THERMAL AND ELECTRICAL CONDUCTIVITIES OF SINGLE-CRYSTAL MOLYBDENUM AT HIGH TEMPERATURES. Peletskii, V. E.; Druzhinin, V. P.; Sobol, Ya. G. (Inst. for High Temperatures, Moscow). High Temp. - High Pressures; 2: 167-70(1970).

The thermal conductivity of single-crystal molybdenum was measured from 1200 to 2200°K by the longitudinal heat flow method on 70 mm long, 8 mm in diameter, cylindrical specimens heated at one end by an electron beam. The temperatures were measured with an optical pyrometer. The electrical resistivity was measured on similar specimens up to 2400°K. The measurements were carried out in the [100] direction. The results are compared with other studies on single-crystal and polycrystalline molybdenum. (auth) (UK)

19221 STRUCTURE AND PROPERTIES OF AN [ELECTRODEPOSITED] INDIUM–ZINC ALLOY. Marchenko, N. A.; Terekhova, L. S. Vestn. Kharkov Politekh Inst.; No. 32, 24-8(1968). (In Russian).

The deposition of an In–Zn alloy from ammoniacal tartrate electrolytes is shown to be possible. Certain properties of the alloy, e.g., microhardness, internal stresses, and corrosion resistance were studied in relation to chemical composition; phase compositions were determined by metallographic and x-ray methods. The alloy has a heterogeneous structure consisting of phases with a hexagonal Zn lattice and phases having a lattice differing from both those of Zn and In. Evidence shows that the latter phases may be considered as intermetallic compounds. (Referativnyi Zh.)

19222 DIRECTION OF THE DEVELOPMENT ON REACTOR MATERIALS. STEEL FOR PRESSURE VESSELS. Nomura, Junichi (Japan Steel Works, Ltd., Tokyo). Genshiryoku Kogyo; 16: No. 4, 73-8(Apr 1970). (In Japanese).

The prospects for development of steel plates for water-cooled reactors are described from the viewpoint of economy and safety. The historical aspect of the improvement of pressure vessel steel is described. The future prospects of Types A533 class 2 and 3, quenched and tempered Cr-Mo steel (A542), and Ni-Cr-Mo steel (A543) are examined on the basis of their economy, transition temperature curve, and tensile strength. The development of high-strength steel in Europe and U.S.A. is discussed. Useful materials for five ranges of high temperature are listed. (Japan)

19223 DIRECTION OF THE DEVELOPMENT ON REACTOR MATERIALS. PRESSURE TUBES AND THE MATERIALS. Kimura, Keizo (National Research Inst. for Metals, Tokyo). Genshiryoku Kogyo; 16: No. 4, 82-5(Apr 1970). (In Japanese).

The advanced thermal reactor, being developed in Japan, is moderated by heavy water and cooled with light water. Pressure tubes are used in the reactor core. The requirements for the tubes include small absorption of thermal neutrons, superior high-temperature strength, and high corrosion-resistance. The pressure tubes and materials are described, with emphasis on the ATR. Requirements are given for the pressure tubes, concerning nuclear characteristics, strength, corrosion resistance, metallurgical stability, integrity, erosion, workability, and economy. Design of the pressure tubes including wall thickness is described. Zirconium alloys as the pressure-tube materials are discussed. Zirconium has high corrosion resistance and strength. Zircaloy-2 and -4 and Zr-2.5 Nb alloy are described, and problems with zirconium alloys are reviewed. (Japan)

19224 UNUSUAL ELASTIC PROPERTIES OF GADOLINIUM AND INVAR. Maeda, Takao (Tokyo Univ.). J. Phys. Soc. Jap.: 30: 375-80(Feb 1971).

In order to investigate the anomalous elastic properties relating to the large-volume magnetostriction, Young's and shear moduli of Gd and Invar were measured as a function of temperature and magnetic field. Their bulk moduli were calculated from the measured values. In spite of the fact that the thermoelastic coefficients of the measured moduli were negative for Gd and positive for Invar, the coefficient of the bulk modulus was negative for each of the two, and an analogous strong magnetic effect on the calculated moduli was observed even for magnetically saturated states. The data for Gd are discussed on the basis of the RKKY interaction. (auth)

19225 MEASUREMENT OF THE PARTIAL OUTGASSING FLUX OF Mo and W AT 2000°K. Lesueur, R. (CEA, Saclay, France). Vide; 25: No. 148-149, 177-82(Jul-Oct 1970). (In French).

The residual partial outgassing flux of molybdenum and tungsten samples at 2000°K was investigated. The outgassing time for the gaseous impurities (H_2, CH_4, N_2, CO, O_2, CO_2) contained in the samples was of particular interest in establishing criteria for the choice of materials for various applications. (auth) (France)

19226 ELECTRICAL CONDUCTIVITY CHARACTERISTICS OF THE TWO-PHASE SYSTEMS. Ministr, Z. Pokroky Praskove Met. VUPM; No. 4, 13-45(Apr 1969). (In Czech).

The two-phase systems considered consist of second-phase particles in a base matrix material. Systems studied include metal/nonmetal and metal/metal types (W/Cu, W/Ag, WC/Ag, Ag/Ni, Cu/graphite, Ag/graphite, Al/Al_2O_3, and Ag/SiO_2). Conductivity characteristics are dependent mainly on the volume proportions of the components. 15 references. (Metals Abstr.)

19227 SPECIAL THERMOCOUPLE FOR TEMPERATURE MEASUREMENTS IN LIQUID METAL MEDIA. Seifritz, W. (Technische Univ., Hanover). Atomkernenergie; 17: 72(Feb 1971).

A special type of a thermocouple which can be used as a transducer to measure the temperature of liquid metals, is described. The main difference from conventional thermocouples is the absence of the thermocouple junction which connects the ends of the two wires. A liquid metal medium or, more generally, a medium with a sufficiently good electrical conductivity connects the ends of these wires automatically. This avoids the thermal capacity of the material of the junction constituting the sensitive volume which always gives rise to a characteristic time constant. This thermocouple has a very short response time (almost, prompt response) since the two naked ends of the wires instantaneously "see" the temperature of the bulk fluid between the ends of the two wires. This is an advantage of a thermocouple when used for dynamic measurements. (auth)

19228 Mg-Zr-Pb ALLOYS OF Pb CONCENTRATIONS BELOW OR EQUAL TO 3 PERCENT. STRUCTURAL AND MECHANICAL PROPERTIES. Dabosi, F. (CEA, Saclay, France); Millet, P.; Pegoud, J. Mem. Sci. Rev. Met.; 67: 659-74(Oct 1970). (In French). (CONF-681085-1).

From Meeting on Metallurgy, Paris, France.

A study was made of the structure and mechanical properties at high temperatures of ternary Mg-Zr-Pb alloys containing 0.45% Zr and 0.2 to 3% Pb. After treatment in CO_2 at T > 350°C, some of the Pb precipitates in the form of Zr_5Pb_3, the remainder forming a solid solution with Mg. By comparison with the binary Mg-Zr alloy, a reduced resistance to traction and creep is observed when the Pb content exceeds 1.5%. At all stages of deformation the elongation increases in the presence of lead and breaks are always ductile. Creep resistance of the 1.5% Pb alloy is improved by a 100 hr treatment at 600°C in CO_2. During a hydrogenation treatment a deterioration in the resistance to creep, together with an increased ductility, is observed for a fine-grained structure and the reverse applies when the grain is coarse. (auth) (France)

19229 THERMAL EXPANSION OF Au_4V. Kasai, Naoko; Ogawa, Shinji (Electrotechnical Lab., Tokyo). J. Phys. Soc. Jap.; 30: 736-41(Mar 1971).

Linear thermal expansion α of Au_4V in the ordered and disordered states was measured from 4.2 to 100°K. An anomaly, which corresponds to the magnetic ordering, was found in the ordered state. The magnetic entropy estimated from the magnetic contribution α_m is $(0.55 \pm 0.16)R$, which suggests a magnetic moment of approximately 1 μ_B per V atom. The Curie temperature of the ordered Au_4V is 52 ± 1°K. The electronic contribution to α (α_e) and the lattice contribution α_L in units of $°K^{-1}$ are: $\alpha_e = (0.95 \pm 0.05) \times 10^{-8}$ T and $\alpha_L = (9.6 \pm 0.2) \times 10^{-11} T^3$ ($T \leq 20°K$) in the disordered state and $\alpha_e = (3.65 \pm 0.05) \times 10^{-8}$ T and $\alpha_L = (9.1 \pm 0.3) \times 10^{-6} C_{Debye} (\theta_D = 245)/3R$ ($T \geq 60°K$) in the ordered state. The pressure dependence of Curie temperature $\partial T_c/\partial P$ in the ordered Au_4V is estimated to be +0.2°K/kbar. The Grueneisen constants in both states are estimated. (auth)

Structure and Phase Studies

19230 (CEA-R-3951) INTERMETALLIC DIFFUSION OF PLUTONIUM IN Pu-Cu AND Pu-U SYSTEMS: INFLUENCE OF A THIRD ELEMENT. Jamet, Christian (Commissariat a l'Energie Atomique, Bruyeres-le-Chatel (France). Centre d'Etudes). Oct 1970. 171p. (In French). Dep. NTIS (U. S. Sales Only).

Thesis. Submitted to Univ. of Lyon, Faculte des Sciences, Lyon, France.

After a review of published information on the subject of self-diffusion in plutonium, and of chemical diffusion of plutonium in various metals; the diffusion of plutonium is described in the systems Pu-Cu; Pu_{δ}-Cu; $Pu_{\delta Ga}$-U; and Pu-U in the presence of nickel. It was found in the absence of Ga, only the compounds $PuCu_2$, $PuCu_4$ and $PuCu_{11}$ are formed in the Pu-Cu diffusion zones at a temperature of 500°C and for very long treatments. In the presence of Ga, in the $Pu_{\delta Ga}$-Cu system a new ternary compound $Pu(CuGa)_3$, unknown until now was found for Ga contents of above 2%. It can be isolated as a single phase by melting Pu, Cu, and Ga in an arc furnace. In the ternary equilibrium diagram, this compound shows a region of stability which widens with increasing temperature. There exists a very wide solid solution region for Ga in the binary compound $PuCu_2$ giving $Pu(CuGa)_2$; this region is much smaller in $PuCu_4$. The intermetallic compounds present in the diffusion zones are hard, brittle, and highly sensitive to oxidation. All the heat treatments were carried out with a view to improving the adhesion of electrolytic deposits of copper on the $Pu_{\delta Ga}$. The results can be explained by the difference in the expansion coefficients of copper and plutonium. In the $Pu_{\delta Ga}$-U system a fine nickel layer (of a few microns) may be interposed between the $Pu_{\delta Ga}$ alloy and the metallic uranium, and after heat treatment of 1 hr at 470°C, for the plutonium to diffuse rapidly into the uranium. This leads to a strong, continuous, metallic bond between the two elements (6.5 kg/mm²). The bonding obtained by eutectic soldering at 470°C between the $Pu_{\delta Ga}$ and the nickel, is easy to carry out because of the formation of a layer of well-defined ternary compound, Pu_2Ni_2Ga, appears to be strong (5 to 7 kg/mm²). During this work it has been possible to show the existence of two definite PuNiGa compounds; these were isolated as a single-phase by melting Pu, Ni, and Ga in a sealed tantalum container. (auth)

19231 (NLCO-1051) AN AS-CAST DILUTE URANIUM ALLOY WITH A FINE-GRAINED, RANDOMLY ORIENTED STRUCTURE. Schaich, E. L. (National Lead Co. of Ohio, Cincinnati). Apr 1970. Contract AT(30-1)-1156. 10p. Dep. NTIS.

Several uranium-base dilute alloys were cast and studied in a search for one having a fine grain size and a random orientation in the as-cast condition. Both consumable arc and induction melting were used to make the alloys. One alloy, containing 500 ± 50 ppM Si and 375 ± 50 ppM Cr, was found to have the desired properties. This alloy may warrant consideration as a fuel or shielding material. (auth)

19232 (UCRL-19696) LECTURE 3: NONEQUILIBRIUM DEFECTS IN METALS. Thomas, G. (California Univ., Berkeley. Lawrence Radiation Lab.). Sep 1970. Contract W-7405-eng-48. 38p. (CONF-700934-3). Dep. NTIS.

From 2nd International Conference on the Science of Materials, Tremezzo, Italy.

XUM

A brief outline of individual defects in metals and their interactions and associations is presented. Discussions are included on point defects, line defects, dislocation origins, dislocations occurring during solidification, nucleation of dislocations from impurities, dislocation multiplication, surface defects, and volume defects. (J.R.D.)

19233 STRUCTURAL CHANGING DURING DEGRADATION OF SUPERSATURATED SOLID SOLUTION OF Ta IN Co. **Korchazhkin, V. V.; Zakharova, M. I. Vestn. Mosk. Univ., Ser. III. Fiz. Astron.; 11: 453-6(Jul-Aug 1970). (In Russian).**

Phase studies of the Co–Ta system showed diffusion of Ta into Co at room temperature to 1250°C. Crystal structure changes, taking place at the initial stages of disintegration, in saturated solid solutions of Co–10 wt % Ta were examined using x-ray and electron microscopic analyses. (R.V.J.)

19234 FORMATION OF DIFFUSION LAYERS IN NITRIDED NIOBIUM, TUNGSTEN, AND IRON–SILICON ALLOYS. **Kaplina, G. S.; Loskutov, V. F. Izv. Akad. Nauk SSSR, Metal.; No. 4, 214-17(Jul-Aug 1970). (In Russian).**

Processes in nitrogenation of Nb, W, and Fe–Si alloys were investigated by high temperature roentgenography. The Nb reaction was carried out at 800 to 1000°C, the W reaction at 800°C, and the Fe–Si reaction at 400 to 1000°C. The nitriding medium was ammonia. It was found that the nitrogen diffuses in Nb and W by formation of nitride phases and by increase in these phases. During nitrogenation of Fe–Si alloys diffusion occurs with solid solution formation followed by diffusion. Discrepancies between phase compositions in diffusion layers found on nitrided Nb and W, and phase diagram data can be explained by diffusion under nonequilibrium conditions. (tr-auth)

19235 STRUCTURE OF $ThRe_2$–$GdRe_2$ ($TbRe_2$, $DyRe_2$, $ErRe_2$). **Badaeva, T. A.; Dashevskaya, L. I. Izv. Akad. Nauk SSSR, Metal.; No. 4, 189-93(Jul-Aug 1970). (In Russian).**

Results of x-ray-phase analyses established the presence of a continuous series of solid solutions in systems composed of $ThRe_2$ with $GdRe_2$, $TbRe_2$, $DyRe_2$, and $ErRe_2$ having hexagonal lattices similar to $MgZn_2$. It was confirmed that inside of grains of crystalline Laves phases having the formula AB_2 close values of lattice parameters are found. A continuous series of solid solutions is expected in these phases. A favorable condition also exists for phases in which there is a common element such as Re and the difference between the atomic radius of other elements in the compound as small as in the case of Th and rare earths. Under these conditions, substitution of one of these elements in the A position of formula AB_2 such as displacement of Th by rare earths in $ThRe_2$ is expected. Solid solutions can be expected in compounds of open maximums and between compounds melted incongruently. (tr-auth)

19236 PHASE DIAGRAM OF Bi–Cd–Hg. **Nosek, M. V.; Semibratova, N. M.; Yang-Shuo-Hsiang, G. V. Izv. Akad. Nauk SSSR, Metal.; No. 4, 194-7(Jul-Aug 1970). (In Russian).**

A phase diagram of Bi–Cd–Hg alloys was prepared by DTA, x-ray phase analysis, and by microstructural and microhardness measurements. Two invariant peritectic points were found at 117 ± 2 and 34 ± 2°C. Phase regions and their boundaries in the ternary system were found to conform to the structure of diagrams representing components of its system. (tr-auth)

19237 STRUCTURE OF V–Cr–Zr ALLOYS AT 1150°C. **Eremenko, V. N.; Prima, S. B.; Tret'yachenko, L. A.; Khoruzhaya, V. G. Izv. Akad. Nauk SSSR, Metal.; No. 4, 168-70(Jul-Aug 1970). (In Russian).**

A phase diagram was prepared for the system V–Zr–Cr by metallographic and x-ray investigations at 1150°C. Phase regions established include alpha–the region of solid solutions of Zr in V and Cr; beta–the region of beta Zr solid solution; and gamma–the regions of continuous solid solutions involving compounds such as V_2Zr, and Cr_2Zr having cubic structure which separates into two-phase fields expressed as alpha + gamma and beta + gamma. (tr-auth)

19238 EFFECTS OF Al AND Zr ON PROPERTIES OF Ti_3Sn. **Kornilov, I. I.; Nartova, T. T.; Shirokova, N. I. Izv. Akad. Nauk SSSR, Metal.; No. 4, 174-7(Jul-Aug 1970). (In Russian).**

The thermodynamics of phases in the Ti–Sn system were studied. Ti_3Sn was investigated in the systems Ti–Zr–Sn and Ti–Zr–Al–Sn. Studies of the system Ti_3Sn containing Ti plus 5% Zr plus 5% Al at about 900°C established the existence of a two-phase alpha plus delta phase. At temperatures of 1000 to 1050°C a three-phase region composed of alpha plus delta plus beta was found. A two-phase delta plus beta and a single phase beta also occurs in this temperature range. At Ti contents of >80% a single delta phase exists. (tr-auth)

19239 STRUCTURE AND PROPERTIES OF W–Mo–Nb–Ta ALLOYS CONTAINING 70 WEIGHT PERCENT TUNGSTEN. **Gromova, V. G.; Pryakhina, L. I. Izv. Akad. Nauk SSSR, Metal.; No. 4, 178-83(Jul-Aug 1970). (In Russian).**

The structure and properties of W–Mo–Nb–Ta alloys containing 70 wt % W were investigated. The alloys in this system crystallize to form continuous series of solid solutions. Room temperature hardness test results show that Mo additions reduce hardness of W and its alloys with Ta and Nb whether added with the latter or separately. (tr-auth)

19240 SOLUBILITY OF O IN Hf–Nb ALLOYS. **Shurin, A. K.; Loktionov, V. A. Izv. Akad. Nauk SSSR, Metal.; No. 4, 46-8(Jul-Aug 1970). (In Russian).**

Phase diagrams were prepared for Nb-rich Nb–Hf alloys at 1000 to 1600°C. Solid solutions of O and Hf in Nb in this temperature range occur at equilibrium with NbO, HfO_2 or with the high temperature modification of Hf. Hafnium reduces the solubility of O in Nb. With the content of Hf over 0.005 at. %, O solubility falls to about 0.025 at. % in the 1000 to 1600°C range. Results obtained represent homogeneous alloys; compositions were controlled by thermal conditions. Deviations in results were caused by lack of complete control of O diffusion in the Nb–Hf alloys. This is the apparent reason for errors in overstating the solubility of O in these alloys. (tr-auth)

19241 PHASE DIAGRAMS AND PROPERTIES OF La–Sc ALLOYS. **Naumkin, O. P.; Terekhova, V. F.; Savitskii, E. M. Izv. Akad. Nauk SSSR, Metal.; No. 4, 137-42(Jul-Aug 1970). (In Russian).**

A phase diagram was prepared for La–Sc alloys by physicochemical analysis, microstructural x-ray analyses, and by thermal and dilatometric methods. Complete miscibility is evident in the liquid state and continuous solid solution phases occur between high temperature modifications of gamma-La and beta-Sc. The system is also characterized by eutectoid transformations at 750 ± 5°C and at 233 ± 2°C when the Sc content is about 45 and about 14 at. % respectively. The solubility of Sc at eutectoid transformation temperatures is about 16 at. % in beta–La and approximately 12 at. % in alpha–La. The maximum solubility of La in alpha–Sc is about 15 at. % at 750°C. Small additions of Sc decreased the corrosion rate of La by oxygen in air during eight-month tests at 25°C. (tr-auth)

19242 CRYSTALLIZATION PROCESS IN BINARY SOLID SOLUTIONS OF NICKEL. **Myasnikova, K. P. Izv. Akad. Nauk SSSR, Metal.; No. 4, 143-9(Jul-Aug 1970). (In Russian).**

Selective etching was used in investigations conducted to show that substructurally homogenized alloys reflect the characteristic of melt crystallization and are dependent on melting properties and hardening conditions. Thermal treatments, deformation, and recrystallization have little effect on binary solid solution recrystallization of Ni with Zr, Nb, Mo, Ru, Rh, or Pd. (tr-auth)

19243 CRYSTAL STRUCTURE OF HOLMIUM AND ERBIUM BETWEEN 77 AND 300°K. **Finkel, V. A.; Palatnik, M. I. (Physical-Tech. Inst., Kiev). Zh. Eksp. Teor. Fiz.; 59: 1518-23(Nov 1970). (In Russian).**

The crystal structure of holmium and erbium was measured by low-temperature x-ray crystallography between 77 and 300°K. It was found that anomalous expansion of the hexagonal compact lattices occurs along the hexagonal axis below T_N (132.5°K for Ho and 84°K for Er). A discontinuous change of the linear expansion coefficients for holmium and erbium occurs at T_N ($\Delta\alpha_\perp > 0$, $\Delta\alpha_{||} < 0$). At $T \sim 120$°K, a peak is observed in the temperature curve of the atomic volume of holmium that is related to a variation of topology of the Fermi surface. (auth)

19244 STRUCTURE OF SPUTTERED NIOBIUM FILMS, OBSERVATION OF A F.C.C. PHASE. **Sella, C.; Tertian L.; Deschamps, J. (CNRS, Meudon-Bellevue, France). Rev. Phys. Appl.; 5: 415-22(Jun 1970). (In French).**

From Meeting on Niobium, Paris, France. See CONF-691046.

Sputtering of normally bcc niobium (a = 3.29 Å) on sodium chloride gives amorphous films on cold substrate polycrystalline disoriented films below 100°C, and epitaxial layers with (110)Nb/(100)NaCl, (111)Nb/(100)NaCl and (100)Nb/(100)NaCl orientations between 100 and 400°C. During the first stage of sputtering an abnormal fcc structure (a = 4.42 Å) oriented with (100)/(100)NaCl was observed. It results from the interaction between the metal and the residual gas present in the sputtering chamber or on the substrate surface. Its formation can be avoided by a careful outgassing of the substrate or a purification of the residual atmosphere by a long preliminary sputtering in order to eliminate the active gas. An attempt to specify the nature of this abnormal phase was made and its evolution was studied in the residual atmosphere of the diffractometer up to about 800°C. (auth) (France)

19245 VACANCY QUENCHING IN Nb. Tete, Claude; Lebouche, Michel; Deviot, Bernard. (Ecole Nationale Superieure de la Metallurgie et de l'Idustrie des Mines, Nancy). Rev. Phys. Appl.; 5: 423-5(Jun 1970). (In French).

From Meeting on Niobium, Paris, France. See CONF-691046.

Two types of specimen were studied (12.5 micron thick ribbons and 5/100 mm wires). In both cases, the samples placed in a pyrex tube were degassed in ultrahigh vacuum at 2000°C; before sealing, the tube was filled with helium purified by passing through zeolite at liquid hydrogen temperature. The samples were heated by Joule effect and quenched by cutting off the current; resistivity measurements were made. The ribbons show one stage after isochronous annealing; two stages were observed for the wires. These stages are due to point defects remaining after quenching. (auth) (France)

19246 STUDY OF NIOBIUM BASE REFRACTORY METAL ALLOYS. Allibert, C.; Wicker, A.; Driole, J.; Bonnier, E. (Ecole Nationale Superieure d'Electrochimie et d'Electrometallurgie, Grenoble, France). Rev. Phys. Appl.; 5: 449-53(Jun 1970). (In French).

From Meeting on Niobium, Paris, France. See CONF-691046.

A synthesis of the results concerning the preparation of homogeneous binary Nb base alloys is presented. The method used is based upon electromagnetic separation; this allows the corresponding phase diagrams to be determined. In the Cu–Nb phase diagram, the isothermal sections of the following systems were established: Cu–Nb–W at 1600, 1900, and 2100°C; Cu–Nb–Mo at 1900 and 2100°C; and Ni–Nb–W at 1800 and 1900°C. (auth) (France)

19247 KINETICS OF ISOTHERMAL MARTENSITE TRANSFORMATION DURING THE AGING OF A TERNARY ALLOY CONTAINING 76 PERCENT Fe, 19 PERCENT Ni, AND 5 PERCENT Mo. Courrier, Raymond (Ecole Nationale Superieure de la Metallurgie et de l'Industrie des Mines, Nancy). Compt. Rend., Ser. C; 271: 1514-17(21 Dec 1970). (In French).

During annealing at 420 to 570°C, a precipitate, coherent with the matrix, appears and simultaneously austenite arises at the interfaces, as in Fe-Ni alloys. In the precipitation the exponent n of J. and M. is 2/3 at low temperatures and between 1.00 and 1.60 at temperatures higher than 480°C. It is about 0.90 in the austenite formation. The precipitate does not retain its coherence when the particle size exceeds 200 Å. (auth) (France)

19248 X-RAY STUDY OF FAULTING IN BCC METALS AND ALLOYS. Rothman, R. L.; Cohen, J. B. (Northwestern Univ., Evanston, Ill.). J. Appl. Phys.; 42: 971-9(1 Mar 1971).

Faulting on {211} planes has been reported in filings of many bcc materials based on differences in the broadening of various peaks in the x-ray powder pattern. These experiments have been repeated in this work using (a) recent techniques for correcting for various experimental errors and (b) new derivations of effects of faults on other planes. It is shown that the mean-square strains $\langle \epsilon_L^2 \rangle$ are generally inversely proportional to the distance L normal to the reflection planes. As a result, it is possible to separate effective particle-size (including faulting) and elastic strains from several first-order reflections, rather than with multiple orders. With this approach, the results indicate that there are no faults produced by filing in Fe, β brass, and Mo–Re alloys. For Nb there are faults on {110}, and the concentration varies inversely with the interstitial content. (auth)

19249 COMBINED FIELD-ION AND ELECTRON MICROSCOPE STUDIES OF GRAIN BOUNDARIES IN TUNGSTEN. Loberg, Bengt. Goteborg, Chalmers Tekniska Hogskola [1970]. 15p.

Thesis.

A method is given for the combined observation of the same specimen in both the electron and the field-ion microscope. The influence of the imaging conditions in the field-ion microscope on the observed material was studied. The parameters for (110) tilt boundaries and grain boundary dislocations were also studied. (Sweden)

Radiation Effects

Refer also to abstract 19807.

19250 (AEC-tr-7192) PROPERTIES OF HEAT-RESISTANT STEELS FOLLOWING HIGH-TEMPERATURE REACTOR IRRADIATION. Votinov, S. N.; Prohorov, V. I.; Ostrovsky, Z. E.; Grinchuk, P. P.; Khoudjakov, A. V. Translation of Russian report. 12p. Dep. NTIS.

Results of investigation of radiation embrittlement of age-hardening steels with different intermetallic hardening are reported. The strength characteristics critical point and apparent yield limit over the entire temperature range are substantially lower for irradiated steel and the steels subject to annealing by the irradiation process, compared with the strength values for steel in the original state. For irradiated steel tested in open heating at a temperature close to 350°C, the beginning of a bulge can be observed, characteristic of strain aging. The same temperature range shows a beginning decrease in the plasticity of the steel in inverse proportion to the temperature increase. (J.R.D.)

19251 (AERE-R-6435) SOME OBSERVATIONS ON THE STRUCTURE AND TENSILE PROPERTIES OF AISI TYPE 316 STEEL AS A FUNCTION OF FAST REACTOR IRRADIATION TEMPERATURE. Barton, P. J. (Atomic Energy Research Establishment, Harwell (England)). Jun 1970. 14p. Dep. NTIS (U. S. Sales Only).

Solution treated AISI Type 316 steel strip specimens were irradiated in the Dounreay Fast Reactor to doses of 1.0 to $1.3.10^{22}$ n/cm^{-2} (total), 1.7 to $2.6.10^{21}$ n/cm^{-2} (fission) within the following measured temperature ranges: 420 to 440, 500 to 513, 520 to 533, 560 to 570, and 645 to 650°C. Transmission electron microscopy revealed the presence of voids after irradiation at all these temperatures. Distribution was uniform after irradiation at 420 to 440, 500 to 513, and 520 to 533°C. At higher temperatures it was uneven and concentration was so low that probably helium bubbles and not voids were being observed. From the temperature dependence of void concentration and average diameter it is deduced that the consequent density decrease is maximal after irradiation at 500 to 513°C. Dislocation loops were present for irradiation at all but the highest temperature. They were interstitial and lay on {111} planes with Burgers vectors of the type a/3 ⟨111⟩. At 420 to 440°C all loops were faulted. As irradiation temperature increased, loop concentration decreased and at 520 to 533°C a few unfaulted loops were observed. Yield stress increases estimated from loop and void concentrations are found to be in fair agreement with measured values. (auth)

19252 (COO-1367-36) EFFECT OF ELECTRON IRRADIATION ON THE STRENGTH OF IRON SINGLE CRYSTALS. Sato, A.; Mifune, T.; Meshii, M. (Northwestern Univ., Evanston, Ill.). [1970]. 5p. (CONF-700819-11). Dep. NTIS.

From 2nd International Conference on the Strength of Metals and Alloys, Pacific Grove, Calif.

The effects of electron irradiation on the strength of monocrystalline bcc iron were studied. Experimental and calculated results strongly supported the contention that the inherent lattice hardening determined the low temperature strength of pure iron and perhaps other pure bcc metals. Dilute impurities would cause the softening effect and the impurity hardening effect could be expected only above a critical concentration. The hardening effect found after the electron irradiation and aging was not clearly understood, since the distribution of the radioinduced defects became uncertain after the aging. (G.M.C.)

19253 (WHAN-FR-16) IRRADIATION PRODUCED DEFECTS IN AUSTENITIC STAINLESS STEEL. Brager, H. R.; Straalsund, J. L.; Holmes, J. J.; Bates, J. F. (WADCO Corp., Richland, Wash.). Dec 1970. Contract AT(45-1)-2170. 48p. Dep. NTIS.

The microstructure of annealed AISI Type 304 and Type 316 stainless steels was characterized by transmission electron microscopy as a function of fast reactor irradiation at fluence levels from 4×10^{21} to 7×10^{22} n/cm^2 (E > 0.1 MeV) and at irradiation temperatures from 370 to 700°C. Several irradiation produced defect types were found: voids, Frank faulted loops, perfect loops, dislocation networks, and precipitates. Void number density obeyed a power law relationship to fluence, wherein the exponent increased with increasing temperature and had a mean value near unity. The void size was nearly independent of fluence and increased with increasing temperature. The upper limit irradiation temperature for void formation was about 650 to 700°C. The density and size of Frank faulted loops followed trends similar to those found for voids to temperatures of ~550°C where unfaulted loops, perfect loops, and dislocation networks coexisted. These experimental results do not confirm predictions of recently advanced models of void formation. The major deficiency of these models appears to be the nucleation rate. Accordingly, empirical nucleation rates were used to formulate a diffusion controlled void growth model. This model was found to closely describe experimentally determined void growth kinetics. (auth)

19254 (WHAN-SA-2) EBR-II IRRADIATION EFFECTS OF RUPTURE OF TYPE 316 STAINLESS STEEL. Barker, R. W.; Holmes, J. J. (WADCO Corp., Richland, Wash.). 1 Jul 1970. 11p. (CONF-701102-7). Dep. NTIS.

From Meeting of the American Nuclear Society, Washington, D. C.

XUM

The effects of EBR-II irradiation on the biaxial stress-rupture properties of annealed Type 316 stainless steel were investigated at test temperatures of 1000, 1200, and 1400°F. Tubular specimens having a 0.208 in. dia and 0.008 in. wall were irradiated in Row 7 to a fluence of 1×10^{22} n/cm^2 ($E > 0.1$ MeV) at an irradiation temperature 850 ± 50°F. The composition of the tubing was as follows: 0.081%C, 2.3%Mo, 1.5%Mn, 13.2%Ni, 17.0%Cr, and 0.5%Si. The EBR-II irradiation produced a loss in rupture strength and ductility at all test temperatures and an increase in creep rate at 1000°F. Stress-to-rupture values were reduced about 20% at a test temperature of 1000°F; at 1200°F a 10% loss in strength occurred while at 1400°F the stress-to-rupture was reduced 25%. Ductility was reduced as much as a factor of 0.1 depending on test temperature and test duration. The greatest losses in ductility occurred at 1000 and 1400°F with little effect occurring at 1200°F. Dorn's theta parameter was used to correlate stress rupture data and to describe fracture mode and precipitation. Two distinct fracture modes were observed. At low theta values, (low temperature or short times) the fracture proceeded by a shear mechanism induced by plastic instability. At intermediate theta values, the shear failure also dominated but wedge-type grain boundary failure also contributed to fracture. Considerably more boundary cracking was evident in the irradiated specimen than in the controls. At high theta values, boundary failure dominated fracture in the irradiated specimen while shear failure dominated the fracture process in the control specimens. Both wedge and cavitation boundary failure was found in the irradiated tests while only cavitation was observed in controls. Concurrent with the change in fracture mode, the level of precipitation which occurred during testing of both irradiated and control specimens increased with theta. Both $M_{23}C_6$ and sigma phase developed to an increasing extent with increasing time or temperature. The loss in stress-rupture life found was a function of both ductility and creep rate modification resulting from irradiation. At low theta values the reduced ductility and the increased creep rate controlled the rupture life. At intermediate temperatures little change in creep rate or ductility occurred, thus, rupture life was not greatly changed by irradiation. However, at high theta values, reduced ductility due to helium embrittlement again produced a loss in rupture life. (auth)

19255 NEUTRON IRRADIATION HARDENING IN ALUMINUM-MAGNESIUM ALLOYS. Shiraishi, Kensuke (Japan Atomic Energy Research Inst., Tokai). Trans. Jap. Inst. Metals; 11: 440-1(Nov 1970).

The effect of neutron irradiation on the tensile properties of Al-Mg alloys with 0.6 to 1.5 at. % Mg was investigated. The specimens were irradiated in a fast neutron flux of 2×10^{11} cm^{-2} sec^{-1} to a dose of 3.3×10^{17} cm^{-2}. An increase in yield stress and the appearance of Luders strain were observed following irradiation and increased with increasing Mg content. After annealing at 220 to 250°C the radioinduced changes in the properties of the 0.6 and 1.1 at. % Mg alloys were almost completely recovered but the radioinduced hardening of the 1.5 at. % Mg alloy still remained. (G.M.C.)

19256 SOME OBSERVATIONS OF A REGULAR VOID ARRAY IN HIGH-PURITY MOLYBDENUM IRRADIATED WITH 2-MeV NITROGEN IONS. Evans, J. H. (Atomic Energy Research Establishment, Harwell, Eng.). pp 235-7 of Ion Implantation. Stevenage, Eng.; Peter Peregrinus Ltd. (1970).

From Conference on Ion Implantation, Reading, England. See CONF-700945.

Voids produced in metals by neutron or accelerator irradiation normally form in random fashion in the lattice, but the studies described show that voids in Mo can be found in regular positions relative to one another. These regular positions are related to the crystallography of the lattice, are three-dimensional and, like the parent lattice, form a bcc array. Single-crystal Mo disks were used in the studies, and specimens were irradiated at temperatures of 700 to 900°C to doses of 4×10^{17} to 1×10^{18} 2-MeV N^+ ions, using a Van de Graaff accelerator, followed by electrolytic thinning to examine damaged layers in an electron microscope. It was found that the damage occurred in a layer between ~8,000 and 25,000 Å from the bombarded surface. A regular void array was clearly seen. The lattice parameter of the bcc array was found to be 220 ± 10 Å, and the voids were ~40 Å in diameter. The reason for the formation of this void lattice, or superlattice, is not clear, and it does not seem to have been theoretically predicted. Possible explanations are suggested. (UK)

19257 OBSERVATIONS OF A REGULAR VOID ARRAY IN HIGH-PURITY MOLYBDENUM IRRADIATED WITH 2 MeV NITROGEN IONS. Evans, J. H. (Atomic Energy Research Establishment, Harwell, Eng.). Nature (London); 229: 403-4(5 Feb 1971).

Voids in metals, formed as a result of neutron irradiation or particle bombardments, are usually found to be distributed randomly in the lattice. It was found, however, that voids can take up regular positions in the lattice with respect to each other and it is demonstrated that the voids form a body-centered-cubic superlattice structure with crystallographic axes identical with those of the molybdenum matrix. The voids in this case were formed as a result of particle irradiations but some observations made on neutron irradiated molybdenum indicate that this same void structure may be present in that case as well. The reason for the formation of this void lattice is not clear and, as far as is known, has not been theoretically predicted. The formation could either be a phenomenon where voids are nucleated on an impurity superlattice existing prior to the irradiation, or could be due to interaction between the voids once they are formed causing the voids to climb into "lattice sites" relative to their neighbors, minimizing their free energy by doing so. Because no such interactions can exist between voids in an isotropic lattice the anisotropy of the molybdenum lattice could be an important factor in this mechanism. (auth) (UK)

Ceramics and Cermets

Refer also to abstract 19166.

Corrosion and Erosion

Refer also to abstracts 18592 and 19179.

19258 KINETICS AND MECHANISMS INVOLVED IN THE SILICONIZATION OF Nb AND THE OXIDATION OF NIOBIUM SILICIDES AT LOW PRESSURES AND HIGH TEMPERATURES. Gelain, C.; Cassuto, A.; Le Goff, P. (CNRS Villers-les-Nancy, France). Rev. Phys. Appl.; 5: 545-9(Jun 1970). (In French).

From Meeting on Niobium, Paris, France. See CONF-691046.

Siliconization of niobium ribbons by the heterogeneous decomposition of SiH_4 results from a competition between surface enrichment in silicon and diffusion towards the bulk of the metal. The kinetics of the decomposition process with silicon and the silicides, and the surface transformation during siliconization was studied. In the presence of oxygen, ribbons covered with silicon or silicides show a sharp transition between a passive state, when the surface is covered with SiO_2 to a stationary combustion regime resulting from vaporization of SiO. For a ribbon consisting of a solid solution of silicon in niobium, the speed of the reaction between oxygen and the non-volatile niobium oxide formed on the surface was determined. A model based on the thermodynamic equilibrium of the components is in accordance with experimental results. (auth) (France)

Preparation and Fabrication

Refer also to abstracts 18517 and 19188.

19259 (NLCO-1029) PRODUCTION OF DENSE THORIA. Burkhardt, W.; Briggs, G. G. (National Lead Co. of Ohio, Cincinnati); Clavel, A. L.; White, J. F. (General Electric Co., Cincinnati, Ohio. Nuclear Systems Programs). Jul 1969. Contract AT(30-1)-1156. 85p. Dep. NTIS.

Large-scale techniques were developed for the production of dense thoria. Impure thorium nitrate solutions were treated by solvent extraction using diamyl-amyl phosphonate in kerosene. This purification step was followed by a second using tributyl phosphate in kerosene if the feed was high in uranium. The purified aqueous thorium nitrate was then treated with ammonium hydroxide in a process developed to precipitate the thorium as thorium hydroxide. The thorium hydroxide was dried to a gel and then calcined or sintered to a form suitable for the preparation of dense ThO_2 for vibratory compaction and, by change in conditions, to a sinterable powder. Additionally, the powders were found to be well suited to the production of cold-pressed and extruded shapes. Several hundred tons of thorium were processed by the methods described. All of this material met strict specifications for chemical purity and physical properties, including the requirement for rapid dissolution after irradiation. (auth)

19260 (ORNL-4629) STATUS AND PROGRESS REPORT FOR THORIUM FUEL CYCLE DEVELOPMENT FOR JANUARY 1, 1969-MARCH 31, 1970. Wymer, R. G.; Lotts, A. L. (comps.) (Oak Ridge National Lab., Tenn.). Feb 1971. Contract W-7405-eng-26. 108p. Dep. NTIS.

Thorium fuel cycle progress is reported in six sections. A separate abstract was prepared for each section. (J.R.D.)

For abstracts of individual sections see: 18564, 18624, 19261-19263, and 19288.

19261 (ORNL-4629, pp 14-64) SOL-GEL PROCESS DEVELOPMENT. (Oak Ridge National Lab., Tenn.).
In Status and progress report for thorium fuel cycle development for January 1, 1969–March 31, 1970.

The sol-gel process development studies have been concerned primarily with the preparation of thoria, urania, and plutonia (and their binary mixtures), although many other oxide sols have also been prepared in laboratory studies. A primary current objective is to develop procedures and equipment useful for remotely operated fuel preparation in the Thorium–Uranium Recycle Facility (TURF). The sol-gel process for preparing ThO_2-UO_2 microspheres was previously demonstrated by preparing 120 kg of spheres while operating process equipment at 10 kg/day. Engineering development of the CUSP UO_2 sol process was begun, and approximately 230 kg of UO_2 sol was prepared. Further work was carried out on gel sphere forming development and included studies of variables by factorial experiments, recycle of 2-ethyl-1-hexanol (2EH), sphere preparation from CUSP UO_2 sols, development of fluidized-bed columns, preparation of small (<200-μm-dia) spheres in nonfluidized columns, and preparation of test materials for recycle test elements (RTE's). (auth)

19262 (ORNL-4629, pp 65-82) FUELED-GRAPHITE FABRICATION DEVELOPMENT. (Oak Ridge National Lab., Tenn.).
In Status and progress report for thorium fuel cycle development for January 1, 1969–March 31, 1970.

Equipment was developed for the remote transfer, shape separation, screening, and blending of fuel particles, and the determination of coating anisotropy, density, and size distribution. Remotely operable equipment is described for coating fuel particles with pyrolytic carbon and with silicon carbide. Coating and bonding of fuel for Recycle Test Elements are described. Surface morphologies of carbon coatings are shown and correlated with density. (auth)

19263 (ORNL-4629, pp 99-102) FUNDAMENTAL SOL-GEL STUDIES. (Oak Ridge National Lab., Tenn.).
In Status and progress report for thorium fuel cycle development for January 1, 1969–March 31, 1970.

The nitric acid present in gel spheres reacted with the sorbed alcohol during drying in steam. The rate at which the drying temperature is increased must be both slow and uniform in fixed beds so that the chemical reaction rate can be controlled and heat is not liberated at an excessive rate. A purge of steam through the bed of spheres enhances the desorption and vaporization of the organic reactants and thus reduces the quantity of organic materials that are available for reaction with nitric acid. Carbonaceous materials and other volatiles remaining after drying were removed during firing before any appreciable shrinkage or densification of ThO_2-UO_2 gel spheres occurred; thus no problems are encountered in attaining the density and chemical composition specified for calcined products. (auth)

19264 IMPROVEMENTS RELATING TO NEUTRON-ABSORBING MATERIALS AND METHODS FOR THEIR PRODUCTION. (to Brown Boveri/Krupp Reaktorbau GmbH). British Patent 1,219,696. 20 Jan 1971. Priority date 5 Sep 1968, Germany.

Preparation of neutron-absorbing materials for use in high-temperature reactors is described. The material contains at least one stable boride in a metal matrix. The compound Bn, FeB, and CrB are particularly suitable for incorporation in Cu, Al, or Cu–Ni. (J.R.D.)

19265 ROLE OF CRYSTALLINITY IN THE SINTERING OF URANIA POWDERS. Moorthy, V. K.; Rao, S. V. K. (BARC, Bombay). Trans. Indian Ceram. Soc.; 27: No. 1, 16-30(1968).

The crystallinity in UO_2 powders prepared by the ADU method at 600 to 1600°C and its influence on their sintering behavior at 1000 to 1600°C in hydrogen were studied by x-ray diffraction techniques. Powder patterns were made for the loose powders and back reflection for the sintered pellets. It was noticed that the higher the calcination temperature, the greater was the degree of crystallinity developed in the powders and poorer was their sinterability. The crystallinity of the sintered pellets was mainly dependent on the sintering temperature and crystallinity of the original powder and is not directly related to the sintered density. By sintering pellets of poorly crystalline powders at about 100°C sintered pellets of near theoretical density but with poorly developed crystallinity could be obtained. (Indian Sci. Abstr.)

19266 EVALUATION OF CRYSTALLINITY OF URANIA POWDERS BY STREAMING POTENTIAL STUDIES. Moorthy, V. K.; Rao, S. V. K. (BARC, Bombay). Trans. Indian Ceram. Soc.; 27: No. 1, 31-40(1968).

It has been shown that the sintering behavior of oxides depends on the origin and thermal history of the powders. Physical characteristics of powder such as surface area and particle size were not found to be adequate to explain their sintering behavior. It is also shown that the sinterability is directly related to the crystallinity in the powders. The crystallinity of the powders can be assessed on a comparative basis by determining the streaming potentials. An apparatus was set up to determine the streaming potentials of urania powders. It was found that the slope of the streaming potentials vs velocity of flow plots was a direct indication of the comparative sinterability of the urania powders. (Indian Sci. Abstr.)

19267 CARRIER FOR URANIUM OXIDE PELLETS. (to United Nuclear Corporation). British Patent 1,222,937. 17 Feb 1971. Priority date 4 Oct 1968, United States.

A carrier is described for use during dewaxing and sintering of uranium oxide fuel pellets. A metallic support is included which is resistant to corrosion under operating conditions. The UO_2 pellets are sintered on a corrugated Mo sheet supported by a Mo base. A Mo heat shield is included. The carrier can be used in automatic or semiautomatic fuel pellet production. (J.R.D.)

19268 APPARATUS AND METHOD FOR BLENDING PARTICLES. (to Gulf General Atomic Inc.). British Patent 1,219,220. 13 Jan 1971. Priority date 6 Jun 1968, United States.

Preparation of fuels comprising a blend of fuel and fertile particles is described. The particles are blended together in predetermined ratios. The compaction ratio of the resulting blend is satisfactory and fuel bodies molded in the cavity provided have good dimensional characteristics and particle distribution throughout. (J.R.D.)

19269 MANUFACTURE OF NUCLEAR FUEL ELEMENTS. Kedward, Eric Charles; Kiernan, Brian; Shove, Arthur Godfrey (to Bristol Aerojet Limited). British Patent 1,220,332. 27 Jan 1971. Filed 3 May 1967.

According to this invention, an element of nuclear fuel is manufactured by electroforming in a bath for the electro-deposition of the material of the matrix and containing particles of the fissile material. When this process is carried out the particles are entrapped by the material being electrodeposited so that a composite coating of particles dispersed individually and/or as agglomerates in a metal matrix is built up. The equipment required for the process is simple and the particles of fissile material are suspended in a liquid. Accordingly, the problems of handling the material safely and of decontaminating equipment are likely to be less than when powder metallurgy techniques are employed. Various fissile materials may be used and examples include uranium dioxide and plutonium. The metal matrix may be any metal or metal alloy which is plateable and which has suitable properties for use in a reactor. One such suitable metal is nickel. (UK)

19270 IMPROVEMENTS IN AND RELATING TO THE ELECTRO-DEPOSITION OF COMPOSITE COATINGS. Kedward, Eric Charles; Kiernan, Brian; Duffin, Roger Alan (to Bristol Aerojet Limited). British Patent 1,220,331. 27 Jan 1971. Filed 27 Apr 1967.

A process is given for the electrodeposition of a composite coating which consists of a matrix of chromium or a chromium alloy with ceramic, cermet, or metal particle additions which comprises co-depositing the matrix and particles in a bath which has already been worked for a period greater than eight hours. The necessity of "working in" the bath for a minimum of eight hours is stressed although there is no practical upper limit as the bath may be used continuously thereafter. The example of the deposition of a composite coating of chromium and zirconium diboride onto graphite is described. (UK)

19271 METHODS FOR PREPARING REPLICAS OF SLIP BANDS PRESHADOWED WITH URANIUM OXIDE. Ahearn, J. S. Jr.; Mitchell, J. W. (Univ. of Virginia, Charlottesville). Rev. Sci. Instrum.; 42: 94-8(Jan 1971).

Three reliable methods are described for preparing uranium oxide preshadowed replicas of the surfaces of deformed single crystals of copper alloys. Difficulties experienced in detaching direct carbon replicas from the surfaces of these alloys have been overcome by the use of a parting layer for low resolution and of a chemical treatment for high resolution work. The fine linear source of uranium oxide produces a sharply defined shadowing deposit of high density and low granularity. This deposit is backed by a film of silver or silicon monoxide for high resolution work with the optical microscope and by a carbon film for work with the electron microscope. The advantages of precompared with postshadowing with uranium oxide for quantitative work on slip bands have been established. The methods are simple and convenient and allow high resolution to be achieved in replica microscopy. (auth)

Properties Evaluations

Refer also to abstracts 18416, 18551, 18613, 18624, 19190, 19226, and 19868.

19272 (AI-AEC-12984) HELIUM INJECTION AS A TECHNIQUE FOR STUDYING RARE GAS BEHAVIOR IN CARBIDE FUEL. Ervin, Guy Jr. (Atomics International, Canoga Park, Calif.). 29 Jan 1971. Contract AT(04-3)-824. 27p. Dep. NTIS.

The method of cyclotron injection of helium into fuel and the subsequent observation of the migration of bubbles during annealing was explored as a means of obtaining basic information about fission gas behavior in ceramic nuclear fuel. As a beginning, the method was applied to uranium carbide containing a dispersion of small tungsten particles. Attachment of bubbles to particles was observed by surface replica electron microscopy. Surface replica observation also indicated that there was substantial bubble migration during high temperature annealing. However, it was difficult to obtain quantitative information by the surface replica technique, and it is likely that transmission electron microscopy would be far superior, as was demonstrated in earlier work on tungsten-containing uranium carbide. (auth)

19273 (BNWL-SA-3579) PROPERTIES OF MOLTEN CERAMICS. Bates, J. L.; McNeilly, C. E.; Rasmussen, J. J. (Battelle-Northwest, Richland, Wash. Pacific Northwest Lab.). [1970]. 18p. (CONF-701206-1). Dep. NTIS.

From Conference on Ceramics in Severe Environments, Raleigh, N. C.

Techniques were developed for measuring the volume change on melting, density, melting point, expansivity, surface tension, viscosity, adiabatic compressibility, and thermal diffusivity of molten ceramic materials to 3000°C. Many of these techniques are extensions of general methods used to measure liquids at lower temperatures, with modifications to reflect the severe conditions imposed by the high temperatures. Several of these techniques used to study molten ceramics are described. The associated experimental difficulties and representative results are also presented. Because of space limitations, no attempt was made to present comprehensive review of the potential high temperature, experimental methods or an analysis of the results. (J.R.D.)

19274 CHANGES IN RESIDUAL CARBON CONTENT IN UO$_2$ PELLETS DURING DECARBONIZATION AND INITIAL PHASES OF SINTERING. Landspersky, Hanus; Bezucha, Jaromir (Inst. of Nuclear Research, Rez, Czech.). Jad. Energ.; 16: 408-13 (Dec 1970).

Decarbonization of UO$_2$ pellets compacted with 2% of binders at temperatures between 500 and 800°C was studied at different heating rates, followed by sintering at temperatures up to 1600°C in hydrogen. During the decarbonization, the content of carbon decreased, but at 800°C the residual carbon content still exceeded several times the limit of 100 ppM. At temperatures above 1000°C, the decarbonization continued and at 1200 to 1400°C the residual carbon content reached ~50 ppM. (auth)

19275 RESEARCH AND DEVELOPMENT OF FUEL FOR LIQUID METAL FAST BREEDER REACTOR. Matsumoto, Kenichi (Power Reactor and Nuclear Fuel Development Corp., Tokai, Japan); Muto, Tadashi; Kobayashi, Shigeo. Genshiryoku Kogyo; 16: No. 5, 82-7(Mar 1970). (In Japanese).

Mixed uranium and plutonium oxide fuel is mainly used in Na-cooled fast breeder reactors. Fission products in the irradiated fuel are gaseous, volatile, oxide-, and metallic-form; their behavior depends largely on these particular forms. The temperatures of the fuel under normal reactor operation are about 2500°C at the center and 1000°C at the surface. Therefore, the structure is subjected to changes under a high-temperature gradient. Swelling of the fuel is closely connected with temperature, burnup, fission product gas release, fuel composition, and cladding. (Japan)

19276 TRIAL FABRICATION OF AN Na-BONDING FUEL ROD, AND ITS OUT-OF-PILE TEST. Nishikawa, Kazuyuki; Manabe, Genroku (Furukawa Electric Co. Ltd., Tokyo). FAPIG (Tokyo); No. 56, 281-6(Mar 1970). (In Japanese).

The Na-bonded fuel rod is promising for future fast reactors. However, one problem is the compatibility between cladding and fuel rods. To study this, trial fuel rods were fabricated; the fuel rods were hypostoichiometric, stoichiometric, and hyperstoichiometric UC, and the cladding materials were 316(L) and 347 stainless steel. The test temperature was 700°C in argon atmosphere, with heating times of 500, 1000, and 1500 hours. Observations on the carbon transfer from pellet to cladding were made by microscope, carbon analysis, x-ray analysis, and mechanical tests. In the hyperstoichiometric fuel rods the carbon transfer to cladding was marked, whereas it was little in the other two. In the former case, the dissolution of carbon into the Na was the rate determining factor. Carbon in the hypo- and stoichiometric rods was little changed by heating; it increased in stainless steel. The carbon content in cladding tended to decrease toward the outside. Brittleness occurred in the stainless steel with carbon precipitation. (Japan)

19277 EFFECTS OF ALUMINUM OXIDES ON THE ACTIVATION ENERGY OF CREEP OF NIOBIUM. Osipov, K. A.; Miroshkina, E. M. Izv. Akad. Nauk SSSR, Metal.; No. 4, 111-14(Jul-Aug 1970). (In Russian).

Cast Nb alloys containing 1.62, 1.90, and 2.90 wt % Al$_2$O$_3$ were studied in creep. The oxide was distributed mainly at grain boundaries. The average particle size of oxides on neutral surfaces of the alloys at 450°C was 0.1 to 10 microns. The strengthening effects of the oxide were demonstrated by results of hot hardness tests and creep tests at high temperature. Results of creep tests of Nb containing 1.62 to 2.90 wt % Al$_2$O$_3$ at 850 to 1450°C at 3 to 10.6 kg^2 are included. Creep rates are greatly reduced by the addition of Al$_2$O$_3$. Activation energy at 1200 to 1450°C at tensions of 3 to 9.5 kg/mm^2 averages about 56 kcal/mole for these dispersions. (tr-auth)

19278 NEW METHOD FOR THE STUDY OF UO$_2$ IN A TEMPERATURE GRADIENT. Freund, D.; Sari, C. (Kernforschungszentrum, Karlsruhe, Ger.). Atomwirt., Atomtech.; 15: 573-4(Dec 1970). (In German).

Direct electric heating of UO$_2$ rods permits the study of structural changes through the temperature gradient, such as grain growth, pore migration, formation of stem crystals, and the stationary distribution of fission products. These changes correspond to those observed in reactor fuel elements. The method and results are described. Close to the central channel, Mo and Ru form rings. The Mo and Ru particles grow during changes in the temperature gradient. (H.B.G.)

19279 EQUIPMENT FOR MEASUREMENT OF ELASTICITY MODULUS FOR HOT CELL APPLICATIONS. Sorrentino, Francois (CEN, Grenoble France). Rev. Sci. Instrum.; 42: 191-2(Feb 1971).

An equipment was developed for in-cell determination of Young's modulus of irradiated materials in a continuous manner in the 20 to 1000°C temperature range. Longitudinal vibrations are electrostatically induced and maintained in the sample at its resonance frequency. The equipment was used to check U–C nuclear fuel samples and alloy specimens. (auth)

19280 EXPERIMENTAL DETERMINATION OF THE EMISSIVITY, ELECTRICAL RESISTIVITY, AND THERMAL CONDUCTIVITY OF PYROLYTIC CARBON. Petrov, V. A.; Petrova, I. I.; Chekhovskoi, V. Ya.; Sheindlin, A. E. (Inst. for High Temperatures, Moscow). High Temp. - High Pressures; 2: 155-60(1970).

The total hemispherical emissivity and the spectral emissivity at an effective wavelength $\lambda = 0.65\ \mu m$ have been measured on pyrolytic carbon samples with the radiant surface parallel to the deposition surface in the temperature range 1200 to 2500°K, and with the radiant surface perpendicular to the deposition surface in the temperature range 1100 to 1900°K. The thermal conductivity was measured on the same samples in the direction perpendicular to the deposition surface in the temperature range 1200 to 2500°K, and the electrical resistivity in both directions in the temperature range 300 to 2500°K. (auth) (UK)

19281 EFFECT OF HEAT TREATMENT ON THE ELECTRICAL RESISTIVITY AND THERMAL CONDUCTIVITY OF PYROLYTIC CARBON. Petrov, V. A.; Petrova, I. I.; Chekhovskoi, V. Ya.; Sheindlin, A. E. (Inst. for High Temperatures, Moscow). High Temp. - High Pressures; 2: 161-5(1970).

Measurements are reported of the electrical resistivity and thermal conductivity of pyrolytic carbon specimens subjected to heat treatment (1) at 2873°K for 3 hr, (2) at 3173°K for 2 hr, and (3) at 3373°K for 1 hr. The thermal conductivity was measured in the direction normal to the deposition surface and found to decrease with temperature up to 1600 to 1800°K and then to rise. This effect is attributed to the presence of microcracks. The electrical resistivity was measured in the directions normal and parallel to the deposition surface. (auth) (UK)

19282 VARIATIONAL BOUNDS OF THE ELASTIC MODULI OF TWO-PHASE MATERIALS. Yeh, Robert H. T. (State Univ. of New York, Buffalo). J. Appl. Phys.; 42: 1101-3(1 Mar 1971).

Previously derived variational bounds [R. H. T. Yeh, J. Appl. Phys. 41, 3353 (1970)] for Young's modulus are compared with experimental results on WC–Co alloy. The agreement is satisfactory. Numerical examples are given to illustrate the usefulness of these bounds for fiber-reinforced materials. (auth)

XUM

19283 RELATIONSHIP BETWEEN ELECTRIC RESISTANCE OF ZIRCONIA CERAMICS AND POROSITY. Rutman, D. S.; Maurin, A. F.; Taksis, G. A.; Toropov, Yu. S. Refractories (USSR) (Engl. Transl.); No. 6, 371-4(Jun 1970).
Translated from Ogneupory, No. 6, 36-9(Jun 1970).

The effects of the porosity of specimens of zirconium dioxide as a function of the electric resistance were determined at various temperatures. Zirconium dioxide containing 99.94% ZrO_2, and chemical purity grade calcium oxide were used. After stabilizing calcination of the mixtures of oxides in the ratio 0.87 ZrO_2 and 0.13 CaO at 1750°C, the phase composition according to the results of x-ray analysis consists of a cubic solid solution with a lattice parameter of a = 5.122 Å. The stabilized zirconia was ground to obtain particles <15 μ. It was treated with 6% by weight of a 10% aqueous solution of polyvinyl alcohol and ground through a screen of 10,000 apertures/cm^2 with naphthalene powder in amounts required to obtain the required porosity. The specimens in the form of cylinders were pressed at 1000 kg/cm^2. The height of the fired (1670°C) specimens was 0.9 to 1.0 cm, the cross-sectional area was 0.9 to 1.0 cm^2, and the true porosity varied from 5 to 48%. On the basis of the results of the investigations it is possible to assume a relationship between the electric resistance and the porosity for zirconia ceramic specimens, if the discrepancy in the results recalculated for dense specimens does not exceed the accuracy of the experimental determinations of the resistivity. (J.R.D.)

Structure and Phase Studies

19284 INTERACTION OF SAMARIUM AND STRONTIUM OXIDES. Lopato, L. M.; Kherak, R.; Shevchenko, O. V.; Kushchevskii, A. E. (Inst. of Problems in Material Studies, Kiev). Dopov. Akad. Nauk Ukr. RSR, Ser. B; No. 11, 1007-9(Nov 1970). (In Ukrainian).

On the basis of data of high-temperature x-ray and differential thermal analyses, a part of the phase diagram was plotted in a temperature range of 1300 to 2000°C for the system Sm_2O_3–SrO with the content of strontium oxide up to 25 mole %. Solid solutions on the Sm_2O_2 A-form base were established to form in a wide range. The temperature boundaries for the mentioned solid solutions were also determined. Similar results were obtained in the systems Gd_2O_3–SrO, Dy_2O_3–SrO and in the corresponding systems with CaO. (auth)

19285 STUDIES OF THE EUROPIUM–OXYGEN–FLUORINE AND SAMARIUM–OXYGEN–FLUORINE SYSTEMS. Bedford, R. G.; Catalano, E. (Univ. of California, Livermore). J. Solid State Chem.; 2: 585-92(Dec 1970).

A portion of the ternary system Eu–Eu_2O_3–EuF_3 has been investigated by equilibrating EuO–EuF_3 and EuO–EuF_2 mixtures at 1500°C and examining the products with a polarizing microscope and by x-ray diffraction. The composition at the liquid–solid boundary was not measured directly, but has been estimated. A phase diagram is presented for that part of the system studied. No ternary compounds are formed with europium in an oxidation state lower than +3 in samples cooled from 1500°C. Several compositions of the Eu_2O_3–EuF_3 and Sm_2O_3–SmF_3 binary systems were examined using differential thermal analysis and x-ray powder diffraction. In these systems, at least one intermediate phase (and probably two or more) in addition to LnOF is stable. These additional phases all lie on the fluoride side of LnOF. At temperatures above 600°C, solid solutions extend from approximately $LnO_{0.8}F_{1.4}$ to $LnO_{0.6}F_{1.8}$. (auth)

19286 MIXED RARE EARTH SULFIDES WITH THE GENERAL FORMULA $LL'S_3$ [L = La, Ce, Pr, Nd, AND L' = LANTHANIDES AND Y]. Vovan, Tien; Carre, Daniel; Khodadad, Parviz (Paris Univ.). Compt. Rend., Ser. C.; 271: 1571-3(21 Dec 1970). (In French).

The mixed rare earth sulfides with the general formula $LL'S_3$ (L = La, Ce, Pr, Nd and L' = lanthanides and Y) were prepared at temperatures of 1450 and 1000°C. They form solid solutions, cubic solutions of Th_3P_4 type at high temperatures and orthorhombic solutions of type $Gd_2S_3\alpha$ at low temperatures. Three new phases were observed at low temperature: a monoclinic phase, $TmCeS_3$ of the type ($P2_1$ or $P2_{1/m}$); an orthorhombic phase, $YbNdS_3$ of the type ($B22_12$); another orthorhombic phase of the $YScS_3$ type. The crystal parameters are given and structure aspects of these various phases discussed. (auth) (France)

Radiation Effects

Refer also to abstracts 19769, 20735, 20736, 20747, and 20836.

19287 (AECL–3690) OXYGEN: METAL RATIO EFFECTS IN $(U,Pu)O_2$ FUELS. Jeffs, Alan T. (Atomic Energy of Canada Ltd., Chalk River (Ontario). Chalk River Nuclear Labs.). Aug 1970. 18p. (CONF-701001-16). Dep. NTIS (U. S. Sales Only).
From 4th International Conference on Plutonium and Other Actinides, Santa Fe, N. Mex.

A test is described in which six $(U,Pu)O_2$ fuel elements were irradiated with oxygen-metal ratios in the range 1.99 to 2.04. Post-irradiation examination results are presented and discussed in terms of the effects of temperature gradient on oxygen redistribution in the fuel and the effects of oxygen-metal ratio on fission product gas release and structural alterations. The major effect noted was on gas release which was an order of magnitude greater for $(U,Pu)O_{2.04}$ than for $(U,Pu)O_{2.00}$. Oxygen was found to move up the thermal gradient in hyperstoichiometric specimens. (auth)

19288 (ORNL–4629, pp 82-98) IRRADIATION OF HTGR FUELS. (Oak Ridge National Lab., Tenn.).
In Status and progress report for thorium fuel cycle development for January 1, 1969–March 31, 1970.

Capsule design and other preparations were made for accelerated testing of coated-particle fuels in the Engineering Test Reactor. Recycle Test Elements, prototypical of full-scale HTGR fuel elements, are being fueled for irradiation in the Peach Bottom Reactor. Several types of coated ThO_2 and UO_2 particles in various combinations will be irradiated to demonstrate performance of products produced by processes proposed for use in TURF, and to provide fuel for reprocessing studies. Good integrity to 6×10^{21} neutrons/cm^2 was shown by bonded beds of coated particles prepared with a pitch binder loaded with 40% graphite or a combination of 29% graphite and 29% carbon black. Blended beds of loose particles shrank during irradiation more than expected from coating densification. (auth)

19289 (WHAN-FR–24) IRRADIATION OF BORON CARBIDE PELLETS AND POWDERS IN HANFORD THERMAL REACTORS. Pitner, A. L; Russcher, G. E. (WADCO Corp., Richland, Wash.). Dec 1970. Contract AT(45-1)-2170. 40p. Dep. NTIS.

Natural boron carbide pellets and powders were irradiated in Hanford thermal production reactors at 500 to 1200°F to a maximum average ^{10}B burnup of 18% ($\sim 26 \times 10^{20}$ captures/cc). Sample forms were 65, 80, and 99% TD pellets and 60 and 80% TD powders. Calculations of exposure conditions for these specimens have shown significant differences in their ^{10}B depletion profiles. The high density materials exhibit greater peak-to-average burnup ratios due to self shielding. The boron burnup analysis has been substantiated by observed differences in microstructures of the irradiated pellets. Metallographic examination disclosed that 99% TD pellets suffered severe damage near the surface but appeared unreacted in the inner core. The 65 and 80% TD pellets experienced radial cracking with no apparent "skin" burnup effect. Powders exhibited the highest gas release rates, increasing from ~10% at 500°F to ~30% at 850°F. Intermediate density pellets (65 and 80% TD) released less gas than the powders. The 99% TD pellets released less gas than any of the other samples ranging from about 5% at 500°F to ~20% at 1200°F. Gas release in the pellets increased rapidly as the irradiation temperature exceeds 1000°F. An analysis of exposure conditions for the specimens tested and those irradiated in other thermal reactors indicated that spectral differences and sample geometry must be considered when evaluating the irradiation behavior of boron carbide. (auth)

19290 (WHAN-SA–15) FISSION GAS BUBBLE PRECIPITATION AND GROWTH IN PuO_2–UO_2 UNDER IRRADIATION. Bullington, D. C.; Leggett, R. D. (WADCO Corp., Richland, Wash.). 13 Jul 1970. 9p. (CONF-701001–14). Dep. NTIS.
From 4th International Conference on Plutonium and Other Actinides, Santa Fe, N. Mex.

The intergranular pore density was determined at two axial positions in a mixed oxide fuel pin irradiated in EBR-II to a peak burnup of 1 percent of the heavy atoms. The pore size was approximately that calculated, however, no dependence of pore size distribution with local temperature or temperature gradient was found. The volumetric average intergranular pore volume was found to be greater in the fuel operating at the lowest burnup rate. The study indicated that unetched fuel is more suitable for measurement of spacial pore distributions than etched samples. (auth)

19291 IRRADIATION TESTS WITH VIBROCOMPACTED $(Th/U)O_2$ PARTICLES. Herren, M. (Kernforschungsanlage, Juelich, Ger.); Neeb, K. H.; Peehs, M.; Reichardt, K.; Thiele, B. Atomkernenergie; 17: 133-6(Mar 1971). (In German).

In five irradiation tests, 10 fuel rods were irradiated to 10,000 MWd/t (U + Th). Fuel rods show all structures between original microspheres and highly densified material. Normally 30 to 40%

XUM

of fission gases were dissolved during operation. Chemical reactions between cladding and fuel could not be detected in selected fuel rods. (auth)

Plastics and Other Materials

Refer also to abstracts 18425, 18430, 18435, 18439, 18441, 18563, 18598, and 19862.

19292 (BNL-50275) CONCRETE-POLYMER MATERIALS. Third Topical Report. Dikeou, J. T.; Cowan, W. C. (Bureau of Reclamation, Denver, Colo.); Steinberg, M.; (and others) (Brookhaven National Lab., Upton, N. Y.). Jan 1971. 111p. (REC-ERC-71-6). Dep. NTIS.

Research and development of concrete-polymer composite materials for use as new and improved materials of construction are described. The main tasks of the program include (1) evaluation and selection of monomers for incorporation in concrete-polymer composites, (2) development of process techniques for the preparation of the composites, (3) testing and measurement of pertinent physical, mechanical, and chemical properties, (4) development of applications, including preparation and testing of full-scale specimens, and (5) development of preliminary cost estimates for concrete-polymer products. Studies are being made at laboratories on the incorporation of monomers in premixed materials. Two materials, PCC and PC are being studied. The PCC consists of a monomer added to a water portland cement aggregate premix which is subsequently polymerized in place. PC consists of an aggregate bound with a monomer which is premixed and subsequently polymerized. Studies to determine the fundamental structure of the concrete-polymer composites are also underway. The studies include microscopic and petrographic investigations and the formulation of theories and mathematical models for predicting the properties of the composite. (J.R.D.)

19293 (UCRL-50952) THEORY IDENTIFICATION FOR MECHANICAL BEHAVIOR OF POLYSTYRENE BEAD FOAMS. Latter, G.; Dong, R.; St. Lawrence, W. (California Univ., Livermore. Lawrence Radiation Lab.). 13 Oct 1970. 18p. Dep. NTIS.

A series of tension-compression tests with variable test rates and temperatures was conducted on SD 505 polystyrene bead foam of 0.05 and 0.1 g/cm^3. Descriptions are given of the test technique and specimens. A discussion is presented of the applicability of the data for design use and how it might be employed. (auth)

19294 IMPROVEMENTS IN MANUFACTURING SUPPLE SHEETS OF SOUND INSULATING AND RADIATION SHIELDING MATERIALS. (to Etablissements Lemer et Cie SA). French Patent 1,586,185. 5 Jan 1970. Filed 5 Sep 1968. (In French).

Processes for the manufacture of elastic sheets of an elastomer mixed with lead powder are described. The sheets may be used by themselves or coated on elastic or rigid supports. Improvements made consist of providing the machine with the usual raw material feed (wet plastisol powder and filtering process), supplying the means of controlling the thickness of the final product and the flow speed. The distribution pump operates without excessive vibration. The equipment produces a continuous sheet either on a slab or bed or on a moving belt. The machine is also provided with a means of heating and polymerizing the sheet and cutting into the required dimensions. (France)

19295 STUDIES ON THE PROPERTIES OF HEAT RESISTING CONCRETE OF THE SERPENTINE AGGREGATE FOR NEUTRON SHIELDING. Iso, Yasuhiko (Japan Atomic Energy Research Inst., Tokyo); Miyasaka, Shunichi. Semento Konkurito; No. 276, 18-25(Feb 1970). (In Japanese).

The properties of the crushed serpentine aggregates and its concretes for neutron shielding were investigated, and after the geological and chemical surveys, the availability of the serpentines, which were obtained in Saitama, Japan was proved. In addition to the ordinary tests for aggregates and concrete, the specific heat, the coefficient of thermal expansion, and the thermal conductivity of the concretes were determined. In order to study the heat resistance of the concretes, the high-temperature compressive strength was tested under the three different conditions of heating. As the behavior of concrete under thermal cycling was also very important, the thermal growth, the density change, and the dynamic elastic modulus were measured. The serpentine aggregates used in these tests had sufficient availability for neutron shielding concretes. By adding river sand to the concrete, the workability was improved, and the strength and the thermal properties became comparable with river gravel concrete. In the course of heating the serpentine concretes, the strength decreased by 100°C but after that it increased with an increase of temperature. After exceeding 500°C the strength decreased. In the scope of these thermal cycling tests, no thermal growth and other extraordinary phenomena were found; however, in order to guarantee the availability, long-term thermal cycling studies are required. (Japan)

19296 CHANGE OF CONCRETE AGGREGATE PROPERTIES UNDER NEUTRON IRRADIATION. Dubrovskii, V. B.; Pergamenshchik, B. K.; Korenevskii, V. V.; Perevalov, V. S. Beton Zhelezobeton; No. 9, 25-7(Sep 1970). (In Russian).

Results are given of studies of neutron irradiation effects on certain rocks (granite, sandstone, basalt, and limestone) and ore impregnations (chromite and hematite) used for production of concrete shielding. Data were obtained on the relation between the dose effects and expansion of the materials. (tr-auth)

19297 DIRECTION OF THE DEVELOPMENT ON REACTOR MATERIALS. PRESTRESSED CONCRETE FOR THE REACTOR PRESSURE VESSEL. Fujii, Shoichi (Shibaura Inst. of Tech., Tokyo). Genshiryoku Kogyo; 16: No. 4, 79-81(Apr 1970). (In Japanese).

The prestressed concrete pressure vessel (PCPV) is widely used in gas-cooled reactors and also in high-temperature gas-cooled reactors. By prestressing the concrete, an increase in size of reactor containment vessels has become possible. The nature of a prestressed concrete pressure vessel is described and the integral type of nuclear reactor made possible by PCPV, and the advantages of a PCPV lined with steel are discussed. The temperature gradient in the concrete is a problem; for this, either thermal insulation or forced cooling is used. The relaxation and rusting of prestressing wires are also problems. Aggregates of small size concretes are used, which are otherwise similar to ordinary concretes. Stress design and model tests for PCPV are also described. (Japan)

19298 RADIATION PROCESSED WOOD-PLASTIC MATERIALS. Narayanamurti, D.; Jayaraman, M. T.; Thacker, R.; Anantanarayanan, S. (Indian Plywood Industries Research Association, Bangalore, India. Bhabha Atomic Research Centre, Bombay). Wood Sci. Technol.; 4: 226-36(1970).

Specimens of Abies sp. (fir), Pinus longifolia (chir), Vateria indica (vellapine), Dichopsis elliptica (pali) and Mangifera indica (mango) were impregnated with monomers of styrene and methylmethacrylate and irradiated under different conditions. The treated specimens were tested as to their crushing strength, their bending strength and their water absorption. The results first indicate an increase in density due to impregnation. A reduction in moisture absorption and volumetric swelling as compared with untreated controls and an increase in crushing strength were observed. The properties varied due to a nonuniform penetration of the polymer. Further experiments on the resistance against degradation by fungi were carried out and respective results are listed and discussed. (auth)

19299 TREATMENTS OF SOUTHERN PINE WITH VINYL CHLORIDE AND METHYL METHACRYLATE FOR RADIATION-PRODUCED WOOD-PLASTIC COMBINATIONS. Calleton, R. L.; Choong, E. T.; McIlhenny, R. C. (Louisiana State Univ., Baton Rouge). Wood Sci. Technol.; 4: 216-25(1970).

A method was developed for the impregnation of liquid vinyl chloride monomer into wood. Wood-plastic combinations (WPC) prepared from polymethyl methacrylate (PMMA), polyvinyl chloride (PVC), and polyvinyl chloride plasticized with dioctylthalate (DOP + PVC) were found to offer improvements in selected physical properties of wood. The initial anti-swell efficiency (ASE) values of PMMA WPC and DOP + PVC WPC are very high, averaging approximately 87 and 82% respectively after 5 hours of soaking; whereas PVC WPC attained an average of only 53%. After prolonged soaking, the ASE values of all treated wood decreased considerably, indicating no permanent stability was achieved. In hardness, the PMMA WPC attained an average springwood-summerwood rating of 76, the DOP + PVC WPC and the PVC WPC a rating of 69 and 63, respectively; whereas the untreated wood achieved a rating of only 53. (auth)

19300 COMPARATIVE STUDY OF THE EFFECT OF IRRADIATION WITH γ-RAYS AND ACCELERATED ELECTRONS ON THE STRUCTURE AND PROPERTIES OF CIS-BUTADIENE RUBBER. Sobolev, V. S.; Klauzen, N. A.; Zaides, A. L. Kolloid. Zh.; 32: 752-6(Sep-Oct 1970). (In Russian).

The structure and physical and mechanical properties of cis-polybutadiene irradiated with accelerated electrons of 10-MeV energy and γ rays in air and under vacuum were studied. Comparison of the structure and properties of vulcanizates obtained by γ irradiation and with accelerated electrons in air using doses of 2 to 25 MRad has shown that under these conditions the dose rate and type of irradiation have no effect on the structure and properties of cis-polybutadiene. (auth)

PHYSICS (GENERAL)

Astrophysics and Cosmology

Cosmic Ray Exposure Ages

Refer also to abstract 18370.

19301 GAMMA EMITTERS AND EXPOSURE AGE OF THE BOVEDY METEORITE OF THE FALL OF APRIL 25, 1969. Tobailem, J.; Nordemann, D.; Grjebine, T. (Centre National de la Recherche Scientifique, Gif-sur-Yvette, France). Nature (London). Phys. Sci.; 229: 118-19(25 Jan 1971).

The ^{54}Mn, ^{22}Na, ^{60}Co, ^{26}Al, and ^{40}K activities in a 230-g piece of the Bovedy Meteorite were measured by nondestructive low-background γ-ray spectrometry. The results are tabulated and discussed. A low value as compared with other published values of exposure age (0.9 ± 0.3 my) is calculated which suggests a rather complicated history of the original meteoroid. (UK)

19302 STUDY OF THE DISTRIBUTION OF Sc, Ce, AND Eu BETWEEN THE VARIOUS PHASES OF METEORITE MATTER. Lavrukhina, A. K.; Kolesov, G. M.; Kalicheva, I. S.; Akol'zina, L. D. Meteoritika; No. 28, 95-101(1968). (In Russian).

The Sc, Ce, and Eu content in a number of meteorites of different chemical composition was determined by neutron activation. The distribution was consistent with the lithophile character of these elements. However, their content in the metal phase of the Kunashak chondrite was higher than in the nickel–iron meteorites Arus and Sikhote–Alin. The Sc content was about the same in the 11 Sikhote–Alin samples, 1×10^{-9} g per g, which evidently indicates that there is no depth effect in the distribution of cosmogenic Sc. (Geophys. Abstr.)

19303 MERCURY IN METEORITES. Ozerova, N. A.; Aidin'yan, N. Kh.; Kvasha, L. G.; Shikina, N. D. (Inst. of Ore Deposit Geology, Petrography, Mineralogy and Geochemistry, Moscow). Dokl. Akad. Nauk SSSR; 194: 1038-41(11 Oct 1970). (In Russian).

Mercury was determined by a chemical method on 1-gram samples from the meteor collection of the Academy of Sciences. The analytical sensitivity was 1×10^{-6}%. The mercury content was determined in iron and iron-ore meteors. About 100 determinations were carried out, representing about one-half of all the known, analytical values for mercury in meteor samples. The results show that the mercury content was noticeably higher in the meteors as compared with the mercury content of magnetic ores of the Earth's crust. About 60% of the meteor samples contained significantly greater than 1×10^{-5}% mercury, while the Clark number is 7.7×10^{-6}%. The mercury content varied considerably even within a single sample. Iron meteorites showed the lowest mercury content. With an iron content of 8 to 70%, about 60% had a mercury content greater than 1×10^{-5}%, while 80 to 90% of the samples with an iron content less than 8% showed a mercury content greater than 1×10^{-5}%. This type of data can be useful in estimating the composition of the Earth's core. (TTT)

Stars

19304 CALIBRATION OF THE WILSON–BAPPU EFFECT ON THE SUN. Pasachoff, Jay M. (Carnegie Institution of Washington, D. C.). Astrophys. J.; 164: 385-6(1 Mar 1971).

A quantitative assessment of the contribution of very asymmetric spectral profiles from small areas on the solar disk to the mean K-line profile for the Sun is now available. Implications for the Wilson–Bappu effect are indicated. (auth)

19305 LIMB DARKENING FOR YELLOW SUPERGIANTS. Parsons, Sidney B. (Case Western Reserve Univ., Cleveland). Astrophys. J.; 164: 355-8(1 Mar 1971).

Limb-darkening data computed from models in a previously published grid with $T_e = 5400$ to 6600° and $\log g = 1.2$ to 2.4 are presented and discussed. (auth)

19306 SECOND-ORDER PULSATIONS IN POLYTROPES. Simon, Norman R. (Goddard Space Flight Center, New York). Astrophys. J.; 164: 331-40(1 Mar 1971).

A theory due to Eddington is employed to calculate second-order corrections to the usual linear, quasi-adiabatic pulsational amplitudes. Such corrections are necessary in order to evaluate the pulsational stability of stars in thermal imbalance ($dS_0/dt \neq 0$). The second-order quantities are calculated, and their properties discussed, for a wide variety of polytropic models. Subsequently, a number of these models are tested for pulsational stability, and the conclusions drawn in an earlier, more preliminary work are re-evaluated on the basis of the results. In particular, it is found that stars in pre-main-sequence contraction are probably stable against pulsations energized via thermal imbalance. (auth)

19307 ADVANCED EVOLUTION OF POPULATION II STARS. I. RED GIANTS AND THE HELIUM FLASH. Demarque, Pierre; Mengel, John G. (Yale Univ. Observatory, New Haven). Astrophys. J.; 164: 317-30(1 Mar 1971).

Models for red-giant stars of Population II were constructed with emphasis on the determination of the critical mass of the helium core at the onset of the helium flash and on the subsequent development of the flash and core-cooling phase which precedes horizontal-branch evolution. Stars with masses 0.85, 0.60, and 0.502 $M_\odot$ and compositions $(X, Z) = (0.75, 0.001)$ and $(0.75, 0.0001)$ were considered. The effects of including relativistic degeneracy were investigated, together with the effects of the inclusion of neutrino losses due to weak-interaction processes. No mixing between the helium core and the hydrogen-rich envelope was found in any of the models considered. The dependence of the mass of the helium core on total mass and on Z was determined and found to be very weak in both cases. Finally, a tentative explanation for Barnard 29 is suggested. (auth)

19308 MEAN SURFACE FIELDS OF MAGNETIC STARS. Preston, George W. (Carnegie Institution of Washington, D. C.). Astrophys. J.; 164: 309-15(1 Mar 1971).

Estimates of mean surface fields H_s for twenty-eight Ap stars of the Sr–Cr–Eu class with $v \sin i \leq 10$ km sec^{-1} were obtained from measurements of magnetically resolved or broadened absorption lines. The fields so obtained do not appear to be correlated with UBV color indices, Eu II line strengths, or rotational velocities inferred from periods for this group of stars. The frequency distribution of H_s is characterized by a maximum between 2 and 3 kilogauss and a tail that extends beyond 10 kilogauss. Indirect arguments based on effective magnetic fields suggest that mean surface fields may increase systematically with rotational velocity, but observational bias and certain selection effects render this conclusion suspect. (auth)

19309 HIGH-FREQUENCY STELLAR OSCILLATIONS. V. POWER SPECTRA FOR THE CENTRAL STARS OF PLANETARY NEBULAE. Lasker, Barry M. (Cerro Tololo Inter-American Observatory, La Serena, Chile); Hesser, James E. Astrophys. J.; 164: 303-8(1 Mar 1971).

Photoelectric time-series data were used to calculate power spectra for the central stars of sixteen planetary nebulae. No periodic activity was evident in the range from 4 to ~700 seconds. The continua of the power spectra were also examined; no clear differences from those for white dwarfs were evident. (auth)

19310 DETAILED COMPARISON OF THE SPECTRA OF A PLANETARY NUCLEUS AND A WOLF–RAYET STAR. Smith, Lindsey F. (Goddard Space Flight Center, Greenbelt, Md.); Aller, Lawrence H. Astrophys. J.; 164: 275-301(1 Mar 1971).

Comparison of the spectra of BD + 30°3639 and HD 164270 shows that they differ in the width of the lines by a factor of 1.6, and in the strengths of some lines by a factor between 1.4 and 3.3. The similarity of the spectra and most of the differences between them are explicable if the material in the atmospheres of the stars is being radially accelerated (as suggested by Beals) and if HD 164270 is 10 times the mass and 3.3 times the size of BD + 30°3639. It follows that the two objects are indeed of very different population type and that a Wolf–Rayet spectrum can be generated by stars of quite different mass and evolutionary stage. It is shown that the correlation between line width and excitation potential is smooth and unique for each spectrum, thus removing the last of the objections to Beals's model of a radial expanding stratified atmosphere. It is found that violet absorption edges occur if and only if the excitation potential of the lower level is less than a critical value which depends on the ion but which is always greater than or equal to the ionization potential of the previous stage of ionization of the atom concerned; with the provision that absorption lines will be unobservable if the line is weak or blended. (auth)

19311 MINIMUM-LIGHT SPECTRA OF MIRA VARIABLES WITH VERY LONG PERIODS. Wyckoff, Susan; Wehinger, Peter (Univ. of Michigan, Ann Arbor). Astrophys. J.; 164: 383-4(1 Mar 1971).

Low-dispersion near-infrared spectra of seven very cool M-type long-period variables obtained near minimum light are classified and discussed. It is found that none of the spectra exhibits near-infrared VO bands as strong as those observed in the spectrum of R Cas at minimum light. (auth)

19312 MAGNETOHYDRODYNAMIC OSCILLATIONS OF NEUTRON STARS. Hide, R. Nature (London), Phys. Sci.; 229: 114-15(25 Jan 1971).

As a result of a study of free magnetohydrodynamic oscillations in neutron stars, it is tentatively concluded that magnetohydrodynamic oscillations of the interior of a neutron star will be strongly affected by Coriolis forces due to the rotation of the star. If these oscillations can be excited then the magnetic-field pattern outside the star will be subject to oscillations with typical periods (as measured by an observer who rotates with the star) ranging from half the rotation period of the star, π/Ωs (or a somewhat longer period if eddy currents induced in the solid crust and atmosphere produce a "short-period cutoff") to $16\pi^2\Omega a^2\mu\rho/B^2$s $\sim 10^{6\pm4}$ times the rotation period. On the oblique rotator model of pulsars (NSA 23: 10365) these oscillations would manifest themselves as modulations of the main pulsar signals. (UK)

19313 EVIDENCE FOR A COLLAPSAR IN THE BINARY SYSTEM ϵ AUR. Cameron, A. G. W. (Yeshiva Univ., New York. Goddard Inst. for Space Studies, New York). Nature (London); 229: 178-80(15 Jan 1971).

It is suggested that the mysterious secondary component of ϵ Aur is probably not in a prestellar stage of evolution. It is more likely to be a "black hole"—a "collapsar"—formed by a stellar implosion. (auth) (UK)

19314 COLLAPSARS, INFRARED DISKS, AND INVISIBLE SECONDARIES OF MASSIVE BINARY SYSTEMS. Stothers, Richard (Goddard Inst. for Space Studies, New York). Nature (London); 229: 180-3(15 Jan 1971).

It is suggested that the supergiant primary of the eclipsing binary system ϵ Aur is probably a star of high mass burning helium in its core. Cameron's suggestion (Nature 229: 178 (1971)) that the invisible secondary is a massive "collapsar" surrounded by a cool disk of solid particles is thus given further support. A similar object with a disk may be in orbit around the supergiant 89 Her, which has a large infrared excess of unknown origin. The disk could be formed during the initial stage of collapse of the secondary. (auth) (UK)

19315 STUDY OF INTRINSIC POLARIZATION IN Be STARS. Bottemiller, Robert Leland. Columbus, Ohio; Ohio State Univ. (1970). 126p. University Microfilms Order No. 70-26,253.

Thesis.

Polarimetric observations of Be stars were obtained in order to investigate the possible existence of intrinsic polarization. Visual binary systems were observed with one member a Be star of high observed rotational velocity, assumed to maximize the probability of intrinsic polarization, and the other member with a low observed rotational velocity. The latter component, with little or no intrinsic polarization, provides a measure of any interstellar polarization arising along the line of sight from the stellar system to the observer. Since this fraction of the polarization affects the light of both pair members identically, the amount present in the companion's beam may be subtracted vectorially from the primary yielding the amount and position angle of the intrinsic polarization. (TSS) (Diss. Abstr. Int., B)

19316 ACCURACY OF SOME CURRENT OBJECTIVE PRISM STELLAR RADIAL VELOCITIES. Bartko, Frank Jr. Washington Univ. (1970). 380p. University Microfilms Order No. 70-26,668.

Thesis.

A radial-velocity study based on three high-quality plates obtained with the normal-field objective-prism instrument designed by Fehrenbach at the Haute-Provence Observatory is described. Kapetyn's Selected Area number 8 in Cassiopeia is obtained on these plates showing predominately B and A type stars encompassing a range of useable magnitudes from about 6 to 10. Two of the plates are 2 × 2 hour exposures and one a 2 × 4 minute exposure, all yielding a dispersion of about 75 Å/mm near Hγ. On the basis of the present analysis, several improvements and additional radial velocity programs are suggested that appear to be ideally suited for the objective-prism technique. Several appendices also describe an attempt to construct a normal-field prism, a comparator calibration, and a catalog of radial velocities with a brief discussion. (TSS) (Diss. Abstr. Int., B.)

19317 RECTIFICATION AND DETERMINATION OF THE PHOTO-METRIC ELEMENTS OF THE W URSAE MAJORIS TYPE ECLIPSING BINARY STARS AK HERCULIS, FG HYDRAE, DK CYGNI, AB ANDROMEDAE, RZ TAURI, V839 OPHIUCHI, AND V566 OPHIUCHI. Brown, Carl S. Washington, D. C.; Georgetown Univ. (1970). 395p. University Microfilms Order No. 70-26,663.

Thesis.

New rectifications and the determination of new photometric orbital and eclipse elements are presented for the following W Ursae Majoris-type eclipsing binary stars: AK Herculis 5, 9, FG Hydrae 9, DK Cygni 5, 7, 9, AB Andromedae 5, RZ Tauri 5, V839 Ophiuchi 5, 7, and V566 Ophiuchi 5, 7, 9. The numbers following the systems indicate the number of Fourier coefficients carried in each rectification and solution. Previously published individual yellow and blue observations are used in the analysis. (TSS) (Diss. Abstr. Int., B.)

19318 OBSERVED AND PREDICTED INTENSITIES OF ABSORPTION LINES IN MIRA VARIABLES. Morris, Synnoeve Voss. Columbus, Ohio; Ohio State Univ. (1970). 90p. University Microfilms Order No. 70-26,334.

Thesis.

The absorption spectra of the long-period variable stars of the Mira type exhibit many peculiar features that previously have only been discussed in a qualitative way. The purpose of this study was to obtain a quantitative description of the spectrum peculiarities and to see whether the measured peculiarities could be understood in terms of the atmospheric structure of these stars. Thirty-five high-dispersion spectra of M-type stars were employed for the study, both normal giant stars of type M and Mira stars of corresponding spectral types. (TSS) (Diss. Abstr. Int., B)

19319 COOL STAR SPECTRUM SYNTHESIS. Jackson, Bernard Vernon. Bloomington, Ind.; Indiana Univ. (1970). 143p. University Microfilms Order No. 70-26,930.

Thesis.

A procedure based on the Minnaert semi-empirical formula was tested on the solar spectrum obtained from the Utrecht Solar Atlas and gave results consistent with known solar abundances, solar temperature, and electron density. As a further test, the method of spectrum synthesis was used to duplicate a spectrum obtained from a 3300°K effective temperature model by Beebe (1969). The Minnaert formula reproduced the model spectrum exactly, giving elemental abundances within a factor of two of the model and a temperature of 3080°K. Finally, the method was applied to the stars Alpha Herculis and 54 Eridani. Kitt Peak 9 Å/mm spectrograms were reduced to relative intensity and wavelength for a 200-Å region centered on 5385 Å. Synthetic spectra were computed to duplicate observed portions of the stellar spectrograms as in the test cases. Alpha Herculis, a well-known M star, is shown to have relative abundances of iron-group and fifth-period elements similar to those of the Sun. However, 54 Eridani, also an M star, is shown to have a temperature of 3600°K, higher than normal M stars, and an enhancement of fifth-period elements and the iron-group elements Sc, V, Mn, and Co. (TSS) (Diss. Abstr. Int., B)

19320 COALESCENCE OF COLLIDING STARS IN DENSE STELLAR SYSTEMS. Sanders, Robert Hugh. Princeton, N. J.; Princeton Univ. (1970). 57p. University Microfilms Order No. 70-23,633.

Thesis.

Effects of stellar collisions such as mass and energy losses, and the question of whether or not two colliding stars coalesce to form a more massive star, are investigated by numerical calculations utilizing a simple physical model. The results of these calculations are then applied by use of Monte Carlo techniques in a computer simulation of dense stellar systems in order to approximately follow the development of the distribution of stellar masses as the systems evolve. In the simulation of a system with a total mass of 10^8 M$_\odot$, it is found that coalescence does not lead to the buildup of massive stars; whereas, for a 10^7 M$_\odot$ system, there is a pronounced tendency to build up a few very massive stars. The supernovae rate from coalesced stars in 10^8 M$_\odot$ and 10^7 M$_\odot$ systems is incapable of explaining Seyfert galaxy or quasar luminosities. (Diss. Abstr. Int., B)

19321 APPARENT DISTRIBUTION OF PLANETARY NEBULAE AND OPEN STAR CLUSTERS. Akhundova, G. V.; Seidov, Z. F. (Shemakha Astrophysical Observatory, Azerbaidzhan, USSR). Sov. Astron. AJ (Engl. Transl.); 14: 734-6(Jan-Feb 1971).

Translated from Astron. Zh.; 47: 911-14(Jul-Aug 1970).

In a substantial number of cases, far more than for a random distribution, planetary nebulae in the galactic-center region are located inside the boundaries of open star clusters. The number of coincidences is greater for the older clusters. (auth)

19322 PHASE SHIFT BETWEEN THE RADIUS AND TEMPERATURE VARIATIONS IN CEPHEIDS. Kolesnik, I. G. (Central Astronomical Observatory, Kiev). Sov. Astron. AJ (Engl. Transl.); 14: 729-31(Jan-Feb 1971).

Translated from Astron. Zh.; 47: 906-9(Jul-Aug 1970).

An equation relating the relative amplitude of the radius variation of a Cepheid and the phase shift between the radius and temperature functions is derived and applied to compute the phase shift for 44 Cepheids. (auth)

19323 CHEMICAL COMPOSITION OF THE ATMOSPHERES OF TYPE-M SUPERGIANTS. Orlov, M. Ya.; Rodriguez, M. H.; Shavrina, A. V. (Central Astronomical Observatory, Kiev). Sov. Astron. AJ (Engl. Transl.); 14: 690-3(Jan-Feb 1971).

Translated from Astron. Zh.; 47: 859-62(Jul-Aug 1970).

The abundances of several metals in the atmospheres of four type M1-M5 supergiants were derived from a curve-of-growth analysis of high-dispersion spectrograms. A comparison with the Sun's chemical composition indicated an excess V and Sc abundance and a Ni deficiency (relative to Fe). The microturbulence velocities were found to be about 10 km/sec. (auth)

19324 IONIZATION ZONES AROUND NEUTRON STARS: Hα EMISSION, HEATING OF THE INTERSTELLAR MEDIUM, AND THE INFLUENCE ON ACCRETION. Shvartsman, V. F. (State Astronomical Inst., Moscow). Sov. Astron. AJ (Engl. Transl.); 14: 662-8(Jan-Feb 1971).

Translated from Astron. Zh.; 47: 824-31(Jul-Aug 1970).

Extensive ionization zones exist around neutron stars of luminosity $L \gtrsim 10^{28}$ ergs/sec. A substantial proportion of the radiation of the neutron stars would be converted into photons of visible light in these zones. If the Hα emission of such regions were observed, old neutron stars could be detected and the distances to many known x-ray sources and pulsars determined. The intrinsic luminosity of old neutron stars should be caused by accretion; the maximum radiation would fall in the ultraviolet range, since the heating of the gas would restrict the strength of the accretion process to values $L \approx 10^{28}$ to 10^{31} ergs/sec. The ultraviolet radiation and x rays of neutron stars should contribute significantly to the ionization of the interstellar clouds, although such radiation apparently would be incapable of providing more than 10% of the effect observed. (auth)

19325 THEORY OF SUPERNOVA EXPLOSION LIGHT CURVES. Gurevich, L. E.; Rumyantsev, A. A. Sov. Astron. AJ (Engl. Transl.); 14: 645-51(Jan-Feb 1971).

Translated from Astron. Zh.; 47: 804-12(Jul-Aug 1970).

Phenomena occurring in the exterior part of a supernova and in the shell expelled immediately after the explosion process in the central region (core) are discussed. It is shown that the distribution of a shock wave in a medium of decreasing density has a number of peculiarities. In the first place, the wave front is unstable and breaks up into individual small parts which diffuse in the direction of the surface. As a result, the process of the front's exit is drawn out and the power carried by the shock wave is decreased. In the second place, a disturbance produced in the shell is not an ordinary shock wave with a thin front but a shock disturbance with a thick front which includes practically the entire shell. This situation occurs if the duration of the explosion process is $\gtrsim H/s$, where H is the height of a uniform atmosphere and s is the average sound velocity. Then the preceding part of the disturbance, acquiring the steep front of an ordinary shock wave, is able to move out to the surface long in advance of when the rear parts of the disturbance overtake it. Upon the exit of such a shock disturbance having a thick front, the luminosity is less by several orders of magnitude than the maximum value, so that the maximum of the brightness is not connected with the exit of the initial shock wave to the star's surface. The shell which is expelled from the star with parabolic velocity is subsequently accelerated to the observed velocities by the pressure of the radiation passing from the core to the cavity located between it and the shell. At the same time the shell thickens due to the radiation pressure which penetrates within it. During the entire time of the shell widening, until the brightness maximum, the radiation which proceeds from the core to the cavity, exerting pressure on the shell, produces weak shock waves in it, which are capable of transporting the principal energy of the explosion in a time of the order of 10^6 seconds. After the brightness maximum, radiative heat transfer plays an essential role in the transfer of radiation and the luminosity drops off in a time of the order of 10^7 sec owing to the exhaustion of the supply of radiation in the shell. (auth)

19326 EXPLOSION OF A ROTATING STAR AS A SUPERNOVA MECHANISM. Bisnovatyi-Kogan, G. S. (Inst. of Applied Mathematics, Moscow). Sov. Astron. AJ (Engl. Transl.); 14: 652-5(Jan-Feb 1971).

Translated from Astron. Zh.; 47: 813-16(Jul-Aug 1970).

A supernova-explosion mechanism not associated with nuclear detonation is proposed for a rotating star. It involves the transfer of angular momentum from a rapidly rotating neutron star, formed through collapse, to the envelope, where the centrifugal force is nearly equal to the gravitational force. An explosion will result when the centrifugal force inside the envelope exceeds the gravitational force, with a shock wave being generated. Angular momentum will be transferred efficiently if a sufficiently strong magnetic field, $H \approx 3 \times 10^9$ gauss, is present. (auth)

19327 INFRARED LINE EMISSION FROM PLANETARY NEBULAE. Holtz, J. Z.; Geballe, T. R.; Rank, D. M. (Univ. of California, Berkeley). Astrophys. J.; 164: L29-33(15 Feb 1971).

A number of planetary nebulae with large Hβ fluxes were examined for the infrared fine-structure lines of Ne II (12.8 μ), Cl IV (11.5 μ), S IV (10.5 μ), and Ar III (8.9 μ). Emission from S IV (10.5 μ) was detected in NGC 6572, NGC 7009, and NGC 7027. The intensities of the infrared lines due to Ne II and S IV are generally much lower than theoretical considerations have indicated. (auth)

19328 CONFIRMATION OF THE MAGNETIC WHITE DWARF G-195-19. Kemp, James C. (Univ. of Oregon, Eugene); Swedlund, John B.; Wolstencroft, Ramon D. Astrophys. J.; 164: L17-18(15 Feb 1971).

Circularly polarized light from the white dwarf G-195-19, discovered by Angel and Landstreet, was verified. A time average $\langle q \rangle = -(3.0 \pm 0.7) \times 10^{-3}$ was measured over the passband $\lambda\lambda$4000 to 6500, the same in handedness and approximate magnitude as they report. The linear polarization was found to be small, of the order 1% at most. (auth)

19329 DETECTION OF CIRCULAR POLARIZATION IN A SECOND WHITE DWARF. Angel, J. R. P. (Columbia Univ., New York); Landstreet, J. D. Astrophys. J.; 164: L15-16(15 Feb 1971).

The continuum radiation in a band from 3800 to 6000 Å from the white dwarf G195-19 was found to have circular polarization of 0.42 ± 0.04%. (auth)

19330 EMISSION FEATURE OF SILICATE MATERIAL AT 30 μm. Krishna Swamy, K. S. (Tata Inst. of Fundamental Research, Bombay). Nature (London). Phys. Sci.; 229: 149(1 Feb 1971).

A strong broad-emission feature has been observed with a peak around 10 μm in the spectra of many stars (Gillett et al. 1968, Woolf et al. 1969). From the work of Lyon (unpublished) and Oehler et al. (1969) it was found that the spectra of silicates have strong absorption features around 10, 20, and 30 μm. The presence of both the 10- and 20-μm emission feature was found in α-Ori (Low and Krishna Swamy 1970) by narrow-band photometry. A search should now be made for the 30-μm feature in α-Ori and other similar stars to supply further evidence for the silicate dust hypothesis. (UK)

19331 HELIUM PRODUCTION BY PULSATIONALLY UNSTABLE MASSIVE STARS. Talbot, Raymond J.; Arnett, David W. (Rice Univ., Houston, Tex.). Nature (London). Phys. Sci.; 229: 150(1 Feb 1971).

Sites of helium production other than the primaeval fireball are necessary to supply the temporal and/or spatial variations of helium abundance in the Galaxy and in other galaxies. The enrichment of helium over long periods of time by stars of conventional mass was investigated (Thuran, et al. 1965). The theory of another means by which stars in the interval 10^2 to 10^5 $M_\odot$ will eject helium into the interstellar gas is discussed, utilising the knowledge of the mass loss rate whereby the consequences can be calculated. The conditions under which the process is possible are considered. The strength of the theory lies in its basis on quantitative calculations of objects, the physics of which is not especially exotic. The possibility of overproduction of elements heavier than helium will eventually provide an internal check on the theory, but it seems possible that the helium observed in the Galaxy could have been formed in such pulsationally unstable massive stars. (UK)

19332 ULTRAVIOLET AND VISUAL SPECTRA OF γ CASSIOPEIAE. Bohlin, Ralph Charles. Princeton, N. J.; Princeton Univ. (1970). 47p. University Microfilms Order No. 70-23,602.

Thesis.

XUM

A rocket ultraviolet spectrum of γ Cas was obtained with a resolution of about 2 Å between 1060 and 2130 Å on November 14, 1968. The strength of the interstellar Lyman-α absorption line corresponds to an average density of 0.15 atoms cm^{-3} of neutral hydrogen over the 220 pc to γ Cas, while the absence of any observable lines of molecular hydrogen yielded an upper limit of 2.4×10^{-3} molecules cm^{-3}. Possible interstellar absorption lines of C II, N I, and Si II have widths indicating that the low-density gas in which the lines arise may have an exponential velocity distribution with a dispersion of $\sigma = 15$ km sec. OAO and visual spectra covering the wavelength range from 1100 to 5000 Å were also analyzed. The measured amount of Balmer continuous emission can be used to explain the weakness of the He I and other visual photospheric lines if the temperature and optical depth of the circumstellar envelope are known. If γ Cas has an envelope consisting of discrete clouds, each of which has an optical depth of unity at 3647 Å and an electron temperature of 20,000°K, then the Balmer continuous emission is accounted for quantitatively and the line profiles in the ultraviolet and visual can be explained qualitatively. (Diss. Abstr. Int., B)

19333 MASS LOSS FROM STARS. Cameron, A. G. W. Comments Astrophys. Space Phys.; 2: 209-13(Nov-Dec 1970).

There is one aspect of stellar evolution that is extremely poorly understood at the present time and that prevents very accurate calculations from being made of the later stages of stellar evolution; this aspect is mass loss. Using the available knowledge of the solar processes leading to mass loss, the operation of these processes in stars is discussed briefly. (W.D.M.)

19334 UBV PHOTOGRAPHIC PHOTOMETRY OF STARS IN THE REGION AR$_{1950}$: 17h03m TO 17h41m Decl$_{1950}$: $-28.^{0}8$ TO $-33.^{0}4$. I. THE CATALOGUE AND IDENTIFICATION MAPS OF 250 OB AND 101 PHOTOMETRICALLY INTERESTING STARS. **Antalova, A. (Astronomical Inst., Skalnate Pleso, Czech.). Bull. Astron. Inst. Czech.; 21: 331-44(1970).**

The probable early-type stars were found by a blink microscope on ubr plate of the Big Schmidt at Mt. Palomar. Further photometric measurements were made by an iris photometer. The faintest stars observed displayed $m_v = 15.42$m (limited by the UBV brightness of standard stars from NGC 6405/M6). The mean square deviation of the individual colors reached a value of 0.06m. The reduction of the effect of interstellar absorption was carried out by the Q method. Above the reddening line of the B3 V stars there are 250 stars, marked OB. The catalog of the 250 OB stars, apart from photographic data, also gives the accurate equatorial and galactic coordinates of the stars (mean error in right ascension 0.5″ and in declination 0.7″). The catalog number of the OB stars on the identification maps is indicated by larger numerals. For 74 of the OB stars a different dependence of A_V on distance follows from the computation than for the neighboring stars. These stars are denoted in the catalog by OB:. The second group is formed by stars with a B−V index larger than +1.0m and U−B less than +0.3m. These stars are given in the catalog of the 101 photometrically interesting stars. Their catalog numbers on the identification maps are shown by smaller numerals. (auth)

19335 PHOTOELECTRIC ELEMENTS OF THE ECLIPSING SYSTEM WX CEP. **Kandpal, C. D.; Srivastava, J. B. (Uttar Pradesh State Observatory, Naini Tal, India). Bull. Astron. Inst. Czech.; 21: 345-52(1970).**

A new period of 3.378453d for the system WX Cep was obtained using the epoch given by Woodward (1943). Photoelectric elements were computed in U, B, and V colors. Color curves of the system indicate that the primary component is bluer than the secondary. Spectroscopic elements of Sahade and Cesco (1945) were used to get the absolute elements. The system is found to be a detached one. (auth)

19336 PHOTOELECTRIC STUDY OF THE ECLIPSING SYSTEM GG CAS. **Srivastava, J. B.; Kandpal, C. D. (Uttar Pradesh State Observatory, Naini Tal, India). Bull. Astron. Inst. Czech.;** 21: 353-8(1970).

Photometric elements of GG Cas were derived from B, V observations. The primary minimum showed total eclipse, while the secondary minimum is not noticeable. (auth)

19337 PHOTOELECTRIC LIGHT ELEMENTS OF IZ PER. **Srivastava, R. K.; Padalia, T. D. (Uttar Pradesh State Observatory, Naini Tal, India). Bull. Astron. Inst. Czech.; 21: 359-67 (1970).**

The geometrical elements of the system IZ Per were obtained. A slightly refined period of 3.687663d is given. (auth)

19338 EXTRACTION OF ROTATIONAL ENERGY FROM A BLACK HOLE. **Penrose, R. (Birbeck Coll., London); Floyd, R. M. Nature (London) Phys. Sci.; 229: 177-9(8 Feb 1971).**

The possible astrophysical consequencies of the existence of a black hole resulting from the gravitational collapse of a massive body are considered, with special reference as to whether the mass-energy content of a black hole could, under suitable circumstances, be a source of available energy. The extraction of rotational energy from a black hole is here considered not least because the rotational energy of a black hole should, in general, be comparable with its total mass-energy. (UK)

19339 α^2 CANUM VENATICORUM AND THE OBLIQUE ROTATOR THEORY. Pyper, Diane Marie. Santa Cruz, Calif.; Univ. of California (1968). 76p. University Microfilms Order No. 70-23,835.

Thesis.

In order to test the oblique rotator theory, a study of the spectrum, radial velocity, and magnetic variations of α^2 CVn was made on spectrograms obtained with the 120-inch coudé spectrograph and the Zeeman analyzer at Lick Observatory. UBV photometric observations of this star were also obtained. The light and color variations do not agree with those predicted from the effective temperature changes during the cycle. The rare earth line-strength variations are also incompatible with a change in temperature. On the basis of the line intensity and radial velocity variations, the elements are found to fall in three groups: the rare earths; the iron-peak elements (Ti, V, Cr, Mn and Fe); and Mg, Si, and Ca. It is shown that the observed changes in the effective magnetic fields, equivalent widths, and radial velocities for the first two groups can be successfully predicted by an oblique rotator model. The magnetic configuration is represented by a combination of dipole and quadrupole fields with their common axis inclined to the rotational axis by about 50°. The rare earth abundance distribution on the stellar surface has a maximum near one magnetic pole. The lines of the iron-peak elements are double throughout most of the cycle, with an inferred abundance distribution having four maxima distributed approximately along the magnetic equator. The data for Mg, Si, and Ca are also compatible with the oblique rotator model if it is assumed that the distribution of these elements is similar to that of the iron-peak group. The light and color variations cannot be explained by the present model. Possibilities for further work on this subject are discussed. (Diss. Abstr. Int., B)

19340 PHOTOELECTRIC OBSERVATIONS OF FLARE STARS. VI. THE PHOTOMETRY OF FLARES OF EV LAC IN FOUR SPECTRAL REGIONS: U, H_β, G. V. Chugainov, P. F. Izv. Krym. Astrofiz. Observ.; 40: 33-8(1969). (In Russian).

Thirty-one flares were recorded for 66 hours of photoelectric observations of EV Lac with a U filter. It is shown that so high a frequency of recording of flares was caused by two factors: 1) high flare activity of the star; 2) higher probability to detect small flares with a U filter than with a B filter during observations. (W.D.M.)

19341 PHOTOELECTRIC OBSERVATIONS OF AG DRA FROM 1962 TO 1967. **Belyakina, T. S. Izv. Krym. Astrofiz. Observ.; 40: 39-45(1969). (In Russian).**

In the period from 1965 to 1967, three-color photoelectric observations of the symbiotic star AG Dra were carried out in a system similar to UBV. A combined photoelectric light curve was constructed from 1962 to 1967. The light variations of AG Dra were irregular but synchronous in all the regions of the spectrum; the amplitude of light variations is 0.15m for yellow light, 0.30m for blue, and 1.0m for ultraviolet. Results of the observations can be explained assuming that AG Dra is a complex system consisting of a cold star (K5 III), a hot one (T_c = 50,000°), and a gas cloud (T_e = 17,000°, $n_e \geq 10^6$ cm^{-3}). In that case the light variations in all the regions of the spectrum are probably due to the variations of the hot component. It was found that the luminosity of the cold component in system V is 9.75m, the minimum luminosity of the hot component in the same system is 1.40m. The amplitude of light variations of the hot component for yellow light exceeds 2.5m. Its minimum absolute visual magnitude M_V is +4.2m. (auth)

19342 PHYSICAL CONDITIONS IN THE ATMOSPHERE OF P CYGNI. **Astaf'ev, E. R.; Gollandskii, O. P.; Kopylov, I. M. Izv. Krym. Astrofiz. Observ.; 40: 46-64(1969). (In Russian).**

Time variations in the atmosphere of P Cygni were investigated using spectrograms obtained with the 1220-mm reflector of the observatory in 1959 (dispersion − 23 Å/mm) and 1963 (dispersion − 14 and 33 Å/mm). Between 1959 and 1963 only small changes in the spectrum were detected. The picture of the spectrum was in

XUM

general similar to that observed earlier, but dome-shaped emission "humps" forming something like bases of strong hydrogen and helium lines were detected. The origin of the "humps" is not known. Using the intensities of interstellar lines the absolute magnitude of the star, M_V, was estimated as 8.2m according to which $R^* \approx 50\ R_\odot$. The following values for the parameters of the atmosphere were found: the logarithm of the quantity of hydrogen atoms on the second level over 1 cm^2 of the photosphere lg $N_{02}H$ = 15.0; the logarithms of the electron density lg $n_e(n_m)$ = 12.74—according to the Inglis–Teller formula and lg $n_e(H)$ = 14.31—according to the Stark broadening of hydrogen lines; microturbulent velocity v_t = 9 km/sec (1959) and v_t = 19 km/sec (1963) using curves of growth for absorption lines of O II and N II. The obtained Balmer decrement is less steep than that obtained by the Burbidges (1955). It is shown that the increase of radial velocity of absorption components of the lines with the decrease of ionization potential could be explained as an effect of "filling up" of absorption by emission. (auth)

19343 SPECTROSCOPIC STUDIES OF PECULIAR A STARS OF THE MANGANESE GROUP. **Khokhlova, V. L.; Aliev, S.; Rudenko, V. M. Izv. Krym. Astrofiz. Observ.; 40: 65-81(1969). (In Russian).**

High-dispersion spectrograms of manganese stars α And and π Boo A were analyzed. A list of 294 lines within the range $\lambda\lambda$3734 to 4800 Å is given. The electron density was found to be $N_e = 10^{14}$. Using Mihalas theoretical models, θ_{eff} and lg g were determined from the hydrogen line profiles and line intensity of C II λ4267 and Mg II λ4481. For α And, θ_{eff} is 0.36, lg g is 3.5 and for π Boo A, θ_{eff} is 0.40, lg g is 3.5. The turbulent velocity is 3 km/sec for α And and 1.9 km/sec for π Boo A. A He deficiency and strong enhancement of Mn, Ga, Y, and Sc as well as P and Sr in α And were detected. The "stellar" oscillator strengths for some lines of Mn II were derived from the curves of growth. (auth)

19344 BINARY HD 175514. I. **Vitrichenko, F. A. Izv. Krym. Astrofiz. Observ.; 40: 82-95(1969). (In Russian).**

Twelve new radial velocity measurements for HD 175514 were made. Using 7 determinations, a radial velocity curve was obtained. The period of system is $1.62192 \pm 5 \times 10^{-5}$ d. The spectroscopic elements were derived by a least-squares solution. It is shown that this star does not belong to runaway stars. Light variation with the same period was revealed. The star is eclipsing with elliptical components. The light curve was obtained from 361 photoelectric measurements. Photometric elements were derived. Two-dimensional classification for the component with an invisible spectrum was made (B3, −2.8m). Both stars belong to the main sequence. Masses of components are 73 and 15 $M_\odot$. The stars almost fill Rosh's surface. Absolute parameters of the system are given. (auth)

19345 PHOTOELECTRIC OBSERVATIONS OF FLARE STARS. V. RESULTS OF PARTICIPATION IN CO-OPERATIVE PROGRAMS IN 1963–1967. **Chugainov, P. F. Izv. Krym. Astrofiz. Observ.; 40: 26-32(1969). (In Russian).**

Forty-seven flares were recorded during the photoelectric observations made simultaneously with radio observations at Jodrell Bank in 1963–1967. The time of the start and end of observations, the time of flare maxima, and their amplitudes are compiled. The light curves of the flares are given. (auth)

19346 STATISTICAL CHARACTERISTICS OF FLARES OF UV CET-TYPE STARS. **Gershberg, R. E.; Chugainov, P. F. Izv. Krym. Astrofiz. Observ.; 40: 7-25(1969). (In Russian).**

Statistical analysis of more than 90 photoelectric light curves of flares of UV Cet-type stars recorded by different observers was carried out. The time changes of the flare activity of these stars were confirmed. A summary of the following photometric data for considered flares was made: amplitudes at maximum light, energies radiated during the flare, rates of increase of energy output before the maximum, times of flare growth and flare decay, ratios of the rate of flare growth of that of flare decay near the maximum of flare, and some properties of the light curves. The energy radiated by a flare in the blue region was equal to $3 \times 10^{31\pm2}$ ergs and more than half of flares considered radiate $10^{31\pm1}$ ergs. The characteristic rates of increase of energy output of flares were found to be 10^{27} to 3×10^{28} ergs/sec^2. A weak dependence of the flare energy and the rate of increase of energy output before the maximum on the luminosity of the UV Cet-type star was revealed: the brighter the star, the greater the mean energy and duration of the flare occurring on the star. The time of flare growth was 10 to 30 sec for half of the flares and 3 to 100 sec for 90% of the flares. The time of flare decay was 10 to 100 times as large as that of flare growth but, as a rule, the rate of increase of energy output just before the maximum was only 2 to 3 times as large as the rate of decrease of energy output immediately after the maximum. Secondary maxima of strong flares usually arise 6 to 10 minutes later than do the main ones. The recorded flares radiate 0.1 to 1% of the energy of the quiet star radiation. Different criteria of the flare activity are briefly discussed. (auth)

19347 PREDICTED ULTRAVIOLET FLUXES FOR MAIN-SEQUENCE STARS. **Blondelot, E. (Univ., Liege). Bull. Soc. Roy. Sci. Liege; 39: 508-20(1970).**

The comparison of stellar observations in the region of 2600 Å with a group of model atmospheres published recently permits a determination of a scale of effective temperatures. The ultraviolet flux of the main-sequence stars is then calculated, starting with this group of model atmospheres and using an interstellar extinction curve deduced from observations and from data in an appendix. (tr-auth)

Quasi-Stellar, Radio, and X-Ray Sources

Refer also to abstracts 18677 and 18680.

19348 (NP-18666) NEUTRON STARS. Lectures given by Gordon Baym at The Niels Bohr Institut and NORDITA Copenhagen. (Niels Bohr Institutet, Copenhagen (Denmark). Nordisk Institut for Teoretisk Atomfysik, Copenhagen (Denmark)). 1970. 74p. Dep. NTIS (U. S. Sales Only).

A survey is given of the present theoretical understanding of the structure of neutron stars. Topics considered include the atmosphere, nuclear physics of the crust, solid-state aspects of the crust, and superfluidity. (W.D.M.)

19349 (NP-18682) DEEP SKY SURVEY AT 2700 MHZ. Wall, Jasper V. (Australian National Univ., Canberra). 1970. 365p. Dep. NTIS (U. S. Sales Only).

Thesis.

The 210-foot telescope of the A.N.R.A.O. was used in a survey of (i) the +4° to −4° declination zone to a source density of 450/sterad, and (ii) six selected regions to a source density of 2500/sterad. Each of the latter corresponds to a two-colour (B–UV) plate taken by Bolton with the 48-inch Schmidt telescope of Palomar Observatory. The positions of all sources found in the surveys were measured to an accuracy of 15" arc, and the fields were examined on the Palomar Sky Survey prints and the two-colour plates taken by Bolton. The spectra of the sources in the ±4° declination zone catalogue were determined by additional observations at the A.N.R.A.O. at frequencies of 470, 635, 1400, and 5000 MHz, supplemented by low-frequency data from other observatories. The first part of the thesis is a description of the survey, the measurement (at 2700 MHz) of positions and flux densities of the sources, and the programmes of optical identification and spectral observations. In the remainder of the thesis, the statistics of the source spectra are examined, and the 2700-MHz number–flux density relation (between 30/sterad and 2500/sterad) is derived. Comparisons are made with the results from lower frequency surveys. Finally, a simple numerical approach to investigate the significance of number–flux density relations is described. The technique enables the computation of the relation at a given frequency with the incorporation of any geometry, radio luminosity function, type of evolution, or form of radio spectrum. Using the identification and spectral data for the sources in the 2700-MHz survey, the number–flux density relations are computed for two uniform models of the Universe, and the results are compared with the observed relations. The catalogues, data on identifications, and spectral observations are presented as appendices. (auth) (Australia)

19350 RADIO STRUCTURES OF SEVENTY-NINE QUASI-STELLAR OBJECTS. **MacDonald, G. H.; Miley, G. K. (National Radio Astronomy Observatory, Green Bank, W. Va.). Astrophys. J.; 164: 237-47(1 Mar 1971).**

The structures of seventy-nine quasi-stellar sources were studied with the NRAO interferometer at a wavelength of 11.1 cm and with a resolution of up to 3 arc sec. All of them had known redshifts. Thirty-three were unresolved (<7"), ten were slightly resolved, and structures were derived for the remainder. This more than doubles the number of QSOs with known redshifts whose radio structures have been determined. The results are discussed from a morphological viewpoint. (auth)

19351 INTERSTELLAR SCINTILLATION OF PULSAR RADIATION. **Lang, Kenneth R. (Arecibo Observatory, Puerto Rico). Astrophys. J.; 164: 249-64(1 Mar 1971).**

It is demonstrated that the long-term fluctuations in the intensity of pulsar radiation are due to interstellar scintillation. Observed statistical quantities are consistent with a thin-screen model in which the screen is located halfway between the Earth and the pulsar. Decorrelation frequencies are found to be proportional to the fourth power of the observing frequency and inversely proportional to the square of the dispersion measure. Power spectra are nearly Gaussian in form, but have a high-frequency tail that may be power law. Observed pulse broadening is shown to be equivalent to the convolution of the emitted pulse profile with an exponential function for which the e^{-1} decay time is the reciprocal of the decorrelation frequency. Decorrelation times are found to be proportional to the observing frequency and weakly dependent on dispersion measure. Modulation indices are nearly unity and independent of observing frequency in the interval 111 to 606 MHz. Both Rice-squared and lognormal probability distribution functions fit the observed probability distributions of intensity well. The scale size is $\approx 10^{11}$ cm, roughly the size of the first Fresnel zone, and the rms fluctuating number density of electrons is 3×10^{-4} cm^{-3}. The scattering becomes weak above 2000 MHz for nearby pulsars. These scintillation measurements provide estimates for pulsar distances which, when used with known dispersion measures, indicate that the average number density of electrons along the line of sight to the pulsars is 0.03 cm^{-3}. Pulsars must be smaller than 10^{-7} seconds of arc in order to give rise to the observed intensity fluctuations. This size is considerably below the angular size of any observable self-absorbed synchrotron radio source. The relative velocities of the pulsar and/or the interstellar medium with respect to the Earth lie in the range 30 to 200 km sec^{-1}. Pulsars with periods smaller than a few milliseconds will not be detected at frequencies below a few hundred MHz. The minimum detectable angular size of a radio source at a distance of 300 pc is on the order of 10^{-3} seconds of arc at 318 MHz. This limiting size is proportional to the square root of the distance and inversely proportional to the square of the observing frequency. The view that the compact source in the Crab Nebula is the pulsar NP 0532 which has been broadened by interstellar scattering is consistent with these measurements. (auth)

19352 LOW-ENERGY COSMIC X RAYS. **Shukla, P. G.; Wilson, B. G. (Univ. of Calgary, Alberta). Astrophys. J.; 164: 265-73(1 Mar 1971).**

Observations of the diffuse x-ray background down to 0.25 keV obtained during a rocket flight on October 26, 1969 from Resolute Bay, N.W.T., Canada, are presented. Identification and spectral data of a new x-ray object in the Cetus region are also discussed. (auth)

19353 FURTHER HIGH-SENSITIVITY X-RAY SKY SURVEY FROM THE SOUTHERN HEMISPHERE. **Cooke, B. A.; Pounds, K. A. (Univ. of Leicester, Eng.). Nature (London). Phys. Sci.: 229: 144-7(1 Feb 1971).**

The strengths of seven x-ray sources at 1 to 12 keV in the Centaurus–Norma–Lupus region of the sky were measured during high-sensitivity surveys in June 1968 and April 1969. The combined emission from the observed Centaurus sources can account for nine-tenths of the previously unresolved excess galactic x rays in this region of the Milky Way. (auth) (UK)

19354 X-RAY OBSERVATION OF Cen XR-4 AND Nor XR-2. **Rao, U. R.; Chritnis, E. V.; Sharma, D. P.; Prakasaras, A. S.; Jayanthi, U. B. (Physical Research Lab., Ahmedabad, India). Nature (London); 229: 248-50(22 Jan 1971).**

The results are presented of an x-ray astronomy experiment conducted from a Centaure rocket launched from Thumba Equatorial Rocket Launching Station, India at 0035 UT on Dec. 7, 1969. Count rates obtained in a xenon–methane proportional counter are given. The x-ray flux from Cen XR-4 as a function of time and the differential photon spectrum of the Nor XR-2 source are plotted. The similarity between the light intensity of a typical fast nova and the x-ray flux of Cen XR-4 is striking, indicating that Cen XR-4 is a nova-like object. It is also suggested that Nor XR-2 is associated with a supernova remnant and that there is a possibility of its x-ray spectrum favouring a synchrotron emission. (UK)

19355 UPPER LIMIT ON RADIO FLUX FROM THE X-RAY SOURCE Sco X-1 AT 327 MHz. **Apparao, Krishna M. V. (Tata Inst of Fundamental Research, Bombay). Nature (London). Phys. Sci.; 229: 114(25 Jan 1971).**

The x-ray source Sco X-1 was observed with a cylindrical radio telescope at Ootacamund, India at 327 MHz with a bandwidth of 4 MHz. A signal of about 1 flux unit (10^{-26} W m^{-2} s^{-1} Hz^{-1}) was observed when the telescope was centered on Sco X-1. This, however, is less than the expected confusion limit of about 1.5 flux unit for the radio telescope on the basis of 5 times the rms fluctuations caused by background radio sources lying within the beam of the radio telescope. Therefore, the measured value should be the upper limit on the radio flux from Sco X-1 at 327 MHz. This upper limit, together with the flux of Andrew and Purton (NSA 22: 34195) and Ables (NSA 23: 14499), gives an index $\alpha \lesssim 1.2$, if the radio spectrum is expressed in a form $J(\nu) = K\nu^{-\alpha}$, where ν is the frequency and K and α are constants. The source was observed on five days for a total of ten hours and no change in the flux was found. (UK)

19356 RECENT DEVELOPMENTS IN X-RAY ASTRONOMY. **Pounds, K. A. (Univ. of Leicester, Eng.). Nature (London); 229: 303-6(29 Jan 1971).**

In the past two years the number of known cosmic x-ray sources has steadily increased and is now near fifty. The first high-resolution spectroscopic and polarization studies have been reported—though with negative results in each case. On the other hand, the first x-ray pulsar has been discovered, further highly variable sources observed, and several important new identifications made. Recent observations below 1 keV have indicated the probability of numerous bright sources and an excess diffuse x-ray component in this previously unexplored spectral region. These more recent developments in cosmic x-ray astronomy are reviewed and the scene set for the significant changes in the observational situation that are likely to follow the introduction of major satellite instruments over the next few years. (UK)

19357 NEW INTERPRETATION OF EXTRAGALACTIC RADIO SOURCES. **Rees, M. J. (Inst. of Theoretical Astronomy, Cambridge, Eng.). Nature (London); 229: 312-17(29 Jan 1971).**

The hypothesis that the energy involved in extragalactic violent events derives from the rotational energy of a large number of collapsing stars or pulsar-like bodies in galactic nuclei was investigated. It shows that extended radio sources may be produced and energized by low-frequency electromagnetic waves generated in this way. (auth) (UK)

19358 CIRCULAR COMPONENTS OF POLARIZATION IN PULSAR RADIATION. **Graham, D. A. (Manchester Univ., Jodrell Bank, Eng.). Nature (London); 229: 326-7(29 Jan 1971).**

The polarization from pulsars is generally elliptical, but the handiness of the circular component appears to be variable so that the Stokes parameter (V) changes in sign both during an individual pulse and from pulse to pulse. If this variation were completely random, then an integrated profile of V obtained by summing several hundred pulses would be close to zero. In an extended series of observations, it was found that the average V component was significantly different from zero in many pulsars, although it seldom approached the strength of the linear component. The average V component was particularly strong in the pulsars PSR 0329 and PSR 1508. The organized part of the circular polarization was seen to be a general property of pulsar radiation. Further, the present observations of PSR 0329 at 408 and 610 MHz may be combined with observations of single pulses at 240 and 408 MHz to show that this phenomenon is practically independent of frequency, as is the organized part of the linear polarization. (UK)

19359 X-RAY OBSERVATIONS OF PULSARS. **Rappaport, S.; Bradt, H.; Mayer, W. (Massachusetts Inst. of Tech., Cambridge). Nature (London). Phys. Sci.; 229: 40-2(11 Jan 1971).**

The results of an analysis of x-ray data from NP 0532 are presented. Limits on x-ray pulsations from five galactic x-ray sources and ten radio pulsars are also given. (auth) (UK)

19360 POSSIBLE HIGH-FREQUENCY MODULATION OF LIGHT FROM THE CRAB PULSAR. **Sturrock, P. A.; Bracewell, R. N.; Switzer, P. (Stanford Univ., Calif.). Nature (London); 229: 186-7(15 Jan 1971).**

It is shown that the pulsar model proposed by Sturrock (Nature, 227: 465(1970)) predicts a high-frequency modulation of the optical, x-ray, and γ-ray radiation that might be detected in the optical part of the spectrum. Some data from observations of the Crab pulsar made with a 100-inch telescope are discussed. (UK)

19361 EXPERIMENT TO DETECT PULSED γ RAYS FROM THE CRAB NEBULA. **Kinzer, R. L.; Noggle, R. C.; Seeman, N.; Share, G. H. (Naval Research Lab., Washington, D. C.). Nature (London); 229: 187-9(15 Jan 1971).**

It is stated that preliminary results from a balloon-borne experiment flown on Oct. 25, 1969, from Texas, indicate an enhanced γ-ray response in phase with the optical pulses and with an intensity close to that predicted from an extrapolation of the total x-ray emission from the Crab to γ-ray energies. A telescope sensitive to 10- to 150-MeV γ radiation was employed. Details are given of the equipment used and its mode of operation. Measurements were made on spark chamber photographs. Two features were apparent for γ rays arriving at less than 10° from the Crab. The first was an excess of γ-ray events in a 2-ms interval coincident with the primary optical peak and the second an excess in a 1-ms interval about 1.5 ms before the interpulse peak. The results are considered to be probable, but not conclusive, evidence for pulsed γ radiation at 10 MeV from the Crab pulsar. (UK)

19362 RADIO SOURCES ASSOCIATED WITH SCORPIUS X-1. Hjellming, R. M.; Wade, C. M. (National Radio Astronomy Observatory, Green Bank, W. Va.). Astrophys. J.; 164: L1-7 (15 Feb 1971).

Interferometric observations of Sco X-1 at 2695 and 8085 MHz show three radio sources close to the x-ray star. One is 1.3′ NE of the star, and the other is 2.0′ SW of it. The third source coincides in position with the x-ray star; it varies in an irregular manner with a typical time scale of hours. The greatest observed change was an increase in flux density by a factor of more than 60 in 25 hours. All three sources have nonthermal spectra. (auth)

19363 SEARCH FOR TEMPORAL STRUCTURE IN X RAYS FROM SCORPIUS X-1. Boldt, E. A.; Holt, S. S.; Serlemitsos, P. J. (Goddard Space Flight Center, Greenbelt, Md.). Astrophys. J.; 164: L9-13(15 Feb 1971).

The temporal behavior of the x-ray emission from Sco X-1 was investigated from data taken over a continuous 122-second exposure on March 3, 1969 where the count was recorded every 322 μsec. No evidence was found for temporal structure, and upper limits for both periodic and nonperiodic variations over time scales ranging from a fraction of a millisecond to about 1 minute were established. Implications of such a lack of observable short-term x-ray fluctuations are discussed. (auth)

19364 METHOD FOR ESTIMATING THE MASS OF QUASI-STELLAR OBJECTS AND GALAXY NUCLEI WITH REDSHIFTED ABSORPTION LINES. Karitskaya, E. M.; Komberg, B. V. (Inst. of Applied Mathematics, Moscow). Sov. Astron. AJ (Engl. Transl.); 14: 656-61(Jan-Feb 1971).

Translated from Astron. Zh.; 47: 817-23(Jul-Aug 1970).

The possibility, in principle, of determining the masses of quasi-stellar objects and galaxy nuclei whose spectra exhibit absorption lines with a relative redshift is discussed. The shift apparently indicates an infall of material into the central regions of these objects. The quasi-stellar galaxy B194 is used as an illustration. That mass infall is indeed occurring might be demonstrated not only by an observation that $\bar{z}_{abs} > \bar{z}_{em}$ in the spectrum of a given object, but by a relation between $\bar{z}_{i,abs} - \bar{z}_{em}$ and the ionization potential χ_{i-1} whose form corresponds to the accelerated infall of material in the gravitational field of the central body. Calculations for B194 with N_e from 10^6 to 10^9 cm^{-3} yield a mass from 7×10^{44} to 2×10^{43} g, respectively, for this object. A noncontradictory model for the absorbing "envelope" of a quasi-stellar object is outlined. The envelope comprises individual condensations of material whose characteristic size $\alpha \approx 6 \times 10^{16}$ to 6×10^{13} cm and whose mass is <1 $M_\odot$. These condensations should be distributed quite sparsely over the ambient medium (filling factor $\approx 10^4$ to 10^7), so that only a few of them may occur along the line of sight. (auth)

19365 PHYSICAL CONDITIONS IN THE ORION NEBULA FROM OBSERVATIONS OF THE H56α EXCITED-HYDROGEN RADIO LINE. Sorochenko, R. L.; Berulis, I. I. (Lebedev Inst. of Physics, Moscow). Sov. Astron. AJ (Engl. Transl.); 14: 683-9(Jan-Feb 1971).

Translated from Astron. Zh.; 47: 850-8(Jul-Aug 1970).

The H56α radio line of excited hydrogen has been observed at five points in the Orion Nebula (NGC 1976) with a resolution of 1.9′. The departure of the population of the 57th level of the hydrogen atom from an equilibrium population is measured by $b_{57} = 0.88 \pm 0.07$. When allowance is made for stimulated emission under the conditions of nonequilibrium population, the measurements obtained for different radio lines can be reconciled, and independent estimates are afforded of the electron temperature and concentration. The latter parameter should be increased to $N_e = (1.75 \text{ to } 10) \times 10^4$ cm^{-3}, suggesting that material is concentrated in condensations in the nebula. Some enhancement of the efficiency of the adopted collision mechanism is also possible. Evidence is obtained on the distribution of physical conditions in the nebula, indicating that T_e decreases toward the periphery, while the velocities of internal turbulent motion increase. A spherically symmetric model is proposed for the T_e distribution in the nebula, with $T_e(x, y, z) = (8800 \pm 700°K)\ [1 - 0.1(x^2 + y^2 + z^2)^{1/4}$, where x, y, z are the coordinates relative to the center of the nebula in minutes of arc. The agreement between the values of T_e derived from measurements of optical and radio lines is significantly improved. (auth)

19366 FURTHER INVESTIGATIONS OF NH_3 INVERSION RADIATION. Knowles, S. H. (Naval Research Lab., Washington, D. C.); Cheung, A. C. Astrophys. J.; 164: L19-21 (15 Feb 1971).

Ammonia inversion radiation at 1.25 cm was studied in the direction of three galactic-center sources with a parametric amplifier. Upper limits were set on densities in other directions. (auth)

19367 NATURE OF THE OUTBURSTS IN QUASARS AND SEYFERT-GALAXY NUCLEI. Shklovskii, I. S. (Inst. for Space Research, Moscow). Sov. Astron. AJ (Engl. Transl.); 14: 594-601(Jan-Feb 1971).

Translated from Astron. Zh.; 47: 742-51(Jul-Aug 1970).

An analysis of the variations in flux density observed in certain quasars and Seyfert nuclei at centimeter wavelengths indicates that, at early stages in the evolution of the expanding relativistic-particle clouds responsible for the variations, the energy spectrum of the relativistic electrons must have been very steep, with an exponent $\gamma_0 \approx 5$. This spectrum would have been transformed quite rapidly to a spectrum with $\gamma \approx 1$. Outbursts of submillimeter synchrotron radiation lasting ≈1 to 2 weeks would be expected; their amplitude would be large but the intensity should drop steeply with time ($\sim t^{-10}$). Schematic "dynamic spectra" are constructed for the outbursts. The powerful submillimeter radiation of quasars and Seyfert-nuclei may be interpreted as representing a large number of such outbursts with comparatively small amplitude and at different stages in their evolution (as described by their expansion). Energy considerations for the outbursts and the physical conditions prevailing early in their development indicate that the phenomenon is very similar to solar flares, differing from flares primarily in its vastly larger scale. The source of infrared radiation at the nucleus of the Galaxy is of the same nature; it may comprise a large number of comparatively weak outbursts taking place within a volume ≈0.7 pc across. Concurrently with the outbursts of submillimeter radiation, active quasars and Seyfert nuclei would be expected to emit powerful bursts of γ rays with quanta in the energy range 10^6 to 10^9 eV, which might well be observable. The model for quasar and Seyfert nuclei obtained by analyzing the flux variations consists of a plasma body 10^{17} to 10^{18} cm across, whose surface layers have a density of $\approx 10^9$ to 10^{10} cm^{-3} and a field strength of $\approx 10^3$ to 10^4 gauss. The plasma would be in a state of violent turbulent motion. (auth)

19368 OBSERVATIONS OF COMPACT RADIO SOURCES WITH A RADIO INTERFEROMETER HAVING A GREEN BANK–CRIMEA BASELINE. Broderick, J. J. (National Radio Astronomy Observatory, Green Bank, W. Va.); Vitkevich, V. V.; Jauncey, D. L.; (and others). Sov. Astron. AJ (Engl. Transl.); 14: 627-9(Jan-Feb 1971).

Translated from Astron. Zh.; 47: 784-6(Jul-Aug 1970).

The sizes of compact radio sources were measured at 2.8 and 6 cm with a radio interferometer having a Green Bank–Crimea baseline and featuring independent recording of signals. The first results are reported. (auth)

19369 EXTRAGALACTIC RADIO SOURCES. I. RADIO SPECTRA: STATISTICS, INTERPRETATION, CLASSIFICATION. Kuril'chik, V. N. (State Astronomical Inst., Moscow). Sov. Astron. AJ (Engl. Transl.); 14: 630-44(Jan-Feb 1971).

Translated from Astron. Zh.; 47: 787-803(Jul-Aug 1970).

The radio-emission spectra of the extragalactic radio sources in the 3CR catalog are analyzed. The entire range of values for the spectral index observed in these objects can be explained through the justifiable assumption that the relativistic electrons accelerated in galaxy and quasar nuclei have a power-law spectrum with an exponent in the interval $2 < \gamma_0 \leq 2.5$. A classification is presented for all the observed radio spectra. (auth)

19370 COHERENT MECHANISMS OF EMISSION AND THEIR APPLICATION TO PULSARS. II. MASER MECHANISMS OF RADIATION. Ginzburg, V. L.; Zheleznyakov, V. V. (Soviet Academy of Sciences, Moscow). Comments Astrophys. Space Phys.; 2: 197-205(Nov-Dec 1970).

Maser mechanisms are discussed using the transfer equation for the intensity of electromagnetic waves, $dI/dx = A + (B - \mu c)\, I$. Analogous equations are written for the other Stokes parameters. In the equation refraction is neglected and in the following discussion the system is assumed uniform along the path L of the ray (x-axis). (W.D.M.)

19371 MULTIPLE ABSORPTION REDSHIFTS IN QUASARS. Bahcall, John N. (California Inst. of Tech., Pasadena). Comments Astrophys. Space Phys.; 2: 221-6(Nov-Dec 1970).

XUM

The validity of the multiple redshift identifications is discussed, and the measured properties of the absorption spectra are reviewed. Some clues as to the origin of the absorption systems that arise from the failure to find certain kinds of lines are indicated. Six observations are described that could greatly increase the understanding of the origin of the absorption spectra. (W.D.M.)

19372 NONPULSING PULSARS: A STANDARD MODEL FOR THEORY. Michel, F. Curtis (Rice Univ., Houston, Tex.). Comments Astrophys. Space Phys.; 2: 227-31(Nov-Dec 1970).

It is noted that pulsar theories might usefully be intercompared by applying them to a standard model, suggested to be that of an idealized neutron star having its spin axis aligned with a uniform internal magnetic field. Such an object might or might not radiate with high brightness temperatures and might or might not radiate in a pulsed mode. A firm prediction of the behavior of this simple model would seem an essential basis for all serious pulsar theories. (W.D.M.)

19373 THE 1969 SOLAR OCCULTATION OF THE CRAB NEBULA PULSAR NP 0532. Rankin, John Metcalf. Iowa City, Iowa; Univ. of Iowa (1970). 148p. University Microfilms Order No. 70-23,935.

Thesis.

The Crab Nebula pulsar passes within five solar radii of the Sun in June, and observation of its pulse-arrival properties at several frequencies during the occultation offers a new technique for studying the ionization content of the corona. The pulsar was observed using the Arecibo radio telescope during its 1969 occulation, and the concentrated attention that the object received as a result of the occultation experiment has led to a deeper understanding of both the radio-propagation characteristics of the corona and the properties of the pulsar itself. (TSS) (Diss. Abstr. Int., B)

19374 INTERFEROMETRY OF GALACTIC H II REGIONS. Webster, William John Jr. Cleveland; Case Western Reserve Univ. (1969). 100p. University Microfilms Order No. 70-25,928.

Thesis.

The N.R.A.O. interferometer was employed to prepare supersynthesis maps of the galactic H II regions W3(IC1795), DR21, Orion A (M42), and M17 at 11.1 cm. The maps have a resolution that ranges from 7 seconds of arc to 9 seconds of arc depending upon declination, and have the capability of showing all structures whose sizes range from approximately 4 minutes of arc to 7 seconds of arc. Considerable structure was detected. Orion A has 6 components, W3 has 5 components, M17 has 3 components, and DR21 could not be reliably decomposed into components. It is possible to interpret the components as the remnants of the protostar cloud complexes from which the exciting stars of the H II region formed. (Diss. Abstr. Int., B)

19375 PULSARS. Rosenberg, J. Ned. Tijdschr. Natuurk.; 36: 139-50(11 Jun 1970). (In Dutch).

The properties of pulsars are reviewed, with discussions of their periods and pulse duration, pulse form, amplitude variations, observations outside the radio range, distance, preliminary limitations on the model of a pulsar, states in a neutron star, hydrostatic equilibrium, stability, energy loss in a neutron star, and superconductivity and superfluidity. 10 references. (J.S.R.)

19376 OBSERVATIONS OF RADIO EMISSION OF SOURCES 3C 273 AND 3C 279 AT 8 mm. Efanov, V. A.; Moiseev, I. G. Izv. Krym. Astrofiz. Observ.; 40: 3-6(1969). (In Russian).

Observations of the quasars 3C 273 and 3C 279 at 8 mm were carried out with the 22-meter radiotelescope of the Crimean Astrophysical Observatory in October—November 1967. The flux density for 3C 273 was found to be 58 ± 3 flux units and that of 3C 279 was 31 ± 7. During the period from April 1965 to October 1967 the flux density of 3C 273 increased by more than a factor of 1.5. (auth)

19377 HIGH-RESOLUTION SEARCH FOR IRON LINE EMISSION FROM SCO X-1. Pounds, K. A. (Leicester Univ., Eng.). Nature (London) Phys. Sci.; 229: 175-6(8 Feb 1971).

The results from a rocket-borne Bragg crystal spectrometer, designed to detect the resonance ($1s^2\ {}^1S - 1s\ 2p\ {}^1P$) line of Fe XXV (6.70 keV) in the x-ray spectrum of Sco X-1, are reported. These observations, if positive, would provide definite confirmation of the thermal nature of its radiation. It is concluded that the present result is just compatible with the optical, infrared, and broadband x-ray observations, interpreted as the thermal emission from a 6×10^7 °K source with the density and dimensions proposed by Neugebauer et al. (1969). A further crystal spectrometer experiment being prepared with improved sensitivity should further test this agreement. (UK)

19378 RELEVANCE OF VARIABLE NEGATIVE RADIAL VELOCITIES TO MODELS OF SCO X-1. Wilson, Robert E. (South Florida Univ., Tampa). Nature (London) Phys. Sci.; 229: 176-7 (8 Feb 1971).

It is pointed out that the variability of the emission-line radial velocities of Sco X-1 on a time scale of days or even hours with an amplitude of perhaps ± 50 km s^{-1} has a bearing on possible models for Sco X-1. This rapid velocity variation requires the source gas to be in close association with the central physical object, and not simply a detached cloud outside its immediate gravitational influence. It is argued that the generally negative velocities (mean value $\simeq -100$ km s^{-1}) are due either to a true approach velocity for the central object, or a preferential direction of motion in the observer's direction for the gas streams causing the lines. These alternatives are discussed, and it is concluded that the latter has two advantages; it includes a means for generating a very large x-ray luminosity, and it is not in conflict with the proper motion and photometric evidence that Sco X-1 is a member of the Scorpio—Centaurus association. (UK)

19379 LINEAR POLARIZATION OF PULSAR PSR 2218 +47. Shitov, Yu. P. (Lebedev Inst. of Physics, Moscow). Nature (London) Phys. Sci.; 229: 179(8 Feb 1971).

Observations of PSR 2218 + 47 at frequencies near 100 MHz, using the broad-band cross radio telescope at Pushchino, have shown a strong linear polarization. The plane of polarization depends on frequency; this is due to Faraday rotation in the interstellar medium. (auth) (UK)

19380 COMPTON SCATTERING OF MAGNETOHYDRODYNAMIC AND PLASMA WAVES AS A SOURCE OF RADIO EMISSION FROM METAGALACTIC OBJECTS. Getmantsev, G. C. (Radiophysical Research Inst., Gorky, USSR). Nature (London) Phys. Sci.; 229: 199(15 Feb 1971).

Low-frequency waves in a cosmic plasma give rise to a random, spatially nonuniform, electromagnetic field, and high-frequency radio waves can be generated from this field by Compton scattering of relativistic electrons. This could be the explanation of the radio emission from metagalactic sources. (UK)

19381 18 CM OBSERVATIONS OF GALACTIC OH FROM LONGITUDES 128^0 TO 300^0. Manchester, R. N.; Robinson, B. J.; Goss, W. M. (CSIRO, Epping, New South Wales). Aust. J. Phys.; 23: 751-75(1970).

Observations were made of 18-cm OH emission and/or absorption for 12 sources between galactic longitudes 128 and 300°. The OH is seen in emission in five of the sources, and the four Stokes parameters of the emission profiles were measured. A new type of strong wideband OH emission was found near $l^{II} = 284°$. There are two sources where weak emission at 1612 MHz accompanies absorption on the other three lines. The relationship of the OH to nearby HII regions was investigated by position measurements and by a comparison of OH and recombination line radial velocities. (auth) (Australia)

19382 OH (1667) LINE ABSORPTION AT $2° < l^{II} < 4°, -0°30' < b^{II} < 1°$. McGee, R. X.; Brooks, J. W.; Sinclair, M. W.; Batchelor, R. A. (CSIRO, Epping, New South Wales). Aust. J. Phys.; 23: 777-87(1970).

The OH absorption line at 1667 MHz was traced from $l^{II} = 2°$ to 4°15′ near the galactic plane. Line profiles and contours of apparent opacity are presented. The measurements completed the general picture of absorbing hydroxyl gas in the vicinity of the galactic center and suggest the existence of a gradient of radial velocities of values near -136 km sec^{-1} at $l^{II} = 359°$ to values near $+141$ km sec^{-1} at $l^{II} = 3°30'$. (auth) (Australia)

19383 QUASI-STELLAR OBJECTS IN THE PARKES 2700 MHz SURVEY: THE SELECTED REGIONS AND THE $+-4^0$ DECLINATION ZONE. Bolton, J. G. (CSIRO, Epping, New South Wales); Wall, J. V. Aust. J. Phys.; 23: 789-815(1970).

One hundred and thirty-two quasi-stellar objects or possible quasi-stellar objects have been found in the first areas of the Parkes 2700-MHz survey. Identifications for 36 of these have already been published and 67 have been confirmed by spectroscopy or two-color photography. Relationships between the various radio and optical parameters are briefly discussed. (auth) (Australia)

19384 GALACTIC RADIO SOURCES. I. HIGH RESOLUTION 5000 MHz OBSERVATIONS. Goss, W. M. (CSIRO, Epping, New South Wales); Shaver, P. A. Aust. J. Phys., Astrophys. Suppl.; No. 14, 1-75(1970).

Contour maps of 63 regions in the galactic plane are presented.

The half-power beamwidth was 4′ arc at 5000 MHz. Positions and composite flux densities are given for 206 sources. (auth) (Australia)

19385 GALACTIC RADIO SOURCES. II. HIGH RESOLUTION 408 MHz OBSERVATIONS. Shaver, P. A. (Univ. of Sydney); Goss, W. M. Aust. J. Phys., Astrophys. Suppl.; No. 14, 77-131 (1970).

Contour maps of 58 regions showing 408-MHz radioisophotes for over 200 galactic radio sources are presented. Positions and integrated flux densities are listed for all the sources. (auth) (Australia)

19386 GALACTIC RADIO SOURCES. III. SPECTRA AND PHYSICAL CHARACTERISTICS. Shaver, P. A. (Univ. of Sydney); Goss, W. M. Aust. J. Phys., Astrophys. Suppl.; No. 14, 133-96(1970).

Spectral indices for over 250 galactic radio sources were determined from high-resolution observations at 408 and 5000 MHz. About 14% of the sources had nonthermal spectra. A comparison with results from an H109α line survey showed that the line-to-continuum temperature ratios for thermal sources were greater than about 2.5%, and no recombination line above the detectable threshold was found in a nonthermal source. A search for optical emission from the vicinity of the thermal and nonthermal radio sources resulted in positive identifications for one-third of them. In 16 cases the radio contours are shown superimposed on optical photographs. Electron temperatures were determined directly from the 408-MHz brightness distribution for 50 thermal sources and were found to be consistent with values obtained from H109α recombination line work, indicating that any departures from local thermodynamic equilibrium and their effects on the recombination lines are small. Physical properties of the thermal sources were computed, assuming a spherical H II region model. It is shown that H II regions have a strong tendency to cluster, and that the cluster sizes are comparable with those of open star clusters. No H II regions were found with turnover frequencies greater than 1400 MHz, indicating that high-density sources ($N_e > 5 \times 10^3$ cm^{-3} over a region >0.1 pc in extent) are very rare. The largest, least-dense H II regions have shell structure consistent with current ideas about the dynamical effects of radiation pressure on the dust within H II regions. Fifteen new supernova remnants were identified and distances and physical properties computed for them. For the well-resolved supernova remnants the shell thickness is a constant fraction of the diameter. It is shown that supernova remnants are frequently located in OB associations. (auth) (Australia)

19387 RIGHT ASCENSIONS FOR 389 SOUTHERN RADIO SOURCES FROM THE MOLONGLO FAN BEAM SURVEY. Hoskins, D. G.; Murdoch, H. S. (Univ. of Sydney). Aust. J. Phys., Astrophys. Suppl.; No. 15, 1-16(1970).

The results of the Molonglo fan beam survey are given for the region 10h 30m to 18h 30m and 0° to −39°. Improved right ascensions and 408-MHz flux densities are given for Parkes sources in the region. Other sources ≥2 flux units are listed with a few sources down to 1.6 flux units. Comparisons are made with the Parkes accurate positions. A comparison is made of flux densities and right ascensions with the Bologna fan beam survey for a limited region of overlap. (auth) (Australia)

19388 GALACTIC METRE WAVE RADIATION. A TWO-FREQUENCY SURVEY BETWEEN DECLINATIONS +25^0 AND -25^0 AND THE PREPARATION OF A MAP OF THE WHOLE SKY. Landecker, T. L.; Wielebinski, R. (Univ. of Sydney). Aust. J. Phys., Astrophys. Suppl.; No. 16, 1-30(1970).

A survey of the sky between $\delta + 25°$ and $\delta - 25°$ at 85 and 150 MHz is described, made with aerial beams 3.8° × 3.5° and 2.2° × 2.2°. Absolute measurements of aerial temperature are tabulated for points spaced 2°. A computer program is described that has enabled these results to be reduced to brightness temperatures, which are tabulated for the same points. The derivation of the radiation properties of the aerials is described. The 150-MHz brightness temperatures are combined with the results of other surveys to produce a map of the whole sky. 150-MHz brightness temperatures are presented as a map in galactic coordinates and are tabulated at points spaced 5°. (auth) (Australia)

19389 ATLAS OF OH (1667) LINE PROFILES NEAR THE GALACTIC CENTER. McGee, R. X. (CSIRO, Epping, New South Wales). Aust. J. Phys., Astrophys. Suppl.; No. 17, 1-17 (1970).

An atlas of OH absorption line profiles at frequency 1667.358 MHz is given for the region $358°30' \le l^{II} \le 2°30'$, $-0°20' \le b^{II} \le +0°10'$. The aerial beamwidth was 12.2° arc, the frequency resolution 37 kHz, and the radial velocity range −250 to +125 km sec^{-1}. (auth) (Australia)

19390 PARKES HYDROGEN-LINE SURVEY OF THE MILKY WAY. III. A SYNOPTIC VIEW OF THE GALACTIC EQUATOR, l^{II} = 185° TO 63°. Kerr, F. J. (Univ. of Maryland, College Park); Hindman, J. V. Aust. J. Phys., Astrophys. Suppl.; No. 18, 1-8 (1970).

Six velocity–longitude maps are presented that cover the galactic equator from l^{II} = 185° to 63°. The data were obtained from points at 1° intervals of longitude. (auth) (Australia)

19391 PARKES HYDROGEN-LINE SURVEY OF THE MILKY WAY. IV. ABSORPTION BY LOW-LATITUDE CONTINUUM SOURCES IN THE REGION l^{II} = 296° TO 63°.5. Kerr, F. J.; Knapp, Gillian R. (Univ. of Maryland, College Park). Aust. J. Phys., Astrophys. Suppl.; No. 18, 9-41(1970).

A discussion is given of H I line absorption profiles observed in the directions of 39 continuum sources near the galactic plane. Diagrams of the profiles are presented for each source and estimates are made where feasible for the distances to the continuum sources and the optical depths of the intervening hydrogen concentrations. The reliability of such estimates from absorption observations is discussed and some comparisons are made with optical information. (auth) (Australia)

19392 PARKES HYDROGEN-LINE SURVEY OF THE MILKY WAY. V. THE SECTION l^{II} = 190° TO 299°, PERPENDICULAR TRACKS. Hindman, J. V.; Kerr, F. J. Aust. J. Phys., Astrophys. Suppl.; No. 18, 43-61(1970).

A set of H I velocity–latitude maps is presented for scans across the galactic plane in the region l^{II} = 190 to 299° at 5° intervals. The 210-ft telescope was used with a frequency resolution of 36 kHz. (auth) (Australia)

Solar Phenomena

Refer also to abstracts 18720 and 19526.

19393 (CSIRO-Trans-10284) CHROMOSPHERIC PROCESSES DURING FORMATION OF SUNSPOTS. Waldmeier, Max. Translated by M. Fremt (Australian Atomic Energy Commission), from Z. Astrophys.; 14: 91-103(1937). 14p. Dep. NTIS (U. S. Sales Only).

A classification is made of flocculi observed with H_α spectroheliograms, by following the chromospheric processes resulting in the formation of sunspots. The classification is based on the central intensity of H_α and divides the brightness into 10 stages: normal chromosphere; 3 stages of dark flocculi; 4 stages of bright flocculi; and 3 stages of flares (the brightest flocculi being approximately equal in intensity to the smallest flares). Configuration and dimensions are compared. Twelve examples are used to describe the processes taking place during sunspot formation. An explanation of the Doppler effect in a flocculus is given. (Australia)

19394 (LA-tr-70-27) LABORATORY MODELING SIMULATION OF COMET PHENOMENA. Kaimakov, E. A.; Sharkov, V. I. Translated by A. D. Cernicek (Los Alamos Scientific Lab., N. Mex.), from pp 15-20 of Transactions of the 6th Annual All-Union Winter School on Cosmological Physics, 1970. 10p. Dep. NTIS.

Several hypotheses concerning the structure and composition of comet cores are mentioned. Investigations carried out at the Ioffe Institute on the behavior in vacuum of H_2O ices and aqueous solutions of electrolytes at low temperatures are described. The behavior of dust particles as possible contaminants of ice cores is discussed. (W.D.M.)

19395 FORMATION OF RESONANCE LINES IN MULTI-DIMENSIONAL MEDIA. I. SCALING PROPERTIES IN TWO DIMENSIONS. Jones, Harrison P. (Goddard Space Flight Center, Greenbelt, Md.). Astrophys. J.; 164: 341-54(1 Mar 1971).

A method developed by Rybicki is applied to the non-LTE line-transfer problem for some simple two-dimensional temperature variations which crudely represent some aspects of the lateral fine structure of the solar atmosphere. Approximate scaling formulae are found which describe the spatial variation of the source function and its dependence on the geometric properties of the atmosphere. It is shown that the resulting spatial behavior of the emergent radiation can vary with frequency within a single profile as well as from line to line even when the underlying horizontal temperature structure is independent of depth. (auth)

19396 MODEL FOR THE SOURCE OF SOLAR-FLARE X RAYS. Strauss, Federico M.; Papagiannis, Michael D. (Boston Univ.). Astrophys. J.; 164: 369-78(1 Mar 1971).

A solar flare model by Sturrock is used to compute quantita-

XUM

tively the thermal x-ray emission during a small flare. The results are in good agreement with actual x-ray data obtained with the OGO-5 satellite. The microwave and optical emissions are also discussed. (auth)

19397 PARTITION FUNCTIONS IN IONIZING PLASMAS. Fischel, D.; Sparks, W. M. (Goddard Space Flight Center, Greenbelt, Md.). Astrophys. J.; 164: 359-64(1 Mar 1971).

Extensive calculations of partition functions and other gas characteristics were made for plasmas of seven different chemical compositions. The analysis of the results led to an extremely accurate expression of very few terms for the partition function of any ion. The determination of opacities and equations of state for astrophysical and laboratory plasmas depend upon accurate partition functions. It is now a relatively simple calculation to make. The seven cases were six pure gases (H, He, N, O, Ne, Ar) and a solar composition of sixteen elements. The calculations cover an electron-pressure range of 10^{-2} to 10^{7} dyn cm^{-2} and a temperature range of 3,000 to 150,000°K. (auth)

19398 EXISTENCE OF SOLAR-FLARE PLASMAS OF $T \geq 10^{8}$ °K. Kahler, S. (Naval Research Lab., Washington, D. C.). Astrophys. J.; 164: 365-8(1 Mar 1971).

The steady-state rate of energy loss from a solar-flare plasma of 10^{8} °K as proposed by Chubb to explain hard x-ray observations is considered. For large electron densities ($n_e \geq 10^{10}$ cm^{-3}), the total energy requirement is shown to be excessively large; and for small densities ($n_e < 10^{10}$ cm^{-3}), the distribution of electron energies may not be thermally relaxed. (auth)

19399 POLARIZATION MEASUREMENTS OF SOLAR TYPE-III RADIO BURSTS AT 25.3 MHz. Chin, Y. C.; Lusignan, B. B.; Fung, P. C. W. (Stanford Univ., Calif.). Solar Phys.; 16: 135-51(Jan 1971).

The results are reported of 1966, 1968, and 1969 polarization measurements of solar type-III radio-noise bursts made by recording the output of two orthogonally polarized receiving channels and subsequent digital processing of selected data. The processed data yield total intensity, degree of polarization, ellipticity, and polarization ellipse orientation at 1 second intervals. The measurements are made in a 100-Hz bandwidth to minimize the influence of the propagating medium on the measurements. The mean degree of polarization was found to be about 65% in contrast to previous studies that indicated that type III events were more weakly polarized. By assuming that type-III bursts are flare-related, the polarization characteristics of type-III bursts were studied as a function of the solar longitude of the related flares. The relation between type-III-event polarization characteristics and flare importance was also investigated. The significance of polarization measurements in studies of solar radio events is pointed out, and suggestions for further theoretical research are given. (auth)

19400 CHARACTERISTICS OF SOFT SOLAR X-RAY BURSTS. Drake, Jerry F. (Univ. of Iowa, Iowa City). Solar Phys.; 16: 152-85(Jan 1971).

The burst component of the solar x-ray flux in the soft-wavelength range $2 < \lambda < 12$ Å observed from Explorer 33 and Explorer 35 from July 1966 to September 1968 are analyzed. In this period 4028 burst peaks are identified. (W.D.M.)

19401 RELATION OF ENERGETIC SOLAR X RAYS ($h\nu >$ 60 keV) AND HIGH-FREQUENCY MICROWAVES DEDUCED FROM THE PERIODIC BURSTS OF AUGUST 8, 1968 FLARE. Parks, George K. (Univ., Toulouse); Winckler, John R. Solar Phys.; 16: 186-97(Jan 1971).

Correlated sixteen-second periodic bursts were observed during the flash phase of a class 2b solar flare in energetic x rays, microwaves, and euv ionizing radiation. The observations of the periodic structures in the various x-ray energy channels indicate that the structures are predominantly a phenomenon of high-energy electrons, $E > 80$ keV. In view of the fact that the periodic x-ray structures were correlated extensively in microwave and euv frequencies, a plausible conclusion is that these three types of radiation have a common energy source. The acceleration of the energetic electrons must occur deep in the chromosphere where there are sufficient solar constituents that can be ionized to produce the correlated periodic euv radiation. (auth)

19402 ENERGETIC ELECTRONS ASSOCIATED WITH SOLAR FLARES AND THEIR RELATION TO TYPE-I NOISE ACTIVITY. Sakurai, Kunitomo (Goddard Space Flight Center, Greenbelt, Md.). Solar Phys.; 16: 198-207(Jan 1971).

The generation of energetic electrons is always associated with the solar flares which occur within the sunspot groups that are highly active in emitting type-I noise storms. The number of the solar flares which are associated with the distinct electron events observed at the Earth tends to increase in association with the westward movement of these active groups. This tendency is not contradictory to the close association between electron producing solar flares and type-I active regions if one takes into account the limited directivity of type-I noise storms associated with these sunspot groups. The acceleration of the energetic electrons associated with solar flares seems to be closely related to the type-I active regions where the enormous numbers of suprathermal electrons exist and play a role in generating these radio-noise storms. (auth)

19403 LONG-TERM STORAGE OF RELATIVISTIC PARTICLES IN THE SOLAR CORONA. Simnett, George M.; Holt, Stephen S. (Goddard Space Flight Center, Greenbelt, Md.). Solar Phys.; 16: 208-23(Jan 1971).

A model presented shows that large numbers of energetic electrons (0.3 to >10 MeV) and protons (1 to 30 MeV) can be stored in the solar corona at altitudes around 3×10^{5} km for periods in excess of 5 days. Specific reference is made to the time period July 6–16, 1968 as an excellent example of energetic solar particle storage. Time histories of interplanetary charged-particle intensities observed by the IMP-4 and Pioneer 8 satellites are used to substantiate this contention. Detailed reference is also made to solar x-ray, optical, and radio data obtained during the period in question, in addition to interplanetary magnetometer data. This model provides a unique solution to many hitherto-unexplained solar-particle events, and can also account for the lack of prompt-particle emission from certain large solar flares recorded in the past. (auth)

19404 VELOCITY FIELD DISTRIBUTION IN THE SOLAR PHOTOSPHERE. Kalinjak, A. A.; Vassileva, G. J. (Pulkovo Observatory, Moscow). Solar Phys.; 16: 37-9(Jan 1971).

It is suggested that the asymmetric velocity field distribution is evidence for the gravity–acoustic wave propagation due to temporary solar surface deformation. Assuming that the gravitational wavelength of the disturbance is of the order of the solar radius and that the time of propagation is comparable to the duration of observations (3×10^{4} sec), the velocity of propagation of the disturbance is of the order of the sound velocity in the photosphere. (W.D.M.)

19405 TRAPPED GRAVITY WAVES AND THE FIVE-MINUTE OSCILLATIONS OF THE SOLAR ATMOSPHERE. Thomas, John H.; Clark, Patricia Andre; Clark, Alfred Jr. (Univ. of Rochester, N. Y.). Solar Phys.; 16: 51-66(Jan 1971).

The various modes of hydrodynamic waves are considered for a model of the solar atmosphere based on the Bilderberg model and including the effects of ionization. The atmosphere forms a "potential well" for internal gravity waves, since the stability is low at the base (near the convection) and low again in the region of partial ionization in the chromosphere. Calculations show that there are two resonant (trapped) modes of internal gravity waves for horizontal wavelengths based on the scale of the granulation. The properties of these modes are in close agreement with the two modes of oscillation observed by Frazier (1968). Trapped acoustic modes are found to have periods too short to account for the observations. (auth)

19406 ABSORPTION MATRIX IN A NONUNIFORM MAGNETIC FIELD. Rees, David E. (Univ. of Sydney). Solar Phys.; 16: 67-71(Jan 1971).

Beckers (1969) and Staude (1969) give contradictory expressions for the absorption matrix for a normal Zeeman triplet in a nonuniform magnetic field. Beckers' result is shown to be the correct one. (auth)

19407 RELIABILITY OF THE CATANIA SUNSPOT AREA MEASUREMENTS. Godoli, G.; Morgante, O.; Sturiale, M. L. (Osservatorio Astrofisico, Catania, Italy). Solar Phys.; 16: 72-4 (Jan 1971).

In order to evaluate the reliability of sunspot area measurements determined on drawings made using the Cooke refractor, projected areas on drawings made from the prints of the photograms and from projection of the photograms were determined for 1968. (W.D.M.)

19408 BRIGHTNESS TEMPERATURES OF THE QUIET SUN AND NEW MOON AT THE 6 mm WAVELENGTH. Reber, E. E. (Aerospace Corp., El Segundo, Calif.). Contract F04701-69-C-0066. Solar Phys.; 16: 75-86(Jan 1971).

Absolute brightness temperatures and brightness temperature ratios of a quiet region near the center of the solar disk and the central region of the new Moon were measured simultaneously at 6-mm wavelength. The measured quiet-Sun/new-Moon brightness temperature ratios and reported central brightness temperatures of the new Moon confirm the measured brightness temperature of the quiet Sun at the 6-mm wavelength. Reported central brightness temperatures of the new Moon are tabulated and graphed as a function of frequency and wavelength. The equation of a linear regression line for the reported measurements is given for estimating the brightness temperature of the new Moon at any millimeter wavelength. Estimated brightness temperatures of the new Moon and measured quiet-Sun/new-Moon ratios are used to estimate solar brightness temperatures at several millimeter wavelengths. The solar brightness temperatures, the regression line, and the Van de Hulst theoretical model are presented graphically as a function of frequency and wavelength. The regression line equation is given for estimating solar brightness temperatures at any wavelength in the 6- to 1-mm wavelength interval and is solved for the wavelength of the measured ratios. Reported solar brightness temperatures in the millimeter-wavelength region are tabulated. The measured temperatures in the 6- to 1-mm wavelength interval and a linear regression line are presented graphically as a function of frequency and wavelength. The regression line equation is given and solved for the solar brightness temperatures at the 6-mm wavelength. (auth)

19409 SOLAR ENHANCEMENTS AT 1.2-mm WAVELENGTH. Beckman, J. E.; Clark, C. D. (Queen Mary Coll., London). Solar Phys.; 16: 87-102(Jan 1971).

Solar observations through the atmospheric pass-band centered at 250 GHz were made in the form of isophote maps. These show chromospheric features which have higher brightness temperatures than the mean disc temperature by up to 10%. Examination of corresponding maps at lower frequencies and also of Ca II and Hα spectroheliograms reveals that the hot areas lie above photospheric active regions, and are regular features of the chromospheric millimetric emission having stable structure and duration of several weeks. Less-frequently-observed variable enhancements are also described and linked with the formation of the stable active regions. (auth)

19410 SPECTRUM OF THE INNER CORONA OBSERVED DURING THE TOTAL SOLAR ECLIPSE OF MAY 30, 1965. Jefferies, John T.; Orrall, Frank Q.; Zirker, J. B. (Univ. of Hawaii, Honolulu). Solar Phys.; 16: 103-10(Jan 1971).

A series of spectrograms of the inner solar corona were obtained at the total solar eclipse of May 30, 1965 using a fast spectrograph with a circular slit that recorded the spectrum from λ3000 to λ9000 at all position angles around the limb simultaneously. Absolute intensity is given as a function of position angle for the stronger lines and the continuum. In the coronal enhancement or condensation centered at heliocentric position angle 293°, absolute intensity is given for 34 forbidden emission lines and the continuum. (auth)

19411 GREEN-LINE OBSERVATIONS OF THE MARCH 1970 CORONAL ENHANCEMENTS. Fisher, Richard R. (Univ. of Hawaii, Honolulu). Solar Phys.; 16: 111-19(Jan 1971).

Monochromatic observations of a double coronal enhancement were obtained on March 3 and March 17, 1970. These data were used, along with the assumption of cylindrical symmetry, to calculate the emittance of the Fe XIV 5303-Å lines as a function of height. These estimates were then used to find the electron density and the density of ions in the $^2P_{3/2}$ level of the ground state as a function of height above the limb. (auth)

19412 EXCITED LINES IN THE H AND K REGION OF Ca II IN THE SOLAR FLARE ON MARCH 12, 1969. Gallegos, H. Grossi; Molnar, H.; Seibold, J. R. (Observatorio Nacional de Fisica Cosmica, San Miguel, Argentina). Solar Phys.; 16: 120-4 (Jan 1971).

Many excited lines and a remarkable emission in the continuum were observed in the region around the H and K lines during a strong flare. (auth)

19413 CHARACTERISTICS OF THE SOLAR-ACTIVE REGIONS RESPONSIBLE FOR THE GENERATION OF TYPE-III RADIO BURSTS AT HECTOMETRIC FREQUENCIES IN AUGUST 1968. Sakurai, Kunitomo (Goddard Space Flight Center, Greenbelt, Md.). Solar Phys.; 16: 125-34(Jan 1971).

The RAE (Radio Astronomy Explorer) satellite observed enormous numbers of type-III radio bursts at hectometric wavelengths from August 13 to 25, 1968. The drift rate of these bursts reached a maximum around the middle of August 20. This means that the source responsible for these bursts gradually moved on the solar disk in association with the rotation of the Sun. During this period, there were two large active sunspot groups, MacMath Nos. 9593 and 9597, located in the southern hemisphere and adjacent to each other. By examining the observational data on solar flares, type-I noise storm activity, and energetic electron flux increases, it is shown that the active region MacMath No. 9597 is responsible for the generation of these type-III radio bursts. The relation between type-III bursts producing electron beams and type-I noise activity is briefly discussed, and a model of this active region is qualitatively described. (auth)

19414 INTERPLANETARY MAGNETIC FIELD IRREGULARITIES AND THE SOLAR PROTON DIFFUSION MEAN FREE PATH DURING THE FEBRUARY 25, 1969 EVENT. Quenby, J. J.; Sear, J. F. (Imperial Coll. of Science and Tech., London). Planet. Space Sci.; 19: 95-106(Jan 1971).

From local measurements of the interplanetary magnetic field, the mean free path for solar-proton diffusion during the February 25, 1969 event was calculated under three different assumptions. These are that the dominant cause of field irregularity is either (1) shocks and rotational discontinuities, (2) tangential discontinuities, or (3) small amplitude waves. At a particle rigidity of 43 MV, the mean free path along the mean-field direction under the three alternative suggestions is found to be (1) 1×10^{12} cm, (2) 2×10^{13} cm, and (3) 7.4×10^{10} cm, respectively. Analysis of the power spectra of the magnetic fluctuations suggests that most of the power resides in discontinuities, rather than in waves. Comparison of the mean-free-path values obtained from field data with the results of a previous study of the solar-proton time characteristics during the event further suggests that shocks and rotational discontinuities are the most important form of field irregularity contributing to solar-proton diffusion during the event studied. Little rigidity dependence to the mean free path for particles between 43 MV and 1 GV was found in any method of calculation. (auth) (UK)

19415 EVIDENCE OF QUASI-PERIODIC MOVEMENTS IN THE SOLAR CHROMOSPHERE AND CORONA. Durasova, M. S.; Dobrin, M. M.; Yuding, O. I. (Gorky State Univ., USSR). Nature (London). Phys. Sci.; 229: 82-4(18 Jan 1971).

An attempt was made to find a relation between the quasi-periodic fluctuations and solar-active regions using the 22-m telescope with a beam of 2′ and a wavelength of 8 cm. On the basis of the preliminary results it may be surmised that oscillations with periods longer than 500 to 600 sec originate in the active regions of the Sun. At present, the quasi-periodic components of the solar radio emission are being studied with periods between a second and several hours. It is believed that valuable information can be obtained from simultaneous studies of the fluctuations in the photosphere, chromosphere, and corona of the Sun, the solar wind, and the magnetosphere and ionosphere of the Earth. (auth) (UK)

19416 STANDARD VALUES FOR THE SOLAR CONSTANT AND ITS SPECTRAL COMPONENTS. Thekaekara, M. P. (Goddard Space Flight Center, Greenbelt, Md.); Drummond, A. J. Nature (London). Phys. Sci.; 229: 6-9(4 Jan 1971).

Recent high-altitude aircraft, balloon, and spacecraft measurements of the extraterrestrial solar irradiances indicate that the earlier integral wavelength value was too high and that the spectral data derived from ground-based techniques were uncertain. Standard values are proposed with a summary of the supporting evidence. (auth) (UK)

19417 POLARIZATION OF LOCAL SOURCES OF SOLAR RADIO EMISSION AT 4.4 cm. Gel'freikh, G. B.; Peterova, N. G. (Main Astronomical Observatory, Moscow). Sov. Astron. AJ (Engl. Transl.); 14: 553-62(Jan-Feb 1971).

Translated from Astron. Zh.; 47: 689-701(Jul-Aug 1970).

The Large Pulkovo Radio Telescope, with a resolution of 1.5′, was used in a study of six local sources of the slowly changing component of solar radio emission. Their fluxes, degree of circular polarization, and extent are given, making it possible to trace the changes in these characteristics in relation to the development of spot groups and their movement across the disk. The influence of sidelobe effects on the polarization measurements was taken into account by computations. In most cases the degree of polarization did not exceed 15%. However, the extent of regions of polarized emission was usually less than their extent in the unpolarized flux, so that their real degrees of polarization must be considerably greater (probably about 50%). The relatively high degrees of polarization (~40%) registered directly in local sources during the decay of spot groups are probably associated with the more rapid development (disappearance) of the unpolarized emission component for the local source during this period in comparison with the polarized component. Individual local sources in unipolar spots exhibited a sharply expressed directivity of polarized emission in contrast to local sources in groups with a complex structure which exhibited no appreciable degree of polarization directivity. The

XUM

strong directivity for the polarized emission of local sources in unipolar groups may be caused by the screening of low-lying local source emission regions with a high degree of polarization by cold spicules. However, most local source emission is probably unpolarized and the emission region is situated higher in the solar atmosphere. A temporary decrease in the degree of polarization of one of the details in the local source of group 101 observed on March 23, 1967, can be explained in this way (screening by cold matter). (auth)

19418 QUIET-CORONA TEMPERATURE DETERMINED FROM SOFT X-RADIATION FLUX. Zhitnik, I. A.; Krutov, V. V.; Livshits, M. A. (Inst. of Physics, Moscow. Inst. of Terrestrial Magnetism, Ionosphere, and Radio Wave Propagation, Moscow). Sov. Astron. AJ (Engl. Transl.); 14: 563-66(Jan-Feb 1971).

Translated from Astron. Zh.; 47: 702-7(Jul-Aug 1970).

An emission flux at 8 to 14 Å from an area measuring 3′ by 30′, oriented along the solar equator, was measured during the second half of June 1967 (epoch of maximum activity). The collimator slit intercepted very quiet regions on the solar disk. The absolute flux corresponds to a temperature in the undisturbed corona of not less than 1.6×10^6 °K. (auth)

19419 POSSIBLE ROLE OF THE MASER EFFECT IN THE RADAR ECHO FROM THE SUN. Gordon, I. M., Tsytovich, V. N. (Inst. of Radiophysics and Electronics, Kharkov. Lebedev Inst. of Physics, Moscow). Sov. Astron. AJ (Engl. Transl.); 14: 567-70 (Jan-Feb 1971).

Translated from Astron. Zh.; 47: 708-12(Jul-Aug 1970).

Various mechanisms are discussed for the amplification of electromagnetic waves in the turbulent coronal plasma above active regions where radar reflection from the Sun takes place. It is shown that amplification due to induced conversion of plasma pulsations into electromagnetic waves may play an important role in these signal-formation regions. (auth)

19420 DETERMINATION OF TURBULENT VELOCITIES AND DAMPING CONSTANTS IN FACULAE AND IN THE PHOTOSPHERE. Sitnik, G. F.; Mitropol'skaya, O. N. (State Astronomical Inst., Moscow). Sov. Astron. AJ (Engl. Transl.); 14: 571-6(Jan-Feb 1971).

Translated from Astron. Zh.; 47: 713-19(Jul-Aug 1970).

Profiles of three weak Ni and Fe infrared spectral lines were recorded photoelectrically in the case of a facula and the adjacent photosphere, at 12 regions on the solar disk and at different distances from the center. These profiles were represented by the Voigt function with specified parameters. The parameters were used to determine the damping constants and Doppler widths. The damping constants increase both with cos θ, and with the excitation potential, i.e., they increase inward toward the center of the Sun, both in faculae and in the photosphere. They are slightly larger in the faculae than in the photosphere, owing to heavy electron pressure. The turbulent velocity decreases with increasing cos θ both in the faculae and in the photosphere, i.e., it decreases in the inward direction (deeper into the solar interior). This is confirmed by the relationship between the velocity and the excitation potential. In the facular surface areas, the turbulent velocity is lower than in the photosphere, while the reverse holds in deeper-lying layers. This is in agreement with other data available, and with theoretical concepts on the matter. (auth)

19421 10,830-A LINE IN SOLAR ACTIVE REGIONS. Nguyen-Ngan. (State Astronomical Inst., Moscow). Sov. Astron. AJ (Engl. Transl.); 14: 577-81(Jan-Feb 1971).

Translated from Astron. Zh.; 47: 720-5(Jul-Aug 1970).

The results of photoelectric observations of the infrared line λ 10,830 in different active regions are given. The optical thickness at the line center ($\tau_{10,830}$) was determined from the ratio of intensities of the main and weak components. It is shown that the source function in the 10,830 line is determined by the radiation flux from the photosphere. In order to obtain agreement between the ratio of the intensities of the two components and the intensity of the main component it must be assumed that the line is formed only in some inhomogeneities. Several possible explanations are proposed for the helium line enhancement observed in an active region. However, an important role is played by an increase in the percentage of the hot compartment in the active chromosphere. The Doppler width is determined from $\tau_{10,830}$ and the total half-width. It is less than in an undisturbed region. The paper also gives the optical thickness at the center of the D_3 line, computed from the equivalent width in one active region. It agrees well with computations based on observations of the infrared line with an excitation temperature of the 2^3S-2^3P transition $T_{ex} = 4500$°K. (auth)

19422 QUASI-AXISYMMETRIC MODELS OF A MAGNETIC DYNAMO AND THE NATURE OF SOLAR-ACTIVITY CYCLES. Iroshnikov, R. S. (State Astronomical Inst., Moscow). Sov. Astron. AJ (Engl. Transl.); 14: 582-93(Jan-Feb 1971).

Translated from Astron. Zh.; 47: 726-41(Jul-Aug 1970).

A semiphenomenological nonlinear system of equations is derived for the magnetic dynamo problem. It is shown that the turbulent magnetic viscosity for the averaged fields cannot be treated as a parameter that is in any way known. The behavior of models in which the differential rotation depends on latitude alone is analyzed. It is shown that, at least for certain broad classes of systems, the magnetic field decays, regardless of whether its sign is constant or variable. It is concluded that such models are unpromising for explaining the cycles of solar activity. (auth)

19423 SOLAR MILLIMETRE BURSTS AND PROTON EVENTS. Croom, David L. (Air Force Cambridge Research Labs., Bedford, Mass.). Nature (London), Phys. Sci.; 229: 142-3(1 Feb 1971).

The extension of regular observations of solar bursts to wavelengths of less than 20 mm has enabled the complete radio spectrum of several proton events to be studied, and this has led to the identification of several characteristics in the radio events associated with solar proton flares. (auth) (UK)

19424 LINE FORMATION IN MULTIDIMENSIONAL MEDIA. Jones, Harrison Price. Boulder, Colo.; Univ. of Colorado (1970). 283p. University Microfilms Order No. 70-23,726.

Thesis.

The explanation of the nonuniform appearance of the solar disk when viewed in the wavelengths of strong spectrum lines requires theoretical treatment of radiation transport in three spatial dimensions. The mathematical formulation and general numerical approximation methods appropriate to the "non-LTE" formation of spectrum lines in multi-dimensional atmospheres are, therefore, explored in this thesis. (TSS) (Diss. Abstr. Int., B)

19425 INTERPLANETARY DUST STREAMS: OBSERVATION BY SATELLITES AND LIDAR. Silverberg, Eric Clark. College Park, Md.; Univ. of Maryland (1970). 182p. University Microfilms Order No. 70-23,319.

Thesis.

The interplanetary dust data from the orbiting satellites carrying "microphone-type" detectors are studied in detail. It is shown that the dust showers seen by these satellites are related to low-inclination, periodic comets. The orbital parameters of the dust leaving each of the indicated comets are calculated. Certain aspects regarding the atmospheric entry of interplanetary dust are studied. The optical scattering cross section produced in the mesosphere is calculated for several models. The lidar data on the mesosphere is reviewed along with some data of high-altitude resolution. It is shown that lidar methods can be applied to the study of many cometary dust showers. (TSS) (Diss. Abstr. Int., B)

19426 HYDROMAGNETIC STUDIES OF THE SOLAR WIND. Gussenhoven, Mary Susan. Boston; Boston Coll. (1970). 179p. University Microfilms Order No. 70-24,601.

Thesis.

Of the eight nonlinear, hydromagnetic equations describing a one-fluid model of the solar wind, which is inviscid, isothermal, infinitely conducting, time-independent, and independent of azimuth, six are solved explicitly. These solutions are carried out by two independent methods: first, by introducing poloidal and toroidal contributions the magnetic and particle flux conservations equations are immediately solved; second, the eight original equations are written in generalized meridional coordinates (f_1, f_2, ϕ), specifying that one of the coordinates, f_1, be along flow lines. These equations are used to examine two problems. (TSS) (Diss. Abstr. Int., B)

19427 PLANETARY INFLUENCES ON SUNSPOTS. Ferris, G. A. J. J. Brit. Astron. Ass.; 79: 385-8(Aug 1969).

Theories of Wolf, Carrington, Brown, et al. on possible correlations between the positions of the planets and the occurrence of sunspots are reviewed; the most frequently proposed theory — direct tidal action as a cause of sunspots — is examined, with particular reference to the presumed influence of Jupiter. Jupiter's tide-rising force is, however, negligible (only 2×10^{-5} of the value of the tidal effects of the Moon upon the Earth). Revivals of subject theory by Jose (1965), and Wood and Wood (1965) may have stimulated reconsideration of the problem by Bigg (1967), who has completed a special statistical frequency analysis of the Zurich sunspot numbers with respect to Mercury. It is concluded from Bigg's findings that, in any complete theory of sunspots, the position of the planets must be considered, not as a direct cause, but as a factor possibly altering the timing of spot formation. (Meteorol. Geoastrophys. Abstr.)

19428 SIMULTANEOUS OBSERVATIONS OF SOLAR-FLARE ELECTRON SPECTRA IN INTERPLANETARY SPACE AND WITHIN EARTH'S MAGNETOSPHERE. West, H. I. Jr. (Univ. of California, Livermore); Vampola, A. L. Phys. Rev. Lett.; 26: 458-63(22 Feb 1971).

Magnetic electron spectrometers on satellites OGO-V and OV1-19 were used to make simultaneous measurements in interplanetary space and over the polar caps during the intense solar-particle event of April 1969. The absolute intensities and energy spectra measured on the two satellites tracked within experimental error for the entire history of the event. The results are examined in terms of the "open" and "closed" models of the magnetosphere. (auth)

19429 NEUTRINO SPECTROSCOPY OF THE SUN. Zatsepin, G. T.; Kuz'min, V. A. Kosm. Luchi; No. 10, 75-7(1969). (In Russian).

A program of neutrino spectroscopy of the Sun is discussed; two sets of detectors are used: (1) ^{71}Ga, ^{37}Cl (or ^{87}Rb) and ^{7}Li suitable for radiochemistry, and (2) electron detectors in β-process caused by solar neutrinos in the nuclei of ^{2}D, ^{7}Li, etc., and in the process of neutrino–electron scattering. Detectors of the second group measure the flux of ^{8}B neutrinos, and detectors of the first group measure fluxes of pp, ^{7}Be, and ^{13}N, ^{15}O, neutrinos. The radiochemical method with ^{7}Li is suitable for determining the effects of the CNO cycle. The possibilities of using ^{7}Li as a radiochemical detector are discussed. (auth) (Meteorol. Geoastrophys. Abstr.)

19430 RELATIONSHIP BETWEEN SOFT X-RAY AND RADIO EMISSIONS IN THE 20th SOLAR CYCLE. Pinter, S. (Geophysical Inst., Hurbanovo, Czech.); Olmr, J. Bull. Astron. Inst. Czech.: 21: 373-9(1970).

Some correlations between the x radiation flux in the spectral ranges of 44 to 60 Å, 8 to 20 Å, and 1 to 8 Å and the radio emission flux on various frequencies were investigated. A slowly variable component of the soft x radiation was found to be in good correlation with the radio emission slowly variable component at the rising phase of the 20th solar activity cycle. The soft x radiation correlation is dependent on the radio frequency, a better correlation with higher frequencies can be followed. The correlation between soft x radiation and radio radiation is not linear within the whole range of fluxes. Reducing the correlation coefficient value by reducing the radio frequency was proved. (auth)

19431 1970 SOLAR ECLIPSE AS SEEN BY A TORSION PENDULUM. Saxl, Erwin J. (Tensitron, Inc., Harvard, Mass.); Allen, Mildred. Phys. Rev., D; 3: 823-5(15 Feb 1971).

During the solar eclipse of March 7, 1970, readings were taken and recorded electronically of the times required for the torsion pendulum to rotate through a given fixed part of its path, involving both clockwise and counterclockwise motions, on its first swing from rest. Significant variations in these times were observed during the course of the eclipse as well as in the hours just preceding and just following the eclipse itself. Between the onset of the eclipse and its midpoint there is a steady increase in the observed times. After the midpoint the times decrease suddenly and level off promptly to values considerably greater than those observed before the eclipse. Furthermore, before the eclipse there is a periodic variation in these times. This strange periodicity was essentially repeated two weeks later at the same hours, though the actual values were somewhat greater than the earlier ones. These increases in actual values exceed by a factor of 10^{5} those that can be explained by the attraction of the Moon due to its change in position relative to the Sun and Earth. All this leads to the conclusion that classical gravitational theory needs to be modified to interpret these experimental facts. (auth)

19432 WILSON EFFECT IN THE ABSORPTION LINES. Baranovskii, E. A. Izv. Krym. Astrofiz. Observ.; 40: 105-10 (1969). (In Russian).

A displacement of the sunspot border to the limb when passing from the continuum to absorption line was measured in the lines Fe I λ6253, Ti I λ6258, and H_{α}. It is shown that the observed displacement in the lines Fe I 6253 and Ti I 6258 can be caused only by the large transparency of the umbra. The displacement calculated on the basis of Michard's sunspot model is in good agreement with the observed one when regarding the magnitude of these displacements. It was determined from the measurements of displacements of the sunspot border in H_{α} that this line originates at the height of 740 km above the sunspot. On the basis of Chistyakov's (1962) observations, the conclusion is made that the penumbra near the umbra–penumbra boundary has as large a transparency as that of the umbra. (auth)

19433 VELOCITY FIELD ON THE TWO LEVELS IN THE ACTIVE REGION OF JULY 1966. Gopasyuk, S. I. Izv. Krym. Astrofiz. Observ.; 40: 111-26(1969). (In Russian).

Radial velocities in the rapidly developing active region, which appeared on the solar disc on July 4, 1966, were studied. The records of radial velocities were made simultaneously in the Fe I λ5250 Å and Ca I λ6102.7 Å lines with the aid of magnetograph from July 4 to July 7, 1966. It is shown that the radial velocities on both levels have the same sign in the areas covering over 85% of the whole active region. At the appearance of spots, gases are descending almost all over the active region. The velocities of descending gases increase with height. The velocities of ascending and descending gases are increasing at both levels, when the active region develops, but the velocities of descending gases are higher at the lower level, and those of ascending gases are higher at the upper level. Correlation coefficients between the velocities at different levels vary with time. With the active region developing, gases are descending over more and more parts of the region occupied by the magnetic field of south polarity and, at the same time, gases are ascending in the parts with the magnetic field of north polarity. Strong transverse magnetic fields coincide on the whole with the seats of descending gases. (auth)

19434 FORMATION OF ABSORPTION LINES IN THE INHOMOGENEOUS MAGNETIC FIELD. Rachkovskii, D. N. Izv. Krym. Astrofiz. Observ.; 40: 127-37(1969). (In Russian).

The formation of absorption lines in the solar atmosphere with inhomogeneous magnetic field is considered. Transfer equations for the Stokes parameters with the assumption of an inhomogeneous atmosphere and nonuniform magnetic field were derived, taking into account the absorption and line scattering. Some preliminary calculations were made for the case of only true absorption. The effect of magnetic intensification in the Fe I 5250-Å line was about 30%. It was found that the polarization of the line originates in the layers higher than those where the intensity does. (auth)

19435 ABOUT HARD X-RAY EMISSION OF THE SOLAR FLARE ON SEPTEMBER 28, 1961. Gopasyuk, S. I.; Eryushev, N. N.; Neshpor, Yu. I. Izv. Krym. Astrofiz. Observ.; 40: 138-46(1969). (In Russian).

The time changes of the flux density of bremsstrahlung emission of nonrelativistic electrons with the power law differential energy spectrum are considered. The results are compared with the data of x-ray bursts of the solar flare on September 28, 1961. It is shown that it is not possible to explain the observed decay phases of hard x-ray bursts in the different energy regions only by ionization losses in the plasma. The rapid rise and decay of these bursts can be explained assuming that nonrelativistic electrons and plasma are penetrated by the magnetic field, compressing at first and then expanding. In this case the collision loss in the plasma is small. The emission-region parameters and the power law differential energy spectrum were determined. The parameters explain quite well the radio burst of this solar flare at $\lambda = 3.2$ cm, supposing that it is synchrotron emission. (auth)

19436 STRUCTURE OF THE SOLAR RADIO BURSTS AT 10-CM WAVELENGTH. Yurovskii, Yu. F. Izv. Krym. Astrofiz. Observ.; 40: 147-60(1969). (In Russian).

The large radio telescope RT-22 of the Crimean Astrophysical Observatory was used for the observations of radio bursts at 10-cm wavelength. The following conclusions were made on the basis of records of 10-cm radio emission: (1) decrease of the flux density can either precede or follow the pulse burst; (2) a screening of the radio source of the S-component is frequently observed; (3) radio events connected even with a small flare sometimes consist of three parts—a simple pulse burst, postburst decrease, and a secondary burst; (4) position of the regions of radio emission for the pulse bursts differs from that of the sources of secondary bursts; and (5) properties of the secondary burst occurring even after a small flare allow one to consider this burst as a kind of type-IV radio emission. (auth)

19437 EQUATORIAL ZONE OF AVOIDANCE OF SOLAR COSMIC-RAY ARRIVAL. Levitskii, L. S.; Vladimirskii, B. M. Izv. Krym. Astrofiz. Observ.; 40: 161-72(1969). (In Russian).

A revised list of solar proton events was used for investigation of the configuration of magnetic force lines of the interplanetary magnetic field in the plane perpendicular to the ecliptic plane. It is shown that solar protons do not practically penetrate into a

XUM

relatively thin layer on the solar equatorial plane (+2° heliographic latitude). The proportionality between the importance of the radio burst (2800 to 9400 Mc) and the amplitude of the effect in solar cosmic rays is violated in this zone. High-energy solar-particle events are not observed when the Earth is in the region of the equatorial layer (June and December). The delay time between the arrival of solar particles and the beginning of the flare increases for this equatorial zone. The equatorial layer does not completely "isolate" one solar hemisphere from the other, and so the particles from the flares of the northern hemisphere can penetrate into the southern regions and vice versa. The average flux of the particles diminishes but the delay time remains about the same with these particles crossing this layer. There is no evidence of the inclination of the force lines of the interplanetary magnetic field to the south as well as the approach of the Earth to the border of the solar-wind cavity. (auth)

19438 COMPARISON OF ATTENUATION STATISTICS AT 19 AND 37 GHz FOR SUN–EARTH PATHS. Davies, P. G. (SRC Radio and Space Research Station, Slough, Eng.). Electron. Lett.; 7: 51-2(28 Jan 1971).

For 0.2% of the observing time during May–August 1970, the attenuations at 19 and 37 GHz were about 3.8 and 10.2 dB, respectively, the larger value being the maximum measurable with the technique used in the investigation. Previous attenuation statistics published for 19 GHz are updated to cover the period June 1968–August 1970. (auth) (UK)

Galaxies

19439 PHOTO-IONIZATION OF HYDROGEN AND HELIUM. Brown, Robert L. (National Radio Astronomy Observatory, Green Bank, W. Va.). Astrophys. J.; 164: 387-8(1 Mar 1971).

The total cross section for the photo-ionization of helium including transitions to doubly excited (bound–free and free–free) states is calculated for the soft x-ray region. Empirical relations applicable to problems of x-ray heating are derived from a tabulation of σ(He)/σ(H); it is demonstrated that this ratio is not constant at x-ray energies. (auth)

19440 Hβ PHOTOMETRY OF THE NIGHT SKY. Johnson, Hugh M. (Lockheed Missiles and Space Co., Palo Alto, Calif.). Astrophys. J.; 164: 379-82(1 Mar 1971).

A sampling of the night sky with β' photometry shows that a solar-type spectrum around Hβ prevails at high galactic latitudes but Hβ turns into net emission at low galactic latitudes not inside mapped H II regions. The Hβ emission may be a recombination spectrum of interstellar hydrogen ionized outside hot-star H II regions by soft x-rays or cosmic rays. (auth)

19441 MASS–LUMINOSITY RELATION FOR SPIRAL GALAXIES. Pikel'ner, S. B. (State Astronomical Inst., Moscow). Sov. Astron. AJ (Engl. Transl.); 14: 732-3(Jan–Feb 1971).

Translated from Astron. Zh.; 47: 909-11(Jul–Aug 1970).

New and homogeneous material was used to derive an improved mass–luminosity relation for spiral galaxies. (auth)

19442 STRUCTURE OF ABSORBING MATERIAL IN THE SOLAR NEIGHBORHOOD. Starikova, G. A. (State Astronomical Inst., Moscow). Sov. Astron. AJ (Engl. Transl.); 14: 694-9(Jan–Feb 1971).

Translated from Astron. Zh.; 47: 863-9(Jul–Aug 1970).

Some general relationships for the structure of the absorbing material in the solar neighborhood are derived from data on the absorption A_V and distances r for 183 open clusters. In projection on the galactic plane, the strongest absorption with values $\Delta A_l/\Delta r_l > 2.80$ m/kpc occurs in lanes about 800 pc wide parallel to features in the spiral structure of the Galaxy as identified from optical objects. The absorbing material is displaced by about 200 pc from the center line of the spiral features toward the outer edge relative to the galactic center. In the immediate vicinity of the Sun the absorption is greatest in the directions closest to a spiral-arm feature; in these directions the color excesses and distances are less-closely correlated. (auth)

19443 DYNAMICAL PARAMETERS OF GALAXIES AS A CONSEQUENCE OF COSMOLOGICAL TURBULENCE. Ozernoi, L. M.; Chibisov, G. V. (Lebedev Inst. of Physics, Moscow. Moscow Technical Physics Inst.). Sov. Astron. AJ (Engl. Transl.); 14: 615-26(Jan–Feb 1971).

Translated from Astron. Zh.; 47: 769-83(Jul–Aug 1970).

According to ideas developed previously, the formation of most of the galaxies in a hot expanding universe may be associated with the evolution of cosmological turbulence. Protogalaxies will be isolated from the expanding background after their excess kinetic energy has diminished to the virial values. This process is discussed in an adiabatic approximation in which the hydrodynamical damping of the motions is compensated by energy flow from larger scales, including the largest scale of all, where the decline in energy is governed by the cosmological expansion. The basic cosmogonic parameters of galaxies are evaluated, namely: a) the epoch of gravitational isolation of most of the galaxies; b) the radius–mass relation; c) the relation between specific angular momentum (or velocity dispersion) and mass. Spiral galaxies will be formed in regions of the medium having primarily vortical motions, while elliptical galaxies will appear in regions with predominantly irrotational velocities. An expression is obtained for the proportion of the mass contained in the neighborhood of the null lines of the vortical-velocity field. This expression provides an estimate for: d) the proportion of the mass going into elliptical galaxies. In a similar way globular clusters are regarded as gravitationally bound neighborhoods of null lines in the vortical field in the galaxies themselves, yielding an estimate for: e) the mass (relative to the mass of the galaxy) entering into the globular clusters. The numerical values obtained from the dynamical relations are found to depend on a single parameter, the ratio of the total mass density of the metagalaxy to the critical density in a Friedmann model, although the parameters of galaxies of maximum mass depend also on the velocity of the vortical motions at the epoch when the radiation density predominated over the mass density. All the theoretical estimates are found to agree satisfactorily with the observed quantities for values of these parameters consistent with the observations. (auth)

19444 DERIVATION OF MODEL GALAXIES FROM 21-cm LINE PROFILES. I. REDUCTION OF THE PROFILES. Sizikov, V. S. (Leningrad State Univ.). Sov. Astron. AJ (Engl. Transl.); 14: 609-14(Jan–Feb 1971).

Translated from Astron. Zh.; 47: 760-8(Jul–Aug 1970).

New methods are developed to correct 21-cm line profiles in galaxies for the peculiar velocities of the hydrogen and for the antenna beam. (auth)

19445 SHOCK WAVES IN THE SPIRAL ARMS OF Sc GALAXIES. Genkina, L. M. (Astrophysical Inst., Alma-Ata, USSR). Sov. Astron. AJ (Engl. Transl.); 14: 602-8(Jan–Feb 1971).

Translated from Astron. Zh.; 47: 752-9(Jul–Aug 1970).

The dark lanes at the inner edge of the arms in Sc galaxies apparently result from a shock wave in the gas that overtakes the density wave representing the arm. The total pressure of the interstellar gas is determined by the temperature, the macroscopic motions, and the magnetic field. The amount of compression is ascertained by equating the total pressure to the kinetic pressure of the oncoming stream. The fact that a density $N \lesssim 10\ \mathrm{cm}^{-3}$ is observed in the lanes implies that the field in Sc galaxies is three to five times weaker than in our Galaxy, and the velocity dispersion is no more than 1 to 2 km/sec. Behind the shock front the gas is accelerated primarily by the overall potential of the galaxy. The large width observed for the lanes evidently requires that this acceleration be retarded by the gravitation of the gas layer itself. Individual clouds will pass through the shock with hardly any deflection. The flow along the arms will be decelerated by collisions with such clouds, with the gas being transformed into a denser phase. This effect might explain the formation of the dark "feathers" observed in Sc galaxies. In Sb galaxies with a strong magnetic field, where compression in a shock is not very great, the gas will suffer hardly any phase transition when it crosses the spiral arms. Both the clouds and the intercloud gas will experience compression and rarefaction simultaneously, their pressure remaining in equilibrium. The density of clouds located between or above the arms will vary in proportion to the mean density there, $N \approx 0.3\ \mathrm{cm}^{-3}$. In Sc galaxies the compression will be strong, and phase transitions, which are irreversible processes, will take place. The irreversible character of the compression in a shock wave will cause a gradual retardation of the rotation of the gas, resulting in a substantial approach toward the center of a Sc galaxy during the lifetime of the system. In SBc galaxies, if the mass distribution is similar to that in ordinary Sc galaxies, a very strong wave should exist with rapid motion of the gas toward the center. The observations seem to exclude such an effect, suggesting that the density distribution in SB galaxies might be nearly uniform out to the ends of the bar. (auth)

19446 INTERSTELLAR SILICATE EXTINCTION RELATED TO THE 2200A BAND. Huffman, Donald R.; Stapp, James, L. (Univ. of Arizona, Tucson). Nature (London). Phys. Sci.; 229: 45-6(11 Jan 1971).

Small-particle scattering theory (Mie theory) using measured optical constants of graphite produces a peak near 2200Å that has led to the explanation that the peak of the interstellar extinction

XUM

curve is due to graphite. However, vibrations in the crystal lattices of certain silicates exhibit interstellar absorption near $10\mu m^{-1}$ in the infrared. Complex optical constants were determined for the brown enstatite, $(MgFe)SiO_3$, and it is shown that Mie scattering theory using these optical constants can give a peak in the ultraviolet similar to graphite. (UK)

19447 ROLE OF SOFT GALACTIC X RAYS IN THE ALIGNMENT OF INTERSTELLAR GRAINS. **Mack, John E. (Univ. of Houston, Texas). Nature (London). Phys. Sci.; 229: 49-50 (11 Jan 1971).**

X-ray intensities occurring at 0.2 to 0.4 keV in the Galaxy were estimated in order to test the validity of an hypothesis (Wickramasinghe, Nature 228: 540(1970)) concerning the mechanism by which interstellar grains may be lined up in accordance with the requirements of the measurement of interstellar polarization. It is concluded that soft x rays, acting according to the hypothesis, play a negligible part in the alignment of interstellar grains. (UK)

19448 100-MICRON MAP OF THE GALACTIC-CENTER REGION. **Hoffmann, William F.; Frederick, Carl L.; Emery, Roger J. (Goddard Inst. for Space Studies, New York). Astrophys. J.; 164: L23-28(15 Feb 1971).**

A detailed far-infrared map of the galactic-center region was obtained in the spectral interval 75 to 125 μ with a resolution of 6′. An emitting region 2° by 3.6° yielded a total flux density of $7.6 \pm 0.8 \times 10^{-20}$ W m^{-2} Hz^{-1}, a luminosity of 1.2×10^{42} ergs sec^{-1}, and a peak brightness of 7.4×10^{-3} ergs sec^{-1} cm^{-2} μ^{-1} $sterad^{-1}$. Five individual peaks were observed, four of which corresponded to the radio-source positions of Sagittarius A, Sagittarius B2, G−0.6−0.1, and KE 56. The Sgr A and B sources were clearly resolved. These observations support the thermal dust-emission model with most probable dust temperatures in the range 20 to 50°K. (auth)

19449 OPTICAL SPECTRA OF THE NUCLEI OF ELLIPTICAL RADIO GALAXIES. **Disney, M. J. (Steward Observatory, Tucson, Ariz.); Cromwell, R. H. Astrophys. J.; 164: L35-9 (15 Feb 1971).**

Spectrograms were obtained of the nuclei of twelve nearby giant E and S0 galaxies that were previously found to be radio sources. Of the three galaxies observed with "normal" radio spectra (spectral indices of about −0.9) none showed unusual optical features; whereas of the eight with definite radio spectral peculiarities (and classified as "active" by Heeschen) seven have emission lines characteristic of low-excitation planetary nebulae. NGC 3078, for which insufficient radio data exist to define it clearly as active or passive, exhibits no optical emission lines. Unlike radio spectra, the present optical spectra of the active elliptical galaxies do not demonstrate any obvious QSO-like properties. This is true of the emission-line spectra and, at least to an accuracy of 0.2 mag, is true of the continuum energy distributions over the region 3700 to 5000 A. (auth)

19450 INTERSTELLAR DUST: GRAPHITE, IRON, AND SILICATE. **Wickramasinghe, N. C. (Cambridge Univ., Eng.); Nandy, K. Nature (London). Phys. Sci.; 229: 81(18 Jan 1971).**

Reference is made to an earlier report by the authors (Nature, 227: 51(1970)) that the observed interstellar extinction curve may be accounted for by a mixture of graphite, iron, and silicate grains and also to a criticism of this work by Duley (Nature, 227: 1277 (1970)) in which the coincidence between the theoretical curves and the observations are dismissed as fortuitous. It is restated that it was the conductivity ($\sigma = 2nk/\lambda$) that was assumed constant and not the refractive index ($n - ik$) as stated by Duley. Additional measurements of the optical and infrared index of iron are given to support the model originally proposed. The reply by Duley included contends that no additional evidence for the presence of silicates, iron, or graphite in the interstellar medium was presented. It is considered that Wickramasinghe and Nandy have succeeded in finding one solution to the problem when a large and perhaps infinite number of solutions exists. (UK)

19451 X-RAY EMISSION AT ¼ keV BY BREMSSTRAHLUNG SUPRATHERMAL PROTONS. **De Frietas Pacheo, J. A. (Observatoire de Nice, Le Mont-Gros, France). Nature (London). Phys. Sci.; 229: 84-5(18 Jan 1971).**

Brown (Nature, 229: 85(1971)) questioned the results of a previous letter by the present author (Nature, 227: 1230(1970)) concerning the bremsstrahlung of suprathermal protons as the mechanism responsible for the x-ray emission at ¼ keV. In agreement with Brown, the author states that the self-absorption by the gas of the so-called galactic halo and the Metagalaxy is to be neglected since the gas is ionized, but disagrees with him regarding the possibility of the existence of a large flux of suprathermal particles outside the Galaxy. It is calculated that the effective spatial range of suprathermal protons $R < 600$ psc, and in this case it is very difficult to understand how suprathermal particles can leak out of the Galaxy and even fill the halo. The author does not think that the flux of suprathermal particles from the Galaxy can be extended very far from the disk and, therefore, feels that the bremsstrahlung emission produced by these particles cannot be strong enough to explain the isotropic x-ray background. In reply, Brown puts forward arguments from which he concludes that the suprathermal proton bremsstrahlung process remains a viable mechanism for the production of the diffuse isotropic extragalactic background at ¼ keV, but x-ray production in the galactic plane by suprathermal proton bremsstrahlung certainly cannot account for the soft x-ray enhancement apparently present at low galactic latitudes. (UK)

19452 COMPOSITION OF INTERSTELLAR GRAINS. **Gilra, Daya P. (Univ. of Wisconsin, Madison). Nature (London); 229: 237-41(22 Jan 1971).**

Computations show that a mixture of meteoritic silicate, silicon carbide, and graphite particles can explain all the observed properties of interstellar grains. 43 references. (auth) (UK)

19453 SILICA MINERALS IN INTERSTELLAR DUST. **Manning, P. G. (Dept. of Energy, Mines, and Resources, Ottawa). Nature (London). Phys. Sci.; 229: 115-16(25 Jan 1971).**

A brief review of work carried out by Nandy and Seddon (Nature 226: 63(1970)) and by Hoyle and Wickramasinghe (NSA 22: 38677) on the broad interstellar band that occurs in the ultraviolet band at 2200 Å is given, and it is suggested that this band is similar in origin to the 2250-Å band observed in spectra of terrestrial Fe or Al-bearing quartz. (UK)

19454 STELLAR CONTENT OF M82. O'Connell, Robert West. Pasadena, Calif.; California Inst. of Tech. (1970). 191p. University Microfilms Order No. 70-24,308.

Thesis.

The stellar contents of two regions on the peculiar galaxy M82 are investigated by spectral synthesis. One of the regions is identified as the nucleus of the galaxy on the basis of its surface brightness and inferred mass density; the other is spectrally representative of the disk of M82. Narrow-band spectrophotometry for both regions can be satisfactorily interpreted in terms of ordinary kinds of stars and dust prevalent in the solar neighborhood if 10^3 $M_\odot$ of dust is mixed with the stars in the nucleus. There is no evidence for stellar abundance anomalies or the presence of significant amounts of nonstellar radiation except for gaseous emission between 3400 and 11,000 Å. Approximately 50% of the observed Na I λ5892 absorption feature originates in the interstellar medium of M82. The deduced main-sequence luminosity functions for both regions resemble that for the galactic disk in the solar vicinity except that an excess of massive stars ($M_V < -3$) exists in the nucleus and a deficiency, in the disk. Sufficient numbers of hot stars are present in the nucleus to maintain the observed level of nuclear interstellar ionization. The absence of massive stars in the disk is corroborated by photographic and spectroscopic evidence and may be the result of a suppression of star formation by a nuclear disturbance. The mass density inferred from the synthesis for the small disk region observed is much higher than found in typical late-type galaxies. The results of extensive absorption feature index photometry of common galactic stars are also described. (Diss. Abstr. Int., B)

19455 MEASUREMENTS OF HARD X AND GAMMA RADIATION FROM VIRGO A AND CENTAURUS A. Fishman, Gerald Jay. Houston, Tex.; Rice Univ. (1970). 176p. University Microfilms Order No. 70-23,507.

Thesis.

Balloon-borne measurements were made of two nearby radio galaxies, Virgo A and Centaurus A, in the hard x and gamma-ray regions in an effort to relate the radiation to lower energy regions of the electromagnetic spectrum. Measurements of this type will make it possible to evaluate various models of the emission mechanism and energy source of these unusual objects. Possible emission mechanisms and models of radio galaxies are reviewed and discussed. Two of these models would predict copious x-ray emission via the synchrotron process observable in the energy range of the detector. The Virgo A observation in August 1967 found a weak source of x rays in the energy region from 40 to 107 keV. The spectral flux amounted to $1.2 \pm 0.5 \times 10^{-4}$ photons cm^{-2} sec^{-1} keV^{-1}. No radiation was found at higher energies. The Centaurus A observation was made in May 1968. No radiation was detected from that radio galaxy; low upper limits were derived in selected energy regions. The detector was modified with additional active collimation for a second observation of Virgo A in December 1968. This modification limited the field of view to 3°. Radiation was again seen from the region of Virgo A in the energy range from 40 to 95 keV amounting to a corrected flux of $2.1 \pm 0.7 \times 10^{-4}$ photons

XUM

cm^{-2} sec^{-1} keV^{-1}. The two independent observations of Virgo A combine to yield a weighted spectral intensity of $9.9 \pm 2.7 \times 10^{-3}$ keV cm^{-2} sec^{-1} keV^{-1} at 65 keV. The two observations of Virgo A with detectors of different fields of view made it possible to set useful upper-limits to the high-energy radiation from the quasar 3C 273. (TSS) (Diss. Abstr. Int., B)

19456 MULTICOLOR PHOTOMETRY OF THE GALAXY NGC 4254 USING AN IMAGE CONVERTER. **Pronik, I. I.; Chuvaev, K. K. Izv. Krym. Astrofiz. Observ.; 40: 96-104(1969). (In Russian).**

Multicolor photometry of the NGC 4254 galaxy was carried out in seven spectral bands. An image converter on the 2.6-meter Schajn Telescope was used. The spectral energy distribution is the same for the central part (nearly 500 psc in diameter). That is the most dense part of the investigated galaxy where radiation decreases according to the exponential law. Outside of this region the radiation is weaker by one order of magnitude. It is bluer than in the central part and decreases very smoothly with the distance from the center. In the central part of the galaxy, 2 kpsc in diameter, an emission in H_α was observed. Its intensity is no less than 10% of the continuum. At distances 0.7 to 8 kpsc from the center of the galaxy, 38 H II regions were found. In 9 of these regions, emission in nebular lines (O II) was suspected. Comparison of the energy distribution of stellar groups in NGC 628 and NGC 4254 shows that in the latter these groups are bluer. The upper limit of the masses of hydrogen nebulae in NGC 4254 lies between 10^6 and 10^5 $M_\odot$ according to the measurements. Taking into account the possible effect of the discrete structure of nebulae, these figures may be 1.0 to 1.5 orders of magnitude lower. (auth)

19457 NOTES TO THE SCATTERING FROM A CIRCULAR GRAPHITE CORE–ICE MANTLE CYLINDER AT NORMAL INCIDENCE. **Svatos, J. (Charles Univ., Prague). Bull. Astron. Inst. Czech.; 21: 368-72(1970).**

A solution for infinite composite cylinders at normal incidence of light is given. Extinction evaluations for graphite core–dielectric mantle cylinders having dimensions $R_0 = 0.05$ μ, $R = 0.13$ μ are compared with those for graphite core–ice mantle spheres in the infrared region 2 to 3.4 μ. It is shown that these composite cylinders do not follow the interstellar extinction law. (auth)

19458 VARIABILITY OF X-RAY EMISSION FROM M87. Byram, E. T.; Chubb, T. A.; Friedman, H. (Naval Research Lab., Washington, D. C.). Nature (London); 229: 544-6(19 Feb 1971).

The authors first reported x-ray emission from the direction of M87 in 1965 and several measurements were subsequently made. The position of the x-ray source was fixed in declination to ±0.1° by a fan beam scan. The new observation reported in this article places the source inside an error box of 0.1 square degrees that includes M87. Both the flux and the shape of the x-ray spectrum in the present observation differ markedly from previous observations, implying a high degree of variability. Evidence for x-ray emission from the quasar 3C 273 was also obtained, although with much lower statistical significance than for M87. (auth) (UK)

19459 GALACTIC MAGNETIC FIELD AND COSMIC RAYS. Piddington, J. H. (CSIRO, Chippendale, New South Wales). Aust. J. Phys.; 23: 731-50(1970).

The structure of the magnetic field of the Galaxy and other spiral systems and the inseparable problem of the origin of cosmic rays are examined: (1) A variety of evidence is used to show that the galactic field extends far beyond the disk and connects the disk field with a general field fixed in the local system of galaxies. (2) The coronal field extends beyond 10 kpc as an oblique helix that is constantly expanding, and has partially force-free characteristics. (3) As in the case of the disk field, the axi-asymmetric coronal field exercises major control over gas clumping and star formation in the disk. Such a model of spiral arm formation has advantages over gravitational theories. (4) The supernova explosion and neutron star theories of cosmic rays are examined and shown to meet major difficulties. A new model of supernova-shell radio sources is proposed. (5) A massive magnetic rotator at the center may be a major source of cosmic rays in the Galaxy and a proportion of other spirals. (6) A second mechanism of cosmic-ray acceleration is by magnetic pumping by hydromagnetic compression waves. These originate in the central rotator (period $\lesssim$300 yr) and accelerate particles in situ throughout the corona and disk. (auth) (Australia)

Cosmology

19460 ELLIPSOIDAL VELOCITY DISTRIBUTIONS AND A KINETIC THEORY OF NEWTONIAN COSMOLOGICAL MODELS. **Truemper, Manfred (Texas A and M Univ., College Station). Astrophys. J.;164: 223-6(1 Mar 1971).**

A method is given for obtaining all solutions (F,ϕ) of the self-consistency problem for gravitating, collisionless gases (stellar systems) whose residual velocity distribution is of the type $F = \psi(w \cdot Cw)$ with a positive, symmetric, time-dependent matrix C. For any given C one can find a solution of Liouville's and Poisson's equations by solving a fifth-order system of ordinary differential equations. All these solutions are of the cosmological type; i.e., they have constant mean mass density and a mean velocity field which is linear in the Cartesian coordinates. On the other hand, for any homogeneous (generally anisotropic) cosmological model in Newton's theory one can find a self-consistent velocity distribution by solving a system of six linear ordinary differential equations. (auth)

19461 NEWTONIAN BIG-BANG HIERARCHICAL COSMOLOGICAL MODEL. **Wertz, James R. (Univ. of Texas, Austin). Astrophys. J.; 164: 227-36(1 Mar 1971).**

Hierarchical cosmology deals with models having multiple clustering in the matter distribution of the Universe. A continuous representation of a hierarchical universe is introduced and applied, within the framework of Newtonian cosmology, to a more or less realistic model. In general, the mean mass-density is a function of both position and size of the volume considered, and generally decreases with increasing radius. (Observationally, de Vaucouleurs has determined $\rho \propto r^{-1.7}$ in the range $10^{20} < r < 10^{27}$ cm.) Similarly, the Hubble parameter depends on the order of the cluster involved and is, therefore, a function of the density. If a common origin of clusters is assumed, the relative expansion of the Universe may be determined directly from the density–radius relation. For realistic models (big-bang hierarchy with $\rho \propto r^{-\theta}$ at the present epoch), a Hubble law characteristic of the hierarchy and, at least in principle, subject to observational verification is obtained. (For a reasonable choice of parameters, the graph is nearly linear but does not intersect the origin.) The history of such a big-bang hierarchy is briefly discussed. (auth)

19462 BACKGROUND RADIATIONS. **Prilutskii, O. F.; Rozental, I. L.; Shukalov, I. B. (Inst. for Space Research, Moscow). Sov. Astron. AJ (Engl. Transl.); 14: 669-75(Jan-Feb 1971). Translated from Astron. Zh.; 47: 832-40(Jul-Aug 1970).**

The interaction between the isotropic radiations in various wavelength ranges (in particular, radio emission and x rays) is discussed. The analysis rests on the assumption that the bulk of the radiation is generated in extragalactic objects. The transmission of cosmic electrons through photon and magnetic fields is examined. An analysis is made of the energy spectra and intensities of intergalactic electrons and of the radio emission and x rays in the Universe. It is suggested that the isotropic soft x rays (energies of 240 to 280 eV) are produced in the upper layers of the Earth's atmosphere. (auth)

19463 SYMMETRIC COSMOLOGY. **Alfven, H. (Royal Inst. of Tech., Stockholm). Nature (London); 229: 184(15 Jan 1971).**

A reply is made to the criticisms of Hoyle and Steigman (Nature, 224: 477(1969)) concerning symmetric cosmology, and it is claimed that some of the statements made by these authors are incorrect, including: the assumption that Klein's metagalactic model turns inside the Schwarzschild limit; also the assumption that, in this model, the path of photons is long compared with the linear size at the turning; also the comments concerning the postulation of processes giving rise to magnetic fields of the order of 1 to 100 gauss. It is stated that discussion of the symmetric cosmology should not be focussed only on the existence of antimatter. Symmetric cosmology can be regarded as an attempt to ascertain how far astrophysics can be understood only by known laboratory laws and without introducing new laws. (UK)

19464 THERMODYNAMICS AND COSMOLOGY. **Stewart, J. M.; MacCallum, M. A. H.; Sciama, D. W.** Comments Astrophys. Space Phys.; 2: 206-8(Nov-Dec 1970).

One of the most surprising differences between the classical and relativistic kinetic theory of gases is that, in the latter case, an ideal gas whose particles have nonzero rest mass cannot expand adiabatically. In a recent critical commentary, Schucking and Spiegel (1970) questioned the validity of this result. They expressed reservations about some of the assumptions made in its derivation and produced an interesting counterexample that would appear to contradict it. An attempt is made to answer the questions they raise by adducing further considerations suggesting that the result may indeed be valid. Although the effect can be shown to be small in most cosmological situations, its existence is of considerable theoretical importance, and so the doubts concerning its validity should be resolved. (W.D.M.)

19465 GENERAL RELATIVITY AND GRAVITATIONAL COLLAPSE. Sexl, R. U. (Univ., Vienna). Acta Phys. Austr.; Suppl. 7, 308-54(1970).

From 9th Conference on Developments in High Energy Physics, Schladming, Austria. See CONF-700220.

The lectures on general relativity and gravitational collapse treat a summary and experimental tests of general relativity, gravitational waves, the use of exterior forms in Riemannian geometry, and spherically symmetric solutions of Einstein field equations. Gravitational collapse, incompressible matter, the geometry of the Schwarzschild solution, the equation of state at high pressures, and Kruskal space are also considered. (J.F.P.)

19466 PLASMA PHYSICS APPLIED TO COSMOLOGY. Alfven, Hannes (Univ. of California, San Diego, La Jolla). Phys. Today; 24: No. 2, 28-33(Feb 1971).

An attempt is made to approach cosmological electrodynamics in terms of matter, antimatter, and ambiplasma. The main point of the article is that every effort should be made to use to their fullest the established laws of physics instead of searching for new ones. (W.D.M.)

Planetary Phenomena

19467 ATMOSPHERE OF MERCURY. Banks, P. M.; Johnson, H. E.; Axford, W. I. Comments Astrophys. Space Phys.; 2: 214-20(Nov-Dec 1970).

The arguments that can be used to support various atmospheric models are discussed, with the conclusion that a collisionless exosphere represents a minimum condition and that dense atmospheric models may be appropriate. (W.D.M.)

Atomic and Molecular Physics

Refer also to abstracts 18850, 19207–19210, 19949, and 20446.

Atomic, Electron, Ion, and Molecular Beams and Their Reactions

Refer also to abstract 19757.

19468 (INP–710) GEOMETRICAL EFFECTS IN SCATTERING OF IONS BY SURFACE OF SOLIDS. Soszka, Waldemar (Institute of Nuclear Physics, Krakow (Poland)). 1970. 120p. (In Polish). Dep. NTIS (U. S. Sales Only).

The spatial and energy distributions of ions scattered on a target having an ordered structure were investigated. The single and multiple collision approximations are considered. The experiments showed the existence of some geometrical correlations in multiple scattering. These correlations lead to anisotropy of spatial distributions and fine structure of the energy spectra. The considerations take account of the modulation of the primary beam due to the channel capture effect. (auth)

19469 SURFACE AND VACUUM PHYSICS INDEX. VOLUME 5, NO. 12, 1970. Bibliography, Author Index, Subject Index in Alphabetical Order, Cumulative Subject Index in Logical Order. Frankfurt am Main; Zentralstelle fuer Atomkernenergie-Dokumentation (1970). 55p.

This listing includes 188 references on various aspects of surface and vacuum physics. (A.G.W.)

19470 ISOTOPE DEPENDENCE IN K-, L-, AND M-SHELL IONIZATION CROSS SECTIONS BY PROTON AND DEUTERON BOMBARDMENTS. Shima, Kunihiro; Makino, Isao; Sakisaka, Masakatsu (Kyoto Univ.). J. Phys. Soc. Jap.; 30: 611-19(Mar 1971).

Ionization cross sections for Al and Ti K shells, Cu, Mo, and Ag L shells, and W–M shells are presented for incident protons and deuterons in the energy range from 90 to 180 keV/amu. The cross sections are derived from the thick-target yields of the respective characteristic x rays. In contrast to the prediction by the Born approximation, isotope dependence is clearly found in the ionization of each target atom. The cross-section ratios for K and L shells as a function of projectile energy per nucleon line up systematically according to the shell binding energies of target atoms. The magnitudes of the K-shell ionization cross sections are in good agreement with "binding theory" of Brandt et al. This means that, in the present energy range, the ionization cross sections depend strongly on the Coulomb deflection of the incident particle and the transient additional binding energy of the K-shell electron with the incident particle during the collision. (auth)

19471 OPTICAL EMISSION FROM ELECTRON-IRRADIATED THIN FOILS. Dinardo, Robert Philip. Hoboken, N. J.; Stevens Inst. of Tech. (1970). 135p. University Microfilms Order No. 71-1165.

Thesis.

Self-supported (334- to 2000-Å thick) foils of gold, silver, copper, and carbon, and a multiple potassium/carbon foil were studied. Normally incident, monochromatic electron beams of 1.0 μA with energies of 297 keV, 423 keV, 632 keV, and 1.10 MeV were used. The absolute photon intensity emitted in the 2200- to 5800-Å wavelength region was analyzed. The optics consisted essentially of a grating spectrometer, spectral filters, an analyzing polarizer, and a quartz-window photomultiplier. The light intensity was measured as a function of forward angle of emission (15°, 30°, 45°) and degree of polarization (parallel and perpendicular to the plane of the incident electrons and the observed photons). The radiation contributions to the photon intensities were found to be essentially transition radiation and optical bremsstrahlung. The results of the perpendicularly polarized radiation clearly demonstrate characteristics of bremsstrahlung. The results also show that the parallel polarized radiation consisted of both transition radiation and bremsstrahlung, the bremsstrahlung being unpolarized and the transition radiation contribution giving very good agreement with that predicted by theory for gold, silver, and copper. The results confirm the prediction that transition radiation is completely polarized in the plane of incidence at these higher electron energies. The results also confirm the unpolarized nature of optical bremsstrahlung, which has been experimentally found at the lower electron energies but has not been predicted by theory. The experimental results for silver show a relatively pronounced minimum in the spectral distributions of transition radiation. This minimum near 3200 Å is predicted by transition radiation theory and is related to the optical transparency of silver in this wavelength region. The experimental data for the carbon foil have been combined with transition radiation theory in a best fit approach to obtain the optical constants of the foil. The results provide values for the constants between those of graphite and glassy carbon (amorphous). The results for the potassium/carbon multiple foil indicate very little structure in the emission spectra around the plasma frequency. The expected peak was not observed. The contribution of Cherenkov radiation was also considered; however, no indication was observed. (Diss. Abstr. Int., B)

Atomic and Molecular Properties

Refer also to abstracts 18859 and 19757.

19472 (UCRL–50985) EQUATION OF STATE FOR DENSE HYDROGEN FROM ZERO TO 10,000°K. Rogers, F. J.; Neece, G. A.; Hoover, W. G.; Ross, Marvin (California Univ., Livermore. Lawrence Radiation Lab.). 23 Dec 1970. 4p. Dep. NTIS.

The results of theoretical calculations of the energy and pressure of dense hydrogen are presented in graphical form. The molecular equation of state and the metallic equation of state are both calculated using the Debye approximation. (auth)

19473 CHEMICAL INFORMATION FROM PHOTOELECTRON AND CONVERSION-ELECTRON SPECTROSCOPY. Hollander, J. M.; Shirley, D. A. (Univ. of California, Berkeley). Annu. Rev. Nucl. Sci.; 20: 435-66(1970).

The relation between inner-shell atomic electrons and chemical properties and methods for studying this relation are reviewed. Four inner-shell spectroscopies and the chemical parameters that can be derived from each are described briefly: (1) chemical effects on the nuclear decay rate, (2) isomer shifts in Moessbauer spectra, (3) chemical effects on conversion-electron spectra, and (4) chemical shifts in the spectra of photoelectrons from inner shells. The measurement and interpretation of chemical shifts by x-ray photoelectron spectroscopy, especially in atoms and molecules, is discussed. Application of this method to solids is also considered. A special class of new effects, core-level splitting, is pointed out. 66 references. (A.G.W.)

19474 COMMENT ON RELATIVE MAGNETIC SUBSTATE AMPLITUDES IN FOIL EXCITATION OF FAST HYDROGEN ATOMS. Sellin, I. A. (Univ. of Tennessee, Knoxville). Phys. Rev., A; 3: 1512-13(Apr 1971).

If the particle–foil interaction potential governing production of H atoms coherently excited by passage through thin foils obeys the LS coupling scheme applied by Macek (conservation of z components of total orbital and spin angular momenta of the entire particle–foil system, and incoherence of final states of foil con-

XUM

stituents), the ad hoc assumption that random phases prevail among the hydrogenic magnetic substate amplitudes invoked in the interpretation of certain recent experiments is avoided. Arguments concerning relative phases of states of different orbital angular momentum are unaffected. (auth)

19475 VARIATIONAL PRINCIPLES FOR EXPECTATION VALUES APPLIED TO THE GROUND STATE OF THE HELIUM ISOELECTRONIC SEQUENCE. Shustek, L. J.; Krieger, J. B. (Polytechnic Inst. of Brooklyn). Phys. Rev., A; 3: 1253-60 (Apr 1971).

Analytic calculations of the expectation values of r^n, $n = -2, -1, 1, 2$, the kinetic energy, and the charge density at the origin, were performed for two-electron atoms with nuclear charge Z using a variational principle first proposed by Delves. The trial wave function ψ_{0T} was taken as a product of single-particle hydrogenic states with a single variational parameter $\bar{Z}$. In each case the complementary function ψ_{1T} was obtained by exactly solving a differential equation relating ψ_{1T} to both ψ_{0T} and the operator whose expectation value was to be calculated. For $Z \geq 2$, the least accurate results obtained are for $\langle r^2 \rangle$, which are 1.9 and 0.7% lower than the highly accurate values obtained by Pekeris for He and Li^+, respectively. In all cases the reduction in the error obtained using a one-parameter wave function given by the variational principle for minimizing the energy increases as Z increases, and the results are, in many cases, comparable to those given by the Hartree–Fock treatment. A condition proposed by Aranoff and Percus involving the minimization of an auxiliary expression was used to renormalize ψ_{1T}. This method left unchanged or improved the results for all cases considered. (auth)

19476 MINIMA IN ATOMIC CONTINUUM GENERALIZED OSCILLATOR STRENGTHS. Manson, Steven Trent (Georgia State Univ., Atlanta). Phys. Rev., A; 3: 1260-7(Apr 1971).

Minima in continuum generalized oscillator strengths for atoms are found to exist, and their position as a function of energy is discussed. It is shown that an increased energy loss they occur at larger momentum transfer. Calculations are performed for the Na $3s \rightarrow \epsilon p$, K $4s \rightarrow \epsilon p$, and Ar $3p \rightarrow \epsilon d$ transitions. (auth)

19477 LAMB SHIFT AND BINDING ENERGIES OF K ELECTRONS IN HEAVY ATOMS. Desiderio, A. M.; Johnson, W. R. (Univ. of Notre Dame, Ind.). Phys. Rev., A; 3: 1267-75(Apr 1971).

The self-energy of K electrons in atoms with atomic numbers in the range $70 \leq Z \leq 90$ is determined numerically. Detailed theoretical evaluations of K-electron binding energies including all effects of $O(\alpha mc^2)$ are given for the four heavy closed-subshell atoms, W, Hg, Pb, and Rn, in the range considered. With the present values of the electron self-energy, the theoretical K-shell binding energies for these elements are found to agree with experimental determinations to better than 1 part in 10^4. (auth)

19478 ACCURATE NUMERICAL HARTREE–FOCK SELF-CONSISTENT-FIELD WAVE FUNCTIONS FOR RARE-EARTH IONS. Saxena, K. M. S.; Malli, Gulzari (Simon Fraser Univ., British Columbia). Phys. Rev., A; 3: 1278-82(Apr 1971).

Accurate numerical Hartree–Fock (HF) self-consistent-field (SCF) wave functions were calculated for Pr^{3+}, Ce^{2+}, Nd^{3+}, Pr^{2+}, Pm^{3+}, Nd^{2+}, Sm^{3+}, Pm^{2+}, Eu^{3+}, Sm^{2+}, Gd^{3+}, Eu^{2+}, Tb^{3+}, Gd^{2+}, Dy^{3+}, Tb^{2+}, Ho^{3+}, Dy^{2+}, Er^{3+}, Ho^{2+}, Tm^{3+}, and Er^{2+} ions having an f^N electron configuration in their ground-state manifolds. Calculations, in general, have an accuracy of seven significant digits in the total energy. Values of several Hartree–Fock parameters were also obtained from these wave functions. (auth)

19479 POTENTIAL CURVES FOR He_2^+ AND Li_2^+. Bardsley, J. N. (Univ. of Texas, Austin. Univ. of Pittsburgh). Phys. Rev., A; 3: 1317-21(Apr 1971).

Ab initio calculations are presented for several states of He_2^+ and Li_2^+ that are relevant to collision problems. In He_2^+, qualitative agreement is found with the predictions from the analysis of the oscillations and anomalous thresholds in He^+–He collision cross sections. For Li_2^+, the results suggest that the oscillations in Li^+–Li differential scattering cross sections are due to Σ–Π transitions caused by the coupling of electronic and nuclear rotations. (auth)

19480 ROTATIONAL RELAXATION OF HD BELOW 40 K. Prangsma, G. J.; Heemskerk, J. P. J.; Knaap, H. F. P.; Beenakker, J. J. M. (Rijksuniversiteit, Leiden). Physica; 50: 433-43(7 Dec 1970).

Sound absorption measurements are reported for the systems HD, HD–He, and HD–Ne at a number of temperatures between 20.4 and 42.6°K. For HD, the times for relaxation between the rotational and the translational degrees of freedom through collisions with HD and through collisions with He are derived. For HD–Ne, the present method turns out to be inadequate to determine rotational relaxation times. For HD–HD collisions it is found that the collision number, Z_{rot}, has a temperature-independent value of about 10, whereas for HD–He collisions Z_{rot} is about 17. (auth)

19481 HELIUM 2^1S–n^1P METASTABLE TRANSITION PROBABILITIES. Arrathoon, R. (Bell Telephone Labs., Inc., Murray Hill, N. J.). J. Opt. Soc. Amer.; 61: 332-4(Mar 1971).

A pulse-amplitude-modulated form of the Reiche–Ladenburg reabsorption technique was devised to determine relative transition probabilities for a number of spectral lines terminating on the He 2^1S level. The technique provides accurate upward branching ratios from metastable levels. The experimental results indicate that such methods may be used to complement values obtained from detailed current theoretical calculations, even for extensively studied gases such as helium. Absolute gain values for several of the weaker He–Ne visible laser transitions were also determined. (auth)

Positronium, Muonium, and Mesic Atoms and Molecules

Refer also to abstracts 18748, 19851, and 19888.

19482 (NRC-TT-1426) MESOATOMIC PROCESSES AND A MODEL OF LARGE MESIC MOLECULES (REVIEW). Gershtein, S. S.; Petrukhin, V. I.; Ponomarev, L. I.; Prokoshkin, Yu. D. (Joint Inst. for Nuclear Research, Dubna (USSR)). Translated from report JINR-P4-3860. 51p. Dep. NTIS (U. S. Sales Only).

An abstract of this paper, prepared from the original language, appeared as NSA 22: 41289.

19483 PIONIC ATOMS. Backenstoss, G. (Univ., Karlsruhe, Ger. CERN, Geneva). Annu. Rev. Nucl. Sci.; 20: 467-508(1970).

A review of basic properties common to all exotic atoms is followed by description of specific properties of π-mesic atoms. Experimental techniques for production and study of pionic atoms and theoretical approaches are discussed. Results of studies of the electromagnetic properties of pionic atoms and of the strong pion–nucleus interaction are summarized. A brief interpretation of these results is included. 100 references. (A.G.W.)

19484 CORRECTIONS TO THE POSITRONIUM HYPERFINE STRUCTURE OF ORDER $\alpha^2 \ln \alpha^{-1}$. Owen, David Adolph. Baltimore; Johns Hopkins Univ. (1970). 124p. University Microfilms Order No. 70-26,702.

Thesis.

A calculation of the $m\alpha^6 \ln \alpha^{-1}$ contributions to the triplet–singlet splitting of the positronium ground state (the positronium "hyperfine" structure) is presented. The result, $\Delta\nu(\alpha^6 \ln \alpha^{-1}) = \frac{1}{2} m\alpha^6 \ln \alpha^{-1} = 46$ MHz, places the theoretical value for the transition frequency ν approximately two standard deviations above the experimental value. The calculation is performed using a perturbation theory based on the Bethe–Salpeter equation and a wave function obtained by a single iteration from the nonrelativistic Pauli wave function. The contributions of order $m\alpha^6 \ln \alpha^{-1}$ represent recoil corrections arising from low-momentum components of the wave function, and it is found that wave function retardation and pair effects are negligible in this order. However, it is essential that these two effects are taken into account in the interaction kernels. After a systematic study of all relevant terms, it is believed that the only diagrams that contribute to this order are those involving the exchange of one or two virtual transverse photons. For these processes, the integrals encountered can be completely evaluated analytically. Including these contributions, the theoretical total triplet–singlet transition frequency is found to be $\nu^{th} = 2.03427 \times 10^5$ MHz, and the experimental value is $\nu^{exp} = 2.03403(12) \times 10^5$ MHz. (TSS) (Diss. Abstr. Int., B)

19485 REPULSIVE EFFECTS DUE TO THE ABSORPTION IN EXOTIC ATOMS. Krell, Max (Univ., Sherbrooke, Quebec). Phys. Rev. Lett.; 26: 584-7(8 Mar 1971).

An attractive K^--nuclear strong interaction as favored by a recent measurement weakens the atomic binding. The repulsion is due to the absorption in the nucleus and starts to dominate over the strong attraction. It is also against normal perturbation calculational experience that a smaller absorptive potential may produce a higher absorption rate. These highly nonlinear phenomena are displayed. The gradient potential has little influence for kaonic atoms. (auth)

19486 ENERGY SHIFT DUE TO NUCLEAR POLARIZATION IN A HIGH ORBITAL STATE OF MUONIC ATOM. Tanabe, Kosai (Yale Univ., New Haven). Phys. Rev., A; 3: 1282-91(Apr 1971).

The effect of the electromagnetic polarization of the nucleus is considered on the energy levels of the high orbital states in a muonic atom. A simplified calculation is carried out to estimate the approximate dependence of the shifts of the energy levels on the atomic number Z for the orbital states 3s, 3p, and 3d. To do this, a formulation is proposed in which the energy shift is regarded as the amount of energy that flows into the system when approximated second-order electromagnetic interaction between muon and nucleus is adiabatically switched on. The many-body property of the nucleus is formally expressed as the correction term to the photon self-energy part that represents the dielectricity of nuclear matter. Then the formal parallel holds between the present treatment of nuclear polarization and that of vacuum polarization in field theory. The applicability of the theory is restricted to the high orbital state, in which the bound-state wave function is less sensitive to the nuclear polarization effect, and its energy fluctuation is much less than the energy attributed to the muonic state. (auth)

19487 POSITRON ANNIHILATION AND POSITRONIUM BUBBLES IN LIQUID AND SOLID ARGON, KRYPTON, AND XENON. Varlashkin, Paul G. (Louisiana State Univ., Baton Rouge). Phys. Rev., A; 3: 1230-2(Apr 1971).

The angular correlations of photons from positrons annihilating in liquid and solid argon, krypton, and xenon show positronium-bubble formation in the liquid phase but not in the solid. Positronium formation increases with increasing atomic weight while bubble radii decrease with increasing atomic weight. (auth)

Collision Phenomena

Refer also to abstracts 18836, 18872, 19757, and 20537.

19488 (INR-P-1225) CLASSICAL THEORY OF ATOMIC COLLISIONS. II. ELASTIC ATOMIC COLLISIONS. Grazinski, M. (Institute of Nuclear Research, Warsaw (Poland)). 1970. 118p. (In Polish). Dep. NTIS (U. S. Sales Only).

A method for description of elastic atomic collisions based on the concepts of classical physics is given. Part I contains general considerations on scattering resulting from the existence in interacting objects of multipole moments of different order, both constant and varying in time. It has been shown that the exponential decrease of interaction effectiveness is the characteristic feature of dynamic systems. In Part II, which is concerned with physical processes, it is shown that the Ramsauer effect is connected with the dynamic nature of the atomic shell, while the intermolecular forces (van der Waals forces) are determined primarily by the time-averaged multipole moments characteristic of an external atomic shell. On the basis of experimental material concerning elastic scattering, the basic multipole moments of some atoms and molecules are determined. The values of these moments are estimated, and the basic shell frequencies are calculated. It is found that there exists agreement between the results obtained and the concept of atomic structure given by the author previously (according to which electrons in an atom move synchronously over radial trajectories of free fall at definite symmetry and space orientation). It is also illustrated by a number of relevant examples that the classical theory of scattering when combined with the classical theory of the atom enables a quantitative analysis of a wide variety of physical phenomena. (auth)

19489 (NP-18680) APPROXIMATE CROSS SECTIONS AND RATE COEFFICIENTS FOR IONIZATION, EXCITATION, AND RECOMBINATION OF HYDROGENIC IONS AND ATOMS. Rijnhuizen Report 70-61. Mewe, R. (Stichting voor Fundamenteel Onderzoek der Materie, Jutphaas (Netherlands). Instituut voor Plasma-Fysica). Jul 1970. 13p. Dep. NTIS.

The cross sections and rate coefficients for inelastic collisions between electrons and hydrogenic ions or atoms are approximated by analytical expressions for a Maxwellian electron energy distribution. (auth)

19490 (ORNL-4584, pp 92-104) ELECTRON AND ION COLLISION PHYSICS. Compton, R. N.; Anderson, V. E.; Carter, Ada; (and others). (Oak Ridge National Lab., Tenn.).

From Health Physics Division annual progress report for period ending July 31, 1970.

Work done during the period on the following projects is summarized: trapped-electron and SF_6-scavenger studies of electron-impact excitation and ionization of helium, neon, and argon; threshold electron-impact excitation of simple molecules; lifetimes and yields of negative ions from electron reactions with substituted benzenes; attachment rates of thermal electrons to SF_6 and other molecules; mass analysis of ions formed in electron swarm experiments; collisions of slow cesium atoms with NO_2; reactions of low-energy O^- ions with deuterated and normal acetylene, ethylene, and benzene. (A.G.W.)

19491 (ORNL-4584, pp 105-24) ATOMIC AND MOLECULAR RADIATION PHYSICS. Christophorou, L. G.; Anderson, V. E.; Birks, J. B.; (and others). (Oak Ridge National Lab., Tenn.).

From Health Physics Division annual progress report for period ending July 31, 1970.

Work done during the period on the following projects is summarized: use of argon, nitrogen, and ethylene as carrier gases for electron attachment studies; rates of electron attachment to SF_6 and various organic molecules and lifetimes of the negative ions formed; and stopping powers of slow electrons in hydrocarbon vapors. (A.G.W.)

19492 (SC-RR-70-735) TOTAL CROSS SECTION FOR SINGLE ELECTRON LOSS BY Ne AND Ar IN NITROGEN, OXYGEN, AND AIR. Lockwood, Grant J. (Sandia Labs., Albuquerque, N. Mex.). Nov 1970. 22p. Dep. NTIS.

Measurements of the total cross section for electron stripping σ_{01} of Ne and Ar in N_2, O_2, and air are reported in the energy range 25 to 90 keV. For all combinations the cross sections are observed to increase with increasing velocity. The dependence of the σ_{01} cross section on the neutralizing gas was measured by charge exchanging the ions in N_2 or air and their parent gas. In all cases studied, the values of σ_{01} for neutrals formed in their parent gas were less than or equal to the value of σ_{01} for neutrals formed in N_2 or air. As expected, the cross section σ_{01} for Ne in air was found to equal 80% of σ_{01} for Ne in N_2 plus 20% of σ_{01} for Ne in O_2. (auth)

19493 STUDY OF THE EXCITATIONS IN LOW-ENERGY ION-ATOM COLLISIONS USING AN ION-PHOTON COINCIDENCE METHOD. Vassilev, Georges; Baudon, Jacques; Rahmat, Gabriel; Barat, Michel (Paris Univ., Orsay, France). Compt. Rend., Ser. B: 271: 1170-3(21 Dec 1970). (In French).

An experiment is described for studying excitations in ion−atom collisions in which the coincidence between an ion scattered at a given angle and a photon emitted by the excited atom is detected. Preliminary results are given for the He^+-He collision at 300 eV with an angle of 8° and excitation of the 3^3P level with 3889-Å emission (3^3P-2^3S). (tr-auth) (France)

19494 ESTABLISHMENT OF THE COMMON ORIGIN OF THE WAVE FUNCTIONS OF THE V.P.S., BORN, AND IMPULSE APPROXIMATIONS USED FOR CALCULATING THE CROSS SECTIONS OF ELECTRON-HYDROGEN ATOM INTERACTIONS. Felden, Madeleine (Univ., Nancy). Compt. Rend., Ser. B: 271: 1149-51(21 Dec 1970). (In French).

The quantum equation resulting from the general wave function used in the VPS method (Vainshtein, Presnyakov, and Sobelman, Zh. Eksp. Teor. Fiz., 45: 2015(1963) is considered. The VPS, Born, and impulse approximations are shown to have a common origin in the general wave function, the only difference being the different approximations made for the attraction potentials. (tr-auth) (France)

19495 DETERMINATION OF INTERMOLECULAR POTENTIALS BY THE INVERSION OF MOLECULAR BEAM SCATTERING DATA. I. THE INVERSION PROCEDURE. Buck, U. (Max-Planck-Institut fuer Stroemungsforschung, Goettingen, Ger.). J. Chem. Phys.; 54: 1923-8(1 Mar 1971).

A practical solution of the inversion problem within the realms of the WKB approximation is reported. The basic input information is only the measured relative differential cross section, from which the WKB phase function or the classical deflection function is constructed. The absolute potential curve is then determined by the application of a modified Firsov method. The problem of which part of the differential cross section is readily measurable and also suitable for the inversion procedure is studied. A practical procedure is proposed and tested by using a simulated example. (auth)

19496 DETERMINATION OF INTERMOLECULAR POTENTIALS BY THE INVERSION OF MOLECULAR BEAM SCATTERING DATA. II. HIGH RESOLUTION MEASUREMENTS OF DIFFERENTIAL SCATTERING CROSS SECTIONS AND THE INVERSION OF THE DATA FOR Na-Hg. Buck, U.; Pauly, H. (Max-Planck-Institut fuer Stroemungsforschung, Goettingen, Ger.). J. Chem. Phys.; 54: 1929-36(1 Mar 1971).

High-resolution differential scattering cross-section measurements for Na−Hg were made using the method of crossed molecular beams. The experimental arrangement, which has a resolution $\Delta v/v$ in the relative velocity of better than 2%, is described. The

XUM

measured differential scattering cross-section curves show up to eight rainbows. The interaction potential between 3 and 9.5 Å was determined from these data by using the inversion procedure described in Part I. The potential well depth is 8.79×10^{-14} erg, and the minimum is at 4.72 Å. The shape of this potential deviates significantly from that of the simple multiparameter potentials commonly used. (auth)

19497 OPTICAL-MODEL ANALYSIS OF NONREACTIVE COLLISIONS OF REACTIVE MOLECULES: SCATTERING OF K, Rb, AND Cs FROM CCl_4, CH_3I, AND $SnCl_4$. Harris, R. M.; Wilson, J. F. (Harvard Univ., Cambridge, Mass.). J. Chem. Phys.; 54: 2088-2104(1 Mar 1971).

Crossed-beam studies of nonreactive scattering of K, Rb, and Cs atoms from CCl_4, CH_3I, and $SnCl_4$ were carried out and the differential cross sections compared with calculations based on a phenomenological optical model analysis. The models employed make use of a parameterized "reference" potential intended both to represent a multipole expansion of the potential surface of the reactants for internuclear distances greater than the radius of chemical interaction and to provide a systematic means of calculating the real parts of the optical phase shifts. A new semiclassical method for calculating nonreactive differential cross sections for an isotropic central potential (reference) and a parameterized probability of reaction (opacity) function, $P(\beta)$, is presented and applied to the scattering of $M + CCl_4$. It is found that the observed cross sections are consistent with a Lennard–Jones reference potential and a $P(\beta)$ that is a rounded-off step function. A better description of the reactivity for these systems was obtained by expressing the opacity function in terms of y, the reduced distance of closest approach, instead of the impact parameter β. The velocity dependence of the opacity function was virtually removed upon making this transformation, and the reactivity for a given alkali atom was found to resemble a diffuse "black sphere" of radius y_c, the opacity becoming less diffuse in the order Cs < Rb < K. The optical model was extended to include an anisotropic term in the reference potential for analysis of the nonreactive scattering of $M + CH_3I$. The magnitude of the anisotropic term was found to be much larger than that predicted from long-range dispersion forces alone. It is shown that the large anisotropy can account for the sudden decrease in the wide-angle nonreactive scattering, which was previously interpreted as a reaction threshold angle. Probability of reaction functions was derived from the data, and the results were consistent with the steric effect found in experiments that employ oriented CH_3I molecules. The cross sections for $M + SnCl_4$ are interpreted on the basis of orbiting from an "electron jump" potential, which is the adiabatic potential resulting from the crossing of covalent $(M + SnCl_4)$ and ionic $(M + SnCl_4^-)$ curves. Parameters for the potential are extracted from the data and used to estimate the electron affinity of the $SnCl_4$ molecule. The value obtained, 2.1 ± 0.2, is in fair agreement with a recent estimate direct measurement of the threshold for ion-pair formation. (auth)

19498 MOLECULAR COLLISIONS. XIV. FIRST-ORDER APPROXIMATION OF THE GENERALIZED PHASE SHIFT TREATMENT OF ROTATIONAL EXCITATION: ATOM–RIGID-ROTOR. Pattengill, M. D.; Curtiss, C. F.; Bernstein, R. B. (Univ. of Wisconsin, Madison). J. Chem. Phys.; 54: 2197-2207 (1 Mar 1971).

The generalized phase shift approach to the rotational excitation problem, introduced in Paper XII of this series, is applied to the atom–rigid-rotor case in the lowest (first-order) approximation. The treatment involves the computation of generalized action integrals over curved trajectories. Numerical results are presented to illustrate the dependence of the transition probabilities on the usual physical parameters, as well as a new parameter, ζ, which is proportional to the ratio of the moment of inertia of the van der Waals' atom–diatom system to that of the diatomic rotor (and thus to the ratio of the collision time to the diatom rotation time). In the limit $\zeta \rightarrow 0$, the development reduces to the sudden approximation. In the large impact parameter limit (straight-line trajectories), the deviation from the sudden approximation is described by "resonance functions" identical to those obtained implicitly by Van Kranendonk. The numerical results are presented in a manner that illustrates the deviation from each of these two limits. (auth)

19499 DETECTION AND IDENTIFICATION OF TRIPLET STATES OF H_2O BY ELECTRON IMPACT. Trajmar, S.; Williams, W.; Kuppermann, Aron (California Inst. of Tech., Pasadena). J. Chem. Phys.; 54: 2274-5(1 Mar 1971).

The angular behavior of the differential cross section for exciting molecular electronic states by low-energy (8 to 55 eV) electron impact was used to investigate water vapor. At least two singlet–triplet transitions were detected and identified. One is a broad feature having a maximum intensity at about 4.5 eV excitation energy, and the other has a sharp maximum at 9.81 eV. (A.G.W.)

19500 SCATTERING AND CAPTURING BY INVERSE FOURTH-POWER POTENTIAL IN LOW-ENERGY RANGE. Coombs, J. A.; Lin, S. H. (Arizona State Univ., Tempe). J. Chem. Phys.; 54: 2285-7(1 Mar 1971).

The quantum mechanical correction to the classical capture cross section and the applicability of the inverse fourth-power potential in the elastic scattering of charged particles by neutral atoms or nonpolar molecules at very low energies were studied. Values of the total scattering cross sections calculated for E = 0 are compared with extrapolated experimental values for several systems. Only in the e–He system do the calculated and extrapolated values agree; in the other systems the calculated value is 1.5 to 7 times the extrapolated value. When several theoretical calculations of total elastic scattering cross sections for the e–H_2 system are compared with the experimental value for E = 0, only the Hartree–Fock calculations that includes both exchange and polarization gives reasonable agreement with the experimental value. (A.G.W.)

19501 ELASTIC SCATTERING OF POSITRONS BY HYDROGEN MOLECULES. Lodge, J. G.; Darewych, J. W.; McEachran, R. P. (York Univ., Toronto). Can. J. Phys.; 49: 13-19(1 Jan 1971).

Elastic positron–hydrogen-molecule collisions are considered below the first electronic excitation threshold. The interaction of the incoming positron with the hydrogen molecule is represented by a superposition of single-center static and nonspherical polarization potentials. The static potential is expanded to second degree in Legendre polynomials. The Chebyshev polynomials are used to improve the truncated Legendre series approximation and the effect of including the fourth degree contribution is shown to be slight. Positronium formation effects are neglected. Two semiphenomenological polarization potentials are used, and it is shown that the parameters can be suitably adjusted to reproduce the results obtained if the Henry and Lane polarization potential is used. It is shown that the partial Ramsauer–Townsend effect is useful in determining the values of polarization-potential parameters. Total elastic scattering cross sections are given for incoming positron energies between about 0.4 and 14 eV, and the positron annihilation coefficient is given to about 60 eV. (auth) (Canada)

19502 ROTATIONAL EXCITATION OF THE HD MOLECULE BY SLOW ELECTRONS. Hara, Shunsuke (Tokyo Univ.). J. Phys. Soc. Jap.; 30: 819-23(Mar 1971).

Effective cross sections for the rotational excitation of the HD molecule by low-energy electrons (incident energy from 1.0 to 13.6 eV) are calculated for transitions of the rotational state from J = 0 to 1, 2 and from J = 1 to 2. The adiabatic approximation is used to obtain these cross sections. It is found that the rotational excitation cross section with $\Delta J = 2$ is almost the same as the e–H_2 result and that the cross sections with $\Delta J = 1$ are about 10% of those with $\Delta J = 2$ in the above-mentioned energy region. (auth)

19503 CLOSED-CHANNEL SPECTRUM OF THE POSITRON–HYDROGEN REARRANGEMENT COLLISION. Hahn, Yukap; Dirks, Johan F. (Univ. of Connecticut, Storrs). Phys. Rev., A; 3: 1513-16(Apr 1971).

For the positron–hydrogen scattering above the electron-pickup threshold, an improved upper bound on the lowest trajectory of the closed-channel Hamiltonian is obtained and its effect on the bounds on the scattering parameters is clarified. (auth)

19504 FORMATION OF METASTABLE HYDROGEN ATOMS BY CHARGE TRANSFER. Fitzwilson, R. L.; Thomas, E. W. (Georgia Inst. of Tech., Atlanta). Phys. Rev., A; 3: 1305-9 (Apr 1971).

Measurements are presented of the total cross sections for formation of metastable hydrogen atoms by charge transfer as protons traverse targets of helium, argon, nitrogen, and oxygen. Projectile energies range from 4 to 26 keV. An H^+ projectile beam was directed into a cell containing the target gas and emerged into an evacuated region where the metastable-state content was determined. The H(2s) flux was monitored by electric-field mixing of this state with the 2p level and detection of the resulting Lyman-α photon. The relative variation of cross section with projectile energy for targets of He and Ar is in agreement with previous work. For oxygen the cross section increases with energy from 4 to 10 keV and remains constant from 10 to 26 keV; for nitrogen the cross section increases monotonically with increasing energy. (auth)

19505 UNITARITY IN COULOMB SCATTERING. Nuttall, J.; Stagat, R. W. (Texas A and M Univ., College Station). Phys. Rev., A; 3: 1355-8(Apr 1971).

It is demonstrated that the pure-Coulomb t matrix satisfies a modified unitarity condition and that its discontinuity is not zero, as has been asserted elsewhere. (auth)

19506 ABSOLUTE TOTAL CROSS SECTIONS FOR THE SCATTERING OF LOW-ENERGY ELECTRONS BY RUBIDIUM, CESIUM, AND POTASSIUM. **Visconti, Paul J.; Slevin, James A.; Rubin, Kenneth (City Coll., New York). Phys. Rev., A; 3: 1310-17(Apr 1971).**

Using the atom-beam recoil technique, absolute total cross sections were measured for the scattering of electrons in the energy range 0.3 to 9 eV by potassium, rubidium, and cesium. The results of these measurements are in substantial disagreement with the experimental values of Brode, obtained more than 40 years ago. On the other hand, the potassium cross sections agree extremely well with the recent calculations of Karule, and Karule and Peterkop, as well as with the experimental values of Collins et al. For cesium and rubidium, the existing theoretical calculations are not in as good agreement with the results as in the case of potassium. (auth)

19507 MANY-BODY METHODS APPLIED TO ELECTRON SCATTERING FROM ATOMS AND MOLECULES. II. INELASTIC PROCESSES. **Csanak, Gyoergy (Univ. of Southern California, Los Angeles); Taylor, Howard S.; Yaris, Robert. Phys. Rev., A; 3: 1322-8(Apr 1971).**

It is shown how the generalized random-phase approximation, previously used to develop a self-consistent theory of elastic scattering and frequency-dependent polarizability, can be extended to the calculation of inelastic scattering cross sections from the ground state of the target. It is also shown that when calculating electron–atom scattering cross sections, one can simultaneously calculate without much additional work elastic and some specific inelastic scattering cross sections for an electron scattering off a positive-ion target. Improvements to the approximation scheme, using self-consistent perturbation methods, are briefly discussed. (auth)

19508 GENERALIZED HYLLERAAS CALCULATION OF POSITRON–HYDROGEN SCATTERING. **Bhatia, A. K.; Temkin, A.; Drachman, Richard J.; Eiserike, H. (Goddard Space Flight Center, Greenbelt Md.). Phys. Rev., A; 3: 1328-35(Apr 1971).**

A rigorous-bound calculation is performed of positron–hydrogen scattering below the positronium pickup threshold. The correlation function is a generalized Hylleraas function with three nonlinear parameters, which includes a virtual-positronium factor explicitly. Phase shifts are calculated as a function of the number of linear parameters using up to 84 terms. Converged phase shifts can be extrapolated to four significant figures. At three of the seven values of k computed, the results are found to disagree slightly but significantly from Schwartz's results. Final phase shifts are estimated to be accurate to $\pm 2 \times 10^{-4}$ rad. (auth)

19509 POSITRON–ATOM SCATTERING BY THE KOHN AND HARRIS METHODS. **Houston, S. K.; Drachman, Richard J. (Goddard Space Flight Center, Greenbelt, Md.). Phys. Rev., A; 3: 1335-42(Apr 1971).**

The S-wave scattering parameters were calculated for the e^+–H and e^+–He systems below the positronium-formation threshold. The phase shifts were computed using the Harris variational method, and at zero energy the scattering lengths were obtained by the Kohn variational method. For hydrogen, a generalized Hylleraas wave function with three nonlinear parameters was used, giving an upper-bound scattering length $a \leq -2.10278$, agreeing with Schwartz's result $a \leq -2.10$. An extrapolation procedure gives an estimate of $a = -2.1036 \pm 0.0004$. At nonzero energies, agreement with the lower-bound results of Bhatia, Temkin, Drachman, and Eiserike, to better than 0.004 rad is achieved. Since the exact atomic-helium wave function is not known, the situation for helium is less clear; various model-target wave functions are examined using a generalized Hylleraas function with two nonlinear parameters. For the exponential model used by Drachman, the scattering is in close agreement with previous results, but the annihilation-rate parameter Z_{eff} is higher by 15% in poorer agreement with experiment at zero energy. (auth)

19510 TOTAL CROSS SECTIONS FOR INELASTIC SCATTERING OF CHARGED PARTICLES BY ATOMS AND MOLECULES. VI. METASTABLE HELIUM. **Briggs, John S.; Kim, Yong-ki (Argonne National Lab., Ill.). Phys. Rev., A; 3: 1342-8 (Apr 1971).**

Sum rules for the asymptotic Born cross sections were applied to the evaluation of various inelastic-scattering cross sections of metastable He ($2\ ^1S$ and $2\ ^3S$). The ionization cross sections for the two species are similar in magnitude, and each constitutes only a small part of the total cross section for inelastic scattering. Although the first Born approximation is inappropriate for the scattering of slow charged particles, the energy dependence exhibited in the recent experiment by Long and Geballe for the ionization of He($2\ ^3S$) by low-energy electrons ($\leq$16 eV) is compatible with the high-energy behavior predicted by the theory. The exchange correction evaluated from the Mott formula was included in the ionization cross section by electron impact. Optical oscillator strengths for the first three transitions to doubly excited states $[2\ ^1S \rightarrow (2lnl')^1P]$ are also given. (auth)

19511 PHOTOEMISSION AND ELECTRON DETACHMENT IN LOW-ENERGY COLLISIONS OF METASTABLE ATOMS WITH NEGATIVE IONS. **Blaney, Benjamin; Berry, R. Stephen (Univ. of Chicago). Phys. Rev., A; 3: 1349-55(Apr 1971).**

Cross sections for Penning detachment, $X^* + Y^- \rightarrow X + Y + e$, and collision-induced photon emission, $X^* + Y^- \rightarrow X + Y^- + h\nu$, were calculated for collisions of metastable neutral atoms and negative ions at low energies ($E \sim 1$ eV). A semiclassical treatment based on the impact-parameter method and adiabatic electronic interactions was employed. Collisions involving H^* (2^1S), Ca^* (3^1D), and He^* (2^1S) with H^-, O^-, Cl^-, and C were investigated. In all collisions not involving H^* (2^1S), Penning detachment predominates and exhibits cross sections on the order of 10^{-14} cm^2. (auth)

Atomic Theory

19512 (CNRS-CPT-70-P-335, pp IV.16-25) NEW THEORETICAL VALUE FOR LAMB SHIFT. **Lautrup, B. (European Organization for Nuclear Research, Geneva (Switzerland)).**

In Colloquium on computational methods in theoretical physics; Marseilles, France (15 Jun 1970).

The way in which a new value of the Lamb shift was determined from computer calculations of the contributions of the slopes of graphs corresponding to different vertex corrections is shown. (France)

19513 EXTENSIONS OF THE HULTHEN ORBITAL CONCEPT. **Weber, Thomas A.; Weare, John H.; Parr, Robert G. (Johns Hopkins Univ., Baltimore). J. Chem. Phys.; 54: 1865-71(1 Mar 1971).**

Three extensions of the Hulthén representation of atomic orbitals are investigated. In earlier work it was shown that radial functions $0s = N_1[\exp(-\alpha r) - \exp(-\beta r)]\ (1/r)$ and $1p = N_2[\exp(-\gamma r) - \exp(-\delta r)]$ excellently represented 1s and 2p radial functions for atoms. In the present paper, investigations are reported (a) using Hulthén orbitals as the starting point for a perturbation calculation of exact Hartree–Fock orbitals, (b) employing a full Dirichlet-type series $[\Sigma_i \lambda_i \exp(-\mu_i r)]\ (1/r)$ to represent a 1s orbital, and (c) using the Laplace transformation representation for a 1s orbital. (auth)

19514 CALCULATION OF UPPER AND LOWER BOUNDS TO OSCILLATOR STRENGTHS. **Weinhold, Frank (Stanford Univ., Calif.). J. Chem. Phys.; 54: 1874-81(1 Mar 1971).**

A procedure is described for calculating rigorous upper and lower bounds to dipole oscillator strengths and is illustrated numerically with various simple applications to the hydrogen molecular ion. The procedure appears to give a good account of the actual errors that may arise in the conventional method based on energy minimization of the two states. In addition, specific regions of configuration space, important for the oscillator strength but perhaps not for the energy, are singled out and emphasized automatically. (auth)

19515 APPLICATION OF TRUNCATED MULTIPOLAR EXPANSION PAIR FUNCTIONS IN ATOMIC STRUCTURE CALCULATIONS. II. IRREDUCIBLE TENSOR OPERATOR FORM OF THE STRONGLY ORTHOGONAL PAIR FUNCTIONS. REDUCTION OF ORTHOGONALITY CONSTRAINTS. **Jankowski, K. (Simon Fraser Univ., Burnaby, B. C.). Can. J. Phys.; 49: 118-32(1 Jan 1971).**

The truncated multipolar expansion pair functions (TMEPF) defined recently by Jankowski were used to formulate an approach that takes into account correlation effects within a pair of electrons in the presence of an N electron sea in a closed shell configuration. An irreducible tensor operator form of the strongly orthogonal pair function components was derived. The analysis of the expressions obtained leads to a systematic reduction of the orthogonality constraints to be imposed on this class of trial functions. The results of this analysis for several types of pair functions are given. Finally, the method of calculation of matrix elements between orthogonally projected pair function components in terms of radial integrals is presented. (auth) (Canada)

19516 SYMMETRIC INTEGRAL EQUATIONS DERIVED FROM THE FADDEEV EQUATIONS. **Mayer, H. (Univ., Freiburg i. B.). Z. Phys.; 242: 210-19(1971).**

XUM

A way is shown to transform the Faddeev equations of the atomic three-body problem into a set of integral equations with symmetric kernel. The method is treated in more detail for total angular momentum J = 0 and applied to calculating the binding energy of the H^- ion. (auth)

19517 HARTREE–FOCK THEORY WITH EXCHANGE CUT-OFF. Weber, Thomas A.; Parr, Robert G. (Johns Hopkins Univ., Baltimore). Phys. Rev., A; 3: 81-6(Jan 1971).

A new Fock-type operator is defined, which varies between the Hartree and the Hartree–Fock operator depending on a cutoff parameter in the exchange potential. The corresponding pseudo-Hartree–Fock equations require each orbital ϕ_i to behave as asymptotically as $\exp[-(-2\epsilon_i)^{1/2} r]$. Calculations are reported for the Ne atom. (auth)

19518 LENGTH AND VELOCITY FORMULAS IN APPROXIMATE OSCILLATOR-STRENGTH CALCULATIONS. Starace, Anthony F. (Univ. of Chicago). Phys. Rev., A; 3: 1242-5 (Apr 1971).

The matrix element for electric dipole transitions is correctly given by the length formula in the Hartree–Fock, configuration-interaction, and related approximations, which involve the diagonalization of an approximate, but nonlocal, Hamiltonian. (auth)

19519 CRITERION OF COMPLETENESS FOR THE SET OF FUNCTIONS USED IN MATRIX HARTREE–FOCK AND CORRELATION-ENERGY CALCULATIONS. Weissmann, M.; Tolmachev, V. V. (Facultad de Ciencias, Santiago de Chile). Phys. Rev., A; 3: 1291-5(Apr 1971).

A study is made of the completeness of the basis sets used by Clementi and Nesbet for the calculation of atomic Hartree–Fock and correlation energies. A good criterion for completeness is found to be related to the overlap between these sets and the hydrogenic functions that contribute most in many-body perturbation theory. Thus the experience gained in perturbation-theory calculations is shown to be helpful in choosing the best basis sets for the matrix method. Moreover, perturbation calculations can be simplified in those cases where the function space can be adequately approximated by a set of easily integrable functions. (auth)

19520 PERTURBATION OF A DECAYING STATE. More, Richard M. (Univ. of Pittsburgh). Phys. Rev., A; 3: 1217-20 (Apr 1971).

One intuitively expects that a long-lived decaying state must have many properties like those of true eigenstates, with interesting technical modifications to encompass the complex energy. The small change in the complex energy due to the application of a weak perturbation is examined here. (auth)

19521 MINIMA IN GENERALIZED OSCILLATOR STRENGTHS OF HYDROGEN-LIKE ATOMS. Shimamura, Isao (Tokyo Univ.). J. Phys. Soc. Jap.; 30: 824-34(Mar 1971).

Algebraic expressions are obtained for generalized oscillator strengths of hydrogen-like atoms for transitions involving s, p, and d states with principal quantum numbers n of 2, 3, and 4. Zero minima are found for all the transitions involving s states, and their positions are shown to be proportional to the effective charge, the coefficients being tabulated. The transitions from the 1s state sometimes show zero minima if different effective charges are used for the initial and the final states. Even nodeless wave functions can produce zeros owing to the nodes of the spherical Bessel function. Some excitation processes of Ne, Na, Mg, and Ar caused by high-energy charged particles are investigated in the first Born hydrogen-like approximation, and the possibility of finding zero minima in the differential cross sections is discussed; the 3s → 4p transitions of Na and Mg have the most conspicuous zeros of all that are studied. (auth)

Cosmic Radiation

Refer also to abstracts 18643, 19459, 19885, 19905, 19971, 19973, and 20446.

19522 (INR-1231) INTERPRETATION OF THE DATA ON MUONS IN COSMIC RAYS FROM THE POINT OF VIEW OF HIGH ENERGY PHYSICS AND ASTROPHYSICS. Wdowczyk, J. (Institute of Nuclear Research, Warsaw (Poland)). 1970. 108p. (In Polish). Dep. NTIS (U. S. Sales Only).

The possibility of the application of the EAS method in the physics of high-energy interactions and astrophysics is discussed. The discussions are based on the analysis of three physical problems: the mass composition, the dependence of mean transverse momentum on the primary energy, and the multiplicity of pion production at extremely high energies. It is shown that the data on muons in cosmic rays indicate that the beam of high-energy primary cosmic rays contains more protons than the beam at lower energies available for direct investigations ($\sim 10^{10}$ eV). The most likely explanation of this effect is the assumption that the primary nuclei are fragmentated in the vicinity of their sources. On the basis of investigations of the lateral distribution of high-energy muons it is shown that the mean transverse momentum of pions produced in interactions of energies 10^{14} eV is about 0.6 to 0.7 GeV/c. Investigations of the height of the effective muon production level suggest that the mean energy of the nuclear-active particles decreases quickly with depth. The simplest explanation of this phenomenon is that the multiplicity of pion production increases quickly with primary energy. The discussion given shows that by selecting suitable parameters it is possible to obtain information on high-energy cosmic-ray particles and their interactions on the basis of the investigation of cosmic-ray propagation in the atmosphere. (auth)

19523 INFLUENCE OF IONIZATION ON THE SPECTRUM AND CHEMICAL COMPOSITION OF COSMIC RAYS IN THE NONRELATIVISTIC ENERGY RANGE. Sazonov, V. N. (Lebedev Inst. of Physics, Moscow. Moscow Technical Physics Inst.). Sov. Astron. AJ (Engl. Transl.); 14: 676-82(Jan-Feb 1971). Translated from Astron. Zh.; 47: 841-9(Jul-Aug 1970).

Ionization losses during the motion of cosmic rays through the interstellar medium are capable of explaining the observed properties of the spectrum of chemical composition of cosmic rays in the nonrelativistic energy range as compared to the corresponding parameters in the relativistic energy range. (auth)

19524 HEAVY COSMIC RAY NUCLEI. Shapiro, Maurice M.; Silberberg, Rein (Naval Research Lab., Washington, D. C.). Annu. Rev. Nucl. Sci.; 20: 323-92(1970).

A summary of present knowledge of the composition of heavy primary nuclei is divided into the following sections: techniques of detection, identification, and energy estimation; composition; fragmentation of heavy primary nuclei; mean pathlength of cosmic rays in space; primordial composition at cosmic-ray sources and its transformation; nucleosynthesis and cosmic-ray composition; propagation and confinement in the Galaxy; origin; some problems and puzzles; modulation of relative abundances. 312 references. (A.G.W.)

19525 HIGH-RESOLUTION MEASUREMENTS OF SLOWING COSMIC RAYS FROM Fe TO U. O'Sullivan, D. (Univ. of California, Berkeley); Price, P. B.; Shirk, E. K.; (and others). Contract AT(04-3)-34. Phys. Rev. Lett.; 26: 463-6(22 Feb 1971).

Cosmic rays with Z = 40, 44, 52, 71, 77, 78, and 92 slowing in a balloon-borne stack were identified. The values of Z assigned by both Lexan plastic detectors and nuclear emulsions were the same to within two units. Both low- and high-energy heavy cosmic rays are synthesized in the rapid neutron-capture process. (auth)

19526 STRUCTURE OF THE INTERPLANETARY SPACE FROM DATA ON ANNUAL COSMIC-RAY VARIATIONS. Dorman, L. I.; Luzov, A. A.; Mamrukova, V. P. Kosm. Luchi; No. 10, 162-6(1969). (In Russian).

The data of the world cosmic-ray station network and of the aerological probes of the atmosphere during 1958, 1960, and 1963 are used to determine the annual variation of the intensity of the secondary component of the cosmic radiation as a function of the Earth's heliographic latitude. The results are compared to the changes of the magnetic activity K_p index and of the flocculi field area. The cosmic-radiation intensity gradient for the plane normal to the ecliptic plane is computed and a dynamic description of the electromagnetic structure of the space and of its changes in the course of the solar activity cycle is given. (auth) (Meteorol. Geoastrophys. Abstr.)

19527 SYSTEM OF EXPERIMENTAL DATA ENCODING IN COSMIC-RAY VARIATIONS. Pimenov, I. A. Kosm. Luchi; No. 10, 5-11(1969). (In Russian).

Several versions of experimental data coding systems for transfer to punch cards are examined. Packing numerical data in the computer memory is shown to be the most efficient method, reducing the number of cards from 910,000 to 152,000. A sampling method for checking over the correct transfer of data to standard forms is suggested. Estimates allowing an assessment of the population size and the respective sample size are provided. (auth) (Meteorol. Geoastrophys. Abstr.)

19528 PROCESSING OF THE DATA OF COSMIC-RAY STATIONS. Pimenov, I. A. Kosm. Luchi; No. 10, 17-19(1969). (In Russian).

A new instrument to be used in studying cosmic-ray variations (a cosmic-ray station, CRS) is briefly examined, considering the station as a source of information. One version of possible central data processing systems is proposed, the system consisting of 10 CRSs and a computer of high information capacity. The system when realized will accomplish 1) automatic recording of data output from CRS; 2) current analysis of the data obtained and a thorough analysis of the accumulated data; 3) automatic outprint of the results of recording and processing; and 4) computing on programs independent of the directly received data. (auth) (Meteorol. Geoastrophys. Abstr.)

19529 PHASE JUMPS OF DIURNAL VARIATIONS IN COSMIC-RAY INTENSITY. Pankratov, A. K.; Vladimirskii, B. M.; Stepanyan, A. A. Kosm. Luchi; No. 10, 27-9(1969). (In Russian).

The phase jumps of the diurnal variation are considered on the basis of the data of the worldwide network of cosmic-ray stations for the IQSY period. (auth) (Meteorol. Geoastrophys. Abstr.)

19530 NATURE OF THE CHANGES IN COSMIC-RAY DIURNAL VARIATION DURING MAGNETIC STORMS WITH SUDDEN COMMENCEMENT. Vladimirskii, B. M.; Pankratov, A. K.; Stepanyan, A. A. Kosm. Luchi; No. 10, 46-9(1969). (In Russian).

The nature of the changes of cosmic-ray diurnal variation during magnetic storms with sudden commencement is considered. (auth) (Meteorol. Geoastrophys. Abstr.)

19531 A MONTE CARLO CALCULATION OF SPALLATION REACTIONS OF ASTROPHYSICAL INTEREST IN THE M NUCLEI. Schmitt, William Francis. Philadelphia; Univ. of Pennsylvania (1970). 124p. University Microfilms Order No. 70-25,725.

Thesis.

A new model was developed of spallation reactions in the M nuclei (carbon, nitrogen, and oxygen) which is suitable for treatment of reactions induced by alpha particles. The model employs discrete nucleons and two-body nuclear potentials rather than the continuous nuclear density functions and central potentials previously employed. Composite fragments are included as knock-on particles and are tracked through the intranuclear cascade, which is the central portion of the model. Calculations were made of protons of 70 to 420 MeV on carbon, oxygen, and nitrogen and were compared with existing experimental data. In general, good agreement was found. Calculations were also made of alpha particles of 22.5 to 235 MeV/nucleon on carbon, nitrogen, and oxygen and were compared with existing experimental data. In general, good agreement was found. (Diss. Abstr. Int., B)

19532 STUDY OF THE CHARGE SPECTRUM OF EXTREMELY HEAVY COSMIC RAYS USING COMBINED PLASTIC DETECTORS AND NUCLEAR EMULSIONS. Price, P. B. (Univ. of California, Berkeley); Fowler, P. H.; Kidd, J. M.; (and others). Contract AT(04-3)-34. Phys. Rev., D; 3: 815-23(15 Feb 1971).

Tracks of 99 nuclei with $Z > 36$ were analyzed in a stack of Lexan polycarbonate, cellulose triacetate, and nuclear emulsion launched from Palestine, Texas, with an area–time factor of 900 m^2 h. Although the mean deviation in charge assignment between plastics and emulsion was ~3 units, there was no systematic variation. One nucleus with charge estimated to be $Z \approx 96$ ($\beta \approx 0.95$) was identified in all three detectors. Combining all available data, 33 events were found with $Z > 70$, giving for the important ratio $(Z > 83)/(70 \leqq Z \leqq 83)$ the value ~0.3. The weakness of the Pb peak relative to the Pt peak indicates that little radioactive decay of the transbismuth nuclei has occurred. These results favor supernova explosions within the Galaxy as the major source of cosmic rays and suggest that their average lifetime is less than 10^7 yr. (auth)

19533 IS IT WORTH-WHILE TO CONTINUE THE INVESTIGATION OF COSMIC-RAY JETS BY MEANS OF EMULSION METHOD? Gierula, J. Rend. Semin. Mat. Fis. Milano; 39: 60-5(1969)

The merits of the nuclear-emulsion technique as a means of investigating cosmic-ray jets are discussed. The main weaknesses of this technique are said to be: (1) the impossibility to measure precisely the primary energy, (2) the existence of strong biases in finding jets (scanning biases), (3) poor statistics, and (4) the complexity of the target in photographic emulsions. While the validity of these points is conceded, the sometimes-inferred worthlessness of the technique's further use is called into question. It is shown that the precise knowledge of the primary energy or the investigation of only the most drastic qualitative effects is not always necessary, and that large enough statistics can be ensured by the technique of irradiating multiliter blocks of emulsion in balloon flights at considerably lesser costs than by accelerator-investigation methods. Hence, it is felt that there still are good prospects for future investigations of cosmic-ray jets by means of the emulsion method. (IAA)

19534 COSMIC X-RAY BACKGROUND: SOME RESULTS BETWEEN 25 AND 200 keV FROM ESRO R/73 EXPERIMENT (PAYLOAD S-11). Brini, Domenico (Univ., Bologna). Sci. Ind. Spatiales; 6: No. 31, 26-34(1970).

The interest of astronomy in x rays and the experimental problems and techniques related to measurements of the cosmic x-ray background are reviewed. Taking these considerations into account, the design and construction of the apparatus for the R/73 experiment is described, as well as tests and calibrations. The experiment was successfully launched by a Skylark rocket on May 22, 1967 from Sardinia. The resulting intensity of the cosmic x-ray background between 25 and 200 keV is 1.29 ± 0.4 photon/sq cm/sec/sr, that being the energy spectrum qualified by a power law with an exponent of −1.8 ± 0.1, and an anisotropy vs the galactic latitude of less than 11%. (IAA)

19535 ABUNDANCES AND ACCELERATION MECHANISMS OF COSMIC RAYS. Havnes, Ove (Astronomical Inst., Utrecht). Nature (London); 229: 548-9(19 Feb 1971).

Measurements of the chemical composition of cosmic rays have shown that, for most elements, the abundances roughly correspond to their universal abundances. It is pointed out that some systamatic differences occur in the low-energy range, which are correlated with the first ionization potentials of the corresponding elements. The findings reported apparently require more than one type of cosmic-ray source. This is in accordance with the conclusions reached by Comstock (NSA 23: 14656) on the basis of the shape of the energy spectrum at low energies. (UK)

Direct Energy Conversion

Refer also to abstracts 18595, 19548, 19563, and 20768.

19536 (JUL-706-TP) APPLIED MAGNETOHYDRODYNAMICS. ISSUE 6. PARAMETRIC STUDIES AND DIMENSIONING OF NOBLE GAS MHD GENERATORS. Bohn, Th.; Holzapfel, Chr.; Kolb, G. (Kernforschungsanlage, Juelich (West Germany). Institut fuer Technische Physik). Oct 1970. 41p. (In German). Dep. NTIS (U. S. Sales Only).

Several parameters in connection with the total plant loop were considered in designing a MHD Generator for a nuclear MHD power plant. Thus, a limitation was established for the parameters in which it is possible to build the MHD generator without conflicting with the conditions of the other components of the power plant. The two working gases, argon and helium seeded with cesium, were numerically investigated, using a one-dimensional theory. Considering friction losses, the upper limit was calculated for the pressure at which it is possible to gain enough power as a function of Mach number. Several examples of the calculated parameters in the generator are shown. (auth)

19537 EXPERIMENTAL INVESTIGATION SINGLE-WAVE MHD MACHINES. Andreev, A. M.; Glukhikh, V. A.; Kirillov, I. R. Magn. Gidrodin., Akad. Nauk Lat. SSR; No. 4, 98-102 (Oct-Dec 1968). (In Russian).

Results are presented of an experimental investigation of compensation of the longitudinal edge effect in the primary loop of a plane linear induction closed-cycle MHD machine with K–Na alloy (78% K) at the liquid metal temperature 100 to 170°C. The cross section of the steel channel of the machine comprised 5.5 × 69 mm^2. Near the lateral sides of the channel are placed copper busbars 6 × 30 mm^2 in cross section and 210 mm in length. The main coil with the number of poles $2p = 2$ and compensating coils were placed in the magnetic circuit gaps. The compensating coils encompass the operating part of the magnetic circuit. With the different methods of switching on the compensating coils, the operating characteristics of the MHD machine in the pump and generator operating regimes were obtained. Maximum power output in the generator regime constituted ~200 watt, and the maximum velocity of the liquid metal in the generator channel was ~30 m/sec. In the working regime and in the open-circuit regime without the liquid metal, the distribution curves of induction were obtained along the length of the generator for the different methods of compensation. (tr-auth)

19538 INVESTIGATION OF LONGITUDINAL EDGE EFFECT IN PRIMARY CIRCUIT OF LINEAR MHD MACHINES. Andreev, A. M. Magn. Gidrodin., Akad. Nauk Lat. SSR; No. 4, 103-8(Oct-Dec 1968). (In Russian).

The equation is developed for the problem of calculation of the currents and voltages of the different series in disconnected linear induction MHD machines under the following conditions:

XUM

(1) the system of input linear voltages is symmetric, (2) the saturation of inductors is absent, (3) the inductor is symmetric and star-connected. Expressions are obtained for direct, reciprocal, and zero voltage current series. (M.H.R.)

19539 ESTIMATE OF FIELD IN WINDING ZONE OF PLANE LINEAR INDUCTION MHD MACHINES WITH CALCULATION OF FINITENESS OF MAGNETIC PERMEABILITY OF IRON. **Birger, B. L.; Vilnitis, A. Ya.; Gorovits, V. S. Magn. Gidrodin., Akad. Nauk Lat. SSR; No. 4, 109-12(Oct-Dec 1968). (In Russian).**

A solution was found for Maxwell equations for the winding zones of MHD machines. The winding zone was represented in the form of a solid medium with electric and magnetic anisotropy. With such an approach the solution of the Maxwell equations is obtained in elemental transcendental functions, assuming that the permeability of the cam inductor has the final value $\mu_{Fe} \neq \infty$. Solutions were found for two types of windings—band and filled. The form of the solution is such that it is easy to obtain known expressions for the field components in the range $\mu_{Fe} \to \infty$. The proposed method makes it possible to determine the parameters of inductors of a specific performance, allowing for finite magnetic permeability of the iron of the inductor. The method may be used for calculations on inductors with external coils, the pump transformers of the traveling field, the deeply grooved MHD machines, and machines with ferromagnetic channels, and also for calculating parameters of machines with drum-type coils. (tr-auth)

19540 ESTIMATE OF STATIONARY REGIME OF FARADAY SEGMENTED MHD GENERATOR IN NON-RATED INPUT PLASMA PARAMETERS. **Kazachkov, Yu. A. Magn. Gidrodin., Akad. Nauk Lat. SSR; No. 4, 116-18(Oct-Dec 1968). (In Russian).**

The method of solution formulated allows for consideration of the effect of the form of the volt-ampere characteristics of the invertor, operating from the MHD generator, on the response of the channel when the input parameters of the plasma are varied. An example is given that allows a comparison of the responses of the channel during regulation of the load for uniform current or voltage. (tr-auth)

19541 UTILIZATION OF MONTARDY SCHEME WITH SEGMENTED ELECTRODES FOR MHD DEVICES WITH ISOTROPIC CONDUCTING WORKING SUBSTANCES. **Starominskii, L. R.; Tolmach, I. M. Magn. Gidrodin., Akad. Nauk Lat. SSR; No. 4, 152-3(Oct-Dec 1968). (In Russian).**

Experimental proof of the possibility of creation of an MHD pump (generator) with increased voltage is attempted. During the experiment the pattern of potential distribution was obtained on electroconductive paper, which is shown for the left half of the channel (the right part is obtained by rotating the pattern 180 deg. around point O, in the plane of the drawing.) In a figure, the equipotential curve is shown through each 5% of the total voltage. Using the experimentally obtained equipotential curves, the current density lines were constructed. From the diagram it is apparent that, in a significant part of the channel length (with the exception of the current-supply zones), the current density has an important transverse component. This component imposed perpendicularly to the plane of the channel of constant magnetic field produces useful pressure in the longitudinal direction. (M.H.R.)

19542 CURRENT DISTRIBUTION IN MHD CHANNELS WITH SOLID ELECTRODES OF FINITE RESISTANCE. **Kos'kin, Yu. P. Magn. Gidrodin., Akad. Nauk Lat. SSR; No. 4, 113-15(Oct-Dec 1968). (In Russian).**

Equations are developed that permit the evaluation of the current distribution and electric potential in the channel of an electromagnetic pump with solid electrodes, which have a resistance proportional to the resistance of the working fluid. It seems the neglect of the internal resistances of electrodes in the development of engineering MHD designs can lead to intrinsic errors. (tr-auth)

19543 DYNAMIC STABILIZATION OF THE ELECTROTHERMAL INSTABILITY. **Uncles, R. J.; Nelson, A. H. (Imperial Coll. of Science and Tech., London). Plasma Phys.; 12: 917-26(Dec 1970).**

The possibility of stabilizing the electrothermal instability by applying an oscillation to the steady current in an MHD generator is examined. A linear, plane-wave analysis shows that if the frequency of the oscillation is high enough, then the critical Hall parameter is always increased by the oscillation. However, if the oscillation frequency is much smaller than the growth rate calculated without dynamic stabilization, then the amplitude of a perturbation will move outside the linear range during a period. Therefore, the theory does not predict linear stabilization for low oscillation frequencies. (auth) (UK)

19544 HEAT SHIELDED THERMIONIC CONVERTER. **Hobson, Robert R. (to General Electric Co.). U. S. Patent 3,551,708. 29 Dec 1970. Filed 28 Nov 1967.**

The converter described has a collector electrode spaced adjacent to an emitter electrode, the collector electrode being reduced in area to decrease cooling of the emitter electrode and permit the use of heat sources of lower heat density. (Official Gazette)

Fluid Physics

Refer also to abstracts 19543 and 19671.

19545 CHARACTER OF EQUILIBRIUM OF AN INVISCID, INFINITELY CONDUCTING FLUID OF VARIABLE DENSITY IN THE PRESENCE OF A HORIZONTAL MAGNETIC FIELD WITH HALL CURRENT. **Ariel, P. D. (M. R. Engineering Coll., Jaipur, India). J. Plasma Phys.; 4: 523-30(Sep 1970).**

The character of equilibrium of an inviscid, incompressible, infinitely conducting fluid of variable density in the presence of a horizontal magnetic field is investigated, taking into account the effects of Hall currents. The solution is shown to be characterized by a variational principle. Making use of the existence of variational principle the solution is developed in the case of continuously stratified fluid of exponentially varying density confined between two horizontal planes at finite distance, from which the necessary and sufficient conditions of stability are obtained. The Hall currents are found to destabilize the wave-number range which is stable otherwise. (auth) (UK)

19546 EFFECT OF HALL CURRENT AND RESISTIVITY ON THE STABILITY OF A GAS-LIQUID SYSTEM. **Kalra, G. L. (Univ. of Delhi. Flinders Univ., Bedford Park, Australia); Kathuria, S. N.; Hosking, R. J.; Lister, G. G. J. Plasma Phys.; 4: 451-69(Sep 1970).**

The stability of a nonconducting, compressible fluid (gas) flowing across the surface of incompressible conducting fluid (liquid) is discussed. Finite resistivity and Hall current are included in the hydromagnetic equations, together with surface tension. Both subsonic and supersonic flows are treated and some new instabilities are found, together with modifications to real and oscillatory modes obtained in earlier treatments. (auth) (UK)

19547 PENETRATION OF A MAGNETIC FIELD BEHIND A SHOCK-WAVE FRONT. **Sinkevich, O. A. Magn. Gidrodin., Akad. Nauk Lat. SSR; No. 4, 71-4(Oct-Dec 1968). (In Russian).**

The entry of a plane strong gasdynamic shock wave in an external magnetic field is considered. The electric conductivity of the medium in front of the shock wave is negligibly small. For the moments of time during which gasdynamic shock wave parameters do not fluctuate, an analytic expression for magnetic field distribution at the front of the shock was obtained. It is shown that the role of the electromagnetic wave, which moves in front of the shock wave, is unimportant for an infinite medium. It is shown that the magnetic field penetration depth at the shock wave front is determined both by the magnetic field diffusion, and by the rate of motion of the media. (tr-auth)

19548 END EFFECTS IN MAGNETOGASDYNAMIC CHANNELS WITH FINITE-SIZE TERMINAL INSULATORS. **Benenson, E. B. Magn. Gidrodin., Akad. Nauk Lat. SSR; No. 4, 119-23(Oct-Dec 1968). (In Russian).**

End effects (longitudinal edge effects) related to the finite size of the electrodes and insulators, which separate the electrodes from the construction elements with potential equal to zero, are considered. Approximate expressions were obtained for the calculation of end losses in a channel, which give satisfactory agreement with exact formulas in a certain range of geometric parameters. (tr-auth)

19549 COMPRESSION OF MAGNETIC FIELDS BY CYLINDRICAL CONDUCTING ENVELOPES. **Akatnov, N. I.; Kuznetsov, A. P. Magn. Gidrodin., Akad. Nauk Lat. SSR; No. 4, 124-8(Oct-Dec 1968). (In Russian).**

Previously, different problems of the theory and practice of magneto-cumulative generators for the creation of transient magnetic fields of great strength have been studied. The working principle of these generators lies in the fact that magnetic flux is constricted by a hollow metal cylinder. Here, an attempt is made to analyze the constricting motion of the cylinder, inside which magnetic flux was contained. The compression of magnetic flux by an axially-symmetric, infinite, cylindrical, conducting fluid envelope and also leakage within its magnetic field owing to the conductivity of the envelope fluid are examined. The solution obtained considers the influence of the bulging effect in the compression process. (tr-auth)

19550 INVESTIGATION OF FLOW OF CONDUCTING FLUID NEAR A NONCONDUCTING SPHERE IN PRESENCE OF CROSSED ELECTRIC AND MAGNETIC FIELDS. **Kinareevskii, V. A. Magn. Gidrodin., Akad. Nauk Lat. SSR; No. 4, 137-42(Oct-Dec 1968). (In Russian).**

Experiments were performed to fit the velocity field in the vicinity of separate nonconducting spherical particles in a mixture of electroconducting fluids in the presence of crossed electric and magnetic fields upon the essentially inertial character of flow near a stationary sphere. The properties and intensity of circular flow were studied by means of a number of mobile spheres, placed in immediate proximity to the rigidly attached sphere in question, and were recorded by means of a cathetometer. From the results obtained it was assumed that the force, which displaces the sphere and characterizes the velocity profile, depends on the difference of the densities of the sphere and the fluids, the radius of the sphere, velocity head, and hydrostatic pressure at the experimental points. The arithmetic mean of the measurements was calculated according to 50 to 100 measurements at each point, yet the spread of the measurements from the average value did not exceed 5%. It was established that the net velocity field in the vicinity of a nonconducting sphere is the superposition of two flows, one of which is four local vortex cells of which surfaces $r = \text{const.}$ serve as current surfaces, while the other (within the limits of each cell) is directed radially to the surface of the sphere and resembles flow about a rotated disk. Qualitative information concerning the effect of the concentration of solid particles in a conducting fluid on MHD separation processes was obtained. (tr-auth)

19551 INFLUENCE OF DISSIPATIVE PROCESSES IN THE CASING ON THE STABILITY OF THE SURFACE OF A LIQUID METAL CONFINED IN VACUUM BY A VARIABLE MAGNETIC FIELD. **Gubarev, V. F.; Ladikov-Roev, Yu. P. Magn. Gidrodin., Akad. Nauk Lat. SSR; No. 4, 143-51(Oct-Dec 1968). (In Russian).**

The problem of the liquid metal, confined in vacuum by a variable magnetic field of circular polarization with a good conducting sheath, was examined in two-dimensional geometry. The sheath has finite conductivity and the viscous liquid metal infinite conductivity. The method of small perturbations was used. The integro-differential equation was obtained concerning the amplitude of the boundary perturbation $\xi(t)$, which, under the condition that the sheath conductivity tends to infinity and the viscosity of the metal to zero, develops into the Mathieu equation. On the condition that the field frequency ω is sufficiently high and much greater than the oscillation frequency of the metal Ω, an asymptotic equation was obtained based on a small parameter ϵ, equal to ratio of depth of skin layer in the sheath to the characteristic dimension of the problem. It is shown that the effect of the dissipative processes in the sheath is manifested in decrease of rigidity of the system and the damping constant, yet the latter is shown only in the third approximation. (tr-auth)

19552 ONE-DIMENSIONAL FLOW OF MAGNETIZED LIQUID. **Yantovskii, E. I. Magn. Gidrodin., Akad. Nauk Lat. SSR; No. 4, 3-9(Oct-Dec 1968). (In Russian).**

The one-dimensional flow of an incompressible, inviscid conducting fluid in a channel with applied transverse electric and magnetic fields with arbitrary magnetic Reynolds number is considered. Two special cases of constant-velocity flow are considered: (1) the magnetic permeability is decreased inversely proportional to the magnetic field strength, and (2) the permeability decreases linearly as the temperature approaches the Curie point. It is shown that the decrease in permeability may be accompanied by an increase in the total pressure of the fluid, and its heating—by the intensification of the magnetic field. (tr-auth)

19553 UNSTEADY FLOW OF MERCURY IN A TROUGH IN A TRANSVERSE MAGNETIC FIELD. **Amitin, M. B.; Vulis, L. A.; Genkin, A. L.; Kudryashova, L. A. Magn. Gidrodin., Akad. Nauk Lat. SSR; No. 4, 10-18(Oct-Dec 1968). (In Russian).**

Results are presented of experimental and theoretical studies of unsteady flow of liquid metal with an exposed surface in a magnetohydrodynamic trough with $R_m \ll 1$. The experiments conducted include the subcritical and supercritical regimes of unsteady flows, including those with hydraulic jump, with change in magnetic field induction time, the resistances of the external loop, etc. For the subcritical flow regimes the experimental results are compared with the results of numerical calculations. (tr-auth)

19554 RESISTANCE IN FLOW OF LIQUID METALS IN CHANNELS IN A TRANSVERSE MAGNETIC FIELD. **Vulis, L. A.; Gnatyuk, V. V.; Paramonova, T. A.; Fomenko, B. A. Magn. Gidrodin., Akad. Nauk Lat. SSR; No. 4, 19-28(Oct-Dec 1968). (In Russian).**

Experimental data are generalized according to the flow resistance of a liquid metal in channels in transverse magnetic fields. The results of all of the known experiments are considered, mainly in nonconducting channels. The generalization is conducted on the basis of concepts concerning two types of transition from the laminar to the turbulent regime and to their gradual change with flow in a transverse field. A reference formula interpolation is cited, suitable for the description of the experimental data with different orientation of the magnetic field for flows in channels with nonconducting and conducting walls. The results of calculation and experiment are compared for a wide range of Hartmann and Reynolds numbers. (tr-auth)

19555 TWO-DIMENSIONAL FLOW OF ANISOTROPIC CONDUCTING INCOMPRESSIBLE FLUID IN AXIALLY SYMMETRIC CHANNELS WITH LONGITUDINAL-TRANSVERSE MAGNETIC FIELDS. **Gorbatkov, S. A. Magn. Gidrodin., Akad. Nauk Lat. SSR; No. 4, 29-38(Oct-Dec 1968). (In Russian).**

The problem of extended flow of a viscous incompressible gas with Hall effect is considered for closed axially symmetric channels with imposed longitudinally-transverse magnetic fields. The system of equations, obtained as a result of simplifications of the initial system of magnetohydrodynamic equations in the limits of boundary layer theory, is determined by the self-similar method and by the method of local similarity. In the case of small MHD interaction parameters ($S < 0.1$), solutions were obtained analytically through elliptic integrals, but for the average MHD interaction parameters ($S \sim 2$)—numerically. The general characteristic of the derived equation is a decrease of completeness of the profile of the longitudinal velocity with increase of Hall coefficient $\beta = \omega_e \tau_e$ and by decrease of angle α of the slope of the magnetic field to the channel axis, that is explained by decrease of the interaction of the gas stream with the magnetic field. (tr-auth)

19556 EXPERIMENTAL INVESTIGATION OF SUPPRESSION OF TURBULENCE IN TUBES OF SPECIAL CONFIGURATION BY TRANSVERSE MAGNETIC FIELDS. **Branover, G. G.; Vasil'ev, A. S.; Shcherbinin, E. V. Magn. Gidrodin., Akad. Nauk Lat. SSR; No. 4, 39-43(Oct-Dec 1968). (In Russian).**

Experiments are described on the effect of a transverse magnetic field on the behavior of the coefficient of resistance of the region with sudden expansion and pressure on an offset of the wall, in the case when the field induction vector is parallel to the long side of a gap of rectangular cross section. Results are presented also of an experiment with finned tubes located lengthwise of the transverse section along the lines of force of the magnetic field. The decrease in the coefficient of local resistance and the relation of dimensionless pressure on the offset was established from the Stewart number. It was established also that the presence of fins in the tube (parallel to the field) with a given orientation of field and flows does not have an effect on the coefficient of resistance in laminar flow. A sharp reduction of the relative coefficient of resistance in such tubes was discovered. An attempt is made to explain the results of the experiments. (tr-auth)

19557 EMPIRICAL APPROXIMATION OF COEFFICIENT OF HYDRAULIC RESISTANCE IN A MOVING MAGNETIC FIELD. **Dronnik, L. M.; Tolmach, I. M. Magn. Gidrodin., Akad. Nauk Lat. SSR; No. 4, 44-52(Oct-Dec 1968). (In Russian).**

Different determinations of the coefficient of flow resistance in a traveling field are analyzed. Expressions are obtained from the equation of motion for this coefficient under the condition of developing turbulent flow and by the calculation of an arbitrary velocity profile (according to depth), and also a parabolic (according to width) profile. First, an expression is obtained for the coefficient of the hydraulic resistance on the premise that the velocity varies according to arbitrary law along the z axis (the depth of flow). Next, the effect of the velocity profile on the width of flow and on its uniformity according to height is considered. The results of an experimental determination of the coefficient of flow resistance for liquid metal in a traveling magnetic field in the range of slip from 0.11 up to 0.67 at Hartman number $220 \div 530$ and Reynolds number $2 \div 4 \cdot 10^5$. (M.H.R.)

19558 CIRCULATION OF AN AXIALLY SYMMETRIC TURBULENT JET OF ELECTRICALLY CONDUCTING FLUID IN A

LONGITUDINAL MAGNETIC FIELD. Dzhaugashtin, K. E. Magn. Gidrodin., Akad. Nauk Lat. SSR; No. 4, 56-8(Oct-Dec 1968). (In Russian).

A problem concerning the circulation of an axially symmetric turbulent jet stream of electroconducting fluids in a longitudinal magnetic field was examined in a noninductive approach in the limits of semi-empirical turbulence theory. The effect of the magnetic field on the regularity of the growth of the jet is analyzed. The calculations are compared with experiment. (tr-auth)

19559 NEAR-WALL FLOW OF JET OF CONDUCTING FLUID IN TRANSVERSE MAGNETIC FIELD. Ermolaeva, G. K.; Sokovishin, Yu. A. Magn. Gidrodin., Akad. Nauk Lat. SSR; No. 4, 59-63(Oct-Dec 1968). (In Russian).

A plane laminar jet of conducting fluid, flowing from a thin gap in a space with a transverse magnetic field, is considered in a noninductive approach. Equations are obtained in partial derivatives after certain transformations are resolved by implicit difference methods. Exact results are compared with approximations obtained by the Karman–Pol'gauzen method using more profiles and by the method of nearly self-similar equations. It was found that the last method gives results that coincide with the exact ones sufficiently well. According to the Karman–Pol'gauzen method, using profiles of the fifth and sixth orders, it is possible to obtain agreement with the force of friction to within 3%. (tr-auth)

19560 DISTRIBUTION OF ENERGY PULSES IN AXIALLY SYMMETRIC TURBULENT JET OF ELECTRICALLY CONDUCTING FLUID CIRCULATING IN LONGITUDINAL MAGNETIC FIELD. Dzhaugashtin, K. E. Magn. Gidrodin., Akad. Nauk Lat. SSR; No. 4, 64-70(Oct-Dec 1968). (In Russian).

In the limits of semi-empirical turbulence theory, the equilibrium energy pulses for an axially symmetric jet of conducting fluid, circulating in a homogeneous longitudinal magnetic field, are calculated. The effect of the magnetic field on single terms in the equilibrium equation of energy pulses is analyzed. The results of the calculation are compared with experiment. (tr-auth)

19561 LAMINAR FLOW OF A VISCOUS CONDUCTING FLUID BETWEEN PARALLEL WALLS IN MOVING MAGNETIC FIELD. Tropp, E. A. Magn. Gidrodin., Akad. Nauk Lat. SSR; No. 4, 75-82(Oct-Dec 1968). (In Russian).

An asymptotic equation was constructed for the problem of the flow of conducting fluid between parallel walls in a traveling magnetic field by expansion according to the negative power of the Hartmann number. The cases of matched and opposed connecting of inductors of the traveling field are examined, and motion in the channel of the electromagnetic mixing equipment is studied. (tr-auth)

19562 TRANSPORT COEFFICIENTS OF INHOMOGENEOUS SYSTEMS IN ELECTROMAGNETIC FIELDS. Ivanov, U. I. Magn. Gidrodin., Akad. Nauk Lat. SSR; No. 4, 83-92(Oct-Dec 1968). (In Russian).

Three fundamental relations of the transport coefficients of inhomogeneous systems were isolated. In the first group, the relations of these coefficients were combined for the concentration of the system, the shapes of the dispersed particles, and the ratios of transport coefficients of the medium and the particle. Other relations were obtained for the calculation of structure change and transport properties of the substance, which was coupled in the boundary phase. The relation of the transport coefficients of inhomogeneous system is considered separately from the spatial localization of the dispersed particles. (M.H.R.)

19563 DESIGN OF SHORTER MAGNETOHYDRODYNAMIC CHANNELS FOR LIQUID METALS. Schuart, L. Wiss. Z. Tech. Hochsch. Otto von Guericke Magdeburg; 14: 103-6(1970). (In German).

The use of streams of liquid metal in Hall-effect generators offers greater promise than the use of gas plasmas. Experiments with electrical analog apparatus show that end losses in a short channel can be reduced considerably by the insertion of electrically insulating baffles, whose length is parallel to the direction of motion of the liquid, in both ends of the channel. The effects of load factor and magnetic induction on the efficiency of such a device are discussed. (Metals Abstr.)

19564 EFFECT OF PLATE TEMPERATURE OSCILLATIONS ON THE MAGNETOHYDRODYNAMIC THERMAL BOUNDARY LAYER ON A SEMI-INFINITE FLAT PLATE. Mital, V. (Madhav Engineering Coll., Gwalior, India). Indian J. Math.; 10: No. 1, 9-17(1968).

Forced-convection laminar boundary layer flow of a viscous incompressible and electrically conducting fluid from a semi-infinite flat plate, when the plate temperature oscillates in time about a constant nonzero mean while the free stream is isothermal, was studied. An approximate integral method is used to integrate the Navier–Stokes and energy equations. Separate solutions for low- and high-frequency ranges are obtained. It is found that, in the low-frequency range, the oscillating component of the temperature in the boundary layer always lags behind the plate temperature oscillations while the rate of heat transfer has a phase lead. In the high-frequency range the temperature in the boundary layer is of the "shear-wave" type. (Indian Science Abstr.)

19565 STEADY SUPERSONIC FLOW OF A CONDUCTING GAS IN A CHANNEL WITH NONCONDUCTING WALLS IN THE CASE OF WEAK MAGNETOHYDRODYNAMIC INTERACTION. Kholshchevnikova, E. K. Zh. Prikl. Mekh. Tekh. Fiz.; No. 4, 20-9(Jul-Aug 1970). (In Russian).

Flow problems were investigated in the case of low values of the magnetohydrodynamic parameter N in a nonconducting channel. The electric parameters and the mean and local gas dynamic flow parameters were determined for two geometries of the applied magnetic field, as the Hall number and the magnetic Reynolds number changed from 0 to 10. It was found that an increase of the Hall parameter and the magnetic Reynolds number results in the decrease of the Joule dissipation and in the perturbation of the mean gas-dynamic flow characteristics. The gas-dynamic parameters were found to be unevenly distributed near the extremities of the system. The Mach number, M_0, of the unperturbed current was found to affect strongly the gas-dynamic parameters, the perturbations of which exhibited an oscillatory character. An increase of the M_0 is accompanied by a strong increase of the density perturbation, whereby the perturbation of the velocity and pressure remain in the same order of magnitude as in case of low M_0 numbers. (TTT)

19566 CERTAIN MAGNETOHYDRODYNAMIC FLOW PROBLEMS RELATED TO WAVE PROPAGATION. Boguslavskii, Yu. Ya.; Ioffe, A. I.; Statnikov, Yu. G. Zh. Prikl. Mekh. Tekh. Fiz.; No. 4, 30-3(Jul-Aug 1970). (In Russian).

Propagation of waves in an absorbing medium is accompanied by the directional flow of the medium because by losing its energy the wave also loses some of its impulse and these losses are compensated by the flow. In a conducting medium, the impulse losses of the wave are related not only to the viscosity and heat conductivity but also to Joule heat losses, and a magnetic field influences the nature and the structure of the flow. The Landau–Lifshits equations were used to determine the motion of a conducting liquid in a magnetic field, assuming that the dissipative coefficients are constant. The transfer equation is thus reduced to an equation of conservation of entropy. The case of an infinite plane layer of a conductive liquid between flat, solid walls, was considered as the medium in which the wave propagates. The ends of the system were assumed to be closed by nontransparent layers, while the homogeneous layer field is applied in a perpendicular direction. It was found that the velocity profile configuration caused by the wave is similar to that obtained under acoustical flow conditions. The absolute velocity may be increased only at the expense of the increase of the absorption coefficient. (TTT)

19567 NONSTATIONARY ELECTRICALLY CONDUCTING FREE JET IN A TRANSVERSE MAGNETIC FIELD. Bertinov, A. I.; But, D. A. Zh. Prikl. Mekh. Tekh. Fiz.; No. 4, 34-9(Jul-Aug 1970). (In Russian).

The effect of viscous friction on the walls in magnetohydrodynamic flow may be considerably reduced by using free or half-restricted jets of a conducting fluid. In this connection, the nonstationary phenomena occurring in the one-dimensional motion in a plane jet consisting of an incompressible liquid with a transverse magnetic field were investigated. The jet touches the sectional electrodes attached at the upper portion of the inductive circuit. It was assumed that the magnetic Reynolds number and the magnetohydrodynamic interaction parameter were large. When the electric field resulting from the electromagnetic reduction in the channel is much lower than the field due to the upper circuits, the problem may be resolved in the form of the characteristic Cauchy problem of a quasi-linear hyperbolic system of first-order equations, solvable by computer. (TTT)

19568 HYDROMAGNETIC FLOW BETWEEN TWO ROTATING COAXIAL DISKS. Khan, Abdul Aleem (Lucknow Univ., India). Def. Sci. J. (New Delhi); 20: 53-8(Jan 1970).

Steady flow of a viscous, incompressible, and electrically conducting fluid between two parallel coaxial rotating discs with a transverse magnetic field is analyzed, when the discs rotate in the same direction at the same velocity and there is a source at the center. The investigation is limited to the case

XUM

of small magnetic Reynolds numbers. The results are shown graphically and summarized; they are shown to be practical in several applications, such as in designing viscosity pumps, rotating heat exchangers, and air thrust bearings. (IAA)

19569 HALL EFFECT ON THE MOTION OF VISCOUS FLUIDS PAST A FLAT PLATE. Dragos, L. (Univ., Bucharest). Rev. Roum. Math. Pures Appl.; 15: No. 5, 683-92(1970).

The motion of incompressible electroconducting viscous fluids past a finite conducting flat plate, taking the Hall effect into account, is investigated. In the undisturbed motion, the velocity and the magnetic induction have the plate direction. The linearized system leads to a partial derivative equation of order 10, whose solution is represented by a superposition of plane waves. The boundary conditions determine the general solution by means of three functions, f, g, and h, which satisfy a system of integral equations. (IAA)

19570 MAGNETOHYDRODYNAMIC FLOW PAST A SEMI-INFINITE FLAT PLATE WITH TRANSVERSE MAGNETIC FIELD. Mital, V.; Bodas, N. G. (Madhav Engineering Coll., Gwalior, India). Arch. Mech. Stosow.; 22: No. 1, 37-41(1970).

The magnetohydrodynamic flow of an electrically conducting, viscous, and incompressible fluid past an electrically nonconducting, semi-infinite plate with transverse magnetic field is analyzed. Similar solutions of the equation of motion are obtained for the magnetic field varying as the inverse of the square root of the distance along the plate. The flow depends on the interaction parameter N. The differential equation is solved numerically for small values of N, and it is found that the frictional force at the plate increases with the increase in the value of N. (IAA)

19571 COMPLETELY CONSERVATIVE DIFFERENCE SCHEMES FOR THE EQUATIONS OF MAGNETOHYDRODYNAMICS. Popov, Yu. P.; Samarskii, A. A. Zh. Vychisl. Mat. i Mat. Fiz.; 10: 990-8(Jul-Aug 1970) (In Russian).

Difference schemes are considered that approximate the system of MHD equations for a one-dimensional plane nonstationary case. The class of completely conservative schemes was isolated from the general family of difference schemes. For them, not only the difference analogs of the main laws of conservation—mass, momentum, and total energy—are valid (as for usual conservative schemes), but also the series of supplementary balance equations, the necessity of completion of which is dictated by physical considerations. Completely conservative schemes with first- and second-order approximations are constructed. (tr-auth)

Geophysics (Upper Atmosphere)

19572 (IPP-4/80) EDDY CURRENT LOSS THROUGH PULSED MAGNETIC FIELDS. Oswald, B. (Institut fuer Plasmaphysik, G.m.b.H. Garching (West Germany)). Sep 1970. 14p. (In German). Dep. NTIS (U. S. Sales Only).

The eddy-current losses in closed current loops caused by pulsed magnetic fields are calculated. The results may be useful for various applications, such as pulsed magnets, superconducting coils, etc. (auth)

19573 UNIDENTIFIED PLASMA IRREGULARITIES IN THE EQUATORIAL ELECTROJET. Balsey, Ben B. (Environmental Science Services Administration, Boulder, Colo.). Plasma Phys.; 12: 817-19(Oct 1970).

The observed characteristics of an as-yet-unidentified family of plasma irregularities found in the E region of the equatorial ionosphere are reported. The irregularities are casually related to the equatorial electrojet—an electron current flowing parallel to the magnetic dip equator. The characteristics of these non-two-stream irregularities show clearly that they are not generated by the Farley mechanism. Analysis of vhf echoes returned from the non-two-stream irregularities shows features which are listed. The casual mechanism is discussed. (UK)

19574 THE MORPHOLOGY OF BACKSCATTER FROM F-LAYER FIELD-ALIGNED IRREGULARITIES AT MID- AND HIGH-LATITUDES AND THE GENERATION OF THESE IRREGULARITIES. Au, Whitlow W. L. Pullman, Wash.; Washington State Univ. (1970). 250p. University Microfilms Order No. 70-24,971. Thesis.

The results of backscatter from F-layer field-aligned irregularities observed at the University of Queensland (UQ), Stanford University, the Air Force Cambridge Research Laboratories' (AFCRL) Plum Island field site, and Washington State University (WSU) are analyzed. Three latitudinal regions, midlatitude, low-auroral zone, and high auroral zone-polar region, were defined and the morphology of the backscatter returns for each region was determined. A data comparison was performed in which the echoes originating from the various latitudinal regions and observed at the different stations were used. The data comparison uncovered several inconsistencies, some of which include the differences in the range distribution of the echoes, the diurnal behavior of the long-range echoes, the data obtained at WSU and AFCRL (both stations are at approximately the same geomagnetic latitude so their data should be similar), and the difference between the magnetic variation of the Stanford and WSU long-range echoes which originate from about the same location. A summary of the different irregularity properties that should be explained by any generation mechanism is presented. A review of past theories indicated that none of the theories pertinent to the F layer is satisfactory. Three different models involving ionospheric electric fields were proposed to be responsible for the existence of some of the irregularities found in the high-latitude F layer. (TSS) (Diss. Abstr. Int., B)

19575 EXPERIMENTAL STUDY OF THE ION CHEMISTRY AND THERMAL BALANCE IN THE E AND F REGIONS ABOVE WALLOPS ISLAND. Pharo III, M. W.; Scott, L. R.; Mayr, H. G.; Brace, L. H.; Taylor, H. A. Jr. (Goddard Space Flight Center, Greenbelt, Md.). Planet. Space Sci.; 19: 15-25(Jan 1971).

Measurements by a Bennett ion-mass spectrometer and two electrostatic probes aboard NASA rocket flight 18.06 on August 26, 1966, produced altitude profiles of ion composition and concentration and electron concentration and temperature in the E and F regions above Wallops Island, Virginia. These charged-particle measurements, supported by measurements of N_2 concentration and neutral gas temperature (measured twenty minutes earlier by experiments on NASA 18.05), measurements of the extreme uv spectrum, and the 1964 Jacchia model (for the remaining neutral constituents) serve as a basis for determining reaction rates of the primary chemical reactions responsible for the formation of the ionosphere. Electron-temperature measurements and N_2 temperatures and concentrations provided rates for electron and ion cooling. The reaction rates ($cm^3\ sec^{-1}$) of the primary thermospheric processes are given. (auth) (UK)

19576 EVIDENCE OF SOLAR GEOMAGNETIC SEASONAL CONTROL OF THE TOPSIDE IONOSPHERE. Taylor, H. A. Jr. (Goddard Space Flight Center, Greenbelt, Md.). Planet. Space Sci.; 19: 77-93(Jan 1971).

Ion-composition results obtained from the polar-orbiting OGO-4 satellite during 1967–68 reveal a pronounced longitudinal variation in the composition of the topside ionosphere. This variation is in the form of a large scale wobble or shift in the latitudinal distributions of the major topside ions H^+, O^+, He^+, and N^+, observed as the Earth rotates beneath the fixed satellite orbit. Both the location and prominence of distinct ionospheric features, including the O^+–H^+ transition level, the H^+/He^+ ratio, the high-latitude depletion of H^+ and He^+, and the winter bulge in He^+, are found to change significantly between longitudes for which the angle between the Earth–Sun line and the dipole equator has its greatest variation. Similarly, it is found that the ambient-ion concentrations at a given latitude may change by as much as an order of magnitude between contrasting longitudes, even though the altitude and magnetic activity remain nearly constant. The overall result is that seasonal variations, such as the decrease in production of ionization at winter latitudes, are maximized at the location of extreme solar-geomagnetic season. The persistence of the longitudinal asymmetry over a range of local times, seasons, and magnetic conditions reveals that the topside ionosphere is dependent upon a solar-geomagnetic rather than simply a solar-seasonal control. This variation, which may involve large scale transport of both ions and neutral particles, presents an added complication to studies of the topside ionosphere. These results indicate that investigations of both long- and short-term changes in the ion composition must, to be rigorous, take into consideration the solar-geomagnetic seasonal effects. (auth) (UK)

19577 PLASMA STREAMING IN THE MAGNETOSPHERE. Hruska, A. (National Center for Atmospheric Research, Boulder, Colo.). Planet. Space Sci.; 19: 107-11(Jan 1971).

Steady-state streaming of the cold-magnetospheric plasma in the plane of the magnetic equator is discussed. The stream lines coincide with the lines of constant plasma density (N) if the value of |grad N| tends to infinity and/or if the vector grad N is parallel (or antiparallel) to the vector grad (BB_p). (B is the total strength of magnetic field and B_p is irrotational part of B). It is suggested that plasma streams across the plasmapause mainly in the region of the "dusk bulge." The plasma flow across the plasmapause is stronger during geomagnetically quiet periods than during the time periods with high geomagnetic activity. (auth) (UK)

XUM

19578 LIFETIMES AND HEIGHTS OF O(^{1}S) IN PULSATING AURORAE. Moore, J. G. (Air Force Cambridge Research Lab., Bedford, Mass.). Planet. Space Sci.; 19: 119-24(Jan 1971).

Brightness pulsations of the $[\mathrm{O\ I}]_{32}$ and $N_2^+(B^2\Sigma_u^+ - X^2\Sigma_g^+; 0-0)$ emissions are used in a cross-spectral method to determine the mean lifetime of the $^1S_0$ level of O I as a function of the frequency of pulsations. Heights of the pulsating aurorae are determined by relating the measured lifetimes of O I to quenching by O_2 and O in a standard atmosphere. The pulsating aurorae reported here occur in a height range from 88 to 115 km depending on the frequency of pulsations. (auth) (UK)

19579 EXCITATION OF λ6300A (O I) AIRGLOW BY SOFT ELECTRON FLUXES. Nichol, D. G. (Tasmania Univ., Australia). Nature (London) Phys. Sci.; 229: 13-14(4 Jan 1971).

The ionospheric study was based on published and original data from Brisbane (λ = 35°S), Canberra (λ = 44°S), and Hobart (λ = 54°S). The λ6300Å airglow was recorded during 1968–70. A comparison of the data showed that, south of about λ = 50°, a mechanism other than that generally accepted, i.e., that a dissociative recombination of O_2^+ is the source of atoms in the quiet mid-latitude F region, is significant. It is suggested that a semipermanent amount of soft electrons (10 to 30 eV) is present south of about λ = 50°S. The flux densities necessary to explain the airglow are presented, and the effects on 6300Å airglow, 5577Å airglow, temperature gradient, and heating are discussed. (UK)

19580 HYDROMAGNETIC WAVES GENERATED AT THE BOW SHOCK BY TANGENTIAL DISCONTINUITIES IN THE SOLAR WIND. Jaggi, R. K. (National Aeronautics and Space Administration, Houston, Tex.); Wolf, R. A. Phys. Fluids; 14: 648-57(Mar 1971).

The problem of interaction of an inhomogeneity frozen into the solar wind with the bow shock was investigated. These frozen-in tangential discontinuities produce ripples that move along the shock, ripples that can cause magnetosonic waves in the downstream medium. There are five linearly independent types of frozen-in inhomogeneities. Of the five inhomogeneities, those involving changes in the magnitude of density or velocity produce magnetosonic waves of largest amplitude. Other inhomogeneities are substantially less effective in producing magnetosonic waves in the magnetosheath. For normal solar wind parameters, a 10% density inhomogeneity upstream typically produces a magnetosonic wave with $|\delta B| = 0.03\ B_S$ where B_S is the field strength in the magnetosheath. A 30° fluctuation in magnetic field direction upstream typically produces a magnetosonic wave downstream with magnetic amplitude $\simeq 10^{-3}B_S$. However, for certain angles between the upstream magnetic field and the shock, the efficiency of conversion into magnetosonic waves in infinite; i.e., the shock is unstable. (auth)

19581 UPPER BOUND ON PLASMA CONTAINMENT. II. Hurley, James (Univ. of California, Davis). Phys. Fluids; 14: 643-7(Mar 1971).

The problem of the saturation energy of a plasma in a magnetic bottle is considered, taking special care to ensure that the plasma is kept away from the sources of the field of the bottle. (auth)

19582 DUST COMET IN THE SOLAR WIND. Stoops, Emerson FitzSimmons. Los Angeles; Univ. of California (1970). 121p. University Microfilms Order No. 71-713.

Thesis.

The question of the possibility of a comet without a significantly ionized atmosphere interacting with the solar wind due to the presence of a cloud of charged dust grains is examined. The equilibrium potential of the dust grains as they traverse the head region of a comet is examined. It investigates the ratio of forces produced by radiation pressure and aerodynamic drag on the dust grains. It looks at a Ferraro-Rosenbluth type of interaction of the outwardly expanding dust–electron cloud of particles with the solar wind. Findings indicate that an interaction of a dust comet with the solar wind is expected even without the presence of a significantly ionized gas constituent to the conductivity of a comet's atmosphere. It finds that interaction of the dust grain cloud with the solar wind will tend to sharpen the leading edge of a comet, and will aid in producing the illusion that a comet's dust tail emanates from the head region in a direction other than along the Sun-comet radius vector direction. (Diss. Abstr. Int., B)

19583 DENSITY OF CHARGE SOURCES DURING INTERACTION OF CHARGED-PARTICLE FLUXES WITH THE ATMOSPHERE. Osipov, N. K.; Pivovarov, V. G.; Pivovarova, N. B. Kosm. Issled.; 8: 460-2(May-Jun 1970). (In Russian).

The negative-charge density is determined by the charge losses per unit length. At a given electron energy distribution and a given pitch-angle it is possible to obtain an expression for the charge loss as a function of atmosphere density and electron density at infinity (beyond the limits of the atmosphere). With the aid of a computer the negative-charge density was estimated for an isotropic electron flux $I = 10^8\ \mathrm{cm}^{-2}\ \mathrm{sec}^{-1}$. The electron energy was varied from 1 to 40 keV, and the height from 80 to 170 km. In a similar way, estimates of the positive charge were obtained for interaction of proton fluxes with the atmosphere by taking into account charge transfer and stripping reactions with neutral atoms of the atmosphere. The positive-charge density is tabulated for proton energies of 5, 10, 20 and 40 keV at heights of 125 to 400 km. These results are of interest in deriving properties of the ionosphere such as conductivity, thermal conductivity, microstructure of the ionosphere, etc. (TTT)

Low-Temperature Physics and Cryogenic Equipment

Superfluidity

Refer also to abstract 19640.

19584 HEAT AS A PROBE OF SUPERFLUID HELIUM FLOW. Payne, Richard Steven. New Haven; Yale Univ. (1970). 99p. University Microfilms Order No. 70-26,195.

Thesis.

An experiment was performed to prove that a force exists on a heated body that moves relative to the superfluid component of He II. It was shown that, if such a force exists, it should modify the logarithmic decrement of a heated, slowly oscillating cylinder in He II. The decrement of three cylinders was measured as a function of power, as a function of period of oscillation, and as a function of temperature. After a correction, due to a small change in the ordinary viscous damping with heat applied, the data were compared with calculated values of the zero-power decrement and calculated values of the changes in the decrement upon heating. It was found that the data agreed very well with the calculations. Since the theoretical calculations involve no adjustable parameters, it may be concluded that heat can serve as a probe of the relative velocity of a solid body and the superfluid component of He II. (Diss. Abstr., Int. B)

19585 RELATION BETWEEN THE SUPERFLUID-HELIUM BULK VISCOSITIES. Putterman, Seth (Univ. of California, Los Angeles). Phys. Rev. Lett.; 26: 421-2(22 Feb 1971).

The assumption that the superfluid-helium bulk viscosities are connected with internal relaxation processes is shown to lead to a relation between the four bulk viscosities such that only one is left independent. In this case absorption of second sound is independent of the bulk viscosities. (auth)

19586 CONDENSATE IN ^{4}He II AS A PILOT WAVE. Cummings, F. W. (Univ. of California, Riverside). Phys. Lett.; 34A: 196-7(22 Feb 1971).

An equation, resembling Maxwell's equation, derived at T = 0°K shows how the depletion gets dragged along at the condensate (curl-free) velocity, except in a thin region near the walls. Conceptual difficulties concerning boundary conditions in the two-fluid model are then resolved. (auth)

19587 FREE-ION MOBILITY IN He II USING FIELD-EMISSION POINTS. Sitton, D. M.; Moss, F. (Univ. of Virginia, Charlottesville). Phys. Lett.; 34A: 159-60(22 Feb 1971).

Positive and negative ion mobilities were obtained in He II between T_λ and 1.7°K from the characteristics of space-charge-limited discharges near tungsten field-emission points. The data are in agreement with previous measurements. (auth)

Superconductivity

Refer also to abstract 19863.

19588 (JINR–P8-5440) EXPERIMENTAL SOLENOID MADE OF Nb_3Sn STRIP. Anishchenko, N. G.; Bashilov, V. A.; Vasil'ev, V. A.; Khitnikov, B. Z.; Zel'dovich, A. G.; Kuznetsov, K. P.; Makarov, Yu. V.; Polinchik, N. N.; Shishov, Yu. A. (Joint Inst. for Nuclear Research, Dubna (USSR). Lab. of High Energy). 1970. 8p. (In Russian). Dep. NTIS (U. S. Sales Only).

Construction of solenoid is described and the results of its test are given. The solenoid is made of two disks wound of superconducting Nb_3Sn strip 40 mm wide and having an inside diameter of 122 mm. The magnetic field intensity in the center of the solenoid is of 30 kG, critical current being 480 A. (auth)

19589 DISLOCATION MOBILITY IN LEAD AND LEAD-INDIUM ALLOY SINGLE CRYSTALS. Parameswaran, V. R. Evanston, Ill.; Northwestern, Univ. (1970). 150p. University Microfilms Order No. 71-1935.

Thesis.

The dislocation mobility in a soft fcc metal was studied. Previously, it was reported that in the soft metals such as copper, zinc, aluminum, and silver the dislocation velocity varied linearly with stress and the principal damping mechanism acting in the high-velocity region (100 to 1000 cm/sec) was due to interaction with thermal phonons (above 60°K) and conduction electrons (below 60°K). Dislocation velocities in lead single crystals were measured by studying the rate of growth of slip bands generated and propagated by impact stress pulses of a few microseconds duration. The velocity measurements were made at different temperatures varying between 4.2 and 298°K in the normal and superconducting states of lead. A linear relationship between dislocation velocity and stress was observed in the lower stress region as predicted by the damping theories. At high stresses the dislocation velocity was found to increase with stress less than linearly, approaching the shear sound velocity at infinite stress. In the normal state the phonon drag was found to decrease with decreasing temperature, and below 77°K, the electron drag was found to increase with decreasing temperature. In the superconducting state the electron drag was found to be considerably smaller than in the normal state. The values of the damping constants calculated from the slope of the linear regions of the dislocation velocity–stress curves at 298, 77 and 4.2°K agreed with the values obtained from internal friction measurements by other investigators. The deviation from linearity at higher stresses could be due to some additional damping (probably relativistic) experienced by the dislocations moving with velocities near the shear sound velocity. The second part of the experiment was to study dislocation mobility in lead with 10 at. % indium alloy single crystals. Indium was added in order to possibly reduce the Peierls energy in the immediate neighborhood of the dislocation. This reduction should reduce the value of the damping constant at 4.2°K and give a higher dislocation velocity. However, the dislocation velocities observed in the superconducting alloy at 4.2°K were an order of magnitude smaller than the velocities in pure metal. This reduced velocity could be due to the increase in energy loss in the alloy due to reradiation of elastic energy by flutter mechanism. The maximum velocity observed in the experiments was $^3/_4$ of the shear sound velocity. (Diss. Abstr. Int., B)

19590 EFFECT OF OMEGA PHASE REVERSION ON THE SUPERCONDUCTING TRANSITION IN TITANIUM-BASE ALLOYS. Luhman, T. S.; Taggart, R.; Polonis, D. H. (Univ. of Washington, Seattle). Contract AT(45-1)-2225-T13. Scr. Met.; 5: 81-6(Feb 1971). (RLO-2225-13-5).

The superconducting transition behavior of titanium-base alloys in which the omega phase was reverted to the parent beta phase by means of an up-quenching treatment to temperatures above the range of stability of the omega phase was studied. Remanent fluctuations in composition persisted in the beta phase after omega reversion, resulting in a continuous solute enriched matrix which effectively screened the solute-depleted zones, thereby markedly affecting the measured superconducting transition temperature of the up-quenched alloy. (auth)

19591 EUROPHYS APPLIED SUPERCONDUCTIVITY COLLOQUIUM HELD AT SMOLENICE, CZECHOSLOVAKIA, ON 23–27 JUNE 1969. Elektrotech. Cas.; 21: 241-438(1970). (CONF-690652).

Sixteen papers are included on the theory of superconductivity, superconducting magnets, electrical machines, and cables, as well as other applications. A separate abstract was prepared for each paper. (M.H.R.)

For abstracts of individual papers see: 19592–19601 and 19633–19638.

19592 ELECTRODYNAMICS OF SUPERCONDUCTORS. Koppe, H. (Univ., Kiel). Elektrotech. Cas.; 21: 243-8(1970).

From Applied Superconductivity Conference, Smolenice, Czechoslovakia. See CONF-690652.

A simple discussion of the problems of nonequilibrium states in superconductors is given. For the example of London's equations it is shown that, in dealing with nonstationary states, it is not so much a matter of finding time-dependent equations, but of introducing simultaneously the right dissipation terms. In connection with that, a very simplified derivation for the viscosity constant for the flux line motion is given. The influence of the temperature gradient on the flux lines is discussed with the aid of Onsager relations. Simple assumptions lead to the conclusion that the force per volume unit is given by grad p. (auth)

19593 SOME TYPE OF SOLUTIONS FOR THE DIFFUSION OF FLUX INTO TYPE-II SUPERCONDUCTORS. Dichtel, K. (Univ., Kiel). Elektrotech. Cas.; 21: 249-56(1970).

From Applied Superconductivity Conference, Smolenice, Czechoslovakia. See CONF-690652.

An investigation is made of the nonlinear partial differential equation $\partial B/\partial t = \partial/\partial x[B(\partial B/\partial x)]$, which phenomenologically describes the penetration of the flux front into a superconductive half-space $x \geq 0$, with the initial condition $B(x,0) \equiv 0$ and the boundary condition $B(0,t) = B_0(t)$, given by the external field $B_0(t)$. For the solution type, which at a certain place $x = a$ of the half-space passes abruptly into the trivial solution $B(x,t) \equiv 0$, a transformation using this function a(t) representing a characteristic of the partial differential equation is advantageous. The separation method leads then for certain functions a(t) to an ordinary differential equation, which can be easily integrated and which gives a great number of solutions for the various external fields $B_0(t)$. (auth)

19594 THERMODYNAMICS OF TYPE-II SUPERCONDUCTORS. Milleron, P. F.; Fournet, G. (Faculte des Sciences de Paris, Fontenay-aux-Roses, France). Elektrotech. Cas.; 21: 257-71(1970).

From Applied Superconductivity Conference, Smolenice, Czechoslovakia. See CONF-690652.

The definitions of fields and energies, which are usually encountered in the investigation of superconductivity, are mentioned first. The results of phenomenological theories are given briefly and the temperature dependencies of parameters that arise (critical field, Ginzburg–Landau parameter). The investigation of specific heat and thermal conductivity is dealt with. Theoretical values are given and comparisons with experimental ones are made. (auth)

19595 FLUX PINNING. Haasen, P. (Univ., Goettingen, Ger.). Elektrotech. Cas.; 21: 272-5(1970).

From Applied Superconductivity Conference, Smolenice, Czechoslovakia. See CONF-690652.

Based on experimental and theoretical investigations, the fluxoid pinning in the mixed state of a Type-II superconductor by structural heterogeneities is discussed. The following problems are analyzed: interactions between fluxoids and dislocations, grain boundaries, martensitic plates, irradiation zones, precipitates, or ferromagnetic particles. Special emphasis is made on the summation statistics of interactions of both systems. New experiments for the flux creep are also discussed. (auth)

19596 VISUALIZATION OF THE MIXED STATE OF TYPE-II SUPERCONDUCTORS. Essmann, U. (Institut fuer Physik, Stuttgart). Elektrotech. Cas.; 21: 276-80(1970).

From Applied Superconductivity Conference, Smolenice, Czechoslovakia. See CONF-690652.

Into a type-II superconductor the magnetic flux penetrates in a form of separate fluxoids after exceeding the critical magnetic field H_{c1}. Each fluxoid conducts through the probe a flux quantum, the smallest flux that can exist in a superconductor. Experimental possibilities for representing the separate fluxoids and their structure are discussed. A direct representation was made possible by the aid of decoration techniques. The results obtained are discussed and compared with theoretical predictions. (auth)

19597 MACROSCOPIC PHENOMENOLOGICAL ELECTRODYNAMICS OF TYPE-II SUPERCONDUCTORS. Hlasnik, I. Elektrotech. Cas.; 21: 281-302(1970).

From Applied Superconductivity Conference, Smolenice, Czechoslovakia. See CONF-690652.

In the investigation of electromagnetic processes in type-II superconductors (T-II-S), the dimensions of which are substantially larger than London's penetration depth λ, it is often necessary but also sufficient to use simplified macroscopic electrodynamics. Its basis is Maxwell's equations completed by material characteristics indicating the relations between macroscopic averaged values $\bar{E}$, $\bar{D}$, $\bar{J}$, $\bar{B}$, $\bar{H}$. In some cases, mainly in homogeneous T-II-S, these characteristics can be determined on the basis of the solution of Ginzburg–Landau equations (microscopic electrodynamics of T-II-S). However, for most cases of hard T-II-S, which have high critical current densities, these characteristics are determined as empiric relations on an experimental basis. With respect to the large influence of the materials structure and the value of B on these characteristics, a survey is presented of various typical regions and of characteristics valid in them. Their validity limits and the influence of some boundary conditions in hard T-II-S are analyzed. As an illustration for the applicability of T-II-S, macroscopic electrodynamics solutions are given for various electromagnetic processes in T-II-S. (auth)

XUM

19598 BEHAVIOR OF TYPE-II SUPERCONDUCTORS IN TIME-DEPENDENT MAGNETIC FIELDS. Fournet, G.; Mailfert, A. Elektrotech. Cas.; 21: 303-13(1970).

From Applied Superconductivity Conference, Smolenice, Czechoslovakia. See CONF-690652.

The properties of type-II superconductors with strong pinning centers in time-variable magnetic fields are investigated. The electric field and losses are expressed precisely, assuming that the probe is isothermic, that the critical-state law is valid for it, and that the influence of a surface current is taken into account. A formula for the electric field in an arbitrary point of the material is derived for the case that the temperature depends only on the time and not on the position of the point taken into account. (auth)

19599 ON THE QUESTION OF PREPARING SUPERCONDUCTORS WITH HIGH PARAMETERS. Alekseevskii, N. E. (Inst. of Physical Problems, Moscow). Elektrotech. Cas.; 21: 323-35 (1970).

From Applied Superconductivity Conference, Smolenice, Czechoslovakia. See CONF-690652.

The possibility of increasing the critical temperature of superconductors is considered. The properties of Nb_3Al-Nb_3Ge system alloys are investigated. The dependencies of the critical temperature on the thermal treating and the dependencies of the critical field on temperature for an alloy with the contents ~30% Nb_3Ge are given. On the basis of x-ray structural investigations, it was concluded that the high critical temperature of the investigated alloy (20°K) is a consequence of the ordering of aluminum and germanium atoms. The result of such ordering can be the origin of an additional branch of oscillations. The origin of an additional branch of oscillations can immediately lead to an electron–phonon interaction and so increase the critical temperature. The possibilities of increasing the critical temperature by the use of "dimensional quantization" in thin layers are dealt with briefly. (auth)

19600 PROXIMITY EFFECTS BETWEEN MAGNETIC AND SUPERCONDUCTING THIN FILMS. Deutscher, G. (Faculte des Sciences, Orsay, France). Elektrotech. Cas.; 21: 336-44 (1970).

From Applied Superconductivity Conference, Smolenice, Czechoslovakia. See CONF-690652.

After recalling some general properties of normal/superconductor contacts, results obtained in the particular case where N is a conducting magnetic material M are reviewed. Particular attention is paid to local properties near the S/M interface. The situation where M is a ferromagnetic insulator is then discussed. In that case, it is shown that recent experimental results indicate the presence of first-order exchange field effects in S. Possible applications are indicated. (auth)

19601 SUPERCONDUCTING POINT CONTACTS WEAKLY CONNECTING TWO SUPERCONDUCTORS. de Bruyn Ouboter, R.; de Waele, A. Th. A. M. (Kamerlingh Onnes Lab., Leiden). Elektrotech. Cas.; 21: 405-18(1970).

From Applied Superconductivity Conference, Smolenice, Czechoslovakia. See CONF-690652.

Dc and ac interference phenomena in superconducting point contacts weakly connecting two superconductors are reviewed. First, the properties of a single superconducting point contact are discussed. Special attention is paid to the resistive–superconductive region and its current–voltage characteristic. The point contact is treated using a two-fluid model in which the total current is the sum of an ideal Josephson supercurrent and a normal current. It appears that very small shunt capacitances and series inductances play an important role, even in its dc current–voltage characteristic. Primarily, the two cases for which either the total current or the voltage are constants of time are discussed. Secondly, the external magnetic field dependence of the critical current through a double point contact weakly coupling two superconductors, when the self-induced flux in the enclosed area is taken into account, is studied extensively. Its relation with a strongly coupled double point contact in which flux quantization holds is treated. Experimental results are shown and compared with theory. Finally, the properties of double point contacts in the resistive–superconductive region in relation to both the ac and dc Josephson effects are discussed. It is observed that the dc voltage across a double point contact oscillates as a function of the applied magnetic field when a constant current is applied as a function of the applied magnetic field when a constant current is applied through the double point contact. The complete current–voltage–magnetic field dependence can be represented by a corrugated surface. (auth)

19602 EXPERIMENTAL DEMONSTRATION OF THE RIEDEL PEAK. Hamilton, C. A.; Shapiro, Sidney (Univ. of Rochester, N. Y.). Phys. Rev. Lett.; 26: 426-8(22 Feb 1971).

Careful measurements were made of the power and frequency dependence of the ac Josephson steps in a superconducting tunnel junction exposed to microwave radiation. At values of $2\alpha = 2eV_{rf}/hf > 25$, significant deviations from Bessel function behavior $[J_N(2\alpha)]$ begin to occur. These deviations are correctly predicted in the detailed microscopic theory of Werthamer and are a consequence of the logarithmic singularity in the ac Josephson current at $f_J = 4\Delta/h$, i.e., the Riedel peak. (auth)

19603 KONDO EFFECT IN SUPERCONDUCTORS. Mueller-Hartmann, E.; Zittartz, J. (Univ. of California, San Diego, La Jolla). Phys. Rev. Lett.; 26: 428-32(22 Feb 1971).

A self-consistent treatment of the Kondo scattering of conduction electrons from magnetic impurities is presented in order to treat finite concentrations of such impurities in superconductors. The present theory leads to a concentration dependence for the transition temperature which differs markedly from the Abrikosov–Gor'kov result. The theory appears to account nicely for various experimental results. It is also found that superconductivity, under certain circumstances, does not exist at all temperatures below T_c. (auth)

19604 THEORY OF ULTRASONIC ATTENUATION IN V_3Si. Schuster, H.; Klose, W. (Univ., Saarlandes, Saarbruecken, Ger.). Phys. Lett.; 34A: 152-3(22 Feb 1971).

The ultrasonic attenuation coefficient for V_3Si is calculated in the linear chain model for β-W compounds. The result deviates from the free electron value and agrees well with experiment. (auth)

19605 PRESSURE ENHANCEMENT OF SUPERCONDUCTIVITY IN V_3Si. Barisic, S. (Laboratoire de Physique des Solides, Orsay, France). Phys. Lett.; 34A: 188-9(22 Feb 1971).

The pressure enhancement of superconductivity in V_3Si is explained on the basis of a tight-binding band and electron–phonon coupling model. The corresponding problem in transition metals is briefly discussed. (auth)

19606 TOWARD THE SUPERCONDUCTIVITY OF RHODIUM. Mota, A. C.; Black, W. C.; Brewster, P. M.; (and others). (Univ. of California, San Diego, La Jolla). Contract AT(04-3)-34. Phys. Lett.; 34A: 160-1(22 Feb 1971).

Superconducting transition temperatures of Rh–Ir and Rh–Os alloys indicate that the critical temperature of rhodium will be at 0.2 m°K. (auth)

19607 INTERACTION OF 9.3-GHz LONGITUDINAL PHONONS WITH ELECTRONS IN SUPERCONDUCTING FILMS. Cohen, Moshe (Hebrew Univ., Jerusalem); Goldstein, Y.; Abeles, B. Phys. Rev., B; 3: 2223-31(1 Apr 1971).

Previous studies of the interaction of longitudinal phonons with superconducting Al/Pb junctions were extended to include nonuniform strains, arising when the thicknesses of the metal films are not negligible compared to the wavelength of the sound and/or when the wave front makes a small angle θ with the plane of the junction. It is found that nonuniform strains produce an electric field proportional to the strain gradient inside the "local" superconducting Al film. This result confirms the theories of Dessler et al., Herring, and Harrison who calculated the gravity-induced electric fields. The strain-induced field in the aluminum excites electromagnetic waves in the junction that are enhanced due to the traveling-wave interaction in the strip line formed by the junction. The electromagnetic field gives rise to an extra tunneling current that exhibits resonant behavior as a function of the angle θ. In the "nonlocal" Pb films, the interaction of the electrons with the strain wave is described by absorption and emission of phonons, and the extra tunneling current due to this process is essentially independent of θ. This behavior enables one to separate the extra current due to the Al film and that due to the Pb film. The agreement between theory and experiment is found satisfactory. (auth)

19608 ATTENUATION OF LONGITUDINAL ULTRASOUND IN NORMAL AND SUPERCONDUCTING MERCURY SINGLE CRYSTALS. Huang, Helen Chi-hsing. Detroit; Wayne State Univ. (1970). 138p. University Microfilms Order No. 71-418.

Thesis.

The ultrasonic attenuation of longitudinal waves in pure single crystals of mercury in both the normal and superconducting states was investigated using the pulse-echo technique, single transducer, or transmission methods. Measurements were made for frequencies from 10 to 320 MHz in the temperature range of 4.2 to 1.1°K, and with the sound propagating along three different crystallographic directions: the three-fold ([111]), the two-fold ([$\bar{1}$10]) and [3$\bar{1}\bar{1}$] axes. Data were analyzed in the scheme of free electron theory. In the normal state, the ql- and frequency dependence of the attenuation were found to be generally in good agreement with the Pippard free electron attenuation theory. However, in the super-

XUM

conducting state the behavior was not in accord with the BCS theory of superconductivity. The present mercury data suggest that the concept of an electron mean free path, which differed in the normal and superconducting states, could explain the observed frequency-dependent behavior in mercury within the framework of the free electron model. However, an anomalous behavior persisted in the high-frequency limit that can not be accounted for in terms of a single-energy-gap BCS theory, or a physically reasonable multiple-gap model. (TSS) (Diss. Abstr. Int., B)

19609 MAGNETIC FLUX FLOW IN A TYPE-II SUPERCONDUCTOR. Urban, Eugene Willard. University, Ala.; Univ. of Alabama (1970). 74p. University Microfilms Order No. 71-1280.

Thesis.

An experimental study was conducted to measure the flow of magnetic flux through the wall of a specimen of Nb−25% Zr, and thereby to infer the magnetic induction and currents in the material. It was found that if at some magnetic field the specimen were heated to above T_c and recooled, then if the applied field were subsequently changed at a constant rate, the rate of flux flow into or out of the sample would increase linearly with time. If measured at a series of magnetic fields, the rates of these increases, or the flow rate slopes were found to be a smoothly increasing function of average applied field. Calculations based on eight published critical-current-density models did not satisfactorily explain these observations. It was found, however, that the empirical current-density model $J_c = \alpha_c\,(\mu_0 H_{c2} - B/B_0 + B)$ did, in fact, give excellent agreement with the measured flow rate behavior. The experimental and analytical results are described, and the new current density model is compared with earlier ones. (Diss. Abstr. Int., B)

19610 AC AND DC POTENTIALS IN SUPERCONDUCTING PHASE-SLIP STRUCTURES. Kirschman, R. K.; Notarys, H. A.; Mercereau, J. E. (Calif. Inst. of Tech., Pasadena). Phys. Lett.; 34A: 209-11(8 Mar 1971).

Ac and dc potentials accompanying phase slip in weakly superconducting structures of well-defined geometry can be described by a Josephson-like oscillation accompanied by intrinsic dissipation and are completely characterized by critical current and normal-state resistance. (auth)

19611 ANOMALOUS EFFECTS OF LENGTH ON THE FIELD-TRAPPING PROPERTIES OF TYPE-I SUPERCONDUCTING HOLLOW CYLINDERS. Schweitzer, D. G. (Brookhaven National Lab., Upton, N. Y.). Phys. Lett.; 34A: 220-1(8 Mar 1971).

Thin-walled hollow cylinders of type-I superconductors in which the walls are annealed and etched exhibit a maximum in the trapped field with length of the cylinder. The effect does not occur in the same samples when the surfaces are strained. (auth)

19612 SELF-RESONANT CURRENT PEAKS IN JOSEPHSON JUNCTIONS. Blackburn, J. A. (Electronics Research Center, Cambridge, Mass.); Leslie, J. D.; Smith, H. J. J. Appl. Phys.; 42: 1047-54(1 Mar 1971).

The finite-difference scheme described yields solutions of the Josephson phase equation. This simulation technique is used to calculate the self-resonant current peaks of a Josephson junction for the two cases, $R \gg Z_J$ and $R \ll Z_J$, where R is the current drive source resistance and Z_J is the junction impedance. The simulation current peaks are compared with ones derived by a perturbation technique for the same two regimes, and also with experiment. In terms of approximating experimental results, it is found that the perturbation solutions with constant damping, σ, are better than those with constant Q; although at small σ the magnitude and shape of the current peaks do not agree well with observations. However, simulation results at small σ are reasonably consistent with experiment. Simulation results for the case $R \ll Z_J$ indicate that self-limiting will affect the magnetic field dependence of the resonances when $L/\lambda_J \geq 2$, where L is the length of the junction and λ_J is the Josephson penetration depth. (auth)

19613 HALL EFFECT IN A SUPERCONDUCTOR NOT IN THE VORTEX STATE. Rieger, T. J. (Univ. of California, Santa Barbara). Phys. Rev., B; 3: 2253-8(1 Apr 1971).

The Hall electric field inside a superconductor not in the vortex state is calculated using the time-dependent Ginzburg–Landau equations. The field exists only in the skin of the superconductor. Part of the electric field penetrating the material dies out in a London penetration length and part dies out in a coherence length. For an applied magnetic field of 1 G, the field is 10^{-7} to 10^{-8} V/m in most pure superconductors, and is proportional to the square of the applied magnetic field. The gradient of the electrochemical potential is zero, so there is no Hall voltage. The charge density producing the electric field is a dipole layer, a penetration length thick, at the surface of the material. This means that the contact potential has a part that depends quadratically on the applied magnetic field. (auth)

19614 INFLUENCE OF NORMAL-STATE ELECTRICAL RESISTANCE ON THE SUPERCONDUCTING TRANSITION TEMPERATURE OF ULTRATHIN FILMS. Crow, J. E.; Strongin, Myron (Brookhaven National Lab., Upton, N. Y.). Phys. Rev., B; 3: 2365-7(1 Apr 1971).

Recent data showing decreases in the T_c of ultrathin films are reconsidered in the light of results from work on fluctuations in films, which indicate the possibility of a large "pair-breaker" in high-resistance films. (auth)

19615 SUPERCONDUCTIVE TUNNELING INTO BULK GALLIUM SINGLE CRYSTALS. Keister, Jamieson Charles. Washington, D. C.; Georgetown Univ. (1970). 154p. University Microfilms Order No. 70-26,673.

Thesis.

Tunneling into bulk superconductors is discussed as a means for determining the energy gap of the superconductor. Methods for fabricating single-crystal bulk gallium tunnel junctions are described. Over 1000 samples were fabricated. Specimens with tunneling directions ⟨100⟩, ⟨010⟩, ⟨001⟩, and random yielded extrapolated energy gaps ranging from 3.5 to 4.0 KT_c, in basic agreement with the magnitude of energy-gap values obtained by others using different measuring techniques. The energy-gap anisotropy calculated using the best estimates of the energy gap is 5%, in agreement with values obtained by other workers performing tunneling experiments, but in basic disagreement with anisotropies of 20% obtained by other workers using different measuring techniques. However, the extremes of measuring errors in this work could permit an anisotropy of up to 20%. Other results, such as tunneling into round-shaped samples, possible multiple-gap structure, excess subharmonic currents, weak-link behavior, and sample aging effects are discussed. (Diss. Abstr. Int., B)

19616 KAPITZA RESISTANCE BETWEEN DIELECTRICS AND METALS IN THE NORMAL AND SUPERCONDUCTING STATES. Papk, Byung Sub; Narahara, Yoshimasa (Tokyo Univ. of Education). J. Phys. Soc. Jap.; 30: 760-7(Mar 1971).

Change of the Kapitza resistance as a metal goes from the normal state to the superconducting state is estimated in the dielectric/metal junction by extending Little's theory that the interaction between surface waves and conduction electrons contributes to heat transfer in the liquid/solid junction. According to this estimate, no change is expected in the case that sound velocities of the dielectric are larger than those of the metal. The sapphire/indium junction is such a case. The Kapitza resistance of this junction measured from 0.6 to 2.2°K shows, however, a small difference between the normal and the superconducting states of indium, contrary to the above estimation. (auth)

19617 GEOMETRICAL RESONANCE EFFECT IN SPUTTERED SUPERCONDUCTING NIOBIUM. Smith, C. W. (Univ. of Maine, Orono); Miller, N. C. Phys. Lett.; 34A: 147-8(22 Feb 1971).

Geometrical resonances were observed in the electron-tunneling characteristics of rf-sputtered niobium films. The data scale correctly with film thickness and result in a mean Fermi velocity in fair agreement with other measurements. (auth)

19618 SUPERCONDUCTING ALLOY. Fedorov, L. N.; Sokolov, V. I.; Mikhaylov, N. N.; (and others) (to Central Scientific Research Inst. of Ferrous Metallurgy). Russian Patent 243,841. 1 Oct 1969. Filed 22 Dec 1967. (In Russian).

A superconducting alloy containing titanium, niobium, zirconium and tantalum is introduced. To improve the stability of its superconducting properties, iron was added, making the following chemical composition (in %): niobium 31 to 35, zirconium 5 to 8, tantalum 0.5 to 1.5, iron 0.3 to 0.7, and the remainder titanium. (JPRS)

19619 FLUX-FLOW RESISTIVITY AND HALL ANGLE IN PURE TRANSITION-METAL SUPERCONDUCTORS NEAR H_{c2}. Tang, I-ming (Reed Coll., Portland, Oreg.). Phys. Rev., B; 3: 2237-43(1 Apr 1971).

The transport equations in the mixed state of a pure type-II transition-metal superconductor are obtained by noting that the physically observed transport currents (i.e., the electric current and the heat current) in the two-band superconductors near H_{c2} are just the sum of the physical observables in the individual bands. Since the two moving energy gaps in the transition-metal superconductors have essentially the same form as the moving order parameter in the one-band superconductors, the calculational techniques devised by Caroli and Maki for evaluating the

XUM

observable in pure one-band superconductors near H_{c2} can be applied directly to the evaluation of the physical observables in the individual bands of the two-band superconductors near H_{c2}. Using the transport equations with the definitions of the flux-flow resistivity and Hall angles, expressions for these properties are obtained which should be valid for pure transition-metal superconductors near H_{c2}. The two-band expressions are used to analyze the experimental data on the flux-flow resistivity and Hall angle in pure superconducting niobium. (auth)

19620 INTERMEDIATE MIXED STATE OF TYPE-II SUPERCONDUCTORS. Aston, D. R. (Temple Univ., Philadelphia); Dubeck, L. W.; Rothwarf, F. Phys. Rev., B; 3: 2231-6(1 Apr 1971).

For magnetic fields in the range $(1 - D)H_{c1} < H < H_t$, magnetization curves of low-κ type-II Pb–In and In–Bi alloys with nonzero demagnetization coefficients D exhibit a linear dependence of the magnetic moment on applied field. H_{c1} is the lower critical field and H_t is the field at which the linear dependence terminates. For finite D, $H_t < H_{c1}$. This behavior can be explained by a model of alternate regions of superconducting and mixed states. This array may be metastable. The mixed-state regions are all presumed to have the same temperature-dependent fluxoid-lattice spacing characteristic of H_{c1} when $D = 0$. Thus, as the magnetic field is increased isothermally, the mixed-state regions grow until the whole sample has been converted into the mixed state. This model implies the existence of an attractive interaction between flux lines in low-κ materials. (auth)

19621 OSCILLATORY DEPENDENCE OF SUPERCONDUCTIVE CRITICAL TEMPERATURE ON NUMBER OF VALENCY ELECTRONS IN Cu_3Au-TYPE ALLOYS. Havinga, E. E.; Damsma, H.; Van Maaren, M. H. (Philips Research Labs., Eindhoven, Netherlands). J. Phys. Chem. Solids; 31: 2653-62(Dec 1970).

The superconducting critical temperature, magnetic susceptibility, and thermoelectric power of a number of pseudo-binary B_3A-type alloys with Cu_3Au structure were investigated. An oscillatory dependence of the properties on the number of valence electrons per atom was observed. The constituents of the alloys were mainly nontransition metals: for the A elements Ca, Y, La, and Th and for the B elements In, Sn, Tl, and Pb. The results can be explained by taking into account the influence of the scattering of electrons by Bragg planes near the Fermi surface on the electron density of states and on the superconductive interaction parameter. In addition, 13 other Cu_3Au-type compounds with mainly nontransition metals were prepared. The superconductivity of 19 out of the 25 Cu_3Au-type compounds investigated can be fitted into the general scheme of oscillatory behavior of T_c with n. The absence of superconductivity for 5 of the compounds can be ascribed to magnetic interactions. (auth) (UK)

19622 ENHANCEMENT OF SUPERCONDUCTIVITY IN ALUMINUM FILMS. Hauser, J. J. (Bell Telephone Labs., Murray Hill, N. J.). Phys. Rev., B; 3: 1611-16(1 Mar 1971).

Mixtures of Al and Al_2O_3 were sputtered at room temperature, while mixtures of Al and Ge were sputtered at 77°K yielding, respectively, a maximum transition temperature of 2.5 and 3.6°K. The phonon spectrum of an Al film with 3.6 at. % Ge(T_c = 3.48°K) is very similar to that of normal Al (T_c = 1.2°K) and only slightly lower in energy. The magnitude at 0°K and the temperature dependence of the energy gap of the enhanced Al are extremely well fitted by the BCS theory. Density measurements were performed in two different ways on the two mixtures (10 wt % of Al_2O_3 and 10 wt % of Ge) with maximum T_c. Density measurements by a direct-weighing technique yielded a decrease in density of 5.5%. Electron-diffraction experiments showed that the lattice spacing increased from 4.05 (normal aluminum) to 4.19 Å for the most-enhanced aluminum, which corresponds to a 10.5% increase in volume. The observed increase in volume is sufficient to explain the increase in T_c without invoking any other mechanism. (auth)

19623 TUNNELING INTO WEAKLY COUPLED FILMS OF ALUMINUM AND TIN IN PROXIMITY. Vrba, J.; Woods, S. B. (Univ. of Alberta, Edmonton). Phys. Rev., B; 3: 2243-52 (1 Apr 1971).

Tunneling experiments were performed into the N side of N/S (aluminum/tin) proximity sandwiches evaporated at room temperature onto an oxidized aluminum electrode B. The coupling between the N and S films was made weak by allowing slight oxidation to occur at the interface. When B is normal, the normalized tunneling conductance of these junctions in the vicinity of the critical temperature of the proximity sandwich is markedly different from that of junctions formed between B and an ordinary (BCS) superconductor. When B is superconducting and the thickness of the N film is made about $d_N \simeq 100$ Å $\simeq \frac{1}{10} d_S$, where d_S is the thickness of the S film, a double-peaked structure is observed in the tunnel conductance as a function of applied voltage. The properties of the proximity sandwich depend on the amount of oxidation at the N/S interface. Self-consistent calculations were performed using the McMillan model of proximity sandwiches and treating the barrier transmission as a parameter. Comparison of these calculations with the experimental results shows satisfactory quantitative agreement. (auth)

19624 THRESHOLD CURRENTS OF LARGE CROSS-SECTION SUPERCONDUCTORS. Iwasa, Y.; Montgomery, D. B. (Massachusetts Inst. of Tech., Cambridge). J. Appl. Phys.; 42: 1040-6 (1 Mar 1971).

The threshold currents of a variety of multifilament, composite Nb–Ti superconductors, both twisted and untwisted, were measured and the results analyzed. The threshold current is defined as a minimum level of transport current that results in a sample quench following a flux jump. The twisted samples are able to maintain much higher levels of threshold current than the untwisted samples. Flux-jump-induced quenches existed in all samples, but analysis of the results reveals that different heat-transfer regimes were operative in the twisted and untwisted materials. For the case of twisted samples, the magnetic energy released in a flux jump is relatively small, and heat transfer is by nucleate boiling; in untwisted samples, the energy released is much greater, and heat transfer is by film boiling. The threshold current levels computed for both the twisted and untwisted samples agree satisfactorily with the experimental results. (auth)

19625 ENERGY SPECTRUM OF A SUPERCONDUCTOR WITH OVERLAPPING ENERGY BANDS. Fal'ko, I. I. (Kharkov Univ.). Ukr. Fiz. Zh.; 15: 1732-3(Oct 1970). (In Russian).

Pair correlations of electrons with contrasting pulses and spins within not only the same zone but also between electrons belonging to a different zone are considered for the superconducting state. Considerations of interzonal transitions resulted in forming a uniform quasi-particle energy spectrum of the two-zone superconductor. It is shown that two kinds of quasi particles exist with dispersion rules E_1 and E_2 that depend on the topological characteristics of both zones. (tr-auth)

19626 LOCAL MAGNETIZATION MEASUREMENTS ON CYLINDRICAL SAMPLES OF LOW-κ TYPE-II SUPERCONDUCTORS. Ortmann, H.-G.; Heiden, C. (Univ., Muenster, Ger.). Phys. Status Solidi (b); 43: K7-10(1 Jan 1971).

Magnetization measurements were carried out on cylindrical samples of Pb–5 at. % In alloy at 4.2°K. The hysteresis observed in the magnetization curve is partly due to surface pinning. Magnetization profiles (function of position along specimen) were also determined, and the fluctuations observed in the mixed state are discussed. The effects of surface treatments on the profiles were studied. (D.L.C.)

19627 SUPERCONDUCTING ALLOYS BASED ON THE NIOBIUM–TITANIUM–ZIRCONIUM SYSTEM. Polyakova, N. V.; Prokoshin, A. F.; Sergeev, I. P.; Fedotov, L. N. Sb. Tr. Tsent. Nauch.-Issled. Inst. Chern. Met.; No. 71, 158-61(1969). (In Russian).

Results are given from a study of superconducting Nb–Ti–Zr alloys. Determinations were made of the critical current density over a wide range of magnetic fields at 4.2°K for wires of the industrial alloys 65BT, 50BT, and 35BT. (Referativnyi Zh.)

19628 TRANSITION OF NIOBIUM INTO THE SUPERCONDUCTING STATE USING NUCLEAR MAGNETIC RESONANCE. Tret'yakov, B. N.; Kuritsin, V. B. Sb. Tr. Tsent. Nauch.-Issled. Inst. Chern. Met.; No. 71, 177-80(1969). (In Russian).

Nuclear magnetic resonance curves were obtained for Nb at four temperatures in a field of 3.9 kOe. The measurements were used to obtain the temperature dependence of the quantity of normal phase present. In the superconducting state, the primary transition occurs in the regions of Nb with a distorted crystal lattice. (Referativnyi Zh.)

19629 CRITICAL TEMPERATURE OF SUPERCONDUCTING ALLOYS OF THE NIOBIUM–TITANIUM–TANTALUM SYSTEM. Rad'kov, A. I.; Fedotov, L. N. Sb. Tr. Tsent. Nauch.-Issled. Inst. Chern. Met.; No. 71, 164-7(1969). (In Russian).

Results are given of measurements of the superconducting transition temperatures of Nb–Ti–Ta alloys containing 56 to 67 at. % Ti and Ta up to 10 at. %. With increasing Ta content, annealed alloys show a decrease in the transition temperature. (Referativnyi Zh.)

19630 FLUX JUMPS IN NONIDEAL TYPE-II SUPERCONDUCTORS. II. FLUX JUMPS IN Nb–Ti RODS. Takeo,

XUM

Masakatsu (Kyushu Univ., Fukuoka). J. Phys. Soc. Jap.; 30: 697-708(Mar 1971).

Mean power losses produced in a cylindrical specimen, when an external magnetic field along the cylindrical axis is increased with a constant rate, are calculated under an assumption that the temperature inside the specimen is uniform. With the aid of this result, a simplified heat equation to describe the variation of the temperature of the specimen with time is derived. Then, calculations are carried out for several qualities vitally concerned with flux jumps, e.q., the relation between the flux jump field and the sweeping rate, the minimum field for the flux jump, and the jump intervals. In addition, an analysis of temperature fluctuations is worked out under the condition of small heat leakage, and the results are compared qualitatively with the experimental data on Nb−Ti rods. (auth)

19631 SUPERCONDUCTING AND SEMICONDUCTING PHASES OF GRANULAR FILMS. Abeles, B.; Hanak, J. J. (RCA Labs., Princeton, N. J.). Phys. Lett.; 34A: 165-6(22 Feb 1971).

A theoretical upper limit is established for the normal resistivity of a granular superconductor at which superconductivity vanishes. Good agreement is found with the experimental value of 10^{-2} Ω-cm for Al, Mo, W and Be in the form of 30 Å grains embedded in SiO_2. (auth)

Equipment and Devices

19632 CONTINUOUSLY OPERATING ^{4}He EVAPORATION REFRIGERATOR. DeLong, L. E.; Symko, O. G.; Wheatley, J. C. (Univ. of California, San Diego, La Jolla). Rev. Sci. Instrum.; 42: 147-50(Jan 1971).

A simple and compact device was developed to provide continuous, self-regulating refrigeration at approximately 1.3°K. The temperature of the device remains nearly constant, independent of external power, up to a critical power. For a molar flow rate of 10^{-4} moles/sec, the refrigerator can absorb 4.5 mW. Such a refrigerator should be suitable for condensing ^{3}He in a ^{3}He−^{4}He dilution refrigerator. (auth)

19633 BIG SUPERCONDUCTING MAGNETS. Bronca, G. (Centre d'Etudes Nucleaires de Saclay, Gif-sur-Yvette, France). Elektrotech. Cas.; 21: 345-51(1970).

From Applied Superconductivity Conference, Smolenice, Czechoslovakia. See CONF-690652.

After a brief review of the evolution of the applications of superconductors, the list of magnet types now being studied, mainly in high-energy physics, is given. The problems to be solved in building superconducting magnets are reviewed: current density, stabilization, forces and protection, cryogenics. (auth)

19634 SMALL SUPERCONDUCTING COILS AND APPLICATIONS TO PLASMA PHYSICS. Cornish, D. N.; Hancox, R. (Culham Lab., Abingdon, Eng.). Elektrotech. Cas.; 21: 352-62 (1970).

From Applied Superconductivity Conference, Smolenice, Czechoslovakia. See CONF-690652.

The problems and techniques of making superconducting coils of the type used in research laboratories are discussed. The development of single strand NbTi to multi-filament twisted composites and narrow Nb_3Sn layer wound coils to 12.7 mm wide disc type coils is included. Some superconducting applications to the field of plasma physics are briefly described. (auth)

19635 ROTATING ELECTRICAL MACHINES USING SUPERCONDUCTORS. Mailfert, A. Elektrotech. Cas.; 21: 363-9 (1970).

From Applied Superconductivity Conference, Smolenice, Czechoslovakia. See CONF-690652.

The consequences of using superconductors in high- and low-power electrical rotating machines are investigated. First, heteropolar machines are dealt with whereby emphasis is made on eddy-current losses in the superconductive exciting winding. Then, homopolar machines are investigated as to various developed and projected arrangements. Finally, attention is drawn to superconductive flux pumps. (auth)

19636 CRYOGENIC ELECTRICAL ENERGY TRANSMISSION. Klaudy, Peter A. (Technische Hochschule, Graz). Elektrotech. Cas.; 21: 370-95(1970).

From Applied Superconductivity Conference, Smolenice, Czechoslovakia. See CONF-690652.

Due to the progress achieved in the cooling machine and heat insulation techniques, the construction of high-power cables operating at very low temperatures seems to be quite possible. Consequently, in lands where electrical power systems do not yet exist, dc superconducting cables will be of interest due to their high efficiency. The same holds true for very large territories in which medium- and high-voltage lossless dc superconducting cables will be of special importance in meeting the changing energy demands. However, also in ac power systems, superconducting cables working with the generator voltage can be applied profitably when the power rating becomes so large that conventional high-voltage lines cannot be used. Work done in connection with the design of superconducting cables in Graz is reported. (auth)

19637 LARGE SUPERCONDUCTING MEMORIES. Rocher, Y. A. Elektrotech. Cas.; 21: 396-404(1970).

From Applied Superconductivity Conference, Smolenice, Czechoslovakia. See CONF-690652.

The future of superconducting memories is investigated on the basis of results obtained in the framework of two projects oriented to the design of memories with a very large capacity. The advantages and disadvantages of various possible realizations of selection and memory systems with superconductive elements are reviewed. Then a description is given of the details for two projects, an American one (external selection, destructive reading), and a French one (integrated selection, nondestructive reading). The progress in the development of these projects gives prospects that, in the near future, superconducting memories will be designed with a large capacity (10^{7} to 10^{8} bits) with an access time of 1 to 5 μsec. The comparison of the separate price positions for superconducting memories with various types of magnetic memories shows that it is possible to obtain economies in the production and in the control electronics and on the input and output of information that exceed the expenses caused by the cryogenic system. (auth)

19638 SUPERCONDUCTING HF CAVITIES. Passow, C. (Univ., Karlsruhe, Ger.). Elektrotech. Cas.; 21: 419-33(1970).

From Applied Superconductivity Conference, Smolenice, Czechoslovakia. See CONF-690652.

Problems in high-frequency superconductivity are surveyed. Application examples are discussed in accelerator engineering for generating stabilized high-frequency waves, e.g., as in electron microscopy. (auth)

19639 ELECTROMAGNETIC INDUCTION OF ROTATING MAGNETS. Tsien, Thomas Nai-chen. Houston, Tex.; Univ. of Houston (1970). 79p. University Microfilms Order No. 71-2500.

Thesis.

A modified unipolar machine, where the rotor consists of two parallel magnets embedded in a superconducting lead casting, is studied. The voltage-detection circuit is well shielded with superconducting materials and is assured to be in zero magnetic field and insulated from the magnets. The same steady voltage as observed for the ordinary unipolar generator is measured on rotating the magnets inside a soft iron cylindrical shell at 4.2°K. The results disagree with the conventional calculations using the polarization $\vec{P} = (\vec{v} \times \vec{M})/c^2$, but can be explained in terms of $\partial\vec{B}/\partial t$ due to the rotation of the magnets. $\vec{B}$ of the rotating magnets at any time is calculated by treating each magnet as if it were at rest with respect to the circuit. As time passes on, the rotating magnets undergo different orientations to give different values of $\vec{B}$ at the circuit and the resulting $\partial\vec{B}/\partial t$ induces the observed emf. The analysis is extended to show that the unipolar voltage is basically the result of an induction effect, provided the motion of the magnetic sources is followed. (Diss. Abstr. Int., B)

19640 COOLING TO 0,7°K BY APPLICATION OF SUPERFLUID PROPERTIES OF ^{4}He. Severijns, A. P.; Staas, F. A. Ned. Tijdschr. Natuurk.; 36: 105-6(1 May 1970). (In Dutch).

A method for cooling to 0.7°K by application of the superfluid properties of ^{4}He is described. The system is compact and consists of two superconductors containing only superfluid helium divided into two capillaries. (J.S.R.)

19641 CRYOSTAT. Haupt, Justus (to EURATOM). British Patent 1,221,726. 10 Feb 1971. Priority date 22 Jun 1967, Netherlands.

The cryostat described is cooled by the supply of a cryogen, such as liquid helium, from a reservoir. The cryogen is supplied into the cryostat at the bottom by a pipe of internal diameter such that the pressure drop along the pipe is between 1 and 100 torr. The sample for cooling is in direct contact with the cryogen. The internal diameter of the pipe is between 0.4 and 0.6 mm. (M.H.R.)

19642 CALORIMETRIC METHOD FOR THE DETERMINATION OF LOSSES IN PULSED SUPERCONDUCTING MAGNETS

XUM

IN SUPERFLUID HELIUM. Bergmann, Wilfried H. (Argonne National Lab., Ill.). J. Appl. Phys.; 42: 1055-6(1 Mar 1971).

A calorimetric method for the determination of the heat dissipation of small superconducting magnets operated in a pulsed or cycling mode in the range from 1.5 to 2.15°K is reported. Preliminary results are given for a NbTi magnet and the accuracy of the technique is discussed. (auth)

19643 USE OF SUPERCONDUCTING JUNCTIONS IN MAGNETOMETRY. Clarke, J. (Univ. of California, Berkeley). Rev. Phys. Appl.; 5: 32-6(Feb 1970). (UCRL–19030).

A superconducting device that has proved useful in the measurement of electrical currents down to 30 nA, voltages down to 10^{-15} V and magnetic fields down to 10^{-8} gauss is described. Also a type of Josephson junction in which the conventional oxide barrier is replaced by a copper barrier is discussed. (M.H.R.)

19644 HIGH-CURRENT DENSITY SUPERCONDUCTING MAGNETS USING HEAVY CURRENTS. Atherton, D. L. (Ferranti-Packard Ltd., Toronto). Can. J. Phys.; 49: 155-6(1 Jan 1971).

Three 5-cm-inside-diameter superconducting magnets are reported that generate 66 kG at 1250 A, 64 kG at 1360 A, and 56 kG at 1890 A, with current densities of 27,200 A/cm^2, 30,500 A/cm^2, and 42,000 A/cm^2, respectively. Fine filamentary conductors are used. Charge rate sensitivity is reported. (auth) (Canada)

Plasma and Thermonuclear Physics

Confinement and Heating

Refer also to abstract 19727.

19645 (IPP–2/86) PLASMA CONFINEMENT IN THE WIIa-STELLARATOR: A COMPARISON BETWEEN EXPERIMENTAL RESULTS AND THEORETICAL ESTIMATES OF NEOCLASSICAL DIFFUSION. Eckhartt, D. (Institut fuer Plasmaphysik, G.m.b.H. Garching (West Germany)). Jul 1970. 38p. Dep. NTIS (U. S. Sales Only).

Experiments with plasmas generated by contact ionization, photoionization, and electron cyclotron resonance heating in the stellarator WIIa are reviewed. The magnitude of cross-field particle diffusion observed in these experiments is compared with theoretical estimates of "neoclassical" diffusion. The scaling of these estimates from presently available plasma densities and temperatures towards higher temperatures predicts an increase in the diffusion rate, in contrast to what is expected from hydromagnetic theory (Pfirsch–Schlüter coefficient). (auth)

19646 (IPP–4/7) LASER ENERGY NECESSARY FOR INERTIALLY CONFINED NUCLEAR FUSION PLASMA. Hora, H.; Pfirsch, D. (Institut fuer Plasmaphysik, G.m.b.H. Garching (West Germany)). Oct 1970. 8p. (IPP–6/91). Dep. NTIS (U. S. Sales Only).

The gain G of the thermonuclear fusion energy of very dense spherical plasmas heated by lasers in times of about 1 nsec is treated theoretically. Assuming as a pessimistic estimate that fast ions leave the plasma without contributing to fusion neutrons, one finds that for $G = 1$, laser energies of 3×10^7 joules are needed. A kinetic theory for a one-species gas, starting with a gaussian density and velocity profile, yields almost the same result as found by a hydrodynamic model with adiabatic expansion and without fast-ion losses taken into account. Therefore, the even point of $G = 1$ is reached at the well-known value for the laser energy of 4.6×10^6 joules for a D–T reaction. (auth)

19647 (IPP–6/90) A TWO DIMENSIONAL COMPUTER PROGRAMME FOR SOLVING THE MHD EQUATIONS FOR THE THETA PINCH IN A TIME-DEPENDENT COORDINATE SYSTEM. Hertweck, F.; Schneider, W. (Institut fuer Plasmaphysik, G.m.b.H. Garching (West Germany)). Jul 1970. 66p. (IPP–1/110). Dep. NTIS (U. S. Sales Only).

The axial losses of mass and energy at the ends of a theta pinch are investigated. The plasma is described by a one-fluid model with the following assumptions: infinite electric conductivity, electron temperature equal to ion temperature, isotropic pressure, and radial equilibrium. The mechanism by which the disturbance due to mass and energy losses at the end of the theta pinch propagates into the inner part of the vessel is investigated. The relative importance of kinetic energy, heat conduction, and convection for the end losses is calculated. This program is intended as a first step towards a more sophisticated program with a two-fluid model, including anisotropic pressure. (auth)

19648 NEW METHOD OF MAGNETIC PUMPING FOR PLASMA HEATING. Koechlin, F.; Samain, A. (Centre d'Etudes Nucleaires, Fontenay-aux-Roses, France). Phys. Rev. Lett.; 26: 490-5(1 Mar 1971).

A variant of magnetic pumping heating is proposed that makes use of a torsional rather than a compressional magnetic perturbation. It is efficient in large-aspect-ratio toroidal configurations such as Tokamaks. Typically, in this case, it is twice as efficient as the compressional magnetic pumping for magnetic perturbations of the same intensity, while using a working frequency three times smaller. (auth)

19649 SOME NEW RESULTS CONCERNING THE NEARLY RESONANT CONFINEMENT OF PLASMA. Klima, R. (Inst. of Plasma Physics, Prague). Plasma Phys.; 12: 819-21(Oct 1970).

The pressure of the radio-frequency field, which is required to block up the loss cone of a mirror, has been estimated numerically (Watson, 1968 and 1969) with very encouraging results. In this note, a simple analytical estimate is deduced, and it is derived that the rf field pressure can be amplified by means of properly chosen dielectric or plasma slabs. (UK)

19650 ION HEATING BY A MODULATED ELECTRON BEAM. Haas, G. M.; Eisner, M. (Univ. of Houston, Tex.). Phys. Fluids; 14: 606-10(Mar 1971).

The transfer of energy to the plasma ions in the interaction of a modulated electron beam with a beam-formed plasma is found to be dependent on the square root of the plasma density and independent of the ion species. (auth)

19651 SHIELDED SUPPORTS IN TOROIDAL MULTIPOLES. Rusbridge, M. G. (Univ. of Manchester, Eng.). Plasma Phys.; 13: 33-46(Jan 1971).

A simple model for the motion of particles near an x-type neutral line in a magnetic field is described and is applied to evaluate the particle loss rate along the field zero lines associated with a magnetically shielded support. The same model gives an estimate of the electrical conductivity of a field zero line. Using this estimate, the effect of a shielded support on plasma rotating azimuthally around a toroidal machine is discussed; it is shown that the rotating plasma will be brought to rest and an estimate of the slowing-down time is given. On the basis of these estimates it is suggested that shielded supports can in principle improve containment in existing experiments. It does not seem likely that they could be used to support internal conductors in a thermonuclear reactor based on a multipole configuration, but in other situations where the plasma layer is thicker their use may be possible. (auth) (UK)

19652 SOME TOROIDAL EQUILIBRIA FOR PLASMA UNDER MAGNETOELECTRIC CONFINEMENT. Stix, Thomas H. (Weizmann Inst. of Science, Rehovot, Israel). Phys. Fluids; 14: 692-701(Mar 1971).

A powerful negative bias tends to arise spontaneously by the loss, from a toroidal plasma, of suprathermal ions such as Ohmic or cyclotron heating runaway ions or fusion-product protons and alpha particles, whose Larmor radius is vastly larger than that of the electrons also scraped off at the limiting plasma aperture. By this mechanism, strong ion-confining electric fields may be expected to appear at the plasma surface in all toroidal configurations including stellarators, Tokamaks, floating rings, etc. Electrons, restricted to their surfaces of constant total energy, are then also confined. A drift-kinetic description is given of a neutral plasma under such "magnetoelectric confinement" for the interesting special case of purely toroidal magnetic field (i.e., symmetric torus with zero rotational transform). Particle diffusion and the approach to quasisteady state with ambipolar particle loss are discussed. Particular attention is paid to the construction of a two-parameter family of equilibria with density profiles approximating those which, in the succeeding paper, are found favorable to stability. (auth)

19653 RESISTIVE LOADING BY A FINITE PLASMA CYLINDER. Hasti, D. E.; Oakes, M. E.; Schlueter, H. (Univ. of Texas, Austin). J. Plasma Phys.; 4: 787-99(Dec 1970).

The loading resistance of a coil–plasma system operated near the lower hybrid resonance in hydrogen and argon was measured. The results are consistent with the predictions of a theoretical model that includes finite plasma effects. (auth) (UK)

19654 ENERGY BALANCE OF PLASMA IN TOKAMAK-TYPE SYSTEMS. Dnestrovskii, Yu. N.; Kostomarov, D. P. At. Energ. (USSR); 29: 434-8(Dec 1970). (In Russian).

The energy balance of plasma in toroidal Tokamak-type systems in the case of classical energy losses is investigated. The heat-conduction equations for ions and electrons and equations for the magnetic field of the plasma current are solved by computer. The dependence of electron and ion temperatures and energetic duration on plasma sizes, plasma density, magnetic field, and discharge current are studied. The results of calculation are in good agreement with the experimental data. This fact indicates a possible explanation of the plasma energy balance in some regimes by the classical conceptions. (auth)

19655 CONTROL-THEORETIC APPROACH TO THE PLASMA CONFINEMENT PROBLEM. **Wang, P. K. C. (Univ. of California, Los Angeles); Janos, W. A. J. Optimization Theory Appl.; 5: 313-29(Apr 1970).**

The problem of confining a collisionless plasma by means of external electromagnetic fields is formulated as an optimal control or variational problem. The paper begins with a formal development of the equations governing the plasma motion. Then, various mathematical formulations of the confinement problem are discussed. Specific results are obtained for the simplified case where confinement is achieved by means of a spatially uniform, time-varying magnetic field. Physical interpretations of these results are also given. (auth) (IAA)

Diagnostics

Refer also to abstracts 19701 and 19713.

19656 (EP-RR-21) MICROWAVE POWER TRANSMISSION RATIO: ITS USE IN ESTIMATING ELECTRON DENSITY. Vance, C. F. (Australian National Univ., Canberra. Dept. of Engineering Physics). Feb 1969. 17p. Dep. NTIS (U. S. Sales Only).

The effect of a cylindrical plasma on transmission of microwave power between broad-beam antennae is calculated in the geometrical optics approximation. The first part extends Wort's (1963) results to an eccentric plasma not filling the whole discharge tube, and the second part considers possible enhanced transmission due to a lower-density outer plasma. When estimating peak density, the only other parameter that appears to require correcting for is the ratio of discharge-to-tube radius, which can be estimated by other means. (auth) (Australia)

19657 (MATT-Trans-16) INVESTIGATION OF THE MATERIAL BALANCE OF THE PLASMA COLUMN AND THE GAS SHEATH IN THE TOROIDAL APPARATUS-TOKAMAK-3. Gorbunov, E. P.; Kotelnikov, Yu. N.; Kutukov, G. P.; Simonov, V. A. (Gosudarstvennyi Komitet po Ispol'zovaniyu Atomnoi Energii SSSR, Moscow. Institut Atomnoi Energii). Translated for Princeton Univ., N. J. from Zh. Tekh. Fiz.; 36: 1831-41(Oct 1966). 32p. Dep. NTIS.

An abstract of this paper, prepared from the original language, appeared as NSA 21: 18631.

19658 CONDUCTIVITY OF CHARGED PLASMA IN A MAGNETIC FIELD. Pleshanov, A. S. Magn. Gidrodin., Akad. Nauk Lat. SSR; No. 4, 93-7(Oct-Dec 1968). (In Russian).

Expressions are obtained for longitudinal and transverse conductivity and for the tangent of the angle of anisotropy for non-quasi-neutral plasmas. In particular, it is shown that the transverse conductivity of such a plasma in ultrastrong magnetic fields is finite, so that generated power density theoretically may be as large as desired (in contrast to quasi-neutral plasmas, where it is finite). (tr-auth)

19659 ELECTRIC PROBE MEASUREMENTS IN A MOVING AND MAGNETIZED PLASMA. Lindberg, L.; Kristoferson, L. (Royal Inst. of Tech., Stockholm). Plasma Phys.; 12: 831-8 (Nov 1970).

High-impedance electric probes and symmetric and unsymmetric floating double probes were used to measure electric field, potential, density, and temperature in a plasma stream. The plasma was fully ionized, supersonic, and collision-free. It moves in a magnetic field, where the electron gyro radii are of the same order as the probe radii, and where the ion gyro radii are large ($n_e \simeq 10^{19}$ m^{-3}, $v \simeq 3 \times 10^5$ m/s, $T_e \simeq 10$ eV, $B \simeq 0.02$ Vs/m^2). Some aspects of basic theory are briefly discussed, and it is shown that reliable measurements can be obtained under certain conditions. (auth) (UK)

19660 SPACE-CHARGE EFFECTS IN PLASMA-PARTICLE ANALYZERS. Green, T. S. (ESRIN, Frascati, Italy). Plasma Phys.; 12: 877-83(Nov 1970).

The effects of space charge on the energy resolution obtainable with deflection-type analyzers have been considered previously for cylindrical beams. In this analysis the problem of the electric field in a retarding-potential analyzer is considered. It is shown that large longitudinal electric fields can exist when the plate separation L is of the order of λ_s, where $\lambda_s^2 = (mu^2/8\pi ne^2Z^2)$, (m, Ze, u, n are respectively the mass, charge, velocity and density of the beam of particles to be analyzed.) This electric field is larger than the transverse field, which causes radial expansion. Extension of the analysis to two dimensions in a simple case shows, however, that the longitudinal field is much reduced when the beam has a diameter small compared to its length L. (auth) (UK)

19661 ELECTRON TEMPERATURE DETERMINATION IN A LOW-DENSITY HELIUM PLASMA. Schieber, D.; Gavril, S.; Erlicki, M. S. (Technion-Israel Inst. of Tech., Haifa). Plasma Phys.; 12: 897-9(Nov 1970).

A numerical treatment is made of the relative intensities of lines of different multiplicities to obtain electron temperatures for low-density helium plasmas. The results are discussed, and it is concluded that available data on excitation cross sections do not suffice for reliable temperature measurements. (UK)

19662 MEASUREMENT OF THE ENERGY OF THE PLASMA IN THE T-3 INSTALLATION. Mirnov, S. V. This paper was summarized in At. Energ. (USSR); 26: 458(May 1969) as paper No. 301/5068. (In Russian).

Since the plasma pressure may in general be anisotropic, two energy components must be considered: the $E_\perp$ component transverse to the direction of the stabilizing magnetic field, and the longitudinal $E_\perp$ component. The value of $E_\perp$ was determined from the diamagnetic effect of the plasma, while $E_\parallel$ was estimated from the equilibrium displacement of the plasma pinch, on the assumption that the current density in the center was no greater than the value allowed by the Kruskal–Shafranov criterion for $q = 1$. The measuring-transformer circuit for determining the diamagnetic flux $\Delta\Phi$ in the cross section of the plasma is shown. Owing to the great inductance of the excitation winding of the stabilizing magnetic field and the low resistance of the external supply circuits, the problem was reduced to one of measuring the additional current ΔI in the circuit of the excitation winding. (TSS)

19663 FRACTIONAL FRINGE HCN LASER-INTERFEROMETER. Olsen, J. N. (Oak Ridge National Lab., Tenn.). Rev. Sci. Instrum.; 42: 104-6(Jan 1971).

An HCN laser–interferometer is reported with better than $^1/_{100}$ of a fringe phase shift sensitivity at a wavelength of 337 μ. Applied to plasma density measurement this corresponds to electron density line integrals of 3.3×10^{12} cm^{-2} or lower. The fractional fringe technique involves sinusoidally driving the reference path mirror in a focused Michelson interferometer; changes in the effective path length alter the relative magnitude of even and odd harmonics in the resultant interferometer signal. Results are shown from application of this diagnostic to the Burnout V plasma. (auth)

19664 CORRELATION TECHNIQUES IN EXPERIMENTAL PLASMA PHYSICS. Hooper, E. B. Jr. (Yale Univ., New Haven). Plasma Phys.; 13: 1-18(Jan 1971).

The processing of signals by means of correlation techniques is examined from the viewpoint of experimental plasma physics. The mathematical character of correlation analysis is discussed briefly. Applications are considered under five headings: averaging techniques in unstable plasmas, statistics in "turbulent" plasmas, comparisons between measurements (e.g. at different points in plasma), direct measurement of plasma properties, and measurements of dispersion relations and transfer functions in plasmas. Under each of these topics the pertinent literature and procedures are discussed, and additional examples provided. Correlation analysis is compared with spectral analysis to demonstrate the relative advantages of each. (auth) (UK)

19665 SPECTROSCOPIC STUDY OF A CAESIUM DISCHARGE PLASMA. Cussenot, J. R.; Fabry, M.; Vicherat, A. (Laboratoire de Physique des Milieux Ionises, Nancy). Plasma Phys.; 13: 80-4(Jan 1971). (In French).

The effect of the cathode potential fall on the excitation states of ions and neutrals and the electron distribution function in a plasma formed by hot-cathode discharge in saturated cesium vapor were investigated. Plasma emission spectrum diagnostics were used. The resulting temperatures are compared with probe measurements, showing good agreement, and with the theory, showing disagreement, for which an explanation is suggested. (UK)

Kinetics (General)

Refer also to abstract 19466.

19666 CHARACTERISTICS OF A REFLEX ARC: LOW MAGNETIC FIELD MODE. Hooper, E. B. Jr. (Yale Univ., New Haven). Plasma Phys.; 12: 855-75(Nov 1970).

XUM

The low-frequency, rotational oscillation present in a reflex arc at low gas pressures and low magnetic fields is studied experimentally with special use made of correlation techniques. Several new results are obtained: (1) The oscillation frequency and its dependence upon the discharge parameters are shown to be in agreement with the predictions of linearized theory. This result, together with those of previous works, strengthens the identification of the mode as the "E × B instability." (2) The radial transport of electrons due to E × B drifts is obtained directly from the density-potential cross correlation function rather than estimated from the oscillation amplitudes. This transport is compared with the collisional transport both near onset and away from onset; it dominates in both cases, but more so away from onset. To within the experimental accuracy the total radial electron flux across any cylindrical shell around the axis and with radius larger than the cathode is independent of radius. The apparent flux decreases in the ionization region and near the walls where finite Larmor radius effects are important. (3) The radial ion flux as estimated in the fluid approximation is clearly inconsistent with the physical processes operating in the discharge; it is postulated that there is a significant contribution from a high energy tail to the ion distribution function. (auth) (UK)

19667 DECOMPOSITION OF A DECELERATING IONIZING SHOCK. **Sloan, D. M. (Univ. of Strathclyde, Glasgow). J. Plasma Phys.; 4: 531-48(Sep 1970).**

The equations governing the collapse of a cylindrical, ionizing shock in an applied axial magnetic field are solved numerically, using a method involving characteristics. Initially, the collapsing shock accelerates, but subsequently the increasing magnetic forces at the shock produce a retardation and this cools the gas behind the shock. The numerical solution describes the behaviour of the shock until the gas behind ceases to conduct. The decomposition of the ionizing shock is examined. (auth) (UK)

19668 CURRENT SHEET TILT IN A PARALLEL-PLATE RAIL GUN. **Pert, G. J. (Univ. of Alberta, Edmonton). Plasma Phys.; 13: 63-9(Jan 1971).**

Spectrographic and probe measurements of a current sheet in a parallel-plate rail gun are presented. The discharge propagates at 6 cm/μsec into hydrogen at 0.5 torr. The measurements indicate that the sheet is tilted with gas flowing both normally and tangentially to the sheet. As a result of this gas flow, "bubbles" of plasma are periodically formed and detached from the discharge. (auth) (UK)

Kinetics (Experimental)

19669 (NP-18715) PLASMA ACCELERATION BY A TRAVELING ELECTROMAGNETIC FIELD. GENERAL DIAGNOSTICS AND VELOCITY MEASUREMENT. (Office National d'Etudes et de Recherches Aerospatiales, Chatillon-sous-Bagneux (France)). 17 Jun 1969. 44p. (In French). Dep. NTIS (U. S. Sales Only).

The acceleration and ionization processes produced by a traveling electromagnetic field, and the fundamental characteristics (temperature, density, and velocity) of the plasma created, were studied. For this purpose, a device operating in the pulse region and allowing simple diagnostic measurements to be made on the electric and magnetic fields, induced current density, temperature, and velocity, was developed. In addition, another technique was applied that led to the indirect determination of these parameters. The results obtained are analyzed and discussed. A temperature wave propagated with the velocity of the related electric field appears to exist in the vicinity of the ejection plane of the device. (auth) (France)

19670 DETERMINATION AND SHAPING ON THE ION-VELOCITY DISTRIBUTION FUNCTION IN A SINGLE-ENDED Q MACHINE. Andersen, S. A.; Jensen, V. O.; Michelsen, P.; Nielsen, P. (Danish Atomic Energy Commission. Risoe). Phys. Fluids; 14: 728-36(Mar 1971).

An electrostatic energy analyzer with a resolution better than 0.03 eV was constructed. This analyzer was used to determine the ion-velocity distribution function at different densities and plate temperatures in a single-ended Q machine. In all regions good agreement with theoretical predictions based on simple, physical pictures was obtained. It is shown that, within certain limits, the velocity distribution function can be shaped; double-humped distribution functions were obtained. The technique used here is suggested as an accurate method for determination of plasma densities within 10% in single-ended Q machines. (auth)

19671 THEORY OF THE PLANE FLOW OF HIGHLY CONDUCTING PLASMA IN A CHANNEL. Morozov, A. I.; Shubin, A. P. Zh. Prikl. Mekh. Tekh. Fiz.; No. 4, 9-19(Jul-Aug 1970). (In Russian).

Simplified equations were derived for the plane flow of a conducting, quasi-neutral, nonviscous plasma in a channel. The study involved analysis of the flow in a channel with conducting electrode-walls. It was found that when the gas pressure is much higher than the magnetic one, $\beta \gg 1$, the field and current distribution is determined by gas-dynamic factors and the longitudinal electric field perturbations penetrate the stream at the surface symmetrically with respect to the two electrodes; this causes an attenuation of the longitudinal electric field near the input area. The motion of the plasma was also studied under conditions of ideal and poor conductivity. In the inverse boundary case, $\beta \ll 1$, in case of an accelerated movement of the plasma in the channel, an increase of the electric field voltage was observed near the anode, and the flow becomes more sharply nonhomogeneous in the transverse direction. The plasma may be removed from the anode; the criterion for this pulloff was determined. The Joule losses in the $\beta \ll 1$ case were found to be low in comparison with the ratio of the power involved in the discharge; these losses were also found to be independent of the conductivity of the plasma. (TTT)

19672 MEASUREMENT OF PLASMA CONDUCTIVITY FOR ELECTRIC FIELDS LARGER THAN THE RUNAWAY FIELD. Lencioni, D. E. (Univ. of Wisconsin, Madison). Phys. Fluids; 14: 566-9(Mar 1971).

The electrical conductivity parallel to a magnetic field of a hot-ion hydrogen plasma with $n \simeq 10^9$ cm^{-3}, $T_i \simeq 50$ eV, and $T_e \simeq 5$ eV was measured for electric fields larger than the runaway field. The conductivity was found to be proportional to the plasma density with a value much less than Spitzer's conductivity but larger than Buneman's turbulent conductivity. When the current became comparable to the electron thermal current, the conductivity was found to decrease. (auth)

Kinetics (Theoretical)

Refer also to abstract 19397.

19673 (DLR-FB-69-78) COLLISION DOMINATED SHEATH IN WEAKLY IONIZED PLASMAS. PART II. Wahle, P.; Mueller, K. G. (Deutsche Versuchsanstalt fuer Luft- und Raumfahrt E. V., Stuttgart (West Germany)). Dec 1969. 95p. (In German). Dep. NTIS (U. S. Sales Only).

A microscopic sheath model is developed that fulfils the exact boundary conditions at the wall. The momentum transport equations of the charge carriers are modified, and specular reflection of the electrons is included. If a suitable coefficient is introduced in the macroscopic boundary condition of the electrons the macroscopic description proves to be in good agreement with the microscopic models. A calculation of this coefficient is performed. The macroscopic models as developed in the past turn out to represent extreme cases of the microscopic model. Density and potential distribution in the sheath and current—voltage characteristics are calculated for various values of the pertinent parameters. (auth)

19674 (IPP-1/112) HYDROMAGNETIC EQUATIONS FOR ANISTROPIC PLASMAS INCLUDING TRANSPORT EFFECTS. Chodura, R.; Pohl, F. (Institut fuer Plasmaphysik, G.m.b.H. Garching (West Germany)). Sep 1970. 37p. Dep. NTIS (U. S. Sales Only).

A set of hydrodynamic equations is derived for an arbitrary anisotropic plasma, allowing for Coulomb collisions among plasma particles. Using a generalized expansion in Hermite polynomials for the distribution functions of plasma constituents (as described in Oraevskii et al. (1968)) the collision integrals occurring in the hydrodynamic equations are calculated. Explicit results for the coefficients of ion viscosity and heat conductivity of ions and electrons are derived. (auth)

19675 ADIABATIC ELECTRON PLASMA AND ITS EQUATION OF STATE. **Knorr, G.; Nuehrenberg, J. (Univ. of Iowa, Iowa City). Plasma Phys.; 12: 927-33(Dec 1970).**

For slow processes in a collisionless two-component plasma that conserve the adiabatic invariant of the electrons, the equation of motion for electrons is derived. The conservation laws for the whole system are discussed in relation to the equation of state and a consistent distribution function for the electrons. (auth) (UK)

19676 EFFECT OF DISSIPATION DUE TO FIREHOSE INSTABILITY ON PERTURBATION HALF-JET FLOW OF A COLLISIONLESS PLASMA. **Morioka, Shigeki (Ames Research Center, Moffett Field, Calif.); Spreiter, John R. J. Plasma Phys.; 4: 629-41(Sep 1970).**

The effects of dissipation due to a weak firehose instability on steady planar flow of a collisionless plasma are investigated on the basis of the quasi-linear fluid equations. Dissipation terms remain nonlinear even within the perturbation theory, and their effects tend to resemble relaxation effects in an ordinary reacting gas rather than ordinary viscous dissipation. As an example, a steady half-jet flow with aligned magnetic field is considered. It is found that the disturbed field decays within a finite distance for some upstream conditions, but grows without limit for others. (auth) (UK)

19677 SHEATH CRITERION FOR A GROWING SHEATH. **Andrews, J. G. (Central Electricity Generating Board, Marchwood, Eng.). J. Plasma Phys.; 4: 603-6(Sep 1970).**

When a sheath grows into a plasma at a slower speed than the local ion speed of sound, an ion rarefaction wave propagates into the plasma ahead of the sheath. It is shown that, in the frame of reference of the sheath edge, the speed of ions arriving at the sheath edge cannot exceed $(kT_e/M)^{½}$. (auth) (UK)

19678 EXACT ELECTROSTATIC SHOCK SOLUTION FOR A COLLISIONLESS PLASMA. **Smith, A. (Univ. of West Indies, Jamaica). J. Plasma Phys.; 4: 549-61(Sep 1970).**

An exact solution to the steady-state Vlasov equations and Poisson's equation for a one-dimensional plasma of electrons and protons is obtained by splitting the energy equation into two integral equations for the trapped particle distributions. This solution has the properties that the number densities and electric potential are monotonic functions of space and do most of their changing over a distance of the order of the Debye length for electrons. The distributions are everywhere differentiable in phase space and are Maxwellian-like, and in terms of elementary functions. Evidence is given to support stability for restricted shock strengths. (auth) (UK)

19679 ELECTROMAGNETIC RADIATION FROM A LASER-PRODUCED PLASMA EXPANDING INTO A UNIFORM MAGNETIC FIELD. **Dunn, H. Searl; Lubin, Moshe J. (Univ. of Rochester, N. Y.). J. Plasma Phys.; 4: 573-83(Sep 1970).**

A laser-produced plasma expanding in a uniform magnetic field emits far infrared radiation. The time-dependent radiation history is calculated, assuming spherical symmetry, and compared with experiment. General features of the radiation history agree well with experimental observation. However, a detailed comparison is difficult because of the oversimplified theoretical model employed. (auth) (UK)

19680 STEADY-STATE VLASOV EQUATIONS FOR A MONOTONIC ELECTRIC POTENTIAL. **Smith, A. (Univ. of West Indies, Kingston, Jamaica). J. Plasma Phys.; 4: 511-22(Sep 1970).**

A large class of solutions to the steady-state Vlasov equations for a two-component one-dimensional plasma for which the electric potential ϕ is monotonic is shown to exist. Some of these solutions are shock-like in the sense that the particle densities are also monotonic. If the particle and energy densities at infinity are not constraints of the problem, it is shown that there are always solutions for an arbitrary monotonic ϕ, and the solutions themselves contain arbitrary functions. (auth) (UK)

19681 PRECURSOR IONIZATION EFFECTS ON MAGNETOHYDRODYNAMIC SWITCH-ON SHOCK STRUCTURE. **Hoffert, Martin I. (Riverside Research Inst., New York). J. Plasma Phys.; 4: 477-94(Sep 1970).**

The influence of shock-induced precursor ionization on the steady-state structure of switch-on shock waves with nonequilibrium ionization and radiation is examined theoretically. A single-temperature monatomic gas is assumed, together with a Clarke-Ferrari model for photoionization of the upstream gas. It is found that the effect of the precursor depends in general on the ratio of a characteristic precursor length to a characteristic magnetic interaction length. For the slightly ionized case treated in some detail, this ratio is much greater than unity, indicating a precursor-independence for the magnetohydrodynamic shock structure. (auth) (UK)

19682 SUPPRESSION OF RUNAWAY OF ELECTRONS IN A LORENTZ PLASMA. II. CROSSED ELECTRIC AND MAGNETIC FIELDS. **Abraham-Shrauner, Barbara (Washington Univ., St. Louis). J. Plasma Phys.; 4: 441-50(Sep 1970).**

Suppression of runaway of electrons in a weak, uniform electric field in a fully ionized Lorentz plasma by crossed magnetic and electric fields is analysed. A uniform, constant magnetic field parallel to a constant or harmonically time varying electric field does not alter runaway from that in the absence of the magnetic field. For crossed, constant fields the passage to runaway or to free motion as described by constant drift motion and spiral motion about the magnetic field is lengthened in time for strong magnetic fields. The new "runaway" time scale is roughly the ratio of the cyclotron frequency to the collision frequency squared for cyclotron frequencies much greater than the collision frequency. All "runaway" time scales may be given approximately by t_E^2/τ_{eff} where t_E is the characteristic time of the electric field and τ_{eff} is the effective collision time as estimated from the appropriate component of the electrical conductivity. (auth) (UK)

19683 CORRECTIONS FOR SMALL VALUES OF THE LOGARITHM TERM IN THE ELECTRICAL CONDUCTIVITY OF A FULLY IONIZED PLASMA. Viegas, John R. (Ames Research Center, Moffett Field, Calif.). Phys. Fluids; 14: 541-4(Mar 1971).

Correction factors that extend the range of validity of expressions for the electrical conductivity of a fully ionized gas to small values of the logarithm of the ratio of the Debye length to the mean impact parameter for a 90° deflection are developed and compared. (auth)

19684 ASYMPTOTIC THERMOCHEMICAL RELAXATION TIMES IN A DENSE PLASMA. Sajben, M. (McDonnell Douglas Astronautics Co., Huntington Beach, Calif.). Phys. Fluids; 14: 555-65(Mar 1971).

Relaxation processes initiated in a spatially uniform, dense plasma by a sudden change in heavy-particle density, temperature, or a superimposed electric field are considered. Electron-impact ionization and three-body recombination, Ohmic heating, elastic energy transfer between electrons and heavy particles of both types, and inelastic energy loss or release are taken into account. The asymptotic phase of the relaxation process is characterized by one single time scale, which is approximated by using the inverse of the logarithmic derivative of electron temperature evaluated for $t \to \infty$. An exact, algebraic formula for this time scale is derived in terms of partial derivatives of terms found in electron energy and mass conservation equations. Specialization to argon shows that the time scale is governed by inelastic rate processes for low degrees of ionization and by electron-ion elastic energy transfer for high ionization fractions. Numerically computed results can be well approximated by simple formulas that clearly demonstrate the relative importance of various processes present. (auth)

19685 ELECTRIC CONDUCTIVITY OF WEAKLY TURBULENT PLASMAS. Ichikawa, Yoshi H.; Nishikawa, K. (Univ. of Iowa, Iowa City). Phys. Fluids; 14: 569-78(Mar 1971).

The static electric conductivity of weakly turbulent plasmas was examined on the basis of a kinetic equation for the linear response to the one-particle distribution function. Within the regime of neglecting the mode-coupling terms, the high-frequency turbulent fluctuations associated with the electron plasma wave give rise to a modification of the ordinary collisional conductivity through the adiabatic interaction between the particles and the turbulent fluctuations. On the other hand, the low-frequency turbulent fluctuation due to the ion oscillation mode determines the relaxation process in the system through the resonant interaction, and gives rise to a finite conductivity even in the collisionless plasmas. (auth)

19686 MICROSCOPIC THEORY OF DENSITY FLUCTUATIONS AND DIFFUSION IN WEAKLY IONIZED PLASMAS. Williams, R. H.; Chappell, W. R. (Environmental Science Services Administration, Boulder, Colo.). Phys. Fluids; 14: 591-8(Mar 1971).

Kinetic equations for the self and distinct parts of the electron density cross-correlation function are obtained for a partially ionized gas by solving a truncated BBGKY hierarchy in the Markovian limit. Assuming a BGK model for the terms representing collisions with the neutrals, these equations are then used to calculate the self and total electron density cross-correlation functions. The expressions obtained for the correlation functions are valid for stationary, homogeneous, partially ionized plasmas. In equilibrium, the expression for the spectral density reduces to that obtained by Dougherty and Farley. In the limit of zero-collision frequencies, the results of Rostoker and Rosenbluth are recovered. For long times and large probe separations analytical expressions are obtained for the cross correlation functions. It is found that the self-correlation function depends on the electron diffusion coefficient and the total electron correlation function depends on the ambipolar diffusion coefficient. (auth)

19687 LINEAR AND NONLINEAR COLLISIONAL PROCESSES IN A PLASMA. Krishan, S. (Univ. of Tennessee, Knoxville. Oak Ridge National Lab., Tenn.); Selim, A. A. Phys. Fluids; 14: 599-602(Mar 1971).

XUM

Quantum techniques are used to treat the linear and nonlinear collisional processes in a uniform weakly interacting plasma near equilibrium in the absence of external magnetic field. The nonlinear collisional process consists of coupling of two particles to two waves, whereas in the linear collisional case, only one wave is coupled to two particles. It is found that, if the plasmon-mode energy is below its equilibrium level, the nonlinear collisions give rise to growth, and above, it contributes to damping. (auth)

19688 ELECTRON VELOCITY DISTRIBUTION IN A FULLY IONIZED PLASMA UNDER THE ACTION OF CROSSED ELECTRIC AND MAGNETIC FIELDS. Sestak, B. (Technical Univ., Prague). Czech. J. Phys.; 20: 1129-37(1970).

A fully ionized spatially homogeneous plasma is subjected to weak constant crossed electric and magnetic fields, and the velocity distribution function for the electrons is studied. The Fokker–Planck type expression for the Lorentz gas is employed for the collision term in the Boltzmann equation. This equation is solved by direct expansion, and some conditions of convergence of this expansion are obtained. (auth)

19689 SECOND-ORDER HARMONICS FOR A LORENTZ PLASMA IN THE PRESENCE OF A CIRCULAR MAGNETIC FIELD. Pop, Gh. G. Rev. Roum. Math. Pures Appl.; 14: 1323-31(1969). (In French).

The behavior of a plasma in the presence of a magnetic field is studied using the Boltzmann equation. The influence of the second-order Fourier harmonic is emphasized. To achieve this, the terms standing for the second-order approximation under consideration are inserted into the fundamental equations, then the resulting equations for each separate approximation are written, the thus-obtained system being subsequently solved. (Rom. Sci. Abstr.)

19690 DETERMINING THE EQUILIBRIUM OF A ROTATING PLASMA. Patraulea, N. N. Stud. Cercet. Mec. Apl.; 28: 791-801(1969). (In Rumanian).

The relative equilibrium of a system of ions compared to a rotating reference system is discussed, and a method is supplied for constructing the equilibrium diagrams. The method relies on the concept of fictitious load in the relative reference system. (auth) (Rom. Sci. Abstr.)

19691 SOLUTION OF THE BOLTZMANN EQUATION FOR A FULLY IONIZED PLASMA IN AN OSCILLATORY ELECTRIC FIELD AND A MAGNETIC STEADY FIELD. IV. Lupu, Gheorghe (Univ., Cluj). Rev. Roum. Math. Pures Appl.; 15: No. 7, 1011-18(1970).

The distribution functions of electrons in a homogeneous plasma for lf and hf electric fields were studied. The results are compared with those presented in the literature. (IAA)

19692 SOLUTION OF THE BOLTZMANN EQUATION FOR A FULLY IONIZED PLASMA IN AN OSCILLATORY ELECTRIC FLUID AND A MAGNETIC STEADY FIELD. III. Lupu, Gheorghe (Univ., Cluj). Rev. Roum. Math. Pures Appl.; 15: No. 6, 871-6(1970).

A method is described for solving the systems of partial differential equations obtained by the author previously (1969) by expanding the electron distribution function in normalized or unnormalized spherical harmonics. The method is based on a technique of dimensionless parameters of Jancel's (1968) procedures, expanding a distribution function into symmetrical irreducible Cartesian tensors. The application of the method to a particular case of a homogeneous plasma in a unidirectional oscillatory electric field is demonstrated. (IAA)

19693 STARK BROADENING OF HYDROGEN SPECTRAL LINES IN TURBULENT PLASMA. Sholin, G. V. Dokl. Akad. Nauk SSSR; 195: 589-92(21 Nov 1970). (In Russian).

The theory of the Stark broadening of hydrogen spectral lines in a turbulent plasma is developed, considering nonadiabatic effects on the atom of the Langmuir oscillations and the contributions of the single-particle mechanisms of broadening. (R.V.J.)

19694 CLASS OF SOLUTIONS OF QUASI-LINEAR EQUATIONS. Ivanov, A. A. (Inst. of Atomic Energy, Moscow); Teichmann, J. J. Plasma Phys.; 4: 667-76(Dec 1970).

A method for obtaining a class of generalized solutions of the system of quasi-linear equations was developed for the case where the wave vector k and the velocity v of the particles are oriented in a general direction with respect to the magnetostatic field. The method is demonstrated on the case of the quasi-linear relaxation of an ion beam penetrating a cold magnetoplasma. (auth) (UK)

19695 THEORY OF A TEST PARTICLE IN AN INHOMOGENEOUS STATIONARY PLASMA. Cairns, R. A. (Univ. of Glasgow). J. Plasma Phys.; 4: 801-6(Dec 1970).

The motion of a test particle in a plasma whose average properties vary along one direction in space, but are independent of time, is considered. A method is given that enables this problem to be treated similarly to existing theories for a homogeneous plasma. (auth) (UK)

19696 RADIATION FROM A CHARGED PARTICLE IN A MAGNETOPLASMA. Trulsen, J.; Fejer, J. A. (Univ. of California, San Diego, La Jolla). J. Plasma Phys.; 4: 825-41 (Dec 1970).

Two expressions for the power radiated by a charged particle in a homogeneous magnetoplasma are derived, using a method similar to that of Kolomenskii (1953), Eidman (1958) and Liemohn (1965). The first expression is identical with that of Eidman. The reason for the correctness of Eidman's result for dispersive media, in spite of his complete neglect of dispersion in the derivation, is explained. Liemohn, by taking dispersion into account at only one stage of the derivation, obtains a result that disagrees with the present one, often by many orders of magnitude, as illustrated by computations. The second expression is derived by several authors by different methods; it is more suitable for computations than the first one. The radiation bands and their limiting frequencies are discussed systematically. (auth) (UK)

19697 RECOMBINATION PROCESSES DURING THE EXPANSION OF A LASER-PRODUCED PLASMA. Mattioli, M. (CEN, Fontenay-aux-Roses, France). Plasma Phys.; 13: 19-28(Jan 1971).

The decay of a spherical LiH plasma, produced by laser radiation, is considered; three-body and radiative recombinations were taken into account. Freezing of the degree of ionization is possible if the energy transferred to the plasma in the three-body recombination processes is considered. Numerical computations are compared with previously published experimental results. (auth) (UK)

19698 FORMATION OF ION-ACOUSTIC COLLISIONLESS SHOCKS. Sakanaka, P. H.; Chu, C. K.; Marshall, T. C. (Columbia Univ., New York). Phys. Fluids; 14: 611-14(Mar 1971).

Formation of ion-acoustic collisionless shocks was studied by numerically solving the one-dimensional Vlasov equation. The shock propagates at about the local ion-acoustic speed, and faster than the ion-acoustic speed ahead; the oscillations behind the shock show ion-acoustic dispersion. A precursor appears with a speed of 1.6 times the shock speed. Different temperature and density ratios produce qualitatively different flows, and they are analyzed in detail. (auth)

19699 MAGNETIC DIPOLE IN A STATIONARY PLASMA. Fougere, P. F. (Air Force Cambridge Research Labs., L. G. Hanscom Field, Mass.). Phys. Fluids; 14: 640-3(Mar 1971).

The determination of the magnetopause or free boundary of a plasma-free point dipole immersed in a field-free, stationary plasma is treated using a moment technique first introduced by Midgley and Davis. Their results are extended in two ways. First, using their form for the bounding surface, the number of adjustable coefficients is increased from 7 to 27. Second, different forms are introduced in which true cusps are produced along the dipole axis. As the number of adjustable constants is increased, these forms converge toward the exact solution from opposite directions. Extrapolation of these results leads to a value of 0.6222485 for the cusp ratio and 1.41397752 r_0 for the equatorial radius. (auth)

Production

Refer also to abstract 19634.

19700 (NP-18722) SOURCE OF SYNTHESIZED PLASMA. (Office National d'Etudes et de Recherches Aerospatiales, Chatillon-sous-Bagneux (France)). 10 Mar 1970. 54p. (In French). Dep. NTIS (U. S. Sales Only).

A source of slow neutralized ions operating with a weak flux of neutral argon was developed from a Kaufman source whose classical extraction system had been replaced by a single grid. This source produces a plasma beam with a velocity of 10 km/s. At 80 cm from the source a charged-particle density of 5×10^6 cm^{-3} was readily obtained. The electron temperature, which can be reduced to beneath 1000°K (less than that of the neutralizer), is controlled. The characteristics of this source make it very useful for ionospheric flight simulation. (auth) (France)

19701 X-RAY TEMPERATURE MEASUREMENTS OF LASER-PRODUCED PLASMAS. Wolterbeek Muller, B.; Green, T. S. (European Space Research Inst., Frascati, Italy). Plasma Phys.; 13: 73-5(Jan 1971).

The use of a focussed laser beam to produce highly stripped ion species requires the attainment of high temperature in the initially formed plasma (Peacock and Pease, 1969). As part of a programme to produce beams of ions in this way, measurements of the temperature attained when focussing onto various foils were made. The derived temperatures for thin foils of polythene, aluminium, and steel are tabulated and discussed. The data show little apparent sensitivity of the observed temperature on the element being studied and this phenomenon is analysed. (UK)

19702 PRODUCTION OF ENERGETIC HIGHLY IONIZED PLASMA BY LASER IRRADIATION OF LITHIUM HYDRIDE PELLETS. Mattioli, M.; Veron, D. (CEN, Fontenay-aux-Roses, France). Phys. Fluids; 14: 717-21(Mar 1971).

Spherical LiH pellets were utilized as targets for high-power, fast-rising, nanosecond laser pulses. Using different pulse lengths, τ, it was shown that the pellets behave as a continuous source of energetic plasma during a time t_l(called "interaction time") depending on the pellet size and on the laser flux density. For pellets 50μ in diameter and flux densities of 1.5×10^{12} W/cm^2, t_l is 20 nsec; the degree of ionization approaches 100% (about 10^{16} ions in the plasma) and the root-mean-square expansion velocity is 10^7 cm/sec; the total plasma energy is about 0.5 J with an energy transfer efficiency of 10%. The general behavior of the burning process agrees with the extension to small pellets of the theoretical model developed for the case of massive targets. (auth)

19703 EXPANSION OF A LASER-PRODUCED PLASMA INTO A VACUUM. Inoue, N.; Kawasumi, Y.; Miyamoto, K. (Nagoya Univ., Japan). Plasma Phys.; 13: 84-7(Jan 1971).

Radiation from a ruby laser with a maximum power of 80 MW (total energy of 1.2 J) was focused onto a tip of a filament of polyethylene $(CH_2)_n$ with a size of 0.2×0.2mm^2 suspended in a vacuum. About one-tenth of the total energy was absorbed in the target. Measurements were performed with an ion energy analyzer (Eubank and Wilkerson, 1963) set up at an angle of 90° from the laser incidence and with an electrostatic probe with twin electrodes. The ion species in the plasma was C^{2+} only. The distribution of ion energy had a peak at an energy of about 70 eV. A lack of hydrogen species was similar to the results obtained in the case of a lithium hydride plasma (Mattioli and Veron, 1969). It was found by mass analysis of the residual gas that the molecular hydrogen and methane components increased noticeably after a laser shot. The angular dependence of the expanding plasma was observed by measuring ion saturation currents to the probe. No magnetic field was applied. (auth) (UK)

Stability

19704 (NP-18681) KINK INSTABILITY OF A TOROIDAL PLASMA COLUMN. Rijnhuizen Report 70-60. Schuurman, W.; Bobeldijk, C. (Stichting voor Fundamenteel Onderzoek der Materie, Jutphaas (Netherlands). Instituut voor Plasma-Fysica). Jul 1970. 20p. Dep. NTIS (U. S. Sales Only).

A normal-mode stability analysis of a toroidal plasma column is performed in toroidal coordinates, based on the ideal MHD equations. Small perturbations of the equilibrium of a sharp incompressible column surrounded by vacuum and a metal wall are considered up to first order in the inverse aspect ratio. A cylindrical perturbation with azimuthal mode number m turns out to split up into three modes, m and m ± 1, in a torus. One result of the calculation is that the first-order toroidal effect on the growth rate of the instability is zero. (auth)

19705 WARM QUIESCENT PLASMA IN A MINIMUM-B FIELD OBTAINED WITH PERMANENT MAGNETS. Brakenhoff, G. J.; Goede, A. (FOM-Instituut voor Atoom- en Molecuulfysica, Amsterdam). Plasma Phys.; 12: 815-17(Oct 1970).

Stabilization in a minimum-B field created by adding a field of permanent magnets to a magnetic mirror field is reported. At not-too-high field strengths, this is a technically simple method for obtaining a minimum-B configuration. The influence of the minimum-B field on the plasma parameters is tabulated from which it is seen that the most important result is the reduction of the fluctuation level by a factor of 15 due to the stabilizing field. (UK)

19706 EFFECTS OF FORCE-FREE FIELDS ON PLASMA STABILITY: COMMENTS ON A PAPER OF W. SCHUURMAN, C. BOBELDIJK, AND R. F. DE VRIES. Freidberg, J. B.; Weitzner, H.; Weldon, D. (Los Alamos Scientific Lab., N. Mex.). Plasma Phys.; 12: 987-9(Dec 1970).

Recently Schuurman et al. (NSA 23: 51700) have proposed to explain the desirable stability properties of their screw-pinch experiments in terms of the presence of force-free magnetic fields outside the plasma column instead of the vacuum magnetic fields usually assumed. It is usually supposed that the force-free field is created by a secondary plasma of effective zero pressure. Further, it is a convenient idealization to set to zero the density of the secondary plasma as well. The original model that the above authors proposed is followed in this note, and comment is made on the significance of the zero density assumption. It is pointed out that force-free fields automatically create destabilizing effects that may well be far more significant than their stabilizing effects. (UK)

19707 PARASITIC INSTABILITY GENERATED BY STEADY-STATE OSCILLATIONS IN A REFLEX ARC PLASMA. Hooper, E. B. (Yale Univ., New Haven). Plasma Phys.; 12: 990-6 (Dec 1970).

The reflex arc is a low-pressure, magnetized plasma subject to numerous instabilities. Data and discussion concerning an instability driven by the density gradients and fields associated with a primary oscillation are given. That is, the discharge is operated in a region in which it is unstable to a rotating, flute-like mode; the new instability is of higher frequency and different symmetry than the primary mode, and occurs on the leading edge of the flute. Because it is apparently driven by the primary mode, it will be termed a "parasitic oscillation." (auth) (UK)

19708 DENSITY THRESHOLDS FOR THE ONSET OF ANISOTROPY AND LOSS-CONE INSTABILITIES IN HOT ELECTRON PLASMAS. Brambilla, Marco (CEN de Saclay, Gif-sur-Yvette, France). Plasma Phys.; 12: 903-16(Dec 1970).

The Harris dispersion relation for electrostatic waves in a hot anisotropic electron plasma is solved for marginally stable waves. The threshold density for the onset of instabilities is studied as a function of frequency, wavelength, and direction of propagation of the oscillations, magnetic field intensity, and electron velocity distribution function. The results obtained by simple analytic methods are confirmed by a number of numerical solutions of the dispersion relation. (auth) (UK)

19709 FORMATION OF AN AXISYMMETRIC BULGED REGION IN A LONG UNIFORM PLASMA COLUMN. McCartan, J.; Wolf, G. H.; Bodin, H. A. B. (United Kingdom Atomic Energy Authority, Abingdon, Eng.). Plasma Phys.; 12: 885-95(Nov 1970).

The formation of an axisymmetric bulge region located in the midplane of an 8-m-long plasma column is described, and the associated axial plasma flow processes are analysed. The bulge is formed by reducing the external magnetic field, B_2, in the central region with respect to the field, B_1, elsewhere. The experimental results are analysed to give average values of beta and plasma radius which are compared with the predictions of an analytic model and a time dependent one-dimensional MHD calculation. It is shown theoretically that no simple equilibrium is possible for $B_2/B_1 \le \sqrt{\beta}$; experimentally, in such cases, bulges were found to grow continuously over the time of observation. (auth) (UK)

19710 TWO-STREAM INSTABILITY AND ITS CLASSIFICATION INTO ABSOLUTE AND CONVECTIVE FOR HOT PLASMAS. Infeld, E.; Skorupski, A. (Inst. of Nuclear Research, Warsaw). J. Plasma Phys.; 4: 607-15(Sep 1970).

The problem of classification of the two-stream instability for hot plasmas is considered. The method is based on the criterion of Fainberg, Kurilko & Shapiro (1961). The basis of the analysis is the "resonance" distribution, but a modified resonance distribution, leading to better results, is also investigated. The stability limit, classification into absolute and convective instabilities, as well as asymptotic growth rates are given for some chosen values of stream densities and temperatures, and arbitrary stream velocities. A method for finding the maximum temporal growth rates is also outlined. (auth) (UK)

19711 EFFECT OF GYRO-VISCOSITY ON RAYLEIGH-TAYLOR INSTABILITY OF A PLASMA. Nayyar, N. K. (Univ. of Delhi); Trehan, S. K. J. Plasma Phys.; 4: 563-71(Sep 1970).

The effect of finite ion-Larmor radius is considered on the Rayleigh–Taylor instability of a plasma. The macroscopic equations of motion are used where the finite ion-Larmor radius effects are incorporated in the stress tensor. The finite ion-Larmor radius stabilization of the interchange mode is demon-

XUM

strated. For disturbances propagating along the magnetic field, it is found that the inclusion of gyro-viscosity has a stabilizing effect; it increases the critical wavenumber (compared to its value in the absence of gyro-viscosity) beyond which all modes are unstable. (auth) (UK)

19712 STABILITY OF RELATIVISTIC ANISOTROPIC PLASMAS TO PERPENDICULAR MAGNETOSONIC WAVES. Landau, R. W.; Cuperman, S. (Tel-Aviv Univ., Israel). J. Plasma Phys.; 4: 495-510(Sep 1970).

The stability of relativistic anisotropic plasmas to the magnetosonic (or right-hand compressional Alfvén) wave, near the ion cyclotron frequency, propagating perpendicular to the magnetic field, is investigated. For this case, and for wavelengths larger than the ion Larmor radius and large ion plasma frequency ($\omega_{p,+}^2 \gg \Omega_+^2$) the dispersion relation is obtained in a simple form and solved. It is shown that for $T_{||} \neq T_\perp$ (even $T_{||} \gg T_\perp$) no instability occurs. This conclusion applies also to the case of the anisotropic interplanetary medium. A peculiarity of the dispersion relation is noted. Zero-order and first-order terms cancel so that the relation is of second order in one expansion parameter. The nonrelativistic numerical results of Fredericks and Kennel are recovered. (auth) (UK)

19713 FEEDBACK-CONTROLLED STEADY-STATE PLASMA. Brown, Ian G.; Compher, Alan B.; Ehlers, Kenneth W.; (and others) (Univ. of California, Berkeley). Plasma Phys.; 13: 47-61(Jan 1971).

A current-free magnetized plasma with independently variable density and electron temperature was produced and studied. The plasma, which may be either steady-state or pulsed, is generated at one end of a 1.5-m-long vacuum system by a 10-GHz microwave discharge at electron gyroresonance in a dc magnetic field. In the main body of the plasma the magnetic field can be varied from 1 to 10 kG and plasma densities $5 \times 10^8 \lesssim n_e \lesssim 5 \times 10^{11}$ cm^{-3} and temperatures $2 \lesssim T_i \lesssim 20$ eV, $T_i \lesssim 1$ eV can be achieved. All the noble gases, as well as hydrogen, were used at pressures ranging from 2×10^{-5} to 2×10^{-3} torr. Electron plasma waves and ion-acoustic waves were both used for diagnostic purposes. Unless special precautions are taken, the plasma has density fluctuations of 5 to 10%. A feedback control system that uses a rapidly responding adjustment of discharge power was used to significantly reduce these fluctuations. This control will also keep the plasma density steady even in the presence of fluctuations in line voltage or gas feed. (auth) (UK)

19714 STABILITY OF A COLD PLASMA UNDER MAGNETO-ELECTRIC CONFINEMENT. Stix, Thomas H. (Weizmann Inst. of Science, Rehovot, Israel). Phys. Fluids; 14: 702-12(Mar 1971).

Surface modes are examined for a semi-infinite cold plasma immersed in a strong magnetic field. Adjacent to the plasma appear, consecutively in space, an electron sheath, a vacuum gap, and a conducting wall. In addition, a gravitational field simulates the effect of inhomogeneity in the magnetic field. Boundary conditions appropriate to the cold-plasma fluid equations are derived and a dispersion relation obtained which is quartic in frequency. Solutions are given for a variety of cases. It is found that the presence of the electron sheath can stabilize the familiar gravitational flute instability at long wavelengths. However, a new mode, termed the "two-fluid diocotron mode," is uncovered which is unstable for configurations where the vacuum gap exceeds a critical thickness. The critical gap for this mode is, nevertheless, significantly larger than the corresponding gap for the ordinary (i.e., plasma replaced by vacuum) long-wavelength diocotron mode. Applications of the cold-plasma stability criteria are discussed for model plasmas under magnetoelectric confinement suitable for ion stripping and for controlled fusion. (auth)

19715 TIME-AVERAGED DENSITY PROFILE IN THE PRESENCE OF AN m = 2 MODE FINITE-AMPLITUDE INSTABILITY. Daugherty, Thomas L.; Ventrice, Carl A. (Tennessee Tech. Univ., Cookeville). Phys. Fluids; 14: 713-16(Mar 1971).

A weakly ionized plasma column is investigated in the presence of a finite-amplitude instability. The theory of Holter and Johnson is extended to include a finite-amplitude m = 2 mode instability. From the zero harmonic solution to the macroscopic equations, the time-averaged particle density is obtained. Computations are performed on a digital computer to determine the form of the particle density profile in the presence of a helical, m = 2, and mixed-mode instability. The form of the profile is found to have a strong dependence on the magnitude and polarity of the amplitude factors. (auth)

19716 TOKAMAK EQUILIBRIUM. Greene, John M.; Johnson, John L.; Weimer, Katherine E. (Princeton Univ., N. J.). Phys. Fluids; 14: 671-83(Mar 1971).

Axisymmetric hydromagnetic equilibria are obtained from an ideal fluid model by means of an asymptotic expansion in the inverse aspect ratio. The calculation is carried sufficiently far so that the equilibrium condition $J \times B = \nabla p$ is satisfied to second order. This provides expressions for the eccentricity of the constant-pressure surfaces, as well as for their displacements, and for both the magnitude and the curvature of the external field that must be provided to support the equilibrium. Scaling considerations are invoked to show how the external field must be altered to compress the plasma to a smaller major radius and thus obtain additional heating. Elementary hydromagnetic considerations indicate that the configuration may be stable with respect to modes that have the symmetry of the equilibrium. Application is made to a specific compression-heating experiment. (auth)

19717 DYNAMIC STABILIZATION OF A LINEAR z PINCH BY A MAGNETIC QUADRUPOLE. Forman, Peter R.; Haberstich, Albert; Karr, Hugh J.; Phillips, James A.; Schofield, Aldred E. (Los Alamos Scientific Lab., New Mex.). Phys. Fluids; 14: 684-91(Mar 1971).

The effect of high-frequency linear quadrupole magnetic fields on the m = 1 kink instabilities of a z pinch, as proposed by Osovets, is investigated. Short-wavelength instabilities of 5 to 12 cm are observed to be dominant and are not suppressed by the stabilization fields. This is contrary to the reported results of others that the short-wavelength instabilities do not develop if the long wavelengths of the order of the interelectrode distance are stabilized. For the experimental conditions used, magnetohydrodynamic theory predicts stabilization of wavelengths of 20 to 80 cm and reduced growth rate for the shorter wavelengths. The observed instabilities have a reduced growth rate in agreement with theory. (auth)

19718 FREE-BOUNDARY LONG HELICAL WAVELENGTH EQUILIBRIA. Weitzner, Harold (New York Univ., N. Y.). Phys. Fluids; 14: 658-70(Mar 1971).

A straight high-beta helical equilibrium approximating a theta pinch is perturbed into a large-aspect-ratio torus by the addition of other helically symmetric fields in such a way that stability of the torus to most significant modes is unaffected. The ideal magnetohydrodynamic free-boundary model is employed. The straight helical equilibrium is obtained by expansions in the two parameters that are small but of the same order of magnitude, the ratio of helical magnetic field to theta pinch field and the product of helical wave number times plasma column radius. Neither beta nor the distortion of the plasma column from a true cylinder are taken small and the helical fields are principally L = 1. The equilibrium without net z current has desirable stability properties to m = 1 long-wavelength modes, although higher m modes are unstable. The stability conditions are more readily satisfied than earlier ones where it was assumed that the plasma column deformation was small and helical wave number times plasma radius was not small. (auth)

19719 EFFECT OF VELOCITY SPACE DIFFUSION ON THE UNIVERSAL INSTABILITY IN A PLASMA. Ong, R. S. B.; Yu, M. Y. (Cornell Univ., Ithaca, N. Y.). J. Plasma Phys.; 4: 729-38(Dec 1970).

The influence of collisions on the universal instability in a fully ionized inhomogeneous plasma is investigated by means of a simplified Fokker–Planck kinetic equation. For $b = \frac{1}{2}k_y^2R_i^2 \ll 1$, the Fokker–Planck model yields results qualitatively similar to the Bhatnagar–Gross–Krook model, but the two models give different collisional effects in the case where $b \geq 1$. Further, it is shown that collisions in general enhance the temperature gradient instability in a plasma when $b \ll 1$ and reduce it when $b \geq 1$. (auth) (UK)

19720 ION WAVES, DRIFT WAVES, AND INSTABILITY IN A WEAKLY IONIZED MAGNETOPLASMA. Self, S. A. (Stanford Univ., Calif.). J. Plasma Phys.; 4: 693-728(Dec 1970).

A unified treatment is given of low-frequency wave propagation in a weakly ionized magnetoplasma from the fluid equations in which ion inertia is retained. An analysis is made of the instabilities that arise due to the influence of drift of the electrons relative to the ions for three cases: (a) parallel drift, $E \| B$, (b) Hall drift, $E \| B$, and (c) diamagnetic drift, $\nabla n \perp B$. In all cases, an ion-acoustic instability is found while additionally, for (c), there is a drift instability for strong magnetic fields. The instability boundaries in parameter space are delineated. Furthermore, for a transversely bounded plasma, the roots $\omega(k_z$ real) and $k_z(\omega$ real) of the dispersion relations are discussed and related to experimental observables. The results are applied to an interpretation of wave propagation and instability on a cylindrical positive column for which all three types of drift are simultaneously present. The relation of this work to the inertialess theories of the current-convective and crossed-field instabilities is also discussed. (auth) (UK)

19721 DYNAMIC STABILITY OF CLOSED PLASMA CONFIGURATIONS. Wells, Daniel R. (Univ. of Miami, Coral Gables, Fla.). J. Plasma Phys.; 4: 645-65(Dec 1970).

The global stability of closed plasma configurations is related to the dynamical principle of least constraint and the space-time and gauge symmetries of the flow fields. This leads to an entirely new concept of MHD stability that is more basic than stability predictions that rely on a linearized perturbation analysis. The predictions of the theory are compared with recent experimental results obtained in studies of the stability of plasma confinement geometries. The theory predicts the violent "instabilities" of these systems, which are currently attributed to other mechanisms. Several pertinent details of the theory, which are widely misinterpreted, are discussed and clarified. (auth) (UK)

19722 TRANSVERSE ELECTROMAGNETIC INSTABILITIES IN COLLISIONLESS PLASMAS. Davidson, R. C.; Haber, I.; Hammer, D. A. (Naval Research Lab., Washington, D. C.). Phys. Lett.; 34A: 235-6(8 Mar 1971).

Computer simulation experiments are reported that verify the energy constants associated with the nonlinear theory of transverse electromagnetic instabilities. (auth)

19723 STRONG TURBULENCE THEORY OF NONLINEAR STABILIZATION AND HARMONIC GENERATION. Manheimer, Wallace M. (Massachusetts Inst. of Tech., Cambridge). Phys. Fluids; 14: 579-90(Mar 1971).

A nonlinear dispersion relation for dispersionless waves in a one-dimensional plasma is obtained by examining the statistical properties of particle orbits in a random potential. New techniques are developed to deal with trapped particles. It is shown that a linearly unstable plasma stabilizes when the trapping frequency is equal to the growth rate. Also, the density fluctuations set up by the trapped particles are shown to have a power-law dependence in wave number. The theory is able to explain many observations in recent beam–plasma experiments. (auth)

Thermonuclear Processes

19724 (FOA-4-4449) THERMONUCLEAR REACTIONS THROUGH LASER RADIATION OF FUSION MATERIALS. Witalis, Erik (Forsvarets Forskningsanstalt, Stockholm (Sweden)). Jan 1971. 20p. (In Swedish). Dep. NTIS (U. S. Sales Only).

The use of lasers for fusion weapons as well as for hydrogen energy is discussed. Criteria for an exothermic laser-induced fusion process are formulated. An account of known calculations and estimations show that the existing laser systems are several magnitudes too small for direct use of lasers in fusion weapons or for peaceful use of hydrogen energy. However, it is shown that in combination with well-established methods, generation and heating of a plasma with laser radiation would be feasible. Finally, the fields within laser and plasma physics where important developments for laser-induced fusion processes can be expected are given. (Sweden)

19725 (LA-4597) INITIAL EQUILIBRIUM CONFIGURATION OF THE SCYLLAC 5-METER TOROIDAL-SECTOR EXPERIMENT. Ribe, F. L.; Borkenhagen, W. H.; Ellis, W. R.; Hanks, K. S. (Los Alamos Scientific Lab., N. Mex.). Dec 1970. Contract W-7405-eng-36. 6p. Dep. NTIS.

The first portion of the Scyllac θ-pinch experiment to be placed in operation is the 5-meter toroidal sector. It provides a toroidal equilibrium by means of an $l = 1$ helical field (plasma ripple $\delta_1 \approx 1$), produced by capacitor-driven windings, and a small admixture of $l = 0$ field ($\delta_0 \approx 0.1$) produced by flux-shaping annular grooves in the compression coil. The theoretical parameters for the toroidal equilibrium are discussed, and curves of their values applicable to Scyllac are given. Aberration fields produced by the varying image currents of the $l = 1$ windings in the $l = 0$ grooved compression coil wall are discussed and their effects estimated. (auth)

19726 EXPERIMENTAL STUDY OF PLASMA EMISSION FROM A TITANIUM RAIL-TYPE GUN. Inoue, N.; Kawasumi, Y.; Uchida, T. (Nagoya Univ., Japan). Plasma Phys.; 12: 977-83(Dec 1970).

The mechanism of plasma emission from a titanium rail-type gun without an external magnetic field was studied by means of high-speed photography, ion mass and energy spectrometry, and magnetic probe and ion probe measurements. Emission of hydrogen plasma was caused mainly by its drift in a crossed electric and magnetic field at the exit of the gun. On the other hand, the high-mass impurities were accelerated by the magnetic force $j \times B$. (auth) (UK)

19727 MAGNETIC AND DRIFT SURFACES: CURRENT CONFIGURATION OF STELLARATOR FIELD. Miyamoto, Kenro (Nagoya Univ., Japan). Phys. Fluids; 14: 722-7(Mar 1971).

Magnetic surfaces and drift surfaces of a single charged particle of a stellarator field are analyzed by using an average method. The dependence of the rotational transform angle and the magnetic well depth on the parameters of the current configuration of the stellarator field is studied for the case of long and short pitch of the helical windings to find the optimum parameters. The relation of magnetic and drift surfaces is examined and a condition for their small deviation is deduced. The properties of constant $|B|$ surfaces are examined. (auth)

19728 USE OF NITRITES TO OBTAIN AND MAINTAIN A VERY HIGH VACUUM IN THERMONUCLEAR EQUIPMENT. Maslennikov, E. A. (Inst. of Atomic Energy, Moscow). Instrum. Exp. Tech. (USSR) (Engl. Transl.); No. 2, 529-33(Mar-Apr 1970). Translated from Prib. Tekh. Eksp.; No. 2, 187-91(Mar-Apr 1970).

The effects of small leaks of air, and also desorbed gases, on the evacuation rate and limiting evacuations obtained with the aid of nitrites are discussed. Results are given for measurements of the effect of high H_2 flows on the sorption rate of a Ti film. In considering the different designs of Ti evaporators, recommendations are given for their use as a function of the experimental conditions, and evaporator parameters are given. (auth)

19729 PLASMA CONTAINMENT APPARATUS AND METHOD. Stengel, Rudolph F. (to Entropy Ltd.). U. S. Patent 3,551,828. 29 Dec 1970. Filed 1 Jul 1968.

This hollow toroidal enclosure for plasma containment contains a plurality of current-carrying assemblies operable to generate an electromagnetic field within the enclosure, this field being directed substantially tangentially to a circle disposed in the plane of each cross section of the enclosure and unidirectionally about the circle at every point thereof; each current-carrying assembly contains two parallel current-carrying conductors in close, radially spaced proximity to each other and in perpendicular orientation to said cross section. (Official Gazette)

19730 CONTROLLED FUSION RESEARCH AND HIGH-TEMPERATURE PLASMAS. Post, R. F. (Univ. of California, Livermore). Annu. Rev. Nucl. Sci.; 20: 509-88(1970).

An extensive general review of plasma research is given under the following topics: (1) scientific goals of fusion research, (2) magnetic confinement and the origin of plasma instabilities, (3) the fusion plasma—required physical conditions, (4) pressure equilibria in closed and open magnetic systems, (5) magnetic confinement—particle orbits in open and closed systems, (6) plasma instabilities and means for their control, (7) fusion plasma technology, and (8) magnetic confinement—experimental results. (M.O.W.)

Wave Phenomena

Refer also to abstract 19720.

19731 EXPERIMENTAL DISPERSION CURVE FOR LOW-FREQUENCY DRIFT WAVES IN AN INHOMOGENEOUS MAGNETOPLASMA. Keen, B. E.; Aldridge, R. V. (United Kingdom Atomic Energy Authority, Abingdon, Eng.). Plasma Phys.; 12: 839-53(Nov 1970).

Measurements made in an inhomogeneous magnetoplasma to determine the low-frequency drift-wave dispersion curve are reported. The waves in the frequency range 20 to 220 kHz were induced externally by various methods, and were detected by phase-sensitive techniques in order to discern the signal above the noise of the plasma. Separate azimuthal modes $m = 0, +1$, or -1 were propagated in axial homogeneous magnetic fields of 0.75 and 1.00 kG, and the $(\omega - \kappa)$ dispersion curve was obtained for each case. The plasma in these experiments was a hollow-cathode arc discharge running in helium and had an electron temperature of 7.0 ± 0.3 eV and a constant inverse radial scale length $[(1/n_0)(dn_0/dr)] = 0.65 \pm 0.05\ \text{cm}^{-1}$. The experimental results obtained are compared with a modified simple drift-wave theory, which includes both the effects of a finite radial electric field and, also, an ion–neutral collision time. Reasonable agreement is found between the theory and the experimental results. (auth) (UK)

19732 HYDROMAGNETIC-WAVE PROPAGATION IN INHOMOGENEOUS MAGNETIC FIELDS. Lehane, J. A.; Paoloni, F. J. (Univ. of Sydney). Plasma Phys.; 12: 823-30(Nov 1970).

Apart from the case of torsional waves propagating into a

XUM

magnetic "beach" where ion cyclotron resonance is encountered, the study of the propagation of magnetohydrodynamic waves in inhomogeneous magnetic fields has received little attention. Some such results for both torsional waves propagating into magnetic "beaches" and compressional waves into magnetic "cliffs" are presented. The inhomogeneous field used consisted of two uniform fields of different magnitude connected by a transition region, the length of which could be changed. Attention was concentrated on looking for a wave reflected from the field discontinuity. For torsional waves no reflected wave was detected, either for waves of frequency much less than ion cyclotron frequency or for those which encountered ion cyclotron resonance in the low-field region. For compressional waves reflection was observed under some conditions. It was most pronounced when the length of the transition region was not appreciably greater than the wave attenuation length and when the wave was cut off in the high-field region. Values of the reflection coefficient and the phase change at reflection are given. (auth) (UK)

19733 SUPRALUMINOUS WAVES IN A RELATIVISTIC ANISOTROPIC PLASMA. Lee, Martin A. (Univ. of Chicago). Plasma Phys.; 12: 935-51(Dec 1970).

The linearized relativistic Vlasov equation is used to investigate supraluminous waves in a field-free two-component plasma. The ions are immobile; the electrons are described by a spatially homogeneous equilibrium distribution $f_0(p)$, which is anisotropic in momentum space but which satisfies $f_0(p) = f_0(-p)$. For a given wave number k there are, in general, three supraluminous normal modes, all of which propagate without growing or damping. One mode remains transverse for all degrees of anisotropy; the other two are mixed in that they are neither purely longitudinal nor purely transverse. Each mode satisfies a different dispersion relation, the difference depending on k, the degree and direction of anisotropy, and the relativistic properties of $f_0(p)$. The resulting "dispersive" effects are discussed for both a plane wave and a pulsed signal. (auth) (UK)

19734 SPACE-CHARGE WAVES IN A TRAPPED RELATIVISTIC PLASMA. Lerche, I. (Univ. of Chicago). Plasma Phys.; 12: 953-75(Dec 1970).

Equations are set up to describe collective longitudinal plasma waves in a trapped, one-dimensional relativistic plasma. It is shown that, provided the background plasma is immobile, the system is unstable if the relativistic plasma frequency is somewhat higher than the typical "bounce" frequency in the trap. It is further shown that inclusion of a cold, but mobile, background plasma quenches the instability provided only that the thermal plasma frequency is greater than about the relativistic plasma frequency. The calculation was performed in order to ascertain the role that collective plasma waves may play in inhibiting, or enhancing, Fermi acceleration of cosmic rays in astrophysical plasma situations. (auth) (UK)

19735 PROPOSAL FOR MEASURING THE POLOIDAL FIELD IN A TOROIDAL MAGNETIC CONFIGURATION. Etievant, C.; Fidone, I. (CEN, Fontenay-aux-Roses, France). Plasma Phys.; 12: 985-6(Dec 1970).

The problem of the polarization of an electromagnetic wave passing through an inhomogeneous plasma, confined by a magnetic field slowly varying in amplitude and direction along the direction of propagation, is discussed. The magnetic configuration of a large torus in a plane perpendicular to the magnetic axis is considered. Along the minor radius the amplitude and the direction of the total field vary slowly in space because of curvature and the presence of an internal current. (UK)

19736 LONG-WAVELENGTH ION-ACOUSTIC WAVES IN A MAGNETOPLASMA IN A GRAVITATIONAL FIELD. Liu, C. H. (Univ. of Illinois, Urbana). J. Plasma Phys.; 4: 617-27(Sep 1970).

Ion-acoustic waves propagating in a collision-free, gravity-supported plasma in a static magnetic field are studied with a linearized Vlasov equation. The dispersion relation is derived in the limit of vanishing electron to ion mass ratio and wavelength much larger than the Debye length. From this dispersion relation it is shown that the well-known fluid dynamic steepening tendency of waves propagating in the direction of decreasing density is competing with the effect of Landau damping. Depending on the ratio of electron and ion temperatures, the direction of propagation and the strength of the static magnetic field, waves of wavelengths of the order of the scale height or even greater are shown to be damped. Several special cases are discussed. (auth) (UK)

19737 KINETIC THEORY OF THREE-WAVE INTERACTION IN A MAGNETIZED PLASMA. Stenflo, L. (Inst. of Physics, Uppsala). J. Plasma Phys.; 4: 585-93(Sep 1970).

The nonlinear resonant interaction between three waves that propagate in the direction of a constant magnetic field in a homogeneous plasma is considered. A coupled-mode theory, which makes it possible to derive the coupling coefficients within a kinetic description, is developed. (auth) (UK)

19738 NEW DERIVATION OF QUASI-LINEAR THEORY. Klozenberg, J. P.; Bernstein, Ira B. (Imperial Coll. of Science and Tech., London). J. Plasma Phys.; 4: 595-602(Sep 1970).

A new derivation of quasi-linear theory for plasma oscillations is given, subject to the neglect of wave–wave interactions. The theory, which applies equally to damping and growing waves, requires that the individual wave resonances be narrow and the electric field spectrum sufficiently broad. (auth) (UK)

19739 RELATIVISTIC SYNCHROTRON PLASMA ECHO. Ott, E. (Cornell Univ., Ithaca, N. Y.). J. Plasma Phys.; 4: 471-6(Sep 1970).

A self-consistent Vlasov equation treatment will be given for a type of echo that arises due to the relativistic velocity dependence of the gyrofrequency. A relativistic plasma is considered in a homogeneous magnetic field. If at $t = 0$ and $t = T$ a spatially homogeneous external rf electric field is applied perpendicular to B_0, then an echo response is produced at $t = 2T$. The amplitude of the second pulse. (auth) (UK)

19740 NUMERICAL EVALUATION OF THE ELECTROMAGNETIC PROPERTIES OF A HALF-SPACE RELATIVISTIC PLASMA. Imre, Kaya; Ozizmir, Ercument (City Univ., New York). Phys. Fluids; 14: 603-5(Mar 1971).

The results of the linearized theory are numerically evaluated in the case of perpendicularly incident electromagnetic waves on a half-space relativistic plasma. Reflection, transmission, and absorption coefficients are calculated. It is found that the surface absorption is more significant at higher temperatures. The maximum value of the absorption coefficient reaches approximately 26% for $\beta = (mc^2/k_BT) \lesssim 0.1$. The results, however, are not valid near cutoff frequencies due to the breakdown of the linearized theory upon which the present calculations are based. (auth)

19741 INTERPRETATION OF SPATIALLY DECAYING ION-ACOUSTIC WAVES. Hirshfield, J. L.; Jacob, J. H.; Baldwin, D. E. (Yale Univ., New Haven). Phys. Fluids; 14: 615-28(Mar 1971).

Detailed examination is given to circumstances surrounding the excitation and detection of spatially propagating ion-acoustic disturbances in a plasma. For relatively weak damping, a theory is presented to show the major influence on spatial signal evolution engendered by source coupling details, by source geometry, and by three-dimensional ion trajectories. In particular, near- and far-zone regions are identified for a disk source. Fresnel interference can dominate the near zone (within which many experiments are performed), so that serious questions can be raised as to the interpretation of observed decays. For relatively strong decays, the transition to the ballistic, three-dimensional, free-streaming solution is presented. Experiments are presented to illustrate some features of the theory, including measurements of Landau damping with $0.04 < k_i/k_r < 0.2$ for $0.6 < \omega/\omega_{pi} < 1.4$. Observed Fresnel interference patterns are compared with theory. (auth)

19742 SYMMETRY CONSIDERATIONS FOR GRID-LAUNCHED ION-ACOUSTIC WAVES. Bernstein, I. B.; Hirshfield, J. L.; Jacob, J. H. (Yale Univ., New Haven). Phys. Fluids: 14: 628-32(Mar 1971).

Immersion of a fine-mesh grid (or set of parallel grids) into a plasma is widely used to stimulate ion-acoustic waves. The grid structure is usually biased so as to reflect electrons and transmit ions. The effect upon the ions due to applied rf fields in the grid region is to provide some combination of velocity and density modulation. The associated applied electric field perturbations will possess a combination of odd and even spatially symmetric parts, about the plane of symmetry of the grid system. The steady-state solution of the governing differential equation in the ion-acoustic limit is shown to depend critically upon this source symmetry, and to reduce to the usual solution only for the case of odd symmetry. Experiments designed to test these symmetry predictions were carried out using an apparatus described previously, except that a four-grid transmitter was substituted for the three-grid one. The outer two grids were grounded and the inner two grids could be driven either in phase (odd E-field symmetry), or 180° out of phase (even E-

XUM

field symmetry). For odd symmetry, the observed spatial disturbance is similar to that reported previously with clear evidence of Fresnel interference. For even symmetry, wavelike signals are not observed near the grids, indicating a strong decrease in coupling between the free-streaming source ions and an ion-acoustic wave. (auth)

19743 LONGITUDINAL WAVE PROPAGATION IN A PLASMA CONTAINING AN EXTERNAL TIME-DEPENDENT ELECTRIC FIELD. Nunez, Paul L. (KMS Tech. Center, San Diego, Calif.). Phys. Fluids; 14: 633-9(Mar 1971).

Frequency and damping decrements for high-frequency longitudinal oscillations in a plasma containing an external high frequency ($\Omega \gg k\bar{v}_-$) electric field are obtained by means of a time-asymptotic solution to the linearized Vlasov equation, with an approximate collision term included. If the external field frequency is close to $(\omega_{p-}^2 + 3\ k^2\bar{v}_-^2)^{1/2}$, the contribution of the ion motion to Landau damping is significant for small external fields. The threshold field necessary to excite a high-frequency instability in a plasma in which the number of particles in a Debye sphere is very large is obtained. This problem is of interest since laser-induced instabilities may be responsible for an anomalous heating effect in the plasma. (auth)

19744 EXCITATION AND STABILIZATION OF ION-ACOUSTIC WAVES IN AN RF PLASMA. Okamoto, Y.; Tamagawa, H. (Nagoya Univ., Japan). Plasma Phys.; 13: 71-3 (Jan 1971).

Collective interaction between plasma particles in ion-acoustic waves is known to cause Landau damping or Landau growth. In order to study Landau growth it is necessary to have a plasma with a special velocity distribution function such as a double-humped one. Experimental confirmations about the relations between ionic energy distribution functions and ion-acoustic waves in an rf plasma are described. It is concluded that if the energy distribution function for the ions has no minimum (single-humped distribution function, such as the Maxwellian distribution) there is no instability, while the presence of a deep-enough minimum, such as double-hump in the distribution function, leads to the electrostatic instabilities. (UK)

19745 COMPRESSIONAL ALFVEN WAVES IN A NON-UNIFORM PLASMA. Morrow, R.; Brennan, M. H. (Flinders Univ., Australia). Plasma Phys.; 13: 75-9(Jan 1971).

The propagation of Alfvén waves in nonuniform plasmas has recently been treated by a number of authors (Woods, 1962, 1963; Pneuman, 1965; McPherson et al., 1966; Cross et al., 1968 and Davies 1969), and the propagation of helicon waves in nonuniform plasmas has been considered in detail by Blevin and Christiansen (1966, 1968) and Davies and Christiansen (1969). Each of these treatments is limited to a rather small range of frequencies: $\omega \ll \omega_{ci}$ for the compressional Alfvén wave, $\omega \gg \omega_{ci}$ for the helicon wave, and a special case $\omega = \omega_{ci}$ (Cross et al., 1968). The treatment presented here is valid from low frequencies through the ion cyclotron region to frequencies less than 0.1 ω_{ce}, and is applicable to a plasma with an arbitrary density distribution. (auth) (UK)

19746 TIME-OF-FLIGHT STUDY OF WAVES GUIDED BY A PLASMA COLUMN. Demokan, O.; Hsuan, H. C. S.; Lonngren, K. E. (Univ. of Iowa, Iowa City). Plasma Phys.; 13: 29-32 (Jan 1971).

An experiment designed to measure the group velocity of waves guided by a plasma column is described. Using very short high-frequency sine-wave burst signals, a time-of-flight experiment was performed. The dependence of the group velocity on $\langle\omega_{pe}(r)\rangle$ was directly obtained. (auth) (UK)

19747 NONLINEAR WAVE MIXING AT HYBRID FREQUENCIES IN AN INHOMOGENEOUS PLASMA. Fidone, I. (CEN, Fontenay-aux-Roses, France); Teichmann J.; Granata, G. Phys. Fluids; 14: 737-45(Mar 1971).

The nonlinear coupling of waves near the hybrid resonances for a magnetized inhomogeneous plasma is investigated. In this case, the geometric optics approximation is no longer valid and the full wave equations must be used. In contrast to the homogeneous plasma treatment, no synchronism relation for the propagation vectors occurs and nonlinear processes are possible that are absent in the homogeneous case. Two special examples of wave–wave mixing are discussed in detail, namely, harmonic generatio at the upper hybrid frequency and excitation of longitudinal wave of frequency near the lower hybrid. (auth)

19748 DAMPING OF A LARGE-AMPLITUDE ION ACOUSTIC SOLITARY WAVE. Ott, Edward (Cornell Univ., Ithaca, N. Y.). Phys. Fluids; 14: 748-50(Mar 1971).

The damping of a finite amplitude ion-acoustic solitary wave due to ion–neutral collisions is examined. (auth)

19749 BOUNDARY PROBLEM IN A PLASMA. Karunarathne, V. B. (Cambridge Univ., Eng.). J. Plasma Phys.; 4: 807-17(Dec 1970).

An isotropic Vlasov plasma occupies an infinite space, the upper half of which ($y > 0$) is a dielectric. A transverse disturbance is incident normally on the face of the dielectric. The waves that are excited in each half of the space are obtained. It is shown that this result can be extended to cover the reflection problem of any normally incident disturbance in a plasma defined by a dispersion relation $D_1(w,k)$. A few examples are considered, in particular, transverse waves in a plasma streaming normal to the boundary where Cherenkov instability can occur. (auth) (UK)

19750 HIGHER-ORDER APPROXIMATIONS IN THE THEORY OF LONGITUDINAL PLASMA OSCILLATIONS. II. Einaudi, F. (Univ. of Colorado, Boulder); Axford, W. I. J. Plasma Phys.; 4: 819-24(Dec 1970).

The results of a previous analysis (Einaudi and Axford, 1967) in which the nonlinear behavior of one-dimensional electrostatic oscillations in a homogeneous, unbounded, collisionless, and fully ionized plasma was considered, are commented on and extended. The evolution of a monochromatic wave of small, but finite amplitude is studied by expanding the dependent variables as well as the independent variable t in the form of asymptotic series; an ordering parameter ϵ proportional to the initial amplitude of the electric field is introduced. The expansion of the independent variable in such a series allows one to eliminate secular terms from the part of the distribution function that does not depend on the free-streaming terms. This, in turn, allows one to determine corrections to the complex frequency ω. Results of the previous note on nonlinear Landau damping for an initially Maxwellian distribution function are confirmed, but it is indicated that they apply to values of time up to a value τ_1 rather than for all times. One can proceed to larger values of time in the manner of the multiple time-scale method. In particular, it is found that the Landau damping is increased with respect to the linear value only initially during the first time scale. (auth) (UK)

19751 DISCRETE SPECTRA AND DAMPED WAVES IN QUASI-LINEAR THEORY. Vahala, George; Montgomery, David (Univ. of California, Berkeley). J. Plasma Phys.; 4: 677-91(Dec 1970).

The consequences of the quasi-linear equations are explored. Particular attention is paid to the differences between the one-dimensional and the two- and three-dimensional cases, and to the differences between the cases of discrete and continuous wave-number spectra. The possibilities of and problems associated with including damped waves are treated. The relation between conservation laws and the "resonance approximation", in which the limit of zero growth rate for the unstable waves is taken at finite times, is clarified. Numerical solutions for the one-dimensional case with finite growth rate are presented. (auth) (UK)

19752 LONGITUDINAL WAVES IN A PERPENDICULAR COLLISIONLESS PLASMA SHOCK. I. COLD IONS. Gary, S. Peter (University Coll. of North Wales, Bangor); Sanderson, J. J. J. Plasma Phys.; 4: 739-51(Dec 1970).

Electrostatic waves in a Vlasov plasma of unmagnetized ions and magnetized, Maxwellian electrons are considered. The linear dispersion relation is derived for waves in a perpendicular shock such that the most important sources of instability are the $E \times B$ and ∇B electron drifts. For the case of cold ions, propagation perpendicular to the applied magnetic field, and the $E \times B$ drift alone, a numerical analysis of frequency vs. wave number is presented. The effects of the ∇B drift are also considered, and it is shown that the maximum growth rate can be larger than the maximum growth rate for the zero magnetic field ion-acoustic instability under comparable conditions. (auth) (UK)

19753 LONGITUDINAL WAVES IN A PERPENDICULAR COLLISONLESS PLASMA SHOCK. II. VLASOV IONS. Gary, S. Peter (University Coll. of North Wales, Bangor). J. Plasma Phys.; 4: 753-60(Dec 1970).

An analysis of the linear dispersion relation for electrostatic waves in a Vlasov plasma of unmagnetized, Maxwellian ions and magnetized, Maxwellian electrons is presented. The electrons undergo $E \times B$ and ∇B drifts, and the electron β is small. For propagation in the perpendicular direction, maximum growth rates can be substantially larger than those of the zero-magnetic-field ion-acoustic instability. For propagation outside a few degrees from the perpendicular, the dispersion characteristics are essentially those of the ion-acoustic instability. (auth) (UK)

19754 LAGRANGIAN METHODS IN PLASMA DYNAMICS. I. GENERAL THEORY OF THE METHOD OF THE AVERAGED

LAGRANGIAN. Dougherty, J. P. (Univ. of California, San Diego, La Jolla). J. Plasma Phys.; 4: 761-85(Dec 1970).

Whitham's averaged Lagrangian method is used to yield a relativistically covariant formalism for wave packets in a weakly inhomogeneous (and time-dependent) medium. Provided the physics of the medium can be based on a Lagrangian density, a procedure of expansion and averaging is available that gives separate Lagrangians for the dynamics of the background and of the waves. The Euler–Lagrange equations then give immediately the equations of motion for the background, including nonlinear reaction of the waves, and the dispersion relation, equations for ray tracing, conservation of wave action, and nonlinear coupling coefficients for the waves. Many of these results can be interpreted in an illuminating way by considering the corresponding expansion of the canonical four-dimensional stress tensor. (auth) (UK)

19755 EXACT TREATMENT OF COLLISIONAL EFFECTS ON TEMPORAL PLASMA-WAVE ECHOES: FREE-PARTICLE MODEL. Furutani, Y.; Coste, J. (Univ., Paris). J. Plasma Phys.; 4: 843-7(Dec 1970).

In the case of a free-particle plasma with no self-consistent field and with collisions described by the Lenard–Bernstein operator, an exact solution of the temporal echo problem is given. (auth) (UK)

19756 SINGULARITIES OF COUPLED FIELDS IN WARM STRATIFIED PLASMAS. Burman, R. (Univ. of Western Australia, Nedlands). Czech. J. Phys.; 20: 1123-8(1970).

Maxwell's equations coupled to single-fluid hydrodynamic equations are used to describe waves in a warm continuously stratified electron plasma. The behavior of the fields in a coupling region, excited by an incident electron-acoustic wave, is investigated. (auth)

Shielding

Refer also to abstracts 18988, 19294, 19971, 20206, 20226, 20442, and 20733.

19757 (ORNL–4584, pp 58-73) THEORETICAL RADIATION PHYSICS. Neufeld, Jacob; Ritchie, R. H.; Anderson, V. E.; (and others). (Oak Ridge National Lab., Tenn.).

From Health Physics Division annual progress report for period ending July 31, 1970.

Initial results from studies of energy deposition by beams of negative and positive pions in the range 160 to 220 MeV/c in water as a function of depth are reported. A model was developed for estimating the effect of charged particles that stop or are borne within a gas-filled sphere irradiated by neutrons on track-length distribution. Results are shown for 0.5- and 2-MeV neutrons. Calculations of critical dipole moments for electron binding to a nonstationary dipolar system are described briefly. A new method of selecting a best trial function in an extension of a variational method for lower bounds on elastic scattering phase shifts is suggested. Results for electron scattering by atomic hydrogen are shown. A slight generalization of oscillator strength, a rapid method of obtaining potential-energy curves for diatomic molecules, the mfp of relativistic electrons for plasmon excitation, an extension of stopping-power theory for charged particles to include a correction term proportional to the cube of the charge of the incident particle, double-plasmon excitation in reactions of fast charged particles with a free-electron gas, and the coupling of photons with surface plasmons on a dielectric solid are discussed briefly. (A.G.W.)

19758 (ORNL–4584, pp 74-86) INTERACTION OF RADIATION WITH LIQUIDS AND SOLIDS. Arakawa, E. T.; Birkhoff, R. D.; Braundmeier, A. J.; (and others). (Oak Ridge National Lab., Tenn.).

From Health Physics Division annual progress report for period ending July 31, 1970.

Work done during the period on the following projects is summarized: collective effects in the optical properties of cesium, optical properties of MgO and MgF_2 in the soft x-ray region, study of the optical properties of solids by ellipsometry, radiative decay of collective oscillations in metals, radiation damping of surface plasmons from aluminum-coated concave diffraction gratings, effects of coating by diffusion pump oil in efficiency of dielectric-coated concave diffraction gratings, observations of surface roughness, and exo-electron emission during oxygen and water chemisorption on fresh magnesium surfaces. (A.G.W.)

19759 (ORNL–4584, pp 87-91) PHYSICS OF TISSUE DAMAGE. Arakawa, E. T.; Birkhoff, R. D.; Emerson, L. C.; (and others). (Oak Ridge National Lab., Tenn.).

From Health Physics Division annual progress report for period ending July 31, 1970.

Slowing down of Auger electrons produced by reactor irradiation in Ge and W was studied. It was concluded that slowing down in semiconductors differs only slightly from that in metals. No explanation was found for previously noted discrepancies between theory and observations. Optical constants for the following liquids are reported for the photon energy range 4.0 to 10.65 eV: CCl_4, C_6H_{14}, C_6H_{12}, C_6H_{10}, C_6H_8, and C_6H_6. (A.G.W.)

19760 APPROXIMATIONS AND INTERPOLATION RULES FOR RANGES AND RANGE STRAGGLINGS. Schiott, H. E. (Bell Telephone Labs., Inc., Murray Hill, N. J.). Radiat. Eff.; 6: 107-13(Nov 1970).

From International Conference on Ion Implantation in Semiconductors, Thousand Oaks, Calif. See CONF-700544.

Approximations and interpolation rules for ranges and stragglings in amorphous substances are presented. Two energy regions, termed low and intermediate energies, corresponding to the dimensionless energy epsilon in the intervals $0.002 < \epsilon < 0.1$ and $0.5 < \epsilon < 10$, respectively, are defined. For low energies the projected range is approximately proportional to $E^{1/2}$, and for intermediate energies approximately proportional to E. For low energies, approximate stragglings are also obtained. The agreement of the results with accurate range calculations is better than ~10 percent. (auth)

19761 ELECTRIC FIELD EXCITED IN AIR BY PULSED γ QUANTA. Medvedev, Ya. A.; Stepanov, B. M.; Fedorovich, G. V. Zh. Prikl. Mekh. Tekh. Fiz., No. 4, 3-8(Jul-Aug 1970). (In Russian).

The characteristics of the electric field due to the polarization of air during the passage of nonstationary Compton currents, excited by γ-quantum pulses in rarefied air, were investigated; the effect of the field on the motion of the Compton electrons was taken into account. The work included estimation of the amplitude and relaxation time of the field. As a result of the disturbance of the Compton electrons, a polarization electric field is created by directional γ quanta in air. The problem is similar to that studied by W. J. Karzas et al., who investigated the electromagnetic field excited by a nonstationary γ source in the upper atmosphere. The Compton electron flux was assumed to be known and to be proportional with the ratio of the gas-kinetic range of Compton electrons and γ quanta which is about 0.01 and is independent of the altitude. After range of the electrons increases, the slowing-down effect of the thus-created electric field on the motion of the Compton electrons becomes stronger. It was found that electric field changes during the first few moments are determined mostly by the accumulation of polarization charges and the conductivity of the air does not affect the field because the electron density is low. (TTT)

19762 STOPPING POWERS OF GASES AND SOLIDS FOR HEAVY CHARGED PARTICLES. Doke, Tadayoshi (Tokyo Univ.). Oyo Butsuri; 39: 1086-1100(Dec 1970). (In Japanese).

Recent works on the slowing down of heavy charged particles in gases and solids are summarized from the viewpoint of stopping power. First, the limitation of the Bethe stopping-power equation in the low-energy region is discussed, and experimental results for low-energy protons and helium ions are reviewed in detail. Next, problems on effective charges of penetrating atoms having atomic number larger than 15 are described. Lastly, after giving typical stopping-power theories in the path-end region of penetrating particles, experimental results are compared with the theoretical predictions. (auth) (Japan)

19763 EXPERIMENTAL DETERMINATION OF PHOTON ENERGY–ANGLE DISTRIBUTIONS FOR ^{60}Co AFTER PENETRATION OF THICK CONCRETE BARRIERS. Starchman, Dale E.; Hoecker, Frank E. (Univ. of Kansas, Lawrence). Health Phys.; 20: 49-53(Jan 1971).

The number photon spectra of transmitted ^{60}Co γ rays scattered by thick concrete barriers were determined as functions of the angle of scatter and of the barrier thickness under broad-incident-beam conditions. The energy region for which the maximum number of photons occurs shifts toward lower energies with increasing thickness, but the rate of this shift as a function of the thickness of concrete becomes small for thick slabs. When the number of photons is plotted as a function of barrier thickness, it is found that after an initial buildup an "equilibrium" thickness is approached. For greater thicknesses the slope of the curve plotted is a constant. The constants determined for plots corresponding to all angles of scattered radiation greater than 0° with the normal to the surface are equal to one another. (auth) (UK)

19764 GAMMA-RAY SCATTERING BY STRUCTURE SURFACES. Kitazume, Mitsuyuki (Hitachi Ltd., Ibaraki, Japan). Hitachi Hyoron; 52: 499-502(Jun 1970). (In Japanese).

Gamma rays emitted from a point source are scattered by structure surfaces and reach a detection point. An equation that evaluates dose rate at a detection point is derived. In the equation, multiple scattering is taken into consideration by modifying a single-scattering equation with a buildup factor that depends on the energy of scattered γ rays. It was found that the result of calculation is in fairly good agreement with the experimental results on ^{60}Co γ scattering by concrete. This method for calculating dose rate is also applicable to nuclear reactor γ rays that are not monoenergetic. (Japan)

19765 STOPPING CROSS SECTIONS FOR FISSION FRAGMENTS OF ^{252}Cf BY GOLD, SILVER, AND CARBON. Bridwell, L.; Walters, A. L. Jr. (Murray State Univ., Ky.). Phys. Rev., B; 3: 2149-53(1 Apr 1971).

Using ^{252}Cf as a source of heavy ions, the stopping cross sections were determined for stopping media of gold, silver, and carbon. The dependence of stopping cross sections on the nuclear charge of the heavy ions was observed at approximately 1.3 cm/nsec. The results are in reasonable agreement with the theory by Lindhard. In some cases, better agreement can be obtained by using a formula published earlier by Bridwell and Moak. (auth)

19766 LOW-ENERGY ELECTRON BEAM STUDIES IN THIN ALUMINUM FOILS. Garber, F. W.; Nakai, M. Y.; Harter, J. A.; Birkhoff, R. D. (Oak Ridge National Lab., Tenn.). J. Appl. Phys.; 42: 1149-58(1 Mar 1971).

The transmission of normally incident electrons through aluminum vacuum-deposited on a 75-Å aluminum oxide insulator was measured for electrons of energy between 1 eV and 4 keV. Currents to the top layer (65 to 525 Å) and to the metallic bottom layer underlying the insulator were monitored with operational amplifiers in obtaining the transmission characteristic. Below 50 eV the transmission is apparently controlled by the aluminum oxide insulator. Above this energy the absorption increases rapidly until the entire beam current is absorbed in the top layer. At still higher energies the current to the top layer decreases through zero to a value of −1 (normalized). The energy at which the top current goes to zero was found to increase as the thickness of the top layer was increased. These data were analyzed to yield the electron stopping power, which was found to vary from about 3.1 eV/Å at 300 eV to about 4.5 eV/Å at 950 eV when the raw data were corrected for nuclear scattering by a modified version of the Yang scattering theory. (auth)

19767 ENERGY DEPOSITION DISTRIBUTIONS. Roesch, W. C.; Glass, W. A. (Battelle-Northwest, Richland, Wash.). Contract AT(45-1)-1830. Radiat. Res.; 45: 1-7(Jan 1971).

The distribution in the increments to the energy deposited in a small site as a result of the interaction of a primary charged particle with a molecule of the medium varies with the position of the molecule along the track of the particle. It is shown that, nevertheless, the energy deposited in the site can be treated as though it were the result of a compound-Poisson process based on a single, effective distribution in the increments due to individual interactions regardless of the position of the interaction along the track. An expression for the effective distribution is given. The theory is generalized to quantities other than energy deposition. (auth)

19768 SHIELDING EFFECTIVENESS OF CRACKED CONCRETE. Seboek, F. (Technische Univ., Budapest). Kerntechnik; 12: 496-501(Nov 1970). (In German and English).

Formulas are developed for the exact definition of the effects of cracks in a concrete shield, and guidelines are presented on the compensation of these effects. The investigations show that it may be economically advantageous to allow a concrete shield to crack and to shield the resulting excess radiation by other means. These considerations may have far-reaching effects on the theory and the practical design of radiation protection structures. (auth)

Solid-State Physics

Refer also to abstracts 18679, 19469, and 20307.

Radiation Effects

Refer also to abstracts 20165–20169.

19769 (LIB/Trans-307) IMPROVEMENTS IN THE METHODS APPLIED TO THE ALTERATION OF THE PROPERTIES OF TYPE IIb DIAMONDS. Translated by D. Roman (Australian Atomic Energy Commission), from French Patent 1,195,862. 7p. Dep. NTIS (U. S. Sales Only).

The properties of a semiconductor diamond irradiated with beams of charged particles and other beams are described. The color and resistance of the diamond were altered by increasing the number of donor centers in the gem, at the expense of acceptor centers. Charged-particle beams (electrons, positrons, α-particles) affected the outer diamond layers only. A 1-MeV electron beam of flux 2×10^6 electrons/cm^2 was used. Neutrons and gamma beams affected the diamond homogeneously. A neutron beam of pile factor 6 for 45 min increased specific resistance to 2500 Ω/cm (a factor of 20) and removed coloration. The optimum energy range for γ rays was 0.5 to 0.9 MeV, and these provide the best means of irradiation when color alteration is the prime factor. Radiocobalt constitutes a practical source. (Australia)

19770 (NYO–3842-12) RADIATION-INDUCED DEFECTS IN ALKALI HALIDES, AND THEIR ROLE IN RECOMBINATION PROCESSES. Final Report, March 1, 1967–July 15, 1970. Murray, R. B. (Delaware Univ., Newark. Dept. of Physics). 22 Jan 1971. Contract AT(30-1)-3842. 13p. Dep. NTIS.

A summary is presented of research in the following areas: luminescence from (electron + V_K) recombination processes, mechanism of producing vacancy defects, optically stimulated orientation of V_K centers, diffusion of the V_K polaron, and effects of channeling on the scintillation response of NaI(Tl) to heavy ions. (D.L.C.)

19771 TOTAL ANTIRESONANCE IN CaF_2: Dy CRYSTALS WITH COLOR CENTERS. Arkhangelskaya, V. A.; Feofilov, P. P. Opt. Spectrosc. (USSR) (Engl. Transl.); 28: 657-8(Jun 1970).

Translated from Opt. Spektrosk.; 28: 1219-21(Jun 1970).

A study was made of the absorption spectra of CaF_2 : Dy (0.2 mole %) crystals colored by gamma rays and heat-treated to transform the color centers. After heating to 170°C, the spectrum at 77°K showed, besides the asymmetric lines, a narrow symmetric trough at 4475Å in the continuum. The wavelengths and types of antiresonance are listed for the strong and weak interactions of states predicted by theory. The problem of the identity of the interfering states is considered; they are probably the vibrational states of the color center at 450 nm and the Dy ion in the complex center. The problem of explaining the sharp decrease of the effect at 300°K remains. (D.L.C.)

19772 ION IMPLANTATION. Proceedings of the European Conference, Reading, England, September 7–9, 1970. Stevenage, Eng.; Peter Peregrinus Ltd. (1970). 241p. £6. (CONF-700945).

Forty-six papers were presented under the following sectional headings: machines and ion sources; electrical behavior of implanted layers; devices; implantation of noncrystalline materials; compound semiconductors; physical processes; and radiation damage processes. Abstracts are included for all papers. (UK)

For abstracts of individual papers see: 18756, 18857, 18858, 19256, 19773–19808, 19862, and 20165–20169.

19773 INDUSTRIAL-SCALE ION-IMPLANTATION FACILITY. Freeman, J. H.; Caldecourt, L. R.; Done, K. C. W.; Francis, R. J. (Atomic Energy Research Establishment, Harwell, Eng.). pp 36-40 of Ion Implantation. Stevenage, Eng.; Peter Peregrinus Ltd. (1970).

From Conference on Ion Implantation, Reading, England. See CONF-700945.

A description is given of an implantation machine at Harwell that was designed to meet a wide range of industrial doping requirements and to provide a production-scale system permitting technical and economic assessments to be made under realistic conditions. Although intended primarily for repetitive doping operations on a batch scale, the system is suitable for the experimental implantation of individual specimens. The doping technique differs from that generally used in that mechanical scanning of targets through a stationary beam is employed. In this way the problems associated with the electrostatic deflection of intense ion beams are avoided, and large-area samples can be doped without loss of angular definition. Since several semiconductor wafers are normally doped simultaneously, ion-beam heating effects are also reduced. The use of an automated high-voltage target chamber allows the possibility of dopant profile control by continuous energy programming. Provision is also made for the inclusion of sample heating and cooling means. The fast acceleration of the ions to the target chamber potential takes place across a single-gap electrode system. The lens assembly is designed to maintain good angular definition for channelling requirements and also to minimize x-ray production and space-charge "blow-up" of the beam. The beam is continuously sampled on the low-voltage side of the acceleration lens and the signal is used to monitor and control the doping rate. The normal maximum energy of the separator is 40 keV and the maximum target chamber potential is 150 kV, but for many dopants higher energies

XUM

(>300 keV) can readily be achieved by use of multiply charged ions. The principle of target scanning is illustrated. For most elements, beams of mA intensity can be obtained, but the utilizable doping current is ~0.5 mA. Continuous operation for periods of tens of hours is possible with most dopants. (UK)

19774 200-kV ION-IMPLANTATION EQUIPMENT AT MRL, SALFORDS. McGinty, G. K.; Goldsmith, B. J.; Thomas, R. A. (Mullard Research Labs., Redhill, Eng.). pp 41-5 of Ion Implantation. Stevenage, Eng.; Peter Peregrinus Ltd. (1970).

From Conference on Ion Implantation, Reading, England. See CONF-700945.

A description is given of this machine, which consists of a 100-kV Danfysik ion accelerator to which is added an Edwards target chamber for hot and cold implantation and a 100-kV post analysis acceleration stage. The equipment enables implantation to be carried out with a wide range of species and energies, over a wide range of angles, and with considerable choice of implant temperatures. It is intended primarily for semiconductor research under laboratory conditions. Details are given of the basic accelerator, neutral beam experiments, the hot and cold target chamber, and the post-analysis acceleration stage. The machine was used mainly to implant B and P ions into Si slices, although Ne and N ions have been used. Ion energies normally ranged from 20 to 70 kV, and good machine stability was obtained. It is hoped that reliable implanting at 100 kV with the basic machine and up to 200 kV with the additions will be achieved. (UK)

19775 ELECTRICAL BEHAVIOUR OF IMPLANTED LAYERS. Glotin, P. (CENG-LETI, Grenoble, France). pp 46-51 of Ion Implantation. Stevenage, Eng.; Peter Peregrinus Ltd. (1970).

From Conference on Ion Implantation, Reading, England. See CONF-700945.

In semiconductor devices the quantity of interest is not the impurity concentration N_D, but the free-carrier concentration N_S, and in thermal diffusion processes it is assumed that N_D and N_S are equal over the whole of the doped layer. This requires that all chemical impurities must find a position in the lattice where they are electrically active and be ionized in the temperature range of interest. It also requires that lattice disorder is negligible and corresponds to very low concentrations of compensating centers. Such an equality, however, never actually exists, and this is especially so in high impurity concentration regions, as shown for P diffused in Si. Equality of N_S and N_D cannot be assumed in ion-implanted layers. The influence of bombardment damage can be much larger than the influence of chemical impurities, and it is convenient to characterize the result of a given implantation, associated with a given annealing treatment, by the ratio N_S/N_D, referred to as the mean electrical activity per implanted ion. This ratio depends on a large number of parameters which are reviewed. Some of the basic phenomena that occur as the implanted ions slow down and come to rest in a target are discussed, and a description is given of the main methods used to measure the electrical activity of a layer, together with experimental results. 29 references. (UK)

19776 INFLUENCE OF ION-BOMBARDMENT DAMAGE ON ANNEALING BEHAVIOUR OF BORON-IMPLANTED SILICON. Blamires, N. G. (Atomic Energy Research Establishment, Harwell, Eng.). pp 52-6 of Ion Implantation. Stevenage, Eng.; Peter Peregrinus Ltd. (1970).

From Conference on Ion Implantation, Reading, England. See CONF-700945.

Doping of Si can be achieved by ion implantation, followed by an annealing treatment at ~630°C to minimize radiation damage effects and to enable the implanted atom to take up a substitutional lattice position. With boron, only ~7% of an implanted dose of 10^{15} ions/cm^2 is electrically active after annealing at 630°C, and annealing temperatures of ~1000°C are required to achieve full electrical activity; such high temperatures may degrade the properties of the device to be produced. It has been shown, however, that if the B is implanted into a region previously rendered amorphous by Ne bombardment, then a much higher percentage of the B is active after annealing. The results presented in this paper show that there is an optimum Ne dose which can result in nearly 100% B activity after a 650°C anneal. This, however, means adding a further impurity. An alternative method for producing an amorphous zone is to implant the B into a cold Si specimen, and it has been found that the lattice disorder produced by 200-keV B in Si is strongly temperature-dependent from −85°C to room temperature. Electrical measurements on 40- and 200-keV implants have shown that the B electrical yield at 600°C increases with the amount of disorder present, and is greatest when the layer is completely amorphous. Results are presented for determinations of the electrical activity of B doses of 10^{15} and 5×10^{15} ions/cm^2 implanted into Si held at 77°K, for the range of B energies from 10 to 400 keV; a variation of electrical activity with energy was evident, attributed to the degree of amorphism produced in the Si. Among other matters discussed are Hall measurements on 130-keV implants and the reverse anneal effect for 300°K implants. It is concluded that the B electrical activity is critically dependent on the degree of damage in the implanted region. 12 references. (UK)

19777 ELECTRICAL AND ELECTRON MICROSCOPE STUDIES OF ANNEALED ION-IMPLANTED SILICON. Bicknell, R. W. (Plessey Co. Ltd., Towcester, Eng.). pp 57-60 of Ion Implantation. Stevenage, Eng.; Peter Peregrinus Ltd. (1970).

From Conference on Ion Implantation, Reading, England. See CONF-700945.

It is stated that the precise nature of the processes involved during the annealing of ion-implanted Si has not been determined. Attempts are described to correlate structural effects visible by electron microscopy with measured changes in electrical characteristics, such as resistivity, and to give possible explanations for the observed effects. Some results are given for B and P implants at various temperatures. It is concluded that B has a single activation energy covering the usual annealing temperature range of 600 to 1300°K, and that when the damage centers recrystallize there is a possibility of B precipitates forming. Phosphorus, however, shows at least two activation energies, one for P in amorphous Si and another for P outside this zone. Phosphorous does not show precipitation when annealed. The Si lattice in both cases shows large amounts of damage and, when annealed, condenses into either dislocation loops or dislocation networks, depending on the amount of damage incurred by the implantation. (UK)

19778 ELECTRICAL MEASUREMENTS ON SILICON FOLLOWING PHOSPHORUS AND BORON IMPLANTATION AND ANNEALING. Burr, P.; Whitehouse, J. E. (Univ. of Reading, Eng.). pp 61-4 of Ion Implantation. Stevenage, Eng.; Peter Peregrinus Ltd. (1970).

From Conference on Ion Implantation, Reading, England. See CONF-700945.

A procedure was adopted of implanting ions of the same type as the bulk dopant and separating the properties of the layer in analysis of the results using the theory of nonuniform semiconductors, in contrast to the technique of layer isolation by implantation to produce p−n or n−p structures used by other authors. A particular advantage of this technique is that properties of the layer may be deduced immediately after implantation and then after annealing at small temperature intervals up to about 1000°C. When using a junction to isolate the layer, measurements are not usually obtained before heating to 400 to 500°C to first create the junction. The material used in the investigations was ~10Ω/cm float-zoned single-crystal Si. In n-type P-doped material $^{31}P^+$ ions were implanted and in p-type B-doped material $^{11}B^+$ ions were used. For both B and P ions at the energy and doses used, a p-type layer was present immediately after implantation, probably due to the surface layers being virtually amorphous. The electrical measurements were made using conventional dc technique, and isochronal annealing was carried out in a silica tube at temperatures up to 1000°C, the temperature intervals being 50°C. Conductivity and Hall coefficient results are given. By measuring the properties of a sample before and after implantation the properties of the implanted layer alone could be deduced. The way in which the effective number of carriers/cm^2 and the effective mobility, measured at room temperature, vary during annealing is shown graphically. The measurements showed that all samples, irrespective of dose, had the same number of carriers in the implanted layer immediately after implantation. A subsidiary maximum was also observed at an annealing temperature of ~500°C followed by a monotonic increase up to 1000°C. In the case of $^{31}P^+$ implantations in n-type substrates, the layer suddenly became n-type at ~500°C. 15 references. (UK)

19779 ANNEALING EXPERIMENTS ON SILICON LAYERS IMPLANTED WITH 50-keV PHOSPHORUS IONS. Andersson, A.; Swenson, G. (Chalmers Univ. of Tech., Goteborg). pp 65-9 of Ion Implantation. Stevenage, Eng.; Peter Peregrinus Ltd. (1970).

From Conference on Ion Implantation, Reading, England. See CONF-700945.

The aim of the studies described was to investigate the electrical properties of Si layers implanted with 50-keV nonchanneled P ions. Hall-effect and sheet-resistivity measurements were made for a wide temperature range employing various doses and a series of annealing stages. ^{31}P ions were implanted into Si samples using an electromagnetic isotope separator capable of operation up to 60 keV, and the beam was electrostatically scanned so as to obtain homogeneous implantation. Red P was used as charge material in the ion source, and implantations were made at room temperature. The depleted layer between the n-type implanted layer and the p-type base crystal provided the electrical isolation so that the implanted layer could be measured independently of the base crystal. Doses of 10^{13}, 10^{14}, and 10^{15} ions/cm^2 were employed. Using a vibrating reed electrometer, the Hall-effect and sheet-resistivity measurements were made on the implanted layer in the temperature range 300 to 77°K immediately after irradiation and after annealing treatments at successively higher temperatures. For the medium dose, the electrical measurements were extended down to 5°K. Measurements were also carried out using the stripping technique. The effective surface-carrier concentration and the effective mobility were calculated from the sheet resistivity and the sheet Hall coefficient, and calculations of the depth distribution of the volume carrier concentration and mobility were also made. 10 references. (UK)

19780 ELECTRICAL PROPERTIES OF ALKALI IMPLANTS IN SILICON. Bilger, H. R.; Nicolet, M. A.; Meyer, O. (Kernforschungszentrum, Karlsruhe, Ger.). pp 70-3 of Ion Implantation. Stevenage, Eng.; Peter Peregrinus Ltd. (1970).

From Conference on Ion Implantation, Reading, England. See CONF-700945.

A brief review is given of previous work on this subject, followed by a description of some studies on Group I element (Na, Rb, Cs) implants in Si that were made with a view to attempting to answer the following: (a) what is the maximum electrical activity (N_s max) in an isochronal annealing process; (b) how does N_S max depend on the implanted dose; (c) is there any correlation with lattice positions and distributions of the implanted impurities observed with backscattering and channeling techniques; (d) is outdiffusion retarded or stopped by depositing SiO_2 layers on the implanted layers during the annealing process? High resistivity p-type Si was used throughout the experiments, and doses employed were 10^{11} to 2×10^{15} ions/cm^2. The ion energy was 40 keV with target at room temperature. Isochronal annealing was performed in a quartz tube with dry Ar atmosphere at 50°C steps. After implantation, van der Pauw patterns were etched into the samples by use of photoresist techniques. Hall-effect and sheet-resistivity measurements were made to determine the effective surface-carrier concentrations and the effective mobility, and channeling and backscattering measurements were made on Rb- and Cs-implanted samples using a 3-MeV accelerator and a beam of 1-MeV $^4He^+$ ions. The samples were mounted on a goniometer and the energy distribution of backscattered particles measured with a surface-barrier detector. It was found that the electrical measurements were difficult to perform. The maximum electrical activity measured was much below 100%, and for Na a saturation level was not reached for the highest dose used. The Rb and Cs data showed only a weak dependence on implanted dose. For doses smaller than 10^{12}/cm^2, 20 to 30% of the implanted ions were electrically active, for doses of the order of 5×10 $^{13}Cs^+$/cm^2 or 10 $^{14}Rb^+$/cm^2 where backscattering and channeling measurements were possible only 1 to 5% were electrically active. The percentage activity could not be increased by coverage with SiO_2 films during annealing, although a retardation of out-diffusion was observed. This may be a reason why any regular lattice position could not be found. 8 references. (UK)

19781 FORMATION OF INSULATING LAYERS BY USE OF REACTIVE ION BEAMS. Freeman, J. H.; Gard, G. A.; Mazey, D. J.; Stephen, J. H.; Whiting, F. B. (Atomic Energy Research Establishment, Harwell, Eng.). pp 74-80 of Ion Implantation. Stevenage, Eng.; Peter Peregrinus Ltd. (1970).

From Conference on Ion Implantation, Reading, England. See CONF-700945.

SiO_2 and SiN layers were prepared by implanting large doses of $^{16}O^+$ or $^{14}N^+$ ions at energies up to 40 keV into polished Si substrates. Both crystalline and amorphous forms of the nitride could be obtained by suitable control of the beam intensity during implantation, and some properties of these layers are described. The Si specimens, both p- and n-type, were implanted at room temperature with doses of about 2×10^{18} ions/cm^2 of $^{16}O^+$ at 15 to 40 keV or 15 to 25 keV for $^{14}N^+$ in the Harwell Mark I electromagnetic isotope separator. Beam currents of ~1 mA/cm^2 were used. The average temperature rise of the specimens did not exceed ~600°C with the O implants, but was ≫600°C with some of the N implants. Two forms of the nitride were produced—an amorphous low-temperature form at a low current density and a high-temperature form at a high current density. The low-temperature form could be converted to the high-temperature form by exposure to a high-intensity beam for a few seconds. An irreversible color change from yellow to blue accompanied the conversion and was apparently due to crystallization of the amorphous layer at high temperatures. A similar color change could be induced in the amorphous material by heating to >1000°C in a vacuum furnace. Details are given of infrared measurements, electron microscope examination, examination of the Si surface for electron-channeling patterns below the insulating layer, optical interference measurements of layer thickness, and electrical measurements (capacitance and dielectric strength). From the data obtained it is concluded that the techniques cannot be regarded as an alternative to the thermal methods of preparation, since considerable damage is produced in the Si, which is not changed by annealing.' 8 references. (UK)

19782 APPLICATIONS TO SEMICONDUCTOR DEVICES. Beale, J. R. A. (Mullard Research Labs., Redhill, Eng.). pp 81-7 of Ion Implantation. Stevenage, Eng.; Peter Peregrinus Ltd. (1970).

From Conference on Ion Implantation, Reading, England. See CONF-700945.

The applications of ion implantation to Si devices were discussed under the following headings: limitations of existing Si devices (high-frequency performance, high-power performance, tolerance, cost); special features of doping by ion implantation compared with other techniques; examples of applications (resistors, diodes, MOS devices, bipolar transistors); future of ion implantation. 6 references. (UK)

19783 THERMAL PROPERTIES OF HIGH-VALUE GALLIUM- AND BORON-IMPLANTED RESISTORS IN SILICON. Oosthoek, D. P.; den Boer, J. A.; Hofker, W. K. (Philips Research Labs., Amsterdam). pp 88-91 of Ion Implantation. Stevenage, Eng.; Peter Peregrinus Ltd. (1970).

From Conference on Ion Implantation, Reading, England. See CONF-700945.

A possible interesting application of ion implantation is stated to be in the fabrication of large resistors in integrated circuits, employing Ga- or B-implanted Si. The temperature coefficient of the sheet resistivity of low-dose Ga- and B-implanted layers was investigated. The Hall voltage was measured, and the charge carrier density and mobility were calculated as a function of temperature. Implantations were made at an energy of 50 keV with a mass separator adapted for the purpose, at room temperature and at 450°C. Annealing was effected in a N_2 atmosphere, using the isochronous method with temperatures up to 800°C. A silicon-oxide layer minimized surface leakage current. The sheet resistivity at room temperature was measured as a function of annealing temperature. The measurements were made for B and Ga implantations at different doses (5×10^{12} to 10^{14}/cm^2 for B, and 2×10^{13} to 10^{15}/cm^2 for Ga). The sheet resistivity was also measured as a function of the ambient temperature. The temperature coefficient was found to be negative for lower annealing temperatures, but became positive after annealing at high temperatures. This means that an annealing temperature could be found at which the temperature coefficient was zero, and the sheet resistivity was then found to be indifferent to the ambient temperature over an extended range. Values of sheet resistance and its temperature coefficient are compared for diffused, thin-film, and implanted resistors. It was concluded that lattice scattering is the dominant scattering mechanism, and also that the low-temperature coefficient of charge-carrier density just balances the negative temperature coefficient of the mobility caused by lattice scattering. 4 references. (UK)

19784 HIGH-ENERGY BORON IMPLANTATION INTO SILICON. Lecrosnier, D. P.; Pelous, G. P. (Centre National d'Etudes des Telecommunications, Lannion, France). pp 102-6 of Ion Implantation. Stevenage, Eng.; Peter Peregrinus Ltd. (1970).

From Conference on Ion Implantation, Reading, England. See CONF-700945.

Almost all previous ion-implantation studies in semiconductors have been carried out using energies <500 keV, with the result that the implanted ion distribution peak is within 1μ of the surface, giving p—n junctions too near the surface for application to some devices. Stopping processes for high-energy ions in the crystal lattice include electronic processes that are often negligible at low energy, and the question arises as to whether the behavior of high-energy implanted ions is in agreement with that of low-energy ions. A study is described of B implantation in Si at the energy range 0.5 to 1.5 MeV. The study included the effect of annealing temperature on sheet resistance, comparisons of electrical profiles with chemical profiles, and the characteristics of implanted junctions on buried layers. The implantations were performed with a mass-analyzed swept beam from a 2-MeV Van de Graaff accelerator operated with BF_3 in a conventional rf ion source; details of the experimental technique adopted are given. The sample temperature was varied from 77 to 1000°K, and the beam current was about 0.3 μA/cm^2. Doses employed were 10^{12} to 10^{15} ions/cm^2. After annealing in dry Ar at 1000°C, p-type buried layers were found in some samples, and a p—n structure in other samples; there were indications that the shallow n-type layer was p-type before annealing, and if it is assumed that the B ions do not move during annealing, some defects produced by implantation must have acted as acceptor centers. The sheet resistance of implanted layers was measured with four probes, giving the average conductivity of the p-type layer on n-type substrate or vice versa. The carrier concentration was also determined as a function of depth, and a plot of ejected ions of given atomic weight against depth was also obtained. Details are given of the annealing procedure, the carrier concentration profiles, and the characteristics of the p–n junctions. The results showed that the electrical properties of the buried layers were very similar to those at lower energies. The high conductivity shown in implanted B layers at 77°K and at high doses after 400°C annealing was considered potentially attractive for device applications, but further studies are indicated. 11 references. (UK)

19785 APPLICATIONS OF ION IMPLANTATION OUTSIDE THE SEMI-CONDUCTOR AREA. Thompson, M. W. (Univ. of Sussex, Brighton, Eng.). pp 109-15 of Ion Implantation. Stevenage, Eng.; Peter Peregrinus Ltd. (1970).

From Conference on Ion Implantation, Reading, England. See CONF-700945.

Ion implantation is not only an important new method for preparing special solid materials, but can also be a very valuable aid to research, and a survey of some possible applications is presented. In other than semiconductor applications more tolerance can be given to impurities in the ion beam and cheaper apparatus could be used. The general features of ion implantation are first summarized, followed by a discussion of probing techniques for ion-implanted surfaces, and property changes induced by ion implantation, including mechanical properties, electrochemical properties, superconductivity, and electrical conductivity. Brief sections are devoted to rare-gas diffusion in solids, and to nuclear solid-state research. 14 references. (UK)

19786 DOPING OF THIN FILMS BY RECOIL-ATOM IMPLANTATION. Stroud, P. T.; Collins, L. E. (Atomic Weapons Research Establishment, Aldermaston, Eng.). pp 116-19 of Ion Implantation. Stevenage, Eng.; Peter Peregrinus Ltd. (1970).

From Conference on Ion Implantation, Reading, England. See CONF-700945.

The processes involved in recoil-atom implantation are depicted. A thin film of the metal required for doping is deposited over the substrate material and bombarded with energetic inert gas ions; atoms displaced from the metal film then recoil into the substrate, where they become trapped. If the projectile range is greater than the film thickness, atoms from the substrate may recoil back into the metal layer. With regard to applications, it has been found that recoil atom-implanted cermets are more reproducible than those produced by conventional co-deposition techniques, but it has not been possible, so far, to relate the projectile dose to the level of implanted metal atoms, although there is indirect evidence for a critical metal concentration of some tens of at. %. Such levels suggest that the number of recoils is of the same order as the projectile dose. Some preliminary experiments designed to check these estimates are described, and the efficiency of recoil-atom implantation was determined absolutely using radioactive tracer and activation analysis techniques to measure the number of recoil-implanted atoms. In the experimental work, the projected ion was always Ar^+ at doses of 0.1 to 5 mCi/cm^2 and ion energy 80 keV. Among matters studied were the backscattering of O from a silica substrate into an Al film by Ar^+ ions, and the recoil implantation of Al atoms into silica and polythene substrates, also using Ar^+ ions. It was found that the density of O atoms backscattered rose sharply to a saturation value of $\sim 3.4 \times 10^{16}$ $atoms/cm^2$ for incident Ar^+ doses in excess of 2×10^{16} $ions/cm^2$. A simple model is proposed for the transfer rate of atoms between film and substrate. Estimates of the order of the forward-scattering cross section were obtained. Results confirmed that the numbers of implanted recoils were of the same order as the projectile flux, agreeing with earlier electrical measurements on cermet structures. A dose of 2.75 mCi/cm^2 Ar^+ implanted 4.5×10^{16} Al atoms, giving a 40% metal content. Reference is made to Nelson's theory of recoil atom implantation (Radiation Effects 2: 47(1969)), which allows at least order-of-magnitude calculations to be made of implantation for low projectile doses. It is concluded that, although recoil atom implantation is inefficient for the deep implantations required in semiconductor technology, it is quite efficient for doping thin-film structures. It could also have advantages over direct implantation when studying the effects of impurities difficult to ionize. 6 references. (UK)

19787 ION-BEAM IRRADIATION OF GLASSES. Bayly, A. R.; Townsend, P. D. (Univ. of Sussex, Brighton, Eng.). pp 120-2 of Ion Implantation. Stevenage, Eng.; Peter Peregrinus Ltd. (1970).

From Conference on Ion Implantation, Reading, England. See CONF-700945.

Some studies are described on changes in surface features of glass due to ion irradiation. Irradiation produces a physical reshaping of the surface due to sputtering away of material, and this can be controlled to etch or figure the glass. Another effect is to alter the refractive index of the surface layers, and both of these effects were studied. Irradiation was with a 20-keV Ar beam to a dose of $10^{18}/cm^2$. It was found that, after prolonged irradiation, a smooth plane normal to the direction of the incident beam developed, and that an initially plane surface was not degraded by the irradiation. It was also found that, whereas ion-beam irradiation of conventionally polished and etched glass initially emphasizes the cracks produced in this processing, prolonged ion-beam irradiation removes stressed regions and surface scratches. An application discussed is the preparation of optical waveguides for communications signals using flexible glass fibers. Such a waveguide requires that the light be totally internally reflected without loss by scattering at surface cracks, etc. Normal cladding techniques involve an abrupt junction at the reflecting boundary, with scattering losses due to the imperfect interface. It is suggested that the "cladding" might be formed within the fiber by changing the refractive index by ion implantation. As part of the studies the profile of the refractive index change across the boundary region was determined; ions were implanted into silica and the refractive index and apparent layer thickness were determined by ellipsometry. It was found that increasing the dose produced a higher refractive index, independently of the ion species. 5 references. (UK)

19788 EFFECT OF ION IMPLANTATION ON ELECTRICAL PROPERTIES OF SiO_2 FILMS AT HIGH FIELDS. Fritzsche, C. R.; Axmann, A.; Seelewind, H. (Insitut fuer Angewandte Festkoerperphysik, Freiburg, i. B.). pp 123-6 of Ion Implantation. Stevenage, Eng.; Peter Peregrinus Ltd. (1970).

From Conference on Ion Implantation, Reading, England. See CONF-700945.

It has been shown that dielectric breakdown and anodic growth of SiO_2 are closely related, and impact ionization is an essential process in both effects. Studies are described on the influence of P- and N-ion implantation on these effects. Changes in the infrared absorption caused by implantation are also reported, showing that the behavior of thermally grown oxides with regard to structural changes and their influence on electrical properties is not completely comparable with that of anodic oxides. Implantations were made at room temperature and samples were half covered with an impermeable metal sheet during implantation so that comparison of implanted and unimplanted material was possible. Increased dielectric strength of thermally grown oxides was observed after implantation, and it is considered that this property could be still further improved by optimizing implantation dose and energy so that radiation damage is more uniformly distributed. The reason for the increase may be that the displaced Si or O ions increase the number of electron impacts so that the probability of reaching the ionization energy increases. This displacement also appears to facilitate the stretching oscillation of the neighboring Si–O bond, thus lowering the absorption frequency. The ir results indicate, however, that implantation in anodic oxides does not cause disorder in the same sense as in thermally grown oxides. 5 references. (UK)

19789 IMPLANTATION OF COMPOUND SEMICONDUCTORS. Allen, R. M. (Services Electronics Research Lab., Baldock, Eng.). pp 127-34 of Ion Implantation. Stevenage, Eng.; Peter Peregrinus Ltd. (1970).

From Conference on Ion Implantation, Reading, England. See CONF-700945.

Compound semiconductors offer a wide choice of band gap and make good luminescent materials. The choice of band gap makes the materials useful for radiation detectors and emitters. A further advantage is that the electron mobility is often much higher in these materials compared with Si. Preparation of the materials in the form of pure single crystals is, however, in general very difficult, although specimens of reasonable size can usually be obtained; the III–V semiconductors are the easiest to grow. The crucial difference between III–V and II–VI semiconductors is in the nature of their atomic bonding; whereas the former are predominantly covalent, most II–VI compounds are mainly ionic and since semiconducting properties are dependent on covalent bonding this severely limits the potential of implantation in II–VI compounds. The role of defects in compound semiconductors is discussed, and implantation problems are outlined, particularly those arising from the annealing stage. The choice of dopants for compound semiconductors is very wide. For example, a III–V compound should be made p-type by replacement of some of its group III atoms by any of the II A atoms, or by replacement of some group V atoms by IV A atoms, and n-type activity would involve replacement of group III atoms by IV A atoms or V atoms by VI A atoms. Choice of implantation temperature is discussed in detail. Electronic processes are discussed in connection with luminescence, and details are given on the implantation of luminescent centers in GaP and ZnTe. The electrical activity of radiation damage centers in GaAs, ZnTe, and InSb is also discussed. Among other materials discussed for doping are GaAs, InAs, InSb, CdS, CdTe, ZnTe, and SiC, and a summary is given of studies on these. 47 references. (UK)

19790 CATHODOLUMINESCENCE OF ION-IMPLANTED SILICON CARBIDE. Brander, R. W.; Callaghan, M. P.; Todkill, A. (GEC Ltd., Wembley, Eng.). pp 135-7 of Ion Implantation. Stevenage, Eng.; Peter Peregrinus Ltd. (1970).

From Conference on Ion Implantation, Reading, England. See CONF-700945.

The effect of ion implantation and the subsequent annealing schedule on the cathodoluminescence of SiC crystals was studied, using Kr, He, and Ge ions. The ions were implanted into epitaxial layers grown on single-crystal SiC substrates. The dose employed was 10^{14} ions/cm^2 at energies of 160 to 300 keV. Some observations are first presented on light transmission and color. Annealing was carried out at various temperatures up to 1400°C and the cathodoluminescence was measured after each annealing stage. The conductivity type and resistivity were controlled by adding N or B as dopants in the gas stream and in the preparation of the epitaxial layers. For undoped crystals, before annealing, the cathodoluminescence from the implanted region was considerably weaker than the background yellow or green luminescence of the unimplanted area. As the annealing temperature was increased, the implanted region began to show a green cathodoluminescence that increased in intensity with increasing temperature, until after an 800°C anneal this luminescence was considerably brighter than the residual luminescence. The luminescence persisted with further annealing up to 1400°C, but began to decrease at that temperature. The peak positions of the luminescence were independent of implanted ion species. The green luminescence could not be detected in crystals that exhibited strong yellow cathodoluminescence before implantation, but after annealing at 800°C yellow luminescence was observed from an implanted region. As the annealing temperature was increased, the intensity of this luminescence increased, but did not reach its original intensity until after 1400°C annealing. P-type material showed no significant change in the weak luminescence shown before implantation. No evidence of any polytype change was obtained. The main features of the green luminescence spectrum are discussed, in relation to luminescence centers. 6 references. (UK)

19791 DAMAGE STUDIES IN ION-IMPLANTED CdS. Armitage, S. A. (Oxford Univ.). pp 138-42 of Ion Implantation. Stevenage, Eng.; Peter Peregrinus Ltd. (1970).

From Conference on Ion Implantation, Reading, England. See CONF-700945.

The conversion of n-type CdS to p-type is an important step in the fabrication of CdS-based devices. Diffusion doping has not so far been successful in accomplishing the conversion, but non-equilibrium processes such as ion implantation may hold promise of achieving this. Damage to the lattice by heavy-ion bombardment must be taken into account, however, since this may result in defects which could nullify the desired doping, and suitable heat treatment is important. The problem of deciding when the best heat treatment has been applied can be tackled from a number of considerations, each concerned with a particular change caused by the annealing. It is not considered sufficient to rely on purely electrical diagnostic techniques. A more direct way of investigation of the state of the crystal is by the direct interaction of ^{4}He ions in the lattice, although restoration of the lattice to its original state may not produce the desired conductivity. An account is given of results obtained from the method of wide-angle ^{4}He-ion scattering employed at the Chalk River Laboratories, Canada. Backscattering spectra were obtained, for the same incident dose (1 to 5 microcoulombs), with the crystal oriented in a random direction to the He beam and then in a channeling direction, using an electronically controlled goniometer. Spectra are shown for an unimplanted sample, for a S implant of 10^{14} ions/cm^2 at 200 keV, and for a Ne implant of 10^{15} ions/cm^2 at 200 keV. Bismuth-implanted samples (10^{14} ions/cm^2 at 200 keV and also 10^{13} ions/cm^2) were also examined; also P implants of 10^{14} ions/cm^2 at 200 keV. Electrical measurements (resistivity and thermoelectric emf), are also described: Annealing in a S atmosphere appeared to make no significant difference to the amount of S lost from the lattice in the region of 500°C. At 200 keV, implantation damage occurred well below the surface and penetrated to many thousands of Å. No well-defined damage layer, as in the case of random implants into Si, were evident. At the ion doses used, a considerable reduction in lattice disorder was achieved by vacuum annealing at ~600°C. 5 references. (UK)

19792 RADIATION-DAMAGE STUDIES OF BISMUTH-ION-IMPLANTED CdS. Eldridge, G.; Govind, P. K.; Nieman, D. A.; Chernow, F. (Univ. of Colorado, Boulder). pp 143-7 of Ion Implantation. Stevenage, Eng.; Peter Peregrinus Ltd. (1970).

From Conference on Ion Implantation, Reading, England. See CONF-700945.

P-type CdS can be produced by ion implantation; in particular, 25-keV Bi implants at room temperature, using doses of 3×10^{15} to 5×10^{16} ions/cm^2, have been shown to produce high-conductivity p-layers and p-n junctions that emit green light at room temperature. These results were obtained without annealing. A comparison of 50- to 200-keV Bi and 30-keV Xe implants at the 10^{15}/cm^2 level appeared to indicate that radiation-damage effects dominated any chemical effects. Reflection electron diffraction, ion penetration profile, and sheet resistivity measurements are described on CdS crystals implanted with various doses of 25-keV Bi ions at room temperature. All measurements were made on high-resistivity CdS platelets. It appeared than an "amorphous" layer is not formed on the crystal surface following bombardment at room temperature in the dose range 1×10^{15} to 2×10^{16} ions/cm^2 and reflection electron diffraction revealed no observable change in the surface structure of the CdS lattice. It is suggested that high sputtering efficiency tends to inhibit formation of an amorphous layer: it was also considered unlikely that a buried amorphous layer was produced. Range studies showed that Bi-ion penetrations occur in CdS to a depth of 3000 Å. On the basis of a simple model, it was found that with high implantation doses (~10^{16} ions/cm^2) significant doping concentrations can be obtained. Although some channeling may have occurred, the findings were more in favor of a diffusion mechanism. Attempts are being made to ascertain whether the implanted Bi attains its depth through kinematic processes or by diffusion effects. It was also found that ion implantation induces electrical activity to depths greater than 1000 Å. Some studies are also reported on CdS (Bi) diodes. 15 references. (UK)

19793 RADIATION DAMAGE IN II–VI SEMICONDUCTORS. Olley, J. A.; Williams, P. M.; Yoffe, A. D. (Cavendish Lab., Cambridge, Eng.). pp 148-52 of Ion Implantation. Stevenage, Eng.; Peter Peregrinus Ltd. (1970).

From Conference on Ion Implantation, Reading, England. See CONF-700945.

Owing to difficulties encountered in doping II–VI semiconductors, because of autocompensation, the possibility of using ion implantation for type conversion was investigated. The damage produced during implantation, and its subsequent annealing, were studied by means of transmission electron microscopy and optical absorption. Since the luminescent properties of these materials are of great interest, the effects of bombardment and annealing on the exciton structure were also investigated. The specimens employed were thin high-resistivity single-crystal platelets of wurtzite structure. Platelets of ZnS, ZnSe, and CdS were irradiated at room temperature with 5×10^{11} ions/cm^2/sec, and were purposely misaligned to minimize channeling along the large $[11\bar{2}0]$ channel. The crystals were subsequently vacuum annealed at up to 500°C, and were examined at various annealing stages. Some samples were implanted at liquid N_2 temperature. It was considered that, of the materials considered, CdS appeared the most promising since the damage could be annealed out more easily than with ZnS and ZnSe, and no phase change occurs at the optimum annealing temperature of 400°C. The optical properties of CdS can also be successfully recovered after implantation. (UK)

19794 PROPERTIES OF ION-IMPLANTED ZnTe. Marine, J. (LETI-CENG, Grenoble, France). pp 153-7 of Ion Implantation. Stevenage, Eng.; Peter Peregrinus Ltd. (1970).

From Conference on Ion Implantation, Reading, England. See CONF-700945.

Ion implantation is a possible chemical doping process for compound semiconductors. The problem with such materials, and particularly with the II–VI family, is that they are always p- or n-type but never both (except for CdTe). As they are wide-bandgap materials, the injection of carriers by means of p-n junctions will lead to materials showing electroluminescence in the visible spectrum. ZnTe was chosen for the study described since it has a bandgap of 2.26 eV at room temperature, and the metallurgy of its growth is well known, as well as the effect of bulk impurities and defects. Experimental evidence is presented showing that type conversion and pn junction formation in this material can be achieved by Cl-ion implantation and appropriate annealing to remove bombardment damage and put the implanted ions in an electrically active site. ZnTe is always grown p-type, owing to Zn vacancies. As the ion implanted profile is Gaussian in form, in

XUM

order to obtain constant doping on a large thickness, multiple implantations were carried out with different doses and energies. Two series of samples were implanted, the first with Cl ions and the second with Ar ions, in order to determine the effect of bombardment damage and whether the observed conductivity was due to the bombardment or to chemical doping. Implantation was at room temperature and the current density was 2 $\mu A/cm^2$. No type conversion was found before annealing. Annealing was carried out at 500 to 520°C, and this was sufficient to remove the lattice damage and to cause the Cl ions to substitute the Te atoms, thus forming donor centers. Doses ranged from 10^{14} to $10^{15}/cm^2$ at energies of 30 to 120 keV. Details are given of hot-probe measurements, showing that before annealing the implanted layers were always p-type, whereas after annealing the Ar bombarded samples remained p-type and the Cl bombarded were converted to n-type. Photoluminescence spectra were obtained for the Cl-implanted samples, and a new characteristic radiation was observed at 2.206 eV. Electrical characteristics were also determined, including those of diodes, in which MIS (metal-insulator-semiconductor) structures occurred. Electroluminescence was observed from the Cl-formed p-n junctions when biased in the forward direction and the MIS structure also showed electroluminescence when biased in reverse. 8 references. (UK)

19795 CATHODOLUMINESCENCE STUDIES OF TRANSITION-METAL ION-IMPLANTED II–VI COMPOUNDS. Cox, A. F. J. (Signals R and D Establishment, Christchurch, Eng.). pp 158-61 of Ion Implantation. Stevenage, Eng.; Peter Peregrinus Ltd. (1970).

From Conference on Ion Implantation, Reading, England. See CONF-700945.

Implanted epitaxial thin films of ZnS films were studied by examining the luminescence emission spectra under low-energy electron beam excitation. A preliminary survey showed that a classical phosphor activator, such as Ag, did not result in any detectable emission, whereas activators like Mn produced very efficient emission. The ZnS studies were made on epitaxial single-crystal films, which were grown on a Si substrate, and samples were examined for luminescence between 300 and 10°K, using 5- to 10-keV electron-beam excitation at current densities of 10 to 50 $\mu A/cm^2$. A one-meter grating spectrometer was used to study the fine structure of the emission. The Cockcroft–Walton accelerator at Harwell was used for 250-kV ion implantation of the specimens at 300 and 550°K, typical doses of 10^{14} to 10^{15} ions/cm^2 being employed. The ZnS films showed no detectable cathodoluminescence before implantation, but broad-band yellow emission was observed after Mn implantation, with a maximum at 586 nm. The power efficiency for conversion of incident electron energy into optical energy was 0.9%, for an implantation dose of 10^{14} ions/cm^2. A similar but weaker emission band was observed for ZnSe, but the band could not be produced in CdS. Experiments with Tb and Er implantation showed that rare-earth ions could also form luminescence centers on implantation. Indications were obtained that channeling processes are necessary for incorporation of the implanted ion as a luminescence center. Data were obtained on the Stark splitting of the emission lines; ZnS showed somewhat larger splitting than ZnSe. 8 references. (UK)

19796 ION PENETRATION. Dearnaley, G. (Atomic Energy Research Establishment, Harwell, Eng.). pp 162-71 of Ion Implantation. Stevenage, Eng.; Peter Peregrinus Ltd. (1970).

From Conference on Ion Implantation, Reading, England. See CONF-700945.

For almost all applications of ion implantation it is necessary to know the range and depth distribution of ions embedded in the specimen. In semiconductors this determined such parameters as junction depth and also the base width of transistors and the voltage dependence of diode capacitance. The depth distribution also determines the peak impurity concentration and the likelihood of precipitation and degree of lattice strain. In photodiodes and nuclear-particle detectors, the thickness of insensitive heavily doped surface material is important. In most cases a film of oxide, or metal plus oxide, is used as a mask during implantation, and it is necessary to know the maximum range of ions in such material. In other applications of ion implantation the physical properties of the implanted surface, e.g., refractive index, hardness, etc., are likely to be governed by the concentration of impurities introduced, and this depends on the range distribution. It is desirable to be able to calculate range distribution following ion implantation into any given solid at a given temperature, but during measurements of ion ranges it became evident that unforeseen effects took place with single-crystal specimens, including anomalous diffusion processes. The slowing down of the implanted ion may occupy only 10^{-12} sec, but the final distribution of impurities may be modified by much slower diffusion processes, dependent on temperature. It is difficult, though not impossible, to distinguish between these processes experimentally and an attempt is described to examine them, with particular reference to Si. Among matters discussed are energy loss, the behavior of ions in crystalline solids, and variation with ion species and absorber. More information is needed regarding dechanneling mechanisms, anomalous diffusion, the influence of lattice strain on channeled range distributions, and the Z_2 dependence of channeled-energy loss. 26 references. (UK)

19797 LOCATION OF IMPLANTED ATOMS WITHIN THE UNIT CELL OF A CRYSTAL. Davies, J. A. (Univ. of Aarhus, Denmark). pp 172-80 of Ion Implantation. Stevenage, Eng.; Peter Peregrinus Ltd. (1970).

From Conference on Ion Implantation, Reading, England. See CONF-700945.

A discussion is presented on the lattice location of implanted ions, and it is pointed out that the "channeling effect technique" offers a fairly simple experimental method for determining the site of a foreign atom in a crystal. The basic principles of this technique are described and illustrations given on its application to determination of the distribution of various implanted foreign atoms between substitutional and specific interstitial sites in the lattice. Information is summarized on lattice location of various implanted ions in Si and Ge. The technique also provides information on the amount of lattice disorder accompanying implantation. 26 references. (UK)

19798 LATTICE-SITE LOCATION MEASUREMENTS AND THEIR INTERPRETATION. Alexander, R. B. (Clarendon Lab., Oxford). pp 181-6 of Ion Implantation. Stevenage, Eng.; Peter Peregrinus Ltd. (1970).

From Conference on Ion Implantation, Reading, England. See CONF-700945.

Reference was made to the ion-channeling technique for locating implanted foreign atoms in crystal lattices, in which two assumptions are generally made in the interpretation of experimental work. If the foreign atoms are substitutional, the attenuation in interaction yield when the incident beam is channeled is assumed to be the same for both foreign and lattice atoms; on the other hand, if the foreign atoms are interstitial along a particular channeling direction, the channeled beam is assumed to interact "normally" with the foreign atoms and the yield to be the same as that for a nonchanneled beam. This is equivalent to the assumption that the flux of channeled ions, in a plane normal to the channel, is constant across the channel and equal to the flux of a random beam. The validity of these assumptions was examined experimentally and by computer calculation. The first assumption was investigated using a crystal containing foreign atoms wholly on substitutional sites. He ions (1.2 MeV) were backscattered from a Cu–Au crystal in which the Au atoms (~2 at. %) occupies substitutional sites at random in the Cu lattice. With the beam incident to within 0.05° of a ⟨110⟩ axis, the same attenuation in yield was observed for both Au and Cu atoms, thus verifying the assumption. The second assumption is to be investigated with a Ti–O crystal in which the O atoms occupy interstitial sites along the c-axis. A description is given of the computer simulation model. The computer technique has the advantage of being able to study the behavior of F_{max} near the surface, where a considerable depth oscillation can be encountered. Among matters discussed are flux peaking, thermal vibrations, electronic multiple scattering, depth dependence of flux profile, beam collimation, crystal alignment, lattice disorder and oxide films, and beam energy. Among conclusions reached is that yield enhancement from interstitial atoms means that the interpretation of atom location experiments is much less simple than previously thought. On the other hand, if the foreign atoms occupy nonsubstitutional sites either near the center of a channel (corresponding to F_{max}) or near lattice sites, it is possible to locate them fairly accurately. 9 references. (UK)

19799 ELECTRICAL AND ATOM-SITE LOCATION PROPERTIES OF ION-IMPLANTED GERMANIUM. Tinsley, A. W. (Univ. of Surrey, Eng.); Jones, K. C.; Stevens, P. R. C.; George, G. G.; Gunnersen, E. M. pp 187-91 of Ion Implantation. Stevenage, Eng.; Peter Peregrinus Ltd. (1970).

From Conference on Ion Implantation, Reading, England. See CONF-700945.

Room temperature implants of heavy Group III and V ions in Ge were studied including their annealing behavior, using Rutherford backscattering techniques and electrical measurements, where possible, on the same sample. The Rutherford scattering technique was found useful not only for studying the atomic behavior of dopant atoms, but also in the study of radiation damage defects introduced during implantation. The backscatter and electrical measurements examine different, but not necessarily unrelated, properties of the material, and their correlation was examined. Implantations were carried out using the Aldermaston

XUM

isotope separator at energies of 40 and 70 keV, with dose rates of 10^{11} to 10^{13} ions/cm^2/sec. Total doses ranged from 10^{11} to 10^{16} ions/cm^2, and the ions studied were In, Tl, Sb, and Bi. In the Rutherford scattering experiments, analysis of the implanted samples was carried out using a He beam from a 3-MeV Van de Graaff, and details are given of lattice disorder and atom site location measurements. Annealing studies are also described. Reasonable agreement was found between the backscatter results and the electrical measurements. It appeared that the Group III and V dopants become electrically active in the substitutional lattice position and the percentage of implanted ions becoming substitutional appeared to be 70 to 80% after a suitable anneal. Interstitial diffusion of impurities is also discussed. Tl showed rapid substitutional behavior compared with the other ions, which need a higher annealing temperature, and from the high-temperature annealing measurements it would seem that Tl shows a higher solubility in Ge. 12 references. (UK)

19800 NEW METHOD FOR FAST MEASUREMENT OF ION-IMPLANTATION PROFILES. Cahen, O.; Netange, B. (Thomson CSF, Corbeville, France). pp 192 of Ion Implantation. Stevenage, Eng.; Peter Peregrinus Ltd. (1970).

From Conference on Ion Implantation, Reading, England. See CONF-700945.

A method used to measure the profile of the concentration and the mobility of electrically active centers in a thin layer of ion-implanted Si semiconductor is described. The method involved gradual stripping of the layer and at each stripping step measuring the electrical resistance and the Hall voltage. Stripping was carried out by sputtering with a low-energy ion beam, and the sputtering was accomplished without removing the sample from the Hall measurement system. The process is very fast, can be easily automated, and can be used for any semiconductor. A standard commercially available ion gun was used in the sputtering system, which gave a 1 mA/cm^2 1-keV neutralized Ar-ion beam with 2% uniformity over 5 cm diameter and a sputtering rate of 300 Å/min for Si, without excessive heating. At each stripping step measurements were made of the current in the sample, the voltage due to sheet resistance, and the voltage due to the Hall effect. The data were computer processed to give concentration and mobility profiles. (UK)

19801 DISTRIBUTION OF ^{32}P CHANNELED INTO INDIUM ANTIMONIDE. Wilkins, M. A.; Dearnaley, G. (Atomic Energy Research Establishment, Harwell, Eng.). pp 193-7 of Ion Implantation. Stevenage, Eng.; Peter Peregrinus Ltd. (1970).

From Conference on Ion Implantation, Reading, England. See CONF-700945.

Implants in InSb were performed on the Harwell Mark I Electromagnetic Separator, using ^{32}P, and an anodic stripping technique was employed, using a current density of ~1 mA/cm^2. Activity was measured by counting the implanted specimen after removal of each layer and determining differences. All the results were differentiated to give the concentration rather than the fraction of remaining activity as a function of depth. Low dose profiles are shown for 2×10^{12} and 5×10^{12} ions/cm^2 at 40 keV and room temperature; these show little difference in channeled profile, but there was a high degree of channeling. The effect of increasing the dose to 10^{15} ions/cm^2 is also shown. At doses of 10^{14} to 10^{15} ions/cm^2, specimens began to show visible radiation damage, including a "milkiness" similar to that in Si. A diffusion mechanism may also occur. Profiles for higher energies of 100 and 120 keV show that there is still a high degree of channeling. A direct comparison is shown for P profiles implanted under similar conditions into InSb and Si, and it is evident that P is much more penetrating in the former than in the latter, an unexpected result, reasons for which are discussed from the point of view of electronic stopping-power cross sections. A direct comparison is also shown between P implanted into InSb and Cu implanted into Si. Further work is indicated. (UK)

19802 GALLIUM IMPLANTATIONS IN SILICON STUDIED BY PROTON BACKSCATTERING, X-RAY EMISSION, AND HALL EFFECT. Van der Weg, W. F. (Philips Research Labs., Amsterdam); den Boer, J. A.; Satis, F. W.; Onderdelinden, D. pp 198-202 of Ion Implantation. Stevenage, Eng.; Peter Peregrinus Ltd. (1970).

From Conference on Ion Implantation, Reading, England. See CONF-700945.

A method of studying implanted semiconductor samples by the channeling technique, using proton backscattering, in conjunction with soft x-ray emission excited by 140-keV protons, is described. This was applied to Si implanted with 10^{15}/cm^2 Ga ions. Radiation damage was indicated by the energy spectrum of the backscattered protons, but protons scattered from the introduced dopants could not be resolved from the background spectrum; hence the proton-induced characteristic x-ray emission was employed to study the lattice location of the implanted Ga ions. Data for the radiation damage and lattice location of the implanted Ga atoms, as a function of post-impact annealing temperature, are compared with data on surface carrier concentration; for this purpose Hall effect and sheet resistivity measurements were made. Implantations were carried out in a 100-keV mass separator, using 50-keV Ga ions to a total dose of 10^{15}/cm^2, with a current of 0.5 μA and substrate temperatures of 20, 350, and 450°C. The proton beam consisted of 140-keV protons, supplied by an ion accelerator, with a typical current density of 50 nA/mm^2. The target was a P-doped silicon single crystal. Backscattered protons were detected by a Si surface barrier detector, and characteristic x rays were measured with a side-window proportional counter, operated in flow mode using an Ar–methane mixture. The intensity of the Si radiation was much stronger than the radiation from Ga, and hence a 6-μ Al foil was placed between target and counter. The signals of the proton and x-ray detector were fed into a 400-channel pulse-height analyzer. A clover leaf-shaped pattern of diffused contacts was employed in measurements of Hall effect and sheet resistivity. The data indicated that conduction could not have been caused solely by Ga acceptors and the conduction mechanism required further elucidation. It was concluded that the x-ray excitation technique can be applied successfully to locate foreign atoms in a lattice. More measurements on samples implanted at different doses, and at a larger variety of implantation temperatures, are desirable. 7 references. (UK)

19803 MEASUREMENT OF IMPLANTED-BORON CONCENTRATION PROFILES IN SILICON BY THE USE OF HEAVY-ION X-RAY EXCITATION. Cairns, J. A.; Holloway, D. F.; Nelson, R. S. (Atomic Energy Research Establishment, Harwell, Eng.). pp 203-6 of Ion Implantation. Stevenage, Eng.; Peter Peregrinus Ltd. (1970).

From Conference on Ion Implantation, Reading, England. See CONF-700945.

Heavy-ion x-ray production possesses the ability to detect the presence of small amounts of an impurity element as a function of depth below the surface of a solid. The basic principles of the method are described. It is possible to excite the characteristic x rays of low-concentration implanted atoms, and to differentiate from those of the host lattice, by choosing an optimum energy for the projectile ions. Difficulties arise, however, in attempting to apply the technique to determining the concentration distribution of implanted B in Si, particularly due to the excitation of complicating x rays including those from the O atoms, which are always present as oxide on the Si surface. For this reason it is virtually impossible to excite boron K x rays in a totally selective manner. It was found, however, that whenever the projectile ion itself exhibited an x ray similar in energy to that from the target atoms then the composite x-ray yield increased very rapidly with increase in projectile energy. The significance of this is that if a Si specimen containing B at a concentration of 10% is bombarded with 100-keV Ar$^+$ ions, it should give a yield of low-energy x rays that is 80% higher than that from pure silicon, assuming that the work is conducted in a nondispersive manner. With present sensitivities the use of a rather heavily doped Si specimen is necessary. The technique of employing a projectile with similar x-ray energy to that of the target has the advantage of yielding a high x-ray cross section, allowing the bombarding dose to be kept low, and avoiding losses by sputtering. A further advantage in using heavy ions in range distribution studies is that the x rays are generated from within a shallow depth below the surface of the specimen; thus 100-keV Ar$^+$ ion bombardment of a B-doped Si specimen produces boron K x rays arising predominantly from not more than 350 Å below the specimen surface. This takes into account the considerable reduction in x-ray yield due to absorption of the ultra-soft boron K x rays within the Si substrate. This is important since it determines the thickness of Si to be removed between B measurements. In the studies described, the B-implanted samples were subjected to a 100-keV Ar$^+$ ion dose of 0.1 μCi and the resultant x ray yield recorded, and compared with the corresponding argon L x ray yield arising from an identical bombardment of a pure Si standard. The implanted specimens, and the standard, were then subjected to an anodic oxidation and stripping procedure, and the x-ray measurements repeated. The x rays were measured with a variable-geometry proportional counter, using a He–isobutane gas mixture. The procedure was used to measure the B concentration distributions of Si specimens implanted with B at 40, 100, and 300 keV to a dose of 1×10^{17} ions/cm^2. The profiles obtained were in good agreement with theoretical predictions. 6 references. (UK)

19804 COMPUTER-SIMULATED FLUX MEASUREMENTS FOR IONS CHANNELED IN DIAMOND STRUCTURE LATTICES. Massa, I. G. (Univ., Bologna). pp 207-11 of Ion Implantation. Stevenage, Eng.; Peter Peregrinus Ltd. (1970).

From Conference on Ion Implantation, Reading, England. See CONF-700945.

The problem of interpreting the results of ion-channeling experiments for determining the positions of foreign atoms in single-crystal lattices is not as simple as was thought, and the effect of "flux peaking" down a channel is much larger than anticipated. A computer program designed to follow the trajectories of fast ions in crystals was employed to investigate flux peaking. The study was confined to the diamond-type structure. Data are given for a Ge lattice, for several axial positions, for different incident proton energies and various angular resolutions of the incident beam. The effects of electron dispersion are included in the calculations. Some results are also given for Si as host lattice, for purposes of comparison. In addition results are given using ^{4}He as the probing ion. The computer model and program are essentially based on an extension of Feldman's single-string crystal model to many strings. Interaction between the ion and the atom is treated as a binary collision, and scattering of the ion is treated classically using the Moliere approximation to the Thomas–Fermi potential and the impulse approximation in the small-angle limit. The thermal oscillations of the atoms are treated using a Debye model. The standard for comparison was the case of 4-MeV protons channeled in Ge, and factors influencing the shape of the flux distribution which were investigated included the electron dispersion effect, beam energy dependence, beam angular collimation dependence, and Z_1 and Z_2 dependence. The computer simulations indicated that the magnitude and shape of the flux distributions of channeled ions in a crystal lattice depend primarily on the dimensions of the channeling axis, that is, on the continuum potential experienced by the ion. Variations in this basic shape are then dependent on the transverse energy of the ion as it moves down the axis, this being a function of the type of incident ion, type of crystal lattice, beam energy, beam collimation, electron dispersion, etc. 11 references. (UK)

19805 RADIATION DAMAGE IN SILICON DURING ION IMPLANTATION. Nelson, R. S. (Atomic Energy Research Establishment, Harwell, Eng.). pp 212-18 of Ion Implantation. Stevenage, Eng.; Peter Peregrinus Ltd. (1970).

From Conference on Ion Implantation, Reading, England. See CONF-700945.

A review is given of present knowledge of the radiation damage produced in semiconductor materials as a result of ion implantation, with particular reference to the nature of the damage, thermal annealing, and the influence of damage on electrical properties. As the most commonly studied semiconductor materials behave qualitatively in a similar way, the discussion was confined to damage in Si. With regard to the nature of the damage, the effects of heavy and light ions are considered separately. Processes considered under the heading of annealing include recrystallization of the amorphous phase and the growth and annealing of dislocation structures. Electrical properties are discussed in relation to defect structure, recombination centers, dislocations, microtwins, stacking faults, crystallinity, etc. 25 references. (UK)

19806 DISORDER PRODUCED DURING ^{11}B AND ^{12}C IMPLANTATION IN SILICON. Eisen, F. M.; Welsh, B. (North American Rockwell Science Center, Thousand Oaks, Calif.). pp 227-30 of Ion Implantation. Stevenage, Eng.; Peter Peregrinus Ltd. (1970).

From Conference on Ion Implantation, Reading, England. See CONF-700945.

In previous work it was found that in room-temperature implantations of ^{11}B in Si, carried out at a fixed flux, the disorder produced was initially proportional to the square root of the flux, but a transition to a linear dependence occurred at a flux which was a function of the flux used in the implantation. The value of the flux at which the transition occurred decreased as the flux used in implantation was increased. This dependence of disorder on flux was somewhat similar to that previously observed for the damage produced by 42-keV Hg-ion bombardment of Si heavily doped with B, suggesting that perhaps the buildup of B during the ^{11}B implantation affected the dependence of the disorder on the ^{11}B flux. Several experiments designed to explore this possibility are described: (i) measurements of the disorder produced in Si by the implantation of ^{12}C at room temperature at several different fluxes; (ii) intercomparison of the disorder produced by ^{12}C, ^{11}B, and ^{10}B at a current density of 2 μA/cm^2; and (iii) study of the effects of high initial B concentrations in the Si samples on the disorder produced by 200-keV ^{11}B ions and by 60- and 600-keV Kr ions. The disorder measurements were carried out using the channeling–backscattering technique with a 450-keV proton beam, and the disorder scale was established by relating the normalized scattering yield behind the disorder peak to the density of scattering centers required to produce this yield. Amongst the conclusions reached are: (i) in C and B implantations the main influence of variation in flux or projectile ion is a corresponding variation in the flux at which the transition from a square-root to a linear dependence of disorder on flux occurs; (ii) the differences observed in disorder production by ^{12}C, ^{11}B, and ^{10}B are associated principally with the difference in mass and atomic number of the implanted ion and not with differences in their chemical nature; (iii) the introduction of B into Si by diffusion has a relatively small effect on the amount of disorder produced. 5 references. (UK)

19807 VOID FORMATION DURING HIGH-DOSE ION IMPLANTATION AT ELEVATED TEMPERATURES. Hudson, J. A.; Mazey, D. J.; Nelson, R. S. (Atomic Energy Research Establishment, Harwell, Eng.). pp 231-4 of Ion Implantation. Stevenage, Eng.; Peter Peregrinus Ltd. (1970).

From Conference on Ion Implantation, Reading, England. See CONF-700945.

The experimental conditions necessary for the production of voids during ion implantation are outlined, and current theoretical models are discussed. Void formation in Ni during bombardment with 100-keV C$^+$ and Ni$^+$ ions in the temperature range 300 to 650°C is taken as an example. Irradiations were performed in a 150-keV heavy-ion accelerator, at a dose rate of 10^{14} to 10^{15} ions/cm^2/sec and to total doses of 10^{16} to 10^{18} ions/cm^2 and the irradiated foils examined in an electron microscope. The temperature range over which void formation occurred in Ni was 240 to 650°C, the accompanying swelling rising rather quickly up to 350°C, then remaining fairly constant up to 550°C, and finally falling sharply above 600°C. Although swelling is manifested as voids, it is caused by the equivalent interstitial content within the metal. This is produced by extra surface layers that have grown as a consequence of interstitials migrating to the surface, or by radiation induced dislocation loops and lines within the damaged region. Another general feature of void formation was the denudation of voids in the vicinity of grain boundaries. By adding small concentrations of He it was possible to greatly increase void nucleation density. The variation of swelling with temperature is discussed; also denudation in the vicinity of grain boundaries. Similar denudations are found at free surfaces. The significance of void formation during ion implantation lies in the catastrophic effect on the final properties. 7 references. (UK)

19808 TRANSMISSION ELECTRON MICROSCOPE STUDIES OF RADIATION DAMAGE IN SILICON. Davidson, S. M. (Oxford Univ.). pp 238-41 of Ion Implantation. Stevenage, Eng.; Peter Peregrinus Ltd. (1970).

From Conference on Ion Implantation, Reading, England. See CONF-700945.

The many different types of defects observed in ion-implanted Si are discussed, and a technique developed by Ray et al. (Phil. Mag., 20: 1265(1969)) is described, which was used to obtain more information about some of these defects. Silicon slices, of n- and p-type, were irradiated with B$^+$, Al$^+$, N$^+$, P$^+$, Sb$^+$, Ne$^+$, and Si$^+$ ions, using either the Harwell Heavy-Ion Accelerator or Isotope Separator. The ion energies ranged from 40 to 100 keV. Discs were cut from the irradiated areas, annealed in a N$_2$ atmosphere at up to 1000°C, and thinned for observation by strong and weak beam transmission electron microscopy. It was found that the greatest variation in structure occurred with relatively low ion doses, of about an order of magnitude lower than those necessary to form a complete amorphous layer in the unannealed material. With n-type dopants (N$^+$, P$^+$, Sb$^+$) the behavior was generally similar, with small dislocation loops the main feature, although there were some differences. The behavior with B$^+$ and Ne$^+$ was surprisingly rather similar, these being the only ions studied that produced long rod-like defects, with cylindrically symmetric strain fields. With Al$^+$ ions, small loops on steeply inclined planes were observed. At higher doses, many small loops were observed for all ions at 800°C, sometimes annealing at 900°C to form an interface dislocation array. Comparisons are made of results obtained with strong and weak beam microscopy, the latter enabling small defects to be studied more easily than previously. Detailed results are described for B, Al, and N-irradiated Si. 9 references. (UK)

19809 FIRST INTERNATIONAL TOPICAL CONFERENCE ON ION IMPLANTATION IN SEMI-CONDUCTORS, THOUSAND OAKS, CALIFORNIA, MAY 4-7, 1970. Chadderton, Lewis T. (ed.). Radiat. Eff.; 6: 1-318(Nov 1970). (CONF-700544).

Forty papers are presented, which cover the following topics: ion implantation in Si, Ge, and the compound semiconductors (InAs, InSb, GaAs, GaP, and SiC); damage profiles and clusters; electric properties; proton irradiations; enhanced diffusion; disorder; and annealing. Separate abstracts were prepared for all 40 papers. (D.L.C.)

For abstracts of individual papers see: 19760 and 19810–19848.

19810 RADIATION DAMAGE IN SILICON AND GERMANIUM. Corbett, J. W. (State Univ. of New York, Albany). Contract F19628-70-C-0062. Radiat. Eff.; 6: 3-10(Nov 1970).

From International Conference on Ion Implantation in Semiconductors, Thousand Oaks, Calif. See CONF-700544.

A review is presented of the present state of knowledge on the mechanisms of radiation damage production in Si. Cross sections for energy transfer are discussed for 1-MeV particles. The structure of the central zone of the damage region is considered. The correlation of the EPR defects with energy levels is discussed. Divacancies and interstitials are described in some detail. Germanium is briefly considered, and some remarks on theory are given. 95 references. (D.L.C.)

19811 EVIDENCE FOR VACANCY MOTION IN LOW-TEMPERATURE ION-IMPLANTED Si. Vook, F. L.; Stein, H. J. (Sandia Labs., Albuquerque, N. Mex.). Radiat. Eff.; 6: 11-17 (Nov 1970).

From International Conference on Ion Implantation in Semiconductors, Thousand Oaks, Calif. See CONF-700544.

Recent results have reported a strong implantation-temperature dependence between 125°K and room temperature for lattice disorder produced by 200-keV B implantation into Si. Using a previous annealing model incorporating implant temperature and dose rate, a characteristic defect annealing time at the threshold of the crystalline-to-amorphous transition at 173°K for 1 $\mu A/cm^2$ was calculated, which agrees very closely with that for neutral vacancy annealing. In addition, measurements were made of the 1.8-μ infrared absorption band, characteristic of the Si divacancy, following room temperature and 85°K implants of 400-keV ^{11}B or ^{121}Sb ions. Very few divacancies are observed immediately after 85°K implants, but annealing growth of divacancies occurs between 150 and 300°K yielding a density almost equal to that for the same ion fluence at 300°K. These results strongly suggest that, below 300°K, neutral vacancy motion and trapping control both the implantation-temperature dependence of lattice damage production for B implantations and the divacancy formation upon annealing for B and Sb implants. (auth)

19812 INFRARED STUDIES OF THE CRYSTALLINITY OF ION-IMPLANTED Si. Stein, H. J.; Vook, F. L.; Brice, D. K.; Borders, J. A.; Picraux, S. T. (Sandia Labs., Albuquerque, N. Mex.). Radiat. Eff.; 6: 19-26(Nov 1970).

From International Conference on Ion Implantation in Semiconductors, Thousand Oaks, Calif. See CONF-700544.

The crystallinity of ion-implanted silicon has been investigated using ion mass and ion fluence dependences of divacancy formation as measured by the characteristic 1.8-μ absorption band. Room temperature, nonchanneled implants of 400-keV ^{11}B, ^{64}Zn, and ^{121}Sb ions were performed to maximum fluences of 10^{14} ions/cm^2 for Sb and Zn and to 2×10^{15} ions/cm^2 for B. The results are interpreted on the basis of ion energy spent in atomic processes per unit volume, E, within the implanted layer. For $E \leq 10^{19}$ keV/cm^3 the energy to form a divacancy (1.5 ± 0.5 keV) is nearly ion-independent. Maxima appear in the divacancy densities at $\sim 10^{13}$ Sb ions/cm^2 and $\sim 2 \times 10^{13}$ Zn ions/cm^2 where $E \approx 10^{20}$ keV/cm^3. The divacancy density for B implantation did not exhibit a distinct maximum at $E = 10^{20}$ keV/cm^3, but continued to increase with fluence. The B results are attributed to defect motion because divacancies are observed beyond the calculated depth for energy deposition after a high-fluence B implant. In addition to the 1.8-μ band, absorption extending from the band edge to at least 3.5 μ is observed to increase with fluence for all ions. Analysis of the divacancy density data indicates that 1.8-μ band quenching occurs for divacancy concentrations $\geq 7 \times 10^{19}$ cm^{-3}. The results of this investigation are consistent with crystal lattice defect domination of the ion-produced disorder when the energy spent in atomic processes is $\leq 10^{20}$ keV/cm^3 at room temperature, and with amorphous-layer formation when the energy deposition is $\sim 10^{21}$ keV/cm^3 at room temperature, providing the defects remain near the position of the initial energy deposition. (auth)

19813 MODEL FOR THE FORMATION OF AMORPHOUS Si BY ION BOMBARDMENT. Morehead, F. F. Jr.; Crowder, B. L. (IBM Thomas J. Watson Research Center, Yorktown Heights, N. Y.). Radiat. Eff.; 6: 27-32(Nov 1970).

From International Conference on Ion Implantation in Semiconductors, Thousand Oaks, Calif. See CONF-700544.

The effective annealing of ion implantations in Si is aided by the formation of a continuous amorphous layer. The amorphous layer regrows epitaxially at 500 to 600°C and incorporates the dopant in an electrically active, uncompensated form. A phenomenological model is proposed which, with adjustable parameters, accounts for the variation of the critical dose required to produce a continuous amorphous layer by ion bombardment with ion, target, temperature, and, with minor additional assumptions, dose rate. (auth)

19814 DAMAGE PRODUCED BY ION IMPLANTATION IN SILICON. Davidson, S. M.; Booker, G. R. (Oxford Univ., Eng.). Radiat. Eff.; 6: 33-43(Nov 1970).

From International Conference on Ion Implantation in Semiconductors, Thousand Oaks, Calif. See CONF-700544.

Silicon specimens were irradiated with Ne^+, B^+, P^+, and Sb^+ ions. The energy was 80 kV, and the doses were in the range 10^{13} to 10^{16} ions/cm^2. The resulting structural damage was investigated by both scanning (SEM) and transmission (TEM) electron microscopy. The SEM electron channeling pattern method was used to determine the variation of gross damage with ion type, dose, depth below the surface, and annealing treatment. The TEM method was used to study the detailed nature of the defects formed by the annealing. These included dislocations, rod-like structures, microtwins, semipolycrystalline material, misoriented zones, etc. The results are briefly compared with known electrical properties of implanted silicon, and some correlations noted. (auth)

19815 CORRELATION OF ELECTRON MICROSCOPE STUDIES WITH THE ELECTRICAL PROPERTIES OF BORON-IMPLANTED SILICON. Bicknell, R. W. (Plessey Co. Ltd. Caswell, Eng.); Allen, R. M. Radiat. Eff.; 6: 45-9(Nov 1970).

From International Conference on Ion Implantation in Semiconductors, Thousand Oaks, Calif. See CONF-700544.

A number of 1-Ω-cm n-type silicon substrates were implanted with boron at room temperature. Samples from these substrates were annealed at predetermined temperatures between 600°K and 1400°K and four-probe electrical measurements and transmission electron micrographs were taken. An attempt was made to correlate the two studies and it is possible to explain the observed annealing behavior in terms of precipitation during recrystallization and migration of defects. (auth)

19816 DISORDER DECHANNELING OF LOW-ENERGY PROTONS AND ALPHA PARTICLES IN SILICON. Hart, R. R. (Hughes Research Labs., Malibu, Calif.). Radiat. Eff.; 6: 51-6(Nov 1970).

From International Conference on Ion Implantation in Semiconductors, Thousand Oaks, Calif. See CONF-700544.

Dechanneling of low-energy protons (<160 keV) and α particles (<320 keV) from the $\langle 111 \rangle$ channel of Si, resulting from collisions with displaced Si atoms, was investigated by backscattered yield measurements. The total disorder produced by implantation of Si with 40-keV Sb^+ was calculated from the backscattered yields on the basis of the single-scattering theory of dechanneling and agreed within experimental error with that determined by the channeling technique. Single scattering also correctly predicted the energy dependence of dechanneling after implantation of Si with 80-keV Cl^+ and accounted for most of the dechanneling correction necessary for the calculation of the disorder profile, which was produced by 40-keV B^+ in Si at −120°C. Thus, the present results suggest that single scattering gives a good description of the dechanneling of low-energy H_1^+ and He^{2+} from the $\langle 111 \rangle$ Si channel. (auth)

19817 RADIOCHEMICAL DETERMINATION OF DAMAGE PROFILES IN SILICON. Masters, B. J. (IBM Components Div., Hopewell Junction, N. Y.); Fairfield, J. M.; Crowder, B. L. Radiat. Eff.; 6: 57-61(Nov 1970).

From International Conference on Ion Implantation in Semiconductors, Thousand Oaks, Calif. See CONF-700544.

A novel technique for the study of structural damage incurred by single-crystal silicon targets during ion implantation is described. The method is based upon copper decoration of the vacancy-rich damaged region, followed by radiochemical measurement of the resulting copper distribution. Utilizing neutron activation, sharply peaked radiocopper profiles are obtained, which are believed to represent the depth distributions of large, relatively immobile defects such as vacancy clusters, voids, or crystalline faults. A more efficient decoration of isolated vacancy-type defects is realized when ^{64}Cu is employed as a radioisotopic tracer in the decoration step; however, the rapid diffusivity of these smaller species leads to less sharply defined radiocopper profiles. Both the neutron activation and radiotracer modifications of the technique yield damage profiles significantly shallower than the corresponding implanted impurity profiles. (auth)

19818 DISTRIBUTION OF DAMAGE PRODUCED BY ION IMPLANTATION OF SILICON AT ROOM TEMPERATURE. Crowder, B. L.; Title, R. S. (IBM Watson Research Center, Yorktown Heights, N. Y.). Radiat. Eff.; 6: 63-75(Nov 1970).

From International Conference on Ion Implantation in Semiconductors, Thousand Oaks, Calif. See CONF-700544.

Experiments designed to determine the damage distribution produced by energetic heavy ions in Si are described. For low ion doses (10^{11} to 10^{13} cm^{-2}), the location of the damage peak was determined by changes, which were produced by ion damage, in the electrical properties of thin (0.6 μ), uniformly doped Si layers as

XUM

a function of depth. The ratio of the peak position in the damage distribution to the peak position in the ion distribution was determined to be approximately 0.6 ± 0.1 for ^{28}Si (150 keV), ^{31}P (70, 140, 200 keV), ^{11}B (60 keV), and ^{75}As (280 keV). A comparison of carrier removal rates and the number of displaced lattice atoms previously reported from backscattering experiments with He ions indicates that the types of damage produced by ^{28}Si and ^{11}B are different. In the former case, cluster damage (amorphous disordered regions) appears to be an important form of radiation damage, whereas in the latter case, isolated defects are the dominant form of radiation damage for room temperature implantations. Isochronal annealing studies of ^{28}Si and ^{11}B ion damage provide further support for the different nature of radiation defects produced by these species. For high doses (10^{14} to 10^{16} cm^{-2}), the growth of a continuous amorphous Si layer was studied with ESR, optical transmission, and visual observation and stripping studies. The ratio of the location of the damage peak to that of the peak ion concentration was determined to be approximately 0.7 for ^{31}P (140, 280 keV) and 0.8 for ^{75}As (280 keV). From the ESR studies, the number of displaced atoms in amorphous clusters was estimated to be 2800 per 280-keV ^{31}P ion. (auth)

19819 SPATIAL DISTRIBUTION OF ENERGY DEPOSITED INTO ATOMIC PROCESSES IN ION-IMPLANTED SILICON. Brice, D. K. (Sandia Labs., Albuquerque, N. Mex.). Radiat. Eff.; 6: 77-87(Nov 1970).

From International Conference on Ion Implantation in Semiconductors, Thousand Oaks, Calif. See CONF-700544.

A method is given for calculating the spatial distribution of the production of a quantity, Q, averaged over many ions incident randomly on a solid for any energy-dependent interaction between the ions and target atoms. The method is basically a two-step method. First, the spatial distribution of the ions in the solid is followed as the ions lose energy. Then, at each intermediate energy the spatial distribution of Q production is obtained, and the result is integrated over the range of intermediate energies assumed by the ions. Saturation effects are ignored in the procedure so that explicit consideration must be given to saturation effects when applying the method to high-dose cases. Annealing and diffusion effects are also ignored, and the method is restricted in applicability to experimental conditions where annealing and diffusion are unimportant. Results of calculations by this method are presented of the depth distribution of energy ultimately deposited into atomic processes for ^{7}Li, ^{11}B, ^{12}C, ^{14}N, ^{16}O, ^{20}Ne, ^{28}Si, and ^{31}P ions incident randomly on silicon with incident energies in the range of 30 to 400 keV. Migration of the deposited energy through the recoil of struck target atoms has been neglected. Comparison of the results of calculations by this method with moments obtained by Sigmund and coworkers for the equal-mass case indicates that for the ions listed above, and for the energy range considered, this approximation is valid. The calculated depth distributions thus represent the final depth distribution of energy deposited into atomic processes. (auth)

19820 LIFETIME EFFECTS IN ION-IMPLANTED SILICON. Pickar, K. A.; Dalton, J. V. (Bell Telephone Labs, Inc., Murray Hill, N. J.). Radiat. Eff.; 6: 89-94(Nov 1970).

From International Conference on Ion Implantation in Semiconductors, Thousand Oaks, Calif. See CONF-700544.

The damage produced by energetic ions in the space-charge region of diffused p$^+$n junction diodes is studied. By measuring the diode reverse leakage current, J_r, as a function of the implant parameters (ion mass, energy, postanneal temperature, etc.) the characteristics of recombination-generation centers introduced by the implant process can be probed. It is these states that strongly affect the operation of lifetime-dependent devices. The results can be fit by a single-level Shockley–Read–Hall model with the centers lying ~1kT from the center of the gap. They are seen to be closer to the surface than the Lindhard–Scharff–Schiøtt range of the implanted carbon ions. Silicon implants have reverse leakage currents, which are roughly linearly dependent on dose for low doses while carbon and helium implants have highly superlinear dependencies indicating that defects created by separate lighter ions can interact at low doses. The pre-implant reverse leakage current of diodes implanted with 10^{15}/cm^2 300-keV C$^+$ can be substantially but not completely recovered after a 750°C anneal. (auth)

19821 HOT-ELECTRON STUDIES OF LATTICE DAMAGE CREATED IN SILICON BY IMPLANTATION OF 2.8-MeV PROTONS. Sigmon, T. W.; Gibbons, J. F. (Stanford Univ., Calif.). Radiat. Eff.; 6: 95-101(Nov 1970).

From International Conference on Ion Implantation in Semiconductors, Thousand Oaks, Calif. See CONF-700544.

Results are reported of a study of the annealing properties of the ionized defect density associated with the damage created in the silicon lattice by implantation of 2.8-MeV protons at room temperature. In particular, the annealing of damage created by implanting to a level of 4.43×10^{12} protons/cm^2 is reported. The resulting isochronal annealing curve covered the temperature range from 70 to 460°C. Two major annealing stages are discussed, one a broad stage between 70 and 200°C and the other an abrupt annealing stage between 440 and 460°C. In the temperature range 200 to 440°C, the number of ionized defects remained relatively constant. Above 460°C no detectable effects of the proton implantation remained. (auth)

19822 RESISTIVITY AND ANNEALING PROPERTIES OF IMPLANTED Si:H$^+$. Schwuttke, G. H. (International Business Machines Corp., Hopewell Junction, N. Y.); Brack, K.; Gorey, E. F.; Kahan, A.; Lowe, L. F. Radiat. Eff.; 6: 103-6(Nov 1970).

From International Conference on Ion Implantation in Semiconductors, Thousand Oaks, Calif. See CONF-700544.

N- or p-type 1-ohm-cm-resistivity silicon crystals are bombarded with 1-MeV protons to doses greater than 10^{15} H$^+$/cm^2. The crystals are characterized through x-ray topography and surface and in-depth resistivity measurement techniques. Post-bombardment measurements indicate a high-resistance layer (10^4 ohm-cm range) on the silicon surface, extending to 16 μm depth after 1-MeV H$^+$ bombardment. Post-anneal results show that this insulating layer is still stable after 300°C anneal cycles. At higher anneal temperatures the radiation damage starts to anneal out, and at 800°C the crystal returns to its original resistivity. (auth)

19823 ENHANCED DIFFUSION IN ION-IMPLANTED SILICON. Namba, Susumu (Osaka Univ., Japan); Masuda, Kohzoh; Gamo, Kenji; and others. Radiat. Eff.; 6: 115-20(Nov 1970).

From International Conference on Ion Implantation in Semiconductors, Thousand Oaks, Calif. See CONF-700544.

Concentration profiles of 20-keV ion-implanted antimony in silicon single crystals are measured by radioactivation analysis and the enhanced diffusion of antimony is observed. The concentration profiles and the diffusion coefficient of antimony are found to be independent of temperature over the range between 500 and 800°C during ion implantation. The enhancement of diffusion during annealing after room-temperature ion implantation is the same as that during high-temperature ion implantation. The diffusion coefficient is estimated to be 1.1×10^{-15} cm^2/sec for diffusion during high-temperature ion implantation and during annealing after room-temperature ion implantation. The measured concentration profiles agree very well with the calculated concentration profiles. These results are explained on the basis of a vacancy mechanism. (auth)

19824 ENHANCED DIFFUSION OF BORON AND PHOSPHORUS IN SILICON DURING HOT SUBSTRATE ION IMPLANTATION. Tsuchimoto, T.; Tokuyama, T. (Hitachi Ltd., Tokyo, Japan). Radiat. Eff.; 6: 121-9(Nov 1970).

From International Conference on Ion Implantation in Semiconductors, Thousand Oaks, Calif. See CONF-700544.

An enhanced diffusion of boron and phosphorus in silicon during hot-substrate ion implantation was interpreted from the increase of diffusion coefficient in the substrate. Distribution of excess vacancies generated during hot implantation was calculated by solving the diffusion equation for density of vacancies. Experiments were carried out in the following categories: (1) Hot implantation of neutral ions, such as H and Ar ions, into boron- and phosphorus-doped surface layers of substrate silicon. (2) Hot implantation of boron and phosphorus ions into the substrate. Excess diffusion-length and carrier-distribution profiles were measured and compared with results calculated from a simple model. Crystal perfection observed by backscattered He ions indicated favorable results. (auth)

19825 ANTIMONY-IMPLANTED SILICON: A COMPARISON BETWEEN THE TOTAL IMPLANTED CONCENTRATION PROFILE AND THE DONOR CONCENTRATION PROFILE. Nelson, R. S.; Cairns, J. A.; Blamires, N. (Atomic Energy Research Establishment, Harwell, Eng). Radiat. Eff.; 6: 131-4(Nov 1970).

From International Conference on Ion Implantation in Semiconductors, Thousand Oaks, Calif. See CONF-700544.

The total concentration profiles of various doses of antimony, implanted into silicon at 100 keV, were determined by a new technique, using Kr$^+$ ions to detect selectively the antimony (as Sb M x rays) at the expense of the silicon. Since most of these x rays arise from only a few tens of angstroms below the surface of the silicon, the x-ray generation can be used in conjunction with an anodic stripping technique to obtain the antimony depth distribution. These profiles are compared with others, obtained by measuring the donor concentration as a function of depth using standard Hall-effect and conductivity measurements. A significant difference between these profiles was observed, which is thought to be due to the suppression of electrical activity that occurs as the result of lattice damage. Confirmatory evidence is presented in the form of electron microscope observations of the implanted region at various depths below the silicon surface. (auth)

19826 EPR OF SUBSTITUTIONAL GROUP V IMPLANTS IN SILICON. Borders, J. A.; Brower, K. L. (Sandia Labs., Albuquerque, N. Mex.). Radiat. Eff.; 6: 135-40(Nov 1970).

From International Conference on Ion Implantation in Semiconductors, Thousand Oaks, Calif. See CONF-700544.

Group V impurities implanted at 400 keV into silicon were detected in substitutional lattice positions by EPR. Three samples of VFZ, p-type 1200- to 1500-ohm-cm silicon from the same ingot were implanted with ^{75}As, ^{121}Sb, and ^{123}Sb, respectively. The EPR spectrum of each implanted substitutional impurity was observed after annealing the lattice damage. Only the isotope implanted in each sample was seen. Since only those donors that are electrically active can be observed, this technique measures the electrically active fraction of the implanted species. Upon annealing to 970°C, most of the antimony was active whereas only about $^1/_5$ of the arsenic was observed. Comparisons with backscattering results indicate that between 350 and 600°C, ~95% of the implanted antimony is substitutional but ~0% is electrically active. The increase in electrical activity at 600°C is due to the rise of the Fermi level to the donor level as the residual lattice damage anneals. The paramagnetic damage centers observed were those also seen in oxygen-implanted silicon, Si–P3 and Si–P1, but the Si–P3 center was not as well resolved and it grew upon annealing to 200°C. (auth)

19827 LATTICE LOCATION OF HEAVY GROUP III AND V ELEMENTS IMPLANTED INTO Ge. Bjoerkqvist, K.; Sigurd, D.; Fladda, G.; Bjarnholt, G. (Research Inst. for Physics, Stockholm). Contract F 61052-68-C-0062. Radiat. Eff.; 6: 141-8(Nov 1970).

From International Conference on Ion Implantation in Semiconductors, Thousand Oaks, Calif. See CONF-700544.

The channeling-effect technique was used to study lattice location of ions implanted in Ge. Results on group III (In, Tl) and group V (Sb, Bi) elements as well as preliminary results on Pb and Hg are reported. The effects of different implantation temperatures (25 to 600°C) and subsequent anneal treatment were investigated. Comparisons with previous measurements on ion-implanted Si indicate that, though there is strong correlation between results in Si and Ge, differences exist, especially for the group III dopants. (auth)

19828 ION IMPLANTATION IN InAs AND InSb. McNally, P. J. (Ion Physics Corp., Burlington, Mass.). Radiat. Eff.; 6: 149-53(Nov 1970).

From International Conference on Ion Implantation in Semiconductors, Thousand Oaks, Calif. See CONF-700544.

Ion implantation in InAs and InSb with sulfur and zinc ions was used to fabricate p–n junction diodes, which were characterized for their infrared detector properties. Planar mosaic infrared detectors were produced in both materials with good characteristics. Blackbody detectivities (D^*_{BB}) of 2×10^9 cm $\mathrm{Hz}^{1/2}$/watt and 4% uniformity were measured for InAs. Similarly, InSb showed D^*_{BB} values of 1.3×10^{10} cm $\mathrm{Hz}^{1/2}$/watt and 49% uniformity between elements in an array. Experimental range–energy data for zinc in InSb were obtained between 0.2 and 1.8 MeV and compared with predicted values from the LSS theory. Theory predicts a deeper range than experimental values indicate; however, the differences are sufficiently small to make the curves useful for device design. The slopes of the curves indicate that a large component of nuclear stopping predominates in this energy region. (auth)

19829 ANOMALOUSLY HIGH YIELDS OF ELASTICALLY SCATTERED ^{12}C IONS FROM Zr, Hf, Tl, AND Hg ATOMS IMPLANTED INTO SILICON. Domeij, B.; Fladda, G.; Johansson, N. G. E. (Research Inst. for Physics, Stockholm). Radiat. Eff.; 6: 155-9(Nov 1970).

From International Conference on Ion Implantation in Semiconductors, Thousand Oaks, Calif. See CONF-700544.

Silicon single crystals were implanted under various conditions with Zr, Hf, Tl, and Hg. The yield of scattered 1.8-MeV ^{12}C ions was studied as a function of the angle of incidence. Around the $\langle 111 \rangle$ direction, the normal channeling dip was observed. Around the $\langle 110 \rangle$ direction, either a narrow peak or a narrow peak superimposed on a channeling dip was found. The occurrence of the peak is interpreted as being caused by scattering from impurity atoms located in the tetrahedral interstitial holes in the silicon lattice. For a beam entering along a $\langle 111 \rangle$ direction these atoms are screened, but they are fully exposed to a beam entering parallel to a $\langle 110 \rangle$ direction. The implications of this effect with respect to earlier measurements of the lattice location of impurity atoms in silicon and germanium are discussed. A similar effect has recently been observed at the University of Aarhus. (auth)

19830 ANALYSIS OF DISORDER DISTRIBUTIONS IN BORON-IMPLANTED SILICON. Westmoreland, J. E. (California Inst. of Tech., Pasadena); Mayer, J. W.; Eisen, F. H.; Welch, B. Radiat. Eff.; 6: 161-74(Dec 1970).

From International Conference on Ion Implantation in Semiconductors, Thousand Oaks, Calif. See CONF-700544.

Channeling effects on the yield of large-angle backscattered energetic H^+ or He^+ were used to investigate properties of the disorder in Si samples previously implanted with ^{11}B ions at substrate temperatures of –150°C to –50°C. Exposure of the implanted samples to the analyzing beam at room temperature caused a large reduction in the amount of disorder measured. A successive layer-removal technique by anodic oxidation and stripping was used to obtain a depth scale for 1.8-MeV He^+ analyses of lightly disordered samples. The results of additional experiments indicate that for 1-MeV He^+ in Si the aligned stopping power is about 80% of the random stopping power. Measured and calculated values of the minimum yield χ_R for the substrate underlying amorphous layers suggested a plural scattering treatment of dechanneling of the analyzing beam using previously measured values of the critical angle. The scattering center distributions calculated from this treatment of dechanneling are presented for 450-keV H^+ analyses of implants with doses of 1×10^{14} to 1.6×10^{15} 200-keV B ions/cm^2. The distribution calculated from the plural scattering dechanneling approximation is compared with distributions calculated from other treatments for a 1.8-MeV He^+ analysis of a 5×10^{14} 200-keV B ions/cm^2 implant. The plural scattering treatment works fairly well for 200-keV implantations at doses $\leq 8 \times 10^{14}$ ions/cm^2. (auth)

19831 ELECTRICALLY ACTIVE DEFECT ANNEALING IN NEUTRON- AND ION-DAMAGED Si. Stein, H. J. (Sandia Labs., Albuquerque, N. Mex.). Radiat. Eff.; 6: 175-80(Dec 1970).

From International Conference on Ion Implantation in Semiconductors, Thousand Oaks, Calif. See CONF-700544.

Hall-effect and electrical conductivity measurements of defect annealing in 1-ohm-cm n-type and 2-ohm-cm p-type silicon were made following neutron irradiation at ~50°C. Measurements were also made following 400-keV ^{11}B ion implantation into a 100-ohm-cm n-type Si substrate. As the neutron fluence is increased the electrical effects of the damage eventually outweigh those of the chemical dopants, and further changes in the electrical properties become small. Conversely, significant electrical recovery upon annealing begins only when the electrical effects of the remaining damage become comparable to those of the chemical dopants. This condition will occur at higher anneal temperatures for higher fluence irradiations. The neutron fluence dependence of the damage and the annealing is interpreted in terms of the neutron energy per cm^3, E, spent in atomic processes divided by the number/cm^3, N, of electrically active dopants. When $E/N \leq 0.5$ keV the electrical measurements show that the predominant defect annealing occurs below 400°C. However, when $E/N > 0.5$ keV electrical measurements emphasize the annealing at temperatures >400°C. After 500°C annealing, energy levels in neutron-damaged Si are observed at $E_v + 0.1$ and $E_v + 0.15$ eV in p-type and at $E_c - 0.33$ eV in n-type Si. Application of the E/N criteria to room-temperature implant-doped Si predicts that the electrical effects will be dominated by lattice damage even if all the implanted ions are substitutional. (auth)

19832 ENERGY DEPENDENCE AND DEPTH DISTRIBUTION OF LATTICE DISORDER IN ION-IMPLANTED SILICON. Marsden, D. A.; Whitton, J. L. (Atomic Energy of Canada Ltd., Chalk River, Ont.). Radiat. Eff.; 6: 181-5(Dec 1970).

From International Conference on Ion Implantation in Semiconductors, Thousand Oaks, Calif. See CONF-700544.

Silicon single crystals were implanted at room temperature with Xe and I ions in the energy range 20 to 150 keV and with 20- to 50-keV P ions. The lattice disorder induced by these implants was measured by a combination of the channeling and Rutherford-backscattering techniques. The disorder produced by implanting I and Xe ions exhibited a relationship with implantation energy similar to that previously established for bismuth implants. The P-ion implants induced less lattice disorder per incident ion in the energy range studied. Integral depth distributions of the implanted ions and of the lattice disorder were obtained by combining a layer-removal technique with radiotracer implants of 110-keV ^{133}Xe and 40-keV ^{32}P. The depth distributions showed that in both cases the ions penetrate deeper into the crystal than the damage they produce but that the separation is significantly greater for the P implant than for the Xe implant. (auth)

19833 CORRELATION FUNCTIONS IN THE THEORY OF ATOMIC COLLISION CASCADES: ION LOCATION AND THE DISTRIBUTION IN DEPTH AND SIZE OF DAMAGE CLUSTERS. Westmoreland, J. E. (California Inst. of Tech., Pasadena); Sigmund, P. Radiat. Eff.; 6: 187-97(Dec 1970).

From International Conference on Ion Implantation in Semiconductors, Thousand Oaks, Calif. See CONF-700544.

XUM

Simple depth-distribution functions of ion-bombardment damage predict the spatial extension of the cumulative damage caused by a beam of ions. Correlation functions need to be considered when more detailed information is desirable, such as the average size or depth of individual damage clusters, the average location of an ion within its damage cluster, and the fluctuations of these quantities. This paper establishes an integral equation for the pair correlation function, coupling the individual ion range with the deposited energy. This pair correlation function determines the damage caused by all those ions that come to rest at a specific penetration depth. Solutions of the integral equation are found by standard methods. Explicit results are presented for elastic scattering governed by power cross sections. The depth distribution of damage clusters turns out to be significantly narrower than the gross damage distribution at all mass ratios except for $M_1 \ll M_2$, and the size distribution appears insensitive to depth when measured perpendicular to the ion beam, but varies with depth when measured parallel. Predictions on ion location suffer from a surprisingly sensitive dependence on the scattering cross section. A note on the fluctuation of the sputtering yield by individual ions concludes the paper. (auth)

19834 CHANNELING STUDY OF BORON-IMPLANTED SILICON: LIQUID NITROGEN TEMPERATURE IMPLANTATION. North, J. C.; Gibson, W. M. (Bell Telephone Labs., Inc., Murray Hill, N. J.). Radiat. Eff.; 6: 199-203(Dec 1970).

From International Conference on Ion Implantation in Semiconductors, Thousand Oaks, Calif. See CONF-700544.

Silicon samples were boron implanted at 150 keV at liquid-nitrogen temperature to a dose of 3.6×10^{15} cm^2. This dose rendered the implanted layer amorphous as viewed by helium-ion backscattering. Four kinds of room-temperature measurements were made on the same set of samples as a function of the isochronal annealing temperature. The measurements made were the determination of the substitutional boron content by the channeling technique using the ^{11}B (p,α) nuclear reaction, observation of the disorder by helium-ion backscattering, determination of the carrier concentration by van der Pauw–Hall measurements, and the sheet resistivity by four-point probe measurements. These measurements are compared with results from samples implanted at room temperature. The carrier concentration correlates well with the substitutional boron content for both room-temperature and liquid-nitrogen-temperature implantations. Following annealing temperatures in the 600 to 800°C range, a much larger percentage of the boron lies on substitutional lattice sites, and therefore the carrier concentration is larger, if the implantation is done at liquid-nitrogen temperature rather than at room temperature. Following liquid-nitrogen-temperature implantation, reverse annealing is observed from 600 to 800°C in the substitutional boron content, carrier concentration, and sheet resistivity. The boron is more than 90% substitutional after annealing to 1100°C for both the room-temperature and liquid-nitrogen-temperature implantations. The low-temperature implantation produced a buried amorphous layer, and this layer was observed to regrow from both the surface and substrate sides at approximately equal rates. (auth)

19835 LOW-ENERGY BORON AND PHOSPHORUS IMPLANTS IN SILICON. A. ELECTRICAL SHEET MEASUREMENTS. Stumpfi, W.; Kalbitzer, S. (Max Planck Institut fuer Kernphysik, Heidelberg). Radiat. Eff.; 6: 205-10(Dec 1970).

From International Conference on Ion Implantation in Semiconductors, Thousand Oaks, Calif. See CONF-700544.

Silicon wafers were implanted in the ⟨111⟩-direction with 7-keV boron and phosphorus ions at room temperature. Doses between 10^{12} and 10^{16} ions/cm^2 were applied. After successive annealing steps, the electrical properties of the implanted layers were determined by Hall-effect and sheet-resistivity measurements. The annealing characteristics of the implants depend on ion dose and species. Three annealing stages can be distinguished: (I) the temperature range below 500°C, (II) 500 to 700°C, (III) 700 to 900°C. After annealing at 900°C, the apparent electrical yield is proportional to dose for all implants and amounts to ~80% for boron and 40% for phosphorus. Sheet resistivity vs dose curves were derived for the annealing temperature of 400°C and used for the fabrication of position-sensitive detectors. The position characteristics were found to be linear within ~1% for resistive layers as long as 20 cm. (auth)

19836 LOW-ENERGY BORON AND PHOSPHORUS IMPLANTS IN SILICON. B. DOPING PROFILES. Bader, R.; Kalbitzer, S. (Max Planck Institut fuer Kernphysik, Heidelberg). Radiat. Eff.; 6: 211-16(Dec 1970).

From International Conference on Ion Implantation in Semiconductors, Thousand Oaks, Calif. See CONF-700544.

Silicon wafers were implanted in ⟨111⟩ and ⟨110⟩ directions with 6-keV boron ions and 20-keV phosphorus ions at room temperature. Doses of 10^{14} ions/cm^2 were applied. At four different temperatures, 300, 420, 600, and 900°C, a few samples of each type of implant were annealed. Standard electrical techniques combined with successive layer removals were used to determine the depth distribution of electrically active centers. Since the method of using non-type-inverting implanted layers was applied, the local annealing behavior over the whole penetration region could be measured. For both Si(B) and Si(P) implants, the part of the profile beyond ~0.15 μm, i.e. the deeper part of the channeling and the whole supertail region, is unaffected by going from 300 to 900°C. All additional annealing, with respect to the electrical yield, takes place in the amorphous range and the adjacent part of the channeling range. After raising the temperature from 600 to 900°C both B and P profiles undergo diffusion-controlled changes in this latter region. (auth)

19837 ANNEALING CHARACTERISTICS OF HIGHLY DOPED ION-IMPLANTED PHOSPHORUS LAYERS IN SILICON. Shannon, J. M. (Mullard Research Labs., Redhill, Eng.); Ford, R. A.; Gard, G. A. Radiat. Eff.; 6: 217-21(Dec 1970).

From International Conference on Ion Implantation in Semiconductors, Thousand Oaks, Calif. See CONF-700544.

Sheet resistance, stripping, and Hall-effect measurements were made on phosphorus layers implanted into silicon at 40 and 100 keV with doses between 1×10^{15} and 5×10^{16} atoms/cm^2. The implants were made at room temperature and 450°C. After annealing at 650°C, the profile of electrically active phosphorus following a high-dose room temperature implant was found to be flat-topped with a concentration of approximately 5×10^{20} cm^3. Very little diffusion occurred when annealing to 850°C where the free electron concentration increased to approximately 1.5×10^{21} cm^3. Highly doped channeled tails were found when implanting at 450°C along the ⟨110⟩ direction, and damage was being continuously annealed out, preventing the formation of an amorphous phase. The rapid diffusion of the profile into the bulk found when annealing between 650°C and 850°C was speculated to be due to the presence of a dense dislocation entanglement in these layers following a hot implant. (auth)

19838 MEASUREMENTS OF HALL EFFECT AND SHEET RESISTIVITY AS A FUNCTION OF TEMPERATURE ON HOT; PHOSPHORUS IMPLANTS IN SILICON. MacDonald, C. (Aarhus Univ., Denmark); Galster, G. Radiat. Eff.; 6: 223-35(Dec 1970).

From International Conference on Ion Implantation in Semiconductors, Thousand Oaks, Calif. See CONF-700544.

Results of Hall-effect measurements as a function of temperature on a layer formed by hot phosphorus (^{31}P) implant in Si at 400 keV in a random direction are presented; the dose used was 10^{15} ions cm^{-2}. The electrical behavior of the layer as a function of isochronal annealing was examined. A detailed analysis of the measured quantities $n_{s_{eff}}$, the effective surface density of free carriers, and μ_{eff}, the effective mobility, down to 4.2°K is presented using the integral equations: $n_{s_{eff}}(T) = [\int_0^t n(x,T)\mu(x,T)dx]^2/\int_0^t n(x,T)\mu(x,T)^2\,dx$; $\mu_{eff}(T) = \int_0^t n(x,T)\mu(x,T)^2\,dx/\int_0^t n(x,T)\mu(x,T)\,dx$. These formulas were solved numerically, the input data, viz, the distribution of donor centers and compensating damage centers, being assumed from the current literature. Results from this analysis indicate a rather complicated distribution of current flow in the layer as a function of temperature; this suggests that the traditional interpretation of Hall measurements based on a homogeneous distribution model is of questionable validity. (auth)

19839 ELECTRICAL ACTIVITY OF PHOSPHORUS CHANNELED INTO SILICON. Goode, P. D.; Wilkins, M. A.; Dearnaley, G. (Atomic Energy Research Establishment, Harwell, Eng.). Radiat. Eff.; 6: 237-45(Dec 1970).

From International Conference on Ion Implantation in Semiconductors, Thousand Oaks, Calif. See CONF-700544.

The electrical activity of phosphorus ions, implanted at energies between 40 and 400 keV along the ⟨110⟩ axis of silicon crystals, was measured as a function of depth, following a 700°C anneal. The electrical activity, determined by differential electrical sheet conductivity measurements combined with anodic stripping, was found to be close to 100% in both pulled and float-zoned material. In some cases it was possible to compare carrier concentration and impurity-ion distributions within the same specimen, implanted with a mixed dose of ^{31}P and ^{32}P. By radioactive tracer techniques it was shown that dechannelling of phosphorus ions is significantly greater in certain dislocation-free crystals than in other dislocated silicon crystals. Scanning x-ray diffractometer measurements reveal considerably more lattice strain in the former. It is proposed that both effects may arise from vacancy clustering, together with associated decoration by impurity atoms, as a result of the absence of sinks provided by a few dislocations. The degree of channelling of ^{32}P in epitaxially grown ⟨111⟩ silicon was found to exceed that in high-quality bulk-grown crystals. The consequences of this observation, combined with the high electrical activity of channelled phosphorus, are considered briefly. (auth)

19840 DIFFUSION IN ION-IMPLANTED SOLIDS WITH NON-UNIFORM DIFFUSION PARAMETERS. Kelly, R.; Nghi, L. Q. (McMaster Univ., Hamilton, Ont.). Radiat. Eff.; 6: 247-56(Dec 1970).

From International Conference on Ion Implantation in Semiconductors, Thousand Oaks, Calif. See CONF-700544.

There is increasing evidence that diffusion phenomena in ion-implanted solids do not follow normal diffusion kinetics at high doses. For example, diffusion profiles are sometimes found to move towards the surface with increasing temperature, and the diffusion temperature widths tend to be up to a factor of 3 too narrow. Such results can be self-consistently explained by recognizing that the diffusion detrapping energy will ordinarily be greater in the vicinity of the damage mean range than deeper in. One way of treating this analytically is to idealize a bombarded target as consisting of the sequence surface/damage/no-damage. It is shown that the interface damage/no-damage then acts as a nearly impermeable barrier and thus tends to prevent inward motion. Alternatively, one can approximate the detrapping energy as varying continuously with depth, $\Delta H = \Delta H_0(1 - gx)$, the problem then becoming one of solving the equation $\partial C/\partial t = D(\partial^2 C/\partial s^2 - \partial C/s\partial s)$, where $s = \exp(-\Delta H_0 gx/2RT)$. The interesting result now is that the integral concentration follows as having a time-independent shape roughly of the form $\exp(-\Delta H_0 gx/RT)$, so that surface-directed motion again follows naturally provided g is large enough. These arguments also apply to ion depth distributions at high doses which are anomalous with respect either to being too shallow or to being temperature-dependent. It is necessary only to assume that prolonged ion impact on a solid surface causes radiation-enhanced diffusion. 53 references. (auth)

19841 DIFFUSION EFFECTS IN ION-IMPLANTED GERMANIUM. Johansson, N. G. E.; Sigurd, D.; Bjoerkqvist, K. (Research Inst. for Physics, Stockholm). Radiat. Eff.; 6: 257-61(Dec 1970).

From International Conference on Ion Implantation in Semiconductors, Thousand Oaks, Calif. See CONF-700544.

During isochronal anneal sequences the number of Hg, Tl, and Bi atoms implanted into Ge was found to decrease. This decrease occurs for all three species and was observed for samples implanted at room temperature as well as for hot implants (300 to 350°C). The decrease starts at anneal temperatures of 350 to 550°C. Similar results were obtained for In- and Sb-implanted Ge. For samples implanted with Hg to doses leading to amorphous layers, the decrease in the number of implanted atoms seems to be related to the reordering of the amorphous layer. The experiments show that no diffusion of the implanted atoms into the bulk material occurs and the decrease observed is attributed to be a diffusion of the atoms to the surface followed by outdiffusion, thermal etching, or both. (auth)

19842 ELECTRICAL PROPERTIES OF Cd, Zn, AND S ION-IMPLANTED LAYERS IN GaAs. Hunsperger, R. G.; Marsh, O. J. (Hughes Research Labs., Malibu, Calif.). Radiat. Eff.; 6: 263-8 (Dec 1970).

From International Conference on Ion Implantation in Semiconductors, Thousand Oaks, Calif. See CONF-700544.

The electrical properties of cadmium-, zinc-, and sulfur-ion-implanted layers in gallium arsenide were measured by the van der Pauw–Hall technique. Ion implantation was performed with the substrates held at room temperature. The dependence of sheet resistivity, surface carrier concentration, and mobility on ion dose and on post-implantation anneal temperature was determined. In the case of 60-keV Ca^+ ions implanted into n-type substrates, a measurable p-type layer resulted when samples were annealed for 10 minutes at a temperature in the range 600 to 900°C. After annealing at 800 to 900°C for 10 minutes, 100% electrical activity of the Cd ions resulted for ion doses $\leq 10^{14}/cm^2$. The properties of p-type layers produced by implantation of 85-keV Zn^+ ions were similar to those of the 60-keV cadmium-implanted layers, in that no measurable p-type behavior was observed in samples annealed below a relatively high temperature. However, in samples implanted with 20-keV Zn^+ ions a p-type layer was observed after annealing for 10 minutes at temperatures as low as 300°C. Implantation of sulfur ions into p-type GaAs substrates at room temperature resulted in the formation of a high-resistivity n-type layer, even before any annealing was performed. Annealing at temperatures up to 200°C or above 600°C lowered the resistivity of the layer, and annealing in the range 300 to 500°C eliminated the n-type layer. (auth)

19843 PROPERTIES OF ION-IMPLANTED SILICON, SULFUR, AND CARBON IN GALLIUM ARSENIDE. Sansbury, J. D.; Gibbons, J. F. (Stanford Electronics Labs., Calif.). Radiat. Eff.; 6: 269-76(Dec 1970).

From International Conference on Ion Implantation in Semiconductors, Thousand Oaks, Calif. See CONF-700544.

Work is described in which chromium-doped semi-insulating gallium arsenide was successfully doped n-type with ion-implanted silicon and sulfur, and p-type with ion-implanted carbon. A dilute chemical etch was employed in conjunction with differential Hall-effect measurements to obtain accurate profiles of carrier concentration and mobility vs depth in conductive implanted layers. This method has been applied to silicon- and sulfur-implanted layers in both Cr-doped semi-insulating GaAs and high-purity vapor-grown GaAs. In the case of sulfur implants, a strong diffusion enhancement was observed during the annealing, presumably due to fast-diffusing implantation-produced damage. Peak doping levels so far obtained are about 8×10^{17} electrons/cm^3 for silicon implants and 2×10^{17} electrons/cm^3 for sulfur implants. Mobility recovery was observed to be complete except in regions near the surface heavily damaged by the implantation. (auth)

19844 RADIATION DAMAGE BY IMPLANTED IONS IN GaAs AND GaP. Carter, G.; Grant, W. A.; Haskell, J. D.; Stephens, G. A. (Univ. of Salford, Eng.). Radiat. Eff.; 6: 277-84(Dec 1970).

From International Conference on Ion Implantation in Semiconductors, Thousand Oaks, Calif. See CONF-700544.

The production of lattice disorder in GaAs and GaP by Te ions up to 40 keV was investigated. For GaAs, the buildup of damage with implanted ion dose is linear until a saturation level is reached. For GaP, two linear regions are evident; a slow buildup of damage to ≃15% of the saturation level, followed by a faster rate of increase up to the final 100% level. Radiation annealing, for GaP samples, both by the heavy-ion beam during implantation and by the helium beam during backscattering measurements was observed. The annealing temperatures required for reordering the lattice depend on the percentage of damage present. Samples damaged up to the saturation level require annealing at ≃500°C, whereas 300°C is sufficient for samples damaged to $\lesssim$50% of the saturation value. (auth)

19845 ION IMPLANTATION OF BISMUTH INTO GaP. I. PHOTOLUMINESCENCE. Merz, J. L.; Feldman, L. D.; Sadowski, E. A. (Bell Telephone Labs., Inc., Murray Hill, N. J.). Radiat. Eff.; 6: 285-91(Dec 1970).

From International Conference on Ion Implantation in Semiconductors, Thousand Oaks, Calif. See CONF-700544.

Photoluminescence from the bismuth isoelectronic trap implanted into GaP is investigated for various ion doses and annealing conditions. A thin coating of silicon oxide is found to be essential to prevent thermal decomposition of the implanted surface during annealing. In isochronal anneal studies the intensity of the Bi luminescence increases rapidly between 650 and 800°C. For 200-keV implants, the dose for maximum luminescence is $\sim 3.5 \times 10^{12}$ ions/cm^2, corresponding to an average concentration of $\sim 10^{18}/cm^3$. However, for the optimum dose and anneal, one observes only ~10% of the light intensity expected from the estimated number of substitutional ions, and the emitting ions are situated in lattice sites with strong local strain. This strain is evident in the photoluminescence spectrum by the appearance of a strong no-phonon line, which results from an otherwise forbidden transition when strain or an external field is present. The luminescence data are correlated with channeling experiments reported in a companion paper. (auth)

19846 IMPLANTATION OF Bi INTO GaP. II. CHANNELING STUDIES. Feldman, L. C.; Augustyniak, W. M.; Merz, J. L. (Bell Telephone Labs., Inc., Murray Hill, N. J.). Radiat. Eff.; 6: 293-9(Dec 1970).

From International Conference on Ion Implantation in Semiconductors, Thousand Oaks, Calif. See CONF-700544.

The channeling technique was used to investigate the properties of Bi-implanted GaP. Measurements of the crystal disorder for 100-keV room temperature implants indicate a damage vs dose curve corresponding to ~13,000 displacements/ion in the linear region and saturation at $\sim 1.5 \times 10^{13}$ Bi ions/cm^2. Annealing of the radiation damage was observed and indicates two annealing steps at ~450°C for light damage and ~750°C for implants in the $1 \times 10^{14}/cm^2$ range. Difficulties associated with the thermal decomposition of the implanted area were overcome by the use of SiO_x coatings. The experimental details associated with the use of the SiO_x layer and with the use of a ^{12}C beam to obtain better depth and mass resolution in the backscattering spectrum are discussed. The lattice location measurements of the Bi impurity show ~50% of the Bi atoms to be along the ⟨110⟩ string after a 900°C anneal for a $7.5 \times 10^{13}/cm^2$ implant. In addition, the spectra show that ~25% of the Bi atoms have diffused to the surface. Correlations of these

XUM

lattice-location results with measurements of the photoluminescen intensity of the GaP (Bi) isoelectronic trap show an agreement in trend with anneal temperature but indicate a factor of ~10 more substitutional ions in the channeling measurement as compared to the photoluminescence results. (auth)

19847 ION-IMPLANTED JUNCTIONS AND CONDUCTING LAYERS IN SiC. Marsh, O. J.; Dunlap, H. L. (Hughes Research Labs., Malibu, Calif.). Radiat. Eff.; 6: 301-11(Dec 1970).

From International Conference on Ion Implantation in Semiconductors, Thousand Oaks, Calif. See CONF-700544.

N-type conducting layers were formed in n- and p-type hexagonal SiC and n-type cubic SiC by implanting ions from Group V: N, P, Sb, or Bi. The implantations were made at room temperature and with energies ranging from 5 to 300 keV. The implanted layers were evaluated by van der Pauw–Hall effect and sheet resistivity measurements and by scanning electron microscopy for anneal temperatures ranging from 1100 to 1800°C. Type conversion of the implanted layers to n-type was observed after a 750°C anneal. Considerable lattice reordering is suggested from the observed carrier mobility values after annealing at 1600°C. An attempt was made to form p-type layers in n-type SiC by implanting Be, B, Al, Ga, and Tl. Application of anneal procedures identical to those used to form n-type layers did not result in measurable p-type layers. The p–n junctions formed by the donor-implanted layers were evaluated as a function of anneal temperature. After annealing at 1200°C there is direct evidence of a thick semi-insulating region between the n-layer and the substrate, which produces a p–i–n diode characteristic. The thickness of this i-layer can be substantially reduced with additional annealing, resulting in abrupt junction behavior for the diode. Well-annealed p–n junctions were characterized as a function of operating temperature over the range of 23 to 400°C. The forward current–voltage behavior of these diodes is dominated by generation and recombination of the carriers in the depletion layer over most of the temperature range. There is some indication of diffusion currents at the highest temperatures. Avalanche breakdown behavior is observed for reverse bias. The capacitance–voltage behavior of these diodes as a function of frequency and temperature indicates the presence of a deep level that can be explained in terms of the bulk properties of the material. (auth)

19848 EFFECTIVENESS OF DISLOCATION LOOPS AS SITES FOR THE ADSORPTION OF IMPLANTED IONS. Gibbons, J. F. (Stanford Univ., Calif.). Radiat. Eff.; 6: 313-18(Dec 1970).

From International Conference on Ion Implantation in Semiconductors, Thousand Oaks, Calif. See CONF-700544.

It is commonly found that when conventional dopant ions are implanted into a semiconductor, only a fraction of the total number implanted will exhibit the electrical behavior that would be expected for an atom of that type in a regular substitutional position. Semiquantitative calculations are presented, which suggest that many of the implanted ions can be adsorbed on dislocation loops produced when the implanted layer is annealed. The effect is particularly large when there is a significant size mismatch between the implanted ion and the host atom. The theory gives a reasonable fit to experimental results if it is assumed that the adsorbed ions are either electrically inactive or else characterized by relatively large carrier ionization energies. (auth)

19849 MOIRE PATTERNS OF ION IMPLANTATION BY CHANNELING. Hutson, A. R. (Bell Telephone Labs., Inc., Murray Hill, N. J.). J. Appl. Phys.; 42: 1239-40(1 Mar 1971).

Planar channeling in two crystals can be used to form a moiré pattern at the exit face of the first crystal and at the entrance face of the second crystal. The result of this moiré pattern at the interface will be either a deep doping pattern in the second crystal or an exit beam pattern from the second crystal. Rotational or parallel moiré patterns can be created, and a third crystal can be used to create a spot pattern. Two channeling parameters must be considered: critical angle and ratio of Thomas–Fermi diameter of the atomic cores to the spacing between channeling planes. Despite its difficulties, moiré doping offers a method for controlling the spatial properties of doping on a very small scale. (D.L.C.)

19850 CHEMILUMINESCENCE METHOD OF INVESTIGATION OF RADIATION DEFECTS IN ALKALI HALIDES. Tiliks, Yu. E.; Bugaenko, L. T.; Teteris, Ya. A.; (and others) (Inst. of Physics, Riga. Moscow State Univ.). Latv. PSR Zinat. Akad. Vestis, Fiz. Teh. Zinat. Ser.; No. 5, 19-24(1970). (In Russian).

Investigation of chemiluminescence during the dissolution of colored alkali halides in water has shown that the chemiluminescence yield is proportional to the concentration of F centers and does not depend on the hole products in crystals. The proposed origin of chemiluminescence is based on excitation of triplet state of water when thermalization of localized electrons during the dissolution occurs. This method may be used for the determination of concentration of F centers when more than 10^{13} per cm^3, which exceeds the sensitivity of usual optical methods. The colloidal metals and compound electronic centers do not take part in the creation of chemiluminescence. (auth)

19851 INFLUENCE OF DEFECTS ON THE ANGULAR CORRELATION OF POSITRON-ANNIHILATION PHOTONS IN IRRADIATED AND IN DEFORMED IRON. Snead, C. L. Jr. (Brookhaven National Lab., Upton, N. Y.); Goland, A. N.; Kusmiss, J. H.; Huang, H. C.; Meade, R. Phys. Rev., B; 3: 275-84(15 Jan 1971).

Measurements of two-photon angular correlations following positron annihilation in both electron-irradiated and plastically deformed iron were made at room temperature. The changes in the angular correlation observed for both treatments are similar and are attributed to the presence of vacancy-type defects. The changes due to the presence of these defects are analyzed in terms of the enhancement of the probability of annihilation of a positron with conduction electrons relative to annihilation with core electrons. The observed effects saturate with increasing defect concentration for both treatments, the total change being larger at saturation for the deformed specimen than for the irradiated one. This is interpreted as being due to less overlap of the positron wave function with core-electron wave functions at vacancy-agglomerate trapping sites in the deformed specimen than at the single-vacancy sites present in the irradiated sample. Stepwise annealing of the specimens firmly established a vacancy–positron interaction, which tends to localize positrons in the vicinity of vacancies as responsible for the angular correlation changes observed. Arrival of carbon-interstitial impurities at single-vacancy sites completely nullified the vacancy–positron interaction. The capture cross section of a vacancy for a positron in iron is estimated to be about 10×10^{-16} cm^2. A method for deducing this cross section from a combination of lifetime and angular correlation results is presented. Recovery of the single vacancies present in the deformed specimen reduced the effect of the deformation by approximately one-half. Additional annealing to 400°C reduced the effect further, but complete recovery was not achieved for the deformed sample up to this temperature. (auth)

19852 . EPR AND OPTICAL ABSORPTION STUDY OF $BrCl^-$ AND ASSOCIATED CENTERS IN DOPED KCl CRYSTALS. I. Delbecq, Charles J.; Schoemaker, Dirk; Yuster, Philip H. (Argonne National Lab., Ill.). Phys. Rev., B; 3: 473-87(15 Jan 1971).

Correlated optical and EPR studies show that after x- or γ-ray irradiation combined with proper thermal treatment, $BrCl^-$ molecular ions aligned along the six ⟨110⟩ directions are present in crystals of KCl doped with a small amount of KBr. The $BrCl^-$ molecular ions, which have a strong σ-polarized transition at 382 nm and a much weaker but still somewhat σ-polarized transition at 760 nm, are thermally more stable than the V_K centers (Cl_2^-) from which they are formed. The increased thermal stability of $BrCl^-$ is believed to arise primarily because the electronegativity of chlorine is greater than that of bromine. A study of the reorientation kinetics at 88°K reveals that the reorientation of $BrCl^-$ proceeds by 90° jumps as well as 60° jumps, and very probably also by 120° jumps, whereas many homonuclear molecular ions reorient only by 60° jumps. (auth)

19853 OBSERVATION OF X-RAY DIFFUSE SCATTERING FROM NEUTRON-IRRADIATED SILICON. Coy, Richard A. (Kansas State Coll., Pittsburg); Thomas, James E. Jr.; Baldwin, Thomas O. J. Appl. Phys.; 42: 1236-8(1 Mar 1971).

Diffuse and small-angle scattering measurements were made on Si single crystals after irradiation with fast-neutron doses of 5×10^{19} n/cm^2. The anomalously transmitted 220 intensity gave R_H (irradiated)/R_H (unirradiated) = 0.63. The 111 Bragg reflection is compared with Laue data. The diffuse scattering results and the asymmetry of the low-angle side of the reflection are compared with these for Cu, and the probable size of the defect clusters is discussed. No change occurred in the small-angle scattering. (D.L.C.)

19854 ANNEALING OF ELECTRON-IRRADIATED n-TYPE SILICON. I. DONOR CONCENTRATION DEPENDENCE. Kimerling, L. C.; DeAngelis, H. M.; Carnes, C. P. (Air Force Cambridge Research Labs., Bedford, Mass.). Phys. Rev., B; 3: 427-33(15 Jan 1971).

The annealing behavior of electron-irradiated phosphorus-doped silicon of low oxygen content (float zoned and Lopex) was studied by monitoring changes in the carrier concentration with Hall-effect measurements. In isochronal anneals, the E-center annealing stage was observed to shift to higher temperatures as the donor concentration was increased. This behavior was found to be con-

XUM

sistent with a charge-state influence on the stability of the E center. Analysis of the experimental data with respect to a charge-state model suggests an activation energy for recovery of the neutrally charged E center of 0.9 to 1.2 eV. This value is in good agreement with previous annealing studies of Watkins and Corbett and Hirata et al. (auth)

19855 TEMPERATURE DEPENDENCE OF DEFECT PRODUCTION IN KBr AND KCl. I. Comins, J. D. (Univ. of the Witwatersrand, Johannesburg). Phys. Status Solidi (b); 43: 101-11(1 Jan 1971).

The rate of production of defects by ionizing radiation in Harshaw K Br and K Cl was studied as a function of temperature. It is found that the production rate increases in a fairly progressive manner between 81 and about 200°K. A correlation is found between the increases in defect production and a progressive broadening of the V-center absorption envelopes formed at the various temperatures of irradiation. Studies of the growth of the major V centers responsible for these absorption envelopes show that they are interstitial defects. It is considered that the enhanced defect production results from an increased probability of interstitial trapping as the temperature of irradiation is raised and that the interstitial defects are trapped in clusters, either intrinsic or nucleated by impurities. (auth)

19856 MICROWAVE DIELECTRIC MEASUREMENTS OF GAMMA-IRRADIATED FERROELECTRIC AMMONIUM SULFATE. Bodi, A.; Baican, R.; Barbur, I. (Univ. of Cluj). Acta Phys. Pol.; A39: 39-44(1971).

The behavior of the complex dielectric constant of unirradiated and gamma-irradiated ferroelectric ammonium sulfate in the microwave region (X band) as a function of temperature is studied. It is concluded that the ferroelectric transition point is shifted from −35°C (for unirradiated samples) to −47°C (for gamma-irradiated samples). Conclusions are reached regarding the thermodynamic aspects of the transformations and the modifications in the crystalline structure produced by gamma irradiation. (auth)

19857 RESIDUAL RESISTIVITY OF Pb FILMS AFTER IMPLANTATION OF Mn IONS. Geerk, J.; Heim, G.; Kessler, J. (Univ., Karlsruhe, Ger.). Z. Phys.; 242: 86-92(1971). (In German).

The method of ion implantation is applied to doping thin lead films with small amounts of manganese. The incident ion intensity is integrated to determine the concentration of magnetic impurities. A marked increase in film resistivity is caused by radiation damage induced in the host lattice and by resonance scattering of conduction electrons on the magnetic impurity sites. Both effects can be observed separately. (auth)

19858 EXPERIMENTAL VERIFICATION OF GENERATION OF CATION VACANCIES DURING IRRADIATION OF KCl CRYSTALS. Kurakina, E. P.; Melik-Gaikazyan, I. Ya. (Tomsk Polytechnic Inst., USSR). Izv. Vyssh. Ucheb. Zaved., Fiz.; No. 10, 155-6(1970). (In Russian).

Cation vacancies produced by irradiation were studied using a KCl monocrystal irradiated by x rays from a tube with a Mo anticathode at 45 kV and 15 mA. The temperature dependence of the conductivity of crystals irradiated in darkness was studied, as well as that of crystals exposed to x irradiation combined with visible light followed by x irradiation in darkness. Results are given in graphical form. (R.V.J.)

19859 KINETICS OF PROCESSES VARIABLY DISTRIBUTED IN RECOVERY ENERGY. Kreutz, E. W.; Moedl, H.; Pagnia, H. (Technische Hochschule, Darmstadt, Ger.). Z. Angew. Phys.; 30: 269-72(1970).

As an example of such processes, the recovery of radiation-induced nonequilibrium occupancy of surface states on germanium was studied. The thermally stimulated recovery of the surface conductance shows stages that are characteristically dependent on the occupancy of states. The model of a variable Gauss distribution and computer evaluations show good agreement with the experimental observations. (auth)

Physical Properties

Refer also to abstracts 19193, 19280, 19281, and 19283.

19860 QUENCHED-IN RESISTIVITY IN MOLYBDENUM. Suezawa, M.; Kimura, H. (Tohoku Univ., Sendai). Scr. Met.; 5: 121-5(Feb 1971).

An appreciable increase in resistivity was found when high-purity molybdenum was quenched in a liquid helium bath. Although further studies are needed, the present results are most satisfactorily explained by attributing the resistivity increase to quenched-in vacancies. (G.M.C.)

19861 RECOVERY OF FAST NEUTRON IRRADIATED MOLYBDENUM. Hanada, R. (Tohoku Univ., Sendai); Takamura, S.; Okuda, S.; Kimura, H. Trans. Jap. Inst. Metals; 11: 434-9(Nov 1970).

Recovery spectra of Mo, fast-neutron irradiated at 10°K, were determined by an electrical resistivity measurement from stage I to stage III. The effect of radiation doping at room temperature on stages I and II recovery was also investigated, and it was found that recovery was enhanced by the doping. The stage III recovery was studied in only doped and in doped and subsequently low-temperature irradiated specimens. The enhancement phenomenon is discussed in conjunction with the stage III recovery study. (auth)

19862 STRUCTURAL MODELS FOR AMORPHOUS SILICON AND GERMANIUM. Walley, P. A. (Chelsea Coll. of Science and Tech., London). pp 219-26 of Ion Implantation. Stevenage, Eng.; Peter Peregrinus Ltd. (1970).

From Conference on Ion Implantation, Reading, England. See CONF-700945.

The term "amorphous" is essentially qualitative, and is used to describe the degree of disorder in solids which lies between the limits of polycrystallinity and total disorder. Classification as amorphous is usually restricted to those materials which do not naturally form bulk glasses, and only a few materials can be deposited in the amorphous form by the conventional process of vapor quenching on to substrates held at normal temperatures; these include the covalent elements Ge, Si, C, and B. The terms short- and long-range order are explained. In all amorphous solids the first and second coordination numbers are fairly well defined, and atomic nearest-neighbour ordering is what is understood by short-range order. By long-range order is meant that property of translational symmetry possessed by crystals; this is lacking in amorphous solids even on a scale of a few tens of Å units. It is this combination of a well-defined short range order, with an absence of long range order, that makes amorphous solids a class of their own. These concepts are applied to Si and Ge. Studies are described on the range of order in α-Si and α-Ge using electron microscopy and diffraction techniques, and requirements of structural models are discussed under the headings of crystallite approach, distorted lattice approach, and rotated bond approach. The production of amorphous films by ion implantation is discussed. It is concluded that the most likely model to describe the structures of amorphous Si and Ge is a disordered network of regular tetrahedra of atoms. 26 references. (UK)

19863 PRESSURE DEPENDENCE OF THE KONDO RESISTANCE ANOMALY AND THE PAIR BREAKING EFFECT IN La–Ce ALLOYS. Gey, W. (Univ., Karlsruhe, Ger.); Umlauf, E. Z. Phys.; 242: 241-9(1971).

The pressure dependence of the pair breaking effect and of the resistance anomaly was measured in LaCe alloys. The results indicate that the maximum in the pressure-dependent pair breaking effect is due to a monotonic shift of the Kondo temperature T_k with pressure from values $T_k \ll T_{c0}$ to $T_k \gg T_{c0}$, where T_{c0} is the superconducting transition temperature of pure lanthanum. (auth)

19864 GRAPHITE CONDUCTION BAND STATES FROM SECONDARY ELECTRON EMISSION SPECTRA. Willis, R. F.; Feuerbacher, B.; Fitton, B. (European Space Research Organization, Moordwijk, Netherlands). Phys. Lett.; 34A: 231-3 (8 Mar 1971).

Intensity maxima were observed in the SEE spectra of graphite excited by low-energy electrons. Their energies agree with critical points in the conduction band of a recent band structure calculation. Variation of peak intensities with angle of incidence suggests that excitation takes place by direct interband transitions. (auth)

19865 MAGNETIC SUSCEPTIBILITY OF DILUTE Au–V ALLOYS. Van Dam, J. E.; Gubbens, P. C. M. (Kamerlingh Onnes Laboratorium, Leiden). Phys. Lett.; 34A: 185-6(22 Feb 1971).

The low-temperature behavior of the susceptibility of dilute Au−V alloys was studied. It is shown that $\Delta\chi \approx 1 - A(T/T_K)^2$ with a T_K of about 250°K. (auth)

19866 4f ELECTRONIC STATES IN THE METALS Nd, Sm, Dy, AND Er STUDIED BY X-RAY PHOTOEMISSION. Heden, P. O. (Chalmers Univ. of Tech., Goteborg); Loefgren, H.; Hagstroem, S. B. M. Phys. Rev. Lett.; 26: 432-4(22 Feb 1971).

Photoelectron spectra excited by x radiation are reported for

XUM

the band-structure part on clean films of the rare-earth metals Nd, Sm, Dy, and Er. The dominant part of the spectra is due to excitation of 4f electrons. The spectra exhibit a complex and extended structure, which is interpreted in terms of multiplet splitting of the final state in the photoemission process. (auth)

19867 VC, NbC, AND TaC WITH VARYING CARBON CONTENT STUDIED BY ELECTRON SPECTROSCOPY FOR CHEMICAL ANALYSIS. Ramqvist, Lars (Axel Johnson Inst. for Industrial Research, Nynaeshamn, Sweden); Hamrin, Kjell; Johansson, Gunilla; Gelius, Ulrik; Nordling, Carl. J. Phys. Chem. Solids; 31: 2669-72(Dec 1970).

Electron spectroscopic studies by the electron spectroscopy for chemical analysis (ESCA) technique of core-level electrons in VC, NbC, and TaC with varying carbon contents show that the electron transfer from the metal atoms increases with increasing carbon content in the VC phase but decreases in the NbC and TaC phases. The VC phase resembles the TiC phase measured in a previous investigation. The ESCA shifts are compared with heats of formation. (auth) (UK)

19868 ELECTRICAL RESISTIVITY OF NbO. Chandrashekhar, G. V.; Moyo, J.; Honig, J. M. (Purdue Univ., Lafayette, Ind.). J. Solid State Chem.; 2: 528-30(Dec 1970).

The resistivity of NbO_x ($0.99 \le x \le 1.03$) boules containing 3 to 5 grains is reported for the range 77 to 900°K. The material is an excellent conductor with a positive temperature coefficient of resistivity. The results are compared with some earlier work, which seems to require correction, and with unpublished work confirmed by this study. (auth)

19869 HEAT CAPACITY AND MAGNETIZATION OF PRASEODYMIUM METAL IN THE TEMPERATURE REGION 1.2 TO 4.2°K WITH APPLIED MAGNETIC FIELDS UP TO 40,000 G. Stein, R. L.; Butera, R. A. (Univ. of Pittsburgh). J. Solid State Chem.; 2: 503-20(Dec 1970).

The magnetic and thermal properties of two spherical samples of praseodymium were determined over the temperature region 1.2 to 4.2°K in magnetic fields of 40 kG. The zero-applied-magnetic-field heat capacity data indicate the existence of an anomaly centered about 3.4°K and an upturn below 1.4°K. The temperature of the small 3.4°K anomaly decreases as the field is increased. The temperature of the onset of the upturn, as well as its magnitude, increases as the magnetic field is applied. This behavior was exhibited by both samples; however, the absolute magnitude of the heat capacity differed between samples. The magnetization exhibited no unusual behavior at 3.4°K; however, the magnetic moment in a 5000-G applied field increased as the temperature decreased. A remnant moment was detected in one of the samples after the application of a magnetic field. The effect of impurities on the anomaly is discussed. (auth)

19870 COMPTON SCATTERING AND ELECTRON MOMENTUM DENSITY IN BERYLLIUM. Currat, R.; DeCicco, P. D.; Kaplow, Roy (Massachusetts Inst. of Tech., Cambridge). Phys. Rev., B; 3: 243-51(15 Jan 1971).

Compton-scattered x-ray spectra were measured for three orientations of a beryllium single crystal. The reduced profiles were analyzed in terms of the electron momentum distribution. Observed anisotropies can be explained qualitatively in terms of the geometry of the Fermi surface and are in qualitative agreement with earlier positron and x-ray data. The present results show high-momentum components among the valence electrons that are not revealed in the positron experiment nor accounted for by available calculations. In the process of reducing the data to obtain the momentum distribution of the valence electrons, detailed consideration was given to the effects of binding on the Compton scattering by the core electrons. (auth)

19871 PARAMAGNETIC BEHAVIOR OF Fe ATOMS IN SOME INTERMETALLIC COMPOUNDS CONTAINING Y, Lu, AND Gd. Givord, Francoise (CNRS, Grenoble, France). Compt. Rend., Ser. B; 271: 1159-61(21 Dec 1970). (In French).

The variations in the magnetic susceptibilities with respect to temperature of Y_2Fe_{17}, Y_6Fe_{23}, YFe_3, YFe_2, $LuFe_2$, and $GdFe_2$ were measured. A comparison between the magnetic moments of iron and cobalt for alloys containing increasing numbers of rare earth atoms was made. (auth) (France)

19872 SOFT MAGNETIC ALLOYS: THEIR HEAT TREATMENT AND TESTING FOR MAGNETIC PROPERTIES. Eberly, Warren S. (Carpenter Tech. Corp., Reading, Pa.). Metals Eng. Quart.: 11: No. 1, 40-7(Feb 1971).

The magnetic properties achieved after heat treatment of the magnetic core or lamination are presented for the following soft magnetic alloy classes: Ni—Fe alloys (HyMu 800, HyMu 80, High Permeability 49, HyRa 49), Fe—Co alloys, Fe—Si alloys, ferritic stainless steels, commercial irons, and commercially pure irons. (D.L.C.)

19873 POLAR REFLECTION FARADAY EFFECT IN SILVER-BASED DISORDERED ALLOYS. Tracy, John Micheal. Seattle; Univ. of Washington (1970). 116p. University Microfilms Order No. 71-1034.

Thesis.

The polar reflection Faraday effect (PRFE) was measured in α-phase disordered alloys of Ag—Mg and Ag—Cd. The PRFE rotation may be related to the size of the necks on the Fermi surface. In addition, the lifetime of the electron states may be estimated. This information was then applied to the improvement of the understanding of disordered alloys. The PRFE is an excellent method for the study of these alloys because of the high frequency of light (about 3.5×10^{14} Hertz) used. In addition, the results have a simple geometrical interpretation. The curve of rotation versus compositior for Ag—Mg showed a drop from the pure Ag value that is qualitatively in accord with the rigid-band model, although no quantitative comparison was made. Ag—Mg samples were studied with compositions up to 30% Mg. For Ag—Cd, the rotation followed that of Ag—Mg out to 30% Cd, at about which point there was a significant drop-off in the rotation. This was interpreted as a touching of the Fermi surface to the Brillouin zone boundary at the point X in addition to the necks already present at L. The rigid-band expectation for the composition at which this occurs is 33%. Ag—Cd samples were made out to 42% Cd. Lifetime measurements were in rough accord with the values obtained from residual resistivity. It was concluded from the measured lifetimes that the ratio of the smearing of the Fermi energy, due to scattering, to the rigid-band shift of that energy was about 0.2, confirming that these were weak scattering alloys. This is to be expected partly because of the large energy gap in noble metals and the half-filled conduction band. Samples were made as opaque films on glass substrates in a two-source electron-beam evaporation apparatus. This was equipped with film-thickness monitors and automatic evaporation ratio control circuits. The electron beam was electrostatically deflected and the duty cycle on each source determined the evaporation rates. Most samples were analyzed for crystallite size and lattice constant by x-ray diffraction. (Diss. Abstr. Int., B)

19874 MAGNETIC SUSCEPTIBILITIES OF HEXAGONAL Tc–Ru, Tc–Rh, AND Ru–Rh ALLOYS. Isaacs, L. L.; Lam, D. J. (Argonne National Lab., Ill.). J. Phys. Chem. Solids.; 31: 2581-3(Nov 1970).

The magnetic susceptibilities (χ) of the alloys were found to be temperature- and field-independent, within the sensitivity of the measurements (1×10^{-8} cmu/g) over the entire temperature range of 4 to 300°K and magnetic field range of 1 to 11 kOe. The χ values at 300°K are tabulated as a function of average group number. The susceptibility results for the Tc alloys show an average group-number dependence similar to that reported by Booth (Phil. Mag. 17: 205, (1967)) for molybdenum alloys, and the absolute values for Ru—Rh alloys are almost identical. (UK)

19875 PERMANENT MAGNET PROPERTIES OF INTERMETALLIC COMPOUNDS Sm (Fe, Co, Cu)$_5$. Katayama, Toshikazu; Shibata, Tsugio (Electrotechnical Lab., Tokyo). Jap. J. Appl. Phys.; 10: 278-9(Feb 1971).

In the series $SmFe_xCo_{5-x}$, saturation magnetization decreases at first with X, reaching a minimum at X = 0.4. For the series $SmFe_x Co_{3.7-x} Cu_{1.3}$, the magnetization, residual magnetization, and maximum energy product BH increase slightly with x up to 0.4, decreasing rapidly thereafter. Coercive force for the same series increases with x up to 0.6; annealing at 400°C also increases the force. The microstructure of $SmFe_{0.2} Co_{3.5} Cu_{1.3}$ shows areas rich in Sm (Fe, Co)$_5$ and $SmCu_5$. The demagnetization curve of an annealed $SmFe_{0.4} Co_{3.55} Cu_{1.25}$ has a maximum energy product of 9.6×10^6 GOe. (D.L.C.)

Moessbauer Effects and NMR

Refer also to abstracts 18751, 18848, 19220, and 20335.

19876 EXPLORATORY DEUTERON MAGNETIC RESONANCE STUDY OF VANADIUM, NIOBIUM, AND TANTALUM DEUTERIDES. Pedersen, B.; Slotfeldt-Ellingsen, D. (Sentralinstitutt for Industriell Furskning, Oslo). J. Less-Common Metals; 23: 223-7(Feb 1971).

A deuteron magnetic resonance (DMR) study on the Group VA metal deuterides is reported. Despite the fact that unique information can be obtained from the DMR spectra, this is probably the first study of DMR in metal deuterides where the dominating broadening mechanism is the coupling between the quadrupole moment of the deuteron and the electric field gradient at the deuteron site. This note concentrates on showing specifically what information can be obtained from DMR spectra of a few, selected samples. (auth)

19877 MOESSBAUER EFFECT OF THE 129-keV TRANSITION IN ^{195}Pt. Wolbeck, B.; Zioutas, K. (Univ., Bonn). Z. Naturforsch.; 25a: 1779-80(Dec 1970).

The Moessbauer effect of the 129-keV transition in ^{195}Pt was observed. By use of a Ge(Li) detector any contribution from the strong 99-keV Moessbauer line could be eliminated. The width of the resonance absorption line corresponds to the natural line width. The branching ratio in the decay of the 129-keV level was found to be I(129)/I(31) = (5.7 ± 1.6)%. (auth)

19878 NEW PRINCIPLE OF MODULATION IN INVESTIGATIONS OF NUCLEAR MAGNETIC RESONANCE IN FERROMAGNETS. Zalesskii, A. V. (Inst. of Crystallography, Moscow). Instrum. Exp. Tech. (USSR) (Engl. Transl.); No. 2, 492-3(Mar-Apr 1970).

Translated from Prib. Tekh. Eksp.; No. 2, 156-7(Mar-Apr 1970).

The possibility of using magnetic modulation of frequency to record a nuclear magnetic resonance signal in ferromagnets is shown. The modulation is based on the variation of magnetic permeability in a sinusoidal field. Results are presented for ^{57}Fe and ^{61}Ni. (D.L.C.)

19879 ALPHER-RUBIN ULTRASONIC ATTENUATION AND DIPOLAR NUCLEAR-ACOUSTIC-RESONANCE COUPLING IN PURE METALS. Miller, J. G.; Smith, W. D.; Bolef, D. I.; Sundfors, R. K. (Washington Univ., St. Louis). Phys. Rev., B; 3: 1547-56(1 Mar 1971).

Experimental results are presented of measurements of the very small magnetic-field-dependent changes in the attenuation $\Delta\alpha$ of ultrasound (absorptive Alpher–Rubin effect) in pure single crystals of Al, Cu, Nb, and Ta. Measurements were made at 293°K in magnetic fields ranging from 0 to 11 kOe, using both longitudinal and transverse acoustic waves. Variations of $\Delta\alpha$ with both orientation and magnitude of the external magnetic field were studied. Measurements of the dependence of $\Delta\alpha$ on frequency over the range 5 to 250 MHz were made. The results are particularly relevant to the study of induced dipolar coupling in nuclear acoustic resonance. A derivation is given of expressions for the nuclear-acoustic-resonance signal in pure metals. (auth)

Theoretical Physics

Refer also to abstracts 19935, 20066, 20513, and 20523.

19880 SOME INEQUALITIES SATISFIED BY NORMAL-ORDERED MOMENTS. Chand, Prakash (Colorado State Univ., Fort Collins). Lett. Nuovo Cim.; 4: 1068-72(5 Dec 1970).

The concept of coherence indices has the advantage of retaining physical interpretation. Normal-ordered moments can be defined as $g^{\mu,\nu} = \mathrm{Tr}\{a^{\nu}\rho a^{\dagger\mu}\}$ where ρ is the density matrix and a and $a^{\dagger}$ are annihilation and creation operators for photons. A number of inequalities satisfied by the normal-ordered moments are derived. (R.W.R.)

19881 FITTING OF DOUBLE EXPONENTIAL LIFETIME SPECTRA USING A MAXIMUM LIKELIHOOD TECHNIQUE. Lee, G. F.; Jones, G. (Univ. of British Columbia, Vancouver). Nucl. Instrum. Methods; 91: 665-6(1971).

A modification of a previously presented iterative method for fitting double exponential lifetime spectra is presented. A different choice of parameters is shown to reduce the number of iterations required. (auth)

19882 ESTIMATION OF PERTURBATION OF EIGENVALUES OF THE TWO-PARTICLE SCHROEDINGER OPERATOR WITH A HARD-CORE POTENTIAL. Pyzh'yanov, A. M. (Moscow State Univ.). Teor. Mat. Fiz.; 6: 225-9(Feb 1971). (In Russian).

Estimations of the quantity $|\lambda_i - \lambda_i^M|$ are derived, where λ_i and λ_i^M are eigenvalues of operators $H = -\Delta + V(x)$ and $H_M = -\Delta + V_M(x)$; ($x = (x_1,x_2,x_3)$) correspondingly. The function V(x) is singular at $|x| < a$, $a > 0$, and $V_M(x) = \min_x \{M, V(x)\}$, M being a sufficiently large positive number. (auth)

19883 DOES THE ELECTRON CHARGE CHANGE WITH THE AGE OF THE UNIVERSE? Kramarovskii, Ya. M.; Chechev, V. P. (Ioffe Inst. of Physics and Tech., Leningrad). Usp. Fiz. Nauk; 102: 141-8(Sep 1970). (In Russian).

The problems of possible changes of atomic constants with the age of the Universe are considered. Dirac concepts on changes of electron charge are described with the conclusion that, assuming e^2 and M_p (proton mass) remain constant, the Newtonian gravitational constant G varies with time. The invariability of the atomic constants based on Teller, Gamow, Bahcall, and Schmidt arguments indicate that none of the hypotheses or experiments on the relation between the atomic and cosmological constants can yet deny the constancy of the elementary electric charge. (21 references) (R.V.J.)

PHYSICS (HIGH ENERGY)

Particle Interactions and Properties (Experimental)

19884 CLOUD-CHAMBER SEARCH FOR $\frac{1}{3}$e AND $\frac{2}{3}$e QUARKS IN AIR SHOWERS. Hazen, W. E. (Univ. of Michigan, Ann Arbor). Phys. Rev. Lett.; 26: 582-3(8 Mar 1971).

A cloud chamber of horizontal area 0.2 m^2 is being used to observe the ionization by the particles in the vicinity of the center of air showers in the manner of McCusker. No particle tracks with ionization typical of charge $\frac{2}{3}$e or $\frac{1}{3}$e were found in 3200 shower photographs taken with a trigger rate of about one per hour. (auth)

19885 PRESENT ROLE AND PROSPECTIVES OF COSMIC RAYS IN HIGH-ENERGY PHYSICS. Fenyves, Ervin. Rend. Semin. Mat. Fis. Milano; 39: 53-9(1969).

A discussion of the aspects of high-energy physics in cosmic ray research, particularly with respect to the experimental study of elementary particles and their interactions, is presented. For such nuclear studies, the investigation of cosmic ray phenomena would seem reasonable only at energies higher than the accelerator energies available at present. It is pointed out, however, that ideas arisen in cosmic ray physics have led to important discoveries in accelerator physics. On the other hand, the theoretical and experimental results obtained from the rapidly growing research in high-energy physics by means of accelerated particles have been and could still be of even larger importance for further cosmic ray investigations. It is therefore felt that experimental and theoretical information obtained at accelerator energies should be used on a much more extended scale in cosmic ray research, and that a much closer connection should be maintained between these two fields. Further arguments and examples substantiating this view are discussed. (auth) (IAA)

Electromagnetic

19886 (DESY-70/61) PHOTOPRODUCTION OF PION PAIRS WITH HIGH INVARIANT MASS. Alvensleben, H.; Becker, U. J.; Bertram, William K.; (and others) (Deutsches Elektronen-Synchrotron, Hamburg (West Germany). Massachusetts Inst. of Tech., Cambridge). Nov 1970. 10p. Dep. NTIS (U. S. Sales Only).

The yield of $\pi^+\pi^-$ pairs from the reaction $\gamma + C \rightarrow C + \pi^+\pi^-$ in the invariant mass region $0.6 < m < 1.8$ GeV/c^2 was measured. The result, based on 10^5 events, shows that the data, at high energy and very small momentum transfer, exhibit an enhancement in the region $1.3 < m < 1.8$ GeV/c^2. (auth)

19887 PHOTOPRODUCTION OF NEUTRAL K MESONS. Cassel, D. G. (Cornell Univ., Ithaca, N. Y.); Engels, E. Jr.; Entis, A. C.; Sadoff, A. Phys. Lett.; 34B: 223-6(15 Feb 1971).

K_L^0 photoproduction was studied in a spark chamber system at 2.5° to bremsstrahlung beams with maximum energy, E_0, between 5.5 and 9.5 GeV. The yields increase approximately as $E_0^{2.5}$. Characteristics of the yields are compared with K_L photoproduction models. (auth)

19888 MEASUREMENT OF THE MUONIUM HFS SPLITTING AND OF THE MUON MOMENT BY "DOUBLE RESONANCE," AND A NEW VALUE OF α. De Voe, R.; McIntyre, P. M.; Magnon, A.; (and others) (Univ. of Chicago). Phys. Rev. Lett.; 25: 1779-83(28 Dec 1970).

The hyperfine interval $\Delta\nu$ and the muon moment $\mu_\mu = g_\mu' \mu_B/2$ were determined from the frequencies of the two alternative Zeeman transitions in muonium, working at that "magic" field where $\partial\nu_1/\partial B = \partial\nu_2/\partial B = 0$. Extrapolating determinations of $\Delta\nu$ in Kr and Ar to zero pressure, consistent results, yielding jointly $\Delta\nu(0) = 4463.3022(89)$ MHz are obtained. Assuming that $g_j(M)$ is unshifted by collisions, $g_e/g_\mu' = 206.765\ 09(80)$ is obtained, which corresponds to $f_\mu/f_p = 3.183\ 373(13)$. The combination of these results gives $\alpha^{-1} - 137 = 0.036\ 54(30)$ (2.1 ppm in α^{-2}), in good agreement with the recommended value of 0.036 02 (21). (auth)

19889 MEASUREMENTS OF THE ASYMMETRY RATIO OF POSITIVE-PION PHOTOPRODUCTION BY LINEARLY POLARIZED PHOTONS. Kuznetsov, V. M.; Stukov, O. I.; Repenko, E. V.; Kalinin, B. N. (Inst. for Nuclear Physics, Tomsk, USSR). Lett. Nuovo Cim.; 1: 233-4(6 Feb 1971).

A linearly polarized photon beam was used for the reaction $\gamma + p \rightarrow \pi^+ + n$ at 227 to 260 MeV for the purpose of measuring the asymmetry ratio for this process. The asymmetry ratios are listed for angles of 51 to 146°. (J.F.P.)

19890 PHOTOPRODUCTION OF TWO NEUTRAL PIONS FROM HYDROGEN NEAR THRESHOLD. Kitagaki, Toshio; Ohnuki, Yuji; Tanaka, Syo; Homma, Saburo; Abe, Koya (Tohoku Univ., Sendai). J. Phys. Soc. Jap.; 30: 595-601(Mar 1971).

Measurement of the photoproduced two neutral pions from hydrogen was performed up to 730 MeV by detecting both pions by means of their decay gamma rays in coincidence. The differential cross section obtained around 600 MeV is close to zero within the statistics and is consistent with the static model calculation. The cross section around 700 MeV, however, is about 0.25 μb/(sterad)^2 at $\theta_{\pi_1} = \theta_{\pi_2} = 55°$ in the laboratory system. (auth)

Weak

19891 (JINR-P1-5542) SEARCH FOR THE DECAY $\mu^+ \rightarrow e^+ + e^+ + e^-$. Korenchenko, S. M.; Kostin, B. F.; Mitsel'makher, G. V.; Nekrasov, K. G.; Smirnov, V. S. (Joint Inst. for Nuclear Research, Dubna (USSR). Lab. of Nuclear Problems). 1970. 6p. (In Russian). Dep. NTIS (U. S. Sales Only).

The $\mu^+ \rightarrow e^+ + e^+ + e^-$ decay was searched for with the help of a cylindrical spark chamber placed in the 4500-Oe magnetic field. Scintillator counter pulses were displayed on the five-ray oscilloscope screen. With $1.1(10)^{10}$ stopped pions about 300 thousand pairs of pictures were taken. After previous scanning 226 events were selected, measured and calculated by the computer. With the help of the χ^2 criteria the consistency of the taken events to the geometrical requirements and to the kinematics of the $\mu^+ \rightarrow e^+ + e^+ + e^-$ decay was established. The events with such a value of χ^2 when its probability is smaller than 5% were rejected. Besides, the events were considered as background and rejected if the angle between e^+ and e^- was 180° ± 20°, and the energy difference of e^+ and e^- was not larger than 10 to 20 MeV taking into account the energy losses in the target. Such events can be imitated by one positron or electron passing through the whole chamber. As a result, not a single event could be regarded as the $\mu^+ \rightarrow e^+ + e^+ + e^-$ decay. The detection efficiency of the $\mu^+ \rightarrow e^+ + e^+ + e^-$ decay was calculated by the Monte Carlo method taking into account chamber geometry and triggering conditions. The decay matrix element was taken constant. After introducing necessary corrections (for triggering system efficiency, camera dead time, spark chamber efficiency, etc.) the detection efficiency of the $\mu^+ \rightarrow e^+ + e^+ + e^-$ decay was obtained to be $3.4(10)^{-2}$. This permits the upper limit of the branching ratio to be established as $W(\mu^+ \rightarrow e^+ + e^+ + e^-)/W(\mu^+ \rightarrow e^+ + \nu_e + \bar{\nu}_\mu) \leq 6.2 \cdot 10^{-8}$ with a 90% confidence level. (auth)

19892 DETERMINATION OF THE NEUTRINO SPECTRUM IN THE CERN 1967 NEUTRINO EXPERIMENT. Bloess, D.; Pattison, J. B. M.; Plass, G.; (and others) (CERN, Geneva). Nucl. Instrum. Methods; 91: 605-12(1971).

The 1967 neutrino spectrum was derived from the measured flux distribution in the shielding. The precision is ±15% between 1.5 GeV and 2 GeV, ±10% in the range 2–5 GeV, and ±25% above 5 GeV where it depends on the K/π ratio uncertainty. The method of determining the spectrum is described. The result agrees well with predictions from recent pion and kaon production data. (auth)

19893 SEARCH FOR PROTON DECAY AS A TEST OF BARYON CONSERVATION. Dix, Frederick William. Cleveland; Case Western Reserve Univ. (1970). 50p. University Microfilms Order No. 70-25,861.

Thesis.

A large-volume heavy-water Cherenkov detector enclosed in a liquid scintillator anticoincidence shield was used to search for proton decay. The 550 gallons of D_2O used were obtained on loan from the Savannah River Plant of the Atomic Energy Commission. The experimental site was located 1950 feet underground to reduce cosmic ray and other background. A lower limit on the proton lifetime of 3.1×10^{23} years was established, independent of the mode of decay. The results were also interpreted to set an upper limit on the ^8B solar neutrino flux of 9.5×10^8 cm^{-2} sec^{-1}. (Diss. Abstr. Int., B)

19894 MEASUREMENT OF THE ASYMMETRY PARAMETERS FOR THE BETA DECAY OF POLARIZED Λ HYPERONS. Swallow, Earl Connor St. Louis; Washington Univ. (1970). 83p. University Microfilms Order No. 70-26,884.

Thesis.

An experiment was performed at Argonne National Laboratory's Zero Gradient Synchrotron to investigate the $\Delta S = 1$ weak decay

$\Lambda^0 \rightarrow p + e^- + \nu$. Decays of polarized Λ^0 hyperons from the associated production process $\pi^- + p \rightarrow \Lambda^0 + K^0$ at 1025 MeV/c were observed in a magnetic spectrometer consisting of optical spark chambers and counters immersed in the field of a large-gap magnet. The desired leptonic decays were identified by Čerenkov and time-of-flight techniques. Analysis of a preliminary sample of 84 events, obtained from 180,000 spark chamber photographs, gave for the decay asymmetry parameters with respect to the Λ^0 spin $\alpha_e = +0.07 \pm 0.25$, $\alpha_p = -0.22 \pm 0.25$, and $\alpha_\nu = +0.56 \pm 0.25$. The values of the proton and neutrino asymmetry parameters are not in particularly good agreement with the most recent fit to the Cabibbo formulation of the V–A theory of weak interactions: the magnitudes are smaller than expected. These values do not directly contradict the results of any other experiment. (Diss. Abstr. Int., B)

19895 ANALYSIS OF THE PION SPECTRUM OF 35,630 τ^+ DECAYS AT REST. Hoffmaster, James Steven Hoboken, N. J.; Stevens Inst. of Tech. (1970). 41p. University Microfilm Order No. 71-1170.

Thesis.

The energy spectrum of the secondary pions of 35,630 τ^+ decays at rest was examined. It was found to be adequately fitted by the linear form $|M|^2 \propto 1 + \alpha_{\tau^+}[(M_k Q/m_\pi^2)]Y$, $\alpha_{\tau^+} = 0.133 \pm 0.006$. The value of the slope parameter is in good agreement with other experiments and in fair agreement with theoretical predictions. The $\Delta I = 1/2$ rule was found to be significantly violated for charged $K^+ \rightarrow 3\pi$ decays. There is no evidence for CP invariance violation in $\tau^\pm$ decay. (Diss. Abstr. Int., B)

19896 BRANCHING RATIOS FOR $K^+ \rightarrow 3\pi$ DECAYS. Pandoulas, Demetrios G. Hoboken, N. J.; Stevens Inst. of Tech. (1970). 42p. University Microfilsm Order No. 71-1179.

Thesis.

The branching ratios $(\tau'^+/K^+ \rightarrow \text{all})$ and (τ'^+/τ^+) were obtained from a sample of 12,976 K^+ decays including 198 τ'^+ and 693 τ^+ decays. It was found that $(\tau'^+/K^+ \rightarrow \text{all}) = 0.0153 \pm 0.0011$ and that $(\tau'^+/\tau^+) = 0.286 \pm 0.023$. The $(\tau^+/K^+ \rightarrow \text{all})$ branching ratio and the π^+ energy spectrum in τ'^+ decay were also obtained and were found to be in good agreement with the more accurate determinations of other experiments. The branching ratio data suggest a small $\Delta I = 3/2$ admixture in the $K \rightarrow 3\pi$ decay amplitudes. Comparison with various theoretical models shows fair to good agreement between experiment and theory. (Diss. Abstr. Int., B)

19897 K_S^0 CHARGED-TO-NEUTRAL DECAY BRANCHING RATIO: A PRECISION MEASUREMENT. Moffett, David Read Rochester, N. Y.; Univ. of Rochester (1970). 102p. University Microfilms Order No. 71-1411.

Thesis.

A precision measurement of the K_S^0 charged to neutral 2 pion decay branching ratio is described. The result is 2.282 ± 0.043. This is a 5.9 standard deviation violation of the $|\Delta I| = 1/2$ rule predication of 2, (when an electromagnetic correction of -0.006 ± 0.024 is included). The K_S^0 were produced by charge exchange of 2.1 GeV/c K^+ in a beryllium target. Optical spark chambers recorded the decays. An overall correction of 3.3% was applied to the raw scan branching ratio. For reasonable choices of $\delta_2 - \delta_0$, (the difference between the $I = 2$ and $I = 0$ S wave $\pi\pi$ strong interaction phase shifts, at the K^0 mass), the $I = 2$ two pion amplitudes for K^+ and K^0 2 pion decay are comparable. If $|\Delta I| = 5/2$ transitions are assumed to be negligible then $|\delta_2 - \delta_0|$ can be calculated. The result is $|\delta_2 - \delta_0| = 44^{\circ}{}^{+\text{[illegible]}}_{-\text{[illegible]}1^{\circ}}$. (Diss. Abstr. Int., B)

19898 CHARGE ASYMMETRY IN THE MUONIC DECAY OF THE K_2^0. Paciotti, Michael Anthony. Berkeley, Calif.; Univ. of California (1970). 109p. University Microfilms Order No. 71-825.

Thesis.

The charge asymmetry $R \equiv [\Gamma(K_L^0 \rightarrow \pi^-\mu^+\nu_\mu)/\Gamma(K_L^0 \rightarrow \pi^+\mu^-\nu_\mu)]$ is measured to be $1.0098 \pm .0032$. Separation of muons from pions is achieved by passage through 230 grams/cm^2 of aluminum and 870 grams/cm^2 of lead. Positive and negative muons are spatially separated behind the pion filter by application of a magnetic field preceding the aluminum and lead absorber. Data are taken with scintillation counters, and optical thin-plate and thick-plate spark chambers are used for calibration of systematic effects. (Diss. Abstr. Int., B)

Strong (Baryon-Induced)

Refer also to abstracts 20257 and 20258.

19899 (UCRL–20000–NN) NN AND ND INTERACTIONS (ABOVE 0.5 GeV/c): A COMPILATION. Benary, Odette; Price, LeRoy R. (California Univ., Berkeley. Lawrence Radiation Lab.); Alexander, Gideon (Tel Aviv Univ. (Israel)). Aug 1970. 358p. Dep. NTIS.

There are 165 papers compiled reporting pp, np, nn, pd, and nd interactions from 0.5 to 70 GeV/c. Cross sections, angular distributions, and polarizations as well as fits to some of the data are displayed. Included are indices to the papers, as well as a complete listing of the selected data. (auth)

19900 (USIP–70–4) PROTON–PROTON REACTIONS AT 19 GeV/c WITH PRODUCTION OF TWO AND THREE PIONS. Scandinavian Collaboration. (Stockholm Univ. (Sweden). Inst. of Physics). Oct 1970. 47p. (CONF-680809–46). Dep. NTIS (U. S. Sales Only).

From 14th International Conference on High Energy Physics, Vienna, Austria.

25000 4-prong events from an exposure of the CERN 2-meter HBC to a 19-GeV/c proton beam were measured and passed through the CERN THRESH-GRIND computer programs. Fits were obtained to the three channels $\rho\rho \rightarrow \rho\rho\,\pi^+\pi^-$ (1), $\rho\rho \rightarrow n\rho\,\pi^+\pi^+\pi^-$ (2), $\rho\rho \rightarrow \rho\rho\,\pi^+\pi^-\pi^0$ (3). Observed branching of the reactions (1), (2) and (3) into various channels is described. The following cross sections were obtained $\sigma(1) = 1.5 \pm 0.2$ mb, $\sigma(2) = 1.7 \pm 0.3$ mb, $\sigma(3) = 1.7 \pm 0.3$ mb. Some features of the double Regge pole exchange model were tested on the channel $\rho\rho \rightarrow \Delta^{++}\pi^-\rho$. A one-pion exchange calculation indicates that only a part of the low mass enhancement in the $\Delta^{++}\pi^-$ system of reaction (1) can be explained as a kinematic effect resulting from Δ^{++} production in association with diffraction scattering. The angular correlation of the two pions in reaction (1) shows that the reaction is so peripheral that the events can be divided into two well defined classes (i) with the grouping ρ–$(\rho\,\pi^+\pi^-)$ contain- 67% of the sample (ii) with the grouping $(\rho\,\pi^+)$ – $(\rho\,\pi^-)$ containing 33% of the sample. The two groups correspond to charge transfer 0 and 1 respectively. All channels are dominated by resonance production. Observed known resonances, as judged from the mass distribution, account for ~90% of the total cross section of reactions (1) ~70% of (2) and ~65% of reaction (3). (FHS) (Sweden)

19901 (USIP–70–7) STUDY OF PROTON–PROTON INTERACTIONS AT 19 AND 10 GeV/c. Yamdagni, Narendra (Stockholm Univ. (Sweden). Inst. of Physics). Nov 1970. 81p. Dep. NTIS (U. S. Sales Only).

Thesis.

A systematic study of the final state involving four charged particles was made in pictures taken at three exposures to 19 GeV/c proton beam in the CERN 2m hydrogen bubble chamber. The experimental procedure is described, and an outline of the beam set up together with scanning and measuring procedures is given. The study of distortion effects in the geometrical reconstruction of events resulted in a number of improvements in the reconstruction of events. Cross sections and study of possible biases in obtaining them are given. General features of the interactions in terms of single particle distributions are presented, and finally an analysis of the data in terms of various subchannels is performed. A study at 10 GeV/c was made in an exposure of pictures carried out in the Saclay 81 cm hydrogen bubble chamber. The cross section for strange particle production was found to increase rapidly with beam momentum from 4 GeV/c to 25 GeV/c. Interpreted in terms of a quasi two-body peripheral production mechanism the results indicate a preference for nonstrange-meson exchange. In a study of six charged particles, final state resonance production was established in the $(N\pi)$ system. The nucleons are observed to be peripheral in six- and seven-body final states. (FHS) (Sweden)

19902 (USIP–70–8) BUBBLE CHAMBER EXPERIMENTS ON 10 AND 19 GeV/c PROTON–PROTON INTERACTIONS. Holmgren, Sven-Olof (Stockholm Univ. (Sweden). Inst. of Physics). Nov 1970. 74p. Dep. NTIS (U. S. Sales Only).

An analysis of proton–proton interactions at 10 GeV/c and 19 GeV/c based on experiments in hydrogen bubble chambers is presented. Experimental details not published earlier are given. Physical results are summarized and for the 19 GeV/c experiment certain physical results are presented, which have not been published before. (FHS) (Sweden)

19903 MEASUREMENT OF THE NEUTRAL CASCADE HYPERON LIFETIME. Jauch, Delbert Edwin. Corvallis, Oreg.; Oregon State Univ. (1970). 134p. University Microfilms Order No. 70-27,031.

Thesis.

The lifetime of the neutral cascade hyperon was measured. The data were from a scintillator optical spark chamber experiment. The cascades were produced by 1.8-GeV/c K^- mesons incident in 1.0 g/cm^2 of liquid hydrogen. The value $\tau_{\Xi^0} = 2.44^{+\text{[illegible]}}_{-\text{[illegible]}} \times 10^{-10}$ sec was obtained. This is consistent with previous measurements and in agreement with the $\Delta I = 1/2$ rule. Order No. 70-27,031, 134 pages. (Diss. Abstr.)

XUM

19904 NUCLEON–NUCLEON TRIPLE-SCATTERING PARAMETERS 510 TO 670 MeV. Surko, Pamela Hansen. Berkeley, Calif.; Univ. of California (1970). 49p. University Microfilms Order No. 71-849.

Thesis.

The values of the Wolfenstein depolarization parameter D are reported at 670, 600, and 520 MeV for the pp interaction, over the cm angular range 30 to 120°. The transfer depolarization parameter D^t is measured at 600 and 525 MeV in the free np system, over the range 65 to 180° CM. Five points are measured at each energy, with statistical accuracy averaging about ±.1 for D_{pp} and ±.3 for D^t_{np}. D^{pp} is between ½ and 1 at forward scattering angles and drops toward zero at angles greater than 90° CM. It remains positive. D^t_{np} is small and positive at measured angles less than 90° and also at 180°. There is an indication of a possible negative value between 90 and 180°. Predictions of various phase-shift solutions are compared to the data. A polarized neutron/proton beam was produced by elastically scattering the beam of the Berkeley 184'' Cyclotron off deuterium/hydrogen. The polarized beam was elastically scattered off hydrogen and the polarization of the recoil proton analyzed in a carbon-slab and magnetostrictive-wire-chamber array. (Diss. Abstr.)

19905 MULTIPARTICLE PRODUCTION IN LIQUID HYDROGEN AND CARBON BY CHARGED COSMIC-RAY HADRONS OF ENERGY GREATER THAN 70 GeV. Erickson, Kenneth Neil. Fort Collins, Colo.; Colorado State Univ. (1970). 123p. University Microfilms Order No. 71-2440.

Thesis.

The operation of a cosmic ray experiment at Echo Lake, Colorado from March, 1968 to May, 1969 produced 288 and 681 in-geometry interactions respectively from a carbon and a liquid hydrogen target. The energy of these interactions was greater than 70 GeV as measured by an ionization calorimeter. A study was made as to the energy dependence of average charged multiplicity and inelasticity, as well as the multiplicity distributions and the center-of-mass angular distributions of the charged particles in the final state. It was found that the average charged multiplicity increases with energy in very good agreement with the ln E dependence as predicted by the multiperipheral model of Chew and Pignotti. The multiplicity distributions were found to be Poisson in nature, consistent with the predictions of Chew and Pignotti and C. P. Wang. The inelasticity was found to be independent of the primary energy. The center of mass angular distributions were observed to be nonisotropic. Results in hydrogen and carbon were compared with respect to average charged multiplicity and inelasticity. (Diss. Abstr.)

19906 PRODUCTION OF LOW MOMENTUM NEGATIVE PARTICLES BY 70 GeV PROTONS. Antipov, Yu. M.; Denisov, S. P.; Donskov, S. V.; (and others) (Inst. for High Energy Physics, Serpukkov, USSR). Phys. Lett.; 34B: 164-6(1 Feb 1971).

The yields of pions, kaons, antiprotons and antideuterons produced by the 70 GeV protons on Al and Be nuclei at the momenta 10 and 13.3 GeV/c were measured. Gas Cherenkov counters and time-of-flight spectrometers were used for particle identification. (auth)

19907 EXPERIMENTAL COMPARISON OF $\bar{d}p$ AND $\bar{p}d$ TOTAL CROSS SECTIONS. Denisov, S. P.; Donskov, S. V.; Gorin, Yu. P. (Inst. for High Energy Physics, Serpukhov, USSR). Phys. Lett.; 34B: 167-9(1 Feb 1971).

$\bar{d}p$ and $\bar{p}d$ total cross sections were measured at 13.3 and 6.65 GeV/c respectively to check CPT-invariance. The standard transmission technique was used. The difference of $\bar{d}p$ and $\bar{p}d$ total cross sections appeared to be equal 0.2 ± 2.6 mb. In addition $\bar{d}d$ and $\bar{p}p$ total cross sections were obtained. The total cross sections of antineutrons on protons, neutrons and deuterons were derived from the experimental data. (L.B.S.)

19908 ABSORPTION OF Σ^- HYPERONS BY NEON AND FORMATION OF NUCLEAR EXCITED STATES AFTER K^--MESON ABSORPTION. Garrett, Neil Edward Knoxville, Tenn.; Univ. of Tennessee (1970). 83p. University Microfilms Order No. 71-346.

Thesis.

In a bubble-chamber study of stopping Σ^- absorption by neon, the hyperfragment production probability (trapped events) was measured to be 25 ± 5%. The Λ trapping probability was calculated to be ≥25% from a model using an s-state capture mechanism and the experimental Λ momentum distribution from Σ^--neon absorption. Sixty-three percent of the hyperfragments were found to decay yielding no visible energy release. The $\Lambda p/\Lambda n$ stimulated decay ratio for nonmesic decay was 0.25 ± 0.10. Observation of the internal pair production process after K^- absorption in the same mixture was used as a technique to estimate the formation of excited nuclear states. From the number of internal pairs produced, the probability for emission of a single γ-ray (with mean energy ≃8 MeV) after K^--neon reactions was calculated to be ≃100%. Gamma-ray emission arose primarily in conjunction with the conversion reactions of Σ hyperons. (Diss. Abstr. Int., B)

Strong (Meson-Induced)

Refer also to abstracts 20144 and 20162.

19909 (CERN/HERA-70-6) COMPILATION OF CROSS SECTIONS V–K^- INDUCED REACTIONS. Flaminio, E.; Hansen, J. D.; Morrison, D. R. O.; Tovey, N. (European Organization for Nuclear Research, Geneva (Switzerland)). 22 Oct 1970. 212p. Dep. NTIS (U. S. Sales Only).

A compilation of cross sections of reactions produced by negative kaons on targets of protons, neutrons and deuterons is presented. Graphs of the variation of cross section with incident laboratory momentum are plotted. Values for the rate of decrease of cross section with incident momentum are given. (auth)

19910 (LAL–1242) STUDY OF THE COHERENT PRODUCTION ON NUCLEI OF THE $K^-\pi^+\pi^-$ SYSTEMS BY K^- OF 5.5, 10.0, AND 12.7 GeV/c. Fournier, D. (Paris Univ., Orsay (France). Laboratoire de l'Accelerateur Lineaire). Dec 1970. 236p. (In French). Dep. NTIS (U. S. Sales Only).

Thesis.

The results of a study of the coherent production of the $K^-\pi^+\pi^-$ system on the nuclei neon, carbon, fluorine, and bromine are described. Negative kaons of momenta 5.5, 10.0, and 12.7 GeV/c are exposed to the nuclei in three bubble chamber experiments. The properties of the $K^-\pi^+\pi^-$ system including the spin, parity, approximate mass, and density matrix elements are studied. The amplitudes of the decay of this system into $\bar{K}^{*0} + \pi^-$ and $K^- + \rho^0$ are also found. The total cross sections for the interactions of this coherent meson system with nucleons are studied in these experiments. (J.F.P.)

19911 MEASUREMENT OF THE REACTION $\pi^-p \to \pi^0n$ AT LARGE MOMENTUM TRANSFERS. Brockett, W. S. (Case Western Reserve Univ., Cleveland); Corlew, G. T.; Frisken, W. R.; (and others). Phys. Rev. Lett.; 26: 527-30(1 Mar 1971).

Results of an experiment to measure the differential cross section of the reaction $\pi^-p \to \pi^0n$ between the forward and backward peaks are presented. The measurements were made at incident π^- momenta of 3.67 and 4.83 GeV/c. The t range $1.7 \leq |t| \leq 4.9$ (GeV/c)^2 was covered at the lower momentum and $1.8 \leq |t| \leq 7$ (GeV/c)^2 at the higher momentum. At the lower momentum the cross section is essentially constant between $|t| = 2.4$ and 4.8 (GeV/c)^2. (auth)

19912 K^-p ELASTIC SCATTERING AT 14.25 GeV/c. Miller, R. J. (Rutherford High Energy Lab., Chilton, Eng.); Phelan, J. J.; Smith, J. R.; (and others). Phys. Lett.; 34B: 230-2(15 Feb 1971).

The K^-p differential and total elastic cross sections were measured at 14.25 GeV/c. The results were compared with various Regge models. (auth)

19913 STUDY OF 10 GeV/c K^+-NUCLEUS COHERENT INTERACTIONS AND THE Q-NUCLEON CROSS-SECTION. Haguenauer, M. (Ecole Polytechnique, Paris); Michael, W.; Mine, P.; (and others). Phys. Lett.; 34B: 219-22(15 Feb 1971).

Coherent production of $K\pi\pi$, $K\pi\pi\pi$ and $K\pi\pi\pi\pi$ systems is studied using 10-GeV/c K^+ interactions on nuclei. In the $K^+\pi^+\pi^-$ channel the Q^+ enhancement is observed. The Q^+-nucleon interaction cross section is estimated to be 20 ± 8 mb. (auth)

19914 KAON, HYPERON, AND ANTIHYPERON FINAL STATES IN K^+p INTERACTIONS NEAR 13 GeV/c. Berlinghieri, Joel Carl. Rochester, N. Y.; Univ. of Rochester (1970). 185p. University Microfilms Order No. 71-1370.

Thesis.

A K^+p scattering experiment at a kaon beam momentum of 12.7 GeV/c was performed using the rf separated beam at the Brookhaven National Laboratory's 80-inch liquid hydrogen bubble chamber. The results of a study, primarily of the two-pronged plus single Vee topology, are presented here. The cross sections in this topology for K^0, Λ, and $\bar{\Lambda}$ production are given below. 2 charged prongs + K^0, 2.70 ± 0.21 mb 2 charged prongs + Λ 0.16 ± 0.02 mb and 2 charged prongs + $\bar{\Lambda}$ 0.093 ± 0.012. The production mechanism for certain quasi two-body states found in the 2 prongs + K^0 reaction and also the 4 prongs $K^+p\pi^+\pi^-$ reaction were investigated by an analysis of the spatial distribution of the resonant decay products. A search was performed for meson resonances having any one of the following properties: a. strangeness (S) = 2. b. S = 1, isotopic spin (I) = $^{3}/_{2}$. c. S = 1, I = $^{1}/_{2}$, decaying into an antihyperon and a nucleon. Assuming a resonant width (full width at half height) of approximately 150 MeV, the upper limits of the resonant production of these states are 5 μb, 8 μb, and 4 μb respectively. A study of $K^+\pi^-$ elastic and charge exchange scattering was performed using the $K^+p \rightarrow K^+\pi^-\Delta^{++}$ and $K^+p \rightarrow K^0\pi^0\Delta^{++}$ final states. The scattering moments, $\langle Y_1^m \rangle$, (uncorrected for off mass-shell effects) are given. The production characteristics of certain hyperons and antihyperons are also given. (Diss. Abstr.)

19915 $\pi^-p \rightarrow \pi^0n$ CHARGE-EXCHANGE CROSS SECTIONS BETWEEN 90 MeV AND 290 MeV. Bugg, D. V. (Rutherford High Energy Lab., Chilton, Eng.); Bussey, P. J.; Dance, D. R.; (and others). Nucl. Phys.; B26: 588-96(1971).

Measurements were made of the total charge-exchange cross section π^-p to π^0n over the laboratory kinetic energy range 90 to 290 MeV. The data have an absolute accuracy of typically 1%, and were used to determine the pion-nucleon P_{13} phase shift. (auth)

19916 TOTAL CROSS SECTIONS FOR PION–PROTON SCATTERING BETWEEN 70 MeV AND 290 MeV. Carter, A. A. (Cavendish Lab., Cambridge, Eng.): Williams, J. R.: Bugg, D. V.; Bussey, P. J.; Dance, D. R. Nucl. Phys.; B26: 445-60(1971).

Measurements were made of the $\pi^{\pm}$ proton total cross sections over the laboratory kinetic energy range 70 to 290 MeV. The absolute accuracy of the data is generally 0.5%, but decreases to 1% for some points where applied corrections are large or where low particle fluxes limit the statistical accuracy. The parameters of the Δ^0, Δ^{2+} resonance were calculated, and a discussion is included on the limitations placed by Coulomb barrier effects on extracting the basic nuclear phase shifts from data in this energy region. (auth)

19917 BARYON EXCHANGE IN THE REACTIONS $K^-n \rightarrow Y\pi^-$ AT 3 GeV/c. Barloutaud, R. (CEN, Saclay, France); Merrill, D.; Scheuer, J. C.; (and others). Nucl. Phys.; B26: 557-72(1971).

At 3 GeV/c, the total and differential cross sections of the reactions $K^-n \rightarrow Y\pi^-$ were determined for nine S = −1 baryonic states. Backward peaks associated with a dip near u = −0.2 are observed in many cases. They have been interpreted, for the isospin-zero Y-states, in terms of a proton-exchange mechanism. The backward peaks in the reactions $K^-n \rightarrow \Lambda\pi^-$ and $K^-n \rightarrow \Sigma^0\pi^-$ were more quantitatively related to the backward $\pi N \rightarrow N\pi$ differential cross sections at the same energy. This comparison leads to the conclusion that the first reaction is dominated by nucleon exchange, whereas the second one requires a more complex exchange mechanism. (auth)

19918 INVESTIGATION OF THE FORWARD STRUCTURE IN CHARGE-EXCHANGE K^{*0}(890) PRODUCTION. Aguilar-Benitez, M.; Barnes, V. E.; Bassano, D.; (and others) (Brookhaven National Lab., Upton, N. Y.). Phys. Rev. Lett.; 26: 466-9(22 Feb 1971).

An investigation of the reaction $K^-p \rightarrow K^{*0}(890)n$ at 3.9 and 4.6 GeV/c incident momenta is presented. The order-of-magnitude increase in statistics with respect to previous analysis allows an investigation of the K^{*0}(890)-production properties in the very forward region of momentum transfer and also provides a quantitative test of the absorption-modified one-pion exchange model. This model gives an excellent description of the differential cross sections and decay correlations at the two energies. (auth)

19919 MESON PRODUCTION BY THE INTERACTION OF π^+ MESONS WITH PHOTOEMULSION KERNELS AT 185 TO 295 MeV ENERGIES. Batusov, I. A.; Bunyatov, S. A.; Ionita, G.; (and others). An. Stiint. Univ. Al. I. Cuza Iasi, Sect. Ib. Fiz.; 16: 63-7 (1970). (In French).

Meson production by mesons at energies in the 185 to 295 MeV range were investigated and the cross sections for the reactions $\pi + A \rightarrow \pi^- + A' + \ldots$ (1200 cases) and $\pi^+ + A \rightarrow \pi^+ + \pi^- + A' + \ldots$ (56 cases) were found. A marked peak was reported at about 250 MeV that might be ascribed to the double charge exchanging process of π^+ mesons. (Rom. Sci. Abstr.)

19920 BRANCHING RATIOS OF THE A_2^+ MESON OBSERVED IN 7 GeV/c π^+p INTERACTIONS. Alston-Garnjost, M.; Barbaro-Galtieri, A.; Buhl, W. F.; (and others) (Univ. of California, Berkeley). Phys. Lett.; 34B: 156-9(1 Feb 1971).

The observed branching fractions of the A_2^+ produced in the reaction $\pi^+p \rightarrow A_2^+p$ at 7 GeV/c and decaying to $\rho\pi$, $\eta\pi$, $K\bar{K}$ and $\eta'\pi$ are presented. The data show no convincing evidence for the decay $A_2^+ \rightarrow \eta'\pi^+$, the branching fraction being less than 3%. For the other decay modes the values obtained for $\rho\pi$, $\eta\pi$ and $K\bar{K}$ are 0.744 ± 0.029, 0.183 ± 0.026 and 0.072 ±0.012 respectively. (auth)

19921 OBSERVATION OF t-CHANNEL HELICITY CONSERVATION IN DIFFRACTIVE REACTIONS PRODUCING A_1 AND Q-MESONS. Beaupre, J. V.; Boesebeck, K.; Deutschmann, M.; (and others) (Technische, Hochschule, Aachen). Phys. Lett.; 34B: 160-3(1 Feb 1971).

It is shown that helicity is conserved in the t-channel for A_1 and Q-meson production by pions of 8 and 16 GeV/c and kaons of 10 GeV/c, respectively. This is in contrast to evidence for s-channel helicity conservation reported for elastic scattering and rho photoproduction. This difference in behavior of diffractive processes may be due to the fact that there is a change in spin in the former reactions but not in the latter, or, alternatively, to different mechanisms operating in the two cases. (auth)

19922 STRANGE PARTICLES FROM π^-d INTERACTIONS AT 3.15 GeV/c. Watkins, Bruce O. Jr. Logan, Utah; Utah State Univ. (1970). 148p. University Microfilms Order No. 70-26,998. Thesis.

The data for this experiment were collected on film in 1963 at the 72-inch bubble chamber at the Lawrence Radiation Laboratory, Berkeley. About 45,000 pictures (3 views each) were taken of π^- mesons at a laboratory momentum of 3.15 GeV/c into deuterium. The film was scanned for interactions with one or more vees. Neutron cross sections are given for 14 final states. The cross sections were calculated by normalization to previously measured proton interaction final states. The spectator model was assumed to hold. The effective path length was 3.47 events/μb. Two resonances, the K^*(890) and the Σ(1385), are clearly seen. For the final state $\Lambda pK^0\pi^-$, the method of maximum likelihood was used to estimate the amount of Σ(1385). A simple model of phase space plus Breit–Wigner resonance was found to reproduce the distribution of $M(\Lambda\pi^-)$ from this final state rather well. The same approach was used to estimate the amount of K^*(890) and Σ(1385) in the final state $\Lambda nK^+\pi^-$. Density matrix elements were calculated from the angular distribution of the Λ from $\Lambda\pi^-$ pairs in the Σ(1385) mass band for the final state $\Lambda pK^0\pi^-$. The elements were found to be in reasonable agreement with those expected for interactions obeying the Stodolsky–Sakurai model. A prominent enhancement in the mass spectrum of $K\pi\pi$ from two different four-body final states was found at 1200 MeV, the so-called Q-region. However, the plot had only 60 events. (Diss. Abstr.)

19923 η′ PRODUCTION IN π^+d INTERACTIONS FROM THRESHOLD TO 2.4 GeV/c. Rader, Robert Kent Berkeley, Calif.; Univ. of California (1970). 75p. University Microfilms Order No. 71-833. Thesis.

The η′ production was studied as part of an experiment using a π^+ beam incident on deuterium in the 72-in. bubble chamber, with beam momenta from 1.1 to 2.4 GeV/c. The η′ is produced in the reaction $\pi^+d \rightarrow pp\eta'$, and the decay mode $\eta' \rightarrow \pi^+\pi^-\eta$ was observed. The reaction $\pi^+n \rightarrow p\eta'$ is studied by using the spectator model. The cross section for $\pi^+n \rightarrow p\eta'$ is observed to rise to a maximum of about 100 μb at 2.2 GeV cm energy. The production angular distribution develops peripheral peaking with increasing energy. (Diss. Abstr. Int., B)

Particle Interactions and Properties (Theoretical)

General

Refer also to abstract 20446.

19924 (JINR–E2-5579) TRANSFORMATION PROPERTIES OF MASSIVE PARTICLE STATES AT INFINITE MOMENTUM. Robashik, D.; Smorodinskii, Ya. A. (Joint Inst. for Nuclear Research, Dubna (USSR). Lab. of Theoretical Physics). 1971. 15p. Dep. NTIS (U. S. Sales Only).

The well-known result that helicity states of massive particles with infinitive momentum satisfy the same transformation laws as the states of massless particles is derived. The limiting procedure holds $p^2 = m^2$ fixed whereas the spatial momentum tends to infinity. For canonical states at infinite momentum the Wigner rotation $R_W^c(L_k^c,p)$ (where L_k^c is a pure Lorentz transformation) is a rotation around the axis $\hat{k} \times \hat{p}$ with the angle $\alpha = \theta - \theta'$, θ and θ' being the well known angles occurring by the aberration of light. The rotation angle φ appearing by the transformation of the helicity states is in a simple way connected with the angle α. For a general Lorentz transformation it is also possible to calculate the value of the angle φ. (auth)

19925 (NP–18703) HELICITY FORMALISM: A LECTURE COURSE. Osborne, P. M. [nd]. 37p. Dep. NTIS (U. S. Sales Only).

XUM

The lectures on helicity formalism cover the Lorentz group, angular momentum for moving particles, crossing, singularities of helicity amplitudes, transversity amplitudes, density matrices, and Regge poles. (J.F.P.)

19926 (NYO-2262-TA-234) HELICITY POLES, TRIPLE REGGE BEHAVIOR AND SINGLE PARTICLE SPECTRA IN HIGH ENERGY COLLISIONS. DeTar, C. E.; Jones, C. E.; Low, F. E.; Weis, J. H.; Young, J. E. (Massachusetts Inst. of Tech., Cambridge); Tan, Chung-I (Brown Univ., Providence, R. I. Dept. of Physics). [1970]. Contract AT(30-1)-2098. 8p. Dep. NTIS.

Following previous work, the single-particle production spectrum is related, through a generalized optical theorem, to a discontinuity in a six-line amplitude. Assuming only analyticity of the six-line amplitude in its angular momenta, a general expression for the behavior of the production spectrum near the phase space boundary is obtained. To study the asymptotic limit appropriate to this region use is made of analytic continuation to complex helicities. (auth)

19927 STRAIGHT-LINE PARTICLE PATH APPROXIMATION IN THE DESCRIPTION OF HIGH-ENERGY HADRON SCATTERING IN QUANTUM FIELD THEORY. Barbashov, B. M.; Kuleshov, S. P.; Matveev, V. A.; (and others). (Joint Inst. for Nuclear Research, Dubna, USSR). Teor. Mat. Fiz.; 5: 330-42 (Dec 1970). (In Russian).

Asymptotic behavior of high-energy elastic and inelastic amplitudes is studied by means of the functional integration method. The straight-line particle path approximation is formulated which makes it possible to calculate effectively functional integrals. The closed relativistically invariant expressions for both the elastic and inelastic scattering amplitudes are obtained in the scalar nucleon-vector meson interaction model. (auth)

19928 MASS SPECTRA AND MOMENTS FROM CLASSICAL DYNAMICS. Jacobi, Lee William. Hoboken, N. J.; Stevens Inst. of Tech. (1970) 289p. University Microfilms Order No. 71-1172.

Thesis.

The nature of mass spectra in the classical relativistic dynamics of point particles, and the nonrelativistic dynamics of extended point particles are investigated. In each case, the particle possesses internal degrees of freedom, i.e., multipole characteristics such as spin. These theories are classical analogs of quantum theories which are described by infinite component linear wave equations. These equations exhibit mass spectra that are discrete but infinite. Through the use of different classical models, mass relations are derived resembling those of Gell-Mann and Okubo or of Barut and Sternheimer. Also the classical field theoretical origins of some of these mass relations are explored. Nonholonomic constraints are employed to couple the space-time trajectories to the internal variables. The rest mass then depends upon the quantizable classical constants of the motion of the internal variables. Correspondence principle arguments are invoked to show that analogous quantum theories have discrete and infinite mass spectra. Two classical models are examined. The first, that of a spherical top, is characterized by one moment of inertia parameter. For a particle described by any one of three different internal groups, de Sitter, complex Lorentz or conformal, relations are derived which are the analogs of the inverted Majorana spectrum. Since different realizations of some particular internal symmetry yield the same mass relation, the attendant dipole and quadrupole moments are calculated to distinguish the theories from one another. For a more complex spherical top model the classical analog of the physically realistic Sternheimer–Barut mass formula is obtained. Also a second model is analyzed, the symmetric top, a classical spinning object characterized by two moment of inertia parameters. The relativistic mass relation and the corresponding magnetic moment are found in general and for various group realizations. It is also shown how this spectrum originates from the classical field theory of Bhabba and Corben. Next, the spin-isospin classical field theories of Le Couteur, Fierz and Pauli are examined to show that their theories also lead to the mass relation of the symmetric top model. Finally for a symmetric top with unitary spin internal symmetry the classical analog of the Okubo baryon spectrum without the linear term is found. (Diss. Abstr.)

19929 POSITIVE DEFINITE PARTICLE DENSITIES FOR THE POSITIVE FREQUENCY SOLUTIONS OF THE KLEIN–GORDON EQUATION WITH ARBITRARY MASS. Henning, J. J. (Atomic Energy Board, Pretoria); Wolf, W. Z. Phys.; 242: 12-20(1971).

It is shown that the set of kernels introduced previously by Gerlach, Gromes and Petzold can be enlarged considerably. A remark on the theory of massless particles is made. (auth)

19930 UNSTABLE SYSTEM WITH N STATES AND THE PROPAGATOR MATRIX WITH A POLE OF HIGHER ORDER. Lokajicek, M. V. (Joint Inst. of Nuclear Research, Dubna, USSR). Czech. J. Phys.; 19: 925-30(1969).

Starting from the general quantum-mechanical laws, the general form of the mass matrix for a special unstable system with N states and of the propagator with higher order pole is derived. (auth)

19931 s-CHANNEL HELICITY CONSERVATION AND THE STRESS-TENSOR. Jones, H. F. (Imperial Coll. of Science and Tech., London); Salam, A. Phys. Lett.; 34B: 149-51(1 Feb 1971).

The general form of covariant helicity-conserving couplings and their relation to the stress-tensor are discussed. (auth)

19932 QUASI-FREE STATES OF THE C* ALGEBRA OF COMMUTATION RELATIONS. II. Kholevo, A. S. (Mathematics Inst., Moscow). Teor. Mat. Fiz.; 6: 145-50(Feb 1971). (In Russian).

Classification of types and equivalence conditions are given for the primary quasi-free states on the C*-algebra of the CCR. (auth)

19933 DEVELOPMENTS IN HIGH ENERGY PHYSICS. Proceedings of the 9th Conference, Schladming, Austria, 23rd February–7th March 1970. Urban, Paul (ed.). Acta Physica Austriaca, Supplementum VII. Vienna; Springer-Verlag (1970). 637p. $30.00. (CONF-700220).

Eighteen lectures are included. Separate abstracts were prepared for each lecture. (J.F.P.)

For abstracts of individual lectures see: 19465, 19934, 19935, 19954, 19968, 19976–19979, 19991, 19992, 20045, 20046, 20067–20070, and 20107.

19934 O(3,1) ANALYSIS OF CURRENTS AND CURRENT COMMUTATORS. Ruehl, W. (CERN, Geneva) Acta Phys. Austr.; Suppl. 7, 392-442(1970).

From 9th Conference on Developments in High Energy Physics, Schladming, Austria. See CONF-700220.

A current density operator $j_\mu(x)$ between one-particle states $\langle p_2,q_2|j_\mu(o)|p_1,q_1\rangle$ is the simplest example of a covariant (in this case: vector) operator connecting two (in this case: reducible unitary) representations of the group SL(2,C). In these lectures the representation theory of the group SL(2,C) is reviewed. This enables one to derive a decomposition theorem for covariant operators with heuristic arguments. By this theorem one can decompose any covariant operator into a direct integral of irreducible covariant operators, which are defined to connect two irreducible representations of SL(2,C). This formalism is then applied to several problems of physical interest. Current matrix elements are analyzed. The interpretation of the singularities of the Fourier transforms leads to the concept of dynamical groups. Asymptotic expansions of the form factors are obtained. Diagonal matrix elements of current commutators $\int d^4x\, e^{ikx} \langle p,q|[j^a_\mu(x), j^b_\nu(o)]|p,q\rangle$ are analyzed. The singularities of the Fourier transforms are interpreted as Lorentz poles and cuts. Asymptotic expansions in $\nu = kp/M$ are obtained. The photon mass is fixed. The same matrix elements are analyzed in a different fashion such that asymptotic expansions in powers of ν for fixed $k^2/2kp$ result. An interpretation of the singularities of the Fourier transforms leads to a novel picture of inelastic electron-proton scattering. (auth)

19935 REALIZATION OF LIE ALGEBRAS THROUGH RATIONAL FUNCTIONS OF CANONICAL VARIABLES. Doebner, H. D. (Univ., Marburg, Ger. Technical Univ., Clausthal, Ger.); Palev, T. D. Acta Phys. Austr.; Suppl. 7, 597-609(1970).

From 9th Conference on Developments in High Energy Physics, Schladming, Austria. See CONF-700220.

The most general case of the Lie algebras G is considered, namely, an arbitrary G over a field ϕ, which includes the real and complex case. Some properties of associative rings and the mapping of Lie algebras into the canonical quotient division ring are discussed. (J.F.P.)

Electromagnetic

Refer also to abstract 20055.

19936 (CNRS-CPT-70-P-335, pp IV.1-15) ANOMALOUS MAGNETIC MOMENTS OF THE ELECTRON AND THE MUON. de Rafael, E. (European Organization for Nuclear Research, Geneva (Switzerland)).

In Colloquium on computational methods in theoretical physics; Marseilles, France (15 Jun 1970).

The results obtained up until the present time on the anomalous magnetic moments of the electron and the muon, using computers, are reviewed. (France)

XUM

19937 (DEMO-71/2) REMARKS ON THE $\eta \rightarrow \pi^0 \gamma\gamma$ DECAY RATE. Gounaris, G. J.; Verganelakis, A. (Democritus Nuclear Research Center, Athens (Greece)). Jan 1971. 13p. Dep. NTIS (U. S. Sales Only).

It is shown that a duality–FESR method to take into account high mass states in the dispersion relations for $\eta \rightarrow \pi^0\gamma\gamma$ predicts that $\Gamma(\eta \rightarrow \pi^0\gamma\gamma)$ is bigger by a factor of 50 than the prediction of any other model. Such a result seems to be favored by recent experiments. The importance of the method to the decay amplitudes for $\omega \rightarrow 3\pi$, $\eta \rightarrow \pi^+\pi^-\gamma$ and $X \rightarrow \pi^+\pi^-\gamma$ as well as the relevance of the process $ee \rightarrow ee\pi^0\eta$ for the study of the $\eta\pi^0\gamma\gamma$ amplitude is also discussed. (auth)

19938 (JINR–P2-5505) RELATION BETWEEN THE CROSS SECTIONS OF THE PROCESSES $e^- + e^+ \rightarrow e^- + e^+ + A^- + A^+$ AND $\gamma + \gamma \rightarrow A^- + A^+$. Isaev, P. S.; Khleskov, V. I. (Joint Inst. for Nuclear Research, Dubna (USSR). Lab. of Theoretical Physics). 1971. 12p. (In Russian). Dep. NTIS (U. S. Sales Only).

A connection between the cross section of the $e^+ + e^- \rightarrow e^+ + e^- + A^+ + A^-$ and $\gamma + \gamma \rightarrow A^+ + A^-$ processes is established in the lower order of perturbation theory. The kinematics of the collision process $e^+ + e^- \rightarrow e^+ + e^- \leftarrow A^+ + A^-$ is chosen such that the virtual space-like photon is very close to the real photon. It means that the "mass" of the virtual photon is close to zero. It can be expressed by the conditions: $[|k^{12}|/k_0^1]^2 = |(p_+ - p_+^1)^2|/(E_+ - E_+^1)^2| \ll 1$ and $[|k^2|/k_0^2 = |(P_- - P_-^1)^2|/(E_- - E_-^1)^2| \ll 1$ (I). The "transversality" condition of the virtual photon should be added to eq. (I). This can be made by comparing the polarization matrix of the $\gamma + \gamma \rightarrow A^+ + A^-$ process with the polarization matrix of the $A^+ + A^-$ pair creation process in the collision of the virtual photons. The $\gamma + \gamma$ interaction can be studied by using the relation between the two cross sections mentioned. (auth)

19939 (NYO–2262-TA-221) SUPER-EIKONAL MODEL OF DEEP INELASTIC ELECTRON-PROTON SCATTERING. Fried, H. M.; Moreno, Hector (Brown Univ., Providence, R. I. Dept. of Physics). [1969]. 11p. Dep. NTIS.

A field-theoretic model is written to describe the structure function W_2 of deep inelastic e–p scattering. Strict Bjorken scaling is found not to hold; nevertheless the model provides a modest fit to the experimental data. A variant of the Drell–Yan–West relation between the elastic limit of W_2 and the asymptotic fall off of the electromagnetic form factors is obtained. (auth)

19940 IMPULSE APPROXIMATION CALCULATION OF THE POLARIZATION OF THE RECOIL PROTON IN THE REACTION $\gamma + n \rightarrow p + \pi^-$ IN DEUTERIUM. Beneventano, Marcello; d'Angelo, Silio; de Notaristefani, Francesco; (and others). Atti Accad. Naz. Lincei, Rend., Cl. Sci. Fis., Mat. Natur.; 47: 509-13(Dec 1969). (In Italian).

The photoproduction of π^- is studied in the interaction $\gamma + d \rightarrow \pi^- + p + p$. The polarization of the recoil proton is calculated in the impulse approximation. It is concluded from the results that the polarization of the recoil proton in this process is not directly comparable with the polarization obtained on a free neutron. (J.F.P.)

19941 LIGHT-CONE COMMUTATORS AND THE HIGH ENERGY ANNIHILATION $e^+ + e^- \rightarrow \pi$ + HADRONS. Georgelin, Y. (Institut de Physique Nucleaire, Orsay, France); Stern, J.; Jersak, J. Phys. Lett.; 34B: 207-10(15 Feb 1971).

The behavior of the π-meson form-factor and of the process $e^+ + e^- \rightarrow \pi$ + hadrons at high q^2 is discussed in terms of the light-cone properties of the electromagnetic and axial-vector current commutator. (auth)

19942 EFFECTS OF VENEZIANO-MODEL FORM FACTORS ON RATIOS OF LEPTON–PROTON SCATTERING CROSS-SECTIONS. Campbell, J. A. (Univ. of Texas, Austin). Lett. Nuovo Cim.; 1: 242-4(6 Feb 1971).

It is pointed out that one of the uses of R, where R is the ratio of differential or total cross sections of $e^+ + p \rightarrow e^+ + p$ to $e^- + p \rightarrow e^- + p$ interactions, is to determine the form factors for the proton. Expressions for the integral approximation for the form factors are given and discussed. These expressions were obtained from the Veneziano model. A formula for R as a function of E,t, and ξ is given which summarizes the values found in numerical programing. (J.F.P.)

19943 MONTE CARLO CALCULATIONS OF ELECTROMAGNETIC SHOWER TRANSITION EFFECTS. Beck, H. L. (Atomic Energy Commission, New York). Nucl. Instrum. Methods; 91: 525-31(1971).

The rapid change in energy deposition and particle flux that occurs when a 1-GeV-electron-initiated shower developing in lead or iron crosses over into a water medium was studied using a recently developed Monte Carlo code. Agreement with experimental data is quite good. Similar calculations were done for 200-MeV-, 500-MeV-, and 1-GeV-electron-initiated air showers entering iron and aluminum. The calculations indicate that significant changes in energy deposition and flux occur over quite small distances from the boundary; for instance, the transition effect will produce an enhancement of about 20% in the measured gas ionization due to the electromagnetic component of the cosmic radiation when 3-g/cm^2 thick steel-walled ionization chambers are used. The magnitude of the Monte Carlo-calculated transition effects are smaller, however, than predicted in earlier studies which relied on approximation B of shower theory. (auth)

19944 DOES A UNIFORMLY ACCELERATED CHARGE RADIATE? Mariwalla, K. H. (MATSCIENCE, Madras); Vasudevan, R. Lett. Nuovo Cim.; 1: 225-8(6 Feb 1971).

Arguments in favor of the radiation hypothesis of a uniformly accelerated charge are examined to show that the proofs involved are either equally consistent with the absence of radiation or are based on a misconception of the problem. Hyperbolic motion in uniform acceleration from minus infinity to plus infinity, and partly hyperbolic motion in uniform acceleration for a finite period are considered. (J.F.P.)

19945 APPROXIMATE DESCRIPTION OF COULOMB SCATTERING. Lu, P. (Arizona State Univ., Temple). Nuovo Cim.; 1B: 65-72(11 Feb 1971).

The modified WKB method as given previously is applied to the attractive-Coulomb-scattering case for the second order in $\hbar$ following a previous calculation. A previously developed method is used. The improvement of the attractive-Coulomb-scattering cross sections is shown by a numerical example. (auth)

19946 ENERGY AND MOMENTUM IN ELECTROMAGNETIC FIELD FOR CHARGED PARTICLES MOVING WITH CONSTANT VELOCITIES. Boyer, Timothy H. (Univ. of Maryland, College Park). Amer. J. Phys.; 39: 257-70(Mar 1971).

The relation between the Lorentz force and the energy and momentum in the electromagnetic field is illustrated with some striking examples for systems of point charges moving at constant velocities. For these systems, the kinetic energy and momentum associated with particle mass do not change, while the external forces which balance the interparticle Lorentz forces give exactly the rate of change of energy, momentum, and angular momentum in the electromagnetic fields. The present evaluations are noteworthy in that they are exact, and also in that the necessary electromagnetic field integrals over all space are reduced to delta function integrations. In the limiting charge distributions involving infinite energy density at spatial infinity, the connection of the Lorentz force with electromagnetic energy and momentum is lost. (auth)

19947 NON-COPLANAR PROTON–PROTON BREMSSTRAHLUNG CALCULATIONS INCLUDING THE RELATIVISTIC SPIN CORRECTIONS. Liou, M. K.; Cho, K. S. (Univ. of Manitoba, Winnipeg). Nucl. Phys.; A160: 417-27(1971).

The noncoplanar proton–proton bremsstrahlung cross sections are calculated including the relativistic spin corrections. The electromagnetic interaction Hamiltonian obtained by applying the Foldy–Wouthuysen (FW) transformation to the Dirac electromagnetic interaction Hamiltonian to order $\underline{M}^{-2}$ was used. The relativistic spin corrections are found to be important in the high-energy region in the calculation which is performed in the lab system. Including these corrections, the results are in good agreement with experimental data. Further corrections are found to be small. (auth)

19948 TWO PROBLEMS OF THE 3π DECAYS OF THE η MESON. Taggart, Keith Anthony. Cleveland; Case Western Reserve Univ. (1970). 122p. University Microfilms Order No. 71-1756.

Thesis.

Two separate problems concerning the 3π decay modes of the η meson are studied. First, the problem of the asymmetry observed in the decay $\eta \rightarrow \pi^+\pi^-\pi^0$ is considered. Bernstein, Feinberg, and Lee suggested that an asymmetry in the average energies of the charged pions in this decay would be proof of C violation in the electromagnetic interaction among hadrons. Recall, however, that the η is identified as a peak in the invariant mass distribution of three pions from a reaction like $\pi^-p \rightarrow \pi^+\pi^-\pi^0n$. Yuta and Okubo proposed that the observed effect is due to interference between the η channel for this reaction and direct 3π production background processes. The background size and its possible contributions to the asymmetry are calculated using a simple model which takes into account only tree (no closed loops) diagrams with constant vertices and ignores the effects of spin. Here 40% of the background observed in the experiment of Gormley et al. is accounted

XUM

for but it is found that the largest asymmetry which can be produced through interference is 10^{-5} as compared to the experimentally observed 1.5×10^{-2}. It is concluded that if the observed asymmetry persists, then charge conjugation invariance is violated by the decay. These results agree with the analysis of Stein of the experimental background. He concluded that the background could account for an asymmetry of no more than 2.7×10^{-3}. Second, the bound 4π model of the η proposed by Mitra and Ray is considered to see if any light can be shed on the 3π decay modes. It is found that the electromagnetic mixing of the vector and tensor mesons gives an interaction which changes 4π's into 3π's. It is found, too, that the symmetry properties of the final 3π state determine the form of the matrix element. It is concluded that the model gives a qualitatively tenable picture. A detailed calculation of a decay rate must still be done to see if quantitative agreement with experiment can be obtained. (Diss. Abstr.)

19949 DOUBLE SCATTERING OF ELECTROMAGNETIC RADIATION BY BOUND ELECTRONS. Kor, J.; Vachaspati (Allahabad Univ., India). Nuovo Cim.; 1B: 57-64(11 Feb 1971).

Assuming that the interparticle distance is greater than the wavelength of the incident light, it is shown that double-scattering effects are important for the fundamental mode of vibration as well as for the second-harmonic mode of vibration for resonance scattering ($\omega = \omega_0$) of electromagnetic waves by a system of bound electrons of natural frequency ω_0. At resonance, for a slab of 1 cm thickness, double-scattering effects would be comparable to single-scattering effects even for low density of electrons such as $n \sim 10^9/cm^3$. The angular distribution of the double-scattered harmonic wave is shown to be different from that of the single-scattered wave; this fact can be used to find out whether or not double scattering is actually taking place. Moreover, measurement of the intensity of the double-scattered wave can be used to determine the density of electrons in the scattering material. It is also shown that double scattering is negligible both for the fundamental and harmonic waves if resonance is excited by incident radiation of half the natural frequency ($\omega = \omega_0/2$). (auth)

19950 MOTION IN ELECTRIC AND MAGNETIC FIELDS. I. KLEIN–GORDON PARTICLES. Lam, Lui (Columbia Univ., N. Y. Bell Telephone Labs., Murray Hill, N. J.). J. Math. Phys. (N. Y.); 12: 299-303(Feb 1971).

Exact solutions of the Klein–Gordon equation are found for a new solvable configuration of external electromagnetic fields, namely, a static uniform electric field inclined at an arbitrary angle to a static uniform magnetic field of arbitrary strength. Applications are discussed at the end. (auth)

19951 AXIAL-CURRENT DIVERGENCES AND THE REACTIONS $\gamma + \gamma \rightarrow$ PIONS. Aviv, R.; Hari Dass, N. D.; Sawyer, R. F. (Univ. of California, Santa Barbara). Phys. Rev. Lett.; 26: 591-4 (8 Mar 1971).

A symmetry argument is presented that gives a relation between the small-momentum limits of the reactions $\gamma + \gamma \rightarrow$ odd number of pions, as calculated explicitly from a single nucleon (or quark) loop in a theory with a formally conserved axial-vector current. These limits are nonvanishing as a consequence of the Adler anomalies in the divergence of the axial-vector current. It is argued that the relationship derived should be true in any chiral model. The cross section for $\gamma + \gamma \rightarrow \pi^+ + \pi^- + \pi^0$ is calculated in terms of the measured $\pi^0 \rightarrow 2\gamma$ decay rate. (auth)

19952 CLASSICAL SELF-ENERGY OF THE ELECTRON. Datzeff, A. B. (Univ. of Sofia). Phys. Lett.; 34A: 167-8(22 Feb 1971).

On the basis of a definite hypothesis about the material carrier of the electromagnetic field a modified, free of divergences, Coulomb law, as well as an approximate value for the electron radius are obtained. (auth)

19953 HIDDEN MOMENTUM FOR NON-STEADY STATE DEFINED USING A NEW MASS–MOMENT OPERATOR THEOREM FOR DIRAC'S EQUATION. Shockley, W.; Thornber, K. K. (Bell Telephone Labs., Murray Hill, N. J. Stanford Univ., Calif.). Phys. Lett.; 34A: 177-8(22 Feb 1971).

A Dirac electron's mass-moment operator conserves velocity of center of total-closed-system mass when the electron interacts with the nonquantum remainder of the system. As operators, kinetic momentum equals hidden momentum plus rate of change of mass moment, i.e., bodily motion momentum. (auth)

19954 VENEZIANO-LIKE MODEL FOR A TWO-CURRENT AMPLITUDE. Landshoff, P. V. (Cambridge Univ., Eng.). Acta Phys. Austr.; Suppl. 7, 166-79(1970).

From 9th Conference on Developments in High Energy Physics, Schladming, Austria. See CONF-700220.

Some properties of the usual Veneziano beta-function are reviewed. A model is then constructed for an amplitude involving two charged isovector currents. It is found that when one incorporates certain desirable features, in particular the correct Fubini–Gell-Mann fixed pole at $j = 1$, the model automatically satisfies the Bjorken scaling law. It is shown how the model may be extended to describe deep inelastic electron-proton scattering. (auth)

19955 APPLICATION OF GLAUBER THEORY OF MULTIPLE SCATTERING TO PHOTON–NUCLEAR INTERACTIONS. Jurisic, Nikola Kuhbauch. Ithaca, N. Y.; Cornell Univ. (1970). 80p. University Microfilms Order No. 70-23,119.

Thesis.

The Glauber theory of multiple scattering is used to treat several problems involving the interaction of high-energy photons with nuclei. Particular emphasis is placed on the role of vector meson dominance in these reactions. The particular cross sections studied are photoproduction of charged pions from the deuteron, total photon absorption in heavy nuclei, photoproduction of vector mesons and charged pions from heavy nuclei. Also studied are corrections to wide-angle bremsstrahlung arising from the Compton scattering of a photon from a nucleus. As experiments involving photon interactions with nuclei became more refined during the past year, it appeared that they did not agree well with the predictions based on the simple optical model approach using the vector dominance model. It is important to determine whether this is a feature of the optical model calculation, or a real physical effect in disagreement with the vector dominance model. An attempt is made to examine critically the optical model approach. To examine the approximations involved in the optical model approach, the somewhat more fundamental multiple scattering theory was studied and the approximations which reduce it to the optical model were identified. (Diss. Abstr. Int., B)

19956 DOES AN ISOTENSOR ELECTROMAGNETIC CURRENT EXIST. Schwela, D. (Univ., Bonn). Nucl. Phys.; B26: 525-35(1971).

In the framework of previous dispersive calculations on pion-photoproduction, it is shown that the present data on negative-pion photoproduction do not allow the inference of an isotensor electromagnetic current. In view of the importance of the problem, a more significant test is suggested. (auth)

19957 MULTIPOLE ANALYSIS OF PI-ZERO AND PI-PLUS PHOTOPRODUCTION BETWEEN THRESHOLD AND 500 MeV. Noelle, P.; Pfeil, W.; Schwela, D. (Univ., Bonn). Nucl. Phys.; B26: 461-96(1971).

The results are reported of an energy independent multipole analysis of the π^0 and π^+ photoproduction for photon lab energies between 180 and 500 MeV. The isospin parts of the ($l \leq 1$) multipole amplitudes were parametrized, and the ($l \geq 2$) multipoles were included in Born approximation. The imaginary parts of the multipoles for $l \leq 1$ were calculated from the real parts by use of the Watson theorem, the imaginary parts of the ($l = 2$) amplitudes are also assumed to be given by the Born terms multiplied by the tangent of the corresponding πN phase shift. The parameters were fitted from the available differential cross-section, polarization, and asymmetry-ratio data. In the energy region between 200 and 400 MeV for the differential cross sections, only the most recent data measured at Bonn and Orsay were used. A very good and consistent representation of the experimental data was obtained. The energy dependence of the multipole amplitudes was found to be smooth. Discrepancies between our results and several theoretical models occur in all amplitudes considered, in particular in the magnetic dipole $M_{1-}^{(1/2)}$, in the isospin $1/2$ parts of E_{1+} and M_{1+} above resonance, and to some extent also in the magnetic dipole $M_{1+}^{(1/2)}$. The energy dependence of the electric dipole $E_{0+}^{(1/2)}$ appears to be somewhat stronger than predicted by theory. The CERN theoretical πN phase shifts were used except for P_{33} where the new results of a measurement of Carter et al. were taken. Small variations in the P_{33} phase do not alter the nonresonant multipoles significantly. (auth)

19958 CALCULATION OF THE TOTAL CROSS SECTION FOR DOUBLE COMPTON SCATTERING. Ram, Michael; Wang, P. Y. (State Univ. of New York, Buffalo). Phys. Rev. Lett.; 26: 476-9 (22 Feb 1971).

The results of a calculation of the total cross section for double Compton scattering ($\gamma + e \rightarrow \gamma + \gamma + e$) are reported. At very high incident photon energies the total cross section for double Compton scattering becomes larger than that for the usual Compton effect ($\gamma + e \rightarrow \gamma + e$) even though the latter is a lower order process. (auth)

19959 SCALING, DEEP INELASTIC ELECTRON–NUCLEON SCATTERING, AND THE MULTIPERIPHERAL MODEL. Shei, Sun-sheng; Tow, Don M. (Univ. of California, Berkeley). Phys. Rev. Lett.; 26: 470-3(22 Feb 1971).

The Amati–Bertocchi–Fubini–Stanghellini–Tonin multiperipheral model is modified to study deep inelastic electron-nucleon scattering. In particular, the scaling property of the structure functions is derived. The multiperipheral derivation is compared with derivations that use other models. (auth)

19960 KINETICS OF HOT ELECTRONS IN THE QUANTIZING MAGNETIC FIELDS. II. DIFFUSION APPROXIMATION. Kalashnikov, V. P. (Inst. of Physics of Metals, Moscow). Teor. Mat. Fiz.; 6: 279-93(Feb 1971). (In Russian).

On the basis of the nonequilibrium statistical operator the system of equations of momentum density and particle number balance in energetical space is deduced, which determines the kinetics of hot electrons in strong crossed electrical and magnetic fields. In the case of quasielastic scattering the equations obtained are transformed into differential equations describing the diffusion of electrons in energy space. These equations are integrated in the lowest approximation with respect to the relation of the transverse momentum relaxation frequency to the cyclotron motion frequency. (auth)

19961 COMMENTS ON EIKONALIZATION AT HIGH ENERGY. Chang, Shau-jin; Fishbane, Paul M. (Univ. of Illinois, Urbana). Phys. Rev., D; 3: 1047-8(15 Feb 1971).

It was previously shown how s-channel iteration of general kinds of exchanges in high-energy e–e scattering in quantum electrodynamics leads to eikonalization. This result is clarified and its implications are briefly discussed. (auth)

19962 CLASSICAL ELECTRODYNAMICS IN TWO DIMENSIONS: EXACT SOLUTION. Bialynicki-Birula, I. (Univ. of Pittsburgh). Contract AT(30-1)-3829. Phys. Rev., D; 3: 864-6(15 Feb 1971).

The classical electrodynamics of N charged pointlike particles, moving in the space-time of two dimensions, is studied. The exact solution of this model is found, and its properties connected with the Poincaré group in two dimensions are described. In the case of N = 2, our solution reduces to a model of relativistic classical mechanics discovered by Currie and Jordan and by Beard and Fong. Nonlinear generalizations of the model are also discussed. (auth)

Weak

Refer also to abstracts 20039 and 20090.

19963 (JINR–P2-5520) ON THE DECAYS $\pi^+ \to e^+(\mu^+)\nu e^+e^-$. Bardin, D. Yu.; Bilen'kii, S. M.; Mitsel'makher, G. V.; Shumeiko, N. M. (Joint Inst. for Nuclear Research, Dubna (USSR). Lab. of Theoretical Physics). 1970. 28p. (In Russian). Dep. NTIS (U. S. Sales Only).

The integral probability of the process $\pi^+ \to l^+ \nu_l e^+e^-$ is calculated. It is shown that study of the decay $\pi^+ \to e^+ \nu_e e^+e^-$ at different detection thresholds of final charged particles allows the information on γ-parameter (the ratio of the axial form factor to the vector one in the decay $\pi^+ \to e^+ \nu_e \gamma$), on electromagnetic radius of π-meson, and on the sign of $\pi^0 \to 2\gamma$ amplitude to be obtained. (auth)

19964 (KFKI–70-24-HEP) INTRODUCTION TO THE CURRENT–CURRENT THEORY OF THE WEAK INTERACTION. Frenkel, A. (Magyar Tudomanyos Akademia Kozponti Fizikai Kutato Intezete, Budapest). 1970. 88p. Dep. NTIS (U. S. Sales Only).

The status of the modern current–current theory of weak interactions is reviewed, and its predictions are compared with experimental results in elementary particle physics. The strangeness-conserving weak decays, leptonic decays of hadrons, the isotriplet vector current theory, and the Cabibbo octet current theory are considered. Also the nonleptonic weak decays and the PCAC hypothesis are discussed. (J.F.P.)

19965 (NYO–2262-TA-236) OKUBO'S SECOND-CLASS CURRENTS IN K_{l2} AND K_{l3} DECAYS. Kang, Kyungsik; Olshansky, Robert (Brown Univ., Providence, R. I. Dept. of Physics). [1970]. 11p. Dep. NTIS.

The modification of the weak interaction theory recently proposed by Okubo is compared with the current-current weak interaction theory generalized to include local scalar or tensor interactions for K_{l2} and K_{l3} decays. In contrast to the latter type of theory, the existence of Okubo's tensor or scalar densities is difficult to verify from K_{l2} and K_{l3} experiments unless one has a reliable theoretical model for the pure V-A vertices. In particular, various possible explanations for the K_{l3} parameters are discussed. (auth)

19966 ORIGIN OF THE NEUTRINO MASS. Novello, M. (Centro Brasileiro de Pesquisas Fisicas, Buenos Aires. Univ., Geneva). Lett. Nuovo Cim.; 1: 252-4(6 Feb 1971).

It is shown that the neutrino acquires a mass as a result of the fundamental γ interaction that generates the gravitational field. (J.F.P.)

19967 NONLEPTONIC DECAY OF HYPERONS. Hosoya, A.; Tokuda, N. (Tokyo Univ.). Lett. Nuovo Cim.; 1: 235-8(6 Feb 1971).

A simple model is proposed which well explains experiments both for S- and P-wave decays. It is assumed that the weak-interaction Hamiltonian belongs to an octet of SU(3) and the parity-violating (conserving) part satisfies certain relations. The PCAC hypothesis is used. The amplitudes of the nonleptonic decays of the hyperons are calculated on the basis of these assumptions. The corresponding matrix elements are discussed in the rest frame of the pion, and then the pion energy is allowed to go to zero, thereby the three-momenta of the baryons go to infinity automatically. (J.F.P.)

19968 STRUCTURE EFFECTS IN WEAK INTERACTIONS. Pietschmann, H. (Univ., Vienna). Acta Phys. Austr.; Suppl. 7, 588-96(1970).

From 9th Conference on Developments in High Energy Physics, Schladming, Austria. See CONF-700220.

The discussion of structure effects in weak interactions covers nonlocal weak coupling, effects to lowest order in G^2, and higher-order weak interactions. (J.F.P.)

19969 DIVERGENCES OF MASSIVE YANG–MILLS THEORIES. Glashow, S. L.; Iliopoulos, J. (Brookhaven National Lab., Upton, N. Y. Harvard Univ., Cambridge, Mass.). Phys. Rev., D; 3: 1043-5(15 Feb 1971).

A model of weak interactions was previously suggested where the divergences of higher-order amplitudes are properly ordered. It is shown that the introduction of Yang–Mills self-couplings preserves this ordering. It is shown, in particular, that the worst divergences of Feynman amplitudes are like $(g^2\Lambda^2)^n$, despite the fact that individual Feynman diagrams diverge like $(g^2\Lambda^4)^n$. (auth)

19970 APPROXIMATE CHIRAL SYMMETRY AND THE LEAKAGE CONTRIBUTIONS TO THE FUBINI–FURLAN K_{l3} SUM RULE. Lane, Kenneth D. (Univ. of Pennsylvania, Philadelphia). Phys. Rev., D; 3: 968-9(15 Feb 1971).

It is commonly assumed that the leakage terms in the Fubini–Furlan sum rule for the K_{l3} scalar form factor F(t) either are very small or are dominated by contributions from uncharged intermediate states. It is shown that these assumptions are incompatible with results for F(t) based on approximate chiral symmetry. (auth)

Strong (General)

Refer also to abstract 20536.

19971 (ANL–7727) PENETRATION AND CASCADE PHENOMENA. Zgrablich, G. (Argonne National Lab., Ill.). Aug 1970. Contract W-31-109-eng-38. 75p. Dep. NTIS.

This work treats two penetration-phenomena problems at low energies and two at very high energies: The stopping probability in a material of a given thickness is studied. The corresponding integro-differential equation is shown to have a regular solution accounting for a finite number of collisions, and a singular solution representing the contribution from an infinite number of collisions. The general solution is unique if and only if the singular solution is identically zero. The ionization cascade is investigated produced by a charged particle. The distribution of ion-pairs produced is computed and can be approximated by the Landau universal distribution for energy loss by ionization. The mean number of ion pairs conditional on a given energy loss by the primary is shown to be linear and independent of primary energy, varying little with the nature of the absorber. The computed energy loss per ion-pair produced is in good agreement with experiments. Multiple particle production models at cosmic-ray energies and their predictions for quantities such as inelasticity and multiplicity distributions are examined. Special attention is paid to the two-temperature model. The three-dimensional nucleon-pion cascade, is solved by a semianalytical method, practical for numerical computation. The lateral structure function for the nuclear active component of extensive air showers is computed for several values of the incident energy and is compared to Monte Carlo calculations and to experimental results. (auth)

19972 (IFPTH–10/70) GENERAL FORMULATION OF A RELATIVISTIC THEORY OF PARTICLE SUBCONSTITUENTS (QUARKS) IN TERMS OF A FIELD VECTOR INTERACTION. Nitti, L. (Bari Univ. (Italy). Istituto di Fisica. Istituto Nazionale di Fisica Nucleare, Bari (Italy)); Pusterla, M. (Padua Univ. (Italy). Istituto di Fisica. Istituto Nazionale di Fisica Nucleare, Padua (Italy)). Dec 1970. 34p. Dep. NTIS (U. S. Sales Only).

XUM

The topics considered are the general formalism with unequal masses for the λ quark and the n – p doublet, the equal-mass limit, computational techniques for the evaluation of higher perturbative orders, Padé formulas and their applications, and physical predictions. (J.F.P.)

19973 (INSTJ-125) SIMULATION IN SPACE AND TIME OF THE NUCLEAR ACTIVE AND MUON COMPONENTS IN EXTENSIVE AIR SHOWERS FOR PRIMARY ENERGIES FROM 10^5 TO 10^7 GeV. Grieder, P. K. F. (Bern Univ. (Switzerland). Physikalisches Institut. Tokyo Univ. (Japan). Inst. for Nuclear Study). 17 Nov 1970. 81p. Dep. NTIS (U. S. Sales Only).

Three highly detailed shower models are described which imply different high energy multiplicity laws. The excitation of different isobar states and coproduction of one or two fireballs, depending on the type of model, are considered. The isobar component is the same for all models, but the fireball component is different in each case. One model considers the production of a single fireball which is stationary in the center of mass, following a multiplicity which is proportional to $E_{lab}^{1/4}$. The other two models consider the simultaneous production of two fireballs that are moving forward and backward, respectively, in the center of mass. The difference between these two models lies in the energy dependence of the velocities of the two fireballs in the center of mass. The latter is proportional to the square root of the total center of mass energy in one case, and proportional to the fourth root in the other, resulting in an asymptotic multiplicity that goes as $E_{lab}^{1/4}$ and $E_{lab}^{1/3}$, respectively. Nucleon-antinucleon pair production is included in all models. Furthermore, ionization losses are considered for all charged particles and in addition coulomb scattering for muons. The simulation is carried out in three dimensions and time. It is based exclusively on Monte Carlo calculations. The results of extensive calculations are summarized and integral energy spectra and lateral density distributions for the different particles are compared with experimental data. (auth)

19974 COMPLEX ANGULAR MOMENTUM THEORY IN PARTICLE PHYSICS. Drechsler, Wolfgang. Fortschr. Phys.; 18: 305-448(1970).

A critical review of the techniques of complex angular momenta used at present in the Regge theory of strong interactions is presented. After discussing the kinematical singularities of helicity amplitudes, their crossing properties as well as the constraints they satisfy, the reggeization procedure for two-body helicity amplitudes is reviewed in detail. The properties of the generalized Froissart–Gribov continuation are investigated. The factorization properties of Regge pole contributions to a general two-body scattering amplitude are studied and the various mechanisms producing the dip structure of differential cross-sections are discussed. The complications of the reggeization for amplitudes describing unequal-mass reactions at high energies in the forward direction are discussed and a survey of the status of "conspiracies" of singularities in the complex angular momentum plane is given. Both, the group theoretical and the analytical methods are discussed in treating the conspiracy problem. Finally, a review of the present situation is given regarding the influence of branch cuts in the complex angular momentum plane and their phenomenological consideration in various multiple scattering models. It is shown that the multiple scattering correction in the Glauber-eikonal type of approach correspond to cuts in the angular momentum plane which represent absorptive corrections to the single Regge exchanges. It is clear from this discussion that cuts in the complex j-plane, describing multi-Regge pole exchanges, cannot be neglected. (auth)

19975 SCATTERING LENGTHS OF EXOTIC PROCESSES OF HADRON INTERACTIONS. Rekalo, M. P. (Physical-Technical Inst., Kharkov). Ukr. Fiz. Zh.; 15: 1674-80(Oct 1970). (In Russian).

A model is suggested for describing the S-state lengths of π-, η-, K-, $\bar{K}$-meson scattering by nucleons and hyperons. The elastic hadron scattering amplitudes at zero energy are approximated in this model by the contribution of vector mesons in the annihilation channel. The constants of the hadron-vector meson interaction may be determined in terms of only one parameter in the quark model. Predictions of this model are not in agreement with experimental data in cases when scattering length are complex values. (auth)

19976 ABSORPTION CORRECTIONS AND CUTS IN THE REGGE POLE MODEL. Hite, G. E. (Univ., Karlsruhe, Ger.). Acta Phys. Austr.; Suppl. 7, 180-213(1970).

From 9th Conference on Developments in High Energy Physics, Schladming, Austria. See CONF-700220.

The methods presently used to introduce absorption corrections, the ways in which they correspond and differ from cut contributions, and their successful description of the structure of experimental differential cross sections are treated. Complications associated with spin and signature factors are avoided. The lectures concern absorptive corrections, eikonal approximations, and Regge poles, cuts in the complex j-plane, absorptive corrections and Mandelstam cuts, and absorptive Regge pole and cut models. (J.F.P.)

19977 LECTURES ON REGGE PHENOMENOLOGY. Phillips, R. J. N. (Rutherford Lab., Chilton, Eng.). Acta Phys. Austr.; Suppl. 7, 214-64(1970).

From 9th Conference on Developments in High Energy Physics, Schladming, Austria. See CONF-700220.

These lectures are about the comparison of Regge theory (and folklore) with experiment. The properties of Regge-pole exchange amplitudes and the places where simple pole dominance seems to fail are surveyed. Regge cuts, various prescriptions for calculating them, and what experiments are helpful are considered. Finite energy sum rules, their use to predict high energy scattering, and some problems with asymptopia are treated. Duality and the Veneziano model are omitted, to avoid double-counting. (auth)

19978 DUALITY. Kugler, M. (Weizmann Inst. of Science, Rehovot, Israel). Acta Phys. Austr.; Suppl. 7, 443-547(1970).

From 9th Conference on Developments in High Energy Physics, Schladming, Austria. See CONF-700220.

The basic ideas and relation with experiment are stressed in the lectures on duality. It is shown that duality is a very useful tool in investigating the strong interaction. A mathematical introduction to finite-energy sum rules, πN charge exchange, Schmidt circles, definition of a resonance, local duality, the two-component theory of the scattering amplitude, and exchange degeneracy and crossing are considered. Also discussed are duality and SU(3) breaking, duality diagrams, exotics of the second kind, duality and low-energy parameters, exchange degeneracy and experiment, cuts and factorization, and the breaking of duality. The Veneziano formula, structure of resonances in the Veneziano model, attempts to unitarize the Veneziano model, and some applications of the Veneziano model are also covered. (J.F.P.)

19979 SOME REMARKS ON THE QUARK MODEL. Flamm, D. (Institut fuer Hochenergiephysik, Vienna). Acta Phys. Austr.; Suppl. 7, 548-66(1970).

From 9th Conference on Developments in High Energy Physics, Schladming, Austria. See CONF-700220.

The properties of the quark model are reviewed, and the hadron mass spectrum in this model is discussed. The Gell-Mann–Zweig quarks are used in general. (J.F.P.)

19980 SHORT GUIDE TO THE QUARK MODEL. Morpurgo, G. (Univ., Genoa. Istituto Nazionale di Fisica Nucleare, Genoa). Annu. Rev. Nucl. Sci.; 20: 105-46(1970).

A review of the quark model is given. The historical background and main assumptions, states and transition matrix elements for hadron structure, collision problems, relativistic kinematics, difficulties of the model, and the search for quarks are covered. (153 references) (J.F.P.)

19981 CHIRAL INVARIANT DUAL MODEL. Brower, R. C. (CERN, Geneva). Phys. Lett.; 34B: 143-6(1 Feb 1971).

Unequal intercept dual N-point functions are found which satisfy the Adler condition for all the external pion lines. With the no-exotics hypothesis, a chiral invariant model is constructed which, in the linear expansion of the invariants, exactly coincides with the non-linear σ model with ($\frac{1}{2}$, $\frac{1}{2}$) breaking. Factorization yields a unique π, A_1, ρ, f^0 and the standard difficulties with tachyons and ghosts. The model can be extended to axial and vector currents with the correct soft couplings, massive kaons, and higher order dual diagrams. (auth)

19982 SCALING BEHAVIOR IN MULTIPERIPHERAL DYNAMICS. Silverman, Dennis (Princeton Univ., N. J. Univ. of California, San Diego, La Jolla); Tan, Chung-I. Phys. Rev., D; 3: 991-5(15 Feb 1971).

The scaling of the single-particle momentum distribution is demonstrated as a general property of all the multiperipheral models which have been proposed. It is also shown that in these models, pionization is approached as a smooth limit from scaling. The proof is based only on the most general multiperipheral assumption and on Pomeranchuk-pole dominance at high energies. Thus the experimental observation of scaling is required for the validity of any multiperipheral model. (auth)

19983 SCALAR MESONS, HADRON MASSES, AND APPROXIMATE SCALE INVARIANCE. Carruthers, P. (Cornell Univ., Ithaca, N. Y.). Phys. Rev., D; 3: 959-67(15 Feb 1971).

The possible role of a scalar-meson nonet in determining hadron masses by means of generalized Goldberger– Treiman formulas is studied. Existing data on scalar-pseudoscalar meson couplings are analyzed, assuming SU_3-invariant couplings for the unmixed mesons. The d/f ratio for the coupling of octet scalars to the baryon octet is predicted to be the same as in the Gell-Mann–Okubo mass formula. The strength of the transition vacuum → scalar meson (induced by the energy-momentum tensor $\theta_{\mu\nu}$) is measured by the constant F_σ. Denoting the SU_3 singlet scalar meson by σ_0 and the octet η-like scalar by σ_8, $F_{\sigma 0}$ is found to be much larger than $F_{\sigma 8}$, provided that the $\sigma_0 BB$ coupling is not considerably smaller than the $\sigma_8 BB$ coupling. Then $F_{\sigma 0}$ is comparable to the usual pion decay constant F_π. The pseudoscalar octet dispersion relation is not scalar dominated. This result is also suggested by analysis of partial conservation of axial-vector current for the scalar-pseudoscalar system, and consideration of the relation to the underlying scale-invariant limit. Implications for the underlying dynamics are discussed. (auth)

19984 ANOMALIES OF THE AXIAL-VECTOR CURRENT IN TWO DIMENSIONS. Georgi, Howard; Rawls, John M. (Yale Univ., New Haven). Phys. Rev., D; 3: 874-9(15 Feb 1971).

In a world with one space and one time dimension, it is shown that the axial-vector current in a vector-gluon model exhibits anomalies in perturbation theory analogous to those found by Adler in fermion electrodynamics. The analysis is extended to include a four-fermion (Thirring) interaction; this model has been solved exactly by Sommerfield, permitting an explicit verification of the perturbation-theory calculations. In analogy to results in four dimensions, a model is presented in which the anomalous properties of the axial-vector current, both in its divergence and in its commutation relations, follow immediately from the canonical structure of the theory. (auth)

Strong (Baryon No. = 0)

Refer also to abstracts 20107 and 20153.

19985 (DEMO-71/1) IS VENEZIANO MODEL CONSISTENT WITH THE YANG-MILLS COUPLING OF VECTOR MESON FIELDS. Gounaris, G. J. (Democritus Nuclear Research Center, Athens (Greece)). Jan 1971. 9p. Dep. NTIS (U. S. Sales Only).

It is shown that the assumption that the vector-mesons couple like Yang-Mills fields in a chiral Lagrangian model is consistent, in the tree approximation, with the simplest Veneziano model for the amplitudes $\omega \to 3\pi$, $\eta \to \pi^+\pi^-\gamma$ and $X \to \pi^+\pi^-\gamma$. (auth)

19986 (IFVE-STF-70-34) CALCULATION OF BOX DIAGRAM EFFECTS WITH TWO RESONANCES IN THE INTERMEDIATE STATE. Anisovich, V. V.; Kobrinskii, M. N. (Gosudarstvennyi Komitet po Ispol'zovaniyu Atomnoi Energii SSSR, Serpukhov. Institut Fiziki Vysokikh Energii). 1970. 28p. (In Russian). Dep. NTIS (U. S. Sales Only).

The box diagrams with resonances in the intermediate state have singularities, that can lie close to the physical region. The calculation of the singularities of these diagrams is presented in the explicit form for the cases of scalar and vector resonances. The detailed investigation of the conditions, under which the box diagram singularities are close to the physical region, is presented. The effects that appear in given processes were calculated. (auth)

19987 (JINR-P2-5566) SCHMIDT METHOD APPLIED TO SOLVING THE QUASIPOTENTIAL EQUATION. Atanasov, A. (Joint Inst. for Nuclear Research, Dubna (USSR). Lab. of Theoretical Physics). 1971. 8p. (In Russian). Dep. NTIS (U. S. Sales Only).

The Schmidt method for solving the integral equations is applied to the quasipotential equation. An analytical expression is obtained for the dependence between the coupling constant and the ground state for the system of two spinless particles interacting by the scalar meson exchange. Correction of the Born amplitude gives an approximation to the energies. (auth)

19988 PROPERTIES OF REGGE POLES TRAJECTORIES. Shirkov, D. V. (Joint Inst. for Nuclear Research, Dubna, USSR). Usp. Fiz. Nauk; 102: 87-104(Sep 1970). (In Russian).

Experimental data on the Regge pole trajectories obtained for particles (α(t) at t > 0) and for the scattering region of (α(t) at t < 0) were reviewed considering trajectories related, mainly, to the ρ-meson and pion–nucleon trajectories Δ_δ, η_γ, and η_α. Data on the theoretical concepts of spectral presentation, pairing of baryon trajectories by parities, and problems on asymptotics of trajectories were also reviewed. General properties of the Regge trajectories are discussed in the linear approximation and in applications to the Veneziano model. 42 references. (R.V.J.)

19989 WIDTH OF THE RHO MESON BY THE BALAZS METHOD. Antippa, Adel F. Medford, Mass.; Tufts Univ. (1970). 318p. University Microfilms Order No. 71-889.

Thesis.

A systematic study of the Balázs method, as applied to the ρ-bootstrap problem in the 2π system, is made in order to determine its validity. Inelastic effects as estimated from Regge theory are included. It is found that the method becomes well-behaved as the number of poles used to approximate the left-hand cut is increased, in contrast to results obtained previously by Bond, and that the sensitivity of the solutions to the choice of matching point may be largely eliminated by a procedure proposed by Williamson and Everett. The method predicts a ρ mass of somewhere between 680 and 760 MeV as compared to the experimental value of 750 ± 25 MeV, and a ρ half-width of about 150 MeV as compared with the experimental value of about 50 MeV. Next the simultaneous bootstrap of the ρ and f^0 mesons was studied, using the Balázs method. When the exchange of an f^0 with physical parameters is included in the input force, it is found that ore obtains an approximately self-consistent ρ with a mass of 710 MeV and full width of 100 MeV; the degree of self-consistency is somewhat improved if the width is reduced to 66 MeV. One can obtain a simultaneous bootstrap of both the ρ and f^0 with a ρ mass and full width of 710 and 46 MeV, and f^0 mass and full width of 1344 and 112 MeV, respectively. It is believed that the double-bootstrap results are somewhat affected by the approximate treatment of inelastic effects, which involves a discontinuity in the inelasticity function R| near the position of the f^0. These results are based upon taking n, the number of poles approximating the left-hand cut, equal to 7. The use of a large number of poles is important, and it is not at all clear from the n dependence of the calculations that a limiting form of the results is obtained as n becomes large, even with n = 7. And finally a ρ-bootstrap calculation, using the Balázs method, with the input crossed channel amplitude given by the Veneziano representation, was performed. Results for the self-consistent mass and width are in good agreement with experiment. The results are consistent with the amplitude being given by only a single Veneziano term, although they do not exclude the presence of additional terms with lower order asymptotic behavior. (Diss. Abstr.)

19990 HIGH-ENERGY BOUNDS ON SCATTERING AMPLITUDES AND OSCILLATIONS IN THE DIFFRACTION-PEAK REGION. Singh, Virendra (Tata Inst. of Fundamental Research, Bombay). Phys. Rev. Lett.; 26: 530-4(1 Mar 1971).

Rigorous bounds are established on the absorptive part of the scattering amplitude, A(s,t), for t real and within the Lehman–Martin ellipse. This result is used to prove an upper bound on $[d \ln A(s,t)/dt]_{t=0}$, and to show that A(s,t) cannot have a zero in the region $0 > t > -4t_0/(\ln s)^2$ for $s \to \infty$ ($\sqrt{t_0} = 2m_\pi$ for $\pi\pi$, πN, KN, and NN scattering). No assumption is made about the high-energy behavior of the total cross sections. (auth)

19991 SOME EXACT RESULTS ON $\pi\pi$ SCATTERING. Martin, A. (CERN, Geneva). Acta Phys. Austr.; Suppl. 7, 71-90(1970).

From 9th Conference on Developments in High Energy Physics, Schladming, Austria. See CONF-700220.

The discussion of exact results on $\pi + \pi$ scattering covers the basic axiomatic results and absolute limits to the $\pi + \pi$ amplitude, and positivity and linear constraints on the partial waves. (J.F.P.)

19992 SOME RECENT WORK IN REGGE THEORY: REGGE CUTS, THE ABSORPTION MODEL, AND GLAUBER THEORY. Landshoff, P. V. (Cambridge Univ., Eng). Acta Phys. Austr.; Suppl. 7, 145-65(1970).

From 9th Conference on Developments in High Energy Physics, Schladming, Austria. See CONF-700220.

It is assumed that scattering amplitudes possess Regge poles, and an analysis is given of the Regge cuts that are then required by unitarity. This is done using perturbation theory. A derivation is given of the cut structure that arises from the absorption model and from the Glauber model of deuteron scattering. The validity of this derivation, and of these models, is then examined. (auth)

19993 UNITARITY AND CROSSING SYMMETRY IN LOW-ENERGY $\pi-\pi$ SCATTERING. Baier, R. (Univ., Graz); Kuehnelt, H.; Widder, F. Z. Phys.; 242: 157-66(1971).

A method of unitarizing the Veneziano model for $\pi\pi$ scattering, employing exact conditions on partial wave amplitudes which allow a minimization of the violation of crossing symmetry is discussed.

XUM

The structure of the left hand cut ($0 \geq s \geq -32m_\pi^2$) is obtained via crossing symmetry, whereas the far left hand cut is parametrized in terms of several poles, the residues of which serve as free parameters in this model. The existence of unitary and almost crossing symmetric solutions with a resonant I = 0 S-wave is demonstrated. The restrictions on these solutions are, however, not sufficient to single out a unique set. (auth)

19994 POSSIBLE DETERMINATION OF THE OFF-MASS-SHELL S-WAVE $\pi^+\pi^-$ SCATTERING AMPLITUDE. Gutay, L. J.; Scharenguivel, J. H.; McIlwain, R. L. (Purdue Univ., Lafayette, Ind.). Phys. Lett.; 34B: 152-5(1 Feb 1971).

Using somewhat specific assumptions, it is shown that the on-mass-shell P-Wave determines the off-mass-shell dependence of the S-Wave $\pi^+\pi^-$ amplitude. This is used to determine $(2a_0 + a_2)/a_1$ experimentally. (auth)

19995 CHARGE-EXCHANGE REACTIONS IN REGGE-POLE PHENOMENOLOGY. Nicolescu, B.; Dita, P. An. Univ. Bucuresti, Ser. Stiint. Natur., Fiz.; 17: 77-82(1968).

A thorough study was carried out on charge-exchange reactions $p\bar{p} \rightarrow n\bar{n}$ and $pn \rightarrow np$, and the treatment of the model of a singular Regge pole is described, it being in good agreement with the experimental data. The basic assumption considers that at high energies all the dominant Regge trajectories can be approximated by a single modelled Regge trajectory in the $t < o$ area. A trajectory was thereby found which is discontinued at $\alpha(o) \approx 0.2$ corresponding to δ mass. (Rom. Sci. Abstr.)

19996 OPERATORIAL CONSTRUCTION OF MULTIPLE CHARGED-PION AMPLITUDES. Willemsen, Jorge F. (Univ. of Chicago). Nucl. Phys.; B26: 573-87(1971).

It is shown that taking the "chiral symmetry" result $\alpha_\rho(0) - \alpha_\pi(0) = \frac{1}{2}$ as a hypothesis allows straightforward use of the oscillator formalism to construct 4π and 6π amplitudes with no tachyon ghosts, and full Regge behavior. An attempt is made to isolate the features of such schemes, needed to generalize the Lovelace amplitude, lead to problematic results in the multipion amplitudes which are obtained. (auth)

19997 VENEZIANO MODEL FOR THE PROCESS $V_1 + \pi \rightarrow V_2 + \pi$. Levy, Naomi; Singer, Paul (Technion-Israel Inst. of Tech., Haifa). Phys. Rev., D; 3: 1028-34(15 Feb 1971).

A Veneziano model is presented for the scattering of pions on isoscalar vector mesons of arbitrary mass, including photons. In addition to the leading term of the amplitude, satellite terms are allowed. The first ones are determined by the requirements of the absence of daughters and the correct widths for the first resonances in all channels. (auth)

19998 INCLUSION OF INTERFERENCE TERMS IN THE AMATI–BERTOCCHI–FUBINI–STANGHELLINI–TONIN MULTIPERIPHERAL MODEL. Snider, Dale R.; Tow, Don M. (Univ. of California, Berkeley). Phys. Rev., D; 3: 996-1005(15 Feb 1971).

An important class of interference terms is included in the ABFST multiperipheral model by adding an extra term to the inhomogeneous term and to the kernel of the integral equation. This additional term corresponds to the contribution to the 2-to-4 cross section from interchanging one or two pairs of particles from two different vertices. It is found that these interference terms change only slightly the position of the output vacuum pole; although they give a non-negligible contribution to the four-particle production cross section. (auth)

19999 BOOTSTRAP MODELS AND A SPECIAL PROPERTY OF THE UNITARY LIE ALGEBRAS. Andersen, C. M. (Coll. of William and Mary, Williamsburg, Va.); Yellin, Joel. Phys. Rev., D; 3: 846-58(15 Feb 1971).

It is shown that within the dynamical framework of N/D bootstraps, Z = 0 field theories, finite-energy sum rules, or narrow-resonance models, a self-consistent world of mesons of both parities, in which all particles interact symmetrically and belong to representations transforming as adjoint$\oplus$singlet of an arbitrary, compact, simple Lie algebra, may be constructed only for the algebras SU(n). (auth)

20000 KINEMATIC SUPERSTRUCTURES FOR ABNORMAL COUPLINGS IN THE 8-π DUAL AMPLITUDE. Canning, Gerald P.; Jacobs, Matthew A. (Tel Aviv Univ., Israel). Phys. Rev., D; 3: 891-8(15 Feb 1971).

A general method is presented for including abnormal couplings in multiparticle dual amplitudes. Amplitudes are constructed from a sum of terms having kinematic superstructure and dual substructure; and it is shown how a tensorial analysis of the kinematic superstructure in various channels determines the normality of the trajectories involved. As an illustration, a specific solution is given for abnormal couplings in the 8-π amplitude in which the above analysis is carried out in detail, and is compared with previous 6-π amplitudes and four-point amplitudes for spin-1–spin-0 scattering. (auth)

Strong (Baryon No. = 1)

Refer also to abstracts 19988 and 20226.

20001 (DEMO–70/19) A NON LINEAR EQUATION FOR THE CORRELATION FUNCTION BETWEEN AN IMPURITY PARTICLE AND A NUCLEON IN NUCLEAR MATTER. Grypeos, M. E. (Democritus Nuclear Research Center, Athens (Greece)). Aug 1970. 18p. Dep. NTIS (U. S. Sales Only).

A new approach is proposed for the determination of the correlation function between an impurity particle (for example a Λ particle) and one of the particles of an infinite host medium of identical particles (taken to be the nuclear matter). By using an approximate expression in "closed form" for the trial energy of the Λ-particle in its ground state in nuclear matter and applying the variational principle in a suitable way, it is shown that the Λ-nucleon correlation function satisfies a nonlinear integrodifferential equation. This equation is further reduced to a linear integrodifferential equation by using a proper linearization procedure. It is finally shown that for large Λ-nucleon separations an effective (reduced) mass $\mu_{\Lambda N}^*$ for the Λ-nucleon pair can be defined. (auth)

20002 (IFVE-STF/SPK–70-30) DO K-MESON NUCLEI EXIST? Gershtein, S. S.; Shlyapnikov, P. V. (Gosudarstvennyi Komitet po Ispol'zovaniyu Atomnoi Energii SSSR, Serpukhov. Institut Fiziki Vysokikh Energii). 1970. 7p. (In Russian). Dep. NTIS (U. S. Sales Only).

The possibility of K-meson nuclei existence on the assumption of the positive sign of the real part of KN-scattering amplitude at low energies is discussed. (auth)

20003 (JINR–E2-5561) MODEL-INDEPENDENT ANALYSIS OF THE FORWARD $\pi^\pm p$ SCATTERING DATA. Dumbrais, O. V.; Queen, N. M. (Joint Inst. for Nuclear Research, Dubna (USSR)). 1971. 8p. Dep. NTIS (U. S. Sales Only).

A new method is used to analyze the experimental data on forward elastic $\pi^\pm p$ scattering in a model-independent way. The analysis yields a value for the πNN coupling constant, values of parameters describing the asymptotic behavior of the amplitudes, and an accurate prediction of the real parts of the amplitudes at moderate energies. (auth)

20004 (JINR–P13-5516) MONTE CARLO GENERATION OF THE NEUTRAL π^-p INTERACTIONS AT 5 GeV/c IN THE PROPANE BUBBLE CHAMBER. Vinogradov, V. B.; Martinska, G.; Shandor, L. (Joint Inst. for Nuclear Research, Dubna (USSR). Lab. of Nuclear Problems). 1970. 23p. (In Russian). Dep. NTIS (U. S. Sales Only).

The technique and the results of Monte Carlo generation of neutral final states produced in the π^-p interactions at 5 GeV/c with the account of γ-ray detection probability in the 1-meter JINR propane bubble chamber are presented. The results were used in determining the cross sections of the reactions $\pi^-p \rightarrow n + (1,2,3,4,5)\pi^0$, $\pi^-p \rightarrow N^{*\,0}(1236)\pi^0$, $\pi^-p \rightarrow nf^{\,0}(f^0 \rightarrow 2\pi^0)$ and $\pi^-p \rightarrow n\eta\ (\eta \rightarrow 2\gamma)$ at 5 GeV/c. (auth)

20005 LOW-ENERGY DATA, ANALYTICITY, AND THE VIOLATION OF POMERANCHUK'S THEOREM. Wit, R. (CERN, Geneva). Phys. Lett.; 34B: 211-13(15 Feb 1971).

In the case of $\pi^\pm p$ scattering the low-energy data do not seem to agree with the predictions following from the recently introduced parametrizations violating the Pomeranchuk theorem. (auth)

20006 ROLE OF NON-POMERANCHUK REGGE CUTS IN HIGH ENERGY SCATTERING. Vasavada, K. V. (Indiana Univ., Indianapolis. Purdue Univ., Indianapolis). Phys. Lett.; 34B: 214-18(15 Feb 1971).

Some interesting properties of the Regge cuts obtained by multiple exchange of nonPomeranchuk type Regge poles are discussed, and their possible role in explanation of recurring minima and polarizations of high-energy reactions is pointed out. (auth)

20007 REGGE TRAJECTORIES AND THE BETHE-SALPETER EQUATION. Chand, Naresh. Pittsburg; Carnegie-Mellon Univ. (1970). 105p. University Microfilms Order No. 71-914.

Thesis.

Regge trajectories of the bound states of the pion nucleon system in the $I = \frac{1}{2}$ and $\frac{3}{2}$ channels are obtained using the Bethe-Salpeter equation in ladder approximation. In the appropriate signature and parity channels, these are trajectories of the nucleon and the N^* or (3,3) resonance. The Wick rotated BS equation is invariant under

XUM

rotations in four dimensions at zero total center of mass energy. To take advantage of this in the variational calculation, spinor spherical harmonics belonging to irreducible representations of O(4) are constructed. These same functions are used at all center of mass energies, leading to simplification in the calculation of matrix elements. A cutoff is introduced to simplify analytic continuation in angular momentum. It is found that nucleon-exchange force alone cannot bind both N and N*. For binding N, inclusion of the force due to N*-exchange is not found to be important, contrary to the results of N/D calculations, leading one to wonder about the validity of the latter. It is found that the forces due to N and ρ exchange together bind both N and N*. Both trajectories are found to have complex branches. Daughters are found to be separated from the parent trajectory by integers at E = 0 though their trajectories could not be calculated accurately. For the N*, the trajectories of the parent and first daughter are calculated using the N-exchange force alone, and they are found to be smooth, fairly flat and wholly real. In the absence of experimental information, it is not clear whether the trajectories should be wholly real or not in the bound state region. (Diss. Abstr.)

20008 REGGE-POLE MODEL FOR $\pi N \to \omega N$. Matthews, J. A. J.; Moen, I. O. (Univ. of Toronto). Lett. Nuovo Cim.; 1: 255-9(6 Feb 1971).

A Regge pole model for $\pi + N \to \omega + N$ interactions at high energies in terms of ρ, ρ^1, and B exchanges is presented. Linear trajectories with a common slope and the definition $\alpha_{\rho 1}(t) = \alpha_\rho(t) - 1$ are used. The predicted total and differential cross sections and the t dependence of the density matrix elements are shown. It is found that the model gives a satisfactory description of the studied reaction at high energies in the forward direction. (J.F.P.)

20009 NOTE ON THE OBSERVATION OF S^0 MESON. Gemesy, T.; Suranyi, G. (Central Research Inst. for Physics, Budapest). Acta Phys. Acad. Sci. Hung.; 29: 91-2(1970).

In searching for the S^0 meson, the γ rays emerging from the reaction $\pi^+ + n \to p + X^0$, where the unknown particle X^0, which may form an S^0 resonance, decays into four photons can be used. Since there are many channels at the studied energy which give a proton and two π^0s in the final state having different effective masses, in order to use this method of finding the S^0, the possible existence of a background channel which could give a bump as a kinematic effect in the $\pi^0\pi^0$ effective mass distribution at about an energy of 720 MeV must be eliminated. The $\pi^0\pi^0$ effective mass distribution in the channel $\pi^+ + n \to N^{*+} + \pi^0 \to p + 2\pi^0$ is calculated. It is concluded that this channel does not affect the observation of the hypothetical S^0. (J.F.P.)

20010 EFFECTIVE RANGE PARAMETER IN S-WAVE PION-NUCLEON SCATTERING. Achuthan, P.; Hite, G. E.; Hoehler, G. (Univ., Karlsruhe, Ger.). Z. Phys.; 242: 167-78(1971).

The effective range parameter b^- for πN s-wave scattering is calculated from fixed-t dispersion relations, using experimental information for the imaginary parts. The result is compared with that of other calculations, based on Ward identities and phenomenological Lagrangians. It is pointed out that a direct determination of b^- from experimental data is not possible. Since the Δ-propagator is not unique, the Δ-exchange amplitudes are given for a one-parameter class of propagators. (auth)

20011 FINITE-ENERGY SUM RULE AS A TEST OF THE POMERANCHUK THEOREM. Igi, K.; Kuroda, M.; Miyazawa, H. (Tokyo Univ.). Phys. Lett.; 34B: 140-2(1 Feb 1971).

A finite-energy sum rule for π-p scattering lengths, which holds even in the case of $\Delta\sigma(\infty) = \sigma_{\pi^-p}(\infty) - \sigma_{\pi^+p}(\infty) \neq 0$, is used to estimate the magnitude of $\Delta\sigma(\infty)$. A criterion is given of testing the presence of the Pomeranchuk-theorem-violating term. (auth)

20012 PION-NUCLEON PHASE SHIFT ANALYSIS FROM 1.98 TO 3.5 GeV/c. Bransden, B. H.; Ogden, P. J. (Univ. of Durham, Eng.). Nucl. Phys.; B26: 511-24(1971).

Phase-shift analyses of elastic pion-nucleon scattering data were carried out at a number of different values of the pion lab momentum between 1.98 and 3.5 GeV/c. At each momentum the minimization was performed by varying the phase-shift parameters for $l < 5$. Starting value of the parameters were taken from those given by the model of Roychoudhury, Perrin and Bransden and phase-shift parameters for $l \geq 5$ were held fixed to the values provided by that model. The results lend support to the general character of the phase shifts previously found by Roychoudhury et al. (auth)

20013 THEORETICAL MODEL-INDEPENDENT DETERMINATION OF THE REAL PARTS OF THE $K^\pm p$ FORWARD SCATTERING AMPLITUDES. Dumbrais, O. V.; Dumbrais, T. Yu.; Queen, N. M. (Joint Inst. for Nuclear Research, Dubna, USSR). Nucl. Phys.; B26: 497-510(1971).

A new method of analyzing experimental data on kaon-proton scattering is used to obtain an accurate determination of the real parts of the forward scattering amplitudes at moderate energies. The method exploits the known analyticity properties of the scattering amplitude and experimental data in a finite-energy range. However, unlike conventional dispersion-relation calculations, it requires no assumptions about the residues of the hyperon pole terms and the amplitudes in the unphysical and asymptotic regions. A parameter describing the unknown asymptotic behavior of the amplitudes is determined. Its value favors a zero asymptotic limit for the $K^\pm p$ cross-section difference but requires a slower approach to zero than that predicted by conventional Regge-pole models which satisfy the Pomeranchuk theorem. The method can be used in principle to analytically continue the scattering amplitude from the physical region of the Λ-pole. However, a sufficiently accurate model-independent determination of the $KN\Lambda$ coupling constant cannot be obtained in this way using the experimental data which exist at the present time. (auth)

20014 MULTIPARTICLE VENEZIANO FORMULAE CORRESPONDING TO THE INTERACTION OF TWO CLASSES OF HADRONS. Jones, K. (Univ. of Durham, Eng.). Nucl. Phys.; B26: 621-39(1971).

A new class of multiparticle Veneziano formulas corresponding to the interaction of n "elementary" hadrons, where only meson-baryon-baryon couplings are allowed, is derived. The n-point function is again expressible as an (n − 3) dimensional integral as it is for the n-point tree graph. This is the generalization of a model proposed by Burnett and Schwarz. This model has been generalized in a different direction by Mandelstam. The generalizations coincide for the five-point function, but diverge for the six-point and higher functions. A complementary, but seemingly unrelated generalization has already been given. The advantages of the generalization given in this paper are demonstrated. (auth)

20015 MASS OPERATOR IN THE SU(3)-SYMMETRIC STRONG COUPLING THEORY WITH PSEUDOSCALAR MESONS. Tolar, J. (Technical Univ., Prague). Czech. J. Phys.; 20: 1093-1106 (1970).

The SU(3)-symmetric model of a static-baryon octet source interacting with pseudoscalar meson octet fields by the coupling of Yukawa type is considered in the strong coupling limit. Using the result derived earlier that the isobaric states form the basis of the unitary irreducible representation of the dynamical group $G = T_{24} \otimes [SU(3) \otimes SU(2)]$, the mass operator is specified by the kinetic part of the Hamiltonian as a particular element of the universal enveloping algebra of the symmetry group $SU(3) \otimes SU(2)$ acting in the space of isobaric states. (auth)

Strong (Baryon No. ≥ 2)

Refer also to abstracts 19485 and 20490.

20016 (CERN-Trans-70-14) NON-STRANGE BARYON-BARYON RESONANCES. Zul'karneev, R. Ya.; Rozanova, A. M. (Joint Inst. for Nuclear Research, Dubna (USSR)). Translated by B. Hodge and revised by N. Mouravieff (CERN, Geneva, Switzerland), from report JINR-P2-5058. 8p. Dep. NTIS (U. S. Sales Only).

A phase analysis is performed on elastic p + p interactions at 640 MeV with the artificial introduction of strong absorption in the $^1D_2$ and $^3P_2$ states. A comparison with other results shows the existence of a resonance in the pp system with mass = 2050 ± 90 MeV and $J^P = 2^+$. (J.F.P.)

20017 (CERN-Trans-70-15) $pn \to np$, $\bar{p}p \to \bar{n}n$ AND BRANCHING IN THE j-PLANE. Kaidalov, A. B.; Karnakov, B. M. Translated by A. Sanders and revised by N. Mouravieff (CERN, Geneva, Switzerland), from Yadern. Fiz.; 7: 1147-9(1968). 7p. Dep. NTIS (U. S. Sales Only).

It is shown that experimental results for the differential cross section behavior for the reactions $p + n \to n + p$ and $\bar{p} + p \to \bar{n} + n$ can be explained using the complex momenta method taking account of branching in the j-plane. (J.F.P.)

20018 (JINR-P2-5507) DOUBLE DIFFERENTIAL DISTRIBUTION OF PARTICLES PRODUCED IN THE PROTON-NUCLEUS COLLISIONS. Barashenkov, V. S.; Il'inov, A. S.; Sobolevskii, N. M.; Toneev, V. D. (Joint Inst. for Nuclear Research, Dubna (USSR). Lab. of Theoretical Physics). 1970. 14p. (In Russian). Dep. NTIS (U. S. Sales Only).

The results of cascade calculations of the double differential distributions of particles, produced in the proton-nucleus col-

XUM

lisions in the energy range from several dozens of MeV up to several GeV, are compared with experiment and the cross sections calculated by the Bertini method. In general, all these data agree well. The reasons for divergences are discussed in some details. (auth)

20019 (LYCEN–7081) LOW-ENERGY THEOREMS AND π-MESON INTERACTIONS WITH NUCLEI. Figureau, Alain (Lyon Univ. (France). Institut de Physique Nucleaire). Nov 1970. 54p. (In French). Dep. NTIS (U. S. Sales Only).

Thesis.

Current algebra and the partially conserved axial current hypothesis (PCAC) were used to study the interactions of π mesons with nuclei. The low-energy theorems obtained generalize for nuclei, results acquired in elementary particle physics. These theorems were derived from the sum rules in which the amplitudes of the pion processes appear to be the only contributions when the mass of the π meson is assumed to be zero. However, the terms in the sum rule corresponding to the nuclear structure must play an important role in determining the physical amplitudes. These corrections to the low-energy theorems were studied and shown to be computable. They were given a physical interpretation and their relative importance estimated. The elastic scattering of π mesons was considered and generalized for the case of photoproduction. It was concluded that the amplitude given by the low-energy theorem could be considered as the Born approximation of the interaction. The physical amplitude was deduced from it using the pion wave distortion correction. The saturation of the sum rules obtained was in general satisfactory even though this scheme did not consider granularity effects in the nuclear structure. (France)

20020 (USIP–70-5) ONE-PION EXCHANGE MODEL APPLIED TO THE REACTION $pp \rightarrow p\pi^+(\Delta^{++})\pi^-p$ AT 19 GeV/c. Brink, Lars; Holmgren, Sven-Olof (Stockholm Univ. (Sweden). Inst. of Physics). Oct 1970. 19p. Dep. NTIS (U. S. Sales Only).

Predictions of a one pion exchange model (OPE) applied to $\rho\rho \rightarrow \rho\pi^+(\Delta^{++})\rho\pi^-$ at 19 GeV/c are compared to experimental data produced by the Scandinavian collaboration in a bubble chamber experiment using the CERN 2m HBC. Limiting forms of reggeized models are compared to the OPE formulas and used in the interpretation of the results. (auth) (Sweden)

20021 SYMMETRIES AND NUCLEAR FORCES. El-Ghabaty, Sayed Shehata. Detroit; Wayne State Univ. (1970). 71p. University Microfilms Order No. 71-399.

Thesis.

Three problems are investigated dealing with various aspects of the symmetries of nuclear forces. First, considering deviations from charge independence, a simple mass-averaging device is described for the investigation of the effect of the pion mass difference on the nucleon-nucleon interaction. While the mass-difference correction in the one-pion-exchange contribution is known to be significant, it is found that the corresponding correction plays a less significant role in the two-pion-exchange contribution. The effect of difference in the coupling constants is also discussed, and found to be equally significant in the one- and two-pion-exchange contributions. The results of the investigation are summarized in two tables which prescribe an average pion mass and an effective coupling constant for each nucleon-nucleon scattering diagram in different isospin states. In order to show the effect of the pion mass difference, the numerical values of the W matrix coefficients at different angles and energies are given. The applicability of the approach to the ρ-exchange contribution is pointed out. Next, the effect on nuclear forces of the second-order nonlinear term in the pion-nucleon coupling as implied by chiral symmetry is considered. By using the nonderivative coupling, it is found that the nonlinear terms add a short-range force to the usual two-pion-exchange contribution. The use of the nonlinear derivative coupling would yield the same final result because of the equivalence of the two couplings for the total contribution of the two-pion-exchange diagrams. The average pion mass and effective coupling constant to be used with the additional diagrams are derived, and the numerical values of the W matrix coefficients are also given. Finally, the calculation of the one-pion-exchange diagram in the U(6,6) model is presented. From this calculation it is found that the U(6,6) coupling gives essentially the usual one-pion-exchange result except for a multiplying factor which depends on the momentum transfer in the scattering process. An additional contribution, including a spin-orbit force, to the nucleon-nucleon interaction is found. For the purpose of comparison with experimental data, the W matrix coefficients were also calculated, and their values at different angles and energies are presented. These results of the investigation could play an important role in the re-evaluation of the effects of symmetries and deviations from them in the area of nuclear forces. (Diss. Abstr.)

20022 RELATION BETWEEN THE BINDING ENERGY AND SCATTERING PHASE SHIFT. Chong, K. F.; Nogami, Y. (McMaster Univ., Hamilton, Ont.). Amer. J. Phys.; 39: 182-6(Feb 1971).

It is well known in the potential scattering in quantum mechanics that it is, in principle, impossible to obtain information about the binding energy from the scattering phase shift, and vice versa. This is illustrated in a simple way for the case of a nonlocal separable potential. The implications of the "relation" between the deuteron binding energy and the low-energy proton–neutron scattering parameters in the ^3S state are discussed. (auth)

20023 SINGLE-PARTICLE-ENERGY SPECTRUM OF A Λ PARTICLE IN NUCLEAR MATTER. Chong, K. F.; Nogami, Y.; Satoh, E. (McMaster Univ., Hamilton, Ont.). Can. J. Phys.; 48: 2804-8(1 Dec 1970).

The single-particle-energy spectrum of a Λ particle in nuclear matter was examined in the independent-pair approximation, by assuming nonlocal separable potentials for the ΛN interaction. Effects of short-range repulsion in the ΛN interaction on the Λ binding were also examined in terms of separable potentials of rank two. (auth) (Canada)

20024 NUCLEON–NUCLEON SCATTERING IN THE ONE-BOSON-EXCHANGE APPROXIMATION. Martin, Alexander. Hoboken, N. J.; Stevens Inst. of Tech. (1970). 108p. University Microfilms Order No. 71-1175.

Thesis.

Nucleon–nucleon scattering is calculated in the one-boson-exchange approximation using the exchange of the π, η, ϵ, ρ, ω, and ϕ mesons. The parameters of the π, η, ϵ, and ρ exchanges, masses and coupling constants can be accurately estimated from experimental data. The vector meson dominance of the nucleon electromagnetic form factors can establish reliably only a relation between the ω and ϕ coupling constants. Since all other parameters are fixed from other experiments, it is possible to use N-N scattering to estimate the ω and ϕ couplings. A goodness-of-fit criterion is defined and investigated for the two undetermined parameters. The predictions of five models of the ω and ϕ couplings suggested in the literature are calculated. Two of the models lead to disagreement with experiments. Of the three which remain, the proposal that the ϕ is not coupled to nucleons is favored by the goodness of fit criterion. It is known that the one-particle-exchange picture cannot explain the nucleon form factors at large momentum transfers. It has been suggested that the discrepancy be attributed to momentum dependence of the vector meson-nucleon couplings. A method is presented for the inclusion of such effects in N-N scattering. Using a momentum dependence required by nucleon form factors in general worsens the agreement with experiment. (Diss. Abstr.)

20025 ONE-BOSON-EXCHANGE MODEL OF N–N SCATTERING FOR THE 0- TO 3-GeV ENERGY RANGE. Ueda, Tamotsu (Osaka Univ.). Phys. Rev. Lett.; 26: 588-91(8 Mar 1971).

With the use of a dispersion relation and a high-energy cutoff, the model involving π, ρ, ω, η_V, f, and σ (0^+, $I = 0$, 416 MeV) is studied for nucleon–nucleon interactions below 3 GeV. All nucleon–nucleon elastic-scattering data and those for p–p collisions at 0.67, 0.97, and 1.4 GeV are in qualitative agreement with the calculations. (auth)

20026 VERY HIGH-MOMENTUM COMPONENTS IN NUCLEI AND FAR SUBTHRESHOLD PRODUCTION OF QUARKS. Danos, Michael; Gibson, Benjamin F. (National Bureau of Standards, Washington, D. C.). Phys. Rev. Lett.; 26: 473-6(22 Feb 1971).

An estimate, valid for inelastic processes, of the probabilities of the high-momentum components in nuclei resulting from many-body correlations, together with data from Serpukhov, is used to derive upper limits for the quark-production cross section near threshold. (auth)

20027 CALCULATING THE CONTRIBUTIONS OF THE FIRST TWO DIAGRAMS TO THE REACTION AMPLITUDE FOR THREE BODIES. Muscalu, S. An. Univ. Bucuresti, Ser. Stiint. Natur., Fiz.; 16: 95-105(1967). (In Rumanian).

The contribution of the polar and simply squared diagrams to the diffusion amplitude is calculated for the case of inelastic interaction between neutrons and deuterons at low energies. These diagrams are plotted for the case when in the final state the particle pair interacts in both single and triplet states. (Rom. Sci. Abstr.)

20028 ATLAS OF PARTICLE PRODUCTION SPECTRA. Grote, H.; Hagedorn, R.; Ranft, J. Geneva; CERN (1970). 231p.

An atlas of the momentum spectra of secondary particles produced in proton–proton and proton reactions with aluminum,

XUM

beryllium, copper, and lead is presented. The calculations are based on the thermodynamic model. (J.F.P.)

20029 ENERGY DEPENDENCE OF COHERENT PRODUCTION CROSS SECTION IN NUCLEI. Lesniak, H.; Lesniak, L. (CERN, Geneva). Phys. Lett.; 34B: 135-9(1 Feb 1971).

A very simple explanation of the energy dependence of the coherent production cross section of 3π and 5π systems in nuclei by 16 to 200 GeV/c incident pions is presented. The decrease of the longitudinal momentum transfer with increasing energy results in an increase of the coherent cross section. (auth)

20030 ISOSPIN ANALYSIS OF PION AND NUCLEON RESONANCE PRODUCTION IN NN COLLISIONS. Koba, Z.; Moellerud, R.; Veje, L. (Niels Bohr Inst., Copenhagen. Univ. of Copenhagen). Nucl. Phys.; B26: 547-56(1971).

After a brief survey of isospin relations for the general reaction $NN \rightarrow N'N' + k\pi$ ($k = 1, 2, 3, \ldots$), cases of $k = 2, 3$ and resonance formation are discussed. The reaction $NN \rightarrow N'\Delta\pi$ is found particularly suitable for the isospin analysis, and its cross sections are given in terms of various isospin exchange amplitudes. Another eventually feasible example is $NN \rightarrow N'\Delta\rho$. (auth)

20031 CALCULATIONS OF π^+ PRODUCTION IN NUCLEI. Beder, D. S.; Bendix, P. (Univ. of British Columbia, Vancouver). Nucl. Phys.; B26: 597-610(1971).

The π^+ production by (600 MeV) protons incident on nuclei is calculated, using a model which expresses the production rate in terms of a momentum averaged free production rate multiplied by an absorptive attenuation factor. The only free parameter is the normalization of the free $NN \rightarrow NN\pi$ matrix element. This is fit to $pp \rightarrow pn\pi^+$ data; subsequently absorption coefficients are calculated from this same matrix element. The results for $d^2\sigma/dE_\pi d\Omega_\pi$ agree very well with available data on nuclei. (auth)

20032 ONE-PION EXCHANGE MODEL APPLIED TO THE REACTION $pp \rightarrow p\pi^+(\Delta^{++})\pi^-p$ AT 19 GeV/c. Brink, Lars (Inst. of Theoretical Physics, Goteborg); Holmgren, Sven-Olof. Nucl. Phys.; B26: 611-20(1971).

Predictions of a OPE model applied to $pp \rightarrow p\pi^+(\Delta^{++})p\pi^-$ at 19 GeV/c are compared to experimental data produced by the Scandinavian collaboration. Limiting forms of reggeized models are compared to the OPE formulas and used in the interpretation of the results. (auth)

Particle Invariance Principles and Symmetries

General

Refer also to abstracts 20021, 20091, and 20105.

20033 INFINITE-DIMENSIONAL REPRESENTATIONS OF THE LORENTZ GROUP: COMPLEMENTARY SERIES OF REPRESENTATIONS. Carmeli, M. (Aerospace Research Labs., Wright-Patterson AFB, Ohio); Malin, S. J. Math. Phys. (N. Y.); 12: 225-9(Feb 1971).

The method used by Carmeli to obtain another form for the principal series of representations of the group SL(2,C) is extended to the complementary series of representations of that group. As a result, a new form for the complementary series of representations of SL(2,C) is obtained which describes the transformation law of an infinite set of numbers under the group translation in a way which is very similar, but as a generalization, to the way spinors appear in the finite-dimensional case. (auth)

20034 IDENTITY SATISFIED BY THE RACAH COEFFICIENTS OF U(n). Louck, J. D. (Los Alamos Scientific Lab., N. Mex.); Biedenharn, L. C. J. Math. Phys. (N. Y.); 12: 173-7(Feb 1971).

The origin of a well-known relation satisfied by the Racah coefficients of SU(2) is demonstrated to be the associative law of multiplication of the Wigner operators of SU(2). Recognition of this simple fact allows the immediate generalization of this identity to the Racah coefficients of U(n). (auth)

20035 REALIZATIONS OF REPRESENTATIONS OF THE POINCARE GROUP AND ASSOCIATED SIMILARITY TRANSFORMATIONS. Beckers, J. (Univ., Liege). Phys. Rev., D; 3: 952-5(15 Feb 1971).

Recent contributions on canonical and manifestly covariant realizations of the representations of the Poincaré group are discussed. A $2(2j + 1)$-dimensional operator for arbitrary spin j is constructed, permitting simple interpretations and discussions of similarity transformations currently used in the literature. (auth)

20036 CONFORMAL SYMMETRY AND THREE-POINT FUNCTIONS. Schreier, Ethan J. (Massachusetts Inst. of Tech., Cambridge). Contract AT(30-1)-2098. Phys. Rev., D; 3: 980-8 (15 Feb 1971).

The general three-point functions invariant under conformal transformations are constructed for both axial-vector and vector currents. These are used to study the anomalies present in the Ward–Takahashi identities. The axial-vector anomalies are considered in detail and Schwinger terms are calculated using equal-time limits. (auth)

20037 DIMENSION OF OPERATORS IN BROKEN SCALE INVARIANCE. O'Donnell, P. J. (Univ. of Toronto). Phys. Rev., D; 3: 1021-4(15 Feb 1971).

It is shown that if the Hamiltonian can be split into a part which is scale invariant and a part which breaks scale invariance by means of a dilaton, then, if the latter part has a unique dimension, this dimension must be 1 if the vacuum does not realize the invariance under scaling. This implies that there must exist a term which breaks scale invariance in addition to that which breaks chiral $SU(3) \times SU(3)$ symmetry in order to avoid a contradiction with Gell-Mann's argument. (auth)

20038 PHENOMENOLOGICAL ACTIONS FOR SPONTANEOUSLY-BROKEN CONFORMAL SYMMETRY. Ellis, John (CERN, Geneva). Nucl. Phys.; B26: 536-46(1971).

The general form of invariant actions for spontaneously-broken conformal symmetry is discussed using equations due to Callan, Coleman and Jackiw. Previously known rules for constructing conformally covariant derivatives are simply obtained, but not all conformal invariant actions can be obtained using fields and their covariant derivatives. A method due to Wess and Zumino is shown to generate all invariant actions not more than second order in the derivatives of spin 0, ½ and 1 fields. Chiral and conformal invariant actions are discussed. (auth)

Applications (Electromagnetic and Weak)

Refer also to abstract 20535.

20039 APPLICATIONS OF WEAK-INTERACTION HAMILTONIAN TO STRANGENESS-CHANGING AND STRANGENESS-PRESERVING PARITY-VIOLATING PROCESSES. Rao, Jandhyala Subba. Rochester, N. Y.; Univ. of Rochester (1970). 113p. University Microfilms Order No. 71-1419.

Thesis.

Certain models of strong interactions based on the notion of chiral symmetry are studied. In particular, the model of Gell-Mann, Oakes and Renner is applied in conjunction with the hypothesis of Gatto et al., with regard to the divergences in weak interactions to the nonleading divergences in a weak process. It is observed that radiative corrections to the same process have similar divergences and suggest that these divergences can cancel the nonleading divergences in the weak process. It is shown that such a conjecture can be maintained in order g^4 and g^2e^2, in a quark model. It leads to a mass of the intermediate vector boson of about 70 GeV through the constraint $g^2 \approx e^2/2$. In the model of Gell-Mann, Oakes and Renner, the symmetry breaking part of the Hamiltonian is assumed to belong to the $(3,3^*) \oplus (3^*,3)$ representation of $SU(3) \otimes SU(3)$. In the symmetry breaking part of a term is included which belongs to the $(8,1) \oplus (1,8)$ representation. The Gatto hypothesis in this model is shown to yield an incorrect value for the Cabibbo angle. Moreover, with the assumption that the leading divergent term dominates the matrix element for nonleptonic processes it is shown that octet dominance for nonleptonic s and p wave decays follows naturally. It is further shown that the equality of the d/f ratios for the weak and medium-strong mass splittings follows in such a model. Assuming also that the parameters that enter into the matrix elements are numerically not too crucially dependent on the presence of the $(8,1) \oplus (1,8)$ term, a value of the cut-off is obtained from the s-wave nonleptonic decay amplitudes. This value of Λ is 30 GeV, which is larger by a factor of 8 than previous estimates from the $K_L^0 - K_S^0$ mass difference. These previous calculations, however, assumed that the leading divergent term was absent and this is not true in a model with a term of the $(8,1) \oplus (1,8)$ type. Then, the problem of the $K_L^0 - K_S^0$ mass difference is reexamined within the framework of this model. The problem of distinguishing between different weak interaction Hamiltonians is studied by considering the consequences of these Hamiltonians in parity-violating nuclear reactions. It is shown that the vector meson exchange potential, which a priori should be comparable to the pion exchange potential, is in fact suppressed if one believes that Schwinger terms cancel seagull terms. In the process $n + p \rightarrow d + \gamma$, the suppression of the vector meson exchange potential has the effect of suppressing the circular polarization of the photon. However, in $n + d \rightarrow {}^3H + \gamma$ this polarization gets contribu-

XUM

tions from both types of potentials and as a result will be relatively large. The asymmetry coefficient of the photon, however, will still be relatively large in n + p → d + γ because only the pion exchange potential contributes here. (Diss. Abstr.)

20040 NONRELATIVISTIC AND RELATIVISTIC COULOMB AMPLITUDE AS THE MATRIX ELEMENT OF A ROTATION IN O(4,2). Barut, A. O.; Rasmussen, W. (Univ. of Colorado, Boulder). Phys. Rev., D; 3: 956-9(15 Feb 1971).

It is shown that the Coulomb amplitude is the matrix element of the group element $e^{i(\theta+\pi)J_2}$ evaluated in a continuous basis in SO(4,2). The method is applied to the relativistic Kepler problem without spins, but with the recoil corrections included. The form of the amplitude for this case is believed to be new. (auth)

20041 CHIRAL SYMMETRY BREAKING AND THE K_{l3} AND K_{l4} FORM FACTORS. Lane, Kenneth Douglas. Baltimore; Johns Hopkins Univ. (1970). 149p. University Microfilms Order No. 70-26,752.

Thesis.

The hypotheses of current algebra and approximate chiral, or SU(3) × SU(3), symmetry are used to obtain information on several of the form factors describing the semileptonic K_{l3} and K_{l4} decays. For the vector form factors $F_\pm(t)$ of K_{l3} decay, these investigations lead to order-of-magnitude constraints on the values of the parameters $\lambda'_\pm = m_\pi^2(dF_\pm/dt)_{t=0}$. Effects on the K_{l3} decay amplitude due to radiative corrections are reviewed, and these are shown to be quite important for the proper determination of $\lambda'_\pm$. The interpretation of several of the results of K_{l3}-decay experiments could be considerably altered once radiative effects are taken into account. The axial-vector form factors of K_{l4} decay were calculated using current algebra and approximate chiral symmetry. They are obtained in the neglect of terms involving second and higher orders in both the symmetry breaking and the momenta of K- and π-mesons. A model for the symmetry breaking is needed to evaluate matrix elements containing σ-type commutators; the Gell-Mann–Oakes–Renner model is chosen for this purpose. The form factors calculated in this way are found to compare favorably with the available experimental data. (Diss. Abstr. Int., B)

Applications (Strong)

Refer also to abstract 19907.

20042 DYNAMICAL REARRANGEMENT OF SPONTANEOUSLY BROKEN CHIRAL SYMMETRY. Bessler, L. (Univ. of Wisconsin, Milwaukee). Lett. Nuovo Cim.; 1: 247-51(6 Feb 1971).

Some relations are derived in the context of a previous formulation of spontaneously broken chiral symmetry and the assumption of dynamical rearrangement of chiral symmetry for nucleons. Restriction is made to the case of chiral SU(2) × SU(2). (J.F.P.)

20043 RENORMALIZATION OF THE K*Kπ COUPLING IN BROKEN SU_3 SYMMETRY. Brout, R. (Univ. Libre, Brussels); Cleymans, J.; Rodenberg, R. Lett. Nuovo Cim.; 1: 245-6(6 Feb 1971).

It is shown that broken SU(3) properly interpreted gives a better width for K* → K + π decay than was previously found. The relation: $g^2_{K^*K\pi}/g^2_{\rho\pi\pi} = m^2_{K^*}/m^2_\rho$, which shows that the ratio of the couplings is renormalized in the same way as the ratio of the masses, is found. From this the predicted width is Γ(K* → Kπ) = 50 MeV which is in excellent agreement with experiment. (J.F.P.)

20044 ELECTROMAGNETIC CORRECTIONS TO CHIRAL SYMMETRY. Gonzalez, Manuel Angel. Seattle; Univ. of Washington (1970). 126p. University Microfilms Order No. 71-970.

Thesis.

The problem of chiral symmetry breaking by the electromagnetic interaction is studied. A theory invariant under the group generated by the vector and axial-vector currents, that is to say a theory for which among other things $m_\pi = 0$ and $\partial_\mu a^\mu_a = \partial_\mu v^\mu_a = 0$ is used. With this theory one attempts to calculate, to first order in the fine structure constant α, the corrections produced by a minimal electromagnetic coupling to low energy theorems which follow from strict chiral symmetry. Finally, the methods are applied to the study of pion–nucleon scattering at threshold, and an expression is derived for the first order in α correction to the difference between the S-wave scattering lengths a_{π^-p} and a_{π^+n}. (Diss. Abstr.)

20045 ASPECTS OF CHIRAL SYMMETRY. Brenner, B. (DAMTP, Cambridge, Eng.). Acta Phys. Austr.; Suppl. 7, 91-144(1970).

From 9th Conference on Developments in High Energy Physics, Schladming, Austria. See CONF-700220.

The lectures on chiral symmetry proceed inductively from some empirical facts to their significance. The starting point is the Goldberger–Treiman relation. The idea of chiral symmetry, low-energy theorems, generalized Ward identities and chiral Lagrangians, reconstruction of chiral Lagrangians from Adler zeros, and extension to SU(3) × SU(3) are treated. (J.F.P.)

20046 MASS OPERATOR IN THE SU(3)-SYMMETRIC STRONG COUPLING THEORY WITH PSEUDOSCALAR MESONS. Tolar, J. (Univ., Marburg, Ger.). Acta Phys. Austr.; Suppl. 7, 610-19(1970).

From 9th Conference on Developments in High Energy Physics, Schladming, Austria. See CONF-700220.

A consistent formulation of the strong-coupling approximation for the meson–baryon system with SU(3) symmetry according to a previous suggestion for the SU(2)-symmetric system is given. It is shown how the Hamiltonian describing an octet of pseudoscalar mesons coupled to a bare baryon source is transformed to a form allowing perturbation theory in the inverse powers of the coupling constant. The basic properties of the lowest order approximation, the wave functions and the energies of the isobaric states, are treated. (J.F.P.)

20047 ON $\rho \to e^+e^-$, $\varphi \to e^+e^-$ AND $\omega \to e^+e^-$ DECAYS IN BROKEN $SU(6)_W$ SYMMETRY. Giler, S.; Lefik, V.; Tybor, V. (Univ., Lodz, Poland). Acta Phys. Pol.; B1: 87-92(Apr-Jun 1970). (In Russian).

In the frame of broken symmetry $SU(6)_W$ a relation between the widths of the decays $\rho \to e^+e^-$, $\varphi \to e^+e^-$, and $\omega \to e^+e^-$ was obtained conforming well with experiment. The obtained sum rule corresponds to the same phases of the constants of the V → γ transition. (tr-auth)

20048 ON $3/2^+ \to 1/2^+0^-$ DECAYS IN BROKEN $SU(6)_W$ SYMMETRY. Giler, S.; Lefik, V.; Tybor, V. (Univ., Lodz, Poland). Acta Phys. Pol.; B1: 93-5(Apr-Jun 1970). (In Russian).

In the frame of broken $SU(6)_W$ symmetry the correlations among the amplitudes of the decays decuplet $3/2^+$ → octet $1/2^+$ + octet 0^- are obtained conforming well with experiment. (J.F.P.)

20049 ESSENTIAL BREAKING OF SCALE INVARIANCE IN NONLINEAR CHIRAL LAGRANGIAN MODELS. Chen, Min-shih (Yale Univ., New Haven. Brookhaven National Lab., Upton, N. Y.). Phys. Rev., D; 3: 1025-8(15 Feb 1971).

It is shown that, in the conventional chiral SU(2) ⊗ SU(2)-symmetric nonlinear Lagrangian models of pseudoscalar mesons, scale invariance is essentially broken. Although a dilatation current $D^\mu(x)$ generating a scale transformation for the meson fields can be explicitly constructed, it is impossible to choose a canonical frame in which the axial-vector current transforms with scaling dimension 3 under this scale transformation. The conflict between scale invariance and the nonlinear realization of chiral symmetry is exhibited through the chiral nonvariance of the new energy-momentum tensor $\theta^{\mu w}$, which gives $D^\mu(x) = x_\nu\theta^{\mu\nu}(x)$ and $\partial_\mu D^\mu(x) = \theta^\mu_\mu(x)$. Furthermore, it is shown that, in nonlinear models, there is no chiral-symmetric tensor which can approach this new energy-momentum tensor in the free-field limit. (auth)

20050 WAVE EQUATIONS WITH COMPACT AND NONCOMPACT SPECTRUM. Gyuk, I.; Umezawa, H. (Univ. of Wisconsin, Milwaukee). Phys. Rev., D; 3: 898-907(15 Feb 1971).

A unified approach to compact and noncompact wave equations based on the algebra of O(6,C) is presented. The Bhabha and Nambu equations emerge as the simplest possibility for describing multiplets of relativistic particles. Dynamical quantities such as mass, spin, and magnetic moment are evaluated in terms of the spectra of relevant operators. (auth)

20051 IS SU(2) ⊗ SU(2) A BETTER SYMMETRY THAN SU(3)? Cheng, T. P.; Dashen, Roger (Inst. for Advanced Study, Princeton). Phys. Rev. Lett.; 26: 594-7(8 Mar 1971).

Using the πN phase shifts and fixed-t dispersion relations the nucleon matrix element of the current algebra "sigma" term was calculated (to first order in symmetry breaking), and a value of about 110 MeV was found. This is an order of magnitude larger than the prediction of the $(\underline{3},\underline{3}^*) \oplus (\underline{3}^*,\underline{3})$ model for chiral symmetry breaking and it indicates that SU(2) ⊗ SU(2) breaking is comparable to SU(3) breaking. (auth)

Field Theories

General

Refer also to abstract 19952.

20052 (SLAC-Trans-130) SYMMETRIC SPACE OF THE GROUP OF THE MAXWELL EQUATIONS. Wyler, Armand. Translated for Stanford Linear Accelerator Center, Calif., from Compt. Rend.; Ser. A, 269: 743-5(1969). 6p. Dep. NTIS.

A study is made of the group of invariance of the Maxwell equations and of its extension associated with the set of hyperboloids of mass. Calculation of the Poisson kernels on the symmetric spaces leads to a geometric interpretation of the constant $e^2\sqrt{\hbar c}$, for which this theory gives the value 1/137.037. (auth)

20053 f-DOMINANCE OF GRAVITY. Isham, C. J.; Salam, Abdus; Strathdee, J. (International Centre for Theoretical Physics, Trieste, Italy). Phys. Rev., D; 3: 867-73(15 Feb 1971).

A Lagrangian theory is formulated describing the intrinsic mixing of the graviton with a massive 2^+ f meson which interacts universally with hadrons through the stress tensor. The theory is developed as an analog of the well-known $\rho-\gamma$ model of hadron electrodynamics, and in particular a field-current identity is exhibited which equates the massive 2^+ meson with the hadronic energy-momentum tensor. An Einstein-type Lagrangian is used for both spin-2 particles, and general covariance is preserved throughout. The nonlinear coupling of the hadrons to the f meson leads, within the framework of nonpolynomial field theories, to a universal cutoff for strong-interaction physics. (auth)

Quantum Field Theory

Refer also to abstracts 19935, 19944, and 20115.

20054 (CNRS-CPT-70-P-335) COLLOQUIUM ON COMPUTATIONAL METHODS IN THEORETICAL PHYSICS, MARSEILLES, FRANCE, JUNE 15-19, 1970. (Centre National de la Recherche Scientifique, Marseilles (France). Centre de Physique Theorique). 1970. 153p. (In English and French). (CONF-700638).

Eleven papers were presented, grouped in four chapters: methods of computation, Pade approximants and particle physics, statistical mechanics, and quantum electrodynamics. Only the three constituting the fourth chapter were abstracted. (auth)

For abstracts of individual papers see: 19512, 19936, and 20055.

20055 (CNRS-CPT-70-P-335, pp IV.26-38) EVALUATION OF THE ELECTRON ANOMALOUS MAGNETIC MOMENT BY COMPUTER. Calmet, J. (Centre National de la Recherche Scientifique, Marseilles (France). Centre de Physique Theorique).

In Colloquium on computational methods in theoretical physics; Marseilles, France (15 Jun 1970).

A method for computing renormalized radiative corrections in quantum electrodynamics is presented. Combinatorial analysis using FORTRAN is used to generate the Feynman diagrams. Algebraic calculations from these diagrams are made with a functional framework existing within the LISP program. A numerical evaluation of the multidimensional integrals of the Feynman parameters obtained succeeds these calculations. A LISP program which extracts from the Feynman amplitudes their contributions to the anomalous magnetic moments of the electron and the muon, is described. The contributions, free of uv divergence, are treated and then the internal divergences subtracted. An L.S.D. routine is used to evaluate the multidimensional integrals. The programs were verified by calculating the contribution of the α^2 term for the electron; they allow all the contributions of the α^3 term of the anomalous magnetic moment to be calculated. They are used with the UNIVAC 1108. (France)

20056 (DESY-70/62) RENORMALIZATION OF THEORIES WITH BROKEN SYMMETRY. Symanzik, K. (Deutsches Elektronen-Synchrotron, Hamburg (West Germany)). Nov 1970. 71p. Dep. NTIS (U. S. Sales Only).

The renormalization of theories with broken symmetry is described from a conservative viewpoint. Only field theories renormalizable in the usual perturbation theoretical sense are considered. The BPH renormalization theory, currents and Ward-Takahashi identities, symmetry breaking by a linear term and by a nonlinear term, ratios of bare coupling constants, calculation of current operators, and spontaneous symmetry breaking are covered. (J.F.P.)

20057 (JINR-E2-5563) A BRIEF REVIEW OF THE REPORTS SUBMITTED TO THE 2nd INTERNATIONAL SYMPOSIUM ON NON-LOCAL QUANTUM FIELD THEORY, AZAU, MARCH 15-24, 1970. Efimov, G. V.; Volkov, M. K. (Joint Inst. for Nuclear Research, Dubna (USSR). Lab. of Theoretical Physics). 1971. 18p. Dep. NTIS (U. S. Sales Only).

The reports submitted to the II International Symposium on Nonlocal Quantum Field Theory are briefly reviewed. (auth)

20058 (JINR-P2-5569) REGULARIZING PROPERTIES OF SUPERPROPAGATORS. Volkov, M. K. (Joint Inst. for Nuclear Research, Dubna (USSR). Lab. of Theoretical Physics). 1971. 21p. (In Russian). Dep. NTIS (U. S. Sales Only).

The regularizing properties of the superpropagators are elucidated. These superpropagators are used in the nonrenormalizable theories describing both the localizable interactions (where it is possible to satisfy the microcausality principle) and the nonlocalizable ones (where only the macrocausality principle can be satisfied). (auth)

20059 (JINR-P4-5547) MOTION OF PARTICLES IN THE FIXED CENTERS FIELD. Amirkhanov, I. V.; Lkhagva, O.; Titov, A. I. (Joint Inst. for Nuclear Research, Dubna (USSR). Lab. of Theoretical Physics). 1970. 19p. (In Russian). Dep. NTIS (U. S. Sales Only).

Motion of an elementary (complex) particle in the field of an arbitrary number of centers is considered. It is shown that the problem is reduced to the solution of a system of algebraic and integral equations, and for its realization the wave functions describing the motion of an elementary (complex) particle in one isolated center are to be known. (auth)

20060 SIXTH-ORDER CHARGE RENORMALIZATION CONSTANT. Brandt, Howard Edward. Seattle; Univ. of Washington (1970). 136p. University Microfilms Order No. 71-948.

Thesis.

As part of the program to establish a finite canonical quantum electrodynamics, the divergent part of the inverse charge renormalization constant, Z_3^{-1}, is calculated in the Feynman gauge to sixth order in the bare charge, disregarding photon self energy insertions. The result is: $(Z_3^{-1})_{\text{div.}} = \alpha_0/2\pi[2/3 + \alpha_0/2\pi - 1/4(\alpha_0/2\pi)^2]\ln M^2/m^2$ where α_0, M, and m are the bare fine structure constant, an infinite mass cutoff, and the mass of the electron respectively. This result is in complete agreement with the important calculation of J. Rosner, who worked in a generalized Landau gauge. The integrals are both fewer and simpler in Feynman gauge. (Diss. Abstr.)

20061 WHEELER-FEYNMAN QUANTUM THEORY. Davies, P. C. W. (Cambridge Univ., Eng.). Nature (London). Phys. Sci.; 229: 20-1(4 Jan 1971).

It is stated that the quantum theory of Wheeler-Feynman direct interparticle action electrodynamics based on a modification of the S-matrix perturbation expansion of conventional QED already reported has now been improved and extended to the full relativistic domain. The results are obtained for an exact expression for S and are thus true for all orders of the perturbation expansion. (UK)

20062 QUANTUM ELECTRODYNAMICS WITH NO PHOTON SELF-ENERGY INSERTIONS. Abdellatif, Refat Ahmed. Seattle; Univ. of Washington (1970). 103p. University Microfilms Order No. 70-19,608.

Thesis.

A theoretical study is made of two aspects of quantum electrodynamics with no photon self-energy insertions (QED). This model QED is known to have fundamental importance for the problem of finiteness of QED. Certain invariance properties of the model under the conformal group are used to derive an expression for $f(\alpha_0)$, the coefficient of the logarithmic divergence in the renormalization constant Z_3^{-1}. The expression obtained for $f(\alpha_0)$ is shown to reproduce the known perturbation expansion up to the second order in α_0. Some ambiguities are encountered in the next order. These ambiguities and prospects for the future are discussed. It is hoped that this approach to the $f(\alpha_0)$ problem will provide a convenient way of finding a closed form for $f(\alpha_0)$. Simple expressions for the one-particle and the two-particle Green's functions are given. It is shown that if one assumes that only the region of small momenta of the exchanged photons is important, then the model QED with no photon self-energy insertions gives the dominant contribution. The Schwinger functional equations are then solved in this approximation to provide the expressions for the Green's functions. These expressions should be useful in calculating asymptotic forms of various QED processes for large energy and small momentum transfer. (Diss. Abstr.)

20063 ANALYTIC PROPERTIES OF NONSTRICTLY LOCALIZABLE FIELDS. Constantinescu, F. (Univ., Munich). J. Math. Phys. (N. Y.); 12: 293-8(Feb 1971).

A class of test functions "minimal with respect to causality" is introduced. The corresponding fields are called local. Tempered and strictly localizable fields are local, but there is a large class of fields that are local but not strictly localizable. For local fields, the analytic properties of vacuum expectation values are studied. The local fields that are not strictly localizable are characterized by an arbitrary fast increase of Wightman functions near the light cone. With an adequate definition of local commutativity, other

XUM

properties of tempered and strictly localizable fields seem to remain valid. (auth)

20064 RELATIVISTIC LAGRANGIAN. Brehme, Robert W. (Wake Forest Univ., Winston-Salem, N. C.). Amer. J. Phys.; 39: 275-80(Mar 1971).

A few aspects of the formulation of the relativistic Lagrangian are discussed with the practical view of working problems in analytic relativistic dynamics. A brief discussion of radiation is included as an example of a nonconservative system in which the Lagrangian formulation is not possible. (auth)

20065 RELATIVISTIC ONE-DIMENSIONAL SQUARE POTENTIAL. Coulter, Byron L.; Adler, Carl G. (East Carolina Univ., Greenville, N. C.). Amer. J. Phys.; 39: 305-9(Mar 1971).

The one-dimensional Dirac equation is applied to the cases of a particle bound in a square well and of a beam of particles impinging upon a square potential. The solutions are compared to the Schrödinger solutions, and the effect of the negative-mass states is discussed. (auth)

20066 GENERALIZED FINITE-MATRIX HAMILTONIANS. Trubatch, S. L. (California State Coll., Long Beach). Amer. J. Phys.; 39: 327-32(Mar 1971).

A Fermion representation is developed for truncated Bose operators. The eigenvalue analysis of finite matrix Hamiltonians becomes transparent by using this representation. Renormalization is discussed independent of infinities for simple separable cases. (auth)

20067 NON-POLYNOMIAL LAGRANGIAN THEORIES. Salam, Abdus (International Centre for Theoretical Physics, Trieste, Italy). Acta Phys. Austr.; Suppl. 7, 1-31(1970).

From 9th Conference on Developments in High Energy Physics, Schladming, Austria. See CONF-700220.

Earlier as well as new results are reviewed for nonpolynomial Lagrangian theories. The methods used, higher orders, and supergraphs are considered. (J.F.P.)

20068 DIFFERENTIABLE MANIFOLDS. Hlawka, E. (Univ., Vienna). Acta Phys. Austr.; Suppl. 7, 265-307(1970).

From 9th Conference on Developments in High Energy Physics, Schladming, Austria. See CONF-700220.

The lecture on differentiable manifolds covers the basic concepts, tangent space, the tangent bundle, vector fields, cotangent fields or Pfaffian forms, orientation of a manifold, Riemann metric, and connexions. (J.F.P.)

20069 CONSTRUCTION OF PHYSICAL STATES IN QUANTUM FIELD THEORY. Streit, L. (Bell Telephone Labs., Inc., Murray Hill, N. J.). Acta Phys. Austr.; Suppl. 7, 355-91(1970).

From 9th Conference on Developments in High Energy Physics, Schladming, Austria. See CONF-700220.

In these lectures general methods are considered rather than a specific model. The problem of physical states in quantum field theory, the Friedrichs method for wave operators, the Lee model as an example of a perturbed ground state, creation and annihilation, approximate dressing transformations, renormalization, and infinite wave function renormalization are treated. (J.F.P.)

20070 ANOMALIES IN WARD IDENTITIES. Kummer, W. (Technische Hochschule, Vienna. Institut fuer Hochenergiephysik, Vienna). Acta Phys. Austr.; Suppl. 7, 567-87(1970).

From 9th Conference on Developments in High Energy Physics, Schladming, Austria. See CONF-700220.

In certain generalized Ward-identities perturbation theory can lead to deviations from the relations derived by canonical field theory. Such a modification caused by the fermion triangle graph in the axial–photon–vertex was discussed in several papers during the last year. An attempt is made to show, also by means of other simple field theoretical models, that the problem of such "anomalies" is by no means solved, since the interpretation of the mathematical equations in terms of experimentally measurable ("renormalized") quantities is still very arbitrary, e.g. sometimes only by abolishing the normal-ordering prescription "anomalies" become "normal" tadpole-contributions. (auth)

20071 TWO-BODY PROBLEM IN QUANTUM FIELD THEORY. Fronsdal, C. (International Centre for Theoretical Physics, Trieste, Italy); Huff, Robert W. Phys. Rev., D; 3: 933-44(15 Feb 1971).

An approach to the relativistic two-body problem that represents a considerable improvement of the Bethe–Salpeter equation is studied. The main advantages are the improved properties of the simple ladder approximation. (a) It has the correct static limit and is in this sense equivalent to the sum of all crossed ladders of the Bethe–Salpeter equation, (b) in the case of massless exchange it is possible to solve analytically and obtain the wave functions and the T matrix in closed form, (c) the system is closed, that is, the two-particle T matrix is unitary. (d) The wave functions admit a complete quantum-mechanical interpretation without compromise of relativistic covariance, the current is conserved, and gauge invariance is respected. (e) The evaluation of physical amplitudes is greatly simplified, as illustrated by positronium decay and the Lamb shift. Both are carried out with full relativistic covariance, and the Lamb-shift calculation in particular is greatly simplified and clarified in comparison with other methods. Most of the results are applicable only to the case of spin-0 or spin-$\frac{1}{2}$ particles interacting through the exchange of a single scalar or vector boson. In particular, the calculations of positronium decay and the Lamb shift are carried out with spinless particles. It is shown, however, that the introduction of photon spin presents no problem and that the Lamb shift can be calculated in a fully gauge-invariant manner. (auth)

20072 LOCAL-LAGRANGIAN QUANTUM FIELD THEORY OF ELECTRIC AND MAGNETIC CHARGES. Zwanziger, Daniel (Weizmann Inst. of Science, Rehovot, Israel). Phys. Rev., D; 3: 880-91(15 Feb 1971).

A local Lagrangian density, depending on a pair of four-potentials A and B, and charged fields ψ_n with electric and magnetic charges e_n and g_n is presented. The resulting local Lagrangian field equations are equivalent to Maxwell's and Dirac's equations. The Lagrangian depends on a fixed four-vector, so manifest isotropy is lost and is regained only for quantized values of $(e_n g_m - g_n e_m)$. This condition results from the requirement that the representation of the Poincaré Lie algebra which results from Poincaré invariance, integrate to a representation of the finite Poincaré group. The finite Lorentz transformation laws of A, B, and ψ_n are presented here for the first time. The familiar apparatus of Lagrangian field theory is applied to yield directly the canonical commutation relations, the energy-momentum tensor, and Feynman's rules. (auth)

20073 QUESTIONS OF LORENTZ INVARIANCE IN FIELD THEORIES WITH INDEFINITE METRIC. Lee, T. D.; Wick, G. C. (Columbia Univ., N. Y.). Phys. Rev., D; 3: 1046-7(15 Feb 1971).

It is pointed out that, contrary to the view expressed by Nakanishi, there is no real reason why one should rigidly follow the so-called "real space-momentum" prescription when "pinching" occurs in a field theory with indefinite metric. Since by adopting the modification introduced by Cutkosky et al., a relativistic and unitary S matrix can be obtained, that should be the obvious choice. (auth)

20074 LORENTZ NONINVARIANCE OF THE COMPLEX-GHOST RELATIVISTIC FIELD THEORY. Nakanishi, Noboru (Brookhaven National Lab., Upton, N. Y.). Phys. Rev., D; 3: 811-14(15 Feb 1971).

It is proved that the complex-ghost relativistic field theory with real space momenta, which was proposed by Lee and Wick and by Lee, is not invariant under real Lorentz transformations in the second-order self-energy part involving a complex-ghost-pair intermediate state. (auth)

20075 MASSLESS LIMIT OF THE MASSIVE YANG–MILLS FIELD. Wong, S. K. (State Univ. of New York, Stony Brook). Contract AT(30-1)-3668B. Phys. Rev., D; 3: 945-52(15 Feb 1971).

The Feynman rules for the massive Yang-Mills field for tree and one-loop diagrams are recast into forms for which the limit as the mass goes to zero can be immediately obtained when the external particles are transversely polarized. Explicit calculations show, however, that the resulting rules cannot be taken to be the correct rules for the massless theory, lest unitarity and Lorentz invariance be violated. (auth)

20076 BEHAVIOR OF COMMUTATOR MATRIX ELEMENTS AT SMALL DISTANCES. II. EQUAL-TIME LIMITS OF CHARGE MOMENTS AND TIME DERIVATIVES. Voelkel, A. H. (Freie Univ., Berlin. Univ., Nijmegen, Netherlands). Phys. Rev., D; 3: 917-28(15 Feb 1971).

From general principles of quantum field theory (especially locality and Poincaré invariance, but without use of the spectrum condition), it is shown that the equal-time limits of current-density commutators exist if the limits for the commutators between one current density and one generalized charge exist. If the equal-time limits of the current-density commutators containing at least one zeroth component exist, then the limits of the space-space components exist also. If the equal-time limits between one current density and the nth time derivative of the generalized charges exist, then also the limits of all time derivatives up to order n of the density commutators exist. Ex-

XUM

plicit expressions for the first time derivative of current-density commutators in terms of the Gell-Mann Σ and meson commutators are derived. (auth)

20077 EQUAL-TIME EQUATION FOR TWO-PARTICLE SYSTEM IN QUANTUM FIELD THEORY. Logunov, A. A.; Savrin, V. I.; Tyurin, N. E.; Khrustalev, O. A. (Inst. of High-Energy Physics, Moscow). Teor. Mat. Fiz.; 6: 157-65(Feb 1971). (In Russian).

It is shown in which way the equal-time formulation of the relativistic two-particle problem in quantum field theory leads to the quasipotential equation and to relativistic generalization of quantum damping theory. (auth)

20078 DYNAMIC THEORY OF VACUUM. Gol'fand, Yu. A. (Lebedev Inst. of Physics, Moscow). Teor. Mat. Fiz.; 6: 180-93 (Feb 1971). (In Russian).

An S-matrix theory is developed in which the "free" Lagrangian L_0 is allowed to possess a complicated structure. The Lagrangian L_0 determines vacuum properties described by Green functions. Scattering is connected with the interaction Lagrangian L_{int}. $L_{int} = 0$ implies $S = 1$, i.e., the absence of the scattering. The functional method of determining Green functions and S-matrix is developed which makes it possible to obtain the S-matrix expansion in powers of function $\varphi(x)$. Coefficients of this expansion are scattering amplitudes. A generalized diagram technique for calculating the S-matrix is constructed. It is shown that under some assumptions about the Lagrangians L_0 and L_{int} S-matrix is unitary and causal. Some physical applications of the theory are discussed. (auth)

20079 NOTE ON A NEW QUANTIZATION; SPIN-HALF PARTICLES WITH AN INFINITE MAXIMUM OCCUPATION NUMBER. Kraev, M. M.; Kademova, K. V. (Inst. of Physics, Sofia). Phys. Lett.; 34B: 147-8(1 Feb 1971).

Free fields are quantized according to new commutation relations. The new quantization leads to spin-half particles having an infinite maximum occupation number. It is pointed out that the new quantization can lead, in particular, to a new treatment of the superconductivity. (auth)

20080 PARASTATISTICS. Stolt, Robert Howard. Boulder, Colo.; Univ. of Colorado (1970). 103p. University Microfilms Order No. 70-23,757.

Thesis.

The first- and second-quantized theories of paraparticles are discussed. The results of Hartle and Taylor in the first-quantized theory are extended to show that all first-quantized paraparticles can be divided into two classes, as particles of finite order and particles of infinite order. The finite-order particles can be classified as parabosons and parafermions of order $p = 1, 2, \ldots$, just as the second-quantized parafields can. The first- and second-quantized descriptions of fixed numbers of paraparticles are compared, and it is shown that, for parabosons and parafermions, the two descriptions are equivalent. The infinite-order particles of the first-quantized theory have no analogue in the present second-quantized theory. The proof utilizes the "ray" formulation—due to Hartle and Taylor—of the first-quantized theory, which removes the redundancy of the generalized ray. For systems of a variable number of particles, the first-quantized theory which follows from the use of the "ray" formalism is seen to be equivalent to the second-quantized theory, and appears to be consistent with reasonable physical requirements. On the other hand, it is shown that a variable-particle theory based on the "generalized ray" formulation of the first-quantized theory cannot be constructed. This is achieved by showing that an absolute selection rule derived by Messiah and Greenberg in the "generalized ray" framework prohibits the creation and destruction of paraparticles. Finally, the several descriptions of variable numbers of paraparticles are examined. Two first-quantized theories can be constructed, one utilizing a Fock space which is the direct sum of the fixed-particle "ray" Hilbert spaces of Hartle and Taylor, the other using a Fock space constructed from the "generalized ray" Hilbert spaces of Messiah and Greenberg. The "ray" theory is seen for the finite-order particles to be equivalent to the second-quantized theory, and it appears to be consistent with reasonable physical requirements. However, it is shown that the "generalized ray" theory cannot consistently describe variable particle systems. This is achieved by showing that an absolute selection rule derived by Messiah and Greenberg in the "generalized ray" framework prohibits the creation and destruction of paraparticles. (Diss. Abstr. Int., B)

20081 PRESENT STATUS OF QUANTUM ELECTRODYNAMICS. Brodsky, Stanley J.; Drell, Sidney D. (Stanford Univ., Calif.). Annu. Rev. Nucl. Sci.; 20: 147-94(1970).

This review of quantum electrodynamics covers the origins of the theory and locality, high-momentum and precision tests of quantum electrodynamics, and limits of the theory. (177 references) (J.F.P.)

20082 GAUGE TRANSFORMATIONS AND LOCAL CHARGES OF QUASIPARTICLES. Khodel, V. A.; Fayans, S. A. (Inst. of Atomic Energy, Moscow). Yadern. Fiz.; 12: 717-24(Oct 1970). (In Russian).

Gauge transformations are used to establish the relation between local charges of quasi-particles. An equation is obtained that generalizes the conventional Ward identity to the case of current nonconservation. On this basis the additional renormalization of the local charges of quasi-particles, due to the nonconservation, is analyzed. (auth)

20083 BOUND STATES OF A RELATIVISTIC TWO-PARTICLE SYSTEM. Atanassov, A. A.; Ivanov, K. I. (Inst. of Science and Mathematics, Plovdiv, Bulgaria). Compt. Rend. Acad. Bulg. Sci.; 23: 911-14(1970).

The Bethe–Salpeter equation is solved for the energies of the bound states of a system of two spinless particles which interact through the scalar field. The method used differs from perturbation theory in that expansion in terms of the coupling constant is not done, while it differs from the variational method in that it is not necessary to seek the solutions of the integral equation. The important point is that the integral equation examined has square-integrable Hermitian kernels, the eigenvalues of which are determined as a function of a parameter. (R.W.R.)

20084 UNNOTICED THEOREM OF RELATIVISTIC MECHANICS. Pietenpol, J. L.; Speisor, D. (Univ. Catholique, Louvain, Belgium). Nature (London) Phys. Sci.; 229: 199-200(15 Feb 1971).

An elementary theorem of relativistic mechanics is established and the difference between the various potentials in relativistic mechanics is illustrated. (UK)

20085 TACHYONS. Swetman, T. P. (Cambridge Univ., Eng.). Phys. Educ.; 6: 1-6(Jan 1971).

Since the epochal publication by Einstein of the first paper on special relativity in 1905 the concept of the velocity of the light barrier has been rendered unavoidable. However it was recently suggested that the existence of particles with velocities greater than light does not contradict special relativity. These particles were called tachyons and the properties that such particles would possess are discussed. Searches which have been made for these particles by various groups are examined and the present position is summarized. It is concluded that a lot of theoretical work has still to be done. The implications for the transfer of information at superluminary velocities if tachyons exist are suggested. (UK)

Gravitation and General Relativity

Refer also to abstracts 19465 and 19966.

20086 SOME PROPERTIES OF CYLINDRICALLY SYMMETRIC EINSTEIN–MAXWELL FIELDS. Safko, John L. (Univ. of South Carolina, Columbia); Witten, Louis. J. Math. Phys. (N. Y.); 12: 257-70(Feb 1971).

Some properties of static cylindrically symmetric universes consisting of gravitational and electromagnetic fields with a central axial mass, charge, or current density are discussed. Of three permissible distinct configurations, general solutions of the appropriate equations are given for two. The properties of the solutions of these two are then examined in greater detail. The equations of motion of test particles (both charged and uncharged) are described for some simple trajectories. The qualitative effect of the magnetic field on uncharged test particle behavior in some instances is noted as well as the qualitative distinction in the behavior of charged and uncharged test particles. The algebraically independent invariants of the Riemann tensor are calculated. A stability analysis is carried out for the two solutions when the system is subjected to radial perturbations. It turns out that both solutions are stable. The stability analysis is carried out by using the equations of the already unified field theory of Rainich, Misner, and Wheeler. (auth)

20087 SCATTERING OF TWO IMPULSIVE GRAVITATIONAL PLANE WAVES. Khan, K. A.; Penrose, R. (Birkbeck Coll., London). Nature (London); 229: 185-6(15 Jan 1971).

It is stated to be a significant theoretical requirement to determine the way in which gravitational waves can scatter one another, and an attempt is presented to try to remedy the paucity of knowledge concerning such scattering. An exact solution of Einstein's vacuum equations is given to represent collision between two impulsive (δ-function) gravitational plane waves, thus facilitating detailed examination of scattering for this case.

XUM

It is found that two gravitational impulsive plane waves approaching each other from different directions will scatter one another, and will cease to be plane after collision. Their pure δ-function becomes modified by the addition of a discontinuity in the curvature, and eventually the focusing effect of each wave on the other results in a singularity in space−time. The discussion might, however, be regarded as rather unrealistic in that pure δ-function waves are unlikely to be found in nature. It would be interesting to examine the case of a collision between two successions of impulsive waves, since this would be a little closer to reality then the simple case considered. (UK)

20088 NONEXISTENCE OF SPHERICALLY SYMMETRIC SOLUTION REPRESENTING VACUUM ELECTROSTATIC FIELD. **Tiwari, R.; Pant, D. N. (Banaras Hindu Univ., India). Phys. Lett.; 33A: 505-6(28 Dec 1970).**

A spherically symmetric solution representing the external field of a localized charge does not exist in Einstein's field theory. (auth)

20089 CONSERVED PARTICLE STRUCTURES IN GENERAL RELATIVITY. **Williams, J. G. (Univ. of Alberta, Edmonton). J. Math. Phys. (N. Y.); 12: 308-13(Feb 1971).**

When general relativity is examined from the point of view of algebraic topology, it is found that the theory exhibits conserved particlelike structures. The number of such particles associated with a given metric is determined by the homotopy class of the metric. It is shown that if the theory is quantized, then the quantum mechanical states corresponding to 1-particle systems in the unquantized theory may have properties similar to fermions. In particular, it is proved that it is possible for wavefunctionals to exist which are double-valued under 2π rotation. (auth)

20090 GRAVITATION AND NEUTRINOS. **Bandyopadhyay, P.; Chaudhuri, P. R. (Indian Statistical Inst., Calcutta). Nuovo Cim.; 1B: 73-84(11 Feb 1971).**

It is well known that gravitational effects can be obtained from the spatial variation of the polarizability of space. It is shown that one can have such polarizability considering that there exists a sea of degenerate neutrinos and antineutrinos in the universe, the neutrino energy density being related with the matter density, and that photons can interact weakly with neutrinos. It is suggested that degenerate neutrinos and antineutrinos in the universe can be considered to be held together in an equilibrium position by the binding force generated by the photon-neutrino weak coupling. This may then give rise to the polarization effect, similar to the polarization effect observed in any dielectric medium. Assuming that the characteristic oscillation frequency of neutrinos is sufficiently large, the polarizability can be considered to be independent of the frequency of light. Thus the sea of degenerate neutrinos and antineutrinos can be taken to behave as a nondispersive medium, and as such, the effect of motion relative to such a medium should be absent in any measurement. Again, from the view-point that the neutrino energy density is related to the matter density, the distribution of degenerate neutrinos and antineutrinos is supposed to be dependent on the distribution of matter. This distribution pattern may then lead to a spatial variation of the polarizability such that the refractive index becomes higher in the vicinity of a massive body. These aspects give rise to gravitational phenomena, and gravitation, in this sense, is considered to be an electromagnetic effect. The role of the principle of equivalence and Mach's principle in this framework were also discussed. Finally, some remarks about the existence of gravitational waves and the possibility of the variation of the gravitational constant G with time were made. (auth)

20091 APPLICATION OF THE SEMIDIRECT PRODUCT OF GROUPS. **Geroch, Robert (Syracuse Univ., N. Y.); Newman, E. T. J. Math. Phys. (N. Y.); 12: 314(Feb 1971).**

A simple example of the application of the semidirect product of groups is presented. (auth)

20092 FUNCTIONAL DESCRIPTION OF QUANTUM ELECTRODYNAMICS IN COULOMB AND FEYNMAN GAUGES. Morawiecki, K. (Univ. of Wroclaw). Acta Phys. Pol.; A39: 45-58 (1971).

The off-mass shell generalization of scattering amplitudes in quantum electrodynamics (QED) is considered. It is shown that different ways of extrapolating scattering amplitudes produce different gauges. For the extrapolations corresponding to Feynman and Coulomb gauges respective unitarity and causality conditions are formulated. The formal solution of these conditions coincide with the conventional S-matrix in both gauges. The equivalence of general classes of gauges specified by the parameters α_μ, Λ and M to the Coulomb gauge is given. In the proof of equivalence the functional integration over nontransversal degrees of freedom is used. The formula connecting any Coulomb Green function with the transversal parts of an infinite set of Feynman Green functions is derived. (auth)

20093 SHORT-RANGED SCALAR GRAVITY IN EINSTEIN'S THEORY. **Das, A. (Simon Fraser Univ., Burnaby, B. C.). J. Math. Phys. (N. Y.); 12: 232-4(Feb 1971).**

The class of conformally flat universe satisfying Einstein's field equations is dealt with from a new point of view. It is shown that this class involves a scalar or pseudoscalar field that necessarily satisfies a meson-type field equation. This scalar gravity does not act at a distance, so to say, but supplies cohesive forces inside the source structure. Furthermore, the scalar field may involve spin-zero, massive quanta if quantized. Three exact solutions of this class are furnished here. (auth)

20094 COVARIANT GREEN FUNCTIONS OF THE NEUTRAL SCALAR MESON, PHOTON, AND ELECTRON IN WEAK GRAVITATIONAL FIELDS. **Carver, James Richard. Hoboken, N. J.; Stevens Inst. of Tech. (1970). 102p. University Microfilms Order No. 71-1160.**

Thesis.

By applying the proper-time method to a scalar field in interaction with a weak gravitational field, the coordinate-gauge arbitrariness of the linearized gravitational theory is treated as the counterpart of electromagnetic gauge. The calculation of the scalar Green function is developed in terms of the weak-field potentials and shown to possess manifest coordinate-gauge covariance; the explicit contribution of the coordinate-gauge function isolated by such a procedure is evaluated. The presentation of the vierbeine formulation of the linearized theory treats the arbitrariness in orienting local Lorentz frames with respect to the background metric as beine-gauge. Coordinate- and beine-gauge separations of the first-order vierbeine and auxiliary fields define the beine-gauge functions and lead to the modified versions of the Mandelstam-DeWitt path-dependent line integrals. The vierbeine formalism is used to obtain local equations of the Green functions of both the electromagnetic and Dirac fields in interaction with a weak gravitational field. The proper-time method is adapted to calculations of the local one-photon as well as the second- and first-order-differential one-electron Green functions in terms of the first-order vierbeine and auxiliary fields and the weak-field potentials. The gauge separations allow the isolation and evaluation of the contributions from both the coordinate- and beine-gauge functions and permit expressions of the first-order contributions to the Green functions in terms of the gauge-invariant weak-field potentials. Gauge-invariant potentials are constructed for the example of constant curvature. The exact expression obtained for the typical scalar Green function exhibits the expected singularities of the flat space time case. (Diss. Abstr. Int., B)

20095 STATE FUNCTIONAL AND PHENOMENON OF TIME IN QUANTIZED GRAVITATION. **Thomas, Lawrence Eldon. New Haven; Yale Univ. (1970). 128p. University Microfilms Order No. 70-26,828.**

Thesis.

Problems in the Hamiltonian formulation and canonical quantization of general relativity are considered. The Hamiltonian formulation of general relativity involves a set of constraints among the field variables which are to be satisfied in addition to modified Hamilton equations. In the DeWitt quantum theory of relativity, these constraints become functional differential equations for the wave functional in order that the theory have dynamical content. An integral representation method is described for obtaining eigenfunctions of simple quantum mechanical problems. The method is generalized in order to obtain an approximate wave functional solution to the constraint equations of general relativity. This method accommodates time independent perturbation theory as well as a particular iterative process whereby the wave functional is systematically approximated. In addition, the question is discussed whether it is possible in the classical theory of relativity to construct invariant generators having vanishing Poisson brackets with the constraints and involving the metric field and positive finite powers of the conjugate momentum field components. These generators could be used to effect contact transformations sending solutions of the field equations into new solutions. The quantum analogs of these quantities could serve to generate new wave functional solutions from given ones. Simple necessary conditions for the existence of these quantities are formulated. Using these conditions, it is found that no such generators exist. Their nonexistence corroborates a conjecture, first made by DeWitt, that the wave functional for quantum relativity is unique. Finally, an explicit approximate wave functional is displayed for quan-

tum relativity, as well as additional evidence for its uniqueness. Using this functional, the dynamics of a simple "quantum geometric" model is discussed. The model illustrates the phenomenological nature of space-time in the quantum theory of relativity. (Diss. Abstr.)

20096 NEW STATIONARY GRAVITATIONAL FIELDS FROM STATIC FIELDS. Misra, R. M.; Pandey, D. B. (Univ. of Gorakhpur, India). Phys. Lett.; 34A: 245-6(8 Mar 1971).

A method is discussed by which one can generate stationary axially symmetric fields from static axially symmetry fields. (auth)

20097 4th TEST OF THE GENERAL RELATIVITY THEORY. Mociutchi, C.; Neagu, E. An. Stiint. Univ. Al. I. Cuza Iasi, Sect. Ib. Fiz.; 15: 170-80(1969). (In Rumanian).

The 4th test of the relativity theory is enlarged upon with the help of the metric $ds^2 = c^2(1 - \mu/r)^2\, dt^2 - (1 - \mu/r)^{-2}\, dr^2 - r^2(d\theta^2 + \sin^2\theta d\phi)^2$ where $\mu = kM/c^2$, k the constant of universal attraction and c the vacuum velocity of light. A method developed by D. K. Ross and L. I. Schiff is used together with Schapiro's hypotheses. (Rom. Sci. Abstr.)

20098 NEW LINEAR GRAVITATION THEORY. III. Gottlieb, I.; Mociutchi, C.; Segal, A.; Tatomir, D.; Teodorescu, V. An. Stiint. Univ. Al. I. Cuza Iasi, Sect. Ib. Fiz.; 15: 1-6(1969). (In German).

Starting from the generalized impulse expression of a particle moving in a gravific field with a tensor potential A_{ik} : $Pi = p_k(\delta_i^k + XA_i^k)$, p_k being the usual four-dimensional impulse, $X = c^{-2}\sqrt{k}$ and δ_i^k the Kronecker tensor, an accurate expression is found for the spectrum lines displacement in a gravific field. Using the general procedures of quantum mechanics, the Klein–Gordon equations, the Dirac equation and the electromagnetic wave equation are found, as well as the neutrino equation for the existence of the gravific field. For the propagation velocity of electromagnetic waves in a static gravific field the expression $u = c(1 + x\varphi)$ is found and a change in their direction takes place according to a similar pattern with the media with $n = (1 + x\varphi)^{-1}$ refractive index. Only for the deviation of light beams in the gravific field of a sphere having the mass M, a value is found which is half the magnitude obtained by the general relativity theory. (Rom. Sci. Abstr.)

20099 CAN THE ENERGY OF A WEAK GRAVITATIONAL FIELD BECOME NEGATIVE? Robinson, David C.; Winicour, Jeffrey (Aerospace Research Labs., Wright-Patterson AFB, Ohio). Phys. Rev., D; 3: 840-5(15 Feb 1971).

The energy-momentum linkages for asymptotically flat solutions of Einstein's equations are considered as functionals of the metric field variables. When the metric components are varied, it is found that the extrema of the rest mass occur only when its value is zero. By considering the weak-field limit, flat space-time is shown to be a local minimum. The implications of this result for the sign of the weak-field energy are discussed, and the effects of nongravitational sources are investigated. (auth)

20100 TORSION-FREE WORLD LINES IN CURVED SPACE-TIME. Karlov, L. (Univ. of Sydney); Rindler, W. Phys. Rev., D; 3: 1035-6(15 Feb 1971).

A torsion-free world line is shown to correspond to a particle whose three-acceleration vector points in a fixed direction relative to its Fermi-transported local inertial rest frame. In flat space-time this is equivalent to the three-acceleration vector pointing in a constant direction. (auth)

20101 NEAR-FIELD APPROXIMATION FOR STRONG GRAVITATIONAL FIELDS. Morgan, Thomas A. (California Inst. of Tech., Pasadena). Phys. Rev., D; 3: 800-10(15 Feb 1971).

The essential features of the near-field approximation for strong gravitational fields are elucidated by developing the approximation (i) in first order for quasistatic systems; (ii) to arbitrary order for nonrotating systems with axial symmetry; and (iii) by sketching the approximation for rotating, axially symmetric systems. The restrictions, placed by Einstein's equations, on the time dependence of the "multipole moments" of a system which is isolated from other bodies of empty space are exhibited. These restrictions are statements of the global conservation of energy and linear momentum. In Newtonian theory they would state that, for an isolated system, $(d/dt)A_0 = 0$ and $(d^2/dt^2)A_1 = 0$ where A_0, A_1 are multipole moments. The principal assumption made is simply that a near-field zone exists for the systems which we consider (i.e., $L/\lambda < 1$). It is not, in any sense, assumed that the gravitational fields are weak. The contracted Bianchi identity $G^{\nu}_{0;\nu} \equiv 0$ plays a crucial role in the analysis since it implies, for a quasistationary system, that if the empty-space field equations $G_{\mu\nu} = 0$ are obeyed in order n, then $[(-g)^{½} G_0^i]_{,i} = 0$ is obeyed in order n + 1. This in turn implies the existence of a vanishing surface integral which restricts the time dependence of the quasistationary field in each order. It is shown that there are close similarities between strong gravitational fields and electromagnetic fields in the near-field approximation. For example, just as the first effect of a quasistatic electromagnetic field is to induce a magnetic field, so the first effect of a quasistatic gravitational field is to induce a magneticlike field, whose potentials are g_{0i}. (auth)

Scattering Theory

Refer also to abstracts 19925, 20078, 20092, and 20531.

20102 (NP-18705) REGGE POLE THEORY AND DUALITY. Brout, R. [nd]. 149p. Dep. NTIS (U. S. Sales Only).

These lectures on Regge pole theory and duality cover the kinematics, crossing, Regge poles, the experimental situation, finite-energy sum rules, the Veneziano model, and diffraction scattering. (J.F.P.)

20103 (NP-18707) LECTURES ON THE THREE-PARTICLE SCATTERING PROBLEM. Kowalski, K. L. Spring 1969. 193p. Dep. NTIS (U. S. Sales Only).

The lectures on the three-body scattering problem treat for nonrelativistic scattering the formulation of well-defined integral equations, standard methods of analysis and approximation to these equations, models, and on-shell analytic properties of N/D calculations for scattering below the three-particle threshold. For relativistic scattering straightforward extensions of off-shell techniques, one-mass methods, models for production and decay amplitudes and three-body final-state enhancements are discussed. (J.F.P.)

20104 (NYO-2262-TA-231) METHOD OF EXTENDING THE BLANKENBECLER–SUGAR–LOGUNOV–TAVKHELIDZE APPROXIMATION TO THE BETHE–SALPETER EQUATION. Chen, T. C. (Brown Univ., Providence, R. I. Dept. of Physics); Raman, K. (Wesleyan Univ., Middletown, Conn. Dept. of Physics). Sep 1970. 20p. Dep. NTIS.

A systematic method of obtaining accurate solutions to the Bethe–Salpeter (BS) equation, with the Blankenbecler–Sugar–Logunov–Tavkhelidze (BSLT) equation as the lowest-order approximation, is proposed. For the equal-mass scattering problem, where the difference between the BS and the BSLT amplitudes is the most marked, the first-order correction gives good agreement with the BS amplitude. The method is also applied to the unequal-mass scattering problem when the mass ratio is the pion–nucleon mass ratio. Here the BSLT amplitude itself is a good approximation to the BS amplitude. (auth)

20105 CROSSING SYMMETRIC EXPANSIONS OF PHYSICAL SCATTERING AMPLITUDES: THE O(2,1) GROUP AND LAME FUNCTIONS. MacFadyen, N. W.; Winternitz, P. (Carnegie-Mellon Univ., Pittsburgh). J. Math. Phys. (N. Y.); 12: 281-93 (Feb 1971).

An explicitly symmetric 2-variable expansion, convergent in the physical regions of both the s and t channels, is obtained for 2-body relativistic scattering amplitudes. Use is made of a symmetric mapping of the variables s and t onto a 2-dimensional hyperboloid, leading to an expansion in terms of Lamé functions, which are the basis functions for an irreducible representation of the group O(2,1) in the parametrization. (auth)

20106 NONSPECULAR SCATTERING FROM A ROUGH SURFACE. Singhal, S. P. (Louisiana State Univ., Baton Rouge). Lett. Nuovo Cim.; 4: 1079-82(5 Dec 1970).

It is generally assumed that the scattering from a surface is specular such that its lifetime depends only on the bulk scattering. There is some nonspecular scattering from a rough surface, however, and this scattering may depend on some quantities which do not affect the bulk scattering. A rough surface is here treated as a small variation from a smooth surface so that the problem of solving the Schrödinger equation with the boundary condition that the wave function vanishes at the rough surface can be transformed to a problem with the smooth surface. The probability of nonspecular reflection is calculated for various angles of incidence and wave vectors. The effect of a magnetic field is also examined. (R.W.R.)

20107 INTRODUCTION TO THE USE OF NON-LINEAR TECHNIQUES IN S-MATRIX THEORY. Atkinson, D. (CERN, Geneva). Acta Phys. Austr.; Suppl. 7, 32-70(1970).

XUM

From 9th Conference on Developments in High Energy Physics, Schladming, Austria. See CONF-700220.

Lectures on problems in S-matrix theory that involve nonlinear function equations are given. The contraction mapping principle, the space of continuous function, principle-value integrals, the space of Hoelder continuous functions, applications to Shirkov equations, the Manderstam equations, and inelastic unitarity are treated. Pion-pion interactions are considered. (J.F.P.)

20108 EXISTENCE OF WAVE OPERATORS IN TIME-DEPENDENT POTENTIAL SCATTERING FOR LONG-RANGE POTENTIALS. **Manoukian, E. B.; Prugovecki, E.** (Univ. of Toronto). Can. J. Phys.; 49: 102-7(1 Jan 1971).

The existence of physical asymptotic states and wave operators is derived for potentials which for $r \to \infty$ decrease faster than $r^{-\alpha}$ for some $\alpha > 1/2$ and $\alpha > 3/4$, respectively. (auth) (Canada)

20109 MULTIPERIPHERAL NONFRACTORIZATION, SIGNATURE, AND TOLLER-ANGLE-VARIABLE CUTS. **Dash, Jan W.** (Univ. of Washington, Seattle). Phys. Rev., D; 3: 1016-21 (15 Feb 1971).

It is shown that the assumption of a multi-Froissart-Gribov definition of signature for multiparticle amplitudes coupled with the existence of discontinuities of internal Regge-residue coupling functions in Toller-angle variables in general gives rise to a nonfactorizable expression for the asymptotic behavior of the full amplitude, even when the signatured amplitudes factorize. Factorizability occurs only in certain exceptional cases, including strict exchange degeneracy. The formalism can be cast into a two-vector form, however, which does factorize in a matrix sense. Chew-Goldberger-Low-type equations thus become 2 × 2 matrix equations in general. Multi-Froissart-Gribov formalism problems involving analyticity and unitarity of multiparticle amplitudes are ignored. (auth)

20110 DIVERGENT REGGE HELICITY SUMS, DISTRIBUTIONS, AND TOLLER ANGLES. **Dash, Jan W.** (Univ. of Washington, Seattle). Phys. Rev., D; 3: 1012-15(15 Feb 1971).

Divergent infinite-helicity sums appearing in complex J continuations of multiparticle unitarity equations including the Faddeev equations, and in the multi-Froissart-Gribov formalism are made convergent by regarding the amplitude as a distribution in the Toller azimuthal angles conjugate to the helicities. Some aspects of dynamical calculations using this formalism are discussed. (auth)

20111 DOES MULTIPLE REGGEON EXCHANGE PRODUCE AN EIKONAL-TYPE FORMULA? Muzinich, I. J. (Brookhaven National Lab., Upton, N. Y.); Tiktopoulos, George; Treiman, S. B. Phys. Rev., D; 3: 1041-3(15 Feb 1971).

An attractive possibility, much discussed recently, suggests that multiple Reggeon exchange produces a scattering amplitude of the eikonal form. This matter is investigated on a simple example. The anticipated eikonal structure does not emerge. (auth)

20112 RELATIVISTIC EIKONAL APPROXIMATION. **Tiktopoulos, George; Treiman, S. B.** (Princeton Univ., N. J.). Phys. Rev. D; 3: 1037-40(15 Feb 1971).

Earlier claims in support of the eikonal approximation to generalized ladder graph amplitudes are withdrawn—for the case of scalar-scalar interactions. Justification of the eikonal formula is provided, however, for the more interesting situation where the exchanged objects are vector particles. (auth)

20113 CROSSED-CHANNEL PARTIAL-WAVE EXPANSIONS AND THE BETHE-SALPETER EQUATION. **Saunders, L. M.** (Princeton Univ., N. J.); Saxton, O. H. N.; **Tan, Chung-i.** Contracts AF 49(638)-1545; NYO-2262TA-226. Phys. Rev., D; 3: 1005-11(15 Feb 1971).

The Bethe-Salpeter equation for the direct-channel absorptive part of the scattering amplitude is analyzed in the ladder approximation to investigate the relationship between SO(1,3) and SO(1,2) crossed-channel partial-wave analyses. The SO(1,2) expansion, used when the momentum transfer Q is spacelike, is studied in detail in the limit $Q_\mu \to 0$. The connection between the SO(1,3) and SO(1,2) partial-wave amplitudes at $Q_\mu = 0$ is obtained explicitly, as is the familiar result that a Toller pole is equivalent to an infinite sequence of integrally spaced Regge poles at $Q_\mu = 0$. (auth)

20114 GROUP-THEORETICAL CONSTRUCTION OF DUAL AMPLITUDES. **Clavelli, L.; Ramond, P.** (National Accelerator Lab., Batavia, Ill.). Phys. Rev., D; 3: 988-90(15 Feb 1971).

General group-theoretical requirements for the construction of factorizable, dual N-point functions are presented. Dual amplitudes for the scattering of arbitrary numbers of spinning particles are built as an example of this approach. (auth)

20115 VALIDITY OF THE REGGE EIKONAL MODEL. **Cicuta, G. M.; Sugar, R. L.** (Univ. of California, Santa Barbara). Contract AT(30-1)-4204. Phys. Rev., D; 3: 970-80(15 Feb 1971).

A detailed study is made of the scattering of two high-energy particles which interact via the exchange of ladders. The legs of the ladders are attached to the world lines of the incident particles in all possible ways. Working to lowest order in the coupling constant for the Regge trajectory and residue functions, it is found that the leading Regge-pole term arising from single-ladder-exchange exponentiates, and the Regge eikonal model is obtained. (auth)

20116 CAUSALITY AND ANALYTICITY IN FORMAL SCATTERING THEORY. **Minerbo, Gerald** (Adelphi Univ., Garden City, N. Y.). Phys. Rev., D; 3: 928-32(15 Feb 1971).

The connection between causality and analyticity in scattering theory is formulated in terms of Hilbert-space concepts. The usual rules of nonrelativistic quantum mechanics are assumed to hold for the "in" and "out" states of the scattering system. It is shown that there is a (physically verifiable) causality condition which implies that each diagonal S-matrix element $S_{\alpha\alpha}(E)$ must be the limit of an analytic function of the energy E, regular in ImE > 0. The implications for partial-wave amplitudes and for the forward scattering amplitude in elastic two-body collisions are discussed. (auth)

20117 LINEAR DEPENDENCES AND THE MULTILOOP VENEZIANO AMPLITUDE. **Kaku, Michio** (Univ. of California, Berkeley). Phys. Rev., D; 3: 908-16(15 Feb 1971).

By using the identities of Brower and Weis, several apparent inconsistencies associated with twisting the Sciuto three-Reggeon vertex are clarified. By using these results, all linear dependences are eliminated from planar, nonplanar, and overlapping n-loop amplitudes and shown to have only a minor effect. The Thorn projection operator is reduced to a hypergeometric function in the number operator and finally to a rational function. The equivalence of these techniques with the projected propagator of Gross and Schwarz and Ida is demonstrated. (auth)

20118 SYMMETRY, UNITARITY, AND GEOMETRY IN ELECTROMAGNETIC SCATTERING. **Waterman, P. C.** (MITRE Corp., Bedford, Mass.). Phys. Rev., D; 3: 825-39(15 Feb 1971).

Upon defining vector spherical partial waves $\{\psi_n\}$ as a basis, a matrix equation is derived describing scattering for general incidence on objects of arbitrary shape. With no losses present, the scattering matrix is then obtained in the symmetric, unitary form $S = -\hat{Q}'^{*}\hat{Q}^{*}$, where (perfect conductor) $\hat{Q}$ is the Schmidt orthogonalization of $Q_{nn'} = (k/\pi) \int d\sigma \cdot [(\nabla \times \mathrm{Re}\psi_n) \times \psi_{n'}]$, integration extending over the object surface. For quadric (separable) surfaces, Q itself becomes symmetric, effecting considerable simplification. A secular equation is given for constructing eigenfunctions of general objects. Finally, numerical results are presented and compared with experimental measurements. (auth)

20119 NON-WIENER CONTINUAL INTEGRALS. **Berezin, F. A.** (Moscow State Univ.). Teor. Mat. Fiz.; 6: 194-212(Feb 1971). (In Russian).

The Feynman continual integral and some other similar integrals over the phase-space paths are considered, by means of which the Cauchy problem for Schrödinger equation can be solved and the S-matrix and statistical sum can be calculated. Connections of these integrals with operator symbols are established. In particular, it is shown that the integrals of the considered type depend strongly on approximations of finite multiplicity. The relation of the Feynman integral with the Wick formula is discussed. (auth)

20120 METHOD OF COHERENT STATES AND FACTORIZATION OF DUAL AMPLITUDES. **Kvinikhidze, A. N.; Markovski, B. L.; Stoyanov, D. Ts.; Tavkhelidze, A. N.** (Joint Inst. of Nuclear Research, Dubna, USSR. Tbilisi State Univ., USSR). Teor. Mat. Fiz.; 6: 166-79(Feb 1971). (In Russian).

Factorization of the N-point dual amplitudes is achieved by using the method of coherent states. The diagram technique is developed for constructing N-point dual amplitudes with the aid of finite number of operators. (auth)

20121 NAKANISHI REPRESENTATION. **Zharinov, V. V.** (Moscow Engineering-Physics Inst.). Teor. Mat. Fiz.; 6: 151-6(Feb 1971). (In Russian).

The Nakanishi representation is proved and the estimate of the growth of amplitude within analyticity region is obtained for a large class of Feynman diagrams. (auth)

20122 IMPACT PARAMETER REPRESENTATION FOR THE OFF-ENERGY-SHELL SCATTERING AMPLITUDE. **Abul-Magd,**

A. Y.; Simbel, M. H. (International Atomic Energy Agency, Trieste, Italy. International Centre for Theoretical Physics, Trieste, Italy). Z. Phys.; 241: 124-9(1971).

The unitarized Born approximation for the scattering amplitude, suggested previously, is considered in the short wavelength limit. It is found that its on-energy-shell component is equivalent to the well-known impact parameter representation developed by Glauber. An approximate expression is then derived for the off-energy-shell scattering amplitude on the basis of the unitarized Born approximation which is expected to be as accurate as the Glauber approximation. (auth)

20123 SOME RENORMALIZATION PROBLEMS OF S-MATRIX IN KADYSHEVSKII'S p-REPRESENTATION. Borelevski, Z. (Joint Inst. for Nuclear Research, Dubna, USSR). Acta Phys. Pol.; B1: 155-63(Apr-Jun 1970). (In Russian).

A method of renormalization of certain elements of the S-matrix in the Kadyshevskii p-representation for the Lagrangian $L(x) = e : J^4(x):$ is proposed. It is found that in this representation only the lines of modified Feynman diagrams, corresponding to quasiparticles, are renormalized. (tr-auth)

20124 PATTERNS OF EXCHANGE DEGENERACIES. Mandula, Jeffrey (Inst. for Advanced Study, Princeton, N. J.); Weyers, Jacques; Zweig, George. Contract AT(11-1)-68. Annu. Rev. Nucl. Sci.; 20: 289-322(1970).

The discussion of exchange degeneracies treats the classificatory aspect. Particles and trajectories in different multiplets are classified, f/d and other coupling ratios are fixed, and representative mixing angles are obtained. The structure of the deviations is discussed. It is assumed that the exchange forces are primarily due to single-particle exchange. Duality and its applications are covered. Also exchange degeneracy equations including meson and baryon trajectories and their couplings are discussed. (J.F.P.)

Particle Accelerators

Refer also to abstracts 18607, 18737, 18757, 18839, 19087, 19773, 19774, and 20450.

20125 (BNL-15430) DESIGN STUDY OF A COLD MAGNET SYNCHROTRON (CMS). van Steenbergen, A. (comp. and ed.) (Brookhaven National Lab., Upton, N. Y.). Oct 1970. 192p. Dep. NTIS.

Results of a conceptual design study for a proton synchrotron using either superconducting or cryogenically cooled pure aluminum magnets for the energy range 100 to 150 GeV are presented and discussed. (W.H.K.)

20126 (CERN-Trans-70-9) VACUUM SYSTEM FOR THE 70-GeV PROTON SYNCHROTRON. Artemov, A. D.; Bogdanov, P. V.; Bulgakov, M. K.; Popkovich, A. V.; Pronin, O. D.; Rogozinskii, V. G.; Ryabov, V. V.; Ushkov, V. L. (Gosudarstvennyi Komitet po Ispol'zovaniyu Atomnoi Energii SSSR, Serpukhov. Institut Fiziki Vysokikh Energii). Translated by M. Besroukoff (CERN, Geneva, Switzerland), from report IFVE-SKU-69-100. 30p. (In French). Dep. NTIS (U. S. Sales Only).

Data are given for the construction of the vacuum chamber as well as the assembling and adjustment of the vacuum system for the 70-GeV proton synchrotron. A vacuum of $2(10)^{-6}$ torr was obtained using titanium electric discharge pumps of the type NEM-300. (tr-auth)

20127 (CERN-Trans-70-12) SOME RESULTS ON THE COMPLEX ADJUSTMENT AND START-UP OF THE IHEP PROTON SYNCHROTRON. Ado, Yu. M.; Zhuravlev, A. A.; Logunov, A. A.; (and others) (Gosudarstvennyi Komitet po Ispol'zovaniyu Atomnoi Energii SSSR, Serpukhov. Institut Fiziki Vysokikh Energii). Translated by A. T. Sanders and revised by N. Mouravieff (CERN, Geneva, Switzerland), from report IFVE-SKU-69-88. 19p. Dep. NTIS (U. S. Sales Only).

A brief history of the construction and commissioning of the Serpukhov 70-GeV proton synchrotron is given, and the main parameters of the accelerator are listed. A short description of the adjustments of the ring magnet system, injection system, vacuum system, rf system, and beam observation system is given. Also, the method and results of the initial start-up of the accelerator are outlined. (W.H.K.)

20128 (IFVE-SEF-70-22) HIGH-PRESSURE GAS TARGET COOLED BY LIQUID NITROGEN. Denisov, S. P.; Nekrasov, A. N.; Stoyanova, D. A.; Sytnik, V. V. (Gosudarstvennyi Komitet po Ispol'zovaniyu Atomnoi Energii SSSR, Serpukhov. Institut Fiziki Vysokikh Energii). 1970. 28p. (In Russian). Dep. NTIS (U. S. Sales Only).

A 3 m gas target for work with hydrogen, deuterium, and helium at pressures up to 75 atm and at the temperature of boiling liquid nitrogen (T = 78°K) is described. The target is used for the experiments at the 70 GeV accelerator. The gas density: ~7.5 g/cm^2 for H_2, ~15 g/cm^2 for D_2 and ~13 g/cm^2 for He can be achieved. The accuracy of the density determination is ~0.5% for H_2 and He, and ~0.7% for D_2. The full thickness of the windows is 2 g/cm^2. (auth)

20129 (INR-P-1218) 10-MeV PROTON LINEAR ACCELERATOR AT SWIERK. Dzyura, E.; Grabovski, V.; Yanushevski, Yu.; (and others) (Institute of Nuclear Research, Warsaw (Poland)). 1970. 13p. (In Russian). Dep. NTIS (U. S. Sales Only).

The main technical data of the 9.7 MeV proton linear accelerator built in the I.N.R. at Swierk are given. The modifications introduced to the Martini-Warner program for numerical calculation of electromagnetic field and resonant frequencies of resonators are mentioned. The basic troubles of the start-up period of the accelerator are described. (auth)

20130 (JINR-P9-5453) EXTERNAL INJECTION AND ACCELERATION OF THE BEAM TO THE FINAL RADIUS IN THE ELECTRON MODEL OF THE RING CYCLOTRON WITH STRONG FOCUSING. Glazov, A. A.; Kol'ga, V. V.; Novikov, D. L.; Onischenko, L. M. (Joint Inst. for Nuclear Research, Dubna (USSR). Lab. of Nuclear Problems). 1970. 19p. (In Russian). Dep. NTIS (U. S. Sales Only).

The results of experimental investigations of the external injection of the beam into the electron model of the ring cyclotron and its acceleration to the final radius are presented. Improvements resulting from the investigation of the beam in the electron model have allowed the electron beam with an average current of about 600 μ A to be accelerated to the final radius. (auth)

20131 (JINR-P9-5535) ON THE PROBLEM OF ION ACCELERATION BY THE ELECTRON RING IN THE DECREASING MAGNETIC FIELD. Ivanov, I. N.; Perel'shtein, E. A.; Sarantsev, V. P. (Joint Inst. for Nuclear Research, Dubna (USSR)). 1970. 11p. (In Russian). Dep. NTIS (U. S. Sales Only).

The problem of keeping the ions in the potential well of the electron ring when accelerating it in the decreasing magnetic field is considered. (auth)

20132 (LA-4593) DYNAMIC MEASUREMENT OF STOPBAND IN LAMPF 805 MHz ACCELERATOR STRUCTURES AT HIGH POWER USING HYBRID COMPUTER TECHNIQUES. Jameson, R. A.; Wallace, J. D. (Los Alamos Scientific Lab., N. Mex.). Jan 1971. Contract W-7405-eng-36. 5p. Dep. NTIS.

A method, using a hybrid computer, of performing high-speed stopband calculations on the 805 MHz side coupled linac is discussed. Results of both transient and steady-state cases are included. (Stopband is defined as frequency spacing between the normal excitation mode of the structure and the next higher mode, minus the frequency spacing between the normal mode and the next lower mode. The next higher and lower modes are taken as the nearest strongly excited modes as determined by the point drive and symmetry.) (auth)

20133 (NP-18671) [EXPERIMENTS WITH ACCELERATOR BEAMS]. Annual Report, 1969. Bergstroem, I. (ed.) (Stockholm Univ. (Sweden). Research Inst. for Physics). Dec 1969. 192p. Dep. NTIS (U. S. Sales Only).

The year 1969 is the first year when the four beam facilities have worked satisfactorily. Mainly because of limited beam quality of the 225 cm and 80 cm cyclotrons, the nuclear research program concentrated on in-beam gamma spectroscopy. The technical efforts were concentrated on pulsing the external beams in the time region between the natural pulse distance of about 125 ns and 10 s. The possibility of supplying nearby hospitals with shortlived radioactive isotopes which can not be produced in reactors was investigated. The joint OSIRIS (isotope separator on-line the Studsvik reactor) project has continued and promising phase. By joining the groups a project of high international quality has been realized. The heavy ion on-line isotope separator, PINGIS, was successfully tested for the first time in realistic experiments. The load on the isotope separator for studies of atomic lifetimes and for making ion implantation in semiconductors was large. The van de Graaff machine mainly was used for the localization of ions implanted in Ge and Si and electrical measurements on ion implanted semiconductors. The double focusing 50 cm beta spectrometer was used for continued studies of beta decay of tritium. A careful systematic investigation was also performed on the difference between positron and electron single and multiple scattering. (auth) (Sweden)

20134 (ORNL-4584, pp 187-97) HPRR AND ACCELERATOR OPERATIONS. Haywood, F. F.; Ward, D. R.; Littleton, C. P.; (and others). (Oak Ridge National Lab., Tenn.).

XUM

From Health Physics Division annual progress report for period ending July 31, 1970.

Results from a new target assembly promise greater neutron yields and longer life for tritium targets for accelerators, especially those used for the $T(d,n)^4He$ reaction. The DOSAR Low Energy Accelerator (DLEA) and the 3-MV Van de Graaff are used extensively in these studies and in most other dosimetry research. The HPRR was operated routinely and without fault. The annual disassembly and inspection revealed no detectable change in the core materials. In July 1970, the seventh intercomparison study in dosimetry was held, using the HPRR as the radiation source, and participants included dosimetrists from four foreign countries. (auth)

20135 (RHEL/R-201) THE PRESENT STATUS OF POLARIZED TARGETS AT THE RUTHERFORD LABORATORY. Nicholas, D. J.; Banks, P. H. T.; Cragg, D. A. (Rutherford High Energy Lab., Chilton (England)). Oct 1970. 24p. Dep. NTIS (U. S. Sales Only). UK 5s.

The polarized proton target in operation on Nimrod during 1970 is described. The target is based on dynamic polarization of protons in neodymium-doped lanthanum magnesium nitrate crystals. Details are given of several techniques novel to polarized targets in current use including a new NMR system devised for the present target. Proton polarization, as measured by this NMR system, is compared with that measured by nuclear scattering techniques. (auth) (UK)

20136 (SC-DR-70-872) REBA: A PULSED ELECTRON BEAM GENERATOR. Johnson, D. L. (Sandia Labs., Albuquerque, N. Mex.). Dec 1970. 33p. Dep. NTIS.

A new electron beam generator, called REBA (Relativistic Electron Beam Accelerator), was designed and constructed. REBA produces 43 kA beams of 3.2 MeV electrons in 70 nsec pulses at a rate of up to 40 shots per day. A unique feature of REBA is that a single Marx generator can pulse charge either of two Blumlein transmission lines and thus provides two independent sources of electrons for experimenters. The research and design considerations and the preliminary operating parameters of REBA are discussed. Preliminary electron beam measurements are also presented. (auth)

20137 ACCEPTANCE CALCULATIONS FOR THE AUSTRALIAN NATIONAL UNIVERSITY MODEL EN (HVEC) TANDEM ACCELERATOR. Merrill, N. H.; Whineray, S. (Australian National Univ., Canberra). Nucl. Instrum. Methods; 91: 613-19 (1971).

The phase space acceptance of an HVEC Model EN tandem accelerator has been calculated under the usual operating conditions. (auth)

20138 BEAM MAPPING METHOD. Akselsson, R.; Johansson, T. B. (Lund Inst. of Tech., Sweden). Nucl. Instrum. Methods; 91: 663-4(1971).

A method to examine the particle distribution in a beam by moving a small probe in it and measuring the characteristic X-rays derived from the probe is described. (auth)

20139 INFLUENCE OF A TOROIDAL ELECTRIC FRINGING FIELD ON THE TRAJECTORIES OF CHARGED PARTICLES IN A THIRD ORDER APPROXIMATION. Matsuda, H. (Osaka Univ.). Nucl. Instrum. Methods; 91: 637-47(1971).

The trajectory of charged particles in the fringing field of a toroidal condenser (including a cylindrical condenser) is calculated and all ion optical effects of the fringing field including the effect of the curved field boundary are described in the transfer matrix representation. All radial effects are calculated in a third order and all axial effects in a second order approximation. (auth)

20140 DOPPLER SHIFT STUDIES WITH SELECTED RECOIL DIRECTIONS. Pronko, J. G.; Lindgren, R. A.; Bromley, D. A. (Yale Univ., New Haven). Contract AT(30-1)-3223. Nucl. Instrum. Methods; 91: 659-61(1971).

By utilizing a specific set of charged particle-gamma ray coincidence configurations and orienting a relatively thin target such that the ions recoil in the plane of the target, inherent difficulties often encountered in Doppler shift attenuation measurements are eliminated. (auth)

20141 PROTON HOLE STATES EXCITED BY MONOENERGETIC GAMMA-QUANTA. Wene, C.-O. (Lund Inst. of Tech., Sweden). Nucl. Instrum. Methods; 91: 547-53(1971).

An experiment is described where elements that can be procured in thin foils, are irradiated with monoenergetic gamma quanta from the reaction $^7Li(p,\gamma)^8Be$. The energies of the photoprotons from the foil are measured with silicon surface barrier detectors. The conditions under which these protons give information about proton hole states are discussed. Results from runs on a foil of natural copper are given. (auth)

20142 IMPROVED ELECTRON ACCELERATOR. (to Thomson-CSF). British Patent 1,213,684. 25 Nov 1970. Priority date 21 Nov 1967, France.

An electron accelerator capable of continuous operation on the order of 100 MeV is described. The accelerator consists of one or more cavity resonators through which the beam is passed in parallel paths a number of times. Semicircular magnetic deflectors redirect the beam back through the resonance cavity. (C.E.S.)

20143 BALL-LOADED HIGH ENERGY PARTICLE BEAM DUMP. Walz, Dieter R. (to United States Atomic Energy Commission). U. S. Patent 3,534,811. 20 Oct 1970. Filed 18 Dec 1968.

A beam dump comprised of a tank loaded with small solid aluminum balls in point-to-point contact for stopping a high-energy particle beam and for dissipating the beam energy to cooling water flowing through the tank is described. (auth)

20144 PRODUCTION OF AN INITIALLY PURE K^0 BEAM OF KNOWN MOMENTUM. Aubert, J. J.; (CERN, Geneva); Niebergall, F.; Stier, H. E.; (and others). Nucl. Instrum. Methods; 91: 595-600(1971).

Apparatus is described which selects electronically K^+ interactions in liquid hydrogen which produce K^0 in the reaction $K^+p \rightarrow K^0p\pi^+$. The directions of all 3 particles of the final state are measured in wire chambers. These measurements determine the K^0 production vertex and decay vertex and the K^0 momentum to a precision of $\pm 3 \times 10^{-2}$, and thus the eigentime of K^0. Calibration measurements using $K^0 \rightarrow \pi^+\pi^-$ decays are described. The apparatus has been designed for a study of the time dependent $K^0 \rightarrow \pi e \nu$ and $K^0 \rightarrow \pi^+\pi^-\pi^0$ decay rates. (auth)

20145 THEORY OF RESONANT INTEGER EXTRACTION FROM SYNCHROTRONS. Month, M. (Brookhaven National Lab., Upton, N. Y.). Nucl. Instrum. Methods; 91: 627-31(1971).

Resonant slow extraction at an integer ν value has been successfully implemented at the CERN proton synchrotron. The general theory underlying this method of particle extraction is presented. It is shown how the resonance is excited with sextupole magnets in combination with a single quadrupole magnet. The effect of the single quadrupole magnet in stabilizing the equilibrium orbit at an integer ν value is discussed. Finally expressions for the extraction efficiency and the emittance of the extracted beam are obtained. (auth)

20146 ULTRAHIGH VACUUM CHAMBER OF THE ISR AT CERN. Samuel, R. L. (European Organization for Nuclear Research, Geneva). Ind. At.; 14: No. 7-8, 21-31(Jul-Aug 1970). (In French).

The UHV chamber of the ISR at CERN is a tubular structure of some 2 km in length (average interior diameter 160 mm) and designed to operate at a pressure lower than 10^{-9} torr. An austenitic stainless steel, specially treated, has been chosen. The tubes of quasi-elliptical section are formed by hydraulic pressure. Strict specifications cover the manufacture of bakeable flanges, metal bellows, valves, as well as the fabrication of chamber units. A thorough inspection is required, in particular, for leak detection. A thorough baking system allows the chamber to be heated up to 300°C, and newly developed operating techniques have shown that it is possible to achieve pressures lower than 10^{-10} torr with a reduced pumping time. The first trials with proton beams are scheduled for January 1971. (auth) (France)

20147 METHOD OF CALCULATING WAVEGUIDES WITH SIMPLE PERIODICAL STRUCTURES. Voisin, Gilles (Lyon Univ., Villeurbanne, France). Compt. Rend., Ser. B; 271: 1133-6(9 Dec 1970). (In French).

A formalism is developed explaining the properties of a periodic structure formed by the juxtaposition along the Oz axis of cylindrical elements parallel to this axis and alternately of type I and II. This formalism is then applied to the interdigital structure and avoids the localized constants model. (France)

20148 USE OF A PULSED VAN DE GRAAFF ACCELERATOR AND TIME-OF-FLIGHT TECHNIQUES TO REDUCE BACKGROUNDS IN (α,γ) SPECTROSCOPY EXPERIMENTS. Jaszczak, Ronald J. (Oak Ridge National Lab., Tenn.); Macklin, R. L.; Dunnam, F. E.; Van Rinsvelt, H. A.; Bloomer, R. H. Rev. Sci. Instrum.; 42: 44-8(Jan 1971).

A pulsed beam of alpha particles from a 5.5 MeV Van de Graaff accelerator has been used to study radiative capture reactions. Time-of-flight techniques are used to discriminate against neutrons produced when the beam interacts with collimator-target contaminants, as well as against beam independent background due to cosmic rays. With a beam pulse of less than 4 nsec (FWHM) duration and a repetition rate of 2 MHz, a portion of the $^{34}S(\alpha,\gamma)^{38}Ar$ excitation function was examined near $E_\alpha = 3.6$ MeV and the background found to be an approximate factor of 15 below that of the effective dc excitation function. In addition it is demonstrated that an angular distribution taken on resonance by this method requires substantially less background subtraction. The method has also been successfully applied to radiative capture studies in which the incident beam energy is above the neutron threshold for the target nuclei. (auth)

20149 FAST NEUTRON CAPTURE CROSS SECTION FACILITY. Macklin, R. L. (Oak Ridge National Lab., Tenn.); Allen, B. J. Nucl. Instrum. Methods; 91: 565-71(1971).

The Total Energy Weighting technique has been applied to measure fast neutron capture in small separated stable isotope samples at the Oak Ridge Electron Linear Accelerator (ORELA). Nonhydrogenous liquid scintillators provide low backgrounds below about 2.5 MeV neutron energy with time resolution better than 2 ns and gamma cascade efficiency typically 15% per neutron captured. The 40 m flight path permits neutron energy resolution ranging from $E_n/600$ at several keV (moderator thickness limited) to about $E_n/400$ at 2 MeV. On line data processing via multiple access computer allows (disc) storage to be reduced from over 4×10^6 channels to ≈190,000. The usual corrections for sample thickness, purity, deadtime, and a transformation to capture cross section vs neutron energy aré accomplished offline in a larger digital computer. (auth)

20150 ION ANALYSIS OF rf-EXCITED DEUTERIUM ION SOURCES. Stark, D. S.; Manley, A. W. J. (Services Electronics Research Lab., Baldock, Eng.). Nucl. Instrum. Methods; 91: 301-5(1971).

Measurements were made of the D_1^+, D_2^+, and D_3^+ ion output from glass- and alumina-walled rf ion sources designed for use in high-output sealed-off D/T neutron generators. Although the ion source in a sealed-off neutron generator necessarily contains a large, cooled metal surface to absorb high-power secondary electrons from the ion accelerator region, the air-cooled glass-walled ion source gave 60% D_1^+ for 200 W coupled into the plasma while the liquid-cooled alumina-walled version yielded 60% D_1^+ at 270 W and 90% D_1^+ at 560 W. The effects of several factors upon the composition of the extracted ions are reported. (auth)

20151 ABERRATIONS OF ASYMMETRIZED QUADRUPOLE LENSES. Szabo, Gy. (Inst. of Nuclear Research, Debrecen, Hungary); Ovsyannikova, L. P. Nucl. Instrum. Methods; 91: 407-11(1971).

The trajectory equation of combined asymmetrized quadrupole lenses is given in third-order approximation. To illustrate the general features, aberration curves are computed for the Gaussian image plane in the case of an electrostatic singlet. (auth)

20152 THE CALCULATED PROPERTIES OF A THREE-ELECTRODE "SINGLE" LENS. Kostka, P. (Central Research Inst. for Physics, Budapest). Nucl. Instrum. Methods; 91: 413-15(1971).

The focusing parameters of an electrostatic three-electrode single lens of given geometry were determined. Diagrams and data of the focusing action and aberration of the lens are given. The lens operates in accordance with the calculations. (auth)

20153 SCATTERING OF REAL PIONS ON EACH OTHER. Csonka, P. L. (Univ. of Oregon, Eugene). Nucl. Instrum. Methods; 91: 469-76(1971).

The feasibility of scattering real pions on each other is discussed. Estimates (based on machine parameters now realized or planned) are given for scattering in minirings when the pion energies are low; for self-clashing and head-on colliding of pion beams when their laboratory energy is high. A pi-pi scattering experiment with a miniring, which may be performed at LAMPF, is described. (auth)

20154 PROGRESS REPORT ON THE NAL ACCELERATOR. Cole, F. T. (National Accelerator Lab., Batavia, Ill.). Particle Accel.; 2: 1-11(Jan 1971).

Progress is reviewed on the proton synchrotron under construction at the National Accelerator Laboratory. The components of the accelerator are given brief descriptions and their present status is presented. (auth) (UK)

20155 EQUILIBRIUM FRACTION MEASUREMENTS OF HEAVY IONS IN FLUOROCARBON STRIPPERS. Ryding, G.; Wittkower, A.; Rose, P. H. (High Voltage Engineering Corp., Burlington, Mass.). Particle Accel.; 2: 13-16(Jan 1971).

Equilibrium fractions of bromine ions at 12 MeV and iodine ions at 3 and 12 MeV were measured in fluorocarbons. The mean charge was found to be appreciably higher in these vapors than in gases such as oxygen—but not as high as in a carbon foil. The use of fluorocarbons as the terminal stripper material for a large tandem accelerator will allow particles to be accelerated at a higher mean charge thereby increasing the useful energy range of these machines. (auth) (UK)

20156 INTERDIGITAL H-TYPE (IH) STRUCTURE, AN ACCELERATING STRUCTURE FOR LOW ENERGY BEAMS. Bres, M.; Chabert, A.; Foret, F.; Tran, D. T.; Voisin, G. (Univ., Lyon). Particle Accel.; 2: 17-29(Jan 1971).

After a brief description of the structure, its main characteristics are deduced from the results of a series of experiments and discussed from a theoretical point of view. Its practical use in an accelerator is considered and illustrated by the outlines of the Lyon heavy-ion linear accelerator project. (auth) (UK)

20157 LONGITUDINAL EFFECTS OF COLLIDING BEAM SPACE CHARGE FORCES IN ELECTRON-POSITRON STORAGE RINGS WITH CROSSING ANGLES. Rees, John R. (Stanford Univ., Calif.). Particle Accel.; 2: 31-7(Jan 1971).

In electron-positron storage rings in which the orbits of the colliding beams cross at a substantial angle, a phase-dependent longitudinal force is exerted on the particles of each beam by the bunches of the other. The effects of this force on both incoherent and coherent longitudinal particle motion are investigated. These effects impose a limit on the number of particles which can be stored in a bunch in such storage rings and the limit is independent of the crossing angle (provided the crossing angle is sufficiently large) and of the rf accelerating system parameters. The limit is imposed by the requirement for stability of coherent particle motions. (auth) (UK)

20158 EXPERIMENTAL PROGRAMME AT THE CERN INTERSECTING STORAGE RINGS. Jentschke, W. (Deutsches Elektronen-Synchrotron, Hamburg). Nature (London) Phys. Sci.; 229: 133-41(1 Feb 1971).

This year the intersecting storage rings at CERN will make available to physicists a new energy range reaching a maximum which will be equivalent to 2,000 GeV. The first experiments that are planned are described. (auth) (UK)

20159 MATRIX METHOD FOR THREE-ELEMENT EXTRACTION SYSTEMS. Paul, Arthur C. (Univ. of California, Berkeley). Particle Accel.; 2: 69-73(Jan 1971).

The matrix-method calculation of the properties of a three-element regenerative extraction system for a synchrocyclotron is discussed. It is shown that the three-element-system stability calculation can be conveniently parameterized in matrix formalism separating the perturbation strengths from the field geometry. (auth) (UK)

20160 EFFECTS OF MAGNETIC LENS ABERRATION IN HIGH-CURRENT LINEAR ACCELERATORS. Woods, C. H.; Freis, R. P. (Univ. of California, Livermore). Particle Accel.; 2: 57-68(Jan 1971).

The geometrical aberration inherent in several different magnetic lens structures is calculated and compared. Two of these satisfy the given definition of a thin lens. Beam transport is considered through perfect and imperfect lenses, and it is shown that beams can be compensated by adjusting the radial density distribution to match the lens aberration and that uncompensated high-current beams may become hollow through self interaction. (auth) (UK)

20161 STUDY ON THE CHOICE OF PARAMETERS FOR A HIGH ENERGY ELECTRON RING ACCELERATOR. Bovet, C.; Pellegrini, C. (Univ. of California, Berkeley). Particle Accel.; 2: 45-56(Jan 1971).

The production of high energy (multi-GeV) proton beams by an electron ring accelerator is considered. Both the final energy and intensity of the proton beam depend on the choice of parameters for the electron ring. Possible sets of parameters, consistent with all the known requirements of ring stability, and which optimize the energy and (or) the intensity of the proton beam, are presented. (auth) (UK)

20162 ENERGY AND ANGULAR RESOLUTION IN PION-PION SCATTERING AND OTHER COLLIDING BEAM EXPERIMENTS. Csonka, Paul L. (Univ. of Oregon, Eugene). Particle Accel.; 2: 39-44(Jan 1971).

In certain types of colliding beam experiments, the interaction region may contain particles within a wide momentum range. The measurement of the energy and angle dependence of the cross section under these circumstances is described. Pion-pion scattering in a miniring is given as an example. (auth) (UK)

XUM

20163 USE OF A WIRE SPARK CHAMBER TO MEASURE THE BEAM PROFILE OF A SYNCHROCYCLOTRON. Vishnaykov, V. V.; Demyanov, A. V.; Roganov, V. S.; Safroshkina, A. S.; Sinaev, A. N. (Joint Inst. for Nuclear Research, Dubna, USSR). Instrum. Exp. Tech. (USSR) (Engl. Transl.); No. 2, 339-41(Mar-Apr 1970).
Translated from Prib. Tekh. Eksp.; No. 2, 32-4(Mar-Apr 1970).

An apparatus is described for measuring the profile of particles in a synchrocyclotron beam. It consists of a wire spark chamber with ferrite rings and an AI-4096 multichannel analyzer. Both chamber electrodes are of wire, each containing 128 strands. Data are obtained simultaneously on both projections of the beam profile. The recording process can be monitored during a measurement. (auth)

20164 MEASUREMENT OF HARMONIC COMPONENTS OF FIELDS OF STANDARD MAGNETIC QUADRUPOLE LENSES. Kats, M. M.; Khasanov, F. M. Instrum. Exp. Tech. (USSR) (Engl. Transl.); No. 2, 335-8(Mar-Apr 1970).
Translated from Prib. Tekh. Eksp.; No. 2, 29-32(Mar-Apr 1970).

An exact formula for the sensitivity of a harmonic coil and the results of measurements of the harmonic components of fields of standard magnetic quadrupole lenses ML-15V, ML-16, ML-17 in the region far from the edges of the lenses are presented. Such lenses can be used for producing separated beams of high-energy particles. (auth)

20165 IMPLANTATION MACHINES. Freeman, J. H. (Atomic Energy Research Establishment, Harwell, Eng.). pp 1-18 of Ion Implantation. Stevenage, Eng.; Peter Peregrinus Ltd. (1970).
From Conference on Ion Implantation, Reading, England. See CONF-700945.

It is emphasized that the technique of ion implantation poses some rather special machine problems, and has led to a number of interesting and novel accelerator designs and a considerable amount of ion source development, but the scope of research in this field is still limited by the availability and suitability of machines. It is also essential to recognize that implantation will only become an industrial feasibility if reliable production machines are available. Ion doping can be carried out with a wide range of equipment, from simple glow discharge to very high-energy accelerator equipment. The brief review given is restricted to machines where performance lies within the energy range 10 to 600 keV and beam currents of 1 μA to 1 mA, and to systems that incorporate some means of beam analysis. The subject is reviewed under the following headings: General accelerator considerations; accelerator configurations; beam analysis; use of multiply charged ions; large area implantations; target chambers; current measurement; and ion-beam heating effects. Amongst machines discussed are conventional accelerators with beam analysis at high voltage, accelerators with target chamber at high voltage, the Aarhus 600-keV accelerator, the Accelerators Inc. 200-keV implanter, the 500-keV Cockcroft-Walton accelerator, the Ion Physics Corp. Van de Graaff accelerator, the "Scandinavian" low-output isotope separator, the Harwell medium-output isotope separator, the Grenoble accelerator with analysis at high voltage, the Hughes Aircraft Corp. accelerator with target at high voltage, and the Waklin isotope separator incorporating crossed-field-beam analyser. 16 references. (UK)

20166 ION SOURCES FOR ION IMPLANATION. Camplan, J. (CNRS, Orsay, France). pp 19-25 of Ion Implantation. Stevenage, Eng.; Peter Peregrinus Ltd. (1970).
From Conference on Ion Implantation, Reading, England. See CONF-700945.

It is pointed out that the choice of an ion source from amongst the large number of available sources is not an obvious matter, and the purpose of this paper is to help the ion implanter to choose the most convenient source. Since plasma ion sources appear to be more convenient than any other type, some of the fundamental aspects of plasma behaviour are also discussed. Amongst source considerations discussed are intensity, emittance, brightness, efficiency, energy spread, cleanliness, versatility, energy consumption, and lifetime. 17 references. (UK)

20167 IMPROVED HIGH-BEAM-CURRENT ION IMPLANTER. Bahrami, H.; Chernow, F.; Dennison, D.; Eldridge, G. (Univ. of Colorado, Boulder. Univ. Instruments Corp., Boulder, Colorado). pp 26-8 of Ion Implantation. Stevenage, Eng.; Peter Peregrinus Ltd. (1970).
From Conference on Ion Implantation, Reading, England. See CONF-700945.

The ion implanter described can provide beam energies of 50 to 300 keV, with usable beam currents up to 1 mA. It was designed for a mass resolution of 510 at mass 210, giving <1 part in 10^7 contamination from next nearest mass numbers, and separation is not dependent on the energy of momentum of the ions. The source material can be solid or gaseous and can be rapidly changed without breaking vacuum, and the system is small and can be pumped from atmospheric to operating pressure in <30 min. The overall system is described and details are given of the quadrupole mass filter employed, the ion source assembly, and the extraction and focusing lenses. The quadrupole provides strong focussing for the slow moving beam, which would otherwise suffer from space charge effects, and at 50 kV the acceleration tube extracts over 80% of the ions leaving the quadrupole. Full current saturation is achieved at 100 kV. A single source assembly was used for over 20 different elements, including B and P, and operated with a minimum of outgassing. The stainless-steel source rods, however, rapidly deteriorated in operation and could only be used several times. Improvements are desirable to the extraction and focussing lens system. 3 references. (UK)

20168 FINE-FOCUSSED ION MACHINE WITH APPLICATIONS TO IMPLANATION, MICROSCOPY, AND MACHINING. Hill, A. R. (Mullard Research Labs., Redhill, Eng.). pp 29-32 of Ion Implantation. Stevenage, Eng.; Peter Peregrinus Ltd. (1970).
From Conference on Ion Implantation, Reading, England. See CONF-700945.

It was thought that fine focused ion beams might be used in the fabrication of micro-circuits, such as for etching purposes or for implanting impurities into a semiconductor. In both cases, the required patterns would be generated by suitable deflection of the fine beam rather than by the use of masks flooded with a broad beam. Another field of application might be the use of the ion beam as an analysis tool, such as an ion probe. It was found possible to make a successful fine-focused ion-beam machine, of maximum ion energy 100 keV. Within the range 15 to 30 keV, focused ion sports of 1 μ were obtained with a current density of 0.25 A/cm^2, this appearing to be limited by the optical quality of the ion source and the spherical aberration of the lens. The machine was operated as a fine-focused ion implanter, a micro-etching device, and a scanning microscope. Results indicated that implantation of most of the components of a microcircuit with a fine-focused beam might be a practical possibility. A general description of the machine is given, together with details of factors limiting performance, ion source, secondary electron current detection, and spot size measurements. 3 references. (UK)

20169 CALUTRON-TYPE ION SOURCE FOR USE IN AN ION-IMPLANTATION MACHINE. Trotel, J. (Thomson CFS, Corbeville; France). pp 33-5 of Ion Implantation. Stevenage, Eng.; Peter Peregrinus Ltd. (1970).
From Conference on Ion Implantation, Reading, England. See CONF-700945.

An ion implantation system is described that employs a calutron-type ion source. This system was built specifically for use in ion implantation work. The source is the only part held at high voltage (40 to 150 kV), the whole of the acceleration being carried out in a single gap directly at the source exit. Details of the method of operation of the source are given. It has been extensively used for the production of B ions from B_2O_3, and P ions from red phosphorus. Maintenance of the source consists of changing the filament every 20 hours and clearing the acceleration gap region about every 100 hours. Amongst the results obtained with this system are: n-p diodes with no channel effect, 10 Ω/□P layers for transistor emitters, and diffused base and implanted emitter transistors with $\beta = 40$ at 5 mA. (UK)

20170 DISPLACEMENT OF THE CENTER OF THE ORBIT IN A CYCLOTRON DUE TO THE VARIATION IN THE VOLTAGE ALONG THE ACCELERATING GAP. Krasnov, N. N.; Ognev, A. A.; Ponomarev, A. A. (Physical-Power Engineering Inst., Obninsk, USSR). Instrum. Exp. Tech. (USSR) (Engl. Transl.); No. 2, 332-4(Mar-Apr 1970).
Translated from Prib. Tekh. Eksp.; No. 2, 27-9(Mar-Apr 1970).

It is shown that the variation in the accelerating voltage along the D's of a cyclotron leads to a displacement of the center of the orbit. An approximate formula for estimating this is obtained. Experimental data relating to the determination of this displacement in the Power Physics Institute's cyclotron are presented. (auth)

20171 MEASURING THE COULOMB FREQUENCY-SHIFT OF BETATRON OSCILLATIONS. Koshkarev, D. G.; Nikolaev, V. I. (Inst. of Theoretical and Experimental Physics, Moscow). Instrum. Exp. Tech. (USSR) (Engl. Transl.); No. 2, 327-31(Mar-Apr 1970).
Translated from Prib. Tekh. Eksp.; No. 2, 23-6(Mar-Apr 1970).

It is shown that the Coulomb frequency-shift of betatron oscillations in ring accelerators can be measured with a resonant beam intensification by a quadrupole field. Briefly described is also the apparatus which has been used in the experiment with the 7 GeV accelerator at the Institute of Theoretical and Experimental Physics. The results of measuring the Coulomb frequency-shift are presented. (auth)

20172 LINEAR ION ACCELERATOR WITH SPATIALLY HOMOGENEOUS STRONG FOCUSING. **Kapchinskii, I. M.; Teplyakov, V. A. (Inst. of Theoretical and Experimental Physics, Moscow. Inst. of High Energy Physics, Serpukhov, USSR). Instrum. Exp. Tech. (USSR) (Engl. Transl.); No. 2, 322-6(Mar-Apr 1970).**
Translated from Prib. Tekh. Eksp.; No. 2, 19-22(Mar-Apr 1970).

A linear ion accelerator is suggested, in which focusing and acceleration is accomplished by means of a h-f electric field generated by a long line of four conducting wires. The accelerator contains no drift tubes. The advantages of this accelerator are its relative simple design, the small transverse dimensions, and the possibility of an essential reduction of injection energy without influencing the high intensity of the accelerated beam. (auth)

20173 SENSITIVITY OF A SECONDARY-EMISSION-TYPE ACCELERATED-ELECTRON-BEAM POSITION MONITOR. **Angelov, B. P.; Prudnikov, I. A.; Toropov, A. S.; Khokhlov, V. K. Instrum. Exp. Tech. (USSR) (Engl. Transl.); No. 2, 342-4(Mar-Apr 1970).**
Translated from Prib. Tekh. Eksp.; No. 2, 34-6(Mar-Apr 1970).

The paper describes an accelerated-electron-beam position monitor whose action is based on secondary electron emission from the surfaces of thin metal foils pierced by a beam of high-energy electrons. The method and results of experimental determination of the monitor's sensitivity are set forth. The monitor can be used to determine beam positions accurate to ±0.2 mm; 1.8% of the beam particles interact with the foils. (auth)

20174 PLASMA BOUNDARY OF AN ION SOURCE. **Lapitskii, Yu. Ya. (Inst. of Theoretical and Experimental Physics, Moscow). Instrum. Exp. Tech. (USSR) (Engl. Transl.); No. 2, 345-7(Mar-Apr 1970).**
Translated from Prib. Tekh. Eksp.; No. 2, 37-9(Mar-Apr 1970).

The brightness of a pulsed beam of hydrogen ions is found to be 3 A/(mrad · cm)^2 for an ion current of 60 mA (pulse length 40 μsec, pulse repetition frequency 7 cps). If an equipotential region in which expansion of the plasma takes place is introduced between the ion source and the extracting electrode, the brightness of the beam diminishes. The results are obtained in an ion source with a cathode needle. (auth)

20175 GAS-FILLED MASS SEPARATOR FOR INVESTIGATIONS OF HEAVY-ION REACTION PRODUCTS. **Bacho, I.; Bogdanov, D. D.; Darotsi, Sh.; (and others) (Joint Inst. of Nuclear Research, Dubna, USSR). Instrum. Exp. Tech. (USSR) (Engl. Transl.); No. 2, 353-7(Mar-Apr 1970).**
Translated from Prib. Tekh. Eksp.; No. 2, 43-7(Mar-Apr 1970).

A gas-filled mass separator is described which has been designed for investigations of the short-lived products of nuclear reactions induced by heavy ions. Using a He-filled separator, a resolution of ~3% (with respect to Hρ) was obtained for ^{103}Ag; the focusing efficiency was 15 to 20%. The separator parameters were also investigated for air filling. The magnetic rigidity was measured for recoil ions of the mass range 84 to 149. An anomalous decrease of equilibrium charge was observed when passing over to rare-earth elements: for Dy this decrease amounts to about 15%. The filling of the inner 4f electron shell results in a reduction of the electron loss cross section. (auth)

20176 DEVICE FOR MEASURING TOTAL PROTON CROSS SECTIONS OF REACTIONS. **Khomyakov, G. K.; Matyash, P. P.; Skakun, N. A.; Strashinskii, A. G. (Physical-Technical Inst., Kharkov). Instrum. Exp. Tech. (USSR) (Engl. Transl.); No. 2, 361-3(Mar-Apr 1970).**
Translated from Prib. Tekh. Eksp.; No. 2, 50-2(Mar-Apr 1970).

A device for measuring total proton cross sections of reactions by the beam attenuation method is described. The reaction ^{3}He(d,p)^{4}He is used to obtain a low intensity proton beam with a low energy component less than 10^{-4}. The use of a collimating system of thin plastic scintillation films permitted the noise produced by protons scattered from structural elements of the device to be reduced significantly. (auth)

20177 DATA DISPLAY SYSTEM FOR USE WITH VISUAL DETECTORS. **Railton, R. (Univ. of Glasgow). Nucl. Instrum. Methods; 91: 517-20(1971).**

The problems of data display for experiments using fast-cycling accelerators are discussed, and a system for displaying numbers in BCD is described. A parallel system with the information appearing in numeric form is also presented, along with the performance of both devices. (auth)

20178 FERRITE BIAS REGULATOR FOR A SYNCHROTRON RESONATOR. **Smith, Bob H. (to United States Atomic Energy Commission). U. S. Patent 3,543,171. 24 Nov 1970. Filed 3 Mar 1969.**

A ferrite bias regulator for a synchrotron resonator controls the resonant frequency of a ferrite tuned cavity in a synchrotron. The ferrite bias regulator supplies a regulated biasing current to a coil, inductively coupled to the ferrite material in the synchrotron cavity, thereby varying the permeability of the ferrite material so as to match or track the resonant frequency of the cavity to the frequency sweep of the particle accelerating electrical field of the synchrotron. The ferrite bias regulator has a high voltage power supply and a low voltage, high current power supply. The high voltage is supplied to overcome the back emf of the unsaturated ferrite at the beginning of the sweep, and the high current is supplied to saturate the ferrite at the end of the sweep. Smooth current transfer is an inherent property of the regulator. The direction of the current passing through the coil is reversed every other sweep, so that the full hysteresis loop of the ferrite is utilized, thereby increasing the range of tuning frequencies obtainable from the ferrite bias regulator. (auth)

20179 PHASE ANGLE MEASUREMENT SYSTEM FOR DETERMINING AND CONTROLLING THE RESONANCE OF THE RADIO FREQUENCY ACCELERATING CAVITIES FOR HIGH ENERGY CHARGED PARTICLE ACCELERATORS. **Kovarik, Vincent J. (to United States Atomic Energy Commission). U. S. Patent 3,543,147. 24 Nov 1970. Filed 29 Mar 1968.**

Discriminating means responsive to the forward and reflected waves in a co-axial cable for determining whether the radio-frequency accelerating cavities for high energy accelerators are in or out of resonance are described. By measuring the phase angle difference between the forward and reflected waves the discriminator can be centrally located away from the accelerating cavities. The system also measures the reactive component of the accelerating cavities for the proper tuning thereof. (auth)

20180 PARTICLE IDENTIFICATION BY AN IMPROVED TIME-OF-FLIGHT SYSTEM. **Udo, F. (CERN, Geneva). Nucl. Instrum. Methods; 91: 521-4(1971).**

It is shown that time-of-flight measurements are feasible in particle beams with intensities up to 6 × 10^6 particles sec^{-1}. Good mass separation is achieved under these conditions at incident momenta up to 2 GeV/c by using a dual time-of-flight system. Possible applications of the principle at substantially higher momenta are discussed. (auth)

20181 SELF-CONSISTENT CLUSTERS OF OSCILLATING HEAVY PARTICLES IN AN ACCELERATOR. **Vlasov, A. D. Zh. Prikl. Mekh. Tekh. Fiz.; No. 4, 140-2(Jul-Aug 1970). (In Russian).**

In a projection on the transverse plane, self-consistent constant-density clusters describe circles of ellipses and oscillate sinusoidally along the axis of the spheroid. An infinite number of particle distributions along the half-axes of the transverse ellipses is possible. The problem of the stationary equilibrium filling up the rotational ellipsoid (or spheroid) by particles which carry out sinusoidal oscillations of given angular frequencies at the axes of the spheroid was examined, in order to clarify the situation prevailing in a linear accelerator with charged particle (proton) clusters. The findings may apply equally to clouds of cosmic dust or star agglomerations. The derivations indicated that self-consistent spheroidal, constant-density clusters consisting of heavy particles or bodies could indeed exist. (TTT)

20182 APPARATUS FOR PRODUCING A PULSATED BEAM OF CHARGED PARTICLES. **Roche, Michel (to Commissariat a l'Energie Atomique). British Patent 1,217,598. 31 Dec 1970. Priority date 31 Oct 1967, France.**

An accelerator beam pulsing system is described. The deflecting system comprises a multiplate electrostatic deflection system where the plates are connected in series by delay lines for synchronized beam pulsing. (W.H.K.)

20183 SWITCHED LINEAR ACCELERATION TECHNIQUE FOR MICROPARTICLES. **McDonnell, J. A. M. (Univ. of Kent, Eng.). Rev. Sci. Instrum.; 42: 274-5(Feb 1971).**

A variation of the configuration and operation of the linear accelerator is suggested, which is particularly suited to the acceleration of solid particles. It is pointed out that the modifications would lead to a drastic reduction in instrument cost

XUM

and an enhancement of the scope of linear accelerator techniques. Other advantages compared to the Van de Graaff accelerator are pointed out. (L.B.S.)

20184 ELECTRONICALLY-CONTROLLED PNEUMATIC TUBE SYSTEM FOR ACTIVATION ANALYSIS AT A PARTICLE ACCELERATOR. Kayser, K.; Nolte, H.; Reich, H. (Physikalisch-Technische Bundesanstalt, Brunswick). Nucl. Instrum. Methods; 92: 93-6(1971). (In German).

The pneumatic tubular post of 9 m length installed on the Braunschweig 140 MeV electron synchrotron is working automatically for short-time and semiautomatically for long-time irradiation. In the latter case one sample can be irradiated during the measurement of a second. Special attention was paid to the exact positioning of the flat samples on the places for irradiation and for measurement. The transport time is less than 2 sec. The irradiation time, the interim between irradiation and measurement, and the measuring time can be controlled separately. (auth)

20185 PARAMETERS WHICH CHARACTERIZE THE DESIGN OF A WINDOWLESS GAS TARGET. Del Bianco, W.; Boridy, E. (Univ. of Montreal). Nucl. Instrum. Methods; 92: 111-23(1971).

The theory relevant to the flow of gases through tubes and orifices has been reviewed and presented in a form suitable for practical applications. The viscous flow of gases through tubes and orifices has been measured for He, N_2, and Ar. The results compare favorably with the theory and the results of other experiments. A four-stage windowless gas target has been designed and its performance evaluated. Overall pressure ratios of the order of 10^7 for He and 3×10^8 for N_2 and Ar have been obtained. (auth)

20186 USKORITILI. VYPUSK XII. (Accelerators. Number 12). Val'dner, O. A. (ed.). Moscow; Atomizdat (1970). 208p.

A collection of 35 articles on the theory and development of high-current linear accelerators is presented. Bunching calculations are given, and certain theoretical aspects of electrodynamic separation of highly relativistic particles are worked out. Experimental investigations of h-f characteristics of accelerating systems of electron linear accelerators and waveguides used in electrodynamic separators are described. (tr-auth)

20187 LIQUID DEUTERIUM TARGET FOR THE PRODUCTION OF A MONOENERGETIC NEUTRON BEAM. Bubb, I. F. (Univ. of Manitoba, Winnipeg). Nucl. Instrum. Methods; 92: 29-32(1971).

A cryogenic liquid deuterium target has been constructed for use in the production of a "monoenergetic" neutron beam by the D(p,n)2p reaction. The cryostat is refrigerated by liquid helium which is continuously transferred to the cryostat at low rates (≈1.0 l/h). When used with protons of energies between approximately 20 and 50 MeV, the peak in the neutron energy spectrum lies in the energy range 18 to 47 MeV. The neutron beam is used in an experimental program for measuring neutron cross sections. (auth)

20188 SMALL SOURCE FOR MULTIPLY CHARGED HEAVY IONS. Prelec, K.; Isaila, M. (Princeton-Pennsylvania Accelerator, Princeton, N. J.). Nucl. Instrum. Methods; 92: 1-6(1971).

A small, compact ion source of the P.I.G. type is described, with a pulsed magnetic field and end extraction. The source has been tested with N, CO, Ne, A, Kr and Xe and ion spectra are presented. Pulsed currents of C^{2+}, N^{3+}, Ne^{3+}, A^{3+}, Kr^{3+} and Xe^{4+} to Xe^{6+} between a few tens and one hundred μA or more were obtained, with an extraction aperture of 0.75 mm diameter. Although the relative yields of multiply charged ions are lower than from ion sources with side extraction, the described source has certain advantages as to its small size and low total power consumption. (auth)

20189 EXPERIMENTAL TECHNIQUES FOR PHOTON SCATTERING BELOW 140 MeV. Mehlig, D.; Czock, K.-H.; Ahrens, J.; Borchert, H.; Ziegler, B. (Max-Planck-Institut fuer Kernphysik, Mainz). Z. Physik; 241: 166-78(1971). (In German).

The facilities for photon scattering experiments at the Mainz electron linear accelerator are described. They include an energy analyzing system, the bremsstrahlung target and a photon spectrometer (NaI-crystals). The question of background elimination is discussed. The scattered photon spectrum from a carbon target is presented. (auth)

20190 ELECTRONUCLEAR BREEDING. Davidenko, V. A. At. Energ. (USSR); 29: 158-62(Sep 1970). (In Russian).

Energy and economic considerations on electronuclear breeding are discussed. The conclusion on insolvency of the idea to produce nuclear fuel by charged-particle accelerators is drawn. (21 references.) (auth)

20191 ELECTRONUCLEAR METHOD OF NEUTRON GENERATION AND FISSILE MATERIAL PRODUCTION. Vasil'kov, R. G.; Gol'danskii, V. I.; Dzhelepov, V. P.; Dmitrievskii, V. P. At. Energ. (USSR); 29: 151-8(Sep 1970). (In Russian).

The possibility of applying the electronuclear method of free neutron production to nuclear power technology is considered from the most general standpoint. The method consists in neutron emission by heavy nuclei when absorbing protons (deuterons) accelerated up to high energies. A brief review of relevant experimental evidence concerning neutron emission by highly excited nuclei and neutron multiplication in targets is given. Some known designs of electronuclear facilities based upon proton or deuteron accelerators with beam powers up to 100 MW are discussed. The main difficulties in the development of a high current accelerating system that would be able to provide the ample accelerated particle currents (~0.1 A at energies of the order of 1 GeV) needed for the electronuclear method are briefly analyzed. Speculation about the inherent features of such electronuclear reactors and neutron generators and their possible role for applied and scientific aims as well as their use in conjunction with ordinary nuclear reactors in particular, fast breeders, is included. (auth)

20192 STORAGE RINGS WITH COLLIDING BEAMS. Waloschek, P. (Deutsches Elektronen-Synchrotron, Hamburg). Kerntechnik; 12: 525-7(Dec 1970). (In German and English).

Some of the world's biggest storage ring projects are described; the main parameters of these machines are summarized in a table. (R.W.R.)

20193 POSITRON–ELECTRON STORAGE RING ADONE. Amman, F. (CNEN, Frascati, Italy). Kerntechnik; 12: 528-30(Dec 1970).

A short account of the construction of the 1.5-GeV electron–positron storage ring ADONE, now operating in the Frascati National Laboratory, is given; the technological problems involved, various aspects of beam stability, and the experience of the first period of operation are presented. (19 references) (auth)

20194 STANFORD STORAGE RING. Richter, B. (Stanford Univ., Calif.). Kerntechnik; 12: 531-3(Dec 1970).

The Stanford Positron– Electron Asymmetric Ring is a single storage ring having two long low-beta insertions to achieve high luminosity at the interaction points. The design luminosity is a maximum at 2 GeV, each beam, where it equals 10^{32} cm^{-2} s^{-1}. The project is described, and the ring parameters are given. (auth)

20195 CAMBRIDGE ELECTRON ACCELERATOR BYPASS. Voss, G. A. (Cambridge Electron Accelerator Lab., Mass.). Kerntechnik; 12: 534-5(Dec 1970).

In the "CEA Bypass Project" use is made of the existing 6-GeV electron synchrotron for accumulation and storage of counter-rotating electron and positron beams. This is made possible through the addition of a positron source and injector, a system for damping betatron oscillations, and an improved vacuum system. Beams of electrons and positrons collide at the midpoint of a beam-transport system, which bypasses roughly one-sixth of the synchrotron magnets. Extra-strong focusing at the interaction point, enclosed in a large solid-angle on-line detector, produces large luminosities. (auth)

20196 DESY-DOUBLE STORAGE RING (DORIS). Steffen, K. (Deutsches Elektronen-Synchrotron, Hamburg). Kerntechnik; 12: 536-40(Dec 1970). (In German and English).

A 3-GeV electron–positron double storage ring at the German Electron-Synchrotron (DESY) is described. In the double ring, the two beams orbit in opposite directions and collide nearly head-on in two crossing points. The conception of the project as it evolved from the requirement of high luminosity is described, and several technical problems are treated in some detail. (auth)

20197 ELECTRON BEAM CURRENT MONITORING SYSTEM. Pruitt, J. S. (National Bureau of Standards, Washington, D. C.). Nucl. Instrum. Methods; 92: 285-97(1971).

A beam current monitoring system used with the NBS electron linac is described in detail. The system consists of a water-cooled Faraday cup designed to dissipate the energy in a 1 cm diameter, 100 kW beam of 100 MeV electrons, and a non-intercepting ferrite loaded toroidal coil. The ferrite is used for continuous-duty monitoring and can be calibrated in absolute units with the Faraday cup. The Faraday cup errors were measured with an absolute accuracy of better than 0.1% by bucking the Faraday cup current against the beam current, using the ferrite monitor as a null detector. The Faraday cup losses are about 0.5% at 30 MeV and decrease to less than 0.1% at 120 MeV. These losses are attributed to backscatter of high energy electrons from the front face of the cup. In addition, it is shown that secondary electrons produced by Møller scattering in the Faraday cup entrance foils may lead to spurious measurements of beam current, and a correction for this effect is derived. (auth)

20198 BOL NUCLEAR RESEARCH PROJECT. Koerts, L. A. Ch.; Mulder, K.; Oberski, J. E. J.; van Dantzig, R. (Inst. for Nuclear Physics Research, Amsterdam). Nucl. Instrum. Methods; 92: 157-60(1971).

A multidetector system has been built for detailed investigations of nuclear reactions. The equipment is designed to perform kinematically complete coincidence experiments. A survey of the system and its main characteristics is given. (auth)

20199 ELECTRONICS OF THE BOL-SYSTEM. Oberski, J. E. J. (Inst. for Nuclear Physics Research, Amsterdam); Mulder, K.; Koerts, L. A. Ch.; (and others). Nucl. Instrum. Methods; 92: 177-87(1971).

The 64-fold digital and analog electronics of the multi-parameter nuclear reaction measuring system BOL is described from an experimentalist's point of view. The digitized measurements are fed event-wise into a PDP8 computer. Up to four-fold coincidences can be accumulated. (auth)

20200 BOL COMPUTER-HARDWARE CONFIGURATION. Oberski, J. E. J. (Inst. for Nuclear Physics Research, Amsterdam); van Dantzig, R.; Mulder, K.; (and others). Nucl. Instrum. Methods; 92: 189-91(1971).

Three computers, two PDP8's and an EL-X8, are linked to the BOL nuclear multi-detector system. The coupling between them, including appropriate display-units allows on-line and off-line visualization of several aspects of the experimental data generated by the detection system. (auth)

20201 SCATTERING CHAMBER OF THE BOL-SYSTEM. Mulder, K.; van Dantzig, R.; Oberski, J. E. J.; (and others) (Inst. for Nuclear Physics Research, Amsterdam). Nucl. Instrum. Methods; 92: 161-72(1971).

A spherical scattering chamber for 64 solid state detector telescopes in fixed positions is described. The scattering chamber has been constructed to allow detection of multiparticle processes with high efficiency (13% of 4π) and good angular resolution (1°). This combination was possible using ΔE-detectors of the "Checkerboard" type. The geometry was calculated to allow optimal homogeneous density for measurements as a function of the angular variables for both single and multiple events. (auth)

20202 DATA ACQUISITION WITH THE BOL NUCLEAR DETECTION SYSTEM. van Dantzig, R. (Inst. for Nuclear Physics Research, Amsterdam); Oberski, J. E. J.; Mulder, K.; (and others). Nucl. Instrum. Methods; 92: 199-203(1971).

The acquisition of nuclear reaction data using the BOL-detection system involves three interacting computers. Data are either stored on magnetic tape for off-line analysis or directly processed on-line depending on various circumstances. Procedures for experiment-control and -checking are briefly described. (auth)

20203 ANALYSIS OF MULTIDIMENSIONAL NUCLEAR DATA (BOL). I. van Dantzig, R. (Inst. for Nuclear Physics Research, Amsterdam); Koerts, L. A. Ch.; Oberski, J. E. J.; (and others). Nucl. Instrum. Methods; 92: 205-13(1971).

Various data processing procedures are described which have been developed for the analysis of nuclear data obtained with the BOL detection system. The great amount of data stored on magnetic tape and their multidimensional character required the development of some unconventional data-handling techniques. (auth)

20204 BEAM INJECTION SYSTEM FOR THE TERMINAL ION SOURCE OF THE ELECTROSTATIC GENERATOR. Isoya, A.; Kato, N. (Kyushu Univ., Fukuoka). Nucl. Instrum. Methods; 92: 215-20(1971).

A new type of beam injection system for the terminal ion source which has been used in the electrostatic generator in Kyushu University is described. Design and performance are described of the whole system, which consists of the magnetic ion source, the ion selector by means of the quadrupole magnetic lens, the preacceleration gap, and the electrostatic deflector. (auth)

20205 MAGNET SYSTEMS FOR THE TRANSPORT OF ION BEAMS WITH NO CHANGE IN PROPERTIES. Tautz, M. F. (Univ. of Victoria, B. C.). Nucl. Instrum. Methods; 92: 263-8 (1971).

Magnet systems are discussed which are achromatic and which have 2×2 optical transfer matrices equal to plus or minus one times the unit matrix. The characteristics of systems consisting of four quadrupoles or four bending magnets are described. (auth)

20206 MUON ENERGY LOSSES AND STRAGGLING FOR HIGH ENERGY MUONS. Roe, B. P. (Univ. of Michigan, Ann Arbor). Nucl. Instrum. Methods; 92: 257-61(1971).

The non-Gaussian nature of energy loss straggling is examined. At NAL large muon shields must be designed to reduce flux by about a factor of 10^{12}. Fortunately it is shown here that on the long range end, the straggling falls off much faster than Gaussian and the amount of shielding needed is significantly reduced. (auth)

20207 TEST-PROCEDURES FOR THE MULTIDETECTOR BOL-SYSTEM. Sonnemans, M. A. A. (Inst. for Nuclear Physics Research, Amsterdam); van Dantzig, R.; Mulder, K.; (and others). Nucl. Instrum. Methods; 92: 193-7(1971).

The application of Checkerboard detectors allows cross section measurement without solid angle defining slits. Special techniques for testing these detectors and for adjusting the accompanying electronic circuitry are presented. The test results demonstrate the diversity, reliability and accuracy of nuclear reaction data obtainable with the Checkerboard detectors. (auth)

20208 TRANSISTOR CONTROL ELEMENT FOR THE CURRENT REGULATION OF A PULSED MAGNET POWER SUPPLY. Depping, F. (CERN, Geneva). Kerntechnik; 12: 551-5(Dec 1970). (In German and English).

A transistor bank used as the control element for the current regulation of a pulsed power supply for deflection magnets (septum magnets) is described. Design and construction details are shown. (auth)

20209 CERN INTERSECTING STORAGE RINGS. Johnsen, K. (CERN, Geneva). Kerntechnik; 12: 541-3(Dec 1970).

A general description is given of the 300-m-diameter CERN Intersecting Storage Rings facility, its current status, and the preparations being made for the experimental program after its completion in mid-1971. Protons from the CERN proton synchrotron at energies between 8 and 28 GeV are stored in each of two rings at design currents of 20 A. Collisions take place at 8 regions where the two rings are interlaced. Special features of the vacuum system, magnetic field and r-f system and problems of the intense beams are discussed. (auth)

20210 STORAGE OF MULTICHARGED IONS IN RELATIVISTIC ELECTRON BEAM. Iovnovich, M. L.; Fiks, M. M. At. Energ. (USSR); 29: 429-33(Dec 1970). (In Russian).

The storing process of ionized atoms in a ring of relativistic electrons is considered. Neutral atoms penetrating into the ring are ionized as a result of collisions with electrons and captured by the electric field of the ring. Time dependence of the density of ions with various charges is given. Electron losses in the storing process due to collisions with heavy particles are determined. (2 figures, 7 references) (auth)

20211 SCATTERING CHAMBER FOR PHYSICAL STUDIES USING ELECTRON BEAMS. Gusev, E. A. (Tomsk Polytechnic Inst., USSR). Izv. Vyssh. Ucheb. Žaved., Fiz.; No. 10, 129-31 (1970). (In Russian).

An experimental device consisting of a radiation source, scattering counter, and magnetic spectrometer was used for studying electron transport through confined media. The design of the scattering chamber enabled investigations of the flux of electrons passing through a target at an angle of ±35° to the incident beam axis. The order of error of the device was ±0.1°. (R.V.J.)

20212 SMALL FURNACE DESIGNED FOR BOMBARDING SPECIMENS IN ACCELERATORS WITHIN THE TEMPERATURE RANGE 700 TO 1500°C. Whitmell, D. S. (Atomic Energy Research Establishment, Harwell, Eng.). J. Phys., E (London); 4: 151-2(Feb 1971).

A furnace has been designed to allow small specimens to be bombarded in accelerators to temperatures up to 1400 to 1500°C. It has a fast time response. Ion beam currents are measured by scanning the beam on to a peripheral collector which is not subject to significant stray currents from the heater. (auth) (UK)

20213 HYPERTRON-30 ELECTRON ACCELERATOR FOR THE RADIATION CURING OF PAINT-COATING. Arakawa, Kazuo (Matsushita Electric Industrial Co. Ltd., Osaka). Purasuchikku Materiaru; 11: No. 2, 52-6(Feb 1970). (In Japanese).

The Hypertron-30 300-keV electron electrostatic accelerator for radiation curing of paint coatings is described. (TSS) (Japan)

20214 COLLECTOR MONITORS FOR ELECTRON BEAMS. Bewley, D. K. (Hammersmith Hospital, London). Phys. Med. Biol.; 16: 131-3(Jan 1971).

A collector monitor is described for use with a 2 MeV electrostatic generator, together with a modified design for an 8 MeV linear accelerator. With a relative fluence of unity, the sensitivity to electrons in the range 1 to 10 MeV is about 8 ×

XUM

10^{-12} A cm^{-2} for 100 rad/min. The point of failure with both was at an irradiated equivalent of more than 1000 megarads to tissue. The advantages of this type of monitor in electron beam therapy are discussed, in relation to an ionization chamber. (UK)

20215 CONTRIBUTION TO THE THEORY OF TRANSVERSE INSTABILITY IN A SECTIONAL LINEAR ACCELERATOR. Kurilko, V. I.; Tolstoluzhskii, A. P. This paper was summarized in At. Energ. (USSR); 28: 498-9(Jun 1970) as paper No. 401/5295. (In Russian).

The theory of transverse instability is examined taking account of the interaction of the accelerated beam with the space harmonics of the field of defocusing oscillations. Equations for the transverse motion of the electron bunch are presented and discussed. (W.H.K.)

20216 INTRODUCTION OF A CONTROLLED ENERGY-MODE IN THE U-150-2 CYCLOTRON OF THE INSTITUTE OF NUCLEAR PHYSICS OF THE UzbSSR ACADEMY OF SCIENCES. Irisbaev, K. N.; Uzakov, Ya. M.; Kurganov, B. G.; (and others). This paper was summarized in At. Energ. (USSR); 26: 459-60(May 1969) as paper No. 303/5074. (In Russian).

A system of coils for magnetic field corrections in the U-150-2 cyclotron is described. Three pairs of coils (central, peripheral, and outer) and four pairs of azimuthal coils are used. (W.H.K.)

20217 THREE-SECTOR FOCUSING MAGNETIC PRISMS WITH r^{-1} FIELD. PART 3. FOCUSING OF CHARGED PARTICLE BEAMS WITH POINT SOURCE. Fedoseev, E. P. (Inst. of Atomic Energy, Moscow). Kernenergie; 13: 178-81(Jun 1970). (In Russian).

Focusing of charged-particle beams from a point source in the three-sector magnetic prism with r^{-1} field is considered. Basic relations for the image parameters are derived. A new ion-optical scheme for a stigmatic-focusing mass analyzer having high resolution is found. (auth)

20218 NEW METHOD FOR RECORDING THE BEAM OF ENERGETIC PARTICLES. II. ETL ELECTROMAGNETIC ISOTOPE MASS SEPARATOR. Nakai, Akira. Denki Shikensho Iho; 34: 582-7(1970). (In Japanese).

A silver-coated graphite plate is proposed for recording the beam-intensity distribution of energetic particles. The principle of the recording is based on the sputtering of silver by the incident particles. The plate clearly records the beam profile over a wide range of beam intensity. The recorded beam-intensity distribution is analyzed quantitatively by measuring the light reflected from the plate. The plate is applicable to any sort of beam. Several advantages of beam recording using the proposed plate over the conventional methods are described. The plate is easy to prepare in a laboratory. Also shown are some examples of recording the beam in the electromagnetic isotope mass separator. (auth)

20219 RADIATION IN LINEAR SYSTEMS WITH CROSS FOCUSING. Grishin, V. K. Vestn. Mosk. Univ., Ser. III. Fiz. Astron.; No. 6, 106-7(Nov-Dec 1968). (In Russian).

The stabilization of relativistic electron beams in linear accelerators in the plane perpendicular to the motion produces various radiative effects. For any focusing devices radiative effects become more noticeable with an increase of particle energy. In order to evaluate these effects, an attempt was made to study relativistic electrons ($\gamma \gg 1$) moving along the z axis, at the velocity $\nu_z \sim c$ with the force $F_x = -k \cdot x$ acting in the perpendicular direction $\underline{x}$. The problem was studied for conditions where F_x was small and the variations of the magnitude of the absolute velocity due to the transverse motion was also small, i.e., $\nu \sim \nu_z$. (R.V.J.)

20220 INTENSE ELECTRON BEAM AUTOACCELERATION. Kazanskii, L. N.; Kiseltsov, A. V.; Lebedev, A. N. At. Energ. (USSR); 30: 26-31(Jan 1971). (In Russian).

The process of autoacceleration of intense electron beams by passive elements is discussed. Autoacceleration means an energy redistribution in the beam, i.e. acceleration of a part of the beam at the expense of the energy of other particles. The results of the calculation of the relativistic electron beam autoacceleration in a cylindrical cavity are presented. (auth)

20221 DISTORTION OF THE STRUCTURE OF THE MAGNETIC FIELD OF AN ACCELERATOR BY THE CONDUCTING COATINGS OF THE CHAMBER. Nepokrytykh, Yu. A. (Tomsk Polytechnical Inst., USSR). Izv. Vyssh. Ucheb. Zaved., Aviats. Tekh.; No. 5, 138-40(1970). (In Russian).

Use of waveguide resonances for cyclic acceleration systems requires knowledge of the effect of conducting materials on the magnetic field distribution within the accelerating chamber; therefore, the influence of thin, conductive coatings deposited on the walls of the chamber was determined. In view of the thinness of the layer, it was assumed that the depthwise distribution within the coating was uniform, and that the effect is exerted only in the horizontal direction. The radial and azimuthal fields were calculated by the sine law, with the phase inhomogeneity of the prompt magnetic field also taken into account. The largest distortion of the field was found to occur during the first period of acceleration. The calculated values were checked experimentally by placing foils between the poles. It was concluded that conducting layers indeed distort the magnetic field distribution, and that the effect of conducting walls in the space between the poles must be calculated and then corrected. (TTT)

20222 SPRAY CURRENT STABILIZER CIRCUIT FOR PRESSURIZED VAN DE GRAAFF GENERATOR. Kadar, Imre; Koltay, Ede. ATOMKI (At. Kut. Intez.) Kozlem.; 12: 161-3 (Nov 1970). (In Hungarian).

A spray current stabilizer circuit has been built with the following parameters: voltage range, $1.5 \text{ kV} < U_A < 40 \text{ kV}$; dynamic resistance 8.10^{10} ohm; current adjustable between 25 μA and 1 mA. (auth)

20223 CALCULATION OF THE ACCEPTANCE FOR ION OPTICAL SYSTEMS. Szabo, Gyula. ATOMKI (At. Kut. Intez.) Kozlem.; 12: 153-9(Nov 1970). (In Hungarian).

An analytical method is presented for calculating the acceptance of ion optical systems which can be described by transfer matrices. The method is applied to determine the acceptance of asymmetrized quadrupole singlets. (auth)

20224 EXPERIMENTAL STUDIES OF THE AUTORESONANCE ELECTRON ACCELERATION. Ishkov, A. P. (Tomsk Polytechnic Inst., USSR). Izv. Vyssh. Ucheb. Zaved., Fiz.; No. 2, 136-8(1970). (In Russian).

Experimental studies were made with autoresonance acceleration of electrons by an electromagnetic wave 10 cm in range with a phase velocity of 1.14 C. The design of the device and the diagram of the magnetic field intensity as a function of the injection intensity are included. The FWHM of the energy spectra of the accelerated electrons was 12%. The energy of the accelerated electrons at an accelerating field energy of 5 kV/cm was 0.320 MeV, which was in agreement with the theoretical value of 0.450 MeV for an ideal field distribution in the accelerating space. (R.V.J.)

20225 ACCELERATOR AT BATAVIA: THE NEXT STEP IN HIGH-ENERGY PHYSICS. Hammond, Allen L. Science; 171: 362-4(29 Jan 1971).

The National Accelerator Laboratory is described. The design and present state of construction of the various components are reviewed, the important problems to be investigated with this machine are discussed, and the experimental facilities available are outlined. (R.W.R.)

20226 ABSORBED DOSE AND DOSE EQUIVALENT FROM NEGATIVELY AND POSITIVELY CHARGED PIONS IN THE ENERGY RANGE 10 TO 2000 MeV. Alsmiller, R. G. Jr.; Armstrong, T. W.; Bishop, Barbara L. (Oak Ridge National Lab., Tenn.). Nucl. Sci. Eng.; 43: 257-66(Mar 1971).

Nucleon–meson cascade calculations have been carried out for broad beams of monoenergetic negatively and positively charged pions normally incident on a semi-infinite slab of tissue 30-cm thick, and the absorbed doses and dose equivalents as a function of depth in the tissue are presented. Results are given for incident energies of 10, 30, 84, 150, 500, 1000, and 2000 MeV. For the lower incident energies ($\lesssim 84$ MeV), the pion range is <30 cm in tissue, and peaks in the absorbed doses and dose equivalents, due to the reaction products produced by the nuclear capture of the stopped negatively charged pions and to the decay products of the stopped positively charged pions, are clearly evident. (auth)

PHYSICS (NUCLEAR)

Neutron Interactions with Matter

Refer also to abstracts 18618, 18738, 18870, 20150, 20187, and 20191.

20227 (AAEC/TM-565) REVIEW OF GAMMA-RAY TRANSITIONS FROM keV NEUTRON CAPTURE. Allen, B. J. (Australian Atomic Energy Commission Research Establishment, Lucas Heights). Sep 1970. 36p. (CONF-700102-4). Dep. NTIS (U. S. Sales Only).

From Annual Meeting of the American Physical Society, Chicago, Ill.

The study of gamma rays from neutron capture in the keV energy region provides information on the properties of individual resonances with keV spacing in light nuclei or nuclei near closed shells, and on the average behavior of resonances in heavy nuclei. The effects of p and d-wave capture can be investigated across the periodic table, as can the neutron capture mechanisms. A variety of techniques are applicable in this energy range and these, with the results obtained, are reviewed. 65 references. (auth)

20228 (CSIRO-Trans-10095) SMALL-SIZE NEUTRON TUBE OF UNG-1 TYPE. Bespalov, D. F.; Mints, A. Z.; Shkol'nikov, A. S. Translated by B. Bergmanis (Australian Atomic Energy Commission), from Tr., Vses. Nauch.-Issled. Inst. Yadern. Geofiz. Geokhim.; No. 1, 134-43(1968). 13p. Dep. NTIS (U. S. Sales Only).

An abstract of this article, prepared from the original, appeared as NSA 24: 8829(1970). (Australia)

20229 (INR-1186) MINIGASKET: A CODE FOR THERMAL NEUTRON SCATTERING LAW IN POLYCRYSTALS. Arkuszewski, Jacek (Institute of Nuclear Research, Warsaw (Poland)). 1970. 124p. Dep. NTIS (U. S. Sales Only).

This computer code is patterned on part of the General Atomic code GASKET, which pertains to two dynamical modes of the scattering system: isotropic harmonic vibration with continuous frequency spectrum and free translation. The scattering law $S(\alpha,\beta)$ for such a system is calculated in incoherent approximation by direct numerical Fourier transformation from the intermediate scattering function averaged over the monatomic polycrystal. Some improvements are introduced to the GASKET numerical procedure. The paper contains a sample case: the scattering-law calculations for the continuous component of the Haywood phonon distribution function for H bound in H_2O. The code is written in ALGOL for the GIER computer. (auth)

20230 (JAERI-Memo-4116) GRAPH: A COMPUTER PROGRAM FOR PLOTTING EXPERIMENTAL DATA IN NEUDADA SYSTEM. Nakagawa, Tsuneo; Igarasi, Sin-iti (Japan Atomic Energy Research Inst., Tokyo). Aug 1970. 39p. (In Japanese). Dep. NTIS (U. S. Sales Only).

GRAPH is a computer program for plotting of numerical data of NEUDADA system. Transmission format, which is one of the output formats of the NEUDADA system, is used as the input data for the computer program GRAPH. This program is written in FORTRAN IV language, and is available for both IBM 360/75 I and FACOM 230-60 computers, associated with a CALCOMP plotter. By using this program, one is able to obtain several types of graphs plotted for experimental data; for example, graphs of the differential cross sections for scattering or graphs of the excitation function for reactions. (auth) (Japan)

20231 (JAERI-Memo-4167) JAPANESE LIST OF REQUESTS FOR MEASUREMENT. [PART] II. Igarasi, Sin-iti (Japan Atomic Energy Research Inst., Tokyo). Oct 1970. 23p. (In Japanese). Dep. NTIS (U. S. Sales Only).

The Japanese requests for nuclear data to be measured, which were compiled by the JNDC and submitted to the EANDC in September 1970, are presented. (Japan)

20232 (JINR-P3-5392) EXPERIMENTS WITH ULTRACOLD NEUTRONS. Groshev, L. V.; Dvoretskii, V. N.; Demidov, A. M.; Lushchikov, V. I.; Panin, Yu. N.; Pokotilovskii, Yu. N.; Strelkov, A. V.; Shapiro, F. L. (Joint Inst. for Nuclear Research, Dubna (USSR). Lab. of Neutron Physics). 1970. 16p. (In Russian). Dep. NTIS (U. S. Sales Only).

A possibility for extraction of ultracold neutrons from a stationary reactor is shown. The spectra and diffusion length of ultracold neutrons are given. The results of preliminary measurements of neutron storage time in closed containers are presented. (auth)

20233 (ORNL-tr-2409) ELF PROGRAM: DESCRIPTION OF UTILIZATION. Gervaise, Francois (Commissariat a l'Energie Atomique, Fontenay-aux-Roses (France). Centre d'Etudes Nucleaires). Translated for Oak Ridge National Lab., Tenn., from report CEA-Note-N-1361. 29p. Dep. NTIS.

The ELF program performs Monte Carlo calculations of neutron transport in cylindrical and spherical geometry. Some improvements in the characteristics of ELF and its auxiliary programs are described, and examples of program input data and results are presented. (H.D.R.)

20234 (PH-4) OPTIMUM THICKNESS OF SINGLE CRYSTAL NEUTRON MONOCHROMATORS. Said, K. I.; Sarah, J. J. (Atomic Energy Commission, Baghdad (Iraq). Nuclear Research Inst.). Oct 1970. 10p. Dep. NTIS (U. S. Sales Only).

The optimum thickness of a copper single crystal neutron monochromator was measured experimentally and comparison with theoretical predictions shows reasonable agreement. Knowledge of the crystal's mosaic spread is necessary for these calculations and suggestions for further work are made. (auth)

20235 (RPI-328-211) MONTE CARLO EVALUATION OF MULTIPLE SCATTERING AND RESOLUTION EFFECTS IN DOUBLE-DIFFERENTIAL NEUTRON SCATTERING CROSS SECTION MEASUREMENTS. Bischoff, F. G.; Yeater, M. L. (Rensselaer Polytechnic Inst., Troy, N. Y.); Moore, W. E. (Knolls Atomic Power Lab., Schenectady, N. Y.). [1970]. Contract AT(30-3)-328. 64p. Dep. NTIS.

Thesis. Submitted to Rensselaer Polytechnic Inst., Troy, N. Y., by F. G. Bischoff.

A Monte Carlo computer code MSC was developed which is of general usefulness in analyzing double-differential neutron scattering measurements. This code is equivalent to a three dimensional solution of the neutron transport equation for finite geometries. It is available for two geometrical configurations (slab geometry and tubular geometry), and is readily adapted to other geometrical configurations. Resolution effects are calculated in detail by including full time dependence in the calculation and considering individually the various factors which contribute to the experimental resolution. MSC uses statistical weights as a means to improve the convergence of the Monte Carlo Method by forcing scattering collisions; the statistical estimation technique used allows every collision to contribute to every scattered energy and angular bin. Options were developed which treat rigorously the coherent and incoherent elastic scattering from polycrystals. Scattered energy and angle are sampled at each Monte Carlo collision by means of a method which samples alpha and beta from the scattering law. This sampling technique is exact within the framework of numerical integration and interpolation. It permits full kernel calculations, yet requires the storage of only two dimensional arrays. Use of MSC has made it possible to obtain good scattering results with relatively thick samples for several materials, notably water, polyethylene, and uranium carbide. Some examples are given of the verification of the methods used. Experience gained by the use of MSC is summarized. 22 references. (auth)

20236 (TID-25648) NEUTRON TRANSPORT THEORY WITH A COMPLETELY DEGENERATE ENERGY TRANSFER KERNEL. Watts, James Fred (Virginia Polytechnic Inst., Blacksburg). May 1968. 118p. Dep. NTIS.

Thesis.

An analytic solution of the time-dependent neutron transport equation in slab geometry is found for a completely degenerate energy transfer kernel and a 1/v total cross section. The time dependence is removed from the transport equation by a Laplace transformation and the solution of the homogeneous form of the transformed equation is expanded using the singular eigenfunction expansion method of Case. A superposition of the elementary solutions of the homogeneous transformed equation is used to construct a solution of the inhomogeneous equation with the expansion coefficients determined by the boundary conditions. The time dependence is recovered by the inverse Laplace transform where the path of integration is deformed to the left as far as possible. To demonstrate the method of solution, three problems are outlined: an albedo problem, a two adjacent half-space problem, and an initial value problem. An exact eigenvalue condition is derived in the solution of the initial value problem and the eigenvalues are calculated. 14 references. (auth)

20237 (UCRL-50400(Vol.9)) INTEGRATED SYSTEM FOR PRODUCTION OF NEUTRONICS AND PHOTONICS CALCULATIONAL CONSTANTS. VOLUME 9. THRESHOLDS OF NUCLEAR REACTIONS INDUCED BY NEUTRONS, PHOTONS, PROTONS,

XUM

DEUTERONS, TRITONS, AND ALPHA PARTICLES. Howerton, Robert J. (California Univ., Livermore. Lawrence Radiation Lab.). 24 Sep 1970. 304p. Dep. NTIS.

The thresholds for nuclear reactions induced by neutrons, photons, protons, deuterons, tritons, and alpha particles are tabulated. The threshold of a reaction is defined to be the minimum kinetic energy of an impinging particle such that the reaction is energetically possible. Thus, a nonzero threshold exists only if the Q-value of the reaction is negative and all exoergic reactions have zero thresholds. It is often useful to have ready reference to the Q-values of exoergic reactions so the negative of the Q-value is entered in the tables for such reactions. (auth)

20238 (UJV-2488-F) SINGLE-CRYSTAL FILTERS OF THERMAL NEUTRONS. Mikula, P.; Michalec, R.; Chalupa, B.; Sedlakova, L.; Dvorak, J. (Ceskoslovenska Akademie Ved, Rez. Ustav Jaderneho Vyzkumu). [1970]. 12p. Dep. NTIS (U. S. Sales Only).

The possibility of using single crystal bismuth and silicon filters supported by the experimental results of the transmission of neutrons in the wavelength region from $\lambda = 0.30 - 1.77$ Å is discussed. (auth)

20239 TIME AND SPACE DEPENDENT STUDIES IN BERYLLIUM OXIDE. Tewari, S. P.; Trikha, S. K. (Univ. of Delhi). J. Nucl. Energy; 24: 387-401(Nov 1970).

Using the Placzek scattering kernel, with $\theta_D = 950$°K, time and space dependent neutron spectra studies were made in beryllium oxide. In each case, the appropriate Boltzmann operator was diagonalized to obtain its eigenvalues and eigenfunctions, using which, neutron spectra were evaluated. The results of the study of slowing down of neutrons in an assembly with $B^2 = 0.059$ cm^{-2} are compared with recent experimental results. Both the slowing down relaxation time τ_s, and the heating up relaxation time τ_H are ~250 μsec, in beryllium oxide assembly with $B^2 = 0.01$ cm^{-2}. This result is qualitatively different from that for beryllium. Space dependent spectra studies were performed at natural and higher absorptions. Only one discrete mode exists up to nearly 2.5 times the natural absorption. The calculated diffusion length agrees well with the experimental results. It was found that the space dependence of neutron spectrum, due to a high energy source is quite different from that due to a low energy source. As absorption of the medium is increased, the build up of neutrons increases in the first Bragg peak while it decreases in the second Bragg peak. (auth) (UK)

20240 PULSED-SOURCE INVESTIGATIONS ON GRAPHITE SYSTEMS. Bull, S. R.; Dance, K. D.; Connolly, T. J. (Stanford Univ., Calif.). J. Nucl. Energy; 24: 473-7(Dec 1970).

The thermal diffusion coefficient was measured in solid graphite systems as a preliminary to measurements in systems containing cavities. The pulsed-source technique was employed and the results are in agreement with those of previous experimenters. A discussion is given of the problems associated with interpretation of the data in terms of diffusion parameters and of some implications regarding the value of $\lambda^* = (v\Sigma_t)_{min}$. (auth) (UK)

20241 DECONVOLUTION OF THE OBSERVED BEAM IN THE ELASTIC SCATTERING OF SLOW NEUTRONS. Deltour, J. (Univ., Liege); Konstantinovic, J. Solid State Commun.; 8: 1799-1802(15 Nov 1970). (In French).

The observed beam in critical neutron scattering is approximated by a Voight function. The resolution function is determined by an extrapolation for $q \rightarrow 0$ and it is then analytically deconvoluted. The diffusion function obtained in the case of Fe exhibits a width at half height depending on the power 2.5 of q as was theoretically predicted. (auth) (UK)

20242 TIME-DEPENDENT THERMALIZATION OF NEUTRONS IN AN EINSTEIN SOLID WITH APPLICATION TO ZIRCONIUM HYDRIDE. von Baltz, Ralph (Univ., Karlsruhe, Ger.). Atomkernenergie; 16: 201-5(1970). (In German).

The Einstein model of a solid is investigated in terms of its neutron thermalization properties. It is shown that the energy mode concept is valid although there is no corresponding discrete time eigenvalue. Thermalization in zirconium hydride may be explained by the Einstein model for times $\tau < 30$ μsec, whereas for longer times the influence of the Debye part of the lattice vibrations dominates. This effect is discussed with the aid of the Heavy Crystal and the Heavy Gas model. (auth)

20243 SLOW-NEUTRON SCATTERING FROM A PARTICLE SYSTEM IN AN ELECTROMAGNETIC WAVE. I. BASIC CONSIDERATIONS. GENERAL EXPRESSION FOR THE CROSS-SECTION. Weil, J. W. (Univ. of Innsbruck). Acta Phys. Pol.; A39: 85-6 (1971).

A general expression for the structure factor, and, therefore, the double-differential slow-neutron scattering cross section, for scattering of neutrons by particles moving in an electromagnetic wave is derived. (auth)

20244 SINGLY BENT GRAPHITE MONOCHROMATORS FOR NEUTRONS. Riste, T. (Institutt for Atomenergi, Kjeller. Norway). Nucl. Instrum. Methods; 86: 1-4(1970).

The performance of singly bent graphite monochromators of radius of curvature R = 79 cm has been studied. At $\lambda = 1.86$ Å a maximum reflectivity of 0.74 was measured. The focussing property was used in decreasing the area of the reflected beam relative to the undeflected one. At distance 2R from the crystal a gain of 3.8 for the neutron flux was measured, this being an indication of the obtainable flux enhancement at the sample position by using a bent monochromator. The merits of bent monochromators are pointed out in neutron crystal spectrometer setups and as a replacement for bent guide tubes. (auth)

20245 NEUTRON TRANSMISSION STUDY THROUGH SIMPLE BENT CONDUCTING TUBE. Bobbio, A.; Vaciago, C. (Politecnico, Turin). Nucl. Instrum. Methods; 91: 429-37(1971).

The neutron distribution at the exit window of a simple bent neutron conducting tube is studied using the Monte Carlo method. The method is also applied to obtain the neutron energy spectra and the transmission on exit from the tube, and to discuss the optimal size of a cold-neutron source. A statistical law relating the average number $\bar{n}$ of neutron reflections inside the tube to the wavelength λ is obtained in a particular case. (auth)

20246 USER'S MANUAL FOR PALLAS CODE. Takeuchi, Kiyoshi (Ship Research Inst., Tokyo). Senpaku Gijutsu Kenkyujo Hokoku; 7: 235-49(Sep 1970). (In Japanese).

The computer code, PALLAS-2D-CY, has been written in FORTRAN IV language for an IBM 360 model 75 computer to solve the steady-state neutron integral transport equation by the numerical integration method, which has been presented by the same author. This code calculates the directional flux density of neutrons as a function of energy in two-dimensional multilayered cylindrical geometry. The limitations on some of the inputs are as follows: number of energy groups ≤50; number of material regions ≤16; number of spatial meshes ≤1200; number of angular meshes = 24. The execution time is about 20 minutes in the case of a problem having 10 energy groups, 4 material regions, 987 spatial meshes, and 24 angular meshes, without inelastic scattering data. (auth) (Japan)

20247 INELASTIC NEUTRON SCATTERING FROM SOLID BENZENE. Logan, K. W.; Trevino, S. F.; Prask, H. J.; Gault, J. D. (Feltman Research Labs., Dover, N. J.). J. Chem. Phys.; 53: 3417-20(1 Nov 1970).

Neutron scattering spectra from polycrystalline benzene were obtained at temperatures between 77 and 270°K. These measurements are compared to recent calculations of spectra using a lattice frequency distribution based on optically determined force constants. The results at different temperatures are discussed, and qualitative agreement between calculated and measured cross sections at lower temperatures is obtained. (auth)

20248 THERMAL NEUTRON DIFFUSION AT THE ICE-WATER PHASE TRANSITION. Williams, P. M.; Munno, F. J. (Univ. of Maryland, College Park). Nucl. Sci. Eng.; 43: 120-2(Jan 1971).

Some recent pulsed-neutron experiments on neutron diffusion in water are discussed in the framework of Fermi's analysis for neutron scattering from chemically bonded hydrogen using Eyring's model. It is concluded that a recently reported discontinuity in the thermal neutron diffusion at the ice-water phase transition is caused by factors occurring in the range 0°C to 10°C. (J.W.R.)

Nuclear Properties and Reactions, A≤ 5

Refer also to abstracts 18647, 20298, 20423, 20511, and 20546.

20249 (ITF-70-51-E) CALCULATION OF THE BINDING ENERGY AND THE WAVE FUNCTION OF ^{3}He BY THE HARMONIC POLYNOMIAL METHOD. Kharchenko, V. F.; Kuzmichev, V. E. (Akademiya Nauk Ukrainskoi SSR, Kiev. Institut Teoreticheskoi Fiziki). 1970. 28p. Dep. NTIS (U. S. Sales Only).

The problem of the bound state of the system consisting of two protons and one neutron (nucleus ^{3}He) with the central interaction between nucleons is considered in the approximation using the expansion of the wave function in terms of the harmonic polynomials. The Coulomb interaction between nucleons, which causes the state with isospin T = $^3/_2$ to be admixed into the ^{3}He wave function, is taken into consideration. For the expansion coefficients the set of coupled differential equations is obtained. In the approximation taking into account the harmonics with K = 0 and 2, the binding energy and the wave functions of ^{3}He are calculated for the square-well potential. On the basis of the wave function obtained, the values for the probabilities of the S′ states with T = $^1/_2$ and with T = $^3/_2$, the electromagnetic form factors, and the root-mean-square radii are obtained. Calculations are also done for ^{3}H. (auth)

20250 (JINR–P2-5496) CONTRIBUTION OF THE EXCHANGE MECHANISM IN THE BACKWARD SCATTERING OF PROTONS ON LIGHT NUCLEI AND d + ^{4}He → ^{3}He + ^{3}H REACTION. Kopeliovich, B. Z.; Potashnikova, I. K. (Joint Inst. for Nuclear Research, Dubna (USSR). Lab. of Nuclear Problems). 1970. 16p. (In Russian). Dep. NTIS (U. S. Sales Only).

The role of the exchange mechanism in the backward scattering of protons on light nuclei is discussed. The results of calculations for dependence of P – ^{4}He backward scattering cross section on proton kinetic energy T_p in lab. system are presented. Since numerical agreement obtained for ^{4}He does not prove the dominance of the pole diagrams, other confirmations are needed. Such confirmation would be, of course, the existence of dips in the energy dependence of p – ^{4}He and p – ^{3}He backward cross sections. From isotopic invariance it follows also that for the pole diagrams, cross sections of p – ^{3}He backward scattering and the p + ^{3}H → n + ^{3}He charge exchange reaction must be equal, but the p – ^{3}H backward scattering should be suppressed. It is desirable also to measure the polarization effects in the above reactions. Such effects should be suppressed in the case of dominance of one of the diagrams. The cross section for d + ^{4}He → ^{3}H + ^{3}He reaction was calculated under the same assumptions. This reaction is interesting from the point of view of isotopic invariance. (auth)

20251 (NP–18678) THREE-NUCLEON CALCULATIONS USING THE FADDEEV EQUATIONS. Malfliet, Rudi (Utrecht Rijksuniversiteit (Netherlands)). 27 Apr 1970. 105p. Dep. NTIS (U. S. Sales Only).

Thesis.

The Faddeev equations are solved by numerical integration, and the results are compared with those of other methods. The properties of the three-nucleon system using simple local potentials are investigated to see whether some conclusions obtained for separable potentials remain valid. This includes a study of the influence of a repulsive core in the two-particle interaction on the three-particle bound-state energy. Then, off-shell effects on three-body observables are studied, together with an investigation of the sensitivity of these three-particle observables to two-particle data. Local potentials with tensor forces and soft cores are used. The binding energy, wave function, and doublet scattering length are calculated and discussed. (R.W.R.)

20252 CONNECTION BETWEEN THE RMS CHARGE RADII AND σ_b^{E1} FOR TRINUCLEONS. Mathur, V. S.; Lagu, A. V. (Banaras Hindu Univ., India). Proc. Indian Nat. Sci. Acad., Part A; 36: 140-5(May 1970).

The connection between the rms charge radii of ^{3}H and ^{3}He and the bremsstrahlung-weighted E1 cross sections of photodisintegration of these nuclei is seen more clearly when both the nucleons are considered to be "extended" particles. It seems to provide independent evidence for the positive value of the slope of the neutron charge form factor. Comparisons are also made in the case of the nuclei ^{2}D and ^{4}He between the experimental values of σ_b^{E1} and the corresponding values calculated from their observed rms charge radii considering and ignoring the neutron charge distribution. (auth)

20253 EQUIVALENT POTENTIALS FOR PION–ALPHA SCATTERING. McDonald, Lawrence Joseph. Minneapolis; Univ. of Minnesota (1969). 114p. University Microfilms Order No. 70-15,775.

Thesis.

A theoretical investigation of pion-nucleus scattering was made to determine the corresponding equivalent potential, using Watson's two-body direct-interaction model. Multiple scattering terms are not included so the potential is simply a sum over the scattering from each bound nucleon. Shell model wave functions describe these nucleons while the impulse approximation is used to replace bound nucleon scattering with a free nucleon scattering matrix calculated off its energy shell. This is evaluated analytically from the experimental pion-nucleon phase shifts, assuming a separable interaction. The resultant equivalent potential is both nonlocal and energy dependent. Numerical calculations were made for the special case on pion-alpha scattering at 24 MeV. The equivalent potential is found to be attractive in both the S and P partial waves. This is a consequence of the P_{33} resonance at 1238 MeV, and the mixing among partial waves due to the difference between pion-nucleon and pion-alpha center of mass reference frames. Experimental evidence indicates the S-wave potential should be repulsive. This disagreement points out the need to suppress the P_{33} partial wave for strongly bound nucleons and suggests the free nucleon scattering matrix does not adequately represent scattering from bound nucleons. Taking nucleon correlations into account is a possible way of eliminating this disagreement. (Diss. Abstr. Int., B)

20254 RETARDATION FUNCTIONS FOR DEUTERON PHOTODISINTEGRATION. PART II. Haemaelaeinen, R. M. K.; Peltola, E. I. (Jyvaeskylae Univ., Finland. Univ. of Helsinki). Ann. Acad. Sci. Fenn., Ser. A VI; No. 332, 1-11(1970).

Several methods for studying the effect of the omission or inclusion of retardation are analyzed. The interaction-dependent method is discussed by taking into account the difference between the initial and the final-state potentials. Numerical values of the transition amplitudes and the cross-section parameters for the electric dipole transition are calculated for laboratory energies of the n-p-system E of 10 MeV to 300 MeV. The results corresponding to the exact matrix elements of the operator $-e/\mu c\ A \cdot p$, as well as their long-wavelength approximations, differ by a noticeable amount from the customary non-retarded results. One can conclude from the present and some earlier calculations, that the retardation problem cannot be solved without satisfactory knowledge of the internucleon currents. (auth) (Finland)

20255 PION CAPTURE IN ^{4}He. Ziock, K. O. H. (CERN, Geneva); Cernigoi, C.; Gorini, G. Phys. Lett.; 33B: 471-3(7 Dec 1970).

Spectra have been measured of protons, deuterons, and tritons emitted following the capture of negative pions in ^{4}He. The proton spectrum agrees with existing calculations but the deuteron spectrum does not. (auth)

20256 ^{3}He–^{3}H CHARGE FORM FACTOR AND THE ^{3}He COULOMB ENERGY. Friar, J. L. (Univ. of Washington, Seattle). Nucl. Phys.; A156: 43-52(1970).

A formula for the Coulomb energy difference of ^{3}He and ^{3}H is derived on the assumption that the trinucleon S-state wave function and the symmetric part of the S′- and D-state wave functions can be represented as a linear superposition of Gaussians. The formula contains only experimentally measured quantities, since the nuclear physics can be parameterized directly in terms of the observed ^{3}He and ^{3}H charge form factors. The effect of two-body correlations is also discussed. The result for the Coulomb energy difference is 0.64 ± 0.01 MeV. (auth)

20257 NEUTRON–PROTON BREMSSTRAHLUNG AT 14.4 MeV. Furic, M.; Valkovic, V.; Miljanic, D.; Tomas, P.; Antolkovic, B. (Inst. Ruder Boskovic, Zagreb). Nucl. Phys.; A156: 105-12(1970).

A kinematically complete experiment on the neutron-proton bremsstrahlung at a neutron energy of 14.4 MeV was performed. Protons and neutrons were detected on opposite sides of the neutron beam. Protons were identified and their energy measured. The associated particle method and the neutron-proton time-of-flight difference were used to reduce the background. An upper limit of 400 $\mu b \cdot sr^{-2}$ was found for the neutron-proton bremsstrahlung differential cross section at the detector setting $\theta_p = \theta_n = 30°$. (auth)

20258 THE INTERACTION OF HIGH ENERGY NEUTRONS WITH HYDROGEN NUCLEI. A HIGH PRECISION MEASUREMENT OF THE NEUTRON–PROTON CROSS SECTION IN THE ENERGY RANGE 500 keV TO 21 MeV. Clements, P. J. Oxford; Oxford Univ. (1970). 145p.

Thesis.

The neutron-proton total cross section was measured over a continuous energy range between 500 keV and 21 MeV. The results were combined into seventeen contiguous energy groups, the weighted mean cross section in each group varying in accuracy from .2% at 1 MeV to 3% at 20 MeV. The experiment was performed using the neutron time-of-flight spectrometer on the Harwell 2.8 m synchrocyclotron, the neutrons being produced in an evaporation spectrum by the deflection of the 140 MeV internal proton beam onto a tungsten target. Cross section values were derived from the ratios of transmission of pairs of samples containing the same amount of carbon, the samples used being toluene (C_7H_8), 2-2-4 trimethylpentane (C_8H_{18}) and reactor grade graphite. Below 7 MeV the n-p total cross section can be accurately represented by a six parameter effective range expansion. Five of the parameters can be calculated from the results of other experiments, but the remaining parameter, the singlet effective range r_0, must be inferred from the results of p-p scattering experiments by assuming the validity of the hypothesis of charge independence. This inferred value of r_{0_s} can be compared with the value derived from high precision n-p total cross section measurements to provide a test of charge independence. The results of the most recent set of n-p total cross sections measurements

XUM

by Engelke et al.(Phys. Rev. 129.324.1963) and Lebowitz (thesis 1965) lead to a value r_{0_s} = 2.72 ± .06 ± .07 F, where the first error is due to the uncertainties in the cross section measurements and the second is due to uncertainties in the other effective range parameters. This result is in agreement with the charge independence prediction but in disagreement with the results of earlier measurements, which when grouped together lead to a value r_{0_s} = 2.99 ± .09 ± .06 F. The results of the present experiment lead to a value r_{0_s} = 2.59 ± .09 ± .05 F, in agreement with the results of Engelke et al and Lebowitz and the charge independent prediction, but in disagreement with the results of earlier measurements. It has recently been suggested (Hrehuss, G. Y.; Czibok, T. Phys. Lett. 28: B 585(1969)) that the n-p total cross section between ~400 keV and ~10 MeV does not vary monotonically with energy, but exhibits fluctuations of up to ~70 mb about a smooth curve. The results of the present measurement show no evidence for any such fluctuation of magnitude greater than the ~6 mb allowed by the statistical uncertainties on the cross section values. The n-p total cross section is widely used as a standard in neutron flux measurements. The results of the present cross section measurement, taken together with the most reliable earlier data, allow calculation of the total cross section with an uncertainty of ±.2% in the energy range of 100 eV to 7 MeV and ±.3% in the range 14 MeV to 30 MeV. The uncertainty is rather higher between 7 MeV and 14 MeV where no accurate measurements exist to check the calculations. (UK)

20259 TRITON BINDING ENERGY CALCULATIONS IN A HARMONIC OSCILLATOR BASIS. **Jackson, A. D. (State Univ. of New York, Stony Brook. Univ. of California, Berkeley); Lande, A.; Sauer, P. U. Nucl. Phys.; A156: 1-9(1970).**

The triton binding energy is calculated in a harmonic oscillator basis using a single term separable potential and the Reid soft-core potential. (auth)

20260 COMPARISON OF p−p AND n−p QUASI-FREE SCATTERING IN p + d → p + p + n REACTION. Valkovic, V.; Rendic, D.; Otte, V. A.; Phillips, G. C. (Rice Univ., Houston, Tex.). Phys. Rev. Lett.; 26: 394-6(15 Feb 1971).

Proton−proton and proton−neutron quasi-elastic scattering-process contributions were measured simultaneously at a proton energy of 12 MeV with $\theta_{1p} = -30°$, $\theta_{2p} = \theta_n = 30°$. The ratio of the peak cross section $(\sigma_{np}/\sigma_{pp})_{exp}$ was found to be 2.0 ± 0.2, while the simple impulse approximation predicts $(\sigma_{np}/\sigma_{pp})_{imp}$ =1.3. No Coulomb effects were found to be significant. (auth)

20261 NUCLEON ELASTIC SCATTERING BY ^{4}He WITH NONLOCAL SEPARABLE POTENTIALS. Barguil, J.; Pigeon, J.; Fayard, C.; Lamot, G.-H.; El Baz, E. (Univ., Lyon). Nuovo Cim.; 1A: 285-92(21 Jan 1971).

Neutron or proton elastic scattering by ^{4}He below 22 MeV is studied with the use of a one-term nonlocal separable potential. The theoretical phase shifts obtained are in very good agreement with the experimental data. The nuclear potential, chosen identical for the neutron and for the proton, gives nearly identical parameters. (auth)

20262 LIGHT-NUCLEI INTERACTIONS WITH A POLARIZED ^{3}He TARGET. Hardy, Donald McCoy. Houston, Tex.; Rice Univ. (1970). 127p. University Microfilms Order No. 70-23,519. Thesis.

The asymmetries in the scattering of ^{4}He particles from ^{3}He particles were measured at 79.3°c.m. and 114.0°c.m. in the energy range 7.5 to 18.0 MeV. A phase shift analysis of ^{4}He−^{3}He scattering incorporating the presently available polarization data was performed for ^{3}He laboratory beam energies ranging from 5.7 to 13.5 MeV. Data for the scattering of ^{3}He from polarized ^{3}He at 66.0°c.m. in the energy range 9.3 to 17.5 MeV are also reported. Asymmetries in the elastic scattering of deuterons from polarized ^{3}He at five center of mass scattering angles in the energy range 4.8 to 11.9 MeV were also measured, as well as the proton asymmetries at two laboratory angles for the ^{3}He(d,p)^{4}He reaction conducted with a polarized ^{3}He target. Comparisons are made of the existing polarization data for d- ^{3}He elastic scattering and for the ^{3}He(d,p)^{4}He reaction. (Diss. Abstr. Int., B)

20263 THE SCATTERING AND BREAKUP OF VECTOR POLARIZED DEUTERONS ON HELIUM. Keller, Leon Gregory. Madison, Wis.; Univ. of Wisconsin (1970). 133p. University Microfilms Order No. 70-8300. Thesis.

Vector polarized deuterons from a tandem accelerator were used to measure the vector analyzing power in the elastic scattering of deuterons from ^{4}He. Data were taken at nine deuteron energies from 3 to 11 MeV, in steps of 1 MeV, for center-of-mass angles between 22 and 152°. Prominent peaks in the angular distributions were seen at all energies and an increase in the complexity of the angular distributions was observed with increasing deuteron energy. The vector polarization data at 90° in the center-of-mass provide unambiguous evidence against p-wave resonances below 11 MeV. A phase shift analysis was carried out at each energy where measurements were made. It was found that particle waves up to f-waves were required to reproduce the data above 8 MeV. Only the two well known d-wave resonances were seen. The p-wave phase shifts were found to be small. The asymmetry of protons from the breakup of the polarized deuterons was measured at 8.5, 10, and 11 MeV deuteron energy for laboratory angles between 17.8 and 88.2°. Large asymmetries were seen for protons in the peak at the high energy end of the spectrum. This peak is usually interpreted as evidence for a final state interaction in the n-^{4}He system, corresponding to the ^{5}He resonance seen in n-^{4}He scattering at 0.96 MeV in the center-of-mass. A modified distorted wave calculation was carried out at 10 MeV deuteron energy under the assumption that a (d,p) stripping mechanism is primarily responsible for the high energy peak. The calculation provides a qualitative fit to the data but detailed agreement is lacking. (Diss. Abstr. Int., B)

20264 IZOTOPY: SPRAVOCHNYE TABLITSY. TOM I V II. (Isotopes: Reference Tables. Volumes I and II). Selinov, I. P. Moscow; Izdatel'stvo Nauka (1970). 1241p.

The three volumes of Isotopes cover the data on the basic properties of stable and radioactive isotopes from Z = 1 to 105. The tabulated data include the symbols of all isotopes and isomers with half life of T ≥ 1mc, types of conversions, nuclear moments, half lives, α- and β-particle energy, γ-ray energy, and nuclear reactions producing isotopes. The first volume deals with the reference tables for isotopes Z = 1 to 62, the second volume includes isotopes Z = 62 to 105 and the third volume enumerates the list of references. (R.V.J.)

Nuclear Properties and Reactions, 6≤A≤19

Refer also to abstracts 18718, 18750, 20264, 20309, 20337, 20838, 20353, 20368, 20372, 20445, 20447, 20448, 20450, 20494, 20497, 20505, 20512, 20522, and 20530.

20265 (CEA-R-4117) STUDY OF REACTIONS ^{9}Be + t BELOW THE COULOMB BARRIER. Ulpat, Jean-Pierre; Pornet, Jacqueline; Bertrand, Francoise (Commissariat a l'Energie Atomique, Limeil-Brevannes (France). Centre d'Etudes). Jan 1971. 25p. (In French). Dep. NTIS (U. S, Sales Only).

Angular distributions and absolute cross sections were measured for the reactions ^{9}Be(t,α_0)^{8}Li and ^{9}Be(t,α_1)^{8}Li* using several values of triton energy in the 0.3 to 1 MeV range. A single nuclear transfer mechanism was assumed, and the D.W.B.A. code Julie fit the data. (France)

20266 (DEMO-70/25) ESTIMATE OF THE BINDING ENERGY OF ^{16}O WITH MATRIX ELEMENTS OF EFFECTIVE INTERACTION. Grypeos, M. E. (Democritus Nuclear Research Center, Athens (Greece)). Dec 1970. 12p. Dep. NTIS (U. S. Sales Only).

An estimate of the binding energy of ^{16}O nucleus is given using matrix elements of effective interaction determined by means of a variational method with a "healing condition". A "minimum condition" is also derived for these matrix elements. (auth)

20267 (EUR-4538) MEASUREMENTS OF NEUTRON ELASTIC SCATTERING FROM CARBON IN THE ENERGY REGION OF 0.50 TO 2.00 MeV. Ahmed, N.; Coppola, M.; Knitter, H.-H. (European Atomic Energy Community, Geel (Belgium). Central Nuclear Measurements Bureau). 1970. 32p. Dep. NTIS (U. S. Sales Only). EUR FF 5.60.

Differential cross sections for the elastic scattering of neutrons from carbon were measured at primary energies between 0.50 and 2.00 MeV in steps of 50 keV. The experimental cross sections were fitted with a five term Legendre polynomial expansion. The obtained B_L-coefficients were then fitted with suited functions of the energy in order to obtain a smooth dependence of the differential cross sections on the primary neutron energy, using a limited number of parameters. A set of recommended differential elastic cross section curves, based on the present measurements, is given. Integrated elastic cross sections were derived from the fitted B_0-coefficients and are compared with earlier results of other workers. 18 references. (auth)

20268 (JINR-P4-5479) SPACE DISTRIBUTION OF THE α-CLUSTERS IN THE LIGHT NUCLEI. Abdinov, O. B.; Barashenkov, V. S. (Joint Inst. for Nuclear Research, Dubna (USSR). Lab. of Theoretical Physics). 1970. 8p. (In Russian). Dep. NTIS (U. S. Sales Only).

Those characteristics of particles (produced in high-energy interactions of protons with carbon nuclei) that are the most sensitive to the form of the space distribution of α clusters are studied in the framework of the intranuclear cascade model. The angular distribution of the resulting α particles is one of those features which depends weakly on other cascade-model parameters. The analysis of experimental data obtained at 660 MeV shows that the model with peripheral distribution is the most preferable; however, more accurate measurements must be performed to draw more detailed conclusions on this point. (auth)

20269 (N–70–37365) TESTS OF EVALUATED BERYLLIUM (n,2n) CROSS SECTIONS BY ANALYSIS OF 1.4-eV FLUX IN WATER FOR AN AMERICIUM–BERYLLIUM SOURCE ENCLOSED IN BERYLLIUM SPHERES. Fieno, Daniel; Alexander, Roger L.; Ford, C. Hubbard (National Aeronautics and Space Administration, Cleveland, Ohio. Lewis Research Center). Sep 1970. 40p. (NASA-TN-D–5995; E–5444). NTIS.

Measurements in water of the neutron flux distributions at indium resonance energy, with Be shells enclosing an Am–Be neutron source, were made to test quantitatively two evaluated sets of (n,2n) cross sections for ^{9}Be. Transport-theory calculations of the experimental flux distributions were made using cross sections from these two evaluations of the decay modes of the ^{9}Be(n,2n) reaction. The first evaluation is based on the cross-section program GAM-II in which the data files are based on the same cross-section evaluation employed for the current ENDF/B library for Be. The second evaluation is based on Perkins' detailed studies of the reactions that contribute to the Be(n,2n) cross section. Calculations using GAM-II data were in poor agreement with the present experiments, whereas calculations using Perkins' data were in good agreement. (auth) (STAR)

20270 (NP–18626) STUDY OF THE DECAY OF THE 16.11-MeV LEVEL OF ^{12}C INTO 3 α PARTICLES. Kong-A-Siou, Dy-Holm (Grenoble Univ. (France)). 1970. 83p. (In French). Dep. NTIS (U. S. Sales Only).

Thesis.

Accurate measurements were made on the disintegration spectra of the ^{12}C nucleus into 3 α particles. In order to suppress normalization problems, three parametric spectra were simultaneously measured. The coincidence methods were used. The use of an IBM 360–50 disc memory allowed the results obtained to be treated under the best conditions. In the analysis of the experimental results, maximum use was made of the known experimental data (partial disintegration widths, ($\alpha-\alpha$) scattering phase shifts); and a minimum number of parameters was introduced. In general, the form of the experimental spectra was good for the angular momentum $l = 2$ relative to the $\alpha-{}^{8}$Be channel. The variation in the population of the Dalitz domain, closely linked to the entry channel, is compatible with a significant contribution of the $S = 1$ spin channel of the entry channel. However, the contribution of the $S = 2$ spin channel is not zero—(channel $S = 1$)/(channel $S = 2$) = 5. The sequential reaction hypothesis (a single interaction in the final state) led to a satisfactory interpretation of the experimental results. The fact that the results were analyzed without introducing either direct production or backscattering indicates that such mechanisms are negligible for the 16.11-MeV level of ^{12}C. (France)

20271 (NP–18628) THE STUDY OF THE (2p–1h) COMPONENTS OF THE EXCITED STATES OF ^{17}O AND ^{29}Si BY DOUBLE STRIPPING REACTIONS. Lemaire, Marie-Claude (Lyon Univ. (France)). 1970. 108p. (In French). Dep. NTIS (U. S. Sales Only).

Thesis.

Proton double-stripping reactions at 18 MeV (He-3, proton) with ^{15}N and ^{27}Al were studied experimentally in order to investigate the population of ^{17}O and ^{29}Si levels. The principles and the techniques used in DWBA cross-section calculations for two-nucleon transfer reactions were recalled; the methods behind the choice of optical parameters were indicated. The experimental results and the spectroscopic information that may be deduced from the DWBA analysis of the angular distributions were presented. The selectivity of these two stripping reactions experimentally demonstrates the intensity of the (2p–1h) force in the wave functions of the different excited levels of ^{17}O and ^{29}Si. (France)

20272 NEUTRON POLARIZATION FOR (d,n) REACTIONS IN THE 1p SHELL. Meier, Michael McDaniel. Durham, N. C.; Duke Univ. (1969). 180p. University Microfilms Order No. 70-20,277.

Thesis.

Neutron polarization data for eleven (d,n) reactions, each involving the transfer of an $l = 1$ proton, were obtained in the bombarding energy range 2.8 to 4.0 MeV for the target nuclei ^{10}B, ^{11}B, ^{13}C, ^{14}N and ^{15}N. Also, an earlier measurement by Sawers (1966) of the ^{12}C(d,n$_0$) reaction over this energy range was extended down to 1.80 MeV. Most of the polarization distributions obtained have qualitative features which do not change appreciably as a function of bombarding energy, implying the dominance of a direct mechanism for these transitions. Also, similarities in the polarization patterns of some of the $j = \frac{1}{2}$ transitions were observed. The ^{14}N(d,n$_0$) reaction is chosen as a subject for analysis, and deuteron optical model wavefunctions for a DWBA analysis are generated by an extensive analysis of existing elastic scattering data for ^{14}N(d,d). An automatic search program, which corrects the experimental cross section for average compound elastic effects is described. This code was used to extract numerous sets of optical model parameters. Subsequent DWBA calculations show that the parameter sets may be classified into several families, each family being comprised of a number of parameter sets which give rise to similar DWBA predictions. One of these families, corresponding to an optical potential with $V_0 \sim 100$ MeV, $r_0 \sim 1.6$ fm, when used for DWBA calculations, predicts polarization which is in reasonable agreement with experiment. Spectroscopic factors derived from calculations using sets from this family are in reasonable agreement with theoretical values. A study of calculational sensitivities of the DWBA cross section and polarization to variations of other parameters provides a critique of the assumptions involved in the calculations as well as some insight into the features observed in several of the other (d,n) reactions. The sign of the polarization at forward angles is not consistently j-dependent. This point seems to be partially explained by the fact that an extremely diverse set of Q-values (–0.2 to 13 MeV) is sampled in this data. The j-dependence of the polarization at forward angles was seen in the experiment and the calculations to be somewhat ambiguous. Experimentally, five of six $j = \frac{1}{2}$ transfers are observed to have large negative polarizations at forward angles. The sixth, a reaction with a very high Q-value (13.73 MeV) exhibits a polarization with the opposite sign. Such an effect is suggested in the DWBA calculations. (Diss. Abstr. Int., B)

20273 ^{7}Li(^{3}He,d)^{8}Be AND ^{7}Li(^{3}He,p)^{9}Be REACTIONS. Dixon, R. L.; Edge, R. D. (Univ. of South Carolina, Columbia). Nucl. Phys.; A156: 33-42(1970).

Angular distributions for the reaction ^{7}Li(^{3}He,d) to the ^{8}Be ground state and first excited state (2.90 MeV) were measured at 10 MeV, and distorted wave stripping calculations were made. Spectroscopic factors were deduced and are in fair agreement with those obtained from the effective-interaction calculations of Cohen and Kurath. Angular distributions for the reaction ^{7}Li(^{3}He,p) to the ground and first three excited states of ^{9}Be(1.67, 2.43, and 3.03 MeV) were measured at 10 MeV. DWBA double-stripping calculations do not predict the observed angular distributions. (auth)

20274 ANALYSIS OF INELASTIC SCATTERING OF ALPHA PARTICLES IN REGION Z = 12 TO 40. Gonchar, V. Yu.; Zheltonog, K. S.; Yushkov, A. V. Izv. Akad. Nauk Kaz. SSR, Ser. Fiz.-Mat.; No. 6, 3-19(Nov–Dec 1969). (In Russian).

A systematic analysis of experimental data on inelastic scattering of medium-energy alpha particles is performed from the diffraction point of view. Excitation of 2^+ and 3^- levels for nickel-58 and for 45 other nuclei in the A = 7 to 140 region for alpha energies of 21 to 100 MeV was studied. Parameters of the APB model were found. The existence of collective effects was considered in the analysis. (auth) (TSS)

20275 SEQUENTIAL REACTION ^{11}B(p,α)2α. Goulard, G. (Univ. of Laval, Quebec). Can. J. Phys.; 48: 2341-56(15 Oct 1970). (In French).

An extensive study is made of the formula derived for the differential cross section of a sequential reaction $A + B \rightarrow C^* \rightarrow D + G^* \rightarrow D + E + F$. Numerical results are obtained for incident energies of 163 keV, 680 keV, 2 MeV, 2.65 MeV and compared with different experimental data. (auth) (Canada)

20276 PHOTONEUTRONS FROM ^{13}C AT PHOTON ENERGIES UP TO 14 MeV. Fukuda, K. (Radiation Center of Osaka Prefecture, Sakai, Japan). Nucl. Phys.; A156: 10-18(1970).

The photoneutron yield of ^{13}C was measured as a function of the maximum bremsstrahlung energy up to 14.5 MeV. The cross section for the ^{13}C(γ,n)^{12}C reaction was obtained by using the inverted matrix method of Penfold and Leiss. The integrated cross sections from threshold to 10 MeV and to 14 MeV are 2 and 16 MeV · mb, respectively. These values are in agreement with earlier experiments. The cross-section curve shows peaks at 6.2, 7.5, 8.2, 9.1, 11 and 13 MeV, the last two being in the pygmy resonance energy region. The angular distributions of photoneutrons were measured at different values of $E_{\gamma max}$. The data were analyzed for the distribution of neutrons from each peak. The significant features of the cross-section curve and the angular distributions of neutrons from the peaks are discussed and compared

XUM

with the theoretical ones reported by several authors. The integrated cross section from the threshold to 10 MeV is much smaller than those calculated on the basis of a pure single-particle model. The neutrons in the pygmy resonance energy region follow a $1 + 0.46 \sin^2 \theta$ angular distribution, while a $1 + 1.5 \sin^2 \theta$ distribution is expected from the single-particle picture of the pygmy resonance. These discrepancies are interpreted in terms of the mixing of core excitations and single-particle excitations. (auth)

20277 GIANT DIPOLE RESONANCES IN ^{11}C AND ^{15}O OBSERVED WITH THE REACTIONS $^{10}B(p,\gamma)^{11}C$ AND $^{14}N(p,\gamma)^{15}O$. Kuan, H. M.; Hasinoff, M.; O'Connell, W. J.; Hanna, S. S. (Stanford Univ., Calif.). Nucl. Phys.; A151: 129-53(1970).

The giant dipole resonances in ^{11}C and ^{15}O were studied with the capture reactions $^{10}B(p,\gamma_0)^{11}C$ ($E_p = 2.6 - 17.0$ MeV) and $^{14}N(p,\gamma_0)^{15}O$ ($E_p = 2.2 - 19.0$ MeV). Some similarity is observed between the giant dipole resonances in ^{11}C and ^{12}C and between those in ^{15}O and ^{16}O. The average (γ,p_0) cross sections for ^{11}C and ^{15}O are smaller by a factor of about 3 than those for ^{12}C and ^{16}O. However, the dipole strength is more spread out in ^{11}C and ^{15}O than in ^{12}C and ^{16}O. A comparison of results from $^{15}N(\gamma,p_0)^{14}C$ and $^{15}O(\gamma,p_0)^{14}N$ suggests the contribution of $T = 3/2$ states in the former reaction but not in the latter. The yields of the reactions $^{10}B(p,\gamma_1)^{11}C^*$ and $^{14}N(p,\gamma_1 + \gamma_2)^{15}O^*$ are relatively weak and only estimates of their upper limits are obtained. For the sharp, low-lying resonances at $E_p = 2.35$ and 2.48 MeV in $^{14}N(p,\gamma_0)^{15}O$ previous assignments of $5/2^-$ and $3/2^-$ are confirmed. For the resonance at $E_p = 4.20$ MeV $3/2^+$ is obtained. (auth)

20278 OPTICAL-MODEL ANALYSIS OF ELASTIC τ SCATTERING ON THE NUCLEI WITH A = 15 TO 18 AT 11 MeV. Bohne, W.; Homeyer, H.; Lettau, H.; Morgenstern, H.; Scheer, J. (Hahn-Meitner Institut fuer Kernforschung, Berlin). Nucl. Phys.; A156: 93-6(1970).

Differential cross sections for the scattering of τ-particles on ^{15}N, ^{16}O, ^{17}O, ^{18}O are measured at 11 MeV and analyzed in terms of the optical model. The potential parameters arrived at show systematic trends as a function of the nuclear mass, with the exception of ^{16}O where anomalies are observed. (auth)

20279 STUDIES OF SOME SUB-COULOMB DEUTERON-INDUCED REACTIONS ON ^{13}C AND ^{12}C. **Putt, Graeme D. (Univ. of Melbourne. Univ. of British Columbia, Vancouver). Nucl. Phys.;** A161: **547-64(1971).**

Isotopically enriched ^{13}C targets were bombarded with deuterons of energy 0.4 to 0.85 MeV. Differential cross sections were measured for the $^{13}C(d,p_0)$, (d,t_0), (d,α_0), and (d,α_1) reactions in the form of an excitation function at 90° (lab) and angular distributions at bombarding energies of 0.41, 0.51, 0.61, 0.71, and 0.81 MeV. They were also measured for the $^{12}C(d,p_0)$ reaction at 0.41 and 0.51 MeV. These data were compared with the predictions of single and two-nucleon transfer DWBA calculations and Hauser–Feshbach statistical theory calculations. The (d,p) reactions can be described by the deuteron stripping mechanism but the (d,α) reactions proceed almost exclusively through broad overlapping levels of the compound nucleus. The (d,t) reaction appears to be an interference mixture of both these processes. (auth)

20280 IS THE GROUND STATE ROTATIONAL BAND CUT OFF IN ^8Be? Bouten, M.; Bouten, M. C.; Depuydt, H.; Schotsmans, L. (SCK/CEN, Mol, Belg.). Phys. Lett.; 33B: 457-9 (7 Dec 1970).

A PHF calculation has been carried out for the ground-state rotational band in ^8Be. The results indicate that the band has no cut-off at L = 4 in the SU_3 model but continues to higher values of L. (auth)

20281 ANGULAR CORRELATIONS IN INELASTIC NEUTRON SCATTERING BY CARBON AT 15.0 MeV. **Spaargaren, D.; Jonker, C. C. (Vrije Univ., Amsterdam). Nucl. Phys.; A161: 354-74(1971).**

The $^{12}C(n,n'\gamma)^{12}C$ reaction was studied at 15.0 MeV. Absolute neutron-gamma angular correlation data were taken with the γ detector in the reaction plane and perpendicular to that plane. The neutron spin-flip probabilities were determined. Differential elastic and inelastic neutron scattering cross sections and the differential cross section of the 4.44 MeV deexcitation γ rays were obtained simultaneously during the angular correlation experiment. The results are compared with other experimental determinations and theoretical predictions. No significant differences between neutron and proton scattering were found. (auth)

20282 CALCULATIONS FOR STRIPPING ON DOUBLY MAGIC NUCLEI. King, K.; McKellar, B. H. J. (Univ. of Sydney). Aust. J. Phys.; 23: 453-63(Aug 1970).

The (d,p) reactions leading to the $d_{5/2}$ ground states of ^{17}O, ^{89}Sr, and ^{91}Zr were analyzed using the BHMM theory of deuteron stripping. Average parameters were used for the scattered neutron wavefunction while proton parameters were derived from optical model analyses of elastic scattering data at appropriate energies. The agreement with experiment is good when incident deuteron energies are above the Coulomb barrier. The spectroscopic factors relating to the final states $^{17}O(1d_{5/2})$, $^{89}Sr(2d_{5/2})$, and $^{91}Zr(2d_{5/2})$ were found to be 0.45, 0.70, and 0.65 respectively, with an uncertainty of ±0.10. (auth) (Australia)

20283 CROSS SECTIONS OF CHARGED PARTICLE REACTIONS YIELDING POSITRON UNSTABLE RADIOISOTOPES. Roughton, Norbert Allen. St. Louis; St. Louis Univ. (1969). 102p. University Microfilms Order No. 70-20,423.

Thesis.

The measurement of activation cross sections for nuclear reactions involving charged particles is a long neglected field of activity. Until very recently, these measurements were not considered of sufficient interest or pertinence to the understanding of nuclear processes to warrant detailed study. Presently, however, the need for such measurements has increased considerably because of the importance of these reactions in the evolution of stars and consequent nucleosynthesis of the elements. In addition, the rate of energy generation in thermonuclear reactions depends ultimately on the cross-sections for reactions between various nuclear species. The number of possible reactions which participate in the above processes is very large and the number of cross-sections measured to date is very small, due mostly to lack of sufficient experimental technique to permit rapid accumulation of large amounts of cross-section data. A method is discussed for the measurement of cross-sections for a particular class of reaction: those which yield positron unstable radioisotopes. The number of such reactions out of all the possibilities available in stellar interiors is considerable. A technique for the measurement of these cross sections using the annihilation of the positron as a reaction signature is evolved and presented. The technique is novel in that measurements can be performed during accelerator bombardment; hitherto this was prohibited due to strong radiation environments in the vicinity of the target. Thus measurements of cross sections were usually limited to those reactions producing long half-lived radioisotopes, whereas many such isotopes have very short half-lives. The technique evolved here is thus particularly important in the study of reactions leading to the latter type of radioproduct. The measurements performed here involve the detection of positron annihilation γ-rays in fast time coincidence, and are demonstrated by measuring the cross sections for the following reactions: $^{12}C(d,n)^{13}N$, $^{24}Mg(d,n)^{25}Al$, $^{32}S(d,n)^{33}Cl$, and $^{32}S(d,\alpha)^{30}P$. The variation of cross-section with energy is measured over the incident deuteron energy range of about 2–3.2 MeV, using the SLU cyclotron as a deuteron accelerator. In addition, the calculation of a reaction rate under stellar conditions using one of the measured cross-sections is demonstrated. (Diss. Abstr. Int., B)

20284 FORMATION OF THE $^6Li_{gs}$ AND THE ^6Li, 3.56 MeV, T = 1 STATE IN THE $^{19}F(^3He,^6Li)^{16}O_{gs}$ REACTION. Klages, W. J.; Duhm, H. H.; Yoshida, H.; Schumacher, P. E.; Detraz, C. (Max-Planck-Institut fuer Kernphysik, Heidelberg). Nucl. Phys.; A156: 65-73(1970).

The $^{19}F(^3He,^6Li)^{16}O_{gs}$ angular distributions were measured for ^6Li, 1^+, T = 0 ground state and the ^6Li, 0^+, T = 1, 3.56 MeV level at $E_{^3He} = 28$ MeV. The angular distributions show pronounced diffraction patterns which are reasonably fitted by zero and finite-range DWBA calculations. The intensity ratio for both states in ^6Li is very close to the expected value for coupling a ^3He and a triton cluster to either a singlet or a triplet state. The absolute magnitudes of the $(^3He,^6Li)$ cross sections may be understood in terms of separating the shell-model configuration s^4p^2 into $(s^3 + sp^2)$. (auth)

20285 ANGULAR DISTRIBUTION OF TRITONS FROM THE $^{11}B(n,t)^9Be$ REACTION AT 14.4 MeV. **Miljanic, D.; Valkovic, V.; Rendic, D.; Furic, M. (Inst. Ruder Boskovic, Zagreb). Nucl. Phys.; A156: 193-8(1970).**

The angular distribution of tritons from the (n,t) reaction on ^{11}B was measured at the neutron bombarding energy of 14.4 MeV. The results obtained were compared with the DWBA predictions. The shape of the (n,t) angular distribution is reasonably well reproduced by the DWBA calculations, while the absolute values are in disagreement. (auth)

20286 CONFIGURATION MIXING CALCULATIONS IN THE HARTREE–FOCK REPRESENTATION. **Kakkar, I.; Mehta, G. K.; Waghmare, Y. R. (Indian Inst. of Tech., Kanpur). Nucl. Phys.; A156: 199-211(1970).**

The results of shell-model calculations in the Hartree–Fock basis for the low-energy excited states of ^{18}O, ^{18}F and ^{10}Be nuclei are presented. The calculations were carried out using the effective Yale interaction of Shakin et al. and the Sussex interaction of Elliott et al. It was found that the calculated Hartree–Fock

XUM

spectra are compressed compared to the experimental spectra in all cases. It is also observed that in the restricted configuration space the Hartree–Fock and the harmonic oscillator wave functions give very similar results. (auth)

20287 POLARIZATION OF PROTONS FROM THE $^{12}C(d,p)^{13}C$ REACTION AT $E_d = 12.4$ MeV. Budzanowski, A.; Freindl, L.; Karcz, W.; Lazarska, B.; Zipper, W. (Inst. of Nuclear Physics, Krakow. Jagellonian Univ., Krakow. Silesian Univ., Katowice, Poland). Nucl. Phys.; A161: 610-20(1971).

The polarization of protons from the $^{12}C(d,p)^{13}C$ reaction at $E_d = 12.4$ MeV was measured for the ground state and first excited state transitions. The results obtained were compared with the vector analyzing power (VAP) data for the same reaction and at the same energy of the incident deuterons. An attempt to fit the polarization data with the DWBA theory is also presented. (auth)

20288 THE RATIO OF THE $^6Li(n,\alpha)$ TO $^{10}B(n,\alpha)$ CROSS-SECTIONS FROM 10 eV TO 80 keV AND RECOMMENDED VALUES OF THE $^{10}B(n,\alpha)$ CROSS-SECTION. Sowerby, M. G.; Patrick, B. H.; Uttley, C. A.; Diment, K. M. (Atomic Energy Research Establishment, Harwell, Eng.). J. Nucl. Energy; 24: 323-36(Oct 1970).

The ratio of the $^6Li(n,\alpha)$ to $^{10}B(n,\alpha)$ cross sections was measured in the energy range 10 eV – 80 keV using the Harwell linear accelerator time-of-flight spectrometer. By combining the ratio data with values of the $^6Li(n,\alpha)$ cross section deduced from an accurate total cross-section measurement, the $^{10}B(n,\alpha)$ cross section was obtained. This was compared with the cross section determined from recent measurements of the total and scattering cross sections of ^{10}B. All these data were fitted by an analytical expression, the form of which was derived from theoretical arguments, using a least squares fitting procedure and it was found that up to 200 keV, the $^{10}B(n,\alpha)$ cross section $\sigma_{n\alpha}(^{10}B)$ is given by $\sigma_{n\alpha}(^{10}B) = (13.837/\sqrt{E}) - 0.312 - 1.014 \times 10^{-2} \sqrt{E} + (2.809 \times 10^5)/(\sqrt{E}[(170.3 - E)^2 + 2.243 \times 10^4])$ barns where E is in keV. (auth) (UK)

20289 DISPUTED 2.86 MeV LEVEL OF ^{10}B. Srivastava, M. L.; Sah, J. P. (Lucknow Univ., India). Curr. Sci. (India); 39: 273-4(20 Jun 1970).

Neutrons from the reaction $^9Be(d,n)^{10}B$ were detected by nuclear emulsions at angles of 0, 90, and 150° to the deuteron beam. A 0.2 mg Be target was bombarded with 650-keV deuterons. Besides the ground state, levels were seen at excitations of 0.73, 1.76, 2.19, 2.85, and 3.69 MeV. The disputed state at 2.85 MeV was clearly resolved. (R.W.R.)

20290 CALCULATION OF NUCLEON–NUCLEUS SCATTERING PROCESSES. II. Weidenmueller, Hans A. (Institut fuer Theoretische Physik, Heidelberg). Comments Nucl. Particle Phys.; 4: 69-74(Mar-Apr 1970).

The shell-model approach is used to interpret the experimental results on compound nuclear resonances. A one-particle–one-hole model is used to discuss the compound nucleus ^{16}O. The cross section for the (γ,p) reaction is examined from 12 to 25 MeV. Although the shell-model approach leads to a semiquantitative understanding of the data, many questions remain open. (R.W.R.)

20291 SPINS AND PARITIES OF HIGHLY EXCITED STATES IN ^{24}Mg. Gobbi, A.; Maurenzig, P. R.; Chua, L.; (and others) (Yale Univ., New Haven). Phys. Rev. Lett.; 26: 396-9(15 Feb 1971).

From a study of the reaction $^{12}C(^{16}O,\alpha_1)^{24}Mg(\alpha_2)^{20}Ne$ spins and parities were measured for states in ^{24}Mg at the following excitation energies (in MeV): 12.10 (4^+), 12.45 (7^-), 13.07 (5^-), 14.41 (4^+), 16.07 (6^+), and 16.59 (6^+). Branching ratios were measured for several states in ^{24}Mg with $13 \le E_{exc} \le 23$ MeV decaying to the following states in ^{20}Ne: 0^+ (ground state), 2^+ (1.63 MeV), and 4^+ (4.25 MeV). These results permit the elimination of several postulated structures for the states in question. (auth)

20292 STATES IN ^{10}B FROM ELASTIC SCATTERING OF ALPHAS BY ^6Li. Balakrishnan, M.; Mehta, M. K.; Divatia, A. S. (Bhabha Atomic Research Centre, Bombay). Nuovo Cim.; 1A: 205-16(21 Jan 1971).

The elastic scattering of alpha particles from ^6Li was studied in the incident alpha energy range between 3.30 and 5.00 MeV. A shape analysis of the resonance structures near 3.502 and 4.250 MeV (alpha energies) leads to the assignments $J^\pi = 2^-$ or 4^- and $J^\pi = 2^+$, respectively, for the levels in ^{10}B at 6.56 and 7.01 MeV. The total widths of these two levels are found to be (26 ± 3) keV and (110 ± 15) keV, respectively, in the center-of-mass system. (auth)

20293 TENSOR POLARIZATION AND DIFFERENTIAL CROSS SECTION FOR THE $^9Be(d,d)^9Be$ ELASTIC SCATTERING AT LOW ENERGIES. Djaloeis, A.; Cords, H.; Nurzynaski, J. (Australian National Univ., Canberra). Nucl. Phys.; A163: 131-44(1971).

Spin tensor moments $\langle T_{20}\rangle$, $\langle T_{21}\rangle$, $\langle T_{22}\rangle$ and the absolute differential cross sections for the $^9Be(d,d)^9Be$ elastic scattering measured at low deuteron energies are compared with the theoretical calculations based on the optical model containing spin-orbit and tensor T_R interactions. The Hauser–Feshbach statistical theory has been used to account for the compound nucleus processes. (auth)

20294 MAGNETIC MONOPOLE TRANSITIONS IN ELECTRON SCATTERING. Borie, E.; Drechsel, Dieter (Univ., Frankfurt am Main). Phys. Rev. Lett.; 26: 195-7(25 Jan 1971).

The electroexcitation cross section for the second-order magnetic monopole transition $0^+ \rightarrow 0^-$ is calculated for ^{16}O. It is assumed that the spectrum of intermediate excited states is complete and that energy loss may be neglected. If these approximations are valid, it should be possible to observe this transition. (auth)

20295 EFFECT OF INTERMEDIATE COUPLING IN PHOTO- AND ELECTROEXCITATION OF ^{12}C NUCLEUS. Goncharova, N. G.; Yudin, N. P. (Inst. of Nuclear Physics, Moscow). Yadern. Fiz.; 12: 725-31(Oct 1970). (In Russian).

The levels $J = 1^-, 2^-, 3^-$, and $T = 1$ of the ^{12}C nucleus are calculated in the intermediate-coupling approximation. The photo- and electroexcitation of the nucleus are discussed. (auth)

20296 FORM FACTORS AND FINE STRUCTURE OF THE GIANT RESONANCE IN ^{12}C NUCLEUS. Gul'karov, I. S. (Tashkent Polytechnic Inst.). Yadern. Fiz.; 12: 694-9(Oct 1970). (In Russian).

Form factors and fine structure of the giant resonance in the ^{12}C nucleus, measured by means of inelastic electron scattering, are compared with the predictions of the Brown model and of the dynamical collective theory. There is a quantitative disagreement between the measured value of the form factor and the calculated value. As for the fine structure, the calculations in framework of the dynamical collective model are in better agreement with the experiment than the calculations based on the shell model. It thus appears that a theoretical account of coupling of the giant dipole resonance with quadrupole vibrations of the nuclear surface is important. (auth)

20297 NEUTRON POLARIZATION IN THE REACTION $^{12}C(d,n)^{13}N$ AT $E_d = 6.4$ MeV. Babenko, N. P.; Domkin, V. D. Yadern. Fiz.; 12: 692-3(Oct 1970). (In Russian).

Neutron polarization in the reaction $^{12}C(d,n)^{13}N$ was measured for the ground state and for the first excited state of the ^{13}N nucleus at the deuteron energy $E_d = 6.4$ MeV. (auth)

20298 BINDING ENERGY OF LIGHT NUCLEI AND NUCLEON–NUCLEON POTENTIAL. Rybachenko, V. F.; Sadovoi, A. A. Yadern. Fiz.; 12: 710-16(Oct 1970). (In Russian).

Through the use of the K-harmonics method, an upper limit is found for the binding energy of a series of light nuclei (up to ^{40}Ca) for singlet and triplet even potentials V_{13} and V_{31} having a small repulsive core. The agreement of calculated values of energies and radii of the nuclei with the experimental values is considerably improved as compared with calculated values of these quantities for potentials without any core. The repulsive V_{33} potential acting in odd-l states improves the results obtained. (auth)

20299 SPIN DEPENDENCE IN THE REACTIONS $^{16}O(p,t)^{14}O$ AND $^{16}O(p,^3He)^{14}N$. Fleming, D. G.; Hardy, J. C.; Cerny, Joseph (Univ. of California, Berkeley). Nucl. Phys.; A162: 225-38 (1971).

The reactions $^{16}O(p,t)^{14}O$ and $^{16}O(p,^3He)^{14}N$ have been studied at 43.7 MeV and 54.1 MeV bombarding energies. Several recent J^π, T assignments have been confirmed, and a pair of states at 9.72 MeV in ^{14}O and 12.50 MeV in ^{14}N have been established as (2^+), T = 1 analogs. The relative spectroscopic strengths for the transfer reactions were compared with predictions from (1p) shell wave functions, and the necessity for a 70% reduction of the S = 1 transition intensity relative to that for S = 0 was indicated. This effect was related to the spin and isospin dependence of the interaction potential. (auth)

20300 THREE-ALPHA FINAL STATE INTERACTIONS WITH FADDEEV THEORY. McMahan, Clyde Alex. Houston, Tex.; Rice Univ. (1970). 90p. University Microfilms Order No. 70-23,555.

Thesis.

An exactly soluble model of the decay of a 2^+ particle into three identical strongly interacting 0^+ particles is used to investigate the reaction $^{11}B(p,\alpha)2\alpha$ at proton energy of 2.65 MeV with the parent particle being the 18.37 MeV state of ^{12}C. The strong final state interactions are described by equations of the Faddeev

XUM

type with separable two-body interactions to represent the ground and first excited states of ^{8}Be. It is necessary to use a mixed ^{12}C initial configuration to reproduce the experimentally observed interference effects. The fit to the data is improved by the approximate inclusion of the Coulomb phase shifts. The decay is primarily through the ground and first excited states of ^{8}Be with little evidence for direct three-body decay. (Diss. Abstr. Int., B)

20301 REACTION MECHANISM OF THE ^{16}O + d REACTIONS. Davison, N. E.; Dawson, W. K.; Roy, G.; McDonald, W. J. (Univ. of Alberta, Edmonton). Can. J. Phys.; 48: 2235-53(1 Oct 1970).

The reactions ^{16}O(d,d)^{16}O, ^{16}O(d,p)^{17}O, and ^{16}O(d,n)^{17}F were studied in the deuteron energy range 4.00–6.00 MeV in order to determine to what extent current theories can satisfactorily describe these reactions. It was found that the theoretical curves from both the optical and DWBA models fit the experimental data significantly better when the deuteron optical-model potentials were obtained using a spin-orbit potential in the analysis of the elastic scattering data. Spectroscopic factors obtained for the ground and first-excited states of ^{17}O and ^{17}F using the DWBA theory are in satisfactory agreement with theoretical predictions and with values obtained by previous workers. Small, but nonzero, spectroscopic factors were obtained for the states at 3.058 and 3.846 MeV excitation in ^{17}O using data measured in this work and in previous experiments. The sum of the calculated direct interaction and compound-nucleus cross sections is in good agreement with experimental data for all states studied, whether they were populated primarily by direct or compound-nucleus reactions. The calculated compound-nucleus lifetimes are also in agreement with values obtained for an analysis of the fluctuations in the yield curves. (auth) (Canada)

20302 EVALUATION PROCESS AND CORRECTIONS IN THE STUDY OF THE INTERNAL BREMSSTRAHLUNG SPECTRUM ACCOMPANYING THE POSITIVE BETA DECAY OF ^{11}C. Berenyi, D.; Scharbert, T.; Vatai, E. (Inst. of Nuclear Research, Debrecen, Hungary). Acta Phys. Acad. Sci. Hung.; 28: 337-56 (1970).

The evaluation and correction procedure for the differential internal bremsstrahlung (IB) spectrum (at 90° between the direction of the beta particle and IB gamma quantum) from the superallowed positron emitter ^{11}C (21 min) is described. First a short outline of the theory and the details of the actual experimental arrangement are given and also a comparison is drawn between the theory and the experiment. The whole procedure for the treatment of the experimental data is given and the following corrections are considered in detail: correction for the Compton distribution in the scintillation spectrum, that for the photopeak efficiency and the gamma absorption as well as for beta absorption and concidence efficiency and, finally, for the finite energy resolution of the gamma detector. A number of other corrections and disturbing effects have also been considered shortly. A discussion of the results and the possible errors concludes the article. (auth)

20303 SOME INITIAL AND FINAL REACTION MECHANISMS IN THE ^{10}B + ^{3}He SYSTEM AT 1.38 AND 1.60 MeV. Bennett, Gary Lee. Pullman, Wash.; Washington State Univ. (1970). 140p. University Microfilms Order No. 70-24,974.

Thesis.

Differential excitation functions at 145° laboratory angle were measured for the reactions ^{10}B(^{3}He,d)^{11}C(g.s.), ^{10}B(^{3}He,p) ^{12}C(16.106), ^{10}B(^{3}He,p) ^{12}C(15.109), ^{10}B(^{3}He,α) ^{9}B(2.330), and ^{10}B(^{3}He,α)^{9}B(g.s.) between 1.20 and 1.85 MeV bombarding energies. No sharp, well-defined resonant behavior was observed. Angular distributions of the reactions ^{10}B(^{3}He,d)^{11}C(g.s.), ^{10}B(^{3}He,p)^{12}C (16.106), and ^{10}B(^{3}He,p)^{12}C(15.109) were measured at a bombarding energy of 1.38 MeV which would correspond to formation of ^{13}N(22.7). The angular distributions for the two proton groups could be described in terms of a direct interaction and compound nucleus formation. The general shape of the angular distribution of the ground-state deuteron could also be described in this manner. It was not possible to assign the compound nucleus contribution to any known level in ^{13}N. Dual and triple coincidence spectra for the ^{10}B(^{3}He,p$\alpha\alpha\alpha$) reaction were measured at a bombarding energy of 1.60 MeV. A partial angular correlation function based on the dual coincidence data for ^{10}B(^{3}He,p)^{12}C(16.106)(α)^{8}Be(2.90) could be fitted with combined direct-interaction and compound-nucleus model. The 10 dual-coincidence spectra taken for the angular correlation measurement indicate that the interactions among the final-state systems modulate very strongly the distribution of events in the available phase space volume. The observed triple coincidence spectrum shows that ^{12}C(16.106) decays preferentially by a sequential process through ^{8}Be(g.s.) and ^{8}Be(2.90). This is consistent with a two-body cluster model description of ^{12}C(16,106). Simultaneous four-body breakup from ^{10}B + ^{3}He or simultaneous three-body breakup from ^{12}C(16.106) must contribute less than 15% of the triple coincidence events if they occur at all. (Diss. Abstr. Int., B)

20304 APPLICATION OF THE FULL SINGLE PAIR MODEL AND THE METHOD OF HARMONIC POLYNOMIALS TO THE STUDY OF CORE DISTORTION IN ^{6}Li. Richardson, Roger Hugh. New York; Fordham Univ. (1969). 113p. University Microfilms Order No. 70-11,449.

Thesis.

The Full Single Pair Model of Malik was applied to the study of core distortion in ^{6}Li. Careful consideration was given to treating the effects of the Pauli Exclusion Principle correctly. It was found that while the core distortion predicted by the model had little effect on either the energy or the magnetic dipole moment, a very significant contribution to the electric quadrupole moment was indicated. Numerical calculations were performed using potentials due to Volkov and Brink and Boeker. Auxiliary expressions for the contributions to all matrix elements from a tensor force were also obtained. A striking feature of the results was the very large contribution of the exchange integrals arising from the Exclusion Principle. In many cases, these contributions were found to dominate the matrix elements. In evaluating the matrix elements, a new procedure for handling harmonic oscillator shell model calculations was developed. This procedure, called the Method of Harmonic Polynomials, has the following features: 1) It provides the analog of the Moshinsky brackets for use with uncoupled product state wave functions. 2) It makes feasible the direct reduction of arbitrary matrix elements to Talmi integrals, for both central and tensor forces. Since no transformation brackets or auxiliary Racah coefficients are required, it seems practical to tabulate, once and for all the coefficients of the various Talmi integrals for both central and tensor forces, for all the matrix elements one might reasonably require. A representative table is given. Both of the above features may be generalized to the case in which the particles have different masses and move in different oscillator wells. (Diss. Abstr. Int., B)

20305 A STUDY OF THE VECTOR ANALYZING POWER IN DEUTERON STRIPPING REACTIONS ON ^{16}O, ^{52}Cr, ^{54}Fe, AND ^{90}Zr. Bjorkholm, Paul James. Madison, Wis.; Univ. of Wisconsin (1970). 152p. University Microfilms Order No. 70-8268.

Thesis.

Polarized deuterons were used to study deuteron stripping reactions and deuteron elastic scattering on targets of ^{16}O, ^{52}Cr, ^{54}Fe, and ^{90}Zr at laboratory angles between 15 and 150° for deuteron energies between 8 and 12 MeV. The azimuthal asymmetry of the outgoing particles was measured to determine the vector analyzing power of the reactions and scattering. The elastic scattering cross sections and vector analyzing powers were analyzed to obtain deuteron optical model potentials. These potentials were used for distorted wave Born approximation (DWBA) calculations of the cross section, vector analyzing power, and proton polarization of the (d,p) reactions. The calculations qualitatively reproduced the vector analyzing power in all cases except for ^{16}O(d,p) ^{17}O(E_x = 0.87 MeV). A comparison of the calculations and data was used to determine the total angular momentum (j) for states in the residual nuclei. All j-assignments are in agreement with previous assignments except for the assignment to the 3.80 MeV level in ^{55}Fe. This level is assigned $\frac{1}{2}^{-}$. Tentative assignments of $j = \frac{7}{2}^{+}$ were made to levels at E_x = 3.814 MeV in ^{55}Fe and E_x = 3.70 MeV in ^{53}Cr. The state at E_x = 2.21 MeV in ^{91}Zr was tentatively assigned $j = \frac{9}{2}^{+}$. These tentative assignments are contrary to shell model predictions. The DWBA calculations also reproduced the observed total angular momentum dependence of the $l = 1$ transitions and the polarization of the protons from the ^{52}Cr(d,p)^{53}Cr and ^{90}Zr(d,p)^{91}Zr reactions. (Diss. Abstr. Int., B)

20306 MO TRANSITIONS IN SPHERICAL NUCLEI. Bell, Donald A. Manhattan, Kan.; Univ. of Kansas (1969). 77p. University Microfilms Order No. 70-10,997.

Thesis.

For light even–even nuclei, $A < 40$, the 0^{-} to 0^{+} transition probability was calculated for the ($\gamma\gamma$), (γe), and (ee) processes. The assumption is made that the 0^{-} state decays through the giant dipole states. The resonance states were calculated according to Brown and Bolsterli particle-hole theory. This was done in both the Tamm–Dancoff (TD) approximation, and Random Phase approximation. In the TD approximation, various potentials were used to calculate the energy levels and eigenvectors to determine the potential dependence in the transition probability. Results for the 0^{-} state at 10.937 MeV in ^{16}O gives a value of 1×10^{-5} for the branching ratio $B(MO,\gamma\gamma)/B(M1)$. The possibility of measuring the (γe) and (ee) processes in ^{16}O are more or less excluded by the exceedingly small value of the branching ratio B(MO, γe or ee)/B(M1). The results of calculations on ^{12}C, ^{28}Si, and ^{32}S are also presented. (Diss. Abstr. Int., B)

Nuclear Properties and Reactions, $20 \leq A \leq 89$

Refer also to abstracts 18679, 18747, 18753, 18754, 20133, 20141, 20264, 20271, 20274, 20282, 20283, 20291, 20298, 20305, 20306, 20368, 20372, 20374, 20417, 20435, 20445, 20447, 20448, 20450, 20471, 20497, 20505, 20522, 20524, and 20530.

20307 (AECL–3667) PHYSICS DIVISION PROGRESS REPORT, JANUARY 1–MARCH 31, 1970. (Atomic Energy of Canada Ltd., Chalk River (Ontario). Chalk River Nuclear Labs.). 114p. (PR-P–85). Dep. CFSTI (U. S. Sales Only). AECL $2.00.

Work performed by the nuclear physics branch, the general physics branch, the neutron physics branch, the theoretical physics branch, and the mathematics and computation branch at the physics division of AECL in the period January 1 to March 31, 1970 is reported. (J.W.R.)

20308 $^{31}P(p,\gamma)^{32}S$ REACTION IN THE PROTON ENERGY REGION 1800-2000 keV. Viitasalo, M.; Fant, B. (Helsinki Univ.). Soc. Sci. Fenn., Comment. Phys.-Math.; 38: 101-13 (1970).

The $^{31}P(p,\gamma)^{32}S$ reaction was studied in the region of E_p = 1800–2000 keV using a 40 cm^3 Ge(Li) detector. The broad resonance at 1890 keV was found to split into several narrow ones. Decay schemes of resonances within the range and the branching ratios of bound states were determined. Resonance state spins 2^+, 1^-, and 2^+ are proposed for the resonances at 1971 keV, 1977 keV, and 1985 keV. (auth) (Finland)

20309 SMALL-ANGLE j DEPENDENCE OF (α,p) REACTIONS. Glenn, J. E.; Zafiratos, C. D.; Zaidins, C. S. (Univ. of Colorado, Boulder). Phys. Rev. Lett.; 26: 328-31(8 Feb 1971).

The small-angle j dependence of (α,p) reactions for $l = 1$ and $l = 2$ reactions is discussed. The small-angle effect appears to persist for cases where the large-angle j dependence is small or absent. (auth)

20310 ELASTIC SCATTERING OF 23-MeV ALPHA PARTICLES BY ^{40}Ca. Labie, E.; Lega, J.; Macq, P. C. (Univ., Louvain, Belgium). Ann. Soc. Sci. Brux. Ser. I; 83: 371–4(28 Dec 1969). (In French).

The elastic scattering of 23-MeV α particles by ^{40}Ca was studied to confirm an isolated low-energy resonance previously observed near 24 MeV. The differential cross section was measured, and the results obtained are tabulated and graphed. The absolute cross-section scale is accurate to ±5.5%. (R.W.R.)

20311 OPTICAL MODEL FOR PROTON SCATTERING FROM ^{40}Ca. Thomas, G. L.; Sinha, B. C. (King's Coll., London). Phys. Rev. Lett.; 26: 325-8(8 Feb 1971).

A six-parameter optical model for proton elastic scattering from ^{40}Ca is developed in which the real part of the potential is generated from a matter distribution that reproduces the single-particle binding energies and electron elastic-scattering cross sections. If a Gaussian nucleon–nucleon force is used, an optimum range (squared) of 4.5 ± 0.4 fm^2 is extracted. Improved fits are obtained with a density-dependent effective interaction. (auth)

20312 METHOD FOR THE STUDY OF SHORT-LIVED NUCLEAR ISOMERS. Cox, A. J.; Kearin, M. J. (Univ. of Aston, Birmingham, Eng.). J. Inorg. Nucl. Chem.; 32: 3950-3(Dec 1970).

A technique was developed for the measurement of the isomeric cross-section ratio of short-lived isomers. The isomers ^{38}K produced by the $^{39}K(n,2n)^{38}K$ reaction using 14.7 MeV neutrons was studied and the ratio found to be 0.46 ± 0.03. (UK)

20313 TOTAL CONVERSION COEFFICIENT AND γ-LINE OF THE 13.34 keV LEVEL IN ^{73}Ge. Riegel, D.; Vester, K. P. (Freien Univ., Berlin). Z. Phys.; 241: 188-90(1971).

The total conversion coefficient of the lowest excited state in ^{73}Ge was measured to be $\alpha_{tot} = 1310 \pm 60$, which is close to the theoretically predicted value 1080 of Hager and Seltzer for a pure E2 transition. The energy of the γ-line is (13.34 ± 0.04) keV. A calculation, based on the experimental data, shows that the Moessbauer effect on this level is measurable. (auth)

20314 PROPERTIES OF NUCLEAR LEVELS AND TRANSITIONS IN ODD COPPER ISOTOPES. PART I. THE $^{58}Ni(p,\gamma)^{59}Cu$ REACTION. Holmberg, P.; Kiuru, A. (Univ. of Helsinki). Soc. Sci. Fenn., Comment. Phys.-Math.; 40: 77-81(Sep 1970).

Branching ratios for resonance states and bound states in ^{59}Cu are reported. At E_p = 1424 keV the angular distribution of gamma rays was measured. The analysis of results are in agreement with the following spin and parity assignments for levels in ^{59}Cu: g.s. $\frac{3}{2}^-$; 490.8 keV, $\frac{1}{2}$; 914.0 keV, $\frac{5}{2}^-$; 1988.9 keV, $\frac{5}{2}^{(-)}$. The measured Q-value for the $^{58}Ni(p,\gamma)^{59}Cu$ reaction is 3418.0 ± 1.4 keV. (auth) (Finland)

20315 AN INVESTIGATION OF THE ^{28}Si NUCLEUS BY THE $^{27}Al(p,\gamma)^{28}Si$ REACTION. Forsblom, I. (Univ. of Helsinki). Soc. Sci. Fenn., Comment. Phys.-Math.; 40: 65-76(Sep 1970).

The gamma decay of nine resonances in the $^{27}Al(p,\gamma)^{28}Si$ reaction in the proton energy range E_p = 1370–1600 keV was investigated and energies and branching ratios of several bound states were determined. Spins and parities are proposed for the following resonance states: 1439 keV 1^-, 1456 keV $4^{(-)}$, 1502 keV 2^+, 1565 keV 4^+ and 1578 keV 2^+ and ≥ 4 (this state is a doublet); and for the following bound states: 8327 keV 1^+, 9480 keV 2^+, 10181 keV 3^-, 10210 keV 2^+ and 10591 keV 2^+. (auth) (Finland)

20316 INVESTIGATION OF THE FIRST T = 2 STATE OF THE ^{32}S NUCLEUS FROM THE REACTION $^{31}P(p,\gamma)^{32}S$. Gales, Sydney; Langevin, Michel; Maison, Jean-Marie; Vernotte, Jean (Paris Univ., Orsay, France). Compt. Rend., Ser. B; 271: 970-3(2 Nov 1970). (In French).

A $12{,}050 \pm 4$ keV level was observed in the $^{31}P(p,\gamma)^{32}S$ reaction using 3289 ± 3 keV protons. The arguments presented favor the attribution of the characteristics 0^+, T = 2 to the level, which correspond to the first T = 2 state of the ^{32}S nucleus. (auth) (France)

20317 ELECTROMAGNETIC TRANSITIONS IN ^{37}Cl FOLLOWING THE β^- DECAY OF ^{37}S. Klotz, G.; Walter, G. (Centre de Recherches Nucleaires, Strasbourg). Nucl. Phys.; A156: 28-32 (1970). (In French).

Gamma-rays following the β-decay of ^{37}Cs were measured with a 40 cm^3 Ge(Li) counter. Two lines were detected at 3103.3 ± 0.3 keV and 3741.8 ± 0.4 keV with relative intensities of 99.7% and 0.3% respectively. They are attributed to ground state de-excitations of the corresponding levels in ^{37}Cl; for the feeding β-transitions one finds log ft = 4.37 and 6.08, respectively. No transition from a state at 3708 ± 4 keV has been observed, with an upper limit of 0.02%. (auth)

20318 GAMMA-RAY POLARIZATION MEASUREMENTS IN ^{22}Na. Baxter, A. M.; Gillespie, B. W. J.; Kuehner, J. A. (McMaster Univ., Hamilton, Ont.). Can. J. Phys.; 48: 2434-46(15 Oct 1970).

The $^{19}F(\alpha,n\gamma)^{22}Na$ reaction was studied using a Ge(Li) single-crystal polarimeter in addition to conventional Ge(Li) counters to elucidate certain spin, parity, and multipole-mixing ratio assignments to low levels of ^{22}Na. The 1.984 MeV level, which had previously been assigned 2+ or 3+, was shown not to be 3+ and, while 2+ is favored by the experiment, the evidence tends to suggest a problem in the interpretation of the properties of this level. The 2.572 MeV level is shown most likely to have spin and parity 2+. The J = 2 level at 3.059 MeV is clearly established as having even parity. In several cases limits on mixing ratios are obtained. These results cast doubt on certain model identifications made recently in ^{22}Na. (auth) (Canada)

20319 TRANSITION RATES IN ^{29}P. Monahan, C. F.; Evans, H. C.; Montague, J. H.; Paulson, W. R.; Zuk, W. M. (Queen's Univ., Kingston, Ont.). Can. J. Phys.; 48: 2683-91(15 Nov 1970).

Lifetimes of three of the low-lying excited states in ^{29}P, populated in the $^{28}Si(p,\gamma)$ reaction, were determined using the Doppler shift attenuation method. The mean lifetimes of states at 4.085, 1.956, and 1.385 MeV were found to be 15 ± 4, 370 ± 80, and 200 ± 60 fs. Angular distribution measurements were performed on gamma rays resulting from the decay of the 4.085 MeV resonance level. The decay was found to go via states at 3.107 MeV (3%), 1.956 MeV (54%), and 1.385 MeV (43%). The spin of the resonance level was uniquely assigned as $\frac{7}{2}$ and the multipole mixing ratios of the 2.129 and 1.385 MeV transitions as $+0.17 \pm 0.05$ and $+0.303 \pm 0.050$ respectively. The consequent transition rates indicate that the parity of the resonance level is positive. (auth) (Canada)

20320 PROPERTIES OF LOW-LYING STATES IN ^{43}Sc. Ball, G. C. (Atomic Energy of Canada Ltd., Chalk River, Ont.); Forster, J. S.; Ingebretsen, F.; Monahan, C. F. Can. J. Phys.; 48: 2735-50(15 Nov 1970). (AECL–3712).

The $^{40}Ca(\alpha,p\gamma)^{43}Sc$ reaction at E_α = 11.8 to 15.5 MeV was used to investigate the level structure of ^{43}Sc below 4.2 MeV excitation. Level energies and decay schemes were determined from proton–gamma coincidence spectra obtained using an annular surface barrier detector positioned near 180° and two 40 cm^3 Ge(Li) detectors. Angular correlations were measured in the same configuration using an array of six 12.7×15.2 cm NaI(Tl) detectors mounted on the Chalk River LOTUS goniometer. Twelve new levels were observed in ^{43}Sc and information on the spins, branching ratios, and gamma-ray multipole mixing ratios of these and several other excited states was obtained. The results are compared with recent theoretical predictions of Johnstone. In par-

XUM

ticular, levels at 1931 and 2552 keV, 1830 keV and 1883 keV were tentatively assigned as the $\frac{9}{2}^{+}$ and probable $\frac{11}{2}^{+}$ members of the $k^{\pi} = \frac{3}{2}^{+}$ band, the $(fp)^{3}$, $J^{\pi} = \frac{11}{2}^{-}$ state, and the $\frac{9}{2}^{-}$ member of the $k^{\pi} = \frac{3}{2}^{-}$ band, respectively. (auth) (Canada)

20321 EXCITED 0^{+} STATES IN ^{52}Fe, ^{54}Fe, ^{56}Ni, AND ^{58}Ni FROM THE (p,t) REACTION. Suehiro, T.; Ishizaki, Y.; Ogata, H.; (and others) (Tokyo Univ.). Phys. Lett.; 33B: 468-70(7 Dec 1970).

Excited O^{+} states have been observed at 4.14, 2.54, 4.99 and 2.94 MeV in ^{52}Fe, ^{54}Fe, ^{56}Ni, and ^{58}Ni, respectively, in the (p,t) reaction. A shell model interpretation of these O^{+} levels is given in terms of four particle(hole)−m hole(particle) configurations. (auth)

20322 REACTION MECHANISM FOR PROTON SCATTERING ON ^{60} ^{64}Ni AND ^{66} ^{68}Zn. Berinde, A.; Martalogu, N.; Neamu, I.; (and others). (Inst. for Atomic Physics, Bucharest). Nucl. Phys.; A161: 529-46(1971).

Elastic and inelastic scattering of protons from ^{60,64}Ni and ^{66,68}Zn exciting the first 2^{+} states was investigated for the bombarding energy range 4 to 8 MeV. For explanation of the measured excitation functions and angular distributions the direct interaction, statistical compound nucleus formation, and resonant excitation via isobaric analogue states are needed. Theoretical off-resonance differential cross sections calculated by means of the optical model, the statistical model, and DWBA, with average optical-model parameters, are in good agreement with the experimental results. The contribution of the statistical compound nucleus formation decreases very much above the (p,n) threshold. The p_1 angular distributions measured on analogue resonances suggest interference effects. Off-resonance ^{64}Ni(p,$p_1\gamma$) angular correlations were also measured. They are well described by contributions from both the direct interaction and compound nucleus formation. (auth)

20323 ANGULAR CORRELATION MEASUREMENTS OF THE FIRST THREE EXCITED STATES IN ^{29}P. Forster, J. S.; Broude, C.; Davies, W. G. (Atomic Energy of Canada Ltd., Chalk River, Ont.). Nucl. Phys.; A161: 375-84(1971).

Alpha-gamma coincidences were measured for the ^{32}S(p,$\alpha\gamma$)^{29}P reaction at E_p = 14.0 MeV using method II geometry of Litherland and Ferguson. The excitation energy of the third excited state of ^{29}P was measured to be 2.424 ± 0.012 MeV. The spins of the first three excited states were found to be: 1.38 MeV, $\frac{3}{2}$; 1.96 MeV, $\frac{5}{2}$; 2.42 MeV, $\frac{3}{2}$. Branching ratios and multipole mixing ratios for the first three excited states are: 1.38 → 0, 100%, $\delta = 0.07 \pm 0.07$ or $1.5^{+0.3}_{-0.4}$; 1.96 → 0, 91 ± 2%, E2; 1.96 → 1.38, 9 ± 2%, $\delta = -0.14 \pm 0.09$; 2.42 → 0, 83 ± 3%, $\delta = -0.23 \pm 0.03$ or $3.3^{+0.4}_{-0.2}$; 2.42 → 1.38, 12 ± 2%, $\delta = 0.15 \pm 0.14$; 2.42 → 1.96, 5 ± 2%, δ not measured. (auth)

20324 LOW-LYING LEVELS IN SOME SPHERICAL AND ROTATIONAL NUCLIDES BY COULOMB EXCITATION AND RADIATIVE CAPTURE OF THERMAL NEUTRONS. McClure, Donald Allan. Rolla, Mo.; Univ. of Missouri (1969). 143p. University Microfilms Order No. 70-21,253.

Thesis.

The work presented was performed in order to obtain additional information on the level schemes and decay properties of several nuclei in an attempt to explain the observations in terms of an applicable nuclear model. Various nuclear models are discussed. A general review from the classical point of view of the Coulomb excitation reaction is discussed and the thermal-neutron-capture reaction is outlined. The experimental equipment and procedure in the ramper method of energy determination is outlined. This method allows the measurement of γ-ray energies to an accuracy of ≈0.1 keV in many cases and therefore increases the chances for an unambiguous placement of the γ ray in a level scheme. A method for the accurate determination of the analyzing system dead time is also presented. The exclusive use of Ge(Li) detectors is made in both singles and coincidence γ-ray studies. A series of measurements on the singles and coincidence γ-ray spectra as well as the conversion electron spectra following the decay of ^{66}Ge is presented. This nucleus decays primarily by allowed beta transitions permitting the determination of the quantum mechanical parameters of many of the states in ^{66}Ga. This nuclide is expected to exhibit excited states being primarily single-particle in nature. The shell model structure of these states could lead to the occurrence of forbidden M1 transitions and indeed the first excited state of ^{66}Ga does exhibit a retarded M1 transition as reflected in its 21 nsec lifetime. Measurements of the de-excitation γ rays following Coulomb excitation of the low-lying levels in ^{105}Pd are presented. Attempts to describe this nucleus in terms of Nilsson orbitals have been largely unsuccessful. A description of the low-lying levels in terms of the core-excitation model is presented. The agreement between the experimental observations and the predictions of the core-excitation model is somewhat less than satisfying. However, accurate B(E2)↑ transition probabilities are presented which may be compared to a more extensive theoretical treatment. The thermal-neutron-capture reaction ^{186}W(n,γ)^{187}W is discussed. Both high-energy and low-energy γ rays were observed using both singles and coincidence γ-ray spectroscopic techniques in an attempt to construct an unambiguous level scheme. The resulting low-lying energy levels are discussed in terms of the Nilsson model including the Coriolis band mixing terms. Evidence is presented for the existence of Coriolis mixed states built on the $[512]\frac{3}{2}^{-}$, and $[510]\frac{1}{2}^{-}$ intrinsic states. The results of the model-predicted energy level sequence and γ-ray branching ratios are discussed. (Diss. Abstr. Int., B)

20325 PROTON INDUCED REACTIONS ON ^{23}Na AT E_p = 1000−1800 keV. Luukko, A.; Holmberg, P.; Kiuru, A. (Helsinki Univ.). Soc. Sci. Fenn., Comment. Phys.-Math.; 38: 115-22 (1970).

Yield measurements were performed for ^{23}Na(p,p′)^{23}Na, ^{23}Na(p,α_0)^{20}Ne, ^{23}Na(p,α')^{20}Ne and ^{23}Na(p,γ)^{24}Mg reactions in the proton energy region E_p = 1000−1800 keV. Twenty-eight resonances were detected. For six (p,α_0)-resonances the angular distribution of α_0-particles was measured. These measurements, complemented by radiative width considerations, suggest the following assignments for the resonances: 1^{-}, 2^{+} at E_p = 1091 keV, 1^{-} at 1284 keV and 1^{-}, 3^{-} at 1458 keV. (auth) (Finland)

20326 EVIDENCE FOR VIBRATIONAL EXCITED STATES IN ^{32}S. Ingebretsen, F. (Atomic Energy of Canada Ltd., Chalk River, Ont.); Sargent, B. W.; Ferguson, A. J.; (and others). Nucl. Phys.; A161: 433-48(1971).

The 0_2^{+}, 2_2^{+}, and 4_1^{+} states at 3781, 4283, and 4461 keV respectively in ^{32}S were studied, with emphasis on the latter two. The spin and parity of 4^{+} was confirmed for the 4461 keV state. The γ energies of the $4_1^{+} \rightarrow 2_1^{+}$ and $2_1^{+} \rightarrow 0_1^{+}$ transitions were determined as 2229.4 ± 1.2 and 2231.7 ± 1.0 keV, respectively. The lifetimes of the 4_1^{+} and 2_1^{+} states were measured by the Doppler-shift attenuation method as 0.21 ± 0.06 and 0.35 ± 0.06 ps, respectively. The $2_2^{+} \rightarrow 0_1^{+}$ and $2_2^{+} \rightarrow 2_1^{+}$ transitions have a branching ratio of 5.9 ± 0.3, and the latter is pure E2 within the experimental error. The strengths of the $2_1^{+} \rightarrow 0_1^{+}$, $0_2^{+} \rightarrow 2_1^{+}$, $2_2^{+} \rightarrow 2_1^{+}$, and $4_1^{+} \rightarrow 2_1^{+}$ transitions are respectively 7 ± 1, 15 ± 4, 7.3 ± 0.7, and 12 ± 3 W.u. These values suggest that the 2_1^{+} level is a one-phonon vibrational state and that the 0_2^{+}, 2_2^{+}, and 4_1^{+} levels make up a predominately two-phonon vibrational triplet. (auth)

20327 HALF-LIVES, FISSION YIELDS, AND NEUTRON EMISSION PROBABILITIES OF ^{87}Se AND ^{88}Se, AND EVIDENCE FOR ^{87}As. Kratz, J.-V.; Herrmann, G. (Univ., Mainz). J. Inorg. Nucl. Chem.; 32: 3713-23(Dec 1970).

Short-lived selenium nuclides were produced by thermal neutron induced fission of ^{235}U and separated chemically by a rapid hydride-volatilization procedure. Half-lives of 5.85 ± 0.15 and 1.4 ± 0.3 sec and fractional cumulative fission yields of 41 ± 7 and 24 ± 6 per cent were obtained for ^{87}Se and ^{88}Se respectively, via neutron counting of their daughter-products 55 sec ^{87}Br and 16 sec ^{88}Br. Evidence for the existence of ^{87}As was found from a slight growth of the ^{87}Se activity, corresponding to a half-life of 0.6 ± 0.3 sec and a fractional cumulative yield of 4 ± 2 per cent for ^{87}As. The yields of ^{87}As, ^{87}Se and ^{88}Se fit the systematics of charge distribution in the fission of ^{235}U by thermal neutrons. ^{87}Se and ^{88}Se were identified as delayed-neutron precursors. The neutron emission probabilities, 0.25 ± 0.06 per cent for ^{87}Se and 0.15 ± 0.09 per cent for ^{88}Se, are lower than expected. (auth) (UK)

20328 DWBA CALCULATIONS FOR (d,p) REACTIONS INCLUDING THE D-STATE OF THE DEUTERON. Delic, G.; Robson, B. A. (Australian National Univ., Canberra). Nucl. Phys.; A156: 97-104(1970).

The effect of the deuteron D-state on DWBA calculations for deuteron stripping was studied for l = 1 transitions in the ^{52}Cr(d,p)^{53}Cr reaction leading to the ground ($\frac{3}{2}^{-}$) and 0.57 MeV ($\frac{1}{2}^{-}$) states. The D-state was included in an exact treatment using a soft-core neutron-proton potential and the corresponding deuteron wave function of Reid. The effect upon the j-dependence of the differential cross sections and the corresponding vector and tensor analyzing powers was investigated. (auth)

20329 GAMMA-RAY DIFFERENTIAL CROSS SECTIONS FROM INELASTIC NEUTRON SCATTERING. Boring, John Wayne. Lexington, Ky.; Univ. of Kentucky (1969).

Thesis.

A measurement that should provide a check of the validity of the statistical model for predicting inelastic neutron cross sections is the measurement of the differential cross sections for the production of the de-excitation gamma rays. In addition to checking the validity of this model, these measurements are ex-

XUM

pected to provide information about the interaction of the incident neutrons at the nuclear surface, i.e., information about the shape of the nuclear potential. Such measurements may also be used to infer possible spin assignments for excited states. The differential cross sections for the production of six gamma rays by inelastic neutron scattering have been measured for an incident neutron energy of 2.9 MeV. The following gamma rays were observed: 0.85 MeV from ^{56}Fe, 1.374 MeV from ^{24}Mg, 0.861 MeV from ^{55}Mn, 1.18 MeV from ^{55}Mn, 0.536 MeV from ^{206}Pb, and 0.814 MeV from ^{206}Pb. The differential cross section measurements were made for the angular range 0–90°. The angular resolution was approximately ±15°, and the spread in energy of the incident neutron beam was around 170 kev. The gamma rays were detected by a shielded $1\frac{1}{2}$ in. dia. × 1 in. NaI(Tl) scintillator. A pulsed-beam neutron source permitted the use of time-of-flight techniques for discrimination against neutron-induced and other background. The absolute neutron flux measurements were made by counting the recoil ^{3}He particles from the D(d,n)^{3}He reaction. Pronounced anisotropies are observed in the angular distributions of the six gamma rays, especially the 1.374 MeV gamma ray from ^{24}Mg. The uncertainties in the absolute cross section measurements were approximately 10%. The experimental cross section measurements indicated that the statistical model in conjunction with the diffuse surface complex potential well is quite adequate in predicting total cross sections for the production of gamma rays by inelastic neutron scattering for the instances checked in the present experiment, but was unable to reproduce adequately the shape of the angular distribution of the 1.374 MeV gamma ray from ^{24}Mg. In order to obtain the agreement in total cross sections it was necessary to use in the calculations orbital angular momentum quantum numbers up to $l = 3$ for the incoming and outgoing neutrons. The differential cross section measurements for the production of the 0.861 MeV and 1.18 MeV gamma rays from ^{55}Mn permitted the establishment of possible spins for the 0.983 MeV and 1.289 MeV levels in ^{55}Mn. (Diss. Abstr. Int., B)

20330 ^{28}Si ENERGY LEVELS NEAR 13.245 MeV FROM THE REACTIONS ^{27}Al(p,γ)^{28}Si AND ^{27}Al(p,α)^{24}Mg. Huck, A.; Baumann, P.; Walter, G. (CNRS, Strasbourg). J. Phys. (Paris); 31: 869-70(Oct 1970). (In French).

The characteristics of the resonances in the reaction ^{27}Al + p at an energy $E_p = 1724$ keV were studied for different exit channels. In this way the existence of two distinct levels ($J^\pi = 3^-$, $J^\pi = 5^-$) in ^{28}Si at 13.245 ± 2 keV was confirmed. (auth) (France)

20331 POLARIZATION MEASUREMENTS FOR PROTON ELASTIC SCATTERING FROM ^{88}Sr, ^{89}Y, ^{92}Zr, $^{92\ 94}$Mo, AND $^{118\ 120}$Sn NEAR ISOBARIC ANALOG RESONANCES. **Ellis, Jerry Lynn. Madison, Wis.; Univ. of Wisconsin (1970). 113p. University Microfilms Order No. 70-8282.**

Thesis.

The polarization of elastically scattered protons was measured near isobaric analog resonances. The targets and energy ranges are: ^{88}Sr(4.5–8.6 MeV), ^{89}Y(5.7–6.4 MeV), ^{92}Zr(4.6–8.6 MeV), ^{92}Mo(4.1–8.7 MeV), ^{94}Mo(4.5–8.5 MeV), ^{118}Sn(7.0–12.1 MeV), and ^{120}Sn(7.3–7.8 MeV). The measurements were made at mean scattering angles of 109.2 and 137.6°. The measurements on ^{88}Sr, ^{92}Zr, ^{92}Mo, ^{94}Mo and ^{118}Sn were made to determine the total angular momenta J of the isobaric analogs of several low-lying states of ^{89}Sr, ^{93}Zr, ^{93}Mo, ^{95}Mo, and ^{119}Sn, respectively. Several disagreements with previous J- and l-assignments were found. The measurements on ^{118}Sn and ^{120}Sn near 7 MeV were made to determine the elastic width for the isobaric analogs of the lowest $\frac{3}{2}^+$ states in ^{119}Sn and ^{121}Sn. The J-values for these states were known from previous polarization measurements. The measurements on the spin-$\frac{1}{2}$ target ^{89}Y were made to determine the relative amplitudes of the $\frac{1}{2}^+$ and $\frac{3}{2}^+$ components of the 1^- state at 1.374 MeV in ^{90}Y. The results show an almost pure $s_{1/2}$ configuration. (Diss. Abstr. Int., B)

20332 PHOTONEUTRON CROSS SECTIONS FOR ^{32}S. **Anderson, D. W.; Bureau, A. J.; Cook, B. C.; Englert, T. J.; Schramm, R. E. (Ames Lab., Iowa). Nucl. Phys.; A156: 74-82(1970).**

The cross section for the ^{32}S(γ,n)^{31}S reaction plus the ^{32}S(γ,2n)^{30}S reaction was measured from threshold to 62 MeV using least-structure analysis of the bremsstrahlung yield curve. Maxima in this cross section appear at 20.3 ± 0.4 MeV, 23.3 ± 0.3 MeV, 27.4 ± 0.5 MeV, 32.1 ± 0.5 MeV, 39.3 ± 0.7 MeV and 58.4 ± 1.0 MeV. The cross section integrated to 62 MeV is 158 ± 7 MeV · mb. The cross section for the ^{32}S(γ,pn)^{30}P plus ^{32}S(γ,d)^{30}P reactions plus the ^{32}S(γ,2n)^{30}S reaction was also measured. Structure occurs at 23.7 ± 0.4 MeV, 25.7 ± 0.4 MeV, 27.4 ± 0.4 MeV, 29.4 ± 0.5 MeV, 32.0 ± 0.5 MeV, 35.4 ± 0.5 MeV, 50.4 ± 0.8 MeV and 55.9 ± 1.0 MeV. The cross section integrated to 62 MeV is 65 ± 5 MeV · mb. (auth)

20333 STATIC MOMENTS OF 2_1^+ STATES IN LIGHT DOUBLY EVEN NUCLEI. **Zamick, Larry (Weizmann Inst. of Science, Rehovot, Israel). Nucl. Phys.; A154: 191-201(1970).**

Quite general arguments indicate that if the shell-model picture holds or even if one allows for effective charge corrections, then the quadrupole moment of the first excited state of ^{48}Ti should be small, and the magnetic moment of the first excited state of ^{54}Fe should be large, compared to the rotational value. These results are contrary to recent experiments. A comparison is made between perturbation theory and matrix diagonalization in the space two holes and three holes and one particle, for ^{54}Fe and ^{54}Co. One gets less magnetic quenching with matrix diagonalization in ^{54}Fe (hence the deviation from experiment is more) than with perturbation theory. The possibility that the lowest 2_1^+ state in ^{54}Fe is mostly a 3p-1h state is ruled out. Corrections to the quasiparticle approximation i.e., the use of the magnetic moment of one hole (^{55}Co) to calculate the magnetic moment two holes (^{54}Fe), are calculated, and again tends to reduce the quenching. The J = 7 J = 0 splitting of two holes –^{54}Co– is less than that of two particles –^{42}Sc– by 400 keV but in perturbation theory the admixture of 3h-1p in ^{54}Co goes in the wrong direction by 600 keV. It is shown however that with matrix diagonalization the J = 0 state of ^{54}Co gets pushed down much less than in perturbation theory, so that this 600 keV additional discrepancy is erased. A triplet of levels at 2.5 MeV in ^{54}Fe is analyzed to consist of a (mostly) 2h J = 4 state, a 3h-1p particle J = 2 state, and 4h-2p J = 0 state. A bare realistic interaction puts the 4h-2p state much too high in energy but an interaction chosen to fit single-particle energy shifts gives excellent agreement. (auth)

20334 ELECTRON-SCATTERING STUDY OF THE CHANGE OF THE CHARGE RADII OF NUCLEI OF IRON AND NICKEL ISOTOPES. **Litvinenko, A. S.; Shevchenko, N. G.; Afanas'ev, N. G.; (and others) (Physical-Technical Inst., Kiev). JETP Lett. (USSR) (Engl. Transl.); 12: 269-71(20 Oct 1970).**

Translated from Zh. Eksp. Teor. Fiz., Pis'ma Red.; 12: 389-93(20 Oct 1970).

Cross sections were measured for elastic scattering of 225-MeV electrons from ^{54}Fe, ^{56}Fe, ^{58}Fe, ^{58}Ni, and ^{62}Ni. The parameters C and t of the Fermi distribution and their changes following addition of nucleons were determined. The isotopic shifts of the radius for pairs of the nuclei are discussed. (D.L.C.)

20335 SPIN DEPENDENCE OF THE NEUTRON-CAPTURE CROSS SECTION OF VANADIUM AND THE INTERNAL MAGNETIC FIELD AT VANADIUM NUCLEI. **Postma, H.; Vanneste, L.; Sailor, V. L. (Brookhaven National Lab., Upton, N. Y.). Phys. Rev., B; 3: 128-30(1 Jan 1971).**

The spin dependence of the neutron-capture cross section of vanadium at 0.115 eV was measured with the aid of polarized neutrons and polarized vanadium nuclei. It is concluded that the capture cross section of ^{51}V is mainly related to spin $J = I - \frac{1}{2}$. In addition, it is shown that the internal field at the vanadium nuclei is less than 4 kOe in very pure vanadium, which apparently does not become ferromagnetic down to 0.06°K. (auth)

20336 ISOBARIC ANALOG PAIR ^{57}Fe–^{57}Co. **Braendle, H.; Wylie, W. R.; Zamboni, F.; Zych, W. (Univ., Zurich). Nucl. Phys.; A151: 211-24(1970).**

Analog states were identified as resonances in (p,γ) and (p,p) reactions on ^{56}Fe in the proton energy ranges 1.2 to 1.6 and 3.7 to 4.3 MeV, respectively. Excitation functions, a level diagram of ^{57}Co, and the Coulomb displacement energy ΔE_c are given. (auth)

20337 STATIC QUADRUPOLE MOMENTS IN A = 18 TO 38 NUCLEI AS PREDICTED IN THE SHELL MODEL. **Wildenthal, B. H. (Michigan State Univ., East Lansing); McGrory, J. B.; Glaudemans, P. W. M. Phys. Rev. Lett.; 26: 96-9(11 Jan 1971).**

The static electric quadrupole moments of the ground and first excited states of nuclei in the sd shell are calculated from shell-model wave functions. The relative values of experimentally known moments of ground states are well reproduced by the calculations as are the relative values of the measured moments of $J^\pi = 2^+$ first excited states. However, the absolute experimental values of the ground-state and excited-state moments cannot be reproduced simultaneously with a single choice of effective charge. (auth)

20338 SCATTERING OF FAST NEUTRONS BY ^{12}C, ^{54}Fe, ^{56}Fe, ^{58}Ni, AND ^{60}Ni. **Boschung, P.; Lindow, J. T.; Shrader, E. F. (Case Western Reserve Univ., Cleveland). Nucl. Phys.; A161: 593-609(1971).**

Differential elastic and inelastic neutron scattering cross sections were measured for ^{12}C, ^{54}Fe, ^{58}Ni, and ^{60}Ni between 4.0 and 5.6 MeV. The ^{54}Fe, ^{56}Fe, ^{58}Ni, and ^{60}Ni elastic cross sections were compared with predictions of the optical model using standard sets of parameters for the potential. Inelastic angular dis-

XUM

tributions were calculated assuming the statistical model and, in addition, for each first excited state a direct reaction contribution was calculated using the DWBA. The agreement between theory and experiment is satisfactory. (auth)

20339 HALF-LIVES OF SOME FISSION PRODUCT NUCLIDES. Baba, S.; Baba, N.; Natsume, H. (Japan Atomic Energy Research Inst., Tokai). J. Inorg. Nucl. Chem.; 33: 589-95(Feb 1971).

Many nuclides are produced in nuclear fission that are hardly available in any other way. In the course of a study of the proton-induced fission of ^{238}U, the fission product nuclides with medium half-lives (^{72}Zn, ^{86}Rb, ^{89}Sr, ^{91}Y, ^{99}Mo, ^{112}Pd, ^{115}Cd, ^{115m}Cd, ^{129m}Te, ^{136}Cs, ^{140}Ba, ^{141}Ce, ^{143}Pr, ^{147}Nd, ^{149}Pm, ^{153}Sm, ^{156}Eu, ^{161}Tb) were repeatedly separated and their yields determined by measuring their radioactivity. Their half-lives were then determined with good precision using a least-squares analysis of the beta decay curves. The resulting half-lives are summarized and compared with values previously reported. 80 references. (UK)

20340 DETAILS OF THE CRITICAL STUDY OF THE INTERNAL BREMSSTRAHLUNG SPECTRUM FROM ^{32}P. Berenyi, D.; Varga, D. (Inst. of Nuclear Research, Debrecen, Hungary). Acta Phys. Acad. Sci. Hung.; 29: 1-26(1970).

On the basis of a critical analysis of the measuring conditions and the evaluation process in the measurement of the internal bremsstrahlung (IB), an experimental study of the integral IB spectrum from ^{32}P was carried out. To eliminate the sources of possible systematic errors both in the measurement and in the evaluation, special care was devoted to the following items. 1) To check the effect of external bremsstrahlung (EB), the magnetic deflection and the "classical" absorption method for the elimination of direct electrons of the source were applied in the same experiment. 2) The detector efficiency (photopeak efficiency) for the correction of the spectrum was determined experimentally using the IAEA, Vienna, standards with known activities (errors from 1 to 3%). 3) The correction for the detector resolution was carried out by a previous method instead of that mostly used. 4) With the geometrical arrangement of the experiment a low Compton distribution (relative to the photopeak) in the spectra of the monoenergetic gamma rays was provided with practically no backscatter peak. 5) The theoretical spectrum was converted into pulse-height distribution. 6) The experimental and theoretical spectrum shape was compared by normalization of the distributions to avoid errors, arising from the absolute determination of beta activity of the source. As a result of the investigation, the observed maximum deviation of the experimental distribution from the Nilsson-corrected KUB theory of IB was about 6% in the energy region from 60 to 1060 keV. Even if the possible maximum errors are taken into consideration, the deviation from the KUB-Nilsson theory cannot be more than 15% in the above region in contrast with e.g. recent contradictory results in one of which a deviation amounting to 30 to 40% from the KUB-Nilsson theory was observed in the region from about 100 to 800 keV, while an agreement was found for higher energies up to about 1200 keV, and in the other an increasing disagreement with the above mentioned theory was indicated from 500 keV towards the higher energies up to about 1300 to 1400 keV (the deviation is about 80% at 1000 keV). At the same time, the present measurements definitely disprove the considerable disagreements (the greatest disagreement ever observed from the theory in an IB study) which were found in the only earlier experiment of this kind where the direct electrons from the source were prevented to reach the gamma-ray detector by applying a magnetic field. (auth)

20341 CHARGED PION PHOTOPRODUCTION ON ^{27}Al NUCLEUS. Grishaev, I. A.; Lapin, N. I.; Nikiforov, V. I.; Pugachev, G. D.; Shramenko, B. I. (Physical-Technical Inst., Kharkov). Yadern. Fiz.; 12: 680-1(Oct 1970). (In Russian).

Experimental results are given for charged-pion photoproduction on the ^{27}Al nucleus by bremsstrahlung γ quanta with energy $E_{\gamma\ max} = 313$ MeV. The charged pions were detected by means of nuclear emulsions. The yield of π^+ and π^- mesons with the kinetic energies 25 to 65 MeV at angles less than 120° in the lab system was measured. The results obtained are discussed in framework of the optical model. (auth)

20342 TENSOR POLARIZATION OF DEUTERONS FROM THE Mg(d,d)Mg ELASTIC SCATTERING AT 7.0 MeV. Djaloeis, A.; Nurzynski, J. (Australian National Univ., Canberra). Nucl. Phys.; A163: 113-30(1971).

The spin tensors moments $\langle T_{20}\rangle$, $\langle T_{21}\rangle$ and $\langle T_{22}\rangle$ of deuterons emitted from the Mg(d,d)Mg elastic scattering reaction have been measured. The average deuteron energy $(\bar{E}_d)$ at the centre of the effective target thickness was 7.0 MeV. The angular dependence of the deuteron tensor polarization has been obtained for angles between 15° and 90° (lab) in steps of 7.5°. Optical-model analyses without and with the inclusion of the Hauser–Feshbach theory have been performed. In all cases, combinations of central potential with spin-orbit interaction were found inadequate to reproduce the data. The addition of a small attractive and long-ranged tensor interaction T_R resulted in a considerably improved fit. Inclusion of a T_L tensor interaction was redundant. (auth)

20343 ENERGY LEVELS IN ^{74}Ge FROM THE DECAY OF ^{74}Ga. Camp, David C. (Univ. of California, Livermore); Fielder, David R.; Foster, Bruce P. Nucl. Phys.; A163: 145-60(1971).

The γ-ray decay scheme and nuclear energy levels in ^{74}Ge have been studied from the decay of ^{74}Ga using a high-resolution 38 cm^3 Ge(Li) detector. The half-life of ^{74}Ga was determined to be 8.25 ± 0.05 min using chemically separated sources. Energies and intensities are given for 97 γ-ray transitions of which 77 are placed in proposed level scheme containing 29 levels. Log ft values are deduced from the relative γ-ray intensities, and spin and parity values are proposed for some of the levels. (auth)

20344 COUPLED-CHANNEL ANALYSIS OF α-PARTICLE SCATTERING FROM THE 5.23 MeV UNNATURAL PARITY STATE OF ^{24}Mg. Singh, P. P.; High, M. D.; Malmin, R. E.; Devins, D. W. (Indiana Univ., Bloomington). Nucl. Phys.; A163: 289-98(1971).

A coupled-channel analysis of the inelastic scattering of 40–80 MeV α-particles from the 3^+ 5.23 MeV state of ^{24}Mg, assuming a rotation–vibration nuclear structure model, successfully reproduced the trend on the angular distribution as a function of the bombarding energy. (auth)

20345 ELECTRON ELASTIC SCATTERING ON ^{64}Zn AND ^{66}Zn NUCLEI. Afanas'ev, V. D.; Afanas'ev, N. G.; Medyanik, V. M.; (and others). Yadern. Fiz.; 12: 673-9(Oct 1970). (In Russian).

The cross sections for electron elastic scattering at 150 and 225 MeV were measured for scattering angles 45 to 110°. Charge distribution parameters in ^{64}Zn and ^{66}Zn are obtained in high-energy and modified Born approximation from the data evaluation. Large increases of the surface-thickness parameter and of the mean square radius of ^{64}Zn are observed, as compared to ^{64}Ni. It is shown that this result may be considered, on the one hand, as a consequence of the redistribution of the charge density in ^{64}Zn to conserve spherical symmetry, and on the other, as a consequence of the deformation of the ^{64}Zn nucleus, the deformation parameter being $\beta \approx 0.23$. (auth)

20346 CALCULATIONS OF CROSS SECTIONS FOR INELASTIC INTERACTION OF NEUTRONS WITH NUCLEI ACCOMPANIED BY THE EMISSION OF PROTONS AND α PARTICLES. Savel'ev, A. E.; Aver'yanov, I. K.; Dzyuba, B. M. Yadern. Fiz.; 12: 704-9 (Oct 1970). (In Russian).

The total cross sections for the (n,p) and (n,α) reactions in a number of light and intermediate nuclei are calculated by using the Hauser–Feshbach method. Incident neutron energies are considered from the thresholds of the above reactions up to ~14 MeV. Optical and statistical parameters are chosen from the condition of satisfactory description of elastic scattering of particles and reactions (n,γ) and (n,n′) and (n,2n). Quite reasonable agreement of theoretical results with experimental ones shows that, for the case of the nuclei considered and at $E_n \lesssim 14$ MeV, the (n,p) and (n,α) reactions proceed mainly via compound-nucleus formation. (auth)

20347 STUDY OF THE EXCITED STATES OF ^{46}V USING THE (^{3}He,t) REACTION. Fadner, W. L.; Farwell, L. C.; Green, R. E. L.; Hayakawa, S. I.; Kraushaar, J. J. (Univ. of Colorado, Boulder). Nucl. Phys.; A162: 239-58(1971).

Differential cross sections were measured for the ^{46}Ti(^{3}He,t)^{46}V reaction at 37.7 MeV using solid-state detectors with an energy resolution of about 100 keV. Angular distributions were obtained for 16 levels in ^{46}V ranging from the 0^+ ground state to 4.01 MeV. The data were compared to both macroscopic and microscopic distorted-wave calculations where a tensor force was included in the effective two-body interaction. Definite J, π assignments could be made to five states including the 0^+(0.0), 2^+(0.97) and 4^+(2.00) isobaric analog states. The spin and parity assignments for ten other levels could be restricted to two or three possibilities. The resulting level scheme differed appreciably from that predicted by shell-model calculations involving just the $f_{7/2}$ nucleons, but the general ordering of the levels was in approximate agreement. (auth)

20348 ANGULAR CORRELATION STUDIES IN ^{34}S. Mulhern, P. J.; Jones, G. D.; Main, I. G.; (and others) (Univ. of Liverpool). Nucl. Phys.; A162: 259-72(1971).

The states of ^{34}S up to 5.4 MeV excitation have been studied by particle-γ-ray angular correlation experiments using the reaction ^{31}P(α,p)^{34}S. Spin assignments of 4, 3, 2 and 1 have been made to the levels at 4.688 MeV, 4.874 MeV, 5.318 MeV and 5.380 MeV, respectively. Spin assignments to levels below 4.9 MeV have been confirmed. Branching ratios have been determined for all but one of the states and multipole mixing ratios for all but one of the observed transitions. The results are discussed in relation to various models. (auth)

20349 LIFETIME MEASUREMENTS IN sd SHELL NUCLEI. V. MEAN LIVES OF ^{31}S AND ^{38}K LEVELS. Engmann, R. (Rijksuniversiteit, Utrecht); Ehrmann, E.; Brandolini, F.; Signorini, C. Nucl. Phys.; A162: 295-304(1971).

Lifetime measurements have been performed in ^{31}S and ^{38}K. From DAS $\alpha\gamma$ coincidence measurements with the ^{32}S(^{3}He,$\alpha\gamma$)^{31}S reaction mean lives of τ_m = 720 ± 180 and 320 ± 80 fs were found for the levels at E_x = 1.25 and 2.23 MeV in ^{31}S, respectively. Similarly, with the ^{39}K(^{3}He,$\alpha\gamma$)^{38}K reaction the mean lives of the ^{38}K levels at E_x = 1.70 and 2.40 MeV were both found as τ_m = 54 ± 25 fs. From the coincidence measurements excitation energies are deduced. With the recoil P-distance method applied to the ^{35}Cl(α,n)^{38}K reaction, the mean life of the 0.46 MeV level in ^{38}K was measured as τ_m = 740 ± 160 ps. Detailed information on transition matrix elements is extracted from γ-ray transition strengths and from β-decay. Experimental results are compared with the results of many-particle shell-model calculations. (auth)

20350 IDENTIFICATION OF PARTICLE-HOLE MULTIPLETS IN ^{40}Sc. Schulz, N.; Alford, W. P.; Jamshidi, A. (Univ. of Rochester, N. Y.). Nucl. Phys.; A162: 349-52(1971).

A number of levels in ^{40}Sc below 3.5-MeV excitation were identified in a high-resolution study of the ^{40}Ca(^{3}He,t) reaction. The states of the $f_{7/2}-d_{3/2}^{-1}$ multiplet are assigned by comparison with the spectrum of ^{40}K. Evidence for the identification of states of the $p_{3/2}-d_{3/2}^{-1}$ multiplet is also obtained. (auth)

20351 STRUCTURE OF POSITIVE PARITY STATES OF ^{20}Ne. Arima, A. (State Univ. of New York, Stony Brook. Tokyo Univ.); Strottman, D. Nucl. Phys.; A162: 423-37(1971).

The positive-parity spectrum of ^{20}Ne is studied using a complete sd basis with additional two- and four-hole states. The effect of promoting two particles to the 2p-1f shell is also examined. A central interaction is assumed that the unperturbed energies of the particle-hole states are taken as free parameters. E2 transition rates and quadrupole moments are calculated and compared with experiment. Agreement with known energy levels is good, but the calculated E2 transition rate from the second 0^+ state to the first 2^+ state is too small. (auth)

20352 DECAY STUDIES OF TRANSITIONAL NUCLEI ^{86}Sr, ^{148}Sm, AND ^{151}Eu. Ford, James Wilburn Jr. Nashville; Vanderbilt Univ. (1970). 155p. University Microfilms Order No. 70-24,863.
Thesis.

Some isotopes in the transition regions between spherical and permanently deformed nuclei are compared with theories of current nuclear models. The nuclei ^{86}Sr, ^{148}Sm and ^{151}Eu represent isotopes in the zone between the single-particle description of the shell model and the collective description of the rotational model. In an attempt to understand better the build-up of the "collective-like" behavior in the single-particle region to vibrational region (^{86}Sr) and the vibrational region to rotational region (^{148}Sm and ^{151}Eu) several experiments were carried out on these nuclei. Extensive gamma-ray singles experiments and gamma-gamma two-parameter coincidence experiments were performed on the decay of $^{86}\mathrm{Y} \xrightarrow{EC,B^+} {}^{86}\mathrm{Sr}$, the decay of the isomer state and ground state of $^{148}\mathrm{Pm} \xrightarrow{B^-} {}^{148}\mathrm{Sm}$, and the decay of $^{151}\mathrm{Gd} \xrightarrow{EC} {}^{151}\mathrm{Eu}$. Improved energy and intensity measurements were made on the gamma-ray spectrums of these three isotopes. Coincidence experiments were used to construct detailed nuclear energy levels for the isotopes. The use of the measured gamma-ray intensities and published conversion electron intensities provided the means of assigning spin and parity to some of these levels. Comparison of the experimental results with theoretical calculations based on several nuclear models is shown to provide poor quantitative agreement. However, qualitatively the low-lying positive and negative parity states of ^{86}Sr are found to agree with the shell model if proton excitations are considered. The isotope ^{148}Sm was found to agree with the general features of the vibrational model. The interpretation of the states in ^{151}Eu are not clear; although, collective behavior is definitely observed. The results indicate that although the current models do provide some phenomenological insight into the structure of these nuclei, they are not adequate in their present form to describe the experimental observations. (Diss. Abstr. Int., B)

20353 APPLICATION OF CORIOLIS-COUPLING MODEL TO ODD-ODD NUCLEI IN THE 2s-1d AND 1f-2p SHELLS. Wasielewski, Paul Francis. New Haven; Yale Univ. (1970). 113p. University Microfilms Order No. 70-25,124.
Thesis.

The strong-coupling collective rotational model of Bohr and Mottelson is used to calculate the energy level spectra and electromagnetic properties of odd-odd nuclei in the 2s-1d and 1f-2p shells. The model places the last odd neutron and odd proton in Nilsson orbitals generated by the axially-symmetric deformed core. The model Hamiltonian consists of the collective rotational energy, including the Coriolis term, plus the Nilsson Hamiltonians of the two odd particles plus a residual interaction between them. The wave functions are obtained by diagonalizing this Hamiltonian on a basis consisting of the rotational bands built on all the allowed single-particle states within the major shell. Magnetic dipole moments, electric quadrupole moments, and M1 and E2 transition rates are calculated. Calculations were performed for ^{18}F, ^{22}Na, ^{26}Al, ^{30}P, ^{46}Sc, and ^{56}Mn. Agreement with the experimental spectrum is poor for ^{18}F. For ^{22}Na, agreement with the experimental spectrum and electromagnetic properties is good for states below 2 MeV, but too many states are predicted between 2 and 4 MeV. For ^{26}Al, there is good agreement with the experimental energy spectrum, but there are discrepancies in the transition rates between low-lying levels. For ^{30}P, the experimental spectrum is well reproduced below 4 MeV, but transition rates from states between 2 and 4 MeV do not agree with experiment. For ^{46}Sc and ^{56}Mn, the theoretical results are in fair accord with existing experimental data, but there is not enough data available to provide an adequate test of the model. (Diss. Abstr. Int., B)

20354 NUCLEAR DATA SHEETS. Nucl. Data, Sect. B; 5: No. 2, B.5.i-B.5.204(Feb 1971).

Nuclear structure information from nuclear reactions and decay studies for A = 84, 85, 86, and 113 nuclei is presented. The adopted level schemes are shown and adopted values of all experimental qualities that were used in constructing the level schemes are given. Experimental results collected from all sources are presented in a form for easy comparison. Reference lists are given which contain all references used in preparing the A-chains. (J.W.R.)

20355 NUCLEAR RESONANCE SCATTERING OF BREMSSTRAHLUNG. Wilson, Henry Hamilton. Boston; Boston Univ. (1970). 237p. University Microfilms Order No. 70-23,132.
Thesis.

Nuclear resonance fluorescence induced by bremsstrahlung from a 3-MeV Van de Graaff accelerator was used in a study of the excited levels of stable nuclei. Scattering, absorption and angular distribution measurements were performed. The results were compared with those of nuclear models. The basic quantity measured in the scattering experiment is $g\Gamma_0(\Gamma_0/\Gamma)W(\theta)$ where Γ is the full width of the excited level, Γ_0 is the partial width for the decay of the level to the ground state, g is the statistical factor and $W(\theta)$ is the angular distribution factor. The quantity $g\Gamma_0(\Gamma_0/\Gamma)W(\theta)$ will be referred to as the raw width. Zinc, gallium, germanium, arsenic, selenium, bromine, strontium, yttrium and antimony were searched for possible resonances and the maximum widths were calculated when no resonance was observed. Several new resonances were observed in ^{69}Ga, ^{75}As, ^{89}Y, ^{121}Sb and ^{123}Sb. The 0.872 and 1.107 MeV levels of ^{69}Ga were determined to have raw widths of 0.9 ± 0.3 and 6.6 ± 1.3 MeV respectively. Three weak resonances were observed in ^{75}As at 0.86, 1.07 and 1.35 MeV with raw widths of 1.4 ± 0.3, 1.9 ± 0.7 and 3.0 ± 0.6 MeV respectively. The resonances observed in antimony at 1.381, 1.630 and 1.720 MeV with raw widths of 15 ± 4, 3.5 ± 1.8 and 18 ± 8 MeV were attributed to ^{121}Sb. The resonances observed at 1.028 and 1.520 MeV with raw widths of 7.8 ± 2.4 and 8.3 ± 2.5 MeV were assigned to ^{123}Sb while another observed at 1.807 MeV with a raw width of 11 ± 7 MeV could not be assigned. The yttrium and sodium results are discussed separately below. The basic quantity determined by the absorption measurement is $g\Gamma_0$. Original measurements were performed in ^{55}Mn, ^{59}Co and ^{89}Y. The 1.527, 1.884, 2.192, 2.252 and 2.564 MeV levels of ^{55}Mn were determined to have values of $g\Gamma_0$ of 5 ± 2, 53 ± 8, 17 ± 4, 14 ± 4 and 54 ± 14 MeV respectively. The 1.190 MeV level of ^{59}Co was determined to have $g\Gamma_0 = 9 + 3$ MeV. The 2.124 MeV level of ^{11}B was measured as having $\Gamma_0 = \Gamma = 110 \pm 10$ MeV. Angular distribution measurements were performed on the 2.982 MeV level of ^{23}Na, the 1.507 MeV level of ^{89}Y and the 1.527, 1.884 and 2.564 MeV levels of ^{55}Mn. The ^{55}Mn results were essentially isotropic which could only aid in the rejection of a $\frac{9}{2}$ spin assignment for these levels. In the ^{23}Na nucleus, Γ_0 for the 2.078 MeV level was measured as 0.8 ± 0.4 MeV and Γ_0/Γ as 0.11 ± 0.08. The 2.391 MeV level was given an upper limit of 1.1 MeV. Comparison of this value with Doppler shift lifetimes supports $J = \frac{1}{2}$ for this level. The width of the 2.640 MeV level was measured as $\Gamma_0 = \Gamma = 3.6 \pm 1.2$ MeV with $J^\pi = \frac{1}{2}^-$ being supported by comparison with the Doppler shift measurements. The angular distribution measurement of the 2.982 MeV level indicated $J^\pi = \frac{5}{2}^+$ with $\delta = +2.6 = 0.4$ for the ground state decay. Γ_0/Γ was measured as

0.56 ± 0.05 leading to $\Gamma_0 = 58 \pm 15$ MeV and $\Gamma = 104 \pm 26$ MeV as the results of the scattering and absorption measurements. Some Nilsson model transition probabilities were calculated for this nucleus. For the 1.507 MeV level of ^{89}Y, the angular distribution results and comparison of the widths obtained with inelastic electron scattering results determined J^π to be $\frac{3}{2}^-$ with $\delta = -0.13 \pm 0.01$. The widths for this level were measured as $\Gamma_0 = \Gamma = 22 \pm 4$ MeV. The widths of the 1.744 MeV level were measured as 0.5 ± 0.2 MeV whose good agreement with the electron scattering results confirms $J^\pi = \frac{5}{2}^-$ for this level. A resonance with a raw width of 30 ± 15 MeV was noted corresponding to the 2.52 MeV level. (Diss. Abstr. Int., B)

20356 DETERMINATION OF ENERGY LEVELS IN STABLE NUCLEI BY NEUTRON INELASTIC SCATTERING. French, W. R. Jr.; Wehrbein, W. M.; Goss, D.; Gasper, J. K. (Nebraska Wesleyan Univ., Lincoln). Amer. J. Phys.; 39: 131-4(Feb 1971).

Neutron inelastic scattering experiments are conceptually simple yet instructive. The energy levels of some stable nuclei were determined by measuring the energies of the gamma radiation produced by the (n,n′γ) reaction with the target nuclei. The source of neutrons was a Pu−Be source. The gamma spectra were obtained with a Ge(Li) detector and a 4096 channel analyzer. A computer program was used to determine the channel locations of the gammas and to calculate their energies. Besides the measurement of energy levels of the detector material (Ge), levels were measured in Fe, Al, Mg, Pb, Na, Cl, Zn, and Cu. (auth)

20357 GAMMA-RAY TRANSITIONS IN ^{29}P. Williams, Roy Prentis Jr. New Orleans; Tulane Univ. (1970). 75p. University Microfilms Order No. 70-24,560.
Thesis.

A study was made at the 1.381 MeV resonance of the ^{28}Si(p,γ)^{29}P reaction. Lifetimes of the resonance level and of the first and second excited states in ^{29}P were determined using the Doppler Shift Attenuation Method, to be 0.013, 0.24, and 0.39, respectively. Accurate energies were determined for the four gamma rays seen at this resonance and for the three energy levels involved. Angular distribution measurements yielded an unambiguous spin assignment of $\frac{7}{2}$ for the resonance level, and the gamma ray branching ratio of this level was obtained. (Diss. Abstr. Int., B)

20358 GAMMA–GAMMA ANGULAR CORRELATIONS IN ^{64}Cu. Wellborn, Colvin Clarke. New Orleans; Tulane Univ. (1970). 78p. University Microfilms Order No. 70-24,558.
Thesis.

The ^{64}Ni(p,n)^{64}Cu reaction was used to populate levels in ^{64}Cu up to 633 keV excitation. Proton bombarding energy was between 3.0 and 3.1 MeV; the target was Ni metal (98% ^{64}Ni) evaporated onto a graphite backing. Angular correlation and distribution measurements were made on several cascades giving evidence for spin assignments for the states at 0, 159, 278, 344, 362, and 663 keV excitation. Detection systems included two lithium-drifted germanium detectors and one NaI(Tl) scintillator. The assignments are compared with other work on this nucleus and arguments are given for a possible shell-model interpretation of the results. (Diss. Abstr. Int., B)

20359 STUDIES OF RESONANCES IN ^{23}Na, ^{26}Mg, ^{41}K, ^{55}Mn, AND ^{59}Co. Stergakos, Elias Peter. Blacksburg, Va.; Virginia Polytechnic Inst. (1970). 60p. University Microfilms Order No. 70-24,221.
Thesis.

The isotopes ^{23}Na, ^{26}Mg, ^{41}K, ^{55}Mn and ^{59}Co were activated by the use of a well collimated, ^{10}B filtered neutron beam from a reactor. An analysis of the induced activity versus ^{10}B filter thickness permitted studies of individual resonances of the target elements. With the assumption of a "1/E" energy dependence for the neutron flux in the beam, it was possible to obtain resonance integrals and partial widths for radiative capture for the individual resonances. The results were normalized to the resonance integral and thermal cross section of gold. Little work of this character has been done previously for these nuclides so that comparative results are not generally available. However, those values that were in the literature, did agree reasonably well with the results. A consistency check obtained by using the values calculated in this work to compute the thermal absorption cross sections showed that the computed cross sections were smaller than or equal to the tabulated absorption cross sections of the elements. Since additional contributions from other resonances would add on to the calculated values, the fact that the tabulated thermal cross sections were not exceeded is in the correct direction. (Diss. Abstr. Int., B)

20360 MUONIC X RAYS AND CAPTURE γ RAYS IN ^{89}Y. Kessler, D. (Carleton Univ., Ottawa); McKee, R. J.; Hargrove, C. K.; Hincks, E. P.; Anderson, H. L. Can. J. Phys.; 48: 3029-37(15 Dec 1970).

The main mu-atomic transition energies in ^{89}Y were measured with a high-resolution Ge(Li) spectrometer. The nuclear charge parameters of yttrium were derived by fitting the observed transition energies to those obtained by numerically solving the Dirac equation, using a radially symmetric Fermi charge distribution. The line intensities were also measured and shown to agree reasonably well with the results of a cascade calculation. Finally, the energies and intensities of the most prominent capture γ rays were measured. Most of these γ rays could be assigned to known transitions in the strontium isotopes 86 through 89. (auth) (Canada)

20361 DECAY OF ^{62}Co ISOMERS AND ^{62}Cu. Eskola, K.; Siivola, A. (Univ. of Helsinki). Ann. Acad. Sci. Fenn., Ser. A VI; No. 329, 1-12(1970).

Excited states of the nucleus ^{62}Ni were studied through the decay of ^{62}Co isomers and ^{62}Cu. The sources were produced through (n,p) reactions on natural nickel metal and through the decay of a source of ^{62}Zn. A total of fourteen excited states were observed in ^{62}Ni. These are at 1172.9, 2048.1, 2301.7, 2336, 3158, 3176, 3256, 3270, 3277, 3369, 3519, 4055, 4063 and 4444 keV. The spins of the ^{62}Co isomers are thought to be 2 and 5 with even parity. (auth) (Finland)

Nuclear Properties and Reactions, A ≥ 90

Refer also to abstracts 18480, 18596, 18703, 18724, 18735, 18737, 18753, 18754, 18772, 19166, 19877, 20133, 20264, 20274, 20282, 20305, 20324, 20327, 20329–20331, 20339, 20352, 20354–20356, 20436, 20431, 20486, 20497, 20499, 20505, 20524, 20530, 20547, 20548, and 20819.

20362 (ANL-7747) PROMPT-NEUTRON SPECTRA AND DELAYED-NEUTRON SPECTRA FROM FISSION: SOME COMMENTS ON CURRENT KNOWLEDGE. Jaffey, Arthur H. (Argonne National Lab., Ill.). Nov 1970. Contract W-31-109-eng-38. 34p. Dep. NTIS.

Work on energy spectra of prompt and delayed fission neutrons is surveyed. The survey covers prompt-neutron spectra for ^{235}U, ^{233}U, ^{239}Pu, ^{241}Pu, ^{238}U, and ^{232}Th irradiated by thermal and high-energy neutrons, and for spontaneous fission of ^{252}Cf, ^{240}Pu, ^{242}Pu, and ^{244}Cm. Although delayed neutron investigations have concentrated on ^{235}U, these spectra are poorly known, with insufficient information for extrapolating to other nuclides. Further, reactor-dynamics calculations indicate that the spectral uncertainties can be important for reactor physics. Many measurements have been made of prompt-neutron spectra, but there is extensive disagreement (outside of statistical error) among these, most likely due to systematic errors in energy calibration of the neutron detectors. Though large shifts in the spectra used in calculations can have important effects in reactor physics, the actual spectra probably do not differ markedly from some average of existing results. Definitive measurements on either prompt- or delayed-neutron spectra would require large undertakings. Data on variation of spectra with neutron-bombarding energy (E_n) are relatively poor. A more reliable value of $d\overline{E}/dE_n$ ($\overline{E}$ = mean energy of fission neutrons) is derivable by evaluating $(d\overline{E}/d\overline{\nu}_p)(d\overline{\nu}_p)/dE_n)$, where $\overline{\nu}_p$ = number of prompt neutrons per fission. Terrell's semitheoretical relation, now experimentally substantiated, yields $d\overline{E}/d\overline{\nu}_p$, and measured values of $d\overline{\nu}_p/dE_n$ are available. 56 references. (auth)

20363 (AWRE-O-86/70) EVALUATION OF $\overline{\nu}$ FOR ^{239}Pu. Mather, D. S.; Bampton, P. F. (Atomic Weapons Research Establishment, Aldermaston (England)). Dec 1970. 18p. (EANDC (UK)-125-AL). Dep. NTIS (U. S. Sales Only).

Data available before July 1970 on direct measurements of $\overline{\nu}$ for the neutron-induced fission of ^{239}Pu are considered, and an evaluation consisting of a set of four straight lines specifying the variation of $\overline{\nu}$ with neutron energy is produced for entry in a new data file DFN-269. (auth)

20364 (BNL-tr-401) RELATIVE MEASUREMENTS OF $\overline{\nu}$ IN THE ^{235}U AND ^{239}Pu FISSION INDUCED BY RESONANCE NEUTRONS. Ryabov, Yu. V.; Sik, So Don; Chikov, N.; Yaneva, N. (Joint Inst. for Nuclear Research, Dubna (USSR)).

Translated by S. J. Amoretty (Brookhaven National Lab., Upton, N. Y.), from report JINR-P3-5297. 21p. Dep. NTIS.

The variation in the average number of neutrons per fission event from resonance to resonance in ^{235}U and ^{239}Pu was examined. Measurements were performed using time-of-flight techniques in the U.I.N.R. fast pulsed reactor. Results of the measurements are presented and discussed. 30 references. (H.D.R.)

20365 (CEA-CONF-1657) STUDY OF (p,d) REACTIONS ON ^{118}Sn AND ^{119}Sn WITH POLARIZED PROTONS. Escudie, J. L.; Gosset, J.; Kamitsubo, H.; Lombard, R.; Mayer, B. (Commissariat a l'Energie Atomique, Saclay (France). Centre d'Etudes Nucleaires). 1970. 2p. (CONF-700911-10). Dep. NTIS (U. S. Sales Only).

From 3rd International Symposium on Polarization Phenomena in Nuclear Reactions, Madison, Wis.

A polarized proton beam was used to induce (p,d) reactions in ^{118}Sn and ^{119}Sn at 24.5 MeV. The cross sections and asymmetries were measured for the transitions to the ground state and the first five levels of ^{117}Sn, and to the ground state and the first excited state of ^{118}Sn. In the ^{118}Sn(p,d)^{117}Sn reaction, three transitions occur with $l = 2$; the j-dependence of the asymmetry for $l = 2$ is shown. The asymmetries for $j = 3/2$ are nearly always negative while the asymmetries for $j = 5/2$ are nearly always positive; the two curves are in phase opposition at forward angles. A D.W.B.A. calculation was performed with optical-potential parameters. These parameters were obtained by fitting the elastic scattering cross sections for both proton and deuteron channels and the polarization for elastic scattering in the proton channel. The agreement of D.W.B.A. predictions with the experimental results is impressive for the $l = 0$ transition. The fit is good for $l = 2$ transitions, but not so good for the asymmetries in $l = 4$ and $l = 5$ transitions although the oscillations are well reproduced. Better fits can be obtained with different optical potential parameters for either the $l = 4$ or the $l = 5$ transitions, but not both. The asymmetry is more sensitive to the optical potential parameters for large l values than for small l values. (auth) (France)

20366 (IEA-211) PHOTOFISSION CROSS SECTIONS OF URANIUM AND THORIUM NEAR THRESHOLD. Mafra, O. Y.; Kuniyoshi, S.; Bianchini, F. G. (Instituto de Energia Atomica, Sao Paulo (Brazil)). May 1970. 17p. Dep. NTIS (U. S. Sales Only).

Using monochromatic gamma rays from (n,γ) reactions, the photofission cross section behavior for natural uranium and thorium was determined in the 5 to 10 MeV energy interval. "Bumps" around the energies of 6 and 6.6 MeV for uranium and around 6.7 and 7.6 MeV for thorium were found. The existence of this structure in the photofission cross section near the threshold is in accordance with Bohr's theory about the excitation of rotational states. (auth)

20367 (INR-P-1216) EQUILIBRIUM DEFORMATIONS OF THE GROUND AND EXCITED STATES IN THE RARE-EARTH NUCLEI. Stepien-Rudzka, W. (Institute of Nuclear Research, Warsaw (Poland)). 1970. 12p. Dep. NTIS (U. S. Sales Only).

The equilibrium deformations of the ground and excited states in nuclei in the rare-earth region are calculated using the new Nilsson model. The residual interactions are taken into account in the form of pairing forces. Comparison is made with previous calculations of similar type together with a suggestion of applying the idea of different deformations in ground and excited states of this same nucleus in analogue state physics. (auth)

20368 (JAERI-Memo-4189) TABLE OF HALF-LIFE, GAMMA-RAY ENERGY, AND INTENSITY OF RADIOISOTOPES. Kumagai, Katsuaki (Japan Atomic Energy Research Inst., Tokyo). Nov 1970. 31p. (In Japanese). Dep. NTIS (U. S. Sales Only).

The gamma-ray energies and the intensities of a number of radioactive nuclei are presented graphically. The radioactive nuclei, which have the half-life of 3.5 sec to 1.12×10^{11} year, are arranged by the order of half-life, and their gamma-ray energies are plotted together with their intensities. Photopeaks in gamma-ray spectra can be easily assigned from this table. (auth) (Japan)

20369 (JINR-P3-5528) PRODUCTION OF SPONTANEOUSLY FISSIONING ISOMERS OF URANIUM, PLUTONIUM, AND AMERICIUM IN THE NEUTRON REACTIONS. Gangrskii, Yu. P.; Nagy, T.; Vinnay, I.; Kovacs, I. (Joint Inst. for Nuclear Research, Dubna (USSR). Lab. of Nuclear Reactions). 1970. 10p. Dep. NTIS.

The cross sections of production of spontaneously fissioning isomers ^{238}U, ^{242}Pu, ^{243}Am in the reaction (n,n′) and ^{242}Am in the reaction (n,2n) were measured. The upper limits of the production of fissioning isomers ^{231}Th, ^{234}U, ^{237}U, ^{238}Pu in the reaction (n,2n) were obtained. The time-of-flight method and neutrons from the reactions ^{3}H + d and ^{9}Be + d were used. (auth)

20370 (JINR-P7-5512) EXPERIMENTS ON MEASUREMENT OF THE COMPOUND NUCLEUS LIFETIME IN THE W(^{22}Ne,f) REACTION. Karamyan, S. A.; Oganesyan, Yu. Ts.; Normuratov, F. (Joint Inst. for Nuclear Research, Dubna (USSR). Lab. of Nuclear Reactions). 1970. 17p. (In Russian). Dep. NTIS (U. S. Sales Only).

The decreasing of the shadow depth in the angular distribution of the fission fragments is found when bombarding the W single crystal with the ^{22}Ne ions of 115-174 MeV energy. This fact is connected with the final lifetime of a compound nucleus from this reaction. The similar effect is not observed for the W(^{16}O,f) reaction at 137 MeV energy ions. The approximate value of the compound nucleus lifetime in the W(^{22}Ne,f) reaction at $E_i = 174$ MeV is 2.5×10^{-18} sec. The main uncertainty of the mentioned value is connected with the fact that there is a set of fissionable compound nuclei with different A in bombarding the natural mixture of W isotopes. (auth)

20371 (JINR-P7-5584) ON THE DELAYED FISSION OF SOME NEUTRON-DEFICIENT ATOMIC NUCLEI. Skobelev, N. K. (Joint Inst. for Nuclear Research, Dubna (USSR). Lab. of Nuclear Reactions). 1971. 10p. (In Russian). Dep. NTIS (U. S. Sales Only).

A possible explanation of the nature of spontaneously fissionable products having a half-life of about 60 s, 1.4 min and 2.6 min connected with the ^{228}Np (^{227}Np), ^{232}Am and ^{234}Am isotopes decay, is analyzed. An observed sharp increase of the probability that these nuclei decay by fissioning can be explained by the delayed fission of the corresponding daughter nuclei of uranium and plutonium from the excited states produced in the electron capture of mother nuclei of ^{228}Np, ^{232}Am and ^{234}Am. (auth)

20372 (KFK-1249) $\beta-\gamma$ (CP)-ASYMMMETRY COEFFICIENTS IN ISOSPIN FORBIDDEN ALLOWED MIXED β TRANSITIONS. Behrens, H. (Kernforschungszentrum, Karlsruhe (West Germany). Institut fuer Experimentelle Kernphysik). Jul 1970. 18p. (CONF-700807-5). Dep. NTIS (U. S. Sales Only).

From Conference on Angular Correlations in Nuclear Disintegration, Delft, The Netherlands.

During the past years a large amount of $\beta-\gamma$ (CP)-asymmetry coefficients have been measured for mixed β-transitions in which the Fermi matrix elements were isospin forbidden. In the following a compilation of all experimental results, their average for the different nuclei, the calculated Fermi matrix elements, isospin impurity coefficients and effective Coulomb matrix elements is given. Where the experimental accuracy should be improved is discussed. (auth)

20373 (LIB-Trans-300) RESEARCH REPORT ON THE MEASUREMENT OF THE AVERAGE NUMBER OF PROMPT NEUTRONS AND OF THE RELATIVE CROSS SECTIONS FOR THE FISSION OF ^{235}U AND ^{239}Pu INDUCED BY NEUTRONS WITHIN THE 0.3 AND 1.4 MeV ENERGY RANGES. Soleilhav, M.; Decarsin, J. P.; Frehaut, J.; Gauriau, J.; Mosinski, G.; Beau, M.; Bertrand, R.; Chardine; Ottoz, A. Translated by P. J. Newton (Australian Atomic Energy Commission Research Establishment, Lucas Heights), from French report. 21p. Dep. NTIS (U. S. Sales Only).

The existence of a structure below 0.7 MeV for $\bar{\nu}_p = f(E)$ in ^{235}U was confirmed, and evidence was obtained of another hump between 0.7 and 1.4 MeV. For ^{239}Pu $\bar{\nu}_p = f(E)$ was very close to a straight line with the possibility of a slight hump near 0.4 MeV. The fission cross section for ^{239}Pu/^{235}U was obtained and approximated that obtained by Davey (1968). Divergence above this value was attributed to lack of data for the 1 to 1.5 MeV region hitherto. Time-of-flight spectra for fissions induced by the neutrons from ^{7}Li(p,n)^{7}Be with 2.7 MeV protons are shown. (Australia)

20374 (NP-18597) ANGULAR CORRELATION STUDIES OF CONVERSION ELECTRONS FROM ^{154}Gd, OF NUCLEAR ELECTRONS FROM ^{48}V AND OF BREMSSTRAHLUNG FROM UNPOLARIZED ELECTRONS. Koopmann, Edzard William (Technische Hogeschool, Delft (Netherlands)). 1970. 74p. Dep. NTIS (U. S. Sales Only).

Thesis.

The influence of the physical condition of the source on the attenuation of the 1276-keV(γ) − 123-keV(γ) directional correlation in ^{154}Gd was investigated. For a europium chloride source surrounded by air, the attenuation of the directional correlation depended on the humidity of the air. For those cases in which the $\gamma-e^-$ and the $\gamma-\gamma$ directional correlations were measured under the same source conditions, good agreement with the theoretical prediction was obtained for the K-shell particle parameter of the 123-keV E2 transition in ^{154}Gd. The $\beta-\gamma$ circular polarization correlation in ^{48}V was measured with a sector-focusing magnetic beta-ray spectrometer, which was used throughout the work reported here. The use of this spectrometer strongly reduces the systematic errors that are inevitable when an anthracene crystal is used. The resulting value of the asymmetry parameter ($A = -0.080 \times 0.023$) supports the validity of the so-called Conserved Vector Current theory. The suggestion that non-nuclear electrons might show an a priori polarization in their interaction was investigated by the measurement of the circular polarization of high-energy bremsstrahlung produced by such electrons. One experiment was performed with the internal conversion electrons from the 662-keV transition in ^{137m}Ba, and another, with electrons of about 2 MeV from a Van de Graaff electron accelerator. The degrees of circular polarization were $(0.0 \pm 5.3) \times 10^{-2}$ and $+(2.9 \pm 2.9) \times 10^{-2}$, respectively, so that no evidence was obtained for violation of parity conservation in electromagnetic interactions. (auth)

20375 (NP-18624) STUDY OF THE TRANSFER MECHANISMS IN THE REACTIONS ^{209}Bi(^{12}C)^{210}At, ^{211}At, ^{210}Po AND ^{209}Bi(^{14}N)^{211}At USING THE RECOIL METHOD. Gardes, Daniel (Paris Univ., Orsay (France)). 1970. 49p. (In French). Dep. NTIS (U. S. Sales Only).

Thesis.

The recoil nuclei from the transfer reactions resulting from the bombardment of a Bi target with C and N ions were studied. The cross sections, angular distributions and recoil paths at certain angles for the radionuclides ^{211}At, ^{210}At, and ^{210}Po were determined A preferential emission of ^{210}At at small angles after the bombardment of Bi with ^{12}C revealed a compound-nucleus mechanism at energies below 80 MeV. With ^{12}C projectiles transfer mechanisms involving α particles or ^{3}He were observed, in particular at high energies. In the case of α-particle transfer the ^{213}At nucleus formed is excited to a sufficiently high energy to evaporate two neutrons subsequently. In the case of ^{3}He transfer, a neutron is emitted by the ^{212}At. ^{4}He transfer followed by the evaporation of 3 neutrons is envisaged in the production of ^{210}At. Two other types of transfer were observed and are responsible for the production of ^{210}Po: the simple transfer of a proton and the transfer of a deuteron followed by the evaporation of a neutron. Certain aspects of the angular distributions are difficult to explain, the most distinct of these aspects being the appearance of a maximum at 17.5° in the laboratory system for all the distributions obtained using ^{12}C projectiles. (France)

20376 (ORNL-tr-2428) NEW TRANSURANIUM ELEMENT FOUND IN NATURE. Nikitin, Andrei. Translated by Francois Kertesz (Oak Ridge National Lab., Tenn.), from Nauka Zhizn; No. 5, 102-7(1970). 12p. Dep. NTIS.

An outline of the discovery of element 108, named sergenium, in samples of volcanic rock is presented. The element is proposed to have chemical properties similar to osmium and a half-life of 4 to 5×10^6 years. (C.E.S.)

20377 (WAPD-TM-971) EVALUATION OF THE RADIATIVE NEUTRON CAPTURE CROSS SECTIONS OF ^{232}Th FOR THE RANGE 0.0 eV TO 15 MeV (LWBR DEVELOPMENT PROGRAM). Steen, N. M. (Bettis Atomic Power Lab., Pittsburgh, Pa.). Dec 1970. Contract AT(11-1)-Gen-14. 94p. Dep. NTIS.

An evaluation of the radiative neutron capture cross sections of ^{232}Th in the range 0.0 eV to 15 MeV was performed. The result is a fully parameterized representation of $\sigma_{n\gamma}(E)$. Of primary interest is the p-wave strength function, which is found to be $(0.914 \pm 0.1) \times 10^{-4}$ for a 3-degree-of-freedom model and $(1.044 \pm 0.1) \times 10^{-4}$ when one degree of freedom is used in the fluctuation of Γ_{n1}. The 2200 m/s cross section is found to be 7.345 ± 0.05 barns with a g-factor of 0.9956. The infinite dilute integral is 85.24 barns. These data were used to reanalyze the ThO$_2$ integral measurements of Hardy and Palowitch ($0.4 \le \sqrt{S/M} \le 1.0$) starting from the experimental activation rates. The resulting experimental and calculated integrals show excellent agreement, as do the calculated and experimental values of I/I_0 for ^{232}Th metal rods with $2.0 \le \sqrt{S/M} \le 7.0$. The reanalysis of the ThO$_2$ integral experiments resulted in a reduction of the experimental integrals of up to 3.5 percent. 52 references. (auth)

20378 ISOBARIC ANALOG STUDIES IN THE OSMIUM AND PLATINUM MASS REGION. Wiesen, Marilyn. New Brunswick, N. J.; Rutgers-The State Univ. (1970). 209p. University Microfilms Order No. 70-16,959.

Thesis.

Isobaric analog states of ^{189,191,193}Os and ^{195,197,199}Pt were studied as compound-nucleus resonances in ^{189,191,193}Ir and ^{195,197,199}Au by proton scattering from isotopically enriched ^{188,190,192}Os and ^{194,196,198}Pt targets. ^{188,190,192}Os(d,p) studies were also performed; the energies of the levels populated in the parent nuclei, ^{189,191,193}Os, by the deuteron stripping reactions were identified up to ~2.0 MeV excitation energy. Parameters for the resonances observed in elastic proton scattering were extracted using a modified R-matrix theory which can treat overlapping resonances; linear energy-dependent optical-model phase shifts are included in order to describe the non-resonant background. Spectroscopic factors for the analogs of the $^9\!/_2{}^+$ states in the odd-mass Pt isotopes were calculated. The sensitivity of these computations to the various input parameters is investigated. Similarities between the results and those found in the Pb isotopes, in particular the non-fragmentation of the $g_{9/2}$ neutron single-particle strengths in the Pt isotopes, are discussed. Off-resonant yields to the first 2^+ states of the even-mass Os and Pt isotopes, at proton energies below the ground-state analog region, are accurately described by semi-classical Coulomb excitation cross sections. Throughout the energy regions where strong resonant structure is observed in the elastic scattering channel, all the 2^+ excitation functions exhibit pronounced interference patterns at backward angles; the nature of this behavior is discussed. Predominantly in the ground-state analog regions, resonant structure is seen in the yields to higher excited states (4^+ and second 2^+ states, etc.). In contrast, bands of states centered at ~4.0 MeV excitation energy in ^{194}Pt and ^{196}Pt are only observed at proton energies corresponding to the formation of the $^9\!/_2{}^+$ analogs of ^{195}Pt and ^{197}Pt. Coulomb displacement energies, deduced from analyses of the analog resonances observed in elastic scattering, are compared with the predictions of a uniform, spherical charge-distribution model. Deviations from this model, attributed to deformation in these transitional nuclei, are considered in terms of a uniform, ellipsoidal charge-distribution. Coulomb displacement energy systematics are also extended to this general region of the periodic table. (Diss. Abstr. Int., B)

20379 ACTIVATION MEASUREMENTS OF THE CROSS SECTION OF THE REACTION ^{147}Pm(n,γ)^{148g}Pm FOR REACTOR NEUTRONS. Cabell, M. J. (Atomic Energy Research Establishment, Harwell, Eng.). J. Inorg. Nucl. Chem.; 32: 3433-40(Nov 1970).

The effective cross section of this reaction was measured for reactor neutrons. The ^{197}Au and ^{59}Co monitors were used to determine the 2200 m/sec neutron fluxes in the spectra employed, and cadmium ratio measurements for gold and the silver-cobalt activity ratio method were used to determine the epithermal indices. The amounts of ^{148g}Pm formed, and the amounts of ^{147}Pm from which they were formed, were both determined after purification of the irradiated material. Gamma-spectrometry was used for the former purpose, and the $4\pi\beta-\gamma$ tracer method, with ^{46}Sc as the tracer, was used for the latter. The cross section of the reaction for Maxwellian neutrons ($\sigma_0 g$) and its reduced resonance integral (Σ') were found to be 96.0 ± 1.8 barns respectively. (auth) (UK)

20380 TWO-QUASIPARTICLE LEVELS OF ^{176}Yb. **Grigor'ev, E. P. (Leningrad State Univ.). Izv. Akad. Nauk SSSR, Ser. Fiz.; 34: 901-3(1970). (In Russian).**

The literature data is reviewed in order to reach definite conclusions on the quantum characteristics of ^{176}Yb levels and the ground state of ^{176}Tm. It is argued that the 95.9-keV transition from the 12-second isomeric level is an E1 transition, and that the spin and parity of the 1050-keV level is 8^- with the probability that this is a two-quasineutron level. Agreement was obtained between the experimental and calculated values of the rotational level energies of 565.0 and 954.2 keV for the ground band with quantum characteristics of 6^+ and 8^+. In this way the evidence is reviewed to assign quantum characteristics to all the observed levels of ^{176}Yb and to the ground state of ^{176}Tm. Thus in ^{176}Yb the 2960-keV level is 8^+, the 2090-keV level is 6^+, the 1050.1-keV level is 8^-, the 954.2 keV level is 8^+, the 565.0-keV level is 6^+, the 262.1-keV level is 4^+, and the 82.13-keV level is 2^+ and the ground state of ^{176}Yb is 0^+. The ground state of ^{176}Tm is 7^+. (TTT)

20381 THE 3.0 MN ISOMER OF ^{138}Cs. **Carraz, Louis-Claude; Blachot, Jean; Monnand, Edouard; Moussa, Andre (CEA, Grenoble, France). Compt. Rend., Ser. B; 271: 545-8(14 Sep 1970). (In French).**

An isomer of 3.0 mn of ^{138}Cs was discovered. The β^- decay of this isomer leads to a metastable level of ^{138}Ba ($T_{1/2}$ = 0.8 μs). (auth) (France)

20382 THE DECAY OF ^{232}Np. **Hollstein, M.; Muenzel, H.; Pfennig, G.; Reuter-Weiss, R. (Kernforschungszentrum, Karlsruhe, Ger.). J. Inorg. Nucl. Chem.; 32: 3159-63(Oct 1970).**

The decay of ^{232}Np was studied by γ-spectroscopy. This nuclide decays predominantly by electron capture with a half-life of 14.7 ± 0.3 min. Eight new transitions and two levels above 1.051 MeV were found for the daughter nucleus ^{232}U. The energy and relative intensity of fifteen γ-lines, EC- and γ-branching intensities are given. A decay scheme is proposed. (auth) (UK)

20383 VALIDITY OF THE NILSSON MODEL FOR PROTON STATES IN THE REGION A = 151 TO 155. Burke, D. G.; Waddington, J. C.; Tippett, J. C. (McMaster Univ., Hamilton, Ont.). Phys. Lett.; 33B: 460-2(7 Dec 1970).

The spectroscopic factors for (α,t) reaction studies of ^{151}Pm, ^{153}Eu, and ^{155}Eu show that the Nilsson model in its simplest form excellently explains the observed proton states in this mass region where the structure of neutron states is extremely complex. (auth)

20384 DECAY OF ^{90}Kr AND ^{90}Rb. Mason, J. F.; Johns, M. W. (McMaster Univ., Hamilton, Ont.). Can. J. Phys.; 48: 2056-82 (1 Sep 1970).

The decay of 32 s ^{90}Kr and 154 s ^{90}Rb was studied using NE102 beta detectors and NaI(Tl) and Ge(Li) gamma-ray detectors, singly and in coincidence. Thirteen excited states of ^{90}Rb involving 35 transitions were identified with excitation energies of 0.1064, 0.1215, 0.2419, 0.3557, 0.6144, 0.6610, 0.7408, 0.8375, 1.2402, 1.6740(1^+), 1.7798(1^+), 2.1261(1^+) and 3.0937(1^+) MeV. The 256 s isomeric state at an excitation of 0.1064 MeV (probably 4−) feeds high spin states of ^{90}Sr at 2.2068, 2.4972, 2.5712, 2.9275, 3.5835, 4.1485, 4.3355, and 5.0397 MeV with a total intensity of 12%. The 154 s ground state of ^{90}Rb feeds many low spin states in ^{90}Sr, including the levels at 0.8315, 1.6555, 1.8921, 2.5271, 3.0385, 3.3833, 3.4497, 3.8985, 4.0325, 4.0360, 4.1360, 4.3660, 4.6466, 4.891, 4.921, 4.964, 5.070, 5.091, 5.163, 5.1876, 5.2540, 5.285, and 5.3336 MeV. Sixty-four transitions in ^{90}Sr were classified in this manner. The decay energy of ^{90}Kr is 4.41 ± 0.03 MeV. (auth) (Canada)

20385 DIRECTIONAL CORRELATIONS OF GAMMA RAYS IN ^{152}Sm AND ^{152}Gd MEASURED BY MEANS OF TWO Ge (Li) COUNTERS. Barrette, J.; Barrette, M.; Boutard, A.; Lamoureux, G.; Monaro, S. (Univ. of Montreal). Can. J. Phys.; 48: 2011-22 (1 Sep 1970).

Directional correlation measurements were performed with two Ge(Li) counters on several γ rays in coincidence with the 121.78 and 334.31 keV γ transitions which de-excite the first 2^+ levels in ^{152}Sm and ^{152}Gd, respectively. A total of 20 $\gamma-\gamma$ directional correlations, 13 in the ^{152}Sm nucleus and 7 in the ^{152}Gd nucleus, was measured simultaneously. Several of the $\gamma-\gamma$ directional correlations involved gamma transitions of weak intensity, for example the (688.66−121.78), (1457.4−121.78), and (1528.16−121.78 keV cascades in ^{152}Sm and the (586.29−334.31) and (1089.73−334.31) keV cascades in ^{152}Gd. Among the various results which could be extracted from these measurements, the most interesting appears to be the determination of a nearly pure E2 character for the 688.66, 964.01, 1112.04, and 867.33 keV gamma transitions. The first two γ rays de-excite the 2^+ β- and γ-vibrational levels to the 2^+ ground-state rotational level at 121.78 keV in ^{152}Sm, whereas the last two γ rays de-excite the 3^+ γ-vibrational level to the 2^+ and 4^+ (at 366.44 keV) ground-state rotational levels in ^{152}Sm. (auth) (Canada)

20386 ANGULAR DISTRIBUTION OF GAMMA RAYS RESULTING FROM POLARIZED ^{124}Sb, ^{192}Ir, AND ^{194}Ir. Sites, James R.; Steyert, W. A. (Los Alamos Scientific Lab., N. Mex.). Nucl. Phys.; A156: 19-27(1970).

A ^{3}He−^{4}He dilution refrigerator coupled with adiabatic demagnitization was used to polarize ^{124}Sb, ^{192}Ir and ^{194}Ir dissolved in an iron foil. The angular distributions of the emitted γ-rays are measured. The magnitude of the ^{124}Sb magnetic moment is determined to be $\pm(1.42 \pm 0.1)\mu_N$. The angular momentum carried off in many of the β-decays and a number of γ-decay mixing ratios in the daughter nuclei are reported. These results include the observation that 67 ± 12% of the 2313 keV ^{124}Sb β-rays carry off 2 units of angular momentum, an unusually large proportion. Also, in the 2091 keV E1 γ-rays of ^{124}Te, there is a 0.07 ± 0.03 M2 amplitude admixture. (auth)

20387 REVISED LEVEL SCHEME OF ^{199}Hg FOLLOWING COULOMB EXCITATION. Kalish, Rafael (Massachusetts Inst. of Tech., Cambridge. Univ. of Wisconsin, Madison. Technion-Israel Inst. of Tech., Haifa); Borchers, R. R.; Kugel, H. W. Nucl. Phys.; A161: 637-49(1971).

Gamma transitions of ^{199}Hg were investigated following Coulomb excitation with oxygen ions at different bombarding energies. Angular distributions with and without coincidence with backscattered oxygen ions were measured. Ge(Li) γ spectra were measured in triple coincidence with γ rays and backscattered particles. A level is reported at 413.5 keV and assigned a spin of $\frac{5}{2}^-$. A spin of $\frac{3}{2}^-$ is assigned to the level at 403.4 keV instead of the $\frac{1}{2}^-$ spin assigned previously. B(E2)↑ values measured relative to B(E2)↑(158.37 keV) = 0.375(17) are 0.248(15), 0.170(20), and 0.099(16) for the 208.3, 403.4, and 413.5 keV transitions, respectively. The measured mixing ratios are −0.65(25) and +0.32(2) for the 208.3 ($\frac{3}{2}^- \rightarrow \frac{1}{2}^-$) and 403.4 ($\frac{3}{2}^- \rightarrow \frac{1}{2}^-$ keV transitions, respectively. The revised decay scheme is presented and discussed. The same experimental techniques were used to Coulomb excite ^{201}Hg. No γ transitions up to an energy of 1000 keV in coincidence with 60 million backscattered particles could be seen when an 85% ^{201}Hg enriched target was bombarded with 33-MeV ^{16}O ions. (auth)

20388 ^{141}Nd LEVELS EXCITED FROM ^{141}Pm(21 MIN) DISINTEGRATION. Charvet, A.; Duffazt, R.; Emsallem, A.; Chery, R. (Univ., Lyon). J. Phys. (Paris); 31: 737-42(Aug-Sep 1970). (In French).

The decay of ^{141}Pm($T_{½}$ = 21 min) was studied using Ge(Li) and Si(Li) detectors. The energies and intensities of the γ transitions, the intensities of the conversion lines, the $\gamma-\gamma$ coincidence spectra and the sum spectrum obtained with a well-type Ge(Li) detector were measured. According to the results, 11 levels were established having the following energies (in keV); 193.7 keV ($\frac{1}{2}^+$); 1 223.3($\frac{5}{2}^+$); 1 345.4($\frac{5}{2}^-$, $\frac{7}{2}^-$); 1 564.7; 1 596.9($\frac{3}{2}^+$, $\frac{5}{2}^+$); 1 820.2; 1 897.0: 1 967.4($\frac{7}{2}^+$); 2 073.5($\frac{3}{2}^+$; $\frac{3}{2}^+$); 2 109.4($\frac{5}{2}^+$, $\frac{7}{2}^+$) and 2 247. The decay scheme accounts for 19 of the 24 transitions observed. The half-life of the first excited level was found to be (1.17 ± 0.15) 10^{-9} second. The Q-value of the decay ^{141}Pm → ^{141}Nd was determined to be 3 730 ± 40 keV. The nature of excited states of ^{141}Nd are discussed in terms of the conventional nuclear models. (auth) (France)

20389 THE FORMATION RATIO OF ^{236}Np ISOMERS IN ^{238}U DEUTERON INTERACTIONS. Fleury, Alain; Larrea, Francoise; Simonoff, Gabriel (Bordeaux Univ., Gradignan, France). Compt. Rend., Ser. B; 271: 1116-18(30 Nov 1970). (In French).

The variations in the ratio of the ^{236}Np isomers formed in the reaction ^{238}U(d,4n)^{236}Np between 20 and 65 MeV, were investigated with respect to incident energy and angular momentum. The isomer of half-life 22 hours was detected by measuring the activity of its daughter product ^{236}Pu, while the isomer of half-life 5000 years was analyzed by mass spectrometry. The isomeric ratios increase successively with increasing incident particle energy. (auth) (France)

20390 STUDY OF HIGH ENERGY REACTIONS WITH Ho AND Tm. Demeyer, A.; Chery, R.; Chevarier, Noelle; Chevarier, A.; Tousset, J.; Tran Minh Duc (Lyon Univ., Villeurbanne, France). J. Phys. (Paris); 31: 847-54(Oct 1970). (In French).

Cross sections for the reactions (α,xn) and [(α,xn) + (α,p(x−1)n)] produced by alpha particles impact with ^{169}Tm and ^{165}Ho were measured for energies up to 150 MeV. Excitation functions were calculated in terms of a statistical theory using a spin level density parameter and the pre-equilibrium model of Griffin. (auth) (France)

20391 NATURAL ALPHA RADIOACTIVITY OF SAMARIUM. Gupta, M. C.; MacFarlane, R. D. (McMaster Univ., Hamilton, Can.). J. Inorg. Nucl. Chem.; 32: 3425-32(Nov 1970).

The half-life and alpha particle energy of ^{147}Sm were remeasured using a high resolution cylindrical ionization chamber. The alpha decay of ^{148}Sm was also detected and the results are consistent with those obtained independently by Korolev. Alpha decay from ^{146}Sm and ^{149}Sm was not observed. The results for ^{148}Sm and ^{149}Sm are not in agreement with those obtained by Karras. (auth) (UK)

20392 ANOMALOUS ^{96}Zr RESONANCE INTEGRAL TO THERMAL ACTIVATION CROSS-SECTION RATIO AND THE NEUTRON ACTIVATION RESONANCE INTEGRAL OF ^{94}Zr AND ^{96}Zr. Ricabarra, M. D.; Turjanski, R.; Ricabarra, G. H. (Comision Nacional de Energia Atomica, Buenos Aires). Can. J. Phys.; 48: 2362-70(15 Oct 1970).

Values of the reduced activity resonance integral relative to the thermal cross section, I'/σ_0, of ^{96}Zr and ^{94}Zr were determined relative to gold by measuring cadmium ratios in a reactor spectrum. Due to the anomalous characteristics of ^{96}Zr a measurement of I'/σ_0 for ^{96}Zr was undertaken in a "quasi" thermal spectrum. ^{96}Zr and ^{94}Zr activation resonance integrals were also determined by measuring the ratio of effective activation cross section of zirconium to ^{55}Mn. International Atomic Energy Agency (IAEA)-calibrated gamma sources were used to determine the samples' absolute activities. A lithium-drifted germanium γ-ray spectrometer was used in all cases to resolve the activities of the irradiated samples. The results for ^{96}Zr are $I'/\sigma_0 = 879 \pm 96$, $I' = 4.97 \pm 0.50$ b, and $\sigma_0 = 5.7 \pm 1.0$ mb; for ^{94}Zr, $I'/\sigma_0 = 587 \pm 0.05$, $I' = 0.369 \pm 0.037$ b, and derived $\sigma_0 = 63 \pm 8$ mb. I'/σ_0 for ^{96}Zr is an order of magnitude or more greater than that found for stable isotopes. This suggests that almost 100% of the activation resonance integral of ^{96}Zr consists of p-neutron captures. This fact is not consistent with the present knowledge of p-strength functions in the 90 < A < 130 mass region. (auth) (Canada)

20393 FISSION OF ^{238}U INDUCED BY NEUTRONS AT ENERGIES NEAR THE THRESHOLD. Lo Nigro, S.; Milone, C. (Univ., Catania, Italy. Istituto Nazionale di Fisica Nucleare, Catania, Italy). Lett. Nuovo Cim.; 4: 808-10(24 Oct 1970).

Angular distributions of the fragments from neutron fission of ^{238}U near the threshold were calculated for the case where the fission occurs through several states in such a way that statistical considerations on K values are possible; the K distribution was assumed as Gaussian. In the range $1.35 < E_n < 1.55$ MeV the calculated angular distributions disagree with the experimental ones and do not explain the large change of the anisotropy ratio vs E_n

found experimentally. It is concluded that a statistical distribution of K values near threshold is unlikely. (R.W.R.)

20394 STUDYING THE MECHANISM OF THE ^{114}Sn(γ,p)^{113}In REACTION IN THE REGION OF THE GIANT DIPOLE RESONANCE. Brovtsyn, V. K.; Osokina, R. M. (All-Union Research Inst. of Nuclear Geophysics and Geochemistry, Moscow). Izv. Akad. Nauk SSSR, Ser. Fiz.; 34: 927-30(1970). (In Russian).

From experimental studies on cross sections of (γ,p) reactions for nuclei with $Z > 30$, it follows that, as a rule, the cross-section maximum is at an energy a few MeV above the maximum of the giant dipole resonance. This fact was surprising until it was explained that the emission of photoprotons by nuclei with $N > Z$ is associated with the excitation of isobaric-analog dipole states with isospin $T = T_0 + 1$ (T_0 = isospin of ground state), the decay of which by the neutron route is forbidden by the selection rules on isotopic spin. At the same time shell calculations of the photodecomposition of a number of even tin isotopes showed via a model of a "quasi-direct" photoeffect that a noticeable cross section for the emission of photoprotons should be expected in the case of light tin isotopes with isospin $T = T_0$ in the region of the giant dipole resonance. Hence, a series of measurements was undertaken to determine the yield of the ^{114}Sn(γ,p)^{113}In* reaction with respect to the yield of the ^{124}Sn(γ,n)-^{123}Sn reaction at excitation energies from 12 to 22 MeV. Samples enriched to 63.2% in the ^{114}Sn were used. The probability of the (γ,p) reaction was found to be negligibly small up to a gamma energy of 16 MeV, and considerably below the calculated value at higher gamma energies. Thus, the experimental results do not confirm the predictions of the "quasi-direct" photoeffect, which indicated a significant cross section for the (γ,p) reaction with ^{114}Sn in the region of the giant dipole resonance. Configurations with states of a more complex nature must also play an essential role in photodecomposition reactions. (TTT)

20395 NUMBER OF RESONANCES TO BE ADOPTED FOR OBTAINING PRACTICALLY RELIABLE CROSS SECTION CURVES. Takano, Hideki; Katsuragi, Satoru; Ishiguro, Yukio; Nakagawa, Masayuki (Japan Atomic Energy Research Inst., Tokai). J. Nucl. Sci. Technol. (Tokyo); 7: 592-5(Nov 1970).

In order to obtain reliable cross-section curves a practicable limit for the number of resonances λ to be considered must be set. The conditions to be fulfilled determining this limit are presented. The dependence of various cross sections of Pu and U on λ and temperature is given. The number of resonances λ that should satisfy all conditions for reliable s-wave cross sections are tabulated for ^{235}U, ^{238}U, and ^{239}Pu for temperatures of 300, 900, and 2100°K. (R.W.R.)

20396 FINE STRUCTURE IN HIGHLY EXCITED ANALOG STATES. Goulard, B. (Laval Univ., Quebec); Fallieros, S. Can. J. Phys.; 48: 2210-11(15 Sep 1970).

The nature of the fine structure surrounding analog states at relatively high excitations is discussed and compared with the corresponding structure at lower energies. (auth) (Canada)

20397 DETERMINATION OF THE NUCLEAR MAGNETIC MOMENT OF ^{203}Hg BY MEANS OF OPTICAL PUMPING AND POLARIZATION OF THE $^2S_{½}$ GROUND STATE OF EVEN ISOTOPES OF THE MERCURY ION BY STEPWISE ELECTRON EXCITATION. King, Richard Lien-chao. New York; New York Univ. (1970). 130p. University Microfilms Order No. 70-19,009.

Thesis.

A direct measurement of the ratio of the nuclear g values of ^{201}Hg and ^{203}Hg was obtained by optical pumping of the 6s^2 $^1S_0$ atomic ground state. The result is g(^{201}Hg)/g(^{203}Hg) = −1.09984(18). The sign results from a prior spectroscopic experiment. Without diamagnetic corrections the nuclear magnetic moment of the 47-d radioisotope ^{203}Hg is $^{203}\mu = 0.83549(13)\ \mu_N$ if the value $^{201}\mu = -0.553144(9)\ \mu_N$ is used for ^{201}Hg. The effect of distributed nuclear magnetization gives a hfs anomaly $^{203}\Delta^{201} = 0.0064(1)$. The pile-produced (n,$\gamma$) reaction was electromagnetically enriched such that the ratio of ^{203}Hg to ^{201}Hg was unity within a factor of two. The number of atoms of ^{203}Hg in the resonance cell was approximately 10^{13}—10^{14} have been used with prior optical pumping experiments of mercury. The 6s $^2S_{½}$ ground ionic state of even isotopes of mercury was polarized in a stepwise excitation process from the atomic 6s $^1S_0$ ground state via the metastable 6s6p $^3P_2$ state. The latter was optically pumped with circularly polarized 6461-Å (6s7s $^3S_1-{}^3P_2$) radiation. Paramagnetic resonance, observed by monitoring the change in intensity of the relatively intense 2815-Å (5d^{9}6s^2 $^2D_{½}$−5d^{10}6s $^2S_{½}$) electric-quadrupole resonance radiation, was used to determine the polarization of the even-isotope ground-state ion to be 15%. If spin angular momentum is conserved, this process should yield highly polarized electrons. (Diss. Abstr. Int., B)

20398 ALPHA-GAMMA ANGULAR CORRELATION AND HYPERFINE INTERACTION IN THE DECAY OF ^{249}Cf. Falk, F.; Linnfors, A.; Orre, B.; Thun, J. E. (Univ. of Uppsala). Phys. Scr.; 1: 13-19(1970).

The angular correlation between the main α transition (5.81 MeV) and the following 388-keV E1 gamma transition (and in one case also the 333-keV E1 transition branching from the same level) in the decay of $^{249}_{98}$Cf to $^{245}_{96}$Cm has been studied. Thin sources were used. The recoiling daughter ions were allowed to escape into vacuum. The strong hyperfine interaction perturbing the correlation in this case was neutralized by a longitudinal decoupling field with a strength of some kilogauss. The unperturbed values of the A_{22} coefficients do not support the mixing ratios ($L = 0$, $L = 2$, $L = 4$) from the Bohr−Froeman−Mottelson theory. The correlation was also studied in silver and nickel surroundings where it was found to be almost unperturbed. In an insulator a strong perturbation was found which was not influenced by the longitudinal field. (auth) (Sweden)

20399 ISOMER SHIFT AND QUADRUPOLE SPLITTING OF THE 2$^+$-ROTATIONAL STATE IN ^{174}Yb. Henning, W.; Baehre, G.; Kienle, P. (Technische Univ., Munich). Z. Phys.; 241: 138-49(1971).

The change of the charge radius and the quadrupole moment of the 2$^+$-rotational state of ^{174}Yb were determined from Moessbauer measurements. Comparison with ^{170}Yb reveals slightly increasing rigidity at constant equilibrium deformation if two neutron pairs are added. Theoretical predictions are discussed, in connection with additional experimental data. (auth)

20400 DIRECTIONAL CORRELATIONS OF SOME γ-RAY CASCADES IN ^{200}Hg. Hattula, J.; Helppi, H.; Kantele, J. (Univ. of Jyvaeskylae, Finland). Z. Phys.; 241: 117-23(1971).

Directional correlation functions of 10 γ-ray cascades in ^{200}Hg were measured using a ^{200}Tl source and a Ge(Li)−NaI(Tl) coincidence spectrometer arrangement. Values of the mixing parameter δ for several transitions are determined and the spin assignments for the following levels in ^{200}Hg are established (level energies are given in keV): 1029.4 (0^+), 1254.2 (2^+), 1573.7 (2^+), 1593.4 (2^+), 1641.5 (2^+), 1730.9 (2^+) and 1775.6 (3^+). (auth)

20401 LEVEL STRUCTURE OF ^{120}Sn FROM THE DECAY OF ^{120}In AND ^{120}Sb ISOMERS. Liukkonen, E.; Hattula, J. (Univ of Jyvaeskylae, Finland). Z. Phys.; 241: 150-65(1971).

Gamma rays in the decay of the 3.2 s (1^+) and 44 s ($4,5^+$) ^{120}In isomers and the 15.9 min (1^+) and 5.8 d (8^-) ^{120}Sb isomers were investigated using Ge(Li) spectrometers and prompt and delayed Ge(Li)−NaI(Tl) coincidence techniques. The constructed level scheme of ^{120}Sn contains 18 levels at the following energies (keV): 0 (0^+), 1171.6 (2^+), 1875.6 (0^+), 2096.9 (1,2,3), 2160.7 (0^+), 2195.0 (4^+), 2284.8 (5^-), 2355.6 (2^+), 2421.2 (1,2,3), 2466.3 (4^+), 2482.1 (7^-), 2643.5 (4^+), 3058.6 (4^+), 3179.7 (4^+), 3349.9 ($3,4^+$), 3440 ($3,4^+$), 3447.6 ($5,6^+$) and 3777 (4^+). The levels are compared with the levels obtained from recent charged-particle reaction studies and the structure of ^{120}Sn is briefly discussed in view of the latest quasiparticle calculations. (auth)

20402 INVESTIGATION OF GAMMA RADIATION OF ISOMERS ^{110m}In AND ^{110}In. Burmistrov, V. R.; Didorenko, V. A.; Andreev, Yu. A. Izv. Akad. Nauk Kaz. SSR, Ser. Fiz.-Mat.; No. 6, 77-85(Nov-Dec 1969). (In Russian).

The γ spectra from the decays of ^{110m}In and ^{110g}In were studied using Ge(Li) detectors with an energy resolution of 5 keV at 662 keV. A total of 40 gamma transitors were observed with 34 being seen for the first time. The results agree with the decay mode of the ^{110}Cd 2221-keV level as proposed from ^{110m}Ag decay studies, but disagree with the proposed mode for the 2926-keV level. A level at 2561.4 keV was confirmed, but the previously proposed level at 1716 keV was not seen. A new level at 3526.2 keV is proposed. (tr-auth)

20403 ISOMER SHIFTS AND CHANGES OF THE NUCLEAR CHARGE RADII IN ^{99}Ru AND ^{101}Ru. Potzel, W. (Technische Univ., Munich); Wagner, F. E.; Moessbauer, R. L.; Kaindl, G.; Seltzer, H. E. Z. Phys.; 241: 179-87(1971).

The recoilless nuclear γ resonance of the 127 keV γ-rays of ^{101}Ru was observed in ruthenium metal, RuO$_2$ and [Ru(NH$_3$)$_4$HSO$_3$)$_2$]. By comparison of the isomer shifts observed in these materials for the 127 keV absorption line with the corresponding shifts of the 90 keV γ-rays of ^{99}Ru one obtains $\delta\langle r^2\rangle[127\ \text{keV}]/\delta\langle r^2\rangle[90\ \text{keV}] = 1.78 \pm 0.26$ for the ratio of the changes of the mean square nuclear charge radii between the first excited and the ground states in these nuclei. An estimate of electron density differences based on free-ion relativistic self-consistent field calculations yields $\delta\langle r^2\rangle/\langle r^2\rangle[90\ \text{keV}] \approx +1.4 \cdot 10^{-3}$ for ^{99}Ru and $\delta\langle r^2\rangle/\langle r^2\rangle[127\ \text{keV}] \approx +2.4 \cdot 10^{-3}$ for the ^{101}Ru case. These results are discussed in terms of the core excitation model. (auth)

20404 DIRECTIONAL CORRELATIONS OF GAMMA-RAY CASCADES IN ^{103}Rh. George, M. C. (Alabama A and M Univ., Normal); Mukerji, A. Can J. Phys.; 48: 2699-2706(15 Nov 1970).

The directional correlations of the 557−53-keV and the 444−53-keV gamma-ray cascades observed in the decay of ^{103}Ru were studied. Dilute liquid sources ($RuCl_2$ in HCl) of varying activity and of predetermined correlation times τ_c were used. The unperturbed angular correlation functions were evaluated to be: 557−53 keV $W(\theta) = 1 + (-0.1310 \pm 0.0140)P_2(\cos\theta) + (-0.046 \pm 0.050)P_4(\cos\theta)$; 444−53 keV $W(\theta) = 1 + (0.121 \pm 0.060)P_2(\cos\theta) + (0.08 \pm 0.10)P_4(\cos\theta)$. Spins and parities of the 650- and 537-keV levels of ^{103}Rh deduced from the analysis of the experimental data and consistent with the restriction of the 53-keV gamma as an M1 transition, indicated by internal conversion coefficient results, are discussed. (auth) (Canada)

20405 DECAY OF ^{155}Ho. Torres, Jean-Philippe; Paris, Pierre; Lecouturier, Daniel (CNRS, Orsay, France). Compt. Rend., Ser. B; 271: 806-8(12 Oct 1970). (In French).

Semiconductor detectors and a magnetic spectrograph were used to study the transitions between the excited levels of ^{155}Dy observed in the decay of ^{155}Ho. An energy level scheme is proposed. (auth) (France)

20406 FRACTIONAL CUMULATIVE YIELD OF 2.6-MIN ^{99m}Nb FROM LOW ENERGY NEUTRON FISSION OF ^{233}U, ^{235}U, ^{238}U, AND SPONTANEOUS FISSION OF ^{252}Cf. Harbour, R. M.; Troutner, D. E. (Univ. of Missouri, Columbia. Oak Ridge National Lab., Tenn.). J. Inorg. Nucl. Chem.; 33: 1-8(Jan 1971).

Rapid chemical separations of niobium and zirconium from molybdenum were used to measure the fractional cumulative yields of 2.6 min ^{99m}Nb from thermal-neutron fission of ^{233}U and ^{235}U, the epithermal-neutron fission of ^{238}U and the spontaneous fission of ^{252}Cf. The yields are 0.29 ± 0.02, 0.31 ± 0.02, 0.30 ± 0.03 and 0.29 ± 0.03, respectively. The half-life of the long-lived isomer of ^{99}Nb was remeasured and found to be 2.6 ± 0.2 min. The fraction of ^{99}Zr decaying to 2.6 min ^{99m}Nb was found to be 0.30 ± 0.04. The measured yields are consistent with the expected charge distribution for each fission process if it is assumed that most of the independently produced ^{99}Nb is formed as the short-lived high-spin ground state. (auth) (UK)

20407 DECAY OF ^{113m}In. Goodier, I. W.; Hughes, F. H.; Woods, M. J. (National Physical Lab., Teddington, Eng.). Int. J. Appl. Radiat. Isotop.; 21: 678-9(Nov 1970).

The total internal conversion coefficient and the half-life of ^{113m}In, obtained by elution of a ^{113}Sn column, were measured. Aliquots of stock solution of ^{113m}In were measured in a calibrated high-pressure ionization chamber to determine the γ-quanta emission rate and in a $4\pi\beta$ proportional counter to obtain the conversion electron emission rate. The half-life was obtained by following the decay of ^{113m}In in two samples both over a six cycle period in the high pressure ionization chamber. Possible sources of error are discussed. Six production models of the ionization chambers used (NPL 1383 A) were checked for variation of sensitivity to γ emitters of energy above 300 keV and were found to be within the ±1% tolerance. (UK)

20408 THE ^{125}Sb–^{125}Te DECAY. Nagpal, T. S.; Gaucher, R. E. (Bishop's Univ., Lennoxville, Quebec). Can. J. Phys.; 48: 2978-83(15 Dec 1970).

The γ and internal conversion transitions in the ^{125}Sb−^{125}Te decay were examined with Ge(Li) and Si(Li) spectrometers. The measurements of their energies, intensities, K-conversion coefficients, and K/L ratios are used to construct a decay scheme of ^{125}Sb. (auth) (Canada)

20409 DOPPLER SHIFT ATTENUATION STUDIES IN HEAVY NUCLEI. Stokstad, R. G.; Fraser, I. A.; Greenberg, J. S.; Sie, S. H.; Bromley, D. A. (Yale Univ., New Haven). Contract AT(30-1)-3223. Nucl. Phys.; A156: 145-69(1970).

The Doppler shift attenuation method for measuring nuclear lifetimes was previously used primarily in studies of light nuclei. An extension of this technique to the heavy, rare earth nuclei is described. Doppler broadened γ-ray line shapes, observed in Coulomb excitation studies utilizing heavy ions incident on thick ^{150}Nd and ^{152}Sm targets, were analyzed using a two-parameter phenomenological representation for the stopping power suggested by Warburton et al. Good fits were obtained to line shapes observed in transitions from nine different levels with mean lifetimes varying from about 1 ps to 16 ps. The lifetimes deduced from the line-shape analyses are in excellent accord with those established from measured Coulomb excitation probabilities if a value of α = 1.25 ± 0.14 ps is used for the average characteristic electronic stopping time for Nd and Sm ions recoiling in thick Nd and Sm targets. The Lindhard-Scharff estimate for α is about 10% larger than this value and deviates in the direction suggested by the results of Moak and Brown obtained in stopping power measurements for iodine ions in various materials. The present measurements also indicate that, for heavy ions with initial recoil velocities greater than c/137, the theory of Lindhard, Scharff and Schiøtt provides a reliable estimate of the parameter K_e/K_n, representing the ratio of electronic and nuclear stopping power. The phenomenological representation for the stopping power is compared with a calculation based on work by Lindhard et al., and by Blaugrund which considers the effects of nuclear scattering on the direction and magnitude of the recoil-ion velocity. The effects of cascade feeding of a level on the deduced lifetime are examined. It is concluded that the phenomenological approach of Warburton et al., which has been employed previously in measurements on light nuclei, can also be used effectively for analyzing the Doppler broadened γ-ray line shapes which may be observed following heavy-ion induced excitation of nuclei in the medium and heavy mass regions. (auth)

20410 $^{115}In(n,\gamma)^{116}In$ REACTION. Lone, M. A.; Earle, E. D.; Bartholomew, G. A. (Atomic Energy of Canada Ltd., Chalk River, Ont.). Nucl. Phys.; A156: 113-32(1970).

High-energy γ-rays following neutron capture at thermal energies and at the 1.46, 3.86, 9.12, 12.1, 23.0, 39.9 and (46.3 + 48.6) eV resonances in natural In are examined. Details of the level structure of ^{116}In are deduced and the partial radiation widths of primary transitions determined. The neutron separation energy is found to be 6781 + 3 keV. Strength functions are derived E1 and M1 transitions. The E1 strength is found to remain constant and the M1 strength to decrease with γ-ray energy from 5.2 to 6.7 MeV. (auth)

20411 LOW-INTENSITY GAMMA RAYS IN ^{90}Nb DECAY. Tucker, A. B.; Simmons, S. O. (Ames Lab., Iowa). Nucl. Phys.; A156: 83-92(1970).

Gamma rays de-exciting levels in ^{90}Zr populated in the decay of ^{90}Nb were analyzed with a Ge(Li) spectrometer. To enhance photopeaks from the weak transitions observed in recently reported conversion electron studies, the Compton background from the strong high-energy lines in the spectrum was suppressed by partially surrounding the Ge(Li) detector with a NaI(Tl) scintillator operated in anticoincidence. Energies, intensities, K-conversion coefficients, and probable multipolarities were determined for 13 transitions. These transitions are placed in a decay scheme which includes 10 excited states in ^{90}Zr. (auth)

20412 PRODUCTION OF SPONTANEOUSLY FISSIONING ISOMERS ^{242}Am AND ^{244}Am BY SLOW NEUTRON CAPTURE. Dalhsuren, B.; Flerov, G. N.; Gangrskii, Yu. P.; Lasarev, Yu. A.; Markov, B. N.; Nguyen Cong Khanh (Joint Inst. for Nuclear Research, Dubna, USSR). Nucl. Phys.; A148: 492-6(1970).

The spontaneously fissioning isomers ^{242}Am and ^{244}Am were produced by slow neutron capture. The cross sections of isomer production were measured at different neutron energies. The correlation between isomer formation and prompt fission was observed. This correlation is discussed on the basis of the two-humped fission barrier hypothesis. (auth)

20413 NUCLEAR ORIENTATION OF ^{59}Fe IN RARE-EARTH DOUBLE-NITRATE CRYSTALS. Tschanz, J. F.; Sapp, R. C. (Univ. of Kansas, Lawrence). Phys. Rev., C; 2: 2168-75(Dec 1970).

Anisotropic emission of 1.10- and 1.29-MeV γ rays from ^{59}Fe oriented in clear single crystals of Ce−Zn and Nd−Zn nitrates cooled by adiabatic demagnetization was studied as a function of temperature in fields of 0 and 250 Oe. From the temperature dependence of the γ anisotropy is extracted an estimate of the nuclear magnetic dipole moment of the ground state of ^{59}Fe of $(1.1 \pm 0.2)\mu_N$. Analysis of the data in terms of the currently accepted spin sequence $\frac{3}{2}(\beta)\frac{3}{2}(\gamma)\frac{7}{2}$ for both γ rays, assuming the fraction of ^{59}Fe aligned in zero field is 0.30 ± 0.03, requires either (i) the hypothesis of Fermi contributions in excess of 30% (contrary to conserved-vector-current theory) or, alternatively, (ii) enhancement factors $Q_2 = 5.0 \pm 2.6$ and 6.7 ± 2.4 for intermediate-state reorientation in the 1.10- and 1.29-MeV levels, respectively. Admixtures of M3 radiation of the order 1−4% may also be involved in the interpretation. (auth)

20414 STUDIES IN THE DECAY OF ^{131}Ba REVEALING NUCLEAR PENETRATION EFFECTS IN THE 92 keV TRANSITION IN ^{131}Cs. Hasselgren, L.; Antman, S.; Sahota, H. S.; Thun, J. E. (Uppsala Univ.). Nucl. Phys.; A153: 625-46 (1970).

The γ-ray and internal conversion spectra of the decay of ^{131}Ba to levels in ^{131}Cs were investigated using a Ge(Li) detector and a double-focussing β-ray spectrometer. Accurate transition energies and internal conversion coefficients were deduced using the

XUM

internal conversion data of Horen et al. in conjunction with the results obtained here. Gamma-gamma and electron-γ directional correlation measurements were performed. Unique spin-parity assignments were obtained for all levels in a compiled level scheme using the deduced conversion coefficients, the results from angular correlation measurements and the deduced log ft values. Nuclear penetration effects were found to be present in the 92 keV transition characterized by $\lambda = 23$. (auth)

20415 DECAY SCHEME STUDIES OF 18 min ^{141}Ba AND 11 min ^{142}Ba. **McIsaac, L. D.; Murri, E. L. (Idaho Nuclear Corp., Idaho Falls). Nucl. Phys.; A156: 212-24(1970).**

The decay schemes of ^{141}Ba and ^{142}Ba were studied using high resolution Ge(Li) and Si(Li) detectors. Coincidence measurements were made using NaI(Tl) detectors and a 256 × 256-channel analyzer. Fifty-four γ-rays from ^{141}Ba and 39 from ^{142}Ba were observed. The majority of these are previously unreported. These data establish the existence of levels in the daughter nucleus, ^{141}La, at the following energies: 190.33, 304.18, 467.26, 580.1, 647.89, 826.3, 831.6, 929.4, 1066.4, 1501.4, 1740.8 and 1872.7 keV. Energy levels proposed for ^{142}La occur at 77.59, 255.29, 309.16, 334.97, 363.94, 424.97, 432.22, 599.71, 1078.6, 1204.2 and 1457.7 keV. The K-conversion coefficient of the 77.59 keV transition deexciting the first excited state in ^{142}La was measured to be 2.0 ± 0.4. (auth)

20416 Kα_1 X-RAY ISOTOPIC SHIFT FOR ^{162}Dy$-$^{164}Dy AND THE DIFFERENCES IN NUCLEAR CHARGE RADII OF Dy ISOTOPES. van Eijk, C. W. E.; Schutte, F. (Univ. of Tech., Delft, Netherlands). Nucl. Phys.; A151: 459-64(1970).

The isotopic shift of the Kα_1 X-rays was measured for ^{162}Dy$-$^{164}Dy. The result $\Delta E = (58.1 \pm 3.3)$ MeV was used to normalize optical isotopic shift data. From these normalized data the differences in the nuclear charge radii of all stable Dy isotopes could be obtained. The measurements were performed with a curved-crystal spectrometer in the DuMond geometry. (auth)

20417 ANGULAR DISTRIBUTIONS AND ENERGY SPECTRA OF INTERNAL BREMSSTRAHLUNG EMITTED DURING BETA DECAY OF ^{32}P, ^{90}Y, ^{204}Tl, AND ^{210}Bi. **Beattie, R. J. D.; Byrne, J. (Univ. of Sussex, Brighton, Eng.). Nucl. Phys.; A161: 650-72(1971).**

The spectral distribution of internal bremsstrahlung emitted in the β decay of ^{32}P, ^{90}Y, ^{204}Tl, and ^{210}Bi was measured at seven values of the angle between the electron and the photon. At angles greater than 45° the agreement between experiment and the Coulomb-corrected theory is good for ^{32}P and satisfactory for ^{210}Bi. For ^{90}Y and ^{204}Tl the measured yields were substantially in excess of those predicted theoretically. However, for ^{204}Tl at least, the agreement was significantly improved when the theory is modified to take account of detour transitions according to the prescription of Ford and Martin. The intensity of internal bremsstrahlung at the high-energy limit is considerably in excess of all theoretical predictions for ^{90}Y, ^{204}Tl, and ^{210}Bi. This effect is probably a result of the neglect of the second and higher order Coulomb terms in the theory. (auth)

20418 HIGH RESOLUTION FISSION CROSS SECTION OF ^{235}U FROM 20 eV TO 100 keV. Lemley, J. R.; Keyworth, G. A.; Diven, B. C. (Los Alamos Scientific Lab., N. Mex.). Nucl. Sci. Eng.; 43: 281-5(Mar 1971).

The fission cross section of ^{235}U has been measured with a nominal resolution of 1 nsec/m from 20 eV to 100 keV. Structure is seen over the entire range with fluctuations as great as 40% in the range 10 to 100 keV. These measurements have an average absolute accuracy of 8% and are based upon the ^{6}Li(n,α) cross section. Some questions are raised concerning existing cross sections that assume smooth energy variation in the region of 10 to 50 keV. (auth)

20419 POTENTIAL IDENTIFICATION OF PRODUCTS OF HEAVY-ION-INDUCED NUCLEAR REACTIONS. **Druin, V. A.; Lobanov, Yu. V.; Kharitonov, Yu. P. At. Energ. (USSR); 29: 132-3(Aug 1970). (In Russian).**

The cross section of the (HI,xn)-type reaction for strongly fissionable nuclei is much lower than that of the direct nuclear reaction: identification of the short-lived products on the basis of their excitation functions is, therefore, difficult. As a result, the possibility of whether differences in the angular distributions of the nuclear reaction products could be used to identify the nuclear reaction involved was examined. The recoil nuclei, collected on a special filter, were mechanically transferred to a Si$-$Au surface-barrier α detector. The system allowed efficient recording of α-active isotopes with lifetimes longer than 0.03 sec; a semiconductor detector was used to identify the α emitter by means of time-amplitude analysis, together with half-life measurements. Scattering of recoil atoms in the thick targets strongly affected the measurements. It was found that the reaction products may be identified by measuring the output through 2 collimators without recourse to excitation curves; thus, the reaction mechanism which leads to a given isotope can be identified. If the products of transfer reactions interfere with the study of isotopes generated through a compound nucleus, the latter may be suppressed without undue energy loss. (TTT)

20420 THE COMPOUND NUCLEUS MECHANISM IN ^{11}B AND ^{10}B INTERACTIONS WITH Tn AND U TARGETS. **Fleury, A.; Hubert, F. (Bordeaux Univ., Gradignan, France). J. Phys. (Paris); 31: 855-68(Oct 1970). (In French).**

The excitation functions in the ^{10}B and ^{11}B ion interactions with Th and U nuclei were measured in view of studying the influence of the angular momentum mechanism on the competition between fission and evaporation processes. The calculations were carried out using an optical model for the light particles. The heavier particles and the cross sections were considered in terms of a parabolic potential, and a semi-analytical method was employed to deal with the deexcitation chains. It was found that for nuclei as heavy as Th and U, the results depend strongly on the fission barrier and the level density parameter a_n for an excited non-deformed nucleus and the same parameter at the saddle point a_f. Moreover, it was shown that the ratio a_n/a_f was closer to 1 for heavy nuclei than for the light ones (Bi). The value of $a_n = A/15$ agrees with the experimental data reasonably well. The calculations of the mean energy carried by the neutrons demonstrated that for the projectiles used, the high values of angular momentum do not result in a significant spallation reaction. This is due to the competitions from fission and transfer reactions that are very likely at high values of angular momentum. Finally, these reactions allow highly excited compound nuclei leading to spallation products that are very deficient in neutrons to be obtained. The electron capture in the decay of ^{240}Bk, ^{242}Bk, and ^{236}Am was thus demonstrated. (auth) (France)

20421 THE ABSOLUTE MEASUREMENT OF BETA-DISINTEGRATING NUCLIDES EMITTING CONVERSION ELECTRONS WITH APPRECIABLE PROPORTIONS. **Baba, H.; Baba, S.; Suzuki, T.; Ishikawa, I.; Umezawa, H. (Japan Atomic Energy Research Inst., Tokai). Int. J. Appl. Radiat. Isotop.; 21: 607-17 (10 Oct 1970).**

A new method was proposed for the $4\pi\beta$ and $4\pi\beta-\gamma$ coincidence absolute measurements of nuclides emitting conversion electrons with appreciable proportions. Correction formulas giving the disintegration rate were shown for ^{153}Sm, which can be easily extended to general forms. The validity of the derived formulas was examined by performing $4\pi\beta$, $4\pi\beta-\gamma$ coincidence, and $\beta-\gamma$-coincidence countings for ^{153}Sm, ^{156}Eu and ^{147}Nd, by comparing the resulting values of the disintegration rate with one another and also with those obtained by other methods, and by examining the consistency of the model. It was concluded that the present method gave satisfactory results for the above three nuclides; that is, the disintegration rate could be determined with an uncertainty of only 0.5 percent. (auth) (UK)

20422 THE DECAY OF CADMIUM ISOTOPES OF MASS 100, 101, AND 102 TO ISOMERS IN SILVER. **Hnatowich, D. J.; Hageboe, E.; Kjelberg, A.; Mohr, R.; Patzelt, P. (CERN, Geneva). J. Inorg. Nucl. Chem.; 32: 3137-48(Oct 1970).**

Mass-separated samples of ^{100}Cd, ^{101}Cd, and ^{102}Cd were produced in the ISOLDE isotope separator facility on line to the CERN 600 MeV synchro-cyclotron. The half-life of ^{100}Cd is 1.1 ± 0.3 min. The existence of the previously reported 15 min half-life for ^{101}Cd and 30 min half-life for ^{102}Cd was not confirmed. The ^{100}Cd does not decay appreciably to the previously known 8 min ^{100}Ag but, instead, to an isomer of half-life 2.3 ± 0.1 min. An isomer in ^{101}Ag at an energy of 273.2 ± 0.7 keV was established. This isomer is a $\frac{1}{2}$-state and decays via an E3 transition to a $\frac{7}{2}^+$ level 97.7 keV above the $\frac{9}{2}^+$ ground state. It was established that in ^{102}Ag, the 8 min isomer is the upper isomer above the 13 min ground state. The isomer energy is 9.3 ± 0.4 keV. (auth) (UK)

20423 FORM FACTORS AND THE CIRCULAR POLARIZATION OF X-RAYS FROM NUCLEAR REACTIONS. Epstein, G. N.; McKellar, B. H. J. (Univ. of Sydney, Australia). Aust. J. Phys.; 23: 601-3(Aug 1970).

The circular polarization of the 396 keV γ-ray from ^{175}Lu, the 482 keV γ-ray from ^{181}Ta, and the γ-ray radiative capture of thermal neutrons by protons were calculated using a dipole form for the vector factor. The choice of form factors has a negligible effect on predictions. (Australia)

20424 SPECIFIC GAMMA-RAY CONSTANT AND GAMMA SPECTRUM OF ^{192}Ir. **Ninkovic, M.; Mladjenovic, M. (Boris Kidrich Inst. of Nuclear Sciences, Belgrade). Atompraxis; 16: 313-16(Sep-Oct 1970).**

The photon spectrum from decay of ^{192}Ir was measured with a

Ge(Li) counter, having a volume of 14 cm^3 and resolution of 3.2 keV at the ^{60}Co energies. Using the published data on the mass energy absorption coefficient of air, total specific gamma ray constant Γ was calculated and a value of (0.468 ± 0.034) Rh^{-1} Ci^{-1} m^2 was obtained. (auth)

20425 ^{152g}Eu AND ^{226}Ra RELATIVE γ-RAY INTENSITIES FOR RAPID EFFICIENCY CALIBRATIONS OF Ge(Li) DETECTORS. Mowatt, R. S. (Atomic Energy of Canada Ltd., Chalk River, Ont.). Can. J. Phys.; 48: 2606-10(1 Nov 1970).

The relative intensities of γ rays following the decay of ^{152}Eu and ^{226}Ra (in equilibrium with its decay products) were studied in order to obtain rapid efficiency calibrations of Ge(Li) detectors. (auth) (Canada)

20426 DECAY OF ^{180}Lu TO THE LEVELS OF ^{180}Hf. Gujrathi, S. C.; D'Auria, J. M. (Simon Fraser Univ., Burnaby, British Columbia). Nucl. Phys.; A161: 410-32(1971).

The decay of ^{180}Lu was studied with Ge(Li) and scintillation spectrometers. The sources were produced using 14.8-MeV neutrons with both natural and enriched targets of hafnium. A half-life of 5.3 ± 0.3 min was observed for the decay of ^{180}Lu while the energies and relative intensities of 19 associated γ rays were determined to an accuracy of at least 500 eV. Beta-decay branches of 2.7 ± 0.15, 2.0 ± 0.15, and 1.5 ± 0.1 MeV were determined with the highest energy group populating the third member of the ground state rotational band of ^{180}Hf. This information along with the results of $\gamma\gamma$ and $\beta\gamma$ coincidence studies was combined and a decay scheme for ^{180}Lu is proposed. The levels of ^{180}Hf populated in this decay lie at energies of 93.308 ($I = 2^+$, $K = 0$), 308.549 ($I = 4^+$, $K = 0$), 1200.2 ($I = 2^+$, $K = 2$), 1292.0 ($I = 3^+$, $K = 2$), 1375.5, 1527.6, 1539.4, and 1608.4 ($I = 4^+$, $K = 4$) keV; the exhibited level pattern and decay modes are discussed in terms of the unified model. Additional information is also provided on the decay of ^{180m}Hp and ^{179m}Hf. (auth)

20427 ELECTROMAGNETIC TRANSITIONS FROM LEVELS IN THE BETA-VIBRATIONAL BAND OF ^{174}Hf. Ejiri, H.; Hagemann, G. B. (Univ. of Copenhagen). Nucl. Phys.; A161: 449-70(1971).

The E0, M1, and E2 matrix elements were obtained for the interband transitions between levels with spins up to 6 in the beta-vibrational and the ground-state bands of ^{174}Hf by studying the following nuclear reactions: $^{174}Hf(\alpha,\alpha')^{174}Hf$, $^{175}Lu(p,2n\gamma)^{174}Hf$, $^{172}Yb(\alpha,2n\gamma)^{174}Hf$, and $^{172}Yb(\alpha,2ne)^{174}Hf$. The interband E2 transition matrix elements are well explained in terms of a coupling of the beta vibration with the rotation. The ratios of the E0 to E2 matrix elements for interband transitions between states of the same spin are fairly constant over spins $I = 0$ to 6. On the other hand, the M1 to E2 ratios for these transitions increase rapidly with the increase of spin. The observed transition matrix elements are discussed in the framework of the collective model including the rotation-vibration interaction. (auth)

20428 DECAY SCHEME OF 25 MIN ^{131g}Te. Macias, E. S.; Walters, W. B. (Massachusetts Inst. of Tech., Cambridge). Nucl. Phys.; A161: 471-80(1971).

The nuclear level structure of ^{131}I was investigated by studying the γ rays emitted in the decay of 25 min ^{131g}Te. The γ rays were detected with Ge(Li) detectors. A total of 42 γ rays were attributed to ^{131g}Te, of which 21 were previously unknown. All but one γ ray was placed in the proposed decay scheme. The half-life of the 149.8 keV level was determined to be 0.76 ± 0.05 ns. The levels are compared to those previously reported from reaction studies. (auth)

20429 DETERMINATION OF THE DECAY CONSTANT FOR SPONTANEOUS FISSION OF ^{238}U. Leme, M. P. T. (CNEN, Sao Paulo, Brazil); Renner, C.; Cattani, M. Nucl. Instrum. Methods; 91: 577-9(1971).

The fission track method is used to determine the decay constant λ_F for spontaneous fission of ^{238}U. This method requires the following measurements: (a) number of spontaneous fission tracks of ^{238}U, (b) number of induced fission tracks of ^{235}U due to thermal neutrons and (c) the thermal neutron flux. The direct neutron flux determination is avoided by measuring instead the activity induced by this flux in a material with cross section that obeys the 1/v law. Samples of natural uranium in contact with mica sheets remained sealed about four years. The decay constant was found to be $\lambda_F = (7.30 \pm 0.16) \times 10^{-17}$ y^{-1}. (auth)

20430 IDENTIFICATION OF μs-ISOMERS AMONG PRIMARY FISSION PRODUCTS. Grueter, J. W.; Sistemich, K.; Armbruster, P.; Eidens, J.; Lawin, H. (Kernforschungsanlage, Juelich, Ger.). Phys. Lett.; 33B: 474-6(7 Dec 1970).

The emitters of isomeric X and γ rays ($t_{½} = 0.1 - 100$ μ sec) among primary fission products in ^{235}U-thermal neutron fission have been identified. A remarkable accumulation of isomers at $N = 58$, 59, and at $N \approx 82$ has been observed. Shape isomerism may explain the pile-up at $N = 58$, 59. (auth)

20431 LEVELS IN ^{238}Pu FROM THE DECAY OF ^{238}Np. Winter, W. J. B.; Wapstra, A. H.; Goudsmit, P. F. A.; Konijn, J. (Instituut voor Kernphysisch Onderzoek, Amsterdam). Nucl. Phys.; A161: 521-8(1971).

Gamma rays following the β decay of ^{238}Np are placed in a decay scheme which, in addition to known levels of the ground state, β and γ vibrational and octupole state bands, and the previously unknown spin-3 member of the last band, shows new levels at 962.3, 985.2, 1082.2, and 1202.0 keV. They are interpreted as spin 1, 2, 3, and 4 states of $K^\pi = 1^-$, 3^-, and 4^- bands of which the band heads are predicted by Soloviev and Siklos to occur at 1.1 and 0.9 MeV. (auth)

20432 ONE-PHONON OCTUPOLE VIBRATION OF ^{151}Eu. Bernstein, E. M.; Boss, G. R.; Hardie, G.; Shamu, R. E. (Western Michigan Univ., Kalamazoo). Phys. Lett.; 33B: 465-7(7 Dec 1970).

A multiplet based on the one-phonon octupole vibration of ^{151}Eu has been observed near 900 keV by inelastic deuteron scattering. The magnitude of the splitting and the relative intensities of the multiplet states are consistent with the weak-coupling model. (auth)

20433 PARITY IRREGULARITIES IN THE 279-keV γ TRANSITION OF ^{203}Tl. De Saintignon, P.; Chabre, M. (Institut des Sciences Nucleaires, Grenoble, France). Phys. Lett.; 33B: 463-4(7 Dec 1970). (In French).

The circular polarization of 279-keV gamma transition emitted by unpolarized nuclei of ^{203}Tl has been measured and the result is: $P_\gamma = (-0.30 \pm 0.18) \times 10^{-4}$. (auth)

20434 γ-DECAY OF PROTON-PARTICLE NEUTRON-HOLE STATES IN ^{208}Bi. Proetel, D.; Dost, M.; Grosse, E.; Koerner, H. J.; von Brentano, P. (Max-Planck-Institut fuer Kernphysik, Heidelberg). Nucl. Phys.; A161: 565-92(1971).

The reaction $^{208}Pb(p,n\gamma)^{208}Bi$ at incident proton energies between 7.0 and 11.0 MeV was used to excite proton-particle neutron hole states in ^{208}Bi and to study their γ decay. In-beam $\gamma\gamma$ coincidence measurements were made utilizing two Ge(Li) detectors combined with on-line computer analysis. By this means a decay scheme for the levels in ^{208}Bi below $E_x \approx 2$ MeV was established and several new spin assignments are suggested. A qualitative discussion of the observed gamma branching ratios and their relation to the single-particle transition strengths in the neighbouring nuclei ^{207}Pb and ^{209}Bi is given. The importance of these ratios in determining configuration admixture among the particle-hole multiplets is pointed out. (auth)

20435 EXCITATION OF SHORT-LIVED ISOMERIC ACTIVITIES IN ^{77}Se, ^{122}Sb, ^{137}Ba, ^{167}Er, AND ^{179}Hf USING 14.5-MeV NEUTRONS. Rurarz, E.; Haratym, Z.; Pietrzykowski, M.; Sulik, A. (Inst. of Nuclear Research, Swierk, Poland). Acta Phys. Pol.; B1: 415-22(Oct-Dec 1970).

The cross sections for the production of short-lived isomeric states in ^{77}Se, ^{122}Sb, ^{137}Ba, ^{167}Er, and ^{179}Hf through the (n,2n) and (n,n') reactions by using 14.5-MeV neutrons are given. The (n,n'γ) cross sections are reported for the first time. Estimates have been obtained for isomeric ratios and spin cut-off parameter using the Huizenga and Vandenbosch method and the Gilbert and Cameron level-density model. (auth)

20436 STUDIES OF ^{95}Ru AND ^{94}Ru WITH THE ^{96}Ru(p,d) AND (p,t) REACTIONS. Ball, J. B. (Oak Ridge National Lab., Tenn.). Nucl. Phys.; A160: 225-36(1971).

The level structure of ^{95}Ru was investigated with the ^{96}Ru(p,d) reaction at a proton energy of 31.5 MeV. Experimental angular distributions are compared with distorted-wave Born approximation calculations to extract spin, parity and spectroscopic-factor assignments for the levels observed up to about 3.5 MeV of excitation. The ground state of ^{95}Ru is observed to be reached by $l = 2$ transfer which is consistent with the $\frac{5}{2}^+$ assignment expected from shell-model considerations. The measured Q-values for the (p,d) and (p,t) reactions result in a new value for the mass of ^{95}Ru and a determination of the previously unmeasured mass of ^{94}Ru. (auth)

20437 STRUCTURE OF CROSS SECTION OF THE PHOTONEUTRON REACTION ON THE ^{208}Pb NUCLEUS IN THE REGION OF A GIANT DIPOLE RESONANCE. Ishkhanov, B. S.; Kapitonov, I. M.; Lazutin, E. V.; Piskarev, I. M.; Shevchenko, O. P. (Inst. of Nuclear Physics, Moscow). Yadern. Fiz.; 12: 682-91(Oct 1970). (In Russian).

In the cross section for photoneutron production for the ^{208}Pb nucleus in the region of the giant dipole resonance a number of peaks with widths of 200 to 400 keV were observed. Interpretation of the structure obtained remains open. (auth)

20438 EFFECTS OF CORRECTION MATRIX ELEMENTS FOR THE FIRST FORBIDDEN β^- TRANSITION IN ^{198}Au. Bogdan, D.; Kyrzhan, N.; Protsop, K.; Vyts, I. (Inst. of Atomic Physics, Bucharest). Yadern. Fiz.; 12: 700-3(Oct 1970). (In Russian).

Observables and the ft value for the first β-transition in ^{198}Au are calculated using the Bhüring formalism. Agreement between theory and experiment is improved by using the correction matrix elements. (auth)

20439 THERMAL NEUTRON ACTIVATION CROSS SECTIONS OF ^{132}Ba(n,γ)^{133m}Ba AND ^{134}Ba(n,γ)^{135m}Ba REACTIONS. Ishii, Taka (Kyoto Univ.). Sci. Rep. Kyoto Prefect. Univ. (Natur. Sci., Living Sci., Welfare Sci.); No. 20, 1-4(Nov 1969).

The thermal neutron activation cross sections (σ_{act}) of ^{132}Ba (n,γ)^{133m}Ba and ^{134}Ba(n,γ)^{135m}Ba reactions have been determined from the analysis of the gamma-ray spectra of Ba activities which were produced by irradiating the natural Ba isotopes with thermal neutrons in a reactor. The spectra were measured by using a 22 cm^3 coaxial type Ge(Li) detector. By adopting the known value of σ_{act} (^{130}Ba) = 10 ± 1 b, the cross sections σ_{act} (^{132}Ba → ^{133m}Ba) = 0.98 ± 0.15 b and σ_{act}(^{134}Ba → ^{135m}Ba) = 0.33 ± 0.06 b were obtained. (auth) (Japan)

20440 ANALYSIS OF THE DEPENDENCE OF $\bar{\eta}$ ON THE NEUTRON ENERGY ON THE BASIS OF THE FISSION ENERGY BALANCE. Vorob'eva, V. G.; D'yachenko, P. P.; Kuz'minov, B. D.; Sergachev, A. I.; Smirenkina, L. D. At. Energ. (USSR); 29: 130-1(Aug 1970). (In Russian).

Although a large volume of experimental data has been accumulated on the dependence of the number of prompt neutrons $\bar{\eta}$ on the neutron energy E_n involved in the fission process, the values of the various authors differ widely. Therefore, this correlation was analyzed on the basis of the energy balance, the mass and kinetic-energy distribution measurements of the fragments for the case of the fission of ^{232}Th, ^{235}U, and ^{238}U by neutrons with energies up to $E_n \approx 6$ MeV were also considered. The curves derived from these calculations agree with the experimental data and thus confirm that the change of the mean fission energy due to charge redistribution $\Delta E_f^Z = 0$, which means that there is no charge redistribution between the fragments. The energy dependence of $\bar{\eta}$ was plotted for the fissioning of ^{235}U, ^{238}U, and ^{232}Th. The reliability of the curves increases toward the lower values of ΔE_n. The method is sufficiently sensitive to local changes of ~0.5% in the value of $\bar{\eta}$. (TTT)

20441 NOTE ON BAND MIXING IN ^{154}Gd. Keller, G. E.; Zganjar, E. F. (Louisiana State Univ., Baton Rouge). Nucl. Phys.; A153: 647-51(1970).

The relative intensities of the γ-rays emitted in the decay of ^{154}Eu were measured using Ge(Li) detectors. The E2 components of the intensities of transitions from the K = 2 and K = 0 vibrational bands to the ground state rotational bands were used to calculate ratios of reduced E2 transition probabilities and the corresponding band-mixing parameters. The band mixing of the K = 2 and the K = 0 vibrational bands could not be described by a two-parameter analysis. (auth)

20442 SLOWING DOWN OF FISSION FRAGMENTS IN VARIOUS ABSORBERS. Mueller, R.; Goennenwein, F. (Univ., Tuebingen, Ger.). Nucl. Instrum. Methods; 91: 357-63(1971).

The slowing-down of fission fragments from the spontaneous fission of ^{252}Cf was studied in the absorbers Au, Ag, Cu, Al, and C and in plastic material (Formvar). The energy degradation of the mean light and heavy fragment after passage through self-supporting foils of different thicknesses was measured using semiconductor detectors. The measurements were carried through in an energy range where electronic collisions predominate, the lower energy limit being approximately 20 and 30 MeV for the heavy and light fragments, respectively. Comparison with existing theories shows the specific energy loss to be higher than the predicted one. (auth)

20443 SPONTANEOUS-FISSION HALF-LIFE OF ^{258}Fm AND NUCLEAR INSTABILITY. Hulet, E. K. (Univ. of California, Livermore); Wild, J. F.; Lougheed, R. W.; (and others). Phys. Rev. Lett.; 26: 523-6(1 Mar 1971).

A spontaneous-fission activity decaying with a half-life of 380 ± 60 μsec, identified as ^{258}Fm, was discovered among the recoil products from the bombardment of ^{257}Fm with 12.5-MeV deuterons. The sharply decreasing spontaneous-fission lifetimes of nuclei with N > 152 show a determined trend contrary to theoretical predictions. The exceedingly short half-life of ^{258}Fm leads to the conclusion that even–even nuclei in the immediate region beyond N = 158 are becoming catastrophically unstable toward fission. (auth)

20444 ^{238}Pu NEUTRON FISSION IN SUB-BARRIER ENERGY RANGE. Ermagambetov, S. B.; Smirenkin, G. N. At. Energ. (USSR); 29: 422-4(Dec 1970). (In Russian).

The energy dependence of the ^{238}Pu fission cross section in the neutron energy range 2.5 keV $\lesssim E_n \lesssim$ 2.5 MeV was measured by using the T (p,n) reaction with an electrostatic generator. The barrier being equal to ~0.5 MeV, the fission cross section in the earlier unexplored range $E_n \lesssim$ 0.05 MeV, is shown to increase considerably and, in the plateau region, reaches values of ~2 b. An analysis of the fission curve in the low-energy region shows that the probabilities of ^{238}Pu fission by s- and p-neutrons are approximately the same. 2 figures, 14 references. (auth)

20445 INTERMEDIATE STRUCTURES IN NEUTRON CROSS SECTIONS. Sukhoruchkin, S. I. At. Energ. (USSR); 29: 187-94 (Sep 1970). (In Russian).

Experimental data on neutron cross sections and neutron strength functions of light and medium-weight nuclei are given. These data show systematic deviations from the statistical approach to individual neutron levels. The structures obtained are intermediate as to the spacing of compound nucleus levels and the spacing of single-particle levels in the optical model. Some of these intermediate structures are well described with the help of doorway states with three quasi-particle configurations. 11 figures, 31 references. (auth)

20446 ANNUAL REVIEW OF NUCLEAR SCIENCE. VOLUME 20. Segre, Emilio (ed.). Palo Alto, Calif.; Annual Reviews Inc. (1970). 619p. $10.00.

Separate abstracts for each of the 13 articles were prepared. (R.W.R.)

For abstracts of individual papers see: 18796, 19473, 19483, 19524, 19730, 19980, 20081, 20124, 20447–20450, and 20708.

20447 NEUTRON CAPTURE GAMMA-RAY SPECTROSCOPY. Motz, H. T. (Los Alamos Scientific Lab., N. Mex.). Annu. Rev. Nucl. Sci.; 20: 1-38(1970).

After an introduction to the major features of neutron-capture gamma-ray spectroscopy, the techniques used in various measurements are reviewed; these include measurements of gamma-ray energies and intensities, prompt and delayed coincidences, gamma–gamma angular correlations, conversion-electron spectra, and polarization effects. Measurements at both resonance and high neutron energies are described. The determination of level schemes and cross sections is discussed. Results of measurements on transition probabilities and photonuclear reactions are presented, and expected future developments in this field are mentioned. 452 references. (R.W.R.)

20448 LOW-ENERGY PHOTONUCLEAR REACTIONS. Firk, F. W. K. (Yale Univ., New Haven). Annu. Rev. Nucl. Sci.; 20: 39-78(1970).

The general properties of the reaction between nuclei and photons of less than 30 MeV are reviewed. The effects of nuclear deformation on the dipole state are recounted. Recent theoretical and experimental developments are discussed. The effects of isospin on the dipole state are considered. 127 references. (R.W.R.)

20449 NUCLEAR EXPLOSIONS AS A NUCLEAR PHYSICS TOOL. Diven, B. C. (Los Alamos Scientific Lab., N. Mex.). Annu. Rev. Nucl. Sci.; 20: 79-104(1970).

Underground nuclear explosions are used as a scientific tool for studying meteorological and seismic phenomena and for the production of new nuclides by multiple neutron capture. The method of heavy-element production in nuclear explosions, particularly the thermonuclear explosions, is discussed in detail, and the advantages and limitations of the method are presented. Nuclear physics experiments performed from 1965 to 1970 with underground nuclear explosions are described and the future work required for cross-section measurements with explosion sources of neutron energies below 20 eV are mentioned. (L.C.L.)

20450 ALPHA-PARTICLE TRANSFER REACTIONS. Bethge, Klaus (Univ., Heidelberg. Univ. of Pennsylvania, Philadelphia). Annu. Rev. Nucl. Sci.; 20: 255-88(1970).

Because of the high binding energy of the alpha particle, α-transfer reactions result in nuclear-structure information regarding the correlation of nucleons inside nuclei. Lithium-induced reactions are dealt with in some detail, and the experimental results from heavier projectiles are surveyed. The theoretical description is far from satisfying although important steps toward understanding the processes have been taken. The attempts to describe an α-transfer process in terms of the DWBA theory, suitably modified, as well as some phenomenological approaches to describe the reaction mechanism, are reviewed. 194 references. (R.W.R.)

20451 ALPHA DECAY OF NEUTRON-DEFICIENT RADON AND POLONIUM ISOTOPES. Hornshoej, P. (Univ. of Aarhus, Denmark); Wilsky, K.; Hansen, P. G.; Lindahl, A.; Nielsen, O. B. Nucl. Phys.; A163: 277-88(1971).

The use of mass-separated samples of neutron-deficient radon isotopes, produced at the ISOLDE on-line mass-separator facility at the CERN 600 MeV synchrocyclotron, has permitted precise half-life determinations and unambiguous mass assignments for a range of light radon isotopes. Alpha/EC-branching ratios are extracted for several radon and polonium isotopes through the use of genetic relationships. The systematics of the α-widths is discussed. (auth)

20452 ^{170}Lu → ^{170}Yb DECAY. Bonch-Osmolovskaya, N. A. (Joint Inst. of Nuclear Research, Dubna, USSR); Ballund, H.; Plochocki, A.; Preibisz, Z.; Zglinski, A. Nucl. Phys.; A162: 305-29(1971).

The ^{170}Lu → ^{170}Yb decay was studied using Ge(Li) detectors and a six-gap β-ray spectrometer. The single γ-ray spectrum and eγ, $\gamma\gamma$ and ee coincidence spectra were measured. Some tentative levels were confirmed and several new ones established. Evidence is given for the existence of several $I^\pi K = 0^+0$ excited states as well as of the associated rotational states. (auth)

20453 TRANSITION RATES IN ^{192}Au. **Hoeglund, A. (Univ. of Stockholm); Malmskog, S. G.; Baecklin, A.; Fogelberg, B.; Jonson, B. Nucl. Phys.; A163: 311-15(1971).**

From data obtained with a double-lens electron coincidence spectrometer and iron-yoke double-focusing spectrometers, the half-life of the 31.6 keV level in ^{192}Au has been determined to be 0.69 ± 0.02 nsec, and the de-exciting transition has been found to have a multipolarity of M1 + (0.66 ± 0.05)% E2. The E2 part of this transition is strongly enhanced, being of the same order as for the $2^+ \rightarrow 0^+$ transition in ^{192}Pt. The half-lives of the 306.5 and 157.2 keV levels in ^{192}Au were found to be <0.18 ns and <0.05 ns, respectively. (auth)

20454 LIFETIME AND g-FACTOR OF THE 74.8 keV STATE OF ^{100}Rh. **Reno, R. C.; Fishbein, M.; Hohenemser, C. (Brandeis Univ., Waltham, Mass.). Nucl. Phys.; A163: 161-5(1971).**

The lifetime and g-factor of the 74.8-keV state of ^{100}Rh were redetermined with the result that $T_{1/2}$ = 214.5 ± 2.0 nsec and g = 2.141 ± 0.015. (auth)

20455 ISOMER RATIO MEASUREMENTS FOR ^{91}Mo, ^{137}Ce, AND ^{141}Nd PRODUCED BY (γ,n) AND (γ,3n) REACTIONS. Haustein, P. E.; Voigt, A. F. (Ames Lab., Iowa). J. Inorg. Nucl. Chem.; 33: 289-94(Feb 1971).

Isomer ratios for the reactions $^{A+1}Z(\gamma,n)^{A}Z$ and $^{A+3}Z(\gamma,3n)^{A}Z$, (^{A}Z = ^{91}Mo, ^{137}Ce, and ^{141}Nd) were deduced from residual radioactivity measurements of separated targets irradiated with 70-MeV bremsstrahlung. More uniform production of the ^{A}Z isomeric pair states was observed by the (γ,3n) reaction than by the (γ,n) reaction. This behavior is discussed in terms of the nuclear photoabsorption process and the neutron emission modes of the compound nucleus. (auth) (UK)

20456 DECAY OF ^{223}Ra AND ITS DAUGHTER PRODUCTS. I. THE DECAY OF ^{223}Ra. Davidson, W. F.; Connor, R. D. (Univ. of Manitoba, Winnipeg). Nucl. Phys.; A149: 363-84(1970).

The Ge(Li) γ-ray spectrum of ^{223}Ra was found to consist of 32 γ-rays whose energies and absolute quantum intensities were determined. The α-ray spectrum was studied using Au(Si) detectors. Conversion line studies ≈0.1% resolution in momentum on the Chalk River $\pi\sqrt{2}$ β-spectrometer yielded the multipolarities of the following more prominent transitions (keV): 110.8 (E2), 122.30 (M1 + 1.8% E2), 144.19 (M1 + 1.5% E2), 154.18 (M1), 158.62 (M1 + 3.8% E2), 269.41 (M1 + 2.4% E2), 323.88 (M1 + 3% E2) and 338.30 (M1 + <9% E2). With solid-state detectors in both channels, $\alpha-\gamma$ directional correlations on the cascades 5.603 MeV α-269.4 keV γ, 5.712 MeV α-144.2 keV γ and 5.712 MeV α-154.2 keV γ yielded the following parameters respectively: $A_{22} = 0.195 \pm 0.045$, $A_{44} = 0.005 \pm 0.048$; $A_{22} = 0.322 \pm 0.042$, $A_{44} = -0.074 \pm 0.050$; $A_{22} = -0.099 \pm 0.029$, $A_{44} = 0.008 \pm 0.033$. The correlations and multipolarities suggest most probable assignments of the spins and parities of the first seven levels in ^{219}Rn as $\frac{5}{2}^+$(g.s.), $\frac{7}{2}^+$(4.4 keV), $\frac{5}{2}^+$(14.4 keV), $\frac{5}{2}^+$ or $\frac{7}{2}^+$(126.7 keV), $\frac{5}{2}^+$(158.6 keV), $\frac{3}{2}^+$ (269.4 keV) and $\frac{3}{2}^+$ or $\frac{5}{2}^+$(338.3 keV) respectively. A decay scheme involving 19 excited states is proposed. The introduction of two new levels at 342.9 keV and 447.0 keV is discussed. (auth)

20457 DETERMINATION OF EXPERIMENTAL VALUES OF INTERNAL CONVERSION MATRIX ELEMENTS. **Grigor'ev, V. N.; Feresin, A. P. (Ioffe Inst. of Physics and Tech., Leningrad). Yadern. Fiz.; 12: 665-72(Oct 1970). (In Russian).**

Anomalous coefficients of internal conversion of some unhindered E1 transitions in the region of heavy and rare-earth nuclei are analyzed. Experimental values of nuclear parameters and internuclear matrix elements for transitions under investigation are given. (auth)

20458 QUEST FOR SUPERHEAVIES. **Schiffer, J. P. (Argonne National Lab., Ill.). Comments Nucl. Particle Phys.; 4: 90-3(Mar-Apr 1970).**

Recent developments in the search for superheavy nuclides in nature are reviewed. Some methods for artificial production of these nuclides are discussed. The importance of the discovery of these nuclides is explained. (R.W.R.)

20459 LEVEL STRUCTURES ^{91}Rb AND ^{91}Sr AS POPULATED IN BETA DECAY. Mason, J. F.; Johns, M. W. (McMaster Univ., Hamilton, Ont.). Can. J. Phys.; 48: 2895-2905(15 Dec 1970).

The decay of 7.9 s ^{91}Kr and its 58 s daughter ^{91}Rb were studied with Ge(Li) plastic and NaI(Tl) detectors, singly and in coincidence, to determine the properties of states in ^{91}Kr, ^{91}Rb, and ^{91}Sr. The energies and intensities of 9 gamma rays following the decay of ^{91}Kr were measured, locating levels at excitations of 0.1086, 0.5068, 0.7218, and 1.6154 MeV in ^{91}Rb. $\beta-\gamma$ coincidence measurements involving the 0.1086, 0.5068, and 0.6132 MeV transitions have established the ^{91}Kr$-^{91}$Rb mass differences as 5.08 ± 0.10 MeV. The energies and intensities of 36 gamma rays following the decay of ^{91}Rb were measured, identifying levels in ^{91}Sr at 0.0931, 0.4392, 1.0414, 1.2306, 1.9426, 2.0643, 2.344, 2.6574, 2.9257, 3.6932, 3.737, 3.752, 3.935, 4.0785, 4.252, 4.265, and 4.497 MeV. The lifetime of the 0.093 MeV state is 91 ± 3 ns. The states at 2.6574, 3.6932, 4.0785, and 4.265 have negative parity. (auth) (Canada)

20460 INTERNAL CONVERSION COEFFICIENTS OF THE 392-keV γ-RAY AND HALF-LIFE OF THE ISOMERIC STATE IN ^{113}In. Hansen, H. H.; De Roost, E.; Mouchel, D.; Vaninbroukx, R. (EURATOM, Geel, Belg.). Int. J. Appl. Radiat. Isotop.; 22: 1-8 (Jan 1971).

The conversion process of the 392 keV γ-transition of ^{113m}In was reinvestigated using two accurate counting methods. The emission rate of conversion electrons was measured with a 4πe$-$X coincidence method using a proportional gas flow counter together with two NaI(Tl) crystals or a Si(Li) detector. The emission rate of the K-shell conversion electrons was determined with a magnetic β-spectrometer and a high resolution Si(Li) detector in an electron X-ray coincidence arrangement. The γ-ray emission rate of all sources was determined with a calibrated NaI(Tl) γ-ray spectrometer. From these measurements the total internal conversion coefficient, α, that for the K-shell, α_K, and the conversion ratio R = K/(L + M + ...) were deduced. A second less accurate value for the ratio R was taken from recorded electron spectra. The results obtained from the measurements with 12 different sources are: $\alpha = 0.540 \pm 0.007$, $\alpha_K = 0.437 \pm 0.007$, and $R = 4.24 \pm 0.07$. The errors stated are discussed in some detail. The half-life of the isomeric state ^{113m}In was determined with a proportional gas flow counter (electrons) and two different NaI(Tl) crystals (γ-rays). The result obtained from measurements with 12 sources is $T_{1/2}$ = (99.47 ± 0.07) min. (auth) (UK)

20461 NUCLEAR ENERGY LEVELS IN EVEN ISOTOPES OF TELLURIUM FROM (ALPHA, XN GAMMA) REACTIONS ON THE SEPARATED TIN ISOTOPES. Warner, Ray Allen. Davis, Calif.; Univ. of California (1969). 147p. University Microfilms Order No. 70-25,158.

Thesis.

Excited states of the even-mass nuclei from ^{114}Te through ^{126}Te were produced in (α, xn) reactions (x = 2, 3, 4) with α-particle energies ranging from 25 to 70 MeV. Over 80 distinct transitions were observed, and 35 of these were assigned to the above nuclides with the aid of measurements of relative intensities, time distributions, excitation functions, angular distributions, and energy systematics. Evidence is presented for a 13-ns isomer in ^{126}Te. All other Te nuclei studied, deexcite completely with half lives ≲3 ns at least 96% of the time. The energy levels deduced, vary smoothly between isotopes, contrary to earlier findings. Angular distribution data are compared with calculations based on the Draper–Lieder analysis of side feeding, and reveal further systematics among the isotopes. (Diss. Abstr. Int., B)

20462 GYROMAGNETIC RATIOS OF EXCITED STATES IN ^{191}Ir. Owens, Williams Richard. Cleveland; Case Western Reserve Univ. (1969). 98p. University Microfilms Order No. 70-25,840.

Thesis.

The Moessbauer effect was observed for the first time in the 82 keV gamma ray of ^{191}Ir. The magnetic hyperfine splitting of this Moessbauer line was also observed with a ^{191}Pt source diffused into an iron foil. The splitting, combined with the accurately known gyromagnetic ratio of the ground state (3/2) level of ^{191}Ir, determined the internal magnetic field on the iridium nucleus and the gyromagnetic ratio of the 82 keV (1/2) level. These values are H_{eff} = 1557 ± 52 kOe. and g(1/2) = 0.03 ± .05. The angular correlation of the 410 keV–129 keV cascade was studied for the first time. The cascade is a strong one and shows a large anistropy. The Legendre polynomial coefficients were determined to be $A_2 = 0.658 \pm .018$ and $A_4 = 0.028 \pm .023$. The per-

XUM

turbed angular correlation of the cascade was studied with the source of ^{191}Pt diffused into an iron lattice whose domains were aligned perpendicular to the plane of the detectors with a C shaped electromagnet. To be sure of the exact internal magnetic field, the same sample that was used in the Moessbauer effect experiment was utilized. Using the integral rotation method, the observed rotation was found to be −0.229 ± .013, which corresponds to a gyromagnetic ratio for the 129 keV (5/2) level of g(5/2) = 0.22 ± .02. The lifetimes of the 82 keV and 129 keV levels were determined by single line Moessbauer experiments to be 5.3 ± .7 nsec. and 0.144 ± .010 nsec. respectively. Electronic delayed coincidence measurements of the 82 keV state meanlife yielded 5.5 ± .5 nsec. and 5.9 ± .2 nsec. for gamma-x ray and electron-x ray coincidences respectively. The gamma ray energy spectrum of ^{191}Pt was studied with a high resolution GeLi spectrometer. Results were in general agreement with previously published work. The observed g factors are compared with various models applicable to this nucleus. An inconsistency is noted in the symmetric rotor model usually applied to explain the observed energy levels of ^{191}Ir. (Diss. Abstr. Int., B)

20463 EXCITATION OF NUCLEAR ENERGY LEVELS BY ELECTRONS AND PHOTONS FOR 167 ≤ A ≤ 197 BETWEEN 2.3 AND 3.5 MeV. Johnson, William T. K. Washington, D. C.; American Univ. (1970). 155p. University Microfilms Order No. 70-24,279.

Thesis.

The nuclear energy levels of four nuclei, two in the deformed region (^{167}Er and ^{179}Hf) and two in the transition region (^{191}Ir and ^{197}Au), were studied by isomer production with electrons and photons produced with a 4-MeV electron Van de Graaff accelerator. Thirty-four levels, twenty-eight previously unobserved, were detected from 2.3 to 3.5 MeV. In twenty-one cases the multipolarity of the upward transition from the ground state could be determined by comparing a factor obtained from the ratio of electron to photon cross sections for an individual level to that obtained from a distorted wave Born approximation calculation of electroexcitation. All but one of these transitions was found to be M1 + E2, the other was E1. Uncertainties in the experimental points due mainly to stripping of the individual state contributions to the total cross section made it impossible to resolve between M1 or E2 or to determine a mixing ratio. Two levels in ^{179}Hf were thought to be populated by an E0 transition because of the absence of a measurable photon cross section. The eight states in ^{167}Er and fourteen states in ^{179}Hf are fitted into bands based upon the Nilsson model for band structure. Several bands in each nucleus are needed to explain the number of states observed. Lack of previous information on states in this energy region did not allow more than gross speculation on the band structure. The states observed in ^{191}Ir and ^{197}Au are discussed in light of models which apply to this region presented in the recent literature. The only E1 transition was observed in ^{197}Au. The widths of the states are compared to the single-particle estimates for all nuclei. The purity of the decay mode measured made it possible to accurately measure the half-life of isomers which were found to be 2.28 ± .03 sec, 18.77 ± .08 sec, 4.88 ± .04 sec, and 7.85 ± .04 sec for ^{167m}Er, ^{179m}Hf, ^{191m}Ir, and ^{197m}Au, respectively. Half-life measurements were also made for three other isomers; they were ^{77m}Se − 17.60 ± .15 sec, ^{79m}Br − 4.97 ± .10 sec, and ^{183m}W − 5.55 ± .25 sec. The measurements are compared to previously published values. In light of the lack of additional information on states in this region further work is recommended by this method of analysis extended to other nuclei and over a larger excitation energy region and to other methods such as Coulomb excitation and neutron capture. The newer Ge(Li) detectors have opened large areas for exploration by the latter two techniques. Because of the very selective nature of the states observed with this study in that they must be connected to both the ground state by L ≤ 2 and to the isomeric state, only a few of the many states present are observed. This is very useful in nuclei like ^{167}Er where the density of states is very high. Unfortunately this method is limited to only the few nuclei which have an isomeric level so that although this method is very useful for these few nuclei complete coverage studies must be made by other techniques. (Diss. Abstr. Int., B)

20464 MEASUREMENT OF THE ACTIVATION CROSS SECTION OF ^{176}Lu USING γ RAYS FROM A ^{60}Co RADIATION SOURCE. Veres, A.; Pavlicsek, I. (Inst. of Isotopes, Budapest). Acta Phys. Acad. Sci. Hung.; 28: 419-29(1970).

The activation cross-section of ^{176}Lu and σ_{Lu}/σ_{In} ratio for several 1.3−80 kCi ^{60}Co γ-sources has been determined. The values found on the basis of isomer activity are σ_{Lu} = 23−47 nb and σ_{Lu}/σ_{In} = 0.65−0.93. The partial widths of the activation levels are estimated from the integrated cross-section values for ^{115}In, 1.08 MeV level: $\Gamma_0 = 3.4 \cdot 10^{-3}$ eV and $\Gamma_m = 0.2 \cdot 10^{-3}$ eV and for ^{176}Lu: $g\Gamma_m \approx 10^{-4}$ eV. (auth)

20465 STUDY OF THE DECAY OF ^{145}Sm BY Ge(Li) DETECTOR TECHNIQUES. Berenyi, D. (Inst. of Nuclear Research, Debrecen, Hungary); Szalay, A.; Varga, D.; Molnar, F.; Uchrin, J. Acta Phys. Acad. Sci. Hung.; 28: 431-4(1970).

The gamma rays from the decay of ^{145}Sm were studied by Ge(Li) semiconductor detector techniques in a low background chamber. The gamma energies and intensities obtained are 61.4 ± 0.5 keV(100), 120.8 ± 2.0 keV($1.1 \cdot 10^{-2}$) and 492.5 ± 1.5 keV($2.5 \cdot 10^{-2}$). That the 120.8 keV gamma rays belong to the decay under investigation was not uniquely determined. (auth)

20466 SHAPES OF RARE-EARTH NUCLEI. Aponick, Athony A. Jr. New Haven; Yale Univ. (1970). 192p. University Microfilms Order No. 70-25,079.

Thesis.

Precision studies of the inelastic scattering alpha particles from selected rare earth nuclei were interpreted to yield quantitative determinations of the hexadecapole term in the mass distributions of these nuclei in addition to the now familiar, and dominant, quadrupole term. Cross sections for scattering to the 0_+, 2_-, and 4_+ states of the ground state rotational bands of ^{154}Sm, ^{166}Er, and ^{176}Yb were measured at 27.5, 30.0, and 32.5 MeV incident alpha particle energy, and over the angular range from 20 to 140 degrees. These data were analyzed with a theory which models the nucleus as a rigid rotor, and the interaction as a deformed, complex optical potential. The parameters of the undeformed potential were determined from an optical model analysis of elastic scattering from the essentially spherical nuclide ^{148}Sm, measured over the same angle and energy ranges. The analysis of the data has as its foundation the utilization of the interferences among Coulomb excitation and nuclear quadrupole and hexadecapole inelastic scattering amplitudes leading to the lower members of the ground state band. The characteristically different energy dependence of these interfering amplitudes has led to a determination of the deformation parameters of both mass and charge distributions of these nuclei. The parameters so determined simultaneously fit the data obtained at all three incident energies. They were, moreover, in complete accord with parameters previously extracted from fixed energy 50 MeV inelastic alpha particle scattering data. Considerable credence is therefore given to the interpretation of this parametrization as a physical representation of the nuclear shape. (Diss. Abstr. Int., B)

20467 NUCLEAR DATA SHEETS. Nucl. Data, Sect. B; 4: No. 6, B.4.i-B.4.697(Sep 1970).

The available experimental data pertaining to the nuclear structure of even-A nuclei from A = 230 through A = 242 are compiled. The adopted decay schemes and other properties are discussed and compared with theory. Reference lists to all the sources of data are presented. (J.W.K.)

20468 NUCLEAR STRUCTURE AND HYPERFINE FIELD STUDIES WITH ^{95}Mo. Bond, Peter Danford. Cleveland; Case Western Reserve Univ. (1969). 129p. University Microfilms Order No. 70-25,939.

Thesis.

Excitation functions for (α,xn) and (α,αn) reactions on niobium foil were measured. The decay of 60 day ^{95m}Tc produced in this manner was used to investigate the energies and spins of levels in ^{95}Mo. Angular correlations of the two strongest gamma−gamma cascades were measured to be $W(\theta) = 1-(.292 \pm .005)P_2(\cos\theta) - (.001 \pm .006)P_4(\cos\theta)$ for 582-204 cascade and $W(\theta) = 1 - (.196 \pm .006)P_2(\cos\theta) - (.003 \pm .008)P_4(\cos\theta)$ for the 835-204 cascade. The mixing ratio of the 582 gamma ray was found to be $\delta = -.20 \pm .02$. Delayed coincidence techniques were used to measure the mean life of the 204 keV level to be $\tau = 1.09 \pm .02$ nanoseconds. The gyromagnetic ratio of the 204 keV level, measured by the time integral reversed field at a fixed angle method, was found to be g = −.26 ± .02. Hyperfine fields at solute molybdenum nuclei in iron and nickel hosts were measured by diffusing technetium into a ferromagnetic foil and using perturbed angular correlation techniques. The internal fields at 55°C were found to be B(Mo in Fe) = (−236,000 ± 19,000) gauss and B(Mo in Ni) = (−29,900 ± 5,000) gauss. An anharmonic vibrator theory of spherical nuclei was applied to odd mass nuclei in the region 87 ≤ A ≤ 99 and the success of this model in predicting nuclear structure is discussed with emphasis upon ^{95}Mo. (Diss. Abstr. Int., B)

20469 COULOMB EXCITATION STUDIES OF ^{134}Ba, ^{136}Ba, ^{138}Ba, AND ^{150}Nd. Kerns, John Richard. Pittsburgh; Univ. of Pittsburgh (1969). 93p. University Microfilms Order No. 70-11,816.

Thesis.

Using ^{16}O and α beams, the angular distribution of the ratio of scattered ions exciting the first 2_+ state to elastically scattered ions was measured. Values of the reduced transition probability B(E2, $0_+ \rightarrow 2_+$) and the static quadrupole moment Q_{2+} of the first

2_+ state were determined. The B(E2, $0_+ \rightarrow 2_+$) values obtained are .672 ± .016, .418 ± .011, .221 ± .009 and 2.72 ± .06 $e^2 \cdot barn^2$, for ^{134}Ba, ^{136}Ba, ^{138}Ba, and ^{150}Nd, respectively. The static quadrupole moments of the first 2_+ state of these nuclei are found to be −.58 ± .26, −.08 ± .36, −.11 ± .15, and −1.34 ± .54 e · barn, respectively. (Diss. Abstr. Int., B)

20470 NEW NUCLIDE, ^{145}Xe: MEASUREMENT OF ITS FRACTIONAL CUMULATIVE YIELD FROM THERMAL NEUTRON FISSION OF ^{235}U. Wolfsberg, Kurt (Los Alamos Scientific Lab., N. Mex.). J. Inorg. Nucl. Chem.; 33: 587-9(Feb 1971).

Experimental details are given of the determination of ^{145}Pr which required very high decontamination of praseodymium due to its low abundance relative to other descendants of krypton and xenon fission products. The half-life of ^{145}Xe was estimated to be 0.9 ± 0.3 sec; the emanating power calculated to be >0.85 and the fractional cumulative yield calculated to be $2.0^{+0.45}_{-0.20} \times 10^{-6}$. These results are discussed. (UK)

20471 MEASUREMENTS OF TRANSITION PROBABILITIES IN SOME MIDDLE-WEIGHT NUCLEI. Kuebbing, Richard Andrew. Cleveland; Case Western Reserve Univ. (1970). 70p. University Microfilms Order No. 70-25,882.

Thesis.

The level schemes of ^{92}Nb and ^{94}Nb were studied via the (p,n) reaction on separated zirconium targets. The pulsed beam of the ORNL 6 MeV Van de Graaff was used to measure the lifetimes of excited states of these nuclei. The 140.4 keV state in ^{94}Nb was found to have a half-life of (36.8 ± 0.4) nanoseconds by measuring the decay of the 99.4 keV gamma ray after the production of the state by the pulsed beam. The 226 keV state in ^{92}Nb was found to have a half-life of (5.2 ± 0.7) microseconds by measuring the decay of the 90.7 keV gamma ray in the same manner. The spins and parities of these states imply that they should be E1 transitions. They are slower however than Weisskopf estimates by factors of 8×10^{-6} and 6×10^{-8} respectively. A simple explanation of this hindrance is proposed by invoking the shell model. A study of the decay of ^{80}Br to the levels of ^{80}Kr was made to test the phonon character of the 0^+ excited state of ^{80}Kr. A search was made for the decay of this state by EO conversion electron as predicted by Reiner. The energy spectrum of electrons from this source in coincidence with other radiation was measured but no peak was seen. Methods for increasing the sensitivity of the experiment are discussed. (Diss. Abstr. Int., B)

20472 CONVERSION ELECTRON MEASUREMENTS IN THE DECAY OF ^{156}Tb. McMillan, D. J. (Vanderbilt Univ., Nashville); Hamilton, J. H.; Mladjenovic, M.; Manthuruthil, J. C.; Pinajian, J. J. Z. Phys.; 241: 103-16(1971).

The conversion electron spectrum from the decay of ^{156}Tb to ^{156}Gd was measured with an iron, double-focusing spectrometer. The K conversion coefficient of the 1222.4 keV transition was measured relative to the K conversion coefficient of the 661.6 keV transition in ^{137}Cs and found to be 0.00174 ± 0.00013. This result was used to normalize electron and gamma-ray data to obtain the K conversion coefficients of 33 transitions in ^{156}Gd. The 1009.6 and 1040.6 keV transitions have large E0 components. (auth)

20473 M/L AND (N + O + ...)/M CONVERSION RATIOS FOR M1 + E2 TRANSITIONS. Milanovic, J.; Stepic, R.; Krpic, D. (Boris Kidric Inst., Belgrade. Faculty of Sciences, Belgrade). Fizika (Zagreb); 2: 109-11(1970).

Internal conversion ratios M/L and (N + O + . . .)/M for four M1 + E2 transitions and one pure M1 transition were measured for Z = 63 to 83 in the energy range 77 to 239 keV. The M/L ratios showed good agreement with other experiments and with theory. The (N + O + . . .)/M ratios differed slightly from earlier measurements. (R.W.R.)

20474 DECAY SCHEME OF ^{146}Eu. Mester, A. An. Univ. Bucuresti, Ser. Stiint. Natur., Fiz.; 16: 107-24(1967). (In Rumanian).

A new decay scheme of $^{146}_{63}$Eu from β decay and K capture is given. It relies on the available experimental data and also considers the table of energy coincidences. A new scheme, in good agreement with experiment, is obtained. (Rom. Sci. Abstr.)

20475 (p,n) CROSS SECTIONS AND THE STRENGTH FUNCTIONS FOR 3- TO 5.5-MeV PROTONS ON In AND ON Sn ISOTOPES. Johnson, C. H.; Kernell, R. L. (Oak Ridge National Lab., Tenn.). Phys. Rev., C; 2: 639-55(Aug 1970).

The (p,n) reaction cross sections were measured to ±4% for 3- to 5.5-MeV protons on ^{117,119,120,122,124}Sn and on natural Sn and In. Analyses with a conventional optical-model potential were made in the energy regions where the (p,n) cross sections are nearly equal to the total absorption cross sections. These analyses show that the energy dependence in the real well is about three times greater for 5- to 10-MeV protons than it is for 10- to 61-MeV protons. The best-fit potential for 3- to 5.5-MeV protons on the Sn isotopes has a surface absorptive layer about half as thick as at 10 MeV. The In strength functions are fitted by increasing both the width and depth of the imaginary part of this potential by about 25%. The Q value for ^{120}Sn(p,n)^{120}Sb was found to be −3465 ± 7 keV. (auth)

20476 RESONANT NEUTRON CAPTURE IN ^{175}Lu. Wasson, O. A.; Chrien, R. E. (Brookhaven National Lab., Upton, N. Y.). Phys. Rev., C; 2: 675-89(Aug 1970).

A study of the neutron-capture reaction mechanism for radiative capture of resonant-energy neutrons has been made for ^{175}Lu(n,γ)^{176}Lu. The statistical distribution of the partial radiation widths over 11 neutron resonances is inconsistent with a χ^2 distribution with one degree of freedom. No correlations are observed between the γ-ray partial widths and the reduced neutron widths of either the capturing or final states. Neither is there any significant correlation among the individual γ-ray widths. Such facts indicate that neither channel capture nor doorway states contribute strongly to the neutron-capture process in the region above the neutron binding energy. However, there is a small but significant departure from a purely statistical compound-nuclear process. Final states unreported in previous experiments are observed. In addition, the spins of 11 resonances, as well as limitations on the spins of the low-lying final states are determined. (auth)

20477 DEFORMATION PARAMETERS IN ^{154}Sm AND ^{148}Sm OBTAINED FROM COUPLED-CHANNEL ANALYSIS OF PROTON SCATTERING. Brown, P. H.; Stoler, P. (Rensselaer Polytechnic Inst., Troy, N. Y.). Phys. Rev., C; 2: 765-7(Aug 1970).

Differential cross sections for 16-MeV protons scattering from ^{154}Sm and ^{148}Sm were reanalyzed using the coupled-channel computer program JUPITOR-1 written by Tamura. The results of this analysis yield a better fit to the data using a value of β_2 = 0.250 for ^{154}Sm than with the value of 0.351 obtained from Coulomb excitation studies. The same optical-model parameters which were used for ^{154}Sm yield a good fit for ^{148}Sm with vibrational deformation parameters $\beta_2 = 0.120$ and $\beta_3 = 0.150$. (auth)

Nuclear Theory

Refer also to abstracts 20019, 20021, 20082, 20106, 20133, 20337, and 20367.

20478 (INR-P–1230) PENETRATION OF A TWO-DIMENSIONAL FISSION BARRIER. Szymanski, Z.; Sobiczewski, A.; Zielinska-Pfabe, M. (Institute of Nuclear Research, Warsaw (Poland)). 1970. 7p. (CONF-700815–6). Dep. NTIS (U. S. Sales Only).

From Conference on the Properties of Nuclei Far from the Region of Beta Stability, Leysin, Switzerland.

The dynamical aspects of fission treated as a two-dimensional process with quadrupole and hexadecapole degrees of freedom are discussed in the framework of microscopic theory. The inclusion of the hexadecapole degree of freedom decreases the spontaneous-fission half-lives by a few orders. (auth)

20479 (JAERI-Memo–4138) MANUAL FOR JUPITOR-1 (SUPPLEMENT). Wakai, Masamiti; Igarasi, Sin-iti; Mikoshiba, Osamu; Yamaji, Shuhei (Japan Atomic Energy Research Inst., Tokyo). Sep 1970. 61p. (In Japanese). Dep. NTIS (U. S. Sales Only).

As supplement to "Manual for JUPITOR-1 (JAERI-memo 3833)," the output calculated with a computer is presented for seven examples. In example 1, all the intermediate output possible is given, with some remarks. In cases where the output is large, only the portion up to midway is given, the rest being omitted. The computers used are HITAC 5020E for the intermediate output in example 1, and FACOM 230-60 for the other examples. (auth) (Japan)

20480 (JINR–E7-5499) VALIDITY OF THE ALEXANDER AND SIMONOFF SEMIEMPIRICAL RULE IN THE REGION 100 ≤ A ≤ 150. Neubert, W. (Joint Inst. for Nuclear Research, Dubna (USSR). Lab. of Nuclear Reactions). 1970. 9p. Dep. NTIS (U. S. Sales Only).

The Alexander and Simonoff semiempirical rule concerning the maximum position of the cross section for (H. I., xn) reactions is checked. The validity of this relation in the medium mass region 100 ≤ A ≤ 150 is shown on the basis of 19 well established excitation functions. (auth)

20481 (JINR-P4-5457) TABLES OF THE WAVE FUNCTIONS OF THE SINGLE-PARTICLE STATES OF THE TRANSURANIUM

XUM

REGION DEFORMED NUCLEI IN THE SAXON–WOODS POTENTIAL. Gareev, F. A.; Ivanova, S. P.; Shirikova, N. Yu. (Joint Inst. for Nuclear Research, Dubna (USSR). Lab. of Theoretical Physics). 1970. 47p. (In Russian). Dep. NTIS (U. S. Sales Only).

Tables of the energies and wave functions of nuclei in the region of $230 < A < 250$ are listed. (auth)

20482 (RFP-Trans-72) NUCLEAR PHYSICS: REMARKS ON THE VALUES OF NUCLEAR RADIATION FROM ALPHA RADIOACTIVITY. Ambrosino, George; Piatier, Henri. Translated for Dow Chemical Co., Golden, Colo., from Compt. Rend.; 232: 401-1 (1951). 3p. Dep. NTIS.

20483 NUCLEAR COLLECTIVE MOTION. MODELS AND THEORY. Rowe, D. J. London; Methuen and Co. Ltd. (1970). 368p. 110s.

The subject is presented under the following headings; phenomenological models (general trends and coupling schemes, the collective vibrational model, the unified model for vibrations, the vibrating potential model (VPM), the E_1 photoresonance, the collective rotational model, the unified model for rotations, the moment of inertia), microscopic theories (Hartree–Fock self-consistent field theory: spherical nuclei, Hartree–Fock self-consistent field theory: deformed nuclei, pairing-force theory, the Tamm-Dancoff approximation or simple particle-hole theory, an equations-of-motion method, the random phase approximation or sophisticated particle-hole theory, time-dependent Hartree–Fock (TDHF) theory, the microscopic foundations of the unified vibrational model). (UK)

20484 TABLE OF E0 CONVERSION PROBABILITY ELECTRONIC FACTORS. Bell, D. A.; Aveledo, C. E.; Davidson, M. G.; Davidson, J. P. (Univ. of Kansas, Lawrence). Can. J. Phys.; 48: 2542-70(1 Nov 1970).

The electronic factor of the electric monopole conversion probability as a function of the atomic charge number Z and transition energy k for K, L_I, and L_{II} shells is presented in tabular form. The table lists factors over a range of k/mc^2 from 0.1 to 5.0 units in increments of 0.1 units and from $Z = 40$ to $Z = 102$ in steps of $\Delta Z = 2$. The factors are calculated relativistically and include corrections for finite nuclear size and bound state atomic screening. (auth) (Canada)

20485 TWO-NUCLEON REACTION MATRIX OFF THE ENERGY-SHELL. Mukhopadhyay, Susanta Kumar. Pittsburgh; Carnegie-Mellon Univ. (1970). 117p. University Microfilms Order No. 70-17,143.

Thesis.

Many-body theories seem to abound in off-energy-shell effects about which very little is known experimentally. In order to get a feeling for the importance of the off-shell behavior of the two-nucleon transition matrix T, a formalism was developed which calculates the entire T-matrix starting from the symmetric part σ of the half-shell T. An underlying potential is assumed (but is never made explicit) and the formalism is restricted to partial-wave channels which neither have any bound state nor are coupled. The arbitrariness in the T-matrix appears as the continuation of the phase shift function, a function of one variable, into two dimensions. Moreover, in the formalism any assumptions regarding the high-energy behavior of the phase shifts and the off-shell behavior of the T-matrix are neatly separated. Assuming definite high-energy behaviors for the phase shifts and a particular one-parameter functional form for σ some preliminary reaction matrix calculations were done for nuclear matter and finite nuclei. The results are fairly insensitive to the high-energy behavior of the phase shifts as expected. However, the off-shell behavior appears to be as important as the consideration of higher order diagrams in the many-body theory. (Diss. Abstr. Int., B)

20486 ISOTOPE-SHIFT OF NUCLEAR CHARGE DISTRIBUTIONS, STATISTICAL THEORY OF DEFORMED NUCLEI, AND VALIDITY OF THE STRUTINSKY SHELL CORRECTION THEORY. Lin, Wing-fai. San Diego, Calif.; Univ. of California (1970). 101p. University Microfilms Order No. 70-23,289.

Thesis.

The energy-density formalism is applied to the study of the isotope shift of nuclear charge distributions. It allows one to determine the part of the shift due to a statistical change in the proton densities. The study is improved by a shell-model calculation based on the Thomas-Fermi potential. The charge distributions are in relatively good agreement with experiment. However, the present model cannot reproduce the part of the shift due to non-monotonic changes in charge distributions. These non-monotonic effects are of a more complicated origin; they are of the same order of magnitude as the statistical shifts. In the case of the pair of ^{40}Ca-^{48}Ca the results are consistent with shifts calculated in self-consistent (Hartree–Fock) methods. The changes in binding energy of $_{114}X^{298}$ under deformation into prolate spheroidal shapes were calculated using the statistical theory of nuclei. The density is restricted only by the requirement that each equidense surface is a spheroid. It is found that the energy is minimized when the density has an approximately uniform surface thickness around the nucleus. To first order the change in binding energy is given well by the liquid-drop model but at large deformation the statistical theory predicts less drop in energy and consequently a slightly more stable nucleus. Realistic shell-model potentials are used to test Strutinsky's method. It is found that the results are strongly dependent on the shell-smearing parameter as well as the order of the curvature correction for smearing. No unambiguous values can be obtained for the shell correction, even with the effect of the continuum properly included. As a result, the Strutinsky theory should be regarded only as a reasonable recipe to be used in combination with Nilsson potentials. (Diss. Abstr. Int., B)

20487 INTEGRAL EQUATION FOR THE N-PARTICLE RESOLVENT OPERATOR. Avishai, Y. (Weizmann Inst. of Science, Rehovot, Israel). Nucl. Phys.; A161: 621-4(1971).

The N-particle problem was studied through the resolvent operator G of the Hamiltonian. On iterating the so-called second resolvent identity, an integral equation with a connected kernel satisfied by G is arrived at. (auth)

20488 SHORT-RANGE CORRELATIONS AND PARITY IMPURITIES. Gari, M.; Kuemmel, H.; Zabolitzky, J. G. (Ruhr-Univ., Bochum, Ger.). Nucl. Phys.; A161: 625-36(1971).

Two problems arising in calculating parity-violating effects in nuclei are discussed: the lack of reliable information on (i) weak parity-violating NN potentials and (ii) strong NN potentials at short relative distances and their influence on nuclear structure (short-range correlations). It is shown how to compute the latter reliably with the result that the parity admixtures depend strongly on the nucleon–nucleon potentials used. From this it was concluded that the determination of the weak NN forces cannot be separated from the determination of the short-range behavior of strong NN potentials. (auth)

20489 CALCULATIONS OF FISSION PARAMETERS BASED ON A MOLECULAR MODEL OF FISSION. Thind, K. S.; Tomlinson, R. H. (McMaster Univ., Hamilton, Ont.). Can. J. Phys.; 48: 3016-2(15 Dec 1970).

A "molecular model" of fission, in which a fragment separation of 4.0 fm defines the scission point, is proposed. Using the fragment separation distance as a free parameter, the sum of the Coulomb and deformation energies for the scission configuration is minimized. This provides a method for calculating the kinetic energies of fragments both at the scission point and at infinite separation. The fragment deformation energies were also calculated. (auth) (Canada)

20490 CROSS-SECTIONS OF HIGH-ENERGY PARTICLES ON ATOMIC NUCLEI. Eliseev, S. M. (Joint Inst. for Nuclear Research, Dubna, USSR). Acta Phys. Pol.; B1: 83-6(Apr-Jun 1970). (In Russian).

It is shown that Glauber theory may be used for the calculation of the total, elastic, and inelastic cross sections for interactions of pions and protons with nuclei at and above several hundred MeV. (tr-auth)

20491 INTERACTION OF SHOCK WAVES WITH FLUCTUATIONS OF NUCLEAR MATTER. Toktarov, K. Izv. Akad. Nauk Kaz. SSR, Ser. Fiz.-Mat.; No. 6, 1-3(Nov-Dec 1969). (In Russian).

The hydrodynamic mechanism of fragmentation, represented as a fluctuation in the density of nuclear matter, was used to study knock-out interactions on nuclei by the shock wave of high-energy particles. An estimate of the quantity of deuterons and tritons emitted in fragmentations according to this model was obtained. It was noted that in order to explain high-energy fragments in knock-out reactions, relativistic considerations must be used in formulating the shock wave. (auth) (TSS)

20492 DIAGONALIZATION OF PAIRED $S = 0$, $T = 1$ CHARGE-SYMMETRICAL HAMILTONIAN. Afanas'ev, G. N. Izv. Akad. Nauk Kaz. SSR, Ser. Fiz.-Mat.; No. 6, 46-8(Nov–Dec 1969). (In Russian).

Some previous results of diagonalization are discussed. The possibility of storing average values of the quasi-projection, isospin, and Casimir R_5 operators is considered. (tr-auth)

20493 NEUTRON–PROTON CORRELATIONS IN LIGHT NUCLEI AND THE CLASSIFICATION OF STATES OF GROUP R_5. Afanas'ev, G. N. Izv. Akad. Nauk Kaz. SSR, Ser. Fiz.-Mat.; No. 6, 19-28(Nov-Dec 1969). (In Russian).

The symmetry properties of the S = 0, T = 1 Hamiltonian were studied. The physical basis of group R_5 with diagonal N, T_0, T^2 was constructed. The problem of the fourth quantum number was decided. (tr-auth)

20494 CENTRAL NUCLEON–NUCLEON POTENTIALS AND THE BEHAVIOUR OF THE GROUND STATE WAVE FUNCTION OF ^{6}Li. **Afzal, S. A.; Ali, S. (Atomic Energy Centre, Dacca, Pakistan). Nucl. Phys.; A157: 363-8(1970).**

The central nucleon–nucleon potentials employed in recent years in the resonating group studies of light nuclei were analyzed. In the course of this analysis, it was observed that although some of these potentials produce low-energy nucleon–nucleon scattering data not too unsatisfactorily, there is still scope for a somewhat better fit to the data with central potentials. The sensitivity of the radial wave function of an assumed $\alpha - d$ structure of the ground state of ^{6}Li to different central potentials that fit the low-energy two-body scattering data with varying degrees of accuracy was explored, and the significance of the explicit distortion effect in terms of the behaviour of the potentials used in the $\alpha - d$ model of ^{6}Li was also discussed. (auth)

20495 CORE-PARTICLE COUPLING IN THE ODD-MASS ISOTOPES OF ANTIMONY. **Sen, S.; Sinha, B. K. (Saha Inst. of Nuclear Physics, Calcutta). Nucl. Phys.; A157: 497-519(1970).**

The different low-energy properties of the odd-mass Sb isotopes from A = 115 to A = 125 were calculated in a core-particle coupling model in which the 51st proton in the $2d_{5/2}$, $1g_{7/2}$, $2d_{3/2}$, $3s_{1/2}$ and $1h_{11/2}$ single-particle states outside the Z = 50 closed shell is coupled to the quadrupole and octupole excitations of the doubly even Sn core. Calculated results were compared with recent experimental findings. (auth)

20496 CORE-POLARIZATION EFFECTS IN CHARGE-EXCHANGE REACTIONS; APPLICATION TO ^{58}Ni(^{3}He,t). **Madsen, V. A. (Oregon State Univ., Corvallis); Brown, V. R.; Becchetti, F.; Greenlees, G. W. Contract AT(11-1)-1265. Phys. Rev. Lett.; 26: 454-8(22 Feb 1971).**

The formal relationship between tensor-force distorted-wave Born approximation theory and β decay is stated. Data on the reaction ^{58}Ni(^{3}He,t) are given and compared with the cross section calculated with model wave functions adjusted to account for the known retardation in the ^{58}Cu positron decay. The calculated (^{3}He,t) cross section is also retarded but to an extent sensitively dependent on the tensor strength and the configurations present. (auth)

20497 REEXAMINATION OF THE DWBA METHOD IN THE DEUTERON STRIPPING REACTION. **Kubo, Ken-ichi (Tokyo Univ.). Progr. Theor. Phys. (Kyoto); 44: 929-51(Oct 1970).**

In the framework of the distorted-wave Born approximation (DWBA), the effects of the term ($V_{pA} - U_{pB}$), which is neglected in the usual DWBA calculations, are investigated by taking a simple case of the (d,p) reaction with a closed-shell target nucleus and also by assuming that the above term is replaced by $-U_{pn}$, where U_{pn} is the potential affecting the outgoing proton from the captured neutron. Detailed numerical investigations are performed for various residual states which involve ^{13}C (1p), ^{13}C(2s), ^{17}O(1d), ^{41}Ca(1f), ^{41}Ca(2p), ^{91}Zr(3s), and ^{91}Zr(2d). (auth)

20498 STATISTICAL DETERMINATION OF MEAN LIFETIMES FOR A RADIOACTIVE SPECIES. **Vogel, Amelitta. Bul. Inst. Politeh. Gheorghe Gheorghiu-Dej Bucuresti; 32: 43-57(Mar-Apr 1970). (In Rumanian).**

The problems connected with the statistics of the determination of the mean half-life of a single radioactive species are studied. The arguments are relatively simple; and the conclusions statistically arrived at are valid for a whole series of physical phenomena, the law of which is mathematically expressed by an exponential function. The problem of the determination of mean lifetimes in the case of elemental particles is particularly important. (auth)

20499 MODEL OF NUCLEAR PHOTOFISSION. **Updegraff, William Edward. Athens, Ohio; Ohio Univ. (1969). 119p. University Microfilms Order No. 70-15,293.**
Thesis.

The process of symmetric binary photofission is investigated by applying the dynamic collective model to the extremely deformed nuclear shapes that must exist during any fission process. The dynamic collective model as used here consists of a combination of the Steinwedel–Jensen photonuclear model and the Bohr–Wheeler liquid-drop model. This combination is possible since the requirements of a variable difference density $\Delta\eta = \rho p - \rho_n$ and a constant total density of $\rho_0 = \rho_p + \rho_n$ can be fulfilled simultaneously. The nuclear system is described by a single-parameter surface $R = R_s (1 + \beta P_2 (\cos\theta))$ before separation of the fragments and by the fragment separation distance x after separation is achieved. The charge-density oscillation eigenfrequencies were calculated; the mass parameter and moment of inertia were determined. Ultimately, cross sections were calculated using standard perturbation theory in the electric-dipole approximation. It was found that only the very lowest eigenfrequency level could contribute significantly to the cross sections at incident photon energies for the order 10 to 20 MeV. As the nucleus deformed, this lowest level tended to zero and about 11 MeV energy was transferred into kinetic energy. The values of the mass parameter and moment of inertia were found to agree with the spherical values and the values at the scission point. Neither function indicated drastic behavior although both are significant functions of β. The theoretical cross sections showed a whole series of resonances that overlapped as the fissionability increased. A qualitative comparison was made with experimental symmetric binary photofission cross sections (^{238}U(γ,f)^{115}Cd) by fitting the theoretical resonances to Breit–Wigner shapes and then broadening the individual resonances by adding an arbitrary width of 0.5 MeV to each width in an attempt to include the broadening effects of all other channels. The resulting comparison showed that the experimental and theoretical cross sections were of the same order of magnitude and that, by judicious choice of the fissionability, the two spectra could be made to coincide at energies up to the threshold of (γ,nf) reactions. Since no other channels besides symmetric fission were considered, these results indicate the model is successful. The present work seems to be unique in that this is the first time that quantitative predictions have been made. (TSS) (Diss. Abstr. Int., B)

20500 SEPARATION OF THE CENTER-OF-MASS MOTION IN THE NUCLEAR MANY-BODY PROBLEM. SKETCH OF AN ALGEBRAIC APPROACH. **Miglietta, F. (Univ., Pavia, Italy. Istituto Nazionale di Fisica Nucleare, Pavia, Italy). Lett. Nuovo Cim.; 4: 1088-90(5 Dec 1970).**

After separation of the cms motion the wave function for an N-particle system depends on only 3(N − 1) coordinates and not 3N. Until now nuclear physics has used wave functions depending on 3N coordinates instead of 3(N − 1) ones, and invented ad hoc rules for eliminating the so-called "spurious" states of cms motion. This paper describes an algebraic approach to the problem of constructing an antisymmetrized basis of wave functions for the relative motion which depends correctly on 3(N − 1) coordinates. (R.W.R.)

20501 CORRECTION TO THE DIRECT TRANSFER REACTION OF HEAVY ION. **Suzuki, Takehiko (Shizuoka Univ., Japan). Progr. Theor. Phys. (Kyoto); 44: 1118-20(Oct 1970).**

The second-order correction to the direct transfer process described in the DWBA amplitude is evaluated for heavy-ion reactions. If the exponential function decreases slowly with increasing l, the second-order contribution is not negligible; the DWBA approach is, therefore, unjustified. Such a situation may conceivably arise from the comparatively short wavelength of the incident heavy ion. (R.W.R.)

20502 MANY-BODY PROBLEM OF ATTRACTIVE FERMIONS WITH ARBITRARY SPIN IN ONE DIMENSION. **Takahashi, Minoru (Tokyo Univ.). Progr. Theor. Phys. (Kyoto); 44: 899-904(Oct 1970).**

A set of coupled integral equations that determine the ground-state energy of N fermions with arbitrary spin attracting via a delta-function potential are obtained. In the case of spin ½ the equations derived are equivalent to those of Gaudin. (auth)

20503 STRUKTURA YADRA. (Nuclear Structure). **Begzhanov, R. B. (ed.). Tashkent; Izdatel'stvo Fan Uzbekskoi SSR (1969). 296p.**

In this compilation of nine monographs, the principles of the phenomenological theory of the excited states of atomic nuclei and the theory of the interaction of nucleons in nuclei are reported. It is shown that the energies of the excited states and probabilities of electromagnetic transitions in even–even, odd, and odd–odd nuclei can be described by a small number of parameters characterizing the form of the nucleus in the ground state and its deformability. Quasi-rotational bands in even–even and odd spherical nuclei are studied. The nature of pair interactions in the final nuclei and the Coriolis interaction in superfluid atomic nuclei, as well as the structure of nuclei determined by electron elastic and inelastic scattering, are thoroughly investigated. (tr-auth)

20504 SOLVABLE QUANTUM-MECHANICAL MODEL WITH NONLINEAR TRANSFORMATION LAWS. **Velo, G. (Univ., Bologna); Wess, J. Nuovo Cim.; 1A: 177-87(1 Jan 1971).**

XUM

A quantum-mechanical model with three degrees of freedom and a nonlinearly realized Lorentz group is solved exactly. Moreover, it is shown that, even after breaking the symmetry by a linearly transforming term, the model remains solvable. In both cases the spectrum of the Hamiltonian is investigated and found to be positive. (auth)

20505 DESCRIPTION OF THE NUCLEAR-CONFIGURATION INTERACTION PROBLEM USING STATISTICAL ENSEMBLES. **Ullah, N. (Univ. of Toronto). Nuovo Cim., 1A: 49-57(1 Jan 1971).**

A statistical theory is developed to treat the configuration-interaction problem for the ground state of the nucleus. The true ground-state wave function is broken into a dominant component and a part that can be treated statistically. Expressions are obtained for the average and the mean-square deviation of the expectation value of some operator in the ground state by using a simple model for the distribution of the coefficients of the statistical components. Within this framework it is shown why the Hartree–Fock approximation should provide a better basis for the configuration-interaction calculations. Some numerical examples are also presented. (auth)

20506 RADIAL DEPENDENCE OF THE P_1 INTERACTION IN THE SCHEMATIC MODEL. **Fujii, S.; Morita, K. (Nihon Univ., Tokyo). Phys. Lett.; 33B: 453-6(7 Dec 1970).**

Electro-excitations of $J^\pi = 1^-$, T = 0 levels in self-conjugate closed shell nuclei are calculated, assuming that the radial part of the separable potential of $Y_1 \cdot Y_1$ type has one node or more and, making a removal of the spurious mode in the schematic model. (auth)

20507 VALIDITY OF RANDOM MATRIX THEORIES FOR MANY-PARTICLE SYSTEMS. **French, J. B. (Univ. of Rochester, N. Y.); Wong, S. S. M. Phys. Lett.; 33B: 449-52(7 Dec 1970).**

The assumption of statistical independence of matrix elements leads to ensembles of Hamiltonians which involve simultaneous interactions between many particles. Then, for example, the resultant (semicircular) spectra are quite different from the Gaussian spectra found for ensembles properly restricted to involve only two-body interactions. (auth)

20508 TENSOR FORCE FORMALISM FOR INELASTIC SCATTERING, CHARGE EXCHANGE, AND KNOCK-OUT REACTIONS. **Love, W. G.; Parish, L. J. (Florida State Univ., Tallahassee). Nucl. Phys.; A157: 625-45(1970).**

A representation of the two-body tensor force is presented that may easily be used in inelastic scattering, charge exchange and knock-out reactions as well as Slater-type structure calculations. The relevant formulas are cast into the general formalism given by Satchler. Explicit formulas are given for both the direct and knock-out form factors so that the tensor force may be incorporated directly into existing distorted-wave programs. A brief discussion is given regarding the influence of the tensor force on various transitions, and some sample DWBA calculations are presented. The effects of recoil were neglected. (auth)

20509 SEPARABLE SINGLE-PARTICLE POTENTIAL IN SHELL-MODEL CALCULATIONS EXTENDED TO THE CONTINUUM. **Jeukenne, J. P.; Stancu, Fl. (Univ. Liege). Nucl. Phys.; A157: 646-60(1970).**

The definition recently discussed by Stingl and Kirson for a microscopically founded single-particle potential was extended. The resulting potential is described by an operator of finite rank. The potential scattering phase shift was analyzed. When a harmonic oscillator basis for the bound states is used, the analytical expressions for the transition amplitude and the wave function are considerably simplified. They are reduced to those that can be obtained in the case of a simple separable operator. It is shown that the phase shifts for all orbital angular momenta l decrease with energy. Restrictions imposed by this result on the use of the potential in the shell-model calculations extended to the continuum are discussed and possible improvements are suggested. (auth)

20510 MULTICHANNEL TREATMENT OF RESONANT REACTIONS USING THE QUASIPARTICLE METHOD. **Weiss, Ulrich (Univ., Stuttgart). Nucl. Phys.; A156: 53-64(1970).**

A multichannel resonant reaction formalism is introduced using the quasiparticle method of Grassberger and Sandhas. Contrary to Feshbach's projection operator approach the method can, without difficulty, take the Pauli principle correctly into account and treat rearrangement processes. The direct transition amplitude and the closed channel bound states obey exact one-dimensional integral equations. The generalized potentials occurring in them are calculable via an iteration scheme which should rapidly converge in most cases of physical interest. Thus the level shift and level width are finally expressed by accessible quantities. (auth)

20511 SEPARABLE APPROACH TO THE MUTUAL SCATTERING OF CLUSTERS. **Kukulin, V. I.; Neudatchin, V. G. (Moscow State Univ.). Nucl. Phys.; A157: 609-24(1970).**

A new class of one-term separable potentials for cluster-cluster (d, t, α) scattering is proposed. The analytical form of the potential form factors for the proposed potentials was obtained directly from the cluster representation of the shell-model wave functions with the corresponding shell-model parameters, and thus a single analytical expression was taken for all (essential) partial waves for the given pair of nuclei. In particular, the S-, D- and G-scattering phases in the ^{4}He-^{4}He system and the S-phase for ^{4}He-d scattering were investigated. A quite adequate description of the phase shifts and radial wave functions in the continuum was obtained. This was due to the fact that in the systems concerned only one (quasi)-stationary state predominates in a given scattering channel. A very simple general relation connecting the positions of the zeros of the phase shifts and the zeros of the oscillator Laguerre polynomials in the momentum representation valid for different partial waves and different cluster pairs is given. Application of the proposed potentials to other two- and three-cluster systems is discussed. (auth)

20512 CHARGE ASYMMETRY OF NUCLEON WIDTHS OF THE LOWEST T = 3/2 STATES OF ^{13}N AND ^{13}C. **Arima, A.; Yoshida, S. (Rutgers—The State Univ., New Brunswick, N. J.). Nucl. Phys.; A161: 492-520(1971).**

The isospin-forbidden widths of the lowest T = $^3\!/_2$ states of ^{13}N and ^{13}C were calculated by including isospin mixing due to Coulomb interaction and charge-dependent nuclear forces in the first-order perturbation approximation. The widths were obtained by using the Feshbach formula with the continuum-state wave function distorted by an optical potential. The widths are sensitive to the exchange character of the charge-independent nuclear potential. The absolute magnitude of the widths, and the charge asymmetry in the branching ratio to the ground and first excited states of ^{12}C were found to be compatible with the theoretical results, and the presence of a charge-dependent nuclear force is not essential for this agreement. (auth)

20513 ANALYTIC INTERPOLATION OF THE EIGENVALUES OF AN ASYMMETRIC ROTATOR. **Talman, J. D. (Univ. of Western Ontario, London. Univ. of Copenhagen). Nucl. Phys.; A161: 481-91(1971).**

The behavior of eigenvalues of the asymmetric rotator as functions of a continuous variable z = I(I + 1) was considered. The eigenvalue problem for the Hamiltonian matrix in a basis of eigenstates of I^2 and I_3, where I_3 is parallel to one of the principal moments of inertia, was studied by transforming it to a Sturm-Liouville problem. A proper eigenvalue problem is obtained only if I_3 is parallel to the largest or smallest moment of inertia. In this case an eigenvalue λ is an analytic function for z in the neighborhood of the real axis, but may have branch points off the real axis, and that λ is real for z real. The behavior of the eigenvalues as the intermediate moment of inertia approaches one of the others is considered in some detail. (auth)

20514 COMPARISON OF HARTREE–FOCK, SLATER, AND THOMAS–FERMI APPROXIMATIONS. **Nemeth, J. (Lab. of Nuclear Physics, Orsay, France). Nucl. Phys.; A156: 183-92 (1970).**

The energy and density distributions of nuclei are calculated with density dependent effective forces in Hartree–Fock, Slater and Thomas–Fermi approximations. The results are compared and the validity of the Slater and Thomas–Fermi approximations, for certain purposes, is examined. (auth)

20515 FORMATION REGION OF INTERNAL CONVERSION COEFFICIENTS. **Band, I. M.; Sliv, L. A.; Trzhaskovskaya, M. B. (Ioffe Inst. of Physics and Tech., Leningrad). Nucl. Phys.; A156: 170-82(1970).**

The inner part of the atom is shown to be of major importance in the formation of internal conversion coefficients (ICC) in all the atomic shells including the outermost ones. The radius r_{ef} of this region is determined by the expression $r_{ef} \lessapprox (l + 1)(l + 2)/\alpha Z$ for the orbital quantum number l. In order to show this r_{ef} was calculated for all the shells in atoms Z = 72, 30, 18 for conversion electron energies ϵ ranging from 1.001 mc^2 to 1.1 mc^2. The results obtained provice justification to the idea of chemical environment analysis with the aid of ICC. They show that measurements of ICC can be used for determining the electron density close to the origin. (auth)

20516 DESCRIPTION OF NUCLEAR REACTIONS IN THE HARMONIC OSCILLATOR SHELL-MODEL FUNCTION SCHEME. **Hackenbroich, Hans H. (Univ., Cologne). Nucl. Phys.; A156: 133-44(1970).**

The general reaction theory formalism given by Heiss and

Hackenbroich—based on the Kohn variational principle—is applied to the case that the two reaction partners in every channel are described in the harmonic oscillator shell model. One of them should be large so that translational invariance may be neglected; the other one consists of a maximum number of four nucleons so that its wave function is given by the translationally invariant shell model without difficulty. The Hamiltonian used in this theory is composed from the elementary nucleon–nucleon interactions. It is shown how some matrix elements of this Hamiltonian can be computed; these matrix elements are the basic quantities in the reaction equation. (auth)

20517 NUCLEAR SCREENING TENSORS AND THE ORBITAL CONTRIBUTION TO THE NUCLEAR SPIN COUPLING TENSOR. **Love, I. (Univ. of Zambia, Lusaka). Mol. Phys.; 19: 733-6 (Nov 1970).**

Part of the nuclear spin coupling between two nuclear moments arises from the coupling of the moments via the orbital angular momenta of the electrons. Pople (NSA 12: 9380) gave an expression for the isotropic coupling constant J^{orb}. An alternative expression is given here derived from the effective Hamiltonian for the coupling of two nuclear magnetic moments. It is stated that Pople's expression is incorrect. The accuracy of measurements of the anisotropic part of the nuclear shielding tensor, as used for the present expression, J^{orb}, is discussed. (UK)

20518 CONDITION FOR THE NEUTRON CAPTURE CROSS-SECTION AS MEASURED BY ACTIVATION TO BE INDEPENDENT OF HALF-LIFE. **Ryves, T. B. (National Physical Lab., Teddington, Eng.). Int. J. Appl. Radiat. Isotop.; 21: 567-8(Sep 1970).**

It is shown that when measuring neutron capture cross sections by the activation method under certain simple conditions an exact knowledge of the half-life of the induced activity is not needed. By way of example the case of ^{90}Y is discussed. (UK)

20519 PROPOSED POLARIZED-TARGET-BEAM TEST FOR $^3S_1$–$^3S_1$ RADIATIVE TRANSITIONS IN THERMAL n–p CAPTURE. **Breit, G.; Rustgi, M. L. (State Univ. of New York, Buffalo). Nucl. Phys.; A161: 337-53(1971).**

The development of techniques for producing polarized-proton targets and polarized-neutron beams may make it possible to set an upper limit on the probability of transitions from the $^3S_1$ states in the continuum of the low-energy n + p system to the $^3S_1$ part of the deuteron ground state. The absence of such transitions was assumed in traditional theories of the thermal-energy neutron capture, as a consequence of the orthogonality of two eigenfunctions of a Schrödinger equation corresponding to two different energies. The applicability of this reasoning to the physical situation is discussed with the conclusion that it is not necessarily valid even apart from the slight effect of the admixture of the $^3D_1$ to the $^3S_1$ state. The density matrix of the colliding particles with arbitrarily assigned polarization vectors of beam and target was then used to calculate the angular distribution and degree of polarization of the capture gamma rays. If the whole of the approximately 9% "interaction effect" of Austern is to be accounted for by $^3S_1 \rightarrow {}^3S_1$ transitions, without any modification of the spin-flip transition intensity, asymmetries in the gamma angular distribution ranging from 23 to 1.98% at a geometric-mean target-beam polarization of 0.954 to 0.577 respectively may be found. Larger or smaller effects may result depending on whether the spin-flip transitions are inhibited or enhanced by n–p interaction and structure effects. Appreciable effects on gamma polarization are expected under conditions leading to appreciable gamma angular distribution effects. (auth)

20520 ODD-EVEN STAGGERING OF NUCLEAR RADII. **Reehal, Balbir S. (Wheeling Coll., W. Va.); Sorensen, Raymond A. Nucl. Phys.; A161: 385-400(1971).**

The odd-even staggering of nuclear radii, as observed in isotope shifts of atomic and mu-atomic spectra, was calculated using the pairing-plus-quadrupole model. The experimental effect is qualitatively explained on the basis that the mean square deformation β^2 associated with the zero-point motion of quadrupole vibrations is greater for even than for odd nuclei. The radius change is related to a change in β^2 using the incompressible fluid model. The theoretical value of $\Delta\beta^2$ is obtained by computing $\langle Q^2\rangle$ for even and for odd nuclei, using BCS wave functions with ground state correlations admixed in perturbation theory by the quadrupole force, and properly blocking the ground state correlation admixtures, in the case of an odd nucleus, by the odd quasiparticle. Near the end of the shell, instead of BCS, a one- and two-particle calculation is done. In addition, the contribution of blocking to the odd-even mass differences is discussed. (auth)

20521 RELATION BETWEEN BELYAEV–ZELEVINSKII AND MARUMORI BOSON EXPANSIONS. **Marshalek, Eugene R. (Univ. of Notre Dame, Ind.). Nucl. Phys.; A161: 401-9(1971).**

If Beliaev–Zelevinsky boson expansions are carried to infinite order, all matrix elements of fermion operators are preserved and hence also the Pauli principle. Given such an expansion, one may easily construct a Marumori expansion having the same physical subspace. It is shown that the usual Beliaev–Zelevinsky expansion is a generalization to the fermion-pair algebra of the Holstein-Primakoff expansion used for the SU(2) algebra. (auth)

20522 ABSORPTION MODEL FOR DIRECT TRANSFER REACTIONS. **Dobes, J. (Nuclear Research Inst., Rez, Czech.). Nucl. Phys.; A157: 661-72(1970).**

A simple model for direct transfer reactions was investigated. The transition amplitude was evaluated by means of the geometric mean (Sopkovich) formula with the sharp cut-off model for elastic scattering. An easy numerical computation removing a number of approximations adopted in previous papers was performed. The model was tested for some (d,p) and (p,d) reactions. Satisfactory agreement with experimental angular distributions and reasonable spectroscopic factors was obtained. (auth)

20523 MANY-BODY FORCES. Chanmugam, Ganesar. Waltham, Mass.; Brandeis Univ. (1970). 113p. University Microfilms Order No. 70-17,117.

Thesis.

Electromagnetic and nuclear many-body forces are discussed. A method of obtaining electromagnetic many-body forces acting between elementary charged particles using a canonical transformation is described. The Hamiltonian so derived is more general than that derived previously by Primakoff and Holstein. Rough estimates show that three-body forces must be taken into account to obtain agreement between theory and experiment in the spectra of small Z atoms. The use of this three-body potential in a (non relativistic) electron gas leads to divergences which are shown not to occur when screening is taken into account. The three-body potential gives important contributions to the ground-state energy of such a non-relativistic electron gas in the high density limit. However, the non-relativistic model is inadequate to describe the electron gas as relativistic effects become important at such high densities. A theory of a relativistic degenerate electron gas taking screening into account is formulated and its longitudinal and transverse dielectric constants are calculated. These may be used (in the future) to determine the effects of many-body forces in a relativistic degenerate plasma. The various methods used to derive nuclear many-body forces and the experimental evidence for their existence are reviewed. The effects of many-body potentials on the ground state energy of a zero temperature many fermion system are determined. It is found that three-body forces give significant contributions to the equation of state of a neutron star at densities $\gtrsim 10^{15}$ gm/cm^3. The effects of three-body forces on various physical properties of neutron stars are briefly discussed. Finally, Zeldovich's theorem on matter at ultra high densities is criticized and it is suggested that the (calculated) speed of sound for such high-density matter will not exceed that of light if many-body forces are taken into account. (Diss. Abstr. Int., B)

20524 UNIFIED MODEL OF DEFORMED ODD–ODD NUCLEI FOR NUCLEAR DATA GENERATION. Fu, Chia-yao. Knoxville, Tenn.; Univ. of Tennessee (1970). 80p. University Microfilms Order No. 70-20,306.

Thesis.

A unified model of deformed odd-odd nuclei was formulated as an aid in nuclear data generation and analysis with emphasis on obtaining information for the calculation of gamma-ray production cross sections. The model employs products of single-particle Nilsson wave functions as basis functions. The coupling of angular momenta of the odd nucleons is assumed to obey the Gallagher–Moszkowski coupling rules. The matrix elements of the proton-neutron residual interaction potential are evaluated with the use of oscillator brackets. The validity of the model was established by computing and comparing with experimental data nuclear energy levels and/or gamma-ray transition probabilities for ^{24}Na, ^{28}Al, ^{166}Ho, ^{182}Ta, and ^{238}Np. The calculated results compare quite well with experiment. Special attention was given to the establishment of an efficient computational method. By inputing calculated level characteristics and gamma-ray transition probabilities to a cascade model, gamma-ray production cross sections can be computed. (Diss. Abstr. Int., B)

20525 PROPERTIES OF REAL RPA MATRICES AND A SIMPLE DIAGONALIZATION PROCEDURE. **Ullah, N.; Rowe, D. J. (Univ. of Toronto). Nucl. Phys.; A163: 257-64(1971).**

In practical situations it transpires that the matrix elements that occur in the eigenvalue equations for non-hermitian matrices of RPA (random-phase approximation) form are almost invariably

XUM

real. It is shown that real RPA matrices have special properties which can be exploited to reduce the non-hermitian RPA eigenvalue equations to eigenvalue equations for a symmetric matrix of half the dimensions. Furthermore, it is shown that the elements of this matrix are real in all practical situations. (auth)

20526 COMPUTATION OF MOSHINSKY BRACKETS BY DIRECT DIAGONALIZATION. Talman, J. D. (Univ. of Western Ontario, London, Can. Univ. of Copenhagen); Lande, A. Nucl. Phys.; A163: 249-56(1971).

A simple and significantly more rapid method for calculating Moshinsky brackets is presented. It consists of diagonalizing a linear combination of the one-particle energy and angular momentum operators h_1, h_2, l_1^2, l_2^2 in the basis of relative and c.m. wave functions. The Moshinsky brackets are then the components of the eigenvectors. The required matrix elements are given for arbitrary orthogonal coordinate transformations, thereby including the unequal mass or frequency cases. (auth)

20527 APPROXIMATION FOR THE ROTATION-VIBRATION TRANSITION REGION. Kamlah, A. (Kernforschungszentrum, Karlsruhe, Ger.). Nucl. Phys.; A163: 166-92(1971).

An approximation is proposed for the collective energies and the wave functions in the rotation-vibration transition region of atomic nuclei in microscopic models. In the vibrational and rotational limiting cases this approximation coincides with former treatments. (auth)

20528 DYNAMICS OF THE OPTICAL MODEL. Brown, G. E. (State Univ. of New York, Stony Brook. NORDITA, Copenhagen). Comments Nucl. Particle Phys.; 4: 75-80(Mar-Apr 1970).

The nucleon–nucleon interaction can be represented by a density-dependent G matrix because of the large contribution from tensor forces. The average strength of the interaction thus obtained is about right. It is the imaginary part of the optical potential, however, which involves the dynamics of the system. This can be calculated from energy-conserving transitions in which the incident particle excites vibrations. The results of these calculations yield a possible explanation of why the absorption is roughly constant in the region from 0 to 30 MeV. (R.W.R.)

20529 ANGULAR ANISOTROPY AND FISSIONABILITY OF NUCLEI. Smirenkin, G. N.; Tishin, A. S. (Physical Energy Inst., Moscow). Yadern. Fiz.; 12: 746-52(Oct 1970). (In Russian).

The effect of nuclear fissionability on the angular anisotropy of fission is studied in the framework of the statistical theory. It is shown that this effect, which was not taken into account in the analysis of experimental data in general, considerably affects the angular distributions of fragments and parameters obtained from the analysis. Regions where the conventional, widely distributed approximation are valid are shown. (auth)

20530 PRIMENENIE CHISLENNYKH METODOV DLYA RASCHETA NEITRONNYKH SECHENII. (Use of Numerical Methods for Neutron Cross Section Calculations). Marchuk, G. I.; Kolesov, V. E. Moscow; Atomizdat (1970). 304p.

Numerical methods of solution of the Schroedinger equation in the framework of the optical model of the nucleus were developed which permitted simple calculation on present-day computers. These methods were used for calculation of neutron cross sections and independent bound states. A comparison of the value of the theoretical cross section with the experimental values is made. The results are tabulated for a broad range of nuclear energy and mass. (tr-auth)

20531 DEUTERON–NUCLEUS COLLISIONS IN THE MULTI-GeV REGION. Faeldt, Goeran (CERN, Geneva); Pilkuhn, H. Ann. Phys. (N. Y.); 58: 454-503(Jun 1970).

A generalization of Glauber theory is used to describe nuclear scattering of relativistic deuterons. The nucleus is described by the Woods–Saxon nuclear density function; and the deuteron, by a Gaussian wave function. The new approximation method is stable over the whole nuclear spectrum and has correction terms of about 10%. Elastic scattering, deuteron dissociation, and deuteron stripping are considered in both coherent and incoherent modes. Scattering with meson production is also treated. (R.W.R.)

20532 NUCLEAR STRUCTURE. II. THE SINGLE-NUCLEON POTENTIAL. Baranger, Michel (Massachusetts Inst. of Tech., Cambridge). Comments Nucl. Particle Phys.; 4: 81-9(Mar-Apr 1970).

Since the single-nucleon potential is a theoretical notion which cannot be measured directly, its definition must be based, at least in part, on convenience. The single-nucleon potential concept is first compared with experiment. Solutions of the Schroedinger equation for this potential do not yield the observed energy levels, and one is forced to distinguish between levels which are "of single-particle character" and those which are not. The best potential U to use in Brueckner calculations is discussed. It is concluded that the low part of the particle spectrum should be given by $\langle a|U|a\rangle = \Sigma_D \langle aD|G(\epsilon_D + \eta)|aD\rangle$, where the available energy is off-shell, while the high-lying spectrum is best left as purely kinetic ($\langle a|U|a\rangle = 0$). (R.W.R.)

20533 DIAGRAM APPROACH TO POLARIZATION EFFECTS IN THE STRIPPING AND PICK-UP REACTIONS. Khangulyan, V. A.; Kolybasov, V. M. (Inst. of Theoretical and Experimental Physics, Moscow). Yadern. Fiz.; 12: 732-45(Oct 1970). (In Russian).

Polarization effects in stripping and pick-up reactions are considered by assuming that the main contribution to the amplitude of the process is given by the pole diagram and by those diagrams the spin structure of which is the same as that of triangle diagrams corresponding to the interactions in initial and final states. New relations are obtained connecting the asymmetry of the particle emission in reactions on polarized targets, and the polarization of recoil nuclei in reactions with nonpolarized initial particles with the polarization of outgoing light particles. To make the exposition more general, results are also given relating to asymmetry in the case of a polarized incident beam; though known before, these results are obtained here by more simple and universal methods, which allow one to formulate clearly the assumptions necessary for the validity of one or another relation. (auth)

20534 NEUTRON DISTRIBUTION IN NUCLEI. Huefner, Joerg; Weidenmueller, Hans A. Comments Nucl. Particle Phys.; 4: 121-5(May-Jun 1970).

Experiments involving isobaric analog resonances make it possible to measure the nuclear mass distribution using essentially the well-known Coulomb interaction. Information on the mass distribution is obtained by comparing the charge distributions of a nuclear state and its analog. The method for doing this, as well as the corrections to the initial results required, are described. (R.W.R.)

20535 MIRROR TRANSITIONS AND SECOND CLASS CURRENTS. Lipkin, H. J. (Weizmann Inst. of Science, Rehovot, Israel). Phys. Lett.; 34B: 202-6(15 Feb 1971).

Theoretical implications of observed mirror asymmetry in nuclear beta decay are examined, taking into account CP violation and internal symmetries. The second class induced tensor current is shown not to be responsible for the observed asymmetry, which must be the result of multinucleon or meson exchange effects. The result is general and holds for all values of momentum transfer. Possible two-nucleon transitions are discussed. Mirror asymmetry in the $\Sigma - \Lambda$ decay cannot be produced by SU(3) octet currents or single quark currents in the quark model even if such second class currents exist. (auth)

20536 WHAT IS THE RADIUS OF A NUCLEUS? Wilson, Richard. Comments Nucl. Particle Phys.; 4: 116-20(May-Jun 1970).

The various values for the radius of the nucleus determined from different measurements are discussed. It is not yet clear whether there is a real difference between the radii of the neutron and proton distributions. A procedure for obtaining cross sections for the scattering of unstable particles by nucleons is described. (R.W.R.)

20537 GENERALIZED IMPULSE APPROXIMATION. Cosgrove, Christine M. Washington, D. C.; Georgetown Univ. (1970). 101p. University Microfilms Order No. 70-26,655.

Thesis.

The impulse approximation, originally introduced by Chew for the calculation of nuclear scattering cross sections and recently applied to molecular processes by Henderson, is reformulated using time dependent S matrix theory. The exact scattering operator for a particle-complex target system is expanded via a formula operator expansion, $e^{-\beta(A+B)} = e^{-\beta A} - e^{-\beta B} V(A,B)$ where $V(A,B)V_{\dagger}(A,B) = 1$. When the commonly assumed form of V, $V(A,B) = e^{\beta^2 c_2} e^{\beta^3 c_3}$ ....., is limited to second order in β, the exact S operator may be expressed in terms of the product of the impulse approximation scattering operator, S^{IA}, and exponential operator of order β^2. This provides an improvement over the simple impulse approximation; $S \sim e^{\beta^2 [K,U]} - S^{IA} e^{-\beta [K,U]}$, where K is the total kinetic energy of the system and U is the energy associated with the binding forces of the target. When the target particle is assumed to be harmonically bound, the resulting matrix elements of the modified impulse approximation become a linear superposition of the known impulse amplitudes. The matrix elements are valid to second order in the ratio of the collision time to the period of the internal motion of the target, a quantity which is small under the assumptions of the impulse approximation. Higher order corrections to the impulse approximation are discussed briefly. In the ensuing development new insight is offered regarding the problems of unitarity and energy conservation which are not maintained simultaneously in the impulse approximation. (Diss. Abstr.)

20538 CALCULATIONS ON THE THREE-NUCLEON SYSTEM USING A SEPARABLE EXPANSION OF LOCAL POTENTIALS. **Harms, E. (Fairfield Univ., Conn.); Laroze, L. Nucl. Phys.; A160: 449-59(1971).**

A separable expansion for local potentials called the unitary pole expansion (UPE) has been applied to the singlet-S soft-core Reid potential. The separable potentials obtained are used in conjunction with a separable tensor potential to calculate the triton binding energy, the nd doublet scattering length, and the nd phase shifts in the $1/2^+$ state above and below break up. The convergence of the UPE is good especially for repulsive terms. The one term approximation (UPA) gives a triton energy differing by 0.04 MeV and a doublet scattering length differing by 0.14 fm from the values found for the local potential. The calculated phase shifts are in good agreement with the phase-shift analysis of Van Oers and Seagrave. (auth)

20539 JOST FUNCTION OF A NON-LOCAL POTENTIAL. **Warke, C. S.; Bhaduri, R. K. (McMaster Univ., Hamilton, Ont.). Nucl. Phys.; A162: 289-94(1971).**

An exact relation for the Jost function of a central nonlocal potential U(r,r′) in the S-state is derived in terms of Fredholm determinants. This is a generalization of the relation given by Jost and Pais for a local potential. (auth)

20540 HOLE POTENTIAL ENERGY IN NUCLEAR MATTER CALCULATIONS. **Mahaux, C. (Univ., Heidelberg). Nucl. Phys.; A163: 299-310(1971).**

The choice of the potential energy U for hole states in a Bethe–Brueckner calculation of nuclear matter is discussed. The U-dependence of the two- and three-hole line contributions. It is proposed that the choice of U is largely arbitrary, the numerical result being fairly insensitive to it. The main U-dependence arises from the Bethe–Faddeev three-body correlation terms. In particular, there is no need to require self-consistency. (auth)

20541 ANGULAR MOMENTUM PROJECTION APPROACH TO NUCLEAR ROTATIONS IN THE RARE-EARTH REGION: AN ILLUSTRATION FOR ^{152}Sm. **Ansari, A.; Nair, S. C. K. (Saha Inst. of Nuclear Physics, Calcutta). Nucl. Phys.; A163: 56-64 (1971).**

For the description of the rotational properties of rare-earth nuclei, the feasibility of angular momentum projections after a variational calculation of the intrinsic band wave function is explored, similar to what has been attempted for sd shell nuclei. As an illustrative example some results for ^{152}Sm in the pairing-plus-quadrupole force model are presented. These projection results are then compared with the corresponding ones in the more conventional semiclassical approaches and with experimental data. It is found that the results for the rotational energies are similar to the cranking model predictions. (auth)

20542 MESON EXCHANGE CURRENTS IN NUCLEAR WEAK AND ELECTROMAGNETIC INTERACTIONS. **Chemtob, M. (Univ. of Copenhagen); Rho, M. Nucl. Phys.; A163: 1-55(1971).**

Meson theory is applied to the study of the exchange magnetic moment and Gamow–Teller operators. Contributions due to the exchange of one pion and of vector mesons are considered and their detailed expressions are given in terms of a general classification of the operators. The one-pion-exchange process is separated into Born and non-Born parts corresponding respectively to the Born and non-Born parts in the process of weak or photoproduction of a pion by the nucleon. The results of low-energy theorems for this process enable one to reach a model-independent description of the non-Born parts. Corrections to the soft-pion limit are studied by means of simple dynamical models: a phenomenological Lagrangian for the weak current and the Chew–Low model for the e.m. current. The exchange operators due to the exchange of ρ- and ω-mesons are evaluated in the vector dominance model. The applications are concerned with the exchange effect in the isovector and isoscalar magnetic moments of ^{3}He and ^{3}H and in the Gamow–Teller matrix element for ^{3}H β-decay. The results are obtained with the dominant S-state with a Gaussian radial function. Their dependence on short-range correlations described in terms of Jastrow factors are discussed. The exchange corrections are found to be too small for the current wave functions of the trinucleons. Other agencies that may account for the remaining discrepancies are discussed briefly. (auth)

20543 MICROSCOPIC BASES OF COLLECTIVITY IN LIGHT NUCLEI. Friedman, Marvin Irwin. New Haven; Yale Univ. (1970). 283p. University Microfilms Order No. 70-25,266. Thesis.

In an attempt to elucidate the microscopic bases of collectivity in light nuclei, individual-particle model calculations were performed using both realistic and non-realistic nuclear models with the aid of angular momentum projection techniques. Matrix methods for projection from several "intrinsic" states of the nucleus are discussed and developed. In addition, a polynomial projection method which is extremely useful in considering systems of neutrons and protons is introduced. It allows for treatment of the Hilbert spaces of the two nucleon states as separate entities, which may, at conclusion, be combined into the Hilbert space of the entire nucleus. The phenomenological pairing-plus-quadrupole nucleon–nucleon interaction is studied in $(\underline{j})^n$ neutron configurations, $7/2 \le \underline{j} \le 15/2$. The $\underline{n}$-body Hamiltonian operator is parameterized in terms of its two-body matrix elements, enabling further calculations, for any given scalar operator, to be performed simply with the specification of its matrix elements. Complete, exact spectra are obtained for the $(\underline{j})^n$ configurations through the application of the matrix projection techniques. Eigen-functions are analyzed in seniority space with particular regard toward the exhibition of collective properties. Various experimentally observed phenomena are attributed to the nature of the simple, but basic, phenomenological forces. One- and two-particle/hole excitations are considered as a mechanism for "scattering" nucleons across the finite energy gap appearing between occupied and unoccupied Hartree–Fock deformed orbitals of even–even, N = Z nuclei in the $2\underline{s}$ – $1\underline{d}$ shell. Admixtures of these configurations to the Hartree–Fock state are found to be minimal and inadequate to account for the discrepancies between theoretically predicted and experimentally observed states of the nucleus. They do, however, give qualitative explanation to the low-energy excited nuclear configurations found to lie within or above the quasi-rotational Hartree–Fock spectrum. Shape-mixing calculations are discussed as a means of correctly predicting properties of eigenstates in the low-energy region of excitation. It is suggested that the objectionable use of a single deformed nuclear configuration as input to the calculations, rather than as output, may be eliminated by variation of the wave functions after projection, rather than before. (Diss. Abstr. Int., B)

20544 POSSIBILITY OF STUDYING THE DIFFERENCE BETWEEN PROTON AND NEUTRON DISTRIBUTIONS IN NUCLEI BY QUASI-FREE SCATTERING REACTIONS. Kabachnik, Nikolai M. Ann. Ist. Super. Sanita; 6: 9-15(1970).

The possibility of studying the difference between proton and neutron distributions in nuclei by means of (e,e′p) and (e,e′n) quasifree reactions, is suggested and analyzed. (auth)

20545 FINITE NUCLEAR SIZE CHARGE MODEL EFFECTS IN THE SMALL ANGLE MULTIPLE SCATTERING OF HIGH ENERGY ELECTRONS. Spight, Lonnie Dean. Reno, Nev.; Univ. of Nevada (1970). 239p. University Microfilms Order No. 70-12,980.

Thesis.

The modification of the small angle (≲6°) multiple scattering distribution of high energy (≳250 MeV) electrons due to the finite size of the charge distribution of target nuclei is determined as an additive correction term to the Molière point nucleus multiple scattering solution. The Mott single scattering cross section used in the small angle approximation form is modified by multiplicative factors to account for atomic electron shielding and the finite size of the target nuclei. Inelastic and scattering effects produced by the atomic electrons are incorporated into the definition of the multiple scattering characteristic angle; inelastic nuclear effects are taken into account by a multiplicative factor to the elastic form factor. First and second Born approximation forms for the single scattering cross section are shown to differ negligibly for the small angle electron scattering case under consideration. An heuristic step function (Olbert) form factor calculation is performed to determine the lower bound in the tail of the multiple scattering distribution allowable for realistic form factors. Four different methods of evaluating the nuclear correction term for general form factors are established. The first two methods use expansion techniques to determine series approximations for the correction term. The first expansion method is a general high energy method; the second is designed specifically for the lower end of the high energy spectrum. The second two methods utilize Hankel and Fourier cosine transforms of the nuclear form factor to establish integral representations for the correction term. In principle these transform methods provide for exact evaluations valid for the general high energy range, but for particular form factors approximative techniques usually prove expedient. These transform methods are representative of a class of evaluation methods; to the extent that they are exactly solvable they give identical results. In general they give results in good agreement with those obtained by the

XUM

first expansion method. Detailed calculations for seven specific form factors suggested by large angle single scattering experiments reported in the literature are made using each of the four methods developed for evaluating the correction term. The form factors used are: (1) Gaussian, (2) hollow Gaussian, (3) Yukawa II, (4) exponential, (5) modified exponential, (6) and (7) hollow exponential I and II. The procedure for obtaining the solutions for other form factors is straightforward. Numerical calculations of the distribution functions for the various methods and models for a number of specific target elements were made; extensive representative graphical results for sulfur targets are presented. In conclusion the four methods are compared and evaluated and the procedures to be followed when other form factors and other effects are selected for treatment are discussed. (Diss. Abstr. Int., B)

20546 UNRESTRICTED VARIATIONAL METHOD ON LIGHT NUCLEI. Urban, L. (Research Group for Theoretical Physics, Budapest). Acta Phys. Acad. Sci. Hung.; 28: 375-80(1970).

A general variational procedure based on the method of steepest descent in Hilbert space is given for the calculation of some nuclear levels. As an example the ^{4}He ground state is calculated. (auth)

20547 MICROSCOPIC INVESTIGATION OF THE COLLECTIVE MODEL OF NUCLEI. Abraham, P. M. Boulder, Colo.; Univ. of Colorado (1970). 114p. University Microfilms Order No. 70-23,679.

Thesis.

A model of deformed even−even nuclei is described in which the nucleus is assumed to be made up of a rotating core and an even number of valence nucleons. The intrinsic motion of the valence nucleons is assumed to be strongly coupled to the nuclear rotation so that the total Hamiltonian of the system may be obtained as consisting of three parts: the Hamiltonian of the rotating core, the intrinsic Hamiltonian describing the motion of the valence nucleons, and the rotation-particle interaction. The rotation-particle interaction is considered in the first and second order. Since the rotation-particle interaction gives rise to coupling between rotational bands with $\Delta K = \pm 1$ in the first order and $\Delta K = \pm 2$ in the second order, the eigenfunctions of the total Hamiltonian are taken to be superpositions of the usual adiabatic wave functions. The valence nucleons are considered to be moving in an axially symmetric deformed field and interacting via the pairing force. The intrinsic energies are obtained in the so-called quasiparticle model by constructing a two-quasiparticle basis for the intrinsic wave functions. The total energy matrix is set up by operating the Hamiltonian on a truncated K space and with the help of a few collective parameters. The energy eigenvalues are obtained by an exact diagonalization of the total energy matrix and the rotational levels built on two-quasiparticle spectra are extracted. Detailed numerical calculations are done on the ground state rotational levels of ^{158}Dy, ^{164}Er, ^{168}Yb, ^{170}Hf and ^{174}Hf. The calculated rotational levels are fit to all known experimental levels. For all the nuclei studied the experimental rotational levels are reproduced with a root mean square deviation of 0.1 – 5. keV. The inclusion of the second order rotation-particle interaction improves substantially the fit between the calculated and observed level energies, especially when levels of extremely high ($I \sim 18$) angular momentum are considered. A method of calculating the generalized decoupling parameters is obtained by expressing the intrinsic angular momentum projection operators as a sum of single particle operators. Reasonably good agreement is obtained between the calculated decoupling parameters and that obtained from the rotational energy systematics. (Diss. Abstr. Int., B)

20548 THE VALIDITY OF THE UNIFIED NUCLEAR MODEL AND ITS APPLICATION TO SEVERAL ODD-MASS ISOTOPES. Clemens, James Theodore. Brooklyn; Polytechnic Inst. (1970). 168p. University Microfilms Order No. 70-26,034.

Thesis.

In an attempt to increase the understanding of the low-energy structure of nuclei in the spherical regions of the nuclear mass spectrum, a theoretical investigation of the low-energy modes of nuclear excitation is presented. Based upon the assumption of the existence of residual two-body interactions in addition to the average nuclear shell model potential a microscopic many-body nuclear Hamiltonian is proposed. Specifically, it is assumed that the residual two-body interaction is composed of the sum of a pairing interaction and multipole−multipole interactions. By subsequent introduction of the Bogolgiubov quasi-particle transformation technique and the Random Phase Approximation, it is demonstrated that for even−even nuclei the low-energy modes of excitation are of a collective phonon nature and for odd-mass nuclei the low-energy modes are due to a coupling of quasiparticle and collective phonon modes of excitation. This approach thus gives one a microscopic insight into the earlier conceptual approaches of the phenomenological unified nuclear model. Using this new microscopic model, the M1 and E2 electro-magnetic transition rates and the static electric quadrupole and magnetic dipole moments are derived. In addition, the model is also used to analyse the one-nucleon transfer reactions. Within the framework of the Zero-Range Distorted Wave Born Approximation cross section magnitudes (spectroscopic factors) are derived, along with spectroscopic sum rules and energy center of gravity theorems. These equations are extremely important since they allow one to quickly analyse experimental one-nucleon transfer reaction data. The application of this microscopic theory for the analysis of the odd-mass molybdenum isotope series (^{93,95,97,99}Mo) is discussed. This isotope series is chosen since, 1) shell model calculations, which should be best suited in this mass region have failed to accurately portray the low energy structure; and, 2) the even−even neighboring nuclei exhibit quadrupole vibrational spectra. By analyzing the existing one-nucleon transfer reaction data via the derived spectroscopic sum rules and energy center of gravity theorems estimates of the effective quasi-particle excitation energies, E_j, and the structure constants, U_j, V_j, are obtained. These are then used to obtain a best fit between theory and experiment with regard to the excitation energies, spins, parities, the one-nucleon transfer reaction spectroscopic factors, and the electromagnetic transition rares and static multipole moments. The application of the microscopic model to ^{93,97,99}Mo has demonstrated the fundamental importance of the single quasiparticle phonon coupling interaction, and the influence of the shell structure on the values of the collective phonon excitation energies. Specifically, the observed variation of the quasi-particle energies with mass now offers an explanation for the sharp drop in the collective phonon excitation energy between ^{98}Mo and ^{100}Mo. The structure of ^{95}Mo, however, had to be explained by the coupling of three quasi-particles to the collective phonons, thus demonstrating the mutual effects of the shell structure and the collective structure. In all cases considered the agreement between theory and experiment is very good, thereby, indicating the fundamental importance of the quasi-particle phonon coupling interaction and lending a great deal of support to the validity of the microscopic two-body pairing and multipole-multipole residual interactions upon which the coupling was derived. (Diss. Abstr. Int., B)

REACTOR TECHNOLOGY

Commercial Power Reactors

Refer also to abstracts 18359 and 19275.

20549 (AEC-tr-7187) NUCLEAR POWER PLANTS. Baturov, B. B.; Koryaki, Yu. I. Translation of Russian report. 56p. Dep. NTIS.

The development of nuclear power plants in the U.S.S.R. is reviewed. Design characteristics and operating histories are discussed. Future development plans are described. (D.C.C.)

20550 (NP-18677) ELECTRICAL GENERATION AND ASSOCIATED DEVELOPMENTS WITH ATOMIC ENERGY. Bainbridge, G. R. (United Kingdom Atomic Energy Authority, Risley (England). [Reactor Group]). Oct 1969. 26p. Dep. NTIS (U. S. Sales Only).

The possibilities for the exploitation of nuclear power in Australia are discussed. An outline is given of the stages in the development of commercial nuclear power in other countries. A general introduction to nuclear power station characteristics is followed by more detailed consideration of the SGHWR. The relative merits of natural U and of enriched U designs are discussed. (UK)

20551 PUTTING INTO SERVICE REACTOR CONTROLLING EQUIPMENT AT THE NUCLEAR POWER STATION OBRIGHEIM LTD. Aleite, Werner (Siemens AG, Erlangen, Ger.). At. Strom; 16: 161-5(Nov-Dec 1970). (In German).

Some tests made and experiences obtained during the first year of operation are reviewed. Recommendations and improvements on the control equipment of future pressurized-water reactors are described. (auth)

20552 INCREASE OF SERVICE RELIABILITY AND MAINTENANCE. Hofmann, Werner (Kernkraftwerk GmbH, Lingen, Ger.). At. Strom; 16: 166-71(Nov-Dec 1970). (In German).

The relations between reliability, availability, and safety of equipment and machinery are analyzed by pointing out the essential magnitudes of influence. The principal features of an increase of service reliability by redundance with and without maintenance are explained quantitatively and qualitatively. In this connection the problem of obtaining reliability characteristics of components is also dealt with. 9 references. (auth)

20553 FINLAND'S POWER ECONOMY FROM 1970 THROUGH 2000. Nevanlinna, Lasse. Teknikka; 1: No. 11, 56-8; 63-6 (1970). (In Finish).

The growth of the consumption of electrical power is closely related to the growth of the national economy. Despite the construction of new power plants, Finland will have to import electrical power. New power plants will be of the nuclear type except for smaller installations. The Scandinavian power network will be enlarged for better cooperation. (auth)

20554 DISMANTLING FACILITY FOR THE LUCENS IRRADIATED FUEL ASSEMBLIES. Ribaux, P. A. (Charmilles Engineering Works Ltd., Geneva). Neue Tech., B; 12: 107-9(Jun 1970).

Description of the Lucens irradiated fuel dismantling facility operating under water is presented. Structural parts are cut by shears and dismantling is carried out with special tools. (auth)

20555 PRODUCTION AND ASSEMBLY OF THE MUEHLEBERG PRESSURE VESSEL. Straub, H.; Ammann, H. (Gebrueder Sulzer AG, Winterthur, Switzerland). Neue Tech., B; 12: 94-101(Jun 1970). (In German).

The manufacture and erection of the first reactor pressure vessel fabricated in Switzerland is described. The technical details and problems are discussed in detail. (auth)

20556 SIMPLIFIED SURVEY OF DESIGN FEATURES AND DEVELOPMENT LINES OF NUCLEAR POWER STATIONS. Bachl, H. Energie; 22: 120-1; 138(1970). (In German).

A diagram demonstrates the development of nuclear power stations with respect to technical features. Coolant and number of coolant loops are located on the abscissa. (INIS)

20557 PRESTRESSED CONCRETE REACTOR PRESSURE VESSEL FOR THE FORT ST. VRAIN REACTOR. Buttemer, D. R.; Rockenhauser, W.; Schuetzenduebel, W. G. Energie; 22: 234-8(1970). (In German). (CONF-691114-5).

From 90th Annual Meeting on American Society of Mechanical Engineers, Los Angeles, Calif.

The Fort St. Vrain reactor is the first nuclear power station in the U.S.A. which was supplied with a pressure vessel composed of prestressed concrete which encloses the primary cooling system. The construction and the layout of the pressure vessel and its components are described. (INIS)

20558 PROOF OF REACTOR COMPONENT IN HELIUM ATMOSPHERE. Bromkamp, K. H.; Kolditz, J. BBC-Nachr.; 52: 260-3(1970). (In German).

Construction requirements for AVR due to the helium cooling system are described. Various designs for the special operating conditions are outlined for some components of the primary coolant circuit: coolant gas blower with oil supply and frequency transformer, shutdown set-up, coolant gas shutter, valves, and seals for helium tightness. (INIS)

20559 NUCLEAR POWER PLANT IN LOVIISA. Numminen, Kalevi. Teknikka; 1: No. 11, 70-4(1970). (In Finish).

Finland's first nuclear power plant in Loviisa, having a power of 440 MW, is scheduled to be operative in 1976. The reactor and essential parts of the machinery will be bought from the Soviet Union. The cooling water is taken directly from the sea. The advantage of a heavy-water reactor is that more control is gained. The whole installation will cost 500 million Finnmarks. (auth)

20560 LINGEN NUCLEAR POWER STATION. Deublein, O. Elektrotech. Z.; A90: 492-4(26 Sep 1969). (In German).

The Lingen plant contains a 252 MW BWR with 96% availability over 48 months in which steam from the reactor is fed through heat exchangers to generate secondary steam. This is superheated in an oil-fired superheater to 530°C and then fed to the turbine. (UKAEA Info. Bulletin)

20561 WURGASSEN NUCLEAR POWER STATION. Vennemann, J. Elektrotech. Z.; A90: 501-4(26 Sep 1969). (In German).

A 640-MW BWR reactor being built at Wuergassen on the Weser River for the Preussische Elektrizitats-AG and becoming critical early 1972 is described. Order for complete installation, including first supply of fuel, was awarded to the Allgemeine Elektrizitats-Gesellschaft AEG-Telefunken. Thermal capacity is 1912 MW, saturated steam production is 3507 t/hr at 285°C and $p = 695\ N/cm^2$. The 86 t of U fuel is distributed in 444 fuel elements, arranged quadratically. Mean enrichment of fuel is 2.6%. (UKAEA Info. Bulletin)

20562 FROM SAINT-LAURENT TO VANDELLOS. Gardon, Pierre-Maurice; Ghilbert, Emile; Petiau, Michel. Acier; 35: 225-33(May 1970).

The methods adopted and the materials used in the construction of Saint Laurent units 1 and 2 nuclear power stations in France, and Vandellos nuclear power station in Spain are described. The same French firm was responsible for the construction of all three stations which are of the same type: uranium-fueled, graphite-moderated and gas-cooled. (auth)

20563 CONSTRUCTION OF THE NUCLEAR POWER PLANT. CONSTRUCTION IN THE GENKAI NUCLEAR POWER PROJECT. Hasegawa, S. (Kyushu Electric Power Co. Inc., Fukuoka). Genshiryoku Kogyo; 16: No. 8, 20-5(Aug 1970). (In Japanese).

The power station, employing a PWR of 559 MW(e), will be completed in 1975 and construction is scheduled to start at the end of 1970, while civil engineering works have already been started. The Genkai nuclear power station is described with emphasis on the civil engineering works. Outline of the power station, including construction schedule, location; site conditions, including geology, earthquake, meteorology, sea; the arrangement, including reactor plant, coolant conduit, sea bank, plant facilities; and the civil engineering works to be performed are described. (Japan)

20564 CONSTRUCTION OF THE NUCLEAR POWER PLANT. CONSTRUCTION IN THE ATR(FUGEN) PROJECT. Kawaguchi, Keizo (Power Reactor and Nuclear Fuel Development Corp., Tokyo); Tanaka, Kentaro; Takemura, T. Genshiryoku Kogyo; 16: No. 8, 11-19(Aug 1970). (In Japanese).

Tsuruga Peninsula in Fukui Prefecture has been decided as the site of prototype ATR(Fugen), which is within the site of the existing JAPCO Tsuruga nuclear power station. The ATR will be completed in 1974, with construction started in 1970. The ATR with power outputs of 165 to 200 MW(e) is D_2O moderated and boiling light-water cooled, with natural uranium plus plutonium as the fuel with a Pu self-sustaining cycle. The following

XUM

are described with emphasis on the civil-engineering works: an outline of the ATR plant, including reactor and associated facilities; civil engineering works, including site investigations, site leveling and (cooling etc.) water supplies; and building constructions, including housing buildings and the seismic design. (Japan)

20565 CONSTRUCTION OF THE NUCLEAR POWER PLANT. CONSTRUCTION IN THE ONAGAWA NUCLEAR POWER PROJECT. Taguchi, Yoshibumi; Watanabe, Yoshio (Tohoku Electric Power Co. Ltd., Sendai). Genshiryoku Kogyo; 16: No. 8, 26-32(Aug 1970). (In Japanese).

The power station, employing a BWR of 524 MW(e), will be completed in 1975, with construction started in February 1971. The Onagawa Power Reactor is described with emphasis on the civil-engineering works. An outline of the power station, including the site, No. 1 plant (524 MW(e)) and construction schedule; buildings and structures; and safety aspects of the civil engineering works are described. (Japan)

20566 PLAN FOR TAKAHAMA NUCLEAR POWER STATION. Hamaguchi, Shunichi (Kansai Electric Power Co. Inc., Osaka). Sangyo To Denki; No. 212, 12-23(May 1970). (In Japanese).

An 826-megawatt nuclear power station is being built by the Kansai Electric Power Company. The new plant is located at Takahama which is about 45 kilometers southwest of Mihama where the two preceding Kansai Electric nuclear power plants—Mihama No. 1 and No. 2—are being constructed. The Takahama site is characterized by the remoteness from population centers, the sound, hard-rock foundation for structures, and the favorable conditions of geology, seismology and meteorology. The nuclear steam generating plant which is designed and constructed by Westinghouse includes a PWR and three closed reactor coolant loops connected in parallel to the reactor vessel, each containing a reactor coolant pump and a steam generator. The turbine of TC-6F-40 design is provided by Mitsubishi. Takahama includes several safety measures normally associated with PWRs, such as high and low-pressure injection systems, the core-flooding tank sometimes known as an accumulator, container spray system, and the closed cycle cooling system for reactor building. Actual construction of the plant began in December, 1969. Initial fuel loading into Unit 1 is scheduled in September, 1973, and commercial operation in August, 1974. (Japan)

20567 800 MW BRUNSBUETTEL NUCLEAR POWER STATION. Kornbichler, H.; Ringeis, W. Atomwirt., Atomtech.; 15: 191-202(Apr 1970). (In German).

The BWR power station is being built on a site originally bought for a coal or oil fired station and a BWR was preferred to a PWR for economic reasons. The reactor has an output of 2,292 MW(t) and 805 MW(e) and a net efficiency of 33.6%. Fuel is UO_2 in Zircaloy-2 cans and its total weight 103.74 t with an average enrichment of 2.6%. There are 532 fuel elements and 129 control rods. Steam is generated at 67 ata and 281.5°C. Details of layout, heat flow diagram, steam generators, steam separators, pumps and electrical plant are presented. (Fuel Abstr.)

20568 NEW GERMAN NUCLEAR POWER STATIONS UNDER CONSTRUCTION. Atomwirt., Atomtech.; 15: 169-71(Apr 1970). (In German).

In West Germany six nuclear power stations with a total capacity of 890 MW(e) are in operation, six with a capacity of 2,560 MW(e) under construction and a further four with a capacity of 2,300 MW(e) should be started in 1970 or early 1971. Progress reports are given of the compact sodium cooled nuclear reactor plant (20 MW(e)), Niederaichbach heavy water pressure tube (100 MW(e)), Schleswig-Holstein (high temperature, helium cooled and helium turbine, 22 MW(e)), Biblis (PWR, 1145 MW(e)), Stade (PWR, 630 MW(e)) and Wurgassen (BWR, 640 MW(e)) nuclear power stations. (Fuel Abstr.)

Operation and Economics

20569 (DOCKET-1155-100) LA CROSSE BOILING WATER REACTOR. Plant Electrical Power Failure. (Dairyland Power Cooperative, La Crosse, Wis.). 5 Feb 1971. 2p. (DPC-71-1). Dep. NTIS.

20570 (DOCKET-1155-101) LA CROSSE BOILING WATER REACTOR. Forced Plant Shutdown Resulting From a Low Flow Scram Caused by Forced Circulation Pump 1B Trip. (Dairyland Power Cooperative, La Crosse, Wis.). 6 Feb 1971. 2p. (DPC-71-2). Dep. NTIS.

20571 (DOCKET-1155-102) LA CROSSE BOILING WATER REACTOR. Monthly Operating Report, November 1970. (Dairyland Power Cooperative, La Crosse, Wis.). 23 Feb 1971. Contract AT(11-1)-851. 31p. (DPC-851-18). Dep. NTIS.

20572 (DOCKET-1155-103) LA CROSSE BOILING WATER REACTOR. Unplanned Reactor Shutdown. (Dairyland Power Cooperative, La Crosse, Wis.). 17 Feb 1971. 2p. (DPC-71-3). Dep. NTIS.

An unplanned reactor shutdown caused by a leaking check valve on a control rod drive accumulator is described. The leaking check valve permitted hydraulic oil to flow back to the charging supply header, thereby decreasing the accumulator pressure. The decreasing accumulator pressure actuated the shutdown. Corrective maintenance is described. (D.C.C.)

20573 (DOCKET-1155-104) LA CROSSE BOILING WATER REACTOR. Monthly Operating Report, December 1970. (Dairyland Power Cooperative, La Crosse, Wis.). 2 Mar 1971. Contract AT(11-1)-851. 31p. (DPC-851-19). Dep. NTIS.

20574 (DOCKET-50003-65) INDIAN POINT STATION, UNIT NO. 1. Semiannual Operations Report No. 16, April 1–September 30, 1970. (Consolidated Edison Co. of New York, Inc., New York). 57p. Dep. NTIS.

20575 (DOCKET-50010-78) DRESDEN NUCLEAR POWER STATION, UNIT 1. Annual Report, 1970. (Commonwealth Edison Co., Chicago, Ill.). 26 Jan 1971. 23p. Dep. NTIS.

20576 (DOCKET-50010-79) DRESDEN NUCLEAR POWER STATION, UNIT 1. Crack in a 4 Inch Stainless Steel Pipe of the Primary Piping System. (Commonwealth Edison Co., Chicago, Ill.). 5 Mar 1971. 3p. Dep. NTIS.

20577 (DOCKET-50016-100) ENRICO FERMI ATOMIC POWER PLANT, UNIT 1. [Operations] Report, September 1970. (Power Reactor Development Co., Detroit, Mich.). 17 Feb 1971. 14p. (PRDC-EF-85). Dep. NTIS.

20578 (DOCKET-50029-143) YANKEE NUCLEAR POWER STATION. Operation Report No. 121, January 1971. (Yankee Atomic Electric Co., Westboro, Mass.). 19 Feb 1971. 7p. Dep. NTIS.

20579 (DOCKET-50029-145) YANKEE NUCLEAR POWER STATION. Faulty Removal of Spent Fuel Assembly. (Yankee Atomic Electric Co., Boston, Mass.). 4 Sep 1969. 2p. Dep. NTIS.

20580 (DOCKET-50133-45) HUMBOLDT BAY POWER PLANT, UNIT NO. 3. Failure of Emergency Condenser Condensate Return Valve to Operate. (Pacific Gas and Electric Co., San Francisco, Calif.). 12 Feb 1971. 3p. Dep. NTIS.

20581 (DOCKET-50133-48) HUMBOLDT BAY POWER PLANT, UNIT NO. 3. Operations Report, July 1–December 1970. (Pacific Gas and Electric Co., San Francisco, Calif.). 4 Mar 1971. 20p. Dep. NTIS.

20582 (DOCKET-50146-68) SAXTON REACTOR. License No. DPR-4; Technical Specifications Change Request No. 41. (Saxton Nuclear Experimental Corp., Pa.). 10 Feb 1971. 6p. Dep. NTIS.

Proposed mid-life core configuration changes for Core III are presented. The fuel elements involved in the changes consist of UO_2 and PuO_2-UO_2 rods. (D.C.C.)

20583 (DOCKET-50155-68) BIG ROCK POINT NUCLEAR PLANT. Semiannual Report of Operations, July 1–December 31, 1970. (Consumers Power Co., Jackson, Mich.). 18 Feb 1971. 13p. Dep. NTIS.

20584 (DOCKET-50171-78) PEACH BOTTOM ATOMIC POWER STATION, UNIT 1. Failure of Primary System Stop Valve to Close. (Philadelphia Electric Co., Pa.). 11 Aug 1969. 2p. Dep. NTIS.

20585 (DOCKET-50213-99) CONNECTICUT YANKEE ATOMIC POWER PLANT. Operation Report No. 71-1, January 1971. (Connecticut Yankee Atomic Power Co., Haddam). 22 Feb 1971. Contract AT(30-1)-3250. 10p. (NYO-3250-56). Dep. NTIS.

20586 (DOCKET-50219-123) OYSTER CREEK NUCLEAR POWER PLANT, UNIT NO. 1. Noncompliance with Provisions of Technical Specifications Revealed by Inspections. (Division of Compliance (AEC), Washington, D. C.). 9 Sep 1970. 3p. Dep. NTIS.

20587 (DOCKET-50220-58) NINE MILE POINT NUCLEAR STATION. Third Semiannual Report of Operation, July 1–December 31, 1970. (Niagara Mohawk Power Corp., Syracuse, N. Y.). 18 Feb 1971. 22p. Dep. NTIS.

20588 (DOCKET-50237-143) DRESDEN NUCLEAR POWER STATION, UNIT 2. Technical Specifications Revision. (Commonwealth Edison Co., Chicago, Ill.). 18 Feb 1971. 1p. Dep. NTIS.

Revised information concerning the operation status of the standby gas treatment system during the operations incident of January 5, 1971 is presented. (D.C.C.)

20589 (DOCKET-50244-64) ROBERT EMMETT GINNA NUCLEAR POWER PLANT, UNIT NO. 1. Status Report on Recommendations Regarding Technical Specification Violation, July 6, 1970. (Rochester Gas and Electric Corp., N. Y.). 17 Feb 1971. 2p. Dep. NTIS.

Corrective actions to prevent a recurrence of the July 6, 1970 operations incident are presented. The incident involved primary coolant dilution. (D.C.C.)

20590 (DOCKET-50244-65) ROBERT EMMETT GINNA NUCLEAR POWER PLANT, UNIT NO. 1. Failure of 1A Diesel Generator to Start. (Rochester Gas and Electric Corp., N. Y.). 24 Feb 1971. 2p. Dep. NTIS.

20591 (DOCKET-50244-66) ROBERT EMMETT GINNA NUCLEAR POWER PLANT, UNIT NO. 1. Semiannual Report No. 2, April 26, 1970–December 25, 1970. (Rochester Gas and Electric Corp., N. Y.). 23 Feb 1971. 25p. Dep. NTIS.

20592 (DOCKET-50245-55) MILLSTONE NUCLEAR POWER STATION, UNIT 1. Abnormal Occurrences No. A0-71-3 and No. A0-71-4. (Millstone Point Co., Hartford, Conn.). 19 Feb 1971. 1p. Dep. NTIS.

Excessive operating times for valves on the cleanup system are described during November 4, 1970 testing. Failure of the return valve to the reactor from the cleanup system on December 8, 1970 is discussed. (D.C.C.)

20593 (DOCKET-50249-57) DRESDEN NUCLEAR POWER STATION, UNIT 3. Technical Specifications on Radioactivity in Liquid Storage Exceeded. (Commonwealth Edison Co., Chicago, Ill.). 12 Feb 1971. 4p. Dep. NTIS.

20594 (DOCKET-50261-51) H. B. ROBINSON UNIT NO. 2. Abnormal Occurrence Report. (Carolina Power and Light Co., Raleigh, N. C.). 9 Feb 1971. 1p. Dep. NTIS.

The release of approximately 300 gallons of liquid waste while the liquid waste release monitor was inoperable is described. The liquid waste release monitor had been removed from service so that the detector volume chamber might be cleaned. Corrective action is described. (D.C.C.)

20595 (DOCKET-50263-56) MONTICELLO NUCLEAR GENERATING PLANT, UNIT 1. Unsuccessful Efficiency Testing of a Standby Gas Treatment System Particulate Filter. (Northern States Power Co., Minneapolis, Minn.). 23 Feb 1971. 2p. Dep. NTIS.

20596 THERMODYNAMIC ANALYSIS OF SATURATED STEAM CYCLES AND OF DIRECT THERMAL CYCLES FOR NUCLEAR POWER STATIONS. Haiduc, C.; Licsandru, E. Stud. Cercet. Energ. Electroteh.; 20: 307-22(1970). (In Rumanian).

The complex equations were developed for the net and thermal outputs of nuclear power stations as functions of a large number of parameters of the heat cycles, of the reactor, and of the steam generator. The results of the thermodynamic analysis of the two cycles are included, emphasis being placed on the possibility of optimizing the parameters of various types of nuclear power stations with thermal neutron reactors or with fast breeding reactors. (auth) (Rom. Sci. Abstr.)

20597 NUCLEAR COSTS: THE FUTURE LOOKS BETTER. Wright, J. H. Elec. World; 173: No. 6, 26-9(9 Feb 1970).

A construction survey of nuclear vs fossil plant costs is presented. (Fuel Abstr.)

20598 COST OF LARGE NUCLEAR POWER PLANTS. Elec. World; 173: No. 11, 57(16 Mar 1970).

Cost of large nuclear power plants is now ~$225/kW, according to figures supplied to AEC by Philadelphia Electric for its 2130 MW Limerick Generating Station and Public Service E & G for its 2176 MW Newbold Island Station. Three years ago costs were only $133/kW for Peach Bottom 2 and 3. (Fuel Abstr.)

20599 CALCULATION OF FUEL COSTS OF A NUCLEAR POWER PLANT. Roth, E. Atomwirt., Atomtech.; 16: 91-6 (Feb 1971). (In German).

A method is proposed that, with a minimum of effort, allows the exact calculation of fuel cost for nuclear power stations. Because of its simplicity, the method can be applied frequently in practice. Moreover, the method can be adapted to any type of fuel charges even under annual variations of the load factor. Income and expenses for fissionable material are computed for the time of transaction, independent of the actual time that the fuel elements remain in the reactor. Although especially developed for Austrian conditions, the method can be applied to other situations. (tr-auth)

Safety and Siting

Refer also to abstracts 18526 and 18974.

20600 (DOCKET-1155-105) LA CROSSE BOILING WATER REACTOR. Reactor Vessel Stresses in Lamination Region. (Dairyland Power Cooperative, La Crosse, Wis.). 27 Apr 1970. 3p. Dep. NTIS.

20601 (DOCKET-50010-80) DRESDEN NUCLEAR POWER STATION, UNIT 1. Additional Information Relative to Clarification of Technical Specifications. (Commonwealth Edison Co., Chicago, Ill.). 3 Mar 1971. 15p. Dep. NTIS.

Additional information on Dresden Power Reactor Unit 1 is presented under the following headings: primary system leak detection; administrative controls; containment leak rate test surveillance; and emergency condenser system. (D.C.C.)

20602 (DOCKET-50016-99) ENRICO FERMI ATOMIC POWER PLANT, UNIT 1. Request for Technical Specifications Change No. 24. (Power Reactor Development Co., Detroit, Mich.). 25 Feb 1971. 18p. Dep. NTIS.

Revised technical specifications concerning secondary containment requirements for sections of primary Na service system piping are presented. (D.C.C.)

20603 (DOCKET-50016-101) ENRICO FERMI ATOMIC POWER PLANT, UNIT 1. Amended Request for Authorization of Change No. 16 in the Technical Specifications. (Power Reactor Development Co., Detroit, Mich.). 25 Feb 1971. 39p. Dep. NTIS.

Revised technical specifications concerning the use of the fuel and repair building for processing irradiated Core A fuel subassemblies are presented. (D.C.C.)

20604 (DOCKET-50016-102) ENRICO FERMI ATOMIC POWER PLANT, UNIT 1. License No. DPR-9. Technical Specifications Change No. 20. (Division of Reactor Licensing (AEC), Washington, D. C.). 9 Mar 1970. 1p. Dep. NTIS.

A temporary change is described for technical specifications concerning the requirement for the core holddown mechanism position. The change is proposed until Core A fuel subassemblies are replaced. (D.C.C.)

20605 (DOCKET-50029-144) YANKEE NUCLEAR POWER STATION. License No. DPR-3; Technical Specifications Change No. 88. (Division of Reactor Licensing (AEC), Washington, D. C.). 29 Aug 1969. 4p. Dep. NTIS.

Revised technical specifications are presented which allow the use of the single-assembly spent fuel cask for transferring irradiated fuel from the reactor vessel to the spent fuel pit. (D.C.C.)

20606 (DOCKET-50029-146) YANKEE NUCLEAR POWER STATION. License No. DPR-3; Technical Specifications Change No. 87. (Division of Reactor Licensing (AEC), Washington, D. C.). 9 Sep 1969. 2p. Dep. NTIS.

Revised technical specifications are presented which provide for a Nuclear Safety Audit and Review Committee. The purpose of the committee is to review and verify plant operations, maintenance, and modifications. (D.C.C.)

20607 (DOCKET-50130-7) PATHFINDER GENERATING PLANT, SIOUX FALLS, SOUTH DAKOTA. Provisional Operating License No. DPR-11, Amendment 50 (Includes Request for a Dismantling Order with Dismantling Plan). (Northern States Power Co., Minneapolis, Minn.). 26 Feb 1971. 45p. Dep. NTIS.

20608 (DOCKET-50133-46) HUMBOLDT BAY POWER PLANT, UNIT NO. 3. License No. DPR-7: Addendum B to Technical Specifications Proposed Change No. 27. (Pacific Gas and Electric Co., San Francisco, Calif.). 23 Feb 1971. 3p. Dep. NTIS.

Revised technical specifications concerning control rod withdrawal times are presented. Maximum velocity of the control rod drives is measured. (D.C.C.)

20609 (DOCKET-50146-69) SAXTON REACTOR. Request for Approval to Use Subassemblies (503-4-32 and 33) Without a Flux Thimble. (Saxton Nuclear Experimental Corp., Pa.). 18 Aug 1970. 1p. Dep. NTIS.

XUM

20610 (DOCKET-50155-67) BIG ROCK POINT NUCLEAR PLANT. License No. DPR-6; Proposed Technical Specifications Change No. 24, Additional Information. (Consumers Power Co., Jackson, Mich.). 16 Feb 1971. 22p. Dep. NTIS.

Hot-cell examinations were conducted on two fuel rods from the Intermediate Performance Centermelt Assembly D-50 (8 × 8 array, 0.570 in. o.d., Zircaloy-2 clad UO_2 pellet fuel), to investigate the cause of multiple-rod failures and to monitor the fuel performance after achieving 10,000 MWD/T rod average exposure. Assembly D-50 was the only one of six original assemblies in the former USAEC–EURATOM PA-50 irradiation program that was continued in operation after the initial 3 months' operation on all six assemblies. The cause of the severe clad deterioration was determined to be accelerated corrosion on the rod outside surface driven by local overheating of the cladding. Grain growth (ASTM 12.5 to 12) in the Zircaloy structure adjacent to the deterioration indicated temperatures of 1200 to 1300°F (650° to 700°C) were reached. Excessive crud deposition and high surface heat fluxes were the main factors involved in creating the high temperature conditions. No burn-up related deterioration or other unusual behavior was noted in the two rods examined. (auth)

20611 (DOCKET-50155-69) BIG ROCK POINT NUCLEAR PLANT. License No. DPR-6; Technical Specifications Change No. 23. (Division of Reactor Licensing (AEC), Washington, D. C.). 22 Feb 1971. 3p. Dep. NTIS.

Revised technical specifications for operations with two auxiliary Sb–Be neutron sources in the core are presented. (D.C.C.)

20612 (DOCKET-50155-70) BIG ROCK POINT NUCLEAR PLANT. License No. DPR-6; Technical Specifications Change No. 25. (Division of Reactor Licensing (AEC), Washington, D. C.). 25 Feb 1971. 3p. Dep. NTIS.

Revised technical specifications concerning the use of Type 2A control elements are presented. Design parameters of Type 2A control elements are included. (D.C.C.)

20613 (DOCKET-50155-71) BIG ROCK POINT NUCLEAR PLANT. License No. DPR-6; Proposed Technical Specifications Change No. 27, Additional Information. (Consumers Power Co., Jackson, Mich.). 26 Feb 1971. 3p. Dep. NTIS.

Revised trip limits for the safety system sensors and containment spray system sensors are listed. The testing schedule for the core spray system sensors is described. Weld inspection requirements for cooling system piping are discussed. (D.C.C.)

20614 (DOCKET-50155-72) BIG ROCK POINT NUCLEAR PLANT. License No. DPR-6; Proposed Technical Specifications Change No. 27, Additional Information. (Consumers Power Co., Jackson, Mich.). 2 Mar 1971. 3p. Dep. NTIS.

Additional information concerning the backup core spray nozzle is presented. The potential core flow blockage from failure of the backup core spray nozzle is analyzed. (D.C.C.)

20615 (DOCKET-50155-74) BIG ROCK POINT NUCLEAR PLANT. Reworking of Orifices. (Consumers Power Co., Jackson, Mich.). 9 Mar 1971. 2p. Dep. NTIS.

20616 (DOCKET-50155-75) BIG ROCK POINT NUCLEAR PLANT. Flows Associated with Core Spray and Containment Spray Systems. (Consumers Power Co., Jackson, Mich.). 5 Mar 1971. 2p. Dep. NTIS.

20617 (DOCKET-50213-98) CONNECTICUT YANKEE ATOMIC POWER PLANT. Operational Environmental Radiation Monitoring Program. Summary Report, January–December 1970. (Connecticut Yankee Atomic Power Co., Hartford). 17 Feb 1971. 25p. Dep. NTIS.

20618 (DOCKET-50219-124) OYSTER CREEK NUCLEAR POWER PLANT, UNIT NO. 1. Radiation Emergency Plan. (Jersey Central Power and Light Co., Morristown, N. J.). 17 Apr 1968. 21p. Dep. NTIS.

20619 (DOCKET-50219-125) OYSTER CREEK NUCLEAR POWER PLANT, UNIT NO. 1. Control Rod Drives. (Division of Reactor Licensing (AEC), Washington, D. C.). 20 May 1970. 2p. Dep. NTIS.

Testing and monitoring procedures for control rod drives are described. Control rod insertion times and performance requirements are listed. (D.C.C.)

20620 (DOCKET-50220-59) NINE MILE POINT NUCLEAR STATION. Provisional Operating License No. DPR-17, Amendment 2 (Authorization for Power Increase to 1850 Megawatts (Thermal)). (Division of Reactor Licensing (AEC), Washington, D. C.). 3 Mar 1971. 76p. Dep. NTIS.

20621 (DOCKET-50220-60) NINE MILE POINT NUCLEAR STATION. Modification of Start-up Procedure. (Niagara Mohawk Power Corp., Syracuse, N. Y.). 26 Jun 1970. 1p. Dep. NTIS.

20622 (DOCKET-50244-60) ROBERT EMMETT GINNA NUCLEAR POWER PLANT, UNIT NO. 1. Report of Stud Failure. (Rochester Gas and Electric Corp., N. Y.). 10 Dec 1970. 38p. Dep. NTIS.

20623 (DOCKET-50244-61) ROBERT EMMETT GINNA NUCLEAR POWER PLANT, UNIT NO. 1. Provisional Operating License No. DPR-18: Request for Revision of Technical Specifications Change No. 8. (Rochester Gas and Electric Corp., N. Y.). 17 Feb 1971. 5p. Dep. NTIS.

Revised technical specifications concerning control rod bank insertion limits and required shutdown margin are presented. (D.C.C.)

20624 (DOCKET-50244-62) ROBERT EMMETT GINNA NUCLEAR POWER PLANT, UNIT NO. 1. Petition Requesting Operation at a Higher Power Level, Amendment 1 (Includes Technical Supplement Accompanying Application to Increase Power, Amendment 1). (Rochester Gas and Electric Corp., N. Y.). 19 Feb 1971. 69p. Dep. NTIS.

Coolant loss accident conditions and emergency core cooling system requirements for operations at increased power are presented. (D.C.C.)

20625 (DOCKET-50244-63) ROBERT EMMETT GINNA NUCLEAR POWER PLANT, UNIT NO. 1. Spent Fuel Pool Charcoal Filter System. (Rochester Gas and Electric Corp., N. Y.). 3 Feb 1971. 7p. Dep. NTIS.

20626 (DOCKET-50245-56) MILLSTONE NUCLEAR POWER STATION, UNIT 1. Environmental Radiation Survey Program Semiannual Report, July 1–December 31, 1970. (ICN/Tracerlab, Waltham, Mass.). 17 Feb 1971. 67p. Dep. NTIS.

For Millstone Point Co., Wethersfield, Conn.

20627 (DOCKET-50249-58) DRESDEN NUCLEAR POWER STATION, UNIT 3. Facility Operating License No. DPR-25; Technical Specifications (Appendix A) Change No. 1. (Division of Reactor Licensing (AEC), Washington, D. C.). 16 Feb 1971. 5p. Dep. NTIS.

Revised technical specifications concerning release rates for gaseous radioactive effluents are presented. (D.C.C.)

20628 (DOCKET-50249-59) DRESDEN NUCLEAR POWER STATION, UNIT 3. Summary Technical Report of Primary Containment Leak Rate Test. (Commonwealth Edison Co., Chicago, Ill.). 11 Feb 1971. 25p. Dep. NTIS.

20629 (DOCKET-50249-60) DRESDEN NUCLEAR POWER STATION, UNIT 3. Facility Operating License No. DPR-25, Amendment 1. (Division of Reactor Licensing (AEC), Washington, D. C.). 2 Mar 1971. 11p. Dep. NTIS.

Authorization for operations at maximum power level of 2527 MW(t) is presented. (D.C.C.)

20630 (DOCKET-50250-39) TURKEY POINT PLANT, UNITS NO. 3 AND NO. 4. Preliminary Safety Analysis Report, [Amendment 31], Suppl. 31 (Includes Final Safety Analysis Report, Rev. 10). (Florida Power and Light Co.). 16 Feb 1971. 64p. (DOCKET-50251-35). Dep. NTIS.

An analysis of coolant loss accident conditions resulting from a pipe rupture in the cooling system is presented. (D.C.C.)

20631 (DOCKET-50250-40) TURKEY POINT PLANT, UNITS NO. 3 AND NO. 4. Preliminary Safety Analysis Report, [Amendment 32], Suppl. 32 (Includes Final Safety Analysis Report, Rev. 11). (Florida Power and Light Co.). 25 Feb 1971. 65p. (DOCKET-50251-36). Dep. NTIS.

Revised and additional design parameters of the Turkey Point Power Reactor Units 3 and 4 are presented. (D.C.C.)

20632 (DOCKET-50250-41) TURKEY POINT PLANT, UNITS NO. 3 AND NO. 4. Preliminary Safety Analysis Report, [Amendment 33], Suppl. 33 (Includes Final Safety Analysis Report, Rev. 12). (Florida Power and Light Co.). 3 Mar 1971. 33p. (DOCKET-50251-37). Dep. NTIS.

Additional information on design parameters and operation aspects of Turkey Point Power Reactor Units 3 and 4 is presented. (D.C.C.)

20633 (DOCKET-50254-28) QUAD-CITIES STATION, UNITS 1 AND 2. Preoperational Environmental Monitoring (Thermal) of

the Mississippi River, July 1969–June 1970. (Industrial Bio-Test Labs., Inc., Northbrook, Ill.). 25 Feb 1971. 169p. (DOCKET-50265-24). Dep. NTIS.
For Commonwealth Edison Co., Chicago, Ill.

20634 (DOCKET-50254-29) QUAD-CITIES STATION, UNITS 1 AND 2. Preliminary Safety Analysis Report, Amendment 17. (Commonwealth Edison Co., Chicago, Ill. Iowa-Illinois Gas and Electric Co., Davenport, Iowa). 1 Mar 1971. 54p. (DOCKET-50265-25). Dep. NTIS.
Additional information on the reactor requested by the Division of Reactor Licensing is presented. (D.C.C.)

20635 (DOCKET-50254-30) QUAD-CITIES STATION, UNITS 1 AND 2. Preliminary Safety Analysis Report, Amendment 18. (Commonwealth Edison Co., Chicago, Ill. Iowa-Illinois Gas and Electric Co., Davenport, Iowa). 1 Mar 1971. 116p. (DOCKET-50265-26). Dep. NTIS.
Additional geological and meteorological data for the reactor site and surrounding area are presented. (D.C.C.)

20636 (DOCKET-50254-31) QUAD-CITIES STATION, UNITS 1 AND 2. Preliminary Safety Analysis Report, Amendment 20. (Commonwealth Edison Co., Chicago, Ill. Iowa-Illinois Gas and Electric Co., Davenport, Iowa). 2 Mar 1971. 5p. (DOCKET-50265-27). Dep. NTIS.
Temperature transients for the core under design basis accident conditions with operating emergency core cooling system are plotted. (D.C.C.)

20637 (DOCKET-50255-33) PALISADES PLANT. Preliminary Safety Analysis Report, Amendment 21 (Includes Additions and Revisions to Final Safety Analysis Report). (Consumers Power Co., Jackson, Mich.). 1 Mar 1971. 13p. Dep. NTIS.
Design modifications for the condenser cooling system and the liquid radwaste system are presented. Cooling towers for the condenser cooling system and a zero-release liquid waste system are described. (D.C.C.)

20638 (DOCKET-50259-22) BROWNS FERRY NUCLEAR PLANT, UNITS 1, 2, AND 3. Preliminary Safety Analysis Report, Amendment 11 (Includes Additions and Revisions to Final Safety Analysis Report). (Tennessee Valley Authority, Chattanooga. Office of Power). 23 Feb 1971. 320p. (DOCKET-50260-22; DOCKET-50296-21). Dep. NTIS.
Revised and additional design parameters of tne Browns Ferry Power Reactor Units 1, 2, and 3 are presented. Design and fabrication requirements for the pressure vessels are described. (D.C.C.)

20639 (DOCKET-50261-52) H. B. ROBINSON UNIT NO. 2. Technical Specifications Proposed Change to Make Allowance for Use of Respiratory Protective Equipment. (Carolina Power and Light Co., Raleigh, N. C.). 19 Feb 1971. 8p. Dep. NTIS.

20640 (DOCKET-50263-55) MONTICELLO NUCLEAR GENERATING PLANT, UNIT 1. Operation at 1670 Mw Thermal Approved. (Division of Reactor Licensing (AEC), Washington, D. C.). 18 Feb 1971. 2p. Dep. NTIS.

20641 (DOCKET-50266-42) POINT BEACH NUCLEAR PLANT, UNITS 1 AND 2. KEWAUNEE NUCLEAR POWER PLANT. Environmental Radiation Survey Annual Report, July 1969–June 1970. (Wisconsin Dept. of Health and Social Services, Madison). 28 Sep 1970. 27p. (DOCKET-50301-27; DOCKET-50305-18). Dep. NTIS.
For Wisconsin Electric Power Co., Milwaukee and Wisconsin Michigan Power Co., Appleton, Wis.

20642 (DOCKET-50267-26) FORT ST. VRAIN NUCLEAR GENERATING STATION, UNIT 1. Emergency Core Cooling. (Public Service Co. of Colorado, Denver). 18 Feb 1971. 2p. Dep. NTIS.

20643 (DOCKET-50267-27) FORT ST. VRAIN NUCLEAR GENERATING STATION, UNIT 1. Preliminary Safety Analysis Report, Amendment 18. (Public Service Co. of Colorado, Denver). 18 Feb 1971. 470p. Dep. NTIS.
Revised design parameters of the Fort St. Vrain Power Reactor Unit 1 are presented. Included also are additional data on the reactor requested by the Division of Reactor Licensing. Recorded data for the environmental radiation surveillance program during July to September 1970 are listed. (D.C.C.)

20644 (DOCKET-50271-38) VERMONT YANKEE NUCLEAR POWER STATION. Preliminary Safety Analysis Report, Amendment 20 (Includes Additional Revisions to Final Safety Analysis Report). (Vermont Yankee Nuclear Power Corp., Rutland). 11 Feb 1971. 69p. Dep. NTIS.
Revised design parameters of the Vermont Yankee Power Reactor are presented. Included also are additional data on the reactor requested by the Division of Reactor Licensing. (D.C.C.)

20645 (DOCKET-50271-39) VERMONT YANKEE NUCLEAR POWER STATION. Draft Detailed Statement on the Environmental Considerations. (Division of Reactor Licensing (AEC), Washington, D. C.). 18 Feb 1971. 205p. Dep. NTIS.
Information concerning chemical, radioactive, and thermal discharges from the reactor is presented. The effects of reactor operations on the environment are analyzed. (D.C.C.)

20646 (DOCKET-50271-40) VERMONT YANKEE NUCLEAR POWER STATION. Preliminary Safety Analysis Report, Amendment 21 (Includes Additional Revisions to Final Safety Analysis Report). (Vermont Yankee Nuclear Power Corp., Rutland). 25 Feb 1971. 3p. Dep. NTIS.
Additional heat transfer calculations for coolant loss accident conditions in the reactor are presented. The coolant loss conditions relate to a double ended recirculation pipe break incident. (D.C.C.)

20647 (DOCKET-50271-41) VERMONT YANKEE NUCLEAR POWER STATION. Preliminary Safety Analysis Report, Amendment 22 (Includes Additional Revisions to Final Safety Analysis Report). (Vermont Yankee Nuclear Power Corp., Rutland). 25 Feb 1971. 25p. Dep. NTIS.
Additional information is presented concerning seismic stress restraints for Class 1 piping system, interaction of the drywell base with the exterior concrete, and safety aspects of instrument lines. Containment structure pressure and temperature distributions from steam leaks are analyzed. (D.C.C.)

20648 (DOCKET-50280-34) SURRY POWER STATION, UNITS 1 AND 2. Preliminary Safety Analysis Report, Amendment 18. (Virginia Electric and Power Co., Richmond). 15 Feb 1971. 56p. (DOCKET-50281-34). Dep. NTIS.
Revised information concerning the construction permit and operating license is presented. Financial statements for the Virginia Electric and Power Company are included. (D.C.C.)

20649 (DOCKET-50280-35) SURRY POWER STATION, UNITS 1 AND 2. Preliminary Safety Analysis Report, Amendment 19 (Includes Additions and Revisions to Final Safety Analysis Report, Part B). (Virginia Electric and Power Co., Richmond). 2 Mar 1971. 131p. (DOCKET-50281-35). Dep. NTIS.
Revised and additional design parameters of the Surry Power Reactor Units 1 and 2 are presented. (D.C.C.)

20650 (DOCKET-50285-42) FORT CALHOUN STATION, UNIT NO. 1. Preliminary Safety Analysis Report, Amendment 23 (Includes Final Safety Analysis Report, Suppl. No. 6). (Omaha Public Power District, Nebr.). 18 Feb 1971. 531p. Dep. NTIS.
Revised design parameters of the Fort Calhoun Power Reactor Unit 1 are presented. Included also are additional data on the reactor requested by the Division of Reactor Licensing. (D.C.C.)

20651 (DOCKET-50293-36) PILGRIM NUCLEAR POWER STATION. Preliminary Safety Analysis Report, Amendment 20 (Includes Additions and Revisions to Final Safety Analysis Report). (Boston Edison Co., Mass.). 11 Feb 1971. 130p. Dep. NTIS.
Revised design parameters of the Pilgrim Power Reactor are presented. Included also are additional data on the reactor requested by the Division of Reactor Licensing. (D.C.C.)

20652 (DOCKET-50293-37) PILGRIM NUCLEAR POWER STATION. Power Piping, Withdrawal of Some Recommendations Dated January 12, 1971. (Boston Edison Co., Mass.). 12 Feb 1971. 3p. Dep. NTIS.
Modified recommendations concerning welds in primary piping are presented. (D.C.C.)

20653 (DOCKET-50293-38) PILGRIM NUCLEAR POWER STATION. Preoperational Environmental Radiation Survey Program. Summary Report through August 31, 1970. (ICN/Tracerlab, Waltham, Mass.). Jan 1971. 43p. Dep. NTIS.
For Boston Edison Co., Mass.

20654 (DOCKET-50293-39) PILGRIM NUCLEAR POWER STATION. Preliminary Safety Analysis Report, Amendment 21 (Includes Additions and Revisions to Final Safety Analysis Report). (Boston Edison Co., Mass.). 26 Feb 1971. 21p. Dep. NTIS.
Revised design parameters of the Pilgrim Power Reactor are

XUM

presented. Included also are additional data on the reactor requested by the Division of Reactor Licensing. (D.C.C.)

20655 (DOCKET-50295-24) ZION STATION, UNITS 1 AND 2. Containment Spray Systems Full Flow Ring Header Tests. (Commonwealth Edison Co., Chicago, Ill.). 10 Mar 1971. 4p. (DOCKET-50304-24). Dep. NTIS.

20656 (DOCKET-50298-13) COOPER NUCLEAR STATION. Preliminary Safety Analysis Report, Amendment 7. Final Safety Analysis Report, Vol. 1. (Consumers Public Power District, Columbus, Nebr.). 26 Feb 1971. 400p. Dep. NTIS.

Information on the Cooper Power Reactor is presented under the following broad topics: station site and environment; and reactor. (D.C.C.)

20657 (DOCKET-50298-14) COOPER NUCLEAR STATION. Preliminary Safety Analysis Report, Amendment 7. Final Safety Analysis Report, Vol. 2. (Consumers Public Power District, Columbus, Nebr.). 26 Feb 1971. 242p. Dep. NTIS.

Information on Cooper Power Reactor is presented under the following broad topics: reactor coolant system; containment; and core standby cooling system. (D.C.C.)

20658 (DOCKET-50298-15) COOPER NUCLEAR STATION. Preliminary Safety Analysis Report, Amendment 7. Final Safety Analysis Report, Vol. 3. (Consumers Public Power District, Columbus, Nebr.). 26 Feb 1971. 349p. Dep. NTIS.

Information on the Cooper Power Reactor is presented under the heading of control and instrumentation. (D.C.C.)

20659 (DOCKET-50298-16) COOPER NUCLEAR STATION. Preliminary Safety Analysis Report, Amendment 7. Final Safety Analysis Report, Vol. 4. (Consumers Public Power District, Columbus, Nebr.). 26 Feb 1971. 214p. Dep. NTIS.

Information on Cooper Power Reactor is presented under the following broad topics: electrical power systems; radioactive waste systems; auxiliary systems; and power conversion systems. (D.C.C.)

20660 (DOCKET-50298-18) COOPER NUCLEAR STATION. Preliminary Safety Analysis Report, Amendment 7. Final Safety Analysis Report, Vol. 6. (Consumers Public Power District, Columbus, Nebr.). 21 Feb 1971. 276p. Dep. NTIS.

Information on Cooper Power Reactor is presented under the following broad topics: pressure integrity of piping and equipment pressure parts; technical specifications; and structural loading criteria. (D.C.C.)

20661 (DOCKET-50298-19) COOPER NUCLEAR STATION. Preliminary Safety Analysis Report, Amendment 7. Final Safety Analysis Report, Vol. 7. (Consumers Public Power District, Columbus, Nebr.). 26 Feb 1971. 307p. Dep. NTIS.

Information on Cooper Power Reactor is presented under the following broad topics: quality assurance program; conformance to AEC general design criteria; station nuclear safety operational analysis; station research, development, and further information, requirements and resolutions; and inservice inspection program. (D.C.C.)

20662 (DOCKET-50298-20) COOPER NUCLEAR STATION. Preliminary Safety Analysis Report, Amendment 7. Annual Report, 1969. (Consumers Public Power District, Columbus, Nebr.). 26 Feb 1971. 30p. Dep. NTIS.

Financial data on the owners of the Cooper Power Reactor are presented in support of the application for operating license. The 1969 Annual Report of the Consumers Public Power District is included. (D.C.C.)

20663 (DOCKET-50301-28) POINT BEACH NUCLEAR PLANT, UNIT NO. 2. Proposed Facility Operating License No. DPR-27. (Division of Reactor Licensing (AEC), Washington, D. C.). 2 Mar 1971. 10p. Dep. NTIS.

20664 (DOCKET-50305-19) KEWAUNEE NUCLEAR POWER PLANT. Technical Specifications. Preliminary Safety Analysis Report, Amendment 8. (Wisconsin Public Service Corp., Green Bay). 25 Feb 1971. 140p. Dep. NTIS.

20665 (DOCKET-50309-27) MAINE YANKEE ATOMIC POWER STATION. Preliminary Safety Analysis Report, Amendment 18. (Maine Yankee Atomic Power Co., Westboro, Mass.). 8 Feb 1971. 76p. Dep. NTIS.

Revised design parameters of the Maine Yankee Power Reactor are presented. Included also are additional data on the reactor requested by the Division of Reactor Licensing. (D.C.C.)

20666 (DOCKET-50309-28) MAINE YANKEE ATOMIC POWER STATION. Preliminary Safety Analysis Report, Amendment 19. (Maine Yankee Atomic Power Co., Westboro, Mass.). 22 Feb 1971. 51p. Dep. NTIS.

Additional data on the Maine Yankee Power Reactor requested by the Division of Reactor Licensing are presented. (D.C.C.)

20667 (DOCKET-50309-29) MAINE YANKEE ATOMIC POWER STATION. Environmental Report, Addenda. (Maine Yankee Atomic Power Co., Westboro, Mass.). 24 Feb 1971. 18p. Dep. NTIS.

20668 (DOCKET-50321-16) EDWIN I. HATCH NUCLEAR PLANT, UNITS 1 AND 2. Environmental Report. (Georgia Power Co., Atlanta). 15 Feb 1971. 111p. (DOCKET-50366-8). Dep. NTIS.

Information concerning chemical, radioactive, and thermal discharges from the reactor is presented. The effects of reactor operations on the environment are analyzed. (D.C.C.)

20669 (DOCKET-50321-17) EDWIN I. HATCH NUCLEAR PLANT, UNIT 1. Supplementary Information to the Preliminary Safety Analysis Report. (Georgia Power Co., Atlanta). 3 Mar 1971. 20p. Dep. NTIS.

Geological data required for the stack site are presented. Design parameters for the stack are included. (D.C.C.)

20670 (DOCKET-50324-19) BRUNSWICK STEAM ELECTRIC PLANT, UNITS 1 AND 2. Small Steam Line Break. Design Report No. 8. (Carolina Power and Light Co., Raleigh, N. C.). 26 Feb 1971. 42p. (DOCKET-50325-19). Dep. NTIS.

20671 (DOCKET-50338-27) NORTH ANNA POWER STATION, UNIT 1. Construction Permit No. CPPR-77. (Division of Reactor Licensing (AEC), Washington, D. C.). 19 Feb 1971. 4p. Dep. NTIS.

20672 (DOCKET-50339-26) NORTH ANNA POWER STATION, UNIT 2. Construction Permit No. CPPR-78. (Division of Reactor Licensing (AEC), Washington, D. C.). 19 Feb 1971. 4p. Dep. NTIS.

20673 (DOCKET-50341-27) ENRICO FERMI ATOMIC POWER PLANT, UNIT 2. Preliminary Safety Analysis Report, Amendment 17. (Detroit Edison Co., Mich.). 22 Feb 1971. 39p. Dep. NTIS.

Additional data on the reactor requested by the Division of Reactor Licensing are presented. (D.C.C.)

20674 (DOCKET-50348-16) JOSEPH M. FARLEY NUCLEAR PLANT, UNITS 1 AND 2. Preliminary Safety Analysis Report, Amendment 10. (Alabama Power Co., Birmingham). 22 Jan 1971. 421p. (DOCKET-50364-10). Dep. NTIS.

Revised design parameters of the Joseph M. Farley Power Reactor Units 1 and 2 are presented. Included also are additional data on the reactor requested by the Division of Reactor Licensing. (D.C.C.)

20675 (DOCKET-50352-11) LIMERICK GENERATING STATION, UNITS 1 AND 2. Preliminary Safety Analysis Report, Amendment 4, Suppl. 4. (Philadelphia Electric Co., Pa.). 24 Feb 1971. 118p. (DOCKET-50353-11). Dep. NTIS.

Revised design parameters of the Limerick Power Reactor Units 1 and 2 are presented. Included also are additional data on the reactor requested by the Division of Reactor Licensing. (D.C.C.)

20676 (DOCKET-50354-11) NEWBOLD ISLAND NUCLEAR GENERATING STATION, UNITS 1 AND 2. Environmental Report; Construction Permit Stage. (Public Service Electric and Gas Co., Newark, N. J.). 27 Jan 1971. 70p. (DOCKET-50355-11). Dep. NTIS.

Information concerning chemical, radioactive, and thermal discharges from the reactor is presented. The effects of reactor operations on the environment are analyzed. (D.C.C.)

20677 (DOCKET-50361-15) SAN ONOFRE NUCLEAR GENERATING STATION, UNITS 2 AND 3. Preliminary Safety Analysis Report, Amendment 7. (Southern California Edison Co., Los Angeles. San Diego Gas and Electric Co., Calif.). 12 Feb 1971. 251p. (DOCKET-50362-14). Dep. NTIS.

Revised design parameters of the San Onofre Power Reactor Units 2 and 3 are presented. Included also are additional data on the reactor requested by the Division of Reactor Licensing. (D.C.C.)

20678 (DOCKET-50363-12) FORKED RIVER NUCLEAR GENERATING STATION, UNIT 1. Preliminary Safety Analysis Report, Amendment 6. (Jersey Central Power and Light Co., Morristown, N. J.). 19 Feb 1971. 181p. Dep. NTIS.

Revised design parameters of the Forked River Power Reactor Unit 1 are presented. Included also are additional data on the reactor requested by the Division of Reactor Licensing. (D.C.C.)

20679 (DOCKET-50369-6) McGUIRE NUCLEAR STATION, UNITS 1 AND 2. Environmental Report. (Duke Power Co., Charlotte, N. C.). 9 Mar 1971. 167p. (DOCKET-50370-5). Dep. NTIS.

Information concerning radioactive and thermal discharges from the reactor is presented. The effects of reactor operations on the environment are analyzed. (D.C.C.)

20680 (DOCKET-50376-9) AGUIRRE NUCLEAR PLANT, UNIT NO. 1. Preliminary Facility Description and Safety Analysis Report, Amendment 2. (Puerto Rico Water Resources Authority, San Juan). 1 Mar 1971. 349p. Dep. NTIS.

Revised and additional design parameters of the Aguirre Power Reactor Unit 1 are presented. (D.C.C.)

20681 (DOCKET-RESARA-1) [WESTINGHOUSE NUCLEAR STEAM SUPPLY SYSTEM]. Reference Safety Analysis Report, Vol. 1. (Westinghouse Electric Corp., Pittsburgh, Pa. PWR Systems Div.). 11 Sep 1970. 604p. Dep. NTIS.

Information on Westinghouse pressurized-water power reactors is included under the following main headings: site and environment; reactor; reactor coolant system; containment; and engineered safety features. (D.C.C.)

20682 (DOCKET-RESARA-2) [WESTINGHOUSE NUCLEAR STEAM SUPPLY SYSTEM]. Reference Safety Analysis Report, Vol. 2. (Westinghouse Electric Corp., Pittsburgh, Pa. PWR Systems Div.). 11 Sep 1970. 506p. Dep. NTIS.

Information on Westinghouse pressurized-water power reactors is included under the following main headings: instrumentation and control; electrical systems; auxiliary systems; steam and power conversion; waste disposal and radiation protection; conduct of operations; initial tests and operations; safety analysis; and quality assurance program. (D.C.C.)

20683 EFFECTS OF NUCLEAR POWER PLANTS ON THE ENVIRONMENT. Vuorinen, Antti; Toivola, Ahti. Teknikka; 1: No. 11, 79-81; 84-6(1970). (In Finish).

Radioactive material can leak from a nuclear power plant mainly through the cooling water and through the air. The primary circuit of the reactor is protected by a shield of steel. In case of malfunction, the air and water purifying equipment must be able to cope with the additional load. All accidents known so far have happened to experimental reactors, not to commercial power plants. Nuclear power plants, because their efficiency is lower than that of conventional ones, put out more heat with the cooling water. This has to be taken into account in order to prevent damage to the environment. (auth)

20684 MEASURES PROVIDED AT THE MUEHLEBERG NUCLEAR POWER PLANT FOR PROTECTION OF THE POPULATION. Hentschel, G. H. (AG Brown, Boveri and Cie, Baden, Ger.). Neue Tech., B; 12: 102-6(Jun 1970). (In German).

Among the measures taken to protect the public against the possible radiological effects of operating a nuclear power plant are the provision of plant protective systems, waste management systems, engineered safeguards and due allowance for natural disasters. Only the last three of these are described in relation to their main design principles and performance characteristics. (4 references) (auth)

20685 RIVERS CANNOT TAKE UP HEAT AT CHOICE. 13 GW AT THE UPPER RHINE. Marguerre, F. Handelsblatt; 25: No. 105, 19(5 Jun 1970). (In German).

Using the example of the Rhine between Karlsruhe and Mainz which may be representative for the whole FRG, various parameters such as water passage, and uptake capacity of the Rhine for waste heat of conventional power plants (6500 MW), light water reactors (4200 MW), and Advanced Gas Cooled Reactors (5800 MW) under continuous full-load are calculated. The calculations are only valid if all power plants are obliged to use waste heat cooling. (INIS)

20686 ACTIVITIES OF ELECTRICITE DE FRANCE IN ATMOSPHERIC POLLUTION CONTROL. De Retz, B. (Electricite de France, Saint-Denis). Ann. Mines; No. 11, 31-44(Nov 1970). (In French).

Both conventional thermal power stations and nuclear power stations are considered with regard to the following problems: nature and origin of the pollutants discharged into the atmosphere; methods used to prevent atmospheric pollution; and most important result obtained. The problems which might arise in the operation of the future conventional thermal power stations are reviewed. (France)

20687 PROPOSALS OF THE GERMAN ATOMIC FORUM ON RESEARCH PROGRAMS ON REACTOR SAFETY. Atomwirt., Atomtech.; 16: 73-4(Feb 1971). (In German).

To assess the safety of nuclear power plants, the German Atomic Forum proposes the formation of a committee constituted by approximately 12 persons representing the applicant, nuclear industry, assessors, research, and government. In particular, the Atomic Forum proposes a research and development program emphasizing the following points: safety philosophy, especially for near-urban sites; federal standards for site selection; establishment of statistical methods for determination of accident probability; evaluation of accidents; evaluation of liabilities and damages in case of accidents; improvement of existing test methods for early recognition of defective components; intensive research in the field of rupture mechanics, especially with respect to containment vessels; emission of radioactive material; and eleven other aspects of reactor safety. (H.B.G.)

20688 AUTHORIZATION PROCEDURES, SITE EVALUATION, AND SAFETY CRITERIA. Wirtz, K. (Kernforschungszentrum, Karlsruhe, Ger.). Atomwirt., Atomtech.; 16: 70-2(Feb 1971). (In German).

In relation to the proposed nuclear power station at Ludwigshafen, problems concerning suburban power stations are discussed as to: authorization procedures, site evaluation, and safety criteria. Thus far, all nuclear power stations erected in West Germany fulfilled completely all expectations with respect to safety and site. Neither during normal operation nor during assumed maximum credible accidents did radiation levels in the environment exceed the established dose values. In fact, dose values for radioactive substances emitted into the atmosphere during normal operation were mostly lower than permissible by a factor of 1000. (H.B.G.)

20689 PROPOSALS OF THE GERMAN ATOMIC FORUM ON LEGAL ATOMIC AUTHORIZATION PROCEDURES. Atomwirt., Atomtech.; 16: 72-3(Feb 1971). (In German).

To accelerate and to simplify authorization procedures for nuclear power plants, the reactor safety commission, as an honorary body, should be relieved of all routine work. Only new designs or new reactor components should be submitted to its scrutiny. The reactor safety commission should have at least two representatives each of fields such as mechanical and structural engineering, reactor physics and hydrodynamics, measuring and control techniques, process techniques and chemistry, operation of power stations, radiation protection, and accident analysis. The honorary commission should be supported by a permanent bureau of professional staff that assesses details of submitted proposals. The commission possesses only advisory capacity; therefore, each member can express his own opinion. To prevent delays, industry could submit newly designed parts to the commission prior to submitting the entire project. (H.B.G.)

Steam and Power Conversion Systems

20690 GAS TURBINE IN PUBLIC ELECTRICITY SUPPLY AND ITS FUTURE PROSPECTS. Deuster, G. (Stadtwerke. AG, Oberhausen, Ger.). Elektrizitaetswirtschaft.; 69: No. 5, 138-45 (1970). (In German).

After a review of the open and closed gas turbines the conclusion that the open gas turbine will be increasingly used for peak load operation is presented. Due to the change in the availability of fuels, particularly natural gas, there are strong incentives for the increasing use of the open gas turbine. There are also great opportunities for wider application in the gas–steam combination. In the heat-electric station there are interesting possibilities for both the open and the closed gas turbine. The closed gas turbine in combination with a gas-cooled high-temperature reactor is described. (INIS)

20691 INTERCONNECTED GRID SYSTEM IN THE SEVENTIES. NUCLEAR POWER STATIONS MAKE TROUBLE. Meister, R. Handelsblatt; 25: No. 105, 20(6 Jun 1970). (In German).

Activities and problems of interconnected utilities are discussed. Aspects in the Federal Republic of Germany are described. Growth of turbosets for nuclear power stations is reviewed. (INIS)

Power Reactor Development

Refer also to abstracts 18830 and 19191.

XUM

20692 (CONF-700816-(Vol.1), pp 289-316) OVERVIEW OF LMFBR PROGRAM AT HANFORD. Nemzek, T. A. (Richland Operations Office (AEC), Wash.).

From 11. AEC air cleaning conference; Richland, Wash. (31 Aug 1970).

In Proceedings of the eleventh AEC air cleaning conference.

An overview of the LMFBR development program is presented. The role of the Hanford site in the LMFBR program is described. Design parameters and development schedule for the FFTF are presented. (D.C.C.)

20693 (GEAP-13649) DESIGN AND TESTING OF THE SEFOR FAST REACTIVITY EXCURSION DEVICE (FRED). McKeehan, E. R. (General Electric Co., Sunnyvale, Calif. Breeder Reactor Development Operation). Oct 1970. Contract AT(04-3)-540. 68p. Dep. NTIS.

The primary objective of FRED design is to provide a reliable device that can rapidly move a poison slug from the reactor core at a predictable rate regarding the time and the desired conditions. To accomplish this objective, a pneumatically actuated device was designed and extensively tested. This device has demonstrated reliable and reproducible performance and has many inherent safety features which are discussed. In reviewing the design of the FRED and the reactor operations with the FRED, the most significant items considered are discussed in detail. (auth)

20694 NUCLEAR REACTOR THERMOELECTRIC POWER PLANT. Zogran, Raymond N.; Weems, Sterling J.; Estrada, Herbert Jr.; Nichols, Julian C. (to Westinghouse Electric Corp.). U. S. Patent 3,537,910. 3 Nov 1970. Filed 2 Aug 1967.

A nuclear reactor is coupled with a thermoelectric generator in a plant for underwater application. The plant is constructed for long-term unattended operation, and for positioning on the ocean floor near the location of the power consumer. Operation of the plant requires no moving parts after steady state conditions have been achieved. The arrangement consists essentially of an assembly of thermoelectric elements mounted on U-tubes attached to the head of a reactor vessel. Primary coolant flows by natural circulation from the reactor core through the inside of the U-tubes to supply heat to the thermoelectric elements. (auth)

20695 GAS COOLED NUCLEAR REACTOR. Shaw, James William Westgarth; Coast, Geoffrey, Briody, Ronald Francis (to United Kingdom Atomic Energy Authority). U. S. Patent 3,544,425. 1 Dec 1970. Priority date 28 Nov 1966, Great Britain.

A nuclear reactor core composed of columns of graphite moderator has a re-entrant moderator coolant plenum defined by a diaphragm above the core. Fuel element charge tubes extend through the apertures in the diaphragm to the core. All thermal expansion transversely of the core is tied to that of the concrete pressure vessel. The core is supported on a number of plates carried by pillars cast into the concrete. The apertures in the diaphragm are tied to the expansion of the pressure vessel. Thus there is no significant differential thermal expansion transversely of the core. (auth)

20696 WHITE PAPER ON ATOMIC ENERGY, THE 14th FEATURING EVENTS IN FISCAL 1969. Genshiryoku Hakusho; No. 14, 184p(Jul 1970). (In Japanese).

The white paper on atomic energy in Japan is presented in the following: development of power reactors, including ATR and FBR and foreign types; nuclear power stations, and their domestic manufacture; nuclear fuels, dealing with the aspects of domestic production; N. S. Mutsu; utilization of RIs etc.; research and development on food irradiations, nuclear fusion and uranium enrichment; research reactors; atomic-energy safety in power reactors, RIs, etc.; environmental radioactivities, international cooperation; and training of atomic-energy personnel. (Japan)

20697 NUCLEAR REACTOR CORE CONSTRUCTION. Schluderberg, Donald C. (to Babcock and Wilcox Co.). U. S. Patent 3,546,068. 8 Dec 1970. Filed 1 Nov 1967.

A steam-cooled nuclear reactor core is defined by a lattice of radially spaced, parallel, fuel-containing pins that have exterior surfaces radially dimensioned to reduce the coolant flow area, and thereby increase the flow velocity and heat transfer rate along axial length zones of the pins where the rate of heat generation is above a certain value. (auth)

20698 ADVANCED GAS COOLED REACTOR WITH STEAM-GENERATORS WITHIN THE WALL OF THE PRESTRESSED CONCRETE PRESSURE VESSEL. Kley, H. BBC-Nachr.; 52: 223-7(1970). (In German).

A description is given of an improved type of the advanced gas cooled reactor. The chief characteristic is a more compact construction which resulted from laying the steam generators inside of the wall of the prestressed concrete pressure vessel. (INIS)

20699 NUCLEAR GAS TURBINES. Proceedings of the International Conference, London, 8–9 April 1970. London; British Nuclear Energy Society (1970). 200p. 120s. (CONF-700430).

Sixteen papers concerning the development of direct cycle gas turbine power reactors are presented. A separate abstract is included for each paper. (UK)

For abstracts of individual papers see: 20700–20703, 20712, 20765, 20766, and 20770–20778.

20700 PRELIMINARY EVALUATION OF DESIGN PRINCIPLES FOR NUCLEAR POWER PLANTS WITH HIGH-TEMPERATURE REACTOR AND GAS TURBINE CYCLES. Foester, S. (Kernforschungsanlage, Juelich, Ger.). pp 11-27 of Nuclear Gas Turbines. London; British Nuclear Energy Society (1970).

From Conference on Nuclear Gas Turbines, London, England. See CONF-700430.

For HTR–GT power plants many plant arrangements are possible. Those best suited to fulfill the requirements of realization, availability, safety and electricity generating costs must be found. A reduced number of 23 overall designs has been compiled systematically so that a comparison and an examination of different plant arrangements can be made. Nonintegrated, partially integrated, full integrated and special designs with arrangement of the whole plant in an air cooling tower are covered. The typical design features of the main plant components are explained and compared. The criterions chosen are: realization, availability, safety and plant costs. Critical examinations were made for the plants to be built as either a demonstration plant, as commercial plants for the near and far future and as ideal plant. The comparisons show that the plant characteristics vary considerably with the overall plant design. With the assumptions made for the evaluation of the characteristics of the different plant design, best overall plant characteristics are expected for non-integrated designs. For commercial power plants, designs with air-cooling system and plant arrangement in the air-cooling tower are attractive. (auth) (UK)

20701 HELIUM TURBINES FOR MK III GAS COOLED REACTORS: THE KEY DEVELOPMENT PROBLEMS. Kronberger, H. (United Kingdom Atomic Energy Authority, Risley, Eng.). pp 135-42 of Nuclear Gas Turbines. London; British Nuclear Energy Society (1970).

From Conference on Nuclear Gas Turbines, London, England. See CONF-700430.

One of the steps envisaged in the further development of gas cooled reactors is the introduction of the direct gas turbine cycle. In the case of helium cooled reactors this step involves raising the gas temperature to a level where the gas turbine cycle would show a sufficient economic advantage over the steam cycle. There is at present not enough information to permit a reliable assessment of the likely savings in generating cost in relation to the steam cycle reactor. In particular it is difficult to determine the temperature which should be aimed at: there is probably an optimum temperature above which the increase of turbine efficiency and reduction of heat exchanger size is more than outweighed by difficulty of design of the reactor and fuel, by the use of expensive circuit, insulation and blade materials, and by frequent maintenance. It is thought that with reasonable extrapolation of present technology this temperature might be at least 850°C. Such a plant might show a discounted saving of about £5/kW compared with the steam cycle plant. This figure needs to be supported by a design study and kept up to date by an investigation of the performance of the proposed materials. The main areas of development required, are discussed. Items of work which could be started now at relatively modest cost, and which are important to improve the assessment and focus subsequent detailed development are described. (auth) (UK)

20702 SYSTEMATIC APPROACH TO THE DESIGN AND DEVELOPMENT OF HTR GAS TURBINE POWER STATIONS. Bradney, D. H.; Andrews, E. G. David (Rolls-Royce Ltd., Derby, Eng.). pp 143-51 of Nuclear Gas Turbines. London; British Nuclear Energy Society (1970).

From Conference on Nuclear Gas Turbines, London, England. See CONF-700430.

Examination of the technical and economic case for HTR-GT power stations shows that achievement of the evident benefits is dependent on economic design and cost-effective development practices. An objective method of determining the optimum station design is explained, some of the more important design variables are discussed, and the design selected by this method in a preliminary study is described in some detail. The requirements for cost-effective development of the direct cycle system are then defined, and various development methods are examined in a preliminary operational analysis that identifies the development process to be preferred both from the point of view of strict economy and from market considerations. (auth) (UK)

20703 DRAGON PROJECT ENGINEERING STUDIES ON THE DIRECT CYCLE HTR. Hosegood, S. B.; Lockett, G. E.; McIver, R. F. (Atomic Energy Establishment, Winfrith, Eng.). pp 161-79 of Nuclear Gas Turbines. London; British Nuclear Energy Society (1970).

From Conference on Nuclear Gas Turbines, London, England. See CONF-700430.

A limited amount of effort in the Dragon Project has become available for study of Direct Cycle HTR systems. As a basis for these studies a reactor and plant layout has been evolved, which is intended to combine the best features of fully integrated and non-integrated arrangements. With machines sized at currently assumed feasibility limits, this arrangement would provide a gross output of 1,000 MW(e) from two generators per reactor. The design has been used as a basis for sizing components, identifying problem areas and assessing the effects of heat exchanger performance, pressure drops, design configurations, and gas temperature limits. (auth) (UK)

Kinetics and Dynamics

Refer also to abstracts 20446 and 20787.

20704 (ANL-7673) INFLUENCE OF A PREDOMINANTLY OXIDE FUEL LOADING ON THE DYNAMIC BEHAVIOR OF EBR-II. EBR-II Project. Campise, A. V. (Argonne National Lab., Ill.). Oct 1970. Contract W-31-109-eng-38. 90p. Dep. NTIS.

The AIROS-IIA dynamic-simulation digital code was used to study the behavior of future EBR-II cores containing predominantly oxide fuel. The response of predominantly oxide cores is considered with and without Doppler feedbacks. The study concludes that the future dynamic behavior of EBR-II with loadings of predominantly oxide fuel is predictable, safe, and well within the range of present operating experience. (auth)

20705 (WCAP-3385-55) SAXTON CORE II NUCLEAR OPERATIONS SUMMARY. Thompson, R. L.; Impink, A. J.; Colombo, R. W. (Westinghouse Electric Corp., Pittsburgh, Pa. Nuclear Fuel Div.). Dec 1970. 98p. (EURAEC-2108). Dep. NTIS.

The Saxton Core II fuel loading consisted of nine central PuO_2–UO_2 fuel assemblies and twelve outer enriched UO_2 fuel assemblies. The mixed oxide contained 6.6 w/o PuO_2 in natural UO_2. The mixed-oxide rods were clad with Zircaloy-4 with the exception of a few special test rods clad with stainless steel. Core II operated for 9,390 EFPH before shutdown. During the operation, periodic measurements were made to determine the system reactivity, control rod and boron worth, flux and power distributions, burnup, and temperature, pressure, and power coefficients. The results of these measurements are presented and compared to analytic predictions. (H.D.R.)

20706 TEMPERATURE FIELDS IN FUEL ELEMENT ROD BUNDLES DURING VARIABLE HEAT TRANSFER AT THE PERIPHERY BETWEEN FUEL ELEMENT SURFACE AND COOLANT. Wolf, L. Waerme; 74: 169-82(1969). (In German).

A heat source distribution variable as a function of radius and azimuth and a heat transfer coefficient variable as a function of azimuth between fuel-cladding, cladding-coolant are presented. (Fuel Abstr.)

20707 SOME COMMENTS ON HTGCR PHYSICS. Yasukawa, Shigeru (Japan Atomic Energy Research Inst., Tokai). Genshiryoku Kogyo; 16: No. 10, 10-16(Oct 1970). (In Japanese).

The nuclear properties of a high temperature gas cooled reactor (HTGCR) were studied. The effect of the chemical bond of graphite on thermal neutron spectrum was large and reduced the absorption cross-section of ^{235}U by 14% at room temperature. The effect also reduced the absorption in C/Pu system by 64% at high temperature. Fast neutron spectrum was distorted from the 1/E distribution because of the low degree of slowing down. The effect of the spectrum distortion due to resonance absorption resulted in the difference of 5.2% in multiplication factor. These effects should be reevaluated at every step of burnup. Multi-group approximation must be taken into consideration in the calculation of the power distribution in a core. To analyze the nuclear properties of a HTGCR, the ratios of the atoms of graphite to U(q), to Th(n), to Pu(p), and to ^{235}U(s) were introduced. The optimum value of q was 200 to 500 for the HTGCR with slightly enriched U at 4 to 8% enrichment. The optimum values of q as well as S for highly enriched U–Th fuel were 2000 to 4000, and the value of n was 300. The optimum value of the average power density in a core was 8 w/cm^3. The age peaking factor was 1.5 with any kind of fuel. (Japan)

20708 FAST BREEDER REACTORS. Haefele, W.; Faude, D.; Fischer, E. A.; Laue, H. J. (Kernforschungszentrum, Karlsruhe, Ger.). Annu. Rev. Nucl. Sci.; 20: 393-434(1970).

The development of fast breeder reactors is reviewed. Design parameters of existing fast breeder reactors and critical assemblies are listed. Physics calculations related to fast breeder reactors are described. Design problems with fuel elements for fast reactors are analyzed. (219 references) (D.C.C.)

20709 ENERGY MODAL SYNTHESIS METHOD IN FAST REACTOR ANALYSIS. Kiguchi, Takashi (Hitachi Central Research Lab., Kawasaki, Japan); An, Shigehiro; Oyama, Akira. Nucl. Sci. Eng.; 43: 328-40(Mar 1971).

The energy modal synthesis method is applied to the computation of the neutron-multiplication factor, the sodium-void coefficient, and the spatial-power distribution of an idealized fast reactor configuration. The method is formulated by means of the variational principle and the error estimator is introduced by the expansion technique of the trial functions in the eigenfunction series. In the space-independent case, the sodium-void coefficient and its error are obtained very accurately by the linear combination of two modes, and the optimal two modes are chosen by the physical consideration. In the one-dimensional case, the continuous-type and the discontinuous-type energy modal synthesis method are formulated. In both cases the infinite-medium spectra and some supplementary modes are used as the trial energy modes. The results of a few-mode synthesis give a good estimate of the reactor parameters, and the error can be evaluated successfully by the error estimator. (auth)

Control Systems

Refer also to abstracts 18646, 20766, and 20777.

20710 (DP-1244) COMPUTER PROGRAM FOR CORRELATION AND SPECTRAL ANALYSIS OF REACTOR FLOW DATA. Harris, S. Dyer (Du Pont de Nemours (E. I.) and Co., Aiken, S. C. Savannah River Lab.). Jan 1971. Contract AT(07-2)-1. 32p. Dep. NTIS.

The computer program for correlation and spectral analysis of reactor flow data operates on stationary time series data to obtain any or all of the following statistics: mean, variance, standard deviation, probability density function, autocorrelation and cross-correlation functions, and the frequency spectrum (Fourier transform). The program is limited to two data records, each up to 2000 points in length. These limits could be increased to accommodate longer records. Statistics that have a functional variation are presented graphically with the option provided for detailed listing of functional values. The program can be expanded to include other operations on the data by adding the appropriate subroutine package, the data set being available in common storage. 5 references. (auth)

20711 (WHAN-FR-37) IN-CORE REGENERATIVE THERMAL NEUTRON DETECTORS FOR NUCLEAR REACTORS. Bunch, W. L.; Jackson, C. N. Jr.; Spear, W. G.; Wood, M. R. (WADCO Corp., Richland, Wash.). Dec 1970. Contract AT(45-1)-2170. 65p. Dep. NTIS.

Computer studies and preliminary experiments conducted at a Hanford "K" Reactor, and subsequent tests at the ETR, demonstrated the greatly reduced burnup characteristics and subsequent long life performance of a regenerative coating material (90% ^{234}U and 10% ^{235}U) in developmental thermal neutron detectors. Prototypic sensors exhibited significantly longer life performance, with the sensitivity remaining within 10% of a median value for exposure of 3.5×10^{21} nvt at a flux of 3.3×10^{14} nv (thermal) in the ETR. This performance surpassed a comparable usable lifetime of the typical ^{235}U fission chamber by a factor of 15. The regenerative detector achieved this longer operating life without sacrificing other desirable features such as robust signal strength, prompt response and a broad dynamic range. Prototypic sensors evidenced a neutron sensitivity of approximately 1×10^{-18} A per nv (thermal) with a gamma sensitivity of approximately 1×10^{-14} A per R/hr for a relatively small device (about 0.250-in. diameter by 3.0-in. long). The ETR experiments afforded a direct performance comparison of the regenerative concept device with three other common in-core thermal neutron detectors. The test capsule contained eight neutron sensors representing regenerative, fully enriched ^{235}U, and ^{130}Rh self-powered types, along with a gamma sensor. (auth)

XUM

20712 POWER LEVEL CONTROL OF A CLOSED LOOP GAS TURBINE, BY NATURAL TRANSFER OF GAS BETWEEN THE LOOP AND AUXILIARY TANKS. Bitsch, D. (Societe pour l'Industrie Atomique, Paris); Chaboseau, J. pp 111-15 of Nuclear Gas Turbines. London; British Nuclear Energy Society (1970).

From Conference on Nuclear Gas Turbines, London, England. See CONF-700430.

The variation of the gas investment of a closed loop gas turbine may be obtained by a simple way, using the natural transfer of gas between the loop and auxiliary tanks conveniently connected to the loop. A parametric study of the load range which can be obtained by this way and some corresponding transients results are presented. (auth) (UK)

20713 EKSPLUATATSIYA PRIBOROV I REGULYATOROV NA ATOMNYKH ELEKTROSTANTSIYAKH. (Instrumentation and Control Operations of Nuclear Power Plants). Popov, A. F. Moscow; Atomizdat (1970). 192p.

Instrumentation and systems for the control and regulation of nuclear power plants are described. Methods used for the maintenance and testing of equipment in an ionizing radiation environment are discussed. (34 references) (tr-auth)

20714 NUCLEAR REACTORS. Gilbert, Charles Philip; Nicholson, Frank David (to the United Kingdom Atomic Energy Authority). British Patent 1,221,309. 3 Feb 1971. Filed 22 Nov 1967.

The invention relates to the reactivity control arrangements for reactors in which tubes for conducting coolant and for housing nuclear fuel extend through and are spaced from a calandria tank (a closed vessel with internal tubes, called calandria tubes). In such a reactor where the calandria tank contains the moderator there is means for introducing neutron absorbing gas into at least some of the interpasses bounded by coolant conducting tubes and calandria tubes. By this means the need for introducing extra neutron absorption material into the core is avoided and also the neutron absorption gas is introduced to very effective regions of the reactor core. (UK)

Shielding

20715 PROBLEMS IN THE PRODUCTION AND ASSEMBLY OF SAFETY VESSELS (CONTAINMENT). Straub, H.; Ramseyer, F. (Gebrueder Sulzer AG, Winterthur, Switzerland). Neue Tech., B; 12: 85-93(Jun 1970). (In German).

Besides the main technical data, a brief description of the design, manufacture, transport, erection, quality control and leakrate test is given. Comprehensive technical details are thereby abandoned in favor of other particularly interesting problems. (auth)

Cooling Systems

Refer also to abstracts 18876 and 19223.

20716 (CEA-R-4118) DETECTION OF LOCAL BOILING IN LIGHT WATER REACTORS. Deiss, Marcel; Janot, Pierre (Commissariat a l'Energie Atomique, Saclay (France). Centre d'Etudes Nucleaires). Jan 1971. 51p. (In French). Dep. NTIS (U. S. Sales Only).

The characteristics of local boiling in the Siloette reactor of the nuclear center at Grenoble was studied. The influence of various parameters was examined in view of defining a simple criterion characteristic of the phenomena. Two methods of detection are described: detection by correlation with neutron noise and the attenuation of an acoustic or ultrasonic signal in traversing a layer of bubbles. (auth) (France)

20717 (JPRS-52384) WATER PUMP FOR PRESSURE-COOLING REACTOR IN ATOMIC POWERPLANT. Turetskii, L. I.; Gryzlov, A. G.; Pugacheva, T. F.; Puzyrev, L. K. Translated from Teploenergetika; No. 12, 8-10(1970). 8p. NTIS.

The types, operating characteristics, and costs of primary coolant circulation pumps for pressurized water reactors are discussed. A comparison of efficiency, reliability, maintenance requirements, size, and cost of the various types indicates that the axial pump is superior. (H.D.R.)

20718 (LIB/Trans-308) FRIGG CIRCUIT: WATER CHEMISTRY UNDER INVESTIGATION. Heetveld, A. (Allmanna Svenska Electriska A. B., Vasteras). Translated by S. Watkins for Australian Atomic Energy Commission, from report ASEA-KAUC-68-3. 7p. Dep. NTIS (U. S. Sales Only).

Water-chemical data obtained from thermal experiments with the Frigg circuit loops correlated with the expected analysis for the Marviken Power-Station. Parameters were: pH dropped from 9.2 to 7.4; electrical conductivity of water at 15°C dropped from 2.1 to 1.2 μS. cm^{-1} (it was possible to hold it at 2 μS. cm^{-1} for the greater part of the experiment—that it did not fall below 1 μS. cm^{-1} was attributed to the breaks in purification flow, and otherwise low flow (0.2 to 0.15 Kg. S^{-1}) through the ion exchanger); water's oxygen content $\leq$0.02 ppm; water's chloride ion content 0.03 ppm; water's content of filterable corrosion products of iron 0.09 to 0.11 ppm. (Australia)

20719 (ORNL-TM-3308) STATIC SEALS AND THEIR APPLICATION IN WATER-COOLED NUCLEAR REACTOR SYSTEMS. (Oak Ridge National Lab., Tenn. Franklin Inst. Research Labs., Philadelphia, Pa.). Mar 1971. Contract W-7405-eng-26; Subcontract 3058. 69p. Dep. NTIS.

Information relative to six types of static seals commonly used in the primary cooling systems of nuclear reactor is compiled. This information includes a description of each type of seal, its material of construction, design features, operating experience, and advantages and disadvantages. The types covered include spiral-wound asbestos-filled gaskets, hollow metallic O-rings, Belleville spring type of gasketed joints, integrated elastomer and metal retainer gaskets, and solid metal gaskets with heavy cross sections. Omega, canopy, and lip seals are discussed briefly, and information on flange design for gasketing is also presented. (27 references) (auth)

20720 (SAN-781-1) DESIGN GUIDE FOR LMFBR SODIUM PIPING. (Braun (C. F.) and Co., Alhambra, Calif.). 1 Feb 1971. Contract AT(04-3)-781. 415p. Dep. NTIS.

The Piping Design Guide for LMFBR Sodium Piping is intended to provide up-to-date technology for design and analysis of sodium piping systems. It is part of the LMFBR program plan to develop the overall technology for eventual construction and operation of fast breeder sodium cooled demonstration power plants. It incorporates applicable provisions of current codes along with new criteria and procedures to direct and assist the designer in solving the complex problems posed by the development of LMFBR technology. Periodic revision of this document is contemplated to keep pace with the rapidly developing technology. (auth)

20721 (SAN-781-110) LMFBR SYSTEM REQUIREMENTS FOR SODIUM PIPING. Technical Report 110. (Braun (C. F.) and Co., Alhambra, Calif.). 25 Oct 1968. Contract AT(04-3)-781. 34p. (CFB-4122-110). Dep. NTIS.

The proposed scope of the Piping Design Guide is defined by establishing tentative LMFBR system requirements for the design of Na piping. The requirements cover operating conditions, both steady state and transient, piping geometry, preheat, thermal insulation, leak detection, interfaces, and quality and reliability assurance. (auth)

20722 (SAN-781-214) REVIEW OF PIPING FAILURE EXPERIENCE. Technical Report 214. (Braun (C. F.) and Co., Alhambra, Calif.). 28 Mar 1969. Contract AT(04-3)-781. 52p (CFB-4122-214). Dep. NTIS.

The findings and conclusions of a study of piping failures are summarized. The failure mechanisms and potential causes of failure in LMFBR sodium piping systems, as well as the means for preventing them, are studied. The information developed will be factored into appropriate chapters of the Piping Design Guide. 76 references. (auth)

20723 (SAN-781-217) REVIEW OF PIPING AND PRESSURE VESSEL CODE DESIGN CRITERIA. Technical Report 217. (Braun (C. F.) and Co., Alhambra, Calif.). 18 Apr 1969. Contract AT(04-3)-781. 55p. (CFB-4122-217). Dep. NTIS.

A review of existing and past U. S. codes for the design of pressure vessels and piping systems is presented. An evaluation is made to determine their applicability to LMFBR environment. 12 references. (auth)

20724 (UNC-5235) STUDY OF FAILURE THEORIES AS RELATED TO LMFBR PIPING SYSTEMS. (United Nuclear Corp., Elmsford, N. Y. Research and Engineering Center. Braun (C. F.) and Co., Alhambra, Calif.). 31 Jan 1969. Contract AT(04-3)-781. 104p. (SAN-781-210; CFB-4122-210). Dep. NTIS.

The identification of the major stress or strain governed failure mechanisms (excluding corrosion, wear, or metallurgical considerations) is studied. The present state-of-the-art methods to predict the imminence of failure by these mechanisms are reviewed. The additional work necessary to select bases and methods upon which design criteria (loads, stresses, or strains) might be established is analyzed. For many of the failure mechanisms studied, recommendations regarding the applicability of methods or design bases for LMFBR piping systems are presented. 76 references. (auth)

20725 (WHAN-SA-46) INDUSTRIAL EFFORTS TO SATISFY DESIGN CRITERIA. Snow, A. (WADCO Corp., Richland, Wash.). 5 Oct 1970. Contract AT(45-1)-2170. 14p. (CONF-700942-1). Dep. NTIS.

From Joint Petroleum Mechanical Engineering and Pressure Vessel and Piping Division Conference, Denver, Colo.

Design requirements and stress limits for pressure vessels and piping systems of liquid metal-cooled reactors are analyzed. Design requirements for the FFTF piping systems and pressure vessel are described. (D.C.C.)

20726 WATER TREATMENT IN A PLANT FOR TESTING FUEL ELEMENTS. Di Pietro, Roberto; Gadda, Ferdinando; Ronchetti, Camillo (CISE, Milan). Termotecnica (Milan); 24: 540-6(Dec 1970). (In Italian).

Characteristics of the coolant in water reactors are briefly reviewed. The possibility of using water with addition of a small amount of NH_3 as coolant of the CIRENE reactor is considered. First experimental results—obtained with an experimental loop—are reported on the concentration of crud and the production of radiolytic gases when the loop water is added with a few ppM of ammonia. (9 references) (auth)

20727 THERMAL INSULATION WITH ENERGY RECOVERY FOR NUCLEAR REACTOR VESSELS. (to Electricite de France). French Patent 1,591,051. 27 Apr 1970. Filed 9 Apr 1968. (In French).

Equipment intended to be used as thermal insulation in conjunction with prestressed concrete nuclear reactor vessels of the integrated exchanger type in which carbon gas is used to carry away the heat is described. The thermal insulation may be considered as a surface exchanger between a heat conducting support and a cold fluid under forced convection cooling the support. This fluid is obtained by tapping off hot fluid from the enclosure and cooling it in such a way that energy recovery is possible; it is then injected through the laminated stack constituting the porous heat insulation. The cold fluid feed consists of a fluid jacket bounded by a metal sheet with a sealed skin; the heat insulation is attached to this sheet. (auth) (France)

20728 PHYSICAL MODEL ON THE BOILING PROCESS IN THE POWER NUCLEAR REACTOR. Haiduc, C.; Vinitchi, V. Stud. Cercet. Energ. Electroteh.; 20: No. 1, 33-42(1970). (In Rumanian).

A qualitative physical model of the boiling process on nuclear fuel cylindrical elements is developed for a natural flow. The experimental evidence collected on a heat loop as to the effect of the element inclination on the diagram $q = f(\Delta t)$ of boiling in the natural flow case is supplied. Experimental data on the boiling hysteresis on cylindrical elements are supplied and the explanation of the phenomenon is offered by the complex variation of the liquid undercooling during the heat flow variation. (auth) (Rom. Sci. Abstr.)

20729 IS NEON MORE ECONOMICAL THAN HELIUM AS COOLING GAS IN THTR? Bonka, H.; Weissfloch, R. (RWTH, Aachen). Atomwirt., Atomtech.; 15: 585-6(Dec 1970). (In German).

Theoretically, nuclear power stations with high-temperature reactors and gas turbines in the primary circuits should have lower construction costs for gases with higher mass numbers. A comparison between He and Ne as cooling gas was performed and results showed that the higher cost of Ne, as compared to He, cannot be overcome by the lower costs of turbines as well as condensers. (H.B.G.)

20730 DISPERSION OF RADIOACTIVITY IN A CLOSED COOLANT SYSTEM. Kushneriuk, S. A. (Chalk River Nuclear Labs., Ont.). Nucl. Sci. Eng.; 43: 247-56(Mar 1971).

Solutions are obtained for the concentration of radioactive nuclide on the walls and in the radially mixed fluid transporting the nuclide, when the fluid circulates in a closed loop system. The differential equations, which describe the mass balance of of the nuclide in the system and on which the solutions are based, take into account nuclide sorption-desorption on the system walls (at constant rates) and a source which releases the radioactive nuclide (fission product) into the stream. (auth)

Fuels

20731 (AECL-3780) CLOSING THE CREDIBILITY GAP IN NUCLEAR FUEL COSTS. Haywood, L. R. (Atomic Energy of Canada Ltd., Chalk River (Ontario). Chalk River Nuclear Labs.). Dec 1970. 10p. Dep. NTIS (U. S. Sales Only).

Canadian fuel fabrication experience is now sufficiently extensive to give confidence in the integrity of CANDU fuel fabrication costs. An analysis and comparison of the factors affecting the present and projected fabrication cost of both CANDU and LWR fuels is presented and CANDU fuels are shown to be likely to retain their considerable fabricating cost advantage. It is also shown that countries that are about to initiate a nuclear power program will be able to operate their fuel fabrication plants with the benefits of mass production if the fuel is of the CANDU type. 2 references. (auth)

20732 (AERE-R-6516) CALCULATION OF STRESS IN FAST REACTOR FUEL ELEMENTS. Matthews, J. R. (Atomic Energy Research Establishment, Harwell (England)). Sep 1970. 12p. Dep. NTIS (U. S. Sales Only).

Estimates of the stresses generated by the restraint of a swelling fuel by its cladding and from other sources are necessary to predict lifetimes of existing fuel element designs and to optimize new configurations. Mathematical models have been developed to enable uniaxial creep and swelling data of both fuel and cladding materials to be used in the calculation of the mechanical behavior of cylindrical fast reactor fuel elements. These models are applied to a hypothetical fast reactor fuel element. The variables of fuel power density, clad temperature, clad creep properties and fuel element dimension are examined and their effects on fuel element stresses calculated. 6 references. (auth)

20733 (BNWL-1523) CALCULATION OF ^{236}Pu AND ^{238}Pu IN THE DISCHARGE FUEL OF LIGHT WATER POWER REACTORS. Prezbindowski, D. L. (Battelle-Northwest, Richland, Wash. Pacific Northwest Lab.). Sep 1970. Contract AT(45-1)-1830. 71p. Dep. NTIS.

The Pu isotopes produced in light water reactors emit a variety of α and γ radiations and neutrons from spontaneous fission. The exact magnitude and character of radiation being produced by the recycle of enriched Pu fuel dictates the amount and kind of shielding required for the fuel fabrication process. A study has been performed to determine the isotopic composition of discharged fuel produced by LWR's. Particular emphasis was placed on the determination of ^{236}Pu and ^{238}Pu concentrations since data on these isotopes are not as plentiful as data on the other Pu isotopes. 15 references. (auth)

20734 (DP-Report-489) SAFETY ASPECTS OF THE REPLACEMENT ELEMENTS IN THE SECOND CHARGE OF THE DRAGON REACTOR. Project DRAGON. Price, M. S. T.; Smith, E. (Atomic Energy Establishment, Winfrith (England)). Dec 1966. 29p. Dep. NTIS (U. S. Sales Only).

The replacement elements for the Dragon Second Charge are described briefly, particularly high-lighting safety aspects. It is concluded that running Charge 2 at 20 MW(th), i.e., full power, will not represent a significant hazard. (auth)

20735 (HPR-127) IRRADIATION BEHAVIOUR AND POST-IRRADIATION EXAMINATION OF SWEDISH TEST FUEL ASSEMBLY IFA-30. Junkrans, S.; Olsson, T.; Knudsen, K. D. (Institutt for Atomenergi, Halden (Norway). OECD Halden Reaktor Prosjekt). Sep 1970. 24p. Dep. NTIS (U. S. Sales Only).

Post-irradiation examination was performed on the nine fuel rods of test fuel assembly IFA-30 (S) which was irradiated in the Halden Boiling Heavy Water Reactor (HBWR) to an average burnup of 5800 MWd/t U. The fuel rods were made of Zircaloy-2 cladding containing sintered UO_2 pellets enriched to 5 w/o ^{235}U of total uranium. The performance of the assembly was very satisfactory thereby confirming the suitability of the design and fabrication methods. (auth)

20736 (HPR-132) UKAEA FUEL TEST ASSEMBLIES IRRADIATED IN HBWR, 1964-1966. Bridge, D. G.; Cordall, D.; Evans, D. M.; Garlick, A.; Greenwood, A. L.; Livesey, D. J.; Pearson, P. E. (Institutt for Atomenergi, Halden (Norway). OECD Halden Reaktor Prosjekt). 5 Feb 1970. 147p. (TRG-Report-1804). Dep. NTIS (U. S. Sales Only).

Irradiation experiments in the Halden BWR on eleven UKAEA fuel test assemblies are described and the results of post-irradiation examination on six of the assemblies are reported. (auth)

20737 WATER TEMPERATURE DISTRIBUTION IN THE CASSETTES OF THE WATER-COOLED AND WATER-MODERATED REACTOR (VVER). Baum, V. A.; Bekmuradov, O. Izv. Akad. Nauk Turkm. SSR, Ser. Fiz.-Tekh., Khim. Geol. Nauk; No. 4, 57-64(1970). (In Russian).

An attempt is made to calculate the temperature distribution in reactor fuel elements without using the linear approximation $I_0[(P/X_0)X]$. (auth) (INIS)

20738 FUEL HANDLING AT AN ADVANCED GAS COOLED REACTOR. Wendt, P. BBC-Nachr.; 52: 254-9(1970). (In German).

The AGR has a desirable characteristic in the continuous fuel change on-load. Therefore different set-ups are necessary which are described in detail. The fuel handling is discussed using the flowsheet of a fuel column and an absorber rod. (INIS)

20739 CERAMICS IN NUCLEAR TECHNOLOGY. **Berggren, G.** **Interceram (Luebeck, Ger.); 18: 183(1969).**

Total estimated output of energy in the European Common Market countries up to 2000 A.D. is shown graphically. By 1990 it is forecast that half the energy will be from nuclear sources. A metal-clad fuel element would permit a reactor to operate with a temperature of 700° at the core outlet; with an all-ceramic core this temperature could be increased to 1000°, with an increase in efficiency of ≤50%. (Fuel Abstr.)

20740 EXPERIMENTAL VIBRATION CHARACTERISTICS OF A B. W. R. FUEL ASSEMBLY. **Ferrucci, Napoleone; Pitimada, Domenico** **(CNEN, Rome).** **Termotecnica (Milan); 24: 577-88(Dec 1970).**

Experiments were carried out in order to develop a qualitative understanding of lateral vibration characteristics of rods assembled in a BWR fuel assembly. Experimental tests which were performed in air are described. The investigation was intended to determine: (1) end fixity of single rod supported at the end plates; (2) vibration mode shapes and corresponding in air resonant frequencies of individual assembled rods excited at various points by a sinusoidal force; (3) differences in the directional dynamic behavior because of the lack of symmetry on spacers; and (4) dynamic behavior of individual assembled rods excited at various points by random forces. (auth)

20741 DISTENTION PRESSURE OF FISSIONABLE MATERIAL AT HIGH BURNUP RATES IN FUEL RODS FOR FAST BREEDER REACTORS. **Plitz, H.** **(AEG-Telefunken, Grossweizheim, Ger.).** **Atomwirt., Atomtech.; 15: 578-9(Dec 1970).** **(In German).**

The internal pressure of a fuel element comprises four components: the initial gas pressure; the pressure of gaseous fission products, which is assumed to increase linearly with time; the constant fuel distention pressure existing as long as free volume is available in the fuel element; and the solid body distention pressure existing after all free volume disappears. To obtain an upper and a lower limit for the fuel distention pressure, computer programs were developed under two assumptions. In the first one, the four internal pressure components are treated as partial pressures. In the second one, the gas pressure is neglected. Results of the theoretical computations are compared with available experimental data. (H.B.G.)

Auxiliary and Emergency Systems

Refer also to abstracts 18385 and 18563.

20742 (DP-Report-496) EXPERIMENTS WITH STAND PIPE CLOSURE AND STAND PIPE-CHARGE MACHINE CONNECTIONS FOR PROPOSED HTGC POWER REACTOR. **Project DRAGON.** **Woodley, H. J.** **(Atomic Energy Establishment, Winfrith (England)).** **Jan 1967. 21p. Dep. NTIS (U. S. Sales Only).**

Experiments were made with a test rig which simulates a method of sealing that has been suggested for use with stand pipe closures and charge machine connections for the proposed HTGC Power Reactor. The system employs large size flange face and piston type elastomer seals outside the normal range of manufacture and experience. Results obtained with flange face seals were satisfactory and showed that a certain amount of angular misalignment of flange faces could be tolerated. Satisfactory results were obtained from the piston seals after modifications were carried out whereby it was possible to apply controlled seal compression. (auth)

20743 NUCLEAR POWER PLANT WITH WET-STEAM GENERATOR AND STEAM DRYING SYSTEM. **Mayer, Hans; Bobmann, Werner** **(to Siemens AG.).** **U. S. Patent 3,544,424. 1 Dec 1970. Priority date 28 Dec 1966, Germany.**

A nuclear power plant with a pressurized-water reactor or boiling-water reactor for producing steam for a turbine is provided with a system which dries the generated wet steam by means of two mutually spaced separators. One of them is a pre-separator, such as a baffle structure, and is mounted in the steam plenum chamber of the wet-steam generating boiler or tank of the reactor. The other main separator is located in the steam line just ahead of the turbine and consists of a centrifugal water-from-steam separator such as a cyclone. (auth)

Operation and Economics

20744 (DOCKET-50231-72) SOUTHWEST EXPERIMENTAL FAST OXIDE REACTOR. **Malfunction of a Safety System Trip Relay.** **(General Electric Co., Sunnyvale, Calif. Breeder Reactor Development Operation).** **2 Mar 1971. 4p. Dep. NTIS.**

20745 (DP-Report-450) HTR FUEL DISPOSAL STUDY. **Project DRAGON.** **Wharton, J.; Thornhill, A. P.** **(United Kingdom Atomic Energy Authority, Risley (England). Engineering Group); Chapman, E. S.** **(United Kingdom Atomic Energy Authority, Sellafield (England). Production Group).** **Jul 1966. 36p. (EG-Report-(47)R). Dep. NTIS (U. S. Sales Only).**

The handling of fuel from a single Dragon-type H.T.G.C. power reactor is considered. The study compares the relative costs of a selected number of alternative methods of storage of the feed and breed fuels discharged from a conceptual 532 MW(e) reactor. The methods considered are storage of whole fuel elements and various processes to reduce the volume of the fuel before storage. It is found that the reduced volume schemes are less safe and cost more than any saving made in storage space. Interim cooling of the fuel within the reactor building for the first 200 days after discharge is recommended, followed by canning of whole fuel elements, and their transfer to a gas-cooled facility in a separate building for long-term storage. This route provides the solution with maximum flexibility and minimum capital cost. 20 references. (auth)

20746 (JUL-644-RG) EVALUATION OF RESULTS OF A STUDY OF THE Th–^{233}U FUEL CYCLE FOR THERMAL REACTORS. **High-Temperature Reactors, Heavy-Water Reactors, Molten-Salt Reactors.** **Hemmersmeier, F.; Kraemer, H.; Wagemann, K.** **(Kernforschungsanlage, Juelich (West Germany). Institut fuer Reaktorentwicklung).** **Feb 1970. 124p. (In German). Dep. NTIS (U. S. Sales Only).**

The reference designs of a 600 and 1200 MW(e) high temperature reactor, 600 and 1200 MW(e) thorium heavy-water reactor, and molten salt reactor to be used in the evaluation of their suitability for conversion to breeder reactors are outlined. The three reactor concepts are compared with respect to fuel cycle and energy production costs, installation costs, construction materials and methods, and the present technical state for the construction. The methods used for nuclear and thermodynamic calculations are given and compared. The development potential of each reactor concept is evaluated. (J.S.R.)

20747 (NP-18668) OECD HIGH-TEMPERATURE REACTOR PROJECT DRAGON. **Eleventh Annual Report, 1969-1970.** **(Organization for Economic Co-operation and Development, Paris (France)).** **197p. Dep. NTIS (U. S. Sales Only).**

The operation of the Dragon Reactor Experiment proceeded with few interruptions, except for the recharging of fuel elements, during the first half of the period from April 1, 1969 to March 31, 1970, despite the existence of serious corrosion in the primary circuit heat exchangers. During the year the manufacture of two complete new sets of heat exchangers (one with mild steel and the other with Incoloy 800 tubes) was completed and the sets were delivered to Winfrith. New secondary circuit pumps were also procured to reduce the flow instability on the secondary side of these heat exchangers, and to increase their heat removal capacity to 25 MW. Because of a high incidence of tube failures at the end of the irradiation of Core 7, and because the new pumps were available, it was decided to bring forward the program for the installation of the new mild steel heat exchangers and the secondary circuit modification. This work was begun at the end of October, 1969, and completed in March, 1970, when the reactor was restarted for the irradiation of Core 8 of the Third Charge. In the first part of the period, 1969/70, up to the end of October, the Reactor operated for the equivalent of 130 days at full power with three shutdowns for refuelling. In the course of this program a number of interesting irradiations were completed including those on early thorium cycle fuels which had been irradiated for approximately 500 days at power without an unacceptable deterioration in their fission product retention. The irradiation of the first tentative designs of power reactor fuel pins for a period of about 140 days was also completed with full success, and new irradiations of more up-to-date designs of tubular interacting and hollow rod fuel pins were begun. Reference coated particle fuel specimens for low enriched uranium power reactor cycles which had been irradiated from the start of the Third Charge had, during irradiation, accumulated up to 200 days full power irradiation with burnups in some specimens exceeding 4% FIMA. The only failures observed occurred in low porosity kernels, no deterioration being apparent in specimens with recommended 20% kernel porosity. At the same time, in external irradiation experiments, the investigation of dimensional changes and creep data on various appropriate types of graphite and pyrocarbon over a fully representative range of temperatures was continued, and the fast neutron doses relevant to commercial fuel cycles were fully covered. Accumulated burn-up and fast neutron dose irradiations were also started in European research reactors on low enriched uranium coated particle fuel specimens, both loose and in graphite matrices. Within the period under review these specimens had reached the half-way mark in their irradiation without apparent deterioration. An important aspect of the Project's work, relating to the safety of power reactors, is concerned with the migration of fission products from fuel elements. An important loop experiment in the PEGASE Reactor at Cadarache, was initiated to supplement the studies done in the Reactor Experiment in this connection. The Project continued to manufacture the bulk of the fuel required for the Reactor Experiment. In addition sufficient capacity was found to be available to manufacture low enriched uranium coated particle fuel for reactor physics experiments to be carried out by the CEA. In November 1969, all the Dragon Signatories signed an Agreement for an extension of the Project to the end of March, 1973. (auth)

20748 (PEL–199) COMPARISON OF ENRICHED AND NATURAL URANIUM POWER REACTORS. (Atomic Energy Board, Pelindaba, Pretoria (South Africa)). Sep 1970. 50p. Dep. NTIS (U. S. Sales Only).

Using South African ground rules, the enriched reactor systems appear capable of generating electricity at a unit cost up to 20 per cent lower than the natural U systems. Therefore, on purely economic grounds the obvious choice of reactor for South Africa's first nuclear power station is one of the three light water cooled versions: BWR, PWR or SGHWR. Although there are doubts about the long term integrity of pressure vessels, the BWR and PWR are the only two economic systems which can be considered fully proven at present, and the study shows that their capital and operating costs are so close that they must be considered identical. If safety and local content emerge as issues of overriding importance, consideration should be given to the SGHWR. If complete independence from an overseas enriched uranium supply is considered to be essential, the increase in running costs could amount to R30 million over the lifetime of the reactor. In this case the choice would then have to be made between the PHWR and CANDU systems. The absence of operating experience with the PHWR, and the fact that its pressure vessel thickness puts it on the fringe of present-day fabrication and inspection techniques, tends to weight the decision in favour of the CANDU system. 14 references. (auth)

20749 TECHNICAL AND ECONOMIC ASSESSMENT OF DIFFERENT NUCLEAR PLANT TYPES. Dibelius, G. Mitt. Ver. Grosskesselbetr.; 49: 367-75(Dec 1969). (In German).

Technical and economic comparisons are made of light-water cooled, heavy-water cooled, advanced gas-cooled, high-temperature, and fast breeder reactors, their electricity generating costs as a function of process efficiency, the effect of single or dual circuits, and temperature level of the working medium. (Fuel Abstr.)

20750 ANALYSIS OF THE EFFICIENCY OF NUCLEAR FUEL CYCLES FOR HEAVY-WATER MODERATED REACTORS IN THE SPECIFIC CONDITIONS OF THE SOCIALIST REPUBLIC OF ROMANIA. Haiduc, C.; Constantinescu, L.; Mihai, D. Stud. Cercet. Energ. Electroteh.; 20: 259-72(1970). (In Rumanian).

A mathematical model was worked up for analyzing the efficiency of the fuel cycles of nuclear reactors together with the appropriate program for use on the CIFA-102 digital computer. The results derived from the use of the above model for heavy-water moderated reactors in the conditions prevailing in Romania are reported. (auth) (Rom Sci Abstr.)

20751 DEVELOPMENTS IN NUCLEAR POWER ECONOMICS. Sporn, P. Elec. World; 173: No. 5, 21(2 Feb 1970).

Problems facing the industry are: the shallowness of design thinking (except in the field of safety); long construction schedules; steep rise in plant costs; failure to hold down electricity costs; environmental pollution. Costs data are presented. (Fuel Abstr.)

20752 MATHEMATICAL MODEL FOR ESTIMATING THE EFFICIENCY OF NUCLEAR FUEL CYCLES OF FAST BREEDING REACTORS. Haiduc, C. Stud. Cercet. Energ. Electroteh.; 19: 741-8(1969). (In Rumanian).

The mathematical model relies on a two-stage fast breeder and two distinct fuel cycles, viz. for the active and for the breeding stages. Equations are also supplied for determining the optimum structure of a system of thermal and fast breeding reactors assuming one or several types of thermal reactors. (auth) (Rom. Sci. Abstr.)

20753 GAME THEORY APPLIED TO PLUTONIUM COST. Jansen, P. (Kernforschungszentrum, Karlsruhe, Ger.). Atomwirt., Atomtech.; 15: 569-72(Dec 1970). (In German).

For various types of future nuclear power stations, competitive position is strongly determined by plutonium cost. Since insufficient plutonium markets exist at the present time to permit predictions about cost developments, theoretical considerations must be applied for strategic and optimal planning. For this purpose, mathematical game theory represents a useful tool. It leads to the conclusion that, for the assessment of the competitive position of fast breeder reactors, a plutonium cost must be assumed that corresponds to its value for recirculation in converters. Discussed are plutonium cost and reactor strategies, plutonium cost in light water reactors, the game theory, application of the game theory to economic exchange of material, competitive position of fast breeders, mixed strategies, and assessment of closed systems. (H.B.G.)

Safety and Siting

Refer also to abstract 20782.

20754 (AERE-R-6481) CAESIUM BEHAVIOUR IN LIQUID SODIUM: THE EFFECT OF CARBON. Clough, W. S.; Wade, S. W. (Atomic Energy Research Establishment, Harwell (England)). Jul 1970. 20p. Dep. NTIS (U. S. Sales Only).

On the basis of previous thermodynamic calculations and experimental work, cesium has been identified as the most volatile major fission product with respect to release from liquid sodium into the gas phase. Sorption of the cesium by graphite has been shown to be very effective in reducing the volatility of the cesium. The formation of stable cesium–graphite compounds reduces the escaping tendency of cesium to less than that of iodine in liquid sodium. The cesium forms two compounds, one of which is relatively unstable in liquid sodium and is probably a surface adsorption compound. The more stable fraction of the adsorbed cesium is probably a lamellar cesium–graphite compound and is almost fully stable in vacuum at 500°C in the absence of sodium. The rate of reaction for the breakdown of the more stable cesium–graphite compound in sodium was measured over a range of temperatures, and the corresponding activation energy was calculated. Graphite was found to be equally effective for cesium sorption when it is used in the gas phase above the liquid sodium. Charcoal was found to be even more efficient than graphite in trapping cesium, and the cesium–charcoal compound which is formed is almost fully stable in sodium at 500°C and in air at the same temperature. Pre-treatment of the charcoal with sodium at 500°C for 3 days had little effect on its performance with respect to cesium sorption. (auth)

20755 (ANL/EBR–8) LEAKRATE TESTING OF THE EBR-II REACTOR BUILDING. EBR-II Project. Buschman, Henry W. (Argonne National Lab., Ill. Argonne National Lab., Idaho Falls, Idaho). Oct 1969. Contract W-31-109-eng-38. 26p. Dep. NTIS.

The results of leakrate testing of the EBR-II reactor building are summarized. The existing leakrate criteria are presented and discussed. It is recommended that the leakrate criterion for each individual building penetration be revised. The revised criteria are based on the size of the penetration to a greater extent than before. Although the allowable leakage for many of the penetrations is increased, the revised criteria continue to ensure that the total leakage from the reactor building will not exceed 1000 ft^3/day (at reference conditions of 36.2 psia and 32°F) with a differential pressure of 24 psig. (One thousand cubic feet per day was the criterion that had previously been established in the Hazard Summary Report as the total allowable.) Comparison of the new criteria with leakrate data from past testing shows that there will be little difficulty meeting the new criteria with present testing techniques. This comparison also shows that when a leak exists that can clearly be detected, the criteria are sufficiently restrictive to require identification and subsequent repair of the leak. (auth)

20756 (CONF-700816–(Vol.1), pp 9-25) ATTENUATION CONCEPT FOR EVALUATING RELEASE OF RADIOIODINE FOLLOWING A LOSS-OF-COOLANT ACCIDENT. Walker, D. H. (Idaho Nuclear Corp., Idaho Falls).

From 11. AEC air cleaning conference; Richland, Wash. (31 Aug 1970).

In Proceedings of the eleventh AEC air cleaning conference.

In evaluating the suitability of pressurized water reactor sites in the United States, the release of radioactivity in the event of a loss-of-coolant accident is one of the major considerations. Doses from released radioactivity at the site boundary must be shown to be less than the guidelines set forth in Title 10, Part 100 of the Code of

XUM

Federal Regulations. For the loss-of-coolant accident, the criteria in the guidelines regarding radioiodine isotopes are most restrictive at the site boundary. The effects of various processes, including those of reactor safety system operation, on the amount of radioiodine escaping from the reactor containment vessel are discussed. Estimates of the magnitude of the radioiodine attenuation and the uncertainties associated with the estimates for each of the sequential events in the transport of radioactivity from the fuel through the containment to the environment can be conveniently represented on an iodine attenuation diagram. The distances to the site boundary needed to meet dose guidelines for specified weather conditions can also be represented on the diagram to assist in evaluating the adequacy of a reactor site. Iodine attenuation diagrams are presented for a typical large pressurized-water reactor. Iodine attenuation by various processes or safety systems, during each of the events in the radioiodine transport sequence, is indicated for the maximum credible loss-of-coolant accident condition (as defined in Title 10, Section 100 of the Code of Federal Regulations), and for expected loss-of-coolant accident conditions. Programs now planned or in progress in the U. S. for studying radioiodine release and characteristics in a coolant loss accident are summarized. 10 references. (auth)

20757 (CONF-700816-(Vol.1), pp 26-48) COMPARISONS OF AEROSOL EXPERIMENTS WITH A MODEL USED IN REACTOR SITING EVALUATION. Greenfield, M.; Koontz, R.; Johnson, R.; Morewitz, H. (Atomics International, Canoga Park, Calif.).

From 11. AEC air cleaning conference; Richland, Wash. (31 Aug 1970).

In Proceedings of the eleventh AEC air cleaning conference.

The theoretical basis of the HAA-3 aerosol agglomeration code is described. The code solutions have been compared successfully against sodium oxide aerosol experiments in two test chambers which differ by a factor of 50 in volume ratio. Since the large vessel is approximately the height of the primary vaults of a typical Liquid Metal Fast Breeder Reactor (LMFBR), HAA-3 can be confidently used in the evaluation of potential aerosol releases from hypothetical LMFBR accidents. The application of HAA-3 to LMFBR containment studies is discussed. 24 references. (auth)

20758 (CONF-700816-(Vol.1), pp 72-101) ESTIMATION OF AEROSOL CONCENTRATION IN A NUCLEAR REACTOR CONTAINMENT AFTER AN ACCIDENT. Davis, R. J.; Gill, J. S. (Oak Ridge National Lab., Tenn.).

From 11. AEC air cleaning conference; Richland, Wash. (31 Aug 1970).

In Proceedings of the eleventh AEC air cleaning conference.

Results are presented which demonstrate that the particle size distribution of the form: $dn/dV = AV^{-2}$ (where n is number concentration, V is particle volume, and A is related to the maximum and minimum particle volumes in the distribution, according to: $A = 1/(V_{min}^{-1} - V_{max}^{-1})$;) does describe aerosols of interest in nuclear safety. Information is also presented regarding the dependence of V_{min} on environment; aerosol age seems to be the most important variable. The effect of the increase in V_{min} with time on the concentration-time behavior in a containment was estimated. Steam condensation experiments demonstrated that particle deposition occurs by thermophoresis in condensing steam. Particle growth and enhanced settling also must occur in condensing steam. The effect of deposition by thermophoresis on the concentration-time behavior in a containment was estimated. Finally, some estimates of aerosol particle concentration vs time in water-cooled reactor containments resulting from all the growth and deposition processes considered are presented. 14 references. (auth)

20759 (CONF-700816-(Vol.1), pp 346-55) CHARACTERIZATION OF ENERGY RELEASE AND AEROSOL BEHAVIOR FROM SODIUM SPRAY FIRES. Granger, J.; Nelson, C.; Silberberg, M. (Atomics International, Canoga Park, Calif.).

From 11. AEC air cleaning conference; Richland, Wash. (31 Aug 1970).

In Proceedings of the eleventh AEC air cleaning conference.

In liquid metal cooled reactors, there remains the remote possibility of sodium leakage into environments containing oxygen. In the case of a spray discharge, a significant energy release can result. Concurrent with these "fires" is the formation of an aerosol which contains radioactive substances. A knowledge of the aerosol characteristics, the energy release, and the resultant leaked mass is required for effective safeguards analysis and design. Previous work in the area of spray fire has neglected the chemical nature of the reaction products, and the geometry and dispersion of the spray. An experimental setup is described for measuring the rate of sodium injected from different sized jets into variable oxygen environments. As the sodium is injected, measurements of oxygen consumption, pressure rise, and gas and wall temperature changes are made, all as a function of time. Measurements of the aerosol concentration, chemical form, fallout rate, and particle size distributions are made after the injected sodium has burned. Experimental results verify that pressure pulses resulting from a spray fire may be significant, but are probably much lower than presently assumed. Agglomeration of the sodium oxide was found to be rapid, and an aerosol distribution of large particles forms within seconds of formation. The factors controlling the rapid agglomeration of the oxide are discussed. (auth)

20760 (CONF-700816-(Vol.1), pp 356-72) BEHAVIOR OF IODINE IN SODIUM SYSTEMS. Goldin, Abraham S.; Trindade, Helena A.; Lee, Sang Hoon; First, Melvin W. (Harvard School of Public Health, Boston, Mass.).

From 11. AEC air cleaning conference; Richland, Wash. (31 Aug 1970).

In Proceedings of the eleventh AEC air cleaning conference.

Knowledge of the behavior of fission product iodine in a sodium or sodium compound environment is important in evaluating the potential hazards from both normal operations and accident conditions in a sodium-cooled breeder reactor system. The evolution of radioiodine ^{131}I from a sodium peroxide system as a function of time, temperature, and carrier gas (nitrogen) flow rate was studied. Virtually no iodine was volatilized at 250°C, and a very small amount, of the order of 10^{-3}% per hour, at 630°C. Substantially greater amounts of iodine were volatilized at 725°C and 830°C. The data are consistent with the hypothesis that the mechanism of transfer is distillation of sodium iodide, and that elemental iodine is not produced in this system. The detection method was gamma counting of radioiodine absorbed in bubblers containing sodium hydroxide–sodium thiosulfate solutions. The collection efficiency of a single bubbler was found to be about 98%, and 0.003 μCi could be detected easily in a one-minute count. When 30 μCi was used in a run, therefore, a transfer of 0.01% could be measured. Preliminary investigations of the uptake of iodine in nitrogen from molten sodium were made. These studies are needed to predict the movement of fission product iodine from cladding breaks or from vented fuel elements. 4 references. (auth)

20761 (CONF-700816-(Vol.1), pp 373-92) BEHAVIOR OF IODINE IN THE PRESENCE OF SODIUM OXIDE AEROSOLS. Baurmash, L.; Nelson, C.; Granger, J.; Koontz, R. (Atomics International, Canoga Park, Calif.).

From 11. AEC air cleaning conference; Richland, Wash. (31 Aug 1970).

In Proceedings of the eleventh AEC air cleaning conference.

The agglomeration of iodine-131 and sodium oxide particulates has been studied for two types of hypothetical Liquid Metal Fast Breeder Reactor (LMFBR) accidents. In the first test, the iodine was in the form of sodium iodide-131, and was released simultaneously with sodium oxide aerosol produced from a pool fire. In the second, the sodium oxide aerosol was released into an atmosphere containing molecular iodine-131 vapor. The first type of release simulates an incident in which the fission product iodine has reacted to form sodium iodide before the accident. The released aerosol consists of sodium oxide and sodium iodide-131. Observations of the airborne concentration, fallout rate, plating rate, and particle size show that the sodium iodide-131 was agglomerated with the sodium oxide, and the aerosol behaved as though it were one material. The second experiment simulates a fuel accident in which fission products are released separately from the oxide. As the sodium oxide aerosol particles were mixed with iodine-131 vapor, the oxide rapidly scavenged a large fraction of the available iodine, reducing the free molecular iodine concentration by a factor of 10^3 in a few minutes. The molecular iodine activity was preferentially associated with the smaller sodium oxide particles. The sedimentation, filtration, and plating rates were measured, and the iodine and the mixed aerosol behaved as had been noted previously. A plating rate was also established for the iodine vapor before the oxide was released. A small residual amount of unagglomerated iodine was detected, which was not identifiable as molecular iodine. The particulate oxide–iodine aerosol was filterable, with an efficiency better than 0.99, while the unagglomerated iodine compound could not be filtered by a molecular membrane filter. (auth)

20762 (JAERI-Memo-4194) CORE TEMPERATURE ANALYSES FOR LOSS-OF-COOLANT ACCIDENTS OF LIGHT WATER REACTOR BY THE COMPUTER CODE NURLOC-1.0. Mitake, S.; Nogaito, T.; Hatta, H.; Nabeta, T.; Fukuda, A.; Shimegi, N. (Japan Atomic Energy Research Inst., Tokyo). Nov 1970. 126p. (In Japanese). Dep. NTIS (U. S. Sales Only).

Results of accident analyses for a commercial power reactor by the digital computer program NURLOC-1.0, which was developed to show thermal conditions of a reactor core under a loss-of-coolant accident, are described. By these analyses, some features of

XUM

the code are also made clear. The following information was obtained: (1) In the course of an accident, some portion of the core melts. Heat to cause melting is supplied mainly by the metal-water reaction. (2) Metal-water reaction is controlled strongly by the steam generation rate. (3) It takes a great deal of computational time to simulate an accident for a whole core which includes structures such as core support grids or plate. (auth) (Japan)

20763 (JAERI-Memo-4229) A STUDY REPORT OF NUCLEAR SAFETY EXPERIMENTAL PROGRAM. NO. 4. Ishikawa, Hiroshi; Ishikawa, Michio; Sako, Kiyoshi; Tomii, Kakuzo; Nakahara, Yasuaki (Japan Atomic Energy Research Inst., Tokyo). Nov 1970. 101p. (In Japanese). Dep. NTIS (U. S. Sales Only).

Activities in the NSRR (Nuclear Safety Research Reactor) program for the period of April to October 1970 are described. With the safety analysis for NSRR and also with design and calculation, the contents are the following: summary of the progress in the period; design studies on NSRR and facilities; core physics calculations; kinetic calculations; experimental pre-analysis; safety analysis; and experiments on fast reactor fuels. 10 references. (Japan)

20764 (NP-18487) APPRECIATION OF FAST REACTOR SAFETY (1970). (United Kingdom Atomic Energy Authority, Risley (England). Authority Health and Safety Branch). 200p. (AHSB(S)R-188). Dep. NTIS (U. S. Sales Only).

Various aspects of sodium-cooled fast reactors which affect their potential safety are discussed. Separate chapters review problems in: (1) kinetic behavior; (2) cooling failure in a subassembly; (3) excursion behavior; (4) molten fuel; (5) evaluation of containment explosion potential; (6) containment; (7) decay heat rejection; (8) sodium-water reactions; (9) instrumentation; (10) fire hazards and precautions; (11) fuel handling; (12) fission product behavior in sodium. (H.D.R.)

20765 DYNAMIC STUDIES OF GAS TURBINE FAST REACTORS. Sarlos, G.; Broido, J. H.; Dupont, J. F.; Telleschi, P.; Tiberini, A. (Swiss Federal Inst. for Reactor Research, Wurenligen, Switzerland). pp 95-102 of Nuclear Gas Turbines. London; British Nuclear Energy Society (1970).

From Conference on Nuclear Gas Turbines, London, England. See CONF-700430.

A description of a compressible flow, transient analysis code developed for the calculation of depressurization accidents in gas turbine fast reactors is presented. Illustrative results taken from test cases are given. The code has been shown capable of following transients over a wide range of time constants and representing a variety of circuit configurations. (auth) (UK)

20766 CONTROL AND SAFETY STUDIES FOR AN HTR GAS TURBINE SYSTEM. Dean, J. R.; Preinreich, G.; Soubelet, G. C. (Atomic Energy Establishment, Winfrith, Eng.). pp 103-10 of Nuclear Gas Turbines. London; British Nuclear Energy Society (1970).

From Conference on Nuclear Gas Turbines, London, England. See CONF-700430.

Descriptions are given of a digital code GASPAR and an analog model with which steady state part-load conditions and kinetics performance, respectively, can be determined for high temperature reactor gas turbine systems. Exploratory studies have been made of a reference design operating under temperature or helium inventory control, after sudden loss of generator load, and during depressurisation. (auth) (UK)

20767 OPERATIONAL CONDITIONS FOR AFTERHEAT REMOVAL OF A GAS-COOLED REACTOR WITH DIRECT CYCLE. Telleschi, P. (Eidgenoessische Institut fuer Reaktorforschung, Wuerenlingen, Switzerland); Sarlos, G.; Frutschi, H. U. Atomkernenergie; 17: 137-9(Mar 1971). (In German).

The afterheat removal at low pressures, e.g., after a depressurization incident, is an important design problem in gas-cooled reactors and particularly in gas-cooled fast breeders. In the case of a fast breeder power plant employing a direct gas turbine cycle the use of the turbogroups for emergency cooling is proposed. Results obtained with a code investigating the plant response under emergency cooling conditions are presented. (auth)

Power Conversion Systems

20768 MAGNETOPLASMADYNAMIC ENERGY CONVERSION IN NUCLEAR POWER STATIONS. Bartsch, G.; Johannsen, K. Waerme; 74: 158-69(1969). (In German).

Known and probable advantages are the absence of rotating parts, efficiencies of up to 50%, and power densities of 10–20 MW/m^3. Converter volume should reduce capital costs. Gas cooled HTRs should be able to produce gas of the required high temperature. The design and operating parameters are detailed. (Fuel Abstr.)

20769 SEPARATION OF STEAM AND WATER IN BOILING-WATER REACTORS AND STEAM GENERATORS. Graebener, Karl-Heinz; Mieville, Bernd; Kison, Harald (AEG-Telefunken, Grosswelzheim, Ger.). At. Strom; 16: 172-5(Nov-Dec 1970). (In German).

Commencing with the requirements for a steam separator system for nuclear steam generators, a coarse separator system is introduced which incorporates the AEG trap cyclone and which has been tested in different trial arrangements and has already been successfully used in boiling-water reactors. The separator can be installed in the boiling water reactor or in the steam generator for a pressurized-water reactor above the core unit or the bank of tubes, or in the trap space. The mode of operation, characteristics and also the relations between the various parameters are described. (2 references) (auth)

20770 POWER CYCLES FOR HELIUM COOLED HIGH TEMPERATURE NUCLEAR REACTORS. Worley, N. G.; Campbell, J. W. E. (Babcock and Wilcox Ltd., London). pp 1-10 of Nuclear Gas Turbines. London; British Nuclear Energy Society (1970).

From Conference on Nuclear Gas Turbines, London, England. See CONF-700430.

Helium cooled power station reactors are being designed for reactor outlet temperatures of about 800°C. For such a temperature level there is a choice of power cycle, steam or direct gas turbine, and it appears that the factors influencing the choice are complex. The efficiency levels available are roughly comparable but the gas turbine has a most complex primary circuit with a large heat transfer area which to a considerable degree offset the advantages of the system. A number of possibilities are discussed and analyzed, including combined cycles which do not appear to be promising. (auth) (UK)

20771 TECHNICAL FEASIBILITY AND FUTURE OF NUCLEAR HELIUM GAS TURBINES. Gasparovic, N. (Technical Univ., Delft, Netherlands). pp 28-35 of Nuclear Gas Turbines. London; British Nuclear Energy Society (1970).

From Conference on Nuclear Gas Turbines, London, England. See CONF-700430.

A nuclear gas turbine is characterized thermodynamically by operating a gas turbine cycle within the direct cycle loop of the reactor. The use of the direct cycle has both advantages and disadvantages, and in the particular case when He constitutes the working fluid the disadvantages are serious in respect to safety precautions. Further with He, high maximum temperatures are required to achieve the necessary efficiencies and this demands internally insulated ducts which for He, have a very low power transport capacity. Only if integrated design is employed can the safety requirements be fulfilled with respect to the possible depressurization accident. He gas turbine power plants cannot deliver higher power per unit than steam power plants. (auth) (UK)

20772 GAS TURBO-MACHINERY FOR HELIUM COOLED REACTORS. Hurst, J. N.; Rendall, C. V. A.; Sandeman, W. A.; Yates, D. A. (Rolls-Royce Ltd., Derby, Eng.). pp 43-50 of Nuclear Gas Turbines. London; British Nuclear Energy Society (1970).

From Conference on Nuclear Gas Turbines, London, England. See CONF-700430.

The construction of an economic nuclear gas turbine plant will make heavy demands on some aspects of gas turbine technology. Problems have been encountered but none will be insoluble. Applied research will, however, be necessary to determine the best solution. The design and development requirements of the turbomachinery are presented. Consideration is also given to the starting, control and safety aspects. Means of starting and controlling the plant are described. Solutions proposed to those safety problems which are peculiar to the gas turbine system are presented. (auth) (UK)

20773 HIGH PRESSURE INDIRECT CO$_2$ CLOSED-CYCLE GAS TURBINES. Strub, R. A.; Frieder, A. J. (Brown Boveri-Sulzer Turbomachinery Ltd., Zurich). pp 51-61 of Nuclear Gas Turbines. London; British Nuclear Energy Society (1970).

From Conference on Nuclear Gas Turbines, London, England. See CONF-700430.

The relative merits of an indirect CO$_2$ gas turbine cycle in the case of gas-cooled fast breeders are underlined, showing that this type of gas is well suited to such application. The supplementary heat exchanger He/CO$_2$ seems to be fully justified by increasing markedly the safety of the plant and by providing easier maintenance of the various components of the gas turbine circuit. It is believed that for future gas-cooled fast breeders and even for high

XUM

temperature gas-cooled reactors CO_2-indirect cycles could be advantageous by replacing steam cycles or even direct He cycles. (auth) (UK)

20774 SIMPLE, COMPACT, NUCLEAR GAS TURBINE FOR INTEGRATION IN THE REACTOR VESSEL. Maillet, E. (CEA, Paris). pp 62-71 of Nuclear Gas Turbines. London; British Nuclear Energy Society (1970).

From Conference on Nuclear Gas Turbines, London, England. See CONF-700430.

Helium turbines for HTR were originally designed with low compression ratios and pressure drops. However to limit the reactor and heat exchanger inlet temperature to a desirable level of 500°C or below, this compression ratio must be increased between 3.5 and 4.5 with three compressors. On the other hand, factors of reliability and reduction of investment costs may lead to a temporary limitation of the upper temperature to about 850°C and to the use of two compressors, the optimum pressure ratio in this case lying between 3 and 3.5. In support of this option towards simplification, the dimensions characterizing the main components are given for 600 MW(e) units. Studies on integration of the circuit may demand heat exchangers with an efficiency of 0.85 only. However it is necessary to design more compact turbomachines. This can be achieved by developing the technique of axial machine bladings towards higher flow rate and pressure coefficients. High efficiency modern centrifugal compressors may be associated with axial compressors and even combined with turbines in certain cases. Several examples of these ideas are given for helium and heavy gas turbines of power 600 MW(e) and possibly higher. (auth) (UK)

20775 HEAT EXCHANGERS FOR GAS TURBINE FAST REACTORS. Lys, L. A.; Von Allmen, I. (Swiss Federal Inst. for Reactor Research, Wurelingen, Switzerland). pp 77-86 of Nuclear Gas Turbines. London; British Nuclear Energy Society (1970).

From Conference on Nuclear Gas Turbines, London, England. See CONF-700430.

The use of large regenerators and coolers clearly affects the efficiency of gas turbine fast reactor plants. This equipment, however, generally represents a significant cost item and therefore it is necessary to determine a compromise between the cost savings resulting from the increased efficiency and the capital expenditure for the equipment required. The work which has been performed by the Swiss Federal Institute for Reactor Research with the participation of Swiss industry with the aim of selecting the proper design of the regenerator and coolers is reviewed. (auth) (UK)

20776 DEVELOPMENT OF A SPECIFICATION FOR HEAT EXCHANGER PLANT TO SUIT A GAS TURBINE HTR. Warner, P. C.; Longstaff, T. N. (Clarke Chapman and Co., Ltd., Gateshead, Eng.). pp 87-94 of Nuclear Gas Turbines. London; British Nuclear Energy Society (1970).

From Conference on Nuclear Gas Turbines, London, England. See CONF-700430.

Specifications for the heat exchanger equipment to be included in a closed cycle gas turbine scheme using a high temperature reactor are described. The timing of development is reviewed. The thermodynamic parameters are discussed, as well as those factors which influence the mechanical layout of the primary circuit and reactor. It is shown that a specification to serve as the basis of a development programme for the heat exchanger equipment can be arrived at using either tubular or plate type configuration. (auth) (UK)

20777 DEVELOPMENT OF COMPONENTS FOR NUCLEAR POWER STATIONS WITH HELIUM TURBINES. Bammert, K. (Technische Univ., Hanover). pp 121-34 of Nuclear Gas Turbines. London; British Nuclear Energy Society (1970).

From Conference on Nuclear Gas Turbines, London, England. See CONF-700430.

A report on some components of He turbine plants for nuclear power stations with high temperature gas-cooled reactors is presented. The start-up behavior and the control action which are of great importance for the use of gas turbines in nuclear power stations are considered. As the heat exchanging apparatus, e.g., recuperators and coolers, add to a large extent to the total amount of investment, some proposals on advantageous designs are submitted. An account of the particularities of the heat removal of gas turbines for dry air cooling systems is given. (auth) (UK)

20778 HELIUM CLOSED-CYCLE GAS TURBINE INTEGRATED WITH A HIGH TEMPERATURE REACTOR. Burylo, P. (English Electric-AEI Turbine Generators Ltd., Whetstone, Eng.). pp 180-90 of Nuclear Gas Turbines. London; British Nuclear Energy Society (1970).

From Conference on Nuclear Gas Turbines, London, England. See CONF-700430.

Mechanical and aerodynamic features of a 300 MW closed-cycle gas turbine, being one of four in an integrated arrangement with a 1200 MW(e) high temperature helium cooled reactor, are described. An important feature of the proposed design is the use of well proven materials and techniques in order to achieve maximum reliability. Unlike the steam turbine, the gas turbine has tremendous possibilities for further development. (auth) (UK)

20779 DYNAMIC BEHAVIOR OF COUNTER-FLOW HEAT EXCHANGERS OF NUCLEAR POWER PLANTS WITH GAS TURBINE AT STEP CHANGE OF INLET TERMPERATURES. Dietrich, R. (Brown Boveri/Krupp Reaktorbau GmbH, Mannheim, Ger.). Atomkernenergie; 17: 34-8(Feb 1971). (In German).

A method is given which permits the calculation of the frequency response and the step response of the gas outlet temperatures of counter-flow heat exchangers of nuclear power plants with gas turbine. The partial differential equations describing the relation between the temperatures of the hot gas, the tube wall, and the cold gas are specified. Based on these equations the relations for calculating the frequency response and the step response of the gas outlet temperatures at a step change of the inlet temperatures are determined by means of Laplace Transform. As an example for the application of the developed method, the frequency response and the step response of the gas outlet temperatures of the counter-flow heat exchanger of a 600 MW(e) nuclear power plant with gas turbine are calculated for a step change of the inlet temperature of the hot gas. (auth)

20780 PRELIMINARY EXPERIMENTS OF A HEAT EXCHANGER IN HELIUM UNDER HIGH-PRESSURE AT THE KFA JUELICH. Groehn, H. G.; Scholz, F.; Tuerk, G. (Kernforschungsanlage, Juelich, Ger.). Atomwirt., Atomtech.; 15: 576-7 (Dec 1970). (In German).

At the high pressure gas channel of the KFA Juelich, preliminary experiments were performed on heat exchangers and other components of high-temperature reactors in He under pressure up to 40 bar and temperatures up to 400°C. The channel contained a tube assembly through which cooling water flowed while the outside was exposed to hot He. Determined were the pressure decrement in the gas and the heat conduction. Results showed that within the range of Reynold's numbers from 10^4 to 10^5 an excellent agreement exists between values obtained for air and for He. Therefore, the similarity theory for heat exchange was found valid and experience gained with air could be applied satisfactorily to the He arrangement. (H.B.G.)

Research and Test Reactors

Refer also to abstracts 18627, 18704, 18732, 18765, 20134, 20692, and 20725.

20781 (AAEC/M-10) REACTOR HIFAR: THE CONTROL ARM CIRCUITS. Sinclair, W. J. (Australian Atomic Energy Commission Research Establishment, Lucas Heights). May 1970. 32p. Dep. NTIS (U. S. Sales Only).

The operation of the control arm circuits in the HIFAR reactor and their relation to other control and safety circuits are described. A description is given of lifting magnet circuits, power supply, operation, master gearbox and control arm position interlocks, downward drive, misalignment of the transmission system, maintenance, and drop testing. (Australia)

20782 (CONF-700816-(Vol.1), pp 102-27) LARGE SCALE AIR CLEANING TESTS IN THE CONTAINMENT SYSTEMS EXPERIMENT. McCormack, J. D.; Hilliard, R. K. (Battelle-Northwest, Richland, Wash. Pacific Northwest Lab.).

From 11. AEC air cleaning conference; Richland, Wash. (31 Aug 1970).

In Proceedings of the eleventh AEC air cleaning conference.

Results of five CSE experiments in which an internal recirculating air-cleaning loop was run in steam-air atmospheres are presented. The loop was composed of a commercial sized heat exchanger, demister, filters and charcoal beds. Variables investigated were loop flow, atmospheric temperature, component arrangement and aerosol source term. The observed removal of iodine, cesium, uranium, and methyl iodide from the typical water cooled reactor post-accident atmospheres is compared to a model which assumes a well mixed gas space. 14 references. (auth)

20783 (CONF-700816-(Vol.1), pp 317-45) VENTILATION SYSTEMS FOR THE FFTF. Shaver, B. O. (WADCO Corp., Richland, Wash.).

From 11. AEC air cleaning conference; Richland, Wash. (31 Aug 1970).

In Proceedings of the eleventh AEC air cleaning conference.

The Fast Flux Test Facility (FFTF) is a coordinated facility for investigation into the behavior of fuels and structural materials subjected to high, fast neutron flux prototypic of fast reactor environments. Heat is removed from the reactor by circulation of liquid sodium coolant through the reactor and associated heat exchanger systems. The heat energy is rejected to the atmosphere without power recovery. Since the primary mission of the reactor is to provide reliable fast flux testing, closely controlled and instrumented environmental conditions are a primary objective. The heating and ventilation system provides the required environmental conditions within FFTF for all air and nitrogen spaces and, by filtration of the exhaust air, controls the release of contaminants discharged to the environment. Features of the FFTF ventilation systems are described. (auth)

20784 (DOCKET-50184-26) NATIONAL BUREAU OF STANDARDS REACTOR. Fuel Element Head Locking Bar Pin. (National Bureau of Standards, Washington, D. C.). 26 Feb 1971. 10p. Dep. NTIS.

20785 (DOCKET-50184-27) NATIONAL BUREAU OF STANDARDS REACTOR. Primary System Inlet Strainer: Follow-up Report. (National Bureau of Standards, Washington, D. C.). 10 Mar 1971. 9p. Dep. NTIS.

On January 9, 1971, it was discovered that the wire mesh assembly and two reinforcing bars of the primary system inlet strainer had torn loose from the strainer basket and were washed downstream. Procedures for locating and recovering the missing equipment are described. (D.C.C.)

20786 (DOCKET-50231-71) SOUTHWEST EXPERIMENTAL FAST OXIDE REACTOR. License No. DR-15; Replacement Pages for Revision No. 1 of Technical Specifications Proposed Change No. 4. (General Electric Co., Sunnyvale, Calif. Breeder Reactor Development Operation). 10 Feb 1971. 6p. Dep. NTIS.

Revised information concerning the calculation of power coefficient of reactivity at constant inlet temperature and constant flow is presented. Inspection procedures for fuel elements are described. (D.C.C.)

20787 (GAMD-10231) REVIEW OF GULF GENERAL ATOMIC SUPPORT OF THE HIGH TEMPERATURE LATTICE TEST REACTOR PROGRAM. Brown, J. R.; Mathews, D. R.; Chryssikos, T. N. (Gulf General Atomic, Inc., San Diego, Calif.). 24 Nov 1970. Contract AT(04-3)-167. 34p. Dep. NTIS.

The HTLTR experimental program has been involved with measurements on Lattices 1 and 2. The experimental program on each lattice involves measurements of k_∞ and the thorium Doppler coefficient at various temperatures up to 1000°C. At room temperature, measurements of central cell absorption rates are made using foil-activation techniques for use in the subsequent data reduction. A separate set of room-temperature experiments were performed in the Physical Constants Test Reactor with Lattice 2 to evaluate the experimental techniques used in the HTLTR and their underlying theoretical basis. 3 references. (auth)

20788 (JAERI-Memo-4215) ANALYSIS OF FAST CRITICAL EXPERIMENTS AND A REVISION OF THE JAERI-FAST SET. Takano, Hideki; Hasegawa, Akira; Katsuragi, Satoru (Japan Atomic Energy Research Inst., Tokyo). Feb 1971. 68p. (In Japanese). Dep. NTIS (U. S. Sales Only).

The standard critical assemblies were analyzed using the JAERI-Fast Set. The integral quantities analyzed are effective multiplication factors, spectral indices, material worths, and perturbation cross sections. Problems involved in various group constants of the set were examined. Revisions of the set were made according to the above examination. It is concluded that the revised JAERI-Fast Set can be applied for analyses of experiments as well as design studies. 29 references. (auth) (Japan)

20789 (ORNL-TM-2893(Vol.1)(Rev.)) TOWER SHIELDING REACTOR II DESIGN AND OPERATIONS REPORT: VOL. 1 DESCRIPTION. Holland, L. B. (Oak Ridge National Lab., Tenn.). 16 Feb 1971. 104p. Dep. NTIS.

The TSR-II has been approved for operation at the Tower Shielding Facility at 100 kW and is mainly used for basic shielding research. Volume 1 of the Design and Operation Report is concerned with operation up to a maximum power level of 1 MW. Included are discussions and descriptions of: (1) site and facility; (2) reactor; (3) reactor physics; (4) core heat transfer; (5) heat-removal system; (6) instrumentation; and (7) waste disposal. (H.D.R.)

20790 (WHAN-FR-22) SIMULATION OF PIPING LENGTHS IN SODIUM SYSTEMS. Gunby, A. L. (WADCO Corp., Richland, Wash.). Dec 1970. Contract AT(45-1)-2170. 38p. Dep. NTIS.

Several models for sodium piping were examined using example pipe sizes and example flow and temperature transients. A reference model (alternating central difference and three-point backward differences at each axial mesh point) was selected to describe the effect of pipe wall stored heat on coolant thermal transients. Model simplifications were investigated. The investigation resulted in a model using a transport delay in series with a single-node for stored heat effects with sodium and metal volumes altered by appropriate fractions. (3 references) (auth)

20791 POST-IRRADIATION STUDY OF BR-5 STANDARD FUEL ELEMENTS CONTAINING URANIUM MONOCARBIDE. Ibragimov, Sh. Sh.; Men'shikova, T. S.; Ladygin, A. Ya.; (and others). At. Energ. (USSR); 30: 3-7(Jan 1971). (In Russian).

A number of BR-5 standard fuel elements with UC as fuel was studied after irradiation. The fuel burnup was 0.8, 2.0 and 3.0% of heavy atoms. The fuel elements show satisfactory compatibility and are found to remain hermetic after a long period of irradiation. UC swelling is observed to be 1.9 ± 0.4% per 1% of heavy atoms burnup with 98% of gas fission fragments remaining in the lattice. Metallography makes it clear that UC_2 gradually vanishes with the increase of burnup. The interaction zones are found to form at both sides of the cladding. Mechanical properties of cladding material change with a ductility drop up to 5 to 0.5%. (13 references) (auth)

20792 ABSOLUTE MEASUREMENT OF REACTOR POWER BY NEUTRON NOISE ANALYSIS. Oliverira, J. Costa (Laboratorio do Fisica e Engenharia Nucleares, Sacavem, Portugal). J. Nucl. Energy; 24: 525-6(Dec 1970).

The application of a new technique for the determination of power spectral density to the absolute power measurement of the critical assembly ERMINE is described. The results show the usefulness of the method to the calibration of low power reactors. (UK)

20793 SODIUM-VOID EXPERIMENT IN UNIT k-INFINITY CORE. Yasuno, Takehiko (Japan Atomic Energy Research Inst., Tokai); Nakagawa, Masatoshi; Hirota, Jitsuya. J. Nucl. Sci. Technol. (Tokyo); 7: 642-4(Dec 1970).

The results of measurements on the capture and scattering effects on the sodium-void coefficient in the Fast Critical Assembly IV-2 are presented. The results are compared with one-dimensional diffusion and transport theory calculations. (H.D.R.)

20794 SPACE-TIME REACTOR KINETICS STUDIES WITH THE UNIVERSITY OF FLORIDA SPERT ASSEMBLY. Diaz, Nils J. Gainesville, Fla.; Univ. of Florida (1969). 284p. University Microfilms Order No. 70-11,739.

Thesis.

A large-in-one-space dimension, side reflected, highly multiplicative ($k_{eff} \sim 0.99$) subcritical assembly was designed and calibrated. The University of Florida SPERT Assembly (UFSA) is a light-water moderated subcritical facility fueled by 4.81% enriched UO_2 pellets encased in stainless steel tubes of 0.465 inch outside diameter (SPERT F-1 Fuel). The fuel arrays are contained in a rectangular tank, 8 feet long, 39 inches high, and of variable width. The core was 6.5 inches wide and 30 inches high. The effective multiplication constant of the assembly was determined to be 0.990 ± .003. The assembly is equipped with nuclear instrumentation capable of automatic scram action. For the kinetics studies, a fast data acquisition system was developed to handle accurately the very high, time-changing count rate encountered in the measurements. The space-time kinetics studies were performed by analyzing the propagation of a fast neutron burst introduced at one end of the assembly, in the absence of inherent feedback effects. The experimental results are compared with the results obtained from the two-group, space-time dependent, one-dimensional diffusion theory scheme known as the WIGLE program. A stringent test of the model is provided by a combined analysis in the time and the frequency domain. Spatial effects in large cores are clearly demonstrated. (Diss. Abstr. Int., B)

20795 REACTIVITY MEASUREMENTS OF THE ASTRA-CORE AFTER INSTALLATION OF A BERYLLIUM REFLECTOR. Nedelik, A.; Gruenwald, H. (Oesterreichische Studiengesellschaft fuer Atomenergie GmbH, Siebersdorf, Austria). Atomkernenergie; 17: 46-8(Feb 1971). (In German).

Replacing of the graphite-reflector by metallic Be elements caused an essential increase of photoneutron-density in the subcritical reactor. A series of simple measurements showed however, that the influence on period-measurements is negligible, provided the power level is chosen properly. Comparative measurements were made in water- and Be-reflected cores to check the relative shape of the inhour-curve. Calibration in absolute

XUM

reactivity units was obtained by using the Xe-poisoning of the core. (auth)

20796 MEASUREMENTS ON BERYLLIUM-REFLECTED CORE OF THE ASTRA REACTOR. Burtscher, A. (Reaktorzentrum, Seibersdorf, Austria). Atomkernenergie; 17: 49-52 (Feb 1971). (In German).

The originally used graphite reflector elements of the ASTRA reactor had to be replaced because of excessive dimensional changes due to radiation damage. The new reflector elements are uncanned Be metal. The reactivity gain of a 4 × 7 core configuration having one row of 9 Be elements at each side of the core was 4% $\Delta k/k$ compared with the graphite reflected core. Because of the (γ,n)- and $(n,2n)$-reactions with the Be, the neutron density in the subcritical reactor core with fully inserted control rods is high enough to be registered by the DC-channels of the reactor instrumentation, even after extended shut down periods. During a reactor start up, the DC-channels measure a few hundred watts reactor power if criticality is approached. Thermal flux values of 1.2×10^{13} cm^{-2} s^{-1} were measured at the Be reflector in the center plane of the core; the ratio $\Phi_0/\Phi_S(E > 1$ MeV) is 15. Compared with the core configuration used with the graphite reflector, the fast neutron beams outside the reactor shielding has decreased by a factor of 3 to 4. (auth)

20797 INFLUENCE OF A HEAVY WATER TANK ON REACTIVITY MEASUREMENTS ON MTR-CORES. Roethemeyer, H. (Physikalisch-Technische Bundesanstalt, Brunswick). Atomkernenergie; 17: 39-45(Feb 1971).

The "Research- and Measuring Reactor" of the Physikalisch-Technische Bundesanstalt (FMRB) is operated with two MTR-cores weakly coupled by a heavy water tank. The reactivity-parameters of the two uncoupled cores facing the tank are discussed. They are determined by means of asymptotic period and pulsed source measurements. Results are given of shutdown and excess reactivity measurements, control rod calibrations and the reactivity contribution of the heavy water tank as a function of heavy water height. The attempt was made to avoid systematic errors caused by the heavy water reflector by the measurement of spatial averages. When subcriticality is achieved by means of control rods the known effect of increasing reduced generation time with increasing subcriticality is observed. But decreasing the heavy water level shows a decreasing neutron generation time with increasing subcriticality. 26 references. (auth)

20798 MEASUREMENT OF THE NEUTRON SPECTRUM AT A BEAM HOLE OF THE FRJ-1 REACTOR IN THE ENERGY RANGE FROM 10 keV TO 10 MeV. Bachner, E. (Kernforschungsanlage, Juelich, Ger.) Krisch, O.; Long, H. Atomkernenergie; 17: 88-92(Mar 1971). (In German).

The measurement of the neutron spectrum at the port of a horizontal beam hole of the FRJ-1 is described. The spectrum in the energy range from 10 keV to 1.5 MeV was measured with a low pressure cloud chamber. For the energy distribution between 1.0 and 10.1 MeV a scattering chamber was used. 14 references. (auth)

20799 MEASURING AND CONTROLLING EQUIPMENT FOR D_2O CRITICAL ASSEMBLY. Yokota, Minoru (Fuji Electric Co. Ltd., Tokyo). FAPIG (Tokyo); No. 56, 257-62(Mar 1970). (In Japanese).

The D_2O Critical Assembly is installed with the measuring and controlling equipment, consisting of (1) process measuring equipment, (2) control circuit and (3) safety protection circuit. The process measuring equipment is mostly contained in a control room consisting of light water system, nitrogen gas system, and heavy water system in which special attention is paid to leak tightness and corrosion resistance. The combination of control consoles and vertical panels with semi-graphic display is used to facilitate central monitoring and controlling. Two kinds of reactivity control are available. One changes the position of control rods, and another regulates heavy water level in a core tank. These are interlocked with each other and not permitted to act simultaneously. To provide safety protection, several interlocks are prepared, among which the starting interlock system can be bypassed with a key locked switch. The safety system also includes 11 scram sensory circuits. Upon the actuation by scram signals, the circuits call the attention of operators with lamps and buzzers, cause four safety rods to be scrammed, and simultaneously dump heavy water into a tank. (Japan)

20800 NUCLEAR INSTRUMENTATION. Takeuchi, Shoko (Fujitsu Ltd., Tokyo). FAPIG (Tokyo); No. 56, 262-5(Mar 1970). (In Japanese).

To monitor and control the reactor from startup to full power, the D_2O Critical Assembly is provided with nuclear measuring and data handling equipment which consists of six channels; two for startup system, one for linear system, one for safety system, one for logarithmic output system, and one for gamma ray system. The detectors in each of six channels are arranged around a core tank, so that an electrical signal converted from thermal neutron flux can be fed to the control room. To avoid the influence of noise, all the nuclear instrumentation cables are passed through copper ducts. In case of the failure of the measuring device or the reactor output exceeding nominal value, the central signalling system in the control room calls the attention of operators with visual and acoustic signals, at the same time the shut down signal is sent out to the reactor. In the DCA instrumentation, recently developed integrated circuits are employed, and semi-conductors are fully applied, therefore the equipment is small and has high performance and high reliability. Maintenance, inspection and the interchange of parts are easy because the modules of the standard AEC 5 in size are adopted. (Japan)

20801 HEAVY WATER, LIGHT WATER, AND GAS SYSTEMS FOR DCA. Nomi, Mitsuhiko (Ebara Mfg. Co. Ltd., Tokyo). FAPIG (Tokyo); No. 56, 254-7(Mar 1970). (In Japanese).

The heavy water, light water and gas systems for the D_2O Critical Assembly (DCA) are described; DCA is for the development of ATR, D_2O moderated and light-water cooled. (1) Heavy water system. D_2O is used as moderator and reflector. The system consists of three subsystems, viz. rapid and slow D_2O supplies and D_2O purification. By the rapid subsystem, an approximate level of D_2O in the DCA tank is attained, and then the slow subsystem is used. The problem of D_2O leakage is also described. (2) Light water system. A test region is in the middle of the core tank, through which light water is circulated. The temperature of light water can be varied from ordinary temperature to 80°C. A purification subsystem is also used. (3) Gas system. Nitrogen gas is used to prevent the contact between D_2O and air, etc. Finally, the injection of D_2O and the deuterium-treatment of ion-exchange resins are described. (Japan)

20802 HOUSING BUILDING FOR THE D_2O CRITICAL ASSEMBLY. Matsumoto, Katsumi (Shimizu Construction Co. Ltd., Tokyo). FAPIG (Tokyo); No. 56, 267-71(Mar 1970). (In Japanese).

The housing building for DCA was built in the form of an L, with the DCA room as the center; surrounding the DCA room are auxiliary (laboratories etc.) and machinery rooms. The primary requirement for the DCA room is high gas-tightness to prevent the spread of an accident of the DCA. The components of the housing building are nearly all of concrete. The DCA-room portion is a two-story structure with one basement; the first and second floors contain DCA, and the D_2O tanks etc. are in the basement. Then, adjoining the DCA room are a fuel-handling room, fuel storage, and light-water and gas system rooms. Access into the DCA room is generally through an air-tight shield door. The housing building for DCA is described in the following: arrangement of the housing building; the process of construction carried out; and the problems and tests of the gas-tightness. (Japan)

20803 THEORETICAL SPECTRUM-THRESHOLD DETECTOR DATA CORRELATION IN EBR-II. Kamphouse, J. L.; Stuart, R. L.; Moteff, J. (General Electric Co., Cincinnati). Contract AT(40-1)-2847. J. Nucl. Mater.; 39: 1-17(Apr 1971).

An experimental and computer program to further examine the neutron environment in the Experimental Breeder Reactor-II (EBR-II) has been completed. Monte Carlo and S_4 Transport methods were used to determine the neutron spectrum at various positions in the EBR-II core and blanket regions. Response functions for the threshold detectors $^{58}Ni(n,p)^{58}Co$ and $^{54}Fe(n,p)^{54}Mn$ were determined for each position and the corresponding predicted induced activities are compared with experimental results. Based on combinations of calculated neutron spectra, experimental detector responses, and cross section end points an empirical differential cross section was determined for the $^{46}Ti(n,p)^{46}Sc$ threshold reaction. Spectrum averaged cross sections for the three threshold reactions which have been determined at various positions in this facility suggest that significant errors in fast neutron fluences will result if the usual fission spectrum averaged cross sections are used. 13 references. (auth)

20804 NEUTRON-PULSE PROPAGATION IN MULTIPLYING ASSEMBLIES. Golay, M. W.; Cady, K. B. (Cornell Univ., Ithaca, N. Y.). Nucl. Sci. Eng.; 43: 303-14(Mar 1971).

Axial neutron-pulse propagation experiments were conducted in cylindrical cores of the Cornell University Zero Reactor (ZPR). Energy-dependent neutron diffusion theory is found to provide a good prediction of the kinetic behavior of the assemblies. At short times the reactor response is that of an infinitely long reactor, and at long times exponential decay of Helmholtz spatial modes is observed. A space-independent pulse propagation velocity is not observed in most of the assemblies. Such a result is obtained only in infinitely long assemblies, and in most finite-length cores end-effect contamination cannot be neglected. In the Laplace transform domain the neutron density wave dispersion relations are obtained when the transform variable ξ is imaginary in the cores which would be prompt-subcritical if they were infinitely long. When ξ is real, the inverse attenuation length which would be measured in a static exponential experiment in an assembly uniformly poisoned by an absorber of strength ξ/v is obtained. The agreement between the measured parameters and the predictions of diffusion theory improves as the neutron multiplication of the assembly decreases due to decreased end-effect contamination of the infinitely long assembly response. The effective multiplication of an assembly is seen to decrease due to spectral hardening as $|\xi|$ increases when $\mathrm{Re}(\xi)$ is non-negative. This effect is reflected in the variation of the dispersion parameters with ξ. (auth)

Rocket and Space Reactors

Refer also to abstract 19195.

20805 (N–70–39420) AUXILIARY AND LOOP FOR REMOVAL OF DECAY HEAT FROM A SPACE POWER REACTOR. Turney, George E.; Petrick, Edward J. (National Aeronautics and Space Administration, Cleveland, Ohio. Lewis Research Center). Sep 1970. 33p. (NASA-TM-X–2077; E–5579). NTIS.

An auxiliary radiator loop with sodium coolant was investigated as a possible means for removing decay heat from a proposed 2.17-megawatt space power reactor. Based on a selected set of operating conditions and assumptions, minimum areas were determined for the auxiliary loop heat exchanger and radiator. The minimum auxiliary heat exchanger surface area was determined to be 0.64 sq ft (0.594 sq m), and the minimum auxiliary radiator surface area was 37.7 sq ft (3.50 sq m). Based on these areas, the maximum temperature of the auxiliary radiator was about 1760 R (978 K). The flow rates and temperatures of sodium in the auxiliary loop were determined as a function of time after reactor shutdown for reactor operating times of 1 year and 1 day. A significant conclusion from the preliminary study is that the size (and/or mass) of the auxiliary loop is relatively small. (auth) (STAR)

20806 GASEOUS NUCLEAR ROCKET ENGINE. McLafferty, George H. (to U. S. Air Force). U. S. Patent 3,546,069. 8 Dec 1970. Filed 15 May 1968.

A vortex stabilized gaseous nuclear rocket engine in which helium gas is injected into a vortex tube to form a buffer layer between the outer periphery of a fuel and the inner surface of a propellant is described. (auth)

20807 NUCLEAR POWER PLANT FOR A SPACE STATION. Fiebelmann, Peter; Neu, Helmut; Buzzi, Umberto (to EURATOM). British Patent 1,220,554. 27 Jan 1971. Priority date 24 May 1968, Germany.

HEAT PIPES—design parameters for thermionic reactor shielding cooling
NUCLEAR AUXILIARY POWER SYSTEMS—design parameters of thermionic reactor system with heat pipe cooling of radiation shield
SHIELDING—cooling system for thermionic reactor, description of heat pipe for (H.D.R.)

20808 NUCLEAR POWER PLANT FOR A SPACE STATION. Fiebelmann, Peter; Neu, Helmut; Buzzi, Umberto (to EURATOM). British Patent 1,220,644. 27 Jan 1971. Priority date 24 May 1968, Germany.

HEAT PIPES—protection of, description of radiator plates for
NUCLEAR AUXILIARY POWER SYSTEMS—design of thermionic reactor system with heat pipe protection by radiator plate
RADIATOR—design parameter of plate type, for protection of heat pipes (H.D.R.)

20809 NUCLEAR REACTOR WITH HEAT PIPES. Neu, Helmut; Fiebelmann, Peter (to EURATOM). British Patent 1,220,553. 27 Jan 1971. Priority date 21 May 1968, Germany.

HEAT PIPES—design parameters of dual crossed axes, for thermionic reactors
NUCLEAR AUXILIARY SYSTEMS—core configuration for thermionic reactor with dual crossed-axis heat pipe system (H.D.R.)

20810 AIRCRAFT NUCLEAR PROPULSION SYSTEM. Kappus, Peter G.; Long, William H. (to General Electric Co.). U. S. Patent 3,547,380. 15 Dec 1970. Filed 18 Sep 1967.

A nuclear power plant includes a closed reactor circuit within which a medium heated by the nuclear reactor transfers energy to a propulsion fluid in a two-step process, the first step being a mechanical transformation and the second step being a thermal transformation of energy. (auth)

20811 ENGINEERING STUDY OF THE COLLOID-FUELED REACTOR CONCEPT. Tang, Y. S.; Stefanko, J. S.; Dickson, P. W.; Drawbaugh, D. W. (Westinghouse Electric Corp., Pittsburgh). J. Spacecraft Rockets; 8: 129-33(Feb 1971).

A concept using colloid fuel, vortex chamber cavity is described. The reactor uses particulate fuel with a composition (1U–10Zr)C where uranium is ^{233}U. The fuel is fed to the cavity by hydrogen gas. The cavity, a compressed vortex chamber, has an L/D ratio of 0.15 in the fuel region. Beryllium is used as the reflector material and is contained in a titanium-alloy (Ti–Al–V) pressure vessel. The reactor is designed for ground test purpose and would generate a 45,000 kg (100,000 lb) thrust with a specific impulse of 1200 sec. The over-all dimensions of the pressure vessel are approximately 240 cm (95 in.) dia and 240 cm (95 in.) in length. The engine weighs 19,000 kg (41,000 lb). (13 references) (auth)

Process Heat and Desalination Reactors

Refer also to abstract 18565.

20812 (TID–25653) ABSTRACTS OF LITERATURE ON THE DISTILLATION OF SEAWATER AND ON THE USE OF NUCLEAR ENERGY FOR DESALTING. Research and Development Progress Report No. 589. Johnsson, K. O.; Hammond, R. P.; Wond, Chung-ming; Sieder, Everett N. (Office of Saline Water, Washington, D. C.). Sep 1970. 280p. GPO $2.00.

Abstracts of desalination literature generally available to the public are listed. The bibliography list is divided into nine categories of desalination information; a single bibliographic entry may be listed in as many as three categories. A keyword index and an author index are provided. Each bibliographic entry includes the following information: author, title, corporate author, number of pages, number of figures, number of references, publication data, document number or journal reference, an informative abstract of less than 200 words, and a list of selected keywords to describe the contents. (D.C.C.)

Marine and Portable Power Reactors

20813 (CEA-CONF–1727) THERMIONIC REACTOR: NEUTRONIC STUDY OF A LIGHT WATER MODERATED CORE. Schwartz, Jean-Pierre (Commissariat a l'Energie Atomique, Saclay (France). Centre d'Etudes Nucleaires). 1970. 6p. (CONF-701039–1). Dep. NTIS (U. S. Sales Only).

From Thermionic Conversion Specialist Conference, Miami Beach, Fla.

A program was undertaken at the CEA Center at Saclay in order to define the neutronic properties, diode geometry (axial heterogeneity), and calculation methods related to diode materials such as Mo, W and Ti. This program involves both mathematical analysis and a critical experiment. The two problems are being tackled: a code is being developed and a thermionic reactor mockup is being constructed at the Cadarache EOLE facility. From the results, it is expected to obtain the data necessary for the design of the neutronics of a core based on a 300 W converter, located undersea in a 100 kW reactor. (auth) (France)

20814 (DOCKET-50238–78) N. S. SAVANNAH. Safety Analysis Summary: Defueling. (Maritime Administration, Washington, D. C.). 12 Feb 1971. 52p. Dep. NTIS.

20815 (DOCKET-50238–144) N. S. SAVANNAH. Safety Analysis Summary, Defueling Pages Inadvertently Omitted. (Maritime Administration, Washington, D. C.). 2 Mar 1971. 4p. Dep. NTIS.

20816 (JPRS–52443) VENTILATION AND AIR CONDITIONING ON ATOMIC SHIPS. Features of Design and Installation. Zubarov, D. L.; Ruban, V. M. Translation of Ventilyatsiya i

Konditsionirovanie Vozdukha na Atomnykh Sudakh. Leningrad; Izdatel'stov Sudostroenie (1968). 325p. NTIS.

The design and installation of ventilation and air conditioning systems on atomic powered ships and on the vessels that service them are described. For compartments of the "strict regime zone" (reactor room, turbine room) and compartments of the "free regime zone" (quarters, service and living areas), the required data are presented concerning the health requirements on the atmosphere, selection and justification of the schematic diagrams of special systems and air supply systems, equipment to be used, etc. Particular attention is devoted to the problems that are specific for the stated systems from the viewpoint of ensuring radiation safety measures to prevent the formation and spreading of radioactive contaminants in the air, purification of contaminated air and its venting into the atmosphere, and design features of the equipment of individual assemblies. The features of the equipment and design of air conditioning systems on atomic powered icebreakers are examined. Systems for ventilation, conditioning, purification, and regeneration of air on nuclear submarines are described. 134 references. (auth)

20817 SUBMERSIBLE NUCLEAR REACTOR PLANT. Flaherty, Robert; Ott, David G. (to Westinghouse Electric Corp.). U. S. Patent 3,547,778. 15 Dec 1970. Filed 24 Jul 1967.

A thermoelectric nuclear power plant suitable for underseas operation includes a nuclear reactor, the fuel elements of which are metal-clad ceramic nuclear fuel rods surrounded by tubular thermoelectric generating devices. The reactor core consists of cylindrical fuel assemblies clamped to a plate at their upper ends and separated and guided by a similar plate at their lower ends. These plates are bolted to the ends of a thick-walled cylindrical barrel which serves both as a neutron reflector and as the main structural member of the reactor which is controlled by the rotation of cylindrical drums mounted with their axes parallel to the axis of the core. Rotation of the drums replaces a neutron-reflecting material close to the core with a neutron absorber. The primary coolant of the reactor is de-ionized water which convectively cools the outer surfaces of the fuel assemblies, and transfers this heat to the sea through the tube walls of a heat exchanger which surrounds and is supported by the reflector barrel. The water is circulated by a submersible motor driven propeller-type pump. (auth)

Production Reactors

Refer also to abstract 20190.

Reactor Theory

Kinetics

Refer also to abstract 20377, 20709, 20730, and 20804.

20818 (AAEC/TM-553) A STUDY OF SOME HEAVY WATER MODERATED NATURAL URANIUM SYSTEMS USING THE WIMS CODE. Rose, E. K. (Australian Atomic Energy Commission Research Establishment, Lucas Heights). Aug 1970. 27p. Dep. NTIS (U. S. Sales Only).

The Winfrith code WIMS was used to study some heavy water moderated, natural uranium single-rod lattices and multi-rod clusters. Comparisons of k_{eff} values and some reaction rates with results from other computational methods currently available are reported. (auth) (Australia)

20819 (JAERI-Memo-4165) ^{239}Pu FISSION PRODUCT YIELDS AND THEIR INFLUENCE ON FAST REACTOR CHARACTERISTICS. Hasegawa, Akira; Tone, Tatsuzo; Katsuragi, Satoru (Japan Atomic Energy Research Inst., Tokyo). Oct 1970. 81p. (In Japanese). Dep. NTIS (U. S. Sales Only).

Considering the incident neutron energy dependence of ^{239}Pu fission products (F.P.) mass-yield curve, pseudo fission product cross sections were produced and the effects on the long-term burnup characteristics of a typical fast reactor were examined. It is shown that detailed study of local structure around the peaks of yield curve rather than the valley is essential, and the variation of the yield due to incident neutron energy should be taken into account, especially, for predicting characteristics after high burnup. For producing the F. P. group constants in the future, the status for the yield data and Benzi's procedure of evaluating F.P. neutron capture cross sections were reviewed in detail. 54 references. (auth) (Japan)

20820 (KFKI-71-4) PRODGROUP: A PROGRAM FOR THE PRODUCTION OF MULTIGROUP REACTOR CONSTANTS FROM THE EVALUATED NUCLEAR DATA AVAILABLE AT IAEA. Vertes, P. (Magyar Tudomanyos Akademiya Kozponti Fizikai Kutato Intezete, Budapest). [1968]. 26p. Dep. NTIS (U. S. Sales Only).

The evaluated nuclear data files available at IAEA are used for generating multigroup constant sets for P_1 equations. The method of data handling and calculation is described and the corresponding computer program is presented. 7 references. (auth)

20821 (TKK-F-A-102) INFORMATION THEORFTICAL ASPECTS OF POWER SPECTRUM MEASUREMENTS IN NUCLEAR REACTORS. Baers, Bruno (Technical Univ. of Helsinki, Otaniemi (Finland). Dept. of Technical Physics). 20 Jan 1970. 45p. Dep. NTIS (U. S. Sales Only).

The relative merits of one- and two-detector techniques in power spectrum measurements on nuclear reactors and the influence of various reactor and detector parameters on three different figures of merit were investigated. Two previously used criteria, the ratio between the correlated and the uncorrelated noise power and the relative accuracy of the correlated part of the spectral density, are less general than the information concept. In the general case the auto- and cross-correlation techniques are complementary and the one cannot replace the other. In the first approximation with specific assumptions the information in a set of power spectrum estimates is determined by one single parameter, the equivalent number of degrees of freedom associated with the power spectrum estimates. Explicit expressions for the statistical uncertainty associated with auto- and crosspower spectra are given based on a space- and energy-independent reactor and detector model. The influence of gamma radiation and of the gamma compensation signal on the statistical accuracy is taken into account. 22 references. (auth) (Finland)

20822 (TKK-F-A-137) ON THE VARIETY AND HIERARCHY OF DATA EXTRACTION METHODS IN NUCLEAR REACTOR NOISE ANALYSIS. Baers, Bruno (Technical Univ. of Helsinki, Otaniemi (Finland). Dept. of Technical Physics). 30 Dec 1970. 23p. Dep. NTIS (U. S. Sales Only).

A review and systematic approach to the data extraction problem in nuclear reactor noise analysis is presented. A large number of signal representations and data extraction methods are obtained by using expansions of the fundamental joint probability and related quantities into sets of observable quantities and by using natural classification criteria specifying the experimental conditions. Most of the previously used and suggested techniques are members of this set. A large number of alternate or modified techniques can be suggested some of which may be of practical interest. The hierarchy of representations given also indicates that the application of information theory to noise problems may be a useful and powerful approach. 37 references. (auth) (Finland)

20823 (TKK-F-A-139) IRESINT 2: A FORTRAN PROGRAM FOR CALCULATION OF RESONANCE INTEGRALS. Wasastjerna, Frej (Technical Univ. of Helsinki, Otaniemi (Finland). Dept. of Technical Physics). 31 Dec 1970. 46p. Dep. NTIS (U. S. Sales Only).

The IBM S/360 FORTRAN IV G program IRESINT 2 is described. The program computes heterogeneous resonance integrals for both fissile and non-fissile nuclides, and for resolved and unresolved resonances. The resolved resonances are computed according to the intermediate resonance approximation with or without interference scattering. The geometry has to be a square or hexagonal lattice of cylindrical fuel rods. 19 references. (auth) (Finland)

20824 INTERNAL BOUNDARY CONDITIONS FOR A RING-SHAPED REACTOR. Stojadinovic, A. (INTERATOM, Bensberg, Ger.). Atomwirt., Atomtech.; 15: 575-6(Dec 1970). (In German).

The internal boundary conditions for a ring-shaped reactor are determined essentially by the geometry of the internal cavity. Boundary conditions are proposed which constitute both a significant simplification and a marked improvement over previously existing conditions. (tr-auth)

20825 LIFETIME AND DELAYED NEUTRON FRACTION OF THERMAL THERMIONIC REACTORS. Trunk, M.; Unger, H. (Stuttgart Univ.). Atomkernenergie; 17: 25-6(Feb 1971). (In German).

The neutron flux and importance function are calculated for a thermal thermionic reactor by multigroup diffusion theory. The mean lifetime of the prompt neutrons and the effective neutron fraction are obtained by means of weighting their influence with the importance function. The prompt neutron lifetime is approximately 10^{-5} s. Leakage effects result in an approximately 20% increase in the effective delayed neutron fraction. The transfer function of the reactor, based on these data, is shown. (auth)

20826 RESONANCE-CAPTURE AND -FISSION IN HIGHLY ENRICHED FUEL-LATTICES. Knapp, J.; Emendoerfer, D.; Hausser, B.; Ruehle, R. (Univ., Stuttgart). Atomkernenergie; 17: 127-32(Mar 1971). (In German).

A calculation of group cross sections for ^{235}U in heterogeneous systems is performed. The neutron fluxes are computed numerically from the Boltzmann-equation. The resonance cross sections can be evaluated with the single-level Breit–Wigner-formula or with a multilevel formulation from Adler. The influence of various moderators is examined. With the multilevel cross sections and the resonance parameters from de Saussure group, cross sections for ^{235}U in the fuel-lattice of a moderated incore-thermionic-reactor (ITR) are computed. These values are necessary for the calculation of temperature coefficients. Especially it is examined, if the ITR-cell can be homogenized in various zones. For this purpose calculations for four zones, for two zones and for a completely homogenized cell are made. 20 references. (auth)

20827 PARAMETER ESTIMATION OF COUPLED REACTORS BY CORRELATION METHODS. Schwalm, D. (EURATOM, Ispra, Italy). Atomkernenergie; 17: 140-2Mar 1971).

The theoretical determination of the parameters of kinetic equations of a system of coupled reactors is a difficult problem for complex geometries. These difficulties can be overcome by measuring the input and output signals of the system and applying correlation methods for multiple-input multiple-output linear dynamical systems. A general representation of the frequency responses of a system of coupled reactors is given. 14 references. (auth)

20828 REFORMULATION OF THE REACTOR KINETICS EQUATIONS. Onega, Ronald J. (Virginia Polytechnic Inst., Blacksburg). Nucl. Sci. Eng.; 43: 345-8(Mar 1971).

Reactor kinetics equations are presented which take into account delayed-neutron emitters and secondary decay processes. Burnup of the delayed-neutron precursors with large absorption cross sections is also considered. (D.C.C.)

20829 TEMPERATURE FORMULATION OF THE SPACE-AVERAGED REACTOR KINETICS EQUATIONS. Kurstedt, H. A. Jr.; Miley, G. H. (Univ. of Illinois, Urbana). Nucl. Sci. Eng.; 43: 319-27(Mar 1971).

Techniques are described for the solution of the space-averaged kinetics equations directly in terms of temperature. A good agreement with single and repetitive pulse experimental data from a TRIGA reactor is demonstrated. The results of the method agree not only with the symmetric portion of the pulse but also with the pulse tail. The required feedback and neutron parameters are determined by conventional techniques; however, the heat-transfer decay constant is normalized to experimental data through measurement of the time-dependent reactivity via a double-pulse method. (auth)

Dynamics

20830 (AAEC/TM-551) CLASSIC: A CODE FOR THE STABILITY AND RESPONSE ANALYSIS OF LINEAR SYSTEMS. Thompson, J. J.; Godfrey, M. (Australian Atomic Energy Commission Research Establishment, Lucas Heights). Jul 1970. 98p. Dep. NTIS (U. S. Sales Only).

CLASSIC is a FORTRAN program for single pass execution on an IBM 360/50H computer. It calculates and plots stability boundaries, frequency response functions and real time responses for pulse, step and ramp inputs, using the classic analytical theory of linear systems. Full details of the program are given, including a complete listing of all subroutines and a sample problem. (Australia)

Experimental Applications

20831 (JAERI-Memo-4238) ANALYSIS OF FLUX MEASUREMENT NEAR STRONG ABSORBER USING VISTA METHOD. I. Takeuchi, Eiji; Akimoto, Masayuki; Takeda, Renzo (Japan Atomic Energy Research Inst., Tokyo). Dec 1970. 35p. (In Japanese). Dep. NTIS (U. S. Sales Only).

Using the VISTA method, strong absorber experiments were carried out at SHE reactor. Analytical results of neutron flux distribution near the strong absorber are described. The analyses are based on the one dimensional S_n transport theory and are done by taking into account flux perturbation due to the presence of foils in the system to be measured. Agreement between experiment and calculation is very good. On the other hand, in the JPDR-II cruciformed control rod design, the boundary condition was obtained using the S_n transport theory computer code in multigroups. 8 references. (auth) (Japan)

20832 (ORNL-TM-3245) ANALYTICAL AND EXPERIMENTAL INVESTIGATION OF THE NEUTRON ENERGY EFFECTS ON REACTOR FLUCTUATION SPECTRA. Ackermann, Norbert Joseph Jr. (Oak Ridge National Lab., Tenn.). Feb 1971. Contract W-7405-eng-26. 128p. Dep. NTIS.

Thesis. Submitted to Univ. of Tennessee, Knoxville.

An analytical and experimental investigation of the neutron energy effects on reactor fluctuation spectra was performed to provide some information about the nonpoint model dependence of reactor noise. A two-energy group, one space point reactor kinetics model was developed using the Langevin conjecture. This model predicted no deviation from the one-energy group, point kinetics model in the frequency range of experimental interest except that the cross power spectral density (CPSD) between the two-energy groups was a complex valued function and that the thermal neutron lifetime could be determined directly from the slope of the curve for the tangent of the phase angle of that CPSD. A reactor noise experiment was performed to investigate these effects using an incore detector that was detecting thermal neutrons in the reactor core and an out-of-core detector that was detecting core fast leakage neutrons in the water shield. The auto power spectral density (APSD) of the incore and out-of-core detectors and the CPSD between the two gave results which were in agreement within the experimental uncertainties. However, the tangent of the CPSD phase angle did not give a slope which agreed with the thermal neutron lifetime of the reactor. (36 references) (auth)

20833 (RCN-132) THEORETICAL AND EXPERIMENTAL STUDY OF A FAST-THERMAL COUPLED REACTOR BY CORRELATION TECHNIQUES. Dalfes, Abdi; Tuerkcan, Erdinc; Dragt, Jan B. (Reactor Centrum Nederland, Petten). Nov 1970. 45p. Dep. NTIS (U. S. Sales Only).

The model proposed by Avery to predict the kinetic behavior of coupled reactors in the mean sense is extended to the determination of the correlation functions between counts given by neutron detectors located in the zones. The agreement between theoretical and experimental results confirms this model. Experiments show that the fast-thermal coupled STEK-4000 core behaves as a two-point reactor for delay times of the order of μs. The correlation functions are measured on-line with a small digital computer. 18 references. (auth) (Netherlands)

Reactor Components, Fuels, and Accessories

Refer also to abstracts 18555, 18568, 18570, 18575, 18576, 18584, 18616, 18641, 18651, 18855, 18863, 18881, 19179, 19189, 19222, 19259, 19260, 19262, 19264, 19267–19269, 19288, 19291, 19297, 19536, 20190, and 20232.

20834 (JAERI-Memo-4205) ESTIMATION OF FISSION PRODUCT DECAY HEAT. Sasamoto, Nobuo; Tasaka, Kanji (Japan Atomic Energy Research Inst., Tokyo). Nov 1970. 46p. (In Japanese). Dep. NTIS (U. S. Sales Only).

Fission product decay heat was estimated and compared with other results. Bateman's equation and its integral form were used repeatedly to get analytically the time dependent concentration of each fission product nucleus. With these data, fission product decay heat was analyzed. In analysis, two kinds of data about released energy at every disintegration of fission product were used, one is the sum of β-ray and γ-ray energy and another is the Q_β-value. As a result of analysis, it was seen that an obvious discrepancy between the results was recognized for the cooling time interval zero to nearly 10^2 second and that the results were in good agreement with others after 10^2 seconds cooling time. The ratio of H_β (β-ray decay heat) to H_γ (γ-ray decay heat) was also analyzed. As a result, it was seen that $H_\beta \simeq H_\gamma$ at zero cooling time, $H_\beta \leqq H_\gamma$ from zero up to 10^7 second cooling time and $H_\beta > H_\gamma$ after 10^7 second cooling time. In addition to the analysis of the decay heat, the progress of studies on fission product decay heat is reviewed. 35 references. (auth) (Japan)

20835 (RT/ING-(70)8) DIGITAL PROGRAMS FOR THERMAL DYNAMICS OF A CYLINDRICAL NUCLEAR FUEL ROD AND A HEAT-EXCHANGER TUBE. Petrarca, S.; Cosimo, E. (Comitato Nazionale per l'Energia Nucleare, Rome (Italy)). 24 Mar 1970. 57p. Dep. NTIS (U. S. Sales Only).

FORTRAN IV digital codes used to study the thermal dynamics of a solid or hollow cylinder, with or without distributed heat generation, are presented. Thermal conductivity and diffusivity of the cylinder are assumed to be constant and the thermal power density is uniform. The surfaces of the cylinder are assumed either insulated or in thermal contact with moving fluids; the heat exchange

XUM

coefficients between the cylinder and the fluid are assumed either constant or linearly dependent on fluids flow rates. The codes apply to the fuel rods of many nuclear reactors, to heat exchanger tubes, to electrically or inductively-heated cylinders or tubes, and to other similar cases. The codes described provide transfer functions from thermal power density and from boundary temperatures and flow rates to the cylinder temperature; moreover, they allow the frequency analysis of the cylinder behavior, by means of Bode diagrams of all the transfer functions concerned. 4 references. (auth)

20836 (WHAN-SA-79) STRUCTURE EVOLUTION IN AN OXIDE FUEL PIN. Christensen, J. A. (WADCO Corp., Richland, Wash.). 27 Oct 1970. Contract AT(45-1)-2170. 11p. (CONF-701037-1). Dep. NTIS.

From Meeting of the American Ceramic Society, San Francisco, Calif.

The development of mixed oxide fuel rods is described. Performance characteristics of PuO_2-UO_2 fuel rods are discussed. Radiation effects on structural changes are analyzed. (D.C.C.)

20837 CORE FOR A NUCLEAR REACTOR. (to Reactor Centrum Nederland). British Patent 1,218,764. 13 Jan 1971. Priority date 12 Jun 1967, Netherlands.

REACTORS—core configuration for, with means for assuring uniform neutron flux distribution (H.D.R.)

20838 NUCLEAR REACTOR REFUELING INSTALLATION. Chevereau, Gerard; Denoit, Daniel; Meunier, Jean; Rouge, Pierre. (to Commissariat a l'Energie Atomique). British Patent 1,219,795. 20 Jan 1971. Priority date 21 Apr 1967, France.

REACTOR LOADING MACHINES—design parameters of gas cooled reactor pressure vessel enclosed

REACTORS, GAS COOLED—loading facility for, design of pressure vessel enclosed (H.D.R.)

20839 IMPROVEMENTS IN AND RELATING TO NUCLEAR REACTORS. Jabsen, Felix Stanley (to Babcock and Wilcox Co.). British Patent 1,220,119. 20 Jan 1971. Priority date 10 May 1967, United States.

REACTOR CONTROL ELEMENTS—drive system for, design of reactor coolant actuated hydraulic (H.D.R.)

20840 NUCLEAR REACTOR WITH INTEGRATED HEAT EXCHANGERS. Chollet, Gerard; Giorgi, Danel; Costes, Didier; Thome, Paul (to Commissariat a l'Energie Atomique). U. S. Patent 3,537,420. 3 Nov 1970. Priority date 24 Feb 1967, France.

In order to permit the withdrawal of any one heat exchanger block from a nuclear reactor of the integrated heat exchanger type in which the pressure vessel is provided with only a small number of extraction openings, the heat exchanger blocks are carried on a rotary support. (auth)

20841 COMPUTER-AIDED TELEOPERATOR SYSTEM. Diederich, Norman Francis. Cleveland; Case Western Reserve Univ. (1970). 195p. University Microfilms Order No. 71-1678. Thesis.

An experimental Teleoperator System is presented which utilizes a general purpose digital computer to assist the operator in performing various tasks. A specific task was selected to test the system. This task involves the use of the teleoperator in the disassembly of a model of a nuclear reactor. Several pieces of equipment were constructed to permit the operator to communicate with the teleoperator system through the computer. These devices are described and their use is detailed. The Computer Aided Teleoperator System utilizes a series of algorithms to perform the necessary control functions. These algorithms along with other special functions can be initiated by the operator from the teletype control console. This function is permitted by a teletype executive control routine which handles this selection. By means of this teletype executive routine the operator can indicate the mode of operation desired including manual, semi-automatic, and fully automatic under the control of another executive routine which is controlled by paper tape. Communication paths have been provided to permit the status of various elements of the manipulator (the prime mover portion of the teleoperator system) to be communicated to the computer. These statuses are evaluated and under certain conditions special action is taken. (Diss. Abstr.)

20842 EQUIPMENT FOR THE REMOTE POSITIONING OF THERMOCOUPLES. Lions, Noel (to Commissariat a l'Energie Atomique). French Patent 1,586,506. 12 Jan 1970. Filed 27 Sep 1968. (In French).

The equipment described allows thermocouples to be placed within or withdrawn from the interior of a nuclear reactor while the reactor is in operation. It consists of a long cylindrical guide tube connected at its open end to the reactor cavity and at its other end to a ferrule which presents a considerable reduction in internal cross section to the tube. This ferrule is fixed in relation to the fuel assemblies. A flexible metallic tube is fitted into the outer tube and the thermocouple cable mounted inside. At the sensitive end the thermocouple cable is fixed to the inner tube by a cable clip. The gripping of the cable closes this clip. (France)

20843 IMPROVEMENTS RELATING TO NUCLEAR REACTOR FUEL ELEMENTS. Campbell, Ronald Hugh (to the United Kingdom Atomic Energy Authority). British Patent 1,221,522. 3 Feb 1971. Filed 16 May 1967.

Nuclear reactor fuel elements are considered of the type which, although sheathed, are adapted for the removal from within the sheathing of gases released by the fuel content during operation. Such a fuel element for a fluid cooled nuclear reactor, being an improvement and modification to a previous patent (NSA 22: 25159), is described. Various configurations of the fuel elements to obtain the most efficient discharge of gaseous fission products are given. (UK)

GENERAL

20844 (AEC-tr-7186) METHOD OF CALCULATING THE COEFFICIENTS OF TURBULENT HEAT TRANSFER IN CHANNELS OF A COMPLEX FORM. Bobkov, V. P.; Ibragimov, M. Kh.; Subbotin, V. I. Translation of Russian report. 16p. Dep. NTIS.

20845 (AECL-3781) A METHOD OF ESTIMATING ERRORS IN EXPERIMENTAL DATA. Blair, J. M. (Atomic Energy of Canada Ltd., Chalk River (Ontario). Chalk River Nuclear Labs.). Dec 1970. 12p. Dep. NTIS (U. S. Sales Only).

20846 (AECL-3784) GAUSFIT: A FORTRAN PROGRAM FOR FITTING GAUSSIAN FUNCTIONS. Wong, P. Y. (Atomic Energy of Canada Ltd., Chalk River (Ontario). Chalk River Nuclear Labs.). Dec 1970. 42p. Dep. NTIS (U. S. Sales Only).

20847 (ANL-Trans-875) CERTAIN BIOLOGICAL PREREQUISITES OF LONGEVITY IN MAMMALS AND MAN. Malinovskii, A. A. Translated for Argonne National Lab., Ill., from Tr. Mosk. Obshchest. Ispyt. Prir., Otd. Biol.; 6: 46-50(1962). 7p. Dep. NTIS.

20848 (BDX-613-233) STATE OF CURE OF PRINTED CIRCUIT BOARDS. Steele, J. W.; Atkinson, K. C. (Bendix Corp., Kansas City, Mo.). Jan 1971. Contract AT(29-1)-613. 21p. Dep. NTIS.

20849 (BDX-613-257) CONFORMAL-COATING. Quarterly Report No. 3, 1970. Moyle, W. F. (Bendix Corp., Kansas City, Mo.). Dec 1970. Contract AT(29-1)-613. 15p. Dep. NTIS.

20850 (BDX-613-265) CONFORMAL-COATING. Quarterly Report No. 4, 1970. Moyle, W. F. (Bendix Corp., Kansas City, Mo.). Dec 1970. Contract AT(29-1)-613. 15p. Dep. NTIS.

20851 (BDX-613-310) POLYMERIC CO-DEPOSITION IN GOLD ELECTROPLATE. Davis, M. V. Jr. (Bendix Corp., Kansas City, Mo.). Contract AT(29-1)-613. 78p. Dep. NTIS.

20852 (BDX-613-324) SOLDERABILITY PROBLEMS CAUSED BY GOLD ELECTROPLATE. Davis, M. V. (Bendix Corp., Kansas City, Mo.). Apr 1969. Contract AT(29-1)-613. 9p. Dep. NTIS.

20853 (BRH/DEP-71-1) MICROWAVE MEASUREMENTS AND NEW TYPES OF DETECTORS FOR EVALUATION OF HEALTH HAZARDS. Swicord, Mays L. (Bureau of Radiological Health, Rockville, Md. Div. of Electronic Products). Jan 1971. 33p. NTIS.

20854 (COO-78-235) INTERACTIONS OF Mn^{++} WITH NUCLEOSIDES, DINUCLEOTIDES AND DNA. Anderson, Janet Askue (Case-Western Reserve Univ., Cleveland, Ohio. Dept. of Biology). Jan 1971. 65p. Dep. NTIS.
Thesis.

20855 (DAE-AR-70) ANNUAL REPORT OF THE DEPARTMENT OF ATOMIC ENERGY, GOVERNMENT OF INDIA 1969-70. (Department of Atomic Energy, Bombay (India)). 1970. 88p. NTIS (U. S. Sales Only).

20856 (GAT-T-999) DETAILED DERIVATIONS OF EQUATIONS USED IN THE LIKELIHOOD RATIO METHOD FOR THE PRECISE AND ACCURATE DETERMINATION OF LATTICE PARAMETERS FOR CUBIC MATERIALS. Beu, K. E.; Musil, F. J.; Whitney, D. R. (Goodyear Atomic Corp., Portsmouth, Ohio). 21 Sep 1962. Contract AT(33-2)-1. 15p. Dep. NTIS.

20857 (GEPP-83) HIGH SENSITIVITY ULTRASONIC TEST SYSTEM FOR WELDS. Fessler, P. A.; Michaud, W. E. (General Electric Co., St. Petersburg, Fla. Neutron Devices Dept.). 11 Nov 1970. Contract AT(29-2)-656. 20p. Dep. NTIS.

20858 (IAEA-INIS-6(Rev.2)) INIS: AUTHORITY LIST FOR CORPORATE ENTRIFS. (International Atomic Energy Agency, Vienna (Austria)). Feb 1971. 210p. Dep. NTIS (U. S. Sales Only).

20859 (IS-T-417) CHEMICAL INTERFERENCES AND IONIZATION IN HIGH TEMPERATURE FLAMES. Becker, Donald Arthur (Ames Lab., Iowa). Nov 1970. Contract W-7405-eng-82. 137p. Dep. NTIS.
Thesis.

20860 (IS-T-419) APPLICATION OF THE AUTOXIDATION OF PHENOLIC COMPOUNDS TO THE ANALYSIS OF CATIONS. Wiedmann, Jerome Lee (Ames Lab., Iowa). Nov 1970. Contract W-7405-eng-82. 162p. Dep. NTIS.
Thesis.

20861 (IS-T-420) STUDY OF THE FERMI SURFACES OF ANTIFERROMAGNETIC CHROMIUM-RICH ALLOYS USING THE DE HAAS-VAN ALPHEN EFFECT. Gutman, Edward Joseph (Ames Lab., Iowa). Feb 1971. Contract W-7405-eng-82. 91p. Dep. NTIS.
Thesis.

20862 (IS-T-427) SURFACE MODES OF VIBRATION AND OPTICAL PROPERTIES OF AN IONIC CRYSTAL SLAB. Jones, William Edward (Ames Lab., Iowa). Feb 1971. Contract W-7405-eng-82. 108p. Dep. NTIS.
Thesis.

20863 (IS-T-430) MEASUREMENT OF THE VOLUME DEPENDENCE OF THE HEAT CAPACITY OF SOLID NEON. Fugate, Robert Quentin (Ames Lab., Iowa). Nov 1970. Contract W-7405-eng-82. 151p. Dep. NTIS.
Thesis.

20864 (IS-T-431) PREPARATION AND CHARACTERIZATION OF SOME ALKANETHIOLATOOSMIUM COMPOUNDS. Schobert, Harold Harris (Ames Lab., Iowa). Nov 1970. Contract W-7405-eng-82. 127p. Dep. NTIS.
Thesis.

20865 (IS-T-432) STRUCTURAL, MAGNETIC, AND SPECTROSCOPIC STUDY OF NICKEL SQUARATE DIHYDRATE. Habenschuss, Michael (Ames Lab., Iowa). Nov 1970. Contract W-7405-eng-82. 224p. Dep. NTIS.
Thesis. Submitted to Iowa State Univ., Ames.

20866 (LA-tr-71-4) STRUCTURE OF THE DETONATION FRONT. Held, Manfred. Translated for Los Alamos Scientific Lab., N. Mex.), from Explosivstoffe; No. 11/12, 241-9(1969). 26p. Dep. NTIS.

20867 (LA-tr-71-10) ON THE STABILITY OF A PLANE STATIONARY SHOCK WAVE. Iordanskii, S. V. Translated by Anna Vakar (Los Alamos Scientific Lab., N. Mex.), from Prikl. Mat. Mekh.; 21: 465-72(1957). 12p. Dep. NTIS.

20868 (MATT-Trans-7) INTERPOLATION DEVICE FOR QUICK EXPLOITATION OF RESISTANCE NETWORKS. Lecroart, H. (Commissariat a l'Energie Atomique, Saclay (France). Centre d'Etudes Nucleaires). Translated for Princeton Univ., N. J. from report PA/IGn/RT-119. 24p. Dep. NTIS.

20869 (NBS-SPEC. PUBL-305(Suppl.1)) PUBLICATIONS OF THE NATIONAL BUREAU OF STANDARDS, 1968-1969. A Compilation of Abstracts and Key Word and Author Indexes. Oberholtzer, Betty L. (National Bureau of Standards, Washington, D. C.). Dec 1970. 497p. GPO $4.50.

20870 (NP-18690) PROJECTIONS OF LAND USE AND PUBLIC FACILITY REQUIREMENTS WITH AND WITHOUT THE ACCELERATOR. Preliminary Report VI. (Real Estate Research Corp., Chicago, Ill.). Mar 1969. 64p.
For Illinois Dept. of Business and Economic Development, Springfield.

20871 (NP-18701) REGISTER OF CURRENT SCIENTIFIC RESEARCH AT SOUTH AFRICAN UNIVERSITIES. (Council for Scientific and Industrial Research, Pretoria (South Africa)). 1970. 232p. (In English and Afrikaans). Dep. NTIS (U. S. Sales Only).

20872 (NP-18708) GAS PRESSURE AND ELECTRON DENSITY IN THE ACTIVE ZONE LEVEL OF HOLLOW CATHODE ARC DISCHARGES. Minoo, Habibollah (Paris Univ., Orsay (France). Laboratoire de Physique des Plasmas). Nov 1970. 15p. (In French). (LP-119). Dep. NTIS (U. S. Sales Only).

20873 (NYO-1368-17) CARBOHYDRATE METABOLISM OF OCULAR TISSUES. Progress Report. (Massachusetts Eye and Ear Infirmary, Boston). [1970]. Contract AT(30-1)-1368. 7p. Dep. NTIS.

XUM

20874 (NYO-2391-126) EXPERIMENTAL PHONON PHYSICS. Progress Report, April 1, 1970–March 31, 1971. Pohl, R. O.; Krumhansl, J. A.; Sievers, A. J. (Cornell Univ., Ithaca, N. Y. Lab. of Atomic and Solid State Physics). Contract AT(30-1)-2391. 16p. Dep. NTIS.

20875 (NYO-3562-3) EFFECTS OF A CHANGE OF TERRAIN ON WIND PROFILES. Final Report, July 1, 1965–August 15, 1968. Blackadar, A. K.; Panofsky, H. A. (Pennsylvania State Univ., University Park. Dept. of Meteorology). 15 Dec 1970. Contract AT(30-1)-3562. 83p. Dep. NTIS.

20876 (NYO-3978-4) PROGRESS REPORT, FEBRUARY 1, 1970–FEBRUARY 1, 1971. Lipsicas, Max (Yeshiva Univ., New York. Belfer Graduate School of Science). Contract AT-(30-1)-3978. 7p. Dep. NTIS.

20877 (NYO-3997-6) ANNUAL PROGRESS REPORT. (Rutgers Univ., New Brunswick, N. J.). 1970. 1p. Dep. NTIS.

20878 (NYO-3997-7) SUMMARY PROGRESS REPORT. (Rutgers Univ., New Brunswick, N. J.). [1970]. 4p. Dep. NTIS.

20879 (NYO-4062-5) THERMODYNAMIC AND TRANSPORT PROPERTIES OF INTERSTITIAL HYDROGEN ISOTOPES IN PALLADIUM. Progress Report, April 1, 1970–December 15, 1970. Brown, John S. (Vermont Univ., Burlington). Contract AT(30-1)-4062. 6p. Dep. NTIS.

20880 (NYO-4176-4) COMPRESSIBILITY OF LIQUID METALS, PARTICULARLY LEAD, FROM THEIR MELTING POINTS TO THEIR CRITICAL REGIONS. Grosse, A. V. (Germantown Labs., Inc., Philadelphia, Pa.). Nov 1970. Contract AT(30-1)-4176. 34p. (GL-1970-14). Dep. NTIS.

20881 (NYO-4176-6) A SIMPLE EMPIRICAL RELATIONSHIP BETWEEN THE COMPRESSIBILITY AND TEMPERATURE OF IDEAL LIQUIDS, COVERING THE RANGE FROM MELTING POINT TO CRITICAL POINT, ND ITS APPLICATION TO MERCURY. Grosse, A. V. (Germantown Labs., Inc., Philadelphia, Pa.). 20 Dec 1970. Contract AT(30-1)-4176. 13p. (GL-1970-15). Dep. NTIS.

20882 (ORNL-TM-3082) CONCENTRATION AND DESALTING OF PROTEIN SOLUTIONS PROGRAM. Progress Report for the Period March 1–May 31, 1970. Hancher, C. W.; Ryon, A. D.; Rogers, F. L. (Oak Ridge National Lab., Tenn.). Mar 1971. 21p. Dep. NTIS.

20883 (ORNL-tr-2355) SEQUENTIAL SAMPLING BY VARIABLES WITH KNOWN VARIANCE OF THE OUTPUT AND A SPECIFICATION RANGE WITH AN UPPER AND LOWER LIMIT FOR THE VARIABLES. Stange, K. Translated by R. Gregg Mansfield (Oak Ridge National Lab., Tenn.), from Biom. Z.; 11: No. 1, 1-24(1969). 24p. Dep. NTIS.

20884 (ORO-4061-1) INTERCHANGE OF ESSENTIAL PROGRAMS BETWEEN DISSIMILAR COMPUTERS. Progress Report. Feustel, Edward Alvin (Rice Univ., Houston, Tex. Dept. of Electrical Engineering). 1 Mar 1971. Contract AT(40-1)-4061. 6p. Dep. NTIS.

20885 (RFP-Trans-74(Pt.1)) PRECIPITATE FORMATION. I. PARTICLE SIZE DISTRIBUTION OF THE BARIUM SULFATE PRECIPITATES CONTAINED IN A RAPID-MIXING APPARATUS. Liteanu, C.; Lingner, H. Translated for Dow Chemical Co., Golden, Colo., from Talanta; 17: 1045-52(1970). 10p. Dep. NTIS.

20886 (RFP-Trans-74(Pt.2)) PRECIPITATE FORMATION. II. EFFECT OF SEVERAL FACTORS UPON THE PARTICLE SIZE DISTRIBUTION IN BARIUM SULFATE PRECIPITATES. Liteanu, Candin; Lingner, Harald. Translated for Dow Chemical Co., Golden, Colo., from Talanta; 17: 1053-8(1970). 8p. Dep. NTIS.

20887 (SC-DR-68-812-B) SIDCAP REPORT NO. 2. SANDIA IMAGE DIGITIZER. Cover, R. K. (Sandia Labs., Albuquerque, N. Mex.). Dec 1970. 31p. Dep. NTIS.

20888 (SC-DR-70-686) COMPARISON OF CBW FM/FM AND DSB/FM TELEMETRY SYSTEMS. Johnson, C. S. (Sandia Labs., Albuquerque, N. Mex.). Dec 1970. 57p. Dep. NTIS.

20889 (SC-DR-70-736) SELECTING A TRANSFORMER CORE MATERIAL FOR A HIGH INDUCTION PULSED APPLICATION. Riedel, A. A. (Sandia Labs., Albuquerque, N. Mex.). Oct 1970. 20p. Dep. NTIS.

20890 (SC-DR-70-867) AERODYNAMIC FORCES AND DYNAMIC STABILITY OF A HIGH-SPEED, MAGNETICALLY SUSPENDED ROCKET SLED. Dodd, H. M. Jr.; Preston, D. L. (Sandia Labs., Albuquerque, N. Mex.). Jan 1971. 54p. Dep. NTIS.

20891 (SC-RR-69-506) STOCHASTIC ANALYSIS OF FRACTURED GLASS. Veneruso, A. F.; Braasch, R. H. (Sandia Labs., Albuquerque, N. Mex.). Dec 1970. 46p. Dep. NTIS.

20892 (SC-RR-70-579) DIRECT METHOD FOR THE DISCRETIZED POISSON EQUATION. Roache, P. J. (Sandia Labs., Albuquerque, N. Mex.). Feb 1971. 47p. Dep. NTIS.

20893 (SC-RR-70-650) TRANSFER FUNCTION MODELS OF DTL AND TTL INTEGRATED CIRCUITS. Daniel, M. E.; O'Connell, L. J. (Sandia Labs., Albuquerque, N. Mex.). Dec 1970. 67p. Dep. NTIS.

20894 (SC-RR-70-766) FRACTURE BRANCHING AND DICING IN STRESSED GLASS. Beauchamp, E. K. (Sandia Labs., Albuquerque, N. Mex.). Jan 1971. 26p. Dep. NTIS.

20895 (SCL-CR-710175) PREDICTION OF FATIGUE LIVES OF 2024-T3 AND 6061-T6 ALUMINUM ALLOYS UNDER BROADBAND RANDOM EXCITATION. Lucke, J.; Brown, G. W. (California Univ., Berkeley). Feb 1971. Contracts 20-5637; AT(29-1)-789. 320p. Dep. NTIS.
For Sandia Labs., Livermore, Calif.

20896 (SCL-T-68-253) BEHAVIOR OF ANODIC COATINGS UNDER THERMAL STRESS. Weigel, Juergen. Translated by B. J. Hazzard for Sandia Labs., Albuquerque, N. Mex., from Fachber. Oberflaechentech.; 23-6(Jan–Feb 1967). 22p. Dep. NTIS.

20897 (TID-25656) RADIOTRACER STUDIES OF NUTRIENT CYCLING PATHWAYS. Stark, N. (Nevada Univ., Reno. Desert Research Inst.). [1971]. 18p. Dep. NTIS.

20898 (TID-25664) RELATIONSHIP OF NITROGEN CONTENT TO THE SUSCEPTIBILITY OF AUSTENITIC STAINLESS STEELS TO STRESS CORROSION. Quarterly Report No. 2, September 1, 1970–November 30, 1970. Clevinger, G. S.; Lytton, Jack L. (Virginia Polytechnic Inst., Blacksburg. Dept. of Metals and Ceramic Engineering). Jan 1971. Contract AT-(40-1)-4052. 23p. Dep. NTIS.

20899 (UCLA-12-810) NEAR-ULTRAVIOLET ABSORPTION BANDS OF TRYPTOPHAN. STUDIES USING HORSERADISH PEROXIDASE ISOENZYMES, BOVINE, AND HORSE HEART CYTOCHROME c, AND N-STEARYL-L-TRYPTOPHAN n-HEXYL ESTER. Strickland, E. Hardin; Horwitz, Joseph; Billups, Carolyn (California Univ., Los Angeles. Lab. of Nuclear Medicine and Radiation Biology); Kay, Ernest; Shannon, Leland M. (California Univ., Riverside. Dept. of Biochemistry); Wilchek, Meir (Weizmann Inst. of Science, Rehovoth (Israel)). [1970]. Contract AT-(04-1)-Gen-12. 47p. Dep. NTIS.

20900 (UCRL-20388) CHARACTERIZATION OF THE MATRIX OF BRITTLE MATRIX COMPOSITES. Holzgraf, James Frederick (California Univ., Berkeley. Lawrence Radiation Lab.). Dec 1970. Contract W-7405-eng-48. 19p. Dep. NTIS.
Thesis.

20901 (UCRL-20393) KAOLINITE DEHYDROXYLATION STUDIES ON COMPACT SPECIMENS. Bandyopadhyay, Gautam (California Univ., Berkeley. Lawrence Radiation Lab.). Dec 1970. Contract W-7405-eng-48. 36p. Dep. NTIS.
Thesis.

20902 (UCRL-20395) STRENGTH OF INTERNALLY STRAINED BRITTLE MATRIX COMPOSITES. Young, Christian A. (California Univ., Berkeley. Lawrence Radiation Lab.). Dec 1970. Contract W-7405-eng-48. 20p. Dep. NTIS.
Thesis.

20903 (UCRL-50978) NEW CONCEPTS FOR GEOGRAPHIC POSITION LOCATORS. Gustavson, M. R.; Salisbury, J. D. (California Univ., Livermore. Lawrence Radiation Lab.). 10 Sep 1970. 27p. Dep. NTIS.

20904 (UCSD-34-P-166-X-2) GENETIC ANALYSIS OF DEVELOPMENT OF SLIME MOLDS. Loomis, William F. Jr. (California Univ., San Diego). Mar 1971. Contract AT(04-3)-34. 7p. Dep. NTIS.

20905 VALUES OF THE FUNDAMENTAL PHYSICAL CONSTANTS ACCORDING TO AGREEMENTS IN 1969. Gorbatsevich, S. V.; Holin, V. M.; Nosal, V. N. Meas. Tech. (USSR)(Engl. Transl.); No. 8, 1124-30(Aug 1970).

Translated from Izmer. Tekh.; No. 8, 9-14(Aug 1970).

CORPORATE AUTHOR INDEX

In the Corporate Author Index, technical report literature is indexed by the organization or institution responsible for issuing the report. Entries are given for all report literature and for published literature for which a corporate author approach is especially desirable, e.g., symposium and conference proceedings.

Each entry under a corporate author gives the publication title and the *NSA* volume and abstract numbers. Report numbers, where applicable, are given in parentheses at the end of the entry.

A

- AKADEMIYA NAUK UKRAINSKOI SSR, KIEV. INSTITUT TEORETICHESKOI FIZIKI.
  - Calculation of binding energy and wave function of ^{3}He by harmonic polynomial method, 25:20249 (ITF-70-51-E)
- AKTIEBOLAGET ATOMENERGI, STUDSVIK (SWEDEN).
  - X-ray powder diffraction with Guinier--Haegg focusing cameras, 25:18826 (AE-409)
- ALABAMA POWER CO., BIRMINGHAM.
  - Joseph M. Farley Nuclear Plant, Units 1 and 2. Preliminary safety analysis report, Amendment 10, 25:20674 (DOCKET-50348-16)
- ALLMANNA SVENSKA ELECTRISKA A. B., VASTERAS.
  - Frigg circuit: water chemistry under investigation, 25:20718 (LIB/Trans-308)
- AMES LAB., IOWA.
  - Application of the autoxidation of phenolic compounds to the analysis of cations, 25:20860 (IS-T-419)
  - Chemical interferences and ionization in high temperature flames, 25:20859 (IS-T-417)
  - Measurement of the volume dependence of the heat capacity of solid neon, 25:20863 (IS-T-430)
  - Preparation and characterization of some alkanethiolatoosmium compounds, 25:20864 (IS-T-431)
  - Structural, magnetic, and spectroscopic study of nickel squarate dihydrate, 25:20865 (IS-T-432)
  - Study of fermi surfaces of antiferromagnetic chromium-rich alloys using de Haas-van Alphen effect, 25:20861 (IS-T-420)
  - Surface modes of vibration and optical properties of an ionic crystal slab, 25:20862 (IS-T-427)
- ARGONNE NATIONAL LAB., IDAHO FALLS, IDAHO.
  - Leakrate testing of EBR-II reactor building, 25:20755 (ANL-EBR-8)
- ARGONNE NATIONAL LAB., ILL.
  - Influence of a predominantly oxide fuel loading on the dynamic behavior of EBR-II. EBR-II Project, 25:20704 (ANL-7673)
  - Leakrate testing of EBR-II reactor building, 25:20755 (ANL-EBR-8)
  - Load-equivalence parameters for dynamic loading of structures in the plastic range, 25:18557 (ANL-7677)
  - Penetration and cascade phenomena, 25:19971 (ANL-7727)
  - Prompt-neutron spectra and delayed-neutron spectra from fission: some comments on current knowledge, 25:20362 (ANL-7747)
  - Pyrochemical processing of fuel materials and scrap containing ^{238}Pu, 25:18492 (ANL-7709)
  - Vaporization dynamics of initially static superheated sodium, 25:19191 (ANL-7706)
- ATLANTIC RICHFIELD CO., PHILADELPHIA, PA.
  - ARC Plant. Scheduling of activities related to construction permit application, 25:18497 (DOCKET-50372-3)
- ATLANTIC RICHFIELD HANFORD CO., RICHLAND, WASH.
  - CPDREV: spare parts inventory control system, 25:18558 (ARH-1474)
- ATOMIC ENERGY BOARD, PELINDABA, PRETORIA (SOUTH AFRICA).
  - Comparison of enriched and natural uranium power reactors, 25:20748 (PEL-199)
- ATOMIC ENERGY COMMISSION, BAGHDAD (IRAQ). NUCLEAR RESEARCH INST.
  - Optimum thickness of single crystal neutron monochromators, 25:20234 (PH-4)
  - Prog. rpt. on preservation of dates by γ-radiation, 10/70, 25:19158 (NP-18679)
- ATOMIC ENERGY ESTABLISHMENT, WINFRITH (ENGLAND).
  - Efficiency of a ^{6}Li glass scintillator detector for fast reactor spectrum measurements, 25:18637 (AEEW-M-898)
  - Experiments with stand pipe closure and stand pipe-charge machine connections for proposed HTGC power reactor, 25:20742 (DP-Report-496)
  - Quality control, inspection, and testing of fuel materials for the two uprated fuel elements, 25:18610 (DP-Report-580)
  - Safety aspects of replacement elements in second charge of Dragon reactor, 25:20734 (DP-Report-489)
- ATOMIC ENERGY OF CANADA LTD., CHALK RIVER (ONTARIO). CHALK RIVER NUCLEAR LABS.
  - A method of estimating errors in experimental data, 25:20845 (AECL-3781)
  - A package of computer programs for the analysis of temperature distribution in three dimensional systems, 25:18577 (AECL-3783)
  - Closing the credibility gap in nuclear fuel costs, 25:20731 (AECL-3780)
  - Gausfit: a fortran program for fitting gaussian functions, 25:20846 (AECL-3784)
  - Oxygen: metal ratio effects in (U,Pu)O$_2$ fuels, 25:19287 (AECL-3690)
  - Prog. rpt. on physics, 1--3/70, 25:20307 (AECL-3667)
- ATOMIC ENERGY RESEARCH ESTABLISHMENT, HARWELL (ENGLAND).
  - Behaviour in the atmosphere of the aerosol from a sodium fire, 25:19167 (AERE-R-6460)
  - Caesium behaviour in liquid sodium: the effect of carbon, 25:19192 (CONF-700816-(Vol.1), pp 393-412)
  - Calculation of stress in fast reactor fuel elements, 25:20732 (AERE-R-6516)
  - Cesium behavior in liquid sodium: effect of carbon, 25:20754 (AERE-R-6481)
  - Code reading of dosemeter films in an automatic densitometer, 25:18797 (AERE-R-6224)
  - Effect of acute x-irradiation on development of eggs of plaice, Pleuronectes platessa, 25:19103 (PG-Report-1013)
  - Structure and tensile properties of steel as function of fast irradiation temperature, 25:19251 (AERE-R-6435)
- ATOMIC WEAPONS RESEARCH ESTABLISHMENT, ALDERMASTON (ENGLAND).
  - Evaluation of anti ν for ^{239}Pu, 25:20363 (AWRE-O-86/70)
  - Present status of the design and testing of radioactive filtration installations and associated aerosol research, 25:18559 (CONF-700816-(Vol.1), pp 128-42)
- ATOMICS INTERNATIONAL, CANOGA PARK, CALIF.
  - Behavior of iodine in the presence of sodium oxide aerosols, 25:20761 (CONF-700816-(Vol.1), pp 373-92)
  - Characterization of energy release and aerosol behavior from sodium spray fires, 25:20759 (CONF-700816-(Vol.1), pp 346-55)
  - Comparisons of aerosol experiments with a model used in reactor siting evaluation, 25:20757 (CONF-700816-(Vol.1), pp 26-48)
  - Helium injection as a technique for studying rare gas behavior in carbide fuel, 25:19272 (AI-AEC-12984)
- AUSTRALIAN ATOMIC ENERGY COMMISSION RESEARCH ESTABLISHMENT, LUCAS HEIGHTS.
  - CLASSIC: code for stability and response analysis of linear systems, 25:20830 (AAEC/TM-551)
  - Reactor HIFAR: control arm circuits, 25:20781 (AAEC/M-10)
  - Review of gamma-ray transitions from keV neutron capture, 25:20227 (AAEC/TM-565)
  - Study of some heavy water moderated natural U systems using WIMS code, 25:20818 (AAEC/TM-553)
- AUSTRALIAN NATIONAL UNIV., CANBERRA.
  - Deep sky survey at 2700 MHz, 25:19349 (NP-18682)
- AUSTRALIAN NATIONAL UNIV., CANBERRA. DEPT. OF ENGINEERING PHYSICS.
  - Microwave power transmission ratio: its use in estimating electron density, 25:19656 (EP-RR-21)

B

- BALLISTIC RESEARCH LABS., ABERDEEN PROVING GROUND, MD.
  - DORF-I: gamma-ray spectrograph shielding studies, 25:18732 (AD-711531)

- BARI UNIV. (ITALY). ISTITUTO DI FISICA.
  - General formulation of relativistic theory of particle subcostituents (quarks) in terms of a field vector interaction, 25:19972 (IFPTH-10/70)
- BATTELLE-NORTHWEST, RICHLAND, WASH. PACIFIC NORTHWEST LAB.
  - Calculation of ^{236}Pu and ^{238}Pu in discharge fuel of light water power reactors, 25:20733 (BNWL-1523)
  - Large scale air cleaning tests in the containment systems experiment, 25:20782 (CONF-700816-(Vol.1), pp 102-27)
  - Prog. rpt. on isotopes development, 8--10/70, 25:18590 (BNWL-1308-4)
  - Properties of molten ceramics, 25:19273 (BNWL-SA-3579)
  - Real-time nuclear fuels inventory and criticality control system, 25:18620 (BNWL-1440)
- BENDIX CORP., KANSAS CITY, MO.
  - Conformal-coating, 25:20849 (BDX-613-257)
  - Conformal-coating, 25:20850 (BDX-613-265)
  - Polymeric co-deposition in gold electroplate, 25:20851 (BDX-613-310)
  - Solderability problems caused by gold electroplate, 25:20852 (BDX-613-324)
  - State of cure of printed circuit boards, 25:20848 (BDX-613-233)
- BERN UNIV. (SWITZERLAND). PHYSIKALISCHES INSTITUT.
  - Simulation in space and time of nuclear active and muon components in extensive air showers for primary energies from 10^5 to 10^7 GeV, 25:19973 (INSJ-125)
- BETTIS ATOMIC POWER LAB., PITTSBURGH, PA.
  - Evaluation of the radiative neutron capture cross sections of ^{232}Th for the range 0.0 eV to 15 MeV (LWBR Development Program), 25:20377 (WAPD-TM-971)
- BOSTON EDISON CO., MASS.
  - Pilgrim Nuclear Power Station. Power piping, withdrawal of some recommendations dated January 12, 1971, 25:20652 (DOCKET-50293-37)
  - Pilgrim Nuclear Power Station. Preliminary safety analysis report, Amendment 20 (includes additions and revisions to final safety analysis report), 25:20651 (DOCKET-50293-36)
  - Pilgrim Nuclear Power Station. Preliminary safety analysis report, Amendment 21 (includes additions and revisions to final safety analysis report), 25:20654 (DOCKET-50293-39)
  - Pilgrim Nuclear Power Station. Preoperational environmental radiation survey program. Summary report through August 31 1970, 25:20653 (DOCKET-50293-38)
- BRAUN (C.F.) AND CO., ALHAMBRA, CALIF.
  - Design guide for LMFBR sodium piping, 25:20720 (SAN-781-1)
  - Failure theories as related to LMFBR piping systems, 25:20724 (UNC-5235)
  - LMFBR system requirements for sodium piping, 25:20721 (SAN-781-110)
  - Review of piping and pressure vessel code design criteria, 25:20723 (SAN-781-217)
  - Review of piping failure experience, 25:20722 (SAN-781-214)
- BROOKHAVEN NATIONAL LAB., UPTON, N. Y.
  - Concrete-polymer materials. Third topical report, 25:19292 (BNL-50275)
  - Design study of a Cold Magnet Synchrotron, 25:20125 (BNL-15430)
  - Safeguards applications for isotopic neutron sources, 25:18619 (BNL-50267)
  - Safeguards glossary, 25:18626 (WASH-1162)
- BROWN UNIV., PROVIDENCE, R. I. DEPT. OF PHYSICS.
  - Helicity poles, triple Regge behavior and single particle spectra in high energy collisions, 25:19926 (NYO-2262-TA-234)
  - Method of extending Blankenbecler--Sugar--Logunov--Tavkhelidze approximation to Bethe--Salpeter equation, 25:20104 (NYO-2262-TA-231)
  - Okubo's second-class currents in K/sub 12/ and K/sub 13/ decays, 25:19965 (NYO-2262-TA-236)
  - Super-eikonal model of deep inelastic electron-proton scattering, 25:19939 (NYO-2262-TA-221)
- BROWN UNIV., PROVIDENCE, R. I. DIV. OF ENGINEERING.
  - Three-dimensional elastic--plastic stress and strain analysis for fracture mechanics. Phase I. Simple flawed specimens, 25:18611 (HSSTP-TR-12)
- BUREAU OF RADIOLOGICAL HEALTH, ROCKVILLE, MD.
  - Biological aspects of laser radiation: a review of hazards, 25:19133 (NP-18714)
  - Cyclotron production of ^{123}I: an evaluation of the nuclear reactions which produce this isotope, 25:18480 (BRH/DMRE-70-4)
  - Review of radium toxicity studies, 25:18979 (BRH/DBE-70-5)
- BUREAU OF RADIOLOGICAL HEALTH, ROCKVILLE, MD. DIV. OF ELECTRONIC PRODUCTS.
  - Inexpensive readout for a commercial thermocouple microwave power density probe, 25:18827 (BRH/DEP-70-31)
  - Microwave measurements and new types of detectors for evaluation of health hazards, 25:20853 (BRH/DEP-71-1)
- BUREAU OF RADIOLOGICAL HEALTH, WINCHESTER, MASS. NORTHEASTERN RADIOLOGICAL HEALTH LAB.
  - Calibration and initial field testing of ^{85}Kr detectors for environmental monitoring around a nuclear fuel reprocessing plant, 25:18638 (CONF-700816-(Vol.1), pp 143-74)
- BUREAU OF RECLAMATION, DENVER, COLO.
  - Concrete-polymer materials. Third topical report, 25:19292 (BNL-50275)

C

- CALIFORNIA INST. OF TECH., PASADENA. ARTHUR A. NOYES LAB. OF CHEMICAL PHYSICS.
  - Puzzles in the diffusion kinetics of the radiation chemistry of aqueous solutions, 25:18447 (CALT-767-P-4-73)
- CALIFORNIA UNIV., BERKELEY.
  - Prediction of fatigue lives of 2024-T3 and 6061-T6 aluminum alloys under broad-band excitation, 25:20895 (SCL-CR-710175)
- CALIFORNIA UNIV., BERKELEY. LAWRENCE RADIATION LAB.
  - Characterization of the matrix of brittle matrix composites, 25:20900 (UCRL-20388)
  - Isolation and genetic characterization of recombination deficient mutants in Saccharomyces cerevisiae, 25:18945 (UCRL-20192)
  - Kaolinite dehydroxylation studies on compact specimens, 25:20901 (UCRL-20393)
  - Lecture 3: nonequilibrium defects in metals, 25:19232 (UCRL-19696)
  - NN and ND interactions (above 0.5 GeV/c), 25:19899 (UCRL-20000-NN)
  - Semiconductor detectors in high-energy physics, 25:18775 (UCRL-20042)
  - Strength of internally strained brittle matrix composites, 25:20902 (UCRL-20395)
- CALIFORNIA UNIV., LIVERMORE. LAWRENCE RADIATION LAB.
  - Equation of state for dense hydrogen from zero to 10,000°K, 25:19472 (UCRL-50985)
  - Integrated system for production of neutronics and photonics calculational constants, 25:20237 (UCRL-50400(Vol.9))
  - New concepts for geographic position locators, 25:20903 (UCRL-50978)
  - Theory identification for mechanical behavior of polystyrene bead foams, 25:19293 (UCRL-50952)
  - Weapons effect display system (WEDS MOD II): prompt effects computer program, 25:18832 (UCRL-50892(Vol.6))
  - Weapons effects display system (WEDS MOD II): mathematical models used for calculations, 25:18831 (UCRL-50892(Vol.1))
- CALIFORNIA UNIV., LOS ANGELES. LAB. OF NUCLEAR MEDICINE AND RADIATION BIOLOGY.
  - Near-uv absorption bands of tryptophan, 25:20899 (UCLA-12-810)
- CALIFORNIA UNIV., RIVERSIDE. DEPT. OF BIOCHEMISTRY.
  - Near-uv absorption bands of tryptophan, 25:20899 (UCLA-12-810)
- CALIFORNIA UNIV., SAN DIEGO.
  - Prog. rpt. on genetic analysis of development of slime molds, 3/71, 25:20904 (UCSD-34-P-166-X-2)
- CAROLINA POWER AND LIGHT CO., RALEIGH, N.C.
  - Brunswick Steam Electric Plant, Units 1 and 2. Small steam line break. Design report No. 8, 25:20670 (DOCKET-50324-19)
  - H. B. Robinson Unit No. 2. Abnormal occurrence report, 25:20594 (DOCKET-50261-51)
  - H. B. Robinson Unit No. 2. Technical specifications proposed change to make allowance for use of respiratory protective equipment, 25:20639 (DOCKET-50261-52)
- CASE WESTERN RESERVE UNIV., CLEVELAND, OHIO. DEPT. OF BIOLOGY.
  - Interactions of Mn^{++} with nucleosides, dinucleotides and DNA, 25:20854 (COO-78-235)
- CENTRE NATIONAL DE LA RECHERCHE SCIENTIFIQUE, MARSEILLES (FRANCE). CENTRE DE PHYSIQUE THEORIQUE.
  - Colloquium on computational methods in theoretical physics, Marseilles, France, 6/70, 25:20054 (CNRS-CPT-70-P-335)
  - Evaluation of the electron anomalous magnetic moment by computer, 25:20055 (CNRS-CPT-70-P-335, pp IV.26-38)
- CESKOSLOVENSKA AKADEMIE VED, REZ. USTAV JADERNEHO VYZKUMU.
  - Problems on sorption equilibrium in ion exchange column for microquantities of radioactive solution in the presence of competing ion, 25:18504 (UJV-2450-Ch)
  - Single-crystal filters of thermal neutrons, 25:20238 (UJV-2488-F)
- CHALMERS TEKNISKA HOGSKOLA, GOTEBORG (SWEDEN).
  - Combined field-ion and electron microscope studies of grain boundaries in tungsten, 25:19249
- COLORADO STATE UNIV., FORT COLLINS. DEPT. OF RADIOLOGY AND RADIATION BIOLOGY.
  - Prog. rpt. on $^{210}PoO_2$ metabolism in ruminants, annual, 1/15/70--1/15/71, 25:18890 (COO-2044-3)
- COMITATO NAZIONALE PER L'ENERGIA NUCLEARE, ROME (ITALY).
  - Analysis of micro constituents in Zr matrix. I, 25:18341 (RT/CHI-(70)14)
  - Digital programs for thermal dynamics of a cylindrical nuclear fuel rod and a heat-exchanger tube, 25:20835 (RT/ING-(70)8)
  - Isotopic analysis of UO_2 and application to stream analysis, 25:18358 (RT/CHI-(70)18)
  - Preparation of complex-group resins and synthesis of phenolic resins with hydroxamic groups. I and II,

- 25:18503 (RT/CHI-(70)25)

COMMISSARIAT A L'ENERGIE ATOMIQUE, BRUYERES-LE-CHATEL (FRANCE). CENTRE D'ETUDES.

- Intermetallic diffusion of plutonium in Pu--Cu and Pu--U systems, 25:19230 (CEA-R-3951)

COMMISSARIAT A L'ENERGIE ATOMIQUE, CHUSCLAN (FRANCE). CENTRE DE PRODUCTION DE PLUTONIUM DE MARCOULE.

- Decladding and dissolution of UO_2 and PuO_2 fuels, clad with stainless steel or Zircaloy, 25:18493 (CEA-Bib-191)

COMMISSARIAT A L'ENERGIE ATOMIQUE, FONTENAY-AUX-ROSES (FRANCE). CENTRE D'ETUDES NUCLEAIRES.

- Analytical methods used by Geochemical Section: water, 25:18339 (CEA-R-3557(2))
- Biochemical considerations on alveolar retention of liquid rare earth aerosols, 25:18889 (CEA-CONF-1676)
- Biological dosimetry of an ultraviolet radiation source using Saccharomyces cerivisiae, 25:18981 (CEA-N-1380)
- Comparative study on whole-body exposure injuries, 25:19012 (CEA-CONF-1695)
- ELF program: description of utilization, 25:20233 (ORNL-tr-2409)
- Hematological and chromosomic aspects of dosimetry in irradiated man, 25:18980 (CEA-CONF-1698)
- Improvement to quantum yield of photocathodes of 56 TVP photomultipliers in red part of spectrum (7000 A), 25:18828 (EUR-CEA-FC-576)
- Radiological accidents rules, 25:18975 (CEA-N-1365)

COMMISSARIAT A L'ENERGIE ATOMIQUE, GRENOBLE (FRANCE). CENTRE D'ETUDES NUCLEAIRES.

- Application of photoelectron spectroscopy to chemical analysis, 25:18338 (CEA-CONF-1725)
- Study and development of cadmium telluride detectors for gamma-ray spectrometry, 25:18733 (CEA-R-4052)

COMMISSARIAT A L'ENERGIE ATOMIQUE, LIMEIL-BREVANNES (FRANCE). CENTRE D'ETUDES.

- Study of reactions ^{9}Be + t below Coulomb barrier, 25:20265 (CEA-R-4117)

COMMISSARIAT A L'ENERGIE ATOMIQUE, SACLAY (FRANCE). CENTRE D'ETUDES NUCLEAIRES.

- Detection of local boiling in light water reactors, 25:20716 (CEA-R-4118)
- Interpolation device for quick exploitation of resistance networks, 25:20868 (MATT-Trans-7)
- Prog. rpt. on physical chemistry service, 7--12/69, 25:18448 (CEA-N-1369)
- Study of (p,d) reactions on ^{118}Sn and ^{119}Sn with polarized protons, 25:20365 (CEA-CONF-1657)
- Thermionic reactor: neutronic study of a light water moderated core, 25:20813 (CEA-CONF-1727)

COMMONWEALTH EDISON CO., CHICAGO, ILL.

- Dresden Nuclear Power Station, Unit 1. Additional information relative to clarification of technical specifications, 25:20601 (DOCKET-50010-80)
- Dresden Nuclear Power Station, Unit 1. Annual report, 1970, 25:20575 (DOCKET-50010-78)
- Dresden Nuclear Power Station, Unit 1. Crack in a 4 inch stainless steel pipe of the primary piping system, 25:20576 (DOCKET-50010-79)
- Dresden Nuclear Power Station, Unit 2. Technical specifications revision, 25:20588 (DOCKET-50237-143)
- Dresden Nuclear Power Station, Unit 3. Summary technical report of primary containment leak rate test, 25:20628 (DOCKET-50249-59)
- Dresden Nuclear Power Station, Unit 3. Technical specifications on radioactivity in liquid storage exceeded, 25:20593 (DOCKET-50249-57)
- Quad-Cities Station, Units 1 and 2. Preliminary safety analysis report, Amendment 18, 25:20635 (DOCKET-50254-30)
- Quad-Cities Station, Units 1 and 2. Preliminary safety analysis report, Amendment 17, 25:20634 (DOCKET-50254-29)
- Quad-Cities Station, Units 1 and 2. Preliminary safety analysis report, Amendment 20, 25:20636 (DOCKET-50254-31)
- Quad-Cities Station, Units 1 and 2. Preoperational environmental monitoring (thermal) of the Mississippi River, July 1969--June 1970, 25:20633 (DOCKET-50254-28)
- Zion Station, Units 1 and 2. Containment spray systems full flow ring header tests, 25:20655 (DOCKET-50295-24)

CONNECTICUT YANKEE ATOMIC POWER CO., HADDAM.

- Connecticut Yankee Atomic Power Plant. Operation report No. 71-1, January 1971, 25:20585 (DOCKET-50213-99)

CONNECTICUT YANKEE ATOMIC POWER CO., HARTFORD.

- Connecticut Yankee Atomic Power Plant. Operational environmental radiation monitoring program. Summary report, January--December 1970, 25:20617 (DOCKET-50213-98)

CONSOLIDATED EDISON CO. OF NEW YORK, INC., NEW YORK.

- Indian Point Station, Unit No. 1. Semiannual operations report No. 16, April 1--September 30, 1970, 25:20574 (DOCKET-50003-65)

CONSUMERS POWER CO., JACKSON, MICH.

- Big Rock Point Nuclear Plant. Flows associated with core spray and containment spray systems, 25:20616 (DOCKET-50155-75)
- Big Rock Point Nuclear Plant. License No. DPR-6; proposed technical specifications Change No. 24, additional information, 25:20610 (DOCKET-50155-67)
- Big Rock Point Nuclear Plant. License No. DPR-6; proposed technical specifications Change No. 27, additional information, 25:20614 (DOCKET-50155-72)
- Big Rock Point Nuclear Plant. License No. DPR-6; proposed technical specifications Change No. 27, additional information, 25:20613 (DOCKET-50155-71)
- Big Rock Point Nuclear Plant. Reworking of orifices, 25:20615 (DOCKET-50155-74)
- Big Rock Point Nuclear Plant. Semiannual report of operations, July 1--December 31, 1970, 25:20583 (DOCKET-50155-68)
- Palisades Plant. Preliminary safety analysis report, Amendment 21 (includes additions and revisions to final safety analysis report), 25:20637 (DOCKET-50255-33)

CONSUMERS PUBLIC POWER DISTRICT, COLUMBUS, NEBR.

- Cooper Nuclear Station. Preliminary safety analysis report, Amendment 7. Final safety analysis report, Vol. 1, 25:20656 (DOCKET-50298-13)
- Cooper Nuclear Station. Preliminary safety analysis report, Amendment 7. Final safety analysis report, Vol. 3, 25:20658 (DOCKET-50298-15)
- Cooper Nuclear Station. Preliminary safety analysis report, Amendment 7. Final safety analysis report, Vol. 4, 25:20659 (DOCKET-50298-16)
- Cooper Nuclear Station. Preliminary safety analysis report, Amendment 7. Annual report, 1969, 25:20662 (DOCKET-50298-20)
- Cooper Nuclear Station. Preliminary safety analysis report, Amendment 7. Final safety analysis report, Vol. 2, 25:20657 (DOCKET-50298-14)
- Cooper Nuclear Station. Preliminary safety analysis report, Amendment 7. Final safety analysis report, Vol. 6, 25:20660 (DOCKET-50298-18)
- Cooper Nuclear Station. Preliminary safety analysis report, Amendment 7. Final safety analysis report, Vol. 7, 25:20661 (DOCKET-50298-19)

CORNELL UNIV., ITHACA, N. Y. LAB. OF ATOMIC AND SOLID STATE PHYSICS.

- Prog. rpt. on experimental phonon physics, 4/70--3/71, 25:20874 (NYO-2391-126)

COUNCIL FOR SCIENTIFIC AND INDUSTRIAL RESEARCH, PRETORIA (SOUTH AFRICA).

- Register of current scientific research at South African universities, 25:20871 (NP-18701)

D

DAIRYLAND POWER COOPERATIVE, LA CROSSE, WIS.

- La Crosse Boiling Water Reactor. Forced plant shutdown resulting from a low flow scram caused by forced circulation pump 1B trip, 25:20570 (DOCKET-1155-101)
- La Crosse Boiling Water Reactor. Monthly operating report, November 1970, 25:20571 (DOCKET-1155-102)
- La Crosse Boiling Water Reactor. Monthly operating report, December 1970, 25:20573 (DOCKET-1155-104)
- La Crosse Boiling Water Reactor. Plant electrical power failure, 25:20569 (DOCKET-1155-100)
- La Crosse Boiling Water Reactor. Unplanned reactor shutdown, 25:20572 (DOCKET-1155-103)

DANISH ATOMIC ENERGY COMMISSION, RISOE. RESEARCH ESTABLISHMENT.

- Thermal neutron spectroscopy using position-sensitive detectors together with fourier correlation time-of-flight and single-crystal techniques, 25:18738 (RISO-229)

DELAWARE UNIV., NEWARK. DEPT. OF PHYSICS.

- Prog. rpt. on radiation induced defects in alkali halides, and their role in recombination processes, final, 3/1/67--7/15/70, 25:19770 (NYO-3842-12)

DEMOCRITUS NUCLEAR RESEARCH CENTER, ATHENS (GREECE).

- A non linear equation for the correlation function between an impurity particle and a nucleon in nuclear matter, 25:20001 (DEMO-70/19)
- Estimate of the binding energy of ^{16}O with matrix elements of effective interaction, 25:20266 (DEMO-70/25)
- Is veneziano model consistent with the yang-mills coupling of vector meson fields, 25:19985 (DEMO-71/1)
- Remarks on the eta $\to \pi^{0} \gamma \gamma$ decay rate, 25:19937 (DEMO-71/2)

DEPARTMENT OF ATOMIC ENERGY, BOMBAY (INDIA).

- Progress report, annual, 1969-70, 25:20855 (DAE-AR-70)

DETROIT EDISON CO., MICH.

- Enrico Fermi Atomic Power Plant, Unit 2. Preliminary safety analysis report, Amendment 17, 25:20673 (DOCKET-50341-27)

DEUTSCHE VERSUCHSANSTALT FUER LUFT- UND RAUMFAHRT E.V., STUTTGART (WEST GERMANY).

- Collision dominated sheath in weakly ionized plasmas. II, 25:19673 (DLR-FB-69-78)

DEUTSCHES ELEKTRONEN-SYNCHROTRON, HAMBURG (WEST GERMANY).

- Photoproduction of pion pairs with high invariant mass, 25:19886 (DESY-70/61)
- Renormalization of theories with broken symmetry, 25:20056 (DESY-70/62)

DIVISION OF COMPLIANCE (AEC), WASHINGTON, D.C.

- Oyster Creek Nuclear Power Plant, Unit No. 1. Noncompliance with provisions of technical specifications revealed by inspections, 25:20586 (DOCKET-50219-123)

XUM

DIVISION OF MATERIALS AND LICENSING (AEC), WASHINGTON, D. C.
West Valley Reprocessing Plant. Comments on nonpropriety portion of Revision 6 to final safety analysis report, 25:18496 (DOCKET-50201-65)
DIVISION OF REACTOR DEVELOPMENT AND TECHNOLOGY (AEC), WASHINGTON, D. C.
Proceedings of the eleventh AEC air cleaning conference held in the Federal Building, Richland, Washington, August 31--September 3, 1970, 25:18525 (CONF-700816-(Vol.1))
DIVISION OF REACTOR LICENSING (AEC), WASHINGTON, D. C.
Big Rock Point Nuclear Plant. License No. DPR-6; technical specifications Change No. 25, 25:20612 (DOCKET-50155-70)
Big Rock Point Nuclear Plant. License No. DPR-6; technical specifications Change No. 23, 25:20611 (DOCKET-50155-69)
Dresden Nuclear Power Station, Unit 3. Facility Operating License No. DPR-25; technical specifications (Appendix A) Change No. 1, 25:20627 (DOCKET-50249-58)
Dresden Nuclear Power Station, Unit 3. Facility Operating License No. DPR-25, Amendment 1, 25:20629 (DOCKET-50249-60)
Enrico Fermi Atomic Power Plant, Unit 1. License No. DPR-9. Technical Specifications Change No. 20, 25:20604 (DOCKET-50016-102)
Monticello Nuclear Generating Plant, Unit 1. Operation at 1670 Mw thermal approved, 25:20640 (DOCKET-50263-55)
Nine Mile Point Nuclear Station. Provisional Operating License No. DPR-17, Amendment 2 (authorization for power increase to 1850 megawatts (thermal)), 25:20620 (DOCKET-50220-59)
North Anna Power Station, Unit 1. Construction Permit No. CPPR-77, 25:20671 (DOCKET-50338-27)
North Anna Power Station, Unit 2. Construction Permit No. CPPR-78, 25:20672 (DOCKET-50339-26)
Oyster Creek Nuclear Power Plant, Unit No. 1. Control rod drives, 25:20619 (DOCKET-50219-125)
Point Beach Nuclear Plant, Unit No. 2. Proposed Facility Operating License No. DPR-27, 25:20663 (DOCKET-50301-28)
Vermont Yankee Nuclear Power Station. Draft detailed statement on the environmental considerations, 25:20645 (DOCKET-50271-39)
Yankee Nuclear Power Station. License No. DPR-3; technical specifications Change No. 87, 25:20606 (DOCKET-50029-146)
Yankee Nuclear Power Station. License No. DPR-3; technical specifications Change No. 88, 25:20605 (DOCKET-50029-144)
DOW CHEMICAL CO., GOLDEN, COLO. ROCKY FLATS DIV.
Recovery of niobium from niobium--uranium alloys: an annotated bibliography, 25:18502 (RFP-1421)
DU PONT DE NEMOURS (E.I.) AND CO., AIKEN, S. C. SAVANNAH RIVER LAB.
Computer program for correlation and spectral analysis of reactor flow data, 25:20710 (DP-1244)
Prog. rpt. on ^{60}Co power and heat sources, 7--9/70, 25:18591 (DP-1254)
Zeolite prefilter to reduce pluggage in zeolite cesium removal column, 25:18621 (DP-1245)
DUKE POWER CO., CHARLOTTE, N.C.
McGuire Nuclear Station, Units 1 and 2. Environmental report, 25:20679 (DOCKET-50369-6)

E

EUROPEAN ATOMIC ENERGY COMMUNITY.
Measurements of neutron elastic scattering from carbon in energy region of 0.50 to 2.00 MeV, 25:20267 (EUR-4538)
EUROPEAN ATOMIC ENERGY COMMUNITY, GEEL (BELGIUM). CENTRAL NUCLEAR MEASUREMENTS BUREAU.
Measurements of neutron elastic scattering from carbon in energy region of 0.50 to 2.00 MeV, 25:20267 (EUR-4538)
EUROPEAN ORGANIZATION FOR NUCLEAR RESEARCH, GENEVA (SWITZERLAND).
Anomalous magnetic moments of the electron and the muon, 25:19936 (CNRS-CPT-70-P-335, pp IV.1-15)
Compilation of cross sections V--K^- induced reactions, 25:19909 (CERN-HERA-70-6)
New theoretical value for Lamb shift, 25:19512 (CNRS-CPT-70-P-335, pp IV.16-25)

F

FLORIDA POWER AND LIGHT CO.
Turkey Point Plant, Units No. 3 and No. 4. Preliminary safety analysis report, [Amendment 31], Suppl. 31 (includes final safety analysis report, Rev. 10), 25:20630 (DOCKET-50250-39)
Turkey Point Plant, Units No. 3 and No. 4. Preliminary safety analysis report, Amendment 32, Suppl. 32 (includes final safety analysis report, Rev. 11), 25:20631 (DOCKET-50250-40)
Turkey Point Plant, Units No. 3 and No. 4. Preliminary safety analysis report, Amendment 33, Suppl. 33 (includes final safety analysis report, Rev. 12), 25:20632 (DOCKET-50250-41)
FORSKNINGSRADENS LABORATORIUM, STUDSVIK (SWEDEN).
Mass spectrometric studies on negative ion--molecule reactions of nitroethylene, 25:18428 (NP-18676)
FORSVARETS FORSKNINGSANSTALT, STOCKHOLM (SWEDEN).
Thermonuclear reactions through laser radiation of fusion materials, 25:19724 (FOA-4-4449)
FORUM ATOMIQUE EUROPEEN.
Future of reprocessing in Europe, 25:18500 (NP-18669)
FRANKLIN INST. RESEARCH LABS., PHILADELPHIA, PA.
Static seals and their application in water-cooled nuclear reactor systems, 25:20719 (ORNL-TM-3308)

G

GENERAL ELECTRIC CO., CINCINNATI, OHIO. NUCLEAR SYSTEMS PROGRAMS.
Production of dense thoria, 25:19259 (NLCO-1029)
GENERAL ELECTRIC CO., ST. PETERSBURG, FLA. NEUTRON DEVICES DEPT.
High sensitivity ultrasonic test system for welds, 25:20857 (GEPP-83)
GENERAL ELECTRIC CO., SUNNYVALE, CALIF. BREEDER REACTOR DEVELOPMENT OPERATION.
Design and testing of the SEFOR Fast Reactivity Excursion Device (FRED), 25:20693 (GEAP-13649)
Southwest Experimental Fast Oxide Reactor. License No. DR-15; replacement pages for Revision No. 1 of technical specifications Proposed Change No. 4, 25:20786 (DOCKET-50231-71)
Southwest Experimental Fast Oxide Reactor. Malfunction of a safety system trip relay, 25:20744 (DOCKET-50231-72)
GEOLOGICAL SURVEY, DENVER, COLO.
Radiochemical analysis of water from wells, springs, and streams in central Nevada, 25:18522 (USGS-474-97)
GEORGIA INST. OF TECH., ATLANTA. ENGINEERING EXPERIMENT STATION.
Prog. rpt. on radiation chemistry of mono-substituted aromatic compounds, 1/15/70--1/15/71, 25:18450 (ORO-3519-8)
GEORGIA POWER CO., ATLANTA.
Edwin I. Hatch Nuclear Plant, Unit 1. Supplementary information to the preliminary safety analysis report, 25:20669 (DOCKET-50321-17)
Edwin I. Hatch Nuclear Plant, Units 1 and 2. Environmental report, 25:20668 (DOCKET-50321-16)
GEORGIA UNIV., ATHENS. SCHOOL OF FOREST RESOURCES.
Prog. rpt. on bioaccumulation of gamma-emitting radionuclides in white-tailed deer, annual, 2/70--1/71, 25:18935 (ORO-3905)
GERMANTOWN LABS., INC., PHILADELPHIA, PA.
Compressibility of liquid metals, particularly lead, from their melting points to their critical regions, 25:20880 (NYO-4176-4)
Simple empirical relationship between compressibility and temperature of ideal liquids, 25:20881 (NYO-4176-6)
GESELLSCHAFT FUER KERNFORSCHUNG m.b.H., KARLSRUHE (WEST GERMANY).
Plutonium-documentation, Vol. 4, No. 12, 1970, 25:19166
GOODYEAR ATOMIC CORP., PORTSMOUTH, OHIO.
Detailed derivations of equations used in the likelihood ratio method for the precise and accurate determination of lattice parameters for cubic materials, 25:20856 (GAT-T-999)
GOSUDARSTVENNYI KOMITET PO ISPOL'ZOVANIYU ATOMNOI ENERGII SSSR, MOSCOW. INSTITUT ATOMNOI ENERGII.
Material balance of plasma column and gas sheath in toroidal apparatus-Tokamak-3, 25:19657 (MATT-Trans-16)
GOSUDARSTVENNYI KOMITET PO ISPOL'ZOVANIYU ATOMNOI ENERGII SSSR, SERPUKHOV. INSTITUT FIZIKI VYSOKIKH ENERGII.
Calculation of box diagram effects with two resonances in the intermediate state, 25:19986 (IFVE-STF-70-34)
Device with snap-off diode for compensation of influence of pulse amplitude spread of scintillation and Cherenkov counters, 25:18639 (IFVE-SEF-69-44)
Do K-meson nuclei exist, 25:20002 (IFVE-STF/SPK-70-30)
High-pressure gas target cooled by liquid nitrogen, 25:20128 (IFVE-SEF-70-22)
Results on complex adjustment and start-up of the IHEP proton synchrotron, 25:20127 (CERN-Trans-70-12)
Time resolution of scintillation counters, 25:18640 (IFVE-SEF-70-23)
Vacuum system for the 70-GeV proton synchrotron, 25:20126 (CERN-Trans-70-9)
GRENOBLE UNIV. (FRANCE).
Decay of 16.11-MeV level of ^{12}C into 3 α particles, 25:20270 (NP-18626)
Study and development of cadmium telluride detectors for gamma-ray spectrometry, 25:18733 (CEA-R-4052)
GRONINGEN RIJKSUNIVERSITEIT (NETHERLANDS).
Hyperthyroidism, radioiodine and thereafter, 25:19062 (NP-18693)
GULF GENERAL ATOMIC, INC., SAN DIEGO, CALIF.
Review of Gulf General Atomic support of the High Temperature Lattice Test Reactor program, 25:20787 (GAMD-10231)

H

- HARVARD SCHOOL OF PUBLIC HEALTH, BOSTON, MASS.
  - Behavior of iodine in sodium systems, 25:20760 (CONF-700816-(Vol.1), pp 356-72)
  - Comparison of equations used in the design of fission gas adsorption beds, 25:18560 (CONF-700816-(Vol.1), pp 207-15)
  - Design of fission gas holdup systems, 25:18561 (CONF-700816-(Vol.1), pp 216-23)
  - Heat transfer of sodium compounds deposited on surfaces from aerosols, 25:18562 (CONF-700816-(Vol.1), pp 413-24)
  - Optical properties of sodium aerosols, 25:19193 (CONF-700816-(Vol.1), pp 425-44)
  - Sodium aerosol filtration studies, 25:18563 (CONF-700816-(Vol.1), pp 445-58)
- HARVARD UNIV., BOSTON, MASS. HARVARD AIR CLEANING LAB.
  - Proceedings of the eleventh AEC air cleaning conference held in the Federal Building, Richland, Washington, August 31--September 3, 1970, 25:18525 (CONF-700816-(Vol.1))
- HELSINKI UNIV. (FINLAND).
  - Polonium and radiolead in some land animals in Finland, 25:18929 (NYO-3446-14, Paper 26)
- HELSINKI UNIV. (FINLAND). DEPT. OF RADIOCHEMISTRY.
  - Body burden of ^{137}Cs and radiation dose of population group in Finnish Lapland, 25:18987 (NYO-3446-14, Paper 29)
  - Chemical and radioactive environmental problems in Finland, 25:18931 (NYO-3446-14, Paper 30)
  - Environmental γ-radiation dose rate in Finnish Lapland and Southern Finland, 25:18986 (NYO-3446-14, Paper 28)
  - Polonium and radiolead in some aqueous ecosystems in Finland, 25:18930 (NYO-3446-14, Paper 27)
  - Prog. rpt. on radioactive foodchains in subarctic environment, annual, 8/15/69--8/14/70, 25:18928 (NYO-3446-14)
  - Radionuclides in plants and reindeer meat in Lapland, 25:18932 (NYO-3446-14, Paper 31)
  - Stable lead and radiolead in air filter samples, 25:18933 (NYO-3446-14, Paper 32)

I

- ICN/TRACERLAB, WALTHAM, MASS.
  - Millstone Nuclear Power Station, Unit 1. Environmental radiation survey program semiannual report, July 1--December 31, 1970, 25:20626 (DOCKET-50245-56)
  - Pilgrim Nuclear Power Station. Preoperational environmental radiation survey program. Summary report through August 31 1970, 25:20653 (DOCKET-50293-38)
- IDAHO NUCLEAR CORP., IDAHO FALLS.
  - Attenuation concept for evaluating release of radioiodine following a loss-of-coolant accident, 25:20756 (CONF-700816-(Vol.1), pp 9-25)
  - SCANS: spectra calculation from activated nuclide sets, 25:18641 (IN-1446)
- ILLINOIS DEPT. OF BUSINESS AND ECONOMIC DEVELOPMENT, SPRINGFIELD.
  - Projections of land use and public facility requirements with and without the accelerator, 25:20870 (NP-18690)
- INDUSTRIAL BIO-TEST LABS., INC., NORTHBROOK, ILL.
  - Quad-Cities Station, Units 1 and 2. Preoperational environmental monitoring (thermal) of the Mississippi River, July 1969--June 1970, 25:20633 (DOCKET-50254-28)
- INSTITUT FUER PLASMAPHYSIK, G.M.B.H. GARCHING (WEST GERMANY).
  - Computer programme for solving MHD equations for theta pinch in time-dependent coordinate system, 25:19647 (IPP-6/90)
  - Eddy current loss through pulsed magnetic fields, 25:19572 (IPP-4/80)
  - Hydromagnetic equations for anistropic plasmas including transport effects, 25:19674 (IPP-1/112)
  - Laser energy necessary for inertially confined nuclear fusion plasma, 25:19646 (IPP-4/7)
  - Plasma confinement in WIIa-stellarator, 25:19645 (IPP-2/86)
- INSTITUTE OF NUCLEAR PHYSICS, KRAKOW (POLAND).
  - Automated systems and electronics for the Krakow--Dubna slow-neutron inverted-geometry spectrometer KD SOG-1, 25:18734 (INP-727)
  - Geometrical effects in scattering of ions by surface of solids, 25:19468 (INP-710)
- INSTITUTE OF NUCLEAR RESEARCH, KRAKOW (POLAND).
  - Calibration of radiometric probes for soil density measurements, 25:18815 (INP-715)
- INSTITUTE OF NUCLEAR RESEARCH, WARSAW (POLAND).
  - 10-MeV proton linear accelerator at Swierk, 25:20129 (INR-P-1218)
  - Beta spectrometer with a Si(Li) detector in homogeneous magnetic field, 25:18736 (INR-P-1227)
  - Classical theory of atomic collisions. II, 25:19488 (INR-P-1225)
  - Equilibrium deformations of the ground and excited states in the rare-earth nuclei, 25:20367 (INR-P-1216)
  - Interpretation of the data on muons in cosmic rays from the point of view of high energy physics and astrophysics, 25:19522 (INR-1231)
  - Measurement of high-energy γ-ray spectra in a strong neutron flux, 25:18735 (INR-1224)
  - MINIGASKET: code for thermal neutron scattering law in polycrystals, 25:20229 (INR-1186)
- INSTITUTO DE ENERGIA ATOMICA, SAO PAULO (BRAZIL).
  - Photofission cross sections of uranium and thorium near threshold, 25:20366 (IEA-211)
- INSTITUTT FOR ATOMENERGI, HALDEN (NORWAY). OECD HALDEN REAKTOR PROSJEKT.
  - Irradiation behavior and post-irradiation examination of Swedish test assembly IFA-30, 25:20735 (HPR-127)
  - UKAEA fuel test assemblies irradiated in HBWR, 1964--66, 25:20736 (HPR-132)
- INSTITUTT FOR ATOMENERGI, KJELLER (NORWAY).
  - Chemical analysis of high burn-up PuO_2 fuel, 25:18356 (KR-140)
- INTERNATIONAL ATOMIC ENERGY AGENCY, VIENNA (AUSTRIA).
  - Conference on uranium exploration geology, Vienna, 4/70, 25:18529 (STI/PUB-277)
  - INIS: authority list for corporate entries, 25:20858 (IAEA-INIS-6(Rev.2))
- INTERNATIONAL CARBON, INC., PARIS (FRANCE).
  - Evaluation of activated carbon supported isotope exchange techniques for containment atmosphere purification, 25:18385 (CONF-700816-(Vol.1), pp 278-88)
- INTERNATIONAL UNION OF PURE AND APPLIED- CHEMISTRY.
  - III Polish analytical conference, Warsaw, 9/68, 25:18334 (CONF-680946-(Absts.))
- ION PHYSICS CORP., BURLINGTON, MASS.
  - Penetration of a two-dimensional fission barrier, 25:20478 (INR-P-1230)
- IOWA-ILLINOIS GAS AND ELECTRIC CO., DAVENPORT, IOWA.
  - Quad-Cities Station, Units 1 and 2. Preliminary safety analysis report, Amendment 20, 25:20636 (DOCKET-50254-31)
  - Quad-Cities Station, Units 1 and 2. Preliminary safety analysis report, Amendment 17, 25:20634 (DOCKET-50254-29)
  - Quad-Cities Station, Units 1 and 2. Preliminary safety analysis report, Amendment 18, 25:20635 (DOCKET-50254-30)
- IOWA STATE UNIV. OF SCIENCE AND TECHNOLOGY, AMES.
  - Structural, magnetic, and spectroscopic study of nickel squarate dihydrate, 25:20865 (IS-T-432)
- ISTITUTO NAZIONALE DI FISICA NUCLEARE, BARI (ITALY).
  - General formulation of relativistic theory of particle subcostituents (quarks) in terms of a field vector interaction, 25:19972 (IFPTH-10/70)
- ISTITUTO NAZIONALE DI FISICA NUCLEARE, PADUA (ITALY).
  - General formulation of relativistic theory of particle subcostituents (quarks) in terms of a field vector interaction, 25:19972 (IFPTH-10/70)

J

- JAPAN ATOMIC ENERGY RESEARCH INST., TOKYO.
  - Analysis of fast critical experiments and revision of JAERI-fast set, 25:20788 (JAERI-Memo-4215)
  - Analysis of flux measurement near strong absorber using VISTA method. I, 25:20831 (JAERI-Memo-4238)
  - Core temperature analyses for loss-of-coolant accidents of light water reactor, 25:20762 (JAERI-Memo-4194)
  - Estimation of fission product decay heat, 25:20834 (JAERI-Memo-4205)
  - GRAPH: computer program for plotting experimental data in NEUDADA system, 25:20230 (JAERI-Memo-4116)
  - Japanese list of requests for measurement. II, 25:20231 (JAERI-Memo-4167)
  - Manual for JUPITOR-1 (Supplement), 25:20479 (JAERI-Memo-4138)
  - Plutonium-239 fission product yields and their influence on fast reactor characteristics, 25:20819 (JAERI-Memo-4165)
  - Prog. rpt. on health and safety at Oarai Research Establishment, 7--9/70, 25:18983 (JAERI-Memo-4216)
  - Prog. rpt. on nuclear safety experimental program, 4--10/70, 25:20763 (JAERI-Memo-4229)
  - Survey list of accident, hazard, and abnormality in nuclear facilities, 25:19013 (JAERI-Memo-4240)
  - Table of half-life, γ-ray energy, and intensity of radioisotopes, 25:20368 (JAERI-Memo-4189)
- JERSEY CENTRAL POWER AND LIGHT CO., MORRISTOWN, N. J.
  - Forked River Nuclear Generating Station, Unit 1. Preliminary safety analysis report, Amendment 6, 25:20678 (DOCKET-50363-12)
  - Oyster Creek Nuclear Power Plant, Unit No. 1. Radiation emergency plan, 25:20618 (DOCKET-50219-124)
- JOINT INST. FOR NUCLEAR RESEARCH, DUBNA (USSR).
  - Investigation of the model of the 2-meter streamer chamber of the SCM-200 assembly, 25:18774 (JINR-P13-5529)
  - Ion acceleration by electron ring in decreasing magnetic field, 25:20131 (JINR-P9-5535)
  - Mesoatomic processes and model of large molecules (review), 25:19482 (NRC-TT-1426)
  - Model-independent analysis of forward π^{+-}p scattering data, 25:20003 (JINR-E2-5561)

XUM

Non-strange baryon--baryon resonances, 25:20016 (CERN-Trans-70-14)
Relative measurements of anti ν in the ^{235}U and ^{239}Pu fission induced by resonance neutrons, 25:20364 (BNL-tr-401)
JOINT INST. FOR NUCLEAR RESEARCH, DUBNA (USSR). LAB. OF HIGH ENERGY.
Experimental solenoid made of Nb_3Sn strip, 25:19588 (JINR-P8-5440)
Method of searching for the kink and determining the track parameters of particles scattered in a bubble chamber, 25:18773 (JINR-P1-5540)
JOINT INST. FOR NUCLEAR RESEARCH, DUBNA (USSR). LAB. OF NEUTRON PHYSICS.
Experiments with ultracold neutrons, 25:20232 (JINR-P3-5392)
JOINT INST. FOR NUCLEAR RESEARCH, DUBNA (USSR). LAB. OF NUCLEAR PROBLEMS.
Contribution of exchange mechanism in backward scattering of protons on light nuclei and $d + {}^4He \to {}^3He + {}^3H$ reaction, 25:20250 (JINR-P2-5496)
External injection and acceleration of the beam to the final radius in the electron model of the ring cyclotron with strong focusing, 25:20130 (JINR-P9-5453)
Magnetic field of thick finite dc solenoids, 25:18829 (JINR-P9-5441)
Monte Carlo generation of neutral π^-p interactions at 5 GeV/c in propane bubble chamber, 25:20004 (JINR-P13-5516)
Search for the decay $\mu^+ \to e^+ + e^+ + e^-$, 25:19891 (JINR-P1-5542)
Two-dimensional analyzer for half life measurements of nucleus of excited states, 25:18642 (JINR-P13-5485)
JOINT INST. FOR NUCLEAR RESEARCH, DUBNA (USSR). LAB. OF NUCLEAR REACTIONS.
Delayed fission of some neutron-deficient atomic nuclei, 25:20371 (JINR-P7-5584)
Experiments on measurement of compound nucleus lifetime in W(^{22}Ne,f) reaction, 25:20370 (JINR-P7-5512)
Production of spontaneously fissioning isomers of U, Pu, and Am in neutron reactions, 25:20369 (JINR-P3-5528)
Validity of Alexander and Simonoff semiempirical rules in region 100 less than or equal to A less than or equal to 150, 25:20480 (JINR-E7-5499)
JOINT INST. FOR NUCLEAR RESEARCH, DUBNA (USSR). LAB. OF THEORETICAL PHYSICS.
Brief review of reports submitted to 2nd international symposium on nonlocal quantum field theory, Azau, 3/70, 25:20057 (JINR-E2-5563)
Decays $\pi^+ \to e^+(\mu^+)\nu e^+e^-$, 25:19963 (JINR-P2-5520)
Double differential distribution of particles produced in the proton-nucleus collisions, 25:20018 (JINR-P2-5507)
Motion of particles in the fixed centers field, 25:20059 (JINR-P4-5547)
Regularizing properties of superpropagators, 25:20058 (JINR-P2-5569)
Relation between cross sections of processes $e^- + e^+ \to e^- + e^+ + A^- + A^+$ and $\gamma + \gamma \to A^- + A^+$, 25:19938 (JINR-P2-5505)
Schmidt method applied to solving the quasipotential equation, 25:19987 (JINR-P2-5566)
Space distribution of the α-clusters in the light nuclei, 25:20268 (JINR-P4-5479)
Table of wave functions of single-particle states of transuranium region deformed nuclei in Saxon--Woods potential, 25:20481 (JINR-P4-5457)
Transformation properties of massive particle states at infinite momentum, 25:19924 (JINR-E2-5579)

K

KARLSRUHE UNIV. (WEST GERMANY).
Material transport in plant foods with regard to radioactive contamination and decontamination, 25:18892 (NP-18641)
KERNFORSCHUNGSANLAGE, JUELICH (WEST GERMANY). INSTITUT FUER MEDIZIN.
Dosimetry of incorporated tritium and ^{125}I, 25:18984 (JUL-688-ME)
KERNFORSCHUNGSANLAGE, JUELICH (WEST GERMANY). INSTITUT FUER REAKTORENTWICKLUNG.
Evaluation of results of a study of the Th--^{233}U fuel cycle for thermal reactors, 25:20746 (JUL-644-RG)
KERNFORSCHUNGSANLAGE, JUELICH (WEST GERMANY). INSTITUT FUER TECHNISCHE PHYSIK.
Applied magnetohydrodynamics. VI, 25:19536 (JUL-706-TP)
KERNFORSCHUNGSZENTRUM, KARLSRUHE (WEST GERMANY). INSTITUT FUER EXPERIMENTELLE KERNPHYSIK.
Beta--γ (CP)-asymmetry coefficients in isospin forbidden allowed mixed β transitions, 25:20372 (KFK-1249)
KERNFORSCHUNGSZENTRUM, KARLSRUHE (WEST GERMANY). INSTITUT FUER RADIOCHEMIE.
Formation of chelates and adduct chelates in the extraction of trivalent americium and californium, 25:18498 (KFK-1298)
KNOLLS ATOMIC POWER LAB., SCHENECTADY, N. Y.
Monte Carlo evaluation of multiple scattering and resolution effects in double-differential neutron scattering cross section measurements, 25:20235 (RPI-328-211)

L

LOS ALAMOS SCIENTIFIC LAB., N. MEX.
Dynamic measurement of stopband in LAMPF 805 MHz accelerator structures at high power using hybrid computer techniques, 25:20132 (LA-4593)
Initial equilibrium configuration of Scyllac 5-meter toroidal-sector experiment, 25:19725 (LA-4597)
Plutonium and strontium in soil near Technical Area 21, Los Alamos Scientific Laboratory, Los Alamos, New Mexico, 25:18985 (LA-4563)
LUND UNIV. (SWEDEN). DEPT. OF PHYSICS.
Photometric mass determination in nuclear emulsion on cosmic ray carbon. I, 25:18643 (NP-18672)
LYON UNIV. (FRANCE).
Excited states of ^{17}O and ^{29}Si, 25:20271 (NP-18628)
LYON UNIV. (FRANCE). FACULTE DES SCIENCES.
Intermetallic diffusion of plutonium in Pu--Cu and Pu--U systems, 25:19230 (CEA-R-3951)
LYON UNIV. (FRANCE). INSTITUT DE PHYSIQUE NUCLEAIRE.
Low-energy theorems and π-meson interactions with nuclei, 25:20019 (LYCEN-7081)

M

MAGYAR TUDOMANYOS AKADEMIA KOZPONTI FIZIKAI KUTATO INTEZETE, BUDAPEST.
Introduction to the current--current theory of the weak interaction, 25:19964 (KFKI-70-24-HEP)
Neutron dosimetry by semiconductor detectors and hydrogenous radiator assembly, 25:18798 (KFKI-70-29-HP)
PRODGROUP: program for production of multigroup reactor constants, 25:20820 (KFKI-71-4)
MAINE YANKEE ATOMIC POWER CO., WESTBORO, MASS.
Maine Yankee Atomic Power Station. Environmental report, Addenda, 25:20667 (DOCKET-50309-29)
Maine Yankee Atomic Power Station. Preliminary safety analysis report, Amendment 18, 25:20665 (DOCKET-50309-27)
Maine Yankee Atomic Power Station. Preliminary safety analysis report, Amendment 19, 25:20666 (DOCKET-50309-28)
MARITIME ADMINISTRATION, WASHINGTON, D. C.
N. S. Savannah. Safety analysis summary: defueling, 25:20814 (DOCKET-50238-78)
N. S. Savannah. Safety analysis summary, defueling pages inadvertently omitted, 25:20815 (DOCKET-50238-144)
MASSACHUSETTS EYE AND EAR INFIRMARY, BOSTON.
Prog. rpt. on carbohydrate metabolism of ocular tissues, annual, 1970, 25:20873 (NYO-1368-17)
MASSACHUSETTS INST. OF TECH., CAMBRIDGE.
Helicity poles, triple Regge behavior and single particle spectra in high energy collisions, 25:19926 (NYO-2262-TA-234)
Photoproduction of pion pairs with high invariant mass, 25:19886 (DESY-70/61)
MICHIGAN STATE UNIV., EAST LANSING.
Prog. rpt. on radiation and chemical-induced molecular damages, annual, 6/70--5/71, 25:19090 (COO-1704-22)
MICHIGAN STATE UNIV., EAST LANSING. DEPT. OF CHEMISTRY.
ESR study of IO_2F^- radical in γ-irradiated single crystals of potassium oxyfluoroiodate, 25:18420 (COO-1385-34)
MILLSTONE POINT CO., HARTFORD, CONN.
Millstone Nuclear Power Station, Unit 1. Abnormal occurrences No. AO-71-3 and No. AO-71-4, 25:20592 (DOCKET-50245-55)
MILLSTONE POINT CO., WETHERSFIELD, CONN.
Millstone Nuclear Power Station, Unit 1. Environmental radiation survey program semiannual report, July 1--December 31, 1970, 25:20626 (DOCKET-50245-56)

N

NATIONAL AERONAUTICS AND SPACE ADMINISTRATION, CLEVELAND, OHIO. LEWIS RESEARCH CENTER.
Auxiliary and loop for removal of decay heat from a space power reactor, 25:20805 (N-70-39420)
Tests of evaluated beryllium (n,2n) cross sections, 25:20269 (N-70-37365)
NATIONAL BUREAU OF STANDARDS, WASHINGTON, D. C.
National Bureau of Standards Reactor. Fuel element head locking bar pin, 25:20784 (DOCKET-50184-26)
National Bureau of Standards Reactor. Primary system inlet strainer: follow-up report, 25:20785 (DOCKET-50184-27)
Prog. rpt. on activation analysis, annual, 7/69--6/70, 25:18366 (NBS-TN-548)
Prog. rpt. on analytical mass spectrometry, annual, 7/69--6/70, 25:18357 (NBS-TN-546)
Publications of the National Bureau of Standards, 1968--69, 25:20869 (NBS-SPEC. PUBL-305(Suppl.1))

NATIONAL COUNCIL ON RADIATION PROTECTION AND MEASUREMENTS, WASHINGTON, D.C.
Basic radiation protection criteria, 25:19008 (NCRP-39)
Protection against neutron radiation, 25:19007 (NCRP-38)
NATIONAL LEAD CO. OF OHIO, CINCINNATI.
Dilute uranium alloy with a fine-grained, randomly oriented structure, 25:19231 (NLCO-1051)
Production of dense thoria, 25:19259 (NLCO-1029)
NAVAL AEROSPACE MEDICAL RESEARCH LAB., PENSACOLA, FLA.
Astronauts' radiation exposure on first lunar landing mission, Apollo XI, 25:18978 (AD-711316)
NEBRASKA UNIV., LINCOLN. DEPT. OF CHEMISTRY.
Prog. rpt. on halogen atom reactions activated by radiative neutron capture and /sup 82m/Br and /sup 130m/I isomeric transition, annual, 2/70--2/71, 25:18483 (COO-1617-27)
NEVADA UNIV., RENO. DESERT RESEARCH INST.
Radiotracer studies of nutrient cycling pathways, 25:20897 (TID-25656)
NIAGARA MOHAWK POWER CORP., SYRACUSE, N. Y.
Nine Mile Point Nuclear Station. Modification of start-up procedure, 25:20621 (DOCKET-50220-60)
Nine Mile Point Nuclear Station. Third semiannual report of operation, July 1--December 31, 1970, 25:20587 (DOCKET-50220-58)
NIELS BOHR INSTITUTET, COPENHAGEN (DENMARK).
Neutron stars, 25:19348 (NP-18666)
NORDISK INSTITUT FOR TEORETISK ATOMFYSIK, COPENHAGEN (DENMARK).
Neutron stars, 25:19348 (NP-18666)
NORTH AMERICAN CARBON, INC., COLUMBUS, OHIO.
Evaluation of activated carbon supported isotope exchange techniques for containment atmosphere purification, 25:18385 (CONF-700816-(Vol.1), pp 278-88)
NORTHERN STATES POWER CO., MINNEAPOLIS, MINN.
Monticello Nuclear Generating Plant, Unit 1. Unsuccessful efficiency testing of a standby gas treatment system particulate filter, 25:20595 (DOCKET-50263-56)
Pathfinder Generating Plant, Sioux Falls, South Dakota. Provisional Operating License No. DPR-11, Amendment 50 (includes request for a dismantling order with dismantling plan), 25:20607 (DOCKET-50130-7)
NORTHWESTERN UNIV., EVANSTON, ILL.
Effect of electron irradiation on the strength of iron single crystals, 25:19252 (COO-1367-36)
NUCLEAR FUEL SERVICES, INC., ROCKVILLE, MD.
West Valley Reprocessing Plant. Technical specification Change No. 13, request for hearing, 25:18494 (DOCKET-50201-63)
NUCLEAR FUEL SERVICES, INC., WEST VALLEY, N.Y.
West Valley Reprocessing Plant. Request for possession limit of 5 x 10^{-3} curies of ^{85}Sr, 25:18495 (DOCKET-50201-64)

O

OAK RIDGE NATIONAL LAB., TENN.
Analytical and experimental investigation of the neutron energy effects on reactor fluctuation spectra, 25:20832 (ORNL-TM-3245)
Applied dosimetry research, 25:18799 (ORNL-4584, pp 165-86)
Atomic and molecular radiation physics, 25:19491 (ORNL-4584, pp 105-24)
Compatibility tests for selection of radioisotope heat source compounds, 25:18592 (ORNL-4298)
Computer program for calculating, tabulating, and plotting outgassing rates of selected gases, 25:19195 (ORNL-TM-3220)
Disposal by hydraulic fracturing, 25:18622 (ORNL-4584, pp 11-15)
Disposal in natural salt formations, 25:18623 (ORNL-4584, pp 16-36)
Dose estimation studies related to peaceful uses of nuclear explosives, 25:18989 (ORNL-4584, pp 42-56)
Dosimetry for human exposures and radiobiology, 25:18990 (ORNL-4584, pp 129-51)
Earthquakes and reactor safety, 25:18556 (ORNL-4584, pp 41)
Electron and ion collision physics, 25:19490 (ORNL-4584, pp 92-104)
Engineering, economic, and safety evaluation, 25:18526 (ORNL-4584, pp 37-40)
Estimation of aerosol concentration in a nuclear reactor containment after an accident, 25:20758 (CONF-700816-(Vol.1), pp 72-101)
Fate of trace elements and radionuclides in terrestrial environment, 25:18521 (ORNL-4584, pp 1-10)
Fueled-graphite fabrication development, 25:19262 (ORNL-4629, pp 65-82)
Fundamental sol-gel studies, 25:19263 (ORNL-4629, pp 99-102)
Health Physics Division annual progress report for period ending 7/31/70, 25:18988 (ORNL-4584)
HPRR and accelerator operations, 25:20134 (ORNL-4584, pp 187-97)
Interaction of radiation with liquids and solids, 25:19758 (ORNL-4584, pp 74-86)
Internal dose estimation, 25:18991 (ORNL-4584, pp 200-22)
Irradiation of HTGR fuels, 25:19288 (ORNL-4629, pp 82-98)
List of AEC radioisotope customers with summary of radioisotope shipments, FY 1970, 25:18593 (ORNL-IIC-32)
Optimum turbine exhaust pressure for use of a single-effect, vertical-tube still desalting plant with a steam turbine-generator, 25:18565 (ORNL-TM-3291)
Physics of tissue damage, 25:19759 (ORNL-4584, pp 87-91)
Process demonstration and ^{233}U distribution, 25:18624 (ORNL-4629, pp 1-9)
Prog. rpt. on Concentration and Desalting of Protein Solutions Program, 3--5/70, 25:20882 (ORNL-TM-3082)
Prog. rpt. on isotope kilowatt program, 12/31/70, 25:18594 (ORNL-TM-3292)
Radiation safety practices: Operation HENRE, 25:18982 (CEX-65.05)
Sol-gel process development, 25:19261 (ORNL-4629, pp 14-64)
Spectrometry research and development, 25:18644 (ORNL-4584, pp 152-64)
Static seals and their application in water-cooled nuclear reactor systems, 25:20719 (ORNL-TM-3308)
Status and progress report for thorium fuel cycle development for January 1, 1969--March 31, 1970, 25:19260 (ORNL-4629)
Theoretical radiation physics, 25:19757 (ORNL-4584, pp 58-73)
Thorium--Uranium Recycle Facility, 25:18564 (ORNL-4629, pp 10-13)
Tower Shielding Reactor II design and operation report: Vol. 1 description, 25:20789 (ORNL-TM-2893(Vol.1)(Rev.))
OESTERREICHISCHE STUDIENGESELLSCHAFT FUER ATOMENERGIE G.M.B.H., SEIBERSDORF.
Recent developments in radioactive waste management, 25:18625 (SGAE-RT-35/1970)
OFFICE NATIONAL D'ETUDES ET DE RECHERCHES AEROSPATIALES, CHATILLON-SOUS-BAGNEUX (FRANCE).
Plasma acceleration by traveling electromagnetic field, 25:19669 (NP-18715)
Source of synthesized plasma, 25:19700 (NP-18722)
OFFICE OF SALINE WATER, WASHINGTON, D. C.
Abstracts of literature on the distillation of seawater and on the use of nuclear energy for desalting, 25:20812 (TID-25653)
OLD DOMINION COLL., NORFOLK, VA.
Use of radioisotopes for studies on the ecology of tick vectors of disease. Final progress report, April 1, 1966--December 31, 1970, 25:18934 (ORO-3514-10)
OMAHA PUBLIC POWER DISTRICT, NEBR.
Fort Calhoun Station, Unit No. 1. Preliminary safety analysis report, Amendment 23 (includes final safety analysis report, Suppl. No. 6), 25:20650 (DOCKET-50285-42)
ORGANIZATION FOR ECONOMIC CO-OPERATION AND DEVELOPMENT, PARIS (FRANCE).
Prog. rpt. on high-temperature reactor, annual, 1969--70, 25:20747 (NP-18668)

P

PACIFIC GAS AND ELECTRIC CO., SAN FRANCISCO, CALIF.
Humboldt Bay Power Plant, Unit No. 3. Failure of emergency condenser condensate return valve to operate, 25:20580 (DOCKET-50133-45)
Humboldt Bay Power Plant, Unit No. 3. License No. DPR-7: Addendum B to technical specifications Proposed Change No. 27, 25:20608 (DOCKET-50133-46)
Humboldt Bay Power Plant, Unit No. 3. Operations report, July 1--December 1970, 25:20581 (DOCKET-50133-48)
PADUA UNIV. (ITALY). ISTITUTO DI FISICA.
General formulation of relativistic theory of particle subcostituents (quarks) in terms of a field vector interaction, 25:19972 (IFPTH-10/70)
PADUCAH GASEOUS DIFFUSION PLANT, KY.
Isotopic integrity for UF_6 field samples, 25:18340 (KY-626)
PANAMETRICS, INC., WALTHAM, MASS.
Prog. rpt. on ultrasonic thermometry in LMFBR systems, 7--9/70, 25:18830 (NYO-3906-12)
PARIS UNIV., ORSAY (FRANCE).
Transfer mechanisms in reactions ^{209}Bi(^{12}C) and ^{209}Bi(^{14}N), 25:20375 (NP-18624)
PARIS UNIV., ORSAY (FRANCE). LABORATOIRE DE L'ACCELERATEUR LINEAIRE.
Study of the coherent production on nuclei of $K^- \pi^+ \pi^-$ systems by K^- of 5.5, 10.0, and 12.7 GeV/c, 25:19910 (LAL-1242)
PARIS UNIV., ORSAY (FRANCE). LABORATOIRE DE PHYSIQUE DES PLASMAS.
Gas pressure and electron density in the active zone level of hollow cathode arc discharges, 25:20872 (NP-18708)
PENNSYLVANIA STATE UNIV., UNIVERSITY PARK. DEPT. OF METEOROLOGY.
Prog. rpt. on effects of a change of terrain on wind profiles, final, 7/1/65--8/15/68, 25:20875 (NYO-3562-3)

XUM

PHILADELPHIA ELECTRIC CO., PA.
- Limerick Generating Station, Units 1 and 2. Preliminary safety analysis report, Amendment 4, Suppl. 4, 25:20675 (DOCKET-50352-11)
- Peach Bottom Atomic Power Station, Unit 1. Failure of primary system stop valve to close, 25:20584 (DOCKET-50171-78)

POWER REACTOR DEVELOPMENT CO., DETROIT, MICH.
- Enrico Fermi Atomic Power Plant, Unit 1. Amended request for authorization of Change No. 16 in the technical specifications, 25:20603 (DOCKET-50C16-101)
- Enrico Fermi Atomic Power Plant, Unit 1. Operations report, September 1970, 25:20577 (DOCKET-50016-100)
- Enrico Fermi Atomic Power Plant, Unit 1. Request for technical specifications Change No. 24, 25:20602 (DOCKET-50016-99)

PUBLIC HEALTH SERVICE, LAS VEGAS, NEV. SOUTHWESTERN RADIOLOGICAL HEALTH LAB.
- Radioiodine field studies with synthetic aerosols, 25:18926 (CONF-700816-(Vol.1), pp 49-71)

PUBLIC SERVICE CO. OF COLORADO, DENVER.
- Fort St. Vrain Nuclear Generating Station, Unit 1. Emergency core cooling, 25:20642 (DOCKET-50267-26)
- Fort St. Vrain Nuclear Generating Station, Unit 1. Preliminary safety analysis report, Amendment 18, 25:20643 (DOCKET-50267-27)

PUBLIC SERVICE ELECTRIC AND GAS CO., NEWARK, N.J.
- Newbold Island Nuclear Generating Station, Units 1 and 2. Environmental report; construction permit stage, 25:20676 (DOCKET-50354-11)

PUERTO RICO WATER RESOURCES AUTHORITY, SAN JUAN.
- Aguirre Nuclear Plant, Unit No. 1. Preliminary facility description and safety analysis report, Amendment 2, 25:20680 (DOCKET-50376-9)
- La Crosse Boiling Water Reactor. Reactor vessel stresses in lamination region, 25:20600 (DOCKET-1155-105)

R

REACTOR CENTRUM NEDERLAND, PETTEN.
- Separation of gram-amounts of lanthanides by cation exchange, using an aqueous solution of α-hydroxyisobutyric acid as an eluant, 25:18501 (RCN-131)
- Theoretical and experimental study of a fast-thermal coupled reactor by correlation techniques, 25:20833 (RCN-132)

REAL ESTATE RESEARCH CORP., CHICAGO, ILL.
- Projections of land use and public facility requirements with and without the accelerator, 25:20870 (NP-18690)

RENSSELAER POLYTECHNIC INST., TROY, N. Y.
- Monte Carlo evaluation of multiple scattering and resolution effects in double-differential neutron scattering cross section measurements, 25:20235 (RPI-328-211)

RICE UNIV., HOUSTON, TEX. DEPT. OF ELECTRICAL ENGINEERING.
- Prog. rpt. on interchange of essential programs between dissimilar computers, annual, 3/71, 25:20884 (ORO-4061-1)

RICHLAND OPERATIONS OFFICE (AEC), WASH.
- Overview of LMFBR program at Hanford, 25:20692 (CONF-700816-(Vol.1), pp 289-316)

ROCHESTER GAS AND ELECTRIC CORP., N. Y.
- Robert Emmett Ginna Nuclear Power Plant, Unit No. 1. Failure of 1A diesel generator to start, 25:20590 (DOCKET-50244-65)
- Robert Emmett Ginna Nuclear Power Plant, Unit No. 1. Petition requesting operation at a higher power level, Amendment 1 (includes technical supplement accompanying application to increase power, Amendment 1), 25:20624 (DOCKET-50244-62)
- Robert Emmett Ginna Nuclear Power Plant, Unit No. 1. Provisional Operating License No. DPR-18: request for revision of technical specifications Change No. 8, 25:20623 (DOCKET-50244-61)
- Robert Emmett Ginna Nuclear Power Plant, Unit No. 1. Report of stud failure, 25:20622 (DOCKET-50244-60)
- Robert Emmett Ginna Nuclear Power Plant, Unit No. 1. Semiannual report No. 2, April 26, 1970--December 25, 1970, 25:20591 (DOCKET-50244-66)
- Robert Emmett Ginna Nuclear Power Plant, Unit No. 1. Spent fuel pool charcoal filter system, 25:20625 (DOCKET-50244-63)
- Robert Emmett Ginna Nuclear Power Plant, Unit No. 1. Status report on recommendations regarding technical specification violation, July 6, 1970, 25:20589 (DOCKET-50244-64)

RUTGERS UNIV., NEW BRUNSWICK, N. J.
- Prog. rpt., 3 yrs, 1968--1970, 25:20878 (NYO-3997-7)
- Prog. rpt., annual, 1970, 25:20877 (NYO-3997-6)

RUTHERFORD HIGH ENERGY LAB., CHILTON (ENGLAND).
- Present status of polarized targets at the Rutherford Laboratory, 25:20135 (RHEL/R-201)

S

SAN DIEGO GAS AND ELECTRIC CO., CALIF.
- San Onofre Nuclear Generating Station, Units 2 and 3. Preliminary safety analysis report, Amendment 7, 25:20677 (DOCKET-50361-15)

SANDIA LABS., ALBUQUERQUE, N. MEX.
- Aerodynamic forces and dynamic stability of high-speed, magnetically suspended rocket sled, 25:20890 (SC-DR-70-867)
- Comparison of CBW FM/FM and DSB/FM telemetry systems, 25:20888 (SC-DR-70-686)
- Direct method for discretized Poisson equation, 25:20892 (SC-RR-70-579)
- Effects of load conditions on long term radioisotope thermoelectric generator operation, 25:18595 (SC-RR-70-854)
- Fracture branching and dicing in stressed glass, 25:20894 (SC-RR-70-766)
- REBA: pulsed electron beam generator, 25:20136 (SC-DR-70-872)
- Sandia image digitizer, 25:20887 (SC-DR-68-812-B)
- Selecting a transformer core material for a high induction pulsed application, 25:20889 (SC-DR-70-736)
- Stochastic analysis of fractured glass, 25:20891 (SC-RR-69-506)
- Total cross section for single electron loss by Ne and Ar in nitrogen, oxygen, and air, 25:19492 (SC-RR-70-735)
- Transfer function models of DTL and TTL integrated circuits, 25:20893 (SC-RR-70-650)
- Ultrasonic characterization and computerized analysis of graphite billets, 25:18613 (SC-DR-70-693)

SANDIA LABS., LIVERMORE, CALIF.
- Prediction of fatigue lives of 2024-T3 and 6061-T6 aluminum alloys under broad-band excitation, 25:20895 (SCL-CR-710175)

SAXTON NUCLEAR EXPERIMENTAL CORP., PA.
- Saxton Reactor. License No. DPR-4; technical specifications Change Request No. 41, 25:20582 (DOCKET-50146-68)
- Saxton Reactor. Request for approval to use subassemblies (503-4-32 and 33) without a flux thimble, 25:20609 (DOCKET-50146-69)

SCHOOL OF AEROSPACE MEDICINE, BROOKS AFB, TEX.
- Reduction of radiation hazard in tritium method of measuring total body water, 25:18977 (AD-702155)

SOUTHERN CALIFORNIA EDISON CO., LOS ANGELES.
- San Onofre Nuclear Generating Station, Units 2 and 3. Preliminary safety analysis report, Amendment 7, 25:20677 (DOCKET-50361-15)

STATE UNIV. OF NEW YORK, STONY BROOK.
- Prog. rpt. on slip initiation and microdynamics of flow in tungsten, 1--12/70, 25:19194 (NYO-4073-4)

STICHTING VOOR FUNDAMENTEEL ONDERZOEK DER MATERIE, JUTPHAAS (NETHERLANDS). INSTITUUT VOOR PLASMA-FYSICA.
- Approximate cross sections and rate coefficients for ionization, excitation, and recombination of hydrogenic ions and atoms, 25:19489 (NP-18680)
- Kink instability of toroidal plasma column, 25:19704 (NP-18681)

STOCKHOLM UNIV. (SWEDEN). INST. OF PHYSICS.
- Bubble chamber experiments on 10 and 19 GeV/c proton--proton interactions, 25:19902 (USIP-70-8)
- Construction and examination of a gas scintillation detector, 25:18645 (USIP-70-1)
- Distortion effects in geometrical reconstruction of events in CERN 2m Hydrogen Bubble Chamber, 25:18777 (USIP-70-6)
- Hardware system for measurements of bubble chamber films on-line, 25:18776 (USIP-70-3)
- One-pion exchange model applied to reaction pp → $p\pi^+(\Delta^{++})\pi^-p$ at 19 GeV/c, 25:20020 (USIP-70-5)
- Proton--proton interactions at 19 and 10 GeV/c, 25:19901 (USIP-70-7)
- Proton--proton reactions at 19 GeV/c with production of two and three pions, 25:19900 (USIP-70-4)

STOCKHOLM UNIV. (SWEDEN). RESEARCH INST. FOR PHYSICS.
- Prog. rpt. on experiments with accelerator beams, annual, 1969, 25:20133 (NP-18671)

T

TECHNICAL UNIV. OF HELSINKI, OTANIEMI (FINLAND). DEPT. OF TECHNICAL PHYSICS.
- Information theoretical aspects of power spectrum measurements in nuclear reactors, 25:20821 (TKK-F-A-102)
- IRESINT 2: program for calculation of resonance integrals, 25:20823 (TKK-F-A-139)
- Variety and hierarchy of data extraction methods in nuclear reactor noise analysis, 25:20822 (TKK-F-A-137)

TECHNISCHE HOGESCHOOL, DELFT (NETHERLANDS).
- Angular correlation studies of conversion electrons from ^{154}Gd, of nuclear electrons from ^{48}V and of Bremsstrahlung from unpolarized electrons, 25:20374 (NP-18597)

TEL AVIV UNIV. (ISRAEL).
- NN and ND interactions (above 0.5 GeV/c), 25:19899 (UCRL-20000-NN)

TENNESSEE UNIV., KNOXVILLE.
- Analytical and experimental investigation of the neutron energy effects on reactor fluctuaticn spectra, 25:20832 (ORNL-TM-3245)

TENNESSEE VALLEY AUTHORITY, CHATTANOOGA. OFFICE OF POWER.
  Browns Ferry Nuclear Plant, Units 1, 2, and 3. Preliminary safety analysis report, Amendment 11 (includes additions and revisions to final safety analysis report), 25:20638 (DOCKET-50259-22)
TEXAS AGRICULTURAL AND MECHANICAL UNIV., COLLEGE STATION.
  Prog. rpt. on,on-line alpha and proton decay spectrometry, annual, 1970, 25:18737 (ORO-3820-7)
TOKYO UNIV. (JAPAN). INST. FOR NUCLEAR STUDY.
  Simulation in space and time of nuclear active and muon components in extensive air showers for primary energies from 10^5 to 10^7 GeV, 25:19973 (INSJ-125)

U

UNITED KINGDOM ATOMIC ENERGY AUTHORITY, RISLEY (ENGLAND). AUTHORITY HEALTH AND SAFETY BRANCH.
  Appreciation of fast reactor safety (1970), 25:20764 (NP-18487)
  Risk evaluation for any curie release spectrum and any dose-risk relationship, 25:18974 (AHSB(S)R-192)
UNITED KINGDOM ATOMIC ENERGY AUTHORITY, RISLEY (ENGLAND). ENGINEERING GROUP.
  HTR fuel disposal study, 25:20745 (DP-Report-450)
UNITED KINGDOM ATOMIC ENERGY AUTHORITY, RISLEY (ENGLAND). REACTOR GROUP.
  Electrical generation and associated developments with atomic energy, 25:20550 (NP-18677)
  Solubility of carbon in sodium, 25:19196 (TRG-Report-1906)
UNITED KINGDOM ATOMIC ENERGY AUTHORITY, SELLAFIELD (ENGLAND). PRODUCTION GROUP.
  Effect of acute x-irradiation on development of eggs of plaice, Pleuronectes platessa, 25:19103 (PG-Report-1013)
  HTR fuel disposal study, 25:20745 (DP-Report-450)
UNITED NUCLEAR CORP., ELMSFORD, N. Y. RESEARCH AND ENGINEERING CENTER.
  Failure theories as related to LMFBR piping systems, 25:20724 (UNC-5235)
UNIVERSIDADE FEDERAL DO RIO DE JANEIRO (BRAZIL). INSTITUTO DE BIOFISICA.
  Radioactivity in the diet of the inhabitants of the Brazilian regions of elevated natural radiation, 25:18927 (NP-18670)
UTRECHT RIJKSUNIVERSITEIT (NETHERLANDS).
  Three-nucleon calculations using the Faddeev equations, 25:20251 (NP-18678)

V

VERMONT UNIV., BURLINGTON.
  Prog. rpt. on thermodynamic and transport properties of interstitial hydrogen isotopes in palladium, 4/1/70--12/15/70, 25:20879 (NYO-4062-5)
VERMONT YANKEE NUCLEAR POWER CORP., RUTLAND.
  Vermont Yankee Nuclear Power Station. Preliminary safety analysis report, Amendment 20 (includes additional revisions to final safety analysis report), 25:20644 (DOCKET-50271-38)
  Vermont Yankee Nuclear Power Station. Preliminary safety analysis report, Amendment 22 (includes additional revisions to final safety analysis report), 25:20647 (DOCKET-50271-41)
  Vermont Yankee Nuclear Power Station. Preliminary safety analysis report, Amendment 21 (includes additional revisions to final safety analysis report), 25:20646 (DOCKET-50271-40)
VIRGINIA ELECTRIC AND POWER CO., RICHMOND.
  Surry Power Station, Units 1 and 2. Preliminary safety analysis report, Amendment 18, 25:20648 (DOCKET-50280-34)
  Surry Power Station, Units 1 and 2. Preliminary safety analysis report, Amendment 19 (includes additions and revisions to final safety analysis report, Part B), 25:20649 (DOCKET-50280-35)
VIRGINIA POLYTECHNIC INST., BLACKSBURG.
  Neutron transport theory with a completely degenerate energy transfer kernel, 25:20236 (TID-25648)
VIRGINIA POLYTECHNIC INST., BLACKSBURG. DEPT. OF METALS AND CERAMIC ENGINEERING.
  Prog. rpt. on relationship of nitrogen content to susceptibility of austenitic stainless steels to stress corrosion, 9--11/70, 25:20898 (TID-25664)

W

WADCO CORP., RICHLAND, WASH.
  Application of aqueous technology to LMFBR separations processes. Program plan for Task T-1: solvent performance, 25:18505 (WHAN-FR-32)
  EBR-II irradiation effects of rupture of Type-316 stainless steel, 25:19254 (WHAN-SA-2)
  Fission gas bubble precipitation and growth in PuO_2--UO_2 under irradiation, 25:19290 (WHAN-SA-15)
  Gas-flow method for detection of fast neutrons in reactors, 25:18646 (WHAN-SA-73)
  In-core regenerative thermal neutron detectors for nuclear reactors, 25:20711 (WHAN-FR-37)
  Industrial efforts to satisfy design criteria, 25:20725 (WHAN-SA-46)
  Irradiation of boron carbide pellets and powders in Hanford thermal reactors, 25:19289 (WHAN-FR-24)
  Irradiation produced defects in austenitic stainless steel, 25:19253 (WHAN-FR-16)
  Simulation of piping lengths in sodium systems, 25:20790 (WHAN-FR-22)
  Structure evolution in an oxide fuel pin, 25:20836 (WHAN-SA-79)
  Ventilation systems for the FFTF, 25:20783 (CONF-700816-(Vol.1), pp 317-45)
WASHINGTON STATE UNIV., PULLMAN. RESEARCH DIV.
  Prog. rpt. on polymer grafting to inorganic substrates, annual, 2/69--1/70, 25:18421 (RLO-2098-1)
WASHINGTON UNIV., SEATTLE. SCHOOL OF MEDICINE.
  Prog. rpt. on lymphocyte formation, life span, fate, and potential for repopulating hemopoietic tissues of irradiated animals, 1/71, 25:18919 (RLO-2225-T-16-1)
WEIZMANN INST. OF SCIENCE, REHOVOTH (ISRAEL).
  Near-uv absorption bands of tryptophan, 25:20899 (UCLA-12-810)
WESLEYAN UNIV., MIDDLETOWN, CONN. DEPT. OF PHYSICS.
  Method of extending Blankenbecler--Sugar--Logunov--Tavkhelidze approximation to Bethe--Salpeter equation, 25:20104 (NYO-2262-TA-231)
WESTINGHOUSE ELECTRIC CORP., PITTSBURGH, PA. ASTRONUCLEAR LAB.
  W-MESHER: a computer program to analytically partition a two-dimensional figure, 25:18578 (WANL-TME-2721)
WESTINGHOUSE ELECTRIC CORP., PITTSBURGH, PA. NUCLEAR FUEL DIV.
  Saxton Core II fuel performance evaluation. Part II. Evaluation of mass spectrometric and radiochemical analyses of irradiated Saxton plutonium fuel, 25:18359 (WCAP-3385-56(Pt.2))
  Saxton Core II nuclear operations summary, 25:20705 (WCAP-3385-55)
WESTINGHOUSE ELECTRIC CORP., PITTSBURGH, PA. PWR SYSTEMS DIV.
  Westinghouse Nuclear Steam Supply System. Reference safety analysis report, Vol. 2, 25:20682 (DOCKET-RESARA-2)
  Westinghouse Nuclear Steam Supply System. Reference safety analysis report, Vol. 1, 25:20681 (DOCKET-RESARA-1)
WISCONSIN DEPT. OF HEALTH AND SOCIAL SERVICES, MADISON.
  Point Beach Nuclear Plant, Units 1 and 2. Kewaunee Nuclear Power Plant. Environmental radiation survey annual report, July 1969--June 1970, 25:20641 (DOCKET-50266-42)
WISCONSIN ELECTRIC POWER CO., MILWAUKEE.
  Point Beach Nuclear Plant, Units 1 and 2. Kewaunee Nuclear Power Plant. Environmental radiation survey annual report, July 1969--June 1970, 25:20641 (DOCKET-50266-42)
WISCONSIN MICHIGAN POWER CO., APPLETON, WIS.
  Point Beach Nuclear Plant, Units 1 and 2. Kewaunee Nuclear Power Plant. Environmental radiation survey annual report, July 1969--June 1970, 25:20641 (DOCKET-50266-42)
WISCONSIN PUBLIC SERVICE CORP., GREEN BAY.
  Kewaunee Nuclear Power Plant. Technical specifications. Preliminary safety analysis report, Amendment 8, 25:20664 (DOCKET-50305-19)

Y

YANKEE ATOMIC ELECTRIC CO., BOSTON, MASS.
  Yankee Nuclear Power Station. Faulty removal of spent fuel assembly, 25:20579 (DOCKET-50029-145)
YANKEE ATOMIC ELECTRIC CO., WESTBORO, MASS.
  Yankee Nuclear Power Station. Operation report No. 121, January 1971, 25:20578 (DOCKET-50029-143)
YESHIVA UNIV., NEW YORK. BELFER GRADUATE SCHOOL OF SCIENCE.
  Prog. rpt., annual, 2/70--2/71, 25:20876 (NYO-3978-4)

Z

ZENTRALSTELLE FUER ATOMKERNENERGIE-DOKUMENTATION, FRANKFURT AM MAIN (WEST GERMANY).
  Surface and vacuum physics index, Vol. 5, No. 12, 1970, 25:19469

XUM

PERSONAL AUTHOR INDEX

Authors' names are indexed in the form appearing in the abstracted publication. Each entry under an author's name gives the publication title and the *NSA* volume and abstract numbers. Report numbers, where applicable, are given in parentheses at the end of the entry.

Because of problems involved in the mechanical preparation of this index, all accent marks are omitted. The following changes in spelling have been introduced to reduce some of the confusion which might result from omitting the accents:

Germanic ä appears as ae
Germanic ö oe
Germanic ü ue
Scandinavian ø oe

A

ABBATI, A., Indium-113m--DTPA in the study of the kidney, 25:19039
ABDELLATIF, Refat Ahmed, Quantum electrodynamics with no photon self-energy insertions, 25:20062
ABDINOV, O. B., Space distribution of the α-clusters in the light nuclei, 25:20268 (JINR-P4-5479)
ABDURAKHIMOV, A. U., Method of searching for the kink and determining the track parameters of particles scattered in a bubble chamber, 25:18773 (JINR-P1-5540)
ABE, Isamu, Honeycomb block used for collimation of radiations and method of manufacturing the same, 25:18656
ABE, Koya, Photoproduction of two neutral pions from hydrogen near threshold, 25:19890
ABE, Mitsuyuki, Effect of radiotherapy on the urinary amino acids, 25:19063
ABELES, B., Interaction of 9.3-GHz longitudinal phonons with electrons in superconducting films, 25:19607
  Superconducting and semiconducting phases of granular films, 25:19631
ABRAHAM, P. M., Microscopic investigation of the collective model of nuclei, 25:20547
ABRAHAM-SHRAUNER, Barbara, Suppression of runaway of electrons in Lorentz plasma. II, 25:19682
ABUL-MAGD, A. Y., Impact parameter representation for the off-energy-shell scattering amplitude, 25:20122
ACHMATOWICZ-SZMAJKE, Teresa, Radiation induced graft terpolymerization of poly(ethylene terephthalate). III, 25:18429
ACHUTHAN, P., Effective range parameter in S-wave pion--nucleon scattering, 25:20010
ACKERMANN, Norbert Joseph Jr., Analytical and experimental investigation of the neutron energy effects on reactor fluctuation spectra, 25:20832 (ORNL-TM-3245)
ACKERSON, B., Analysis of a breakup using mean track width and blob measurements, 25:18795
ADACHI, Hiromichi, Survey list of accident, hazard, and abnormality in nuclear facilities, 25:19013 (JAERI-Memo-4240)
ADAIR III, T. W., Thermomagnetic torque in deuterium gas, 25:18403
ADAMIYA, T. V., Evaluating the mobility of surface O in several oxides and their mixtures by means of O isotope exchange. I, 25:18388
ADAMS, M. F., Prog. rpt. on polymer grafting to inorganic substrates, annual, 2/69--1/70, 25:18421 (RLO-2098-1)
ADLER, Carl G., Relativistic one-dimensional square potential, 25:20065
ADLER, H. H., Interpretation of color relations in sandstone as a guide to uranium exploration and ore genesis, 25:18553
ADO, Yu. M., Results on complex adjustment and start-up of the IHEP proton synchrotron, 25:20127 (CERN-Trans-70-12)
AFANAS'EV, B. P., Selection of conditions for rotation irradiation on gamma-therapeutic apparatus Rokus, 25:19067
AFANAS'EV, G. N., Diagonalization of paired S = 0, T = 1 charge-symmetrical Hamiltonian, 25:20492
  Neutron--proton correlations in light nuclei and classification of states of group R_5, 25:20493
AFANAS'EV, N. G., Electron elastic scattering on ^{64}Zn and ^{66}Zn nuclei, 25:20345
  Electron-scattering study of the change of the charge radii of nuclei of iron and nickel isotopes, 25:20334
AFANAS'EV, V. D., Electron elastic scattering on ^{64}Zn and ^{66}Zn nuclei, 25:20345
AFANASEV, V. F., Resolving power of silicon surface-barrier counters, 25:18672
AFZAL, S. A., Ground state wave function of ^{6}Li, 25:20494
AGUILAR-BENITEZ, M., Investigation of the forward structure in charge-exchange K^{*0}(890) production, 25:19918
AHEARN, J. S. Jr., Methods for preparing replicas of slip bands preshadowed with uranium oxide, 25:19271
AHMED, M. S. H., Prog. rpt. on preservation of dates by γ-radiation, 10/70, 25:19158 (NP-18679)
AHMED, M. Y. Y., Effects of gamma radiation on cotton leaf worm, 25:19097
AHMED, N., Measurements of neutron elastic scattering from carbon in energy region of 0.50 to 2.00 MeV, 25:20267 (EUR-4538)
AHRENS, J., Experimental techniques for photon scattering below 140 MeV, 25:20189
AIDIN'YAN, N. Kh., Mercury in meteorites, 25:19303
AINSWORTH, E. John, Acute lethality and recovery of goats after 1 MVp x-irradiation, 25:19115
AKATNOV, N. I., Compression of magnetic fields by cylindrical conducting envelopes, 25:19549
AKHMEROV, R. V., Electron detection with a shower detector, 25:18786
AKHUNDOVA, G. V., Apparent distribution of planetary nebulae and open star clusters, 25:19321
AKIMOTO, Masayuki, Analysis of flux measurement near strong absorber using VISTA method. I, 25:20831 (JAERI-Memo-4238)
AKIMOVA, T. G., Methods for electrophoretic and chromatographic analysis of azo compounds. III, 25:18347
AKKI, S. B., Separation of bismuth(III) from other ions by cation exchange chromatography, 25:18520
AKOL'ZINA, L. D., Study of distribution of Sc, Ce, and Eu between the various phases of meteorite matter, 25:19302
AKSELSSON, R., Beam mapping method, 25:20138
ALAKAEVA, L. A., Titrimetric determination of the rare earth elements with 1,2-dihydroxybenzene-3,5-disulphonic acid, 25:18348
ALBRECHT, J. M., Cementation of Nb by Ti and Cr silicides for the production of protective coatings, 25:19175
ALDRIDGE, R. V., Dispersion curve for drift waves in inhomogeneous magnetoplasma, 25:19731
ALEITE, Werner, Putting into service reactor controlling equipment, 25:20551
ALEKSEEVSKII, N. E., Preparing superconductors with high parameters, 25:19599
ALEXANDER, Gideon, NN and ND interactions (above 0.5 GeV/c), 25:19899 (UCRL-20000-NN)
ALEXANDER, R. B., Lattice-site location measurements and their interpretation, 25:19798
ALEXANDER, Roger L., Tests of evaluated beryllium (n,2n) cross sections, 25:20269 (N-70-37365)
ALEXANDROV, A. M., Velocity field of turbulent fluid flow in a longitudinal streamline of clusters of rods, 25:18576 (AEC-tr-7189)
ALFES, H., Intestinal absorption of metallic mercury, 25:18369
ALFORD, W. P., Identification of particle-hole multiplets in ^{40}Sc, 25:20350
ALFVEN, H., Symmetric cosmology, 25:19463
ALFVEN, Hannes, Plasma physics applied to cosmology, 25:19466
ALHERITIERE, E., Research and development of new high temperature resistant Nb alloys, 25:19218
ALI, M. Khalil, Regional pulmonary function in metastatic carcinoma to the lung studied with ^{133}Xe, 25:19048
ALI, S., Ground state wave function of ^{6}Li, 25:20494
ALIEV, S., Spectroscopic studies of peculiar A stars of Mn group, 25:19343
ALI-ZADE, D. G., Pulse amplitude discriminators based on avalanche transistors, 25:18847
ALLAN, D. L., Analysis with a Po--Be source, 25:18368

ALLEN, B. J., Fast neutron capture cross section facility, 25:20149
Review of gamma-ray transitions from keV neutron capture, 25:20227 (AAEC/TM-565)
ALLEN, Mildred, 1970 solar eclipse as seen by torsion pendulum, 25:19431
ALLEN, R. M., Electrical properties of boron-implanted silicon, 25:19815
Implantation of compound semiconductors, 25:19789
ALLER, Lawrence H., Comparison of spectra of planetary nucleus and Wolf--Rayet star, 25:19310
ALLIBERT, C., Study of niobium base refractory metal alloys, 25:19246
ALSMILLER, R. G. Jr., Absorbed dose and dose equivalent from negatively and positively charged pions in the energy range 10 to 2000 MeV, 25:20226
ALSTON-GARNJOST, M., Branching ratios of the A_2^+ meson observed in 7 GeV/c π^+p interactions, 25:19920
AL-UTHMAN, Hilmi Sabir, Effect of x-irradiation on blowfly, 25:19098
ALVENSLEBEN, H., Photoproduction of pion pairs with high invariant mass, 25:19886 (DESY-70/61)
ALVES FILHO, Mario, Radiations, 25:18971
AMALDI, U. Jr., Spectral distributions of fast and slow components in a liquid scintillator, 25:18678
AMBROSINO, George, Nuclear physics: remarks on the values of nuclear radiation from alpha radioactivity, 25:20482 (RFP-Trans-72)
AMBRUS, Julian L., Proliferation of donor spleen and bone-marrow cells in the spleens and bone marrows of unirradiated and irradiated adult mice, 25:19129
AMER, Soheir M., Cytogenetic studies on effect of chronic gamma irradiation on Vicia faba, 25:18950
AMIRKHANOV, I. V., Motion of particles in the fixed centers field, 25:20059 (JINR-P4-5547)
AMITIN, M. B., Unsteady flow of mercury in a trough in a transverse magnetic field, 25:19553
AMMAN, F., Positron--electron storage ring ADONE, 25:20193
AMMANN, H., Production and assemby of the Muehleberg pressure vessel, 25:20555
AN, Shigehiro, Energy modal synthesis method in fast reactor analysis, 25:20709
ANANTANARAYANAN, S., Radiation processed wood-plastic materials, 25:19298
ANCELLIN, J., Buildup of radionuclides in marine species, 25:18894
ANDERSEN, C. M., Bootstrap models and special property of unitary Lie algebras, 25:19999
ANDERSEN, S. A., Ion-velocity distribution function in a single-ended Q machine, 25:19670
ANDERSON, D. H., Barium and Sr in silicates, 25:18335
ANDERSON, D. W., Photoneutron cross sections for ^{32}S, 25:20332
ANDERSON, H. L., Muonic x rays and capture gamma rays in ^{89}Y, 25:20360
ANDERSON, Janet Askue, Interactions of Mn^{++} with nucleosides, dinucleotides and DNA, 25:20854 (COO-78-235)
ANDERSON, V. E., Atomic and molecular radiation physics, 25:19491 (ORNL-4584, pp 105-24)
Electron and ion collision physics, 25:19490 (ORNL-4584, pp 92-104)
Theoretical radiation physics, 25:19757 (ORNL-4584, pp 58-73)
ANDERSSON, A., Annealing experiments on Si layers implanted with 50-keV P ions, 25:19779
ANDERSSON, Bengt, Histopathology of late radiolesions, 25:19124
ANDO, Atsushi, Distribution to organs of ^{131}I--erythrosine B, 25:19060
ANDO, Masao, Seeking for the merits of a nuclear iron mill, 25:19182
ANDRE, Garnier, Radioactive aerosol sampling device, 25:18877
ANDREEV, A. M., Experimental investigation single-wave MHD* machines, 25:19537
Investigation of longitudinal edge effect in primary circuit of linear MHD machines, 25:19538
ANDREEV, D. S., Elimination of correlation effects in the detection of gamma quanta, 25:18669
ANDREEV, Yu. A., Investigation of gamma radiation of isomers /sup 110m/In and ^{110}In, 25:20402
ANDREWS, E. G. David, Systematic approach to the design and development of HTR gas turbine power stations, 25:20702
ANDREWS, J. G., Sheath criterion for a growing sheath, 25:19677
ANGEL, J. R. P., Detection of circular polarization in a second white dwarf, 25:19329
ANGELINO, G., Real gas effects in carbon dioxide cycles, 25:18587
ANGELOV, B. P., Sensitivity of a secondary-emission-type accelerated-electron-beam position monitor, 25:20173
ANGER, H. O., Lung function studies using short-lived /sup 81m/Kr and the scintillation camera, 25:19056
ANGER, Hal O., Myocardial uptake studies with ^{129}Cs and the scintillation camera, 25:19055
ANGERMAN, C. L., Prog. rpt. on ^{60}Co power and heat sources, 7--9/70, 25:18591 (DP-1254)
ANISHCHENKO, N. G., Experimental solenoid made of Nb$_3$Sn strip, 25:19588 (JINR-P8-5440)
ANISOVICH, V. V., Calculation of box diagram effects with two resonances in the intermediate state, 25:19986 (IFVE-STF-70-34)
ANSARI, A., Angular momentum projection approach to nuclear rotations in rare-earth region, 25:20541
ANTALOVA, A., UBV photographic photometry of stars. I, 25:19334
ANTIPOV, Yu. M., Production of low momentum negative particles by 70 GeV protons, 25:19906
ANTIPPA, Adel F., Width of the rho meson by the Balazs, 25:19989
ANTMAN, S., Decay of ^{131}Ba, 25:20414
ANTOKU, Shigetoshi, Protective effect of AET against fast neutron and x-ray irradiation, 25:19029
ANTOLKOVIC, B., Neutron--proton bremsstrahlung at 14.4 MeV, 25:20257
APONICK, Athony A. Jr., Shapes of rare-earth nuclei, 25:20466
APPARAO, Krishna M. V., Upper limit on radio flux from Sco X-1 at 327 MHz, 25:19355
APPLEBY, A., Scavenging of the molecular hydrogen yield from water irradiated with tritium β particles, 25:18458
ARAKAWA, E. T., Interaction of radiation with liquids and solids, 25:19758 (ORNL-4584, pp 74-86)
Physics of tissue damage, 25:19759 (ORNL-4584, pp 87-91)
ARAKAWA, Kazuo, Hypertron-30 electron accelerator for the radiation curing of paint-coating, 25:20213
Mass spectrometric studies on negative ion--molecule reactions of nitroethylene, 25:18428 (NP-18676)
ARAKI, Fumio, Studies on the bone marrow of a-bomb exposed in hiroshima by autoradiography, 25:19134
ARAKI, Kimiko, Effects of x-irradiation on ^{14}C-pyruvate metabolism in rat thymocytes, 25:18902
ARCHULETA, R. J., Efficiency of channel electron multipliers for electrons of 1 to 50 keV, 25:18659
ARIEL, P. D., Equilibrium of inviscid, infinitely conducting fluid in horizontal magnetic field with Hall current, 25:19545
ARIMA, A., Charge asymmetry of nucleon widths of lowest T = 3/2 states of ^{13}N and ^{13}C, 25:20512
Structure of positive parity states of ^{20}Ne, 25:20351
ARKHANGELSKAYA, V. A., Total antiresonance in CaF$_2$: Dy crystals with color centers, 25:19771
ARKUSZEWSKI, Jacek, MINIGASKET: code for thermal neutron scattering law in polycrystals, 25:20229 (INR-1186)
ARMBRUSTER, P., Gas-filled magnetic separators, 25:18851
Identification of μs-isomers among primary fission products, 25:20430
ARMITAGE, B. H., Analysis with a Po--Be source, 25:18368
ARMITAGE, S. A., Damage studies in ion-implanted CdS, 25:19791
ARMSTRONG, Carla L., Computer program for calculating, tabulating, and plotting outgassing rates of selected gases, 25:19195 (ORNL-TM-3220)
ARMSTRONG, D. D., Supercollimation of negative ion beams with apertures, 25:18842
ARMSTRONG, T. W., Absorbed dose and dose equivalent from negatively and positively charged pions in the energy range 10 to 2000 MeV, 25:20226
ARNETT, David W., Helium production by pulsationally unstable massive stars, 25:19331
ARONOFF, Elihu J., Radiation curable paint containing a vinyl ester binder resin having pendant diester groups, 25:18439
ARRATHOON, R., Helium 2^{1}S--n^{1}P metastable transition probabilities, 25:19481
ARSLANOVA, S. V., Pyruvic acid content of cells of cotton plants following γ irradiation, 25:18918
ARTEMOV, A. D., Vacuum system for the 70-GeV proton synchrotron, 25:20126 (CERN-Trans-70-9)
ASHBURN, William L., Digital and analog processing of Anger camera data with a dedicated computer-controlled system, 25:18730
ASRIYAN, N. S., Radioinduced anomalies in cotton pollen, 25:18955
ASTAF'EV, E. R., Physical conditions in atmosphere of P Cygni, 25:19342
ASTON, D. R., Intermediate mixed state of Type-II superconductors, 25:19620
ASYEE, Future of reprocessing in Europe, 25:18500 (NP-18669)
ASZALOS, Z., Morphological changes in nervous system (of cats) induced by ionizing radiation, 25:19109
ATANASOV, A., Schmidt method applied to solving the quasipotential equation, 25:19987 (JINR-P2-5566)
ATANASSOV, A. A., Bound states of a relativistic two-particle system, 25:20083
ATHERTON, D. L., High-current density superconducting magnets using heavy currents, 25:19644
ATKINSON, D., Use of non-linear techniques in S-matrix theory, 25:20107
ATKINSON, K. C., State of cure of printed circuit boards, 25:20848 (BDX-613-233)
AU, Whitlow W. L., Morphology of backscatter from F-layer field-aligned irregularities, 25:19574
AUBERT, J. J., Large-area wire spark chambers with two-coordinate read-out and ferrite core memory, 25:18790
Production of initially pure K^0 beam of known momentum, 25:20144
AUBRY, J., Cementation of Nb by Ti and Cr silicides for the production of protective coatings, 25:19175

AUCHAPT, Jacqueline M., Decladding and dissolution of UO_2 and PuO_2 fuels, clad with stainless steel or Zircaloy, 25:18493 (CEA-Bib-191)
AUCHAPT, Pierre R., Decladding and dissolution of UO_2 and PuO_2 fuels, clad with stainless steel or Zircaloy, 25:18493 (CEA-Bib-191)
AUGUSTYNIAK, W. M., Implantation of Bi into GaP. II, 25:19846
AULOV, V. A., Application of the method of radiothermoluminescence for the investigation of high-temperature relaxation in polyethylene, 25:18435
AVDONINA, E. N., Processes for the destruction of the n-hexane molecule due to the action of tritium recoil atoms, 25:18487
AVELEDO, C. E., Table of E0 conversion probability electronic factors, 25:20484
AVER'YANOV, I. K., Calculations of cross sections for inelastic interaction of neutrons with nuclei accompanied by emission of protons and α particles, 25:20346
AVIO, C. M., Behavior of a stabilized cellular strain cultured in a medium contaminated with ^{137}Cs. III, 25:18904
AVISHAI, Y., Integral equation for the N-particle resolvent operator, 25:20487
AVIV, R., Axial-current divergences and the reactions $\gamma + \gamma \rightarrow$ pions, 25:19951
AXFORD, W. I., Atmosphere of Hg, 25:19467
Higher-order approximations in theory of longitudinal plasma oscillations. II, 25:19750
AXMANN, A., Effect of ion implantation on electrical properties of SiO_2 films at high fields, 25:19788

B

BABA, H., Absolute measurement of beta-disintegrating nuclides, 25:20421
BABA, N., Half-lives of some fission product nuclides, 25:20339
BABA, S., Absolute measurement of beta-disintegrating nuclides, 25:20421
Half-lives of some fission product nuclides, 25:20339
BABCOCK, Dale F., Dual temperature isotope exchange process, 25:18514
Dual temperature isotope exchange process, 25:18512
Dual temperature isotope exchange process, 25:18513
BABENKO, N. P., Neutron polarization in the reaction $^{12}C(d,n)^{13}N$ at E/sub d/ = 6.4 MeV, 25:20297
BABESHKIN, A. M., Gamma-radiolysis of tin oxides, 25:18470
BABICH, Valentin Grigorievich, Weight and radioactive concentation of aerosols, 25:18685
BACHL, H., Simplified survey of design features and development lines of nuclear power stations, 25:20556
BACHNER, E., Measurement of neutron spectrum at beam hole of FRJ-1 reactor in energy range from 10 keV to 10 MeV, 25:20798
BACHO, I., Gas-filled mass separator for investigations of heavy-ion reaction products, 25:20175
BACHURIN, V. I., Effect of microwaves on revascularization of the blood supply in free skin grafts, 25:19104
BACKENSTOSS, G., Pionic atoms, 25:19483
BADAEVA, T. A., Structure of $ThRe_2$--$GdRe_2$ ($TbRe_2$, $DyRe_2$, $ErRe_2$), 25:19235
BADER, R., Low-energy B and P implants in Si. B, 25:19836
BADGETT, Charles O., Radiation fill gauge, 25:18820
BAECKLIN, A., Transition rates in ^{192}Au, 25:20453
BAEHRE, G., Isomer shift and quadrupole splitting of the 2^+-rotational state in ^{174}Yb, 25:20399
BAERS, Bruno, Information theoretical aspects of power spectrum measurements in nuclear reactors, 25:20821 (TKK-F-A-102)
Variety and hierarchy of data extraction methods in nuclear reactor noise analysis, 25:20822 (TKK-F-A-137)
BAHCALL, John N., Multiple absorption redshifts in quasars, 25:19371
BAHRAMI, H., Improved high-beam-current ion implanter, 25:20167
BAICAN, R., Microwave dielectric measurements of gamma-irradiated ferroelectric ammonium sulfate, 25:19856
BAIER, R., Unitarity and crossing symmetry in low-energy π--π scattering, 25:19993
BAILEY, Peter, Corpus allatum size and ovarian environment in irradiated cucumber fly, 25:19096
BAILLET, Francois, Place of implantation in tongue and floor of mouth cancer, 25:19080
BAINBRIDGE, G. R., Electrical generation and associated developments with atomic energy, 25:20550 (NP-18677)
BAKER, R. A., Ultrasonic characterization and computerized analysis of graphite billets, 25:18613 (SC-DR-70-693)
BAKH, N. A., Effect of temperature and oxygen on the composition of the γ-radiolysis products of isooctane (2,2,4-trimethylpentane), 25:18471
BALAKRISHNAN, M., States in ^{10}B from elastic scattering of alphas by ^6Li, 25:20292
BALDWIN, D. E., Interpretation of spatially decaying ion-acoustic waves, 25:19741
BALDWIN, T., Sodium aerosol filtration studies, 25:18563 (CONF-700816-(Vol.1), pp 445-56)
BALDWIN, Thomas O., Observation of x-ray diffuse scattering from neutron-irradiated silicon, 25:19853
BALKAS, Turgut I., Radiation chemistry of aqueous solutions of $CFCl_3$, CF_2Cl_2, and CF_3Cl, 25:18460
BALL, G. C., Properties of low-lying states in ^{43}Sc, 25:20320
BALL, J. B., Studies of ^{95}Ru and ^{94}Ru with the $^{96}Ru(p,d)$ and (p,t) reactions, 25:20436
BALLUND, H., Lutetium-170 → ^{170}Yb decay, 25:20452
BALSEY, Ben B., Unidentified plasma irregularities in the equatorial electrojet, 25:19573
BAMMERT, K., Development of components for nuclear power stations with helium turbines, 25:20777
BAMPTON, P. F., Evaluation of anti ν for ^{239}Pu, 25:20363 (AWRE-O-86/70)
BAND, I. M., Formation region of internal conversion coefficients, 25:20515
BANDYOPADHYAY, Gautam, Kaolinite dehydroxylation studies on compact specimens, 25:20901 (UCRL-20393)
BANDYOPADHYAY, P., Gravitation and neutrinos, 25:20090
BANERJEE, K., Possible utilization of the Carnegie-Mellon synchrocyclotron for cancer therapy, 25:19087
BANEVER, Carol, Growth of the human liver: a preliminary scan study, 25:19061
BANKS, P. H. T., Present status of polarized targets at the Rutherford Laboratory, 25:20135 (RHEL/R-201)
BANKS, P. M., Atmosphere of Hg, 25:19467
BANNISTER, Roger, Place of isotope encephalography by the lumbar route in neurological diagnosis, 25:19043
BARANGER, Michel, Nuclear structure. II, 25:20532
BARANOVSKII, E. A., Wilson effect in the absorption lines, 25:19432
BARASHENKOV, V. S., Double differential distribution of particles produced in the proton-nucleus collisions, 25:20018 (JINR-P2-5507)
Space distribution of the α-clusters in the light nuclei, 25:20268 (JINR-P4-5479)
BARAT, Michel, Excitations in low-energy ion--atom collisions, 25:19493
BARBARO-GALTIERI, A., Branching ratios of the A_2^+ meson observed in 7 GeV/c π^+p interactions, 25:19920
BARBASHOV, B. M., Straight-line particle path approximation in description of high-energy hadron scattering, 25:19927
BARBUR, I., Microwave dielectric measurements of gamma-irradiated ferroelectric ammonium sulfate, 25:19856
BARDIN, D. Yu., Decays $\pi^+ \rightarrow e^+(\mu^+)\nu e^+e^-$, 25:19963 (JINR-P2-5520)
BARDOLLE, J., Study of the oxidation of Nb, 25:19177
BARDSLEY, J. N., Potential curves for He_2^+ and Li_2^+, 25:19479
BARDYUKOV, Yu. V., 180-liter xenon bubble chamber, 25:18783
BARGUIL, J., Nucleon elastic scattering by ^4He, 25:20261
BARIL, Marcel, Application of electrostatic mirrors in the elimination of chromatic effect in magnetic spectrometers. II, 25:18875
BARISIC, S., Pressure enhancement of superconductivity in V_3Si, 25:19605
BARKAI-GOLAN, Rivka, Control of Penicillium--digitatum in inoculated citrus fruits, 25:19162
BARKER, R. W., EBR-II irradiation effects of rupture of Type-316 stainless steel, 25:19254 (WHAN-SA-2)
BARLOUTAUD, R., Baryon exchange in reactions $K^-n \rightarrow Y\pi^-$ at 3 GeV/c, 25:19917
BARNABY, C. F., Calibration of whole-body counter, 25:18695
Follow-up of thyroid carcinoma by whole-body counting, 25:19035
BARNES, V. E., Investigation of the forward structure in charge-exchange $K^{*0}(890)$ production, 25:19918
BARNETT, Mark, How to protect patient and physician during x-ray examinations. I, 25:19010
BARRALL, Raymond C., Distribution and dosimetry of /sup 113m/In colloid, 25:18994
BARRETTE, J., Directional correlations of gamma rays in ^{152}Sm and ^{152}Gd, 25:20385
BARRETTE, M., Directional correlations of gamma rays in ^{152}Sm and ^{152}Gd, 25:20385
BARTHOLOMEW, G. A., Reaction $^{115}In(n,\gamma)^{116}In$, 25:20410
BARTKO, Frank Jr., Accuracy of some current objective prism stellar radial velocities, 25:19316
BARTON, C. J., Dose estimation studies related to peaceful uses of nuclear explosives, 25:18989 (ORNL-4584, pp 42-56)
BARTON, J. C., Improved ringing coil pulse encoders, 25:18868
BARTON, P. J., Structure and tensile properties of steel as function of fast irradiation temperature, 25:19251 (AERE-R-6435)
BARTSCH, G., Magnetoplasmadynamic energy conversion in nuclear power stations, 25:20768
BARUT, A. O., Nonrelativistic and relativistic Coulomb amplitude as matrix element of rotation in O(4,2), 25:20040
BARZ, A., Properties of ultra high vacuum extractor gages, 25:18838
BASHILOV, V. A., Experimental solenoid made of Nb_3Sn strip, 25:19588 (JINR-P8-5440)
BASSANO, D., Investigation of the forward structure in charge-exchange $K^{*0}(890)$ production, 25:19918
BATCHELOR, R. A., OH (1667) line absorption, 25:19382
BATES, J. F., Irradiation produced defects in austenitic

stainless steel, 25:19253 (WHAN-FR-16)
BATES, J. L., Properties of molten ceramics, 25:19273 (BNWL-SA-3579)
BATUROV, B. B., Nuclear power plants, 25:20549 (AEC-tr-7187)
BATUSOV, I. A., Meson production by interaction of π^+ mesons wfth photoemulsion kernels at 185 to 295 MeV energies, 25:19919
BAUDON, Jacques, Excitations in low-energy ion--atom collisions, 25:19493
BAUM, J. W., Dose equivalent meter designs, 25:18809
BAUM, John W., Pressurized gas monitor for low level radioactive gases, 25:18744
BAUM, V. A., Water temperature distribution in cassettes of water-cooled and water-moderated reactor (VVER), 25:20737
BAUMANN, P., Silicon-28 energy levels near 13.245 MeV, 25:20330
BAUMGAERTEL, G., Simultaneous determination of Pu(IV) and nitric acid, 25:18350
BAURMASH, L., Behavior of iodine in the presence of sodium oxide aerosols, 25:20761 (CONF-700816-(Vol.1), pp 373-92)
BAXTER, A. M., Gamma-ray polarization measurements in ^{22}Na, 25:20318
BAYLY, A. R., Ion-beam irradiation of glasses, 25:19787
BAZIN, J. P., Dosimetry of the gastro-intestinal tract, 25:19141
BEACH, S. A., Effect of acute x-irradiation on development of eggs of plaice, Pleuronectes platessa, 25:19103 (PG-Report-1013)
BEALE, J. R. A., Applications to semiconductor devices, 25:19782
BEATTIE, R. J. D., Angular distributions and energy spectra of internal bremsstrahlung emitted during beta decay of ^{32}P, ^{90}Y, ^{204}Tl, and ^{210}Bi, 25:20417
BEAU, M., Research report on measurement of average number of prompt neutrons, 25:20373 (LIB/Trans-300)
BEAUCHAMP, E. K., Fracture branching and dicing in stressed glass, 25:20894 (SC-RR-70-766)
BEAUPRE, J. V., t-channel helicity conservation in diffractive reactions producing A_1 and Q-mesons, 25:19921
BEAVERS, J. B., Effects of gamma irradiation or the chemosterilant, tepa, on the citrus red mite and its progeny, 25:19100
BECCHETTI, F., Core-polarization effects in charge-exchange reactions; application to ^{58}Ni(^{3}He,t), 25:20496
BECK, H. L., Monte Carlo calculations of electromagnetic shower transition effects, 25:19943
BECKA, J., Utilization of electroslag welding in the production of steel pressure vessels for nuclear reactors, 25:19181
BECKER, David V., Evaluation of spleen size during routine liver imaging with /sup 99m/Tc and the scintillation camera, 25:19057
BECKER, Donald A., Prog. rpt. on activation analysis, annual, 7/69--6/70, 25:18366 (NBS-TN-548)
BECKER, Donald Arthur, Chemical interferences and ionization in high temperature flames, 25:20859 (IS-T-417)
BECKER, Klaus, Applied dosimetry research, 25:18799 (ORNL-4584, pp 165-86)
  New trends in personnel dosimetry, 25:18811
BECKER, U. J., Photoproduction of pion pairs with high invariant mass, 25:19886 (DESY-70/61)
BECKERS, J., Realizations of representations of Poincare group, 25:20035
BECKMAN, J. E., Solar enhancements at 1.2-mm wavelength, 25:19409
BEDER, D. S., Calculations of π^+ production in nuclei, 25:20031
BEDFORD, R. G., Studies of the europium--oxygen--fluorine and samarium--oxygen--fluorine systems, 25:19285
BEENAKKER, J. J. M., Rotational relaxation of HD below 40 K, 25:19480
BEETEM, W. A., Radiochemical analysis of water from wells, springs, and streams in central Nevada, 25:18522 (USGS-474-97)
BEGZHANOV, R. B., Nuclear structure, 25:20503
BEHRENS, H., Beta--γ (CP)-asymmetry coefficients in isospin forbidden allowed mixed β transitions, 25:20372 (KFK-1249)
BEKAURI, N. G., Investigation of aromatic hydrocarbons of supsinskaya petroleum and their catalytic conversion in the presence of irradiated catalysts, 25:18444
BEKH, A. D., High speed magnetic-chip memory in a scanning robot for measurement of chamber photographs, 25:18780
BEKKER, A. A., Gamma-radiolysis of tin oxides, 25:18470
BEKMURADOV, O., Water temperature distribution in cassettes of water-cooled and water-moderated reactor (VVER), 25:20737
BELCARZ, E., Beta spectrometer with a Si(Li) detector in homogeneous magnetic field, 25:18736 (INR-P-1227)
  Beta spectrometer with Si(Li) detector in homogeneous magnetic field, 25:18767
BELL, D. A., Table of E0 conversion probability electronic factors, 25:20484
BELL, Donald A., M0 transitions in spherical nuclei, 25:20306
BELL, G. D., Risk evaluation for any curie release spectrum and any dose-risk relationship, 25:18974 (AHSB(S)R-192)
BELL, Ronald L., Enhanced scintigraphic information display using computer-generated ratio techniques, 25:19053
BELLIAN, J. G., Radiation hazards in industry, 25:18973
BELOUSOV, A. S., Cherenkov total-absorption spectrometer, 25:18787
BELYAKINA, T. S., Photoelectric observations of AG Dra from 1962 to 1967, 25:19341
BENAKIS, Achille, New gels used in liquid scintillation, 25:18687
BENARY, Odette, NN and ND interactions (above 0.5 GeV/c), 25:19899 (UCRL-20000-NN)
BENDER, Myron L., Mechanisms of monofunctional and bifunctional catalysis of an ester hydrolysis. The kinetics of methyl 2,6-dicarboxybenzoate hydrolysis, 25:18400
BENDIX, P., Calculations of π^+ production in nuclei, 25:20031
BENENSON, E. B., End effects in magnetogasdynamic channels with finite-size terminal insulators, 25:19548
BENEVENTANO, Marcello, Impulse approximation calculation of the polarization of the recoil proton in the reaction $\gamma + n \to p + \pi^-$ in deuterium, 25:19940
BENNETT, Gary Lee, Reaction mechanisms in ^{10}B + ^{3}He system at 1.38 and 1.60 MeV, 25:20303
BENNINGHOVEN, A., Tandem mass spectrometer for secondary ion studies, 25:18841
BENTON, E. V., Method for development of volume tracks in dielectric nuclear track detectors, 25:18708
BERANGER, G., Contamination of Nb by O during electrolytic polishing and annealing under vacuum, 25:19171
BERENYI, D., Distorting effect of the absorbers for the semiconductor and scintillation gamma-ray spectra, 25:18771
  Effect of thin foils on the spectrum of monoenergetic electrons, 25:18770
  Internal bremsstrahlung spectrum accompanying positive beta decay of ^{11}C, 25:20302
  Internal bremsstrahlung spectrum from ^{32}P, 25:20340
  Study of decay of ^{145}Sm, 25:20465
BEREZIN, F. A., Non-Wiener continual integrals, 25:20119
BERG, C., Silicon detector as absolute gamma dosimeter, 25:18806
BERGER, David S., Elective irradiation of the neck lymphatics for squamous cell carcinomas of the nasopharynx and oropharynx, 25:19084
BERGER, K.-H., VEB RFT Messelektronik Dresden linear amplifier/analyzer VA-V-100, 25:18873
BERGGREN, G., Ceramics in nuclear technology, 25:20739
BERGMANN, Wilfried H., Determination of losses in pulsed superconducting magnets in superfluid He, 25:19642
BERGSTROEM, I., Prog. rpt. on experiments with accelerator beams, annual, 1969, 25:20133 (NP-18671)
BERINDE, A., Reaction mechanism for proton scattering on ^{60} ^{62}Ni and ^{64} ^{66}Zn, 25:20322
BERLIN, A., Neutron flux measurement by counting the associated ^{3}He particles from T(p,n) reaction, 25:18647
BERLINER, Ernst, Kinetics of iodination of sodium phenylpropiolate, 25:18397
BERLINGHIERI, Joel Carl, Kaon, hyperon, and antihyperon final states in K^+p interactions near 13 GeV/c, 25:19914
BERNARDET, H., Measurements and calibrations at pressures between 10^{-5} and 10^{-12} torr, 25:18878
  Operation of the gages with a screened collector, 25:18837
BERNDT, C. W., Weapons effects display system (WEDS MOD II): mathematical models used for calculations, 25:18831 (UCRL-50892(Vol.1))
BERNSTEIN, E. M., One-phonon octupole vibration of ^{151}Eu, 25:20432
BERNSTEIN, I. B., Symmetry considerations for grid-launched ion-acoustic waves, 25:19742
BERNSTEIN, Ira B., New derivation of quasi-linear theory, 25:19738
BERNSTEIN, R. B., Molecular collisions. XIV, 25:19498
BERRY, R. Stephen, Photoemission and electron detachment in low-energy collisions of metastable atoms with negative ions, 25:19511
BERTHOLLET, Pierre, Analytical methods used by Geochemical Section: water, 25:18339 (CEA-R-3557(2))
BERTIE, J. E., Infrared and Raman spectra and vibrational assignment of methylene cyclopropane-h_6 and -d_6, 25:18402
BERTIN, A., Response of large volume NE-213 liquid scintillators to electrons and protons, 25:18655
BERTINOV, A. I., Nonstationary electrically conducting free jet in a transverse magnetic field, 25:19567
BERTRAM, William K., Photoproduction of pion pairs with high invariant mass, 25:19886 (DESY-70/61)
BERTRAND, Francoise, Study of reactions ^{9}Be + t below Coulomb barrier, 25:20265 (CEA-R-4117)
BERTRAND, R., Research report on measurement of average number of prompt neutrons, 25:20373 (LIB/Trans-300)
BERULIS, I. I., Physical conditions in the Orion Nebula, 25:19365
BESPALOV, D. F., Small-size neutron tube of UNG-1 type, 25:20228 (CSIRO-Trans-10095)
BESSING, Reinhold, Moisture determination in solids by neutron radiation, 25:18362

XUM

BESSLER, L., Dynamical rearrangement of spontaneously broken chiral symmetry, 25:20042
BETHGE, Klaus, Alpha-particle transfer reactions, 25:20450
BETHOUX, O., Niobium base superconductors, 25:19219
BETTENHAUSEN, R., Evaluation of an LN_2-temperature solid state spectrometer for rocket borne experiments, 25:18654
BEU, K. E., Detailed derivations of equations used in the likelihood ratio method for the precise and accurate determination of lattice parameters for cubic materials, 25:20856 (GAT-T-999)
BEVINGTON, P. R., High performance linear emitter follower, 25:18860
BEWLEY, D. K., Monitors for electron beams, 25:20214
BEYSTER, J. R., Safeguards applications for isotopic neutron sources, 25:18619 (BNL-50267)
BEZUCHA, Jaromir, Changes in residual carbon content in UO_2 pellets during decarbonization and initial phases of sintering, 25:19274
BHACCA, N. S., Structure of nitroform in various solvents, 25:18391
BHADURI, R. K., Jost function of a non-local potential, 25:20539
BHARATHAN, K. G., Radioactivity in the diet of population of the Kerala coast, 25:19143
BHATIA, A. K., Generalized Hylleraas calculation of positron--hydrogen scattering, 25:19508
BIALYNICKI-BIRULA, I., Classical electrodynamics in two dimensions: exact solution, 25:19962
BIANCASTELLI, R., Spectral distributions of fast and slow components in a liquid scintillator, 25:18678
BIANCHINI, F. G., Photofission cross sections of uranium and thorium near threshold, 25:20366 (IEA-211)
BICKNELL, R. W., Electrical and electron microscope studies of annealed ion-implanted silicon, 25:19777
  Electrical properties of boron-implanted silicon, 25:19815
BIEDENHARN, L. C., Identity satisfied by Racah coefficients of U(n), 25:20034
BIELER, Julianne, Effect of x rays on developing cysticercoids of Hymenolepis microstoma, 25:19095
BILELLO, J. C., Prog. rpt. on slip initiation and microdymamics of flow in tungsten, 1--12/70, 25:19194 (NYO-4073-4)
BILEN'KII, S. M., Decays $\pi^+ \to e^+(\mu^+)\nu e^+e^-$, 25:19963 (JINR-P2-5520)
BILGER, H. R., Electrical properties of alkali implants in silicon, 25:19780
BILLUPS, Carolyn, Near-uv absorption bands of tryptophan, 25:20899 (UCLA-12-810)
BIRGER, B. L., Estimate of field in winding zone of plane linear induction MHD machines, 25:19539
BIRKHOFF, R. D., Interaction of radiation with liquids and solids, 25:19758 (ORNL-4584, pp 74-86)
  Low-energy electron beam studies in thin aluminum foils, 25:19766
  Physics of tissue damage, 25:19759 (ORNL-4584, pp 87-91)
BIRKS, J. B., Atomic and molecular radiation physics, 25:19491 (ORNL-4584, pp 105-24)
BISCHOFF, F. G., Monte Carlo evaluation of multiple scattering and resolution effects in double-differential neutron scattering cross section measurements, 25:20235 (RPI-328-211)
BISHOP, Barbara L., Absorbed dose and dose equivalent from negatively and positively charged pions in the energy range 10 to 2000 MeV, 25:20226
BISHOP, D. E., Ultrasonic characterization and computerized analysis of graphite billets, 25:18613 (SC-DR-70-693)
BISNOVATYI-KOGAN, G. S., Explosion of a rotating star as a supernova mechanism, 25:19326
BITSCH, D., Power level control of a closed loop gas turbine, by natural transfer of gas between the loop and auxiliary tanks, 25:20712
BJARNHOLT, G., Lattice location of heavy group III and V elements implanted into Ge, 25:19827
BJOERKQVIST, K., Diffusion effects in ion-implanted germanium, 25:19841
  Lattice location of heavy group III and V elements implanted into Ge, 25:19827
BJORKHOLM, Paul James, Deuteron stripping reactions on ^{16}O, ^{52}Cr, ^{54}Fe, and ^{90}Zr, 25:20305
BLACHOT, Jean, Isomer of ^{138}Cs, 25:20381
BLACK, S. C., Radioiodine field studies with synthetic aerosols, 25:18926 (CONF-700816-(Vol.1), pp 49-71)
BLACK, W. C., Toward the superconductivity of rhodium, 25:19606
BLACKADAR, A. K., Prog. rpt. on effects of a change of terrain on wind profiles, final, 7/1/65--8/15/68, 25:20875 (NYO-3562-3)
BLACKBURN, J. A., Self-resonant current peaks in Josephson junctions, 25:19612
BLAHD, W. H., Scintillation camera in the dynamic evaluation of renal disorders, 25:19046
BLAIR, J. M., A method of estimating errors in experimental data, 25:20845 (AECL-3781)
BLAMIRES, N., Antimony-implanted silicon, 25:19825
BLAMIRES, N. G., Influence of ion-bombardment damage on annealing behaviour of boron-implanted silicon, 25:19776
BLANEY, Benjamin, Photoemission and electron detachment in low-energy collisions of metastable atoms with negative ions, 25:19511
BLOESS, D., Determination of neutrino spectrum in CERN 1967 neutrino experiment, 25:19892
BLOKHIN, M. A., X-ray spectral apparatus (review), 25:18673
BLOMEKE, J. O., Disposal in natural salt formations, 25:18623 (ORNL-4584, pp 16-36)
BLOMQVIST, G., Hardware system for measurements of bubble chamber films on-line, 25:18776 (USIP-70-3)
BLONDELOT, E., Predicted ultraviolet fluxes for main-sequence stars, 25:19347
BLOOMER, R. H., Use of a pulsed Van de Graaff accelerator and time-of-flight techniques to reduce backgrounds in (α,γ) spectroscopy experiments, 25:20148
BLUE, James W., Cyclotron production of ^{123}I: an evaluation of the nuclear reactions which produce this isotope, 25:18480 (BRH/DMRE-70-4)
BOBBIO, A., Neutron transmission study through simple bent conducting tube, 25:20245
BOBELDIJK, C., Kink instability of toroidal plasma column, 25:19704 (NP-18681)
BOBKOV, V. P., Method of calculating the coefficients of turbulent heat transfer in channels of a complex form, 25:20844 (AEC-tr-7186)
BOBLETER, O., Distribution of Np in nitric acid solution containing uranyl ion, 25:18519
BOBMANN, Werner, Nuclear power plant with wet-steam generator and steam drying system, 25:20743
BOCCALARI, M., Mechanical and metallurgical steel/Zr junctions, 25:19183
BODAS, N. G., Magnetohydrodynamic flow past a semi-infinite flat plate with transverse magnetic field, 25:19570
BODI, A., Microwave dielectric measurements of gamma-irradiated ferroelectric ammonium sulfate, 25:19856
BODIN, H. A. B., Formation of an axisymmetric bulged region in a long uniform plasma column, 25:19709
BOERBOOM, A. J. H., Diffusion coefficients of isotopic mixtures of CO and N_2, 25:18604
BOESEBECK, K., t-channel helicity conservation in diffractive reactions producing A_1 and Q-mesons, 25:19921
BOGDAN, D., Correction matrix elements for the first forbidden β^- transition in ^{198}Au, 25:20438
BOGDANOV, D. D., Gas-filled mass separator for investigations of heavy-ion reaction products, 25:20175
BOGDANOV, P. V., Vacuum system for the 70-GeV proton synchrotron, 25:20126 (CERN-Trans-70-9)
BOGUSLAVSKII, Yu. Ya., Certain magnetohydrodynamic flow problems related to wave propagation, 25:19566
BOHLIN, Ralph Charles, Ultraviolet and visual spectra of γ Cassiopeiae, 25:19332
BOHN, Th., Applied magnetohydrodynamics. VI, 25:19536 (JUL-706-TP)
BOHNE, W., Elastic tau scattering on nuclei with $A = 15$ to 18 at 11 MeV, 25:20278
BOISOT, P., Contamination of Nb by O during electrolytic polishing and annealing under vacuum, 25:19171
BOLDT, E. A., Search for temporal structure in x rays from Scorpius X-1, 25:19363
BOLEF, D. I., Alpher--Rubin ultrasonic attenuation and dipolar nuclear-acoustic-resonance coupling in pure metals, 25:19879
BOLOGOVA, G. S., Glucose and oxalic acid methods of γ-radiation dosimetry, 25:18808
BOL'SHAKOV, K. A., Extraction for separation and isolation of rare metals, 25:18510
BOLTON, J. G., Quasi-stellar objects in the Parkes 2700 MHz survey, 25:19383
BONCH-OSMOLOVSKAYA, N. A., Lutetium-170 $\to$ ^{170}Yb decay, 25:20452
BOND, Peter Danford, Nuclear structure and hyperfine field studies with ^{95}Mo, 25:20468
BOND, V. P., Negative pions: their possible use in radiotherapy, 25:19078
BONIFORTI, R., Isotopic analysis of UO_2 and application to stream analysis, 25:18358 (RT/CHI-(70)18)
BONKA, H., Is neon more economical than helium as cooling gas in THTR, 25:20729
BONNER, W. P., Fate of trace elements and radionuclides in terrestrial environment, 25:18521 (ORNL-4584, pp 1-10)
BONNIER, E., Present state of the bibliography on Nb and its alloys, 25:19165
  Study of niobium base refractory metal alloys, 25:19246
BONTE, Frederick J., Image aberrations produced by multichannel collimators for a scintillation camera, 25:18660
BOOKER, G. R., Damage produced by ion implantation in silicon, 25:19814
BOOTH, R. S., Dose estimation studies related to peaceful uses of nuclear explosives, 25:18989 (ORNL-4584, pp 42-56)
BORCHERS, R. R., Revised level scheme of ^{199}Hg following Coulomb excitation, 25:20387
BORCHERT, H., Experimental techniques for photon scattering below 140 MeV, 25:20189
BORDERS, J. A., Crystallinity of ion-implanted Si, 25:19812
  EPR of substitutional group V implants in Si, 25:19826
BORELEVSKI, Z., Renormalization of S-matrix in Kadyshevskii's p-representation, 25:20123
BORELLO, A., Analysis of micro constituents in Zr matrix.

I, 25:18341 (RT/CHI-(70)14)
BORESI, A. P., Theory for free vibration of orthotropic shells of revolution, 25:18568
BORESKOV, G. K., Kinetic isotopic effect of the oxidation of hydrogen on ferric oxide, 25:18386
BORGARDT, F. G., Structure of nitroform in various solvents, 25:18391
BORIDY, E., Windowless gas target, 25:20185
BORIE, E., Magnetic monopole transitions in electron scattering, 25:20294
BORING, John Wayne, Gamma-ray differential cross sections from inelastic neutron scattering, 25:20329
BORKENHAGEN, W. H., Initial equilibrium configuration of Scyllac 5-meter toroidal-sector experiment, 25:19725 (LA-4597)
BORNMANN, G., Intestinal absorption of metallic mercury, 25:18369
BOS, L., Equipment for sampling sodium, 25:18336
BOSCHUNG, P., Scattering of fast neutrons by ^{12}C, ^{54}Fe, ^{56}Fe, ^{58}Ni, and ^{60}Ni, 25:20338
BOSIO, C., Spectral distributions of fast and slow components in a liquid scintillator, 25:18678
BOSS, G. R., One-phonon octupole vibration of ^{151}Eu, 25:20432
BOSTER, T. A., Soft x rays from collisions of 1 MeV H_2^+ and 500 keV Ar^+ with carbon, 25:18836
BOTTEMILLER, Robert Leland, Study of intrinsic polarization in be stars, 25:19315
BOULTER, Frank, Removing matter from filter elements, 25:18572
BOUTAINE, J., Neutron radiography, 25:18615
BOUTARD, A., Directional correlations of gamma rays in ^{152}Sm and ^{152}Gd, 25:20385
BOUTEN, M., Is ground state rotational band cut off in ^{8}Be, 25:20280
BOUTEN, M. C., Is ground state rotational band cut off in ^{8}Be, 25:20280
BOVARD, P., Pollution and hydrobiology of fresh water, 25:18937
BOVET, C., Study on the choice of parameters for a high energy electron ring accelerator, 25:20161
BOWDEN, M. J., Radiation-induced solid-state polymerization in some methacrylates, 25:18445
BOWIE, S. H. U., Some geological concepts for consideration in the search for uranium provinces and major uranium deposits, 25:18550
  World uranium deposits, 25:18531
BOX, W. D., Compatibility tests for selection of radioisotope heat source compounds, 25:18592 (ORNL-4298)
BOYD, R. E., Short lived radiopharmacuetícals, 25:19054
BOYER, Timothy H., Energy and momentum in electromagnetic field for charged particles moving with constant velocities, 25:19946
BOYETT, R. H., Applied dosimetry research, 25:18799 (ORNL-4584, pp 165-86)
BOZHKO, D. F., Thermal stability of monoisopropylbiphenyl, 25:18377
BRAASCH, R. H., Stochastic analysis of fractured glass, 25:20891 (SC-RR-69-506)
BRACE, L. H., Ion chemistry and thermal balance in E and F regions above Wallops Island, 25:19575
BRACEWELL, R. N., High-frequency modulation of light from Crab pulsar, 25:19360
BRACK, K., Resistivity and annealing properties of implanted $Si:H^+$, 25:19822
BRADNEY, D. H., Systematic approach to the design and development of HTR gas turbine power stations, 25:20702
BRADSHAW, R. L., Disposal in natural salt formations, 25:18623 (ORNL-4584, pp 16-36)
BRADT, H., X-ray observations of pulsars, 25:19359
BRAENDLE, H., Isobaric analog pair ^{57}Fe--^{57}Co, 25:20336
BRAGER, H. R., Irradiation produced defects in austenitic stainless steel, 25:19253 (WHAN-FR-16)
BRAKENHOFF, G., Warm quiescent plasma in minimum-B field, 25:19705
BRAMBILLA, Marco, Density thresholds for onset of anisotropy loss-cone instabilities, 25:19708
BRANDER, R. W., Cathodoluminescence of ion-implanted silicon carbide, 25:19790
BRANDOLINI, F., Mean lives of ^{31}S and ^{38}K levels, 25:20349
BRANDT, Howard Edward, Sixth-order charge renormalization constant, 25:20060
BRANOVER, G. G., Suppression of turbulence in tubes by transverse magnetic fields, 25:19556
BRANSDEN, B. H., Pion--nucleon phase shift analysis from 1.98 to 3.5 GeV/c, 25:20012
BRAUNDMEIER, A. J., Interaction of radiation with liquids and solids, 25:19758 (ORNL-4584, pp 74-86)
BREHME, Robert W., Relativistic Lagrangian, 25:20064
BREIT, G., Proposed polarized-target-beam test for $^3S_1$--$^3S_1$ radiative transitions in thermal n--p capture, 25:20519
BRENNAN, James T., Effects of fast neutrons on human skin, 25:19149
BRENNAN, M. H., Compressional Alfven waves in nonuniform plasma, 25:19745
BRENNER, B., Aspects of chiral symmetry, 25:20045
BRENT, Robert L., Response of the $9^1/_2$-day-old-rat embryo to variations in exposure rate of 150 R x-irradiation, 25:19117
BRES, M., Interdigital H-type (IH) structure, an accelerating structure for low energy beams, 25:20156
BREWSTER, P. M., Toward the superconductivity of rhodium, 25:19606
BREYER, B., Attenuation of proportional counter pulses by pulse shaping networks, 25:18700
BRICE, D. K., Crystallinity of ion-implanted Si, 25:19812
  Spatial distribution of energy deposited into atomic processes in ion-implanted silicon, 25:19819
BRIDGE, D. G., UKAEA fuel test assemblies irradiated in HBWR, 1964--66, 25:20736 (HPR-132)
BRIDWELL, L., Stopping cross sections for fission fragments of ^{252}Cf by gold, silver, and carbon, 25:19765
BRIGGS, G. G., Production of dense thoria, 25:19259 (NLCO-1029)
BRIGGS, John S., Total cross sections for inelastic scattering of charged particles by atoms and molecules. VI, 25:19510
BRINI, Domenico, Cosmic x-ray background, 25:19534
BRINK, Lars, One-pion exchange model applied to reaction pp + $p\pi^+(\Delta^{++})\pi^-p$ at 19 GeV/c, 25:20020 (USIP-70-5)
  One-pion exchange model applied to reaction pp + $p\pi^+(\Delta^{++})\pi^-p$ at 19 GeV/c, 25:20032
BRIODY, Ronald Francis, Gas cooled nuclear reactor, 25:20695
BRISAC, Michael, Improvements in shielding containers, 25:18633
BROCKETT, W. S., Measurement of reaction $\pi^- + \pi^0 n$ at large momentum transfers, 25:19911
BRODERICK, J. J., Observations of compact radio sources, 25:19368
BRODSKY, Stanley J., Present status of quantum electrodynamics, 25:20081
BROIDO, J. H., Dynamic studies of gas turbine fast reactors, 25:20765
BROMKAMP, K. H., Proof of reactor component in helium atmosphere, 25:20558
BROMLEY, D. A., Doppler shift attenuation studies in heavy nuclei, 25:20409
  Doppler shift studies with selected recoil directions, 25:20140
BRONCA, G., Big superconducting magnets, 25:19633
BROOKS, A. L., Metaphase chromosome aberrations in Chinese hamster liver cells in vivo after single acute ^{60}Co exposure, 25:18960
BROOKS, J. W., OH (1667) line absorption, 25:19382
BROUDE, C., Angular correlation measurements of first three excited states in ^{29}P, 25:20323
BROUT, R., Regge pole theory and duality, 25:20102 (NP-18705)
  Renormalization of $K^*K\pi$ coupling in broken SU_3 symmetry, 25:20043
BROVCHENKO, V. G., Circuits for the identification of neutrons, 25:18667
BROVTSYN, V. K., Mechanism of $^{114}Sn(\gamma,p)^{113}In$ reaction, 25:20394
BROWER, K. L., EPR of substitutional group V implants in Si, 25:19826
BROWER, R. C., Chiral invariant dual model, 25:19981
BROWN, Allan, X-ray powder diffraction with Guinier--Haegg focusing cameras, 25:18826 (AE-409)
BROWN, Carl S., Rectification and determination of the photo-metric elements of W Ursae Majoris type eclipsing binary stars, 25:19317
BROWN, D. P., Gas-flow method for detection of fast neutrons in reactors, 25:18646 (WHAN-SA-73)
BROWN, G. E., Dynamics of the optical model, 25:20528
BROWN, G. W., Prediction of fatigue lives of 2024-T3 and 6061-T6 aluminum alloys under broad-band excitation, 25:20895 (SCL-CR-710175)
BROWN, Ian G., Feedback-controlled steady-state plasma, 25:19713
BROWN, J. R., Review of Gulf General Atomic support of the High Temperature Lattice Test Reactor program, 25:20787 (GAMD-10231)
BROWN, John S., Prog. rpt. on thermodynamic and transport properties of interstitial hydrogen isotopes in palladium, 4/1/70--12/15/70, 25:20879 (NYO-4062-5)
BROWN, M. D., Spectrometry research and development, 25:18644 (ORNL-4584, pp 152-64)
BROWN, P. H., Deformation parameters in ^{154}Sm and ^{148}Sm, 25:20477
BROWN, Robert L., Photo-ionization of hydrogen and helium, 25:19439
BROWN, V. R., Core-polarization effects in charge-exchange reactions; application to $^{58}Ni(^3He,t)$, 25:20496
BRUECHER, E., Exchange reactions of central atoms in lanthanide--aminopolycarboxylate complexes. III, 25:18412
BRUNO, Fred P., New dose calibrator for nuclear medicine, 25:18723
BRUNVOLL, J., Symmetry coordinates, harmonic force field, and mean amplitudes for light and heavy dibenzene Cr, 25:18392
BRUSENTSEVA, S. A., Salt effect during pulsed radiolysis of neutral water and alkaline solutions, 25:18474
BRUSTAD, Tor, Time scale for radioprotection by and permeation of glycerol in anoxic cells of E. coli B, 25:19022
BRUTTO, E., Mechanical and metallurgical steel/Zr junctions, 25:19183

XUM

BRYANT, Peter J., Cell lineage relationships in the imaginal wing disc of Drosophila melanogaster, 25:18967
BRZOSKO, J. S., Measurement of high-energy γ-ray spectra in a strong neutron flux, 25:18735 (INR-1224)
BUBB, I. F., Liquid deuterium target for the production of a monoenergetic neutron beam, 25:20187
BUCHET, R., Introduction to medical neutron radiography, 25:19034 (AEC-tr-7219)
BUCK, U., Intermolecular potentials by inversion of molecular beam scattering data. I, 25:19495
  Intermolecular potentials by inversion of molecular beam scattering data. II, 25:19496
BUCKLEY, J. P., Use of ^{14}C as a secondary counting standard for ^{35}S, 25:18364
BUDINGER, Thomas F., Myocardial uptake studies with ^{129}Cs and the scintillation camera, 25:19055
BUDZANOWSKI, A., Polarization of protons from ^{12}C(d,p)^{13}C reaction at E/sub d/ = 12.4 MeV, 25:20287
BUEB, B., Data acquisition and analysis system for nuclear physics, 25:18852
BUGAENKO, L. T., Chemiluminescence method of investigation of radiation defects in alkali halides, 25:19850
BUGG, D. V., Pi$^-$p $\rightarrow$ π^0n charge-exchange cross sections between 90 MeV and 290 MeV, 25:19915
  Total cross sections for pion--proton scattering between 70 MeV and 290 MeV, 25:19916
BUHL, W. F., Branching ratios of the A_2^+ meson observed in 7 GeV/c π^+p interactions, 25:19920
BULGAKOV, M. K., Vacuum system for the 70-GeV proton synchrotron, 25:20126 (CERN-Trans-70-9)
BULGAKOV, N. N., Kinetic isotopic effect of the oxidation of hydrogen on ferric oxide, 25:18386
BULL, S. R., Pulsed-source investigations on graphite systems, 25:20240
BULLINGTON, D. C., Fission gas bubble precipitation and growth in PuO$_2$--UO$_2$ under irradiation, 25:19290 (WHAN-SA-15)
BUNCH, W. L., In-core regenerative thermal neutron detectors for nuclear reactors, 25:20711 (WHAN-FR-37)
BUNYATOV, S. A., Meson production by interaction of π^+ mesons with photoemulsion kernels at 185 to 295 MeV energies, 25:19919
BURCH, P. R. J., Prenatal radiation exposure and childhood cancer, 25:19089
BUREAU, A. J., Photoneutron cross sections for ^{32}S, 25:20332
BURGMER, W., Efficiency of a 180° coincidence spectrometer for extended sources, 25:18758
BURKE, D. G., Validity of Nilsson model for proton states in region A = 151 to 155, 25:20383
BURKHARDT, W., Production of dense thoria, 25:19259 (NLCO-1029)
BURKHART, Andre, Apparatus for producing a voltage, 25:18721
BURMAN, R., Singularities of coupled fields in warm stratified plasmas, 25:19756
BURMISTROV, V. R., Investigation of gamma radiation of isomers /sup 110m/In and ^{110}In, 25:20402
BURR, P., Electrical measurements on silicon following phosphorus and boron implantation and annealing, 25:19778
BURTSCHER, A., Measurements on Be-reflected core of ASTRA reactor, 25:20796
BURYLO, P., Helium closed-cycle gas turbine integrated with a high temperature reactor, 25:20778
BUSCHMAN, Henry W., Leakrate testing of EBR-II reactor building, 25:20755 (ANL-EBR-8)
BUSSEY, P. J., Pi$^-$p $\rightarrow$ π^0n charge-exchange cross sections between 90 MeV and 290 MeV, 25:19915
  Total cross sections for pion--proton scattering between 70 MeV and 290 MeV, 25:19916
BUSSO, L., Solid state detector telescope for charged photoparticles, 25:18675
BUT, D. A., Nonstationary electrically conducting free jet in a transverse magnetic field, 25:19567
BUTALA, Sharon Smock, Effect of far-red and blue light on maleic hydrazide-induced chromosomal aberrations in Vicia faba, 25:18962
BUTERA, R. A., Heat capacity and magnetization of praseodymium metal in the temperature region 1.2 to 4.2°K with applied magnetic fields up to 40,000 G, 25:19869
BUTLER, H. M., Radiation safety practices: Operation HENRE, 25:18982 (CEX-65.05)
BUTTEMER, D. R., Prestressed concrete reactor pressure vessel for Fort St. Vrain reactor, 25:20557
BUZZI, Umberto, Nuclear power plant for a space station, 25:20807
  Nuclear power plant for a space station, 25:20808
BYAKOV, V. M., An observation on the nature of intermediate particles in the radiolysis of aqueous solutions of oxygen, 25:18477
BYRAM, E. T., Variability of x-ray emission from M87, 25:19458
BYRNE, J., Angular distributions and energy spectra of internal bremsstrahlung emitted during beta decay of ^{32}P, ^{90}Y, ^{204}Tl, and ^{210}Bi, 25:20417
BYRON, J. W., Pre-irradiation action of TAB, 25:19026

C

CABELL, M. J., Cross section of reaction ^{147}Pm(n,γ)/sup 148g/Pm, 25:20379
CACHIN, Y., Telecobalt therapy for carcinoma of laryngopharynx, 25:18998
CADY, K. B., Neutron-pulse propagation in multiplying assemblies, 25:20804
CAHEN, O., Fast measurement of ion-implantation profiles, 25:19800
CAIRNS, J. A., Antimony-implanted silicon, 25:19825
  Measurement of implanted-boron concentration profiles in silicon, 25:19803
CAIRNS, R. A., Theory of a test particle in an inhomogeneous stationary plasma, 25:19695
CALDECOURT, L. R., Industrial-scale ion-implantation facility, 25:19773
CALDWELL, Richard A., Secondary deuterium isotope effects on triplet excitation transfer. Deuterium position and sensitizer effects, 25:18406
CALLAGHAN, M. P., Cathodoluminescence of ion-implanted silicon carbide, 25:19790
CALLETON, R. L., Treatments of southern pine with vinyl chloride and methyl methacrylate for radiation-produced wood-plastic combinations, 25:19299
CALMET, J., Evaluation of the electron anomalous magnetic moment by computer, 25:20055 (CNRS-CPT-70-P-335, pp IV.26-38)
CAMERON, A. G. W., Collapsar in binary system epsilon Aur, 25:19313
  Mass loss from stars, 25:19333
CAMERON, J., Alio Ghelle radioactive mineral occurrence in Bur region of Republic of Somalia, 25:18541
CAMP, David C., Energy levels in ^{74}Ge from decay of ^{74}Ga, 25:20343
CAMPBELL, J. A., Effects of Veneziano-model form factors on ratios of lepton--proton scattering cross-sections, 25:19942
CAMPBELL, J. L., Coincidence technique for study of Ge(Li) detector profiles, 25:18759
  Efficiency calibration of semiconductor x ray detectors, 25:18715
CAMPBELL, J. W. E., Power cycles for helium cooled high temperature nuclear reactors, 25:20770
CAMPBELL, Robert C., Preparation of noninfectious arbovirus antigens by sucrose--acetone extraction of gamma-irradiated tissue, 25:18924
CAMPBELL, Ronald Hugh, Improvements relating to nuclear reactor fuel elements, 25:20843
CAMPISE, A. V., Influence of a predominantly oxide fuel loading on the dynamic behavior of EBR-II. EBR-II Project, 25:20704 (ANL-7673)
CAMPLAN, J., Ion sources for ion implanation, 25:20166
CANNING, Gerald P., Kinematic superstructures for abnormal couplings in δ-π dual amplitude, 25:20000
CAPLAN, Robert H., Thyroid uptake of radioactive iodine. A reevaluation, 25:19051
CARLESI, O., Ionizing radiation effects on neuroblast cultivated in vitro, 25:19120
CARLTON, J. E., Rapid separation of generator-produced ^{68}Ga from EDTA eluate, 25:18482
CARMELI, M., Infinite-dimensional representations of Lorentz group, 25:20033
CARNELL, K. H., Estimation of the size of bubbles in a bubble chamber by contrast measurement, 25:18792
CARNES, C. P., Annealing of electron-irradiated n-type silicon. I. Donor concentration dependence, 25:19854
CARNEVALE, E. H., Prog. rpt. on ultrasonic thermometry in LMFBR systems, 7--9/70, 25:18830 (NYO-3906-12)
CARRAZ, Louis-Claude, Isomer of ^{138}Cs, 25:20381
CARRE, Daniel, Mixed rare earth sulfides, 25:19286
CARRUTHERS, P., Scalar mesons, hadron masses, and approximate scale invariance, 25:19983
CARTER, A. A., Total cross sections for pion--proton scattering between 70 MeV and 290 MeV, 25:19916
CARTER, Ada, Electron and ion collision physics, 25:19490 (ORNL-4584, pp 92-104)
CARTER, G., Radiation damage by implanted ions in GaAs and GaP, 25:19844
CARVALHO, Fabiano C., Activity of ionizing radiation on fertile eggs of Triatomideos-Rhodnius prolixus, 25:19099
CARVER, James Richard, Green functions of neutral scalar meson, photon, and electron in weak gravitational fields, 25:20094
CARVER, M. B., A package of computer programs for the analysis of temperature distribution in three dimensional systems, 25:18577 (AECL-3783)
CASH, Bernard L., DORF-I: gamma-ray spectrograph shielding studies, 25:18732 (AD-711531)
CASON, J. L., Portable neutron radiographic camera using ^{252}Cf, 25:18617
CASSEL, D. G., Photoproduction of neutral K mesons, 25:19887
CASSUTO, A., Kinetics and mechanisms involved in the siliconization of Nb and the oxidation of niobium silicides at low pressures and high temperatures, 25:19258
CASTRO, Joseph R., Place of implantation in tongue and floor of mouth cancer, 25:19080

CATALANO, E., Studies of the europium--oxygen--fluorine and samarium--oxygen--fluorine systems, 25:19285
CATTANI, M., Decay constant for spontaneous fission of ^{238}U, 25:20429
CAVALIER, Guy, Analytical methods used by Geochemical Section: water, 25:18339 (CEA-R-3557(2))
CAVALLERI, G., Extension of Ramo's theorem as applied to induced charge in semiconductor detectors, 25:18710
CERNIGOI, C., Pion capture in ^{4}He, 25:20255
CERNY, Joseph, Spin dependence in the reactions ^{16}O(p,t)^{14}O and ^{16}O(p,^{3}He)^{14}N, 25:20299
CHABERT, A., Interdigital H-type (IH) structure, an accelerating structure for low energy beams, 25:20156
CHABOSEAU, J., Power level control of a closed loop gas turbine, by natural transfer of gas between the loop and auxiliary tanks, 25:20712
CHABRE, M., Parity irregularities in 279-keV γ transition of ^{203}Tl, 25:20433
CHADDERTON, Lewis T., First international topical conference on ion implantation in semi-conductors, Thousand Oaks, California, May 4--7, 1970, 25:19809
CHAIKOVSKII, V. G., Measurement limits of exposure dose rate by gas-discharge counters, 25:18664
CHAKHAVA, O. V., Influence of ionizing radiation on natural immunity, 25:18922
CHAKRABORTI, D., 1-(2-carboxy-4-sulphonatophenyl)-3-hydroxy-3-phenyltriazene as spectrophotometric reagent for Cu(II) and Pd(II) in Fe, Mo, and V, 25:18342
CHALUPA, B., Single-crystal filters of thermal neutrons, 25:20238 (UJV-2488-F)
CHAND, Naresh, Regge trajectories and the Bethe-Salpeter equation, 25:20007
CHAND, Prakash, Some inequalities satisfied by normal-ordered moments, 25:19880
CHANDRASHEKHAR, G. V., Electrical resistivity of NbO, 25:19868
CHANG, Shau-jin, Comments on eikonalization at high energy, 25:19961
CHANMUGAM, Ganesar, Many-body forces, 25:20523
CHAPMAN, E. S., HTR fuel disposal study, 25:20745 (DP-Report-450)
CHAPPELL, W. R., Density fluctuations and diffusion in weakly ionized plasmas, 25:19686
CHARDINE, Research report on measurement of average number of prompt neutrons, 25:20373 (LIB/Trans-300)
CHARPAK, G., Evolution of the automatic spark chambers, 25:18796
CHARVET, A., Neodymium-141 levels excited from ^{141}Pm(21 min) disintegration, 25:20388
CHASE, R. L., Dose equivalent meter designs, 25:18809
CHASSAGNE, Daniel, Place of implantation in tongue and floor of mouth cancer, 25:19080
CHAUDHURI, P. R., Gravitation and neutrinos, 25:20090
CHECHEV, V. P., Does the electron charge change with the age of the Universe, 25:19883
CHEKA, J. S., Applied dosimetry research, 25:18799 (ORNL-4584, pp 165-86)
  Dosimetry for human exposures and radiobiology, 25:18990 (ORNL-4584, pp 129-51)
CHEKHOVSKOI, V. Ya., Effect of heat treatment on the electrical resistivity and thermal conductivity of pyrolytic carbon, 25:19281
  Emissivity, electrical resistivity, and thermal conductivity of pyrolytic carbon, 25:19280
CHEMTOB, M., Meson exchange currents in nuclear weak and electromagnetic interactions, 25:20542
CHEN, Min-shih, Essential breaking of scale invariance in nonlinear chiral Lagrangian models, 25:20049
CHEN, P. Y. P., Discontinuous finite elements in thermal analysis, 25:18573
CHEN, T. C., Method of extending Blankenbecler--Sugar--Logunov--Tavkhelidze approximation to Bethe--Salpeter equation, 25:20104 (NYO-2262-TA-231)
CHEN, W. L., Dosimetry for human exposures and radiobiology, 25:18990 (ORNL-4584, pp 129-51)
CHENAULT, Roger, Reading thermoluminescent dosimeters, 25:18804
CHENG, T. P., Is SU(2) x SU(2) a better symmetry than SU(3), 25:20051
CHEPELEV, V. V., Scintillation characteristics of pure and activated cadmium iodide crystals, 25:18665
CHERNENKO, A. A., Theory of pulse radiolysis in an electric field, 25:18469
CHERNIKOVA, O. P., Effect of space-flight factors on Crepis-capillaris seeds, 25:18953
CHERNOW, F., Improved high-beam-current ion implanter, 25:20167
  Radiation-damage studies of bismuth-ion-implanted CdS, 25:19792
CHERY, R., High energy reactions with Ho and Tm, 25:20390
  Neodymium-141 levels excited from ^{141}Pm(21 min) disintegration, 25:20388
CHEUNG, A. C., Further investigations of NH$_3$ inversion radiation, 25:19366
CHEVARIER, A., High energy reactions with Ho and Tm, 25:20390
CHEVARIER, Noelle, High energy reactions with Ho and Tm, 25:20390
CHEVEREAU, Gerard, Nuclear reactor refuelling installation, 25:20838
CHIACCHIERINI, Richard P., Review of radium toxicity studies, 25:18979 (BRH/DBE-70-5)
CHIBISOV, G. V., Dynamical parameters of galaxies as a consequence of cosmological turbulence, 25:19443
CHIKOV, N., Relative measurements of anti ν in the ^{235}U and ^{239}Pu fission induced by resonance neutrons, 25:20364 (BNL-tr-401)
CHIN, Y. C., Polarization of solar Type-III radio bursts at 25.3 MHz, 25:19399
CHIPPERFIELD, Alan R., Binding of americium and plutonium to bone glycoproteins, 25:18899
CHO, K. S., Non-coplanar proton--proton bremsstrahlung calculations including the relativistic spin corrections, 25:19947
CHO, S. W., Determination of percent contents of U and Th in natural radioactive ores by γ-ray spectrometry, 25:18365
  Semi-empirical efficiency curve for thin Ge(Li) detector at low energies, 25:18725
CHODURA, R., Hydromagnetic equations for anistropic plasmas including transport effects, 25:19674 (IPP-1/112)
CHOI, In Kap, Thermal decomposition of bis-hexanitroazobenzene and pyrolysis of urania gel. I. and II, 25:18378
CHOI, Jae Ho, Chemical effects of nuclear isomeric transformation of /sup 80m/Br in bromobenzene, 25:18490
CHOLLET, Gerard, Nuclear reactor with integrated heat exchangers, 25:20840
CHONG, K. F., Relation between the binding energy and scattering phase shift, 25:20022
  Single-particle-energy spectrum of a Λ particle in nuclear matter, 25:20023
CHOONG, E. T., Treatments of southern pine with vinyl chloride and methyl methacrylate for radiation-produced wood-plastic combinations, 25:19299
CHOUMOFF, P. S., Measurements and calibrations at pressures between 10^{-8} and 10^{-12} torr, 25:18878
  Operation of the gages with a screened collector, 25:18837
CHRIEN, R. E., Resonant neutron capture in ^{175}Lu, 25:20476
CHRISTE, Karl O., Matrix-isolation study of the low-pressure pyrolysis and ultraviolet photolysis of dimethyl peroxides and of CF$_3$OCl, 25:18394
CHRISTENSEN, E. R., Application of one-dimensional transport theory to the subsurface gamma-scatter density probe, 25:18816
CHRISTENSEN, J. A., Structure evolution in an oxide fuel pin, 25:20836 (WHAN-SA-79)
CHRISTIAN, J. E., 4π liquid-scintillation whole-body counter. II, 25:18649
CHRISTOPHOROU, L. G., Atomic and molecular radiation physics, 25:19491 (ORNL-4584, pp 105-24)
CHRITNIS, E. V., X-ray observation of Cen XR-4 and Nor XR-2, 25:19354
CHRYSSIKOS, T. N., Review of Gulf General Atomic support of the High Temperature Lattice Test Reactor program, 25:20787 (GAMD-10231)
CHU, C. K., Formation of ion-acoustic collisionless shocks, 25:19698
CHU, Patricia, Myocardial uptake studies with ^{129}Cs and the scintillation camera, 25:19055
CHUA, L., Spins and parities of highly excited states in ^{24}Mg, 25:20291
CHUANG, L. A., Measurement of absorbed dose rate from terrestrial background radiation in Hong Kong, 25:19006
CHUBB, T. A., Variability of x-ray emission from M87, 25:19458
CHUGAINOV, P. F., Photoelectric observations of flare stars. V, 25:19345
  Photoelectric observations of flare stars. VI, 25:19340
  Statistical characteristics of flares of UV Cet-type stars, 25:19346
CHUNG, M. K., Determination of percent contents of U and Th in natural radioactive ores by γ-ray spectrometry, 25:18365
  Semi-empirical efficiency curve for thin Ge(Li) detector at low energies, 25:18725
CHUVAEV, K. K., Multicolor photometry of galaxy NGC 4254 using image converter, 25:19456
CICUTA, G. M., Validity of Regge eikonal model, 25:20115
CIMERMAN, M., Attenuation of proportional counter pulses by pulse shaping networks, 25:18700
CIZERON, C., Deformation and rupture of Nb between -196°C and 20°C, 25:19217
  Study of the changes in the mechanical properties of Nb with different impurity contents between 20 and 850°C, 25:19212
CLARK, Alfred Jr., Trapped gravity waves and the five-minute oscillations of the solar atmosphere, 25:19405
CLARK, C. D., Solar enhancements at 1.2-mm wavelength, 25:19409
CLARK, Howell R., Acid and metal salt catalyzed hydrolyses of PO$_2$F$_2^-$ and PO$_3$F^{2-}, 25:18373
CLARK, Howell Rieke, Metal-ion catalyzed and metal-ion-assisted fluoride hydrolyses, 25:18375
CLARK, Patricia Andre, Trapped gravity waves and the five-minute oscillations of the solar atmosphere, 25:19405
CLARKE, J., Superconducting junctions in magnetometry, 25:19643
CLAUSING, R. E., Computer program for calculating,

XUM

tabulating, and plotting outgassing rates of selected gases, 25:19195 (ORNL-TM-3220)
CLAUSS, A., Hydrogen embrittlement of Nb base alloys, 25:19216
  Preparation of high purity niobium base alloys, 25:19186
CLAVEL, A. L., Production of dense thoria, 25:19259 (NLCO-1029)
CLAVELLI, L., Group-theoretical construction of dual amplitudes, 25:20114
CLAVENNA, L. R., Interaction of N_2 with (100) W, 25:19208
CLEMENS, James Theodore, Unified nuclear model and application to odd-mass isotopes, 25:20548
CLEMENT, J. C., 250 meter neutron time-of-flight facility, 25:18742
CLEMENTS, P. J., Interaction of high energy neutrons with hydrogen nuclei, 25:20258
CLEVINGER, G. S., Prog. rpt. on relationship of nitrogen content to susceptibility of austenitic stainless steels to stress corrosion, 9--11/70, 25:20898 (TID-25664)
CLEYMANS, J., Renormalization of $K^*K\pi$ coupling in broken SU_3 symmetry, 25:20043
CLINE, J. E., Determination of relative photopeak efficiency and system linearity for Ge(Li) gamma-ray spectrometers, 25:18747
CLOKE, Robert L., Inexpensive readout for a commercial thermocouple microwave power density probe, 25:18827 (BRH/DEP-70-31)
CLOOS, O., Automatic compensating instrument for measuring low electric direct currents, 25:18834
CLOUGH, W. S., Behaviour in the atmosphere of the aerosol from a sodium fire, 25:19167 (AERE-R-6460)
  Caesium behaviour in liquid sodium: the effect of carbon, 25:19192 (CONF-700816-(Vol.1), pp 393-412)
  Cesium behavior in liquid sodium: effect of carbon, 25:20754 (AERE-R-6481)
COAST, Geoffrey, Gas cooled nuclear reactor, 25:20695
COCHRAN, J. A., Calibration and initial field testing of ^{85}Kr detectors for environmental monitoring around a nuclear fuel reprocessing plant, 25:18638 (CONF-700816-(Vol.1), pp 143-74)
COHEN, J. B., X-ray study of faulting in bcc metals and alloys, 25:19248
COHEN, Moshe, Interaction of 9.3-GHz longitudinal phonons with electrons in superconducting films, 25:19607
COLE, F. T., Progress report on NAL accelerator, 25:20154
COLLINS, L. E., Doping of thin films by recoil-atom implantation, 25:19786
COLOMBETTI, Lelio G., Distribution and dosimetry of /sup 113m/In colloid, 25:18994
COLOMBO, R. W., Saxton Core II nuclear operations summary, 25:20705 (WCAP-3385-55)
COMINS, J. D., Temperature dependence of defect production in KBr and KCl. I, 25:19855
COMPHER, Alan B., Feedback-controlled steady-state plasma, 25:19713
COMPTON, R. N., Electron and ion collision physics, 25:19490 (ORNL-4584, pp 92-104)
CONDE, J. F. G., Quality control, inspection, and testing of fuel materials for the two uprated fuel elements, 25:18610 (DP-Report-580)
CONNOLLY, T. J., Pulsed-source investigations on graphite systems, 25:20240
CONNOR, R. D., Decay of ^{223}Ra and its daughter products. I, 25:20456
CONSTANTINESCU, F., Analytic properties of nonstrictly localizable fields, 25:20063
CONSTANTINESCU, L., Analysis of efficiency of nuclear fuel cycles for heavy-water moderated reactors in specific conditions of socialist republic of Romania, 25:20750
COOK, B. C., Photoneutron cross sections for ^{32}S, 25:20332
COOKE, B. A., Further high-sensitivity x-ray sky survey from the southern hemisphere, 25:19353
COOMBS, J. A., Scattering and capturing by inverse fourth-power potential in low-energy range, 25:19500
COPPOLA, M., Measurements of neutron elastic scattering from carbon in energy region of 0.50 to 2.00 MeV, 25:20267 (EUR-4538)
CORBETT, J. W., Radiation damage in silicon and germanium, 25:19810
CORDALL, D., UKAEA fuel test assemblies irradiated in HBWR, 1964--66, 25:20736 (HPR-132)
CORDS, H., Tensor polarization and differential cross section for ^{9}Be(d,d)^{9}Be elastic scattering at low energies, 25:20293
COREY, J. C., Miscible displacement measurements within laboratory columns using the gamma-photoneutron method, 25:18523
CORI, Carl F., Glucose 6-phosphatase deficiency: mechanisms of genetic control and biochemistry, 25:19128
CORLEW, G. T., Measurement of reaction $\pi^- + \pi^0 n$ at large momentum transfers, 25:19911
CORNELIUS, Eugene A., Scan evidence of organ involution and improvement of hypersplenism in Hodgkin's disease following splenic artery ligation, 25:19058
CORNISH, D. N., Small superconducting coils and applications to plasma physics, 25:19634
CORNWELL, J. C., Chemical analysis of tellurite--tellurate compounds, 25:18351
CORSINI, A., 5,7-dihalo-8-hydroxyquinoline complexes of U(VI), 25:18374
COSGROVE, Christine M., Generalized impulse approximation, 25:20537
COSIMO, E., Digital programs for thermal dynamics of a cylindrical nuclear fuel rod and a heat-exchanger tube, 25:20835 (RT/ING-(70)8)
COSTA, S., Solid state detector telescope for charged photoparticles, 25:18675
COSTE, J., Treatment of collisional effects on temporal plasma-wave echoes, 25:19755
COSTES, Didier, Nuclear reactor with integrated heat exchangers, 25:20840
COULTER, Byron L., Relativistic one-dimensional square potential, 25:20065
COURRIER, Raymond, Kinetics of isothermal martensite transformation during aging of ternary alloy containing 76 percent Fe, 19 percent Ni, and 5 percent Mo, 25:19247
COVER, R. K., Sandia image digitizer, 25:20887 (SC-DR-68-812-B)
COWAN, Robert J., Selenomethionine ^{75}Se thymus scans in myasthenia gravis, 25:19049
COWAN, W. C., Concrete-polymer materials. Third topical report, 25:19292 (BNL-50275)
COWSER, K. E., Disposal by hydraulic fracturing, 25:18622 (ORNL-4584, pp 11-15)
  Dose estimation studies related to peaceful uses of nuclear explosives, 25:18989 (ORNL-4584, pp 42-56)
  Engineering, economic, and safety evaluation, 25:18526 (ORNL-4584, pp 37-40)
COX, A. F. J., Cathodoluminescence of transition-metal ion-implanted II--VI compounds, 25:19795
COX, A. J., Method for study of short-lived nuclear isomers, 25:20312
COY, Richard A., Observation of x-ray diffuse scattering from neutron-irradiated silicon, 25:19853
CRAGG, D. A., Present status of polarized targets at the Rutherford Laboratory, 25:20135 (RHEL/R-201)
CRAIG, E. C., 4π liquid-scintillation whole-body counter. II, 25:18649
CRAMER, C. F., Computer programs for calculation of liquid-scintillation data, 25:18693
CRESPI PORRO, R., Cerebral gliomas. I, 25:19065
CREWS, Quintous E., Comparative evaluation of the sequential use of irradiation and surgery in primary tumors of the oral cavity, oropharynx, larynx, and hypopharynx, 25:19083
CROMWELL, R. H., Optical spectra of the nuclei of elliptical radio galaxies, 25:19449
CROOM, David L., Solar millimetre bursts and proton events, 25:19423
CROUSE, R. S., Compatibility tests for selection of radioisotope heat source compounds, 25:18592 (ORNL-4298)
CROW, J. E., Influence of normal-state resistance on superconducting transition temperature of ultrathin films, 25:19614
CROW, V. L., Real-time nuclear fuels inventory and criticality control system, 25:18620 (BNWL-1440)
CROWDER, B. L., Distribution of damage produced by ion implantation of silicon at room temperature, 25:19818
  Model for formation of amorphous Si by ion bombardment, 25:19813
  Radiochemical determination of damage profiles in silicon, 25:19817
CROWDER, Samuel E., Leak testing chromatographic radium sources: radon emanation technique, 25:19016
CSANAK, Gyoergy, Many-body methods applied to electron scattering from atoms and molecules. II, 25:19507
CSER, F., Investigations of radiation-induced solid-state polymerization. XXVI, 25:18431
CSONKA, P. L., Scattering of real pions on each other, 25:20153
CSONKA, Paul L., Energy and angular resolution in pion--pion scattering and other colliding beam experiments, 25:20162
CUMMINGS, F. W., Condensate in ^{4}He II as pilot wave, 25:19586
CUPERMAN, S., Stability of relativistic anisotropic plasmas to perpendicular magnetosonic waves, 25:19712
CURL, Ruth, List of AEC radioisotope customers with summary of radioisotope shipments, FY 1970, 25:18593 (ORNL-IIC-32)
CURRAT, R., Compton scattering and electron momentum density in beryllium, 25:19870
CURTISS, C. F., Molecular collisions. XIV, 25:19498
CUSSENOT, J. R., Spectroscopic study of a caesium discharge plasma, 25:19665
CYVIN, S. J., Symmetry coordinates, harmonic force field, and mean amplitudes for light and heavy dibenzene Cr, 25:18392
CZOCK, K.-H., Experimental techniques for photon scattering below 140 MeV, 25:20189
CZUBEK, Jan A., Calibration of radiometric probes for soil density measurements, 25:18815 (INP-715)

D

DABOSI, F., Magnesium--Zr--Pb alloys of Pb concentrations below or equal to 3 percent, 25:19228
DALE, P. W., Automatic scanner for nuclear emulsions,

25:18690
DALFES, Abdi, Theoretical and experimental study of a fast-thermal coupled reactor by correlation techniques, 25:20833 (RCN-132)
DALHSUREN, B., Production of spontaneously fissioning isomers ^{242}Am and ^{244}Am, 25:20412
DALIBARD, G., Study of the oxidation of Nb, 25:19177
DALKHSUREN, B., Spark fission-fragment counter, 25:18671
DALTON, A. W., Effects of elastic scattering on the low energy neutron detection efficiency of a lithium glass and boron-loaded liquid scintillator, 25:18716
DALTON, J. V., Lifetime effects in ion-implanted silicon, 25:19820
DAMKJAAR NIELSEN, Meta, Plasma renin measured by radioimmunoassay for angiotensin, 25:18920
DAMSMA, H., Oscillatory dependence of T/sub c/ on number of valency electrons in Cu_3Au-type alloys, 25:19621
DANCE, D. R., Pi$^-$p + π^0n charge-exchange cross sections between 90 MeV and 290 MeV, 25:19915
  Total cross sections for pion--proton scattering between 70 MeV and 290 MeV, 25:19916
DANCE, K. D., Pulsed-source investigations on graphite systems, 25:20240
D'ANGELO, Silio, Impulse approximation calculation of the polarization of the recoil proton in the reaction γ + n + p + π^- in deuterium, 25:19940
DANIEL, M. E., Transfer function models of DTL and TTL integrated circuits, 25:20893 (SC-RR-70-650)
DANIEL, S. H., Recoil tritium reactions with trimethylfluorosilane. A study on parameters affecting hot-atom substitution reactions, 25:18484
DANILOV, V. I., Magnetic field of thick finite dc solenoids, 25:18829 (JINR-P9-5441)
DANON, J., Electron paramagnetic resonance of electron-irradiated $K_3Rh(CN)_6$ in a KCl lattice, 25:18462
DANOS, Michael, Very high-momentum components in nuclei and far subthreshold production of quarks, 25:20026
DAREWYCH, J. W., Elastic scattering of positrons by hydrogen molecules, 25:19501
DAROTSI, Sh., Gas-filled mass separator for investigations of heavy-ion reaction products, 25:20175
DAS, A., Short-ranged scalar gravity in Einstein's theory, 25:20093
DAS, H. A., Separation of gram-amounts of lanthanides by cation exchange, using an aqueous solution of α-hydroxyisobutyric acid as an eluant, 25:18501 (RCN-131)
DASH, Jan W., Divergent Regge helicity sums, distributions, and Toller angles, 25:20110
  Multiperipheral nonfractorization, signature, and Toller-angle-variable cuts, 25:20109
DASHEN, Roger, Is SU(2) x SU(2) a better symmetry than SU(3), 25:20051
DASHEVSKAYA, L. I., Structure of $ThRe_2$--$GdRe_2$ ($TbRe_2$, $DyRe_2$, $ErRe_2$), 25:19235
DATZEFF, A. B., Classical self-energy of the electron, 25:19952
DAUGHERTY, Thomas L., Time-averaged density profile in finite-amplitude instability, 25:19715
D'AURIA, J. M., Decay of ^{180}Lu to levels of ^{180}Hf, 25:20426
DAVIDENKO, V. A., Electronuclear breeding, 25:20190
DAVIDSON, J. P., Table of E0 conversion probability electronic factors, 25:20484
DAVIDSON, M. G., Table of E0 conversion probability electronic factors, 25:20484
DAVIDSON, R. C., Transverse electromagnetic instabilities in collisionless plasmas, 25:19722
DAVIDSON, S. M., Damage produced by ion implantation in silicon, 25:19814
  Transmission electron microscope studies of radiation damage in silicon, 25:19808
DAVIDSON, W. F., Decay of ^{223}Ra and its daughter products. I, 25:20456
DAVIES, J. A., Location of implanted atoms within the unit cell of a crystal, 25:19797
DAVIES, P. C. W., Wheeler--Feynman quantum theory, 25:20061
DAVIES, P. G., Attenuation statistics at 19 and 37 GHz for Sun--Earth paths, 25:19438
DAVIES, W. G., Angular correlation measurements of first three excited states in ^{29}P, 25:20323
DAVIS, Lawrence W., Brain and liver scans in the evaluation of lung cancer patients, 25:19047
DAVIS, M. V., Solderability problems caused by gold electroplate, 25:20852 (BDX-613-324)
DAVIS, M. V. Jr., Polymeric co-deposition in gold electroplate, 25:20851 (BDX-613-310)
DAVIS, R. J., Estimation of aerosol concentration in a nuclear reactor containment after an accident, 25:20758 (CONF-700816-(Vol.1), pp 72-101)
DAVISON, N. E., Reaction mechanism of the ^{16}O + d reactions, 25:20301
DAWSON, W. K., Reaction mechanism of the ^{16}O + d reactions, 25:20301
DEAN, J. R., Control and safety studies for an htr gas turbine system, 25:20766
DEANGELIS, H. M., Annealing of electron-irradiated n-type silicon. I. Donor concentration dependence, 25:19854
DEARNALEY, G., Distribution of ^{32}P channeled into indium antimonide, 25:19801
  Electrical activity of phosphorus channeled into silicon, 25:19839
  Ion penetration, 25:19796
DEBRAY, Werner, Method of preoxidizing nuclear reactor components of zirconium alloys, 25:19180
DE BRUYN, Ouboter R., Superconducting point contacts weakly connecting two superconductors, 25:19601
DECARSIN, J. P., Research report on measurement of average number of prompt neutrons, 25:20373 (LIB/Trans-300)
DECHAMPS, Michel, Zirconium oxidation under a low oxygen pressure, 25:19178
DECICCO, P. D., Compton scattering and electron momentum density in beryllium, 25:19870
DEFOREST, S. E., Efficiency of channel electron multipliers for electrons of 1 to 50 keV, 25:18659
DE FRIETAS PACHEO, J. A., X-ray emission at $^1/_4$ keV by bremsstrahlung suprathermal protons, 25:19451
DEGOWIN, Richard L., Studies of recovery of erythropoiesis after irradiation as a function of the cellularity of the endocolonized spleen, 25:19125
DE GUARRINI, F., Measurements of neutron spectrum of Am--Be source, 25:18761
DEISS, Marcel, Automatic adjustment of reactivity meter, 25:18855
  Detection of local boiling in light water reactors, 25:20716 (CEA-R-4118)
DEKNUDT, Gh., Rate of translocations induced in spermatogonia of mice by two x-irradiation exposures separated by varying time intervals, 25:18958
DE LAGUNA, Wallace, Disposal by hydraulic fracturing, 25:18622 (ORNL-4584, pp 11-15)
DELBECQ, Charles J., EPR and optical absorption study of $BrCl^-$ and associated centers in doped KCl crystals. I, 25:19852
DEL BIANCO, W., Windowless gas target, 25:20185
DE LEEUW, S., New spectrometer for in-core neutron spectrum measurements or low α activity detection, 25:18741
DE LEEUW-GIERTS, G., New spectrometer for in-core neutron spectrum measurements or low α activity detection, 25:18741
DELIC, G., DWBA calculations for (d,p) reactions, 25:20328
DELMAS, J., Transfer of radionuclides to plants by irrigation, 25:18938
DELONG, L. E., Continuously operating ^{3}He evaporation refrigerator, 25:19632
DELTOUR, J., Deconvolution of the observed beam in the elastic scattering of slow neutrons, 25:20241
DELZER, W., Effect of 6-azauridine on labelling index and mean grain count of Ehrlich-carcinoma ascites cells, 25:18888
DEMARQUE, Pierre, Advanced evolution of Population II stars. I, 25:19307
DEMAYO, Adrian, Secondary deuterium isotope effects on ionization in benzoic, o-toluic, mesitoic, and phenylacetic acid systems, 25:18409
DEME, S., Neutron dosimetry by semiconductor detectors and hydrogenous radiator assembly, 25:18798 (KFKI-70-25-HP)
DEMEYER, A., High energy reactions with Ho and Tm, 25:20390
DEMIDOV, A. M., Experiments with ultracold neutrons, 25:20232 (JINR-P3-5392)
DEMOKAN, O., Time-of-flight study of waves guided by a plasma column, 25:19746
DEMUYNCK, J., Isomeric transitions, 25:18753
DEMYANOV, A. V., Use of a wire spark chamber to measure the beam profile of a synchrocyclotron, 25:20163
DENARDO, Gerald L., Enhanced scintigraphic information display using computer-generated ratio techniques, 25:19053
DEN BOEF, R., Chemical analysis of high burn-up PuO_2 fuel, 25:18356 (KR-140)
DEN BOER, J. A., Gallium implantations in Si studied by proton backscattering, x-ray emission, and Hall effect, 25:19802
  Position sensitive detector telescopes for charged particles used in the BOL-system, 25:18757
  Thermal properties of high-value gallium- and boron-implanted resistors in silicon, 25:19783
DENEKAMP, J., Response of mouse epidermal cells to single and divided doses of fast neutrons, 25:19092
DENERT, E., Pseudorandom pulse generator for a uniform amplitude distribution with discrete lines, 25:18853
DENISOV, S. P., Experimental comparison of anti dp and anti pd total cross sections, 25:19907
  High resolution differential Cherenkov counters, 25:18794
  High-pressure gas target cooled by liquid nitrogen, 25:20128 (IFVE-SEF-70-22)
  Production of low momentum negative particles by 70 GeV protons, 25:19906
DENNISON, D., Improved high-beam-current ion implanter, 25:20167
DENOIT, Daniel, Nuclear reactor refuelling installation, 25:20836
DE NOTARISTEFANI, Francesco, Impulse approximation calculation of the polarization of the recoil proton in the reaction γ + n + p + π^- in deuterium, 25:19940
DEPPING, F., Transistor control element for the current regulation of a pulsed magnet power supply, 25:20208
DEPUYDT, H., Is ground state rotational band cut off in

^{8}Be, 25:20280
DER, R. C., Soft x rays from collisions of 1 MeV H_2^+ and 500 keV Ar^+ with carbon, 25:18836
DE RAFAEL, E., Anomalous magnetic moments of the electron and the muon, 25:19936 (CNRS-CPT-70-P-335, pp IV.1-15)
DEREBCHINSKII, A. I., Spark chamber with graphite electrodes, 25:18785
DE RETZ, B., Activities of Electricite de France in atmospheric pollution control, 25:20686
DE ROOST, E., Isomeric state in ^{113}In, 25:20460
DERVIEUX, Bernard, Analysing an amplitude spectrum, 25:18652
DE SAINTIGNON, P., Parity irregularities in 279-keV γ transition of ^{203}Tl, 25:20433
DESCHAMPS, J., Structure of sputtered niobium films, observation of a fcc phase, 25:19244
DESIDERIO, A. M., Lamb shift and binding energies of K electrons in heavy atoms, 25:19477
DETAR, C. E., Helicity poles, triple Regge behavior and single particle spectra in high energy collisions, 25:19926 (NYO-2262-TA-234)
DETRAZ, C., Formation of ^{6}Li/sub g s / and ^{6}Li, 3.56 MeV, T = 1 state, 25:20284
DEUBLEIN, O., Lingen nuclear power station, 25:20560
DEUSTER, G., Gas turbine in public electricity supply and its future prospects, 25:20690
DEUTSCHER, G., Proximity effects between magnetic and superconducting thin films, 25:19600
DEUTSCHMANN, M., t-channel helicity conservation in diffractive reactions producing A_1 and Q-mesons, 25:19921
DEVINS, D. W., Coupled-channel analysis of α-particle scattering from the 5.23 MeV natural parity state of ^{24}Mg, 25:20344
DEVIOT, Bernard, Vacancy quenching in Nb, 25:19245
DE VOE, R., Measurement of the muonium hfs splitting and of the muon moment by double resonance, and a new value of α, 25:19888
DE WAELE, A. Th. A. M., Superconducting point contacts weakly connecting two superconductors, 25:19601
DEWAN, John T., Multiple detector neutron logging technique, 25:18874
DE WIT, R., Chemical analysis of high burn-up PuO_2 fuel, 25:18356 (KR-140)
DIAZ, Nils J., Space--time reactor kinetics studies with the Univ. of Florida SPERT assembly, 25:20794
DIBELIUS, G., Technical and economic assessment of different nuclear plant types, 25:20749
DI CASA, Michele, Some Italian meteorites trace elements content by nondestructive neutron activation analysis, 25:18370
DICHTEL, K., Diffusion of flux into Type-II superconductors, 25:19593
DICKSON, P. W., Engineering study of the colloid-fueled reactor concept, 25:20811
DIDORENKO, V. A., Investigation of gamma radiation of isomers /sup 110m/In and ^{110}In, 25:20402
DIEDERICH, Norman Francis, Computer-aided teleoperator system, 25:20841
DIETRICH, R., Dynamic behavior of counter-flow heat exchangers of nuclear power plants with gas turbine at step change of inlet termperatures, 25:20779
DIETRICK, William, Early use of xenografts as a biologic dressing in burn trauma, 25:19020
DIEVAL, Michel, System for measuring radiation doses, 25:18805
DIGE, Ulrik, Radiation-induced osteogenic sarcoma, 25:19140
DIKEOU, J. T., Concrete-polymer materials. Third topical report, 25:19292 (BNL-50275)
DIMENT, K. M., Ratio of ^{6}Li(n,α) to ^{10}B(n,α) cross-sections, 25:20288
DINARDO, Robert Philip, Optical emission from electron-irradiated thin foils, 25:19471
DI PIETRO, Roberto, Water treatment in a plant for testing fuel elements, 25:20726
DIPRIMIO, J., Possible utilization of the Carnegie-Mellon synchrocyclotron for cancer therapy, 25:19087
DIRKS, Johan F., Closed-channel spectrum of the positron--hydrogen rearrangement collision, 25:19503
DI ROCCO, James V., Radiation detection devices, 25:18682
DISDIER, R., Transfer of radionuclides to plants by irrigation, 25:18938
DISNEY, M. J., Optical spectra of the nuclei of elliptical radio galaxies, 25:19449
DITA, P., Charge-exchange reactions in Regge-pole phenomenology, 25:19995
DIVATIA, A. S., States in ^{10}B from elastic scattering of alphas by ^{6}Li, 25:20292
DIVEN, B. C., High resolution fission cross section of ^{235}U from 20 eV to 100 keV, 25:20418
  Nuclear explosions as a nuclear physics tool, 25:20449
DIX, Frederick William, Search for proton decay as a test of baryon conservation, 25:19893
DIXON, R. L., Reactions ^{7}Li(^{3}He,d)^{8}Be and ^{7}Li(^{3}He,p)^{9}Be, 25:20273
DJALOEIS, A., Tensor polarization and differential cross section for ^{9}Be(d,d)^{9}Be elastic scattering at low energies, 25:20293
  Tensor polarization of deuterons from Mg(d,d)Mg elastic scattering at 7.0 MeV, 25:20342
DMITRIEV, A. B., Low-activated trigger chamber containing ^{3}He, 25:18662
DMITRIEVSKII, V. P., Electronuclear method of neutron generation and fissile material production, 25:20151
DNESTROVSKII, Yu. N., Energy balance of plasma in Tokamak-type systems, 25:19654
DOBES, J., Absorption model for direct transfer reactions, 25:20522
DOBRIN, M. M., Evidence of quasi-periodic movements in the solar chromosphere and corona, 25:19415
DOBROWOLSKI, J., Radiobiological and radioecological aspects of radioactive pollution of earth atmosphere, 25:18941
DODD, H. M. Jr., Aerodynamic forces and dynamic stability of high-speed, magnetically suspended rocket sled, 25:20890 (SC-DR-70-867)
DOEBNER, H. D., Realizations of Lie algebras through rational functions of canonical variable, 25:19935
DOKE, Tadayoshi, Stopping powers of gases and solids for heavy charged particles, 25:19762
DOLIN, P. I., Primary radiolysis reactions of nonalkaline aqueous solutions of pyrimidine bases, 25:18475
DOMEIJ, B., Anomalously high yields of elastically scattered ^{12}C from atoms implanted into silicon, 25:19829
DOMKIN, V. D., Neutron polarization in the reaction ^{12}C(d,n)^{13}N at E/sub d/ = 6.4 MeV, 25:20297
DONATI, Jean Roger, Automatic goniometer, 25:18861
DONE, K. C. W., Industrial-scale ion-implantation facility, 25:19773
DONG, R., Theory identification for mechanical behavior of polystyrene bead foams, 25:19293 (UCRL-50952)
DONSKOV, S. V., Experimental comparison of anti dp and anti pd total cross sections, 25:19907
  High resolution differential Cherenkov counters, 25:18794
  Production of low momentum negative particles by 70 GeV protons, 25:19906
  Time resolution of scintillation counters, 25:18640 (IFVE-SEF-70-23)
DORMAN, L. I., Structure of the interplanetary space from data on annual cosmic-ray variations, 25:19526
DOST, M., Gamma-decay of proton-particle neutron-hole states in ^{208}Bi, 25:20434
DOUGHERTY, J. P., Lagrangian methods in plasma dynamics. I, 25:19754
DOUZON, Jean, Analysing an amplitude spectrum, 25:18652
DOWDEY, J. Edward, Image aberrations produced by multichannel collimators for a scintillation camera, 25:18660
DRACHMAN, Richard J., Generalized Hylleraas calculation of positron--hydrogen scattering, 25:19508
  Positron--atom scattering by Kohn and Harris methods, 25:19509
DRAGOS, L., Hall effect on the motion of viscous fluids past a flat plate, 25:19569
DRAGT, Jan B., Theoretical and experimental study of a fast-thermal coupled reactor by correlation techniques, 25:20833 (RCN-132)
DRAKE, Jerry F., Characteristics of soft solar x-ray bursts, 25:19400
DRAWBAUGH, D. W., Engineering study of the colloid-fueled reactor concept, 25:20811
DRECHSEL, Dieter, Magnetic monopole transitions in electron scattering, 25:20294
DRECHSLER, Wolfgang, Complex anguler momentum theory in particle physics, 25:19974
DRELL, Sidney D., Present status of quantum electrodynamics, 25:20081
DRESIA, Heinrich, Moisture determination in solids by neutron radiation, 25:18362
DRIOLE, J., Present state of the bibliography on Nb and its alloys, 25:19165
  Study of niobium base refractory metal alloys, 25:19246
DRONNIK, L. M., Empirical approximation of coefficient of hydraulic resistance in a moving magnetic field, 25:19557
DROZDOV, V. E., Calculation of efficiency of γ-irradiators, 25:18571
DRUIN, V. A., Potential identification of products of heavy-ion-induced nuclear reactions, 25:20419
DRUMMOND, A. J., Standard values for the solar constant and its spectral components, 25:19416
DRUZHININ, V. P., Thermal and electrical conductivities of single-crystal molybdenum at high temperatures, 25:19220
DRYANOVSKI, P., Influence of antibody formation on permeability of erythrocytes, 25:18900
DUBECK, L. W., Intermediate mixed state of Type-II superconductors, 25:19620
DUBININA, L. G., Effect of space-flight factors on Crepis-capillaris seeds, 25:18953
DUBROVSKII, V. B., Change of concrete aggregate properties under neutron irradiation, 25:19296
DUCOFF, H. S., Partial-body irradiation of larvae of Tenebrio molitor, 25:19094
DUFFAZT, R., Neodymium-141 levels excited from ^{141}Pm(21 min) disintegration, 25:20388
DUFFIN, Roger Alan, Deposition of composite coatings, 25:19270
DUHM, H. H., Formation of ^{6}Li/sub g s / and ^{6}Li, 3.56 MeV, T = 1 state, 25:20284

DUL'KIN, I. N., Heat transfer in pool boiling of water and Freon-113 on cylindrical rod, 25:18585
DUMBRAIS, O. V., Model-independent analysis of forward π^{+-}p scattering data, 25:20003 (JINR-E2-5561)
  Real parts of the K^{+-}p forward scattering amplitudes, 25:20013
DUMBRAIS, T. Yu., Real parts of the K^{+-}p forward scattering amplitudes, 25:20013
DUNAEV, L. M., Calculation of efficiency of γ-irradiators, 25:18571
DUNAITSEV, A. F., Electron energy measurement by the shower spectrometer, 25:18779
DUNLAP, H. L., Ion-implanted junctions and conducting layers in SiC, 25:19847
DUNN, H. Searl, Electromagnetic radiation from a laser-produced plasma expanding into a uniform magnetic field, 25:19679
DUNNAM, F. E., Use of a pulsed Van de Graaff accelerator and time-of-flight techniques to reduce backgrounds in (α,γ) spectroscopy experiments, 25:20148
DUPLISHCHEVA, A. P., Influence of ionizing radiation on natural immunity, 25:18922
DUPONT, J. F., Dynamic studies of gas turbine fast reactors, 25:20765
DURAND, Roger, Economics of the various methods available for preparing Nb, 25:19187
DURASOVA, M. S., Evidence of quasi-periodic movements in the solar chromosphere and corona, 25:19415
DVORAK, J., Single-crystal filters of thermal neutrons, 25:20238 (UJV-2488-F)
DVORETSKII, V. N., Experiments with ultracold neutrons, 25:20232 (JINR-P3-5392)
D'YACHENKO, P. P., Dependence of anti ν on neutron energy on basis of fission energy balance, 25:20440
DYAKONOV, V. P., Pulse amplitude discriminators based on avalanche transistors, 25:18847
DYMENT, J., Present status of the design and testing of radioactive filtration installations and associated aerosol research, 25:18559 (CONF-700816-(Vol.1), pp 128-42)
DYSON, E. D., Effect of acute x-irradiation on development of eggs of plaice, Pleuronectes platessa, 25:19103 (PG-Report-1013)
DZHAUGASHTIN, K. E., Circulation of an axially symmetric turbulent jet of electrically conducting fluid in a longitudinal magnetic field, 25:19558
  Distribution of energy pulses in jet of conducting fluid in longitudinal magnetic field, 25:19560
DZHELEPOV, V. P., Electronuclear method of neutron generation and fissile material production, 25:20191
DZYUBA, B. M., Calculations of cross sections for inelastic interaction of neutrons with nuclei accompanied by emission of protons and α particles, 25:20346
DZYURA, E., 10-MeV proton linear accelerator at Swierk, 25:20129 (INR-P-1218)

E

EARLE, E. D., Reaction ^{115}In(n,γ)^{116}In, 25:20410
EASTON, D. S., Computer program for calculating, tabulating, and plotting outgassing rates of selected gases, 25:19195 (ORNL-TM-3220)
EBELS, E. J., Enzymehistochemical maturation of the cerebellar cortex of rats after early postnatal x irradiation, 25:19114
EBERLY, Warren S., Soft magnetic alloys: their heat treatment and testing for magnetic properties, 25:19872
ECKHARTT, D., Plasma confinement in WIIa-stellarator, 25:19645 (IPP-2/86)
EDDY, William C. Jr., Passive device for determining relative rotation, 25:18822
EDGE, R. D., Reactions ^{7}Li(^{3}He,d)^{8}Be and ^{7}Li(^{3}He,p)^{9}Be, 25:20273
EDMONDS, C. J., Follow-up of thyroid carcinoma by whole-body counting, 25:19035
EFANOV, V. A., Observations of radio emission of sources 3C 273 and 3C 279 at 8 mm, 25:19376
EFIMOV, G. V., Brief review of reports submitted to 2nd international symposium on nonlocal quantum field theory, Azau, 3/70, 25:20057 (JINR-E2-5563)
EGAMBERDIEV, A., Mitosis process in meristematic cells of cotton under the action of gamma rays and dimethyl sulfate, 25:18954
EGELSTAFF, P. A., New time-of-flight analyzer for neutron scattering, 25:18765
EGLAND, R. J., Origin of complex electron spin resonance spectra of γ-irradiated polycrystalline n-alkyl iodides with even number of carbon atoms per molecule, 25:18424
EGOROVA, Z. S., Action of ionizing radiation on the structure and properties of the copolymer of styrene with 2-ethylhexyl acrylate, 25:18436
EHLERS, Kenneth W., Feedback-controlled steady-state plasma, 25:19713
EHRHART, J. C., Biochemical considerations on alveolar retention of liquid rare earth aerosols, 25:18889 (CEA-CONF-1676)
EHRMANN, E., Mean lives of ^{31}S and ^{38}K levels, 25:20349
EIDE, I., Renal excretion of ^{51}Cr-EDTA, 25:18893
EIDENS, J., Gas-filled magnetic separators, 25:18851
  Identification of μs-isomers among primary fission products, 25:20430
EINAUDI, F., Higher-order approximations in theory of longitudinal plasma oscillations. II, 25:19750
EISEN, F. H., Analysis of disorder distributions in boron-implanted silicon, 25:19830
EISEN, F. M., Disorder produced during ^{11}B and ^{12}C implantation in silicon, 25:19806
EISENBERG, R. A., Antibody inhibition of the immune response: experimental analysis of the site of action in vivo, 25:18923
EISERIKE, H., Generalized Hylleraas calculation of positron--hydrogen scattering, 25:19508
EISNER, M., Ion heating by a modulated electron beam, 25:19650
EJIRI, H., Electromagnetic transitions from levels in the beta-vibrational band of ^{174}Hf, 25:20427
EL-BADRY, E. A., Effects of gamma radiation on cotton leaf worm, 25:19097
EL BAZ, E., Nucleon elastic scattering by ^{4}He, 25:20261
ELDRIDGE, G., Improved high-beam-current ion implanter, 25:20167
  Radiation-damage studies of bismuth-ion-implanted CdS, 25:19792
EL-GHABATY, Sayed Shehata, Symmetries and nuclear forces, 25:20021
ELIAS, Cezar A., Activity of ionizing radiation on fertile eggs of Triatomideos-Rhodnius prolixus, 25:19099
ELISEEV, S. M., Cross-sections of high-energy particles on atomic nuclei, 25:20490
ELISEEV, S. S., Oxidation-reduction processes in the systems $ReCl_5$--UO_2Cl_2 ($UOCl_3$), 25:18384
ELLIS, Frank, Afterloading techniques, 25:19076
ELLIS, Jerry Lynn, Proton elastic scattering from ^{88}Sr, ^{89}Y, ^{92}Zr, ^{92} ^{94}Mo, and ^{118} ^{120}Sn, 25:20331
ELLIS, John, Phenomenological actions for spontaneously-broken conformal symmetry, 25:20038
ELLIS, Robert E., Purification of polonium, 25:18509
ELLIS, W. R., Initial equilibrium configuration of Scyllac 5-meter toroidal-sector experiment, 25:19725 (LA-4597)
EL'MANOVA, N. A., Oxidation-reduction processes in the systems $ReCl_5$--UO_2Cl_2 ($UOCl_3$), 25:18384
EMENDOERFER, D., Resonance-capture and -fission in highly enriched fuel-lattices, 25:20826
EMERSON, L. C., Physics of tissue damage, 25:19759 (ORNL-4584, pp 87-91)
EMERY, E. W., Response of mouse epidermal cells to single and divided doses of fast neutrons, 25:19092
EMERY, Roger J., 100-micron map of galactic center region, 25:19448
EMPSON, F. M., Disposal in natural salt formations, 25:18623 (ORNL-4584, pp 16-36)
EMSALLEM, A., Neodymium-141 levels excited from ^{141}Pm(21 min) disintegration, 25:20388
ENGELS, E. Jr., Photoproduction of neutral K mesons, 25:19887
ENGLERT, T. J., Photoneutron cross sections for ^{32}S, 25:20332
ENGLUND, Bjoern, Construction and examination of a gas scintillation detector, 25:18645 (USIP-70-1)
ENGMANN, R., Mean lives of ^{31}S and ^{38}K levels, 25:20349
ENTIS, A. C., Photoproduction of neutral K mesons, 25:19887
EPSTEIN, G. N., Form factors and polarization of x-rays from nuclear reactions, 25:20423
EREMENKO, V. N., Structure of V--Cr--Zr alloys at 1150°C, 25:19237
ERICKSON, Kenneth Neil, Multiparticle production in liquid H and C by charged cosmic-ray hadrons, 25:19905
ERLICKI, M. S., Electron temperature determination in a low-density helium plasma, 25:19661
ERLIK, A., Lifetime measurements of alpha emitters in the millisecond region, 25:18703
ERMAGAMBETOV, S. B., Plutonium-238 neutron fission in sub-barrier energy range, 25:20444
ERMOLAEVA, G. K., Near-wall flow of jet of conducting fluid in transverse magnetic field, 25:19559
ERTL, Harald H., Dosimetry of incorporated tritium and ^{125}I, 25:18984 (JUL-688-ME)
ERVIN, Guy Jr., Helium injection as a technique for studying rare gas behavior in carbide fuel, 25:19272 (AI-AEC-12984)
ERYUSHEV, N. N., Hard x-ray emission of solar flare on Sept. 28, 1961, 25:19435
ESCUDIE, J. L., Study of (p,d) reactions on ^{118}Sn and ^{119}Sn with polarized protons, 25:20365 (CEA-CONF-1657)
ESKOLA, K., Decay of ^{62}Co isomers and ^{62}Cu, 25:20361
ESPINASSE, Pierre, Radiation detecting device, 25:18688
ESSMANN, U., Visualization of mixed state of Type-II superconductors, 25:19596
ESTOURNEL, R., Exposure of man to natural and artificial sources of ionizing radiations, 25:19137
ESTRADA, Herbert Jr., Nuclear reactor thermoelectric power plant, 25:20694
ETIEVANT, C., Measuring poloidal field in toroidal magnetic configuration, 25:19735
EVANS, D. M., UKAEA fuel test assemblies irradiated in HBWR, 1964--66, 25:20736 (HPR-132)
EVANS, H. C., Transition rates in ^{29}P, 25:20319
EVANS, J. H., Regular void array in high-purity Mo irradiated with 2-MeV N^{+} ions, 25:19256

XUM

Void array in high-purity Mo irradiated with 2 MeV nitrogen ions, 25:19257
EVANS, Titus C., Mitotic inhibition and its relation to survival in S-180 ascites tumor cells in vivo following fractionated exposures of x-radiation, 25:19091
EVSEEV, A. G., Relation of radiation cross-linking in special purpose elastomers to additions of chloroalkanes of various structures, 25:18434

F

FABRI, G., Extension of Ramo's theorem as applied to induced charge in semiconductor detectors, 25:18710
FABRICHNYI, P. B., Gamma-radiolysis of tin oxides, 25:18470
FABRY, M., Spectroscopic study of a caesium discharge plasma, 25:19665
FADNER, W. L., Excited states of ^{46}V, 25:20347
FAELDT, Goeran, Deuteron--nucleus collisions in the multi-GeV region, 25:20531
FAIRFIELD, J. M., Radiochemical determination of damage profiles in silicon, 25:19817
FALK, F., Decay of ^{249}Cf, 25:20398
FAL'KO, I. I., Energy spectrum of a superconductor with overlapping energy bands, 25:19625
FALLIEROS, S., Fine structure in highly excited analog states, 25:20396
FANT, B., Reaction ^{31}P(p,γ)^{32}S, 25:20308
FARKAS, Erzsebet, Elimination of oxidation induced by gamma irradiation in aqueous pharmaceuticals, 25:18472
FARWELL, L. C., Excited states of ^{46}V, 25:20347
FASTOVSKII, V. G., Heat transfer in pool boiling of water and Freon-113 on cylindrical rod, 25:18585
FAUDE, D., Fast breeder reactors, 25:20708
FAYANS, S. A., Gauge transformations and local charges of quasiparticles, 25:20082
FAYARD, C., Nucleon elastic scattering by ^{4}He, 25:20261
FAYARD, Florence, Discussion of the elementary reactions of radiolysis of methane in the gaseous phase, 25:18449 (ORNL-tr-2386)
FAYOS, Juan V., Radiation therapy of carcinoma of the tonsillar region, 25:19085
FEDOROV, L. N., Superconducting alloy, 25:19618
FEDOROVA, T. A., Influence of ionizing radiation and radio-protectors on the antihyaluronidase activity of blood serum and tissue permeability in rats, 25:19031
FEDOROVICH, G. V., Electric field excited in air by pulsed γ quanta, 25:19761
FEDOSEEV, E. P., Three-sector focusing magnetic prisms with r^{-1} field. III, 25:20217
FEDOTOV, L. N., Critical temperature of superconducting alloys of Nb--Ti--Ta system, 25:19629
  Superconducting alloys based on Nb--Ti--Zr system, 25:19627
FEINAUER, Dieter, Formation of chelates and adduct chelates in the extraction of trivalent americium and californium, 25:18498 (KFK-1298)
FEJER, J. A., Radiation from a charged particle in a magnetoplasma, 25:19696
FEL, N. S., Primary radiolysis reactions of nonalkaline aqueous solutions of pyrimidine bases, 25:18475
FELDEN, Madeleine, Origin of wave functions of approximations used calculating cross sections of electron--H atom interactions, 25:19494
FELDMAN, L. C., Implantation of Bi into GaP. II, 25:19846
  Ion implantation of Bi into GaP. I, 25:19845
FELSTEINER, J., Lifetime measurements of alpha emitters in the millisecond region, 25:18703
FENDLER, J. H., Radiation chemistry of aqueous solutions of $CFCl_3$, CF_2Cl_2, and CF_3Cl, 25:18460
FENDLEY, T. T., Prog. rpt. on bioaccumulation of gamma-emitting radionuclides in white-tailed deer, annual, 2/70--1/71, 25:18935 (ORO-3905)
FENRICK, H. W., Growth and decay of alkyl radicals in γ-irradiated alkyl iodides at 77°K, 25:18461
FENYVES, Ervin, Cosmic rays in high-energy physics, 25:19885
FEOFILOV, P. P., Total antiresonance in CaF_2: Dy crystals with color centers, 25:19771
FERESIN, A. P., Determination of experimental values of internal conversion matrix elements, 25:20457
FERGUSON, A. J., Evidence for vibrational excited states in ^{32}S, 25:20326
FERGUSON, D. E., Weapons effects display system (WEDS MOD II): mathematical models used for calculations, 25:18831 (UCRL-50892(Vol.1))
FERNANDEZ POLO, J. A., Genesis of uraniferous deposits in metasediments in Province of Salamanca, 25:18547
FERRADINI, C., Effect of food preirradiation on the fecundity of two insects: mealy bugs (Pseudaulacaspis pentagona Targ.) and Indian-meal moths (Plodia interpunctella Huebn.), 25:19159
FERRARI, T., Micrologic integrated circuit for monitoring correlation in pulse sequences, 25:18701
FERRARO, John R., Low-frequency vibrations of inorganic and coordination compounds, 25:18419
FERRERO, L., Solid state detector telescope for charged photoparticles, 25:18675
FERRIS, G. A. J., Planetary influences on sunspots, 25:19427
FERRUCCI, Napoleone, Experimental vibration characteristics of BWR fuel assembly, 25:20740
FESSLER, P. A., High sensitivity ultrasonic test system for welds, 25:20857 (GEPP-83)
FEUERBACHER, B., Graphite conduction band states from secondary electron emission spectra, 25:19864
FEUSTEL, Edward Alvin, Prog. rpt. on interchange of essential programs between dissimilar computers, annual, 3/71, 25:20884 (ORO-4061-1)
FIDONE, I., Measuring poloidal field in toroidal magnetic configuration, 25:19735
  Nonlinear wave mixing at hybrid frequencies in an inhomogeneous plasma, 25:19747
FIEBELMANN, Peter, Nuclear power plant for a space station, 25:20807
  Nuclear power plant for a space station, 25:20808
  Nuclear reactor with heat pipes, 25:20809
FIELD, S. B., Response of mouse epidermal cells to single and divided doses of fast neutrons, 25:19092
FIELD, Stanley B., Effects of fast neutrons on human skin, 25:19149
FIELDER, David R., Energy levels in ^{74}Ge from decay of ^{74}Ga, 25:20343
FIENO, Daniel, Tests of evaluated beryllium (n,2n) cross sections, 25:20269 (N-70-37365)
FIGLIK, Kenneth G., Method of inhibiting the corrosion of tantalum by liquid lithium, 25:19168
FIGUERA, A. S., Absolute γ-ray efficiency of 50 cm^3 Ge(Li) detector, 25:18702
FIGUREAU, Alain, Low-energy theorems and π-meson interactions with nuclei, 25:20019 (LYCEN-7081)
FIKS, M. M., Storage of multicharged ions in relativistic electron beam, 25:20210
FILATOV, A. I., Measurement limits of exposure dose rate by gas-discharge counters, 25:18664
FINKEL, V. A., Crystal structure of Ho and Er between 77 and 300°K, 25:19243
FINSTON, Roland A., Distribution and dosimetry of /sup 113m/In colloid, 25:18994
FIRK, F. W. K., Low-energy photonuclear reactions, 25:20448
FIRST, M. W., Sodium aerosol filtration studies, 25:18563 (CONF-700816-(Vol.1), pp 445-58)
FIRST, Melvin W., Behavior of iodine in sodium systems, 25:20760 (CONF-700816-(Vol.1), pp 356-72)
  Heat transfer of sodium compounds deposited on surfaces from aerosols, 25:18562 (CONF-700816-(Vol.1), pp 413-24)
  Proceedings of the eleventh AEC air cleaning conference held in the Federal Building, Richland, Washington, August 31--September 3, 1970, 25:18525 (CONF-700816-(Vol.1))
FISCHEL, D., Partition functions in ionizing plasmas, 25:19397
FISCHER, E. A., Fast breeder reactors, 25:20708
FISCHER, J., Position sensitive detector for a magnetic spectrograph, 25:18681
  Pyrochemical processing of fuel materials and scrap containing ^{239}Pu, 25:18492 (ANL-7709)
FISCHOTTER, Peter, Moisture determination in solids by neutron radiation, 25:18362
FISHBANE, Paul M., Comments on eikonalization at high energy, 25:19961
FISHBEIN, M., Lifetime and g-factor of 74.8 keV state of ^{100}Rh, 25:20454
FISHER, Ch., Problems of protection in the industrial utilization of the radioelements, 25:18996
FISHER, Richard R., Green-line observations of Mar. 1970 coronal enhancements, 25:19411
FISHMAN, Gerald Jay, Measurements of hard x and γ radiation from Virgo A and Centaurus A, 25:19455
FITTON, B., Graphite conduction band states from secondary electron emission spectra, 25:19864
FITZGERALD, Lawrence T., Coordinate measuring device for radium applications, 25:19004
FITZWILSON, R. L., Formation of metastable hydrogen atoms by charge transfer, 25:19504
FLADDA, G., Anomalously high yields of elastically scattered ^{12}C from atoms implanted into silicon, 25:19829
  Lattice location of heavy group III and V elements implanted into Ge, 25:19827
FLAHERTY, Robert, Submersible nuclear reactor plant, 25:20817
FLAMANT, Y., Wired arithmetic computer for particle identification, 25:18718
FLAMINIO, E., Compilation of cross sections V--K^- induced reactions, 25:19909 (CERN-HERA-70-6)
FLAMM, D., Some remarks on the Quark model, 25:19979
FLEISCHAKER, Barbara, Evaluation of phototoxicity of salicylanilides and similar compounds by photohemolysis, 25:18913
  Red blood cell hemolysis by photosensitizing compounds, 25:18914
FLEMING, D. G., Spin dependence in the reactions ^{16}O(p,t)^{14}O and ^{16}O(p,^{3}He)^{14}N, 25:20299
FLEROV, G. N., Production of spontaneously fissioning isomers ^{242}Am and ^{244}Am, 25:20412
FLETCHER, Gilbert H., Comparative evaluation of the sequential use of irradiation and surgery in primary tumors of the oral cavity, oropharynx, larynx, and

hypopharynx, 25:19083
Elective irradiation of the neck lymphatics for squamous cell carcinomas of the nasopharynx and oropharynx, 25:19084
FLETCHER, Larry L., Radiation hardened transistor circuit, 25:18879
FLEURY, A., Boron-11 and ^{10}B interactions with Th and U, 25:20420
FLEURY, Alain, Ratio of ^{236}Np isomers in ^{238}U deuteron interactions, 25:20389
FLORENCE, T. M., Spectrophotometric determination of U(VI), 25:18352
FLOYD, R. M., Extraction of rotational energy from a black hole, 25:19338
FOESTER, S., Preliminary evaluation of design principles for nuclear power plants with high-temperature reactor and gas turbine cycles, 25:20700
FOGELBERG, B., Transition rates in ^{192}Au, 25:20453
FOMENKO, B. A., Resistance in flow of liquid metals in channels in a transverse magnetic field, 25:19554
FOMINA, N. V., Radiothermal isomerization of alkyl bromides, 25:18438
FOMINYKH, V. I., Two-dimensional analyzer for half life measurements of nucleus of excited states, 25:18642 (JINR-P13-5485)
FORD, C. Hubbard, Tests of evaluated beryllium (n,2n) cross sections, 25:20269 (N-70-37365)
FORD, James Wilburn Jr., Decay studies of transitional nuclei ^{88}Sr, ^{148}Sm, and ^{151}Eu, 25:20352
FORD, R. A., Annealing characteristics of highly doped ion-implanted phosphorus layers in silicon, 25:19837
FORESTIER, H., Hydrogen embrittlement of Nb base alloys, 25:19216
Preparation of high purity niobium base alloys, 25:19186
FORET, F., Interdigital H-type (IH) structure, an accelerating structure for low energy beams, 25:20156
FORMAN, Peter R., Dynamic stabilization of a linear z pinch, 25:19717
FORSBLOM, I., Investigation of ^{28}Si by $^{27}Al(p,\gamma)^{28}Si$, 25:20315
FORSTER, J. S., Angular correlation measurements of first three excited states in ^{29}P, 25:20323
Properties of low-lying states in ^{43}Sc, 25:20320
FORTNER, R. J., Soft x rays from collisions of 1 MeV H_2^+ and 500 keV Ar^+ with carbon, 25:18836
FOSS, M. H., Possible utilization of the Carnegie-Mellon synchrocyclotron for cancer therapy, 25:19087
FOSTER, Bruce P., Energy levels in ^{74}Ge from decay of ^{74}Ga, 25:20343
FOUGERE, P. F., Magnetic dipole in a stationary plasma, 25:19699
FOULQUIER, L., Pollution and hydrobiology of fresh water, 25:18937
FOURNET, G., Behavior of Type-II superconductors in time-dependent magnetic fields, 25:19598
Thermodynamics of Type-II superconductors, 25:19594
FOURNIER, D., Study of the coherent production on nuclei of $K^- \pi^+ \pi^-$ systems by K^- of 5.5, 10.0, and 12.7 GeV/c, 25:19910 (LAL-1242)
FOWLER, P. H., Charge spectrum of extremely heavy cosmic rays, 25:19532
FOX, J. G., Possible utilization of the Carnegie-Mellon synchrocyclotron for cancer therapy, 25:19087
FRANC, L., Modification of NLZ 716a-T pulse height analyzer, 25:18862
FRANCIS, C. W., Fate of trace elements and radionuclides in terrestrial environment, 25:18521 (ORNL-4584, pp 1-10)
FRANCIS, R. J., Industrial-scale ion-implantation facility, 25:19773
FRANCOIS, P. E., Phosphorescent components in CsI(Tl) and CsI(Na), 25:18648
FRANGHYAN, A. A., Superhigh-energy particle detector based on using the radiation of a particle in a laminar medium, 25:18781
FRANKEVICH, E. L., Stabilized ions and the formation of cross links in the radiolysis of polybutadiene, 25:18467
FRANKLIN, Paul, Weapons effect display system (WEDS MOD II): prompt effects computer program, 25:18832 (UCRL-50892(Vol.6))
FRASER, I. A., Doppler shift attenuation studies in heavy nuclei, 25:20409
FREDERICK, Carl L., 100-micron map of galactic center region, 25:19448
FREEMAN, J. H., Formation of insulating layers by use of reactive ion beams, 25:19781
Implantation machines, 25:20165
Industrial-scale ion-implantation facility, 25:19773
FREHAUT, J., Research report on measurement of average number of prompt neutrons, 25:20373 (LIB/Trans-300)
FREIDBERG, J. B., Effects of force-free fields on plasma stability, 25:19706
FREINDL, L., Polarization of protons from $^{12}C(d,p)^{13}C$ reaction at E/sub d/ = 12.4 MeV, 25:20287
FREIRE-MAIA, Newton, Abortions, chromosomal aberrations, and radiation, 25:18969
FREIS, R. P., Effects of magnetic lens aberration in high-current linear accelerators, 25:20160
FRENCH, J. B., Validity of random matrix theories for many-particle systems, 25:20507
FRENCH, W. R. Jr., Determination of energy levels in stable nuclei by neutron inelastic scattering, 25:20356
FRENKEL, A., Introduction to the current--current theory of the weak interaction, 25:19964 (KFKI-70-24-HEP)
FREUND, D., New method for the study of UO_2 in a temperature gradient, 25:19278
FREUND, Jean-Pierre, An electric generator with thermopiles and radioelements, 25:18598
Isotopic electric generator using thermoelectric elements, 25:18605
FREYTAG, E., Measurements of high doses with glass dosimeters, 25:18802
FRIAR, J. L., Helium-3--^3H charge form factor and ^3He Coulomb energy, 25:20256
FRIED, H. M., Super-eikonal model of deep inelastic electron-proton scattering, 25:19939 (NYO-2262-TA-221)
FRIED, W., Accelerated regeneration of transplanted hematopoietic stem cells in irradiated mice pretreated with cyclophosphamide, 25:19127
FRIED, Walter, Factors regulating the proliferation and migration of hematopoietic stem cells, 25:19126
FRIEDER, A. J., High pressure indirect CO_2 closed cycle gas turbines, 25:20773
FRIEDMAN, H., Variability of x-ray emission from M87, 25:19458
FRIEDMAN, Marvin Irwin, Microscopic bases of collectivity in light nuclei, 25:20543
FRIES, E., Comparison between the oxidation of Nb and that of a Nb base alloy (P353M), 25:19172
FRIES, J. F., Deformation and rupture of Nb between -196°C and 20°C, 25:19217
Study of the changes in the mechanical properties of Nb with different impurity contents between 20 and 850°C, 25:19212
FRIESE, T., Pseudorandom pulse generator for a uniform amplitude distribution with discrete lines, 25:18853
FRISKEN, W. R., Measurement of reaction $\pi^- + \pi^0 n$ at large momentum transfers, 25:19911
FRITZSCHE, C. R., Effect of ion implantation on electrical properties of SiO_2 films at high fields, 25:19788
FROEHLICH, K., Polymeric chromium(III) complexes arising from neutron irradiation of crystalline potassium chromate. I, 25:18486
FRONSDAL, C., Two-body problem in quantum field theory, 25:20071
FRUTSCHI, H. U., Operational conditions for afterheat removal of a gas-cooled reactor with direct cycle, 25:20767
FU, Chia-yao, Unified model of deformed odd--odd nuclei for nuclear data generation, 25:20524
FUBINI, A., Energy calibration of Ge(Li) spectrometer, 25:18714
FUEKI, Kenji, Photoisomerization of maleate radical anions produced in 2-methyltetrahydrofuran by γ irradiation at 77°K, 25:18457
FUGATE, Robert Quentin, Measurement of the volume dependence of the heat capacity of solid neon, 25:20863 (IS-T-430)
FUJII, S., Radial dependence of P_1 interaction in schematic model, 25:20506
FUJII, Shoichi, Direction of development on reactor materials, 25:19297
FUKUDA, A., Core temperature analyses for loss-of-coolant accidents of light water reactor, 25:20762 (JAERI-Memo-4194)
FUKUDA, K., Photoneutrons from ^{13}C, 25:20276
FUKUDA, Kiyoshi, Recent improvements in fluoro-glass dosimeter, 25:18810
FUKUDA, Masasi, Effect of radiotherapy on the urinary amino acids, 25:19063
FUKUMOTO, Tsutomu, Studies on the fluidized bed calcination of high level radioactive liquid wastes, 25:18630
FULLER, E. L. Jr., Uniform, nonporous thoria, 25:18416
FUNG, P. C. W., Polarization of solar Type-III radio bursts at 25.3 MHz, 25:19399
FUNK, R., Protection of Nb against oxidation, 25:19176
FURAEVA, L. P., Influence of ionizing radiation and radio-protectors on the antihyaluronidase activity of blood serum and tissue permeability in rats, 25:19031
FURIC, M., Neutron--proton bremsstrahlung at 14.4 MeV, 25:20257
Reaction $^{11}B(n,t)^9Be$ at 14.4 MeV, 25:20285
FURUKAWA, T., Study on curved pipe steam generator, 25:18586
FURUTANI, Y., Treatment of collisional effects on temporal plasma-wave echoes, 25:19755
FUSCHINI, E., Use of a checker board counter in blocking experiments, 25:18679

G

GABELMAN, J. W., Metallotectonic control of uranium distribution, 25:18543
Speculations on the uranium ore fluid, 25:18552
GADDA, Ferdinando, Water treatment in a plant for testing fuel elements, 25:20726
GAGNON, W. F., Scavenging of the molecular hydrogen yield from water irradiated with tritium β particles, 25:18458
GALES, Sydney, First T = 2 state of ^{32}S, 25:20316
GALLEGOS, H. Grossi, Excited lines in H and K region of Ca II in flare on Mar. 12, 1969, 25:19412

XUM

GALPERIN, L. N., Discrete frequency sweep in a synthesizer for nuclear magnetic resonance spectroscopy, 25:18848
GALSTER, G., Hall effect and sheet resistivity as function of temperature on P implants in Si, 25:19838
GAMMAGE, R. B., Uniform, nonporous thoria, 25:18416
GAMMEL, Reinhold, Measuring and analyzing methods with multi-channel analyzer VAS 4096, 25:18674
GAMO, Kenji, Enhanced diffusion in ion-implanted silicon, 25:19823
GANGLOFF, A., Geology of principal uraniferous districts studied by CEA, 25:18534
GANGRSKII, Yu. P., Production of spontaneously fissioning isomers ^{242}Am and ^{244}Am, 25:20412
  Production of spontaneously fissioning isomers of U, Pu, and Am in neutron reactions, 25:20369 (JINR-P3-5528)
  Spark fission-fragment counter, 25:18671
GANICHEV, G. I., Radiation resistance of type ZnS + ^{10}B detectors to neutrons, 25:18880
GANZER, U., Radiation treatment of tumors, 25:19071
  X irradiation of animal tumors, 25:19075
GARBER, F. W., Low-energy electron beam studies in thin aluminum foils, 25:19766
GARD, G. A., Annealing characteristics of highly doped ion-implanted phosphorus layers in silicon, 25:19837
  Formation of insulating layers by use of reactive ion beams, 25:19781
GARDES, Daniel, Transfer mechanisms in reactions ^{209}Bi(^{12}C) and ^{209}Bi(^{14}N), 25:20375 (NP-18624)
GARDNER, Alvis H., DORF-I: gamma-ray spectrograph shielding studies, 25:18732 (AD-711531)
GARDON, Pierre-Maurice, From Saint-Laurent to Vandellos, 25:20562
GAREEV, F. A., Table of wave functions of single-particle states of transuranium region deformed nuclei in Saxon--Woods potential, 25:20481 (JINR-P4-5457)
GARI, M., Short-range correlations and parity impurities, 25:20488
GARINA, K. P., Effect of space flight factors on barley seeds, 25:18952
GARLAND, J. A., Behaviour in the atmosphere of the aerosol from a sodium fire, 25:19167 (AERE-R-6460)
GARLICK, A., UKAEA fuel test assemblies irradiated in HBWR, 1964--66, 25:20736 (HPR-132)
GARNETT, J. L., Radiation-induced copolymerization of styrene and cellulose at low dose rates, 25:18446
GARRETT, Neil Edward, Absorption of Σ^- hyperons by neon and formation of nuclear excited states after K$^-$-meson absorption, 25:19908
GARY, S. Peter, Longitudinal waves in a perpendicular collisionless plasma shock. II, 25:19753
  Longitudinal waves in a perpendicular collisionless plasma shock. I, 25:19752
GASPARINI, G. M., Preparation of complex-group resins and synthesis of phenolic resins with hydroxamic groups. I and II, 25:18503 (RT/CHI-(70)25)
GASPAROVIC, N., Technical feasibility and future of nuclear helium gas turbines, 25:20771
GASPER, J. K., Determination of energy levels in stable nuclei by neutron inelastic scattering, 25:20356
GATTI, E., Extension of Ramo's theorem as applied to induced charge in semiconductor detectors, 25:18710
GAUCHER, Jean-Claude, Stationary detector for visual display, 25:18689
GAUCHER, R. E., The ^{125}Sb--^{125}Te decay, 25:20408
GAULT, J. D., Inelastic neutron scattering from solid benzene, 25:20247
GAURIAU, J., Research report on measurement of average number of prompt neutrons, 25:20373 (LIB/Trans-300)
GAVRIL, S., Electron temperature determination in a low-density helium plasma, 25:19661
GAWLOWSKI, Janusz, Effect of ammonia on the ion reactions in the radiolysis of ethylene in the gas phase, 25:18452
  Nitrogen sensitized gas phase γ-radiolysis of ethylene, 25:18455
GEBALLE, T. R., Infrared line emission from planetary nebulae, 25:19327
GEERK, J., Residual resistivity of Pb films after implantation of Mn ions, 25:19857
GEHRKE, R. J., Determination of relative photopeak efficiency and system linearity for Ge(Li) gamma-ray spectrometers, 25:18747
GELAIN, C., Kinetics and mechanisms involved in the siliconization of Nb and the oxidation of niobium silicides at low pressures and high temperatures, 25:19258
GEL'BSHTEIN, A. I., Evaluating the mobility of surface O in several oxides and their mixtures by means of O isotope exchange. I, 25:18388
GEL'FREIKH, G. B., Polarization of local sources of solar radio emission at 4.4 cm, 25:19417
GELIUS, Ulrik, VC, NbC, and TaC studied by electron spectroscopy for chemical analysis, 25:19867
GEMESY, T., Observation of S^0 meson, 25:20009
GENKIN, A. L., Unsteady flow of mercury in a trough in a transverse magnetic field, 25:19553
GENKINA, L. M., Mass--luminosity relation for spiral galaxies, 25:19441
GEORGE, G. G., Electrical and atom-site location properties of ion-implanted germanium, 25:19799
GEORGE, M. C., Directional correlations of gamma-ray cascades in ^{103}Rh, 25:20404
GEORGELIN, Y., Light-cone commutators and high energy annihilation $e^+ + e^- \to \pi$ + hadrons, 25:19941
GEORGI, Howard, Anomalies of the axial-vector current in two dimensions, 25:19984
GEROCH, Robert, Application of the semidirect product of groups, 25:20091
GERSHBERG, R. E., Statistical characteristics of flares of UV Cet-type stars, 25:19346
GERSHTEIN, S. S., Do K-meson nuclei exist, 25:20002 (IFVE-STF/SPK-70-30)
  Mesoatomic processes and model of large molecules (review), 25:19482 (NRC-TT-1426)
GERVAISE, Francois, ELF program: description of utilization, 25:20233 (ORNL-tr-2409)
GESCHIER, R., Hydrogen embrittlement of Nb base alloys, 25:19216
  Preparation of high purity niobium base alloys, 25:19186
GETMANTSEV, G. C., Compton scattering of MHD and plasma waves as source of radio emission, 25:19380
GEY, W., Pressure dependence of Kondo resistance anomaly and pair breaking effect in La--Ce alloys, 25:19863
GHELARDI, M., Behavior of a stabilized cellular strain cultured in a medium contaminated with ^{137}Cs. III, 25:18904
GHILBERT, Emile, From Saint-Laurent to Vandellos, 25:20562
GHYS, R., Evidence of thyroid function using radioactive iodine, 25:19041
GIACCONI, R., Rocket payload using focusing x-ray optics for the observation of soft cosmic x-rays, 25:18680
GIBBONS, J. F., Effectiveness of dislocation loops as sites for the adsorption of implanted ions, 25:19848
  Lattice damage created in Si by implantation of 2.8-MeV protons, 25:19821
  Properties of ion-implanted Si, S, and C in GaAs, 25:19843
GIBSON, Benjamin F., Very high-momentum components in nuclei and far subthreshold production of quarks, 25:20026
GIBSON, W. M., Channeling study of B-implanted Si, 25:19834
GIERLIK, E., Measurement of high-energy γ-ray spectra in a strong neutron flux, 25:18735 (INR-1224)
GIERULA, J., Investigation of cosmic-ray jets by emulsion method, 25:19533
GIESE, J., Plasma renin measured by radioimmunoassay for angiotensin, 25:18920
GIESLER, G. C., Spurious peaks produced by Compton scattering in Ge(Li)--Ge(Li) coincidence gamma-ray spectrometer systems, 25:18754
GILBERT, Charles Philip, Nuclear reactors, 25:20714
GILER, S., Decays in broken SU(6)/sub W/ symmetry, 25:20047
  Decays in broken SU(6)/sub W/ symmetry, 25:20048
GILL, J. S., Estimation of aerosol concentration in a nuclear reactor containment after an accident, 25:20758 (CONF-700816-(Vol.1), pp 72-101)
GILLESPIE, B. W. J., Gamma-ray polarization measurements in ^{22}Na, 25:20318
GILOT-DELHALLE, J., Repairing processes of chromosome aberrations induced by γ rays in Nigella, 25:18951
GILRA, Daya P., Composition of interstellar grains, 25:19452
GILSON, Albert J., Scintillation of a vascular rim in subdural hematoma, 25:19059
GINZBURG, V. L., Coherent mechanisms of emission and their application to pulsars. II, 25:19370
GIORGI, Danel, Nuclear reactor with integrated heat exchangers, 25:20840
GIROURY, Andre, Analysing an amplitude spectrum, 25:18652
GISLON, R., Characteristics of implanted p--n junctions by C(V,f) measurements, 25:18857
GITSCH, E., Radioisotope surgery in gynecology, 25:19070
GIVEN, Fred T. Jr., Rectovaginal fistula. A review of 20 years'experience in a community hospital, 25:19138
GIVORD, Francoise, Paramagnetic behavior of Fe atoms in some intermetallic compounds containing Y, Lu, and Gd, 25:19871
GLAGOLEVA, N. S., Investigation of the model of the 2-meter streamer chamber of the SCM-200 assembly, 25:18774 (JINR-P13-5529)
GLASHOW, S. L., Divergences of massive Yang--Mills theories, 25:19969
GLASS, J. C., Studies of anomalous water in carbonic anhydrase, 25:18884
GLASS, W. A., Energy deposition distributions, 25:19767
GLAUDEMANS, P. W. M., Static quadrupole moments in A = 18 to 38 nuclei, 25:20337
GLAZOV, A. A., External injection and acceleration of the beam to the final radius in the electron model of the ring cyclotron with strong focusing, 25:20130 (JINR-P9-5453)
GLENN, J. E., Small-angle j dependence of (α,p) reactions, 25:20309
GLOTIN, P., Electrical behaviour of implanted layers, 25:19775
GLUECKSOHN-WAELSCH, Solome, Glucose 6-phosphatase deficiency: mechanisms of genetic control and biochemistry, 25:19128
GLUKHIKH, V. A., Experimental investigation single-wave MHD machines, 25:19537
GLUKHOV, I. A., Oxidation-reduction processes in the

systems $ReCl_5$--UO_2Cl_2 ($UOCl_3$), 25:18384
GNATYUK, V. V., Resistance in flow of liquid metals in channels in a transverse magnetic field, 25:19554
GOBBI, A., Spins and parities of highly excited states in ^{24}Mg, 25:20291
GODFREY, M., CLASSIC: code for stability and response analysis of linear systems, 25:20830 (AAEC/TM-551)
GODOLI, G., Reliability of Catania sunspot area measurements, 25:19407
GOEDE, A., Warm quiescent plasma in minimum-B field, 25:19705
GOENNENWEIN, F., Slowing down of fission fragments in various absorbers, 25:20442
GOFMAN, J. W., Fluoroscopic radiation and risk of lung cancer following therapy of tuberculosis, 25:19068
GOKHALE, G. S., Orientation system for balloon-borne payloads, 25:18677
GOLAND, A. N., Influence of defects on the angular correlation of positron-annihilation photons in irradiated and in deformed iron, 25:19851
GOLAY, M. W., Neutron-pulse propagation in multiplying assemblies, 25:20804
GOL'DANSKII, V. I., Electronuclear method of neutron generation and fissile material production, 25:20191
GOLDEN, D. E., Energy modulated high energy resolution electron spectrometer, 25:18762
GOLDIN, Abraham S., Behavior of iodine in sodium systems, 25:20760 (CONF-700816-(Vol.1), pp 356-72)
GOLDSMITH, B. J., 200-kV ion-implantation equipment at MRL, Salfords, 25:19774
GOLDSMITH, William A., System for computer processing of radiopharmaceutical disbursement information, 25:19050
GOLDSTEIN, Y., Interaction of 9.3-GHz longitudinal phonons with electrons in superconducting films, 25:19607
GOL'FAND, Yu. A., Dynamic theory of vacuum, 25:20078
GOLLANDSKII, O. P., Physical conditions in atmosphere of P Cygni, 25:19342
GOLOVANOVA, T. A., Effect of antilymphocytic sera on the hemopoietic tissue, 25:18921
GONCHAR, V. Yu., Analysis of inelastic scattering of alpha particles in region Z = 12 to 40, 25:20274
GONCHAROVA, N. G., Effect of intermediate coupling in photo and electroexcitation of ^{12}C nucleus, 25:20295
GONZALEZ, Manuel Angel, Electromagnetic corrections to chiral symmetry, 25:20044
GOOD, P. D., Quality control, inspection, and testing of fuel materials for the two uprated fuel elements, 25:18610 (DP-Report-580)
GOODE, P. D., Electrical activity of phosphorus channeled into silicon, 25:19839
GOODIER, I. W., Decay of /sup 113m/In, 25:20407
GOPAL-AYENGAR, A. R., Radioactivity in the diet of population of the Kerala coast, 25:19143
GOPASYUK, S. I., Hard x-ray emission of solar flare on Sept. 28, 1961, 25:19435
  Velocity field on two levels in active region of July 1966, 25:19433
GORBATKOV, S. A., Flow of conducting fluid in channels with longitudinal--transverse magnetic fields, 25:19555
GORBATSEVICH, S. V., Values of the fundamental physical constants according to agreements in 1969, 25:20905
GORBUNOV, E. P., Material balance of plasma column and gas sheath in toroidal apparatus-Tokamak-3, 25:19657 (MATT-Trans-16)
GORDON, I. M., Role of maser effect in radar echo from sun, 25:19419
GORENSTEIN, P., Rocket payload using focusing x-ray optics for the observation of soft cosmic x-rays, 25:18680
GOREY, E. F., Resistivity and annealing properties of implanted Si:H^+, 25:19822
GORIN, Yu. P., Experimental comparison of anti dp and anti pd total cross sections, 25:19907
  High resolution differential Cherenkov counters, 25:18794
GORINA, D. O., Extraction separation of Mo from Re and its determination with 5,7-dibromo-8-quinolinol, 25:18353
GORING, D. A. I., Temperature dependence of the 1555 cm^{-1} infrared absorption band in liquid D_2O, 25:18401
GORINI, G., Pion capture in ^{4}He, 25:20255
GORIZONTOVA, M. P., Effect of esculamine on permeability of the membranes of nuclei and mitochondria in cells of irradiated animals, 25:19025
GOROVITS, V. S., Estimate of field in winding zone of plane linear induction MHD machines, 25:19539
GORYAEV, N. M., Investigation of the effect of ionizing radiation on the structure and properties of modified capron fibers, 25:18425
GOSS, D., Determination of energy levels in stable nuclei by neutron inelastic scattering, 25:20356
GOSS, W. M., Galactic radio sources. I, 25:19384
  Galactic radio sources. II, 25:19385
  Galactic radio sources. III, 25:19386
  Observations of galactic OH, 25:19381
GOSSET, J., Study of (p,d) reactions on ^{118}Sn and ^{119}Sn with polarized protons, 25:20365 (CEA-CONF-1657)
GOTTLIEB, I., New linear gravitation theory. III, 25:20098
GOUDSMIT, P. F. A., Levels in ^{238}Pu from decay of ^{238}Np, 25:20431
GOULARD, B., Fine structure in highly excited analog states, 25:20396
GOULARD, G., Sequential reaction $^{11}B(p,\alpha)2\alpha$, 25:20275
GOUMNEROVA, L., Alpha-spectroscopy determination of concentrations of radon daughters in air, 25:18363
GOUNARIS, G. J., Is veneziano model consistent with the yang-mills coupling of vector meson fields, 25:19985 (DEMO-71/1)
  Remarks on the eta → π^0 γ γ decay rate, 25:19937 (DEMO-71/2)
GOVIND, P. K., Radiation-damage studies of bismuth-ion-implanted CdS, 25:19792
GRABOVSKI, V., 10-MeV proton linear accelerator at Swierk, 25:20129 (INR-P-1218)
GRAEBENER, Karl-Heinz, Separation of steam and water in boiling-water reactors and steam generators, 25:20769
GRAF, G., Studies of anomalous water in carbonic anhydrase, 25:18884
GRAHAM, D. A., Circular components of polarization in pulsar radiation, 25:19358
GRAHAM, H. M., Suppression of populations of pink bollworm by releases of gamma-irradiated moths in field cages, 25:19102
GRAHAM, John B., Mast cell identification of radiation fistulas, 25:19139
GRAHAM, Kenneth D., Image aberrations produced by multichannel collimators for a scintillation camera, 25:18660
GRAHAM, Ruth M., Mast cell identification of radiation fistulas, 25:19139
GRANATA, G., Nonlinear wave mixing at hybrid frequencies in an inhomogeneous plasma, 25:19747
GRANGER, J., Behavior of iodine in the presence of sodium oxide aerosols, 25:20761 (CONF-700816-(Vol.1), pp 373-92)
  Characterization of energy release and aerosol behavior from sodium spray fires, 25:20759 (CONF-700816-(Vol.1), pp 346-55)
GRANT, W. A., Radiation damage by implanted ions in GaAs and GaP, 25:19844
GRAUBY, A., Fixation and migration in soils of products of fission and activation, 25:18528
  Transfer of radionuclides to plants by irrigation, 25:18938
GRAZINSKI, M., Classical theory of atomic collisions. II, 25:19488 (INR-P-1225)
GREBE, S. F., Use of radioisoxope generators in nuclear medicine, 25:18885
GREEN, James F., Reduction of radiation hazard in tritium method of measuring total body water, 25:18977 (AD-702155)
GREEN, R. E., Miscible displacement measurements within laboratory columns using the gamma-photoneutron method, 25:18523
GREEN, R. E. L., Excited states of ^{46}V, 25:20347
GREEN, T. S., Space-charge effects in plasma-particle analyzers, 25:19660
  X-ray temperature measurements of laser-produced plasmas, 25:19701
GREENBERG, J. S., Doppler shift attenuation studies in heavy nuclei, 25:20409
GREENE, John M., Tokamak equilibrium, 25:19716
GREENFIELD, M., Comparisons of aerosol experiments with a model used in reactor siting evaluation, 25:20757 (CONF-700816-(Vol.1), pp 26-48)
GREENLEES, G. W., Core-polarization effects in charge-exchange reactions; application to $^{58}Ni(^3He,t)$, 25:20496
GREENWOOD, A. L., UKAEA fuel test assemblies irradiated in HBWR, 1964--66, 25:20736 (HPR-132)
GREGORY, S. A., Accelerated regeneration of transplanted hematopoietic stem cells in irradiated mice pretreated with cyclophosphamide, 25:19127
GREGORY, Stephanie A., Factors regulating the proliferation and migration of hematopoietic stem cells, 25:19126
GREIMANN, L. F., Finite element analysis of plate bending with transverse shear deformation, 25:18575
GRENIER, Raymond P., Radiation detection devices, 25:18682
GRENON, Michel, Uranium enrichment by gaseous diffusion or ultracentrifugation, 25:18609
GRESSER, J., Operation of sampling spark chambers, 25:18778
GRIEDER, P. K. F., Simulation in space and time of nuclear active and muon components in extensive air showers for primary energies from 10^5 to 10^7 GeV, 25:19973 (INSJ-125)
GRIFFITHS, R., Calculated total efficiencies of coaxial Ge(Li) detectors, 25:18755
GRIGOR'EV, E. P., Two-quasiparticle levels of ^{176}Yb, 25:20380
GRIGOR'EV, V. N., Determination of experimental values of internal conversion matrix elements, 25:20457
GRINCHUK, P. P., Properties of heat-resistant steels following high-temperature reactor irradiation, 25:19250 (AEC-tr-7192)
GRISHAEV, I. A., Charged pion photoproduction on ^{27}Al nucleus, 25:20341
GRISHIN, V. K., Radiation in linear systems with cross focusing, 25:20219
GRISSOM, John Thomas, Improvements in or relating to timekeeping systems with a radioactive timekeeping standard, 25:18819
GRJEBINE, T., Gamma emitters and exposure age of the Bovedy meteorite, 25:19301

GROEHN, H. G., Preliminary experiments of a heat exchanger in He under high-pressure, 25:20780
GROMOV, V. V., Radiation damage in selenates of divalent metals, 25:18479
GROMOVA, V. G., Structure and properties of W--Mo--Nb--Ta alloys, 25:19239
GROSHEV, L. V., Experiments with ultracold neutrons, 25:20232 (JINR-P3-5392)
GROSS, Cordell E., Coordinate measuring device for radium applications, 25:19004
GROSSE, A. V., Compressibility of liquid metals, particularly lead, from their melting points to their critical regions, 25:20880 (NYO-4176-4)
Simple empirical relationship between compressibility and temperature of ideal liquids, 25:20881 (NYO-4176-6)
GROSSE, E., Gamma-decay of proton-particle neutron-hole states in ^{208}Bi, 25:20434
GROTE, H., Atlas of particle production spectra, 25:20028
GRUBB, W. B., Joint transduction of separate extrachromosomal drug resistance determinants in Staphylococcus aureus E169, 25:19157
GRUBNER, Otto, Design of fission gas holdup systems, 25:18561 (CONF-700816-(Vol.1), pp 216-23)
GRUENWALD, H., Reactivity measurements of ASTRA-core after installation of Be reflector, 25:20795
GRUETER, J. W., Gas-filled magnetic separators, 25:18851
Identification of µs-isomers among primary fission products, 25:20430
GRUHLE, W., Efficiency of a 180° coincidence spectrometer for extended sources, 25:18758
GRUND, Frank M., Studies of recovery of erythropoiesis after irradiation as a function of the cellularity of the endocolonized spleen, 25:19125
GRUNEWALD, Ralph, 4π liquid-scintillation whole-body counter. II, 25:18649
GRYPEOS, M. E., A non linear equation for the correlation function between an impurity particle and a nucleon in nuclear matter, 25:20001 (DEMO-70/19)
Estimate of the binding energy of ^{16}O with matrix elements of effective interaction, 25:20266 (DEMO-70/25)
GRYZLOV, A. G., Water pump for pressure-cooling reactor in atomic powerplant, 25:20717 (JPRS-52384)
GUBAREV, V. F., Influence of dissipative processes in casing on stability of surface of liquid metal, 25:19551
GUBBENS, P. C. M., Magnetic susceptibility of dilute Au--V alloys, 25:19865
GUEGUENIAT, P., Contamination of marine species by ^{106}Ru and ^{95}Zr, 25:18939
GUETLICH, P., Polymeric chromium(III) complexes arising from neutron irradiation of crystalline potassium chromate. I, 25:18486
GUGIC, P., Semiconductive detectors of ionizing radiation, 25:18694
GUIDOTTI, G. R., Analysis of micro constituents in Zr matrix. I, 25:18341 (RT/CHI-(70)14)
GUILLE, J., Hydrogen embrittlement of Nb base alloys, 25:19216
GUILLOT, Francois, Apparatus for producing a voltage, 25:18721
GUILLOUD, J. C., Theoretical and experimental study of centrifugation within fixed walls of a gaseous binary mixture, 25:18597
GUISAN, Michel, Digital and analog processing of Anger camera data with a dedicated computer-controlled system, 25:18730
GUJRATHI, S. C., Decay of ^{180}Lu to levels of ^{180}Hf, 25:20426
GULAKOV, I. R., Contribution of the scintillator to the resolution of a spectrometer using the single-electron method, 25:18745
GUL'KAROV, I. S., Form factors and fine structure of giant resonance in ^{12}C nucleus, 25:20296
GUNBY, A. L., Simulation of piping lengths in sodium systems, 25:20790 (WHAN-FR-22)
GUNNERSEN, E. M., Electrical and atom-site location properties of ion-implanted germanium, 25:19799
Prototype semiconductor gamma-camera, 25:18699
GUPTA, M. C., Natural alpha radioactivity of Sm, 25:20391
GUPTA, S. K., Constants of the charged particle identifier, 25:18705
GUREVICH, L. E., Theory of supernova explosion light curves, 25:19325
GURSKY, H., Rocket payload using focusing x-ray optics for the observation of soft cosmic x-rays, 25:18680
GUSEV, E. A., Scattering chamber for physical studies using electron beams, 25:20211
GUSSENHOVEN, Mary Susan, Hydromagnetic studies of the solar wind, 25:19426
GUSTAVSON, M. R., New concepts for geographic position locators, 25:20903 (UCRL-50978)
GUTAY, L. J., Off-mass-shell S-wave $\pi^+\pi^-$ scattering amplitude, 25:19994
GUTMAN, Edward Joseph, Study of fermi surfaces of antiferromagnetic chromium-rich alloys using de Haas-van Alphen effect, 25:20861 (IS-T-420)
GYUK, I., Wave equations with compact and noncompact spectrum, 25:20050

H

HAALAND, J., Chemical analysis of high burn-up PuO_2 fuel, 25:18356 (KR-140)
HAAS, G. M., Ion heating by a modulated electron beam, 25:19650
HAASEN, P., Flux pinning, 25:19595
HABENSCHUSS, Michael, Structural, magnetic, and spectroscopic study of nickel squarate dihydrate, 25:20865 (IS-T-432)
HABER, I., Transverse electromagnetic instabilities in collisionless plasmas, 25:19722
HABERSTICH, Albert, Dynamic stabilization of a linear z pinch, 25:19717
HACKENBROICH, Hans H., Nuclear reactions in harmonic oscillator shell-model function scheme, 25:20516
HAEFELE, W., Fast breeder reactors, 25:20708
HAEHN, J., Considerations on the mechanism of sulfurous radiation protection agents, 25:19021
HAEMAELAEINEN, R. M. K., Retardation functions for deuteron photodisintegration. II, 25:20254
HAGE, S. J., Polaroid film in radiation dosimetry and survey, 25:19005
HAGEBOE, E., Decay of Cd isotopes, 25:20422
HAGEDORN, R., Atlas of particle production spectra, 25:20028
HAGEMANN, G. B., Electromagnetic transitions from levels in the beta-vibrational band of ^{174}Hf, 25:20427
HAGEMANN, Ronald F., Mitotic inhibition and its relation to survival in S-180 ascites tumor cells in vivo following fractionated exposures of x-radiation, 25:19091
HAGSTROEM, S. B. M., 4f electronic states in the metals Nd, Sm, Dy, and Er studied by x-ray photoemission, 25:19866
HAGUENAUER, M., Study of 10 GeV/c K$^+$-nucleus coherent interactions and Q-nucleon cross-section, 25:19913
HAHN, Yukap, Closed-channel spectrum of the positron--hydrogen rearrangement collision, 25:19503
HAIDUC, C., Analysis of efficiency of nuclear fuel cycles for heavy-water moderated reactors in specific conditions of socialist republic of Romania, 25:20750
Mathematical model for estimating the efficiency of nuclear fuel cycles of fast breeding reactors, 25:20752
Physical model on the boiling process in the power nuclear reactor, 25:20728
Thermodynamic analysis of saturated steam cycles and of direct thermal cycles for nuclear power stations, 25:20596
HAIGHT, R. C., Method for improving heavy ion spectra in scattering experiments, 25:18750
HALEY, J. R., Pyrochemical processing of fuel materials and scrap containing ^{238}Pu, 25:18492 (ANL-7709)
HALL, J. W., New time-of-flight analyzer for neutron scattering, 25:18765
HALLOPEAU, C., Development of a radioactive marine periphytal community, 25:18936
HAMAGUCHI, Shunichi, Plan for Takahama Nuclear Power Station, 25:20566
HAMILTON, C. A., Experimental demonstration of Riedel peak, 25:19602
HAMILTON, J. H., Conversion electron measurements in decay of ^{156}Tb, 25:20472
HAMMARSTROEM, Lars, Radiopathology of ^{241}Am. I, 25:18901
HAMMER, D. A., Transverse electromagnetic instabilities in collisionless plasmas, 25:19722
HAMMOND, Allen L., Accelerator at Batavia: the next step in high-energy physics, 25:20225
HAMMOND, R. P., Abstracts of literature on the distillation of seawater and on the use of nuclear energy for desalting, 25:20812 (TID-25653)
HAMPTON, R. B., Effects of gamma irradiation or the chemosterilant, tepa, on the citrus red mite and its progeny, 25:19100
HAMRIN, Kjell, VC, NbC, and TaC studied by electron spectroscopy for chemical analysis, 25:19867
HANADA, R., Recovery of fast neutron irradiated molybdenum, 25:19861
HANAK, J. J., Superconducting and semiconducting phases of granular films, 25:19631
HANCHER, C. W., Prog. rpt. on Concentration and Desalting of Protein Solutions Program, 3--5/70, 25:20882 (ORNL-TM-3082)
HANCOX, R., Small superconducting coils and applications to plasma physics, 25:19634
HANKS, K. S., Initial equilibrium configuration of Scyllac 5-meter toroidal-sector experiment, 25:19725 (LA-4597)
HANNA, S. S., Giant dipole resonances in ^{11}C and ^{15}O, 25:20277
HANSEN, H. H., Isomeric state in ^{113}In, 25:20460
HANSEN, J. D., Compilation of cross sections V--K$^-$ induced reactions, 25:19909 (CERN-HERA-70-6)
HANSEN, J. E., Prog. rpt. on isotopes development, 8--10/70, 25:18590 (BNWL-1308-4)
HANSEN, M. F., Effects of gamma-radiation on the pathogenicity of Histomonas meleagridis, 25:19156
HANSEN, P. G., Alpha decay of neutron-deficient radon and polonium isotopes, 25:20451
HARA, Shunsuke, Rotational excitation of HD molecule by slow electrons, 25:19502
HARATYM, Z., Excitation of short-lived isomeric activities

in ^{77}Se, ^{122}Sb, ^{137}Ba, ^{167}Er, and ^{179}Hf using 14.5-MeV neutrons, 25:20435
HARBOUR, R. M., Yield of /sup 99m/Nb from fission of ^{233}U, ^{235}U, ^{238}U and ^{252}Cf, 25:20406
HARDIE, G., One-phonon octupole vibration of ^{151}Eu, 25:20432
HARDIMAN, J. P., Efficiency of a ^{6}Li glass scintillator detector for fast reactor spectrum measurements, 25:18637 (AEEW-M-898)
HARDY, Donald McCoy, Light-nuclei interactions with a polarized ^{3}He target, 25:20262
HARDY, Gy., Investigations of radiation-induced solid-state polymerization. XXVI, 25:18431
  Investigations of radiation-induced-solid state polymerization. XXVII, 25:18432
HARDY, J. C., Spin dependence in the reactions $^{16}O(p,t)^{14}O$ and $^{16}O(p,{}^{3}He)^{14}N$, 25:20299
HARGROVE, C. K., Muonic x rays and capture gamma rays in ^{89}Y, 25:20360
HARI DASS, N. D., Axial-current divergences and the reactions $\gamma + \gamma \to$ pions, 25:19951
HARLEY, N. H., Detection limits for radionuclides in the analysis of multi-component gamma ray spectrometer data, 25:18746
HARMS, E., Calculations on the three-nucleon system using a separable expansion of local potentials, 25:20538
HARMUT, Magda, Direct counting of ^{47}Ca and ^{85}Sr in biological samples, 25:18997
HARPER, John W., Reduction of radiation hazard in tritium method of measuring total body water, 25:18977 (AD-702155)
HARRIS, B., Rocket payload using focusing x-ray optics for the observation of soft cosmic x-rays, 25:18680
HARRIS, R. M., Optical-model analysis of nonreactive collisions of reactive molecules, 25:19497
HARRIS, S. Dyer, Computer program for correlation and spectral analysis of reactor flow data, 25:20710 (DP-1244)
HARSHMAN, E. N., Uranium ore rolls in United States, 25:18545
HART, Edwin J., Device for producing and monitoring hydrated electrons, 25:18854
HART, R. R., Disorder dechanneling of low-energy protons and alpha particles in silicon, 25:19816
HARTENBOWER, D. L., Scintillation camera in the dynamic evaluation of renal disorders, 25:19046
HARTER, J. A., Low-energy electron beam studies in thin aluminum foils, 25:19766
HARUTYUNYAN, F. R., Superhigh-energy particle detector based on using the radiation of a particle in a laminar medium, 25:18781
HASCHKE, J., Control of tritium in water and sewage, 25:18360
HASEGAWA, Akira, Analysis of fast critical experiments and revision of JAERI-fast set, 25:20788 (JAERI-Memo-4215)
  Plutonium-239 fission product yields and their influence on fast reactor characteristics, 25:20819 (JAERI-Memo-4165)
HASEGAWA, Masayoshi, Iron and steel used for nuclear reactors, 25:19200
HASEGAWA, S., Construction of nuclear power plant, 25:20563
HASINOFF, M., Giant dipole resonances in ^{11}C and ^{15}O, 25:20277
HASKELL, J. D., Radiation damage by implanted ions in GaAs and GaP, 25:19844
HASS, A. Curtis, Reproductive factors associated with radiotherapy of malignant lymphomas, 25:19147
HASSELGREN, L., Decay of ^{131}Ba, 25:20414
HASTI, D. E., Resistive loading by a finite plasma cylinder, 25:19653
HATANO, Yoshihiko, Uncharged transient species in radiation chemistry, 25:18454
HATFIELD, M., Possible hazard from nuclear submarine corrosion products, 25:19014
HATONO, Sotaro, Honeycomb block used for collimation of radiations and method of manufacturing the same, 25:18856
HATTA, H., Core temperature analyses for loss-of-coolant accidents of light water reactor, 25:20762 (JAERI-Memo-4194)
HATTULA, J., Directional correlations of some γ-ray cascades in ^{200}Hg, 25:20400
  Level structure of ^{120}Sn from decay of ^{120}In and ^{120}Sb isomers, 25:20401
HAUPT, Justus, Cryostat, 25:19641
HAUSER, J. J., Enhancement of superconductivity in aluminum films, 25:19622
HAUSSER, B., Resonance-capture and -fission in highly enriched fuel-lattices, 25:20826
HAUSTEIN, P. E., Isomer ratio measurements for ^{91}Mo, ^{137}Ce, and ^{141}Nd produced by (γ,n) and $(\gamma,3n)$ reactions, 25:20455
HAVINGA, E. E., Oscillatory dependence of T/sub c/ on number of valency electrons in Cu_3Au-type alloys, 25:19621
HAVNES, Dve, Abundances and acceleration mechanisms of cosmic rays, 25:19535
HAWES, Norman L., Two radiation-induced chromosomal inversions in mice (Mus musculus), 25:18968
HAWKINS, R. H., Miscible displacement measurements within laboratory columns using the gamma-photoneutron method, 25:18523
  Zeolite prefilter to reduce pluggage in zeolite cesium removal column, 25:18621 (DP-1245)
HAYAKAWA, S. I., Excited states of ^{46}V, 25:20347
HAYASHI, Koichiro, Dissociative electron capture process of methyl vinyl ether in organic glasses, 25:18456
HAYASHI, S., Uranium occurrences in small sedimentary basins in Japan, 25:18546
HAYES, R. L., Rapid separation of generator-produced ^{68}Ga from EDTA eluate, 25:18482
HAYES, Thomas P., Brain and liver scans in the evaluation of lung cancer patients, 25:19047
HAYWOOD, F. F., HPRR and accelerator operations, 25:20134 (ORNL-4584, pp 187-97)
  Radiation safety practices: Operation HENRE, 25:18982 (CEX-65.05)
HAYWOOD, L. R., Closing the credibility gap in nuclear fuel costs, 25:20731 (AECL-3780)
HAZEN, W. E., Cloud-chamber search for $^{1}/_{3}e$ and $^{2}/_{3}e$ quarks in air showers, 25:19884
HEATH, R. L., Determination of relative photopeak efficiency and system linearity for Ge(Li) gamma-ray spectrometers, 25:18747
HECHT, F., Distribution of Np in nitric acid solution containing uranyl ion, 25:18519
HEDEN, P. O., 4f electronic states in the metals Nd, Sm, Dy, and Er studied by x-ray photoemission, 25:19866
HEEMSKERK, J. P. J., Rotational relaxation of HD below 40 K, 25:19480
HEETVELD, A., Frigg circuit: water chemistry under investigation, 25:20718 (LIB/Trans-308)
HEIDBREDER, E., Properties of thin spark chambers with the admixture of carbohydrates to the spark chamber gas, 25:18657
HEIDEN, C., Local magnetization measurements on cylindrical samples of low-kappa type-II superconductors, 25:19626
HEIGWER, G., Automatic compensating instrument for measuring low electric direct currents, 25:18834
HEIM, G., Residual resistivity of Pb films after implantation of Mn ions, 25:19857
HEJL, V., Thermodynamic conditions of the origin of uraninites, 25:18551
HEKIMYAN, G. A., Superhigh-energy particle detector based on using the radiation of a particle in a laminar medium, 25:18781
HELD, Manfred, Structure of the detonation front, 25:20866 (LA-tr-71-4)
HELPPI, H., Directional correlations of some γ-ray cascades in ^{200}Hg, 25:20400
HEMMERSMEIER, F., Evaluation of results of a study of the Th--^{233}U fuel cycle for thermal reactors, 25:20746 (JUL-644-RG)
HEMPEL, Franklin Glenn, Visually evoked potentials from the laser-irradiated rabbit retina, 25:19132
HENDRICKS, William D., DORF-I: gamma-ray spectrograph shielding studies, 25:18732 (AD-711531)
HENDRY, Innes Craig, Improvements in or relating to neutron radiography apparatus, 25:18618
HENKE, G., Intestinal absorption of metallic mercury, 25:18369
HENNING, J. J., Positive definite particle densities for solutions of Klein--Gordon equation, 25:19929
HENNING, W., Isomer shift and quadrupole splitting of the 2^{+}-rotational state in ^{174}Yb, 25:20399
HENTSCHEL, G. H., Measures provided at the Muehleberg nuclear power plant for protection of the population, 25:20684
HERKENRATH, H., Heat transfer values for water in steam generators with forced convection and reactor channels at pressures of 170 to 215 bar, 25:18581
HERRE, F., Safety aspects in the design of WAK, 25:18566 (ORNL-tr-2370)
HERREN, M., Irradiation tests with vibrocompacted $(Th/U)O_2$ particles, 25:19291
HERRMANN, G., Half-lives of ^{87}Se and ^{88}Se, 25:20327
HERRY, J., Wired arithmetic computer for particle identification, 25:18718
HERTWECK, F., Computer programme for solving MHD equations for theta pinch in time-dependent coordinate system, 25:19647 (IPP-6/90)
HESSE, M., Improvement to quantum yield of photocathodes of 56 TVP photomultipliers in red part of spectrum (7000 A), 25:18828 (EUR-CEA-FC-576)
HESSER, James E., High-frequency stellar oscillations. V, 25:19309
HICKS, Harald P., Method of and apparatus for the measurement of physical characteristics of x-rays, 25:18651
HIDE, R., Magnetohydrodynamic oscillations of neutron stars, 25:19312
HIGATSBERGER, Michael J., Method of and apparatus for the measurement of physical characteristics of x-rays, 25:18651
HIGH, M. D., Coupled-channel analysis of α-particle scattering from the 5.23 MeV natural parity state of ^{24}Mg, 25:20344
HILL, A. R., Fine-focussed ion machine with applications to implantation, microscopy, and machining, 25:20168
HILL, Martin J., Acid-catalyzed isomerization of cis-1-phenyl-1,3-butadiene and cis-1-methyl-3-phenylallyl alcohol, 25:18405

HILLIARD, R. K., Large scale air cleaning tests in the containment systems experiment, 25:20782 (CONF-700816-(Vol.1), pp 102-27)
HINCKS, E. P., Muonic x rays and capture gamma rays in ^{89}Y, 25:20360
HINDEL, Robert, Scintillation detector indicating system, 25:18713
HINDMAN, J. V., Parkes hydrogen-line survey of the Milky Way. V, 25:19392
  Parkes hydrogen-line survey of the Milky Way. III, 25:19390
HINDS, Edward C., Dental care and oral hygiene before and after treatment. Radiation caries, 25:19079
HINDS, William C., Optical properties of sodium aerosols, 25:19193 (CONF-700816-(Vol.1), pp 425-44)
HIROTA, Jitsuya, Sodium-void experiment in unit k-infinity core, 25:20793
HIRSHFIELD, J. L., Interpretation of spatially decaying ion-acoustic waves, 25:19741
  Symmetry considerations for grid-launched ion-acoustic waves, 25:19742
HISSINK, M., Analysis of oxygen and hydrogen in sodium, 25:18863
  Equipment for sampling sodium, 25:18336
HITE, G. E., Absorption corrections and cuts in the Regge pole model, 25:19976
  Effective range parameter in S-wave pion--nucleon scattering, 25:20010
HJELLMING, R. M., Radio sources associated with Scorpius X-1, 25:19362
HLASNIK, I., Macroscopic phenomenological electrodynamics of Type-II superconductors, 25:19597
HLAWKA, E., Differentiable manifolds, 25:20068
HNATOWICH, D. J., Decay of Cd isotopes, 25:20422
HOBSON, Robert R., Heat shielded thermionic converter, 25:19544
HOEBERECHTS, A. M. E., Position sensitive detector telescopes for charged particles used in the BOL-system, 25:18757
HOECKER, Frank E., Photon energy--angle distributions for ^{60}Co after penetration of concrete, 25:19763
HOEDE, D., Separation of gram-amounts of lanthanides by cation exchange, using an aqueous solution of α-hydroxyisobutyric acid as an eluant, 25:18501 (RCN-131)
HOEGLUND, A., Transition rates in ^{192}Au, 25:20453
HOEHLEIN, G., Californium-252 as a neutron source, 25:18481
HOEHLER, G., Effective range parameter in S-wave pion--nucleon scattering, 25:20010
HOFFERT, Martin I., Precursor ionization effects on magnetohydrodynamic switch-on shock structure, 25:19681
HOFFMANN, William F., 100-micron map of galactic center region, 25:19448
HOFFMASTER, James Steven, Analysis of the pion spectrum of 35,630 tau$^+$ decays at rest, 25:19895
HOFKER, W. K., Position sensitive detector telescopes for charged particles used in the BOL-system, 25:18757
  Thermal properties of high-value gallium- and boron-implanted resistors in silicon, 25:19783
HOFMANN, Werner, Increase of service reliability and maintenance, 25:20552
HOHENEMSER, C., Lifetime and g-factor of 74.8 keV state of ^{100}Rh, 25:20454
HOLAN, T., Beta therapy with ^{90}Sr in plastic induration of the penis, 25:19072
HOLDREN, G. R., Rate constants for reaction of hydrogen atoms in aqueous solutions, 25:18459
HOLIN, V. M., Values of the fundamental physical constants according to agreements in 1969, 25:20905
HOLLAND, L. B., Tower Shielding Reactor II design and operation report: Vol. 1 description, 25:20789 (ORNL-TM-2893(Vol.1)(Rev.))
HOLLANDER, J. M., Chemical information from photoelectron and conversion-electron spectroscopy, 25:19473
HOLLIDAY, J., Quality control, inspection, and testing of fuel materials for the two uprated fuel elements, 25:18610 (DP-Report-580)
HOLLOWAY, D. F., Measurement of implanted-boron concentration profiles in silicon, 25:19803
HOLLSTEIN, M., Decay of ^{232}Np, 25:20382
HOLMBERG, P., Nuclear levels and transitions in odd Cu isotopes. I, 25:20314
  Proton reactions on ^{23}Na, 25:20325
HOLMES, H. F., Uniform, nonporous thoria, 25:18416
HOLMES, J. J., EBR-II irradiation effects of rupture of Type-316 stainless steel, 25:19254 (WHAN-SA-2)
  Irradiation produced defects in austenitic stainless steel, 25:19253 (WHAN-FR-16)
HOLMGREN, S. O., Hardware system for measurements of bubble chamber films on-line, 25:18776 (USIP-70-3)
HOLMGREN, Sven-Olof, Bubble chamber experiments on 10 and 19 GeV/c proton--proton interactions, 25:19902 (USIP-70-8)
  One-pion exchange model applied to reaction $pp \to p\pi^+(\Delta^{++})\pi^-p$ at 19 GeV/c, 25:20020 (USIP-70-5)
  One-pion exchange model applied to reaction $pp \to p\pi^+(\Delta^{++})\pi^-p$ at 19 GeV/c, 25:20032
HOLT, S. S., Search for temporal structure in x rays from Scorpius X-1, 25:19363
HOLT, Stephen S., Long-term storage of relativistic particles in the solar corona, 25:19403
HOLTZ, J. Z., Infrared line emission from planetary nebulae, 25:19327
HOLTZ, Robert E., Vaporization dynamics of initially static superheated sodium, 25:19191 (ANL-7706)
HOLZAPFEL, Chr, Applied magnetohydrodynamics. VI, 25:19536 (JUL-706-TP)
HOLZGRAF, James Frederick, Characterization of the matrix of brittle matrix composites, 25:20900 (UCRL-20388)
HOMEYER, H., Elastic tau scattering on nuclei with A = 15 to 18 at 11 MeV, 25:20278
HOMMA, Saburo, Photoproduction of two neutral pions from hydrogen near threshold, 25:19890
HONG, C. Y., Determination of percent contents of U and Th in natural radioactive ores by γ-ray spectrometry, 25:18365
HONIG, J. M., Electrical resistivity of NbO, 25:19868
HOOPER, E. B., Parasitic instability generated by steady-state oscillations in a reflex arc plasma, 25:19707
HOOPER, E. B. Jr., Characteristics of a reflex arc: low magnetic field mode, 25:19666
  Correlation techniques in experimental plasma physics, 25:19664
HOOVER, W. G., Equation of state for dense hydrogen from zero to 10,000°K, 25:19472 (UCRL-50985)
HOPKINS, B. J., Relationship between surface potential and electronegativity for adsorption on tungsten single crystals, 25:19207
  Work function changes due to adsorption of Cl, Br, and I on W single crystal surfaces, 25:19209
HORA, H., Laser energy necessary for inertially confined nuclear fusion plasma, 25:19646 (IPP-4/7)
HORNBAKER, Edwin D., Radiation curable polyvinyl chloride composition containing triallyl isocyanurate, 25:18437
HORNSHOEJ, P., Alpha decay of neutron-deficient radon and polonium isotopes, 25:20451
HORTON, J. H., Zeolite prefilter to reduce pluggage in zeolite cesium removal column, 25:18621 (DP-1245)
HORWITZ, Joseph, Near-uv absorption bands of tryptophan, 25:20899 (UCLA-12-810)
HOSEGOOD, S. B., Dragon project engineering studies on the direct cycle HTR, 25:20703
HOSKING, R. J., Effect of Hall current and resistivity on stability of gas--liquid system, 25:19546
HOSKINS, D. G., Right ascensions for 389 sourthern radio sources, 25:19387
HOSOYA, A., Nonleptonic decay of hyperons, 25:19967
HOUSSIN, B., Deformation and rupture of Nb between -196°C and 20°C, 25:19217
HOUSTON, S. K., Positron--atom scattering by Kohn and Harris methods, 25:19509
HOWE, Clifton D., Regional pulmonary function in metastatic carcinoma to the lung studied with ^{133}Xe, 25:19048
HOWE, I., Unimolecular decomposition of tcluene and cycloheptatriene molecular ions, 25:18393
HOWERTON, Robert J., Integrated system for production of neutronics and photonics calculational constants, 25:20237 (UCRL-50400(Vol.9))
HOWES, J. H., Characteristics of large-area ion-implanted p--n junctions for detectors, 25:18756
HRUSKA, A., Plasma streaming in the magnetosphere, 25:19577
HSUAN, H. C. S., Time-of-flight study of waves guided by a plasma column, 25:19746
HUANG, H. C., Influence of defects on the angular correlation of positron-annihilation photons in irradiated and in deformed iron, 25:19851
HUANG, Helen Chi-hsing, Attenuation of longitudinal ultrasound in normal and superconducting mercury single crystals, 25:19608
HUBERT, F., Boron-11 and ^{10}B interactions with Th and U, 25:20420
HUCK, A., Silicon-28 energy levels near 13.245 MeV, 25:20330
HUDSON, J. A., Void formation during high-dose ion implantation at elevated temperatures, 25:19807
HUEBNER, Klaus, Improvements in threshold dosimeters, 25:18803
HUEFNER, Joerg, Neutron distribution in nuclei, 25:20534
HUFF, Robert W., Two-body problem in quantum field theory, 25:20071
HUFFMAN, Donald R., Interstellar silicate extinction related to 2200A band, 25:19446
HUGHES, F. H., Decay of /sup 113m/In, 25:20407
HULET, E. K., Spontaneous-fission half-life of ^{258}Fm and nuclear instability, 25:20443
HULTH, P. O., Hardware system for measurements of bubble chamber films on-line, 25:18776 (USIP-70-3)
HUMSKI, K., β-deuterium isotope effect in solvolysis of 1,2-dimethyl-exo-2-norbornyl p-nitrobenzoate, 25:18413
HUNSPERGER, R. G., Electrical properties of Cd, Zn, and S ion-implanted layers in GaAs, 25:19842
HURLEY, James, Upper bound on plasma containment. II, 25:19581
HURLEY, James R., Evaluation of spleen size during routine liver imaging with /sup 99m/Tc and the scintillation camera, 25:19057
HURST, Gail H., Mechanisms of monofunctional and bifunctional catalysis of an ester hydrolysis. The kinetics of methyl 2,6-dicarboxybenzoate hydrolysis, 25:18400

HURST, J. N., Gas turbo-machinery for helium cooled reactors, 25:20772
HUTSON, A. R., Moire patterns of ion implantation by channeling, 25:19849

I

IANOVICH, M., Magnetic field of thick finite dc solenoids, 25:18829 (JINR-P9-5441)
IANTUONO, A., Evaluation of an LN_2-temperature solid state spectrometer for rocket borne experiments, 25:18654
IAPTEFF, B., Measurements and calibrations at pressures between 10^{-5} and 10^{-12} torr, 25:18678
IBRAGIMOV, M. Kh., Method of calculating the coefficients of turbulent heat transfer in channels of a complex form, 25:20844 (AEC-tr-7186)
IBRAGIMOV, Sh. Sh., Post-irradiation study of BR-5 standard fuel elements containing UC, 25:20791
ICHIKAWA, Yoshi H., Electric conductivity of weakly turbulent plasmas, 25:19685
IGARASI, Sin-iti, GRAPH: computer program for plotting experimental data in NEUDADA system, 25:20230 (JAERI-Memo-4116)
 Japanese list of requests for measurement. II, 25:20231 (JAERI-Memo-4167)
 Manual for JUPITOR-1 (Supplement), 25:20479 (JAERI-Memo-4138)
IGI, K., Finite-energy sum rule as a test of the Pomeranchuk theorem, 25:20011
IGNATOV, D. V., Oxidation of Mo at 500 to 1000°C and pressures of 10^{-3} to -1 torr, 25:19169
IIDA, Yoshihiro, Movements of generating vapour bubble in saturated pool boiling. I, 25:18582
IKELAAR, P., Data collector for a coinidence experiment, 25:18872
IL'INOV, A. S., Double differential distribution of particles produced in the proton-nucleus collisions, 25:20018 (JINR-P2-5507)
ILIOPOULOS, J., Divergences of massive Yang--Mills theories, 25:19969
IMAI, Ryukichi, Direction of development on a nuclear fuel cycle, 25:19189
IMHOF, H., Spleen scintigraphy with /sup 113m/In-labeled erythrocytes, 25:19036
IMPINK, A. J., Saxton Core II nuclear operations summary, 25:20705 (WCAP-3385-55)
IMRE, Kaya, Electromagnetic properties of a half-space relativistic plasma, 25:19740
INFELD, E., Two-stream instability and classification into absolute and convective, 25:19710
INGAMELLS, C. O., Barium and Sr in silicates, 25:18335
INGEBRETSEN, F., Evidence for vibrational excited states in ^{32}S, 25:20326
 Properties of low-lying states in ^{43}Sc, 25:20320
INOUE, N., Expansion of a laser-produced plasma into a vacuum, 25:19703
 Plasma emission from titanium rail-type gun, 25:19726
INOUYE, T., Square root transform for the analysis of quantum fluctuations in spectrum data, 25:18739
IOFFE, A. I., Certain magnetohydrodynamic flow problems related to wave propagation, 25:19566
IONITA, G., Meson production by interaction of π^+ mesons with photoemulsion kernels at 185 to 295 MeV energies, 25:19919
IORDANSKII, S. V., Stability of a plane stationary shock wave, 25:20867 (LA-tr-71-10)
IOVNOVICH, M. L., Storage of multicharged ions in relativistic electron beam, 25:20210
IRIE, Masahiro, Dissociative electron capture process of methyl vinyl ether in organic glasses, 25:18456
IRISBAEV, K. N., Introduction of controlled energy-mode in U-150-2 cyclotron of Inst. of Nuclear Physics of UzbSSR Academy of Sciences, 25:20216
IROSHNIKOV, R. S., Quasi-axisymmetric models of a magnetic dynamo and the nature of solar-activity cycles. I, 25:19422
ISAACS, L. L., Magnetic susceptibilities of hexagonal Tc--Ru, Tc--Rh, and Ru--Rh alloys, 25:19874
ISAEV, P. S., Relation between cross sections of processes $e^- + e^+ + e^- + e^+ + A^- + A^+$ and $\gamma + \gamma + A^- + A^+$, 25:19938 (JINR-P2-5505)
ISAILA, M., Small source for multiply charged heavy ions, 25:20188
ISHAM, C. J., f-dominance of gravity, 25:20053
ISHIGURO, Yukio, Number of resonances to be adopted for obtaining practically reliable cross section curves, 25:20395
ISHII, Taka, Thermal neutron activation cross sections of $^{132}Ba(n,\gamma)$/sup 133m/Ba and $^{134}Ba(n,\gamma)$/sup 135m/Ba reactions, 25:20439
ISHII, Yukifumi, Chronic granulocytic leukemia with special reference to A-bomb survivors, 25:18963
ISHIKAWA, Hiroshi, Prog. rpt. on nuclear safety experimental program, 4--10/70, 25:20763 (JAERI-Memo-4229)
ISHIKAWA, I., Absolute measurement of beta-disintegrating nuclides, 25:20421
ISHIKAWA, Michio, Prog. rpt. on nuclear safety experimental program, 4--10/70, 25:20763 (JAERI-Memo-4229)
 Survey list of accident, hazard, and abnormality in nuclear facilities, 25:19013 (JAERI-Memo-4240)
ISHIZAKI, Y., Excited 0^+ states in ^{52}Fe, ^{54}Fe, ^{56}Ni, and ^{58}Ni from (p,t) reaction, 25:20321
ISHIZUKA, Hiroshi, Process for the separation of hafnium contained in zirconium, 25:18499 (LIB/Trans-330)
ISHKHANOV, B. S., Structure of cross section of photoneutron reaction on ^{208}Pb nucleus in the region of a giant dipole resonance, 25:20437
ISHKOV, A. P., Experimental studies of the autoresonance electron acceleration, 25:20224
ISMAGILOV, Z. R., Kinetic isotopic effect of the oxidation of hydrogen on ferric oxide, 25:18386
ISO, Yasuhiko, Properties of heat resisting concrete for neutron shielding, 25:19295
ISOYA, A., Beam injection system for the terminal ion source of the electrostatic generator, 25:20204
ITO, Akihide, Effects of introducing nuclear energy into the aluminum industry, 25:19184
ITO, Akihiko, Radiation-induced polycondensation of furfural in the presence of alkyl halide, 25:18430
IVANOV, A. A., Class of solutions of quasi-linear equations, 25:19694
IVANOV, I. N., Ion acceleration by electron ring in decreasing magnetic field, 25:20131 (JINR-P9-5535)
IVANOV, K. I., Bound states of a relativistic two-particle system, 25:20083
IVANOV, S. N., Effect of biological properties of plant on ^{90}Sr contents in yield, 25:18597
IVANOV, U. I., Transport coefficients of inhomogeneous systems in electromagnetic fields, 25:19562
IVANOV, V. I., Microdosimetry (physical aspects and fundamental problems), 25:18993
IVANOVA, S. P., Table of wave functions of single-particle states of transuranium region deformed nuclei in Saxon--Woods potential, 25:20481 (JINR-P4-5457)
IVANSHIN, Yu. I., Electron energy measurement by the shower spectrometer, 25:18779
IWAO, Hiroyuki, Influence of ^{60}Co γ-ray on potato, 25:19160
IWASA, Y., Threshold currents of large cross-section superconductors, 25:19624
IYENGAR, V. S., Orientation system for balloon-borne payloads, 25:18677

J

JAAKKOLA, T., Environmental γ-radiation dose rate in Finnish Lapland and Southern Finland, 25:18986 (NYO-3446-14, Paper 28)
JABSEN, Felix Stanley, Improvements in and relating to nuclear reactors, 25:20839
JACKSON, A. D., Triton binding energy calculations, 25:20259
JACKSON, Bernard Vernon, Cool star spectrum synthesis, 25:19319
JACKSON, C. N. Jr., In-core regenerative thermal neutron detectors for nuclear reactors, 25:20711 (WHAN-FR-37)
JACKSON, Herbert L., Reproductive factors associated with radiotherapy of malignant lymphomas, 25:19147
JACKSON, W., Compensating the effect of surface irregularities in high-energy radiotherapy, 25:19066
JACOB, J. H., Interpretation of spatially decaying ion-acoustic waves, 25:19741
 Symmetry considerations for grid-launched ion-acoustic waves, 25:19742
JACOBI, Lee William, Mass spectra and moments from classical dynamics, 25:19928
JACOBS, D. G., Engineering, economic, and safety evaluation, 25:18526 (ORNL-4584, pp 37-40)
JACOBS, Matthew A., Kinematic superstructures for abnormal couplings in 8-π dual amplitude, 25:20000
JAFFE, Norman, Irradiation of the liver in children: acute effects enhanced by concomitant chemotherapeutic administration, 25:18999
JAFFEY, Arthur H., Prompt-neutron spectra and delayed-neutron spectra from fission: some comments on current knowledge, 25:20362 (ANL-7747)
JAGGI, R. K., Hydromagnetic waves generated at the bow shock, 25:19580
JAMESON, R. A., Dynamic measurement of stopband in LAMPF 805 MHz accelerator structures at high power using hybrid computer techniques, 25:20132 (LA-4593)
JAMET, Christian, Intermetallic diffusion of plutonium in Pu--Cu and Pu--U systems, 25:19230 (CEA-R-3951)
JAMMET, H., Comparative study on whole-body exposure injuries, 25:19012 (CEA-CONF-1695)
 Radiological accidents rules, 25:18975 (CEA-N-1365)
JAMSHIDI, A., Identification of particle-hole multiplets in ^{40}Sc, 25:20350
JANEWAY, Richard, Selenomethionine ^{75}Se thymus scans in myasthenia gravis, 25:19049
JANKOWSKI, K., Application of truncated multipolar expansion pair functions in atomic structure calculations. II, 25:19515
JANOS, W. A., Control-theoretic approach to the plasma confinement problem, 25:19655
JANOT, Pierre, Detection of local boiling in light water reactors, 25:20716 (CEA-R-4118)
JANSEN, P., Game theory applied to plutonium cost, 25:20753
JANSSON, Per-Aake, Mass spectral data processing. II,

XUM

25:18835

JASZCZAK, Ronald J., Proton recoil monitor for neutron flux measurements, 25:18763

Use of a pulsed Van de Graaff accelerator and time-of-flight techniques to reduce backgrounds in (α,γ) spectroscopy experiments, 25:20148

JAUCH, Delbert Edwin, Measurement of the neutral cascade hyperon lifetime, 25:19903

JAUNCEY, D. L., Observations of compact radio sources, 25:19368

JAYANTHI, U. B., X-ray observation of Cen XR-4 and Nor XR-2, 25:19354

JAYARAMAN, M. T., Radiation processed wood-plastic materials, 25:19298

JAYARAMAN, S., Partial-body irradiation of larvae of Tenebrio molitor, 25:19094

JEANNE, F., Present state of the bibliography on Nb and its alloys, 25:19165

JEFFERIES, John T., Spectrum of inner corona during eclipse of May 30, 1965, 25:19410

JEFFS, Alan T., Oxygen: metal ratio effects in $(U,Pu)O_2$ fuels, 25:19287 (AECL-3690)

JENCEK, L., Significance of radioactive isotopes in building structures, 25:18599

JENCKS, William P., Reactions of acetylimidazole and acetylimidazolium ion with nucleophilic reagents, 25:18398

JENKINS, J. H., Prog. rpt. on bioaccumulation of gamma-emitting radionuclides in white-tailed deer, annual, 2/70--1/71, 25:18935 (ORO-3905)

JENSEN, V. O., Ion-velocity distribution function in a single-ended Q machine, 25:19670

JENTSCHKE, W., Experimental programme at CERN intersecting storage rings, 25:20158

JERSAK, J., Light-cone commutators and high energy annihilation $e^+ + e^- \to \pi +$ hadrons, 25:19941

JESSE, Richard H. Jr., Elective irradiation of the neck lymphatics for squamous cell carcinomas of the nasopharynx and oropharynx, 25:19084

JESSUP, Gordon L., Review of radium toxicity studies, 25:18979 (BRH/DBE-70-5)

JEUKENNE, J. P., Separable single-particle potential in shell-model calculations, 25:20509

JIMENEZ-ZAMUDIO, Luis Antonio, Studies on the initiation and regulation of antibody formation to sheep red blood cells in mice, 25:18925

JOENSSON, G., Photometric mass determination in nuclear emulsion on cosmic ray carbon. I, 25:18643 (NP-18672)

JOERGENSEN, M., Plasma renin measured by radioimmunoassay for angiotensin, 25:18920

JOH, Hiroshi, Influence of defects in 80 mm thickness steel plates for weld quality, 25:19202

JOHANNSEN, K., Magnetoplasmadynamic energy conversion in nuclear power stations, 25:20768

JOHANSSON, Gunilla, VC, NbC, and TaC studied by electron spectroscopy for chemical analysis, 25:19867

JOHANSSON, N. G. E., Anomalously high yields of elastically scattered ^{12}C from atoms implanted into silicon, 25:19829

Diffusion effects in ion-implanted germanium, 25:19841

JOHANSSON, T. B., Beam mapping method, 25:20138

JOHNS, M. W., Decay of ^{90}Kr and ^{90}Rb, 25:20384

Level structures of ^{91}Rb and ^{91}Sr as populated in beta decay, 25:20459

JOHNSEN, K., CERN intersecting storage rings, 25:20209

JOHNSON, C. H., (p,n) cross sections and the strength functions for protons on In and on Sn isotopes, 25:20475

JOHNSON, C. S., Comparison of CBW FM/FM and DSB/FM telemetry systems, 25:20888 (SC-DR-70-686)

JOHNSON, D. A., Spectrophotometric determination of U(VI), 25:18352

JOHNSON, D. L., REBA: pulsed electron beam generator, 25:20136 (SC-DR-70-872)

JOHNSON, H. E., Atmosphere of Hg, 25:19467

JOHNSON, Hugh M., Hβ photometry of the night sky, 25:19440

JOHNSON, James E., Prog. rpt. on $^{210}PoO_2$ metabolism in ruminants, annual, 1/15/70--1/15/71, 25:18890 (COO-2044-3)

JOHNSON, John L., Tokamak equilibrium, 25:19716

JOHNSON, R., Comparisons of aerosol experiments with a model used in reactor siting evaluation, 25:20757 (CONF-700816-(Vol.1), pp 26-48)

JOHNSON, R. J. R., Comparison of the effect of hyperbaric oxygen and oxygen plus 5 percent CO_2 on tissue circulation and oxygenation, 25:19023

JOHNSON, Robert Carey, Ultraviolet light mutation induction during synchronous replication in E. coli, 25:18966

JOHNSON, W. R., Lamb shift and binding energies of K electrons in heavy atoms, 25:19477

JOHNSON, William T. K., Excitation of nuclear levels by electrons and photons for 167 less than or equal to A less than or equal to 197, 25:20463

JOHNSSON, K. O., Abstracts of literature on the distillation of seawater and on the use of nuclear energy for desalting, 25:20812 (TID-25653)

JONES, Arthur W., Effect of x rays on developing cysticercoids of Hymenolepis microstoma, 25:19095

JONES, C. E., Helicity poles, triple Regge behavior and single particle spectra in high energy collisions, 25:19926 (NYO-2262-TA-234)

JONES, G., Fitting of double exponenial lifetime spectra using a maximum likelihood technique, 25:19881

JONES, G. D., Angular correlation studies in ^{34}S, 25:20348

JONES, H. F., s-channel helicity conservation and the stress-tensor, 25:19931

JONES, Harrison P., Formation of resonance lines in multidimensional media. I, 25:19395

JONES, Harrison Price, Line formation in multidimensional media, 25:19424

JONES, K., Multiparticle Veneziano formulae corresponding to interaction of two classes of hadrons, 25:20014

JONES, K. C., Electrical and atom-site location properties of ion-implanted germanium, 25:19799

JONES, Mark M., Acid and metal salt catalyzed hydrolyses of $PO_2F_2^-$ and PO_3F^{2-}, 25:18373

JONES, William Edward, Surface modes of vibration and optical properties of an ionic crystal slab, 25:20862 (IS-T-427)

JONKER, C. C., Angular correlations in inelastic neutron scattering by carbon at 15.0 MeV, 25:20281

JONSON, B., Transition rates in ^{192}Au, 25:20453

JOON, K., Chemical analysis of high burn-up PuO_2 fuel, 25:18356 (KR-140)

JOSHI, P. V., Size determination of airborne plutonium particles by autoscintigraphy, 25:18976

JOSSO, E., Structure and properties of the binary Nb--Ti, Nb--Mo, and Nb--Zr solid solutions, 25:19215

JOWETT, C. W., Relationship between surface potential and electronegativity for adsorption on tungsten single crystals, 25:19207

Work function changes due to adsorption of Cl, Br, and I on W single crystal surfaces, 25:19209

JOWITT, D., Measurement of $^{238}U/^{235}U$ fission ratios in Zebra, 25:18704

JUILLARD, G., Telecobalt therapy for carcinoma of laryngopharynx, 25:18998

JUNKRANS, S., Irradiation behavior and post-irradiation examination of Swedish test assembly IFA-30, 25:20735 (HPR-127)

JURISIC, Nikola Kuhbauch, Application of Glauber theory to photon--nuclear interactions, 25:19955

K

KABACHNIK, Nikolai M., Difference between proton and neutron distributions in nuclei, 25:20544

KABAKCHI, A. M., Determination of the radiation yield of nitrite ions in the irradiation of sodium nitrate solutions in the small-dose region, 25:18463

KABAKCHI, S. A., Evidence of the occurrence of monomolecular reactions in the radiolysis of aqueous solutions of oxygen, 25:18476

KADAR, Imre, Spray current stabilizer circuit for pressurized van de Graaff generator, 25:20222

KADEMOVA, K. V., Spin-half particles with an infinite maximum occupation number, 25:20079

KAETSU, Isao, Radiation-induced polycondensation of furfural in the presence of alkyl halide, 25:18430

KAHAN, A., Resistivity and annealing properties of implanted $Si:H^+$, 25:19822

KAHLER, S., Existence of solar-flare plasmas of T greater than or equal to 10^8 °K, 25:19398

KAHN, Guinter, Evaluation of phototoxicity of salicylanilides and similar compounds by photohemolysis, 25:18913

Red blood cell hemolysis by photosensitizing compounds, 25:18914

KAIDALOV, A. B., $pn \to np$, anti $pp \to$ anti nn and branching in j-plane, 25:20017 (CERN-Trans-70-15)

KAIMAKOV, E. A., Laboratory modeling simulation of comet phenomena, 25:19394 (LA-tr-70-27)

KAINDL, G., Isomer shifts and changes of nuclear charge radii in ^{99}Ru and ^{101}Ru, 25:20403

KAJI, Harumi, Study of chemical behavior of recoil atoms due to (γ,γ') process, 25:18488

KAKAURIDZE, D. B., Electron energy measurement by the shower spectrometer, 25:18779

KAKKAR, I., Configuration mixing calculations in Hartree--Fock representation, 25:20286

KAKU, Michio, Linear dependences and multiloop Veneziano amplitude, 25:20117

KALASHNIKOV, V. P., Kinetics of hot electrons in quantizing magnetic fields. II, 25:19960

KALBITZER, S., Low-energy B and P implants in Si. B, 25:19836

Low-energy B and P implants in Si. A, 25:19835

KALICHEVA, I. S., Study of distribution of Sc, Ce, and Eu between the various phases of meteorite matter, 25:19302

KALININ, B. N., Measurements of the asymmetry ratio of positive-pion photoproduction by linearly polarized photons, 25:19889

KALINYAK, A. A., Velocity field distribution in the solar photosphere, 25:19404

KALISH, Rafael, Revised level scheme of ^{199}Hg following Coulomb excitation, 25:20387

KALLO, A., Investigations of radiation-induced solid-state polymerization. XXVI, 25:18431

KALRA, G. L., Effect of Hall current and resistivity on stability of gas--liquid system, 25:19546

KALYAZIN, E. T., An observation on the nature of intermediate particles in the radiolysis of aqueous solutions of oxygen, 25:18477
KAMADA, Nanao, Chronic granulocytic leukemia with special reference to A-bomb survivors, 25:18963
KAMITSUBO, H., Study of (p,d) reactions on ^{118}Sn and ^{119}Sn with polarized protons, 25:20365 (CEA-CONF-1657)
KAMIYAMA, Teiji, Direction of development on a nuclear fuel cycle, 25:18555
KAMLAH, A., Approximation for the rotation-vibration transition region, 25:20527
KAMPHOUSE, J. L., Theoretical spectrum-threshold detector data correlation in EBR-II, 25:20803
KANDPAL, C. D., Photoelectric elements of eclipsing system WX Cep, 25:19335
  Photoelectric study of eclipsing system GG Cas, 25:19336
KANG, Kyungsik, Okubo's second-class currents in K/sub 12/ and K/sub 13/ decays, 25:19965 (NYO-2262-TA-236)
KANTELE, J., Directional correlations of some γ-ray cascades in ^{200}Hg, 25:20400
  Semiconductor detector telescope electron spectrometer, 25:18760
KAPCHINSKII, I. M., Linear ion accelerator with spatially homogeneous strong focusing, 25:20172
KAPITONOV, I. M., Structure of cross section of photoneutron reaction on ^{208}Pb nucleus in the region of a giant dipole resonance, 25:20437
KAPLAN, Henry S., Production and repair of radiochemical damage in Escherichia coli deoxyribonucleic acid; its modification by culture conditions and relation to survival, 25:18912
KAPLINA, G. S., Diffusion in nitrided Nb, W, and Fe--Si alloys, 25:19234
KAPLOW, Roy, Compton scattering and electron momentum density in beryllium, 25:19870
KAPPUS, Peter G., Aircraft nuclear propulsion system, 25:20810
KARABALAEV, U., Thickening of wool fibers under the influence of ionizing radiation, 25:19121
KARAMYAN, S. A., Experiments on measurement of compound nucleus lifetime in W(^{22}Ne,f) reaction, 25:20370 (JINR-P7-5512)
KARATAEV, V. D., Device for studying electron backscattering from layers of materials, 25:18823
KARCZ, W., Polarization of protons from ^{12}C(d,p)^{13}C reaction at E/sub d/ = 12.4 MeV, 25:20287
KARGIN, V. A., Application of the method of radiothermoluminescence for the investigation of high-temperature relaxation in polyethylene, 25:18435
KARHAUSEN, L., Dosimetry of the gastro-intestinal tract, 25:19141
KARITSKAYA, E. M., Estimating mass of quasi-stellar objects and galaxy nuclei, 25:19364
KARLOV, L., Torsion-free world lines in curved space--time, 25:20100
KARNAKOV, B. M., pn + np, anti pp + anti nn and branching in j-plane, 25:20017 (CERN-Trans-70-15)
KARPOV, V. L., Action of ionizing radiation on the structure and properties of the copolymer of styrene with 2-ethylhexyl acrylate, 25:18436
KARR, Hugh J., Dynamic stabilization of a linear z pinch, 25:19717
KARUNARATHNE, V. B., Boundary problem in a plasma, 25:19749
KARZHAVIN, Yu. A., Investigation of the model of the 2-meter streamer chamber of the SCM-200 assembly, 25:18774 (JINR-P13-5529)
KASAI, Naoko, Thermal expansion of Au_4V, 25:19229
KASATKINA, L. A., Isotopic exchange in carbon monoxide molecules on zinc and iron oxides, 25:18387
KASPAR, J., Thermodynamic conditions of the origin of uraninites, 25:18551
KASPEREK, K., Uses of a research reactor for medical investigations, 25:18886
KASYMOV, A., Radiotoxin fractionation and investigations on their biological properties, 25:18915
KATAYAMA, Toshikazu, Permanent magnet properties of intermetallic compounds Sm (Fe, Co, Cu)$_5$, 25:19875
KATHURIA, S. N., Effect of Hall current and resistivity on stability of gas--liquid system, 25:19546
KATO, Masao, Detection of radiation emitted from moving sources. I, 25:18692
  Trends in utilization of radiations and radioisotopes, 25:18608
KATO, N., Beam injection system for the terminal ion source of the electrostatic generator, 25:20204
KATS, M. M., Measurement of harmonic components of fields of standard magnetic quadrupole lenses, 25:20164
KATSANOS, N. A., Theory of chemical effects produced by isomeric transition of /sup 82m/Br in liquid organic systems, 25:18489
KATSUBE, Yutaka, Effect of Tween 80 on strand breaks of E. coli DNA irradiated in situ, 25:19027
KATSUMOTO, Tomiyasu, Honeycomb block used for collimation of radiations and method of manufacturing the same, 25:18856
KATSURAGI, Satoru, Analysis of fast critical experiments and revision of JAERI-fast set, 25:20788 (JAERI-Memo-4215)
  Number of resonances to be adopted for obtaining practically reliable cross section curves, 25:20395
  Plutonium-239 fission product yields and their influence on fast reactor characteristics, 25:20819 (JAERI-Memo-4165)
KATZ, R., Analysis of a breakup using mean track width and blob measurements, 25:18795
KAULEN, D. R., Effect of antilymphocytic sera on the hemopoietic tissue, 25:18921
KAURANEN, P., Environmental γ-radiation dose rate in Finnish Lapland and Southern Finland, 25:18986 (NYO-3446-14, Paper 28)
  Polonium and radiolead in some aqueous ecosystems in Finland, 25:18930 (NYO-3446-14, Paper 27)
  Polonium and radiolead in some land animals in Finland, 25:18929 (NYO-3446-14, Paper 26)
KAURANEN, Pentti, Stable lead and radiolead in air filter samples, 25:18933 (NYO-3446-14, Paper 32)
KAVANAGH, T. M., Soft x rays from collisions of 1 MeV H_2^+ and 500 keV Ar^+ with carbon, 25:18836
KAWAGUCHI, Keizo, Construction of nuclear power plant, 25:20564
KAWASUMI, Y., Expansion of a laser-produced plasma into a vacuum, 25:19703
  Plasma emission from titanium rail-type gun, 25:19726
KAY, Ernest, Near-uv absorption bands of tryptophan, 25:20899 (UCLA-12-810)
KAYSER, K., Electronically-controlled pneumatic tube system for activation analysis at a particle accelerator, 25:20184
KAZACHKOV, Yu. A., Estimate of stationary regime of Faraday segmented MHD generator in non-rated input plasma parameters, 25:19540
KAZANSKII, L. N., Intense electron beam autoacceleration, 25:20220
KAZANSKII, V. D., EPR study on stable H atoms on γ-irradiated clinoptilolites containing La, Mg, and K ions, 25:18423
KAZNOVSKII, S. P., Boiling of liquids on fine wire under natural convection conditions, 25:18583
KEARIN, M. J., Method for study of short-lived nuclear isomers, 25:20312
KEDWARD, Eric Charles, Deposition of composite coatings, 25:19270
  Manufacture of nuclear fuel elements, 25:19269
KEEN, B. E., Dispersion curve for drift waves in inhomogeneous magnetoplasma, 25:19731
KEISTER, Jamieson Charles, Superconductive tunneling into bulk gallium single crystals, 25:19615
KELKAR, D. N., Size determination of airborne plutonium particles by autoscintigraphy, 25:18976
KELLER, G. E., Band mixing in ^{154}Gd, 25:20441
KELLER, Leon Gregory, The scattering and breakup of vector polarized deuterons on helium, 25:20263
KELLY, R., Diffusion in ion-implanted solids with nonuniform diffusion parameters, 25:19840
KELLY, T. M., Scintillation decay spectrometer for resolving subnanosecond lifetimes, 25:18696
KELLY, W. H., Spurious peaks produced by Compton scattering in Ge(Li)--Ge(Li) coincidence gamma-ray spectrometer systems, 25:18754
KEMP, James C., Confirmation of magnetic white dwarf G-195-19, 25:19328
KENNEDY, William R., Plutonium and strontium in soil near Technical Area 21, Los Alamos Scientific Laboratory, Los Alamos, New Mexico, 25:18985 (LA-4563)
KERBEL, Sheldon J., Radiation sensitive notch pattern detection system, 25:18818
KERN, H., DNA synthesis after irradiation with high doses of x-rays and spindle inhibition, 25:18910
KERNELL, R. L., (p,n) cross sections and the strength functions for protons on In and on Sn isotopes, 25:20475
KERNS, John Richard, Coulomb excitation studies of ^{134}Ba, ^{136}Ba, ^{138}Ba, and ^{150}Nd, 25:20469
KEROE, E. A., Determination of ^{15}N by emission spectroscopy, 25:18344
KERR, F. J., Parkes hydrogen-line survey of the Milky Way. V, 25:19392
  Parkes hydrogen-line survey of the Milky Way. IV, 25:19391
  Parkes hydrogen-line survey of the Milky Way. III, 25:19390
KERSHNER, Carl J., Purification of polonium, 25:18509
KESSLER, D., Muonic x rays and capture gamma rays in ^{89}Y, 25:20360
KESSLER, J., Residual resistivity of Pb films after implantation of Mn ions, 25:19857
KESSLER, W. V., 4π liquid-scintillation whole-body counter. II, 25:18649
KEYWORTH, G. A., High resolution fission cross section of ^{235}U from 20 eV to 100 keV, 25:20418
KHAN, Abdul Aleem, Hydromagnetic flow between two rotating coaxial disks, 25:19568
KHAN, Faiz M., Use of electron filter to reduce skin dose in cobalt teletherapy, 25:19082
KHAN, J. M., Soft x rays from collisions of 1 MeV H_2^+ and 500 keV Ar^+ with carbon, 25:18836
KHAN, K. A., Scattering of two impulsive gravitational plane waves, 25:20087
KHANGULYAN, V. A., Diagram approach to polarization effects in the stripping and pick up reactions, 25:20533
KHARCHENKO, V. F., Calculation of binding energy and wave function of ^{3}He by harmonic polynomial method,

25:20249 (ITF-70-51-E)
KHARITONOV, S. E., Spectrometric scintillation equipment of commercial application for radioactive logging of boreholes in ore deposits, 25:18814 (CSIRO-Trans-9992)
KHARITONOV, Yu. P., Potential identification of products of heavy-ion-induced nuclear reactions, 25:20419
KHASANOV, F. M., Measurement of harmonic components of fields of standard magnetic quadrupole lenses, 25:20164
KHERAK, R., Interaction of samarium and strontium oxides, 25:19284
KHITNIKOV, B. Z., Experimental solenoid made of Nb_3Sn strip, 25:19588 (JINR-P8-5440)
KHLESKOV, V. I., Relation between cross sections of processes $e^- + e^+ + e^- + e^+ + A^- + A^+$ and $\gamma + \gamma + A^- + A^+$, 25:19938 (JINR-P2-5505)
KHODADAD, Parviz, Mixed rare earth sulfides, 25:19286
KHODEL, V. A., Gauge transformations and local charges of quasiparticles, 25:20082
KHOKHLOV, V. K., Sensitivity of a secondary-emission-type accelerated-electron-beam position monitor, 25:20173
KHOKHLOVA, V. L., Spectroscopic studies of peculiar A stars of Mn group, 25:19343
KHOLEVO, A. S., Quasi-free states of C* algebra of commutation relations. II, 25:19932
KHOLIN, V. N., Spectrometric scintillation equipment of commercial application for radioactive logging of boreholes in ore deposits, 25:18814 (CSIRO-Trans-9992)
KHOLSHCHEVNIKOVA, E. K., Steady supersonic flow of conducting gas in channel in case of weak MHD interaction, 25:19565
KHOMYAKOV, G. K., Device for measuring total proton cross sections of reactions, 25:20176
KHOPKAR, P. K., Effect of ionic media on stability constants of chloride, nitrate, and thiocyanate complexes of Am(III) and Eu(III), 25:18371
KHOPKAR, S. M., Separation of bismuth(III) from other ions by cation exchange chromatography, 25:18520
KHORAVA, I. S., Investigation of aromatic hydrocarbons of supsinskaya petroleum and their catalytic conversion in the presence of irradiated catalysts, 25:18444
KHORUZHAYA, V. G., Structure of V--Cr--Zr alloys at 1150°C, 25:19237
KHOUDJAKOV, A. V., Properties of heat-resistant steels following high-temperature reactor irradiation, 25:19250 (AEC-tr-7192)
KHRIPIN, L. A., Reduction of uranium tetrafluoride vapors by certain metals, 25:18372
KHRUSTALEV, O. A., Equal-time equation for two-particle system in quantum field theory, 25:20077
KIDD, J. M., Charge spectrum of extremely heavy cosmic rays, 25:19532
KIENLE, P., Isomer shift and quadrupole splitting of the 2^+-rotational state in ^{174}Yb, 25:20399
KIERNAN, Brian, Deposition of composite coatings, 25:19270
Manufacture of nuclear fuel elements, 25:19269
KIESZKOWSKI, Z., Radiological protection of out-patients, 25:19009
KIGUCHI, Takashi, Energy model synthesis method in fast reactor analysis, 25:20709
KILNA, R., Nearly resonant confinement of plasma, 25:19649
KIM, E. G., Semi-empirical efficiency curve for thin Ge(Li) detector at low energies, 25:18725
KIM, Hi Gyu, Thermoluminescent properties of Korean natural quartz for possible use in γ-ray dosimetry, 25:18813
KIM, Yong-ki, Total cross sections for inelastic scattering of charged particles by atoms and molecules. VI, 25:19510
KIMERLING, L. C., Annealing of electron-irradiated n-type silicon. I. Donor concentration dependence, 25:19854
KIMURA, H., Quenched-in resistivity in molybdenum, 25:19860
Recovery of fast neutron irradiated molybdenum, 25:19861
KIMURA, Keizo, Direction of development on reactor materials, 25:19223
KINAREEVSKII, V. A., Flow of conducting fluid near nonconducting sphere in crossed electric and magnetic fields, 25:19550
KING, K., Calculations for stripping on doubly magic nuclei, 25:20282
KING, Richard Lien-chao, Determination of nuclear magnetic moment of ^{203}Hg, 25:20397
KING ASSIS, Benedito G., Activity of ionizing radiation on fertile eggs of Triatomideos-Rhodnius prolixus, 25:19099
KINZER, R. L., Experiment to detect pulsed γ rays from Crab Nebula, 25:19361
KIRILLOV, I. R., Experimental investigation single-wave MHD machines, 25:19537
KIRILLOV, P. K., Discrete frequency sweep in a synthesizer for nuclear magnetic resonance spectroscopy, 25:18848
KIRSCHMAN, R. K., Ac and dc potentials in superconducting phase-slip structures, 25:19610
KISLETSOV, A. V., Intense electron beam autoacceleration, 25:20220
KISON, Harald, Separation of steam and water in boiling-water reactors and steam generators, 25:20769
KITAGAKI, Toshio, Photoproduction of two neutral pions from hydrogen near threshold, 25:19890
KITAMURA, Kanae, Effect of radiotherapy on the urinary amino acids, 25:19063
KITAZUME, Mitsuyuki, Gamma-ray scattering by structure surfaces, 25:19764
KIURU, A., Nuclear levels and transitions in odd Cu isotopes. I, 25:20314
Proton reactions on ^{23}Na, 25:20325
KJELBERG, A., Decay of Cd isotopes, 25:20422
KJEMS, Joergen, Thermal neutron spectroscopy using position-sensitive detectors together with fourier correlation time-of-flight and single-crystal techniques, 25:18738 (RISO-229)
KLADNITSKAYA, E. N., Method of searching for the kink and determining the track parameters of particles scattered in a bubble chamber, 25:18773 (JINR-P1-5540)
KLAGES, W. J., Formation of ^{6}Li/sub g s / and ^{6}Li, 3.56 MeV, T = 1 state, 25:20284
KLAUDY, Peter A., Cryogenic electrical energy transmission, 25:19636
KLAUZEN, N. A., Comparative study of effect of irradiation with γ-rays and accelerated electrons on structure and properties of cis-butadiene rubber, 25:19300
KLEINE-TEBBE, E., Electric equipment for fuel element handling at ESSOR reactor in EURATOM Nuclear Research Centre, Ispra, Italy, 25:18627
KLEY, H., Advanced gas cooled reactor with steam-generators within the wall of the prestressed concrete pressure vessel, 25:20698
KLOPFER, Oskar E., Radiation curable polyvinyl chloride composition containing triallyl isocyanurate, 25:18437
KLOSE, W., Theory of ultrasonic attenuation in V_3Si, 25:19604
KLOTZ, G., Electromagnetic transitions in ^{37}Cl, 25:20317
KLOZENBERG, J. P., New derivation of quasi-linear theory, 25:19738
KNAAP, H. F. P., Rotational relaxation of HD below 40 K, 25:19480
KNAJFL, J., Passage of iron(III) cyanoferrate through the gastrointestinal tract of rats, 25:18887
KNAPP, Gillian R., Parkes hydrogen-line survey of the Milky Way. IV, 25:19391
KNAPP, J., Resonance-capture and -fission in highly enriched fuel-lattices, 25:20826
KNIGHT, J. A. Jr., Prog. rpt. on radiation chemistry of mono-substituted aromatic compounds, 1/15/70--1/15/71, 25:18450 (ORO-3519-8)
KNILL, G., Characteristics of large-area ion-implanted p--n junctions for detectors, 25:18756
KNISPEL, Gerard, Study and development of cadmium telluride detectors for gamma-ray spectrometry, 25:18733 (CEA-R-4052)
KNITTER, H.-H., Measurements of neutron elastic scattering from carbon in energy region of 0.50 to 2.00 MeV, 25:20267 (EUR-4538)
KNORR, G., Adiabatic electron plasma and its equation of state, 25:19675
KNOSPE, W. H., Accelerated regeneration of transplanted hematopoietic stem cells in irradiated mice pretreated with cyclophosphamide, 25:19127
KNOSPE, William H., Factors regulating the proliferation and migration of hematopoietic stem cells, 25:19126
KNOWLES, S. H., Further investigations of NH_3 inversion radiation, 25:19366
KNUDSEN, K. D., Irradiation behavior and post-irradiation examination of Swedish test assembly IFA-30, 25:20735 (HPR-127)
KNYAZEV, V. M., Spark gap for operation with spark chambers, 25:18782
KOBA, Z., Isospin analysis of pion and nucleon resonance production in NN collisions, 25:20030
KOBAYASHI, Kiyoshi, Movements of generating vapour bubble in saturated pool boiling. I, 25:18582
KOBAYASHI, Masao, Gamma irradiation in medicinal plant breeding. II, 25:19151
KOBAYASHI, Shigeo, Research and development of fuel for liquid metal fast breeder reactor, 25:19275
KOBRINSKII, M. N., Calculation of box diagram effects with two resonances in the intermediate state, 25:19986 (IFVE-STF-70-34)
KOCHESHKOV, K. A., Radiothermal isomerization of alkyl bromides, 25:18438
KOCHMANSKA, Anna, Effect of prolonged fractionated x-ray irradiation on the generation cycle of small intestine crypt cells in mice, 25:19122
KOCIAN, P., Properties of ultra high vacuum extractor gages, 25:18838
KOECHLIN, F., New method of magnetic pumping for plasma heating, 25:19648
KOEHLER, Conrad F. Jr., Technique for attaching a vacuum tight window to a curved surface, 25:18712
KOEHLER, Dale Roland, Improvements in or relating to timekeeping systems with a radioactive timekeeping standard, 25:18819
KOENIG, W., Measurement of coal dust concentrations in pipelines using radioactive isotopes, 25:18606
KOEPPL, G. W., Solvent isotope effects upon proton transfer from the hydronium ion, 25:18395
Vibrational analyses of liquid water and the hydronium ion in aqueous solution, 25:18399
KOERNER, H. J., Gamma-decay of proton-particle neutron-hole states in ^{208}Bi, 25:20434
KOERTS, L. A. Ch., Analysis of multidimensional nuclear data (BOL). I, 25:20203

BOL nuclear research project, 25:20198
Electronics of the BOL-system, 25:20199
KOEVER, A., Effect of thin foils on the spectrum of monoenergetic electrons, 25:18770
KOKES, A., Pulse sequence identifier, 25:18866
KOLB, G., Applied magnetohydrodynamics. VI, 25:19536 (JUL-706-TP)
KOLDITZ, J., Proof of reactor component in helium atmosphere, 25:20558
KOLESNIK, I. G., Phase shift between the radius and temperature variation in Cepheids, 25:19322
KOLESOV, B. M., Radiation resistance of type ZnS + ^{10}B detectors to neutrons, 25:18880
KOLESOV, G. M., Study of distribution of Sc, Ce, and Eu between the various phases of meteorite matter, 25:19302
KOLESOV, V. E., Use of numerical methods for neutron cross section calculations, 25:20530
KOL'GA, V. V., External injection and acceleration of the beam to the final radius in the electron model of the ring cyclotron with strong focusing, 25:20130 (JINR-P9-5453)
KOLTAY, Ede, Spray current stabilizer circuit for pressurized van de Graaff generator, 25:20222
KOLYBASOV, V. M., Diagram approach to polarization effects in the stripping and pick up reactions, 25:20533
KOMAR, I. N., Structure and stabilities of free radicals formed in γ-irradiated glycine, 25:18478
KOMBERG, B. V., Estimating mass of quasi-stellar objects and galaxy nuclei, 25:19364
KON, Hideo, Comparison of electrical discharge with γ-radiation for the production of free radicals in lyophilized proteins, 25:18906
KONDRASHEVA, E. P., Measurement limits of exposure dose rate by gas-discharge counters, 25:18664
KONDRATEV, L. G., Circuits for the identification of neutrons, 25:18667
KONG-A-SIOU, Dy-Holm, Decay of 16.11-MeV level of ^{12}C into 3 α particles, 25:20270 (NP-18626)
KONIJN, J., Levels in ^{238}Pu from decay of ^{238}Np, 25:20431
KONOVALOV, O. G., Spark chamber with graphite electrodes, 25:18785
KONSTANTINOVIC, J., Deconvolution of the observed beam in the elastic scattering of slow neutrons, 25:20241
KOONTZ, R., Behavior of iodine in the presence of sodium oxide aerosols, 25:20761 (CONF-700816-(Vol.1), pp 373-92)
Comparisons of aerosol experiments with a model used in reactor siting evaluation, 25:20757 (CONF-700816-(Vol.1), pp 26-48)
KOOPMANN, Edzard William, Angular correlation studies of conversion electrons from ^{154}Gd, of nuclear electrons from ^{48}V and of Bremsstrahlung from unpolarized electrons, 25:20374 (NP-18597)
KOPELIOVICH, B. Z., Contribution of exchange mechanism in backward scattering of protons on light nuclei and d + ^{4}He $\rightarrow$ ^{3}He + ^{3}H reaction, 25:20250 (JINR-P2-5496)
KOPPE, H., Electrodynamics of superconductors, 25:19592
KOPYLOV, I. M., Physical conditions in atmosphere of P Cygni, 25:19342
KOR, J., Double scattering of electromagnetic radiation by bound electrons, 25:19949
KORCHAZHKIN, V. V., Structural changing during degradation of supersaturated solid solution of Ta in Co, 25:19233
KORENCHENKO, S. M., Search for the decay $\mu^+ \rightarrow e^+ + e^+ + e^-$, 25:19891 (JINR-P1-5542)
KORENEVSKII, V. V., Change of concrete aggregate properties under neutron irradiation, 25:19296
KORNBICHLER, H., 800 MW Brunsbuettel nuclear power station, 25:20567
KORNIENKO, T. P., Mechanism of radiation polymerization of vinyl monomers in the presence of mineral additions, 25:18442
KORNILOV, I. I., Effects of Al and Zr on properties of Ti$_3$Sn, 25:19238
KOROTAEV, S. K., Boiling of liquids on fine wire under natural convection conditions, 25:18583
KOROVIN, S. S., Extraction for separation and isolation of rare metals, 25:18510
KORPUSOV, G. V., Determination of the distribution constants of trivalent cerium in extraction by neutral alkyl phosphonates, 25:18516
KORSUNSKII, M. I., Electrostatic spectrometer of charged particle beams with ring focussing in the field of a cylindrical condenser, 25:18849
KORYAKI, Yu. I., Nuclear power plants, 25:20549 (AEC-tr-7187)
KOSHKAREV, D. G., Measuring the Coulomb frequency-shift of betatron oscillations, 25:20171
KOS'KIN, Yu. P., Current distribution in mhd channels with solid electrodes of finite resistance, 25:19542
KOSTIAL, Krista, Direct counting of ^{47}Ca and ^{85}Sr in biological samples, 25:18997
KOSTIN, B. F., Search for the decay $\mu^+ \rightarrow e^+ + e^+ + e^-$, 25:19891 (JINR-P1-5542)
KOSTKA, P., Calculated properties of a three-electrode ''single'' lens, 25:20152
KOSTOMAROV, D. P., Energy balance of plasma in Tokamak-type systems, 25:19654
KOTELNIKOV, Yu. N., Material balance of plasma column and gas sheath in toroidal apparatus-Tokamak-3, 25:19657 (MATT-Trans-16)
KOVACH, J. L., Evaluation of activated carbon supported isotope exchange techniques for containment atmosphere purification, 25:18385 (CONF-700816-(Vol.1), pp 278-88)
KOVACS, I., Production of spontaneously fissioning isomers of U, Pu, and Am in neutron reactions, 25:20369 (JINR-P3-5528)
KOVARIK, Vincent J., Phase angle measurement system for determining and controlling the resonance of the radio frequency accelerating cavities for high energy charged particle accelerators, 25:20179
KOVDA, G. A., Survey of development on technology of processing uranium ore in U.S.S.R, 25:18491 (AEC-tr-7190)
KOWALCZYKOWA, Janina, Influence of bis(-3-hydroxypropyl) trisulfide on the peripheral blood in rats irradiated with large doses of x-rays, 25:19131
KOWALSKI, K. L., Three-particle scattering problem, 25:20103 (NP-18707)
KOYANAGI, Takami, Fundamental studies on radiation thickness gauge. V, 25:18825
KOYCHEV, K., Influence of antibody formation on permeability of erythrocytes, 25:18900
KOZEKI, Moribumi, Study on curved pipe steam generator, 25:18586
KOZLOV, A. P., Selection of conditions for rotation irradiation on gamma-therapeutic apparatus Rokus, 25:19067
KOZLOV, V. T., Relation of radiation cross-linking in special purpose elastomers to additions of chloroalkanes of various structures, 25:18434
Stabilized ions and the formation of cross links in the radiolysis of polybutadiene, 25:18467
KRAEMER, H., Evaluation of results of a study of the Th--^{233}U fuel cycle for thermal reactors, 25:20746 (JUL-644-RG)
KRAEV, M. M., Spin-half particles with an infinite maximum occupation number, 25:20079
KRAINER, E., Practical testing with colour radiography, 25:18612 (LIB/Trans-324)
KRAMAROVSKII, Ya. M., Does the electron charge change with the age of the Universe, 25:19883
KRASHIN, D. I., Change of properties of silica gel under action of gamma irradiation, 25:18427
KRASNOV, N. N., Displacement of the center of the orbit in a cyclotron due to the variation in the voltage along the accelerating gap, 25:20170
KRATOCHVIL, J., Solubility of carbon dioxide in heavy water at pressures up to 40 atm, 25:18418
KRATZ, J.-V., Half-lives of ^{87}Se and ^{88}Se, 25:20327
KRAUSHAAR, J. J., Excited states of ^{46}V, 25:20347
KREBS, Adolph T., Bubble chamber pictures as a means of demonstrating radiation distribution in biological systems, 25:18995
KRELL, Max, Repulsive effects due to the absorption in exotic atoms, 25:19485
KRESGE, A. J., Solvent isotope effects upon proton transfer from the hydronium ion, 25:18395
Vibrational analyses of liquid water and the hydronium ion in aqueous solution, 25:18399
KREUTZ, E. W., Kinetics of processes variably distributed in recovery energy, 25:19859
KRIEGER, J. B., Variational principles for expectation values applied to the ground state of the helium isoelectronic sequence, 25:19475
KRISHAN, S., Linear and nonlinear collisional processes in a plasma, 25:19687
KRISHNAMURTHY, G. T., Scintillation camera in the dynamic evaluation of renal disorders, 25:19046
KRISHNA SWAMY, K. S., Emission feature of silicate material at 30 μm, 25:19330
KRISHNASWAMY, V., Calculation of the dose distribution about ^{252}Cf needles in tissue, 25:19003
KRISTIANSSON, K., Photometric mass determination in nuclear emulsion on cosmic ray carbon. I, 25:18643 (NP-18672)
KRISTOFERSON, L., Electric probe measurements in a moving and magnetized plasma, 25:19659
KRITSKAYA, D. A., Kinetics for the radiation polymerization of solid acrylonitrile in the regions of phase transitions, 25:18440
KRONBERGER, H., Helium trubines for mk iii gas cooled reactors: the key development problems, 25:20701
KRPIC, D., Conversion ratios for M1 + E2 transitions, 25:20473
KRUMHANSL, J. A., Prog. rpt. on experimental phonon physics, 4/70--3/71, 25:20874 (NYO-2391-126)
KRUTOV, V. V., Quiet-corona temperature determined from soft x-radiation flux, 25:19418
KUAN, H. M., Giant dipole resonances in ^{11}C and ^{15}O, 25:20277
KUBO, Ken-ichi, DWBA method in deuteron stripping reaction, 25:20497
KUDRYASHOVA, L. A., Unsteady flow of mercury in a trough in a transverse magnetic field, 25:19553
KUEBBING, Richard Andrew, Transition probabilities in middle-weight nuclei, 25:20471
KUEHNELT, H., Unitarity and crossing symmetry in low-energy π--π scattering, 25:19993
KUEHNER, A. V., Dose equivalent meter designs, 25:18809
KUEHNER, J. A., Gamma-ray polarization measurements in

XUM

^{22}Na, 25:20318
KUEMMEL, H., Short-range correlations and parity impurities, 25:20488
KUGEL, H. W., Revised level scheme of ^{199}Hg following Coulomb excitation, 25:20387
KUGLER, M., Some remarks on the Quark model, 25:19978
KUHN, E., Simultaneous determination of Pu(IV) and nitric acid, 25:18350
KUJAK, Richard, Thyroid uptake of radioactive iodine. A reevaluation, 25:19051
KUKRAL, H., Molybdenum-disk-to-glass seal, 25:19188
KUKULIN, V. I., Mutual scattering of clusters, 25:20511
KULESHOV, S. P., Straight-line particle path approximation in description of high-energy hadron scattering, 25:19927
KULESZA, Romuald, Effect of O-enriched inspired air, on survival of mice irradiated with 500, 550, and 600 R, 25:19123
KULL, L. A., Safeguards applications for isotopic neutron sources, 25:18619 (BNL-50267)
KULLANDER, S., Readout of wire spark chamber by delay lines, 25:18793
KULYAKO, Yu. M., Decomposition of ammonium uranyl pentafluoride on heating, 25:18380
KUMAGAI, Katsuaki, Table of half-life, γ-ray energy, and intensity of radioisotopes, 25:20368 (JAERI-Memo-4189)
KUMAR, Sampath Sadhu, Chemical effects of radiation in benzene--bromobenzene solutions, 25:18451
KUMMER, W., Anomalies in Ward identities, 25:20070
KUMTA, U. S., Radiation sensitivity and biochemical characteristics of microflora of Bombay duck (Harpodon nehereus), 25:19163
KUNIYOSHI, S., Photofission cross sections of uranium and thorium near threshold, 25:20366 (IEA-211)
KUNTE, P. K., Orientation system for balloon-borne payloads, 25:18677
KUNZE, R., Scintillation decay of several fast organic scintillators, 25:18656
KUNZLE-LUTZ, M., Retention of inhaled Pu oxide, 25:18895
KUPPERMANN, Aron, Detection and identification of triplet states of H_2O by electron impact, 25:19499
  Puzzles in the diffusion kinetics of the radiation chemistry of aqueous solutions, 25:18447 (CALT-767-P-4-73)
KURAKINA, E. P., Experimental verification of generation of cation vacancies during irradiation of KCl crystals, 25:19858
KURBAKOV, V. I., Device for studying electron backscattering from layers of materials, 25:18823
KURGANOV, B. G., Introduction of controlled energy-mode in U-150-2 cyclotron of Inst. of Nuclear Physics of UzbSSR Academy of Sciences, 25:20216
KURI, Zen-ichiro, Photoisomerization of maleate radical anions produced in 2-methyltetrahydrofuran by γ irradiation at 77°K, 25:18457
KURIHARA, Hiroyoshi, Development of inspection methods and techniques for nuclear facilities, 25:19019
KURIL'CHIK, V. N., Extragalactic radio sources. I. Radio spectra, 25:19369
KURILKO, V. I., Transverse instability in sectional linear accelerator, 25:20215
KURITSIN, V. B., Transition of niobium into the superconducting state using nuclear magnetic resonance, 25:19628
KURIYAMA, Etuko, Influence of ^{60}Co γ-ray on potato, 25:19160
KURODA, M., Finite-energy sum rule as a test of the Pomeranchuk theorem, 25:20011
KURODA, Rokuro, Reversed-phase thin-layer chromatography of metal ions, 25:18337
KUROSU, Kenji, Study on curved pipe steam generator, 25:18586
KURSKII, Alexandr Kuzmich, Weight and radioactive concentration of aerosols, 25:18685
KURSTEDT, H. A. Jr., Temperature formulation of the space-averaged reactor kinetics equations, 25:20829
KUSHCHEVSKII, A. E., Interaction of samarium and strontium oxides, 25:19284
KUSHNERIUK, S. A., Dispersion of radioactivity in a closed coolant system, 25:20730
KUSMISS, J. H., Influence of defects on the angular correlation of positron-annihilation photons in irradiated and in deformed iron, 25:19851
KUSWA, Glenn W., Sensitive fast response electron detector, 25:18711
KUTSIAVA, N. G., Investigation of aromatic hydrocarbons of supsinskaya petroleum and their catalytic conversion in the presence of irradiated catalysts, 25:18444
KUTUKOV, G. P., Material balance of plasma column and gas sheath in toroidal apparatus-Tokamak-3, 25:19657 (MATT-Trans-16)
KUZMICHEV, V. E., Calculation of binding energy and wave function of ^{3}He by harmonic polynomial method, 25:20249 (ITF-70-51-E)
KUZ'MIN, V. A., Neutrino spectroscopy of the Sun, 25:19429
KUZ'MINOV, B. D., Dependence of anti ν on neutron energy on basis of fission energy balance, 25:20440
KUZMINOV, Ya. S., Scintillation counter with LiI(Eu) crystal for registering thermal neutrons, 25:18661
KUZNETSOV, A. P., Compression of magnetic fields by cylindrical conducting envelopes, 25:19549
KUZNETSOV, E. V., 180-liter xenon bubble chamber, 25:18783
KUZNETSOV, K. P., Experimental solenoid made of Nb_3Sn strip, 25:19588 (JINR-P8-5440)
KUZNETSOV, P. S., Investigation of the model of the 2-meter streamer chamber of the SCM-200 assembly, 25:18774 (JINR-P13-5529)
KUZNETSOV, V. M., Measurements of the asymmetry ratio of positive-pion photoproduction by linearly polarized photons, 25:19889
KVASHA, L. G., Mercury in meteorites, 25:19303
KVINIKHIDZE, A. N., Method of coherent states and factorization of dual amplitudes, 25:20120
KYRZHAN, N., Correction matrix elements for the first forbidden β^- transition in ^{198}Au, 25:20438

L

LABIE, E., Elastic scattering of 23-MeV alpha particles by ^{40}Ca, 25:20310
LACOMBE, P., Contamination of Nb by O during electrolytic polishing and annealing under vacuum, 25:19171
  Deformation and rupture of Nb between -196°C and 20°C, 25:19217
  Study of the changes in the mechanical properties of Nb with different impurity contents between 20 and 850°C, 25:19212
LADIKOV-ROEV, Yu. P., Influence of dissipative processes in casing on stability of surface of liquid metal, 25:19551
LADYGIN, A. Ya., Post-irradiation study of BR-5 standard fuel elements containing UC, 25:20791
LAENSIMAEKI, Marja, Stable lead and radiolead in air filter samples, 25:18933 (NYO-3446-14, Paper 32)
LAFLEUR, Philip D., Prog. rpt. on activation analysis, annual, 7/69--6/70, 25:18366 (NBS-TN-548)
LAFUMA, J., Radiological accidents rules, 25:18975 (CEA-N-1365)
LAGOWSKA-ZLOTORZYCKA, Maria, Reversion of rough to smooth forms in Brucella abortus. I, 25:18970
LAGU, A. V., Connection between the RMS charge radii and sigma/sub b//sup E1/ for trinucleons, 25:20252
LALANNE, C. M., Telecobalt therapy for carcinoma of laryngopharynx, 25:18998
LALOY, Paul, Determining position of a radioactive source, 25:18567
LAM, D. J., Magnetic susceptibilities of hexagonal Tc--Ru, Tc--Rh, and Ru--Rh alloys, 25:19874
LAM, Lui, Motion in electric and magnetic fields. I, 25:19950
LAMBERT, R. J. W., Preventive medicine in the nuclear submarine programme, 25:18972
LAMBRECHT, R. M., Scintillation decay spectrometer for resolving subnanosecond lifetimes, 25:18696
LAMOT, G.-H., Nucleon elastic scattering by ^{4}He, 25:20261
LAMOUREUX, G., Directional correlations of gamma rays in ^{152}Sm and ^{152}Gd, 25:20385
LAMPE, Isadore, Radiation therapy of carcinoma of the tonsillar region, 25:19085
  Radiotherapeutic principles and viewpoints, 25:19081
LAMPTON, Michael, Feedback control of proportional counter gain, 25:18658
LANDAU, R. W., Stability of relativistic anisotropic plasmas to perpendicular magnetosonic waves, 25:19712
LANDAUD, G., Readout of wire spark chamber by delay lines, 25:18793
LANDE, A., Computation of Moshinsky brackets by direct diagonalization, 25:20526
  Triton binding energy calculations, 25:20259
LANDECKER, T. L., Galactic metre wave radiation, 25:19388
LANDSHOFF, P. V., Some recent work in Regge theory: Regge cuts, the absorption model, and Glauber theory, 25:19992
  Veneziano-like model for a two-current amplitude, 25:19954
LANDSPERSKY, Hanus, Changes in residual carbon content in UO_2 pellets during decarbonization and initial phases of sintering, 25:19274
LANDSTREET, J. D., Detection of circular polarization in a second white dwarf, 25:19329
LANE, Kenneth D., Approximate chiral symmetry and leakage contributions to Fubini--Furlan K/sub 13/ sum rule, 25:19970
LANE, Kenneth Douglas, Chiral symmetry breaking and the K/sub 13/ and K/sub 14/ form factors, 25:20041
LANG, Kenneth R., Interstellar scintillation of pulsar radiation, 25:19351
LANGEVIN, Michel, First T = 2 state of ^{32}S, 25:20316
LANGKAU, R., Scintillation decay of several fast organic scintillators, 25:18656
LANSIART, Alain, Particle detector, 25:18698
  Recording diffraction patterns, 25:18859
  Stationary detector for visual display, 25:18689
LANZOLA, E., Radioactivity of foods in Province of Pavia, 25:18942
LAPIN, N. I., Charged pion photoproduction on ^{27}Al nucleus, 25:20341
LAPITSKII, Yu. Ya., Plasma boundary of an ion source, 25:20174
LAPSHIN, V. G., Device with snap-off diode for compensation of influence of pulse amplitude spread of scintillation and Cherenkov counters, 25:18639 (IFVE-SEF-69-44)

LAROZE, L., Calculations on the three-nucleon system using a separable expansion of local potentials, 25:20538
LARREA, Francoise, Ratio of ^{236}Np isomers in ^{238}U deuteron interactions, 25:20389
LARSSON, Boerje, Histopathology of late radiolesions, 25:19124
LASAREV, Yu. A., Production of spontaneously fissioning isomers ^{242}Am^{f} and ^{244}Am, 25:20412
LASKER, Barry M., High-frequency stellar oscillations. V, 25:19309
LASKORIN, B. N., Survey of development on technology of processing uranium ore in U.S.S.R, 25:18491 (AEC-tr-7190)
LATTER, G., Theory identification for mechanical behavior of polystyrene bead foams, 25:19293 (UCRL-50952)
LAU, S. Y., Measurement of absorbed dose rate from terrestrial background radiation in Hong Kong, 25:19006
LAUE, H. J., Fast breeder reactors, 25:20708
LAUTRUP, B., New theoretical value for Lamb shift, 25:19512 (CNRS-CPT-70-P-335, pp IV.16-25)
LAVRUKHINA, A. K., Study of distribution of Sc, Ce, and Eu between the various phases of meteorite matter, 25:19302
LAWIN, H., Identification of μs-isomers among primary fission products, 25:20430
LAZAREV, Yu. A., Spark fission-fragment counter, 25:18671
LAZARSKA, B., Polarization of protons from ^{12}C(d,p)^{13}C reaction at E/sub d/ = 12.4 MeV, 25:20287
LAZUTIN, E. V., Structure of cross section of photoneutron reaction on ^{208}Pb nucleus in the region of a giant dipole resonance, 25:20437
LEBEDEV, A. N., Intense electron beam autoacceleration, 25:20220
LEBOUCHE, Michel, Vacancy quenching in Nb, 25:19245
LECOUTURIER, Daniel, Decay of ^{155}Ho, 25:20405
LECROART, H., Interpolation device for quick exploitation of resistance networks, 25:20868 (MATT-Trans-7)
LECROSNIER, D. P., High-energy boron implantation into silicon, 25:19784
LEE, Chul, Thermoluminescent properties of Korean natural quartz for possible use in γ-ray dosimetry, 25:18813
LEE, G. F., Fitting of double exponenial lifetime spectra using a maximum likelihood technique, 25:19881
LEE, Hee Yong, Thermoluminescent properties of Korean natural quartz for possible use in γ-ray dosimetry, 25:18813
LEE, Joseph Y. C., Polymerization of arylacetylenic compounds, 25:18441
LEE, Martin A., Supraluminous waves in a relativistic anisotropic plasma, 25:19733
LEE, Sang Hoon, Behavior of iodine in sodium systems, 25:20760 (CONF-700816-(Vol.1), pp 356-72)
LEE, Sang Soo, Detection of ^{235}U fission fragments by solid state track recorder using cellulose nitrate, 25:18724
LEE, T. D., Questions of Lorentz invariance in field theories with indefinite metric, 25:20073
LEEPER, Dennis B., Mitotic inhibition and its relation to survival in S-180 ascites tumor cells in vivo following fractionated exposures of x-radiation, 25:19091
LEFEBVRE, J. C., Biochemical considerations on alveolar retention of liquid rare earth aerosols, 25:18889 (CEA-CONF-1676)
LEFIK, V., Decays in broken SU(6)/sub W/ symmetry, 25:20047
Decays in broken SU(6)/sub W/ symmetry, 25:20048
LEFUR, R., Telecobalt therapy for carcinoma of laryngopharynx, 25:18998
LEGA, J., Elastic scattering of 23-MeV alpha particles by ^{40}Ca, 25:20310
LEGGETT, R. D., Fission gas bubble precipitation and growth in PuO_2--UO_2 under irradiation, 25:19290 (WHAN-SA-15)
LE GO, R., Comparative study on whole-body exposure injuries, 25:19012 (CEA-CONF-1695)
Radiological accidents rules, 25:18975 (CEA-N-1365)
LE GO, Roland, Biological dosimetry of an ultraviolet radiation source using Saccharomyces cerivisiae, 25:18981 (CEA-N-1380)
Hematological and chromosomic aspects of dosimetry in irradiated man, 25:18980 (CEA-CONF-1698)
LE GOFF, P., Kinetics and mechanisms involved in the siliconization of Nb and the oxidation of niobium silicides at low pressures and high temperatures, 25:19258
LEHANE, J. A., Hydromagnetic-wave propagation in inhomogeneous magnetic fields, 25:19732
LEHMANN, A. R., Double-strand breaks in DNA of mammalian cell after x-irradiation, 25:18911
LEHR, Pierre, Zirconium oxidation under a low oxygen pressure, 25:19178
LEITNER, E., First results of lung function diagnostic methods in nuclear medicine, 25:19044
LEKSELL, Lars, Histopathology of late radiolesions, 25:19124
LEMAIRE, H., Application of photoelectron spectroscopy to chemical analysis, 25:18338 (CEA-CONF-1725)
LEMAIRE, Marie-Claude, Excited states of ^{17}O and ^{29}Si, 25:20271 (NP-18628)
LEME, M. P. T., Decay constant for spontaneous fission of ^{238}U, 25:20429
LEMLEY, J. R., High resolution fission cross section of ^{235}U from 20 eV to 100 keV, 25:20418
LENC, J. F., Pyrochemical processing of fuel materials and scrap containing ^{239}Pu, 25:18492 (ANL-7709)
LENCIONI, D. E., Measurement of plasma conductivity for electric fields larger than the runaway field, 25:19672
LEONARD, A., Radiation-induced translocations in spermatogonia of mice, 25:18948
Rate of translocations induced in spermatogonia of mice by two x-irradiation exposures separated by varying time intervals, 25:18958
LEONG, George F., Acute lethality and recovery of goats after 1 MVp x-irradiation, 25:19115
LEONOV, V. F., Amplifier for semiconductor gamma detectors, 25:18668
LEONTIADIS, I. L., Theory of chemical effects produced by isomeric transition of /sup 82m/Br in liquid organic systems, 25:18489
LEQUAIS, Jean, Stationary detector for visual display, 25:18689
LERCH, Irving A., Response of Photobacterium fischeri MAV exposed to an ultra high dose-rate pulsed electron beam, 25:19154
LERCHE, I., Space-charge waves in a trapped relativistic plasma, 25:19734
LEROY, Marcel, Radiation detecting device, 25:18688
LESHCHENKO, S. S., Action of ionizing radiation on the structure and properties of the copolymer of styrene with 2-ethylhexyl acrylate, 25:18436
LESKOVEC, R. A., High performance linear emitter follower, 25:18860
LESLIE, J. D., Self-resonant current peaks in Josephson junctions, 25:19612
LESNIAK, H., Energy dependence of coherent production cross section in nuclei, 25:20029
LESNIAK, L., Energy dependence of coherent production cross section in nuclei, 25:20029
LESUEUR, R., Measurement of partial outgassing flux of Mo and W at 2000°K, 25:19225
LETTAU, H., Elastic tau scattering on nuclei with A = 15 to 18 at 11 MeV, 25:20278
LEVAN, H., Polaroid film in radiation dosimetry and survey, 25:19005
LEVCHENKO, Yu. D., Velocity field of turbulent fluid flow in a longitudinal streamline of clusters of rods, 25:18576 (AEC-tr-7189)
LEVENTHAL, J. J., Study of calibration, resolution, and transmission of electrostatic velocity selector, 25:18843
LEVITSKII, L. S., Equatorial zone of avoidance of solar cosmic-ray arrival, 25:19437
LEVKOVICH, A. D., Contribution of the scintillator to the resolution of a spectrometer using the single-electron method, 25:18745
LEVY, N., Three-dimensional elastic--plastic stress and strain analysis for fracture mechanics. Phase I. Simple flawed specimens, 25:18611 (HSSTP-TR-12)
LEVY, Naomi, Veneziano model for process $V_1 + \pi \to V_2 + \pi$, 25:19997
LICSANDRU, E., Thermodynamic analysis of saturated steam cycles and of direct thermal cycles for nuclear power stations, 25:20596
LIKHONINA, E. A., Methods for electrophoretic and chromatographic analysis of azo compounds. III, 25:18347
LILIENFELD, Pedro, Beta-absorption-impactor aerosol mass monitor, 25:18821
LIN, S. H., Scattering and capturing by inverse fourth-power potential in low-energy range, 25:19500
LIN, Wing-fai, Isotope-shift of nuclear charge distributions, 25:20486
LINDAHL, A., Alpha decay of neutron-deficient radon and polonium isotopes, 25:20451
LINDBERG, L., Electric probe measurements in a moving and magnetized plasma, 25:19659
LINDBERG, Robert D., Elective irradiation of the neck lymphatics for squamous cell carcinomas of the nasopharynx and oropharynx, 25:19084
LINDEMAN, H., Lifetime measurements of alpha emitters in the millisecond region, 25:18703
LINDGREN, R. A., Doppler shift studies with selected recoil directions, 25:20140
LINDOW, J. T., Scattering of fast neutrons by ^{12}C, ^{54}Fe, ^{56}Fe, ^{58}Ni, and ^{60}Ni, 25:20338
LINGNER, H., Precipitate formation. I, 25:20885 (RFP-Trans-74(Pt.1))
LINGNER, Harald, Precipitate formation. II, 25:20886 (RFP-Trans-74(Pt.2))
LINNFORS, A., Decay of ^{249}Cf, 25:20398
LIONS, Noel, Remote positioning of thermocouples, 25:20842
LIOU, M. K., Non-coplanar proton--proton bremsstrahlung calculations including the relativistic spin corrections, 25:19947
LIPKIN, H. J., Mirror transitions and second class currents, 25:20535
LIPOVSKII, A. A., Investigation of complex formation in the system UO_2^{2+}--H_2SO_4--HF--TOA, 25:18381
LIPSICAS, Max, Prog. rpt., annual, 2/70--2/71, 25:20876 (NYO-3978-4)
LIPSKI, Slawomir, Effect of O-enriched inspired air, on survival of mice irradiated with 500, 550, and 600 R, 25:19123

LISCIA, A., Mechanical and metallurgical steel/Zr junctions, 25:19183
LISTER, G. G., Effect of Hall current and resistivity on stability of gas--liquid system, 25:19546
LITEANU, C., Precipitate formation. I, 25:20885 (RFP-Trans-74(Pt.1))
LITEANU, Candin, Precipitate formation. II, 25:20886 (RFP-Trans-74(Pt.2))
LITTLE, H. W., Distribution of types of uranium deposits and favorable environments for uranium explorations, 25:18532
LITTLEFIELD, Peter S., Pressurized gas monitor for low level radioactive gases, 25:18744
LITTLETON, C. P., HPRR and accelerator operations, 25:20134 (ORNL-4584, pp 187-97)
LITVINENKO, A. S., Electron-scattering study of the change of the charge radii of nuclei of iron and nickel isotopes, 25:20334
LIU, C. H., Long-wavelength ion-acoustic waves in a magnetoplasma in a gravitational field, 25:19736
LIUKKONEN, E., Level structure of ^{120}Sn from decay of ^{120}In and ^{120}Sb isomers, 25:20401
LIVESEY, D. J., UKAEA fuel test assemblies irradiated in HBWR, 1964--66, 25:20736 (HPR-132)
LIVSHITS, M. A., Quiet-corona temperature determined from soft x-radiation flux, 25:19418
LKHAGVA, O., Motion of particles in the fixed centers field, 25:20059 (JINR-P4-5547)
LO, C. C., Spark gap trigger amplifier with 1-msec recovery time, 25:18791
LOBANOV, Yu. V., Potential identification of products of heavy-ion-induced nuclear reactions, 25:20419
LOBERG, Bengt, Combined field-ion and electron microscope studies of grain boundaries in tungsten, 25:19249
LOCKER, A., Radioprotective effects of psychotropic drugs, 25:19028
LOCKETT, G. E., Dragon project engineering studies on the direct cycle HTR, 25:20703
LOCKWOOD, Grant J., Total cross section for single electron loss by Ne and Ar in nitrogen, oxygen, and air, 25:19492 (SC-RR-70-735)
LODGE, J. G., Elastic scattering of positrons by hydrogen molecules, 25:19501
LOEBACH, E., Tandem mass spectrometer for secondary ion studies, 25:18841
LOEFGREN, H., 4f electronic states in the metals Nd, Sm, Dy, and Er studied by x-ray photoemission, 25:19866
LOGAN, K. W., Inelastic neutron scattering from solid benzene, 25:20247
LOGSDON, Donald F. Jr., Reduction of radiation hazard in tritium method of measuring total body water, 25:18977 (AD-702155)
LOGUNOV, A. A., Equal-time equation for two-particle system in quantum field theory, 25:20077
  Results on complex adjustment and start-up of the IHEP proton synchrotron, 25:20127 (CERN-Trans-70-12)
LOKAJICEK, M. V., Unstable system with N states and propagator matrix, 25:19930
LOKTIONOV, V. A., Solubility of O in Hf--Nb alloys, 25:19240
LOMBARD, R., Study of (p,d) reactions on ^{118}Sn and ^{119}Sn with polarized protons, 25:20365 (CEA-CONF-1657)
LONE, M. A., Reaction ^{115}In(n,γ)^{116}In, 25:20410
LONG, H., Measurement of neutron spectrum at beam hole of FRJ-1 reactor in energy range from 10 keV to 10 MeV, 25:20798
LONG, William H., Aircraft nuclear propulsion system, 25:20810
LONG II, Thomas Veach, Resonance phosphorescence, Raman scattering, and decomposition of hexaamminechromium(III) salts utilizing He--Ne laser excitation, 25:18404
LONGSON, B., Solubility of carbon in sodium, 25:19196 (TRG-Report-1906)
LONGSTAFF, T. N., Development of a specification for heat exchanger plant to suit a gas turbine htr, 25:20776
LO NIGRO, S., Fission of ^{238}U induced by neutrons at energies near threshold, 25:20393
LONNGREN, K. E., Time-of-flight study of waves guided by a plasma column, 25:19746
LOOMIS, William F. Jr., Prog. rpt. on genetic analysis of development of slime molds, 3/71, 25:20904 (UCSD-34-P-166-X-2)
LOPATO, L. M., Interaction of samarium and strontium oxides, 25:19284
LORENZI, P., Micrologic integrated circuit for monitoring correlation in pulse sequences, 25:18701
LORENZI, R., Readout of wire spark chamber by delay lines, 25:18793
LOS, J., Diffusion coefficients of isotopic mixtures of CO and N_2, 25:18604
  Residence time measurements for surface ionization of K on W, 25:19210
LOSKUTOV, V. F., Diffusion in nitrided Nb, W, and Fe--Si alloys, 25:19234
LOTTS, A. L., Status and progress report for thorium fuel cycle development for January 1, 1969--March 31, 1970, 25:19260 (ORNL-4629)
LOUCK, J. D., Identity satisfied by Racah coefficients of U(n), 25:20034
LOUGHEED, R. W., Spontaneous-fission half-life of ^{258}Fm and nuclear instability, 25:20443
LOVE, I., Nuclear screening tensors and nuclear spin coupling tensor, 25:20517
LOVE, W. G., Inelastic scattering, charge exchange, and knock-out reactions, 25:20508
LOVEDAY, George Christopher, Detecting apparatus for radiation, 25:18686
LOW, F. E., Helicity poles, triple Regge behavior and single particle spectra in high energy collisions, 25:19926 (NYO-2262-TA-234)
LOWE, L. F., Resistivity and annealing properties of implanted Si:H^+, 25:19822
LU, P., Approximate description of Coulcmb scattering, 25:19945
LUBIN, Moshe J., Electromagnetic radiation from a laser-produced plasma expanding into a uniform magnetic field, 25:19679
LUCKE, J., Prediction of fatigue lives of 2024-T3 and 6061-T6 aluminum alloys under broad-band excitation, 25:20895 (SCL-CR-710175)
LUENING, K. G., Testing for recessive lethals in mice, 25:18956
LUHMAN, T. S., Effect of omega phase reversion on the superconducting transition in titanium-base alloys, 25:19590
LUK'YANOVA, L. A., Reduction of uranium tetrafluoride vapors by certain metals, 25:18372
LUNAU, Wigand, Moisture determination in solids by neutron radiation, 25:18362
LUND, J. O., Plasma renin measured by radioimmunoassay for angiotensin, 25:18920
LUPU, Gheorghe, Solution of Boltzmann equaticn for fully ionized plasma in oscillatory electric fluid and magnetic steady field. III, 25:19692
  Solution of Boltzmann equation for fully ionized plasma in oscillatory electric field and magnetic steady field. IV, 25:19691
LUSHCHIKOV, V. I., Experiments with ultracold neutrons, 25:20232 (JINR-P3-5392)
LUSIGNAN, B. B., Polarization of solar Type-III radio bursts at 25.3 MHz, 25:19399
LUTSENKO, S. M., Effect of microwaves on revascularization of the blood supply in free skin grafts, 25:19104
LUTZ, M., Pulmonary retention and disposal of plutonium oxide, 25:18891 (LF-tr-46)
LUUKKO, A., Proton reactions on ^{23}Na, 25:20325
LUX, B., Protection of Nb against oxidation, 25:19176
LUZOV, A. A., Structure of the interplanetary space from data on annual cosmic-ray variations, 25:19526
LYNN, K. R., γ-irradiation of dilute solutions of chymotrypsin: protein substrates, 25:18907
LYNN, P. P., Finite element analysis of plate bending with transverse shear deformation, 25:18575
LYNNWORTH, L. C., Prog. rpt. on ultrasonic thermometry in LMFBR systems, 7--9/70, 25:18830 (NYO-3906-12)
LYS, L. A., Heat exchangers for gas turbine fast reactors, 25:20775
LYSENKO, Z. V., Data transmission in measurement-computing complex of the Joint Inst. for Nuclear Research, 25:18845
LYSKOVICH, A. B., Scintillation characteristics of pure and activated cadmium iodide crystals, 25:18665
LYTTON, Jack L., Prog. rpt. on relationship of nitrogen content to susceptibility of austenitic stainless steels to stress corrosion, 9--11/70, 25:20898 (TID-25664)

M

MA, Benjamin M., Reactor stress analysis in nuclear engineering education, 25:18616
MACCALLUM, M. A. H., Thermodynamics and cosmology, 25:19464
MACDONALD, C., Hall effect and sheet resistivity as function of temperature on P implants in Si, 25:19838
MACDONALD, G. H., Radio structures of seventy-nine quasi-stellar objects, 25:19350
MACFADYEN, N. W., Crossing symmetric expansions of physical scattering amplitudes: O(2,1) group and Lame functions, 25:20105
MACFARLANE, R. D., Natural alpha radioactivity of Sm, 25:20391
MACFARLANE, Ronald D., Prog. rpt. on on-line alpha and proton decay spectrometry, annual, 1970, 25:18737 (ORO-3820-7)
MACGREGOR, G. A., Evaluation of an LN_2-temperature solid state spectrometer for rocket borne experiments, 25:18654
MACHADO, J. Ottilio L., Activity of ionizing radiation on fertile eggs of Triatomideos-Rhodnius prolixus, 25:19099
MACIAS, E. S., Decay scheme of 25 min /sup 131g/Te, 25:20428
MACK, John E., Role of soft galactic x rays in the alignment of interstellar grains, 25:19447
MACKENZIE, I. K., Coincidence technique for study of Ge(Li) detector profiles, 25:18759
MACKLIN, R. L., Fast neutron capture cross section facility, 25:20149
  Proton recoil monitor for neutron flux measurements, 25:18763

Use of a pulsed Van de Graaff accelerator and time-of-flight techniques to reduce backgrounds in (α,γ) spectroscopy experiments, 25:20148
MACQ, P. C., Elastic scattering of 23-MeV alpha particles by ^{40}Ca, 25:20310
MADSEN, V. A., Core-polarization effects in charge-exchange reactions; application to ^{58}Ni(^{3}He,t), 25:20496
MAEDA, Kenjiro, Studies on the fluidized bed calcination of high level radioactive liquid wastes, 25:18630
MAEDA, Takao, Unusual elastic properties of Gd and Invar, 25:19224
MAFRA, O. Y., Photofission cross sections of uranium and thorium near threshold, 25:20366 (IEA-211)
MAGDON, E., Effect of 6-azauridine on labelling index and mean grain count of Ehrlich-carcinoma ascites cells, 25:18888
MAGNON, A., Measurement of the muonium hfs splitting and of the muon moment by double resonance, and a new value of α, 25:19888
MAHAUX, C., Hole potential energy in nuclear matter calculations, 25:20540
MAIER, I., Structure and stabilities of free radicals formed in γ-irradiated glycine, 25:18478
MAILFERT, A., Behavior of Type-II superconductors in time-dependent magnetic fields, 25:19598
Rotating electrical machines using superconductors, 25:19635
MAILLET, E., Simple, compact, nuclear gas turbine for integration in the reactor vessel, 25:20774
MAIN, I. G., Angular correlation studies in ^{34}S, 25:20348
MAISON, Jean-Marie, First T = 2 state of ^{32}S, 25:20316
MAJKRZAK, Charles P., Hydrospace energy converter, 25:18600
MAJUMDAR, A. K., 1-(2-carboxy-4-sulphonatophenyl)-3-hydroxy-3-phenyltriazene as spectrophotometric reagent for Cu(II) and Pd(II) in Fe, Mo, and V, 25:18342
MAKAROV, Yu. V., Experimental solenoid made of Nb_3Sn strip, 25:19588 (JINR-P8-5440)
MAKINO, Isao, Isotope dependence in K-, L-, and M-shell ionization cross sections by proton and deuteron bombardments, 25:19470
MALARBET, Jean-Louis, Biological dosimetry of an ultraviolet radiation source using Saccharomyces cerivisiae, 25:18981 (CEA-N-1380)
MALARODA, R., Measurements of neutron spectrum of Am--Be source, 25:18761
MALFLIET, Rudi, Three-nucleon calculations using the Faddeev equations, 25:20251 (NP-18678)
MALIN, S., Infinite-dimensional representations of Lorentz group, 25:20033
MALININ, V. F., Possibility for determining porosity, density, and mineral composition of rocks by gamma-ray absorption, 25:18524
MALINOVSKII, A. A., Certain biological prerequisites of longevity in mammals and man, 25:20847 (ANL-Trans-875)
MALJKOVIC, Tea, Direct counting of ^{47}Ca and ^{85}Sr in biological samples, 25:18997
MALLI, Gulzari, Accurate numerical Hartree--Fock self-consistent-field wave functions for rare-earth ions, 25:19478
MALMIN, R. E., Coupled-channel analysis of α-particle scattering from the 5.23 MeV natural parity state of ^{24}Mg, 25:20344
MALMQVIST, L., Photometric mass determination in nuclear emulsion on cosmic ray carbon. I, 25:18643 (NP-18672)
MALMSKOG, S. G., Transition rates in ^{192}Au, 25:20453
MALONEY, C. R. C., Comparison of switching speeds of implant auto-registered and diffused mist, 25:18858
MALYSHEV, E. K., Low-activated trigger chamber containing ^{3}He, 25:18662
MAMRUKOVA, V. P., Structure of the interplanetary space from data on annual cosmic-ray variations, 25:19526
MANABE, Genroku, Trial fabrication of an Na-bonding fuel rod, and its out-of-pile test, 25:19276
MANCHESTER, R. N., Observations of galactic OH, 25:19381
MANDULA, Jeffrey, Patterns of exchange degeneracies, 25:20124
MANHEIMER, Wallace M., Nonlinear stabilization and harmonic generation, 25:19723
MANLEY, A. W. J., Ion analysis of rf-excited deuterium ion sources, 25:20150
MANNING, P. G., Silica minerals in interstellar dust, 25:19453
MANOUKIAN, E. B., Wave operators in time-dependent potential scattering for long-range potentials, 25:20108
MANSON, Steven Trent, Minima in atomic continuum generalized oscillator strengths, 25:19476
MANTHURUTHIL, J. C., Conversion electron measurements in decay of ^{156}Tb, 25:20472
MANYUKOV, B. A., Computation of kinematic parameters of electron tracks in bubble chambers, 25:18784
MARAFANTE, E., Arylsulfatase activity in the urine of the irradiated rat, 25:18905
MARCAL, P. V., Three-dimensional elastic--plastic stress and strain analysis for fracture mechanics. Phase I. Simple flawed specimens, 25:18611 (HSSTP-TR-12)
MARCHENKO, N. A., Structure and properties of an [electrodeposited] In--Zn alloy, 25:19221
MARCHETTI, R., Radioactivity of foods in Province of Pavia, 25:18942
MARCHUK, G. I., Use of numerical methods for neutron cross section calculations, 25:20530
MARCUS, Future of reprocessing in Europe, 25:18500 (NP-18669)
MARGUERRE, F., Rivers cannot take up heat at choice. 13 GW at the upper Rhine, 25:20685
MARHIC, C., Comparison between the oxidation of Nb and that of a Nb base alloy (P353M), 25:19172
MARIK, P., Modification of NLZ 716a-T pulse height analyzer, 25:18862
MARINE, J., Properties of ion-implanted ZnTe, 25:19794
MARIWALLA, K. H., Does a uniformly accelerated charge radiate, 25:19944
MARKOV, B. N., Production of spontaneously fissioning isomers ^{242}Am and ^{244}Am, 25:20412
Spark fission-fragment counter, 25:18671
MARKOV, Konstantin Petrovich, Weight and radioactive concentation of aerosols, 25:18685
MARKOVSKI, B. L., Method of coherent states and factorization of dual amplitudes, 25:20120
MARNER, W. J., Heat transfer to a Bingham plastic in the entrance region of a circular tube, 25:18588
MARONI, C., Use of a checker board counter in blocking experiments, 25:18679
MARSDEN, D. A., Energy dependence and depth distribution of lattice disorder in ion-implanted silicon, 25:19832
MARSH, O. J., Electrical properties of Cd, Zn, and S ion-implanted layers in GaAs, 25:19842
Ion-implanted junctions and conducting layers in SiC, 25:19847
MARSHAL, C. J., Precipitation conditions in the uranyl nitrate--ammonium hydroxide system, 25:18379
MARSHALEK, Eugene R., Relation between Belyaev--Zelevinskii and Marumori boson expansions, 25:20521
MARSHALL, H. P., Structure of nitroform in various solvents, 25:18391
MARSHALL, T. C., Formation of ion-acoustic collisionless shocks, 25:19698
MARTALOGU, N., Reaction mechanism for proton scattering on ^{60,64}Ni and ^{66,68}Zn, 25:20322
MARTIN, A., Some exact results on $\pi\pi$ scattering, 25:19991
MARTIN, Alexander, Nucleon--nucleon scattering in the one-boson-exchange approximation, 25:20024
MARTIN, D. T., Phosphorescent components in CsI(Tl) and CsI(Na), 25:18648
MARTIN, E. C., Radiation-induced copolymerization of styrene and cellulose at low dose rates, 25:18446
MARTINSKA, G., Monte Carlo generation of neutral $\pi^{-}p$ interactions at 5 GeV/c in propane bubble chamber, 25:20004 (JINR-P13-5516)
MARUYAMA, Masatomo, Reprocessing of spent fuel, 25:18631
MASLENNIKOV, E. A., Use of nitrites to obtain and maintain a very high vacuum in thermonuclear equipment, 25:19728
MASLENNIKOV, S. I., Device for multiparametric investigation of nuclear fission, 25:18670
MASLENNIKOVA, N. V., Effect of γ-radiation on amino acid composition of muscular tissue of fish, 25:19110
MASON, J. F., Decay of ^{90}Kr and ^{90}Rb, 25:20384
Level structures of ^{91}Rb and ^{91}Sr as populated in beta decay, 25:20459
MASSA, I., Use of a checker board counter in blocking experiments, 25:18679
MASSA, I. G., Computer-simulated flux measurements for ions channeled in diamond structure lattices, 25:19804
MASTERS, B. J., Radiochemical determination of damage profiles in silicon, 25:19817
MASUDA, Kohzoh, Enhanced diffusion in ion-implanted silicon, 25:19823
MASYAGIN, V. E., Electrostatic spectrometer of charged particle beams with ring focussing in the field of a cylindrical condenser, 25:18849
MATHER, D. S., Evaluation of anti ν for ^{239}Pu, 25:20363 (AWRE-O-86/70)
MATHEWS, D. R., Review of Gulf General Atomic support of the High Temperature Lattice Test Reactor program, 25:20787 (GAMD-10231)
MATHIE, F., First results of lung function diagnostic methods in nuclear medicine, 25:19044
MATHUR, V. S., Connection between the RMS charge radii and sigma/sub b//sup E1/ for trinucleons, 25:20252
MATOBA, M., Stabilization of spectrum with no reference peaks, 25:18867
MATOS DIAS, J. M., Uranium deposits in Portugal, 25:18537
MATOUS, J., Solubility of carbon dioxide in heavy water at pressures up to 40 atm, 25:18418
MATSUDA, H., Influence of a toroidal electric fringing field on the trajectories of charged particles in a third order approximation, 25:20139
MATSUMOTO, Katsumi, Housing building for D_2O critical assembly, 25:20802
MATSUMOTO, Kenichi, Research and development of fuel for liquid metal fast breeder reactor, 25:19275
MATTERN, Ullrich, Method of preoxidizing nuclear reactor components of zirconium alloys, 25:19180
MATTHEWS, J. A. J., Regge-pole model for $\pi N \to \omega N$, 25:20008
MATTHEWS, J. R., Calculation of stress in fast reactor fuel elements, 25:20732 (AERE-R-6516)
MATTIOLI, M., Production of plasma by laser irradiation of lithium hydride pellets, 25:19702
Recombination processes during the expansion of a laser-

XUM

produced plasma, 25:19697
MATTOS ASSUMPCAO, H., Activity of ionizing radiation on fertile eggs of Triatomideos-Rhodnius prolixus, 25:19099
MATVEEV, V. A., Straight-line particle path approximation in description of high-energy hadron scattering, 25:19927
MATYASH, P. P., Device for measuring total proton cross sections of reactions, 25:20176
MATYUSHIN, A. T., Investigation of the model of the 2-meter streamer chamber of the SCM-200 assembly, 25:18774 (JINR-P13-5529)
MATYUSHIN, V. T., Investigation of the model of the 2-meter streamer chamber of the SCM-200 assembly, 25:18774 (JINR-P13-5529)
MAUDERLI, Walter, Coordinate measuring device for radium applications, 25:19004
  New dose calibrator for nuclear medicine, 25:18723
MAURA, Giancarlo, Detection of traces of transition metals by formation of peroxy compounds and sorption on a chelating resin, 25:18343
MAURENZIG, P. R., Spins and parities of highly excited states in ^{24}Mg, 25:20291
MAURIN, A. F., Relationship between electric resistance of zirconia ceramics and porosity, 25:19283
MAVINKURVE, S. S., Radiation sensitivity and biochemical characteristics of microflora of Bombay duck (Harpodon nehereus), 25:19163
MAXIA, Vera, Some Italian meteorites trace elements content by nondestructive neutron activation analysis, 25:18370
MAYAHI, M. F., Prog. rpt. on preservation of dates by γ-radiation, 10/70, 25:19158 (NP-18679)
MAYER, B., Study of (p,d) reactions on ^{118}Sn and ^{119}Sn with polarized protons, 25:20365 (CEA-CONF-1657)
MAYER, H., Symmetric integral equations derived from Faddeev equations, 25:19516
MAYER, Hans, Nuclear power plant with wet-steam generator and steam drying system, 25:20743
MAYER, I., EPR spectra of irradiated solid glycine, 25:18468
MAYER, J. W., Analysis of disorder distributions in boron-implanted silicon, 25:19830
MAYER, W., X-ray observations of pulsars, 25:19359
MAYNARD, C. Douglas, Selenomethionine ^{75}Se thymus scans in myasthenia gravis, 25:19049
MAYNARD, George Herbert, Removing matter from filter elements, 25:18572
MAYR, H. G., Ion chemistry and thermal balance in E and F regions above Wallops Island, 25:19575
MAZEY, D. J., Formation of insulating layers by use of reactive ion beams, 25:19781
  Void formation during high-dose ion implantation at elevated temperatures, 25:19807
MAZOT, P., Study of hardening due to interstitials between 20 and 1200°C in Nb and Nb alloys, 25:19213
MCALLISTER, J. D., Possible utilization of the Carnegie-Mellon synchrocyclotron for cancer therapy, 25:19087
MCCARTAN, J., Formation of an axisymmetric bulged region in a long uniform plasma column, 25:19709
MCCLAIN, W. C., Earthquakes and reactor safety, 25:18556 (ORNL-4584, pp 41)
MCCLURE, Donald Allan, Low-lying levels in spherical and rotational nuclides, 25:20324
MCCLURG, G. R., Thermomagnetic torque in deuterium gas, 25:18403
MCCORMACK, J. D., Large scale air cleaning tests in the containment systems experiment, 25:20782 (CONF-700816-(Vol.1), pp 102-27)
MCCREADY, V. R., Prototype semiconductor gamma-camera, 25:18699
MCDONALD, Lawrence Joseph, Equivalent potentials for pion--alpha scattering, 25:20253
MCDONALD, W. J., Reaction mechanism of the ^{16}O + d reactions, 25:20301
MCDONNELL, J. A. M., Switched linear acceleration technique for microparticles, 25:20183
MCEACHRAN, R. P., Elastic scattering of positrons by hydrogen molecules, 25:19501
MCGEE, R. X., Atlas of OH (1667) line profiles near the galactic center, 25:19389
  OH (1667) line absorption, 25:19382
MCGINNESS III, John Edward, Vibrational entropy of the dilute silver-gold system, 25:18367
MCGINTY, G. K., 200-kV ion-implantation equipment at MRL, Salfords, 25:19774
MCGRORY, J. B., Static quadrupole moments in A = 18 to 38 nuclei, 25:20337
MCHARRIS, Wm. C., Spurious peaks produced by Compton scattering in Ge(Li)--Ge(Li) coincidence gamma-ray spectrometer systems, 25:18754
MCILHENNY, R. C., Treatments of southern pine with vinyl chloride and methyl methacrylate for radiation-produced wood-plastic combinations, 25:19299
MCILWAIN, R. L., Off-mass-shell S-wave $\pi^+\pi^-$ scattering amplitude, 25:19994
MCINTYRE, P. M., Measurement of the muonium hfs splitting and of the muon moment by double resonance, and a new value of α, 25:19888
MCISAAC, L. D., Decay scheme of ^{141}Ba and ^{142}Ba, 25:20415
MCIVER, R. F., Dragon project engineering studies on the direct cycle HTR, 25:20703
MCKEE, R. J., Muonic x rays and capture gamma rays in ^{89}Y, 25:20360
MCKEEHAN, E. R., Design and testing of the SEFOR Fast Reactivity Excursion Device (FRED), 25:20693 (GEAP-13649)
MCKELLAR, B. H. J., Calculations for stripping on doubly magic nuclei, 25:20282
  Form factors and polarization of x-rays from nuclear reactions, 25:20423
MCLAFFERTY, F. W., Unimolecular decomposition of toluene and cycloheptatriene molecular ions, 25:18393
MCLAFFERTY, George H., Gaseous nuclear rocket engine, 25:20806
MCLAUGHLIN, Ernest O., Radiation curable paint containing a vinyl ester binder resin having pendant diester groups, 25:18439
MCMAHAN, Clyde Alex, Three-alpha final state interactions with Faddeev theory, 25:20300
MCMAHON, James J., Head and neck exposures from Panoramix roentgenography, 25:19001
MCMILLAN, D. J., Conversion electron measurements in decay of ^{156}Tb, 25:20472
MCNALLY, P. J., Ion implantation in InAs and InSb, 25:19828
MCNEILLY, C. E., Properties of molten ceramics, 25:19273 (BNWL-SA-3579)
MCNELIS, D. N., Radioiodine field studies with synthetic aerosols, 25:18926 (CONF-700816-(Vol.1), pp 49-71)
MCNELLES, L. A., Efficiency calibration of semiconductor x ray detectors, 25:18715
MCRAE, J., Lung function studies using short-lived /sup 81m/Kr and the scintillation camera, 25:19056
MEADE, R., Influence of defects on the angular correlation of positron-annihilation photons in irradiated and in deformed iron, 25:19851
MEDVECZKY, L., Audiovisual discrimination for track measurements in emulsions, 25:18728
  Processing of thin emulsions, 25:18729
MEDVEDEV, A. S., Radiation damage in selenates of divalent metals, 25:18479
MEDVEDEV, Ya. A., Electric field excited in air by pulsed γ quanta, 25:19761
MEDYANIK, V. M., Electron elastic scattering on ^{64}Zn and ^{66}Zn nuclei, 25:20345
MEE, L. K., RNA synthesis primed by γ-irradiated chromatin templates, 25:18916
MEHLIG, D., Experimental techniques for photon scattering below 140 MeV, 25:20189
MEHTA, G. K., Configuration mixing calculations in Hartree--Fock representation, 25:20286
MEHTA, M. K., States in ^{10}B from elastic scattering of alphas by ^{6}Li, 25:20292
MEIER, Michael McDaniel, Neutron polarization for (d,n) reactions in the 1p shell, 25:20272
MEIER, S., Steady-state, two-dimensional temperature distributions in single fuel element pellet and adjacent cladding due to axial varying heat transfer coefficients, 25:18589
MEISEL, Werner, Instrument representing Moessbauer spectra, 25:18743
MEISTER, R., Interconnected grid system in the seventies. Nuclear power stations make trouble, 25:20691
MELIK-GAIKAZYAN, I. Ya., Experimental verification of generation of cation vacancies during irradiation of KCl crystals, 25:19858
MELKERSSON, Sune, Mass spectral data processing. II, 25:18835
MELONI, C., Radioactivity of foods in Province of Pavia, 25:18942
MELONI, Sandro, Some Italian meteorites trace elements content by nondestructive neutron activation analysis, 25:18370
MENGEL, John G., Advanced evolution of Population II stars. I, 25:19307
MEN'SHIKOVA, T. S., Post-irradiation study of BR-5 standard fuel elements containing UC, 25:20791
MERCEREAU, J. E., Ac and dc potentials in superconducting phase-slip structures, 25:19610
MERRER, Robert J., Biamperometric titration of hexacyanoferrate(III), Fe(III), Cu(II), Ce(IV), and I, 25:18346
MERRIGAN, J. A., Scintillation decay spectrometer for resolving subnanosecond lifetimes, 25:18696
MERRILL, D., Baryon exchange in reactions K^-n + $Y\pi^-$ at 3 GeV/c, 25:19917
MERRILL, N. H., Acceptance calculations for Australian EN HVEC tandem accelerator, 25:20137
MERRIMAN, Sandra H., Computer program for calculating, tabulating, and plotting outgassing rates of selected gases, 25:19195 (ORNL-TM-3220)
MERZ, J. L., Implantation of Bi into GaP. II, 25:19846
  Ion implantation of Bi into GaP. I, 25:19845
MESHII, M., Effect of electron irradiation on the strength of iron single crystals, 25:19252 (COO-1367-36)
MESTER, A., Decay scheme of ^{146}Eu, 25:20474
METIVIER, H., Retention of inhaled Pu oxide, 25:18895
METZGER, G., Operation of sampling spark chambers, 25:18778
MEUNIER, Jean, Nuclear reactor refuelling installation, 25:20838
MEWE, R., Approximate cross sections and rate coefficients

for ionization, excitation, and recombination of hydrogenic ions and atoms, 25:19489 (NP-18680)
MEYER, D., Electrical properties of alkali implants in silicon, 25:19780
MICHAEL, W., Study of 10 GeV/c K^+-nucleus coherent interactions and Q-nucleon cross-section, 25:19913
MICHALEC, R., Single-crystal filters of thermal neutrons, 25:20238 (UJV-2488-F)
MICHAUD, W. E., High sensitivity ultrasonic test system for welds, 25:20857 (GEPP-83)
MICHEL, F. Curtis, Nonpulsing pulsars, 25:19372
MICHELSEN, P., Ion-velocity distribution function in a single-ended Q machine, 25:19670
MICHON, G., Milk as a vector of radioactive nuclides, 25:18943
MICLUTIA, M., Beta therapy with ^{90}Sr in plastic induration of the penis, 25:19072
MIETTINEN, J. K., Body burden of ^{137}Cs and radiation dose of population group in Finnish Lapland, 25:18987 (NYO-3446-14, Paper 29)
Polonium and radiolead in some aqueous ecosystems in Finland, 25:18930 (NYO-3446-14, Paper 27)
Polonium and radiolead in some land animals in Finland, 25:18929 (NYO-3446-14, Paper 26)
Radionuclides in plants and reindeer meat in Lapland, 25:18932 (NYO-3446-14, Paper 31)
MIETTINEN, Jorma K., Chemical and radioactive environmental problems in Finland, 25:18931 (NYO-3446-14, Paper 30)
Prog. rpt. on radioactive foodchains in subarctic environment, annual, 8/15/69--8/14/70, 25:18928 (NYO-3446-14)
MIEVILLE, Bernd, Separation of steam and water in boiling-water reactors and steam generators, 25:20769
MIFUNE, T., Effect of electron irradiation on the strength of iron single crystals, 25:19252 (COO-1367-36)
MIGLIETTA, F., Separation of center-of-mass motion in nuclear many-body problem, 25:20500
MIGUNOV, B. B., Spectrometric scintillation equipment of commercial application for radioactive logging of boreholes in ore deposits, 25:18814 (CSIRO-Trans-9992)
MIHAI, D., Analysis of efficiency of nuclear fuel cycles for heavy-water moderated reactors in specific conditions of socialist republic of Romania, 25:20750
MIKHAEL, Evon, Cytogenetic studies on effect of chronic gamma irradiation on Vicia faba, 25:18950
MIKHAYLOV, N. N., Superconducting alloy, 25:19618
MIKHEEV, V. S., Strength and plasticity of Ti--Nb--Zr alloys at -196 and +20°C, 25:19206
MIKHEIKIN, I. D., EPR study on stable H atoms on γ-irradiated clinoptilolites containing La, Mg, and K ions, 25:18423
MIKHLIN, E. B., Determination of the distribution constants of trivalent cerium in extraction by neutral alkyl phosphonates, 25:18516
MIKOSHIBA, Osamu, Manual for JUPITOR-1 (Supplement), 25:20479 (JAERI-Memo-4138)
MIKULA, P., Single-crystal filters of thermal neutrons, 25:20238 (UJV-2488-F)
MILANOVIC, J., Conversion ratios for M1 + E2 transitions, 25:20473
MILEY, G. H., Temperature formulation of the space-averaged reactor kinetics equations, 25:20829
MILEY, G. K., Radio structures of seventy-nine quasi-stellar objects, 25:19350
MILJANIC, D., Neutron--proton bremsstrahlung at 14.4 MeV, 25:20257
Reaction ^{11}B(n,t)^{9}Be at 14.4 MeV, 25:20285
MILLER, G. L., Position sensitive detector for a magnetic spectrograph, 25:18681
MILLER, J. G., Alpher--Rubin ultrasonic attenuation and dipolar nuclear-acoustic-resonance coupling in pure metals, 25:19879
MILLER, John M., Regional pulmonary function in metastatic carcinoma to the lung studied with ^{133}Xe, 25:19048
MILLER, N. C., Geometrical resonance effect in sputtered superconducting niobium, 25:19617
MILLER, R. J., K^-p elastic scattering at 14.25 GeV/c, 25:19912
MILLER, Suzanne H., Studies of recovery of erythropoiesis after irradiation as a function of the cellularity of the endocolonized spleen, 25:19125
MILLERON, P. F., Thermodynamics of Type-II superconductors, 25:19594
MILLET, P., Magnesium--Zr--Pb alloys of Pb concentrations below or equal to 3 percent, 25:19228
MILNE, J. M., Quality control, inspection, and testing of fuel materials for the two uprated fuel elements, 25:18610 (DP-Report-580)
MILONE, C., Fission of ^{238}U induced by neutrons at energies near threshold, 25:20393
MINE, P., Study of 10 GeV/c K^+-nucleus coherent interactions and Q-nucleon cross-section, 25:19913
MINERBO, Gerald, Causality and analyticity in formal scattering theory, 25:20116
MINEV, L., Alpha-spectroscopy determination of concentrations of radon daughters in air, 25:18363
MINISTR, Z., Electrical conductivity characteristics of the two-phase systems, 25:19226
MINOO, Habibollah, Gas pressure and electron density in the active zone level of hollow cathode arc discharges, 25:20872 (NP-18708)
MINTS, A. Z., Small-size neutron tube of UNG-1 type, 25:20228 (CSIRO-Trans-10095)
MIREK, Teresa, Influence of bis(-3-hydroxypropyl) trisulfide on the peripheral blood in rats irradiated with large doses of x-rays, 25:19131
MIRNOV, S. V., Measurement of energy of plasma in T-3 installation, 25:19662
MIROSHKINA, E. M., Effects of aluminum oxides on the activation energy of creep of niobium, 25:19277
MIRZAKARIMOV, A. M., Hydrochloric acid extraction of Mo from tailings of Uzbekistan coal ash treated by sulfuric acid, 25:18508
MISHCHENKO, Yu. A., Evaluating the mobility of surface O in several oxides and their mixtures by means of O isotope exchange. I, 25:18388
MISHIMA, Yoshitsugu, Direction of development on reactor materials, 25:19179
MISRA, R. M., New stationary gravitational fields from static fields, 25:20096
MISTRY, K. B., Radioactivity in the diet of population of the Kerala coast, 25:19143
MITAKE, S., Core temperature analyses for loss-of-coolant accidents of light water reactor, 25:20762 (JAERI-Memo-4194)
MITAL, V., Effect of plate temperature oscillations on MHD thermal boundary layer, 25:19564
Magnetohydrodynamic flow past a semi-infinite flat plate with transverse magnetic field, 25:19570
MITANI, Iwao, Distribution to organs of ^{131}I--erythrosine B, 25:19060
MITCHELL, J. W., Methods for preparing replicas of slip bands preshadowed with uranium oxide, 25:19271
MITROFANOV, K. P., Resonance recording of ^{57}Co γ quanta, 25:18751
MITROFANOVA, G. N., Influence of the conditions of preliminary treatment on the energy of the bonding of oxygen on lanthanum oxide, 25:18389
MITROPOL'SKAYA, O. N., Turbulent velocities and damping constants in faculae and in photosphere, 25:19420
MITSEL'MAKHER, G. V., Decays $\pi^+ + e^+(\mu^+)\nu e^+e^-$, 25:19963 (JINR-P2-5520)
Search for the decay $\mu^+ + e^+ + e^+ + e^-$, 25:19891 (JINR-P1-5542)
MITSUISHI, Nobuo, Studies on the fluidized bed calcination of high level radioactive liquid wastes, 25:18630
MITTEMPERGHER, M., Exhalative-supergenic uranium mineralization in quaternary alkaline volcanic rocks of central Italy, 25:18542
Uranium ore genesis in Permian and Lower Triassic of Italian Alps, 25:18548
MITUS, Anna, Irradiation of the liver in children: acute effects enhanced by concomitant chemotherapeutic administration, 25:18999
MIYAMOTO, K., Expansion of a laser-produced plasma into a vacuum, 25:19703
MIYAMOTO, Kenro, Magnetic and drift surfaces: current configuration of stellarator field, 25:19727
MIYASAKA, Shunichi, Properties of heat resisting concrete for neutron shielding, 25:19295
MIYASHITA, Kyoichi, Measuring calorific value of petroleum, 25:18817
MIYATA, Haruo, Synthesis of (o-oxalophenylazo)chromotropic acid and stability constant of its Th chelate, 25:18382
MIYAZAKI, Tetsuo, Photoisomerization of maleate radical anions produced in 2-methyltetrahydrofuran by γ irradiation at 77°K, 25:18457
MIYAZAWA, H., Finite-energy sum rule as a test of the Pomeranchuk theorem, 25:20011
MIYOSHI, Shigeru, Influence of defects in 80 mm thickness steel plates for weld quality, 25:19202
MIZOGUCHI, T., Gas recoil neutron spectrometer with electronic collimation by rise-time discrimination, 25:18749
MIZUHO, M., Gas recoil neutron spectrometer with electronic collimation by rise-time discrimination, 25:18749
MLADJENOVIC, M., Conversion electron measurements in decay of ^{156}Tb, 25:20472
Specific gamma-ray constant and gamma spectrum of ^{192}Ir, 25:20424
MOCIUTCHI, C., 4th test of general relativity theory, 25:20097
New linear gravitation theory. III, 25:20098
MOEDL, H., Kinetics of processes variably distributed in recovery energy, 25:19859
MOELLERUD, R., Isospin analysis of pion and nucleon resonance production in NN collisions, 25:20030
MOELLMANN, H., Intestinal absorption of metallic mercury, 25:18369
MOEN, I. O., Regge-pole model for $\pi N + \omega N$, 25:20008
MOERK-MOERKENSTEIN, P., Heat transfer values for water in steam generators with forced convection and reactor channels at pressures of 170 to 215 bar, 25:18581
MOESSBAUER, R. L., Isomer shifts and changes of nuclear charge radii in ^{99}Ru and ^{101}Ru, 25:20403
MOFFETT, David Read, K/sub S/^{0} charged-to-neutral decay branching ratio, 25:19897
MOHAN, N., Green's function analysis of SF_6 and related molecules, 25:18408
MOHR, R., Decay of Cd isotopes, 25:20422
MOISEEV, I. G., Observations of radio emission of sources 3C 273 and 3C 279 at 8 mm, 25:19376

MOKRUSHIN, A. D., Possible use of positron annihilation to study chemisorption, 25:18415
MOLLIMARD, D., Study of the oxidation of Nb, 25:19177
MOLNAR, F., Study of decay of ^{148}Sm, 25:20465
MOLNAR, H., Excited lines in H and K region of Ca II in flare on Mar. 12, 1969, 25:19412
MOLODYKH, E. I., Thermal stability of monoisopropylbiphenyl, 25:18377
MONAHAN, C. F., Properties of low-lying states in ^{43}Sc, 25:20320
  Transition rates in ^{29}P, 25:20319
MONARO, S., Directional correlations of gamma rays in ^{152}Sm and ^{152}Gd, 25:20385
MONKELIS, M. R., W-MESHER: a computer program to analytically partition a two-dimensional figure, 25:18578 (WANL-TME-2721)
MONNAND, Edouard, Isomer of ^{138}Cs, 25:20381
MONTAGNON, J. R., Evaluation of activated carbon supported isotope exchange techniques for containment atmosphere purification, 25:18385 (CONF-700816-(Vol.1), pp 278-88)
MONTAGUE, J. H., Transition rates in ^{29}P, 25:20319
MONTGOMERY, D. B., Threshold currents of large cross-section superconductors, 25:19624
MONTGOMERY, David, Discrete spectra and damped waves in quasi-linear theory, 25:19751
MONTH, M., Theory of resonant integer extraction from synchrotrons, 25:20145
MOORE, C., Computer programs for calculation of liquid-scintillation data, 25:18693
MOORE, J. G., Lifetimes and heights of O(^{1}S) in pulsating aurorae, 25:19578
MOORE, P. W., Polyethylene ampoule containers for radiation-sterilised parenteral solutions, 25:19164
MOORE, W. E., Monte Carlo evaluation of multiple scattering and resolution effects in double-differential neutron scattering cross section measurements, 25:20235 (RPI-328-211)
MOORE, Wellington Jr., Biological aspects of laser radiation: a review of hazards, 25:19133 (NP-18714)
MOORTHY, V. K., Evaluation of crystallinity of urania powders by streaming potential studies, 25:19266
  Role of crystallinity in the sintering of urania powders, 25:19265
MORANDI, G., Prospects and limits of employment of resistance strain gauges in radioactive environment, 25:18883
MORAWIECKI, K., Functional description of quantum electrodynamics in Coulomb and Feynman gages, 25:20092
MORE, Richard M., Perturbation of a decaying state, 25:19520
MOREHEAD, F. F. Jr., Model for formation of amorphous Si by ion bombardment, 25:19813
MORENO, D. S., Effects of gamma irradiation or the chemosterilant, tepa, on the citrus red mite and its progeny, 25:19100
MORENO, Hector, Super-eikonal model of deep inelastic electron-proton scattering, 25:19939 (NYO-2262-TA-221)
MORERE, J. L., Effect of food preirradiation on the fecundity of two insects: mealy bugs (Pseudaulacaspis pentagona Targ.) and Indian-meal moths (Plodia interpunctella Huebn.), 25:19159
MOREWITZ, H., Comparisons of aerosol experiments with a model used in reactor siting evaluation, 25:20757 (CONF-700816-(Vol.1), pp 26-48)
MORGAN, James M. Jr., Proceedings of the eleventh AEC air cleaning conference held in the Federal Building, Richland, Washington, August 31--September 3, 1970, 25:18525 (CONF-700816-(Vol.1))
MORGAN, Thomas A., Near-field approximation for strong gravitational fields, 25:20101
MORGANTE, O., Reliability of Catania sunspot area measurements, 25:19407
MORGENSTERN, H., Elastic tau scattering on nuclei with A = 15 to 18 at 11 MeV, 25:20278
MORGENTHALER, A. C., CPDREV: spare parts inventory control system, 25:18558 (ARH-1474)
MORIOKA, Shigeki, Effect of dissipation due to firehose instability on perturbation half-jet flow of a collisionless plasma, 25:19676
MORISSET, A., Riverbed pollution. Development of equipment simulating natural flow, 25:18940
MORITA, K., Radial dependence of P_1 interaction in schematic model, 25:20506
MORIYA, Masatoshi, Thickness measurement by radiation manufacturing automobile tires, 25:18824
MOROZOV, A. I., Theory of the plane flow of highly conducting plasma in a channel, 25:19671
MOROZOV, V. A., Apparatus for measuring the lifetime of induced nuclear conditions in the nano- and subnanosecond range, 25:18691
  Two-dimensional analyzer for half life measurements of nucleus of excited states, 25:18642 (JINR-P13-5485)
MORPURGO, G., Short guide to the quark model, 25:19980
MORRIS, Synnoeve Voss, Intensities of absorption lines in Mira variables, 25:19318
MORRISON, D. R. O., Compilation of cross sections V--K- induced reactions, 25:19909 (CERN-HERA-70-6)
MORROW, R., Compressional Alfven waves in nonuniform plasma, 25:19745
MORUCCI, Jean-Pierre, Recording diffraction patterns, 25:18859
MORVAN, P., Light pen used for nuclear data processing, 25:18844
MOSELEY, Robert D. Jr., How to protect patient and physician during x-ray examinations. I, 25:19010
MOSER, Kenneth M., Digital and analog processing of Anger camera data with a dedicated computer-controlled system, 25:18730
MOSINSKI, G., Research report on measurement of average number of prompt neutrons, 25:20373 (LIB/Trans-300)
MOSS, Alfred Jefferson, The influence of energy deprivation on the repair of radiation induced DNA damage, 25:18908
MOSS, F., Free-ion mobility in He II using field-emission points, 25:19587
MOSTAFA, I. Y., Cytogenetic studies on effect of chronic gamma irradiation on Vicia faba, 25:18950
MOTA, A. C., Toward the superconductivity of rhodium, 25:19606
MOTEFF, J., Theoretical spectrum-threshold detector data correlation in EBR-II, 25:20803
MOTZ, H. T., Neutron capture gamma-ray spectroscopy, 25:20447
MOUCHEL, D., Isomeric state in ^{113}In, 25:20460
MOUSSA, Andre, Isomer of ^{138}Cs, 25:20381
MOUTSCHEN-DAHMEN, J., Repairing processes of chromosome aberrations induced by γ rays in Nigella, 25:18951
MOUTSCHEN-DAHMEN, M., Repairing processes of chromosome aberrations induced by γ rays in Nigella, 25:18951
MOWATT, R. S., Europium-152g and ^{226}Ra relative γ-ray intensities, 25:20425
MOYLE, W. F., Conformal-coating, 25:20849 (BDX-613-257)
  Conformal-coating, 25:20850 (BDX-613-265)
MOYO, J., Electrical resistivity of NbO, 25:19868
MOZSA, Szabolcs, Hematologic examinations of chronic radiation load of radiologists, 25:19142
MUEHL, A., Determination of ^{15}N by emission spectroscopy, 25:18344
MUEHLLEHNER, G., Tomographic scintillation camera, 25:18697
MUELLER, K. G., Collision dominated sheath in weakly ionized plasmas. II, 25:19673 (DLR-FB-69-78)
MUELLER, R., Slowing down of fission fragments in various absorbers, 25:20442
MUELLER-HARTMANN, E., Kondo effect in superconductors, 25:19603
MUENZEL, H., Decay of ^{232}Np, 25:20382
MUJEEB, Kazi Abdul, Gamma radiation effects on Phaseolus vulgaris L. and seed radiosensitivity determinations for other species, 25:18946
MUKERJI, A., Directional correlations of gamma-ray cascades in ^{103}Rh, 25:20404
MUKHOPADHYAY, Susanta Kumar, Two-nucleon reaction matrix off the energy-shell, 25:20485
MULDER, K., BOL computer-hardware configuration, 25:20200
  BOL nuclear research project, 25:20198
  Data acquisition with the BOL nuclear detection system, 25:20202
  Electronics of the BOL-system, 25:20199
  Scattering chamber of the BOL-system, 25:20201
  Test-procedures for multidetector BOL-system, 25:20207
MULHERN, P. J., Angular correlation studies in ^{34}S, 25:20348
MUNAS, A. F., Improved ringing coil pulse encoders, 25:18868
MUNCK, O., Plasma renin measured by radioimmunoassay for angiotensin, 25:18920
MUNIZ, R. P. A., Electron paramagnetic resonance of electron-irradiated $K_3Rh(CN)_6$ in a KCl lattice, 25:18462
MUNNO, F. J., Thermal neutron diffusion at the ice-water phase transition, 25:20248
MURAKAMI, Yukio, Trends in the utilization of radiations and radioisotopes. new applications and the problems, 25:18607
MURAMATSU, Susumu, Late appearing radiation injury. I, 25:19105
MURATBEKOV, M. B., Role of charged particles and excited molecules in the radiolytic oxidation of n-heptane by molcular oxygen, 25:18466
MURDOCH, H. S., Right ascensions for 389 sourthern radio sources, 25:19387
MURRAY, R. B., Prog. rpt. on radiation induced defects in alkali halides, and their role in recombination processes, final, 3/1/67--7/15/70, 25:19770 (NYO-3842-12)
MURRI, E. L., Decay scheme of ^{141}Ba and ^{142}Ba, 25:20415
MUSARRA, Joseph S., System for computer processing of radiopharmaceutical disbursement information, 25:19050
MUSCALU, S., Calculating the contributions of the first two diagrams to the reaction amplitude for three bodies, 25:20027
MUSIL, F. J., Detailed derivations of equations used in the likelihood ratio method for the precise and accurate determination of lattice parameters for cubic materials, 25:20856 (GAT-T-999)
MUSZYNSKI, G., Safety aspects in the design of WAK, 25:18566 (ORNL-tr-2370)
MUTO, Tadashi, Research and development of fuel for liquid metal fast breeder reactor, 25:19275
MUTOH, Yuhei, Recent improvements in fluoro-glass dosimeter, 25:18810

MUZINICH, I. J., Does multiple Reggeon exchange produce an eikonal-type formula, 25:20111
MYASNIKOVA, K. P., Crystallization process in binary solid solutions of nickel, 25:19242
MYERS, George Rodney, Comparison of the ultraviolet spectra and polymerization of some dimethacrylamides and N-isobutyrylmethacrylamides, 25:18433
MYERS, D. H., Earthquakes and reactor safety, 25:18556 (ORNL-4584, pp 41)
MYUMINOV, T. M., Apparatus for measuring the lifetime of induced nuclear conditions in the nano- and subnanosecond range, 25:18691

N

NABETA, T., Core temperature analyses for loss-of-coolant accidents of light water reactor, 25:20762 (JAERI-Memo-4194)
NAGAKURA, Tadashi, Method for the solidification of radioactive waste, 25:18634
NAGAOKA, Y., Flocculation treatment of radioactive contaminated sea water. I, 25:18518
NAGATANI, Toshio, Study of chemical behavior of recoil atoms due to (γ,γ') process, 25:18488
NAGPAL, T. S., The ^{125}Sb--^{125}Te decay, 25:20408
NAGY, T., Production of spontaneously fissioning isomers of U, Pu, and Am in neutron reactions, 25:20369 (JINR-P3-5528)
NAIR, S. C. K., Angular momentum projection approach to nuclear rotations in rare-earth region, 25:20541
NAITO, Yasuo, Experimental studies on the correlation between lethal effect in fractionated irradiation and the recovery of bone marrow cells in mice, 25:19108
NAKAGAWA, Masatoshi, Sodium-void experiment in unit k-infinity core, 25:20793
NAKAGAWA, Masayuki, Number of resonances to be adopted for obtaining practically reliable cross section curves, 25:20395
NAKAGAWA, Tsuneo, GRAPH: computer program for plotting experimental data in NEUDADA system, 25:20230 (JAERI-Memo-4116)
NAKAHARA, Yasuaki, Prog. rpt. on nuclear safety experimental program, 4--10/70, 25:20763 (JAERI-Memo-4229)
NAKAI, Akira, New method for recording beam of energetic particles. II, 25:20218
NAKAI, M. Y., Low-energy electron beam studies in thin aluminum foils, 25:19766
NAKAJIMA, Kentaro, Direction of development on a nuclear fuel cycle, 25:18570
NAKAMURA, Kenji, Reversed-phase thin-layer chromatography of metal ions, 25:18337
NAKAMURA, Yasuji, Plutonium: thermal utilization techniques, 25:19198
NAKANE, Ryohei, Present state and problems in the development of gaseous diffusion technique, 25:18602
NAKANISHI, Noboru, Lorentz noninvariance of the complex-ghost relativistic field theory, 25:20074
NAKANISHI, Sumio, Survival and repopulation of hemopoietic tissues of irradiated mice transplanted with bone marrow cells from cyclophosphamide treated donors, 25:19112
NAMBA, Susumu, Enhanced diffusion in ion-implanted silicon, 25:19823
NANDY, K., Interstellar dust: graphite, Fe, and silicate, 25:19450
NARAHARA, Yoshimasa, Kapitza resistance between dielectrics and metals in the normal and superconducting states, 25:19616
NARAYANAMURTI, D., Radiation processed wood-plastic materials, 25:19298
NARAYANANKUTTY, P., Effect of ionic media on stability constants of chloride, nitrate, and thiocyanate complexes of Am(III) and Eu(III), 25:18371
NARIAI, Hideki, Study on curved pipe steam generator, 25:18586
NARTOVA, T. T., Effects of Al and Zr on properties of Ti_3Sn, 25:19238
NASARYAN, A. A., Superhigh-energy particle detector based on using the radiation of a particle in a laminar medium, 25:18781
NASH, Donald J., Radiation-induced cataracts in genetically differentiated mice, 25:19116
NATSUME, H., Half-lives of some fission product nuclides, 25:20339
NAUMKIN, O. P., Phase diagrams and properties of La--Sc alloys, 25:19241
NAVRATIL, James D., Recovery of niobium from niobium--uranium alloys: an annotated bibliography, 25:18502 (RFP-1421)
NAYLOR, Donald William, Removing matter from filter elements, 25:18572
NAYYAR, N. K., Effect of gyro-viscosity on Rayleigh--Taylor instability of a plasma, 25:19711
NAZHAT, N. B., Growth and decay of alkyl radicals in γ-irradiated alkyl iodides at 77°K, 25:18461
NEAGU, E., 4th test of general relativity theory, 25:20097
NEAMU, I., Reaction mechanism for proton scattering on ^{60} ^{64}Ni and ^{66} ^{68}Zn, 25:20322
NEDELIK, A., Reactivity measurements of ASTRA-core after installation of Be reflector, 25:20795
NEEB, K. H., Irradiation tests with vibrocompacted $(Th/U)O_2$ particles, 25:19291
NEECE, G. A., Equation of state for dense hydrogen from zero to 10,000°K, 25:19472 (UCRL-50985)
NEEL, James V., Evaluation of the effects of chemical mutagens on man: the long road ahead, 25:18965
NEKIPELOV, V. N., Isotopic exchange in carbon monoxide molecules on zinc and iron oxides, 25:18387
NEKRASOV, A. N., High-pressure gas target cooled by liquid nitrogen, 25:20128 (IFVE-SEF-70-22)
NEKRASOV, K. G., Search for the decay $\mu^+ + e^+ + e^+ + e^-$, 25:19891 (JINR-P1-5542)
NELSON, A. H., Dynamic stabilization of the electrothermal instability, 25:19543
NELSON, Arne, Long term effects of radioactive fallout, 25:19148
NELSON, C., Behavior of iodine in the presence of sodium oxide aerosols, 25:20761 (CONF-700816-(Vol.1), pp 373-92)
  Characterization of energy release and aerosol behavior from sodium spray fires, 25:20759 (CONF-700816-(Vol.1), pp 346-55)
NELSON, Neal S., Review of radium toxicity studies, 25:18979 (BRH/DBE-70-5)
NELSON, P. A., Pyrochemical processing of fuel materials and scrap containing ^{238}Pu, 25:18492 (ANL-7709)
NELSON, R. S., Antimony-implanted silicon, 25:19825
  Measurement of implanted-boron concentration profiles in silicon, 25:19803
  Radiation damage in silicon during ion implantation, 25:19805
  Void formation during high-dose ion implantation at elevated temperatures, 25:19807
NEMETH, J., Comparison of Hartree--Fock, Slater, and Thomas--Fermi approximations, 25:20514
NEMZEK, T. A., Overview of LMFBR program at Hanford, 25:20692 (CONF-700816-(Vol.1), pp 289-316)
NEPOKRYTYKH, Yu. A., Distortion of the structure of the magnetic field of an accelerator by the conducting coatings of the chamber, 25:20221
NESHPOR, Yu. I., Hard x-ray emission of solar flare on Sept. 28, 1961, 25:19435
NESMEYANOV, An. N., Gamma-radiolysis of tin oxides, 25:18470
NETA, P., Rate constants for reaction of hydrogen atoms in aqueous solutions, 25:18459
NETANGE, B., Fast measurement of ion-implantation profiles, 25:19800
NEU, Helmut, Nuclear power plant for a space station, 25:20808
NEU, Helmut, Nuclear power plant for a space station, 25:20807
  Nuclear reactor with heat pipes, 25:20809
NEUBERT, W., Validity of Alexander and Simonoff semiempirical rules in region 100 less than or equal to A less than or equal to 150, 25:20480 (JINR-E7-5499)
NEUDATCHIN, V. G., Mutual scattering of clusters, 25:20511
NEUFELD, Jacob, Theoretical radiation physics, 25:19757 (ORNL-4584, pp 58-73)
NEUHAUS, Otto W., Stimulated uptake of α-aminoisobutyric acid in rat liver following whole-body γ-irradiation, 25:19024
NEVANLINNA, Lasse, Finland's power economy from 1970 through 2000, 25:20553
NEVSKII, B. V., Survey of development on technology of processing uranium ore in U.S.S.R, 25:18491 (AEC-tr-7190)
NEWMAN, E. T., Application of the semidirect product of groups, 25:20091
NGHI, L. Q., Diffusion in ion-implanted solids with nonuniform diffusion parameters, 25:19840
NGUYEN CONG, Khan, Spark fission-fragment counter, 25:18671
NGUYEN CONG KHANH, Production of spontaneously fissioning isomers ^{242}Am and ^{244}Am, 25:20412
NGUYEN DIN THY, Method of searching for the kink and determining the track parameters of particles scattered in a bubble chamber, 25:18773 (JINR-P1-5540)
NGUYEN-NGAN, 10,830-A line in solar active regions, 25:19421
NICHOL, D. G., Excitation of lambda6300A (O I) airglow by soft electron fluxes, 25:19579
NICHOLAS, D. J., Present status of polarized targets at the Rutherford Laboratory, 25:20135 (RHEL/R-201)
NICHOLS, Julian C., Nuclear reactor thermoelectric power plant, 25:20694
NICHOLSON, Frank David, Nuclear reactors, 25:20714
NICHOLSON, M., Computer programs for calculation of liquid-scintillation data, 25:18693
NICOLESCU, B., Charge-exchange reactions in Regge-pole phenomenology, 25:19995
NICOLET, M. A., Electrical properties of alkali implants in silicon, 25:19780
NIEBERGALL, F., Large-area wire spark chambers with two-coordinate read-out and ferrite core memory, 25:18790
  Production of initially pure K^0 beam of known momentum, 25:20144
NIEDZIELSKI, Jan, Effect of ammonia on the ion reactions in the radiolysis of ethylene in the gas phase, 25:18452
  Nitrogen sensitized gas phase γ-radiolysis of ethylene, 25:18455

XUM

NIELSEN, O. B., Alpha decay of neutron-deficient radon and polonium isotopes, 25:20451
NIELSEN, P., Ion-velocity distribution function in a single-ended Q machine, 25:19670
NIEMAN, D. A., Radiation-damage studies of bismuth-ion-implanted CdS, 25:19792
NIKIFOROV, V. I., Charged pion photoproduction on ^{27}Al nucleus, 25:20341
NIKITIN, Andrei, New transuranium element found in nature, 25:20376 (ORNL-tr-2428)
NIKITINA, S. A., Investigation of complex formation in the system UO$_2$$^{2+}$--H$_2SO_4$--HF--TOA, 25:18381
NIKOLAEV, V. I., Measuring the Coulomb frequency-shift of betatron oscillations, 25:20171
NIKOLOV, O. T., Structure and stabilities of free radicals formed in γ-irradiated glycine, 25:18478
NILSSON, Agnar, Radiopathology of ^{241}Am. I, 25:18901
NININGER, R. D., Uranium reserves, future demand, and extent of exploration problem, 25:18530
NINKOVIC, M., Specific gamma-ray constant and gamma spectrum of ^{192}Ir, 25:20424
NISHIKAWA, K., Electric conductivity of weakly turbulent plasmas, 25:19685
NISHIKAWA, Kazuyuki, Trial fabrication of an Na-bonding fuel rod, and its out-of-pile test, 25:19276
NITTI, L., General formulation of relativistic theory of particle subcostituents (quarks) in terms of a field vector interaction, 25:19972 (IFPTH-10/70)
NITZE, H. R., Radiation treatment of tumors, 25:19071
  X irradiation of animal tumors, 25:19075
NOBLE, Paul Jr., Structure of nitroform in various solvents, 25:18391
NODVIK, R. J., Saxton Core II fuel performance evaluation. Part II. Evaluation of mass spectrometric and radiochemical analyses of irradiated Saxton plutonium fuel, 25:18359 (WCAP-3385-56(Pt.2))
NOELLE, P., Multipole analysis of pi-zero and pi-plus photoproduction between threshold and 500 MeV, 25:19957
NOGAITO, T., Core temperature analyses for loss-of-coolant accidents of light water reactor, 25:20762 (JAERI-Memo-4194)
NOGAMI, Y., Relation between the binding energy and scattering phase shift, 25:20022
  Single-particle-energy spectrum of a Λ particle in nuclear matter, 25:20023
NOGGLE, R. C., Experiment to detect pulsed γ rays from Crab Nebula, 25:19361
NOLIBE, D., Retention of inhaled Pu oxide, 25:18895
NOLIBE, Petravy G., Pulmonary retention and disposal of plutonium oxide, 25:18891 (LF-tr-46)
NOLTE, H., Electronically-controlled pneumatic tube system for activation analysis at a particle accelerator, 25:20184
NOMI, Mitsuhiko, Heavy water, light water, and gas systems for DCA, 25:20801
NOMURA, Junichi, Direction of development on reactor materials, 25:19222
NORDEMANN, D., Gamma emitters and exposure age of the Bovedy meteorite, 25:19301
NORDLING, Carl, VC, NbC, and TaC studied by electron spectroscopy for chemical analysis, 25:19867
NORMURATOV, F., Experiments on measurement of compound nucleus lifetime in W(^{22}Ne,f) reaction, 25:20370 (JINR-P7-5512)
NORTH, G. R., Study of calibration, resolution, and transmission of electrostatic velocity selector, 25:18843
NORTH, J. C., Channeling study of B-implanted Si, 25:19834
NORTON, M. G., Infrared and Raman spectra and vibrational assignment of methylene cyclopropane-h$_6$ and -d$_6$, 25:18402
NOSAL, V. N., Values of the fundamental physical constants according to agreements in 1969, 25:20905
NOSEK, M. V., Phase diagram of Bi--Cd--Hg, 25:19236
NOTARYS, H. A., Ac and dc potentials in superconducting phase-slip structures, 25:19610
NOTEA, A., Ge(Li) spectrometer as a point detector, 25:18676
NOVELLO, M., Origin of the neutrino mass, 25:19966
NOVIKOV, D. L., External injection and acceleration of the beam to the final radius in the electron model of the ring cyclotron with strong focusing, 25:20130 (JINR-P9-5453)
NOVIKOV, G. F., Stabilized ions and the formation of cross links in the radiolysis of polybutadiene, 25:18467
NOVIKOV, V. P., Thermal stability of monoisopropylbiphenyl, 25:18377
NOVIKOVA, K. F., Influence of solar activity on the blood fibrinolytic system, 25:19145
NUEHRENBERG, J., Adiabatic electron plasma and its equation of state, 25:19675
NULAND, Sherwin B., Scan evidence of organ involution and improvement of hyperspleniam in Hodgkin's disease following splenic artery ligation, 25:19058
NUMMINEN, Kalevi, Nuclear power plant in Loviisa, 25:20559
NUNEZ, Paul L., Longitudinal wave propagation in a plasma, 25:19743
NURZYNASKI, J., Tensor polarization and differential cross section for ^{9}Be(d,d)^{9}Be elastic scattering at low energies, 25:20293
NURZYNSKI, J., Tensor polarization of deuterons from Mg(d,d)Mg elastic scattering at 7.0 MeV, 25:20342
NUSYNOWITZ, Martin L., System for computer processing of radiopharmaceutical disbursement information, 25:19050
NUTTALL, J., Unitarity in coulomb scattering, 25:19505
NYITRAI, K., Investigations of radiation-induced-solid state polymerization. XXVII, 25:18432

O

OAKBERG, E. F., New concept of spermatogonial stem-cell renewal in the mouse and its relationship to genetic effects, 25:18959
OAKENFULL, David G., Reactions of acetylimidazole and acetylimidazolium ion with nucleophilic reagents, 25:18398
OAKES, M. E., Resistive loading by a finite plasma cylinder, 25:19653
OBERHOLTZER, Betty L., Publications of the National Bureau of Standards, 1968--69, 25:20869 (NBS-SPEC. PUBL-305(Suppl.1))
OBERSKI, J. E. J., Analysis of multidimensional nuclear data (BOL). I, 25:20203
  BOL computer-hardware configuration, 25:20200
  BOL nuclear research project, 25:20198
  Data acquisition with the BOL nuclear detection system, 25:20202
  Electronics of the BOL-system, 25:20199
  Scattering chamber of the BOL-system, 25:20201
O'BRIEN, K., Monte-Carlo unfolding of neutron spectra, 25:18740
O'BRIEN, P., Efficiency calibration of semiconductor x ray detectors, 25:18715
O'CONNELL, L. J., Transfer function models of DTL and TTL integrated circuits, 25:20893 (SC-RR-70-650)
O'CONNELL, Robert West, Stellar content of M82, 25:19454
O'CONNELL, W. J., Giant dipole resonances in ^{12}C and ^{16}O, 25:20277
ODA, Fumihiko, Studies on the fluidized bed calcination of high level radioactive liquid wastes, 25:18630
ODAR, S., Polymeric chromium(III) complexes arising from neutron irradiation of crystalline potassium chromate. I, 25:18486
ODER, R., Temperature dependence of the 1555 cm^{-1} infrared absorption band in liquid D$_2$O, 25:18401
O'DONNELL, J. H., Radiation-induced solid-state polymerization in some methacrylates, 25:18445
O'DONNELL, P. J., Dimension of operators in broken scale invariance, 25:20037
O'FERRALL, R. A. More, Solvent isotope effects upon proton transfer from the hydronium ion, 25:18395
  Vibrational analyses of liquid water and the hydronium ion in aqueous solution, 25:18399
OGANESYAN, Yu. Ts., Experiments on measurement of compound nucleus lifetime in W(^{22}Ne,f) reaction, 25:20370 (JINR-P7-5512)
OGATA, H., Excited 0^+ states in ^{52}Fe, ^{54}Fe, ^{56}Ni, and ^{58}Ni from (p,t) reaction, 25:20321
OGAWA, Shinji, Thermal expansion of Au$_4$V, 25:19229
OGDEN, P. J., Pion--nucleon phase shift analysis from 1.98 to 3.5 GeV/c, 25:20012
OGNEV, A. A., Displacement of the center of the orbit in a cyclotron due to the variation in the voltage along the accelerating gap, 25:20170
OGREN, P. J., Growth and decay of alkyl radicals in γ-irradiated alkyl iodides at 77°K, 25:18461
  Origin of complex electron spin resonance spectra of γ-irradiated polycrystalline n-alkyl iodides with even number of carbon atoms per molecule, 25:18424
OGUMA, Koichi, Reversed-phase thin-layer chromatography of metal ions, 25:18337
OHARA, Kanji, Survival and repopulation of hemopoietic tissues of irradiated mice transplanted with bone marrow cells from cyclophosphamide treated donors, 25:19112
OHKITA, Takeshi, Survival and repopulation of hemopoietic tissues of irradiated mice transplanted with bone marrow cells from cyclophosphamide treated donors, 25:19112
OHNUKI, Yuji, Photoproduction of two neutral pions from hydrogen near threshold, 25:19890
OHYAMA, Harumi, Effects of x-irradiation on ^{14}C-pyruvate metabolism in rat thymocytes, 25:18902
OKAMOTO, Y., Excitation and stabilization of ion-acoustic waves in RF plasma, 25:19744
OKAMURA, Seizo, Dissociative electron capture process of methyl vinyl ether in organic glasses, 25:18456
OKOLOVICH, V. N., Device for multiparametric investigation of nuclear fission, 25:18670
OKUBO, Takayoshi, Studies on the fluidized bed calcination of high level radioactive liquid wastes, 25:18630
OKUDA, S., Recovery of fast neutron irradiated molybdenum, 25:19861
OKUMURA, Y., Application of the modulation transfer function to reduce unsharpness in scintigrams, 25:18650
OLIVERIRA, J. Costa, Absolute measurement of reactor power by neutron noise analysis, 25:20792
OLIVO, O. M., Ionizing radiation effects on neuroblast cultivated in vitro, 25:19120
OLLEY, J. A., Radiation Damage in II--VI semiconductors,

25:19793
OLMR, J., Relationship between soft x-ray and radio emissions in the 20th solar cycle, 25:19430
OLSEN, J. N., Fractional fringe HCN laser-interferometer, 25:19663
OLSHANSKY, Robert, Okubo's second-class currents in K/sub 12/ and K/sub 13/ decays, 25:19965 (NYO-2262-TA-236)
OLSON, Robert Elmer, Method and apparatus for improving counting statistics in radioactive sampling apparatus, 25:18683
OLSSON, T., Irradiation behavior and post-irradiation examination of Swedish test assembly IFA-30, 25:20735 (HPR-127)
ONDERDELINDEN, D., Gallium implantations in Si studied by proton backscattering, x-ray emission, and Hall effect, 25:19802
ONEGA, Ronald J., Reformulation of the reactor kinetics equations, 25:20828
ONG, R. S. B., Effect of velocity space diffusion on the universal instability in a plasma, 25:19719
ONISCHENKO, L. M., External injection and acceleration of the beam to the final radius in the electron model of the ring cyclotron with strong focusing, 25:20130 (JINR-P9-5453)
OOSTHOEK, D. P., Thermal properties of high-value gallium- and boron-implanted resistors in silicon, 25:19783
O'REILLY, R. J., Joint transduction of separate extrachromosomal drug resistance determinants in Staphylococcus aureus E169, 25:19157
OREKHOV, V. D., Determination of the radiation yield of nitrite ions in the irradiation of sodium nitrate solutions in the small-dose region, 25:18463
ORLOV, M. Ya., Composition of atmospheres of Type-M supergiants, 25:19323
ORMEROD, M. G., Double-strand breaks in DNA of mammalian cell after x-irradiation, 25:18911
ORRALL, Frank Q., Spectrum of inner corona during eclipse of May 30, 1965, 25:19410
ORRE, B., Decay of ^{249}Cf, 25:20398
ORTMANN, H.-G., Local magnetization measurements on cylindrical samples of low-kappa type-II superconductors, 25:19626
ORVINI, Edoardo, Some Italian meteorites trace elements content by nondestructive neutron activation analysis, 25:18370
OSBORNE, P. M., Helicity formalism: a lecture course, 25:19925 (NP-18703)
OSIPOV, K. A., Effects of aluminum oxides on the activation energy of creep of niobium, 25:19277
OSIPOV, N. K., Density of charge sources during interaction of charged-particle fluxes with the atmosphere, 25:19583
OSOKINA, R. M., Mechanism of ^{114}Sn(γ,p)^{113}In reaction, 25:20394
OSTLE, D., Criteria for selection of exploration areas in United Kingdom, 25:18554
OSTROVSKY, Z. E., Properties of heat-resistant steels following high-temperature reactor irradiation, 25:19250 (AEC-tr-7192)
O'SULLIVAN, D., High-resolution measurements of slowing cosmic rays from Fe to U, 25:19525
OSWALD, B., Eddy current loss through pulsed magnetic fields, 25:19572 (IPP-4/80)
OSZUSZKY, F. J. P., Recent developments in radioactive waste management, 25:18625 (SGAE-RT-35/1970)
OTT, David G., Submersible nuclear reactor plant, 25:20817
OTT, E., Relativistic synchrotron plasma echo, 25:19739
OTT, Edward, Damping of a large-amplitude ion acoustic solitary wave, 25:19748
OTTE, V. A., Comparison of p--p and n--p quasi-free scattering in p + d → p + p + n reaction, 25:20260
OTTOZ, A., Research report on measurement of average number of prompt neutrons, 25:20373 (LIB/Trans-300)
OVAKIMOV, V. G., Influence of ionizing radiation and radioprotectors on the antihyaluronidase activity of blood serum and tissue permeability in rats, 25:19031
OVCHINNIKOV, A. K., Radiation resistance of type ZnS + ^{10}B detectors to neutrons, 25:18880
OVERMAN, R. F., Miscible displacement measurements within laboratory columns using the gamma-photoneutron method, 25:18523
OVSYANNIKOVA, L. P., Aberrations of asymmetrized quadrupole lenses, 25:20151
OWEN, David Adolph, Corrections to the positronium hyperfine structure of order $\alpha^2 \ln\alpha^{-1}$, 25:19484
OWEN, L. N., Bone tumours in man and animals, 25:19136
OWENS, Williams Richard, Gyromagnetic ratios of excited states in ^{191}Ir, 25:20462
OYAMA, Akira, Energy modal synthesis method in fast reactor analysis, 25:20709
OZAKI, Takeshi, Synthesis of (o-oxalophenylazo)chromotropic acid and stability constant of its Th chelate, 25:18382
OZERNOI, L. M., Dynamical parameters of galaxies as a consequence of cosmological turbulence, 25:19443
OZEROVA, N. A., Mercury in meteorites, 25:19303
OZIZMIR, Ercument, Electromagnetic properties of a half-space relativistic plasma, 25:19740
OZONO, Noboru, Chronic granulocytic leukemia with special reference to A-bomb survivors, 25:18963

P

PACILIO, N., Micrologic integrated circuit for monitoring correlation in pulse sequences, 25:18701
PACIOTTI, Michael Anthony, Charge asymmetry in the muonic decay of the K_2^0, 25:19898
PADALIA, T. D., Photoelectric light elements of IZ Per, 25:19337
PADOVA, R., Control of Penicillium--digitatum in inoculated citrus fruits, 25:19162
PAEDA, R. I., Teflon and aluminum cells with windows for liquid scintillation detectors, 25:18666
PAGE, Norbert P., Acute lethality and recovery of goats after 1 MVp x-irradiation, 25:19115
PAGETTI, Jacques, Electrochemical properties of Nb, 25:19170
PAGNIA, H., Kinetics of processes variably distributed in recovery energy, 25:19859
PALATNIK, M. I., Crystal structure of Ho and Er between 77 and 300°K, 25:19243
PALEV, T. D., Realizations of Lie algebras through rational functions of canonical variable, 25:19935
PANDEY, D. B., New stationary gravitational fields from static fields, 25:20096
PANDOULAS, Demetrios G., Branching ratios for $K^+ \to 3\pi$ decays, 25:19896
PANDULA, Egon, Elimination of oxidation induced by gamma irradiation in aqueous pharmaceuticals, 25:18472
PANIN, Yu. N., Experiments with ultracold neutrons, 25:20232 (JINR-P3-5392)
PANKRATOV, A. K., Nature of the changes in cosmic-ray diurnal variation during magnetic storms with sudden commencement, 25:19530
  Phase jumps of diurnal variations in cosmic-ray intensity, 25:19529
PANOFSKY, H. A., Prog. rpt. on effects of a change of terrain on wind profiles, final, 7/1/65--8/15/68, 25:20875 (NYO-3562-3)
PANT, D. N., Nonexistence of spherically symmetric solution representing vacuum electrostatic field, 25:20088
PAOLONI, F. J., Hydromagnetic-wave propagation in inhomogeneous magnetic fields, 25:19732
PAPADAKIS, E. P., Prog. rpt. on ultrasonic thermometry in LMFBR systems, 7--9/70, 25:18830 (NYO-3906-12)
PAPADOPOULOS, L., Spectral distributions of fast and slow components in a liquid scintillator, 25:18678
PAPAGIANNIS, Michael D., Model for the source of solar-flare x rays, 25:19396
PAPENFUSS, Morris E., Radiation hardened transistor circuit, 25:18879
PAPK, Byung Sub, Kapitza resistance between dielectrics and metals in the normal and superconducting states, 25:19616
PAPP, J., EPR study on stable H atoms on γ-irradiated clinoptilolites containing La, Mg, and K ions, 25:18423
PARAMESWARAN, V. R., Dislocation mobility in lead and lead--indium alloy single crystals, 25:19589
PARAMONOVA, T. A., Resistance in flow of liquid metals in channels in a transverse magnetic field, 25:19554
PARIS, Pierre, Decay of ^{159}Ho, 25:20405
PARISH, L. J., Inelastic scattering, charge exchange, and knock-out reactions, 25:20508
PARKER, R. P., Prototype semiconductor gamma-camera, 25:18699
PARKS, George K., Relation of energetic solar x rays and high-frequency microwaves, 25:19401
PARMENTIER, N., Comparative study on whole-body exposure injuries, 25:19012 (CEA-CONF-1695)
PARR, Robert G., Extensions of Hulthen orbital concept, 25:19513
  Hartree--Fock theory with exchange cutoff, 25:19517
PARSONS, Sidney B., Limb darkening for yellow supergiants, 25:19305
PASACHOFF, Jay M., Calibration of the Wilson--Bappu effect on the Sun, 25:19304
PASQUALINI, L., Solid state detector telescope for charged photoparticles, 25:18675
PASQUIER, Ch., Biochemical considerations on alveolar retention of liquid rare earth aerosols, 25:18889 (CEA-CONF-1676)
PASSE, Jean, Coaxial cable, 25:18881
PASSOJA, A., Semiconductor detector telescope electron spectrometer, 25:18760
PASSOW, C., Superconducting hf cavities, 25:19638
PASTERNACK, B. S., Detection limits for radionuclides in the analysis of multi-component gamma ray spectrometer data, 25:18746
PATCH, D. R., Prog. rpt. on ultrasonic thermometry in LMFBR systems, 7--9/70, 25:18830 (NYO-3906-12)
PATRAULEA, N. N., Determining the equilibrium of a rotating plasma, 25:19690
PATRICK, B. H., Ratio of ^{6}Li(n,α) to ^{10}B(n,α) cross-sections, 25:20288
PATTENGILL, M. D., Molecular collisions. XIV, 25:19498
PATTERSON, J. A., Character of United States uranium resources, 25:18536
PATTISON, J. B. M., Determination of neutrino spectrum in

XUM

CERN 1967 neutrino experiment, 25:19892
PATZELT, A., Safety aspects in the design of WAK, 25:18566 (ORNL-tr-2370)
PATZELT, P., Decay of Cd isotopes, 25:20422
PAUKER, S., Transfer properties of ^{252}Cf and their use for source preparation, 25:18596
PAUL, Arthur C., Matrix method for three-element extraction systems, 25:20159
PAULSEN, A., Neutron flux measurement by counting the associated ^{3}He particles from T(p,n) reaction, 25:18647
PAULSON, W. R., Transition rates in ^{29}P, 25:20319
PAULUS, Klaus O., Material transport in plant foods with regard to radioactive contamination and decontamination, 25:18892 (NP-18641)
PAULY, H., Intermolecular potentials by inversion of molecular beam scattering data. II, 25:19496
PAVLICSEK, I., Measurement of activation cross section of ^{176}Lu, 25:20464
PAVLOV, A. F., Device for multiparametric investigation of nuclear fission, 25:18670
PAYNE, Richard Steven, Heat as a probe of superfluid helium flow, 25:19584
PEARCE, Clyde E., Thermoluminescence: a better way to monitor radiation exposure, 25:18812
PEARSON, Neal, A ^{14}C kinetic isotope effect study of nucleophilic substitution reactions of p-substituted benzyl chlorides, 25:18407
PEARSON, P. E., UKAEA fuel test assemblies irradiated in HBWR, 1964--66, 25:20736 (HPR-132)
PEDERSEN, B., Exploratory deuteron magnetic resonance study of V, Nb, and Ta deuterides, 25:19876
PEENS, M., Irradiation tests with vibrocompacted $(Th/U)O_2$ particles, 25:19291
PEGOUD, J., Magnesium--Zr--Pb alloys of Pb concentrations below or equal to 3 percent, 25:19228
PELETSKII, V. E., Thermal and electrical conductivities of single-crystal molybdenum at high temperatures, 25:19220
PELLEGRINI, C., Study on the choice of parameters for a high energy electron ring accelerator, 25:20161
PELLIONISZ, P., Statistical chopper method for separation of elastic and inelastic scattered neutrons in time-of-flight experiments, 25:18764
PELOUS, G. P., High-energy boron implantation into silicon, 25:19784
PELTOLA, E. I., Retardation functions for deuteron photodisintegration. II, 25:20254
PENCHEV, N. P., Participation of radiogenic neon in the formation of the Earth's atmosphere, 25:18527
PENNA FRANCA, Eduardo, Radioactivity in the diet of the inhabitants of the Brazilian regions of elevated natural radiation, 25:18927 (NP-18670)
PENROSE, Dana Jo Burge, Resonance phosphorescence, Raman scattering, and decomposition of hexaamminechromium(III) salts utilizing He--Ne laser excitation, 25:18404
PENROSE, R., Extraction of rotational energy from a black hole, 25:19338
  Scattering of two impulsive gravitational plane waves, 25:20087
PENTSAK, G. M., Scintillation characteristics of pure and activated cadmium iodide crystals, 25:18665
PEPINO, A. T., Early use of xenografts as a biologic dressing in burn trauma, 25:19020
PERELMUTER, M., Geometry changes in the limit analysis of axisymmetric intersecting shells, 25:18569
PEREL'SHTEIN, E. A., Ion acceleration by electron ring in decreasing magnetic field, 25:20131 (JINR-P9-5535)
PERESIE, R. J., Secondary deuterium isotope effects on triplet excitation transfer. Deuterium position and sensitizer effects, 25:18406
PEREVALOV, V. S., Change of concrete aggregate properties under neutron irradiation, 25:19296
PERGAMENSHCHIK, B. K., Change of concrete aggregate properties under neutron irradiation, 25:19296
PERRIN, C., Study of the oxidation of Nb, 25:19177
PERRIN, Charles L., Relative leaving abilities and isotope effects in electrophilic aromatic substitution, 25:18414
PERSCHKE, H., Determination of ^{15}N by emission spectroscopy, 25:18344
PERT, G. J., Current sheet tilt in a parallel-plate rail gun, 25:19668
PERTSEV, A. N., Contribution of the scintillator to the resolution of a spectrometer using the single-electron method, 25:18745
PESKOV, O. L., Investigation of heat-transfer crisis in a bunch of fuel element simulators under natural circulation conditions, 25:18584
PETEROVA, N. G., Polarization of local sources of solar radio emission at 4.4 cm, 25:19417
PETERS, E., Kinetics of copper(II)- and copper(I)-catalyzed deuterium exchange in sulfuric and perchloric acid solutions, 25:18390
PETERS, R. F., Metaphase chromosome aberrations in Chinese hamster liver cells in vivo after single acute ^{60}Co exposure, 25:18960
PETIAU, Michel, From Saint-Laurent to Vandellos, 25:20562
PETIT, George S., Corrosion-resistant uranium, 25:19185
PETRARCA, S., Digital programs for thermal dynamics of a cylindrical nuclear fuel rod and a heat-exchanger tube, 25:20835 (RT/ING-(70)8)
PETRESCU, M., Tin self-diffusion in In--48 percent Sn liquid alloy at pre-solidification temperatures, 25:19199
PETRICK, Edward J., Auxiliary and loop for removal of decay heat from a space power reactor, 25:20805 (N-70-39420)
PETROV, V. A., Effect of heat treatment on the electrical resistivity and thermal conductivity of pyrolytic carbon, 25:19281
  Emissivity, electrical resistivity, and thermal conductivity of pyrolytic carbon, 25:19280
PETROVA, I. I., Effect of heat treatment on the electrical resistivity and thermal conductivity of pyrolytic carbon, 25:19281
  Emissivity, electrical resistivity, and thermal conductivity of pyrolytic carbon, 25:19280
PETRUKHIN, V. I., Mesoatomic processes and model of large molecules (review), 25:19482 (NRC-TT-1426)
PEYRESBLANQUES, H., Neutron dosimetry in plants treating irradiated fuels, 25:18800 (SC-T-71-3009)
PFEIL, W., Multipole analysis of pi-zero and pi-plus photoproduction between threshold and 500 MeV, 25:19957
PFENNIG, G., Decay of ^{232}Np, 25:20382
PFEUFER, G., Absolute γ-ray efficiency of 50 cm^{3} Ge(Li) detector, 25:18702
PFIRSCH, D., Laser energy necessary for inertially confined nuclear fusion plasma, 25:19646 (IPP-4/7)
PHARO III, M. W., Ion chemistry and thermal balance in E and F regions above Wallops Island, 25:19575
PHELAN, J. J., $K^{-}p$ elastic scattering at 14.25 GeV/c, 25:19912
PHILLIPS, G. C., Comparison of p--p and n--p quasi-free scattering in $p + d \to p + p + n$ reaction, 25:20260
PHILLIPS, James A., Dynamic stabilization of a linear z pinch, 25:19717
PHILLIPS, R. J. N., Lectures on Regge phenomenology, 25:19977
PHILLIPS, Rita J. S., Mutagenic effectiveness of fast neutrons in male and female mice, 25:18949
PHILLIPS, Rodney M., X-ray-induced changes in function and structure of the rat parotid gland, 25:19119
PHILLIPS, Theodore L., Effects of fast neutrons on human skin, 25:19149
PIATIER, Henri, Nuclear physics: remarks on the values of nuclear radiation from alpha radioactivity, 25:20482 (RFP-Trans-72)
PICAT, P., Riverbed pollution. Development of equipment simulating natural flow, 25:18940
PICHUZHKIN, V. I., Effect of temperature and oxygen on the composition of the γ-radiolysis products of isooctane (2,2,4-trimethylpentane), 25:18471
PICK, J., Solubility of carbon dioxide in heavy water at pressures up to 40 atm, 25:18418
PICKAR, K. A., Lifetime effects in ion-implanted silicon, 25:19820
PICRAUX, S. T., Crystallinity of ion-implanted Si, 25:19812
PIDDINGTON, J. H., Galactic magnetic field and cosmic rays, 25:19459
PIEPGRAS, U., Scintigraphic detection of pathological processes within spinal cord space following intravenous administration of radioisotopes, 25:19042
PIERQUIN, Bernard, Place of implantation in tongue and floor of mouth cancer, 25:19080
PIETENPOL, J. L., Unnoticed theorem of relativistic mechanics, 25:20084
PIETRZYKOWSKI, M., Excitation of short-lived isomeric activities in ^{77}Se, ^{122}Sb, ^{137}Ba, ^{167}Er, and ^{179}Hf using 14.5-MeV neutrons, 25:20435
PIETSCH, R., Investigation of extraction of Th, Pb, and Fe(III) as caproic acid compounds, 25:18506
PIETSCHMANN, H., Structure effects in weak interactions, 25:19968
PIGEON, J., Nucleon elastic scattering by ^{4}He, 25:20261
PIKEL'NER, S. B., Shock waves in the spiral arms of Sc galaxies, 25:19445
PILIPENKO, A. T., Study of the fluorescent niobium complex with hydrogen peroxide and sulphonaphtholazoresorcinol, 25:18349
PILIPOVICH, Donald, Matrix-isolation study of the low-pressure pyrolysis and ultraviolet photolysis of dimethyl peroxides and of CF_3OCl, 25:18394
PILKUHN, H., Deuteron--nucleus collisions in the multi-GeV region, 25:20531
PIMENOV, I. A., Processing of the data of cosmic-ray stations, 25:19528
  System of experimental data encoding in cosmic-ray variations, 25:19527
PINAJIAN, J. J., Conversion electron measurements in decay of ^{156}Tb, 25:20472
PINTER, S., Relationship between soft x-ray and radio emissions in the 20th solar cycle, 25:19430
PIPEROV, N. B., Participation of radiogenic neon in the formation of the Earth's atmosphere, 25:18527
PISKAREV, I. M., Structure of cross section of photoneutron reaction on ^{208}Pb nucleus in the region of a giant dipole resonance, 25:20437
PITIMADA, Domenico, Experimental vibration characteristics of BWR fuel assembly, 25:20740
PITNER, A. L, Irradiation of boron carbide pellets and

powders in Hanford thermal reactors, 25:19289 (WHAN-FR-24)
PIVOVAROV, V. G., Density of charge sources during interaction of charged-particle fluxes with the atmosphere, 25:19583
PIVOVAROVA, N. B., Density of charge sources during interaction of charged-particle fluxes with the atmosphere, 25:19583
PLACCI, A., Apparatus for detection and energy measurement of muonic and pionic x-rays, 25:18748
  Response of large volume NE-213 liquid scintillators to electrons and protons, 25:18655
PLASS, G., Determination of neutrino spectrum in CERN 1967 neutrino experiment, 25:19892
PLAVNIK, G. M., Investigation of the effect of ionizing radiation on the structure and properties of modified capron fibers, 25:18425
PLESHANOV, A. S., Conductivity of charged plasma in a magnetic field, 25:19658
PLESTER, D. W., Sterilizing processes in plastics, 25:19161
PLITZ, H., Distention pressure of fissionable material at high burnup rates in fuel rods for fast breeder reactors, 25:20741
PLOCHOCKI, A., Beta spectrometer with a Si(Li) detector in homogeneous magnetic field, 25:18736 (INR-P-1227)
  Beta spectrometer with Si(Li) detector in homogeneous magnetic field, 25:18767
  Lutetium-170 + ^{170}Yb decay, 25:20452
PLOCK, C. E., Voltammetry of Np(VI)--propionate complexes at rotated glassy carbon electrode, 25:18376
PLOTNIKOVA, M. V., Resonance recording of ^{57}Co γ quanta, 25:18751
PLUSKAL, O., Uranium mineralization in Bohemian Massif, 25:18535
POCKER, Y., Acid-catalyzed isomerization of cis-1-phenyl-1,3-butadiene and cis-1-methyl-3-phenylallyl alcohol, 25:18405
PODZOROVA, E. A., Determination of the radiation yield of nitrite ions in the irradiation of sodium nitrate solutions in the small-dose region, 25:18463
POEYHOENEN, L., Scanning of placenta with /sup 99m/Tc, 25:19045
POHL, F., Hydromagnetic equations for anistropic plasmas including transport effects, 25:19674 (IPP-1/112)
POHL, R. O., Prog. rpt. on experimental phonon physics, 4/70--3/71, 25:20874 (NYO-2391-126)
POKOTILOVSKII, Yu. N., Experiments with ultracold neutrons, 25:20232 (JINR-P3-5392)
POLACCO, E., Apparatus for detection and energy measurement of muonic and pionic x-rays, 25:18748
POLESE, E., Behavior of a stabilized cellular strain cultured in a medium contaminated with ^{137}Cs. III, 25:18904
POLINCHIK, N. N., Experimental solenoid made of Nb$_3$Sn strip, 25:19588 (JINR-P8-5440)
POLONIS, D. H., Effect of omega phase reversion on the superconducting transition in titanium-base alloys, 25:19590
POLUEKTOV, N. S., Titrimetric determination of the rare earth elements with 1,2-dihydroxybenzene-3,5-disulphonic acid, 25:18348
POLYAKOV, V. N., Data transmission in measurement-computing complex of the Joint Inst. for Nuclear Research, 25:18845
POLYAKOVA, N. V., Superconducting alloys based on Nb--Ti--Zr system, 25:19627
POLYAKOVA, R. S., Investigation of W--Mo--Nb alloys containing 30 percent W, 25:19205
POLYANIN, L. N., Heat and mass transfer of rods in a turbulent liquid, 25:18580
POMANSKII, A. A., Practical possibilities of using gallium and lithium as solar neutrino detectors, 25:18720
POMERANTSEV, A. A., Low-activated trigger chamber containing ^{3}He, 25:18662
POMPIDOU, Alain, Biological dosimetry of an ultraviolet radiation source using Saccharomyces cerivisiae, 25:18981 (CEA-N-1380)
POMYTKIN, A. P., Space distribution of radicals during γ-irradiation of methanol at 77°K, 25:18464
PONOMAREV, A. A., Displacement of the center of the orbit in a cyclotron due to the variation in the voltage along the accelerating gap, 25:20170
PONOMAREV, A. N., Kinetics for the radiation polymerization of solid acrylonitrile in the regions of phase transitions, 25:18440
PONOMAREV, L. I., Mesoatomic processes and model of large molecules (review), 25:19482 (NRC-TT-1426)
POP, Gh. G., Second-order harmonics for Lorentz plasma in presence of circular magnetic field, 25:19689
POPHAM, Mary G., Dosimetry of ^{67}Ga in hybrid rats, 25:18992
POPKOVICH, A. V., Vacuum system for the 70-GeV proton synchrotron, 25:20126 (CERN-Trans-70-9)
POPOV, A. F., Instrumentation and control operations of nuclear power plants, 25:20713
POPOV, Yu. P., Completely conservative difference schemes for the equations of magnetohydrodynamics, 25:19571
POPOVSKII, V. V., Kinetic isotopic effect of the oxidation of hydrogen on ferric oxide, 25:18386
PORNET, Jacqueline, Study of reactions ^{9}Be + t below Coulomb barrier, 25:20265 (CEA-R-4117)
PORROT, Emile, Reading thermoluminescent dosimeters, 25:18804
PORTAL, Guy, Reading thermoluminescent dosimeters, 25:18804
POST, R. F., Controlled fusion research and high-temperature plasmas, 25:19730
POSTMA, H., Spin dependence of the neutron-capture cross section of vanadium and the internal magnetic field at vanadium nuclei, 25:20335
POSTON, J. W., Dosimetry for human exposures and radiobiology, 25:18990 (ORNL-4584, pp 129-51)
  Spectrometry research and development, 25:18644 (ORNL-4584, pp 152-64)
POTASHNIKOVA, I. K., Contribution of exchange mechanism in backward scattering of protons on light nuclei and d + ^{4}He + ^{3}He + ^{3}H reaction, 25:20250 (JINR-P2-5496)
POTZEL, W., Isomer shifts and changes of nuclear charge radii in ^{99}Ru and ^{101}Ru, 25:20403
POUNDS, K. A., Further high-sensitivity x-ray sky survey from the southern hemisphere, 25:19353
  High-resolution search for Fe line emission from Sco X-1, 25:19377
  Recent developments in x-ray astronomy, 25:19356 .
POZDEEV, V. V., Gamma-radiolysis of tin oxides, 25:18470
  Radiothermal isomerization of alkyl bromides, 25:18438
PRAKASARAS, A. S., X-ray observation of Cen XR-4 and Nor XR-2, 25:19354
PRANGSMA, G. J., Rotational relaxation of HD below 40 K, 25:19480
PRASK, H. J., Inelastic neutron scattering from solid benzene, 25:20247
PREIBISZ, Z., Lutetium-170 + ^{170}Yb decay, 25:20452
PREINREICH, G., Control and safety studies for an htr gas turbine system, 25:20766
PRELEC, K., Small source for multiply charged heavy ions, 25:20188
PRESTON, D. L., Aerodynamic forces and dynamic stability of high-speed, magnetically suspended rocket sled, 25:20890 (SC-DR-70-867)
PRESTON, George W., Mean surface fields of magnetic stars, 25:19308
PREZBINDOWSKI, D. L., Calculation of ^{236}Pu and ^{238}Pu in discharge fuel of light water power reactors, 25:20733 (BNWL-1523)
PRICE, LeRoy R., NN and ND interactions (above 0.5 GeV/c), 25:19899 (UCRL-20000-NN)
PRICE, M. S. T., Safety aspects of replacement elements in second charge of Dragon reactor, 25:20734 (DP-Report-489)
PRICE, P. B., Charge spectrum of extremely heavy cosmic rays, 25:19532
  High-resolution measurements of slowing cosmic rays from Fe to U, 25:19525
PRIGENT, Raymond, Reading thermoluminescent dosimeters, 25:18804
PRILUTSKII, O. F., Background radiations, 25:19462
PRIMA, S. B., Structure of V--Cr--Zr alloys at 1150°C, 25:19237
PROCHAZKA, Z., Use of linear accelerator in irradiation of Dictyocaulus viviparus larvae, 25:19101
PROESCH, U., Considerations on the mechanism of sulfurous radiation protection agents, 25:19021
PROETEL, D., Gamma-decay of proton-particle neutron-hole states in ^{208}Bi, 25:20434
PROHOROV, V. I., Properties of heat-resistant steels following high-temperature reactor irradiation, 25:19250 (AEC-tr-7192)
PROKERT, Konrad, Improvements in threshold dosimeters, 25:18803
PROKOP'EV, E. P., Possible use of positron annihilation to study chemisorption, 25:18415
PROKOSHIN, A. F., Superconducting alloys based on Nb--Ti--Zr system, 25:19627
PROKOSHKIN, D. A., Diffusion coefficients for binary Nb alloys, 25:19204
PROKOSHKIN, Yu. D., Differential-threshold Cherenkov detector, 25:18788
  Mesoatomic processes and model of large molecules (review), 25:19482 (NRC-TT-1426)
PROKSCH, E., Radiation hardening of commercial polyester resins, 25:18443
PROKSCH, G., Determination of ^{15}N by emission spectroscopy, 25:18344
PRONIK, I. I., Multicolor photometry of galaxy NGC 4254 using image converter, 25:19456
PRONIN, O. D., Vacuum system for the 70-GeV proton synchrotron, 25:20126 (CERN-Trans-70-9)
PRONKO, J. G., Doppler shift studies with selected recoil directions, 25:20140
PROTSOP, K., Correction matrix elements for the first forbidden β^- transition in ^{198}Au, 25:20438
PRUDHOMME, Jean, Biological dosimetry of an ultraviolet radiation source using Saccharomyces cerivisiae, 25:18981 (CEA-N-1380)
PRUDNIKOV, I. A., Sensitivity of a secondary-emission-type accelerated-electron-beam position monitor, 25:20173
PRUGOVECKI, E., Wave operators in time-dependent potential scattering for long-range potentials, 25:20108
PRUITT, J. S., Electron beam current monitoring system, 25:20197
PRYAKHINA, L. I., Structure and properties of W--Mo--Nb--Ta

alloys, 25:19239

PUGACHEV, G. D., Charged pion photoproduction on ^{27}Al nucleus, 25:20341

PUGACHEVA, T. F., Water pump for pressure-cooling reactor in atomic powerplant, 25:20717 (JPRS-52384)

PULLIAINEN, E., Polonium and radiolead in some land animals in Finland, 25:18929 (NYO-3446-14, Paper 26)

PURTYMUN, William D., Plutonium and strontium in soil near Technical Area 21, Los Alamos Scientific Laboratory, Los Alamos, New Mexico, 25:18985 (LA-4563)

PUSTERLA, M., General formulation of relativistic theory of particle subcostituents (quarks) in terms of a field vector interaction, 25:19972 (IFPTH-10/70)

PUSTOVOITOVA, T. G., Strength and plasticity of Ti--Nb--Zr alloys at -196 and +20°C, 25:19206

PUTNAM, G. E., SCANS: spectra calculation from activated nuclide sets, 25:18641 (IN-1446)

PUTNAM, M. H., SCANS: spectra calculation from activated nuclide sets, 25:18641 (IN-1446)

PUTT, Graeme D., Sub-Coulomb deuteron-induced reactions on ^{13}C and ^{12}C, 25:20279

PUTTERMAN, Seth, Relation between the superfluid-helium bulk viscosities, 25:19585

PUZYREV, L. K., Water pump for pressure-cooling reactor in atomic powerplant, 25:20717 (JPRS-52384)

PYPER, Diane Marie, Alpha^{2} Canum Venaticorum and the oblique rotator theory, 25:19339

PYZH'YANOV, A. M., Perturbation of eigenvalues of two-particle Schroedinger operator with hard-core potential, 25:19862

Q

QUEEN, N. M., Model-independent analysis of forward π^{+-}p scattering data, 25:20003 (JINR-E2-5561)
  Real parts of the K^{+}-p forward scattering amplitudes, 25:20013

QUENBY, J. J., Interplanetary magnetic field irregularities and solar proton diffusion, 25:19414

QUILLIN, Robert M., Methods for the enhancement of skin sparing in ^{60}Co teletherapy, 25:19086

R

RACHKOVSKII, D. N., Formation of absorption lines in the inhomogeneous magnetic field, 25:19434

RADER, Robert Kent, eta' production in π^{+}d interactions from threshold to 2.4 GeV/c, 25:19923

RAD'KOV, A. I., Critical temperature of superconducting alloys of Nb--Ti--Ta system, 25:19629

RADVAN, Rostislav, Course of pulmonary ascariasis in an irradiated organism. III, 25:19032

RAE, J. B., Code reading of dosemeter films in an automatic densitometer, 25:18797 (AERE-R-6224)

RAFF, R. A. V., Prog. rpt. on polymer grafting to inorganic substrates, annual, 2/69--1/70, 25:18421 (RLO-2098-1)

RAFLA, S., Major surgery after radical radiotherapy. Indications and complications, 25:19088

RAHMAT, Gabriel, Excitations in low-energy ion--atom collisions, 25:19493

RAHOLA, Tua, Body burden of ^{137}Cs and radiation dose of population group in Finnish Lapland, 25:18987 (NYO-3446-14, Paper 29)
  Radionuclides in plants and reindeer meat in Lapland, 25:18932 (NYO-3446-14, Paper 31)

RAI, Charanjit, 2-substituted naphth(1,2)oxazole scintillators, 25:18731

RAILTON, R., Data display system for use with visual detectors, 25:20177

RAISSON, G., Oxidation and pest phenomena in $NbAl_3$, 25:19174

RAITSIMRING, A. M., Space distribution of radicals during γ-irradiation of methanol at 77°K, 25:18464

RAKOV, Z. G., Decomposition of ammonium uranyl pentafluoride on heating, 25:18380

RAKUSHINA, N. I., Heat transfer in pool boiling of water and Freon-113 on cylindrical rod, 25:18585

RAM, Michael, Calculation of total cross section for double Compton scattering, 25:19958

RAMAN, K., Method of extending Blankenbecler--Sugar--Logunov--Tavkhelidze approximation to Bethe--Salpeter equation, 25:20104 (NYO-2262-TA-231)

RAMASWAMY, K., Green's function analysis of SF_6 and related molecules, 25:18408

RAMOND, P., Group-theoretical construction of dual amplitudes, 25:20114

RAMQVIST, Lars, VC, NbC, and TaC studied by electron spectroscopy for chemical analysis, 25:19667

RAMSEYER, F., Problems in production and assembly of safety vessels (containment), 25:20715

RANCHENKOV, G. M., Change of properties of silica gel under action of gamma irradiation, 25:18427

RANDOLPH, H. W., Sampling by laminar flow entrainment to prevent wall effects, 25:18717

RANFT, J., Atlas of particle production spectra, 25:20028

RANK, D. M., Infrared line emission from planetary nebulae, 25:19327

RANKIN, John Metcalf, The 1969 solar occultation of the Crab Nebula pulsar NP 0532, 25:19373

RANNAUD, J.-Cl., Pulmonary retention and disposal of plutonium oxide, 25:18891 (LF-tr-46)

RAO, Jandhyala Subba, Applications of weak-interaction Hamiltonian to strangeness-changing and strangeness-preserving parity-violating processes, 25:20039

RAO, S. R., Alkaline earth elements in marine sediments off Tarapur coast, 25:18354

RAO, S. V. K., Evaluation of crystallinity of urania powders by streaming potential studies, 25:19266
  Role of crystallinity in the sintering of urania powders, 25:19265

RAO, U. R., X-ray observation of Cen XR-4 and Nor XR-2, 25:19354

RAPPAPORT, I., Early use of xenografts as a biologic dressing in burn trauma, 25:19020

RAPPAPORT, S., X-ray observations of pulsars, 25:19359

RASMUSSEN, J. J., Properties of molten ceramics, 25:19273 (BNWL-SA-3579)

RASMUSSEN, W., Nonrelativistic and relativistic Coulomb amplitude as matrix element of rotation in O(4,2), 25:20040

RATHJE, W., Advantages and limitations of diagnostic nuclear medicine, 25:19037

RAVENTOS, Antolin, Brain and liver scans in the evaluation of lung cancer patients, 25:19047
  Effects of fast neutrons on human skin, 25:19149

RAWLS, John M., Anomalies of the axial-vector current in two dimensions, 25:19984

RAZOV, V. I., Two-dimensional analyzer for half life measurements of nucleus of excited states, 25:18642 (JINR-P13-5485)

REBER, E. E., Brightness temperatures of quiet Sun and new Moon at 6 mm, 25:19408

RED'KIN, V. S., Electrostatic spectrometer of charged particle beams with ring focussing in the field of a cylindrical condenser, 25:18849

REEHAL, Balbir S., Odd--even staggering of nuclear radii, 25:20520

REES, David E., Absorption matrix in a nonuniform magnetic field, 25:19406

REES, John R., Longitudinal effects of colliding beam space charge forces in electron--positron storage rings with crossing angles, 25:20157

REES, M. J., New interpretation of extragalactic radio sources, 25:19357

REEVES III, M., Engineering, economic, and safety evaluation, 25:18526 (ORNL-4584, pp 37-40)

REICH, H., Electronically-controlled pneumatic tube system for activation analysis at a particle accelerator, 25:20184

REICHARDT, K., Irradiation tests with vibrocompacted $(Th/U)O_2$ particles, 25:19291

REIER, Melvin, Absolute gamma-ray intensity measurements of a SNAP-15A heat source, 25:18601

REINHARDT, K., Influence of hypothermia on the radiation effect in healthy and cancer tissue, 25:19093

REIST, Parker C., Optical properties of sodium aerosols, 25:19193 (CONF-700816-(Vol.1), pp 425-44)

REKALO, M. P., Scattering lengths of exotic processes of hadron interactions, 25:19975

RENDALL, C. V. A., Gas turbo-machinery for helium cooled reactors, 25:20772

RENDIC, D., Comparison of p--p and n--p quasi-free scattering in $p + d \to p + p + n$ reaction, 25:20260
  Reaction $^{11}B(n,t)^{9}Be$ at 14.4 MeV, 25:20285

RENNER, C., Decay constant for spontaneous fission of ^{238}U, 25:20429

RENO, R. C., Lifetime and g-factor of 74.8 keV state of ^{100}Rh, 25:20454

REPENKO, E. V., Measurements of the asymmetry ratio of positive-pion photoproduction by linearly polarized photons, 25:19889

REUTER-WEISS, R., Decay of ^{232}Np, 25:20382

RHO, M., Meson exchange currents in nuclear weak and electromagnetic interactions, 25:20542

RIALLAND, Jean-Francois, Contribution to the study of the electrochemical properties of indium amalgams, 25:19190 (AI-Trans-287)

RIBAUX, P. A., Dismantling facility for Lucens irradiated fuel assemblies, 25:20554

RIBE, F. L., Initial equilibrium configuration of Scyllac 5-meter toroidal-sector experiment, 25:19725 (LA-4597)

RICABARRA, G. H., Resonance integral of ^{94}Zr and ^{96}Zr, 25:20392

RICABARRA, M. D., Resonance integral of ^{94}Zr and ^{96}Zr, 25:20392

RICCABONA, G., First results of lung function diagnostic methods in nuclear medicine, 25:19044

RICHARDSON, G. L., Application of aqueous technology to LMFBR separations processes. Program plan for Task T-1: solvent performance, 25:18505 (WHAN-FR-32)

RICHARDSON, Roger Hugh, Core distortion in ^{6}Li, 25:20304

RICHMOND, C. A., Suppression of populations of pink bollworm by releases of gamma-irradiated moths in field cages, 25:19102

RICHTER, B., Stanford storage ring, 25:20194

RIEDEL, A. A., Selecting a transformer core material for a high induction pulsed application, 25:20889 (SC-DR-70-736)

RIEDINGER, M., Operation of sampling spark chambers, 25:18778

RIEGEL, D., Total conversion coefficient and γ-line of the

13.34 keV level in ^{73}Ge, 25:20313
RIEGER, T. J., Hall effect in a superconductor not in the vortex state, 25:19613
RIESZ, Peter, Comparison of electrical discharge with γ-radiation for the production of free radicals in lyophilized proteins, 25:18906
RIGAUT, Henri, System for measuring radiation doses, 25:18805
RIKIMARU, Shigeho, Distribution to organs of ^{131}I--erythrosine B, 25:19060
RINALDI, Gilberto, Detection of traces of transition metals by formation of peroxy compounds and sorption on a chelating resin, 25:18343
RINDLER, W., Torsion-free world lines in curved space--time, 25:20100
RING, C., Data acquisition and analysis system for nuclear physics, 25:18852
RINGEIS, W., 800 MW Brunsbuettel nuclear power station, 25:20567
RISLEY, John S., Magnetic field measurements using an electron beam and an electrostatic analyzer, 25:18865
RISTE, T., Singly bent graphite monochromators for neutrons, 25:20244
RITCHIE, R. H., Theoretical radiation physics, 25:19757 (ORNL-4584, pp 58-73)
RITTER, Evelyn F., Technique for attaching a vacuum tight window to a curved surface, 25:18712
ROACHE, P. J., Direct method for discretized Poisson equation, 25:20892 (SC-RR-70-579)
ROBASHIK, D., Transformation properties of massive particle states at infinite momentum, 25:19924 (JINR-E2-5579)
ROBERT, Jack, Contribution to the study of the electrochemical properties of indium amalgams, 25:19190 (AI-Trans-287)
ROBERTSON, D. S., Uranium: its geological occurrence as a guide to exploration, 25:18549
ROBINSON, B. J., Observations of galactic OH, 25:19381
ROBINSON, David C., Can the energy of a weak gravitational field become negative, 25:20099
ROBSON, B. A., DWBA calculations for (d,p) reactions, 25:20328
ROCHE, Michel, Apparatus for producing a pulsated beam of charged particles, 25:20182
ROCHER, Y. A., Large superconducting memories, 25:19637
ROCKENHAUSER, W., Prestressed concrete reactor pressure vessel for Fort St. Vrain reactor, 25:20557
RODARTE-RAMON, Ubaldo Sergio, Isolation and genetic characterization of recombination deficient mutants in Saccharomyces cerevisiae, 25:18945 (UCRL-20192)
RODENBERG, R., Renormalization of K*Kπ coupling in broken SU$_3$ symmetry, 25:20043
RODERICK, Thomas H., Producing and detecting paracentric chromosomal inversions in mice, 25:18947
  Two radiation-induced chromosomal inversions in mice (Mus musculus), 25:18968
RODIER, J., Exposure of man to natural and artificial sources of ionizing radiations, 25:19137
RODRIGUEZ, M. H., Composition of atmospheres of Type-M supergiants, 25:19323
ROE, B. P., Muon energy losses and straggling for high energy muons, 25:20206
ROEMER, M., Use of radioisotope generators in nuclear medicine, 25:18885
ROESCH, W. C., Energy deposition distributions, 25:19767
ROETHEMEYER, H., Influence of heavy water tank on reactivity measurements on MTR-cores, 25:20797
ROGANOV, V. S., Use of a wire spark chamber to measure the beam profile of a synchrocyclotron, 25:20163
ROGERS, F. J., Equation of state for dense hydrogen from zero to 10,000°K, 25:19472 (UCRL-50985)
ROGERS, F. L., Prog. rpt. on Concentration and Desalting of Protein Solutions Program, 3--5/70, 25:20882 (ORNL-TM-3082)
ROGERS, Lester, Transport of radioactive material: accidents and insurance coverage, 25:19017
ROGERS, Max T., ESR study of IO$_2$F$^-$ radical in γ-irradiated single crystals of potassium oxyfluoroiodate, 25:18420 (COO-1385-34)
ROGOZINSKII, V. G., Vacuum system for the 70-GeV proton synchrotron, 25:20126 (CERN-Trans-70-9)
ROGOZKIN, V. D., Influence of ionizing radiation and radioprotectors on the antihyaluronidase activity of blood serum and tissue permeability in rats, 25:19031
ROHDE, J. F. M., Equipment for sampling sodium, 25:18336
ROIZEN, L. I., Heat transfer in pool boiling of water and Freon-113 on cylindrical rod, 25:18585
ROKHLOV, N. I., Resonance recording of ^{57}Co γ quanta, 25:18751
ROKITYANSKII, V. I., Biophysical mechanisms of ultraviolet radiation, 25:18903
ROLLAG, M. D., Metaphase chromosome aberrations in Chinese hamster liver cells in vivo after single acute ^{60}Co exposure, 25:18960
ROLLE, R., Determination of radon daughters on filters by a simple liquid scintillation technique, 25:18768
ROMANOVA, N. I., Effect of space flight factors on barley seeds, 25:18952
RONCHETTI, Camillo, Water treatment in a plant for testing fuel elements, 25:20726
ROQUES, B., Cementation of Nb by Ti and Cr silicides for the production of protective coatings, 25:19175
ROSE, E. K., Study of some heavy water moderated natural U systems using WIMS code, 25:20818 (AAEC/TM-553)
ROSE, P. H., Equilibrium fraction measurements of heavy ions in fluorocarbon strippers, 25:20155
ROSENBERG, J., Pulsars, 25:19375
ROSS, C. P., Prog. rpt. on ^{60}Co power and heat sources, 7--9/70, 25:18591 (DP-1254)
ROSS, Marvin, Equation of state for dense hydrogen from zero to 10,000°K, 25:19472 (UCRL-50985)
ROSSI, A., Indium-113m--DTPA in the study of the kidney, 25:19039
ROSSI, Harald H., Biophysical aspects of high LET irradiation, 25:19077
ROSSI-TORELLI, M., Behavior of a stabilized cellular strain cultured in a medium contaminated with ^{137}Cs. III, 25:18904
ROTH, E., Calculation of fuel costs of a nuclear power plant, 25:20599
ROTHMAN, R. L., X-ray study of faulting in bcc metals and alloys, 25:19248
ROTHWARF, F., Intermediate mixed state of Type-II superconductors, 25:19620
ROTOLANTE, Ralph Allen, Multiparameter coincidence experiment and levels of ^{185}Re, 25:18772
ROUGE, Pierre, Nuclear reactor refuelling installation, 25:20838
ROUGHTON, Norbert Allen, Cross sections of charged particle reactions yielding positron unstable radioisotopes, 25:20283
ROUX, F., Diffusion in the binary systems Ti--Nb, Zr--Nb, V--Nb, Mo--Nb, W--Nb, 25:19214
ROUX, Georges, Recording diffraction patterns, 25:18859
  Stationary detector for visual display, 25:18689
ROWE, D. J., Nuclear collective motion, 25:20483
  Properties of real RPA matrices and a simple diagonalization procedure, 25:20525
ROY, G., Reaction mechanism of the ^{16}O + d reactions, 25:20301
ROY, Robert Michael McGregor, Some effects of ionizing radiation of Vicia faba, 25:19153
ROZANOV, A. N., 180-liter xenon bubble chamber, 25:18783
ROZANOVA, A. M., Non-strange baryon--baryon resonances, 25:20016 (CERN-Trans-70-14)
ROZEN, I. V., Change of properties of silica gel under action of gamma irradiation, 25:18427
ROZENFELD, Martin, Digital search method for computing isodose curves, 25:19000
ROZENTAL, I. L., Background radiations, 25:19462
ROZHDESTVENSKAYA, E. D., Influence of solar activity on the blood fibrinolytic system, 25:19145
ROZOVSKII, Yu. G., Methods for electrophoretic and chromatographic analysis of azo compounds. III, 25:18347
RUBAN, V. M., Ventilation and air conditioning on atomic ships, 25:20816 (JPRS-52443)
RUBIN, Kenneth, Absolute total cross sections for scattering of low-energy electrons by Rb, Cs, K, 25:19506
RUDENKO, V. M., Spectroscopic studies of peculiar A stars of Mn group, 25:19343
RUDENKO, V. N., Device for studying electron backscattering from layers of materials, 25:18823
RUDNICKI, Tadeusz, Effect of prolonged fractionated x-ray irradiation on the generation cycle of small intestine crypt cells in mice, 25:19122
RUEGG, F. C., Circuit which expands the count storage capacity of a multichannel analyzer, 25:18869
RUEHL, W., O(e,l) analysis of currents and current commutators, 25:19934
RUEHLE, R., Resonance-capture and -fission in highly enriched fuel-lattices, 25:20826
RUETER, W., Electric equipment for fuel element handling at ESSOR reactor in EURATOM Nuclear Research Centre, Ispra, Italy, 25:18627
RUFF, M. D., Effects of gamma-radiation on the pathogenicity of Histomonas meleagridis, 25:19156
RUMI, V. A., Radioinduced anomalies in cotton pollen, 25:18955
RUMYANTSEV, A. A., Theory of supernova explosion light curves, 25:19325
RURARZ, E., Excitation of short-lived isomeric activities in ^{77}Se, ^{122}Sb, ^{137}Ba, ^{167}Er, and ^{179}Hf using 14.5-MeV neutrons, 25:20435
RUSAKOV, S. V., Cherenkov total-absorption spectrometer, 25:18787
RUSBRIDGE, M. G., Shielded supports in toroidal multipoles, 25:19651
RUSSCHER, G. E., Irradiation of boron carbide pellets and powders in Hanford thermal reactors, 25:19289 (WHAN-FR-24)
RUSSELL, Liane B., Definition of functional units in a small chromosomal segment of the mouse and its use in interpreting the nature of radiation-induced mutations, 25:18957
RUSTGI, M. L., Proposed polarized-target-beam test for $^3S_1$--$^3S_1$ radiative transitions in thermal n--p capture, 25:20519
RUTMAN, D. S., Relationship between electric resistance of zirconia ceramics and porosity, 25:19283
RYABOV, Nikolai Vasilievich, Weight and radioactive concentation of aerosols, 25:18685
RYABOV, V. V., Vacuum system for the 70-GeV proton

synchrotron, 25:20126 (CERN-Trans-70-9)
RYABOV, Yu. V., Relative measurements of anti ν in the ^{235}U and ^{239}Pu fission induced by resonance neutrons, 25:20364 (BNL-tr-401)
RYBACHENKO, V. F., Binding energy of light nuclei and nucleon--nucleon potential, 25:20298
RYDING, G., Equilibrium fraction measurements of heavy ions in fluorocarbon strippers, 25:20155
RYHAGE, Ragnar, Mass spectral data processing. II, 25:18835
RYKALIN, V. I., Device with snap-off diode for compensation of influence of pulse amplitude spread of scintillation and Cherenkov counters, 25:18639 (IFVE-SEF-69-44)
RYON, A. D., Prog. rpt. on Concentration and Desalting of Protein Solutions Program, 3--5/70, 25:20882 (ORNL-TM-3082)
RYVES, T. B., Neutron capture cross-section measured by activation independent of half-life, 25:20518
RYZEWSKI, Jan, Effect of O-enriched inspired air, on survival of mice irradiated with 500, 550, and 600 R, 25:19123

S

SAAS, A., Fixation and migration in soils of products of fission and activation, 25:18528
SADOFF, A., Photoproduction of neutral K mesons, 25:19887
SADOVOI, A. A., Binding energy of light nuclei and nucleon--nucleon potential, 25:20298
SADOWSKI, E. A., Ion implantation of Bi into GaP. I, 25:19845
SAFKO, John L., Some properties of cylindrically symmetric Einstein--Maxwell fields, 25:20086
SAFROSHKINA, A. S., Use of a wire spark chamber to measure the beam profile of a synchrocyclotron, 25:20163
SAH, J. P., Disputed 2.86 MeV level of ^{10}B, 25:20289
SAHOTA, H. S., Decay of ^{131}Ba, 25:20414
SAID, K. I., Optimum thickness of single crystal neutron monochromators, 25:20234 (PH-4)
SAILOR, V. L., Spin dependence of the neutron-capture cross section of vanadium and the internal magnetic field at vanadium nuclei, 25:20335
SAITO, Hideo, Detection of radiation emitted from moving sources. I, 25:18692
SAJBEN, M., Asymptotic thermochemical relaxation times in a dense plasma, 25:19684
SAKANAKA, P. H., Formation of ion-acoustic collisionless shocks, 25:19698
SAKISAKA, Masakatsu, Isotope dependence in K-, L-, and M-shell ionization cross sections by proton and deuteron bombardments, 25:19470
SAKO, Kiyoshi, Prog. rpt. on nuclear safety experimental program, 4--10/70, 25:20763 (JAERI-Memo-4229)
  Survey list of accident, hazard, and abnormality in nuclear facilities, 25:19013 (JAERI-Memo-4240)
SAKURAI, A., Flocculation treatment of radioactive contaminated sea water. I, 25:18518
SAKURAI, Kunitomo, Characteristics of solar-active regions responsible for Type-III radio bursts in Aug 1968, 25:19413
  Energetic electrons associated with flares and relation to Type-I noise activity, 25:19402
SALADIN, J. X., Method for improving heavy ion spectra in scattering experiments, 25:18750
SALAM, A., s-channel helicity conservation and the stress-tensor, 25:19931
SALAM, Abdus, f-dominance of gravity, 25:20053
  Non-polynomial Lagrangian theories, 25:20067
SALISBURY, J. D., New concepts for geographic position locators, 25:20903 (UCRL-50978)
SAMAIN, A., New method of magnetic pumping for plasma heating, 25:19648
SAMANT, A. B., Heat transfer to a Bingham plastic in the entrance region of a circular tube, 25:18588
SAMARSKII, A. A., Completely conservative difference schemes for the equations of magnetohydrodynamics, 25:19571
SAMUEL, R. L., Ultrahigh vacuum chamber of ISR at CERN, 25:20146
SAMYGIN, V. K., Blood changes in dinitrochlorbenzol-sensitized dogs after irradiation, 25:19030
SANDEMAN, W. A., Gas turbo-machinery for helium cooled reactors, 25:20772
SANDERS, Robert Hugh, Coalescence of colliding stars in dense stellar systems, 25:19320
SANDERSON, J. J., Longitudinal waves in a perpendicular collisionless plasma shock. I, 25:19752
SANNA, R., Monte-Carlo unfolding of neutron spectra, 25:18740
SANSBURY, J. D., Properties of ion-implanted Si, S, and C in GaAs, 25:19843
SAPANKEVICH, A., Investigation of heat-transfer crisis in a bunch of fuel element simulators under natural circulation conditions, 25:18584
SAPP, R. C., Nuclear orientation of ^{59}Fe in rare-earth double-nitrate crystals, 25:20413
SARAEVA, V. V., Effect of temperature and oxygen on the composition of the γ-radiolysis products of isooctane (2,2,4-trimethylpentane), 25:18471
  Role of charged particles and excited molecules in the radiolytic oxidation of n-heptane by molcular oxygen, 25:18466
SARAH, J. J., Optimum thickness of single crystal neutron monochromators, 25:20234 (PH-4)
SARANTSEV, V. P., Ion acceleration by electron ring in decreasing magnetic field, 25:20131 (JINR-P9-5535)
SARGENT, B. W., Evidence for vibrational excited states in ^{32}S, 25:20326
SARGOOD, A. J., Relationship between surface potential and electronegativity for adsorption on tungsten single crystals, 25:19207
SARI, C., New method for the study of UO$_2$ in a temperature gradient, 25:19278
SARLOS, G., Dynamic studies of gas turbine fast reactors, 25:20765
  Operational conditions for afterheat removal of a gas-cooled reactor with direct cycle, 25:20767
SAROPULU, M., Mitosis process in meristematic cells of cotton under the action of gamma rays and dimethyl sulfate, 25:18954
SASA, Matsuko, Changes of membrane permeabilities of erythrocytes by radiation. I, 25:19107
SASAMOTO, Nobuo, Estimation of fission product decay heat, 25:20834 (JAERI-Memo-4205)
SATIS, F. W., Gallium implantations in Si studied by proton backscattering, x-ray emission, and Hall effect, 25:19802
SATO, A., Effect of electron irradiation on the strength of iron single crystals, 25:19252 (COO-1367-36)
SATO, Fumiaki, Late appearing radiation injury. I, 25:19105
SATO, Otomaru, Detection of radiation emitted from moving sources. I, 25:18692
SATOH, E., Single-particle-energy spectrum of a Λ particle in nuclear matter, 25:20023
SAUER, P. U., Triton binding energy calculations, 25:20259
SAUNDERS, L. M., Crossed-channel partial-wave expansions and Bethe--Salpeter equation, 25:20113
SAVEL'EV, A. E., Calculations of cross sections for inelastic interaction of neutrons with nuclei accompanied by emission of protons and α particles, 25:20346
SAVITSKII, E. M., Phase diagrams and properties of La--Sc alloys, 25:19241
SAVRIN, V. I., Equal-time equation for two-particle system in quantum field theory, 25:20077
SAVVIN, S. B., Methods for electrophoretic and chromatographic analysis of azo compounds. III, 25:18347
SAWADA, Shozo, Protective effect of AET against fast neutron and x-ray irradiation, 25:19029
SAWYER, R. F., Axial-current divergences and the reactions $\gamma + \gamma \to$ pions, 25:19951
SAXENA, K. M. S., Accurate numerical Hartree--Fock self-consistent-field wave functions for rare-earth ions, 25:19478
SAXL, Erwin J., 1970 solar eclipse as seen by torsion pendulum, 25:19431
SAXTON, O. H. N., Crossed-channel partial-wave expansions and Bethe--Salpeter equation, 25:20113
SAYLOR, William L., Methods for the enhancement of skin sparing in ^{60}Co teletherapy, 25:19086
SAZONOV, L. A., Influence of the conditions of preliminary treatment on the energy of the bonding of oxygen on lanthanum oxide, 25:18389
SAZONOV, V. N., Influence of ionization losses on spectrum and composition of cosmic rays, 25:19523
SCHAEFER, Hermann J., Astronauts' radiation exposure on first lunar landing mission, Apollo XI, 25:18978 (AD-711316)
SCHAEFER, Lothar, Symmetry coordinates, harmonic force field, and mean amplitudes for light and heavy dibenzene Cr, 25:18392
SCHAICH, E. L., Dilute uranium alloy with a fine-grained, randomly oriented structure, 25:19231 (NLCO-1051)
SCHARBERT, T., Internal bremsstrahlung spectrum accompanying positive beta decay of ^{11}C, 25:20302
SCHARENGUIVEL, J. H., Off-mass-shell S-wave $\pi^+\pi^-$ scattering amplitude, 25:19994
SCHARF, Karl, Spectrophotometric measurement of ferric ion concentration in ferrous sulphate (Fricke) dosemeter, 25:18801
SCHECTER, D. J., Prog. rpt. on polymer grafting to inorganic substrates, annual, 2/69--1/70, 25:18421 (RLO-2098-1)
SCHEER, J., Elastic tau scattering on nuclei with A = 15 to 18 at 11 MeV, 25:20278
SCHEIWE, John P., Passive device for determining relative rotation, 25:18822
SCHEUER, J. C., Baryon exchange in reactions $K^-n \to Y\pi^-$ at 3 GeV/c, 25:19917
SCHICHA, H., Uses of a research reactor for medical investigations, 25:18886
SCHIEBER, D., Electron temperature determination in a low-density helium plasma, 25:19661
SCHIFFER, J. P., Quest for superheavies, 25:20458
SCHILB, J. D., Pyrochemical processing of fuel materials and scrap containing ^{238}Pu, 25:18492 (ANL-7709)
SCHILLER, P., Determination of low silver content in drugs by low-energy gamma-ray stimulated characteristic radiation, 25:18355
SCHIOTT, H. E., Approximations and interpolation rules for

ranges and range stragglings, 25:19760
SCHLOSSER, Kurt, Treatment and disposal of radioactive waste. I, 25:18515
SCHLUDERBERG, Donald C., Nuclear reactor core construction, 25:20697
SCHLUETER, H., Resistive loading by a finite plasma cylinder, '25:19653
SCHMIDT, Klaus H., Device for producing and monitoring hydrated electrons, 25:18854
SCHMIDT, L. D., Interaction of N_2 with (100) W, 25:19208
SCHMIDT, W., Efficiency of a 180° coincidence spectrometer for extended sources, 25:18758
SCHMIT, M., Wired arithmetic computer for particle identification, 25:18718
SCHMITT, F., Operation of sampling spark chambers, 25:18778
SCHMITT, William Francis, A Monte Carlo calculation of spallation reactions of astrophysical interest in the M nuclei, 25:19531
SCHNEIDER, A., Measurement of coal dust concentrations in pipelines using radioactive isotopes, 25:18606
SCHNEIDER, W., Computer programme for solving MHD equations for theta pinch in time-dependent coordinate system, 25:19647 (IPP-6/90)
SCHOBERT, Harold Harris, Preparation and characterization of some alkanethiolatoosmium compounds, 25:20864 (IS-T-431)
SCHOEMAKER, Dirk, EPR and optical absorption study of $BrCl^-$ and associated centers in doped KCl crystals. I, 25:19852
SCHOFIELD, Aldred E., Dynamic stabilization of a linear z pinch, 25:19717
SCHOLZ, F., Preliminary experiments of a heat exchanger in He under high-pressure, 25:20780
SCHOLZ, Kenneth L., Cyclotron production of ^{123}I: an evaluation of the nuclear reactions which produce this isotope, 25:18480 (BRH/DMRE-70-4)
SCHOTSMANS, L., Is ground state rotational band cut off in ^{9}Be, 25:20280
SCHRAMM, R. E., Photoneutron cross sections for ^{32}S, 25:20332
SCHREIER, Ethan J., Conformal symmetry and three-point functions, 25:20036
SCHRODER, L. J., Radiochemical analysis of water from wells, springs, and streams in central Nevada, 25:18522 (USGS-474-97)
SCHUART, L., Design of shorter magnetohydrodynamic channels for liquid metals, 25:19563
SCHUETZENDUEBEL, W. G., Prestressed concrete reactor pressure vessel for Fort St. Vrain reactor, 25:20557
SCHULER, Robert H., Radiation chemistry of aqueous solutions of $CFCl_3$, CF_2Cl_2, and CF_3Cl, 25:18460
  Rate constants for reaction of hydrogen atoms in aqueous solutions, 25:18459
SCHULTZ, J., Variations in the makeup of lens insoluble proteins, 25:18909
SCHULZ, N., Identification of particle-hole multiplets in ^{46}Sc, 25:20350
SCHULZE, K. P., Safety aspects in the design of WAK, 25:18566 (ORNL-tr-2370)
SCHUMACHER, P. E., Formation of ^{6}Li/sub g s / and ^{6}Li, 3.56 MeV, T = 1 state, 25:20284
SCHUSTER, H., Theory of ultrasonic attenuation in V_3Si, 25:19604
SCHUTTE, F., X-ray isotopic shift for ^{162}Dy--^{164}Dy, 25:20416
SCHUURMAN, W., Kink instability of toroidal plasma column, 25:19704 (NP-18681)
SCHWALM, D., Parameter estimation of coupled reactors by correlation methods, 25:20827
SCHWARTZ, Jean-Pierre, Thermionic reactor: neutronic study of a light water moderated core, 25:20813 (CEA-CONF-1727)
SCHWARTZ, Robert J., Pile-up discrimination technique, 25:18840
SCHWEITZER, D. G., Field-trapping properties of Type-I superconducting hollow cylinders, 25:19611
SCHWELA, D., Does an isotensor electromagnetic current exist, 25:19956
  Multipole analysis of pi-zero and pi-plus photoproduction between threshold and 500 MeV, 25:19957
SCHWUTTKE, G. H., Resistivity and annealing properties of implanted $Si:H^+$, 25:19822
SCIAMA, D. W., Thermodynamics and cosmology, 25:19464
SCOPPA, P., Arylsulfatase activity in the urine of the irradiated rat, 25:18905
SCOTT, L. R., Ion chemistry and thermal balance in E and F regions above Wallops Island, 25:19575
SEALAND, O. M., Disposal by hydraulic fracturing, 25:18622 (ORNL-4584, pp 11-15)
SEAR, J. F., Interplanetary magnetic field irregularities and solar proton diffusion, 25:19414
SEAR, R., Dual detector system for thyroid uptake measurement, 25:18898
SEARLE, A. G., Mutagenic effectiveness of fast neutrons in male and female mice, 25:18949
SEBOEK, F., Shielding effectiveness of cracked concrete, 25:19768
SEDLAKOVA, L., Single-crystal filters of thermal neutrons, 25:20238 (UJV-2488-F)
SEELEWIND, H., Effect of ion implantation on electrical properties of SiO_2 films at high fields, 25:19788
SEEMAN, N., Experiment to detect pulsed γ rays from Crab Nebula, 25:19361
SEGAL, A., New linear gravitation theory. III, 25:20098
SEGAL, Y., Wires as thermal neutron probes, 25:18707
SEGRE, Emilio, Annual review of nuclear science. Volume XX, 25:20446
SEIBOLD, J. R., Excited lines in H and K region of Ca II in flare on Mar. 12, 1969, 25:19412
SEIDOV, Z. F., Apparent distribution of planetary nebulae and open star clusters, 25:19321
SEIFRITZ, W., Special thermocouple for temperature measurements in liquid metal media, 25:19227
SELEVANOV, Yu. F., Boiling of liquids on fine wire under natural convection conditions, 25:18583
SELEZNEV, V. P., Decomposition of ammonium uranyl pentafluoride on heating, 25:18380
SELF, S. A., Ion waves, drift waves, and instability in a weakly ionized magnetoplasma, 25:19720
SELIM, A. A., Linear and nonlinear collisional processes in a plasma, 25:19687
SELINOV, I. P., Isotopes: reference tables. I and II, 25:20264
SELLA, C., Structure of sputtered niobium films, observation of a fcc phase, 25:19244
SELLIN, I. A., Comment on relative magnetic substate amplitudes in foil excitation of fast hydrogen atoms, 25:19474
SELTZER, H. E., Isomer shifts and changes of nuclear charge radii in ^{99}Ru and ^{101}Ru, 25:20403
SEMENOV, V. A., Clinical aspects and treatment of radiation combined injuries, 25:19033
SEMIBRATOVA, N. M., Phase diagram of Bi--Cd--Hg, 25:19236
SEN, S., Core-particle coupling in isotopes of antimony, 25:20495
SENATOR, A., Position sensitive detector for a magnetic spectrograph, 25:18681
SERGACHEV, A. I., Dependence of anti ν on neutron energy on basis of fission energy balance, 25:20440
SERGEEV, I. P., Superconducting alloys based on Nb--Ti--Zr system, 25:19627
SERLEMITSOS, P. J., Search for temporal structure in x rays from Scorpius X-1, 25:19363
SESTAK, B., Electron velocity distribution in a fully ionized plasma under the action of crossed electric and magnetic fields, 25:19688
SETHI, S. K., Compton-suppressed low level gamma-ray scintillation spectrometer, 25:18752
SEUGE, J., Effect of food preirradiation on the fecundity of two insects: mealy bugs (Pseudaulacaspis pentagona Targ.) and Indian-meal moths (Plodia interpunctella Huebn.), 25:19159
SEVERIJNS, A. P., Cooling to 0.7°K by application of superfluid properties of ^{4}He, 25:19640
SEVERIN, N. F., Electron detection with a shower detector, 25:18786
SEXL, R. U., General relativity and gravitational collapse, 25:19465
SEYNAEVE, Future of reprocessing in Europe, 25:18500 (NP-18669)
SHAGALOVA, E. D., Effect of biological properties of plant on ^{90}Sr contents in yield, 25:18897
SHAH, S. M., Alkaline earth elements in marine sediments off Tarapur coast, 25:18354
SHAKARASHVILI, T. S., Investigation of aromatic hydrocarbons of supsinskaya petroleum and their catalytic conversion in the presence of irradiated catalysts, 25:18444
SHAMU, R. E., One-phonon octupole vibration of ^{151}Eu, 25:20432
SHANDOR, L., Monte Carlo generation of neutral $\pi^- p$ interactions at 5 GeV/c in propane bubble chamber, 25:20004 (JINR-P13-5516)
SHANNON, J. M., Annealing characteristics of highly doped ion-implanted phosphorus layers in silicon, 25:19837
SHANNON, Leland M., Near-uv absorption bands of tryptophan, 25:20899 (UCLA-12-810)
SHAPIRO, F. L., Experiments with ultracold neutrons, 25:20232 (JINR-P3-5392)
SHAPIRO, Lewis, Alopecia mucinosa: treatment and prognosis, 25:19073
SHAPIRO, Maurice M., Heavy cosmic ray nuclei, 25:19524
SHAPIRO, Sidney, Experimental demonstration of Riedel peak, 25:19602
SHARE, G. H., Experiment to detect pulsed γ rays from Crab Nebula, 25:19361
SHARKIS, A. A., Teflon and aluminum cells with windows for liquid scintillation detectors, 25:18666
SHARKOV, V. I., Laboratory modeling simulation of comet phenomena, 25:19394 (LA-tr-70-27)
SHARMA, D. P., X-ray observation of Cen XR-4 and Nor XR-2, 25:19354
SHAVER, B. O., Ventilation systems for the FFTF, 25:20783 (CONF-700816-(Vol.1), pp 317-45)
SHAVER, P. A., Galactic radio sources. I, 25:19384
  Galactic radio sources. II, 25:19385
  Galactic radio sources. III, 25:19386
SHAVRINA, A. V., Composition of atmospheres of Type-M supergiants, 25:19323
SHAW, C. B., Portable neutron radiographic camera using ^{252}Cf, 25:18617
SHAW, James William Westgarth, Gas cooled nuclear reactor,

25:20695
SHCHERBININ, E. V., Suppression of turbulence in tubes by transverse magnetic fields, 25:19556
SHEI, Sun-sheng, Scaling, deep inelastic electron--nucleon scattering, and the multiperipheral model, 25:19959
SHEINDLIN, A. E., Effect of heat treatment on the electrical resistivity and thermal conductivity of pyrolytic carbon, 25:19281
  Emissivity, electrical resistivity, and thermal conductivity of pyrolytic carbon, 25:19280
SHELINE, Glenn E., Effects of fast neutrons on human skin, 25:19149
SHERBOURNE, A. N., Geometry changes in the limit analysis of axisymmetric intersecting shells, 25:18569
SHEVCHENKO, N. G., Electron-scattering study of the change of the charge radii of nuclei of iron and nickel isotopes, 25:20334
SHEVCHENKO, O. P., Structure of cross section of photoneutron reaction on ^{208}Pb nucleus in the region of a giant dipole resonance, 25:20437
SHEVCHENKO, O. V., Interaction of samarium and strontium oxides, 25:19284
SHIBA, Mayayoshi, Survey list of accident, hazard, and abnormality in nuclear facilities, 25:19013 (JAERI-Memo-4240)
SHIBATA, Tsugio, Permanent magnet properties of intermetallic compounds Sm (Fe, Co, Cu)$_5$, 25:19875
SHIELDS, William R., Prog. rpt. on analytical mass spectrometry, annual, 7/69--6/70, 25:18357 (NBS-TN-546)
SHIFRINA, S. S., Effect of biological properties of plant on ^{90}Sr contents in yield, 25:18897
SHIGA, Tetsuo, Mass spectrometric studies on negative ion--molecule reactions of nitroethylene, 25:18428 (NP-18676)
SHIHABI, Zakariya, Stimulated uptake of α-aminoisobutyric acid in rat liver following whole-body γ-irradiation, 25:19024
SHIKINA, N. D., Mercury in meteorites, 25:19303
SHIMA, Kunihiro, Isotope dependence in K-, L-, and M-shell ionization cross sections by proton and deuteron bombardments, 25:19470
SHIMAMURA, Isao, Minima in generalized oscillator strengths of hydrogen-like atoms, 25:19521
SHIMAZAKI, Shozo, Effect of ionizing radiation on the vascular system in transplanted rat tumor, 25:19111
SHIMEGI, N., Core temperature analyses for loss-of-coolant accidents of light water reactor, 25:20762 (JAERI-Memo-4194)
SHIMOMURA, Hiroko, Influence of ^{60}Co γ-ray on potato, 25:19160
SHIPP, Erik, Corpus allatum size and ovarian environment in irradiated cucumber fly, 25:19096
SHIRAISHI, Kensuke, Neutron irradiation hardening in aluminum--magnesium alloys, 25:19255
  Precipitation hardening of Al--2.2wt. percent Li alloy after neutron irradiation, 25:19201
SHIRAKURA, Ichiro, Modification of radiosensitivity of Ehrlich ascites carcinoma cells in vivo. I, 25:19130
SHIRIKOVA, N. Yu., Table of wave functions of single-particle states of transuranium region deformed nuclei in Saxon--Woods potential, 25:20481 (JINR-P4-5457)
SHIRK, E. K., High-resolution measurements of slowing cosmic rays from Fe to U, 25:19525
SHIRKOV, D. V., Properties of Regge poles trajectories, 25:19988
SHIRLEY, D. A., Chemical information from photoelectron and conversion-electron spectroscopy, 25:19473
SHIROKOVA, N. I., Effects of Al and Zr on properties of Ti_3Sn, 25:19238
SHISHOV, Yu. A., Experimental solenoid made of Nb_3Sn strip, 25:19588 (JINR-P8-5440)
SHITOV, Yu. P., Linear polarization of pulsar PSR 2218 + 47, 25:19379
SHKLOVSKII, I. S., Nature of the outbursts in quasars and Seyfert-galaxy nuclei, 25:19367
SHKOL'NIKOV, A. S., Small-size neutron tube of UNG-1 type, 25:20228 (CSIRO-Trans-10095)
SHLEIEN, B., Calibration and initial field testing of ^{85}Kr detectors for environmental monitoring around a nuclear fuel reprocessing plant, 25:18638 (CONF-700816-(Vol.1), pp 143-74)
SHLYAPNIKOV, P. V., Computation of kinematic parameters of electron tracks in bubble chambers, 25:18784
  Do K-meson nuclei exist, 25:20002 (IFVE-STF/SPK-70-30)
SHNYREV, G. D., Strength and plasticity of Ti--Nb--Zr alloys at -196 and +20°C, 25:19206
SHOCKLEY, W., Hidden momentum for non-steady state defined, 25:19953
SHOLIN, G. V., Stark broadening of hydrogen spectral lines in turbulent plasma, 25:19693
SHOVE, Arthur Godfrey, Manufacture of nuclear fuel elements, 25:19269
SHRADER, E. F., Scattering of fast neutrons by ^{12}C, ^{54}Fe, ^{56}Fe, ^{58}Ni, and ^{60}Ni, 25:20338
SHRAMENKO, B. I., Charged pion photoproduction on ^{27}Al nucleus, 25:20341
SHTAN, A. S., Radiation technology. IV, 25:18870
SHTANKO, V. F., Radiation damage in selenates of divalent metals, 25:18479
SHUBIN, A. P., Theory of the plane flow of highly conducting plasma in a channel, 25:19671
SHUBIN, V. N., Evidence of the occurrence of monomolecular reactions in the radiolysis of aqueous solutions of oxygen, 25:18476
SHUKALOV, I. B., Background radiations, 25:19462
SHUKLA, P. G., Low-energy cosmic x rays, 25:19352
SHUMEIKO, N. M., Decays $\pi^+ \to e^+(\mu^+)\nu e^+e^-$, 25:19963 (JINR-P2-5520)
SHURIN, A. K., Solubility of O in Hf--Nb alloys, 25:19240
SHUSTEK, L. J., Variational principles for expectation values applied to the ground state of the helium isoelectronic sequence, 25:19475
SHUVALOV, R. S., Time resolution of scintillation counters, 25:18640 (IFVE-SEF-70-23)
SHVARTSMAN, V. F., Ionization zones around neutron stars, 25:19324
SIDOROV, L. V., Time--amplitude converter for the nanosecond range, 25:18846
SIE, S. H., Doppler shift attenuation studies in heavy nuclei, 25:20409
SIEDER, Everett N., Abstracts of literature on the distillation of seawater and on the use of nuclear energy for desalting, 25:20812 (TID-25653)
SIEGEL, G., Considerations on the mechanism of sulfurous radiation protection agents, 25:19021
SIEVERS, A. J., Prog. rpt. on experimental phonon physics, 4/70--3/71, 25:20874 (NYO-2391-126)
SIGEL, Richard M., Evaluation of spleen size during routine liver imaging with /sup 99m/Tc and the scintillation camera, 25:19057
SIGMON, T. W., Lattice damage created in Si by implantation of 2.8-MeV protons, 25:19821
SIGMUND, P., Correlation functions in theory of atomic collision cascades, 25:19833
SIGNORINI, C., Mean lives of ^{31}S and ^{38}K levels, 25:20349
SIGURD, D., Diffusion effects in ion-implanted germanium, 25:19841
  Lattice location of heavy group III and V elements implanted into Ge, 25:19827
SIIVOLA, A., Decay of ^{62}Co isomers and ^{62}Cu, 25:20361
SIK, So Don, Relative measurements of anti ν in the ^{235}U and ^{239}Pu fission induced by resonance neutrons, 25:20364 (BNL-tr-401)
SILBERBERG, M., Characterization of energy release and aerosol behavior from sodium spray fires, 25:20759 (CONF-700816-(Vol.1), pp 346-55)
SILBERBERG, Rein, Heavy cosmic ray nuclei, 25:19524
SILLER, V., Uses of a research reactor for medical investigations, 25:18886
SILVER, G. L., Disproportionation coefficients of Pu, 25:18383
SILVERBERG, Eric Clark, Interplanetary dust streams: observation by satellites and lidar, 25:19425
SILVERMAN, Dennis, Scaling behavior in multiperipheral dynamics, 25:19982
SIMBEL, M. H., Impact parameter representation for the off-energy-shell scattering amplitude, 25:20122
SIMMONS, S. D., Low-intensity gamma rays in ^{90}Nb decay, 25:20411
SIMNETT, George M., Long-term storage of relativistic particles in the solar corona, 25:19403
SIMON, D., Study of the oxidation of Nb, 25:19177
SIMON, Norman R., Second-order pulsations in polytropes, 25:19306
SIMONOFF, Gabriel, Ratio of ^{236}Np isomers in ^{238}U deuteron interactions, 25:20389
SIMONOV, V. A., Material balance of plasma column and gas sheath in toroidal apparatus-Tokamak-3, 25:19657 (MATT-Trans-16)
SINAEV, A. N., Use of a wire spark chamber to measure the beam profile of a synchrocyclotron, 25:20163
SINCLAIR, M. W., OH (1667) line absorption, 25:19382
SINCLAIR, W. J., Reactor HIFAR: control arm circuits, 25:20781 (AAEC/M-10)
SINGER, Paul, Veneziano model for process $V_1 + \pi \to V_2 + \pi$, 25:19997
SINGER, Ralph M., Vaporization dynamics of initially static superheated sodium, 25:19191 (ANL-7706)
SINGH, P. P., Coupled-channel analysis of α-particle scattering from the 5.23 MeV natural parity state of ^{24}Mg, 25:20344
SINGH, Virendra, High-energy bounds on scattering amplitudes and oscillations in the diffraction-peak region, 25:19990
SINGHAL, S. P., Nonspecular scattering from a rough surface, 25:20106
SINGSAAS, Bjoern, Time scale for radioprotection by and permeation of glycerol in anoxic cells of E. coli B, 25:19022
SINHA, B. C., Optical model for proton scattering from ^{40}Ca, 25:20311
SINHA, B. K., Core-particle coupling in isotopes of antimony, 25:20495
SINKEVICH, O. A., Penetration of a magnetic field behind a shockwave front, 25:19547
SISTEMICH, K., Identification of μs-isomers among primary fission products, 25:20430
SITES, James R., Gamma rays from polarized ^{124}Sb, ^{192}Ir, and ^{194}Ir, 25:20386
SITNIK, G. F., Turbulent velocities and damping constants in faculae and in photosphere, 25:19420
SITTON, D. M., Free-ion mobility in He II using field-

emission points, 25:19587
SIXTA, Vaclav, Use of silica gel for the separation of traces of uranium, 25:18345
SIZIKOV, V. S., Derivation of model galaxies from 21-cm line profiles. I, 25:19444
SKAKUN, N. A., Device for measuring total proton cross sections of reactions, 25:20176
SKOBELEV, N. K., Delayed fission of some neutron-deficient atomic nuclei, 25:20371 (JINR-P7-5584)
SKOBLA, J., Determination of low silver content in drugs by low-energy gamma-ray stimulated characteristic radiation, 25:18355
SKOBLO, V. A., Change of properties of silica gel under action of gamma irradiation, 25:18427
SKOKOVA, A. A., Radioinduced anomalies in cotton pollen, 25:18955
SKORUPSKI, A., Two-stream instability and classification into absolute and convective, 25:19710
SLAMA, G., Formation and structure of aluminide base protective coatings on Nb and its alloys, 25:19173
SLAPA, M., Beta spectrometer with a Si(Li) detector in homogeneous magnetic field, 25:18736 (INR-P-1227)
  Beta spectrometer with Si(Li) detector in homogeneous magnetic field, 25:18767
SLEVIN, James A., Absolute total cross sections for scattering of low-energy electrons by Rb, Cs, K, 25:19506
SLIV, L. A., Formation region of internal conversion coefficients, 25:20515
SLOAN, D. M., Decomposition of a decelerating ionizing shock, 25:19667
SLOTFELDT-ELLINGSEN, D., Exploratory deuteron magnetic resonance study of V, Nb, and Ta deuterides, 25:19876
SLOVOKHOTOVA, N. A., Application of the method of radiothermoluminescence for the investigation of high-temperature relaxation in polyethylene, 25:18435
SMIRENKIN, G. N., Angular anisotropy and fissionability of nuclei, 25:20529
  Plutonium-238 neutron fission in sub-barrier energy range, 25:20444
SMIRENKINA, L. D., Dependence of anti ν on neutron energy on basis of fission energy balance, 25:20440
SMIRNOV, V. S., Search for the decay $\mu^+ + e^+ + e^+ + e^-$, 25:19891 (JINR-P1-5542)
SMITH, A., Exact electrostatic shock solution for a collisionless plasma, 25:19678
  Steady-state Vlasov equations for monotonic electric potential, 25:19680
SMITH, Bob H., Ferrite bias regulator for a synchrotron resonator, 25:20178
SMITH, C. W., Geometrical resonance effect in sputtered superconducting niobium, 25:19617
SMITH, D. G., Calibration and initial field testing of ^{85}Kr detectors for environmental monitoring around a nuclear fuel reprocessing plant, 25:18638 (CONF-700816-(Vol.1), pp 143-74)
SMITH, E., Safety aspects of replacement elements in second charge of Dragon reactor, 25:20734 (DP-Report-489)
SMITH, H. J., Coincidence technique for study of Ge(Li) detector profiles, 25:18759
  Self-resonant current peaks in Josephson junctions, 25:19612
SMITH, J. R., K^-p elastic scattering at 14.25 GeV/c, 25:19912
SMITH, Joe N. Jr., Residence time measurements for surface ionization of K on W, 25:19210
SMITH, Kendric C., Production and repair of radiochemical damage in Escherichia coli deoxyribonucleic acid; its modification by culture conditions and relation to survival, 25:18912
SMITH, Lindsey F., Comparison of spectra of planetary nucleus and Wolf--Rayet star, 25:19310
SMITH, R. F., Isotopic integrity for UF$_6$ field samples, 25:18340 (KY-626)
SMITH, T., Calibration of whole-body counter, 25:18695
  Follow-up of thyroid carcinoma by whole-body counting, 25:19035
SMITH, W. D., Alpher--Rubin ultrasonic attenuation and dipolar nuclear-acoustic-resonance coupling in pure metals, 25:19879
SMOAK, William M., Scintillation of a vascular rim in subdural hematoma, 25:19059
SMORODINSKII, Ya. A., Transformation properties of massive particle states at infinite momentum, 25:19924 (JINR-E2-5579)
SNEAD, C. L. Jr., Influence of defects on the angular correlation of positron-annihilation photons in irradiated and in deformed iron, 25:19851
SNIDER, Dale R., Interference terms in Amati--Bertocchi--Fubini--Stanghellini--Tonin multiperipheral model, 25:19998
SNOW, A., Industrial efforts to satisfy design criteria, 25:20725 (WHAN-SA-46)
SOARES DE ANDRADE, A. A., Uranium deposits in Portugal, 25:18537
SOBICZEWSKI, A., Penetration of a two-dimensional fission barrier, 25:20478 (INR-P-1230)
SOBOL, Ya. G., Thermal and electrical conductivities of single-crystal molybdenum at high temperatures, 25:19220
SOBOLEV, V. S., Comparative study of effect of irradiation with γ-rays and accelerated electrons on structure and properties of cis-butadiene rubber, 25:19300
SOBOLEVSKII, N. M., Double differential distribution of particles produced in the proton-nucleus collisions, 25:20018 (JINR-P2-5507)
SOBR, J., Solubility of carbon dioxide in heavy water at pressures up to 40 atm, 25:18418
SODD, Vincent J., Cyclotron production of ^{123}I: an evaluation of the nuclear reactions which produce this isotope, 25:18480 (BRH/DMRE-70-4)
SOERENSEN, H., Low-grade uranium deposits in agpaitic nepheline syenites, south Greenland, 25:18539
  Occurrence of uranium in alkaline igneous rocks, 25:18540
SOFER, D. H., Specific γ-ray constant of radon, 25:19002
SOKOLOV, I. B., Effect of irradiation dose rate and manner of preparation of samples on the kinetics of radical build-up in aniline, 25:18465
SOKOLOV, V. I., Superconducting alloy, 25:19618
SOKOLOV, V. S., Strength and plasticity of Ti--Nb--Zr alloys at -196 and +20°C, 25:19206
SOKOLOVSKAYA, L. A., Methods for electrophoretic and chromatographic analysis of azo compounds. III, 25:18347
SOKOLOVSKII, V. D., Influence of the conditions of preliminary treatment on the energy of the bonding of oxygen on lanthanum oxide, 25:18389
SOKOLOWSKI, Janusz, Automated systems and electronics for the Krakow--Dubna slow-neutron inverted-geometry spectrometer KD SOG-1, 25:18734 (INP-727)
SOKOVISHIN, Yu. A., Near-wall flow of jet of conducting fluid in transverse magnetic field, 25:19559
SOLEILHAV, M., Research report on measurement of average number of prompt neutrons, 25:20373 (LIB/Trans-300)
SOLOVEV, V. E., Discrete frequency sweep in a synthesizer for nuclear magnetic resonance spectroscopy, 25:18848
SOMIKOV, A. V., Amplifier for semiconductor gamma detectors, 25:18668
SOMOGYI, Gy., Investigations on alpha radiography with plastic track detectors, 25:18727
SONENSHINE, Daniel E., Use of radioisotopes for studies on the ecology of tick vectors of disease. Final progress report, April 1, 1966--December 31, 1970, 25:18934 (ORO-3514-10)
SONG, Kwang Suk, Detection of ^{235}U fission fragments by solid state track recorder using cellulose nitrate, 25:18724
SONNEMANS, M. A. A., Test-procedures for multidetector BOL-system, 25:20207
SONODA, M., Stabilization of spectrum with no reference peaks, 25:18867
SOOBY, Donna L., Reproductive factors associated with radiotherapy of malignant lymphomas, 25:19147
SORENSEN, C. M., Analysis of a breakup using mean track width and blob measurements, 25:18795
SORENSEN, Raymond A., Odd--even staggering of nuclear radii, 25:20520
SORI, Naoyuki, Honeycomb block used for collimation of radiations and method of manufacturing the same, 25:18856
SOROCHENKO, R. L., Physical conditions in the Orion Nebula, 25:19365
SORRENTINO, Francois, Equipment for measurement of elasticity modulus for hot cell applications, 25:19279
SOSZKA, Waldemar, Geometrical effects in scattering of ions by surface of solids, 25:19468 (INP-710)
SOTHMAN, R. D., Radiation-induced solid-state polymerization in some methacrylates, 25:18445
SOTTAN, A. Jr., Measurement of high-energy γ-ray spectra in a strong neutron flux, 25:18735 (INR-1224)
SOUBELET, G. C., Control and safety studies for an htr gas turbine system, 25:20766
SOVOCOOL, G. W., Secondary deuterium isotope effects on triplet excitation transfer. Deuterium position and sensitizer effects, 25:18406
SOWERBY, M. G., Ratio of ^{6}Li(n,α) to ^{10}B(n,α) cross-sections, 25:20288
SPAARGAREN, D., Angular correlations in inelastic neutron scattering by carbon at 15.0 MeV, 25:20281
SPARANO, Ottorino, Method of obtaining artificial genetic improvements in plants, 25:18964
SPARKS, W. M., Partition functions in ionizing plasmas, 25:19397
SPEAR, W. G., Gas-flow method for detection of fast neutrons in reactors, 25:18646 (WHAN-SA-73)
  In-core regenerative thermal neutron detectors for nuclear reactors, 25:20711 (WHAN-FR-37)
SPEISOR, D., Unnoticed theorem of relativistic mechanics, 25:20084
SPENCER, R. P., Self-volume standards for Schilling tests and other in vitro bulk liquid counting, 25:18361
SPENCER, Richard P., Growth of the human liver: a preliminary scan study, 25:19061
  Scan evidence of organ involution and improvement of hypersplenism in Hodgkin's disease following splenic artery ligation, 25:19058
SPENCER, W., Analysis with a Po--Be source, 25:18368
SPERGEL, Philip, Radiation detection devices, 25:18682
SPIGHT, Lonnie Dean, Small angle multiple scattering of high energy electrons, 25:20545
SPITSYN, V. I., Investigation of the effect of ionizing radiation on the structure and properties of modified

XUM

capron fibers, 25:18425
SPITSYN, Vict. I., Radiation damage in selenates of divalent metals, 25:18479
SPOGLIA, U., Characteristics of implanted p--n junctions by C(V,f) measurements, 25:18857
SPORN, P., Developments in nuclear power economics, 25:20751
SPOWART, Alexander Rollo, Improvements in or relating to neutron radiography apparatus, 25:18618
SPRAGUE, Estel D., Evidence for hydrogen atom abstraction by methyl radicals in the solid state at 77°K, 25:18426
SPREITER, John R., Effect of dissipation due to firehose instability on perturbation half-jet flow of a collisionless plasma, 25:19676
SRIVASTAVA, D. S., Distorting effect of the absorbers for the semiconductor and scintillation gamma-ray spectra, 25:18771
  Investigations on alpha radiography with plastic track detectors, 25:18727
SRIVASTAVA, J. B., Photoelectric elements of eclipsing system WX Cep, 25:19335
  Photoelectric study of eclipsing system GG Cas, 25:19336
SRIVASTAVA, M. L., Disputed 2.86 MeV level of ^{10}B, 25:20289
SRIVASTAVA, R. K., Photoelectric light elements of IZ Per, 25:19337
ST. JOHN, Karl M., Radiation sensitive notch pattern detection system, 25:18818
ST. LAWRENCE, W., Theory identification for mechanical behavior of polystyrene bead foams, 25:19293 (UCRL-50952)
STAAS, F. A., Cooling to 0.7°K by application of superfluid properties of ^{4}He, 25:19640
STADLER, Janice, Radiation-induced cataracts in genetically differentiated mice, 25:19116
STAGAT, R. W., Unitarity in coulomb scattering, 25:19505
STANCU, Fl., Separable single-particle potential in shell-model calculations, 25:20509
STANGE, K., Sequential sampling by variables with known variance of the output and a specification range with an upper and lower limit for the variables, 25:20883 (ORNL-tr-2355)
STAPP, James, L., Interstellar silicate extinction related to 2200A band, 25:19446
STARACE, Anthony F., Length and velocity formulas in approximate oscillator-strength calculations, 25:19518
STARCHMAN, Dale E., Photon energy--angle distributions for ^{60}Co after penetration of concrete, 25:19763
STARIKOVA, G. A., Structure of absorbing material in the solar neighborhood, 25:19442
STARK, D. S., Ion analysis of rf-excited deuterium ion sources, 25:20150
STARK, N., Radiotracer studies of nutrient cycling pathways, 25:20897 (TID-25656)
STAROMINSKII, L. R., Montardy scheme with segmented electrodes for MHD devices, 25:19541
STAS, Konstantin Nikolaevich, Weight and radioactive concentation of aerosols, 25:18685
STATNIKOV, Yu. G., Certain magnetohydrodynamic flow problems related to wave propagation, 25:19566
STECHER, P., Protection of Nb against oxidation, 25:19176
STEELE, J. W., State of cure of printed circuit boards, 25:20848 (BDX-613-233)
STEEN, N. M., Evaluation of the radiative neutron capture cross sections of ^{232}Th for the range 0.0 eV to 15 MeV (LWBR Development Program), 25:20377 (WAPD-TM-971)
STEFANI, S., Polaroid film in radiation dosimetry and survey, 25:19005
STEFANKO, J. S., Engineering study of the colloid-fueled reactor concept, 25:20811
STEFFEN, K., DESY-double storage ring Doris, 25:20196
STEIGER-SHAFRIR, N. H., Transfer properties of ^{252}Cf and their use for source preparation, 25:18596
STEIN, H. J., Crystallinity of ion-implanted Si, 25:19812
  Defect annealing in neutron- and ion-damaged Si, 25:19831
  Vacancy motion in low-temperature ion-implanted Si, 25:19811
STEIN, R. L., Heat capacity and magnetization of praseodymium metal in the temperature region 1.2 to 4.2°K with applied magnetic fields up to 40,000 G, 25:19869
STEINBERG, M., Concrete-polymer materials. Third topical report, 25:19292 (BNL-50275)
STEINWANDTER, H., Distribution of Np in nitric acid solution containing uranyl ion, 25:18519
STENFLO, L., Kinetic theory of three-wave interaction in a magnetized plasma, 25:19737
STENGEL, Rudolph F., Plasma containment apparatus and method, 25:19729
STENSGAARD, R., Position sensitive detector for a magnetic spectrograph, 25:18681
STEPANOV, B. M., Electric field excited in air by pulsed γ quanta, 25:19761
STEPANYAN, A. A., Nature of the changes in cosmic-ray diurnal variation during magnetic storms with sudden commencement, 25:19530
  Phase jumps of diurnal variations in cosmic-ray intensity, 25:19529
STEPHEN, J. H., Formation of insulating layers by use of reactive ion beams, 25:19781
STEPHENS, G. A., Radiation damage by implanted ions in GaAs and GaP, 25:19844
STEPHENSON, J., Automatic scanner for nuclear emulsions, 25:18690
STEPIC, R., Conversion ratios for M1 + E2 transitions, 25:20473
STEPIEN-RUDZKA, W., Equilibrium deformations of the ground and excited states in the rare-earth nuclei, 25:20367 (INR-P-1216)
STERGAKOS, Elias Peter, Resonances in ^{23}Na, ^{26}Mg, ^{41}K, ^{55}Mn, and ^{59}Co, 25:20359
STERN, J., Light-cone commutators and high energy annihilation $e^+ + e^- \to \pi$ + hadrons, 25:19941
STERN, William K., Evolution of an abnormal light test reaction, 25:19150
STEVENS, P. R. C., Electrical and atom-site location properties of ion-implanted germanium, 25:19799
STEWART, J. M., Thermodynamics and cosmology, 25:19464
STEYERT, W. A., Gamma rays from polarized ^{124}Sb, ^{192}Ir, and ^{194}Ir, 25:20386
STIEDING, Lothar, Method of preoxidizing nuclear reactor components of zirconium alloys, 25:19180
STIER, H. E., Production of initially pure K^0 beam of known momentum, 25:20144
STIJFHOORN, D. E., Chemical analysis of high burn-up PuO_2 fuel, 25:18356 (KR-140)
STILL, Edwin T., Acute lethality and recovery of goats after 1 MVp x-irradiation, 25:19115
STIPANICIC, P. N., Distribution of U deposits with sedimentary control in Argentina, 25:18544
STIX, Thomas H., Stability of a cold plasma under magnetoelectric confinement, 25:19714
  Toroidal equilibria for plasma under magnetoelectric confinement, 25:19652
STOCK, John T., Biamperometric titration of hexacyanoferrate(III), Fe(III), Cu(II), Ce(IV), and I, 25:18346
STOENNER, A., Measurement of coal dust concentrations in pipelines using radioactive isotopes, 25:18606
STOJADINOVIC, A., Internal boundary conditions for a ring-shaped reactor, 25:20824
STOJADINOVIC, S., Passage of iron(III) cyanoferrate through the gastrointestinal tract of rats, 25:18887
STOKER, G. C., Ultrasonic characterization and computerized analysis of graphite billets, 25:18613 (SC-DR-70-693)
STOKSTAD, R. G., Doppler shift attenuation studies in heavy nuclei, 25:20409
STOLARCZYK, Lech, Radiation induced graft terpolymerization of poly(ethylene terephthalate). III, 25:18429
STOLER, P., 250 meter neutron time-of-flight facility, 25:18742
  Deformation parameters in ^{154}Sm and ^{148}Sm, 25:20477
STOLL, Roger, An electric generator with thermopiles and radioelements, 25:18598
  Isotopic electric generator using thermoelectric elements, 25:18605
STOLL, W., Plutonium technology, 25:18517
STOLT, Robert Howard, Parastatistics, 25:20080
STOLZ, Werner, Improvements in threshold dosimeters, 25:18803
STONEKING, J. E., Theory for free vibration of orthotropic shells of revolution, 25:18568
STOOPS, Emerson FitzSimmons, Dust comet in the solar wind, 25:19582
STOTHERS, Richard, Collapsars, infrared disks, and invisible secondaries of massive binary systems, 25:19314
STOYANOV, D. Ts., Method of coherent states and factorization of dual amplitudes, 25:20120
STOYANOVA, D. A., High-pressure gas target cooled by liquid nitrogen, 25:20128 (IFVE-SEF-70-22)
STRAALSUND, J. L., Irradiation produced defects in austenitic stainless steel, 25:19253 (WHAN-FR-16)
STRASHINSKII, A. G., Device for measuring total proton cross sections of reactions, 25:20176
STRATHDEE, J., f-dominance of gravity, 25:20053
STRAUB, H., Problems in production and assembly of safety vessels (containment), 25:20715
  Production and assemby of the Muehleberg pressure vessel, 25:20555
STRAUSS, Federico M., Model for the source of solar-flare x rays, 25:19396
STRAUSSER, Yale E., Scintillation-type ion detector employing a secondary emitter target surrounding the ion path, 25:18722
STREIT, L., Construction of physical states in quantum field theory, 25:20069
STRELKOV, A. V., Experiments with ultracold neutrons, 25:20232 (JINR-P3-5392)
STRENG, W., Pseudorandom pulse generator for a uniform amplitude distribution with discrete lines, 25:18853
STRICKLAND, E. Hardin, Near-uv absorption bands of tryptophan, 25:20899 (UCLA-12-810)
STROKAN, N. B., Resolving power of silicon surface-barrier counters, 25:18672
STRONGIN, Myron, Influence of normal-state resistance on superconducting transition temperature of ultrathin films, 25:19614
STROTTMAN, D., Structure of positive parity states of ^{20}Ne, 25:20351
STROUD, P. T., Doping of thin films by recoil-atom

implantation, 25:19786
STRUB, R. A., High pressure indirect CO_2 closed cycle gas turbines, 25:20773
STUART, R. L., Theoretical spectrum-threshold detector data correlation in EBR-II, 25:20803
STUKOV, O. I., Measurements of the asymmetry ratio of positive-pion photoproduction by linearly polarized photons, 25:19889
STUMPFI, W., Low-energy B and P implants in Si. A, 25:19835
STURIALE, M. L., Reliability of Catania sunspot area measurements, 25:19407
STURROCK, P. A., High-frequency modulation of light from Crab pulsar, 25:19360
SUBBOTIN, V. I., Boiling of liquids on fine wire under natural convection conditions, 25:18583
  Method of calculating the coefficients of turbulent heat transfer in channels of a complex form, 25:20844 (AEC-tr-7186)
  Velocity field of turbulent fluid flow in a longitudinal streamline of clusters of rods, 25:18576 (AEC-tr-7189)
SUBRAMANIAN, R. V., Prog. rpt. on polymer grafting to inorganic substrates, annual, 2/69--1/70, 25:18421 (RLO-2098-1)
SUBRAMANIAN, S., ESR study of IO_2F^- radical in γ-irradiated single crystals of potassium oxyfluoroiodate, 25:18420 (COO-1385-34)
SUDARIKOV, B. N., Decomposition of ammonium uranyl pentafluoride on heating, 25:18380
SUEHIRO, T., Excited 0^+ states in ^{52}Fe, ^{54}Fe, ^{56}Ni, and ^{58}Ni from (p,t) reaction, 25:20321
SUEZAWA, M., Quenched-in resistivity in molybdenum, 25:19860
SUGAR, Eva, Radiologic presentation of the forms of pelvic fracture, 25:19040
SUGAR, R. L., Validity of Regge eikonal model, 25:20115
SUGIHARA, Yoshio, Studies on the bone marrow of a-bomb exposed in hiroshima by autoradiography, 25:19134
SUGIURA, Toshio, Mass spectrometric studies on negative ion--molecule reactions of nitroethylene, 25:18428 (NP-18676)
SUH, D. W., Semi-empirical efficiency curve for thin Ge(Li) detector at low energies, 25:18725
SUHR, N. H., Barium and Sr in silicates, 25:18335
SUIT, Herman D., Experimental evaluation of tumor bed effect for C3H mouse mammary carcinoma and for C3H mouse fibrosarcoma, 25:19118
SUKHORUCHKIN, S. I., Intermediate structures in neutron cross sections, 25:20445
SUKHOV, F. F., Application of the method of radiothermoluminescence for the investigation of high-temperature relaxation in polyethylene, 25:18435
SULCEK, Zdenek, Use of silica gel for the separation of traces of uranium, 25:18345
SULIK, A., Excitation of short-lived isomeric activities in ^{77}Se, ^{122}Sb, ^{137}Ba, ^{167}Er, and ^{179}Hf using 14.5-MeV neutrons, 25:20435
SULLIVAN, Jeremiah J., Astronauts' radiation exposure on first lunar landing mission, Apollo XI, 25:18978 (AD-711316)
SUNDFORS, R. K., Alpher--Rubin ultrasonic attenuation and dipolar nuclear-acoustic-resonance coupling in pure metals, 25:19879
SURANYI, G., Observation of S^0 meson, 25:20009
SURKO, Pamela Hansen, Nucleon-nucleon triple-scattering parameters 510 to 670 MeV, 25:19904
SUTRA-FOURCADE, Y., Neutron dosimetry in plants treating irradiated fuels, 25:18800 (SC-T-71-3009)
SUTTER, G., Operation of sampling spark chambers, 25:18778
SUZUKI, Katsuhiko, Analysis of radiosensitivity by modification of DNA metabolism, 25:19155
SUZUKI, T., Absolute measurement of beta-disintegrating nuclides, 25:20421
SUZUKI, Tadao, Honeycomb block used for collimation of radiations and method of manufacturing the same, 25:18856
SUZUKI, Takehiko, Correction to the direct transfer reaction of heavy ion, 25:20501
SUZUKI, Toshimi, Photoisomerization of maleate radical anions produced in 2-methyltetrahydrofuran by γ irradiation at 77°K, 25:18457
SVATOS, J., Scattering from a circular graphite core--ice mantle cylinder at normal incidence, 25:19457
SVEDIN, U., Hardware system for measurements of bubble chamber films on-line, 25:18776 (USIP-70-3)
SVELTO, V., Extension of Ramo's theorem as applied to induced charge in semiconductor detectors, 25:18710
SVINGOR, E., Distorting effect of the absorbers for the semiconductor and scintillation gamma-ray spectra, 25:18771
SVIRIDENKO, V. E., Boiling of liquids on fine wire under natural convection conditions, 25:18583
SVITEL, J., Determination of low silver content in drugs by low-energy gamma-ray stimulated characteristic radiation, 25:18355
SVOBODA, M., Numerical calculation of one-dimensional unstationary temperature and stress fields, 25:18579
SWALLOW, Earl Connor, Asymmetry parameters for beta decay of polarized Λ hyperons, 25:19894
SWEDLUND, John B., Confirmation of magnetic white dwarf G-195-19, 25:19328
SWENSON, G., Annealing experiments on Si layers implanted with 50-keV P ions, 25:19779
SWETMAN, T. P., Tachyons, 25:20085
SWICORD, Mays L., Microwave measurements and new types of detectors for evaluation of health hazards, 25:20853 (BRH/DEP-71-1)
SWITZER, P., High-frequency modulation of light from Crab pulsar, 25:19360
SYMANZIK, K., Renormalization of theories with broken symmetry, 25:20056 (DESY-70/62)
SYMKO, O. G., Continuously operating ^{3}He evaporation refrigerator, 25:19632
SYRE, R., Research and development of new high temperature resistant Nb alloys, 25:19218
SYTNIK, V. V., High-pressure gas target cooled by liquid nitrogen, 25:20128 (IFVE-SEF-70-22)
SZABO, Gy., Aberrations of asymmetrized quadrupole lenses, 25:20151
SZABO, Gyula, Calculation of the acceptance for ion optical systems, 25:20223
SZALAY, A., Study of decay of ^{145}Sm, 25:20465
SZARVAS, P., Exchange reactions of central atoms in lanthanide--aminopolycarboxylate complexes. III, 25:18412
SZAWLOWSKI, Theodore H., 2-substituted naphth(1,2)oxazole scintillators, 25:18731
SZEGO, L., Precipitation conditions in the uranyl nitrate--ammonium hydroxide system, 25:18379
SZY, Sandor, Radiologic presentation of the forms of pelvic fracture, 25:19040
SZYMANSKI, Z., Penetration of a two-dimensional fission barrier, 25:20478 (INR-P-1230)
SZYMCZAK, M., Beta spectrometer with a Si(Li) detector in homogeneous magnetic field, 25:18736 (INR-P-1227)
  Beta spectrometer with Si(Li) detector in homogeneous magnetic field, 25:18767

T

TABARDEL-BRIAN, Renee, Neutron dosimetry in plants treating irradiated fuels, 25:18800 (SC-T-71-3009)
TADA, Masabumi, Direction of development on reactor materials, 25:18574
TAFT, R. W., Secondary hydrogen--deuterium isotope effects in the fluorine nuclear magnetic resonance shifts of methyl-p-fluorophenylcarbonium ions, 25:18396
TAGGART, Keith Anthony, Two problems of the 3π decays of the eta meson, 25:19948
TAGGART, R., Effect of omega phase reversion on the superconducting transition in titanium-base alloys, 25:19590
TAGUCHI, Shigetoshi, Effects of x-irradiation on ^{14}C-pyruvate metabolism in rat thymocytes, 25:18902
TAGUCHI, Yoshibumi, Construction of nuclear power plant, 25:20565
TAILLEFER, R., Base-catalyzed protium--deuterium exchange in bicyclo[2.2.1]heptanones, 25:18411
TAKADA, Akikazu, Proliferation of donor spleen and bone-marrow cells in the spleens and bone marrows of unirradiated and irradiated adult mice, 25:19129
TAKADA, Mamoru, Measuring calorific value of petroleum, 25:18817
TAKADA, Yumiko, Proliferation of donor spleen and bone-marrow cells in the spleens and bone marrows of unirradiated and irradiated adult mice, 25:19129
TAKAGI, Yutaka, Male sterility in oil rape induced by gamma-irradiation, 25:19152
TAKAHASHI, Hidesuke, Histological and cytological changes of cervical cancer during the linear accelerator irradiation therapy, 25:19064
TAKAHASHI, Hiroshi, Survival and repopulation of hemopoietic tissues of irradiated mice transplanted with bone marrow cells from cyclophosphamide treated donors, 25:19112
TAKAHASHI, Minoru, Many-body problem of attractive fermions with arbitrary spin in one dimension, 25:20502
TAKAI, Yuriko, Influence of ^{60}Co γ-ray on potato, 25:19160
TAKAMURA, S., Recovery of fast neutron irradiated molybdenum, 25:19861
TAKANO, Hideki, Analysis of fast critical experiments and revision of JAERI-fast set, 25:20788 (JAERI-Memo-4215)
  Number of resonances to be adopted for obtaining practically reliable cross section curves, 25:20395
TAKASHIMA, Tsutomu, Distribution to organs of ^{131}I--erythrosine B, 25:19060
TAKEDA, Renzo, Analysis of flux measurement near strong absorber using VISTA method. I, 25:20831 (JAERI-Memo-4238)
TAKEI, Mitsuo, Direction of development on a nuclear fuel cycle, 25:18603
TAKEMURA, T., Construction of nuclear power plant, 25:20564
TAKEO, Masakatsu, Flux jumps in nonideal type-II superconductors. II, 25:19630
TAKEUCHI, Eiji, Analysis of flux measurement near strong absorber using VISTA method. I, 25:20831 (JAERI-Memo-4238)
TAKEUCHI, Katsumi, Effect of radiotherapy on the urinary amino acids, 25:19063
TAKEUCHI, Kiyoshi, User's manual for PALLAS code, 25:20246
TAKEUCHI, Shoko, Nuclear instrumentation, 25:20800

XUM

TAKSIS, G. A., Relationship between electric resistance of zirconia ceramics and porosity, 25:19283
TALBOT, Jean, Electrochemical properties of Nb, 25:19170
TALBOT, Raymond J., Helium production by pulsationally unstable massive stars, 25:19331
TALMAN, J. D., Analytic interpolation of the eigenvalues of an asymmetric rotator, 25:20513
  Computation of Moshinsky brackets by direct diagonalization, 25:20526
TAL'ROZE, V. L., Kinetics for the radiation polymerization of solid acrylonitrile in the regions of phase transitions, 25:18440
TALYSHINSKII, R. R., Effect of laser beam on bone, 25:19146
TAMAGAWA, H., Excitation and stabilization of ion-acoustic waves in RF plasma, 25:19744
TAMM, E. I., Cherenkov total-absorption spectrometer, 25:18787
TAMPLIN, A. R., Fluoroscopic radiation and risk of lung cancer following therapy of tuberculosis, 25:19068
TAMSKY, Morgan Jerome, Thermally stimulated currents from gamma-irradiated organic polymers, 25:18422
TAMURA, Tsuneo, Disposal by hydraulic fracturing, 25:18622 (ORNL-4584, pp 11-15)
  Fate of trace elements and radionuclides in terrestrial environment, 25:18521 (ORNL-4584, pp 1-10)
TAN, Chung-I, Helicity poles, triple Regge behavior and single particle spectra in high energy collisions, 25:19926 (NYO-2262-TA-234)
TAN, Chung-i., Crossed-channel partial-wave expansions and Bethe--Salpeter equation, 25:20113
  Scaling behavior in multiperipheral dynamics, 25:19982
TAN, F. C., Barium and Sr in silicates, 25:18335
TANABE, Kosai, Energy shift due to nuclear polarization in a high orbital state of muonic atom, 25:19486
TANAKA, Kentaro, Construction of nuclear power plant, 25:20564
TANAKA, Norimoto, Modification of radiosensitivity of Ehrlich ascites carcinoma cells in vivo. I, 25:19130
TANAKA, Syo, Photoproduction of two neutral pions from hydrogen near threshold, 25:19890
TANG, I-ming, Flux-flow resistivity and Hall angle in pure transition-metal superconductors near H/sub c2/, 25:19619
TANG, Y. S., Engineering study of the colloid-fueled reactor concept, 25:20811
TANG, Yi-noo, Recoil tritium reactions with trimethylfluorosilane. A study on parameters affecting hot-atom substitution reactions, 25:18484
TARASENKO, A. T., Influence of ionizing radiation and radio-protectors on the antihyaluronidase activity of blood serum and tissue permeability in rats, 25:19031
TASAKA, Kanji, Estimation of fission product decay heat, 25:20834 (JAERI-Memo-4205)
TATCHER, M., Lifetime measurements of alpha emitters in the millisecond region, 25:18703
TATOMIR, D., New linear gravitation theory. III, 25:20098
TAUTZ, M. F., Magnet systems for the transport of ion beams with no change in properties, 25:20205
TAVKHELIDZE, A. N., Method of coherent states and factorization of dual amplitudes, 25:20120
TAYLOR, D. M., Dosimetry of ^{67}Ga in hybrid rats, 25:18992
TAYLOR, David M., Binding of americium and plutonium to bone glycoproteins, 25:18899
TAYLOR, H. A. Jr., Ion chemistry and thermal balance in E and F regions above Wallops Island, 25:19575
  Solar geomagnetic seasonal control of topside ionosphere, 25:19576
TAYLOR, Howard S., Many-body methods applied to electron scattering from atoms and molecules. II, 25:19507
TAYLOR, James F., Acute lethality and recovery of goats after 1 MVp x-irradiation, 25:19115
TAYLOR, M. C., Proton recoil monitor for neutron flux measurements, 25:18763
TAYLOR, Raymond A., Nuclear radiation digital dose measuring system, 25:18684
TEBRA, W., Data collector for a coinidence experiment, 25:18872
TEFFT, Melvin, Irradiation of the liver in children: acute effects enhanced by concomitant chemotherapeutic administration, 25:18999
TEICHMANN, J., Class of solutions of quasi-linear equations, 25:19694
TEICHMANN J., Nonlinear wave mixing at hybrid frequencies in an inhomogeneous plasma, 25:19747
TELLES, Norman C., Review of radium toxicity studies, 25:18979 (BRH/DBE-70-5)
TELLESCHI, P., Dynamic studies of gas turbine fast reactors, 25:20765
  Operational conditions for afterheat removal of a gas-cooled reactor with direct cycle, 25:20767
TEMKIN, A., Generalized Hylleraas calculation of positron--hydrogen scattering, 25:19508
TENG, K., Computer programs for calculation of liquid-scintillation data, 25:18693
TENGROTH, Bjoern, Medical aspects of the use of lasers, 25:19074
TEODORESCU, V., New linear gravitation theory. III, 25:20098
TEODOSIC, V., Dead-time correction for any distribution of input events, 25:18706
TEPLYAKOV, V. A., Linear ion accelerator with spatially homogeneous strong focusing, 25:20172
TEREKHOVA, L. S., Structure and properties of an [electrodeposited] In--Zn alloy, 25:19221
TEREKHOVA, V. F., Phase diagrams and properties of La--Sc alloys, 25:19241
TERRASI, F., Energy calibration of Ge(Li) spectrometer, 25:18714
TERTIAN L., Structure of sputtered niobium films, observation of a fcc phase, 25:19244
TETE, Claude, Vacancy quenching in Nb, 25:19245
TETERIS, Ya. A., Chemiluminescence method of investigation of radiation defects in alkali halides, 25:19850
TEWARI, S. P., Studies in Be oxide, 25:20239
THACKER, R., Radiation processed wood-plastic materials, 25:19298
THEKAEKARA, M. P., Standard values for the solar constant and its spectral components, 25:19416
THIELE, B., Irradiation tests with vibrocompacted (Th/U)O$_2$ particles, 25:19291
THIND, K. S., Calculations of fission parameters based on a molecular model of fission, 25:20489
THOMAS, E. W., Formation of metastable hydrogen atoms by charge transfer, 25:19504
THOMAS, G., Lecture 3: nonequilibrium defects in metals, 25:19232 (UCRL-19696)
THOMAS, G. L., Optical model for proton scattering from ^{40}Ca, 25:20311
THOMAS, James E. Jr., Observation of x-ray diffuse scattering from neutron-irradiated silicon, 25:19853
THOMAS, John H., Trapped gravity waves and the five-minute oscillations of the solar atmosphere, 25:19405
THOMAS, Lawrence Eldon, State functional and phenomenon of time in quantized gravitation, 25:20095
THOMAS, P. B., Scintillation camera in the dynamic evaluation of renal disorders, 25:19046
THOMAS, R. A., 200-kV ion-implantation equipment at MRL, Salfords, 25:19774
THOME, Paul, Nuclear reactor with integrated heat exchangers, 25:20840
THOMPSON, J. A., Secondary hydrogen--deuterium isotope effects in the fluorine nuclear magnetic resonance shifts of methyl-p-fluorophenylcarbonium ions, 25:18396
THOMPSON, J. J., CLASSIC: code for stability and response analysis of linear systems, 25:20830 (AAEC/TM-551)
  Discontinuous finite elements in thermal analysis, 25:18573
THOMPSON, M., 5,7-dihalo-8-hydroxyquinoline complexes of U(VI), 25:18374
THOMPSON, M. W., Applications of ion implantation outside the semi-conductor area, 25:19785
THOMPSON, R. L., Saxton Core II nuclear operations summary, 25:20705 (WCAP-3385-55)
THORLEY, A. W., Solubility of carbon in sodium, 25:19196 (TRG-Report-1906)
THORNBER, K. K., Hidden momentum for non-steady state defined, 25:19953
THORNGATE, J. H., Spectrometry research and development, 25:18644 (ORNL-4584, pp 152-64)
THORNHILL, A. P., HTR fuel disposal study, 25:20745 (DP-Report-450)
THUN, J. E., Decay of ^{131}Ba, 25:20414
  Decay of ^{249}Cf, 25:20398
TIBERINI, A., Dynamic studies of gas turbine fast reactors, 25:20765
TIKHONOV, K. A., Discrete frequency sweep in a synthesizer for nuclear magnetic resonance spectroscopy, 25:18848
TIKTOPOULOS, George, Does multiple Reggeon exchange produce an eikonal-type formula, 25:20111
  Relativistic eikonal approximation, 25:20112
TILIKS, Yu. E., Chemiluminescence method of investigation of radiation defects in alkali halides, 25:19850
TIMBERLAKE, J. W., Secondary hydrogen--deuterium isotope effects in the fluorine nuclear magnetic resonance shifts of methyl-p-fluorophenylcarbonium ions, 25:18396
TIMMONS, Richard B., Kinetic isotope effects in reactions of bromine atoms with CH$_4$ and CD$_4$, 25:18410
TIMOFEEVA, T. V., Radiation resistance of type ZnS + ^{10}B detectors to neutrons, 25:18880
TINSLEY, A. W., Electrical and atom-site location properties of ion-implanted germanium, 25:19799
TIPPETT, J. C., Validity of Nilsson model for proton states in region A = 151 to 155, 25:20383
TISHCHENKO, M. A., Titrimetric determination of the rare earth elements with 1,2-dihydroxybenzene-3,5-disulphonic acid, 25:18348
TISHIN, A. S., Angular anisotropy and fissionability of nuclei, 25:20529
TISNEK, N. I., Resolving power of silicon surface-barrier counters, 25:18672
TITANI, Yoiti, Effect of Tween 80 on strand breaks of E. coli DNA irradiated in situ, 25:19027
TITLE, R. S., Distribution of damage produced by ion implantation of silicon at room temperature, 25:19818
TITOV, A. I., Motion of particles in the fixed centers field, 25:20059 (JINR-P4-5547)
TITOV, Yu. I., Electron detection with a shower detector, 25:18786
TITTEL, O., Improvement to quantum yield of photocathodes of 56 TVP photomultipliers in red part of spectrum

(7000 A), 25:18828 (EUR-CEA-FC-576)
TIWARI, R., Nonexistence of spherically symmetric solution representing vacuum electrostatic field, 25:20088
TOBA, H. H., Effects of gamma irradiation or the chemosterilant, tepa, on the citrus red mite and its progeny, 25:19100
TOBAILEM, J., Gamma emitters and exposure age of the Bovedy meteorite, 25:19301
TODKILL, A., Cathodoluminescence of ion-implanted silicon carbide, 25:19790
TOEI, Kyoji, Synthesis of (o-oxalophenylazo)chromotropic acid and stability constant of its Th chelate, 25:18382
TOIVOLA, Ahti, Effects of nuclear power plants on the environment, 25:20683
TOKTAROV, K., Interaction of shock waves with fluctuations of nuclear matter, 25:20491
TOKUDA, N., Nonleptonic decay of hyperons, 25:19967
TOKUYAMA, T., Enhanced diffusion of B and P in Si during ion implantation, 25:19824
TOLAR, J., Mass operator in SU(3)-symmetric strong coupling theory with pseudoscalar mesons, 25:20015
  Mass operator in the SU(3)-symmetric strong coupling theory with pseudoscalar mesons, 25:20046
TOLKACH, P. N., Contribution of the scintillator to the resolution of a spectrometer using the single-electron method, 25:18745
TOLKACHEV, V. A., Destruction of free radicals in irradiated organic crystals, 25:18473
  Effect of irradiation dose rate and manner of preparation of samples on the kinetics of radical build-up in aniline, 25:18465
TOLMACH, I. M., Empirical approximation of coefficient of hydraulic resistance in a moving magnetic field, 25:19557
  Montardy scheme with segmented electrodes for MHD devices, 25:19541
TOLMACHEV, V. V., Criterion of completeness for set of functions used in matrix Hartree--Fock and correlation-energy calculations, 25:19519
TOLSTOLUZHSKII, A. P., Transverse instability in sectional linear accelerator, 25:20215
TOMANEK, J., Use of linear accelerator in irradiation of Dictyocaulus viviparus larvae, 25:19101
TOMAS, P., Neutron--proton bremsstrahlung at 14.4 MeV, 25:20257
TOMII, Kakuzo, Prog. rpt. on nuclear safety experimental program, 4--10/70, 25:20763 (JAERI-Memo-4229)
TOMLINSON, R. H., Calculations of fission parameters based on a molecular model of fission, 25:20489
TOMPKINS, Edythalena, Review of radium toxicity studies, 25:18979 (BRH/DBE-70-5)
TOMS, M. E., Computer analysis to obtain neutron spectra from an organic scintillator, 25:18766
TONAPETYAN, S. G., Spark chamber with graphite electrodes, 25:18785
TONE, Tatsuzo, Plutonium-239 fission product yields and their influence on fast reactor characteristics, 25:20819 (JAERI-Memo-4165)
TONEEV, V. D., Double differential distribution of particles produced in the proton-nucleus collisions, 25:20018 (JINR-P2-5507)
TOOLE, James F., Selenomethionine ^{75}Se thymus scans in myasthenia gravis, 25:19049
TORBENKO, V. P., Clinical aspects and treatment of radiation combined injuries, 25:19033
TORGOMYAN, G. B., Superhigh-energy particle detector based on using the radiation of a particle in a laminar medium, 25:18781
TORIKAI, Ayako, Photoisomerization of maleate radical anions produced in 2-methyltetrahydrofuran by γ irradiation at 77°K, 25:18457
TOROPOV, A. S., Sensitivity of a secondary-emission-type accelerated-electron-beam position monitor, 25:20173
TOROPOV, Yu. S., Relationship between electric resistance of zirconia ceramics and porosity, 25:19283
TORRES, Jean-Philippe, Decay of ^{155}Ho, 25:20405
TOUSSET, J., High energy reactions with Ho and Tm, 25:20390
TOVEY, N., Compilation of cross sections V--K^- induced reactions, 25:19909 (CERN-HERA-70-6)
TOW, Don M., Interference terms in Amati--Bertocchi--Fubini--Stanghellini--Tonin multiperipheral model, 25:19998
  Scaling, deep inelastic electron--nucleon scattering, and the multiperipheral model, 25:19959
TOWN, Christopher D., Production and repair of radiochemical damage in Escherichia coli deoxyribonucleic acid; its modification by culture conditions and relation to survival, 25:18912
TOWNSEND, P. D., Ion-beam irradiation of glasses, 25:19787
TOYAMA, Masaaki, Thickness measurement by radiation manufacturing automobile tires, 25:18824
TRACY, John Micheal, Polar reflection Faraday effect in silver-based disordered alloys, 25:19873
TRAJMAR, S., Detection and identification of triplet states of H_2O by electron impact, 25:19499
TRAN, D. T., Interdigital H-type (IH) structure, an accelerating structure for low energy beams, 25:20156
TRAN MINH DUC, High energy reactions with Ho and Tm, 25:20390
TRAPANI, A., Neutron flux measurement by counting the associated ^{3}He particles from T(p,n) reaction, 25:18647
TREHAN, S. K., Effect of gyro-viscosity on Rayleigh--Taylor instability of a plasma, 25:19711
TREIMAN, S. B., Does multiple Reggeon exchange produce an eikonal-type formula, 25:20111
  Relativistic eikonal approximation, 25:20112
TRET'YACHENKO, L. A., Structure of V--Cr--Zr alloys at 1150°C, 25:19237
TRET'YAKOV, B. N., Transition of niobium into the superconducting state using nuclear magnetic resonance, 25:19628
TREVINO, S. F., Inelastic neutron scattering from solid benzene, 25:20247
TRIKHA, S. K., Studies in Be oxide, 25:20239
TRINDADE, Helena A., Behavior of iodine in sodium systems, 25:20760 (CONF-700816-(Vol.1), pp 356-72)
TRINKL, Gabriele, Vapor pressure of Gd(III)-bromide according to cup method of W. Fischer, 25:18417
TROBAUGH, F. E. Jr., Accelerated regeneration of transplanted hematopoietic stem cells in irradiated mice pretreated with cyclophosphamide, 25:19127
TROBAUGH, Frank E. Jr., Factors regulating the proliferation and migration of hematopoietic stem cells, 25:19126
TROKHAN, A. M., Electron gun having an electron output from a vacuum into gas, 25:18850
TROPP, E. A., Laminar flow of a viscous conducting fluid between parallel walls in moving magnetic field, 25:19561
TROSKO, James E., Prog. rpt. on radiation and chemical-induced molecular damages, annual, 6/70--5/71, 25:19090 (COO-1704-22)
TROTEL, J., Calutron-type ion source for use in an ion-implantation machine, 25:20169
TROTT, N. G., Dosimetry of ^{67}Ga in hybrid rats, 25:18992
TROUTNER, D. E., Yield of /sup 99m/Nb from fission of ^{233}U, ^{235}U, ^{238}U and ^{252}Cf, 25:20406
TRUBATCH, S. L., Generalized finite-matrix Hamiltonians, 25:20066
TRUEMPER, Manfred, Ellipsoidal velocity distributions and a kinetic theory of Newtonian cosmological models, 25:19460
TRULSEN, J., Radiation from a charged particle in a magnetoplasma, 25:19696
TRUNK, M., Lifetime and delayed neutron fraction of thermal thermionic reactors, 25:20825
TRUSOVA, V. P., Glucose and oxalic acid methods of γ-radiation dosimetry, 25:18808
TRZHASKOVSKAYA, M. B., Formation region of internal conversion coefficients, 25:20515
TSCHANZ, J. F., Nuclear orientation of ^{59}Fe in rare-earth double-nitrate crystals, 25:20413
TSIEN, Thomas Nai-chen, Electromagnetic induction of rotating magnets, 25:19639
TSIRIN, E. Kh., Blood changes in dinitrochlorbenzol-sensitized dogs after irradiation, 25:19030
TSISEK, Z., Device with snap-off diode for compensation of influence of pulse amplitude spread of scintillation and Cherenkov counters, 25:18639 (IFVE-SEF-69-44)
TSOLOV, V., Influence of antibody formation on permeability of erythrocytes, 25:18900
TSUBOKAWA, Tadashi, Gamma irradiation in medicinal plant breeding. II, 25:19151
TSUCHIMOTO, T., Enhanced diffusion of B and P in Si during ion implantation, 25:19824
TSUCHIMOTO, Taiso, Chronic granulocytic leukemia with special reference to A-bomb survivors, 25:18963
TSUPKO-SITNIKOV, V. M., Two-dimensional analyzer for half life measurements of nucleus of excited states, 25:18642 (JINR-P13-5485)
TSURUOKA, Kazuo, Heat resisting metal, 25:19197
TSVETKOV, Yu. D., Space distribution of radicals during γ-irradiation of methanol at 77°K, 25:18464
TSYGANOV, A. D., Possible use of positron annihilation to study chemisorption, 25:18415
TSYTOVICH, V. N., Role of maser effect in radar echo from sun, 25:19419
TUCKER, A. B., Low-intensity gamma rays in ^{90}Nb decay, 25:20411
TUERK, G., Preliminary experiments of a heat exchanger in He under high-pressure, 25:20780
TUERKCAN, Erdinc, Theoretical and experimental study of a fast-thermal coupled reactor by correlation techniques, 25:20833 (RCN-132)
TUMANYAN, M. A., Influence of ionizing radiation on natural immunity, 25:18922
TURBA, E., Indium-113m--DTPA in the study of the kidney, 25:19039
TURETSKII, L. I., Water pump for pressure-cooling reactor in atomic powerplant, 25:20717 (JPRS-52384)
TURIEL, I., Evaluation of an LN_2-temperature solid state spectrometer for rocket borne experiments, 25:18654
TURIN, M., Use of Hall probes in inhomogeneous magnetic fields, 25:18833
TURJANSKI, R., Resonance integral of ^{94}Zr and ^{96}Zr, 25:20392
TURNEY, George E., Auxiliary and loop for removal of decay heat from a space power reactor, 25:20805 (N-70-39420)
TWIGG, Homer L., How to protect patient and physician during x-ray examinations. I, 25:19010

TYBOR, V., Decays in broken SU(6)/sub W/ symmetry, 25:20047
  Decays in broken SU(6)/sub W/ symmetry, 25:20048
TYURIN, N. E., Equal-time equation for two-particle system in quantum field theory, 25:20077
TZIANABOS, Theodore, Preparation of noninfectious arbovirus antigens by sucrose--acetone extraction of gamma-irradiated tissue, 25:18924

U

UCHIDA, T., Plasma emission from titanium rail-type gun, 25:19726
UCHIDA, Yoshihisa, Measuring calorific value of petroleum, 25:18817
UCHINO, Haruto, Chronic granulocytic leukemia with special reference to A-bomb survivors, 25:18963
UCHRIN, J., Study of decay of ^{145}Sm, 25:20465
UDO, F., Particle identification by an improved time-of-flight system, 25:20180
UEDA, Tamotsu, One-boson-exchange model of N--N scattering for the 0- to 3-GeV energy range, 25:20025
UGUZZONI, A., Use of a checker board counter in blocking experiments, 25:18679
UHER, E., Problems on sorption equilibrium in ion exchange column for microquantities of radioactive solution in the presence of competing ion, 25:18504 (UJV-2450-Ch)
UJHELYI, Cs., Effect of thin foils on the spectrum of monoenergetic electrons, 25:18770
ULLAH, N., Description of the nuclear-configuration interaction problem using statistical ensembles, 25:20505
  Properties of real RPA matrices and a simple diagonalization procedure, 25:20525
ULPAT, Jean-Pierre, Study of reactions ^{9}Be + t below Coulomb barrier, 25:20265 (CEA-R-4117)
UL'YANOV, M. I., Clinical aspects and treatment of radiation combined injuries, 25:19033
UMEK, H., Spleen scintigraphy with /sup 113m/In-labeled erythrocytes, 25:19036
UMEZAWA, H., Absolute measurement of beta-disintegrating nuclides, 25:20421
  Wave equations with compact and noncompact spectrum, 25:20050
UMLAUF, E., Pressure dependence of Kondo resistance anomaly and pair breaking effect in La--Ce alloys, 25:19863
UNCLES, R. J., Dynamic stabilization of the electrothermal instability, 25:19543
UNDERHILL, Dwight, Design of fission gas holdup systems, 25:18561 (CONF-700816-(Vol.1), pp 216-23)
UNDERHILL, Dwight W., Comparison of equations used in the design of fission gas adsorption beds, 25:18560 (CONF-700816-(Vol.1), pp 207-15)
UNGER, H., Lifetime and delayed neutron fraction of thermal thermionic reactors, 25:20825
UPDEGRAFF, William Edward, Model of nuclear photofission, 25:20499
UPTON, J. W. Jr., Gas-flow method for detection of fast neutrons in reactors, 25:18646 (WHAN-SA-73)
URANO, Muneyasu, Experimental evaluation of tumor bed effect for C3H mouse mammary carcinoma and for C3H mouse fibrosarcoma, 25:19118
  Modification of radiosensitivity of Ehrlich ascites carcinoma cells in vivo. I, 25:19130
URAZGALIEV, A., Thickening of wool fibers under the influence of ionizing radiation, 25:19121
URBAN, Eugene Willard, Magnetic flux flow in a Type-II superconductor, 25:19609
URBAN, L., Unrestricted variational method on light nuclei, 25:20546
URBAN, Paul, Conference on developments in high energy physics, Schladming, Austria, 2--3/70, 25:19933
URLI, N. B., Characteristics of implanted p--n junctions by C(V,f) measurements, 25:18857
URTH, A., Problems concerning radiotherapy and curietherapy in dentistry, 25:19069
USAMI, Akira, Curve power factors and its radiation-induced changes in silicon photovoltaic cells, 25:18882
USHAKOV, P. A., Velocity field of turbulent fluid flow in a longitudinal streamline of clusters of rods, 25:18576 (AEC-tr-7189)
USHKOV, V. L., Vacuum system for the 70-GeV proton synchrotron, 25:20126 (CERN-Trans-70-9)
UTTLEY, C. A., Ratio of ^{6}Li(n,α) to ^{10}B(n,α) cross-sections, 25:20288
UYTTENHOVE, J., Isomeric transitions, 25:18753
UZAKOV, Ya. M., Introduction of controlled energy-mode in U-150-2 cyclotron of Inst. of Nuclear Physics of UzbSSR Academy of Sciences, 25:20216

V

VAALAMO, P., Scanning of placenta with /sup 99m/Tc, 25:19045
VACCA, G., Dosimetry of the gastro-intestinal tract, 25:19141
VACHASPATI, Double scattering of electromagnetic radiation by bound electrons, 25:19949
VACIAGO, C., Neutron transmission study through simple bent conducting tube, 25:20245
VACIRCA, Salvatore John, Predicting body doses due to diagnostic radiography, 25:19038
VAHALA, George, Discrete spectra and damped waves in quasi-linear theory, 25:19751
VAL'DNER, O. A., Accelerators. XII, 25:20186
VALKOVIC, V., Comparison of p--p and n--p quasi-free scattering in p + d + p + p + n reaction, 25:20260
  Neutron--proton bremsstrahlung at 14.4 MeV, 25:20257
  Reaction ^{11}B(n,t)^{9}Be at 14.4 MeV, 25:20285
VAMPOLA, A. L., Solar-flare electron spectra in space and within Earth's magnetosphere, 25:19428
VAN ANTWERP, Walter R., DORF-I: gamma-ray spectrograph shielding studies, 25:18732 (AD-711531)
VANCE, C. F., Microwave power transmission ratio: its use in estimating electron density, 25:19656 (EP-RR-21)
VAN DAM, J. E., Magnetic susceptibility of dilute Au--V alloys, 25:19865
VAN DANTZIG, R., Analysis of multidimensional nuclear data (BOL). I, 25:20203
  BOL computer-hardware configuration, 25:20200
  BOL nuclear research project, 25:20198
  Data acquisition with the BOL nuclear detection system, 25:20202
  Scattering chamber of the BOL-system, 25:20201
  Test-procedures for multidetector BOL-system, 25:20207
VAN DER GRIENT, Anton Jacobus, Hyperthyroidism, radioiodine and thereafter, 25:19062 (NP-18693)
VAN DER WEG, W. F., Gallium implantations in Si studied by proton backscattering, x-ray emission, and Hall effect, 25:19802
VAN DER WIEL, M. J., Data collector for a coinidence experiment, 25:18872
VAN DYKE, Donald, Myocardial uptake studies with ^{129}Cs and the scintillation camera, 25:19055
VAN EIJK, C. W. E., X-ray isotopic shift for ^{162}Dy--^{164}Dy, 25:20416
VANINBROUKX, R., Isomeric state in ^{113}In, 25:20460
VANLAER, Marcel, Economics of the various methods available for preparing Nb, 25:19187
VAN MAAREN, M. H., Oscillatory dependence of T/sub c/ on number of valency electrons in Cu_3Au-type alloys, 25:19621
VANNESTE, L., Spin dependence of the neutron-capture cross section of vanadium and the internal magnetic field at vanadium nuclei, 25:20335
VAN RINSVELT, H. A., Use of a pulsed Van de Graaff accelerator and time-of-flight techniques to reduce backgrounds in (α,γ) spectroscopy experiments, 25:20148
VAN STEENBERGEN, A., Design study of a Cold Magnet Synchrotron, 25:20125 (BNL-15430)
VAN STIGT, Ch. A., Separation of gram-amounts of lanthanides by cation exchange, using an aqueous solution of α-hydroxyisobutyric acid as an eluant, 25:18501 (RCN-131)
VARGA, D., Effect of thin foils on the spectrum of monoenergetic electrons, 25:18770
  Internal bremsstrahlung spectrum from ^{32}P, 25:20340
  Study of decay of ^{145}Sm, 25:20465
VARLASHKIN, Paul G., Positron annihilation and positronium bubbles in liquid and solid Ar, Kr, and Xe, 25:19487
VARSHNEYA, N. C., Theory of radiation detection through supercooled liquid, 25:18709
VASAVADA, K. V., Role of non-Pomeranchuk Regge cuts in high energy scattering, 25:20006
VASIL'EV, A. S., Suppression of turbulence in tubes by transverse magnetic fields, 25:19556
VASIL'EV, A. V., Glucose and oxalic acid methods of γ-radiation dosimetry, 25:18808
VASIL'EV, V. A., Experimental solenoid made of Nb_3Sn strip, 25:19588 (JINR-P8-5440)
VASIL'EVA, E. V., Diffusion coefficients for binary Nb alloys, 25:19204
VASIL'KOV, R. G., Electronuclear method of neutron generation and fissile material production, 25:20191
VASSILEV, Georges, Excitations in low-energy ion--atom collisions, 25:19493
VASSIL'EVA, G. J., Velocity field distribution in the solar photosphere, 25:19404
VASUDEVAN, R., Does a uniformly accelerated charge radiate, 25:19944
VATA, I., Energy calibration of Ge(Li) spectrometer, 25:18714
VATAI, E., Internal bremsstrahlung spectrum accompanying positive beta decay of ^{11}C, 25:20302
VAURAMO, E., Scanning of placenta with /sup 99m/Tc, 25:19045
VEJE, L., Isospin analysis of pion and nucleon resonance production in NN collisions, 25:20030
VELIKOV, V., Alpha-spectroscopy determination of concentrations of radon daughters in air, 25:18363
VELNER, S., Wires as thermal neutron probes, 25:18707
VELO, G., Solvable quantum-mechanical model with nonlinear transformation laws, 25:20504
VENERUSO, A. F., Stochastic analysis of fractured glass, 25:20891 (SC-RR-69-506)
VENNEMANN, J., Wurgassen nuclear power station, 25:20561
VENTRICE, Carl A., Time-averaged density profile in finite-amplitude instability, 25:19715
VERCAEMER, C., Hydrogen embrittlement of Nb base alloys, 25:19216

VERES, A., Measurement of activation cross section of ^{176}Lu, 25:20464
VERESHCHINSKII, I. V., Determination of the radiation yield of nitrite ions in the irradiation of sodium nitrate solutions in the small-dose region, 25:18463
VERGANELAKIS, A., Remarks on the eta $\rightarrow \pi^0 \gamma \gamma$ decay rate, 25:19937 (DEMO-71/2)
VERGASOVA, L. L., Diffusion coefficients for binary Nb alloys, 25:19204
VERNHES, C., Exposure of man to natural and artificial sources of ionizing radiations, 25:19137
VERNOTTE, Jean, First T = 2 state of ^{32}S, 25:20316
VERON, D., Production of plasma by laser irradiation of lithium hydride pellets, 25:19702
VERONDINI, E., Use of a checker board counter in blocking experiments, 25:18679
VERTES, P., PRODGROUP: program for production of multigroup reactor constants, 25:20820 (KFKI-71-4)
VERTUT, Jean, Improvements in shielding containers, 25:18633
VESTER, K. P., Total conversion coefficient and γ-line of the 13.34 keV level in ^{73}Ge, 25:20313
VICHERAT, A., Spectroscopic study of a caesium discharge plasma, 25:19665
VIEGAS, John R., Corrections of logarithm term in electrical conductivity of a fully ionized plasma, 25:19683
VIGNES, A., Diffusion in the binary systems Ti--Nb, Zr--Nb, V--Nb, Mo--Nb, W--Nb, 25:19214
  Formation and structure of aluminide base protective coatings on Nb and its alloys, 25:19173
  Oxidation and pest phenomena in NbAl$_3$, 25:19174
VIITASALO, M., Reaction ^{31}P(p,γ)^{32}S, 25:20308
VILLASANA, Edward, Radiochemical analysis of water from wells, springs, and streams in central Nevada, 25:18522 (USGS-474-97)
VILNITIS, A. Ya., Estimate of field in winding zone of plane linear induction MHD machines, 25:19539
VILQUIN, A., Buildup of radionuclides in marine species, 25:18894
  Experimental contamination of marine species by soluble and insoluble forms of ^{106}Ru in seawater, 25:18944
  Residual contamination of mussels, 25:18896
VINITCHI, V., Physical model on the boiling process in the power nuclear reactor, 25:20728
VINKLER, E. G., Theory of pulse radiolysis in an electric field, 25:18469
VINNAY, I., Production of spontaneously fissioning isomers of U, Pu, and Am in neutron reactions, 25:20369 (JINR-P3-5528)
VINOGRADOV, V. B., Monte Carlo generation of neutral π^-p interactions at 5 GeV/c in propane bubble chamber, 25:20004 (JINR-P13-5516)
VINOGRADOVA, A. P., Action of ionizing radiation on the structure and properties of the copolymer of styrene with 2-ethylhexyl acrylate, 25:18436
VISCONTI, Paul J., Absolute total cross sections for scattering of low-energy electrons by Rb, Cs, K, 25:19506
VISHNAYKOV, V. V., Use of a wire spark chamber to measure the beam profile of a synchrocyclotron, 25:20163
VISSER, Age T., Meter for measuring RMS values of pulsed current signals, 25:18839
VITALE, A., Response of large volume NE-213 liquid scintillators to electrons and protons, 25:18655
VITKEVICH, V. V., Observations of compact radio sources, 25:19368
VITOUX, D., Method for improving heavy ion spectra in scattering experiments, 25:18750
VITRICHENKO, F. A., Binary HD 175514. I, 25:19344
VLADIMIRSKII, B. M., Equatorial zone of avoidance of solar cosmic-ray arrival, 25:19437
  Nature of the changes in cosmic-ray diurnal variation during magnetic storms with sudden commencement, 25:19530
  Phase jumps of diurnal variations in cosmic-ray intensity, 25:19529
VLASOV, A. D., Self-consistent clusters of oscillating heavy particles in an accelerator, 25:20181
VOELKEL, A. H., Behavior of commutator matrix elements at small distances. II, 25:20076
VOETS, P., Scintigraphic detection of pathological processes within spinal cord space following intravenous administration of radioisotopes, 25:19042
VOGEL, Amelitta, Statistical determination of mean lifetimes for a radioactive species, 25:20498
VOIGT, A. F., Isomer ratio measurements for ^{91}Mo, ^{137}Ce, and ^{141}Nd produced by (γ,n) and (γ,3n) reactions, 25:20455
VOISIN, G., Interdigital H-type (IH) structure, an accelerating structure for low energy beams, 25:20156
VOISIN, Gilles, Method of calculating waveguides with simple periodical structures, 25:20147
VOITENKO, Yu. G., High speed magnetic-chip memory in a scanning robot for measurement of chamber photographs, 25:18780
VOLKAR, Martin Anthony, Charge-state distributions of boron ions and carbon ions by recoil spectrometry, 25:18485
VOLKOV, A. S., Statistical error of counting rate of a gas-discharge counter, 25:18663
VOLKOV, M. K., Brief review of reports submitted to 2nd international symposium on nonlocal quantum field theory, Azau, 3/70, 25:20057 (JINR-E2-5563)
  Regularizing properties of superpropagators, 25:20058 (JINR-P2-5569)
VOLKOVA, A. I., Study of the fluorescent niobium complex with hydrogen peroxide and sulphonaphtholazoresorcinol, 25:18349
VOLODIN, V. D., Investigation of the model of the 2-meter streamer chamber of the SCM-200 assembly, 25:18774 (JINR-P13-5529)
VOMERO, S., Preparation of complex-group resins and synthesis of phenolic resins with hydroxamic groups. I and II, 25:18503 (RT/CHI-(70)25)
VON ALLMEN, I., Heat exchangers for gas turbine fast reactors, 25:20775
VON BACKSTROEM, J. W., Roessing uranium deposit near Swakopmund, South West Africa, 25:18538
VON BALTZ, Ralph, Time-dependent thermalization of neutrons, 25:20242
VON BRENTANO, P., Gamma-decay of proton-particle neutron-hole states in ^{208}Bi, 25:20434
VON HAHN, H. E. A., Kinetics of copper(II)- and copper(I)-catalyzed deuterium exchange in sulfuric and perchloric acid solutions, 25:18390
VON WANGENHEIM, K.-H., DNA synthesis after irradiation with high doses of x-rays and spindle inhibition, 25:18510
VOOK, F. L., Crystallinity of ion-implanted Si, 25:19812
  Vacancy motion in low-temperature ion-implanted Si, 25:19811
VOROBEV, M. G., Low-activated trigger chamber containing ^{3}He, 25:18662
VOROB'EVA, V. G., Dependence of anti ν on neutron energy on basis of fission energy balance, 25:20440
VOSS, G. A., Cambridge electron accelerator bypass, 25:20195
VOSTEEN, K.-H., Radiation treatment of tumors, 25:19071
VOTINOV, S. N., Properties of heat-resistant steels following high-temperature reactor irradiation, 25:19250 (AEC-tr-7192)
VOVAN, Tien, Mixed rare earth sulfides, 25:19286
VRBA, J., Tunneling into weakly coupled films of aluminum and tin in proximity, 25:19623
VRBENSKY, J., Utilization of electroslag welding in the production of steel pressure vessels for nuclear reactors, 25:19181
VSEVOLODOV, E. B., Thickening of wool fibers under the influence of ionizing radiation, 25:19121
VUGMAN, N. V., Electron paramagnetic resonance of electron-irradiated K$_3$Rh(CN)$_6$ in a KCl lattice, 25:18462
VUGTS, H. F., Diffusion coefficients of isotopic mixtures of CO and N$_2$, 25:18604
VULIS, L. A., Resistance in flow of liquid metals in channels in a transverse magnetic field, 25:19554
  Unsteady flow of mercury in a trough in a transverse magnetic field, 25:19553
VUORINEN, Antti, Effects of nuclear power plants on the environment, 25:20683
VYTSE, I., Correction matrix elements for the first forbidden β^- transition in ^{198}Au, 25:20438

W

WADACHI, Y., Flocculation treatment of radioactive contaminated sea water. I, 25:18518
WADDINGTON, J. C., Validity of Nilsson model for proton states in region A = 151 to 155, 25:20383
WADDOUPS, I. G., Effects of load conditions on long term radioisotope thermoelectric generator operation, 25:18595 (SC-RR-70-854)
WADE, C. M., Radio sources associated with Scorpius X-1, 25:19362
WADE, S. W., Caesium behaviour in liquid sodium: the effect of carbon, 25:19192 (CONF-700816-(Vol.1), pp 393-412)
  Cesium behavior in liquid sodium: effect of carbon, 25:20754 (AERE-R-6481)
WAGEMANN, K., Evaluation of results of a study of the Th--^{233}U fuel cycle for thermal reactors, 25:20746 (JUL-644-RG)
WAGHMARE, Y. R., Configuration mixing calculations in Hartree--Fock representation, 25:20286
WAGNER, F. E., Isomer shifts and changes of nuclear charge radii in ^{99}Ru and ^{101}Ru, 25:20403
WAHLE, P., Collision dominated sheath in weakly ionized plasmas. II, 25:19673 (DLR-FB-69-78)
WAKAI, Masamiti, Manual for JUPITOR-1 (Supplement), 25:20479 (JAERI-Memo-4138)
WAKID, A. M., Effects of gamma radiation on cotton leaf worm, 25:19097
WALDMEIER, Max, Chromospheric processes during formation of sunspots, 25:19393 (CSIRO-Trans-10284)
WALISZEWSKI, Jerome A., System for computer processing of radiopharmaceutical disbursement information, 25:19050
WALKER, D. H., Attenuation concept for evaluating release of radioiodine following a loss-of-coolant accident, 25:20756 (CONF-700816-(Vol.1), pp 9-25)
WALKER, David Marshall, Multiple gamma scattering in Ge, 25:18726
WALL, J. V., Quasi-stellar objects in the Parkes 2700 MHz survey, 25:19383
WALL, Jasper V., Deep sky survey at 2700 MHz, 25:19349

XUM

(NP-18682)
WALLACE, J. D., Dynamic measurement of stopband in LAMPF 805 MHz accelerator structures at high power using hybrid computer techniques, 25:20132 (LA-4593)
WALLEY, P. A., Structural models for amorphous silicon and germanium, 25:19862
WALOSCHEK, P., Storage rings with colliding beams, 25:20192
WALTER, G., Electromagnetic transitions in ^{37}Cl, 25:20317
  Silicon-28 energy levels near 13.245 MeV, 25:20330
WALTERS, A. L. Jr., Stopping cross sections for fission fragments of ^{252}Cf by gold, silver, and carbon, 25:19765
WALTERS, W. B., Decay scheme of 25 min /sup 131g/Te, 25:20428
WALTHER, F., DNA synthesis after irradiation with high doses of x-rays and spindle inhibition, 25:18910
WALZ, Dieter R., Ball-loaded high energy particle beam dump, 25:20143
WANG, James Y. N., Method of inhibiting the corrosion of tantalum by liquid lithium, 25:19168
WANG, P. K. C., Control-theoretic approach to the plasma confinement problem, 25:19655
WANG, P. Y., Calculation of total cross section for double Compton scattering, 25:19958
WAPSTRA, A. H., Levels in ^{238}Pu from decay of ^{238}Np, 25:20431
WARD, D. R., HPRR and accelerator operations, 25:20134 (ORNL-4584, pp 187-97)
WARD, Eileen, Effect of acute x-irradiation on development of eggs of plaice, Pleuronectes platessa, 25:19103 (PG-Report-1013)
WARKE, C. S., Jost function of a non-local potential, 25:20539
WARNER, P. C., Development of a specification for heat exchanger plant to suit a gas turbine htr, 25:20776
WARNER, R. A., Spurious peaks produced by Compton scattering in Ge(Li)--Ge(Li) coincidence gamma-ray spectrometer systems, 25:18754
WARNER, Ray Allen, Energy levels in even isotopes of tellurium, 25:20461
WASASTJERNA, Frej, IRESINT 2: program for calculation of resonance integrals, 25:20823 (TKK-F-A-139)
WASIELEWSKI, Paul Francis, Application of Coriolis--coupling model to odd--odd nuclei, 25:20353
WASSON, O. A., Resonant neutron capture in ^{175}Lu, 25:20476
WATANABE, Ikuo, Cultured cells and radiobiology, 25:19106
WATANABE, Ryoji, Present state of non-ferrous metallic material for reactor use, 25:19203
WATANABE, Yoshio, Construction of nuclear power plant, 25:20565
WATERMAN, P. C., Symmetry, unitarity, and geometry in electromagnetic scattering, 25:20118
WATKINS, Bruce O. Jr., Strange particles from π^-d interactions at 3.15 GeV/c, 25:19922
WATTERS, R. L., Prog. rpt. on ^{210}PoO$_2$ metabolism in ruminants, annual, 1/15/70--1/15/71, 25:18890 (COO-2044-3)
WATTS, James Fred, Neutron transport theory with a completely degenerate energy transfer kernel, 25:20236 (TID-25648)
WDOWCZYK, J., Interpretation of the data on muons in cosmic rays from the point of view of high energy physics and astrophysics, 25:19522 (INR-1231)
WEARE, John H., Extensions of Hulthen orbital concept, 25:19513
WEBER, Christian H., Digital pulse stabilization at low coincidence count rates, 25:18871
WEBER, Thomas A., Extensions of Hulthen orbital concept, 25:19513
  Hartree--Fock theory with exchange cutoff, 25:19517
WEBSTER, William John Jr., Interferometry of galactic H II regions, 25:19374
WEEMS, Sterling J., Nuclear reactor thermoelectric power plant, 25:20694
WEGENER, Kurt, Osteodystrophy after inhalation of ^{222}Rn, 25:19144
WEGNER, H. E., Supercollimation of negative ion beams with apertures, 25:18842
WEHINGER, Peter, Minimum-light spectra of Mira variables with very long periods, 25:19311
WEHRBEIN, W. M., Determination of energy levels in stable nuclei by neutron inelastic scattering, 25:20356
WEIDENMUELLER, Hans A., Calculation of nucleon--nucleus scattering processes. II, 25:20290
  Neutron distribution in nuclei, 25:20534
WEIGEL, Fritz, Vapor pressure of Gd(III)-bromide according to cup method of W. Fischer, 25:18417
WEIGEL, Juergen, Behavior of anodic coatings under thermal stress, 25:20896 (SCL-T-68-253)
WEIL, J. W., Slow-neutron scattering from particle system in an electromagnetic wave. I, 25:20243
WEIMER, Katherine E., Tokamak equilibrium, 25:19716
WEINHOLD, Frank, Calculation of upper and lower bounds to oscillator strengths, 25:19514
WEINZIERL, Peter, Method of and apparatus for the measurement of physical characteristics of x-rays, 25:18651
WEIS, J. H., Helicity poles, triple Regge behavior and single particle spectra in high energy collisions, 25:19926 (NYO-2262-TA-234)
WEISH, P., Radioprotective effects of psychotropic drugs, 25:19028
WEISS, E. R., Scintillation camera in the dynamic evaluation of renal disorders, 25:19046
WEISS, J. J., RNA synthesis primed by γ-irradiated chromatin templates, 25:18916
WEISS, Ulrich, Multichannel treatment of resonant reactions using the quasiparticle method, 25:20510
WEISSENBERG, Gustav, Thermoluminescent dosimeter for repetitive analysis, 25:18807
WEISSFLOCH, R., Is neon more economical than helium as cooling gas in THTR, 25:20729
WEISSMAN, I. L., Antibody inhibition of the immune response: experimental analysis of the site of action in vivo, 25:18923
WEISSMANN, M., Criterion of completeness for set of functions used in matrix Hartree--Fock and correlation-energy calculations, 25:19519
WEITZNER, H., Effects of force-free fields on plasma stability, 25:19706
WEITZNER, Harold, Free-boundary long helical wavelength equilibria, 25:19718
WELCH, B., Analysis of disorder distributions in boron-implanted silicon, 25:19830
WELDON, D., Effects of force-free fields on plasma stability, 25:19706
WELFARE, F. G., Optimum turbine exhaust pressure for use of a single-effect, vertical-tube still desalting plant with a steam turbine-generator, 25:18565 (ORNL-TM-3291)
WELFORD, W. T., Contrast and shape of bubble images in bubble chambers with brightfield illumination, 25:18789
  Estimation of the size of bubbles in a bubble chamber by contrast measurement, 25:18792
WELLBORN, Colvin Clarke, Gamma--gamma angular correlations in ^{64}Cu, 25:20358
WELLMAN, Henry N., Cyclotron production of ^{123}I: an evaluation of the nuclear reactions which produce this isotope, 25:18480 (BRH/DMRE-70-4)
WELLS, Daniel R., Dynamic stability of closed plasma configurations, 25:19721
WELSH, B., Disorder produced during ^{11}B and ^{12}C implantation in silicon, 25:19806
WENDT, P., Fuel handling at an advanced gas cooled reactor, 25:20738
WENE, C.-O., Proton hole states excited by monoenergetic gamma-quanta, 25:20141
WERNER, Abraham, Comments on shielding by the lead shot method, 25:19011
WERNER, Louis B., Precipitation method of recovering element 95 from contaminants, 25:18507
WERSTIUK, N. H., Base-catalyzed protium--deuterium exchange in bicyclo[2.2.1]heptanones, 25:18411
WERTZ, James R., Newtonian big-bang hierarchical cosmological model, 25:19461
WERY, M., Data acquisition and analysis system for nuclear physics, 25:18852
WESS, J., Solvable quantum-mechanical model with nonlinear transformation laws, 25:20504
WEST, H. I. Jr., Solar-flare electron spectra in space and within Earth's magnetosphere, 25:19428
WESTMORELAND, J. E., Analysis of disorder distributions in boron-implanted silicon, 25:19830
  Correlation functions in theory of atomic collision cascades, 25:19833
WEYERS, Jacques, Patterns of exchange degeneracies, 25:20124
WHARTON, J., HTR fuel disposal study, 25:20745 (DP-Report-450)
WHEATLEY, J. C., Continuously operating ^{3}He evaporation refrigerator, 25:19632
WHEELER, C. M., RNA synthesis primed by γ-irradiated chromatin templates, 25:18916
WHINERAY, S., Acceptance calculations for Australian EN HVEC tandem accelerator, 25:20137
WHITE, Frederick H. Jr., Comparison of electrical discharge with γ-radiation for the production of free radicals in lyophilized proteins, 25:18906
WHITE, J. F., Production of dense thoria, 25:19259 (NLCO-1029)
WHITEHOUSE, J. E., Electrical measurements on silicon following phosphorus and boron implantation and annealing, 25:19778
WHITESIDE, H. C. M., Uraniferous precambrian conglomerates of South Africa, 25:18533
WHITING, F. B., Formation of insulating layers by use of reactive ion beams, 25:19781
WHITMELL, D. S., Small furnace designed for bombarding specimens in accelerators within temperature range 700 to 1500°C, 25:20212
WHITNEY, D. R., Detailed derivations of equations used in the likelihood ratio method for the precise and accurate determination of lattice parameters for cubic materials, 25:20856 (GAT-T-999)
WHITTAKER, E. L., Radioiodine field studies with synthetic aerosols, 25:18926 (CONF-700816-(Vol.1), pp 49-71)
WHITTON, J. L., Energy dependence and depth distribution of lattice disorder in ion-implanted silicon, 25:19832
WICK, G. C., Questions of Lorentz invariance in field theories with indefinite metric, 25:20073
WICK, Gerald L., Is there a safe radiation limit, 25:19018

WICKER, A., Study of niobium base refractory metal alloys, 25:19246
WICKRAMASINGHE, N. C., Interstellar dust: graphite, Fe, and silicate, 25:19450
WIDDER, F., Unitarity and crossing symmetry in low-energy π--π scattering, 25:19993
WIDERA, R., Neutron flux measurement by counting the associated ^{3}He particles from T(p,n) reaction, 25:18647
WIEDMANN, Jerome Lee, Application of the autoxidation of phenolic compounds to the analysis of cations, 25:20860 (IS-T-419)
WIEGAND, Clyde E., Semiconductor detectors in high-energy physics, 25:18775 (UCRL-20042)
WIELEBINSKI, R., Galactic metre wave radiation, 25:19388
WIESEN, Marilyn, Isobaric analog studies in the osmium and platinum mass region, 25:20378
WIKSTROEM, Sten, Mass spectral data processing. II, 25:18835
WILCHEK, Meir, Near-uv absorption bands of tryptophan, 25:20899 (UCLA-12-810)
WILD, J. F., Spontaneous-fission half-life of ^{258}Fm and nuclear instability, 25:20443
WILDENTHAL, B. H., Static quadrupole moments in A = 18 to 38 nuclei, 25:20337
WILHELMI, Z., Measurement of high-energy γ-ray spectra in a strong neutron flux, 25:18735 (INR-1224)
WILKINS, M. A., Distribution of ^{32}P channeled into indium antimonide, 25:19801
  Electrical activity of phosphorus channeled into silicon, 25:19839
WILLARD, J. E., Growth and decay of alkyl radicals in γ-irradiated alkyl iodides at 77°K, 25:18461
  Origin of complex electron spin resonance spectra of γ-irradiated polycrystalline n-alkyl iodides with even number of carbon atoms per molecule, 25:18424
WILLEMSEN, Jorge F., Operatorial construction of multiple charged-pion amplitudes, 25:19996
WILLIAMS, Clyde M., New dose calibrator for nuclear medicine, 25:18723
WILLIAMS, Ffrancon, Evidence for hydrogen atom abstraction by methyl radicals in the solid state at 77°K, 25:18426
WILLIAMS, J. G., Conserved particle structures in general relativity, 25:20089
WILLIAMS, J. R., Total cross sections for pion--proton scattering between 70 MeV and 290 MeV, 25:19916
WILLIAMS, N., Position sensitive detector for a magnetic spectrograph, 25:18681
WILLIAMS, P. M., Radiation Damage in II--VI semiconductors, 25:19793
  Thermal neutron diffusion at the ice-water phase transition, 25:20248
WILLIAMS, R. H., Density fluctuations and diffusion in weakly ionized plasmas, 25:19686
WILLIAMS, Roy Prentis Jr., Gamma-ray transitions in ^{29}P, 25:20357
WILLIAMS, W., Detection and identification of triplet states of H_2O by electron impact, 25:19499
WILLIS, R. F., Graphite conduction band states from secondary electron emission spectra, 25:19864
WILLITTS, T. R., Large-area wire spark chambers with two-coordinate read-out and ferrite core memory, 25:18790
WILSKY, K., Alpha decay of neutron-deficient radon and polonium isotopes, 25:20451
WILSON, B. G., Low-energy cosmic x rays, 25:19352
WILSON, Henry Hamilton, Nuclear resonance scattering of Bremsstrahlung, 25:20355
WILSON, J. F., Optical-model analysis of nonreactive collisions of reactive molecules, 25:19497
WILSON, Mary H., Kinetics of iodination of sodium phenylpropiolate, 25:18397
WILSON, Richard, What is the radius of a nucleus, 25:20536
WILSON, Robert E., Relevance of variable negative radial velocities to models of Sco X-1, 25:19378
WINCKLER, John R., Relation of energetic solar x rays and high-frequency microwaves, 25:19401
WINICOUR, Jeffrey, Can the energy of a weak gravitational field become negative, 25:20099
WINSTON, M. A., Scintillation camera in the dynamic evaluation of renal disorders, 25:19046
WINTER, W. J. B., Levels in ^{239}Pu from decay of ^{239}Np, 25:20431
WINTERNITZ, P., Crossing symmetric expansions of physical scattering amplitudes: O(2,1) group and Lame functions, 25:20105
WIRTZ, K., Authorization procedures, site evaluation, and safety criteria, 25:20688
WIT, R., Low-energy data, analyticity, and violation of Pomeranchuk's theorem, 25:20005
WITALIS, Erik, Thermonuclear reactions through laser radiation of fusion materials, 25:19724 (FOA-4-4449)
WITCOFSKI, Richard L., Selenomethionine ^{75}Se thymus scans in myasthenia gravis, 25:19049
WITTEN, Louis, Some properties of cylindrically symmetric Einstein--Maxwell fields, 25:20086
WITTKOWER, A., Equilibrium fraction measurements of heavy ions in fluorocarbon strippers, 25:20155
WITTMER, P., Data acquisition and analysis system for nuclear physics, 25:18852
WOLBECK, B., Moessbauer effect of 129-keV transition in ^{195}Pt, 25:19877
WOLF, G. H., Formation of an axisymmetric bulged region in a long uniform plasma column, 25:19709
WOLF, L., Steady-state, two-dimensional temperature distributions in single fuel element pellet and adjacent cladding due to axial varying heat transfer coefficients, 25:18589
  Temperature fields in fuel element rod bundles during variable heat transfer at the periphery between fuel element surface and coolant, 25:20706
WOLF, R. A., Hydromagnetic waves generated at the bow shock, 25:19580
WOLF, W., Positive definite particle densities for solutions of Klein--Gordon equation, 25:19929
WOLFSBERG, Kurt, New nuclide, ^{145}Xe, 25:20470
WOLLESWINKEL, J., Residence time measurements for surface ionization of K on W, 25:19210
WOLSCHRIJN, Rolf A., Measurement of alpha contamination on surface of fissile element, 25:18636
WOLSTENCROFT, Ramon D., Confirmation of magnetic white dwarf G-195-19, 25:19328
WOLTERBEEK MULLER, B., X-ray temperature measurements of laser-produced plasmas, 25:19701
WOND, Chung-ming, Abstracts of literature on the distillation of seawater and on the use of nuclear energy for desalting, 25:20812 (TID-25653)
WONG, C. Y., Measurement of absorbed dose rate from terrestrial background radiation in Hong Kong, 25:19006
WONG, P. Y., Gausfit: a fortran program for fitting gaussian functions, 25:20846 (AECL-3784)
WONG, S. K., Massless limit of massive Yang--Mills field, 25:20075
WONG, S. S. M., Validity of random matrix theories for many-particle systems, 25:20507
WOOD, M. R., In-core regenerative thermal neutron detectors for nuclear reactors, 25:20711 (WHAN-FR-37)
WOODLEY, H. J., Experiments with stand pipe closure and stand pipe-charge machine connections for proposed HTGC power reactor, 25:20742 (DP-Report-496)
WOODS, C. H., Effects of magnetic lens aberration in high-current linear accelerators, 25:20160
WOODS, M. J., Decay of /sup 113m/In, 25:20407
WOODS, S. B., Tunneling into weakly coupled films of aluminum and tin in proximity, 25:19623
WORLEY, N. G., Power cycles for helium cooled high temperature nuclear reactors, 25:20770
WRIGHT, A. G., Improved ringing coil pulse encoders, 25:18868
WRIGHT, George G., Preparation of noninfectious arbovirus antigens by sucrose--acetone extraction of gamma-irradiated tissue, 25:18924
WRIGHT, J. H., Nuclear costs: the future looks better, 25:20597
WRIGHT, James F., Review of radium toxicity studies, 25:18979 (BRH/DBE-70-5)
WRIGHT, James Francis, Pathologic effects of continuous ^{90}Sr ingestion in mice, 25:19113
WRIGHT, Ralph R., Corrosion-resistant uranium, 25:19185
WRIGHT, W. H., Generalized pulse height distribution for the electron multiplier, 25:18864
WYCKOFF, Susan, Minimum-light spectra of Mira variables with very long periods, 25:19311
WYLER, Armand, Symmetric space of group of Maxwell equations, 25:20052 (SLAC-Trans-130)
WYLIE, W. R., Isobaric analog pair ^{57}Fe--^{57}Co, 25:20336
WYMER, R. G., Status and progress report for thorium fuel cycle development for January 1, 1969--March 31, 1970, 25:19260 (ORNL-4629)

Y

YADA, Hisashi, Fuji electromagnetic flowmeters for liquid sodium, 25:18876
YAKOVLEV, B. S., Stabilized ions and the formation of cross links in the radiolysis of polybutadiene, 25:18467
YAMADA, Kaneo, Influence of defects in 80 mm thickness steel plates for weld quality, 25:19202
YAMADA, Takeshi, Effects of x-irradiation on ^{14}C-pyruvate metabolism in rat thymocytes, 25:18902
YAMAJI, Shuhei, Manual for JUPITOR-1 (Supplement), 25:20479 (JAERI-Memo-4138)
YAMAMOTO, Kazuhiko, Effects of ^{60}Co gamma rays on lysozyme in aqueous solution, 25:18917
YAMANISHI, Kiyoshi, Gamma irradiation in medicinal plant breeding. II, 25:19151
YAMAOKA, Hitoshi, Mass spectrometric studies on negative ion--molecule reactions of nitroethylene, 25:18428 (NP-18676)
YAMAZAKI, Masao, Direction of development on a nuclear fuel cycle, 25:18570
YAMAZAKI, Tomohisa, Gamma irradiation in medicinal plant breeding. II, 25:19151
YAMAZAKI, Yasaburo, Survey list of accident, hazard, and abnormality in nuclear facilities, 25:19013 (JAERI-Memo-4240)
YAMDAGNI, N., Distortion effects in geometrical reconstruction of events in CERN 2m Hydrogen Bubble Chamber, 25:18777 (USIP-70-6)
YAMDAGNI, Narendra, Proton--proton interactions at 19 and 10 GeV/c, 25:19901 (USIP-70-7)

XUM

YANEVA, N., Relative measurements of anti ν in the ^{235}U and ^{239}Pu fission induced by resonance neutrons, 25:20364 (BNL-tr-401)
YANG-SHUO-HSIANG, G. V., Phase diagram of Bi--Cd--Hg, 25:19236
YANO, Y., Lung function studies using short-lived /sup 81m/Kr and the scintillation camera, 25:19056
YANO, Yukio, Myocardial uptake studies with ^{129}Cs and the scintillation camera, 25:19055
YANTOVSKII, E. I., One-dimensional flow of magnetized liquid, 25:19552
YANUSHEVSKI, Yu., 10-MeV proton linear accelerator at Swierk, 25:20129 (INR-P-1218)
YARIS, Robert, Many-body methods applied to electron scattering from atoms and molecules. II, 25:19507
YASHIRO, Hideo, Honeycomb block used for collimation of radiations and method of manufacturing the same, 25:18856
YASUDA, Tokuichi, Genetic effect of radiation in mankind and statistical genetics, 25:18961
YASUKAWA, Shigeru, Some comments on HTGCR physics, 25:20707
YASUNO, Takehiko, Sodium-void experiment in unit k-infinity core, 25:20793
YATES, D. A., Gas turbo-machinery for helium cooled reactors, 25:20772
YAWATARI, Kei, Influence of ^{60}Co γ-ray on potato, 25:19160
YEATER, M. L., Monte Carlo evaluation of multiple scattering and resolution effects in double-differential neutron scattering cross section measurements, 25:20235 (RPI-328-211)
YEH, Robert H. T., Variational bounds of the elastic moduli of two-phase materials, 25:19282
YELLIN, Joel, Bootstrap models and special property of unitary Lie algebras, 25:19999
YERGIN, P. F., 250 meter neutron time-of-flight facility, 25:18742
YOFFE, A. D., Radiation Damage in II--VI semiconductors, 25:19793
YOKOTA, Minoru, Measuring and controlling equipment for D_2O critical assembly, 25:20799
YOKOTA, Ryosuke, Recent improvements in fluoro-glass dosimeter, 25:18810
YOKOTA, Toshitsugu, Kinetic isotope effects in reactions of bromine atoms with CH_4 and CD_4, 25:18410
YONEZAWA, Toshio, Iron and steel used for nuclear reactors, 25:19200
YONNET, J., Readout of wire spark chamber by delay lines, 25:18793
YOO, K. J., Determination of percent contents of U and Th in natural radioactive ores by γ-ray spectrometry, 25:18365
YOSHIDA, H., Formation of ^{6}Li/sub g s / and ^{6}Li, 3.56 MeV, T = 1 state, 25:20284
YOSHIDA, Hiroshi, Dissociative electron capture process of methyl vinyl ether in organic glasses, 25:18456
YOSHIDA, S., Charge asymmetry of nucleon widths of lowest T = 3/2 states of ^{13}N and ^{13}C, 25:20512
YOSHIHARA, Kenji, Study of chemical behavior of recoil atoms due to (γ,γ') process, 25:18488
YOUNG, Christian A., Strength of internally strained brittle matrix composites, 25:20902 (UCRL-20395)
YOUNG, F. C., Absolute γ-ray efficiency of 50 cm³ Ge(Li) detector, 25:18702
YOUNG, J. E., Helicity poles, triple Regge behavior and single particle spectra in high energy collisions, 25:19926 (NYO-2262-TA-234)
YOUNGDAHL, Carl K., Load-equivalence parameters for dynamic loading of structures in the plastic range, 25:18557 (ANL-7677)
YU, M. Y., Effect of velocity space diffusion on the universal instability in a plasma, 25:19719
YUDIN, N. P., Effect of intermediate coupling in photo and electroexcitation of ^{12}C nucleus, 25:20295
YUDING, O. I., Evidence of quasi-periodic movements in the solar chromosphere and corona, 25:19415
YULO, T., Variations in the makeup of lens insoluble proteins, 25:18909
YUROVSKII, Yu. F., Structure of the solar radio bursts at 10-cm wavelength, 25:19436
YUSA, Hideo, Design of fission gas holdup systems, 25:18561 (CONF-700816-(Vol.1), pp 216-23)
  Heat transfer of sodium compounds deposited on surfaces from aerosols, 25:18562 (CONF-700816-(Vol.1), pp 413-24)
YUSHKOV, A. V., Analysis of inelastic scattering of alpha particles in region Z = 12 to 40, 25:20274
YUSTER, Philip H., EPR and optical absorption study of BrCl- and associated centers in doped KCl crystals. I, 25:19852

Z

ZABIYAKIN, G. I., Data transmission in measurement-computing complex of the Joint Inst. for Nuclear Research, 25:18845
ZABOLITZKY, J. G., Short-range correlations and parity impurities, 25:20488
ZABRODIN, V. A., Discrete frequency sweep in a synthesizer for nuclear magnetic resonance spectroscopy, 25:18848
ZAFIRATOS, C. D., Small-angle j dependence of (α,p) reactions, 25:20309
ZAGORSKI, Zbigniew Pawel, Self-absorption of Cherenkov light as a quantitative indicator of radiolysis progress, 25:18453
ZAIDES, A. L., Comparative study of effect of irradiation with γ-rays and accelerated electrons on structure and properties of cis-butadiene rubber, 25:19300
ZAIDINS, C. S., Small-angle j dependence of (α,p) reactions, 25:20309
ZAITSEV, A. A., Oxidation of Mo at 500 to 1000°C and pressures of 10^{-3} to -1 torr, 25:19169
ZAJC, A., Significance of radioactive isotopes in building structures, 25:18599
ZAKHAROVA, M. I., Structural changing during degradation of supersaturated solid solution of Te in Co, 25:19233
ZAKI, M. M., Effects of gamma radiation on cotton leaf worm, 25:19097
ZAKIROVA, L. S., Radiotoxin fractionation and investigations on their biological properties, 25:18915
ZALESKI, Tadeusz, Automated systems and electronics for the Krakow--Dubna slow-neutron inverted-geometry spectrometer KD SOG-1, 25:18734 (INP-727)
ZALESSKII, A. V., New principle of modulation in investigations of nuclear magnetic resonance in ferromagnets, 25:19878
ZAMBONI, F., Isobaric analog pair ^{57}Fe--^{57}Co, 25:20336
ZAMICK, Larry, Static moments in light doubly even nuclei, 25:20333
ZASHKVARA, V. V., Electrostatic spectrometer of charged particle beams with ring focussing in the field of a cylindrical condenser, 25:18849
ZATSEPIN, G. T., Neutrino spectroscopy of the Sun, 25:19429
ZAVATTINI, E., Apparatus for detection and energy measurement of muonic and pionic x-rays, 25:18748
ZEBRO, Tadeusz, Influence of bis(-3-hydroxypropyl) trisulfide on the peripheral blood in rats irradiated with large doses of x-rays, 25:19131
ZECCA, A., Energy modulated high energy resolution electron spectrometer, 25:18762
ZEKE, J., Utilization of electroslag welding in the production of steel pressure vessels for nuclear reactors, 25:19181
ZEL'DOVICH, A. G., Experimental solenoid made of Nb_3Sn strip, 25:19588 (JINR-P8-5440)
ZELENCHUKOVA, T. G., Mechanism of radiation polymerization of vinyl monomers in the presence of mineral additions, 25:18442
ZELIKSON, D. L., Electron gun having an electron output from a vacuum into gas, 25:18850
ZEMCIK, T., Experimental apparatus for investigation of Moessbauer effect, 25:18769
ZENKEVICH, B. A., Investigation of heat-transfer crisis in a bunch of fuel element simulators under natural circulation conditions, 25:18584
ZGANJAR, E. F., Band mixing in ^{154}Gd, 25:20441
ZGLINSKI, A., Lutetium-170 → ^{170}Yb decay, 25:20452
ZGRABLICH, G., Penetration and cascade phenomena, 25:19971 (ANL-7727)
ZHARIKOV, G. P., High speed magnetic-chip memory in a scanning robot for measurement of chamber photographs, 25:18780
ZHARINOV, V. V., Nakanishi representation, 25:20121
ZHAROVSKII, F. G., Extraction separation of Mo from Re and its determination with 5,7-dibromo-8-quinolinol, 25:18353
ZHEBENTYAEV, A. I., Study of the fluorescent niobium complex with hydrogen peroxide and sulphonaphtholazoresorcinol, 25:18349
ZHELEZNYAKOV, V. V., Coherent mechanisms of emission and their application to pulsars. II, 25:19370
ZHELTONOG, K. S., Analysis of inelastic scattering of alpha particles in region Z = 12 to 40, 25:20274
ZHEREBETSKII, S. K., Scintillation characteristics of pure and activated cadmium iodide crystals, 25:18665
ZHITNIK, I. A., Quiet-corona temperature determined from soft x-radiation flux, 25:19418
ZHURAVLEV, A. A., Results on complex adjustment and start-up of the IHEP proton synchrotron, 25:20127 (CERN-Trans-70-12)
ZHURAVLEV, O. K., Amplifier for semiconductor gamma detectors, 25:18668
ZIEGLER, B., Experimental techniques for photon scattering below 140 MeV, 25:20189
ZIELINSKA-PFABE, M., Penetration of a two-dimensional fission barrier, 25:20478 (INR-P-1230)
ZIEMER, P. L., 4π liquid-scintillation whole-body counter. II, 25:18649
ZIGMAN, S., Variations in the makeup of lens insoluble proteins, 25:18909
ZIMEK, Zbigniew, Self-absorption of Cherenkov light as a quantitative indicator of radiolysis progress, 25:18453
ZIOCK, K. O. H., Pion capture in ^{4}He, 25:20255
ZIOUTAS, K., Moessbauer effect of 129-keV transition in ^{195}Pt, 25:19877
ZIPPER, W., Polarization of protons from ^{12}C(d,p)^{13}C reaction at E/sub d/ = 12.4 MeV, 25:20287
ZIRKER, J. B., Spectrum of inner corona during eclipse of May 30, 1965, 25:19410

ZITTARTZ, J., Kondo effect in superconductors, 25:19603
ZOGRAN, Raymond N., Nuclear reactor thermoelectric power plant, 25:20694
ZOLOTOV, Yu. A., Liquid--liquid extraction of metal-halide complexes depending on their composition and structure. I, 25:18511
ZONDERHUIS, J., Separation of gram-amounts of lanthanides by cation exchange, using an aqueous solution of α-hydroxyisobutyric acid as an eluant, 25:18501 (RCN-131)
ZUBAROV, D. L., Ventilation and air conditioning on atomic ships, 25:20816 (JPRS-52443)
ZUBOV, P. I., Relation of radiation cross-linking in special purpose elastomers to additions of chloroalkanes of various structures, 25:18434
ZUK, W. M., Transition rates in ^{29}P, 25:20319
ZUL'KARNEEV, R. Ya., Non-strange baryon--baryon resonances, 25:20016 (CERN-Trans-70-14)
ZWANZIGER, Daniel, Local-Lagrangian quantum field theory of electric and magnetic charges, 25:20072
ZWEIG, George, Patterns of exchange degeneracies, 25:20124
ZYCH, W., Isobaric analog pair ^{57}Fe--^{57}Co, 25:20336
ZYLICZ, J., Beta spectrometer with a Si(Li) detector in homogeneous magnetic field, 25:18736 (INR-P-1227)
  Beta spectrometer with Si(Li) detector in homogeneous magnetic field, 25:18767

SUBJECT INDEX

Cross references are included in cumulative subject indexes and in *Subject Headings Used by the USAEC Division of Technical Information* (USAEC report TID-5001).

The reader is also referred to *Guide to Abstracting and Indexing for Nuclear Science Abstracts* (USAEC report TID-4576).

Most headings in the subject index are specific materials, things, and processes. The headings are followed by modifiers that describe the properties of, or processes applied to, the headings.

All index entries cite *NSA* volume and abstract numbers; volume number precedes the colon and the abstract number follows it. The designation (R) following the abstract number indicates a progress report; (P) indicates a patent; and (T) indicates a translation. Abstracts for reports other than progress reports carry no letter designation. Report numbers, where applicable, are included in parentheses after the abstract number of the citation. Published literature (journal article or book) can be identified by the absence of a report number.

Ideas presented in the original literature, rather than key words, have been indexed. The indexers have selected what seemed the most probable and logical place to look for typical information. Since it is not always possible to anticipate where a user would look for information, the cumulative indexes include numerous cross references. Consideration of synonymous or closely related terms will prove valuable.

Information is indexed for the greatest use to the greatest number of users. This requires that a topic be indexed to headings that most specifically describe it and not ordinarily to the headings that describe its ultimate use or to the general class headings that include the specific headings. For example, information on boiler design for the Fermi Fast Breeder Reactor would be indexed under the headings BOILERS and FERMI FAST BREEDER REACTOR but not necessarily under the headings REACTORS, FAST or REACTORS, BREEDER.

General or broad headings are reserved for general summaries, reviews, comprehensive reports, and similar literature.

Subject Heading Styles

Generally, the direct form of subject entry is used rather than inverted headings; e.g., AMINO ACIDS rather than ACIDS, AMINO; HELIUM ISOTOPES He-4 rather than HELIUM—ISOTOPES He-4 or HELIUM—He-4 ISOTOPES. Note, however, that in some cases parenthetic modifying terms or inverted headings such as NEUTRONS, FAST, are used where the alphabetical arrangement of a direct entry would cause information to be scattered. In addition, organic compounds are usually entered in the index in the inverted form to facilitate grouping like or related compounds with the parent compounds; e.g., BENZENE, BROMO- rather than BROMOBENZENE. In general, the nomenclature used is that of the subject indexes to *Chemical Abstracts.*

Alphabetization

Subject headings are alphabetized word by word. Parenthetic qualifiers, numbers, and Greek letters within subject headings are disregarded in alphabetizing unless there are two or more headings that are otherwise identical, in which case the qualifier, numerical progression, or spelled names for the Greek letters determine the order.

Examples:

M-Capture
  see ELECTRON CAPTURE
MAGNESIUM
MAGNESIUM ALLOYS AND SYSTEMS
MANGANESE FLUORIDES
MANGANESE FLUORIDES MnF_2
MESONS
MESONS (π)
MESONS (ρ)
1-PENTANOL
2-PENTANOL

Modifying Phrases

The modifiers appearing under a subject heading are written specifically to show the relation between the item being indexed and the heading. The modifier therefore contains a maximum of useful information. Although the modifier begins with the word judged to be of greatest use to the greatest number of users, there is still need for the searcher to consider all modifiers under the heading(s) of interest.

Modifiers usually form meaningful phrases when combined with the subject heading. Some are intended to be read following the subject heading, e.g., the entry HYDROGEN—sorption by charcoal should be read "hydrogen sorption by charcoal." As a result of placing the important word first, however, many modifiers must be rearranged for smooth reading, e.g., FORMALDEHYDE—yields in radiolysis of ethyl ether, effects of deuterium on, should be read "effects of deuterium on formaldehyde yields in radiolysis of ethyl ether" and URANIUM—crystal structure of, effect of cooling rate on allotropic transformations in, should be read "effect of cooling rate on allotropic transformations in crystal structure of uranium."

Special characters are added to modifiers in the fields of physics and reactor technology; if the modifier does not establish the experimental or theoretical character of a reference, a symbol (E), (T), or (E/T) is placed immediately after the modifying phrase and before the abstract number.

Physical States and Configurations of Materials

The specific physical state, if other than normal, or the geometric configuration of the material is included in the modifying phrase; e.g., information on liquid metals is indexed under the specific metal with "liquid" in the modifier and carbon crucibles is indexed under CARBON with "crucibles" appropriately placed in the modifier. The information on carbon crucibles is also indexed under CRUCIBLES.

Nomenclature of Inorganic Compounds

Inorganic compounds are indexed to subject headings in the direct form. Cations are listed in the order of increasing valence for polycationic salts of varying valence and in alphabetic order for polycationic salts in which all cations have the same valence; e.g., SODIUM ALUMINUM SILICATES and POTASSIUM SODIUM SULFATES. If more than one anionic species is presented in a compound, the anions are arranged alphabetically, e.g., BERYLLIUM FLUORIDE HYDROXIDES.

Nomenclature of Organic Compounds

Organic compounds are indexed by subject headings based on the indexes to *Chemical Abstracts* except in the area of enzymes, in which specific enzymes, named according to the 1964 recommendations of the International Union of Biochemistry, are used. In many cases nonproprietary names for drugs are used as subject headings, and cross references are made from the systematic chemical names. Subject headings for hormones appear in the inverted style at HORMONES.

Nomenclature of Life Sciences

Subject headings for plants are names of phyla with one exception: members of the Phylum Tracheophyta are indexed under class or subclass names. Scientific names (genus and species) are used as the initial, or file, word in the modifying phrase. Scientific names are omitted only when the name is not available in the literature or cannot be found in available references.

Subject headings for animals are the names of phyla with the following exceptions: (1) members of Phylum Arthropoda and Phylum Chordata are indexed under appropriate class name, and (2) common names are used for members of Class Mammalia.

Subject headings are entered for various classes of commodities, and specific products are identified in the file-word position of the modifier. In the following examples, approved subject headings are capitalized and typical modifier file words are listed in lower case.

Example 1	Example 2
CEREALS	MEATS
bread	beef
flour	fish
oats	mutton
rice	pork
rye	poultry
wheat	seafood

Diseases, pathological conditions, and in vitro studies of atypical cells and tissues are indexed under subject headings for the organism affected, under the appropriate anatomical structure of physiological phenomenon affected, and under the appropriate disease heading. Subject headings for diseases (defined as any deviation from the norm) are DISEASES; DISEASES, INFECTIOUS; DISEASES, NEOPLASTIC; DISEASES, PHYSIOLOGICAL; DISEASES, PLANT; and DISEASES, TRAUMATIC.

Diseases of mixed etiology are treated in the following manner: neoplastic diseases that are also classified as infectious or physiological are indexed under DISEASES, NEOPLASTIC; diseases in which a microorganism is the etiologic agent are classified under DISEASES, INFECTIOUS; physiological anomalies that are neither neoplastic nor infectious are indexed under DISEASES, PHYSIOLOGICAL; the acute radiation syndrome, nonspecific radiation injuries, trauma, and wounds or incisions inflicted mechanically are indexed under DISEASES, TRAUMATIC.

Specific diseases or pathological conditions are named in the file-word position of the modifier, in the author's terminology, and are set off from the remainder of the modifier by commas. Neoplasms are designated as benign or malignant in the file-word position when more specific information is not available.

Multicomponent Alloys and Other Systems

Multicomponent alloys and systems, except well-known trade names, are indexed under a subject heading for each component in the form "element systems" for nonmetals or "element alloys and systems" for metals. The modifier begins with element symbols for each component arranged alphabetically. In addition, if significance is placed on the base metal of the alloy, this is indicated by adding "-base" to the element symbol.

Example: A 1.5C, 12Cr, 0.25V, 0.8Mo, bal Fe alloy is indexed as

```
CARBON SYSTEMS
  C--Cr--Fe-base--Mo--V, ...
CHROMIUM ALLOYS AND SYSTEMS
  C--Cr--Fe-base--Mo--V,...
IRON ALLOYS AND SYSTEMS
  C--Cr--Fe-base--Mo--V, ...
MOLYBDENUM ALLOYS AND SYSTEMS
  C--Cr--Fe-base--Mo--V, ...
VANADIUM ALLOYS AND SYSTEMS
  C--Cr--Fe-base--Mo--V, ...
```

Well-known alloys, such as ZIRCALOY-2, are indexed under the trade name; cross references from each component of the alloy to the trade name appear in cumulative indexes.

Multicomponent systems in which nonmetallic elements are present in large percentage and which are commonly referred to as systems or mixtures are indexed in a manner similar to alloys.

Example: A tungsten–silicon preparation is indexed as

```
TUNGSTEN ALLOYS AND SYSTEMS
  Si--W, ...
SILICON SYSTEMS
  Si--W, ...
```

Multicompound systems and mixtures of inorganic compounds are indexed under the subject heading for each component compound; the modifiers begin with an alphabetical listing of compound formulas.

Example: A lead titanate–lead zirconate mixture is indexed as

```
LEAD TITANATES
  PbTiO3 --PbZrO3
LEAD ZIRCONATES
  PbTiO3 --PbZrO3
```

XUM

A mixed system of compounds and elements is indexed by a combined form of the preceding conventions; e.g., a dispersion of copper and alumina would be indexed as

ALUMINUM OXIDES
  Al_2O_3--Cu, ...
COPPER ALLOYS AND SYSTEMS
  Al_2O_3--Cu, ...

Mixtures of organic compounds are indexed under subject headings for each component of the mixture; the modifiers begin with an alphabetical listing of compound names.

Example:

ACETIC ACID
  acetic acid--BF_3, ...
BORON FLUORIDES
  acetic acid--BF_3, ...

Example:

BENZENE, CHLORO-
  bromophenol--chlorobenzene, ...
PHENOL, BROMO-
  bromophenol--chlorobenzene, ...

If modifiers for alloys and systems are included with other modifiers under the same subject heading, they are filed last.

Example:

CARBON SYSTEMS
  deposition on nuclear fuel particles
  molecular structure of
  neutron total cross section for
  sorptive properties for xenon
  Young's modulus for
  Al--C--Cr, superconductivity in
  B--C, phase studies for
  C--U--Zr, fabrication and physical properties of

Nomenclature of High Energy Physics

Information on particle-particle events is indexed under subject headings for the specific particles involved. The modifier file word *interactions* is followed by the specific interaction written in symbolic form. Particle nomenclature and symbols follow that of Rosenfeld, et al. *Data on Particles and Resonant States,* UCRL-8030 (latest revision). For consistency the incident particle is always written first. The mass (in MeV) of a resonance state is included in parentheses after the symbol to avoid ambiguity. Hyperfragments are indicated in modifiers as in the following examples: Λ-He^5, Σ-H^3, $\Lambda\Lambda$-Be^{10}. The superscript on the right indicates the total number of baryons in the composite system.

Examples:

MESONS (π^-)
  interactions $\pi^- + p \rightarrow \Lambda + K^+ + \pi^-$ at 6 GeV/c in hydrogen bubble chamber, $\Lambda K(1700)$ enhancement in, (E)
BARYONS, RESONANCE (N^*)
  production of $\Delta^{++}(1236)$ and $\Delta^0(1236)$ from $K^- + p \rightarrow K^- + p + \pi^+ + \pi^-$ interactions at 2.63 and 2.70 GeV/c, (E)
HYPERFRAGMENTS
  binding energy of $\Lambda\Lambda$-He^6, three-body α--Λ--Λ model for

Subject headings are also provided for specific models and theories.

Examples:

ELEMENTARY PARTICLE MODELS (TRIPLET)
  hadron total cross sections in quark, numerical analysis of
CURRENT ALGEBRA
  PCAC hypothesis for A_1 and rho dominance in $\pi \rightarrow e + \nu + \gamma$ decay
REGGE POLE THEORY
  predictions for polarization in $K^- + p \rightarrow$ anti $K^0 + n$, $\pi^- + p \rightarrow \pi^0 + n$, and $\pi^- + p \rightarrow$ eta $+ n$ interactions at high energies
SYMMETRY GROUPS
  $SU(2) \times SU(4)$ intermediate-coupling model for nucleon and hyperon isobars

Nomenclature of Reactor Technology

Subject headings for reactors are of three types:

(1) Specific reactors, e.g., ARGONNE RESEARCH REACTOR, SAXTON POWER REACTOR

(2) Reactors having a common physics or engineering characteristic, e.g., REACTORS, FAST; REACTORS, ORGANIC-COOLED; REACTORS, PRESSURIZED-WATER

(3) Reactors having a common purpose, e.g., REACTORS, POWER; REACTORS, RESEARCH

Information on specific reactors, type (1), is indexed under the one specific subject heading. Information on classes or types of reactors, types (2) (characteristics) and (3) (purpose), is indexed under all applicable headings. For example, information on a heavy-water-moderated organic-cooled power reactor is indexed under REACTORS, HEAVY WATER-MODERATED; REACTORS, ORGANIC-COOLED; and REACTORS, POWER.

Subject headings exist for selected reactor components, e.g., REACTOR FUEL ELEMENTS. When applicable, headings for components are indexed even though they may have been included in a modifier under a type (1) or (2) heading. The materials in reactor components are indexed when the information is peculiar to the material.

Modifier file words under reactor headings are of two primary types: one type expresses reactor characteristics, e.g., reactivity; the other, components, e.g., control rod. If no subject heading appears for a reactor component, the heading REACTORS is used, and the component is used as the modifier file word.

A

- **ACCELERATORS**
  - accelerating cavities of, distortion of magnetic fields due to conducting coatings on, 25:20221
  - beam dumps for, aluminum ball-loaded, 25:20143(P)
  - beam position monitor for electron, sensitivity of secondary-emission detector, 25:20173
  - beam pulser for, design of electrostatic deflection, 25:20182(P)
  - beam transport systems for, magnet system for achromatic, 25:20205
  - betatron oscillations in circular, measurement of Coulomb frequency-shift of, 25:20171
  - cavity resonator tuning in high-energy, phase-angle measurement system for, 25:20179(P)
  - data display systems for fast-cycling, design and performance of, 25:20177
  - description of continuously operating 100-MeV electron, with multiple beam passage through cavity resonators, 25:20142(P)
  - design and performance of autoresonance electron, 25:20224
  - design of REBA 3.2-MeV 43-kA electron, 25:20136 (SC-DR-70-872)
  - magnetic fields of, distortion due to conducting coatings of accelerating cavity, 25:20221
  - operation of autoacceleration, for intense electron beams, 25:20220
  - performance as neutron sources for reactor fuel breeding, 25:20190
  - performance for ion implantation at 10 to 600 keV, review, 25:20165
  - stripper gases for tandem, measurement of heavy-ion charge states for fluorocarbon, 25:20155
- **ACCIDENTS**
  - handling neutron exposure, guidelines for, 25:19007 (NCRP-38)
  - radiation, comparison of dosimetric, clinical, and therapeutic aspects of whole-body exposures in, 25:19012 (CEA-CONF-1695)
  - radiation, insurance coverage and liability for, in USA, 25:19017
  - radiation, rules for clinical and therapeutic procedures following, 25:18975 (CEA-N-1365)
  - radiation, summary of 347, 25:19013 (JAERI-Memo-4240)
- **ACETAMIDE**
  - radiolysis of aqueous perchloric acid solutions of, rate constants for reactions of hydrogen atoms produced by γ, 25:18459
- **ACETIC ACID**
  - radiolysis of aqueous perchloric acid solutions of, rate constants for reactions of hydrogen atoms produced by γ, 25:18459
- **ACETIC ACID, BROMO-**
  - radiolysis of aqueous perchloric acid solutions of, rate constants for reactions of hydrogen atoms produced by γ, 25:18459
- **ACETIC ACID, [(CARBOXYMETHYLIMINO)BIS(ETHYLENENITRILO)]TETRA-**
  - effectiveness of metastable indium-113-labeled, for kidney scanning, comparison of mercury-197-labeled chlormerodrin with, 25:19039
- **ACETIC ACID, (ETHYLENEDINITRILO)TETRA-**
  - effects on repair processes following γ-radioinduced chromosome aberrations in Nigella damascena seeds, 25:18951
  - excretion of chromium-51-labeled, by kidneys of dogs, 25:18893
- **ACETONE**
  - radiolysis of aqueous perchloric acid solutions of, rate constants for reactions of hydrogen atoms produced by γ, 25:18459
  - radiolysis of crystals of, processes for annealing of free radicals formed by, 25:18473
- **ACETONITRILE**
  - radiation effects on solid, isotope effects and activation energy of hydrogen atom abstraction process in γ, 25:18426
  - radiolysis of aqueous perchloric acid solutions of, rate constants for reactions of hydrogen atoms produced by γ, 25:18459
- **ACETYLENE**
  - oxygen-ion reactions at 0 to 2 eV with deuterated and normal, rates of, 25:19490 (ORNL-4584, pp 92-104)
- **ACETYLENE, DIPHENYL-**
  - radioinduced polymerization of, properties of products from γ, 25:18441
- **ACRIFLAVINE**
  - effects on Brucella abortus, frequency of mutagenic, 25:18970
- **ACRYLAMIDE**
  - radioinduced polymerization in aqueous solutions in presence of unsaturated dicarboxylic acids, 25:18429
  - radioinduced polymerization of solid, NMR studies on kinetics of, 25:18448(R) (CEA-N-1369)
  - radiolysis of aqueous solutions of, 25:18429
- **ACRYLAMIDE, N,2-DIMETHYL-**
  - dimers, radioinduced polymerization of, NMR studies on products from, 25:18433
- **ACRYLAMIDE, N-ISOBUTYRYL-N,2-DIMETHYL-**
  - radioinduced polymerization of, NMR studies on products from, 25:18433
- **ACRYLAMIDE, N-ISOBUTYRYL-2-METHYL-**
  - radioinduced polymerization of, NMR studies on products from, 25:18433
- **ACRYLAMIDE, 2-METHYL-N-PHENYL-**
  - dimers, radioinduced polymerization of, NMR studies on products from, 25:18433
- **ACRYLAMIDE, N-ISOBUTRYL-2-METHYL-N-PHENYL-**
  - radioinduced polymerization of, NMR studies on products from, 25:18433
- **ACRYLIC ACID, 2-ETHYLHEXYL ESTER**
  - poly(2-ethylhexyl acrylate)--polystyrene, radiation effects on crosslinking and properties of, γ, 25:18436
- **ACRYLIC ACID, METHYL ESTER**
  - glass textiles--methyl acrylate, radiation effects on mechanical properties of, γ, 25:18421(R) (RLO-2098-1)
- **ACRYLONITRILE**
  - radioinduced polymerization in graphite, mechanical properties of products from γ, 25:18421(R) (RLO-2098-1)
  - radioinduced polymerization of solid, in regions of phase transitions, kinetics of electron, 25:18440
- **ACTINIDES**
  - retention of aerosols of liquid, in alveolar lipoprotein of monkeys and rats, use of lanthanum-140 to demonstrate stability of complex formed following in vitro and in vivo, 25:18889 (CEA-CONF-1676)
- **ACTIVATION ANALYSIS**
  - computer program for peak finding and integration in, 25:18366(R) (NBS-TN-548)
  - developments in, 25:18870
  - equipment for photon, 25:18366(R) (NBS-TN-548)
  - neutron generator for 3-MeV neutron, 25:18366(R) (NBS-TN-548)
  - research progress on, 25:18366(R) (NBS-TN-548)
- **ADSORPTION SEPARATION PROCESSES**
  - efficiency for removing krypton-85 from radioactive off-gases, equations for calculating, 25:18560 (CONF-700816-(Vol.1), pp 207-15)
  - equipment for fission gas, method for calculating efficiency of, 25:18561 (CONF-700816-(Vol.1), pp 216-23)
- **AEROSOL GENERATORS**
  - design for preparation of iodine-131-labeled diatomaceous earth aerosols, 25:18926 (CONF-700816-(Vol.1), pp 49-71)
  - design for preparation of radioisotope-labeled aerosols, 25:18525 (CONF-700816-(Vol.1))
- **AEROSOLS**
  - conference on generation, transport, and removal from environment of radioactive, 25:18525 (CONF-700816-(Vol.1))
  - filtration of radioactive and toxic, design and testing of equipment for, 25:18559 (CONF-700816-(Vol.1), pp 128-42)
  - mass monitoring in air, beta-absorption impactor for, 25:18821
  - release of radioactive, from liquid metal cooled fast breeder reactor during accident conditions, (E/T), 25:20757 (CONF-700816-(Vol.1), pp 26-48)
  - release of radioactive, in water cooled reactor containment systems during accident conditions, (E/T), 25:20758 (CONF-700816-(Vol.1), pp 72-101)
  - removal of radioactive, by water cooled reactor containment system filters during coolant loss accident conditions, 25:20782 (CONF-700816-(Vol.1), pp 102-27)
  - sampling of radioactive, air sampler for, 25:18877(P)
- **AET**
  - effects on uptake of α-aminoisobutyric acid, inulin, orotic acid, and phosphorus-32 by tissues of γ-irradiated rats, 25:19024
  - radioprotective effects of, on hematopoiesis, intestines, and survival of mice, comparison of whole-body fast-neutron and x, 25:19029
- **AGUIRRE POWER REACTOR, UNIT 1**
  - design parameters of, revised and additional data on, 25:20680 (DOCKET-50376-9)
  - operations aspects of, revised and additional data on, 25:20680 (DOCKET-50376-9)
- **AIR**
  - analysis for aerosols, beta-absorption-impactor mass monitor for, 25:18821
  - cascade showers in, Monte Carlo calculations of transition effects at aluminum and iron interfaces for 200-MeV- to 1-GeV-electron-initiated, 25:19943
  - flow through channels containing smooth packed rods, resistance and velocity fields in turbulent, 25:18576(T) (AEC-tr-7189)
  - neon-atom reactions at 25 to 90 keV with, total cross section for single electron loss in, (E), 25:19492 (SC-RR-70-735)
  - photon reactions with, electric field excited by pulsed gamma, 25:19761
  - radon daughter content in, α-spectroscopic method for determining, 25:18363
- **AIR SAMPLERS**
  - design for radioactive aerosols, 25:18877(P)
  - development for measuring particle concentrations and

XUM

radioactivity concentrations of alpha-active aerosols, 25:18685(P)

AIRGLOW
excitation of lambda6300 (O I) in, by soft electrons, (E/T), 25:19579

ALANINE, 2-METHYL-
radiation effects on uptake by rat kidney, liver, muscles, and spleen, effects of AET and cysteamine on γ, 25:19024

ALANINE, PHENYL-
radiation effects on, in relation to physiological damage in cells, biophysical mechanisms of uv, 25:18903

ALBUMINS
effects on reactivity of γ-irradiated solutions of chymotrypsin, 25:18907

ALGAE
radioisotope accumulation by marine, effects of physico-chemical form on, 25:18894
radioisotope content of chlorophyll-A in marine, in contaminated ecosystem, cerium-144 and cesium-137, 25:18936
radioisotope content of marine, following radioactive waste disposal, 25:18939

ALKALI METAL HALIDES
radioinduced defects in crystals of, studies of recombination processes of, 25:19770(R) (NYO-3842-12)
radioinduced F centers in, chemiluminescence--dissolution method for study of, 25:19850

ALKYL BROMIDES
radioinduced isomerization at 150 to 240°C, 25:18438
radiolysis at 150 to 240°C, 25:18438

ALKYL CHLORIDES
effects on radioinduced crosslinking of elastomers, 25:18434

ALKYL HALIDES
effects on radioinduced polymerization of 2-furaldehyde, 25:18430

ALPHA DECAY
energy release from, (T), 25:20482(T) (RFP-Trans-72)

ALPHA PARTICLES
channeling in silicon, effects of disorder produced by ion implantation on, 25:19816
detection and measurement in aerosols, detector for, 25:18685(P)
dose to human population on Kerala coast, India from food, 25:19143
effects on human population following chronic internal and external exposure, natural background low-dose, 25:18927 (NP-18670)
effects on semiconducting diamonds, 25:19769(T) (LIB/Trans-307)
hazards to human populations following polonium-210 pasture contamination, suggested revision of MPC values on basis of potential, 25:18890(R) (COO-2044-3)
reactions (α,2ne) and (α,2nγ) with ytterbium-172 at 20.5 MeV, energy levels of hafnium-174 from, (E), 25:20427
reactions (α,γ) with nuclei, background reduction for spectroscopy of, 25:20148
reactions (α,nγ) with fluorine-19, γ-ray polarization in, (E), 25:20318
reactions (α,p) with carbon-12, magnesium-26, nickel-62, and silicon-28 at 35.5 MeV, DWBA analysis of j dependence in angular distributions from, (E), 25:20309
reactions (α,p) with phosphorus-31 at 11.0 MeV, p--γ angular correlations from, (E), 25:20348
reactions (α,pγ) with calcium-40 at 11.8 to 15.5 MeV, p-γ coincidence spectra from, (E), 25:20320
reactions (α,t) with neodymium-150, samarium-152, and samarium-154, proton states from, (E/T), 25:20383
reactions (α,xn) and (α,pxn) with holmium-165 and thulium-169 up to 150 MeV, cross sections for, (E), 25:20390
reactions of 22.5- to 235-MeV/N cosmic, with carbon, nitrogen, and oxygen, (E), 25:19531
reactions with nuclei, tables of thresholds for, (E), 25:20237 (UCRL-50400(Vol.9))
scattering by A = 7 to 140 nuclei, model analysis of inelastic, 25:20274
scattering by calcium-40 at 23.1 MeV, differential cross sections for elastic, (E), 25:20310
scattering by erbium-166, samarium-154, and ytterbium-176 at 27.5 to 32.5 MeV, cross sections for inelastic, (E), 25:20466
scattering by hafnium-174 at 15 MeV, energy level transitions from inelastic, (E), 25:20427
scattering by helium-4, separable potentials for, 25:20511
scattering by lithium-6 at 3.30 to 5.00 MeV, excitation functions for elastic, (E), 25:20292
scattering by polarized helium-3 at 7.5 to 18 MeV, asymmetries in, (E), 25:20262
scattering by silicon at 5 MeV, blocking patterns from elastic, (E), 25:18679
scattering by the 5.23-MeV level in magnesium-24 at 40.2 to 79.5 MeV, angular distribution and optical-model parameters for inelastic, (E), 25:20344

ALPHA SOURCES
content in ground waters of central Nevada, 25:18522 (USGS-474-97)
monitoring on reactor fuel element surfaces, ionization chamber for, 25:18636(P)

ALPHA SPECTROMETERS
development of liquid scintillation, for determination of radon daughters on filters, 25:18768
development of proportional--surface-barrier coincidence, for low-level alpha sources, 25:18741

ALUMINUM
cascade showers in, Monte Carlo calculations of transition effects at air interface for 200-MeV- to 1-GeV-electron-initiated, 25:19943
chromatographic behavior in hydrochloric acid--thiocyanate mixture on Amberlite LA-2, 25:18337
determination in natural waters from uranium mining operations, method for, 25:18339 (CEA-R-3557(2))
determination using azo compounds, photometric, 25:18347
deuteron reactions at 180 to 360 keV with, cross sections for K-shell ionization in, (E), 25:19470
effect on hydrolysis of potassium phosphorodifluoridate, catalytic, 25:18373
effects as additive on properties of intermetallic Ti_3Sn, 25:19238
effects on fluoride hydrolysis, catalytic, 25:18375
electron reactions at 80 keV with, radiative decay spectra from, (E), 25:19758 (ORNL-4584, pp 74-86)
electron transmission through foils of, at 1 eV to 4 keV, (E), 25:19766
fission fragment stopping power, energy loss, and range in, (E), 25:20442
gamma spectra distortion in absorbers of, 25:18771
implantation of recoil atoms of, in silica and polythene substrates by argon-ion bombardment, 25:19786
laser-beam reactions with foils of, plasma production in, 25:19701
phonon interactions with electrons in superconducting films in junctions, (E/T), 25:19607
preparation and properties for use as matrix for neutron-absorbing borides, 25:19264(P)
production of, effects of nuclear power on economics of, 25:19184
properties of wire screens of, for use as thermal insulation in radioisotope-fueled thermoelectric systems, 25:18594(R) (ORNL-TM-3292)
proton reactions at 70 GeV, yields and differential cross sections for π^-, K^-, anti p, and anti d production in, (E), 25:19906
proton reactions at 90 to 180 keV with, cross sections for K-shell ionization in, (E), 25:19470
proton reactions at high energies, atlas of hadron momentum spectra from, (T), 25:20028
separation of bismuth from, by cation exchange chromatography, 25:18520
superconducting and semiconducting phase of, embedded in SiO_2 films, 25:19631
superconductivity in films of, enhancement by Al_2O_3 and germanium additions, 25:19622
tunneling into weakly coupled films of, and superconducting tin in proximity, 25:19623
ultrasonic attenuation in single crystals of, Alpher--Rubin effect of magnetic field on, 25:19879

ALUMINUM ALLOYS AND SYSTEMS
fatigue lives of 2024-T3 and 6061-T6, under broad-band excitation, prediction of, 25:20895 (SCL-CR-710175)
properties for use as fuel cladding, 25:19203
Al--Al_2O_3, electric conductivity of two-phase, 25:19226
Al--Cr--Nb--Si--Sn--Ti, properties for use as protective coating on niobium, 25:19176
Al--epoxy resins, radiation effects on bonding in, γ, 25:18421(R) (RLO-2098-1)
Al--Ge--Nb, properties of intermetallic system Nb_3Al--Nb_3Ge, for high parameter superconductors, (E), 25:19599
Al--Nb, crystal structure of intermetallic coatings of, on niobium and niobium alloys, 25:19173
Al--Nb, oxidation of intermetallic $NbAl_3$ coatings of, at 600 to 1400°C, kinetics of pest-type, 25:19174
Al--Nb--Si--Sn--Ti, properties for use as protective coating on niobium, 25:19176
Al-base--Li, hardening in neutron irradiated, mechanisms of precipitation, 25:19201
Al-base--Mg, radiation effects on tensile properties of, fast neutron, 25:19255

ALUMINUM IONS
implantation in silicon at 40 to 100 keV, electron microscopic studies of defects induced in, 25:19808
implantation in silicon carbide at 5 to 300 keV, properties of conducting layers and p--n junctions formed by, (E), 25:19847

ALUMINUM ISOTOPES Al-26
abundance in Bovedy meteorite, (E), 25:19301
energy levels of, calculation using strong-coupling rotational model, (T), 25:20353

ALUMINUM ISOTOPES Al-27
energy levels from neutron inelastic scattering, (E), 25:20356
helium-3 elastic scattering at 18 MeV, optical-model analysis of angular distributions from, (E/T), 25:20271 (NP-18628)
helium-3 reactions (He-3,p) at 18 MeV, DWBA analysis of angular distributions from, (E/T), 25:20271 (NP-18628)
neutron inelastic scattering by, γ energies from fast, (E), 25:20356
neutron reactions (n,p) and (n,α) up to 14 MeV, Hauser--

  Feshbach analysis of excitation functions for, (E/T), 25:20346
 photon reactions at 313 MeV endpoint energy, meson (π^-) and (π^+) energy spectra and π^-/π^+ ratio from, (E), 25:20341
 proton reactions (p,α) and (p,γ) at 1.7 MeV, excitation functions for, (E), 25:20330
 proton reactions up to several GeV, cascade calculations of double differential distributions of particles from, (T), 25:20018 (JINR-P2-5507)
ALUMINUM ISOTOPES Al-28
 energy levels of, calculation using unified model, 25:20524
ALUMINUM OXIDES
 physical properties of molten, to 3000°C, equipment and methods for measuring, 25:19273 (BNWL-SA-3579)
 thermal properties of layers of, 25:20896(T) (SCL-T-68-253)
 Al_2O_3--Nb-base, creep of dispersion-strengthened, at 850 to 1450°C, 25:19277
 Al_2O_3--polyethylene, radiation effects on electrical and mechanical properties of, γ, 25:18421(R) (RLO-2098-1)
 Al--Al_2O_3, electric conductivity of two-phase, 25:19226
AMERICIUM
 binding to glycoprotein in bovine bones, mechanism of, 25:18899
 complexes with 4,4,4-trifluoro-1-(2-thienyl)-1,3-butanedione, stability of, effects of adduct-forming agents on, 25:18498 (KFK-1298)
 complexes with chloride, nitrate, and thiocyanate, stability constants for, effects of ionic media on, 25:18371
 separation from aqueous solutions by solvent extraction, chelate formation in, 25:18498 (KFK-1298)
 separation from iron and fission products by precipitation, 25:18507(P)
AMERICIUM ISOTOPES Am-232
 electron-capture decay of, delayed fission of plutonium-232 from, (T), 25:20371 (JINR-P7-5584)
AMERICIUM ISOTOPES Am-234
 electron-capture decay of, delayed fission of plutonium-234 from, (T), 25:20371 (JINR-P7-5584)
AMERICIUM ISOTOPES Am-241
 determination in irradiated plutonium dioxide--uranium dioxide fuels as measure of burnup, 25:18359 (WCAP-3385-56(Pt.2))
 distribution in tissues of mice following intravenous injection, autoradiographic study of, 25:18901
 neutron capture at 0.2 to 20 eV with fission isomer excitation, cross section and prompt-to-isomer fission ratio for, (E), 25:20412
AMERICIUM ISOTOPES Am-242
 fission of isomeric, half-life for spontaneous, (E), 25:20412
 production of spontaneously fissioning isomeric, in (n,2n) reactions, cross sections for, (E), 25:20369 (JINR-P3-5528)
AMERICIUM ISOTOPES Am-243
 determination in irradiated plutonium dioxide--uranium dioxide fuels as measure of burnup, 25:18359 (WCAP-3385-56(Pt.2))
 neutron capture at 0.2 to 20 eV with fission isomer excitation, cross section and prompt-to-isomer fission ratio for, (E), 25:20412
 neutron reactions (n,n') and (n,2n) with, cross sections for production of spontaneously fissioning isomers in, (T), 25:20369 (JINR-P3-5528)
 production of spontaneously fissioning isomeric, in (n,n') reactions, cross sections for, (E), 25:20369 (JINR-P3-5528)
AKERICIUM ISOTOPES Am-244
 fission of isomeric, half-life for spontaneous, (E), 25:20412
AMIDE POLYMERS
 radiation effects on structure and mechanical properties of Capron, effects of surface modification and additives on electron, 25:18425
AMINO ACIDS
 radiation effects on composition of, of protein of fish muscles, effects of dose on ionizing, 25:19110
 radiation effects on excretion of, in human urine following therapy for malignant tumors, 25:19063
AMINOPTERIN
 effects on radiosensitivity of yeast cells, 25:19155
AMMETERS
 description for measuring rms values of pulsed current signals, 25:18839(P)
 design of low-current dc, 25:18834
AMMONIA
 detection of, in direction of three galactic-center radio sources, (E), 25:19366
 effects on coolant chemistry in water cooled reactor loops, (E), 25:20726
 effects on ion reactions in radiolysis of gaseous ethylene, 25:18452
 radiolysis of, absorption spectra of ions produced by electron pulse, 25:18448(R) (CEA-N-1369)
 yields from γ radiolysis of aniline, effects of additives on, 25:18450(R) (ORO-3519-8)
AMMONIUM HYDROXIDES
 reactions with thorium nitrates to prepare thorium hydroxide, 25:19259 (NLCO-1029)
 NH_4OH--$UO_2(NO_3)_2$, precipitation in, effects of uranium concentration on composition of precipitate formed by, 25:18379
AMMONIUM SULFATES
 radiation effects on dielectric constant and ferroelectric transition of single crystals of, gamma, 25:19856
AMMONIUM TARTRATES
 use as electrolyte for deposition of indium--zinc alloys, 25:19221
AMMONIUM URANYL FLUORIDES
 thermal decomposition of, thermodynamics of, 25:18380
AMPLIFIERS
 design and operation of fast-recovery-time trigger, for spark chambers, 25:18791
 design and operation of VA-V-100 linear amplifier/analyzer with specifications, 25:18873
 design of transistor, for semiconductor detector, 25:18668
ANALYTICAL CHEMISTRY
 conference on, Warsaw, September 10--14, 1968, 25:18334 (CONF-680946-(Absts.))
ANGIOSPERMIDAE
 Allium cepa, radiosensitivity of seeds of, in comparison to other species, effects of dose on γ, 25:18946
 Avena sp., strontium-90 uptake by, 25:18897
 Betula sp., radioisotope content of, in Finnish Lapland during 1968 and 1969, 25:18932 (NYO-3446-14, Paper 31)
 Brassica napus, radioinduced male sterility in, γ, 25:19152
 Citrullus vulgaris, radiosensitivity of seeds of, in comparison to other species, effects of dose on γ, 25:18946
 Crepis capillaris, aberrations induced in chromosomes of, during space flight, effects of ethylenimine on, 25:18953
 Datura tatula, radioinduced mutations in, γ, 25:19151
 Euphorbia lagascae, radiosensitivity of seeds of, in comparison to other species, effects of dose on γ, 25:18946
 Gossypium sp., radiation effects on chromosomes and mitosis in roots of, and combined effects of dimethyl sulfate following seed exposure, γ, 25:18954
 Gossypium sp., radiation effects on dehydrogenase activity and pyruvic acid content of cell mitochondria and nuclei in, γ, 25:18918
 Gossypium sp., radiation effects on pollen of, effects of, on meiosis in embryonic tissues, γ, 25:18955
 Hordeum sp., strontium-90 uptake by, 25:18897
 Hordeum vulgare, aberrations induced in chromosomes of, during space flight, 25:18952
 Lupinus sp., strontium-90 uptake by, 25:18897
 Lycospersicum esculentum, radiosensitivity of seeds of, in comparison to other species, effects of dose on γ, 25:18946
 Nigella damascena, radioinduced chromosome aberrations in seeds of, effects of chelating agents on repair processes following cobalt-60 γ, 25:18951
 Phaseolus vulgaris, radioinduced mutations in, for chlorophyll, effects of dose on γ, 25:18946
 Phaseolus vulgaris, radiosensitivity of seeds of, in comparison to other species, effects of dose on γ, 25:18946
 Phleum pratense, strontium-90 uptake by, 25:18897
 Pisum sativum, radiosensitivity of seeds of, in comparison to other species, effects of dose on γ, 25:18946
 Salix sp., radioisotope content of, in Finnish Lapland during 1968 and 1969, 25:18932 (NYO-3446-14, Paper 31)
 Secale sp., strontium-90 uptake by, 25:18897
 Solanum sp., radioinduced production of toxin in, 25:18915
 Solanum sp., radioisotope removal from tissue of, methods for, 25:18892 (NP-18641)
 Trifolium sp., strontium-90 uptake by, 25:18897
 Vaccinium sp., radioisotope content of, in Finnish Lapland during 1968 and 1969, 25:18932 (NYO-3446-14, Paper 31)
 Vicia faba, chromosome aberrations induced in, by maleic hydrazide and x radiation, effects of blue, green, and infrared light on, 25:18962
 Vicia faba, radiation effects on carbon-14-labeled carbon dioxide assimilation and distribution and chlorophyll content in, x, 25:19153
 Vicia faba, radioinduced chromosome aberrations in, chronic γ, 25:18950
 Vicia faba, radiosensitivity of seeds of, in comparison to other species, effects of dose on γ, 25:18946
 Vicia sp., strontium-90 uptake by, 25:18897
 Zea mays, growth of roots of, effects of radiotoxins on, 25:18915
 Zea sp., strontium-90 uptake by, 25:18897
ANILINE
 radiolysis at 77 to 120°K, yields from electron pulse and γ, 25:18465
 radiolysis of, effects of additives on yields from γ, 25:18450(R) (ORO-3519-8)
ANIMALS
 book: Bone Tumors in Man and Animals, 25:19136
ANTHELMINTICS
 effectiveness in treatment of ascariasis in lungs of x-

XUM

- irradiated mice, 25:19032

ANTHRACENE
- effects on hemolysis of uv-irradiated erythrocytes, 25:18914
- effects on yields from γ radiolysis of aniline, 25:18450(R) (ORO-3519-8)

ANTIBIOTICS
- effectiveness in treatment of ascariasis in lungs of x-irradiated mice, 25:19032

ANTIBODIES
- content of serum of calves, effects of, on permeability of erythrocytes to phosphorus-32, 25:18900
- effects on immune reactions of x-irradiated mice to sheep red blood cells, 25:18923

ANTIGENS
- preparation of noninfectious arbovirus, from irradiated infected mouse tissues, 25:18924

ANTIMONY
- chromatographic behavior in hydrochloric acid--thiocyanate mixture on Amberlite LA-2, 25:18337
- separation of bismuth from, by cation exchange chromatography, 25:18520

ANTIMONY ALLOYS AND SYSTEMS
- In--Sb, ion implantation in, review, 25:19789
- In--Sb, phosphorus-ion channeling profile in InSb, 25:19801
- In--Sb, zinc-ion implantation and range at 0.2 to 1.8 MeV in, for infrared detector fabrication, 25:19828

ANTIMONY HALIDES
- separation by solvent extraction, effects of charge, composition, and structure on, 25:18511

ANTIMONY IONS
- effects on silicon at 400 keV, annealing of defects induced in, 25:19811
- implantation in germanium at 30 to 40 keV, channeling study of lattice location of, 25:19827
- implantation in germanium at 40 and 70 keV, electric properties and lattice location of, 25:19799
- implantation in silicon at 20 keV, enhanced diffusion in, 25:19823
- implantation in silicon at 40 keV, effects on channeling of low-energy alpha particles and protons, 25:19816
- implantation in silicon at 40 to 100 keV, electron microscopic studies of defects induced in, 25:19808
- implantation in silicon at 400 keV, divacancy and amorphous-layer formation in, 25:19812
- implantation in silicon at 400 keV, EPR of substitutional atoms from, 25:19826
- implantation in silicon at 80 keV, electron microscopic studies of damage from, 25:19814
- implantation in silicon carbide at 5 to 300 keV, properties of conducting layers and p--n junctions formed by, (E), 25:19847
- implantation into silicon at 100 keV, comparison of total and donor profiles of, 25:19825

ANTIMONY ISOTOPES Sb-115
- core-particle coupling in, (T), 25:20495

ANTIMONY ISOTOPES Sb-117
- core-particle coupling in, (T), 25:20495

ANTIMONY ISOTOPES Sb-119
- core-particle coupling in, (T), 25:20495

ANTIMONY ISOTOPES Sb-120
- beta and electron-capture decay of ground-state and isomeric, γ singles and coincidence spectra from, (E), 25:20401

ANTIMONY ISOTOPES Sb-121
- core-particle coupling in, (T), 25:20495
- electron paramagnetic resonance of implanted, in silicon, 25:19826
- energy levels from gamma resonance scattering, widths for, (E), 25:20355

ANTIMONY ISOTOPES Sb-123
- core-particle coupling in, (T), 25:20495
- electron paramagnetic resonance of implanted, in silicon, 25:19826
- energy levels from gamma resonance scattering, widths for, (E), 25:20355
- neutron reactions (n,2n) at 14.5 MeV, cross sections and gamma spectra from, (E), 25:20435

ANTIMONY ISOTOPES Sb-124
- beta decay of polarized, γ-ray angular distributions from, (E), 25:20386
- nuclear magnetic moment of, (E), 25:20386

ANTIMONY ISOTOPES Sb-125
- beta decay of, γ and conversion electron spectra from, (E), 25:20408
- content of plants in Finnish Lapland during 1968 and 1969, 25:18932 (NYO-3446-14, Paper 31)
- core-particle coupling in, (T), 25:20495

ANTINEOPLASTIC DRUGS
- toxicity in liver of children, synergistic effects of radiotherapy on, 25:18999

ARACHNIDA
- Amblyomma sp., carbon-14 content of larvae of, following inoculation of females with labeled glucose, 25:18934(R) (ORO-3514-10)
- Amblyomma sp., population dynamics in different habitats, use of radioisotopes for determining, 25:18934(R) (ORO-3514-10)
- Dermacentor sp., carbon-14 content of larvae of, following inoculation of females with labeled glucose, 25:18934(R) (ORO-3514-10)
- Dermacentor sp., population dynamics in different habitats, use of radioisotopes for determining, 25:18934(R) (ORO-3514-10)
- Haemaphysalis sp., carbon-14 content of larvae of, following inoculation of females with labeled glucose, 25:18934(R) (ORO-3514-10)
- Haemaphysalis sp., population dynamics in different habitats, use of radioisotopes for determining, 25:18934(R) (ORO-3514-10)
- Panonychus citri, radiation effects on fecundity of, effects of dose and TEPA on γ, 25:19100
- Panonychus citri, radioinduced mutations in sperm of, effects of dose and TEPA on γ, 25:19100

ARGON
- electron reactions with, autoionizing states and negative-ion resonances from, 25:19490 (ORNL-4584, pp 92-104)
- energy-level transitions in, continuum generalized oscillator strengths for 3p--epsilon d, (T), 25:19476
- energy-level transitions in, minima in generalized oscillator strengths for, (T), 25:19521
- performance as carrier gas for electron attachment studies, 25:19491 (ORNL-4584, pp 105-24)
- plasma of, asymptotic thermochemical relaxation processes in, 25:19684
- plasma of, partition functions for, (T), 25:19397
- plasma of, resistive loading in rf heating of, (E/T), 25:19653
- positron annihilation in liquid and solid, positronium-bubble formation and angular correlation of photons from, 25:19487
- proton reactions at 5 to 26 keV with, total cross sections for formation of metastable hydrogen atoms by charge exchange in, (E), 25:19504
- reactions with nitrogen and oxygen molecules at 25 to 90 keV, total cross sections for single electron loss in, (E), 25:19492 (SC-RR-70-735)
- sorption by nonporous thorium oxides, effects of surface water on, 25:18416

ARGON IONS
- effects on glass at 20 keV, 25:19787
- implantation in silicon at 260 keV, damage profiles from, 25:19817
- implantation in silicon at 50 keV, effects on impurity diffusion, 25:19824
- implantation in zinc telluride at 30 to 120 keV, properties induced by, 25:19794
- reactions with carbon at 500 keV, x-ray spectra from, 25:18836
- recoil-atom implantation by 80-keV, into substrates from thin aluminum films, 25:19786
- use of 100-keV, to excite x rays in boron-implanted silicon for implantation profile measurement, 25:19803

ARGONNE SYNCHROTRON (ZGS)
- magnet power supply for, meter for measuring rms values of pulsed current signals from, 25:18839(P)

ARSENIC
- chromatographic behavior in hydrochloric acid--thiocyanate mixture on Amberlite LA-2, 25:18337

ARSENIC HALIDES
- separation by solvent extraction, effects of charge, composition, and structure on, 25:18511

ARSENIC IONS
- implantation in silicon at 280 keV, damage distribution from, 25:19818
- implantation in silicon at 400 keV, EPR of substitutional atoms from, 25:19826

ARSENIC ISOTOPES As-75
- electron paramagnetic resonance of implanted, in silicon, 25:19826
- energy levels from gamma resonance scattering, widths for, (E), 25:20355

ARSENIC ISOTOPES As-87
- yield in uranium-235 thermal neutron fission, (E), 25:20327

ARYLSULPHATASE
- radiation effects on activity of, in rat urine, whole-body x, 25:18905

ASPHALT
- radioactive waste fixation in, method for intermediate-level, 25:18634

ASTRONAUTS
- radiation dose to Apollo XI, during moon landing, Ilford G.5 and K.2 nuclear emulsion measurement of, 25:18978 (AD-711316)

ATLANTIC RICHFIELD REPROCESSING PLANT
- construction permit application for, scheduling of activities related to, 25:18497 (DOCKET-50372-3)

ATMOSPHERE
- contamination by gaseous effluents from nuclear power plants, computer methods for evaluating, 25:18526 (ORNL-4584, pp 37-40)
- lead-210 content of ground-level, in Finland, effects of geographical location, meteorological conditions, and season on, 25:18933 (NYO-3446-14, Paper 32)
- radiation monitoring of, at UKAEA facilities, methods for, 25:18635
- radioactive aerosol removal from, methods for, 25:18525 (CONF-700816-(Vol.1))
- radioactive contamination of, effects of fallout and wastes from reactor power plants on, 25:18941

radioactivity monitoring of, calibration and testing of detectors for krypton-85, 25:18638 (CONF-700816-(Vol.1), pp 143-74)
radioisotope content in, origin of neon-21 and neon-22, (E/T), 25:18527
ATMOSPHERES
spectral line formation in multi-dimensional, (T), 25:19424
ATOMIC BEAMS
intensity profile of, development of method for measuring and recording, 25:20218
ATOMIC CLOUDS
radiation dose estimates for human populations resulting from transient passage of, 25:18989 (ORNL-4584, pp 42-56)
ATOMIC ENERGY, LEGAL ASPECTS
book: Problems of Protection in Industrial Utilization of Radioelements, 25:18996
radiation protection of personnel, federal and state, 25:18973
regulations covering shipment of radioactive materials in USA, 25:19017
treaty for non-proliferation of nuclear weapons, standards for safeguards methods in relation to, 25:19019
ATOMIC PHYSICS
bibliography on surface and vacuum physics, 25:19469
ATOMIC STRUCTURE
calculations of, use of truncated multipolar expansion pair functions in, 25:19515
integral equations for three-body problem in, derivation from Faddeev equations, 25:19516
ATOMS
charged-particle reactions at very low energies with, inverse fourth-power potential in calculation of cross sections for capture and elastic scattering in, 25:19500
electron binding energy in Z = 70 to 90, K-shell, (T), 25:19477
electron inelastic scattering by, generalized random phase approximation for calculation of, 25:19507
energy levels of, perturbation effects on long-lived decaying states, (T), 25:19520
energy of, completeness criteria for functions used in matrix Hartree--Fock and correlation-energy calculations of, 25:19519
energy-level transitions in, calculation of minima in generalized oscillator strengths for, using hydrogen-like wave functions, 25:19521
energy-level transitions in, calculation of upper and lower bounds to oscillator strengths for dipole, 25:19514
energy-level transitions in, generalization of oscillator strength for, 25:19757 (ORNL-4584, pp 58-73)
energy-level transitions in, length and velocity formulas in calculation of approximate oscillator strengths for electric dipole, 25:19518
energy-level transitions in, minima in atomic continuum generalized oscillator strengths for, (T), 25:19476
ion reactions with, ion--photon coincidence method for study of excitation in, 25:19493
Lamb shift in Z = 70 to 90, (T), 25:19477
photon reactions with inner-shell electrons of, review of chemical information from, 25:19473
reactions with diatomic molecules, generalized phase shift approach to rotational excitation in, 25:19498
scattering by atoms, inversion procedure for determination of intermolecular potentials from differential cross sections for, (T), 25:19495
wave functions for, calculation using Hartree--Fock theory with exchange cutoff, 25:19517
wave functions for, extensions of Hulthen representation of orbital, 25:19513
AURORAE
oxygen heights and lifetimes in frequency-dependent pulsating, at 88 to 115 km, atomic, (E/T), 25:19578
AUSTRALIA
nuclear power plant development in, prospects for, 25:20550 (NP-18677)
AUTORADIOGRAPHY
detector for alpha, cellulose nitrate track, 25:18799 (ORNL-4584, pp 165-86)
detectors for alpha, performance of plastic track, 25:18727
AVES
Lagopus lagopus, radioisotope content of bones and soft tissues of, in Finland, 25:18929 (NYO-3446-14, Paper 26)
Lagopus mutus, radioisotope content of bones and soft tissues of, in Finland, 25:18929 (NYO-3446-14, Paper 26)
Meleagris sp., radiation effects on pathogenicity of Histomonas meleagridis in, γ, 25:19156
AVR REACTOR
cooling system for, design requirements for components of helium cooled, 25:20558
6-AZAURIDINE
effects on radiosensitivity of Ehrlich ascites cells following incubation in tritium-labeled thymidine, 25:18888
AZO COMPOUNDS
preparation for use in electrophoretic and chromatographic determination of elements, 25:18347
AZOBENZENE, HEXANITRO-
thermal decomposition of, kinetics of, 25:18378
AZULENE
electron reactions with, attachment rates for, 25:19491 (ORNL-4584, pp 105-24)

B

BABOONS
plutonium oxide retention in lungs of, following inhalation, effects of washing on, 25:18895
BACTERIOPHAGES
radiation effects on frequency of transduction of drug resistance determinants by lysates of, in Staphylococcus aureus E169, uv, 25:19157
BARIUM
chromatographic behavior in hydrochloric acid--thiocyanate mixture on Amberlite LA-2, 25:18337
determination in minerals and rocks by isotope dilution mass spectrometric, neutron activation, gravimetric, and other spectrometric methods, 25:18335
separation of bismuth from, by cation exchange chromatography, 25:18520
sorption by monocrystalline tungsten, effects of adatom surface potential and adsorbate electronegativity on, 25:19207
BARIUM ISOTOPES Ba-131
capture decay of, γ and conversion electron spectra and angular correlations from, (E), 25:20414
BARIUM ISOTOPES Ba-132
neutron capture by, cross sections and gamma spectra from thermal, (E), 25:20439
BARIUM ISOTOPES Ba-134
energy levels from Coulomb excitation, transition probability and quadrupole moment of first 2^+, (E), 25:20469
neutron capture by, cross sections and gamma spectra from thermal, (E), 25:20439
BARIUM ISOTOPES Ba-136
energy levels from Coulomb excitation, transition probability and quadrupole moment of first 2^+, (E), 25:20469
BARIUM ISOTOPES Ba-137
neutron inelastic scattering at 14.5 MeV, cross sections and gamma spectra from, (E), 25:20435
BARIUM ISOTOPES Ba-138
energy levels from Coulomb excitation, transition probability and quadrupole moment of first 2^+, (E), 25:20469
half-life of isomeric, (E), 25:20381
neutron reactions (n,2n) at 14.5 MeV, cross sections and gamma spectra from, (E), 25:20435
BARIUM ISOTOPES Ba-140
half-life, (E), 25:20339
BARIUM ISOTOPES Ba-141
beta decay of, γ singles and coincidence spectra from, (E), 25:20415
BARIUM ISOTOPES Ba-142
beta decay of, γ singles and coincidence spectra from, (E), 25:20415
BARIUM SELENATES
radiolysis of powders of, γ, 25:18479
BARIUM SULFATES
particle size in precipitates of, factors influencing, 25:20886(T) (RFP-Trans-74(Pt.2))
precipitation of, particle size distribution in, 25:20885(T) (RFP-Trans-74(Pt.1))
BARYONS
decay of decuplet $3/2^+$, broken SU(6)/sub W/ symmetry for correlations among amplitudes of octet $1/2^+$ baryon and octet 0^- meson production from, (T), 25:20048
interactions with mesons, multiparticle Veneziano formula for, 25:20014
interactions with pseudoscalar meson octet fields, mass operator in SU(3) symmetric strong coupling theory for, (T), 25:20015
production of octet $1/2^+$, from decay of decuplet $3/2^+$ baryons, broken SU(6)/sub W/ for, (T), 25:20048
BARYONS, RESONANCE (N*)
decay $\Delta^{++}(1900) \to \Delta^{++}(1236) + \pi^+ + \pi^-$ in hydrogen bubble chamber, (E), 25:19902 (USIP-70-8)
parity and spin of pp(2050) in $p + \bar{p} \to p + p$ interactions at 640 MeV, phase analysis study of, (T), 25:20016(T) (CERN-Trans-70-14)
production in anti N-, N-, and π-initiated cosmic EAS at 10^5 to 10^7 GeV, models for, (T), 25:19973 (INSJ-125)
production of Δ and N in $p + p \to 2p + \pi^+ + \pi^-$ and $p + p \to n + p + 2\pi^+ + \pi^-$ interactions at 19 GeV/c in hydrogen bubble chamber, 25:19900 (USIP-70-4)
production of Δ and N* in four-prong $p + p$ interactions at 19 GeV/c in hydrogen bubble chamber, (E), 25:19901 (USIP-70-7)
production of Δ in $p + p \to 2p + \pi^+ + \pi^- + \pi^0$ interactions at 19 GeV/c in hydrogen bubble chamber, (E), 25:19900 (USIP-70-4)
production of $\Delta(1236)$ and N(1650) in six-prong $p + p$ interactions at 10 GeV/c in hydrogen bubble chamber, (E), 25:19902 (USIP-70-8)
production of $\Delta^{++}(1900)$ in $p + p \to \Delta^{++}(1900) + n$

XUM

  interactions at 19 GeV/c in hydrogen bubble chamber, (E), 25:19902 (USIP-70-8)
  production of pp(2050) in p + p → p + p interactions at 640 MeV, phase analysis study of, (T), 25:20016(T) (CERN-Trans-70-14)
BARYONS, RESONANCE (Y*)
  production of Σ(1385) and Σ(1650) in six-prong p + p interactions at 10 GeV/c in hydrogen bubble chamber, (E), 25:19902 (USIP-70-8)
  production of Σ(1385) in π^- + d at 3.15 GeV/c in deuterium bubble chamber, (E), 25:19922
BASALT
  radiation effects on properties of, for use in concrete shielding aggregates, neutron, 25:19296
BATTERIES
  electric potential of aqueous mercury-sodium carbonate, 25:19190(T) (AI-Trans-287)
BEAM SEPARATORS
  characteristics of wave guide, 25:20186
  harmonic components of fields of magnetic quadrupole lens, measurement of, 25:20164
BEARS
  radioisotope content of bones and soft tissues of, in Finland, 25:18929 (NYO-3446-14, Paper 26)
BENZENE
  electron reactions with substituted, lifetimes and yields of negative ions from, 25:19490 (ORNL-4584, pp 92-104)
  neutron inelastic scattering spectra at 77 to 270°K, comparison with calculations, (E/T), 25:20247
  optical constants in photon energy range 4.0 to 10.65 eV for, 25:19759 (ORNL-4584, pp 87-91)
  oxygen-ion reactions at 0 to 2 eV with deuterated and normal, rates of, 25:19490 (ORNL-4584, pp 92-104)
  yields from γ radiolysis of aniline, effects of additives on, 25:18450(R) (ORO-3519-8)
  benzene--Br, radiation effects on liquid and solid, labeled organic yields from neutron, 25:18483(R) (COO-1617-27)
  benzene--bromobenzene, radiolysis of, yields from γ, 25:18451
  benzene--bromobenzene--Crystal Violet, radiolysis of, yields from γ, 25:18451
  benzene--hexane--Li_2CO_3, radiation effects on, yields from reactions of tritium recoil atoms from neutron, 25:18487
  benzene--I, iodine-128 or iodine-130 isomeric transitions or radiative neutron capture in liquid and solid, organic yields from, 25:18483(R) (COO-1617-27)
  benzene--IBr, radiation effects on liquid and solid, labeled organic yields from, 25:18483(R) (COO-1617-27)
  benzene--ICl, radiation effects on liquid and solid, labeled organic yields from neutron, 25:18483(R) (COO-1617-27)
BENZENE, ALKYL-
  alkylbenzene--I, radiation effects on, at 77 and 298°K, organic yields from neutron, 25:18483(R) (COO-1617-27)
  alkylbenzene--ICl, radiation effects on, at 77 and 298°K, isotope effects and yields from neutron, 25:18483(R) (COO-1617-27)
BENZENE, BROMO-
  radiolysis of, yields from γ, 25:18451
  benzene--bromobenzene, radiolysis of, yields from γ, 25:18451
  benzene--bromobenzene--Crystal Violet, radiolysis of, yields from γ, 25:18451
  Br--bromobenzene, bromine-80 isomeric transition in, chemical effects from, 25:18490
  Br--bromobenzene, radiation effects on, comparison of yields from bromine-80 isomeric transition with neutron, 25:18490
BENZENE, 1-CHLORO-2,4-DINITRO-
  effects on x-radiosensitivity of leukocyte count of dogs, 25:19030
BENZENE, p-DICHLORO-
  neutron incoherent scattering on, measurements of thermal, 25:18738 (RISO-229)
BENZOIC ACID
  radiolysis of aqueous perchloric acid solutions of, rate constants for reactions of hydrogen atoms produced by γ, 25:18459
p-BENZOQUINONE
  electron reactions with, formation and lifetimes of negative ions from, 25:19491 (ORNL-4584, pp 105-24)
  benzoquinone--cholesterol acrylate, radioinduced polymerization of, 25:18432
BERYLLIUM
  chromatographic behavior in hydrochloric acid--thiocyanate mixture on Amberlite LA-2, 25:18337
  effects on fluoride hydrolysis, catalytic, 25:18375
  electron momentum distribution in single crystal of, Compton-scattering x-ray study of anisotropic, (E/T), 25:19870
  electron reactions at 80 keV with, radiative decay spectra from, (E), 25:19758 (ORNL-4584, pp 74-86)
  photon reactions at 5.5 to 9.5 GeV, counter--spark chamber study of differential cross sections for K_2^0 production in, 25:19887
  proton reactions at 70 GeV, yields and differential cross sections for π^-, K^-, anti p, and anti d production in, (E), 25:19906
  proton reactions at high energies, atlas of hadron momentum spectra from, (T), 25:20028
  reactions with uranium tetrafluoride vapors, production of uranium trifluoride by, 25:18372
  superconducting and semiconducting phase of, embedded in SiO_2 films, 25:19631
BERYLLIUM ALLOYS AND SYSTEMS
  properties for use as fuel cladding, 25:19203
BERYLLIUM IONS
  implantation in silicon carbide at 5 to 300 keV, properties of conducting layers and p--n junctions formed by, (E), 25:19847
BERYLLIUM ISOTOPES Be-8
  rotational band of, PHF calculation for ground-state, (T), 25:20280
BERYLLIUM ISOTOPES Be-9
  deuteron elastic scattering at 5 to 7 MeV, deuteron tensor polarization and differential cross sections for, (E), 25:20293
  deuteron reactions (d,n) at 650 keV, energy spectra from, (E), 25:20289
  energy levels from lithium-7 (He-3,d) reactions, spectroscopic factors for, (E), 25:20273
  neutron reactions (n,2n) with, cross sections for, (E), 25:20269 (N-70-37365)
  triton reactions (t,α) at 0.3 to 1 MeV, angular distributions and differential cross sections for, (E), 25:20265 (CEA-R-4117)
BERYLLIUM ISOTOPES Be-10
  energy levels of, shell-model calculations using Hartree--Fock basis, (T), 25:20286
BERYLLIUM OXIDES
  compatibility with refractory metal and superalloy capsule materials at high temperatures, 25:18592 (ORNL-4298)
  neutron spectra in, time and space dependent calculations for, (T), 25:20239
BERYLLIUM SELENATES
  radiolysis of powders of, γ, 25:18479
BETA DECAY
  asymmetry coefficients in isospin-forbidden mixed, β-γ, 25:20372 (KFK-1249)
  asymmetry in, CP violation and internal symmetries for second-class currents for mirror, (T), 25:20535
  meson exchange currents in, (T), 25:20542
BETA PARTICLES
  detection of, design of split-anode proportional counter for, 25:18698(P)
  dose of, methods for calculating, 25:18984 (JUL-688-ME)
  dose to human population on Kerala coast, India from food, 25:19143
  dose to man during use of tritium as label for total body water determinations, methods for reducing, 25:18977 (AD-702155)
  dosimetry at 30 keV to 2 MeV photoluminescent glass dosimeters for, 25:18810
  dosimetry of, development of thermoluminescent dosimeters capable of repetitive analysis for, 25:18807(P)
  effects on bones, bone marrow, and hematopoietic tissues of mice following ingestion of strontium-89, carcinogenic, 25:19113
  effects on water, mechanism for scavenging effects of copper ions on hydrogen yields from, 25:18458
  spectra of, effects of thin foils on distortion of, 25:18770
BETA SOURCES
  content in ground waters of central Nevada, 25:18522 (USGS-474-97)
  content of aerosols in Finland, 25:18931 (NYO-3446-14, Paper 30)
  determination of, 2-substituted naphth(1,2)oxazole solutes for liquid scintillation, 25:18731(P)
  effectiveness of strontium-90, for therapy of plastic induration of human penis, 25:19072
BETA SPECTROMETERS
  description of sector-focusing magnetic, 25:20374 (NP-18597)
  design and performance of energy-moderated high energy-resolution, 25:18762
  design and performance of semiconductor telescope, for beta and conversion electron spectra above 0.4 MeV, 25:18760
  design of conversion electron--gamma, for lifetime measurements of energy levels in subnanosecond range, 25:18691
  design of magnetic, using lithium-drifted silicon detector, 25:18736 (INR-P-1227)
  design of magnetic, with lithium-drifted silicon detector, 25:18767
  spectra distortion in semiconductor, effects of thin foils on, 25:18770
BIBLIOGRAPHIES
  on desalination, annotated, 25:20812 (TID-25653)
  on National Bureau of Standards publications, 1968--1969, 25:20869 (NBS-SPEC. PUBL-305(Suppl.1))
  on niobium and niobium alloys, 25:19165
  on plutonium with appendix on transplutonium elements, Dec. 1970, 25:19166
  on surface and vacuum physics, 25:19469
BIG ROCK POINT POWER REACTOR
  containment spray system for, flow rates for, 25:20616 (DOCKET-50155-75)
  containment spray system sensors for, revised trip limits

for, 25:20613 (DOCKET-50155-71)
  control elements for, revised technical specifications for Type 2A, 25:20612 (DOCKET-50155-70)
  core spray nozzle for, potential core flow blockage from failure of backup, 25:20614 (DOCKET-50155-72)
  emergency core cooling system for, flow rates for, 25:20616 (DOCKET-50155-75)
  emergency core cooling system for, reworking of spray orifices for, 25:20615 (DOCKET-50155-74)
  fuel elements for, post-irradiation examination of failed Zircaloy 2 clad uranium oxide (UO_2) rod type, 25:20610 (DOCKET-50155-67)
  neutron sources for, revised technical specifications for two auxiliary antimony--beryllium, 25:20611 (DOCKET-50155-69)
  operations history for July to December 1970, 25:20583 (DOCKET-50155-68)
  piping systems for, weld inspection requirements for, 25:20613 (DOCKET-50155-71)
  safety system sensors for, revised trip limits for, 25:20613 (DOCKET-50155-71)
BINDING ENERGY
  of light nuclei, calculations with several nucleon--nucleon potentials, (T), 25:20298
BIOLOGICAL MATERIALS
  analysis for trace elements by activation, 25:18886
  analysis of standard, for trace elements by neutron activation, 25:18366(R) (NBS-TN-548)
  electron distribution in, analysis of bubble chamber tracks to determine 7.7 MeV, 25:18995
BIOLOGICAL MODELS
  development for determining cesium-137 and strontium-90 contamination of plants during irrigation, 25:18938
  development of computerized, for studies of river bed pollution, 25:18940
  development of human embryo, for radiation dose calculations, 25:18990 (ORNL-4584, pp 129-51)
BIPHENYL
  effects on survival of Penicillium digitatum inoculated in oranges, combined effects of gamma radiation, heat, and, 25:19162
  effects on yields from γ radiolysis of aniline, 25:18450(R) (ORO-3519-8)
BIPHENYL, ISOPROPYL-
  thermal stability of, 25:18377
BIPYRIDINE
  effects on repair processes following γ-radioinduced chromosome aberrations in Nigella damascena seeds, 25:18951
BISMUTH
  chromatographic behavior in hydrochloric acid--thiocyanate mixture on Amberlite LA-2, 25:18337
  diffusion of implanted, in germanium, during annealing, 25:19841
  performance of single crystals of, for neutron filter, 25:20238 (UJV-2488-F)
  photoluminescence of implanted, in gallium phosphide, (E), 25:19845
  separation from other elements by cation exchange chromatography, 25:18520
BISMUTH ALLOYS AND SYSTEMS
  Bi--Cd--Hg, phase studies of, 25:19236
  Bi--In, magnetization curves of intermediate mixed state of Type-II superconducting, 25:19620
BISMUTH HALIDES
  separation by solvent extraction, effects of charge, composition, and structure on, 25:18511
BISMUTH IONS
  implantation in cadmium sulfide at 200 keV, annealing of, 25:19791
  implantation in cadmium sulfide at 25 keV, 25:19792
  implantation in gallium phosphide at 100 and 200 keV, channeling study of damage induced by, 25:19846
  implantation in germanium at 30 to 40 keV, channeling study of lattice location of, 25:19827
  implantation in germanium at 40 and 70 keV, electric properties and lattice location of, 25:19799
  implantation in silicon carbide at 5 to 300 keV, properties of conducting layers and p--n junctions formed by, (E), 25:19847
BISMUTH ISOTOPES Bi-208
  gamma decay of proton-particle neutron-hole states of, from lead-208 (p,nγ) reactions, (E), 25:20434
BISMUTH ISOTOPES Bi-209
  carbon-12 reactions (C-12,α) at 120 MeV, energy spectra from, (E), 25:18737(R) (ORO-3820-7)
  carbon-12 reactions (C-12,xn) with, excitation functions for, (E), 25:18737(R) (ORO-3820-7)
  carbon-12 reactions at 71 and 86 MeV, cross sections, angular distributions, and recoil paths for astatine-210 and -211 and polonium-210 from, (E/T), 25:20375 (NP-18624)
  nitrogen-14 reactions at 78 and 100 MeV, cross sections, angular distributions, and recoil paths for astatine-211 from, (E/T), 25:20375 (NP-18624)
  proton reactions up to several GeV, cascade calculations of double differential distributions of particles from, (T), 25:20018 (JINR-P2-5507)
BISMUTH ISOTOPES Bi-212
  decay in SNAP-15A heat source, measurement of gamma spectra from, 25:18601
  energy-level transitions in, internal conversion ratios for M1 + E2, (E), 25:20473
BISMUTH ISOTOPES Bi-214
  gamma emission from, use for leak testing radium-226 applicators, 25:19016
BISMUTH OXIDES
  oxygen mobility in, oxygen-18 exchange studies of surface, 25:18388
  Bi_2O_3--MoO_3, oxygen mobility in, oxygen-18 exchange studies of surface, 25:18388
BLACK HOLES
  energy from, extraction of rotational, (T), 25:19338
  evidence for, in binary system epsilon Aur, (T), 25:19313
  evidence for, in binary systems epsilon Aur and 89 Her, (T), 25:19314
BLADDER
  radiation dose calculations for human, from radioisotopes excreted in urine, 25:18991 (ORNL-4584, pp 200-22)
BLOOD
  analysis for mercury by neutron activation, 25:18369
  cesium-129 uptake by coronary, in canine and human myocardium, scanning studies on, 25:19055
  fibrinolytic activity of, in rheumatic patients, effects of solar activity on, 25:19145
  radiation effects on peripheral, of rats, effects of trithiodipropanol on x, 25:19131
BLOOD CELLS
  radiation effects on, of medical personnel, review of effects of small doses, 25:19142
BLOOD PLASMA
  renin content of, radioimmunoassay method for measuring, 25:18920
BLOOD SERUM
  effects of antilymphocytic, on stem cells of irradiated mice, 25:18921
BLOOD VESSELS
  radiation effects on human, following therapy for cerebral gliomas, 25:19065
  radiation effects on restoration of, in skin grafts on man and rabbits, microwave, 25:19104
  radiodiagnosis of diseases of, of human brain using percutaneous retrograde arteriography, 25:19040
BLOWERS
  design requirements for helium cooled reactor, 25:20558
BODY FLUIDS
  determination of total water using tritium tracer, beta dose reduction in, 25:18977 (AD-702155)
BOILERS
  design codes and standards in U.S. for liquid metal cooled fast breeder reactor, 25:20723 (SAN-781-217)
  design for radioisotope-fueled organic Rankine cycle power system, 25:18594(R) (ORNL-TM-3292)
  flow in curved tubes in, heat transfer in two-phase, 25:18586
BOILING
  detection in water cooled reactors, methods for local, (E), 25:20716 (CEA-R-4118)
  model for free convection, effect of heat source configuration on, 25:20728
BONE MARROW
  radiation dose calculations for human, from radioisotopes deposited in lungs, 25:18991 (ORNL-4584, pp 200-22)
  radiation effects on cells of, in mice, correlation of lethality and recovery with fractionated γ, 25:19108
  radiation effects on proliferation of cells of, in bone marrow and spleen of mice, effects of dose on x, 25:19129
  radiation effects on, of man following exposure from atomic bombing in Hiroshima, autoradiography studies on, 25:19134
  radioinduced chromosome aberrations in human, radiation dosimetry using, 25:18980 (CEA-CONF-1698)
  scanning of human, using indium-113m colloid, 25:18994
  transplantation from mice treated with cyclophosphamide to γ-irradiated mice, effects of, 25:19112
BONES
  book: Bone Tumors in Man and Animals, 25:19136
  glycoprotein binding to americium and plutonium in bovine, mechanisms for, 25:18899
  radiation effects on human, comparison of gas and solid-state laser, 25:19146
  radioinduced osteodystrophy of human following inhalation of radon-222, 25:19144
  radioinduced sarcomas in human clavicle following post-operative therapy for breast malignancies, 25:19140
  radioisotope content of human, in Finland, 25:18931 (NYO-3446-14, Paper 30)
BORON
  determination by isotope dilution methods, 25:18358 (RT/CHI-(70)18)
  determination by nuclear track method, 25:18366(R) (NBS-TN-548)
  diffusion in silicon during hot-substrate ion implantation, 25:19824
BORON CARBIDES
  radiation effects on pellets and powders of, relations of density with neutron, 25:19289 (WHAN-FR-24)
BORON CHLORIDES
  electron reactions with, threshold excitation and slow-electron production in, 25:19490 (ORNL-4584, pp 92-104)

XUM

BORON IONS
- effects on electric properties of n-type silicon at 400 keV, annealing of, 25:19831
- effects on silicon at 200 and 400 keV, annealing of defects induced in, 25:19811
- implantation in silicon and germanium at 10 to 40 keV, to produce p-n junctions as radiation detectors, 25:18756
- implantation in silicon at 0.5 to 1.5 MeV, electric properties produced by, 25:19784
- implantation in silicon at 10 to 400 keV, effects of radiation damage and amorphous state on electric properties of, 25:19776
- implantation in silicon at 150 keV and liquid-nitrogen temperature, channeling and electrical measurements in annealing of, 25:19834
- implantation in silicon at 200 and 300 keV, channeling study of depth distribution of lattice disorder induced in, 25:19830
- implantation in silicon at 30 to 400 keV, calculated spatial distributions of damage from, 25:19819
- implantation in silicon at 40 keV, effects on channeling of low-energy alpha particles and protons, 25:19816
- implantation in silicon at 40 to 100 keV, electron microscopic studies of defects induced in, 25:19808
- implantation in silicon at 400 keV, divacancy and amorphous-layer formation in, 25:19812
- implantation in silicon at 50 keV, correlation of electron microscopic and electric property studies after annealing, 25:19815
- implantation in silicon at 50 to 150 keV, effects on impurity diffusion, 25:19824
- implantation in silicon at 6 keV, electric profiles after annealing of, 25:19836
- implantation in silicon at 60 keV, damage distribution from, 25:19818
- implantation in silicon at 7 keV, annealing and electric properties of implanted layers, 25:19835
- implantation in silicon at 80 keV, electron microscopic studies of damage from, 25:19814
- implantation in silicon carbide at 5 to 300 keV, properties of conducting layers and p--n junctions formed by, (E), 25:19847
- implantation in silicon diodes at 300 keV, effects on carrier lifetime, 25:19820
- implantation in silicon, annealing effects on, 25:19777
- implantation in silicon, electrical properties before and after annealing, 25:19778
- implantation in silicon, lattice disorder produced in, 25:19806
- implantation layers in silicon at 50 keV, temperature coefficient of sheet resistivity of, 25:19783
- implantations in silicon at 15 keV, electric capacitance of, 25:18857
- implantations in silicon at 40 to 300 keV, heavy-ion X-ray excitation measurements of profiles of, 25:19803
- production by calutron-type ion source, 25:20169

BORON ISOTOPES B-10
- chemical states of recoil, from carbon-13 (d,α) reactions, 25:18485
- deuteron reactions (d,n) at 2.8 to 4 MeV, neutron polarization in, (E), 25:20272
- energy levels from alpha resonances in lithium-6, resonance parameters and spin--parity assignments for, (E), 25:20292
- energy levels from beryllium-9 (d,n) reactions, (E), 25:20289
- helium-3 reactions $(He\text{-}3,\alpha)$, (He-3,d), and (He-3,p) at 1.2 to 1.9 MeV, analysis for reaction mechanisms in, (E), 25:20303
- neutron reactions (n,α) up to 200 keV, cross section for, (E), 25:20288
- proton reactions (p,γ) at 2.6 to 17 MeV, cross sections for, (E), 25:20277
- reactions with thorium-232 and uranium, analysis of compound nucleus mechanism in, (E/T), 25:20420

BORON ISOTOPES B-11
- deuteron reactions (d,n) at 2.8 to 4 MeV, neutron polarization in, (E), 25:20272
- energy levels from gamma resonance absorption, widths for, (E), 25:20355
- neutron reactions (n,t) at 14.4 MeV, angular distributions for, (E), 25:20285
- proton reactions $(p,3\alpha)$ at 163 keV to 2.65 MeV, differential cross sections for, (T), 25:20275
- proton reactions (p,α) 2α at 2.65 MeV, analysis of three-alpha final state interactions using Faddeev method, (T), 25:20300
- proton reactions (p,α) and $(p,3\alpha)$ at 163 keV, cross sections and alpha spectra from, (E), 25:20270 (NP-18626)
- reactions with thorium-232 and uranium, analysis of compound nucleus mechanism in, (E/T), 25:20420

BORON NITRIDES
- preparation and properties for incorporation in metals for neutron absorbers, 25:19264(P)

BORON SYSTEMS
- B--C--Hf--Nb-base--W--Zr, properties for use at high temperatures, 25:19218

BOSONS
- expansions of [illegible]lation between Beliaev--Zelevinsky and Marumori, 25:20521
- interactions of spinless, by scalar meson exchange, Schmidt method for solution of quasipotential equation for two-body, (T), 25:19987 (JINR-P2-5566)
- motion of Klein--Gordon spin-0, in solvable configuration of electromagnetic fields, (T), 25:19950
- production of octet 0^-, in decay of decuplet $3/2^+$ baryons, broken SU(6)/sub W/ for, (T), 25:20048
- scattering of spin-zero, approximate solution to Bethe--Salpeter equation for, (T), 25:20104 (NYO-2262-TA-231)
- theory for arbitrary-mass, positive definite particle densities for positive frequency solutions of Klein--Gordon equation in, (T), 25:19929
- theory for para-, first- and second-quantized statistical, 25:20080

BOSONS, INTERMEDIATE-VECTOR
- mass of, Hamiltonian for divergences in weak interactions for, (T), 25:20039

BRAIN
- radiation effects on maturation of cerebellar cortex in rats, postnatal x, 25:19114
- radiodiagnosis of subdural hematoma with vascular rim in human, comparison of mercury-203-labeled chlormerodrin and technetium-99m labeled-pertechnetate for, 25:19059
- radiodiagnosis of vascular diseases of human, using percutaneous retrograde arteriography, 25:19040
- radioinduced histological changes in, of cats and rats, 25:19109
- radioinduced injuries of goat, high-energy proton, 25:19124
- scanning of human, preparation of technetium-99m-labeled sodium pertechnetate for, 25:19054

BRASS
- faulting in filings of, β-x-ray diffraction search for, 25:19248

BRAZIL
- radiation effects on human populations in, following residence in areas of high natural alpha background, 25:18927 (NP-18670)

BREMSSTRAHLUNG
- production of wide-angle, in photon Compton scattering by nuclei, Glauber theory of multiple scattering for corrections for, (T), 25:19955
- reactions (γ,d), (γ,n), $(\gamma,2n)$ and (γ,pn) with sulfur-32 at 15 to 62 MeV, resonance structure in cross sections for, (E), 25:20332
- reactions (γ,n) and $(\gamma,3n)$ at 70 MeV, isomer ratios in production of molybdenum-91, cerium-137, and neodymium-141 by, 25:20455
- reactions (γ,n) with carbon-13 up to 14 MeV, angular distributions and integrated cross sections for, (E), 25:20276
- reactions (γ,p) with tin-114 at 12 to 22 MeV, excitation functions for, (E/T), 25:20394
- reactions (γ,xn) with lead-208 at 35 MeV endpoint energy, excitation functions, spectra, and integrated cross sections for, (E/T), 25:20437
- reactions wth aluminum-27 at 313 MeV endpoint energy, meson (π^-) and (π^+) energy spectra and π^-/π^+ ratio from, (E), 25:20341

BREN OPERATION
- radiation safety program for, 25:18982 (CEX-65.05)

BROMINE
- meson (K^-) reactions at 10 GeV/c in bubble chamber, $K^-\pi^+\pi^-$ system coherent production and total cross sections for $K^-\pi^+\pi^- + N$ interactions in, (E), 25:19910 (LAL-1242)
- sorption by monocrystalline tungsten, effects of adatom surface potential and adsorbate electronegativity on, 25:19207
- sorption by monocrystalline tungsten, effects on work function, 25:19209

BROMINE ISOTOPES Br-78
- isomeric transitions in, gamma spectra from, (E), 25:18753

BROMINE ISOTOPES Br-79
- half-life of isomeric, 25:20463

BROMINE ISOTOPES Br-80
- chemical states of recoil, in bromine--bromobenzene systems, 25:18490
- isomeric transition in bromine--bromobenzene systems, chemical effects from, 25:18490
- reactions of recoils of, with liquid and solid benzene--iodine systems, labeled organic yields from, 25:18483(R) (COO-1617-27)

BROMINE ISOTOPES Br-82
- beta decay of, gamma spectra from, (E), 25:18747
- isomeric transition in gaseous bromine--bromomethane systems, organic yields from, 25:18483(R) (COO-1617-27)
- isomeric transitions in bromine--organic compound systems, theory of chemical effects from, 25:18489
- reactions of recoils of, with liquid and solid benzene--iodine systems, labeled organic yields from, 25:18483(R) (COO-1617-27)

BROMINE SYSTEMS
- benzene--Br, radiation effects on liquid and solid, labeled organic yields from neutron, 25:18483(R) (COO-1617-27)
- Br--bromobenzene, bromine-80 isomeric transition in, chemical effects from, 25:18490
- Br--bromobenzene, radiation effects on, comparison of yields from bromine-80 isomeric transition with

- neutron, 25:18490
- Br--bromomethane, radiation effects on gases of, effects of pressure on organic yields from reactions of recoil bromine-80 or bromine-82 produced by isomeric transitions or neutron, 25:18483(R) (COO-1617-27)
- Br--organic compounds, bromine-82 isomeric transitions in, theory of chemical effects from, 25:18489

BROWNS FERRY POWER REACTOR, UNIT 1
- design parameters of, revised and additional data on, 25:20638 (DOCKET-50259-22)
- operations aspects of, revised and additional data on, 25:20638 (DOCKET-50259-22)
- pressure vessel for, design and fabrication requirements for, 25:20638 (DOCKET-50259-22)

BROWNS FERRY POWER REACTOR, UNIT 2
- design parameters of, revised and additional data on, 25:20638 (DOCKET-50259-22)
- operations aspects of, revised and additional data on, 25:20638 (DOCKET-50259-22)
- pressure vessel for, design and fabrication requirements for, 25:20638 (DOCKET-50259-22)

BROWNS FERRY POWER REACTOR, UNIT 3
- design parameters of, revised and additional data on, 25:20638 (DOCKET-50259-22)
- operations aspects of, revised and additional data on, 25:20638 (DOCKET-50259-22)
- pressure vessel for, design and fabrication requirements for, 25:20638 (DOCKET-50259-22)

BRUNSBUETTEL POWER REACTOR
- design parameters of, 25:20567

BRUNSWICK POWER REACTOR, UNIT 1
- containment structure for, effects of steam line break on, 25:20670 (DOCKET-50324-19)

BRUNSWICK POWER REACTOR, UNIT 2
- containment structure for, effects of steam line break on, 25:20670 (DOCKET-50324-19)

BRYOPHYTA
- radioisotope contamination of fresh water, technique for study of, 25:18937

BUBBLES
- images in bubble chambers with bright-field illumination, contrast and shape of, 25:18789
- nucleation in pool boiling, mechanisms of, 25:18582

BUTADIENE POLYMERS
- radiation effects on structure and properties of, gamma and electron, 25:19300
- radiolysis at 77°K, concentration of cross links and stabilized ions from γ, 25:18467

BUTADIYNE, DIPHENYL-
- radioinduced polymerization of, properties of products from γ, 25:18441

BUTANE, 1-BROMO-
- radioinduced isomerization at 150 to 240°C, 25:18438

BUTANE, IODO-
- radiation effects on glasses of, at 77°K, kinetics of decay of alkyl radicals produced by γ, 25:18461

1,3-BUTANEDIONE, 4,4,4-TRIFLUORO-1-(2-THIENYL)-
- complexes with americium, stability of, effects of adduct-forming agents on, 25:18498 (KFK-1298)
- complexes with californium, stability of, 25:18498 (KFK-1298)

1-BUTANOL
- radiolysis of aqueous perchloric acid solutions of, rate constants for reactions of hydrogen atoms produced by γ, 25:18459

2-BUTANOL
- radiolysis of aqueous perchloric acid solutions of, rate constants for reactions of hydrogen atoms produced by γ, 25:18459

1-BUTENE, 2-METHYL-
- reactions with iodine at 25°C, kinetics of, 25:18483(R) (COO-1617-27)

2-BUTENE, 2-METHYL-
- reactions with iodine at 25°C, kinetics of, 25:18483(R) (COO-1617-27)

BUTYRIC ACID
- radiolysis of aqueous perchloric acid solutions of, rate constants for reactions of hydrogen atoms produced by γ, 25:18459

C

CABLES
- description of MKSB, for computer data links, 25:18845
- design of superconducting, studies for, 25:19636

CADMIUM
- analysis of high-purity, for gold, manganese, and iron by photon activation, 25:18366(R) (NBS-TN-548)
- chromatographic behavior in hydrochloric acid--thiocyanate mixture on Amberlite LA-2, 25:18337
- effects on Staphylococcus aureus E169, use of uv-irradiated transducing phage lysates to determine chromosomal relation of determinants for sensitivity, 25:19157
- separation of bismuth from, by cation exchange chromatography, 25:18520

CADMIUM ALLOYS AND SYSTEMS
- Ag--Cd, polar-reflection Faraday effect in α-phase disordered, Fermi surface and band lifetime from, 25:19873
- Bi--Cd--Hg, phase studies of, 25:19236

CADMIUM IONS
- implantation in n-type gallium arsenide at 60 keV, annealing effects on electric properties of implanted layers, 25:19842

CADMIUM ISOTOPES Cd-100
- decay of, half-life and γ spectra for, (E), 25:20422

CADMIUM ISOTOPES Cd-101
- decay of, γ spectra from, (E), 25:20422

CADMIUM ISOTOPES Cd-102
- decay of, γ spectra from, (E), 25:20422

CADMIUM ISOTOPES Cd-110
- energy levels from indium-110 decay, (E), 25:20402

CADMIUM ISOTOPES Cd-115
- half-lives of ground-state and isomeric, (E), 25:20339

CADMIUM SULFIDES
- ion implantation in, review, 25:19789
- ion implantations in, 25-keV bismuth, 25:19792
- ion implantations in, helium-ion backscattering study of annealing of 200-keV, 25:19791
- radiation damage from ion implantations in single-crystal platelets of, anealing and luminescent effects of, 25:19793

CADMIUM TELLURATES
- $CdTeO_3$--$CdTeO_4$, analysis for hexavalent tellurium and total tellurium by automatic amperometric and potentiometric titrations, 25:18351

CADMIUM TELLURIDES
- ion implantation in, review, 25:19789
- preparation and properties of semiconductor detectors of, 25:18733 (CEA-R-4052)

CADMIUM TELLURITES
- $CdTeO_3$--$CdTeO_4$, analysis for hexavalent tellurium and total tellurium by automatic amperometric and potentiometric titrations, 25:18351

CALCIUM
- abundance in α^2 CVn, (E), 25:19339
- abundance in Type-M supergiant, (E), 25:19323
- chromatographic behavior in hydrochloric acid--thiocyanate mixture on Amberlite LA-2, 25:18337
- determination in marine sediments off Tarapur Coast, 25:18354
- determination in natural waters from uranium mining operations, method for, 25:18339 (CEA-R-3557(2))
- reactions with negative ions at 1 eV of metastable atoms of, cross sections for electron detachment and photon emission in, (T), 25:19511
- separation of bismuth from, by cation exchange chromatography, 25:18520

CALCIUM FLUORIDES
- radioinduced color centers in dysprosium-doped crystals of, total antiresonance induced by heat treatment of gamma, 25:19771

CALCIUM IONS
- spectra of Ca II in solar flare of Mar. 12, 1969, excited H and K, (E), 25:19412

CALCIUM ISOTOPES Ca-40
- alpha differential elastic scattering cross sections at 23.1 MeV, angular distributions from, (E), 25:20310
- alpha reactions (α,pγ) at 11.8 to 15.5 MeV, p-γ coincidence spectra from, (E), 25:20320
- deuteron reactions (d,p) at 10 and 11 MeV, DWBA calculations of angular distributions and overlap integrals from, (T), 25:20497
- deuteron reactions (d,p) at 12 MeV, model for, (T), 25:20522
- helium-3 reactions (He-3,t) at 28 MeV, differential cross sections for, (E), 25:20350
- nuclear radii and density distributions for, statistical-ensemble calculations of, (T), 25:20505
- proton elastic scattering at 30 to 45.5 MeV, optical-model analysis of angular distributions from, (E/T), 25:20311
- proton reactions (p,d) at 27.5 MeV, model for, (T), 25:20522
- proton reactions up to several GeV, cascade calculations of double differential distributions of particles from, (T), 25:20018 (JINR-P2-5507)

CALCIUM ISOTOPES Ca-47
- content of excreta and tissues of rats, comparison of direct and treated-sample determinations of, 25:18997

CALCIUM PHOSPHATES
- properties as flocculant in treatment of radioactively contaminated seawater, 25:18518

CALCIUM SELENATES
- radiolysis of powders of, γ, 25:18479

CALIFORNIUM
- complexes with 5,7-dichloro-8-quinolinol, 4,4,4-trifluoro-1-(2-thienyl)-1,3-butanedione, or 8-quinolinol, stability of, 25:18498 (KFK-1298)
- separation from aqueous solutions by solvent extraction, chelate formation in, 25:18498 (KFK-1298)

CALIFORNIUM ISOTOPES Cf-249
- alpha decay of, α-γ angular correlations in, (E), 25:20398

CALIFORNIUM ISOTOPES Cf-252
- fission of, fractional cumulative yield of niobium-99m from spontaneous, (E), 25:20406
- fission of, spectra of fragments from spontaneous, (E), 25:20442
- neutron flux from, calibration of, 25:18590(R) (BNWL-

XUM

1308-4)
  properties and uses as neutron source, 25:18481
  radiation dose distribution in tissue from implanted point sources of, (T), 25:19003
  self-transfer properties of, for neutron source preparation, 25:18596
  uses as source for portable neutron radiographic camera, 25:18617
CALUTRONS
  use in ion implantation machine, 25:20169
CAMBRIDGE SYNCHROTRON
  beam bypass for storage rings at, operation of, 25:20195
CAMERAS
  development of portable neutron radiographic, using californium-252 source, 25:18617
CANALS
  excavation of interoceanic, using nuclear explosives, radiological safety of, 25:18989 (ORNL-4584, pp 42-56)
CARBAMIC ACID, DIETHYLDITHIO-
  effects on repair processes following γ-radioinduced chromosome aberrations in Nigella damascena seeds, 25:18951
CARBOHYDRATES
  metabolism in eyes, relation to cataract formation, 25:20873(R) (NYO-1368-17)
CARBON
  alpha-particle spallation reactions at 22.5 to 235 MeV/N with, cosmic, (E), 25:19531
  content in uranium dioxide pellets, effects of decarbonization and sintering at 500 to 1600°C on, 25:19274
  cosmic hadron reactions above 70 GeV, multiparticle production in, (E), 25:19905
  deposition on sol-gel particles of thorium dioxide and uranium dioxide, fluidized bed method for, 25:19262 (ORNL-4529, pp 65-82)
  effects of surface impurity of, on ionization of potassium by polycrystalline tungsten, 25:19210
  effects on calcining of plutonium oxide--uranium dioxide gel spheres, 25:19263 (ORNL-4629, pp 99-102)
  effects on cesium reactions with liquid sodium, (E), 25:19192 (CONF-700816-(Vol.1), pp 393-412)
  electric conductivity of pyrolytic, at 300 to 2500°K, 25:19280
  electric conductivity of pyrolytic, effects of high-temperature heat treatments on, 25:19281
  electron reactions at 0.3 to 1.1 MeV with thin foils of, photon emission spectra from, 25:19471
  emissivity of pyrolytic, at 1200 to 2500°K, total hemispherical, 25:19280
  fission fragment stopping power, energy loss, and range in, (E), 25:20442
  fission-fragment stopping in, cross sections for californium-252, (E), 25:19765
  ion reactions at 1 MeV, x-ray spectra from H_2^+, 25:18836
  ion reactions at 500 keV, x-ray spectra from Ar^+, 25:18836
  mass determination of cosmic-ray, using nuclear emulsions, 25:18643 (NP-18672)
  meson (K^-) reactions at 10 GeV/c in bubble chamber, $K^-\pi^+\pi^-$ system coherent production and total cross sections for $K^-\pi^+\pi^- + N$ interactions in, (E), 25:19910 (LAL-1242)
  microstructure of fuel particle coatings of, 25:19262 (ORNL-4629, pp 65-82)
  neutron elastic scattering at 0.5 to 2 MeV, differential cross sections for, (E), 25:20267 (EUR-4538)
  photon reactions at 5.8 to 6.6 GeV/c, magnetic spectrometer study of (1550) enhancement in mass spectrum for π^+--π^- pairs produced in, (E), 25:19886 (DESY-70/61)
  proton spallation reactions at 70 to 420 MeV with, cosmic, (E), 25:19531
  solubility in sodium at 600 to 950°C, 25:19196 (TRG-Report-1906)
  thermal conductivity of pyrolytic, at 1200 to 2500°K, 25:19280
  thermal conductivity of pyrolytic, effects of high-temperature heat treatments on, 25:19281
CARBON BLACK
  carbon black--polyethylene, radiation effects on electrical and mechanical properties of, γ, 25:18421(R) (RLO-2098-1)
  carbon black--polystyrene, radiation effects on electrical and mechanical properties of, γ, 25:18421(R) (RLO-2098-1)
CARBON DIOXIDES
  determination of free, in natural waters from uranium mining operations, method for, 25:18339 (CEA-R-3557(2))
  diffusion from molybdenum and tungsten at 2000°K, 25:19225
  effects on oxygen enhancement of radiosensitivity of human tumors, 25:19023
  performance as working fluid in complex and simple power cycles, 25:18587
  radiation effects on assimilation and distribution of carbon-14-labeled, in Vicia faba, x, 25:19153
  radiolysis of, absorption spectra of ions produced by electron pulse, 25:18448(R) (CEA-N-1369)
  solubility in heavy water at pressures to 40 atm and 30 to 80°C, 25:18418
CARBON IONS
  channeling in ion-implanted silicon at 1.8 MeV, 25:15829
  channeling of 2-MeV, in bismuth-implanted gallium phosphide, 25:19846
  effects on nickel at 100 keV and 300 to 650°C, void formation in, 25:19807
  implantation in gallium arsenide, electric profiles of implanted layers after annealing, 25:19843
  implantation in silicon at 30 to 400 keV, calculated spatial distributions of damage from, 25:19819
  implantation in silicon diodes at 300 keV, effects on carrier lifetime, 25:19820
  implantation in silicon, lattice disorder produced in, 25:19806
  reactions with calcium, helium, and hydrogen metastable atoms at 1 eV of C^-, cross sections for electron detachment and photon emission in, (T), 25:19511
CARBON ISOTOPES C-11
  beta decay of, evaluation and correction procedure for internal bremsstrahlung spectrum in, 25:20302
  energy levels from boron-11 (p,γ) reactions, spin-parity assignment and width for giant dipole, (E), 25:20277
CARBON ISOTOPES C-12
  alpha reactions (α,p) at 35.5 MeV, DWBA analysis of j dependence in angular distributions from, (E), 25:20309
  chemical states of recoil 5.01-MeV, from carbon-12 (d,d) reactions, 25:18485
  deuteron elastic scattering at 0.4 to 0.85 MeV, cross sections and angular distributions for, (E), 25:20279
  deuteron reactions (d,α), (d,p), and (d,t) at 0.4 to 0.85 MeV, cross sections and angular distributions for, (E), 25:20279
  deuteron reactions (d,d) with, 5.01-MeV carbon-12 recoil ions charge-state distribution from, 25:18485
  deuteron reactions (d,n) at 2 to 3.2 MeV, cross-section measurements by detection of positron annihilation γ rays, (E), 25:20283
  deuteron reactions (d,n) at 6.4 MeV, neutron spectra and polarizations from, (E), 25:20297
  deuteron reactions (d,p) at 12 and 26 MeV, model for, (T), 25:20522
  deuteron reactions (d,p) at 12.4 MeV, polarization of protons from, (E/T), 25:20287
  deuteron reactions (d,p) at 9 MeV, DWBA calculations of angular distributions from, (T), 25:20497
  electron inelastic scattering at 200 MeV, form factors and spectra in giant resonance region from, (E/T), 25:20296
  energy level at 16.11 MeV, decay to 3 alpha particles of, 25:20270 (NP-18626)
  energy levels of, calculation of magnetic monopole transition probabilities for, (T), 25:20306
  energy levels of, intermediate-coupling calculation of, (T), 25:20295
  neutron inelastic scattering at 15 MeV, neutron-gamma angular correlations in inelastic, (E), 25:20281
  neutron scattering at 4.0 to 5.6 MeV, angular distributions and cross sections for, (E/T), 25:20338
  nuclear charge form factors for, (T), 25:20295
  oxygen-16 reactions (O-16,α) at 48.0 to 58.3 MeV with sequential α decay, α--α angular correlations and spectra from, (E), 25:20291
  proton reactions (p,α) at 660 MeV, intranuclear-cascade-model calculations of angular distributions from, (T), 25:20268 (JINR-P4-5479)
  proton reactions up to several GeV, cascade calculations of double differential distributions of particles from, (T), 25:20018 (JINR-P2-5507)
  reactions (C-12,α) with bismuth-209 at 120 MeV, energy spectra from, (E), 25:18737(R) (CRO-3820-7)
  reactions (C-12,xn) with bismuth-209, excitation functions for, (E), 25:18737(R) (ORO-3820-7)
  reactions with bismuth-209 at 71 and 86 MeV, cross sections, angular distributions, and recoil paths for astatine-210 and -211 and polonium-210 from, (E/T), 25:20375 (NP-18624)
CARBON ISOTOPES C-13
  deuteron elastic scattering at 0.4 to 0.85 MeV, cross sections and angular distributions for, (E), 25:20279
  deuteron reactions (d,α) with, boron-10 recoil charge-state distribution from, 25:18485
  deuteron reactions (d,α), (d,p), and (d,t) at 0.4 to 0.85 MeV, cross sections and angular distributions for, (E), 25:20279
  deuteron reactions (d,n) at 2.8 to 4 MeV, neutron polarization in, (E), 25:20272
  energy levels of, charge asymmetry of nucleon widths of lowest $T = {}^3/_2$, 25:20512
  photon reactions (γ,n) up to 14 MeV, angular distributions and integrated cross sections for, (E), 25:20276
CARBON ISOTOPES C-14
  content of man in Finland from natural sources, 25:18931 (NYO-3446-14, Paper 30)
  effects on nucleophilic substitution reactions of para-substituted benzyl chlorides, 25:18407
  use as secondary counting standard in measurement of sulfur-35, 25:18364
  use as tracer for ecological studies on ticks, 25:18934(R) (ORO-3514-10)

CARBON MONOXIDES
  diffusion from molybdenum and tungsten at 2000°K, 25:19225
  diffusion in isotopic mixtures incorporating carbon-12, carbon-13, oxygen-16, and oxygen-18, effects of temperature on, 25:18604
  oxygen-18 exchange in molecules of, on iron or zinc oxides, 25:18387
  CO--N, diffusion in isotopic mixtures of, incorporating carbon-12, carbon-13, oxygen-16, and oxygen-18, effects of temperature on, 25:18604
CARBON SYSTEMS
  B--C--Hf--Nb-base--W--Zr, properties for use at high temperatures, 25:19218
  C--Hf--Mo--Nb-base--W, properties for use at high temperatures, 25:19218
  C--Nb-base--Ti--V--W--Zr, oxidation morphology and rates in air at 800 to 950°C, 25:19172
CARBON TETRACHLORIDE
  alkali-metal-atom scattering by, crossed-beam measurements and optical-model analysis of, 25:19497
  optical constants in photon energy range 4.0 to 10.65 eV for, 25:19759 (ORNL-4584, pp 87-91)
CARBONATES
  determination in natural waters from uranium mining operations, method for, 25:18339 (CEA-R-3557(2))
CARBONIC ANHYDRASE
  reactions of anomalous water in anhydrated, directional correlation studies on, 25:18884
CARDIAC PACEMAKERS
  heat source for, dose rates from implanted plutonium-238, 25:18590(R) (BNWL-1308-4)
CASCADE SHOWERS
  calculations for π^+ and π^- dose to tissues at 10 to 2000 MeV, 25:20226
  production of ionization, from charged particle interactions in absorber, properties of ion pairs in, (T), 25:19971 (ANL-7727)
  transition effects in, Monte Carlo calculations of, 25:19943
CASEIN
  effects on reactivity of γ-irradiated solutions of chymotrypsin, 25:18907
CATALYSTS
  radiation effects on, in conversion of aromatic hydrocarbons, γ, 25:18444
CATHODE-RAY TUBES
  light pen for, 25:18844
CATIONS
  determination by spectrophotometry using autoxidation of phenolic compounds, 25:20860 (IS-T-419)
CATS
  cesium-137 content of bobcats (Lynx rufus) in Southeast USA during 1969, relation of ingestion of cotton rats to, 25:18935(R) (ORO-3905)
  radioinduced histological changes in brain of, classification of, 25:19109
CATTLE
  antibody content of serum of, effects of, on permeability of erythrocytes to phosphorus-32, 25:18900
  polonium-210 metabolism by, following ingestion as oxide, coefficients for transfer to meat and milk during, 25:18890(R) (COO-2044-3)
CAVITY RESONATORS
  conducting coatings on, distortion of accelerator magnetic fields due to, 25:20221
  description of interdigital H-type linac, 25:20156
  development of superconducting hf, 25:19638
  tuning in high-energy accelerators, phase-angle measurement system for, 25:20179(P)
  tuning of synchrotron, ferrite bias regulator for, 25:20178(P)
CELL MEMBRANES
  radiation effects on permeability of, in erythrocytes of rabbits, x, 25:19107
  radiation effects on permeability of, in rat thymus to magnesium ions, protective effects of esculamine against x, 25:19025
CELLS
  effects of pulmonary macrophage, on plutonium oxide particle retention following inhalation by rabbits, 25:18891(T) (LF-tr-46)
  labeling Ehrlich ascites, with tritium-labeled thymidine, effects of 6-azauridine on, 25:18888
  radiation effects on generation cycle of crypt, in small intestine of mice, effects of chronic fractionated x, 25:19122
  radiation effects on mitosis and survival of ascites, of mice, effects of dose fractionation on x, 25:19091
  radiation effects on proliferation of, in bone marrow and spleen of mice, effects of dose on x, 25:19129
  radiation effects on regeneration of stem, in mice, effects of dose and shielding on x, 25:19126
  radiation effects on replication of, in endocolonized mouse spleen, tritium tracer study of x, 25:19125
  radiation effects on survival of epidermal, of mice, effects of dose fractionation on RBE for fast neutron, 25:19092
  radiation effects on, in relation to effects on aromatic amino acids, biophysical mechanisms of uv, 25:18903
  radiation effects on, microdosimetry studies of, 25:18993
  radioinduced double-strand breaks in DNA in mammalian, 25:18911
  regeneration of hematopoietic stem, following transplantation into x-irradiated mice treated with cyclophosphamide, 25:19127
  repopulation of hematopoietic, in γ-irradiated mice, effects of transplants of bone marrow from mice treated with cyclophosphamide on, 25:19112
CELLS, CULTURED
  radiation effects at molecular level on mammalian, synergistic effects of chemicals on biological expression of uv, 25:19090(R) (COO-1704-22)
  radiation effects at molecular level on mammalian, progress report on repair of uv, 25:19090(R) (COO-1704-22)
  radiation effects on morphology and function of, from cesium-137-contaminated media, 25:18904
  radiation effects on neuroblast, from chickens, effects of dose on x, 25:19120
  radiation effects on, review of, 25:19106
  radioinduced chromosome aberrations in, effects of hypothermia on, 25:19093
CELLS, L
  radioinduced breaks in DNA of, effects of energy deprivation on repair of x, 25:18908
CELLULOSE
  radioinduced graft polymerization with styrene at low dose rates, γ, 25:18446
CENTRIFUGATION
  efficiency of fixed-wall confined, for separation of components of binary gaseous mixtures, 25:18597
CENTRIFUGES
  evaluation of zonal, for determining distribution and particle size of trace elements in soils, 25:18521 (ORNL-4584, pp 1-10)
CERAMIC MATERIALS
  deposition of chromium-matrix composite coatings of, method for electro-, 25:19270(P)
  radioinduced polymerization of acrylic or vinyl monomers in porous, ion exchange properties of products from γ, 25:18421(R) (RLO-2098-1)
CERIUM
  abundance in meteorites, (E), 25:19302
  compatibility with refractory metal and superalloy capsule materials at high temperatures, 25:18592 (ORNL-4298)
  determination by biamperometric titration with mercury perchlorate, 25:18346
  determination of trace amounts of, by formation of colored peroxy compounds and sorption on chelating resin, 25:18343
  determination using 4,5-dihydroxy-m-benzenedisulfonic acid, in presence of Eriochrome Cyanine R, titrimetric, 25:18348
  separation from nitric acid solutions by solvent extraction using alkyl phosphonates, 25:18516
  separation from seawater by flocculation, 25:18518
CERIUM ALLOYS AND SYSTEMS
  Ce--La-base, Kondo resistance anomaly and superconducting transition temperature of, effects of pressure on, (E/T), 25:19863
CERIUM BORIDES
  compatibility with refractory metal and superalloy capsule materials at high temperatures, 25:18592 (ORNL-4298)
CERIUM FLUORIDES
  compatibility with refractory metal and superalloy capsule materials at high temperatures, 25:18592 (ORNL-4298)
CERIUM IONS
  wave functions for, accurate numerical Hartree--Fock self-consistent field, 25:19478
CERIUM ISOTOPES Ce-137
  production by photon reactions (γ,n) and (γ,3n) at 70 MeV, isomer ratios in, 25:20455
  uptake by plants during irrigation, development of model simulating, 25:18938
CERIUM ISOTOPES Ce-138
  photon reactions (γ,n) at 70 MeV, isomer ratios from, 25:20455
CERIUM ISOTOPES Ce-140
  photon reactions (γ,3n) at 70 MeV, isomer ratios from, 25:20455
CERIUM ISOTOPES Ce-141
  half-life, (E), 25:20339
CERIUM ISOTOPES Ce-144
  accumulation by marine organisms, effects of physico-chemical form on, 25:18894
  content of chlorophyll-A in marine algae following contamination of ecosystem, 25:18936
  content of man in Finland from artificial sources, 25:18931 (NYO-3446-14, Paper 30)
  effects on development of marine periphytal ecosystem, 25:18936
  removal from plant tissue, methods for, 25:18892 (NP-18641)
  use as tracer for ecological studies on ticks, 25:18934(R) (ORO-3514-10)
CERIUM OXIDES
  compatibility with refractory metal and superalloy capsule materials at high temperatures, 25:18592

(ORNL-4298)

CERIUM SULFIDES
- compatibility with refractory metal and superalloy capsule materials at high temperatures, 25:18592 (ORNL-4298)

CERMETS
- deposition of chromium-matrix composite coatings of, method for electro-, 25:19270(P)

CERN SYNCHROTRON
- beam extraction from, theory of resonant integer, 25:20145
- experimental facility for particle identification, time-of-flight, 25:20180
- experimental facility for production of initially pure K^0 beam of known momentum, 25:20144
- experimental facility for, design and performance of spark chamber with ferrite-core memory, 25:18790
- magnet power supplies for, design of transistor control element for current regulation of pulsed, 25:20208
- storage rings at, description of intersecting, 25:20209

CESIUM
- determination in high-burnup plutonium dioxide fuel by isotope dilution mass spectrometry, 25:18356 (KR-140)
- electron scattering at 0.3 to 9 eV by, absolute total cross sections for, (E), 25:19506
- optical properties of, collective effects in, (E), 25:19758 (ORNL-4584, pp 74-86)
- plasma of, spectroscopic diagnostics in discharge, 25:19665
- properties of encapsulated fission product, for use as process radiation source, 25:18590(R) (BNWL-1308-4)
- reactions with liquid sodium, effects of carbon on, (E), 25:19192 (CONF-700816-(Vol.1), pp 393-412)
- reactions with nitrogen oxide up to 14 eV, negative-ion production in, 25:19490 (ORNL-4584, pp 92-104)
- scattering by carbon tetrachloride, iodomethane, and tin chloride, crossed-beam measurements and optical-model analysis of, 25:19497
- separation from rubidium by solvent extraction, review on, 25:18510
- separation from seawater by flocculation, 25:18518
- sorption by monocrystalline tungsten, effects of adatom surface potential and adsorbate electronegativity on, 25:19207
- volatility in liquid sodium, effects of carbon adsorbers on, (E), 25:20754 (AERE-R-6481)

CESIUM IONS
- implantation in silicon at 40 keV, electrical properties of, 25:19780

CESIUM ISOTOPES Cs-129
- production by cyclotron irradiation of sodium iodide for use in radiodiagnosis, 25:19055

CESIUM ISOTOPES Cs-131
- energy levels from barium-131 decay, spin-parity assignments for, (E), 25:20414
- energy-level transitions from barium-131 decay, multipole mixing ratios, conversion coefficients, and nuclear penetration effects in, (E), 25:20414

CESIUM ISOTOPES Cs-133
- use as tracer in directional correlation studies of anomalous water in bovine carbonic anhydrase, 25:18884

CESIUM ISOTOPES Cs-136
- half-life, (E), 25:20339

CESIUM ISOTOPES Cs-137
- accumulation by marine organisms, effects of physico-chemical form on, 25:18894
- beta decay of, gamma spectra with spurious peaks from Compton scattering between γ--γ coincidence detectors in, (E), 25:18754
- content of bobcats (Lynx rufus) and cotton rats in Southeast USA during 1969, 25:18935(R) (ORO-3905)
- content of chlorophyll-A in marine algae following contamination of ecosystem, 25:18936
- content of food and milk in Pavia, Italy from 1964 to 1966, 25:18942
- content of food chains in Finland, 25:18931 (NYO-3446-14, Paper 30)
- content of human bones and tissues, milk, and rainwater in Finland, 25:18931 (NYO-3446-14, Paper 30)
- content of man in Finland, 25:18931 (NYO-3446-14, Paper 30)
- content of man in Finland during 1960 to 1970, 25:18986 (NYO-3446-14, Paper 28)
- content of muscle samples from deer in Southeast USA during 1969, 25:18935(R) (ORO-3905)
- content of plants in Finnish Lapland during 1968 and 1969, 25:18932 (NYO-3446-14, Paper 31)
- content of reindeer herders in Finnish Lapland, effects on whole-body γ dose, 25:18987 (NYO-3446-14, Paper 29)
- content of reindeer meat in Finnish Lapland during 1966 to 1970, 25:18932 (NYO-3446-14, Paper 31)
- determination in irradiated plutonium dioxide--uranium dioxide fuels as measure of burnup, 25:18359 (WCAP-3385-56(Pt.2))
- distribution in soils from cesium-137-tagged tulip tree forest, (E), 25:18521 (ORNL-4584, pp 1-10)
- distribution in White Oak Creek sediments, (E), 25:18521 (ORNL-4584, pp 1-10)
- effects on development of marine periphytal ecosystem, 25:18936
- performance as gamma source for radiometric rock analysis, 25:18524
- recovery from reprocessed fuels, computer evaluation of economics of, 25:18590(R) (BNWL-1308-4)
- removal from plant tissue, methods for, 25:18892 (NP-18641)
- separation from radioactive waste by zeolite prefilter, 25:18621 (DP-1245)
- transport from fallout through soil-plant-animal food chains in Southeast USA, mechanisms for, 25:18935(R) (ORO-3905)
- transport from pastures to milk to man, 25:18943
- use for implant therapy, evaluation of applicators and methods for, 25:19076

CESIUM ISOTOPES Cs-138
- beta decay of isomeric, half-life for, (E), 25:20381

CHARCOAL
- effects on radioisotope removal from reactor containment systems by isotope exchange, catalytic, 25:18385 (CONF-700816-(Vol.1), pp 278-88)
- sorptive properties for gaseous cesium in liquid sodium, (E), 25:20754 (AERE-R-6481)

CHARGED-PARTICLE BEAMS
- focusing of point-source, using three-sector magnetic prisms with 1/r field, 25:20217
- intensity profile of, development of method for measuring and recording, 25:20218
- trajectories in asymmetrized quadrupole electrostatic lenses, aberrations in, 25:20151

CHARGED PARTICLES
- acceleration of solid, switched linear accelerator technique for, 25:20183
- detection and identification of, calculation of constants for telescope detectors for, 25:18705
- energy deposition distribution in single events, compound-Poisson calculations of, (T), 25:19767
- identification of, development of hard-wired arithmetic computer for, 25:18718
- interactions in absorber, properties of ion pairs in ionization cascade production in, (T), 25:19971 (ANL-7727)
- motion in inhomogeneous stationary plasma, theory for test-particle, 25:19695
- motion of Klein--Gordon spin-0, in solvable configuration of electromagnetic fields, (T), 25:19950
- motion with constant velocities in electromagnetic field, Lorentz force relation with energy and momentum for, (T), 25:19946
- radiation of uniformly accelerated, (T), 25:19944
- reactions with atoms and nonpolar molecules at very low energies, inverse fourth-power potential in calculation of cross sections for capture and elastic scattering in, 25:19500
- reactions with free-electron gases, double-plasmon excitation in, 25:19757 (ORNL-4584, pp 58-73)
- scattering by helium metastable atoms, total cross sections for inelastic, (T), 25:19510
- spectra measurements from photonuclear reactions, semiconductor telescope detector for, 25:18675
- stopping of, Z^3 correction in theory of, 25:19757 (ORNL-4584, pp 58-73)
- trajectories of, third order approximation for effects of toroidal electric fringing field on, 25:20139

CHLORIDES
- complexes with americium and europium, stability constants for, effects of ionic media on, 25:18371
- determination in natural waters from uranium mining operations, method for, 25:18339 (CEA-R-3557(2))
- yields from electron pulse and γ radiolysis of aqueous solutions of chlorofluoromethanes, effects of ethylene on, 25:18460

CHLORINE
- neutron inelastic scattering by, γ energies from fast, (E), 25:20356
- sorption by monocrystalline tungsten, effects of adatom surface potential and adsorbate electronegativity on, 25:19207
- sorption by monocrystalline tungsten, effects on work function, 25:19209

CHLORINE IONS
- implantation in silicon at 80 keV, effects on channeling of low-energy alpha particles and protons, 25:19816
- implantation in zinc telluride at 30 to 120 keV, properties induced by, 25:19794
- reactions with calcium, helium, and hydrogen metastable atoms at 1 eV of Cl^-, cross sections for electron detachment and photon emission in, (T), 25:19511

CHLORINE ISOTOPES
- energy levels from neutron inelastic scattering, (E), 25:20356

CHLORINE ISOTOPES Cl-37
- energy levels and transitions from sulfur-37 decay, (E), 25:20317

CHLORMERODRIN
- effectiveness of mercury-197-labeled, for kidney scanning, comparison of indium-113m-labeled DTPA with, 25:19039

CHLOROPHYLL
- radiation effects on content of, in leaves of Vicia faba, x, 25:19153
- radioisotope content of, in marine algae in contaminated ecosystem, cerium-144 and cesium-137, 25:18936

CHOLESTEROL
- acetate, phase studies on, 25:18431
- acrylate, radioinduced polymerization of, 25:18432
- acrylate, radioinduced polymerization of, phase studies on products from γ, 25:18431
- propionate, phase studies on, 25:18431
- benzoquinone--cholesterol acrylate, radioinduced polymerization of, 25:18432
- cholesterol acrylate--cholesterol propionate, radioinduced polymerization of, 25:18432

CHROMATIN
- radiation effects on template activity for RNA synthesis, γ, 25:18916

CHROMATOGRAPHY
- radioactive material on moving bands in, scintillation detector for studying local concentration of, 25:18688(P)

CHROMITES
- radiation effects on properties of, for use in concrete shielding aggregates, neutron, 25:19296

CHROMIUM
- abundance in Type-M supergiant, (E), 25:19323
- chromatographic behavior in hydrochloric acid--thiocyanate mixture on Amberlite LA-2, 25:18337
- complexes of, radioinduced production of chromium-51-labeled mono- and polynuclear, in aqueous solutions of neutron-irradiated potassium chromate, 25:18486
- determination in Italian meteorites by nondestructive neutron activation, 25:18370
- determination of trace amounts of, by formation of colored peroxy compounds and sorption on chelating resin, 25:18343
- reactions with uranium tetrafluoride vapors, 25:18372

CHROMIUM ALLOYS AND SYSTEMS
- Fermi surface of antiferromagnetic, de Haas-van Alphen effects study of, 25:20861 (IS-T-420)
- Al--Cr--Nb--Si--Sn--Ti, properties for use as protective coating on niobium, 25:19176
- Cr--Fe--Nb--Si, properties for use as protective coating on niobium, 25:19176
- Cr--Ti-base, superconducting transition temperature in, effects of omega phase reversion on, 25:19590
- Cr--V--Zr, phase studies of, 25:19237
- Cr--ZrB_2, deposition on graphite, method for electro-, 25:19270(P)

CHROMIUM BORIDES
- preparation and properties for incorporation in metals for neutron absorbers, 25:19264(P)

CHROMIUM ISOTOPES Cr-51
- chemical states of recoil, in aqueous solutions of neutron-irradiated potassium chromate, 25:18486

CHROMIUM ISOTOPES Cr-52
- deuteron elastic scattering at 8 to 12 MeV using polarized beam, cross section and vector analyzing power for, (E), 25:20305
- deuteron reactions (d,p) at 8 MeV, effect of deuteron D-state in DWBA analysis of, (T), 25:20328
- deuteron reactions (d,p) at 8 to 12 MeV using polarized beams, cross sections and vector analyzing power for, (E), 25:20305

CHROMIUM SILICIDES
- deposition on niobium by pack cementation for corrosion protection, 25:19175

CHROMOSOMES
- aberration induction in Crepis capillaris seed, during space flight, effects of ethylenimine on, 25:18953
- aberrations induced in barley, during space flight, 25:18952
- aberrations induced in Vicia faba, by maleic hydrazide and x radiation, effects of blue, green, and infrared light on, 25:18962
- radioinduced aberrations in human, in comparison with mutagenic chemicals, evaluation of, 25:18965
- radioinduced aberrations in, of human sperm following therapy for malignant lymphomas, reproductive factors in, 25:19147
- radioinduced aberrations of human bone marrow, radiation dosimetry using, 25:18980 (CEA-CONF-1698)
- radioinduced aberrations of metaphase, in hamster liver cells, effects of hepatectomy on γ, 25:18960
- radioinduced aberrations of Vicia faba, chronic γ, 25:18950
- radioinduced aberrations of, in bone marrow cells of leukemia patients, effects of exposure to atomic bomb on frequency of, 25:18963
- radioinduced aberrations of, in cotton roots and combined effects of dimethyl sulfate, 25:18954
- radioinduced aberrations of, in cultured cells and plant seeds, effects of hypothermia on, 25:19093
- radioinduced aberrations of, in humans in relation to frequency of abortion, effects of dose on, 25:18969
- radioinduced aberrations of, in man exposed to atomic bombing in Japan, statistics of, 25:18961
- radioinduced aberrations of, in seeds of Nigella damascena, effects of chelating agents on repair processes following cobalt-60 γ, 25:18951
- radioinduced inversions in, of mice, whole-body x, 25:18968
- radioinduced mutations in DNA specific, in synchronous cultures of Escherichia coli, uv, 25:18966
- radioinduced paracentric inversion aberrations of, in hybrid male mice, detection of x, 25:18947
- radioinduced translocation aberrations of, in spermatogonia of mice, fast neutron, 25:18949
- radioinduced translocation aberrations of, in spermatogonia of mice, effects of dose fractionation on rate of x, 25:18958
- radioinduced translocation aberrations of, in spermatogonia of mice, review of kinetics of x, 25:18948

CHROMOSPHERE
- fluctuations in, quasi-periodic, (E), 25:19415
- gravity waves and five-minute oscillations in, trapped, (T), 25:19405
- microwave emission at 1.2 mm, enhancements of, (E), 25:19409
- sunspot formation in, processes occurring during, (E/T), 25:19393(T) (CSIRO-Trans-10284)

CHRONOMETERS
- development of radiometric, using gamma emitter with half-life $>10^4$ years, 25:18819(P)

CHYMOTRYPSIN
- radiation effects on reactivity of dilute solutions of, effects of protein substrate on, 25:18907

CIRCUITS
- curing printed board, procedure for determining degree of, 25:20848 (BDX-613-233)
- design of ringing coil pulse encoders, 25:18868
- exploitation of resistance, interpolation device for quick, 25:20868(T) (MATT-Trans-7)
- fabrication of micro-, fine-focused ion machine for, 25:20168
- models of DTL and TTL integrated, transfer function, 25:20893 (SC-RR-70-650)
- radiation hardening of transistor, equipment and method for, 25:18879(P)

CIRCULATORY SYSTEM
- radiation effects on, in transplanted Walker carcinoma tumors in rats, 25:19111

CLINOPTILOLITE
- radiation effects on samples containing lanthanum, magnesium, or potassium ions, EPR spectral study of stable hydrogen atoms from γ, 25:18423

CLOPENTHIXOL
- radioprotective effects of, on mice, whole-body cobalt-60 γ, 25:19028

COAL
- ash from, separation of molybdenum from, 25:18508
- density of air--powder mixtures of, measurements in pipelines using strontium-90 sources, 25:18606

COATINGS
- deposition of chromium-matrix composite, method for electro-, 25:19270(P)
- deposition of, thickness measurement and control in, 25:20850 (BDX-613-265)
- thickness of conformal, microwave system for measuring, 25:20849 (BDX-613-257)

COAXIAL CABLES
- development of radiation hardened, for use in reactor core, 25:18881(P)

COBALT
- abundance in Type-M supergiant, (E), 25:19323
- chromatographic behavior in hydrochloric acid--thiocyanate mixture on Amberlite LA-2, 25:18337
- determination in Italian meteorites by nondestructive neutron activation, 25:18370
- magnetic moments in alloys with rare earths, 25:19871
- reactions of cobalt-60-enriched, with superalloy fuel capsule materials at high temperatures, 25:18591(R) (DP-1254)
- reactions with refractory metal and superalloy fuel capsule materials in air at high temperatures, 25:18591(R) (DP-1254)
- separation of bismuth from, by cation exchange chromatography, 25:18520

COBALT ALLOYS AND SYSTEMS
- magnetic properties of soft magnetic, effects of heat treatments on, 25:19872
- Co--Cu--Fe--Sm, magnetic properties of $Sm(Fe,Co,Cu)_5$, (E), 25:19875
- Co--Fe--Sm, magnetization of SmFe/sub x/Co/sub 5-x, saturation, (E), 25:19875
- Co--WC, elastic modulus of two-phase, variational bounds of, (T), 25:19282
- Co-base--Ta, crystal structure of solid solutions of, during degradation, 25:19233
- Co-base--Ta, phase studies of solid solutions of, 25:19233

COBALT ALUMINATES
- compatibility with refractory metal and superalloy fuel capsule materials at high temperatures, 25:18591(R) (DP-1254)

COBALT ISOTOPES Co-54
- energy level of, magnetic moment of first 2^+, (T), 25:20333

COBALT ISOTOPES Co-56
- beta and electron-capture decay of, gamma spectra from, (E), 25:18747

COBALT ISOTOPES Co-57
- energy levels from iron-56 proton elastic scattering and (p,γ) reactions, isobaric analog, (E), 25;20336

COBALT ISOTOPES Co-59
- energy levels from gamma resonance absorption, widths

XUM

  - for, (E), 25:20355
  - neutron capture by, resonance integrals and partial widths of resonances in, (E), 25:20359
- COBALT ISOTOPES Co-60
  - abundance in Bovedy meteorite, (E), 25:19301
  - content of fresh water fish, molluscs, and mosses in France, technique for study of, 25:18937
  - properties for use in nondestructive testing of isotopic heat sources, 25:18590(R) (BNWL-1308-4)
- COBALT ISOTOPES Co-62
  - beta decay of ground-state and isomeric, γ spectra from, (E), 25:20361
  - nuclear spin and parity of ground-state and isomeric, (E), 25:20361
- COBALT MAGNESIUM OXIDES
  - compatibility with refractory metal and superalloy fuel capsule materials at high temperatures, 25:18591(R) (DP-1254)
- COBALT OXIDES
  - compatibility with refractory metal and superalloy capsule materials at high temperatures, 25:18591(R) (DP-1254)
  - compatibility with rhenium under welding conditions, 25:18591(R) (DP-1254)
- COINCIDENCE CIRCUITS
  - data acquisition system for, for atomic collision studies, 25:18872
  - design for fission studies, 25:18670
  - design of conversion electron--gamma, for lifetime measurements of energy levels in subnanosecond range, 25:18691
  - design of γ-γ, for lifetime measurements of nuclear energy levels, 25:18642 (JINR-P13-5485)
- COINCIDENCE MEASUREMENTS
  - method for improving heavy-ion spectra in scattering experiments, 25:18750
  - peaks produced by Compton scattering between detectors, spurious, 25:18754
- COLLIMATORS
  - design for negative ion beams, 25:18842
  - development of electronic, for gas recoil neutron spectrometry, 25:18749
  - fabrication of honeycomb, 25:18856(P)
- COLLISION PROCESSES
  - theory of atomic elastic, classical, 25:19488 (INR-P-1225)
- COMETS
  - composition of cores of, laboratory simulation studies, (E), 25:19394(T) (LA-tr-70-27)
  - dust streams from, interplanetary, (E), 25:19425
  - solar-wind interaction with non-ionized dust, (T), 25:19582
  - structure of cores of, laboratory simulation studies, (E), 25:19394(T) (LA-tr-70-27)
- COMPOSITE MATERIALS
  - elastic modulus of fiber-reinforced, variational bounds of, (T), 25:19282
  - strength of internally strained brittle matrix, 25:20902 (UCRL-20395)
- COMPOSITE PARTICLES
  - motion in fixed-centers field, system of algebraic and integral equations for, (T), 25:20059 (JINR-P4-5547)
- COMPTON EFFECT
  - cause of spurious peaks in γ-ray coincidence experiments, 25:18754
- COMPUTER PROGRAMS
  - ALSPIS, for peak finding and integration in activation analysis, 25:18366(R) (NBS-TN-548)
  - CLASSIC, for stability and response analysis of linear systems, FORTRAN IV for IBM 360, 25:20830 (AAEC/TM-551)
  - CPDREV, for spare parts inventory, FORTRAN for Univac 1108, 25:18558 (ARH-1474)
  - ELF, for neutron transport in cylindrical and spherical geometry, (T), 25:20233(T) (ORNL-tr-2409)
  - for anomalous magnetic moment of electron and meson (μ), in LISP for UNIVAC 1108, 25:20055 (CNRS-CPT-70-P-335, pp IV.26-38)
  - for calculation of one-dimensional transient temperature and elastic thermal stress fields, FORTRAN IV for CDC 6600, 25:18579
  - for data analysis for liquid scintillation detectors, in FORTRAN IV, 25:18693
  - for lateral structure function of N-component of cosmic EAS, in FORTRAN IV, 25:19971 (ANL-7727)
  - for monitoring reactor flow systems, 25:20710 (DP-1244)
  - for plasma confinement in theta pinches, 25:19647 (IPP-6/90)
  - for renormalized radiative corrections to quantum electrodynamics, in FORTRAN and LISP for UNIVAC 1108, 25:20055 (CNRS-CPT-70-P-335, pp IV.26-38)
  - for Weapons Effects Display System for mapping prompt effects of nuclear explosions, 25:18832 (UCRL-50892(Vol.6))
  - GAUSFIT, for fitting Gaussian functions, in FORTRAN, 25:20846 (AECL-3784)
  - GRAPH, for plotting numerical data of NEUDADA system, in FORTRAN IV for IBM 360/75 I and FACOM 230-60 with CALCOMP platter, 25:20230 (JAERI-Memo-4116)
  - interchange of essential, between dissimilar, 25:20884(R) (ORO-4061-1)
  - IRESINT 2, for calculation of heterogeneous resonance integrals in reactor lattices, FORTRAN IV for IBM 360, 25:20823 (TKK-F-A-139)
  - JUPITOR-1 supplement, for coupled-channels calculations of nuclear reactions, for HITAC 5020E and FACOM 230-60, 25:20479 (JAERI-Memo-4138)
  - MINIGASKET, for calculating the thermal-neutron scattering law in polycrystals, in Algol for GIER computer, 25:20229 (INR-1186)
  - OUTGAS, for calculating outgassing rates of selected gases, FORTRAN for IBM 360/75 or 360/91, 25:19195 (ORNL-TM-3220)
  - PALLAS-2D-CY, for solving steady-state neutron integral transport equation, in FORTRAN IV for IBM 360/75, 25:20246
  - PATHWAY, for simulating transport of nuclear power plant stack-released radioisotopes in food chains, FORTRAN IV, 25:18526 (ORNL-4584, pp 37-40)
  - PRODGROUP, for production of multigroup reactor constants, 25:20820 (KFKI-71-4)
  - SCANS, for determining reactor flux spectra from foil activation measurements, in FORTRAN IV for IBM 360, 25:18641 (IN-1446)
  - TRUMP, for analysis of temperature distribution in complex three-dimensional systems, 25:18577 (AECL-3783)
  - W-MESHER, for calculating temperature distribution on heat transfer surfaces, FORTRAN IV for CDC 6600, 25:18578 (WANL-TME-2721)
- COMPUTERS
  - description of PDP 8--EL-X8, for BOL multidector system for nuclear reaction studies, 25:20200
  - development of hard-wired arithmetic, for particle identification, 25:18718
  - programming for analysis of ultrasonic test results from graphite, 25:18613 (SC-DR-70-693)
  - programming for real-time control of criticality and inventory of fissionable materials, 25:18620 (BNWL-1440)
  - scanner for CDC 160A, for digitizing and processing two-dimensional drawings, 25:20887 (SC-DR-68-812-B)
- CONCRETES
  - density and water content of, radiometric method for measuring, 25:18599
  - development and properties of prestressed, for reactor pressure vessels, 25:19297
  - neutron attenuation by, fast, 25:19007 (NCRP-38)
  - photon penetration of thick barriers of, energy--angle distributions for cobalt-60, 25:19763
  - properties of heat-resisting, for use as neutron shielding, 25:19295
  - radiation effects on aggregates for, neutron, 25:19296
  - radioactive waste fixation in, method for intermediate-level, 25:18634
  - shielding effectiveness of cracked, (T), 25:19768
  - shielding properties of, used for buildings on Hiroshima and Nagasaki, 25:18990 (ORNL-4584, pp 129-51)
  - concrete--plastics, development, preparation, properties, and testing of, produced by radioinduced polymerization, 25:19292 (BNL-50275)
- CONNECTICUT YANKEE POWER REACTOR
  - operations history for January 1971, 25:20585 (DOCKET-50213-99)
  - site for, environmental radiation surveys during January to December 1970, 25:20617 (DOCKET-50213-98)
- CONSTANTS AND CONVERSION FACTORS
  - values of fundamental physical, 1969 agreement on, 25:20905
- CONTAINMENT SYSTEMS EXPERIMENT
  - aerosol removal in, performance of containment system filters under coolant loss conditions for radioactive, (E), 25:20782 (CONF-700816-(Vol.1), pp 102-27)
- CONVERSION ELECTRONS
  - detection of, $4\pi\beta$ and $4\pi\beta$-γ coincidence methods for, 25:20421
- COOPER POWER REACTOR
  - auxiliary systems for, preliminary safety analysis of, 25:20659 (DOCKET-50298-16)
  - containment systems for, preliminary safety analysis of, 25:20657 (DOCKET-50298-14)
  - control systems for, preliminary safety analysis of, 25:20658 (DOCKET-50298-15)
  - cooling system for, preliminary safety analysis of, 25:20657 (DOCKET-50298-14)
  - design parameters for, preliminary safety analysis of, 25:20661 (DOCKET-50298-19)
  - design parameters of, preliminary safety analysis of, 25:20656 (DOCKET-50298-13)
  - electrical systems for, preliminary safety analysis of, 25:20659 (DOCKET-50298-16)
  - emergency core cooling system for, preliminary safety analysis of, 25:20657 (DOCKET-50298-14)
  - inspection program for, inservice, 25:20661 (DOCKET-50298-19)
  - instrumentation for, preliminary safety analysis of, 25:20658 (DOCKET-50298-15)
  - operations aspects for, preliminary safety analysis of, 25:20661 (DOCKET-50298-19)
  - owners of, financial statements of, 25:20662 (DOCKET-50298-20)
  - piping systems for, fabrication and pressure integrity of, 25:20660 (DOCKET-50298-18)

  quality assurance program for, 25:20661 (DOCKET-50298-19)
  radioactive waste disposal system for, preliminary safety analysis of, 25:20659 (DOCKET-50298-16)
  site for, preliminary safety analysis of, 25:20656 (DOCKET-50298-13)
  steam and power conversion systems for, preliminary safety analysis of, 25:20659 (DOCKET-50298-16)
  structures for, stress loading requirements for Class 1, 25:20660 (DOCKET-50298-18)
  technical specifications for, 25:20660 (DOCKET-50298-18)
COPPER
  chromatographic behavior in hydrochloric acid--thiocyanate mixture on Amberlite LA-2, 25:18337
  coating with stainless steel by sputtering for radiation source prototype development, 25:18590(R) (BNWL-1308-4)
  determination by biamperometric titration with mercury perchlorate, 25:18346
  determination in Italian meteorites by nondestructive neutron activation, 25:18370
  determination in presence of other ions and in ternary mixtures with metals by spectrophotometry using 1-(2-carboxy-4-sulfonatophenyl)-3-hydroxy-3-phenyltriazene, 25:18342
  determination in zirconium alloy simultaneously with molybdenum, polarographic, 25:18341 (RT/CHI-(70)14)
  determination using azo compounds, photometric, 25:18347
  deuteron reactions at 180 to 360 keV with, cross sections for L-shell ionization in, (E), 25:19470
  effects of divalent ions of, on yields of hydrogen from β radiolysis of water, 25:18458
  effects of divalent or monovalent ions of, on deuterium exchange with hydrogen in perchloric or sulfuric acid solutions, 25:18390
  electron reactions at 0.3 to 1.1 MeV with thin foils of, photon emission spectra from, 25:19471
  fission fragment stopping power, energy loss, and range in, (E), 25:20442
  heat transfer by rods of, to pool boiling Freon-113 and water, 25:18585
  neutron inelastic scattering by, γ energies from fast, (E), 25:20356
  photon reaction (γ,p) at 17.6 MeV, proton spectra from, 25:20141
  preparation and properties for use as matrix for neutron-absorbing borides, 25:19264(P)
  proton reactions at 90 to 180 keV with, cross sections for L-shell ionization in, 25:19470
  proton reactions at high energies, atlas of hadron momentum spectra from, (T), 25:20028
  separation of bismuth from, by cation exchange chromatography, 25:18520
  slip initiation in monocrystalline, 25:19194(R) (NYO-4073-4)
  thickness optimization of single crystals of, for use as neutron monochromator, 25:20234 (PH-4)
  ultrasonic attenuation in single crystals of, Alpher--Rubin effect of magnetic field on, 25:19879
  use in radiochemical decoration method for measuring damage profiles in ion-implanted silicon, 25:19817
COPPER ALLOYS AND SYSTEMS
  surfaces of deformed monocrystalline, preparation of replicas preshadowed with uranium oxide for analysis of, 25:19271
  Au--Cu-base, helium-ion backscattering from crystal of, 25:19798
  Co--Cu--Fe--Sm, magnetic properties of Sm(Fe,Co,Cu)$_5$, (E), 25:19875
  Cu--epoxy resins, radiation effects on bonding in, γ, 25:18421(R) (RLO-2098-1)
  Cu--Ga--Pu, phase studies of, 25:19230 (CEA-R-3951)
  Cu--graphite, electric conductivity of two-phase, 25:19226
  Cu--Mo--Nb-base, phase studies of isothermal sections of, at 1900 and 2100°C, 25:19246
  Cu--Mo--Zr, analysis for copper and molybdenum, simultaneous polarographic, 25:18341 (RT/CHI-(70)14)
  Cu--Nb-base, phase studies of, 25:19246
  Cu--Nb-base--W, phase studies of isothermal sections of, at 1600, 1900, and 2100°C, 25:19246
  Cu--Ni, properties for use as matrix for neutron-absorbing, 25:19264(P)
  Cu--Pu, diffusion of plutonium in, at 500°C, effects of gallium on, 25:19230 (CEA-R-3951)
  Cu--stainless steel, radiation effects on bonding in, γ, 25:18421(R) (RLO-2098-1)
  Cu--W, electric conductivity of two-phase, 25:19226
  Cu-base--Si, slip initiation in monocrystalline, 25:19194(R) (NYO-4073-4)
COPPER FERROCYANIDES
  properties as flocculant in treatment of radioactively contaminated seawater, 25:18518
COPPER ISOTOPES
  energy levels from neutron inelastic scattering, (E), 25:20356
COPPER ISOTOPES Cu-59
  energy levels from nickel-58 (p,γ) reactions, spin-parity assignments for, (E), 25:20314
COPPER ISOTOPES Cu-62
  beta and electron-capture decay of, γ spectra from, (E), 25:20361
COPPER ISOTOPES Cu-64
  energy levels from nickel-64 (p,n) reactions, spin assignments for, (E), 25:20358
  proton reactions up to several GeV, cascade calculations of double differential distributions of particles from, (T), 25:20018 (JINR-P2-5507)
COSMIC PARTICLES
  acceleration mechanisms for primary, (E/T), 25:19535
  composition of heavy primary, review, 25:19524
  composition of primary, effects of ionization losses on, (T), 25:19523
  composition of, (E/T), 25:19535
  detection of Z = 40, 44, 52, 71, 77, 78, 92 nuclei in, (E), 25:19525
  energy spectra of primary, effects of ionization losses on, (T), 25:19523
  hadron reactions with carbon above 70 GeV, multiparticle production in, (E), 25:19905
  interactions of primary, (T), 25:19522 (INR-1231)
  interactions with protons above 70 GeV, multiparticle production in, (E), 25:19905
  mass determination of carbon, using nuclear emulsions, 25:18643 (NP-18672)
  origin of heavy primary, review, 25:19524
  propagation of heavy primary, review, 25:19524
  reactions of protons and alpha particles with carbon, nitrogen, and oxygen, spallation, (E), 25:19531
  spectra of extragalactic electrons, (T), 25:19462
  spectra of extremely heavy, charge, (E), 25:19532
COSMIC RADIATION
  acceleration of primary, (T), 25:19459
  dosimetry during Apollo XI flight using Ilford G.5 and K.2 nuclear emulsions, 25:18978 (AD-711316)
  effects on ionization of interstellar hydrogen, (E/T), 25:19440
  intensity of x-ray background, between 25 and 200 keV from ESRO R/73 experiment, 25:19534
  intensity variations of secondary, determination of structure of interplanetary space from, (E), 25:19526
  intensity variations of, data processing system for, 25:19527
  intensity variations of, data processing system for, 25:19528
  intensity variations of, magnetic storm effects on diurnal, (E), 25:19530
  intensity variations of, phase jumps of diurnal, (E), 25:19529
  origin of primary, (T), 25:19459
  propagation in atmosphere, (T), 25:19522 (INR-1231)
  research in, role and perspectives for particle interaction studies from, (E), 25:19885
COSMIC RADIO SOURCES
  ammonia inversion radiation in direction of three galactic-center, (E), 25:19366
  detection between declinations +25° and -25° at 85 and 150 MHz, (E), 25:19388
  dimensions of compact, long-base-line interferometry for, (E), 25:19368
  flux densities for 206 galactic, 5000-MHz observations of, 25:19384
  flux densities of 200 galactic, 408-MHz observations of, 25:19385
  hydrogen absorption profiles in directions of 39 continuum, (E), 25:19391
  model for extragalactic, featuring collapsing stars in galactic nuclei, (T), 25:19357
  number--flux density relations for, (E), 25:19349 (NP-18682)
  positions for 206 galactic, (E), 25:19384
  positions of 200 galactic, (E), 25:19385
  radio-emission mechanism for extragalactic, Compton scattering of plasma waves as, (T), 25:19380
  right ascensions for 389 southern, (E), 25:19387
  spectra and physical characteristics of galactic, (E), 25:19386
  spectra of three, associated with Sco X-1, (E), 25:19362
  survey of, at 2700 MHz, (E), 25:19349 (NP-18682)
COSMIC SHOWERS
  jets of, merits of nuclear-emulsion technique for investigation of, 25:19533
  meson (μ) component in anti N-, N-, and π-initiated EAS at 10^6 to 10^7 GeV, models for, (T), 25:19973 (INSJ-125)
  mesons (μ) lateral distribution in, (T), 25:19522 (INR-1231)
  mesons (π) production in, (T), 25:19522 (INR-1231)
  nuclear-active component in anti N-, N-, and π-initiated EAS at 10^6 to 10^7 GeV, models for, (T), 25:19973 (INSJ-125)
  nuclear-active component of EAS, computer program for lateral structure function of, 25:19971 (ANL-7727)
  nuclear-active component of EAS, pion links method for lateral structure function for three-dimensional, (T), 25:19971 (ANL-7727)
  quarks in center of, cloud-chamber search for, 25:19884
COSMIC X-RAY SOURCES
  Cen XR-4, x-ray flux from, (E), 25:19354
  Cyg X-1, intensity at 0.5 to 1.2 keV, (E), 25:18680
  detection of, (T), 25:19356
  flux from seven, in Cen--Nor--Lup region, (E), 25:19353

Nor XR-2, x-ray flux from, (E), 25:19354
observation of, rocket payload using focusing optics for, 25:18680
Sco X-1, radio sources associated with, (E), 25:19362
Sco X-1, search for iron line emission from, 25:19377
Sco X-1, search for temporal structure in x rays from, (E), 25:19363
Sco X-1, upper limit on radio flux from, (E), 25:19355
Sco X-1, variable negative radial velocity models for, 25:19378
spectra of, in Cetus, (E), 25:19352
telescopes for, development of orientation system for balloon-borne, 25:18677
x-ray pulsations from, (E), 25:19359

COSMOLOGY
expansion of ideal gas of nonzero rest mass, adiabatic, (T), 25:19464
gravitational collapse in, lectures on general relativity theory for, (T), 25:19465
matter--antimatter in, plasma aspects of, 25:19466
model for, Newtonian big-bang hierarchical, (T), 25:19461
models for, ellipsoidal velocity distributions and kinetic theory of Newtonian, (T), 25:19460
symmetric, discussion on, (T), 25:19463
turbulence in early universe, effects on galactic parameters, (T), 25:19443

COUMARIN, 8-[[BIS(2-HYDROXYETHYL)AMINO]METHYL]-6,7-DIHYDROXY-4-METHYL-
radioprotective effects of, on cell membrane in rat thymus, x, 25:19025
radioprotective effects of, on liver mitochondria membranes in mice, x, 25:19025

CRAB NEBULA
gamma emission from, detection of pulsed, (E), 25:19361

CRITICAL ASSEMBLIES
containment building for DCA, design layout of, 25:20802
control system for DCA, instrumentation for, 25:20800
control system for DCA, operation of, 25:20799
cooling system for DCA, design of, 25:20801
kinetics of coupled fast--thermal STEK, correlation technique determinations of, (E/T), 25:20833 (RCN-132)
moderator system for DCA, design of, 25:20801
physics parameters of fast, JAERI-Fast Set analysis of, (T), 25:20788 (JAERI-Memo-4215)
power of ERMINE, neutron noise analysis technique for measurement of, 25:20792
sodium void coefficient for FCA core IV-2, neutron capture and scattering effects on, (E/T), 25:20793

CROSS SECTIONS
plotting of numerical, computer code for, 25:20230 (JAERI-Memo-4116)
scattering, for unstable particles on nucleons, methods for determining, (T), 25:20536

CRYOSTATS
design of, using liquid helium, 25:19641(P)

CRYSTAL STRUCTURE
equations for likelihood ratio method for determination of lattice parameters for cubic materials, 25:20856 (GAT-T-999)

CRYSTAL VIOLET
benzene--bromobenzene--Crystal Violet, radiolysis of, yields from γ, 25:18451

CRYSTALS
ion channeling in diamond-type, computer simulation of flux-peaking effect in, 25:19804
ion channeling in foreign atom-implanted, testing of assumptions in, 25:19798
ion implantation in, creation of moire patterns by channeling in, 25:19849
ion implants in, channeling method for lattice location of, 25:19797
neutron critical scattering in, deconvolution of resolution function for slow, 25:20241
optical properties of ionic slab, 25:20862 (IS-T-427)

CULTURE MEDIA
effects on repair of x-radioinduced single-chain breaks in DNA of Escherichia coli, 25:18912
effects on survival of log-phase and stationary-phase x-irradiated Escherichia coli, 25:18912

CUPFERRON
effects on repair processes following γ-radioinduced chromosome aberrations in Nigella damascena seeds, 25:18951

CURIUM BROMIDES
sublimation and vaporization of, thermodynamics of, 25:18417

CURIUM ISOTOPES Cm-242
determination in irradiated plutonium dioxide--uranium dioxide fuels as measure of burnup, 25:18359 (WCAP-3385-56(Pt.2))

CURIUM ISOTOPES Cm-244
determination in irradiated plutonium dioxide--uranium dioxide fuels as measure of burnup, 25:18359 (WCAP-3385-56(Pt.2))

CURRENT ALGEBRA
commutation relations in, primary quasi-free states on C* algebra of, 25:19932
commutators for π and hadron production in $e^+ + e^-$ interactions at high energies, light-cone properties of axial-vector and electromagnetic, 25:19941
commutators for π form factor, light-cone properties of axial-vector and electromagnetic, 25:19941
current--current theory of weak interactions in, review of, 25:19964 (KFKI-70-24-HEP)
currents and current commutators in O(3,1), 25:19934
currents and current commutators in O(3,1), for singularities of Fourier transforms for inelastic $e + p$ interactions, 25:19934
decay $K \to \pi + l + \nu$ and $K \to 2\pi + l + \nu$ in, form factors for, 25:20041
low-energy theorems for π elastic scattering by nuclei and π photoproduction on nuclei, 25:20019 (LYCEN-7081)

CYCLOBUTENEDIONE, DIHYDROXY-
nickel salt, structure and magnetic and spectroscopic properties of, 25:20865 (IS-T-432)

1,3-CYCLOHEXADIENE
optical constants in photon energy range 4.0 to 10.65 eV for, 25:19759 (ORNL-4584, pp 87-91)

CYCLOHEXANE
optical constants in photon energy range 4.0 to 10.65 eV for, 25:19759 (ORNL-4584, pp 87-91)

CYCLOHEXANE, UNDECAFLUORO(TRIFLUOROMETHYL)-
radiolysis of, NMR studies on radicals produced by γ and uv, 25:18448(R) (CEA-N-1369)

CYCLOHEXENE
optical constants in photon energy range 4.0 to 10.65 eV for, 25:19759 (ORNL-4584, pp 87-91)

CYCLONE SEPARATORS
design parameters of steam, for water cooled power reactors, 25:20769
operation characteristics of trap, for water cooled power reactors, 25:20769

CYCLOPENTANE
cyclopentane--I, iodine-128 or iodine-130 isomeric transitions or radiative neutron capture in liquid and solid, organic yields from, 25:18483(R) (COO-1617-27)
cyclopentane--ICl, iodine-128 isomeric transitions or neutron capture in liquid and solid, labeled organic yields from, 25:18483(R) (COO-1617-27)

CYCLOPHOSPHAMIDE
effects on regeneration of hemopoietic stem cells following transplantation into x-irradiated mice, 25:19127
effects on repopulation of mouse bone marrow transplants in γ-irradiated mice, 25:19112

CYCLOTRONS
beam injection in electron model of ring, with strong focusing, 25:20130 (JINR-P9-5453)
beam orbit displacement due to variation in voltage along accelerating gap, 25:20170
development of Swedish, 1969, 25:20133(R) (NP-18671)
experimental facilities for Texas A and M, sample gas transport spectrometry system, 25:18737(R) (ORO-3820-7)
experimental facility for, electromagnetic mass separator, 25:20175
magnetic field correction in U-150-2, system of coils for, 25:20216
operation of electron model of ring, with strong focusing, 25:20130 (JINR-P9-5453)
research at Swedish, 1969, 25:20133(R) (NP-18671)

CYSTEAMINE
effects on uptake of α-aminoisobutyric acid, inulin, orotic acid, and phosphorus-32 by tissues of γ-irradiated rats, 25:19024
radioprotective effects of, on serum antihyaluronidase activity and tissue permeability in skin of rats, γ, 25:19031

CYSTINE
radiation effects on, in relation to physiological damage in cells, biophysical mechanisms of uv, 25:18903

CYTIDINE, 2'-DEOXY-
metabolism in lymphocytes, tritium tracer study of effects of phytohemagglutinin on, 25:18919(R) (RLO-2225-T-16-1)

D

DATA ACQUISITION SYSTEMS
description of analog and digital electronics for BOL nuclear multidetection system, 25:20199
description of computer-based, for BOL nuclear detection system, 25:20202
design of logic interfaces for, in nuclear physics, 25:18852
development of computer, for radiopharmaceutical disbursement and inventory, 25:19050
transmission system for computer-based, 25:18845

DATA DISPLAY SYSTEMS
computer program for Weapons Effects Display System for prompt effects, 25:18832 (UCRL-50892(Vol.6))
computer programs for Weapons Effects Display System, mathematical models for development of, 25:18831 (UCRL-50892(Vol.1))
description of multicolored, for radioisotope scanners, 25:18653(P)
design and performance for fast-cycling accelerators, 25:20177
development for stationary scintillation cameras, 25:18689(P)

DATA PROCESSING SYSTEMS
- description for BOL nuclear detection sysfem, 25:20203
- operation of cosmic-ray, 25:19528
- operation of cosmic-ray, 25:19527

DATA TABULATIONS
- cross sections for $K^- + p$, $K^- + n$, and $K^- + d$ interactions at high energies, 25:19909 (CERN-HERA-70-6)
- cross sections, angular distributions, and polarizations for N + N and N + d interactions, 25:19899 (UCRL-20000-NN)
- fundamental physical constants, 1969 agreement on values of, 25:20905
- nuclear data sheets for A = 84, 85, 86, and 113, 25:20354
- nuclear data sheets for even A = 230 through 242 nuclei, 25:20467
- nuclear reactions induced by neutrons, photons, protons, deuterons, tritons, and alpha particles, tables of thresholds for, (E), 25:20237 (UCRL-50400(Vol.9))
- on β-γ asymmetry coefficients in isospin-forbidden mixed beta transitions, 25:20372 (KFK-1249)
- radioisotope half-lives, gamma energies and intensities, 25:20368 (JAERI-Memo-4189)
- wave functions of single-particle states of deformed transuranium nuclei, 25:20481 (JINR-P4-5457)

DECAY SCHEMES
- nuclear data sheets for A = 84, 85, 86, and 113, 25:20354
- nuclear data sheets for even A = 230 through 242 nuclei, 25:20467

DEER
- cesium-137 content of muscles of reindeer in Finnish Lapland during 1966 to 1970, 25:18932 (NYO-3446-14, Paper 31)
- radioisotope content of bones and soft tissues of, in Finland, 25:18929 (NYO-3446-14, Paper 26)
- radioisotope content of muscle samples from, in Southeast USA during 1969, 25:18935(R) (ORO-3905)

DEHYDROGENASES
- radiation effects on activity of, in cells of cotton plants, γ, 25:18918

DENSIMETERS
- calibration of radiometric, for soils, 25:18815 (INP-715)
- calibration of subsurface gamma-scatter, using one-dimensional transport theory, 25:18816
- design and performance of beta-absorption-impactor, for monitoring mass concentration of particulate matter in air, 25:18821

DESALTING
- bibliography on, annotated, 25:20812 (TID-25653)
- plant design for, steam turbine exhaust pressure optimization in nuclear, 25:18565 (ORNL-TM-3291)

DETONATION WAVES
- structure of, 25:20866(T) (LA-tr-71-4)

DEUTERIUM
- concentration by dual-temperature exchange between hydrogen sulfide and water, 25:18512(P)
- concentration by dual-temperature exchange between hydrogen sulfide and water, 25:18513(P)
- concentration by dual-temperature exchange between hydrogen sulfide and water, 25:18514(P)
- effects on acid-catalyzed isomerization of cis-1-methyl-3-phenylallyl alcohol and cis-1-phenyl-1,3-butadiene, 25:18405
- effects on decay of alkyl radicals produced by γ radiation effects on iodoalkane glasses at 77°K, 25:18461
- effects on electrophilic aromatic substitution, role of leaving abilities of electrophiles in, 25:18414
- effects on emission and absorption spectra of $Cr(NH_3)_6^{3+}$, 25:18404
- effects on fluorine NMR spectra of p-fluorophenylmethylcarbonium ions, 25:18396
- effects on harmonic force field, mean amplitudes, and symmetry coordinates for dibenzene chromium, 25:18392
- effects on hydrogen atom abstraction process in γ-irradiated solid acetonitrile, 25:18426
- effects on hydrolysis of methyl 3-nitrophthalate, methyl 6-nitrophthalate, or methyl 1,2,3-benzenetricarboxylate, 25:18400
- effects on iodination of sodium phenylpropiolate, kinetic studies on solvent, 25:18397
- effects on ionization in benzoic, o-toluic, mesitoic, and phenylacetic acid systems, 25:18409
- effects on ir and Raman spectra of methylenecyclopropane, 25:18402
- effects on ir spectra of water, 25:18401
- effects on kinetics of reactions of hydrogen atoms produced by γ irradiation of organic solutes in aqueous perchloric acid solutions, 25:18459
- effects on low-pressure pyrolysis and uv photolysis of methyl peroxide and other methane derivatives, 25:18394
- effects on oxidation of hydrogen on ferric oxide, 25:18386
- effects on photosensitized trans-cis isomerization of β-methylstyrene, 25:18406
- effects on proton transfer from hydronium ions in water, kinetic studies on solvent, 25:18395
- effects on reaction rates of oxygen ions with acetylene, benzene, and ethylene at 0 to 2 eV, 25:19490 (ORNL-4584, pp 92-104)
- effects on reactions of amines with acetylimidazolium ions, solvent, 25:18398
- effects on reactions of bromine atoms with methane, 25:18410
- effects on solvolysis of 1,2-dimethyl-exo-2-norbornyl p-nitrobenzoate in dioxane--water system, 25:18413
- effects on spectra of polycrystals of iodoethane, ESR studies on, 25:18424
- effects on unimolecular decomposition of molecular ions of toluene and cycloheptatriene, 25:18393
- effects on vibrational spectra of liquid water and hydronium ions, 25:18399
- exchange between hydronium ions and water, 25:18399
- exchange between hydronium ions and water, 25:18395
- exchange with hydrogen in bicyclo[2.2.1]heptanones, 25:18411
- exchange with hydrogen in deuterated sulfuric acid--heavy water solutions of trinitromethane, kinetics of, 25:18391
- exchange with hydrogen in perchloric or sulfuric acid solutions, catalytic effects of cupric or cuprous ions on, 25:18390
- photodisintegration of, analysis of retardation in, (T), 25:20254
- photodisintegration of, bremsstrahlung-weighted E1 cross sections for, (T), 25:20252
- proton reactions (p,2p) and (p,np) at 12 MeV, impulse-approximation analysis of coincidence spectra from, (E), 25:20260
- target of liquid, for D(p,n) neutron source, 25:20187
- targets of, design of high-pressure, 25:20128 (IFVE-SEF-70-22)
- thermomagnetic torque in gaseous, at 100 to 350°K, isotopic effects in, 25:18403

DEUTERIUM HYDRIDES
- electron reactions at 1.0 to 13.6 eV with, effective cross sections for rotational excitation in, (T), 25:19502
- rotational relaxation time below 40°K, sound absorption measurements of, 25:19480
- DH--He, rotational relaxation time below 40°K, sound absorption measurements of, 25:19480
- DH--Ne, sound absorption measurements below 40°K, 25:19480

DEUTERON SOURCES
- yields of rf-excited, ion analysis of, 25:20150

DEUTERONS
- binding energy of, relation of phase shift for p + n interactions at low energies with, (T), 25:20022
- interactions anti d + d at 13.3 GeV/c, total cross sections for, 25:19907
- interactions anti n + d at 6.65 GeV/c, total cross sections for, 25:19907
- interactions anti p + d at 6.65 GeV/c, test of CPT invariance from total cross sections for, 25:19907
- interactions $\gamma + d \to \pi^- + p + p$, impulse approximation calculation of recoil proton polarization in, (T), 25:19940
- interactions γ + d at high energies, Glauber theory of multiple scattering for cross sections of π^- and π^+ production in, (T), 25:19955
- interactions $K^- + d$ at high energies, compilation of cross sections for, (E), 25:19909 (CERN-HERA-70-6)
- interactions n + d at 0.5 to 70 GeV/c, compilation of cross sections, angular distributions, and polarizations for, (E), 25:19899 (UCRL-20000-NN)
- interactions of, Glauber model for Regge cuts in amplitudes of, (T), 25:19992
- interactions p + d at 0.5 to 70 GeV/c, compilation of cross sections, angular distributions, and polarizations for, (E), 25:19899 (UCRL-20000-NN)
- interactions $\pi^- + d$ at 3.15 GeV/c in deuterium bubble chamber, neutron cross sections and K*(890), Σ(1385), and Kππ(1200) enhancement in, (E), 25:19922
- reactions (α,p) with helium-4 at 8.5 to 11 MeV using polarized beam, proton asymmetries from, (E), 25:20263
- reactions (d,4n) with uranium-238 at 20 to 65 MeV, isomer ratio in, (E), 25:20389
- reactions (d,α) with carbon-13, boron-10 recoil charge-state distribution from, 25:18485
- reactions (d,α) with sulfur-32 at 2 to 32 MeV, cross-section measurement by detection of positron annihilation γ rays, (E), 25:20283
- reactions (d,α), (d,p), and (d,t) with carbon-12 and carbon-13 at 0.4 to 0.85 MeV, angular distributions and cross sections for, (E), 25:20279
- reactions (d,d) with carbon-12, 5.01-MeV carbon-12 ions recoil charge-state distribution from, 25:18485
- reactions (d,n) and (d,p) with oxygen-16 at 4 to 6 MeV, DWBA and optical-model analyses of, (E/T), 25:20301
- reactions (d,n) with beryllium-9 at 650 keV, energy spectra from, (E), 25:20289
- reactions (d,n) with boron-10, boron-11, carbon-13, nitrogen-14, and nitrogen-15 at 2.8 to 4 MeV, neutron polarization in, (E), 25:20272
- reactions (d,n) with carbon-12 at 6.4 MeV, neutron spectra and polarizations from, (E), 25:20297
- reactions (d,n) with carbon-12, magnesium-24, and sulfur-32 at 2 to 3.2 MeV, cross-section measurements by

- detection of positron annihilation γ rays, (E), 25:20283
- reactions (d,p) with calcium-40, carbon-12, oxygen-16, and zirconium-90, DWBA calculations of angular distributions and overlap integrals from, (T), 25:20497
- reactions (d,p) with carbon-12 at 12.4 MeV, polarization of protons from, (E/T), 25:20287
- reactions (d,p) with carbon-12, calcium-40, oxygen-16, and silicon-28 at 12 to 26 MeV, model for, (T), 25:20522
- reactions (d,p) with chromium-52 at 8 MeV, effect of deuteron D-state in DWBA analysis of, (T), 25:20328
- reactions (d,p) with chromium-52, iron-54, oxygen-16, and zirconium-90 at 8 to 12 MeV using polarized beam, cross sections and vector analyzing powers for, (E), 25:20305
- reactions (d,p) with nitrogen-14 at 3 MeV and 45°, energy spectra from, (E), 25:18718
- reactions (d,p) with oxygen-16, strontium-88, and zirconium-90, analysis using BHMM theory, (T), 25:20282
- reactions (d,p) with oxygen-16, use in determining niobium oxidation, 25:19171
- reactions (d,p) with polarized helium-3 at 4.8 to 11.9 MeV, asymmetries in, (E), 25:20262
- reactions (d,t) with helium-4, pole-diagram analysis of exchange mechanism in, (T), 25:20250 (JINR-P2-5496)
- reactions n + d at low energies, contributions of first two diagrams to amplitude of three-body inelastic, (T), 25:20027
- reactions with metals at 180 to 360 keV, ratios of inner-shell ionization cross sections for, to corresponding proton-bombardment cross sections, 25:19470
- reactions with nuclei, tables of thresholds for, (E), 25:20237 (UCRL-50400(Vol.9))
- scattering by beryllium-9 at 5 to 7 MeV, tensor polarization and differential cross sections for elastic, (E), 25:20293
- scattering by carbon-12 and carbon-13 at 0.4 to 0.85 MeV, angular distributions and cross sections for elastic, (E), 25:20279
- scattering by chromium-52, iron-54, oxygen-16, and zirconium-90 at 8 to 12 MeV using polarized beams, cross sections and vector analyzing powers for elastic, (E), 25:20305
- scattering by europium-151 at 12 MeV, inelastic, (E), 25:20432
- scattering by helium-4 at 3 to 11 MeV using polarized beam, vector analyzing power for elastic, (E), 25:20263
- scattering by helium-4, separable potentials for, 25:20511
- scattering by magnesium at 7.0 MeV, tensor polarization in elastic, (E), 25:20342
- scattering by nuclei in multi-GeV region, Glauber theory of, (T), 25:20531
- scattering by oxygen-16 at 4 to 6 MeV, DWBA and optical-model analyses of elastic, (E/T), 25:20301
- scattering by polarized helium-3 at 4.8 to 11.9 MeV, asymmetries in elastic, (E), 25:20262

DEUTERONS (anti d)
- interactions anti d + d at 13.3 GeV/c, total cross sections for, 25:19907
- interactions anti d + p at 13.3 GeV/c, test of CPT invariance from total cross sections for, 25:19907
- production in proton reactions with aluminum and beryllium at 70 GeV, yields and differential cross sections for, (E), 25:19906

DIAMONDS
- radiation effects on color and resistance of semiconducting Type IIb, 25:19769(T) (LIB/Trans-307)

DIATOMACEOUS EARTH
- preparation of iodine-131-labeled aerosols of, for atmosphere dispersion studies, 25:18926 (CONF-700816-(Vol.1), pp 49-71)

DIDO REACTORS
- control arm drive circuits for HIFAR, operation manual for, 25:20781 (AAEC/M-10)

DIET
- radioactivity of human, on Kerala coast, India, 25:19143
- radioisotope content of human, in high natural background areas in Brazil, 25:18927 (NP-18670)

DIFFERENTIAL EQUATIONS
- solution of discretized Poisson, error vector propagation method for, 25:20892 (SC-RR-70-579)
- solution of reactor kinetics, for delayed neutron emitters and secondary decay processes in, (T), 25:20828
- solution of temperature formulation of space averaged reactor kinetics, (E/T), 25:20829

DIFFRACTION GRATINGS
- performance of dielectric-coated, (E), 25:19758 (ORNL-4584, pp 74-86)

DIFFUSION
- theory for ion-implanted solids with nonuniform diffusion parameters, 25:19840

DIODES
- capacitance of ion-implanted silicon p-n, 25:18857
- fabrication of silicon p--n junction, by ion implantation, 25:19828

DIPHENYLAMINE
- yields from γ radiolysis of aniline, effects of additives on, 25:18450(R) (ORO-3519-8)

DISEASES
- radiodiagnosis in patients with myasthenia gravis, use of selenium-75-labeled selenomethionine scanning for, 25:19049

DISEASES, INFECTIOUS
- ascariasis, treatment of pulmonary, in x-irradiated mice, effectiveness of active immunization, anthelmintics, and antibiotics for, 25:19032

DISEASES, NEOPLASTIC
- book: Bone Tumors in Man and Animals, 25:19136
- cancer, frequency of human thyroid, in Norway, effects of iodine-131 content of milk on, 25:19135
- carcinomas, iodine-131 retention in man with thyroid, use of whole-body counting for measuring, 25:19035
- carcinomas, radiation effects on growth of C3H mammary, following transplantation into mice, evaluation of tumor bed effect for x, 25:19118
- carcinomas, radioinduced, in lungs following fluoroscopy and pneumothorax therapy in patients with tuberculosis history, x, 25:19068
- carcinomas, radioinduced, in mastoid glands and paranasal sinuses of man following ingestion or injection of radium-226, relation of dose and time to, 25:18979 (BRH/DBE-70-5)
- carcinomas, radiotherapy of human cervical, effects on cells and tissues following linear accelerator, 25:19064
- carcinomas, radiotherapy of human mouth, effectiveness of γ and x, 25:19081
- carcinomas, radiotherapy of human tonsil, effectiveness of cobalt-60 γ, 25:19085
- carcinomas, radiotherapy of mouse skin, effects of synchronized treatment using fluorouracil on survival after x, 25:19075
- carcinomas, use of radioisotope scanning in pre- and postoperative surgery of gynecological, 25:19070
- Ehrlich ascites tumor, radiation effects on survival of transplanted, in mice, combined effects of immunization and x, 25:19130
- fibrosarcomas, radiation effects on growth of C3H, following transplantation into mice, evaluation of tumor bed effect for x, 25:19118
- gliomas, radiotherapy of human cerebral, vascular proliferation following, 25:19065
- Hodgkin's disease, radiodiagnosis of spleen involvement in human, use of technetium-99m for, 25:19058
- leukemia, occurrence in man exposed to atomic bombing on Hiroshima and Nagasaki, 25:18990 (ORNL-4584, pp 129-51)
- leukemia, radioinduced chromosome aberrations in bone marrow cells of patients with, effects of exposure to atomic bomb on frequency of, 25:18963
- leukemia, radioinduced, in man following ingestion or injection of radium-226, relation of dose and time to, 25:18979 (BRH/DBE-70-5)
- lymphomas, radiotherapy of malignant, in man, reproductive factors in, 25:19147
- malignant, occurrence in children exposed in utero to atomic bombing at Hiroshima and Nagasaki, 25:19089
- malignant, radiation effects on man following surgery for, laser, 25:19074
- malignant, radioinduced, in bones, bone marrow, and hematopoietic tissues of mice following ingestion of strontium-89, 25:19113
- malignant, radioinduced, in human thyroid following inhalation of iodine-131, relation of dose to probability of, 25:18974 (AHSB(S)R-192)
- malignant, radioinduced, in man following dental therapy, etiology and prevention of, 25:19069
- malignant, radioinduced, in man following ingestion or injection of radium-224, relation of dose and time to, 25:18979 (BRH/DBE-70-5)
- malignant, radiotherapy of human breast, development of osteosarcoma in clavicle following post-operative, 25:19140
- malignant, radiotherapy of human head, neck, and pelvic, review of complications necessitating surgery following high-dose, 25:19088
- malignant, radiotherapy of human larynx and pharynx, comparison of effectiveness of cobalt-60 γ, with surgery, 25:18998
- malignant, radiotherapy of human mouth and tongue, effectiveness of iridium-192 applicators for γ, 25:19080
- malignant, radiotherapy of human mouth, methods for dental care and oral hygiene before, during, and following, 25:19079
- malignant, radiotherapy of human, afterloading techniques for implant, 25:19076
- malignant, radiotherapy of human, characteristics of 440-MeV proton beam for, 25:19087
- malignant, radiotherapy of human, effects of LET on effectiveness of ionizing, 25:19077
- malignant, radiotherapy of human, use of lead glass filters for protection of skin during γ, 25:19086
- malignant, radiotherapy of human, use of tin radiation filters for protection of skin during γ, 25:19082
- malignant, radiotherapy of liver, in children, acute toxicity of antineoplastic drug theory during,

25:18999
  malignant, radiotherapy of pelvic, mast cell studies on vaginal fistulas following, 25:19139
  malignant, radiotherapy of primary, of human larynx, mouth, and pharynx, comparison of effectiveness of, with surgery, 25:19083
  malignant, radiotherapy, evaluation of negative pion beams for, 25:19078
  metastases, effects of lung, on regional lung function, use of xenon-133 scanning in evaluation of, 25:19048
  metastases, radiodiagnosis of human brain and liver, in patients with lung neoplasms, use of pretreatment radioisotope scanning for, 25:19047
  metastases, radiotherapy of human neck lymph node, x, 25:19084
  osteosarcomas, radioinduced, in man following postoperative therapy for breast malignancies, 25:19140
  osteosarcomas, radiotherapy of femoral, in man, effects of localized hypothermia and ischemia on skin reactions following, 25:19093
  radiodiagnosis of human, review of methods for, 25:19037
  sarcomas, radioinduced, in bones of dogs, man, and mice, following ingestion or injection of radium-226, relation of dose and time to, 25:18979 (BRH/DBE-70-5)
  tumors, radiosensitivity of, effects of oxygen and oxygen plus carbon dioxide on, 25:19023
  tumors, radiotherapy of human head and neck, effects of mitotic synchronization with fluorouracil on effectiveness of x, 25:19071
  tumors, radiotherapy of human, effects of, on amino acid excretion, 25:19063
  Walker carcinosarcomas, radiation effects on circulatory system in transplanted, in rats, 25:19111

DISEASES, PHYSIOLOGICAL
  alopecia mucinosa, radiotherapy of human, further management and prognosis following soft x, 25:19073
  cataracts, radioinduced, in inbred and hybrid mice, effects of dose on x, 25:19116
  dermatitis, radiation effects on man following treatment of, laser, 25:19074
  edema, radioinduced, in human skin, uv, 25:19150
  embolisms, radiodiagnosis of pulmonary, using scintillation camera with xenon-133 source, performance of computer-generated ratio method for data display in, 25:19053
  emphysema, radiodiagnosis of pulmonary, using scintillation camera with xenon-133 source, performance of computer-generated ratio method for data display in, 25:19053
  fistulas, radioinduced rectovaginal, in man following therapy, surgical methods for repair of, 25:19138
  fistulas, radioinduced, in human vagina following therapy for pelvic malignancies, mast cell studies on, 25:19139
  hydrocephalus, radiodiagnosis of communicating, use of iodine-131-labeled human serum albumin by lumbar injection for, 25:19043
  hyperthyroidism, radiodiagnosis in man, use of iodine-131 thyroid uptake for, 25:19051
  hyperthyroidism, radiotherapy of human, using internal iodine-131, review of effectiveness of, 25:19062 (NP-18693)
  hypothyroidism, radiodiagnosis in man, use of iodine-131 thyroid uptake for, 25:19051
  ischemia, effects on skin reactions following radiotherapy of osteosarcomas in human femur, 25:19093
  ischemia, effects on tissues of irradiated rodents, 25:19093
  myocardial infarction, radiodiagnosis of canine and human, using cesium-129, 25:19055
  osteodystrophy, radioinduced human, following inhalation of radon-222, 25:19144
  plastic induration, radiotherapy of, in human penis, effectiveness of strontium-90 β, 25:19072
  radiodiagnosis in spinal canal, effectiveness of myeloscintigraphy with intravenously injected mercury-197 or technetium-99m for, 25:19042
  radiodiagnosis of human, review of methods for, 25:19037
  radiodiagnosis of vascular, of human brain using percutaneous retrograde arteriography, 25:19040
  rheumatism, solar activity effects on fibrinolytic activity in human, 25:19145
  splenomegaly, radiodiagnosis of human, effectiveness of metastable technetium-99 scanning for, 25:19057

DISEASES, PLANTS
  radioinduced mutations for increased resistance to, effects of dose and seed exposure on γ, 25:18964(P)

DISEASES, TRAUMATIC
  burns, treatment of human, effectiveness of frozen irradiated pigskin xenografts for, 25:19020
  crush syndrome, clinical aspects and treatment of, in dogs with acute radiation sickness, 25:19033
  hematoma, radiodiagnosis of subdural, with vascular rim, comparison of mercury-203-labeled chlormerodrin and technetium-99m labeled pertechnetate for, 25:19059
  radiation injuries, diagnosis in man, criteria for, 25:19008 (NCRP-39)
  radiation injuries, dosimetric, clinical, and therapeutic aspects of accidental whole-body, 25:19012 (CEA-CONF-1695)
  radiation injuries, estimation of probability of, in human populations following radioisotope release to atmosphere during reactor accidents, 25:18974 (AHSB(S)R-192)
  radiation injuries, occurrence in human skin following fast neutron therapy of neoplasms, 25:19149
  radiation injuries, occurrence in liver of children following therapy, effects of antineoplastic drugs on severity of, 25:18999
  radiation injuries, prevention and treatment of human mouth, induced by therapy, 25:19079
  radiation injuries, rules for clinical and therapeutic procedures for, to man, 25:18975 (CEA-N-1365)
  radiation sickness, clinical aspects and treatment of acute, in dogs with crush syndrome, 25:19033

DISPERSION RELATIONS
  effective-range parameter for S-wave π + N interactions from fixed-t, 25:20010

DISPLACEMENT GAGES
  rotation, development of passive radioactive device for determining relative, 25:18822(P)

DOGS
  chromium-51-labeled EDTA excretion by kidneys of, 25:18893
  radiation effects on leukocyte count of, sensitizing effects of dinitrochlorobenzol on x, 25:19030
  radiodiagnosis of myocardial infarction in, cesium-129 scanning method for, 25:19055
  radium-226 carcinogenicity and dosimetry in, following injection, review of, 25:18979 (BRH/DBE-70-5)
  scanning of pancreas of, effectiveness of iodine-131-labeled erythrosine B for, 25:19060
  treatment of combined crush syndrome and radiation sickness in, clinical aspects for, 25:19033

DOLOMITES
  composition, density, and porosity of, determination by gamma absorption, 25:18524

DRESDEN POWER REACTOR, UNIT 1
  administrative control for, technical specifications for, 25:20601 (DOCKET-50010-80)
  containment system for, leak rate test surveillance for, 25:20601 (DOCKET-50010-80)
  cooling system for, leak detection requirements for primary, 25:20601 (DOCKET-50010-80)
  emergency condenser systems for, technical specifications for, 25:20601 (DOCKET-50010-80)
  operations history for 1970, 25:20575 (DOCKET-50010-78)
  operations incident of February 3, 1971, crack in Type 304 stainless steel pipe of primary piping system, 25:20576 (DOCKET-50010-79)

DRESDEN POWER REACTOR, UNIT 2
  operations incident of January 5, 1971, revised information for standby gas treatment system test status, 25:20588 (DOCKET-50237-143)

DRESDEN POWER REACTOR, UNIT 3
  containment structure for, integrated leak rate testing of, 25:20628 (DOCKET-50249-59)
  operations incident of February 2, 1971, excessive radioactivity in liquid waste storage tanks, 25:20593 (DOCKET-50249-57)
  power level for, authorization for 2527 MW(t) maximum, 25:20629 (DOCKET-50249-60)
  radioactive effluents from, revised technical specifications for release rates of gaseous, 25:20627 (DOCKET-50249-58)

DRUGS
  analysis for silver by x-ray fluorescence, comparison of americium-241, gadolinium-153, and iodine-125 sources for, 25:18355

DUSTS
  streams of interplanetary, cometary origin of, (E), 25:19425

DYSPROSIUM
  electron band structure of, x-ray photoelectron study of 4f levels in, 25:19866

DYSPROSIUM ALLOYS AND SYSTEMS
  Dy--Re--Th, crystal structure of intermetallic compounds of, 25:19235

DYSPROSIUM IONS
  effects on antiresonance in absorption spectra of color centers in heat-treated gamma-irradiated calcium fluoride crystals, 25:19771
  wave functions for, accurate numerical Hartree--Fock self-consistent field, 25:19478

DYSPROSIUM ISOTOPES
  charge radii in A = 156 to 164, differences in, (E), 25:20416
  isotopic shift for 162-164, K x-ray, (E), 25:20416

DYSPROSIUM ISOTOPES Dy-155
  energy levels and transitions from holmium-155 decay, (E), 25:20405

DYSPROSIUM ISOTOPES Dy-158
  energy levels of, calculation using microscopic collective model, (T), 25:20547

E

EARTHQUAKES
  detection at ORNL Station ORT from Aug. 1969 to Aug. 1970, station operation for, 25:18556 (ORNL-4584, pp 41)
  effects on West Valley Processing Plant design criteria,

XUM

25:18496 (DOCKET-50201-65)
ECOSYSTEMS
  nutrient cycling in tropical forest, tracer studies, 25:20897 (TID-25656)
  radiation effects on growth of marine periphytal, contaminated with cerium-144 and cesium-137, 25:18936
  radioactive contamination of, effects of fallout and wastes from reactor power plants on, 25:18941
  radioisotope accumulation in aquatic, in Finland, 25:18930 (NYO-3446-14, Paper 27)
  ruthenium-106 contamination of marine, comparison between soluble and insoluble, 25:18944
EDWIN I. HATCH POWER REACTOR, UNIT 1
  effluents from, effects on environment of chemical, radioactive, and thermal, 25:20668 (DOCKET-50321-16)
  stack disposal system for, design parameters and site geological data for main, 25:20669 (DOCKET-50321-17)
EDWIN I. HATCH POWER REACTOR, UNIT 2
  effluents from, effects on environment of chemical, radioactive, and thermal, 25:20668 (DOCKET-50321-16)
EGGS
  radiation effects on assassin bug, effects of nutrition on, 25:19099
  radiation effects on development and survival of fish, effects of dose on x, 25:19103 (PG-Report-1013)
  radiation effects on production of, by cotton leaf worm exposed as pupae, γ, 25:19097
  radioisotope content of tick, following inoculation of females, 25:18934(R) (ORO-3514-10)
ELASTOMERS
  preparation of lead powder-incorporating sheets of, for shielding and acoustic insulation, 25:19294(P)
  radioinduced crosslinking of, effects of chloroalkanes on, 25:18434
ELECTRIC ARCS
  oscillations in reflex, with low magnetic fields, 25:19666
  plasma instabilities in reflex, effects of steady-state oscillations on, (E/T), 25:19707
ELECTRIC CHARGES
  constancy of electron, (T), 25:19883
ELECTRIC DISCHARGE
  effects on production of free radicals in lyophilized proteins in comparison to effects of γ radiation, 25:18906
  electron density and gas pressure in active zone level of hollow cathode, 25:20872 (NP-18708)
  spectroscopic diagnostics of cesium in, 25:19665
ELECTRIC FIELDS
  electron kinetics in strong crossed magnetic and, diffusion approximation for hot, (T), 25:19960
ELECTRIC GENERATORS
  development of closed cycle gas turbine, for gas cooled power reactors, 25:20690
  performance of, using superconducting elements, 25:19635
ELECTRIC POWER
  development of cryogenic energy transmission systems, 25:19636
  economics of nuclear power plant-generated, in aluminum production, 25:19184
  production rates in radioisotope thermoelectric converters, effects on long-term converter operation, 25:18595 (SC-RR-70-854)
ELECTRIC PROBES
  performance of floating double, for plasma jet diagnostics, 25:19659
ELECTRODYNAMICS
  solution for N charged particles in two dimensions in classical, exact, 25:19962
  symmetry for, semidirect product for invariance group in, (T), 25:20091
ELECTROJETS
  plasma irregularities in equatorial, vhf echoes from, 25:19573
ELECTROMAGNETIC FIELDS
  charged-particle motion in solvable configuration of, Klein--Gordon spin-0, (T), 25:19950
  charged-particle motion with constant velocities in, Lorentz force relation with energy and momentum for, (T), 25:19946
  Coulomb law for, modified divergence-free, (T), 25:19952
  Einstein--Maxwell equations for, properties of cylindrically symmetric, (T), 25:20086
  electron self-energy in, divergenceless classical, (T), 25:19952
  Maxwell equations for, symmetric space of group of, 25:20052(T) (SLAC-Trans-130)
ELECTROMAGNETIC LENSES
  charged-particle beam motion in, effects of aberration on high-current, 25:20160
  charged-particle focusing in three-sector magnetic prisms with 1/r fields, image parameters for, 25:20217
  harmonic components of fields of quadrupole, measurement of, 25:20164
  ion beam acceptance of asymmetrized quadrupole singlet, calculation of, 25:20223
ELECTROMAGNETIC WAVES
  interactions with toroidal plasma, polarization in, (T), 25:19735
  neutron scattering by particles moving in, slow, (T), 25:20243
  propagation in half-space relativistic plasma, (T), 25:19740
  propagation in warm stratified electron plasma, singularities of coupled fields in, (T), 25:19756
  scattering by bound electrons, double scattering effects in, (T), 25:19949
ELECTRON BEAMS
  interactions with plasma, ion heating in, (T), 25:19650
  monitor for 2- to 8-MeV, design of collector, 25:20214
  position monitoring of, sensitivity of metal foil secondary-emission detector for, 25:20173
ELECTRON GAS
  charged-particle reactions with, double-plasmon excitation in, 25:19757 (ORNL-4584, pp 58-73)
  ground-state energy of, calculation using three-body forces, (T), 25:20523
ELECTRON MICROSCOPES
  use in combination with field ion microscopes in tungsten grain boundary studies, 25:19249
ELECTRON MULTIPLIER TUBES
  efficiency of channel, for electron detection at 1 to 50 keV, 25:18659
  pulse height distribution for, calculations of generalized, 25:18864
ELECTRON-RING ACCELERATORS
  design parameters for high-energy proton, 25:20161
  ion acceleration in electron ring in decreasing magnetic field, 25:20131 (JINR-P9-5535)
  ion storage in rings of, positive, 25:20210
ELECTRON SOURCES
  design of gun-type, for injection into gases at atmospheric pressures through differential window, 25:18850
ELECTRONS
  acceleration in solar flares, relation to Type-I noise activity, (E), 25:19402
  density from 80 to 170 km in ionosphere, interaction mechanisms of, (E/T), 25:19583
  detection and energy measurement up to 15 GeV/c, shower spectrometer for, 25:18779
  detection and monitoring of hydrated, equipment for, 25:18854(P)
  detection at 1 to 50 keV, efficiency of channel electron multiplier for, 25:18659
  detection of high-energy, resolution of Cherenkov shower detector for, 25:18786
  detection of, response of NE-213 liquid scintillator for, 25:18655
  distribution in biological materials, analysis of bubble chamber tracks to determine, 25:18995
  effects of pulsed, on 2-propanol, effects of alkoxy radicals on, 25:18448(R) (CEA-N-1369)
  effects of pulsed, on alkaline solutions and neutral water, 25:18474
  effects of pulsed, on ammonia and carbon dioxide, absorption spectra of ions produced by, 25:18448(R) (CEA-N-1369)
  effects of pulsed, on aniline at 83 and 120°K, yields from, 25:18465
  effects of pulsed, on aqueous solutions of chlorofluoromethanes, effects of ethylene on halide yields from, 25:18460
  effects of pulsed, on aqueous solutions of nickel chlorides, nickel perchlorates, nickel sulfates, and uranyl perchlorates, hydrogen yields from, 25:18448(R) (CEA-N-1369)
  effects of pulsed, on aqueous solutions of potassium bromates or potassium iodates, spectra of radicals produced by, 25:18448(R) (CEA-N-1369)
  effects of pulsed, on aqueous solutions of thymine, 25:18475
  effects of pulsed, on p-bromophenol in ethanol solutions, hydrogen yields from, 25:18448(R) (CEA-N-1369)
  effects on Capron fibers, effects of surface modification and additives on, 25:18425
  effects on curing of resin-type coatings, 25:18439(P)
  effects on cyanorhodate ions in potassium chloride host lattice, 25:18462
  effects on hardening of polyester resins, 25:18443
  effects on iron at 2.5 MeV, positron interactions with vacancies induced in, (E/T), 25:19851
  effects on nematode larvae, effects of dose on attenuating, 25:19101
  effects on phosphorus-doped n-type silicon at 1 MeV, annealing of E centers induced in, (E/T), 25:19854
  effects on polymerization of frozen acrylonitrile, 25:18440
  effects on semiconducting diamonds, 25:19769(T) (LIB/Trans-307)
  effects on skin during high energy radiotherapy, 25:19066
  effects on strength of monocrystalline bcc iron, 25:19252 (COO-1367-36)
  effects on structure and properties of cis-butadiene rubber, 25:19300
  effects on survival of Photobacterium, effects of dose rate per pulse on, 25:19154
  electric charge of, constancy of, (T), 25:19883
  electromagnetic-wave scattering by bound, double scattering effects in, (T), 25:19949
  emission of exo-, during oxygen and water chemisorption on magnesium surfaces, 25:19758 (ORNL-4584, pp 74-86)

- emission spectra of graphite conduction band states, secondary, 25:19864
- interactions $e + e$ at high energies in quantum electrodynamics, eikonalization for, 25:19961
- interactions $e + N$, multiperipheral model for scaling property of structure functions for deep inelastic, (T), 25:19959
- interactions $e + p \to e + p$, effects of Veneziano-model form factors on ratios of cross sections for $e^{+} + p \to e^{+} + p$ interactions and, (T), 25:19942
- interactions $e + p$, O(3,1) analysis of currents and current commutators for singularities of Fourier transforms for inelastic, (T), 25:19934
- interactions $e + p$, super-eikonal model for structure function of deep inelastic, (T), 25:19939 (NYO-2262-TA-221)
- interactions $e + p$, Veneziano-like model for two-current amplitude of deep inelastic, (T), 25:19954
- interactions $e^{+} + e^{-} \to e^{+} + e^{-} + A^{+} + A^{-}$, lower order of perturbation theory for cross section relation of $\gamma + \gamma \to A^{+} + A^{-}$ interactions with, (T). 25:19938 (JINR-P2-5505)
- interactions $e^{+} + e^{-}$ at high energies, light-cone properties of axial-vector and electromagnetic current commutators for π and hadron production in, (T), 25:19941
- interactions $\gamma + e \to \gamma + e$, approximate description of attractive, (T), 25:19945
- interactions $\gamma + e \to \gamma + \gamma + e$, total cross sections for double Compton, (T), 25:19958
- interactions with nonquantum subsystem in nonsteady state, mass--momentum operator in Dirac equation for hidden momentum in, (T), 25:19953
- interactions with weak gravitational fields, covariant Green functions of, (T), 25:20094
- kinetics in strong crossed electric and magnetic fields, diffusion approximation for, (T), 25:19960
- magnetic moment of, computer program for anomalous, (T), 25:20055 (CNRS-CPT-70-P-335, pp IV.26-38)
- magnetic moment of, review of anomalous, (T), 25:19936 (CNRS-CPT-70-P-335, pp IV.1-15)
- production of hydrated, equipment for, 25:18854(P)
- radius of, divergenceless electromagnetic field for classical, (T), 25:19952
- reactions (e,γ) with tungsten at 0.662 and 2 MeV, gamma circular polarization from, (E), 25:20374 (NP-18597)
- reactions of relativistic, mean free path for plasmon excitation in, 25:19757 (ORNL-4584, pp 58-73)
- reactions with aluminum, beryllium, and magnesium films at 80 keV, radiative decay spectra from, (E), 25:19758 (ORNL-4584, pp 74-86)
- reactions with argon, helium, and neon, autoionizing states and negative-ion resonances from, 25:19490 (ORNL-4584, pp 92-104)
- reactions with boron trichloride, threshold excitation and slow-electron production in, 25:19490 (ORNL-4584, pp 92-104)
- reactions with deuterium hydrides at 1.0 to 13.6 eV, effective cross sections for rotational excitation in, (T), 25:19502
- reactions with hydrogen atoms, origin of wave functions for calculating cross sections for, 25:19494
- reactions with hydrogenic atoms and ions, analytical expressions for approximate cross sections for excitation, ionization, and recombination in, 25:19489 (NP-18680)
- reactions with molecules at thermal energies, attachment rates for, 25:19490 (ORNL-4584, pp 92-104)
- reactions with nonstationary dipolar systems, critical dipole moments for electron binding in, 25:19757 (ORNL-4584, pp 58-73)
- reactions with organic molecules, attachment rates and lifetimes of negative ions from, 25:19491 (ORNL-4584, pp 105-24)
- reactions with substituted benzenes, lifetimes and yields of negative ions from, 25:19490 (ORNL-4584, pp 92-104)
- reactions with sulfur hexafluoride, attachment rates for, (E), 25:19491 (ORNL-4584, pp 105-24)
- reactions with thin foils at 0.3 to 1.1 MeV, photon emission spectra from, 25:19471
- reactions with water vapor at 8 to 55 eV, detection and identification of triplet states excited by, (E), 25:19499
- scattering by atoms and molecules, generalized random phase approximation for calculation of inelastic, 25:19507
- scattering by carbon-12 at 200 MeV, form factors and spectra in giant resonance region from inelastic, (E/T), 25:20296
- scattering by cesium, potassium, and rubidium at 0.3 to 9 eV, absolute total cross sections for, (E), 25:19506
- scattering by helium at 0 to 60 eV, performance of energy-moderated high-resolution beta spectrometer for, 25:18762
- scattering by hydrogen atoms, lower bounds on phase shifts for elastic, 25:19757 (ORNL-4584, pp 58-73)
- scattering by layers of materials, device for studying back-, 25:18823
- scattering by nuclei above 250 MeV, effect of finite nuclear size on small-angle multiple, (T), 25:20545
- scattering by nuclei with nucleon emission, analysis for nuclear neutron and proton distributions by quasi-free, (T), 25:20544
- scattering by oxygen-16 at 50 to 200 MeV, cross sections for M0 transitions in inelastic, (T), 25:20294
- scattering by zinc-64 and -66 at 150 and 225 MeV, differential cross sections and form factors for elastic, (E), 25:20345
- slowing down in germanium and tungsten, 25:19759 (ORNL-4584, pp 87-91)
- spectra of extragalactic, (T), 25:19462
- stopping in hydrocarbon vapors, 25:19491 (ORNL-4584, pp 105-24)
- storage of relativistic, in solar corona, (E/T), 25:19403
- transmission through aluminum foils at 1 eV to 4 keV, (E), 25:19766

ELECTROPHORESIS
- radioactive material on moving bands in, scintillation detector for studying local concentration of, 25:18688(P)

ELECTROSTATIC ANALYZERS
- calibration and performance of 127° cylindrical, 25:18843
- design with ring focusing in field of cylindrical condenser, 25:18849
- performance as magnetometer using electron beam, 25:18865
- space-charge effects on use for plasma diagnostics, 25:19660

ELECTROSTATIC FIELDS
- theory for vacuum, nonexistence of spherically symmetric solution in, (T), 25:20088

ELECTROSTATIC GENERATORS
- description of 300-keV electron, for radiation curing of paints, 25:20213
- design of Marx, for REBA 3.2-MeV 43-kA electron accelerator, 25:20136 (SC-DR-70-872)
- ion sources for, beam injection system for terminal, 25:20204

ELECTROSTATIC LENSES
- aberration curves for asymmetrized quadrupole, 25:20151
- charged-particle trajectories in toroidal, third order approximation for fringing field effects on, 25:20139
- focusing parameters of three-electrode, calculation and verification of, 25:20152

ELEMENT 114
- binding energy of A = 298 isotope of, calculation using statistical theory, 25:20486

ELEMENTARY PARTICLE MODELS
- absorption, Regge cuts for scattering amplitudes in, 25:19992
- dual-sigma, N-point functions for mesons in chiral-symmetric, 25:19981
- eikonal, structure function of deep inelastic $e + p$ interactions in super-, 25:19939 (NYO-2262-TA-221)
- fireball, multiple particle production in strong interactions at very high energies in, 25:19971 (ANL-7727)
- Glauber, Regge cuts for amplitudes of deuteron interactions in, 25:19992
- multiperipheral, inclusion of interference terms in, 25:19998
- multiperipheral, scaling behavior in, 25:19982
- multiperipheral, scaling property of structure functions for deep inelastic $e + N$ interactions in, 25:19959
- one-pion exchange, forward structure in $K^{-} + p \to K^{*0}(890) + n$ interactions at 3.9 and 4.6 GeV/c in hydrogen bubble chamber for test of absorption-modified, (E/T), 25:19918
- one-pion-exchange, for $p + p \to p + \pi^{+}(\Delta^{++}) + \pi^{-} + p$ interactions at 19 GeV/c, 25:20020 (USIP-70-5)
- two-temperature, multiple particle production in strong interactions at very high energies in, 25:19971 (ANL-7727)
- vector gluon, divergence of axial-vector current in, 25:19984
- Veneziano, consistency with Yang--Mills coupling of vector meson fields for eta $\to \pi^{+} + \pi^{-} + \gamma$, $\omega \to 3\pi$, and $X^{0} \to \pi^{+} + \pi^{-} + \gamma$ decays, 25:19985 (DEMO-71/1)
- Veneziano, for pion--vector meson interactions, 25:19997
- Veneziano, group-theoretical construction of N-point, 25:20114
- Veneziano, method of uniterization with crossing symmetry for $\pi + \pi$ interactions at low energies in, 25:19993
- Veneziano, proton form factor effects on ratios of $e^{-} + p \to e^{-} + p$ and $e^{+} + p \to e^{+} + p$ interaction cross sections in, 25:19942
- Veneziano, two-current amplitude of deep inelastic $e + p$ interactions in, 25:19954

ELEMENTARY PARTICLE MODELS (BOOTSTRAP)
- meson (rho) and (f) mass and width in, Balazs method for, 25:19989
- symmetry algebra SU(n) for mesons in, 25:19999

ELEMENTARY PARTICLE MODELS (TRIPLET)
- currents for mirror asymmetry in $\Sigma \to \Lambda + e + \nu$ decay in, single-quark, 25:20535
- hadron mass spectra in quark, review of, 25:19979
- theory in terms of field vector interaction for quark, general formulation of relativistic, 25:19972 (IFPTH-10/70)
- theory of quark, review of, 25:19980
- weak-interaction Hamiltonian for divergences in quark,

XUM

25:20039
ELEMENTARY PARTICLES
  couplings of, relation of stress-tensor to s-channel helicity-conserving, 25:19931
  gravitation for, short-ranged scalar gravity in Einstein theory of, (T), 25:20093
  helicity formalism for, lectures on, 25:19925 (NP-18703)
  interactions at high energies, helicity poles and triple Regge behavior in single-particle production spectrum from, (T), 25:19926 (NYO-2262-TA-234)
  interactions of massive, at infinite momentum, helicity transformation for, (T), 25:19924 (JINR-E2-5579)
  interactions of, role and perspectives of cosmic ray research for study of, (E), 25:19885
  lectures on, (T), 25:19933
  Lie algebras for, realization through rational functions of canonical variables for, 25:19935
  mass of unstable system with N states in, matrix for, (T), 25:19930
  mass spectra of, moments from classical dynamics for, (T), 25:19928
  motion in fixed-centers field, system of algebraic and integral equations for, (T), 25:20059 (JINR-P4-5547)
  propagator for unstable system with N states in, matrix for, (t), 25:19930
  strong interactions at very high energies, two-temperature and fireball models for multiple particle production in, (T), 25:19971 (ANL-7727)
  strong interactions of, lectures on absorption corrections and cuts in Regge pole model for, (T), 25:19976
  strong interactions of, lectures on duality for, (T), 25:19978
  strong interactions of, lectures on Regge phenomenology for, (T), 25:19977
  strong interactions of, model for S-state scattering lengths of exotic, (T), 25:19975
  strong interactions of, review of complex angular momentum in Regge pole theory of, (T), 25:19974
  weak interactions of, Hamiltonian for intermediate-vector boson mass and quark model for divergences in, (T), 25:20039
  weak interactions of, review of current--current theory of, (T), 25:19964 (KFKI-70-24-HEP)
  weak interactions of, structure effects in, (T), 25:19968
  weak interactions of, Yang--Mills model of, 25:19969
ELEMENTARY PARTICLES (TRIPLET)
  production of quarks in nucleon reactions with nuclei at high energies, very high-momentum nuclear components for cross section upper limits for far subthreshold, (T), 25:20026
  search for quarks in air showers using cloud chamber, (E), 25:19884
ELEMENTS
  determination by photoelectron spectroscopy, 25:18338 (CEA-CONF-1725)
EMBRYOS
  radiation dosimetry in, development of mathematical models for, 25:18990 (ORNL-4584, pp 129-51)
  radiation effects on growth and incidence of malformations of rat, effects of exposure rate and protracted dose on x, 25:19117
EPOXY RESINS
  Ag--epoxy resins, radiation effects on bonding in, γ, 25:18421(R) (RLO-2098-1)
  Al--epoxy resins, radiation effects on bonding in, γ, 25:18421(R) (RLO-2098-1)
  Cu--epoxy resins, radiation effects on bonding in, γ, 25:18421(R) (RLO-2098-1)
ERBIUM
  chromatographic behavior in hydrochloric acid--thiocyanate mixture on Amberlite LA-2, 25:18337
  crystal structure at 77 to 300°K, expansion in, (E/T), 25:19243
  electron band structure of, x-ray photoelectron study of 4f levels in, 25:19866
ERBIUM ALLOYS AND SYSTEMS
  Er--Re--Th, crystal structure of intermetallic compounds of, 25:19235
ERBIUM IONS
  implantation in zinc sulfide and selenide films at 250 kV, cathodoluminescence effects of, 25:19795
  wave functions for, accurate numerical Hartree--Fock self-consistent field, 25:19478
ERBIUM ISOTOPES Er-164
  energy levels of, calculation using microscopic collective model, (T), 25:20547
ERBIUM ISOTOPES Er-166
  alpha inelastic scattering at 27.5 to 32.5 MeV, cross sections for, (E), 25:20466
  nuclear mass distribution of, hexadecapole term in deformation parameter for, (E/T), 25:20466
ERBIUM ISOTOPES Er-167
  energy levels from electro- and photoexcitation, transition multipolarities for, (E), 25:20463
  half-life of isomeric, 25:20463
  neutron inelastic scattering at 14.5 MeV, cross sections and gamma spectra from, (E), 25:20435
ERBIUM ISOTOPES Er-168
  neutron reactions (n,2n) at 14.5 MeV, cross sections and gamma spectra from, (E), 25:20435
ERYTHROCYTES
  effects of sheep, on radiation effects on immune reactions in mice, 25:18925
  labeling with metastable indium-113 for spleen scintigraphy, methods for, 25:19036
  phosphorus-32 permeability of calf, effects of antibody content of serum on, 25:18900
  radiation effects on content of potassium and sodium in, of rabbits, x, 25:19107
  radioinduced hemolysis of, effects of photosensitizing compounds on uv, 25:18914
  radioinduced hemolysis of, effects of salicylanilide on uv, 25:18913
ERYTHROPOIESIS
  radiation effects on recovery of, in endocolonized mouse spleen, 25:19125
ERYTHROSINE B
  evaluation of iodine-131-labeled, for scanning canine pancreas, 25:19060
ESTERS
  polymers, radiation hardening of, 25:18443
  glass textiles--polyesters, radiation effects on mechanical properties of, γ, 25:18421(R) (RLO-2098-1)
ETHANE, IODO-
  radiation effects on glasses of deuterated and normal, at 77°K, kinetics of decay of ethyl radicals produced by γ, 25:18461
  radiation effects on polycrystals of deuterium- and/or iodine-129-labeled, ESR studies on spectra produced by, 25:18424
ETHANOL
  radiolysis of aqueous perchloric acid solutions of, rate constants for reactions of hydrogen atoms produced by γ, 25:18459
  ethanol--N_2O, radiolysis of solutions of, precursors of free radicals and hydrogen in, 25:18448(R) (CEA-N-1369)
ETHENESULFONIC ACID
  sodium salt, radioinduced polymerization in porous ceramics and firebrick, ion exchange properties of products from γ, 25:18421(R) (RLO-2098-1)
ETHER, METHYL VINYL
  radiation effects on glasses of 3-methylhexane or tetrahydro-2-methylfuran containing, at 77°K, ESR studies on dissociative electron capture in γ, 25:18456
ETHYLENE
  effects on halide yields from electron pulse and γ radiolysis of aqueous solutions of chlorofluoromethanes, 25:18460
  effects on radioinduced grafting of ethylene terephthalate polymers in aqueous solutions of acrylamide or methacrylamide, 25:18429
  oxygen-ion reactions at 0 to 2 eV with deuterated and normal, rates of, 25:19490 (ORNL-4584, pp 92-104)
  performance as carrier gas for electron attachment studies, 25:19491 (ORNL-4584, pp 105-24)
  radiolysis of gaseous, effects of ammonia on ion reactions in γ, 25:18452
  ethylene--N, radiolysis of, reaction mechanisms of γ, 25:18455
ETHYLENE, CHLORO-, POLYMERS
  radioinduced thermally stimulated currents in, γ, 25:18422
  2-(hydroxylmethyl)-1,3-propanediol trimethacrylate--polychloroethylene, radiation effects on curing of, 25:18437(P)
  polychloroethylene--triallyl-s-triazine-2,4,6-(1H,3H,5H)-trione, radiation effects on curing of, 25:18437(P)
ETHYLENE, NITRO-
  ionization of, mass-spectrometric studies on, 25:18428 (NP-18676)
  radioinduced polymerization of, mass-spectrometric studies on initiating species in, 25:18428 (NP-18676)
ETHYLENE POLYMERS
  aluminum recoil-atom implantation in substrates of, by argon-ion bombardment of films, 25:19786
  laser-beam reactions with foils of, plasma production in, 25:19701
  neutron attenuation in borated, fast, 25:19007 (NCRP-38)
  plasma of, expansion of laser-produced, (E), 25:19703
  radiation effects on reactions of containers of, with water, γ, 25:19164
  radioinduced thermally stimulated currents in, γ, 25:18422
  radioinduced thermoluminescence of, relation of α-relaxation to γ, 25:18435
  Al_2O_3--polyethylene, radiation effects on electrical and mechanical properties of, γ, 25:18421(R) (RLO-2098-1)
  carbon black--polyethylene, radiation effects on electrical and mechanical properties of, γ, 25:18421(R) (RLO-2098-1)
  glass textiles--polyethylene, radiation effects on mechanical properties of, γ, 25:18421(R) (RLO-2098-1)
ETHYLENE, TETRAFLUORO-, POLYMERS
  development of asbestos-treated filters of, for collecting sodium aerosols, 25:18563 (CONF-700816-(Vol.1), pp 445-58)
  radioinduced thermally stimulated currents in, γ, 25:18422

- ETHYLENIMINE
  - effects on chromosome aberrations and mutations in Crepis capillaris seeds exposed to space flight, 25:18953
- EUMYCOTA
  - Dictyostelium discoideum, development of, genetic study of, 25:20904(R) (UCSD-34-P-166-X-2)
  - Penicillium digitatum, radiation effects on survival of spores of, inoculated in oranges, combined effects of biphenyl, heat, and cobalt-60 γ, 25:19162
  - Saccharomyces cerevisiae, radioinduced mutations in, isolation of recombination deficient uv and x, 25:18945 (UCRL-20192)
  - Saccharomyces cerivisiae, radiation effects on survival of, uv dosimetry using, 25:18981 (CEA-N-1380)
  - yeasts, radiosensitivity of, effects of aminopterin on, 25:19155
- EUROPE
  - radioactive waste management in western, development of methods for, 25:18625 (SGAE-RT-35/1970)
- EUROPIUM
  - abundance in meteorites, (E), 25:19302
  - complexes with chloride, nitrate, and thiocyanate, stability constants for, effects of ionic media on, 25:18371
  - determination in high-burnup plutonium dioxide fuel by isotope dilution mass spectrometry, 25:18356 (KR-140)
- EUROPIUM ALLOYS AND SYSTEMS
  - Eu--EuF_3--Eu_2O_3, phase studies at 1500°C, 25:19285
- EUROPIUM FLUORIDES
  - Eu--EuF_3--Eu_2O_3, phase studies at 1500°C, 25:19285
- EUROPIUM IONS
  - wave functions for, accurate numerical Hartree--Fock self-consistent field, 25:19478
- EUROPIUM ISOTOPES Eu-146
  - beta and electron-capture decay of, (E), 25:20474
- EUROPIUM ISOTOPES Eu-151
  - energy levels from gadolinium-151 decay, model analysis of, (E/T), 25:20352
  - energy levels of, inelastic deuteron scattering study of one-phonon octupole vibration in collective, (E), 25:20432
- EUROPIUM ISOTOPES Eu-152
  - decay of, relative γ-ray intensities from, 25:20425
- EUROPIUM ISOTOPES Eu-153
  - energy levels of proton states from samarium-152 (α,t) reactions, (E/T), 25:20383
  - energy-level transitions in, internal conversion ratios for M1 + E2, (E), 25:20473
- EUROPIUM ISOTOPES Eu-154
  - beta decay of, γ spectra from, (E), 25:20441
  - beta decay of, γ--γ and γ--e^- directional correlations in, (E), 25:20374 (NP-18597)
- EUROPIUM ISOTOPES Eu-155
  - energy levels of proton states from samarium-154 (α,t) reactions, (E/T), 25:20383
- EUROPIUM ISOTOPES Eu-156
  - beta decay of, conversion electron spectra from, 25:20421
  - half-life, (E), 25:20338
  - half-life, (E), 25:20339
- EUROPIUM OXIDES
  - Eu--EuF_3--Eu_2O_3, phase studies at 1500°C, 25:19285
- EUROPIUM TELLURATES
  - $Eu_2(TeO_3)_3$--$Eu_2(TeO_4)_3$, analysis for hexavalent tellurium and total tellurium by automatic amperometric and potentiometric titration, 25:18351
- EUROPIUM TELLURITES
  - $Eu_2(TeO_3)_3$--$Eu_2(TeO_4)_3$, analysis for hexavalent tellurium and total tellurium by automatic amperometric and potentiometric titration, 25:18351
- EXPERIMENTAL BREEDER REACTOR-II
  - containment building for, revised leakrate testing criteria for, 25:20755 (ANL-EBR-8)
  - dynamic characteristics of, effects of oxide fuel loading on, (T), 25:20704 (ANL-7673)
  - neutron spectra in, distribution of fast, (E/T), 25:20803
- EXPONENTIAL PILES
  - kinetics of UFSA, studies of space-time, (E/T), 25:20794
  - neutron pulse propagation in Cornell University ZPR, (E/T), 25:20804
- EYES
  - radiation effects on composition of lens proteins in, x, 25:18909
  - radioinduced lesions in retinas of rabbit, mechanisms of, light evoked electric responses in ruby laser, 25:19132
  - radiosensitivity of human, laser, 25:19133 (NP-18714)

F

- FALLOUT
  - effects on Japanese fishermen 14 years after exposure from Bikini nuclear tests, long-term, 25:19148
  - monitoring of, mathematical models for computer programs for Weapons Effects Display System for, 25:18831 (UCRL-50892(Vol.1))
- FAST FLUX TEST FACILITY
  - core vessel for, design requirements and stress limits for, 25:20725 (WHAN-SA-46)
  - design parameters of, 25:20692 (CONF-700816-(Vol.1), pp 289-316)
  - development schedule for, 25:20692 (CONF-700816-(Vol.1), pp 289-316)
  - nuclear materials control at, computerized real-time method for, 25:18620 (BNWL-1440)
  - piping systems for, design requirements and stress limits for, 25:20725 (WHAN-SA-46)
  - ventilation systems for, design parameters of, 25:20783 (CONF-700816-(Vol.1), pp 317-45)
- FAST TEST REACTOR
  - core vessel for, design requirements and stress limits for, 25:20725 (WHAN-SA-46)
  - piping system for, stored heat and thermal transients in liquid sodium, (T), 25:20790 (WHAN-FR-22)
  - piping systems for, design requirements and stress limits for, 25:20725 (WHAN-SA-46)
  - ventilation systems for, design parameters of, 25:20783 (CONF-700816-(Vol.1), pp 317-45)
- FECES
  - radioisotope content of rat, comparison of direct and treated-sample determinations of, 25:18997
- FERMI FAST BREEDER REACTOR
  - buildings for, revised technical specifications for processing irradiated Core A fuel subassemblies in fuel and repair, 25:20603 (DOCKET-50016-101)
  - core holddown mechanism for, temporarily revised technical specifications for position of, 25:20604 (DOCKET-50016-102)
  - operations history for September 1970, 25:20577 (DOCKET-50016-100)
  - piping for, revised technical specifications for secondary containment requirements of primary liquid sodium service, 25:20602 (DOCKET-50016-99)
- FERMI POWER REACTOR, UNIT 2
  - design parameters of, requested additional information on, 25:20673 (DOCKET-50341-27)
  - operations aspects of, requested additional information on, 25:20673 (DOCKET-50341-27)
- FERMIONS
  - decay of decuplet $3/2^+$, broken SU(6)/sub W/ symmetry for correlations among amplitudes of octet $1/2^+$ baryon and octet 0^- meson production from, (T), 25:20048
  - energy of attractive many-body system of, ground-state, (T), 25:20502
  - production of octet $1/2^+$, from decay of decuplet $3/2^+$ baryons, broken SU(6)/sub W/ for, (T), 25:20048
  - structures of conserved, in general relativity theory, (T), 25:20089
  - theory for para-, first- and second-quantized statistical, 25:20080
- FERMIUM ISOTOPES Fm-258
  - fission of, half-life for spontaneous, (E), 25:20443
- FERRICYANIDES
  - determination by biamperometric titration with mercury perchlorate, 25:18346
- FIELD EMISSION MICROSCOPES
  - use in combination with electron microscopes in tungsten grain boundary studies, 25:19249
- FIELD THEORY
  - Einstein unified, nonexistence of spherically symmetric solution for vacuum electrostatic field in, 25:20088
- FILTERS
  - cleaning of, method for vacuum, 25:18572(P)
  - design and testing of HEPA, for ventilation systems in radioactive and toxic process buildings, 25:18559 (CONF-700816-(Vol.1), pp 128-42)
  - development of asbestos-treated Teflon, for collecting sodium aerosols, 25:18563 (CONF-700816-(Vol.1), pp 445-58)
  - efficiency of zeolite pre-, for removal of cesium-137 from radioactive wastes, 25:18621 (DP-1245)
  - performance of water cooled reactor containment system, during coolant loss accident conditions, 25:20782 (CONF-700816-(Vol.1), pp 102-27)
- FINLAND
  - cesium-137 content of reindeer herders in, effects on whole-body γ dose, 25:18987 (NYO-3446-14, Paper 29)
  - fallout content of food chains and man in, 25:18931 (NYO-3446-14, Paper 30)
  - lead-210 activity in ground-level atmosphere in, effects of geographical location, meteorological conditions, and season on, 25:18933 (NYO-3446-14, Paper 32)
  - power production in, forecast of 1970 to 2000, 25:20553
  - radiation dose to man in, from natural and artificial gamma sources, 25:18986 (NYO-3446-14, Paper 28)
  - radioisotope accumulation in aquatic ecosystems of, 25:18930 (NYO-3446-14, Paper 27)
  - radioisotope content of plants and reindeer meat during 1966 to 1970, 25:18932 (NYO-3446-14, Paper 31)
  - radioisotope content of terrestrial birds and mammals of, 25:18929 (NYO-3446-14, Paper 26)
  - radioisotope transport through food chains in, 25:18928(R) (NYO-3446-14)
- FIRES
  - aerosols from sodium, behavior of atmospheric, 25:19167 (AERE-R-6460)
- FISSION
  - barrier in spontaneous, effect of hexadecapole term on penetration of two-dimensional, (T), 25:20478 (INR-P-1230)
  - molecular model of, (T), 25:20489

- neutron spectra from, review of delayed and prompt, 25:20362 (ANL-7747)

FISSION FRAGMENTS
- angular anisotropy of, effect of fissionability on, (T), 25:20529
- angular distributions from neutron fission of uranium-238 at 1.20 to 2.66 MeV, (T), 25:20393
- buildup in reactors, semiconductor detector for selectively monitoring, 25:18651(P)
- detection of uranium-235, using cellulose nitrate track detectors, 25:18724
- detection of, coincidence circuit for, 25:18670
- detection of, spark chamber for, 25:18671
- energy of mean light and heavy, after slow-down in aluminum, carbon, copper, Formvar, gold, and silver, (E), 25:20442
- stopping of californium-252, in carbon, gold, and silver as function of ion nuclear charge, (E), 25:19765

FISSION PRODUCTS
- beta decay of, time-dependent heat energy release from, (T), 25:20834 (JAERI-Memo-4205)
- deposition in reactor cooling systems, (T), 25:20730
- diffusion from ceramic fuels, effects of neutron irradiation and temperature on, 25:19287 (AECL-3690)
- diffusion in gas cooled reactor fuel elements, (E), 25:20747(R) (NP-18668)
- distribution in reactor cooling systems, (T), 25:20730
- distribution in uranium dioxide rods, effects of temperature gradients on, 25:19278
- fixation in soils in France, review of factors influencing, 25:18528
- gamma decay of, time-dependent heat energy release from, (T), 25:20834 (JAERI-Memo-4205)
- isomers in uranium-235--thermal neutron primary, microsecond, 25:20430
- properties of encapsulated, for use as process radiation sources, 25:18590(R) (BNWL-1308-4)
- release from liquid metal cooled fast breeder reactor during accident conditions, (E/T), 25:20757 (CONF-700816-(Vol.1), pp 26-48)
- release from pressurized water reactors during coolant loss accidents, 25:20756 (CONF-700816-(Vol.1), pp 9-25)
- removal from sodium coolant, effects of carbon on cesium, (E), 25:20754 (AERE-R-6481)
- separation of americium from, by precipitation, 25:18507(P)

FISSIONABLE MATERIAL
- deposition of composites containing, to form fuel elements, method for electro-, 25:19269(P)
- fabrication of fuel elements of, incorporating fertile materials, design of equipment for, 25:19268(P)

FLOWMETERS
- development of electromagnetic, for liquid sodium, 25:18876

FLUID FLOW
- magnetohydrodynamic free jet, in transverse magnetic field, (T), 25:19567
- magnetohydrodynamic laminar viscous, between parallel walls in moving magnetic field, 25:19561
- magnetohydrodynamic one-dimensional, 25:19552
- magnetohydrodynamic peripheral, in transverse magnetic field, (T), 25:19559
- magnetohydrodynamic two-dimensional anisotropic conducting incompressible, in axially symmetric channels, (T), 25:19555
- magnetohydrodynamic viscous, Hall effect on motion past flat plate of, (T), 25:19569
- magnetohydrodynamic, between two rotating coaxial disks, (T), 25:19568
- magnetohydrodynamic, circulation of axially symmetric turbulent jet in, (T), 25:19558
- magnetohydrodynamic, effect of plate temperature oscillations on thermal boundary layer on semi-infinite flat plate in, (T), 25:19564
- magnetohydrodynamic, empirical determination of coefficient of hydraulic flow resistance in traveling magnetic field, (T), 25:19557
- magnetohydrodynamic, energy pulse distribution in axially symmetric turbulent jet in, (T), 25:19560
- magnetohydrodynamic, equilibrium of variable density flows with Hall current, (T), 25:19545
- magnetohydrodynamic, magnetic field compression by cylindrical conducting envelopes in, (T), 25:19549
- magnetohydrodynamic, near nonconducting sphere in crossed electric and magnetic fields, (T), 25:19550
- magnetohydrodynamic, past semi-infinite flat plate with transverse magnetic field, (T), 25:19570
- magnetohydrodynamic, transport coefficients of inhomogeneous systems in, (T), 25:19562
- magnetohydrodynamic, turbulence suppression in tubes by transverse magnetic fields, (E/T), 25:19556
- magnetohydrodynamic, wave propagation in, 25:19566

FLUIDIZED BEDS
- development for use in carbon coating of particulate thorium dioxide and uranium dioxide, 25:19262 (ORNL-4629, pp 65-82)
- development for use in sol-gel process, 25:19261 (ORNL-4629, pp 14-64)

FLUORIDES
- determination in natural waters from uranium mining operations, method for, 25:18339 (CEA-R-3557(2))
- hydrolysis of, catalytic effects of metal ions on, 25:18375
- yields from electron pulse and γ radiolysis of aqueous solutions of chlorofluoromethanes, effects of ethylene on, 25:18460

FLUORINE
- meson (K^-) reactions at 10 GeV/c in bubble chamber, $K^-\pi^+\pi^-$ system coherent production and total cross sections for $K^-\pi^+\pi^- + N$ interactions in, (E), 25:19910 (LAL-1242)

FLUORINE ISOTOPES F-17
- energy levels from oxygen-16 (d,n) reactions, spectroscopic factors for, (E/T), 25:20301

FLUORINE ISOTOPES F-18
- energy levels of, calculation using strong-coupling rotational model, (T), 25:20353
- energy levels of, shell-model calculations using Hartree--Fock basis, (T), 25:20286

FLUORINE ISOTOPES F-19
- alpha reactions $(\alpha,n\gamma)$ with, γ-ray polarization in, (E), 25:20318
- helium-3 reactions (He-3,Li-6) at 28 MeV, angular distributions for, (E), 25:20284

FLUOROCARBONS
- performance as stripper gas for heavy-ion tandem accelerator, 25:20155

FLUPENTHIXOL
- radioprotective effects of, on mice, whole-body cobalt-60 γ, 25:19028

FOOD
- contamination by gaseous effluents from nuclear powerplants, PATHWAY computer program for evaluating, 25:18526 (ORNL-4584, pp 37-40)
- effects of radiation processed, on fecundity of mealy bugs and Indian meal moths, 25:19159
- radioisotope content of, in Pavia, Italy from 1964 to 1966, cesium-137 and strontium-90, 25:18942

FOOD CHAINS
- iodine-131 transport through plant--cow--milk--man, following release during nuclear explosions, 25:18926 (CONF-700816-(Vol.1), pp 49-71)
- radioisotope accumulation in aquatic, in Finland, 25:18930 (NYO-3446-14, Paper 27)
- radioisotope content of, in Finland, 25:18931 (NYO-3446-14, Paper 30)
- radioisotope transport through soil--plant--man in Brazil, 25:18927 (NP-18670)
- radioisotope transport through soil-vegetation-wild animal, in Southeast USA, 25:18935(R) (ORO-3905)
- radioisotope transport through, in Finland, 25:18928(R) (NYO-3446-14)

FORKED RIVER POWER REACTOR, UNIT 1
- design parameters of, revised and additional data on, 25:20678 (DOCKET-50363-12)
- operations aspects of, revised and additional data on, 25:20678 (DOCKET-50363-12)

FORT CALHOUN POWER REACTOR, UNIT 1
- design parameters of, revised and additional data on, 25:20650 (DOCKET-50285-42)
- operations aspects of, revised and additional data on, 25:20650 (DOCKET-50285-42)

FORT ST. VRAIN POWER REACTOR, UNIT 1
- design parameters of, revised and additional data on, 25:20643 (DOCKET-50267-27)
- emergency core cooling system for, additional design requirements and modifications for, 25:20642 (DOCKET-50267-26)
- operations aspects of, revised and additional data on, 25:20643 (DOCKET-50267-27)
- pressure vessel for, design parameters and fabrication of prestressed concrete, 25:20557
- site for, environmental radiation survey during July to September 1970, 25:20643 (DOCKET-50267-27)

FREE RADICALS
- annealing in irradiated organic crystals, processes in, 25:18473
- radioinduced production in lyophilized proteins, comparison to electric discharge induced, γ, 25:18906

FRUITS
- dates, radiation processing for eradication of insects infesting stored, effectiveness of γ, 25:19158(R) (NP-18679)
- dates, radiation processing of, effectiveness of γ, 25:19158(R) (NP-18679)
- oranges, radiation processing of, combined effects of biphenyl, heat, and cobalt-60 γ, 25:19162

FUEL CAPSULES
- safety of heat source, isotopes kilowatt program for evaluation of, 25:18594(R) (ORNL-TM-3292)

2-FURALDEHYDE
- radioinduced polymerization of, effects of alkyl halides on, 25:18430

FURAN, TETRAHYDRO-2-METHYL-
- radiation effects on glasses of, containing diethyl maleate, dimethyl maleate, or maleic acid at 77°K, photoisomerization of maleate radicals produced by γ, 25:18457
- radiation effects on glasses of, containing methyl vinyl ether at 77°K, ESR studies on dissociative electron capture in γ, 25:18456

  - N_2O--tetrahydro-2-methylfuran, radiolysis of solutions of, precursors of free radicals and hydrogen in, 25:18448(R) (CEA-N-1369)
- FURNACES
  - design of accelerator target, 25:20212

G

- GADOLINIUM
  - compatibility with refractory metal and superalloy capsule materials at high temperatures, 25:18592 (ORNL-4298)
  - elastic moduli of, effects of magnetic field on temperature-dependent, (E/T), 25:19224
- GADOLINIUM ALLOYS AND SYSTEMS
  - Fe--Gd, magnetic susceptibility of $GdFe_2$, 25:19871
- GADOLINIUM BROMIDES
  - sublimation and vaporization of, thermodynamics of, 25:18417
  - vapor pressure of, 25:18417
- GADOLINIUM IONS
  - wave functions for, accurate numerical Hartree--Fock self-consistent field, 25:19478
- GADOLINIUM ISOTOPES Gd-151
  - electron-capture decay of, γ singles and coincidence spectra from, (E), 25:20352
- GADOLINIUM ISOTOPES Gd-152
  - energy-level transitions in, direction correlations and multipolarities for, (E), 25:20385
- GADOLINIUM ISOTOPES Gd-154
  - energy levels from europium-152 decay, transition probabilities and band mixing parameters for, (E), 25:20441
- GADOLINIUM ISOTOPES Gd-156
  - energy-level transitions from terbium-156 decay, K-conversion coefficients for, (E), 25:20472
- GADOLINIUM TELLURATES
  - $Gd_2(TeO_3)_3$--$Gd_2(TeO_4)_3$, analysis for hexavalent tellurium and total tellurium by automatic amperometric and potentiometric titrations, 25:18351
- GADOLINIUM TELLURITES
  - $Gd_2(TeO_3)_3$--$Gd_2(TeO_4)_3$, analysis for hexavalent tellurium and total tellurium by automatic amperometric and potentiometric titrations, 25:18351
- GAGES AND METERS
  - description of neutron radiometric, for measuring calorific value of petroleum flowing in pipeline, 25:18817(P)
- GALAXIES
  - hydrogen distribution in NGC 4254, (E), 25:19456
  - hydrogen-line profiles of model, 21-cm, (T), 25:19444
  - mass of nuclei of redshifted, (E/T), 25:19364
  - mass--luminosity relation for spiral, (T), 25:19441
  - parameters of, as consequence of cosmological turbulence, (T), 25:19443
  - photometry of NGC 4254, multicolor, (E), 25:19456
  - shock waves in spiral arms of Sc, (E/T), 25:19445
  - stellar content of M82, (E), 25:19454
  - x-ray emission from M87, variability of, (E), 25:19458
- GALLIUM
  - abundance in α And, (E), 25:19343
  - chromatographic behavior in hydrochloric acid--thiocyanate mixture on Amberlite LA-2, 25:18337
  - effects on diffusion of plutonium in copper--plutonium and plutonium--uranium alloys at 500°C, 25:19230 (CEA-R-3951)
  - separation from indium by solvent extraction, review on, 25:18510
  - superconducting tunneling into bulk single crystals of, (E), 25:19615
- GALLIUM ALLOYS AND SYSTEMS
  - Cu--Ga--Pu, phase studies of, 25:19230 (CEA-R-3951)
  - Ga--In, transformation into pulverulent state, mechanisms for, 25:19190(T) (AI-Trans-287)
- GALLIUM ARSENIDES
  - ion implantation in chromium-doped and pure, electric profiles of implanted layers after annealing, 25:19843
  - ion implantation in, annealing effects on electric properties of implanted layers, 25:19842
  - ion implantation in, review, 25:19789
  - tellurium-ion implantation in, annealing of lattice disorder induced by, 25:19844
- GALLIUM IONS
  - implantation in silicon carbide at 5 to 300 keV, properties of conducting layers and p--n junctions formed by, (E), 25:19847
  - implantation layers in silicon at 50 keV, temperature coefficient of sheet resistivity of, 25:19783
  - implantations in silicon at 50 keV, proton bombardment and Hall-effect study of, 25:19802
- GALLIUM ISOTOPES Ga-66
  - energy levels from germanium-66 decay, model analysis of, (E/T), 25:20324
- GALLIUM ISOTOPES Ga-67
  - radiation dosimetry for intravenously administered citrate-incorporated, in rats, 25:18992
- GALLIUM ISOTOPES Ga-68
  - purification of generator-produced, by ion exchange separation from EDTA eluate, 25:18482
  - uses in medicine, 25:18482
- GALLIUM ISOTOPES Ga-69
  - energy levels from gamma resonance scattering, widths for, (E), 25:20355
- GALLIUM ISOTOPES Ga-74
  - beta decay of, beta and gamma spectra, half-life, and log ft of, (E), 25:20343
- GALLIUM PHOSPHIDES
  - bismuth-ion implantation at 100 and 200 keV in, channeling study of damage induced by, 25:19846
  - bismuth-ion implantation at 200 keV in, photoluminescence of implanted ions, (E), 25:19845
  - ion implantation in, review, 25:19789
  - tellurium-ion implantation in, annealing of lattice disorder induced by, 25:19844
- GAMMA CAMERAS
  - design and performance of position-sensitive lithium-drifted germanium, for radiodiagnosis, 25:18699
  - performance for dynamic studies of kidneys using combined iodine-131 and technetium-99m, 25:19046
  - performance for localization of human placentas following administration of technetium-99m, 25:19045
- GAMMA RADIATION
  - detection at 122 keV to 9.17 MeV, absolute efficiency of lithium-drifted germanium detector for, 25:18702
  - detection of low-energy, semi-empirical efficiency curve for lithium-drifted germanium detectors for, 25:18725
  - detection of pulsed, from Crab Nebula, (E), 25:19361
  - detection of, calculations of efficiencies of coaxial lithium-drifted germanium detectors for, 25:18755
  - detection of, design of split-anode proportional counter for, 25:18698(P)
  - detection of, elimination of correlation effects in, 25:18669
  - detection of, position-sensitive scintillation detector for, 25:18686(P)
  - dose distribution in tissues from implanted californium-252 point source, (T), 25:19003
  - dose to human population on Kerala coast, India from food, daily, 25:19143
  - dose to man in Finland from natural and artificial sources, 25:18986 (NYO-3446-14, Paper 28)
  - dose to organs of rats after gallium-67 citrate injection, 25:18992
  - dosimetry for rotational therapy, criteria for planning, 25:19067
  - dosimetry for therapy of neoplasms of human larynx and pharynx, 25:18998
  - dosimetry in radon therapy, correction factor for, 25:19002
  - dosimetry in therapy using applicators, use of computer calculations for, 25:19004
  - dosimetry of, development of thermoluminescent dosimeters capable of repetitive analysis for, 25:18807(P)
  - dosimetry of, properties of Korean natural quartz thermoluminescent dosimeters for, 25:18813
  - dosimetry of, silicon detector for absolute, 25:18806
  - dosimetry using Polaroid film, evaluation and survey of, 25:19005
  - effectiveness for therapy of carcinomas of human mouth, effects of dose on, 25:19081
  - effectiveness for therapy of carcinomas of human tonsils, 25:19085
  - effectiveness for therapy of neoplasms of human larynx and pharynx, comparison of, with surgery, 25:18998
  - effectiveness for therapy of neoplasms of human mouth and tongue, 25:19080
  - effects on 2,2,4-trimethylpentane, effects of oxygen and temperature on products from, 25:18471
  - effects on activity and chemical composition of lysozyme in aqueous solutions, 25:18917
  - effects on activity of dehydrogenases and content of pyruvic acid in cell mitochondria and nuclei of cotton plants, 25:18918
  - effects on adult life span and egg production of cotton leaf worm exposed as pupae, 25:19097
  - effects on aniline at 77°K, yields from, 25:18465
  - effects on aniline, effects of additives on yields from, 25:18450(R) (ORO-3519-8)
  - effects on aqueous solutions of chlorofluoromethanes, effects of ethylene on halide yields from, 25:18460
  - effects on aqueous solutions of sodium nitrate, 25:18463
  - effects on arbovirus activity in mouse tissues for preparation of noninfectious antigens, 25:18924
  - effects on benzene, bromobenzene, Crystal Violet, and their mixtures, 25:18451
  - effects on bonding of epoxy resins to metals, 25:18421(R) (RLO-2098-1)
  - effects on bone marrow cells in mice, correlation of lethality and recovery with fractionated, 25:19108
  - effects on catalyst used for conversion of aromatic hydrocarbons, 25:18444
  - effects on chlorophyll and seeds of beans, effects of dose on frequency and spectrum of mutagenic, 25:18946
  - effects on chromatin template activity for RNA synthesis, 25:18916
  - effects on chromosomes and mitosis in roots of cotton and combined effects with dimethyl sulfate, 25:18954
  - effects on chromosomes of Nigella damascena seeds, effects of chelating agents on repair processes following aberrant cobalt-60, 25:18951
  - effects on chromosomes of Vicia faba, aberrant chronic cobalt-60, 25:18950

XUM

effects on corpus allatum size in female Dacus cucumis, whole-body cobalt-60, 25:19096
effects on cytology of embryonic tissues of cotton following exposure of pollen, 25:18955
effects on Datura tatula, mutagenic, 25:19151
effects on dielectric constant of ferroelectric ammonium sulfate single crystals, 25:19856
effects on diethyl maleate, dimethyl maleate, or maleic acid in glasses of tetrahydro-2-methylfuran at 77°K, photoisomerization of maleate radicals produced by, 25:18457
effects on dysprosium-doped calcium fluoride crystals, total antiresonance induced by heat treatment in, 25:19771
effects on electrical and mechanical properties of carbon black and polyethylene or polystyrene systems and aluminum oxide and polyethylene systems, 25:18421(R) (RLO-2098-1)
effects on ethylene--nitrogen systems, reaction mechanisms of, 25:18455
effects on fertility of transplanted ovaries in female Dacus cucumis, cobalt-60, 25:19096
effects on food of mealy bugs and Indian meal moths as reflected in fecundity, 25:19159
effects on gaseous ethylene, effects of ammonia on ion reactions in, 25:18452
effects on germination, nutritive elements, storage life, and water content of potatoes, effects of dose on, 25:19160
effects on glycine, structure and stability of radicals from, 25:18478
effects on grafting of styrene to cellulose at low dose rates, 25:18446
effects on hardening of polyester resins, 25:18443
effects on hematopoiesis and survival of mice, effects of transplants of bone marrow cells from mice treated with cyclophosphamide on, 25:19112
effects on heptane, effects of nitrous oxide and oxygen on yields from, 25:18466
effects on human skin during therapy of neoplasms, effectiveness of lead glass filters for protection against, 25:19086
effects on iodoalkane glasses at 77°K, kinetics of decay of alkyl radicals produced by, 25:18461
effects on life span of mice, effects of dose on, 25:19105
effects on mechanical properties of glass fibers and methyl acrylate, methyl methacrylate, polyesters, polyethylene, or styrene, 25:18421(R) (RLO-2098-1)
effects on metaphase chromosomes of hamster liver cells, effects of hepatectomy on aberrant, 25:18960
effects on methanol at 77°K, space distribution of radicals from, 25:18464
effects on methyl vinyl ether in glasses of 3-methylhexane or tetrahydro-2-methylfuran at 77°K, ESR studies on dissociative electron capture in, 25:18456
effects on mice, protective effects of clopenthixol, flupenthixol, mesoridazine, and thioridazine against whole-body cobalt-60, 25:19028
effects on mice, use of functional units in small chromosome segments for interpretation of mutagenic, 25:18957
effects on morphology and function of cultured cells from cesium-137-contaminated media, 25:18904
effects on oil rape, mutagenic, 25:19152
effects on organic polymers, thermally stimulated currents from, 25:18422
effects on organic solutes in aqueous perchloric acid, rate constants for reactions of hydrogen atoms produced by, 25:18459
effects on oxidation of aqueous pharmaceutical solutions, elimination of, 25:18472
effects on pathogenicity of Histomonas meleagridis in turkeys, 25:19156
effects on Penicillium digitatum inoculated in oranges, combined effects of biphenyl, heat, and, 25:19162
effects on plants, effects of dose and seed exposure on mutagenic, 25:18964(P)
effects on poly(2-ethylhexyl acrylate)--polystyrene, 25:18436
effects on polybutadiene at 77°K, concentration of cross links and stabilized ions from, 25:18467
effects on polycrystals of deuterium- and/or iodine-129-labeled iodoethane, ESR studies on spectra produced by, 25:18424
effects on polymerization of acrylic or vinyl monomers in porous ceramics and firebrick, ion exchange properties of products from, 25:18421(R) (RLO-2098-1)
effects on polymerization of acrylonitrile in graphite, mechanical properties of products from, 25:18421(R) (RLO-2098-1)
effects on polymerization of cholesterol acrylate, 25:18431
effects on polymerization of dimethylamides and N-isobutyrylmethacrylamides, 25:18433
effects on polymerization of diphenylacetylene or diphenylbutadiyne, properties of products from, 25:18441
effects on polymerization of some solid methacrylates, 25:18445
effects on polymerization of styrene with methyl methacrylate in presence of silica gel or magnesium oxide, 25:18442
effects on populations of pink bollworm following release of exposed moths, inhibitory, 25:19102
effects on potassium chloride single crystals doped with bromide, properties of BrCl⁻ molecule-ion center induced in, 25:19852
effects on potassium dioxodifluoroiodate, ESR studies on radicals produced by, 25:18420 (COO-1385-34)
effects on production of free radicals in lyophilized proteins in comparison to effects of electric discharge, 25:18906
effects on reactions of water with polyethylene containers, 25:19164
effects on reactivity of dilute solutions of chymotrypsin,, effects of protein substrate on, 25:18907
effects on seeds of beans, Euphorbia, onions, peas, tomatoes, Vicia, and watermelon, effects of dose on, 25:18946
effects on selenates, 25:18479
effects on semiconducting diamonds, 25:19769(T) (LIB/Trans-307)
effects on serum antihyaluronidase activity and tissue permeability of skin in rats, protective effects of mercamine and serotonin against stimulatory, 25:19031
effects on silicon solar cells, 25:18882
effects on skin during therapy of neoplasms, effectiveness of tin radiation filters for protection against, 25:19082
effects on solid acetonitrile, isotope effects and activation energy of hydrogen atom abstraction process in, 25:18426
effects on solid glycine, ESR studies on, 25:18468
effects on sorptive properties of silica gel, 25:18427
effects on sperm of citrus red mites, effects of dose and TEPA on mutagenic, 25:19100
effects on storage life and wholesomeness of dates, effects of dose on, 25:19158(R) (NP-18679)
effects on storage life and wholesomeness of fish, 25:19163
effects on strand breaks in DNA in Escherichia coli, protective effects of Polysorbate 80 against, 25:19027
effects on structure and properties of cis-butadiene rubber, 25:19300
effects on survival of Aeromonas, Achromobacter, Micrococcus, Proteus, and Vibrio species of bacteria, effects of dose on, 25:19163
effects on survival of insects infesting stored dates, effects of dose on, 25:19158(R) (NP-18679)
effects on systems of molecular iodine-131 and pentane, 1-pentene, or 2-pentene, yields from, 25:18483(R) (COO-1617-27)
effects on thermoluminescence of polyethylene, relation of α-relaxation to, 25:18435
effects on tin monoxide and dioxide, products from, 25:18470
effects on undecafluoro(trifluoromethyl)cyclohexane, NMR studies on radicals produced by, 25:18448(R) (CEA-N-1369)
effects on uptake of α-aminoisobutyric acid, inulin, orotic acid, and phosphorus-32 by tissues of rats, effects of AET and cysteamine on, 25:19024
effects on uptake of labeled 2'-deoxy-5-iodouridine by bone marrow cells in mice, 25:19108
effects on viability of eggs of mites, effects of dose and TEPA on, 25:19100
emission from Cen A and Virgo A, (E), 25:19455
energy spectra of SNAP-15A heat source, germanium crystal measurements of, 25:18601
monitoring in liquid streams, laminar flow sample cell for continuous, 25:18717
penetration of concrete barriers, energy-angle distributions for cobalt-60, 25:19763
reactions (γ,f) with thorium-232 and uranium at 5 to 10 MeV, cross section structure near threshold for, (E), 25:20366 (IEA-211)
reactions with air, electric field excited by pulsed, 25:19761
scattering by lutetium-176 using cobalt-60 source, isomeric activation cross section for, (E), 25:20464
scattering by structure surfaces, 25:19764
spectra of, effect of absorbers on distortion of, 25:18771

GAMMA SOURCES
efficiency of irradiation facility, equation for calculating, 25:18571
leak testing radium-226, by gamma counting radon daughters, 25:19016
performance of americium-241, gadolinium-153, and iodine-125, for x-ray fluorescence determination of silver in drugs, 25:18355
uses in underwater radiography, design of equipment for, 25:18614(P)

GAMMA SPECTROMETERS
design and performance of Compton-suppressed low-level scintillation, for extended samples, 25:18752
design of liquid, for fast neutron capture cross section measurements, 25:20149
detection limits for radioisotopes, calculation of, 25:18746
development of cadmium telluride, 25:18733 (CEA-R-4052)

efficiency of 180° coincidence, for extended positron sources, 25:18758
multiple scattering in lithium-drifted germanium, 25:18726
peaks produced by Compton scattering in coincidence, elimination of spurious, 25:18754
photopeaks efficiency and system linearity for lithium-drifted germanium, determination of relative, 25:18747
resolution of scintillation, single-electron method for measuring photopeak, 25:18745
shielding studies on DORF pulsed reactor, 25:18732 (AD-711531)
spectra distortion in semiconductor and scintillation, effects of absorbers on, 25:18771
GAMMA SPECTROSCOPY
review of neutron-capture, (E/T), 25:20447
GAS FLOW
magnetohydrodynamic plane, theory of highly conducting plasma, 25:19671
magnetohydrodynamic steady supersonic, in channel with nonconducting walls and weak MHD interaction, (T), 25:19565
magnetohydrodynamic, end effects in channels with finite-size terminal insulators, (T), 25:19548
magnetohydrodynamic, Hall current and resistivity effects on stability of gas--liquid system, (T), 25:19546
magnetohydrodynamic, magnetic field penetration at shock wave front, 25:19547
magnetohydrodynamic, stabilization of electrothermal instabilities in channel, (T), 25:19543
GASEOUS DIFFUSION PROCESS
development for uranium enrichment, status of Japanese, 25:18602
evaluation for production of enriched uranium requirements to 1980, 25:18609
GASES
expansion of nonzero rest-mass ideal, adiabatic, (T), 25:19464
ion stopping in, review, (E/T), 25:19762
separation of components of binary mixtures of, efficiency of fixed-wall confined centrifugal, 25:18597
GASTROINTESTINAL TRACT
iron-59-labeled ferricyanide transport through, effects of time on, 25:18887
radiation dosimetry in human, following ingestion of radionuclides, mathematical model for, 25:19141
GENES
loci for radioinduced mutations controlling glucose-6-phosphatase activity, 25:19128
radioinduced somatic cross-over in, of Drosophila melanogaster, effects of x, on cell lineage patterns of wing disc, 25:18967
GENETIC TRANSFER
radiation effects on frequency of transduction, of drug resistance determinants by phage lysates in Staphylococcus aureus E169, uv, 25:19157
GEOMAGNETIC FIELDS
solar-wind interaction with, effect on topside ionosphere ion composition, (E/T), 25:19576
GERMANIUM
amorphous state in, structure of, 25:19862
chromatographic behavior in hydrochloric acid--thiocyanate mixture on Amberlite LA-2, 25:18337
diffusion of implanted atoms in, during annealing, 25:19841
electron slowing down in, 25:19759 (ORNL-4584, pp 87-91)
ion implantation at 30 to 40 keV in, channeling study of lattice location of implanted atoms from, 25:19827
ion implants in, electric properties and lattice location of indium, thallium, antimony, and bismuth, 25:19799
ion implants in, lattice locations of, 25:19797
neutron inelastic scattering by, γ energies from fast, (E), 25:20356
radiation damage mechanisms in, review of, 25:19810
radioinduced surface conductance in, annealing recovery of uv and x, (T), 25:19859
reactions with uranium tetrafluoride vapors, 25:18372
GERMANIUM ALLOYS AND SYSTEMS
Al--Ge--Nb, properties of intermetallic system Nb_3Al--Nb_3Ge, for high parameter superconductors, (E), 25:19599
GERMANIUM HALIDES
separation by solvent extraction, effects of charge, composition, and structure on, 25:18511
GERMANIUM IONS
implantation in silicon carbide at 160 to 300 keV, effects on cathodoluminescence, 25:19790
GERMANIUM ISOTOPES
energy levels from neutron inelastic scattering, (E), 25:20356
GERMANIUM ISOTOPES Ge-66
beta and electron-capture decay of, γ and conversion electron spectra from, (T), 25:20324
GERMANIUM ISOTOPES Ge-73
energy-level transition from arsenic-73 decay, total conversion coefficient for, (E), 25:20313
GERMANIUM ISOTOPES Ge-74
energy levels from gallium-74 decay, spins and parities of, (E), 25:20343
GERMANIUM SILICIDES
properties for use in thermopiles for radioisotope-fueled power systems, 25:18598(P)

GLASS
analysis for thallium by photon activation, 25:18366(R) (NBS-TN-548)
analysis of standard, for trace elements by neutron activation, 25:18366(R) (NBS-TN-548)
bend strengths of, effects of water content on uniaxial, 25:20900 (UCRL-20388)
bonding to molybdenum, method for, 25:19188
effectiveness of lead, for skin protection during γ therapy, 25:19086
fracture branching and dicing in stressed, 25:20894 (SC-RR-70-766)
fracture of, stochastic analysis of surface area of particles from, 25:20891 (SC-RR-69-506)
radiation effects on surfaces and refractive index of, 20-keV argon-ion, 25:19787
use of Raschig rings of borosilicate, for control of criticality in uranium-233 storage, 25:18624 (ORNL-4629, pp 1-9)
glass--$MoSi_2$, properties for use as protective coating on niobium, 25:19176
GLASS TEXTILES
glass textiles--methyl acrylate, radiation effects on mechanical properties of, γ, 25:18421(R) (RLO-2098-1)
glass textiles--methyl methacrylate, radiation effects on mechanical properties of, γ, 25:18421(R) (RLO-2098-1)
glass textiles--polyesters, radiation effects on mechanical properties of, γ, 25:18421(R) (RLO-2098-1)
glass textiles--polyethylene, radiation effects on mechanical properties of, γ, 25:18421(R) (RLO-2098-1)
glass textiles--styrene, radiation effects on mechanical properties of, γ, 25:18421(R) (RLO-2098-1)
GLOSSARIES
on nuclear materials safeguards, 25:18626 (WASH-1162)
GLOVE BOXES
design for handling plutonium nitrate, engineering drawings for, 25:18628
design of destructible, 25:18629(P)
GLUCOSE
radiolysis of aqueous solutions of, yield relations for dosimetry by gamma, 25:18808
GLUCOSE 6-PHOSPHATASE
activity in mice, effects of radioinduced mutations on control of, 25:19128
GLYCEROL
radiolysis of crystals of, processes for annealing of free radicals formed by, 25:18473
radioprotective effects of, on anoxic cells of Escherichia coli, effects of time scale on x, 25:19022
GLYCINE
radiolysis of solid, ESR spectra of radicals from γ, 25:18468
radiolysis of solid, structure and stability of radicals from γ, 25:18478
GLYCOPROTEINS
binding to americium and plutonium in bovine bones, mechanisms for, 25:18899
GOATS
polonium-210 metabolism by, following ingestion as oxide, coefficients for transfer to meat and milk during, 25:18890(R) (COO-2044-3)
radiation effects on brain of, high-energy proton, 25:19124
radiation effects on, effects of dose fractionation on recovery from 1 MV x, 25:19115
GOLD
chromatographic behavior in hydrochloric acid--thiocyanate mixture on Amberlite LA-2, 25:18337
deposition by cyanide electrolysis, polymeric codeposition in, 25:20851 (BDX-613-310)
determination in high-purity cadmium by photon activation, 25:18366(R) (NBS-TN-548)
determination in silver-base alloys by neutron activation, 25:18367
electron reactions at 0.3 to 1.1 MeV with thin foils of, photon emission spectra from, 25:19471
fission fragment stopping power, energy loss, and range in, (E), 25:20442
fission-fragment stopping in, cross sections for californium-252, (E), 25:19765
soldering parts coated with, problems in, 25:20852 (BDX-613-324)
GOLD ALLOYS AND SYSTEMS
Ag-base--Au, vibrational entropy of dilute solutions of, neutron activation method for determination of, 25:18367
Au--Cu-base, helium-ion backscattering from crystal of, 25:19798
Au-base--V, magnetic susceptibility at 2 to 300°K, Kondo temperature from, 25:19865
Au-base--V, thermal expansion of Au_4V in magnetically ordered and disordered states, 25:19229
GOLD ISOTOPES Au-192
energy levels from mercury-192 decay, half-lives and transition rates for, (E), 25:20453
GOLD ISOTOPES Au-197
energy levels from electro- and photoexcitation, transition multipolarities for, (E), 25:20463
half-life of isomeric, 25:20463
neutron capture at 3.0 to 6.5 MeV, gamma spectra from,

XUM

(E), 25:18735 (INR-1224)

GOLD ISOTOPES Au-198
- beta decay of, calculations of observables and log-ft values using correction matrix elements for first forbidden, (T), 25:20438

GOLD ORES
- distribution, history, and mineralogy of South African, 25:18533

GONIOMETERS
- development of automatic, with high resolving power for study of solids by small-angle diffraction of x rays, 25:18861(P)

GRANITES
- radiation effects on properties of, for use in concrete shielding aggregates, neutron, 25:19296

GRAPHITE
- abundance in interstellar materials, (T), 25:19452
- coating with chromium--zirconium diboride layers, electrolytic method for, 25:19270(P)
- electron band structure of, secondary-electron emission spectral study of conduction band in, 25:19864
- light extinction due to interstellar, (E), 25:19446
- light scattering from interstellar ice particles with cores of, (T), 25:19457
- oxygen desorption from, kinetics of, 25:18448(R) (CEA-N-1369)
- presence in interstellar grains, evidence for, (E/T), 25:19450
- radiation effects on electrical and mechanical properties of resin-laminated cloth of, γ, 25:18421(R) (RLO-2098-1)
- radiation effects on mechanical properties of, fast neutron, (E), 25:20747(R) (NP-18668)
- radiation effects on stability of, relations of binders and fillers with in-pile, 25:19288 (ORNL-4629, pp 82-98)
- radioinduced polymerization of acrylonitrile in, mechanical properties of products from γ, 25:18421(R) (RLO-2098-1)
- sorptive properties for gaseous cesium in liquid sodium, (E), 25:20754 (AERE-R-6481)
- structure of, development of automatic goniometers with high resolving power for x-ray diffraction studies of, 25:18861(P)
- ultrasonic testing of, computerized system for, 25:18613 (SC-DR-70-693)

GRAPHITE SYSTEMS
- neutron thermal diffusion coefficient for, measurement using pulsed source, (E), 25:20240
- Ag--graphite, electric conductivity of two-phase, 25:19226
- Cu--graphite, electric conductivity of two-phase, 25:19226

GRAVITATION
- effects in degenerate sea of anti ν and ν, spatial polarizability for, (T), 25:20090
- Einstein field equations in, short-ranged scalar gravity in, 25:20093
- quantization of, time and state functional in, 25:20095
- theory of, linear, 25:20098

GRAVITATIONAL COLLAPSE
- lectures on, 25:19465
- radio-source model featuring, of stars in galactic nuclei, (T), 25:19357

GRAVITATIONAL FIELDS
- Einstein--Maxwell equations for, properties of cylindrically symmetric, (T), 25:20086
- electron interactions with weak, covariant Green functions of, (T), 25:20094
- energy of weak, negative, 25:20099
- generation of stationary, from axially symmetric static vacuum field equations, (T), 25:20096
- meson interactions with weak, covariant Green functions of neutral scalar, (T), 25:20094
- near-field approximation for strong, 25:20101
- photon interactions with weak, covariant Green functions of, (T), 25:20094
- photon interactions with, neutrino mass from, (T), 25:19966

GRAVITATIONAL RADIATION
- graviton mixing with f meson, Lagrangian theory for, 25:20053
- interactions with impulsive gravitational waves, exact solution of Einstein vacuum equations for, (T), 25:20087

GROUND WATERS
- radioactivity in central Nevada, gross alpha and beta, 25:18522 (USGS-474-97)
- tritium content in central Nevada, 25:18522 (USGS-474-97)

GROUP THEORY
- BMS group in general relativity theory, semidirect product for, 25:20091
- invariance group for electrodynamics and linearized general relativity theory in, semidirect product for, 25:20091
- invariance group of Maxwell equations in, symmetric space of, 25:20052(T) (SLAC-Trans-130)
- Poincare, canonical and covariant representations of, 25:20035

GUANIDINE, 2-MERCAPTOETHYL-
- radioprotective effects of, on intestines in mice, comparison of whole-body fast neutrons and x, 25:19029

GUINEA PIGS
- radiation effects on cellular recovery in lymphoid tissues of, 25:18919(R) (RLO-2225-T-16-1)

GYROSCOPES
- relative rotation in, development of passive radioactive device for determining, 25:18822(P)

H

H.B. ROBINSON POWER REACTOR, UNIT 2
- operations incident of February 1, 1971, inoperable liquid waste monitor during liquid waste release, 25:20594 (DOCKET-50261-51)
- personnel for, revised technical specifications for use of respiratory protective equipment by, 25:20639 (DOCKET-50261-52)

HI REGIONS
- absorption profiles for, in directions of 39 continuum sources, (E), 25:19391
- velocity--latitude maps of, for region l/sup II/ = 190 to 299°, (E), 25:19392
- velocity--longitude maps of, in region l/sup II/ = 185 to 63°, (E), 25:19390

HII REGIONS
- distribution in NGC 4254, (E), 25:19456
- spectra and physical characteristics of galactic, (E), 25:19386
- structure in W3, DR21, Orion A, and M17, (E), 25:19374

HADRONS
- decay of,, weak-interaction Hamiltonian for octet dominance for nonleptonic s- and p-wave, (T), 25:20039
- interactions at high energies, straight-line particle-path approximation in quantum field theory for elastic and inelastic, (T), 25:19927
- interactions with hadrons at very high energies, two-temperature and fireball models for multiple particle production in, (T), 25:19971 (ANL-7727)
- interactions with hadrons, lectures on absorption corrections and cuts in Regge pole model for, (T), 25:19976
- interactions with hadrons, lectures on duality for, (T), 25:19978
- interactions with hadrons, lectures on Regge phenomenology for, (T), 25:19977
- interactions with hadrons, model for S-state scattering lengths of exotic, (T), 25:19975
- interactions with hadrons, review of complex angular momentum in Regge pole theory of, (T), 25:19974
- interactions with protons above 70 GeV, multiparticle production in, (E), 25:19905
- mass formulas for, test of approximate scale invariance from, 25:19983
- mass spectra of, review of quark model for, (T), 25:19979
- mass splittings of, weak-interaction Hamiltonian for d/f ratios for weak and medium-strong, (T), 25:20039
- production in p + p interactions and proton reactions with aluminum, beryllium, copper, and lead at high energies, atlas of momentum spectra for, (T), 25:20028
- reactions with carbon above 70 GeV, multiparticle production in, (E), 25:19905
- symmetry for, lectures on chiral, (T), 25:20045

HAFNIUM
- chromatographic behavior in hydrochloric acid--thiocyanate mixture on Amberlite LA-2, 25:18337
- separation from zirconium by double chloride extraction, 25:18499(T) (LIB/Trans-330)

HAFNIUM ALLOYS AND SYSTEMS
- B--C--Hf--Nb-base--W--Zr, properties for use at high temperatures, 25:19218
- C--Hf--Mo--Nb-base--W, properties for use at high temperatures, 25:19218
- Hf--Nb--O, phase studies of, 25:19240
- Hf--Nb-base, superconductivity of, relations with microstructure, 25:19219

HAFNIUM IONS
- implantation in silicon at 40 keV, carbon-ion channeling study of, 25:19829

HAFNIUM ISOTOPES Hf-170
- energy levels of, calculation using microscopic collective model, (T), 25:20547

HAFNIUM ISOTOPES Hf-174
- alpha inelastic scattering at 15 MeV, energy level transitions from, (E), 25:20427
- energy levels of, calculation using microscopic collective model, (T), 25:20547
- energy levels of, E0, M1, and E2 matrix elements for interband transitions between, (E), 25:20427

HAFNIUM ISOTOPES Hf-179
- decay of metastable, (E), 25:20426
- energy levels from electro- and photoexcitation, transition multipolarities for, (E), 25:20463
- half-life of isomeric, 25:20463

HAFNIUM ISOTOPES Hf-180
- decay of metastable, (E), 25:20426
- energy levels from lutetium-180 beta decay, (E), 25:20426
- neutron reactions (n,2n) at 14.5 MeV, cross sections and gamma spectra from, (E), 25:20435

  neutron reactions (n,p) at 14.8 MeV, production of lutetium-180 in, (E), 25:20426
HAIR
  radiation effects on thickness of, of sheep, ionizing, 25:19121
HALDEN BOILING REACTOR
  fuel elements in, radiation testing of SGHWR-type during 1964 to 1966, (E), 25:20736 (HPR-132)
  fuel elements in, radiation testing of Zircaloy-2 clad uranium oxide (UO_2), (E), 25:20735 (HPR-127)
HAMBURG ELECTRON SYNCHROTRON (DESY)
  storage ring DORIS at, design of, 25:20196
HAMSTERS
  radioinduced aberrations of metaphase chromosomes in liver cells of, effects of hepatectomy on γ, 25:18960
HASTELLOY C
  reactions with cobalt in air at high temperatures, 25:18591(R) (DP-1254)
  reactions with metallic cobalt-60 at high temperatures, 25:18591(R) (DP-1254)
HASTELLOY X
  oxidation by air at 1000 to 1125°C, 25:18591(R) (DP-1254)
  properties for use as capsule material for radioisotope heat sources, evaluation of high-temperature, 25:18592 (ORNL-4298)
  reactions with cobalt in air at high temperatures, 25:18591(R) (DP-1254)
  reactions with metallic cobalt-60 at high temperatures, 25:18591(R) (DP-1254)
HAYNES 25 ALLOY
  oxidation by air at 1000 to 1125°C, 25:18591(R) (DP-1254)
  properties for use as capsule material for radioisotope heat sources, evaluation of high-temperature, 25:18592 (ORNL-4298)
  reactions with cobalt in air at high temperatures, 25:18591(R) (DP-1254)
  reactions with metallic cobalt-60 at high temperatures, 25:18591(R) (DP-1254)
HAYNES 188 ALLOY
  oxidation by air at 1000 to 1125°C, 25:18591(R) (DP-1254)
HEALTH PHYSICS
  research at ORNL, July 31, 1970, 25:18988(R) (ORNL-4584)
HEART
  cesium-129 uptake by blood in canine and human, scanning studies on, 25:19055
HEAT EXCHANGERS
  description of intermediate and secondary, for sodium-cooled fast breeder reactors, 25:18574
  design parameters for direct cycle gas turbines, 25:20775
  design requirements for direct cycle gas turbines, 25:20776
  supports for, description of rotating, 25:20840(P)
  thermodynamics of tube type, FORTRAN 4 computer programs for calculation of, 25:20835 (RT/ING-(70)8)
HEAT EXCHANGERS (GAS-GAS)
  development of dry air, for direct cycle gas turbine helium cooled power reactors, 25:20777
  gas outlet temperatures of reactor counter-flow, effects of step change of inlet temperatures on, (T), 25:20779
HEAT EXCHANGERS (GAS-LIQUID)
  heat transfer performance of high temperature reactor, in high pressure helium, (E), 25:20780
HEAT PIPES
  design and testing for use in radioisotope-fueled thermoelectric systems, 25:18594(R) (ORNL-TM-3292)
  design parameters for thermionic reactor shielding cooling, 25:20807(P)
  design parameters of dual crossed axis, for thermionic reactors, 25:20809(P)
  protection of, description of radiator plates for, 25:20808(P)
HEAT-RESISTING ALLOYS AND METALS
  properties for use in gas-cooled reactors, 25:19197
HEAT SOURCES
  compatibility testing of compounds for radioisotope, program for, 25:18592 (ORNL-4298)
  design 30 kW cobalt-60, 25:18591(R) (DP-1254)
HEAT TRANSFER
  analysis of transient, discontinuous finite element method for, 25:18573
  calculation of liquid sodium piping system, (T), 25:20790 (WHAN-FR-22)
  coefficient of turbulent, in complex channels, (T), 25:20844(T) (AEC-tr-7186)
  mechanisms of boiling, role of bubble generation mode in, 25:18582
HEAT TRANSFER SYSTEMS
  coolant chemistry in FRIGG loop, control of water, (E), 25:20718(T) (LIB/Trans-308)
HEATED EFFLUENTS
  effects on Rhine River of nuclear and conventional steam power plants, 25:20685
  environmental effects from, 25:20683
HELIUM
  abundance in α And, (E), 25:19343
  burning in red giants, flash, (T), 25:19307
  charged-particle inelastic scattering by metastable atoms of, total cross sections for, (T), 25:19510
  diffusion of bubbles of, in tungsten-uranium carbide during annealing at 800 to 1500°C, 25:19272 (AI-AEC-12984)
  effects on void formation in nickel bombarded with 100-keV carbon and nickel ions, 25:19807
  electron reactions with, autoionizing states and negative-ion resonances from, 25:19490 (ORNL-4584, pp 92-104)
  electron scattering at 0 to 60 eV, performance of energy-modulated high-resolution beta spectrometer for, 25:18762
  energy-level transitions in, optical oscillator strengths for, (T), 25:19510
  energy-level transitions of, probabilities for 2^1S--n^1p, (E), 25:19481
  expectation values for, variational principles for analytic calculation of, 25:19475
  helium-ion reactions at 300 eV with, ion--photon coincidence study of excitation in, 25:19493
  ionization of interstellar, by soft x rays, (T), 25:19439
  nucleosynthesis in pulsationally unstable massive stars, (T), 25:19331
  plasma of, electron temperature determination in low density, (T), 25:19661
  plasma of, partition functions for, (T), 25:19397
  positron scattering by, calculation using Kohn and Harris variational methods, 25:19509
  proton reactions at 5 to 26 keV with, total cross sections for formation of metastable hydrogen atoms by charge exchange in, (E), 25:19504
  reactions with negative ions at 1 eV of metastable atoms of, cross sections for electron detachment and photon emission in, (T), 25:19511
  targets of, design of high-pressure, 25:20128 (IFVE-SEF-70-22)
HELIUM IONS
  abundance of He^+ in topside ionosphere, solar-geomagnetic seasonal control of, (E/T), 25:19576
  channeling in boron-implanted silicon at 1 and 1.8 MeV, 25:19830
  channeling in copper--gold crystal, 25:19798
  implantation in silicon carbide at 160 to 300 keV, effects on cathodoluminescence, 25:19790
  implantation in silicon diodes at 300 keV, effects on carrier lifetime, 25:19820
  potential-energy curves for diatomic He_2^+, (T), 25:19479
  reactions with helium at 300 eV, ion--photon coincidence study of excitation in, 25:19493
  stopping in gases and solids, review, (E), 25:19762
HELIUM ISOTOPES He-3
  alpha scattering at 7.5 to 18 MeV using polarized target, asymmetries in, (E), 25:20262
  Coulomb energy difference relative to tritium, (T), 25:20256
  deuteron elastic scattering at 4.8 to 11.9 MeV using polarized target, asymmetries in, (E), 25:20262
  deuteron reactions (d,p) at 4.8 to 11.9 MeV using polarized target, proton asymmetries in, (E), 25:20262
  helium-3 scattering at 9.3 to 17.5 MeV using polarized target, asymmetries in, (E), 25:20262
  nuclear binding energy, Coulomb energy, form factors, magnetic moments, radii, and wave functions for, harmonic-polynomial calculations of, (T), 25:20249 (ITF-70-51-E)
  photodisintegration of, bremsstrahlung-weighted E1 cross sections for, (T), 25:20252
  proton scattering at backward angles, pole-diagram analysis of exchange mechanism in, (T), 25:20250 (JINR-P2-5496)
  reactions (He-3,α), (He-3,d), and (He-3,p) with boron-10 at 1.2 to 1.9 MeV, analysis for reaction mechanisms in, (E), 25:20303
  reactions (He-3,d) and (He-3,p) at 10 MeV, angular distributions for, (E), 25:20273
  reactions (He-3,d) with neodymium-150, proton states from, (E/T), 25:20383
  reactions (He-3,Li-6) with fluorine-19 at 28 MeV, angular distributions for, (E), 25:20284
  reactions (He-3,p) with aluminum-27 and nitrogen-15 at 18 MeV, DWBA analysis of angular distributions from, (E/T), 25:20271 (NP-18628)
  reactions (He-3,t) with calcium-40 at 28 MeV, differential cross sections for, (E), 25:20350
  reactions (He-3,t) with nickel-58, core-polarization effects on cross section for, (T), 25:20496
  reactions (He-3,t) with titanium-46 at 37.7 MeV, differential cross sections for, (E), 25:20347
  scattering by aluminum-27 and nitrogen-15 at 18 MeV, optical-model analysis of angular distributions from elastic, (E/T), 25:20271 (NP-18628)
  scattering by nitrogen-15, oxygen-16, oxygen-17, and oxygen-18 at 11 MeV, optical-model analysis of elastic, (E/T), 25:20278
HELIUM ISOTOPES He-4
  alpha scattering by, separable potentials for, (T), 25:20511
  condensate in liquid II, as pilot wave, (T), 25:19586
  deuteron elastic scattering at 3 to 11 MeV using polarized beam, vector analyzing power for, (E), 25:20263

XUM

  deuteron reactions (d,p) at 8.5 to 11 MeV using polarized beam, proton asymmetries from, (E), 25:20263
  deuteron reactions (d,t) with, pole-diagram analysis of exchange mechanism in, (T), 25:20250 (JINR-P2-5496)
  deuteron scattering by, separable potentials for, (T), 25:20511
  energy level of, variation calculation of ground-state, (T), 25:20546
  ion mobility in liquid II, using field-emission points, 25:19587
  meson (π) scattering at 24 MeV, equivalent potential for, (T), 25:20253
  meson (π^-) capture by, proton, deuteron, and triton spectra from, 25:20255
  neutron elastic scattering below 22 MeV, phase shifts calculated from one-term nonlocal separable potentials for, (T), 25:20261
  photodisintegration of, bremsstrahlung-weighted E1 cross sections for, (T), 25:20252
  proton elastic scattering below 22 MeV, phase shifts calculated from one-term nonlocal separable potentials for, (T), 25:20261
  proton scattering at backward angles, pole-diagram analysis of exchange mechanism in, (T), 25:20250 (JINR-P2-5496)
  superfluid bulk viscosities in, relation between, (T), 25:19585
  superfluid flow in, heat as probe of, (E), 25:19584
  superfluid properties of, use for cooling to 0.7°K, 25:19640
  tritium scattering by, separable potentials for, (T), 25:20511
HELIUM SYSTEMS
  DH--He, rotational relaxation time below 40°K, sound absorption measurements of, 25:19480
HEMATITES
  radiation effects on properties of, for use in concrete shielding aggregates, neutron, 25:19296
HEMATOPOIESIS
  radiation effects on, in mice, effects of dose and shielding on x, 25:19126
HEPTANE
  radiolysis of, effects of nitrous oxide and oxygen on yields from γ, 25:18466
HEXANE
  optical constants in photon energy range 4.0 to 10.65 eV for, 25:19759 (ORNL-4584, pp 87-91)
  reactions with recoil tritium atoms in benzene, products from, 25:18487
  benzene--hexane--Li_2CO_3, radiation effects on, yields from reactions of tritium recoil atoms from neutron, 25:18487
HEXANE, IODO-
  radiation effects on glasses of, at 77°K, kinetics of decay of alkyl radicals produced by γ, 25:18461
HEXANE, 3-METHYL-
  radiation effects on glasses of, containing methyl vinyl ether at 77°K, ESR studies on dissociative electron capture in γ, 25:18456
HEXANOIC ACID
  use in extraction of iron, lead, and thorium, 25:18506
1-HEXANOL, 2-ETHYL-
  performance as recycling extractant, in CUSP process for uranum dioxide sols, 25:19261 (ORNL-4629, pp 14-64)
HIGH-ENERGY PHYSICS
  lectures on, (T), 25:19933
  research in, role and perspectives of cosmic rays in, (E), 25:19885
HIGH-TEMPERATURE GAS-COOLED REACTOR EXPERIMENT
  fuel elements for, safety aspects of second charge, 25:20734 (DP-Report-489)
  operation during April 1969 to March 1970, 25:20747(R) (NP-18668)
HIGH-TEMPERATURE LATTICE TEST REACTOR
  kinetics of thorium oxide (ThO_2)--uranium carbide (UC_2) fueled HTGR Lattice 1 in, (E/T), 25:20787 (GAMD-10231)
HIROSHIMA
  atomic bombing of, radiation effects on bone marrow of human babies and man following, autoradiography studies on, 25:19134
  neoplasm incidence in children exposed in utero to atomic bombing at, 25:19089
HOISTS
  design parameters of service structures, for reactor construction, 25:20562
HOLMIUM
  crystal structure at 77 to 300°K, expansion in, (E/T), 25:19243
  determination using 4,5-dihydroxy-m-benzenedisulfonic acid, in presence of Eriochrome Cyanine R, titrimetric, 25:18348
HOLMIUM IONS
  wave functions for, accurate numerical Hartree--Fock self-consistent field, 25:19478
HOLMIUM ISOTOPES Ho-155
  decay of, γ and β^+ spectra from, (E), 25:20405
HOLMIUM ISOTOPES Ho-165
  alpha reactions (α,xn) and (α,pxn) up to 150 MeV, cross sections for, (E), 25:20390
  energy-level transitions in, internal conversion ratios for M1 + E2, (E), 25:20473
HOLMIUM ISOTOPES Ho-166
  energy levels of, calculation using unified model, 25:20524
HORMONES
  labeling of, for use in diagnostic nuclear medicine, review of, 25:19037
HORMONES, THYROID
  thyroxin, use of radioiodine-labeled triiodothyronine and, for in vitro thyroid function studies, 25:19041
  triiodothyronine, use of radioiodine-labeled thyroxine and, for in vitro thyroid function studies, 25:19041
HOT CELLS
  decontamination of TURF, 25:18564 (ORNL-4629, pp 10-13)
HUMBOLDT BAY POWER REACTOR
  control rod drives for, revised technical specifications for maximum velocity of, 25:20608 (DOCKET-50133-46)
  operations history for July to December 1970, 25:20581 (DOCKET-50133-48)
  operations incidents of February 5 and February 7, 1971, failure of emergency condenser condensate return valve, 25:20580 (DOCKET-50133-45)
HUMIDITY
  effects on behavior of sodium fire aerosols in atmosphere, 25:19167 (AERE-R-6460)
HYALURONATE LYASE
  radiation effects on activity of serum, in rats, protective effects of mercamine and serotonin against γ, 25:19031
HYDROCARBONS
  conversion of petroleum aromatic, in presence of irradiated catalysts, 25:18444
  electron stopping powers of vapors of, 25:19491 (ORNL-4584, pp 105-24)
  radiolysis of, yields of hot hydrogen atoms from, 25:18454
HYDROCHLORIC ACID
  solvent properties for molybdenum, 25:18508
HYDROFLUORIC ACID
  corrosive effects on niobium, 25:19170
HYDROGEN
  determination in sodium coolant systems of fast reactors, equipment for, 25:18863
  diffusion from molybdenum and tungsten at 2000°K, 25:19225
  effects of surface impurity of, on ionization of potassium by polycrystalline tungsten, 25:19210
  effects on ductility of molybdenum--niobium alloys, 25:19216
  effects on ductility of niobium--titanium alloys, 25:19216
  effects on ductility of niobium--zirconium alloys, 25:19216
  electron elastic scattering by atomic, lower bounds on phase shifts for, 25:19757 (ORNL-4584, pp 58-73)
  electron reactions with atomic, analytical expressions for approximate cross sections for excitation, ionization, and recombination in, 25:19489 (NP-18680)
  electron reactions with atomic, origin of wave functions for calculation of cross sections for, 25:19494
  energy levels of atomic, relative magnetic substates in foil-excited, (T), 25:19474
  equation of state for dense molecular and metallic, at 0 to 10,000°K, (T), 25:19472 (UCRL-50985)
  ionization of interstellar, by soft x rays or cosmic rays, (E/T), 25:19440
  ionization of interstellar, by soft x rays, (T), 25:19439
  Lamb shift in, quantum field theory for, 25:20071
  Lamb shift in, review of, (T), 25:19512 (CNRS-CPT-70-P-335, pp IV.16-25)
  neutron capture by, effect of form factor in calculation of γ circular polarization from thermal, (T), 25:20423
  neutron total cross section at 500 keV to 21 MeV, (E), 25:20258
  nuclear magnetic resonance measurements in gaseous and liquid, near critical point, 25:20876(R) (NYO-3978-4)
  oxidation on ferric oxide, effects of deuterium on, 25:18386
  plasma of, conductivity in electric fields larger than runaway field, (E), 25:19672
  plasma of, partition functions for, (T), 25:19397
  plasma of, resistive loading in rf heating of, (E/T), 25:19653
  plasma of, Stark broadening of spectral lines in turbulent, (T), 25:19693
  positron annihilation rate for molecular, (T), 25:19501
  positron elastic scattering at 0.4 to 14 eV by molecular, total cross sections for, (T), 25:19501
  positron reactions with atomic, closed-channel spectrum for rearrangement in, (T), 25:19503
  positron scattering at low energies by atomic, generalized Hylleraas calculation of phase shifts for, 25:19508
  positron scattering by atomic, calculation using Kohn and Harris variational methods, 25:19509
  reactions of atomic, produced by γ irradiation of organic solutes in aqueous perchloric acid solutions, kinetics of, 25:18459
  reactions of hot atoms of, in radiolysis of compounds, 25:18454
  reactions with negative ions at 1 eV of metastable atoms of, cross sections for electron detachment and photon

    emission in, (T), 25:19511
  spectra of atoms of, in, 25:18423
  targets of, design of high-pressure, 25:20128 (IFVE-SEF-70-22)
  yields from β radiolysis of water, mechanism for scavenging effects of copper ions on production of, 25:18458
  yields from γ radiolysis of aniline, effects of additives on, 25:18450(R) (ORO-3519-8)
  yields from γ radiolysis of heptane, effects of nitrous oxide and oxygen on, 25:18466
HYDROGEN IONS (H^-)
  binding energy of ground state of, (T), 25:19516
  reactions with calcium, helium, and hydrogen metastable atoms at 1 eV, cross sections for electron detachment and photon emission in, (T), 25:19511
HYDROGEN IONS (H_2^+)
  energy-level transitions in, calculation of upper and lower bounds to oscillator strengths for dipole, 25:19514
  reactions with carbon at 1 MeV, x-ray spectra from, 25:18836
HYDROGEN ISOTOPES
  thermodynamic and transport properties of interstitial, in palladium, 25:20879(R) (NYO-4062-5)
HYDROGEN PEROXIDES
  complexes with niobium and 4-[(2,4-dihydroxyphenyl)azo]-1-naphthalenesulfonic acid, fluorescent and spectrophotometric studies on, 25:18349
HYDROGEN SULFIDES
  determination in natural waters from uranium mining operations, method for, 25:18339 (CEA-R-3557(2))
  deuterium exchange between, and water, dual-temperature process for, 25:18513(P)
  deuterium exchange between, and water, dual-temperature process for, 25:18512(P)
  deuterium exchange between, and water, dual-temperature process for, 25:18514(P)
HYDROMAGNETIC WAVES
  effects of galactic, on cosmic-ray acceleration, (T), 25:19459
  propagation in Earth's bow shock, 25:19580
  propagation in inhomogeneous magnetic fields, (E), 25:19732
  scattering of, in extragalactic radio sources, Compton, (T), 25:19380
HYDROXYL (HO)
  radio emission from, between 128 and 300°, 18-cm observations of, 25:19381
  radio spectral absorption line at 1667 MHz near galactic center, (E), 25:19382
  radio spectral absorption lines at 1667.358 MHz in galactic center region due to, (E), 25:19389
HYPERFRAGMENTS
  decay in bubble chamber, $\Lambda p/\Lambda n$ ratio for nonmesic, (E), 25:19908
  production in Σ^- absorption by neon at rest in bubble chamber, probability for, (E), 25:19908
HYPERONS
  decay of, model for S- and P-wave nonleptonic, (T), 25:19967
  decay $\Sigma \to \Lambda + e + \nu$, SU(3) octet currents and single-quark currents for mirror asymmetry in, (T), 25:20535
  production in $K^+ + p$ interactions at 12.7 GeV/c in hydrogen bubble chamber, properties of, (E), 25:19914
HYPERONS (ANTIPARTICLES)
  production in $K^+ + p$ interactions at 12.7 GeV/c in hydrogen bubble chamber, properties of, (E), 25:19914
HYPERONS (Λ)
  binding energy in nuclear matter, effects of short-range repulsion in $\Lambda + N$ interactions on, (T), 25:20023
  correlation with nucleons in nuclear matter, nonlinear equation for function for, (T), 25:20001 (DEMO-70/19)
  coupling with octet of pseudoscalar mesons, mass operator in SU(3) symmetric, (T), 25:20046
  decay $\Lambda \to p + e^- + \nu$, asymmetry parameters for, (E), 25:19894
  energy spectrum in nuclear matter, independent-pair approximation for single-particle, (T), 25:20023
  interactions $\Lambda + N$, effects on Λ binding energy in nuclear matter from short-range repulsion in, (T), 25:20023
  production in $K^+ + p$ interactions at 12.7 GeV/c in hydrogen bubble chamber, cross sections for, 25:19914
HYPERONS (anti Λ)
  production in $K^+ + p$ interactions at 12.7 GeV/c in hydrogen bubble chamber, cross sections for, 25:19914
HYPERONS (Σ)
  coupling with octet of pseudoscalar mesons, mass operator in SU(3) symmetric, (T), 25:20046
HYPERONS (Σ^-)
  absorption by neon at rest in bubble chamber, hyperfragment production probability from, (E), 25:19908
HYPERONS (Ξ)
  coupling with octet of pseudoscalar mesons, mass operator in SU(3) symmetric, (T), 25:20046
HYPERONS (Ξ^0)
  lifetime of, scintillator optical spark chamber study of, (E), 25:19903

I

ICE
  light scattering from interstellar particles of, with graphite cores, (T), 25:19457
  neutron scattering by hydrogen bound in, calculations for Haywood phonon distribution function of thermal, (T), 25:20229 (INR-1186)
  properties under vacuum at low temperatures of clean and dirty, (E), 25:19394(T) (LA-tr-70-27)
IGNEOUS ROCKS
  thorium mineralization and occurrence in alkaline, 25:18540
  uranium mineralization and occurrence in alkaline, 25:18540
  uranium mineralization in quaternary alkaline, of central Italy, exhalative-supergenic, 25:18542
IMMUNE REACTIONS
  radiation effects on cellular and humoral factors of, ionizing, 25:18922
  radiation effects on, in mice, effects of mouse spleen cells and sheep erythrocytes on, 25:18925
  radiation effects on, of mice to sheep red blood cells, effects of antisheep red blood cell antibodies on x, 25:18923
  suppression in rats, effectiveness of antilymphocytic serum for, 25:18919(R) (RLO-2225-T-16-1)
IMMUNIZATION
  effectiveness in treatment of ascariasis in lungs of x-irradiated mice, 25:19032
  effects on permeability of calf erythrocytes to phosphorus-32, 25:18900
  effects on x radiosensitivity of transplanted Ehrlich ascites tumor cells in mice, 25:19130
IMPACT SHOCK
  effects on deformation of structures in plastic range, relations with effective load and total impulse, 25:18557 (ANL-7677)
INCONEL X
  properties for use as capsule material for radioisotope heat sources, evaluation of high-temperature, 25:18592 (ORNL-4298)
INCONEL 600
  compatibility with cobalt aluminate at 1000 to 1200°C, 25:18591(R) (DP-1254)
  compatibility with cobalt magnesium oxide at 1000 to 1200°C, 25:18591(R) (DP-1254)
  compatibility with cobalt oxides at 1000 to 1200°C, 25:18591(R) (DP-1254)
  reactions with cobalt in air at high temperatures, 25:18591(R) (DP-1254)
  reactions with metallic cobalt-60 at high temperatures, 25:18591(R) (DP-1254)
INDIA
  annual report of department of Atomic Energy in, 25:20855 (DAE-AR-70)
  radioactivity of human diet on Kerala coast, 25:19143
INDIAN POINT POWER REACTOR, UNIT 1
  operations history for April to September 1970, 25:20574 (DOCKET-50003-65)
INDIUM
  chromatographic behavior in hydrochloric acid--thiocyanate mixture on Amberlite LA-2, 25:18337
  complexes, radiation effects on, reaction of recoil of indium isomers in γ, 25:18488
  Kapitza resistance of junction with sapphire, effects of superconducting transition on, (E/T), 25:19616
  neutron capture at 3.0 to 6.5 MeV, gamma spectra from, (E), 25:18735 (INR-1224)
  proton reactions (p,n) at 3 to 5.5 MeV, cross sections and strength functions for, (E), 25:20475
  separation from gallium by solvent extraction, review on, 25:18510
INDIUM ALLOYS AND SYSTEMS
  Bi--In, magnetization curves of intermediate mixed state of Type-II superconducting, 25:19620
  Ga--In, transformation into pulverulent state, mechanisms for, 25:19190(T) (AI-Trans-287)
  Hg--In, electrochemical properties of, 25:19190(T) (AI-Trans-287)
  In--Pb, dislocation mobility in normal and superconducting single crystals of, (E), 25:19589
  In--Pb, magnetization curves of intermediate mixed state of Type-II superconducting, 25:19620
  In--Pb-base, magnetization of superconducting cylinders of, local, 25:19626
  In--Sb, ion implantation in, review, 25:19789
  In--Sb, phosphorus-ion channeling profile in InSb, 25:19801
  In--Sb, zinc-ion implantation and range at 0.2 to 1.8 MeV in, for infrared detector fabrication, 25:19828
  In--Sn, diffusion of tin in fused eutectics of, 25:19199
  In--Zn, crystal structure of electrodeposited, 25:19221
  In--Zn, properties of electrodeposited, 25:19221
INDIUM ARSENIDES
  ion implantation in, review, 25:19789
  sulfur-ion implantation at 400 keV in, for infrared detector fabrication, 25:19828

XUM

INDIUM IONS
  implantation in germanium at 30 to 40 keV, channeling study of lattice location of, 25:19827
  implantation in germanium at 40 and 70 keV, electric properties and lattice location of, 25:19799
INDIUM ISOTOPES In-110
  beta and electron-capture decay of ground-state and isomeric, γ spectra from, (E), 25:20402
INDIUM ISOTOPES In-113
  distribution of metastable, in rabbits following injection as colloid in comparison to distribution of metastable technetium-113--tin-113 colloid, 25:18994
  dosimetry of metastable, in human bone marrow, liver, and spleen, 25:18994
  effectiveness of DTPA-incorporated, for kidney scanning, comparison of mercury-197-labeled chlormerodrin with, 25:19039
  effectiveness of erythrocyte-incorporated metastable, for liver scintigraphy, 25:19036
  isomeric transition in, half-life and internal conversion coefficients for, (E), 25:20460
  isomeric transition in, half-life and internal conversion coefficient for, (E), 25:20407
  production of metastable, for use in scanning, use of tin-113 generator for, 25:18865
INDIUM ISOTOPES In-114
  reactions of recoil isomers of, in γ-irradiated indium complexes, 25:18488
INDIUM ISOTOPES In-115
  neutron capture up to 50 eV, γ spectra from, (E), 25:20410
  reactions of recoil isomers of, in γ-irradiated indium complexes, 25:18488
INDIUM ISOTOPES In-116
  energy levels from indium-115 neutron capture, spins, widths, and strength functions for, (E), 25:20410
  reactions of recoil isomers of, in γ-irradiated indium complexes, 25:18488
INDIUM ISOTOPES In-120
  beta decay of ground-state and isomeric, γ singles and coincidence spectra from, (E), 25:20401
INDIUM TELLURATES
  $In_2(TeO_3)_3$--$In_2(TeO_4)_3$, analysis for hexavalent tellurium and total tellurium by automatic amperometric and potentiometric titrations, 25:18351
INDIUM TELLURITES
  $In_2(TeO_3)_3$--$In_2(TeO_4)_3$, analysis for hexavalent tellurium and total tellurium by automatic amperometric and potentiometric titrations, 25:18351
INDUSTRIAL MANAGEMENT
  spare parts inventory control system for, computer program for, 25:18558 (ARH-1474)
INFORMATION RETRIEVAL SYSTEMS
  authority list for corporate entries for INIS, 25:20858 (IAEA-INIS-6(Rev.2))
INFRARED RADIATION
  effects on aberrations induced in chromosomes of Vicia faba by maleic hydrazide and x radiation, 25:18962
  emission from epsilon Aur and 89 Her, (T), 25:19314
  emission from galactic-center region, (E), 25:19448
  emission from planetary nebulae, (E), 25:19327
INFRARED SPECTROSCOPY
  book: Low-Frequency Vibrations of Inorganic and Coordination Compounds, 25:18419
INORGANIC COMPOUNDS
  book: Low-Frequency Vibrations of Inorganic and Coordination Compounds, 25:18419
INSECTA
  Dacus cucumis, radiation effects on corpus allatum size in female, whole-body cobalt-60 γ, 25:19096
  Dacus cucumis, radiation effects on transplanted ovaries in female, cobalt-60 γ, 25:19096
  Drosophila melanogaster, radiation effects on cell lineage patterns in imaginal wing disc of, somatic x, 25:18967
  Pectinophora gossypiella, radiation effects on populations of larvae of, following release of exposed moths, γ, 25:19102
  Phaenicia sericata, radiation effects on adult, larval, and pupal stages of, x, 25:19098
  Plodia interpunctella, effects of irradiated food on fecundity of, 25:19159
  Pseudaulacaspis pentagona, effects of irradiated food on fecundity of, 25:19159
  radiosterilization of date-infesting, γ, 25:19158(R) (NP-18679)
  Rhodnius prolixus, radiation effects on eggs of, effects of nutrition on, 25:19099
  Spodoptera exigua, radiation effects on adult life span and egg production of, exposed as pupae, γ, 25:19097
  Tenebrio molitor, radiation effects on pupation and survival of larvae of, effects of partial shielding on x, 25:19094
INSTRUMENTS
  development of radiometric, 25:18870
INTERNAL CONVERSION
  coefficients for E1 transitions in A = 175 to 243 nuclei, 25:20457
  coefficients for, effect of inner atomic shells on, (T), 25:20515
  coefficients of, efficiency of lithium-drifted germanium detector coincidence method for measuring K, 25:18759
  electric monopole conversion probability in, table of electron factors for, 25:20484
INTERSTELLAR MATERIAL
  alignment of grains in, effects of soft x rays on, (T), 25:19447
  composition of grains, mixed, (T), 25:19452
  light absorption in graphite and silicate, (E), 25:19446
  light scattering from graphite core--ice mantle cylinders in, (T), 25:19457
  model for, featuring mixture of iron, graphite, and silicate for extinction curve, (E/T), 25:19450
  photo-ionization of, by soft x rays, (T), 25:19439
  silica minerals in, (E), 25:19453
  structure of light-absorbing, in solar neighborhood, (E), 25:19442
INTESTINES
  radiation effects on generation cycle of crypt cells in small, of mice, effects of chronic fractionated x, 25:19122
INULIN
  radiation effects on uptake by rat kidney, liver, muscles, and spleen, effects of AET and cysteamine on γ, 25:19024
INVARIANCE PRINCIPLES
  charge conjugation violation in eta $\to \pi^+ + \pi^- + \pi^0$ decay asymmetry, (T), 25:19948
  CP violation for second-class currents for mirror asymmetry in beta decay, (T), 25:20535
  parity-violating nuclear reactions, weak-interaction Hamiltonians for, (T), 25:20039
  scale invariance in nonlinear chiral Lagrangian models for pseudoscalar, 25:20049
  scale invariance test from hadron mass formulas, approximate, 25:19983
  scale invariance, dimension of operators in broken, 25:20037
INVERTEBRATES
  radioisotope content of aquatic, in Finland, 25:18930 (NYO-3446-14, Paper 27)
IODINE
  determination by biamperometric titration with mercury perchlorate, 25:18346
  metabolism in man, biological model for, 25:18991 (ORNL-4584, pp 200-22)
  reactions with 2-methyl-1-butene, 2-methyl-2-butene, 1-pentene, cis-2-pentene, and trans-2-pentene at 25°C, kinetics of, 25:18483(R) (COO-1617-27)
  reactions with liquid sodium in liquid metal cooled fast breeder reactor systems, (E), 25:20760 (CONF-700816-(Vol.1), pp 356-72)
  sorption by monocrystalline tungsten, effects of adatom surface potential and adsorbate electronegativity on, 25:19207
  sorption by monocrystalline tungsten, effects on work function, 25:19209
IODINE BROMIDES
  benzene--IBr, radiation effects on liquid and solid, labeled organic yields from, 25:18483(R) (COO-1617-27)
IODINE CHLORIDES
  alkylbenzene--ICl, radiation effects on, at 77 and 298°K, isotope effects and yields from neutron, 25:18483(R) (COO-1617-27)
  benzene--ICl, radiation effects on liquid and solid, labeled organic yields from neutron, 25:18483(R) (COO-1617-27)
  cyclopentane--ICl, iodine-128 isomeric transitions or neutron capture in liquid and solid, labeled organic yields from, 25:18483(R) (COO-1617-27)
IODINE IONS
  implantation in silicon at 20 to 150 keV, energy dependence of lattice disorder induced in, 25:19832
IODINE ISOTOPES I-123
  production in cyclotrons, evaluation of techniques for, 25:18480 (BRH/DMRE-70-4)
IODINE ISOTOPES I-125
  radiation dose distribution from point source, methods for calculating, 25:18984 (JUL-688-ME)
IODINE ISOTOPES I-128
  isomeric transition in liquid and solid benzene--iodine systems, organic yields from, 25:18483(R) (COO-1617-27)
  reactions of recoils of, with iodine or iodine chloride in alkylbenzenes, benzene, or cyclopentane, labeled organic yields from, 25:18483(R) (COO-1617-27)
  reactions of recoils of, with pentane, 1-pentene, and 2-pentene, labeled organic yields from, 25:18483(R) (COO-1617-27)
IODINE ISOTOPES I-129
  effects on spectra of polycrystals of iodoethane, ESR studies on, 25:18424
IODINE ISOTOPES I-130
  isomeric transition in liquid and solid benzene--iodine systems, organic yields from, 25:18483(R) (COO-1617-27)
  reactions of recoils of, with iodine or iodine chloride in alkylbenzenes, benzene, or cyclopentane, labeled organic yields from, 25:18483(R) (COO-1617-27)
  reactions of recoils of, with iodomethane and pentane, 1-pentene, and 2-pentene, labeled organic yields from, 25:18483(R) (COO-1617-27)

IODINE ISOTOPES I-131
  content of milk in Norway, 25:19135
  dose to human thyroid from milk in Norway, relation of frequency of cancer to, 25:19135
  effectiveness for internal treatment of hyperthyroidism in man, review of, 25:19062 (NP-18693)
  energy levels from decay of 25-min tellurium-131g, (E), 25:20428
  inhalation by man following release to atmosphere during reactor accidents, relation of activity to probability of development of thyroid neoplasms following, 25:18974 (AHSB(S)R-192)
  reactions with liquid sodium in liquid metal cooled fast breeder reactor systems, (E), 25:20760 (CONF-700816-(Vol.1), pp 356-72)
  release from pressurized water reactors during coolant loss accidents, 25:20756 (CONF-700816-(Vol.1), pp 9-25)
  retention in man with thyroid carcinoma, use of whole-body counting for measuring, 25:19035
  transport from pastures to milk to man, 25:18943
  transport of aerosol-incorporated, through plant--cow--milk--man food chains following nuclear explosions, 25:18926 (CONF-700816-(Vol.1), pp 49-71)
  uptake by thyroid gland, dual detector system for measuring, 25:18898
  uptake by thyroid in man, diagnosis of hyperthyroidism and hypothyroidism using, 25:19051
  use for diagnosis of communicating hydrocephalus by lumbar administration, 25:19043
  use for scanning kidneys for blood circulation and function, combined use of metastable technetium-99-labeled pertechnetate with, 25:19046
  use of erythrosine B- incorporated, for scanning canine pancreas, 25:19060
IODINE ISOTOPES I-132
  uptake by thyroid gland, dual detector system for measuring, 25:18898
IODINE SYSTEMS
  alkylbenzene--I, radiation effects on, at 77 and 298°K, organic yields from neutron, 25:18483(R) (COO-1617-27)
  benzene--I, iodine-128 or iodine-130 isomeric transitions or radiative neutron capture in liquid and solid, organic yields from, 25:18483(R) (COO-1617-27)
  cyclopentane--I, iodine-128 or iodine-130 isomeric transitions or radiative neutron capture in liquid and solid, organic yields from, 25:18483(R) (COO-1617-27)
  I--1-pentene, radiation effects on, organic yields from reactions of recoil iodine-128 from neutron, 25:18483(R) (COO-1617-27)
  I--2-pentene, radiation effects on, organic yields from reactions of recoil iodine-128 from neutron, 25:18483(R) (COO-1617-27)
  I--pentane, radiation effects on, organic yields from reactions of recoil iodine-128 produced from neutron, 25:18483(R) (COO-1617-27)
  iodine-131--1-pentene, radiolysis of, yields from γ, 25:18483(R) (COO-1617-27)
  iodine-131--2-pentene, radiolysis of, yields from γ, 25:18483(R) (COO-1617-27)
  iodine-131--pentane, radiolysis of, yields from γ, 25:18483(R) (COO-1617-27)
ION-ACOUSTIC WAVES
  damping of large-amplitude solitary, effect of ion--neutral collisions on, (T), 25:19748
  excitation and stabilization in rf plasma, 25:19744
  excitation by grids in plasma, symmetry considerations for, (T), 25:19742
  propagation in collisionless gravity-supported magnetoplasma, (T), 25:19736
  propagation in plasma, detection of spatially decaying, 25:19741
ION BEAMS
  charge exchange stripper gases for heavy, performance of fluorocarbon, 25:20155
  collimation of negative, with apertures, 25:18842
  interactions with magnetoplasmas, quasi-linear solutions for, 25:19694
  reactions (HI,xn) with fissionable nuclei, product identification by means of angular distributions, (E), 25:20419
  transport with no change of properties, magnet system for, 25:20205
ION EXCHANGE MATERIALS
  cesium-137 removal by zeolite prefilter, efficiency of, 25:18621 (DP-1245)
ION SOURCES
  beam injection system for terminal, in electrostatic generator, 25:20204
  description of fine-focused, for ion implantation, micro-etching, and microscopy, 25:20168
  description of high-beam-current, for ion implantation, 25:20167
  design and performance of heavy-, review of, 25:20450
  design and performance of PIG, for multiply charged heavy ions, 25:20188
  ion yields of rf-excited deuterium, atomic, diatomic, and triatomic, 25:20150
  performance for ion implantation at 10 to 600 keV, review, 25:20165
  plasma boundary of, 25:20174
  properties for ion implantation, review, 25:20166
  use of calutron-type, in ion immplantation machine, 25:20169
IONOSPHERE
  charged-particle densities from 80 to 400 km in, interaction mechanisms of electron and proton, (E/T), 25:19583
  E region, ion chemistry and thermal balance in, above Wallops Island, (E), 25:19575
  F region, backscatter irregularities at midlatitude and low- and high-auroral zone, morphology and generation of, (E/T), 25:19574
  F region, ion chemistry and thermal balance in, above Wallops Island, (E), 25:19575
  ion variations in topside, solar-geomagnetic seasonal control of primary, (E/T), 25:19576
IONS
  channeling in crystals with implanted foreign atoms, testing of assumptions in, 25:19798
  channeling in diamond-type lattices, computer simulation of flux-peaking effect in, 25:19804
  detection of, scintillation detector with secondary electron emitter for, 25:18722(P)
  effects on silicon, model for amorphous-layer formation in, 25:19813
  effects on solids, range--damage correlation functions for predicting, (T), 25:19833
  effects on zinc sulfide, zinc selenide, and cadmium sulfide, annealing of, 25:19793
  electron reactions with one-electron, analytical expressions for approximate cross sections for excitation, ionization, and recombination in, 25:19489 (NP-18680)
  energy-level transitions in, calculation of upper and lower bounds to oscillator strengths for dipole, 25:19514
  expectation values for two-electron, variation principles for analytic calculation of, 25:19475
  implantation facility, description of industrial-scale, 25:19773
  implantation in compound semiconductors, review, 25:19789
  implantation in crystals, channeling method for lattice location of, 25:19797
  implantation in crystals, creation of moire patterns by channeling in, 25:19849
  implantation in semiconductors, first international topical conference at Thousand Oaks, Calif., May 4--7, 1970, 25:19809
  implantation in semiconductors, review of electric properties of doped layers produced in, 25:19775
  implantation in semiconductors, review of range and depth distributions in, 25:19796
  implantation in silicon devices, survey, 25:19782
  implantation in silicon, copper-decoration method for determination of damage from, 25:19817
  implantation in silicon, review of damage from, 25:19805
  implantation in solids, European conference on, Reading, England, Sept. 7 to 9, 1970, 25:19772
  implantation in solids, survey of possible uses of, 25:19785
  implantation machine, description of 200-kV, 25:19774
  implantation profile in silicon, ion-beam stripping--electrical method for measuring, 25:19800
  improvement of heavy, coincidence method for energy spectra of, 25:18750
  mass identification in electron swarm experiments, apparatus for, 25:19490 (ORNL-4584, pp 92-104)
  range in amorphous substances, approximations and interpolation rules for calculation of, 25:19760
  reactions with atoms, ion--photon coincidence method for study of excitation in, 25:19493
  scattering by solid surfaces, angular and energy distributions from, 25:19468 (INP-710)
  sorption of implanted, on dislocation loops in semiconductors during annealing, (T), 25:19848
  stopping by carbon, gold, and silver of heavy, cross sections as function of ion nuclear charge for, (E), 25:19765
  stopping in gases and solids, review, (E/T), 25:19762
IRIDIUM
  chromatographic behavior in hydrochloric acid--thiocyanate mixture on Amberlite LA-2, 25:18337
  compatibility with cobalt aluminate at high temperatures, 25:18591(R) (DP-1254)
  compatibility with cobalt magnesium oxide at high temperature, 25:18591(R) (DP-1254)
  compatibility with cobalt oxide at high temperatures, 25:18591(R) (DP-1254)
  detection in low-energy cosmic radiation, (E), 25:19525
  effects on corrosion of tantalum by liquid lithium, inhibition, 25:19168(P)
IRIDIUM ALLOYS AND SYSTEMS
  Ir--Rh, superconducting properties of fcc solid solutions of, (E), 25:19606
IRIDIUM ISOTOPES Ir-191
  energy levels from electro- and photoexcitation, transition multipolarities for, (E), 25:20463
  energy levels of, lifetimes and gyromagnetic ratios of, (E), 25:20462
  energy-level transitions in, internal conversion ratios for M1 + E2, (E), 25:20473

XUM

  - half-life of isomeric, 25:20463
- IRIDIUM ISOTOPES Ir-192
  - beta decay of polarized, γ-ray angular distributions from, (E), 25:20386
  - gamma emission from, total specific γ-ray constant for, 25:20424
  - γ spectra of, (E), 25:20424
  - use for implant therapy, evaluation of applicators and methods for, 25:19076
- IRIDIUM ISOTOPES Ir-194
  - beta decay of polarized, γ-ray angular distributions from, (E), 25:20386
- IRON
  - abundance in α^2 CVn, (E), 25:19339
  - cascade showers in, Monte Carlo calculations of transition effects at water interface for 1-GeV-electron-initiated, 25:19943
  - cascade showers in, Monte Carlo calculations of transition effects at air interface for 200-MeV- to 1-GeV-electron-initiated, 25:19943
  - chromatographic behavior in hydrochloric acid--thiocyanate mixture on Amberlite LA-2, 25:18337
  - determination by biamperometric titration with mercury perchlorate, 25:18346
  - determination in high-purity cadmium by photon activation, 25:18366(R) (NBS-TN-548)
  - determination in natural waters from uranium mining operations, method for, 25:18339 (CEA-R-3557(2))
  - determination in presence of palladium and vanadium by spectrophotometry using 1-(2-carboxy-4-sulfonatophenyl)-3-hydroxy-3-phenyltriazene, 25:18342
  - effects of small additions on superconductivity of Nb--Ta--Ti--Zr alloys, 25:19618(P)
  - effects on separation of strontium from aqueous solutions by cation exchange, 25:18504 (UJV-2450-Ch)
  - faulting in filings of, x-ray diffraction search for, 25:19248
  - magnetic moments in alloys with rare earths, 25:19871
  - neutron inelastic scattering by, γ energies from fast, (E), 25:20356
  - positron annihilation in deformed and irradiated, effects of vacancies on two-photon angular correlation of, (E/T), 25:19851
  - presence in interstellar grains, evidence for, (E/T), 25:19450
  - production in Japan, use of nuclear energy for, 25:19182
  - properties for use in heat block-shields in radioisotope-fueled thermoelectric systems, 25:18594(R) (ORNL-TM-3292)
  - radiation effects on strength of monocrystalline bcc, electron, 25:19252 (COO-1367-36)
  - reactions with uranium tetrafluoride vapors, 25:18372
  - separation from lead and thorium by extraction as caproate into chloroform, 25:18506
  - separation of americium from, by precipitation, 25:18507(P)
  - separation of bismuth from, by cation exchange chromatography, 25:18520
  - use in reactor construction, review of considerations for, 25:19200
- IRON ALLOYS AND SYSTEMS
  - magnetic properties of soft magnetic, effects of heat treatments on, 25:19872
  - Co--Cu--Fe--Sm, magnetic properties of Sm(Fe,Co,Cu)$_5$, (E), 25:19875
  - Co--Fe--Sm, magnetization of SmFe/sub x/Co/sub 5-x, saturation, (E), 25:19875
  - Cr--Fe--Nb--Si, properties for use as protective coating on niobium, 25:19176
  - Fe--Gd, magnetic susceptibility of GdFe$_2$, 25:19871
  - Fe--Lu, magnetic susceptibility of LuFe$_2$, 25:19871
  - Fe--Ni, elastic moduli of Invar, effects of magnetic field on temperature-dependent, (E/T), 25:19224
  - Fe--Y, magnetic susceptibility of Y$_2$Fe$_{17}$, Y$_6$Fe$_{23}$, YFe$_3$, and YFe$_2$, 25:19871
  - Fe-base--Mo--Ni, phase transformation during aging, kinetics of martensitic, 25:19247
- IRON BORIDES
  - preparation and properties for incorporation in metals for neutron absorbers, 25:19264(P)
- IRON FERRICYANIDES
  - transport of iron-59-labeled, through gastrointestinal tract of rats, effects of time on, 25:18887
- IRON ISOTOPES
  - energy levels from neutron inelastic scattering, (E), 25:20356
- IRON ISOTOPES Fe-52
  - energy level from iron-54 (p,t) reaction, excited 0$^+$, (E/T), 25:20321
- IRON ISOTOPES Fe-54
  - charge radius of, electron elastic scattering study of, (E), 25:20334
  - deuteron elastic scattering at 8 to 12 MeV using polarized beam, cross section and vector analyzing power for, (E), 25:20305
  - deuteron reactions (d,p) at 8 to 12 MeV using polarized beams, cross sections and vector analyzing power for, (E), 25:20305
  - energy level from iron-56 (p,t) reaction, excited 0$^+$, (E/T), 25:20321
  - energy level of, magnetic moment of first 2$^+$, (T), 25:20333
  - neutron reactions (n,α) up to 14 MeV, Hauser--Feshbach analysis of excitation functions for, (E/T), 25:20346
  - neutron scattering at 4.0 to 5.6 MeV, angular distributions and cross sections for, (E/T), 25:20338
  - nuclear magnetic moment of, (E), 25:20413
  - proton reactions (p,t) at 51.9 MeV, excited 0$^+$ state in iron-52 from, (E/T), 25:20321
- IRON ISOTOPES Fe-55
  - content of food chains in Finland, 25:18931 (NYO-3446-14, Paper 30)
  - content of man in Finland during 1960 to 1970, 25:18986 (NYO-3446-14, Paper 28)
- IRON ISOTOPES Fe-56
  - charge radius of, electron elastic scattering study of, (E), 25:20334
  - neutron inelastic scattering at 2.9 MeV, γ-ray differential cross sections for, (E), 25:20329
  - neutron scattering at 4.0 to 5.6 MeV, angular distributions and cross sections for, (E/T), 25:20338
  - proton elastic scattering at 3.7 to 4.3 MeV, angular distributions for, (E), 25:20336
  - proton reactions (p,γ) at 1.2 to 1.6 MeV, angular distributions for, (E), 25:20336
  - proton reactions (p,t) at 51.9 MeV, excited 0$^+$ state in iron-54 from, (E/T), 25:20321
- IRON ISOTOPES Fe-57
  - nuclear magnetic resonance spectrum of, magnetic modulation of frequency in, 25:19878
- IRON ISOTOPES Fe-58
  - charge radius of, electron elastic scattering study of, (E), 25:20334
- IRON ISOTOPES Fe-59
  - transport of ferricyanide-incorporated, through gastrointestinal tract in rats, effects of time on, 25:18887
- IRON OXIDES Fe$_2$O$_3$
  - effects on oxygen-18 exchange in carbon monoxide molecules, catalytic, 25:18387
- IRON OXIDES Fe$_3$O$_4$
  - effects on oxygen-18 exchange in carbon monoxide molecules, catalytic, 25:18387
- IRON SILICIDES
  - reactions with nitrogen at 400 to 1000°C, diffusion and nitrogenation, 25:19234
- IRRADIATION FACILITIES
  - description of 200-kV ion-implantation machine, 25:19774
  - description of industrial-scale ion-implantation, 25:19773
  - developments in, 25:18870
  - efficiency of gamma, equation for calculating, 25:18571
- ISOTOPE DILUTION ANALYSIS
  - developments in mass-spectrometric, 25:18357(R) (NBS-TN-546)
- ISOTOPE SEPARATION METHODS
  - development of dual-temperature liquid--gas, 25:18514(P)
  - development of dual-temperature liquid--gas, 25:18512(P)
  - development of dual-temperature liquid--gas, 25:18513(P)
  - efficiency of fixed-wall centrifugal, comparison with ultracentrifugation, 25:18597
- ISOTOPES
  - book: Isotopes: Reference Tables. Volumes I and II, 25:20264

J

- JAPAN
  - iron production in, use of nuclear energy for, 25:19182
  - nuclear energy development in, review of fiscal 1969, 25:20696
  - nuclear fuel cycle development in, 25:18555
  - radiation monitoring programs at Oarai Research Establishment during 1970, 25:18983(R) (JAERI-Memo-4216)
  - safeguards methods for nuclear facilities in, 25:19019
- JAPANESE ADVANCED THERMAL REACTOR
  - pressure tubes for, properties of zirconium alloy, 25:19223
- JOSEPH M. FARLEY POWER REACTOR, UNIT 1
  - design parameters of, revised and additional data on, 25:20674 (DOCKET-50348-16)
  - operations aspects of, revised and additional data on, 25:20674 (DOCKET-50348-16)
- JOSEPH M. FARLEY POWER REACTOR, UNIT 2
  - design parameters of, revised and additional data on, 25:20674 (DOCKET-50348-16)
  - operations aspects of, revised and additional data on, 25:20674 (DOCKET-50348-16)

K

- KAOLINITES
  - dehydroxylation on compact specimens, 25:20901 (UCRL-20393)
- KEWAUNEE POWER REACTOR
  - site for, environmental radiation survey during July 1969 to June 1970, 25:20641 (DOCKET-50266-42)
  - technical specifications for, 25:20664 (DOCKET-50305-19)
- KIDNEYS
  - analysis for mercury by neutron activation, 25:18369

  - radiation effects on uptake of α-aminoisobutyric acid, inulin, orotic acid, and phosphorus-32 by rat, effects of AET and cysteamine on γ, 25:19024
  - scanning for blood circulation and function, combined use of iodine-131-labeled Hippuran and metastable technetium-99-labeled pertechnetate with γ cameras for, 25:19046
  - scanning of human, comparison of indium-113m-labeled DTPA with mercury-197-labeled chlormerodrin for, 25:19039
- KRYPTON
  - positron annihilation in liquid and solid, positronium-bubble formation and angular correlation of photons from, 25:19487
- KRYPTON IONS
  - implantation in boron-doped silicon at 60 and 600 keV, lattice disorder produced in, 25:19806
  - implantation in silicon carbide at 160 to 300 keV, effects on cathodoluminescence, 25:19790
- KRYPTON ISOTOPES Kr-80
  - energy levels from bromine-80 decay, (E), 25:20471
- KRYPTON ISOTOPES Kr-81
  - production of metastable, using rubidium-81 generator for use in radiodiagnosis, 25:19056
  - use of metastable, for human lung scanning, 25:19056
- KRYPTON ISOTOPES Kr-85
  - content of natural gas produced in Gasbuggy Project during 1969, hazards to man from, 25:18989 (ORNL-4584, pp 42-56)
  - monitoring around fuel reprocessing plants, calibration and testing of detectors for, 25:18638 (CONF-700816-(Vol.1), pp 143-74)
  - monitoring of trace amounts in gases, scintillation detector for, 25:18744(P)
  - removal from radioactive off-gases, equations for calculating efficiency of fission gas adsorption beds for, 25:18560 (CONF-700816-(Vol.1), pp 207-15)
- KRYPTON ISOTOPES Kr-90
  - beta decay of, β and γ singles and coincidence spectra from, (E), 25:20384
- KRYPTON ISOTOPES Kr-91
  - beta decay of, γ spectra from, (E), 25:20459
- KYUSHU POWER REACTOR, UNIT 1
  - buildings and structures for, design parameters and construction schedule for, 25:20563
  - design parameters of, 25:20563
  - site for, preparation of, 25:20563

L

- LA CROSSE BOILING-WATER REACTOR
  - operations history for December 1970, 25:20573 (DOCKET-1155-104)
  - operations history for November 1970, 25:20571 (DOCKET-1155-102)
  - operations incident of February 11, 1971, unplanned shutdown from leaking control rod drive accumulator check valve, 25:20572 (DOCKET-1155-103)
  - operations incident of January 20, 1971, plant electrical power failure, 25:20569 (DOCKET-1155-100)
  - operations incident of January 29, 1970, unplanned shutdown from low flow trip of forced circulation pump, 25:20570 (DOCKET-1155-101)
  - pressure vessel for, stresses in laminated region of, 25:20600 (DOCKET-1155-105)
- LABORATORY FURNITURE
  - design of process hoods for handling plutonium nitrate solutions, 25:18628
- LANTHANUM
  - abundance in Type-M supergiant, (E), 25:19323
  - chromatographic behavior in hydrochloric acid--thiocyanate mixture on Amberlite LA-2, 25:18337
  - determination using 4,5-dihydroxy-m-benzenedisulfonic acid, in presence of Eriochrome Cyanine R, titrimetric, 25:18348
  - determination using azo compounds, photometric, 25:18347
- LANTHANUM ALLOYS AND SYSTEMS
  - Ce--La-base, Kondo resistance anomaly and superconducting transition temperature of, effects of pressure on, (E/T), 25:19863
  - La--Sc, phase studies of, 25:19241
  - properties of, 25:19241
- LANTHANUM ISOTOPES La-140
  - use to demonstrate retention of actinide and lanthanide liquid aerosols in alveolar lipoproteins of monkeys and rats in vitro and in vivo, 25:18889 (CEA-CONF-1676)
- LANTHANUM ISOTOPES La-141
  - energy-level transitions from barium-141 decay, conversion coefficients and multipolarities for, (E), 25:20415
- LANTHANUM ISOTOPES La-142
  - energy levels from barium-142 decay, conversion coefficients and multipolarities for, (E), 25:20415
- LANTHANUM OXIDES
  - oxygen isotope exchange on, effects of conditions of preliminary treatment on rate of homomolecular, 25:18389
- LANTHANUM TELLURATES
  - $La_2(TeO_3)_3$--$La_2(TeO_4)_3$, analysis for hexavalent tellurium and total tellurium by automatic amperometric and potentiometric titrations, 25:18351
- LANTHANUM TELLURITES
  - $La_2(TeO_3)_3$--$La_2(TeO_4)_3$, analysis for hexavalent tellurium and total tellurium by automatic amperometric and potentiometric titrations, 25:18351
- LARVAE
  - radiation effects on development and survival of fish, effects of dose on x, 25:19103 (PG-Report-1013)
  - radiation effects on pupation and survival of Tenebrio, effects of partial shielding on x, 25:19094
  - radioinduced attenuation of nematode, effects of dose on electron and x, 25:19101
  - radioinduced suppression of populations of pink bollworm, following release of exposed moths, γ, 25:19102
  - radioisotope content of tick, following inoculation of females, 25:18934(R) (ORO-3514-10)
  - radiosensitivity of Phaenicia sericata, effects of age on x, 25:19098
- LARYNX
  - radiotherapy of neoplasms of human, comparison of effectiveness of cobalt-60 γ, with surgery, 25:18998
  - radiotherapy of neoplasms of human, comparison of effectiveness of, with surgery, 25:19083
- LASER RADIATION
  - effects on human bones, comparison of gas and solid-state laser, 25:19146
  - effects on light evoked electric responses of eyes of rabbits, mechanisms of ruby, 25:19132
  - effects on man following dermatology, neoplastic surgery, or neurosurgery, 25:19074
  - interactions with plasma, energy requirements for inertially confined, (T), 25:19646 (IPP-4/7)
  - interactions with plasma, far-infrared radiations from, 25:19679
  - reactions with foils, plasma production in, 25:19701
  - reactions with lithium hydride targets, plasma production in, 25:19702
  - reactions with solid targets, plasma expansion into vacuum from, (E), 25:19703
- LASERS
  - hazards to man, review of, 25:19133 (NP-18714)
  - performance of HCN laser interferometer, for plasma diagnostics, 25:19663
  - use for production of thermonuclear reactions, 25:19724 (FOA-4-4449)
- LEAD
  - cascade showers in, Monte Carlo calculations of transition effects at water interface for 1-GeV-electron-initiated, 25:19943
  - chromatographic behavior in hydrochloric acid--thiocyanate mixture on Amberlite LA-2, 25:18337
  - compressibility from melting point to critical regions, 25:20880 (NYO-4176-4)
  - dislocation mobility in normal and superconducting single crystals of, (E), 25:19589
  - gamma spectra distortion in absorbers of, 25:18771
  - incorporation in elastomeric shielding materials, method for, 25:19294(P)
  - magnetic-field-trapping properties of hollow cylinders of, anomalous length effects in, 25:19611
  - manganese-ion implantation at 250 keV in films of, effects on electric conductivity, 25:19857
  - neutron inelastic scattering by, γ energies from fast, (E), 25:20356
  - phonon interactions with electrons in superconducting films in junctions, (E/T), 25:19607
  - proton reactions at high energies, atlas of hadron momentum spectra from, (T), 25:20028
  - separation from iron and thorium by extraction as caproate into chloroform, 25:18506
  - separation of bismuth from, by cation exchange chromatography, 25:18520
- LEAD ALLOYS AND SYSTEMS
  - In--Pb, dislocation mobility in normal and superconducting single crystals of, (E), 25:19589
  - In--Pb, magnetization curves of intermediate mixed state of Type-II superconducting, 25:19620
  - In--Pb-base, magnetization of superconducting cylinders of, local, 25:19626
  - Mg-base--Pb--Zr, crystal structure of phases in dilute, 25:19228
  - Mg-base--Pb--Zr, mechanical properties of dilute, effects of heat treatments in carbon dioxide on, 25:19228
  - Pb--Styrofoam, gamma shielding properties of composites of, 25:19011
- LEAD HALIDES
  - separation by solvent extraction, effects of charge, composition, and structure on, 25:18511
- LEAD IONS
  - implantation in germanium at 30 to 40 keV, channeling study of lattice location of, 25:19827
- LEAD ISOTOPES
  - energy levels from neutron inelastic scattering, (E), 25:20356
- LEAD ISOTOPES Pb-206
  - neutron inelastic scattering at 2.9 MeV, γ-ray differential cross sections for, (E), 25:20329
- LEAD ISOTOPES Pb-207
  - nitrogen-14 reactions (N-14,xn) with, excitation functions for total neutron emission for, (E), 25:18737(R) (ORO-3820-7)
  - proton reactions up to several GeV, cascade calculations of double differential distributions of particles from,

XUM

(T), 25:20018 (JINR-P2-5507)

LEAD ISOTOPES Pb-208
- nuclear radii of, statistical ensemble calculations of, (T), 25:20505
- photon reactions (γ,xn) at 35 MeV endpoint energy, excitation functions, spectra, and integrated cross sections for, (E/T), 25:20437
- proton reactions (p,nγ) at 7 to 11 MeV, proton-particle neutron-hole states in bismuth-208 from, (E), 25:20434

LEAD ISOTOPES Pb-210
- accumulation in aquatic ecosystems in Finland, 25:18930 (NYO-3446-14, Paper 27)
- activity of natural in ground level atmosphere in Finland, 25:18933 (NYO-3446-14, Paper 32)
- beta decay of, angular distribution and energy spectra of internal bremsstrahlung emitted during, (E/T), 25:20417
- content of food chains in Finland, 25:18931 (NYO-3446-14, Paper 30)
- content of man in Finland during 1960 to 1970, 25:18986 (NYO-3446-14, Paper 28)
- content of terrestrial birds and mammals of Finland, comparison of bone and soft tissue, 25:18929 (NYO-3446-14, Paper 26)
- use as natural tracer for lead uptake from atmosphere by man, 25:18933 (NYO-3446-14, Paper 32)

LEAD ISOTOPES Pb-212
- decay in SNAP-15A heat source, measurement of gamma spectra from, 25:18601

LEAD ISOTOPES Pb-214
- gamma emission from, use for leak testing radium-226 applicators, 25:19016

LEUKOCYTES
- radiation effects on count of dogs, sensitizing effects of dinitrochlorobenzol on x, 25:19030
- radiation effects on count of goat, correlation of x, with recovery from radiation injury, 25:19115

LEVEL INDICATORS
- development of radiometric, for determining amounts of fill materials in vessels, 25:18820(P)

LICHENS
- Cladonia sp., radioisotope content of, in Finnish Lapland during 1968 and 1969, 25:18932 (NYO-3446-14, Paper 31)

LIFE SPANS
- radiation effects on, of cotton leaf worm exposed as pupae, γ, 25:19097
- radiation effects on, of mice, effects of dose on γ, neutron, and x, 25:19105

LIMERICK POWER REACTOR, UNIT 1
- design parameters of, revised and additional data on, 25:20675 (DOCKET-50352-11)
- operations aspects of, revised and additional data on, 25:20675 (DOCKET-50352-11)

LIMERICK POWER REACTOR, UNIT 2
- design parameters of, revised and additional data on, 25:20675 (DOCKET-50352-11)
- operations aspects of, revised and additional data on, 25:20675 (DOCKET-50352-11)

LIMESTONE
- radiation effects on properties of, for use in concrete shielding aggregates, neutron, 25:19296

LINEAR ACCELERATORS
- beam current monitoring system for NBS, performance of, 25:20197
- beam instability in sectional theory of transverse, 25:20215
- beam stabilization in electron, radiative effects accompanying, 25:20219
- beam transport in high-current electron, effects of magnetic lens aberration on, 25:20160
- cavity resonators for LAMPF, dynamic measurements of stopband in, 25:20132 (LA-4593)
- cavity resonators for low-energy, interdigital H-type, 25:20156
- charge-particle clusters in, self-consistent oscillating, 25:20181
- description of Swierk 10-MeV proton, 25:20129 (INR-P-1218)
- design modifications for acceleration of solid particles, 25:20183
- design of ion, with no drift tubes, 25:20172
- development of high-current, 25:20186
- experimental facilities for Mainz electron, for photon scattering below 140 MeV, 25:20189
- experimental facility for ORELA, for fast neutron capture cross section measurements, 25:20149
- theory of high-current, 25:20186

LINEAR ENERGY TRANSFER
- effects on therapeutic effectiveness of radiations for treatment of human neoplasms, 25:19077
- measurement of, development of proportional detector for, 25:18644 (ORNL-4584, pp 152-64)

LINGEN POWER REACTOR
- operation of summary of, 25:20560

LIPOPROTEINS
- aerosol retention in, alveolar, of monkeys and rats, use of lanthanum-140 to demonstrate stability of complex formed following in vitro and in vivo actinide and lanthanide liquid, 25:18889 (CEA-CONF-1676)

LIQUID FLOW
- boiling in free convection, effect of heat source configuration on, 25:20728
- magnetohydrodynamic channel resistance in, in transverse magnetic field, 25:19554
- magnetohydrodynamic unsteady, of mercury in trough in transverse magnetic field, (E/T), 25:19553
- magnetohydrodynamic, effect of dissipative processes in sheath on stability of surface of liquid metal, 25:19551
- magnetohydrodynamic, Hall current and resistivity effects on stability of gas--liquid system, (T), 25:19546

LIQUID METAL FAST BREEDER REACTOR
- accidents in, analysis of aerosols of sodium oxide and sodium iodide released from sodium combustion, 25:20761 (CONF-700816-(Vol.1), pp 373-92)
- accidents in, analysis of radioactive aerosol release from, (E/T), 25:20757 (CONF-700816-(Vol.1), pp 26-48)
- accidents in, analysis of release of sodium oxide aerosols from sodium combustion, (E), 25:20759 (CONF-700816-(Vol.1), pp 346-55)
- boilers for, review of U.S. design codes and standards for, 25:20723 (SAN-781-217)
- coolant for, characteristics of iodine in liquid sodium, (E), 25:20760 (CONF-700816-(Vol.1), pp 356-72)
- coolant vaporization in, effects of superheating on, 25:19191 (ANL-7706)
- development program for, review of economics and objectives of, 25:20692 (CONF-700816-(Vol.1), pp 289-316)
- fuel for, solvent performance in Purex Process for reprocessing of, 25:18505 (WHAN-FR-32)
- fuels for, development and performance of plutonium oxide--uranium oxide, 25:19275
- neutron flux measurements in, development of beryllium-9 gas flow activation detector for, 25:18646 (WHAN-SA-73)
- piping systems for, design guide for liquid sodium, 25:20720 (SAN-781-1)
- piping systems for, design requirements for, 25:20721 (SAN-781-110)
- piping systems for, failure mechanisms and incidents for, 25:20722 (SAN-781-214)
- piping systems for, failure mechanisms and theories for, (T), 25:20724 (UNC-5235)
- piping systems for, review of U.S. design codes and standards for, 25:20723 (SAN-781-217)
- pressure vessels for, review of U.S. design codes and standards for, 25:20723 (SAN-781-217)
- radioactive effluents from, analysis of accident release of aerosol, (E/T), 25:20757 (CONF-700816-(Vol.1), pp 26-48)
- thermometry system for, development of ultrasonic, 25:18830(R) (NYO-3906-12)

LIQUIDS
- radiolysis of, self-absorption of Cherenkov light as indicator of progress of, 25:18453

LITHIUM
- corrosive effects on tantalum, effects of iridium on inhibition of, 25:19168(P)

LITHIUM ALLOYS AND SYSTEMS
- Al-base--Li, hardening in neutron irradiated, mechanisms of precipitation, 25:19201

LITHIUM CARBONATES
- benzene--hexane--Li_2CO_3, radiation effects on, yields from reactions of tritium recoil atoms from neutron, 25:18487

LITHIUM HYDRIDES
- plasma of, expansion of laser-produced, (E), 25:19703
- plasma of, production by laser irradiation of solid targets, 25:19702
- plasma of, recombination processes in laser-produced, 25:19697

LITHIUM IONS
- implantation in silicon at 30 to 400 keV, calculated spatial distributions of damage from, 25:19819
- potential-energy curves for diatomic Li_2^+, (T), 25:19479

LITHIUM ISOTOPES Li-6
- alpha elastic scattering at 3.30 to 5.00 MeV, excitation functions for, (E), 25:20292
- energy levels from fluorine-19 (He-3,Li-6) reactions, (E), 25:20284
- neutron reactions (n,α) at 10 eV to 80 keV, ratio of cross section to boron-10 (n,α) cross section, (E), 25:20288
- nuclear core distortion in, analysis using full single pair model and harmonic polynomials method, 25:20304
- wave function of, effects of central potentials on ground state, 25:20494

LITHIUM ISOTOPES Li-7
- helium-3 reactions (He-3,d) and (He-3,p) at 10 MeV, angular distributions for, (E), 25:20273

LITHIUM PERCHLORATES
- radiolysis of aqueous solutions of, electron pulse, 25:18474

LIVER
- radiation effects on uptake of α-aminoisobutyric acid, inulin, orotic acid, and phosphorus-32 by rat, effects of AET and cysteamine on γ, 25:19024
- radioinduced aberrations of metaphase chromosomes in cells of hamster, effects of hepatectomy on γ, 25:18960
- radioinduced injuries of, in children, synergistic

  - effects of antineoplastic drugs on, 25:18999
  - radioinduced production of toxin in rat, 25:18915
  - scanning in human children for measurement of hepatic growth, 25:19061
  - scanning of human, evaluation of spleen size during, using technetium-99m, 25:19057
- LOOPS
  - design for testing organic Rankine cycle working fluids, 25:18594(R) (ORNL-TM-3292)
- LOS ALAMOS AREA (N. MEX.)
  - radiation monitoring during 1970, 25:18985 (LA-4563)
- LOS ALAMOS MESON PHYSICS FACILITY
  - linear accelerator for, dynamic measurements of stopband in, 25:20132 (LA-4593)
- LOVIISA POWER REACTOR
  - construction of, schedule and cost of, 25:20559
  - design parameters of, 25:20559
- LUCENS REACTOR
  - maintenance of, description of remote handling equipment for irradiated fuel assemblies dismantling, 25:20554
- LUNGS
  - ascariasis in, of x-irradiated mice, effectiveness of active immunization, anthelmintics, and antibiotics for treatment of, 25:19032
  - function of human, use of technetium-99-labeled sulfur colloids and xenon-133 for studying, 25:19044
  - plutonium oxide retention in, of baboons following inhalation, effects of washing on, 25:18895
  - radioinduced carcinoma in, following fluoroscopy and pneumothorax therapy in patients with tuberculosis history, x, 25:19068
  - scanning for regional function in patients with metastatic carcinomas, use of xenon-133 for, 25:19048
  - scanning of human, preparation of technetium-99m-labeled macroaggregated iron hydroxide for, 25:19054
  - scanning of human, using krypton-81m, 25:19056
- LUTETIUM
  - detection in low-energy cosmic radiation, (E), 25:19525
- LUTETIUM ALLOYS AND SYSTEMS
  - Fe--Lu, magnetic susceptibility of $LuFe_2$, 25:19871
- LUTETIUM ISOTOPES Lu-170
  - beta decay of, gamma and conversion electron spectra and log ft for, (E), 25:20452
- LUTETIUM ISOTOPES Lu-175
  - gamma circular polarization from, effect of form factor in calculation for, (T), 25:20423
  - neutron capture by, mechanism and resonance parameters for, (E), 25:20476
  - proton reactions (p,2nγ) at 12 MeV, energy levels of hafnium-174 from, (E), 25:20427
- LUTETIUM ISOTOPES Lu-176
  - photon scattering using cobalt-60 source, isomeric activation cross section for, (E), 25:20464
- LUTETIUM ISOTOPES Lu-180
  - beta decay of, coincidence and gamma spectrometric studies on, (E), 25:20426
  - production by hafnium-180 (n,p) reactions at 14.8 MeV, (E), 25:20426
- LYMPH NODES
  - radiotherapy of metastases of pharyngeal carcinomas in human neck, methods for x, 25:19084
- LYMPHOCYTES
  - metabolism in, tritium tracer study of deoxycytidine and thymidine, 25:18919(R) (RLO-2225-T-16-1)
  - radiation effects on incorporation of carbon-14-labeled pyruvate into tricarboxylic acid cycle in rat, in-vitro x, 25:18902
  - radiation effects on life span and potential for repopulating hemopoietic tissues, 25:18919(R) (RLO-2225-T-16-1)
- LYNX
  - radioisotope content of bones and soft tissues of, in Finland, 25:18929 (NYO-3446-14, Paper 26)
- LYSOZYME
  - radioinduced inactivation of, in aqueous solution, relation of alteration of chemical composition to γ, 25:18917

M

- MC GUIRE POWER REACTOR, UNIT 1
  - effluents from, effects on environment of radioactive and thermal, 25:20679 (DOCKET-50369-6)
  - effluents from, effects on environment of radioactive and thermal, 25:20679 (DOCKET-50369-6)
- MAGNESIUM
  - abundance in α^2 CVn, (E), 25:19339
  - chromatographic behavior in hydrochloric acid--thiocyanate mixture on Amberlite LA-2, 25:18337
  - determination in natural waters from uranium mining operations, method for, 25:18339 (CEA-R-3557(2))
  - deuteron elastic scattering at 7.0 MeV, deuteron tensor polarization from, (E), 25:20342
  - effects on fluoride hydrolysis, catalytic, 25:18375
  - electron reactions at 80 keV with, radiative decay spectra from, (E), 25:19758 (ORNL-4584, pp 74-86)
  - energy-level transitions in, minima in generalized oscillator strengths for, (T), 25:19521
  - neutron inelastic scattering by, γ energies from fast, (E), 25:20356
  - separation of bismuth from, by cation exchange chromatography, 25:18520
  - sorptive properties for oxygen and water, relation of exoelectron emission to, 25:19758 (ORNL-4584, pp 74-86)
- MAGNESIUM ALLOYS AND SYSTEMS
  - properties for use as fuel cladding, 25:19203
  - Ag--Mg, polar-reflection Faraday effect in α-phase disordered, Fermi surface and band lifetime from, 25:19873
  - Al-base--Mg, radiation effects on tensile properties of, fast neutron, 25:19255
  - Mg-base--Pb--Zr, crystal structure of phases in dilute, 25:19228
  - Mg-base--Pb--Zr, mechanical properties of dilute, effects of heat treatments in carbon dioxide on, 25:19228
- MAGNESIUM ALUMINUM OXIDES
  - physical properties of molten, to 3000°C, equipment and methods for measuring, 25:19273 (BNWL-SA-3579)
- MAGNESIUM FLUORIDES
  - optical properties of, (E), 25:19758 (ORNL-4584, pp 74-86)
- MAGNESIUM ISOTOPES
  - energy levels from neutron inelastic scattering, (E), 25:20356
- MAGNESIUM ISOTOPES Mg-24
  - alpha decay of, branching ratios for, (E), 25:20291
  - alpha inelastic scattering from the 5.23-MeV level at 40.2 to 79.5 MeV, angular distribution and optical-model parameters for, (E), 25:20344
  - deuteron reactions (d,n) at 2 to 3.2 MeV, cross-section measurements by detection of positron annihilation γ rays, (E), 25:20283
  - energy levels from carbon-12 (O-16,α) reactions, spin-parity assignments for, (E), 25:20291
  - neutron inelastic scattering at 2.9 MeV, γ-ray differential cross sections for, (E), 25:20329
  - oxygen-16 inelastic scattering at 22 MeV, relative cross sections from, (E), 25:18750
- MAGNESIUM ISOTOPES Mg-26
  - alpha reactions (α,p) at 35.5 MeV, DWBA analysis of j dependence in angular distributions from, (E), 25:20309
  - neutron capture by, resonance integrals and partial widths of resonances in, (E), 25:20359
- MAGNESIUM LANTHANUM NITRATES
  - targets of neodymium-doped, development of polarized proton, 25:20135 (RHEL/R-201)
- MAGNESIUM OXIDES
  - effects on radioinduced polymerization of styrene with methyl methacrylate, 25:18442
  - optical properties of, (E), 25:19758 (ORNL-4584, pp 74-86)
- MAGNET COILS
  - acceleration by traveling electromagnetic fields, diagnostics of, (E), 25:19669 (NP-18715)
  - eddy-current losses from pulsed magnetic fields, (T), 25:19572 (IPP-4/80)
  - fabrication and testing of superconducting, (E), 25:19588 (JINR-P8-5440)
  - fabrication of small superconducting, 25:19634
  - magnetic fields of thick finite d-c, 25:18829 (JINR-P9-5441)
  - uses of small superconducting, in plasma physics, 25:19634
- MAGNETIC ANALYZERS
  - chromatic aberrations in, elimination of, 25:18875
- MAGNETIC FIELDS
  - compression by cylindrical conducting envelopes, (T), 25:19549
  - effects on thermal capacity of praseodymium at 1.2 to 4.2°K, 25:19869
  - electron kinetics in strong crossed electric and, diffusion approximation for hot, (T), 25:19960
  - irregularities of interplanetary, effect on solar-proton diffusion during Feb. 25, 1969 event, (E/T), 25:19414
  - measurement using electron beam and electrostatic analyzer, 25:18865
  - strength of mean, at surfaces of Ap, (E), 25:19308
  - structure of galactic, (T), 25:19459
  - Zeeman triplet in nonuniform, absorption matrix for normal, (T), 25:19406
- MAGNETIC MATERIALS
  - heat treatment effects on properties of soft magnetic alloys, review, 25:19872
- MAGNETIC MIRROR MACHINES
  - plasma diagnostics in Burnout V, fractional fringe HCN laser interferometer for, 25:19663
- MAGNETIC MIRRORS
  - plasma confinement in, effect of rf fields on loss cone, 25:19649
  - plasma stabilization in minimum-B fields, warm quiescent, 25:19705
- MAGNETIC MONOPOLES
  - quantum field theory for, local-Lagrangian, 25:20072
- MAGNETIC SEPARATORS
  - design of gas-filled, for heavy-ion reaction products, 25:20175
- MAGNETIC STORMS
  - effects on cosmic-ray diurnal variations, (E), 25:19530
  - effects on fibrinolytic activity in rheumatic patients, inhibitory, 25:19145

XUM

MAGNETOHYDRODYNAMIC GENERATORS
- current distribution in channels of, with solid electrodes of finite resistance, 25:19542
- design of rare gas, for nuclear power plant, parametric study of, 25:19536 (JUL-706-TP)
- design of shorter channels for Hall-effect, using liquid metals, 25:19563
- edge effect in primary circuit of linear, longitudinal, (T), 25:19538
- end effects in channels with finite-size terminal insulators, (T), 25:19548
- gas flow in, stabilization of electrothermal instabilities in, (T), 25:19543
- magnetic field calculations in winding zone of plane linear induction, allowing for finite permeability of iron, 25:19539
- Montardy scheme use with segmented electrodes for, with isotropic conducting working substances, 25:19541
- primary loops of, compensation of longitudinal edge effect in, 25:19537
- stationary regime of Faraday segmented, in non-rated plasma input parameters, (T), 25:19540

MAGNETOHYDRODYNAMICS
- equations of, completely conservative difference schemes for, (T), 25:19571

MAGNETOMETERS
- errors in Hall probe, in inhomogeneous fields, 25:18833
- properties of superconducting junctions as, 25:19643

MAGNETOSPHERE
- electron spectra in, from April 1969 solar flare, (E), 25:19428
- plasma streaming in plane of magnetic equator, steady-state cold, (T), 25:19577
- solar wind interactions with, hydromagnetic waves in bow shock, 25:19580

MAGNETS
- electromagnetic induction of rotating superconducting, 25:19639
- fabrication problems of large superconducting, 25:19633
- heat dissipation in pulsed superconducting, colorimetric method for determination of, (E), 25:19642
- performance of high-current-density superconducting, using heavy currents, 25:19644
- power supplies for, design of transistor control element for current regulation of pulsed, 25:20208
- properties of quadrupole and bending, for ion beam transport systems, 25:20205

MAINE YANKEE POWER REACTOR
- design parameters of, requested additional information on, 25:20666 (DOCKET-50309-28)
- design parameters of, revised and additional data on, 25:20665 (DOCKET-50309-27)
- effluents from, effects on environment of chemical, radioactive, and thermal, 25:20667 (DOCKET-50309-29)
- operations aspects of, requested additional information on, 25:20666 (DOCKET-50309-28)
- operations aspects of, revised and additional data on, 25:20665 (DOCKET-50309-27)

MALEIC ACID
- radiation effects on glasses of tetrahydro-2-methylfuran containing, at 77°K, photoisomerization of maleate radicals produced by γ, 25:18457

MALEIC ACID, DIETHYL ESTER
- radiation effects on glasses of tetrahydro-2-methylfuran containing, at 77°K, photoisomerization of maleate radicals produced by γ, 25:18457

MALEIC ACID, DIMETHYL ESTER
- radiation effects on glasses of tetrahydro-2-methylfuran containing, at 77°K, photoisomerization of maleate radicals produced by γ, 25:18457

MALONIC ACID
- radiolysis of aqueous perchloric acid solutions of, rate constants for reactions of hydrogen atoms produced by γ, 25:18459

MAMMALIA
- longevity in, biological prerequisites of, 25:20847(T) (ANL-Trans-875)
- mutation induction in, evaluation of chemical, 25:18965
- radiation effects on survival of rodent, effects of artificial hypothermia and ischemia on lethal whole-body, 25:19093

MAN
- book: Bone Tumors in Man and Animals, 25:19136
- cesium-137 content of reindeer herders in Finnish Lapland, effects on whole-body γ dose, 25:18987 (NYO-3446-14, Paper 29)
- fibrinolytic activity in blood of, with rheumatism, effects of solar activity on, 25:19145
- indium-113m dosimetry in bone marrow, liver, and spleen of, following injection as colloid for scanning, 25:18994
- iodine-131 dose to thyroid of, from milk produced in Norway, relation of frequency of cancer to, 25:19135
- iodine-131 retention in, with thyroid carcinoma, use of whole-body counting for measuring, 25:19035
- iodine-131 uptake by thyroid in, use for diagnosis of hyperthyroidism and hypothyroidism, 25:19051
- iodine-131 uptake by thyroid of, following release to atmosphere during nuclear explosions, 25:18926 (CONF-700816-(Vol.1), pp 49-71)
- lead inhalation by, use of natural lead-210 in atmosphere as tracer for study of, 25:18933 (NYO-3446-14, Paper 32)
- leukemia incidence in, exposed to atomic bombing on Hiroshima and Nagasaki, 25:18990 (ORNL-4584, pp 129-51)
- liver scanning in children for estimation of hepatic growth, 25:19061
- neoplasm incidence in children exposed in utero to atomic bombing at Hiroshima and Nagasaki, 25:19089
- neutron dose to, maximum permissible fast, 25:19007 (NCRP-38)
- radiation dose to body of, during diagnostic radiography, method for measurement of x, 25:19038
- radiation dose to tissues of head and neck of, during dental radiography using intracavitary machine, x, 25:19001
- radiation dose to, during diagnostic radiography, methods for reducing, 25:19009
- radiation dose to, during use of tritium as label for total body water determinations, methods for reducing β, 25:18977 (AD-702155)
- radiation dose to, establishment of limits for maximum permissible, 25:19018
- radiation dose to, exposed to atomic bombing on Hiroshima and Nagasaki, methods for estimation of fast neutron and γ, 25:18990 (ORNL-4584, pp 129-51)
- radiation dose to, following external exposure or ingestion of radioisotopes released during nuclear excavation, 25:18989 (ORNL-4584, pp 42-56)
- radiation dose to, from accidental intake of nuclear submarine corrosion products, 25:19014
- radiation dose to, from artificial and natural sources, 25:19137
- radiation dose to, from internally-deposited radioisotopes, methods for calculation of, 25:18991 (ORNL-4584, pp 200-22)
- radiation dose to, in Finland from natural and artificial gamma sources, 25:18986 (NYO-3446-14, Paper 28)
- radiation dose to, in Finland from natural sources, 25:18931 (NYO-3446-14, Paper 30)
- radiation dose to, in homes heated with Gasbuggy gas, methods for calculation of, 25:18989 (ORNL-4584, pp 42-56)
- radiation dose to, maximum permissible external and internal, 25:19008 (NCRP-39)
- radiation dose to, maximum permissible for medical, 25:19008 (NCRP-39)
- radiation dose to, on Kerala coast, India, from food, daily, 25:19143
- radiation dose to, residing in trajectory of atomic cloud released during underground nuclear explosion, 25:18989 (ORNL-4584, pp 42-56)
- radiation dosimetry in gastrointestinal tract of, following ingestion of radionuclides, mathematical model for, 25:19141
- radiation effects on abortion frequency in, in relation to chromosome aberrations, effects of dose on, 25:18969
- radiation effects on bone marrow of, following exposure from atomic bombing in Hiroshima, autoradiography studies on, 25:19134
- radiation effects on bones of, comparison of gas and solid-state in vitro laser, 25:19146
- radiation effects on Japanese, 14 years after exposure from Bikini nuclear test, long-term, 25:19148
- radiation effects on revascularization of therapeutic skin grafts on, microwave, 25:19104
- radiation effects on, effects of age, dose, dose rate, and sex on pathological, 25:19008 (NCRP-39)
- radiation effects on, effects of dose on carcinogenic and leukemogenic, 25:18971
- radiation effects on, environmental, 25:18941
- radiation effects on, following chronic internal and external exposure to natural background α, 25:18927 (NP-18670)
- radiation effects on, following dermatology, neurosurgery, or neoplastic surgery, laser, 25:19074
- radiation effects on, review of laser, 25:19133 (NP-18714)
- radiation hazards to, following polonium-210 pasture contamination, suggested revision of MPC values on basis of potential α, 25:18890(R) (COO-2044-3)
- radiation hazards to, from nuclear submarine corrosion products, 25:19014
- radiation injuries to skin of, mechanisms of pathogenesis following uv, 25:19150
- radiation injury of, rules for clinical and therapeutic procedures for, 25:18975 (CEA-N-1365)
- radiation protection of skin of, during therapy, use of lead glass radiation filters for γ, 25:19086
- radiation protection of skin of, during therapy, use of tin in radiation filters for γ, 25:19082
- radiodiagnosis of lung disorders in, using krypton-81m, 25:19056
- radiodiagnosis of myocardial infarction in, cesium-129 scanning method for, 25:19055
- radiodiagnosis of spleen involvement in Hodgkin's disease, 25:19058
- radioinduced aberrations in sperm of, following therapy for malignant lymphomas, reproductive factors in, 25:19147
- radioinduced chromosome aberrations in bone marrow cells

of, effects of exposure to atomic bomb on frequency of, 25:18963
  radioinduced histological changes in brain of, classification of, 25:19109
  radioinduced injuries of liver in children of, during therapy, effects of antineoplastic drugs on, 25:18999
  radioinduced injuries of skin of, effects of dose, dose fractionation, and time on fast neutron, 25:19149
  radioinduced injuries to, during radiodiagnosis, programmed instruction course on methods for protection against, 25:19010
  radioinduced mutations in, exposed to atomic bombing in Japan, statistics of, 25:18961
  radioinduced neoplasms of thyroid in, following inhalation of iodine-131 released to atmosphere during reactor accidents, methods for calculation of probability of, 25:18974 (AHSB(S)R-192)
  radioinduced neoplastic lesions in, following dental therapy, etiology and prevention of, 25:19069
  radioinduced osteosarcomas in clavicle of, following post-operative therapy for breast malignancies, 25:19140
  radioinduced rectovaginal fistulas in, following therapy, surgical methods for repair of, 25:19138
  radioinduced sterility in, following therapy for malignant lymphomas, reproductive factors in, 25:19147
  radioinduced vaginal fistulas in, following therapy for pelvic malignancies, mast cells studies on, 25:19139
  radioinduced vascular proliferation in cerebrum of, following therapy for cerebral gliomas, 25:19065
  radioisotope contamination of, rules for clinical and therapeutic procedures for internal, 25:18975 (CEA-N-1365)
  radioisotope content of bones and tissues of, in Finland, 25:18931 (NYO-3446-14, Paper 30)
  radioisotope content of, in Finland, during 1960 to 1970, 25:18986 (NYO-3446-14, Paper 28)
  radioisotope ingestion by, following accidental contamination of pastures, 25:18943
  radiotherapy of alopecia mucinosa in, further management and prognosis following soft x, 25:19073
  radiotherapy of carcinomas of mouth in, effectiveness of γ and x, 25:19081
  radiotherapy of carcinomas of tonsils in, effectiveness of γ, 25:19085
  radiotherapy of cervical carcinomas in, cytology and histology of cells following linear accelerator, 25:19064
  radiotherapy of head and neck tumors of, effects of mitotic synchronization with fluorouracil on survival following x, 25:19071
  radiotherapy of hyperthyroidism in, review of effectiveness of iodine-131 for internal, 25:19062 (NP-18693)
  radiotherapy of lymph node metastases from pharyngeal carcinomas in, use of whole-neck exposure for x, 25:19084
  radiotherapy of neoplasms in, afterloading techniques for implant, 25:19076
  radiotherapy of neoplasms of head, neck, and pelvis of, review of complications necessitating surgery following high-dose, 25:19088
  radiotherapy of neoplasms of larynx and pharynx of, comparison of effectiveness of cobalt-60 γ, with surgery, 25:18998
  radiotherapy of neoplasms of mouth and tongue in, effectiveness of iridium-192 applicators for γ, 25:19080
  radiotherapy of neoplasms of mouth of, dental care and oral hygiene before, during, and following, 25:19079
  radiotherapy of osteosarcomas in femur of, effects of localized hypothermia and ischemia on skin reactions following, 25:19093
  radiotherapy of primary neoplasms of larynx, mouth, and pharynx of, comparison of effectiveness of, with surgery, 25:19083
  radium-224 carcinogenicity and dosimetry in, following ingestion or injection, review of, 25:18979 (BRH/DBE-70-5)
  radium-226 carcinogenicity and dosimetry in, following ingestion or injection, review of, 25:18979 (BRH/DBE-70-5)
  shielding organs of, during therapy, development of lead shot filled Styrofoam shields for γ, 25:19011
  treatment of burns on, effectiveness of frozen irradiated pigskin xenografts for, 25:19020
MANGANESE
  abundance in α And, (E), 25:19343
  abundance in α^2 CVn, (E), 25:19339
  chromatographic behavior in hydrochloric acid--thiocyanate mixture on Amberlite LA-2, 25:18337
  determination in high-purity cadmium by photon activation, 25:18366(R) (NBS-TN-548)
  determination in Italian meteorites by nondestructive neutron activation, 25:18370
  determination in natural waters from uranium mining operations, method for, 25:18339 (CEA-R-3557(2))
  reactions with dinucleotides, DNA, and nucleosides, 25:20854 (COO-78-235)
  separation of bismuth from, by cation exchange chromatography, 25:18520
MANGANESE IONS
  implantation in lead films at 250 keV, effects on electric conductivity, 25:19857
  implantation in zinc sulfide and selenide films at 250 kV, cathodoluminescence effects of, 25:19795
MANGANESE ISOTOPES Mn-54
  abundance in Bovedy meteorite, (E), 25:19301
  content of fresh water fish, molluscs, and mosses in France, technique for study of, 25:18937
  content of plants in Finnish Lapland during 1968 and 1969, 25:18932 (NYO-3446-14, Paper 31)
MANGANESE ISOTOPES Mn-55
  energy levels at 0.983 and 1.289 MeV from neutron inelastic scattering, spin assignments for, (E), 25:20329
  energy levels from gamma resonance absorption, widths for, (E), 25:20355
  neutron capture by, resonance integrals and partial widths of resonances in, (E), 25:20359
  neutron inelastic scattering at 2.9 MeV, γ-ray differential cross sections for, (E), 25:20329
MANGANESE ISOTOPES Mn-56
  energy levels of, calculation using strong-coupling rotational model, (T), 25:20353
MARITIME PRESSURIZED-WATER REACTOR
  fuel element removal from, additional safety analysis information for, 25:20815 (DOCKET-50238-144)
  fuel removal procedures for, safety analysis of, 25:20814 (DOCKET-50238-78)
MASS SPECTROGRAPHY
  developments in, review on, 25:18357(R) (NBS-TN-546)
MASS SPECTROMETERS
  characteristics of gas-filled magnetic, for studying heavy fast recoils from nuclear reactions, 25:18851
  chromatic aberrations in, elimination of, 25:18875
  data processing system for, off-line computer, 25:18835
  design of tandem, for secondary ion studies, 25:18841
  detectors for, design and performance of position-sensitive proportional, 25:18681
  development of recoil time-of-flight, at Texas A and M Univ, 25:18737(R) (ORO-3820-7)
MATERIALS TESTING
  methods for elastic--plastic strain and stress analysis for fracture in flawed specimens, 25:18611 (HSSTP-TR-12)
MATHEMATICAL PHYSICS
  normal-ordered moments in, inequalities satisfied by, (T), 25:19880
MATTER, ANTI-
  role in symmetric cosmology, (T), 25:19463
MEATS
  fish, radiation processing of Bombay duck, survival of spoilage bacteria following γ, 25:19163
  polonium-210 transfer to, of cattle and goats following ingestion as oxide, coefficients for, 25:18890(R) (COO-2044-3)
  reindeer, cesium-137 content in Finnish Lapland during 1966 to 1970, 25:18932 (NYO-3446-14, Paper 31)
MECHANICS
  theory for relativistic, theorem and potentials in, 25:20084
MEDICAL PERSONNEL
  radiation effects on blood cells of, review of effects of small doses on, 25:19142
  radiation protection of, during insertion of radioapplicators, evaluation of afterloading techniques for, 25:19076
  radioinduced injuries to, during radiodiagnosis, programmed instruction course on methods for protection against, 25:19010
MEDICAL SUPPLIES
  radiation processing of plastic, 25:19161
MEDICINE
  diagnosis in nuclear, review of, 25:19037
  radioisotope production for use in, generators for, 25:18885
  radioisotope use in clinical, for improvement of surgical efficiency, methods for, 25:19070
  rules for clinical and therapeutic procedures following accidental external irradiation or internal radioactive contamination, 25:18975 (CEA-N-1365)
MEIOSIS
  radiation effects on, in embryonic tissues of cotton following pollen exposure, γ, 25:18955
MEMORY DEVICES
  description of high-speed magnetic-chip, in scanning robot for measurement of bubble chamber particle tracks, 25:18780
  description of superconducting, and their development, 25:19637
MERCAPTO GROUP
  radioprotective effects of compounds containing, mechanisms of, 25:19021
MERCURY
  chromatographic behavior in hydrochloric acid--thiocyanate mixture on Amberlite LA-2, 25:18337
  compressibility from melting point to critical point, 25:20881 (NYO-4176-6)
  contents in meteorites from Russian collection, 25:19303
  determination in blood and kidneys by neutron activation, 25:18369
  diffusion of implanted, in germanium, during annealing,

  25:19841
  flow in trough in transverse magnetic field, unsteady, (E/T), 25:19553
  scattering by sodium atoms, crossed-beam measurements of differential cross sections and intermolecular potentials for, 25:19496
  separation of bismuth from, by cation exchange chromatography, 25:18520
  ultrasonic attenuation in normal and superconducting single crystals of, longitudinal, (E/T), 25:19608
MERCURY (PLANET)
  atmosphere of, models for, (T), 25:19467
MERCURY ALLOYS AND SYSTEMS
  Bi--Cd--Hg, phase studies of, 25:19236
  Hg--In, electrochemical properties of, 25:19190(T) (AI-Trans-287)
  Hg--Na_2Co_3, electric potential of aqueous solutions of, 25:19190(T) (AI-Trans-287)
MERCURY IONS
  implantation in germanium at 30 to 40 keV, channeling study of lattice location of, 25:19827
  implantation in silicon at 40 keV, carbon-ion channeling study of, 25:19829
MERCURY ISOTOPES
  hyperfine structure anomaly in, (E), 25:20397
  polarization of ground state of even-A, using paramagnetic resonance, (E), 25:20397
MERCURY ISOTOPES Hg-197
  effectiveness of chlormerodrin-incorporated, for kidney scanning, comparison of indium-113m-labeled DTPA with, 25:19039
  effectiveness of intravenously injected chlormerodrin-incorporated, for myeloscintigraphy, 25:19042
MERCURY ISOTOPES Hg-199
  oxygen-16 inelastic scattering at 25 and 33 MeV, energy levels from Coulomb excitation by, (E), 25:20387
MERCURY ISOTOPES Hg-200
  energy levels from thallium-200 decay, spin assignments for, (E), 25:20400
  energy-level transitions from thallium-200 decay, mixing parameters for, (E), 25:20400
MERCURY ISOTOPES Hg-201
  oxygen-16 inelastic scattering at 33 MeV, Coulomb excitation by, (E), 25:20387
MERCURY ISOTOPES Hg-203
  nuclear magnetic moment of, (E), 25:20397
  use as tracer for determining mercury contamination of fish in Finland, 25:18931 (NYO-3446-14, Paper 30)
  use of chlomerodrin incorporated, for radiodiagnosis of subdural hematoma, 25:19059
MESIC ATOMS
  energy levels of μ^-, effects of nuclear polarization on 3s, 3p, and 3d, (T), 25:19486
  energy-level shifts and widths in K^-, repulsive effects of nuclear absorption on, 25:19485
  meson (K^-) absorption in nucleus of repulsive effects from, 25:19485
  properties of π^-, review, (E/T), 25:19483
  x-ray spectra from yttrium-89 μ^-, (E), 25:20360
  x-rays from μ^- and π^-, target-detector assembly for detection and measurement of, 25:18748
MESIC MOLECULES
  model for large, 25:19482(T) (NRC-TT-1426)
MESONS
  couplings of scalar and pseudoscalar, analysis of SU(3)-invariant, 25:19983
  dual model with chiral symmetry for, 25:19981
  exchange in interactions of two spinless bosons, Schmidt method for solution of quasipotential equation for, (T), 25:19987 (JINR-P2-5566)
  interactions of spinless, by scalar meson exchange, Schmidt method for solution of quasipotential equation for two-body, (T), 25:19987 (JINR-P2-5566)
  interactions with baryons, multiparticle Veneziano formula for, 25:20014
  interactions with nucleons, scalar nucleon--vector meson interaction model for elastic and inelastic amplitudes of, (T), 25:19927
  interactions with π, Veneziano model for vector, 25:19997
  interactions with static baryon octet source, mass operator in SU(3) symmetric strong coupling theory for, (T), 25:20015
  interactions with weak gravitational fields, covariant Green functions of, (T), 25:20094
  production of octet 0^-, in decay of decuplet $3/2^+$ baryons, broken SU(6)/sub W/ for, (T), 25:20048
  production of vector, in photon reactions with heavy nuclei at high energies, Glauber theory of multiple scattering for cross sections for, (T), 25:19955
  symmetry algebra SU(n) in bootstrap models for, 25:19999
  symmetry SU(2) x SU(2) for pseudoscalar, breaking of scale invariance in nonlinear Lagrangian models of chiral, 25:20049
MESONS (eta)
  coupling with baryons, mass operator in SU(3) symmetric, (T), 25:20046
  decay eta → $\pi^0 + 2\gamma$, duality--finite-energy-sum-rule method for width of, (T), 25:19937 (DEMO-71/2)
  decay eta → $\pi^+ + \pi^- + \gamma$, Yang--Mills coupling of vector meson fields consistency with Veneziano model for, (T), 25:19985 (DEMO-71/1)
  decay eta → $\pi^+ + \pi^- + \pi^0$, charge conjugation violation from asymmetry in, (T), 25:19948
  decay of, bound 4π model for 3π, (T), 25:19948
  exchange in N + N interactions, one-boson-exchange approximation for, (T), 25:20024
MESONS (f)
  mass and width of, Balazs method for bootstrap for, (T), 25:19989
  mixing with graviton, Lagrangian theory for, 25:20053
MESONS (K)
  coupling with baryons, mass operator in SU(3) symmetric, (T), 25:20046
  decay K → $2\pi + l + \nu$, current algebra and chiral symmetry breaking for axial-vector form factors for, (T), 25:20041
  decay K → $\pi + l + \nu$, current algebra and chiral symmetry breaking for vector form factors for, (T), 25:20041
  decay K → $\pi + l + \nu$, incompatibility of chiral symmetry and leakage contributions to Fubini--Furlan sum rule for, 25:19970
  decay K → $\pi + \mu + e$, Okubo second-class currents in, (T), 25:19965 (NYO-2262-TA-236)
  decay of, Okubo second-class currents in two-body leptonic, (T), 25:19965 (NYO-2262-TA-236)
  interactions K + N at high energies, bounds on amplitudes and oscillations in diffraction-peak region for, (T), 25:19990
  interactions K + N at low energies, existence of K-mesic nuclei from assumption of positive sign of real part of amplitude of, (T), 25:20002 (IFVE-STF/SPK-70-30)
MESONS (K^-)
  absorption by neon in bubble chamber, production of excited states from, (E), 25:19908
  interactions $K^- + d$ at high energies, compilation of cross sections for, (E), 25:19909 (CERN-HERA-70-6)
  interactions $K^- + n \to \Lambda + \pi^-$ at 3 GeV/c, nucleon exchange in, (E/T), 25:19917
  interactions $K^- + n \to \Sigma^0 + \pi^-$ at 3 GeV/c, baryon exchange in, (E/T), 25:19917
  interactions $K^- + n \to V + \pi^-$ at 3 GeV/c, total and differential cross sections for, (E/T), 25:19917
  interactions $K^- + n$ at high energies, compilation of cross sections for, (E), 25:19909 (CERN-HERA-70-6)
  interactions $K^- + p \to K^{*0}(890) + n$ at 3.9 and 4.6 GeV/c in hydrogen bubble chamber, test of absorption-modified one-pion exchange model for forward structure in, (E/T), 25:19918
  interactions $K^- + p \to K^- + p$ at 14.25 GeV/c in hydrogen bubble chamber, differential and total cross sections for, (E), 25:19912
  interactions $K^- + p \to p + Q^-$ at 10 GeV/c, t-channel helicity conservation in diffractive, (E), 25:19921
  interactions $K^- + p$ at high energies, compilation of cross sections for, (E), 25:19909 (CERN-HERA-70-6)
  interactions $K^- + p$, model-independent determination of real parts of amplitudes for, 25:20013
  production in proton reactions with aluminum and beryllium at 70 GeV, yields and differential cross sections for, (E), 25:19906
  reactions with bromine, carbon, and fluorine at 10 GeV/c in bubble chamber, $K^-\pi^+\pi^-$ system coherent production and total cross sections for $K^-\pi^+\pi^- + N$ interactions in, (E), 25:19910 (LAL-1242)
  reactions with neon at 5.5 and 12.7 GeV/c in bubble chamber, $K^-\pi^+\pi^-$ system coherent production and total cross sections for $K^-\pi^+\pi^- + N$ interactions in, (E), 25:19910 (LAL-1242)
MESONS (K^0)
  decay $K^0 \to \pi^+ + \pi^-$, eigentime distribution for, 25:20144
  decay $K_1{}^0 \to 2\pi^0$, optical spark chamber study of branching ratio for, (E), 25:19897
  decay $K_1{}^0 \to \pi^+ + \pi^-$, optical spark chamber study of branching ratio for, (E), 25:19897
  decay $K_2{}^0 \to \pi^-(\text{eta}^+) + \mu^+(\mu^-) + \nu$, scintillation counter and spark chamber study of charge asymmetry ratio for, (E), 25:19898
  mass difference ($K_2{}^0 - K_1{}^0$), weak-interaction Hamiltonian for, (T), 25:20039
  production in $K^+ + p$ interactions at 12.7 GeV/c in hydrogen bubble chamber, cross sections for, 25:19914
  production of $K_2{}^0$ in photon reactions with beryllium at 5.5 to 9.5 GeV, counter--spark chamber study of differential cross sections for, (E), 25:19887
  production of pure beam of, target--detector system for, 25:20144
MESONS (K^+)
  decay $K^+ \to 3\pi$ at rest, π energy spectrum and $\Delta I = {}^1/_2$ rule violation in, (E>, 25:19895
  decay $K^+ \to 3\pi$, π^+ energy spectrum and branching ratios for, (E), 25:19896
  decay $\pi^+ \to \mu^+ + \nu$, determination of neutrino spectrum in, (E), 25:19892
  interactions $K^+ + p \to \Delta^{++} + K^{*0}(1420)$, $K^{*0}(1420) \to K^+ + \pi^-$ at 12.7 GeV/c in hydrogen bubble chamber, cross sections and production mechanism for, (E), 25:19914
  interactions $K^+ + p \to \Delta^{++} + K^{*0}(890)$, $K^{*0}(890) \to K^+(K^0) + \pi^-(\pi^0)$ at 12.7 GeV/c in hydrogen bubble chamber, cross sections and production mechanism for, (E), 25:19914
  interactions $K^+ + p \to K^0 + \Delta^{++}(1236)$ at 12.7 GeV/c in hydrogen bubble chamber, cross sections and production mechanism for, (E), 25:19914

interactions $K^+ + p \to K^+(K^0) + \pi^-(\pi^0) + \Delta^{++}$ at 12.7 GeV/c in hydrogen bubble chamber, $K^+ + \pi^- \to K^+(K^0) + \pi^-(\pi^0)$ interactions in, (E), 25:19914

interactions $K^+ + p \to K^+(K^0) + \pi^-(\pi^0)$, $K^+ + p \to K^+(K^0) + \pi^-(\pi^0) + \Delta^{++}$ interactions at 12.7 GeV/c in hydrogen bubble chamber for, (E), 25:19914

interactions $K^+ + p \to p + K^{*+}(890)$, $K^{*+}(890) \to K^0 + \pi^+$ at 12.7 GeV/c in hydrogen bubble chamber, cross sections and production mechanism for, (E), 25:19914

interactions $K^+ + p$ at 12.7 GeV/c in hydrogen bubble chamber, upper limits for meson resonance production in, (E), 25:19914

interactions $K^+ + p$ at 12.7 GeV/c in hydrogen bubble chamber, hyperon and antihyperon production properties in, (E), 25:19914

interactions $K^+ + p$ at 12.7 GeV/c in hydrogen bubble chamber, K^0, Λ, and anti Λ production cross sections for, (T), 25:19914

interactions $K^+ + p$, model-independent determination of real parts of amplitudes for forward, 25:20013

reactions with nuclei at 10 GeV/c in heavy-liquid bubble chambers, $Q^+(1275)$ enhancement and K(890) in coherent production of $K^+\pi^+\pi^-$ system in, (E), 25:19913

reactions with nuclei at 10 GeV/c in heavy-liquid bubble chamber, cross sections and momentum transfer distributions for coherent production of $K2\pi$, $K3\pi$, and $K4\pi$ systems in, (E), 25:19913

reactions with nuclei at 10 GeV/c in heavy-liquid bubble chambers, cross sections for $Q^+(1275) + N$ interactions in nucleus in, (E/T), 25:19913

MESONS (μ)

distribution in cosmic showers, lateral, (T), 25:19522 (INR-1231)

energy loss and straggling in iron for design of NAL shielding, calculations of, 25:20206

magnetic moment determination from Zeeman transitions in muonium, (E), 25:19888

magnetic moment of, computer program for anomalous, (T), 25:20055 (CNRS-CPT-70-P-335, pp IV.26-38)

magnetic moment of, review of anomalous, (T), 25:19936 (CNRS-CPT-70-P-335, pp IV.1-15)

MESONS (μ^-)

capture by yttrium-89, γ spectra from, (E), 25:20360

reactions with chemical compounds, review of processes in, 25:19482(T) (NRC-TT-1426)

MESONS (μ^+)

decay $\mu^+ \to 2e^+ + e^-$, upper limit for branching ratio for, (E), 25:19891 (JINR-P1-5542)

MESONS (ω)

decay $\omega \to 3\pi$, Yang--Mills coupling of vector meson fields consistency with Veneziano model for, (T), 25:19985 (DEMO-71/1)

decay $\omega \to e^+ + e^-$, sum rule for width of, (T), 25:20047

exchange in N + N interactions, one-boson-exchange approximation for, (T), 25:20024

production in four-prong p + p interactions at 19 GeV/c in hydrogen bubble chamber, (E), 25:19901 (USIP-70-7)

production in $p + p \to 2p + \pi^+ + \pi^- + \pi^0$ interactions at 19 GeV/c in hydrogen bubble chamber, (E), 25:19900 (USIP-70-4)

MESONS (phi)

decay phi $\to e^+ + e^-$, sum rule for width of, (T), 25:20047

exchange in N + N interactions, one-boson-exchange approximation for, (T), 25:20024

MESONS (π)

bound states (π--N), Bethe--Salpeter equation in ladder approximation for Regge trajectories of, (T), 25:20007

coupling constant difference effects on π exchange in N + N interactions, (T), 25:20021

coupling constant for πNN, from model-independent analysis of forward elastic $\pi^- + p$ and $\pi^+ + p$ interactions, (T), 25:20003 (JINR-E2-5561)

coupling of πN, effect on nuclear forces of second-order nonlinear term in, (T), 25:20021

coupling with baryons, mass operator in SU(3) symmetric, (T), 25:20046

exchange in N + N interactions, calculation of one-pion-exchange diagram in U(6,6) for, 25:20021

exchange in N + N interactions, effects of mass and coupling-constant differences on, (T), 25:20021

exchange in N + N interactions, one-boson-exchange approximation for, (T), 25:20024

form factor of, light-cone properties of axial-vector and electromagnetic current commutators for, (T), 25:19941

interactions of charged, oscillator formalism for construction of amplitudes for multi-particle, 25:19996

interactions of, kinematic superstructures for abnormal couplings in multiparticle dual amplitude of, 25:20000

interactions $\pi + N \to \omega + N$ at high energies, Regge pole model for differential and total cross sections and t dependence of density matrix elements for forward, (T), 25:20008

interactions $\pi + N$ at 1.98 to 3.5 GeV/c, phase shift analyses of elastic, (T), 25:20012

interactions $\pi + N$ at high energies, bounds on amplitudes and oscillations in diffraction-peak region for, (T), 25:19990

interactions $\pi + N$ at high energies, non-Pomeranchuk Regge cuts for minima and polarization in elastic and charge-exchange, (T), 25:20006

interactions $\pi + N$ at threshold, electromagnetic corrections to chiral symmetry for S-wave scattering lengths for, (T), 25:20044

interactions $\pi + N$, fixed-t dispersion relations for effective-range parameter for S-wave, (T), 25:20010

interactions $\pi + N$, nucleon matrix elements in chiral symmetry breaking calculations from phase shifts and dispersion relations for, 25:20051

interactions $\pi + p$, test of Pomeranchuk theorem from finite-energy sum rules for, 25:20011

interactions $\pi + \pi$ at high energies, bounds on amplitudes and oscillations in diffraction-peak region for, (E), 25:19990

interactions $\pi + \pi$ at low energies, method of uniterizing Veneziano model with crossing symmetry for, (T), 25:19993

interactions $\pi + \pi$ in colliding beams, feasibility using mini-rings, (T), 25:20153

interactions $\pi + \pi$, exact basic axiomatic results, absolute limits to amplitude, and positivity and linear constraints on partial waves for, (T), 25:19991

interactions $\pi + \pi$, interference terms in multiperipheral model for, 25:19998

interactions $\pi + \pi$, lectures on nonlinear techniques in S-matrix theory for, (T), 25:20107

interactions $\pi + \pi$, operation of mini-ring for colliding beam, 25:20162

interactions with nuclei at several hundred MeV, cross-section calculations using Glauber theory, (T), 25:20490

interactions with vector mesons, Veneziano model for, 25:19997

mass difference effects on π exchange in N + N interactions, (T), 25:20021

production in cosmic showers, (T), 25:19522 (INR-1231)

production in $e^+ + e^-$ interactions at high energies, light-cone properties of axial-vector and electromagnetic current commutators for, (T), 25:19941

production in $K^+ \to 3\pi$ decays, energy spectrum for, (E), 25:19895

production in photon reactions with nuclei, low-energy theorems for, 25:20019 (LYCEN-7081)

radius of, $\pi^+ \to e^+ + \nu + e^+ + e^-$ decay for electromagnetic, (T), 25:19963 (JINR-P2-5520)

Regge trajectories for, review of, (E), 25:19988

scattering by helium-4 at 24 MeV, equivalent potential for, (T), 25:20253

scattering by nuclei, low-energy theorems for elastic, (T), 25:20019 (LYCEN-7081)

symmetry for, dynamical rearrangement of spontaneously broken SU(2) x SU(2), 25:20042

symmetry for, lectures on chiral, (T), 25:20045

MESONS (π^-)

capture by helium-4, proton, deuteron, and triton spectra from, 25:20255

dose to tissues at 10 to 2000 MeV, calculation of, 25:20226

energy deposition in water at 160 to 220 MeV/c as function of depth, 25:19757 (ORNL-4584, pp 58-73)

evaluation for radiotherapy, 25:19078

interactions $\pi^- + d$ at 3.15 GeV/c in deuterium bubble chamber, neutron cross sections and $K^*(890)$, $\Sigma(1385)$, and $K\pi\pi(1200)$ enhancement in, (E), 25:19922

interactions $\pi^- + p \to \Delta^0(1236) + \pi^0$ at 5 GeV/c in propane bubble chamber, cross sections from Monte Carlo generation of, (T), 25:20004 (JINR-P13-5516)

interactions $\pi^- + p \to n + \text{eta}$, eta $\to 2\gamma$ at 5 GeV/c in propane bubble chamber, cross sections from Monte Carlo generation of, (T), 25:20004 (JINR-P13-5516)

interactions $\pi^- + p \to n + f^0$, $f^0 \to 2\pi^0$ at 5 GeV/c in propane bubble chamber, cross sections from Monte Carlo generation of, (T), 25:20004 (JINR-P13-5516)

interactions $\pi^- + p \to n + m\pi^0$ at 5 GeV/c in propane bubble chamber, cross sections from Monte Carlo generation of, (T), 25:20004 (JINR-P13-5516)

interactions $\pi^- + p \to p + A_1^-$ at 16 GeV/c, t-channel helicity conservation in diffractive, (E), 25:19921

interactions $\pi^- + p \to \pi^0 + n$ at 3.67 and 4.83 GeV/c at large momentum transfers, differential cross sections of, (E), 25:19911

interactions $\pi^- + p \to \pi^0 + n$ at 90 to 290 MeV, P-wave phase shift from total cross sections for, (E/T), 25:19915

interactions $\pi^- + p \to \pi^- + p$, amplitudes and πNN coupling constant from model-independent analysis of forward, (T), 25:20003 (JINR-E2-5561)

interactions $\pi^- + p$ at 70 to 290 MeV, Δ resonance parameters from total cross sections for, (E), 25:19916

interactions $\pi^- + p$ at low energies, analyticity and Pomeranchuk theorem violation predictions for, (T), 25:20005

interactions $\pi^+ + \pi^-$, determination of off-mass-shell S-wave amplitude of, 25:19994

photoproduction of π^---π^+ pairs in field of aluminum-27 at 313 MeV endpoint energy, π^- and π^+ energy spectra and π^-/π^+ ratio from, (E), 25:20341

production in $\gamma + d \to \pi^- + p + p$ interactions, impulse approximation calculation of recoil proton polarization for, (T), 25:19940

production in $\gamma + d$ interactions at high energies,

XUM

Glauber theory of multiple scattering for cross sections of, (T), 25:19955
- production in photon reactions with heavy nuclei at high energies, Glauber theory of multiple scattering for cross sections for, (T), 25:19955
- production in proton reactions with aluminum and beryllium at 70 GeV, yields and differential cross sections for, (E), 25:19906
- production in π^+ reactions with nuclei at 185 to 295 MeV in emulsions, cross sections for, (E), 25:19919
- production of $\pi^+ - \pi^-$ pairs in γ reactions with carbon at 5.8 to 6.6 GeV/c, magnetic spectrometer study of (1550) enhancement in mass spectrum for, (E), 25:19886 (DESY-70/61)
- reactions with chemical compounds, review of processes in, 25:19482(T) (NRC-TT-1426)
- reactions with nuclei at 16 to 200 GeV/c, energy dependence of cross sections for coherent production of 3π and 5π systems in, (E/T), 25:20029

MESONS (π^0)
- decay $\pi^0 \to 2\gamma$, $\pi^+ \to e^+ + \nu + e^+ + e^-$ decay for sign of amplitude of, (T), 25:19963 (JINR-P2-5520)
- production in $\gamma + p \to p + 2\pi^0$ at 550 to 730 MeV, differential cross sections for, (E), 25:19890

MESONS (π^+)
- decay $\pi^+ \to e^+ + \nu + e^+ + e^-$, ratio of axial to vector form factor for $\pi^+ \to e^+ + \nu + \gamma$ decay, π electromagnetic radius, and sign of amplitude of $\pi^0 \to 2\gamma$ decay from, (T), 25:19963 (JINR-P2-5520)
- decay $\pi^+ \to e^+ + \nu + \gamma$, $\pi^+ \to e^+ + \nu + e^+ + e^-$ decay for ratio of axial to vector form factor for, (T), 25:19963 (JINR-P2-5520)
- decay $\pi^+ \to e^+(\mu^+) + \nu + e^+ + e^-$, integral probability of, (T), 25:19963 (JINR-P2-5520)
- decay $\pi^+ \to \mu^+ + \nu$, determination of neutrino spectrum in, (E), 25:19892
- dose to tissues at 10 to 2000 MeV, calculation of, 25:20226
- energy deposition in water at 160 to 220 MeV/c as function of depth, 25:19757 (ORNL-4584, pp 58-73)
- interactions $\pi^+ + n \to p + \text{eta}'$ at 1.1 to 2.4 GeV/c in deuterium bubble chamber, cross sections and angular distributions for, (E), 25:19923
- interactions $\pi^+ + n \to p + S^0$, elimination of background for, (T), 25:20009
- interactions $\pi^+ + p \to A_2^+ + p$ at 7 GeV/c, decay branching ratios of A_2 from, (E), 25:19920
- interactions $\pi^+ + p \to p + A_1^+$ at 8 and 16 GeV/c, t-channel helicity conservation in diffractive, (E), 25:19921
- interactions $\pi^+ + p \to \pi^+ + p$, amplitudes and πNN coupling constant from model-independent analysis of forward, (T), 25:20003 (JINR-E2-5561)
- interactions $\pi^+ + p$ at 70 to 290 MeV, Δ resonance parameters from total cross sections for, (E), 25:19916
- interactions $\pi^+ + p$ at low energies, analyticity and Pomeranchuk theorem violation predictions for, (T), 25:20005
- interactions $\pi^+ + \pi^-$, determination of off-mass-shell S-wave amplitude of, 25:19994
- photoproduction of π^---π^+ pairs in field of aluminum-27 at 313 MeV endpoint energy, π^- and π^+ energy spectra and π^-/π^+ ratio from, (E), 25:20341
- production in $\gamma + d$ interactions at high energies, Glauber theory of multiple scattering for cross sections of, (T), 25:19955
- production in $\gamma + p \to \pi^+ + n$ interactions at 227 to 260 MeV and 51 to 146°, asymmetry ratios for, (E), 25:19889
- production in $K^+ \to 3\pi$ decay, energy spectrum for, (E), 25:19896
- production in photon reactions with heavy nuclei at high energies, Glauber theory of multiple scattering for cross sections for, (T), 25:19955
- production in proton reactions with nuclei at 600 MeV, classical absorptive-gas model for, 25:20031
- production in π^+ reactions with nuclei at 185 to 295 MeV in emulsions, cross sections for, (E), 25:19919
- production of $\pi^+ - \pi^-$ pairs in γ reactions with carbon at 5.8 to 6.6 GeV/c, magnetic spectrometer study of (1550) enhancement in mass spectrum for, (E), 25:19886 (DESY-70/61)
- reactions with nuclei at 185 to 295 MeV in emulsions, cross sections for π^- and π^+ production in, (E), 25:19919

MESONS (rho)
- coupling constant difference effects on rho exchange in N + N interactions, (T), 25:20021
- decay rho $\to e^+ + e^-$, sum rule for width of, (T), 25:20047
- exchange in N + N interactions, effects of mass and coupling-constant differences on, (T), 25:20021
- exchange in N + N interactions, one-boson-exchange approximation for, (T), 25:20024
- mass and width of, Balazs method for bootstrap for, (T), 25:19989
- mass difference effects on rho exchange in N + N interactions, (T), 25:20021
- production in four-prong p + p interactions at 19 GeV/c in hydrogen bubble chamber, (E), 25:19901 (USIP-70-7)
- production of rho^0 in $p + p \to n + p + 2\pi^+ + \pi^-$ interactions at 19 GeV/c in hydrogen bubble chamber, (T), 25:19900 (USIP-70-4)
- production of rho$^+$ in $p + p \to 2p + \pi^+ + \pi^- + \pi^0$ interactions at 19 GeV/c in hydrogen bubble chamber, (E), 25:19900 (USIP-70-4)
- Regge trajectories for, review of, (E), 25:19988

MESONS (X^0)
- decay $X^0 \to \pi^+ + \pi^- + \text{eta}$ in deuterium bubble chamber, (E), 25:19923
- decay $X^0 \to \pi^+ + \pi^- + \gamma$, Yang--Mills coupling of vector meson fields consistency with Veneziano model for, (T), 25:19985 (DEMO-71/1)
- production in $\pi^+ + n \to p + \text{eta}'$ interactions at 1.1 to 2.4 GeV/c in deuterium bubble chamber, cross sections and angular distributions for, (E), 25:19923

MESONS, RESONANCE
- decay $A_2^+ \to \text{eta} + \pi$, branching fraction for, (E), 25:19920
- decay $A_2^+ \to \text{eta}' + \pi$, branching fraction for, (E), 25:19920
- decay $A_2^+ \to K + \text{anti } K$, branching fraction for, (E), 25:19920
- decay $A_2^+ \to \text{rho} + \pi$, branching fraction for, (E), 25:19920
- decay $K^* \to K + \pi$, coupling renormalization in broken SU(3) for width of, (T), 25:20043
- decay $K^{*0}(890) \to K^- + \pi^+$ in hydrogen bubble chamber, test of absorption-modified one-pion exchange model for, (E/T), 25:19918
- decay $K^-\pi^+\pi^- \to \text{anti } K^*(K^-) + \pi^-(\text{rho}^0)$ in bubble chamber, amplitudes of, (E), 25:19910 (LAL-1242)
- decay of A_2^+ from $\pi^+ + p \to A_2^+ + p$ interactions at 7 GeV/c, branching ratios for, (E), 25:19920
- exchange of epsilon in N + N interactions, one-boson-exchange approximation for, (T), 25:20024
- interactions $K^-\pi^+\pi^- + N$ in K^- reactions with bromine, carbon, fluorine, and neon at 5.5 to 12.7 GeV/c in bubble chamber, (E), 25:19910 (LAL-1242)
- interactions $Q^+(1275) + N$ in nucleus in K^+ reactions with nuclei at 10 GeV/c in heavy-liquid bubble chamber, cross sections for, (E/T), 25:19913
- mass and width of $Q^+(1275)$ enhancement in coherent production of $K^+\pi^+\pi^-$ system in K^+ reactions with nuclei at 10 GeV/c in heavy-liquid bubble chambers, (E), 25:19913
- production in $K^+ + p$ interactions at 12.7 GeV/c in hydrogen bubble chamber, upper limits for, (E), 25:19914
- production of broad (1550) enhancement in $\pi^+ - \pi^-$ mass spectrum from γ reactions with carbon at 5.8 to 6.6 GeV/c, magnetic spectrometer study of, (E), 25:19886 (DESY-70/61)
- production of $K^*(890)$ and $K\pi\pi(1200)$ enhancement in $\pi^- + d$ interactions at 3.15 GeV/c in deuterium bubble chamber, (E), 25:19922
- production of $K^{*0}(890)$ in $K^- + p \to K^{*0}(890) + n$ interactions at 3.9 and 4.6 GeV/c in hydrogen bubble chamber, test of absorption-modified one-pion exchange model for forward structure in, (E/T), 25:19918
- production of K(890) and $Q^+(1275)$ enhancement in $K^+\pi^+\pi^-$ system in K^+ reactions with nuclei at 10 GeV/c in heavy-liquid bubble chamber, (E), 25:19913
- production of $K^-\pi^+\pi^-$ system in K^- reactions with bromine, carbon, fluorine, and neon at 5.5 to 12.7 GeV/c in bubble chamber, coherent, (E), 25:19910 (LAL-1242)
- production of S^0 in $\pi^+ + n \to p + S^0$ interactions, elimination of background for, (T), 25:20009
- production of single heavy, in π-initiated cosmic EAS at 10^6 to 10^7 GeV, models for, (T), 25:19973 (INSJ-125)
- production of two scalar and vector, in intermediate state of anti p + p interactions, calculation of box-diagram effect for, (T), 25:19986 (IFVE-STF-70-34)
- properties of $K^-\pi^+\pi^-$ system in K^- reactions with bromine, carbon, fluorine, and neon at 5.5 to 12.7 GeV/c in bubble chamber, (E), 25:19910 (LAL-1242)

MESORIDAZINE
- radioprotective effects of, on mice, whole-body cobalt-60 γ, 25:19028

METALLURGICAL EQUIPMENT
- development for in-cell measurement of Young's modulus for irradiated fuels or reactor materials, 25:19279

METALS
- abundance in Type-M supergiant, (E), 25:19323
- analysis of high-purity, for thallium by photon activation, 25:18366(R) (NBS-TN-548)
- defects in, lecture on behavior of nonequilibrium, 25:19232 (UCRL-19696)
- nuclear-acoustic-resonance coupling in pure, equations for, (T), 25:19879
- temperature of liquid, development of open-ended thermocouples for measuring, 25:19227

METEORITES
- age for Bovedy, cosmic-ray exposure, (E), 25:19301
- analysis for trace elements by nondestructive neutron activation, 25:18370
- element abundance in, cerium, europium, and scandium, (E), 25:19302
- gamma emission from Bovedy, (E), 25:19301
- mercury contents in Russian collection, 25:19303

METHACRYLAMIDE
- dimers, radioinduced polymerization of, NMR studies on

products from, 25:18433
radioinduced polymerization in aqueous solutions in presence of unsaturated dicarboxylic acids, 25:18429
METHACRYLIC ACID
barium salt, radioinduced polymerization of solid monohydrate, ESR studies on γ, 25:18445
radioinduced polymerization of solid, ESR studies on γ, 25:18445
zinc salt, radioinduced polymerization of solid, ESR studies on γ, 25:18445
METHACRYLIC ACID, 3-CHLORO-2-HYDROXYPROPYL ESTER
3-chloro-2-hydroxypropyl methacrylate--trimethylamine, radioinduced polymerization in porous ceramics and firebrick, ion exchange properties of products from γ, 25:18421(R) (RLO-2098-1)
METHACRYLIC ACID, METHYL ESTER
glass textiles--methyl methacrylate, radiation effects on mechanical properties of, γ, 25:18421(R) (RLO-2098-1)
methyl methacrylate--styrene, radioinduced polymerization of, effects of magnesium oxide and silica gel on γ, 25:18442
METHACRYLIC ACID, METHYL ESTER, POLYMERS
radioinduced thermally stimulated currents in, γ, 25:18422
METHACRYLIC ACID, OCTADECYL ESTER
radioinduced polymerization of solid, ESR studies on γ, 25:18445
METHANE
diffusion from molybdenum and tungsten at 2000°K, 25:19225
radiolysis of, G values and mechanisms for, 25:18449(T) (ORNL-tr-2386)
METHANE, BROMO-
Br--bromomethane, radiation effects on gases of, effects of pressure on organic yields from reactions of recoil bromine-80 or bromine-82 produced by isomeric transitions or neutron, 25:18483(R) (COO-1617-27)
METHANE, CHLOROTRIFLUORO-
heat transfer from heated copper rods to, in pool boiling, 25:18585
radiolysis of aqueous solutions of, effects of ethylene on halide yields from electron pulse and γ, 25:18460
METHANE, DICHLORODIFLUORO-
radiolysis of aqueous solutions of, effects of ethylene on halide yields from electron pulse and γ, 25:18460
METHANE, IODO-
alkali-metal-atom scattering by, crossed-beam measurements and optical-model analysis of, 25:19497
iodomethane--1-pentene, radiation effects on, organic yields from reactions of recoil iodine-128 produced from neutron, 25:18483(R) (COO-1617-27)
iodomethane--2-pentene, radiation effects on, organic yields from reactions of recoil iodine-128 produced from neutron, 25:18483(R) (COO-1617-27)
iodomethane--pentane, radiation effects on, organic yields from reactions of recoil iodine-128 produced from neutron, 25:18483(R) (COO-1617-27)
METHANE, TRICHLOROFLUORO-
radiolysis of aqueous solutions of, effects of ethylene on halide yields from electron pulse and γ, 25:18460
METHANOL
radiolysis at 77°K, space distribution of radicals from γ, 25:18464
radiolysis of aqueous perchloric acid solutions of, rate constants for reactions of hydrogen atoms produced by γ, 25:18459
radiolysis of crystals of, processes for annealing of free radicals formed by, 25:18473
METHYL SULFATES
effects on chromosomes and mitosis in roots of cotton and combined effects with γ radiation, 25:18954
MICE
americium-241 distribution in tissues of, following intravenous injection, autoradiographic study of, 25:18901
ascariasis in lungs of x-irradiated, effectiveness of anthelmintics, antibiotics, and immunization for, 25:19032
radiation effects on bone marrow cells in, correlation of lethality and recovery with fractionated γ, 25:19108
radiation effects on erythrocyte and leukocyte counts in peripheral blood and on survival of, effects of oxygen content of inspired air and dose on x, 25:19123
radiation effects on generation cycle of crypt cells in small intestine of, effects of chronic fractionated x, 25:19122
radiation effects on hematopoiesis and survival of, effects of transplants of bone marrow cells from mice treated with cyclophosphamide on γ, 25:19112
radiation effects on hematopoiesis, intestines, and survival of, comparison of protective effects of AET against whole-body fast neutron and x, 25:19029
radiation effects on immune reactions in, effects of mouse spleen cells and sheep erythrocytes on, 25:18925
radiation effects on immune reactions of, effects of transplants of bone marrow, embryonic liver, and spleen on, 25:18921
radiation effects on immune reactions of, to sheep red blood cells, effects of anti-sheep red blood cell antibodies on x, 25:18923
radiation effects on intestines of, protective effects of MEG against whole-body fast neutrons and x, 25:19029
radiation effects on life span of, effects of dose on γ, neutron, and x, 25:19105
radiation effects on mitosis and survival of ascites cells of, effects of dose fractionation on x, 25:19091
radiation effects on permeability of liver mitochondria membranes in, to manganese-54, protective effects of esculamine against x, 25:19025
radiation effects on proliferation of cells in bone marrow and spleen of, x, 25:19129
radiation effects on regeneration of stem cells in, effects of dose and shielding on x, 25:19126
radiation effects on survival of spermatogonia of, in relation to mutation frequency, effects of dose on x, 25:18959
radiation effects on survival of transplanted Ehrlich ascites tumor cells in, combined effects of immunization and x, 25:19130
radiation effects on survival of, following therapy for skin cancer, effects of synchronized treatment with fluorouracil on, 25:19075
radiation effects on, effects of phentolamine and propranolol on protective effects of typhoid-paratyphoid vaccine against x, 25:19026
radiation effects on, protective effects of clopenthixol, flupenthixol, mesoridazine, and thioridazine against whole-body cobalt-60 γ, 25:19028
radioinduced cataracts in eyes of inbred and hybrid, effects of dose on x, 25:19116
radioinduced chromosome inversions in, whole-body x, 25:18968
radioinduced inversion aberrations in male germ cells of, x, 25:18947
radioinduced lethal mutations in, methods for testing 14-MeV neutron, 25:18956
radioinduced mutations in, control of enzyme activity by, 25:19128
radioinduced mutations in, use of functional units in small chromosome segments for interpretation of γ, neutron, and x, 25:18957
radioinduced neoplasms of bones, bone marrow, and hematopoietic tissues in, following ingestion of strontium-89, 25:19113
radioinduced translocation aberrations of chromosomes in spermatogonia of, review of x, 25:18948
radioinduced translocation aberrations of chromosomes in spermatogonia of, effects of dose fractionation on rate of x, 25:18958
radiosensitivity of primordial oogonia and spermatogonia in, fast neutron, 25:18949
radium-226 carcinogenicity and dosimetry in, following injection, review of, 25:18979 (BRH/DBE-70-5)
MICROWAVE EQUIPMENT
waveguides with simple periodic structure, method of calculating, 25:20147
MICROWAVES
cosmic background, interactions with other background radiations, (T), 25:19462
detection and measurement of, design of readout for thermocouple power density probe for, 25:18827 (BRH/DEP-70-31)
effects on revascularization of blood supply in skin grafts on rabbits and man, 25:19104
emission from chromosphere at 1.2 mm, enhancements of, (E), 25:19409
hazards from, detectors for evaluation of, 25:20853 (BRH/DEP-71-1)
interactions with cylindrical plasma, transmission in, (T), 25:19656 (EP-RR-21)
reflection from corona, maser effect in, (T), 25:19419
MILITARY PERSONNEL
radiation protection of nuclear submarine, medical programs for, 25:18972
MILK
iodine-131 content in Norwegian, relation of frequency of thyroid cancer to, 25:19135
polonium-210 transfer to, of cattle and goats following ingestion as oxide, coefficients for, 25:18890(R) (COO-2044-3)
radioisotope content of, following accidental contamination of pastures, 25:18943
radioisotope content of, in Finland, 25:18931 (NYO-3446-14, Paper 30)
radioisotope content of, in Pavia, Italy from 1964 to 1966, cesium-137 and strontium-90, 25:18942
MILKY WAY
infrared map of center region of, (E), 25:19448
light-absorbing material in solar neighborhood, structure of, (E), 25:19442
magnetic field in, structure of, (T), 25:19459
mapping of H I regions in region l/sup II/ = 185 to 63°, (E), 25:19390
mapping of H I regions in region l/sup II/ = 190 to 299°, (E), 25:19392
photometry of night sky in, Hβ, (E), 25:19440
radio spectral absorption lines of hydroxyl at 1667.358 MHz in center region, (E), 25:19389
radio survey between declinations +25° and -25°, (E), 25:19388
x-ray background in southern, origin of, (E), 25:19353
x-ray background in, origin of 0.25-keV, (T), 25:19451

XUM

- MILLSTONE POINT POWER REACTOR, UNIT 1
  - operations incident of December 8, 1970, failure of cleanup system return valve, 25:20592 (DOCKET-50245-55)
  - operations incident of November 4, 1970, excessive operating times for cleanup system valves, 25:20592 (DOCKET-50245-55)
  - site for, environmental radiation survey during July to December 1970, 25:20626 (DOCKET-50245-56)
- MINERALS
  - analysis for barium and strontium by isotope dilution mass spectrometric, neutron activation, gravimetric, and other spectrometric methods, 25:18335
  - prospecting for, development of methods for seabed, 25:18590(R) (BNWL-1308-4)
- MITOCHONDRIA
  - radiation effects on permeability of membranes of mouse liver, to manganese-54, protective effects of esculamine against x, 25:19025
- MITOSIS
  - radiation effects on, in cotton roots, and combined effects of dimethyl sulfate, 25:18954
  - radioinduced delay of, in ascites cells of mice, effects of dose fractionation on x, 25:19091
- MOESSBAUER SPECTROMETERS
  - calibration of cobalt-57, G--M resonance detector for, 25:18751
  - description of, having two detectors, 25:18743(P)
  - operation of, review of, 25:18769
- MOISTURE GAGES
  - development of neutron radiometric, for solids, 25:18362(P)
- MOLECULES
  - atom reactions with diatomic, generalized phase shift approach to rotational excitation in, 25:19498
  - charged-particle reactions at very low energies with nonpolar, inverse fourth-power potential in calculation of cross sections for capture and elastic scattering in, 25:19500
  - electron inelastic scattering by, generalized random phase approximation for calculation of, 25:19507
  - electron reactions with nonstationary dipolar, critical dipole moments for electron binding in, 25:19757 (ORNL-4584, pp 58-73)
  - energy-level transitions in, generalization of oscillator strength for, 25:19757 (ORNL-4584, pp 58-73)
  - photon reactions with inner-shell electrons of, review of chemical information from, 25:19473
  - potential energy curves for diatomic, method for calculation of, 25:19757 (ORNL-4584, pp 58-73)
  - scattering cross sections of, S-matrix theory for reformulation of generalized impulse approximation for, (T), 25:20537
- MOLLUSCA
  - mussels, ruthenium-106 content of flesh and shells of, effects of cooking on, 25:18896
  - radioisotope contamination of fresh water, technique for study of, 25:18937
- MOLYBDENUM
  - bonding to glass, method for, 25:19188
  - chromatographic behavior in hydrochloric acid--thiocyanate mixture on Amberlite LA-2, 25:18337
  - degasification at 2000°K, measurement of rate of, 25:19225
  - determination in high-burnup plutonium dioxide fuel by isotope dilution mass spectrometry, 25:18356 (KR-140)
  - determination in presence of palladium and copper or vanadium by spectrophotometry using 1-(2-carboxy-4-sulfonatophenyl)-3-hydroxy-3-phenyltriazene, 25:18342
  - determination in presence of rhenium by extraction photometry using 5,7-dibromo-8-quinolinol, 25:18353
  - determination in zirconium alloy simultaneously with copper, polarographic, 25:18341 (RT/CHI-(70)14)
  - determination of trace amounts of, by formation of colored peroxy compounds and sorption on chelating resin, 25:18343
  - deuteron reactions at 180 to 360 keV with, cross sections for L-shell ionization in, (E), 25:19470
  - electric conductivity of quenched, mechanism for, 25:19860
  - electric conductivity of single-crystal, at 1200 to 2200°K, 25:19220
  - grain growth of fission-product, in uranium dioxide rods, effects of thermal gradients on, 25:19278
  - properties for use as capsule material for radioisotope heat sources, evaluation of high-temperature, 25:18592 (ORNL-4298)
  - properties for use as support base and sheets used in uranium dioxide pellet dewaxing and sintering, 25:19267(P)
  - proton reactions at 90 to 180 keV with, cross sections for L-shell ionization in, 25:19470
  - radioinduced production of void regular arrays in single crystals of, 2-MeV nitrogen ion, 25:19256
  - radioinduced voids in, distribution of 2-MeV nitrogen ion, 25:19257
  - reactions with oxygen at 500 to 1000°C and low pressure, 25:19169
  - recovery of fast-neutron-irradiated, electric conductivity study of effects of defect doping on, 25:19861
  - separation from sulfuric acid-treated coal ash by solvent extraction using hydrochloric acid, 25:18508
  - superconducting and semiconducting phase of, embedded in SiO_2 films, 25:19631
  - thermal conductivity of single-crystal, at 1200 to 2200°K, 25:19220
- MOLYBDENUM ALLOYS AND SYSTEMS
  - magnetic properties of soft magnetic, effects of heat treatments on, 25:19872
  - C--Hf--Mo--Nb-base--W, properties for use at high temperatures, 25:19218
  - Cu--Mo--Nb-base, phase studies of isothermal sections of, at 1900 and 2100°C, 25:19246
  - Cu--Mo--Zr, analysis for copper and molybdenum, simultaneous polarographic, 25:18341 (RT/CHI-(70)14)
  - Fe-base--Mo--Ni, phase transformation during aging, kinetics of martensitic, 25:19247
  - Mo--Nb, crystallization of solid-solution, mechanisms of, 25:19242
  - Mo--Nb, diffusion in solid-solution, at 1100 to 1800°C, effects of molybdenum content on reciprocal, 25:19204
  - Mo--Nb, diffusion in, kinetics of, 25:19214
  - Mo--Nb--Ta--W-base, mechanical properties of, effects of composition on, 25:19239
  - Mo--Nb-base, embrittlement by hydrogen, effects of interstitial solutes on, 25:19216
  - Mo--Nb-base, mechanical properties of solid solutions of, 25:19215
  - Mo--Nb-base, preparation of high-purity, by electron beam melting, 25:19186
  - Mo--PuO_2, separation of plutonium from, pyrochemical methods for, 25:18492 (ANL-7709)
  - Mo--Re, faulting in filings of, x-ray diffraction search for, 25:19248
  - Mo--Ta--W, properties of, microstructural and physical, 25:19205
- MOLYBDENUM ISOTOPES Mo-91
  - production by photon reactions (γ,n) and (γ,3n) at 70 MeV, isomer ratios in, 25:20455
- MOLYBDENUM ISOTOPES Mo-92
  - photon reactions (γ,n) at 70 MeV, isomer ratios from, 25:20455
  - proton elastic scattering at 4.1 to 8.7 MeV, polarization in, (E), 25:20331
- MOLYBDENUM ISOTOPES Mo-93
  - energy levels from molybdenum-92 proton elastic scattering, spin assignments for isobaric analog, (E), 25:20331
  - energy levels of, calculation using unified model, (T), 25:20548
- MOLYBDENUM ISOTOPES Mo-94
  - photon reactions (γ,3n) at 70 MeV, isomer ratios from, 25:20455
  - proton elastic scattering at 4.5 to 8.6 MeV, polarization in, (E), 25:20331
- MOLYBDENUM ISOTOPES Mo-95
  - energy levels from molybdenum-94 proton elastic scattering, spin assignments for isobaric analog, (E), 25:20331
  - energy levels from technetium-95m decay, spins, lifetimes, and gyromagnetic ratios for, (E), 25:20468
  - energy levels of, calculation using unified model, (T), 25:20548
- MOLYBDENUM ISOTOPES Mo-97
  - energy levels of, calculation using unified model, (T), 25:20548
- MOLYBDENUM ISOTOPES Mo-99
  - energy levels of, calculation using unified model, (T), 25:20548
  - half-life, (E), 25:20339
- MOLYBDENUM OXIDES
  - oxygen mobility in, oxygen-18 exchange studies of surface, 25:18388
  - Bi_2O_3--MoO_3, oxygen mobility in, oxygen-18 exchange studies of surface, 25:18388
- MOLYBDENUM SILICIDES
  - glass--$MoSi_2$, properties for use as protective coating on niobium, 25:19176
- MONKEYS
  - aerosol retention in alveolar lipoproteins of, use of lanthanum-140 to demonstrate stability of complex formed following in vitro and in vivo actinide and lanthanide liquid, 25:18889 (CEA-CONF-1676)
- MONOMERS
  - development for incorporation and polymerization in concrete, 25:19292 (BNL-50275)
  - radioinduced polymerization of, in wood, equipment for gamma, 25:19299
- MONTICELLO POWER REACTOR, UNIT 1
  - operations incident of January 27, 1971, efficiency testing of standby gas treatment system filter, 25:20595 (DOCKET-50263-56)
  - power level for, license for operation at maximum 1670 MW(t), 25:20640 (DOCKET-50263-55)
- MOON
  - radio brightness temperatures of new, at millimeter wavelengths, (E), 25:19408
- MOUTH
  - radiotherapy of neoplasms of human, comparison of effectiveness of, with surgery, 25:19083
  - radiotherapy of neoplasms of human, dental care and oral hygiene before, during, and following, 25:19079

MUEHLEBERG POWER REACTOR
engineered safeguards for, 25:20684
pressure vessel for, manufacturing and fabrication problems with steel, 25:20555
radioactive waste disposal systems for, 25:20684

MUONIUM
hyperfine structure splitting determination from Zeeman transitions of muonium, (E), 25:19888
spectra of, μ magnetic moment and muonium hyperfine structure determination from Zeeman, (E), 25:19888

MUSCLES
radiation effects on uptake of α-aminoisobutyric acid, inulin, orotic acid, and phosphorus-32 by rat, effects of AET and cysteamine on γ, 25:19024

MUTAGENS
effects of chemical, on human populations, evaluation of, 25:18965

MUTATIONS
frequency in Crepis capillaris seeds exposed to space flight, effects of ethylenimine on, 25:18953
induced in Brucella abortus by acriflavine or nitrous acid, frequency of rough to smooth reversion, 25:18970
radioinduced lethal, in mice, methods for testing 14-MeV neutron, 25:18956
radioinduced male sterile, in rape plants, γ, 25:19152
radioinduced recombination deficient yeast, isolation of uv and x, 25:18945 (UCRL-20192)
radioinduced reversion in yeast, frequency of uv and x, 25:18945 (UCRL-20192)
radioinduced reversion, in Brucella abortus uv, 25:18970
radioinduced, for studies of the genetic control of enzyme activity, 25:19128
radioinduced, in beans for chlorophyll, effects of dose on γ, 25:18946
radioinduced, in Datura tatula, γ, 25:19151
radioinduced, in man exposed to atomic bombing in Japan, effects of dose on frequency of, 25:18961
radioinduced, in mice, use of functional units in small chromosome segments for interpretation of γ, neutron, and x, 25:18957
radioinduced, in plants for flower, fruit, and root quality and disease resistance, effects of dose and seed exposure on γ, 25:18964(P)
radioinduced, in sperm of citrus red mites, effects of dose and TEPA on γ, 25:19100
radioinduced, in spermatogonia of mice in relation to cell survival, effects of dose on frequency of x, 25:18959
radioinduction at specific loci in oocytes and spermatogonia of mice by fast neutron, 25:18949

N

NAGASAKI
neoplasm incidence in children exposed in utero to atomic bombing at, 25:19089

NAPHTHALENE
effects on yields from γ radiolysis of aniline, 25:18450(R) (ORO-3519-8)

2,7-NAPHTHALENEDISULFONIC ACID, 3-(CARBOXYCARBONYLPHENYLAZO)-4,5-DIHYDROXY-
reactions with thorium, stability of complexes from, 25:18382

1-MAPHTHALENESULFONIC ACID, 4-[(2,4-DIHYDROXYPHENYL)AZO]-
complexes with niobium and hydrogen peroxide, fluorescent and spectrophotometric studies on, 25:18349

1,4-NAPHTHOQUINONE
electron reactions with, formation and lifetimes of negative ions from, 25:19491 (ORNL-4584, pp 105-24)

NAPHTH[1,2-d]OXAZOLE, 2-(2-FURYL)-
performance as solute for liquid scintillation beta counting, 25:18731(P)

NAPHTH[1,2-d]OXAZOLE, 2-(1-NAPHTHYL)-
performance as solute for liquid scintillation beta counting, 25:18731(P)

NAPHTH[1,2-d]OXAZOLE, 2-(2-NAPHTHYL)-
performance as solute for liquid scintillation beta counting, 25:18731(P)

NAPHTH[1,2-d]OXAZOLE, 2-PHENYL-
performance as solute for liquid scintillation beta counting, 25:18731(P)

NATIONAL ACCELERATOR LABORATORY SYNCHROTRON
design and construction of, review of, 25:20225
development of, status of, 25:20154
economic impact on surrounding area, 25:20870 (NP-18690)
experimental facilities and research program at, review of, 25:20225
shielding design for, energy loss and straggling of mesons (μ) in iron for, 25:20206

NATURAL BACKGROUND RADIATION
effects of high-level, on human populations in Brazil, 25:18927 (NP-18670)
effects on man, 25:19008 (NCRP-39)
measurement of absorbed dose in soils from, in Hong Kong, 25:19006
radiation dose to man from, in Finland, 25:18986 (NYO-3446-14, Paper 28)

NATURAL GAS
radioisotope content of, from Gasbuggy well, estimate of home occupancy factor from, 25:18989 (ORNL-4584, pp 42-56)

NAVIGATIONAL INSTRUMENTS
position locator, new concepts for geographic, 25:2090 (UCRL-50978)

NBS RESEARCH REACTOR
cooling system inlet strainer for, locating and recovery procedures for missing equipment of, 25:20785 (DOCKET-50184-27)
fuel elements for, design modifications for locking bar pin of, 25:20784 (DOCKET-50184-26)
operations incident of February 2, 1971, fuel element head locking bar pin failure, 25:20784 (DOCKET-50184-26)

NEBULAE
electron temperatures in Orion, (E), 25:19365
physical conditions in Orion, from H56α line observations, 25:19365

NEMATODA
Dictyocaulus viviparus, radioinduced attenuation of larvae of, effects of dose on electron and x, 25:19101

NEODYMIUM
determination in high-burnup plutonium dioxide fuel by isotope dilution mass spectrometry, 25:18356 (KR-140)
determination using 4,5-dihydroxy-m-benzenedisulfonic acid, in presence of Eriochrome Cyanine R, titrimetric, 25:18348
electron band structure of, x-ray photoelectron study of 4f levels in, 25:19866

NEODYMIUM IONS
wave functions for, accurate numerical Hartree--Fock self-consistent field, 25:19478

NEODYMIUM ISOTOPES Nd-141
energy levels from promethium-141 decay, (E), 25:20388
production by photon reactions (γ,n) and (γ,3n) at 70 MeV, isomer ratios in, 25:20455

NEODYMIUM ISOTOPES Nd-142
photon reactions (γ,n) at 70 MeV, isomer ratios from, 25:20455

NEODYMIUM ISOTOPES Nd-144
photon reactions (γ,3n) at 70 MeV, isomer ratios from, 25:20455

NEODYMIUM ISOTOPES Nd-147
beta decay of, conversion electron spectra from, 25:20421
half-life, (E), 25:20338
half-life, (E), 25:20339

NEODYMIUM ISOTOPES Nd-148
determination in irradiated plutonium dioxide--uranium dioxide fuels as measure of burnup, 25:18359 (WCAP-3385-56(Pt.2))

NEODYMIUM ISOTOPES Nd-150
alpha reactions (α,t), proton states from, (E/T), 25:20383
energy levels from Coulomb excitation, lifetime measurements for, (E), 25:20409
energy levels from Coulomb excitation, transition probability and quadrupole moment of first 2^+, (E), 25:20469
helium-3 reactions (He-3,d), proton states from, (E/T), 25:20383
sulfur-32 scattering at 94 to 110 MeV with Coulomb excitation, Doppler shift attenuation in γ spectra from, (E), 25:20409

NEODYMIUM TELLURATES
$Nd_2(TeO_3)_3$--$Nd_2(TeO_4)_3$, analysis for hexavalent tellurium and total tellurium by automatic amperometric and potentiometric titrations, 25:18351

NEODYMIUM TELLURITES
$Nd_2(TeO_3)_3$--$Nd_2(TeO_4)_3$, analysis for hexavalent tellurium and total tellurium by automatic amperometric and potentiometric titrations, 25:18351

NEON
electron reactions with, autoionizing states and negative-ion resonances from, 25:19490 (ORNL-4584, pp 92-104)
energy-level transitions in, minima in generalized oscillator strengths for, (T), 25:19521
hyperon (Σ^-) absorption at rest in bubble chamber, hyperfragment production probability from, (E), 25:19908
meson (K^-) absorption at rest in bubble chamber, production of excited nuclear states from, (E), 25:19908
meson (K^-) reactions at 5.5 and 12.7 GeV/c in bubble chamber, $K^-\pi^+\pi^-$ system coherent production and $K^-\pi^+\pi^- + N$ interactions in, (E), 25:19910 (LAL-1242)
plasma of, partition functions for, (T), 25:19397
production of excited, in K^- absorption by neon in bubble chamber, (E), 25:19908
properties of atomic, calculation using Hartree--Fock theory with exchange cutoff, 25:19517
reactions with air, nitrogen, and oxygen molecules at 25 to 90 keV, total cross sections for single electron loss in, (E), 25:19492 (SC-RR-70-735)
thermal capacity of solid, temperature and volume dependence of, 25:20863 (IS-T-430)

NEON IONS
effects on electric properties of boron-implanted silicon, 25:19776
implantation in cadmium sulfide at 200 keV, annealing of, 25:19791

  implantation in silicon at 30 to 400 keV, calculated spatial distributions of damage from, 25:19819
  implantation in silicon at 40 to 100 keV, electron microscopic studies of defects induced in, 25:19808
  implantation in silicon at 80 keV, electron microscopic studies of damage from, 25:19814
NEON ISOTOPES Ne-20
  alpha decay of excited states from sodium-20 beta decay, alpha spectra from, (E), 25:18737(R) (ORO-3820-7)
  energy levels of, structure of positive-parity, (T), 25:20351
NEON ISOTOPES Ne-21
  origin of atmospheric, (E/T), 25:18527
NEON ISOTOPES Ne-22
  origin of atmospheric, (E/T), 25:18527
  reactions (Ne-22,f) with tungsten at 115 to 174 MeV, compound-nucleus lifetime in, (E), 25:20370 (JINR-P7-5512)
NEON SYSTEMS
  DH--Ne, sound absorption measurements below 40°K, 25:19480
NEPTUNIUM
  complexes of hexavalent, with sodium propionate, voltammetric study of, 25:18376
  separation from nitric acid solutions by anion exchange, effects of uranyl ion on, 25:18519
NEPTUNIUM ISOTOPES Np-227
  electron-capture decay of, delayed fission of uranium-227 from, (T), 25:20371 (JINR-P7-5584)
NEPTUNIUM ISOTOPES Np-228
  electron-capture decay of, delayed fission of uranium-228 from, (T), 25:20371 (JINR-P7-5584)
NEPTUNIUM ISOTOPES Np-232
  electron-capture decay of, γ spectra and half-life for, (E), 25:20382
NEPTUNIUM ISOTOPES Np-237
  determination in irradiated plutonium dioxide--uranium dioxide fuels as measure of burnup, 25:18359 (WCAP-3385-56(Pt.2))
NEPTUNIUM ISOTOPES Np-238
  beta decay of, gamma spectra from, (E), 25:20431
  energy levels of, calculation using unified model, 25:20524
NEUTRINOS
  emission from sun, development of gallium chloride and lithium chloride detectors for detection of, 25:18720
  emission from sun, upper limit on flux from boron-8 in, (E), 25:19893
  gravitational effects in sea of degenerate anti ν and, spatial polarizability for, (T), 25:20090
  mass of, photon interactions with gravitational field for, (T), 25:19966
  spectroscopy of solar, program for, 25:19429
NEUTRINOS (ANTI ν)
  gravitational effects in sea of degenerate ν and, spatial polarizability for, (T), 25:20090
NEUTRINOS (ν/sub μ/)
  spectra from K^+ and π^+ decays, μ^+ flux measurement for determination of, (E), 25:19892
NEUTRON BEAMS
  intensity profile of, development of method for measuring and recording, 25:20218
  transmission through simple bent conducting tubes, calculation of, 25:20245
NEUTRON CHOPPERS
  operation of statistical, for separation of elastic and inelastic scattered neutrons in time-of-flight measurements, 25:18764
NEUTRON CROSS SECTIONS
  book: Use of Numerical Methods for Neutron Cross Section Calculations (in Russian), 25:20530
  compilation of Japanese requests for measurements, 25:20231 (JAERI-Memo-4167)
  measurement of capture, condition for independence from half-life of product in activation, 25:20518
  measurements of scattering, Monte Carlo code for evaluation of double-differential, (E/T), 25:20235 (RPI-328-211)
NEUTRON MONOCHROMATORS
  performance of singly bent graphite, 25:20244
  thickness of copper single crystal, optimum, 25:20234 (PH-4)
NEUTRON SOURCES
  characteristics and safety of, 25:19007 (NCRP-38)
  design and operation of UNG-1 tube-type, for well logging, 25:20228(T) (CSIRO-Trans-10095)
  design, development, and handling of isotopic, for use in nuclear materials safeguards assay, 25:18619 (BNL-50267)
  development of (d,xn) and (p,xn), for nuclear power technology, 25:20191
  development of cold, from stationary reactors, 25:20232 (JINR-P3-5392)
  developments in, 25:18870
  evaluation for medical radiography, 25:19034(T) (AEC-tr-7219)
  ion sources for T(d,n), rf, 25:20150
  preparation of californium-252, self-transfer properties for, 25:18596
  radiation hazards during operation of high-yield, 25:18982 (CEX-65.05)
  spectra of americium--beryllium, use of nuclear emulsions and proton recoil spectrometer for measurement of, 25:18761
  target for D(p,n), design of liquid deuterium, 25:20187
  targets for T (d,n), development of, 25:20134 (ORNL-4584, pp 187-97)
NEUTRON SPECTROMETERS
  data collection system for time-of-flight, 25:18765
  design and performance of Fourier correlation time-of-flight, for thermal neutrons, 25:18738 (RISO-229)
  design and performance of triple-axis crystal, for thermal neutrons, 25:18738 (RISO-229)
  design of 250-meter time-of-flight, with liquid scintillation detector, 25:18742
  design of JINR, for microdynamics of condensed matter, 25:18734 (INP-727)
  development of gas recoil fast, with electronic collimation by rise-time discrimination, 25:18749
  development of proportional--surface-barrier coincidence, for in-core spectrum measurements, 25:18741
  pulse-height analysis of organic scintillation, 25:18766
  spectra unfolding for multisphere, Monte Carlo method for, 25:18740
NEUTRON SPECTROSCOPY
  method using statistical chopper for separation of elastic and inelastic scattered neutrons in time-of-flight, 25:18764
NEUTRON STARS
  atmosphere of, (T), 25:19348 (NP-18666)
  crust of, nuclear physics of, (T), 25:19348 (NP-18666)
  crust of, solid-state aspects of, (T), 25:19348 (NP-18666)
  ionization zones around, (T), 25:19324
  matter accretion by, (T), 25:19324
  model featuring explosions of, supernova, (T), 25:19326
  oscillations of, magnetohydrodynamic, (T), 25:19312
  properties of, review on, (T), 25:19375
  superfluidity in, (T), 25:19348 (NP-18666)
  ultraviolet emission from ionization zones around, (T), 25:19324
NEUTRONS
  capture by cobalt-59, magnesium-26, manganese-55, potassium-41, and sodium-23, resonances integrals and partial widths of resonances in, (E), 25:20359
  capture by indium-115 up to 50 eV, γ spectra from, (E), 25:20410
  capture by nuclei, review of energy-level transitions from keV, 25:20227 (AAEC/TM-565)
  capture by nuclei, review of gamma spectroscopy of, 25:20447
  capture by thorium-232 at 0 to 15 MeV, cross sections and resonance integrals for, (E/T), 25:20377 (WAPD-TM-971)
  capture by vanadium at 0.115 eV spin dependence of cross section for, 25:20335
  detection by lithium glass and boron-loaded liquid scintillator, effects of elastic scattering on efficiency of, 25:18716
  detection in gamma background, scintillation detector circuits for, 25:18667
  detection of, measurement of proton-recoil tracks in nuclear emulsions for, 25:18728
  dosimetry in fuel reprocessing plants, radiation detectors for, 25:18800(T) (SC-T-71-3009)
  dosimetry in phantoms, calculation of encapsulated californium-252, 25:18990 (ORNL-4584, pp 129-51)
  dosimetry in rabbits and rats, development of phantoms for, 25:18990 (ORNL-4584, pp 129-51)
  dosimetry of, performance of semiconductor detectors and hydrogeneous radiator assembly for, 25:18798 (KFKI-70-29-HP)
  effects on benzene--hexane--lithium carbonate mixtures, yields from reactions of tritium recoil atoms from, 25:18487
  effects on bromine or iodine bromides in liquid and solid benzene, isotope effects and labeled organic yields from, 25:18483(R) (COO-1617-27)
  effects on bromine--bromobenzene system, 25:18490
  effects on electric properties of n- and p-type silicon, annealing of, 25:19831
  effects on fission gas release and oxygen distribution in plutonium dioxide--uranium dioxide fuels, 25:19287 (AECL-3690)
  effects on gaseous bromine--bromomethane, effects of pressure on organic yields from reactions of recoil bromine-80 or bromine-82 produced from, 25:18483(R) (COO-1617-27)
  effects on hardening of polyester resins, 25:18443
  effects on iodine and pentane, 1-pentene, or 2-pentene, organic yields from reactions of recoil iodine-128 produced from, 25:18483(R) (COO-1617-27)
  effects on iodine or iodine chloride in liquid or solid alkylbenzenes, benzene, or cyclopentane, isotope effects and yields from, 25:18483(R) (COO-1617-27)
  effects on iodomethane and pentane, 1-pentene, or 2-pentene, organic yields from reactions of recoil iodine-128 produced from, 25:18483(R) (COO-1617-27)
  effects on life span of mice, effects of dose on, 25:19105
  effects on mice, use of functional units in small chromosome segments for interpretation of mutagenic, 25:18957
  effects on microstructure and tensile properties of Type

316 stainless steel, relations with irradiation temperature at 420 to 650°C, 25:19251 (AERE-R-6435)
effects on potassium chromates crystals, separation and chemical properties of polynuclear recoil products from, 25:18486
effects on semiconducting diamonds, 25:19769(T) (LIB/Trans-307)
effects on shielding properties of concrete aggregate components, 25:19296
effects on structure of plutonium oxide (PuO_2)--uranium oxide (UO_2) rods, 25:20836 (WHAN-SA-79)
effects on structure of uranium carbide (UC), 25:20791
energy in reactor cores, effects on noise spectra of, (E/T), 25:20832 (ORNL-TM-3245)
filters for, single-crystal bismuth and silicon, 25:20238 (UJV-2488-F)
flux distribution near absorbers, VISTA technique for measurements of, 25:20831 (JAERI-Memo-4238)
flux measurement from proton reactions (p,n) with tritium, associated particle method for, 25:18647
flux measurements in reactors, beryllium-9 gas flow activation detector for, 25:18646 (WHAN-SA-73)
flux monitoring of, helium-3 ionization detector for in-core, 25:18662
interactions anti n + n at 6.65 GeV/c, total cross sections for, 25:19907
interactions $\gamma + n \to p + \pi^-$, test for existence of isotensor electromagnetic current from, (T), 25:19956
interactions $K^- + n \to \Lambda + \pi^-$ at 3 GeV/c, nucleon exchange in, (E/T), 25:19917
interactions $K^- + n \to \Sigma^0 + \pi^-$ at 3 GeV/c, baryon exchange in, (E/T), 25:19917
interactions $K^- + n \to V + \pi^-$ at 3 GeV/c, total and differential cross sections for, (E/T), 25:19917
interactions K^- + n at high energies, compilation of cross sections for, (E), 25:19909 (CERN-HERA-70-6)
interactions n + d at 0.5 to 70 GeV/c, compilation of cross sections, angular distributions, and polarizations for, (E), 25:19899 (UCRL-20000-NN)
interactions n + n at 0.5 to 70 GeV/c, compilation of cross sections, angular distributions, and polarizations for, (E), 25:19899 (UCRL-20000-NN)
interactions $n + p \to 3p + \gamma$, weak-interaction Hamiltonian for photon polarization in, (T), 25:20039
interactions $n + p \to d + \gamma$, weak-interaction Hamiltonian for photon polarization in, (T), 25:20039
interactions n + p at 14.4 MeV with bremsstrahlung production, cross sections for, (E), 25:20257
interactions n + p at 525 and 600 MeV at 65 to 180°, transfer depolarization parameter for, (E), 25:19904
interactions $p + n \to n + p$, complex momenta method with branching in j-plane for differential cross sections of, (T), 25:20017(T) (CERN-Trans-70-15)
interactions $p + n \to n + p$, singular Regge pole model for, (T), 25:19995
interactions p + n at 0.5 to 70 GeV/c, compilation of cross sections, angular distributions, and polarizations for, (T), 25:19899 (UCRL-20000-NN)
interactions p + n at low energies, relation between deuteron binding energy and phase shift for, (T), 25:20022
interactions $\pi^+ + n \to p$ + eta' at 1.1 to 2.4 GeV/c in deuterium bubble chamber, cross sections and angular distributions for, (E), 25:19923
interactions $\pi^+ + n \to p + S^0$, elimination of background for, (T), 25:20009
noise analysis of, power measurement in critical assemblies by, 25:20792
photoproduction in heavy water, measurement of water displacement in soils by, 25:18523
production in π^- + d interactions at 3.15 GeV/c in deuterium bubble chamber, cross sections for, (E), 25:19922
reactions (n,2n) with beryllium-9, cross sections for, (E), 25:20269 (N-70-37365)
reactions (n,α) with boron-10 up to 200 keV, cross section for, (E), 25:20288
reactions (n,α) with lithium-6 at 10 eV to 8 keV, ratio of cross section to boron-10 (n,α) cross section, (E), 25:20288
reactions (n,f) with plutonium-238 at 2.5 keV to 2.5 MeV, cross sections for, (E), 25:20444
reactions (n,f) with plutonium-239 and uranium-235, average neutron production by resonance, (E), 25:20364(T) (BNL-tr-401)
reactions n + d at low energies, contributions of first two diagrams to amplitude of three-body inelastic, (T), 25:20027
reactions with gas-filled spheres at 0.5 and 2 MeV, track-length distributions in, 25:19757 (ORNL-4584, pp 58-73)
reactions with nuclei, tables of thresholds for, (E), 25:20237 (UCRL-50400(Vol.9))
resonance integrals for zirconium-94 and -96, (E), 25:20392
scattering by helium-4 below 22 MeV, phase shifts calculated from one-term nonlocal separable potentials for elastic, (T), 25:20261
scattering by particles moving in an electromagnetic wave, (T), 25:20243
scattering by uranium carbide, vanadium, and water, evaluation of double-differential, (E/T), 25:20235 (RPI-328-211)
scattering in crystals, deconvolution of resolution function for critical slow, 25:20241
spectra in beryllium oxide, time and space dependent calculations for, (T), 25:20239
thermalization in zirconium hydride, Einstein model of, (T), 25:20242
transport equation for slab geometry, solution using completely degenerrte energy transfer kernel, (T), 25:20236 (TID-25648)
transport in cylindrical and spherical geometry, improvements in ELF code for Monte Carlo calculations of, (T), 25:20233(T) (ORNL-tr-2409)
transport of, computer program for solving steady-state integral equation for, (T), 25:20246
uses in radiography, review on, 25:18615

NEUTRONS (anti n)
interactions anti n + d at 6.65 GeV/c, total cross sections for, 25:19907
interactions anti n + n at 6.65 GeV/c, total cross sections for, 25:19907
interactions anti n + p at 6.65 GeV/c, total cross sections for, 25:19907

NEUTRONS, COLD
production from stationary reactors, diffusion length, spectra, and storage time from, (E), 25:20232 (JINR-P3-5392)
transmission through simple bent conducting tubes, calculation of, 25:20245

NEUTRONS, DELAYED
fraction for in-core thermionic thermal reactors, effective, (T), 25:20825
spectra from neutron-induced and spontaneous fission, review of, 25:20362 (ANL-7747)

NEUTRONS, EPITHERMAL
capture by americium-241 and -243 at 0.2 to 20 eV with fission isomer excitation, cross section and prompt-to-isomer fission ratio in, (E), 25:20412
capture by lutetium-175, mechanism and resonance parameters for, (E), 25:20476
reactions (n,f) with uranium-238, fractional cummulative yield of niobium-99m from, (E), 25:20406

NEUTRONS, FAST
capture by gold-197, indium, and tantalum at 3.0 to 6.5 MeV, gamma spectra from, (E), 25:18735 (INR-1224)
capture by protons, $^3S_1$-$^3S_1$ radiative transitions in, 25:20519
dose distribution in tissues from implanted californium-252 point source, (T), 25:19003
dosimetry in tissues for 0.5 to 400 MeV, absorbed and equivalent, 25:19007 (NCRP-38)
dosimetry methods for, 25:19007 (NCRP-38)
effects on hematopoiesis, intestines, and survival of mice, comparison of protective effects of AET against whole-body x and, 25:19029
effects on human skin, effects of dose, dose fractionation, and time on pathological, 25:19149
effects on intestines of mice, protective effects of MEG against whole-body, 25:19029
effects on mechanical properties of graphite, (E), 25:20747(R) (NP-18668)
effects on mechanical properties of Type 316 stainless steel at 1000 to 1400°F, 25:19254 (WHAN-SA-2)
effects on mice, methods for testing lethal mutagenic, 25:18956
effects on microstructure of annealed Types 304 and 316 stainless steels at 370 to 700°C, 25:19253 (WHAN-FR-16)
effects on oocytes and spermatogonia of mice, mutagenic, 25:18949
effects on silicon single crystals, x-ray diffuse and small-angle scattering study of, 25:19853
effects on survival of epidermal cells of mice, effects of dose fractionation on RBE for, 25:19092
effects on tensile properties of aluminum-magnesium alloys, 25:19255
flux measurements from ORELA, performance of proton recoil monitor using silicon surface barrier detector for, 25:18763
flux spectra from foil activation measurements in reactors, computer program for determining, (T), 25:18641 (IN-1446)
production of, nuclear reactions for, 25:19007 (NCRP-38)
protection against 0.5 to 400 MeV, National Council on Radiation Protection recommendations for, 25:19007 (NCRP-38)
reactions (n,2n) with antimony-123, barium-138, erbium-168, hafnium-180, and selenium-78 at 14.5 MeV, cross sections and gamma spectra from, (E), 25:20435
reactions (n,2n) with potassium-39 at 14.7 MeV, isomeric cross-section ratio for, 25:20312
reactions (n,α) with iron-54 up to 14 MeV, Hauser--Feshbach analysis of excitation functions for, (E/T), 25:20346
reactions (n,f) with plutonium-239, fission product yields from, (T), 25:20819 (JAERI-Memo-4165)
reactions (n,f) with thorium-232 and uranium-235 and -238 at energies up to 6 MeV, energy-balance analysis of dependence of number of prompt neutrons on bombarding energy for, (T), 25:20440
reactions (n,f) with uranium-235 and plutonium-239 at 0.3

XUM

to 1.4 MeV, relative cross sections and number of prompt neutrons for, 25:20373(T) (LIB/Trans-300)
reactions (n,f) with uranium-238 at 1.20 to 2.66 MeV, fragment angular distributions from, (T), 25:20393
reactions (n,p) and (n,α) with aluminum-27 up to 14 MeV, Hauser--Feshbach analysis of excitation functions for, (E/T), 25:20346
reactions (n,p) with hafnium-180 at 14.8 MeV, production of lutetium-180 in, (E), 25:20426
reactions (n,p) with nickel-58 up to 14 MeV, Hauser--Feshbach analysis of excitation functions for, (E/T), 25:20346
reactions (n,t) with boron-11 at 14.4 MeV, angular distributions for, (E), 25:20285
reactions with hydrogen at 500 keV to 21 MeV, total cross section for, (E), 25:20258
reactions with nuclei at 0.1 to 10.0 MeV, intermediate structure in total cross sections for, (E/T), 25:20445
reactions with tissues to 400 MeV, 25:19007 (NCRP-38)
scattering by barium-137, erbium-167, and selenium-77 at 14.5 MeV, cross sections and gamma spectra from inelastic, (E), 25:20435
scattering by carbon at 0.5 to 2 MeV, differential cross sections for elastic, (E), 25:20267 (EUR-4538)
scattering by carbon-12 at 15 MeV, neutron--gamma angular correlations in inelastic, (E), 25:20281
scattering by carbon-12, iron-54, iron-56, nickel-58, and nickel-60 at 4.0 to 5.6 MeV, angular distributions and cross sections for, (E/T), 25:20338
scattering by iron-56,, lead-206, magnesium-24, and manganese-55 at 2.9 MeV, γ-ray differential cross sections for inelastic, (E), 25:20329
scattering by Z = 11 to 82 nuclei, γ energies from inelastic, (E), 25:20356
spectra in liquid metal cooled reactor, distribution of, (E/T), 25:20803
spectra measurements of, efficiency of lithium-6 glass scintillation detector for in-core, 25:18637 (AEEW-M-898)

NEUTRONS, FISSION
yields of plutonium-239, summary of, (E), 25:20363 (AWRE-O-86/70)

NEUTRONS, INTERMEDIATE
reactions (n,f) with uranium-235 at 20 eV to 100 keV, high-resolution cross section for, (E), 25:20418

NEUTRONS, PILE
capture by promethium-147, cross section and resonance integral for, (E), 25:20379
effects on ductility of stainless steel at high temperatures, 25:19250(T) (AEC-tr-7192)
effects on pellets and powders of boron carbide, 25:19289 (WHAN-FR-24)

NEUTRONS, PROMPT
lifetime in in-core thermionic thermal reactors, (T), 25:20825
spectra from neutron-induced and spontaneous fission, review of, 25:20362 (ANL-7747)
yield dependence on bombarding energy for neutron fission of thorium-232 and uranium-235 and -238 at energies up to 6 MeV, energy-balance analysis of, (T), 25:20440
yields of plutonium-239, summary of, (E), 25:20363 (AWRE-O-86/70)

NEUTRONS, THERMAL
capture by barium-132 and -134, cross sections and gamma spectra from, 25:20439
capture by hydrogen, effect of form factor in calculation of γ circular polarization from, (T), 25:20423
capture by tungsten-186, γ spectra from, (E), 25:20324
capture by zirconium-94 and -96, cross sections for, (E), 25:20392
detection of, response of europium-activated lithium iodide scintillation detectors for, 25:18661
diffusion coefficient in graphite systems, measurement using pulsed source, (E), 25:20240
diffusion in water, analysis in ice--water phase transition region, 25:20248
effects on boron-10--zinc sulfide scintillation detectors, 25:18680
flux mapping in reactors, performance of in-core regenerative detectors for, (E), 25:20711 (WHAN-FR-37)
flux measurements of, calculation of radioactivity of wire activation detectors for, 25:18707
flux spectra from foil activation measurements in reactors, computer program for determining, (T), 25:18641 (IN-1446)
reactions (n,f) with uranium-233 and -235, fractional cumulative yield of niobium-99m from, (E), 25:20406
reactions (n,f) with uranium-235, microsecond isomers in primary products of, 25:20430
reactions (n,f) with uranium-235, yield of xenon-145 from, (E), 25:20470
reactions (n,f) with uranium-235, yields of arsenic-87, selenium-87, and selenium-88 in, (E), 25:20327
scattering by hydrogen bound in ice, calculations for Haywood phonon distribution function of, (T), 25:20229 (INR-1186)
scattering by p-dichlorobenzene, measurements of, 25:18738 (RISO-229)
scattering by solid benzene at 77 to 270°K, inelastic, (E/T), 25:20247
scattering from terbium, measurements of critical magnetic, 25:18738 (RISO-229)
scattering in polycrystals, computer program for calculating law of, (T), 25:20229 (INR-1186)

NEVADA TEST SITE
radiation monitoring of Operation Bren area, 25:18982 (CEX-65.05)

NEWBOLD ISLAND POWER REACTOR, UNIT 1
effluents from, effects on environment of chemical, radioactive, and thermal, 25:20676 (DOCKET-50354-11)

NEWBOLD ISLAND POWER REACTOR, UNIT 2
effluents from, effects on environment of chemical, radioactive, and thermal, 25:20676 (DOCKET-50354-11)

NICHROME
thermal loading to induce water boiling on wires of, parameters for critical, 25:18583

NICKEL
abundance in Type-M supergiant, (E), 25:19323
chromatographic behavior in hydrochloric acid--thiocyanate mixture on Amberlite LA-2, 25:18337
effects on diffusion of plutonium in plutonium--uranium alloys at 500°C, 25:19230 (CEA-R-3951)
properties for use in heat block-shields in radioisotope-fueled thermoelectric systems, 25:18594(R) (ORNL-TM-3292)
radioinduced void formation at 300 to 650°C, 100-keV carbon- and nickel-ion, 25:19807
separation of bismuth from, by cation exchange chromatography, 25:18520

NICKEL 200
oxidation by air at 1000 to 1125°C, 25:18591(R) (DP-1254)

NICKEL ALLOYS AND SYSTEMS
magnetic properties of soft magnetic, effects of heat treatments on, 25:19872
properties of N-155 and Ni-O-Nel, for use as capsule material for radioisotope heat sources, 25:18592 (ORNL-4298)
Ag--Ni, electric conductivity of two-phase, 25:19226
Cu--Ni, properties for use as matrix for neutron-absorbing, 25:19264(P)
Fe--Ni, elastic moduli of Invar, effects of magnetic field on temperature-dependent, (E/T), 25:19224
Fe-base--Mo--Ni, phase transformation during aging, kinetics of martensitic, 25:19247
Nb--Ni, crystallization of solid-solution, mechanisms of, 25:19242
Nb-base--Ni--W, phase studies of isothermal sections of, at 1800 and 1900°C, 25:19246
Ni--Pu--U, phase studies of, 25:19230 (CEA-R-3951)
Ni--Zr, crystallization of solid-solution,' mechanisms of, 25:19242

NICKEL CHLORIDES
radiolysis of aqueous solutions of, hydrogen yields from electron pulse, 25:18448(R) (CEA-N-1369)

NICKEL IONS
effects on nickel at 100 keV and 300 to 650°C, void formation in, 25:19807

NICKEL ISOTOPES NI-56
energy level from nickel-58 (p,t) reaction,, excited 0^+, (E/T), 25:20321

NICKEL ISOTOPES NI-58
charge radius of, electron elastic scattering study of, (E), 25:20334
energy level from nickel-60 (p,t) reaction, excited 0^+, (E/T), 25:20321
helium-3 reactions (He-3,t) with, core-polarization effects in cross section for, (T), 25:20496
neutron reactions (n,p) up to 14 MeV, Hauser--Feshbach analysis of excitation functions for, (E/T), 25:20346
neutron scattering at 4.0 to 5.6 MeV, angular distributions and cross sections for, (E/T), 25:20338
proton reactions (p,γ) at 1.4 MeV, γ-ray angular distribution and Q-value for, (E), 25:20314
proton reactions (p,t) at 51.9 MeV, excited 0^+ state in nickel-56 from, (E/T), 25:20321

NICKEL ISOTOPES NI-59
proton reactions up to several GeV, cascade calculations of double differential distributions of particles from, (T), 25:20018 (JINR-P2-5507)

NICKEL ISOTOPES NI-60
neutron scattering at 4.0 to 5.6 MeV, angular distributions and cross sections for, (E/T), 25:20338
proton reactions (p,t) at 51.9 MeV, excited 0^+ state in nickel-58 from, (E/T), 25:20321
proton scattering at 4.25 to 8.47 MeV, angular distributions and excitation functions for, (E), 25:20322

NICKEL ISOTOPES NI-61
nuclear magnetic resonance spectrum of, magnetic modulation of frequency in, 25:19878

NICKEL ISOTOPES NI-62
alpha reactions (α,p) at 35.5 MeV, DWBA analysis of j dependence in angular distributions from, (E), 25:20309
charge radius of, electron elastic scattering study of, (E), 25:20334
energy levels from cobalt-62 and copper-62 decays, (E), 25:20361

NICKEL ISOTOPES NI-64
proton reactions (p,n) at 3 MeV, γ--γ angular correlations from, (E), 25:20358
proton scattering at 4.25 to 8.47 MeV, angular

  distributions and excitation functions for, (E), 25:20322
NICKEL PERCHLORATES
  radiolysis of aqueous solutions of, hydrogen yields from electron pulse, 25:18448(R) (CEA-N-1369)
NICKEL SULFATES
  radiolysis of aqueous solutions of, hydrogen yields from electron pulse, 25:18448(R) (CEA-N-1369)
NINE MILE POINT POWER REACTOR
  operations history for July to December 1970, 25:20587 (DOCKET-50220-58)
  power increase to 1850 MW(t), revised technical specifications and safety evaluation for, 25:20620 (DOCKET-50220-59)
  startup procedures for, modification of, 25:20621 (DOCKET-50220-60)
NIOBIUM
  bibliography on, 25:19165
  coating with chromium silicide by pack cementation for corrosion protection, 25:19175
  coating with intermetallic aluminides, crystal structure of, 25:19173
  coating with silicon by decomposition of silicon hydride, effects of oxygen on, 25:19258
  coating with titanium silicide by pack cementation for corrosion protection, 25:19175
  complexes with hydrogen peroxide and 4-[(2,4-dihydroxyphenyl)azo]-1-naphthalenesulfonic acid, fluorescent and spectrophotometric studies on, 25:18349
  conference on properties and uses of, Paris, Oct. 20 to 21, 1969, 25:19211
  corrosion by acid and alkaline solutions, mechanisms of, 25:19170
  corrosion by hydrofluoric acid, 25:19170
  corrosion protection of, development of coatings for, 25:19176
  crystal structure of sputtered films of, on sodium chloride, 25:19244
  deformation and rupture at -196 and 20°C, effects of interstitial impurities on plastic, 25:19217
  determination in presence of tantalum using hydrogen peroxide and 4-[(2,4-dihydroxyphenyl)azo]-1-naphthalenesulfonic acid, fluorimetric, 25:18349
  faulting in filings of, x-ray diffraction study of, 25:19248
  hardening at 20 to 1200°C in vacuum, effects of interstitial impurities on, 25:19213
  heating and quenching of, effects on vacancies, 25:19245
  magnetic flux-flow resistivity and Hall angle in pure superconducting, two-band expressions for, (T), 25:19619
  mechanical properties of, effects of interstitial impurities on, 25:19212
  oxidation during annealing and electropolishing, determination by deuteron reactions with oxygen, 25:19171
  oxidation morphology and rates in air at 800 to 950°C, 25:19172
  oxidation of, effects of pressure and temperature on morphology and kinetics of, 25:19177
  passivation in deaerated sodium hydroxide, tests for, 25:19170
  preparation of, economics of methods for, 25:19187
  properties for use as capsule material for radioisotope heat sources, evaluation of high-temperature, 25:18592 (ORNL-4298)
  reactions with nitrogen at 800 to 1000°C, diffusion and nitrogenation, 25:19234
  resonance effect in sputtered superconducting, geometrical, (T), 25:19617
  separation from acid solutions by ion exchange on phenolic resins, 25:18503 (RT/CHI-(70)25)
  separation from niobium—uranium alloys, bibliography on, 25:18502 (RFP-1421)
  separation from seawater by flocculation, 25:18518
  superconducting transition of, NMR study of temperature dependence of quantity of normal phase in, 25:19628
  ultrasonic attenuation in single crystals of, Alpher—Rubin effect of magnetic field on, 25:19879
NIOBIUM ALLOYS AND SYSTEMS
  bibliography on, 25:19165
  coating with intermetallic aluminides, crystal structure of, 25:19173
  hardening at 20 to 1200°C in vacuum, effects of interstitial impurities on. 25:19213
  properties for use as fuel cladding, 25:19179
  Al_2O_3--Nb-base, creep of dispersion-strengthened, at 850 to 1450°C, 25:19277
  Al--Cr--Nb--Si--Sn--Ti, properties for use as protective coating on niobium, 25:19176
  Al--Ge--Nb, properties of intermetallic system Nb_3Al—Nb_3Ge, for high parameter superconductors, (E), 25:19599
  Al--Nb, crystal structure of intermetallic coatings of, on niobium and niobium alloys, 25:19173
  Al--Nb, oxidation of intermetallic $NbAl_3$ coatings of, at 600 to 1400°C, kinetics of pest-type, 25:19174
  Al--Nb--Si--Sn--Ti, properties for use as protective coating on niobium, 25:19176
  B--C--Hf--Nb-base--W--Zr, properties for use at high temperatures, 25:19218
  C--Hf--Mo--Nb-base--W, properties for use at high temperatures, 25:19218
  C--Nb-base--Ti--V--W--Zr, oxidation morphology and rates in air at 800 to 950°C, 25:19172
  Cr--Fe--Nb--Si, properties for use as protective coating on niobium, 25:19176
  Cu--Mo--Nb-base, phase studies of isothermal sections of, at 1900 and 2100°C, 25:19246
  Cu--Nb-base, phase studies of, 25:19246
  Cu--Nb-base--W, phase studies of isothermal sections of, at 1600, 1900, and 2100°C, 25:19246
  Hf--Nb--O, phase studies of, 25:19240
  Hf--Nb-base, superconductivity of, relations with microstructure, 25:19219
  Mo--Nb, crystallization of solid-solution, mechanisms of, 25:19242
  Mo--Nb, diffusion in solid-solution, at 1100 to 1800°C, effects of molybdenum content on reciprocal, 25:19204
  Mo--Nb--Ta--W-base, mechanical properties of, effects of composition on, 25:19239
  Mo--Nb-base, embrittlement by hydrogen, effects of interstitial solutes on, 25:19216
  Mo--Nb-base, mechanical properties of solid solutions of, 25:19215
  Mo--Nb-base, preparation of high-purity, by electron beam melting, 25:19186
  Nb--Ni, crystallization of solid-solution, mechanisms of, 25:19242
  Nb--Pd, crystallization of solid-solution, mechanisms of, 25:19242
  Nb--Rb, crystallization of solid-solution, mechanisms of, 25:19242
  Nb--Ru, crystallization of solid-solution, mechanisms of, 25:19242
  Nb--Ta, diffusion in solid-solution, at 1100 to 1800°C, effects of tantalum content on reciprocal, 25:19204
  Nb--Ta--Ti, superconducting transition temperature of, 25:19629
  Nb--Ta--Ti--Zr, effects of iron additions on superconducting properties of, 25:19618(P)
  Nb--Ti, diffusion in solid-solution, at 1100 to 1800°C, effects of titanium content on reciprocal, 25:19204
  Nb--Ti, diffusion in, kinetics of, 25:19214
  Nb--Ti, magnetic flux jumps in superconducting, (E/T), 25:19630
  Nb--Ti, superconductivity of, relations with microstructure, 25:19219
  Nb--Ti, threshold currents of large cross-section superconducting, 25:19624
  Nb--Ti--Zr, superconducting properties of, 25:19627
  Nb--U, separation of niobium from, bibliography en, 25:18502 (RFP-1421)
  Nb--V, diffusion in solid-solution, at 1100 to 1800°C, effects of vanadium content on reciprocal, 25:19204
  Nb--V, diffusion in, kinetics of, 25:19214
  Nb--W, diffusion in solid-solution, at 1100 to 1800°C, effects of tungsten content on reciprocal, 25:19204
  Nb--W, diffusion in, kinetics of, 25:19214
  Nb--Zr, diffusion in solid-solution, at 1100 to 1800°C, effects of zirconium content on reciprocal, 25:19204
  Nb--Zr, diffusion in, kinetics of, 25:19214
  Nb--Zr, magnetic flux flow in superconducting, 25:19609
  Nb-base--Ni--W, phase studies of isothermal sections of, at 1800 and 1900°C, 25:19246
  Nb-base--Sn, superconductivity of, relations with microstructures, 25:19219
  Nb-base--Ti, embrittlement by hydrogen, effects of interstitial solutes on, 25:19216
  Nb-base--Ti, mechanical properties of solid solutions of, 25:19215
  Nb-base--Ti, preparation of high-purity, by vacuum arc melting, 25:19186
  Nb-base--Ti--Zr, plasticity and strength of, at -196 and 20°C, 25:19206
  Nb-base--Zr, embrittlement by hydrogen, effects of interstitial solutes on, 25:19216
  Nb-base--Zr, mechanical properties of solid solutions of, 25:19215
  Nb-base--Zr, preparation of high-purity, by electron beam melting, 25:19186
  Nb-base--Zr, properties for use in Japanese ATR pressure tubes, 25:19223
  Nb-base--Zr, superconductivity of, relations with microstructure, 25:19219
NIOBIUM CARBIDES
  electron band structure of, ESCA study of, 25:19867
NIOBIUM DEUTERIDES
  deuteron magnetic resonance study of, exploratory, 25:19876
NIOBIUM ISOTOPES Nb-90
  beta and electron-capture decay of, γ spectra from, (E), 25:20411
NIOBIUM ISOTOPES Nb-92
  energy levels from zirconium-92 (p,n) reactions, lifetimes of, (E), 25:20471
NIOBIUM ISOTOPES Nb-94
  energy levels from zirconium-94 (p,n) reactions, lifetimes of, (E), 25:20471
NIOBIUM ISOTOPES Nb-99
  yields of isomeric, in uranium-233, -235, and -238 neutron fission and californium-252 spontaneous

fission, (E), 25:20406

NIOBIUM OXIDES
  electric conductivity of NbO/sub x/ at 77 to 900°K, (E), 25:19868

NIOBIUM SILICIDES
  reactions with oxygen at high pressures and temperatures, 25:19258

NITRATES
  complexes with americium and europium, stability constants for, effects of ionic media on, 25:18371
  determination in natural waters from uranium mining operations, method for, 25:18339 (CEA-R-3557(2))

NITRIC ACID
  determination simultaneously with plutonium by conductivity and density measurements, 25:18350

NITRITES
  use in vacuum systems for thermonuclear devices, 25:19728
  yields from γ radiolysis of aqueous solutions of sodium nitrate, 25:18463

NITROGEN
  alpha-particle spallation reactions at 22.5 to 235 MeV/N with, cosmic, (E), 25:19531
  analysis for nitrogen-15 by emission spectroscopy, 25:18344
  argon-atom reactions at 25 to 90 keV with molecular, total cross sections for single electron loss in, (E), 25:19492 (SC-RR-70-735)
  determination by photon activation, 25:18366(R) (NBS-TN-548)
  diffusion from molybdenum and tungsten at 2000°K, 25:19225
  diffusion of molecular, in isotopic mixtures incorporating nitrogen-14 and nitrogen-15, 25:18604
  effects of surface impurity of, on ionization of potassium by polycrystalline tungsten, 25:19210
  neon-atom reactions at 25 to 90 keV with molecular, total cross sections for single electron loss in, (E), 25:19492 (SC-RR-70-735)
  performance as carrier gas for electron attachment studies, 25:19491 (ORNL-4584, pp 105-24)
  plasma of, partition functions for, (T), 25:19397
  proton reactions at 5 to 26 keV with molecular, total cross sections for formation of metastable hydrogen atoms by charge exchange in, (E), 25:19504
  proton spallation reactions at 70 to 420 MeV with, cosmic, (E), 25:19531
  reactions with (100) crystal planes of tungsten, kinetics of, 25:19208
  reactions with iron silicide at 400 to 1000°C, 25:19234
  reactions with niobium at 800 to 1000°C, 25:19234
  reactions with tungsten at 800°C, 25:19234
  sorption by nonporous thorium oxides, effects of surface water on, 25:18416

NITROGEN IONS
  effects of implanted, on electric properties of silica films, 25:19788
  effects on production of regular void arrays in molybdenum single crystals at 2 MeV, 25:19256
  effects on void distribution in high-purity molybdenum at 2-MeV, 25:19257
  implantation in silicon at 15 to 25 keV for insulating layer formation, 25:19781
  implantation in silicon at 30 to 400 keV, calculated spatial distributions of damage from, 25:19819
  implantation in silicon at 40 to 100 keV, electron microscopic studies of defects induced in, 25:19808
  implantation in silicon carbide at 5 to 300 keV, properties of conducting layers and p--n junctions formed by, (E), 25:19847

NITROGEN IONS (N^+)
  abundance in topside ionosphere, solar-geomagnetic seasonal control of, (E/T), 25:19576

NITROGEN ISOTOPES N-13
  energy levels of, charge asymmetry of nucleon widths of lowest $T = {}^3/_2$, 25:20512

NITROGEN ISOTOPES N-14
  deuteron reactions (d,n) at 2.8 to 4 MeV, neutron polarization in, (E), 25:20272
  deuteron reactions (d,p) at 3 MeV and 45°, energy spectra from, (E), 25:18718
  energy levels from oxygen-16 (p,He-3) reactions, isobaric analog, (E), 25:20299
  proton reactions (p,γ) at 2.2 to 19 MeV, cross sections for, (E), 25:20277
  reactions (N-14,xn) with lead-207, excitation functions for total neutron emission for, (E), 25:18737(R) (ORO-3820-7)
  reactions with bismuth-209 at 78 and 100 MeV, cross sections, angular distributions, and recoil paths for astatine-211 from, (E/T), 25:20375 (NP-18624)

NITROGEN ISOTOPES N-15
  determination in low concentration range by emission spectroscopy, 25:18344
  deuteron reactions (d,n) at 2.8 to 4 MeV, neutron polarization in, (E), 25:20272
  helium-3 elastic scattering at 11 MeV, optical-model analysis of, (E/T), 25:20278
  helium-3 elastic scattering at 18 MeV, optical-model analysis of angular distributions from, (E/T), 25:20271 (NP-18628)
  helium-3 reactions (He-3,p) at 18 MeV, DWBA analysis of angular distributions from, (E/T), 25:20271 (NP-18628)

NITROGEN OXIDES NO_2 OR N_2O_4
  cesium-atom reactions up to 14 eV with, negative-ion production in, 25:19490 (ORNL-4584, pp 92-104)

NITROGEN OXIDES N_2O
  effects on yields from γ radiolysis of heptane, 25:18466
  ethanol--N_2O, radiolysis of solutions of, precursors of free radicals and hydrogen in, 25:18448(R) (CEA-N-1369)
  N_2O--tetrahydro-2-methylfuran, radiolysis of solutions of, precursors of free radicals and hydrogen in, 25:18448(R) (CEA-N-1369)

NITROGEN SYSTEMS
  CO--N, diffusion in isotopic mixtures of, incorporating carbon-12, carbon-13, oxygen-16, and oxygen-18, effects of temperature on, 25:18604
  ethylene--N, radiolysis of, reaction mechanisms of γ, 25:18455

NITROUS ACID
  effects on Brucella abortus, frequency of mutagenic, 25:18970

NORTH ANNA POWER REACTOR, UNIT 1
  construction of, permit for, 25:20671 (DOCKET-50338-27)

NORTH ANNA POWER REACTOR, UNIT 2
  construction of, permit for, 25:20672 (DOCKET-50339-26)

NOVO VORONEZH POWER REACTOR, UNIT 1
  fuel element assemblies of, calculation of coolant temperature distribution in, (T), 25:20737

NUCLEAR AUXILIARY POWER SYSTEMS
  core configuration for thermionic reactor with dual crossed axis heat pipe system, 25:20809(P)
  design of mercury vapor turbine-type, for undersea operation, 25:18600(P)
  design of thermionic reactor system with heat pipe protection by radiator plate, 25:20808(P)
  design parameters of thermionic reactor system with heat pipe cooling of radiation shield, 25:20807(P)
  design parameters of uranium oxide (UO_2) fueled water cooled thermionic, for underwater operation, 25:20817(P)
  shutdown cooling of space reactor, sodium loop and radiator for, (T), 25:20805 (N-70-39420)

NUCLEAR ELECTRIC MOMENTS
  quadrupole, for A = 18 to 38 nuclei as predicted by the shell model, (T), 25:20337

NUCLEAR EMULSIONS
  meson (π^+) reactions with nuclei at 185 to 295 MeV in emulsions, cross sections for π^- and π^+ production in, (E), 25:19919
  particle track analysis for mass determination of cosmic-ray carbon, 25:18643 (NP-18672)
  particle track analysis using mean track width and blob measurements in breakup event, 25:18795
  particle tracks in, development of automatic scanner for, 25:18690
  particle tracks in, for neutron detection, measurement of proton-recoil, 25:18728
  performance of Ilford-K2, for measurement of neutron spectrum from americium--beryllium source, 25:18761
  processing of thin, 25:18729

NUCLEAR ENGINEERING
  curriculum for, objectives and content of stress analysis, 25:18616

NUCLEAR EXPLOSIONS
  effects of, computer program for Weapons Effects Display System for mapping prompt, 25:18832 (UCRL-50892(Vol.6))
  effects of, mathematical models for computer programs for Weapons Effects Display System for mapping prompt, 25:18831 (UCRL-50892(Vol.1))

NUCLEAR EXPLOSIONS, UNDERGROUND
  detection at ORNL Station ORT from Aug. 1969 to Aug. 1970, station operation for, 25:18556 (ORNL-4584, pp 41)
  hazards to human populations from fallout release during, 25:18989 (ORNL-4584, pp 42-56)
  uses in nuclear physics, 25:20449

NUCLEAR ISOMERS
  lifetimes of, system for measuring ms and μs, 25:18753
  production in nuclear reactions, method for measurement of cross-section ratio for, 25:20312

NUCLEAR MAGNETIC MOMENTS
  nuclear spin coupling tensor for, orbital contribution to, (T), 25:20517

NUCLEAR MAGNETIC RESONANCE
  acoustic coupling in pure metals, equations for, (T), 25:19879
  frequency modulation in ferromagnets, magnetic, 25:19878

NUCLEAR MATERIALS MANAGEMENT
  methods for criticality and inventory control in, computerized real-time, 25:18620 (BNWL-1440)
  neutron sources for nondestructive assay in, 25:18619 (BNL-50267)
  safeguards for, relation of non-proliferation treaty to, 25:19019

NUCLEAR MATTER
  hole potential energy in, 25:20540
  hyperon (Λ) binding energy in, effects of short-range repulsion in $\Lambda + N$ interactions on, (T), 25:20023
  hyperon (Λ) in, nonlinear equation for correlation function between nucleon and, (T), 25:20001 (DEMO-

70/19)
  hyperon (Λ) single-particle-energy spectrum in, independent-pair approximation for, (T), 25:20023
NUCLEAR MODELS
  book: Nuclear Collective Motion. Models and Theory, 25:20483
  collective, microscopic description of, (T), 25:20547
  Nilsson, of proton states in A = 151 to 155 region, 25:20383
  optical, calculation of nuclear-reaction dynamics in, (T), 25:20528
  optical, for photon reactions with nuclei at high energies, 25:19955
  shell, extension to continuum of separable single-particle potential in, 25:20509
  shell, prediction of static quadrupole moments of A = 18 to 38 nuclei by, (T), 25:20337
  symmetric model with nonlinear transformation laws, exact solution of quantum-mechanical, (T), 25:20504
  unified, validity of, (T), 25:20548
NUCLEAR PARTICLES
  identification of, development of hard-wired arithmetic computer for, 25:18718
NUCLEAR PHYSICS
  book: Annual Review of Nuclear Science, Vol. 20, 25:20446
  research at AECL from January 1, 1970 through March 31, 1970, 25:20307(R) (AECL-3667)
  research in Sweden, 1969, 25:20133(R) (NP-18671)
NUCLEAR POWER PLANTS
  construction costs of, comparison with conventional steam power plants of, 25:20597
  construction in Finland, forecast of 1970 to 2000, 25:20553
  construction of, cost increases for, 25:20598
  control systems for, reliability and maintenance requirements of redundant, 25:20552
  development in Australia, prospects for, 25:20550 (NP-18677)
  development in U.S.S.R, 25:20549(T) (AEC-tr-7187)
  development of, graph illustration of, 25:20556
  economics of, problems in, 25:20751
  effluents from, activities in France for control of air pollution from, 25:20686
  effluents from, environmental effects from radioactive and thermal, 25:20683
  magnetohydrodynamic generators for, parametric design study of rare-gas, 25:19536 (JUL-706-TP)
  operation histories of U.S.S.R, 25:20549(T) (AEC-tr-7187)
  operation of, computer methods for evaluating environmental effects of, 25:18526 (ORNL-4584, pp 37-40)
  power cycles for, thermodynamic analysis of optimum, (T), 25:20596
  power grid system in Germany for, requirements for interconnected, 25:20691
  thermal effluents from, effects on Rhine River of, 25:20685
  turbines for desalination, optimum exhaust pressure for, 25:18565 (ORNL-TM-3291)
NUCLEAR REACTION ANALYSIS
  development of, use of beryllium-polonium as source in, 25:18368
NUCLEAR REACTIONS
  alpha transfer in heavy-ion, review of, (E/T), 25:20450
  analysis of high-energy knock-out, using hydrodynamic model, (T), 25:20491
  core polarizaion effects in, (T), 25:20496
  coupled-channels calculations of, supplement to manual for computer code for, (T), 25:20479 (JAERI-Memo-4138)
  cross sections for (heavy-ion, xn), validity of Alexander--Simonoff semiempirical rule in A = 100 to 150 region for, (T), 25:20480 (JINR-E7-5499)
  cross sections for γ production, unified model of deformed nuclei for, (T), 25:20524
  cross sections for neutron capture, condition for half-life independence in activation measurement of, 25:20518
  description of resonant, using multichannel treatment and quasiparticle method, (T), 25:20510
  description using harmonic oscillator shell-model function scheme, (T), 25:20516
  identification of heavy-ion, by means of product angular distributions, (E), 25:20419
  model for direct transfer, 25:20522
  parity violation in, weak-interaction Hamiltonian for, (T), 25:20039
  radioisotope production in charged-particle induced, method for cross-section measurement of positron-unstable, 25:20283
  tables of thresholds for, (E), 25:20237 (UCRL-50400(Vol.9))
  tensor force in charge-exchange and knock-out, formalism of two-body, 25:20508
NUCLEAR REACTIONS (DIRECT)
  DWBA description of heavy-ion, second-order corrections to, (T), 25:20501
  pick-up, diagram approach to polarization effects in, (T), 25:20533
  stripping, diagram approach to polarization effects in, (T), 25:20533
  theory of (d,p) stripping, effects of neglecting certain terms in DWBA, (T), 25:20497
NUCLEAR STRUCTURE
  book: Nuclear Structure (in Russian), 25:20503
  calculations for light nuclei, unrestricted variation method for, (T), 25:20546
  collectivity in light nuclei, microscopic bases of, (T), 25:20543
  configuration interactions using statistical ensembles, calculations of, (T), 25:20505
  in rare-earth region, Nilsson model calculations of equilibrium deformations in, 25:20367 (INR-P-1216)
  mass distribution in nuclei, determination using isobaric analog resonances, (T), 25:20534
  nucleon-nucleon potentials in light, analysis of central, 25:20494
  odd-even staggering of nuclear radii, 25:20520
  quasi-particles in, gauge transformations and local charges of, (T), 25:20082
  single-nucleon potentials in, appropriate choice of, (T), 25:20532
NUCLEAR THEORY
  angular momentum projection approach to nuclear rotation in the rare-earth region, 25:20541
  approximation for the rotation-vibration transition region, 25:20527
  book: Nuclear Collective Motion. Models and Theory, 25:20483
  boson expansions in, relation between Beliaev--Zelevinsky and Marumori, 25:20521
  calculation of the three-nucleon system using a separable expansion of local potentials, 25:20538
  computation of Moshinsky brackets by direct diagonalization, 25:20526
  forces in, π exchange effects on N + N interactions and πN coupling effects on, 25:20021
  generalized impulse approximation of scattering, 25:20537
  Hamiltonian function in, diagonalization of S = 0, T = 1 charge-symmetrical, 25:20492
  Hartree-Fock, Slater, and Thomas-Fermi approximations in, comparison of, 25:20514
  Jost function of a nonlocal potential, 25:20539
  many-body forces in, 25:20523
  many-body problems in, algebraic approach to correct separation of center-of-mass motion in, 25:20500
  many-body system of attractive fermions with arbitrary spin in one dimension, ground-state energy of, 25:20502
  many-particle systems in, validity of random matrix treatment for, 25:20507
  meson exchange currents in weak and electromagnetic interactions, 25:20542
  neutron-proton correlations in light nuclei, analysis using R5 group, 25:20493
  nuclear radii, results of different methods for determining, 25:20536
  nucleon-nucleon interactions, weak parity-violating and strong potentials in, 25:20488
  properties of real RPA matrices and a simple diagonalization procedure, 25:20525
  Strutinsky method in, validity of, 25:20486
  three-body problem in, calculations using Faddeev equations, 25:20251 (NP-18678)
  two-nucleon reaction matrix in, off-shell, 25:20485
NUCLEI
  alpha decay of, total energy release from, (T), 25:20482(T) (RFP-Trans-72)
  alpha inelastic scattering by A = 7 to 140, model analysis of, 25:20274
  alpha reactions (α,γ), background reduction for spectroscopy of, 25:20148
  binding energies of light, calculations with several nucleon--nucleon potentials for, (T), 25:20298
  charge distribution in, isotope shift of, (T), 25:20486
  deuteron scattering in multi-GeV region, Glauber theory of, (T), 25:20531
  electron quasi-free scattering with nucleon emission, analysis for nuclear neutron and proton distributions by, (T), 25:20544
  electron small-angle multiple scattering above 250 MeV, effect of finite nuclear size on, (T), 25:20545
  energy levels of A equals 18 to 32, electric quadrupole moments for ground and first-excited, 25:20337
  energy levels of self-conjugate closed-shell, calculation using schematic model with separable potential, 25:20506
  energy levels of, conversion electron--gamma coincidence system for subnanosecond measurements of lifetimes of, 25:18691
  energy levels of, γ-γ coincidence circuit for lifetime measurements of, 25:18642 (JINR-P13-5485)
  energy-level transitions in A = 175 to 243, internal conversion coefficients and matrix elements for E1, (E), 25:20457
  energy-level transitions in radioactive, tables of energies and intensities of, (E), 25:20368 (JAERI-Memo-4189)
  existence of K-mesic, from assumption of positive sign of real part of amplitude of K + N interactions at low energies, (T), 25:20002 (IFVE-STF/SPK-70-30)

XUM

  half-lives of, table of, (E), 25:20368 (JAERI-Memo-4189)
  heavy-ion reactions (HI,xn) with fissionable, product identification by means of angular distributions, (E), 25:20419
  mass distribution in, determination using isobaric analog resonances, (T), 25:20534
  meson (K^+) reactions at 10 GeV in heavy-liquid bubble chambers, $Q^+(1275)$ enhancement and K(890) in coherent production of $K^+\pi^+\pi^-$ systems in, (E), 25:19913
  meson (K^+) reactions at 10 GeV/c in heavy-liquid bubble chamber, cross sections and momentum transfer distributions for coherent production of $K2\pi$, $K3\pi$, and $K4\pi$ systems in, (E), 25:19913
  meson (K^+) reactions at 10 GeV/c in heavy-liquid bubble chambers, cross sections for $Q^+(1275)$ + N interactions in nucleus in, (E/T), 25:19913
  meson (π) elastic scattering by, low-energy theorems for, (T), 25:20019 (LYCEN-7081)
  meson (π) interactions at several hundred MeV, cross-section calculations using Glauber theory, (T), 25:20490
  meson (π^-) reactions at 16 to 200 GeV/c, energy dependence of cross sections for coherent production of 3π and 5π systems in, (E/T), 25:20029
  meson (π^+) reactions at 185 to 295 MeV in emulsions, cross sections for π^- and π^+ production in, (E), 25:19919
  neutron and proton distributions in, use of quasi-free scattering reactions for analysis of, (T), 25:20544
  neutron capture by, review of energy-level transitions from keV, 25:20227 (AAEC/TM-565)
  neutron capture by, review of gamma spectroscopy of, 25:20447
  neutron total cross sections at 0.1 to 10.0 MeV, intermediate structure in, (E/T), 25:20445
  nucleon reactions at high energies, very high-momentum nuclear components for cross section upper limits for far subthreshold production of quarks in, (T), 25:20026
  photon reactions (γ,n) up to 30 MeV, review of, (E/T), 25:20448
  photon reactions at high energies, Glauber theory of multiple scattering for cross sections for total photon absorption and vector meson and π^- and π^+ production in, (T), 25:19955
  photon reactions at high energies, optical model for, (T), 25:19955
  photon reactions with, low-energy theorems for π production in, (T), 25:20019 (LYCEN-7081)
  photon scattering by, Glauber theory of multiple scattering for corrections to wide-angle bremsstrahlung from Compton, (T), 25:19955
  proton interactions at several hundred MeV, cross-section calculations using Glauber theory, (T), 25:20490
  radii of light, calculations with several nucleon--nucleon potentials for, (T), 25:20298
  radii of, odd-even staggering of, 25:20520
  reactions with nuclei at 600 MeV, classical absorptive-gas model for calculation of meson (π^+) production in, 25:20031
  rotation of rare-earth, angular momentum projection approach to, (T), 25:20541
  rotation-vibration transition region of, approximation for, (T), 25:20527
  scattering cross sections of, S-matrix theory for reformulation of generalized impulse approximation for, (T), 25:20537
  spectra of extremely heavy primary cosmic, charge, (E), 25:19532
NUCLEIC ACID, DEOXYRIBO-
  characterization of mitochondrial molecules of isogenic wild-type and vegetative-petite diploid strains, 25:20878(R) (NYO-3997-7)
  molecular topology during cell cycle in synchronous cultures, 25:20877(R) (NYO-3997-6)
  radiation effects on replication of, in synchronous cultures of Escherichia coli, mutagenic uv, 25:18966
  radiation effects on synthesis of, in Oenothera and wheat, x, 25:18910
  radioinduced breaks in double strand, of murine lymphoma cells, x, 25:18911
  radioinduced breaks in L cell, effects of energy deprivation on repair of x, 25:18908
  radioinduced single-chain breaks in Escherichia coli, effects of culture medium on repair of x, 25:18912
  radioinduced strand breaks in, in Escherichia coli, protective effects of Polysorbate 80 against cobalt-60 γ, 25:19027
NUCLEIC ACID, RIBO-
  radiation effects on chromatin templates for synthesis of, γ, 25:18916
NUCLEONS
  bound states (π--N), Bethe--Salpeter equation in ladder approximation for Regge trajectories of, (T), 25:20007
  correlation with Λ in nuclear matter, nonlinear equation for function for, (T), 25:20001 (DEMO-70/19)
  coupling constant for πNN, from model-independent analysis of forward elastic π^- + p and π^+ + p interactions, (T), 25:20003 (JINR-E2-5561)
  coupling of πN, effect on nuclear forces of second-order nonlinear term in, (T), 25:20021
  coupling with octet of pseudoscalar mesons, mass operator in SU(3) symmetric, (T), 25:20046
  interactions e + N, multiperipheral model for scaling property of structure functions for deep inelastic, (T), 25:19959
  interactions K + N at high energies, bounds on amplitudes and oscillations in diffraction-peak region for, (T), 25:19990
  interactions K + N at low energies, existence of K-mesic nuclei from assumption of positive sign of real part of amplitude of, (T), 25:20002 (IFVE-STF/SPK-70-30)
  interactions $K^-\pi^+\pi^-$ + N in K^- reactions with bromine, carbon, fluorine, and neon at 5.5 to 12.7 GeV/c in bubble chamber, (E), 25:19910 (LAL-1242)
  interactions Λ + N, effects on Λ binding energy in nuclear matter from short-range repulsion in, (T), 25:20023
  interactions N + N → N' + Δ + π, isospin analysis of, (T), 25:20030
  interactions N + N → N + Δ + rho, isospin analysis of, (T), 25:20030
  interactions N + N → N + N* + π, isospin analysis of, (T), 25:20030
  interactions N + N → N + N* + rho, isospin analysis of, (T), 25:20030
  interactions N + N at 0 to 3 GeV, one-boson-exchange model of elastic, (E/T), 25:20025
  interactions N + N at high energies, bounds on amplitudes and oscillations in diffraction-peak region for, (T), 25:19990
  interactions N + N, calculation of one-pion-exchange diagram in U(6,6) for, 25:20021
  interactions N + N, effects of mass and coupling-constant differences on π and rho exchange contributions to, (T), 25:20021
  interactions N + N, one-boson-exchange approximation for, (T), 25:20024
  interactions N + N, parity-violating and strong potentials in, 25:20488
  interactions π + N → ω + N at high energies, Regge pole model for differential and total cross sections and t dependence of density matrix elements for forward, (T), 25:20008
  interactions π + N at 1.98 to 3.5 GeV/c, phase shift analyses of elastic, (T), 25:20012
  interactions π + N at high energies, bounds on amplitudes and oscillations in diffraction-peak region for, (T), 25:19990
  interactions π + N at high energies, non-Pomeranchuk Regge cuts for minima and polarization in elastic and charge-exchange, (T), 25:20006
  interactions π + N at threshold, electromagnetic corrections to chiral symmetry for S-wave scattering lengths for, (T), 25:20044
  interactions π + N, fixed-t dispersion relations for effective-range parameter for S-wave, (T), 25:20010
  interactions π + N, nucleon matrix elements in chiral symmetry breaking calculations from phase shifts and dispersion relations for, 25:20051
  interactions $Q^+(1275)$ + N in nucleus in K^+ reactions with nuclei at 10 GeV/c in heavy-liquid bubble chamber, cross sections for, (E/T), 25:19913
  interactions with vector mesons, scalar nucleon--vector meson interaction model for elastic and inelastic amplitudes for, (T), 25:19927
  mass of, dynamical rearrangement of spontaneously broken SU(2) x SU(2) chiral symmetry for relation for, (T), 25:20042
  reactions with nuclei at high energies, very high-momentum nuclear components for cross section upper limits for far subthreshold production of quarks in, (T), 25:20026
  Regge trajectories for, review of, (E), 25:19988
  three-body systems of, calculation using a separable expansion of local potentials, (T), 25:20538

O

OBRIGHEIM POWER REACTOR (GERMANY)
  control system for, design parameters and performance of, 25:20551
1-OCTANOL
  radiolysis of crystals of, processes for annealing of free radicals formed by, 25:18473
OOCYTES
  radioinduced specific locus mutations in, of mice, frequency of fast neutron, 25:18949
ORES
  analysis for thorium and uranium by gamma spectrometry or neutron activation, 25:18365
  analysis for uranium using 2-[(5-bromo-2-pyridyl)azo]-5-(diethylamino)phenol, spectrophotometric, 25:18352
  analysis of, scintillation spectroscopy equipment for radiometric borehole, 25:18814(T) (CSIRO-Trans-9992)
ORGANIC ACIDS
  effectiveness for removal of radioisotopes from plant tissue, 25:18892 (NP-18641)
  radiolysis of aqueous solutions of unsaturated dicarboxylic, effects on grafting of acrylamide and methacrylamide of, 25:18429

ORGANIC COMPOUNDS
- Br--organic compounds, bromine-82 isomeric transitions in, theory of chemical effects from, 25:18489

ORGANIC COMPOUNDS, FLUORO-
- hydrolysis of, catalytic effects of metal ions on, 25:18375

ORNL FAST BURST REACTOR
- operation, 1969--1970, 25:20134 (ORNL-4584, pp 187-97)

OROTIC ACID
- radiation effects on uptake by rat kidney, liver, muscles, and spleen, effects of AET and cysteamine on γ, 25:19024

OSMIUM ALLOYS AND SYSTEMS
- Os--Rh, superconducting properties of fcc solid solutions of, (E), 25:19606

OSMIUM CHLORIDES
- reactions with alkanethiols, properties of alkanethiolatoosmium compounds from, 25:20864 (IS-T-431)

OSMIUM ISOTOPES Os-189
- energy levels from osmium-188 proton scattering, spectroscopic factors for isobaric analog, (E), 25:20378

OSMIUM ISOTOPES Os-191
- energy levels from osmium-190 proton scattering, spectroscopic factors for isobaric analog, (E), 25:20378

OSMIUM ISOTOPES Os-193
- energy levels from osmium-192 proton scattering, spectroscopic factors for isobaric analog, (E), 25:20378

OSTEICHTHYES
- Clupea harengus, radioisotope content of, in Finland, 25:18930 (NYO-3446-14, Paper 27)
- Coregonus albula, radioisotope content of, in Finland, 25:18930 (NYO-3446-14, Paper 27)
- Coregonus lavaretus, radioisotope content of, in Finland, 25:18930 (NYO-3446-14, Paper 27)
- Esox lucius, radioisotope content of, in Finland, 25:18930 (NYO-3446-14, Paper 27)
- Gadus sp., radiation effects on amino acid composition of protein of muscles of, ionizing, 25:19110
- Leuciscus rutilus, radioisotope content of, in Finland, 25:18930 (NYO-3446-14, Paper 27)
- Lota vulgaris, radioisotope content of, in Finland, 25:18930 (NYO-3446-14, Paper 27)
- Pleuronectes platessa, radiation effects on development and survival of eggs of, effects of dose on x, 25:19103 (PG-Report-1013)
- radioisotope contamination of fresh water, technique for study of, 25:18937
- Salmo salar, radioisotope content of, in Finland, 25:18930 (NYO-3446-14, Paper 27)
- Salmo trutta, radioisotope content of, in Finland, 25:18930 (NYO-3446-14, Paper 27)
- Silurus sp., radiation effects on amino acid composition of protein of muscles of, ionizing, 25:19110

OVARIES
- radiation effects on transplanted, in female Dacus cucumis, γ, 25:19096

OXALIC ACID
- radiolysis of aqueous perchloric acid solutions of, rate constants for reactions of hydrogen atoms produced by γ, 25:18459
- radiolysis of aqueous solutions of, yield relations for dosimetry by gamma, 25:18808

OXYGEN
- alpha-particle spallation reactions at 22.5 to 235 MeV/N with, cosmic, (E), 25:19531
- argon-atom reactions at 25 to 90 keV with molecular, total cross sections for single electron loss in, (E), 25:19492 (SC-RR-70-735)
- desorption from graphite, kinetics of, 25:18448(R) (CEA-N-1369)
- determination in liquid sodium, equipment for sampling in, 25:18336
- determination in sodium coolant systems of fast reactors, equipment for, 25:18863
- determination of dissolved, in natural waters from uranium mining operations, method for, 25:18339 (CEA-R-3557(2))
- effects of surface impurity of, on ionization of potassium by polycrystalline tungsten, 25:19210
- effects on products from γ radiolysis of 2,2,4-trimethylpentane, 25:18471
- effects on radiosensitivity of human tumors, effects of carbon dioxide on enhancement of, 25:19023
- effects on x-radiosensitivity of mice, 25:19123
- effects on yields from γ radiolysis of heptane, 25:18466
- excitation of lambda6300 (O I), ionospheric soft electron, (E/T), 25:19579
- heights and lifetimes of atomic, at 88 to 115 km in frequency-dependent pulsating aurorae, (E/T), 25:19578
- mobility of surface, in bismuth oxide, molybdenum oxide, and bismuth molybdate, oxygen-18 exchange studies, 25:18388
- neon-atom reactions at 25 to 90 keV with molecular, total cross sections for single electron loss in, (E), 25:19492 (SC-RR-70-735)
- plasma of, partition functions for, (T), 25:19397
- proton reactions at 5 to 26 keV with molecular, total cross sections for formation of metastable hydrogen atoms by charge exchange in, (E), 25:19504
- proton spallation reactions at 70 to 420 MeV with, cosmic, (E), 25:19531
- radiolysis of aqueous solutions of, monomolecular reactions in, 25:18476
- radiolysis of aqueous solutions of, reactions of intermediates in, 25:18477
- reactions with intermetallic $NbAl_3$ coatings at 600 to 1400°C, kinetics of pest-type, 25:19174
- reactions with molybdenum at 500 to 1000°C and low pressure, 25:19169
- reactions with niobium and niobium alloys at 800 to 950 in air, morphology and rates of, 25:19172
- reactions with niobium silicide and silicon coatings on niobium at high pressures and temperatures, 25:19258
- reactions with zirconium at low pressures, model for, 25:19178
- separation from polonium by vaporization, 25:18509(P)
- sorption by monocrystalline tungsten, effects of adatom surface potential and adsorbate electronegativity on, 25:19207
- sorption on magnesium surfaces, exoelectron emission during, 25:19758 (ORNL-4584, pp 74-86)

OXYGEN IONS
- implantation in silicon at 15 to 40 keV for insulating layer formation, 25:19781
- implantation in silicon at 30 to 400 keV, calculated spatial distributions of damage from, 25:19819

OXYGEN IONS (O^+)
- abundance in topside ionosphere, solar-geomagnetic seasonal control of, (E/T), 25:19576

OXYGEN IONS (O^-)
- reactions with calcium, helium, and hydrogen metastable atoms at 1 eV, cross sections for electron detachment and photon emission in, (T), 25:19511
- reactions with deuterated and normal acetylene, benzene, and ethylene at 0 to 2 eV, rates of, 25:19490 (ORNL-4584, pp 92-104)

OXYGEN ISOTOPES
- exchange on lanthanum oxide, effects of conditions of preliminary treatment on rate of homomolecular, 25:18389

OXYGEN ISOTOPES O-14
- energy levels from oxygen-16 (p,t) reactions, isobaric analog, (E), 25:20299

OXYGEN ISOTOPES O-15
- energy levels from nitrogen-14 (p,γ) reactions, spin-parity assignments and widths for giant dipole, (E), 25:20277

OXYGEN ISOTOPES O-16
- binding energy of, calculation using matrix elements of the effective interaction, (T), 25:20266 (DEMO-70/25)
- deuteron elastic scattering at 4 to 6 MeV, DWBA and optical-model analyses of, (E/T), 25:20301
- deuteron elastic scattering at 8 to 12 MeV using polarized beam, cross section and vector analyzing power for, (E), 25:20305
- deuteron reactions (d,n) and (d,p) at 4 to 6 MeV, DWBA and optical-model analyses of, (E/T), 25:20301
- deuteron reactions (d,p) at 12 MeV, model for, (T), 25:20522
- deuteron reactions (d,p) at 7.73 and 12 MeV, DWBA calculations of angular distributions and overlap integrals from, (T), 25:20497
- deuteron reactions (d,p) at 8 to 12 MeV using polarized beams, cross sections and vector analyzing power for, (E), 25:20305
- deuteron reactions (d,p) with, analysis using BHMM theory, (T), 25:20282
- deuteron reactions (d,p) with, use on determining niobium oxidation, 25:19171
- electron inelastic scattering at 50 to 200 MeV, cross sections for M0 transitions in, (T), 25:20294
- energy levels of, calculation of magnetic monopole transition probabilities for, (T), 25:20306
- helium-3 elastic scattering at 11 MeV, optical-model analysis of, (E/T), 25:20278
- nuclear radii and single-particle energies for statistical-ensemble calculations of, (T), 25:20505
- photon reactions (γ,p) at 12 to 25 MeV, shell-model analysis of excitation function for, (T), 25:20290
- proton reactions (p,t) and (p,He-3) at 43.7 and 54.1 MeV, angular distributions for, (E), 25:20299
- reaction (O-16,α) with carbon-12 at 48.0 to 58.3 MeV with sequential α decay, α--α angular correlations and spectra from, (E), 25:20291
- reactions (O-16,xn) with thallium-205, excitation functions for total neutron emission for, (E), 25:18737(R) (ORO-3820-7)
- scattering by magnesium-24 at 22 MeV, relative cross sections from inelastic, (E), 25:18750
- scattering by mercury-199 and mercury-201 at 25 and 33 MeV, Coulomb excitation by, (E), 25:20387
- scattering by samarium-152 at 60 MeV with Coulomb excitation, Doppler shift attenuation in γ spectra from, (E), 25:20409

OXYGEN ISOTOPES O-17
- energy levels from nitrogen-15 (He-3,p) reactions, spin-parity assignments for, (E/T), 25:20271 (NP-18628)
- energy levels from oxygen-16 (d,p) reactions, spectroscopic factors for, (E/T), 25:20301

  helium-3 elastic scattering at 11 MeV, optical-model analysis of, (E/T), 25:20278
OXYGEN ISOTOPES O-18
  energy levels of, shell-model calculations using Hartree--Fock basis, (T), 25:20286
  exchange in bismuth oxide, molybdenum oxide, and bismuth molybdate, 25:18388
  exchange in carbon monoxide molecules on iron or zinc oxides, 25:18387
  exchange in isomerization of cis-1-methyl-3-phenylallyl alcohol, 25:18405
  helium-3 elastic scattering at 11 MeV, optical-model analysis of, (E/T), 25:20278
OXYGEN SYSTEMS
  Hf--Nb--O, phase studies of, 25:19240
OYSTER CREEK POWER REACTOR, UNIT 1
  control rod drives for, testing and monitoring procedures for, 25:20619 (DOCKET-50219-125)
  radiation emergency plan for, 25:20618 (DOCKET-50219-124)
  technical specifications for, violations during January to May 1970, 25:20586 (DOCKET-50219-123)

P

PACKAGING
  regulations for radioactive materials and radioisotopes for shipment by air, rail, truck, or water in USA, 25:19017
PAINTS
  radioinduced curing of resin, electron, 25:18439(P)
  radioinduced curing of, 300-keV electron electrostatic accelerator for, 25:20213
PALISADES POWER REACTOR
  cooling system for, design modifications for cooling towers in condenser, 25:20637 (DOCKET-50255-33)
  radioactive waste disposal system for, design modifications for zero-release liquid, 25:20637 (DOCKET-50255-33)
PALLADIUM
  chromatographic behavior in hydrochloric acid--thiocyanate mixture on Amberlite LA-2, 25:18337
  determination in high-burnup plutonium dioxide fuel by isotope dilution mass spectrometry, 25:18356 (KR-140)
  determination in presence of other ions and in ternary mixtures with metals by spectrophotometry using 1-(2-carboxy-4-sulfonatophenyl)-3-hydroxy-3-phenyltriazene, 25:18342
  determination using azo compounds, photometric, 25:18347
  optical properties of, (E), 25:19758 (ORNL-4584, pp 74-86)
PALLADIUM ALLOYS AND SYSTEMS
  Nb--Pd, crystallization of solid-solution, mechanisms of, 25:19242
PALLADIUM ISOTOPES Pd-105
  energy levels from Coulomb excitation, model analysis of, (E/T), 25:20324
PALLADIUM ISOTOPES Pd-112
  half-life, (E), 25:20339
PANCREAS
  scanning of canine, effectiveness of iodine-131-labeled erythrosine B for, 25:19060
PAROTID GLANDS
  radiation effects on function and structure of rat, x, 25:19119
PARTICLE TRACKS
  analysis of breakup event in nuclear emulsions, 25:18795
  analysis of bubble chamber, on-line CDC 8090 computer system for, 25:18776 (USIP-70-3)
  analysis of dielectric track detector, for measurement of uranium-238--uranium-235 fission ratio in reactor, 25:18704
  analysis of electron, in heavy-liquid bubble chambers, 25:18784
  analysis of nuclear emulsion, automatic scanner for, 25:18690
  energy deposition in small sites in charged-particle, compound-Poisson calculations of, (T), 25:19767
  measurement of nuclear emulsion proton-recoil, for neutron detection, 25:18728
PARTICLE TRAJECTORIES
  calculations for asymmetrized quadrupole electrostatic lenses, 25:20151
PARTICLES
  stopping in materials, integro--differential equations for probability of, (T), 25:19971 (ANL-7727)
PATHOGENICITY
  radiation effects on, of Histomonas meleagridis in turkeys, γ, 25:19156
PEACH BOTTOM POWER REACTOR, UNIT 1
  operations incident of August 6, 1969, failure of primary system stop valve to close, 25:20584 (DOCKET-50171-78)
PENICILLIN
  effects on Staphylococcus aureus E169, use of uv-irradiated transducing phage lysates to determine chromosomal relation of determinants for sensitivity, 25:19157
PENIS
  radiotherapy of plastic induration of human, effectiveness of strontium-90 β, 25:19072
PENTANE
  I--pentane, radiation effects on, organic yields from reactions of recoil iodine-128 produced from neutron, 25:18483(R) (COO-1617-27)
  iodine-131--pentane, radiolysis of, yields from γ, 25:18483(R) (COO-1617-27)
  iodomethane--pentane, radiation effects on, organic yields from reactions of recoil iodine-128 produced from neutron, 25:18483(R) (COO-1617-27)
PENTANE, 1-IODO-
  radiation effects on glasses of, at 77°K, kinetics of decay of alkyl radicals produced by γ, 25:18461
PENTANE, 2,2,4-TRIMETHYL-
  radiolysis of, effects of oxygen and temperature on products from γ, 25:18471
1-PENTENE
  reactions with iodine at 25°C, kinetics of, 25:18483(R) (COO-1617-27)
  I--1-pentene, radiation effects on, organic yields from reactions of recoil iodine-128 from neutron, 25:18483(R) (COO-1617-27)
  iodine-131--1-pentene, radiolysis of, yields from γ, 25:18483(R) (COO-1617-27)
  iodomethane--1-pentene, radiation effects on, organic yields from reactions of recoil iodine-128 produced from neutron, 25:18483(R) (COO-1617-27)
2-PENTENE
  reactions with iodine at 25°C, kinetics of, 25:18483(R) (COO-1617-27)
  I--2-pentene, radiation effects on, organic yields from reactions of recoil iodine-128 from neutron, 25:18483(R) (COO-1617-27)
  iodine-131--2-pentene, radiolysis of, yields from γ, 25:18483(R) (COO-1617-27)
  iodomethane--2-pentene, radiation effects on, organic yields from reactions of recoil iodine-128 produced from neutron, 25:18483(R) (COO-1617-27)
PERCHLORIC ACID
  radiolysis of organic solutes in aqueous solutions of, rate constants for reactions of hydrogen atoms produced by γ, 25:18459
PERSONNEL
  book: Problems of Protection in Industrial Utilization of Radioelements, 25:18996
  radiation dose to hands, forearms, skin, organs, tissues, and whole-body of, maximum permissible, 25:19008 (NCRP-39)
  radiation hazards to inexperienced, from x-ray equipment, 25:18971
  radiation hazards to, from industrial and medical equipment, regulations for protection against, 25:18973
  radiation injury in accidents, comparison of dosimetry, clinical, and therapy aspects of, 25:19012 (CEA-CONF-1695)
  radioinduced osteodystrophy in uranium mining, following inhalation of radon-222, 25:19144
  safety procedures for, during Operation Bren, 25:18982 (CEX-65.05)
PERTURBATION THEORY
  divergence condition for axial-vector current in vector gluon model with Thirring interaction, 25:19984
PETROLEUM
  calorific value of flowing, neutron radiometric gage for measuring, 25:18817(P)
PHANTOMS
  development of rabbit and rat, for neutron dosimetry, 25:18990 (ORNL-4584, pp 129-51)
  radiation dose distribution in, extrapolation ionization detector for measurement of, 25:18644 (ORNL-4584, pp 152-64)
PHARMACEUTICALS
  disbursement and inventory of radioisotope-labeled, development of computer data system for, 25:19050
  production of short-lived radio-, for scanning, review on, 25:19054
  radioactivity assay in, ionization chamber for, 25:18723
  radioinduced oxidation of aqueous solutions of, evaluation of protective agents for elimination of γ, 25:18472
PHARYNX
  radiotherapy of neoplasms of human, comparison of effectiveness of cobalt-60 γ, with surgery, 25:18998
  radiotherapy of neoplasms of human, comparison of effectiveness of, with surgery, 25:19083
PHENOL
  radiolysis of crystals of, processes for annealing of free radicals formed by, 25:18473
PHENOL, p-BROMO-
  radiolysis of ethanol solutions of, yields of hydrogen from electron pulse, 25:18448(R) (CEA-N-1369)
PHENOL, 2-[(5-BROMO-2-PYRIDYL)AZO]-5-(DIETHYLAMINO)-
  uses for spectrophotometric determination of uranium, 25:18352
PHENOTHIAZINE
  effects on hemolysis of uv-irradiated erythrocytes, 25:18914
PHENTOLAMINE
  effects on radioprotective action of TAB vaccine on x-irradiated mice, 25:19026
p-PHENYLENEDIAMINE, N,N,N',N'-TETRAMETHYL-
  effects on yields from γ radiolysis of aniline,

- 25:18450(R) (ORO-3519-8)

PHONONS
- physics of, Cornell Univ. research on experimental, 25:20874(R) (NYO-2391-126)

PHOSPHATE ROCKS
- analysis for uranium using 2-[(5-bromo-2-pyridyl)azo]-5-(diethylamino)phenol, spectrophotometric, 25:18352

PHOSPHATES
- determination in natural waters from uranium mining operations, method for, 25:18339 (CEA-R-3557(2))

PHOSPHONIC ACID, METHYL-, DIISOOCTYL ESTER
- solvent properties for cerium, 25:18516

PHOSPHONIC ACID, METHYL-, DIISOPENTYL ESTER
- solvent properties for cerium, 25:18516

PHOSPHORIC ACID
- analysis for uranium using 2-[(5-bromo-2-pyridyl)azo]-5-(diethylamino)phenol, spectrophotometric, 25:18352

PHOSPHORIC ACID, TRIBUTYL ESTER
- radiation effects on solvent properties of, in Purex Process, 25:18505 (WHAN-FR-32)

PHOSPHORODIFLUORIDATES
- hydrolysis of, catalytic effects of metal salts and acids on, 25:18373

PHOSPHOROFLUORIDATES
- hydrolysis of, catalytic effects of metal salts and acids on, 25:18373

PHOSPHORS
- development of organic gel, for scintillation detectors, 25:18687(P)
- scintillation lifetime measurements of, spectrometer for subnanosecond, 25:18696

PHOSPHORUS
- abundance in α And, (E), 25:19343
- diffusion in silicon during hot-substrate ion implantation, 25:19824
- distribution and forms of, in sediments and soils, (E), 25:18521 (ORNL-4584, pp 1-10)

PHOSPHORUS IONS
- channeling in indium antimonide at 40 to 120 keV, tracer study of distribution of, 25:19801
- effects of implanted, on electric properties of silica films, 25:19788
- implantation in cadmium sulfide at 200 keV, annealing of, 25:19791
- implantation in silicon at 20 keV, electric profiles after annealing of, 25:19836
- implantation in silicon at 20 to 50 keV, energy dependence and depth distribution of lattice disorder induced in, 25:19832
- implantation in silicon at 200 and 300 keV, damage profiles from, 25:19817
- implantation in silicon at 25 to 100 keV, effects on impurity diffusion, 25:19824
- implantation in silicon at 30 to 400 keV, calculated spatial distributions of damage from, 25:19819
- implantation in silicon at 40 and 100 keV, annealing characteristics of implanted layers, 25:19837
- implantation in silicon at 40 to 100 keV, electron microscopic studies of defects induced in, 25:19808
- implantation in silicon at 40 to 400 keV along (110) axis, electric profiles after annealing of, (E), 25:19839
- implantation in silicon at 400 keV, Hall-effect and resistivity measurements as function of temperature on implanted layers, 25:19838
- implantation in silicon at 50 keV, electrical properties and annealing of, 25:19779
- implantation in silicon at 7 keV, annealing and electric properties of implanted layers, 25:19835
- implantation in silicon at 70 to 280 keV, damage distribution from, 25:19818
- implantation in silicon at 80 keV, electron microscopic studies of damage from, 25:19814
- implantation in silicon carbide at 5 to 300 keV, properties of conducting layers and p--n junctions formed by, (E), 25:19847
- implantation in silicon, annealing effects on, 25:19777
- implantation in silicon, electrical properties before and after annealing, 25:19778
- implantations in silicon at 15 keV, electric capacitance of, 25:18857
- production by calutron-type ion source, 25:20169

PHOSPHORUS ISOTOPES P-29
- energy levels from silicon-28 (p,γ) reactions, lifetimes, spin assignments, and γ branching ratio, (E), 25:20357
- energy levels from silicon-28 (p,γ) reactions, lifetimes for, (E), 25:20319
- energy-level transitions from silicon-28 (p,γ) reactions, multipole mixing ratios for, (E), 25:20319

PHOSPHORUS ISOTOPES P-30
- energy levels of, calculation using strong-coupling rotational model, (T), 25:20353

PHOSPHORUS ISOTOPES P-31
- alpha reactions (α,p) at 11.0 MeV, p--γ angular correlations from, (E), 25:20348
- proton reactions (p,γ) at 1.555 MeV, energy levels of sulfur-32 from, 25:20326
- proton reactions (p,γ) at 1.8 to 2 MeV, analysis of resonances in, (E), 25:20308

PHOSPHORUS ISOTOPES P-32
- beta decay of, angular distribution and energy spectra of internal bremsstrahlung emitted during, (E/T), 25:20417
- beta decay of, internal bremsstrahlung spectra from, (E), 25:20340
- channeling in indium antimonide at 40 to 120 keV, tracer study of distribution of, 25:19801
- diffusion into calf erythrocytes, effects of antibody and sialic acid content of serum on, 25:18900
- energy levels from sulfur-32 $(p,\alpha\gamma)$ reactions at 14 MeV, angular correlation measurements of, (E), 25:20323
- radiation effects on uptake by rat kidney, liver, muscles, and spleen, effects of AET and cysteamine on γ, 25:19024
- use as tracer for ecological studies on ticks, 25:18934(R) (ORO-3514-10)

PHOTOELECTRIC CELLS
- description of light pen for data processing, 25:18844

PHOTOFISSION
- cross sections for symmetric binary, from dynamic collective model, (T), 25:20499

PHOTOGRAPHIC FILM
- processing of, radiometric notch-sensitive cuing system for, 25:18818(P)
- uses of color, in x radiography, 25:18612(T) (LIB/Trans-324)

PHOTOMULTIPLIER TUBES
- cathode-follower circuit with feedback for, design of linear, 25:18860
- efficiency of PM 56 TVP, improvement of, 25:18828 (EUR-CEA-FC-576)

PHOTONS
- interactions $\gamma + d \to \pi^- + p + p$, impulse approximation calculation of recoil proton polarization in, (T), 25:19940
- interactions $\gamma + d$ at high energies, Glauber theory of multiple scattering for cross sections of π^- and π^+ production in, (T), 25:19955
- interactions $\gamma + e \to \gamma + e$, approximate description of attractive, (T), 25:19945
- interactions $\gamma + e \to \gamma + \gamma + e$, total cross sections for double Compton, (T), 25:19958
- interactions $\gamma + \gamma \to A^+ + A^-$, lower order of perturbation theory for cross section relation of $e^+ + e^- \to e^+ + e^- + A^+ + A^-$ interactions with, (T), 25:19938 (JINR-P2-5505)
- interactions $\gamma + \gamma \to \pi^+ + \pi^- + \pi^0$, axial-current divergences in calculations of, 25:19951
- interactions $\gamma + n \to p + \pi^-$, test for existence of isotensor electromagnetic current from, (T), 25:19956
- interactions $\gamma + p \to n + \pi^+$ at threshold to 500 MeV, multipole analysis of, (T), 25:19957
- interactions $\gamma + p \to p + 2\pi^0$ at 550 to 730 MeV, differential cross sections for, (E), 25:19890
- interactions $\gamma + p \to p + \pi^0$ at threshold to 500 MeV, multipole analysis of, (T), 25:19957
- interactions $\gamma + p \to \pi^+ + n$ interactions at 227 to 260 MeV and 51 to 146°, symmetry ratios for, (E), 25:19889
- interactions of, matrix element of rotation in O(4,2) for amplitude of Coulomb, 25:20040
- interactions with gravitational field, neutrino mass from, (T), 25:19966
- interactions with weak gravitational fields, covariant Green functions of, (T), 25:20094
- polarization in $n + p \to d + \gamma$ and $n + d \to 3p + \gamma$ interactions, weak-interaction Hamiltonian for, (T), 25:20039
- production of wide-angle, in photon Compton scattering by nuclei, Glauber theory of multiple scattering for corrections for, (T), 25:19955
- reactions (γ,f) with uranium-238, cross sections from dynamic collective model of, 25:20499
- reactions $(\gamma,n)p$ with deuterium, analysis of retardation in, (T), 25:20254
- reactions (γ,p) with copper at 17.6 MeV, proton spectra from, 25:20141
- reactions (p,n) with nuclei up to 30 MeV, review of, (E), 25:20448
- reactions with beryllium at 5.5 to 9.5 GeV, counter--spark chamber study of differential cross sections for K_2^0 production in, (E), 25:19887
- reactions with carbon at 5.8 to 6.6 GeV/c, magnetic spectrometer study of (1550) enhancement in mass spectrum for $\pi^+ - \pi^-$ pairs produced in, (E), 25:19886 (DESY-70/61)
- reactions with deuterium, helium-3, helium-4, and tritium, bremsstrahlung-weighted E1 cross sections for disintegration, (T), 25:20252
- reactions with dielectric solids, photon--plasmon coupling in, 25:19757 (ORNL-4584, pp 58-73)
- reactions with heavy nuclei at high energies, Glauber theory of multiple scattering for cross sections for total photon absorption and vector meson and π^- and π^+ production in, (T), 25:19955
- reactions with nuclei at high energies, optical model for, (T), 25:19955
- reactions with nuclei, low-energy theorems for π production in, (T), 25:20019 (LYCEN-7081)
- reactions with nuclei, tables of thresholds for, (E), 25:20237 (UCRL-50400(Vol.9))
- scattering below 140 MeV, Mainz electron linear accelerator experimental facilities for, 25:20189
- scattering by nuclei, Glauber theory of multiple

scattering for corrections to wide-angle bremsstrahlung from Compton, (T), 25:19955
PHOTOSPHERE
fluctuations in, quasi-periodic, (E), 25:19415
gravity waves and five-minute oscillations in, trapped, (T), 25:19405
motion in, velocity field distribution in, (E), 25:19404
turbulent velocities and damping constants in, (E), 25:19420
PILGRIM POWER REACTOR
design parameters of, revised and additional data on, 25:20651 (DOCKET-50293-36)
design parameters of, revised and additional data on, 25:20654 (DOCKET-50293-39)
operations aspects of, revised and additional data on, 25:20651 (DOCKET-50293-36)
operations aspects of, revised and additional data on, 25:20654 (DOCKET-50293-39)
piping systems for, requirements of welds in, 25:20652 (DOCKET-50293-37)
site for, environmental survey through August 1970, 25:20653 (DOCKET-50293-38)
PINCH DEVICES
design of Scyllac 5-meter toroidal sector, equilibrium configuration for, 25:19725 (LA-4597)
plasma confinement in theta-, computer program for calculating, 25:19647 (IPP-6/90)
plasma equilibrium in toroidal, high-beta, (T), 25:19718
PINCH EFFECT
plasma instability in screw, effect of force-free fields on, (T), 25:19706
plasma stabilization in linear z, by quadrupole magnetic fields, 25:19717
PIPES
design codes and standards in U.S. for liquid metal cooled fast breeder reactor, 25:20723 (SAN-781-217)
design for plutonium nitrate solution handling facility, 25:18628
design guide for liquid sodium, in liquid metal cooled fast breeder reactors, 25:20720 (SAN-781-1)
design requirements for liquid metal cooled reactors, 25:20725 (WHAN-SA-46)
design requirements for liquid sodium cooled fast breeder reactor, 25:20721 (SAN-781-110)
failure of liquid metal cooled fast breeder reactor, mechanisms and theories for, (T), 25:20724 (UNC-5235)
failure of liquid sodium cooled fast breeder reactor, mechanisms and incidents for, 25:20722 (SAN-781-214)
heat transfer characteristics of, (T), 25:20790 (WHAN-FR-22)
neutron transmission through simple bent conducting, calculations of, 25:20245
stress limits for liquid metal cooled reactor, 25:20725 (WHAN-SA-46)
PLACENTA
localization of human, use of metastable technetium-99 and γ cameras for, 25:19045
PLANETARY NEBULAE
distribution in open star clusters, (E), 25:19321
infrared line emission from, (E), 25:19327
spectra of HD 184738, comparison to star BD + 30°3639, (E), 25:19310
spectra of sixteen central stars of, power, (E/T), 25:19309
PLANETS
effects on sunspots, (T), 25:19427
PLANTS
radioinduced mutations in, for flower, fruit, and root quality and disease resistance, effects of dose and seed exposure on, 25:18964(P)
radioisotope content of Southeast USA, 25:18935(R) (ORO-3905)
radioisotope uptake by, during irrigation, development of model for determining, 25:18938
PLASMA
boundary sheath criterion for, ion speed effects on, (T), 25:19677
boundary sheath dynamics in weakly ionized, microscopic model for collision-dominated, (T), 25:19673 (DLR-FB-69-78)
charged-particle motion in inhomogeneous stationary, theory for test-, 25:19695
collision processes in, quantum theory for linear and nonlinear, (T), 25:19687
conductivity of charged, in magnetic field, (T), 25:19658
conductivity of fully ionized, logarithm term for electric, (T), 25:19683
conductivity of hot hydrogen, in electric fields larger than runaway field, (E), 25:19672
conductivity of weakly turbulent, electric, (T), 25:19685
confinement by external electromagnetic fields, (T), 25:19655
confinement in magnetic bottles, upper bounds of, (T), 25:19581
confinement in magnetic mirrors, effect of rf fields on loss cone, 25:19649
confinement in theta pinches, computer program for calculating, 25:19647 (IPP-6/90)
confinement in tokamak-type devices, energy balance in, (T), 25:19654
confinement in toroidal devices, equilibria in, (T), 25:19652
confinement in toroidal multipoles with shielded supports, (T), 25:19651
confinement in WIIa stellarator, neoclassical diffusion, (E/T), 25:19645 (IPP-2/86)
diagnostics in Burnout V, fractional fringe HCN laser interferometer for, 25:19663
diagnostics of cesium discharge, spectroscopic, 25:19665
diagnostics of laser-produced, x-ray temperature, 25:19701
diagnostics of low-temperature helium, electron temperature, (T), 25:19661
diagnostics of Tokamak-3, material balance, (E), 25:19657(T) (MATT-Trans-16)
diagnostics of, correlation techniques for, 25:19664
diagnostics of, space-charge effects on electrostatic analyzers, 25:19660
diagnostics using microwaves, electron density, (T), 25:19656 (EP-RR-21)
electron beam interactions with, ion heating in, (T), 25:19650
electron density fluctuations and diffusion in weakly ionized, microscopic theory of, 25:19686
electron distribution function for fully ionized, in steady magnetic fields, (T), 25:19691
electron runaway in fully ionized Lorentz, suppression by crossed electric and magnetic fields, (T), 25:19682
electron velocity distribution in fully ionized, in crossed electric and magnetic fields, (T), 25:19688
electron--ion recombination processes in laser-produced lithium hydride, 25:19697
equilibrium in Tokamak-type devices, axisymmetric hydromagnetic, (T), 25:19716
equilibrium in toroidal theta pinch, high-beta, (T), 25:19718
equilibrium of rotating, (T), 25:19690
expansion of laser-produced, into vacuum, (E), 25:19703
flow in channel, theory of highly conducting plane, 25:19671
heating by lasers, energy requirements for inertially confined, (T), 25:19646 (IPP-4/7)
heating by magnetic pumping, torsional magnetic perturbation in, (T), 25:19648
heating by modulated electron beams, ion, (T), 25:19650
heating near lower hybrid resonance, resistive loading in, (E/T), 25:19653
ion beam interactions with magneto-, quasi-linear solutions for, 25:19694
ion velocity distribution function in single-ended Q devices, shaping of, (E), 25:19670
ionizing, partition functions in, (T), 25:19397
kinetic theory in circular magnetic fields, Boltzmann equation for, (T), 25:19689
kinetic theory in steady magnetic fields, Boltzmann equation for, 25:19692
kinetic theory of collisional anisotropic, hydromagnetic equations for, 25:19674 (IPP-1/112)
kinetics of collisionless two-component, equation of state for adiabatic electron, 25:19675
kinetics of two-component, steady-state Vlasov equations for monotonic electric potential, 25:19680
magnetic dipoles in stationary, free boundary of, (T), 25:19699
oscillations in homogeneous collisionless, electrostatic, (T), 25:19750
oscillations in, quasi-linear theory of, (T), 25:19738
production by laser irradiation of foils, x-ray temperature measurements for, 25:19701
production of lithium hydride, by laser irradiation of solid targets, 25:19702
production of steady-state, feedback control of, (E), 25:19713
production of, source for space flight simulation, 25:19700 (NP-18722)
properties in reflex arcs in low magnetic fields, 25:19666
properties of astrophysical, containing matter and antimatter, (T), 25:19466
radiations from homogeneous magnetized, (T), 25:19696
radiations from laser-produced, far-infrared, 25:19679
relaxation processes in dense argon, asymptotic thermochemical, 25:19684
research on, review of, 25:19730
shock wave production in collisionless, ion-acoustic, (T), 25:19698
shock wave propagation in collisionless, numerical solutions for electrostatic, 25:19678
shock wave propagation in, decomposition of decelerating ionizing, (T), 25:19667
shock wave structure in, precursor ionization effects on MHD, (T), 25:19681
spectral-line broadening in turbulent hydrogen, Stark, (T), 25:19693
stability in closed configurations, magnetohydrodynamic, (T), 25:19721
stability in reflex arcs, effects of steady-state oscillations on, (E/T), 25:19707
stability of cold, under magnetoelectric confinement, 25:19714
stability of collisionless, transverse electromagnetic,

(T), 25:19722
stability of column, formation of axisymmetric bulged region in, (E/T), 25:19709
stability of fully ionized inhomogeneous, effect of velocity space diffusion on universal, (T), 25:19719
stability of hot electron, density thresholds for onset of anisotropy and loss-cone, (T), 25:19708
stability of hot, classification of two-stream, (T), 25:19710
stability of relativistic anisotropic, to perpendicular magnetosonic waves, (T), 25:19712
stability of screw-pinch, effects of force-free fields on, (T), 25:19706
stability of toroidal, normal-mode analysis of kink, 25:19704 (NP-18681)
stability of weakly ionized magneto-, low-frequency, (T), 25:19720
stability of, effect of gyro-viscosity on Rayleigh--Taylor, 25:19711
stability of, time-averaged density profile in m = 2 mode finite-amplitude, (T), 25:19715
stabilization in minimum-B fields, warm quiescent, 25:19705
stabilization of discharge, feedback-control, (E), 25:19713
stabilization of linear z-pinch, by magnetic quadrupoles, 25:19717
stabilization of, strong turbulence theory for nonlinear, 25:19723
wave coupling at hybrid frequencies in inhomogeneous, nonlinear, (T), 25:19747
wave damping in, effect of ion--neutral collisions on large-amplitude ion-acoustic, (T), 25:19748
wave damping in, quasi-linear theory for, 25:19751
wave echoes in relativistic, frequency effects on, (T), 25:19739
wave echoes in, collisional effects on temporal, (T), 25:19755
wave excitation and stabilization in rf, ion-acoustic, 25:19744
wave excitation by grids in, ion-acoustic, (T), 25:19742
wave excitation in, strong turbulence theory for harmonic, 25:19723
wave interactions in magnetized, kinetic theory of three-, 25:19737
wave interactions with boundary of, transmission and reflection of, 25:19749
wave interactions with cylindrical, transmission of microwaves, (T), 25:19656 (EP-RR-21)
wave interactions with toroidal, polarization of electromagnetic, (T), 25:19735
wave packets in weakly inhomogeneous, Lagrangian formalism for, 25:19754
wave propagation in collisionless gravity-supported magneto-, ion-acoustic, (T), 25:19736
wave propagation in collisionless Vlasov, dispersion relations for, 25:19752
wave propagation in collisionless Vlasov, dispersion relations for electrostatic, 25:19753
wave propagation in column, group velocity of, 25:19746
wave propagation in electric-field-immersed, damping of hf longitudinal, (T), 25:19743
wave propagation in half-space relativistic, electromagnetic, (T), 25:19740
wave propagation in inhomogeneous magnetic fields, hydromagnetic, (E), 25:19732
wave propagation in inhomogeneous magneto-, dispersion curve for drift, 25:19731
wave propagation in nonuniform, compressional Alfven, (T), 25:19745
wave propagation in relativistic anisotropic, supraluminous, (T), 25:19733
wave propagation in stratified electron, singularities of coupled fields in, (T), 25:19756
wave propagation in trapped relativistic, space-charge, (T), 25:19734
wave propagation in weakly ionized magneto-, unified theory for drift and ion, 25:19720
wave propagation in, detection of spatially decaying ion-acoustic, 25:19741

PLASMA ACCELERATORS
jet current sheet tilt in parallel-plate rail-type, 25:19668
performance of titanium rail-type, (E), 25:19726

PLASMA JETS
acceleration by traveling electromagnetic fields, diagnostics of, (E), 25:19669 (NP-18715)
diagnostics of magnetized, using floating double electric probes, (E), 25:19659
flow of collisionless, effect of dissipation from firehose instability on perturbation half-jet, (T), 25:19676

PLASMAPAUSE
plasma streaming across dusk bulge in, relation to geomagnetic activity, (T), 25:19577

PLASTICS
fission fragment energy loss in, (E), 25:20442
radiation processing of medical supplies of, 25:19161
concrete--plastics, development, preparation, properties, and testing of, produced by radioinduced polymerization, 25:19292 (BNL-50275)
plastics--wood, physical properties of, 25:19299
plastics--wood, properties of radiation processed, mechanical and physical, 25:19298

PLATES
bending with transverse shear deformation, finite element method for analysis of, 25:18575
plasticity of circular, under uniform pressure, analysis of dynamic, 25:18557 (ANL-7677)
thickness measurements of moving, theory of operation of radiometric gages for, 25:18825

PLATINUM
chromatographic behavior in hydrochloric acid--thiocyanate mixture on Amberlite LA-2, 25:18337
detection in low-energy cosmic radiation, (E), 25:19525
thermal loading to induce water boiling on wires of, parameters for critical, 25:18583

PLATINUM ISOTOPES Pt-195
energy levels from platinum-194 proton scattering, spectroscopic factors for isobaric analog, (E), 25:20378
Moessbauer spectrum of 129-keV energy-level transition in, branching ratio from, 25:19877

PLATINUM ISOTOPES Pt-197
energy levels from platinum-196 proton scattering, spectroscopic factors for isobaric analog, (E), 25:20378

PLATINUM ISOTOPES Pt-199
energy levels from platinum-198 proton scattering, spectroscopic factors for isobaric analog, (E), 25:20378

PLATYHELMINTHES
Hymenolepis microstoma, radiation effects on development of cysticercoids of, x, 25:19095

PLOWSHARE PROJECT
radiological safety of interoceanic canal construction using nuclear explosives, 25:18989 (ORNL-4584, pp 42-56)
radiological safety of natural gas produced by Gasbuggy for home heating and production of petrochemicals, 25:18989 (ORNL-4584, pp 42-56)

PLUTONIUM
bibliography on, Dec. 1970, 25:19166
binding to glycoprotein in bovine bones, mechanism of, 25:18899
cost in reactor fuel cycles, game theory calculations of, 25:20753
determination in high-burnup plutonium dioxide fuel by isotope dilution mass spectrometry, 25:18356 (KR-140)
determination simultaneously with nitric acid by conductivity and density measurements, 25:18350
development of fuels of, technology for, 25:19198
disproportionation reactions of tetravalent and pentavalent, oxidation states of products from, 25:18383
fuel cycles for, development of, 25:19189
separation from fuel mateials and plutonium dioxide scrap by pyrochemical methods, 25:18492 (ANL-7709)
separation from spent fuels, 25:18517

PLUTONIUM ALLOYS AND SYSTEMS
Cu--Ga--Pu, phase studies of, 25:19230 (CEA-R-3951)
Cu--Pu, diffusion of plutonium in, at 500°C, effects of gallium on, 25:19230 (CEA-R-3951)
Ni--Pu--U, phase studies of, 25:19230 (CEA-R-3951)
Pu--U, diffusion of plutonium in, at 500°C, effects of nickel on, 25:19230 (CEA-R-3951)
Pu--U, diffusion of plutonium in, at 500°C, effects of gallium on, 25:19230 (CEA-R-3951)

PLUTONIUM ISOTOPES Pu-232
fission from electron-capture decay of americium-232, delayed, (T), 25:20371 (JINR-P7-5584)

PLUTONIUM ISOTOPES Pu-234
fission from electron-capture decay of americium-234, delayed, (T), 25:20371 (JINR-P7-5584)

PLUTONIUM ISOTOPES Pu-236
content in water cooled reactor irradiated fuel elements, 25:20733 (BNWL-1523)
decay in SNAP-15A heat source, measurement of gamma spectra from, 25:18601
determination in irradiated plutonium dioxide--uranium dioxide fuels as measure of burnup, 25:18359 (WCAP-3385-56(Pt.2))

PLUTONIUM ISOTOPES Pu-238
content in water cooled reactor irradiated fuel elements, 25:20733 (BNWL-1523)
content of soil at Los Alamos Area, N. Mex, 25:18985 (LA-4563)
decay in SNAP-15A heat source, measurement of gamma spectra from, 25:18601
determination in irradiated plutonium dioxide--uranium dioxide fuels as measure of burnup, 25:18359 (WCAP-3385-56(Pt.2))
energy levels from neptunium-239 beta decay, (E), 25:20431
neutron fission at 2.5 keV to 2.5 MeV, cross sections for, (E), 25:20444
production of spontaneously fissioning isomeric, in (n,2n) reactions, upper limits for cross sections for, (E), 25:20369 (JINR-P3-5528)
radiation dose from implanted heat source of, 25:18590(R) (BNWL-1308-4)
separation from fuel materials and scrap by pyrochemical methods, 25:18492 (ANL-7709)

XUM

PLUTONIUM ISOTOPES Pu-239
content of soil at Los Alamos Area, N. Mex, 25:18985 (LA-4563)
determination in irradiated plutonium dioxide--uranium dioxide fuels as measure of burnup, 25:18359 (WCAP-3385-56(Pt.2))
distribution of oxide particles of, following inhalation by rabbits, role of pulmonary macrophages in, 25:18891(T) (LF-tr-46)
fission of, summary of neutron yields from, (E), 25:20363 (AWRE-O-86/70)
neutron cross sections for, number of resonances necessary for calculating s-wave, (T), 25:20395
neutron fission at 0.3 to 1.4 MeV, cross section relative to uranium-235 and average number of prompt neutrons for, (E), 25:20373(T) (LIB/Trans-300)
neutron fission of, average neutron production by resonance, (E), 25:20364(T) (BNL-tr-401)
neutron fission of, fission product yields from fast, (T), 25:20819 (JAERI-Memo-4165)
neutron reactions (n,2n) with, upper limits for cross sections for production of spontaneously fissioning isomers in, (E), 25:20369 (JINR-P3-5528)
size of airborne particles containing, autoscintigraphy method for measuring, 25:18976
PLUTONIUM ISOTOPES Pu-242
neutron reactions (n,n') with, cross sections for production of spontaneously fissioning isomers in, (E), 25:20369 (JINR-P3-5528)
production of spontaneously fissioning isomeric, in (n,n') reactions, cross sections for, (E), 25:20369 (JINR-P3-5528)
PLUTONIUM NITRATES
handling of, design of glove boxes for, 25:18628
PLUTONIUM OXIDES
distribution of particles of plutonium-239, following inhalation by rabbits, role of pulmonary macrophages in, 25:18891(T) (LF-tr-46)
retention of particles of, in lungs of baboons, effects of washing on, 25:18895
size of airborne particles of plutonium-239, autoscintigraphy methods for measurement of, 25:18976
plutonium oxides--uranium oxides, development and performance of fuels of, for liquid metal fast breeder reactors, 25:19275
PLUTONIUM OXIDES PuO_2
analysis of pyrocarbon--silicon carbide-coated, by isotope dilution mass spectrometry and gamma spectrometry, 25:18356 (KR-140)
purification of, pyrochemical methods for, 25:18492 (ANL-7709)
separation of plutonium from, by pyrochemical methods, 25:18492 (ANL-7709)
Mo--PuO_2, separation of plutonium from, pyrochemical methods for, 25:18492 (ANL-7709)
PuO_2--UO_2, analysis of irradiated, for cesium-137, neodymium-148, and transuranium elements as measure of burnup, 25:18359 (WCAP-3385-56(Pt.2))
PuO_2--UO_2, production of, problems in, 25:18517
PuO_2--UO_2, radiation effects on fission gas release and oxygen distribution in, neutron, 25:19287 (AECL-3690)
PuO_2--UO_2, radiation effects on intergranular pore density of fuel pins of, in-pile, 25:19290 (WHAN-SA-15)
PuO_2--UO_2, radiation effects on structure of, neutron, 25:20636 (WHAN-SA-79)
PuO_2--UO_2, reprocessing of stainless steel-clad or Zircaloy-clad, chemical, electrolytic, and mechanical methods for, 25:18493 (CEA-Bib-191)
PuO_2--ZrO_2, separation of plutonium from, pyrochemical methods for, 25:18492 (ANL-7709)
PNEUMATIC SYSTEMS
design for sample transfer for activation analysis at Braunschweig 140-MeV electron synchrotron, 25:20184
POINT BEACH POWER REACTOR, UNIT 1
site for, environmental radiation survey during July 1969 to June 1970, 25:20641 (DOCKET-50266-42)
POINT BEACH POWER REACTOR, UNIT 2
operation of, proposed issuance of license for, 25:20663 (DOCKET-50301-28)
site for, environmental radiation survey during July 1969 to June 1970, 25:20641 (DOCKET-50266-42)
POLARIMETERS
description for helicity measurements, 25:20374 (NP-18597)
POLLEN
radiation effects on, of cotton, effects of, on meiosis in embryonic tissues, γ, 25:18955
POLONIUM
separation of oxygen from, by vaporization, 25:18509(P)
POLONIUM HALIDES
separation by solvent extraction, effects of charge, composition, and structure on, 25:18511
POLONIUM ISOTOPES Po-196
alpha decay of, alpha spectra, half-life, and branching ratio for, (E), 25:20451
POLONIUM ISOTOPES Po-197
alpha decay of, alpha spectra, half-life, and branching ratio for, (E), 25:20451
POLONIUM ISOTOPES Po-198
alpha decay of, alpha spectra, half-life, and branching ratio for, (E), 25:20451
POLONIUM ISOTOPES Po-199
alpha decay of, alpha spectra, half-life, and branching ratio for, (E), 25:20451
POLONIUM ISOTOPES Po-200
alpha decay of, alpha spectra, half-life, and branching ratio for, (E), 25:20451
POLONIUM ISOTOPES Po-201
alpha decay of, alpha spectra, half-life, and branching ratio for, (E), 25:20451
POLONIUM ISOTOPES Po-202
alpha decay of, alpha spectra, half-life, and branching ratio for, (E), 25:20451
POLONIUM ISOTOPES Po-210
accumulation in aquatic ecosystems in Finland, 25:18930 (NYO-3446-14, Paper 27)
content of food chains in Finland, 25:18931 (NYO-3446-14, Paper 30)
content of man in Finland during 1960 to 1970, 25:18986 (NYO-3446-14, Paper 28)
content of pastures, suggested revision of MPC values for, 25:18890(R) (COO-2044-3)
content of terrestrial birds and mammals of Finland, comparison of bone and soft tissue, 25:18929 (NYO-3446-14, Paper 26)
metabolism by cattle and goats following ingestion in oxide form, coefficients for transfer to meat and milk during, 25:18890(R) (COO-2044-3)
POLONIUM ISOTOPES Po-214
alpha decay of, half-life measurement of, 25:18703
POLONIUM ISOTOPES Po-215
alpha decay of, half-life measurement of, 25:18703
POLYCRYSTALS
neutron scattering in, computer program for calculating law of thermal, (T), 25:20229 (INR-1186)
POLYSACCHARIDES
radioprotective effects of, 25:18922
POLYSORBATE 80
radioprotective effects of, on DNA strand breaks in Escherichia coli, cobalt-60 γ, 25:19027
POPULATIONS
radiation dose to human, establishment of limits for maximum permissible, 25:19018
radiation dose to human, from artificial and natural sources, 25:19137
radiation dose to human, from consumer products containing radioisotopes, analysis of procedures for control of external and cumulative, 25:19015
radiation dose to human, on Kerala coast, India, from food, daily, 25:19143
radiation dose to, following release of radioisotopes to atmosphere during reactor accidents, methods for calculation of, 25:18974 (AHSB(S)R-192)
radioinduced mutations in human, in comparison with chemicals, evaluation of, 25:18965
POROSIMETERS
development of neutron radiometric, for well logging, 25:18674(P)
PORPHYRINS
effects on hemolysis of uv-irradiated erythrocytes, 25:18914
POSITRONIUM
decay of, quantum field theory for two-photon, 25:20071
formation in liquid and solid argon, krypton, and xenon, bubbles associated with, 25:19487
hyperfine structure of ground-state, corrections to, (T), 25:19484
POSITRONS
annihilation in irradiated and deformed iron, effects of vacancies on two-photon angular correlation of, (E/T), 25:19851
annihilation in liquid and solid argon, krypton, and xenon, positronium-bubble formation and angular correlation of photons from, 25:19487
annihilation of, study of chemisorption of various substances by, 25:18415
annihilation rate in hydrogen molecules, (T), 25:19501
effects on semiconducting diamonds, 25:19769(T) (LIB/Trans-307)
interactions $e^+ + e^- \to e^+ + e^- + A^+ + A^-$, lower order of perturbation theory for cross section relation of $\gamma + \gamma \to A^+ + A^-$ interactions with, (T), 25:19938 (JINR-P2-5505)
interactions $e^+ + e^-$ at high energies, light-cone properties of axial-vector and electromagnetic current commutators for π and hadron production in, (T), 25:19941
interactions $e^+ + p \to e^+ + p$, effects of Veneziano-model form factors on ratios of cross sections for $e^- + p \to e^- + p$ interactions and, (T), 25:19942
reactions with hydrogen atoms, closed-channel spectrum for rearrangement in, (T), 25:19503
scattering by helium and hydrogen atoms, calculation using Kohn and Harris variational methods, 25:19509
scattering by hydrogen atoms at low energies, generalized Hylleraas calculation of phase shifts for, 25:19508
scattering by hydrogen molecules at 0.4 to 14 eV, total cross sections for elastic, (T), 25:19501
POTASSIUM
determination in natural waters from uranium mining operations, method for, 25:18339 (CEA-R-3557(2))

  electron reactions at 0.3 to 1.1 MeV with thin multiple-layer foils with carbon, photon emission spectra from, 25:19471
  electron scattering at 0.3 to 9 eV by, absolute total cross sections for, (E), 25:19506
  energy-level transitions in, continuum generalized oscillator strengths for 4s--epsilon p, (T), 25:19476
  ionization on tungsten surfaces, effects of impurities on residence time for, 25:19210
  radiation effects on content of, in erythrocytes of rabbits, 25:19107
  scattering by carbon tetrachloride, iodomethane, and tin chloride, crossed-beam measurements and optical-model analysis of, 25:19497
POTASSIUM BROMATES
  radiolysis of aqueous solutions of, absorption spectra of bromate radicals produced by electron pulse, 25:18448(R) (CEA-N-1369)
POTASSIUM BROMIDES
  radioinduced V centers in single crystals of, temperature dependence of production of x, (E), 25:19855
POTASSIUM CHLORIDES
  radioinduced $BrCl^-$ molecule-ion center in bromide-doped single crystals of, properties of gamma and x, 25:19852
  radioinduced cation vacancies in single crystals of, electric conductivity study of x, (E), 25:19858
  radioinduced V centers in single crystals of, temperature dependence of production of x, (E), 25:19855
POTASSIUM CHROMATES
  radiation effects on crystals of, separation and chemical properties of polynuclear recoil products from neutron, 25:18486
POTASSIUM CYANORHODATES
  radiation effects on, in potassium chloride lattice, EPR studies on electron, 25:18462
POTASSIUM DIOXODIFLUOROIODATES
  radiation effects on single crystals of, ESR studies on radicals produced by γ, 25:18420 (COO-1385-34)
POTASSIUM IODATES
  radiolysis of aqueous solutions of, absorption spectra of iodate radicals produced by electron pulse, 25:18448(R) (CEA-N-1369)
POTASSIUM ISOTOPES K-38
  energy levels from chlorine-35 (α,n) reactions, lifetime of, (E), 25:20349
  energy levels from potassium-39 (He-3,α) reactions, lifetime of, (E), 25:20349
POTASSIUM ISOTOPES K-39
  neutron reactions (n,2n) at 14.7 MeV, isomeric cross-section ratio for, (E), 25:20312
POTASSIUM ISOTOPES K-40
  abundance in Bovedy meteorite, (E), 25:19301
  content of human diet on Kerala coast, India, 25:19143
  content of man in Finland from natural sources, 25:18931 (NYO-3446-14, Paper 30)
  content of muscle samples from deer in Southeast USA during 1969, 25:18935(R) (ORO-3905)
POTASSIUM ISOTOPES K-41
  neutron capture by, resonance integrals and partial widths of resonances in, (E), 25:20359
POTASSIUM PYROSULFITES
  effects on radioinduced oxidation of pharmaceuticals, 25:18472
POWER CYCLES
  design and development of radioisotope-fueled organic Rankine, 25:18594(R) (ORNL-TM-3292)
  design of radioisotope-fueled mercury vapor turbine-type, for use as undersea power source, 25:18600(P)
  development of steam and direct cycle gas turbine, for helium cooled power reactors, 25:20770
  performance of carbon dioxide, calculations of complex and simple, 25:18587
POWER PLANTS
  structural plate bending in, finite element method for analysis of, 25:18575
POWER SUPPLIES
  control element for current regulation of pulsed magnet, design of transistor, 25:20208
  current signals from pulsed, meter for measuring rms values of, 25:18839(P)
PRASEODYMIUM
  determination using 4,5-dihydroxy-m-benzenedisulfonic acid, in presence of Eriochrome Cyanine R, titrimetric, 25:18348
  thermal capacity at 1.2 to 4.2°K, effects of magnetic fields up to 40 kG on, 25:19869
PRASEODYMIUM IONS
  wave functions for, accurate numerical Hartree--Fock self-consistent field, 25:19478
PRASEODYMIUM ISOTOPES Pr-143
  half-life, (E), 25:20339
PREAMPLIFIERS
  design for G--M detector readout for TSEE dosimeter, 25:18644 (ORNL-4584, pp 152-64)
  design for spark counter readout system for thin-film dielectric track detectors, 25:18644 (ORNL-4584, pp 152-64)
PREGNANCY
  radiation effects on frequency of spontaneous termination of human, in relation to chromosome aberrations, 25:18969
PRESSURE VESSELS
  design codes and standards in U.S. for liquid metal cooled fast breeder reactor, 25:20723 (SAN-781-217)
  design parameters of gas cooled reactor prestressed concrete, 25:20557
  development of prestressed concrete reactor, 25:19297
  fabrication of gas cooled reactor prestressed concrete, 25:20557
  fabrication of steel, problems with, 25:20555
  manufacture of steel, problems with, 25:20555
  properties of steel, for water reactor, 25:19222
  thermal insulation for reactor prestressed concrete, design of laminated porous, 25:20727(P)
  welding of steel, review of electroslag method for, 25:19181
PROMETHIUM
  determination in high-burnup plutonium dioxide fuel by gamma spectrometry, 25:18356 (KR-140)
  separation from seawater by flocculation, 25:18518
PROMETHIUM IONS
  wave functions for, accurate numerical Hartree--Fock self-consistent field, 25:19478
PROMETHIUM ISOTOPES Pm-141
  beta and electron-capture decay of, γ and internal conversion spectra from, (E), 25:20388
PROMETHIUM ISOTOPES Pm-147
  neutron capture in reactor spectrum, cross section and resonance integral for, (E), 25:20379
  purification by cation exchange using α-hydroxyisobutyric acid as eluant, 25:18501 (RCN-131)
PROMETHIUM ISOTOPES Pm-148
  beta decay of, γ singles and coincidence spectra from, (E), 25:20352
PROMETHIUM ISOTOPES Pm-149
  half-life, (E), 25:20338
  half-life, (E), 25:20339
PROMETHIUM ISOTOPES Pm-151
  energy levels of proton states from neodymium-150 (He-3,d) and (α,t) reactions, (E/T), 25:20383
PROMETHIUM OXIDES
  Pm_2O_3--Sm_2O_3, phase studies of, 25:19273 (BNWL-SA-3579)
PROPANE, 1-IODO-
  radiation effects on glasses of, at 77°K, kinetics of decay of alkyl radicals produced by γ, 25:18461
1,2-PROPANEDIOL, 2-(HYDROXYMETHYL)-
  2-(hydroxymethyl)-1,3-propanediol trimethacrylate--polychloroethylene, radiation effects on curing of, 25:18437(P)
1-PROPANOL
  radiolysis of aqueous perchloric acid solutions of, rate constants for reactions of hydrogen atoms produced by γ, 25:18459
2-PROPANOL
  radiolysis of aqueous perchloric acid solutions of deuterated and normal, rate constants for reactions of hydrogen atoms produced by γ, 25:18459
  radiolysis of, effects of alkoxy radicals on electron pulse, 25:18448(R) (CEA-N-1369)
1-PROPANOL, 2-METHYL-
  radiolysis of aqueous perchloric acid solutions of, rate constants for reactions of hydrogen atoms produced by γ, 25:18459
1-PROPANOL, TRITHIODI-
  effects on x-radiation effects on peripheral blood of rats, 25:19131
PROPENE POLYMERS
  radioinduced thermally stimulated currents in, γ, 25:18422
PROPIONIC ACID
  radiolysis of aqueous perchloric acid solutions of, rate constants for reactions of hydrogen atoms produced by γ, 25:18459
  sodium salt, complexes with hexavalent neptunium, voltammetric study of, 25:18376
PROPRANOLOL
  effects on radioprotective action of TAB vaccine on x-irradiated mice, 25:19026
PROTEINS
  concentration and desalting of solutions of, 25:20882(R) (ORNL-TM-3082)
  radiation effects on composition of lens insoluble, in young and old animals, x, 25:18909
  radiation effects on production of free radicals in lyophilized, comparison of, to effects of electric discharge, γ, 25:18906
PROTON BEAMS
  characteristics of 440-MeV, for use in therapy of human malignancies, 25:19087
  monitoring of particle distribution in, x-ray fluorescence probe for, 25:20138
PROTON CROSS SECTIONS
  measurement of total, target chamber for, 25:20176
PROTON SPECTROMETERS
  performance of recoil, for measurement of neutron spectrum from americium--beryllium source, 25:18761
PROTONS
  abundance in topside ionosphere, solar-geomagnetic seasonal control of, (E/T), 25:19576
  channeling in boron-implanted silicon at 450 keV, 25:19830

XUM

channeling in silicon, effects of disorder produced by ion implantation on, 25:19816
decay of, Cherenkov detector search for, (E), 25:19893
density from 125 to 140 km in ionosphere, interaction mechanisms of, (E/T), 25:19583
detection of, response of NE-213 liquid scintillator for, 25:18655
diffusion mean free path during Feb. 25, 1969 solar event, effect of interplanetary magnetic-field irregularities on, (E/T), 25:19414
effects on brain of goats, effects of dose and energy on pathological, 25:19124
effects on silicon at 1 MeV, annealing of insulating surface layers formed in, 25:19822
effects on silicon diodes at 2.8 MeV, annealing of ionized defects induced in, 25:19821
form factor effects on ratios of $e^- + p \to e^- + p$ and $e^+ + p \to e^+ + p$ interaction cross sections, Veneziano model for, (T), 25:19942
implantation in silicon at 50 keV, effects on impurity diffusion, 25:19824
interactions anti $d + p$ at 13.3 GeV/c, test of CPT invariance from total cross sections for, 25:19907
interactions anti $n + p$ at 6.65 GeV/c, total cross sections for, 25:19907
interactions anti $p + p \to 2\pi(2\gamma)$, calculation of box-diagram effect with two resonances in intermediate state for, (T), 25:19986 (IFVE-STF-70-34)
interactions anti $p + p \to 2\pi(2\gamma)$, calculation of box-diagram effect with two resonances in intermediate state for, (T), 25:19986 (IFVE-STF-70-34)
interactions anti $p + p \to 4K$, calculation of box-diagram effect with two resonances in intermediate state for, (T), 25:19986 (IFVE-STF-70-34)
interactions anti $p + p \to$ anti $n + n$, complex momenta method with branching in j-plane for differential cross sections of, (T), 25:20017(T) (CERN-Trans-70-15)
interactions anti $p + p \to$ anti $n + n$, singular Regge pole model for, (T), 25:19995
interactions anti $p + p$ at 6.65 GeV/c, total cross sections for, 25:19907
interactions $e + p \to e + p$, effects of Veneziano-model form factors on ratios of cross sections for $e^+ + p \to e^+ + p$ interactions and, (T), 25:19942
interactions $e + p$, O(3,1) analysis of currents and current commutators for singularities of Fourier transforms for inelastic, (T), 25:19934
interactions $e + p$, super-eikonal model for structure function of deep inelastic, (T), 25:19939 (NYO-2262-TA-221)
interactions $e + p$, Veneziano-like model for two-current amplitude of deep inelastic, (T), 25:19954
interactions $e^+ + p \to e^+ + p$, effects of Veneziano-model form factors on ratios of cross sections for $e^- + p \to e^- + p$ interactions and, (T), 25:19942
interactions $\gamma + p \to n + \pi^+$ at threshold to 500 MeV, multipole analysis of, (T), 25:19957
interactions $\gamma + p \to p + 2\pi^0$ at 550 to 730 MeV, differential cross sections for, (E), 25:19890
interactions $\gamma + p \to p + \pi^0$ at threshold to 500 MeV, multipole analysis of, (T), 25:19957
interactions $\gamma + p \to \pi^+ + n$ interactions at 227 to 260 MeV and 51 to 146°, symmetry ratios for, (E), 25:19889
interactions $K^+ + p \to \Delta^{++} + K^{*0}(1420)$, $K^{*0}(1420) \to K^+ + \pi^-$ at 12.7 GeV/c in hydrogen bubble chamber, cross sections and production mechanism for, (E), 25:19914
interactions $K^+ + p \to \Delta^{++} + K^{*0}(890)$, $K^{*0}(890) \to K^+(K^0) + \pi^-(\pi^0)$ at 12.7 GeV/c in hydrogen bubble chamber, cross sections and production mechanism for, (E), 25:19914
interactions $K^- + p \to K^{*0}(890) + n$ at 3.9 and 4.6 GeV/c in hydrogen bubble chamber, test of absorption-modified one-pion exchange model for forward structure in, (E/T), 25:19918
interactions $K^+ + p \to K^0 + \Delta^{++}(1236)$ at 12.7 GeV/c in hydrogen bubble chamber, cross sections and production mechanism for, (E), 25:19914
interactions $K^- + p \to K^- + p$ at 14.25 GeV/c in hydrogen bubble chamber, differential and total cross sections for, (E), 25:19912
interactions $K^+ + p \to K^+(K^0) + \pi^-(\pi^0) + \Delta^{++}$ at 12.7 GeV/c in hydrogen bubble chamber, $K^+ + \pi^- \to K^+(K^0) + \pi^-(\pi^0)$ interactions in, (E), 25:19914
interactions $K^+ + p \to K^+(K^0) + \pi^-(\pi^0)$, $K^+ + p \to K^+(K^0) + \pi^-(\pi^0) + \Delta^{++}$ interactions at 12.7 GeV/c in hydrogen bubble chamber for, (E), 25:19914
interactions $K^+ + p \to p + K^{*+}(890)$, $K^{*+}(890) \to K^0 + \pi^+$ at 12.7 GeV/c in hydrogen bubble chamber, cross sections and production mechanism for, (E), 25:19914
interactions $K^- + p \to p + Q^-$ at 10 GeV/c, t-channel helicity conservation in diffractive, (E), 25:19921
interactions $K^+ + p$ at 12.7 GeV/c in hydrogen bubble chamber, hyperon and antihyperon production properties in, (E), 25:19914
interactions $K^+ + p$ at 12.7 GeV/c in hydrogen bubble chamber, K^0, Λ, and anti Λ production cross sections for, (T), 25:19914
interactions $K^+ + p$ at 12.7 GeV/c in hydrogen bubble chamber, upper limits for meson resonance production in, (E), 25:19914
interactions $K^- + p$ at high energies, compilation of cross sections for, (E), 25:19909 (CERN-HERA-70-6)
interactions $K^+ + p$, model-independent determination of real parts of amplitudes for forward, 25:20013
interactions $K^- + p$, model-independent determination of real parts of amplitudes for, 25:20013
interactions $n + p \to 3p + \gamma$, weak-interaction Hamiltonian for photon polarization in, (T), 25:20039
interactions $n + p \to d + \gamma$, weak-interaction Hamiltonian for photon polarization in, (T), 25:20039
interactions $n + p$ at 14.4 MeV with bremsstrahlung production, cross sections for, (E), 25:20257
interactions $n + p$ at 525 and 600 MeV at 65 tc 180°, transfer depolarization parameter for, (E), 25:19904
interactions of suprathermal cosmic, x-ray emission from, (T), 25:19451
interactions $p + d$ at 0.5 to 70 GeV/c, compilation of cross sections, angular distributions, and polarizations for, (E), 25:19899 (UCRL-20000-NN)
interactions $p + n \to n + p$, complex momenta method with branching in j-plane for differential cross sections of, (T), 25:20017(T) (CERN-Trans-70-15)
interactions $p + n \to n + p$, singular Regge pole model for, (T), 25:19995
interactions $p + n$ at 0.5 to 70 GeV/c, compilation of cross sections, angular distributions, and polarizations for, (T), 25:19899 (UCRL-20000-NN)
interactions $p + n$ at low energies, relation between deuteron binding energy and phase shift for, (T), 25:20022
interactions $p + p \to 2p + \pi^+ + \pi^- + \pi^0$ at 19 GeV/c in hydrogen bubble chamber, Δ, ω, and rho$^+$ production and cross sections for, (E), 25:19900 (USIP-70-4)
interactions $p + p \to 2p + \pi^+ + \pi^-$ at 19 GeV/c in hydrogen bubble chamber, Δ, N, and meson resonance production in, (E), 25:19901 (USIP-70-7)
interactions $p + p \to 2p + \pi^+ + \pi^-$ at 19 GeV/c in hydrogen bubble chamber, Δ and N resonance production and cross sections for, (E), 25:19900 (USIP-70-4)
interactions $p + p \to \Delta +$ rho $+ N$ at 19 GeV/c in hydrogen bubble chamber, (E), 25:19902 (USIP-70-8)
interactions $p + p \to \Delta^{++} + p + \pi^-$ at 19 GeV/c, OPE and Regge models for, (E/T), 25:20032
interactions $p + p \to \Delta^{++} + \pi^- + p$ at 19 GeV/c in hydrogen bubble chamber, (E), 25:19902 (USIP-70-8)
interactions $p + p \to \Delta^{++}(1900) + n$ at 19 GeV/c in hydrogen bubble chamber, (E), 25:19902 (USIP-70-8)
interactions $p + p \to n + p + 2\pi^+ + \pi^-$ at 19 GeV/c in hydrogen bubble chamber, Δ, N, and rho^0 resonance production and cross sections for, (E), 25:19900 (USIP-70-4)
interactions $p + p \to p + p$ at 640 MeV, phase analysis study of pp(2050) resonance in, (T), 25:20016(T) (CERN-Trans-70-14)
interactions $p + p \to p + p(n) + \pi^+ + \pi^-(\pi^+) + \pi^0(\pi^-)$ at 19 GeV/c in hydrogen bubble chamber, Δ, N, and meson resonance production in, (E), 25:19901 (USIP-70-7)
interactions $p + p \to p + \pi^+(\Delta^{++}) + \pi^- + p$ at 19 GeV/c, one-pion-exchange model for, (E), 25:20020 (USIP-70-5)
interactions $p + p$ at 0.5 to 70 GeV/c, compilation of cross sections, angular distributions, and polarizations for, (E), 25:19899 (UCRL-20000-NN)
interactions $p + p$ at 10 GeV, (E), 25:19901 (USIP-70-7)
interactions $p + p$ at 10 GeV/c in hydrogen bubble chamber, baryon resonance production and cross sections in six-prong, (E), 25:19902 (USIP-70-8)
interactions $p + p$ at 19 GeV/c in hydrogen bubble chamber, cross sections for inelastic, (E), 25:19902 (USIP-70-8)
interactions $p + p$ at 520 to 670 MeV at 30 to 120°, Wolfenstein depolarization parameter for, (E), 25:19904
interactions $p + p$ at high energies, atlas of hadron momentum spectra from, (T), 25:20028
interactions $\pi + p$, test of Pomeranchuk theorem from finite-energy sum rules for, 25:20011
interactions $\pi^+ + p \to A_2^+ + p$ at 7 GeV/c, decay branching ratios of A_2 from, (E), 25:19920
interactions $\pi^- + p \to \Delta^0(1236) + \pi^0$ at 5 GeV/c in propane bubble chamber, cross sections from Monte Carlo generation of, (T), 25:20004 (JINR-P13-5516)
interactions $\pi^- + p \to n +$ eta, eta $\to 2\gamma$ at 5 GeV/c in propane bubble chamber, cross sections from Monte Carlo generation of, (T), 25:20004 (JINR-P13-5516)
interactions $\pi^- + p \to n + f^0$, $f^0 \to 2\pi^0$ at 5 GeV/c in propane bubble chamber, cross sections from Monte Carlo generation of, (T), 25:20004 (JINR-P13-5516)
interactions $\pi^- + p \to n + m\pi^0$ at 5 GeV/c in propane bubble chamber, cross sections from Monte Carlo generation of, (T), 25:20004 (JINR-P13-5516)
interactions $\pi^- + p \to p + A_1^-$ at 16 GeV/c, t-channel helicity conservation in diffractive, (E), 25:19921
interactions $\pi^+ + p \to p + A_1^+$ at 8 and 16 GeV/c, t-channel helicity conservation in diffractive, (E), 25:19921
interactions $\pi^- + p \to \pi^0 + n$ at 3.67 and 4.83 GeV/c at large momentum transfers, differential cross sections of, (E), 25:19911
interactions $\pi^- + p \to \pi^0 + n$ at 90 to 290 MeV, P-wave phase shift from total cross sections for, (E/T), 25:19915
interactions $\pi^+ + p \to \pi^+ + p$, amplitudes and πNN coupling constant from model-independent analysis of forward, (T), 25:20003 (JINR-E2-5561)

interactions $\pi^- + p \to \pi^- + p$, amplitudes and πNN coupling constant from model-independent analysis of forward, (T), 25:20003 (JINR-E2-5561)
interactions $\pi^- + p$ at 70 to 290 MeV, Δ resonance parameters from total cross sections for, (E), 25:19916
interactions $\pi^+ + p$ at 70 to 290 MeV, Δ resonance parameters from total cross sections for, (E), 25:19916
interactions $\pi^+ + p$ at low energies, analyticity and Pomeranchuk theorem violation predictions for, (T), 25:20005
interactions $\pi^- + p$ at low energies, analyticity and Pomeranchuk theorem violation predictions for, (T), 25:20005
interactions with cosmic hadrons above 70 GeV, multiparticle production from, (E), 25:19905
interactions with nuclei at several hundred MeV, cross-section calculations using Glauber theory, (T), 25:20490
lifetime of, Cherenkov detector study of lower limit on, (E), 25:19893
neutron capture by, $^3S_1$-$^3S_1$ radiative transitions in thermal, 25:20519
$p + p \to p + p + \gamma$ at 10 to 157 MeV, relativistic spin corrections for noncoplanar, (T), 25:19947
polarization in carbon-12 (d,p) reactions at 12.4 MeV, (E/T), 25:20287
polarization of recoil, in $\gamma + d \to \pi^- + p + p$ interactions, impulse approximation calculation of, (T), 25:19940
reactions (γ,p) with oxygen-16 at 12 to 25 MeV, shell-model analysis of excitation function for, (T), 25:20290
reactions (p,2nγ) with lutetium-175 at 12 MeV, energy levels of hafnium-174 from, (E), 25:20427
reactions (p,2p) and (p,np) with deuterium at 12 MeV, impulse-approximation analysis of coincidence spectra from, (E), 25:20260
reactions (p,3α) with boron-11 at 163 keV to 2.65 MeV, differential cross sections for, (T), 25:20275
reactions (p,α) 2α with boron-11 at 2.65 MeV, analysis of three-alpha final state interaction using Faddeev method, (T), 25:20300
reactions (p,α) and (p,3α) with boron-11 at 163 keV, cross sections and alpha spectra from, (E), 25:20270 (NP-18626)
reactions (p,α) and (p,γ) with aluminum-27 at 1.7 MeV, excitation functions for, (E), 25:20330
reactions (p,α) and (p,γ) with sodium-23 at 1 to 1.8 MeV, analysis of resonances in, (E), 25:20325
reactions (p,α) with carbon-12 at 660 MeV, intranuclear-cascade-model calculations of angular distributions from, (T), 25:20268 (JINR-P4-5479)
reactions (p,$\alpha\gamma$) with sulfur-32 at 14 MeV, angular correlations in, (E), 25:20323
reactions (p,d) and (p,t) with ruthenium-96 at 31.5 MeV, Q-values and angular distributions for, (E), 25:20436
reactions (p,d) with calcium-40 at 27.5 MeV, model for, (T), 25:20522
reactions (p,d) with tin-118 and -119 at 24.5 MeV, DWBA analysis of cross-section and asymmetry angular distributions from polarized, (E), 25:20365 (CEA-CONF-1657)
reactions (p,γ) with boron-10 at 2.6 to 17 MeV, cross sections for, (E), 25:20277
reactions (p,γ) with iron-56 at 1.2 to 1.6 MeV, angular distributions for, (E), 25:20336
reactions (p,γ) with nickel-58 at 1.4 MeV, γ-ray angular distributions and Q-value for, (E), 25:20314
reactions (p,γ) with nitrogen-14 at 2.2 to 19 MeV, cross sections for, (E), 25:20277
reactions (p,γ) with phosphorus-31 at 1.55 MeV, energy levels of sulfur-32 from, 25:20326
reactions (p,γ) with phosphorus-31 at 1.8 to 2 MeV, analysis of resonances in, (E), 25:20308
reactions (p,γ) with silicon-28 at 1.4 MeV, γ spectra and angular distributions for, (E), 25:20357
reactions (p,γ) with silicon-28 near 2 MeV, angular distributions for, (E), 25:20319
reactions (p,n) with natural indium and tin and on tin isotopes, cross sections and strength functions for, (E), 25:20475
reactions (p,n) with nickel-64 at 3 MeV, γ--γ angular correlations from, (E), 25:20358
reactions (p,n) with tritium at 2.56 MeV, associated particle method for measuring neutron flux from, 25:18647
reactions (p,nγ) with lead-208 at 7 to 11 MeV, proton-particle neutron-hole states in bismuth-208 from, (E), 25:20434
reactions (p,t) and (p,He-3) at 43.7 and 54.1 MeV, angular distributions for, (E), 25:20299
reactions (p,t) with iron-54, iron-56, nickel-58, and nickel-60 at 51.9 MeV, 25:20321
reactions of 70- to 420-MeV cosmic, with carbon, nitrogen, and oxygen, (E), 25:19531
reactions with aluminum and beryllium at 70 GeV, yields and differential cross sections for π^-, K^-, anti p, and anti d production in, (E), 25:19906
reactions with aluminum, beryllium, copper, and lead at high energies, atlas of hadron momentum spectra from, (T), 25:20028
reactions with argon, helium, nitrogen, and oxygen at 4 to 26 keV, total cross sections for formation of metastable hydrogen atoms by charge exchange in, (E), 25:19504
reactions with metals at 90 to 180 keV, ratios of inner-shell ionization cross sections for, to corresponding deuteron-bombardment cross sections, 25:19470
reactions with nuclei at 600 MeV, classical absorptive-gas model for calculation of meson (π^+) production in, 25:20031
reactions with nuclei up to several GeV, cascade calculations of double differential distributions of particles from, (T), 25:20018 (JINR-P2-5507)
reactions with nuclei, tables of thresholds for, (E), 25:20237 (UCRL-50400(Vol.9))
scattering by calcium-40 at 30 to 45.5 MeV, optical-model analysis of angular distributions from elastic, (E/T), 25:20311
scattering by helium-3 and -4 at backward angles, pole-diagram analysis of exchange mechanism in, (T), 25:20250 (JINR-P2-5496)
scattering by helium-4 below 22 MeV, phase shifts calculated from one-term nonlocal separable potentials for elastic, (T), 25:20261
scattering by iron-56 at 3.7 to 4.3 MeV, angular distributions for elastic, (E), 25:20336
scattering by molybdenum-92, molybdenum-94, strontium-88, tin-118, tin-120, and zirconium-92 at 4 to 12 MeV, polarization in elastic, (E), 25:20331
scattering by nickel-60, nickel-64, zinc-66, and zinc-68 at 4.25 to 8.47 MeV, angular distributions and excitation functions for, (E), 25:20322
scattering by samarium-148 and -154 at 16 MeV, differential cross sections and deformation parameters for, (E/T), 25:20477
scattering by sodium-23 at 1 to 1.8 MeV, analysis of resonances in inelastic, (E), 25:20325
scattering by sulfur-32 at 9.275 MeV, evidence for vibrational excited states from inelastic, (E), 25:20326
stopping in gases and solids, review, (E), 25:19762
storage of relativistic, in solar corona, (E/T), 25:19403
targets of polarized, development of neodymium-doped lanthanum magnesium nitrate, 25:20135 (RHEL/R-201)
zone of avoidance in interplanetary space of solar, equatorial, (E/T), 25:19437

PROTONS (anti p)
interactions anti $p + d$ at 6.65 GeV/c, test of CPT invariance from total cross sections for, 25:19907
interactions anti $p + p \to 4K$, calculation of box-diagram effect with two resonances in intermediate state for, (T), 25:19986 (IFVE-STF-70-34)
interactions anti $p + p \to$ anti $n + n$, complex momenta method with branching in j-plane for differential cross sections of, (T), 25:20017(T) (CERN-Trans-70-15)
interactions anti $p + p \to$ anti $n + n$, singular Regge pole model for, (T), 25:19995
interactions anti $p + p$ at 6.65 GeV/c, total cross sections for, 25:19907
production in proton reactions with aluminum and beryllium at 70 GeV, yields and differential cross sections for, (E), 25:19906

PROTOTYPE ADVANCED THERMAL REACTOR
buildings and structures for, design parameters and construction schedule for, 25:20564
design parameters of, 25:20564
site for, preparation of, 25:20564

PROTOZOA
Histomonas meleagridis, radiation effects on pathogenicity of, in turkeys, γ, 25:19156

PSORALEN
effects on hemolysis of uv-irradiated erythrocytes, 25:18914

PULSARS
model for nonpulsing, standard, (T), 25:19372
NP 0532, detection of pulsed gamma rays from, (E), 25:19361
NP 0532, high-frequency modulation of light from, (E), 25:19360
NP 0532, maser mechanism for radiation emission in, (T), 25:19370
NP 0532, solar occultation of, (E), 25:19373
NP 0532, x-ray pulsations from, (E), 25:19359
polarization of, circular components of, (E), 25:19358
properties of, review on, (T), 25:19375
PSR 0329, polarization in, (E), 25:19358
PSR 1508, polarization in, (E), 25:19358
PSR 2218 + 47, linear polarization of, (E), 25:19379
radiation emission mechanism for, maser action in, (T), 25:19370
scintillation of, interstellar, (E/T), 25:19351
x-ray pulsations from, (E), 25:19359

PULSE ANALYZERS
circuit for expanding count storage capacity, 25:18869
description of reference-signal comparison, for use with proportional detectors, 25:18652(P)
design and operation of VA-V-100 linear amplifier/analyzer with specifications, 25:18873
design modification of NLZ 716a-T, in NZG 312-T

  - spectrometer, 25:18862
  - gain stabilization for spectrum with no reference peaks, method for, 25:18867
  - operation and uses of VAS 4096 multichannel, 25:18674
  - testing of, pseudorandom pulse generator for, 25:18853
- PULSE CONVERTERS
  - design and performance of time-to-amplitude, for nanosecond range, 25:18846
  - design modification of analog-to-digital, for pulse stabilization at low coincidence count rates, 25:18871
  - pulse sequence identifier for time-to-pulse height, 25:18866
- PULSE DISCRIMINATORS
  - description for pulse pile-up prevention, 25:18840(P)
  - design and performance of, based on avalanche transistors, 25:18847
  - development of rise-time, for electronic collimation, 25:18749
- PULSE GENERATORS (ELECTRONICS)
  - development of pseudorandom, for uniform amplitude distributions with discrete lines for testing pulse-height analyzers, 25:18853
- PULSE SHAPERS
  - circuits for compensation of pulse spread for improved time resolution, 25:18639 (IFVE-SEF-69-44)
  - pulse attenuation by, proportional detector, 25:18700
- PUMPS
  - performance characteristics of primary coolant, for pressurized water reactors, 25:20717(T) (JPRS-52384)
- PUPAE
  - radiosensitivity of Phaenicia sericata, effects of age on x, 25:19098
- PUREX PROCESS
  - solvent performance in LMFBR fuel reprocessing by, 25:18505 (WHAN-FR-32)
- 3,6-PYRIDAZINEDIONE, 1,2-DIHYDRO-
  - effects on chromosomes of root cells of Vicia faba, effects of blue, green, and infrared light on aberrant, 25:18962
- PYRUVIC ACID
  - radiation effects on content of, in cell mitochondria and nuclei of cotton plants, γ, 25:18918
  - radiation effects on incorporation of carbon-14-labeled, into tricarboxylic acid cycle in rat thymocytes, in vitro x, 25:18902

Q

- Q DEVICES
  - ion velocity distribution function in single-ended, shaping of, (E), 25:19670
- QUAD CITIES POWER REACTOR, UNIT 1
  - core for, temperature transients during design basis accident conditions for, 25:20636 (DOCKET-50254-31)
  - design parameters of, requested additional data on, 25:20634 (DOCKET-50254-29)
  - operations aspects of, requested additional data on, 25:20634 (DOCKET-50254-29)
  - site for, additional geological and meteorological data for, 25:20635 (DOCKET-50254-30)
  - site for, environmental temperature survey during July 1969 to June 1970, 25:20633 (DOCKET-50254-28)
- QUAD CITIES POWER REACTOR, UNIT 2
  - core for, temperature transients during design basis accident conditions for, 25:20636 (DOCKET-50254-31)
  - design parameters of, requested additional data on, 25:20634 (DOCKET-50254-29)
  - operations aspects of, requested additional data on, 25:20634 (DOCKET-50254-29)
  - site for, additional geological and meteorological data for, 25:20635 (DOCKET-50254-30)
  - site for, environmental temperature survey during July 1969 to June 1970, 25:20633 (DOCKET-50254-28)
- QUANTUM ELECTRODYNAMICS
  - charge renormalization constant in, sixth-order, 25:20060
  - conference on computational methods in, 25:20054 (CNRS-CPT-70-P-335)
  - gauge transformations and local charges of quasi-particles, (T), 25:20082
  - Green functions for, model with no photon self-energy insertions for, 25:20062
  - radiative corrections to, computer programs for renormalized, 25:20055 (CNRS-CPT-70-P-335, pp IV.26-38)
  - renormalization constant in, model with no photon self-energy insertions for coefficient of logarithmic divergence in, 25:20062
  - scattering amplitudes in Coulomb and Feynman gauges in, functional description of, 25:20092
  - theory of, relativistic extension of Wheeler--Feynman, 25:20061
  - theory of, review of, 25:20081
  - Ward identities in, anomalies in, 25:20070
- QUANTUM FIELD THEORY
  - Bethe--Salpeter equation for relation between SO(1,3) and SO(1,2) crossed-channel partial-wave analyses, 25:20113
  - bound states of relativistic two-particle system, solution of Bethe--Salpeter equation for, (T), 25:20083
  - current-density commutators in, equal-time limits of, 25:20076
  - field quantization for spin-half particles with infinite maximum occupation number, 25:20079
  - fields in, analytic properties of nonstrictly localizable, 25:20063
  - formulation of local Lagrangian, for electric and magnetic charges, 25:20072
  - interactions in, generalized finite-matrix Hamiltonians for, 25:20066
  - Lagrangian theories in, review of nonpolynomial, 25:20067
  - Lorentz invariance in indefinite-metric, 25:20073
  - Lorentz noninvariance of complex-ghost relativistic, 25:20074
  - manifolds in, lecture on differentiable, 25:20068
  - particle motion in fixed-centers field in, system of algebraic and integral equations for, 25:20059 (JINR-P4-5547)
  - physical states in, lectures on construction of, 25:20069
  - renormalization of theories with broken symmetry in, 25:20056 (DESY-70/62)
  - superpropagators in nonrenormalizable, regularizing properties of, 25:20058 (JINR-P2-5569)
  - theory for nonlocal, review of, 25:20057 (JINR-E2-5563)
  - two-body problem in, equal-time formulation of, 25:20077
  - two-body problem in, relativistic, 25:20071
  - vacuum in, S-matrix theory for, 25:20078
  - Ward identities in, anomalies in, 25:20070
  - Yang--Mills field in, massless limit of massive, 25:20075
  - Yang--Mills model of weak interactions, massive, 25:19969
- QUANTUM MECHANICS
  - computation of Moshinsky brackets by direct diagonalization, 25:20526
  - Dirac equation in, one-dimensional square potential in, 25:20065
  - eigenvalues of asymmetric rotator in, analytic interpolation of, 25:20513
  - Hamiltonians in, generalized finite-matrix, 25:20066
  - Lie algebras for, realization through rational functions of canonical variables for, 25:19935
  - properties of real RPA matrices and a simple diagonalization procedure, 25:20525
  - Schroedinger operator with hard-core potential in, perturbation of eigenvalues of two-particle, 25:19882
- QUARTZ
  - thermoluminescence properties of Korean natural, for gamma dosimetry, 25:18813
- QUASARS
  - identification of, in Parkes 2700-MHz survey, (E), 25:19383
  - luminosity of, failure of supernova rate from coalesced stars to explain, (T), 25:19320
  - mass of, (E/T), 25:19364
  - radiation emission from 3C 273, high-energy, (E), 25:19455
  - radio flux densities for 3C 273 and 3C 279, (E), 25:19376
  - radio flux density variations of, (E), 25:19367
  - radio structures of seventy-nine, (E), 25:19350
  - spectra of, classification of radio, (E), 25:19369
  - spectra of, multiple absorption redshifts in, (T), 25:19371
  - x-ray emission from 3C 273, (E), 25:19458
- 8-QUINOLINOL
  - complexes with californium, stability of, 25:18498 (KFK-1298)
  - effects on repair processes following γ-radioinduced chromosome aberrations in Nigella damascena seeds, 25:18951
- 8-QUINOLINOL, 5,7-DIBROMO-
  - complexes with hexavalent uranium, structure of product precipitated from aqueous acetone solutions of, 25:18374
- 8-QUINOLINOL, 5,7-DICHLORO-
  - complexes with californium, stability of, 25:18498 (KFK-1298)
  - complexes with hexavalent uranium, structure of product precipitated from aqueous acetone solutions of, 25:18374

R

- RABBITS
  - indium-113m uptake by bone marrow of, following injection as colloid, 25:18994
  - plutonium-239 distribution in, following inhalation in oxide aerosols, role of pulmonary macrophages in, 25:18891(T) (LF-tr-46)
  - radiation effects on content of potassium and sodium in erythrocytes of, x, 25:19107
  - radiation effects on revascularization of blood supply in skin grafts on, microwave, 25:19104
  - radioinduced lesions in retinas of eyes of, mechanisms of light evoked electric responses in ruby laser, 25:19132

RADIATION
- book: Bone Tumors in Man and Animals, 25:19136
- dose to human population from consumer products containing radioisotopes, analysis of procedures for control of external and cumulative, 25:19015
- dose to human populations from artificial and natural sources, 25:19137
- dosimetry of human gastrointestinal tract following ingestion of radionuclides, mathematical model for, 25:19141
- effects of nuclear explosion, on frequency of chromosome aberrations in bone marrow cells of leukemia patients exposed in Hiroshima and Nagasaki, 25:18963
- effects on abortion frequency in humans in relation to incidence of chromosome aberrations, effects of dose on, 25:18969
- effects on alkali metal halide crystals, studies of defect recombination processes in, 25:19770(R) (NYO-3842-12)
- effects on alkali metal halides, chemiluminescence--dissolution method for study of defects induced in, 25:19850
- effects on amino acid composition of protein of fish muscles, ionizing, 25:19110
- effects on blood cells of medical personnel, review of effects of small doses, 25:19142
- effects on blood vessels in human cerebrum following therapy for cerebral gliomas, 25:19065
- effects on bone marrow of human babies and man following exposure from atomic bombing in Hiroshima, autoradiography studies on, 25:19134
- effects on bones and other tissues of human mouth, pathological, 25:19079
- effects on cells, microdosimetry studies of, 25:18993
- effects on cellular and humoral factors of natural immunity, ionizing, 25:18922
- effects on cellular recovery in lymphoid tissues of guinea pigs, 25:18919(R) (RLO-2225-T-16-1)
- effects on chromosomes in cultured cells and plant seeds, effects of hypothermia on aberrant, 25:19093
- effects on chromosomes of man exposed to atomic bombing in Japan, statistics of aberrant, 25:18961
- effects on circulatory system in transplanted Walker carcinoma tumors in rats, 25:19111
- effects on crosslinking of elastomers, effects of chloroalkanes on, 25:18434
- effects on cultured cells, review of, 25:19106
- effects on curing resins of poly(vinyl halides) and polyfunctional allyl or vinyl monomers, 25:18437(P)
- effects on fertile eggs of assassin bugs, effects of nutrition on, 25:19099
- effects on histology of brain of cats and man, ionizing, 25:19109
- effects on human bones following post-operative therapy for breast malignancies, 25:19140
- effects on human populations in comparison with chemicals, evaluation of mutagenic, 25:18965
- effects on immune reactions of mice, effects of transplants of bone marrow, embryonic liver, and spleen on, 25:18921
- effects on liver of children, combined effects of antineoplastic drugs and pathological, 25:18999
- effects on man following accidental exposure, rules for clinical and therapeutic procedures for external, 25:18975 (CEA-N-1365)
- effects on man, effects of age, dose, dose rate, and sex on pathological, 25:19008 (NCRP-39)
- effects on man, effects of dose on carcinogenic and leukemogenic, 25:18971
- effects on methane, G values and mechanisms for, 25:18449(T) (ORNL-tr-2386)
- effects on mice, effects of antigen-reactive mice spleen cells on, in combination with sheep erythrocytes, 25:18925
- effects on nitric oxide in ethanol and tetrahydro-2-methylfuran solutions, precursors of free radicals and hydrogen in, 25:18448(R) (CEA-N-1369)
- effects on organic crystals, annealing of free radicals from, 25:18473
- effects on plastic medical supplies, sterilizing, 25:19161
- effects on polymerization of 2-furaldehyde, effects of alkyl halides on, 25:18430
- effects on polymerization of solid acrylamide, NMR studies on kinetics of, 25:18448(R) (CEA-N-1369)
- effects on skin reactions on man following therapy for femoral osteosarcoma, effects of hypothermia and ischemia on, 25:19093
- effects on survival of malignant and normal cells in man, effects of LET on, 25:19077
- effects on thickness of hair of sheep, ionizing, 25:19121
- effects on tissues of rodents, effects of artificial hypothermia and ischemia on lethal whole-body, 25:19093
- effects on toxin production in biological materials, 25:18915
- effects on yeast cells, effects of aminopterin on, 25:19155

RADIATION CHEMISTRY
- diffusion kinetics in, 25:18447 (CALT-767-P-4-73)
- radiolysis of liquids, self-absorption of Cherenkov light as indicator of progress of, 25:18453
- reactions of uncharged transient species in, 25:18454
- theory of pulse radiolysis in electric field, 25:18469

RADIATION DETECTORS
- calculation of constants for telescope, for particle identification, 25:18705
- circuit for monitoring correlation in pulse sequences from, micrologic integrated, 25:18701
- data processing system for telescope, for particle identification, 25:18718
- dead-time correction for, 25:18706
- description of dual, for measuring iodine-131 and iodine-132 uptake by thyroid, 25:18898
- development for measuring particle concentrations and radioactivity concentrations of alpha-active aerosols, 25:18685(P)
- development of gallium chloride and lithium chloride, for solar neutrino detection, 25:18720
- geometric arrangement for elimination of correlation effects in gamma detection, 25:18669
- performance of superhigh-energy resonance-radiation, 25:18781
- pulse pile-up discrimination circuitry for, 25:18840(P)
- sensitivity of secondary-emission, for monitoring position of electron beams, 25:20173
- theory of supercooled liquid, based on crystallization along particle track, 25:18709
- window attachment to curved surface of, method for vacuum-tight, 25:18712

RADIATION DETECTORS, ACTIVATION
- activity evaluating device for in-pile, 25:18719(P)
- calculation of radioactivity of wire, for thermal neutron flux measurements, 25:18707
- data from in-pile, computer program for processing, 25:18641 (IN-1446)
- development of beryllium-9 gas flow, for in-core neutron flux measurements, 25:18646 (WHAN-SA-73)

RADIATION DETECTORS, BUBBLE CHAMBER
- bubble contrast and shape in, with bright-field illumination, 25:18789
- bubble size measurement by image contrast in brightfield illuminations, 25:18792
- design of 180-liter xenon, 25:18783
- distortion effects in geometrical reconstruction of events in CERN 2-m hydrogen, 25:18777 (USIP-70-6)
- particle tracks in heavy-liquid, analysis of electron, 25:18784
- particle tracks in, high-speed magnetic-chip memory in scanning robot for measurement of, 25:18780
- particle tracks in, on-line CDC 8090 computer system for analysis of, 25:18776 (USIP-70-3)
- particle tracks in, searching for kinks and determining parameters for scattering, 25:18773 (JINR-P1-5540)
- performance in 7.7 MeV-electron distribution determinations in biological materials, 25:18995

RADIATION DETECTORS, CHERENKOV
- design and performance for total-absorption spectroscopy with KRS-6 single-crystal radiator, 25:18787
- design and performance of high resolution differential, 25:18794
- design of differential--threshold, 25:18788
- development of shower, for electron energy measurement up to 15 GeV/c, 25:18779
- pulse shaper circuit for improved time resolution, 25:18639 (IFVE-SEF-69-44)
- resolution of shower, for high-energy electrons, 25:18786

RADIATION DETECTORS, CRYSTAL
- performance of germanium, for measuring gamma spectra from SNAP-15A heat source, 25:18601

RADIATION DETECTORS, DIELECTRIC TRACK
- design of cellulose nitrate, for detection of uranium-235 fission fragments, 25:18724
- development of, 25:18799 (ORNL-4584, pp 165-86)
- particle track analysis for measurement of uranium-238--uranium-235 fission ratio in reactors, 25:18704
- particle track etching in, method for volume, 25:18708
- particle tracks in thin-film, preamplifier for spark counter for readout of, 25:18644 (ORNL-4584, pp 152-64)
- performance of cellulose nitrate, for alpha particle autoradiography, 25:18799 (ORNL-4584, pp 165-86)
- performance of plastic, for alpha radiography, 25:18727

RADIATION DETECTORS, FISSION CHAMBER
- performance of in-core regenerative, for thermal neutron flux mapping in reactors, (E), 25:20711 (WHAN-FR-37)

RADIATION DETECTORS, FISSION FOIL
- review of, 25:18811

RADIATION DETECTORS, GEIGER-MUELLER
- calibration and testing for krypton-85 monitoring in atmosphere, 25:18638 (CONF-700816-(Vol.1), pp 143-74)
- count rate limits for, effects of various counter parameters on, 25:18664
- count rates of, statistical errors in, measurement of, 25:18663
- preamplifier for TSEE dosimeter readout, 25:18644 (ORNL-4584, pp 152-64)

RADIATION DETECTORS, IONIZATION CHAMBER
- calibration and testing for krypton-85 monitoring in atmosphere, 25:18638 (CONF-700816-(Vol.1), pp 143-74)
- count rate limits for, effects of various counter

- parameters on, 25:18664
- count rates of, statistical errors in, measurement of, 25:18663
- design for bulk assay of mCi amounts of radiopharmaceuticals, 25:18723
- design of compensated helium-3, for in-core neutron flux monitoring, 25:18662
- development for measuring alpha contamination on reactor fuel element surfaces, 25:18636(P)
- development for measuring total integrated dose, 25:18805(P)
- development of array of, for high spatial resolution, 25:18682(P)
- development of extrapolation, for measuring dose distribution in phantoms, 25:18644 (ORNL-4584, pp 152-64)
- readout circuit for, logarithmic, 25:18721(P)

RADIATION DETECTORS, PROPORTIONAL
- design and performance of position-sensitive helium-3 resistant-wire, for thermal neutron spectroscopy, 25:18738 (RISO-229)
- design and performance of position-sensitive, for magnetic spectrographs, 25:18681
- design of laminar flow, for continuous monitoring of gamma activity in liquid streams, 25:18717
- design of spherical tissue-equivalent, with dose equivalent readout, 25:18809
- design of split-anode, for beta and gamma detection, 25:18698(P)
- development for LET measurements, 25:18644 (ORNL-4584, pp 152-64)
- development of gas recoil, with electronic collimation for fast neutron spectroscopy, 25:18749
- development of multiwire, review of, 25:18796
- gain stabilization for, feedback system for, 25:18658
- performance of boron trifluoride, for personnel neutron dosimetry, 25:18800(T) (SC-T-71-3009)
- pulse analyzer for use in prospecting, reference-signal comparison, 25:18652(P)
- pulse shapers for, pulse attenuation by, 25:18700

RADIATION DETECTORS, SCINTILLATION
- calibration and testing for krypton-85 monitoring in atmosphere, 25:18638 (CONF-700816-(Vol.1), pp 143-74)
- characteristics of pure and activated cadmium iodide, 25:18665
- circuit for, ringing coil pulse encoder, 25:18868
- circuitry for proper positioning of scintillation points on cathode-ray tubes, design of, 25:18713(P)
- circuits for neutron discrimination in gamma background, 25:18667
- data analysis for liquid, computer programs for, 25:18693
- description of plastic, for monitoring trace amounts of radioactive gases, 25:18744(P)
- description of position-sensitive, for gamma rays, 25:18686(P)
- design and performance of xenon gas, 25:18645 (USIP-70-1)
- design for radiometric well logging, 25:18814(T) (CSIRO-Trans-9992)
- design of time-of-flight, for particles with momenta up to 2 GeV/c, 25:20180
- design with secondary electron emitter, for detection of ion beams, 25:18722(P)
- development for dose rate measurements, 25:18684(P)
- development for studying local concentration of radioactive material on moving band, 25:18688(P)
- development of fast response miniature electron, for use with small energy analyzer, 25:18711
- development of organic gel, 25:18687(P)
- development of position-sensitive, 25:18713(P)
- development of shower, for electron energy measurement up to 15 GeV/c, 25:18779
- development with sample rotation for improving counting statistics, 25:18683(P)
- efficiency of lithium glass and boron-loaded liquid, effects of elastic scattering on low-energy neutron detection, 25:18716
- efficiency of lithium-6 glass, for in-core fast neutron spectra measurements, 25:18637 (AEEW-M-898)
- orientation system for balloon-borne cosmic X-ray telescopes, development of, 25:18677
- performance for measurement of high-energy gamma spectra in strong neutron fluxes, 25:18735 (INR-1224)
- performance of liquid, for determination of radon daughters on filters, 25:18768
- performance of multisphere europium-activated lithium-6 iodide, for personnel neutron dosimetry, 25:18800(T) (SC-T-71-3009)
- performance of stilbene, for measurement of neutron spectra from americium--beryllium source, 25:18761
- performance of thallium-activated sodium iodide, in Compton-suppressed low-level gamma spectrometers for extended samples, 25:18752
- phosphorescence of thallium-activated and sodium-activated cesium iodide, 25:18648
- pulse shaper circuit for improved time resolution, 25:18639 (IFVE-SEF-69-44)
- pulse-height analysis of organic, for neutron spectroscopy, 25:18766
- radiation effects on boron-10--zinc sulfide, thermal neutron, 25:18880
- resolution for spectroscopy, single-electron method for measuring photopeaks, 25:18745
- response of europium-activated lithium iodide, to thermal neutrons, 25:18661
- response of NE-213 liquid, to electrons and protons, 25:18655
- sample cells for liquid, performance of aluminum and Teflon, 25:18666
- scintillation decay of fast organic, 25:18656
- scintillation lifetime measurements of, spectrometer for subnanosecond, 25:18696
- solutes for liquid, for beta counting, 2-substituted naphth(1,2)oxazole, 25:18731(P)
- spectral distributions in NE213 liquid, time dependence of, 25:18678
- time resolution calculations for, 25:18640 (IFVE-SEF-70-23)

RADIATION DETECTORS, SEMICONDUCTOR
- amplifier for, design of transistor, 25:18668
- characteristics of large-area ion-implanted p-n junctions, 25:18756
- design and performance of telescope, for photonuclear reaction studies, 25:18675
- development and operation of, 25:18694
- development and use in high-energy physics, review on, 25:18775 (UCRL-20042)
- development for monitoring selected fission fragments in reactor cores, 25:18651(P)
- development of cadmium telluride, for gamma spectroscopy, 25:18733 (CEA-R-4052)
- fabrication of position-sensitive, by ion implantation in silicon, 25:19835
- performance for neutron dosimetry, using sandwiched polyethylene--aluminum radiator, 25:18798 (KFKI-70-29-HP)
- space charge in, extension of Ramo's theorem to fixed, 25:18710

RADIATION DETECTORS, SEMICONDUCTOR (GERMANIUM)
- calibration of lithium-drifted, europium-152 and radium-226 relative intensities for, 25:20425
- calibration of lithium-drifted, method for improved energy, 25:18714
- characteristics of position-sensitive lithium-drifted, for γ cameras, 25:18699
- efficiencies of coaxial lithium-drifted, calculations of, 25:18755
- efficiency as a point detector, calibration of, 25:18676
- efficiency calibration for 1- to 100-keV x radiation from radioactive sources, 25:18715
- efficiency curve for thin lithium-drifted, for low-energy gamma rays, semi-empirical, 25:18725
- efficiency of 50 cm^3 lithium-drifted, for gamma radiation at 122 keV to 9.17 MeV, 25:18702
- efficiency of lithium-drifted, for measurement of K conversion coefficients, coincidence-collimation technique for, 25:18759
- fabrication of lithium-drifted, for gamma spectroscopy, 25:18772
- multiple scattering in lithium-drifted, for gamma spectroscopy, 25:18726
- operation and performance of lithium-drifted, for gamma spectroscopy, 25:18772
- peaks from Compton scattering between lithium-drifted coincidence, elimination of spurious, 25:18754
- performance in system for measuring lifetimes of isomeric energy levels, 25:18753
- photopeak, efficiency of lithium-drifted, determination of relative, 25:18747
- pulse analyzer for, operation and uses of VAS 4096 multichannel, 25:18674

RADIATION DETECTORS, SEMICONDUCTOR (SILICON)
- calculation of constants for telescope, for particle identification, 25:18705
- circuits for surface-barrier, for half-life measurements of alpha emitters in ms range, 25:18703
- design and performance for absolute gamma dosimetry, 25:18806
- design and performance of surface-barrier--lithium-drifted telescope, for beta spectroscopy, 25:18760
- efficiency calibration for 1- to 100-keV x radiation from radioactive sources, 25:18715
- performance for measuring nuclear cross sections and particle energy spectra in BOL system, test procedures for, 25:20207
- performance for neutron dosimetry, using polyethylene radiator, 25:18798 (KFKI-70-29-HP)
- performance of position-sensitive checkerboard, in blocking experiments, 25:18679
- performance of position-sensitive telescope, for BOL nuclear detection system, 25:18757
- performance of rocket-borne lithium-drifted, for solar x-ray spectroscopy at 4 to 40 keV, 25:18654
- performance of surface barrier, in proton recoil system for neutron flux measurements in ORELA, 25:18763
- resolution of surface-barrier, 25:18672

RADIATION DETECTORS, SPARK CHAMBER
- amplifier with 1 msec recovery time for, design and operation of trigger, 25:18791
- BCD code display system for optical, 25:20177
- design and performance for fission fragment detection, 25:18671

  design and performance with graphite electrodes, 25:18785
  design and performance with two-coordinate readout and ferrite-core memory, 25:18790
  design of multiwire, for synchrocyclotron beam profile measurements, 25:20163
  development of 2-meter streamer, 25:18774 (JINR-P13-5529)
  development of automatic, review of, 25:18796
  electric discharge circuit for, spark-gap high-voltage, 25:18782
  operation of sampling, 25:18778
  properties of thin, with carbohydrate mixtures in filling gas, 25:18657
  readout system for wire, delay line, 25:18793
RADIATION DOSE
  calculations for human populations during nuclear excavation, 25:18989 (ORNL-4584, pp 42-56)
  calculations for human populations in trajectory of atomic cloud released during underground nuclear explosion, 25:18989 (ORNL-4584, pp 42-56)
  calculations for human populations residing in homes heated with Gasbuggy gas, 25:18989 (ORNL-4584, pp 42-56)
  maximum permissible environmental, medical, and occupational external and internal, 25:19008 (NCRP-39)
  maximum permissible neutron, for human skin, fetuses, and personnel, recommendations of National Council on Radiation Protection, 25:19007 (NCRP-38)
  maximum permissible, human populations, establishment of, 25:19018
RADIATION DOSIMETERS
  calibration of nuclear accident, intercomparison study for, 25:20134 (ORNL-4584, pp 187-97)
  characteristics, economics, and uses of, for personnel monitoring, 25:18973
  development of ionization chamber, 25:18805(P)
  performance for 0.5 to 400 MeV neutrons, 25:19007 (NCRP-38)
RADIATION DOSIMETERS, BIOLOGICAL
  evaluation of bone marrow chromosome, 25:18980 (CEA-CONF-1698)
  performance of Saccharomyces cerivisiae as uv, 25:18981 (CEA-N-1380)
RADIATION DOSIMETERS, CHEMICAL
  description for use in radiosterilization or radiopasteurization at high dose levels, 25:18803(P)
  development of bromobenzene--Crystal Violet, for γ, 25:18451
  equations for glucose and oxalic acid, 25:18808
  readout calibration for Fricke, spectrophotometric, 25:18801
RADIATION DOSIMETERS, EXOELECTRON
  characteristics of beryllium oxide, 25:18799 (ORNL-4584, pp 165-86)
  development of, 25:18799 (ORNL-4584, pp 165-86)
  readout equipment for, preamplifier for G--M, 25:18644 (ORNL-4584, pp 152-64)
  review of, 25:18811
RADIATION DOSIMETERS, PHOTOGRAPHIC FILM
  performance for measurement of radiation dose to human body during diagnostic x radiography, 25:19038
  performance for personnel neutron dosimetry, 25:18800(T) (SC-T-71-3009)
  performance of Polaroid, for γ and x, 25:19005
  readout of, automatic densitometer for coded, 25:18797 (AERE-R-6224)
RADIATION DOSIMETERS, PHOTOLUMINESCENT
  development of glass, for beta dosimetry at 30 keV to 2 MeV, 25:18810
  performance of glass, for high gamma doses, 25:18802
RADIATION DOSIMETERS, THERMOLUMINESCENT
  description of, 25:18812
  development of foil, capable of repetitive analysis, 25:18807(P)
  performance for measurement of radiation dose to human body during diagnostic x radiography, 25:19038
  properties of Korean natural quartz, for gamma dosimetry, 25:18813
  readout equipment and method using increasing temperature stages, 25:18804(P)
RADIATION DOSIMETRY
  developments in, 25:18870
  methods for personnel, review of, 25:18811
  physical constants determination for micro-, 25:18993
RADIATION FILTERS
  effectiveness of lead glass, for protection of human skin during therapy using cobalt-60, 25:19086
  effectiveness of tin, for protection of human skin during cobalt-60 γ therapy, 25:19082
  feasibility of tissue-equivalent wax, for compensating surface irregularity effects in high energy electron radiotherapy, 25:19066
  performance bismuth and silicon single-crystal, for neutrons, 25:20238 (UJV-2488-F)
RADIATION MONITORING
  book: Problems of Protection in Industrial Utilization of Radioelements, 25:18996
  programs at Oarai Research Establishment, Japan, during 1970, 25:18983(R) (JAERI-Memo-4216)
RADIATION PROTECTION
  developments in, 25:18870
  methods for outpatients by reducing dose during radiodiagnosis, 25:19009
  methods for, during medical diagnosis, programmed training in, 25:19010
  methods for, following accidental contamination of pastures, 25:18943
  procedures evaluation for radiometric devices available to public, 25:19015
  recommendations of National Council on Radiation Protection for, 25:19008 (NCRP-39)
  recommendations of National Council on Radiation Protection for neutron, 25:19007 (NCRP-38)
  regulations for industrial and medical personnel, federal and state, 25:18973
RADIATION RATE METERS
  development of scintillation detector, 25:18684(P)
RADIATION SOURCES
  development of advanced, 25:18590(R) (BNWL-1308-4)
  development of isotopic, 25:18870
  dose curves for, use of computer calculations for, 25:19000
  positioning in industrial radiography equipment, device for exact, 25:18567(P)
  radiation from moving, characteristics of detection of, 25:18692
RADIATION TARGET CANS
  design for testing HTGR recycle fuels, 25:19288 (ORNL-4629, pp 82-98)
RADIATION TARGET CHAMBERS
  description for Doppler shift studies with selected recoil directions, 25:20140
  design for BOL nuclear detection system, 25:20201
  design for electron scattering studies, 25:20211
  design for studying (γ,p) reactions, 25:20141
  design for total proton cross section measurements, 25:20176
RADIATION TARGETS
  design of furnace for high-temperature, 25:20212
  design of high pressure gas, cooled by liquid nitrogen, 25:20128 (IFVE-SEF-70-22)
  design of liquid deuterium, for D(p,n) neutron source, 25:20187
  design of secondary-particle, for meson (π) interactions, 25:20153
  design of windowless gas, optimization of, 25:20185
  development of polarized proton, of neodymium-doped lanthanum magnesium nitrate crystals, 25:20135 (RHEL/R-201)
  development of tritium, for T (d,n) neutron sources, 25:20134 (ORNL-4584, pp 187-97)
RADIATORS
  design of space vehicle liquid sodium, for shutdown cooling of reactors, 25:20805 (N-70-39420)
  design parameter of plate type, for protection of heat pipes, 25:20808(P)
RADIO ASTRONOMY
  map of entire sky, (E), 25:19388
RADIO GALAXIES
  gamma emission from Cen A and Virgo A, (E), 25:19455
  spectra of nuclei of elliptical, optical, (E), 25:19449
  spectra of, classification of radio, (E), 25:19369
  x-ray emission from Cen A and Virgo A, (E), 25:19455
RADIO WAVES
  attenuation of solar, at 19 and 37 GHz, (E), 25:19438
  emission during 20th solar cycle, relation to soft x rays, (E), 25:19430
  emission from spot groups, polarization of, (E), 25:19417
RADIOACTIVE CONTAMINATION
  effects of environmental, on man, 25:18941
  model for river, development of computer, 25:18940
RADIOACTIVE MATERIALS
  book: Problems of Protection in Industrial Utilization of Radioelements, 25:18996
  release in accidents, summary of 347 cases of, 25:19013 (JAERI-Memo-4240)
  shipping of, design of fire- and shock-resistant shielded containers for, 25:18633(P)
  shipping of, design of fire-resistant container for, 25:18632(P)
  shipping, insurance coverage and safety of, 25:19017
RADIOACTIVE MINERALS
  occurrence in Bur region of Republic of Somalia, 25:18541
RADIOACTIVE WASTE
  disposal in sea, contamination of algae following, 25:18939
  disposal in terrestial environment, effects on radioisotope and trace element content in soils, (E), 25:18521 (ORNL-4584, pp 1-10)
  disposal of high- and low-level solidified, in Lyons, Kans. salt mine, feasibility study of facility for, 25:18623 (ORNL-4584, pp 16-36)
  disposal of intermediate-level, Japanese methods for solidification for, 25:18634
  disposal of liquid, by deep underground hydraulic fracturing, (E), 25:18622 (ORNL-4584, pp 11-15)
  disposal of nuclear submarine, hazards of, 25:19014
  disposal of, review of methods for economic, 25:18570
  disposal systems for power reactors, design requirements of, 25:20684

  disposal to environment, UKAEA methods for control of, 25:18635
  environmental effects from, 25:20683
  krypton-85 removal from gaseous, equations for calculating efficiency of fission gas adsorption beds for, 25:18560 (CONF-700816-(Vol.1), pp 207-15)
  management methods for, development of western European, 25:18625 (SGAE-RT-35/1970)
  processing and disposal of, 25:18515
  processing of, recovery of plutonium-238 in, 25:18492 (ANL-7709)
  removal from Fast Flux Test Facility off-gases, method for calculating efficiency of adsorption beds for, 25:18561 (CONF-700816-(Vol.1), pp 216-23)
  separation of cesium-137 from, efficiency of zeolite prefilter for, 25:18621 (DP-1245)
  solidification of high-level, by fluidized bed calcination, 25:18630

RADIOAPPLICATORS
  dose calculations for radium-226, use of computers for γ, 25:19004
  effectiveness of iridium-192, for therapy of neoplasms of human mouth and tongue, 25:19080
  implantation using afterloading techniques, 25:19076
  leak testing radium-226, by gamma counting radon daughters, 25:19016

RADIOCHEMICAL PROCESSING PLANTS
  design and operation of Karlsruhe WAK, safety aspects of, 25:18566(T) (ORNL-tr-2370)
  design and safety of, at Tokai, Japan, 25:18631
  development of Japanese, 25:18570
  maintenance, operation, and safety procedures for TURF, 25:18564 (ORNL-4629, pp 10-13)
  radiation dosimetry at, detectors for neutron, 25:18800(T) (SC-T-71-3009)

RADIOFREQUENCY SPECTROMETERS
  circuit for NMR, discrete frequency sweep synthesizer, 25:18848

RADIOGRAPHY, BIOMEDICAL
  conference, abstracts of papers presented, 25:19052
  developments in, 25:18870
  effectiveness of percutaneous retrograde arteriography for diagnosis of vascular diseases of brain, 25:19040
  neutron source evaluation for, 25:19034(T) (AEC-tr-7219)
  radiation dose to man during diagnostic, method for measurement of x, 25:19038
  radiation dose to tissues of human head and neck during dental, using intracavitary machine, x, 25:19001

RADIOGRAPHY, INDUSTRIAL
  development of neutron camera for, using californium-252 source, 25:18617
  developments in, 25:18870
  equipment for neutron, design of, 25:18618(P)
  equipment for underwater, design of, 25:18614(P)
  method for color film, using x radiation, 25:18612(T) (LIB/Trans-324)
  method[illegible] uses of neutron, review on, 25:18615
  radiation source position in, device for determining exact, 25:18567(P)

RADIOIMMUNOASSAY
  method for measuring content of plasma renin by quantitation of angiotensin I, 25:18920

RADIOISOTOPE SCANNERS
  data display system for, 25:19053
  data display system for scintillation, multicolored, 25:18653(P)
  image enhancement in, use of modulation transfer function for, 25:18650

RADIOISOTOPES
  book: Isotopes: Reference Tables. Volumes I and II, 25:20264
  book: Problems of Protection in Industrial Utilization of Radioelements, 25:18996
  determination in mixtures, calculation of lower limits of detection for gamma spectroscopic, 25:18746
  determination in radiopharmaceuticals, ionization chamber for mCi, 25:18723
  determination in urine, self-volume standards for, 25:18361
  disbursement and inventory of, development of computer data system for, 25:19050
  dosimetry of internally-deposited, use of human phantoms and computer calculations based on decay schemes for, 25:18991 (ORNL-4584, pp 200-22)
  half-lives of, statistical determination of mean, (T), 25:20498
  half-lives of, table of, (E), 25:20368 (JAERI-Memo-4189)
  hazards of corrosion-product, from nuclear submarines, 25:19014
  hazards to public from consumer products containing, analysis of procedures for control of, 25:19015
  incorporation in hormones for use in diagnostic nuclear medicine, 25:19037
  production and use in Japan, review on, 25:18607
  production of medium- and short-lived, in research reactors for use in biological and medical studies, 25:18886
  removal from man, rules for clinical and therapeutic procedures for, 25:18975 (CEA-N-1365)
  sales and shipments of USAEC-produced, list of Fy 1970 customers for, 25:18593 (ORNL-IIC-32)
  shipping, insurance coverage and safety of, 25:19017
  transport in food chains of nuclear power plant stack-released, PATHWAY computer program for simulating, 25:18526 (ORNL-4584, pp 37-40)
  transport through food chains in Finland, 25:18928(R) (NYO-3446-14)
  uptake and transport in plant tissues, (E/T), 25:18892 (NP-18641)
  use as heat source for mercury turbogenerators for undersea operation, 25:18600(P)
  use for diagnosis in nuclear medicine, review of, 25:19037
  use for improvement of surgical efficiency in gynecology, methods for, 25:19070
  use for tracer studies on ecology and population dynamics of ticks, 25:18934(R) (ORO-3514-10)
  uses in Japanese industry, review on, 25:18608
  uses in measuring density and water content of concretes and soils, review of, 25:18599

RADIOMETRIC ANALYSIS
  developments in, 25:18870
  standards for, evaluation of self-volume, 25:18361

RADIOPRESERVATION
  dosimeter for use in high dose level, 25:18803(P)

RADIOPROTECTIVE COMPOUNDS
  action mechanisms of SH-containing, 25:19021

RADIOSTERILIZATION
  dosimeter for use in high dose level, 25:18803(P)

RADIOTHERAPY
  dose curve calculations for, use of computers in, 25:19000
  effectiveness for carcinomas of human mouth, 25:19081
  effectiveness for treatment of neoplasms of head, neck, and pelvis, 25:19088
  effectiveness for treatment of neoplasms of human larynx, mouth, or pharynx, comparison of effectiveness of high-dose, with surgery, 25:19083
  effectiveness in patients with lung neoplasms, use of pretreatment radioisotope scanning of brain and liver for metastases in evaluation of, 25:19047
  effectiveness of, effects of LET on, 25:19077
  evaluation of meson π^-, 25:19078
  methods for prevention of neoplastic lesions following dental, 25:19069
  planning for rotational, criteria for, 25:19067
  surface irregularities in high energy electron, use of wax retraction for compensating effects of, 25:19066

RADIUM
  performance as gamma source for radiometric rock analysis, 25:18524
  use for implant therapy, evaluation of applicators and methods for, 25:19076

RADIUM ISOTOPES Ra-223
  alpha decay of, alpha and gamma spectra and α--γ angular correlations from, (E), 25:20456

RADIUM ISOTOPES Ra-224
  carcinogenicity in man, following ingestion or injection, 25:18979 (BRH/DBE-70-5)
  radiation dose to man following ingestion or injection of, review of, 25:18979 (BRH/DBE-70-5)

RADIUM ISOTOPES Ra-226
  alpha decay of, relative γ-ray intensities from, (E), 25:20425
  carcinogenicity in dogs, man, and mice, following ingestion or injection, 25:18979 (BRH/DBE-70-5)
  content of human diet, placental tissues, and teeth in high natural background areas in Brazil, 25:18927 (NP-18670)
  content of man in Finland from natural sources, 25:18931 (NYO-3446-14, Paper 30)
  determination in marine sediments off Tarapur Coast, 25:18354
  radiation dose to dogs, man, and mice following ingestion or injection of, review of, 25:18979 (BRH/DBE-70-5)

RADIUM ISOTOPES Ra-228
  content of human diet on Kerala coast, India, 25:19143
  content of man in Finland from natural sources, 25:18931 (NYO-3446-14, Paper 30)

RADON
  gamma constants for radiotherapy applicators of, specific, 25:19002

RADON ISOTOPES Rn-200
  alpha decay of, alpha spectra, half-life, and branching ratio for, (E), 25:20451

RADON ISOTOPES Rn-201
  alpha decay of, alpha spectra, half-life, and branching ratio for, (E), 25:20451

RADON ISOTOPES Rn-202
  alpha decay of, alpha spectra, half-life, and branching ratio for, (E), 25:20451

RADON ISOTOPES Rn-203
  alpha decay of, alpha spectra, half-life, and branching ratio for, (E), 25:20451

RADON ISOTOPES Rn-204
  alpha decay of, alpha spectra, half-life, and branching ratio for, (E), 25:20451

RADON ISOTOPES Rn-205
  alpha decay of, alpha spectra, half-life, and branching ratio for, (E), 25:20451

RADON ISOTOPES Rn-206
  alpha decay of, alpha spectra, half-life, and branching ratio for, (E), 25:20451

- RADON ISOTOPES Rn-207
  - alpha decay of, alpha spectra, half-life, and branching ratio for, (E), 25:20451
- RADON ISOTOPES Rn-208
  - alpha decay of, alpha spectra, half-life, and branching ratio for, (E), 25:20451
- RADON ISOTOPES Rn-218
  - alpha decay of, half-life measurement of, 25:18703
- RADON ISOTOPES Rn-219
  - energy levels from radium-223 decay, spins and parities of, (E), 25:20456
- RADON ISOTOPES Rn-222
  - content of man in Finland from natural sources, 25:18931 (NYO-3446-14, Paper 30)
  - decay scheme for, 25:19016
  - determination of content in air of daughters of, by alpha spectroscopy, 25:18363
  - determination of daughters of, method for alpha spectrometric, 25:18768
  - effects on osteodystrophy in man following inhalation, 25:19144
- RAINWATER
  - fallout content of, in Finland, 25:18931 (NYO-3446-14, Paper 30)
- RARE EARTH ISOTOPES
  - energy levels of, Nilsson model calculations of equilibrium deformations of, (T), 25:20367 (INR-P-1216)
  - nuclear rotation in, angular momentum projection approach to, (T), 25:20541
- RARE EARTH SULFIDES
  - phase studies of mixed binary, 25:19286
- RARE EARTHS
  - abundance in α^2 CVn, (E), 25:19339
  - determination using 4,5-dihydroxy-m-benzenedisulfonic acid, in presence of Eriochrome Cyanine R, titrimetric, 25:18348
  - retention of aerosols of liquid, in alveolar lipoprotein of monkeys and rats, use of lanthanum-140 to demonstrate stability of complex formed following in vitro and in vivo, 25:18889 (CEA-CONF-1676)
  - separation by solvent extraction, review on, 25:18510
  - separation of fission product, by cation exchange using α-hydroxyisobutyric acid as eluant, 25:18501 (RCN-131)
- RARE GASES
  - diffusion in solids, 25:19785
- RATS
  - aerosol retention in alveolar lipoproteins of, use of lanthanum-140 to demonstrate stability of complex formed following in vitro and in vivo actinide and lanthanide liquid, 25:18889 (CEA-CONF-1676)
  - cesium-137 content of cotton, in Southeast USA during 1969, 25:18935(R) (ORO-3905)
  - gallium-67 radiation dose to, following intravenous administration as citrate, 25:18992
  - iron-59-labeled iron ferricyanide transport through gastrointestinal tract of, 25:18887
  - mercury content in blood and kidneys of, neutron activation determination of, 25:18369
  - radiation effects on arylsulphatase activity in urine of, whole-body x, 25:18905
  - radiation effects on circulatory system in transplanted Walker carcinoma tumors in, revascularization following, 25:19111
  - radiation effects on function and structure of parotid glands in, x, 25:19119
  - radiation effects on growth and incidence of malformations of embryos of, effects of exposure rate and protracted dose on x, 25:19117
  - radiation effects on incorporation of carbon-14-labeled pyruvate into tricarboxylic acid cycle in thymocytes of, in-vitro x, 25:18902
  - radiation effects on maturation of cerebellar cortex in, postnatal x, 25:19114
  - radiation effects on peripheral blood of, effects of trithiodipropanol on x, 25:19131
  - radiation effects on permeability of cell membranes in thymus of, to magnesium ions, protective effects of esculamine against x, 25:19025
  - radiation effects on serum antihyaluronidase activity and skin permeability of, protective effects of mercamine and serotonin against γ, 25:19031
  - radioactive corrosion product sorption by intestine of, 25:19014
  - radioisotope content of excreta and tissues of, comparison of direct and treated-sample determinations of, 25:18997
- REACTIVITY
  - measurement of, automatic adjustment of simulated source for analog meters for, 25:18855(P)
- REACTOR CONTAINMENT STRUCTURES
  - fabrication of steel, procedures for, 25:20715
  - testing of steel, procedures for, 25:20715
- REACTOR CONTAINMENT SYSTEMS
  - aerosol distribution in water cooled reactor, effects of accident conditions on radioactive, (E/T), 25:20758 (CONF-700816-(Vol.1), pp 72-101)
  - aerosol removal by water cooled reactor, effects of coolant loss accident conditions on radioactive, (E), 25:20782 (CONF-700816-(Vol.1), pp 102-27)
  - tritium removal by isotope exchange, catalytic effects of activated carbon on, 25:18385 (CONF-700816-(Vol.1), pp 278-88)
  - xenon-133 removal by isotope exchange, catalytic effects of activated carbon on, 25:18385 (CONF-700816-(Vol.1), pp 278-88)
- REACTOR CONTROL ELEMENTS
  - drive system for, design of reactor coolant actuated hydraulic, 25:20839(P)
  - materials for, preparation of improved, 25:19264(P)
- REACTOR CONTROL SYSTEMS
  - book: Instrumentation and Control Operations of Nuclear Power Plants, in Russian, 25:20713
  - design requirements of pressurized water reactor, 25:20551
  - development of flowing gas for direct cycle gas turbine gas cooled power reactor, 25:20712
  - development of flowing gas, for direct cycle gas turbine helium cooled power reactor, 25:20777
  - maintenance requirements of redundant, 25:20552
  - reliability of redundant, 25:20552
- REACTOR EXPERIMENTAL FACILITIES
  - data collection system for neutron time-of-flight, 25:18765
  - neutron spectra at beam hole of Merlin, (E), 25:20798
- REACTOR FUEL ELEMENTS
  - alpha sources on surfaces of, ionization chamber for monitoring, 25:18636(P)
  - cladding for, development of high-temperature, 25:19179
  - cladding for, properties of alloys of aluminum, beryllium, magnesium, vanadium, and zirconium for use as, 25:19203
  - compatibility of sodium-bonded uranium carbide, with Type 316 and 347 stainless steel cladding at 700°C, 25:19276
  - composition of water cooled irradiated, calculation of plutonium-236 and plutonium-238, 25:20733 (BNWL-1523)
  - degasification rates for, computer program for calculation of, 25:19195 (ORNL-TM-3220)
  - design of metal sheathed, with means for fission gas removal, 25:20843(P)
  - design parameters for cylinder shaped fast, calculation of stresses for optimum, (T), 25:20732 (AERE-R-6516)
  - development of fast breeder, problems with, 25:20708
  - dismantling of irradiated assemblies, description of remote handling equipment for, 25:20554
  - elasticity of irradiated, equipment for in-cell measurement of modulus of, 25:19279
  - fabrication costs for CANDU and water cooled reactors, 25:20731 (AECL-3780)
  - fission product migration from HTGR-type, (E), 25:20747(R) (NP-18668)
  - handling of gas cooled, equipment and procedures for on-load, 25:20738
  - heat transfer crisis for natural circulation water-cooled bundles of, equation for calculation of, 25:18584
  - heat transfer from, discontinuous finite element method for analysis of transient, 25:18573
  - internal pressure limits at high burnup rates for, (E/T), 25:20741
  - performance of ceramic, effects on power plant economics of, 25:20739
  - preparation by electroforming in baths, description of method for, 25:19269(P)
  - quality control and testing of uranium carbide and uranium carbide--zirconium carbide, 25:18610 (DP-Report-580)
  - radiation effects on intergranular pore density of plutonium dioxide--uranium dioxide pin-type, in-pile, 25:19290 (WHAN-SA-15)
  - radiation effects on structure of plutonium oxide (PuO_2)--uranium oxide (UO_2) rod type, neutron, 25:20836 (WHAN-SA-79)
  - radiation effects on uranium carbide (UC), neutron, 25:20791
  - radiation testing of Zircaloy clad uranium oxide (UO_2), in Halden during 1964 to 1966, (E), 25:20736 (HPR-132)
  - radiation testing of Zircaloy clad uranium oxide (UO_2), dimensional changes, fission gas release, microstructure changes, and burnup from, (E), 25:20735 (HPR-127)
  - storage of spent HTGR-type, methods for long-term, (T), 25:20745 (DP-Report-450)
  - stress in cylinder shaped fast, effect of design parameters on, (T), 25:20732 (AERE-R-6516)
  - temperature distribution at cladding--coolant interface during variable heat transfer, (T), 25:20706
  - thermodynamics of solid or hollow cylinder, FORTRAN 4 computer programs for calculation of, 25:20835 (RT/ING-(70)8)
  - vibration characteristics of end supported, simulation of, (E), 25:20740
- REACTOR FUELS
  - analysis by isotope dilution mass spectrometry, 25:18356 (KR-140)
  - burnup analysis of oxide, mass-spectrometric and radiochemical, 25:18359 (WCAP-3385-56(Pt.2))
  - cycle development for, program for, 25:19260(R) (ORNL-4629)
  - cycle development for, review of worldwide, 25:18603
  - cycle development in Japan, 25:18555
  - cycles for fast breeders, model for optimization of, (T), 25:20752

XUM

- cycles for heavy water moderated reactors in Romania, model for analysis of, 25:20750
- cycles for power reactors, calculation of costs of, 25:20599
- cycles for power reactors, game theory calculations of plutonium cost in, 25:20753
- cycles for thermal breeder reactors, economics of thorium-uranium-233, (T), 25:20746 (JUL-644-RG)
- fission product decay in, time-dependent heat energy release from, (T), 25:20834 (JAERI-Memo-4205)
- preparation of blended fertile and fissile particulate, design of equipment for, 25:19268(P)
- processing of spent, world trend in methods for, 25:18570
- production by breeding in charged-particle accelerators, feasibility of, 25:20190
- radiation testing of coated particle, for high temperature gas cooled reactors, 25:20747(R) (NP-18668)
- reprocessing in Europe, economics and methods of, 25:18500 (NP-18669)
- reprocessing of, recovery of plutonium-238 in, 25:18492 (ANL-7709)
- separation of plutonium from spent, 25:18517
- temperature distribution in clad pellet-type, effects of coefficient of heat transfer on, 25:18589

REACTOR LOADING MACHINES
- design for Essor reactor, 25:18627
- design parameters for gas cooled reactor on-load, 25:20738
- design parameters of gas cooled reactor pressure vessel enclosed, 25:20838(P)

REACTOR SAFETY
- research activities in Japan, summary of April to October 1970, 25:20763(R) (JAERI-Memo-4229)
- research programs on, proposals for German, 25:20687

REACTORS
- accidents in, radiation dose to man from radioisotopes released in, 25:18974 (AHSB(S)R-192)
- coaxial cable for use in, development of radiation hardened, 25:18881(P)
- components for, preoxidation method for zirconium alloy, 25:19180(P)
- coolant flow in rod-packed channels in, resistance and velocity fields in turbulent, 25:18576(T) (AEC-tr-7189)
- cooling systems for, computer program for monitoring, 25:20710 (DP-1244)
- cooling systems of, fission product deposition and distribution in, (T), 25:20730
- core configuration for, with means for assuring uniform neutron flux distribution, 25:20837(P)
- core configuration for, with tube arrangement for introduction of gaseous poison, 25:20714(P)
- core for, equipment for remote positioning of thermocouples in, 25:20842(P)
- dynamics analysis of, CLASSIC code for stability and frequency response calculations in, 25:20830 (AAEC/TM-551)
- fission fragment buildup in, semiconductor detector for selectively monitoring, 25:18651(P)
- heat exchanger supports for, description of rotating, 25:20840(P)
- kinetics equations for, analysis of delayed neutron emitters and secondary decay processes in, (T), 25:20828
- kinetics equations for, temperature formulation of space averaged, (E/T), 25:20829
- kinetics of coupled fast--thermal, correlation technique determinations of, (E/T), 25:20833 (RCN-132)
- kinetics parameters of coupled core, correlation method for analysis of, 25:20827
- maintenance of, development of teletype actuated computer operated remote handling equipment for, 25:20841
- materials for, methods for stress analysis of, 25:18616
- neutron flux distribution near absorbers in, VISTA technique for measurements of, (E/T), 25:20831 (JAERI-Memo-4238)
- neutron flux monitoring in, method for measuring activities of activation probe bodies for, 25:18719(P)
- neutron flux spectra from foil activation measurements in, computer program for determining, (T), 25:18641 (IN-1446)
- neutron transport in cylindrical annular, internal boundary conditions of, (T), 25:20824
- noise analysis in, review of data extraction methods for, 25:20822 (TKK-F-A-137)
- noise measurement in, information theory aspects of, 25:20821 (TKK-F-A-102)
- noise spectra in, effects of neutron energy on, (E/T), 25:20832 (ORNL-TM-3245)
- physics calculations for, PRODGROUP code for production of multigroup constants for, 25:20820 (KFKI-71-4)
- pressure vessels for, development of prestressed concrete, 25:19297
- reactivity measurement of, automatic adjustment of simulated source of analog meter for, 25:18855(P)
- structural plate bending in, finite element method for analysis of, 25:18575

REACTORS, AGR-TYPE
- design with steam generators in wall of prestressed concrete pressure vessel, 25:20698
- economics of power, comparison with other common reactor types of, 25:20749
- fuel element handling in, equipment and procedures for on-load, 25:20738

REACTORS, AIRCRAFT
- design parameters of closed cycle helium cooled, with wing mounted propulsion turbines, 25:20810(P)

REACTORS, BOILING
- economics of power, comparison with other common reactor types of, 25:20749
- fuel elements for, lateral vibration characteristics of, (E), 25:20740

REACTORS, BREEDER
- coolant depressurization incidents in gas cooled, performance of emergency core cooling systems following, (T), 25:20767
- core design for steam cooled, with increased coolant flow in central region, 25:20697(P)
- development of fast, review of, 25:20708
- economics of power, comparison with other common reactor types of, 25:20749
- fuel cycles for thermal, economics of thorium--uranium-233, (T), 25:20746 (JUL-644-RG)
- fuel cycles for, model for optimization of, (T), 25:20752
- fuel elements for, internal pressure limits at high burnup rates in, (E/T), 25:20741
- heat exchangers for sodium-cooled fast, description of intermediate and secondary, 25:18574
- kinetics of fast, (T), 25:20708
- power cycles for, thermodynamic analysis of optimum, (T), 25:20596

REACTORS, CANDU-TYPE
- fuel elements for, fabrication costs for, 25:20731 (AECL-3780)

REACTORS, FAST
- coolant depressurization incidents in gas cooled, performance of emergency core cooling systems following, (T), 25:20767
- coolant for, method for determining hydrogen and oxygen content in, sodium, 25:18863
- coolant loss accident conditions for direct cycle gas turbine gas cooled, computer program analysis of, 25:20765
- core design for steam cooled, with increased coolant flow in central region, 25:20697(P)
- development of breeder, review of, 25:20708
- economics of power, comparison with other common reactor types of, 25:20749
- fuel cycles for, model for optimization of, (T), 25:20752
- fuel elements for, calculation of stresses for optimum design parameters of cylinder shaped, (T), 25:20732 (AERE-R-6516)
- fuel elements for, internal pressure limits at high burnup rates in, (E/T), 25:20741
- heat exchangers for direct cycle gas turbine helium cooled, optimum design parameters of, 25:20775
- heat exchangers for sodium-cooled breeder, description of intermediate and secondary, 25:18574
- kinetics of breeder, (T), 25:20708
- physics calculations for, energy modal synthesis method for, (T), 25:20709
- physics characteristics of, effects of plutonium-239 fission product yields on, (T), 25:20819 (JAERI-Memo-4165)
- power cycles for, thermodynamic analysis of optimum, (T), 25:20596
- safety of sodium cooled, review of problems in, 25:20764 (NP-18487)

REACTORS, FLUID-FUELED
- design parameters of uranium-233 colloid fueled concept, with vortex fuel containment, 25:20811

REACTORS, GAS-COOLED
- control requirements for direct cycle gas turbine power, computer program analysis of, 25:20766
- control system for direct cycle gas turbine power, development of flowing gas, 25:20777
- control system for direct cycle gas turbine power, development of flowing gas, 25:20712
- coolant depressurization incidents in fast breeder, performance of emergency core cooling systems following, (T), 25:20767
- coolant loss accident conditions for direct cycle gas turbine fast, computer program analysis of, 25:20765
- coolant loss accident conditions for direct cycle gas turbine power, computer program analysis of, 25:20766
- coolants for, economic comparison of helium and neon, (T), 25:20729
- core design for, with improved alignment between fuel channels and fuel charge tubes, 25:20695(P)
- design parameters for 1000 MW(e) integrated and non-integrated direct cycle gas turbine, analysis of optimum, 25:20703
- design parameters for high temperature power, with direct cycle gas turbines, 25:20700
- design parameters of aircraft closed cycle helium, with wing mounted propulsion turbines, 25:20810(P)
- design parameters of direct cycle gas turbine power, analysis of optimum economic, 25:20702

development of direct cycle gas turbine power, 25:20699
development of direct cycle gas turbine power, analysis of optimum economic, 25:20701
economics of power, comparison with other common reactor types of, 25:20749
electric generators for power, development of closed cycle gas turbine, 25:20690
fuel cladding for high-temperature, development of materials for, 25:19179
fuel cycle for high temperature, economics of thorium--uranium-233, (T), 25:20746 (JUL-644-RG)
fuel elements for high temperature, methods for long-term storage of spent, (T), 25:20745 (DP-Report-450)
heat exchangers for direct cycle gas turbine fast, optimum design parameters of, 25:20775
heat exchangers for direct cycle gas turbine power, development of dry air, 25:20777
heat exchangers for direct cycle high temperature gas turbine power, design requirements for, 25:20776
heat exchangers for high temperature, heat transfer characteristics of, (E), 25:20780
heat exchangers for, effects of step change of gas inlet temperatures on gas outlet temperatures of counter-flow, (T), 25:20779
kinetics of thorium oxide (ThO_2)--uranium carbide (UO_2) fueled, (E/T), 25:20787 (GAMD-10231)
loading facility for, design of pressure vessel enclosed, 25:20838(P)
materials for, properties of heat-resisting alloy and metal, 25:19197
physics parameters for high temperature, 25:20707
power conversion systems for, design and operating parameters of magnetoplasmadynamic, (T), 25:20768
power cycles for power, comparison of steam and direct gas turbine, 25:20770
pressure vessels for, thermal insulation for prestressed concrete, 25:20727(P)
stand pipe closure and loading machine connections for high temperature, elastomer O-ring seals for, (E), 25:20742 (DP-Report-496)
turbines for 1200 MW(e), design requirements for integrated direct cycle gas, 25:20778
turbines for power, design requirements for direct cycle gas, 25:20772
turbines for power, design requirements for integrated direct cycle gas, 25:20774
turbines for power, development of direct cycle gas, 25:20771
turbines for power, development of indirect cycle carbon dioxide, 25:20773

REACTORS, GAS-FUELED
design of vortex stabilized rocket, with helium gas buffer layer between fuel and propellant, 25:20806(P)

REACTORS, GERMANY
construction of power, proposals of authorization procedures for, 25:20689
construction of power, status of, 25:20568
safety of power, proposals for research programs on, 25:20687
safety of, German authorization procedures, site evaluation, and criteria for, 25:20688

REACTORS, HEAVY WATER-MODERATED
economics of power, comparison with other common reactor types of, 25:20749
fuel cycle efficiency in Romania, model for analysis of, 25:20750
fuel cycle for, economics of thorium--uranium-233, (T), 25:20746 (JUL-644-RG)
multiplication factors for natural uranium lattices in, WIMS code analysis of effective, (T), 25:20818 (AAEC/TM-553)
reactivity of thorium oxide (ThO_2)--uranium oxide (UO_2) lattices in, effects of thorium-232 capture cross section on, (E/T), 25:20377 (WAPD-TM-971)

REACTORS, HETEROGENEOUS
neutron resonance integrals for, IRESINT 2 code for calculation of, 25:20823 (TKK-F-A-139)

REACTORS, LIQUID METAL-COOLED
coolant for, method for determining hydrogen and oxygen content in, sodium, 25:18863
core vessels for, design requirements and stress limits for, 25:20725 (WHAN-SA-46)
fission product removal from sodium cooled, effects of carbon on cesium, (E), 25:20754 (AERE-R-6481)
piping systems for, design requirements and stress limits for, 25:20725 (WHAN-SA-46)
safety of sodium cooled fast, review of problems in, 25:20764 (NP-18487)
shutdown cooling of space, sodium loop and radiator for, 25:20805 (N-70-39420)

REACTORS, MARITIME
air conditioning systems for, design and installation of, 25:20816(T) (JPRS-52443)

REACTORS, MOLTEN-SALT
fuel cycle for, economics of thorium--uranium-233, (T), 25:20746 (JUL-644-RG)

REACTORS, POWER
construction in Germany of, authorization procedures proposals for, 25:20689
construction of German, status of, 25:20568
containment structures for, procedures for fabrication and testing of steel, 25:20715
control requirements for direct cycle gas turbine helium cooled, computer program analysis of, 25:20766
control system for direct cycle gas turbine gas cooled, development of flowing gas, 25:20712
control system for direct cycle gas turbine helium cooled, development of flowing gas, 25:20777
control systems for, methods for maintenance and testing of, 25:20713
coolant boiling in, qualitative physical model of, (E/T), 25:20728
coolant chemistry in CIRENE, effects of ammonia additions on, (E), 25:20726
coolant loss accident conditions for direct cycle gas turbine helium cooled, computer program analysis of, 25:20766
design of thermoelectric generator, for underwater operation, 25:20694(P)
design parameters for 1000 MW(e) integrated and non-integrated direct cycle gas turbine gas cooled, analysis of optimum, 25:20703
design parameters for direct cycle gas turbine gas cooled, analysis of optimum economic, 25:20702
design parameters for high temperature gas cooled, with direct cycle gas turbines, 25:20700
development in Japan, review of fiscal 1969, 25:20696
development of direct cycle gas turbine gas cooled, 25:20699
development of direct cycle gas turbine helium cooled, analysis of optimum economic, 25:20701
economics in South Africa, comparison of enriched and natural uranium systems, (T), 25:20748 (PEL-199)
economics of, effects of ceramic fuel element performance on, 25:20739
economics of, effects of reactor type and power conversion system design on, (T), 25:20749
electric generators for gas cooled, development of closed cycle gas turbine, 25:20690
fuel cycles for, calculation of costs of, 25:20599
fuel cycles for, game theory calculations of plutonium cost in, 25:20753
fuel elements of water cooled, calculation of plutonium-236 and plutonium-238 in irradiated, 25:20733 (BNWL-1523)
heat exchangers for direct cycle gas turbine helium cooled, development of dry air, 25:20777
heat exchangers for direct cycle high temperature gas turbine gas cooled, design requirements for, 25:20776
heat exchangers for, effects of step change of gas inlet temperatures on gas outlet temperatures of counter-flow, (T), 25:20779
kinetics of light water moderated thermionic, for undersea operation, 25:20813 (CEA-CONF-1727)
neutron capture and fission in uranium-235 fueled thermionic, cross sections and resonance parameters for, (T), 25:20826
neutron lifetime and delayed neutron fraction in thermionic, prompt, (T), 25:20825
physics parameters for high temperature gas cooled, 25:20707
power conversion systems for, design and operating parameters of magnetoplasmadynamic, (T), 25:20768
power cycles for helium cooled, comparison of steam and direct cycle gas turbine, 25:20770
safety analysis of Westinghouse pressurized water, reference guide for, 25:20682 (DOCKET-RESARA-2)
safety analysis of Westinghouse pressurized water, reference guide for, 25:20681 (DOCKET-RESARA-1)
safety of, German authorization procedures, site evaluation, and criteria for, 25:20688
safety of, proposals for German research programs on, 25:20687
steam separator for water cooled, design parameters and operation characteristics of trap cyclone, 25:20769
steam separator system for water cooled, 25:20743(P)
turbines for 1200 MW(e) helium cooled, design requirements for integrated direct cycle gas, 25:20778
turbines for helium cooled, design requirements for direct cycle gas, 25:20772
turbines for helium cooled, design requirements for integrated direct cycle gas, 25:20774
turbines for helium cooled, development of direct cycle gas, 25:20771
turbines for helium cooled, development of indirect cycle carbon dioxide, 25:20773

REACTORS, PRESSURIZED-WATER
control system for, design requirements of, 25:20551
coolant loss accidents in, analysis of radioiodine release from, 25:20756 (CONF-700816-(Vol.1), pp 9-25)
core for, reactivity coefficient, control rod worths, burnup, and power distribution in plutonium oxide (PuO_2)--uranium oxide (UO_2), (E/T), 25:20705 (WCAP-3385-55)
economics of power, comparison with other common reactor types of, 25:20749
pumps for, performance characteristics of primary coolant, 25:20717(T) (JPRS-52384)
radioactive effluents from, effects of coolant loss accidents on release of radioiodine, 25:20756 (CONF-700816-(Vol.1), pp 9-25)
safety analysis of Westinghouse power, reference guide for, 25:20681 (DOCKET-RESARA-1)

safety analysis of Westinghouse power, reference guide for, 25:20682 (DOCKET-RESARA-2)

REACTORS, PROCESS HEAT
bibliography on desalination, annotated, 25:20812 (TID-25653)

REACTORS, RESEARCH
experimental facilities for DORF pulsed, shielding of gamma spectrometer, 25:18732 (AD-711531)
fuel elements for U.S.S.R. BR-5, radiation effects on uranium carbide (UC), 25:20791
handling equipment for Essor, design of, 25:18627
kinetics of beryllium reflected core for ASTRA, (E), 25:20796
neutron spectra at beam hole of Merlin, (E), 25:20798
reactivity of ASTRA, effects of beryllium reflector on subcritical, (E), 25:20795
reactivity of FMRB uncoupled cores, effects of heavy water reflector tank on, (E), 25:20797

REACTORS, ROCKET
design of vortex stabilized gaseous core, with helium gas buffer layer between fuel and propellant, 25:20806(P)
design parameters of uranium-233 colloid fueled concept, with vortex fuel containment, 25:20811

REACTORS, SUPERHEATING
core design for steam cooled, with increased coolant flow in central region, 25:20697(P)

REACTORS, THERMAL
fuel cycles for breeder, economics of thorium--uranium-233, (T), 25:20746 (JUL-644-RG)
neutron flux mapping in, performance of in-core regenerative detectors for, (E), 25:20711 (WHAN-FR-37)
neutron lifetime and delayed neutron fraction in thermionic, prompt, (T), 25:20825
power cycles for, thermodynamic analysis of optimum, (T), 25:20596

REACTORS, U.S.S.R.
design parameters of, 25:20549(T) (AEC-tr-7187)
development of, 25:20549(T) (AEC-tr-7187)

REACTORS, WATER-COOLED
accidents in, analysis of radioactive aerosol release from, (E/T), 25:20758 (CONF-700816-(Vol.1), pp 72-101)
containment system for, analysis of accidents release of radioactive aerosols in, (E/T), 25:20758 (CONF-700816-(Vol.1), pp 72-101)
containment system for, effects of coolant loss conditions on performance of air cleaning equipment for, (E), 25:20782 (CONF-700816-(Vol.1), pp 102-27)
coolant boiling in, methods for detection of local, (E), 25:20716 (CEA-R-4118)
coolant chemistry in, control of, (E), 25:20718(T) (LIB/Trans-308)
coolant heat transfer in, effects of turbulence around fuel rods on, 25:18580
coolant loss accidents in, analysis of radioactive aerosol removal by containment system filters during, (E), 25:20782 (CONF-700816-(Vol.1), pp 102-27)
coolant loss accidents in, NURLOC-1.0 code analyses of core temperatures following, 25:20762 (JAERI-Memo-4194)
cooling systems of, review of static seals for primary, 25:20719 (ORNL-TM-3308)
design parameters of uranium oxide (UO_2) fueled thermionic, for underwater operation, 25:20817(P)
economics of power, comparison with other common reactor types of, 25:20749
fuel elements for, fabrication costs for, 25:20731 (AECL-3780)
fuel elements of power, calculation of plutonium-236 and plutonium-238 in irradiated, 25:20733 (BNWL-1523)
pressure vessels for, performance and properties of steel, 25:19222
steam separator for power, design parameters and operation characteristics of trap cyclone, 25:20769
steam separator system for power, 25:20743(P)

REACTORS, WATER-MODERATED
kinetics of thermionic power, for undersea operation, 25:20813 (CEA-CONF-1727)

RECOILS
detection of heavy, from heavy-ion nuclear reactions, gas-filled magnetic separator for, 25:18851
implantation in substrates by rare gas-ion bombardment, 25:19786

REFRIGERATION
design of system of, using superfluid properties of helium-4, 25:19640
equipment for, helium-4 evaporation, 25:19632

REGGE POLE THEORY
absorption corrections and cuts for strong interactions in, lectures on, 25:19976
angular momentum for strong interactions in, review of complex, 25:19974
cuts for minima and polarization in elastic and charge-exchange π + N interactions in, non-Pomeranchuk, 25:20006
cuts for scattering amplitudes in, absorption and Glauber models for, 25:19992
dual amplitudes in, method of coherent states for factorization of N-point, 25:20120
duality for strong interactions in, lectures on, 25:19978
duality in, lectures on, 25:20102 (NP-18705)
duality--finite-energy-sum-rule method for width of eta → π^0 + 2γ decay in, 25:19937 (DEMO-71/2)
eikonal model in, validity of, 25:20115
exchange degeneracies in, review of patterns of, 25:20124
model for anti p + p → anti n + n and p + n → p + n interactions in, singular-pole, 25:19995
model for forward π + N → ω + N interactions at high energies in, differential and total cross sections and t dependence of density matrix elements in, 25:20008
moments method with branching in j-plane for differential cross sections of p + n → n + p and anti p + p → anti n + n interactions in, complex, 25:20017(T) (CERN-Trans-70-15)
multiperipheral nonfactorization, signature, and Toller-angle variable cuts in, 25:20109
poles in single-particle production spectrum from high-energy interactions in, triple asymptotic limit for, 25:19926 (NYO-2262-TA-234)
Pomeranchuk theorem violation predictions for π^- + p and π^+ + p interactions at low energies, 25:20005
scattering amplitude with eikonal structure from multiple Reggeon exchange in, 25:20111
scattering amplitudes in, divergent helicity sums in multiparticle, 25:20110
strong interactions in, lectures on, 25:19977
trajectories in, review of rho, π, and N, (E), 25:19588
trajectories of bound states of π--N systems in, Bethe--Salpeter equation in ladder approximation for, 25:20007

RELATIVE BIOLOGICAL EFFECTIVENESS
calculation for fast neutrons relative to 250 kV x rays, 25:19092

RELATIVITY THEORY
charged-particle radiation in, uniformly accelerated, 25:19944
Einstein field equations in general, short-ranged scalar gravity in, 25:20093
Einstein unified field theory in, nonexistence of spherically symmetric solution for vacuum electrostatic field in, 25:20088
Einstein--Maxwell field equations in, properties of cylindrically symmetric, 25:20086
fermion structures in general, conserved, 25:20089
gravitational collapse in general, lectures on, 25:19465
Lagrangian function in special, formulation of, 25:20064
mechanics in, theorem and potentials for, 25:20084
quantization of general, time and state functional in, 25:20095
space-time in, torsion-free world lines in curved, 25:20100
symmetry for general, semidirect product for BMS group in, 25:20091
symmetry for linearized general, semidirect product for invariance group in, 25:20091
test of general, metric for 4th, 25:20097

REMOTE-HANDLING EQUIPMENT
design for Essor reactor, 25:18627
design parameters for irradiated fuel assemblies dismantling, 25:20554
design parameters of thermocouples, for in-core positioning, 25:20842(P)
development of teletype actuated computer operated, for reactor maintenance, 25:20841

RENIN
content in blood plasma, radioimmunoassay method for measuring, 25:18920

REPRODUCTIVE SYSTEM
radiation effects on human male, following therapy for malignant lymphomas, 25:19147

REPUBLIC OF SOUTH AFRICA
power reactor economics in, comparison of enriched and natural uranium, (T), 25:20748 (PEL-199)
scientific research in universities of, 25:20871 (NP-18701)

RESINS
fission fragment energy loss in, (E), 25:20442
properties of phenolic, with hydroxamic group for purification of uranium solutions, 25:18503 (RT/CHI-(70)25)
radiation effects on curing of thermally stable vinyl halide, 25:18437(P)
radiation effects on mechanical properties of graphite cloth laminates of, γ, 25:18421(R) (RLO-2098-1)
radiation hardening of polyester, 25:18443
radioinduced crosslinking of vinyl ester, for coatings, electron, 25:18439(P)

RESISTORS
electric conductivity of gallium- and boron-implanted layers in silicon, temperature coefficient of, 25:19783

RETICULO-ENDOTHELIAL SYSTEM
scanning of human, preparation of technetium-99-labeled rhenium sulfide colloid for, 25:19054

RHENIUM
analysis for molybdenum by extraction photometry using 5,7-dibromo-8-quinolinol, 25:18353
chromatographic behavior in hydrochloric acid--thiocyanate mixture on Amberlite LA-2, 25:18337
compatibility of fuel capsules of, with cobalt oxides under welding conditions, 25:18591(R) (DP-1254)
compatibility with cobalt aluminate at high temperatures,

XUM

  25:18591(R) (DP-1254)
  compatibility with cobalt magnesium oxide at high temperature, 25:18591(R) (DP-1254)
  compatibility with cobalt oxide at high temperatures, 25:18591(R) (DP-1254)
  reactions with cobalt in air at high temperatures, 25:18591(R) (DP-1254)
RHENIUM ALLOYS AND SYSTEMS
  Dy--Re--Th, crystal structure of intermetallic compounds of, 25:19235
  Er--Re--Th, crystal structure of intermetallic compounds of, 25:19235
  Gd--Re--Th, crystal structure of intermetallic compounds of, 25:19235
  Mo--Re, faulting in filings of, x-ray diffraction search for, 25:19248
  Re--Tb--Th, crystal structure of intermetallic compounds of, 25:19235
  Re--W, thermal loading to induce boiling on wires of, parameters for critical, 25:18583
  Re--W-base, reactions with cobalt in air at high temperatures, 25:18591(R) (DP-1254)
RHENIUM CHLORIDES
  reactions with uranyl chloride, mechanisms of, 25:18384
RHENIUM ISOTOPES Re-185
  energy-level transitions in, intensities of, (E), 25:18772
RHINE RIVER
  heating of, effects of nuclear and steam power plants thermal effluents on, 25:20685
RHODIUM
  chromatographic behavior in hydrochloric acid--thiocyanate mixture on Amberlite LA-2, 25:18337
  superconductivity of, possibility of, 25:19606
RHODIUM ALLOYS AND SYSTEMS
  Ir--Rh, superconducting properties of fcc solid solutions of, (E), 25:19606
  Nb--Rb, crystallization of solid-solution, mechanisms of, 25:19242
  Os--Rh, superconducting properties of fcc solid solutions of, (E), 25:19606
  Rh--Ru, magnetic susceptibility at 4 to 300°K, 25:19874
  Rh--Tc, magnetic susceptibility at 4 to 300°K, 25:19874
RHODIUM ISOTOPES Rh-100
  energy level at 74.8 keV from palladium-100 decay, half-life and g-factor for, (E), 25:20454
RHODIUM ISOTOPES Rh-102
  half life of metastable, 25:18590(R) (BNWL-1308-4)
RHODIUM ISOTOPES Rh-103
  energy levels from ruthenium-103 decay, spin-parity assignments for, (E), 25:20404
RIVERS
  radioactive contamination of, development of computer model for study of, 25:18940
ROBERT E. GINNA POWER REACTOR, UNIT 1
  control rods for, revised technical specifications for insertion limits and shutdown margin for, 25:20623 (DOCKET-50244-61)
  coolant loss accident conditions for, calculation at increased power of, 25:20624 (DOCKET-50244-62)
  emergency core cooling system requirements for, calculation at increased power of, 25:20624 (DOCKET-50244-62)
  fuel element storage pool for, design parameters of charcoal filter system for spent, 25:20625 (DOCKET-50244-63)
  operations history for April to December 1970, 25:20591 (DOCKET-50244-66)
  operations incident of January 25, 1971, failure of 1A diesel generator to start, 25:20590 (DOCKET-50244-65)
  operations incident of July 6, 1970, corrective actions for primary coolant dilution, 25:20589 (DOCKET-50244-64)
  pumps for, failure of support stud for cooling system, 25:20622 (DOCKET-50244-60)
ROCKETS
  aerodynamic forces and dynamic stability of high-speed magnetically suspended, 25:20890 (SC-DR-70-867)
ROCKS
  analysis for barium and strontium by isotope dilution mass spectrometric, neutron activation, gravimetric, and other spectrometric methods, 25:18335
  analysis for trace amounts of uranium after chromatographic separation on silica gel column, spectrophotometric, 25:18345
RODS
  heat transfer from nonuniformly heated, in turbulent liquids, equation for calculation of, 25:18580
ROTORS
  use of superconductors in rotating electric machines, 25:19635
RUBBER
  thickness measurement for manufacture of tires, beta backscatter gage for, 25:18824
RUBIDIUM
  electron scattering at 0.3 to 9 eV by, absolute total cross sections for, (E), 25:19506
  scattering by carbon tetrachloride, iodomethane, and tin chloride, crossed-beam measurements and optical-model analysis of, 25:19497
  separation from cesium by solvent extraction, review on, 25:18510
RUBIDIUM IONS
  implantation in silicon at 40 keV, electrical properties of, 25:19780
RUBIDIUM ISOTOPES Rb-86
  half-life, (E), 25:20339
RUBIDIUM ISOTOPES Rb-87
  content of man in Finland from natural sources, 25:18931 (NYO-3446-14, Paper 30)
RUBIDIUM ISOTOPES Rb-90
  beta decay of, β and γ singles and coincidence spectra from, (E), 25:20384
  energy levels from krypton-90 decay, (E), 25:20384
RUBIDIUM ISOTOPES Rb-91
  beta decay of, γ spectra from, (E), 25:20459
  energy levels from krypton-91 decay, (E), 25:20459
RUPTURE
  mechanics of flawed specimen, three-dimensional elastic--plastic strain and stress analysis of, 25:18611 (HSSTP-TR-12)
RUTHENIUM
  chromatographic behavior in hydrochloric acid--thiocyanate mixture on Amberlite LA-2, 25:18337
  detection in low-energy cosmic radiation, (E), 25:19525
  determination in high-burnup plutonium dioxide fuel by isotope dilution mass spectrometry, 25:18356 (KR-140)
  grain growth of fission-product, in uranium dioxide rods, effects of thermal gradients on, 25:19278
  separation from seawater by flocculation, 25:18518
RUTHENIUM ALLOYS AND SYSTEMS
  Nb--Ru, crystallization of solid-solution, mechanisms of, 25:19242
  Rh--Ru, magnetic susceptibility at 4 to 300°K, 25:19874
  Ru--Tc, magnetic susceptibility at 4 to 300°K, 25:19874
RUTHENIUM ISOTOPES Ru-94
  nuclear mass, (E), 25:20436
RUTHENIUM ISOTOPES Ru-95
  energy levels and transitions from ruthenium-96 (p,d) reactions, (E), 25:20436
RUTHENIUM ISOTOPES Ru-96
  proton reactions (p,d) and (p,t) at 31.5 MeV, Q-values and angular distributions for, (E), 25:20436
RUTHENIUM ISOTOPES Ru-99
  energy levels of, isomer shifts and changes in nuclear charge radii between, (E), 25:20403
RUTHENIUM ISOTOPES Ru-100
  proton reactions up to several GeV, cascade calculations of double differential distributions of particles from, (T), 25:20018 (JINR-P2-5507)
RUTHENIUM ISOTOPES Ru-101
  energy levels of, isomer shifts and changes in nuclear charge radii between, (E), 25:20403
  isomeric transitions in, gamma spectra from, (E), 25:18753
RUTHENIUM ISOTOPES Ru-103
  beta decay of, γ-γ angular correlations for, (E), 25:20404
RUTHENIUM ISOTOPES Ru-106
  accumulation by marine organisms, effects of physico-chemical form on, 25:18894
  content of flesh and shells of mussels, effects of cooking on, 25:18896
  content of man in Finland from artificial sources, 25:18931 (NYO-3446-14, Paper 30)
  content of marine algae following radioactive waste disposal, 25:18939
  content of organisms in seawater, comparison between soluble and insoluble forms of, 25:18944
  content of plants in Finnish Lapland during 1968 and 1969, 25:18932 (NYO-3446-14, Paper 31)

S

S-MATRIX
  element renormalization for, Kadyshevskii p-representation for, 25:20123
  theory for interactions $\pi + \pi$, lectures on nonlinear techniques in, 25:20107
  theory for, lectures on nonlinear techniques in, 25:20107
  vacuum theory in dynamic, 25:20078
SAINT LAURENT-DES-EAUX REACTOR (EDF-4)
  construction of, design parameters of service structures for, 25:20562
SAINT LAURENT-DES-EAUX REACTOR, UNIT 2
  construction of, design parameters of service structures for, 25:20562
SALICYLANILIDE
  effects on hemolysis of uv-irradiated erythrocytes, 25:18914
  toxicity evaluation using photohemolysis of erythrocytes, 25:18913
SALT DEPOSITS
  radioactive waste disposal in Lyons, Kans., feasibility study of facility for high- and low-level solidified, 25:18623 (ORNL-4584, pp 16-36)
SAMARIUM
  chromatographic behavior in hydrochloric acid--thiocyanate mixture on Amberlite LA-2, 25:18337
  determination in high-burnup plutonium dioxide fuel by

XUM

  isotope dilution mass spectrometry, 25:18356 (KR-140)
  electron band structure of, x-ray photoelectron study of 4f levels in, 25:19866
SAMARIUM ALLOYS AND SYSTEMS
  Co--Cu--Fe--Sm, magnetic properties of $Sm(Fe,Co,Cu)_5$, (E), 25:19875
  Co--Fe--Sm, magnetization of SmFe/sub x/Co/sub 5-x, saturation, (E), 25:19875
SAMARIUM FLUORIDES
  SmF_3--Sm_2O_3, phase studies of, 25:19285
SAMARIUM IONS
  wave functions for, accurate numerical Hartree--Fock self-consistent field, 25:19478
SAMARIUM ISOTOPES Sm-145
  electron-capture decay of, γ spectra from, (E), 25:20465
SAMARIUM ISOTOPES Sm-146
  energy levels from europium-146 beta and electron-capture decay, (E), 25:20474
SAMARIUM ISOTOPES Sm-147
  alpha decay of, α energy and half-life for, (E), 25:20391
SAMARIUM ISOTOPES Sm-148
  alpha decay of, α energy and half-life for, (E), 25:20391
  energy levels from promethium-148 decay, model analysis of, (E/T), 25:20352
  proton elastic and inelastic scattering at 16 MeV, differential cross sections and deformation parameters for, (E/T), 25:20477
SAMARIUM ISOTOPES Sm-149
  alpha decay of, search for, 25:20391
SAMARIUM ISOTOPES Sm-152
  energy levels, from Coulomb excitation lifetime measurements for, (E), 25:20409
  energy-level transitions in, direction correlations and multipolarities for, (E), 25:20385
  nuclear rotation in, angular momentum projection approach to, (T), 25:20541
  oxygen-16 scattering at 60 MeV with Coulomb excitation, Doppler shift attenuation in γ spectra from, (E), 25:20409
  sulfur-32 scattering at 94 to 110 MeV with Coulomb excitation, Doppler shift attenuation in γ spectra from, (E), 25:20409
SAMARIUM ISOTOPES Sm-153
  beta decay of, conversion electron spectra from, 25:20421
  half-life, (E), 25:20338
  half-life, (E), 25:20339
SAMARIUM ISOTOPES Sm-154
  alpha inelastic scattering at 27.5 to 32.5 MeV, cross sections for, (E), 25:20466
  nuclear mass distribution of, hexadecapole term in deformation parameter for, (E/T), 25:20466
  proton elastic and inelastic scattering at 16 MeV, differential cross sections and deformation parameters for, (E/T), 25:20477
SAMARIUM OXIDES
  physical properties of molten, to 3000°C, equipment and methods for measuring, 25:19273 (BNWL-SA-3579)
  Pm_2O_3--Sm_2O_3, phase studies of, 25:19273 (BNWL-SA-3579)
  Sm_2O_3-base--SrO, phase diagram at 1300 to 2000°C, 25:19284
  SmF_3--Sm_2O_3, phase studies of, 25:19285
SAMPLING
  method of sequential, by variables with known variance of output and specification range with upper and lower limit for variables, 25:20883(T) (ORNL-tr-2355)
SAN ONOFRE POWER REACTOR, UNIT 2
  operations aspects of, revised and additional data on, 25:20677 (DOCKET-50361-15)
SAN ONOFRE POWER REACTOR, UNIT 3
  design parameters of, revised and additional data on, 25:20677 (DOCKET-50361-15)
  design parameters of, revised and additional data on, 25:20677 (DOCKET-50361-15)
  operations aspects of, revised and additional data on, 25:20677 (DOCKET-50361-15)
SANDSTONE
  radiation effects on properties of, for use in concrete shielding aggregates, neutron, 25:19296
SAPPHIRES
  Kapitza resistance of junction with indium, effects of superconducting transition on, (E/T), 25:19616
SAXTON POWER REACTOR
  fuel elements for, proposed changes for Core 3 plutonium oxide (PuO_2)--uranium oxide (UO_2) and uranium oxide (UO_2) rod type, 25:20582 (DOCKET-50146-68)
  fuel subassemblies for, technical specifications for operation without center rod position flux thimbles, 25:20609 (DOCKET-50146-69)
  fuels for, burnup of plutonium oxide (PuO_2)--uranium oxide (UO_2), 25:18359 (WCAP-3385-56(Pt.2))
  operation of, performance of plutonium oxide (PuO_2)--uranium oxide (UO_2) core in, (E/T), 25:20705 (WCAP-3385-55)
SCANDIUM
  abundance in α And, (E), 25:19343
  abundance in meteorites, (E), 25:19302
  abundance in Type-M supergiant, (E), 25:19323
  chromatographic behavior in hydrochloric acid--thiocyanate mixture on Amberlite LA-2, 25:18337
  determination in Italian meteorites by nondestructive neutron activation, 25:18370
SCANDIUM ALLOYS AND SYSTEMS
  La--Sc, phase studies of, 25:19241
  properties of, 25:19241
SCANDIUM ISOTOPES Sc-40
  energy levels from calcium-40 (He-3,t), particle-hole multiplet, (E), 25:20350
SCANDIUM ISOTOPES Sc-43
  energy levels from calcium-40 (α,p) reactions, spin-parity assignments for, (E), 25:20320
  energy-level transitions from calcium-40 (α,p) reactions, multipole mixing and γ branching ratios for, (E), 25:20320
SCANDIUM ISOTOPES Sc-46
  energy levels of, calculation using strong-coupling rotational model, (T), 25:20353
SCATTERING
  amplitudes for interaction of two classes of hadrons, multiparticle Veneziano formula for, 25:20014
  amplitudes of multiparticle, kinematic superstructure for abnormal couplings in dual, 25:20000
  amplitudes of, absorption and Glauber models for Regge cuts in, 25:19992
  amplitudes of, Bethe--Salpeter equation for relation between SO(1,3) and SO(1,2) crossed-channel partial-wave expansions of, 25:20113
  amplitudes of, functional description in quantum electrodynamics for Coulomb and Feynman gauges for, 25:20092
  amplitudes of, group-theoretical construction of N-point, 25:20114
  amplitudes of, impact-parameter representation for off-energy-shell, 25:20122
  amplitudes of, Lame functions for O(2,1) group for crossing symmetric expansions of physical, 25:20105
  amplitudes of, linear dependence of multiloop Veneziano, 25:20117
  amplitudes of, method of coherent states for factorization of N-point dual, 25:20120
  amplitudes of, relativistic eikonal approximation for, 25:20112
  Bethe--Salpeter equation for spin-zero particle, approximate solution to, (T), 25:20104 (NYO-2262-TA-231)
  eigenvalues of asymmetric rotator from, analytic interpolation of, 25:20513
  Feynman diagrams for, Nakanishi representation and amplitude increase in analyticity region for, 25:20121
  Feynman integrals in, continual, 25:20119
  generalized impulse approximation for molecular and nuclear scattering, (T), 25:20537
  helicity formalism for, lectures on, 25:19925 (NP-18703)
  matrix equation for electromagnetic, symmetry and unitarity, 25:20118
  N-particle resolvent operator in, integral equation for, 25:20487
  nonspecular, by rough surfaces, (T), 25:20106
  phase shifts for elastic, variational method for lower bounds on, 25:19757 (ORNL-4584, pp 58-73)
  potential, existence of wave operators in time-dependent long-range, 25:20108
  potentials for cluster-cluster, separable, (T), 25:20511
  tensor force in inelastic, formalism of two-body, 25:20508
  theory for three-body, lectures on, 25:20103 (NP-18707)
  theory of, relation between analyticity and causality in formal, 25:20116
  unitarity condition for pure-Coulomb t matrix in, 25:19505
SCHIZOMYCOTA
  Achromobacter sp., radiation effects on survival of, effects of dose on γ, 25:19163
  Aeromonas sp., radiation effects on survival of, effects of dose on γ, 25:19163
  Brucella abortus, mutations induced in, by acriflavine or nitrous acid, frequency of rough to smooth reversion, 25:18970
  Brucella abortus, radioinduced reversion mutations in, frequency of uv, 25:18970
  Escherichia coli, radiation effects on anoxic cells of, effects of time scale on protective effects of glycerol against x, 25:19022
  Escherichia coli, radiation effects on survival of log-phase and stationary-phase, effects of culture medium on x, 25:18912
  Escherichia coli, radioinduced mutations in synchronous cultures of, during DNA replication, uv, 25:18966
  Escherichia coli, radioinduced strand breaks in DNA of, protective effects of Polysorbate 80 against cobalt-60 γ, 25:19027
  Micrococcus sp., radiation effects on survival of, effects of dose on γ, 25:19163
  Photobacterium fischeri, radiation effects on survival of, effects of dose rate per pulse on electron, 25:19154
  Proteus sp., radiation effects on survival of, effects of dose on γ, 25:19163
  Staphylococcus aureus E169, drug resistance determinants in, use of uv-irradiated transducing phage lysates to determine chromosomal relation of, 25:19157

- Staphylococcus aureus E169, frequency of transduction of drug resistance determinants in, by uv-irradiated lysates of typing phage 80,, 25:19157
- use of intestinal, for preparation of antigens for stimulating natural immunity, 25:18922
- Vibrio sp., radiation effects on survival of, effects of dose on γ, 25:19163

SCINTILLATION
- lifetime measurements of, spectrometer for subnanosecond, 25:18696

SCINTILLATION CAMERAS
- data processing system for Anger, computer-based, 25:18730
- design of tomographic, 25:18697
- development of stationary, with visual data display, 25:18689(P)
- image aberrations produced by multichannel collimators, 25:18660

SEALS AND GLANDS
- design requirements for helium cooled reactor, 25:20558
- operating characteristics of static seals for water cooled reactor systems, review of, 25:20719 (ORNL-TM-3308)
- performance of elastomer O-ring, for HTGR-type reactor stand pipe connections, (E), 25:20742 (DP-Report-496)

SEAWATER
- decontamination of fission product-contaminated, by flocculation, 25:18518
- ruthenium-106 contamination of organisms in, comparison of soluble and insoluble, 25:18944

SEDIMENTARY DEPOSITS
- uranium deposit distribution in South America, relations with geology, 25:18544

SEED
- germination of barley, effects of space flight on, 25:18952
- radiation effects on DNA synthesis in Oenothera and wheat, x, 25:18910
- radiation effects on, of fruits, grasses, and vegetables, effects of moisture content on mutagenic γ, 25:18964(P)
- radioinduced chromosome aberrations in plant, effects of hypothermia on, 25:19093
- radiosensitivity of Euphorbia, onion, pea, tomato, Vicia, and watermelon, effects of dose on γ, 25:18946

SEISMIC WAVES
- measurement of earthquake- and underground nuclear explosion-generated, Aug. 1969 to Aug. 1970 ORNL Station ORT results for, 25:18556 (ORNL-4584, pp 41)

SELENIUM
- chromatographic behavior in hydrochloric acid--thiocyanate mixture on Amberlite LA-2, 25:18337

SELENIUM HALIDES
- separation by solvent extraction, effects of charge, composition, and structure on, 25:18511

SELENIUM ISOTOPES Se-75
- electron-capture decay of, gamma spectra from, (E), 25:18747
- use of selenomethionine-incorporated, for scanning thymus gland, 25:19049

SELENIUM ISOTOPES Se-77
- half-life of isomeric, 25:20463
- neutron inelastic scattering at 14.5 MeV, cross sections and gamma spectra from, (E), 25:20435

SELENIUM ISOTOPES Se-78
- neutron reactions (n,2n) at 14.5 MeV, cross sections and gamma spectra from, (E), 25:20435

SELENIUM ISOTOPES Se-87
- half-life and neutron emission probability of, (E), 25:20327
- yield in uranium-235 thermal neutron fission, (E), 25:20327

SELENIUM ISOTOPES Se-88
- half-life and neutron emission probability of, (E), 25:20327
- yield in uranium-235 thermal neutron fission, (E), 25:20327

SEMICONDUCTOR JUNCTIONS
- characteristics of large-area ion-implanted p-n, as radiation detectors, 25:18756
- properties of ion-implanted p--n silicon carbide, (E), 25:19847

SEMICONDUCTORS
- implanted-ion sorption on dislocation loops in, during annealing, (T), 25:19848
- ion implantation in compound, review, 25:19789
- ion implantation in, 200-kV machine for, 25:19774
- ion implantation in, European conference on, Reading, England, Sept. 7 to 9, 1970, 25:19772
- ion implantation in, first international topical conference at Thousand Oaks, Calif., May 4--7, 1970, 25:19809
- ion implantation in, review of range and depth distribution in, 25:19796
- ion-implanted layers in, review of electric properties of, 25:19775

SEROTONIN
- radioprotective effects of, on serum antihyaluronidase activity and tissue permeability in skin of rats, γ, 25:19031

SERPENTINE
- properties of crushed, for use as neutron shielding, 25:19295

SERPUKHOV SYNCHROTRON
- startup of, discussion of initial, 25:20127(T) (CERN-Trans-70-12)
- vacuum system for, 25:20126(T) (CERN-Trans-70-9)

SEWAGE
- analysis for tritium, 25:18360

SEYFERT GALAXIES
- luminosity of, failure of supernova rate from coalesced stars to explain, (T), 25:19320
- radio flux density variations of, (E), 25:19367

SF MATERIALS ACCOUNTING
- glossary of safeguards terms for use in, 25:18626 (WASH-1162)

SHALE DEPOSITS
- radioactive waste disposal in deep underground, hydraulic fracturing studies for, 25:18622 (ORNL-4584, pp 11-15)

SHEEP
- radiation effects on thickness of hair of, ionizing, 25:19121

SHELLS (GEOMETRY)
- plasticity of reinforced, under uniform pressure, analysis of dynamic, 25:18557 (ANL-7677)
- plasticity of ring-loaded circular cylindrical, analysis of dynamic, 25:18557 (ANL-7677)
- stress limit of internally-loaded axisymmetric intersecting, method for calculating, 25:18569
- vibration of revolving orthotropic, theory for free, 25:18568

SHIELDED CONTAINERS
- design of fire- and shock-resistant, 25:18633(P)
- design of fire-resistant, for shipping radioactive materials, 25:18632(P)

SHIELDING
- cooling system for thermionic reactor, description of head pipe for, 25:20807(P)
- design of heat block, for Rankine cycle thermoelectric converter heat source, 25:18594(R) (ORNL-TM-3292)
- development of lead shot in shaped Styrofoam, for protection of human organs during therapy, γ, 25:19011

SHIELDING MATERIALS
- preparation of lead powder-containing elastomeric, equipment and method for, 25:19294(P)

SHIPPING
- safety of radioactive material, in USA, 25-year review of, 25:19017

SHIPS
- air conditioning systems for nuclear powered, design and installation of, 25:20816(T) (JPRS-52443)

SHOCK WAVES
- magnetic field penetration of front of, (T), 25:19547
- production in collisionless plasma, ion-acoustic, (T), 25:19698
- propagation in collisionless plasma, numerical solutions for electrostatic, 25:19678
- propagation in plasma, decomposition of decelerating ionizing, (T), 25:19667
- stability of plane stationary, 25:20867(T) (LA-tr-71-10)
- structure in plasma, precursor ionization effects on MHD, (T), 25:19681

SIALIC ACIDS
- content of serum of calves, effects of, on permeability of erythrocytes to phosphorus-32, 25:18900

SILANE, FLUOROTRIMETHYL-
- reactions with recoil tritium atoms, parameter effects on, 25:18484

SILICATES
- abundance in interstellar materials, (T), 25:19452
- light extinction due to interstellar, (E), 25:19446
- presence in interstellar grains, evidence for, (E/T), 25:19450
- spectra of, emission, (E/T), 25:19330

SILICON
- abundance in α^2 CVn, (E), 25:19339
- alpha elastic scattering at 5 MeV, blocking patterns from, (E), 25:18679
- alpha-particle channeling in, effects of disorder produced by ion implantation on, 25:19816
- amorphous state in, structure of, 25:19862
- antimony ion-implantation in, comparison of total and donor profiles of 100-keV, 25:19825
- boron implantation profiles in, heavy-ion x-ray excitation measurements of, 25:19803
- boron-ion implantation at 150 keV and liquid-nitrogen temperature in, channeling and electrical measurements in annealing of, 25:19834
- boron-ion implantation at 200 and 300 keV in, channeling study of lattice disorder induced in, 25:19830
- boron-ion implantation at 6 keV in, electric profiles after annealing of, 25:19836
- boron-ion implantation in, correlation of electron microscopic and electric property studies of annealed 50-keV, 25:19815
- carbon-ion channeling in ion-implanted, 25:19829
- deposition on niobium by decomposition of silicon hydride, effects of oxygen on, 25:19258
- determination in natural waters from uranium mining operations, method for, 25:18339 (CEA-R-3557(2))
- electric conductivity of gallium- and boron-implanted layers in, temperature coefficient of, 25:19783
- ion implantation at 0.5 to 1.5 MeV, electric properties

XUM

  produced by boron, 25:19784
  ion implantation at 20 to 150 keV in, energy dependence and depth distributions of lattice disorder induced in, 25:19832
  ion implantation at 400 keV in, annealing of defects induced in, (E), 25:19811
  ion implantation at 400 keV in, EPR of substitutional antimony and arsenic from, 25:19826
  ion implantation at 7 keV in, annealing and electric properties of implanted layers, 25:19835
  ion implantation damage in, divacancy and amorphous-layer formation in 400-keV antimony, boron, and zinc, 25:19812
  ion implantation damage in, electron microscopic studies of 80-keV, 25:19814
  ion implantation for insulating layer formation, nitrogen and oxygen, 25:19781
  ion implantation in boron-doped single crystals of, enhanced diffusion in 20-keV, 25:19823
  ion implantation in, calculated spatial distributions of damage from 30- to 400-keV, 25:19819
  ion implantation in, effects of radiation damage and amorphous state on electric activity of boron, 25:19776
  ion implantation in, electrical properties and annealing of 50-keV phosphorus, 25:19779
  ion implantation in, enhanced diffusion of boron and phosphorus during hot-substrate, 25:19824
  ion implantation in, flux dependence of lattice disorder produced in boron, carbon, and krypton, 25:19806
  ion implantation in, review of range and depth distribution in, 25:19796
  ion implantation profile measurement, ion-beam stripping--electrical method for, 25:19800
  ion implantations in, electrical properties before and after annealing of boron and phosphorus, 25:19778
  ion implantations in, electrical properties of 40-keV alkali-metal, 25:19780
  ion implantations in, electron-microscopic and electrical studies of annealing of boron and phosphorus, 25:19777
  ion implantations in, studies of 50-keV gallium, 25:19802
  ion implants in, lattice locations of, 25:19797
  performance of single crystals of, for neutron filter, 25:20238 (UJV-2488-F)
  phosphorus-ion implantation along (110) axis at 40 to 400 keV in, electric profiles after annealing of, (E), 25:19839
  phosphorus-ion implantation at 20 keV in, electric profiles after annealing of, 25:19836
  phosphorus-ion implantation at 40 and 100 keV in, annealing characteristics of implanted layers, 25:19837
  phosphorus-ion implantation at 400 keV in, Hall-effect and resistivity measurements as function of temperature on implanted layers, 25:19838
  proton channeling in, effects of disorder produced by ion implantation on, 25:19816
  radiation damage distribution in ion-implanted, 25:19818
  radiation damage from ion implantation, review, 25:19805
  radiation damage from ion implantations at 40 to 100 keV in, electron microscopic studies of, 25:19808
  radiation damage mechanisms in, review of, 25:19810
  radiation damage profiles in ion-implanted, radiochemical copper-decoration method for measuring, 25:19817
  radiation effects on electric properties of n- and p-type, annealing of boron-ion and neutron, 25:19831
  radiation effects on single crystals of, x-ray diffuse and small-angle scattering study of fast-neutron, 25:19853
  radioinduced amorphous layers in, model for formation of ion, 25:19813
  radioinduced E centers in phosphorus-doped n-type, annealing of 1-MeV electron, (E/T), 25:19854
  radioinduced insulating surface layers in, annealing of 1-MeV proton, 25:19822
SILICON CARBIDES
  abundance in interstellar materials, (T), 25:19452
  ion implantation at 5 to 300 keV in, properties of conducting layers and p--n junctions formed by, (E), 25:19847
  ion implantation effects on cathodoluminescence of epitaxial, annealing of, 25:19790
  ion implantation in, review, 25:19789
SILICON HYDRIDES
  decomposition for deposition of silicon on niobium, effects of oxygen on, 25:19258
SILICON IONS
  implantation in gallium arsenide, electric profiles of implanted layers after annealing, 25:19843
  implantation in silicon at 150 keV, damage distribution from, 25:19818
  implantation in silicon at 280 keV, damage profiles from, 25:19817
  implantation in silicon at 30 to 400 keV, calculated spatial distributions of damage from, 25:19819
  implantation in silicon at 40 to 100 keV, electron microscopic studies of defects induced in, 25:19808
  implantation in silicon diodes at 300 keV, effects on carrier lifetime, 25:19820
SILICON ISOTOPES Si-28
  alpha reactions (α,p) at 35.5 MeV, DWBA analysis of j dependence in angular distributions from, (E), 25:20309
  deuteron reactions (d,p) at 15 MeV, model for, (T), 25:20522
  energy levels from aluminum-27 (p,γ) reactions, spin-parity assignments for, (E), 25:20315
  energy levels near 13.245 MeV from aluminum-27 proton resonance, (E), 25:20330
  energy levels of, calculation of magnetic monopole transition probabilities for, (T), 25:20306
  proton reactions (p,γ) at 1.4 MeV, γ spectra and angular distributions for, (E), 25:20357
  proton reactions (p,γ) near 2 MeV, angular distributions for, (E), 25:20319
SILICON ISOTOPES Si-29
  energy levels from aluminum-27 (He-3,p) reactions, spin-parity assignments for, (E/T), 25:20271 (NP-18628)
SILICON JUNCTIONS
  capacitance of ion-implanted p-n diodes, 25:18857
  ion implantation in, survey, 25:19782
  radiation damage in diodes, annealing of ionized defects in 2.8-MeV proton, 25:19821
  radiation effects on carrier lifetime in diffused p--n diodes, 300-keV ion, 25:19820
SILICON NITRIDES
  formation of insulating layers of, in silicon by nitrogen-ion implantation, 25:19781
SILICON OXIDES
  abundance in interstellar dust, (E), 25:19453
  aluminum recoil-atom implantation in substrates of, by argon-ion bombardment of films, 25:19786
  effects of colloidal, on radioinduced polymerization of styrene with methyl methacrylate, 25:18442
  formation of insulating layers of, in silicon by oxygen-ion implantation, 25:19781
  ion implantation effects on electric properties of films of, at high fields, 25:19788
  radiation effects on refractive index of, ion, 25:19787
  radiation effects on sorptive properties of colloidal, γ, 25:18427
SILICON SYSTEMS
  Al--Cr--Nb--Si--Sn--Ti, properties for use as protective coating on niobium, 25:19176
  Al--Nb--Si--Sn--Ti, properties for use as protective coating on niobium, 25:19176
  Cr--Fe--Nb--Si, properties for use as protective coating on niobium, 25:19176
  Cu-base--Si, slip initiation in monocrystalline, 25:19194(R) (NYO-4073-4)
SILTS
  analysis of marine, for radium-226, strontium, and calcium, 25:18354
  radioisotope content in White Oak Creek, cesium-137 and strontium-90, (E), 25:18521 (ORNL-4584, pp 1-10)
SILVER
  chromatographic behavior in hydrochloric acid--thiocyanate mixture on Amberlite LA-2, 25:18337
  determination in drugs by x-ray fluorescence, comparison of americium-241, gadolinium-153, and iodine-125 sources for, 25:18355
  determination in silver-base alloys by neutron activation, 25:18367
  deuteron reactions at 180 to 360 keV with, cross sections for L-shell ionization in, (E), 25:19470
  electron reactions at 0.3 to 1.1 MeV with thin foils of, photon emission spectra from, 25:19471
  fission fragment stopping power, energy loss, and range in, (E), 25:20442
  fission-fragment stopping in, cross sections for californium-252, (E), 25:19765
  proton reactions at 90 to 180 keV with, cross sections for L-shell ionization in, 25:19470
  separation of bismuth from, by cation exchange chromatography, 25:18520
SILVER ALLOYS AND SYSTEMS
  Ag--Cd, polar-reflection Faraday effect in α-phase disordered, Fermi surface and band lifetime from, 25:19873
  Ag--epoxy resins, radiation effects on bonding in, γ, 25:18421(R) (RLO-2098-1)
  Ag--graphite, electric conductivity of two-phase, 25:19226
  Ag--Mg, polar-reflection Faraday effect in α-phase disordered, Fermi surface and band lifetime from, 25:19873
  Ag--Ni, electric conductivity of two-phase, 25:19226
  Ag--SiO_2, electric conductivity of two-phase, 25:19226
  Ag--W, electric conductivity of two-phase, 25:19226
  Ag--WC, electric conductivity of two-phase, 25:19226
  Ag-base--Au, vibrational entropy of dilute solutions of, neutron activation method for determination of, 25:18367
SILVER IONS
  implantation in zinc sulfide and selenide films at 250 kV, cathodoluminescence effects of, 25:19795
SILVER ISOTOPES Ag-100
  decay of ground-state and isomeric, half-lives for, (E), 25:20422
SILVER ISOTOPES Ag-101
  decay of ground-state and isomeric, half-lives for, (E), 25:20422

energy-level transitions from cadmium-101 decay, internal conversion coefficients for, (E), 25:20422
SILVER ISOTOPES Ag-102
decay of isomeric, half-life for, (E), 25:20422
SILVER OXIDES
Ag--SiO$_2$, electric conductivity of two-phase, 25:19226
SIOUX FALLS POWER REACTOR
dismantling of, procedures and technical specifications for, 25:20607 (DOCKET-50130-7)
SKIN
radiation effects on permeability of rat, protective effects of mercamine and serotonin against γ, 25:19031
radiation effects on revascularization of transplanted, on man and rabbits, microwave, 25:19104
radiation injuries to human, mechanisms of pathogenesis following uv, 25:19150
radiation protection of human, during γ therapy, use of lead glass filters for, 25:19086
radiation protection of human, during γ therapy, use of tin filters for, 25:19082
radioinduced injuries of human, effects of dose, dose fractionation, and time on fast neutron, 25:19149
radiosensitivity of human, laser, 25:19133 (NP-18714)
SLURRIES
heat transfer to Bingham plastic-type, in circular tube entrances, calculation of forced-convection, 25:18588
SODIUM
analysis for hydrogen and oxygen, equipment for, 25:18863
analysis of liquid, equipment for sampling in, 25:18336
cesium volatility in liquid, effects of carbon adsorbers on, (E), 25:20754 (AERE-R-6481)
combustion of liquid, analysis of aerosols of sodium oxide released from, (E), 25:20759 (CONF-700816-(Vol.1), pp 346-55)
combustion of liquid, analysis of aerosols of sodium iodide and sodium oxide release from, 25:20761 (CONF-700816-(Vol.1), pp 373-92)
combustion of, behavior of atmospheric aerosols from, 25:19167 (AERE-R-6460)
determination in Italian meteorites by nondestructive neutron activation, 25:18370
determination in natural waters from uranium mining operations, method for, 25:18339 (CEA-R-3557(2))
energy-level transitions in, continuum generalized oscillator strengths for 3s--epsilon p, (T), 25:19476
energy-level transitions in, minima in generalized oscillator strengths for, (T), 25:19521
filtering of aerosols of, accidentally released from LMFBR, testing of materials for, 25:18563 (CONF-700816-(Vol.1), pp 445-58)
flow rate of liquid, electromagnetic flowmeter for measurement of, 25:18876
optical properties of aerosols of, measurements of, 25:19193 (CONF-700816-(Vol.1), pp 425-44)
properties for use as reactor coolant, 25:19179
radiation effects on content of, in erythrocytes of rabbits, 25:19107
reactions of liquid, with cesium, effects of carbon on, (E), 25:19192 (CONF-700816-(Vol.1), pp 393-412)
reactions with iodine in liquid metal cooled fast breeder reactor systems, (E), 25:20760 (CONF-700816-(Vol.1), pp 356-72)
scattering by mercury atoms, crossed-beam measurements of differential cross sections and intermolecular potentials for, 25:19496
solvent properties for carbon at 600 to 950°C, 25:19196 (TRG-Report-1906)
thermal conductivity of deposited aerosol combustion products of, equipment and method for measurement of, 25:18562 (CONF-700816-(Vol.1), pp 413-24)
vaporization kinetics of initially static superheated, 25:19191 (ANL-7706)
SODIUM ACID CARBONATES
production in sodium fires, effects of atmospheric humidity on, 25:19167 (AERE-R-6460)
SODIUM CARBONATES
production in sodium fires, effects of atmospheric humidity on, 25:19167 (AERE-R-6460)
Hg--Na$_2$Co$_3$, electric potential of aqueous solutions of, 25:19190(T) (AI-Trans-287)
SODIUM CHLORIDES
niobium films on, crystal structure of sputtered, 25:19244
H$_2$O--NaCl, boiling on thermally-loaded wires, critical parameters for, 25:18583
SODIUM HYDROXIDES
reactions with niobium, anodic, 25:19170
SODIUM IODIDES
release of aerosol, by liquid metal cooled fast breeder reactor during sodium combustion accidents, 25:20761 (CONF-700816-(Vol.1), pp 373-92)
SODIUM IONS
implantation in silicon at 40 keV, electrical properties of, 25:19780
SODIUM ISOTOPES Na-20
beta decay of, β--ν angular correlations in, (E), 25:18737(R) (ORO-3820-7)
beta decay of, ft values and half-life for, (E), 25:18737(R) (ORO-3820-7)
SODIUM ISOTOPES Na-22
abundance in Bovedy meteorite, (E), 25:19301
energy levels from fluorine-19 (α,nγ) reactions, spin-parity assignments for, (E), 25:20318
energy levels of, calculation using strong-coupling rotational model, (T), 25:20353
energy-level transitions from fluorine-19 (α,nγ) reactions, multipole mixing ratios for, (E), 25:20318
SODIUM ISOTOPES Na-23
energy levels from gamma resonance scattering, widths for, (E), 25:20355
energy levels from neutron inelastic scattering, (E), 25:20356
neutron capture by, resonance integrals and partial widths of resonances in, (E), 25:20359
neutron inelastic scattering by, γ energies from fast, (E), 25:20356
proton inelastic scattering at 1 to 1.8 MeV, analysis of resonances in, (E), 25:20325
proton reactions (p,α) and (p,γ) at 1 to 1.8 MeV, analysis of resonances in, (E), 25:20325
SODIUM ISOTOPES Na-24
energy levels of, calculation using unified model, 25:20524
SODIUM NITRATES
displacement of water in soil columns by heavy water-dissolved, measurement by gamma-photoneutron reactions, 25:18523
radiolysis of aqueous solutions of, yields of nitrite ions from γ, 25:18463
SODIUM OXIDES
release of aerosol, by liquid metal cooled fast breeder reactor during sodium combustion accidents, 25:20761 (CONF-700816-(Vol.1), pp 373-92)
release of aerosol, from liquid metal cooled fast breeder reactors during sodium combustion accidents, (E), 25:20759 (CONF-700816-(Vol.1), pp 346-55)
SOILS
cesium-137 distribution in cesium-137-tagged tulip tree forest, (E), 25:18521 (ORNL-4584, pp 1-10)
contamination by gaseous effluents from nuclear power plants, computer methods for evaluating, 25:18526 (ORNL-4584, pp 37-40)
density and water content of, radiometric method for measuring, 25:18599
density measurements of, calibration of radiometric densimeters for, 25:18815 (INP-715)
fission product fixation in, of France, review of factors influencing, 25:18528
neutron attenuation by, fast, 25:19007 (NCRP-38)
radioactive contamination of, in Hong Kong, spectrometric method for measuring absorbed dose from background, 25:19006
radioisotope content in vicinity of Los Alamos, N. Mex, 25:18985 (LA-4563)
radioisotope content of Southeast USA, 25:18935(R) (ORO-3905)
water displacement in, by heavy water and heavy water--sodium nitrate solutions, gamma-photoneutron reaction measurements for determination of, 25:18523
SOL-GEL PROCESS
development for production of plutonium dioxide, thorium dioxide, and uranium dioxide sols, 25:19261 (ORNL-4629, pp 14-64)
SOLAR ACTIVE REGIONS
formation of stable, (E), 25:19409
radio emission from, polarization of, (E), 25:19417
radio-burst generation from, Type-III, (E), 25:19413
relation to quasi-periodic oscillations of corona and chromosphere, (E), 25:19415
spectra of, 10,830-A line in ir, (E), 25:19421
velocity fields on two levels in July 1966, (E), 25:19433
SOLAR CELLS
radiation effects on curve power factors of silicon, γ, 25:18882
SOLAR CORONA
charged-particle storage in, relativistic, (E/T), 25:19403
electron and ion densities on Mar. 3 and 17, 1970, (E), 25:19411
electron densities in, from occultation of NP 0532, (E), 25:19373
fluctuations in, quasi-periodic, (E), 25:19415
microwave reflection from, maser effect in, (T), 25:19419
spectra of inner, observed during total eclipse of May 30, 1965, (E), 25:19410
temperature of quiet, determined from soft x-ray flux, (E), 25:19418
SOLAR DISTURBANCES
effects on fibrinolytic activity in rheumatic patients, inhibitory, 25:19145
turbulent velocities and damping constants in faculae, (E), 25:19420
SOLAR FLARES
electron spectra of Apr. 1969, observations in interplanetary space and magnetosphere, (E), 25:19428
electrons associated with, relation to Type-I noise activity, (E), 25:19402
emission of x rays, microwaves, and euv in Aug. 8, 1968, (E), 25:19401
energy losses from 10^{8}°K plasma in, (E/T), 25:19398

XUM

  proton propagation in interplanetary space from, (E/T), 25:19437
  radio burst associated with Sept. 28, 1961, (E), 25:19435
  radio bursts associated with, millimeter, (E), 25:19423
  spectra of Mar. 12, 1969, excited lines in H and K region of Ca II in, (E), 25:19412
  x-ray emission from Sept. 28, 1961, hard, (E), 25:19435
  x-ray emission from, model for, (E/T), 25:19396

SOLAR PARTICLES
  proton-diffusion mean free path during Feb. 25, 1969 event, effect of interplanetary magnetic-field irregularities on, (E/T), 25:19414
  zone of avoidance in interplanetary space, equatorial, (E/T), 25:19437

SOLAR RADIO BURSTS
  characteristics of, associated with proton flares, (E), 25:19423
  emission during flare of Sept. 28, 1961, (E), 25:19435
  polarization measurements on Type-III, at 25.3 MHz, 25:19399
  production of Type-III, in Aug. 1968, (E), 25:19413
  relation of Type-I, to energetic electrons, (E), 25:19402
  relation to x rays in flare of Aug. 8, 1968, (E), 25:19401
  structure of, at 10 cm, (E), 25:19436

SOLAR SYSTEM
  dust streams in, cometary origin of, (E), 25:19425

SOLAR WIND
  hydromagnetic studies of, (T), 25:19426
  interaction with geomagnetic field, effect on topside ionosphere ion composition, (E/T), 25:19576
  interaction with non-ionized dust comet, (T), 25:19582
  interactions with magnetosphere, hydromagnetic waves in bow shock, 25:19580

SOLAR X-RAY BURSTS
  characteristics of soft, (E), 25:19400
  relation to microwaves in flare of Aug. 8, 1968, (E), 25:19401

SOLID STATE PHYSICS
  research at AECL from January 1, 1970 through March 31, 1970, 25:20307(R) (AECL-3667)

SOLIDS
  diffusion in ion-implanted, with nonuniform diffusion parameters, (T), 25:19840
  ion implantation in, European conference on, Reading, England, Sept. 7 to 9, 1970, 25:19772
  ion implantation in, fine-focused ion machine for, 25:20168
  ion implantation in, review of range and depth distribution in, 25:19796
  ion implantation in, survey of possible uses of, 25:19785
  ion implantation machines, review of, 25:20165
  ion range and stragglings in amorphous, approximations and interpolation rules for calculation of, 25:19760
  ion scattering by surfaces of, angular and energy distributions from, 25:19468 (INP-710)
  ion stopping in, review, (E/T), 25:19762
  moisture content in, neutron radiometric gage for determination of, 25:18362(P)
  photon reactions with inner-shell electrons of, review of chemical information from, 25:19473
  radiation damage in, range correlation functions for predicting ion, (T), 25:19833
  sorptive properties of, use of positron annihilation to study chemi-, 25:18415
  structure of, development of automatic goniometers with high resolving power for x-ray diffraction studies of, 25:18861(P)

SOLUTIONS
  radiolysis of aqueous, diffusion kinetics in pulse, 25:18447 (CALT-767-P-4-73)

SOLVENT EXTRACTION PROCESSES
  development for rare metals, 25:18510

SOUND
  absorption of, preparation of lead powder-containing elastomers for, 25:19294(P)

SOUTHWEST EXPERIMENTAL FAST OXIDE REACTOR
  fuel elements for, inspection procedures for, 25:20786 (DOCKET-50231-71)
  operations incident of February 21, 1971, malfunction of safety system trip relay, 25:20744 (DOCKET-50231-72)
  power coefficient of reactivity for, calculation at constant flow and constant inlet temperature, 25:20786 (DOCKET-50231-71)
  reactivity excursions in, design and testing of FRED device for initiation of fast, 25:20693 (GEAP-13649)

SPACE
  electron spectra in interplanetary, from April 1969 solar flare, (E), 25:19428
  structure of interplanetary, from annual cosmic-ray intensity variations, (E), 25:19526

SPACE FLIGHT
  effects on chromosomes of barley, effects of seed exposure on aberrant, 25:18952
  effects on chromosomes of Crepis capillaris seeds, effects of ethylenimine on aberrant, 25:18953
  simulation of, plasma source for, 25:19700 (NP-18722)

SPECTROMETERS
  detectors for magnetic, design and performance of position-sensitive proportional, 25:18681

SPECTROSCOPY
  chemical interferences in flame, 25:20859 (IS-T-417)
  data filtering for, square root transform for, 25:18739
  development of photoelectron, for determination of most elements, 25:18338 (CEA-CONF-1725)

SPERM
  radioinduced chromosome aberrations in human, following therapy for malignant lymphomas, reproductive factors in, 25:19147

SPERMATOGONIA
  radiation effects on survival of, in mice in relation to mutation frequency, effects of dose on x, 25:18959
  radioinduced specific locus mutations in, of mice, frequency of fast neutron, 25:18949
  radioinduced translocation of chromosomes in, of mice, review of x, 25:18948
  radioinduced translocation of chromosomes in, of mice, effects of dose fractionation on rate of x, 25:18958

SPLEEN
  radiation effects on cell replication in endocolonized mouse, tritium tracer study of x, 25:19125
  radiation effects on proliferation of cells of, in bone marrow and spleen of mice, effects of dose on x, 25:19129
  radiation effects on uptake of α-aminoisobutyric acid, inulin, orotic acid, and phosphorus-32 by rat, effects of AET and cysteamine on γ, 25:19024
  scanning of human, for evaluation of organ involvement in Hodgkin's disease, 25:19058
  scintigraphy using metastable indium-113-labeled erythrocytes, 25:19036
  size of human, method for evaluation of, during routine liver scanning using technetium-99m, 25:19057

SPUTTERING
  development of methods of, for production of thin film radiation sources, 25:18590(R) (BNWL-1308-4)

STACK DISPOSAL
  effects on site environment of nuclear power plant, computer methods for evaluating, 25:18526 (ORNL-4584, pp 37-40)
  monitoring at Los Alamos Scientific Lab. during 1970, 25:18985 (LA-4563)
  monitoring for trace amounts of radioactive gases, scintillation detector for, 25:18744(P)

STAINLESS STEEL
  compatibility of cladding of Types 316 and 347, with sodium-bonded uranium carbide fuel rods at 700°C, 25:19276
  corrosion of austenitic, effects of nitrogen on susceptibility to stress, 25:20898(R) (TID-25664)
  deposition on copper by sputtering, for radiation source prototype development, 25:18590(R) (BNWL-1308-4)
  joining to Zircaloy to form reactor components, coextrusion and rolling methods for, 25:19183
  magnetic properties of soft magnetic, effects of heat treatments on, 25:19872
  properties of Types 304 and 316, for use in sodium-cooled fast breeder reactor heat exchangers, 25:18574
  radiation effects on ductility of USSR, high temperature in-pile, 25:19250(T) (AEC-tr-7192)
  radiation effects on mechanical properties of Type 316, at 1000 to 1400°F, fast neutron, 25:19254 (WHAN-SA-2)
  radiation effects on microstructure and tensile properties of Type 316, relations of irradiation temperature at 420 to 650°C with neutron, 25:19251 (AERE-R-6435)
  radiation effects on microstructure of annealed Types 304 and 306, at 370 to 700°C, fast neutron, 25:19253 (WHAN-FR-16)
  Cu--stainless steel, radiation effects on bonding in, γ, 25:18421(R) (RLO-2098-1)

STANFORD LINEAR ACCELERATOR
  storage ring for, design of SPEAR, 25:20194

STAR CLUSTERS
  nebulae distribution in open, planetary, (E), 25:19321

STARS
  atmosphere analysis for α Her and 54 Eri, (E/T), 25:19319
  atmosphere of P Cyg, physical conditions in, (E), 25:19342
  collisions in dense systems, coalescence during, (T), 25:19320
  darkening data for yellow-supergiant, limb-, (E/T), 25:19305
  element abundances in α^2 CVn, (E), 25:19339
  evidence for black hole in epsilon Aur system, (T), 25:19313
  flares in UV Cet-type, statistical characteristics of, (E), 25:19346
  flares in, photoelectric and radio observations of, (E), 25:19345
  helium production in pulsationally unstable massive, (T), 25:19331
  light curve for AG Dra, (E), 25:19341
  light curve for HD 175514, (E), 25:19344
  light polarization in Be, intrinsic, (E), 25:19315
  light polarization in white-dwarf, detection of circular, (E), 25:19329
  light polarization of white-dwarf, detection of circular, (E), 25:19328

  magnetic fields at surfaces of 28 Ap, mean, (E), 25:19308
  magnetic-field variations in α^2 CVn, (E), 25:19339
  mass losses during evolution of, (T), 25:19333
  metal abundances in Type-M supergiant, (E), 25:19323
  models for red-giant, critical mass at helium flash, (T), 25:19307
  phase shift between radius and temperature variations for 44 Cepheids, (E), 25:19322
  photoelectric elements of WX Cep, (E), 25:19335
  photometric elements of HD 175514, (E), 25:19344
  photometric elements of W Ursae Majoris eclipsing binary, rectification and determination of, (E), 25:19317
  photometry of α^2 CVn, (E), 25:19339
  photometry of GG Cas, (E), 25:19336
  photometry of IZ Per, (E), 25:19337
  photometry of OB, in region α = 17h 03m to 17h 41m; d = −28.8° to 33.4°, (E), 25:19334
  properties of epsilon Aur and 89 Her, (T), 25:19314
  pulsations in polytropes, second-order, (T), 25:19306
  spectra of α And and π Boo A, (E), 25:19343
  spectra of α^2 CVn, (E), 25:19339
  spectra of BD + 30°3639, comparison to planetary HD 164270, (E), 25:19310
  spectra of γ Cas, ultraviolet and visual, (E), 25:19332
  spectra of Mira variables with very long periods, minimum-light, (E), 25:19311
  spectra of, silicate emission feature at 30 μm in, (E/T), 25:19330
  spectral absorption lines in Mira-variable, (E), 25:19318
  spectrum synthesis for cool, method for, (E/T), 25:19319
  ultraviolet fluxes for main-sequence, prediction of, 25:19347
  velocities of, in Selected Area 8, radial, (E), 25:19316
  velocity of α^2 CVn, radial, (E), 25:19339
STATISTICS
  error estimation in experimental data, numerical method for, 25:20845 (AECL-3781)
  maximum likelihood method for fitting of double exponential lifetime spectra, 25:19881
  paraparticles in, first- and second-quantized theories of, 25:20080
STEAM
  separator system, description of, 25:20743(P)
  separators for, design parameters and operation characteristics of, 25:20769
  H_2O--steam, heat transfer from flowing, in curved tubes, 25:18586
STEAM-GENERATING HEAVY-WATER-MODERATED REACTOR
  fuel elements for, radiation testing of prototype, (E), 25:20736 (HPR-132)
STEAM POWER PLANTS
  construction costs of, comparison with nuclear power plants of, 25:20597
  effluents from, activities in France for control of air pollution from, 25:20686
  power grid system in Germany for, requirements for interconnected, 25:20691
  thermal effluents from, effects on Rhine River of, 25:20685
STEEL
  laser-beam reactions with foils of, plasma production in, 25:19701
  magnetic properties of soft magnetic, effects of heat treatments on, 25:19872
  properties for use in sodium-cooled fast breeder reactor heat exchangers, 25:18574
  properties of Types A533, A542, and A543, for use in pressure vessels, 25:19222
  thermal loading to induce water boiling on wires of, parameters for critical, 25:18583
  use in reactor construction, review of considerations for, 25:19200
  welding of reactor pressure vessels of, review of electroslag method for, 25:19181
  welding of thick plates of, effects of defects on weld quality in, 25:19202
STELLAR FLARES
  light curves for, in EV Lac, (E), 25:19340
  light curves for, photoelectric observations of, (E), 25:19345
  statistical characteristics of, in UV Cet-type stars, (E), 25:19346
STELLARATORS
  charged-particle motion in, magnetic and drift surfaces in, (T), 25:19727
  magnetic and drift surfaces in, (T), 25:19727
  plasma confinement in WIIa, neoclassical diffusion, (E/T), 25:19645 (IPP-2/86)
STORAGE RINGS
  beam bypass for CEA, operation of, 25:20195
  beam motion in electron--positron colliding beam, longitudinal effects of space charge forces on, 25:20157
  description of CERN ISR, 25:20209
  design of DORIS, at DESY, 25:20196
  design of mini-rings, for meson (π) interactions, 25:20153
  design of SPEAR, review of, 25:20194
  design parameters for colliding-beam, tables of, 25:20192
  operation and development of ADONE, review of, 25:20193
  operation and performance of mini-ring, for π + π scattering studies, 25:20162
  research at CERN ISR, summary of planned high-energy, 25:20158
  vacuum chamber of CERN ISR, design of ultrahigh, 25:20146
STRAIN GAGES
  performance of resistance, in radioactive environments, 25:18883
STREPTOMYCIN
  effects on Staphylococcus aureus E169, use of uv-irradiated transducing phage lysates to determine chromosomal relation of determinants for sensitivity, 25:19157
STRESS
  analysis of three-dimensional elastic--plastic, for fracture in flawed specimens, 25:18611 (HSSTP-TR-12)
STRONTIUM
  abundance in α And, (E), 25:19343
  chromatographic behavior in hydrochloric acid--thiocyanate mixture on Amberlite LA-2, 25:18337
  compatibility with refractory metal and superalloy capsule materials at high temperatures, 25:18592 (ORNL-4298)
  determination in marine sediments off Tarapur Coast, 25:18354
  determination in minerals and rocks by isotope dilution mass spectrometric, neutron activation, gravimetric, and other spectrometric methods, 25:18335
  properties of encapsulated fission product, for use as process radiation source, 25:18590(R) (BNWL-1308-4)
  separation from aqueous solutions by cation exchange, effects of iron on, 25:18504 (UJV-2450-Ch)
  separation from seawater by flocculation, 25:18518
  separation of bismuth from, by cation exchange chromatography, 25:18520
STRONTIUM FLUORIDES
  compatibility with refractory metal and superalloy capsule materials at high temperatures, 25:18592 (ORNL-4298)
STRONTIUM ISOTOPES Sr-85
  content of excreta and tissues of rats, comparison of direct and treated-sample determinations of, 25:18997
  removal from plant tissue, methods for, 25:18892 (NP-18641)
STRONTIUM ISOTOPES Sr-86
  energy levels from yttrium-86 decay, model analysis of, (E/T), 25:20352
STRONTIUM ISOTOPES Sr-87
  production of metastable, for use in scanning, use of yttrium-87 generator for, 25:18885
STRONTIUM ISOTOPES Sr-88
  deuteron reactions (d,p) with, analysis using BHMM theory, (T), 25:20282
  proton elastic scattering at 4.5 to 8.6 MeV, polarization in, (E), 25:20331
STRONTIUM ISOTOPES Sr-89
  energy levels from strontium-88 proton elastic scattering, spin assignments for isobaric analog, (E), 25:20331
  half-life, (E), 25:20339
  transport from pastures to milk to man, 25:18943
STRONTIUM ISOTOPES Sr-90
  accumulation in harvested agricultural plants, effects of calcium content on, 25:18897
  content of food and milk in Pavia, Italy from 1964 to 1966, 25:18942
  content of food chains in Finland, 25:18931 (NYO-3446-14, Paper 30)
  content of fresh water fish, molluscs, and mosses in France, technique for study of, 25:18937
  content of human bones and tissues, cereals, milk, and rainwater in Finland, 25:18931 (NYO-3446-14, Paper 30)
  content of man in Finland during 1960 to 1970, 25:18986 (NYO-3446-14, Paper 28)
  content of soil at Los Alamos Area, N. Mex, 25:18985 (LA-4563)
  distribution in harvested agricultural plants, effects of calcium on, 25:18897
  distribution in White Oak Creek sediments, (E), 25:18521 (ORNL-4584, pp 1-10)
  energy levels from rubidium-90 decay, (E), 25:20384
  properties for use as heat source in thermopile-type power systems, 25:18598(P)
  removal from plant tissue, methods for, 25:18892 (NP-18641)
  transport from pastures to milk to man, 25:18943
  uptake by plants during irrigation, development of model simulating, 25:18938
  use as tracer for ecological studies on ticks, 25:18934(R) (ORO-3514-10)
  uses as radiation source for measuring density of air-coal dust mixtures in pipelines, 25:18606
STRONTIUM ISOTOPES Sr-91
  energy levels from rubidium-91 decay, (E), 25:20459
STRONTIUM OXIDES
  compatibility with refractory metal and superalloy capsule materials at high temperatures, 25:18592 (ORNL-4298)
  Sm_2O_3-base--SrO, phase diagram at 1300 to 2000°C,

  25:19284
STRONTIUM SILICIDES
  compatibility with refractory metal and superalloy capsule materials at high temperatures, 25:18592 (ORNL-4298)
STRONTIUM TITANATES
  compatibility with refractory metal and superalloy capsule materials at high temperatures, 25:18592 (ORNL-4298)
STRUCTURAL BEAMS
  plasticity of centrally-loaded, analysis of dynamic, 25:18557 (ANL-7677)
STRUCTURES
  design parameters of service, for reactor construction, 25:20562
  loading of, load-equivalence parameters for plastic-range dynamic, 25:18557 (ANL-7677)
STYRENE
  radioinduced graft polymerization with cellulose at low dose rates, γ, 25:18446
  glass textiles--styrene, radiation effects on mechanical properties of, γ, 25:18421(R) (RLO-2098-1)
  methyl methacrylate--styrene, radioinduced polymerization of, effects of magnesium oxide and silica gel on γ, 25:18442
STYRENE POLYMERS
  mechanical properties of bead foams of SD 505, effects of temperature and test rates on, 25:19293 (UCRL-50952)
  radioinduced thermally stimulated currents in, γ, 25:18422
  carbon black--polystyrene, radiation effects on electrical and mechanical properties of, γ, 25:18421(R) (RLO-2098-1)
  Pb--Styrofoam, gamma shielding properties of composites cf, 25:19011
  poly(2-ethylhexyl acrylate)--polystyrene, radiation effects on crosslinking and properties of, γ, 25:18436
SUBMARINE REACTORS
  corrosion products from, hazards of radioactive, 25:19014
SUBMARINES
  air conditioning systems for nuclear powered, design and installation of, 25:20816(T) (JPRS-52443)
  radiation protection of personnel on nuclear, medical programs for, 25:18972
SUCCINIC ACID
  radiolysis of aqueous perchloric acid solutions of, rate constants for reactions of hydrogen atoms produced by γ, 25:18459
  radiolysis of crystals of, processes for annealing of free radicals formed by, 25:18473
SULFATES
  determination in natural waters from uranium mining operations, method for, 25:18339 (CEA-R-3557(2))
SULFONAMIDES
  effects on hemolysis of uv-irradiated erythrocytes, 25:18914
SULFUR
  determination in natural waters from uranium mining operations, method for, 25:18339 (CEA-R-3557(2))
SULFUR FLUORIDES
  electron reactions at thermal energies with, attachment rates for, 25:19490 (ORNL-4584, pp 92-104)
  electron reactions with, attachment rates for, (E), 25:19491 (ORNL-4584, pp 105-24)
  molecular oscillations of, Green's function analysis of effects of sulfur-34 on, 25:18408
SULFUR IONS
  implantation in cadmium sulfide at 200 keV, annealing of, 25:19791
  implantation in gallium arsenide, electric profiles of implanted layers after annealing, 25:19843
  implantation in indium arsenide at 400 keV for infrared detector fabrication, 25:19828
  implantation in p-type gallium arsenide at 100 keV, annealing effects on electric properties of implanted layers, 25:19842
SULFUR ISOTOPES S-31
  energy levels from sulfur-32 (He-3,α) reactions, lifetimes of, (E), 25:20349
SULFUR ISOTOPES S-32
  deuteron reactions (d,α) at 2 to 3.2 MeV, cross-section measurements by detection of positron annihilation γ rays, (E), 25:20283
  deuteron reactions (d,n) at 2 to 3.2 MeV, cross-section measurements by detection of positron annihilation γ rays, (E), 25:20283
  energy level from phosphorus-32 (p,γ) reactions, spin-parity assignment for first T = 2, (E), 25:20316
  energy levels from phosphorus-31 (p,γ) reactions at 1.555 MeV, (E), 25:20326
  energy levels of, calculation of magnetic monopole transition probabilities for, (T), 25:20306
  photon reactions (γ,d), (γ,n), (γ,2n), and (γ,pn) at 15 to 62 MeV, resonance structure in cross sections for, (E), 25:20332
  proton inelastic scattering at 9.275 MeV, evidence for vibrational excited states from, (E), 25:20326
  proton reactions (p,$\alpha\gamma$) at 14 MeV, angular correlations in, (E), 25:20323
  scattering by neodymium-150 and samarium-152 at 94 to 110 MeV with Coulomb excitation, Doppler shift attenuation in γ spectra from, (E), 25:20409
SULFUR ISOTOPES S-34
  effects on molecular constants of sulfur fluorides, 25:18408
  energy levels from phosphorus-31 (α,p) reactions, spins and gamma branching ratios for, (E), 25:20348
SULFUR ISOTOPES S-35
  determination of, use of carbon-14 as secondary counting standard in, 25:18364
SULFUR ISOTOPES S-37
  beta decay of, γ spectra from, (E), 25:20317
SUN
  atmosphere of, absorption matrix for normal Zeeman triplet in, (T), 25:19406
  eclipse of Mar. 7, 1970 as studied with torsion pendulum, 25:19431
  mass-loss processes in, (T), 25:19333
  neutrino emission from, development of gallium chloride and lithium chloride detectors for detection of, 25:18720
  neutrino flux from boron-8 in, upper limit on, (E), 25:19893
  neutrino spectroscopy of, program for, 25:19429
  plasma in, partition functions for ionizing, (T), 25:19397
  radiation constant of, (E), 25:19416
  radio brightness temperatures at millimeter wavelengths, (E), 25:19408
  radio emission from, attenuation at 19 and 37 GHz, (E), 25:19438
  spectra of, calibration of Wilson--Bappu effect in, (E), 25:19304
  spectra of, formation of absorption lines in, (E/T), 25:19434
  spectral energy distribution of, (E), 25:19416
  spectral line formation in atmosphere of, (T), 25:19424
  spectral resonance lines in atmosphere of, formation of, (T), 25:19395
SUNSPOTS
  area measurements on, reliability of Catania, (E), 25:19407
  cycles of, quasi-axisymmetric models of magnetic dynamo in, (T), 25:19422
  formation of, chromospheric processes during, (E/T), 25:19393(T) (CSIRO-Trans-10284)
  formation of, effects of planets on, (T), 25:19427
  spectra of, Wilson effect in absorption lines in, (E), 25:19432
  transparency of umbra and penumbra of, (E), 25:19432
SUPERCONDUCTIVITY
  conference on applied, Smolenice, Czechoslovakia, 6/69, 25:19591
SUPERCONDUCTORS
  critical temperature dependence on number of valence electrons in Cu_3Au-type alloys, oscillatory, (E/T), 25:19621
  electrodynamics of Type-II, macroscopic phenomenclogical, 25:19597
  electrodynamics of, (T), 25:19592
  energy spectra of, with overlapping energy bands, 25:19625
  Hall effect in, not in vortex state, (T), 25:19613
  Josephson effect in, demonstration of Riedel peak in, (E), 25:19602
  Josephson junctions in, self-resonant current peaks in, (T), 25:19612
  Kapitza resistance of junction with dielectric, effects of transition to normal state on, (E/T), 25:19616
  Kondo effect in, (T), 25:19603
  magnetic flux diffusion into Type-II, types of solutions for, 25:19593
  magnetic flux jumps in nonideal Type-II, (T), 25:19630
  magnetic flux-flow resistivity and Hall angle in pure transition-metal, near H/sub c2/, (T), 25:19619
  magnetic fluxoid pinning in mixed state of Type-II, 25:19595
  magnetic fluxoids in mixed state of Type-II, visualization of, (T), 25:19596
  magnetic-field-trapping properties of Type-I cylinders, anomalous length effects in, 25:19611
  phase slip in structures of weak, ac and dc potentials in, (T), 25:19610
  properties of superconducting points contacts weakly connecting two, 25:19601
  properties of Type-II, in time-dependent magnetic fields, 25:19598
  proximity effects between magnetic and superconducting thin films, 25:19600
  thermodynamics of Type-II, 25:19594
  transition temperature of ultrathin films, effect of normal-state resistance on, (T), 25:19614
  use in high-current-density magnets, 25:19644
  use of junctions of, in magnetometry, 25:19643
SUPERFLUIDITY
  occurrence in neutron stars, (T), 25:19348 (NP-18666)
SUPERNOVA REMNANTS
  identification of fifteen new, (E), 25:19386
SUPERNOVAE
  cosmic primary production in heavy, (T), 25:19532
  light curves for, (T), 25:19325
  mechanism for, featuring explosions of rotating stars,

XUM

(T), 25:19326
SURFACE WATERS
  contamination by gaseous effluents from nuclear power plants, computer methods for evaluating, 25:18526 (ORNL-4584, pp 37-40)
  temperature distribution in Walker Branch Watershed (Tennessee), measurement of, 25:18521 (ORNL-4584, pp 1-10)
SURFACES
  bibliography on surface and vacuum physics, 25:19469
  roughness measurements of, method for, 25:19758 (ORNL-4584, pp 74-86)
  scattering from rough, probabilities for nonspecular, (T), 25:20106
SURGERY
  techniques for gynecological, using radioisotopes, 25:19070
SURRY POWER REACTOR, UNIT 1
  construction of, revised permit application for, 25:20648 (DOCKET-50280-34)
  design parameters of, revised and additional data on, 25:20649 (DOCKET-50280-35)
  operation of, revised license application for, 25:20648 (DOCKET-50280-34)
  operations aspects of, revised and additional data on, 25:20649 (DOCKET-50280-35)
  owners of, financial statements of, 25:20648 (DOCKET-50280-34)
SURRY POWER REACTOR, UNIT 2
  construction of, revised permit application for, 25:20648 (DOCKET-50280-34)
  design parameters of, revised and additional data on, 25:20649 (DOCKET-50280-35)
  operation of, revised license application for, 25:20648 (DOCKET-50280-34)
  operations aspects of, revised and additional data on, 25:20649 (DOCKET-50280-35)
  owners of, financial statements of, 25:20648 (DOCKET-50280-34)
SWITCHES
  properties of superconducting point contacts weakly connecting two superconductors, 25:19601
SYMMETRY GROUPS
  beta decay in, second-class currents for mirror asymmetry in, 25:20535
  breaking of chiral, for form factors for $K \to \pi + l + \nu$ and $K \to 2\pi + l + \nu$ decays, 25:20041
  broken, renormalization of quantum field theories with, 25:20056 (DESY-70/62)
  chiral symmetry for hadrons, lectures on, 25:20045
  chiral, for S-wave scattering lengths for $\pi + N$ interactions at threshold, electromagnetic corrections to, 25:20044
  conformal transformations of three-point functions for axial-vector and vector currents, 25:20036
  conformal, phenomenological actions for spontaneously broken, 25:20038
  O(2,1), Lame functions for, crossing symmetric expansions of physical scattering amplitudes in, 25:20105
  O(4,2), Coulomb amplitude as matrix element of rotation in, 25:20040
  O(6,C) algebra, wave equations with compact and noncompact spectrum in, 25:20050
  SL(2,C), representations of, complementary series of, 25:20033
  SU(2) x SU(2) chiral, dynamical rearrangement of spontaneously broken, 25:20042
  SU(2) x SU(2), comparison with SU(3) for $\pi + N$ interactions, 25:20051
  SU(6)/sub W/, production of octet $1/2^+$ baryons and octet 0^- mesons in decay of decuplet $3/2^+$ baryons in broken, (T), 25:20048
  SU(n) algebra for mesons in bootstrap model, 25:19999
  U(6,6), meson (π) exchange in N + N interactions in, calculation of one-pion-exchange diagram for, 25:20021
  U(n), Racah coefficients of, identity satisfied by, 25:20034
SYMMETRY GROUPS SU(3)
  coupling renormalization for width of $K^* \to K + \pi$ decay in broken, 25:20043
  mass operator in strong coupling theory for static baryon octet source interacting with pseudoscalar meson octet fields in, 25:20015
  mass operator in, for baryon coupling with pseudoscalar meson octet, 25:20046
  octet currents for mirror asymmetry in $\Sigma \to \Lambda + e + \nu$ decay in, 25:20535
SYNCHROCYCLOTRONS
  beam extraction system for, matrix method for three-element regenerative, 25:20159
  beam profile monitor for, multiwire spark chamber, 25:20163
  experimental facilities for BOL nuclear research project, analog and digital electronics for, 25:20199
  experimental facilities for BOL nuclear research project, position-sensitive detector telescopes for, 25:18757
  experimental facilities for BOL nuclear research project, multidetector, 25:20198
  experimental facilities for BOL nuclear research project, design of scattering chamber for, 25:20201
  experimental facilities for BOL nuclear research project computer-hardware configuration for, 25:20200
SYNCHROTRONS
  beam extraction from, theory of resonant integer, 25:20145
  cavity resonator ferrite bias regulator for, 25:20178(P)
  cavity resonator tuning in high-energy, phase-angle measurement system for, 25:20179(P)
  design study for 100- to 150-GeV proton, using superconducting or cryogenically cooled aluminum magnets, 25:20125 (BNL-15430)
  evaluation of Carnegie--Mellon proton, for use in radiotherapy, 25:19087
  experimental facility for Braunschweig 140-MeV electron, pneumatic system for activation analysis, 25:20184
SYSTEMS FOR NUCLEAR AUXILIARY POWER (SNAP-15)
  heat source for, measurement of gamma spectra of, 25:18601

T

TACHYONS
  theory for, review of, (T), 25:20085
TAKAHAMA POWER REACTOR, UNIT 1
  design parameters of, 25:20566
TANTALUM
  corrosion by liquid lithium, effects of iridium on inhibition of, 25:19168(P)
  neutron capture at 3.0 to 6.5 MeV, gamma spectra from, (E), 25:18735 (INR-1224)
  properties for use as capsule material for radioisotope heat sources, evaluation of high-temperature, 25:18592 (ORNL-4298)
  ultrasonic attenuation in single crystals of, Alpher--Rubin effect of magnetic field on, 25:19879
TANTALUM ALLOYS AND SYSTEMS
  Co-base--Ta, crystal structure of solid solutions of, during degradation, 25:19233
  Co-base--Ta, phase studies of solid solutions of, 25:19233
  Mo--Nb--Ta--W-base, mechanical properties of, effects of composition on, 25:19239
  Mo--Ta--W, properties of, microstructural and physical, 25:19205
  Nb--Ta, diffusion in solid-solution, at 1100 to 1800°C, effects of tantalum content on reciprocal, 25:19204
  Nb--Ta--Ti, superconducting transition temperature of, 25:19629
  Nb--Ta--Ti--Zr, effects of iron additions on superconducting properties of, 25:19618(P)
TANTALUM CARBIDES
  electron band structure of, ESCA study of, 25:19867
TANTALUM DEUTERIDES
  deuteron magnetic resonance study of, exploratory, 25:19876
TANTALUM ISOTOPES Ta-181
  gamma circular polarization from, effect of form factor in calculation for, (T), 25:20423
TANTALUM ISOTOPES Ta-182
  energy levels of, calculation using unified model, 25:20524
  use for implant therapy, evaluation of applicators and methods for, 25:19076
TD-NICKEL
  reactions with cobalt in air at high temperatures, 25:18591(R) (DP-1254)
TD-NICKEL CHROMIUM
  reactions with cobalt in air at high temperatures, 25:18591(R) (DP-1254)
TECHNETIUM ALLOYS AND SYSTEMS
  Rh--Tc, magnetic susceptibility at 4 to 300°K, 25:19874
  Ru--Tc, magnetic susceptibility at 4 to 300°K, 25:19874
TECHNETIUM ISOTOPES Tc-95
  beta and electron-capture decay of isomeric, γ--γ angular correlations from, (E), 25:20468
TECHNETIUM ISOTOPES Tc-99
  effectiveness of inhaled sulfur-colloid-incorporated, for determining lung function in man, 25:19044
  effectiveness of pertechnetate-incorporated metastable, for myeloscintigraphy in man following intravenous injection, 25:19042
  preparation of macroaggregated iron hydroxide-incorporated metastable, for use in lung perfusion studies, 25:19054
  preparation of rhenium sulfide colloid-incorporated, for scanning of reticulo-endothelial system, 25:19054
  preparation of sodium pertechnetate-incorporated metastable, for brain scanning, 25:19054
  production of metastable, for use in scanning, use of molybdenum-99 generator for, 25:18885
  use for scanning kidneys for blood circulation and function, combined use of iodine-131-labeled Hippuran with, 25:19046
  use of metastable, for diagnosis of communicating hydrocephalus by lumbar administration, 25:19043
  use of metastable, for diagnosis of spleen involvement in Hodgkin's disease, 25:19058
  use of metastable, for evaluation of human spleen size during liver scanning, 25:19057
  use of metastable, for localization of human placenta by γ camera scanning, 25:19045

XUM

use of pertechnetate incorporated metastable, for radiodiagnosis of subdural hematoma, 25:19059

TELEMETERING SYSTEMS
  comparison of CBW FM/FM and DSB/FM, 25:20888 (SC-DR-70-686)

TELLURIUM
  chromatographic behavior in hydrochloric acid--thiocyanate mixture on Amberlite LA-2, 25:18337
  detection in low-energy cosmic radiation, (E), 25:19525
  determination in cadmium, indium, rare earth, and zinc tellurate-tellurite compounds, 25:18351
  determination of hexavalent, in cadmium, indium, rare earth, and zinc tellurate-tellurite compounds, 25:18351

TELLURIUM HALIDES
  separation by solvent extraction, effects of charge, composition, and structure on, 25:18511

TELLURIUM IONS
  implantation in gallium phosphide and arsenide at 20 and 40 keV, lattice disorder induced by, 25:19844

TELLURIUM ISOTOPES Te-114
  energy levels from tin (α,xn) reactions, (E), 25:20461

TELLURIUM ISOTOPES Te-116
  energy levels from tin (α,xn) reactions, (E), 25:20461

TELLURIUM ISOTOPES Te-118
  energy levels from tin (α,xn) reactions, (E), 25:20461

TELLURIUM ISOTOPES Te-120
  energy levels from tin (α,xn) reactions, (E), 25:20461

TELLURIUM ISOTOPES Te-122
  energy levels from tin (α,xn) reactions, (E), 25:20461

TELLURIUM ISOTOPES Te-124
  energy levels from tin (α,xn) reactions, (E), 25:20461
  energy-level transitions from antimony-124 decay, multipole mixing ratios for, (E), 25:20386

TELLURIUM ISOTOPES Te-125
  energy levels and transitions from antimony-125 decay, (E), 25:20408

TELLURIUM ISOTOPES Te-126
  energy levels from tin (α,xn) reactions, (E), 25:20461

TELLURIUM ISOTOPES Te-129
  half-life of isomeric, (E), 25:20339

TELLURIUM ISOTOPES Te-131
  beta decay of 25-min isomer of, gamma spectra from, (E), 25:20428

TEMPERATURE
  calculation of transient fields of, FORTRAN program for numerical, 25:18579
  distribution in fuel pellets and cladding, effects of coefficient of heat transfer on, 25:18589
  distribution on heat transfer surfaces, W-MESHER computer program for calculation of, 25:18578 (WANL-TME-2721)

TERBIUM
  neutron critical magnetic scattering from, measurements of thermal, 25:18738 (RISO-229)

TERBIUM ALLOYS AND SYSTEMS
  Re--Tb--Th, crystal structure of intermetallic compounds of, 25:19235

TERBIUM IONS
  implantation in zinc sulfide and selenide films at 250 kV, cathodoluminescence effects of, 25:19795
  wave functions for, accurate numerical Hartree--Fock self-consistent field, 25:19478

TERBIUM ISOTOPES Tb-156
  decay of, conversion electron spectra from, (E), 25:20472

TERBIUM ISOTOPES Tb-160
  exchange between terbium ions and terbium--aminopolycarboxylate complexes, 25:18412

TERBIUM ISOTOPES Tb-161
  half-life, (E), 25:20338
  half-life, (E), 25:20339

TEREPHTHALIC ACID, POLYETHYLENE ESTERS
  radioinduced grafting in aqueous solutions containing acrylamide or methacrylamide saturated with ethylene, 25:18429

TETRACYCLINE
  effects on hemolysis of uv-irradiated erythrocytes, 25:18914
  effects on Staphylococcus aureus E169, use of uv-irradiated transducing phage lysates to determine chromosomal relation of determinants for sensitivity, 25:19157

THALLIUM
  chromatographic behavior in hydrochloric acid--thiocyanate mixture on Amberlite LA-2, 25:18337
  determination in glass and high-purity metals by photon activation, 25:18366(R) (NBS-TN-548)
  diffusion of implanted, in germanium, during annealing, 25:19841

THALLIUM IONS
  implantation in germanium at 30 to 40 keV, channeling study of lattice location of, 25:19827
  implantation in germanium at 40 and 70 keV, electric properties and lattice location of, 25:19799
  implantation in silicon at 40 keV, carbon-ion channeling study of, 25:19829
  implantation in silicon carbide at 5 to 300 keV, properties of conducting layers and p--n junctions formed by, (E), 25:19847

THALLIUM ISOTOPES Tl-200
  beta and electron-capture decay of, γ-γ directional correlations for, 25:20400

THALLIUM ISOTOPES Tl-203
  energy-level transition of, gamma-ray polarization in 279-keV, (E), 25:20433

THALLIUM ISOTOPES Tl-204
  beta decay of, angular distribution and energy spectra of internal bremsstrahlung emitted during, (E/T), 25:20417

THALLIUM ISOTOPES Tl-205
  oxygen-16 reactions (O-16,xn) with, excitation functions for total neutron emission for, (E), 25:18737(R) (ORO-3820-7)

THALLIUM ISOTOPES Tl-208
  decay in SNAP-15A heat source, measurement of gamma spectra from, 25:18601

THERMAL CONDUCTIVITY CELLS
  development for measuring heat transfer of deposited sodium compounds, 25:18562 (CONF-700816-(Vol.1), pp 413-24)

THERMAL INSULATION
  design of laminated porous, for gas cooled reactor vessels, 25:20727(P)

THERMAL STRESSES
  calculation of elastic fields of, FORTRAN program for numerical, 25:18579

THERMIONIC CONVERTERS
  design of heat-shielded, 25:19544(P)

THERMOCOUPLES
  development for temperature measurements in liquid metals, 25:19227
  positioning in reactor cores, equipment for remote, 25:20842(P)
  readout for microwave power density probe of, design of, 25:18827 (BRH/DEP-70-31)

THERMODYNAMICS
  expansion of ideal gas of nonzero rest mass, adiabatic, (T), 25:19464

THERMOELECTRIC CONVERTERS
  design and testing of 2-kW radioisotope-fueled, 25:18594(R) (ORNL-TM-3292)
  design of radioisotope-fueled, 25:18605(P)
  design of strontium-90-fueled, with germanium silicide thermopiles, 25:18598(P)
  operation of radioisotope-fueled, effects of load conditions and temperature on long-term, 25:18595 (SC-RR-70-854)

THERMOMETRY
  development of instruments for ultrasonic, for LMFBR, 25:18830(R) (NYO-3906-12)

THERMONUCLEAR EXPLOSIONS
  uses in nuclear physics, 25:20449

THERMONUCLEAR REACTIONS
  production using lasers, review of, 25:19724 (FOA-4-4449)

THERMONUCLEAR REACTORS
  design of toroidal, 25:19729(P)
  plasma confinement and equilibrium in toroidal, (T), 25:19652
  plasma confinement in toroidal multipoles with shielded supports, (T), 25:19651
  plasma energy balance in tokamak-type systems, (T), 25:19654
  research on, review of, 25:19730
  vacuum systems for, use of nitrites for, 25:19728

THERMOPILES
  design for use in radioisotope-fueled generators, 25:18605(P)

THICKNESS GAGES
  design of beta backscatter, for manufacture of rubber tires, 25:18824
  development of beta backscatter, 25:18823
  operation of radiometric, on moving plates, theory of, 25:18825

THIOCYANATES
  complexes with americium and europium, stability constants for, effects of ionic media on, 25:18371

THIORIDAZINE
  radioprotective effects of, on mice, whole-body cobalt-60 γ, 25:19028

THORIUM
  chromatographic behavior in hydrochloric acid--thiocyanate mixture on Amberlite LA-2, 25:18337
  determination in radioactive ores by gamma spectrometry or neutron activation, 25:18365
  determination using azo compounds, photometric, 25:18347
  effects on fluoride hydrolysis, catalytic, 25:18375
  effects on hydrolysis of potassium phosphorodifluoridate and sodium phosphorofluoridate, catalytic, 25:18373
  mineralization and occurrence in alkaline igneous rocks, 25:18540
  reactions with (o-oxalophenylazo)chromotropic acid, stability of complexes from, 25:18382
  separation from iron and lead by solvent extraction as caproate into chloroform, 25:18506
  separation of bismuth from, by cation exchange chromatography, 25:18520

THORIUM ALLOYS AND SYSTEMS
  Dy--Re--Th, crystal structure of intermetallic compounds of, 25:19235
  Er--Re--Th, crystal structure of intermetallic compounds of, 25:19235

- Gd--Re--Th, crystal structure of intermetallic compounds of, 25:19235
- Gd--Re--Th, crystal structure of intermetallic compounds of, 25:19235
- Re--Tb--Th, crystal structure of intermetallic compounds of, 25:19235

THORIUM CARBIDES
- preparation of coated particles of, for in-pile irradiation, 25:19288 (ORNL-4629, pp 82-98)

THORIUM DEPOSITS
- occurrence of low-grade, in south Greenland, 25:18539

THORIUM HIGH-TEMPERATURE REACTOR
- coolants for, economic comparison of helium and neon, (T), 25:20729

THORIUM HYDROXIDES
- conversion to thorium dioxide by calcination or sintering, 25:19259 (NLCO-1029)

THORIUM ISOTOPES Th-226
- dosimetry in man, use of decay scheme data and computer calculations for, 25:18991 (ORNL-4584, pp 200-22)

THORIUM ISOTOPES Th-228
- content of human diet, placental tissues, and teeth in high natural background areas in Brazil, 25:18927 (NP-18670)

THORIUM ISOTOPES Th-231
- production of spontaneously fissioning isomeric, in (n,2n) reactions, upper limits for cross sections for, (E), 25:20369 (JINR-P3-5528)

THORIUM ISOTOPES Th-232
- boron-10 reactions with, analysis of compound nucleus mechanism in, (E/T), 25:20420
- boron-11 reactions with, analysis of compound nucleus mechanism in, (E/T), 25:20420
- neutron capture at 0 to 15 MeV, cross sections and resonance integrals for, (E/T), 25:20377 (WAPD-TM-971)
- neutron fission at energies up to 6 MeV, energy-balance analysis of dependence of number of prompt neutrons on bombarding energy for, (T), 25:20440
- neutron reactions (n,2n) with, upper limits for cross sections for production of spontaneously fissioning isomers in, (E), 25:20369 (JINR-P3-5528)
- photofission at 5 to 10 MeV, cross section structure near threshold for, (E), 25:20366 (IEA-211)

THORIUM NITRATES
- purification by solvent extraction from impure solutions, 25:19259 (NLCO-1029)
- reactions with ammonium hydroxide to prepare thorium hydroxide, 25:19259 (NLCO-1029)

THORIUM OXIDES
- analysis for uranium using 2-[(5-bromo-2-pyridyl)azo]-5-(diethylamino)phenol, spectrophotometric, 25:18352
- coating of sol-gel particles of, fluidized bed method for carbon, 25:19262 (ORNL-4629, pp 65-82)

THORIUM OXIDES ThO$_2$
- preparation of coated particles of, for in-pile irradiation, 25:19288 (ORNL-4629, pp 82-98)
- production of dense, methods for large-scale, 25:19259 (NLCO-1029)
- radiation effects on compacted clad fuel rods of, at 10,000 MWd/t, 25:19291
- sorptive properties of nonporous, for argon, nitrogen, and water vapor, effects of surface water on, 25:18416
- ThO$_2$--UO$_2$, calcining of gel spheres of, effects of carbon on, 25:19263 (ORNL-4629, pp 99-102)
- ThO$_2$--UO$_2$, coating of sol-gel particles of, fluidized bed method for carbon, 25:19262 (ORNL-4629, pp 65-82)
- ThO$_2$--UO$_2$, preparation of coated particles of, for in-pile irradiation, 25:19288 (ORNL-4629, pp 82-98)
- ThO$_2$--UO$_2$, preparation of microspheres of, engineering scale demonstrations on, 25:19261 (ORNL-4629, pp 14-64)
- ThO$_2$--UO$_2$, preparation of microspheres of, incorporating uranium-233, 25:18624 (ORNL-4629, pp 1-9)
- ThO$_2$--UO$_3$, drying of gel spheres of, development of optimum methods for, 25:19263 (ORNL-4629, pp 99-102)
- ThO$_2$--UO$_3$, preparation of sols of, by extraction from nitrate solutions using Amberlite LA-2, 25:19261 (ORNL-4629, pp 14-64)

THULIUM IONS
- wave functions for, accurate numerical Hartree--Fock self-consistent field, 25:19478

THULIUM ISOTOPES Tm-169
- alpha reactions (α,xn) and (α,pxn) up to 150 MeV, cross sections for, (E), 25:20390
- energy-level transitions in, internal conversion ratios for M1 + E2, (E), 25:20473

THULIUM ISOTOPES Tm-170
- performance as gamma source for radiometric rock analysis, 25:18524

THULIUM ISOTOPES Tm-176
- nuclear spin and parity of, 25:20380

THULIUM TELLURATES
- Tm$_2$(TeO$_3$)$_3$--Tm$_2$(TeO$_4$)$_3$, analysis for hexavalent tellurium and total tellurium by automatic amperometric and potentiometric titrations, 25:18351

THULIUM TELLURITES
- Tm$_2$(TeO$_3$)$_3$--Tm$_2$(TeO$_4$)$_3$, analysis for hexavalent tellurium and total tellurium by automatic amperometric and potentiometric titrations, 25:18351

THYMIDINE
- metabolism in lymphocytes, tritium tracer study of effects of phytohemagglutinin on, 25:18919(R) (RLO-2225-T-16-1)

THYMINE
- radiolysis of aqueous solutions of, electron pulse, 25:18475

THYMUS GLAND
- scanning in patients with myasthenia gravis for diagnosis of neoplasms, use of selenium-75-labeled selenomethionine for, 25:19049

THYROID GLAND
- function of human, use of radioiodine-labeled thyroxine and triiodothyronine for in vitro studies on, 25:19041
- iodine isotope uptake by, dual detector system for measuring, 25:18898
- iodine-131 dose to human, from milk in Norway, relation of frequency of cancer to, 25:19135
- iodine-131 uptake by human, effects of thyroid diseases on, 25:19051

TIN
- chromatographic behavior in hydrochloric acid--thiocyanate mixture on Amberlite LA-2, 25:18337
- magnetic-field-trapping properties of hollow cylinders of, anomalous length effects in, 25:19611
- properties as radiation filters for skin protection during γ therapy, 25:19082
- proton reactions (p,n) at 3 to 5.5 MeV, cross sections and strength functions for, (E), 25:20475
- separation of bismuth from, by cation exchange chromatography, 25:18520
- tunneling into weakly coupled films of aluminum and superconducting, in proximity, 25:19623

TIN ALLOYS AND SYSTEMS
- Al--Cr--Nb--Si--Sn--Ti, properties for use as protective coating on niobium, 25:19176
- Al--Nb--Si--Sn--Ti, properties for use as protective coating on niobium, 25:19176
- In--Sn, diffusion of tin in fused eutectics of, 25:19199
- Nb-base--Sn, superconductivity of, relations with microstructures, 25:19219
- Sn--Ti, properties of intermetallic Ti$_3$Sn, effects of aluminum and zirconium additions on, 25:19238

TIN CHLORIDES
- alkali-metal-atom scattering by, crossed-beam measurements and optical-model analysis of, 25:19497

TIN HALIDES
- separation by solvent extraction, effects of charge, composition, and structure on, 25:18511

TIN ISOTOPES Sn-114
- photon reactions (γ,p) at 12 to 22 MeV, excitation functions for, (E/T), 25:20394

TIN ISOTOPES Sn-117
- proton reactions (p,n) at 3 to 5.5 MeV, cross sections and strength functions for, (E), 25:20475

TIN ISOTOPES Sn-118
- proton elastic scattering at 7 to 12.1 MeV, polarization in, (E), 25:20331
- proton reactions (p,d) at 24.5 MeV, DWBA analysis of cross-section and asymmetry angular distributions from polarized, (E), 25:20365 (CEA-CONF-1657)

TIN ISOTOPES Sn-119
- energy levels from tin-118 proton elastic scattering, spin assignments for isobaric analog, (E), 25:20331
- proton reactions (p,d) at 24.5 MeV, DWBA analysis of cross-section and asymmetry angular distributions from polarized, (E), 25:20365 (CEA-CONF-1657)
- proton reactions (p,n) at 3 to 5.5 MeV, cross sections and strength functions for, (E), 25:20475

TIN ISOTOPES Sn-120
- energy levels from antimony-120 and indium-120 decays, spin-parity assignments for, (E), 25:20401
- proton elastic scattering at 7.3 to 7.8 MeV, polarization in, (E), 25:20331
- proton reactions (p,n) at 3 to 5.5 MeV, cross sections and strength functions for, (E), 25:20475

TIN ISOTOPES Sn-121
- energy levels from tin-120 proton elastic scattering, widths for isobaric analog, (E), 25:20331

TIN ISOTOPES Sn-122
- proton reactions (p,n) at 3 to 5.5 MeV, cross sections and strength functions for, (E), 25:20475

TIN ISOTOPES Sn-124
- proton reactions (p,n) at 3 to 5.5 MeV, cross sections and strength functions for, (E), 25:20475

TIN OXIDES
- radiolysis of SnO and SnO$_2$, effects of dose on products from γ, 25:18470

TIRES
- manufacture of, beta backscatter thickness gage for, 25:18824

TISSUES
- neutron interactions with, fast, 25:19007 (NCRP-38)
- radiation dose distribution in, from implanted californium-252 point sources, (T), 25:19003
- radiation dose to, calculation of 10- to 2000-MeV π^+ and π^-, 25:20226
- radiation effects on rodent, effects of artificial hypothermia and ischemia on lethal whole-body, 25:19093
- radioisotope content of human, in Finland, 25:18931 (NYO-3446-14, Paper 30)
- radioisotope content of rat, comparison of direct and treated-sample determinations of, 25:18997

XUM

- radiosensitivity of malignant and normal in man, effects of LET on ionizing, 25:19077

TITANIUM
- abundance in α^2 CVn, (E), 25:19339
- abundance in Type-M supergiant, (E), 25:19323
- chromatographic behavior in hydrochloric acid--thiocyanate mixture on Amberlite LA-2, 25:18337
- determination of trace amounts of, by formation of colored peroxy compounds and sorption on chelating resin, 25:18343
- deuteron reactions at 180 to 360 keV with, cross sections for K-shell ionization in, (E), 25:19470
- effects on fluoride hydrolysis, catalytic, 25:18375
- proton reactions at 90 to 180 keV with, cross sections for K-shell ionization in, (E), 25:19470
- reactions with uranium tetrafluoride vapors, production of uranium trifluoride by, 25:18372
- separation of bismuth from, by cation exchange chromatography, 25:18520

TITANIUM ALLOYS AND SYSTEMS
- Al--Cr--Nb--Si--Sn--Ti, properties for use as protective coating on niobium, 25:19176
- Al--Nb--Si--Sn--Ti, properties for use as protective coating on niobium, 25:19176
- C--Nb-base--Ti--V--W--Zr, oxidation morphology and rates in air at 800 to 950°C, 25:19172
- Cr--Ti-base, superconducting transition temperature in, effects of omega phase reversion on, 25:19590
- Nb--Ta--Ti, superconducting transition temperature of, 25:19629
- Nb--Ta--Ti--Zr, effects of iron additions on superconducting properties of, 25:19618(P)
- Nb--Ti, diffusion in solid-solution, at 1100 to 1800°C, effects of titanium content on reciprocal, 25:19204
- Nb--Ti, diffusion in, kinetics of, 25:19214
- Nb--Ti, magnetic flux jumps in superconducting, (E/T), 25:19630
- Nb--Ti, superconductivity of, relations with microstructure, 25:19219
- Nb--Ti, threshold currents of large cross-section superconducting, 25:19624
- Nb--Ti--Zr, superconducting properties of, 25:19627
- Nb-base--Ti, embrittlement by hydrogen, effects of interstitial solutes on, 25:19216
- Nb-base--Ti, mechanical properties of solid solutions of, 25:19215
- Nb-base--Ti, preparation of high-purity, by vacuum arc melting, 25:19186
- Nb-base--Ti--Zr, plasticity and strength of, at -196 and 20°C, 25:19206
- Sn--Ti, properties of intermetallic Ti_3Sn, effects of aluminum and zirconium additions on, 25:19238
- Ti-base--V, superconducting transition temperature in, effects of omega phase reversion on, 25:19590

TITANIUM ISOTOPES Ti-46
- helium-3 reactions (He-3,t) at 37.7 MeV, differential cross sections for, (E), 25:20347

TITANIUM SILICIDES
- deposition on niobium by pack cementation for corrosion protection, 25:19175

TOHOKU POWER REACTOR, UNIT 1
- buildings and structures for, design parameters and construction schedule for, 25:20565
- design parameters of, 25:20565
- site for, preparation of, 25:20565

TOKAMAK DEVICES
- plasma column and gas sheath in T-3, material balance of, 25:19657(T) (MATT-Trans-16)
- plasma energy balance in, (T), 25:19654
- plasma energy in T-3, circuit and technique for measurement of, 25:19662
- plasma equilibria in, axisymmetric hydromagnetic, (T), 25:19716
- plasma heating by magnetic pumping in, torsional magnetic perturbation method for, (T), 25:19648

TONSILS
- radiotherapy of carcinomas of human, effectiveness of γ, 25:19085

TOWER SHIELDING FACILITY
- design parameters of TSR-II for operation at 1 MW, 25:20789 (ORNL-TM-2893(Vol.1)(Rev.))

TOXINS
- radioinduced, in potatoes and rat liver, effects on corn root growth of, 25:18915

TRACE ELEMENTS
- content and distribution in sediments and soils, (E), 25:18521 (ORNL-4584, pp 1-10)
- determination in biological materials by activation, 25:18886

TRACER TECHNIQUES
- development of radioactive and Rhodamine B dye, for measuring hydraulic fracturing of underground shales, 25:18622 (ORNL-4584, pp 11-15)
- methods for biology and medicine, 25:18886

TRANSACTINIDE ELEMENTS
- existence of element 108 in nature, 25:20376(T) (ORNL-tr-2428)
- production of, review of means for, (T), 25:20458
- search for, review of, (T), 25:20458

TRANSFORMERS
- core materials for, evaluation of Supermendur and Silectron Steel, 25:20889 (SC-DR-70-736)

TRANSISTORS
- fabrication using ion implantation and calutron-type ion source, 25:20169
- radiation hardening of circuits containing, equipment and method for, 25:18879(P)
- switching speeds of diffused and ion-implanted MIS, comparison, (E/T), 25:18858

TRANSITION METALS
- magnetic flux-flow resistivity and Hall angle in pure superconducting, two-band expressions for, (T), 25:19619
- superconductivity in, pressure enhancement of, (T), 25:19605

TRANSPORT THEORY
- use of one-dimensional, for calibration of subsurface gamma-scatter densimeter, 25:18816

TRANSURANIUM ELEMENTS
- bibliography on, Dec. 1970, 25:19166
- nuclear wave functions for single-particle states in deformed, tables of, 25:20481 (JINR-P4-5457)
- production in nuclear explosions, 25:20449

s-TRIAZINE-2,4,6(1H,3H,5H)-TRIONE, TRIALLYL-
- polychloroethylene--triallyl-s-triazine-2,4,6-(1H,3H,5H)-trione, radiation effects on curing of, 25:18437(P)

TRICARBOXYLIC ACID CYCLE
- radiation effects on incorporation of carbon-14-labeled pyruvate into, in rat thymocytes, 25:18902

TRIETHYLENEPHOSPHORAMIDE
- effects on fecundity of γ-irradiated citrus red mites, 25:19100
- effects on γ-radioinduced mutations in sperm of citrus red mites, 25:19100

TRIMETHYLAMINE
- 3-chloro-2-hydroxypropyl methacrylate--trimethylamine, radioinduced polymerization in porous ceramics and firebrick, ion exchange properties of products from γ, 25:18421(R) (RLO-2098-1)

TRIOCTYLAMINE
- complexes with uranyl fluorides and sulfates in hydrofluoric and sulfuric acids, spectra and structure of, 25:18381

TRITIUM
- binding energy of, calculation using harmonic oscillator basis, (T), 25:20259
- content in ground waters of central Nevada, 25:18522 (USGS-474-97)
- content of natural gas produced in Gasbuggy Project during 1969, hazards to man from, 25:18989 (ORNL-4584, pp 42-56)
- content of rainwater in Finland, 25:18931 (NYO-3446-14, Paper 30)
- Coulomb energy difference relative to helium-3, (T), 25:20256
- determination in water and sewage, 25:18360
- effects on proton transfer from hydronium ions in water, kinetic studies on solvent, 25:18395
- exchange between hydronium ions and water, 25:18395
- exchange with hydrogen in water, catalytic effects of activated carbon GX 133 on, 25:18385 (CONF-700816-(Vol.1), pp 278-88)
- incorporation in Ehrlich ascites cells as labeled thymidine, effects of 6-azauridine on, 25:18888
- nuclear binding energy, Coulomb energy, form factors, magnetic moments, radii, and wave functions for, harmonic-polynomial calculations of, (T), 25:20249 (ITF-70-51-E)
- nuclear binding energy, doublet scattering length, and wave function for, Faddeev calculations of, (T), 25:20251 (NP-18678)
- photodisintegration of, bremsstrahlung-weighted E1 cross sections for, (T), 25:20252
- proton reactions (p,n) at 2.56 MeV, associated particle method for measuring neutron flux from, 25:18647
- radiation dose distribution from point source, methods for calculating, 25:18984 (JUL-688-ME)
- radiation hazards during handling of large amounts of, 25:18982 (CEX-65.05)
- reactions of recoil atoms of, with hexane in benzene, products from, 25:18487
- reactions of recoil, with fluorotrimethylsilane, 25:18484
- targets for T (d,n) neutron sources, development of, 25:20134 (ORNL-4584, pp 187-97)
- use as tracer for ecological studies on ticks, 25:18934(R) (ORO-3514-10)
- use as tracer to determine total body water in man, methods for reducing radiation dose from, 25:18977 (AD-702155)

TRITONS
- binding energy of, using a separable expansion of local potentials, (T), 25:20538
- reactions with beryllium-9 at 0.3 to 1 MeV, angular distributions and differential cross sections for, (E), 25:20265 (CEA-R-4117)
- reactions with nuclei, tables of thresholds for, (E), 25:20237 (UCRL-50400(Vol.9))
- scattering by helium-4, separable potentials for, 25:20511

TRYPTOPHAN
- radiation effects on, in relation to physiological damage

    in cells, biophysical mechanisms of uv, 25:18903
  spectra of, near-uv absorption band, 25:20899 (UCLA-12-810)
TUBES
  neutron transmission through simple bent conducting, calculations of, 25:20245
TUNGSTEN
  chromatographic behavior in hydrochloric acid--thiocyanate mixture on Amberlite LA-2, 25:18337
  degasification at 2000°K, measurement of rate of, 25:19225
  deuteron reactions at 180 to 360 keV with, cross sections for M-shell ionization in, (E), 25:19470
  electron slowing down in, 25:19759 (ORNL-4584, pp 87-91)
  grain boundaries in, combined electron and field ion microscope determination of, 25:19249
  neon-22 reactions (Ne-22,f) at 115 to 174 MeV, compound-nucleus lifetime in, (E), 25:20370 (JINR-P7-5512)
  potassium surface ionization on, effects of impurities on residence time for, 25:19210
  properties for use as capsule material for radioisotope heat sources, evaluation of high-temperature, 25:18592 (ORNL-4298)
  proton reactions at 90 to 180 keV with, cross sections for M-shell ionization in, (E), 25:19470
  reactions of (100) crystal planes of, with nitrogen, 25:19208
  reactions with cobalt in air at high temperatures, 25:18591(R) (DP-1254)
  reactions with nitrogen at 800°C, diffusion and nitrogenation, 25:19234
  slip initiation in monocrystalline, 25:19194(R) (NYO-4073-4)
  sorptive properties for atoms of other elements, relations with adatom surface potential and adsorbate electronegativity, 25:19207
  sorptive properties for bromine, chlorine, and iodine, relations with work function, 25:19209
  superconducting and semiconducting phase of, embedded in SiO_2 films, 25:19631
  thermal loading to induce water boiling on wires of, parameters for critical, 25:18583
TUNGSTEN ALLOYS AND SYSTEMS
  Ag--W, electric conductivity of two-phase, 25:19226
  B--C--Hf--Nb-base--W--Zr, properties for use at high temperatures, 25:19218
  C--Hf--Mo--Nb-base--W, properties for use at high temperatures, 25:19218
  C--Nb-base--Ti--V--W--Zr, oxidation morphology and rates in air at 800 to 950°C, 25:19172
  Cu--Nb-base--W, phase studies of isothermal sections of, at 1600, 1900, and 2100°C, 25:19246
  Cu--W, electric conductivity of two-phase, 25:19226
  Mo--Nb--Ta--W-base, mechanical properties of, effects of composition on, 25:19239
  Mo--Ta--W, properties of, microstructural and physical, 25:19205
  Nb--W, diffusion in solid-solution, at 1100 to 1800°C, effects of tungsten content on reciprocal, 25:19204
  Nb--W, diffusion in, kinetics of, 25:19214
  Nb-base--Ni--W, phase studies of isothermal sections of, at 1800 and 1900°C, 25:19246
  Re--W, thermal loading to induce boiling on wires of, parameters for critical, 25:18583
  Re--W-base, reactions with cobalt in air at high temperatures, 25:18591(R) (DP-1254)
  UC-base--W, diffusion of helium bubbles in, during annealing at 800 to 1500°C, 25:19272 (AI-AEC-12984)
TUNGSTEN CARBIDES
  Ag--WC, electric conductivity of two-phase, 25:19226
  Co--WC, elastic modulus of two-phase, variational bounds of, (T), 25:19282
TUNGSTEN ISOTOPES W-183
  half-life of isomeric, 25:20463
TUNGSTEN ISOTOPES W-186
  neutron capture by, γ spectra from thermal, (E), 25:20324
TUNGSTEN ISOTOPES W-187
  energy levels from tungsten-186 thermal neutron capture, model analysis of, (E/T), 25:20324
TURBINES
  design requirements for direct cycle gas, for helium cooled power reactors, 25:20772
  design requirements for integrated direct cycle gas, for helium cooled power reactors, 25:20774
  design requirements for integrated direct cycle gas, for 1200 MW(e) helium cooled reactors, 25:20778
  development of direct cycle gas, for helium cooled power reactors, 25:20771
  development of indirect cycle carbon dioxide, for helium cooled power reactors, 25:20773
  exhaust pressure for, calculation of optimum, 25:18565 (ORNL-TM-3291)
TURKEY POINT POWER REACTOR, UNIT 3
  coolant loss accident conditions for, safety analysis of, 25:20630 (DOCKET-50250-39)
  design parameters of, revised and additional data on, 25:20631 (DOCKET-50250-40)
  design parameters of, revised and additional data on, 25:20632 (DOCKET-50250-41)
  operations aspects of, revised and additional data on, 25:20631 (DOCKET-50250-40)
  operations aspects of, revised and additional data on, 25:20632 (DOCKET-50250-41)
TURKEY POINT POWER REACTOR, UNIT 4
  coolant loss accident conditions for, safety analysis of, 25:20630 (DOCKET-50250-39)
  design parameters of, revised and additional data on, 25:20631 (DOCKET-50250-40)
  design parameters of, revised and additional data on, 25:20632 (DOCKET-50250-41)
  operations aspects of, revised and additional data on, 25:20631 (DOCKET-50250-40)
  operations aspects of, revised and additional data on, 25:20632 (DOCKET-50250-41)
TYROSINE
  radiation effects on, in relation to physiological damage in cells, biophysical mechanisms of uv, 25:18903
TZM (MOLYBDENUM ALLOY)
  compatibility with cobalt aluminate at 1000°C, 25:18591(R) (DP-1254)
  compatibility with cobalt magnesium oxide at 1000°C, 25:18591(R) (DP-1254)
  compatibility with cobalt oxide at 1000°C, 25:18591(R) (DP-1254)
  properties for use as capsule material for radioisotope heat sources, evaluation of high-temperature, 25:18592 (ORNL-4298)

U

ULTRACENTRIFUGATION
  evaluation for production of enriched uranium requirements to 1980, 25:18609
ULTRASONIC TESTING
  method for locating discontinuities in graphite structures, description of computerized, 25:18613 (SC-DR-70-693)
ULTRAVIOLET RADIATION
  dosimetry using survival of Saccharomyces cerivisiae, 25:18981 (CEA-N-1380)
  effects on aromatic amino acids in relation to physiological damage in cells, biophysical mechanisms of, 25:18903
  effects on Brucella abortus, frequency of mutagenic, 25:18970
  effects on cultured mammalian cells, progress report on repair of molecular, 25:19090(R) (COO-1704-22)
  effects on cultured mammalian cells, synergistic effects of chemicals on biological expression of molecular, progress report on, 25:19090(R) (COO-1704-22)
  effects on DNA specific chromosomes in synchronous cultured Escherichia coli, mutagenic, 25:18966
  effects on erythrocytes, effects of photosensitizing compounds on hemolytic, 25:18914
  effects on erythrocytes, effects of salicylanilide on hemolytic, 25:18913
  effects on frequency of transduction of drug resistance determinants by phage lysates in Staphylococcus aureus E169, 25:19157
  effects on human skin, effects of, on light test reaction 24 hours following exposure, 25:19150
  effects on mitotic segregation in recombination deficient mutants of yeast, 25:18945 (UCRL-20192)
  effects on reversion in mutants of yeast, 25:18945 (UCRL-20192)
  effects on surface conductance of germanium, annealing recovery of, (T), 25:19859
  effects on undecafluoro(trifluoromethyl)cyclohexane, NMR studies on radicals produced by, 25:18448(R) (CEA-N-1369)
UNITED STATES
  seismic activity in southeastern, computerized history of, 25:18556 (ORNL-4584, pp 41)
URACIL, 5-FLUORO-
  effects on survival of x-irradiated mice following therapy for skin cancer, effects of synchronized treatment on, 25:19075
  effects on survival time in man following radiotherapy for tumors of head and neck, 25:19071
URANINITES
  occurrence in South African auriferous conglomerates, 25:18533
  origin of, thermodynamic conditions for, 25:18551
URANIUM
  boron-10 reactions with, analysis of compound nucleus mechanism in, (E/T), 25:20420
  boron-11 reactions with, analysis of compound nucleus mechanism in, (E/T), 25:20420
  chromatographic behavior in hydrochloric acid--thiocyanate mixture on Amberlite LA-2, 25:18337
  complexes with 5,7-dihalo-8-hydroxyquinoline, structure of product precipitated from aqueous acetone solutions of, 25:18374
  detection in low-energy cosmic radiation, (E), 25:19525
  determination by isotope dilution methods, 25:18358 (RT/CHI-(70)18)
  determination by nuclear track method, 25:18366(R) (NBS-TN-548)
  determination in natural waters from uranium mining operations, method for, 25:18339 (CEA-R-3557(2))
  determination in radioactive ores by gamma spectrometry

XUM

- or neutron activation, 25:18365
- determination in rocks and water after chromatographic separation on silica gel column, spectrophotometric, 25:18345
- determination of trace amounts of, by formation of colored peroxy compounds and sorption on chelating resin, 25:18343
- determination using 2-[(5-bromo-2-pyridyl)azo]-5-(diethylamino)phenol, spectrophotometric, 25:18352
- distribution in Earth's crust, relations with geology, 25:18549
- distribution of, metallotectonic zoning of, 25:18543
- enrichment by gaseous diffusion or ultracentrifugation, worldwide requirements for, 25:18609
- enrichment by gaseous diffusion, Japanese developments in, 25:18602
- enrichment for reactor fuel, review of worldwide status of, 25:18603
- mineralization and occurrence in alkaline igneous rocks, 25:18540
- mineralization in Bohemian Massif, Czechoslovakia, 25:18535
- mineralization in quaternary alkaline volcanic rocks of central Italy, exhalative-supergenic, 25:18542
- photofission at 5 to 10 MeV, cross section structure near threshold for, (E), 25:20366 (IEA-211)
- preparation of corrosion-resistant uranium dioxide-coated, by heating at 500 to 650°C, 25:19185(P)
- purification of acid solutions of, properties of phenolic resins with hydroxamic group for, 25:18503 (RT/CHI-(70)25)
- separation from ores, survey of Russian developments in, 25:18491(T) (AEC-tr-7190)
- separation of bismuth from, by cation exchange chromatography, 25:18520
- sorption by monocrystalline tungsten, effects of adatom surface potential and adsorbate electronegativity on, 25:19207

URANIUM ALLOYS AND SYSTEMS
- grain structure of as-cast chromium- and silicon-containing, randomly oriented fine, 25:19231 (NLCO-1051)
- Nb--U, separation of niobium from, bibliography on, 25:18502 (RFP-1421)
- Ni--Pu--U, phase studies of, 25:19230 (CEA-R-3951)
- Pu--U, diffusion of plutonium in, at 500°C, effects of gallium on, 25:19230 (CEA-R-3951)
- Pu--U, diffusion of plutonium in, at 500°C, effects of nickel on, 25:19230 (CEA-R-3951)

URANIUM CARBIDES
- compatibility of sodium-bonded fuel rods of, with Types 316 and 347 stainless steel cladding at 700°C, 25:19276
- elasticity of irradiated fuel elements of, equipment for in-cell measurement of modulus of, 25:19279
- neutron scattering by, Monte Carlo code for evaluation of double-differential, (E/T), 25:20235 (RPI-328-211)
- preparation of coated particles of, for in-pile irradiation, 25:19288 (ORNL-4629, pp 82-98)
- quality control and testing of fuel elements of, 25:18610 (DP-Report-580)
- radiation effects on structure of, neutron, 25:20791
- UC--ZrC, quality control and testing of fuel elements of, 25:18610 (DP-Report-580)
- UC-base--W, diffusion of helium bubbles in, during annealing at 800 to 1500°C, 25:19272 (AI-AEC-12984)

URANIUM DEPOSITS
- conference on exploration geology of, Vienna, April 13 to 17, 1970, 25:18529 (STI/PUB-277)
- distribution and mineralization of Canadian, 25:18532
- distribution and occurrence of world wide, 25:18531
- distribution in sedimentary rocks in South America, relations with geology, 25:18544
- distribution, geology, and occurrence in western US, 25:18536
- exploration for Canadian, 25:18532
- exploration in UK, criteria for selection of areas for, 25:18554
- geology and mineralization in Swakopmund, South West Africa, 25:18538
- geology and occurrence in Portugal, 25:18537
- geology and occurrence of roll-type, in US, 25:18545
- geology and origin in metasediments in Province of Salamanca, Spain, 25:18547
- geology of sedimentary formations and vein-type, CEA studies of, 25:18534
- mineralization of, speculations on ore fluid properties for, 25:18552
- occurrence and origin in sandstone, relations with color, 25:18553
- occurrence in small sedimentary basins in Japan, 25:18546
- occurrence of low-grade, in south Greenland, 25:18539
- occurrence of, relations with geology, 25:18550
- prospecting and development of Japanese, 25:18555
- uranium mineralization in Bohemian Massif, Czechoslovakia, 25:18535

URANIUM FLUORIDES UF_3
- production by reduction of uranium tetrafluoride vapors by metals, effects of impurities on, 25:18372

URANIUM FLUORIDES UF_4
- reduction of vapors of, by metals, effects of impurities on uranium trifluoride produced by, 25:18372

URANIUM FLUORIDES UF_6
- analysis for uranium isotopes, sampling procedures for mass spectrometric, 25:18340 (KY-626)

URANIUM ISOTOPES
- determination in uranium dioxide, 25:18358 (RT/CHI-(70)18)
- determination in uranium hexafluoride, sampling procedures for mass spectrometric, 25:18340 (KY-626)

URANIUM ISOTOPES U-227
- fission from electron-capture of neptunium-227, delayed, (T), 25:20371 (JINR-P7-5584)

URANIUM ISOTOPES U-228
- fission from electron-capture decay of neptunium-228, delayed, (T), 25:20371 (JINR-P7-5584)

URANIUM ISOTOPES U-232
- energy levels and transitions from neptunium-232 decay, (E), 25:20382

URANIUM ISOTOPES U-233
- criticality in storage tanks, development of methods for control of, 25:18624 (ORNL-4629, pp 1-9)
- distribution and storage of, operation of ORNL facility for, 25:18624 (ORNL-4629, pp 1-9)
- neutron fission of, fractional cumulative yield of niobium-99m from thermal, (E), 25:20406

URANIUM ISOTOPES U-234
- production of spontaneously fissioning isomeric, in (n,2n) reactions, upper limits for cross sections for, (E), 25:20369 (JINR-P3-5528)

URANIUM ISOTOPES U-235
- neutron capture and fission in thermionic reactor cores, cross sections and resonance parameters for, (T), 25:20826
- neutron cross sections for, number of resonances necessary for calculating s-wave, (T), 25:20395
- neutron fission at 0.3 to 1.4 MeV, cross section relative to plutonium-239 and average number of prompt neutrons for, (E), 25:20373(T) (LIB/Trans-300)
- neutron fission at 20 eV to 100 keV, high-resolution cross section for, (E), 25:20418
- neutron fission at energies up to 6 MeV, energy-balance analysis of dependence of number of prompt neutrons on bombarding energy for, (T), 25:20440
- neutron fission of, average neutron production by resonance, (E), 25:20364(T) (BNL-tr-401)
- neutron fission of, fractional cumulative yield of niobium-99m from thermal, (E), 25:20406
- neutron fission of, microsecond isomers in primary products of thermal, 25:20430
- neutron fission of, yield of xenon-145 from thermal, (E), 25:20470
- neutron fission of, yields of arsenic-87, selenium-87, and selenium-88 in thermal, (E), 25:20327
- neutron reactions (n,2n) with, upper limits for cross sections for production of spontaneously fissioning isomers in, (E), 25:20369 (JINR-P3-5528)

URANIUM ISOTOPES U-237
- production of spontaneously fissioning isomeric, in (n,2n) reactions, upper limits for cross sections for, (E), 25:20369 (JINR-P3-5528)

URANIUM ISOTOPES U-238
- deuteron reactions (d,4n) at 20 to 65 MeV, isomer ratio in, (E), 25:20389
- fission of, fission track measurement of decay constant for spontaneous, 25:20429
- neutron cross sections for, number of resonances necessary for calculating s-wave, (T), 25:20395
- neutron fission at 1.20 to 2.66 MeV, fragment angular distributions from, (T), 25:20393
- neutron fission at energies up to 6 MeV, energy-balance analysis of dependence of number of prompt neutrons on bombarding energy for, (T), 25:20440
- neutron fission of, fractional cumulative yield of niobium-99m from epithermal, (E), 25:20406
- neutron reactions (n,2n) with, upper limits for cross sections for production of spontaneously fissioning isomers in, (E), 25:20369 (JINR-P3-5528)
- neutron reactions (n,n') with, cross sections for production of spontaneously fissioning isomers in, (E), 25:20369 (JINR-P3-5528)
- photofission cross sections from dynamic collective model of, (T), 25:20499
- production of spontaneously fissioning isomeric, in (n,n') reactions, cross sections for, (E), 25:20369 (JINR-P3-5528)
- proton reactions up to several GeV, cascade calculations of double differential distributions of particles from, (T), 25:20018 (JINR-P2-5507)

URANIUM MINERALS
- occurrence in Portugal, 25:18537

URANIUM ORES
- geology, occurrence, and origin in Italian Alps, 25:18548
- processing of, survey of Russian developments in, 25:18491(T) (AEC-tr-7190)

URANIUM OXIDES
- preparation for shadowing replicas of surfaces of deformed monocrystalline copper alloys, 25:19271
- plutonium oxides--uranium oxides, development and performance of fuels of, for liquid metal fast breeder reactors, 25:19275

URANIUM OXIDES UO$_2$
- analysis for uranium isotopes, 25:18358 (RT/CHI-(70)18)
- carbon content of pellets of, effects of decarbonization and sintering at 500 to 1600°C on, 25:19274
- coating of sol-gel particles of, fluidized bed method for carbon, 25:19262 (ORNL-4629, pp 65-82)
- crystal structure changes in rods of, direct heating studies on effects of temperature gradients on, 25:19278
- dewaxing and sintering of pellet-type fuels of, design of molybdenum support base and sheets for, 25:19267(P)
- physical properties of molten, to 3000°C, equipment and methods for measuring, 25:19273 (BNWL-SA-3579)
- preparation of coated particles of, for in-pile irradiation, 25:19288 (ORNL-4629, pp 82-98)
- preparation of microspheres of, from CUSP sols, 25:19261 (ORNL-4629, pp 14-64)
- preparation of sols of, by extraction from nitrate solutions using Amberlite LA-2, 25:19261 (ORNL-4629, pp 14-64)
- preparation of sols of, CUSP process flowsheets for, 25:19261 (ORNL-4629, pp 14-64)
- pyrolysis of gel shards and beads of, gas chromatographic analysis of gases evolved by, 25:18378
- radiation effects on compacted clad fuel rods of, at 10,000 MWd/t, 25:19291
- radiation effects on reactor fuels of, (E), 25:20735 (HPR-127)
- reprocessing of stainless steel-clad or Zircaloy-clad, chemical, electrolytic, and mechanical methods for, 25:18493 (CEA-Bib-191)
- sinterability of powdered, effects of crystallinity on, 25:19265
- sinterability of powdered, effects of crystallinity on, 25:19266
- stability at 300 to 900°K and pressures of 1 to 10000 atm, thermodynamic properties of, 25:18551
- PuO$_2$--UO$_2$, analysis of irradiated, for cesium-137, neodymium-148, and transuranium elements as measure of burnup, 25:18359 (WCAP-3385-56(Pt.2))
- PuO$_2$--UO$_2$, production of, problems in, 25:18517
- PuO$_2$--UO$_2$, radiation effects on fission gas release and oxygen distribution in, neutron, 25:19287 (AECL-3690)
- PuO$_2$--UO$_2$, radiation effects on intergranular pore density of fuel pins of, in-pile, 25:19290 (WHAN-SA-15)
- PuO$_2$--UO$_2$, radiation effects on structure of, neutron, 25:20836 (WHAN-SA-79)
- PuO$_2$--UO$_2$, reprocessing of stainless steel-clad or Zircaloy-clad, chemical, electrolytic, and mechanical methods for, 25:18493 (CEA-Bib-191)
- ThO$_2$--UO$_2$, calcining of gel spheres of, effects of carbon on, 25:19263 (ORNL-4629, pp 99-102)
- ThO$_2$--UO$_2$, coating of sol-gel particles of, fluidized bed method for carbon, 25:19262 (ORNL-4629, pp 65-82)
- ThO$_2$--UO$_2$, preparation of coated particles of, for in-pile irradiation, 25:19288 (ORNL-4629, pp 82-98)
- ThO$_2$--UO$_2$, preparation of microspheres of, engineering scale demonstrations on, 25:19261 (ORNL-4629, pp 14-64)
- ThO$_2$--UO$_2$, preparation of microspheres of, incorporating uranium-233, 25:18624 (ORNL-4629, pp 1-9)

URANIUM OXIDES UO$_3$
- stability at 300 to 900°K and pressures of 1 to 10000 atm, thermodynamic properties of, 25:18551
- ThO$_2$--UO$_3$, drying of gel spheres of, development of optimum methods for, 25:19263 (ORNL-4629, pp 99-102)
- ThO$_2$--UO$_3$, preparation of sols of, by extraction from nitrate solutions using Amberlite LA-2, 25:19261 (ORNL-4629, pp 14-64)

URANIUM OXIDES U$_3$O$_8$
- production from South African auriferous and uraniferous conglomerates, 1952 to 1968, 25:18533
- production of, economics of worldwide, 25:18530
- stability at 300 to 900°K and pressures of 1 to 10000 atm, thermodynamic properties of, 25:18551

URANIUM RESERVES
- estimates of worldwide, to year 2000, 25:18530

URANYL CHLORIDES
- reactions with rhenium chloride, mechanisms of, 25:18384

URANYL FLUORIDES
- complexes with trioctylamine in hydrofluoric and sulfuric acids, spectra and structure of, 25:18381

URANYL NITRATES
- effects on distribution of neptunium between nitric acid and anion exchanger, 25:18519
- NH$_4$OH--UO$_2$(NO$_3$)$_2$, precipitation in, effects of uranium concentration on composition of precipitate formed by, 25:18379

URANYL PERCHLORATES
- radiolysis of aqueous solutions of, hydrogen yields from electron pulse, 25:18448(R) (CEA-N-1369)

URANYL SULFATES
- complexes with trioctylamine in hydrofluoric and sulfuric acids, spectra and structure of, 25:18381

UREA
- radiation effects on excretion of, in human urine following therapy for malignant tumors, 25:19063

URIDINE, 2'-DEOXY-5-IODO-
- radiation effects on uptake of labeled, by bone marrow cells of mice, whole-body fractionated γ, 25:19108

URINE
- analysis for radioisotopes, self-volume standards for, 25:18361
- radiation effects on amino acid excretion in human, following therapy for malignant tumors, 25:19063
- radiation effects on arylsulphatase activity in, of rats, whole-body x, 25:18905
- radioisotope content of rat, comparison of direct and treated-sample determinations of, 25:18997

UROCHORDATA
- radioisotope accumulation by marine, effects of physicochemical form on, 25:18894

V

VACCINES
- radioprotective effects of typhoid-paratyphoid, on mice, effects of phentolamine and propranolol on x, 25:19026

VACUUM
- bibliography on surface and vacuum physics, 25:19469

VACUUM GAGES
- calibration at 10^{-8} to 10^{-12} torr, equipment and method for, 25:18878
- operation of ionization, with screened collector down to 10^{-12} torr, 25:18837
- performance of modified extractor, down to 10^{-12} torr, 25:18838

VACUUM SYSTEMS
- degasification rates for high, computer program for calculation of, 25:19195 (ORNL-TM-3220)
- nitrite use in, for thermonuclear research, 25:19728

VAGINA
- radioinduced fistulas in human, following therapy for pelvic malignancies, mast cell studies on, 25:19139

VALVES
- design requirements for helium cooled reactor, 25:20558

VAN DE GRAAFF ACCELERATORS
- beam injection in EN tandem, phase space acceptance calculations for, 25:20137
- circuit for pressurized, spray current stabilizer, 25:20222
- development of Swedish, 1969, 25:20133(R) (NP-18671)
- experimental facility for alpha radiative capture spectroscopy, 25:20148
- operation of ORNL 3-MeV, 1969--1970, 25:20134 (ORNL-4584, pp 187-97)
- research at Swedish, 1969, 25:20133(R) (NP-18671)

VANADIUM
- abundance in α^2 CVn, (E), 25:19339
- abundance in Type-M supergiant, (E), 25:19323
- chromatographic behavior in hydrochloric acid--thiocyanate mixture on Amberlite LA-2, 25:18337
- determination in presence of palladium and copper, molybdenum, or iron by spectrophotometry using 1-(2-carboxy-4-sulfonatophenyl)-3-hydroxy-3-phenyltriazene, 25:18342
- determination of trace amounts of, by formation of colored peroxy compounds and sorption on chelating resin, 25:18343
- determination using azo compounds, photometric, 25:18347
- magnetic field at nuclei in very pure, (E), 25:20335
- neutron capture at 0.115 eV, spin dependence of cross section for, (E), 25:20335
- neutron scattering by, Monte Carlo code for evaluation of double-differential, (E/T), 25:20235 (RPI-328-211)
- separation of bismuth from, by cation exchange chromatography, 25:18520

VANADIUM ALLOYS AND SYSTEMS
- properties for use as fuel cladding, 25:19203
- Au-base--V, magnetic susceptibility at 2 to 300°K, Kondo temperature from, 25:19865
- Au-base--V, thermal expansion of Au$_4$V in magnetically ordered and disordered states, 25:19229
- C--Nb-base--Ti--V--W--Zr, oxidation morphology and rates in air at 800 to 950°C, 25:19172
- Cr--V--Zr, phase studies of, 25:19237
- Nb--V, diffusion in solid-solution, at 1100 to 1800°C, effects of vanadium content on reciprocal, 25:19204
- Nb--V, diffusion in, kinetics of, 25:19214
- Ti-base--V, superconducting transition temperature in, effects of omega phase reversion on, 25:19590

VANADIUM CARBIDES
- electron band structure of, ESCA study of, 25:19867

VANADIUM DEUTERIDES
- deuteron magnetic resonance study of, exploratory, 25:19876

VANADIUM ISOTOPES V-46
- energy levels from titanium-46 (He-3,t) reactions, spin and parity of, (E), 25:20347

VANADIUM ISOTOPES V-48
- beta and electron-capture decay of, β--γ circular polarization correlations in, (E), 25:20374 (NP-18597)

VANADIUM SILICIDES
- superconductivity in V$_3$Si, pressure enhancement of, (T), 25:19605
- ultrasonic attenuation in V$_3$Si, theory of, 25:19604

VANDELLOS POWER REACTOR
- construction of, design parameters of service structures for, 25:20562

VEGETABLES
- potatoes, radiation processing of, effects of, on

XUM

- germination and storage qualities of, 25:19160

VENTILATION
- design of shipboard systems of, 25:20816(T) (JPRS-52443)
- design parameters for liquid metal cooled fast test reactors, 25:20783 (CONF-700816-(Vol.1), pp 317-45)
- equipment for radioactive and toxic process buildings, design and testing of HEPA filter, 25:18559 (CONF-700816-(Vol.1), pp 128-42)
- installation of shipboard systems of, 25:20816(T) (JPRS-52443)

VERMONT YANKEE POWER REACTOR
- containment structure for, effects of steam leaks on pressure and temperature distributions in, 25:20647 (DOCKET-50271-41)
- coolant loss accident in, heat transfer calculations for, 25:20646 (DOCKET-50271-40)
- design parameters of, revised and additional data on, 25:20644 (DOCKET-50271-38)
- effluents from, effects on environment of chemical, radioactive, and thermal, 25:20645 (DOCKET-50271-39)
- instrument lines for, safety aspects of, 25:20647 (DOCKET-50271-41)
- operations aspects of, revised and additional data on, 25:20644 (DOCKET-50271-38)
- piping system for, earthquake stress restraints for Class 1, 25:20647 (DOCKET-50271-41)
- structures for, force loadings on concrete, 25:20647 (DOCKET-50271-41)

VIBRATIONS
- characteristics of end supported fuel elements, simulation of, 25:20740
- theory for free, for revolving orthotropic shells, 25:18568

VINBLASTINE
- effects on hematopoietic stem cells in x-irradiated mice, 25:19126

VIRUSES
- arbovirus, radioinduced inactivation of, in mouse tissues for preparation of noninfectious antigens, 25:18924

VITAMIN B GROUP
- cyanocobalamin, radioinduced oxidation of aqueous solutions of, evaluation of protective agents for elimination of, 25:18472

W

WATER
- analysis for elements during uranium mining operations, 25:18339 (CEA-R-3557(2))
- analysis for trace amounts of uranium after chromatographic separation on silica gel column, spectrophotometric, 25:18345
- analysis for tritium, 25:18360
- analysis for uranium using 2-[(5-bromo-2-pyridyl)azo]-5-(diethylamino)phenol, spectrophotometric, 25:18352
- boiling on thermally-loaded wires, critical parameters for, 25:18583
- cascade showers in, Monte Carlo calculations of transition effects at iron and lead interfaces for 1-GeV-electron-initiated, 25:19943
- deuterium exchange between, and hydrogen sulfide, dual-temperature process for, 25:18512(P)
- deuterium exchange between, and hydrogen sulfide, dual-temperature process for, 25:18514(P)
- deuterium exchange between, and hydrogen sulfide, dual-temperature process for, 25:18513(P)
- displacement in soil columns by heavy water solutions of sodium nitrate, measurement by gamma-photoneutron reactions, 25:18523
- displacement in soil columns by heavy water, measurement by gamma-photoneutron reactions, 25:18523
- heat transfer from heated copper rods to, in pool boiling, 25:18585
- heat transfer to high-pressure, flowing in tubes, graphs on, 25:18581
- meson (π) energy deposition in, at 160 to 220 MeV/c as function of depth, 25:19757 (ORNL-4584, pp 58-73)
- neutron attenuation by, fast, 25:19007 (NCRP-38)
- neutron diffusion coefficient in ice--water phase transition region, 25:20248
- neutron scattering by, Monte Carlo code for evaluation of double-differential, (E/T), 25:20235 (RPI-328-211)
- radiation effects on reactions of, with polyethylene containers, γ, 25:19164
- radiation monitoring of, at UKAEA facilities, methods for, 25:18635
- radiolysis of oxygen-containing, monomolecular reactions in, 25:18476
- radiolysis of oxygen-containing, reactions of intermediates in, 25:18477
- radiolysis of, diffusion kinetics in pulse, 25:18447 (CALT-767-P-4-73)
- radiolysis of, mechanism for scavenging effects of copper ions on yields of hydrogen from β, 25:18458
- radiolysis of, salt effect in electron pulse, 25:18474
- reactions of anomalous, in carbonic anhydrase, directional correlation studies on, 25:18884
- sorption by monocrystalline tungsten, effects of adatom surface potential and adsorbate electronegativity on, 25:19207
- sorption by nonporous thorium oxides, effects of surface water on, 25:18416
- sorption on magnesium surfaces, exoelectron emission during, (E), 25:19758 (ORNL-4584, pp 74-86)
- H_2O--NaCl, boiling on thermally-loaded wires, critical parameters for, 25:18583
- H_2O--steam, heat transfer from flowing, in curved tubes, 25:18586

WATER-d_2
- displacement of water in soil columns by, measurement by gamma-photoneutron reactions, 25:18523
- solvent properties for carbon dioxide at pressures to 40 atm and 30 to 80°C, 25:18418
- spectra of, effects of temperature on ir, 25:18401

WATER-t
- removal from reactor containment air by isotope exchange, catalytic effects of activated carbon GX 133 on, 25:18385 (CONF-700816-(Vol.1), pp 278-88)

WATER VAPOR
- electron reactions at 8 to 55 eV with, detection and identification of triplet states excited by, (E), 25:19499

WAXES
- use of time-equivalent, for compensating effects of surface irregularities in high energy radiotherapy, 25:19066

WELDING
- method for steel reactor pressure vessels, review of electroslag, 25:19181

WELDS
- inspection of, design of equipment for underwater radiographic, 25:18614(P)
- testing of electron beam, in stainless steel parts, semi-automatic ultrasonic system for, 25:20857 (GEPP-83)

WELL LOGGING
- equipment for, design and operation of tube-type neutron source, 25:20228(T) (CSIRO-Trans-10095)
- equipment for, scintillation spectrometer, 25:18814(T) (CSIRO-Trans-9992)
- equipment to correct inaccurate responses due to changes in borehole environment, 25:18874(P)

WEST VALLEY PROCESSING PLANT
- design criteria for, effects of earthquakes and tornadoes on, 25:18496 (DOCKET-50201-65)
- safety specifications for, request for hearing on No. 13, 25:18494 (DOCKET-50201-63)
- waste treatment at, request for possession limits of 5 x 10^{-3} Ci of strontium-85 for tracer studies on, 25:18495 (DOCKET-50201-64)

WHOLE-BODY COUNTERS
- calibration of, 25:18695
- development of 4π liquid scintillation, for gamma and positron emitters, 25:18649

WIND
- effects on West Valley Processing Plant design criteria, 25:18496 (DOCKET-50201-65)
- profiles for surface layer, effects of terrain changes on, 25:20875(R) (NYO-3562-3)

WOLVERINES
- radioisotope content of bones and soft tissues of, in Finland, 25:18929 (NYO-3446-14, Paper 26)

WOLVES
- radioisotope content of bones and soft tissues of, in Finland, 25:18929 (NYO-3446-14, Paper 26)

WOOD
- plastics--wood, physical properties of, 25:19299
- plastics--wood, properties of radiation processed, mechanical and physical, 25:19298

WUERGASSEN POWER REACTOR
- design parameters of, 25:20561

X

X RADIATION
- detection and measurement of 1- to 100-keV, efficiency calibration of germanium and silicon detectors for, 25:18715
- detection of mesic atom (μ and π), design and performance of target--detector assembly for, 25:18748
- detection of soft cosmic, rocket-borne proportional detector using focusing optics for, 25:18680
- detection of, design of split-anode proportional counter for, 25:18698(P)
- dose control during diagnostic use, 25:19010
- dose to tissues of human head and neck during dental radiography using intracavitary machine, 25:19001
- dosimetry of, silicon detector for absolute, 25:18806
- dosimetry using Polaroid film, evaluation and survey of, 25:19005
- effectiveness for therapy of carcinomas of human mouth, effects of dose on, 25:19081
- effectiveness for therapy of head and neck tumors in man following mitotic synchronization with fluorouracil, 25:19071
- effectiveness for therapy of lymph node metastases in human neck, 25:19084
- effects of high doses of, on DNA synthesis in seeds of Oenothera and wheat, 25:18910
- effects of soft galactic, on alignment of interstellar grains, (T), 25:19447
- effects on activity of arylsulphatase in urine of rats,

whole-body, 25:18905
effects on adult, larval, and pupal stages of blowfly, 25:19098
effects on anoxic cells of Escherichia coli, effects of time scale on protective effects of glycerol against, 25:19022
effects on carbon-14-labeled carbon dioxide assimilation and distribution and chlorophyll content in Vicia faba, 25:19153
effects on cell lineage patterns in imaginal wing disc of Drosophila, somatic, 25:18967
effects on cell replication in endocolonized mouse spleen, tritium tracer study, 25:19125
effects on chromosomes in male germ cells of mice, aberrant, 25:18947
effects on chromosomes in spermatogonia of mice, effects of dose fractionation on aberrant, 25:18958
effects on chromosomes in spermatogonia of mice, review of aberrant, 25:18948
effects on chromosomes of root cells of Vicia faba, effects of blue, green, and infrared light on aberrant, 25:18962
effects on composition of lens insoluble proteins, 25:18909
effects on development and survival of fish eggs, effects of dose on, 25:19103 (PG-Report-1013)
effects on development of cysticercoids of Hymenolepis (tapeworm), 25:19095
effects on DNA of L cells, effects of energy deprivation on repair of breaks following, 25:18908
effects on double-strand breaks in DNA in mammalian cells, 25:18911
effects on erythrocyte and leukocyte counts in peripheral blood and on survival of mice, effects of oxygen content of inspired air and dose on, 25:19123
effects on function and structure of parotid glands in rats, 25:19119
effects on generation cycle of crypt cells in small intestine of mice, effects of chronic fractionated, 25:19122
effects on goats, effects of dose fractionation on recovery from 1 MV, 25:19115
effects on growth and incidence of malformations of rat embryos, effects of exposure rate and protracted dose on, 25:19117
effects on growth of tumors following transplantation of fibrosarcomas and mammary carcinomas in tissues of mice, evaluation of tumor bed effect for, 25:19118
effects on hematopoiesis, intestines, and survival of mice, comparison of protective effects of AET against whole-body fast neutron and, 25:19029
effects on immune reactions of mice to sheep red blood cells, effects of anti-sheep red blood cell antibodies on, 25:18923
effects on inbred and hybrid mice, effects of dose on cataractogenic, 25:19116
effects on incorporation of carbon-14-labeled pyruvate into tricarboxylic acid cycle in rat thymocytes in vitro, 25:18902
effects on induction of chromosome inversions in mice, whole-body, 25:18968
effects on intestines of mice, protective effects of MEG against whole-body, 25:19029
effects on leukocyte count of dogs, sensitizing effects of dinitrochlorobenzol on, 25:19030
effects on life span of mice, effects of dose on, 25:19105
effects on lungs following fluoroscopy and pneumothorax therapy in patients with tuberculosis history, 25:19068
effects on maturation of cerebellar cortex in rats, postnatal, 25:19114
effects on membrane content of potassium and permeability of erythrocytes in rabbits, 25:19107
effects on mice, effects of phentolamine and propranolol on protective effects of typhoid-paratyphoid vaccine against, 25:19026
effects on mice, use of functional units in small chromosome segments for interpretation of mutagenic, 25:18957
effects on mitosis and survival of ascites cells of mice, effects of dose fractionation on, 25:19091
effects on mitotic segregation in recombination deficient mutants of yeast, 25:18945 (UCRL-20192)
effects on nematode larvae, effects of dose on attenuating, 25:19101
effects on peripheral blood of rats, effects of trithiodipropanol on, 25:19131
effects on permeability of cell membranes in rat thymus to magnesium ions, protective effects of esculamine against, 25:19025
effects on permeability of membranes of liver mitochondria to manganese-54 in mice, protective effects of esculamine against, 25:19025
effects on potassium bromide and chloride, temperature dependence of defect production in, (E), 25:19855
effects on potassium chloride single crystals doped with bromide, properties of BrCl- molecule-ion center induced in, 25:19852
effects on potassium chloride single crystals, cation vacancies induced in, (E), 25:19858
effects on proliferation of cells in bone marrow and spleen of mice, effects of dose on, 25:19129
effects on pupation and survival of larvae of Tenebrio, effects of partial shielding on, 25:19094
effects on regeneration of hematopoietic stem cells of mice following transplantation, effects of cyclophosphamide on, 25:19127
effects on regeneration of stem cells of mice, effects of dose and shielding on, 25:19126
effects on reversion in mutants of yeast, 25:18945 (UCRL-20192)
effects on single-chain breaks in DNA of Escherichia coli, effects of culture medium on repair of, 25:18912
effects on structure of chicken embryo neuroblast cells, effects of dose on, 25:19120
effects on surface conductance of germanium, annealing recovery of, (T), 25:19859
effects on survival of log-phase and stationary-phase Escherichia coli, effects of culture medium on, 25:18912
effects on survival of mice following therapy for skin cancer, effects of synchronized treatment with fluorouracil on, 25:19075
effects on survival of spermatogonia of mice in relation to mutation frequency, effects of dose on, 25:18959
effects on survival of transplanted Ehrlich ascites tumor cells in mice, combined effects of immunization and, 25:19130
emission at 0.25 keV as bremsstrahlung of suprathermal protons, (T), 25:19451
emission during 20th solar cycle of soft, relation to radio emissions, (E), 25:19430
emission from Cen A and Virgo A, (E), 25:19455
emission from solar flares, mechanism for, (E/T), 25:19398
emission from solar flares, model for, (E/T), 25:19396
emission of hard, during solar flare of Sept. 28, 1961, (E), 25:19435
flux of soft, from quiet corona, (E), 25:19418
hazards to patients and personnel during medical diagnosis, programmed instruction course on methods for protection against, 25:19010
intensity of cosmic background, between 25 and 200 keV from ESRO R/73 experiment, 25:19534
interactions of cosmic background, with other background radiations, (T), 25:19462
interactions of soft, with interstellar hydrogen and helium, ionization by, (T), 25:19439
interactions with interstellar hydrogen, ionization during, (E/T), 25:19440
observations of cosmic background, above 0.25 keV, (E), 25:19352
reactions with inner-shell electrons of atoms and molecules, review of chemical information from, 25:19473
use for therapy of alopecia mucinosa in man, further management and prognosis following, 25:19073
uses in radiography for nondestructive testing using color film, 25:18612(T) (LIB/Trans-324)

X-RAY ASTRONOMY
  developments in, (T), 25:19356

X-RAY CAMERAS
  design of Guinier--Haegg, for x-ray powder diffraction, 25:18826 (AE-409)

X-RAY DIFFRACTOMETERS
  design for shortening exposure time, 25:18859(P)

X-RAY EQUIPMENT
  hazards to inexperienced personnel, 25:18971

X-RAY SPECTROMETERS
  description of Johann-type crystal, for studying ion reactions with carbon, 25:18836
  design and performance of target--detector assembly for mesic atom, 25:18748
  development and uses of, review on, 25:18673
  performance of rocket-borne lithium-drifted silicon, at 4 to 40 keV, 25:18654

XENON
  positron annihilation in liquid and solid, positronium-bubble formation and angular correlation of photons from, 25:19487
  uses for fission product, evaluation of large-scale, 25:18590(R) (BNWL-1308-4)

XENON IONS
  implantation in silicon at 20 to 150 keV, energy dependence and depth distributon of lattice disorder induced in, 25:19832

XENON ISOTOPES Xe-131
  exchange with xenon-133 in sodium xenate or xenon fluoride, catalytic effects of activated carbons on, 25:18385 (CONF-700816-(Vol.1), pp 278-88)

XENON ISOTOPES Xe-133
  effectiveness of intravenously injected, for determining lung function in man, 25:19044
  exchange with xenon-131 in sodium xenate or xenon fluoride, catalytic effects of activated carbons on, 25:18385 (CONF-700816-(Vol.1), pp 278-88)
  removal from reactor containment air by isotope exchange, catalytic effects of activated carbon on, 25:18385 (CONF-700816-(Vol.1), pp 278-88)
  use for lung scanning in patients with metastatic carcinomas for evaluation of regional function, 25:19048

XUM

XENON ISOTOPES Xe-145
  half-life of, (E), 25:20470
  yield in uranium-235 thermal neutron fission, (E), 25:20470

Y

YANKEE POWER REACTOR
  fuel element shipping cask for, revised technical specifications for use of spent, 25:20605 (DOCKET-50029-144)
  operations aspects of, revised technical specifications for audit and review committee for, 25:20606 (DOCKET-50029-146)
  operations history for January 1971, 25:20578 (DOCKET-50029-143)
  operations incident of August 18, 1969, faulty removal of spent fuel assembly, 25:20579 (DOCKET-50029-145)
YTTERBIUM
  chromatographic behavior in hydrochloric acid--thiocyanate mixture on Amberlite LA-2, 25:18337
YTTERBIUM ISOTOPES Yb-168
  energy levels of, calculation using microscopic collective model, (T), 25:20547
YTTERBIUM ISOTOPES Yb-170
  energy levels from lutetium-170 decay, spin and parity for, (E), 25:20452
YTTERBIUM ISOTOPES Yb-172
  alpha reactions (α,2ne) and (α,2nγ) at 20.5 MeV, energy levels of hafnium-174 from, 25:20427
YTTERBIUM ISOTOPES Yb-174
  energy level of, isomer shift and quadrupole splitting of 2^+ rotational, (E), 25:20399
YTTERBIUM ISOTOPES Yb-176
  alpha inelastic scattering at 27.5 to 32.5 MeV, cross sections for, (E), 25:20466
  energy levels of, spin-parity assignments for two-quasiparticle, 25:20380
  nuclear mass distribution of, hexadecapole term in deformation parameter for, (E/T), 25:20466
YTTERBIUM TELLURATES
  $Yb_2(TeO_3)_3$--$Yb_2(TeO_4)_3$, analysis for hexavalent tellurium and total tellurium by automatic amperometric and potentiometric titrations, 25:18351
YTTERBIUM TELLURITES
  $Yb_2(TeO_3)_3$--$Yb_2(TeO_4)_3$, analysis for hexavalent tellurium and total tellurium by automatic amperometric and potentiometric titrations, 25:18351
YTTRIUM
  abundance in α And, (E), 25:19343
  chromatographic behavior in hydrochloric acid--thiocyanate mixture on Amberlite LA-2, 25:18337
  determination using 4,5-dihydroxy-m-benzenedisulfonic acid, in presence of Eriochrome Cyanine R, titrimetric, 25:18348
  separation from seawater by flocculation, 25:18518
YTTRIUM ALLOYS AND SYSTEMS
  Fe--Y, magnetic susceptibility of Y_2Fe_{17}, Y_6Fe_{23}, YFe_3, and YFe_2, 25:19871
YTTRIUM ISOTOPES Y-86
  beta and electron-capture decay of, γ singles and coincidence spectra from, (E), 25:20352
YTTRIUM ISOTOPES Y-89
  energy levels from gamma resonance scattering, widths for, (E), 25:20355
  meson (μ^-) capture by, γ spectra from, 25:20360
  proton elastic scattering at 5.7 to 6.4 MeV, polarization in, (E), 25:20331
  x-ray spectra from μ-mesic atoms of, 25:20360
YTTRIUM ISOTOPES Y-90
  beta decay of, angular distribution and energy spectra of internal bremsstrahlung emitted during, (E/T), 25:20417
  energy levels from yttrium-89 proton elastic scattering, spin assignments for isobaric analog, (E), 25:20331
YTTRIUM ISOTOPES Y-91
  half-life, (E), 25:20339
YTTRIUM TELLURATES
  $Y_2(TeO_3)_3$--$Y_2(TeO_4)_3$, analysis for hexavalent tellurium and total tellurium by automatic amperometric and potentiometric titrations, 25:18351
YTTRIUM TELLURITES
  $Y_2(TeO_3)_3$--$Y_2(TeO_4)_3$, analysis for hexavalent tellurium and total tellurium by automatic amperometric and potentiometric titration, 25:18351

Z

ZINC
  chromatographic behavior in hydrochloric acid--thiocyanate mixture on Amberlite LA-2, 25:18337
  determination using azo compounds, photometric, 25:18347
  neutron inelastic scattering by, γ energies from fast, (E), 25:20356
  separation of bismuth from, by cation exchange chromatography, 25:18520
ZINC ALLOYS AND SYSTEMS
  In--Zn, crystal structure of electrodeposited, 25:19221
  In--Zn, properties of electrodeposited, 25:19221
ZINC IONS
  implantation in indium antimonide at 400 keV for infrared detector fabrication, 25:19828
  implantation in n-type gallium arsenide at 20 and 85 keV, annealing effects on electric properties of implanted layers, 25:19842
  implantation in silicon at 400 keV, divacancy and amorphous-layer formation in, 25:19812
  range in indium antimonide at 0.2 to 1.8 MeV, 25:19828
ZINC ISOTOPES
  energy levels from neutron inelastic scattering, (E), 25:20356
ZINC ISOTOPES Zn-63
  beta and electron-capture decay of, gamma spectra with spurious peaks from Compton scattering between γ--γ coincidence detectors in, (E), 25:18754
ZINC ISOTOPES Zn-64
  electron elastic scattering at 150 and 225 MeV, differential cross sections and form factors for, (E), 25:20345
ZINC ISOTOPES Zn-66
  electron elastic scattering at 150 and 225 MeV, differential cross sections and form factors for, (E), 25:20345
  proton scattering at 4.25 to 8.47 MeV, angular distributions and excitation functions for, (E), 25:20322
ZINC ISOTOPES Zn-68
  proton scattering at 4.25 to 8.47 MeV, angular distributions and excitation functions for, (E), 25:20322
ZINC ISOTOPES Zn-72
  half-life, (E), 25:20339
ZINC OXIDES
  effects on oxygen-18 exchange in carbon monoxide molecules, catalytic, 25:18387
ZINC SELENIDES
  ion implantations in thin films of, cathodoluminescence effects of 250-kV transition-metal, 25:19795
  radiation damage from ion implantations in single-crystal platelets of, anealing and luminescent effects of, 25:19793
ZINC SULFIDES
  ion implantations in thin films of, cathodoluminescence effects of 250-kV transition-metal, 25:19795
  radiation damage from ion implantations in single-crystal platelets of, anealing and luminescent effects of, 25:19793
ZINC TELLURATES
  $ZnTeO_3$--$ZnTeO_4$, analysis for hexavalent tellurium and total tellurium by automatic amperometric and potentiometric titrations, 25:18351
ZINC TELLURIDES
  ion implantation in, review, 25:19789
  ion implantations in, studies of chlorine- and argon-, 25:19794
ZINC TELLURITES
  $ZnTeO_3$--$ZnTeO_4$, analysis for hexavalent tellurium and total tellurium by automatic amperometric and potentiometric titrations, 25:18351
ZION POWER REACTOR, UNIT 1
  containment spray system for, full flow testing requirements of, 25:20655 (DOCKET-50295-24)
ZION POWER REACTOR, UNIT 2
  containment spray system for, full flow testing requirements of, 25:20655 (DOCKET-50295-24)
ZIRCALOY
  joining to stainless steel to form reactor components, coextrusion and rolling methods for, 25:19183
ZIRCALOY-2
  properties for use in Japanese ATR pressure tubes, 25:19223
ZIRCALOY-4
  properties for use in Japanese ATR pressure tubes, 25:19223
ZIRCONIUM
  abundance in Type-M supergiant, (E), 25:19323
  chromatographic behavior in hydrochloric acid--thiocyanate mixture on Amberlite LA-2, 25:18337
  detection in low-energy cosmic radiation, (E), 25:19525
  determination in high-burnup plutonium dioxide fuel by isotope dilution mass spectrometry, 25:18356 (KR-140)
  determination using azo compounds, photometric, 25:18347
  effect on hydrolysis of potassium phosphorodifluoridate, catalytic, 25:18373
  effects as additive on properties of intermetallic Ti_3Sn, 25:19238
  effects on fluoride hydrolysis, catalytic, 25:18375
  oxidation at low oxygen pressures, model for, 25:19178
  reactions with uranium tetrafluoride vapors, production of uranium trifluoride by, 25:18372
  separation from acid solutions by ion exchange on phenolic resins, 25:18503 (RT/CHI-(70)25)
  separation from hafnium by double chloride extraction, 25:18499(T) (LIB/Trans-330)
  separation from seawater by flocculation, 25:18518
  separation of bismuth from, by cation exchange chromatography, 25:18520
ZIRCONIUM ALLOYS AND SYSTEMS
  oxidation of reactor components of, method for protective, 25:19180(P)
  properties for use as fuel cladding, 25:19179

  properties for use as fuel cladding, 25:19203
  B--C--Hf--Nb-base--W--Zr, properties for use at high temperatures, 25:19218
  C--Nb-base--Ti--V--W--Zr, oxidation morphology and rates in air at 800 to 950°C, 25:19172
  Cr--V--Zr, phase studies of, 25:19237
  Cu--Mo--Zr, analysis for copper and molybdenum, simultaneous polarographic, 25:18341 (RT/CHI-(70)14)
  Mg-base--Pb--Zr, crystal structure of phases in dilute, 25:19228
  Mg-base--Pb--Zr, mechanical properties of dilute, effects of heat treatments in carbon dioxide on, 25:19228
  Nb--Ta--Ti--Zr, effects of iron additions on superconducting properties of, 25:19618(P)
  Nb--Ti--Zr, superconducting properties of, 25:19627
  Nb--Zr, diffusion in solid-solution, at 1100 to 1800°C, effects of zirconium content on reciprocal, 25:19204
  Nb--Zr, diffusion in, kinetics of, 25:19214
  Nb--Zr, magnetic flux flow in superconducting, 25:19609
  Nb-base--Ti--Zr, plasticity and strength of, at -196 and 20°C, 25:19206
  Nb-base--Zr, embrittlement by hydrogen, effects of interstitial solutes on, 25:19216
  Nb-base--Zr, mechanical properties of solid solutions of, 25:19215
  Nb-base--Zr, preparation of high-purity, by electron beam melting, 25:19186
  Nb-base--Zr, properties for use in Japanese ATR pressure tubes, 25:19223
  Nb-base--Zr, superconductivity of, relations with microstructure, 25:19219
  Ni--Zr, crystallization of solid-solution, mechanisms of, 25:19242
ZIRCONIUM BORIDES
  Cr--ZrB_2, deposition on graphite, method for electro-, 25:19270(P)
ZIRCONIUM CARBIDES
  UC--ZrC, quality control and testing of fuel elements of, 25:18610 (DP-Report-580)
ZIRCONIUM HYDRIDES
  neutron thermalization in, Einstein model of, (T), 25:20242
ZIRCONIUM IONS
  implantation in silicon at 40 keV, carbon-ion channeling study of, 25:19829
ZIRCONIUM ISOTOPES Zr-90
  deuteron elastic scattering at 8 to 12 MeV using polarized beam, cross section and vector analyzing power for, (E), 25:20305
  deuteron reactions (d,p) at 10 MeV, DWBA calculations of angular distributions and overlap integrals from, (T), 25:20497
  deuteron reactions (d,p) at 8 to 12 MeV using polarized beams, cross sections and vector analyzing power for, (E), 25:20305
  deuteron reactions (d,p) with, analysis using BHMM theory, (T), 25:20282
  energy levels from niobium-90 decay, spin-parity assignments for, (E), 25:20411
  energy levels of, fine structure surrounding analog, (T), 25:20396
  level transitions from niobium-90 decay, external conversion coefficients and multipolarities for, (E), 25:20411
ZIRCONIUM ISOTOPES Zr-92
  proton elastic scattering at 4.5 to 8.6 MeV, polarization in, (E), 25:20331
ZIRCONIUM ISOTOPES Zr-93
  energy levels from zirconium-92 proton elastic scattering, spin assignments for isobaric analog, (E), 25:20331
ZIRCONIUM ISOTOPES Zr-94
  neutron thermal activation cross sections and resonance integrals for, (E), 25:20392
ZIRCONIUM ISOTOPES Zr-95
  accumulation by marine organisms, effects of physico-chemical form on, 25:18894
  content of man in Finland from artificial sources, 25:18931 (NYO-3446-14, Paper 30)
  content of marine algae following radioactive waste disposal, 25:18939
  content of plants in Finnish Lapland during 1968 and 1969, 25:18932 (NYO-3446-14, Paper 31)
  removal from plant tissue, methods for, 25:18892 (NP-18641)
ZIRCONIUM ISOTOPES Zr-96
  neutron thermal activation cross sections and resonance integrals for, (E), 25:20392
ZIRCONIUM OXIDES
  analysis for uranium using 2-[(5-bromo-2-pyridyl)azo]-5-(diethylamino)phenol, spectrophotometric, 25:18352
  electric conductivity of calcium oxide-stabilized, relations with porosity, 25:19283
  PuO_2--ZrO_2, separation of plutonium from, pyrochemical methods for, 25:18492 (ANL-7709)

XUM

REPORT NUMBER INDEX

Reports, conference papers and proceedings, numbered translations, and patents are included in this index. Each item is listed by report number; this is followed by the abstract number and a brief notation regarding public availability. The index entries show which reports are on file in the institutions listed on the back of the front cover (Dep.), which reports have been published in open-literature journals (journal citation), and which reports can be purchased (source and price). Whenever a report is identified by more than one number, the availability is given under the primary number, and a cross reference is given under the secondary report number.

The report number codes apply to USAEC reports unless designated otherwise. Non-USAEC reports are identified by parenthetical notes after the report codes; e.g., (non-AEC), (British), (Canadian), (French). The note (Misc.) identifies the codes used for both USAEC and non-USAEC reports. Patents are listed under the heading "PATENTS"; the country of origin is included in parentheses.

A comprehensive list of both USAEC and non-USAEC report codes is contained in the latest revision of TID-85, *Report Number Series Used by the Division of Technical Information in Cataloging Reports*. This information is also included in the Cumulative Report Number Index (issued annually).

Availability of USAEC Reports

All USAEC Reports abstracted in *Nuclear Science Abstracts* are available through one or more of the following sources:

(1) University and public libraries in the United States. A list of these organizations appears on the inside front cover of each issue of *NSA*.

(2) NCR Microcard Editions in Microcard and micronegative form. Orders and inquiries should be sent to: Order Processing Department, 365 South Oak Street, West Salem, Wisconsin 54669.

(3) National Technical Information Service, U. S. Department of Commerce, Springfield, Virginia 22151.

(4) Superintendent of Documents, U. S. Government Printing Office, Washington, D. C. 20402.

(5) National Cash Register Co., P. O. Box 3111, Oak Ridge, Tenn. 37830, in micronegative form. Purchase details available on request.

Availability of Non-USAEC Reports

U. S. Reports. Reports of U. S. Government agencies are available to the public from the National Technical Information Service (NTIS). If specific availability is not shown, inquiries may be directed to NTIS.

Non-U. S. Reports. Reports of atomic energy organizations of other countries are available from NTIS for U. S. sale only. Specific availability in the country of origin is shown, when known, at the report number entry. Otherwise, inquiries should be made to the organizations listed below:

AUSTRALIA

Australian Atomic Energy Commission Research Establishment. Available upon request from the Library, Australian Atomic Research Establishment, Private Mail Bag, Sutherland, New South Wales, Australia.

BELGIUM

Centre d'Étude de l'Energie Nucléaire. Available upon request to individuals and organizations from the Centre d'Etude de l'Energie Nucléaire (C.E.N.), Studiecentrum voor Kernenergie (S.C.K.), Technical Information Dept., MOL-DONK (Belgium).

CERN

CERN European Organization for Nuclear Research. Available without charge from CERN European Organization for Nuclear Research, Geneva 23, Switzerland. Copies are deposited in libraries throughout the world.

FRANCE

Commissariat a l'Energie Atomique. Inquiries for reports numbered 1-2199 should be addressed to Service Central de Documentation du C.E.A., Centre d'Etudes Nucléaires de Saclay, Boîte postale n° 2, 91. GIF-sur-YVETTE, FRANCE. Reports numbered 2200 and above are available from La Documentation Française, 31 quai Voltaire, 75, PARIS (7e), FRANCE.

Service Central de Protection contre les Rayonnements Ionisants. Copies are available from Ministère de la Santé Publique, Service Central de Protection contre les Rayonnements Ionisants, B.P. n° 78 Le Vesinet (France) Telex 25667.

GERMANY

Deutsches Elektronen-Synchrotron DESY. Copies are available from Deutsches Elektronen-Synchrotron DESY, Dokumentation, 2000 Hamburg 52, Notkestieg 1, Germany.

Gesellschaft für Kernforschung mbH (KFK). Copies are available from Gesellschaft für Kernforschung mbH, 75 Karlsruhe, Postfach 947, Germany. Copies are also deposited in many national nuclear centers in the world.

Kernforschungsanlage. Copies may be ordered from Zentralbibliothek der Kernforschungsanlage Jülich, Jülich, Bundesrepublik Deutschland.

Hahn-Meitner-Institute für Kernforschung. Available without charge from Hahn-Meitner-Institute für Kernforschung Ber-

XUM

lin, Bibliothek, Glienicker Strasse 100, 1 Berlin 39, Germany. Copies are deposited in many national nuclear centers in the world.

Johann-Wolfgang-Goethe Universität, Frankfurt Am Main, Institut für Kernphysik, (IKF). Copies are available from Gmelin Institut, 40–42 Varrentrappstrasse, Frankfurt (Main), West Germany.

ISRAEL

Israel Atomic Energy Commission. Available without charge from Israel Atomic Energy Commission, Soreq Nuclear Research Centre, Yavne, Israel.

ITALY

Centro Informazioni Studi Esperienze (CISE). For sale at CISE Press Office, Casella Postale 3986, Milano, Italy. Copies are deposited in the libraries of various nuclear centers in Italy and abroad.

Comitato Nazionale per l'Energia Nucleare. Copies are available from Comitato Nazionale per l'Energia Nucleare, Divisione Affari Internazionali e Studi Economici, Ufficio Pubblicazioni, Via Belisario, 15, Roma, Italy.

JAPAN

Japan Atomic Energy Research Institute (JAERI). Available from the Staff Supply Cooperative of Japan Atomic Energy Research Institute (JAERI), Tokai-mura, Naka-gun, Ibaraki-ken, Japan. Copies are deposited in depositories in Tokyo, Nagoya, and Osaka.

Nagoya University. Copies are available from Research Information Center, Institute of Plasma Physics, Nagoya University, Nagoya, Japan.

University of Tokyo. Available free of charge from Institute for Nuclear Study, University of Tokyo, Tanashi-Machi, Kitatama-gun, Tokyo, Japan.

NETHERLANDS

Reactor Centrum Nederland. For sale by Reactor Centrum Nederland, 112 Scheveningseweg, 's-Gravenhage, The Netherlands. Copies are deposited in university libraries in Holland and in many national nuclear centers in the world.

NEW ZEALAND

Institute of Nuclear Sciences. Copies are available from Librarian, N. Z. Institute of Nuclear Sciences, D.S.I.R., Private Bag, Lower Hutt, New Zealand. Copies are deposited in other countries.

PAKISTAN

Atomic Energy Center. Copies are available from Atomic Energy Center, P. O. Box 658, Lahore, (West Pakistan).

POLAND

Reports of the Polish nuclear institutes are published by the Nuclear Energy Information Center of the Government Commissioner for Use of Nuclear Energy. Copies are available free of charge from Nuclear Energy Information Center, Palace of Culture and Science, Warsaw, Poland.

SPAIN

Junta de Energia Nuclear. "JEN" reports are available without charge from Servicio de Documentation, Junta de Energia Nuclear, Ciudad Universitaria, Madrid (3), España.

SWITZERLAND

Eidgenössisches Institut für Reaktorforschung. "EIR" reports are available from Eidgenössisches Institut für Reaktorforschung, c/o Bibliothek, 5303 Würenlingen/Switzerland.

TURKEY

Turkish Atomic Energy Commission. Copies are available free of charge from T.A.E.C., Çekmece Nuclear Research Center, P. O. Box 1, Airport, Istanbul, Turkey.

Conferences

Published conference proceedings as well as individual unpublished papers from conferences are included in this index. A CONF number is assigned to the conference if published proceedings are received and also if only a single paper is received. The base number used is year-month-sequence. Thus, the number CONF-650101 indicates that the conference was held in 1965, in January, and that this was the first January 1965 conference so received. This number would be assigned to complete published proceedings. If individual papers are received, the base number is extended to include a paper number, e.g., CONF-650101-1. As additional papers are received, they will be assigned consecutive numbers in the series, CONF-650101-1, CONF-650101-2, etc. This numbering system ensures that all papers received from a conference will be associated with that conference in this index.

If published proceedings are received after the receipt of individual papers, the complete proceedings will be abstracted and the abstract number will appear in this index with the base CONF number.

Abbreviations Used in Availability Column

AECL	Reports of the Atomic Energy of Canada Limited are for sale by the Scientific Document Distribution Office, Atomic Energy of Canada Limited, Chalk River, Ontario, Canada.
CFSTI	See NTIS
DENM	Reports of the Atomic Energy Commission Research Establishment, Risö, are available on exchange from the Library, Danish Atomic Energy Commission, Risö, Roskilde, Denmark. Also for sale at the price shown from Jul. Gjellerup, Booksellers, 87 Sölvgade, Kobenhavn K., Denmark. Reports of Danatom are available on loan from Research Establishment, Risö, Roskilde, Denmark. Copies are available from Danatom, Aurehojvej 2, Hellerup, Denmark.
Dep.	AEC reports so designated are maintained in the organizations listed on the inside front cover of *NSA*. Prior to July 1, 1965, reports were deposited either in printed copy form or in microform. After that time, all reports have been in the form of micronegatives. Reports from other countries so designated are available in the United States at the organizations listed on the inside front cover of *NSA*.

XUM

DTIE	Available from the U. S. Atomic Energy Commission, Division of Technical Information Extension, P. O. Box 62, Oak Ridge, Tennessee 37830. (Conference papers are available on loan only.)
EM	Blueprints of AEC engineering drawings are available from NTIS, U. S. Department of Commerce, Springfield, Virginia 22151. Current prices of the CAPE-packages may be obtained from this address. TID-4100, available from the Division of Technical Information Extension, P. O. Box 62, Oak Ridge, Tennessee 37830, contains information on all the CAPE-packages for sale.
EUR	For sale by Centrale de vente des publications des Communautés européennes 37, rue Glesener-Luxembourg.
GPO	For sale by the Superintendent of Documents, Government Printing Office, Washington, D. C. 20402.
IAEA	Available from the International Atomic Energy Agency, Vienna, Austria, and from its sales agencies in various countries throughout the world. A list of these agencies is found in each STI/DOC and STI/PUB publication.
NORW	Reports from Forsvarets Forskningsinstitutt are available from Norwegian Defense Research Establishment, Library, P. O. Box 25, Kjeller, Norway. "KR" reports are available on an exchange basis from the Library, Institutt for Atomenergi, Box 40, Kjeller, Norway. Reports of the Norwegian Reactor School are available from the Library, Institutt for Atomenergi, P. O. Box 40, Kjeller, Norway.
NRC	For sale by the National Research Council of Canada, Ottawa, Ontario, Canada.
NTIS	For sale by the National Technical Information Service (NTIS), U. S. Department of Commerce, Springfield, Virginia 22151 at the following prices for eye legible copy: 1–300 pages $3.00 301–600 pages $6.00 601–900 pages $9.00 Documents over 900 pages have special prices which may be obtained from NTIS. Microfiche copy of each separately bound document can be purchased for $0.95. Reports issued by organizations outside the United States will be sold by NTIS *only to purchasers within the United States.* Purchasers outside the United States may acquire such reports from the sources described elsewhere in these columns.
OECD	Available from O. E. C. D., Publications 2, rue, André-Pascal, 75 Paris 16^{e}, France, and from its sales agencies in various countries throughout the world. A list of these agencies is found in each OECD publication.
SWED	"AE" reports are for sale from Aktiebolaget Atomenergi, Library Section, Box 43041, Stockholm 43, Sweden. Microcopy of these reports is available from the International Documentation Center, Tumba, Sweden. Reports of the VDDIT-series may be obtained from Aktiebolaget Atomenergi, Information Office, Scientific and Technical Information, Box 43041, Stockholm 43, Sweden. Other series are not generally available to the public. Organizations in the Atomic Energy field may obtain copies from Aktiebolaget Atomenergi.
UK	United Kingdom Atomic Energy Authority reports generally may be purchased from Her Majesty's Stationery Office, P. O. Box 569, London S.E.1. Copies of many UKAEA reports (particularly earlier ones) may be purchased in microcopy form from Micro Methods Ltd., East Ardsley, Wakefield, Yorkshire, England. Copies of UKAEA reports are deposited with the National Lending Library for Science and Technology and 10 public libraries in England; with the USAEC and (through USAEC) with NTIS; and in most national nuclear centers throughout the world. In the USA, UKAEA reports are available on a subscription basis, by subject category, from UNIPUB, Inc., P. O. Box 433, New York, N. Y. 10016, USA.
UN	Mail orders should be directed to the Sales Section, Room 1059, United Nations Headquarters, New York, New York 10017.
ZAED	Available from Zentralstelle für Atomkernenergie Dokumentation, 6000 Frankfurt/Main 90, P. O. Box 901069, Westendstr. 21, West Germany

Report No.	Abstract No.	Availability
AAEC/M-	(Australian)	
10	25-20781	Dep. NTIS (U. S. Sales Only), 32p.
AAEC/TM-	(Australian)	
551	25-20830	Dep. NTIS (U. S. Sales Only), 98p.
553	25-20818	Dep. NTIS (U. S. Sales Only), 27p.
565	25-20227	Dep. NTIS (U. S. Sales Only), 36p.
AD-	(Misc.)	
702155	25-18977	CFSTI, 11p.
711316	25-18978	NTIS, 32p.
711531	25-18732	NTIS, 42p.
AE-	(Non-AEC)	
409	25-18826	Dep. NTIS (U. S. Sales Only), 101p.
AEC-tr-		
7186	25-20844	Dep. NTIS
7187	25-20549	Dep. NTIS
7189	25-18576	Dep. NTIS
7190	25-18491	Dep. NTIS
7192	25-19250	Dep. NTIS
7219	25-19034	Dep. NTIS
AECL-	(Canadian)	
3667	25-20307	Dep. CFSTI (U. S. Sales Only). AECL $2.00, 114p.
3690	25-19287	Dep. NTIS (U. S. Sales Only), 18p.
3712	25-20320	Can. J. Phys.; 48: 2735-50(15 Nov 1970)
3780	25-20731	Dep. NTIS (U. S. Sales Only), 10p.
3781	25-20845	Dep. NTIS (U. S. Sales Only), 12p.
3783	25-18577	Dep. NTIS (U. S. Sales Only), 37p.
3784	25-20846	Dep. NTIS (U. S. Sales Only), 42p.
AEEW-M-	(British)	
898	25-18637	Dep. NTIS (U. S. Sales Only). UK 5s. 6d, 21p.
AERE-R-	(British)	
6224	25-18797	Dep. NTIS (U. S. Sales Only). UK 2s. 6d, 13p.
6435	25-19251	Dep. NTIS (U. S. Sales Only), 14p.
6460	25-19167	Dep. NTIS (U. S. Sales Only), 14p.
6481	25-20754	Dep. NTIS (U. S. Sales Only), 20p.
6516	25-20732	Dep. NTIS (U. S. Sales Only), 12p.
AHSB(S)R-	(British)	
188	25-20764	See NP-18487
192	25-18974	Dep. NTIS (U. S. Sales Only), 20p.
AI-AEC-		
12984	25-19272	Dep. NTIS, 27p.
AI-Trans-	(Misc.)	
287	25-19190	Dep. NTIS
ANL-		
7673	25-20704	Dep. NTIS, 90p.
7677	25-18557	Dep. NTIS, 71p.
7706	25-19191	Dep. NTIS, 34p.
7709	25-18492	Dep. NTIS, 49p.
7727	25-19971	Dep. NTIS, 75p.
7747	25-20362	Dep. NTIS, 34p.
ANL-EBR-		
8	25-20755	Dep. NTIS, 26p.
ANL-Trans-		
875	25-20847	Dep. NTIS
ARH-		
1474	25-18558	Dep. NTIS, 54p.
AWRE-O-	(British)	
86/70	25-20363	Dep. NTIS (U. S. Sales Only). UK 3s, 18p.
B-	(Misc.)	
6	25-19158	See NP-18679
BDX-		
613-233	25-20848	Dep. NTIS, 21p.
613-257	25-20849	Dep. NTIS, 15p.
613-265	25-20850	Dep. NTIS, 15p.
613-310	25-20851	Dep. NTIS, 78p.
613-324	25-20852	Dep. NTIS, 9p.
BNL-		
15430	25-20125	Dep. NTIS, 192p.
50267	25-18619	Dep. NTIS, 121p.
50275	25-19292	Dep. NTIS, 111p.
BNL-tr-		
401	25-20364	Dep. NTIS
BNWL-		
1308-4	25-18590	Dep. NTIS, 41p.
1440	25-18620	Dep. NTIS, 199p.
1523	25-20733	Dep. NTIS, 71p.
BNWL-SA-		
3579	25-19273	Dep. NTIS, 18p.
BRH/DBE-	(Non-AEC)	
70-5	25-18979	NTIS, 31p.
BRH/DEP-	(Non-AEC)	
70-31	25-18827	NTIS, 13p.
71-1	25-20853	NTIS, 33p.
BRH/DMRE-	(Non-AEC)	
70-4	25-18480	NTIS, 40p.
BRL-MR-	(Non-AEC)	
2045	25-18732	See AD-711531
CALT-		
767-P-4-73	25-18447	Dep. NTIS, 28p.
CAPE-		
1752	25-18628	EM
CEA-Bib-	(French)	
191	25-18493	Dep. NTIS (U. S. Sales Only), 185p.
CEA-CONF-	(French)	
1657	25-20365	Dep. NTIS (U. S. Sales Only), 2p.
1676	25-18889	Dep. NTIS (U. S. Sales Only), 9p.
1695	25-19012	Dep. NTIS (U. S. Sales Only), 31p.
1698	25-18980	Dep. NTIS, 26p.
1725	25-18338	Dep. NTIS (U. S. Sales Only), 16p.
1727	25-20813	Dep. NTIS (U. S. Sales Only), 6p.
CEA-N-	(French)	
1365	25-18975	Dep. NTIS (U. S. Sales Only), 61p.
1369	25-18448	Dep. NTIS (U. S. Sales Only), 60p.
1380	25-18981	Dep. NTIS (U. S. Sales Only), 11p.
CEA-R-	(French)	
3557(2)	25-18339	Dep. NTIS (U. S. Sales Only), 189p.
3951	25-19230	Dep. NTIS (U. S. Sales Only), 171p.
4052	25-18733	Dep. NTIS (U. S. Sales Only), 85p.
4117	25-20265	Dep. NTIS (U. S. Sales Only), 25p.
4118	25-20716	Dep. NTIS (U. S. Sales Only), 51p.
CERN-HERA-	(European Organization for Nuclear Research)	
70-6	25-19909	Dep. NTIS (U. S. Sales Only), 212p.
CERN-Trans-	(European Organization for Nuclear Research)	
70-9	25-20126	Dep. NTIS (U. S. Sales Only)
70-12	25-20127	Dep. NTIS (U. S. Sales Only)
70-14	25-20016	Dep. NTIS (U. S. Sales Only)
70-15	25-20017	Dep. NTIS (U. S. Sales Only)
CEX-		
65.05	25-18982	Dep. NTIS, 34p.
CFB-		
4122-110	25-20721	See SAN-781-110
4122-210	25-20724	See UNC-5235
4122-214	25-20722	See SAN-781-214
4122-217	25-20723	See SAN-781-217
CNRS-CPT-	(French)	
70-P-335	25-20054	
CONF-660807-	(Symposium on Neutron Monitoring for Radiological Protection, Vienna, Austria, Aug. 29, 1966)	
41	25-18800	See SC-T-71-3009
CONF-670461-	(7th Meeting of Radiologist Doctors of Latin Origin and 1st Congress of the European Association of Radiology, Barcelona, Spain, Apr. 2-8, 1967)	
1	25-19012	See CEA-CONF-1695
2	25-18980	See CEA-CONF-1698
CONF-680809-	(14th International Conference on High Energy Physics, Vienna, Austria, Aug. 28-Sept. 5, 1968)	
46	25-19900	See USIP-70-4
CONF-680946-	(3rd Conference on Analytical Chemistry, Warsaw, Poland, Sept. 10, 1968)	
(Absts.)	25-18334	
CONF-681085-	(Meeting on Metallurgy, Paris, France, Oct. 14-17, 1968)	
1	25-19228	Mem. Sci. Rev. Met.; 67: 659-74(Oct 1970)
CONF-690652-	(Applied Superconductivity Conference, Smolenice, Czechoslovakia, June 23-27, 1969)	
	25-19591	Elektrotech. Cas.; 21: 241-438(1970)
CONF-691021-	(12th International Congress of Radiology, Tokyo, Japan, Oct. 6-11, 1969)	

XUM

Report No.	Abstract No.	Availability
(Absts.)	25-19052	Chiba, Japan; National Institute of Radiological Sciences (1969). 613p
CONF-691046-	(Meeting on Niobium, Paris, France, Oct. 20, 1969)	
	25-19211	Rev. Phys. Appl.; 5: 363-610(Jun 1970)
CONF-691114-	(90th Annual Meeting on American Society of Mechanical Engineers, Los Angeles, Calif., Nov. 16-20, 1969)	
5	25-20557	Energie; 22: 234-8(1970)
CONF-700102-	(Annual Meeting of the American Physical Society, Chicago, Ill., Jan. 26-29, 1970)	
4	25-20227	See AAEC/TM-565
CONF-700220-	(9th Conference on Developments in High Energy Physics, Schladming, Austria, Feb. 23-Mar. 7, 1970)	
	25-19933	Vienna; Springer-Verlag (1970). 637p. $30.00
CONF-700319-	(International Meeting on Primary Radiation Effects in Chemistry and Biology, Buenos Aires, Argentina, Mar. 9-14, 1970)	
1	25-18447	See CALT-767-P-4-73
CONF-700412-	(Meeting on The Biology and Ecology of Polonium and Radiolead, Sutton, England, Apr. 30-May 1, 1970)	
1	25-18929	See NYO-3446-14, Paper 26
2	25-18930	See NYO-3446-14, Paper 27
CONF-700429-	(Panel on Uranium Exploration Geology, Vienna, Austria, Apr. 13-17, 1970)	
	25-18529	See STI/PUB-277
CONF-700430-	(Conference on Nuclear Gas Turbines, London, England, Apr. 8-9, 1970)	
	25-20699	London; British Nuclear Energy Society (1970). 200p. 120s
CONF-700505-	(2nd Congress of the International Radiation Protection Association, Brighton, England, May 3-8, 1970)	
16	25-18986	See NYO-3446-14, Paper 28
17	25-18987	See NYO-3446-14, Paper 29
CONF-700544-	(International Conference on Ion Implantation in Semiconductors, Thousand Oaks, Calif., May 4-7, 1970)	
	25-19809	Radiat. Eff.; 6: 1-318(Nov 1970)
CONF-700638-	(Colloquium on Computational Methods in Theoretical Physics, Marseille, France, June 15-19, 1970)	
	25-20054	See CNRS-CPT-70-P-335
CONF-700807-	(Conference on Angular Correlations in Nuclear Disintegration, Delft, The Netherlands, Aug. 17-21, 1970)	
5	25-20372	See KFK-1249
CONF-700815-	(Conference on the Properties of Nuclei Far from the Region of Beta-Stability, Leysin, Switzerland, Aug. 31-Sept. 4, 1970)	
6	25-20478	See INR-P-1230
CONF-700816-	(11th AEC Air Cleaning Conference, Richland, Wash., Aug. 31-Sept. 3, 1970)	
(Vol.1)	25-18525	Dep. NTIS, 458p.
CONF-700819-	(2nd International Conference on the Strength of Metals and Alloys, Pacific Grove, Calif., Aug. 30-Sept. 4, 1970)	
11	25-19252	See COO-1367-36
CONF-700902-	(International Conference on Instrumentation for High Energy Physics, Dubna, U.S.S.R., Sept. 8-12, 1970)	
6	25-18775	See UCRL-20042
CONF-700903-	(4th Foratom Congress on Industrial Aspects of the Nuclear Fuel Cycle in Europe, Stockholm, Sweden, Sept. 21-23, 1970)	
14	25-18625	See SGAE-RT-35/1970
CONF-700911-	(160th National Meeting of the American Chemical Society, Chicago, Ill., Sept. 14-18, 1970)	
10	25-20365	See CEA-CONF-1657
CONF-700931-	(3rd International Symposium on Inhaled Particles, London, England, Sept. 21-23, 1970)	
2	25-18889	See CEA-CONF-1676
CONF-700934-	(2nd International Conference on the Science of Materials, Tremezzo, Italy, Sept. 13-25, 1970)	
3	25-19232	See UCRL-19696
CONF-700942-	(Joint Petroleum Mechanical Engineering and Pressure Vessel and Piping Division Conference, Denver, Colo., Sept. 13-16, 1970)	
1	25-20725	See WHAN-SA-46
CONF-700945-	(Conference on Ion Implantation, Reading, England, Sept. 7-9, 1970)	
	25-19772	Stevenage, Eng.; Peter Peregrinus Ltd. (1970). 241p. Pound 6
CONF-700947-	(2nd Seminar on Soil Mechanics and Foundation Engineering, Lodz, Poland, Sept. 7-10, 1970)	
1	25-18815	See INP-715
CONF-701001-	(4th International Conference on Plutonium and Other Actinides, Santa Fe, N. Mex., Oct. 5-9, 1970)	
14	25-19290	See WHAN-SA-15
16	25-19287	See AECL-3690
CONF-701036-	(Conference on the Doping of Interstitial Elements and Their Influence on the Properties of Metals and Alloys, Grenoble, France, Oct. 29-30, 1970)	
1	25-18338	See CEA-CONF-1725
CONF-701037-	(Meeting of the American Ceramic Society, San Francisco, Calif., Oct. 27-29, 1970)	
1	25-20836	See WHAN-SA-79
CONF-701039-	(Thermionic Conversion Specialist Conference, Miami Beach, Fla., Oct. 26-29, 1970)	
1	25-20813	See CEA-CONF-1727
CONF-701102-	(Meeting of the American Nuclear Society, Washington, D.C., Nov. 15-19, 1970)	
7	25-19254	See WHAN-SA-2
8	25-18646	See WHAN-SA-73
CONF-701206-	Conference on Ceramics in Severe Environments, Raleigh, N.C., Dec. 7-9, 1970)	
1	25-19273	See BNWL-SA-3579
COO-		
78-235	25-20854	Dep. NTIS, 65p.
1367-36	25-19252	Dep. NTIS, 5p.
1385-34	25-18420	Dep. NTIS, 23p.
1617-27	25-18483	Dep. NTIS, 115p.
1704-22	25-19090	Dep. NTIS, 22p.
2044-3	25-18890	Dep. NTIS, 52p.
CSIRO-Trans-	(Australian)	
9992	25-18814	Dep. NTIS (U. S. Sales Only)
10095	25-20228	Dep. NTIS (U. S. Sales Only)
10284	25-19393	Dep. NTIS (U. S. Sales Only)
DAE-AR-	(Indian)	
70	25-20855	NTIS (U. S. Sales Only), 88p.
DEMO-	(Greek)	
70/19	25-20001	Dep. NTIS (U. S. Sales Only), 18p.
70/25	25-20266	Dep. NTIS (U. S. Sales Only), 12p.
71/1	25-19985	Dep. NTIS (U. S. Sales Only), 9p.
71/2	25-19937	Dep. NTIS (U. S. Sales Only), 13p.
DESY-	(German)	
70/61	25-19886	Dep. NTIS (U. S. Sales Only), 10p.
70/62	25-20056	Dep. NTIS (U. S. Sales Only), 71p.
DLR-FB-	(German)	
69-78	25-19673	Dep. NTIS (U. S. Sales Only), 95p.
DOCKET-1155-	(LaCrosse Boiling Water Reactor) (AEC)	
100	25-20569	Dep. NTIS, 2p.
101	25-20570	Dep. NTIS, 2p.
102	25-20571	Dep. NTIS, 31p.
103	25-20572	Dep. NTIS, 2p.
104	25-20573	Dep. NTIS, 31p.
105	25-20600	Dep. NTIS, 3p.
DOCKET-50003-	(Indian Point Station; See Also DOCKET-50247, DOCKET-50286) (Non-AEC)	
65	25-20574	Dep. NTIS, 57p.
DOCKET-50010-	(Dresden Nuclear Power Station; See also DOCKET-50237 and DOCKET-50249) (Non-AEC)	
78	25-20575	Dep. NTIS, 23p.
79	25-20576	Dep. NTIS, 3p.
80	25-20601	Dep. NTIS, 15p.
DOCKET-50016-	(Enrico Fermi Atomic Power Plant) (Non-AEC)	
99	25-20602	Dep. NTIS, 18p.
100	25-20577	Dep. NTIS, 14p.
101	25-20603	Dep. NTIS, 39p.

Report No.	Abstract No.	Availability
102	25-20604	Dep. NTIS, 1p.
DOCKET-50029-	(Yankee Atomic Electric Co.) (Non-AEC)	
143	25-20578	Dep. NTIS, 7p.
144	25-20605	Dep. NTIS, 4p.
145	25-20579	Dep. NTIS, 2p.
146	25-20606	Dep. NTIS, 2p.
DOCKET-50130-	(Pathfinder Atomic Power Plant) (Misc.)	
7	25-20607	Dep. NTIS, 45p.
DOCKET-50133-	(Humboldt Bay Power Plant) (Non-AEC)	
45	25-20580	Dep. NTIS, 3p.
46	25-20608	Dep. NTIS, 3p.
48	25-20581	Dep. NTIS, 20p.
DOCKET-50146-	(Saxton Nuclear Experimental Corporation) (Non-AEC)	
68	25-20582	Dep. NTIS, 6p.
69	25-20609	Dep. NTIS, 1p.
DOCKET-50155-	(Big Rock Point Reactor) (Misc.)	
67	25-20610	Dep. NTIS, 22p.
68	25-20583	Dep. NTIS, 13p.
39	25-20611	Dep. NTIS, 3p.
70	25-20612	Dep. NTIS, 3p.
71	25-20613	Dep. NTIS, 3p.
72	25-20614	Dep. NTIS, 3p.
74	25-20615	Dep. NTIS, 2p.
75	25-20616	Dep. NTIS, 2p.
DOCKET-50171-	(Peach Bottom Atomic Power Station; See also DOCKET-50277 and DOCKET-50278) (Non-AEC)	
78	25-20584	Dep. NTIS, 2p.
DOCKET-50184-	(National Bureau of Standards Reactor) (Non-AEC)	
26	25-20784	Dep. NTIS, 10p.
27	25-20785	Dep. NTIS, 9p.
DOCKET-50201-	(West Valley Reprocessing Plant--Formerly Spent Fuel Processing Plant) (Misc.)	
63	25-18494	Dep. NTIS, 3p.
64	25-18495	Dep. NTIS, 1p.
65	25-18496	Dep. NTIS, 3p.
DOCKET-50213-	(Connecticut Yankee Atomic Power Plant) (Misc.)	
98	25-20617	Dep. NTIS, 25p.
99	25-20585	Dep. NTIS, 10p.
DOCKET-50219-	(Oyster Creek Nuclear Power Plant) (Non-AEC)	
123	25-20586	Dep. NTIS, 3p.
124	25-20618	Dep. NTIS, 21p.
125	25-20619	Dep. NTIS, 2p.
DOCKET-50220-	(Nine Mile Point Nuclear Station) (Non-AEC)	
58	25-20587	Dep. NTIS, 22p.
59	25-20620	Dep. NTIS, 76p.
60	25-20621	Dep. NTIS, 1p.
DOCKET-50231-	(Southwest Experimental Fast Oxide Reactor) (Non-AEC)	
71	25-20786	Dep. NTIS, 6p.
72	25-20744	Dep. NTIS, 4p.
DOCKET-50237-	(Dresden Nuclear Power Station, See also DOCKET-50249) (Non-AEC)	
143	25-20588	Dep. NTIS, 1p.
DOCKET-50238-	(N.S. Savannah Safety Assessment) (Non-AEC)	
78	25-20814	Dep. NTIS, 52p.
144	25-20815	Dep. NTIS, 4p.
DOCKET-50244-	(Robert Emmett Ginna Nuclear Power Plant, Formerly Brookwood Nuclear Station) (Non-AEC)	
60	25-20622	Dep. NTIS, 38p.
61	25-20623	Dep. NTIS, 5p.
62	25-20624	Dep. NTIS, 69p.
63	25-20625	Dep. NTIS, 7p.
64	25-20589	Dep. NTIS, 2p.
65	25-20590	Dep. NTIS, 2p.
66	25-20591	Dep. NTIS, 25p.
DOCKET-50245-	(Millstone Point Nuclear Power Station) (Non-AEC)	
55	25-20592	Dep. NTIS, 1p.
56	25-20626	Dep. NTIS, 67p.
DOCKET-50249-	(Dresden Nuclear Power Station; See also DOCKET-50237) (Non-AEC)	
57	25-20593	Dep. NTIS, 4p.
58	25-20627	Dep. NTIS, 5p.
59	25-20628	Dep. NTIS, 25p.
60	25-20629	Dep. NTIS, 11p.
DOCKET-50250-	(Turkey Point, See also DOCKET-50251) (Non-AEC)	
39	25-20630	Dep. NTIS, 64p.
40	25-20631	Dep. NTIS, 65p.
41	25-20632	Dep. NTIS, 33p.
DOCKET-50251-	(Turkey Point, See also DOCKET-50250) (Non-AEC)	
35	25-20630	See DOCKET-50250-39
36	25-20631	See DOCKET-50250-40
37	25-20632	See DOCKET-50250-41
DOCKET-50254-	(Quad-Cities Station; See also DOCKET-50265) (Non-AEC)	
28	25-20633	Dep. NTIS, 169p.
29	25-20634	Dep. NTIS, 54p.
30	25-20635	Dep. NTIS, 116p.
31	25-20636	Dep. NTIS, 5p.
DOCKET-50255-	(Palisades Plant) (Non-AEC)	
33	25-20637	Dep. NTIS, 13p.
DOCKET-50259-	(Browns Ferry Nuclear Power Station. See also DOCKET-50260 and DOCKET-50296) (Non-AEC)	
22	25-20638	Dep. NTIS, 320p.
DOCKET-50260-	(Browns Ferry Nuclear Power Station. See also DOCKET-50259 and DOCKET-50296) (Non-AEC).	
22	25-20638	See DOCKET-50259-22
DOCKET-50261-	(H. B. Robinson) (Non-AEC)	
51	25-20594	Dep. NTIS, 1p.
52	25-20639	Dep. NTIS, 8p.
DOCKET-50263-	(Monticello Nuclear Generating Plant) (Non-AEC)	
55	25-20640	Dep. NTIS, 2p.
56	25-20595	Dep. NTIS, 2p.
DOCKET-50265-	(Quad-Cities Station; See also DOCKET-50254) (Non-AEC)	
24	25-20633	See DOCKET-50254-28
25	25-20634	See DOCKET-50254-29
26	25-20635	See DOCKET-50254-30
27	25-20636	See DOCKET-50254-31
DOCKET-50266-	(Point Beach Nuclear Plant) (Non-AEC)	
42	25-20641	Dep. NTIS, 27p.
DOCKET-50267-	(Fort St. Vrain Nuclear Generating Station) (Non-AEC)	
26	25-20642	Dep. NTIS, 2p.
27	25-20643	Dep. NTIS, 470p.
DOCKET-50271-	(Vermont Yankee Nuclear Power Station) (Non-AEC)	
38	25-20644	Dep. NTIS, 69p.
39	25-20645	Dep. NTIS, 205p.
40	25-20646	Dep. NTIS, 3p.
41	25-20647	Dep. NTIS, 25p.
DOCKET-50280-	(Surry Power Station, See also DOCKET-50281) (Non-AEC)	
34	25-20648	Dep. NTIS, 56p.
35	25-20649	Dep. NTIS, 131p.
DOCKET-50281-	(Surry Power Station, See also DOCKET-50280) (Non-AEC)	
34	25-20648	See DOCKET-50280-34
35	25-20649	See DOCKET-50280-35
DOCKET-50285-	(Fort Calhoun Station) (Non-AEC)	
42	25-20650	Dep. NTIS, 531p.
DOCKET-50293-	(Pilgrim Nuclear Power Station) (Non-AEC)	
36	25-20651	Dep. NTIS, 130p.
37	25-20652	Dep. NTIS, 3p.
38	25-20653	Dep. NTIS, 43p.
39	25-20654	Dep. NTIS, 21p.
DOCKET-50295-	(Zion Station Nuclear Power Plant. See also DOCKET-50304) (Non-AEC)	
24	25-20655	Dep. NTIS, 4p.
DOCKET-50296-	(Browns Ferry Nuclear Power Station. See also DOCKET-50259 and DOCKET-50260) (Non-AEC)	
21	25-20638	See DOCKET-50259-22
DOCKET-50298-	(Cooper Nuclear Station) (Non-AEC)	
13	25-20656	Dep. NTIS, 400p.
14	25-20657	Dep. NTIS, 242p.
15	25-20658	Dep. NTIS, 349p.
16	25-20659	Dep. NTIS, 214p.
18	25-20660	Dep. NTIS, 276p.
19	25-20661	Dep. NTIS, 307p.
20	25-20662	Dep. NTIS, 30p.
DOCKET-50301-	(Point Beach Nuclear Plant) (Non-AEC)	
27	25-20641	See DOCKET-50266-42
28	25-20663	Dep. NTIS, 10p.
DOCKET-50304-	(Zion Station Nuclear Power Plant. See also DOCKET-50295) (Non-AEC)	
24	25-20655	See DOCKET-50295-24

XUM

Report No.	Abstract No.	Availability
DOCKET-50305-	(Kewaunee Nuclear Power Plant) (Non-AEC)	
18	25-20641	See DOCKET-50266-42
19	25-20664	Dep. NTIS, 140p.
DOCKET-50309-	(Maine Yankee Atomic Power Company) (Non-AEC)	
27	25-20665	Dep. NTIS, 76p.
28	25-20666	Dep. NTIS, 51p.
29	25-20667	Dep. NTIS, 18p.
DOCKET-50321-	(Edwin I. Hatch Nuclear Plant) (Non-AEC)	
16	25-20668	Dep. NTIS, 111p.
17	25-20669	Dep. NTIS, 20p.
DOCKET-50324-	(Brunswick Steam Electric Plant, Units 1 and 2, See also DOCKET-50325) (Non-AEC)	
19	25-20670	Dep. NTIS, 42p.
DOCKET-50325-	(Brunswick Steam Electric Plant, Units 1 and 2, See also DOCKET-50324) (Non-AEC)	
19	25-20670	See DOCKET-50324-19
DOCKET-50338-	(North Anna Power Station; See also DOCKET-50339) (Non-AEC)	
27	25-20671	Dep. NTIS, 4p.
DOCKET-50339-	(North Anna Power Station; See also DOCKET-50338) (Non-AEC)	
26	25-20672	Dep. NTIS, 4p.
DOCKET-50341-	(Enrico Fermi Atomic Power Plant) (Non-AEC)	
27	25-20673	Dep. NTIS, 39p.
DOCKET-50348-	(Joseph M. Farley Nuclear Plant, Units 1 and 2, Formerly Seala Nuclear Plant, See also DOCKET-50364) (Non-AEC)	
16	25-20674	Dep. NTIS, 421p.
DOCKET-50352-	(Limerick Generating Station) (See also DOCKET-50353) (Non-AEC)	
11	25-20675	Dep. NTIS, 118p.
DOCKET-50353-	(Limerick Generating Station) (See also DOCKET-50352) (Non-AEC)	
11	25-20675	See DOCKET-50352-11
DOCKET-50354-	(Newbold Island Nuclear Generating Station) (See also DOCKET-50355) (Non-AEC)	
11	25-20676	Dep. NTIS, 70p.
DOCKET-50355-	(Newbold Island Nuclear Generating Station) (See also DOCKET-50354) (Non-AEC)	
11	25-20676	See DOCKET-50354-11
DOCKET-50361-	(San Onofre Nuclear Generating Station) (Units 2 and 3) (See also Docket-50362) (Docket-50206) (Unit 1) (Non-AEC)	
15	25-20677	Dep. NTIS, 251p.
DOCKET-50362-	(San Onofre Nuclear Generating Station) (Units 2 and 3) (See also Docket-50361) (Docket-50206) (Unit 1) (Non-AEC)	
14	25-20677	See DOCKET-50361-15
DOCKET-50363-	(Forked River Nuclear Station) (Unit 1) (Non-AEC)	
12	25-20678	Dep. NTIS, 181p.
DOCKET-50364-	(Joseph M. Farley Nuclear Plant, Units 1 and 2, See also DOCKET-50348) (Non-AEC)	
10	25-20674	See DOCKET-50348-16
DOCKET-50366-	(Edwin I. Hatch Nuclear Plant, Unit 2, Non-AEC)	
8	25-20668	See DOCKET-50321-16
DOCKET-50369-	(McGuire Nuclear Station) (See also DOCKET-50370) (Non-AEC) (Units 1 and 2)	
6	25-20679	Dep. NTIS, 167p.
DOCKET-50370-	(McGuire Nuclear Station) (See also DOCKET-50369) (Non-AEC) (Units 1 and 2)	
5	25-20679	See DOCKET-50369-6
DOCKET-50372-	(Atlantic Richfield Company) (Non-AEC)	
3	25-18497	Dep. NTIS, 3p.
DOCKET-50376-	(Aguirre Nuclear Plant) (Non-AEC)	
9	25-20680	Dep. NTIS, 349p.
DOCKET-0$_0$400	(Westinghouse Four-Loop Nuclear Steam Supply esign)	
RESARA-		
1	25-20681	Dep. NTIS, 604p.
2	25-20682	Dep. NTIS, 506p.
DP-		
1244	25-20710	Dep. NTIS, 32p.
1245	25-18621	Dep. NTIS, 16p.
1254	25-18591	Dep. NTIS, 27p.

Report No.	Abstract No.	Availability
DP-Report-	(British)	
450	25-20745	Dep. NTIS (U. S. Sales Only), 36p.
489	25-20734	Dep. NTIS (U. S. Sales Only), 29p.
496	25-20742	Dep. NTIS (U. S. Sales Only), 21p.
580	25-18610	Dep. NTIS (U. S. Sales Only), 31p.
DPC-		
71-1	25-20569	See DOCKET-1155-100
71-2	25-20570	See DOCKET-1155-101
71-3	25-20572	See DOCKET-1155-103
851-18	25-20571	See DOCKET-1155-102
851-19	25-20573	See DOCKET-1155-104
E-	(Misc.)	
5444	25-20269	See N-70-37365
5579	25-20805	See N-70-39420
EANDC(UK)-	(European-American Nuclear Data Committee)	
125-AL	25-20363	See AWRE-O-86/70
EG-Report-	(British)	
(47)R	25-20745	See DP-Report-450
EP-RR-	(Australian)	
21	25-19656	Dep. NTIS (U. S. Sales Only), 17p.
EUR-	(European Atomic Energy Community)	
4538	25-20267	Dep. NTIS (U. S. Sales Only). EUR FF 5.60, 32p.
EUR-CEA-FC-	(European Atomic Energy Community)	
576	25-18828	Dep. NTIS (U. S. Sales Only), 23p.
EURAEC-		
2108	25-20705	See WCAP-3385-55
FOA-	(Swedish)	
4-4449	25-19724	Dep. NTIS (U. S. Sales Only), 20p.
GAMD-	(Misc.)	
10231	25-20787	Dep. NTIS, 34p.
GAT-T-		
999	25-20856	Dep. NTIS, 15p.
GEAP-	(Misc.)	
13649	25-20693	Dep. NTIS, 68p.
GEPP-		
83	25-20857	Dep. NTIS, 20p.
GL-		
1970-14	25-20880	See NYO-4176-4
1970-15	25-20881	See NYO-4176-6
HPR-	(Norwegian)	
127	25-20735	Dep. NTIS (U. S. Sales Only), 24p.
132	25-20736	Dep. NTIS (U. S. Sales Only), 147p.
HSSTP-TR-		
12	25-18611	Dep. NTIS, 121p.
IAEA-INIS-	(International Atomic Energy Agency)	
6(Rev.2)	25-20858	Dep. NTIS (U. S. Sales Only), 210p.
IEA-	(Brazilian)	
211	25-20366	Dep. NTIS (U. S. Sales Only), 17p.
IFPTH-	(Italian)	
10/70	25-19972	Dep. NTIS (U. S. Sales Only), 34p.
IFVE-SEF-	(Russian)	
69-44	25-18639	Dep. NTIS (U. S. Sales Only), 17p.
70-22	25-20128	Dep. NTIS (U. S. Sales Only), 28p.
70-23	25-18640	Dep. NTIS (U. S. Sales Only), 15p.
IFVE-SKU-	(Russian)	
69-88	25-20127	For translation see CERN-Trans-70-12
69-100	25-20126	For translation see CERN-Trans-70-9
IFVE-STF-	(Russian)	
70-34	25-19986	Dep. NTIS (U. S. Sales Only), 28p.
IFVE-STF/SPK-	(Russian)	
70-30	25-20002	Dep. NTIS (U. S. Sales Only), 7p.
IN-		
1446	25-18641	Dep. NTIS, 23p.
INP-	(Polish)	
710	25-19468	Dep. NTIS (U. S. Sales Only), 120p.
715	25-18615	Dep. NTIS (U. S. Sales Only), 17p.
727	25-18734	Dep. NTIS (U. S. Sales Only), 15p.
INR-	(Non-AEC)	
1186	25-20229	Dep. NTIS (U. S. Sales Only), 124p.
1224	25-18735	Dep. NTIS (U. S. Sales Only), 12p.
1231	25-19522	Dep. NTIS (U. S. Sales Only), 108p.
INR-P-	(Polish)	
1216	25-20367	Dep. NTIS (U. S. Sales Only), 12p.

Report No.	Abstract No.	Availability
1218	25-20129	Dep. NTIS (U. S. Sales Only), 13p.
1225	25-19488	Dep. NTIS (U. S. Sales Only), 118p.
1227	25-18736	Dep. NTIS (U. S. Sales Only), 10p.
1230	25-20478	Dep. NTIS (U. S. Sales Only), 7p.
INSJ-	(Japanese)	
125	25-19973	Dep. NTIS (U. S. Sales Only), 81p.
IPP-	(Non-AEC)	
1/110	25-19647	See IPP-6/90
1/112	25-19674	Dep. NTIS (U. S. Sales Only), 37p.
2/86	25-19645	Dep. NTIS (U. S. Sales Only), 38p.
4/7	25-19646	Dep. NTIS (U. S. Sales Only), 8p.
4/80	25-19572	Dep. NTIS (U. S. Sales Only), 14p.
6/90	25-19647	Dep. NTIS (U. S. Sales Only), 66p.
6/91	25-19646	See IPP-4/7
IS-T-		
417	25-20859	Dep. NTIS, 137p.
419	25-20860	Dep. NTIS, 162p.
420	25-20861	Dep. NTIS, 91p.
427	25-20862	Dep. NTIS, 108p.
430	25-20863	Dep. NTIS, 151p.
431	25-20864	Dep. NTIS, 127p.
432	25-20865	Dep. NTIS, 224p.
ITF-	(Russian)	
70-51-E	25-20249	Dep. NTIS (U. S. Sales Only), 28p.
JAERI-Memo-	(Japanese)	
4116	25-20230	Dep. NTIS (U. S. Sales Only), 39p.
4138	25-20479	Dep. NTIS (U. S. Sales Only), 61p.
4165	25-20819	Dep. NTIS (U. S. Sales Only), 81p.
4167	25-20231	Dep. NTIS (U. S. Sales Only), 23p.
4189	25-20368	Dep. NTIS (U. S. Sales Only), 31p.
4194	25-20762	Dep. NTIS (U. S. Sales Only), 126p.
4205	25-20834	Dep. NTIS (U. S. Sales Only), 46p.
4215	25-20788	Dep. NTIS (U. S. Sales Only), 68p.
4216	25-18983	Dep. NTIS (U. S. Sales Only), 26p.
4229	25-20763	Dep. NTIS (U. S. Sales Only), 101p.
4238	25-20831	Dep. NTIS (U. S. Sales Only), 35p.
4240	25-19013	Dep. NTIS (U. S. Sales Only), 60p.
JINR-	(Russian)	
E2-5561	25-20003	Dep. NTIS (U. S. Sales Only), 8p.
E2-5563	25-20057	Dep. NTIS (U. S. Sales Only), 18p.
E2-5579	25-19924	Dep. NTIS (U. S. Sales Only), 15p.
E7-5499	25-20480	Dep. NTIS (U. S. Sales Only), 9p.
P1-5540	25-18773	Dep. NTIS (U. S. Sales Only), 19p.
P1-5542	25-19891	Dep. NTIS (U. S. Sales Only), 6p.
P2-5058	25-20016	For translation see CERN-Trans-70-14
P2-5496	25-20250	Dep. NTIS (U. S. Sales Only), 16p.
P2-5505	25-19938	Dep. NTIS (U. S. Sales Only), 12p.
P2-5507	25-20018	Dep. NTIS (U. S. Sales Only), 14p.
P2-5520	25-19963	Dep. NTIS (U. S. Sales Only), 28p.
P2-5566	25-19987	Dep. NTIS (U. S. Sales Only), 8p.
P2-5569	25-20058	Dep. NTIS (U. S. Sales Only), 21p.
P3-5297	25-20364	For translation see BNL-tr-401
P3-5392	25-20232	Dep. NTIS (U. S. Sales Only), 16p.
P3-5528	25-20369	Dep. NTIS, 10p.
P4-3860	25-19482	For translation see NRC-TT-1426
P4-5457	25-20481	Dep. NTIS (U. S. Sales Only), 47p.
P4-5479	25-20268	Dep. NTIS (U. S. Sales Only), 8p.
P4-5547	25-20059	Dep. NTIS (U. S. Sales Only), 19p.
P7-5512	25-20370	Dep. NTIS (U. S. Sales Only), 17p.
P7-5584	25-20371	Dep. NTIS (U. S. Sales Only), 10p.
P8-5440	25-19588	Dep. NTIS (U. S. Sales Only), 8p.
P9-5441	25-18829	Dep. NTIS (U. S. Sales Only), 26p.
P9-5453	25-20130	Dep. NTIS (U. S. Sales Only), 19p.
P9-5535	25-20131	Dep. NTIS (U. S. Sales Only), 11p.
P13-5485	25-18642	Dep. NTIS (U. S. Sales Only), 18p.
P13-5516	25-20004	Dep. NTIS (U. S. Sales Only), 23p.
P13-5529	25-18774	Dep. NTIS (U. S. Sales Only), 13p.
JPRS-	(Non-AEC)	
52384	25-20717	NTIS
52443	25-20816	NTIS
JUL-	(German)	
644-RG	25-20746	Dep. NTIS (U. S. Sales Only), 124p.
688-ME	25-18984	Dep. NTIS (U. S. Sales Only), 37p.
706-TP	25-19536	Dep. NTIS (U. S. Sales Only), 41p.
KFK-	(German)	
1249	25-20372	Dep. NTIS (U. S. Sales Only), 18p.
1298	25-18498	Dep. NTIS (U. S. Sales Only), 73p.
KFKI-	(Hungarian)	
70-24-HEP	25-19964	Dep. NTIS (U. S. Sales Only), 88p.
70-29-HP	25-18798	Dep. NTIS (U. S. Sales Only), 7p.
71-4	25-20820	Dep. NTIS (U. S. Sales Only), 26p.
KR-	(Norwegian)	
140	25-18356	Dep. NTIS (U. S. Sales Only), 25p.
KS-	(Misc.)	
6903	25-18643	See NP-18672
KY-		
626	25-18340	Dep. NTIS, 8p.

Report No.	Abstract No.	Availability
LA-		
4563	25-18985	Dep. NTIS, 5p.
4593	25-20132	Dep. NTIS, 5p.
4597	25-19725	Dep. NTIS, 6p.
LA-tr-		
70-27	25-19394	Dep. NTIS
71-4	25-20866	Dep. NTIS
71-10	25-20867	Dep. NTIS
LAL-	(French)	
1242	25-19910	Dep. NTIS (U. S. Sales Only), 236p.
LF-	(Misc.)	
33	25-18428	See NP-18676
LF-tr-		
46	25-18891	Dep. NTIS
LIB/Trans-	(Australian)	
300	25-20373	Dep. NTIS (U. S. Sales Only)
307	25-19769	Dep. NTIS (U. S. Sales Only)
308	25-20718	Dep. NTIS (U. S. Sales Only)
324	25-18612	Dep. NTIS (U. S. Sales Only)
330	25-18499	Dep. NTIS
LP-	(Misc.)	
119	25-20872	See NP-18708
LYCEN-	(French)	
7081	25-20019	Dep. NTIS (U. S. Sales Only), 54p.
MATT-Trans-		
7	25-20868	Dep. NTIS
16	25-19657	Dep. NTIS
N-	(Misc.)	
70-37365	25-20269	NTIS, 40p.
70-39420	25-20805	NTIS, 33p.
NAMRL-	(Non-AEC)	
1112	25-18978	See AD-711316
NASA-TM-X-	(Misc.)	
2077	25-20805	See N-70-39420
NASA-TN-D-	(Misc.)	
5995	25-20269	See N-70-37365
NBS-SPEC. PUBL-	(Non-AEC)	
305(Suppl. 1)	25-20869	GPO $4.50
NBS-TN-	(Misc.)	
546	25-18357	GPO $1.25
548	25-18366	GPO $1.25
NCRP-	(Non-AEC)	
38	25-19007	NCRP $3.00
39	25-19008	NCRP $2.00
NLCO-		
1029	25-19259	Dep. NTIS, 85p.
1051	25-19231	Dep. NTIS, 10p.
NP-	(AEC File No. for Non-AEC Reports)	
18487	25-20764	Dep. NTIS (U. S. Sales Only), 200p.
18597	25-20374	Dep. NTIS (U. S. Sales Only), 74p.
18624	25-20375	Dep. NTIS (U. S. Sales Only), 49p.
18626	25-20270	Dep. NTIS (U. S. Sales Only), 83p.
18628	25-20271	Dep. NTIS (U. S. Sales Only), 108p.
18641	25-18892	Dep. NTIS (U. S. Sales Only), 105p.
18666	25-19348	Dep. NTIS (U. S. Sales Only), 74p.
18668	25-20747	Dep. NTIS (U. S. Sales Only), 197p.
18669	25-18500	Dep. NTIS (U. S. Sales Only), 136p.
18670	25-18927	Dep. NTIS (U. S. Sales Only), 163p.
18671	25-20133	Dep. NTIS (U. S. Sales Only), 192p.
18672	25-18643	Dep. NTIS (U. S. Sales Only), 70p.
18676	25-18428	Dep. NTIS (U. S. Sales Only), 37p.
18677	25-20550	Dep. NTIS (U. S. Sales Only), 26p.
18678	25-20251	Dep. NTIS (U. S. Sales Only), 105p.
18679	25-19158	Dep. NTIS (U. S. Sales Only), 10p.
18680	25-19489	Dep. NTIS, 13p.
18681	25-19704	Dep. NTIS (U. S. Sales Only), 20p.
18682	25-19349	Dep. NTIS (U. S. Sales Only), 365p.
18690	25-20870	
18693	25-19062	Dep. NTIS (U. S. Sales Only), 148p.
18701	25-20871	Dep. NTIS (U. S. Sales Only), 232p.
18703	25-19925	Dep. NTIS (U. S. Sales Only), 37p.
18705	25-20102	Dep. NTIS (U. S. Sales Only), 149p.
18707	25-20103	Dep. NTIS (U. S. Sales Only), 193p.
18708	25-20872	Dep. NTIS (U. S. Sales Only), 15p.
18714	25-19133	
18715	25-19669	Dep. NTIS (U. S. Sales Only), 44p.
18722	25-19700	Dep. NTIS (U. S. Sales Only), 54p.
NRC-TT-	(Canadian)	
1426	25-19482	Dep. NTIS (U. S. Sales Only)

XUM

Report No.	Abstract No.	Availability
NYO-		
1368-17	25-20873	Dep. NTIS, 7p.
2262-TA-221	25-19939	Dep. NTIS, 11p.
2262-TA-231	25-20104	Dep. NTIS, 20p.
2262-TA-234	25-19926	Dep. NTIS, 8p.
2262-TA-236	25-19965	Dep. NTIS, 11p.
2391-126	25-20874	Dep. NTIS, 16p.
3250-56	25-20585	See DOCKET-50213-99
3446-14	25-18928	Dep. NTIS, 100p.
3562-3	25-20875	Dep. NTIS, 83p.
3842-12	25-19770	Dep. NTIS, 13p.
3906-12	25-18830	Dep. NTIS, 13p.
3978-4	25-20876	Dep. NTIS, 7p.
3997-6	25-20877	Dep. NTIS, 1p.
3997-7	25-20878	Dep. NTIS, 4p.
4062-5	25-20879	Dep. NTIS, 6p.
4073-4	25-19194	Dep. NTIS, 21p.
4176-4	25-20880	Dep. NTIS, 34p.
4176-6	25-20881	Dep. NTIS, 13p.
ORNL-		
4298	25-18592	Dep. NTIS, 187p.
4584	25-18988	Dep. NTIS, 255p.
4629	25-19260	Dep. NTIS, 108p.
ORNL-IIC-		
32	25-18593	Dep. NTIS, 30p.
ORNL-TM-		
2893(Vol.1) (Rev.)	25-20789	Dep. NTIS, 104p.
3082	25-20882	Dep. NTIS, 21p.
3220	25-19195	Dep. NTIS, 149p.
3245	25-20832	Dep. NTIS, 128p.
3291	25-18565	Dep. NTIS, 26p.
3292	25-18594	Dep. NTIS, 26p.
3308	25-20719	Dep. NTIS, 69p.
ORNL-tr-		
2355	25-20883	Dep. NTIS
2370	25-18566	Dep. NTIS
2386	25-18449	Dep. NTIS
2409	25-20233	Dep. NTIS
2428	25-20376	Dep. NTIS
ORO-		
2968-54	25-18426	J. Amer. Chem. Soc.; 93: 787-8(10 Feb 1971)
3514-10	25-18934	Dep. NTIS, 129p.
3519-8	25-18450	Dep. NTIS, 19p.
3820-7	25-18737	Dep. NTIS, 21p.
3905	25-18935	Dep. NTIS, 35p.
4061-1	25-20884	Dep. NTIS, 6p.
PATENTS	(British)	
1,204,162	25-18743	
1,209,512	25-18652	
1,209,788	25-18859	
1,209,826	25-18719	
1,209,844	25-18861	
1,210,047	25-18803	
1,210,350	25-18698	
1,210,756	25-18817	
1,210,984	25-18804	
1,211,122	25-18653	
1,211,316	25-18567	
1,212,118	25-18964	
1,213,478	25-18686	
1,213,684	25-20142	
1,216,061	25-18721	
1,216,561	25-18685	
1,217,277	25-18819	
1,217,515	25-18618	
1,217,598	25-20182	
1,218,096	25-18856	
1,218,124	25-18682	
1,218,296	25-18805	
1,218,764	25-20837	
1,218,884	25-18683	
1,219,220	25-19268	
1,219,696	25-19264	
1,219,795	25-20838	
1,220,119	25-20839	
1,220,331	25-19270	
1,220,332	25-19269	
1,220,553	25-20809	
1,220,554	25-20807	
1,220,644	25-20808	
1,221,309	25-20714	
1,221,522	25-20843	
1,221,726	25-19641	
1,222,081	25-18572	
1,222,189	25-18633	
1,222,196	25-18632	
1,222,937	25-19267	
PATENTS	(French)	
1,195,862	25-19769	For translation see LIB/Trans-307
1,537,218	25-18499	For translation see LIB/Trans-330
1,586,185	25-19294	
1,586,204	25-18877	
1,586,506	25-20842	
1,586,904	25-18689	
1,588,079	25-18855	
1,590,198	25-18881	
1,590,263	25-18688	
1,590,762	25-18687	
1,591,051	25-20727	
1,594,560	25-18614	
1,595,595	25-18629	
1,595,641	25-18598	
PATENTS	(Russian)	
243,841	25-19618	
PATENTS	(U. S.)	
3,521,165	25-18839	
3,524,999	25-18879	
3,525,047	25-18840	
3,526,768	25-18731	
3,531,638	25-18820	
3,531,639	25-18744	
3,531,641	25-18807	
3,531,997	25-18822	
3,532,883	25-18362	
3,532,884	25-18874	
3,532,927	25-18713	
3,534,811	25-20143	
3,535,087	25-18854	
3,535,520	25-18651	
3,535,524	25-18636	
3,537,420	25-20840	
3,537,910	25-20694	
3,538,328	25-18722	
3,539,488	25-18437	
3,541,311	25-18684	
3,541,339	25-18818	
3,542,587	25-18439	
3,543,036	25-18600	
3,543,147	25-20179	
3,543,171	25-20178	
3,544,307	25-18509	
3,544,424	25-20743	
3,544,425	25-20695	
3,546,068	25-20697	
3,546,069	25-20806	
3,547,380	25-20810	
3,547,685	25-19168	
3,547,709	25-19185	
3,547,778	25-20817	
3,549,323	25-18512	
3,549,324	25-18513	
3,549,325	25-18514	
3,551,119	25-18507	
3,551,212	25-18605	
3,551,708	25-19544	
3,551,828	25-19729	
3,556,870	25-19180	
PEL-	(South African)	
199	25-20748	Dep. NTIS (U. S. Sales Only), 50p.
PG-Report-	(British)	
1013	25-19103	Dep. NTIS (U. S. Sales Only), 13p.
PH-	(Swedish)	
4	25-20234	Dep. NTIS (U. S. Sales Only), 10p.
PR-P-	(Canadian)	
85	25-20307	See AECL-3667
PRDC-EF-		
85	25-20577	See DOCKET-50016-100
RCN-	(Dutch)	
131	25-18501	Dep. NTIS (U. S. Sales Only), 72p.
132	25-20833	Dep. NTIS (U. S. Sales Only), 45p.
REC-ERC-		
71-6	25-19292	See BNL-50275
RFP-		
1421	25-18502	Dep. NTIS, 43p.
RFP-Trans-		
72	25-20482	Dep. NTIS
74(Pt.1)	25-20885	Dep. NTIS
74(Pt.2)	25-20886	Dep. NTIS
RHEL/R-	(British)	
201	25-20135	Dep. NTIS (U. S. Sales Only). UK 5s, 24p.
RISO-	(Danish)	
229	25-18738	Dep. NTIS (U. S. Sales Only), 56p.
RLO-		
2098-1	25-18421	Dep. NTIS, 93p.
2225-T-16-1	25-18919	Dep. NTIS, 4p.
2225-13-5	25-19590	Scr. Met.; 5: 81-6(Feb 1971)

Report No.	Abstract No.	Availability
RPI-	(Misc.)	
328-211	25-20235	Dep. NTIS, 64p.
RT/CHI-	(Italian)	
(70)14	25-18341	Dep. NTIS (U. S. Sales Only), 12p.
(70)18	25-18358	Dep. NTIS (U. S. Sales Only), 18p.
(70)25	25-18503	Dep. NTIS (U. S. Sales Only), 30p.
RT/ING-	(Italian)	
(70)8	25-20835	Dep. NTIS (U. S. Sales Only), 57p.
SAM-TR-	(Non-AEC)	
69-82	25-18977	See AD-702155
SAN-		
781-1	25-20720	Dep. NTIS, 415p.
781-110	25-20721	Dep. NTIS, 34p.
781-210	25-20724	See UNC-5235
781-214	25-20722	Dep. NTIS, 52p.
781-217	25-20723	Dep. NTIS, 55p.
SC-DR-		
68-812-B	25-20887	Dep. NTIS, 31p.
70-686	25-20888	Dep. NTIS, 57p.
70-693	25-18613	Dep. NTIS, 62p.
70-736	25-20889	Dep. NTIS, 20p.
70-867	25-20890	Dep. NTIS, 54p.
70-872	25-20136	Dep. NTIS, 33p.
SC-RR-		
69-506	25-20891	Dep. NTIS, 46p.
70-579	25-20892	Dep. NTIS, 47p.
70-650	25-20893	Dep. NTIS, 67p.
70-735	25-19492	Dep. NTIS, 22p.
70-766	25-20894	Dep. NTIS, 26p.
70-854	25-18595	Dep. NTIS, 64p.
SC-T-		
71-3009	25-18800	Dep. NTIS
SCL-CR-		
710175	25-20895	Dep. NTIS, 320p.
SCL-T-		
68-253	25-20896	Dep. NTIS
SGAE-RT-	(Non-AEC)	
35/1970	25-18625	Dep. NTIS (U. S. Sales Only), 13p.
SLAC-Trans-		
130	25-20052	Dep. NTIS
STI/PUB-	(International Atomic Energy Agency)	
277	25-18529	IAEA $10.00
TID-		
25648	25-20236	Dep. NTIS, 118p.
25653	25-20812	GPO $2.00
25656	25-20897	Dep. NTIS, 18p.
25660	25-18419	New York; Plenum Press (1971). 320p. $18.50
25664	25-20898	Dep. NTIS, 23p.
TKK-F-A-	(Finnish)	
102	25-20821	Dep. NTIS (U. S. Sales Only), 45p.
137	25-20822	Dep. NTIS (U. S. Sales Only), 23p.
139	25-20823	Dep. NTIS (U. S. Sales Only), 46p.
TRG-Report-	(British)	
1804	25-20736	See HPR-132
1906	25-19196	Dep. NTIS (U. S. Sales Only), 20p.
UCLA-		
12-810	25-20899	Dep. NTIS, 47p.

Report No.	Abstract No.	Availability
UCRL-		
19030	25-19643	Rev. Phys. Appl.; 5: 32-6(Feb 1970)
19696	25-19232	Dep. NTIS, 38p.
20000-NN	25-19899	Dep. NTIS, 358p.
20042	25-18775	Dep. NTIS, 20p.
20192	25-18945	Dep. NTIS, 76p.
20388	25-20900	Dep. NTIS, 19p.
20393	25-20901	Dep. NTIS, 36p.
20395	25-20902	Dep. NTIS, 20p.
50400(Vol. 9)	25-20237	Dep. NTIS, 304p.
50892(Vol. 1)	25-18831	Dep. NTIS, 26p.
50892(Vol. 6)	25-18832	Dep. NTIS, 346p.
50952	25-19293	Dep. NTIS, 18p.
50978	25-20903	Dep. NTIS, 27p.
50985	25-19472	Dep. NTIS, 4p.
UCSD-		
34-P-166-X-2	25-20904	Dep. NTIS, 7p.
UJV-	(Czechoslovakian)	
2450-Ch	25-18504	Dep. NTIS (U. S. Sales Only), 40p.
2488-F	25-20238	Dep. NTIS (U. S. Sales Only), 12p.
UNC-	(Misc.)	
5235	25-20724	Dep. NTIS, 104p.
USGS-		
474-97	25-18522	Dep. NTIS, 24p.
USIP-	(Swedish)	
70-1	25-18645	Dep. NTIS (U. S. Sales Only), 38p.
70-3	25-18776	Dep. NTIS (U. S. Sales Only), 48p.
70-4	25-19900	Dep. NTIS (U. S. Sales Only), 47p.
70-5	25-20020	Dep. NTIS (U. S. Sales Only), 19p.
70-6	25-18777	Dep. NTIS (U. S. Sales Only), 49p.
70-7	25-19901	Dep. NTIS (U. S. Sales Only), 81p.
70-8	25-19902	Dep. NTIS (U. S. Sales Only), 74p.
WANL-TME-	(Non-AEC)	
2721	25-18578	Dep. NTIS, 140p.
WAPD-TM-	(Misc.)	
971	25-20377	Dep. NTIS, 94p.
WASH-		
1162	25-18626	GPO $0.25
WCAP-	(Misc.)	
3385-55	25-20705	Dep. NTIS, 98p.
3385-56(Pt. 2)	25-18359	Dep. NTIS, 144p.
WHAN-FR-		
16	25-19253	Dep. NTIS, 48p.
22	25-20790	Dep. NTIS, 38p.
24	25-19289	Dep. NTIS, 40p.
32	25-18505	Dep. NTIS, 72p.
37	25-20711	Dep. NTIS, 65p.
WHAN-SA-		
2	25-19254	Dep. NTIS, 11p.
15	25-19290	Dep. NTIS, 9p.
46	25-20725	Dep. NTIS, 14p.
73	25-18646	Dep. NTIS, 14p.
79	25-20836	Dep. NTIS, 11p.

☆U. S. GOVERNMENT PRINTING OFFICE: 1971—436-213/23

XUM

UNITED STATES
ATOMIC ENERGY COMMISSION
P. O. BOX 62
OAK RIDGE, TENNESSEE 37830

OFFICIAL BUSINESS

POSTAGE AND FEES PAID
U. S. ATOMIC ENERGY COMMISSION

UNITE
GOVERNMENT
DIVI
PUBLIC
WASHINGT
OFFICI

STAGE AND FEES PAID
VERNMENT PRINTING OFFICE

UNIVERSITY MICROFILMS
ATTN MRS. MARLENE HURST
MANAGER, PUBLISHER RELATIONS
ANN ARBOR MICHIGAN 48106

1

TECHNICAL PROGRESS REVIEWS

The Division of Technical Information, U. S. Atomic Energy Commission, also publishes three journals on nuclear technology, the Technical Progress Reviews. These journals summarize, evaluate, and reference the progress of development in three important fields. *Nuclear Safety* is a bimonthly journal; the other two are quarterly journals.

Isotopes and Radiation Technology P. S. Baker, A. F. Rupp, and associates, Oak Ridge National Laboratory. Reviews AEC-sponsored projects and related significant worldwide developments in radioisotopes and radiation technology.

Nuclear Safety Wm. B. Cottrell, J. P. Blakely, W. H. Jordan, and associates, Nuclear Safety Information Center, Oak Ridge National Laboratory. Covers topics relevant to the analysis and control of hazards associated with nuclear reactors and with operations involving fissionable materials and the products of nuclear fission.

Reactor Technology Reviews reactor research, development, design practices, operating experience, and aerospace applications, as well as current developments in reactor fuel processing.

Availability

SUBSCRIPTION RATE: The Technical Progress Reviews may be purchased from the Superintendent of Documents, U. S. Government Printing Office, Washington, D. C. 20402: *Nuclear Safety* at $3.50 per year (six issues) or $0.60 per issue; *Reactor Technology* at $3.00 per year (four issues) or $0.75 per issue; *Isotopes and Radiation Technology* at $2.50 per year (four issues) or $0.70 per issue.

POSTAGE: Postpaid within the United States, Canada, Mexico, and all Central and South American countries except Argentina, Brazil, Guyana, French Guiana, Surinam, and British Honduras. For these Central and South American countries and all other countries: add, for each annual subscription, $1.00 for *Nuclear Safety* and $0.75 for each of the other journals; for single issues, add one-fourth of the single-issue price.

REMITTANCE: Payment should be by check, money order, or document coupons and MUST accompany order. Remittances from foreign countries should be made by international money order or draft on an American bank payable to the Superintendent of Documents or by UNESCO book coupons.

XUM

XUM